British Journal of Pharmacology

September 1993

Volume 110 Number 1 pages 1–506

Br. J. Pharmacol. (1993), **110**, 3–17

THIRTEENTH GADDUM MEMORIAL LECTURE

ST GEORGE'S HOSPITAL MEDICAL SCHOOL, LONDON

DECEMBER 1990

Neuronal and endothelium-derived mediators in the modulation of the gastric microcirculation: integrity in the balance

Brendan J.R. Whittle

Department of Pharmacology, Wellcome Research Laboratories, Langley Court, Beckenham, Kent BR3 3BS

Keywords: Microcirculation; noradrenaline; neuropeptide Y; sensory neuropeptides; calcitonin gene-related peptide; endothelial-derived mediators; endothelin; nitric oxide; prostacyclin

Introduction

J.H. Gaddum began his long and most productive career in pharmacology in 1925, when he joined the Wellcome Research Laboratories in Beckenham, under the guidance of J.W. Trevan. It was here that he was exposed to problems in bioassay, the generation of quantitative data and its subsequent mathematical and statistical evaluation. Three years later, when he joined Sir Henry Dale at the National Institute of Medial Research in Hampstead, he retained his enthusiasm for such analytical pharmacology, while developing interests in many other areas including peripheral neuronal regulatory mechanisms and the production and actions of novel local mediators.

Of particular relevance to the theme of this review was his detection in 1931, along with U.S. von Euler, of an unknown depressor substance in extracts of various tissues, particularly the brain and intestine (Euler & Gaddum, 1931). This factor, which they called substance P, for no better reason than this was the letter on the label used on the original standard preparations of the extracts, was more fully characterized in collaboration with H.O. Schild (Gaddum & Schild, 1934). These studies by Gaddum thus initiated the field of pharmacological study on sensory neuropeptides. Only more recently, however, has there been appropriately detailed research on the actions and role of this diverse group of peptides with potent biological properties. As will be discussed later, the sensory neuropeptide, calcitonin gene-related peptide (CGRP), plays an important role in the regulation of gastric mucosal integrity, interacting with other local mediators.

During his time at the College of the Pharmaceutical Society in Bloomsbury, Gaddum also developed and refined techniques to determine the release of neurotransmitters into the perfused vasculature of isolated tissues (Gaddum *et al.*, 1939). It is therefore fitting, in view of his interest in neuronal modulatory processes and the release of local mediators, to describe in this Thirteenth Gaddum Memorial Lecture, our current understanding of the mechanisms that regulate microvascular blood flow in the gastric mucosa. It will become apparent that local neuronal and endothelium-derived factors that affect the microcirculation have a crucial influence on the processes that allow the gastric mucosa to fulfil its secretory function and to resist the continual onslaught of aggressive agents including physiological concentrations of luminal acid, pepsin and bile, and the ingestion of irritants such as ethanol and spicy foods.

The review is based on the Thirteenth Gaddum Memorial Lecture, given by the author at the meeting of the British Pharmacological Society at St. George's Hospital Medical School, London, December 1990

Importance of the gastric microcirculation

The stomach, like all organs in the body, requires an adequate blood flow to maintain its structural and cellular integrity and to conduct its physiological functions. Indeed, because of the extensive metabolic requirements for the elaboration and secretion of hydrogen ions from the parietal cell, gastric mucosal blood flow can be a prime factor in the regulation of gastric secretion. Early studies using aminopyrine or aniline clearance techniques in the dog, cat and rat suggested a close correlation between acid output and mucosal blood flow during stimulation with histamine or pentagastrin (Jacobson *et al.*, 1966; Harper *et al.*, 1968; Main & Whittle, 1973; Kauffman, 1982; Guth & Leung 1987).

It is now known, however, that the clearance of weak bases is not an accurate index of mucosal blood flow under secretory conditions. Using the well-validated hydrogen gas clearance technique in more recent studies, increases in mucosal blood flow were also observed in the rat during stimulation of acid secretion by pentagastrin infusion (Murakami *et al.*, 1982; Leung *et al.*, 1984; Pique *et al.*, 1992a). Furthermore, using both direct visualization of rat submucosal vessels and laser Doppler flowmetry, pentagastrin-stimulated acid secretion was associated with an increase in microvascular perfusion, although a direct correlation between these parameters was not observed (Holm-Rutili & Berglindh, 1986). However, when hydrogen gas clearance was used to determine rat mucosal blood flow, a significant correlation with acid output during pentagastrin stimulation was obtained by others (Pique *et al.*, 1988).

These discrepancies in the degree of mucosal hyperaemia may reflect not only differences in the techniques used to determine blood flow, but also the possibility that different rates of oxygen extraction from the mucosal blood supply may operate under different experimental conditions (Perry *et al.*, 1983). Hence the need for an equivalent degree of local vasodilatation to support active acid secretion under different conditions may not be essential. Apart from the possible local generation of vasoactive waste products of parietal cell stimulation, these local vasodilator responses following

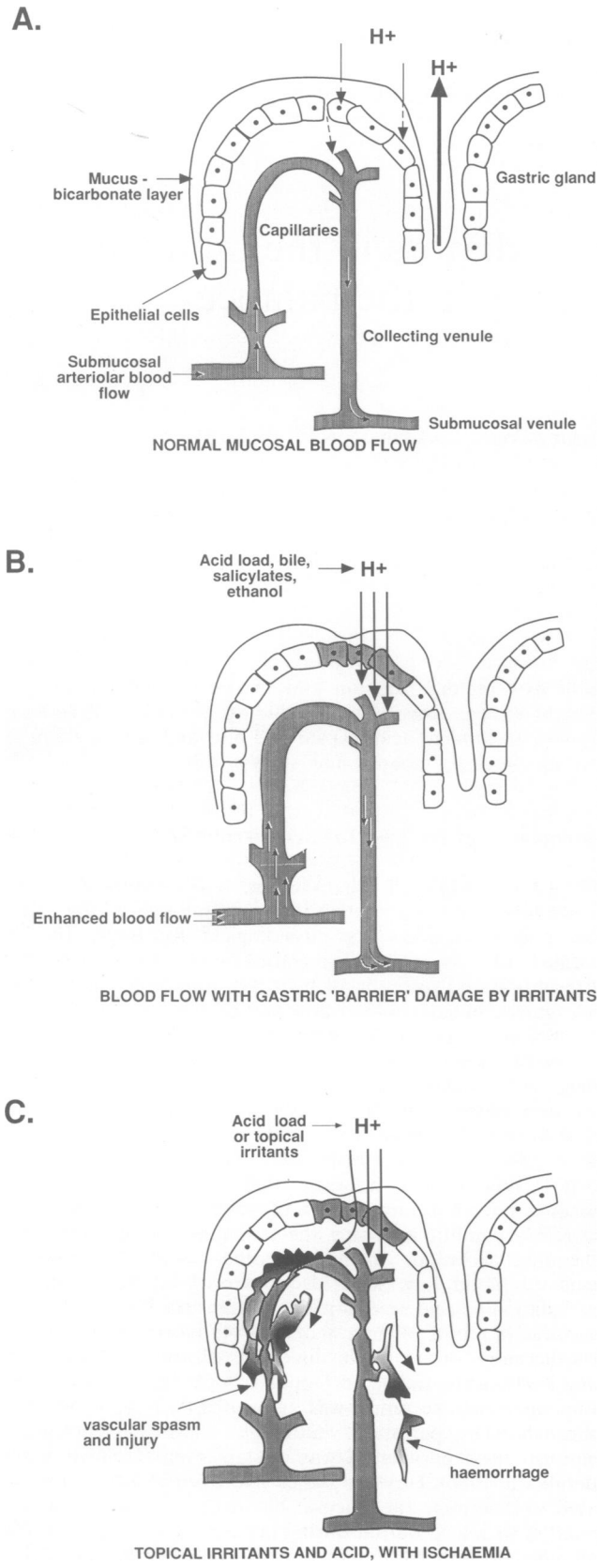

Figure 1 Role of the gastric mucosal microcirculation in removing hydrogen ions that have back-diffused into the mucosal tissue. (A) Under physiological conditions, blood flow will wash out any such hydrogen ions. (B) Following an acid load or topical damage to the, apical mucosa by irritants, the excess intra-mucosal hydrogen ions are removed by an augmented blood flow. (C) Limitation of this blood flow response by vasoconstrictors and ischaemia leads to intramucosal accumulation of acid, provoking haemorrhage and tissue necrosis.

secretory stimulation may reflect the release of vasoactive substances into the microcirculation. Early studies had suggested the involvement of local prostaglandins (Main & Whittle, 1973; 1975) and more recently, adenosine (Gerber & Guth, 1989), but the pharmacological evidence for these substances in secretory vasodilatation cannot now be considered compelling. Thus, the identity of this local vasodilator mediator has remained under investigation up to the present time (Walder *et al.*, 1990; Pique *et al.*, 1992a).

Protective role of mucosal blood flow

An adequate blood flow is also essential for gastric mucosal tissue to withstand the challenge of both endogenous and exogenous aggressors. Thus, blood flow, by providing tissue oxygenation and nutrient delivery, will act to enhance the mucosal defence mechanisms, while an inappropriate reduction in blood flow will lead to mucosal injury or make the tissue more susceptible to damage (Figure 1). Indeed, local ischaemia has consistently been proposed over the past 100 years as a mechanism underlying various forms of gastric damage, ranging from acute gastric erosions to chronic peptic ulceration. The mechanisms by which mucosal blood flow is regulated thus assume significant importance in considering most aspects of the physiology and pathophysiology of the stomach.

An important factor in the relationship between mucosal blood flow, tissue integrity and mucosal defence is the maintenance of intramucosal acid-base neutrality (Kivilaakso *et al.*, 1978). When the mucosal epithelial cell layer is undamaged, only minimal levels of the hydrogen ions that have been actively secreted into the lumen, will diffuse back into the gastric tissue. Under conditions where acidity in the lumen is pH 2 or above, the secretion of bicarbonate and mucus from surface epithelial cells will form an unstirred layer capable of adequately buffering such acid back-diffusion (Allen & Garner, 1980; Flemstrom, 1987). Any remaining hydrogen ions that gain entry into the tissue will be buffered by the bicarbonate derived from the blood or from the alkaline tide generated by parietal cells activity, as well as being removed by microcirculation (Figure 1).

Limitation of mucosal blood flow will, therefore, allow the intramucosal accumulation of hydrogen ions by reducing both their neutralisation and their washout. Should the intramucosal pH drop significantly, then cellular damage will rapidly ensue, either as a direct consequence of the acidic environment of by the subsequent release of tissue-damaging mediators (Figure 1). This situation is exacerbated by high intragastric acid concentrations (an acid load) or following luminal application of weak irritants such as bile salts, ethanol or salicylates, the so-called 'barrier breakers', which disrupt the continuity of surface epithelial cells and enhance back diffusion of acid into mucosal tissue. These latter events may not necessarily lead to deep necrotic damage in the mucosa if there is adequate blood flow to allow buffering and washout of the hydrogen ions (Figure 1). Indeed, many studies show that a hyperaemic response can be provoked by such irritation, perhaps a reflection of a pathophysiological defence mechanism that involves the release of local vasodilator mediators and neuronal pathways (Ritchie, 1975; Whittle, 1977; Druggeman *et al.*, 1979; Holzer *et al.*, 1991a,b; Lippe & Holzer, 1992).

In support of this concept of a protective hyperaemia, are the findings that when the mucosa of rat or dog is exposed to an acidified solution of the mild irritant, taurocholate, limited macroscopic damage can be observed. However, following a reduction in blood flow or concurrent administration of a vasoconstrictor agent such as vasopressin or noradrenaline, deep necrotic damage rapidly occurs (Richie, 1975; Whittle, 1977; 1983). The vasoconstrictor metabolite of arachidonic acid, thromboxane A_2 or its stable epoxy-methano mimetic also potentiates the mucosal injury by acidified bile salts or ethanol in the dog and rat gastric mucosa (Whittle *et al.*,

1981; Esplugues & Whittle, 1988a; Whittle & Esplugues, 1989). In addition, local or systemic infusion of the low molecular weight phospholipid, platelet activating factor (PAF), which reduces mucosal blood flow and causes haemorrhagic erosions in the gastric mucosa (Rosam *et al.*, 1986; Whittle *et al.*, 1986), greatly potentiates mucosal damage brought about by low intraluminal concentrations of ethanol or bile salts (Wallace & Whittle, 1986; Esplugues & Whittle, 1988b). Thus, any limitation of microvascular blood flow can greatly enhance the susceptibility of the mucosa to disruption by topical irritants, as well as itself provoking mucosal injury.

Microvascular ischaemia and injury

Gastric damage which results from inadequate vascular perfusion may reflect the period of relative anoxia and hence disturbances in cell metabolism and integrity. However, such damage may also involve the subsequent local release of tissue-damaging mediators, among which oxygen-derived free radicals are likely candidates (Parks *et al.*, 1982). These highly-labile and reactive moieties have the capacity to disrupt cell membranes by lipid peroxidation of membrane constituents and destroying the interstitial matrix following degradation of collagen and hyaluronic acid (Del Maestro *et al.*, 1980). This cellular injury can induce the further release of endogenous cytotoxic agents, including lysosomal enzymes. Thus, tissue damage may not only occur during the anoxic episode, but appear as subsequent reperfusion injury. Such damage in the stomach following hypovolemic shock is reduced by agents that interfere with free-radical generation, the xanthine oxidase inhibitor, allopurinol, or by free-radical scavengers (Itoh & Guth, 1985).

More direct evidence for the tissue-damaging actions of such oxygen metabolites in gastric tissue has come from studies where local infusion of a superoxide generating system into the rat coeliac artery caused gastric mucosal bleeding, as assessed by the leakage of radiolabelled erythrocytes (Wadhwa & Perry, 1987). Furthermore, local intra-arterial infusion of either hydrogen peroxide, which can form hydroxyl radicals, or a superoxide generating system, induced macroscopically apparent damage in the mucosa, that was attenuated by concurrent administration of catalase or superoxide dismutase, respectively (Esplugues & Whittle, 1989a). In these studies, the initial site of injury was considered to be the microvascular endothelium.

Endothelial cells can regulate mucosal integrity by providing a local diffusion barrier and by the release of factors that interact to modulate tone of the microvascular smooth muscle or affect the processes of cellular adhesion. The role of endothelium-derived mediators in the physiological modulation of mucosal blood flow and integrity in the stomach will therefore be considered further. The influence of neuronally derived vasoactive mediators in the process underlying damage and protection of the gastric mucosa will, however, be initially described.

Neuronal mediators in the gastric mucosa

Noradrenaline and neuropeptide Y

Effects of noradrenaline on gastric blood flow In early studies in cat, intravenous infusion of adrenaline or splanchnic sympathetic stimulation was shown to reduce gastric blood flow (Thompson & Vane, 1953; Reed *et al.*, 1971). Other early studies in the dog demonstrated a reduction in gastric blood flow following parenteral administration of adrenaline or noradrenaline, as determined both by a clearance technique and by electromagnetic flowprobes (Cowley & Code, 1970; Zinner *et al.*, 1975). Likewise, noradrenaline infusion reduced both acid secretion and blood flow in the dog during stimulation with histamine, using venous outflow determinations (Cumming *et al.*, 1963), electromagnetic flowmeters (Nicoloff *et al.*, 1964) and a clearance technique (Jacobson, 1970). This reduction in blood flow by noradrenaline appeared to limit the secretory process rather than to be secondary to the reduction in functional vasodilator drive. Both total gastric and mucosal blood flow were reduced by intravenous administration of noradrenaline in the dog stomach (Varro *et al.*, 1978), while in the gastric chamber preparation of dog stomach *in situ*, noradrenaline increased vascular perfusion pressure, indicating vasoconstriction (Kauffman & Whittle, 1982). Similarly, in the isolated perfused vasculature of the rat and rabbit stomach, vasoconstrictor actions of noradrenaline were also demonstrated (Salvati & Whittle, 1981).

The vasoconstrictor activity of noradrenaline has been observed directly using *in vivo* microscopy techniques in the rat following topical application to the exposed gastric submucosal microvessels (Guth & Smith, 1975a,b; Oren-Wolman & Guth, 1984). More recently, locally infused noradrenaline was shown to induce a dose-dependent reduction in rat gastric mucosal blood flow determined by laser Doppler flowmetry (Tepperman & Whittle, 1991). Submucosal injection of adrenaline, or its application directly to the exposed rat gastric submucosal vessels also reduced laser Doppler flow (Chung *et al.*, 1990; Leung, 1992).

Effects of neuropeptide Y and related peptides In addition to the classical neurotransmitters, sympathetic neurones can synthesize biologically active peptides including the 36 residue vasoconstrictor, neuropeptide Y (NPY; Lundberg & Tatemoto, 1982). NPY has been identified in postganglionic nerves supplying arteries and veins, co-existing with noradrenaline, both being released by sympathetic stimulation (Sundler *et al.*, 1983; Lundberg *et al.*, 1984). In the gastrointestinal tract, NPY-like immunoreactivity has been found in sympathetic nerves associated with blood vessels (Lee *et al.*, 1985; Ekblad *et al.*, 1985) and in enteric neurones originating from the myenteric and submucosal plexus (Furness *et al.*, 1983; Lee *et al.*, 1985; Su *et al.*, 1987). In addition, peptides that are structurally similar to NPY, including pancreatic polypeptide (PP) and polypeptide YY (PYY), are also found in the gut, although primarily in endocrine cells (Lundberg *et al.*, 1982; El-Salhy *et al.*, 1983).

Investigations on the possible physiological role of NPY in the gastro-intestinal tract have included studies on its effects on non-vascular smooth muscle tone (Allen *et al.*, 1987; Hellstrom, 1987; Holzer *et al.*, 1987) and intestinal ion and water transport (Saria & Beubler, 1985). Systemic administration of NPY stimulates duodenal alkaline secretion, through vagal non-cholinergic neuronal mechanisms (Pascaud *et al.*, 1993). The release of immunoreactive-NPY from the rat isolated stomach can be provoked by acetylcholine, probably through nicotinic-receptor stimulation of intrinsic ganglia (McIntosh *et al.*, 1992), while intracerebroventricular administration of NPY stimulated both gastric acid and pepsin secretion through a vagally mediated process (Matsuda *et al.*, 1991). By contrast, injection of NPY into the rat hypothalamic paraventricular nucleus inhibited acid secretion through a mechanism involving the suppression of vagal cholinergic tone following activation of α_2-adrenoceptors, but did not affect gastric mucosal blood flow (Humphreys *et al.*, 1992).

NPY induces vasoconstriction in the vascular beds of the spleen and large and small intestine (Lundberg *et al.*, 1982; Hellstrom, 1987; Westfall *et al.*, 1987; MacLean & Hiley, 1990; Sheikh, 1991). In addition, local intra-arterial infusion of NPY has been shown to reduce rat gastric mucosal blood flow, as determined by laser Doppler flowmetry (Tepperman & Whittle, 1991). Although the structurally related peptide, PP and PYY were effective vasoconstrictors in the cat submandibular gland (Lundberg & Tatemoto, 1982), PYY produced responses as potent but more variable than those to NPY, while PP was minimally active in the rat gastric microcirculation (Tepperman & Whittle, 1991). By contrast, in the

pithed rat, intravenous infusion of NPY elevated blood pressure and induced vasoconstriction in the mesenteric bed, but did not increase vascular resistance in the stomach, as estimated by radiolabelled microspheres (MacLean & Hiley, 1990). The inability of the α_1-adrenoceptor antagonist, prazosin, to overcome the effect of NPY in the gastric circulation (Tepperman & Whittle, 1991) is consistent with other findings in the mesenteric circulation of the rat (Westfall *et al*, 1987), indicating that NPY, like noradrenaline, affects the gastric microcirculation by actions directly on gastric vascular smooth muscle, but through activation of a distinct receptor type.

There is a close anatomical relationship between NPY and noradrenergic neurones in the rat stomach and after treatment with 6-hydroxydopamine to deplete noradrenergic nerves, NPY-containing fibres around blood vessels also disappear (Wang *et al.*, 1987). Although NPY may modulate the actions of noradrenaline by acting either prejunctionally to suppress noradrenaline release or postjunctionally to potentiate the noradrenaline response (Hakanson *et al.*, 1986), this did not occur in the rat gastric microcirculation (Tepperman & Whittle, 1991). Furthermore, unlike its actions on the gastro-epiploic artery, NPY did not potentiate the vasoconstrictor effects of noradrenaline in segments of gastro-epiploic vein (Wahlestedt *et al.*, 1985), nor suppress noradrenaline release (Ekblad *et al.*, 1984). Thus, the nature of the interactions between NPY and noradrenaline in the gut appear to be organ or tissue specific.

Effects of noradrenaline and neuropeptide Y on gastric mucosal integrity Intravenous infusion of noradrenaline for 3 h in the rat potentiated mucosal damage induced by intragastric perfusion of bile salts (Whittle, 1983). In other studies, close-arterial infusion of NPY or noradrenaline for only 10 min, resulted in dose-dependent haemorrhagic damage to the gastric mucosa in the presence of physiological concentrations of luminal acid (Tepperman & Whittle, 1991). As with the microcirculatory actions, the injurious effects of noradrenaline, but not NPY, were inhibited by α_1-adrenoceptor blockade. The substantial vasoconstriction induced by both NPY and noradrenaline is likely to underlie these mucosal injurious actions, which re-inforces the importance of adequate microvascular perfusion even in the absence of local irritants.

It is feasible that elevated levels of noradrenaline following sympathetic stimulation, that could occur under situations of stress, may be associated with any accompanying mucosal injury. In addition, plasma NPY levels are increased after haemorrhagic shock in both rats and pigs (Morris *et al.*, 1987; Lundberg *et al.*, 1987). Since haemorrhagic shock is usually followed by gastric damage and bleeding (Guth & Leung, 1987), the release of NPY may play some role in this type of gastric injury.

Neuronal mechanisms in mucosal vasodilatation and protection

Cholinergic and non-cholinergic processes The direct effects of cholinergic stimulation on the gastric microcirculation may be obscured by concurrent induction of acid secretion and hence an accompanying vasodilatation. However, an increase in mucosal blood flow following vagal stimulation has been observed to precede the secretion of acid, indicating a direct vasodilator action (Martinson, 1965; Guth & Smith, 1975b). The gastric vasodilatation induced by vagal stimulation can be blocked by hexamethonium, and reduced but not abolished by atropine in doses sufficient to abolish the response to acetylcholine (Martinson, 1965; Yano *et al.*, 1983; Kitagawa *et al.*, 1987). This could suggest the release of a vasodilator mediator other than acetylcholine acting on non-muscarinic sites following vagal stimulation.

Local non-adrenergic, non-cholinergic (NANC) neuronal processes within the gastric mucosa modulate its ability to withstand noxious challenge. Thus, local infusion through the left gastric artery of the neurotoxin, tetrodotoxin, which did not itself induce gastric mucosal injury, substantially potentiated the haemorrhagic damage following local administration of PAF (Esplugues *et al.*, 1989). By contrast, pretreatment with atropine or the adrenoreceptor antagonists, phentolamine and propanolol did not augment such mucosal injury, suggesting the involvement of a NANC neuronal pathway (Esplugues & Whittle, 1989b). In further studies, local infusion of tetrodotoxin also potentiated the mucosal injury induced by intra-arterial administration of a vasoconstrictor thromboxane mimetic (Whittle & Esplugues, 1990), as well as that brought about by intragastric application of acidified ethanol (Holzer *et al.*, 1991 a,b), again indicating the involvement of a local neuronal mechanism in the regulation of mucosal integrity.

Sensory neurones The release of vasodilator neuropeptides from afferent sensory neurones, through a local reflex, has been suggested to be a protective mechanism in the gastric mucosa. Much of the early evidence for such a role of sensory neurones came from studies with capsaicin pretreatment (Szolcsanyi & Bartho, 1981; Holzer & Sametz, 1986), a pungent extract of red peppers, (8-methyl-*N*-vanillyl-6-nonenamide), which can deplete primary afferent sensory neurones of their neuropeptide content and cause their functional ablation (Sternini *et al.*, 1987; Green & Dockray, 1988; Holzer, 1991). Thus, capsaicin pretreatment, which itself did not injure the mucosa, enhanced mucosal damage following a number of pro-ulcerogenic procedures including acid distension and pylorus ligation as well as challenge with indomethacin, ethanol and PAF (Szolcsanyi & Bartho, 1981; Holzer & Sametz, 1986; Esplugues *et al.*, 1989; Esplugues & Whittle, 1990).

Another approach to the pharmacological modulation of sensory neuronal activity in the stomach has been the use of opioids. Since the early description of the pro-ulcerogenic potential of morphine (Selye, 1935), administration of opioids, including morphine, has been demonstrated to augment gastric mucosal injury in a variety of experimental models. Thus, relatively low doses of morphine augmented the gastric damage induced by pylorus ligation (Ho *et al.*, 1984) indomethacin administration (Gyires *et al.*, 1985), or restraint stress (Morley *et al.*, 1982; Till *et al.*, 1988). The mechanisms underlying this action of morphine have not been clear and may not be seen in all experimental models. Studies on vascular permeability and analgesia have however suggested that opioids can modulate the activity of primary afferent neurones (Ferreira & Nakamura, 1979; Bartho & Szolcsanyi, 1981; Smith & Buchan, 1984; Lembeck & Donnerer, 1985; Russell *et al.*, 1987). It is therefore feasible that opioids could affect the ability of the mucosa to withstand mucosal injury by exerting a peripheral action on local afferent neuronal mechanisms (Esplugues *et al.*, 1989). Indeed, morphine can augment the gastric mucosal damage and detrimental blood flow changes induced by local infusion of PAF or following challenge with ethanol to a comparable degree as capsaicin pretreatment (Esplugues *et al.*, 1989; Pique *et al.*, 1990; Esplugues & Whittle, 1990). These effects are exerted on peripheral μ-opioid receptors for they were shared by N-methyl morphine that does not penetrate the brain, and were inhibited by administration of naloxone or by the quaternary antagonist, N-methyl nalorphine (Esplugues *et al.*, 1989; Esplugues & Whittle, 1990).

Involvement of calcitonin gene-related peptide The predominant neuropeptide localized by immuno-histochemical techniques in capsaicin-sensitive neurones in the rat stomach is CGRP (Green & Dockray, 1988) and such neurones are found in close proximity to the submucosal microvasculature (Ekblad *et al.*, 1985; Su *et al.*, 1987; Sternini *et al.*, 1987). This neuropeptide occurs principally in the form of α-CGRP

in the sensory neurones innervating gastro-intestinal tissue (Mulderry *et al.*, 1988). Intragastric instillation of capsaicin to stimulate mucosal sensory neurones, induces acute gastric mucosal vasodilatation (Lippe *et al.*, 1989b; Holzer *et al.*, 1990; 1991b; Whittle *et al.*, 1992b). This acute hyperaemia involves the release of CGRP from spinal sensory neurones innervating the gastric mucosa, since it was inhibited by concurrent infusion of the CGRP-receptor antagonist $CGRP_{8-37}$, as well as by selective ablation of pericoeliac nerves by prior application of capsaicin (Li *et al.*, 1991).

Activation of sensory neurones following acid back diffusion induced by intragastric application of acid-ethanol is also considered to be involved in the associated protective increase in gastric mucosal blood flow (Holzer *et al.*, 1991 a,b). This mucosal hyperaemia was not altered by bilateral vagotomy but was abolished by removal of the coeliac-mesenteric ganglionic complex or transection of the greater splanchnic nerves (Holzer & Lippe, 1992). It was also blocked by tetrodotoxin and by morphine administration, as well as by capsaicin desensitization and by local infusion of the antagonist $CGRP_{8-37}$, indicating the involvement of CGRP (Holzer *et al.*, 1991a,b).

Acute mucosal application of capsaicin protected against mucosal damage provoked by ethanol and acid load (Holzer & Lippe, 1988; Holzer *et al.*, 1990; Li *et al.*, 1992). Furthermore, subcutaneous or intra-arterial administration of rat α-CGRP inhibited the gastric injury induced by intragastric instillation of aspirin or ethanol (Maggi *et al.*, 1987; Lippe *et al.*, 1989a). Local infusion of CGRP also prevented the vascular and haemorrhagic injury induced by close-intra-arterial infusion of endothelin-1 (Whittle & Lopez-Belmonte, 1991).

Intravenous infusion of antisecretory doses of rat α-CGRP did not alter rat mucosal blood flow (Leung *et al.*, 1987), whereas intravenous administration of higher doses of CGRP increased blood flow in the rat and rabbit stomach (Dipette *et al.*, 1987; Bauerfeind *et al.*, 1989). Moreover, close-intra-arterial infusion of rat α-CGRP increased resting mucosal blood flow, as determined by hydrogen-gas clearance (Holzer & Guth, 1991; Li *et al.*, 1991) and laser Doppler flowmetry (Whittle *et al.*, 1992b). By contrast, local infusion of the sensory neuropeptides, substance P or neurokinin A, did not elevate resting mucosal blood flow (Holzer & Guth, 1991). Thus, CGRP has the profile of actions compatible with its proposed role as an endogenous vasoactive mediator involved in the regulation of gastric blood flow and integrity.

Endothelium-derived factors – the endothelins

Vascular endothelial cells synthesize a 21-residue peptide known as endothelin-1 (ET-1) which can exert vasoconstrictor actions both *in vitro* and *in vivo* (Yanagisawa *et al.*, 1988; Inoue *et al.*, 1989). Intravenous administration of ET-1 can, however, decrease, increase or exhibit a biphasic action on rat systemic arterial blood pressure depending on the dose used, the level of anaesthesia or the existing blood pressure (Wright & Fozard, 1988; De Nucci *et al.*, 1988; Whittle *et al.*, 1989a,b; Gardiner *et al.*, 1989). Moreover, ET-1 induces the release of prostacyclin and nitric oxide from the vascular endothelium which accounts for the vasodilatation seen in the isolated mesenteric vascular bed (De Nucci *et al.*, 1988). Endothelin-1-like immunoreactivity has been demonstrated in the rat gastric mucosa in both antral and corpus regions (Matsumoto *et al.*, 1989; Takahashi *et al.*, 1990). Much lower levels of immunoreactivity to endothelin-3 (ET-3), which differs from ET-1 by alterations in six amino acids (Inoue *et al.*, 1989) have also been found in the rat stomach (Matsumoto *et al.*, 1989).

Local intra-arterial infusion of picomole quantities of ET-1 induces substantial gastric mucosal vasocongestion and haemorrhagic injury in the rat (Whittle & Esplugues, 1988; Whittle *et al.*, 1989a,b; Whittle & Lopez-Belmonte, 1991). Furthermore, intravenous infusion of ET-1 augments mucosal damage induced by intragastric instillation of ethanol or acid (Wallace *et al.*, 1989a; MacNaughton *et al.*, 1989b; Peskar *et al.*, 1992). ET-1 and ET-3 were equipotent in inducing rat gastric haemorrhage following intravenous infusion (Wallace *et al.*, 1989b). Local intra-arterial infusion of high doses of ET-3 induced vascular lesions in the rat gastric mucosa that involved the venules and capillaries and potentiated the vascular injury induced by acid and ethanol (Morales *et al.*, 1992). Furthermore, an anti-ET-3 serum reduced the extent of mucosal damage induced by intragastric ethanol, suggesting that acute release of endogenous endothelins are involved in such mucosal injury (Morales *et al.*, 1992).

Microcirculatory actions of endothelins

The vasoconstrictor actions of ET-1 have been demonstrated in the perfused vasculature of the rat isolated stomach (Wallace *et al.*, 1989a; Peskar *et al.*, 1992). Furthermore, the vasoconstriction that follows intravascular infusion of ethanol in the rabbit isolated perfused stomach was accompanied by the release of ET-1 into the perfusate, and was inhibited by an anti-ET-1 antibody (Masuda *et al.*, 1992). ET-3 also induced small increases in canine gastric vascular resistance following close-arterial infusion (Wood *et al.*, 1992).

More recently, close intra-arterial infusion of higher doses of ET-1 to the rat stomach *in vivo* has been demonstrated to induce an initial vasodilatation followed by a sustained vasoconstrictor response (Lopez-Belmonte & Whittle, 1993). This vasoconstriction may reflect actions on the ET_A receptor, located on vascular smooth muscle (Arai *et al.*, 1990, Sakurai *et al.*, 1990). By contrast, local infusion of low doses of ET-1 induced only a sustained vasodilatation (Lopez-Belmonte & Whittle, 1993). Whether this reflects a direct vasodilator response through an uncharacterized mechanism, or is the consequence of the release of local vasoactive mediators (De Nucci *et al.*, 1988), perhaps through ET_B receptors located on the vascular endothelium (Masaki *et al.*, 1991) or following endothelial perturbation, will require further evaluation.

Interactions of endothelins in the gastric mucosa

The injurious action of ET-1 on the rat gastric mucosa following its intra-arterial infusion was not inhibited by pretreatment with atropine nor α- and β-adrenoceptor antagonists, indicating no involvement of adrenergic or cholinergic mechanisms (Whittle & Esplugues, 1988). In addition, pretreatment with a 5-lipoxygenase inhibitor had no effect on the mucosal injury, showing that local release of vasoconstrictor leukotrienes (Whittle *et al.*, 1985) did not contribute to the mucosal damage with ET-1 (Whittle & Esplugues, 1988). An increase in PAF formation by the gastric mucosa has been reported to be stimulated by ET-1, along with activation of the fibrinolytic system, while a PAF receptor antagonist attenuated mucosal injury induced ET-1 (Kurose *et al.*, 1992). By contrast, others have found no protection by a PAF receptor antagonist against ET-1 induced mucosal damage (Wallace *et al.*, 1989a). Whether the release of PAF or fibrinolytic activation are secondary responses, perhaps as a consequence of endothelial injury by ET-1, therefore requires consideration.

Inhibition of cyclo-oxygenase by indomethacin augmented the mucosal damage induced by intravenous ET-1 in combination with an acid load or ethanol (MacNaughton *et al.*, 1989b; Wallace *et al.*, 1989a), or following its local infusion (Whittle & Lopez-Belmonte, 1991). Furthermore, capsaicin-pretreatment or morphine administration substantially elevated the mucosal damage provoked by ET-1, while close-arterial infusion of CGRP inhibited the damage (Whittle & Lopez-Belmonte, 1991). These findings suggest an interaction

between the vascular effects of ET-1 and those of sensory neuropeptides and prostaglandins (Figure 2) . This certainly would be applicable under conditions where ET-1 induces mucosal damage through its vasoconstrictor actions, which would be thus offset by the vasodilator actions of endogenous CGRP or prostacyclin released under physiological conditions or in response to ET-1.

Such interactions occur in other microvascular beds, for intravenous infusion of CGRP can reverse the vasoconstrictor action of ET-1 on the rat internal carotid vasculature (Gardiner *et al.*, 1990a), and local CGRP administration reduces the vasoconstriction induced by ET-1 in rabbit skin (Brain *et al.*, 1988). Furthermore, it is of interest that ET-1 can be localized using *in situ* hybridization and immunostaining techniques in both sensory and motor neurones and dorsal root ganglia from human spinal tissue, and can coexist with CGRP and substance P (Giaid *et al.*, 1989). In addition, ET-1 induces depolarization of rat spinal neurones *in vitro*, which can be inhibited by a substance P antagonist (Yoshizawa *et al.*, 1989). These findings may indicate an interaction between ET-1 and such neuropeptides in the modulation of sensory neuronal function.

More recently, however, it has been found that local infusion of low doses of ET-1, that only induce vasodilatation in the gastric microcirculation, can provoke substantial mucosal injury. This hyperaemia may be the consequence of initial damage to the endothelium, since concurrent local infusion of vasodilator doses of CGRP that inhibited mucosal damage paradoxically suppressed the mucosal hyperaemia (Lopez-Belmonte & Whittle, 1993). It would therefore appear that the interactions between ET-1 and CGRP in the mucosal microcirculation are not simply due to opposing vasoactive properties, but may also reflect more-complex events, perhaps involving the release of local mediators and actions on the continuity of the vascular endothelium.

Prostacyclin

The synthesis of the labile vasodilator cyclo-oxygenase product, prostacyclin (PGI_2), from the fatty acid precursor, arachidonic acid, was originally identified in endothelial cells

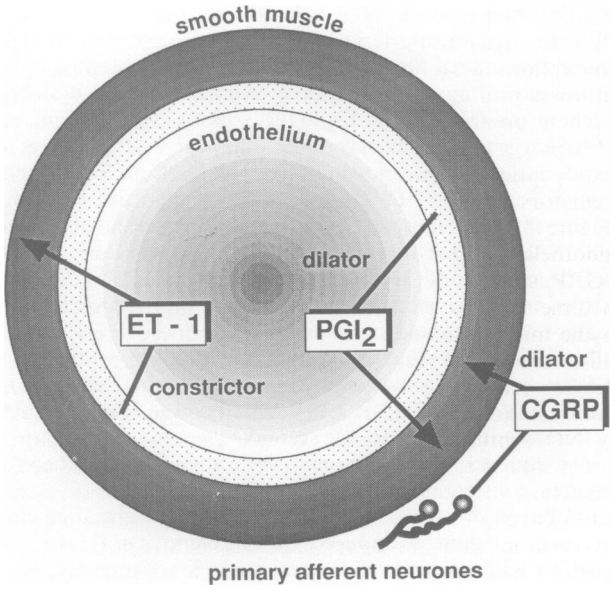

Figure 2 Interactions of the endothelium-derived mediators, endothelin-1 (ET-1) and prostacyclin (PGI_2) and the sensory neuropeptide, calcitonin-gene-related peptide (CGRP) in the mucosal microcirculation. Attenuation of the synthesis or release of the vasodilator mediators, prostacyclin and CGRP respectively, augments ET-1 induced mucosal injury.

(Moncada *et al.*, 1976; Moncada & Vane, 1979). Its formation can be detected in gastric mucosal tissue using bioassay or radioimmunoassay techniques and is inhibited both *in vitro* and *in vivo* by non-steroid anti-inflammatory drugs such as aspirin and indomethacin (Whittle *et al.*, 1980; Whittle & Vane, 1987). Such actions on prostanoid synthesis are likely to contribute to the complex multifactorial mechanisms that underlie the gastric mucosal injury induced by these agents (Whittle *et al.*, 1980; Whittle, 1992).

Prostacyclin can inhibit gastric acid secretion in a number of experimental preparations (Whittle *et al.*, 1978; Gerkens *et al.*, 1978; Kauffman *et al.*, 1979a; Konturek *et al.*, 1980; Whittle, 1981; Shea-Donohue *et al.*, 1982) and can stimulate the secretion of bicarbonate, a luminal protective factor (Whittle *et al.*, 1984). Prostacyclin and its more-stable analogues, like other prostanoids particularly of the E series (Robert *et al.*, 1979), exert potent protective actions against gastric mucosal damage in a number of experimental models (Whittle *et al.*, 1978; Whittle & Boughton-Smith, 1979; Kauffman *et al.*, 1979b; Konturek *et al.*, 1981; 1984).

Effects on the gastric microcirculation

Under resting conditions, intravenous infusion of prostacyclin elevated basal mucosal blood flow (estimated using clearance techniques) in the rat and dog (Whittle *et al.*, 1978; Konturek *et al.*, 1980; Walus *et al.*, 1980). Using radiolabelled microspheres in the dog, infusion of low doses of prostacyclin into the left atrium or directly into the gastric artery increased blood flow in fundic and antral mucosa, (Gerber & Nies, 1982; Einzig *et al.*, 1980), as also found following intravenous infusion in the pig (Gaskill *et al.*, 1982). During partial inhibition of gastric acid secretion induced by prostacyclin in the rat, mucosal blood flow, estimated by a clearance technique, was elevated, whereas at higher doses mucosal blood flow fell, presumably as a consequence of reduced functional vasodilator drive following the substantial secretory inhibition (Whittle *et al.*, 1978). In the dog, acid inhibition by prostacyclin was also accompanied by a fall in mucosal blood flow, but the ratio of these parameters remained unaltered indicating that the vascular changes were secondary to the secretory events (Kauffman *et al.*, 1979a).

Under basal conditions, prostacyclin was a potent vasodilator in the blood-perfused canine gastric circulation *in situ* following close-arterial infusion or bolus injection (Gerkens *et al.*, 1978; Walus *et al.*, 1980; Kauffman & Whittle, 1982) and in the gastric circulation of the isolated stomach of rat and rabbit (Salvati & Whittle, 1981). The stable analogues, 6β-PGI_1 and the 16-phenoxy derivative of prostacyclin, increased the ratio of blood flow to acid output during intravenous infusion of antisecretory doses in the conscious dog (Kauffman *et al.*, 1979b). Both 6β-PGI_1, and carbacyclin also reduced gastric vascular resistance in the dog stomach following intra-arterial injection (Kauffman & Whittle, 1982). Whereas the breakdown product 6-oxo-$PGF_{1\alpha}$ had little effect on gastric mucosal blood flow or vascular resistance, the putative prostacyclin metabolite 6-oxo-PGE_1 was some three to four times less active than prostacyclin as a vasodilator in the dog gastric circulation *in situ* and in the perfused gastric vasculature of rat and rabbit *in vitro* (Kauffman & Whittle, 1982; Salvati & Whittle, 1981).

Increases in local blood flow by prostacyclin would be beneficial in maintaining the functional integrity of gastric tissue and defence mechanisms, especially under conditions of relative ischaemia in the mucosa (Whittle & Vane, 1987). Although net vasodilatation would contribute to the protective actions of the prostaglandins, more local changes in microcirculation may be of greater significance. Studies on mucosal injury and ulceration have pointed to the microvascular endothelium as an initial site of damage resulting from application of the irritant, ethanol (Guth *et al.*, 1984; Szabo *et al.*, 1985; Oates & Hakkinen, 1988). Following challenge

with irritant agents, vascular engorgement can be observed, which is correlated with the stasis of blood flow within the microcirculation. Such microvascular stasis can lead to areas of deep necrosis, a predominant histological characteristic of this damage. Pretreatment with anti-ulcer prostaglandins prevents this microcirculatory stasis and the subsequent development of necrotic lesions (Guth *et al.*, 1984; Pihan *et al.*, 1986). Protection of the gastric microvasculature, either by direct actions on endothelial cell integrity or by the prevention of the release of vasoconstrictor or cytotoxic mediators (Whittle *et al.*, 1985; Boughton-Smith & Whittle, 1988) may, therefore, be an important mechanism that underlies the so-called cytoprotective actions of prostacyclin and other prostanoids.

Nitric oxide

Endothelial cells also release another highly labile humoral vasodilator substance, originally known as endothelium-derived relaxing factor (EDRF), that mediates the vascular relaxation induced by agents such as acetylcholine and bradykinin (Furchgott & Zawadzki 1980; Furchgott, 1984). The release of an endothelium-derived factor in the gastric microcirculation was considered to underlie the vasodilatation induced by local administration of acetylcholine and by vagal stimulation (Kitagawa *et al.*, 1987). It is now known that nitric oxide (NO), accounts for the biological properties of EDRF (Palmer *et al.*, 1987; 1988a; Khan & Furchgott, 1987; Ignarro *et al.*, 1987; Kelm *et al.*, 1988).

NO synthase generates NO from the terminal guanidino nitrogen atoms of L-arginine, through a process where molecular oxygen is also incorporated (Palmer *et al.*, 1988b; Palmer & Moncada, 1989; Leone *et al.*, 1991). The constitutively expressed NO synthase enzyme is calcium-, calmodulin- and NADPH-dependent (Moncada *et al.*, 1991), and has been demonstrated in rat whole stomach and gastric mucosa (Salter *et al.*, 1991; Whittle *et al.*, 1992a). In a study on the cellular distribution of NO synthase in the rat gastric mucosa, epithelial cells separated by elutriation exhibited high levels of constitutive enzyme activity (Brown *et al.*, 1992b). This localization of NO synthase may reflect a non-vascular role for NO in the modulation of mucus or bicarbonate secretion from these cells, which, as in vascular tissue (Gruetter *et al.*, 1979; Moncada *et al.*, 1991) may involve activation of guanylate cyclase and elevation of cyclic GMP. Indeed, application of NO donors or dibutyryl cyclic GMP to the rat gastric mucosa *in vivo* can increase mucus thickness, and these agents can stimulate mucus output from gastric epithelial cells *in vitro* (Brown *et al.*, 1992a; 1993).

The formation of NO is inhibited by L-arginine analogues such as N^G-monomethyl-L-arginine (L-NMMA), as demonstrated in studies *in vitro* on vascular tissue (Palmer *et al.*, 1988b; Rees *et al.*, 1989b). In the rabbit, rat and guinea-pig, L-NMMA increased systemic arterial blood pressure, an effect reversed by L-arginine but not the enantiomer, D-arginine, suggesting that endogenous NO biosynthesis from L-arginine can modulate resting vascular tone *in vivo* (Rees *et al.*, 1989a; Whittle *et al.*, 1989a; Aisaka *et al.*, 1989; Gardiner *et al.*, 1990b). Local infusion of L-NMMA also increased peripheral vascular tone in man (Vallance *et al.*, 1989), while studies with other L-arginine analogues that inhibit NO biosynthesis, such as the more potent N^G-nitro-L-arginine methyl ester (L-NAME) have confirmed the importance of NO in the regulation of systemic arterial blood pressure (Rees *et al.*, 1990).

Effect on the gastric microcirculation

Intravenous administration of L-NMMA dose-dependently reduced resting gastric mucosal blood flow, determined by hydrogen gas clearance (Pique *et al.*, 1989). These effects were not shared by D-NMMA, while L-arginine but not D-arginine reversed these actions. Subsequently, using laser Doppler flowmetry and hydrogen gas clearance, both L-NMMA and L-NAME have been shown to reduce resting mucosal blood flow, confirming the involvement of NO in the regulation of microvascular blood flow (Tepperman & Whittle, 1992; Lippe & Holzer, 1992).

The mucosal hyperaemia induced by intravenous infusion of pentagastrin was attenuated by concurrent infusion of L-NMMA or L-NAME (Walder *et al.*, 1990; Pique *et al.*, 1992a). Pretreatment with low doses of L-NMMA reduced the elevation of mucosal blood flow but had no significant effect on the plateau rates of acid secretion induced by pentagastrin, thus indicating an effect on the microcirculation independent of secretory modulation (Pique *et al.*, 1992a). These findings indicate that NO is a prime mediator of the blood flow changes associated with acid secretion, whereas inhibition of NO biosynthesis appeared to have no direct acute effect on the stimulation of acid secretion. Recent studies, have, however demonstrated the involvement of NO in the process by which acute administration of endotoxin or the cytokine, interleukin 1α can inhibit acid secretion, perhaps through modulation of a neuronal pathway (Martinez-Cuesta *et al.*, 1992; Esplugues *et al.*, 1993a,b).

NO is involved in the gastric mucosal hyperaemia that follows acute normovolemic anaemia induced by haemodilution (Panes *et al.*, 1992). Furthermore, it is possible that excessive NO synthesis contributes to the hyperdynamic splanchnic circulation, including the gastric vasodilatation, observed in portal hypertensive and cirrhotic rats (Pizcueta *et al.*, 1992a,b; Pique *et al.*, 1992b). NO also mediates the gastric mucosal hyperaemia that is associated with renal failure (Quintero & Guth, 1992a,b).

Interactions of NO in the gastric mucosa

Interactions in the microcirculation

Interactions between NO and CGRP in the microvasculature are evident, since chronic capsaicin treatment greatly augments the fall in mucosal blood flow induced by L-NMMA and L-NAME (Tepperman & Whittle, 1992). Furthermore, the acute increase in mucosal blood flow following instillation of capsaicin directly into the gastric lumen, is abolished by concurrent administration of L-NAME (Whittle *et al.*, 1992b). Both NO and CGRP also appear to be involved in the processes underlying the mucosal vasodilatation following sensory nerve activation through acid back-diffusion into the mucosal tissue (Lippe & Holzer, 1992).

These observations may reflect physiological interactions, perhaps of a synergistic nature, between NO and sensory neuropeptides in the modulation of microvascular tone, both mediators acting directly to relax the vascular smooth muscle (Figure 3). There could also be a partial dependence upon endothelial NO for the vascular relaxation induced by CGRP, since CGRP is an endothelium-dependent vasodilator in some vascular beds (Brain *et al.*, 1985). For this to occur in the microcirculation, it would be necessary for CGRP to diffuse from neurones surrounding the vascular smooth muscle to reach the endothelium. However, the mucosal vasodilatation induced by CGRP is only partially attenuated by NO synthase inhibitors (Whittle *et al.*, 1992). Alternatively, like its involvement in NANC neuronally-evoked relaxation of the stomach musculature (Li & Rand, 1990; Boeckxstaens *et al.*, 1991; Desai *et al.*, 1991), NO may be involved in local vascular neuromodulator processes. NO synthase has been detected in neuronal cell bodies and nerve fibres in the myenteric plexus using immunohistochemical techniques (Bredt *et al.*, 1990) and it is possible that NO released from sensory neurones in the stomach could directly relax vascular smooth muscle. One stage in the events leading to neuronal NO biosynthesis and release could be the influx or intracellular mobilization of calcium, as it has been shown

that brain NO synthase can be activated by submicromolar concentrations of calcium (Knowles *et al.*, 1989). NO could also be involved in modulating the activity of sensory neurones or the release of neuropeptides (Figure 3).

Interactions modulating mucosal integrity

In studies on the interactions of local mediators with endogenous NO, administration of L-NMMA induced acute gastric mucosal injury in rats pretreated with indomethacin, using doses of either agent that themselves did not provoke acute mucosal injury. L-NMMA also induced extensive haemorrhagic mucosal injury in rats chronically pretreated with capsaicin. Furthermore, L-NMMA induced deep haemorrhagic necrosis involving virtually all of the mucosal area in rats pretreated concurrently with both indomethacin and capsaicin (Whittle *et al.*, 1990). Such findings indicate a critical interaction between endogenous NO, sensory neuropeptides and prostanoids, all of which appear to subserve a modulator function in the regulation of gastric mucosal integrity (Figure 4). These mediators, which have distinct biochemical origins, may not only exert local vasodilator actions on the microcirculation essential for adequate microvascular blood flow under physiological conditions, but may act to enhance or preserve endothelial cells function and continuity, especially under conditions of challenge.

Capsaicin pretreatment or morphine administration attenuates the protective properties of PGE_2 and its 16, 16-dimethyl analogue against acute gastric challenge, suggesting a permissive role for sensory neuropeptides in the mechanisms of protection by prostanoids (Esplugues & Whittle, 1991; Esplugues *et al.*, 1992). Furthermore, the mucosal injury induced by indomethacin is augmented in capsaicin-pretreated rats, again reflecting interactions between endogenous protective sensory neuropeptides and prostanoids (Holzer & Sametz, 1986; Whittle *et al.*, 1990). However, the mucosal protective actions of a PGE_2 analogue against ethanol-induced injury do not appear to depend on endogenous NO, since they were not inhibited by N^G-nitro-L-arginine (Konturek *et al.*, 1992). By contrast, the protection against ethanol-induced injury by

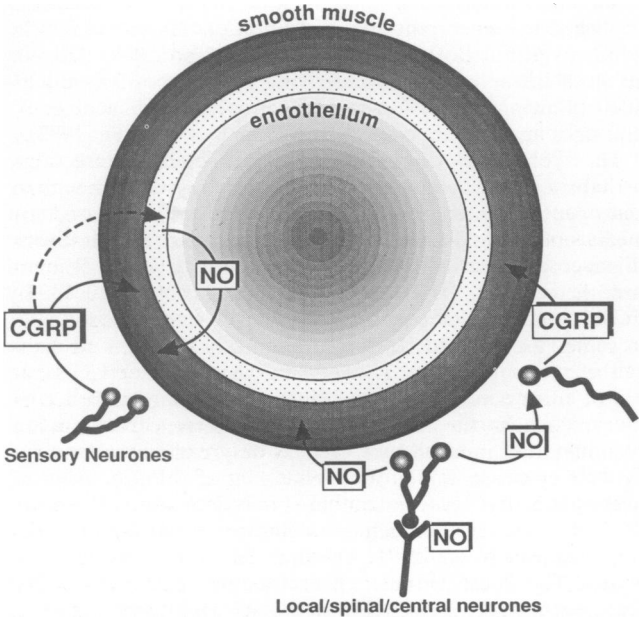

Figure 3 Possible neuronal and vascular interactions between nitric oxide (NO) and calcitonin-gene-related peptide (CGRP) in the modulation of the gastric microcirculation. These mediators may interact not only to affect directly the tone of vascular smooth muscle, but NO may be involved in neuromodulation and the release of the neuropeptide.

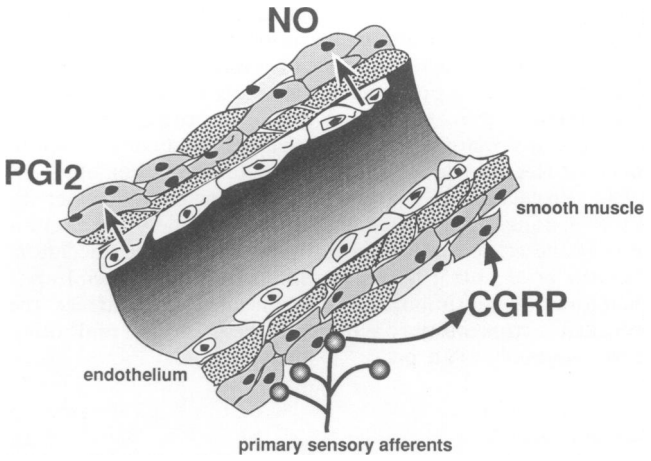

Figure 4 Local mediators, nitric oxide (NO), prostacyclin (PGI_2) and calcitonin gene-related peptide (CGRP) within the gastric mucosal microcirculation contribute through local vasoactive effects and actions on the endothelium, to the regulation of mucosal integrity.

acute intraluminal instillation of capsaicin, is attenuated by N^G-nitro-L-arginine (Peskar *et al.*, 1991), again implying interactions between endogenous neuropeptides and NO in the mechanisms subserving mucosal protection.

NO and the enzymes that form prostacyclin are highly susceptible to attack by free radicals (Moncada & Vane, 1979; Gryglewski *et al.*, 1986; Rubanyi & Vanhoutte, 1986) and interference with the actions of these mediators may be involved in the microvascular injury seen following local release of free radicals. It is pertinent that neutrophils play a role in the genesis of gastric injury, such as that induced by PAF, ischaemia, ethanol or non-steroid anti-inflammatory agents (Smith *et al.*, 1987; Kvietys *et al.*, 1990; Kubes *et al.*, 1990; Wallace *et al.*, 1991). Thus, free radical release from such leukocytes following adhesion to the endothelium may contribute to the microvascular injury by affecting the formation and stability of these endothelial cell mediators. Furthermore, inhibition of NO biosynthesis can promote neutrophil adherence and permeability changes in microvascular endothelium, as demonstrated in the cat mesentery (Kubes *et al.*, 1991; Kubes & Granger, 1992). A reduction in NO formation or its inactivation by free radicals in both endothelial cells and neutrophils (McCall *et al.*, 1989) may therefore serve to initiate or to amplify endothelial injury. Such effects may contribute to the mechanism by which L-NMMA can elevate the intestinal vascular permeability changes seen in acute endotoxin shock that follows the rapid release of PAF and thromboxane (Hutcheson *et al.*, 1990; Boughton-Smith *et al.*, 1990) and indicates a role for constitutive NO in modulating this acute inflammatory response.

Protection and damage by NO in the microvasculature

The release of NO from nitrovasodilator agents either following metabolic transformation as with glyceryl trinitrate and isoamyl nitrite, or spontaneously as with nitroprusside, is responsible for their ability to activate guanylate cyclase, elevate cyclic GMP and relax vascular smooth muscle (Gruetter *et al.*, 1979; Ignarro *et al.*, 1981; Feelisch & Noack, 1987; Feelisch, 1991). Following intragastric application, these nitrovasodilators protect against acute haemorrhagic mucosal injury induced by topical irritants and by intravenous infusion of ET-1 (Kitagawa *et al.*, 1990; MacNaughton *et al.*, 1989a). The nitrosothiol, S-nitroso-*N*-acetyl-penicillamine (SNAP), which spontaneously liberates NO (Ignarro *et al.*, 1981) also protects against acute microvascular injury in the stomach and small intestine induced by endotoxin or PAF (Boughton-Smith *et al.*, 1990; 1992a).

Local administration of glyceryl trinitrate or SNAP in low doses protects the gastric mucosa from damage induced by intra-arterial infusion of ET-1 (Lopez-Belmonte *et al.*, 1993). Such actions of the NO donors could reflect vascular interactions between ET-1 and the locally generated NO in the mucosal microcirculation, on both vascular tone and endothelial integrity. By contrast, mucosal injury was observed after infusion of nitroprusside or higher doses of SNAP, which may indicate cytotoxic actions of high levels of NO on the microvascular endothelium (Lopez-Belmonte *et al.*, 1993). Indeed, the excessive production of NO by an inducible NO synthase in endothelial cells is considered to underlie the reduction in viability of these cells in culture following exposure over a 48 h period to endotoxin and the cytokine, intereferon-α (Palmer *et al.*, 1992), while induction of NO synthesis is also considered to be involved in damage to adenocarcinoma cells (O'Connor & Moncada, 1991) . High concentrations of exogenous NO can suppress prostacyclin synthesis by endothelial cells, which may also reflect cytotoxicity (Doni *et al.*, 1988). In addition, the substantial synthesis of NO by the immunologically-induced NO synthase in macrophages accounts for the cytotoxic actions against tumour cells (Hibbs *et al.*, 1987; 1988; Marletta *et al.*, 1988; Drapier *et al.*, 1988).

Excessive NO production and the induction of NO synthase has been implicated in the cardiovascular crisis and collapse following endotoxaemia in animals and patients (Kilbourn *et al.*, 1990; Thiemermann & Vane, 1990; Fleming *et al.*, 1991; Nava *et al.*, 1991; Petros *et al.*, 1991; Wright *et al.*, 1992). Furthermore, the increase in microvascular permeability, an index of endothelial injury, seen in the rat small and large intestine four to six hours after endotoxin administration is correlated with the corticosteroid-sensitive induction of a calcium-independent NO synthase over this period (Boughton-Smith *et al.*, 1992b). Induction of NO synthase is also associated with inflammation and injury observed in a model of colitis (Boughton-Smith *et al.*, 1992c) and is seen in the inflamed colonic mucosa of patients with ulcerative colitis (Boughton-Smith *et al.*, 1992d). It is feasible that local high concentrations of NO may form tissue destructive species such as hydroxyl moieties derived from the peroxynitrite radical (Beckman *et al.*, 1990) which contribute to the endothelial injury in the microvasculature, leading to mucosal necrosis and ulceration.

A balance of vasoactive factors for mucosal integrity?

The regulation of microvascular tone and integrity is thus of critical importance for the conduct of the physiological responses of the stomach and in the prevention of mucosal injury by both endogenous and exogenous aggressors. Local neuronal activity could provoke the inappropriate release of vasoconstrictor mediators such as noradrenaline or NPY, while stimulation of sensory neurones release the neuropeptide CGRP, involved in protective vasodilatation. Pathological events that enhance the neuronal release of these vasoconstrictor agents, or that depress the release of CGRP and possibly other protective sensory neuropeptides would thus be expected to lead to mucosal injury.

As described, the endothelium is a rich source of local vasoactive mediators capable of modulating tone and integrity in the microcirculation. Thus, the local release of the vasoconstrictor ET-1 may be an initial event in some forms of mucosal injury, or be released as a consequence of endothelial injury, thus augmenting and perpetuating the original insult. Knowledge of the regulatory processes underlying endothelin biosynthesis, and the mechanism of endothelin release in the microcirculation which may only occur under non-physiological conditions, may thus give some indication to its possible involvement in ulcer disease.

Prostacyclin and NO appear to play protective roles within the gastric microcirculation. However, it is apparent that NO may be involved in both physiological and pathological events in the gastric mucosa. Thus, endogenous NO plays an important role in the modulation of mucosal blood flow under resting and stimulated conditions, and has a key interactive role in the regulation of mucosal integrity. However, an excess, unregulated, liberation of NO has also ulcerogenic potential. The factors that regulate the synthesis and release of endogenous NO by the neuronal and endothelial constitutive enzymes, likely to be involved in physiological processes, and by inducible enzymes that may underlie certain pathological events, will thus be of importance to the understanding of tissue integrity. Indeed, it is possible that local toxins produced by the bacterial organism, *Helicobacter pylori* that is implicated in peptic ulceration, could induce an NO synthase in epithelial or other mucosal cells and hence local excess NO or its cytotoxic metabolites may contribute to the mechanisms underlying the associated cellular injury.

A balance between the release or actions of these vasoconstrictor and vasodilator mediators in the microcirculation could be involved in the physiological control of mucosal blood flow, providing a mechanism for the rapid vascular response to the functional needs of the mucosa. The systemic release of vasoactive factors may also influence the tone of the microvasculature. However, it is feasible that the complex interactions between these opposing mediators on vascular tone may only operate to modulate blood flow under conditions of challenge. Furthermore, under physiological conditions, blood flow may be regulated predominantly by only one local vasodilator mediator, with the pharmacological evidence from the use of selective inhibitors being strongest for NO. Interference with NO biosynthesis alone under acute pathological conditions may not, however, be detrimental, since prostacyclin or CGRP can subserve this vasodilator role when necessary. Indeed, inhibition of constitutively formed NO only leads to extensive acute mucosal injury when the synthesis or release of prostanoids and CGRP are concurrently depressed. Alterations in the balance between these vasodilator mediators may thus be implicated in the pathogenesis of peptic ulceration.

A further important physiological role of these mediators may be to preserve endothelial integrity, which in turn could help provide for adequate microvascular blood flow. Indeed, earlier studies had implicated the prevention of microcirculatory injury and stasis as an underlying mechanism of mucosal protection by prostanoids (Guth *et al.*, 1984; Pihan *et al.*, 1986). Moreover, interactions of these diverse local mediators at the level of the endothelial barrier, rather than solely on vascular smooth muscle tone are suggested by analysis of their microcirculatory changes and current actions on mucosal integrity (Whittle & Tepperman, 1991; Tepperman & Whittle, 1992; Lopez-Belmonte & Whittle, 1993). Under conditions of challenge, these endogenous endothelial processes may assume strategic importance in the mechanisms of resistance to mucosal injury. Whereas selective inhibition of either mediator alone does not produce acute mucosal injury, concurrent pharmacological interference with more than one such mediator induces widespread tissue damage (Whittle *et al.*, 1990). An understanding of the properties of these agents that confer endothelial resilience would therefore offer novel approaches to the attenuation of cell injury in the stomach, which could be relevant for other tissues and organs. The interplay between endogenous mediators in the microvasculature in the control of tissue integrity is thus likely to extend beyond influences on local blood flow to encompass even more fundamental regulatory processes at the cellular level.

References

AISAKA, K., GROSS, S.S., GRIFFITH, O.W. & LEVI, R. (1989). N^G-methylarginine, an inhibitor of endothelium-derived nitric oxide synthesis is a potent pressor agent in the guinea-pig: does nitric oxide regulate blood pressure *in vivo*? *Biochem. Biophys. Res. Commun.*, **160,** 881 – 886.

ALLEN, A. & GARNER, A. (1980). Mucus and bicarbonate secretion in the stomach and their possible role in mucosal protection. *Gut*, **21,** 249 – 262.

ALLEN, J.M., HUGHES, J. & BLOOM,S. (1987). Presence, distribution and pharmacological effects of neuropeptide Y in mammalian gastrointestinal tract. *Dig. Dis. Sci.*, **32,** 506 – 512.

ARAI, H., HORI, S., ARAMORI, I., OHKUBO, H. & NAKANISHI, S. (1990). Cloning and expression of a cDNA encoding an endothelin receptor. *Nature*, **348,** 730 – 732.

BARTHO, L. & SZOLCSANYI, J. (1981). Opiate agonists inhibit neurogenic plasma extravasation in the rat. *Eur. J. Pharmacol.*, **73,** 101 – 104.

BAUERFEIND, P., HOF, R., HOF, A., CUCALA, M., SIEFRIST, S., VON RITTER, C., FISCHER, J.A. & BLUM, A.L. (1989). Effects of hCGRP I and II on gastric blood flow and acid secretion in anesthetized rabbits. *Am. J. Physiol.*, **256,** G145 – G149.

BECKMAN, J.S., BECKMAN, T.W., CHEN, J., MARSHALL, P.A. & FREEMAN B.A. (1990). Apparent hydroxyl radical production by peroxynitrite: implications for endothelial injury from nitric oxide and superoxide. *Proc. Natl. Acad. Sci. USA.*, **87,** 1620 – 1624.

BOECKXSTAENS, G.E., PELCKMANS, P.A., BOGERS, J.J., BULT, H., DE MAN, J.G., OSSTERBOSCH, L., HERMAN, A.G. & VAN MAERCKE, Y.M. (1991). Release of nitric oxide upon stimulation of non-adrenergic non-cholinergic nerves in the rat gastric fundus. *J. Pharmacol. Exp. Ther.*, **256,** 441 – 447.

BOUGHTON-SMITH, N.K. & WHITTLE, B.J.R. (1988). Inhibition by 16,16-dimethyl PGE_2 of ethanol-induced gastric mucosal damage and leukotriene B_4 and C_4 formation. *Prostaglandins*, **35,** 945 – 957.

BOUGHTON-SMITH, N.K., DEAKIN, A.M. & WHITTLE, B.J.R. (1992a). Actions of nitric oxide on the acute gastrointestinal damage induced by PAF in the rat. *Agents and Actions*, (Special Conference Issue) ed. Velo, G.P., Whittle, B.J.R., Bray, M.A. C3 – 9.

BOUGHTON-SMITH, N.K., EVANS, S.M., WHITTLE, B.J.R. & MONCADA, S. (1992b). Dexamethasone inhibits endotoxin-induced vascular permeability and nitric oxide synthase in the rat intestine. *Br. J. Pharmacol.*, **107,** 79P.

BOUGHTON-SMITH, N.K., EVANS, S.M., WHITTLE, B.J.R. & MONCADA, S. (1992c) . Induction of colonic nitric oxide synthase in a rat model of colitis. *Gastroenterology*, **102,** A598.

BOUGHTON-SMITH, N.K., EVANS, S.M., COLE, A.T., WHITTLE, B.J.R. & HAWKEY, C.J. (1992d). Increased nitric oxide synthase activity in inflamed colon from ulcerative colitis patients. *Gut*, **33,** S11.

BOUGHTON-SMITH, N.K., HUTCHESON, I., DEAKIN, A.M., WHITTLE, B.J.R. & MONCADA, S. (1990). Protective effect of S-nitroso-N-acetyl-pencillamine in endotoxin-induced acute intestinal damage in the rat. *Eur. J. Pharmacol.*, **191,** 485 – 488.

BRAIN, S.D., TIPPINS, J.R. & WILLIAMS, T.J. (1988). Endothelin induces potent microvascular constriction. *Br. J. Pharmacol.*, **95,** 1005 – 1007.

BRAIN, S.D., WILLIAMS, T.J., TIPPINS, J.R., MORRIS, H.R. & MACINTYRE, I. (1985). Calcitonin gene-related peptide is a potent vasodilator. *Nature*, **313,** 54 – 56.

BREDT, D.S., HWANG, P.M. & SNYDER, S.H. (1990). Localization of nitric oxide synthase indicating a neural role of nitric oxide. *Nature*, **347,** 768 – 770.

BROWN, J.F., HANSON, P.J. & WHITTLE, B.J.R. (1992a). Nitric oxide donors increase mucus gel thickness in rat stomach. *Eur. J. Pharmacol.*, **223,** 103 – 104.

BROWN, J.F., HANSON, P.J. & WHITTLE, B.J.R. (1993). Nitric oxide donors stimulate rat gastric mucus release and epithelial cyclic GMP. *Gastroenterology*, **104,** 47A.

BROWN, J.F., TEPPERMAN, B.L., HANSON, P.J., WHITTLE, B.J.R. & MONCADA, S. (1992b). Differential distribution of nitric oxide synthase between cell fractions isolated from the rat gastric mucosa. *Biochem. Biophys. Res. Commun.*, **184,** 680 – 685.

CHUNG, S.C.S., LEUNG, J.W.C. & LEUNG, F.W. (1990). Effect of submucosal epinephrine injection on local gastric blood flow: a study using laser Doppler flowmetry and reflectance spectrophotometry. *Dig. Dis. Sci.*, **35,** 1008 – 1011.

COWLEY, D.J. & CODE, C.F. (1970). Effects of secretory inhibitors on mucosal blood flow in non-secreting stomach of conscious dogs. *Am. J. Physiol.*, **218,** 270 – 274.

CUMMING, J.D., HAIGH, A.L., HARRIS, E.H.L. & NUTT, M.E. (1963). A study of gastric secretion and blood flow in the anaesthetized dog. *J. Physiol.*, **168,** 219 – 233.

DEL MAESTRO, R., THAW, H.H., BJORK, J., PLANKER, M. & ARFORS, K.-E. (1980). Free radicals as mediators of tissue injury. *Acta. Physiol. Scand.*, **492,** 43 – 57.

DE NUCCI, G., THOMAS, R., D'ORLEANS-JUSTE, P., ANTUNES, E., WALDER, C., WARNER, T.D. & VANE, J.R. (1988). Pressor effects of circulating endothelin are limited by its removal in the pulmonary circulation and by the release of prostacyclin and endothelium-derived relaxing factor. *Proc. Natl. Acad. Sci. USA*, **85,** 9797 – 9800.

DESAI, K.M., SESSA W.C. & VANE, J.R. (1991). Involvement of nitric oxide in the reflex relaxation of the stomach to accommodate food or fluid. *Nature*, **351,** 477 – 479.

DIPETTE, D.J., SCHWARZENBERGER, K., KERR, N. & HOLLAND, O.B. (1987). Systemic and regional hemodynamic effects of calcitonin gene-related peptide. *Hypertension*, **9,** Suppl. III, 142 – 146.

DONI, M.G., WHITTLE, B.J.R., PALMER, R.M.J. & MONCADA, S. (1988). Actions of nitric oxide on the release of prostacyclin from bovine endothelial cells in culture. *Eur. J. Pharmacol.*, **151,** 19 – 25.

DRAPIER, J.-C. & HIBBS, J.B. Jr. (1988). Differentiation of murine macrophages to express non-specific cytotoxicity for tumour cells results in L-arginine-dependent inhibition of mitochondrial iron-sulfur enzymes in the macrophage effector cells. *J. Immunol.*, **140,** 2829 – 2838.

DRUGGEMAN, T.W., WOOD, J.G. & DAVENPORT, H.W. (1979). Local control of blood flow in the dog's stomach. Vasodilatation caused by acid back diffusion following topical application of salicylic acid. *Gastroenterology*, **77,** 736 – 744.

EINZIG, S., RAO, G.H.R. & WHITE J.G. (1980). Differential sensitivity of regional vascular beds in the dog to low-dose prostacyclin infusion. *Can. J. Physiol. Pharmacol.*, **58,** 940 – 946.

EKBLAD, E., EDVINSSON, L., WAHLESTEDT, C., UDDMAN, R., HAKANSON, R. & SUNDLER, F. (1984). Neuropeptide Y co-exists and co-operates with noradrenaline in perivascular nerve fibres. *Regul. Pept.*, **8,** 225 – 235.

EKBLAD, E., EKELUND, M., GRAFFNER, H., HAKANSON, R. & SUNDLER, M. (1985). Peptide-containing nerve fibres in the stomach wall of rat and mouse. *Gastroenterology*, **89,** 73 – 85.

EL-SALHY, M., WILANDER, E., JUNTTI-BERGGREN, L. & GRIMELIUS, L. (1983). The distribution and ontogeny of polypeptide YY (PYY) and pancreatic polypeptide (PP)-immunoreactive cells in the gastrointestinal tract of rat. *Histochemistry*, **78,** 53 – 60.

ESPLUGUES, J.V., BARRACHINA, M.D., CALATAYUD, S., PIQUE, J.M. & WHITTLE, B.J.R. (1993a). Nitric oxide mediates the inhibition by interleukin-1β of pentagastrin-stimulated rat gastric acid secretion. *Br. J. Pharmacol.*, **108,** 9 – 10.

ESPLUGUES, J.V., MARTINEZ-CUESTA, M.A., BARRACHINA, M.D., MORENO, L., PIQUE, J.M. & WHITTLE, B.J.R. (1993b). Reversal by tetrodotoxin and nitric oxide-inhibition of the reduction by endotoxin of pentagastrin-stimulated gastric acid secretion. *Gastroenterology*, **104,** A882.

ESPLUGUES, J.V. & WHITTLE, B.J.R. (1988a). Close-arterial administration of the thromboxane mimetic U-46619 induces damage to the rat gastric mucosa. *Prostaglandins*, **35,** 137 – 148.

ESPLUGUES, J.V. & WHITTLE, B.J.R. (1988b). Gastric mucosal damage induced by local intra-arterial administration of Paf in the rat. *Br. J. Pharmacol.*, **93,** 222 – 228.

ESPLUGUES, J.V. & WHITTLE, B.J.R. (1989a). Gastric damage following local intra-arterial administration of reactive oxygen metabolites in the rat. *Br J. Pharmacol.*, **97,** 1085 – 1092.

ESPLUGUES, J.V. & WHITTLE, B.J.R. (1989b). Mechanisms contributing to gastric motility changes induced by PAF-acether and endotoxin in rats. *Am. J. Physiol.*, **256,** G275 – G282.

ESPLUGUES, J.V. & WHITTLE, B.J.R. (1990). Morphine potentiation of ethanol-induced gastric mucosal damage in the rat. Role of local sensory afferent neurons. *Gastroenterology*, **98,** 82 – 89.

ESPLUGUES, J.V. & WHITTLE, B.J.R. (1991). Peripheral opioid-sensitive mechanisms of mucosal injury and protection. In *Mechanisms of Injury, Protection and Repair of the Upper Gastrointestinal Tract.* ed. Garner, A. & O'Brien, P.E. pp. 115 – 125, Chichester: John Wiley & Sons.

ESPLUGUES, J.V., WHITTLE, B.J.R & MONCADA, S. (1989). Local opioid-sensitive afferent sensory neurones in the modulation of gastric damage induced by Paf. *Br. J. Pharmacol.*, **97,** 579 – 585.

ESPLUGUES, J.V., WHIITLE, B.J.R. & MONCADA, S. (1992). Modulation by opioids and by afferent sensory neurones of prostanoid protection of the rat gastric mucosa. *Br. J. Pharmacol.*, **106,** 846 – 852.

EULER, U.S. VON & GADDUM, J.H. (1931). An unidentified depressor substance in certain tissue extracts. *J Physiol.*, **72,** 74 – 87.

FEELISCH, M. (1991). Correlation between nitric oxide formation during degradation of organic nitrates and activation of guanylate cyclase. *Eur. J. Pharmacol.*, **139,** 19 – 30.

FEELISCH, M. & NOACK, E.A. (1987). The biochemical pathways of nitric oxide formation from nitrovasodilators: appropriate choice of exogenous NO donors and aspects of preparation and handling of aqueous NO solutions. *J. Cardiovasc. Pharmacol.*, **17,** (Suppl. 3), S25 – S33.

FERREIRA, S.H. & NAKAMURA, M. (1979). Prostaglandin hyperalgesia. The peripheral analgesic activity of morphine, enkephalins and opioid antagonists. *Prostaglandins*, **18,** 191 – 200.

FLEMING, I., JULOU-SCHAEFER, G., GRAY, G.A., PARRAT, J.R. & STOCKLET, J.-C. (1991). Evidence that an L-arginine/nitric oxide dependent elevation of tissue cyclic GMP content is involved in depression of vascular reactivity by endotoxin. *Br. J. Pharmacol.*, **103,** 1047 – 1052.

FLEMSTROM, G. (1987). Gastric and duodenal mucosal bicarbonate secretion. In: *Physiology of the Gastrointestinal Tract.* ed. Johnson, L.R. Second Edition, Vol. II pp. 1011 – 1029, New York: Raven Press.

FURCHGOTT, R.F. (1984). The role of endothelium in the responses of vascular smooth muscle to drugs. *Annu. Rev. Pharmacol. Toxicol.*, **24,** 175 – 197.

FURCHGOTT, R.F. & ZAWADZKI, J.V. (1980). The obligatory role of endothelial cells in the relaxation of arterial smooth muscle by acetylcholine. *Nature*, **288,** 373 – 376.

FURNESS, V.B., COSTA, M., EMSON, P.C., HAKANSON, R., MOHIM-ZADEH, E., SUNDLER, F., TAYLOR, I.L. & CHANCE, R.E. (1983). Distribution, pathways and reactions to drug treatment of nerves with neuropeptide Y and pancreatic polypeptide like immunoreactivity in the guinea-pig digestive tract. *Cell Tissue Res.*, **234,** 71 – 92.

GADDUM, J.H. & SCHILD, H. (1934). Depressor substances in extracts of intestine. *J. Physiol.*, **83,** 1 – 14.

GADDUM, J.H., JANG, C.S. & KWIATKOWSKI, H. (1939). The effect on the intestine of the substance liberated by adrenergic nerves in a rabbit's ear. *J. Physiol.*, **96,** 104 – 108.

GARDINER, S.M., COMPTON, A.M. & BENNETT, T. (1989). Regional haemodynamic effects of endothelin-1 in conscious, unrestrained, Wistar rats. *J. Cardiovasc. Pharmacol.*, **13,** Suppl. 5, S202 – 204.

GARDINER, S.M., COMPTON, M., BENNETT, T., KEMP, P.A. & NEY, U. (1990a). Synergistic internal carotid vasodilator effects of human α-calcitonin gene related peptide and nimodipine in conscious rats. *Br. J. Pharmacol.*, **99,** 830 – 834.

GARDINER, S.M., COMPTON, A.M., BENNETT, T., PALMER, R.M.J. & MONCADA, S. (1990b). Control of regional blood flow by endothelium-derived nitric oxide. *Hypertension*, **15,** 486 – 492.

GASKILL, H.V., SIRINEK, K.R. & LEVINE, B.A. (1982). Prostacyclin-mediated gastric cytoprotection is dependent on mucosal blood flow. *Surgery*, **92,** 220 – 225.

GERBER, J.G. & GUTH, P.H. (1989). Role of adenosine in the gastric blood flow response to pentagastrin in the rat. *J. Pharmacol. Exp. Ther.*, **251,** 550 – 556.

GERBER, J.G. & NIES, A.S. (1982). Canine gastric mucosal vasodilation with prostaglandins and histamine analogs. *Dig. Dis. Sci.*, **27,** 870 – 874.

GERKENS, J.F., GERBER, J.G., SHAND, D.G. & BRANCH, R.A. (1978). Effect of PGI_2, PGE_2 and 6-keto-$PGF_{1\alpha}$ on canine gastric blood flow and acid secretion. *Prostaglandins*, **16,** 815 – 823.

GIAID, A., GIBSON, S.J., IBRAHIM, N.B.N., LEGON, S., BLOOM, S.R., YANAGISAWA, M., MASAKI, T., VARNDELL, I.M. & POLAK, J.M. (1989). Endothelin 1, an endothelium-derived peptide is expressed in neurons of the human spinal cord and dorsal root ganglia. *Proc. Natl. Acad. Sci. USA*, **86,** 7634 – 7638.

GREEN, T. & DOCKRAY, G.J. (1988). Characterisation of the peptidergic afferent innervation of the stomach in rat, mouse and guinea-pig. *Neuroscience*, **25,** 181 – 193.

GRUETTER, C.A., BARRY, B.K., MCNAMARA, D.B., GRUETTER, D.Y., KADOWITZ, P.J. & IGNARRO, L.J. (1979). Relaxation of bovine coronary artery and activation of coronary guanylate cyclase by nitric oxide, nitroprusside and a carcinogenic nitrosoamine. *J. Cyclic. Nucl. Res.*, **5,** 211 – 224.

GRYGLEWSKI, R.J., PALMER, R.M.J. & MONCADA, S. (1986). Superoxide anion is involved in the breakdown of endothelium-derived vascular relaxing factor. *Nature*, **320,** 454 – 456.

GUTH, P.H. & LEUNG, F.W. (1987). Physiology of the gastric circulation. In *Physiology of the Gastrointestinal Tract.* Second edition. Vol. II. ed. Johnson, L.R. pp. 1031 – 1053. New York: Raven Press.

GUTH, P.H. & SMITH, E. (1975a). Escape from vasoconstriction in the gastric microcirculation. *Am. J. Physiol.*, **228,** 1893 – 1895.

GUTH, P.H. & SMITH, E. (1975b). Neural control of gastric mucosal blood flow in the rat. *Gastroenterology*, **69,** 935 – 940.

GUTH, P.H., PAULSEN, G. & NAGATA, H. (1984). Histologic and microcirculatory changes in alcohol-induced gastric lesions in the rat. Effect of prostaglandin cytoprotection. *Gastroenterology*, **87,** 1083 – 1090.

GYIRES, K., FURST, S., FARCZADI, E. & MARTON, A. (1985). Morphine potentiates the gastroulcerogenic effect of indomethacin. *Pharmacology*, **30,** 25 – 31.

HAKANSON, R., WAHLSTEDT, C., EKBLAD, E., EDVINSSON, L. & SUNDLER, R. (1986). Neuropeptide Y: co-existence with noradrenaline. Functional implications. *Prog. Brain. Res.*, **68,** 279-287.

HARPER, A.A., REED, J.D. & SMY, J.R. (1968). Gastric blood flow in anaesthetized cats. *J. Physiol.*, **194,** 795-807.

HELLSTROM, P.M. (1987). Mechanisms involved in colonic vasoconstriction and inhibition of motility induced by neuropeptide Y. *Acta Physiol. Scand.*, **129,** 549-556.

HIBBS, J.B. JR., VAVRIN, Z. & TAINTOR, R.R. (1987). L-arginine is required for expression of the activated macrophage effector mechanism causing selective metabolic inhibition in target cells. *J. Immunol.*, **138,** 550-565.

HIBBS, J.B. JR., TAINTOR, R.R., VAVRIN, Z. & RACHLIN, E.M. (1988). Nitric oxide: a cytotoxic activated macrophage effector molecule. *Biochem. Biophys. Res. Commun.*, **157,** 87-94.

HO, M., DAI, S. & OGLE, W. (1984). Decreased acid secretion and gastric lesion production by morphine in rats. *Eur. J. Pharmacol.*, **102,** 117-121.

HOLM-RUTILI, L. & BERGLINDH, T. (1986). Pentagastrin and gastric mucosal blood flow. *Am. J. Physiol.*, **250,** G525-G580.

HOLZER, P. (1991). Capsaicin: Cellular targets, mechanism of action, and selectivity for thin sensory neurones. *Pharmacol. Rev.*, **43,** 143-201.

HOLZER, P. & GUTH, P.H. (1991). Neuropeptide control of rat gastric mucosal blood flow: Increase by calcitonin gene-related peptide and vasoactive intestinal polypeptide, but not subtance P and Neurokinin A. *Circ. Res.*, **68,** 100-105.

HOLZER, P. & LIPPE, I. Th. (1988). Stimulation of afferent nerve endings by intragastric capsaicin protects against ethanol-induced damage of gastric mucosa. *Neuroscience*, **27,** 981-987.

HOLZER, P. & LIPPE, I.T. (1992). Gastric mucosal hyperemia due to acid back diffusion depends on splanchnic nerve activity. Am. *J. Physiol.*, **262,** G505-G509.

HOLZER, P., LIPPE, I. Th., BARTHO, L. & SARIA, A. (1987). Neuropeptide Y, inhibits excitatory enteric neurons supplying the circular muscle of the guinea-pig small intestine. *Gastroenterology*, **92,** 1944-1950.

HOLZER, P., LIVINGSTON, E.H. & GUTH, P.H. (1991a). Sensory neurons signal for an increase in rat gastric mucosal blood flow in the face of pending acid injury. *Gastroenterology*, **101,** 416-423.

HOLZER, P., LIVINGSTON, E.H., SARIA, A. & GUTH, P.H. (1991b). Sensory neurons mediate protective vasodilatation in rat gastric mucosa. *Am. J. Physiol.*, **260,** G363-G370.

HOLZER, P. & PABST, M.A., LIPPE, I. Th., PESKAR, B.M., PESKAR, B.A., LIVINGSTON, E.H. & GUTH, P.H. (1990). Afferent nerve-mediated protection against deep mucosal damage in the rat stomach. *Gastroenterology*, **98,** 838-848.

HOLZER, P. & SAMETZ W. (1986). Gastric mucosal protection against ulcerogenic factors in the rat mediated by capsaicin-sensitive afferent neurones. *Gastroenterology*, **91,** 975-981.

HUMPHREYS, G.A., DAVISON, J.S. & VEALE, W.L. (1992). Hypothalamic neuropeptide Y inhibits gastric acid output in rat: role of the autonomic nervous system. *Am. J. Physiol.*, **263,** G726-G732.

HUTCHESON, I.R., WHITTLE, B.J.R. & BOUGHTON-SMITH, N.K. (1990). Role of nitric oxide in maintaining vascular integrity in endotoxin-induced acute intestinal damage in the rat. *Br. J. Pharmacol.*, **101,** 815-820.

IGNARRO, L.J., BUGA, G.M., WOOD, K.S., BYRNS, R.E. & CHAUDHURI, G. (1987). Endothelium-derived relaxing factor produced and released from artery and vein is nitric oxide. *Proc. Natl. Acad. Sci. USA.*, **81,** 9265-9269.

IGNARRO, L.J., LIPPTON, H., EDWARDS, J.C., BARICOS, W.H., HYMAN, A.L., KADOWITZ, P.J. & GRUETTER, C.A. (1981). Mechanism of vascular smooth muscle relaxation by organic nitrates, nitrites, nitroprusside and nitric oxide: evidence for the involvement of S-nitrosothiols as active intermediates. *J. Pharmacol. Exp. Ther.*, **218,** 739-749.

INOUE, A., YANAGISAWA, M., KIMURA, S., KASUYA, Y., MIYAUCHI, T., GOTO, K. & MASAKI, T. (1989). The human endothelin family: Three structurally and pharmacologically distinct isopeptides predicted by three separate genes. *Proc. Natl. Acad. Sci. USA*, **86,** 2863-2867.

ITOH, M. & GUTH, P.H. (1985). Role of oxygen-derived free radicals in hemorrhagic shock-induced gastric lesions in the rat. *Gastroenterology*, **88,** 1162-1167.

JACOBSON, E.D. (1970). Comparison of prostaglandin E_1 and norepinephrine on the gastric mucosal circulation. *Proc. Soc. Exp. Biol. Med.*, **133,** 516-519.

JACOBSON, E.D., LINFORD, R.H. & GROSSMAN, M.I. (1966). Gastric secretion in relation to mucosal blood flow studied by a clearance technique. *J. Clin. Invest.*, **45,** 1-13.

KAUFFMAN, G.L. (1982). Blood flow and gastric secretion. *Fed. Proc.*, **41,** 2080-2083.

KAUFFMAN, G.L. & WHITTLE, B.J.R. (1982). Gastric vascular actions of prostanoids and the dual effect of arachidonic acid. *Am. J. Physiol.*, **242,** G582-G587.

KAUFFMAN, G.L., WHITTLE, B.J.R., AURES, D., VANE, J.R. & GROSSMAN, M.I. (1979a). Effects of prostacyclin and a stable analogue 6β-PGI_1 on gastric acid secretion, mucosal blood flow and blood pressure in conscious dogs. *Gastroenterology*, **77,** 1301-1306.

KAUFFMAN, G.L., WHITTLE, B.J.R., AURES, D. & GROSSMAN, M.I. (1979b). Gastric antisecretory and cardiovascular actions of a stable 16-phenoxy prostacyclin analogue in the dog. In: *Advances in Prostaglandin and Thromboxane Research*, ed. Samuelsson, B, Ramwell, P.W. & Paoletti, R. pp. 1521–1524. Raven Press: New York.

KELM, M., FEELISCH, M., SPAHR, R., PIPER, H.-M., NOACK, E. & SCHRADER, J. (1988). Quantitative and kinetic characterization of nitric oxide and EDRF released from cultured endothelial cells. *Biochem. Biophys. Res. Commun.*, **154,** 236-244.

KHAN, M.T. & FURCHGOTT, R.F. (1987). Additional evidence that endothelium derived relaxing factor is nitric oxide. In *Pharmacology* ed. Rand, M.J. & Raper, C. pp. 341–344. New York: Elsevier.

KILBOURN, R.G., JUBRAN, A.N., GROSS, S.S., GRIFFITH, O.W., LEVI, R., ADAMS, J. & LODATO, R.F. (1990). Reversal of endotoxin-mediated shock by N^G-methyl-L-arginine, an inhibitor of nitric oxide synthesis. *Biochem. Biophys. Res. Commun.*, **172,** 1132-1138.

KITAGAWA, H., TAKEDA, F. & KOHEI, H. (1987). Endothelium-dependent increases in rat gastric mucosal haemodynamics induced by acetylcholine and vagal stimulation. *Eur. J. Pharmacol.*, **133,** 57-63.

KITAGAWA, H., TAKEDA, F., KOHEI, H. (1990). Effect of endothelium-derived relaxing factor on the gastric lesions induced by HCl in rats. *J. Pharmacol. Exp. Ther.*, **253,** 1133-1137.

KIVILAAKSO, E., FROMM, D. & SILEN, W. (1978). Relationship between ulceration and intramural pH of gastric mucosa during hemorrhagic shock. *Surgery*, **84,** 70-78.

KNOWLES, R.G., PALACIOS, M., PALMER, R.M.J. & MONCADA, S. (1989). Formation of nitric oxide from L-arginine in the central nervous system: a transduction mechanism for stimulation of the soluble guanylate cyclase. *Proc. Natl. Acad. Sci. USA.*, **86,** 5159-5162.

KONTUREK, S.J., BROZOZOWSKI, T., MAJKA, J.K & CZARNOBILSKI, K. (1992). Role of nitric oxide and prostaglandins in sucralfate-induced gastroprotection. *Eur. J. Pharmacol.*, **211,** 277-279.

KONTUREK, S.J., BRZOZOWSKI, T., RADECKI, T. & PIASTUCKI, I. (1984). Comparison of gastric and intestinal antisecretory and protective effects of prostacyclin and its stable thia-imino-analogue (HOE 892) in conscious rats. *Prostaglandins*, **151,** 19-25.

KONTUREK, S.J., ROBERT, A., HANCHER, A.J. & NEZAMIS, J.E. (1980). Comparison of prostacyclin and prostaglandin E_2 on gastric acid secretion, gastrin release and mucosal blood flow in dogs. *Dig. Dis. Sci.*, **25,** 673-679.

KONTUREK, S.J., RADECKI, T., BROZOZOWSKI, T., PIASTUCKI, I., DEMBINSKA-KIEC, A. & ZMUDA. A. (1981). Aspirin-induced gastric ulcers in cats. Prevention by prostacyclin. *Dig. Dis. Sci.*, **26,** 1003-1012.

KUBES, P. & GRANGER, D.N. (1992). Nitric oxide modulates microvascular permeability. *Am. J. Physiol.*, **262,** H611-H615.

KUBES, P., SUZUKI, M. & GRANGER, D.N. (1990). Modulation of PAF-induced leukocyte adherence and increased microvascular permeability. *Am. J. Physiol.*, **259,** G859-G864.

KUBES, P., SUZUKI, M. & GRANGER, D.N. (1991). Nitric oxide: an endogenous modulator of leukocyte adhesion. *Proc. Natl. Acad. Sci. USA.*, **88,** 4651-4655.

KUROSE, I., MIURA, S., FUKUMURA, D., TASHIRO, H., IMAEDA, H., SHIOZAKI, H., SUEMATSU, M., NAGATA, H., SEKIZUKA, E. & TSUCHIYA, M. (1992). Role of platelet activating factor on the fibrinolytic activation in the pathogenesis of gastric mucosal damage induced by endothelin-1. *Gut*, **33,** 868-871.

KVIETYS, P.B., TWOHIG, B., DANZELL, J. & SPECIAN, R.D. (1990). Ethanol-induced injury to the rat gastric mucosa. Role of neutrophils and xanthine oxidase-derived radicals. *Gastroenterology*, **98,** 909-920.

LEE, Y., SHIOSAKA, S ., EMSON, P. C., POWELL, J.F., SMITH, A.D. & TOHYAMA, M. (1985). Neuropeptide Y-like immunoreactive structure in the rat stomach with special reference to the noradrenaline neuron system. *Gastroenterology*, **89,** 118-126.

LEMBECK, F. & DONNERER, J. (1985). Opioid control of the function of primary afferent substance P fibres. *Eur. J. Pharmacol.*, **114,** 241-246.

LEONE, A.M., PALMER, R.M.J., KNOWLES, R.G., FRANCIS, P.L., ASHTON, D.S. & MONCADA, S. (1991). Constitutive and inducible nitric oxide synthases are L-arginine N^G-C^G-dioxygenases. *J. Biol. Chem.*, **266,** 23790-23795.

LEUNG, F.W. (1992). Modulation of autoregulatory escape by capsaicin-sensitive afferent nerves in rat stomach. *Am. J. Physiol.*, **262,** H562-H567.

LEUNG, F.W., GUTH, P.H., SCREMIN, O.U., GOLANSKA, E.M., KAUFFMAN, G.L. Jr. (1984). Regional gastric mucosal blood flow measurements by hydrogen gas clearance in the anaesthetized rat and rabbit. *Gastroenterology*, **87,** 28-36.

LEUNG, F.W., TALLOS, E.G., TACHE, Y.F. & GUTH, P.H. (1987). Calcitonin gene-related peptide inhibits acid secretion without modifying blood flow. *Am. J. Physiol.*, **252,** G215-G218.

LI, C.G. & RAND, M.J. (1990). Nitric oxide and vasoactive intestinal polypeptide mediate non-adrenergic, non-cholinergic inhibitory transmission to smooth muscle of the rat gastric fundus. *Eur. J. Pharmacol.*, **191,** 303-309.

LI, D.S., RAYBOULD, H.E., QUINTERO, E. & GUTH, P.H. (1991). Role of calcitonin gene-related peptide in gastric hyperemic response to intragastric capsaicin. *Am. J. Physiol.*, **261,** G657-G661.

LI, D.S., RAYBOULD, H.E., QUINTERO, E. & GUTH, P.H. (1992). Calcitonin gene-related peptide mediates the gastric hyperemic response to acid back-diffusion. *Gastroenterology*, **102,** 1124-1128.

LIPPE, I.Th. & HOLZER, P. (1992). Participation of endothelium-derived nitric oxide but not prostacyclin in the gastric mucosal hyperaemia due to acid back diffusion. *Br. J. Pharmacol.*, **105,** 708-714.

LIPPE, I.T., LORBACH, M. & HOLZER, P. (1989a). Close arterial infusion of calcitonin gene-related peptide into the rat stomach inhibits aspirin- and ethanol-induced hemorrhagic damage. *Regul. Pept*, **26,** 35-46

LIPPE, I.Th., PABST, M.A. & HOLZER, P. (1989b). Intragastric capsaicin enhances rat gastric acid elimination and mucosal blood flow by afferent nerve stimulation. *Br. J. Pharmacol.*, **96,** 91-100.

LOPEZ-BELMONTE, J. & WHITTLE, B.J.R. (1993). Paradoxical interactions between endothelin-1 and calcitonin gene-related peptide in the rat gastric microcirculation. *Br. J. Pharmacol.*, **108,** 113P.

LOPEZ-BELMONTE, J., WHITTLE, B.J.R. & MONCADA, S. (1993). The actions of nitric oxide donors in the prevention or induction of injury to the rat gastric mucosa. *Br. J. Pharmacol.*, **108,** 73-78.

LUNDBERG, J.M. & TATEMOTO, K. (1982). Pancreatic polypeptide family (APP, BPP, NPY and PYY) in relation to sympathetic vasoconstriction resistant to α-adrenoceptor blockade. *Acta Physiol. Scand.*, **116,** 393-402.

LUNDBERG, J.M., TATEMOTO, K., TERENIUS, L., HELLSTROM, P.M., MITT, V., HOKFELT, T. & HAMBERGER, B. (1982). Localisation of peptide YY (PYY) in gastrointestinal enocrine cells and effects on intestinal blood flow. *Proc. Natl. Acad. Sci. USA*, **79,** 4471-4475.

LUNDBERG, J.M., TERENIUS, L., HOKFELT, T., MARTLING, C.R., TATEMOTO, K., MUTT, V., POLAK, J., BLOOM, S. & GOLDSTEIN, M. (1984). Neuropeptide Y (NPY)-like immunoreactivity in peripheral noradrenergic neurons and effects of NPY on sympathetic function. *Acta Physiol. Scand.*, **116,** 447-480.

LUNDBERG, J.M., PERNOW, J., FRANCO-CERECEDA, A. & RUDEHILL, A. (1987). Effect of antihypertensive drugs on sympathetic vascular control in relation to neuropeptide Y. *J. Cardiovasc. Pharmacol.*, **10** (Suppl. 12), S51–S68.

MAIN, I.H.M. & WHITTLE, B.J.R. (1973). Gastric mucosal blood flow during pentagastrin- and histamine-stimulated acid secretion in the rat. *Br J. Pharmacol.*, **49,** 534-542.

MAIN, I.H.M. & WHITTLE, B.J.R. (1975). Investigation of the vasodilator and antisecretory role of prostaglandins in the rat gastric mucosa by use of non-steroidal anti-inflammatory drugs. *Br. J. Pharmacol.*, **53,** 217-225.

MACLEAN, M.R. & HILEY, C.R. (1990). Effect of neuropeptide Y on cardiac output, its distribution, reginal blood flow and organ vascular resistance in the pithed rat. *Br. J. Pharmacol.*, **99,** 340-342.

MACNAUGHTON, W.K., CIRINO, G. & WALLACE, J.L. (1989a). Endothelium derived relaxing factor (nitric oxide) has protective actions in the stomach. *Life Sci.*, **45,** 1869-1876.

MACNAUGHTON, W.K., KEENAN, C.M., McKNIGHT, G. & WALLACE, J.L. (1989b). The modulation of gastric mucosal integrity endothelin-1 and prostacyclin. *J. Cardiovasc. Pharmacol.*, (Suppl. 5), S118-S122.

MAGGI, C.A., EVANGELISTA, S., GIULIANI, S. & MELI, A. (1987). Anti-ulcer activity of calcitonin gene-related peptide in rats. *Gen. Pharmacol.*, **18,** 33-34.

MARLETTA, M.A., YOON, P.S., IYENGAR, R., LEAF, C.D. & WISHNOK, J.S. (1988). Macrophage oxidation of L-arginine to nitrite and nitrate: Nitric oxide is an intermediate. *Biochemistry*, **27,** 8706-8711.

MARTINEZ-CUESTA, M.A., BARRACHINA, D., PIQUE, J.M., WHITTLE, B.J.R. & ESPLUGUES, J.V. (1992). The role of nitric oxide and platelet-activating factor in the inhibition by endotoxin of pentagastrin-stimulated gastric acid secretion. *Eur. J. Pharmacol.*, **218,** 351-354.

MARTINSON, J. (1965). The effect of graded vagal stimulation on gastric motility, secretion and blood flow in the cat. *Acta Physiol. Scand.*, **62,** 256–262.

MASAKI, T., KIMURA, S., YANAGISAWA, M. & GOTO, K. (1991). Molecular and cellular mechanism of endothelin regulation. Implication for vascular function. *Circulation*, **84,** 1457–1468.

MASUDA, E., KAWANO, S., NAGANO, K., TSUJI, S., ISHIGAMI, Y.,TSUJII, M., HAYASHI, N., FUSAMOTO, H. & KAMADA, T. (1992). Effect of intravascular ethanol on modulation of gastric mucosal integrity, possible role of endothelin-1. *Am. J. Physiol.*, **262,** G785 – G790.

MATSUDA, M., AONO, M., MORIGA, M. & OKUMA, M. (1991). Centrally administered NPY stimulated gastric acid and pepsin secretion by a vagally mediated mechanism. *Regul. Pept*, **35,** 31 – 41.

MATSUMOTO, H., SUZUKI, N., ONDA, H. & FUJINO, M. (1989). Abundance of endothelin-3 in rat intestine, pituitary gland and brain. *Biochem. Biophys. Res. Commun.*, **164,** 74 – 80.

MCCALL, T.B., BOUGHTON-SMITH, N.K., PALMER, R.M.J., WHITTLE, B.J.R. & MONCADA, S. (1989). Synthesis of nitric oxide from L-arginine by neutrophils. Release and interaction with superoxide anion. *Biochem. J.*, **261,** 293 – 296.

MCINTOSH, C.H.S., DADGAR, A. & KWOK, Y.N. (1992). Cholinergic stimulation of neuropeptide Y secretion from the isolated perfused rat stomach. *Regul. Pept*, **39,** 83 – 94.

MONCADA, S., GRYGLEWSKI, R.J., BUNTING, S. & VANE, J.R. (1976). An enzyme isolated from arteries transforms prostaglandin endoperoxides to an unstable substance that inhibits platelet aggregation. *Nature*, **263,** 663 – 665.

MONCADA, S., PALMER, R.M.J. & HIGGS, E.A. (1991) Nitric oxide: physiology, pathophysiology and pharmacology. *Pharmacol. Rev.*, **43,** 109 – 142.

MONCADA, S. & VANE, J.R. (1979). Pharmacology and endogenous roles of prostaglandin endoperoxides, thromboxane A_2, and prostacyclin. *Pharmacol. Rev.*, **30,** 293 – 331.

MORALES, R.W., JOHNSON, B.R. & SZABO, S. (1992). Endothelin induces vascular and mucosal lesions, enhances the injury by HCl/ethanol, and the antibody exerts gastroprotection. *FASEB J.*, **6,** 2354 – 2360.

MORLEY, J.E., LEVINE, A.S. & SILVIS, S.E. (1982). Endogenous opiates and stress ulceration. *Life Sci.*, **31,** 693 – 699.

MORRIS, M.J., KAPOOR, V. & CHALMERS, J.P. (1987). Plasma neuropeptide Y concentration is increased after hemorrhage in conscious rats: Relative contributions of sympathetic nerves and the adrenal medulla. *J. Cardiovasc. Pharmacol.*, **9,** 541 – 545.

MULDERRY, P.K., GHATEI, M.A., SPOKES, R.A., JONES, P., PIERSSON, A.M., HAMID, Q.A., KAUSE, S., AMARA, S.G., BURR, J.M., LEGON, S., POLAK, J.M. & BLOOM, S.R. (1988). Different expression of α-CGRP and β-CGRP by primary sensory neurones and enteric autonomic neurons of the rat. *Neuroscience*, **25,** 195 – 206.

MURAKAMI, M., MORIGA, M., MIYAKE, T. & UCHINO, H. (1982). Contact electrode method in hydrogen gas clearance teehnique: a new method for determination of regional gastric mucosal blood flow in animals and humans. *Gastroenterology*, **82,** 457 – 467.

NAVA, E., PALMER, R.M.J. & MONCADA, S. (1991). Inhibition of nitric oxide synthesis in septic shock: how much is beneficial? *Lancet*, **338,** 1555 – 1557.

NICOLOFF, D.M., PETER, E.T., STONE, N.H. & WANGENSTEEN, O.H. (1964). Effect of catecholamines on gastric secretion and blood flow. *Ann. Surg.*, **159,** 32 – 36.

O'CONNOR, K.J. & MONCADA, S. (1991). Glucocorticoids inhibit the induction of nitric oxide synthase and the related cell damage in adenocarcinoma cells. *Biochim. Biophys. Acta*, **1097,** 227 – 231.

OATES, P.J. & HAKKINEN, J.P. (1988). Studies on the mechanism of ethanol-induced gastric damage in rats. *Gastroenterology*, **94,** 10 – 21.

OREN-WOLMAN, N. & GUTH, P.H. (1984). Adrenergic sensitivity of different-sized gastric submucosal arterioles. *Microvasc. Res.*, **28,** 345 – 351.

PALMER, R.M.J. & MONCADA, S. (1989). A novel citrulline-forming enzyme implicated in the formation of nitric oxide by vascular endothelial cells. *Biochem. Biophys. Res. Commun.*, **158,** 348 – 352.

PALMER, R.M.J., FERRIGE, A.G. & MONCADA, S. (1987). Nitric oxide release accounts for the biological activity of endothelium-derived relaxing factor. *Nature*, **327,** 524 – 526.

PALMER, R.M.J., ASHTON, D.S. & MONCADA, S. (1988a). Vascular endothelial cells synthesise nitric oxide from L-arginine. *Nature*, **333,** 664 – 666.

PALMER, R.M.J., BRIDGE, L., FOXWELL, N.A. & MONCADA, S. (1992). The role of nitric oxide in endothelial cell damage and its inhibition by glucocorticoids. *Br J. Pharmacol.*, **105,** 11 – 12.

PALMER, R.M.J., REES, D.D., ASHTON, D.S. & MONCADA, S. (1988b). L-arginine is the physiological precursor for the formation of nitric oxide in endothelium-dependent relaxation. *Biochem. Biophys. Res. Commun.*, **153,** 1251 – 1256.

PANES, J., CASADEVALL, M., PIQUE, J.M., BOSCH, J., WHITTLE, B.J.R. & TERES, J. (1992). Effects of acute normovolemic anemia on gastric mucosal blood flow in rats: role of nitric oxide. *Gastroenterology*, **103,** 407 – 413.

PARKS, D.A., BULKLEY, G.B.M., GRANGER, D.N., HAMILTON, S.R. & MCCORD, J.M. (1982). Ischemic injury in the cat small intestine: role of superoxide radicals. *Gastroenterology*, **82,** 9 – 15.

PASCAUD, X.B., CHOVET, M., ROZE, C. & JUNIEN, J.L. (1993). Neuropeptide Y and σ receptor agonists act through a common pathway to stimulate duodenal alkaline secretion in rats. *Eur. J. Pharmacol.*, **231,** 389 – 394.

PERRY, M., HAEDICKE, G., BULKLEY, G., KVIETYS, P., GRANGER, D. (1983). Relationship between acid secretion and blood flow in the canine stomach, role of oxygen consumption. *Gastroenterology*, **85,** 529 – 534.

PESKAR, B.M., NOWAK, P. & LAMBRECHT, N. (1992). Effect of prostaglandins and capsaicin on gastric vascular flow and mucosal injury in endothelin-1 treated rats. *Agents & Actions* (Suppl 37), 89 – 91.

PESKAR, B.M., RESPONDEK, M., MULLER, K.M. & PESKAR, B.A. (1991). A role of nitric oxide in capsaicin-induced gastroprotection. *Eur. J. Pharmacol.*, **198,** 113 – 114.

PETROS, A., BENNETT, D. & VALLANCE, P. (1991). Effect of nitric oxide synthase inhibitors on hypotension in patients with septic shock. *Lancet*, **338,** 1557 – 1558.

PIHAN, G., MAJZOUBI, D., HAUDENSCHILD, C., TRIER, J.S. & SZABO, S. (1986). Early microcirculatory stasis in acute gastric mucosal injury in the rat and prevention by 16,16-dimethyl prostaglandin E_2 or sodium thiosulfate. *Gastroenterology*, **91,** 1415 – 1426.

PIQUE, J.M., ESPLUGUES, J.V. & WHITTLE, B.J.R. (1992a). Endogenous nitric oxide as a mediator of gastric mucosal vasodilatation during acid secretion. *Gastroenterology*, **102,** 168 – 174.

PIQUE, J.M., ESPLUGUES, J.V. & WHITTLE, B.J.R. (1990). Influence of morphine or capsaicin pretreatment on rat gastric microcirculatory response to PAF. *Am. J. Physiol.*, **258,** G352 – G357.

PIQUE, J.M., LEUNG, F.W., TAN, H.W., LIVINGSTON, E., SCREMIN, O.U. & GUTH, P.H. (1988). Gastric mucosal blood flow response to stimulation and inhibition of gastric acid secretion. *Gastroenterology*, **95**, 642 – 650.

PIQUE, J.M., PIZCUETA, M.P., BOSCH, J., FERNANDEZ, M., WHITTLE, B.J.R. & MONCADA, S. (1992b). Role of nitric oxide in the hyperdynamic splanchnic circulation of portal hypertensive rats. In: *The Biology of Nitric Oxide. 1. Physiological and Clinical Aspects*. eds. Moncada, S., Marletta, M.A., Hibbs, Jr, J.B. & Higgs, E.A. pp. 60–64. London & Chapel Hill, Portland Press.

PIQUE, J.M., WHITTLE, B.J.R. & ESPLUGUES, J.V. (1989). The vasodilator role of endogenous nitric oxide in the rat gastric microcirculation. *Eur. J. Pharmacol.*, **174**, 293 – 296.

PIZCUETA, M.P., PIQUE, J.M., BOSCH, J., WHITTLE, B.J.R. & MONCADA, S. (1992a) Effects of inhibiting nitric oxide biosynthesis on the systemic and splanchnic circulation of rats with portal hypertension. *Br. J. Pharmacol.*, **105**, 184 – 190.

PIZCUETA, M.P., PIQUE, J.M., FERNANDEZ, M., BOSCH, J., RODES, J., WHITTLE, B.J.R. & MONCADA, S. (1992b). Modulation of the hyperdynamic circulation of cirrhotic rats by nitric oxide inhibition. *Gastroenterology*, **103**, 1909 – 1915.

QUINTERO, E, & GUTH, P.H. (1992a). Nitric oxide-mediated gastric hyperemia decreases ethanol-induced gastric mucosal injury in uraemic rats. *Dig. Dis. Sci.*, **37**, 1324 – 1328.

QUINTERO, E. & GUTH, P.H. (1992b). Renal failure increases gastric mucosal blood flow and acid secretion in rats: role of endothelium-derived nitric oxide. *Am. J. Physiol.*, **263**, G75 – G80.

REED, J.D., SANDERS, D.J. & THORPE, V. (1971). The effect of splanchnic nerve stimulation on gastric acid secretion and mucosal blood flow in the anaesthetized cat. *J. Physiol.*, **214**, 1 – 13.

REES, D.D., PALMER, R.M.J., HODSON, H.F. & MONCADA, S. (1989b). A specific inhibitor of nitric oxide formation from L-arginine attenuates endothelium-dependent relaxation. *Br. J. Pharmacol.*, **96**, 418 – 424.

REES, D.D, PALMER, R.M.J. & MONCADA, S. (1989a). Role of endothelium-derived nitric oxide in the regulation of blood pressure. *Proc. Natl. Acad. Sci. USA*, **86**, 3375 – 3378.

REES, D.D., PALMER, R.M.J., SCHULZ, R., HODSON, H.F. & MONCADA, S. (1990). Characterisation of three inhibitors of endothelial nitric oxide synthase *in vitro* and *in vivo*. *Br. J. Pharmacol.*, **101**, 746 – 752.

RITCHIE, W.P. (1975). Acute gastric mucosal damage induced by bile salts, acid and ischemia. *Gastroenterology*, **68**, 699 – 707.

ROBERT, A., NEZAMIS, J.E., LANCASTER, C. & HANCHAR, A.J. (1979) Cytoprotection by prostaglandins in rats – Prevention of gastric necrosis produced by alcohol, HCl, NaOH, hypertonic NaCl and thermal injury. *Gastroenterology*, **77**, 433 – 443.

ROSAM, A.C., WALLACE, J.L. & WHITTLE, B.J.R. (1986). Potent ulcerogenic actions of platelet-activating factor on the stomach. *Nature*, **319**, 54 – 56.

RUBANYI, G.M. & VANHOUTTE, P.M. (1986). Superoxide anions and hyperoxia inactivate endothelium-derived relaxing factor. *Am. J. Physiol.*, **250**, H822 – H827.

RUSSELL, N.J.W., SCHAIBLE, H-G. & SCHMIDT, R.F. (1987). Opiates inhibit the discharges of fine afferent units from inflamed knee joint of the cat. *Neurosci. Lett.*, **76**, 107 – 112.

SAKURAI, T., YANAGISAWA, M., TAKUWA, Y., MIYAZAKI, H., KIMURA, S., GOTTO, K. & MASAKI, T. (1990). Cloning of cDNA encoding a non-isopeptide selective subtype of the endothelin receptor. *Nature*, **348**, 732 – 735.

SALTER, M., KNOWLES, R.G. & MONCADA, S. (1991) Widespread tissue distribution, species distribution and changes in activity of Ca^{2+}-dependent and Ca^{2+}-independent nitric oxide synthases. *FEBS. Lett.*, **291**, 145 – 149.

SALVATI, P. & WHITTLE, B.J.R. (1981). Investigation of the vascular actions of arachidonate lipoxygenase and cyclo-oxygenase products on the isolated perfused stomach of rat and rabbit. *Prostaglandins*, **22**, 141 – 156.

SARIA, A. & BEUBLER, E. (1985). Neuropeptide Y (NPY) and peptide YY (PYY) inhibit prostaglandin E_2-induced intestinal fluid and electrolyte secretion in the rat jejunum *in vivo*. *Eur. J. Pharmacol.*, **119**, 47 – 52.

SELYE, M. (1935). A syndrome produced by diverse nocuous agents. *Nature*, **138**, 32 – 40.

SHEA-DONOHUE, T., NOMPLEGGI, D., MYERS, L. & DUBOIS, A. (1982). A comparison of the effects of prostacyclin and the 15(S) 15-methyl analogs of PGE_2 and $PGF_{2\beta}$ on gastric parietal and non-parietal secretion. *Dig. Dis. Sci.*, **27**, 17 – 22.

SHEIKH, S.P. (1991). Neuropeptide Y and peptide YY: major modulators of gastrointestinal blood flow and function. *Am. J. Physiol.*, **261**, G701 – G715.

SMITH, T.W. & BUCHAN, P. (1984). Peripheral opioid receptors located on rat saphenous nerve. *Neuropeptides*, **5**, 217 – 220.

SMITH, S.M., HOLM-RUTILI, L., PERRY, M.A., GRISHAM, M.N., ARFORS, K-E., GRANGER, D.N., KVIETYS, P.R. & RUSSEL, J.M. (1987). Role of neutrophils in haemorrhagic shock-induced gastric mucosal injury in the rat. *Gastroenterology*, **93**, 466 – 471.

STERNINI, C., REEVE, J.R. & BRECHA, N. (1987). Distribution characterisation of calcitonin gene-related peptide immunoreactivity in the digestive system of normal and capsaicin-treated rats. *Gastroenterology*, **93**, 852 – 862.

SU, H.C., BISHOP, A.E., POWER, R.F., HAMADA, Y. & POLAK, J.M. (1987). Dual intrinsic and extrinsic origins in CGRP- and NPY-immunoreactive nerves of rat gut and pancreas. *J. Neurosci.*, **7**, 2674 – 2687.

SUNDLER, F., MOGHIMZADEH, E., HAKANSON, R., EKELAND, M. & EMSON, P. (1983). Nerve fibres in the gut and pancreas of the rat displaying neuropeptide-Y immunoreactivity. Intrinsic and extrinsic origin. *Cell Tissue Res.*, **280**, 487 – 493.

SZABO, S., TRIER, J.S., BROWN, A. & SCHNOOR, J. (1985). Early vascular injury and increased vascular permeability in gastric mucosal injury caused by ethanol in the rat. *Gastroenterology*, **88**, 228 – 236.

SZOLCSANYI, J. & BARTHO, L. (1981). Impaired defense mechanism to peptic ulcer in the capsaicin-desensitized rat. In *Gastrointestinal Defense Mechanisms*. ed. Mozsik, G., Hanninen, O. & Javor. *Adv. Physiol. Sci.*, Vol. 29, pp. 39 – 51. Oxford U.K. and Budapest, Hungary: Pergamon Press and Akademiai Kiado.

TAKAHASHI, K., JONES, P.M., KANSE, S.M., LAM, H.-C., SPOKES, R.A., GHATEI, M.A. & BLOOM, S.R. (1990). Endothelin in the gastrointestinal tract: Presence of endothelin like immunoreactivity, endothelin-1 messenger RNA, endothelin receptors and pharmacological effect. *Gastroenterology*, **99**, 1660 – 1667.

TEPPERMAN, B.L. & WHITTLE, B.J.R. (1991). Comparison of the effects of neuropeptide Y and noradrenaline on rat gastric mucosal blood flow and integrity. *Br. J. Pharmacol.*, **102**, 95 – 100.

TEPPERMAN, B.L. & WHITTLE, B.J.R. (1992). Endogneous nitric oxide and sensory neuropeptides interact in the modulation of the rat gastric microcirculation. *Br. J. Pharmacol.*, **105**, 171 – 175.

THIEMERMANN, C. & VANE, J. (1990). Inhibition of nitric oxide synthesis reduces the hypotension induced by bacterial lipopolysaccharides in the rat *in vivo*. *Eur. J. Pharmacol.*, **182**, 591 – 595.

THOMPSON, J.E. & VANE, J.R. (1953). Gastric secretion induced by histamine and its relationship to the rate of blood flow. *J. Physiol.*, **121**, 433 – 444.

TILL, M., GATI, T., RABAI, K., SZOMBATH, D. & SZEKELY, J.I. (1988). Effect of [D-Met^{2}Pro^5]enkephalinamide on gastric ulceration and transmucosal potential difference. *Eur. J. Pharmacol.*, **150**, 325 – 330.

VALLANCE, P., COLLIER, J. & MONCADA, S. (1989). Effects of endothelium-derived nitric oxide on peripheral arteriole tone in man. *Lancet*, **ii**, 997 – 1000.

VARRO, V., DOBRONTE, Z. & SAGI, I. (1978). Inter-relation between gastric blood flow and HCI secretion in dogs. *Acta Med. Acad. Sci. Hung.*, **35**, 1 – 20.

WADHWA, S.S. & PERRY, M.A. (1987). Gastric injury induced by hemorrhage, local ischemia, and oxygen radical generation. *Am. J. Physiol.*, **253**, G129 – G133.

WAHLESTEDT, C., DEVINSSON, L., EKBLAD, G. & HAKANSON, R. (1985). Neuropeptide Y potentiates noradrenaline-evoked vasoconstriction: mode of action. *J. Pharmacol. Exp. Ther.*, **243**, 735 – 741.

WALDER, C.E., THIEMERMANN, C. & VANE, J.R. (1990). Endothelium derived relaxing factor participates in the increased blood flow in response to pentagastrin in the rat stomach mucosa. *Proc. R. Soc.*, **241**, 195 – 200.

WALLACE, J.L., ARFORS, K-E. & McKNIGHT, G.W. (1991). A monoclonal antibody against the CD18 leukocyte adhesion molecule prevents indomethacin-induced gastric damage in the rabbit. *Gastroenterology*, **100**, 878 – 883.

WALLACE, J.L., CIRINO, G., DE NUCCI, G., McKNIGHT, W. & MACNAUGHTON, W.K. (1989a). Endothelin has potent ulcerogenic vasoconstrictor actions in the stomach. *Am. J. Physiol.*, **256**, G661 – 666.

WALLACE, J.L., KEENAN, C.M., MACNAUGHTON, W.K. & MCKNIGHT, G.W. (1989b). Comparison of the effects of endothelin-1 and endothelin-3 on the rat stomach. *Eur. J. Pharmacol.*, **167,** 41 – 47.

WALLACE, J.L. & WHITTLE, B.J.R. (1986). Picomole doses of platelet-activating factor predispose the gastric mucosa to damage by topical irritants. *Prostaglandins*, **31,** 989 – 998.

WALUS, K.M., PAWLIK, W. & KONTUREK, S.J. (1980). Prostacyclin-induced gastric mucosal vasodilatation and inhibition of acid secretion in the dog. *Proc. Soc. Exp. Biol. Med.*, **163,** 228 – 232.

WANG, Y.N., MCDONALD, J.K. & WYATT, R.J. (1987). Immunocytochemical localisation of neuropeptide Y-like immunoreactivity in adrenergic and non-adrenergic neurons of the rat gastro-intestinal tract. *Peptides*, **8,** 145 – 151.

WESTFALL, T.C., CARPENTIER, S., CHEN, X., BEINFELD, M.C., NAES, L. & MELDRUM, M.J. (1987). Prejunctional and postjunctional effects of neuropeptide Y at the noradrenergic neuroeffector junction of the perfused mesenteric arterial bed of the rat. *J. Cardiovasc. Pharmacol.*, **10,** 716 – 722.

WHITTLE, B.J.R. (1977). Mechanisms underlying gastric mucosal damage induced by indomethacin and bile salts and the actions of prostaglandins. *Br. J. Pharmacol.*, **61,** 455 – 460.

WHITTLE, B.J.R. (1980). Actions of prostaglandins on gastric mucosal blood flow. In: *Gastro-Intestinal Mucosal Blood Flow*, ed. Fielding, L.P. pp. 180–191. Edinburgh, New York: Churchill Livingstone.

WHITTLE, B.J.R. (1981). Antisecretory actions of prostacyclin and its analogues on the gastric mucosa. In: *Clinical Pharmacology of Prostacyclin*, ed. Lewis P.J. O'Grady, J. pp. 219–232. New York: Raven Press.

WHITTLE, B.J.R. (1983). The potentiation of taurocholate-induced rat gastric erosions following parental administration of cyclooxygenase inhibitors. *Br. J. Pharmacol.*, **80,** 545 – 551.

WHITTLE, B.J.R. (1992). Unwanted effects of aspirin and related agents on the gastrointestinal tract. In: *Aspirin and other Salicylates*. ed. Vane, J.R. & Botting, R. pp. 465–509. London: Chapman & Hall.

WHITTLE, B.J.R. & BOUGHTON-SMITH, N.K. (1979). 16-Phenoxy prostacyclin analogues potent, selective anti-ulcer compounds. In: *Prostacyclin*, ed. Vane, J.R. & Bergstrom, S. pp. 159–171, New York: Raven Press.

WHITTLE, B.J.R., BOUGHTON-SMITH, N.K. & MONCADA, S. (1992a). Biosynthesis and role of the endothelium-derived vasodilator, nitric oxide, in the gastric mucosa. In: *Neuro-immuno-physiology of the Gastrointestinal Mucosa. Implications for Inflammatory Diseases*. ed. Stead, R.H., Perdue, M.H., Cooke, H., Powell, D.W. & Barrett, K.W. *Ann. NY Acad. Sci.*, **664,** 126 – 139.

WHITTLE, B.J.R., BOUGHTON-SMITH, N.K., MONCADA, S. & VANE, J.R. (1978). Actions of prostacyclin (PGI_2) and its product 6-oxo-$PGF_{1\alpha}$ on the rat gastric mucosa *in vivo* and *in vitro*. *Prostaglandins*, **15,** 955 – 968.

WHITTLE, B.J.R. & ESPLUGUES, J.V. (1988). Induction of rat gastric damage by the endothelium-derived peptide, endothelin. *Br. J. Pharmacol.*, **95,** 1011 – 1013.

WHITTLE, B.J.R. & ESPLUGUES, J.V. (1989). Pro-ulcerogenic eicosanoids and related lipid mediators in gastro-intestinal damage. In: *Advances in Drug Therapy of Gastrointestinal Ulceration*, ed. Garner, A. & Whittle, B.J.R. pp. 165–188. Chichester: J. Wiley and Sons.

WHITTLE, B.J.R. & ESPLUGUES, J.V. (1990). Vascular interactions between endogenous prostanoids and vasoactive peptide mediators in gastric damage. *Advances in Prostaglandin, Thromboxane and Leukotriene Research*, Vol. 21, ed. Samuelsson, B. pp.761–765. New York: Raven Press.

WHITTLE, B.J.R., HIGGS, G.A., EAKINS, K.E., MONCADA, S. & VANE, J.R. (1980). Selective inhibition of prostaglandin production in inflammatory exudates and gastric mucosa. *Nature*, **284,** 271 – 273.

WHITTLE. B.J.R., KAUFFMAN G.L. & BOUGHTON-SMITH. N.K. (1984). Stimulation of gastric alkaline secretion by stable prostacyclin analogues in rat and dog. *Eur. J. Pharmacol.*, **100,** 277 – 283.

WHITTLE, B.J.R., KAUFFMAN, G.L. & MONCADA, S. (1981). Vasoconstriction with thromboxane A_2, induces ulceration of the gastric mucosa. *Nature*, **292,** 472 – 474.

WHITTLE, B.J.R. & LOPEZ-BELMONTE, J. (1991). Interactions between the vascular peptide endothelin-1 and sensory neuropeptides in gastric mucosal injury. *Br. J Pharmacol.*, **102,** 950 – 954.

WHITTLE B.J.R., LOPEZ-BELMONTE, J. & REES, D.D. (1989a). Modulation of the vasodepressor actions of acetylcholine, bradykinin, substance P and endothelin in the rat by a specific inhibitor of nitric oxide formation. *Br. J. Pharmacol.*, **98,** 646 – 652.

WHITTLE B.J.R., LOPEZ-BELMONTE, J. & MONCADA, S. (1990). Regulation of gastric mucosal integrity by endogenous nitric oxide: interactions with prostanoids and sensory neuropeptides in the rat. *Br. J. Pharmacol.*, **99,** 607 – 611.

WHITTLE, B.J.R., LOPEZ-BELMONTE, J. & MONCADA, S. (1992b). Nitric oxide mediates rat mucosal vasodilatation induced by intragastric capsaicin. *Eur J. Pharmacol.*, **218,** 339 – 341.

WHITTLE, B.J.R., OREN-WOLMAN, N. & GUTH, P.H. (1985). Gastric vasoconstrictor actions of leukotriene C_4, $PGF_{2\alpha}$ and thromboxane mimetic U-46619 on rat submucosal microcirculation in vivo. *Am. J. Physiol.*, **248,** G580 – G586.

WHITTLE, B.J.R., PAYNE, A.N. & ESPLUGUES, J.V. (1989b). Cardiopulmonary and gastric ulcerogenic actions of endothelin-1 in the guinea-pig and rat. *J. Cardiovasc. Pharmacol.*, **13** (Suppl 5) S103 – S107.

WHITTLE, B.J.R., MORISHITA, T., OHYA, Y., LEUNG, F.W. & GUTH, P.H. (1986). Microvascular actions of platelet-activating factor on the rat gastric mucosa and submucosa. *Am. J. Physiol.*, **251,** G772 – G778.

WHITTLE, B.J.R. & TEPPERMAN, B.L. (1991). Role of the endogenous vasoactive mediators, nitric oxide, prostanoids and sensory neuropeptides in the regulation of gastric blood flow and mucosal integrity. In: *Mechanism of Injury, Protection and Repair of the Upper Gastrointestinal Tract*. ed. Garner, A. & O'Brien, P.E. pp. 127–137. Chichester: J. Wiley & Sons.

WHITTLE, B.J.R. & VANE, J.R. (1987). Prostanoids as regulators of gastrointestinal function. In: *Physiology of the Gastrointestinal Tract*. ed. Johnson, L.R. Second Edition, Vol. 1. pp. 143–180. New York: Raven Press.

WOOD, J.G., YAN, Z.Y., CHEUNG, L.Y. (1992). Relative potency of endothelin analogues on changes in gastric vascular resistance. *Am. J. Physiol.*, **262,** G977 – G982.

WRIGHT, C.E. & FOZARD, J.R. (1988). Regional vasodilation is a prominent feature of the haemodynamic response to endothelin in anaesthetized spontaneously hypertensive rats. *Eur. J. Pharmacol.*, **155,** 201 – 203.

WRIGHT, C.E., REES, D.D. & MONCADA, S. (1992). Protective and pathological roles of nitric oxide in endotoxin shock. *Cardiovasc. Res.*, **26,** 48 – 57.

YANAGISAWA, M., KURIHARA, H., KIMURA, S., TOMOBE, Y., KOSASHI, M., YAZAKI, Y., GOTO, K. & MASAKI, T. (1988). A potent vasoconstrictor peptide produced by vascular endothelial cells. *Nature*, **323,** 411 – 415.

YANO, S.A., FUIJWARA, Y., OZAKI & HARADA, M. (1983). Gastric blood flow responses to autonomic nerve stimulation and related pharmacological studies in rats. *J. Pharm. Pharmacol.*, **35,** 641 – 646.

YOSHIZAWA, T., KIMURA, S., KANAZAWA, I., UCHIYAMA, Y., YGISAWA, M. & MASAKI, T. (1989). Endothelin localizes in dorsal horn and acts on the spinal neurones: possible involvement of dihydropyridine-sensitive calcium channels and substance P release. *Neurosci. Lett.*, **102,** 179 – 184.

ZINNER, M.J., KERR, J.C. & REYNOLDS, D.G. (1975). Hemodynamic effects of intra-arterial infusions of catecholamine on the canine gastric circulation. *Surgery*, **78,** 381 – 388.

(Received June 12, 1993)

Br. J. Pharmacol. (1993), **110**, 18–19

SPECIAL REPORT

Prevention by an inhibitor of the L-arginine-nitric oxide pathway of the antiarrhythmic effects of bradykinin in anaesthetized dogs

Agnes Vegh, Julius Gy Papp, Laszlo Szekeres & [1]*James R. Parratt

Department of Pharmacology, Albert Szent Gyorgyi Medical University of Szeged, Dom ter 12, POB 115, Szeged, Hungary and *Department of Physiology and Pharmacology, University of Strathclyde, 204 George Street, Glasgow G1 1XW

The intracoronary administration of bradykinin (25 ng kg^{-1} min^{-1}) markedly reduces the severity of arrhythmias that occur during a 25 min occlusion of the left anterior descending coronary artery in chloralose, urethane anaesthetized dogs. This protection was abolished by the prior administration, by the same route, of N^G-nitro-L-arginine methyl ester (L-NAME), an inhibitor of the L-arginine-nitric oxide pathway. The protective effect of bradykinin on reperfusion-induced VF was not affected by L-NAME. These results strongly suggest that the antiarrhythmic effect of bradykinin in this model is mediated by nitric oxide release. It also supports the concept that bradykinin might be a 'primary mediator' of the protective, antiarrhythmic effects of ischaemic preconditioning.

Keywords: Nitric oxide; preconditioning; myocardial ischaemia; bradykinin; N^G-nitro-L-arginine methyl ester (L-NAME); arrhythmias

Introduction In anaesthetized dogs the local intracoronary infusion of bradykinin markedly reduces the severity of life-threatening ventricular arrhythmias that occur during coronary artery occlusion (Vegh *et al.*, 1991). One possible explanation for this protection is that bradykinin releases nitric oxide (NO) and prostacyclin from endothelial cells via stimulation of B_2 receptors (Hecker *et al.*, 1992). Since there is evidence (Vegh *et al.*, 1992b,c) that NO contributes to the pronounced antiarrhythmic effects observed following ischaemic preconditioning, we explored the possibility that this also mediates the antiarrhythmic activity of bradykinin by examining its effects on arrhythmias, and on changes in the degree of the inhomogeneity of conduction, in the presence of an inhibition of the L-arginine-nitric oxide pathway, N^G-nitro-L-arginine methyl ester (L-NAME).

Methods These have been described in detail elsewhere (Vegh *et al.*, 1991; 1992a,c). We used mongrel dogs with a weight in excess of 17 kg, anaesthetized with a mixture of chloralose and urethane (60 and 200 mg kg^{-1} respectively, given i.v.) and ventilated with room air. The anterior descending left coronary artery (LAD) was prepared for occlusion and a small branch of this artery, immediately proximal to the proposed occlusion site, was catheterized for the local administration of bradykinin, saline or L-NAME. ST-segment changes and the degree of inhomogeneity of conduction were recorded from epicardial electrograms and a composite electrode respectively (Vegh *et al.*, 1992c). Blood flow in the left circumflex coronary artery (LCX), a limb lead electrocardiogram, systemic arterial and left ventricular (LV) pressures, and LV$dP/dT$ were recorded on a Medicor R81 recorder. Analysis of ventricular arrhythmias during occlusion and reperfusion, and details of statistical tests used, were as outlined by Vegh *et al.* (1992c).

Bradykinin (25 ng kg^{-1} min^{-1}) was infused into the side branch of the LAD at a rate of 0.075 ml min^{-1} for 15 min prior to occlusion of the artery and throughout the 25 min occlusion period. L-NAME (5 mg kg^{-1}) was given into the same side branch of the coronary artery 20 min before the start of the bradykinin infusion. The results from 15 dogs given bradykinin in the presence of L-NAME, were compared with those from 9 dogs which received intracoronary bradykinin at the same dose (Vegh *et al.*, 1991), but without L-NAME. Both groups were compared with a group of 20 controls in which the LAD was simply occluded for a 25 min period.

Results Even in the presence of L-NAME, bradykinin had no significant haemodynamic effects, neither did it alter the inhomogeneity of conduction or the ST-segment (compare Vegh *et al.*, 1991).

The effect of L-NAME was gradually to increase arterial blood pressure by 22 ± 3 mmHg from a mean pressure of 110 ± 5 mmHg over the next 20 min. There was a slight (−7 ± 3 beats min^{-1}) decrease in heart rate (from 158 ± 6 beats min^{-1}). LV$dP/dt_{max}$ and LVEDP were unchanged but relaxation was enhanced (negative dp/dt_{max}; from −2819 ± 219 to −3539 ± 326 mmHg s^{-1}; $P<0.05$). Although diastolic LCX blood flow was unchanged (123 ± 10 to 124 ± 11 ml min^{-1}) coronary vascular resistance was increased (from 0.83 ± 0.06 to 1.04 ± 0.08; units; $P<0.05$). L-NAME had no effect on the ST-segment recorded from epicardial electrodes or on the degree of inhomogeneity of conduction (56 ± 3 ms before, and 55 ± 3 ms 20 min after, L-NAME).

The haemodynamic changes in these dogs following coronary artery occlusion were similar to those described previously in control dogs not administered either L-NAME or bradykinin (Vegh *et al.*, 1992a). Changes in the inhomogeneity of conduction were more marked in the dogs given bradykinin in the presence of L-NAME compared to those given bradykinin alone (11 ± 3, 54 ± 13 and 89 ± 19 ms respectively 1, 3 and 5 min after coronary occlusion in the bradykinin group and 15 ± 7, 114 ± 18 ($P<0.05$) and 129 ± 20 ms ($P<0.05$) in those dogs given bradykinin in the presence of L-NAME). The marked reduction in ST-segment elevation during occlusion resulting from intracoronary bradykinin administration compared to controls (Vegh *et al.*, 1991) was prevented by L-NAME (1.7 ± 0.4, 3.9 ± 0.5 and 6.1 ± 0.9 mV at 1, 3 and 5 min after occlusion in the bradykinin group but 3.7 ± 0.7, 10.9 ± 1.4 and 13.3 ± 1.5 mV ($P<0.05$) at the same times in those dogs also given bradykinin but in the presence of L-NAME).

[1] Author for correspondence.

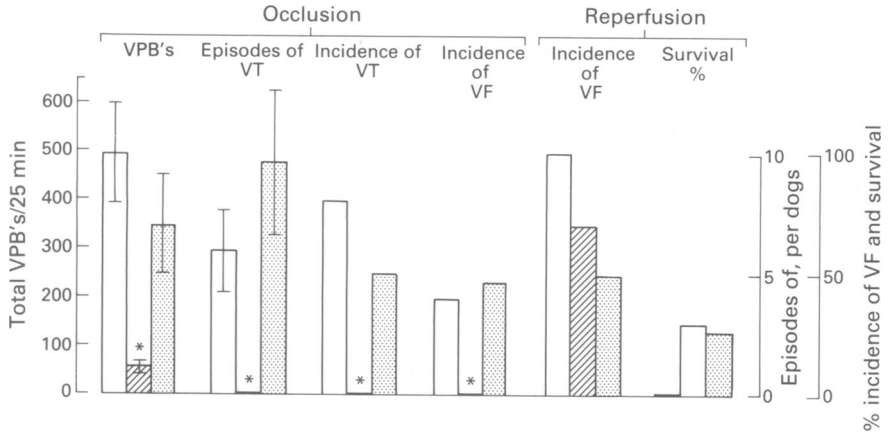

Figure 1 The total number of ventricular premature beats (VPB's), the number of episodes of ventricular tachycardia (VT), the incidences of VT and ventricular fibrillation (VF) and the survival from the combined reperfusion insult, in dogs subjected to a 25 min occlusion of the left anterior descending coronary artery. There was a marked reduction in the severity of ischaemia-induced arrhythmias in dogs administered bradykinin (25 ng kg^{-1} min^{-1}, lined columns, $n = 9$) by intracoronary infusion; this antiarrhythmic effect was largely prevented by the prior administration, by the same route of L-NAME (5 mg kg^{-1}, stippled columns, $n = 15$). In contrast, inhibition of the L-arginine nitric oxide pathway did not influence the protective effect of bradykinin on reperfusion-induced VF or on survival. Control: open columns, $n = 20$. $*P < 0.05$ vs control.

The intracoronary administration of L-NAME resulted in some ectopic activity of 29 ± 14 VPBs over the 20 min period before the start of bradykinin administration. Coronary artery occlusion in those dogs administered bradykinin in the presence of L-NAME resulted in ectopic activity which continued throughout the entire occlusion period (Figure 1). In all there were 344 ± 102 VPB's in contrast to 53 ± 10 in the 9 dogs given only bradykinin. No VT or VF was seen in dogs given only bradykinin (cf. VF in 7/15 and VT in 10/15 in the bradykinin plus L-NAME group). Reperfusion-induced VF and survival from the combined ischaemia reperfusion insult were unaffected by L-NAME.

Discussion These results suggest that the unexpected and pronounced antiarrhythmic effects of locally infused bradykinin under conditions of ischaemia and reperfusion are largely mediated through the release of nitric oxide, since they are markedly attenuated by the prior and local administration of an inhibitor of the L-arginine NO pathway. L-NAME itself does not modify ischaemia-induced arrhythmias (Vegh *et al.*, 1992c). We cannot at present rule out a contribution to this protective effect of prostacyclin, which like NO is also released from endothelial cells by bradykinin and which is also markedly antiarrhythmic in dogs when given by intracoronary administration (Coker & Parratt, 1983). We suggest that this protection is mediated by B_2 receptors since Linz *et al.* (1992) have recently shown that in rat isolated hearts, reperfusion arrhythmias are also reduced by bradykinin and that this protection is prevented by the B_2 antagonist Hoe 140 and by N^G-nitro-L-arginine.

The precise cellular mechanisms of the protective (antiarrhythmic) effects of nitric oxide are unknown but, because the pronounced antiarrhythmic effects of ischaemic preconditioning (Vegh *et al.*, 1992a) are also attenuated by L-NAME (Vegh *et al.*, 1992c) and by methylene blue (Vegh *et al.*, 1992b), an elevation of cyclic GMP within myocytes is one possibility.

This study also raises the possibility that bradykinin is involved in the antiarrhythmic effects of preconditioning; indeed, it might well be a 'primary' mediator. Certainly acid optimum kininogenase enzymes are present in the coronary vessels (Zeitlin *et al.*, 1989), are depleted following ischaemia and may be responsible for the rapid release of kinins that occurs within minutes of the onset of ischaemia (Koide *et al.*, 1993).

This study was supported by a collaborative grant from the Wellcome Trust and by the Hungarian National Scientific Research Foundation. We acknowledge the superb technical skills of Mrs Rozsa Bite.

References

COKER, S.J. & PARRATT, J.R. (1983). Prostacyclin – antiarrhythmic or arrhythmogenic? Comparision of the effects of intravenous and intracoronary prostacyclin and ZK 36374 during coronary artery occlusion and reperfusion in anaesthetised greyhounds. *J. Cardiovasc. Pharmacol.*, **5**, 557–567.

HECKER, M., DAMBACHER, T. & BUSSE, R. (1992). Role of endothelium-derived bradykinin in the control of vascular tone. *J. Cardiovasc. Pharmacol.*, **20**, Suppl 9, 555–561.

KOIDE, A., ZEITLIN, I.J. & PARRATT, J.R. (1993). Kinin formation in ischaemic heart and aorta of rats. *J. Physiol.*, (in press).

LINZ, W., WIEMER, G. & SCHOLKENS, B.A. (1992). ACE-inhibition induced NO-formation in cultural bovine endothelial cells and protects isolated ischemic rat hearts. *J. Mol. Cell. Cardiol.*, **24**, 909–919.

VEGH, A., KOMORI, S., SZEKERES, L. & PARRATT, J.R. (1992a). Antiarrhythmic effects of preconditioning in anaesthetised dogs and rats. *Cardiovasc. Res.*, **26**, 487–495.

VEGH, A., PAPP, J.GY., SZEKERES, L. & PARRATT, J.R. (1992b). The local intracoronary administration of methylene blue prevents the pronounced antiarrhythmic effect of ischaemic preconditioning. *Br. J. Pharmacol.*, **107**, 910–911.

VEGH, A., SZEKERES, L. & PARRATT, J.R. (1991). Local coronary infusions of bradykinin profoundly reduce the severity of ischaemia-induced arrhythmias in anaesthetised dogs. *Br. J. Pharmacol.*, **104**, 294–295.

VEGH, A., SZEKERES, L. & PARRATT, J.R. (1992c). Preconditioning of the ischaemic myocardium: involvement of the L-arginine nitric oxide pathway. *Br. J. Pharmacol.*, **107**, 648–652.

ZEITLIN, I.J., FAGBEMI, O. & PARRATT, J.R. (1989). Enzymes in normally perfused and ischaemic dog hearts which release a substance with kinin like activity. *Cardiovasc. Res.*, **23**, 91–97.

(Received January 25, 1993
Accepted March 19, 1993)

Br. J. Pharmacol. (1993), **110**, 20–22

SPECIAL REPORT

Release-regulating dopamine autoreceptors in human cerebral cortex

Ernesto Fedele, *Gian Carlo Andrioli, *Antonio Ruelle & [1]Maurizio Raiteri

Institute of Pharmacology and Pharmacognosy, University of Genova, Viale Cembrano 4, 16148 Genova and *Division of Neurosurgery, Galliera Hospital, Via A. Volta 8, 16128 Genova, Italy

Slices from fresh specimens of human neocortex which had to be removed during neurosurgery to reach subcortical tumours were labelled with [^{3}H]-dopamine and stimulated electrically. Quinpirole, a selective dopamine D_2 receptor agonist, inhibited the stimulated tritium overflow (EC_{50} = 25 nM; maximal inhibition: about 80% at 10 μM). The selective D_1 receptor agonist, SKF 38393, was inactive up to 10 μM. Quinpirole was antagonized by the D_2 receptor antagonist (−)-sulpiride (apparent pA_2 = 8.26). Thus dopaminergic axon terminals in the human mesocortical pathway possess autoreceptors of the D_2 type.

Keywords: Human neocortex; dopamine release; dopamine autoreceptors; dopamine D_2 receptors

Introduction Receptor heterogeneity bears important implications. The phenomenon favours the development of more selective drugs. However, the increasing evidence that different isoreceptors subserve identical function in different species requires the development of novel drugs based on animal studies to be postponed until the human target receptors are characterized.

Autoreceptors on presynaptic nerve terminals participate in the local control of transmitter release. According to a review by Starke *et al.* (1989), dopamine release-modulating autoreceptors exist in various brain areas of different animal species and belong to the D_2 type. Most studies have been performed in the mesostriatal system, whereas few investigations concern dopamine autoreceptors in the terminal regions of the mesocortical dopaminergic pathway.

With the exception of one study on dopamine autoreceptors in *post-mortem* human striatum (Hetey *et al.*, 1991), no data are available regarding the presence of these release-regulating receptors in human brain. Actually, according to De Keyser (1993), the available data do not support the existence of such presynaptic receptors in man. We have therefore investigated the presence and the pharmacological characteristics of dopamine receptors able to regulate [^{3}H]-dopamine release from electrically-stimulated slices of human neocortex.

Methods Specimens of human cerebral cortex were obtained from patients undergoing neurosurgery to remove subcortical tumours. Samples of frontal (1), temporal (4) and parietal (2) cortex from 5 males and 2 females (aged 32–57 years) were used. After removal, the tissue was kept in ice-cold medium containing (mM): NaCl 125, KCl 3, $MgSO_4$ 1.2, $CaCl_2$ 1.2, $NaHCO_3$ 22, Na_2HPO_4 1 and glucose 10, aerated with O_2/CO_2 (95:5), pH 7.4

Slices (approx. 4 × 4 × 0.4 mm) were incubated (15 min, 37°C) with 0.02 μM [^{3}H]-dopamine in the presence of 0.1 μM 6-nitroquipazine and nisoxetine to prevent false labelling of 5-hydroxytryptaminergic and noradrenergic terminals, respectively. Slices were then transferred into 12 parallel superfusion chambers (1 slice/chamber) and stimulated according to a continuous electrical stimulation protocol (Raiteri *et al.*, 1992).

Each experiment was carried out on tissue obtained from a single patient; full concentration-response curves for the agonist(s), in the presence or in the absence of (−)-sulpiride, along with appropriate controls were done in the same experiment.

[1] Author for correspondence.

The tritium present in each 5 min fraction (see Figure 1) was calculated as a percentage of the total tissue content at the onset of the fraction collected. The evoked ^{3}H overflow in the fraction F_1 and in each fourth fraction collected after addition of the various agonist concentrations (F_2, F_3, F_4, F_5) was calculated by subtracting basal efflux from total efflux in the fraction considered.

The agonist effects on the evoked ^{3}H overflow were evaluated by comparing the ratios F_2/F_1, F_3/F_1, F_4/F_1, F_5/F_1 to the corresponding ratios obtained under control conditions, i.e.

$$\% \text{ change} = 100 \times \left(\frac{F_x/F_1 \text{ agonist}}{\text{average } F_x/F_1 \text{ control}} - 1 \right)$$

No significant differences both in the evoked overflows and in the effects of drugs have been observed among the different cortical areas. Therefore the data obtained from the different experiments were pooled.

The EC_{50} values for quinpirole were determined graphically at the 40% level of inhibition, the maximum effect of the

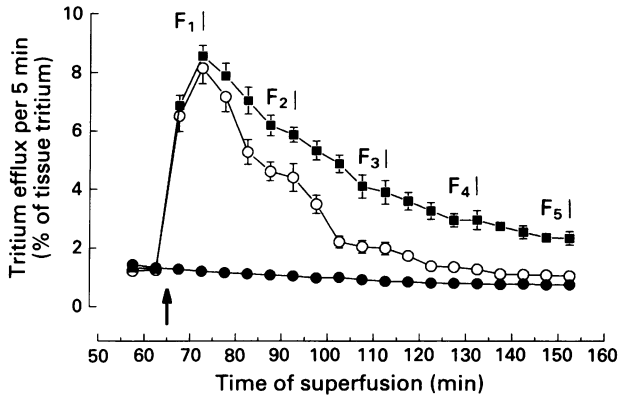

Figure 1 Continuous electrically-evoked release of tritium from human cerebral cortex slices labelled with [^{3}H]-dopamine. Slices were labelled and superfused at 1 ml min^{-1}. Electrical stimulation (3 Hz, 2 ms, 24 mA) was applied from t = 65 (see arrow) to the end of the experiment. Increasing concentrations of agonists (0.01, 0.1, 1 and 10 μM) were added every 20 min (t = 75, 95, 115, 135 min). F_1, F_2, F_3, F_4 and F_5 represent the fractions at which the ^{3}H overflow was calculated. Each point represents the mean ± s.e.mean of 7 experiments in duplicate: (●) spontaneous ^{3}H outflow; (■) evoked ^{3}H efflux; (○) evoked efflux in the presence of quinpirole.

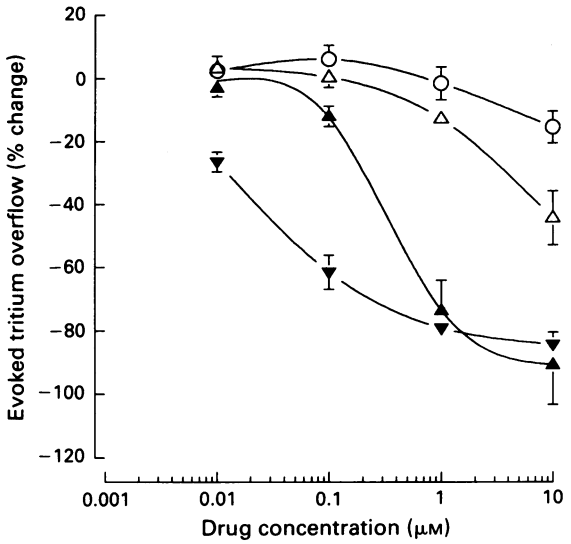

Figure 2 Effects of quinpirole and SKF 38393 on the electrically-evoked tritium overflow from human neocortex slices and antagonism by (−)-sulpiride. Drugs were added every 20 min after the peak of the evoked tritium efflux had been reached. (−)-Sulpiride was present throughout the experiment. For further details see Methods. Means ± s.e.mean of 3–7 experiments in duplicate are shown: (▼) quinpirole; (○) SKF 38393; (▲) quinpirole + 0.1 μM (−)-sulpiride; (△) quinpirole + 1 μM (−)-sulpiride.

agonist being about 80%. The apparent pA_2 values of (−)-sulpiride, calculated according to Furchgott (1972, p. 290) for the two concentrations of the antagonist, were averaged.

Student's *t* test was used to analyse the significance of the difference between two means.

Drugs [^{3}H]-dopamine (specific activity 45 Ci mmol^{-1}) was purchased from Amersham Radiochemical Centre (Buckinghamshire). The following drugs were gifts from the companies indicated: 2,3,4,5-tetrahydro-7,8-dihydroxy-1-phenyl-1H-benzazepine (SKF 38393) (SmithKline Beecham, Surrey); quinpirole (Eli Lilly & Co, Indianapolis, IN, U.S.A.); (−)-sulpiride (Ravizza, Milan, Italy).

Results Figure 1 illustrates the patterns of tritium release from human cortical slices prelabelled with [^{3}H]-dopamine. The spontaneous outflow in the pre-stimulation fraction was 1.294 ± 0.112%. The tritium overflows at F_1, F_2, F_3, F_4 and F_5, under control conditions, amounted to 7.415 ± 0.460, 4.897 ± 0.641, 3.065 ± 0.530, 2.194 ± 0.418 and 1.667 ± 0.299%, respectively. The figure also shows the effects of quinpirole added at increasing concentrations in order to construct concentration-response curves (see Figure 2).

Quinpirole (0.01–10 μM) inhibited the overflow of tritium from slices prelabelled with [^{3}H]-dopamine. The maximal inhibition (about 80%) was reached at 10 μM. The EC_{50} value amounted to 25 nM. No significant changes of tritium overflow were produced by SKF 38393. Addition of (−)-sulpiride (0.1 and 1 μM) shifted to the right the concentration-response curve of quinpirole. The pA_2 average value was 8.26 (8.51 at 1 μM and 8.02 at 0.1 μM).

Under our experimental conditions, (−)-sulpiride, at 1 μM, did not affect on its own the tritium overflow (F_1 = 7.906 ± 1.487; F_2 = 4.864 ± 1.299; F_3 = 3.127 ± 0.184; F_4 = 2.049 ± 0.565; F_5 = 1.482 ± 0.462%; n = 4). The drugs used had no significant effect, on their own, on basal tritium outflow (not shown).

Discussion Mesocortical dopaminergic neurones seem to play an important role in the therapeutic activity of antipsychotics which justifies investigations into the mechanisms regulating the activity of dopaminergic neurones projecting into the cortex. Studies of autoreceptors regulating dopamine release in animal neocortex are surprisingly few (Plantjé *et al.*, 1985; Talmaciu *et al.*, 1986; Hoffman *et al.*, 1988) as compared to those on dopamine autoreceptors in the mesostriatal pathway (see review by Starke *et al.*, 1989). Furthermore, the existence of dopamine autoreceptors in human cortex has not been reported.

Quinpirole, a selective agonist at dopamine D_2 receptors, but not the D_1 agonist SKF 38393, inhibited the overflow of [^{3}H]-dopamine from human neocortex slices. Accordingly, the selective D_2 receptor antagonist (−)-sulpiride prevented the inhibition by quinpirole. The results indicate the existence of dopamine autoreceptors which may be pharmacologically classified as the D_2 type.

An apparent pA_2 value of 8.26 was obtained for (−)-sulpiride as a dopamine autoreceptor antagonist in human cortex. Curiously enough, in spite of the wide use of this drug as a diagnostic D_2 receptor antagonist, to our knowledge the only quantitative evaluation for (−)-sulpiride as a blocker of dopamine autoreceptors was carried out in the rabbit caudate nucleus (pA_2 = 7.84; Starke *et al.*, 1983).

(−)-Sulpiride did not increase, on its own, the evoked overflow of [^{3}H]-dopamine, a result often interpreted as absence of tonic activation. Although a definite conclusion requires further experiments, it is worth noting that (−)-sulpiride behaved similarly in slices of rabbit frontal cortex, whereas it increased [^{3}H]-dopamine overflow in the striatum (Hoffman *et al.*, 1988).

To conclude, the release of dopamine from mesocortical axon terminals in human brain is sensitive to D_2 receptor ligands suggesting the presence of presynaptic autoreceptors of the D_2 type. According to molecular biology studies, subtypes of the D_2 receptor exist in man (De Keyser, 1993); however, a pharmacological subclassification of the dopamine autoreceptor in man will not be possible until novel selective drugs are available.

This work was supported by grants from the Italian M.U.R.S.T. and from the Italian C.N.R.

References

DE KEYSER, J. (1993). Subtypes and localization of dopamine receptors in human brain. *Neurochem. Int.*, **22**, 83–93.

FURCHGOTT. R.F. (1972). The classification of adrenoceptors (adrenergic receptors). An evaluation from the standpoint of receptor theory. In *Handbook of Experimental Pharmacology. Catecholamines*, Vol. XXXIII. ed. Blaschko, H. & Muscholl, E. pp. 283–335, Berlin, Heidelberg, New York: Springer.

HETEY, L., SCHWITZKOWSKY, R., OTT, T. & BARZ, H. (1991). Diminished synaptosomal dopamine (DA) release and DA autoreceptor supersensitivity in schizophrenia. *J. Neural Transm.*, **83**, 25–35.

HOFFMANN, I.S., TALMACIU, R.K., FERRO, C.P. & CUBEDDU, L.X. (1988). Sustained high release at rapid stimulation rates and reduced functional autoreceptors characterize prefrontal cortex dopamine terminals. *J. Pharmacol. Exp. Ther.*, **245**, 761–772.

PLANTJÉ, J.F., DIJCKS, F.A., VERHEIJDEN, P.F.H.M. & STOOF, J.C. (1985). Stimulation of D-2 dopamine receptors in rat mesocortical areas inhibits the release of [^{3}H]dopamine. *Eur. J. Pharmacol.*, **114**, 401–402.

RAITERI, M., BONANNO, G., MAURA, G., PENDE, M., ANDRIOLI, G.C. & RUELLE, A. (1992). Subclassification of release-regulating α_2-autoreceptors in human brain cortex. *Br. J. Pharmacol.*, **107**, 1146–1151.

STARKE, K., SPÄTH, L., LANG, J.D. & ADELUNG, C. (1983). Further functional in vitro comparison of pre- and postsynaptic dopamine receptors in the rabbit caudate nucleus. *Naunyn-Schmied. Arch. Pharmacol.*, **323**, 298–306.

STARKE, K., GÖTHERT, M. & KILBINGER, H. (1989). Modulation of neurotransmitter release by presynaptic autoreceptors. *Physiol. Rev.*, **69**, 864–989.

TALMACIU, R.K., HOFFMANN, I.S. & CUBEDDU, L.X. (1986). DA autoreceptors modulate DA release from the prefrontal cortex. *J. Neurochem.*, **47**, 865–870.

(Received May 27, 1993
Accepted June 1, 1993)

Br. J. Pharmacol. (1993), **110**, 23–28

Electrophysiological effects of Org 7797 in the closed-chest anaesthetized dog

[1]J. Leboeuf, M. Basiez & R. Massingham

Department of Pharmacology, RL. CERM, rue Henri Goudier, 63203 Riom Cedex, France

1 The intravenous electrophysiological effects of a new antifibrillatory agent, Org 7797, were studied in closed chest anaesthetized dogs. Effects of fast sodium and slow calcium-mediated action potentials were also examined in guinea-pig isolated papillary muscle.

2 The major effects of a known antifibrillatory dose of Org 7797 (0.5 mg kg^{-1}) were a protracted slowing of AV nodal conduction (for at least 20 min) and prolongation of the AV nodal functional refractory period. Conduction in the atria and His-Purkinje system (reflected by the St-A and HV intervals) were not significantly modified whilst ventricular conduction (reflected by the QRS interval) and the ventricular functional refractory period were only transiently prolonged. No other electrophysiological changes were seen.

3 A higher dose of Org 7797 (1.5 mg kg^{-1}) slowed conduction at all levels of the myocardium (as evidenced by increases in the St-A, AH, HV and QRS intervals), slightly shortened cardiac repolarization (as assessed from JTc) and decreased Wenckebach rate. Atrial refractory periods were increased whereas effects on ventricular refractory periods were modest.

4 Neither heart rate nor sinus node recovery time were modified by either dose of Org 7797.

5 Org 7797, at a concentration (20 μM) which reduced V_{max} of fast sodium-mediated action potentials in isolated papillary muscle by 83%, did not modify V_{max} of slow calcium-mediated action potentials. It prolonged duration of the latter but did not modify that of the former. However, the plateau phase of both the 'fast' and especially the 'slow' action potentials was prolonged.

6 It is concluded that the main electrophysiological effects of a known antifibrillatory dose of Org 7797 in dogs with normal cardiac function are seen at the level of the AV node, actions which are unlikely to be explained by calcium channel block. Higher doses display a class Ic profile. This preferential action on the AV node may contribute to the control of ventricular rate during atrial fibrillation in the absence of infra-nodal conduction disturbances.

7 These results contrast with those previously obtained in infarcted dogs and might further suggest that myocardial infarction enhances the Class I action of Org 7797.

Keywords: Org 7797; electrophysiology; anaesthetized dog; normal ventricular function

Introduction

Org 7797 ((16α, 17β)-17-methylamino-estra-1,3,5(10-triene-3,16-diol(z)-2 butenedioate) is a new antifibrillatory agent (Janse *et al.*, 1990; Kirchhof *et al.*, 1991) currently undergoing clinical evaluation. Previous electrophysiological studies *in vitro* characterized Org 7797 as a class I drug with a profile more similar to that of the Ic agent propafenone than that of Ia or Ib drugs (Winslow *et al.*, 1989), results which were confirmed *in vivo* using a known antifibrillatory dose (0.5 mg kg^{-1}) (Winslow *et al.*, 1991) in dogs with 5 to 6 day-old myocardial infarcts (Campbell *et al.*, 1991). However, the consistent and potent antifibrillatory actions of Org 7797 observed in rat, canine and porcine models of myocardial ischaemia (Janse *et al.*, 1990; Winslow *et al.*, 1991) are difficult to reconcile with a Ic sodium channel blocking action since agents of this class, which, whilst having proven antiarrhythmic effects, do not appear to prevent, and indeed may exacerbate, ventricular fibrillation during ischaemia both in animals (e.g. Lynch *et al.*, 1987; Timour *et al.*, 1991) and man (The Cardiac Arrhythmia Suppression Trial Investigators, 1989). In addition, although qualitatively similar electrophysiological actions (slowed conduction at all levels of the myocardium) to those induced by propafenone are seen in infarcted dogs (Campbell *et al.*, 1991), Org 7797, whilst being about 4 times more potent than propafenone in these respects, is only equipotent with this agent in controlling 'late' ischaemia-induced tachyarrhythmias in conscious dogs, despite the dependency of these arrhythmias on sodium channel block for their suppression (Marshall & Winslow, 1982). Further discrepancies arise from clinical studies in which intravenous Org 7797 administered to healthy volunteers in a dose (36 mg) similar to that used in the study of Campbell *et al.* (1991) (0.5 mg kg^{-1}) failed to modify QRS duration (Morrison, unpublished). Taken together, these results suggest that the electrophysiological actions of Org 7797 may be different in normal and infarcted hearts. The aim of the present study was, therefore, to evaluate the electrophysiological effects of Org 7797 in dogs with normal cardiac function since no detailed experimental or clinical electrophysiological study has yet been performed in subjects with normal ventricular function. Part of this work has been published in abstract form (Leboeuf *et al.*, 1992).

Methods

Electrophysiological studies in vivo

Beagle dogs of either sex (12–16 kg) were given sodium pentobarbitone (5 mg kg^{-1}, i.v.) to avoid chloralose-induced tremors and alpha-chloralose (100 mg kg^{-1}, i.v.) used for induction and maintenance of the anaesthesia. The trachea was cannulated and the animal artificially respired with room air to maintain arterial blood gases and pH within the physiological range (Po_2, 80–100 mmHg; Pco_2, 35–40 mmHg and pH 7.4 ± 0.5). Three endocavitory electrodes (Plastimed 6F) were positioned with the aid of an image intensifier as described previously (Leboeuf *et al.*, 1989) for

[1] Author for correspondence.

recording of the His-bundle and atrial electrograms and to allow pacing of either atrium or the right ventricle. A limb (Lead II) electrocardiogram (ECG) was recorded from subcutaneous electrodes and arterial blood pressure recorded from the right femoral artery. Records were displayed on a Gould ES 1000 recorder.

Intraventricular conduction time (QRS) and ventricular repolarization time (QT) were measured during normal sinus rhythm. The St-A, AH, and HV intervals (the time between the start of the stimulus artefact and the first deflection of the atrial electrogram, the interval from the first deflection of the atrial electrogram to the start of the largest His deflection and the time between the start of the largest His deflection to the start of the ventricular electrogram, respectively) were measured during atrial pacing at a rate 20% above the spontaneous sinus rate. Atrial, AV nodal and ventricular refractory periods were determined by interpolating an extra stimulus (S2) after every 8th paced stimulus (S1) (pulse width 2 ms; 2 × threshold voltage). The effective refractory period (ERP) was defined as the greatest S1–S2 interval which failed to elicit a propagated response (R2). The functional refractory period (FRP) was taken as the smallest value of R1–R2 (R1 being the propagated response to S1) for any S1–S2. For assessment of the AV junctional refractory periods the reference was the atrial R1–R2 interval rather than the S1–S2 interval.

Anterograde and retrograde Wenckebach rates were determined by progressively increasing the rate of atrial and ventricular pacing respectively until AV conduction block appeared.

Sinus node recovery time (SRT) was defined as the interval between the start of the last atrial complex during pacing and the beginning of the first atrial complex when normal sinus rhythm recommenced. The corrected SRT (cSRT) was measured according to the method of Narula *et al.* (1972) as the difference between the sinus pause duration and the spontaneous cycle length.

The QT and JT (QT–QRS) intervals were corrected for heart rate using the Bazett formula (1920) to give values of QTc ($QT/\sqrt{RR}$) and JTc ($JT/\sqrt{RR}$).

Org 7797 (0.5 mg kg^{-1} followed 35 min later by 1.5 mg kg^{-1}) was administered as intravenous bolus injections in 10 ml saline given over 1 min. Control dogs received two 20 ml injections of saline. Electrophysiological determinations were made prior to drug or vehicle administration and at various times up to 35 min following administration.

Absolute changes from pretreatment values in both the Org 7797 and control groups were determined and compared by Student's *t* test for independent series. A *P* value of $\leqslant 0.05$ was considered significant.

Electrophysiological studies in vitro

Right papillary muscles were removed from male guinea-pigs (Dunkin-Hartley) and pinned to the base of a recording chamber. The preparations were superfused with physiological salt solution containing (mM): NaCl 119, KCl 4.7, $MgCl_2$ 0.56, NaH_2PO_4 1.0, $NaHCO_3$ 25, $CaCl_2$ 2.5 and glucose 22, gassed with carbogen and maintained at a temperature of 37 ± 0.5°C. The tissues were electrically stimulated at a frequency of 0.5 Hz (2 ms duration, 2–3 × threshold voltage). After a 90 min equilibration period, normal 'fast' transmembrane action potentials were recorded using 3 M KCl-filled glass microelectrodes. 'Slow' calcium-mediated action potentials were then elicited by superfusion with salt solution containing 26 mM potassium and 1 μM isoprenaline and after 30 min action potentials again recorded. The tissues were subsequently superfused for 30 min with depolarizing medium containing 20 μM Org 7797 followed by normal medium also containing 20 μM Org 7797 and action potentials recorded at the end of the 30 min drug exposure periods. Action potentials were displayed on an oscilloscope and the signals fed into a Hewlett-Packard 85 microcomputer for measurement and data analysis (using an unpaired *t* test). The parameters measured were resting membrane potential (RMP), action potential amplitude (APH) and the times taken to reach 50 and 90% repolarization (APD_{50} and APD_{90}). The maximum rate of depolarization (V_{max}) was obtained by electronic differentiation. Effective refractory periods were determined by the paired stimulus technique.

Results

The electrophysiological effects of Org 7797 were investigated in 7 dogs and compared to those of its solvent given to 5 dogs (control group). Two of these dogs were unable to follow the pacing stimulus after administration of the higher dose, thereby precluding electrophysiological measurement. These two dogs have therefore been excluded from the study to allow a properly controlled comparison of the effects of the two different doses of Org 7797 used. Table 1 shows mean baseline values of the various parameters obtained prior to drug or saline administration.

Effects of Org 7797 on sinus function

Pretreatment spontaneous rates were 140 ± 8 and 145 ± 11 beats min^{-1} in the Org 7797 and control groups respectively ($n = 5$). Org 7797 did not significantly modify heart rate, sinus node recovery time or corrected sinus node recovery time (Figure 1).

Effects of Org 7797 at the level of the atrium

As shown in Figure 2, 0.5 mg kg^{-1} Org 7797 failed to modify either atrial conduction time or the atrial effective (AERP) or functional (AFRP) refractory periods. In contrast, the higher dose (1.5 mg kg^{-1}) markedly increased St-A (from 30 ± 3 to 52 ± 4 ms) and prolonged both AERP (from 108 ± 4 to 156 ± 12 ms) and AFRP (from 155 ± 8 to 188 ± 15 ms). The effects on the refractory periods appeared shorter lived than the effect on conduction which was still significantly slowed 20 min after administration. Effects on the refractory periods failed to maintain significance at this time.

Effects of Org 7797 on the AV node

Intranodal conduction (AH) was increased by Org 7797 in a dose-dependent manner (Figure 3a) from 56 ± 6 ms pretreatment to 75 ± 3 and 98 ± 8 ms after administration of 0.5 and 1.5 mg kg^{-1}, respectively. These actions were accompanied by lengthening of the functional refractory period from 217 ± 16

Table 1 Baseline values of the electrophysiological parameters in the two groups of animals

	HR	*SRT*	*cSRT*	*QRS*	*St-A*	*AH*	*HV*	*QT*	*JT*	*QTc*	*JTc*	*AERP*	*AFRP*	*AVFRP*	*VERP*	*VFRP*	*AWCK*	*RWCK*
Control	145	580	156	71	34	56	22	244	173	376	266	118	149	244	164	199	301	263
	±11	±43	±26	±2	±3	±6	±1	±10	±11	±8	±7	±7	±6	±12	±7	±10	±10	±35
Org 7797	140	660	138	62	27	56	23	231	168	351	256	104	148	217	138	180	327	220
	±8	±83	±34	±2	±2	±6	±2	±7	±6	±7	±6	±2	±9	±16	±6	±5	±19	±6

Parameters are expressed as mean ± s.e.mean of 5 experiments.

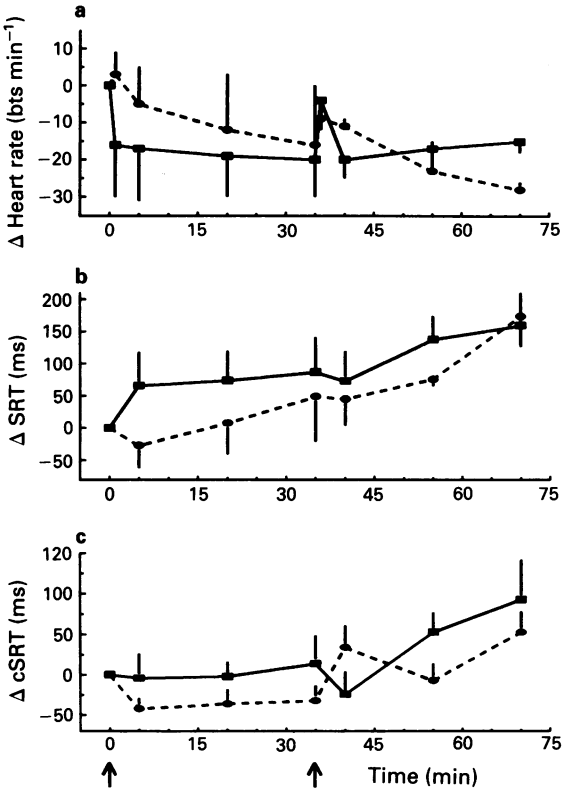

Figure 1 Time course of the effects of Org 7797 on sinus function: (a,b and c) depict changes from pretreatment values in spontaneous heart rate, sinus node recovery time (SRT) and corrected sinus node recovery time respectively. The arrows denote administration of Org 7797 (0.5 followed by 1.5 mg kg^{-1}) (——) or saline (------). Each point is the mean ± s.e.mean of 5 experiments. *$P \leqslant 0.05$ denotes a significant difference from saline-treated animals.

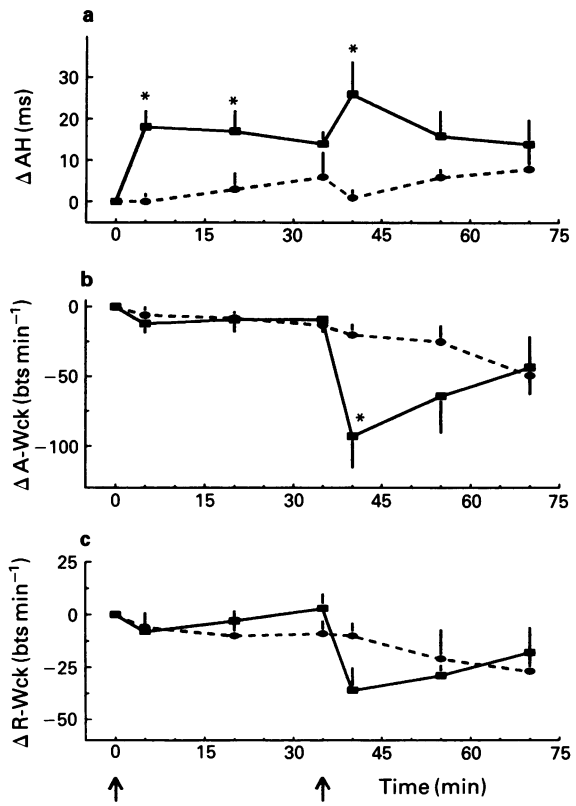

Figure 3 Time course of the effects of Org 7797 on AV nodal function: (a,b and c) depict changes from pretreatment values in AV conduction time (AH), anterograde (A-Wck) and retrograde (R-Wck) Wenckebach rates respectively. The arrows denote administration of Org 7797 (0.5 followed by 1.5 mg kg^{-1}) (——) or saline (------). Each point is the mean ± s.e.mean of 5 experiments. *$P \leqslant 0.05$ denotes a significant difference from saline-treated animals.

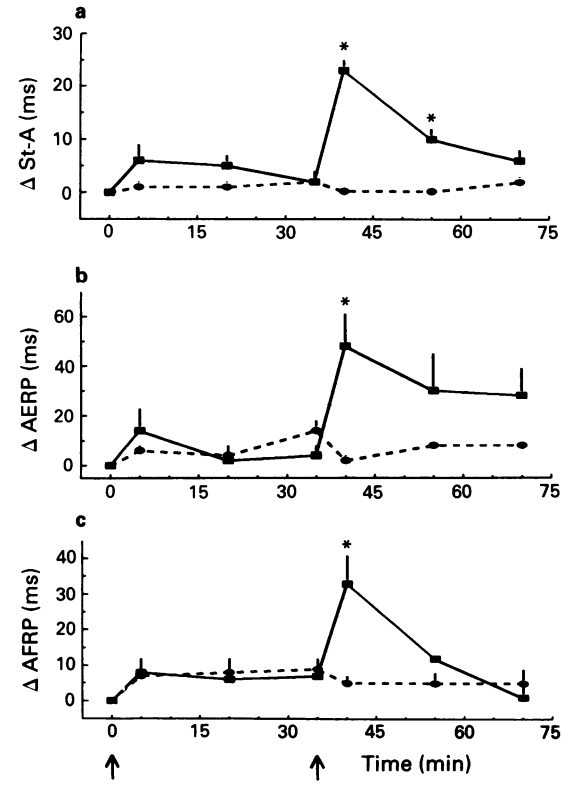

Figure 2 Time course of the effects of Org 7797 at the atrial level: (a,b and c) depict changes from pretreatment values in intraatrial conduction time (St-A), effective (AERP) and functional (AFRP) refractory periods respectively. The arrows denote administration of Org 7797 (0.5 followed by 1.5 mg kg^{-1}) (——) or saline (------). Each point is the mean ± s.e.mean of 5 experiments. *$P \leqslant 0.05$ denotes a significant difference from saline-treated animals.

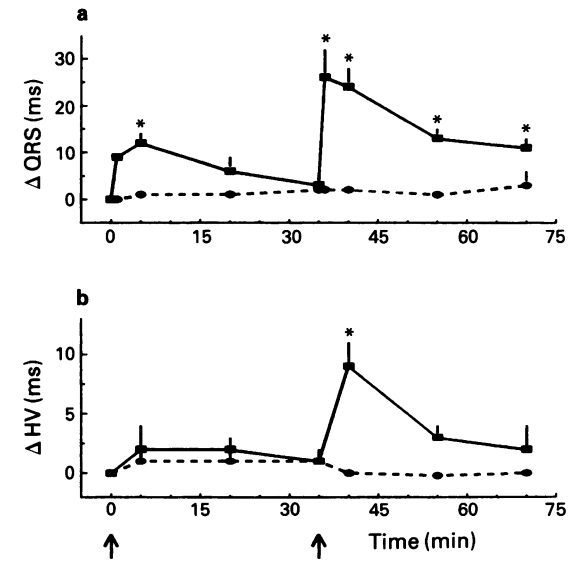

Figure 4 Time course of the effects of Org 7797 on ventricular refractory periods: (a and b) depict changes from pretreatment values in the effective (VERP) and functional (VFRP) refractory periods respectively. The arrows denote administration of Org 7797 (0.5 followed by 1.5 mg kg^{-1}) (——) or saline (------). Each point is the mean ± s.e.mean of 5 experiments. *$P \leqslant 0.05$ denotes a significant difference from saline-treated animals.

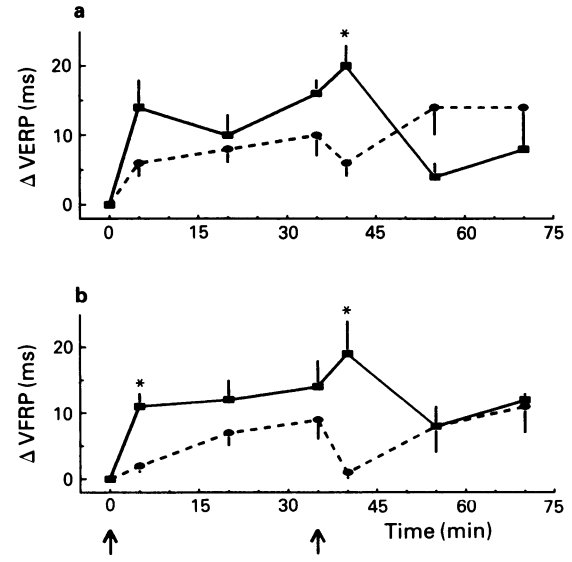

Figure 5 Time course of the effects of Org 7797 at the ventricular level: (a and b) depict changes from pretreatment values in interventricular (QRS) and His-Purkinje (HV) conduction times respectively. The arrows denote administration of Org 7797 (0.5 followed by 1.5 mg kg^{-1}) (——) or saline (------). Each point is the mean ± s.e.mean of 5 experiments. *$P \leq 0.05$ denotes a significant difference from saline-treated animals.

to 248 ± 16 and 262 ± 10 ms respectively (not shown) and were still significant 20 min after administration at the lower dose. However, anterograde and retrograde Wenckebach rates were only decreased at the higher dose (Figure 3b and c).

Effects of Org 7797 at the ventricular level

Org 7797 induced dose-dependent increases in QRS (Figure 4a) and in both the effective (VERP) and functional (VFRP) refractory periods (Figure 5). With the exception of the prolongation in QRS induced by the higher dose, these effects were relatively short-lived. HV was unaltered by the lower dose of Org 7797 but prolonged by the higher dose (Figure 4b).

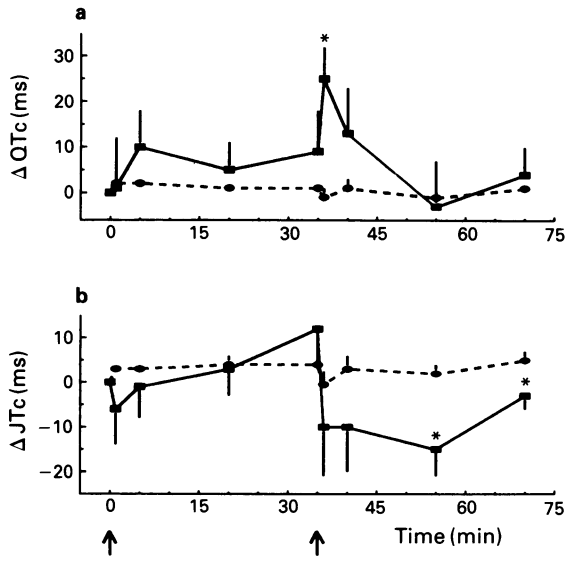

Figure 6 Time course of the effects of Org 7797 at the ventricular repolarization: (a and b) depict changes from pretreatment values in the QTc and JTc intervals respectively. The arrows denote administration of Org 7797 (0.5 followed by 1.5 mg kg^{-1}) (——) or saline (------). Each point is the mean ± s.e.mean of 5 experiments. *$P \leq 0.05$ denotes a significant difference from saline-treated animals.

Table 2 Comparative electrophysiological actions of Org 7797 on 'fast' and 'slow' actions potentials in guinea-pig papillary muscle driven at 0.5 Hz

Fast action potentials [ ] μM	n	*RMP*	*APH*	*APD_{50}*	*APD_{90}*	*V_{max}*	*ERP*
0	24	−83.6 ±0.7	121 ±2	170 ±4	202 ±3	310 ±21	203 ±17
20	24	−82.5 ±0.4	117 ±2	183 ±4 *	204 ±4	53 ±3 ***	>250 ***

Slow action potentials [ ] μM	n	*RMP*	*APH*	*APD_{50}*	*APD_{90}*	*V_{max}*
0	24	−46 ±0.4	78 ±0.9	112 ±4	131 ±3	19.8 ±1
20	24	−45 ±0.5	71 ±0.9 ***	146 ±3 ***	168 ±3 ***	19.6 ±0.8

For abbreviations, see text.
Parameters are expressed as mean ± s.e.mean.
8 action potentials were recorded from each of 3 preparations.
*$P<0.05$; **$P<0.01$; ***$P<0.001$.

Baseline values of QT and JT intervals were in the same range in the control and Org 7797-treated groups (see Table 1). Org 7797, 0.5 mg kg^{-1}, did not significantly modify either the QT or JT intervals (increased by 11 ± 3 and 13 ± 4% respectively compared to 10 ± 8 and 14 ± 11% in the control group). A dose of 1.5 mg kg^{-1} only significantly increased the QT interval at the 5 min time point (by 13 ± 1.5% vs 6 ± 3% in the control group) while the maximum JT interval in the Org 7797-treated group was shorter than that reached in the control group (201 ± 11 vs 229 ± 11 ms). Figure 6a and b illustrates the effects of Org 7797 on QTc and JTc. The lower dose was without effect whilst the higher dose induced a sustained shortening of JTc. QTc was unchanged except for a very transient increase seen immediately following administration of the higher dose.

Electrophysiological effects

The effects of Org 7797 were similar in all 3 preparations studied and the results are summarized in Table 2. Org 7797 (20 μM) slightly prolonged APD_{50} and markedly reduced V_{max} of normal 'fast' action potentials. These effects were accompanied by a small decrease in action potential amplitude and a prolongation of the effective refractory period beyond the limit of measurement. In contrast, V_{max} of 'slow' action potentials was unchanged although a significant decrease in action potential amplitude was observed. In addition marked prolongation of action potential duration (both at the 50 and 90% levels) was observed.

Discussion

In the present study, Org 7797 was given at a dose (0.5 mg kg^{-1}) known to exert marked antifibrillatory actions in both rats and greyhound dogs (Winslow *et al.*, 1991) and subsequently at three times this dose.

The results of this study indicate that the electrophysiological profile of high dose Org 7797 *in vivo* in dogs with normal cardiac function is similar to that reported for other known class Ic sodium channel blocking agents (Harrison, 1985; Karagueuzian *et al.*, 1984; 1985; Schlepper, 1987; Vaughan Williams, 1989). At a dose of 1.5 mg kg^{-1}, Org 7797 rendered 2 out of 7 dogs unable to follow an atrial pacing stimulus of approximately 170 beats min^{-1}. In the remaining dogs, conduction was slowed at all levels of the

myocardium as shown by prolongation of the St-A, AH, HV and QRS intervals, reflecting slowing of conduction in the atria, AV node, His-Purkinje system and ventricular myocardium, respectively. These effects werer accompanied by only modest and transient increases in ventricular and atrial refractory periods and by a slight but definite shortening of cardiac repolarization as assessed from JTc. QTc was, however, essentially unaltered apart from a very transient increase which can be adequately explained by the marked prolongation of the QRS interval seen at this time. The slight shortening of JTc and the inactivity of Org 7797 on the duration of fast action potential *in vitro* seen in the present study are more reminiscent of the effects of class Ib agents such as mexilitine which either have no effect or shorten repolarization *in vivo* (Costard-Jackle & Franz, 1989) and *in vitro* (Vaughan Williams, 1989). The marked decrease of V_{max} (83%) of the fast action potential by Org 7797 in isolated papillary muscle and its lengthening of QRS (52%) *in vivo* suggest pronounced blockade of sodium channels in ventricular tissue following high dose administration.

The electrophysiological effects of the lower (antifibrillatory dose) of Org 7797 were almost exclusively confined to the AV node. At other levels of the myocardium, the only effects which were seen were modest and transient slowing of ventricular conduction (prolongation of QRS of 19%) together with very modest increases in the ventricular refractory periods. These results are in marked contrast to those reported in anaesthetized dogs with 5–6 day old myocardial infarcts (Campbell *et al.*, 1991) in which a similar dose of Org 7797 maximally increased St-A, QRS and HV by 81, 37 and 22% respectively, effects which were still significant 10 min after drug administration. Taken together these result suggest that the sodium channel blocking action of Org 7797 may be enhanced by myocardial infarction, as has been suggested for other class I drugs including propafenone (Seipel & Breithardt, 1978; Connoly *et al.*, 1983a,b) and disopyramide (Marrott *et al.*, 1976; Ross *et al.*, 1978). Despite the failure of low dose Org 7797 to influence conduction markedly in the fast conducting system or in atrial or ventricular muscle, a noticeable and sustained (at least 20 min) slowing of AV nodal conduction was observed (AH was increased by 34%) accompanied by a sustained prolongation (of 14%) of the AV nodal functional refractory period. These results might suggest a blockade of calcium ion channels (Fleckenstein, 1985). However, other calcium-dependent processes in large animals (Fleckenstein, 1985), such as heart rate in the present study and myocardial contractility in previous studies (Winslow *et al.*, 1991; Winslow & Mason, 1992), are not reduced by this dose of Org 7797. Also a concentration of Org 7797 which reduced V_{max} of fast sodium-mediated action potentials in isolated papillary muscle by 83% (at low stimulation frequency) failed to modify V_{max} of slow calcium-mediated action potentials (Table 2) suggesting that marked inhibition of sodium ion channels is not accompanied by blockade of calcium ion channels. This would also be consistent with the observation that the FRP of the atrium changed more rapidly than the ERP. Although action potential amplitude was reduced, this may be explained by inhibition of residual sodium current in the depolarized tissues. These results are puzzling but the action of Org 7797 on AV nodal refractoriness might be explained by effects on currents involved in the plateau phase of the action potential (such as sodium-calcium exchange, sodium or calcium window or potassium currents; Noble, 1992; Hiraoka *et al.*, 1992; January & Moscucci, 1992) since in the present study, the duration of the fast action potential at the level of the plateau phase was lengthened as was the duration of the slow calcium-mediated action potential (see Table 2). Other Ic antiarrhythmic agents such as flecainide, which also prolong AV conduction and refractoriness (e.g. Hodess *et al.*, 1979), have been shown to influence potassium currents (Follmer & Colasky, 1990) whereas Ib drugs which do not slow conduction during normal sinus rhythm have no such effect at therapeutic concentrations (Campbell, 1987). These *in vitro* effects may explain the lengthening of the AV nodal refractory period observed in this study. Janse *et al.* (1990) and Kirchhof *et al.* (1991) have also provided evidence from porcine or canine preparations to suggest that the antifibrillatory effects of Org 7797 may be explained by prolongation of wavelength (the product of conduction velocity and refractory period) at fast frequencies. This preferential prolongation of refractory periods (compared to slowing of conduction) might at least be contributed to by rate-dependent prolongation of repolarization (Winslow & Campbell, 1991). However, explanation for the preferential electrophysiological effects of Org 7797 at the level of the AV node seen in the present study must remain speculative until the effects of Org 7797 on the various ion channels at different levels of the myocardium are elucidated. The picture is also complicated by the known frequency-dependent and concentration-dependent effects of Org 7797 on the inward sodium current (Winslow & Campbell, 1991) both of which would tend to oppose drug-induced prolongation of action potential duration. Nevertheless, the selective effect of this agent on the AV node in an antifibrillatory dose might contribute to the control of ventricular rate during atrial fibrillation in the absence of infra-nodal conduction disturbances.

In conclusion, the results of the present study suggest that the main electrophysiological effects of an antifibrillatory dose of Org 7797 in dogs with normal cardiac function are seen at the level of the AV node. Comparisons with previous studies also indicate that myocardial infarction may enhance the sodium channel blocking activity of this compound.

We should like to thank M.J. Peyrin and M. Robillon for help with the figures and A. Thomas for typing the manuscript.

References

BAZETT, H.C. (1920). An analysis of the time relations of electrocardiograms. *Heart*, **7**, 353–370.

CAMPBELL, T. (1987). Differing electrophysiological effects of class Ia, Ib and Ic antiarrhythmic drugs on guinea-pig sinoatrial node. *Br. J. Pharmacol.*, **91**, 395–401.

CAMPBELL, J.K., MARSHALL, R.J. & WINSLOW, E. (1991). Comparison of the electrophysiological effects of Org 7797, disopyramide, mexiletine and propafenone in anaesthetized dogs with myocardial infarcts. *Br. J. Pharmacol.*, **104**, 433–439.

CONNOLY, S.J., KATES, R.E., LEBSACK, C.S., ECHT, D.S., MASON, J.W. & WINKLE, R.A. (1983a). Clinical efficacy and electrophysiology of oral propafenone for ventricular tachycardia. *Am. J. Cardiol.*, **52**, 1208–1213.

CONNOLY, S.J., KATES, R.E., LEBSACK, C.S., HARRISON, D.C. & WINKLE, R.A. (1983b). Clinical pharmacology of propafenone. *Circulation*, **68**, 589–596.

COSTARD-JACKLE, A. & FRANZ, M.R. (1989). Frequency-dependent antiarrhythmic drug effects on postrepolarization refractoriness and ventricular conduction time in canine ventricular myocardium in vivo. *J. Pharmacol. Exp. Ther.*, **251**, 39–46.

FLECKENSTEIN, A. (1985). Calcium antagonism in heart and vascular smooth muscle. *Med. Res. Rev.*, **5**, 395–425.

FOLLMER, C.H. & COLATSKY, T.J. (1990). Block of delayed rectifier potassium current, IK, by flecainide and E-4031 in cat ventricular myoctyes. *Circulation*, **82**, 289–293.

HARRISON, D.C. (1985). Antiarrhythmic drug classification: new science and practical applications. *Am. J. Cardiol.*, **56**, 185–187.

HIRAOKA, M., SUNAMI, A., FAN, Z. & SAWANOBORI, T. (1992). Multiple ionic mechanisms of early after depolarizations in isolated ventricular myocytes from guinea-pig hearts. *Ann. N.Y. Acad. Sci.*, **644**, 33–47.

HODESS, A.B., FOLLANSBEE, W.P., SPEAR, J.F. & MOORE, E.N. (1979). Electrophysiological effects of a new antiarrhythmic agent, flecainide, on the intact canine heart. *J. Cardiovasc. Pharmacol.*, **1**, 427–439.

JANSE, M.J., WILMS-SCHOPMAN, F. & OPTHOF, T. (1990). Mechanism of antifibrillatory action of Org 7797 in regionally ischemic pig heart. *J. Cardiovasc. Pharmacol.*, **15**, 633–643.

JANUARY, C.T. & MOSCUCCI, A. (1992). Cellular mechanisms of early after depolarizations. *Ann. N.Y. Acad. Sci.*, **644**, 23–32.

KARAGUEUZIAN, H.S., KATOH, T., MCCULLEN, A., MANDEL, W.J. & PETER, T.C. (1984). Electrophysiologic and haemodynamic effects of propafenone a new antiarrhythmic agent on anaesthetized closed chest dogs: a comparative study with lidocaine. *Am. Heart J.*, **107**, 418–424.

KARAGUEUZIAN, H.S., PETER, T.C. & MANDEL, W.J. (1985). Propafenone. In *New Drugs Annuals: Cardiovascular Drugs*. ed. Scriabine, A., Vol. 3, pp. 285–299. New York: Raven Press.

KIRCHHOF, C., WIJFFELS, M., BRUGADA, J., PLANELLAS, J. & ALLESSIE, M. (1991). Mode of action of a new class Ic drug (Org 7797) against atrial fibrillation in conscious dogs. *J. Cardiovasc. Pharmacol.*, **17**, 116–124.

LEBOEUF, J., LAMAR, J.C., MASSINGHAM, R. & PONSONNAILLE, J. (1989). Electrophysiological effects of bepridil and its quaternary derivative CERM 1188 in closed chest anaethetized dogs. A comparison with verapamil and diltiazem. *Br. J. Pharmacol.*, **98**, 1351–1359.

LEBOEUF, J., PLANELLAS, J. & WINSLOW, E. (1992). Electrophysiological effects of Org 7797 in animals and man. *Eur. Heart J.*, **13** (suppl), 213.

LYNCH, J.J., DI CARLO, L.A., MONTGOMERY, D.G. & LUCCHESI, B.R. (1987). Effects of flecainide acetate on ventricular tachyarrhythmia and fibrillation in dogs with recent myocardial infarction. *Pharmacology*, **35**, 181–193.

MARROT, P.K., RUTTLEY, M.S.T., WINTERBOTTAM, J.T. & MUIR, J. (1976). A study of the acute electrophysiological and cardiovascular action of disopyramide in man. *Eur. J. Cardiol.*, **4**, 303–312.

MARSHALL, R.J. & WINSLOW, E. (1982). The effects of sodium channel inhibitors on early arrhythmias associated with acute myocardial ischaemia. In *Early Arrhythmias Resulting from Myocardial Ischaemia. Mechanisms and Prevention by Drugs*. ed. Parratt, J.R., pp. 251–294. London and Basingstoke: Macmillan Press Ltd.

NARULA, O.S., SAMET, P. & JAVIER, R.P. (1972). Significance of the sinus node recovery time. *Circulation*, **45**, 140–158.

NOBLE, D. (1992). Ionic mechanisms determining the timing of ventricular repolarization: significance for cardiac arrhythmias. *Ann. N.Y. Acad. Sci.*, **644**, 1–22.

ROSS, D., VOHRA, J. & SLOMAN, J.G. (1978). Disopyramide in myocardial infarction. *The Lancet*, **ii**, 330.

SCHLEPPER, M. (1987). Propafenone, a review of its profile. *Eur. Heart J.*, **8** (suppl A), 27–32.

SEIPEL, L. & BREITHARDT, G.L. (1978). Electrophysiological effects of mexiletine in man: influence on stimulus-induced ventricular arrhythmias. In *Management of Ventricular Tachycardia: Role of Mexiletine*. ed. Sandoe, E., Julian, D.G. & Bell, J.W. pp. 219–232. Amsterdam, Oxford: Excerpta Medica.

THE CARDIAC ARRHYTHMIA SUPPRESSION TRIAL (CAST) INVESTIGATORS (1989). Increased mortality due to encainide or flecainide in a randomised trial of arrhythmia suppression after myocardial infarction. *N. Engl. J. Med.*, **221**, 406–412.

TIMOUR, Q., AUPETIT, J.-F., LOUFOUA-MOUNDANGA, J., GERENTES-CHASSANGE, I., KIOUEH, I. & FAUCON, G. (1991). Class Ic antiarrhythmic drugs and myocardial ischaemia: study in the pig heart in situ. *Naunyn Schmiedebergs Arch. Pharmacol.*, **343**, 645–651.

VAUGHAN WILLIAMS, E.M. (1989). Classification of antiarrhythmic actions. In *Antiarrhythmic Drugs*. ed. Vaughan Williams, E.M. & Campbell, T.J. pp. 45–67. Berlin: Springer Verlag.

WINSLOW, E., MARTONARA, M. & BELL, P. (1989). Electrophysiologic effects of Org 7797, a new steroidal antiarrhythmic agent: comparison with class 1a, 1c drugs. *J. Cardiavasc. Pharmacol.*, **14**, 205–212.

WINSLOW, E. & CAMPBELL, J.K. (1991). Comparative frequency-dependent effects of three class Ic agents, Org 7797, flecainide, and propafenone, on ventricular action potential duration. *J. Cardiovasc. Pharmacol.*, **18**, 911–917.

WINSLOW, E., CAMPBELL, J.K., BARRON, E., MARSHALL, R.J. & MUIR, A.W. (1991). Effects of Org 7797 on early, late and inducible arrhythmias following coronary artery occlusion in rats and dogs. *Br. J. Pharmacol.*, **104**, 853–858.

WINSLOW, E. & MASON, R. (1992). Comparative hemodynamic effects of Org 7797, flecainide, and propafenone in anaesthetized pigs with developing myocardial infarcts. *J. Cardiovasc. Pharmacol.*, **19**, 435–441.

(Received November 24, 1992
Revised February 10, 1993
Accepted February 25, 1993)

Br. J. Pharmacol. (1993), **110**, 29–35

Characteristics of the bradykinin-induced changes in intracellular calcium ion concentration of single bovine tracheal smooth muscle cells

Katrina A. Marsh & [1]Stephen J. Hill

Department of Physiology & Pharmacology, University of Nottingham Medical School, Queen's Medical Centre, Nottingham NG7 2UH

1 Single bovine tracheal smooth muscle (BTSM) cells were cultured and used to measure bradykinin-induced changes in $[Ca^{2+}]_i$ by dynamic video imaging.

2 Bradykinin (10 pM–10 μM)-induced an increase in $[Ca^{2+}]_i$ over basal levels (69 ± 2 nM; $n = 353$) which was concentration-dependent (log $EC_{50} = -8.7$ M) in the presence of extracellular calcium ions (2 mM). The bradykinin B_2 receptor antagonist, D-Arg[Hyp^3,Thi^{5,8},D-Phe^7]-bradykinin, produced a parallel shift to the right of the bradykinin concentration-response curve (log $EC_{50} = -7.1$ M and -5.8 M in the presence of 1 μM and 10 μM antagonist respectively) yielding an apparent K_D of 26 nM.

3 In the absence of extracellular calcium ions (with 0.1 mM EGTA), bradykinin (10 pM– 10 μM) produced a uniform increase in $[Ca^{2+}]_i$ from a basal level of 33 ± 2 nM ($n = 140$) to approximately 180 nM in BTSM cells indicating an 'all-or-nothing' release of intracellular calcium ions. In the presence of 10 μM D-Arg[Hyp^3,Thi^{5,8},D-Phe^7]-bradykinin no responses could be induced by bradykinin at concentrations below 100 nM. However, at 100 nM and 1 μM bradykinin there was no change in the uniform increase in $[Ca^{2+}]_i$ in these cells previously observed.

4 In both the absence or presence of D-Arg[Hyp^3,Thi^{5,8},D-Phe^7]-bradykinin, there was a concentration-dependent increase in the percentage of cells responding to bradykinin (frequency) under calcium-rich or calcium-free conditions. Individual cells also demonstrated a difference in the sensitivity to any particular concentration of bradykinin.

5 A latency in the response of cells to bradykinin was observed both in calcium-containing and calcium-free conditions.

6 We conclude that bradykinin B_2 receptors are expressed by BTSM cells and are involved in the bradykinin-induced increase in $[Ca^{2+}]_i$. It appears that the increase in $[Ca^{2+}]_i$ can be mediated via a graded influx of calcium ions from the extracellular space or an 'all-or-nothing' release from intracellular stores.

Keywords: Bradykinin; calcium ion mobilisation; trachea; cultured smooth muscle

Introduction

The involvement of intracellular calcium ions in smooth muscle contraction and relaxation is a well recognized phenomenon; however, the mechanisms by which changes in intracellular calcium ion concentration ($[Ca^{2+}]_i$) are obtained within the cell are not completely understood, particularly in the smooth muscle of the airways. An increase in $[Ca^{2+}]_i$ can be mediated either via a release of calcium from intracellular stores (Somylo *et al.*, 1988; Berridge & Irvine, 1989; Irvine, 1990) or via an influx of calcium from the extracellular fluid (Benham & Tsien, 1987; Murray & Kotlikoff, 1991). The release of calcium ions from intracellular stores can be effected by a spasmogen-induced activation of phospholipase C leading to an increase in the production and action of inositol 1,4,5-triphosphate (IP_3: Berridge & Irvine, 1989). It has recently been proposed that, in a number of cell types, including pancreatic acini (Muallem *et al.*, 1989), hepatocytes (Taylor & Potter, 1990; Oldershaw *et al.*, 1991) and HeLa cells (Bootman *et al.*, 1992), the IP_3-mediated release of calcium from intracellular stores is a quantal process where these stores differ in their sensitivity to IP_3.

Bradykinin is a nonapeptide which has been suggested to have an involvement in the pathogenesis of allergic asthma. In addition, elevated levels of this peptide have been observed in asthmatic patients (Christiansen *et al.*, 1987), although the physiological role of bradykinin is unclear. It has been demonstrated that bradykinin can induce an increase in $[Ca^{2+}]_i$ in both human (Murray & Kotlikoff, 1991) and guinea-pig (Farmer *et al.*, 1991a,b) airway smooth muscle cells, but the characteristics of these responses remain to be elucidated. Bradykinin receptors have classically been divided into two subtypes, those of B_1 and B_2, according to the relative potencies of antagonists and agonists (Regoli & Barabe, 1980). However, the receptor by which bradykinin exerts its intracellular effect is unclear. Using cultured cells from the guinea-pig tracheal smooth muscle, Farmer *et al.* (1991b) suggested that the activation of a putative B_3 receptor (Farmer *et al.*, 1989) was responsible for the bradykinin-induced increase in $[Ca^{2+}]_i$ they observed which was insensitive to both B_1 and B_2 receptor antagonists.

We have previously reported that bradykinin can induce an increase in phosphoinositide hydrolysis in cultures of bovine tracheal smooth muscle cells which appears to be mediated via the activation of the bradykinin B_2 receptor (Marsh & Hill, 1992a). In addition, initial studies on single bovine tracheal smooth muscle cells indicated that bradykinin also induced an increase in $[Ca^{2+}]_i$ in the presence and absence of extracellular calcium ions (Marsh & Hill, 1992b,c). We have therefore extended these studies to investigate the characteristics of the bradykinin-induced increase in $[Ca^{2+}]_i$ of single bovine tracheal smooth muscle cells in both calcium-free and calcium-rich conditions using dynamic video imaging. This paper describes the involvement of the bradykinin B_2 receptor in mediating a bradykinin-induced increase

[1] Author for correspondence.

in $[Ca^{2+}]_i$ and the characteristics of this increase by use of calcium-free and calcium-rich experimental conditions. A preliminary account of part of this work has been presented to the British Pharmacological Society (Marsh & Hill, 1993).

Methods

Cell culture

Cultures of bovine tracheal smooth muscle cells were obtained as described previously (Marsh & Hill, 1992a,b,c). Briefly, fresh tracheal smooth muscle denuded of mucosa and connective tissue was chopped into $1mm^3$ pieces and transferred to tissue culture-treated plastic flasks. These explants were then covered with a D-Val-substituted minimum essential medium containing 10% foetal calf serum (FCS) and antibiotics (100 u ml^{-1} penicillin G; 100 $\mu g\ ml^{-1}$ streptomycin; 250 ng ml^{-1} amphotericin B) then maintained at 37°C in 10% CO_2. Smooth muscle cells grew to confluency from the explants and were routinely subcultured by treatment with trypsin (0.05% in versene, Glasgow formula). Using the Hoechst 33258 staining method of Chen (1977), mycoplasmal contamination was shown to be negative. Immunocytochemical analysis using the monoclonal antibody to alpha smooth actin was performed as described previously (Marsh & Hill, 1992a) confirming the identity of the cells as smooth muscle. For image analysis purposes, cells from passages 4 to 10 were seeded at a split ratio of 1:10 onto 22 mm circular glass coverslips in Dulbecco's modified Eagle's medium with 10% FCS and grown for 72 h under the above conditions.

Image analysis

Coverslips with attached cells were washed three times in a physiological saline solution (PSS) containing (in mM): NaCl 145, KCl 5, $MgSO_4$ 1, N-2-hydroxyethylpiperazine-*N'*-2-ethanesulphonic acid (HEPES) 10, glucose 10 and $CaCl_2$ 2, pH 7.4. The cells were then incubated at 37°C for 30 min with PSS containing 10% FCS and 5 μM fura-2 acetoxymethylester; then excess dye was removed by washing with PSS a further 3 times. Coverslips were transferred to a metal holder which was mounted in a heated chamber maintained at 37°C. A volume of 900 μl of PSS was added to the chamber and agents were added directly in a volume of 100 μl PSS. For experiments requiring calcium-free conditions, any PSS added to the chamber was deficient of $CaCl_2$ and supplemented with 0.1 mM EGTA. All coverslips were used within 90 min of the end of the loading time.

Image analysis was performed with MagiCal hardware and TARDIS software supplied by Applied Imaging International Ltd. (Hylton Park, Sunderland, Tyne & Wear) as described previously in detail (Neylon *et al.*, 1990). Briefly, fluorescent images were detected by a Nikon Diaphot epifluorescence microscope with a 10 × quartz objective lens then relayed through an image intensifying charged couple device camera (Photonic Science) to the MagiCal hardware where the images underwent analogue to digital conversion. Images captured were 256 × 256 pixels in size and each frame was averaged 8 times with analogue hardware averaging to reduce camera noise. Incident light of alternating 340 and 380 nm wavelength was supplied to the sample by means of a rotating filter wheel so that the time between image pairs was 1.5 s. Once a sequence of images had been captured they were subjected to a background subtraction. For this purpose, an averaged image of each of the 340 and 380 nm types was captured from an area of the coverslip devoid of any cells using the same parameters as for cell measurements. The 340 nm background was then subtracted from each of the 340 nm images on a pixel-by-pixel basis and similar processing was performed with the 380 nm background and images.

After digital conversion, background-corrected image pairs were ratioed (340/380) on a pixel-by-pixel basis and calcium ion concentration was calculted with a 2-D look up table utilising the Grynkiewicz (1985) equation below

$$[Ca] = K_D\ \beta\ [R - R_{min}/R_{max} - R]$$

where R is the measured ratio and β is the fluorescence ratio at 380 nM of R_{min} to R_{max}. R_{max} and R_{min} values were calculated for calibration purposes by exposing the cells firstly to 20 μM ionomycin in the presence of 10 mM calcium, thus allowing flooding of the cell with calcium and a maximum fluorescence ratio (R_{max}) to be obtained. R_{min} (minimum fluorescence ratio) was calculated by chelation of the free calcium ions with 6 mM EGTA. A dissociation constant (K_D) of 224 nM for fura-2 and calcium at 37°C was incorporated into the 2-D look up table.

Image analysis software performed quantification of mean calcium ion concentration as a function of time (Figure 1a) and whole cell intracellular calcium ion quantification was obtained by outlining each individual cell with a light pen (Figure 1b). Graphical representation was automatically produced from the pixel data contained within the defined region.

Data analysis

Concentration-response curves were fitted to a Hill equation by use of the non-linear programme ALLFIT (DeLean *et al.*, 1978). The equation fitted was

$$\%\ \text{of maximal response} = E_{max} \times D^n/D^n + (EC_{50})^n$$

where D is the agonist concentration, n is the Hill coefficient, EC_{50} is the concentration of agonist giving half maximal response and E_{max} is the maximal stimulation. Apparent dissociation constant (K_D) of the receptor antagonist was determined, assuming competitive antagonism, from shifts in the agonist concentration-response curves using the relationship

$$K_D = D/(K_2/K_1 - 1)$$

where D is the concentration of antagonist, K_1 is the concentration of agonist producing half maximal response and K_2 is the concentration of agonist producing the same response in the presence of antagonist. The data point at each concentration of bradykinin was calculated from accumulated data from a single field of view (containing 4–10 cell) from each of at least six different coverslips each arising from different animals.

Chemicals

D-Arg[Hyp^3,$Thi^{5,8}$,D-Phe^7]-bradykinin, bradykinin acetate and Hoechst 22358 were obtained from Sigma. Anti-alpha smooth muscle actin monoclonal antibody was purchased from Dako Ltd.

Results

Figure 1a demonstrates the time sequence of changes in $[Ca^{2+}]_i$ of cells from a single field of view. An interval of approximately 3 s separates each image and bradykinin (10 nM) was added between the first two frames. The graphical analysis from Figure 1a is shown in Figure 1b where each line on the upper graph represents the changes in intracellular calcium ion concentration from the individual cell defined by the outline of the same colour.

In the presence of extracellular calcium, bradykinin produced a sharp increase in the $[Ca^{2+}]_i$ of bovine tracheal smooth muscle (BTSM) cells which fell to a lower yet elevated over basal level that was maintained for several minutes (Figure 1). On analysis of data from between 26 and 45 cells at each concentration, bradykinin was found to produce a concentration-dependent increase in $[Ca^{2+}]_i$ over basal levels (mean basal level in calcium-rich conditions = 69 ± 2 nM; n = 353: maximum increase =

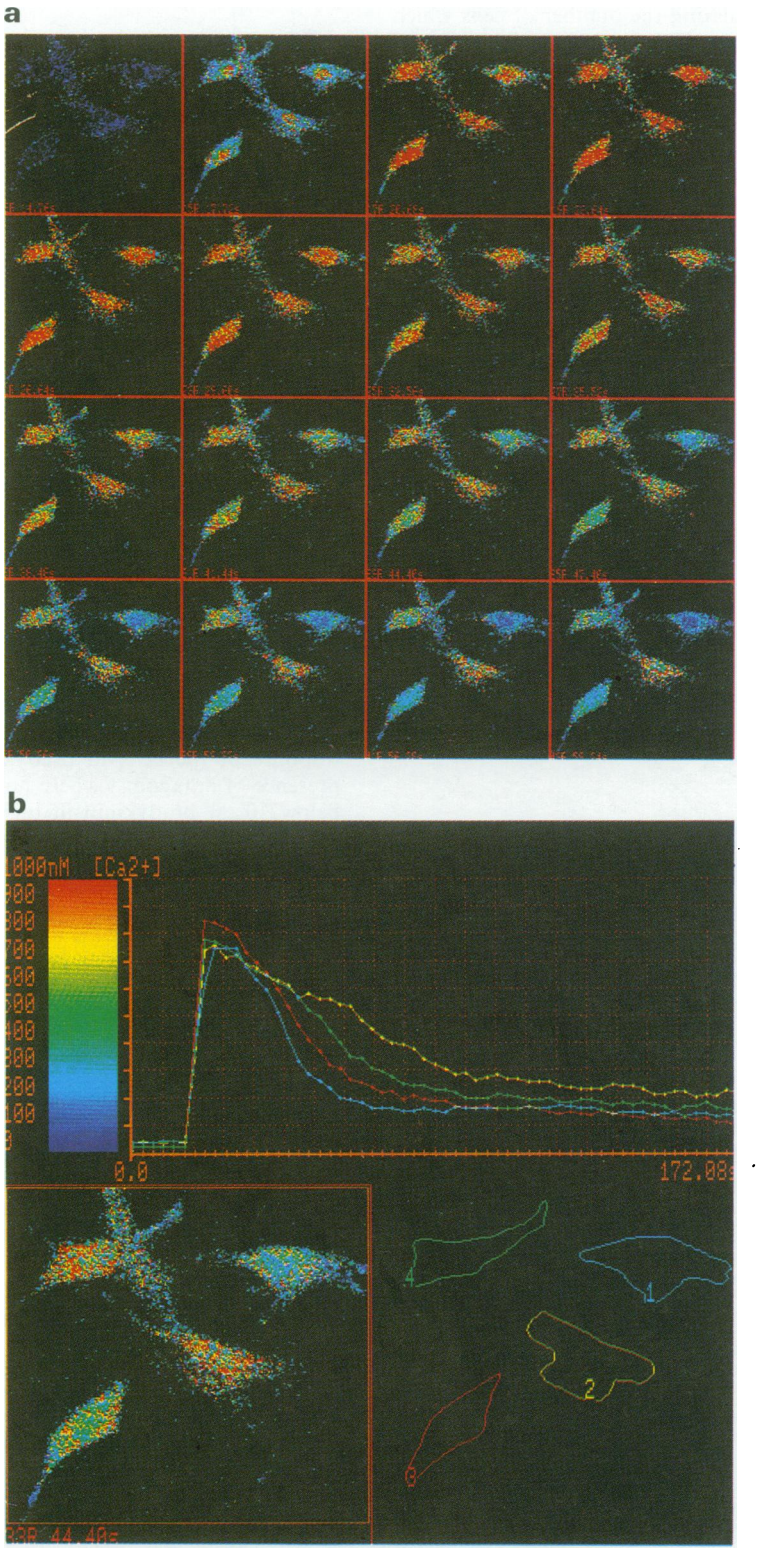

Figure 1 Bradykinin-induced changes in intracellular calcium ion concentration in single bovine tracheal smooth muscle cells in the presence of extracellular calcium ions. (a) Montage of a time sequence of images obtained from the 'MagiCal' image analysis system. A time interval of approximately 3 s separates each image and the different colours represent different intracellular calcium ion concentrations (indicated to the left of the graph in Figure 1b). For evaluation of changes in calcium ion concentration within single cells, one field of view (4–10 cells) was monitored as a representative area from each coverslip. (b) Intracellular calcium ion concentrations for each of the cells were then measured individually as a function of time and are represented by separate traces on the graph. Each coloured trace of the graph (top) represents the data obtained from the cell (shown in the bottom left image) which is outlined by the same colour (bottom right image). Intracellular calcium ion concentrations are represented by the colours indicated to the left of the graph. Bradykinin (100 nM) was added to the bathing medium 15 s after the start of image capture (0 s).

428 ± 45 nM at 1 μM bradykinin; $n = 45$: Figure 2). It became increasingly apparent that not all the cells in any one field of view were responding to bradykinin, particularly at the lower concentrations of this agonist. We therefore analysed further this phenomenon with respect to the frequency of responding cells. This was done by calculating the number of cells which responded to a particular concentration of bradykinin as a percentage of the total number of cells observed at that concentration. By analysing the data in this way we found a concentration-dependent increase in the frequency of response of BTSM cells to bradykinin (Table 1). In light of this observation, data have been calculated from the bradykinin-sensitive cells only in order to evaluate the results as actual cell responses rather than as a function of the frequency of response of the cells. One field of view, containing 4–10 cells, was observed from each of six different coverslips (arising from different animals) for each concentration of bradykinin. The mean increase in $[Ca^{2+}]_i$ of all the cells which responded to each concentration of bradykinin was then calculated.

Evaluating the results in this way we found that the concentration-response curve for bradykinin in the presence of extracellular calcium ions revealed a log EC_{50} value of − 8.7 M (Figure 3). On addition of the bradykinin B_2 receptor antagonist, D-Arg[Hyp^3,Thi^{5,8},D-Phe^7]-bradykinin, 2 min prior to the addition of bradykinin, there was a parallel shift to the right of the bradykinin concentration-response curve

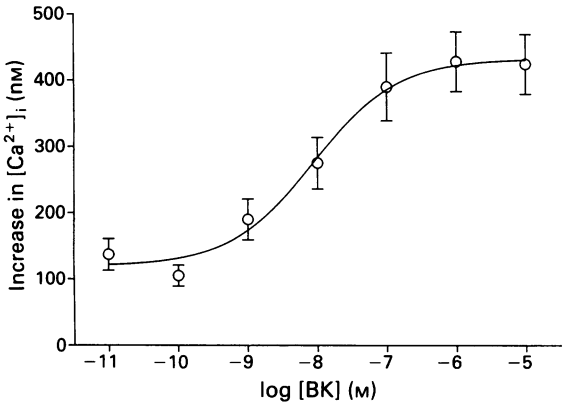

Figure 2 Concentration-response curve to bradykinin (10 pM–10 μM). Values represent the mean increase in intracellular calcium ion concentration over basal levels of all BTSM cells (i.e. bradykinin (BK)-responsive and non-responsive cells) observed. Means of the cell responses ($n = 26–45$ at each concentration of bradykinin) were calculated from at least six fields of view from separate coverslips each arising from different animals. Points show means with s.e.mean.

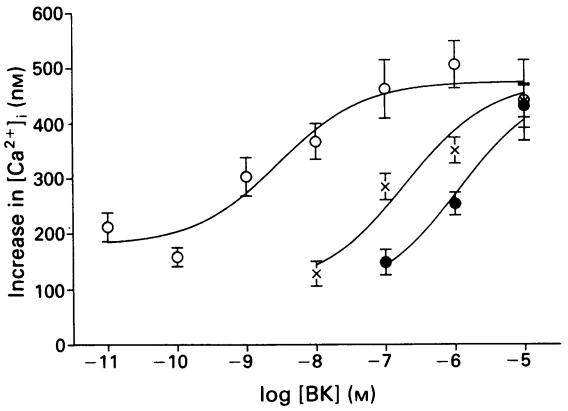

Figure 3 Concentration-response curves to bradykinin (10 pM–10 μM) in the absence (o) and presence of 1 μM (x) or 10 μM (●) D-Arg[Hyp^3,Thi^{5,8},D-Phe^7]-bradykinin added 2 min prior to bradykinin in the presence of extracellular calcium ions. Values represent the mean increase in intracellular calcium ion concentration over basal levels of only the BTSM cells which responded to bradykinin. Means of responding cells ($n = 21–38$ at each concentration) were calculated from at least six fields of view from separate coverslips each originating from different animals. Points show means with s.e.mean.

(Figure 3) indicating competitive antagonism resulting in log EC_{50} values of − 7.1 and − 5.8 in the presence of 1 μM and 10 μM antagonist respectively. These values yielded an apparent K_D of 26 nM for D-Arg[Hyp^3,Thi^{5,8},D-Phe^7]-bradykinin. Table 1 demonstrates the differences in the frequency of response of the cells to bradykinin in the absence and the presence of antagonist where no cell responses were observed below 10 nM bradykinin in the presence of 1 μM antagonist and below 100 nM bradykinin in the presence of 10 μM D-Arg[Hyp^3,Thi^{5,8},D-Phe^7]-bradykinin. No increase in $[Ca^{2+}]_i$ was observed on addition of D-Arg[Hyp^3,Thi^{5,8},D-Phe^7]-bradykinin to the cells (results not shown).

In the absence of extracellular calcium ions there was an increase in $[Ca^{2+}]_i$ above basal levels (mean basal level in calcium-free conditions = 33 ± 2 nM; $n = 140$) in response to bradykinin which returned to basal levels within 90 s (Figure 4). However, as in the presence of extracellular calcium ions, not all cells responded to bradykinin (Figure 4, Table 1). On analysing the data from bradykinin-sensitive cells only, it was revealed that there was a uniform increase in $[Ca^{2+}]_i$ of approximately 180 nM on addition of concentrations of bradykinin between 10 pM and 10 μM bradykinin ($n = 4–22$ for each concentration of bradykinin) indicating the absence of any concentration-response relationship. The

Table 1 Frequency of response of single BTSM cells to various concentrations of bradykinin in calcium-containing (+Ca) and calcium-free conditions (− Ca)

	Frequency of response (%)						
log [BK] (M)	− 11	− 10	− 9	− 8	− 7	− 6	− 5
+ Calcium							
BK alone	65 (24/37)	67 (26/39)	63 (27/43)	75 (21/28)	84 (38/45)	84 (38/45)	96 (25/26)
+ 1 μM antagonist	–	0 (0/20)	0 (0/31)	41 (14/34)	90 (30/33)	96 (26/27)	100 (32/32)
+ 10 μM antagonist	–	0 (0/15)	0 (0/16)	0 (0/30)	15 (4/26)	86 (30/35)	95 (19/20)
− Calcium							
BK alone	18 (7/38)	15 (5/34)	39 (14/36)	34 (13/38)	27 (9/33)	55 (22/40)	67 (20/30)
+ 10 μM antagonist	–	0 (0/8)	0 (0/17)	0 (0/24)	31 (18/59)	39 (22/56)	53 (25/47)

Experiments, as described in the text, were performed in the absence or presence of 1 μM or 10 μM of D-Arg[Hyp^3,Thi^{5,8},D-Phe^7]-bradykinin as indicated. The frequency indicated is calculated from a sample of cells taken from at least six separate coverslips each originating from different animals and is defined as the percentage of the total number of cells observed which respond to bradykinin. Numbers in parentheses indicate the number of cells responding to bradykinin/the total number of cells observed.

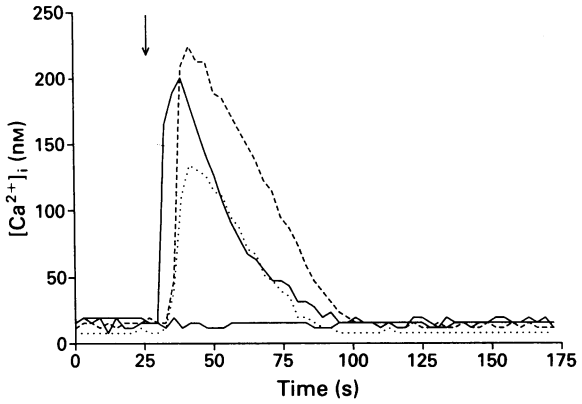

Figure 4 Bradykinin-induced changes in intracellular calcium ion concentration of single BTSM cells in calcium-free conditions (with 0.1 mM EGTA). The arrow indicates the addition of 100 nM bradykinin. Note that one of the four cells was not responsive to 100 nM bradykinin. Intracellular calcium ion concentrations were calculated as in Figure 1.

slope of the linear regression line fitted to the data points did not differ significantly from zero (Figure 5). However, the frequency of response of the cells under calcium-free conditions are shown in Table 1 and although these frequencies are lower than those observed in the presence of extracellular calcium, a concentration-dependent increase in frequency is still apparent. In the presence of 10 μM D-Arg[Hyp^3,Thi^{5,8},D-Phe^7]-bradykinin no responses were observed below a concentration of bradykinin of 100 nM in calcium-free conditions (Table 1). At concentrations of bradykinin of 0.1 and 1 μM there was no statistically significant difference (unpaired t test) between the increases in $[Ca^{2+}]_i$ obtained in the absence or presence of D-Arg[Hyp^3,Thi^{5,8},D-Phe^7]-bradykinin. However, on addition of 10 μM bradykinin a significantly greater increase in $[Ca^{2+}]_i$ was induced in the presence of 10 μM D-Arg[Hyp^3,Thi^{5,8},D-Phe^7]-bradykinin (338 ± 44, $n = 25$) than in the absence of antagonist (193 ± 20, $n = 20$; $P < 0.01$).

In addition to the above observations, it was also noted that there was a difference in the latency of response to bradykinin between cells in any one field of view particularly at the lower concentrations of bradykinin. Figure 6 demonstrates the different latencies of response of 3 cells to 1 nM bradykinin under calcium-free conditions which is representative of the phenomenon observed in both calcium-free and calcium-containing conditions. We do not attribute these latencies to the diffusion of bradykinin across the monolayer as the spatial arrangement of the cells and the temporal aspect of the response are not consistent with a diffusion pattern (results not shown).

A difference in sensitivity was observed between cells to any particular concentration of bradykinin. Figure 7a demonstrates the responses of 2 cells to 0.1, 1, 10 and 1000 pM bradykinin in the presence of extracellular calcium. The cell response depicted by the solid line responds to all four concentrations of bradykinin with increasing amplitude. In contrast the cell represented by the dashed line shows a marginal increase in $[Ca^{2+}]_i$ to 0.1 pM bradykinin, no further increase at 1 pM but additional increases at 10 and 1000 pM bradykinin. In the absence of extracellular calcium ions differences in sensitivity were also observed in response to 0.01, 0.1, 1 and 10 μM bradykinin; however, under these conditions no further increases in $[Ca^{2+}]_i$ were seen on addition of higher concentrations of bradykinin.

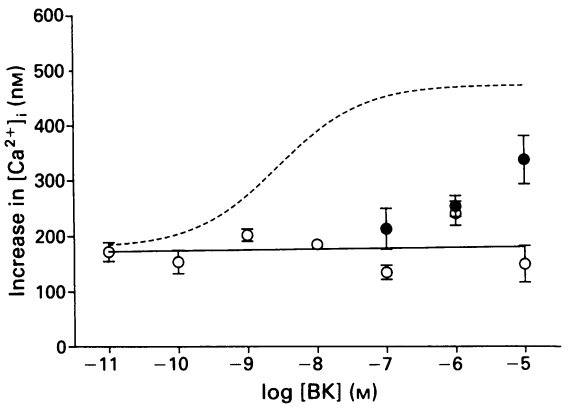

Figure 5 Bradykinin (BK) (10 pM–10 μM)-induced increases in intracellular calcium ion concentrations in calcium-free medium in the absence (○) and presence (●) of 10 μM D-Arg[Hyp^3,Thi^{5,8},D-Phe^7]-bradykinin added 2 min before bradykinin. Means of responding cells ($n = 4$–22 at each concentration) were calculated as for Figure 3. Points are means with s.e.mean. The dashed line represents the concentration-response curve to bradykinin in the presence of extracellular calcium taken from Figure 3 for purposes of comparison. The linear regression line fitted through the data points obtained in the absence of antagonist reveals a Y intercept of 189 nM and a slope of 1.5 which did not differ significantly from zero.

Discussion

This study demonstrates that in the presence of extracellular calcium ions, bradykinin can induce a concentration-dependent increase in the $[Ca^{2+}]_i$ of single bovine tracheal smooth muscle (BTSM) cells. This increase can be attenuated by the bradykinin B_2 receptor antagonist D-Arg[Hyp^3,Thi^{5,8},D-Phe^7]-bradykinin suggesting that the receptor via which bradykinin exerts its effects is the B_2 receptor. This would concur with our previous report that the B_2 receptor mediates the bradykinin-induced increase in phosphoinositide (PI) hydrolysis in these cells (Marsh & Hill, 1992a,b) in that stimulation of the B_2 receptor increases the production of IP_3 which itself can lead to the release of calcium from intracellular stores (Berridge & Irvine, 1989). One of the more striking findings of this study is the uniform increase in $[Ca^{2+}]_i$ induced by all concentrations of bradykinin used in the absence of extracellular calcium. These results would suggest that, in this cell type, bradykinin is able to induce an 'all-or-nothing' release of calcium from the intracellular stores. This therefore suggests that the influx of calcium from the extracellular space (plateau phase of Figure 1b) appears to have a graded component and that the concentration-response curve obtained in the presence of extracellular calcium is a product

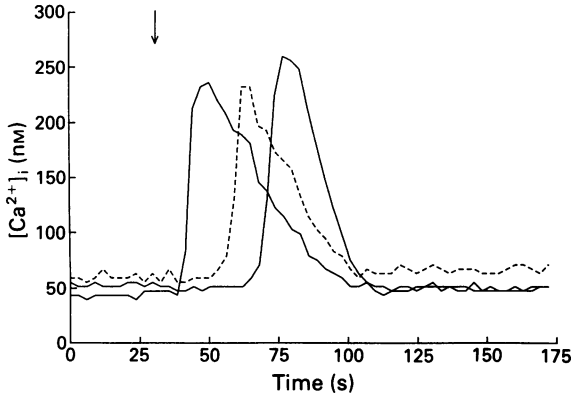

Figure 6 Latencies of individual cells responding to bradykinin in calcium-free conditions. Each trace represents the changes in intracellular calcium ion concentration of individual cells in the same field of view. The three cells represented in the graph responded approximately 7 s, 21 s and 34 s after the addition of 1 nM bradykinin (arrow).

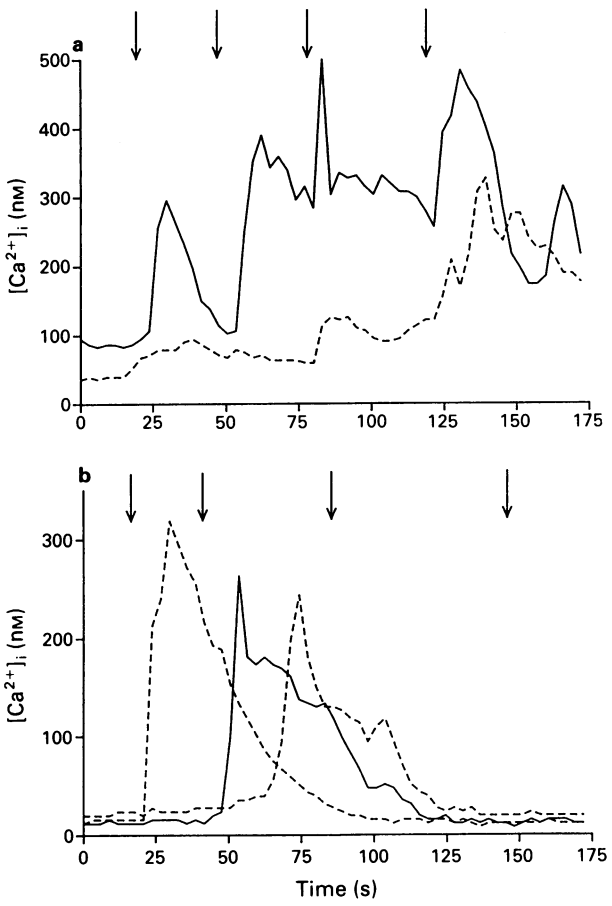

Figure 7 Different sensitivities of individual BTSM cells within a single field of view to bradykinin in (a) calcium-containing medium and (b) calcium-free medium. Arrows represent the sequential additions of (a) 0.1, 1, 10 and 100 pM bradykinin or (b) 0.01, 0.1, 1 and 10 μM bradykinin.

of the graded influx of ions from the extracellular space and an 'all-or-nothing' release of calcium from internal stores.

The characteristics of the 'all-or-nothing' release of calcium in the present study appears to be different from that observed in other cell types (Muallem *et al.*, 1989; Taylor & Potter, 1990; Oldershaw *et al.*, 1991; Bootman *et al.*, 1992). These groups have proposed that the intracellular calcium stores consist of several smaller stores which differ in their sensitivity to IP_3, resulting in the release of only a portion of the stores at low concentrations followed by a further emptying of more stores on application of higher concentrations of IP_3. This is not a phenomenon observed in the present study where it is quite clearly shown in Figure 7b that, in the absence of extracellular calcium ions, once a cell has responded to bradykinin it will not repeat this increase on further additions of higher concentrations of bradykinin. We do not believe this to be a result of desensitization to bradykinin as multiple responses to bradykinin are observed under calcium-rich conditions. It is possible that the calcium release mechanism is sufficiently cooperative within individual BTSM cells to enable a complete emptying of the calcium stores which is consistent with the observation that IP_3-stimulated calcium release can be highly cooperative (Meyer *et al.*, 1988; 1990; Bootman *et al.*, 1992). Interpretation of the results obtained in the present study in calcium-free conditions leads to several suggestions, one being that the intracellular calcium stores within BTSM cells are cooperative but are not compartmentalized. A particular concentration of IP_3 may then trigger a complete emptying of the entire store. If the sensitivity to IP_3 differs from cell to cell, then this could produce the apparent difference in sensitivity to bradykinin. Alternatively, the stores may indeed be compartmentalized yet the bradykinin triggers an 'all-or-nothing' production of IP_3 which releases only a portion of the stores and the different sensitivities observed are due to the differences in sensitivities of the cells to bradykinin.

Another possibility is that the constant amplitude of the bradykinin response seen in this study in calcium-free media may be a consequence of the interaction between IP_3-sensitive and IP_3-insensitive calcium stores which leads to the filling and subsequent transient calcium-induced release of calcium from the latter stores. This mechanism is one which has been proposed to account for the oscillations in $[Ca^{2+}]_i$ observed in a number of cell types (Berridge *et al.*, 1988; Berridge, 1990). Indeed the latency of response of BTSM cells to bradykinin observed in this study would be consistent with this latter hypothesis (Figure 6). If this is the case, then the graded increases observed in the presence of extracellular calcium induced by the higher concentrations of bradykinin must therefore be able to increase $[Ca^{2+}]_i$ directly or to act via IP_3-insensitive stores which are not accessible to calcium released from IP_3-sensitive stores. The graded influx of calcium ions from the extracellular space may also interact synergistically with IP_3 to cause channel opening (Finch *et al.*, 1991) resulting in the calcium mobilized from the stores promoting further calcium release within the cell. However, the exact mechanisms involved in the bradykinin-induced increase in $[Ca^{2+}]_i$ require further intracellular investigation for complete elucidation.

It has been established that the receptor mediating the bradykinin-induced increase in PI hydrolysis is the B_2 receptor (Marsh & Hill, 1992a) and from the present study it is now apparent that this same receptor is involved in the bradykinin-induced increase in $[Ca^{2+}]_i$ in cultured BTSM cells. We have found that in this assay system, as in the PI hydrolysis system, there is no inherent partial agonist activity produced by D-Arg[Hyp^3,Thi^{5,8},D-Phe^7]-bradykinin as has been observed in the guinea-pig lung and tracheal strips (Farmer *et al.*, 1989). The K_D value obtained in BTSM cells in this study for D-Arg[Hyp^3,Thi^{5,8},D-Phe^7]-bradykinin (26 nM) is of the same order of magnitude as those obtained in functional studies using the B_2 receptor-rich system, the rabbit jugular vein (10 nM; Regoli *et al.*, 1990).

We suggested in our previous paper (Marsh & Hill, 1992a) that a species difference exists in the coupling of bradykinin receptors to PI hydrolysis and calcium ion mobilization in airway smooth muscle cells. This was due to the sensitivity of the bradykinin-induced increase in PI hydrolysis to B_2 receptor antagonists in bovine cells (Marsh & Hill, 1992a) and the insensitivity of calcium ion mobilization in guinea-pig cells to B_2 receptor antagonists (Farmer *et al.*, 1991b). The results presented here support the view that there are indeed species differences and bradykinin B_2 receptors in BTSM cells are coupled to both second messenger systems whereas the receptor mediating calcium ion mobilization in guinea-pig cells is not a B_2 receptor and may be a B_3 receptor as suggested by Farmer *et al.* (1991a,b).

The results we obtained of the responses to bradykinin in the presence of 10 μM D-Arg[Hyp^3,Thi^{5,8},D-Phe^7]-bradykinin in calcium-free media (Figure 5) are in the main consistent with what we would expect for the antagonism of an 'all-or-nothing' response. In this case the antagonist abolished the responses to low concentrations of bradykinin (< 100 nM) but did not significantly alter the magnitude of the calcium response of the cells sensitive to 100 mM or 1 μM bradykinin (circa 200 nM). The only possible exception was that 10 μM bradykinin induced an increase in $[Ca^{2+}]_i$ which was significantly higher in the presence of D-Arg[Hyp^3,Thi^{5,8},D-Phe^7]-bradykinin. This response may be a result of the high and perhaps non-specific concentration of bradykinin used or may reflect a further quantal release of intracellular calcium ions. Another possibility is the involvement of B_1 receptors becoming apparent at that concentration of bradykinin under these conditions.

The involvement of B_1 receptors in the bradykinin-induced increase in PI hydrolysis of BTSM cells was found to be very small in that the relative potency of the B_1 agonist des-Arg^9-bradykinin (Regoli & Barabé, 1980) was only 16% of that produced by bradykinin itself (Marsh & Hill, 1992a). However it is of interest to note that initial studies investigating the involvement of the B_1 receptor, using des-Arg^9-bradykinin, in the calcium response of BTSM cells indicates a possible role for the B_1 receptor in calcium ion mobilization. The presence of this receptor in airway smooth muscle from other species is doubted (Farmer *et al.*, 1989) and we are therefore extending our studies to evaluate the possible involvement of this receptor in mediating the bradykinin-induced increase in $[Ca^{2+}]_i$ of BTSM cells.

One curious result produced by this present study is the concentration-dependent change in the frequency of response of the cells to bradykinin in both the absence and presence of extracellular calcium ions. This could be easily explained solely by a difference in the sensitivity of individual cells to bradykinin. This would involve there being few highly sensitive cells in a population which respond to lower concentrations of bradykinin yielding a lower frequency of response, whereas in comparison, the higher frequency of response result from the more abundant, less sensitive cells requiring higher concentrations of bradykinin to produce a detectable response. One possible reason for this heterogeneity of sensitivity could be that the cultures are taken from a full cross section of tracheal smooth muscle which itself may not be homogeneous in its distribution of bradykinin-sensitive cells. To prove or disprove this theory would require precise sectioning of the tracheal smooth muscle and differential culturing of the cells in order to establish whether or not homogeneous cultures can be obtained from a particular section of smooth muscle which may give us some insight into the physiological role of bradykinin in the airways.

We wish to thank the A.F.R.C. for their financial support of this work.

References

BENHAM, C.D. & TSIEN, R.W. (1987). A novel receptor-operated Ca^{2+}-permeable channel activated by ATP in smooth muscle. *Nature*, **328,** 275–278.

BERRIDGE, M.J. (1990). Temporal aspect of calcium signalling. *Adv. Second Messenger Phosphoprotein Res.*, **24,** 108–114.

BERRIDGE, M.J. & IRVINE, R.F. (1989). Inositol phosphates and cell signalling. *Nature*, **341,** 197–205.

BOOTMAN, M.D., BERRIDGE, M.J. & TAYLOR, C.W. (1992). All-or-nothing Ca^{2+} mobilisation from the intracellular stores of single histamine-stimulated HeLa cells. *J. Physiol.*, **450,** 163–178.

CHEN, T.R. (1977). *In situ* detection of mycoplasma contamination in cell cultures by fluorescent Hoechst stain 33258. *Exp. Cell Res.*, **104,** 255–259.

CHRISTIANSEN, S.C., PROUD, D. & COCHRANE, C.G. (1987). Detection of tissue kallikrein in the bronchoalveolar lavage fluid of asthmatic patients. *J. Clin. Invest.*, **79,** 188–197.

DELEAN, A., MUNSON, P.J. & RODBARD, D. (1978). Simultaneous analysis of families of sigmoidal curves: application to bioassay, radioligand assay and physiological dose-response curves. *Am. J. Physiol.*, **235,** E97–E102.

FARMER, S.G., BURCH, R.M., KYLE, D.J., MARTIN, J.A., MEEKER, S.N. & TOGO, J. (1991b). D-Arg[Hyp^3-Thi^5-D-Tic^8]-bradykinin, a potent antagonist of smooth muscle BK_2 receptors and BK_3 receptors. *Br. J. Pharmacol.*, **102,** 785–787.

FARMER, S.G., BURCH, R.M., MEEKER, S.A. & WILKINS, D.E. (1989). Evidence for a pulmonary B_3 bradykinin receptor. *Mol. Pharmacol.*, **36,** 1–8.

FARMER, S.G., ENSOR, J.E. & BURCH, R.M. (1991a). Evidence that cultured airway smooth muscle cells contain bradykinin B_2 and B_3 receptors. *Am. J. Respir. Cell Mol. Biol.*, **4,** 273–277.

FINCH, E.A., TURNER, T.J. & GOLDIN, S.M. (1991). Calcium as a co-agonist of inositol 1,4,5-trisphosphate-induced calcium release. *Science*, **252,** 443–446.

GRYNKIEWICZ, G., POENIE, M. & TSIEN, R.Y. (1985). A new generation of Ca^{2+} indicators with greatly improved fluorescence indicators. *J. Biol. Chem.*, **260,** 3440–3450.

IRVINE, R.F. (1990). 'Quantal' Ca2+ release and the control of Ca2+ entry by inositol phosphates – a possible mechanism. *FEBS*, **263,** 5–9.

MARSH, K.A., & HILL, S.J. (1992a). Bradykinin B_2 receptor-mediated phosphoinositide hydrolysis in bovine cultured tracheal smooth muscle cells. *Br. J. Pharmacol.*, **107,** 443–447.

MARSH, K.A. & HILL, S.J. (1992b). Characteristics of bovine tracheal smooth muscle cells during agonist-induced phosphoinositide hydrolysis and calcium mobilisation. *Am. Rev. Respir. Dis.*, **145,** A371.

MARSH, K.A. & HILL, S.J. (1992c). Bradykinin-induced phosphoinositide hydrolysis and calcium ion mobilisation in cultured bovine tracheal smooth muscle cells. *Br. J. Pharmacol.*, **105,** 66P.

MARSH, K.A. & HILL, S.J. (1993). Characteristics of the bradykinin-induced increase in intracellular calcium ion concentration of single cultured bovine tracheal smooth muscle cells. *Br. J. Pharmacol.* (in press).

MEYER, T., HOLOWKA, D. & STRYER, L. (1988). Highly cooperative opening of calcium channels by inositol 1,4,5-trisphosphate. *Science*, **240,** 653–656.

MEYER, T., WENSEL, T. & STRYER, L. (1990). Kinetics of calcium channel opening by inositol 1,4,5-trisphosphate. *Biochem.*, **29,** 32–37.

MUALLEM, S, PANDOL, S.J. & BEEKER, T.G. (1989). Hormone-evoked calcium release from intracellular stores is a quantal process. *J. Biol. Chem.*, **264,** 205–212.

MURRAY, R.K. & KOTLIKOFF, M.I. (1991). Receptor-activated calcium influx in human airway smooth muscle cells. *J. Physiol.*, **435,** 123–144.

NEYLON, C.B., HOYLAND, J., MASON, W. & IRVINE, R.F. (1990). Spatial dynamics of intracellular calcium in agonist-stimulated vascular smooth muscle cells. *Am. J. Physiol.*, **259,** C657–C686.

OLDERSHAW, K.A., NUNN, D.L. & TAYLOR, C.W. (1991). Quantal Ca^{2+} mobilisation stimulated by inositol 1,4,5-trisphosphate in permeabilised hepatocytes. *Biochem. J.*, **278,** 705–708.

REGOLI, D. & BARABÉ, J. (1980). Pharmacology of bradykinin and related kinins. *Pharmacol. Rev.*, **32,** 1–46.

REGOLI, D., RHALEB, N.-E., DRAPEAU, G. & DION, S. (1990). Kinin receptor subtypes. *J. Card. Pharmac.*, **15,** S30–S38.

SOMLYO, A.P., WALKER, J.W., GOLDMAN, Y.E., TRENTHAM, D.R., KOBAYASHI, S., KITAZAWA, T. & SOMLYO, A.V. (1988). Inositol triphosphate, calcium and muscle contraction. *Phil. Trans. R. Soc. B.*, **320,** 399–404.

TAYLOR, C.W. & POTTER, B.V.L. (1990). The size of inositol 1,4,5-trisphosphate-sensitive Ca^{2+} stores depends on inositol 1,4,5-trisphosphate concentration. *Biochem. J.*, **266,** 189–194.

(Received March 1, 1993
Revised April 19, 1993
Accepted April 22, 1993)

Br. J. Pharmacol. (1993), **110**, 36–42

Lack of effect of L-687,414 ((+)-*cis*-4-methyl-HA-966), an NMDA receptor antagonist acting at the glycine site, on cerebral glucose metabolism and cortical neuronal morphology

[1]R.J. Hargreaves, M. Rigby, D. Smith & R.G. Hill

Department of Pharmacology, Merck Sharp & Dohme Research Laboratories, Neuroscience Research Centre, Terlings Park, Eastwick Road, Harlow, Essex CM20 2QR

1 N-methyl-D-aspartate (NMDA) receptor ion channel antagonists have been reported to cause pronounced increases in cerebral glucose metabolism (CMR_{glc}) and transient reversible vacuolation within pyramidal cortical neurones. The present studies examined in rats the effects of the NMDA receptor antagonist, L-687,414 (**R**-(+)-*cis*-4-methyl-3-amino-1-hydroxypyrolid-2-one; (+)-*cis*-4-methyl-HA-966) on regional CMR_{glc} and cortical neuronal morphology.

2 L-687,414 was given as a steady state intravenous infusion for 4 h in a neuroprotective dose regime of 17.5 mg free base kg^{-1} bolus followed by 225 $\mu g\,kg^{-1}\,min^{-1}$ ($n = 8$) or at the higher dose rate of 35 mg kg^{-1} bolus followed by 440 $\mu g\,kg^{-1}\,min^{-1}$ ($n = 10$). Data were compared to a parallel series of experiments in rats given the NMDA receptor ion channel antagonist, dizocilpine for 4 h in the optimum intravenous neuroprotective dose-regime of 0.12 mg kg^{-1} bolus followed by 1.8 $\mu g\,kg^{-1}\,min^{-1}$ ($n = 8$) or at the higher dose rate of 0.4 mg kg^{-1} bolus followed by 6 $\mu g\,kg^{-1}\,min^{-1}$ ($n = 4$; morphology only studied). A saline-infused group of rats ($n = 8$) were used as controls.

3 CMR_{glc} was studied by use of [^{14}C]-2-deoxyglucose and autoradiography ($n = 4$ each group) whilst plasma drug levels were in a steady state during the final 45 min of the 4 h drug infusion. Effects on cortical neuronal morphology were assessed at the end of the 4 h infusion period using light microscopic techniques ($n = 4–6$ each group).

4 The results showed a selective activation of limbic CMR_{glc} by dizocilpine at optimal neuroprotective dose levels and showed that this dose was at the threshold for the neuronal vacuolation response as 1 of 4 rats showed morphological changes in the pyramidal neurones in the posterior cingulate and retrosplenial cortices. At the higher dose rate of dizocilpine, all 4 animals showed extensive morphological changes in these cortical neurones. In contrast, L-687,414 did not increase limbic CMR_{glc} nor evoke vacuolation when given in the neuroprotective dose-regime or at the higher dosage rate.

5 The findings of the present study suggest that neuroprotection mediated through the NMDA receptor complex can be achieved without changes in CMR_{glc} or cortical neuronal morphology by antagonism at the glycine modulatory site.

Keywords: L-687,414; dizocilpine; NMDA glycine; partial agonist; cerebral glucose metabolism; cortical neuronal morphology

Introduction

Overactivation of N-methyl-D-aspartate (NMDA) receptors by excitatory amino acids released during cerebral ischaemia is thought to result in an excessive calcium influx into neurones that causes cell death (Choi, 1990; Benveniste, 1991). NMDA receptor antagonists have been shown to be neuroprotective in various experimental models of focal ischaemia (McCulloch, 1991) and to protect against excitotoxin-induced CNS nerve cell loss (Foster *et al.*, 1988; 1990). Antagonism of the excitotoxic effects associated with excessive NMDA receptor activation can be achieved by actions at several distinct sites within the NMDA receptor complex (Wong & Kemp, 1991). NMDA antagonists may act within the ion channel controlled by the receptor producing a use-dependent non-competitive blockade, competitively at the glutamate recognition site or at allosteric modulatory sites on the receptor complex where glycine and polyamines are thought to act to enhance NMDA receptor function.

The administration of some non-competitive NMDA receptor channel antagonists (phencyclidine and the related compounds dizocilpine (MK-801) and ketamine) has been shown to increase cerebral glucose metabolism (CMR_{glc}) particularly within the limbic system (Kurumaji *et al.*, 1989; Nehls *et al.*, 1990). The same NMDA receptor channel antagonists have also been shown to induce transient reversible vacuolation in pyramidal neurones in the posterior cingulate and retrosplenial cortices in the rat (Olney *et al.*, 1989), areas of the CNS coincident anatomically with regions in which glucose hypermetabolism is observed (Allen & Iversen, 1990).

L-687,414 (**R**-(+)-*cis*-4-methyl-HA-966) is an NMDA antagonist that acts at the glycine modulatory site of the NMDA receptor complex, but at high concentrations shows characteristics typical of a low efficacy partial agonist (Kemp *et al.*, 1991). L-687,414 has higher affinity and slightly lower intrinsic activity at the glycine site than HA-966 (Foster *et al.*, 1991). L-687,414 has been shown to be active in anticonvulsant tests in rodents (Saywell *et al.*, 1991) and primates (Smith & Meldrum, 1992) and to give significant neuroprotection when given post-occlusion in the rat middle cerebral artery occlusion (MCAO) model of focal cerebral ischaemia (Gill *et al.*, 1991a).

The objectives of the present studies were to examine the effects of neuroprotective dose regimes of L-687,414 on CMR_{glc} and neuronal morphology in comparison with the NMDA receptor channel blocker dizocilpine, the most potent neuroprotective agent yet described (Gill *et al.*, 1991b). The study design mimicked that of experimental studies of focal ischaemia in rats and attempted to simulate some of the conditions that may occur in the clinic where neuroprotective agents might be given by bolus intravenous injection follow-

[1] Author for correspondence.

ed by slow intravenous infusion to sustain plasma concentrations for prolonged periods of time. A preliminary account of part of these studies was given at the XVth International Symposium on Cerebral Blood Flow and Metabolism (Hargreaves *et al.*, 1991).

Methods

Male Sprague-Dawley rats (approximately 260 g body weight) were anaesthetized with isoflurane and the tail artery and lateral tail veins cannulated for blood sampling and the administration of test compounds, radiolabelled tracer or 0.9% saline vehicle. After surgery the animals were placed in a quiet room in open restraining cages (that allow movement but prevent turning to gain access to the vascular cannulae) and allowed to recover for 2 h before dosing.

After recovery the rats were given either L-687,414 or MK-801 intravenously. Groups of rats were given L-687,414 as a 17.5 mg kg^{-1} bolus followed by infusion at 225 $\mu g\ kg^{-1}\ min^{-1}$ ($n = 8$: the neuroprotective dose regime in the rat MCAO model of focal ischaemia (Gill *et al.*, 1991a)) or at the higher dose rate of 35 mg kg^{-1} bolus followed by 440 $\mu g\ kg^{-1}\ min^{-1}$ ($n = 10$). For comparison, groups of rats were given dizocilpine intravenously as a 0.12 mg kg^{-1} bolus followed by infusion at 1.8 $\mu g\ kg^{-1}\ min^{-1}$ ($n = 8$: the optimal neuroprotection regime in the rat MCAO model of focal ischaemia (Gill *et al.*, 1991b)) or the higher dose rate of 0.4 mg kg^{-1} bolus followed by 6 $\mu g\ kg^{-1}\ min^{-1}$ ($n = 4$). As control, a group of rats were given saline (vehicle) as a bolus 1.0 ml kg^{-1} followed by infusion at 4.27 $\mu l\ kg^{-1}\ min^{-1}$, giving an identical dose volume to the animals receiving L-687,414 or dizocilpine. All infusions lasted for 4 h. From each group, 4 rats were used to examine effects on cerebral glucose metabolism and the remainder to study neuronal morphology. In the high dose dizocilpine group, only neuronal morphology was examined. Regional cerebral glucose metabolism was measured during the final 45 min of a 4 h drug infusion and effects on neuronal morphology studied at 4 h, at the end of dosing.

Cardiovascular effects

The blood pressure effects of L-687,414 given in the dosing regimes used in this study were monitored from the tail artery catheter in animals used for neuronal morphology studies. Heart rate was derived from the blood pressure signal. The blood pressure and heart rate effects of dizocilpine were recorded in separate groups of animals ($n = 4$ in each) that were treated identically to the two dizocilpine dose groups used in the present studies.

Plasma drug levels

Plasma levels of L-687,414 in rats from both the low and high dose groups used to study neuronal morphology were measured by high performance liquid chromatography (h.p.l.c.) using fluorescence detection after solid phase extraction and pre-column derivatisation with FMOC chloride. Plasma dizocilpine levels resulting from the present dosing regimes have been reported previously (Gill *et al.*, 1991b). Plasma profiles representative of rats in both of the dizocilpine dosed groups in the present studies were determined by radioimmunoassay (Hichens *et al.*, 1990).

Regional cerebral glucose metabolism ($rCMR_{glc}$)

Measurements of glucose metabolism were limited to a series of structures within the limbic and auditory systems (cerebellar vermis as negative control area) since changes selectively within these structures were shown previously to be characteristic following the administration of NMDA antagonists (Nehls *et al.*, 1988). Autoradiographic studies of $rCMR_{glc}$ were made whilst the plasma levels of L-687,414 and dizocilpine were in a steady state. $rCMR_{glc}$ was measured using the 2-deoxyglucose (2-DG) method essentially as described previously by Sokoloff *et al.* (1977). At 45 min before the end of the drug infusion schedules, approximately 125 $\mu Ci\ kg^{-1}$ [^{14}C]-2-DG was given intravenously in a dose volume of 1 mg kg^{-1} body weight. A blood sample was taken before the administration of [^{14}C]-2-DG and 14 small blood samples were taken afterwards over 45 min. Plasma fractions were separated from the blood samples and assayed for radioactivity and glucose content. At 45 min after administration of label, rats were killed by rapid i.v. injection of pentobarbitone Na (200 mg ml^{-1}) and decapitated. The brain was removed and frozen in isopentane at −45°C. The frozen brain was sectioned (20 μm) in a cryostat and 3 of every 10 sections mounted on coverslips, dried at 60°C and placed in apposition to Hyperfilm along with precalibrated ^{14}C standards. Local tissue levels of ^{14}C were determined by quantitative densitometry. For each region of the brain analysed, 12 bilateral density readings were made on a series of six sections in which the structure was clearly identifiable. Regional cerebral glucose metabolism (CMR_{glc}) was calculated using the standard operational equation from tissue ^{14}C, plasma ^{14}C and plasma glucose levels (Sokoloff *et al.*, 1977).

Neuronal morphology

At the end of the 4 h drug treatment regime the animals were anaesthetized with 60 mg kg^{-1} pentobarbitone Na i.p. and perfused transcardially with ice-cold heparinised saline at 100 mmHg pressure. Following exsanguination with saline the perfusion was changed to freshly prepared 1% paraformaldehyde/1.5% glutaraldehyde in 0.1 M phosphate buffered saline (PBS) at pH 7.4. Once fixed the brain was removed from the skull and allowed to stand in cold fixative for 1 h. The brain was then sliced into 1 mm transverse sections and sampled for the areas of interest (posterior cingulate and retrosplenial cortices) which were kept in fixative at 4°C overnight.

The samples were washed three times with 0.1 M PBS before post-fixation in 1 ml of 1% osmium tetroxide at 4°C overnight. The samples were again washed three times with PBS before dehydration in alcohol, and infiltration with araldite. The samples were embedded and polymerised at 60°C overnight before curing for 12 h and sectioning. Tissue sections (1 μm) were stained with methylene blue/Azure II. Neuronal morphology was assessed by examining the entire area of representative sections through each brain area by light microscopy at × 1000 magnification. Sections were examined by an independent observer who was unaware of the treatments given.

Materials

2-Deoxy-D-[1-^{14}C]-glucose was purchased from Amersham (CFA 728; 50–60 mCi $mmol^{-1}$) together with autoradiographic ^{14}C microscales (31-883 nCi g^{-1}; RPA504L). Autoradiographic film was Hyperfilm β_{max} from Amersham. All other compounds were obtained from Sigma Chemical Co or Fisons Scientific.

Results

Representative plasma profiles for L-687,414 and dizocilpine are shown in Figures 1 and 2. The mean plasma concentrations of L-687,414 over the 4 h dosing period were 19 ± 1 $\mu g\ ml^{-1}$ in the low dose group and 54 ± 3 $\mu g\ ml^{-1}$ in the high dose group. Similarly, the mean plasma concentrations of dizocilpine were 22 ± 6 ng ml^{-1} and 73 ± 8 ng ml^{-1}.

Figure 3 shows that dizocilpine administration caused an immediate dose-related rise in blood pressure that was sustained throughout the drug infusion period. In contrast, L-

687,414 did not affect blood pressure at either the low or high dose level. Dizocilpine also caused a concomitant increase in heart rate (+18%) but no effect was observed with L-687,414 (Figure 4).

Plasma glucose levels at the start of 2-deoxyglucose experiments, 3.25 h after the start of drug or vehicle infusions, were 6.6 ± 0.6 mM (saline), 8.0 ± 0.4 mM (dizocilpine), 7.2 ± 0.4 mM (low dose L-687,414) and 7.8 ± 0.6 mM (high dose L-687,414). The dizocilpine group showed behavioural changes (head weaving, followed by reduced spontaneous activity) but these were not observed in animals given L-687,414.

The effects of L-687,414 and dizocilpine on regional CMR_{glc} are given in Table 1. Dizocilpine administration caused pronounced increases in CMR_{glc} in the hippocampus and entorhinal cortex and throughout the component regions of the Papez circuit (see McCulloch & Iversen, 1991). In contrast, CMR_{glc} was moderately decreased in auditory structures. Unlike dizocilpine, L-687,414 did not evoke increases in limbic CMR_{glc} at either dose level tested. Glucose use appeared slightly depressed at the higher dose of L-687,414 particularly in auditory regions. The studies of neuronal morphology (Figure 5) detected neuronal vacuolation in the pyramidal neurones of the posterior cingulate and retrosplenial cortices of one of 4 rats given dizocilpine at the lower dose level. At the high dose of dizocilpine, all four animals showed extensive neuronal morphological changes (Figure 5c). The neurones appeared swollen with numerous vacuoles evident throughout the cytoplasmic compartment. The changes were most apparent in medium and large sized neurones in layer III of the cortices with small neurones in layer II being unaffected. The glycine site antagonist L-687,414 did not evoke vacuolation at the low or high dose levels (Figure 5b). All neurones showed normal cytoplasmic morphology (dense basophilic even-staining) and were indistinguishable from those of control saline-infused animals (Figure 5a).

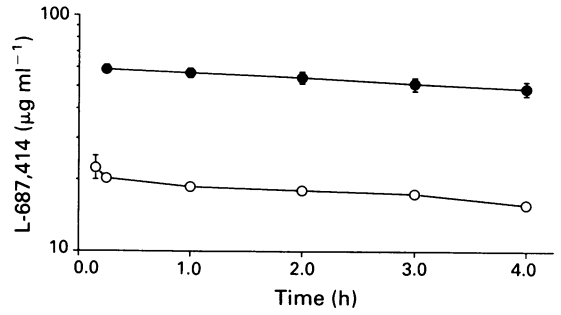

Figure 1 Plasma levels of L-687,414 during intravenous bolus and infusion: (○) 17.5 mg kg^{-1} bolus followed by 225 μg kg^{-1} min^{-1}, mean plasma level is 19 μg ml^{-1}; (●) 35 mg kg^{-1} bolus followed by 440 μg kg^{-1} min^{-1}, mean plasma level is 54 μg ml^{-1}. Points are mean ± s.e.mean. $n = 4$ or 6.

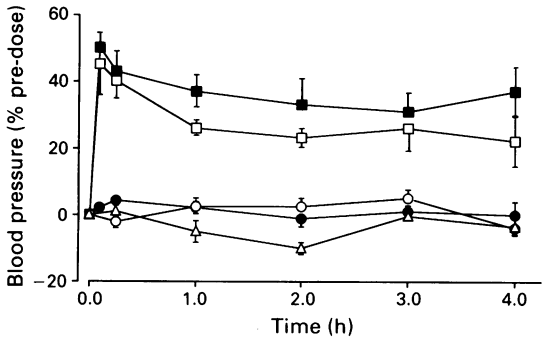

Figure 3 Changes in mean arterial blood pressure during the intravenous bolus injection and infusion of (■) dizocilpine, 0.4 mg kg^{-1} bolus + 6 μg kg^{-1} min^{-1} (104 ± 4); (□) dizocilpine, 0.12 mg kg^{-1} bolus + 1.8 μg kg^{-1} min^{-1} (110 ± 3); (●) L-687,414, 35 mg kg^{-1} bolus + 440 μg kg^{-1} min^{-1} (102 ± 2); (○) L-687,414 17.5 mg kg^{-1} + 225 μg kg^{-1} min^{-1} (104 ± 1); (△) saline, 1.0 ml kg^{-1} + 4.27 μg kg^{-1} min^{-1} (118 ± 2). Starting blood pressures (mmHg ± s.e.mean) are given in parentheses. Data points are mean ± s.e.mean. $n = 4$ or 6.

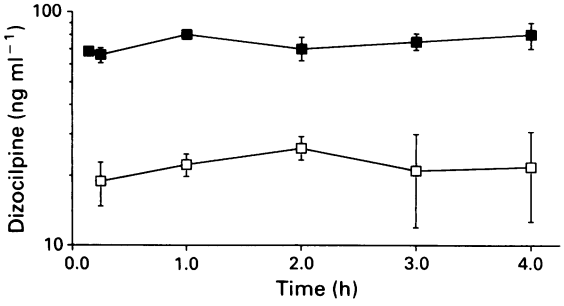

Figure 2 Plasma levels of dizocilpine during intravenous bolus and infusion: (□) 0.12 mg kg^{-1} bolus followed by 1.8 μg kg^{-1} min^{-1}, mean plasma level is 22 ng ml^{-1}; (■) 0.4 mg kg^{-1} bolus followed by 6 μg kg^{-1} min^{-1}, mean plasma level is 73 ng ml^{-1}. Points are mean ± s.e.mean. $n = 3$.

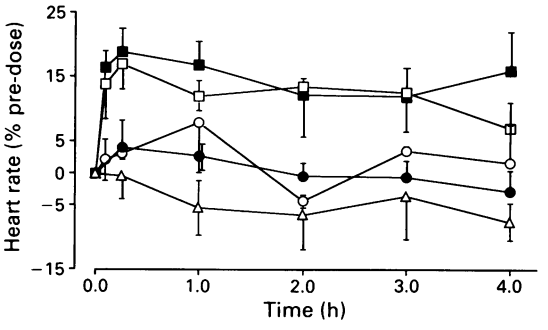

Figure 4 Changes in heart rate during the intravenous bolus injection and infusion of (■) dizocilpine, 0.4 mg kg^{-1} bolus + 6 μg kg^{-1} min^{-1} (416 ± 26); (□) dizocilpine, 0.12 mg kg^{-1} bolus + 1.8 μg kg^{-1} min^{-1} (425 ± 24); (●) L-687,414, 35 mg kg^{-1} bolus + 440 μg kg^{-1} min^{-1} (433 ± 13); (○) L-687,414 17.5 mg kg^{-1} + 225 μg kg^{-1} min^{-1} (370 ± 22). (△) Saline, 1.0 ml kg^{-1} + 4.27 μg kg^{-1} min^{-1} (460 ± 22). Starting heart rates (beats min^{-1} ± s.e.mean) are given in parentheses. Data points are mean ± s.e.mean. $n = 4$ or 6.

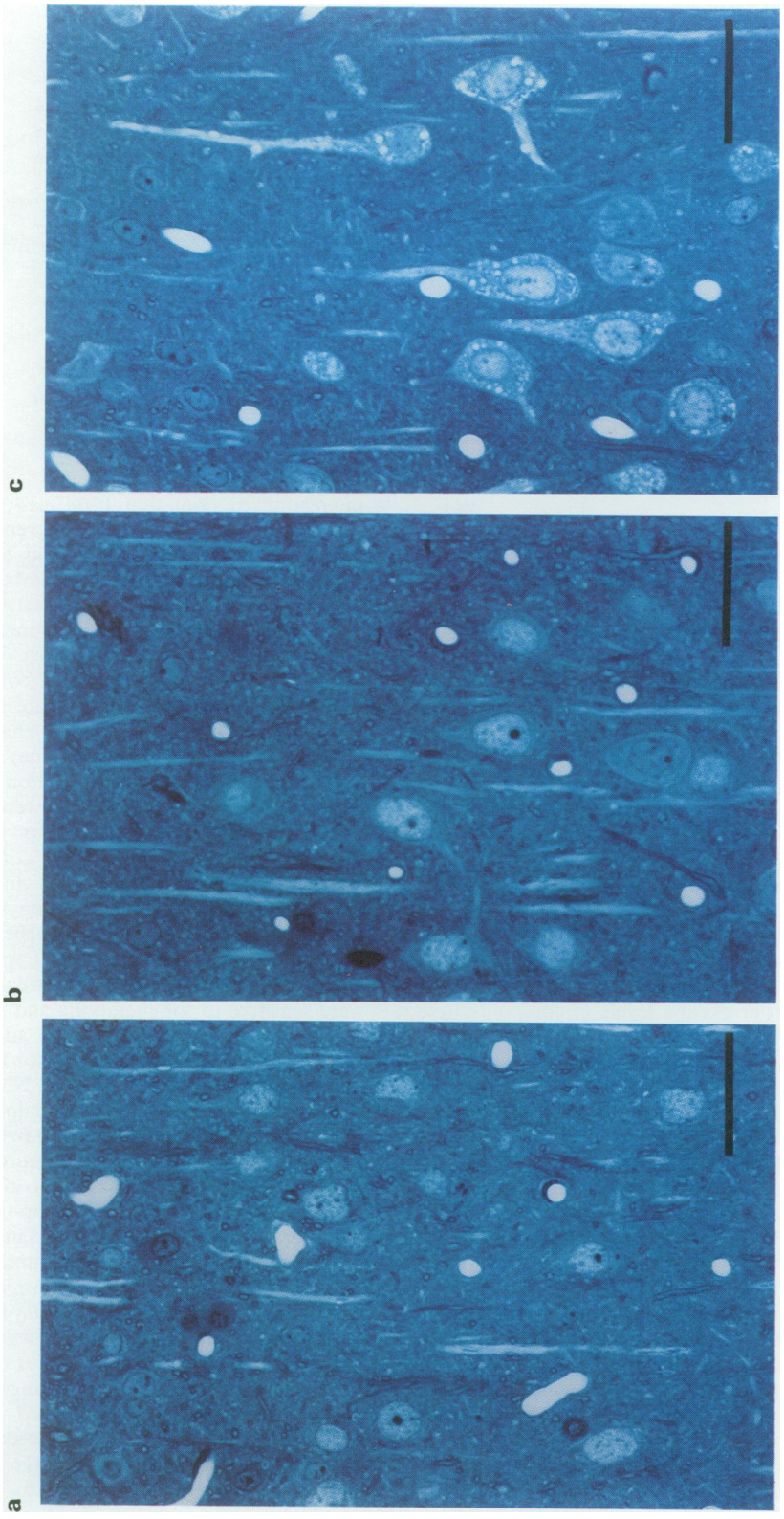

Figure 5 Comparison of the effects of saline (1.0 ml kg^{-1} + 4.67 µl kg^{-1} min^{-1}), L-687,414 (35 mg kg^{-1} bolus + 440 µg kg^{-1} min^{-1}) and dizocilpine (0.4 mg kg^{-1} bolus + 6 µg kg^{-1} min^{-1}) on neuronal morphology in the rat posterior cingulate cortex. In rats given saline (a) and L-687,414 (b) the cytoplasm of medium and large pyramidal neurones is uniformly well stained whereas in rats given dizocilpine (c) it is swollen and pale and shows extensive vacuolation. Bar = 50 µm.

Table 1 Effects of L-687,414 and dizocilpine on regional cerebral glucose metabolism

Region	*Saline*	*Dizocilpine*[a]	*L-687,414*[b]	*L-687,414*[c]
Limbic system				
Hippocampal molecular layer (P)	62 ± 4	110 ± 10**	57 ± 7	52 ± 6
Dentate gyrus	54 ± 3	74 ± 4*	55 ± 5	45 ± 5
Anteroventral thalamic nucleus (P)	90 ± 4	228 ± 39**	85 ± 9	76 ± 12
Posterior cingulate cortex (P)	86 ± 4	179 ± 14**	80 ± 5	57 ± 6
Retrosplenial cortex (P)	68 ± 4	159 ± 22**	80 ± 8	58 ± 6
Entorhinal cortex (P)	48 ± 3	90 ± 8**	52 ± 9	42 ± 6
Auditory system				
Auditory cortex	120 ± 7	100 ± 6	116 ± 7	63 ± 6**
Medial geniculate body	100 ± 10	67 ± 3**	82 ± 4	46 ± 5**
Inferior colliculus	143 ± 18	106 ± 10	143 ± 7	79 ± 5**
Superior olivary nucleus	122 ± 21	108 ± 6	122 ± 7	107 ± 8
Other structures				
Cerebellar vermis	42 ± 3	50 ± 7	41 ± 3	38 ± 4
Caudate	96 ± 8	146 ± 19*	91 ± 3	79 ± 13

[a]Dizocilpine 0.12 mg kg^{-1} followed by infusion of 1.8 μg kg^{-1} min^{-1};
[b]L-687,414; 17.5 mg kg^{-1} followed by infusion of 225 μg kg^{-1} min^{-1}
[c]L-687,414; 35 mg kg^{-1} followed by infusion of 440 μg kg^{-1} min^{-1}
(P) Components of the limbic Papez circuit.
Data are CMR_{glc} (μmol 100 g^{-1} min^{-1}) ± s.e.mean
*$P<0.05$; **$P<0.01$ ANOVA and Dunnett's multiple comparison with respect to saline dosed controls

Discussion

The intravenous infusion of dizocilpine at neuroprotective dose levels was associated with dose-related sustained systemic hypertension and tachycardia in conscious rats. Similar effects have been reported with bolus intravenous doses of ketamine (Traber *et al.*, 1971; White *et al.*, 1982) and with dizocilpine itself (Lewis *et al.*, 1989). These cardiovascular effects are thought to reflect centrally mediated increases in sympathetic nerve activity. Sympathoexcitatory effects were not observed with L-687,414 such that the cardiovascular profile was similar to the saline controls.

Plasma levels of the lower doses of L-687,414 and dizocilpine in the present experiments (19 μg ml^{-1} and 22 ng ml^{-1} respectively) were similar to those (25 μg ml^{-1} and 19 ng ml^{-1} respectively) achieved with the same dosing regimes in the rat MCAO studies of focal ischaemia that were conducted in parallel in our laboratories (Gill *et al.*, 1991a,b). Plasma levels produced by the higher dose levels of L-687,414 (54 μg ml^{-1}) and dizocilpine (73 ng ml^{-1}) exceeded those required for neuroprotection. The slightly lower plasma levels in conscious rats after infusion of L-687,414 in the neuroprotective dose regime probably reflects slightly faster plasma clearance than occurs in the isoflurane anaesthetized animals used for MCAO studies.

The autoradiographic studies of regional CMR_{glc} were made with the plasma drug levels in the steady state, a condition of the 2-deoxyglucose methodology that is rarely met in studies of CMR_{glc} after intravenous bolus injection of test compounds. The results showed that dizocilpine caused pronounced activation of CMR_{glc} in the glutamatergic perforant pathway that projects from the entorhinal cortex and terminates in the dentate gyrus and hippocampus. It has been hypothesized, on the basis that the hippocampus contains a very high density of NMDA receptors, that blockade in this brain region evokes increased input cell firing in an attempt to overcome the block (McCulloch & Iversen, 1991). Since NMDA antagonism with receptor ion channel blocking agents is both non-competitive and use-dependent, this increased firing leads to an intensification of the blockade and increased CMR_{glc} around the limbic Papez circuit (see Table 1).

If this hypothesis is correct then it is clear that the level of blockade that can be achieved with L-687,414 is insufficient to evoke this response despite being effective against focal ischaemia following MCAO. Whatever the mechanism, the present findings show that neuroprotection with NMDA antagonists can be achieved without limbic neuronal activation. It is interesting to note that L-687,414 given to conscious rats at 100 mg free base kg^{-1} intravenously did not stimulate dopamine metabolism (measured as the DOPAC + HVA/dopamine ratio) in the nucleus accumbens within the limbic system or in the striatum. In contrast, dizocilpine at 0.2 mg kg^{-1} intravenously produced a large increase in dopamine turnover in the accumbens, indicative of greatly increased neuronal activity (Hutson, personal communication).

Olney *et al.* (1989) first reported that acute administration of several non-competitive NMDA receptor channel antagonists (phencyclidine, tiletamine and dizocilpine) induced dose-dependent reversible swelling and vacuolation in pyramidal neurones in the rat posterior cingulate and retrosplenial cortices. It has been suggested that there may be age-related changes in the susceptibility of rats to the cortical morphological effects of the NMDA receptor ion channel blockers with responsivity first being observed at 30 days (Sharp *et al.*, 1992) increasing to three months of age (Farber *et al.*, 1992). In the present studies the rats used were approximately 12 weeks old and were age-matched across treatment groups. These rats were sensitive to the metabolic and morphological effects of dizocilpine and thus provided a suitable positive control. There is as yet no published evidence for age-related changes in sensitivity with other classes of NMDA receptor antagonists. Chronic administration of dizocilpine (1 mg kg^{-1} day^{-1} for 14 days) to mature Sprague-Dawley rats (>12 weeks of age) was not associated with neuronal cell loss, suggesting that the vacuolation seen shortly after acute dosing is not a prelude to significant long-term neuronal damage. Only after very high acute doses (5 mg kg^{-1} dizocilpine, s.c.) were a few neurones (<0.5%) found to be irreversibly damaged when CNS tissues were examined 48 h after dosing (Allen & Iversen, 1990; Allen *et al.*, 1991).

The present studies indicate that the doses of dizocilpine required for optimal neuroprotection (Gill *et al.*, 1991b) are at the threshold of those for inducing changes in neuronal morphology since one of four rats showed a vacuolation response. Thus, there is little margin between wanted and unwanted effects with dizocilpine. L-687,414 did not alter cortical neuronal morphology when given to conscious rats in the neuroprotective dose regime (Gill *et al.*, 1991a) or at a higher rate that produced two to threefold higher plasma levels, indicating that it may have a greater therapeutic window. This estimate of the potential therapeutic window with L-687,414 is likely to be a lower limit as no cardiovascular sympathoexcitation, increased CMR_{glc} nor changes in cortical neuronal morphology were detected at either of the plasma

levels tested. It should be noted that the present studies were not designed to investigate the neurotoxic profile of L-687,414 but to establish, by direct comparison with rat MCAO experiments conducted in parallel in our laboratories (Gill *et al.*, 1991a,b), that there is a clear window between neurotoxicity and neuroprotection with L-687,414 that is absent with the NMDA receptor ion channel blocker, dizocilpine. Comparison with another neuroprotection study in which the plasma levels of L-687,414 and dizocilpine were measured suggests that the window for L-687,414 is at least 18 whilst that for dizocilpine is <2 (Rigby *et al.*, 1992). If the total dose of L-687,414 administered over 4 h in the present experiments is used for such comparisons, then the window for L-687,414 appears much larger still.

Scatton and colleagues have shown that SL 82.0715, an NMDA antagonist acting at the polyamine site, does not evoke increased CMR_{glc} nor induce neuromorphological changes in rat CNS (Scatton *et al.*, 1991; Duval *et al.*, 1992). These results, together with those from the present studies, suggest that the potential therapeutic window for NMDA receptor antagonists may depend upon the specific site within the NMDA receptor complex at which the compound acts to reduce activation. This view is supported by our observation that competitive NMDA receptor antagonists acting at the glutamate recognition site are capable of increasing limbic CMR_{glc} and producing cortical neuronal vacuolation but, nevertheless, appear also to have a greater potential therapeutic window than dizocilpine (Hargreaves *et al.*, 1993). The mechanism of vacuolation in cortical neurones is unclear. The anatomical coincidence of morphological changes and increased CMR_{glc} has implicated hypermetabolism in the dizocilpine vacuolation response and several observations support this view. Parallels have been drawn between the morphological changes in neurones after periods of hypermetabolism associated with seizure activity (McCulloch & Iversen, 1991) suggesting that vacuolation may be linked in some way to the CMR_{glc} response. The present studies and those of Duval *et al.* (1992) have shown that L-687,414 and SL 82.0715 do not increase CMR_{glc} in rat brain and do not induce vacuolation in the posterior cingulate and retrosplenial cortical neurones.

The cortical morphological effects of NMDA receptor ion channel blockers have been shown (Olney *et al.*, 1991) to be antagonized by muscarinic antagonists and drugs acting at GABAergic sites (barbiturates, diazepam) indicating an involvement of pathways with these receptor types in the vacuolation response. Sharp *et al.* (1991, 1992) have suggested that drug-induced vacuolar changes and altered intracellular proteins in cortical neurones then act as a stimulus for the later expression of heat shock protein. Importantly, heat shock protein expression appears to be primarily in injured neurones that are destined to survive (Lindsberg *et al.*, 1991; Sharp *et al.*, 1991; Welsh *et al.*, 1991). Thus, neuronal vacuolation can be viewed as an early marker of drug-induced cellular stress. Production of heat shock protein has been shown to be inhibited by agents that prevent vacuolation (Olney *et al.*, 1991) supporting the idea that their pathogenesis is linked to a common mechanism. Olney's findings suggest a specific involvement of cholinergic muscarinic pathways in the response to the NMDA receptor ion channel blockers (Olney *et al.*, 1991). Indeed, the changes in the pattern of coupling of regional cerebral blood flow and glucose metabolism after dizocilpine (Nehls *et al.*, 1990; McCulloch & Iversen, 1991) resemble those that result from stimulation of the fastigial nucleus that is thought to activate ascending cholinergic pathways (Iadecola *et al.*, 1983; Nakai *et al.*, 1983). It is noteworthy that dizocilpine caused profound hyperaemia, in excess of the increase in cerebral blood flow expected as a result of increased metabolic activity in the cingulate cortex (see McCulloch & Iversen, 1991). Heightened blood flow may remove lactate accumulated as a result of the maintenance of intracellular ionic homeostasis by glycolysis during the intense activation of cingulate neurones. Interestingly, following ketamine administration, cerebral blood flow was also found to increase in excess of metabolic demand within the cingulate cortex (Cavazzuti *et al.*, 1987).

Recent studies on the protective effects of haloperidol and rimcazole against heat shock protein induction by phencyclidine and dizocilpine support the involvement of multiple receptor subtypes in the cortical morphological response (Sharp *et al.*, 1992). However, doses of haloperidol in excess of 5 mg kg^{-1} may cause generalized CNS depression. This observation together with those on the protective effects of pretreatment with gaseous anaesthetics (Kurumaji & McCulloch, 1989; Hargreaves & Rigby unpublished observations) indicate that non-specific depression of CNS activity may also be involved in the action of the compounds that antagonize the cortical morphological effects of NMDA receptor ion channel blockers, and could be a means of controlling their potential adverse side-effects. It should be noted, however, that when dizocilpine is given before halothane anaesthesia then protection is not seen (Olney *et al.*, 1991).

It remains to be determined whether the apparent differences in therapeutic window for NMDA receptor antagonists acting at different sites within the receptor complex are due to true differences in side-effect liability or reflect a greater ability to 'fine-tune' the level of blockade so that the neuroprotective and morphological effects can be divorced. Clearly the actions of competitive antagonists acting at the glycine and glutamate recognition sites will be critically influenced by the prevailing concentrations of the endogenous ligands unlike the uncompetitive ion channel blocking agents. Since endogenous brain glycine concentrations are thought to be near saturating for the NMDA glycine site, it may be very difficult with a competitive antagonist acting at this site to achieve the same levels of blockade that can be attained with a channel blocking agent such as dizocilpine. Interpretation of the actions of the glycine site antagonist L-687,414 are complicated somewhat by its partial agonist properties (Kemp *et al.*, 1991). On voltage clamped cultured cortical neurones, L-687,414 antagonized glycine and NMDA responses competitively but reached a plateau of effect at 90% inhibition and showed weak agonist effects (6% of the maximum response to glycine) at high concentrations. Thus, it appears likely that blockade of the NMDA receptor, equivalent to that possible with an NMDA receptor channel blocker, cannot be achieved with L-687,414 and it may be this that restricts its side-effect potential. Further examination of site-related differences in the potential therapeutic window for NMDA antagonists awaits the testing of a brain penetrant, glycine site full antagonist for its neuromorphological and cerebral metabolic effects.

The eventual clinical usefulness of NMDA receptor antagonists in cerebral ischaemia may not be determined by their neuroprotective efficacy but by their adverse CNS side-effects. It has been argued that the enormous potential benefits of successful drug treatment with dizocilpine in stroke victims may outweigh the risk to small numbers of CNS neurones (McCulloch & Iversen, 1991). The present studies, however, suggest that NMDA-mediated neuroprotection can be achieved without increases in CMR_{glc} or changes in cortical neuronal morphology by antagonism at the glycine modulatory site.

We are grateful for the excellent technical assistance given by Aurelio Barranco, Cathy Hurley and Aidan Foster.

References

ALLEN, H.L. & IVERSEN, L.L. (1990). Phencyclidine, dizocilpine and cerebrocortical neurons. *Science*, **247**, 221.

ALLEN, H.L., SMITH, D.W., HARGREAVES, R.J. & IVERSEN, L.L. (1991). The effects of acute and chronic treatment with dizocilpine on neuronal morphology in the rat CNS. In *Neurodegeneration*. ed. Hunter, A.J. & Clark, M. pp. 232–233. London: Academic Press.

BENVENISTE, H. (1991). The excitotoxin hypothesis in relation to cerebral ischaemia. *Cereb. Brain Metabol. Rev.*, **3**, 213–245.

CAVAZZUTI, M., PORRO, C.A., BIRAL, G.P., BENASSI, C. & BARBIERI, G.C. (1987). Ketamine effects on local cerebral blood flow and metabolism in the rat. *J. Cereb. Blood Flow Metab.*, **7**, 806–811.

CHOI, D.W. (1990). Methods for antagonising glutamate neurotoxicity. *Cereb. Brain Metabol. Rev.*, **2**, 105–147.

DUVAL, D., ROOME, N., GAUFFENY, C., NOWICKI, J.P. & SCATTON, B. (1992). SL 82.0715, an NMDA antagonist acting at the polyamine site, does not induce neurotoxic effects on rat cortical neurons. *Neurosci. Letts.*, **137**, 193–197.

FARBER, N.B., PRICE, M.T., LABRUYERE, J., FULLER, T.A. & OLNEY, J.W. (1992). Age dependency of NMDA antagonist neurotoxicity. *Soc. Neurosci. Abs.*, **18**, 1148.

FOSTER, A.C., DONALD, A.E., WILLIS, C.L., TRIDGETT, R., KEMP, J.A. & PRIESTLEY, T. (1990). The glycine site on the NMDA receptor: pharmacology and involvement in NMDA receptor-mediated neurodegeneration. In *Excitatory Amino Acids and Neuronal Plasticity*. ed. Ben-Ari, Y., pp. 93–100. New York: Plenum Press.

FOSTER, A.C., DONALD, A.E., GRIMWOOD, S., LEESON, P.D. & WILLIAMS, B.J. (1991). Activities of 4-methyl derivatives of HA-966 at the glycine site of the N-methyl-D-aspartate receptor from rat brain. *Br. J. Pharmacol.*, **102**, 64P.

FOSTER, A.C., GILL, R. & WOODRUFF, G.N. (1988). Neuroprotective effects of MK-801 *in vivo*: selectivity and evidence for delayed degeneration mediated by NMDA receptor activation. *J. Neurosci.*, **8**, 4745–4754.

GILL, R., HARGREAVES, R.J. & KEMP, J.A. (1991a). Neuroprotective effects of the glycine site antagonist (+)cis-4-methyl-HA-966 (L-687,414) in a rat focal ischaemia model. *J. Cereb. Blood Flow Metab.*, **11**, Suppl. 2, S304.

GILL, R., BRAZELL, C., WOODRUFF, G.N. & KEMP, J.A. (1991b). The neuroprotective action of dizocilpine (MK-801) in the rat middle cerebral artery model of cerebral ischaemia. *Br. J. Pharmacol.*, **103**, 2030–2036.

HARGREAVES, R.J., RIGBY, M., SMITH, D., FOSTER, A., HURLEY, C.J. & HILL, R.G. (1991). L-687,414 ((+)-cis-4-methyl-HA-966), an NMDA receptor antagonist acting at the glycine site, does not alter glucose metabolism or neuronal morphology at neuroprotective dose levels. *J. Cereb. Blood Flow Metab.*, **11**, Suppl. 2, S301.

HARGREAVES, R.J., RIGBY, M., SMITH, D., HILL, R.G. & IVERSEN, L.L. (1993). Competitive as well as uncompetitive N-methyl-D-aspartate receptor antagonists affect cortical neuronal morphology and cerebral glucose metabolism. *Neurochem. Res.*, **18**, 1263–1269.

HICHENS, M., GREBER, T.F. & VYAS, K.P. (1990). A radioimmunoassay for the anticonvulsant and neuroprotective agent MK-801. *J. Immunoassay*, **11**, 477–502.

IADECOLA, C., MRAOVITCH, S., MEELEY, M.P. & REIS, D.J. (1983). Lesions of the basal forebrain in rat selectivity impair the cortical vasodilation elicited from the cerebellar fastigial nucleus. *Brain Res.*, **279**, 41–52.

KEMP, J.A., PRIESTLEY, T., MARSHALL, G.R., LEESON, P.D. & WILLIAMS, B.J. (1991). Functional assessment of the actions of 4-methyl derivatives of HA-966 at the glycine site of the N-methyl-D-aspartate receptor. *Br. J. Pharmacol.*, **102**, 65P.

KURUMAJI, A. & MCCULLOCH, J. (1989). Effects of MK-801 upon local cerebral glucose utilisation in conscious rats and in rats anaesthetised with halothane. *J. Cereb. Blood Flow Metab.*, **9**, 786–794.

KURUMAJI, A., NEHLS, D.G., PARK, C.K. & MCCULLOCH, J. (1989). Effects of NMDA antagonists, MK-801 and CPP, upon local cerebral glucose use. *Brain Res.*, **496**, 268–284.

LEWIS, S.J., BARRES, C., JACOB, H.J., OHTA, H. & BRODY, M.J. (1989). Cardiovascular effects of the N-methyl-D-aspartate receptor antagonist MK-801 in conscious rats. *Hypertension*, **13**, 759–765.

LINDSBERG, P.J., NOWAK, T.S., SIREN, A.-L. & HALLENBECK, J.M. (1991). Heat shock protein (HSP70) expression in focal brain damage. *Soc. Neurosci. Abs.*, **17**, 1083.

MCCULLOCH, J. (1991). Ischaemic brain damage – prevention with competitive and non-competitive antagonists of N-methyl-D-aspartate receptors. *Arzneim-Forschung Drug Res.*, **41**, 319–324.

MCCULLOCH, J. & IVERSEN, L.L. (1991). Autoradiographic assessment of the effects of N-methyl-D-aspartate (NMDA) receptor antagonists *in vivo*. *Neurochem. Res.*, **16**, 951–961.

NAKAI, M., IADECOLA, C., RUGGIERO, D.A., TUCKER, L.W. & REIS, D.J. (1983). Electrical stimulation of cerebellar fastigial nucleus increases cerebral cortical blood flow without change in local metabolism: evidence for an intrinsic system in brain for primary vasodilation. *Brain Res.*, **260**, 35–49.

NEHLS, D.G., KURUMAJI, A., PARK, C.K. & MCCULLOCH, J. (1988). Differential effects of competitive and non-competitive N-methyl-D-aspartate antagonists on glucose use in the limbic system. *Neurosci. Letts.*, **91**, 204–210.

NEHLS, D.G., PARK, C.K., MACCORMACK, A.G. & MCCULLOCH, J. (1990). The effects of N-methyl-D-aspartate receptor blockade with MK-801 upon the relationship between cerebral blood flow and glucose utilisation. *Brain Res.*, **511**, 271–279.

OLNEY, J.W., LABRUYERE, J. & PRICE, M.T. (1989). Pathological changes induced in cerebrocortical neurons by phencyclidine and related drugs. *Science*, **244**, 1360–1362.

OLNEY, J.W., LABRUYERE, J., WANG, G., WOZNIAK, D.F., PRICE, M.T. & SESMA, M.A. (1991). NMDA antagonist neurotoxicity: mechanism and prevention. *Science*, **254**, 1515–1518.

RIGBY, M., BARRANCO, A., SEARLE, C.Y., HARGREAVES, R.J. & HILL, R.G. (1992). Plasma profiles of ligands at the NMDA receptor complex after neuroprotective doses. In *Neurodegeneration*. ed. Hunter, A.J. & Clark, M. p. 232. London: Academic Press.

SAYWELL, K., SINGH, L., OLES, R.J., VASS, C., LEESON, P.D., WILLIAMS, B.J. & TRICKLEBANK, M.D. (1991). The anti-convulsant properties in the mouse of the glycine/NMDA receptor antagonist, L-687,414. *Br. J. Pharmacol.*, **102**, 66P.

SCATTON, B., CUDDENNEC, A., DUVERHER, D., MACKENZIE, E.T., NOWICKI, J.P. & ZIRKOVIC, B. (1991). Effects of SL 82.0715, an NMDA receptor antagonist acting at the polyamine modulatory site, on local cerebral glucose use in rat brain. *J. Cereb. Blood Flow Metab.*, **11**, Suppl. 2, S312.

SHARP, F.R., JASPER, P., HALL, J., NOBLE, L. & SAGAR, S.M. (1991). MK-801 and ketamine induced heat shock protein HSP72 in injured neurons in posterior cingulate and retrosplenial cortex. *Ann. Neurol.*, **30**, 801–809.

SHARP, F.R., WANG, S., BUTMAN, J., KOISTANAHO, J., GRAHAM, S., NOBLE, L. & SAGAR, S.M. (1992). Haloperidol and rimcazole prevent induction of the HPS70 heat shock gene in neurons injured by phencyclidine and MK-801. *Soc. Neurosci. Abs.*, **18**, 1145.

SMITH, S.E. & MELDRUM, B.S. (1992). The glycine-site NMDA receptor antagonist, R-(+)-cis-β-methyl-3-amino-1-hydroxypyrrolid-2-one, L-687,414 is anticonvulsant in baboons. *Eur. J. Pharmacol.*, **211**, 109–111.

SOKOLOFF, L., REIVICH, M., KENNEDY, D., DES ROSIERS, M.H., PATLAK, C.S., PETTIGREW, K.D., SAKURADA, O. & SHINOHARA, M. (1977). The [^{14}C]deoxyglucose method for the measurement of local cerebal glucose utilization: theory, procedure and normal values in the conscious and anaesthetised albino rat. *J. Neurochem.*, **28**, 897–916.

TRABER, D.L., WILSON, R.D. & PRIANO, L.L. (1971). The effect of alpha-adrenergic blockade on the cardiopulmonary response to ketamine. *Anesth. Analg.*, **50**, 737–742.

WELSH, F.A., MOYER, D.J. & HARRIS, V.A. (1991). Relationship between expression of heat shock protein-70 mRNA and histologic injury following focal ischaemia in rat brain. *Soc. Neurosci. Abs.*, **17**, 1084.

WHITE, P.F., WAY, W.L. & TREVOR, A.J. (1982). Ketamine – its pharmacology and therapeutic uses. *Anesthesiology*, **56**, 119–136.

WONG, E.H.F. & KEMP, J.A. (1991). Site for antagonism on the N-methyl-D-aspartate receptor channel complex. *Ann. Rev. Pharmacol. Toxicol.*, **31**, 401–425.

(Received November 20, 1992
Revised April 6, 1993
Accepted May 10, 1993)

Br. J. Pharmacol. (1993), **110**, 43–49

Stimulation of angiogenesis by substance P and interleukin-1 in the rat and its inhibition by NK_1 or interleukin-1 receptor antagonists

[1]Tai-Ping D. Fan, De-En Hu, *Steven Guard, †G. Austin Gresham & *Keith J. Watling

Department of Pharmacology, University of Cambridge, Tennis Court Road, Cambridge CB2 1QJ; *Parke-Davis Neuroscience Research Centre, Addenbrooke's Hospital Site, Hills Road, Cambridge CB2 2QB and †Department of Histopathology, Addenbrooke's Hospital, Cambridge CB2 2QQ

1 Daily administration of 1 nmol substance P or 3 pmol recombinant human interleukin-1 alpha (IL-1α) caused intense neovascularization in a rat sponge model of angiogenesis. Lower doses of substance P (10 pmol) or IL-1α (0.3 pmol) were ineffective when given alone. When combined at these low doses, substance P and IL-1α interacted to produce an enhanced neovascular response.

2 By use of selective tachykinin NK_1, NK_2 and NK_3 receptor agonists, ([Sar^9,Met(O$_2$)^{11}]substance P, [β-Ala^8]neurokinin A(4-10), Succ-[Asp^6,MePhe^8]substance P(6-11) (senktide), respectively), it was established that the activation of NK_1 receptors is most likely to mediate the angiogenic response to substance P in this model.

3 The angiogenic activity of substance P and IL-1α (10 pmol and 0.3 pmol day^{-1}, respectively) was abolished by co-administration of (i) the selective peptide NK_1 receptor antagonist, L-668,169 (1 nmol day^{-1}), (ii) the selective non-peptide NK_1 receptor antagonists, RP 67580 and (±)-CP-96,345 (both at 1 nmol day^{-1}) or (iii) the IL-1 receptor antagonist, IL-1ra, (50 μg day^{-1}). In contrast, the selective NK_2 receptor antagonist, L-659,874 (1 nmol day^{-1}) was ineffective.

4 The angiogenic action of substance P and IL-1α was resistant to modification by mepyramine (1 nmol day^{-1}) and/or cimetidine (10 nmol day^{-1}), indomethacin (7 nmol day^{-1}) or the platelet-activating factor (PAF) antagonist, WEB-2086 (22 nmol day^{-1}), indicating that histamine, prostaglandins and PAF are not likely to be involved in this neovascular response.

5 The inhibition of the substance P/IL-1 angiogenic response by selective NK_1 receptor antagonists or by an IL-1 receptor antagonist demonstrates that angiosuppression can be achieved by blocking the activity of angiogenic factors at the receptor level.

Keywords: Angiogenesis; angiosuppression; substance P; tachykinin receptors; NK_1 receptor antagonists; interleukin-1; interleukin-1 receptor antagonist; rheumatoid arthritis

Introduction

Angiogenesis, the formation and growth of new capillary blood vessels, is an important process in many physiological conditions such as embryonic development and wound healing. However, defects in the controlling mechanism of angiogenesis often result in pathological conditions e.g. rheumatoid synovial hypertrophy, atherosclerosis, proliferative retinopathy and solid tumours. It is now widely recognised that both growth factors and inhibitors are involved in the regulation of vascular growth (see Folkman & Klagsbrun, 1987; Klagsbrun & D'Amore, 1991; Moses & Langer, 1991; Fan & Brem, 1992, for reviews).

The neuropeptides, substance P and calcitonin gene-related peptide (CGRP), are important mediators of inflammation. In addition to their vasodilator activity (Brain & Williams, 1989; Payan, 1989), they are mitogenic for cells derived from the vasculature and connective tissues. For example, substance P stimulates the proliferation of arterial smooth muscle cells, skin fibroblasts, synovial cells and endothelial cells (Nilsson *et al.*, 1985; Lotz *et al.*, 1987; Ziche *et al.*, 1990) and CGRP is mitogenic for endothelial cells (Haegerstrand *et al.*, 1990). These *in vitro* data raise the possibility that substance P and other neuropeptides may be involved in angiogenesis. In support of this hypothesis, substance P has been shown to stimulate neovascularization in rabbit cornea (Ziche *et al.*, 1990).

The interactions between cytokines and inflammatory mediators have been investigated by many groups in the last few years. For example, Lotz *et al.* (1988) demonstrated that substance P increases the production of inflammatory cytokines, including interleukin 1 alpha (IL-1α) by cultured monocytes, while Kimball & Fisher (1988) reported substance P to potentiate IL-1-induced BALB/3T3 fibroblast proliferation. *In vivo*, interactions between IL-1 and CGRP have been shown to induce inflammatory oedema (Buckley *et al.*, 1991). Recently, we presented preliminary evidence that in addition to substance P, other peptides such as CGRP and vasoactive intestinal polypeptide (VIP) also stimulate angiogenesis in a rat sponge model (Fan & Hu, 1991; Hu & Fan, 1991). Furthermore, some of these peptides interact with IL-1α to modulate the neovascular response. Thus, neuropeptides may contribute to the aberrant neovascularization often associated with chronic inflammatory diseases.

In view of the fact that at least three receptor types, termed NK_1, NK_2 and NK_3, are believed to mediate the biological effects of tachykinins (see Guard & Watson, 1991, for review), we have characterized the tachykinin receptor(s) involved in the substance P/IL-1α response, using selective tachykinin receptor agonists and antagonists. In addition, we have examined the effects of indomethacin, a platelet-activating factor (PAF) antagonist and histamine receptor antagonists in order to examine whether the synergistic interaction of substance P and IL-1α is mediated by prostaglandins, PAF or histamine.

[1] Author for correspondence.

Methods

The sponge implant model

Circular sponge discs (1.2 cm diameter) were prepared from a sheet of 5 mm thick polyether foam. A 1.2 cm segment of polythene tubing (1.4 mm internal diameter) was secured to the interior of each sponge disc by means of 5/0 silk sutures so that every sponge disc possessed a central cannula. Before implantation, sponge discs were soaked in 70% ethanol for 2–3 h and then rinsed in sterile phosphate buffered saline (PBS). After squeezing the sponges in a 20 ml syringe to remove excess PBS, they were sterilised by overnight ultraviolet light irradiation.

Implantation of sponge discs was performed with aseptic techniques. Hypnorm (0.5 ml kg^{-1}; 0.315 mg ml^{-1} fentanyl citrate and 10 mg ml^{-1} fluanisone) was used to induce neuroleptanalgesia in male Wistar rats weighing 180–200 g. After the dorsal side had been shaved and wiped with 70% ethanol, a 1 cm dorsal, midline, vertical skin incision was made approximately 4 cm caudal to the occipital ridge. Using a pair of curved scissors, two subcutaneous air-pockets were prepared, one anterior and the other posterior to the incision. Two needle punctures (5 cm apart) were made on top of the pockets. A sterile sponge disc was then inserted into each air-pocket, with the free end of its cannula being exteriorised through the needle puncture. To immobilise the sponge implant, the base of each cannula was sutured to the rat skin. Finally, the skin incision was sutured with two interrupted 5/0 silk stitches, and the cannula was plugged with a sterile polythene stopper so as to prevent overt infection and evaporation of ^{133}Xe-saline during blood flow measurements. The stopper was changed every day and if infection of the implants became apparent, the animals were excluded from the experiments. To prevent the rats from tampering with the cannulae, they were housed individually in plastic cages. Animals were provided with a normal diet and water.

Neovascularisation was assessed as a function of blood flow through the implants over a period of 14 days, by a ^{133}Xe clearance technique (Andrade *et al.*, 1987) and confirmed histologically. Briefly, animals were anaesthetized with Hypnorm as before and 10 µl ^{133}Xe in sterile PBS was injected into the sponges through the cannulae. The washout of radioactivity from the implants was monitored with a gamma scintillation detector. The 6 min ^{133}Xe clearance value was calculated as follows:

$$\%\ ^{133}\text{Xe clearance} = \frac{\text{initial radioactivity} - \text{residual radioactivity at 6 min}}{\text{initial radioactivity}} \times 100\%$$

The validity of this method has recently been established (Fan *et al.*, 1992a,b; Hu *et al.*, 1992; Hu & Fan, 1993). First, we carried out parallel studies of ^{133}Xe clearance and ^{113}Sn microsphere accumulation during sponge-induced angiogenesis. The latter technique enabled us to measure absolute blood flow in the sponges. Second, the ^{133}Xe clearance data have been correlated with the amount of haemoglobin in the sponges. The results from these two studies indicate that measurements of relative blood flow changes in sponge implants by the ^{133}Xe clearance method provide a simple and rapid means to assess new blood vessel formation, when confirmed by histological studies.

Test substances dissolved in PBS were administered through attached cannulae into sponges in a total volume of 50 µl daily, starting on day 1 after implantation, until day 10. To exclude the possible acute effects of the test substances (dilatation or constriction) on the microvasculature, they were given 16–24 h prior to the ^{133}Xe measurements.

Histology

For histology, animals were killed by cervical dislocation and sponges dissected out, carefully removing the cannulae and any adherent fat. The samples were then bisected and fixed in formal saline at 4°C for 1 h. Sections (10 µm) were prepared from paraffin-embedded blocks and stained with haematoxylin and eosin (H&E) or a specific endothelial cell marker *Bandeiraea simplicifolia* lectin I, isolection B_4. The specimens were analysed and recorded on Ektachrome ASA 64T film.

Radioimmunoassay for 6-keto-$PGF_{1\alpha}$

On day 14 after implantation, animals were killed by cervical dislocation and sponges dissected out. Each sponge was placed immediately in 1 ml PBS containing 10 µg ml^{-1} BW755C at 4°C to inhibit further arachidonate metabolism. Sponges were minced in this solution and then centrifuged at 4000 r.p.m. to remove the sponge, cells and debris. The supernatant (sponge fluid) was stored at – 20°C until assay of sponge 6-keto-$PGF_{1\alpha}$ content by a specific radioimmunoassay as described by Fan & Lewis (1984). Unlabelled 6-keto-$PGF_{1\alpha}$, over the concentration range 0.15–80 ng ml^{-1} in 0.1 M tricine buffered saline (TBS) pH 8.0 containing 0.1% gelatin and 0.9% NaCl, was used as standard. Standard or sample (100 µl) was incubated at 4°C for at least 2 h with 100 µl [^{3}H]-6-keto-$PGF_{1\alpha}$ (50 µCi ml^{-1}) and 100 µl antiserum to 6-keto-$PGF_{1\alpha}$ diluted 1/3,000 in TBS. Incubation was terminated by addition of 1.4 ml ammonium calcium sulphate suspension (65% saturated $(NH_4)_2SO_4$, pH 8.0, containing 2.5% $CaSO_4 \cdot 2H_2O$) followed by centrifugation at 2,500 r.p.m. for 10 min. The supernatant was removed by aspiration and the pellet resuspended in 600 µl distilled water before addition of 1.4 ml Instagel scintillant (Packard). After thorough mixing, the gel was allowed to set at 4°C before counting for 1 min in a Packard Tri-Carb 300 scintillation counter. The absolute amount of radioactivity in the gel was counted, the percentage binding calculated and sample values estimated from a standard curve.

Materials

Substance P and [D-Pro^2,D-Phe^7,D-Trp^9]SP were purchased from Peninsula Laboratories, UK. [Sar^9,Met(O$_2$)^{11}]substance P (Drapeau *et al.*, 1987), [β-Ala^8]neurokinin A(4-10) (Rovero *et al.*, 1989) succ-[Asp^6,MePhe^8]substance P(6-11) (senktide)(Wormser *et al.*, 1986), L-668,169 (cyclo[Gln-D-Trp-(NMe)-Phe(R)-Gly(ANC-2·Leu-Met]$_2$) and L-659,874 (Ac-Leu-Met-Gln-Trp-Phe-Gly-NH_2; Williams *et al.*, 1988) were purchased from Cambridge Research Biochemicals, UK. Racemic (±)-CP-96,345 (a mixture of the two enantiomers

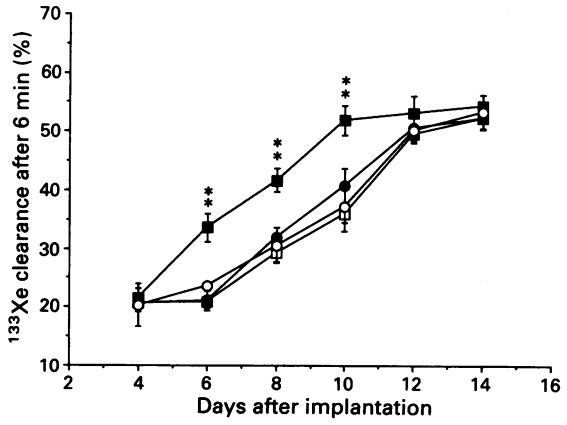

Figure 1 Effect of substance P and interleukin-1α (IL-1α) on sponge-induced angiogenesis. Symbols represent sponges treated daily with PBS alone (□), 10 pmol substance P (○), 0.3 pmol IL-1α (●) or a combination of 10 pmol substance P and 0.3 pmol IL-1α (■); see Methods for details. Each point represents mean data ± s.e.mean from 8–10 animals. $^{**}P < 0.01$ (substance P and IL-1α vs PBS control).

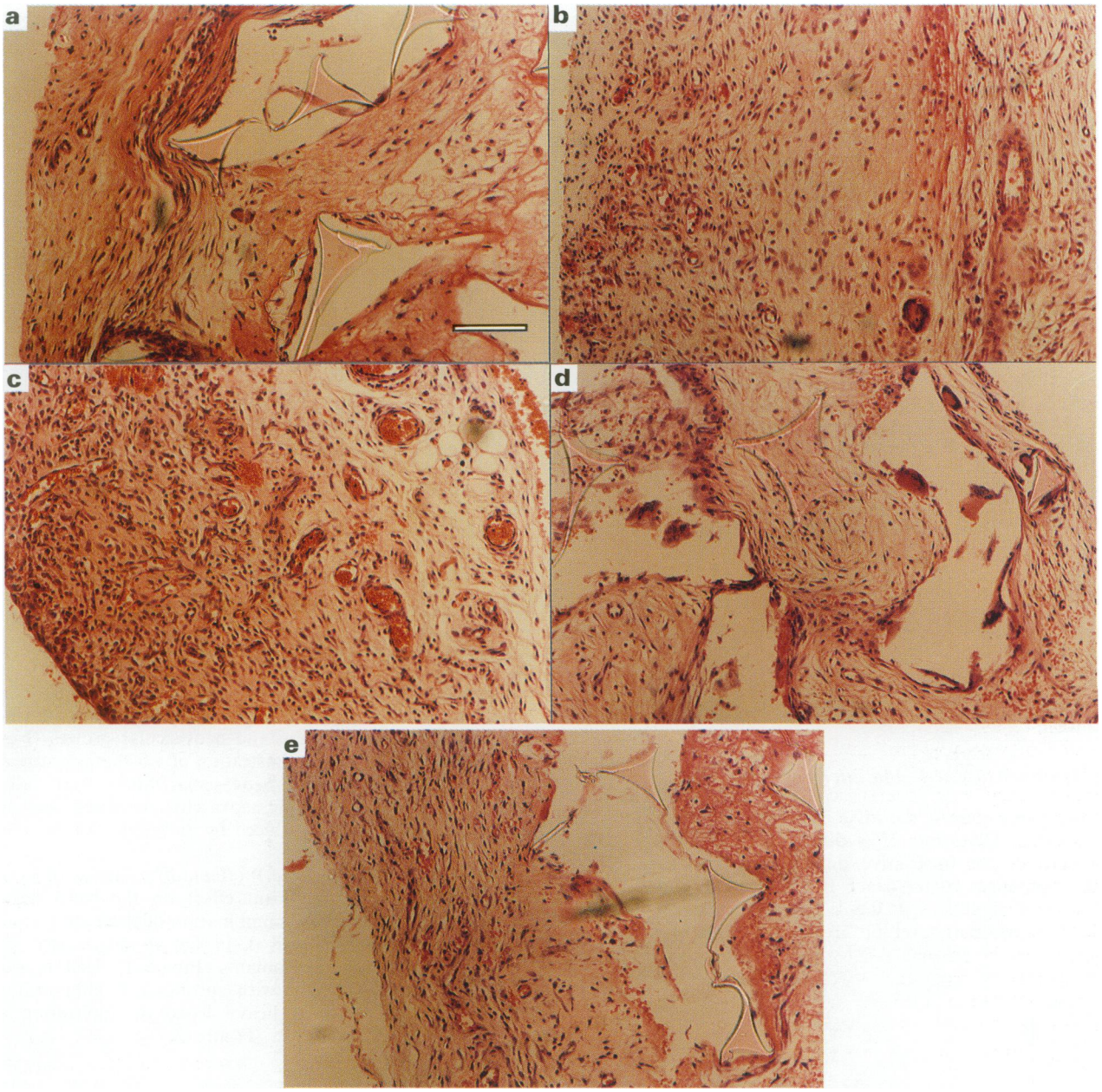

Figure 2 Histological sections of 8 day old sponges illustrating (i) the intense neovascularization induced by substance P alone (1 nmol day^{-1}) or substance P/interleukin-1α (IL-1α) (10 pmol/0.3 pmol day^{-1}), and (ii) the angiosuppressive effect of RP 67580 (1,000 pmol day^{-1}) or IL-1ra (50 μg day^{-1}). All sections were H&E stained and photographed at × 200 magnification. Bar = 100 μm. (a) Sponge treated with PBS; (b) sponge treated with substance P alone; (c) sponge treated with substance P/IL-1α; (d) sponge treated with substance P/IL-1α plus RP 67580; (e) sponge treated with substance P/IL-1α plus IL-1ra.

[(2S,3S) and (2**R**,3**R**)] of the non-peptide NK_1 receptor antagonist (*cis*-2-(diphenylmethyl)-*N*-[(2-methoxyphenyl]-methyl]-1-azabicyclo [2.2.2] octan-3-amine; Snider *et al.*, 1991) and RP 67580 ((3a**R**,7a**R**)-7,7,-diphenyl-2-[1-imino-2-(2-methoxyphenyl)-ethyl] perhydroisoindol-4-one; Garret *et al.*, 1991) were obtained from the Parke-Davis Neuroscience Research Centre, Cambridge. Recombinant human IL-1α, recombinant human IL-1 receptor antagonist (IL-1ra; Hannum *et al.*, 1990), recombinant human basic fibroblast growth factor (bFGF), 6-keto-$PGF_{1\alpha}$ antiserum and the PAF receptor antagonist WEB-2086 (3-[4-(2-chlorphenyl)-9-methyl-6H-thieno [3,2-f] [1,2,4] triazolo-[4,3-a] [1,4]-diazepin-2-yl]-1-(4-morpholinyl)-1-propanone; Casals-Stenzel *et al.*, 1987) were gifts from Dr J. Saklatvala of Strangeways Research Laboratory, Cambridge, Dr R.C. Thompson of Synergen Inc., Colorado, U.S.A., Dr M. Presta, Department of Biomedical Sciences and Biotechnology, University of Brescia, Italy, Dr J. Salmon of Wellcome Research Laboratories, Kent, U.K. and Dr C. Meade of Boehringer Ingelheim, Germany, respectively.

^{133}Xenon injection (10 mCi in 3 ml saline) and [^{3}H]-6-keto-$PGF_{1\alpha}$ (50 mCi ml^{-1}) were obtained from Amersham International plc, UK. Other materials or reagents were purchased from the following companies: polyether foam sheet (R.E. Carpenter & Co., Suffolk, UK); polythene tubings (Portex Ltd., UK); Hypnorm (Janssen Pharmaceuticals, UK); indomethacin, mepyramine and cimetidine (Sigma Chemical Co., UK); specific endothelial cell marker *Bandeiraea simplicifolia* lectin I, isolectin B_4 ($BSL\text{-}B_4$, Vector Laboratories Ltd., Peterborough, UK). Indomethacin, and WEB 2086 were prepared in PBS (calcium and magnesium free, pH 7.4) from a stock solution of 10 mg ml^{-1} in ethanol. All other drugs were made up in PBS daily and sterilized by membrane filtration (0.45 μm) before use.

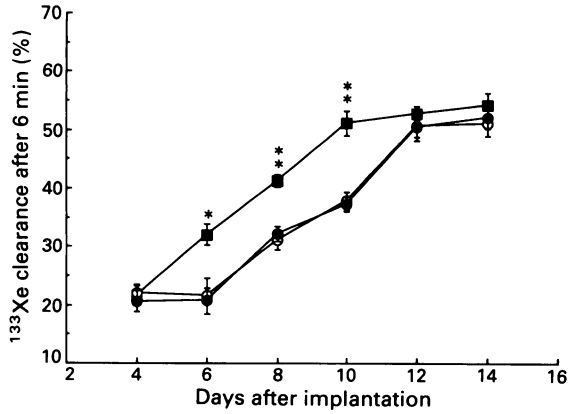

Figure 3 Inhibition of the angiogenic effect of substance P/interleukin-1α (IL-1α) by the substance P antagonist, [D-Pro^2, D-Phe^7, D-Trp^9]substance P. Symbols represent sponges treated daily with substance P/IL-1α (■), substance P/IL-1α plus 100 pmol (●) or 1,000 pmol (○) of the antagonist; see Methods for details. Each point represents mean data ± s.e.mean from 8–10 animals. $*P<0.05$; $**P<0.01$ (substance P/IL-1α plus 1,000 pmol [D-Pro^2, D-Phe^7, D-Trp^9]substance P vs substance P/IL-1α).

Statistical analysis

Statistical analysis of results was performed by a Student's *t* test.

Results

Effects of substance P and interleukin-1α

As shown in Figure 1, the ^{133}Xe clearance in control sponges was between 19% and 22% during the first 6 days after implantation due to passive diffusion of the radioisotope from the sponges. After day 6 the clearance increased such that by day 10 it was 36.0 ± 1.5%, and by day 14 it had reached a maximal level of 52.3 ± 1.7%, which was approaching the clearance obtained in normal rat skin (65–72%).

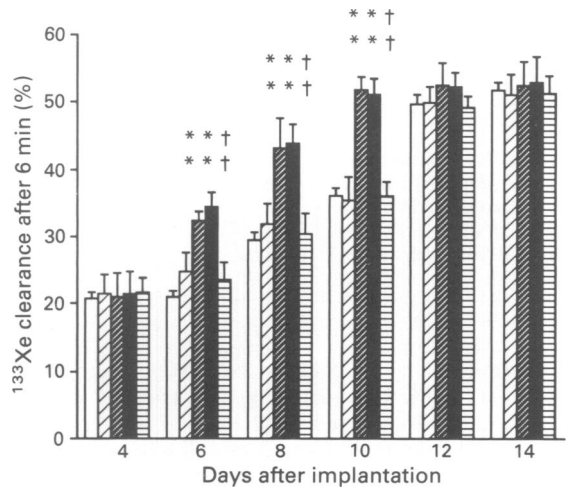

Figure 4 Angiogenic activity of the selective NK_1-receptor agonist [Sar^9,Met(O$_2$)^{11}]SP and its antagonism by the selective NK_1-receptor antagonist, L-668,169. Columns represent sponges treated daily with PBS alone (□), 10 pmol [Sar^9,Met(O$_2$)^{11}]SP (▨), 1,000 pmol [Sar^9,Met(O$_2$)^{11}]SP (▨), 10 pmol [Sar^9,Met(O$_2$)^{11}]SP plus 0.3 pmol interleukin-1α (IL-1α) (■) and 10 pmol [Sar^9,Met(O$_2$)^{11}]SP plus 0.3 pmol IL-1α plus 1,000 pmol L-668,169 (▤). Note that 1,000 pmol L-668,169 alone produced no effect; see Methods for details. Each point represents mean data ± s.e.mean from 6–8 animals. $**P<0.01$ (1,000 pmol [Sar^9,Met(O$_2$)^{11}]SP vs PBS alone: $††P<0.01$ [Sar^9,Met(O$_2$)^{11}]SP/IL-1α vs PBS alone; [Sar^9,Met(O$_2$)^{11}]SP/IL-1α vs [Sar^9,Met(O$_2$)^{11}]SP/IL-1α plus L-668,169).

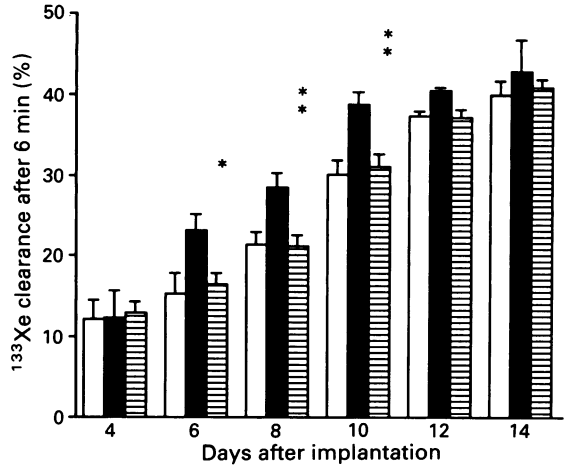

Figure 5 Inhibition of substance P/interleukin-1α (IL-1α)-induced angiogenesis by the non-peptide NK_1 receptor antagonist, RP 67580. Columns represent sponges treated daily with PBS (□), 10 pmol substance P plus 0.3 pmol IL-1α (■) and 10 pmol substance P plus 0.3 pmol IL-1α plus 1,000 pmol RP 67580 (▤). Note that 1,000 pmol RP 67580 alone produced no effect. See Methods for details. Each point represents mean data ± s.e.mean from 6 animals. $*P<0.05$; $**P<0.01$ (substance P/IL-1α plus RP 67580 vs substance P/IL-1α).

Histological studies showed that 8-day-old sponges treated with PBS were encapsulated by connective tissue, but with only little tissue infiltration and neovascular growth (Figure 2a). In contrast, daily administration of 1,000 pmol substance P elicited a substantial neovascularization and cellular infiltration (Figure 2b). This neovascular response was indistinguishable from that produced by daily injection of 3 pmol IL-1α (data not shown).

Lower doses of substance P (10 pmol) or IL-1α (0.3 pmol) alone produced no significant effect on the basal neovascularization. However, the combination of these subthreshold doses of substance P and IL-1α led to accelerated ^{133}Xe clearance by the sponge implants (Figure 1). Histologically, 8-day-old sponges treated with substance P (10 pmol) and IL-1α (0.3 pmol) showed heavy leucocyte infiltration and extensive neovascularisation (Figure 2c).

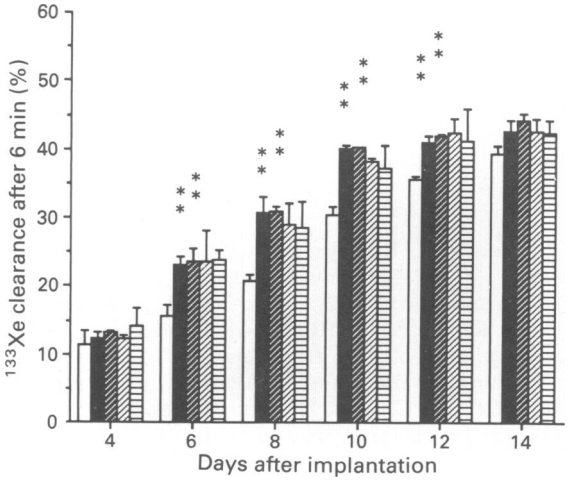

Figure 6 Effect of RP 67580 on angiogenesis induced by interleukin-1α (IL-1α) or bFGF alone. Columns represent sponges treated daily with PBS alone (□), 3 pmol IL-1α (■), 6 pmol bFGF (▨) 3 pmol IL-1α plus 1,000 pmol RP 67580 (▨), and 6 pmol bFGF plus 1,000 pmol RP 67580 (▤); see Methods for details. Each point represents mean data ± s.e.mean from 6 animals. $**P<0.01$ (3 pmol IL-1α vs PBS alone; 6 pmol bFGF vs PBS alone). RP 67580 produced no significant effect on sponges receiving IL-1α or bFGF.

Effects of tachykinin receptor agonists and antagonists

Since the angiogenic response elicited by subthreshold doses of substance P and IL-1α was inhibited by concomitant treatment with 1,000 pmol of the substance P antagonist, [D-Pro^2,D-Phe^7,D-Trp^9]substance P (Figure 3), it was decided to characterize the tachykinin receptors which mediate the angiogenic activity of substance P. Figure 4 shows that daily injection of 1,000 pmol of the selective NK_1 receptor agonist [Sar^9,Met(O$_2$)^{11}]substance P into sponge implants caused a significant increase in ^{133}Xe clearance as compared with controls. Lower doses (10–100 pmol) of [Sar^9,Met(O$_2$)^{11}]substance P did not induce any significant angiogenic response. However, when combined with a subthreshold dose of IL-1α (0.3 pmol), 10 pmol [Sar^9,Met(O$_2$)^{11}]-substance P was sufficient to produce a strong neovascular response similar to that elicited by either 1,000 pmol [Sar^9,Met(O$_2$)^{11}]substance P or 3 pmol IL-1α alone.

The ability of [Sar^9,Met(O$_2$)^{11}]substance P to mimic the angiogenic effect of substance P suggests that NK_1 receptors are likely to be involved. To test this hypothesis, the NK_1 receptor antagonist L-668,169 was used in initial experiments. Since at least 10,000 pmol L-668,169 would be required to inhibit the angiogenic effects of 1,000 pmol [Sar^9,Met(O$_2$)^{11}]-substance P alone, it was decided to test the ability of the antagonist to inhibit the effect of [Sar^9,Met(O$_2$)^{11}]substance P (10 pmol) and IL-1α (0.3 pmol). Figure 4 shows that L-668,169 (1,000 pmol) was able to reduce the elevated ^{133}Xe clearance values of sponges treated with [Sar^9,Met(O$_2$)^{11}]-substance P (10 pmol) and IL-1α (0.3 pmol) to that of controls. Similarly, daily doses of the non-peptide NK_1 receptor antagonist RP 67580 (1,000 pmol) completely antagonized the effect of substance P/IL-1α (Figures 2d and 5). Figure 6 shows that RP 67580 did not block the action of IL-1α. The specificity of NK_1 blockade was further confirmed by the failure of RP 67580 to block the comparable neovascular responses elicited by bFGF (Figure 6). In another series of experiments, a second non-peptide NK_1 receptor antagonist (±)-CP-96,345 (1,000 pmol day^{-1}) was also able to suppress the angiogenic effect of substance P/IL-1α (Figure 7).

In contrast, daily doses of 1,000 pmol of the selective NK_2 receptor agonist [β-Ala^8]NKA(4-10), or the NK_3 receptor agonist, senktide, did not influence the basal neovascular response in the sponges (data not shown). Since [β-Ala^8]NKA(4-10) and senktide display at least 100 times lower affinity than substance P at NK_1 receptors, they were used at 100 times the subthreshold dose of substance P (i.e., 1,000 pmol) in the study of potential interactions between these peptides and IL-1α. However, the combination of these peptides did not modify the basal neovascularization. Likewise, the NK_2 receptor antagonist L-659,874 (1,000 pmol) was ineffective against the angiogenic effect of substance P/IL-1α (data not shown).

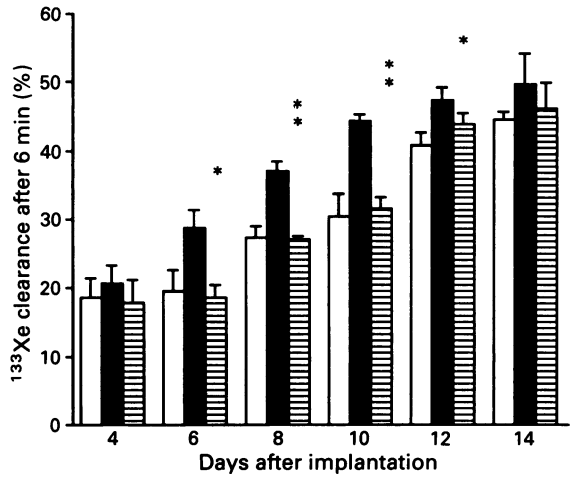

Figure 7 Inhibition of substance P/interleukin-1α (IL-1α)-induced angiogenesis by the non-peptide NK_1 receptor antagonist, (±)-CP-96,345. Columns represent sponges treated daily with PBS alone (□), 10 pmol substance P plus 0.3 pmol IL-1α (■) and 10 pmol substance P plus 0.3 pmol IL-1α plus 1,000 pmol (±)-CP-96,345 (▤); 1,000 pmol (±)-CP-96,345 alone produced no effect; see Methods for details. Each column represents mean data ± s.e.mean from 6–12 animals. $*P<0.05$; $**P<0.01$ (substance P/IL-1α plus (±)-CP-96,345 vs substance P/IL-1α).

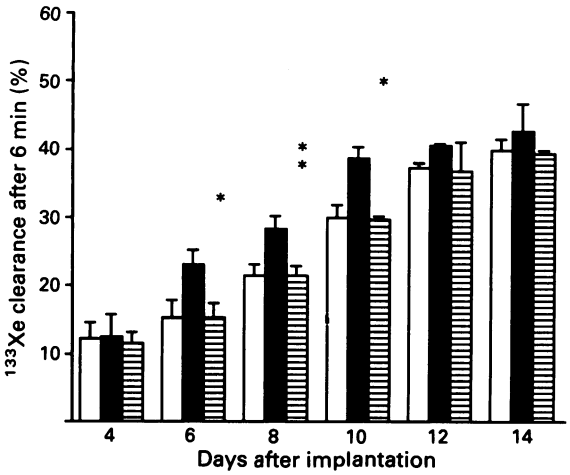

Figure 8 Inhibition of substance P/interleukin-1α (IL-1α)-induced angiogenesis by IL-1 receptor antagonist (IL-1ra). Columns represent sponges treated daily with PBS (□), 10 pmol substance P plus 0.3 pmol IL-1α (■), and 10 pmol substance P plus 0.3 pmol IL-1α plus 50 μg IL-1ra (▤). IL-1ra alone produced no effect; see Methods for details. Each column represents mean data ± s.e.mean from 6 animals. $*P<0.05$; $**P<0.01$ (substance P/IL-1α plus IL-1ra vs substance P/IL-1α).

Effect of IL-1 receptor antagonist

To establish the relative contribution of substance P and IL-1 in the substance P/IL-1α-induced neovascularization, the effect of an IL-1 receptor antagonist (IL-1ra) was examined. Like the NK_1 receptor antagonists (L-668,169, RP 67580 and (±)-CP-96,345), daily administration of 50 μg IL-1ra was able to inhibit the angiogenic effect of substance P/IL-1α (Figures 2e and 8).

Effects of indomethacin, a PAF antagonist and histamine antagonists

To analyse the possible involvement of prostaglandins, PAF and histamine in substance P/IL-1α-induced neovascularization, three different classes of drugs were used. On day 14 after implantation, the 6-keto-PGF$_{1\alpha}$ content in the sponges receiving substance P/IL-1α was elevated by almost 19 fold (376 ± 9 pg per sponge, $n = 6$, $P<0.01$) from that in the sponges receiving PBS alone (20 ± 5 pg per sponge, $n = 6$). When the prostaglandin synthesis inhibitor, indomethacin (7 nmol day^{-1}), was co-administered with the peptides into the sponges, the elevated 6-keto-PGF$_{1\alpha}$ level in these sponges was reduced by 95% (23 ± 8 pg per sponge vs 376 ± 9 pg per sponge, $n = 6$, $P<0.01$). However, indomethacin did not modify new vessel formation as determined by ^{133}Xe clearance (data not shown).

In parallel experiments, daily doses of 22 nmol of the PAF antagonist WEB-2086 had no significant effect (data not shown). Similarly, daily doses of 1 nmol of the H_1-receptor antagonist mepyramine and/or 10 nmol of the H_2-receptor antagonist cimetidine produced no changes on the angiogenesis induced by substance P/IL-1α (data not shown).

Discussion

In this paper, we present two lines of evidence which suggest a role for substance P in angiogenesis. First, a variety of selective tachykinin receptor ligands were able to mimic/antagonize the substance P/IL-1α angiogenic response. Thus, it was found that the angiogenic effect of substance P could be mimicked by the NK_1 selective agonist [Sar^9,$Met(O_2)^{11}$]-substance P, but not by the NK_2 or NK_3 selective agonists (β-Ala^8]-NKA(4-10) and senktide, suggesting that the activation of NK_1 receptors is most likely to mediate this effect of substance P. These results are in agreement with the findings of Ziche *et al.* (1990). Two earlier clinical observations also indicate a role of substance P in angiogenesis. In 1987, Hermanson *et al.* noted an increase in superficial skin wounds of substance P-immunoreactive sensory nerve fibres in connection with blood vessel regeneration. Subsequently, Mantyh and colleagues (1988) reported that in surgical specimens obtained from patients with inflammatory bowel diseases, receptor binding sites for substance P, but not neurokinin A or neurokinin B, were expressed in high concentrations by arterioles, venules and regional lymph nodules.

The other major finding of this paper is that the angiogenic action of substance P/IL-1α can be inhibited by the selective NK_1 receptor antagonists RP 67580 (Garret *et al.*, 1991) and (±)-CP-96,345 (Snider *et al.*, 1991), but not by the NK_2 selective antagonist, L-659,874 (Williams *et al.*, 1988). These observations are of potential clinical relevance in view of a recent report that substance P binding sites, with characteristics of NK_1 receptors, are localized on human synovial endothelial cells (Walsh *et al.*, 1992). This suggests that perivascular nerves containing substance P and substance P binding sites are well placed to play a regulatory role in synovial vasculature. However, the breakdown of this regulatory network may occur in rheumatoid arthritis, as suggested by the work of Levine *et al.* (1984), leading to excessive neovascularization. In such a situation, the blockade of NK_1 receptors in the joint may halt or reverse the progression of the disease. This approach may also have therapeutic implication in the future management of other angiogenic diseases, such as atherosclerosis, diabetic retinopathy and cancer.

Questions remain as to the mechanism by which substance P and IL-1α stimulate blood vessel formation. Both peptides have been shown to stimulate collagenase production by fibroblasts (Lotz *et al.*, 1987; see Payan, 1989), which is vital in the dissolution of the basement membrane of pre-existing blood vessels before angiogenesis can take place. They are also mitogenic for vascular endothelial cells *in vitro* (Ziche *et al.*, 1990; Detmar *et al.*, 1992). In addition, recent studies suggest several levels of interaction between substance P and IL-1 in chronic inflammation. Substance P can stimulate the production of IL-1 and other cytokines by human blood monocytes (Lotz *et al.*, 1988). On the other hand, IL-1 has been shown to increase substance P levels under inflammatory conditions and its gene expression in sympathetic neurones (Arai *et al.*, 1990; Freidin & Kessler, 1991; Hart *et al.*, 1991). Our ability to suppress the substance P/IL-1-induced angiogenesis by the blockade of either NK_1 or IL-1 receptor further illustrates the important interactions between these two peptides in chronic inflammatory diseases. However, IL-1 may play a bi-directional role in angiogenesis. It potentiates the effect of some factors such as substance P, but antagonizes the activity of others, e.g. it inhibits bFGF-induced vessel formation, probably due to its ability to decrease the expression of high-affinity bFGF binding sites on endothelium (Cozzolino *et al.*, 1990).

In an *in vivo* situation, additional factors may also be involved. For example, substance P can release histamine from mast cells (Foreman & Jordan, 1983) and PGE_2 from fibroblasts (Lotz *et al.*, 1987). Furthermore, both IL-1 and substance P are capable of stimulating endothelial cells and neutrophils to produce PAF (Bussolino *et al.*, 1986; Brunelleschi *et al.*, 1990), which could in turn stimulate endothelial cell migration and proliferation (Smither & Fan, 1992) and enhance the sponge-induced angiogenesis (Smither & Fan, 1990). However, the failure of histamine receptor antagonists, indomethacin and the PAF antagonist WEB-2086 to modify the substance P/IL-1α angiogenic response in this model indicates that histamine, prostaglandins and PAF do not play an important role.

In conclusion, the positive interaction between substance P and IL-1α described here underlines the potential importance of these two peptides in the angiogenic cascade leading to a variety of diseases characterized by excessive neovascularization. The successful blockade of the angiogenic response elicited by substance P and IL-1 suggests that in diseases associated with chronic release of these two peptides, nonpeptide NK_1 antagonists or IL-1 receptor antagonists could provide an effective treatment. More importantly, this study demonstrates that angiosuppression can be achieved by blocking the activity of angiogenic factors at the receptor level (Fan & Brem, 1992).

This work was supported by the Wellcome Trust and the British Heart Foundation. We thank Mrs Beverly Wilson and Mr Kwok Kei Chan for their help with histology and Ms Jane Glegg for technical assistance.

References

ANDRADE, S.P., FAN, T.-P.D. & LEWIS, G.P. (1987). Quantitative *in vivo* studies on angiogenesis in a rat sponge model. *Br. J. Exp. Pathol.*, **68**, 755–766.

ARAI, K., LEE, F., MIYAJIMA, A., MIYATAKE, S., ARAI, N. & YOKOTA, T. (1990). Cytokines: coordinators of immune and inflammatory responses. *Annu. Rev. Biochem.*, **59**, 783–836.

BRAIN, S.D. & WILLIAMS, T.J. (1989). Interactions between the tachykinins and calcitonin gene-related peptide lead to the modulation of oedema formation and blood flow in rat skin. *Br. J. Pharmacol.*, **97**, 77–82.

BRUNELLESCHI, S., CENI, E., GIOTTI, A. & FANTOZZI, R. (1990). Tachykinins stimulate lyso-PAF:acetyl-CoA acetyltransferase activity in neutrophils. *Eur. J. Pharmacol.*, **186**, 367–368.

BUCKLEY, T.L., BRAIN, S.D., COLLINS, P.D. & WILLIAMS, T.J. (1991). Inflammatory edema induced by interactions between IL-1 and the neuropeptide calcitonin gene-related peptide. *J. Immunol.*, **146**, 3424–3430.

BUSSOLINO, F., BREVIARIO, F., TETTA, C., AGLIETTA, M., MANTOVANI, A. & DEJENA, E. (1986). Interleukin-1 stimulates platelet-activating factor production in cultured human endothelial cells. *J. Clin. Invest.*, **77**, 2027–2033.

CASALS-STENZEL, J., MUACEVIC, G. & WEBER, K.-H. (1987). Pharmacological actions of WEB 2086, a new specific antagonist of platelet-activating factor. *J. Pharmacol. Exp. Ther.*, **241**, 974–981.

COZZOLINO, F., TORCIA, M., ALDINUCCI, D., ZICHE, M., ALMERIGOGNA, F., BANI, D. & STERN, D.M. (1990). Interleukin 1 is an autocrine regulator of human endothelial cell growth. *Proc. Natl. Acad. Sci. U.S.A.*, **87**, 6487–6491.

DETMAR, M., TENORIO, S., HETTMANNSPERGER, U., RUSZCZAK, Z. & ORFANOS, C.E. (1992). Cytokine regulation of proliferation and ICAM-1 expression of human dermal microvascular endothelial cells in vitro. *Invest. Dermatol.*, **98**, 147–153.

DRAPEAU, G., D'ORLEANS-JUSTE, P., DION, S., RHALEB, N.-E. & REGOLI, D. (1987). Selective agonists for substance P and neurokinin receptors. *Neuropeptides*, **10**, 43–54.

FAN, T.-P.D. & BREM, S. (1992). Angiosuppression. In *The Search for New Anticancer Drugs*. ed. Waring, M.J. & Ponder, B.A.J. pp. 183–227. Dordrecht, Boston, London: Kluwer Academic Publishers.

FAN, T.-P.D. & HU, D.-E. (1991). Modulation of angiogenesis by inflammatory polypeptides. *Int. J. Radiat. Biol.*, **60**, 71.

FAN, T.-P.D., HU, D.-E. & HILEY, C.R. (1992a). Development and validation of a sponge model for quantitative studies on angiogenesis. In *Angiogenesis in Health and Disease*, pp. 317–332. ed. Maragoudakis, M.E., Gullino, P. & Lelkes, P.I. New York & London: Plenum Press.

FAN, T.-P.D., HU, D.-E., SMITHER, R.L. & GRESHAM, G.A. (1992b). Further studies on angiogenesis in a rat sponge model. In: *Angiogenesis*, pp. 308–314. ed. Steiner, R., Weisz, P.B. & Langer, R. Basel: Birkhaüser Verlag AG.

FAN, T.-P.D. & LEWIS, G.P. (1984). Effect of cyclosporin A and inhibitors of arachidonic acid metabolism on blood flow and cyclo-oxygenase products in rat skin allografts. *Br. J. Pharmacol.*, **81,** 261–271.

FOLKMAN, J. & KLAGSBRUN, M. (1987). Angiogenic factors. *Science*, **235,** 442–447.

FOREMAN, J.C. & JORDAN, C.C. (1983). Histamine release and vascular changes induced by neuropeptides. *Agents Actions*, **13,** 105–116.

FREIDIN, M. & KESSLER, J.A. (1991). Cytokine regulation of substance P expression in sympathetic neurons. *Proc. Natl. Acad. Sci. U.S.A.*, **88,** 3200–3203.

GARRET, C., CARRUETTE, A., FARDIN, V., MOUSSAQUI, S., PEYRONEL, J.-F., BLANCHARD, J.-C. & LADURON, P.M. (1991). Pharmacological properties of a potent selective nonpeptide substance P antagonist. *Proc. Natl. Acad. Sci. U.S.A.*, **88,** 10208–10212.

GUARD, S. & WATSON, S.P. (1991). Tachykinin receptor types: classification and membrane signalling mechanisms. *Neurochem. Int.*, **18,** 149–165.

HAEGERSTRAND, A., DALSGAARD, C.-J., JONZON, B., LARSSON, O. & NILSSON, J. (1990). Calcitonin gene-related peptide stimulates proliferation of human endothelial cells. *Proc. Natl. Acad. Sci. U.S.A.*, **87,** 3299–3303.

HANNUM, C.H., WILCOX, C.J., AREND, W.P., JOSLIN, F.G., DRIPPS, D.J., HEIMDAL, P.L., ARMES, L.G., SOMMER, A., EISENBERG, S.P. & THOMPSON, R.C. (1990). Interleukin-1 receptor antagonist activity of a human interleukin-1 inhibitor. *Nature*, **343,** 336–340.

HART, R.P., SHADIACK, A.M. & JONAKAIT, G.M. (1991). Substance P gene expression is regulated by interleukin-1 in cultured sympathetic ganglia. *J. Neurosci. Res.*, **29,** 282–291.

HERMANSON, A., DALSGAARD, C.-J., BJÖRKLUND, H. & LINDBLOM, U. (1987). Sensory reinnervation and sensitivity after superficial skin wounds in human patients. *Neurosci. Lett.*, **74,** 377–382.

HU, D.-E. & FAN, T.-P.D. (1991). Synergistic interaction between bradykinin and interleukin-1 in angiogenesis. *Br. J. Pharmacol.*, **104,** 83P.

HU, D.E. & FAN, T.-P.D. (1993). [Leu^8]des-Arg^9-bradykinin inhibits the angiogenic effect of bradykinin and interleukin-1 in rats. *Br. J. Pharmacol.*, **109,** 14–17.

HU, D.E., HILEY, C.R. & FAN, T.-P.D. (1992). Parallel studies of ^{133}Xe clearance and ^{113}Sn microsphere accumulation during sponge-induced angiogenesis and the effects of interleukin-1α. *Br. J. Pharmacol.*, **106,** 102P.

KIMBALL, E.S. & FISHER, M.C. (1988). Potentiation of IL-1-induced BALB/3T3 fibroblast proliferation by substance P. *Ann. N.Y. Acad. Sci.*, **540,** 681–683.

KLAGSBRUN, M. & D'AMORE, P.A. (1991). Regulators of angiogenesis. *Annu. Rev. Physiol.*, **53,** 217–239.

LEVINE, J.D., CLARK, R., DEVOR, M., HELMS, C., MOSKOWITZ, M.A. & BASBAUM, A.I. (1984). Intraneuronal substance P contributes to the severity of experimental arthritis. *Science*, **226,** 547–549.

LOTZ, M., CARSON, D.A. & VAUGHAN, J.H. (1987). Substance P activation of rheumatoid synoviocytes: neural pathway in pathogenesis of arthritis. *Science*, **235,** 893–895.

LOTZ, M., VAUGHAN, J.H. & CARSON, D.A. (1988). Effects of neuropeptides on production of inflammatory cytokines by human monocytes. *Science*, **241,** 1218–1221.

MANTYH, C.R., GATES, T.S., ZIMMERMAN, R.P., WELTON, M.L., PASSARO, E.P. Jr., VIGNA, S.R., MAGGIO, J.E., KRUGER, L. & MANTYH, P.W. (1988). Receptor binding sites for substance P, but not substance K or neuromedin K, are expressed in high concentrations by arterioles, venules, and lymph nodules in surgical specimens obtained from patients with ulcerative colitis and Crohn disease. *Proc. Natl. Acad. Sci. U.S.A.*, **85,** 3235–3239.

MOSES, M.A. & LANGER, R. (1991). Inhibitors of angiogenesis. *Biotechnology*, **9,** 630–634.

NILSSON, J., VON EULER, A.M. & DALSGAARD, C.-J. (1985). Stimulation of connective tissue cell growth by substance P and substance K. *Nature*, **315,** 61–63.

PAYAN, D.G. (1989). Neuropeptides and inflammation: the role of substance P. *Ann. Rev. Med.*, **40,** 341–352.

ROVERO, P., PESTELLINI, V., RHALEB, N.-E., DION, S., ROUISSI, N., TOUSIGNANT, C., TELEMAQUE, S., DRAPEAU, G. & REGOLI, D. (1989). Structure-activity studies of neurokinin A. *Neuropeptides*, **13,** 263–270.

SMITHER, R.L. & FAN, T.-P.D. (1990). PAF antagonists inhibit angiogenesis in a rat sponge model. *Br. J. Pharmacol.*, **99,** 87P.

SMITHER, R.L. & FAN, T.-P.D. (1992). Effects of platelet-activating factor on endothelial cells and fibroblast in vitro. In: *Angiogenesis*, pp. 230–234. ed. Steiner, R., Weisz, P.B. & Langer, R. Basel: Birkhaüser Verlag AG.

SNIDER, R.M., CONSTANTINE, J.W., LOWE, J.A., III, LONGO, K.P. LEBEL, W.S., WOODY, H.A., DROZDA, S.E., DESAI, M.C., VINICK, F.J., SPENCER, R.W. & HESS, H.-J. (1991). A potent nonpeptide antagonist of the substance P (NK_1) receptor. *Science*, **251,** 435–437.

WALSH, D.A., MAPP, P.I., WHARTON, J., RUTHERFORD, R.A.D., KIDD, B.L., REVELL, P.A., BLAKE, D.R. & POLAK, J.M. (1992). Localisation and characterisation of substance P binding to human synovial tissue in rheumatoid arthritis. *Ann. Rheum. Dis.*, **51,** 313–317.

WILLIAMS, B.J., CURTIS, N.R., MCKNIGHT, A.T., MAGUIRE, J., FOSTER, A. & TRIDGETT, R. (1988). Development of NK-2 selective antagonists. *Regul. Pept.*, **22,** 189.

WORMSER, U., LAUFER, R., HART, Y., CHOREV, M., GILON, C. & SELINGER, Z. (1986). Highly selective agonists for substance P receptor subtypes. *EMBO J.*, **5,** 2805–2808.

ZICHE, M., MORBIDELLI, L., PACINI, M., GEPPETTI, P., ALESSANDRI, G. & MAGGI, C.A. (1990). Substance P stimulates neovascularization *in vivo* and proliferation of cultured endothelial cells. *Microvasc. Res.*, **40,** 264–278.

(Received February 25, 1993
Accepted May 10, 1993)

Br. J. Pharmacol. (1993), **110**, 50–53

Glycine stimulates striatal dopamine release in conscious rats

Gal Yadid, Karel Pacak, Eliahu Golomb, Judith D. Harvey-White, *Daniel M. Lieberman, Irwin J. Kopin & [1]David S. Goldstein

Clinical Neuroscience Branch and *Surgical Neurology Branch, National Institute of Neurological Disorders and Stroke, National Institutes of Health, Bethesda, Maryland 20892, U.S.A.

1 Glycine is an inhibitory neurotransmitter in the spinal cord and brainstem. The mechanism of this inhibition is via binding of glycine to specific receptors, increasing transmembrane Cl^- conductance and hyperpolarizing neurones. Strychnine selectively antagonizes these effects. The role of glycinergic neurones in supraspinal regions is poorly understood.

2 Effects of glycine on release of catecholamines in the striatum were examined by microdialysis in freely-moving rats. Transcription of the genes encoding strychnine-sensitive glycine receptors was assessed in the striatum and substantia nigra, by use of reverse transcription followed by the polymerase chain reaction.

3 Glycine administered via the microdialysis probe dose-dependently increased concentrations of dopamine and its metabolites, dihydroxyphenylacetic acid and homovanillic acid, in the perfusate, indicating increased local release and metabolism of dopamine. Strychnine markedly attenuated these responses. Whereas striatal tissue did not contain mRNA for either the adult or neonatal form of strychnine-sensitive glycine receptor, nigral tissue contained a message for the adult form.

4 The results suggest that dopaminergic cells in the substantia nigra synthesize strychnine-sensitive glycine receptors and transport the receptors to terminals in the striatum. Occupation of the glycine receptors then exerts a net stimulatory effect on striatal dopamine release *in vivo*.

Keywords: Glycine; strychnine; microdialysis; substantia nigra; dopamine; dihydroxyphenylacetic acid (DOPAC); homovanillic acid (HVA); polymerase chain reaction

Introduction

Glycine has long been considered to be an inhibitory neurotransmitter in the central nervous system (Curtis & Malik 1968; Krnjevik, 1974). As with γ-aminobutyric acid (GABA), a prototypical inhibitory transmitter, glycine hyperpolarizes neurones by increasing membrane chloride conductance (Bormann, 1988). Strychnine blocks glycine- but not GABA-induced neuronal inhibition (Young & Snyder, 1973).

In rat striatal slices previously exposed to [^{3}H]-dopamine, both glycine and GABA increase spontaneous [^{3}H]-dopamine release (Giorguieff *et al.*, 1978; Kerwin & Pycock, 1979). Analogously, after loading brain slices from other regions with [^{3}H]-noradrenaline, [^{3}H]-acetylcholine or [^{3}H]-dopamine, addition of glycine to the medium increases release of the radioactivity, and strychnine blocks the glycine-evoked release. These stimulatory effects have been attributed to blockade of local inhibitory interneurones. Recent findings, however, have indicated direct stimulatory effects of glycine on release of endogenous catecholamines from isolated chromaffin cells (Yadid *et al.*, 1991; 1992). Moreover, radioligand binding (Yadid *et al.*, 1989) and autoradiographic studies (unpublished data) have confirmed that chromaffin cells possess strychnine-sensitive glycine receptors. These findings suggest that glycine is not a universally inhibitory neurotransmitter.

The present study was designed to evaluate the effects of glycine on dopamine release in the striatum, by *in vivo* neurochemical and *in vitro* molecular techniques. Although genes encoding strychnine-sensitive glycine receptors are expressed in many brain areas, it was not known whether cells in the substantia nigra contain mRNA for strychnine-sensitive glycine receptors (Malosio *et al.*, 1991). *In vivo* effects of glycine in supraspinal regions have not been reported. The present study applied *in vivo* microdialysis in conscious, freely-moving rats, in order to determine whether glycine affects endogenous dopamine release and turnover in the striatum, and whether the effects are strychnine-sensitive. By use of reverse transcription followed by polymerase chain reaction (RT-PCR), transcription of the genes encoding two forms of strychnine-sensitive glycine receptor (adult and neonatal) was examined in the striatum and substantia nigra.

[1] Author for correspondence.

Methods

Microdialysis

Male Sprague-Dawley rats (230–250 g; $n = 5–9$ per treatment group) were anaesthetized with sodium pentobarbitone (50 mg kg^{-1}, i.p.). A microdialysis probe (4 mm length, 20 kD cutoff value, CMA/10, BAS/Carnegie Medicine, West Lafayette, IN, U.S.A.) was placed stereotaxically (David-Kopf Instruments, Tujunga, CA, USA; incisor bar 3.2 mm below the interaural line) in the anterior striatum (1.0 mm anterior to bregma, 2.5 mm lateral to midline suture, 6.5 mm ventral to dura; Paxinos & Watson, 1982) and cemented to the skull, as previously described (Pacak *et al.*, 1992). Body temperature was maintained with a heating blanket.

Artificial cerebrospinal fluid (aCSF; NaCl 189 mM, $CaCl_2$ 3.37 mM and KCl 3.9 mM, pH 6.3) was pumped through the dialysis probe (1.0 μl min^{-1}) with a microinjection pump (CMA 100, BAS/Carnegie Medicine, West Lafayette, IN, U.S.A.).

Experiments were performed in conscious, unrestrained animals 20–24 h after probe implantation. The dialysate was collected into polyethylene tubes containing 15 μl EDTA/ethanol (0.02/1%). After two 30 min baseline collections, aCSF containing glycine (Sigma, St. Louis, MO, U.S.A.) at various concentrations (0.02–20 mM) was administered, with or without strychnine (10 μM, Sigma, St. Louis, MO, U.S.A.) in the perfusate.

The dialysate samples were injected directly into a high-performance liquid chromatograph coupled to an electromechanical detector. Separation of the cathecholamines and their metabolites was achieved by reverse phase liquid

chromatography (Altex Ion Pair Ultrasphere C-18, 5 μm 4.6 mm ID × 250 mm column, No. 235335), with column temperature 30°C. The mobile phase, consisting of 2.1 l of water, 3.2 g 1-heptanesulphonic acid (No 0-3013, Fisher Scientific, Fairlawn, NJ, USA), 0.2 g EDTA (Fisher No. S-311), 16 ml triethylamine (Fisher No. 0-4884), 12 ml 85% phosphoric acid (Fisher No. A-260-500), and 60 ml acetonitrile (No 015-4 Burdick & Jockson, Muskegon, MI, U.S.A.), was pumped at 0.8 ml min^{-1}.

The detection apparatus included an analytical cell (No CB-100, EiCOM, Kitahatacho Fushimi, Kyoto, Japan) and a detector (No 460, Waters, Millipore, Milford, MA, U.S.A.), with oxidation potential 0.64–0.67 V.

Probe recoveries of dopamine, dihydroxyphenylacetic acid (DOPAC), and homovanillic acid (HVA) were measured in a 22°C water bath.

Statistical analyses included two-way analysis of variance with one repeated measure. A P value less than 0.01 defined statistical significance.

Transcription of genes encoding for glycine receptors

The existence of mRNA encoding the main adult and neonatal forms of the strychnine-binding subunit of glycine receptors was examined by RT-PCR, using the medulla oblongata as a positive control. The striatum, medulla oblongata, and substantia nigra (SN) of rats were dissected and immediately frozen in liquid nitrogen. Striata and SN of six rats were pooled for RNA extraction. RNA was extracted from the frozen tissues as described by Chomczynski & Sacchi (1987), using a commercial solution (RNAzol B, Tel-Test Inc., Friendswood, TX, U.S.A.). The quality of the RNA preparation was examined by electrophoresis of the RNA on a 16% formaldehyde, 1.25% agarose gel, by visualisation of the 28S and 18S bands. Oligonuleotide primers for the genes were synthesized by Lofstrand Labs, Inc. (Gaithersburg, MD, U.S.A.), according to published sequences (Grenningloh *et al.*, 1987; Kuhse *et al.*, 1990). The sequences of the primers for the adult rat 48K subunit glycine receptor (encompassing a cDNA fragment of 542 base pairs) were (upstream) CTTCCTGGATAAGCTTATGGGAAGG and (downstream) CTCTTCCTTCAGGATAAACTGAGGC. The primers for the rat neonatal glycine receptor (encompassing a cDNA fragment of 487 basepairs) were (upstream) GCAAAGACCATGACTCCAGG and (downstream) GCTGCATTGTACAGGTCTGG.

Reverse transcription (RT) with the specific downstream primers was performed for 2 h at 42°C, using 5 μg of total RNA, in a total volume of 20 μl, containing 50 mM Tris-HCl (pH = 8.3), 40 mM KCl, 6 mM $MgCl_2$, 1 mM DTT, 40 u RNAsin (Promega, Madison, WI, U.S.A.), 2 μg bovine serum albumin, 2 μM of the downstream primer, 0.2 mM of each deoxynucleotide, and 5 units of AMV reverse transcriptase (Gibco-BRL, Gaithesburg, MD, U.S.A.). Five microliters of the RT product were subjected to 40 cycles of PCR, using the GeneAmp kit (Cetus-Perkin-Elmer, Norwalk, CT, U.S.A.). Each reaction was carried out in a total volume of 100 μl, containing 25 pmol of each oligonucleotide primer and 2.5 u AmpliTaq DNA polymerase. Each cycle consisted of denaturation at 94°C for 1 min, annealing at 55°C for 90 s, and extension at 72°C for 90 s.

After amplification, 10 μl of the product of each reaction was electrophoresed on a 4-20% Tris-glycine gel (Novex, San Diego, CA, U.S.A.). The gel was stained with ethidium bromide, exposed to u.v. light, and photographed.

Results

Basal microdialysate dopamine, DOPAC, and HVA concentrations averaged 13.5 ± (s.e.mean) 0.50, 2067 ± 131, and 994 ± 102 nmol l^{-1} (n = 20). *In vitro* recoveries of dopamine, DOPAC and HVA averaged 20 ± 1.6, 22 ± 2 and 26 ± 0.5% (n = 6). Applying these recoveries, and correcting for the volume of preservative (15 μl added to 30 μl of microdialysate), estimated extracellular fluid concentrations of dopamine, DOPAC, and HVA were 0.10 ± 0.004, 17.8 ± 0.9, and 5.7 ± 0.6 μmol l^{-1}.

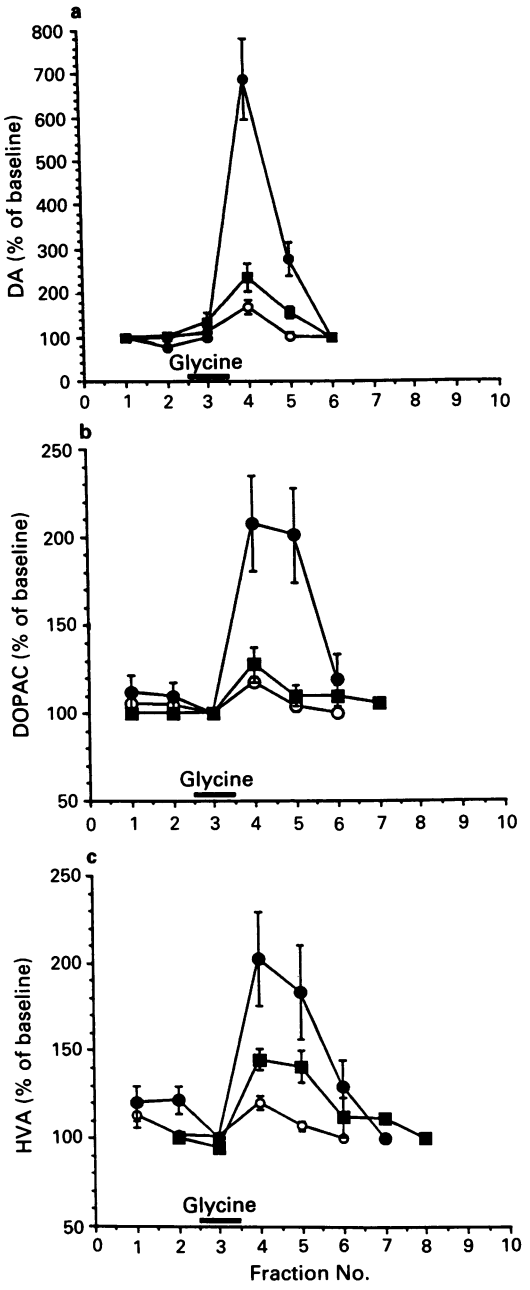

Figure 1 Effects of glycine (0.2 mM, ○; 2 mM, ■; 20 mM, ●) on microdialysate concentrations of dopamine (DA), dihydroxyphenylacetic acid (DOPAC) and homovanillic acid (HVA) in the corpus striatum of conscious rats. The bars indicate the period of glycine administration. Each fraction corresponds to 30 min.

Glycine dose-dependently increased microdialysate dopamine, DOPAC, and HVA levels (Figures 1,2). Although the approximately 9 fold increase in levels of dopamine above baseline was larger than the approximately 3.5 fold increases in levels of metabolites, the absolute increases in dopamine (about 900 nmol l^{-1}) were far smaller than those in the metabolites (about 8000 nmol l^{-1}). The increment in dopamine appeared mostly in a single fraction following glycine, whereas the elevations in metabolites occurred during both the first and second 30 min collections after glycine.

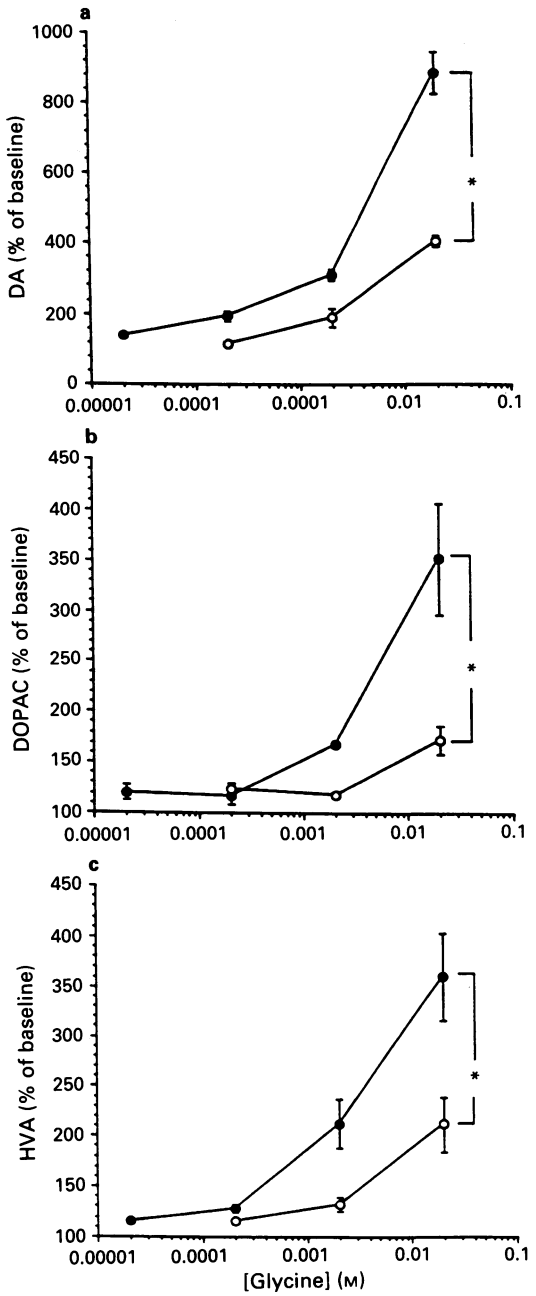

Figure 2 Microdialysate concentrations of dopamine (DA), dihydroxyphenylacetic acid (DOPAC) and homovanillic acid (HVA) after glycine administration with (○) or without (●) strychnine (10 μM). $*P<0.01$.

Strychnine markedly reduced glycine-evoked increases in dialysate dopamine, DOPAC, and HVA levels (Figure 2), shifting the dose-response curves to the right by at least 10 fold.

When striatal RNA was used as a template, we could not detect any RT-PCR product, with primers encompassing a region of the adult form of the glycine receptor, or with those spanning sequences of the neonatal type (Figure 3, lanes 1,4). In contrast, using extracted RNA from SN, a product of the adult glycine receptor, but not the neonatal type could be detected. A single clear band of the expected size (542 and 487 bp for the adult and neonatal types, respectively) was evident in both reactions in which RNA from the medulla, which served as the positive control, was used (Figure 3, lanes 2,5). These bands were evident also after 25 cycles of PCR (data not shown).

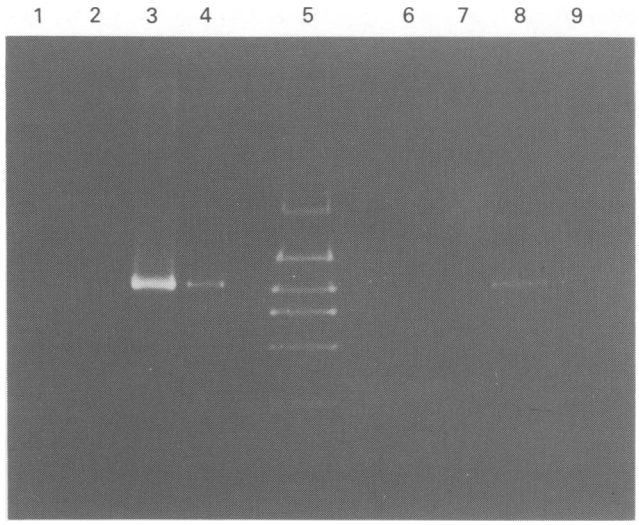

Figure 3 Ethidium bromide stained electrophoresed RT-PCR products of: (lane 1) water blank, amplified with primers encompassing a 542 bp region of the adult-type (48K subunit) glycine receptor; (lane 2) RNA from striatum, with primers encompassing a 542 bp region of the adult-type (48K subunit) glycine receptor; (lane 3) RNA from medulla oblongata, with primers encompassing a 542 bp region of the adult-type (48K subunit) glycine receptor; (lane 4) RNA from the substantia nigra, with primers encompassing a 542 bp region of the adult-type (48K subunit) glycine receptor; (lane 5) gel size markers (band sizes 1000, 700, 500, 400, 300, and 200 bp) (Research Genetics, Hansville, AL, U.S.A.); (lane 6) water blank, with primers encompassing a 487 bp region of the neonatal-type glycine receptor; (lane 7) RNA from striatum, with primers encompassing a 487 bp region of the neonatal-type glycine receptor; (lane 8) RNA from medulla oblongata, with primers encompassing a 487 bp region of the neonatal-type glycine receptor; (lane 9) RNA from the substantia nigra, with primers encompassing a 487 bp region of the neonatal-type glycine receptor.

Discussion

In the present study, glycine administered via a microdialysate probe in the striatum of conscious rats dose-dependently increased dopamine, DOPAC, and HVA concentrations in the dialysate. These results indicate that glycine releases dopamine into the extracellular fluid, with subsequent neuronal reuptake of dopamine and intraneuronal conversion of dopamine to DOPAC and with extraneuronal uptake of dopamine and DOPAC and extraneuronal conversion to HVA. The results therefore indicate that the net effect of glycine in the striatum is to stimulate endogenous dopamine release.

Strychnine attenuated glycine-evoked release of dopamine and its metabolites by at least 90%, suggesting involvement of a strychnine-sensitive receptor. Analogously, glycine stimulates [^{3}H]-noradrenaline release *in vitro* in hippocampal slices (Raiteri *et al.*, 1990; Schmidt & Taylor 1990), stimulates [^{3}H]-acetylcholine release in striatum (Taylor *et al.*, 1988), and stimulates [^{3}H]-dopamine release in ventral tegmentum (Gunglach & Beart., 1982), with all these effects blocked by strychnine.

The concentrations of glycine in the microdialysate that were required to stimulate dopamine release probably substantially exceeded those required to act at striatal effector sites, because the permeable membrane maintains a concentration gradient between the perfusate and the extracellular fluid, and because glycine in the extracellular fluid may be subject to metabolism or cellular uptake before reaching dopaminergic effector sites (Roberts & Anderson, 1979). Thus, administration of glycine directly into the striatum via a cannula attached to the microdialysis probe shifts the glycine concentration-microdialysate dopamine response curve to the left by about 10 fold, compared to the curve

obtained with administration of glycine via the perfusate in the probe (Yadid *et al.*, unpublished observations). At present, the exact relationship between glycine concentrations in the perfusate and endogenous glycine concentrations at striatal effector sites is unclear. The basal glycine concentration in striatal extracellular fluid is about 10 μM (M. Globus, personal communication). When glycine is administered via a cannula attached to the microdialysis probe, the minimum concentration producing significant increments in microdialysate dopamine is about 50 μM, whereas in the present study, the minimum effective concentration of glycine administered via the probe membrane was 200 μM.

Since glycine is thought to be an inhibitory neurotransmitter, one would expect the net stimulatory effect of glycine on striatal dopamine release to occur via an indirect local mechanism. For instance, glycine could inhibit inhibitory interneurones in the striatum; inhibit inhibitory heteroreceptors on dopaminergic terminals; de-inactivate local calcium channels by membrane hypopolarization (Llinas *et al.*, 1983); or increase transmembrane Cl^- conductance in nearby axons (Simmonds, 1983; Raiteri *et al.*, 1990), thereby producing receptor-mediated depolarization rather than hyperpolarization.

Mechanisms requiring the synthesis of strychnine-sensitive glycine receptors within the striatum can be excluded, since we failed to detect expression of genes encoding the two main types of glycine receptor (adult and neonatal types) in the striatum by the highly sensitive method of RT-PCR. Consistent with these results, studies using *in situ* hybridization have reported expression of mRNA encoding strychnine-sensitive glycine receptors in supraspinal structures, but not in the striatum (Malosio *et al.*, 1991). Thus, if glycine releases dopamine via inhibition of local inhibitory mechanisms, the receptors mediating this effect must differ structurally from those already identified or must be associated with axons projecting from sources outside the striatum.

The present results did confirm the expression of mRNA encoding the adult form of strychnine-sensitive glycine receptor in the substantia nigra, which is the source of dopaminergic innervation of the striatum. This result raises the possibility that strychnine-sensitive glycine receptors are transported in the axoplasm from dopaminergic cell bodies in the substantia nigra to dopaminergic terminals in the striatum, and that occupation of the receptors evokes transmitter release from the terminals. Indeed, in substantia nigra zona compacta neurones, glycine was shown to produce a membrane depolarization that was blocked by strychnine (Mercuri *et al.*, 1990). The results therefore suggest a stimulatory effect of what has been thought to be a purely inhibitory neurotransmitter in the central nervous system.

References

BORMANN J. (1988). Patch clamp analysis of GABA- and glycine-gated chloride channels. In *Chloride Channels and Their Modulation by Neurotransmitters and Drugs*. ed. Biggio, G. & Costa, E. pp. 47–61. New York: Raven Press.

CHOMCZYNSKI, P. & SACCHI, N. (1987). Single-step method of RNA isolation by acid guanidinium thiocyanate-phenol-chloroform extraction. *Anal. Biochem.*, **162,** 156–159.

CURTIS, D.R. & MALIK, R. (1968). A pharmacological study of the depression of spinal neurons by glycine and related amino acids. *Exp. Brain Res.*, **6,** 1–21.

GIORGUIEFF, M.F., KEMEL, M.L., GLOWINSKI, J. & BENSON, M.J. (1978). Stimulation of dopamine release by GABA in striatal slices. *Brain Res.*, **139,** 115–130.

GRENNINGLOH, G., RIENITZ, A., SCHMITT, B., METHFESSEL, C., ZENSEN, M., BEYREUTHER, K., GUNDELFINGER, E.D. & BETZ, H. (1987). The strychnine-binding subunit of the glycine receptor shows homology with nicotinic acetylcholine receptor. *Nature*, **328,** 215–220.

GUNDLACH, A.L. & BEART, P.M. (1982). Neurochemical studies of the mesolimbic dopaminergic pathway: glycinergic mechanisms and glycinergic-dopaminergic interactions in the rat ventral tegmentum. *J. Neurochem.*, **38,** 574–581.

KERWIN, R. & PYCOCK, C. (1979). Effect of ω-amino acids on tritiated dopamine release from rat striatum: evidence for a possible glycinergic mechanism. *Biochem. Pharmacol.*, **28,** 2193–2197.

KRNJEVIK, A. (1974). Chemical nature of synaptic transmission in vertebrates. *Physiol. Rev.*, **54,** 418–440.

KUHSE, J., SCMIEDEN, V. & BETZ, H. (1990). A single amino acid exchange alters the pharmacology of neonatal rat glycine receptor subunit. *Neuron*, **5,** 867–73.

LLINAS, R., GREENFIELD, S.A. & JAHNSEN, H. (1983). Electrophysiology of the pars compacta cells in the substentia nigra- a possible mechanism for dendritic release. *Brain Res.*, **294,** 127–132.

MALOSIO, M.L., MARQUEZE-POUEY, B., KUHSE, J. & BETZ, H. (1991). Widespread expression of the glycine receptor subunit mRNA in the adult and developing rat brain. *EMBO J.*, **10,** 2401–2409.

MERCURI, N.B., CALLABRESI, P. & BERNARDI, G. (1990). Effect of glycine on neurons in the rat substantia nigra zone compacta: in vitro electrophysiological study. *Synapse*, **5,** 190–200.

PACAK, K., ARMANDO, I., FUKUHARA, K., PALKOVITS, M., KOPIN, I.J. & GOLDSTEIN, D.S. (1992). Noradrenergic activation in the paraventricular nucleus during acute and chronic immobilization stress in rats: in vivo microdialysis. *Brain Res.*, **589,** 91–96.

PAXINOS, G. & WATSON, C. (1986). *The Rat in Stereotaxic Coordinates*. Orlando, FL: Academic Press.

RAITERI, M., FONTANA, G. & FEDEL, E. (1990). Glycine stimulates [^{3}H]-noradrenaline release by activation of a strychnine-sensitive receptor in rat hippocampus. *Br. J. Pharmacol.*, **184,** 239–250.

ROBERTS, P.J. & ANDERSON, S.D. (1979). Stimulatory effect of L-glutamate and related amino acids on ^{3}H-dopamine release from rat striatum: an in vitro model for glutamate action. *J. Neurochem.*, **32,** 1539–1542.

SCHMIDT, C.J. & TAYLOR, V.L. (1990). Strychnine-sensitive, glycine-induced release of [3H]-norepinephrine from rat hippocampal slices. *J. Neurochem*, **54,** 2077–2081.

SIMMONDS, M.A. (1983). Depolarization responses to glycine, β-alanine and muscimol in isolated optic nerve and cuneate nucleus. *Br. J. Pharmacol.*, **79,** 779–806.

TAYLOR, C.A., TSAI, C. & LEHMANN, J. (1988). Glycine-evoked release of [^{3}H]-acetylcholine from rat striatal slices is independent of the NMDA receptor. *Naunyn-Schmied. Arch. Pharmacol.*, **337,** 552–555.

YADID, G., YOUDIM, M.B.H. & ZINDER, O. (1989). High affinity strychnine binding to adrenal medulla chromaffin cell membranes. *Eur. J. Pharmacol.*, **175,** 365–366.

YADID, G., ZINDER, O. & YOUDIM, M.B.H. (1991). Effect of the prodrug milacemide (2-N-pentylaminoacetamide) on catecholamine secretion from isolated adrenal chromaffin cells. *Br. J. Pharmacol.*, **104,** 760–764.

YADID, G., ZINDER, O. & YOUDIM, M.B.H. (1992). Preferred release of epinephrine by glycine from adrenal chromaffin cells. *Eur. J. Pharmacol.*, **221,** 389–391.

YOUNG, A.B. & SNYDER, S.H. (1973). Strychnine binding associated with receptor of central nervous system. *Proc. Natl. Acad. Sci. U.S.A.*, **70,** 2832–2836.

(Received February 4, 1993
Accepted April 29, 1993)

Br. J. Pharmacol. (1993), **110**, 54–60

Cloning and expression of a fish α_2-adrenoceptor

*†Samuel P.S. Svensson, *Thomas J. Bailey, *Dave J. Pepperl, †Nils Grundström, **Sari Ala-Uotila, **Mika Scheinin, †Jan Olof G. Karlsson & [1,]*John W. Regan

*Departments of Pharmacology & Toxicology, and Physiology and the Program in Neuroscience, College of Pharmacy, University of Arizona, Tucson, AZ 85721, U.S.A.; †Department of Pharmacology, University of Linköping, S-581 85 Linköping, Sweden and **Department of Pharmacology, University of Turku, SF-20520 Turku, Finland

1 Pigment granule aggregation in specialized cells (melanophores) from the skin of teleost fishes has been shown to be mediated by receptors with an α_2-adrenoceptor pharmacology. We now report the cloning of the α_2-F, a fish skin α_2-receptor from the cuckoo wrasse (*Labrus ossifagus*).

2 Degenerate oligonucleotides corresponding to conserved regions of the human α_2-adrenoceptor subtypes were used in a polymerase chain reaction (PCR) with cDNA prepared from mRNA isolated from the skin of the cuckoo wrasse. An 876 base pair (bp) product was obtained that was homologous with that of the human α_2-adrenoceptor and was used to screen a genomic library from the cuckoo wrasse.

3 A clone (pTB17BS) consisting of ~5 kb of genomic DNA was obtained which contained the nucleotide sequence of the initial PCR product. In addition, it contained an open reading frame that encoded a protein of 432 amino acids and ~2 kb of 5'-untranslated sequence.The deduced amino acid sequence of this protein showed 47–57% identity with the human α_2-adrenoceptors and thus appeared to encode a fish α_2-adrenoceptor.

4 In the 5'-untranslated region of the gene, nucleotide sequences were present suggesting that transcription of the α_2-F might be regulated by cyclic AMP, calcium and/or steroids.

5 The α_2-F was expressed in COS-7 cells and radioligand binding studies were performed with [^{3}H]-rauwolscine. The binding was of high affinity and it was saturable with a K_D of 0.8 ± 0.1 nM and a B_{max} of 5.7 ± 1.0 pmol mg^{-1} of protein.

6 Competition curves for the displacement of specific [^{3}H]-rauwolscine binding showed the following order of potency: for agonists, medetomidine > clonidine > *p*-aminoclonidine > B-HT 920 > (−)-noradrenaline; for antagonists, rauwolscine > atipamezole > yohimbine > phentolamine > prazosin.

7 These results show that α_2-F has characteristics of both the human α_2-C10 and α_2-C4 and that it might represent an ancestral α_2-adrenoceptor subtype.

Keywords: Adrenoceptor; G-protein coupled receptor; melanophore; yohimbine; *Labrus ossifagus*

Introduction

Mammalian α_2-adrenoceptors belong to the growing family of G-protein-coupled receptors (Regan & Cotecchia, 1992). The receptor proteins within this family consist of a single polypeptide chain that is postulated to span the cell membrane seven times (Dohlman *et al.*, 1991). To date, three α_2-adrenoceptor subtypes have been identified which mediate a variety of tissue-specific responses including; presynaptic inhibition of neurotransmitter release, smooth muscle contraction, inhibition of lipolysis, inhibition of insulin release and platelet aggregation (Nichols & Ruffolo, 1991). In the skin of many lower vertebrates, such as frogs and fish, receptors with an α_2-adrenoceptor pharmacology, have been shown to mediate pigment granule aggregation in specialized cells called melanophores (Berthelsen & Pettinger, 1977; Andersson *et al.*, 1984). The aggregation, or dispersion, of these granules is responsible for colour changes in these animals. The fact that these changes can be easily evaluated with a photometer or light microscope have made the melanophores from fish skin an ideal model system for functional studies of α_2-adrenoceptors (Karlsson *et al.*, 1989; Svensson *et al.*, 1991a). Although similar in some respects to its mammalian counterparts, the fish melanophore α_2-adrenoceptor has a unique pharmacology. For example, the imidazoline, UK 14304, which is an agonist at mammalian α_2-adrenoceptors, is an antagonist at the α_2-adrenoceptors present in fish melanophores (Karlsson *et al.*, 1989).

We were, therefore, interested in cloning and expressing DNA encoding the fish melanophore α_2-adrenoceptor in order to correlate functional properties of the receptor with its protein structure. Using mRNA isolated from the skin of the cuckoo wrassse, a PCR product was obtained that appeared to encode an α_2-adrenoceptor. This was used to screen a genomic library and a gene was isolated which yielded a complete sequence for the α_2-F. This is the first nonmammalian α_2-adrenoceptor to be cloned and it shows some interesting structural and pharmacological characteristics with respect to the human α_2-adrenoceptor subtypes.

[1] Author for correspondence.

Methods

Reverse transcriptase/polymerase chain reaction

mRNA was isolated from the skin of the cuckoo wrasse (*Labrus ossifagus*) with the Fast Track Kit (Invitrogen). cDNA was synthesized from 100 ng of mRNA in a 20 µl reaction containing 10 mM Tris-HCl pH 8.3, 50 mM KCl, 1.5 mM $MgCl_2$, 0.001% (w/v gelatin, 40 u RNAsin inhibitor (Invitrogen), 0.5 mM dNTP's (Pharmacia), 2 µg random primers (Invitrogen) and 15 u of AMV reverse transcriptase (United States Biochemical). The reaction mix was incubated for 10 min at room temperature, then 60 min at 42°C. It was stopped by heating at 95°C for 5 min.

Oligonucleotide primers were prepared corresponding to the 3rd (primer A) and 7th (primer B) transmembrane domains of the human α_2-adrenoceptors and included a BamHI site (primer A) and a SacII site (primer B) to facilitate cloning. The sequences of the primers are shown below: primers A and B were 16 fold and 4 fold degenerate, respectively.

primer A
5'CGTCC ATCGG GATCC TGTGC GCCAT $C^T/_A{}^C/_G$CC
TGGAC$^C/_A$G$^G/_C$TA3'
primer B
5'GTAGA TCCGC GGGTT GAGCG AGCTG TTGCA
GTAGC CGA$^T/_C/^A/_G$ CCA3'

To the reverse transcriptase reaction, a PCR-mixture containing 100 pmol of primer A, 50 pmol of primer B, 5% dimethylsulphoxide (DMSO) and 1.25 u of AmpliTaq DNA polymerase (Perkin Elmer/Cetus) was added. Sixty cycles of PCR were performed using the following temperature profile: 95°C, 1 min; 50°C, 2 min; 72°C, 3 min. An 876 bp product was obtained and was named CW1. CW1 was cloned into pBluescript SK$^+$ (Stratagene) and the nucleotide sequence of both strands was determined by primer extension and dideoxynucleotide sequencing with Sequenase (United States Biochemical; Sanger *et al.*, 1977).

Southern blot analysis

Genomic DNA was extracted from cuckoo wrasse brains according to the method of Ausubel *et al.* (1988); 10 μg was digested with either EcoRI, HindIII or PstI. The DNA fragments were separated on 1% agarose gels and were blotted on to nitrocellulose filters (Sambrook *et al.*, 1989). The PCR product, CW1, was labelled with ^{32}P by the method of nick translation (Gibco/BRL) and used as a probe. Hybridization was performed overnight at 40°C in 50% formamide, 25 mM KPO_4, 5 × SSC and 0.25% nonfat powdered milk. Final washing conditions were for 30 min at 55°C in 2XSSC/0.1% SDS. Autoradiographs were obtained using Kodak XAR film and overnight exposures at − 70°C.

Construction and screening of a size-selected fish genomic library

EcoRI-digested genomic DNA was fractionated by centrifugation at 20°C for 24 h at 25,000 r.p.m. (SW28 rotor) over a 10–40% sucrose-gradient and DNA fragments ranging in size from 14–18 kb were pooled. These were used to prepare a library in the vector Lambda Dash II (Stratagene), according to the manufacturer's instructions. Approximately 1.4 × 10^6 plaque-forming-units were obtained of which 80% had inserts; without amplification, 400,000 were used to infect SRB-P2 cells at a titer of 20,000 plaques/plate. Nitrocellulose lifts were taken and were screened using the nick-translated ^{32}P-CW1 as a probe (see above). Pre-hybridization was done at 37°C for 2 h in 70 ml of 50% formamide, 1% SDS, 1 M NaCl, and 100 μg ml^{-1} herring sperm DNA. The probe was added (~5 × 10^6 d.p.m. ml^{-1}) and hybridized overnight at 37°C. The filters were washed at 53°C for 90 min in 2 × SSC/0.1% SDS and overnight exposures were made at − 70°C using Kodak XAR film and cassettes containing intensifying screens. A positive signal was found and the responsible clone, TB17, was isolated following 2 additional rounds of plating and screening. TB17 was amplified in plate lysates and DNA was prepared using LambdaSorb (Promega). A 16.5 kb insert was present which hybridized with ^{32}P-CW1 in Southern blot analysis.

Construction of a full-length clone encoding α_2-F

Using Southern blot analysis, a 3 kb BamHI fragment from TB17 was identified which hybridized with ^{32}P-CW1. It was subcloned into pBluescritp SK$^+$ to yield pTB17B and was sequenced. The sequence of CW1 was found within an open reading frame of 1293 bases, but the BamHI fragment began with this open reading frame, presenting the possibility that the coding sequence was short. A BamHI/SacII fragment of pTB17B, which contained 227 bases of the 5'-end of the open reading frame, was used as a probe in a Southern blot of SacII digested TB17. A 2 kb SacII fragment was identified and cloned into pBluescript. The 2 kb SacII fragment was then cloned into SacII-digested pTB17B to yield pTB17BS. [SacII cleaves pTB17B twice: once in the multiple cloning site, just upstream of the BamHI site, and again 227 bases downstream of the BamHI site.] In pTB17BS the open reading frame was extended an additional 57 bases beyond the BamHI site; however, the first methionine in this 1350 base open reading frame was only 3 bases upstream of the BamHI site. The length of open reading frame, therefore, starting with the first ATG (methionine) is 1296 nucleotides.

Construction of a eukaryotic expression vector encoding α_2-F

pTB17BS was used as a template in a PCR reaction with a sense primer containing adjacent SacII and DraI restriction sites (5'CCGCGGTTTAAA . . .), and corresponding to nucleotides − 136 to − 119 of α_2-F (Figure 2), and an antisense primer corresponding to nucleotides 401–423. A 571 bp product was obtained which was cleaved with SacII yielding a 374 bp fragment that was isolated and cloned into SacII digested pTB17BS. This created pA2F which could be cleaved with DraI to yield a 1.5 kb blunt-ended fragment containing the full coding sequence of α_2-F along with 136 bases of 5'-untranslated sequence and 68 bases of 3'-untranslated sequence. The eukaryotic expression vector, pBC 12BI (Cullen, 1987), was digested with HindIII and BamHI, blunt-ended with Klenow, and ligated with the 1.5 kb DraI fragment to give pBCA2F.

Expression and radioligand binding studies

pBCA2F was expressed transiently in COS-7 cells and the binding [^{3}H]-rauwolscine (77.9 Ci mmol^{-1}) to membranes was examined as previously described (Regan *et al.*, 1988). For saturation curve analysis, nonspecific binding was defined with 100 μM phentolamine. For competition curves analysis, a final concentration of 1 nM [^{3}H]-rauwolscine was used. Data were analysed by computer using the logistic function described by Parker & Waud (1971). K_i values were calculated by the Cheng-Prusoff conversion. Protein concentrations were determined by Bradford assay (Biorad).

Drugs

Drugs were obtained as follows: atipamezole and medetomidine were gifts from the Orion Corp./Farmos (Turku, Finland); yohimbine, prazosin, clonidine, (−)-noradrenaline, methoxamine and *p*-aminoclonidine were from Sigma Chemicals (St. Louis, MO, U.S.A.); SKF 104078 (6-chloro-9-[(3-methyl-2-butenyl)oxy]-3-methyl-1H2,3,4,5-tetrahydro-3-benzopine) was a gift from Smith Kline & French (Hearts, UK); phentolamine and guanfacine were gifts from CIBA-Geigy (Basel, Switzerland); UK 14304 (5-bromo-6-*N*-(2-4,5-dihydroimidazolyl) quinoxaline was a gift from Pfizer Central Research (Sandwich, UK); idazoxan was a gift from Reckitt & Colman (Kingston-upon-Hull, UK); B-HT 920 (2-amino-6 ally-5,6,7,8-tetrahydro-4H-thiazolo-[4,5-d]-azepine dihydrochloride) was a gift from Dr Thomae (Biberach, Germany), oxymetazoline was a gift from Astra Draco (Lund, Sweden); rauwolscine was from Carl Roth (Karlsruhe, Germany); [^{3}H]-rauwolscine was from New England Nuclear/Dupont (Boston, MA, U.S.A.).

Results

Cloning and sequence of α_2-F

mRNA was isolated from the skin of the cuckoo wrasse and was used as a template in a polymerase chain reaction (PCR) with degenerate primers from conserved regions of the human α_2-adrenoceptors. An 876 base pair (bp) product was obtained from a set of primers that corresponded to the third and seventh membrane domains of the human α_2-adreno-

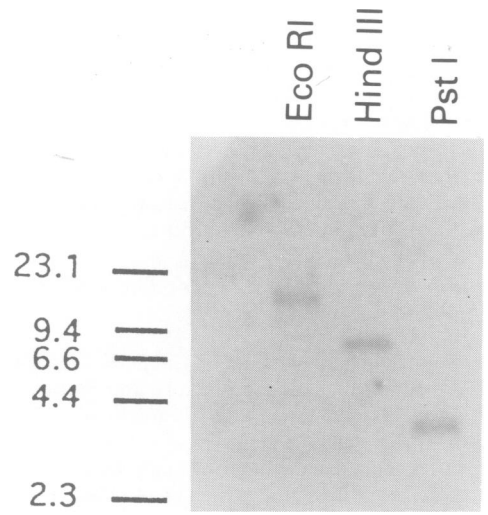

Figure 1 Southern blot of cuckoo wrasse (*Labrus ossifagus*) genomic DNA, digested with the indicated restriction enzymes and probed with ^{32}P-CW1, a PCR-product generated from fish skin mRNA and degenerate primers designed from the mammalian α_2-adrenoceptors. Restriction enzyme digests and blotting conditions were as described in Methods. The positions of molecular size standards are indicated on the left.

ceptors. When sequenced, this PCR product was found to have similarity with the human α_2-adrenoceptors and it could be aligned with them.

Difficulties with the preparation of skin cDNA libraries led to the screening of a genomic library in order to obtain the full coding sequence of this putatative fish α_2-AR. Prior to this, genomic DNA from the cuckoo wrasse was used in a Southern blot with the ^{32}P-labelled PCR product as a probe (Figure 1). Under conditions of moderate stringency (55°C, 2 × SSC) only a single band was present in DNA that had been cleaved with either EcoRI, HindIII or PstI. EcoRI-digested genomic DNA was fractionated by sucrose density gradient centrifugation and DNA in the size range of 14–18 kb was used to make a library in lambda phage. The library was screened with the ^{32}P-labelled PCR product and a phage was cloned with a 16.5 kb genomic insert that hybridized with the probe.

Restriction enzyme mapping, Southern blotting and subcloning resulted in the construction of a plasmid (pTB17BS) that contained a 1350 base open reading frame (ORF) and approximately 2 kb of additional sequence both 5′ and 3′ to the ORF. Figure 2 shows the nucleotide sequence for 2898 bases of this clone and the deduced amino acid sequence for 1296 bases of the ORF. The deduced amino acid sequence codes for a protein of 432 amino acids the beginning of which, was defined as the first ATG (methionine) in the ORF and by the presence of an optimal consensus sequence for the initiation of translation (Kozak, 1980). Within this open reading frame was the sequence of the PCR product that had been obtained from the skin mRNA (nt. 363–1218). The identity of the complete deduced amino acid sequence with the sequences of the human α_2-adrenoceptor subtypes was as follows: α_2-C4, 57%; α_2-C10, 50%; and α_2-C2, 47%. We named this intronless gene from fish as the α_2-F.

Hydropathy analysis (Kyte & Doolittle, 1982) of the deduced amino acid sequence of the α_2-F indicated seven domains of hydrophobic amino acids, each separated by loops of hydrophilic residues. These domains are thought to span the cell membrane and give the receptor a topological structure similar to rhodopsin (Dohlman *et al.*, 1991). This model as applied to the α_2-F is shown in Figure 3. The amino acid sequence identity of the α_2-F compared with other G-protein coupled receptors was highest in these putative transmembrane domains. Amino acid identities in the transmembrane domains between α_2-F and other adrenoceptor receptors are as follows: α_2-C4, 82%, α_2-C10, 77%; α_2-C2, 78%, α_1B, 43%, α_1C, 41%; β_1, 41%; β_2, 38%; β_3, 41%, D_2, 49%. In the third intracellular loop, which represents the most divergent part of the α_2-F as compared with its mammalian counterparts, serines and threonines were found that may represent sites for regulatory phosphorylation by protein kinases such as protein kinase A and β-adrenoceptor kinase (Benovic *et al.*, 1989). As in two of the mammalian α_2-adrenoceptor subtypes, potential sites for N-linked glycosylation (Asn-X-Ser or Asn-X-Thr) were found in the amino terminus.

A variety of nucleotide consensus sequences have been identified that are involved in the transcriptional regulation of eukaryotic genes (Maniatis *et al.*, 1987). In the 5′-untranslated sequence of the α_2-F, two TATA-like sequences are present at nt. − 21 and − 157 which could represent part of the promoter for RNA polymerase. Consensus sequences for other transcription factors that could potentially regulate the expression of the α_2-F were also found in the 5′ untranslated region. As listed in Table 1, these included activation protein-2 (AP-2, Mitchell *et al.*, 1987), adenosine 3′:5′-cyclic monophosphate (cyclic AMP) response element (CRE, Montminy *et al.*, 1990), steroid hormone receptor binding site (SRE, Beato, 1986) and a CAAT-box.

Expression

The ligand recognition properties of the α_2-F were determined in membranes prepared from COS-7 cells that had been transiently transfected with pBCA2F, a plasmid derived from the eukaryotic expression plasmid, pBC12BI and the coding region of the α_2-F (see Methods). In membranes prepared from the transfected COS-7 cells, [^{3}H]-rauwolscine bound in a specific and saturable manner (Figure 4). The binding of [^{3}H]-rauwolscine was linear with protein concentration and reached equilibrium after 20 min (data not shown). The affinity of [^{3}H]-rauwolscine for the α_2-F, as determined by Scatchard analysis of saturation binding data, was 0.8 ± 0.1 nM (K_D) with a B_{max} of 5.7 ± 1.0 pmol mg^{-1} protein. Competition binding studies were used to characterize the pharmacology of the α_2-F (Table 2). The potency series for putative agonists was as follows: medetomidine > clonidine > B-HT 920 > guanfacine > UK14304 > (−)-noradrenaline >> isoprenaline and methoxamine. For putative antagonists, the potency series was: rauwolscine > atipamezole > yohimbine > phentolamine > prazosin. The α_2-F, indeed, has the pharmacological characteristics of an α_2-adrenoceptor.

Table 1 Potential upstream promoter elements in the gene encoding the α_2-F[a]

Promoter	*Sequence*[b]	*Location*[c]	*Activator*
AP-2	CCCCAcaC	− 758/− 749	Cyclic AMP/Ca^{2+}
CRE	aaAGGTCA	− 1040/− 1033	Cyclic AMP
SRE	GGTCt---TGAgC	− 871/− 859	Steroids
CAAT-box	CAAT	− 219/− 216	

[a]Abbreviations: AP-2, activation protein 2; CRE, cyclic AMP response element; SRE, steroid hormone response element.
[b]Nucleotide sequence in the α_2-F, nonhomologous bases are shown in small caps.
[c]According to the nucleotide sequence shown in Figure 2.

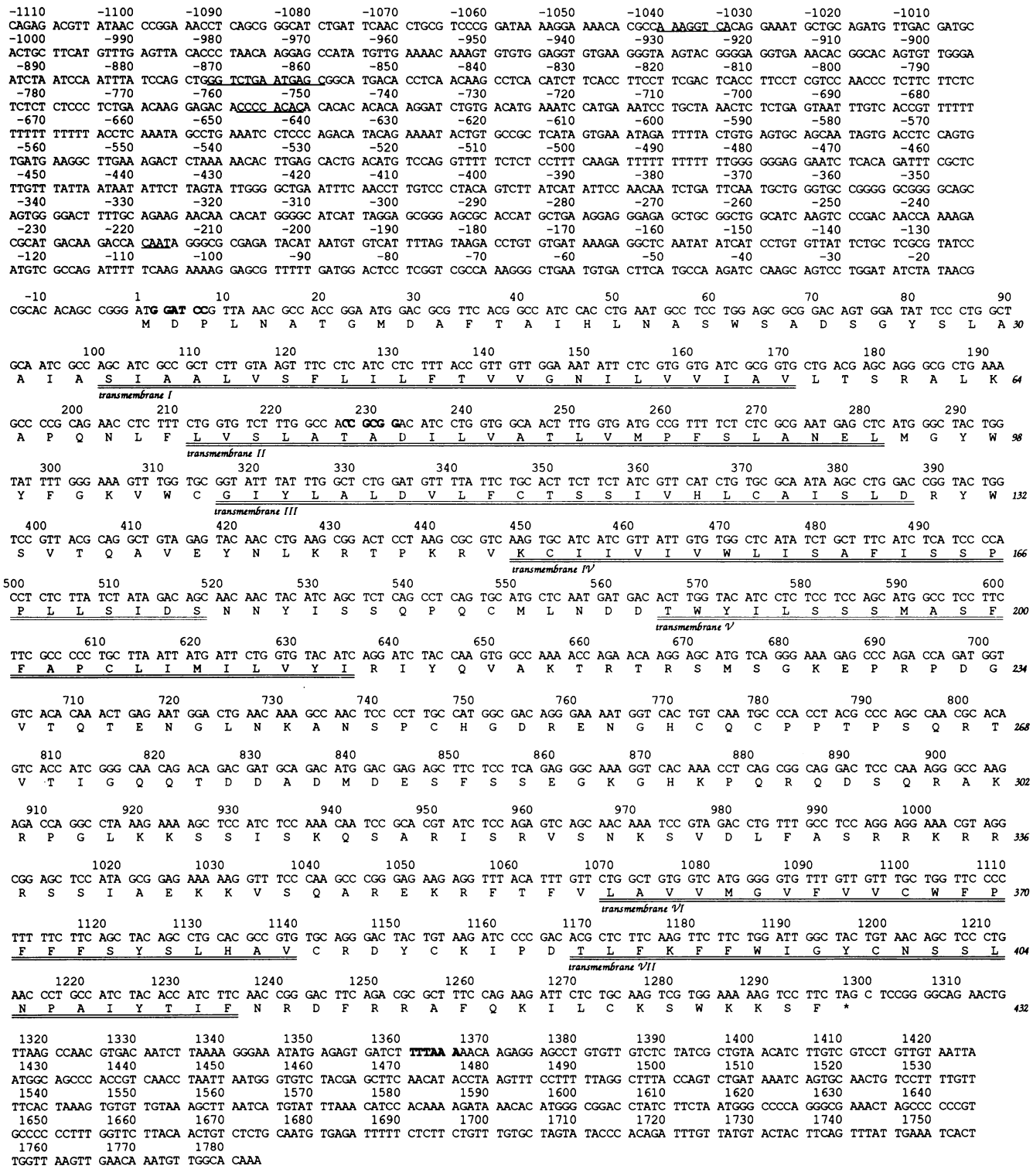

Figure 2 Nucleotide and deduced amino acid sequence of the fish pigment cell α_2-adrenoceptor (α_2-F). Consensus sequences for potential regulators of transcription (Table 1) are indicated by the single underline. Probable transmembrane domains are indicated by the double underlines. Three restriction sites that were used during the cloning procedures are indicated in bold-face type (BamHI, nt. 3–8; SacII, nt. 227–232; DraI, nt. 1361–1366).

Discussion

The α_2-F, an adrenoceptor from the skin of the cuckoo wrasse, has been cloned and heterologous expression in a mammalian cell line has shown a unique pharmacology but one that is characteristic of the α_2-adrenoceptor family. The α_2-F appears to be that receptor in fish skin which controls the aggregation of pigment granules in melanophores. The melanophores of frog skin were one of the first cell types where functional postsynaptic α_2-adrenoceptors were identified (Berthelsen & Pettinger, 1977). Recent work has also identified the presence of postsynaptic α_2-adrenoceptors on the melanophores from several species of teleost fishes (Andersson *et al.*, 1984; Svensson *et al.*, 1989). In functional

Table 2 Binding affinities of adrenoceptor ligands at the α_2-F[a]

Ligand	K_i (nM)
Rauwolscine	0.3 ± 0.05
Atipamezole	0.6 ± 0.1
Yohimbine	1.1 ± 0.2
SKF 104078	24 ± 4
Idazoxan	45 ± 4
Phentolamine	104 ± 12
Prazosin	469 ± 79
UK 14304	1612 ± 218
Medetomidine	46 ± 2
Oxymetazoline	49 ± 12
Clonidine	83 ± 11
p-Aminoclonidine	92 ± 17
B-HT 920	209 ± 13
Guanfacine[b]	1404 ± 149
Noradrenaline	2849 ± 286
Amiloride	23000 ± 3400
Isoprenaline	67468 ± 10417
Methoxamine	87440 ± 23096

[a]As determined in radioligand binding studies using [^{3}H]-rauwolscine (1 nM) and membranes prepared from COS-7 cells transfected with the α_2-F. Data are the means ± s.e.mean for 3 experiments.
[b]$n = 2$.

Table 3 K_i ratios for prazosin/oxymetazoline and prazosin/yohimbine[a]

Subtypes	*Prazosin/ Oxymetazoline*	*Prazosin/ Yohimbine*
α_2A	164	1125
α_2B	0.19	31
α_2C	0.66	44
α_2-F	10	426

[a]Data for the α_2-F are derived from Table 2. Data for the human α_2A (α_2-C10), α_2B (α_2-C2) and α_2C (α_2-C4) are from Harrison *et al.* (1991).

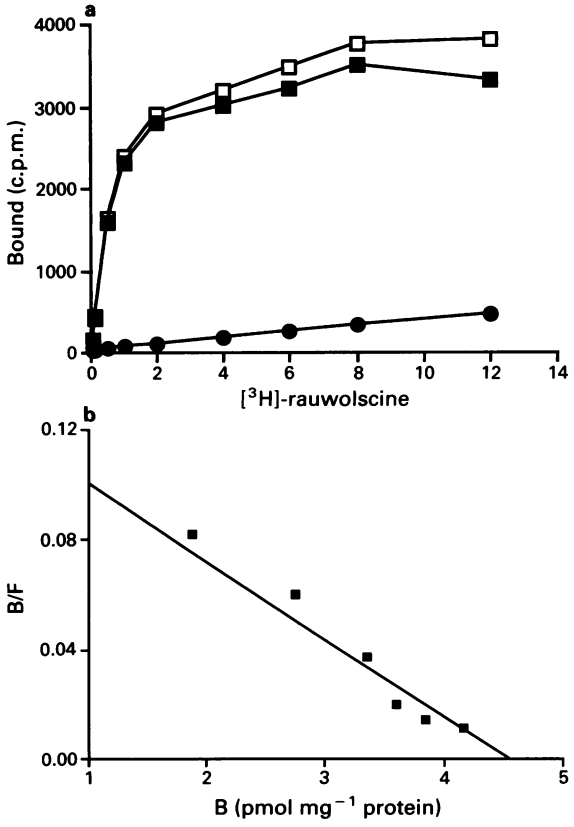

Figure 4 Saturation curve (a) and Scatchard plot (b) for the binding of [^{3}H]-rauwolscine to membranes prepared from COS-7 cells transiently transfected with the α_2-F. A representative experiment is shown, conducted as described in Methods. Total binding (□), nonspecific (●) and specific (■) binding.

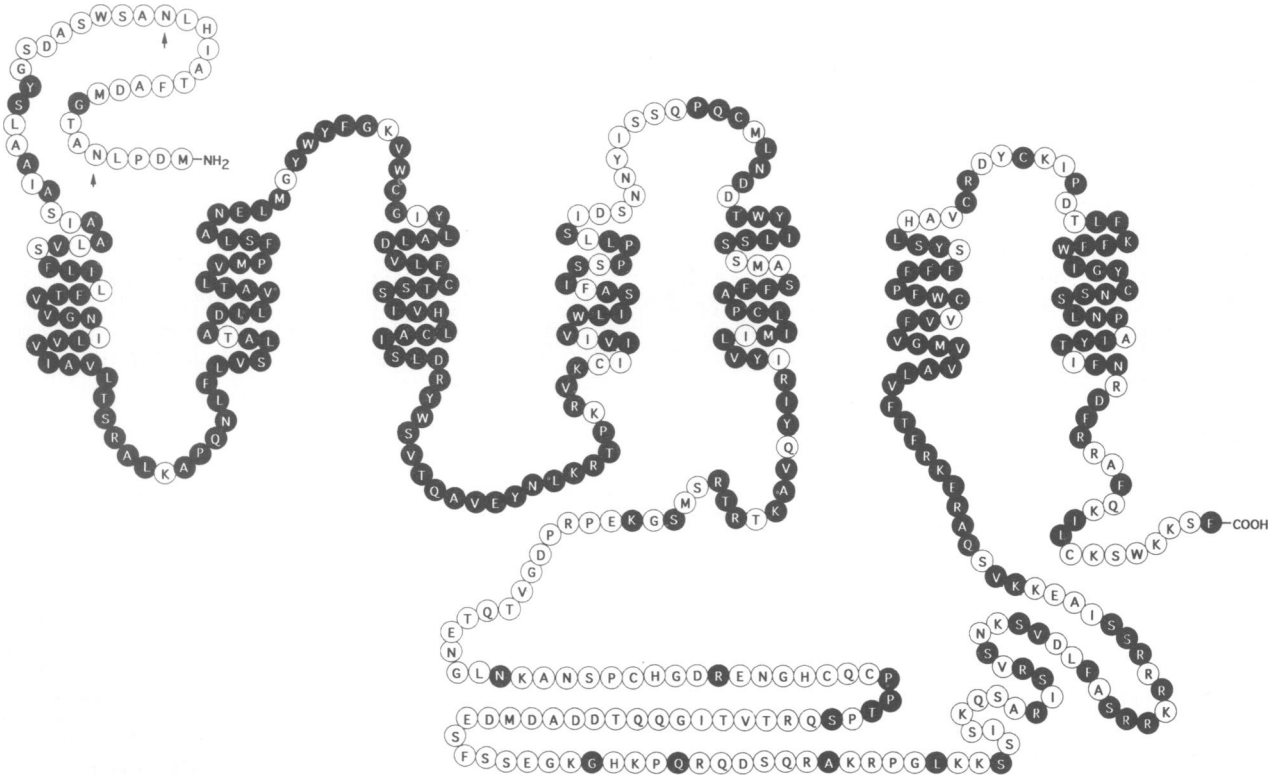

Figure 3 Seven transmembrane domain model for the deduced amino acid sequence of the α_2-F. The circles represent individual amino acids (single letter code). Amino acids that are conversed between the α_2-F and the human α_2-C4 are shown in black. Sites for potential N-linked glycosylation are indicated with arrows.

studies, the melanophore α_2-adrenoceptor is pharmacologically similar to its mammalian counterparts; however, UK 14304, an imidazoline which is a full agonist at mammalian α_2-adrenoceptors, is an antagonist at the α_2-adrenoceptors on melanophores (Karlsson *et al.*, 1989). It was of interest, therefore, to determine the primary sequence of this receptor because differences between it and the mammalian α_2-adrenoceptors might be revealing with respect to what it takes to activate an α_2-adrenoceptor.

Molecular cloning has identified 3 mammalian genes encoding α_2-adrenoceptor subtypes in both man (α_2-C2, α_2-C4, α_2-C10) and rats (Kobilka *et al.*, 1987; Regan *et al.*, 1988; Lomasney *et al.*, 1991; Weinshank *et al.*, 1990; Zeng *et al.*, 1990; Chalberg *et al.*, 1990; Lanier *et al.*, 1991). Based largely on radioligand binding studies, Bylund (1988) has also defined 3 α_2-adrenoceptor subtypes (α_2A, α_2B, α_2C). Biochemical, molecular biological and pharmacological studies have correlated the α_2-C10 with the α_2-A, the α_2-C2 with the α_2B and the α_2-C4 with the α_2C (Lanier *et al.*, 1988; Lorenz *et al.*, 1990; Harrison *et al.*, 1991; Regan & Cotecchia, 1992; Bylund *et al.*, 1992).

The deduced amino acid sequence of the α_2F shows similarity with its mammalian counterparts. Overall sequence identity suggests that α_2-F is most closely related to the α_2-C4 (57% for the α_2-C4 versus 50% for the α_2-C10 and 47% for the α_2-C2). This level of identity is significantly less than has been observed between α_2-adrenoceptor subtypes from more closely related species. For example, there is 88% overall identity between the human α_2-C4 and its equivalent in the rat. With respect to various regions of the mammalian α_2-adrenoceptors, the greatest identity with the α_2-F is in the membrane spanning domains where ligand binding is thought to occur (Dohlman *et al.*, 1991).

Several amino acids that are highly conserved in the adrenoceptor family, and which are thought to be part of the ligand binding site, are also found in the α_2-F. For example, present in the α_2-F are 2 serines in the fifth transmembrane domain and an aspartic acid in the third transmembrane domain which may interact with noradrenaline by way of its catechol hydroxyl groups and amino nitrogen, respectively (Dixon *et al.*, 1988). An amino acid that is not conserved in the α_2-F, as compared with the mammalian α_2-adrenoceptors, is a phenylalanine in the seventh membrane spanning domain. This residue which corresponds to F^{412} in the human α_2-C10 appears to be deleted in the α_2-F (if present, it would be between F^{395} and W^{396}). Interestingly, F^{412} has been shown to be critical in dictating antagonist binding specificity (Suryanarayana *et al.*, 1991). Mutation of F^{412} from phenylalanine to asparagine results in a receptor with low affinity for the α_2-selective antagonist, yohimbine, and high affinity for the β-selective antagonist, alprenolol. In the human β_2-adrenoceptor, an asparagine is present at the equivalent position (N^{312}). Whether the absence of this residue in the α_2-F can explain any of the unusual aspects of its pharmacology remains to be tested.

The transiently expressed α_2-F displayed high affinity and saturable binding with [^{3}H]-rauwolscine as a radioligand. To characterize further the pharmacological profile of the α_2-F, the potency of a variety of adrenoceptor ligands was examined. The α_2-F behaved like an α_2-adrenoceptor. Using regression analyses, the data for the compounds listed in Table 2 showed the best correlation with the human α_2-C4 subtype, perhaps reflecting the greater structural identity of the α_2-F with the α_2-C4. Using the analysis as suggested by Harrison *et al.* (1991), however, somewhat different results were obtained. In this analysis, the ratios of prazosin to oxymetazoline and prazosin to yohimbine are compared: Table 3 lists these ratios. Using the prazosin to oxymetazoline ratio, it is hard to find any good correlation, but using the prazosin to yohimbine ratio, α_2-F appears more like the α_2-C10. This pharmacology, with characteristics of both the α_2-C4 and α_2-C10, suggests that α_2-F is not a simple homologue of the human α_2-C4 and that it might represent a common ancestor. Obviously, more work will be needed to answer this question.

Another question concerns whether or not the α_2-F represents the α_2-receptor controlling the pigment granule aggregation in melanophores. Although the PCR product used to clone the α_2-F was obtained from fish skin, and its sequence was present in the clone, we cannot at this time unequivocally prove that it is the melanophore α_2-adrenoceptor. This is a consequence of the possibility of more than one α_2-receptor being present in the skin. Several lines of evidence suggest, however, that it is the fish melanophore α_2-adrenoceptor. The first is that when the α_2-F was used as a radiolabelled probe, only one hybridizing band was observed in a Southern blot of fish genomic DNA (Figure 1). With similar hybridization and wash conditions, experiments done with a human α_2-C10 probe invariably identified the other α_2-adrenoceptor subtypes in Southern blots of human genomic DNA (Kobilka *et al.*, 1987; Regan & Cotecchia, 1992). A second line of evidence is that the pharmacology of the α_2-F and the melanophore α_2-adrenoceptor are very similar. For example, both receptors are rather insensitive to prazosin (Table 2; Svensson *et al.*, 1993). Additionally, in melanophores Schild plot analysis gave a pA_2 of 6 for UK 14304 which is in good agreement with the K_i obtained for UK 14304 in binding studies with the expressed α_2-F (1.6 μM).

In studies of the functional activity of fish melanophore α_2-adrenoceptor, scales containing the pigment cells are removed from the skin and are maintained in tissue culture. Because the scales are innervated, the process of removing them results in degeneration of the intrinsic sympathetic nerve endings going to the melanophores. With time, there develops a supersensitivity of the α_2-adrenoceptors for noradrenaline which is probably related to the loss of nerve endings (Karlsson *et al.*, 1988; Svensson *et al.*, 1991b).

The molecular mechanism of this denervation supersensitivity is unknown but it could involve increased expression of the α_2-adrenoceptor. It is interesting that there is a consensus sequence for a cyclic AMP response element (CRE) in the 5'-untranslated region of the α_2-F (Table 1). Stimulation of the melanophore α_2-adrenoceptor by noradrenaline decreases intracellular cyclic AMP and causes pigment granule aggregation (Andersson *et al.*, 1984). It is possible, therefore, that loss of a tonic inhibition could raise intracellular cyclic AMP levels and increase receptor expression by increasing transcription. There is precedence for this, the genes for the β_2-adrenoceptor (Collins *et al.*, 1989) and the α_2-C10 (Sakaue & Hoffman, 1991) both contain CRE's and seem to be regulated by their second messenger, i.e. cyclic AMP.

Other promoters may also operate to regulate the expression of the α_2-F. Thus, consensus sequences were found in the 5'-untranslated region of the α_2-F that could lead to regulation of expression by calcium and/or steroids (Table 1). Understanding the possible role of these promoters may do more than just helping us to understand the fish melanophore α_2-adrenoceptor: a consensus site for AP-2 and a CRE have also been found in the 5'-untranslated region of the α_2-C10 (Fraser *et al.*, 1989). It is hoped that future studies on the α_2-F and its gene will provide us with a better understanding of the function, pharmacology and expression of all the members of the α_2-adrenoceptor family.

This work has been supported in part by grants from the National Institutes of Health (R29 EY09355 to J.W.R.), Allergan (to J.W.R.), Eli Lilly & Co. (to J.W.R.), the Arizona Affiliate of the American Heart Association (to J.W.R.), the Swedish Medical Research Council (K90-04X-9350-01G; K92-14P-09297-03A; B91-04R-9599; B92-04X-09474-02B), CFN, the Magnus Bergvall Foundation, the Thyr and Thure Stenemark Foundation, the Ruth Trossebeck's Foundations and the Tore Nilson Foundation, the Nordiska ministerrådet, Orion Corp./Farmos and the Technology Development Centre of Finland.

References

ANDERSSON, R.G.G., KARLSSON, J.O. & GRUNDSTRÖM, N. (1984). Adrenergic nerves and the alpha2-adrenoceptor system regulating melanosome aggregation within fish melanophores. *Acta Physiol. Scand.*, **121,** 173–179.

AUSUBEL, F.M., BRENT, R., KINGSTON, R.E., MOORE, D.D., SEIDMAN, J.G., SMITH, J.A. & STRUHL, K. (1988). In *Short Protocols in Molecular Biology*. Harvard Medical School.

BEATO, M. (1986). Gene regulation by steroid hormones. *Cell*, **56,** 335–344.

BENOVIC, J.L., DEBLASI, A., STONE, W.C., CARON, M.G. & LEFKOWITZ, R.J. (1989). β-Adrenergic receptor kinase: primary structure delineates a multigene family. *Science*, **246,** 235–240.

BERTHELSEN, S. & PETTINGER, W.A. (1977). A functional basis for classification of alpha-adrenergic receptors. *Life Sci.*, **21,** 595–606.

BYLUND, D. (1988). Subtypes of α_2-adrenoceptors: pharmacological and molecular biological evidence converge. *Trends Pharmacol. Sci.*, **9,** 356–361.

BYLUND, D.B., BLAXALL, H.S., IVERSEN, L.J., CARON, M.G., LEFKOWITZ, R.J. & LOMASNEY, J.W. (1992). Pharmacological characteristics of α_2-adrenergic receptors: comparison of pharmacologically defined subtypes with subtypes identified by molecular cloning. *Mol. Pharmacol.*, **42,** 1–5.

CHALBERG, S.C., DUDA, T., RHINE, J.A. & SHARMA, R.K. (1990). Molecular cloning, sequencing and expression of an alpha-2 adrenergic receptor complementary DNA from rat brain. *Mol. Cell. Biochem.*, **97,** 161–172.

COLLINS, S., BOUVIER, M., BOLANOWSKI, M.A., CARON, M.G. & LEFKOWITZ, R.J. (1989). cAMP stimulates transcription of the β_2-adrenergic receptor gene in response to short-term agonist exposure. *Proc. Natl. Acad. Sci. U.S.A.*, **86,** 4853–4857.

CULLEN, B.R. (1987). Use of eukaryotic expression technology in the functional analysis of cloned genes. *Methods Enzymol.*, **152,** 684–704.

DIXON, R.A.F., SIGAL, I.S. & STRADER, C.D. (1988). Structure-function analysis of the β-adrenergic receptor. *Cold Spring Harbor Symp. Quant. Biol.*, **53,** 487–497.

DOHLMAN, H.G., THORNER, J., CARON, M.G. & LEFKOWITZ, R.J. (1991). Model system for the study of seven-transmembrane-segment receptors. *Annu. Rev. Biochem.*, **60,** 653–688.

FRASER, C.M., ARAKAWA, S., MCCOMBIE, W.R. & VENTER, J.C. (1989). Cloning sequence analysis, and permanent expression of a human α_2-adrenergic receptor. *J. Biol. Chem.*, **264,** 11754–11761.

HARRISON, J.K., D'ANGELO, D.D., ZENG, D. & LYNCH, K.R. (1991). Pharmacological characterization of rat α_2-adrenergic receptors. *Mol. Pharmacol.*, **40,** 407–412.

KARLSSON, J.O.G., ANDERSSON, R.G.G., GRUNDSTRÖM, N. & ANDERSSON, R.G.G. (1988). Pronounced supersensitivity of postjunctional alpha adrenoceptors after denervation of fish melanophores. *J. Pharmacol. Exp. Ther.*, **245,** 345–351.

KARLSSON, J.O.G., ANDERSSON, R.G.G. & GRUNDSTRÖM, N. (1989). Characterization of pigment aggregating α_2-adrenoceptors of fish melanophores using different agonists after partial irreversible receptor inactivation. *Br. J. Pharmacol.*, **97,** 222–228.

KOBILKA, B.K., MATSUI, H., KOBILKA, T.S., YANG-FENG, T.L., FRANCKE, U., CARON, M.G., LEFKOWITZ, R.J. & REGAN, J.W. (1987). Cloning, sequencing and expression of the gene coding for the human platelet α_2-adrenergic receptor. *Science*, **238,** 650–656.

KOZAK (1983). Comparison of initiation of protein synthesis in prokaryotes, eukaryotes, and organelles. *Microbiol. Rev.*, **47,** 1–45.

KYTE, J. & DOOLITTLE, R.F. (1982). A simple method for displaying the hydropathic character of a protein. *J. Mol. Biol.*, **157,** 105–132.

LANIER, S.M., HOMCY, C.J., PATENAUDE, C. & GRAHAM, R.M. (1988). Identification of structurally distinct α_2-adrenergic receptors. *J. Biol. Chem.*, **263,** 14491–14496.

LANIER, S.M., DOWNING, S., DUZIC, E. & HOMCY, C.J. (1991). Isolation of rat genomic clones encoding subtypes of the α_2-adrenergic receptor: identification of a unique receptor subtype. *J. Biol. Chem.*, **266,** 10470–10478.

LOMASNEY, J.W., LORENZ, W., ALLEN, L.F., KING, K., REGAN, J.W., YANG-FENG, T.L., CARON, M.G. & LEFKOWITZ, R.J. (1990). Expansion of the α_2-adrenergic receptor family: Cloning and characterization of a human α_2-adrenergic receptor subtype, the gene for which is located on chromosome 2. *Proc. Natl. Acad. Sci. U.S.A.*, **87,** 5094–5098.

LORENZ, W., LOMASNEY, J.W., COLLINS, S., REGAN, J.W., CARON, M.G. & LEFKOWITZ, R.J. (1990). Expression of three α_2-adrenergic receptor subtypes in rat tissues: Implications for α_2-receptors classification. *Mol. Pharmacol.*, **38,** 599–603.

MANIATIS, T., GOODBOURN, S. & FISCHER, J.A. (1987). Regulation of inducible and tissue-specific gene expression. *Science*, **236,** 1237–1245.

MITCHELL, P.J., WANG, C. & TJIAN, R. (1987). Positive and negative regulation of transcription in vitro: enhancer-binding protein AP-2 is inhibited by SV40 T antigen. *Cell*, **50,** 847–861.

MONTMINY, M.R., GONZALES, G.A. & YAMAMOTO, K.K. (1990). Regulation of cAMP-inducible genes by CREB. *Trends Neurosci.*, **13,** 184–188.

NICHOLS, A.J. & RUFFULO, R.R. (1991). Functions mediated by α-adrenoceptors. In *α-Adrenoceptors: Molecular Biology, Biochemistry and Pharmacology*, ed. Ruffolo, R.R. London: Karger.

PARKER, R.B. & WAUD, D.R. (1971). Pharmacological estimation of drug receptor dissociation constant. Statistical evaluation. I. Agonists. *J. Pharmacol. Exp. Ther.*, **177,** 1–12.

REGAN, J.W. & COTECCHIA, S. (1992). The α-adrenergic receptors: New subtypes, pharmacology and coupling mechanism. In *Molecular Biology of G-Protein-Coupled Receptors*. ed. Brann, M.R. pp. 76–112. Boston, MA: Birkhauser Inc.

REGAN, J.W., KOBILKA, T.S., YANG-FENG, T.L., CARON, M.G., LEFKOWITZ, R.J. & KOBILKA, B.K. (1988). Cloning and expression of a human cDNA for an α_2-adrenergic receptor subtype. *Proc. Natl. Acad. Sci. U.S.A.*, **85,** 6301–6305.

SAKAUE, M. & HOFFMAN, B.B. (1991). cAMP regulates transcription of the α_2A adrenergic receptor gene in HT-29 cells. *J. Biol. Chem.*, **266,** 5743–5749.

SAMBROOK, J., FRITSCH, E.F. & MANIATIS, T. (1989). In *Molecular Cloning: a Laboratory Manual*. Cold Spring Harbor, NY: Cold Spring Harbor Laboratory Press.

SANGER, G., NICKLEN, S. & COULSON, A.R. (1977). DNA sequencing with chain terminating inhibitors. *Proc. Natl. Acad. Sci. U.S.A.*, **74,** 5463–5467.

SURYANARAYANA, S., DAUNT, D.A., VON ZASTROW, M. & KOBILKA, B.K. (1991). A point mutation in the seventh hydrophobic domain of the α_2-adrenergic receptor increases its affinity for a family of β receptor antagonists. *J. Biol. Chem.*, **266,** 15488–15492.

SVENSSON, S.P., KARLSSON, J.O.G. & GRUNDSTRÖM, N. (1989). Melanophores in isolated scales of *Labrus bergylta* (Ascanius): innervation and alpha$_2$-adrenoceptor-mediated pigment aggregation. *Comp. Biochem. Physiol.*, **93C,** 247–251.

SVENSSON, S.P.S., MÅRTENSSON, L.G.E., GRUNDSTRÖM, N., ANDERSSON, R.G.G., CRAGOE, E.J. & KARLSSON, J.O.G. (1991a). Antagonistic effect of amiloride on alpha-2 adrenoceptor-mediated pigment aggregation: pharmacological heterogeniety between B-HT 920 and noradrenaline. *J. Pharmacol. Exp. Ther.*, **258,** 447–451.

SVENSSON, S.P.S., ANDERSSON, R.G.G. & KARLSSON, J.O.G. (1991b). Reciprocal changes in sensitivity to MCH and noradrenaline after denervation of teleost melanophores. *Pigment Cell Res.*, **4,** 252–254.

WEINSHANK, R.L., ZGOMBICK, J.M., MACCHI, M., ADHAM, N., LICHTBLAU, H., BRANCHEK, T.A. & HARTIG, P.R. (1990). Cloning, expression, and pharmacological characterization of a human α_2B-adrenergic receptor. *Mol. Pharmacol.*, **38,** 681–688.

ZENG, D.J., HARRISON, J.K., D'ANGELO, D.D., BARBER, C.M., TUCKER, A.L., LU, Z. & LYNCH, K.R. (1990). Molecular characterization of a rat α_2B-adrenergic receptor. *Proc. Natl. Acad. Sci. U.S.A.*, **87,** 3102–3106.

(Received March 1, 1993
Revised May 4, 1993
Accepted May 11, 1993)

Br. J. Pharmacol. (1993), **110**, 61–70

Muscarinic excitatory and inhibitory mechanisms involved in afferent fibre-evoked depolarization of motoneurones in the neonatal rat spinal cord

Takashi Kurihara, Hidenori Suzuki, Mitsuhiko Yanagisawa & [1]Koichi Yoshioka

Department of Pharmacology, Faculty of Medicine, Tokyo Medical and Dental University, Bunkyo-ku, Tokyo 113, Japan

1 The involvement of acetylcholine and muscarinic receptors in spinal synaptic responses evoked by electrical and noxious sensory stimuli was investigated in the neonatal rat spinal cord *in vitro*.

2 Potentials were recorded extracellularly from a ventral root (L3–L5) of the isolated spinal cord, spinal cord-cutaneous nerve, and spinal cord-skin preparations of 1- to 4-day-old rats. Spinal reflexes were elicited by electrical stimulation of the ipsilateral dorsal root or the cutaneous saphenous nerve, or by noxious skin stimulation.

3 Single shock stimulation of supramaximum intensity of a dorsal root induced a mono-synaptic reflex in the corresponding ventral root. Bath-application of the muscarinic agonists, muscarine (0.3–30 μM) and (+)-*cis*-dioxolane (0.1–100 μM), produced an inhibition of the mono-synaptic reflex and a depolarization of motoneurones. Other muscarinic agonists, arecoline (10 nM–10 μM) and oxotremorine (10 nM–1 μM), inhibited the mono-synaptic reflex with little or no depolarization of motoneurones. Repetitive stimulation of the saphenous nerve at C-fibre strength induced a slow depolarizing response lasting about 30 s of the L3 ventral root. This slow ventral root potential (VRP) was also inhibited by arecoline (10 nM–10 μM) and oxotremorine (10 nM–1 μM).

4 In the spinal cord-saphenous nerve-skin preparation, a slow VRP was evoked by application of capsaicin (0.5 μM), bradykinin (3 μM), or noxious heat (47°C) to skin. This slow VRP was depressed by the muscarinic agonists, arecoline (3 μM) and oxotremorine (1 μM).

5 Of the (+)-*cis*-dioxolane-induced inhibition of mono-synaptic reflex and motoneurone depolarization, the M_2 antagonists, AF-DX 116 (0.1–1 μM) and methoctramine (100–300 nM), preferentially blocked the former response, whereas the M_3 antagonists, 4-DAMP (3–10 nM) and *p*-F-HHSiD (0.3–3 μM), preferentially blocked the latter response. AF-DX 116 (0.1–1 μM) and methoctramine (100–300 nM) also effectively antagonized the arecoline- and oxotremorine-induced inhibition of the slow VRP. The pA_2 values of AF-DX 116 and methoctramine against the arecoline-induced inhibition of the mono-synaptic reflex were both 6.79, and that of 4-DAMP against the (+)-*cis*-dioxolane-induced motoneurone depolarization was 8.16.

6 In the spinal cord-cutaneous nerve preparation, the saphenous nerve-evoked slow VRP was augmented by the anticholinesterase, edrophonium (5 μM). AF-DX 116 (1 μM) and methoctramine (100 nM) also potentiated the slow VRP, whereas 4-DAMP (10 nM) depressed the response. 4-DAMP (5–10 nM) depressed the capsaicin-induced slow VRP in the spinal cord-skin preparation.

7 Oxotremorine (0.3 μM) and arecoline (1 μM) markedly depressed the depolarization of motoneurones evoked by application of capsaicin (3 μM) to the spinal cord, whereas they depressed only slightly the depolarization induced by substance P (10 nM).

8 The present study suggests that both excitatory (via M_3-type receptors) and inhibitory (via M_2-type receptors) muscarinic mechanisms are involved in afferent fibre-evoked nociceptive transmissions in the neonatal rat spinal cord.

Keywords: Muscarinic receptor subtypes; nociceptive transmission; spinal cord

Introduction

Cholinergic muscarinic mechanisms have been shown to modulate pain sensation and associated behaviours at the level of the central nervous system in man and experimental animals (for review, see Green & Kitchen, 1986). A number of studies have shown that administration of cholinomimetic drugs to the spinal cord *in vivo* induces antinociceptive effects that can be blocked by muscarinic antagonists, which suggests the presence of a muscarinic analgesic mechanism in the spinal cord (Taylor *et al.*, 1982; Dirksen & Nijhuis, 1983; Yaksh *et al.*, 1985; Gillberg *et al.*, 1989; Hartvig *et al.*, 1989; Smith *et al.*, 1989). However, the precise neuronal mechanisms and the muscarinic receptor subtypes involved are not clear.

Previous studies have shown that in the isolated spinal cord of the neonatal rat cholinoceptor agonists evoke both excitatory and inhibitory muscarinic responses: a depolarization of motoneurones (Evans, 1978; Jiang & Dun, 1986; Newberry & Connolly, 1989; Yoshioka *et al.*, 1990b) and an inhibition of the mono-synaptic reflex (Newberry & Connolly, 1989; Yoshioka *et al.*, 1990b). These responses are presumably mediated by different types of muscarinic receptors (Newberry & Connolly, 1989; Yoshioka *et al.*, 1990b), but their pharmacological properties have not been fully characterized. In isolated spinal cord preparations, activation of primary afferent fibres by either electrical stimulation or peripheral noxious stimulation evokes a depolarization of slow time course in ventral roots (Yanagisawa *et al.*, 1982; Akagi *et al.*, 1985; Otsuka & Yanagisawa, 1988; Nussbaumer *et al.*, 1989; Yanagisawa *et al.*, 1992). There is evidence that this depolarization, hereafter referred to as the slow ventral root potential (VRP), represents a C-fibre-evoked nociceptive response in which tachykininergic primary afferents are

[1] Author for correspondence.

involved (Otsuka & Yanagisawa, 1987). Evidence that the slow VRP involves excitatory amino acid transmitter(s) is also accumulating (Dray & Perkins, 1987; King et al., 1990; Kurihara et al., 1991). Furthermore, Yoshioka et al. (1990b) recently found in an isolated spinal cord-peripheral nerve preparation that conditioning stimulation of the saphenous nerve at C-fibre strength induced a prolonged inhibition of the muscle nerve-evoked mono-synaptic reflex. They suggested that tachykininergic primary afferents contained in the cutaneous nerve excite spinal cholinergic neurones and as a result the released acetylcholine inhibits the mono-synpatic reflex. In support of this, tachykinins have been shown to release acetylcholine from the spinal cord (Kobayashi et al., 1991) and cholinoceptor agonists applied to the spinal cord inhibited the monosynaptic reflex (Newberry & Connolly, 1989; Yoshioka et al., 1990b). Whether the transmitter acetylcholine released by tachykinins also influences the slow VRP, however, is not known.

In this paper we investigated the possible involvement of acetylcholine and muscarinic receptors in spinal nociceptive transmission. To this end, we examined the effects of muscarinic drugs on the slow VRPs evoked by electrical or noxious stimuli and the pharmacological characteristics of the muscarinic receptors that mediate excitatory and inhibitory muscarinic responses in the neonatal rat spinal cord.

Preliminary results of this study have been presented elsewhere (Yoshioka et al., 1990a,b; 1991).

Methods

Preparations

In this study we used the following three types of preparations isolated from Wistar rats aged 1–4 days.

Isolated spinal cord preparation Under ether anaesthesia, the spinal cord below the middle thoracic level together with spinal nerve roots (L3–L5) was isolated, hemisected, and placed in a recording chamber of 0.3 ml volume (Otsuka & Konishi, 1974). The chamber was perfused with artificial cerebrospinal fluid (CSF) at a rate of 2.5 ml min^{-1}. The composition of artificial CSF was as follows (mM): NaCl 138.6, KCl 3.35, $NaHCO_3$ 20.9, glucose 10.0, $CaCl_2$ 1.25 and $MgCl_2$ 1.15. The solution was equilibrated with a gas mixture of 95% O_2:5% CO_2 and the temperature of the solution in the chamber was kept at 27°C. A tight-fitting suction electrode was used for extracellular recording from the ventral root (L3–L5).

Another suction electrode was used for electrical stimulation of the dorsal root of the same segment (single shocks with square pulses of 500 μs in duration and 20–30 V in amplitude, supramaximum for mono-synaptic reflex; positive voltage was applied to the inside of the electrode). Potential changes were recorded on a pen recorder and spinal reflexes of fast time course were stored in a transient memory device and then recorded on the pen recorder with an expanded time-scale.

Isolated spinal cord-saphenous nerve preparation The hemisected spinal cord below the middle thoracic level was isolated together with the attached L3–L5 ventral roots and dorsal roots, the latter remaining connected with the dorsal root ganglia and the femoral and saphenous nerves (Nussbaumer et al., 1989). The saphenous nerve was stimulated supramaximally with one to five pulses of 500 μs duration and 30–40 V intensity at 50 Hz and the potential changes were recorded from the L3 ventral root on a pen recorder. The duration of the saphenous nerve-evoked slow VRP was taken as the time required for the depolarized potential to decay from the peak to 10% of the peak amplitude and the magnitude of the slow VRP was expressed as the integrated area of the depolarization on the chart record. To assess the effects of drugs on the slow VRP, the averaged magnitude of three responses before and after administration of the drugs were compared.

Isolated spinal cord-saphenous nerve-skin preparation This preparation consisted of a hemisected spinal cord that remained connected to the saphenous nerve (see above) and a piece of skin (approximately 5 × 5 mm) of the hind limb (Yanagisawa et al., 1992). The recording chamber was made from Sylgard and consisted of two wells, which were independently perfused at a rate of 2.5 ml min^{-1}. The spinal cord was placed in one well (0.3 ml volume) and the skin was placed with the outside surface upwards in the neighbouring well (0.1 ml volume). The saphenous nerve was led through a break in a thin septum (1 mm width) into the skin well. The break in the septum was sealed with Vaseline. Drugs were either applied to the skin by perfusing the skin well with solutions containing the drugs or injected into the perfusion solution with short pressure pulses as described previously (Otsuka & Yanagisawa, 1988). A heat stimulus was applied by perfusing the skin well with heated solution such that the maximum temperature in the skin well became 47–48°C. The temperature rose soon after starting the perfusion of heated solution (about 5 s), reached maximum in less than 15 s and fell to the original temperature within 30 s after stopping the heat stimulus. Capsaicin and the heat stimulus were applied to the skin at intervals of 40 min while bradykinin was applied at intervals of 1 h to avoid tachyphylaxis. The evoked responses were recorded from the L3 ventral root on a pen recorder. The magnitude of each depolarizing response was estimated as the integrated area as described above. In the experiments using capsaicin as a stimulus the skin was pretreated with prostaglandin E_1 (1 μM) for 3 min to enhance the slow VRP (Yanagisawa et al., 1992).

Esimation of pA_2 values of muscarinic antagonists for inhibition of the mono-synpatic reflex

The pA_2 values of muscarinic antagonists were determined against the arecoline-induced inhibition of the mono-synaptic reflex. Mono-synaptic reflexes were elicited by dorsal root stimulation every 30 s in the isolated spinal cord preparations. Forty to sixty min after perfusing the spinal cord with normal solution, arecoline was applied by perfusion at increasing concentrations in a cumulative manner. A 10 min exposure to each concentration of arecoline was sufficient to obtain a steady inhibitory effect on the mono-synaptic reflex. Then, the spinal cord was perfused with three increasing concentrations of an antagonist with 0.5 logarithmic concentration steps. The spinal cord was allowed to equilibrate for 40–60 min with each concentration of the antagonist and then arecoline was applied as described above. The amplitude of the mono-synaptic reflex at each concentration of arecoline was compared to the average of about six control responses before application of arecoline and concentration-inhibition curves were constructed. The pA_2 values were determined from Arunlakshana-Schild plots by the least square regression analysis (Arunlakshana & Schild, 1959).

Concentration-response curves for the muscarinic depolarization of motoneurones

(+)-*cis*-Dioxolane (Ehlert et al., 1980) was used to evoke a muscarinic depolarizing response of motoneurones in the presence of 0.3 μM tetrodotoxin (TTX). Increasing concentrations of (+)-*cis*-dioxolane were applied for 1 min duration to the isolated spinal cord preparations at intervals of 30–40 min to avoid desensitization. The magnitude of each response was estimated as the integrated area of depolarization. Concentration-depolarization curves were constructed in the absence of an antagonist and then in the presence of increasing concentrations of the antagonist. The spinal cord

was allowed to equilibrate for 40–60 min with each concentration of the antagonist before (+)-*cis*-dioxolane was applied.

Drugs

The following drugs were used: AF-DX 116 (11-[[2-[(diethylamino)methyl]-1-piperidinyl]acetyl]-5,11-dihydro-6H-pyrido [2,3-b] [1,4]benzodiazepine-6-one) was kindly donated by Dr K. Thomae, Biberach, Germany; (+)-*cis*-dioxolane, 4-DAMP (4-diphenylacetoxy-*N*-methyl-piperidine methiodide), *p*-F-HHSiD (*para*-fluoro-hexahydrosiladiphenidol hydrochloride). McN-A-343 (4-[*m*-chlorophenyl carbamoyloxy]-2-butynyltrimethylammonium chloride), and methoctramine tetrahydrochloride were purchased from Research Biochemicals Inc., arecoline hydrobromide, atropine sulphate, capsaicin, gallamine triethiodide, oxotremorine, and pirenzepine dihydrochloride were purchased from Sigma Chemicals; bradykinin and substance P (SP) were purchased from Peptide Institute, Inc., Osaka, Japan; edrophonium chloride was obtained from Kyorin, Tokyo, Japan; protaglandin E_1 was kindly provided by Ono Pharmaceutical Co., Osaka, Japan; TTX was purchased from Sankyo Co., Ltd., Tokyo, Japan. All drugs were dissolved in artificial CSF and applied by superfusion.

Results

Effects of muscarinic agonists in the neonatal rat spinal cord

We examined the effects of muscarinic agonists on the dorsal root-evoked mono-synaptic reflex in the isolated spinal cord preparation and the saphenous nerve-evoked slow VRP in the spinal cord-saphenous nerve preparation. The duration of this slow VRP was 32.0 ± 0.66 s when the saphenous nerve was stimulated with 4 pulses of 30 V intensity ($n = 3$).

Bath-application of muscarinic agonists to the spinal cord evoked two distinct types of response. One type of response was an inhibition of the mono-synaptic reflex (Figure 1) as well as the slow VRP (Figure 2) and the other was a depolarization of motoneurones (Figure 1). Of several muscarinic agonists, (+)-*cis*-dioxolane (0.3–100 μM) and muscarine (0.1–30 μM; data not shown) evoked both types of response, whereas arecoline (10 nM–10 μM) and oxotremorine (10 nM–1 μM) inhibited the mono-synaptic reflex and the slow VRP but induced little or no depolarization of motoneurones (Figure 2). The concentration of arecoline and oxotremorine required to inhibit the mono-synaptic reflex to half of the control were 0.97 ± 0.06 μM ($n = 16$) and 0.32 ± 0.05 μM ($n = 5$), respectively. Both types of response to these muscarinic agonists were completely antagonized by atropine (100 nM; data not shown).

McN-A-343 (1–100 μM), a putative M_1-selective agonist (Hammer & Giachetti, 1982), did not evoke a depolarization of motoneurones. Although it depressed the mono-synpatic reflex at a relatively high concentration (100 μM), this effect was not antagonized by atropine (100 nM; data not shown).

Effects of muscarinic agonists on the slow VRP evoked by noxious skin stimulation

In the spinal cord-saphenous nerve-skin preparation, application of capsaicin (0.5 μM), bradykinin (3 μM), or noxious heat to the skin produced depolarizing responses of motoneurones of slow time course (Figure 3). These responses were markedly depressed by arecoline (3 μM) or oxotremorine (1 μM). Oxotremorine (1 μM) reduced the capsaicin-, bradykinin- and heat-induced responses by 95.3 ± 2.24%, 94.6 ± 1.48%, 91.2 ± 3.35% of the control responses, respectively ($n = 3$).

Effects of muscarinic antagonists on the responses to muscarinic agonists

Muscarinic receptors are pharmacologically classified into M_1, M_2 and M_3 subtypes (for review see Hulme *et al.*, 1990). The M_1 receptor is characterized by a high affinity for pirenzepine (Hammer *et al.*, 1980). The receptors with lower affinities for pirenzepine are further divided into M_2 and M_3 subtypes: the former is sensitive to AF-DX 116 (Giachetti *et al.*, 1986), gallamine (Riker & Wescoe, 1951) and methoctramine (Melchiorre *et al.*, 1987), whereas the latter is sensitive to 4-DAMP (Barlow *et al.*, 1976; Brown *et al.*, 1980) and *p*-F-HHSiD (Lambrecht *et al.*, 1988).

Figures 1 and 2 illustrate the effects of muscarinic antagonists on the excitatory and inhibitory responses to muscarinic agonists. The M_2 antagonists, AF-DX 116

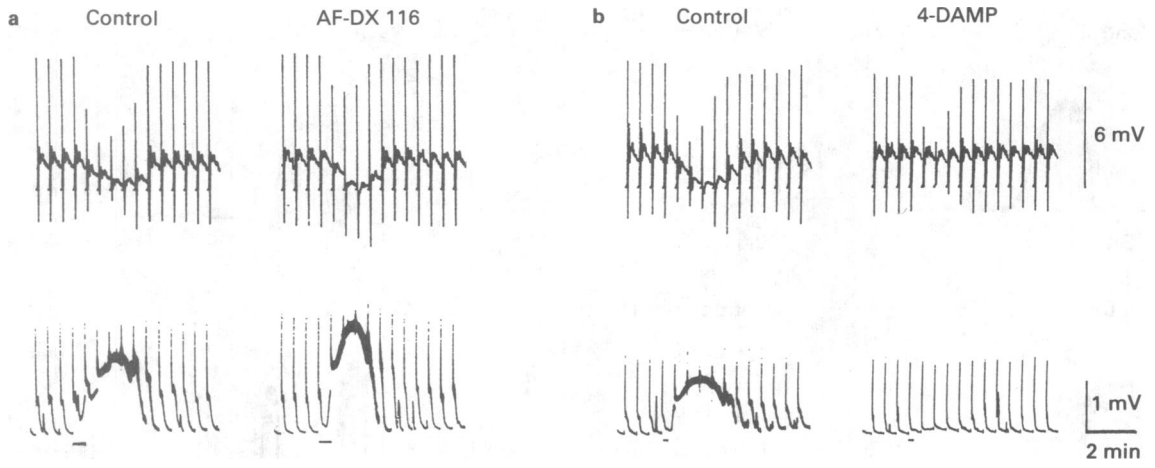

Figure 1 Effects of muscarinic antagonists on (+)-*cis*-dioxolane-evoked responses. Effects of AF-DX 116 (1 μM) (a) and 4-DAMP (5 nM) (b) in normal artificial CSF. (+)-*cis*-Dioxolane was applied at 3 μM for 30 s in (a) and at 10 μM for 10 s in (b) during the periods indicated by bars. Single-shock stimuli of supramaximal intensity were applied to the L4 dorsal root every 30 s and the resulting reflexes were recorded from the ipsilateral ventral root of the same segment. The upper traces show the records of the fast reflex responses during 52 ms post-stimulus periods, which were stored in a memory device in a.c. mode and then recorded on a pen-recorder on a 1000 times expanded time-base. Initial sharp spikes represent the mono-synaptic reflexes. The lower traces show continuous chart records of the d.c. potential. Records in (a) and (b) were taken from different preparations.

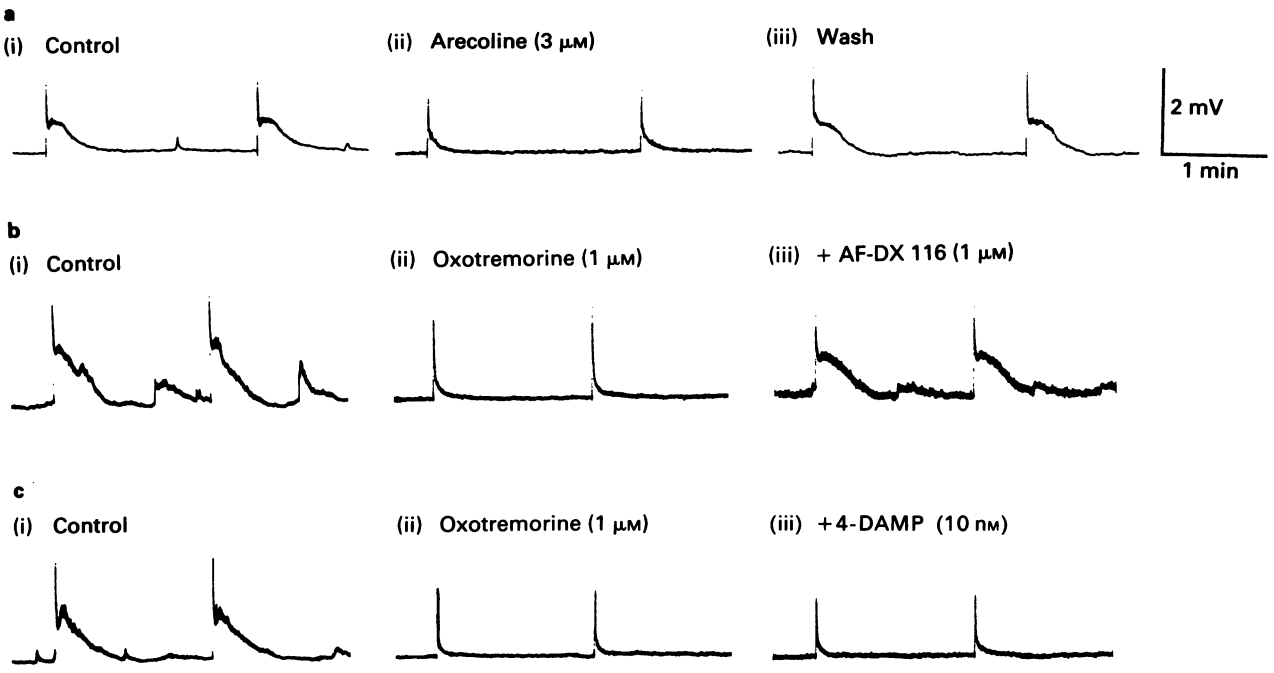

Figure 2 Effects of muscarinic agonists and antagonists on saphenous nerve-evoked slow VRP. (a) Effect of arecoline on the slow VRP evoked by saphenous nerve stimulation. (i) Control responses; (ii) in the presence of arecoline (3 μM); and (iii) after removal of arecoline. (b) Effect of oxotremorine and AF-DX 116 on the slow VRP. (i) Control responses; (ii) in the presence of oxotremorine (1 μM); and (iii) after adding AF-DX 116 (1 μM) in the continued presence of oxotremorine. (c) Effect of oxotremorine and 4-DAMP on the slow VRP. (i) Control responses; (ii) in the presence of oxotremorine (1 μM); and (iii) after adding 4-DAMP (10 nM) in the continued presence of oxotremorine. The saphenous nerve was stimulated every 2 min with 4 shocks in (a) and every 90 s with 2 shocks in (b) and (c) of supramaximal intensity. Records in (a), (b) and (c) were taken from different preparations.

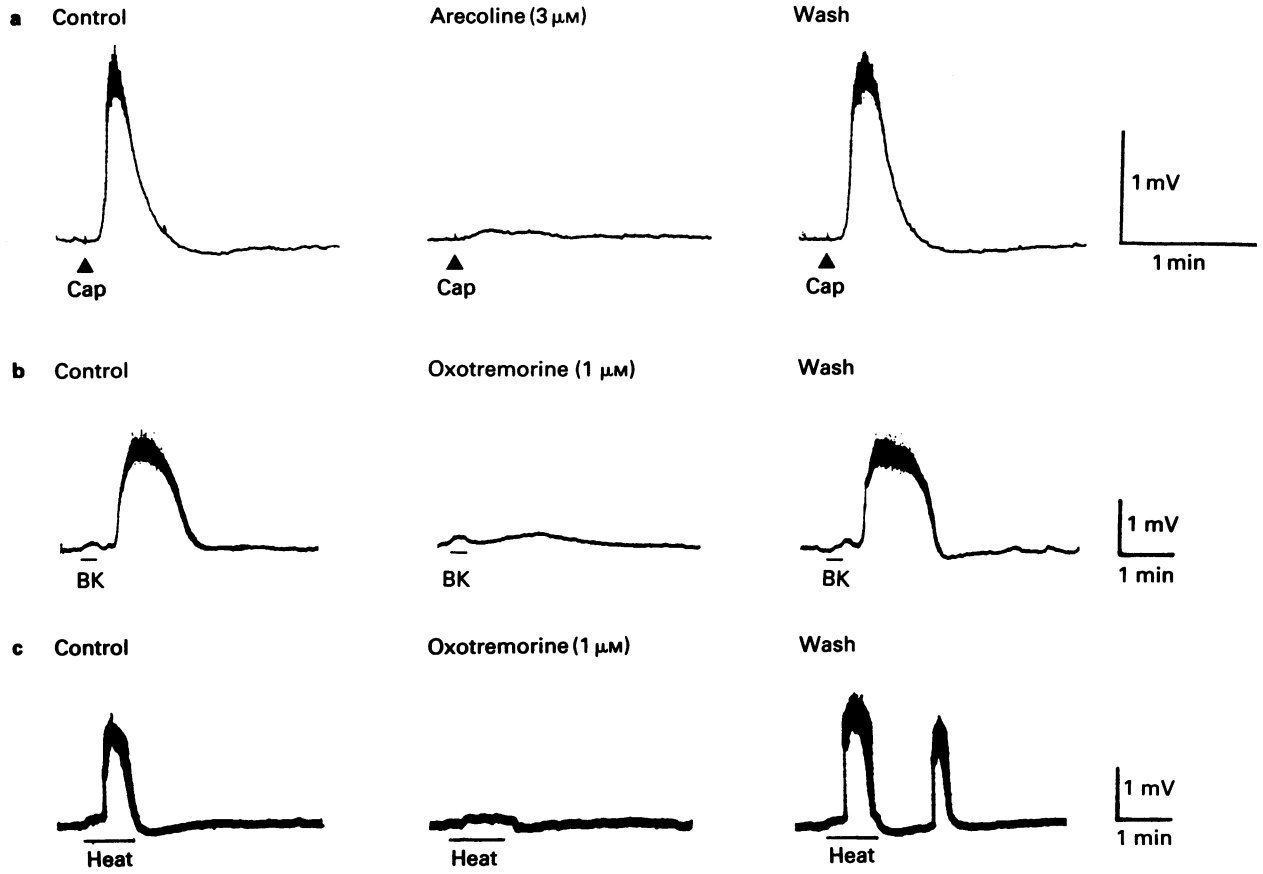

Figure 3 Effects of arecoline and oxotremorine on the slow VRP evoked by noxious skin stimulation in the isolated spinal cord-saphenous nerve-skin preparations. (a) Capsaicin (Cap, 0.5 μM) was applied to the skin with a pressure pulse of 0.45 s duration at (▲). The skin was perfused with artifical CSF containing prostaglandin E_1 (1 μM). (b) Bradykinin (BK, 3 μM) was applied during the periods (20 s) indicated by bars. (c) Heat (47°C) was applied during the periods (1 min) indicated by bars. The records in the middle column were taken after pretreatment of the spinal cord with arecoline or oxotremorine for 30 min. Records in (a), (b), and (c) were taken from different preparations.

(0.1–1 μM; Figures 1a and 2b), methoctramine (100–300 nM; data not shown), and gallamine (5–30 μM; data not shown), reduced the muscarinic inhibition of the mono-synaptic reflex and slow VRP induced by (+)-*cis*-dioxolane, oxotremorine or arecoline. The M_2 antagonists at these concentrations did not reduce the depolarization of motoneurones evoked by (+)-*cis*-dioxolane but often potentiated the response (Figure 1a). On the other hand, the M_3 antagonists, 4-DAMP (3–10 nM; Figures 1b and 2c) and *p*-F-HHSiD (0.1–3 μM; data not shown), did not affect or only slightly reduced the muscarinic inhibition of the monosynaptic reflex and slow VRP. In contrast, these antagonists markedly depressed the (+)-*cis*-dioxolane-evoked motoneurone depolarization (see also Figure 6).

Effects of edrophonium and muscarinic antagonists on the slow VRPs

In the spinal cord-saphenous nerve preparation, the anticholinesterase, edrophonium (5 μM) potentiated the slow VRP evoked by saphenous nerve stimulation (Figure 4a). This potentiating effect became evident within 10 min after starting perfusion of the drug and the slow VRP returned to the control size within 30–60 min after wash-out of the drug.

The M_1 antagonist, pirenzepine (10 nM) had little effect on the slow VRP. However, the M_2 antagonists, AF-DX 116 (1 μM; Figure 4b) and methoctramine (100 nM; data not shown), potentiated the slow VRP. In contrast, the M_3 antagonist 4-DAMP (10 nM, Figure 4c) depressed the slow VRP. Table 1 summarizes the changes of size of the slow VRP produced by edrophonium (5 μM) and the muscarinic antagonists in the presence of edrophonium. The effects of these antagonists could be observed in experiments in normal artificial CSF, but became more pronounced in the presence of edrophonium.

In the spinal cord-saphenous nerve-skin preparation, the M_3 antagonist 4-DAMP (5–10 nM; Figure 4d) also significantly depressed the motoneurone depolarization evoked by application of capsaicin to the skin (−47.9 ± 14.8, % change of the response compared to the control, $n = 3$, $P < 0.05$ by Student's *t* test). 4-DAMP (5–10 nM) also

Table 1 Changes of saphenous nerve-evoked slow VRP by muscarinic drugs

Drugs		*% change*	n
Edrophonium	(5 μM)	77 ± 4**	17
Pirenzepine	(10 nM)	11 ± 1*	4
AF-DX 116	(1 μM)	75 ± 9*	5
4-DAMP	(5 nM)	− 50 ± 9*	3

The areas of depolarization (mV × min) were measured on chart records, and the averages of 3–5 consecutive responses were determined. Each value is the percentage change of the responses induced by each muscarinic drug compared with the control responses. The effects of muscarinic antagonists were tested in the presence of edrophonium (5 μM). Details of the experiments are the same as in Figure 4. Each value represents the mean ± s.e.mean ($n = 3$–17).
*$P < 0.05$; **$P < 0.01$ in comparison with the control responses by Student's *t* test.

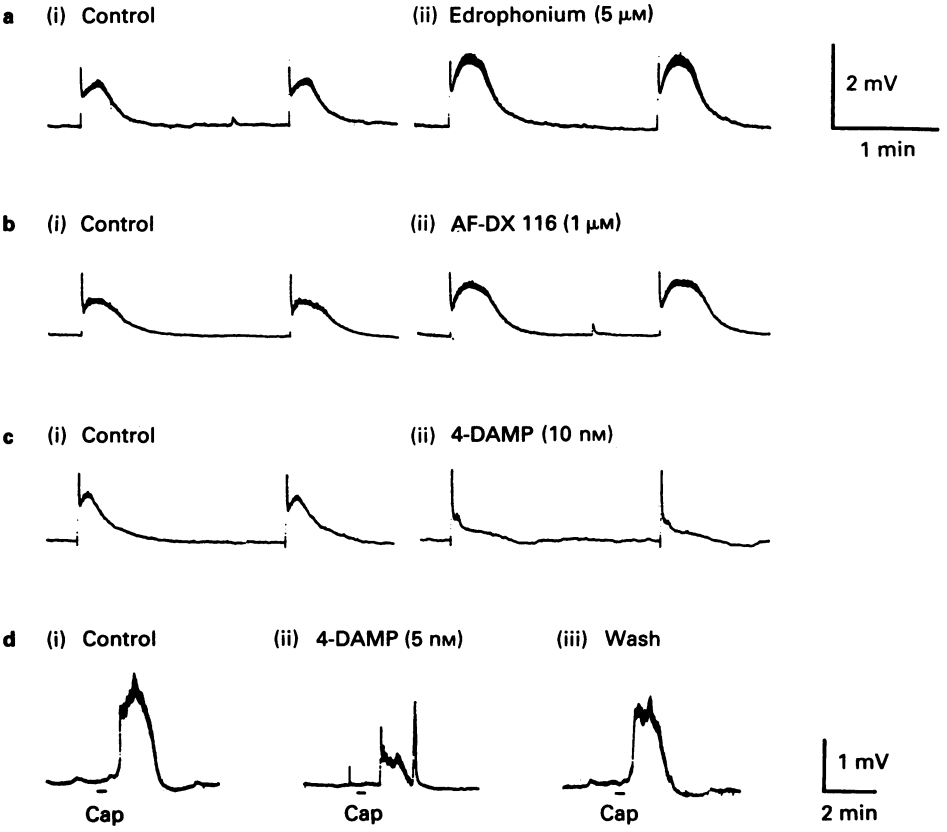

Figure 4 Effects of edrophonium and muscarinic antagonists on the slow VRPs. (a) (i) In normal artificial CSF and (ii) in the presence of edrophonium (5 μM). (b) and (c) (i) In normal artificial CSF containing edrophonium (5 μM) and (ii) after adding AF-DX 116 (1 μM) and 4-DAMP (10 nM), respectively. The saphenous nerve was stimulated every 2 min with 4 shocks in (a) and 2 shocks in (b) and (c) of supramaximal intensity. (d) (i) In normal artificial CSF; (ii) in the presence of 4-DAMP (5 nM); and (iii) after removal of 4-DAMP. Capsaicin (Cap; 0.3 μM) was applied to the skin for 20 s as indicated by bars. Records in (a), (b) and (c) were taken from spinal cord-saphenous nerve preparations and (d) was taken from spinal cord-saphenous nerve-skin preparation.

depressed spontaneous depolarizing activities of motoneurones (data not shown).

Pharmacological analyses of muscarinic responses

Figure 5 illustrates representative concentration-response curves and the Arunlakshana-Schild plot for the arecoline-induced inhibition of the mono-synaptic reflex in the absence or presence of AF-DX 116. The antagonist caused parallel shifts to the right of the concentration-response curve. Similar parallel shifts were obtained with methoctramine (30–300 nM, data not shown), pirenzepine (0.1–3 μM; data not shown), and 4-DAMP (10–100 nM; data not shown). Table 2 summarizes the results of Arunlakshana-Schild plot analysis. The plots were linear within the concentration ranges of the antagonists and the slopes of the regression lines were not significantly different from unity except for 4-DAMP ($P<0.05$ by Student's t test). The variance of 4-DAMP slope about the mean was much less than that of the other antagonists.

Muscarinic receptor-induced depolarization of motoneurones was also analyzed. Figure 6 shows concentration-depolarization curves for (+)-*cis*-dioxolane and the effects of muscarinic antagonists. The experiments were done in the presence of TTX (0.3 μM) to suppress trans-synaptic actions of drugs. 4-DAMP potently inhibited the effect of (+)-*cis*-dioxolane (Figure 6a; $n=4$), but there was a tendency towards a reduction of the slopes of the curves with increasing concentrations of the antagonist. The potency of another M_3 antagonist *p*-F-HHSiD was weak. Furthermore, increasing the concentration of *P*-F-HHSiD beyond 1 μM did not cause a further appreciable shift of the curve to the right (Figure 6b; $n=3$). The effect of the M_1 antagonist, pirenzepine, was also weak (Figure 6c; $n=6$). The M_2 antagonist AF-DX 116 considerably shifted the curve at 0.1 μM but the effect tended to be saturated at 0.3–1 μM (Figure 6d; $n=3$). Owing to the non-parallel shifts of the concentration-response curves it was not possible to obtain pA_2 values for the antagonists.

Effects of arecoline and oxotremorine on substance P- and capsaicin-evoked depolarizations

To obtain information about the mechanisms of the inhibitory muscarinic action on the slow VRPs, effects of oxotremorine and arecoline on the ventral root depolarizations induced by bath-applications of capsaicin (3 μM for 10 s) and SP (10 nM for 10 s) to the spinal cord were examined. In this experiment a relatively high (nearly maximal) concentration of capsaicin and a low (submaximal) concentration of SP were used. At these concentrations the depolarizations induced by these agents were mainly due to trans-synpatic action (Yanagisawa *et al.*, 1980; Yanagisawa & Otsuka, 1990). Oxotremorine (0.3 μM) (Figure 7b) markedly depressed the capsaicin-evoked depolarization (9.80 ± 0.72% of the control response, $n=3$), whereas the SP-evoked depolarization was much less depressed (68.7 ± 4.85% of the control response, $n=3$). Similar results were obtained for the arecoline (1 μM)-induced depression of capsaicin- and SP-evoked depolarizations (data not shown).

Table 2 pA_2 values and slopes of Arunlakshana-Schild plots for muscarinic antagonists against arecoline-induced inhibition of mono-synaptic reflex

Antagonist	*pA_2*	*Slope*	n
Pirenzepine	6.59 ± 0.08	1.07 ± 0.12	4
AF-DX 116	6.79 ± 0.06	1.06 ± 0.15	3
Methoctramine	6.79 ± 0.12	1.04 ± 0.18	3
4-DAMP	8.16 ± 0.19	1.16 ± 0.01	3

Each value represents the mean ± s.e.mean ($n=3$–4). The slopes of regression lines of the Arunlakshana-Schild plots are not significantly different from unity except for 4-DAMP ($P<0.05$ by Student's t test).

Discussion

In this study we showed the existence of two pharmacologically distinct, excitatory and inhibitory, muscarinic receptor-mediated responses in the neonatal rat spinal cord and provided evidence that both types of muscarinic mechanisms are involved in spinal nociceptive transmissions.

Previous studies have shown that the slow VRPs induced by both saphenous nerve stimulation and application of capsaicin to skin were markedly depressed by a tachykinin antagonist spantide (Nussbaumer *et al.*, 1989; Yanagisawa *et al.*, 1992). There is evidence that these slow depolarizing responses represent a component of nociceptive spinal reflexes (Nussbaumer *et al.*, 1989; Yanagisawa *et al.*, 1992).

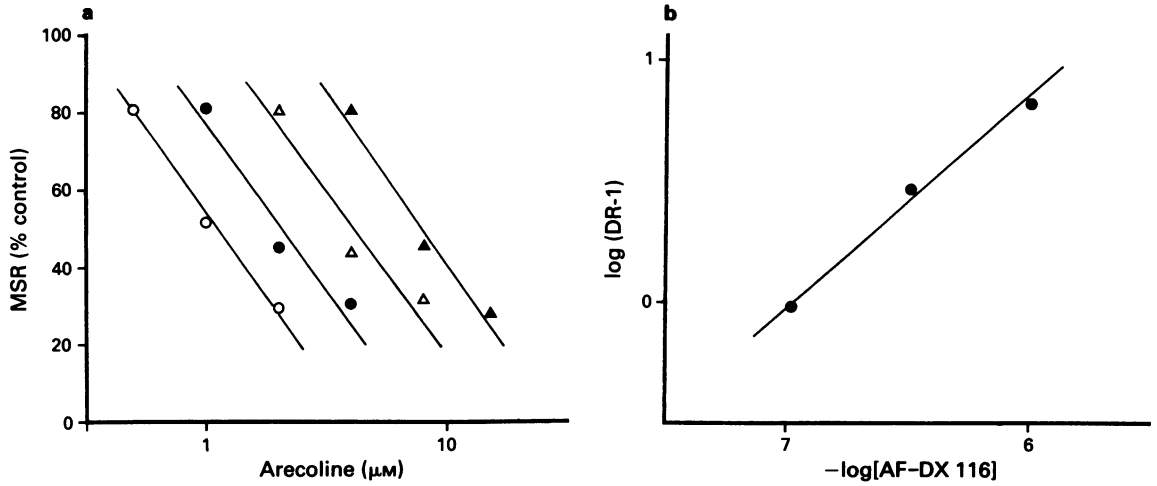

Figure 5 Antagonism by AF-DX 116 of arecoline-induced inhibition of mono-synaptic reflex. (a) Concentration-inhibition curves to arecoline in the absence (○) and in the presence of AF-DX 116 at 0.1 μM (●), 0.3 μM (△) and 1 μM (▲). Ordinate scale: amplitude of mono-synaptic reflex expressed as a percentage of the control reflex amplitude. Abscissa scale: logarithmic concentration of arecoline (see Methods for details). (b) Arunlakshana-Schild plot of log {dose-ratio (DR) − 1} versus − log concentration of AF-DX 116. Each point was derived from the results shown in (a). Data were derived from a single typical experiment but similar results were obtained in 2 other experiments.

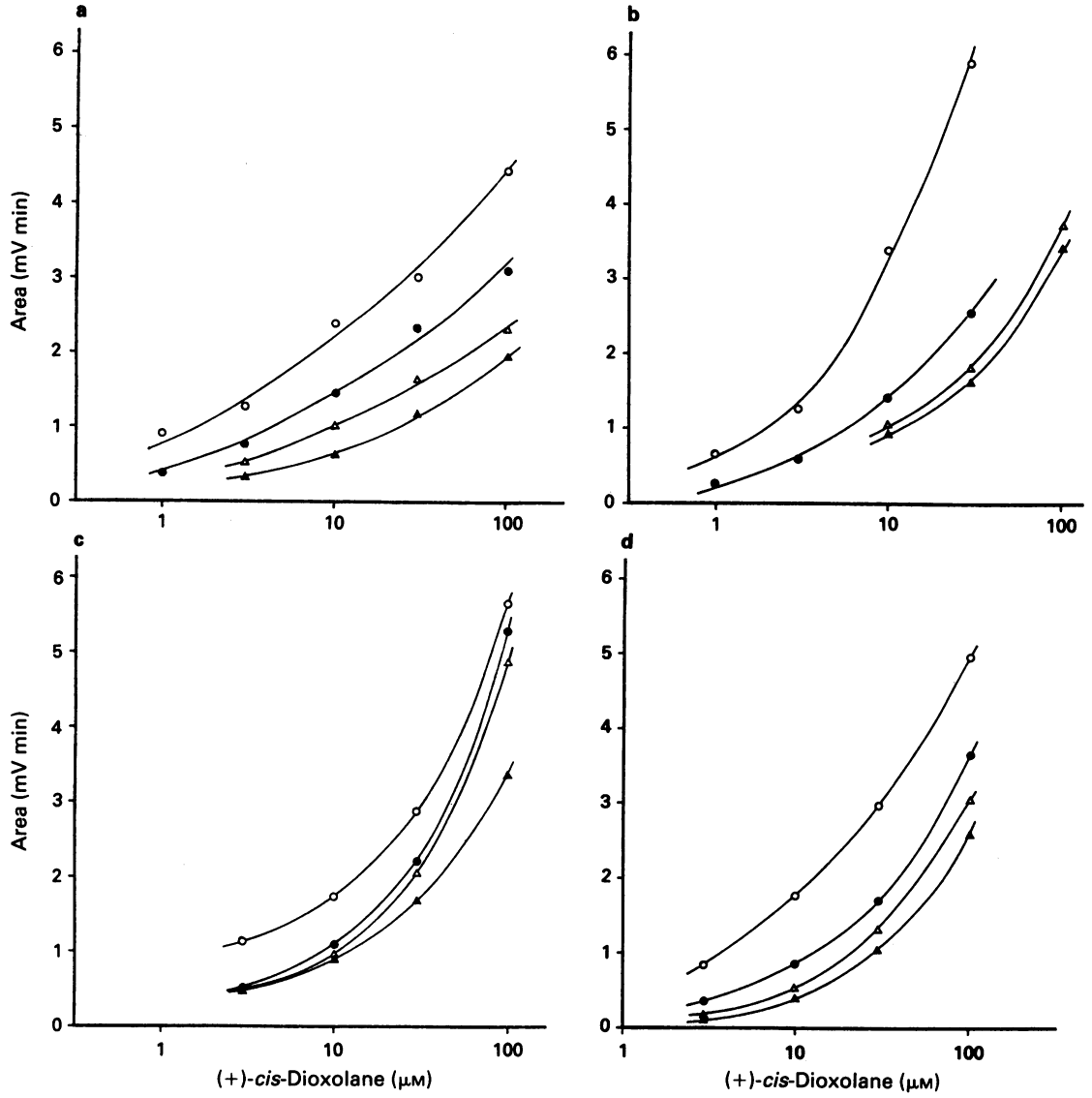

Figure 6 Antagonsim by muscarinic antagonists of (+)-*cis*-dioxolane-induced motoneurone depolarization. Effects of 4-DAMP (a), *p*-F-HHSiD (b), pirenzepine (c) and AF-DX 116 (d). Concentration-depolarization curves to (+)-*cis*-dioxolane were obtained in the presence of tetrodotoxin (TTX, 0.3 μM) and then the effect of each antagonist was examined in the continued presence of TTX. (○) Control in (a), (b), (c) and (d). In (a) 4-DAMP: (●) 1 nM; (△) 3 nM and (▲) 10 nM. In (b) *p*-F-HHSiD: (●) 0.3 μM; (△) 1 μM and (▲) 3 μM. In (c) pirenzepine: (●) 10 nM; (△) 30 nM and (▲) 100 nM. In (d) AF-DX116: (●) 0.1 μM; (△) 0.3 μM and (▲) 1 μM. Ordinate scale: area of depolarization (mV min). Abscissa scale; logarithmic concentration of (+)-*cis*-dioxolane (see Methods for details). Data were derived from a single typical experiment but similar results were obtained in 2–5 other experiments.

In this study we found that the slow VRPs were depressed by oxotremorine and arecoline, which presumably act as M_2 agonists. Furthermore, the saphenous nerve-evoked slow VRP was potentiated by the M_2 antagonists, AF-DX 116 and methoctramine. These results suggest that cholinoceptor inhibitory mechanism, via M_2-type receptors, is involved in the slow VRP and the nociceptive transmissions in the neonatal rat spinal cord. The pA_2 values of muscarinic antagonists against the muscarinic inhibition of the slow VRPs were not obtained since it was difficult to maintain stable responses of the slow VRPs for the period necessary to construct concentration-response curves (about 5–6 h). However, the qualitative analyses suggested that the muscarinic receptors were identical with the M_2 receptors mediating the inhibition of the mono-synaptic reflex.

Gillberg *et al.* (1989) observed that intrathecal application of carbachol to rats induced analgesia and suggested that both M_1 and M_2 receptors were involved since the effect of carbachol was antagonized by similar doses of AF-DX 116 and pirenzepine. At present, however, evidence of the involvement of M_1 receptors in the muscarinic inhibitory responses has not been obtained. Although the putative M_1 agonist McN-A 343 induced an inhibition of the mono-synaptic reflex, this effect was not antagonized by atropine and is therefore probably an action not mediated by muscarinic receptors. Although the M_1 antagonist, pirenzepine, at 0.1–1 μM antagonized the muscarine-evoked inhibition of the mono-synaptic reflex (Yoshioka *et al.*, 1990b), these concentrations would be sufficiently high to block other types of muscarinic receptors.

In an attempt to examine the synaptic site of the muscarinic inhibition of the slow VRPs we compared the depressant effect of oxotremorine on the capsaicin-induced depolarization with that on the SP-induced depolarization. Previous studies have shown that capsaicin applied to the neonatal rat spinal cord produces a depolarization of ventral roots and that the release of tachykinins from primary afferent terminals is involved in the depolarization (Theriault

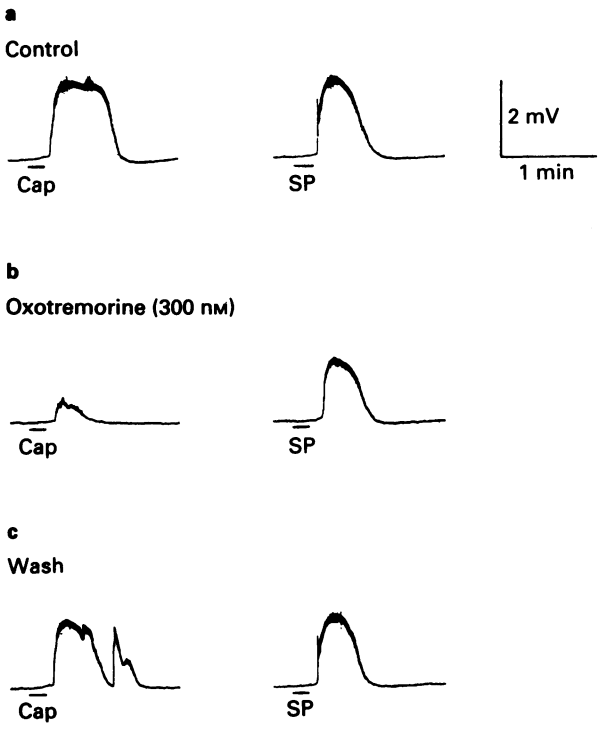

Figure 7 Effects of oxotremorine on the depolarizations evoked by application of capsaicin (Cap) and substance P (SP) to the spinal cord. (a) In normal artificial CSF. (b) In the presence of oxotremorine (300 nM). (c) After removal of oxotremorine. Potentials were recorded from L3 ventral root of an isolated spinal cord preparation. Capsaicin (3 μM for 10 s) and SP (10 nM for 10 s) were applied to the spinal cord alternately at intervals of 30 min.

et al., 1979; Yanagisawa *et al.*, 1980; Yoshioka *et al.*, 1990b). The finding that oxotremorine preferentially inhibited the effect of capsaicin over that of SP suggested that the inhibitory action is primarily due to an inhibition of the release of transmitters including tachykinins from primary afferents. In accord with this notion, Yoshioka *et al.* (1990b) have provided electrophysiological evidence suggesting that the muscarinic inhibition of the mono-synaptic reflex is through a presynaptic mechanism. Furthermore, morphological studies have shown that the dorsal horn of the rat spinal cord contains a dense plexus of choline acetyltransferase-immunoreactive axons and varicosities particularly in lamina III (Barber *et al.*, 1984; Borge & Iversen, 1986; for review see Gillberg *et al.*, 1990), where some cholinergic interneurones form axoaxonic synapses with primary sensory fibres (Ribeiro-da-Silva & Cuello, 1990). Autoradiographic studies have also demonstrated that the substantia gelatinosa of rat spinal cord contains a high density of muscarinic receptors, some of which seem to be localized on terminals of primary sensory fibres (Gillberg & Wiksten, 1986; Gillberg & Askmark, 1991; for review see Gillberg *et al.*, 1990).

The slow VRP induced by saphenous nerve stimulation was potentiated by the anticholinesterase, edrophonium and depressed by the M_3 antagonist, 4-DAMP. Furthermore, the depolarizing response of the ventral root evoked by application of capsaicin to skin was depressed by 4-DAMP. These results suggest that, in addition to M_2 inhibitory muscarinic receptors, excitatory M_3 muscarinic receptors are involved in the nociceptive transmissions.

It is not known how excitatory cholinergic neurones are involved in the neural circuits for the slow VRPS. These cholinergic neurones might be directly activated by tachykininergic C-fibres since tachykinins have been shown to release acetylcholine from the neonatal rat spinal cord (Kobayashi *et al.*, 1991). In addition, however, the neuronal pathways for the slow VRPs seem to contain interneurones releasing excitatory amino acid transmitter(s), since we and other groups have shown that excitatory amino acid antagonists reduce the slow depolarisation evoked by peripheral nerve stimualtion (Dray & Perkins, 1987; King *et al.*, 1990; Kurihara *et al.*, 1991).

The concentration-response curve for arecoline to inhibit the mono-synaptic reflex was shifted in parallel by muscarinic antagonists. The slopes of the Arunlakshana-Schild plots for the antagonists were close to unity. These results suggest that the inhibition of the mono-synaptic reflex was mediated by a homogeneous population of muscarinic receptors. The pA_2 values of pirenzepine (6.59), AF-DX 116 (6.79), 4-DAMP (8.16), for this action are comparable with those for the chronotropic muscarinic action in the guinea-pig atrium, i.e., 6.60, 6.49, and 7.90, respectively (Clague *et al.*, 1985; Eglen & Whiting, 1987). However, the pA_2 value of methoctramine for the monosynaptic reflex inhibition (6.79) is much lower than the value for the atrial chronotropism (7.73) (Melchiorre *et al.*, 1987). These results suggest that the muscarinic receptors mediating inhibition of the mono-synaptic reflex in this preparation are similar to, but not identical with the cardiac type M_2 receptors.

In contrast, the muscarinic antagonists produced non-parallel shift of the concentration-response curves for (+)-*cis*-dioxolane to induce the motoneurone depolarization, suggesting the involvement of multiple muscarinic receptors in the depolarizing action. Newberry & Connolly (1989) also reported that atropine flattened the concentration-response curves for cholinergic agonists to induce motoneurone depolarization. Although the M_1 antagonist, pirenzepine (10 nM) and M_2 antagonist, AF-DX 116 (100 nM) slightly depressed the depolarization, the effects tended to be saturated with higher concentrations of these antagonists. The contribution of M_1 and M_2 receptors to the depolarization therefore seems to be small if any. In contrast, the potent antagonistic effect of 4-DAMP at 1–10 nM on the depolarization is comparable with its effect on the M_3 receptor response of the guinea-pig ileum (pA_2 value: 9.0) (Clague *et al.*, 1985; Eglen & Whiting, 1987). However, the concentrations of another M_3 antagonist *p*-F-HHSiD needed to antagonize the depolarization were high (100 nM–3 μM), when compared with its concentrations of action on the ileal M_3 receptor (pA_2 value: 7.8) (Lambrecht *et al.*, 1988). Furthermore, arecoline and oxotremorine, which exhibit a full agonist activity on the ileum (Clague *et al.*, 1985), had a very weak depolarizing action on motoneurones in the neonatal rat spinal cord. These results suggest that the motoneurone depolarization is mainly mediated by receptors similar to, but not identical with the ileal M_3-type receptors.

Excitatory muscarinic postsynaptic actions on neurones have been reported in a variety of areas in the central nervous system (e.g. hippocampus, olfactory cortex, neocortex, thalamus, and neostriatum) and it has been suggested that the receptor subtypes involved in these actions may be either M_1- or M_2-type (see Nicoll *et al.*, 1990). The present study suggests the existence of an excitatory muscarinic response of central neurones mediated by M_3-type receptors.

We wish to thank Professors M. Otsuka and K. Kubota for encouragement and advice. Part of this work was supported by research grants from the Ministry of Education, Science and Culture, Japan.

References

AKAGI, H., KONISHI, S., OTSUKA, M. & YANAGISAWA, M. (1985). The role of substance P as a neurotransmitter in the reflexes of slow time courses in the neonatal rat spinal cord. *Br. J. Pharmacol.*, **84**, 663–673.

ARUNLAKSHANA, A.D. & SCHILD, H.O. (1959). Some quantitative uses of drug antagonists. *Br. J. Pharmacol. Chemother.*, **14**, 48–58.

BARBER, R.P., PHELPS, P.E., HOUSER, C.R., CRAWFORD, G.D., SALVATERRA, P.M. & VAUGHN, J.E. (1984). The morphology and distribution of neurons containing choline acetyltransferase in the adult rat spinal cord: an immunocytochemical study. *J. Comp. Neurol.*, **229**, 329–346.

BARLOW, R.B., BERRY, K.J., GLENTON, P.A.M., NIKOLAOU, N.M. & SOH, K.S. (1976). A comparison of affinity constants for muscarine-sensitive acetylcholine receptors in guinea-pig atrial pacemaker cells at 29°C and 37°C. *Br. J. Pharmacol.*, **58**, 613–620.

BORGE, L. & IVERSEN, S.D. (1986). Topography of choline acetyltransferase immunoreactive neurons and fibers in the rat spinal cord. *Brain Res.*, **362**, 140–148.

BROWN, D.A., FORWARD, A. & MARSH, S. (1980). Antagonist discrimination between ganglionic and ileal muscarinic receptors. *Br. J. Pharmacol.*, **71**, 362–364.

CLAGUE, R.U., EGLEN, R.M., STRACHAN, A.C. & WHITING, R.L. (1985). Action of agonists and antagonists at muscarinic receptors present on ileum and atria *in vitro*. *Br. J. Pharmacol.*, **86**, 163–170.

DIRKSEN, R. & NIJHUIS, G.M.M. (1983). The relevance of cholinergic transmission at the spinal level to opiate effectiveness. *Eur. J. Pharmacol.*, **91**, 215–221.

DRAY, A. & PERKINS, M.N. (1987). Blockade of nociceptive responses in the neonatal rat spinal cord *in vitro* by excitatory amino acid antagonists. *J. Physiol.*, **382**, 177P.

EGLEN, R.M. & WHITING, R.L. (1987). Competitive and non-competitive antagonism exhibited by 'selective' antagonists at atrial and ileal muscarinic receptor subtypes. *Br. J. Pharmacol.*, **90**, 701–707.

EHLERT, F.J., DUMONT, Y., ROESKE, W.R. & YAMAMURA, H.I. (1980). Muscarinic receptor binding in rat brain using the agonist, [^{3}H]cis methyldioxolane. *Life Sci.*, **26**, 961–967.

EVANS, R.H. (1978). Cholinoceptive properties of motoneurones of the immature rat spinal cord maintained in vitro. *Neuropharmacology*, **17**, 277–279.

GIACHETTI, A., MICHELETTI, R. & MONTAGNA, E. (1986). Cardioselective profile of AF-DX 116, a muscarine M_2 receptor antagonist. *Life Sci.*, **38**, 1663–1672.

GILLBERG, P.-G., ASKMARK, H. & AQUILONIUS, S.-M. (1990). Spinal cholinergic mechanisms. In *Prog. Brain Res.*, ed. Aquilonius, S.-M. & Gillberg, P.-G. pp. 361–370. Amsterdam: Elsevier.

GILLBERG, P.-G. & ASKMARK, H. (1991). Changes in cholinergic and opioid receptors in the rat spinal cord, dorsal root and sciatic nerve after ventral and dorsal root lesion. *J. Neural. Transm.* [Gen Sect.], **85**, 31–39.

GILLBERG, P.-G., GORDH, T., HARTVIG, P., JANSSON, I., PETTERSSON, J. & POST, C. (1989). Characterization of the antinociception induced by intrathecally administered carbachol. *Pharmacol. Toxicol.*, **64**, 340–343.

GILLBERG, P.-G. & WIKSTEN, B. (1986). Effect of spinal cord lesions and rhizotomies on cholinergic and opiate receptor binding site in rat spinal cord. *Acta Physiol. Scand.*, **126**, 575–582.

GREEN, P.G. & KITCHEN, I. (1986). Antinociception opioids and the cholinergic system. *Prog. Neurobiol.*, **26**, 119–146.

HAMMER, R., BERRIE, C.P., BIRDSALL, N.J.M., BURGEN, A.S.V. & HULME, E.C. (1980). Pirenzepine distinguishes between different subclasses of muscarinic receptors. *Nature*, **283**, 90–92.

HAMMER, R. & GIACHETTI, A. (1982). Muscarinic receptor subtypes: M1 and M2 biochemical and functional characterization. *Life Sci.*, **31**, 2991–2998.

HARTVIG, P., GILLBERG, P.-G., GORDH, T. & POST, C. (1989). Cholinergic mechanisms in pain and analgesia. *Trends Pharmacol. Sci. Suppl.*, **10**, 75–79.

HULME, E.C., BIRDSALL, N.J.M. & BUCKLEY, N.J. (1990). Muscarinic receptor subtypes. *Annu. Rev. Pharmacol. Toxicol.*, **30**, 633–677.

JIANG, Z.G. & DUN, N.J. (1986). Presynaptic suppression of excitatory postsynaptic potentials in rat ventral horn neurons by muscarinic agonists. *Brain Res.*, **381**, 182–186.

KING, A.E., THOMPSON, S.W.N. & WOOLF, C.J. (1990). The prolonged postsynaptic depolarizations evoked in ventral horn neurons following stimulation of small-calibre primary afferents in the isolated rat hemisected spinal cord-hindlimb preparation are APV sensitive. *J. Physiol.*, **422**, 7P.

KOBAYASHI, N., SAKUMA, M., YOSHIOKA, K., ONISHI, Y., YANAGISAWA, M., KAWASHIMA, K. & OTSUKA, M. (1991). Substance P-evoked release of acetylcholine from isolated spinal cord of the newborn rat. *Neuroscience*, **45**, 331–337.

KURIHARA, T., YOSHIOKA, K. & OTSUKA, M. (1991). Involvement of excitatory amino acid receptors in the cutaneous nerve-evoked and substance P-evoked depolarizations of rat motoneurons. *Jpn. J. Pharmacol. Suppl.*, **55**, 358P.

LAMBRECHT, G., FEIFEL, R., FORTH, B., STROHMANN, C., TACKE, R. & MUTSCHLER, E. (1988). *p*-Fluoro-Hexahydro-sila-difenidol: The first $M_{2\beta}$-selective muscarinic antagonist. *Eur. J. Pharmacol.*, **152**, 193–194.

MELCHIORRE, C., ANGELI, P., LAMBRECHT, G., MUTSCHLER, E., PICCHIO, M. & WESS, J. (1987). Antimuscarinic action of methoctramine, a new cardioselective M-2 muscarinic receptor antagonist, alone and in combination with atropine and gallamine. *Eur. J. Pharmacol.*, **144**, 117–124.

NEWBERRY, N.R. & CONNOLLY, G.P. (1989). Muscarinic pharmacology of the spinal cord of the neonatal rat *in vitro*. *Neuropharmacology*, **28**, 149–152.

NICOLL, R.A., MALENKA, R.C. & KAUER, J.A. (1990). Functional comparison of neurotransmitter receptor subtypes in mammalian central nervous system. *Physiol. Rev.*, **70**, 513–565.

NUSSBAUMER, J.-C., YANAGISAWA, M. & OTSUKA, M. (1989). Pharmacological properties of a C-fibre response evoked by saphenous nerve stimulation in an isolated spinal cord-nerve preparation of the newborn rat. *Br. J. Pharmacol.*, **98**, 373–382.

OTSUKA, M. & KONISHI, S. (1974). Electrophysiology of mammalian spinal cord *in vitro*. *Nature*, **252**, 733–734.

OTSUKA, M. & YANAGISAWA, M. (1987). Does substance P act as a pain transmitter? *Trends Pharmacol. Sci.*, **8**, 506–510.

OTSUKA, M. & YANAGISAWA, M. (1988). Effect of a tachykinin antagonist on a nociceptive reflex in the isolated spinal cord-tail preparation of the newborn rat. *J. Physiol.*, **395**, 255–270.

RIBEIRO-DA-SILVA, A. & CUELLO, A.C. (1990). Choline acetyltransferase-immunoreactive profiles are presynaptic to primary sensory fibers in the rat superficial dorsal horn. *J. Comp. Neurol.*, **295**, 370–384.

RIKER, W.F. & WESCOE, W.C. (1951). The pharmacology of flaxedil with observations on certain analogs. *Ann. N.Y. Acad. Sci.*, **54**, 373–394.

SMITH, M.D., YANG, X., NHA, J.-Y. & BUCCAFUSCO, J.J. (1989). Antinociceptive effect of spinal cholinergic stimulation: interaction with substance P. *Life Sci.*, **45**, 1255–1261.

TAYLOR, J.E., YAKSH, T.L. & RICHELSON, E. (1982). Agonist regulation of muscarinic acetylcholine receptors in the rat spinal cord. *J. Neurochem.*, **39**, 521–524.

THERIAULT, E., OTSUKA, M. & JESSELL, T. (1979). Capsaicin-evoked release of substance P from primary sensory neurons. *Brain Res.*, **170**, 209–213.

YAKSH, T.L., DIRKSEN, R. & HARTY, G.J. (1985). Antinociceptive effects of intrathecally injected cholinomimetic drugs in the rat and cat. *Eur. J. Pharmacol.*, **117**, 81–88.

YANAGISAWA, M., NAKANO, S. & OTSUKA, M. (1980). Capsaicin-induced depolarization of primary afferent fibers and the release of substance P from isolated rat spinal cord. *Biomed. Res. Suppl.*, **1**, 88–90.

YANAGISAWA, M., OTSUKA, M., KONISHI, S., AKAGI, H., FOLKERS, K. & ROSELL, S. (1982). A substance P antagonist inhibits a slow reflex response in the spinal cord of the newborn rat. *Acta Physiol. Scand.*, **116**, 109–112.

YANAGISAWA, M. & OTSUKA, M. (1990). Pharmacological profile of a tachykinin antagonist, spantide, as examined on rat spinal motoneurones. *Br. J. Pharmacol.*, **100**, 711–716.

YANAGISAWA, M., HOSOKI, R. & OTSUKA, M. (1992). The isolated spinal cord-skin preparation of the newborn rat and effects of some algogenic and analgesic substances. *Eur. J. Pharmacol.*, **220**, 111–117.

YOSHIOKA, K., KURIHARA, T., SUZUKI, H. & OTSUKA, M. (1990a). Different subtypes of muscarinic receptors are involved in two muscarinic responses in neonatal rat spinal cord. *Jpn. J. Pharmacol. Suppl.*, **52**, 359P.

YOSHIOKA, K., SAKUMA, M. & OTSUKA, M. (1990b). Cutaneous nerve-evoked cholinergic inhibition of monosynaptic reflex in the neonatal rat spinal cord: involvement of M_2 receptors and tachykininergic primary afferents. *Neuroscience*, **38**, 195–203.

YOSHIOKA, K., KURIHARA, T. YANAGISAWA, M. & OTSUKA, M. (1991). Facilitatory and inhibitory muscarinic modulation of C fiber-evoked depolarization in the neonatal rat spinal cord. *Neurosci. Res. Suppl.*, **14**, S134.

(Received January 12, 1993
Revised April 13, 1993
Accepted April 20, 1993)

Br. J. Pharmacol. (1993), **110**, 71–76

Mediation by B_1 and B_2 receptors of vasodepressor responses to intravenously administered kinins in anaesthetized dogs

*†Nabil Nakhostine, [1]†Christophe Ribuot, †Daniel Lamontagne, †Réginald Nadeau & [2]*Réjean Couture

*Department of Physiology, Faculty of Medicine, Université de Montréal, Montréal, Québec, Canada H3C 3J7 and †Research Center, Hôpital du Sacré-Coeur de Montréal, Montréal, Québec, Canada H4J 1C5

1 Vasodepressor responses to intravenous (i.v.) injection of bradykinin (BK) and des-Arg^9-BK, a selective B_1 kinin receptor agonist, were characterized following i.v. pretreatment with selective B_1 ([Leu^8]-des-Arg^9-BK) and B_2 (Hoe 140) kinin receptor antagonists in anaesthetized dogs.

2 Des-Arg^9-BK (0.05–3.3 nmol kg^{-1}) produced dose-dependent decreases in mean arterial blood pressure with a ED_{50} 0.4 nmol kg^{-1}. The vasodepressor effects evoked by des-Arg^9-BK (0.6 nmol kg^{-1}) and BK (0.2 nmol kg^{-1}) were greater after i.v. and i.a. injections, respectively.

3 The vasodepressor response to BK (0.6 nmol kg^{-1}) but not to des-Arg^9-BK (0.6 nmol kg^{-1}) was significantly ($P<0.001$) blocked by pretreatment with the B_2 receptor antagonist, Hoe 140.

4 The vasodepressor response to des-Arg^9-BK (0.6 nmol kg^{-1}) but not to BK (0.6 nmol kg^{-1}) was significantly ($P<0.001$) reduced by pretreatment with the selective B_1 receptor antagonist, [Leu^8]-des-Arg^9-BK. Although both B_1 and B_2 receptor antagonists caused a transient fall in blood pressure, their inhibitory action was unlikely to be related to a desensitization mechanism.

5 Inhibition of prostaglandin synthesis with indomethacin prevented the vasodepressor response induced by arachidonic acid (1 mg kg^{-1}, i.v.) but not that to BK or des-Arg^9-BK (0.6 nmol kg^{-1}).

6 These results suggest, firstly, that the vasodepressor responses to i.v. BK and des-Arg^9-BK are mediated by the activation of B_2 and B_1 receptors, respectively; secondly, that prostaglandins are not involved in the vasodepressor responses to kinins. These findings provide pharmacological evidence for the existence of functionally active B_1 receptors in canine cardiovascular homeostasis.

Keywords: Bradykinin; des-Arg^9-BK; kinin receptors; kinin antagonists; blood pressure

Introduction

Bradykinin (BK) is a potent vasodilator the action of which appears to be mediated by the release of an endothelium-derived relaxing factor and/or prostacyclin, resulting from the activation of B_2 receptors on the vascular endothelium (Taylor *et al.*, 1989). Despite the very well known B_2 receptor-mediated vasodepressor effect of kinins (Regoli & Barabé, 1980; Bhoola *et al.*, 1992), the cardiovascular activity of the natural kininase I metabolite, des-Arg^9-BK, which is a selective B_1 receptor agonist, has been less studied. This fact is due in part to the belief that B_1 receptors are not expressed in normal tissues but are synthesized *de novo* during tissue incubation *in vitro* and as a result of inflammation or exposure of tissue to chemical noxious stimuli *in vivo* (Marceau *et al.*, 1983; Bouthillier *et al.*, 1987). For instance, des-Arg^9-BK had no significant effect on the cardiovascular system of rats and rabbits whereas exogenous des-Arg^9-BK lowered mean arterial blood pressure through the activation of peripheral vascular B_1 receptors in rabbits pre-injected intravenously 5 h earlier with a bacterial lipopolysaccharide (Regoli *et al.*, 1981; Marceau *et al.*, 1983; Bouthillier *et al.*, 1987). Nevertheless, under normal conditions, both B_1 and B_2 receptors appear to mediate the vasodilator action of kinins in the canine renal artery *in vitro* (Rhaleb *et al.*, 1989) as well as the vasorelaxation responsible for an increased renal blood flow in the dog *in vivo* (Lortie *et al.*, 1992). In the latter study, mediation of the natriuretic response to intrarenal infusion of BK was ascribed to a tubular B_1 receptor.

Selective antagonists for the B_1 and B_2 receptors are now available. The compound [Leu^8]-des-Arg^9-BK is considered as the prototype antagonist for the B_1 receptor (Regoli & Barabé, 1980) while Hoe 140 (D-Arg-[Hyp^3,Thi^5,D-Tic^7, Oic^8]BK) is the most potent, long-acting and selective B_2 receptor antagonist so far described *in vitro* and *in vivo* (Wirth *et al.*, 1991; Hock *et al.*, 1991; Bao *et al.*, 1991; Lembeck *et al.*, 1991; Rhaleb *et al.*, 1992).

The present study was designed to test the hypothesis that vascular B_1 and B_2 receptors can mediate the vasodepressor response to kinins in the dog under normal conditions. Thus, the selective antagonists of the B_1 ([Leu^8]-des-Arg^9-BK) and B_2 (Hoe 140) receptors were used to characterize kinin receptors that mediate the blood pressure effects of BK and des-Arg^9-BK in anaesthetized dogs. BK-induced vasorelaxation appears to be mediated by prostaglandins in arteries of some species (Barabé *et al.*, 1979; Taylor *et al.*, 1989). Moreover, unlike the endothelial B_2 receptor, canine muscular B_1 and B_2 receptors mediate relaxation of the arterial smooth muscle by promoting the release of prostaglandins (Rhaleb *et al.*, 1989). The second objective of the present study was therefore to examine the contribution of prostaglandins in the vasodepressor response to kinins. A preliminary account of this work has been published in an abstract form (Nakhostine *et al.*, 1992).

Methods

Surgical preparation of the animal

Adult mongrel dogs of either sex ($n=20$) weighing 17.5 ± 0.7 kg were anaesthetized with sodium thiopenone (25 mg kg^{-1}, i.v.) and alpha-chloralose (80 mg kg^{-1} followed by 15–20 mg kg^{-1} h^{-1}, i.v.). The animals were heparinized (200

[1] Present address: Faculté de pharmacie, Université Joseph Fourier, 38700 La Tronche, France.

[2] Author for correspondence at: Département de physiologie, Faculté de médecine, Université de Montreal, C.P. 6128, Succursale A, Montréal, Québec, Canada H3C 3J7.

i.u. kg^{-1}, i.v.) and ventilated artificially with room air through an endotracheal tube by means of a Harvard pump (model 607). The right femoral artery was cannulated with a polyethylene catheter (PE-90) filled with physiological saline to measure the arterial blood pressure. The right and left femoral veins were also cannulated to enable the intravenous infusion or bolus injections of drugs. The data were recorded on a polygraph system (Nihon Kohden, model RM-6000) and the multi speed transmission Harvard apparatus infusion pump (model 940) was used for drug administration.

Care of the animals and haematological analysis

The research protocol and the care of the animals conformed to the guiding principles for animal experimentation as enunciated by the Canadian Council on animal care and approved by the ethical committee of University of Montreal for animal research.

All dogs were housed and maintained at a constant temperature of 20–22°C on a 12 h light/dark cycle (lights on 06 h 00 min–18 h 00 min) and provided with food and water *ad libitum*. Each animal underwent a veterinary medical examination before experimentation. Furthermore, a complete blood analysis was performed on three canine specimens to confirm that these animals were pathogen-free. Haematological analysis was made the day of their arrival at the animal house (initial values) and two weeks later just prior to experimentation. As shown in Table 1, the haematological values of white and red blood cells, haemoglobin, haematrocrit, mean corpuscular volume (MCV), mean corpuscular haemoglobin (MCH), mean corpuscular haemoglobin concentration (MCHC), platelets, sodium, potassium, calcium, glucose, urea, creatinine, alkaline phosphatase, arpartate aminotransferase (GOT) and total protein were all within normal limits.

Experimental protocol

The first series of experiments was designed to measure the i.v. effects of several increasing doses of des-Arg^9-BK (0.05 to 3.3 nmol kg^{-1}) and of three doses of BK (0.2, 0.6 and 2.2 nmol kg^{-1}) on mean arterial blood pressure (MAP). The two kinins were injected to the same animals in a volume of 3 ml followed by a 2 ml saline to wash out the cannula. The interval between injection was 10 min. In addition, the vasodepressor effects induced by BK (0.2 nmol kg^{-1}) and des-Arg^9-BK (0.6 nmol kg^{-1}) were compared after i.v. and i.a. injections.

The second series of experiments aimed to characterize the vasodepressor responses to BK and des-Arg^9-BK with the use of [Leu^8]-des-Arg^9-BK, a B_1 receptor selective antagonist and of Hoe 140, a B_2 receptor selective antagonist. BK or des-Arg^9-BK was injected at the same dose of 0.6 nmol kg^{-1}, (a) before and 3–5 min after the i.v. injection of [Leu^8]-des-Arg^9-BK (6.0 nmol kg^{-1} followed by an infusion of 0.6 nmol kg^{-1} min^{-1} for 5 min); (b) before and 10 min after the i.v. injection of Hoe 140 (4.5 nmol kg^{-1}) or (c) 5 min after the i.v. injection of 5 ml saline followed by an infusion of saline at 7.6 ml min^{-1} for 5 min as control group.

The third series of experiments was to examine the participation of prostaglandins in the BK and des-Arg^9-BK induced vasodepressor responses. Each agonist was tested at a dose of 0.6 nmol kg^{-1}, 1 h after the i.v. injection of either indomethacin (10 mg kg^{-1}) or the vehicle (Trizma base 0.2 M). To ascertain the effectiveness of this treatment, the vasodepressor effect of arachidonic acid (1 mg kg^{-1}) (precursor of prostaglandins) was measured in 2 dogs before and after indomethacin treatment.

Peptides and drugs

Des-Arg^9-BK was purchased from Hukabel Scientific Ltd. Montréal, Québec, Canada. BK, [Leu^8]-des-Arg^9-BK, indomethacin, Trizma base, arachidonic acid and heparin sodium salt were all purchased from Sigma Chemical Co., St-Louis, MO, U.S.A. Hoe 140 was made available from Hoechst AG (Frankfurt, Germany).

Stock solutions of peptides (1–10 mg ml^{-1}) were made in saline, divided into 100 µl aliquots and stored at −20°C until used. Indomethacin was prepared in Trizma base (0.2 M) just before use while arachidonic acid was prepared in 25% ethanol.

Statistical analysis

Values represent the mean ± s.e.mean of (n) animals. Statistical significance of differences between means were calculated with Student's t test for paired samples. Only probability values (P) smaller than 0.05 were considered to be statistically significant.

Table 1 Haematological values for 3 dogs

	Normal values[1]	*Initial values*	*Values before experimentation*
Leukocytes	6.0–18.5 × 10^9 l^{-1}	11.6 ± 0.7	12.7 ± 1.1
Erythrocytes	5.5–8.5 × 10^{12} l^{-1}	7.5 ± 0.9	7.2 ± 0.8
Haemoglobin	133–192 g l^{-1}	172.0 ± 15.6	164.0 ± 14.0
Haematocrit	36.8–54.4%	48.7 ± 4.3	47.2 ± 3.7
MCV	59.9–75.2 fl	65.8 ± 3.4	66.4 ± 3.4
MCH	21.5–27.2 pg	23.2 ± 1.1	23.0 ± 1.0
MCHC	336–383 g l^{-1}	353.0 ± 1.5	347.0 ± 3.2
Platelets	200–900 × 10^9 l^{-1}	375 ± 79	381 ± 59
Sodium	140–170 mmol l^{-1}	151.0 ± 2.5	150.1 ± 1.9
Potassium	3.5–6.7 mmol l^{-1}	4.3 ± 0.2	4.8 ± 0.3
Calcium	2.1–3.1 mmol l^{-1}	2.7 ± 0.04	3.7 ± 0.1
Glucose	3.0–6.5 mmol l^{-1}	5.2 ± 0.4	5.4 ± 0.5
Urea	3.6–9.0 mmol l^{-1}	8.6 ± 2.6	2.7 ± 0.1
Creatinine	85–175 µmol l^{-1}	110.1 ± 8.5	85.0 ± 9.6
Alkaline phosphatase	5–135 Ul^{-1}	33.0 ± 6.1	55.0 ± 18.0
GOT	17–58 Ul^{-1}	37.7 ± 1.8	41.7 ± 7.9
Total proteins	50–80 g l^{-1}	65.3 ± 2.2	59.3 ± 5.8

[1]Normal values are taken from Tvedten (1989).
Abbreviations: MCV, mean corpuscular volume, MCH, mean corpuscular haemoglobin; MCHC, mean corpuscular haemoglobin concentration, GOT, aspartate aminotransferase.

Results

Vasodepressor effects of des-Arg⁹-BK and BK

Baseline mean arterial pressure (MAP) prior to des-Arg⁹-BK or BK injections was 126 ± 5 mmHg ($n = 8$). Des-Arg⁹-BK produced dose-dependent decreases in MAP between 0.05 and 3.3 nmol kg^{-1} ($ED_{50} = 0.4$ nmol kg^{-1}); the maximal fall in MAP (− 41 ± 3 mmHg) was elicited at 2.2 nmol kg^{-1} (Figure 1). The depressor response to 0.6 nmol kg^{-1} des-Arg⁹-BK peaked at 27 ± 2 s post-injection and lasted for 3 to 4 min (Figure 2). The effect of 0.6 nmol kg^{-1} BK on MAP was 1.5 fold geater than that observed with the same dose of des-Arg⁹-BK (− 48 ± 2 mmHg vs − 30 ± 3 mmHg; $P <$ 0.001), while the time course effect was similar for both peptides (Figure 2). The dose of 2.2 nmol kg^{-1} BK produced a vasodepressor response (− 51 ± 5 mmHg, $n = 3$) which was similar to that induced by the dose of 0.6 nmol kg^{-1}. The vasodepressor response to 0.6 nmol kg^{-1} des-Arg⁹-BK was significantly ($P < 0.05$, $n = 6$) greater after i.v. injection than after i.a. administration. In contrast, the changes in MAP elicited by 0.2 nmol kg^{-1} BK was significantly ($P < 0.05$, $n = 6$) higher after i.a. administration (Figure 3). Thus, BK appeared more potent than des-Arg⁹-BK in reducing MAP whatever the route of administration.

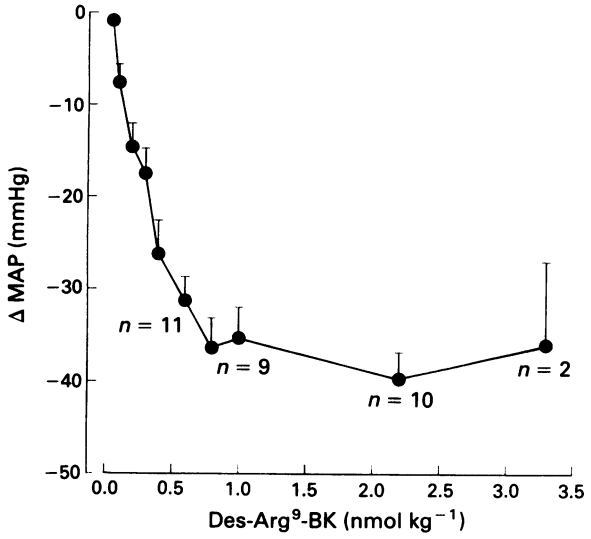

Figure 1 Dose-response curve showing the changes in mean arterial blood pressure (MAP) induced by the i.v. injection of des-Arg⁹-BK in anaesthetized dogs. Values are the mean ± s.e.mean of 8 dogs unless otherwise indicated by n.

Effect of [Leu⁸]-des-Arg⁹-BK, a selective B_1 receptor antagonist

Baseline MAP before [Leu⁸]-des-Arg⁹-BK infusion was 115 ± 4 mmHg ($n = 10$). [Leu⁸]-des-Arg⁹-BK injection (6.0 nmol kg^{-1}) induced a significant ($P < 0.001$, $n = 10$) decrease in MAP (− 38 ± 3 mmHg) which peaked at 27 ± 1 s and returned rapidly to pretreatment value (Figure 4). No tachyphylaxis was observed when des-Arg⁹-BK (0.6 nmol kg^{-1}) or [Leu⁸]-des-Arg⁹-BK (6.0 nmol kg^{-1}) were injected three times at intervals of 10 min (Figure 4). However, the vasodepressor effect of 0.6 nmol kg^{-1} des-Arg⁹-BK was significantly ($P <$ 0.001, $n = 10$) blocked 3–5 min after the i.v. injection of [Leu⁸]-des-Arg⁹-BK (6.0 nmol kg^{-1} plus 0.6 nmol kg^{-1} min^{-1} × 5 min) (Figures 4 and 5). In contrast, [Leu⁸]-des-Arg⁹-BK had no significant effect on the vasodepressor effect elicited by 0.6 nmol kg^{-1} BK (Figure 5).

Effect of Hoe 140, a selective B_2 receptor antagonist

Baseline MAP before Hoe 140 injection was 118 ± 5 mmHg ($n = 10$). The i.v. injection of 4.5 nmol kg^{-1} Hoe 140 significantly ($P < 0.001$, $n = 10$) decreased MAP (− 17 ± 3 mmHg), an effect which peaked at 34 ± 2 s and returned rapidly to pretreatment value (Figure 4). Although no tachyphylaxis occurred when 0.6 nmol kg^{-1} BK was injected three times at intervals of 10 min, the depressor response to 4.5 nmol kg^{-1} Hoe 140 was no longer present after the second and third injections. The decrease in MAP induced by 0.6 nmol kg^{-1} BK was significantly blocked ($P < 0.001$, $n = 10$) 10 min after the prior i.v. injection of 4.5 nmol kg^{-1} Hoe 140 (Figures 4, 6). In contrast, the vasodepressor response to 0.6 nmol kg^{-1} des-Arg⁹-BK remained unaffected by the pre-injection of Hoe 140 (Figure 6). The vasodepressor re-

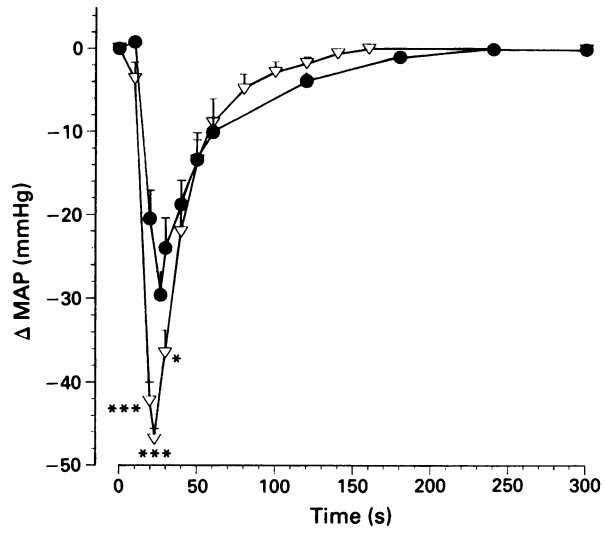

Figure 2 Time course of the changes in mean arterial blood pressure (MAP) induced by the i.v. injection of 0.6 nmol kg^{-1} of either bradykinin (BK) (▽) or des-Arg⁹-BK (●) in anaesthetized dogs. Values are the mean ± s.e.mean of 11 dogs. The statistical significance between bradykinin (BK) and des-Arg⁹-BK is indicated by $*P < 0.05$ and $***P < 0.001$.

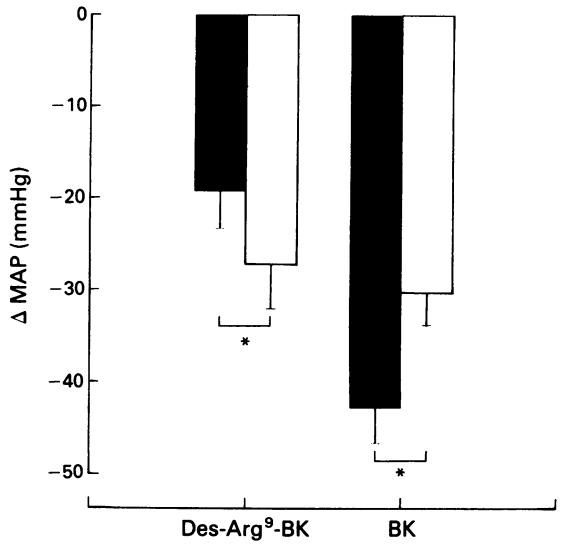

Figure 3 Maximal changes in mean arterial blood pressure (MAP) induced by the i.v. (open columns) or i.a. (solid columns) injection of 0.6 nmol kg^{-1} des-Arg⁹-BK or 0.2 nmol kg^{-1} bradykinin (BK) in anaesthetized dogs. Values are the mean ± s.e.mean of 6 dogs. The statistical significance between i.v. and i.a. values is indicated by $*P < 0.05$.

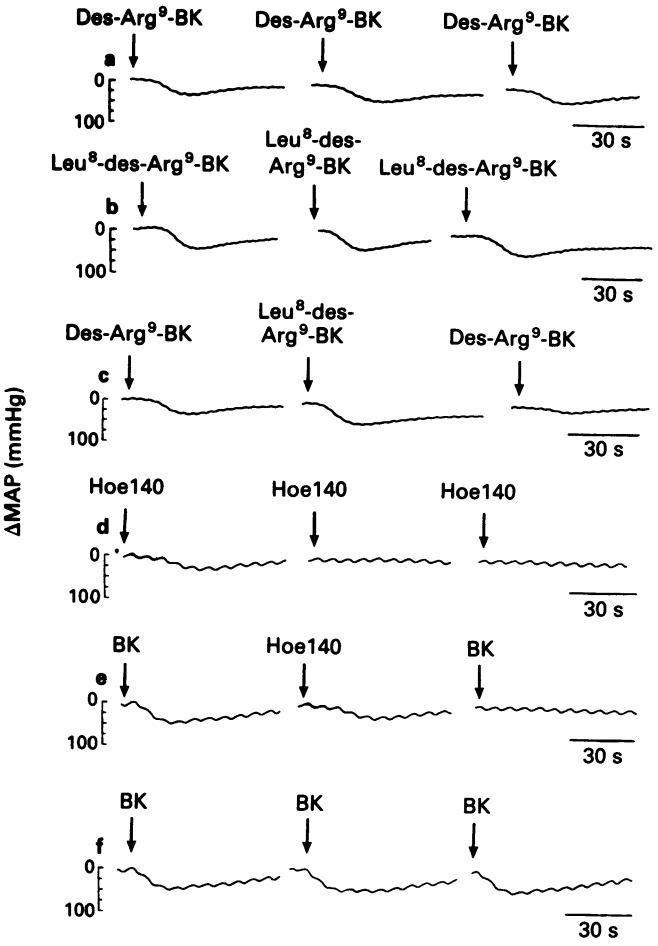

Figure 4 Example of traces showing the vasodepressor effects induced by three i.v. injections of 0.6 nmol kg^{-1} des-Arg^9-BK (a), 6.0 nmol kg^{-1} [Leu^8]-des-Arg^9-BK (b), 4.5 nmol kg^{-1} Hoe 140 (d) and 0.6 nmol kg^{-1} bradykinin (BK) (f). The vasodepressor effect of 0.6 nmol kg^{-1} des-Arg^9-BK is blocked 5 min after the prior i.v. infusion of [Leu^8]-des-Arg^9-BK (6.0 nmol kg^{-1} plus 0.6 nmol kg^{-1} min^{-1} × 5 min) (c). The vasodepressor effect of 0.6 nmol kg^{-1} BK is blocked 10 min after the prior i.v. injection of Hoe 140 (4.5 nmol kg^{-1}) (e). Each injection is separated by a period of 10 min. These experiments were conducted in dogs; haematological values are provided in Table 1.

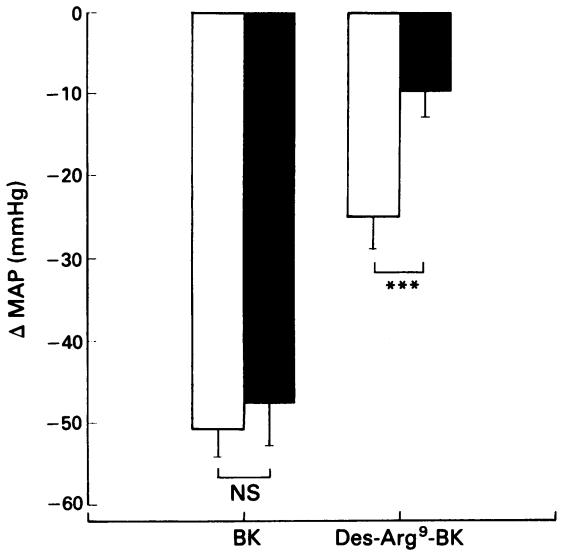

Figure 5 Effects of [Leu^8]-des-Arg^9-BK on the changes in mean arterial blood pressure (MAP) induced by the i.v. injection of 0.6 nmol kg^{-1} bradykinin (BK) or des-Arg^9-BK in anaesthetized dogs. Values are the mean ± s.e.mean of 5 (BK) and 10 (des-Arg^9-BK) dogs in the absence (open columns) and presence (solid columns) of the B_1 receptor antagonist (6.0 nmol kg^{-1} plus 0.6 nmol kg^{-1} min^{-1} for 5 min). Statistical significance is indicated by $***P<0.001$ and NS = not significant.

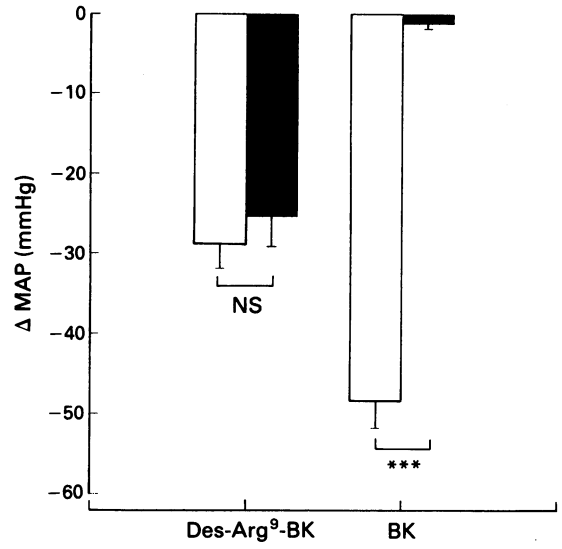

Figure 6 Effects of Hoe 140 on the changes in mean arterial blood pressure (MAP) induced by the i.v. injection of 0.6 nmol kg^{-1} bradykinin (BK) or des-Arg^9-BK in anaesthetized dogs. Values are the mean ± s.e.mean of 10 dogs in the absence (open columns) and presence (solid columns) of the B_2 receptor antagonist (4.5 nmol kg^{-1}). Statistical significance is indicated by $***P<0.001$ and NS = not significant.

sponse to BK was still impaired by 92%, 30 min after the injection of the antagonist (data not shown).

Effect of indomethacin on the vasodepressor responses to BK and des-Arg^9-BK

Baseline MAP before indomethacin treatment was 114 ± 4 mmHg (n = 10). The decrease in MAP to indomethacin injection (− 21 ± 4 mmHg) peaked at 21 ± 2 s and was stable at 109 ± 5 mmHg 1 h later, when BK and des-Arg^9-BK were injected. The indomethacin's vehicle (Trizma base) caused a similar fall in MAP (− 25 ± 3 mmHg) that peaked at 21 ± 1 s and the blood pressure returned to baseline within 5 min.

Indomethacin had no effect on vasodepressor responses to BK or des-Arg^9-BK. In contrast, the vasodepressor effect induced by the i.v. injection of arachidonic acid (1 mg kg^{-1}) was abolished in two animals pretreated with indomethacin (Figure 7).

Discussion

This study has shown that des-Arg^9-BK reduces systemic blood pressure in a dose-dependent manner in the dog. To our knowledge, this is the first species in which des-Arg^9-BK can lower blood pressure under non-pathological conditions. This effect has been well studied in pathological conditions such as following the injection of a sublethal dose of bacterial lipopolysaccharide (endotoxin) in the rabbit (Regoli *et al.*, 1981; Bouthillier *et al.*, 1987; Drapeau *et al.*, 1991b). The vasodepressor response to i.v. injection of BK was smaller than that observed after i.a. administration which is consistent with previous reports showing that 80–95% of the biological activity of BK is inactivated by kininase II during the first passage through the pulmonary circulation (Regoli & Barabé,

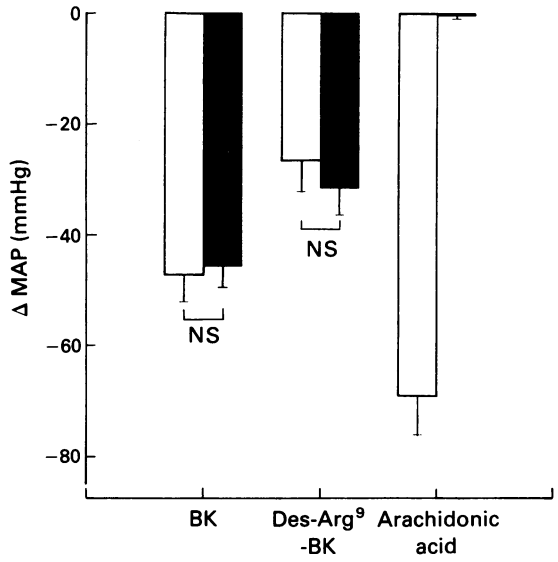

Figure 7 Effects of indomethacin on the changes in mean arterial blood pressure (MAP) induced by the i.v. injection of 0.6 nmol kg^{-1} bradykinin (BK) or des-Arg^9-BK and 1 mg kg^{-1} arachidonic acid in anaesthetized dogs. Values are the mean ± s.e.mean of 10 (kinins) or 2 (arachidonic acid) dogs in the absence (open columns) and presence (solid columns) of indomethacin (10 mg kg^{-1}, i.v. 1 h earlier). NS = not significant.

1980). However, the vasodepressor effect of des-Arg^9-BK described here was significantly greater after i.v. administration, suggesting a slower catabolism of this naturally occurring peptide through the pulmonary circulation compared to BK. This is in agreement with the recent observation that kininase II acts on des-Arg^9-BK at a slow rate and with a low affinity as compared to its action on BK (Drapeau *et al.*, 1991a,b). The higher potency of des-Arg^9-BK after i.v. administration has never been observed previously because in most species (e.g. rabbit, rat and guinea-pig), the selective B_1 receptor agonist has less than 1% of the activity of BK on systemic blood pressure (Regoli & Barabé, 1980; Bhoola *et al.*, 1992). The mechanism of the higher potency of des-Arg^9-BK after i.v. injection awaits elucidation but might be due to changes in the pulmonary circulatory resistance or to the release of an endogenous mediator from the pulmonary circulation which is probably not a prostaglandin.

Infusion of [Leu^8]-des-Arg^9-BK, a selective and competitive antagonist of the B_1 receptor (Regoli & Barabé, 1980), reduced significantly the vasodepressor response to des-Arg^9-BK but not to BK. In contrast, Hoe 140, a selective and potent antagonist of B_2 receptors that was found to inhibit BK-induced hypotensive responses in rats (Wirth *et al.*, 1991; Bao *et al.*, 1991), antagonized only the vasodepressor response to BK. These results suggest that the vasodepressor responses to BK and to des-Arg^9-BK in dogs are mediated by vascular B_2 and B_1 receptors, respectively. Until recently, it was believed that B_1 receptors are not present on vessels isolated from healthy animals. However, it has been demonstrated that the dog isolated renal artery contains a population of functional B_1 receptors involved in the vasodilator action of kinins (Rhaleb *et al.*, 1989). Furthermore, renal B_1 receptors were implicated in the action of BK on increased renal blood flow and sodium excretion in dogs (Lortie *et al.*, 1992).

The fact that [Leu^8]-des-Arg^9-BK and Hoe 140 caused a transient vasodepressor response would suggest that these antagonists maintain partial agonist activities on their respective receptors. In conscious dogs, i.v. administration of Hoe 140 (0.01 and 0.1 mg kg^{-1}) did not affect MAP or HR during a 15 min observation period when recorded indirectly from the tail artery (Wirth *et al.*, 1991). In our study, Hoe 140 ($\sim$6 μg kg^{-1}) caused only a transient decrease of MAP which may have escaped detection in an indirect recording system. It is of particular interest to note that [Leu^8]-des-Arg^9-BK and related selective antagonists at the B_1 receptor are unequivocally devoid of intrinsic activity in most of the reported *in vitro* and *in vivo* systems containing the B_1 receptor (Barabé *et al.*, 1979; Couture *et al.*, 1981; Marceau *et al.*, 1983; Drapeau *et al.*, 1991b). This finding suggests that the functional B_1 receptor described in the present *in vivo* model under non-pathological conditions is somewhat different from the inducible B_1 receptor which has been described under pathological conditions. Further studies are under way to define further the pharmacological profile of this so-called atypical B_1 receptor.

Under the experimental conditions, no tachyphylaxis occurred after repeated injections of the B_1 receptor agonist or antagonist, suggesting that the inhibitory effect of [Leu^8]-des-Arg^9-BK is not due to a desensitization mechanism but to pharmacological antagonism. Similarly, no tachyphylaxis occurred with BK while Hoe 140 produced a small vasodepressor response which could not be reproduced at the second and third injection. Since the direct effect of Hoe 140 on blood pressure is much smaller than that evoked by BK, the blockade of the BK response by Hoe 140 is probably related to a pharmacological antagonism as reported earlier (Wirth *et al.*, 1991; Hock *et al.*, 1991; Lembeck *et al.*, 1991). Hoe 140 did not alter the B_1 receptor response evoked by des-Arg^9-BK in our paradigm and thus appears specific for B_2 receptors.

The finding that [Leu^8]-des-Arg^9-BK and Hoe 140, at doses sufficient to block exogenous des-Arg^9-BK and BK, did not cause increases in baseline arterial blood pressure casts some doubt concerning the contribution of endogenous kinins to blood pressure maintenance in normotensive dogs. One cannot exclude, however, the possibility that kinins might control vascular resistance and blood flow in specific vascular territories or interact with other vasoregulatory mechanisms such as the renin-angiotensin system (Van Den Buuse & Kerkhoff, 1991).

In order to evaluate the role of prostanoids in the peripheral action of BK and des-Arg^9-BK, we investigated the effect of indomethacin, a cyclo-oxygenase inhibitor. The vasodepressor effect of arachidonate, the natural precursor of prostaglandin synthesis, was totally inhibited in the presence of indomethacin, thus confirming the effectiveness of indomethacin in preventing formation of prostaglandins. The action of both BK and des-Arg^9-BK on the systemic circulation was not altered by indomethacin which rules out the participation of prostglandins in this response. This supports the belief that the involvement of prostacyclin/prostaglandins in the vasodilator action of BK is tissue- and species-dependent (Taylor *et al.*, 1989).

In conclusion, des-Arg^9-BK, the naturally occurring bradykinin metabolite, and BK administered intravenously are potent hypotensive peptides in dogs; their action appears to be mediated by peripheral B_1 and B_2 receptors, respectively.

This work was supported by grants from the Medical Research Council of Canada (MRCC) to R.C. and R.N. N.N. holds a studentship from the Fonds pour la Formation de Chercheurs et l'Aide à la Recherche. R.N. is a career investigator of the MRCC. R.C. is a senior scholar and D.L. a junior scholar from the Fonds de la recherche en santé du Québec. We are grateful to Mrs Francine Legault for her technical assistance.

References

BAO, G., QADRI, F., STAUSS, B., STAUSS, H., GOHLKE, P. & UNGER, T. (1991). Hoe 140, a new highly potent and long-acting bradykinin antagonist in conscious rats. *Eur. J. Pharmacol.*, **200,** 179–182.

BARABÉ, J., MARCEAU, F., THÉRIAULT, B., DROUIN, J.-N. & REGOLI, D. (1979). Cardiovascular actions of kinins in the rabbit. *Can. J. Physiol. Pharmacol.*, **57,** 78–91.

BHOOLA, K.D., FIGUEROA, C.D. & WORTHY, K. (1992). Bioregulation of kinins: kallikreins, kininogens, and kininases. *Pharmacol. Rev.*, **44,** 1–80.

BOUTHILLIER, J. DEBLOIS, D. & MARCEAU, F. (1987). Studies on the induction of pharmacological responses to des-Arg^9-bradykinin *in vitro* and *in vivo*. *Br. J. Pharmacol.*, **92,** 257–264.

COUTURE, R., MIZRAHI, J., REGOLI, D. & DEVROEDE, G. (1981). Peptides and the human colon: an in vitro pharmacological study. *Can. J. Physiol. Pharmacol.*, **59,** 957–964.

DRAPEAU, G., CHOW, A. & WARD, P.E. (1991a). Metabolism of bradykinin analogs by angiotensin I converting enzyme and carboxypeptidase N. *Peptides*, **12,** 631–638.

DRAPEAU, G., DEBLOIS, D. & MARCEAU, F. (1991b). Hypotensive effects of Lys-des-Arg^9-bradykinin and metabolically protected agonists of B_1 receptors for kinins. *J. Pharmacol. Exp. Ther.*, **259,** 997–1003.

HOCK, J.F., WIRTH, K., ALBUS, U., LINZ, W., GERHARDS, H.J., WIEMER, G., HENKE, ST, BREIPOHL, G., KÖNIG, W., KNOLLE, J. & SCHÖLKENS, B.A. (1991). Hoe 140 a new potent and long acting bradykinin-antagonist: *in vitro* studies. *Br. J. Pharmacol.*, **102,** 769–773.

LEMBECK, F., GRIESBACHER, T., ECKHARDT, M., HENKE, S., BREIPOHL, G. & KNOLLE, J. (1991). New, long-acting, potent bradykinin antagonists. *Br. J. Pharmacol.*, **102,** 297–304.

LORTIE, M., REGOLI, D., RHALEB, N.-E. & PLANTE, G.E. (1992). The role of B_1- and B_2-kinin receptors in the renal tubular and hemodynamic response to bradykinin. *Am. J. Physiol.*, **262,** R72–R76.

MARCEAU, F., LUSSIER, A., REGOLI, D. & GIROUD, J.P. (1983). Pharmacology of kinins: their relevance to tissue injury and inflammation. A review. *Gen. Pharmacol.*, **14,** 209–229.

NAKHOSTINE, N., COUTURE, R. & NADEAU, R. (1992). Étude pharmacologique des récepteurs B_1 et B_2 des kinines sur le système cardiovasculaire du chien. *Médecine-Sciences* (suppl. 2) **8,** Abstract 176.

REGOLI, D. & BARABÉ, J. (1980). Pharmacology of bradykinin and related kinins. *Pharmacol. Rev.*, **32,** 1–46.

REGOLI, D., MARCEAU, F. & LAVIGNE, J. (1981). Induction of B_1 receptors for kinins in the rabbit by a bacterial lipopolysaccharide. *Eur. J. Pharmacol.*, **71,** 105–115.

RHALEB, N.-E., DION, S., BARABÉ, J. ROUISSI, N., JUKIC, D., DRAPEAU, G. & REGOLI, D. (1989). Receptors for kinins in isolated arterial vessels of dogs. *Eur. J. Pharmacol.*, **162,** 419–427.

RHALEB, N.-E., ROUISSI, N., JUKIC, D., REGOLI, D., HENKE, S., BREIPOHL, G. & KNOLLE, J. (1992). Pharmacological characterization of a new highly potent B_2 receptor antagonist (Hoe 140: D-Arg-[Hyp^3,Thi^5,D-Tic^7,Oic^8]bradykinin). *Eur. J. Pharmacol.*, **210,** 115–120.

TAYLOR, J.E., DEFEUDIS, F.V. & MOREAU, J.P. (1989). Bradykinin-antagonists: therapeutic perspectives. *Drug Develop Res.*, **16,** 1–11.

TVEDTEN, H. (1989). Referral and in-office laboratories. In *Small Animal Clinical Diagnosis by Laboratory Methods*. ed. Willard, M.D., Tvedten, H. & Turnwald, G.H. pp. 1–13. Philadelphia: W.B. Saunders Company.

VAN DEN BUUSE, M. & KERKHOFF, J. (1991). Interaction of bradykinin and angiotensin in the regulation of blood pressure in conscious rats. *Gen. Pharmacol.*, **22,** 759–762.

WIRTH, K., HOCK, F.J., ALBUS, U., LINZ, W., ALPERMANN, H.G., ANAGNOSTOPOULOS, H., HENKE, ST., BREIPOHL, G., KÖNIG, W., KNOLLE, J. & SCHÖLKENS, B.A. (1991). Hoe 140 a new potent and long acting bradykinin-antagonist *in vivo* studies. *Br. J. Pharmacol.*, **102,** 774–777.

(Received September 11, 1992
Revised April 13, 1993
Accepted April 20, 1993)

Br. J. Pharmacol. (1993), **110**, 77–86

Effects of LY274614, a competitive NMDA receptor antagonist, on the micturition reflex in the urethane-anaesthetized rat

M. Yoshiyama, [1]J.R. Roppolo, *K.B. Thor & W.C. de Groat

Department of Pharmacology, School of Medicine, University of Pittsburgh, Pittsburgh PA 15261, U.S.A. and *Division of CNS/GI/GU Research, Lilly Research Laboratories, Eli Lilly and Company, Indianapolis IN 46285, U.S.A.

1 The effects of 3 competitive N-methyl-D-aspartate (NMDA) receptor antagonists, LY274614, LY233536 and LY235723, on the micturition reflex and external urethral sphincter EMG activity, were examined either under isovolumetric conditions or during continuous filling cystometry in urethane-anaesthetized (1.2 g kg^{-1}, s.c.) rats.

2 Intravenous administration of LY274614 (3–30 mg kg^{-1}) inhibited in a dose-dependent fashion both bladder and sphincter activity in the intact rats. In addition, the volume threshold for inducing micturition was increased and voided volume was decreased.

3 Intrathecal administration of LY274614 (0.06–30 μg) similarly inhibited bladder and sphincter activity during cystometry in intact rats.

4 In chronic spinal cord (T_6–T_8) transected rats LY274614 (0.1–30 mg kg^{-1}, i.v.) did not alter bladder activity under isovolumetric conditions but decreased the amplitude of micturition contractions and sphincter EMG activity during cystometry at a dose of 10–30 mg kg^{-1}.

5 The inhibitory effects of i.v. administration of LY274614, on bladder and sphincter activity induced by infusion of chemical irritant (0.1% acetic acid) or saline, were similar; except that a slightly larger dose was needed to inhibit sphincter activity during acetic acid infusion.

6 Peak amplitude of micturition contractions recovered to 50% of control 3 h following i.v. (30 mg kg^{-1}) or i.t. (6 μg) administration of LY274614.

7 Two other chemically related NMDA antagonists, LY233536 and LY235723 produced similar but less potent effects than LY274614 when given i.v.

8 These data indicate that glutamatergic transmitter mechanisms at the level of the spinal cord are important in modulating bladder activity in the intact animal, but that these mechanisms do not contribute to bladder reflexes in the chronic spinal rat. These mechanisms may, however, contribute to sphincter activity in both intact or chronic spinal rats.

Keywords: NMDA receptor antagonist; rat bladder; EMG; external urethral sphincter; glutamate; micturition reflex

Introduction

Reflex micturition is produced by a contraction of the smooth muscle of the urinary bladder and a reciprocal relaxation of bladder neck, urethra, and the external urethral sphincter. However, in rats (Kruse *et al.*, 1993) and to a lesser degree in dog (Nishizawa *et al.*, 1985) the striated muscle of the external urethral sphincter contracts intermittently in high (4–6 Hz) frequency bursts during voiding. This enhanced and pulsatile sphincter activity may aid in expulsion of urine in these animals, while continuous contraction of sphincter prevents urine release. In many species these responses are mediated by a spinobulbospinal reflex pathway that passes through relay centres in the lumbosacral spinal cord and the rostral brain stem (the pontine micturition centre) (de Groat *et al.*, 1992). The reflex pathway is activated by distension of the urinary bladder and subsequent firing in tension receptor afferent fibres that pass through the pelvic nerve to the lumbosacral spinal cord.

Pharmacological studies have implicated a number of neurotransmitters in the central nervous control of micturition (de Groat *et al.*, 1992). Among the putative excitatory transmitters, glutamic acid has attracted the most attention. Microinjection, of glutamic acid or related excitatory amino acids, into the pontine micturition centre or adjacent pontine area, facilitated micturition in the cat (Mallory *et al.*, 1991) and rat (Lumb & Morrison, 1987). Whereas, systemic administration of MK-801, an N-methyl-D-aspartate (NMDA) glutamate receptor antagonist, inhibited bladder and sphincter reflexes in anaesthetized rats (Maggi *et al.*, 1990; Yoshiyama *et al.*, 1991a,b; 1993). MK-801 also blocked the bladder contractions elicited by electrical stimulation of the pontine micturition centre (Suzuki *et al.*, 1991) and depressed the expression of the immediate early gene, c-*fos*, in spinal neurones induced by chemical irritation of the bladder mucosa (Birder & de Groat, 1992). Ligand binding studies have revealed that NMDA receptors are present at various locations along the micturition reflex pathway; including areas in proximity to the lumbosacral parasympathetic nucleus, the urethral sphincter motor nucleus and the pontine micturition centre (Jansen *et al.*, 1990; Shaw *et al.*, 1991).

The present study was undertaken to evaluate further the role of NMDA receptors in the micturition reflex pathway. We have examined the changes in bladder and sphincter activity induced by LY274614, a potent competitive NMDA receptor antagonist (Ornstein *et al.*, 1991), which enters the central nervous system following systemic administration. Two other competitive NMDA receptor antagonists (LY233536 and LY235723) were also examined in a few experiments. Unlike the non-competitive antagonist, MK-801, which blocks the cation channel of the NMDA receptor (Wong *et al.*, 1986), LY274614 acts at the glutamate binding site on the NMDA receptor (Ornstein *et al.*, 1991). In addition, LY274614 is likely to have a more selective action than MK-801 since, in high concentrations, MK-801 is known to block nicotinic acetylcholine receptor channels (Amador & Dani, 1991). The latter effect could alter ganglionic transmission in the peripheral autonomic pathways to the bladder, as well as transmission at the neuromuscular junction, in the striated sphincter muscle and thereby alter micturition reflexes by a peripheral non-glutamatergic mechanism. The

[1] Author for correspondence.

present results with LY274614 confirm and extend the findings with MK-801; indicating that glutamatergic transmission at NMDA receptors has an important facilitatory influence on bladder and sphincter reflexes in the anaesthetized rat. This influence must occur, at least in part, at the level of the lumbosacral spinal cord, since intrathecally administered LY274614 mimicked the effect of systemic administration.

A preliminary account of this work has been presented in an abstract (Yoshiyama *et al.*, 1992).

Methods

Animal preparation

Experiments were performed on 79 female urethane-anaesthetized (1.2 g kg^{-1}, s.c.) Sprague-Dawley rats weighing 170 to 310 g (mean = 240 g). The trachea was cannulated with a polyethylene tube (PE-205) to facilitate respiration; and cannulae (PE-50) were placed in the external jugular vein or femoral vein for intravenous drug administration. A transurethral bladder catheter connected to a pressure transducer was used to record the bladder pressure isovolumetrically with the urethral outlet ligated or to record pressure during cystometry when the bladder was filled with a constant infusion of physiological saline or acetic acid (0.1%) and allowed to empty around the catheter. To evaluate voiding efficiency (% of bladder volume voided) saline was infused into the bladder (0.04 ml min^{-1}) until the peak of a voiding bladder contraction; then the infusion was stopped and the saline voided from the bladder was collected and measured to determine the volume voided. The bladder was then emptied, the residual volume measured and cystometrogram repeated. The procedure was repeated a minimum of three times for each drug dose and control. Continuous cystometry was performed by a constant infusion (0.21 ml min^{-1}) of saline into the bladder to elicit repetitive voidings, which allowed rapid collection of data for a large number of voiding cycles (Maggi *et al.*, 1986). PE-90 and PE-50 cannulae were used for isovolumetric recording and constant infusion cystometry (continuous and single), respectively. For isovolumetric recording, the ureters were tied distally, cut and the proximal ends cannulated (PE-10) and drained externally. The procedure prevented the bladder from filling with urine during the experiment.

Eleven rats were spinalized under halothane anaesthesia. After a T_6–T_8 laminectomy, the dura and spinal cord were cut with scissors, and a sterile sponge (Gelfoam, The Upjohn Company) was placed between the cut ends. The bladders of spinal rats were expressed manually two or three times daily, and perigenital stimulation with a cotton swab was performed to encourage reflex bladder emptying (Mallory *et al.*, 1989). The experiments on spinalized rats were performed 2 to 3 weeks postspinalization.

In 19 rats anaesthetized with urethane (1.2 g kg^{-1}, s.c.), an intrathecal (i.t.) catheter was inserted according to the technique of Yaksh & Rudy, 1976. The occipital crest of the skull was exposed and the atlanto-occipital membrane was incised at the midline using the tip of a 19 gauge needle as a cutting edge. A catheter (PE-10) was inserted through the slit and passed caudally to the L_6-level of the spinal cord. The volume of fluid within the catheter was kept constant at 6 µl. Cumulative dose-response curves were obtained by administering the drugs in 6 µl injections followed by 6 µl flush with artificial CSF at 15 min intervals. At the end of the experiment a laminectomy was performed to verify the location of the catheter tip.

In 23 experiments (5 intact, 5 chronic spinal, 8 intact with i.t. cannulae, and in 5 intact animals with acetic acid infusion

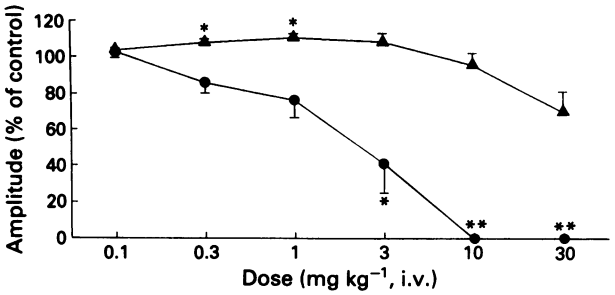

Figure 2 Log dose-response curves showing the effects of increasing doses of LY274614 (0.1–30 mg kg^{-1}, i.v.) on the amplitude of reflex bladder contractions under isovolumetric conditions in the urethane-anaesthetized intact (●) and chronic spinal (▲) rats. Abscissa scale: the cumulative dose of LY274614 (mg kg^{-1}, i.v.) plotted on a log scale. Ordinate scale: contraction amplitude as a % of control. Mean ± s.e.mean is plotted for each point. Data in the intact rat ($n = 5$) shows a dose-dependent significant decrease from control. Dose-response curve in the chronic spinal rat ($n = 5$) shows a small but significant increase at doses of 0.3 and 1 mg kg^{-1}. Individual doses are compared to control by paired t test (*$P<0.05$, **$P<0.001$). As a comparison of dose-response curves between the intact and chronic spinal rats at each dose, significant differences were seen at 0.3–30 mg kg^{-1} (0.3–1 mg kg^{-1}, $P<0.05$; 3 mg kg^{-1}, $P<0.01$; 10–30 mg kg^{-1}, $P<0.001$, unpaired t test).

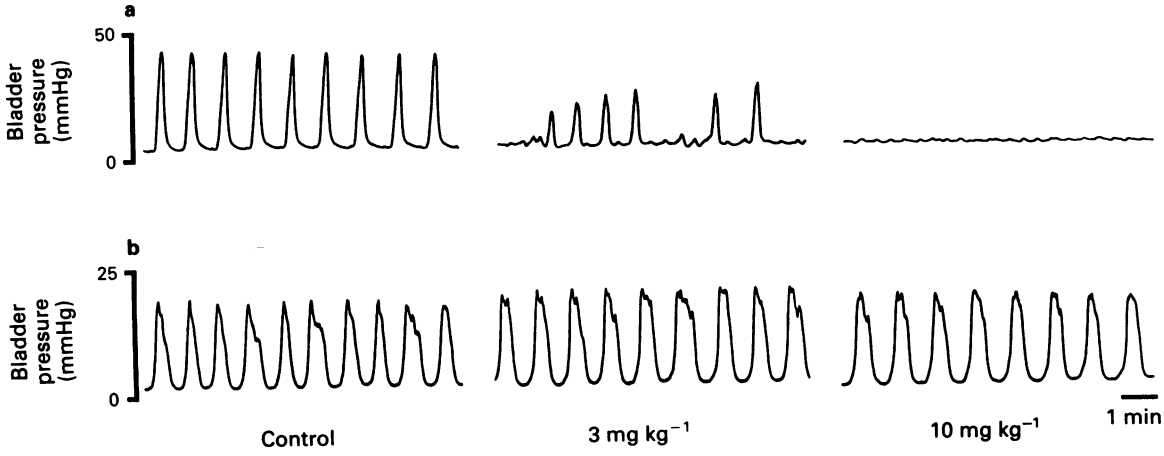

Figure 1 The effects of increasing doses of LY274614 on rhythmic reflex bladder contractions under isovolumetric conditions in the urethane-anaesthetized intact (a) and chronic spinal rats (b). Doses represent total cumulative doses. Note that the amplitude of bladder contractions is reduced by increasing doses of LY274614 (3–10 mg kg^{-1}, i.v.) in the intact rat while a small increase is seen in the chronic spinal rat. The spinal cord was sectioned at the level of T_6–T_8, 3 weeks prior to the experiment.

instead of saline), fine (76 μm) wire EMG electrodes were placed percutaneously in the external urethreal sphincter to record the electrical activity of the striated muscle. A 30 gauge needle with a hooked EMG electrode positioned at the tip was inserted into sphincter approximately 5–10 mm lateral to the urethra and then withdrawn leaving the EMG wires embedded in the muscle (Kruse *et al.*, 1990). The EMG activity obtained was passed through a ratemeter and recorded on chart recorder. The peak firing rate during each micturition contraction was measured.

Acetic acid (0.1%) infusion into the bladder

Acetic acid infused into the bladder was used as a model for bladder irritation (Birder & de Groat, 1992). In 12 experiments, 0.1% acetic acid (pH = 3.5) was infused into the bladder, after recording control bladder contractions induced by normal saline infusion. Control bladder activity during chemical irritation was analyzed 0.5–2.5 h after beginning acetic acid infusion, to allow time for the bladder contractions to stabilize.

Evaluation and statistical analysis

The effects of cumulative doses of LY274614, LY233536 or LY235723 injected at approximately 15 min intervals on the amplitude, duration and frequency of reflex bladder contractions were recorded under isovolumetric conditions with the urethra closed or with it open to allow the bladder to empty. The interval between two voiding cycles, termed the intercontraction interval (Maggi *et al.*, 1986), was also measured during continuous cystometry. During single cystometry, each dose of LY274614 was given 20 min prior to the first test. Two to four records were obtained after each dose. The effects of the drug on volume threshold (V_T) to induce micturition and the volume of fluid released (voided volume; V_V) during each voiding reflex was measured. Based on this value, voiding efficiency (%) ($V_E = 100\ V_V(V_T)^{-1}$) could be estimated. All values are expressed as mean ± s.e.mean. Repeated measures analysis of variance (ANOVA) and Student's *t* test were used when appropriate for statistical data analysis. For all statistical tests, $P<0.05$ was considered significant. The ED_{50} values were calculated from the dose-response curves.

Drugs

Drugs used in these studies included urethane (ethyl carbamate, Sigma), halothane (Ayerst Lab. Inc.), LY274614 ((±)-decahydro-6-(phosphonomethyl)-3-isoquinolinecarboxylic acid), LY233536 ((±)-decahydro-6-(2H-tetrazol-5-ylmethyl)-3-isoquinolinecarboxylic acid) and LY235723 ([cis-(−)]-4-(2H-tetrazol-5-ylmethyl)-2-piperidinecarboxylic acid) (Lilly Res. Lab.). LY274614 was dissolved in a few drops of 1*N* sodium hydroxide and physiological saline for i.v. administration and in artificial CSF (Merlis, 1940; Feldberg & Fleischhauer, 1960) for i.t. injection. LY233536 and LY235723 were dissolved in physiological saline for i.v. administration. Drugs doses were calculated for the salts of each compound.

Results

The effects of LY274614 on bladder reflexes were studied in four different preparations: (1) animals with an intact

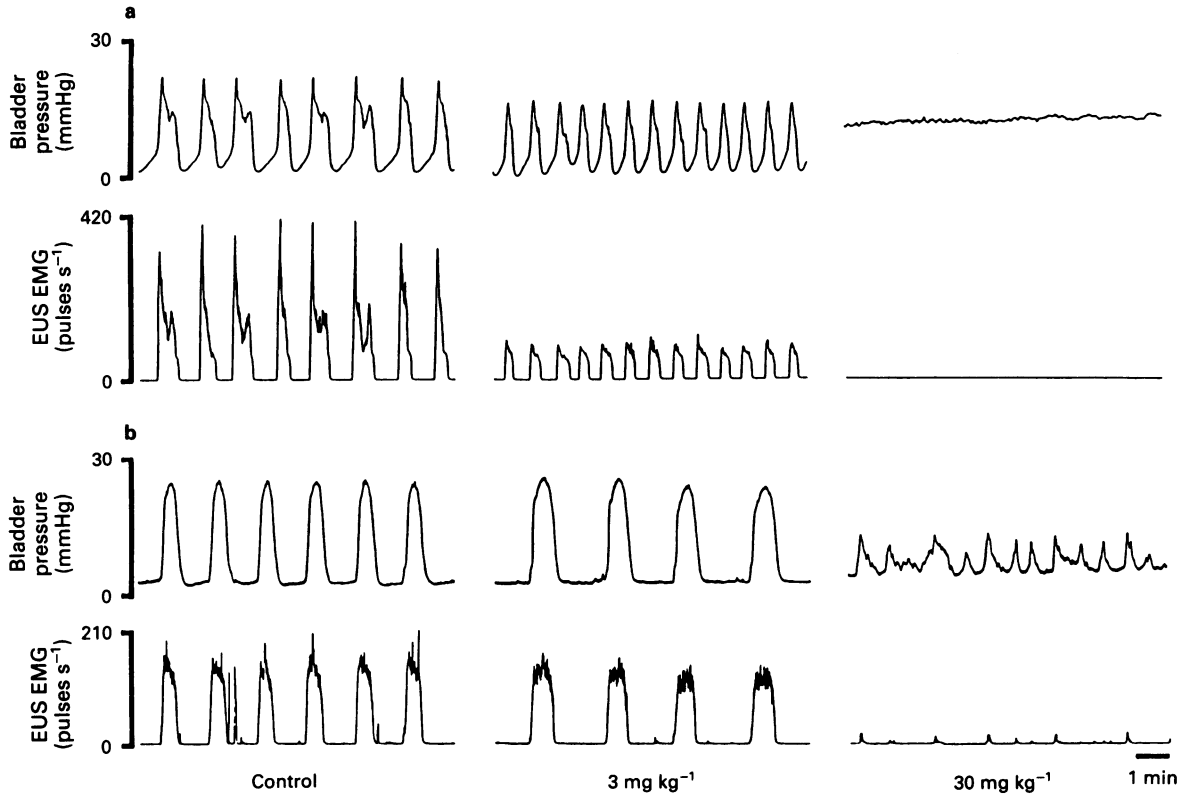

Figure 3 The effects of increasing doses of LY274614 on continuous filling (0.21 ml min^{-1}) cystometry and EMG of the external urethral sphincter muscle in urethane-anaesthetized intact (a) and chronic spinal (b) rats. Doses represent total cumulative doses. Note that the amplitude of micturition contractions and sphincter EMG activity are reduced by increasing doses of LY274614 (3–30 mg kg^{-1}, i.v.) both in the intact and chronic spinal rats. Some bladder and sphincter EMG activity in the chronic spinal rat remained even at the largest dose 30 mg kg^{-1} while those in the intact rat are completely abolished at this dose. Data in the intact rat at 30 mg kg^{-1} show a bladder inhibition with a higher baseline intravesical pressure. The reduction in amplitude of micturition contractions in the chronic spinal animal is probably due to inhibition of external urethral sphincter activity (see Discussion). EUS = external urethral sphincter.

neuraxis (intact) and (2) chronic spinal animals in which the i.v. route of administration was used, (3) intact animals in which drugs were administered intrathecally (i.t.) and (4) intact rats during bladder irritation produced by infusion of 0.1% acetic acid into the bladder. Six parameters of bladder activity were measured: peak amplitude of intravesical pressure, duration and frequency of bladder contractions, intercontraction interval (interval between voids during continuous cystometry), volume threshold for inducing micturition (V_T or bladder capacity) and voided volume (V_V). Based on V_T and V_V, voiding efficiency as percentage of bladder volume ($V_E = 100V_V (V_T)^{-1}$) was estimated. In some experiments the external urethral sphincter EMG activity was also recorded while recording micturition reflexes.

Intact rats

Bladder activity recorded under constant volume conditions ($n = 5$) consisted of rhythmic contractions occurring at peak amplitudes of 27–45 mmHg (mean = 33 mmHg), frequencies of 0.30–0.98 min^{-1} (mean = 0.69 min^{-1}) and durations of 32–43 s (mean = 38 s). The amplitude of bladder contractions was decreased or inhibited completely following the administration of increasing doses of LY274614 (Figure 1a). As shown in the dose-response curve in Figure 2, a significant decrease in amplitude of bladder contractions was seen at doses between 3–30 mg kg^{-1} with an ED_{50} of 2.3 mg kg^{-1}. LY274614 in doses of 0.1–30 mg kg^{-1} did not affect either frequency or duration of bladder contractions.

In 12 animals, urinary bladder contractions recorded during a continuous transurethral infusion (0.21 ml min^{-1}) of saline exhibited peak pressures ranging from 16–107 mmHg (mean = 50 mmHg), duration of 25–198 s (mean = 68 s) and intercontraction interval of 10–302 s (mean = 118 s). The amplitude of micturition contractions was reduced in a dose-dependent manner following the administration of increasing doses of LY274614 (3–30 mg kg^{-1}, i.v.; Figures 3a and 4a) with an ED_{50} of 12.2 mg kg^{-1}. Although changes in intercontraction interval and duration of micturition contractions were seen in some experiments, these changes were not consistent or statistically significant ($n = 12$). In 3 of 12 animals, 30 mg kg^{-1} or higher doses did not completely abolish the rhythmic bladder activity but these doses did reduce amplitude to 48% of control (range: 26–86% of control). In 5 of 9 animals following complete inhibition of rhythmic bladder contractions, baseline bladder pressure was higher than control levels (range: 10–23 mmHg, above control baseline mean = 16 mmHg) (Figure 3a). Sphincter EMG recorded simultaneously with bladder reflex activity was also reduced in a dose-dependent fashion by LY274614 (0.1–30 mg kg^{-1}, $n = 5$) with an ED_{50} of 3.5 mg kg^{-1} (Figures 3a and 4b).

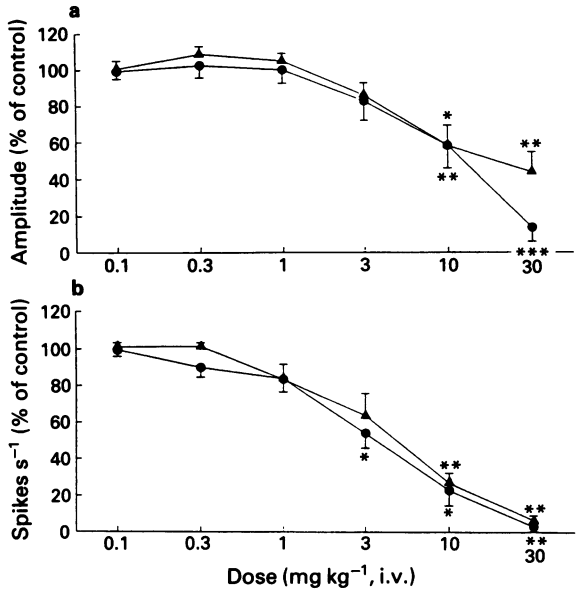

Figure 4 Log dose-response curves showing the effects of increasing doses of LY274614 (0.1–30 mg kg^{-1}, i.v.) on the amplitude of micturition contractions (a) and sphincter EMG (b), during continuous filling (0.21 ml min^{-1}) cystometry in the urethane-anaesthetized intact (●) and chronic spinal (▲) rats. Abscissa scale: the cumulative dose of LY274614 (mg kg^{-1}, i.v.) plotted on a log scale. Ordinate scale: contraction amplitude (a) or peak firing of EMG in spikes s^{-1} (b) as a % of control. Mean ± s.e.mean is plotted for each point. Dose-response curves for amplitude of micturition contractions or sphincter EMG both in the intact ($n = 12$, cystometrograms; $n = 5$, EMG) and chronic spinal ($n = 6$, cystometrograms; $n = 5$, EMG) rats show a significant decrease. Individual doses are compared to control by paired t test (*$P<0.05$, **$P<0.01$, ***$P<0.001$). No significant difference between the pairs of dose-response curves was revealed by two-way repeated measures ANOVA in either (a) or (b).

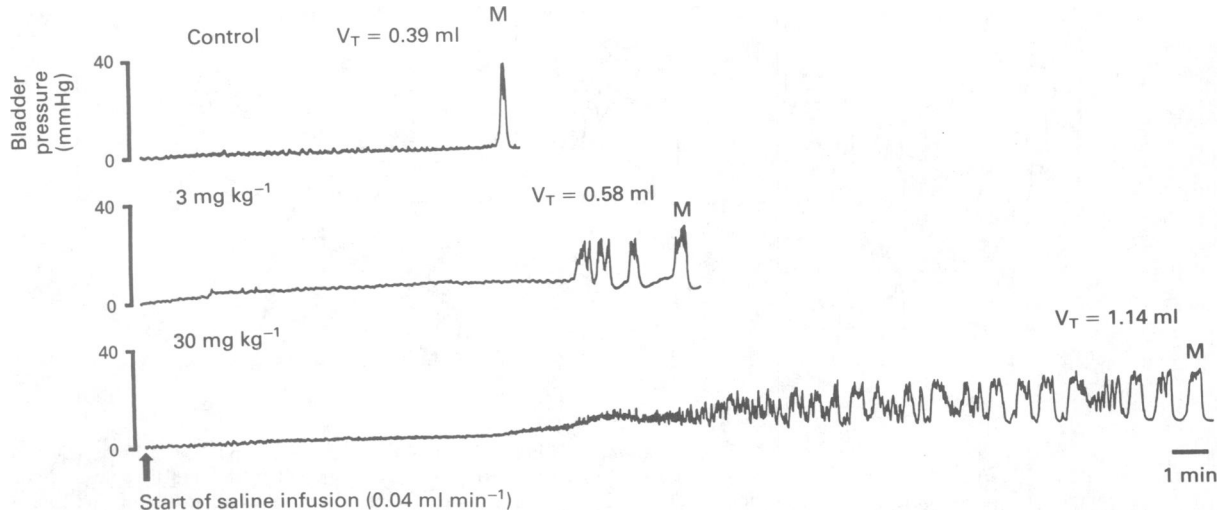

Figure 5 The effects of increasing doses of LY274614 during single filling (0.04 ml min^{-1}) cystometry in the urethane-anaesthetized intact rat. Doses represent total cumulative doses. Note that the interval from the start of saline infusion to the point where micturition occurs was prolonged by increasing doses of LY274614 (3–30 mg kg^{-1}, i.v.). Amplitude of micturition contractions was also reduced by LY274614. M = micturition. V_T = volume threshold.

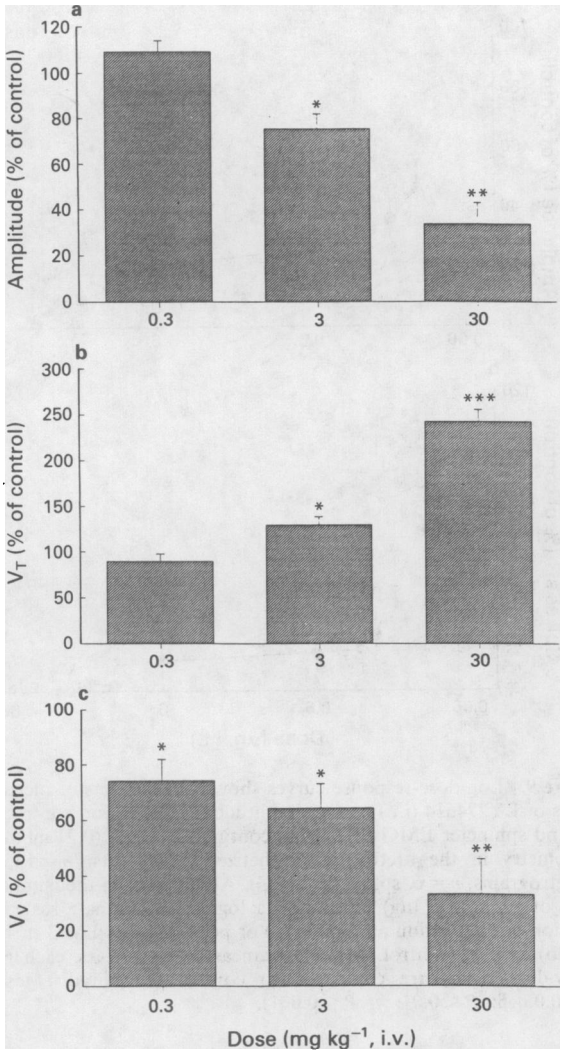

Figure 6 (a) The effect of LY274614 on the amplitude of micturition contraction during single filling (0.04 ml min^{-1}) cystometry in the urethane-anaesthetized intact rats ($n = 5$). LY274614 (0.3–30 mg kg^{-1}, i.v.) decreases the amplitude in a dose-dependent manner similar to the result during continuous filling (0.21 ml min^{-1}) cystometry (Figure 4). There is no statistical difference at each dose between continuous and single cystometry. (b) LY274614 increases V_T (volume threshold) in a dose-dependent manner. (c) LY274614 decreases V_V (voided volume) in a dose-dependent manner. Mean ± s.e.mean is indicated for each column. Individual doses are compared to control by paired t test (*$P<0.05$, **$P<0.01$, ***$P<0.001$).

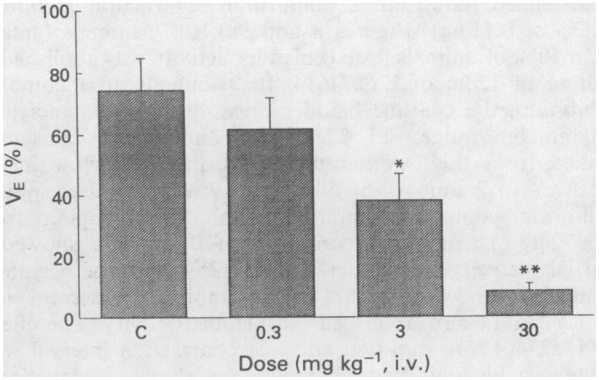

Figure 7 The depressant effect of increasing doses of LY274614 (0.3–30 mg kg^{-1}, i.v.) on the efficiency of voiding during single filling (0.04 ml min^{-1}) cystometry in the urethane-anaesthetized intact rats ($n = 5$). Voiding efficiency (V_E, %) is defined as 100 V_V $(V_T)^{-1}$. Abscissa scale: the dose of LY274614 (mg kg^{-1}, i.v.). Ordinate scale: voiding efficiency (%). Mean ± s.e.mean is plotted for each column. Individual doses are compared to control by paired t test (*$P<0.05$, **$P<0.01$). C = control.

In 5 animals, urinary bladder activity was recorded during cystometry performed using a slower rate of transurethral infusion (0.04 ml min^{-1}) which more closely approximated the rate of urine formation (Sillen, 1980). The bladder was emptied at the end of each cystometrogram. The peak amplitudes of micturition contractions ranged from 26–40 mmHg (mean = 33 mmHg) and durations between 25–45 s (mean = 34 s). These parameters were not significantly different from the measurements obtained during continuous cystometry. LY274614 produced a dose-dependent decrease in the amplitude of micturition contractions (Figures 5 and 6a) similar to the effect during continuous cystometry (Figure 4a). Figure 5 shows that with increasing doses of LY274614 the volume of saline (bladder capacity or volume threshold) to produce a micturition contraction was increased 1.5 and 3 times control levels with 3 and 30 mg kg^{-1} of LY274614, respectively. In addition, as the bladder began to fill, small bladder contractions which did not produce a void were seen prior to micturition (Figure 5). Control V_T and V_V were 0.36–0.60 ml (mean = 0.41 ml) and 0.13–0.53 ml (mean = 0.31 ml), respectively, with a V_E of 74%. Increasing doses of LY274614 increased V_T (Figure 6b) and reduced V_V (Figure 6c). V_E was reduced to 11% of control at the maximal dose of LY274614 (Figure 7).

Chronic spinal rats

In 5 chronic spinal animals, bladder activity recorded under constant volume conditions consisted of rhythmic contractions occurring at peak amplitudes of 10–23 mmHg (mean = 16 mmHg), frequencies of 0.71–1.14 min^{-1} (mean = 0.96 min^{-1}) and durations of 33–41 s (mean = 37 s). As shown in Figure 1b, LY274614, at doses of 0.3 and 1 mg kg^{-1}in this preparation slightly but significantly increased the amplitude of bladder contractions (Figure 2), while the effects of larger doses were not significantly different from control. Doses of LY274614 (0.1–30 mg kg^{-1} i.v.) had no effect on frequency or duration of bladder contractions.

In 6 chronic spinal animals, micturition contractions recorded during a continuous transurethral infusion (0.21 ml min^{-1}) of saline exhibited peak pressures ranging from 10–42 mmHg (mean = 18 mmHg), durations of 24–46 s (mean = 31 s) and intercontraction intervals of 8–42 s (mean = 18 s). Increasing doses of LY274614 (0.1–30 mg kg^{-1}, i.v.) reduced the amplitude of the micturition contractions (Figure 3b). A significant decrease was seen at doses of 10 and 30 mg kg^{-1} of LY274614 (Figure 4a) with an ED_{50} of 18.5 mg kg^{-1}. Durations and intercontraction intervals were not affected by LY274614. Following the 30 mg kg^{-1} dose of LY274614 bladder activity was depressed for the remainder of the experiment (2–8 h). In 5 animals in which sphincter EMG was recorded during cystometry, LY274614 significantly decreased sphincter activity with an ED_{50} of 4.7 mg kg^{-1} (Figures 3b and 4b).

Intact rats: i.t. administration of LY274614

In 13 animals with an intrathecal catheter, voiding reflexes induced by a continuous infusion of saline (0.21 ml min^{-1}) had peak intravesical pressures of 21–127 mmHg (mean = 58 mmHg), intercontraction intervals of 25–317 s (mean = 106 s) and durations of 22–287 s (mean = 92 s). An i.t. administration of LY274614 (0.06–30 μg) produced a

dose-related reduction in micturition contraction amplitude (ED_{50} of 0.11 μg) (Figures 8 and 9a). In 7 animals (greater than 50% of animals tested) bladder activity was abolished at a dose of 12 μg of LY274614. In 9 animals after complete inhibition, the baseline bladder pressure markedly increased (20 mmHg; range: 15–27 mmHg) and saline constantly leaked from the external urethral orifice (overflow incontinence). In 7 animals, bladder activity was measured 5–18 h following complete inhibition with doses ranging from 12–72 μg. During this period, 5 of 7 animals showed a partial recovery of bladder activity (35–141% of beginning control, mean = 71%). In 4 of these animals, a second dose of LY274614 also abolished the bladder activity. The effects of LY274614 on duration and intercontraction interval were quite variable and although a few doses showed a statistically significant decrease, the effects were not dose-dependent. Sphincter EMG recorded simultaneously with bladder reflex activity was also reduced in a dose-dependent fashion by LY274614 (0.06–30 μg, n = 8) (Figures 8 and 9b). A statistically significant reduction in the EMG activity was noted at a dose of 0.12 μg (64.0% of control) with an ED_{50} of 0.16 μg.

Time course of LY274614 effects on amplitude of micturition contractions measured during continuous cystometry

The durartion of bladder inhibition produced by LY274614 was studied following both i.v. and i.t. administration of the drug. During continuous cystometry, a single dose (30 mg kg^{-1}, i.v., $n = 5$ or 6 μg i.t., $n = 5$) of LY274614 was given to each animal and time course of recovery recorded for up to 10 h following drug administration. Figure 10 shows the time course (up to 6 h) of recovery. Some recovery was seen at 2.5 to 3 h following LY274614. In 2 animals following i.v. and in 3 animals following i.t. administration, the amplitude of the micturition contractions had not recovered to control levels for up to 10 h following administration.

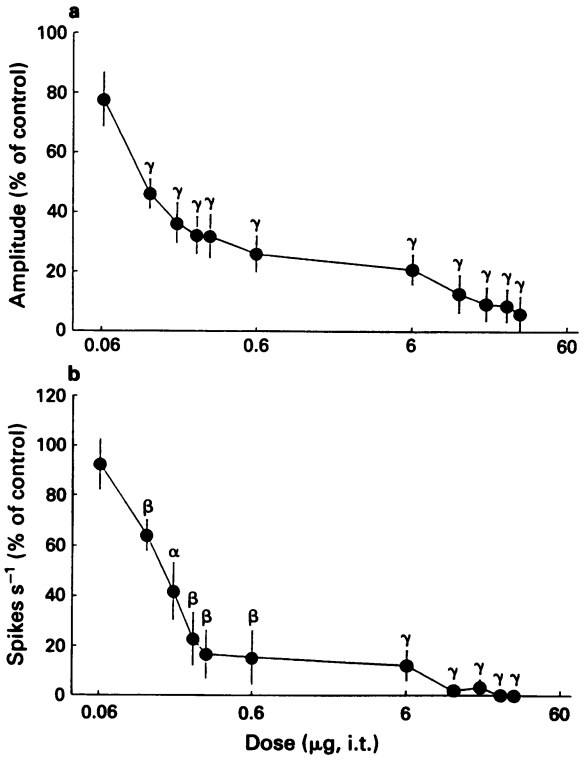

Figure 9 Log dose-response curves showing the effects of increasing doses of LY274614 (i.t.) on the amplitude of micturition contractions (a) and sphincter EMG (b) during continuous filling (0.21 ml min^{-1}) cystometry in the urethane-anaesthetized intact rats ($n = 13$, cystometrograms; $n = 6$, sphincter EMG). Abscissa scale: the cumulative dose of LY274614 (μg) plotted on a log scale. Ordinate scale: contraction of micturition amplitude (a) or peak firing of EMG in spikes s^{-1} (b) as a % control. Mean ± s.e.mean is plotted for each point. Individual doses are compared to control by paired t test (α: $P<0.05$, β: $P<0.01$, γ: $P<0.001$).

Influence of bladder irritation with acetic acid (0.1%) on the effects of LY274614 (i.v.)

Since drugs that suppress the micturition reflex might be used clinically to diminish bladder hyperactivity induced by neurological disorders, a series of experiments was conducted to examine the effect of LY274614 on bladder hyperactivity induced by chemical irritation. In 12 animals, urinary bladder activity was recorded during a continuous transurethral infusion (0.21 ml min^{-1}). Control micturition contractions induced by saline infusion occurred at peak amplitudes of 21–78 mmHg, intercontraction intervals of 35–271 s and durations of 27–86 s (Table 1). Following a control period of 30 min with saline infusion, the infusion solution was switched to 0.1% acetic acid, which had little effect on the amplitude (32–69 mmHg) or duration (25–56 s) of micturition contractions but significantly decreased intercontraction interval (9–83 s) (Table 1). In these animals the amplitude of micturition contractions ($n = 12$) and sphincter EMG activity ($n = 5$) were reduced following the administration of increasing doses of LY274614 (0.1–30 mg kg^{-1} i.v.: Figure 11). The ED_{50}s for these effects were 24.3 mg kg^{-1} and 16.6 mg kg^{-1}, respectively. Although reduction in amplitude of micturition contractions seemed to require a larger dose of LY274614 in the acetic acid-infused bladder (Figure 11a), this effect was

Figure 8 The effects of increasing doses of LY274614 administered by i.t. injection on continuous filling (0.21 ml min^{-1}) cystometry and sphincter EMG in the urethane-anaesthetized intact rat. Doses represent total cumulative doses. Drug injections were made subdurally at the L_6–S_1 level of spinal cord. Note the decrease in the amplitude of the micturition contractions and the sphincter EMG activity following LY274614 (0.12–18 μg). EUS = external urethral sphincter.

Table 1 The effects of acetic acid (0.1%) continuous filling infusion (0.21 ml min^{-1}) to the bladder

Continuous filling cystometrogram	*Amplitude (mmHg)*	*Intercontraction interval* (s)*	*Duration (s)*
Saline	53 ± 5	95 ± 20	41 ± 6
Acetic acid	52 ± 3	27 ± 6	40 ± 3

*Significant difference between 'saline' and 'acetic acid' ($P<0.01$, paired t test). Only the intercontraction interval was changed by acetic acid continuous infusion to the bladder but not the amplitude and duration of micturition contractions. All values are expressed as mean ± s.e.mean ($n = 12$).

not statistically significant (two-way repeated measures ANOVA) from saline infusion. Reduction in sphincter EMG did, however, require a larger dose of LY274614 in the acetic acid infused bladder as compared to saline-infused preparations (Figure 11b). A significant reduction in sphincter EMG was only detected at a dose of 30 mg kg^{-1} (23.2% of control); and a significant difference from the control experiment with saline infusion occurred at 10 mg kg^{-1} (two-way repeated measures ANOVA followed by unpaired t test, $P<0.05$). A significant decrease in duration of micturition contractions was seen at 10 and 30 mg kg^{-1} for acetic acid-infused bladder.

Effects of LY233536 and LY235723 on continuous filling cystometry

Two other competitive NMDA receptor antagonists were studied on micturition reflexes. LY233536 is related chemically to LY274614, while LY235723 is chemically distinct. Both compounds (1–100 mg kg^{-1}, i.v. of LY233536, $n = 5$ or LY235723, $n = 6$) decreased the amplitude of micturition contractions in a dose-dependent manner when studied with continuous cystometry. Micturition contractions were completely inhibited by LY233536 or LY235723 at 100 mg kg^{-1} with ED_{50}s of 18 or 20 mg kg^{-1}, respectively. A significant decrease in amplitude occurred at doses of 10 mg kg^{-1} and larger of LY235723, and 30 mg kg^{-1} and larger of LY233536. These drugs did not change durations or intercontraction intervals with the exception of an increase of these intervals by LY235723 at doses of 1 mg kg^{-1} ($P<0.05$, paired t test) and 3 mg kg^{-1} ($P<0.01$, paired t test).

Discussion

The results of the present study indicate that LY274614, LY233536 and LY235723, competitive NMDA receptor antagonists that enter the central nervous system (CNS) following systemic administration, can inhibit bladder and external urethral sphincter reflexes in the urethane-anaesthetized rat. The site of these inhibitory effects is, at least in part, at the level of the lumbosacral spinal cord and dependent on an intact descending pathway from supraspinal sites. These data support the conclusions that emerged from previous studies with the non-competitive NMDA receptor antagonist, MK-801, that CNS glutamatergic mechanisms involving NMDA receptors are important in modulating bladder and sphincter activities.

Although the block of the micturition reflex produced by MK-801 is at the cationic channel associated with the NMDA receptor complex (Foster & Fagg, 1987) while LY274614, LY233536 and LY235723 block at the recognition site for NMDA, the effects of the drugs are qualitatively similar in most respects. Both LY274614 and MK-801 inhibit bladder and sphincter reflexes when administered either intravenously (i.v.) or intrathecally (i.t.). MK-801 is however more potent (ED_{50} = 0.36 mg kg^{-1}) than LY274614 (ED_{50} = 12.2 mg kg^{-1}) on i.v. administration but LY274614 is more potent on i.t. administration (ED_{50} of MK-801 = 17 μg; of LY274614 = 0.11 μg) (Yoshiyama *et al.*, 1993). LY274614 has a slightly

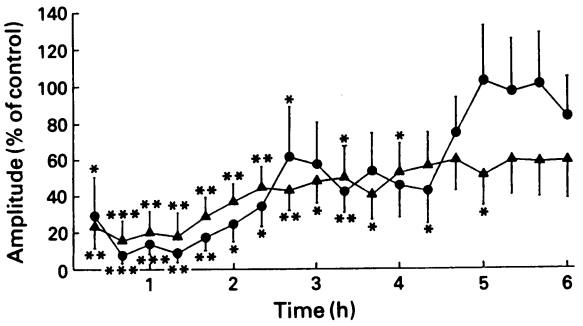

Figure 10 Graph showing the time course of the effect of LY274614 (30 mg kg^{-1} i.v., ●, $n = 6$ and 6 μg i.t., ▲, $n = 6$) on the amplitude of micturition contractions during continuous filling (0.21 ml min^{-1}) cystometry in the urethane-anaesthetized intact rats. Abscissa scale: time scale (h) since LY274614 was administered. Ordinate scale: contraction amplitude as a % of control. Mean ± s.e.mean is plotted for each point. Individual points are compared to control by paired t test (*$P<0.05$, **$P<0.01$, ***$P<0.001$). A comparison between the i.v. and i.t. administration at each period, showed no significant difference up to 6 h. Note that some recovery from LY274614 was seen 2.5 to 3 h after injection but complete recovery was not seen in all animals even 6 h after LY274614.

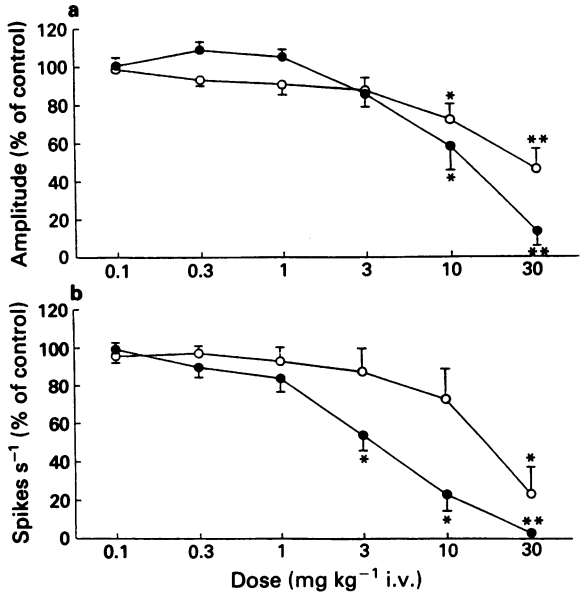

Figure 11 Log dose-response curves showing the effects of increasing doses of LY274614 (i.v.) on the amplitude of micturition contraction (a) and sphincter EMG (b) during continuous filling (0.21 ml min^{-1}) cystometry with either saline (●) or 0.1% acetic acid (○) in intact rats. Abscissa scale: the cumulative dose of LY274614 (mg kg^{-1}, i.v.) plotted on a log scale. Ordinate scale: contraction amplitude (a) or ratemeter output of EMG in spikes s^{-1} as a % control (b). Mean ± s.e.mean is plotted for each point. Dose-response curves both with saline ($n = 12$, cystometrograms; $n = 5$, sphincter EMG) and acetic acid ($n = 12$, cystometrograms; $n = 5$, sphincter EMG) infusion show a statistically significant decrease in amplitude and sphincter EMG peak firing. Individual doses are compared to control by paired t test (*$P<0.01$, **$P<0.001$). There is no significant difference between pairs of dose-response curves with saline or acetic acid infusion in (a) although a significant difference is seen in (b) at a dose of 10 mg kg^{-1} (two-way repeated measured ANOVA followed by unpaired t test, $P<0.05$).

longer time for onset than MK-801 (4–6 min compared to 1–2 min). These differences are consistent with the poorer penetration of LY274614 across the blood-brain barrier and the greater affinity of LY274614 for its binding to the NMDA receptor complex (personal communications with Drs Ornstein & Schoepp), in comparison to MK-801. Similar differences in effective doses of MK-801 and LY274614 were seen by other investigators examining the effects of these NMDA antagonists on pain pathways (Elliott *et al.*, 1991) and on neurotoxic effects of excitatory amino acids and amphetamine (Fuller *et al.*, 1992).

One other qualitative difference between these two drugs was the elevated bladder tone following complete inhibition of bladder contractions with LY274614, seen when bladder reflexes were studied during continuous cystometry. The baseline bladder pressure was high (average 20 mmHg) with LY274614 (i.v. and i.t.), but this was rarely seen with MK-801. Overflow incontinence occurred with both drugs following inhibition of bladder contractions but only with LY274614 was an elevated resting pressure observed. The magnitude of the pressure recorded in the bladder during continuous infusion cystometry depends on two factors, the contractile force of the bladder and the pressure at which the striated and smooth muscle sphincters relax (outlet resistance). Since both LY274614 and MK-801 inhibit micturition contractions, the increase in baseline pressure seen following LY274614 is probably due to some residual urethral resistance reducing flow through the urethra. The exact mechanism of this high resting tone is not known but may represent some differential action of the two drugs on either urethral smooth or striated muscle sphincter activity. Although the mechanism of this elevated bladder pressure was not investigated in the present study one might speculate from *in vitro* data, which shows that MK-801 blocks nicotinic channels in cultured striated muscle cells (Amador & Dani, 1991), that MK-801 may produce a more effective relaxation of external urethral sphincter than LY274614. An alternative explanation would be that MK-801 is more effective in producing relaxation of the smooth muscle of the urethra.

The site of action of LY274614 within the CNS appears to be similar to that proposed for MK-801 (Yoshiyama *et al.*, 1993). Since an i.t. administration of LY274614 or MK-801 at the level of L_6–S_1 spinal cord inhibited bladder and sphincter activity, a spinal site of action is likely. However, the absence of an effect of LY274614 or MK-801 (Yoshiyama *et al.*, 1993) on bladder contractions in chronic spinal animals studied under isovolumetric conditions would suggest that an intact descending pathway from the pontine micturition centre is necessary for the action of the drugs. However, a decrease in sphincter activity with LY274614 or MK-801 was seen both in animals with an intact spinal cord and in chronic spinal cord transected animals; suggesting that NMDA receptor mechanisms are important for both the spinal and supraspinal control of external urethral sphincter activity. It should be noted, however, that LY274614 did partially reduce the amplitude of the micturition contractions in chronic spinal animals when using continuous cystometry with the urethral outlet open. This effect is probably produced by decreased outlet resistance rather than a decrease in bladder contractility since with continuous cystometry, bladder pressure begins to decrease as soon as the urethral outlet relaxes and voiding begins. Furthermore, LY274614, even in very large doses ($> 30\ mg\ kg^{-1}$), produced no decrease in reflex bladder contractions in a group of animals studied with closed bladder outlets (ligated) and at constant bladder volume. In these animals, changes in outlet resistance could not modify bladder pressure since a ligature separates the bladder from the urethra. It is, therefore, concluded that reflex bladder contractions are not reduced by LY274614 in chronic spinal animals.

The lack of effect on bladder contractions in chronic spinal animals with both LY274614 and MK-801 would suggest that neural elements in the spinal bladder reflex pathway including bladder afferent neurones, interneurones and preganglionic efferent neurones do not utilize a glutamatergic NMDA receptor mechanism. On the other hand i.t. administration of very small doses of LY274614 to animals with an intact spinal cord inhibited bladder activity, indicating that the descending limb of the spinobulbospinal micturition reflex pathway (de Groat *et al.*, 1992) may utilize glutamate as a transmitter and must be intact for LY274614 to be effective. However, since the drugs do depress sphincter activity in chronic spinal animals, NMDA receptor-related glutamatergic mechanisms must be involved in the spinal reflex pathway controlling sphincter function. In intact animals, the sphincter activity is suppressed at a lower dose ($ED_{50} = 3.5\ mg\ kg^{-1}$) than bladder activity ($ED_{50} = 12.2\ mg\ kg^{-1}$), which suggests that the drug affects bladder and sphincter by different mechanisms. NMDA receptors in the spinal cord are prominent in the vicinity of the motoneurones which control sphincter, and around the central canal and in the intermediolateral gray (Jansen *et al.*, 1990; Shaw *et al.*, 1991). The latter regions of the cord contain bladder preganglionic neurones or interneurones which are involved in lower urinary tract function (de Groat *et al.*, 1992), and thus are likely to be one site of action of the NMDA antagonists.

Although the present study suggests a spinal site of action for LY274614, an effect on supraspinal pathways is also possible. A supraspinal site of action is supported by receptor binding studies which show that NMDA receptors are present in the brainstem near the pontine micturition centre (Monagham & Cotman, 1985). Further support for a supraspinal site of action is provided by studies from this and other laboratories which examined the effects of neuromodulators at the level of the pontine micturition centre (Lumb & Morrison, 1987; Willette *et al.*, 1988; Mallory *et al.*, 1991). In these studies glutamate was an effective agent in modulating micturition reflexes producing a reduction in V_T when injected directly into the pontine micturition centre. LY274614, much like MK-801 (Yoshiyama *et al.*, 1993), increased the V_T and decreased the V_V when given i.v. and tested using cystometry. The ED_{50} for LY271614 in these experiments is about 30 times that for MK-801: suggesting that LY274614 is less potent than MK-801.

The duration of action of LY274614 following either i.v. or i.t. was long, requiring approximately 4 h for a 50% recovery. These results are consistent with those reported by other laboratories which have evaluated different pharmacological effects of LY274614 (Schoepp *et al.*, 1991; Fuller *et al.*, 1992). We therefore were able to use, in the majority of our studies, cumulative doses of LY274614 given at 15 min intervals with complete dose-response curves usually requiring less than 90 min. This approach could be used since there was no evidence for rapid tolerance development to repeated i.v. administration of LY274614. Following partial or total recovery from LY274614, a second dose of the drug produced the same magnitude of response as seen with the first dose.

The effects of LY274614 on bladder hyperactivity due to bladder irritation was also examined in the present study. Bladder irritation was produced by substituting 0.1% acetic acid for normal saline during a continuous cystometry. In the irritated bladder model, LY274614 reduced the amplitude of micturition contractions and sphincter EMG activity with the dose-response curve for sphincter EMG showing a small shift to the right. The typical effect of LY274614 in reducing bladder and sphincter activity occurred at a slightly higher dose for sphincter EMG activity when the bladder was irritated with acetic acid. The major effect produced by acetic acid was to decrease the intercontraction interval (increase in frequency), and this effect of irritation was not reduced by LY274614. This latter result would be in agreement with our conclusions that neither LY274614 nor MK-801 (Yoshiyama *et al.*, 1993) have any effect on the afferent limb of the micturition reflex or on nociceptive afferents that modulate the reflex. These findings are also consistent with the effects of MK-801 on increased expression of the immediate early gene, c-*fos*, in spinal neurones induced by stimulation of bladder afferents. MK-801

in doses that blocked the micturition reflex did not alter c-*fos* expression elicited by non-noxious distension of the bladder of the rat (Birder & de Groat, 1993). Large doses of MK-801 did reduce by 50% the increased c-*fos* expression induced by chemical irritation of the bladder (Birder & de Groat, 1992). However, this effect was remarkably reduced in spinal transected animals, suggesting that the effect of MK-801 was dependent upon the integrity of supraspinal pathways and was not mediated by direct actions on spinal nociceptive mechanisms.

Although the pharmacology and possible sites of action of LY274614 were the primary focus of this study, two additional competitive NMDA receptor antagonists were examined for their effects on micturition reflexes. LY233536 is chemically similar to LY274614 except that the phosphonic acid moiety is replaced with a tetrazole group, while LY235723 is the (−)-isomer of LY233053, a 4-tetrazolylalkyl substituted piperidine-2-carboxylic acids with competitive NMDA antagonist activity (Schoepp *et al.*, 1990; Ornstein *et al.*, 1991; 1992a,b; Zimmerman *et al.*, 1992). Both LY233536 and LY235723 produced effects, qualitatively similar to those of LY274614 and MK-801, but were less potent in reducing micturition bladder contractions. The reduced potency of these compounds is in agreement with lower NMDA receptor affinity *in vitro* and lower *in vivo* and *in vitro* antagonist activity reported by others (Ornstein *et al.*, 1991). The fact that a variety of compounds which possess a high affinity for NMDA receptors *in vitro* produce profound effects on micturition reflexes, provides a strong support for the idea that glutamatergic mechanisms are important in modulating reflex micturition.

In summary, these experiments suggest that glutamic acid is an important neurotransmitter in the micturition reflex pathway of the rat. This substance acts via NMDA receptors in the lumbosacral spinal cord when descending pathways from the brainstem to the cord are intact. On the other hand, in chronic paraplegic rats when the descending pathways are eliminated, NMDA receptor mediated glutamatergic transmission is not essential for the generation of spinal micturition reflexes. The inhibitory effects of LY274614 on external urethral sphincter, however, still occurred after chronic spinalization; indicating that glutamate is a transmitter in the spinal reflex pathways controlling the urethral sphincter. LY274614 is a long acting NMDA antagonist and may be potentially useful in the treatment of neurogenic bladder hyperactivity. It has the advantage over MK-801 of having fewer phencyclidine-like side effects (Rasmussen, 1991; Rasmussen *et al.*, 1991).

This work was supported by a research grant from Eli Lilly and Company and NIH Grants DK37241 (W.D.), DK42369 (W.D.) and NS21137 (J.R.R.). We would like to acknowledge Dr P.L. Ornstein and Dr D.D. Schoepp of the CNS Research Division of Lilly Research Laboratories (Eli Lilly and Company) for their helpful discussions throughout this study and during preparation of this manuscript.

References

AMADOR, M. & DANI, J.A. (1991). MK-801 inhibition of nicotinic acetylcholine receptor channels. *Synapse*, **7**, 207–215.

BIRDER, L.A. & DE GROAT, W.C. (1992). The effect of glutamate antagonists on c-*fos* expression induced in spinal neurons by irritation of the lower urinary tract. *Brain Res.*, **580**, 115–120.

BIRDER, L.A. & DE GROAT, W.C. (1993). Induction of c-*fos* gene expression in spinal neurons of the rat by nociceptive and non-nociceptive stimulation of the lower urinary tract. *Am. J. Physiol.*, (in press).

DE GROAT, W.C., BOOTH, A.M. & YOSHIMURA, N. (1993). Neurophysiology of micturition and its modification in animal models of human disease. Chapter 8. In *The Autonomic Nervous System*, Vol. 3: *Nervous Control of the Urogenital System*. ed. Maggi, C.A. pp. 227–290. London: Harwood Academic Publishers.

ELLIOTT, K.J., CERBONE, D.J., FOLEY, K.M. & INTURRISI, C.E. (1991). NMDA receptor antagonists are antinociceptive in the mouse formalin model during acute and chronic administration. *Soc. Neurosci. Abstr.*, **17**, 588.

FELDBERG, W. & FLEISCHHAUER, K. (1990). Penetration of bromophenol blue from the perfused cerebral ventricles into the brain tissue. *J. Physiol.*, **150**, 451–462.

FOSTER, A.C. & FAGG, G.E. (1987). Taking apart NMDA receptors. *Nature*, **329**, 395–396.

FULLER, R.W., HEMRICK-LUECKE, S.K. & ORNSTEIN, P.L. (1992). Protection against amphetamine-induced neurotoxicity toward striatal dopamine neurons in rodents by LY274614, an excita-tory amino acid antagonist. *Neuropharmacol.*, **31**, 1027–1032.

JANSEN, K.L.R., FAULL, R.L.M., DRAGUNOW, M. & WALDVOGEL, H. (1990). Autoradiographic localization of NMDA, quisqualate kainic acid receptors in human spinal cord. *Neurosci. Lett.*, **108**, 53–57.

KRUSE, M.N., BELTON, A.L. & DE GROAT, W.C. (1993). Changes in bladder and external urethral sphincter function following spinal cord injury in the rat. *Am. J. Physiol.*, (in press).

KRUSE, M.N., NOTO, H., ROPPOLO, J.R. & DE GROAT, W.C. (1990). Pontine control of the urinary bladder and external urethral sphincter in the rat. *Brain Res.*, **532**, 182–190.

LUMB, B.M. & MORRISON, J.F.B. (1987). An excitatory influence of dorsolateral pontine structures on urinary bladder motility in the rat. *Brain Res.*, **435**, 363–366.

MAGGI, C.A., GIULIANI, S., GIACHETTI, A. & MELI, A. (1990). The effect of MK-801 on the micturition reflex in anesthetized rats. *Eur. J. Pharmacol.*, **181**, 105–109.

MAGGI, C.A., SANTICIOLI, P. & MELI, A. (1986). The nonstop transvesical cystometrogram in urethane-anesthetized rats. *J. Pharmacol. Methods*, **15**, 157–167.

MALLORY, B.S., ROPPOLO, J.R. & DE GROAT, W.C. (1991). Pharmacological modulation of the pontine micturition center. *Brain Res.*, **546**, 310–320.

MALLORY, B., STEERS, W.D. & DE GROAT, W.C. (1989). Electrophysiological study of micturition reflexes in rats. *Am. J. Physiol.*, **257**, R410–R421.

MERLIS, J.K. (1940). The effect of changes in the calcium content of the cerebrospinal fluid on spinal reflex activity in the dog. *Am. J. Physiol.*, **131**, 67–72.

MONAGHAN, D.T. & COTMAN, C.W. (1985). Distribution of *N*-methyl-D-aspartate-sensitive L-[^{3}H]glutamate-binding sites in rat brain. *J. Neurosci.*, **5**, 2909–2919.

NISHIZAWA, O., FUKUDA, T., MATSUZAKI, A., MORIYA, I., HARADA, T. & TSUCHIDA, S. (1985). Role of the sympathetic nerve in bladder and urethral sphincter function during the micturition cycle in the dog evaluated by pressure flow EMG study. *J. Urol.*, **134**, 1259–1261.

ORNSTEIN, P.L., ARNOLD, M.B., AUGENSTEIN, N.K., LEANDER, J.D., LODGE, D. & SCHOEPP, D.D. (1991). Characterization of (−)-LY235959, (−)-LY202157 and (−)-LY235723 as the active isomers of the racemic competitive NMDA antagonists LY274614, LY233536 and LY233053, respectively. *Soc. Neurosci. Abstr.*, **17**, 392.

ORNSTEIN, P.L., SCHOEPP, D.D., ARNOLD, M.B., AUGENSTEIN, N.K., LODGE, D., MILLAR, J.D., CHAMBERS, J., CAMPBELL, J., PASCHAL, J.W., ZIMMERMAN, D.M. & LEANDER, J.D. (1992a). 6-Substituted decahydroisoquinoline- 3-carboxylic acids as potent and selective conformationally constrained NMDA receptor antagonists. *J. Med. Chem.*, **35**, 3547–3560.

ORNSTEIN, P.L., SCHOEPP, D.D., ARNOLD, M.B., JONES, N.D., DEETER, J.B., LODGE, D. & LEANDER, J.D. (1992b). NMDA antagonist activity of (±)-(2SR,4RS)-4-(1H-tetrazol-5-ylmethyl) piperidine-2-carboxylic acid resides with the (−)-2R,4S-isomers. *J. Med. Chem.*, **35**, 3111–3115.

RASMUSSEN, K. (1991). Afferent effects on locus coeruleus in opiate withdrawal. *Prog. Brain Res.*, **88**, 207–216.

RASMUSSEN, K., FULLER, R.W., STOCKTON, M.E., PERRY, K.W. SWINFORD, R.M. & ORNSTEIN, P.L. (1991). NMDA receptor antagonists suppress behaviors but not norepinephrine turnover or locus coeruleus unit activity induced by opiate withdrawal. *Eur. J. Pharmacol.*, **197**, 9–16.

SCHOEPP, D.D., ORNSTEIN, P.L., LEANDER, J.D., LODGE, D., SALHOFF, C.R., ZEMAN, S. & ZIMMERMAN, D.M. (1990). Pharmacological characterization of LY233053: a structurally novel tetrazole-substituted competitive N-methyl-D-aspartic acid antagonist with a short duration of action. *J. Pharmacol. Exp. Ther.*, **255**, 1301–1308.

SCHOEPP, D.D., ORNSTEIN, P.L., SALHOFF, C.R. & LEANDER, J.D. (1991). Neuroprotectant effects of LY274614, a structurally novel systemically active competitive NMDA receptor antagonist. *J. Neural. Transm.* (Gen. Sect.), **85**, 131–143.

SHAW, P.J., INCE, P.G., JOHNSON, M., PERRY, E.K. & CANDY, J. (1991). The quantitative autoradiographic distribution of [^{3}H]MK-801 binding sites in the normal human spinal cord. *Brain Res.*, **539**, 164–168.

SILLEN, U. (1980). Central neurotransmitter mechanisms involved in the control of the urinary bladder function. *Scand. J. Urol. Nephrol. Suppl.*, **58**, 1–45.

SUZUKI, T., BIRDER, L.A., YOSHIYAMA, M., ROPPOLO, J.R. & DE GROAT, W.C. (1991). Electrophysiological studies of the effects of glutamate antagonists (MK801 and CNQX) on the micturition reflex in the rat. *Soc. Neurosci. Abstr.*, **17**, 1002.

WILLETTE, R.N., MORRISON, S., SAPRU, H.N. & REISS, D.J. (1988). Stimulation of opiate receptors in the dorsal pontine tegmentum inhibits reflex contraction of the urinary bladder. *J. Pharmacol. Exp. Ther.*, **244**, 403–409.

WONG, E.H.F., KEMP, J.A., PRIESTLEY, T., KNIGHT, A.R., WOODRUFF, G.N. & IVERSEN, L.L. (1986). The anticonvulsant MK-801 is a potent N-methyl-D-aspartate antagonist. *Proc. Natl. Acad. Sci. U.S.A.*, **83**, 7104–7108.

YAKSH, T.L. & RUDY, T.A. (1976). Chronic catheterization of the spinal subarachnoid space. *Physiol. Behav.*, **17**, 1031–1036.

YOSHIYAMA, M., ROPPOLO, J.R. & DE GROAT, W.C.(1991a). The effects of glutamate receptor antagonists on the micturition reflex in the rat. *Soc. Neurosci. Abstr.*, **17**, 1001.

YOSHIYAMA, M., ROPPOLO, J.R. & DE GROAT, W.C. (1993). Effects of MK-801 on the micturition reflex in the rat – possible sites of action. *J. Pharmacol. Exp. Ther.*, **265**, 844–850.

YOSHIYAMA, M., ROPPOLO, J.R., RIHMLAND, J., BLASTOS, B. & DE GROAT, W.C. (1991b). The effects of MK-801, an NMDA receptor antagonist, on the micturition reflex in the rat. *Neurosci. Lett.*, **126**, 141–144.

YOSHIYAMA, M., ROPPOLO, J.R., THOR. K.B. & DE GROAT, W.C. (1992). The effects of LY-274614, a competitive NMDA receptor antagonist, on the micturition reflex in the rat. *Soc. Neurosci. Abstr.*, **18**, 126.

ZIMMERMAN, D.M., SCHOEPP, D.D., LEANDER, J.D. & ORNSTEIN, P.L. (1992). The discovery and characterization of the competitive NMDA antagonists LY274614, LY233536 and LY233053. *Mol. Neuropharmacol.*, **2**, 77–81.

(Received February 12, 1993
Revised April 4, 1993
Accepted April 20, 1993)

Br. J. Pharmacol. (1993), **110**, 87–94

Membrane current responses to externally-applied ATP in the longitudinal muscle of the chicken rectum

T. Matsuoka, S. Komori & H. Ohashi

Laboratory of Pharmacology, Department of Veterinary Science, Faculty of Agriculture, Gifu University, Gifu 501-11, Japan

1 Membrane current responses to ATP in enzymically-dispersed single smooth muscle cells from the chicken rectum were investigated by the whole-cell voltage clamp technique.

2 In cells dialysed with a KCl-rich solution under voltage clamp at a holding potential of −40 mV, ATP (10 μM) produced an inward current followed by an outward current. When the holding potential was changed to 0 mV and −80 mV, the biphasic current response to ATP was converted to an outward current alone and an inward current alone, respectively.

3 External application of tetraethylammonium (TEA, 5 mM), intracellular dialysis with a CsCl-rich solution, or inclusion of EGTA (10 mM) in the pipette abolished the outward current response to ATP.

4 Neither depletion of Ca^{2+} store with caffeine (10 mM) nor block of voltage-gated Ca^{2+} channels with nifedipine (10 μM) affected the biphasic current response to ATP. After removal of the extracellular Ca^{2+} the outward current response to ATP was abolished.

5 α,β-methylene ATP (100 μM) elicited a current similar to the ATP-induced current. In the presence of α,β-methylene ATP (100 μM), application of ATP (100 μM) was without effect.

6 In CsCl-filled cells, ATP analogues elicited an inward current and the order of potency was ATP ≒ α,β-methylene ATP > ADP >> AMP.

7 Inclusion of GTP γ S (0.2 mM) or GDP β S (2 mM) in the pipette did not affect the ATP-induced inward current in CsCl-filled cells. The reversal potential of the ATP-induced inward current was about 0 mV and was completely inhibited after replacement of the cations in the bath solution by Tris. The reversal potential remained almost unchanged after replacement of Na^+ in the bath solution with 110 mM Ca^{2+}, but shifted in the negative direction after replacement of Na^+ or both Na^+ and Ca^{2+} with glucosamine.

8 The results suggest that ATP acts on P_2 purinoceptors to cause activation of cation channels with selectivity for Ca^{2+} over Na^+. Moreover, it appears that no G-protein-mediated mechanism is involved and increased Ca^{2+} entry through the cation channels causes activation of Ca^{2+}-activated K^+ channels.

Keywords: Smooth muscle; ATP; membrane current: chicken rectum; cationic channel; purinoceptor; voltage-clamp; G-protein

Introduction

Non-adrenergic, non-cholinergic (NANC) neurotransmission occurs in artery (Sneddon & Burnstock, 1985; Suzuki, 1985), vas deferens (Sneddon *et al.*, 1982; Sneddon & Westfall, 1984) and urinary bladder (Hoyle & Burnstock, 1985; Fujii, 1988; Brading & Mostwin, 1989) of several species of mammals. There is considerable evidence that suggests that ATP serves as a transmitter, mediating fast excitatory junction potentials (e.j.ps) in these preparations. Recent studies with the whole-cell voltage clamp technique in enzymatically isolated cells revealed that ATP causes activation of non-selective cation channels leading to membrane depolarization with the necessary properties of the fast excitatory neuromuscular transmitter (ear artery: Benham *et al.*, 1987; Benham & Tsien, 1987; vas deferens: Nakazawa & Matsuki, 1987; Friel, 1988; urinary bladder: Inoue & Brading, 1990).

In the rectum of the fowl, the presence of NANC innervation has been reported (Takewaki & Ohashi, 1977; Komori & Ohashi, 1988a) and the e.j.p. evoked by stimulation of the NANC nerves is very similar in temporal and spatial properties to the fast e.j.p. recorded from the smooth muscle of mammals (Komori & Ohashi, 1982). ATP, when applied locally by pressure ejection from a micropipette, also causes the membrane of the smooth muscle of the chicken rectum to depolarize and the membrane depolarization can mimic the NANC e.j.p. in some respects. However, there are some unfavourable observations for the hypothesis that ATP serves as a transmitter for NANC neuromuscular transmission. A general criterion used to characterize the transmitter is desensitization. In chicken rectum, e.j.ps can be recorded without any noticeable change in amplitude from cells in which desensitization to the depolarizing action of ATP has developed with repetitive application of ATP (Komori & Ohashi, 1988b). Furthermore, a non-hydrolysable ATP analogue, α,β-methylene ATP, which has been shown to activate and then desensitize P_2 purinoceptors in many different cell types of mammals, does not cause selective desensitization of P_2 purinoceptors and therefore does not represent a useful pharmacological tool for the study of the transmitter in NANC neurones in the rectal muscle of the chicken (Komori *et al.*, 1988).

In the present study, membrane currents in response to ATP were measured by use of the whole-cell voltage clamp technique in single smooth muscle cells isolated from the longitudinal muscle layer of the chicken rectum. Some characteristics and intracellular transduction mechanisms of current responses to ATP were investigated for comparison with those in mammalian smooth muscle in which ATP acts on P_2 purinoceptors as an excitatory transmitter.

Methods

Preparation of cells

White Leghorn chickens of either sex, aged 3–6 months (0.8–2.0 kg) were stunned and bled. The rectal region of the

[1] Author for correspondence.

intestine was removed and flushed clean with a physiological salt solution (PSS; composition given in Table 1). The isolated rectum was sectioned lengthwise and pinned serosal side up on a rubber board. Ten to fifteen pieces of muscle strips (about 1 mm in width and 10 mm in length) were dissected from the longitudinal muscle layer of the intestine. The strips were cut into small pieces, about 1 mm square, incubated in a Ca^{2+}-free PSS for 10 min at 37°C and then re-incubated in a mixture of collagenase (1.25 mg ml^{-1}) and papain (4.5 mg ml^{-1}) in a low Ca^{2+} (30 μM) containing-PSS for 60 min at 37°C. After the enzymic digestion, tissue pieces were placed in a fresh 120 μM Ca^{2+}-containing PSS and gently agitated by drawing them in and out of a blunt glass pipette 50–60 times. The resulting suspension was filtered through a fine nylon mesh and centrifuged at 700 r.p.m. for 2 min and the cells were resuspended in 3–5 ml PSS containing 0.5 mM Ca^{2+}. Small aliquots of cell suspension were placed on 10 to 20 cover-glasses and kept in a moist atmosphere at 4°C until use. The isolated cells were used for the experiments on the day they were prepared.

Recording of membrane currents

A cover-glass with cells was placed in a small bath (1.5 ml) on the stage of a microscope (Olympus: CK-2). The organ bath was filled with PSS. Whole-cell current recordings were made at room temperature with standard patch-clamp techniques (Hamill *et al.*, 1981). Patch pipettes had resistances of 3–7 MΩ when filled with pipette solution. Current recordings were made through an amplifier (List; EPC-7) and were displayed on an oscilloscope and stored on FM tape with a recorder (Sony; FFR-3215W) and then replayed onto a thermal array chart recorder (Nihon Kohden: RTA-1100M) for illustration and analysis.

To measure the reversal potential of the ATP-induced current in CsCl-filled cells, the membrane potential was held at − 40 mV and step pulses (200–300 ms in duration) were applied during the application of ATP. For a precise current-voltage relationship, current amplitudes at the test potentials should be measured at a steady conductance level. In practice this was not possible because of the transient nature of the ATP-induced current. The peak amplitude of the ATP-induced current at − 40 mV (I_{ATP-40}) was measured and the amplitudes of ATP-induced currents at the two test potentials were estimated by an extrapolation method using the decay time constant for I_{ATP-40}.

The experimental values in the text are expressed as the mean ± s.e.mean. Statistical significance was tested by Student's unpaired t test and differences were considered significant when $P < 0.05$.

Application of drugs

Extracellular application of a drug was made by replacing the bath solution with the drug-containing solution. Intracellular application of a drug was made by allowing it to diffuse into the cell from patch pipettes filled with the drug-containing pipette solution.

Table 1 Ionic composition of the bathing solutions

	Concentration (mM)				
Bath solution	NaCl	KCl	$MgCl_2$	$CaCl_2$	Glucosamine HCl
PSS	126	6	1.2	2	–
130-Na	130	–	–	–	–
110-Ca	–	–	–	110	–
2-Ca/135-Glu	–	–	–	2	135
0-Ca/135-Glu	–	–	–	–	135

All solutions contained 14 mM glucose and 10.5 mM HEPES. The PSS was adjusted to pH 7.2 with NaOH and the other solutions to pH 7.2 by titration with Tris-(hydroxymethyl)-aminomethane. At this pH, glucosamine (pKa = 8.6) is 96% ionized.

Solutions and drugs

The ionic compositions of salt solutions are present in Table 1.

A KCl-rich patch pipette solution had the following composition (mM): KCl 134, ATP 1, EGTA 0.05, glucose 14, HEPES 10.5 (titrated to pH 7.2 with NaOH). A CsCl-rich pipette solution was prepared by equimolar substitution of KCl with CsCl and adjusted to pH 7.2 by titration with Tris.

Drugs used were adenosine 5'triphosphate magnesium salt (ATP: Sigma), adenosine 5'-disphosphate sodium salt (ADP; Sigma), adenosine 5'-monophosphate sodium salt (AMP; Sigma), α,β-methylene adenosine 5'-triphosphate lithium salt (α,β-methylene ATP; Sigma), carbachol chloride (Tokyo Kasei), caffeine (Wako), guanosine 5'-O-(3-thriotriphosphate) (GTP γ S; Sigma), guanosine 5'-O-(2-thiodiphosphate) (GDP β S; Sigma), glycol etherdiamine tetraacetic acid (EGTA; Wako), D-(+)-glucosamine hydrochloride (Glu; Wako), nifedipine (Tokyo Kasei) and tetraethylammonium chloride (TEA; Wako). All other chemicals used were of reagent grade.

Results

Current responses to externally applied ATP

Single smooth muscle cells from chicken rectum were bathed in PSS and held under voltage-clamp at a holding potential of − 40 mV using pipettes filled with a KCl-rich solution. In a fraction of the cells, spontaneous transient outward currents (STOCs; Benham & Bolton, 1986) were observed.

ATP (10 μM), when applied extracellularly, produced an inward current followed by an outward current. The initial inward current component of the biphasic current response to ATP developed rapidly to reach a peak amplitude within 1 s and was then converted to an outward current (Figure 1). Such a rapid transition from inward to outward current apparently determined the peak amplitude of the inward current which varied from a barely detectable level (about 20 pA) to 0.5 nA ($n = 26$). The outward current reached a peak amplitude of 0.1 to 2.0 nA 0.4 to 2.4 s after the peak of the preceding inward current and then declined to the basal current level within 10 s in the continued presence of ATP. ATP also increased the frequency of STOCs. When application of ATP (10 μM) was repeated at an interval of 3 to 5 min, desensitization to ATP developed and the third or fourth application of ATP produced no detectable current response.

Differentiation between the inward and outward current components of the biphasic ATP response

In cells held at 0 mV, ATP (10 μM) evoked an outward current lasting 4 to 10 s, and the peak amplitude was between 0.2 and 1.6 nA ($n = 5$) (Figure 2a). The frequency and amplitude of STOCs increased during the current response to ATP. When the holding potential was − 80 mV, close to K^+ equilibrium potential, ATP (10 μM) evoked an inward current with a peak amplitude of 100 to 420 pA ($n = 6$) which lasted for about 15 s. Figure 2b shows current responses of a cell to ATP (10 μM) obtained at holding potentials of − 80 mV and − 40 mV. The cell responded with a single inward current at − 80 mV but with a biphasic current at − 40 mV.

When a potassium channel blocker, TEA (5 mM), was added to the bath solution, no outward current was elicited

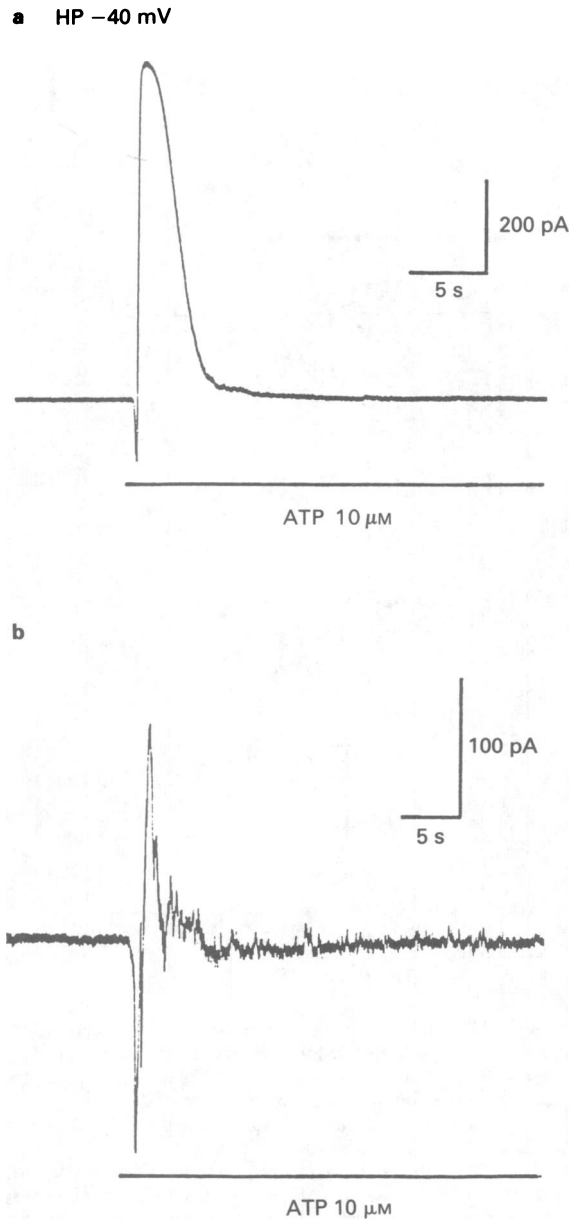

Figure 1 Biphasic current responses to ATP (10 μM) in two different cells held under voltage-clamp at a holding potential of − 40 mV (HP − 40 mV). The cells were dialysed with a KCl-rich pipette solution. (a) A transient small inward current was followed by a relatively large outward current; (b) initial inward and subsequent outward currents with a similar amplitude. In all 26 cells, ATP (10 μM) evoked a biphasic current response although both inward and outward current components varied in shape and amplitude from one cell to another. See text for details.

by ATP (10 μM) in cells held at − 40 mV. After removal of TEA from the bath solution, ATP produced a biphasic current response (Figure 3a). When a CsCl-rich pipette solution to block K^+ current was used, ATP (10 μM) elicited a brief inward current (see Figure 6b and Figure 7). Furthermore, the outward component of the biphasic current to ATP was not observed with 10 mM EGTA in a KCl-rich pipette solution (Figure 3b).

These results strongly suggest that the outward current component of the biphasic ATP response results from activation of K^+ channels which is brought about by a rise in intracellular Ca^{2+} concentration ($[Ca^{2+}]_i$) and the inward current component results from activation of other ion channels which are not regulated by $[Ca^{2+}]_i$.

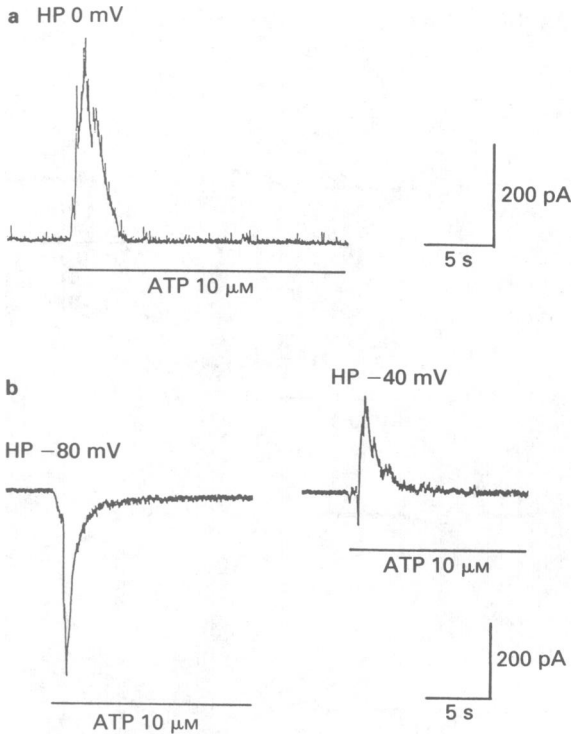

Figure 2 Current responses to ATP (10 μM) at three different holding potentials. KCl-rich pipette solution was used. (a) ATP-induced current response at 0 mV; (b) current responses to ATP at − 80 mV (left), and at − 40 mV (right). Current records in (a) and (b) are from different cells. Note that ATP-induced current response was biphasic at − 40 mV, but simply inward at − 80 mV or outward at 0 mV.

Calcium sources responsible for the ATP-induced K^+ current

Release of Ca^{2+} from intracellular stores produced by bath application of caffeine (10 mM) (Benham & Bolton, 1986) produced a brief outward current with a peak amplitude of 0.1–2.7 nA ($n = 5$) which resulted from opening of Ca^{2+}-activated K^+ channels. STOCs were also abolished by caffeine. In the continued presence of caffeine, application of ATP (10 μM) produced a biphasic current response similar to that seen in normal PSS (Figure 4a). After removal of Ca^{2+} (with addition of 0.5 mM EGTA) from the bath solution. ATP activated only an inward current whereas caffeine (10 mM), applied in the presence of ATP, produced a large outward current (Figure 4b). Readmission of Ca^{2+} to the bath solution resulted in restoration of a biphasic current response to ATP (Figure 4c). A voltage-dependent Ca^{2+} channel blocker, nifedipine (10 μM), when applied in the bath solution, had no noticeable effect on the biphasic ATP response.

These results suggest that a rise in $[Ca^{2+}]_i$ responsible for the ATP-induced outward K^+ current may result from Ca^{2+} influx through a nifedipine-insensitive pathway rather than release of Ca^{2+} from internal Ca^{2+} stores.

Effects of α,β-methylene ATP on the ATP-induced current

Bath application of α,β-methylene ATP (100 μM) induced a biphasic current response resembling the ATP-induced current. A transient inward current was followed by a relatively long-lasting outward current (Figure 5a) and the outward current component was absent in CsCl-filled cells (Figure 5b). Application of ATP (10 or 100 μM) in the presence of α,β-methylene ATP did not evoke a current (Figure 5a,b).

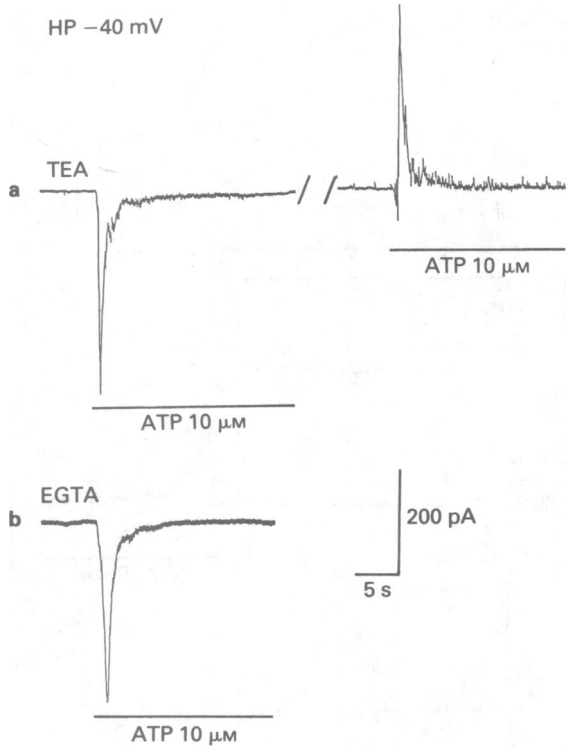

Figure 3 The effect of external TEA and intracellular EGTA on the outward current component of the ATP-induced biphasic current. The cells were voltage-clamped at −40 mV (HP −40 mV) and a KCl-rich pipette solution was used. (a) An inward current alone in response to ATP (10 μM) with extracellular application of TEA (5 mM) (left) and a biphasic current response after removal of TEA (right). (b) An inward current response to ATP (10 μM) with inclusion of EGTA (10 mM) in the pipette solution. Current records in (a) and (b) are from different cells.

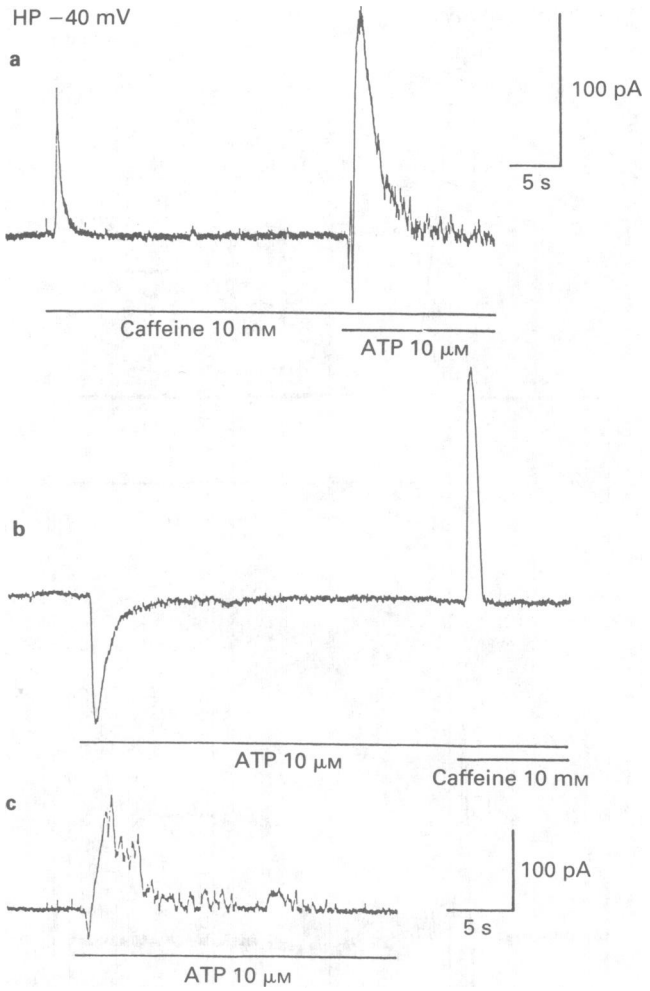

Figure 4 ATP-induced current responses after depletion of the intracellular Ca^{2+} store and in the absence of extracellular Ca^{2+}. The cells were voltage-clamped at −40 mV and a KCl-rich pipette solution was used. (a) A biphasic current response to ATP (10 μM) in the continued presence of caffeine (10 mM) which depleted the intracellular Ca^{2+} stores (see a transient outward current on application of caffeine). (b) An inward current response to ATP (10 μM) and an outward current response to caffeine (10 mM) applied in the continued presence of ATP in a cell bathed in Ca^{2+}-free, with 0.5 mM EGTA-added, PSS. (c) A biphasic current response to ATP (10 μM) after readmission of Ca^{2+} in the bath solution. Current records in (b) and (c) are from the same cell.

Concentration-dependence of the ATP-induced inward current and the effects of ATP analogues

The shape and amplitude of the ATP-induced inward current were less variable in CsCl-filled cells than in cells with KCl-filled pipettes. Thus, the concentration-dependence of the ATP-induced inward current was examined in cells with CsCl-filled pipettes held at −40 mV. Current responses to ATP at various concentrations were obtained from different cells in order to avoid underestimation that might arise from desensitization following repetitive exposure to ATP. ATP at a concentration of 0.1 μM was without effect ($n = 4$), but at concentrations greater than 1 μM, elicited a brief inward current. The peak amplitude of current responses increased in a concentration-dependent manner. The maximum amplitude of 292 ± 28 pA, ($n = 3$) was attained with 100 μM ATP. The concentration required for half the maximum amplitude could not be determined precisely but was in the micromolar range (see Figure 6a).

The effective concentrations of α,β-methylene ATP were also in the micromolar range and the amplitude of peak inward currents induced by 100 μM α,β-methylene ATP was 315 ± 90 pA ($n = 5$), which was not significantly different from that of ATP (100–200 μM)-induced currents. Another ATP derivative, ADP, at 100 μM also produced an inward current with amplitudes of 10 to 40 pA ($n = 3$), but AMP (100 μM) produced no detectable current. Thus, the order of potency in producing the inward current was ATP ≒ α,β-methylene ATP > ADP >> AMP, suggesting that the current response is mediated by P_2 purinoceptors (Burnstock, 1978).

Effects of GTPγS and GDPβS on the ATP-induced inward current

Involvement of a GTP-binding protein in the ATP-induced inward current was tested with a non-hydrolysable GTP analogue, GTPγS, and a non-hydrolysable GDP analogue, GDPβS. These agents are known to affect muscarinic receptor-activated cation channels in intestinal smooth muscle cells (Inoue & Isenberg, 1990; Komori *et al.*, 1992a). With GTPγS (0.2 mM) in the patch pipette solution, there were small and irregular inward currents for several minutes after rupturing the cell membrane. This was not observed with GDPβS. Neither GTPγS (0.2 mM) nor GDPβS (2 mM) affected the ATP (10 μM)-induced inward current and its shape and amplitude were very similar to those in normal cells (Figure 6b): The mean amplitude of the ATP-induced current was 253 ± 53 pA ($n = 11$) in GTPγS-treated cells and 273 ± 64 pA ($n = 10$) in GDPβS-treated cells. Each of the mean values did not significantly differ from the control value of 221 ± 43 pA ($n = 15$) (see Figure 6a).

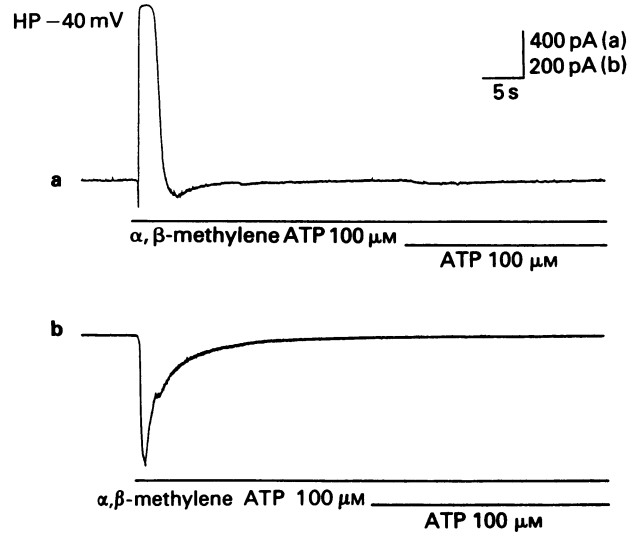

Figure 5 Currents to α,β-methylene ATP and its effect on the response to ATP. The cells were voltage-clamped at − 40 mV. (a) A biphasic current to α,β-methylene ATP (100 μM) in a cell dialysed with KCl-rich pipette solution which blocked the response to ATP (100 μM). (b) An inward current to α,β-methylene ATP (100 μM) which blocked the response to ATP (100 μM) in a cell dialysed with CsCl-rich pipette solution. Note that α,β-methylene ATP induced similar currents to ATP shown in Figures 1 and 6b and rendered the cells insensitive to ATP.

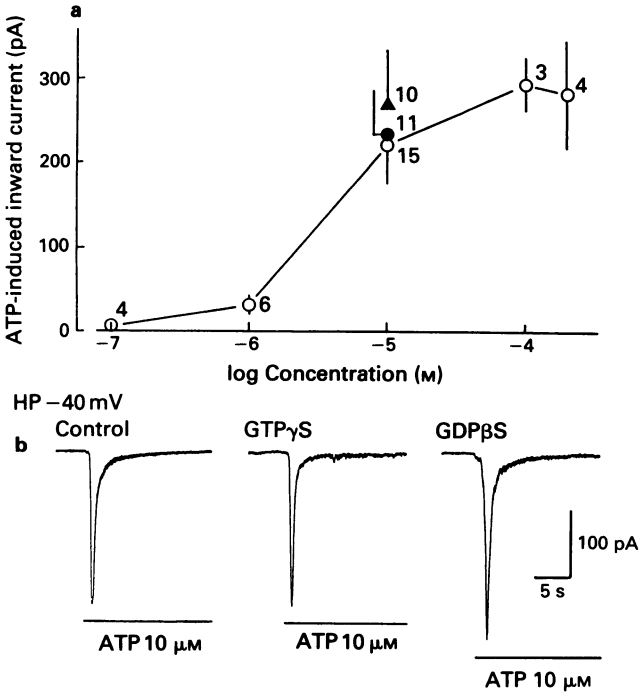

Figure 6 Concentration-dependence and lack of effect of intracellularly-applied GTPγS and GDPβS on the ATP-induced inward current. A CsCl-rich pipette solution was used and cells were voltage-clamped at − 40 mV. Each measurement of ATP-induced currents was made in a different cell. (a) Plot of the peak amplitude of ATP-induced current against ATP concentration in control cells (○). The amplitudes of current responses to 10 μM ATP in GTPγS (0.2 mM)-treated cells (●) and GDPβ (2 mM)-treated cells (▲), are also presented. Each point represents the mean ± s.e.mean. The number of measurements is indicated by numbers close to the points. The concentration-response relationship shows that the concentration required for half maximum response of the ATP-induced inward current is in the micromolar range. (b) Inward current responses to ATP (10 μM) in normal (left), GTPγS (0.2 mM)-treated (middle) and GDPβS (2 mM)-treated cells (right). The GTP analogues were included in the patch pipette solution.

Ionic basis of the ATP-activated current

In an attempt to evaluate the ionic selectivity of the ATP-induced inward current, the reversal potential of the current to ATP (10 μM) was measured in cells dialysed with a CsCl-rich pipette solution and bathed in various extracellular solutions (see Table 1).

Substitution of external cations with Tris, normally a less permeant cation through cationic channels, resulted in abolition of the ATP (10 μM)-induced inward current. After returning to normal PSS ATP evoked an inward current (Figure 7).

Cells were bathed in 130-Na solution (see Table 1), and the membrane potential was stepped from the holding potential of − 40 mV to test potentials of − 10 and + 10 mV during application of ATP (10 μM). Figure 8a shows a typical recording of an ATP-induced current from a cell bathed in 130-Na solution. The ATP-induced current was inward at − 40 and − 10 mV but outward at 10 mV. To estimate the reversal potential of the ATP-induced current, the apparent peak amplitudes of ATP-induced currents at the three different potentials were obtained by an extrapolation method (see Methods). Figure 8c shows a plot of the peak current amplitudes obtained from the recording in Figure 8a against the membrane potential (closed triangles). The current-voltage relationship gave a reversal potential in this cell of + 0.3 mV. In seven cells, the mean reversal potential of the current was 0.4 ± 1.0 mV. According to a modified Goldman-Hodgkin-Katz equation (Fatt & Ginsborg, 1958), the mean reversal potential corresponded to a relative permeability for Na^+ over Cs^+ (P_{Na}/P_{Cs}) of 1.2 (see Table 2). Similar experiments were carried out in cells bathed in PSS. In eight different cells, measurement of the reversal potential of the current gave a mean value of + 4.2 ± 3.0 mV.

With 110 mM $CaCl_2$ in the bath solution (110-Ca solution: Table 1), ATP produced an inward current at the holding potential of − 40 mV, and the peak amplitude was comparable with that evoked in PSS or 130-Na solution. The ATP-induced current was also inward at − 40 and − 10 mV and outward at + 10 mV (Figure 8b and c, closed circles). In four different cells, the mean reversal potential of the current was + 8.0 ± 2.5 mV ($n = 4$) which gives a ratio of permeability of Ca^{2+} to Cs^+ (P_{Ca}/P_{Cs}) of 2.9 (Table 2). With a reduction of the external Ca^{2+} concentration to 2 mM (2-Ca/135-Glu solution; Table 1), ATP still induced an inward current at the holding potential of − 40 mV, but the current amplitude became much smaller than that observed in 110-Ca solution. As illustrated in Figure 9a (also see closed circles in Figure 9c), the ATP-induced current obtained in 2-Ca/135-Glu solution was inward at − 40 mV and outward at − 20 mV. The mean reversal potential was − 31.7 ± 0.4 mV ($n = 7$) which corresponds to a relative

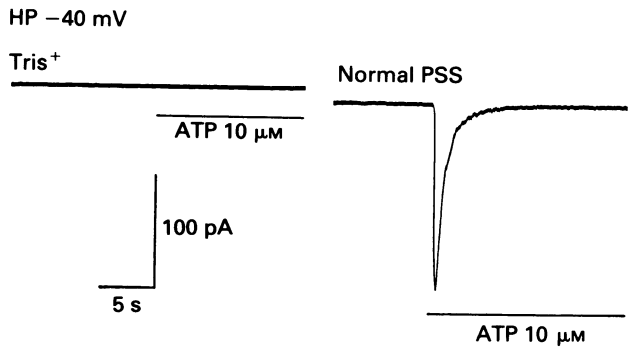

Figure 7 Abolition of ATP-induced inward current by substitution of the external cations with Tris. The cell was held at − 40 mV and CsCl-rich pipette solution was used. No response to bath-applied ATP (10 μM) was observed in the presence of Tris (left) but after returning to normal PSS, ATP elicited an inward current (right).

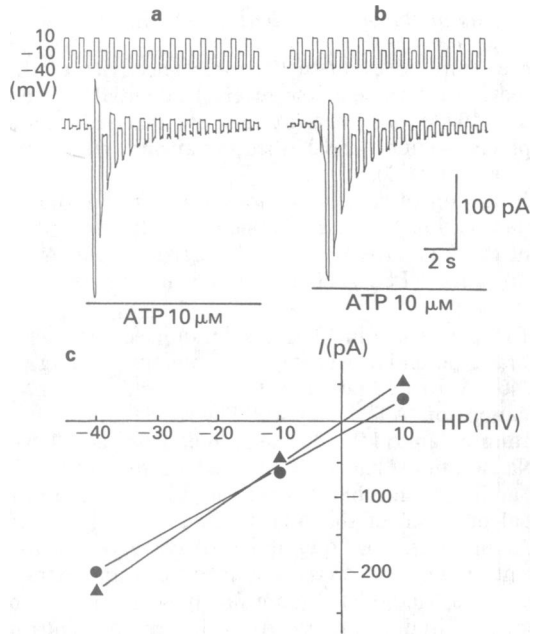

Figure 8 Relationship between the amplitude of the ATP-induced currents and the clamp potential. The cells were dialysed with a CsCl-rich pipette solution and held at − 40 mV. (a and b) Current responses to ATP (10 μM) in cells bathed in 130-Na solution (a) and 110-Ca solution (b) (see Table 1). Test step potentials were − 10 and + 10 mV. Upper traces, voltage step protocol: lower traces, current record. (c) Plot of the amplitude of ATP-induced currents against clamp potential: (▲) from the recording in (a); (●) from that in (b). The current amplitudes at − 10 mV and 10 mV were estimated by an extrapolation method using the decay time constant for the ATP-induced current at − 40 mV (700 ms in (a) and 1250 ms in (b). (see Methods). Lines were drawn by the least-squares method.

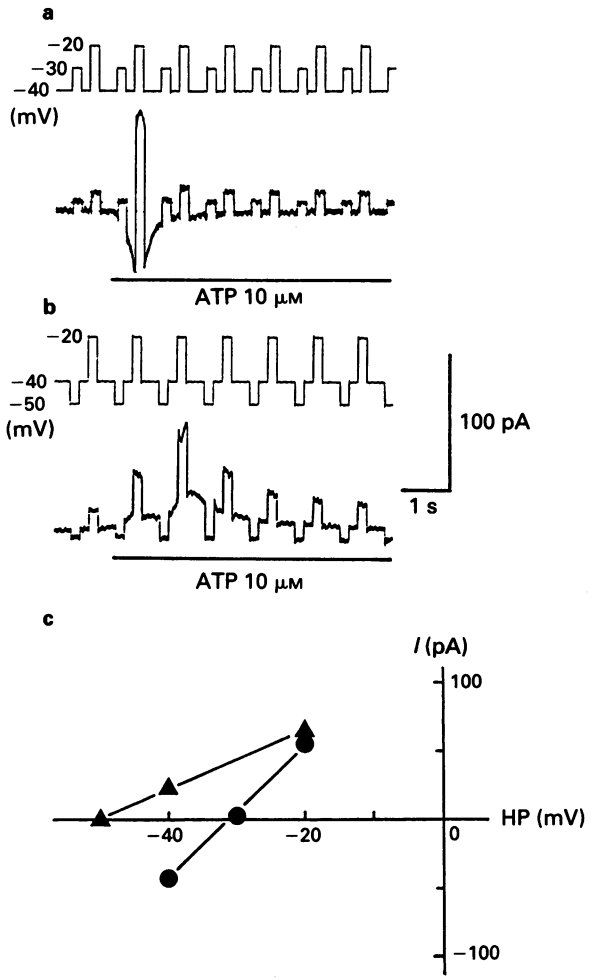

Figure 9 Relationship between the amplitude of the ATP-induced current and the clamp potential. The cells were dialysed with CsCl-rich pipette solution and held at − 40 mV. (a and b) Current responses to ATP (10 μM) in two different cells bathed in 2-Ca/135-Glu (a) and 0-Ca/135-Glu (b) (see Table 1). During application of ATP, the membrane potential was stepped from − 40 mV to test potentials of − 30 and − 20 mV in (a) and to − 50 and − 20 mV in (b). Upper traces, voltage step protocol; lower traces, current record. (c) Plot of the amplitude of ATP-induced currents against clamp potential: (●) and (▲) are from the recordings in (a) and (b) respectively. Lines were drawn by the least-squares method.

Table 2 Reversal potentials of the ATP-induced current

Bath solution	*Reversal potential* (mean ± s.e.mean) (mV)	*Permeability ratio*	
PSS	+4.2 ± 3.0 (n = 8)	–	
130-Na	+0.4 ± 1.0 (n = 7)	PNa/PCs	1.2
110-Ca	+8.0 ± 2.5 (n = 4)	PCa/PCs	2.9
2-Ca/135-Glu	−31.7 ± 0.4 (n = 7)	PCa/PCs	7.1
0-Ca/135-Glu	−46.6 ± 1.5 (n = 3)	PGlu/PCs	0.15

CsCl-rich pipette solution (containing 130 mM CsCl) was used. Permeability ratios were calculated using the mean values of the reversal potential according to a modified Goldman-Hodgkin-Katz equation (Fatt & Ginsborg, 1958). Monovalent ion activities were taken as 0.75 and divalent ion activities as 0.25 (110-Ca solution) or 0.3 (2-Ca/135-Glu solution) (Benham & Tsien, 1987).

permeability for Ca^{2+} over Cs^+ (P_{Ca}/P_{Cs}) of 7.1, if P_{Glu}/P_{Cs} is taken as 0.15 (see below). Further, with removal of external 2 mM $CaCl_2$ (0-Ca/135-Glu solution: Table 1), the ATP-induced current was outward at − 40 and − 20 mV, as shown in Figure 9b and c (closed triangles). With these solutions the mean reversal potential of the current was − 46.6 ± 1.5 mV (n = 3), which was significantly ($P < 0.05$) different from the value (− 31.7 ± 0.4 mV) obtained in 2-Ca/135-Glu solution. The mean reversal potential obtained in 0-Ca/135-Glu solution gives a relative permeability for glucosamine-H^+ over Cs^+ (P_{Glu}/P_{Cs}) of 0.15 (Table 2).

These results suggest that the ATP-induced inward current may be carried by Ca^{2+}-permeable cation channels.

Discussion

The present study shows that in enzyme-dispersed single smooth muscle cells from the longitudinal muscle layer of chicken rectum, ATP induces two types of membrane current. One type appears to flow through cation selective channels and its reversal potential is close to 0 mV in PSS, and the other type passes through K^+ channels which are activated by intracellular Ca^{2+}. Since activation of the cation channels is expected to depolarize the membrane of smooth muscle cells, the inward current described in this paper may underlie the depolarization evoked by ATP in tissue preparations from chicken rectum (Komori & Ohashi, 1988b).

Properties of the ATP-induced outward current

The outward current component of the biphasic response to ATP was blocked by TEA in the bath solution and was not observed at the potassium equilibrium potential (− 80 mV) or if potassium was not present in the pipette and bathing solution. Thus, the outward current to ATP appears to be due to activation of K^+ channels. Since inclusion of EGTA

(10 mM) in the pipette blocked the outward current, the link between ATP receptor and the opening of K^+ channels may be an increase in Ca^{2+} concentration in the cytoplasm. Elevation of $[Ca^{2+}]_i$ caused by increased Ca^{2+} entry across the membrane may play a major role for the activation of K^+ channels, since the ATP-induced outward current was elicited after depletion of intracellular Ca^{2+} stores by caffeine. The outward current was abolished after removal of the extracellular Ca^{2+} with intact caffeine-releasable intracellular Ca^{2+} stores. The Ca^{2+} influx pathway is not the voltage-dependent Ca^{2+} channel because of insensitivity of the Ca^{2+}-activated K^+ current to nifedipine.

In ear artery cells from the rabbit, it has been demonstrated, with a fluorescent Ca^{2+} indicator (Indo-1), that ATP activates Ca^{2+}-permeable nonselective channels, which results in a rise in $[Ca^{2+}]_i$ due to Ca^{2+} entry (Benham, 1989). In the present study, it was shown that the ATP-induced inward current could be carried by calcium ions. In the present work single channel activity was not recorded but it seems likely that the ATP-induced current is carried by Ca^{2+}-permeable cation channels. Ca^{2+} entry then leads to activation of Ca^{2+}-activated K^+ channels. This view is compatible with the finding that the outward current component of the biphasic response to ATP was always preceded by the inward current component. In rabbit jejunal smooth muscle cells, carbachol induces an inward current due to activation of cation channels almost impermeable to Ca^{2+} as well as an outward current due to activation of Ca^{2+}-activated K^+ channels brought about by release of Ca^{2+} from internal stores (Komori & Bolton, 1990). Thus, there is apparently no causal relationship between inward and outward currents. It is worth noting that the outward current is not necessarily preceded by the inward current in this type of smooth muscle cell (Komori & Bolton, 1990).

ATP, unlike caffeine, did not reduce or abolish the activity of STOCs (see Figure 2a) which are considered to represent the sporadic release of Ca^{2+} from intracellular stores (Benham & Bolton, 1986; Bolton & Lim, 1989), suggesting that ATP may not release Ca^{2+} from internal stores in chicken rectal cells. Application of caffeine subsequent to ATP elicited an outward current due to activation of Ca^{2+}-activated K^+ channels which was comparable to that elicited by caffeine alone. Similarly, it has been reported that ATP does not release Ca^{2+} stores in smooth muscle cells dispersed from rabbit ear artery (Benham *et al.*, 1987; Benham, 1989). On the other hand, ATP produces release of Ca^{2+} stores in cultured smooth muscle cells from rat and pig aorta (Tawada *et al.*, 1987; Phaneuf *et al.*, 1987; Droogmans *et al.*, 1991). The existence of a subtype of ATP receptor (P_{2y} purinoceptor), which is coupled to phospholipase C leading to the formation of inositol 1,4,5-trisphosphate mediating the release of Ca^{2+}, has been suggested in turkey erythrocytes (Boyer *et al.*, 1989) and in rat renal cortex (Nanoff *et al.*, 1990). The different effects of ATP on Ca^{2+} stores in many types of cells may be largely due to the existence of two different subtypes of P_2 purinoceptor (P_{2x} and P_{2y}).

Properties of the ATP-induced inward current

The ATP-induced inward current in chicken rectal cells is similar in many properties to that in a variety of smooth muscle cells (rabbit ear artery, Benham *et al.*, 1987; Benham & Tsien, 1987; rat vas deferens, Nakazawa & Matsuki, 1987; Friel, 1988; guinea-pig urinary bladder, Inoue & Brading, 1990). First, there is rapid desensitization of the current. Secondly, the current does not depend on intracellular Ca^{2+}. Thirdly, activation of ion channels responsible for the current is mediated via P_2 purinoceptors and the effective concentration of ATP is in the micromolar range. Fourthly, the current reverses near 0 mV in PSS (with Na^+ as a main cation) and it is carried by cations. Some of these are the properties usually linked with the P_{2x} receptor subtype. In different cell types, however, α,β-methylene ATP is not as potent an agonist as ATP and may or may not block the response to ATP. After exposure to α,β-methylene ATP, ATP is completely ineffective in chicken rectum muscle and guinea-pig urinary bladder muscle (Inoue & Brading, 1990), but it is still effective in rat vas deferens muscle (Friel, 1988). α,β-methylene ATP was as potent as ATP in activating the inward current in smooth muscle cells of chicken rectum and rabbit ear artery, but less potent than ATP in guinea-pig urinary bladder and rat vas deferens. In the present study, permeabilities of Ca^{2+} relative to Na^+ (P_{Ca}/P_{Na}) in the ATP-activated cation channels were estimated to be 2.4 and 5.9 with 110 mM Ca^{2+} and 2 mM Ca^{2+} in the external medium, respectively (see Table 2), which are similar to the values described in rabbit ear artery (Benham & Tsien, 1987). Based on these facts, the ATP receptor subtype in chicken rectum muscle seems closely related to that in rabbit ear artery muscle.

GTPγS and GDPβS, applied in the same way and at the same concentration as in our previous study, where these agents markedly affected the activation of ion channels following stimulation of G-protein-coupled receptors in guinea-pig ileal muscle cells (Komori *et al.*, 1992a), did not modify the ATP-induced inward current. This result suggests no involvement of any G-protein-mediated mechanisms in activation of the cation channels. It seems likely that binding of ATP to the receptor could activate directly ion channels, as described for the nicotinic ACh receptor (Hille, 1984). Benham & Tsien (1987) suggested a direct coupling between ATP binding and channel opening, based on their observations in rabbit ear artery muscle that ATP activates unitary inward currents in outside-out membrane patches but not in cell-attached patches.

A physiological role of ATP

ATP is considered to act as a non-adrenergic, non-cholinergic (NANC) excitatory neuromuscular transmitter in blood vessels, vas deferens and the urinary bladder of some species of mammals (artery, Suzuki & Kou, 1983; Suzuki, 1985; vas deferens, Sneddon & Westfall, 1984; urinary bladder, Fujii, 1988).

The presence of NANC excitatory innervation to the avian rectum has been also reported (Ohashi *et al.*, 1977; Takewaki & Ohashi, 1977; Komori & Ohashi, 1982). The neurotransmitter has not been identified, but ATP and neurotensin have been proposed as candidates (Meldrum & Burnstock, 1985; Komori *et al.*, 1986). Local application of either ATP or neurotensin by means of pressure ejection from micropipettes evokes a brief, monophasic membrane depolarization similar to the e.j.p. (Komori & Ohashi, 1988b; Komori *et al.*, 1992b). Further, patch clamp experiments revealed that both ATP and neurotensin are channel activators with specific membrane receptors. Both agents activate current with a reversal potential close to 0 mV in a quasi-physiological ionic environment (Komori *et al.*, 1992b; the present study). Activation of such currents leads to membrane depolarization. The e.j.p. has been shown to be associated with an increase of membrane conductance with a reversal potential of about −15 mV (Komori & Ohashi, 1988a). Further experiments are required to elucidate the identity of the excitatory transmitter in the chicken rectum.

We would like to thank Dr C.D. Benham (SmithKline Beecham Pharmaceuticals, U.K.) for his helpful suggestions.

References

BENHAM, C.D. (1989). ATP-activated channels gate calcium entry in single smooth muscle cells dissociated from rabbit ear artery. *J. Physiol.*, **419**, 689–701.

BENHAM, C.D. & BOLTON, T.B. (1986). Spontaneous transient outward currents in single visceral and vascular smooth muscle cells of the rabbit. *J. Physiol.*, **381**, 385–406.

BENHAM, C.D., BOLTON, T.B., BYRNE, N.G. & LARGE, W.A. (1987). Action of externally applied adenosine triphosphate on single smooth muscle cells dispersed from rabbit ear artery. *J. Physiol.*, **387**, 473–488.

BENHAM, C.D. & TSIEN, R.W. (1987). A novel receptor-operated Ca^{2+}-permeable channel activated by ATP in smooth muscle. *Nature*, **328**, 275–278.

BOLTON, T.B. & LIM, S.P. (1989). Properties of calcium stores and transient outward currents in single smooth muscle cells of rabbit intestine. *J. Physiol.*, **409**, 385–401.

BOYER, J.L., DOWNES, C.P. & HARDEN, T.K. (1989). Kinetics and activation of phospholipase C by P_{2y} purinergic receptor agonists and guanine nucleotides. *J. Biol. Chem.*, **264**, 884–890.

BRADING, A.F. & MOSTWIN, J.L. (1989). Electrical and mechanical responses of guinea-pig bladder muscle to nerve stimulation. *Br. J. Pharmacol.*, **98**, 1083–1090.

BURNSTOCK, G. (1978). A basis for distinguishing two types of purinergic receptor. In *Cell Membrane Receptors*. pp. 107–118. New York: Raven Press.

DROOGMANS, G., CALLEWAERT, G., DECLERCK, I. & CASTEELS, R. (1991). ATP-induced Ca^{2+} release and Cl^- current in cultured smooth muscle cells from pig aorta. *J. Physiol.*, **440**, 623–634.

FATT, P. & GINSBORG, B.L. (1958). The ionic requirements for the production of action potentials in crustacean muscle fibers. *J. Physiol.*, **142**, 516–543.

FRIEL, D.D. (1988). An ATP-sensitive conductance in single smooth muscle cells from the rat vas deferens. *J. Physiol.*, **401**, 361–380.

FUJII, K. (1988). Evidence for adenosine triphosphate as an excitatory transmitter in guinea-pig, rabbit and pig urinary bladder. *J. Physiol.*, **404**, 39–52.

HAMILL, O.P., MARTY, A., NEHER, E., SAKMANN, B. & SIGWORTH, F.J. (1981). Improved patch-clamp techniques for high-resolution current recording from cells and cell-free membrane patches. *Pflügers Arch.*, **391**, 85–100.

HILLE, B. (1984). *Channels of Excitable Membranes*. Sunderland, Massachusetts: Sinaeur Associates Inc.

HOYLE, C.H.V. & BURNSTOCK, G. (1985). Atropine-resistant excitatory junction potentials in rabbit bladder are blocked by α,β-methylene ATP. *Eur. J. Pharmacol.*, **114**, 239–240.

INOUE, R. & BRADING, A.F. (1990). The properties of the ATP-induced depolarization and current in single cells isolated from the guinea-pig urinary bladder. *Br. J. Pharmacol.*, **100**, 619–625.

INOUE, R. & ISENBERG, G. (1990). Acetylcholine activates non-selective cation channels in guinea-pig ileum through a G-protein. *Am. J. Physiol.*, **258**, C1173–1178.

KOMORI, S. & BOLTON, T.B. (1990). Role of G-proteins in muscarinic receptor inward and outward currents in rabbit jejunal smooth muscle. *J. Physiol.*, **427**, 395–419.

KOMORI, S., FUKUTOME, T. & OHASHI, H. (1986). Isolation of a peptide material showing strong rectal muscle-contracting activity from chicken rectum and its identification as chicken neurotensin. *Jpn. J. Pharmacol.*, **40**, 577–589.

KOMORI, S., KAWAI, M., TAKEWAKI, T. & OHASHI, H. (1992a). GTP-binding protein involvement in membrane currents evoked by carbachol and histamine in guinea-pig ileal muscle. *J. Physiol.*, **450**, 105–126.

KOMORI, S., KWON, S. & OHASHI, H. (1988). Effects of a prolonged exposure to α,β-methylene ATP on non-adrenergic, non-cholinergic excitatory transmission in the rectum of the chicken. *Br. J. Pharmacol.*, **94**, 9–18.

KOMORI, S., MATSUOKA, T., KWON, S., TAKEWAKI, T. & OHASHI, H. (1992b). Membrane potential and current responses to neurotensin in the longitudinal muscle of the rectum of the fowl. *Br. J. Pharmacol.*, **107**, 790–796.

KOMORI, S. & OHASHI, H. (1982). Some characteristics of transmission from non-adrenergic, non-cholinergic excitatory nerves to the smooth muscle of the chicken rectum. *J. Auton. Nerv. Syst.*, **8**, 199–210.

KOMORI, S. & OHASHI, H. (1988a). Some membrane properties of the circular muscle of chicken rectum and its non-adrenergic, non-cholinergic innervation. *J. Physiol.*, **401**, 417–435.

KOMORI, S. & OHASHI, H. (1988b). Membrane potential responses to ATP applied by pressure ejection in the longitudinal muscle of chicken rectum. *Br. J. Pharmacol.*, **95**, 1157–1164.

MELDRUM, L.A. & BURNSTOCK, G. (1985). Investigations into the identity of the non-adrenergic, non-cholinergic excitatory transmission in the smooth muscle of chicken rectum. *Comp. Biochem. Physiol.*, **81**, 307–309.

NAKAZAWA, K. & MATSUKI, N. (1987). Adenosine triphosphate-activated inward current in isolated smooth muscle cells from rat vas deferens. *Pflügers Arch.*, **409**, 644–646.

NANOFF, C., FREISSMUTH, M., TUISL, E. & SCHÜTZ, W. (1990). P_2, but not P_1-purinoceptors mediate formation of 1,4,5-inositol triphosphate and its metabolites via a pertussis toxin-insensitive pathway in the rat renal cortex. *Br. J. Pharmacol.*, **100**, 63–68.

OHASHI, H., NAITO, K., TAKEWAKI, T. & OKADA, T. (1977). Non-cholinergic, excitatory junction potentials in smooth muscle of chicken rectum. *Jpn. J. Pharmacol.*, **27**, 379–387.

PHANEUF, S., BERTA, P., CASANOVA, J. & CAVADORE, J.C. (1987). ATP stimulates inositol phosphates accumulation and calcium mobilization in primary culture of rat aortic myocytes. *Biochem. Biophys. Res. Commun.*, **143**, 454–460.

SNEDDON, P. & BURNSTOCK, G. (1985). ATP as a cotransmitter in rat tail artery. *Eur. J. Pharmacol.*, **106**, 149–152.

SNEDDON, P. & WESTFALL, D.P. (1984). Pharmacological evidence that adenosine triphosphate and noradrenaline are co-transmitters in the guinea-pig vas deferens. *J. Physiol.*, **347**, 561–580.

SNEDDON, P., WESTFALL, D.P. & FEDAN, J.S. (1982). Cotransmitters in the motor nerves of the guinea-pig vas deferens: electrophysiological evidence. *Science*, **218**, 693–695.

SUZUKI, H. (1985). Electrical responses of smooth muscle cells of the rabbit ear artery to adenosine triphosphate. *J. Physiol.*, **359**, 401–415.

SUZUKI, H. & KOU, K. (1983). Electrical components contributing to the nerve-mediated contractions in the smooth muscles of the rabbit ear artery. *Jpn. J. Pharmacol.*, **33**, 743–756.

TAKEWAKI, T. & OHASHI, H. (1977). Non-cholinergic excitatory transmission to intestinal smooth muscle cells. *Nature*, **268**, 749–750.

TAWADA., Y., FURUKAWA, K. & SHIGEKAWA, M. (1987). ATP-induced calcium transient in cultured rat aortic smooth muscle cells. *J. Biochem.*, **102**, 1499–1509.

(Received April 4, 1993
Revised April 19, 1993
Accepted April 21, 1993)

Br. J. Pharmacol. (1993), **110**, 95–98

The positive inotropic effect of compound II, a novel analogue of sotalol, on guinea-pig papillary muscles and single ventricular myocytes

[1]E. White, [2]S.P. Connors, E.W. Gill & [3]D.A. Terrar

University Department of Pharmacology, Mansfield Road, Oxford, OX1 3QT

1 Compound II is a novel analogue of sotalol which has been reported to be free of β-adrenoceptor and L-type calcium channel blocking actions. The effects of compound II on the contraction of guinea-pig papillary muscles (at 2 μM) and single ventricular myocytes (at 100 nM) were investigated.

2 Exposure to compound II caused a significant increase in the contraction of both preparations.

3 Compound II prolonged the action potential of the single myocytes and increased the magnitude of the Ca-activated current which was used as a qualitative indicator of the intracellular calcium transient.

4 The ratio of first/steady state Ca-activated currents evoked by short action potentials was not modified. This may indicate that compound II does not influence the normal functioning of the sarcoplasmic reticulum stores.

5 The observations are consistent with the hypothesis that action potential prolongation by compound II reduces Ca^{2+} extrusion via the Na-Ca exchange. This in turn allows increased uptake of calcium into the sarcoplasmic reticulum stores so that more calcium is available for release by subsequent action potentials, leading to an increase in intracellular calcium transients and contractions.

Keywords: Sotalol; Class III antiarrhythmics; cardiac contraction; sodium-calcium exchange

Introduction

A characteristic of Class III antiarrhythmic agents is their ability to prolong the cardiac action potential (Vaughan Williams, 1970). Prolongation of the action potential has a positive inotropic effect on mammalian heart tissue (see, Boyett *et al.*, 1993). However, studies on the inotropic response to the most commonly used Class III antiarrhythmic agents, amiodarone and sotalol, give conflicting results, possibly because of the secondary negative inotropic actions of these agents (e.g. the blockade of β-adrenoceptors and of L-type calcium channels, see Boyett *et al.*, 1993).

Compound II (1-(4-methanesulphonamidophenoxy)-3-(*N*-methyl 3,4,dichlorophenylethylamino)-2-propanol) is an analogue of sotalol which has been shown to prolong cardiac action potentials with a 1000 fold increase in potency, compared with the parent compound, and is devoid of any β-adrenoceptor blocking activity (Connors *et al.*, 1991; 1992). The mechanism of action of compound II is a specific blocking of the time-dependent delayed rectifier potassium current (I_K).

The purpose of this study was to test the hypothesis that compound II, a Class III antiarrhythmic agent which is free of the negative inotropic properties mentioned above, has a positive inotropic effect on cardiac tissue.

Experiments were carried out on multicellular and single cell preparations of guinea-pig ventricles. The Ca-activated current (thought to be carried by sodium-calcium exchange, Chapman & Noble, 1989) was used as a qualitative indicator of intracellular calcium ($[Ca^{2+}]_i$) transients (Egan *et al.*, 1989; Terrar & White, 1989) which do not alter the timecourse of the $[Ca^{2+}]_i$ transient (Noble & Powell, 1991). This current can also be used as an indicator of calcium uptake and release from the sarcoplasmic reticulum (Terrar & White, 1989; White & Terrar, 1990a,b).

Methods

Guinea-pigs were killed by cervical dislocation following stunning and hearts were excised. Papillary muscles (3.5 mm in length and 0.1–1.0 mm in diameter) were dissected from the free wall of the right ventricle. The base of the Papillary muscle was tied to a bottom support in a vertical bath with silk thread. The tissue was bathed with an oxygenated solution containing (mM): NaCl 118.5, $NaHCO_3$ 14.5, KCl 4.2, $K_2H_2PO_4$ 1.2, $MgSO_4$ 1.2, glucose 11.1 and $CaCl_2$ 2.5. The tendonous end of the muscle was placed under 0.25 g tension. Muscles were stimulated with platinum external electrodes (placed near the base of the muscle) at 1.5–2 times threshold (2 ms duration) at a frequency of 2 Hz, 36°C. Muscles were left to equilibrate for 1 h. Isometric force was measured by an Octromed recorder (MX216). Single guinea-pig ventricular myocytes were isolated as previously described by Powell *et al.* (1980) and Mitchell *et al.* (1984). After isolation, cells were superfused with the solution described above. Myocyte length was measured by analysis of a video image as described by Annetts *et al.* (1990) and White & Terrar (1991). Cells were impaled with microelectrodes containing 0.5 mM K_2SO_4 plus 5 or 10 mM KCl. In experiments where contraction and the $[Ca^{2+}]_i$ transient were abolished by the Ca^{2+} chelator BAPTA (1,2-*bis*(2-aminophenoxy)ethane-*N*, *N*, *N*,-*N*-tetracetic acid, Tsien, 1980), 75 mM BAPTA was added to the electrode filling solution.

Ca-activated currents were evoked by the technique of interrupted action potentials as described by Terrar & White (1989) and White & Terrar (1990a,b). In brief, following 8 full action potentials, action potentials were interrupted by a 300 ms voltage clamp pulse to −40 mV. This procedure

[1] Present address: Department of Physiology, University of Leeds, Leeds.
[2] Present address: Medical Sciences Faculty, Memorial University of Newfoundland, Canada.
[3] Author for correspondence.

evoked the Ca-activated current and by varying the time of action potential interruption it was possible to create an envelope of tail currents which is thought to reflect the $[Ca^{2+}]_i$ transient associated with contraction. Repeating the procedure in the presence of intracellular BAPTA allows the investigation of residual outward currents which may be associated with the repolarization of the cell. Current amplitude and decay were analysed by the VCAN software package provided by Dr J. Dempster.

Experiments carried out on single cells were performed at 36°C at a stimulation frequency of 1 Hz. Levels of statistical significance were tested using paired or unpaired t tests as appropriate.

Results

Initially, the effects of 4 min exposure to 2 μM compound II on the force of contraction of guinea-pig papillary mucles was investigated. This concentration was chosen to produce maximal prolongation of the action potential (Connors *et al.*, 1991; 1992). There was a consistent increase in force in all preparations of 14 ± 4.6% (mean ± s.e.mean, $n = 4$; $P < 0.05$).

The effects of compound II on contraction were further investigated in single guinea-pig ventricular cells. The influence of compound II on action potential duration was studied at 100 nM. The effects on membrane currents (see later) were tested at 1 μM for consistency with a previous study, (Connors *et al.*, 1992). Both doses of drug give maximal prolongation of the action potential (Connors *et al.*, 1992). Following 4 min exposure to 100 nM compound II there was an increase in action potential duration but no change in resting membrane potential (consistent with previous reports, Connors *et al.*, 1992). There was also a significant increase in cell shortening (29 ± 5%, $n = 5$ cells, $P < 0.01$), (Figure 1).

One mechanism to explain the increase in cell shortening upon exposure to compound II is an increase in the $[Ca^{2+}]_i$ transient. Ca-activated tail currents were therefore measured by interrupting action potentials with a 300 ms voltage-clamp to − 40 mV. The sizes of these currents are thought to reflect the level of cytosolic calcium (Egan *et al.*, 1989; Terrar & White, 1989, and see Introduction). Exposure to 1 μM compound II significantly increased the mean action potential duration from 184 ± 16 to 240 ± 22 ms ($P < 0.01$, $n = 7$ cells) and increased the peak Ca-activated current from 1.37 ± 0.27 nA by 23 ± 8% ($P < 0.05$), a mean increase of greater than 300 pA (Figure 2a). Figure 2b shows tail current transients constructed from the envelope of tail currents following interruption of the action potential at different times after the upstroke both before and after exposure to 1 μM compound II (exposure times 2 to 5 min). Tail currents after exposure to compound II were significantly larger at all action potential durations ($P < 0.05$). The increases in the Ca-activated tail currents are consistent with an increase in the $[Ca^{2+}]_i$ transient upon exposure to compound II which may in turn lead to the increase in muscle tension and in single cell shortening reported above.

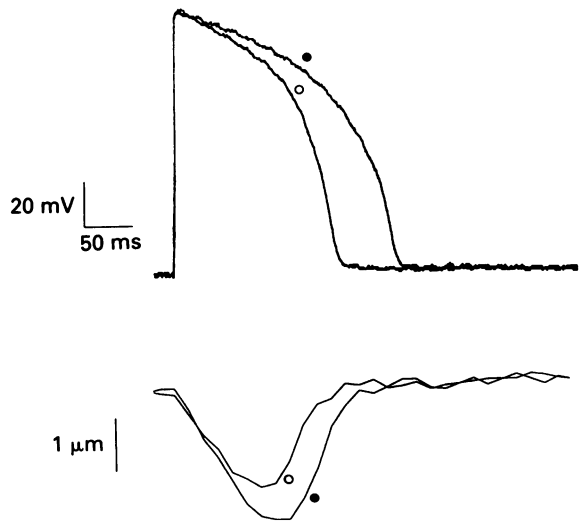

Figure 1 Action potentials (upper traces) and cell shortening (lower traces) from a single guinea-pig ventricular myocyte, before (○) and after (●) exposure to 100 nM compound II. Exposure to compound II increased the duration of the action potential and cell shortening. 1 Hz, 36°C.

When action potentials are interrupted and cytosolic calcium is buffered at a low level by intracellular BAPTA, small time-dependent outward currents remain (Terrar & White, 1989). These currents may be carried by I_K which is activated during the ventricular action potential plateau and which plays an important role in the repolarization of the cell. If this is so, at least part of the apparent increase in inward calcium-activated current might arise from blockade of opposing outward current by compound II. This was tested by applying compound II to cells loaded with intracellular BAPTA (75 mM in the microelectrode). In the absence of compound II, small residual outward currents remained, these currents were abolished by exposure to 1 μM compound II in all the five cells tested (Figure 3). The size of time-dependent current between repolarization and the end of the 300 ms voltage clamp pulse was less than 100 pA. This was considerably smaller than the increase in the calcium-activated tail current reported above when compound II was applied in the absence of BAPTA, but may have led to overestimation of this increase.

It was observed that compound II consistently increased the time constant of decay of the Ca-activated current (Figure 4a, $P < 0.01$, at all action potential durations) but did not change the progressive quickening of the currents as action potential duration increased. An increase in the time-constant of the current would be expected if a small outward current were blocked. It should be noted that increasing the magnitude of the tail current need not increase the time constant of current decay (White & Terrar, 1990b).

Short (12 ms) action potentials (immediately following full action potentials) elicited large Ca-activated currents which subsequently decline to a smaller steady state level on continued stimulation of shortened action potentials. This decline is thought to reflect rundown of the amount of Ca^{2+} stored in the sarcoplasmic reticulum (see Terrar & White, 1989; White & Terrar, 1990a,b). It can be seen from Figure 4b that compound II did not influence the ratio of steady state/first tail current. This observation does not support a direct influence of compound II on the sarcoplasmic reticulum stores.

Discussion

Our observations show that compound II can produce a positive inotropic effect in guinea-pig papillary muscles and an increased shortening in single ventricular myocytes. Compound II is not thought to enhance Ca^{2+} entry via L-type calcium channels at the concentrations used in this study (Connors *et al.*, 1992). It seems possible that the increase in force is a secondary consequence of action potential prolongation. Evidence in support of this interpretation is provided by the experiments where Ca-activated currents were measured during action potentials interrupted with a voltage-clamp pulse to − 40 mV. These observations showed that exposure to compound II increased the $[Ca^{2+}]_i$ transient measured in this way. This would be expected to increase contraction. One possible mechanism for this increase is that action potential prolongation potentiates contraction via the Na:Ca exchange. Action potential prolongation and elevation of the action potential plateau would be expected to reduce

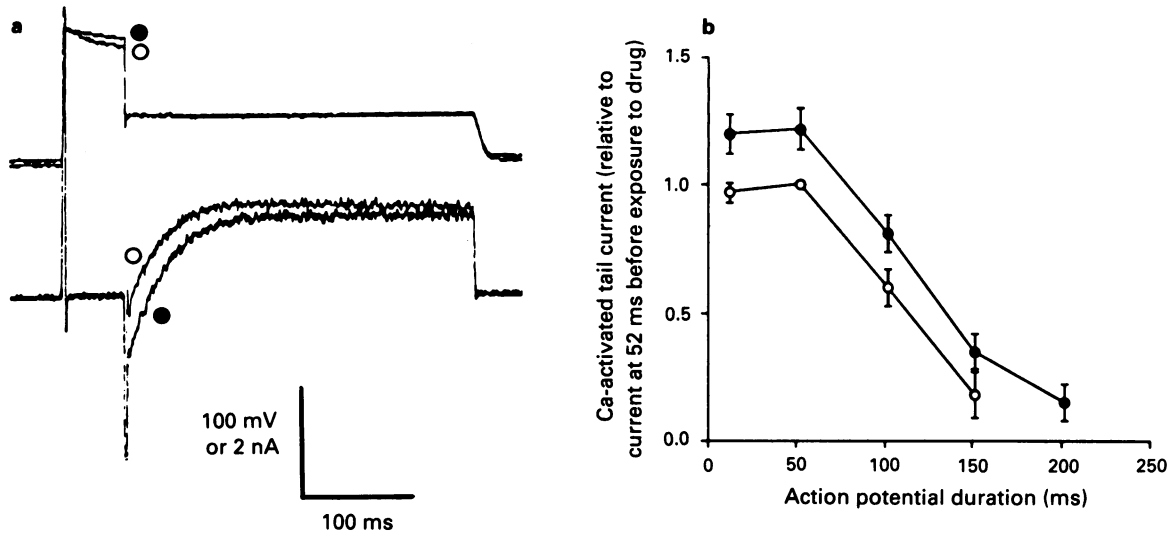

Figure 2 (a) Membrane potential (upper traces), current (lower traces) for an action potential interrupted 52 ms after the upstroke by a 300 ms voltage clamp to − 40 mV in order to evoke Ca-activated current. Records before (○) and after (●) exposure to 1 μM compound II. Compound II elevates the action potential plateau and increases the amplitude of the Ca-activated current. 1 Hz, 36°C. (b) Ca-activated tail current transients before (○) and after (●) exposure to 1 μM compound II (mean ± s.e.mean, $n = 7$ cells). Currents expressed relative to those at 52 ms before exposure to drug (1.0 current = 1.32 ± 0.2 nA, currents greater after exposure, $P < 0.05$ at all durations).

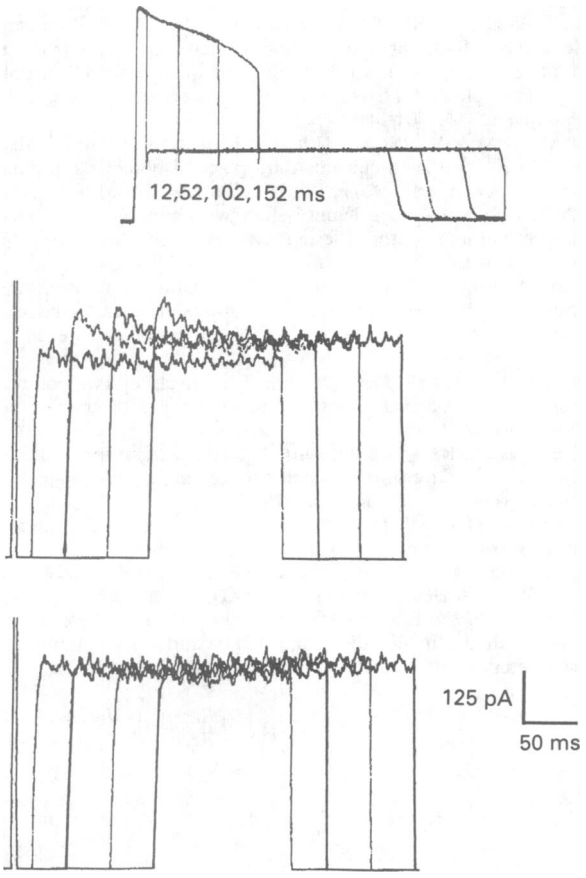

Figure 3 Membrane potential (schematic) (upper traces) and currents in the presence of intracellular BAPTA (75 mM in the microelectrode) before (middle traces) and after (lower traces) exposure to 1 μM compound II. Action potentials were interrupted at varying times indicated by voltage clamping the cell to − 40 mV, in order to evoke small, BAPTA-resistant currents which were abolished by exposure to compound II. 1 Hz, 36°C.

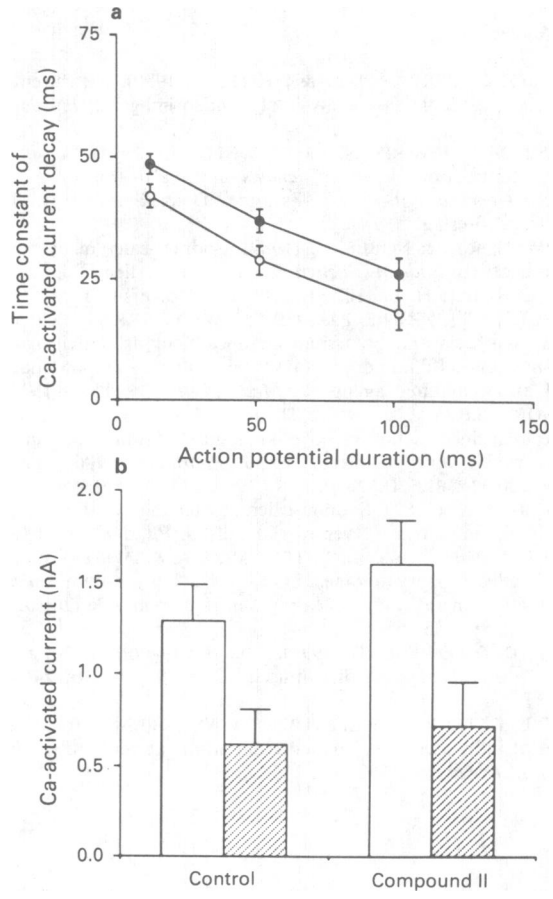

Figure 4 (a) Time constants of Ca-activated current decay before (○) and after (●) exposure to 1 μM compound II, time constants larger after exposure at all durations ($P < 0.01$). (b) First (open columns) and steady state (hatched columns) Ca-activated currents evoked by action potentials of 12 ms duration before and after exposure to 1 μM compound II. Ratio of steady state/first currents not significantly different before (0.41 ± 0.1) and after (0.39 ± 0.09) ($P > 0.05$) exposure to 1 μM drug (mean ± s.e.mean, $n = 7$ cells in a and b).

the driving force of the electrogenic Na:Ca exchange to extrude Ca^{2+} from the cell. Reduced extrusion of Ca^{2+} may then lead to increased loading of intracellular Ca^{2+} stores allowing a greater Ca^{2+} release by the following action potential (see, Boyett *et al.*, 1993).

The above hypothesis does not require any interference by compound II with the normal handling of calcium by the sarcoplasmic reticulum. The ratio of steady state/first Ca-activated currents following abbreviated action potentials is thought to reflect the degree of loading of Ca^{2+} into the sarcoplasmic reticulum (since the stores are loaded to a state determined by normal action potentials at a particular frequency, while maintained stimulation with abbreviated action potentials leads to a progressive decline in stores loading to a new steady state, see Terrar & White, 1989). The ratio of steady state/first Ca-activated current for short interrupted action potentials was unaffected by compound II, unlike the response to caffeine and ryanodine (White & Terrar, 1990a). This is taken as evidence that compound II did not affect normal handling of Ca^{2+} by the sarcoplasmic reticulum.

The effects of compound II on Ca-activated current time constants are qualitatively and quantitatively different from 10 mM caffeine and 10 μM ryanodine which are known to disrupt Ca stores function (see White & Terrar, 1990a). In the light of the above discussion, the most likely interpretation of the increase in time constant of the Ca-activated current on exposure to compound II is block of a small outward time-dependent current.

The progressive decrease in the time constant of the Ca-activated tail currents with increased action potential length (Figure 4a) was not changed by compound II. This supports the hypothesis that the progressive quickening of the currents is not the result of developing outward I_K and is consistent with the explanation for tail current decay given by White & Terrar (1990a).

Our observations show that compound II has a positive inotropic effect on guinea-pig multicellular and single cell preparations. They further indicate that compound II does not influence the normal functioning of the sarcoplasmic reticulum. Our results are consistent with the hypothesis that action potential prolongation leads to reduced Ca^{2+} extrusion by the Na-Ca exchange which in turn leads to increased loading of intracellular stores of Ca^{2+} and subsequently an increase in the $[Ca^{2+}]_i$ transient.

The combination of Class III antiarrhythmic action with a positive intropic effect is potentially clinically useful. Compound II can be listed with the new, more specific, Class III antiarrhythmic agents which share these properties (e.g. E-4031, Wettner *et al.*, 1991 and UK68,798, Tande *et al.*, 1990).

We thank Mrs Nadine Cummings for preparation of cardiac myocytes. This work was supported by The Wellcome Trust and a Rhodes scholarship to S.P.C.

References

ANNETTS, C., TERRAR, D.A. & WHITE, E. (1990). Measurement of cardiac cell length by analysis of a video image. *J. Physiol.*, **430**, 3P.

BOYETT, M.R., HARRISON, S.M. & WHITE, E. (1993). K^+ channels and contraction. In *K^+ Channels in Cardio-vascular Medicine: from Gene to Patient*. ed, Escande, D. & Standen, N. Berlin: Springer-Verlag.

CHAPMAN, R.A. & NOBLE, D. (1989). Sodium-calcium exchange in the heart. In *Sodium-Calcium Exchange*. ed. Allen, T.J.A., Noble, D. & Reuter, H. pp. 102–125. Oxford University Press: Oxford.

CONNORS, S.P., DENNIS, P.D., GILL, E.W. & TERRAR, D.A. (1991). The synthesis and potassium channel blocking activity of some (4-methanesulfonamidophenoxy)propanalmines as potential Class III antiarrhythmic agents. *J. Med. Chem.*, **34**, 1570–1577.

CONNORS, S.P., GILL, E.W. & TERRAR, D.A. (1992). Actions and mechanisms of action of novel analogues of sotalol on guinea-pig and rabbit ventricular cells. *Br. J. Pharmacol.*, **106**, 958–965.

EGAN, T.M., NOBLE, D., NOBLE, S.J., POWELL, T., SPINDLER, A.J. & TWIST, V.W. (1989). Sodium-calcium exchange during the action potential in guinea-pig ventricular cells. *J. Physiol.*, **411**, 639–661.

MITCHELL, M.R., POWELL, T., TERRAR, D.A. & TWIST, V.W. (1984). The effects of ryanodine, EGTA and low sodium on action potentials in rat and guinea-pig ventricular muscle. *Br. J. Pharmacol.*, **81**, 543–550.

NOBLE, D. & POWELL, T. (1991). The slowing of Ca^{2+} signals by Ca^{2+} indicators in cardiac muscle. *Proc. R. Soc.*, B, **246**, 167–172.

POWELL, T., TERRAR, D.A. & TWIST, V.W. (1980). Electrical properties of individual cells isolated from adult rat ventricular myocardium. *J. Physiol.*, **302**, 131–153.

TANDE, P.M., BJORNSTAD, H. & REFSUM, H. (1990). Rate-dependent class III antiarrhythmic action, negative chronotropy and positive inotropy of a novel Ik blocking drug, UK 68,798: Potent in guinea pig but no effect in rat myocardium. *J. Cardiovasc. Pharmacol.*, **16**, 401–410.

TERRAR, D.A. & WHITE, E. (1989). Changes in cytosolic calcium monitored by inward currents during action potentials in guinea-pig ventricular cells. *Proc. R. Soc.*, B, **238**, 171–188.

TSIEN, R.Y. (1980). New calcium buffers with high selectivity against magnesium and protons: design, synthesis and properties of prototype structures. *Biochemistry*, **19**, 2396–2404.

VAUGHAN WILLIAMS, E.M. (1970). Classification of antiarrhythmic drugs. In *Symposium on Cardiac Arrhythmias*. ed. Sandoe, E., Flensted-Jenson, E. & Olson, K.H. Soderaljiie. Sweden: AB Astra.

WHITE, E. & TERRAR, D.A. (1990a). The effects of ryanodine and caffeine on Ca-activated current in guinea-pig ventricular myocytes. *Br. J. Pharmacol.*, **101**, 399–405.

WHITE, E. & TERRAR, D.A. (1990b). The action of strophanthidin on Ca-activated current and contraction in single guinea-pig ventricular myocytes. *Exp. Physiol.*, **75**, 559–572.

WHITE, E. & TERRAR, D.A. (1991). Action potential duration and the inotropic response to reduced extracellular potassium in guinea-pig ventricular myocytes. *Exp. Physiol.*, **76**, 705–716.

WETTNER, E., SCHOLTYSIK, G., SCHAAD, A., HIMMEL, H. & RAVENS, U. (1991). Effects of the new class III antiarrhythmic drug E-4031 on the myocardial contractility and electrophysiological parameters. *J. Cardiovasc. Pharmacol.*, **17**, 480–487.

(Received March 29, 1993
Accepted April 22, 1993)

Br. J. Pharmacol. (1993), **110**, 99–106

Acceleration by chronic treatment with clorgyline of the turnover of brain α_2-adrenoceptors in normotensive but not in spontaneously hypertensive rats

Catalina Ribas, Antonio Miralles & [1]Jesús A. García-Sevilla

Laboratory of Neuropharmacology, Department of Fundamental Biology and Health Sciences, University of the Balearic Islands, E-07071 Palma de Mallorca, Spain

1 The aim of this study was to quantitate and compare the turnover of α_2-adrenoceptors in the cerebral cortex of normotensive Wistar-Kyoto (WKY) and spontaneously hypertensive (SHR) rats, and its modulation during chronic treatment with the monoamine oxidase (MAO) inhibitor, clorgyline.

2 In SHR, the specific binding of the agonist [^{3}H]-UK 14304 and of the antagonist [^{3}H]-RX 821002 was significantly reduced in the brain (B_{max} 15–19% lower) as compared to that in sex- and age-matched WKY rats. In contrast, no significant changes in the K_d values for both radioligands were found between WKY and SHR rats. Therefore, SHR rats offer a genetic model with a lower density of α_2-adrenoceptors in the brain.

3 Chronic treatment (21–35 days) with clorgyline (1 mg kg^{-1}, i.p.) markedly decreased the density of brain α_2-adrenoceptors ([^{3}H]-UK 14304 binding) in Sprague-Dawley (B_{max} reduced by 50%) and in WKY (B_{max} reduced by 30%) rats without any apparent change in the affinity of the radioligand. In contrast, the density of brain α_2-adrenoceptors in SHR was not down-regulated by chronic clorgyline treatment.

4 The recovery of [^{3}H]-UK 14304 binding after irreversible inactivation by N-ethoxycarbonyl-2-ethoxy-1,2-dihydroquinoline (EEDQ; 1.6 mg kg^{-1}) (an alkylating agent for the α_2-adrenoceptor) was assessed in control and clorgyline-treated (1 mg kg^{-1}; i.p. for 7–21 days) WKY and SHR rats to study the process of α_2-adrenoceptor repopulation and to calculate receptor turnover parameters.

5 The simultaneous analysis of receptor recovery curves revealed that the turnover of brain α_2-adrenoceptors in SHR rats was accelerated ($k = 0.141$ day^{-1}; $t_{1/2} = 4.9$ days; $r/k = 40$ fmol mg^{-1} protein) compared to that in WKY rats ($k = 0.085$ day^{-1}; $t_{1/2} = 8.1$ days; $r/k = 54$ fmol mg^{-1} protein) and that the reduced density of cortical α_2-adrenoceptors (B_{max} or r/k values) in SHR was probably due to an abnormal higher receptor degradation ($\Delta k = 66\%$) and not to a decreased receptor synthesis which in fact showed a slight increase ($\Delta r = 24\%$).

6 Treatment with clorgyline (1 mg kg^{-1}, i.p. for 21 days) accelerated the turnover of brain α_2-adrenoceptors in WKY rats ($k = 0.328$ days^{-1}; $t_{1/2} = 2.1$ days; $r/k = 29$ fmol mg^{-1} protein) and the greater increase in receptor degradation ($\Delta k = 286\%$) over receptor synthesis ($\Delta r = 109\%$) led to down-regulation of receptor density ($r/k = 46\%$ lower). In contrast, treatment with clorgyline did not modify significantly the turnover of brain α_2-adrenoceptors in SHR ($k = 0.192$ days^{-1}; $t_{1/2} = 3.6$ days; $r/k = 39$ fmol mg^{-1} protein), indicating that in this genetic model of hypertension, the desensitized α_2-adrenoceptors cannot be further down-regulated by clorgyline treatment and that they lack the expected adaptative increase in receptor synthesis.

Keywords: Spontaneously hypertensive rats (SHR); brain α_2-adrenoceptors; [^{3}H]-UK 14304; [^{3}H]-RX 821002; N-ethoxycarbonyl-2-ethoxy-1,2-dihydroquinoline (EEDQ); receptor turnover; clorgyline

Introduction

Biochemical and functional studies have suggested that endogenous depression is related to α_2-adrenoceptor supersensitivity (García-Sevilla *et al.*, 1986; 1990) and desensitization of these inhibitory receptors has been involved in the mechanism of action of various classes of antidepressant treatments such as tricyclic drugs and monoamine oxidase (MAO) inhibitors (Meana *et al.*, 1992 and other references therein). However, the basic biochemical mechanisms involved in antidepressant-induced down-regulation of the steady state expression of brain α_2-adrenoceptors are poorly understood. Recently long-term treatment with desipramine has been shown to down-regulate the density of α_2-adrenoceptors in the rat brain and to accelerate the turnover of the receptor with a marked increase in its degradation rate (Barturen & García-Sevilla, 1992). The increased α_2-adrenoceptor degradation, which appears to be the result of prolonged receptor activation by endogenous noradrenaline (NA) after inhibition of neuronal uptake by desipramine, could explain the induction of down-regulation of brain α_2-adrenoceptors. Therefore, accelerated α_2-adrenoceptor degradation could be the first change in the metabolism of the receptor induced by specific antidepressant drugs.

The genetic model of the spontaneously hypertensive rats (SHR) of the Wistar-Kyoto (WKY) strain has been associated with dysfunctions of α_2-adrenoceptors which appear to have pathophysiological implications (see Michel *et al.*, 1990). In SHR, the specific binding of [^{3}H]-clonidine to brain α_2-adrenoceptors as well as clonidine-induced mydriasis are reduced when compared to those in sex- and age-matched normotensive WKY rats (Olmos *et al.*, 1991). Therefore, in contrast to the antidepressant-induced receptor down-regulation, the SHR offers a genetic model of down-regulation of α_2-adrenoceptors in the brain (receptor number and function) to assess further biochemical events associated with this relevant receptor regulatory mechanism.

[1] Author for correspondence at: Lab Neurofarmacologia, Dept. Biologia Fonamental i Ciències de la Salut, Universitat de les Illes Balears, Cra. Valldemossa Km 7.5, E-07071 Palma de Mallorca, Spain.

In this context, the present study was designed to quantitate and compare the turnover of brain α_2-adrenoceptors in WKY and SHR rats, and its modulation during treatment with the antidepressant drug, clorgyline, a MAO inhibitor which induces down-regulation of brain α_2-adrenoceptors (Giralt & García-Sevilla, 1989; Menargues *et al.*, 1990), most probably through an indirect mechanism, similar to that described above for desipramine, which involves an increased availability of intraneuronal and/or synaptic NA (L'Heureux *et al.*, 1986; Routledge & Marsden, 1987; Giralt & García-Sevilla, 1989). A preliminary report of this work was given at a meeting of the British Pharmacological Society (London Meeting, September 1992) (Ribas *et al.*, 1992).

Methods

α_2-Adrenoceptor turnover

The irreversible blockade/inactivation of receptors, followed by assessment of the kinetics of reappearance of receptor binding to control levels has been the approach most widely used to study the metabolism of adrenoceptors *in vivo* and *in vitro* (Mahan *et al.*, 1987). The peptide-coupling agent N-ethoxycarbonyl-2-ethoxy-1,2-dihydroquinoline (EEDQ) at a dose of 1.6 mg kg^{-1} was selected as the irreversible antagonist for brain α_2-adrenoceptors (see Barturen & García-Sevilla, 1992 for specific details of EEDQ as a tool to study the turnover of α_2-adrenoceptors). EEDQ appears to alkylate the carboxyl group of an acylamino acid, forming a mixed carbonic anhydride and free quinoline. This mixed carbonic anhydride reacts with a sterically accessible nucleophilic group to inactivate the receptor (Belleau *et al.*, 1969).

Animals and treatments

Male normotensive Wistar-Kyoto (WKY) and spontaneously hypertensive (SHR) rats (200–300 g) (R. Janvier, Le Genest, France) and adult male Sprague-Dawley (SD) rats (250–300 g) were used. The systolic blood pressure, measured by the tail-cuff method, of SHR (196 ± 1 mmHg, $n = 64$) was significantly higher than those of age-matched normotensive WKY (142 ± 1 mmHg, $n = 68$; $P < 0.001$, two-tailed t test) and SD (132 ± 1 mmHg, $n = 12$; $P < 0.001$, two-tailed t test) rats. The animals received a standard diet with water freely available and were housed at 20 ± 2°C with a 12 h light/dark cycle. The animals received i.p. every 24 h either 0.9% saline vehicle or the MAO inhibitor, clorgyline (1 mg kg^{-1}) for 7–35 days (SD rats) or 21 days (WKY and SHR rats). The rats were killed 24 h after the last injection. This dose of clorgyline was considered optimal for induction of brain α_2-adrenoceptor down-regulation (Giralt & García-Sevilla, 1989). EEDQ (1.6 mg kg^{-1}) was dissolved in ethanol and then diluted sequentially with propyleneglycol and purified water (final ratio, 1:1:2, v/v/v) and it was administered i.p. in a single dose. Rats were killed 0.25, 1, 2, 4, 7, 9, 14, 21 and 30 days after EEDQ administration to evaluate the recovery of brain α_2-adrenoceptor density, which allowed estimation of receptor turnover parameters. To study the modulation of α_2-adrenoceptor turnover by clorgyline, EEDQ was injected into rats treated with the antidepressant for 7 days, and treatment was then continued until day 21 (phase 7–21 days, presence or absence of receptor down-regulation in WKY and SHR rats, respectively; see Table 2). The animals were killed by decapitation, the brains rapidly removed and the parietooccipital cortex dissected on ice and stored at − 70°C until assay.

Preparation of membranes

Cortical membranes (P_2 fractions) were prepared by established methods (Giralt & García-Sevilla, 1989) from the parietooccipital cortex. Briefly, after thawing, the tissue samples were homogenized in 5 ml of ice-cold Tris-sucrose buffer (5 mM Tris-HCl, 250 mM sucrose, 1 mM $MgCl_2$; pH 7.4). The homogenates were centrifuged at 1,100 g for 10 min, and the supernatants were then recentrifuged at 40,000 g for 10 min. The resulting pellet was washed twice with 2 ml of fresh incubation buffer (50 mM Tris-HCl, 0.1 mM $MnCl_2$, 0.1% ascorbic acid, pH 7.7 for [^{3}H]-UK 14304 binding assays, or 50 mM Tris-HCl, 0.1% ascorbic acid, pH 7.5 for [^{3}H]-RX 821002 binding assays) (Meana *et al.*, 1989; Miralles *et al.*, 1993). The final pellet was resuspended in an appropriate volume of the incubation buffer to a final protein content of 800–1000 μg ml^{-1}. Protein was determined by the method of Lowry *et al.* (1951) with bovine serum albumin as the standard.

[^{3}H]-UK 14304 and [^{3}H]-RX 821002 binding assays

Total [^{3}H]-UK 14304 binding was measured in 1.1 ml-aliquots (50 mM Tris-HCl, 0.1 mM $MnCl_2$ 0.1% ascorbic acid, pH 7.7) of the cortical membranes which were incubated for 60 min at 25°C with eight concentrations of [^{3}H]-UK 14304 (6×10^{-11} M to 8×10^{-9} M). Total [^{3}H]-RX 821002 binding was also measured in 1.1 ml-aliquots (50 mM Tris-HCl, 0.1% ascorbic acid, pH 7.5) of the membranes which were incubated for 30 min at 25°C with eight concentrations of [^{3}H]-RX 821002 (6×10^{-11} M to 8×10^{-9} M). For both radioligands, nonspecific binding was determined in presence of 10^{-5} M (−)-adrenaline. Specific binding (about 85% at K_d values) was defined as the difference between total binding and nonspecific binding and was plotted as a function of increasing concentrations of the radioligands. Incubations were terminated by diluting the samples with 5 ml of ice-cold Tris incubation buffer (4°C). Membrane-bound [^{3}H]-UK 14304 or [^{3}H]-RX 821002 was measured by vacuum filtration, using a Brandel 48R cell harvester (Biomedical Research & Development Laboratories, U.S.A.), through Whatman GF/C glass fibre filters, which had been presoaked with 0.5% polyethylenimine (Bruns *et al.*, 1983). Then the filters were rinsed twice with 5 ml of incubation buffer, air-dried, transferred to minivials containing 5 ml of OptiPhase 'HiSafe' II cocktail (LKB, England) and counted for radioactivity by liquid scintillation spectrometry at 50% efficiency (Packard model 300C).

Analyses of binding data and statistics

Analyses of saturation isotherms (K_d, dissociation constant; B_{max}, maximum density of binding sites) as well as the fitting of data to the appropriate binding model were performed by computer-assisted nonlinear regression using the EBDA-LIGAND programmes (Munson & Rodbard, 1980; McPherson, 1985). The results were expressed as means ± s.e.mean. One- and two-way analysis of variance (ANOVA), followed by Fisher's LSD or Scheffé's test; and Student's two-tailed t test were used for the statistical evaluations. The level of signficance was $P = 0.05$. To strengthen the comparison between WKY and SHR rats, saturation curves for [^{3}H]-UK 14304 and [^{3}H]-RX 821002 were also simultaneously analysed for best fit using the LIGAND programme. First, the two sets of data (WKY and SHR groups) were analysed separately. Next, they were pooled and analysed simultaneously, and constrained to share two or only one common parameter (K_d and/or B_{max}). The statistical significance of the improvement was determined by the extra sum of squares principle (F-test) as outlined by Munson & Rodbard (1980), with a level of significance of $P = 0.05$. A P value less than 0.05 indicated that the separate fit was much better than the pooled fit (i.e. the fit with one or two shared parameters).

Analyses of α_2-adrenoceptor turnover functions and statistics

For analysis of α_2-adrenoceptor turnover, data from the recovery of brain α_2-adrenoceptor density after irreversible

inactivation by EEDQ were analysed as previously described (Barturen & García-Sevilla, 1992) according to a monoexponential model based on two implicit assumptions (Mauger *et al.*, 1982), that (1) the rate of receptor appearance is constant during the repopulation period (i.e. zero-order process) and (2) receptor disappearance is proportional to the density of receptors at any time (i.e. first-order process). Exponential recovery data were fitted, using the simple nonlinear least squares fitting programme Grafit (Leatherbarrow, 1990), to the equation:

$$[Rt] = r/k\ (1 - e^{-kt}) \qquad \text{(Eq. 1)}$$

where $[Rt]$ is expressed as fmol mg^{-1} protein and represents the receptor number at a given discrete time t; r is the appearance ('synthesis') rate constant of the receptor expressed as fmol mg^{-1} protein day^{-1}, and k is the disappearance ('degradation') rate constant of the receptor, in units of day^{-1}, that allows to estimate the apparent half-life for the receptor ($t_{1/2} = \ln 2/k$). In the present model the ratio r/k represents the density of receptors at steady state towards the system tends after irreversible inactivation of the receptors.

Receptor turnover parameters are expressed as the best fit values ± standard error determined by the matrix inversion method, using the nonlinear regression programme GraFit (Leatherbarrow, 1990). Standard error values determined by nonlinear regression were not used in further formal statistical calculations. Comparisons of experimental data sets for the recovery of α_2-adrenoceptor density were performed by comparing the goodness of fit of a model with and without a set of constraints by means of an F-test. First, the sets of data were analysed separately (with no constraints), the overall value for the sum of squares was the sum of the individual values from each fit and, similarly, the number of degrees of freedom. Next, the sets of data were pooled analysed simultaneously, and constrained to share one or more common parameters, which gave values for the sum of squares and degrees of freedom. The analysis that permitted one or more of the parameters to be shared without a significant increase in the residual variance was taken as the best fit. For further details see Barturen & García-Sevilla (1992) and other references therein.

Drugs

[^{3}H]-UK 14304 (bromoxidine; specific activity, 60–87 Ci $mmol^{-1}$) was purchased from New England Nuclear/Du Pont (U.S.A.) and it was stored at − 30°C. [^{3}H]-RX 821002 (2-methoxyidazoxan; specific activity, 56 Ci $mmol^{-1}$) was purchased from Amersham International plc (U.K.) and it was stored at 2°C. For the binding assays appropriate amounts of the stock solutions were diluted with distilled and purified water (Milli-Q) containing 2.5 mM HCl and 6% ethanol. Other drugs (and their sources) included: (−)-adrenaline bitartrate (Sigma Chemical Co., U.S.A.); EEDQ (N-ethoxycarbonyl-2-ethoxy-1,2-dihydroquinoline) (Sigma); clorgyline HCl (Sigma). Other reagents were obtained from Sigma Chemical Co. (U.S.A.).

Results

Density of α_2-adrenoceptors in the cerebral cortex of WKY and SHR rats

Saturation experiments with the α_2-adrenoceptor agonist [^{3}H]-UK 14304 and the antagonist [^{3}H]-RX 821002 were performed in order to quantitate accurately the density of brain α_2-adrenoceptors in normotensive WKY and spontaneously hypertensive (SHR) rats. In both strains, the specific binding of [^{3}H]-UK 14304 and that of [^{3}H]-RX 821002 were saturable processes of high affinity that revealed the existence of single populations of sites (Table 1, Figure 1). As expected, the density of sites for the antagonist [^{3}H]-RX 821002 (total population of α_2-adrenoceptors) was higher than that obtained for the agonist [^{3}H]-UK 14304 (high-affinity state of the α_2-adrenoceptor; e.g. Meana *et al.*, 1989) (Table 1).

In SHR, the specific binding of [^{3}H]-UK 14304 was reduced in the cerebral cortex (B_{max} 19% lower, $P<0.01$) as compared to that in sex- and age-matched WKY rats (Table 1). Moreover, the simultaneous analysis of multiple saturation isotherms from the WKY and SHR rats further indicated the existence of a decreased number of binding sites for [^{3}H]-UK 14304 ($F[1,12] = 4.98$; $P = 0.045$) with no difference in affinity (K_d values) ($F[1,12] = 0.36$; $P = 0.56$) in the cerebral cortex of SHR (Figure 1a). In SHR, the specific binding of [^{3}H]-RX 821002 was also decreased in the cortex although to a lesser extent (B_{max} 15% lower, $P = 0.056$), and the simultaneous analysis of multiple saturation isotherms from the WKY and SHR rats clearly indicated in this latter strain the existence of a decreased density of sites for [^{3}H]-RX 821002 ($F[1,42] = 8.83$; $P = 0.005$) with no change in receptor affinity ($F[1,42] = 0.16$; $P = 0.69$) (Figure 1b).

Effect of chronic treatment with clorgyline on α_2-adrenoceptors in the cerebral cortex of SD, WKY and SHR rats

Analyses of saturation curves for [^{3}H]-UK 14304 binding to cortical membranes from saline and clorgyline-treated SD rats (1 mg kg^{-1}; i.p. every 24 h for 7, 14, 21, 28, and 35 days) revealed the existence of a time-dependent down-regulation of α_2-adrenoceptor density induced by the antidepressant drug. Thus, short-term treatment for 7 days with clorgyline did not reduce significantly the density of brain α_2-adrenoceptors. In contrast, long-term treatment for 14–35 days clearly induced significant decreases in receptor density with maximal reductions at 21–28 days (B_{max} reduced by 51–54%, respectively; $P<0.001$) (Table 2). Chronic treatment with clorgyline did not alter significantly the binding affinity (K_d values) of [^{3}H]-UK 14304 for the α_2-adrenoceptor (Table 2).

Similarly, long-term treatment of WKY rats with the MAO inhibitor, clorgyline, for 21 days induced down-regulation of the density of brain α_2-adrenoceptors (B_{max} reduced by 30%, $P<0.05$) with no change in receptor

Table 1 Specific binding of [^{3}H]-UK 14304 and [^{3}H]-RX 821002 to brain cortical membranes of normotensive Wistar-Kyoto (WKY) and spontaneously hypertensive (SHR) rats

	Binding parameters		
Radioligand/strain	K_d (nM)	B_{max} (fmol mg^{-1} protein)	n
[^{3}H]-UK 14304			
WKY	1.5 ± 0.1	57 ± 3	10
SHR	1.1 ± 0.3	46 ± 3*	5
[^{3}H]-RX 821002			
WKY	0.5 ± 0.03	81 ± 3†	3
SHR	0.5 ± 0.03	69 ± 4†	3

Neural membranes were incubated at 25°C for 60 min ([^{3}H]-UK 14304) or 30 min ([^{3}H]-RX 821002) with eight concentrations of the radioligands (6×10^{-11} M to 8×10^{-9} M). The specific binding of the radioligands to α_2-adrenoceptors was defined as the difference between total binding and binding in the presence of 10^{-5} M (−)-adrenaline (non-specific binding). Binding parameters (K_d, B_{max}) were determined directly by computer-assisted nonlinear analysis from untransformed data using the EBDA-LIGAND programmes. Each value represents the mean ± s.e.mean of n experiments per group with an animal per experiment.

*$P<0.01$ when compared with the corresponding value in WKY rats (two-tailed t test).

†$P<0.01$ when compared with the corresponding value for [^{3}H]-UK 14304 (two-tailed t test).

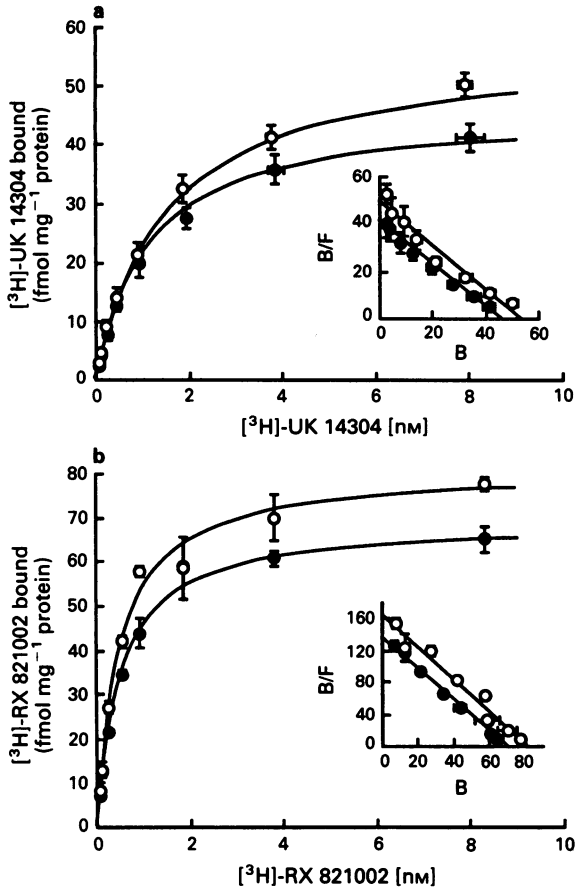

Figure 1 Specific binding of (a) [^{3}H]-UK 14304 and (b) [^{3}H]-RX 821002 to brain cortical membranes of normotensive Wistar-Kyoto (WKY) (○) and spontaneously hypertensive (SHR) (●) rats as a function of increasing concentrations of the radioligand. Data shown are means ± s.e.mean derived from 3–10 experiments per group. See Table 1 for changes in binding parameters. Saturations isotherms also were analysed for best fit as described in Methods. For each radioligand, the simultaneous analysis (LIGAND programme) of the two sets of data (WKY and SHR rats: common K_d and B_{max}) indicated that saturation isotherms were different from each other for both [^{3}H]-UK 14304 ($F[2,12] = 17.54$; $P < 0.0001$) and [^{3}H]-RX 821002 ($F[2,42] = 16.98$; $P < 0.0001$). In both strains of rat, the constraint of the curves to share a common K_d value did not yield a significant increase in the sum of squares ($F[1,12] = 0.36$; $P = 0.56$ for [^{3}H]-UK 14304; and ($F[1,42] = 0.16$; $P = 0.691$ for [^{3}H]-RX 821002) whereas sharing a common B_{max} significantly increased the sum of squares of the fit ($F[1,12] = 4.98$; $P = 0.045$ for [^{3}H]-UK 14304; and ($F[1,42] = 8.83$; $P = 0.005$ for [^{3}H]-RX 821002), which indicated that WKY and SHIR rats differ significantly as to B_{max} but not as to K_d whatever the radioligand used. Inset: Scatchard plots (same data) showing K_d and B_{max} values similar to those reported in Table 1.

affinity (Table 2). In contrast, the density of brain α_2-adrenoceptors in SHR rats was not down-regulated by chronic 21 days clorgyline treatment (Table 2).

α_2-Adrenoceptor turnover in the cerebral cortex of WKY and SHR rats

Treatment of WKY and SHR rats with a single dose of EEDQ (1.6 mg kg^{-1}, i.p.) induced an almost complete reduction in the density of α_2-adrenoceptors in the cerebral cortex (B_{max} for [^{3}H]-UK 14304 reduced more than 95% at 6 h), that was followed by a progressive recovery of the receptor density, as revealed by [^{3}H]-UK 14304 saturation isotherms performed at different times after *in vivo* EEDQ administration (1, 2, 4, 7, 9, 14, 21 and 30 days). The binding affinity of [^{3}H]-UK 14304 for the α_2-adrenoceptor was unaltered during recovery from EEDQ-induced receptor inactivation. These

Table 2 Effects of chronic treatments with clorgyline on the specific binding of [^{3}H]-UK 14304 to brain cortical membranes of normotensive Sprague-Dawley (SD) and Wistar-Kyoto (WKY), and spontaneously hypertensive (SHR) rats

		[^{3}H]-UK 14304		
Strain/Treatment	*Duration* (days)	K_d (nM)	B_{max} (fmol mg^{-1} protein)	n
SD				
Saline		2.1 ± 0.2	70 ± 3	8
Clorgyline	7	2.7 ± 0.2	66 ± 2	3
	14	2.5 ± 0.1	56 ± 2*	3
	21	2.0 ± 0.4	34 ± 2**	3
	28	1.7 ± 0.3	32 ± 2**	3
	35	1.5 ± 0.1	41 ± 1*	3
WKY				
Saline		1.46 ± 0.2	60 ± 4	5
Clorgyline	21	2.10 ± 0.1	42 ± 3*	3
SHR				
Saline		1.37 ± 0.1	45 ± 4	6
Clorgyline	21	2.30 ± 0.3	48 ± 5	3

Clorgyline (1 mg kg^{-1}) was administered i.p., every 24 h for various periods of time. The rats were killed 24 h after the last injection. Other details as for Table 1. Each value represents the mean ± s.e.mean of n experiments per group with an animal per experiment. Two-way ANOVA for B_{max}, but not for K_d values, detected significant differences between strains ($F[2,34] = 3.39$, $P = 0.042$), treatments ($F[1,34] = 9.73$, $P = 0.003$) and for the interaction between strains and treatment ($F[2,34] = 4.10$, $P = 0.025$). One-way ANOVA followed by a multiple comparison test detected a significant decrease in B_{max} after chronic treatment with clorgyline in SD and WKY rats but not in SHR rats ($F[9,30] = 11.92$, $P = 0.0001$).
*$P < 0.05$; **$P < 0.01$ when compared with the corresponding saline-treated group (ANOVA followed by Fisher's LSD or Sheffé's test).

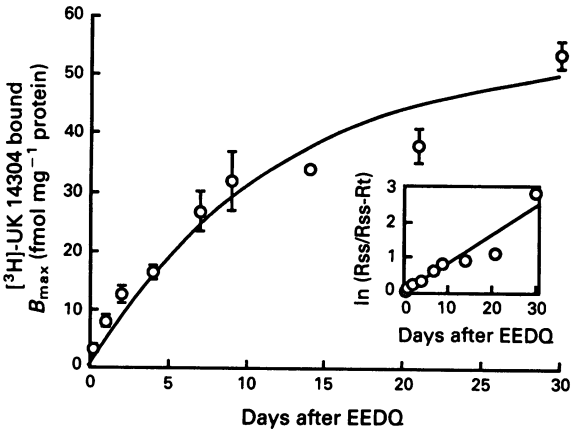

Figure 2 Recovery of α_2-adrenoceptor density in the rat cerebral cortex of normotensive Wistar-Kyoto (WKY) rats after EEDQ-induced receptor inactivation. Data shown are means ± s.e.mean derived from 4 experiments. Other details as for Tables 1 and 3. The B_{max} values were detrmined, for each time, from complete saturation experiments for [^{3}H]-UK 14304 binding using the nonlinear programme LIGAND. Range for K_d values was 0.6 ± 0.1 to 1.6 ± 0.6 nM. ANOVA for K_d values gave $F[9,22] = 1.18$ and $P = 0.35$. The solid line represents the computer-assisted curve fitting of experimental data to the monoexponential model described by the equation $Rt = r/k(1 - e^{-kt})$. Vehicle-treated controls ($B_{max} = 60 \pm 4$ fmol mg^{-1} protein; $K_d = 1.5 \pm 0.2$ nM). Inset: Semilogarithmic plot of the time course for the assessment of α_2-adrenoceptor turnover according to the equation (Mauger *et al.*, 1982): ln [Rss]/[Rss]-[Rt] = kt, where [Rss] and [Rt] are the density of α_2-adrenoceptors in vehicle- and EEDQ-treated rats at time t, respectively. In this linear transformation the slope of the line gives the rate constant of disappearance of the receptor ($k = 0.079$ days^{-1}). The coefficient of correlation is $r = 0.94$. See Table 3 for turnover parameters.

experiments provided the B_{max} values for the analysis of the exponential recovery function (Figure 2).

The quantitative evaluation of the process of α_2-adrenoceptor repopulation in the brain of WKY rats (Figure 2) yielded estimates for the appearance (r) and disappearance (k) rate constants of 4.6 ± 0.5 fmol mg^{-1} protein day^{-1} and 0.085 ± 0.015 day^{-1}, respectively; and a half life ($t_{1/2}$) for the receptor of 8.1 ± 1.5 days (Table 3). The estimated value for the limit of the recovery function (eventual steady state density of α_2-adrenoceptors after complete recovery) was very similar ($r/k = 54$ fmol mg^{-1} protein) to the density of α_2-adrenoceptors obtained in control rats ($B_{max} = 57-60$ fmol mg^{-1} protein) (Tables 1–3 and Figure 3a). Similarly, the quantitative evaluation of α_2-adrenoceptor repopulation in the brain of SHR rats yielded estimates for r and k of 9.6 ± 2.2 fmol mg^{-1} protein day^{-1} and 0.328 ± 0.098 day^{-1}, respectively. The $t_{1/2}$ of the receptor in SHR rats was 2.1 ± 0.7 days and the estimated value for the limit of the recovery function was also very similar ($r/k = 40$ fmol mg^{-1} protein) to the density of α_2-adrenoceptors in control rats ($B_{max} = 45-46$ fmol mg^{-1} protein) (Tables 1–3 and Figure 3b). The simultaneous analysis of experimental data obtained for WKY and SHR rats according to a sole monoexponential function (same r and k values) compared with the analysis without constraints (i.e. independent r and k values for each strain), revealed that the turnover of brain α_2-adrenoceptors in SHR rats was accelerated (increased k value and shorter $t_{1/2}$) compared to that in WKY rats ($F[2,54] = 3.76$, $P = 0.03$) and that the reduced density of cortical α_2-adrenoceptors (B_{max} or r/k values) in hypertensive rats (Tables 1–3) was probably due to an abnormal higher receptor degradation ($\Delta k = 66\%$, $F[1,54] = 3.19$, $P = 0.08$) and not to a decreased receptor synthesis which in fact showed a slight increase ($\Delta r = 24\%$, $F[1,54] = 1.34$, $P = 0.25$) (Table 3 and Figure 3a,b).

Effect of chronic treatment with clorgyline on α_2-adrenoceptor turnover in cerebral cortex of WKY and SHR rats

Long-term treatment with clorgyline for 21 days induced down-regulation of brain α_2-adrenoceptor density in WKY (B_{max} reduced by 30%, $P<0.05$) but not in SHR rats (Table 2). Since clorgyline modulated the steady state expression of brain α_2-adrenoceptors in WKY rats with a pattern of receptor down-regulation, such a pattern might be expected to be the consequence of altered rates of receptor appearance (synthesis) and/or disappearance (degradation). In SHR rats, however, the apparent lack of receptor down-regulation induced by clorgyline might reflect an altered pattern of these receptor regulatory mechanisms. Therefore, α_2-adrenoceptor turnover was assessed during clorgyline treatment (7–21 days) both in WKY and SHR rats.

Similarly to control rats, EEDQ (1.6 mg kg^{-1}, i.p.) treatment in clorgyline-treated WKY and SHR rats (1 mg kg^{-1}, i.p. every 24 h for 7 days) resulted in almost complete reductions (>90% at 6 h) in α_2-adrenoceptor densities in the cerebral cortex (B_{max} for [^{3}H]-UK 14304 binding). In both strains of rat the initial reductions of brain α_2-adrenoceptors were followed by rapid and time-dependent recoveries in receptor density towards control values (i.e. receptor density after 21 days of clorgyline treatment) (Figure 3c,d). The binding affinity of [^{3}H]-UK 14304 for the α_2-adrenoceptor was unaltered during recovery from EEDQ-induced receptor inactivation (Figure 3, legend).

The simultaneous analysis of recovery functions in control and in clorgyline-treated WKY rats, revealed the existence of a marked modulation by the antidepressant of cortical α_2-adrenoceptor turnover function ($F[2,42] = 7.32$, $P = 0.002$) (Table 3, Figure 3a,c). Clorgyline increased significantly the disappearance (degradation) rate constant of the receptor in the brain of WKY rats ($\Delta k = 286\%$, $F[1,42] = 12.7$, $P = 0.0009$), leading to a marked reduction in the half-life of the receptor (control, $t_{1/2} = 8.1$ days; clorgyline, $t_{1/2} = 2.1$ days). Moreover, the appearance (synthesis) rate constant was also increased by clorgyline in WKY rats ($\Delta r = 109\%$, $F[1,42] = 8.53$, $P = 0.0055$). In contrast, the simultaneous analysis of recovery functions in control and in clorgyline-treated SHR rats indicated that the MAO inhibitor did not modify significantly the turnover parameters of brain α_2-adrenoceptors in hypertensive rats ($F[2,42] = 0.78$, $P = 0.46$) (Table 3 and Figure 3b,d). However, it should be noted that in SHR rats clorgyline also tended to accelerate the turnover of brain α_2-adrenoceptors (Table 3).

Table 3 Effect of chronic treatment with clorgyline on α_2-adrenoceptor turnover parameters in the cerebral cortex of normotensive Wistar-Kyoto (WKY) and spontaneously hypertensive (SHR) rats

	Turnover parameters			
Strain/ Treatment	k (day^{-1})	$t_{1/2}$ (days)	r (fmol mg^{-1} protein day^{-1})	r/k (fmol mg^{-1} protein)
WKY				
Saline	0.085 ± 0.015	8.1 ± 1.5	4.6 ± 0.5	54
Clorgyline	0.328 ± 0.098††	2.1 ± 0.7††	9.6 ± 2.2†	29†
SHR				
Saline	0.141 ± 0.024*	4.9 ± 0.9*	5.7 ± 0.7	40
Clorgyline	0.192 ± 0.049	3.6 ± 1.0	7.4 ± 1.2	39

Rats were injected with a single dose of the irreversible antagonist, EEDQ (1.6 mg kg^{-1}, i.p.) and killed after different periods of time to assess the recovery of the specific binding of [^{3}H]-UK 14304 to cortical membranes, which was used as a biochemical index to quantitate the density of α_2-adrenoceptors. Receptor turnover parameters were calculated from data shown in Figure 3 (see Methods). Receptor turnover was assessed in saline-treated rats and during clorgyline (1 mg kg^{-1}, i.p., every 24 h)-induced receptor down-regulation (phase 7–21 days of treatment) (see Table 2). Reappearance of receptors was assessed by nonlinear analysis according to the equation: $Rt = r/k\ (1 - e^{-kt})$, where r is the appearance (synthesis) rate constant, k is the disappearance (degradation) rate constant of the receptor, and the ratio r/k the density of receptors at steady state after irreversible inactivation. $t_{1/2}$ represents the apparent half-life of the receptor and was calculated by the equation: $t_{1/2} = \ln 2/k$. Turnover parameters are expressed as the best fit values ± standard error calculated by the matrix inversion method, using the nonlinear regression programme GraFit (Leatherbarrow, 1990). Statistical comparisons between strains and treatments were made by comparing the goodness of fit of simultaneous analysis with and without a set of constraints (same or different r and k values) by means of an F test. The simultaneous analysis of recovery curves revealed significant differences in α_2-adrenoceptor turnover parameters between WKY and SHR rats ($F[2,54] = 3.76$; $P = 0.03$), and also between saline and clorgyline-treated WKY rats ($F[2,42] = 7.32$, $P = 0.002$) but not between saline and clorgyline-treated SHR rats ($F[2,42] = 0.78$, $P = 0.46$).

*$P = 0.08$ when compared with the corresponding value in WKY rats (F-test).

†$P<0.01$; ††$P<0.001$ when compared with the corresponding saline-treated group (F-test).

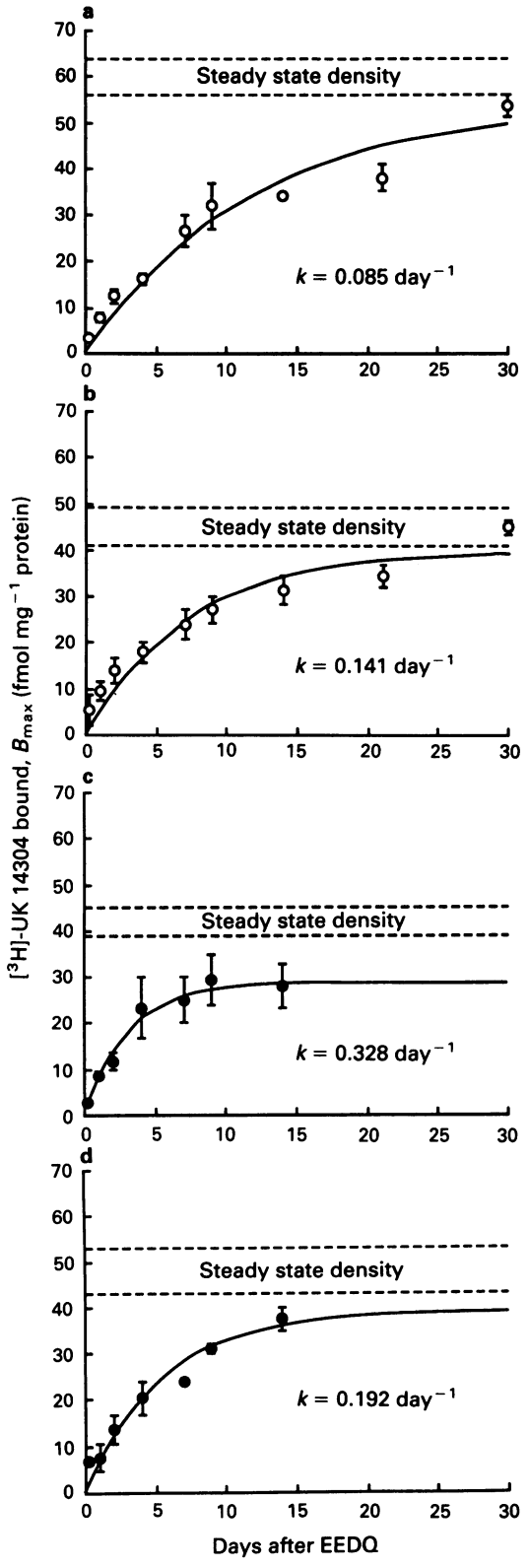

Figure 3 Recovery of α_2-adrenoceptor density (B_{max} for [^{3}H]-UK 14304 binding) in the cerebral cortex of (a,c) normotensive Wistar-Kyoto (WKY) and (b,d) spontaneously hypertensive rats (SHR) after EEDQ-induced receptor inactivation in control rats (a,b) (○) and during clorgyline (1 mg kg^{-1}, i.p., every 24 h)-induced receptor down regulation in WKY but not in SHR rats (c,d) (●) (phase 7–21 days of treatment) (see Table 2). Clorgyline-treated rats were injected with EEDQ (1.6 mg kg^{-1}, i.p.) at day 7 and treatment with clorgyline was continued until 24 h before killing. The B_{max} values were determined from complete saturation experiments for [^{3}H]-UK 14304 using the nonlinear regression programme LIGAND. Other details as for Tables 1 and 3. Data shown are means ± s.e.mean derived from 3–5 experiments. The solid lines represent the computer-assisted curve fitting of experimental data to the monoexponential model described by the equation $Rt = r/k(1 - e^{-kt})$. The dashed horizontal lines show the range (means ± s.e.mean) of receptor density at steady state (i.e. the densities of brain α_2-adrenoceptors in saline- and clorgyline-treated WKY and SHR rats; Table 2). Range for K_d values during recovery was 0.9 ± 0.1 to 1.7 ± 0.2 nM. ANOVA for K_d values (control and clorgyline groups) gave $F[9,99] = 1.70$ and $P = 0.098$. See Table 3 for clorgyline-induced changes in α_2-adrenoceptor turnover parameters.

Discussion

The results of this study are consistent with previous data that demonstrated the existence of a reduced density and sensitivity of brain α_2-adrenoceptors in SHR compared to WKY rats (Olmos *et al.*, 1991). The decrease in the number of receptors detected with both the agonist [^{3}H]-UK 14304 and the antagonist [^{3}H]-RX 821002 was very similar (11 and 12 fmol mg^{-1} protein, respectively), suggesting that the observed alterations in the density and sensitivity of brain α_2-adrenoceptors in SHR involve mainly the high affinity state of the receptor. A reduced α_2-adrenoceptor-mediated autoinhibition of noradrenergic transmission has been demonstrated in the hypothalamus of SHR (Kubo *et al.*, 1986) which results in a potentiation of NA release (Tsuda *et al.*, 1990). This greater release of NA in SHR could explain (through desensitization processes) the decreases in the density and sensitivity of brain α_2-adrenoceptors found in this model of genetic hypertension (Olmos *et al.*, 1991; present results). In this context, the quantitative evaluations of receptor repopulation after EEDQ in the cerebral cortex of WKY and SHR revealed that α_2-adrenoceptor turnover is markedly accelerated (increased degradation and shorter half-life) in hypertensive rats. In contrast, receptor synthesis appears to be rather similar in both strains. These results are in agreement with the reported greater release of NA in the brain of SHR (Kubo *et al.*, 1986; Tsuda *et al.*, 1990) which through sustained activation of α_2-adrenoceptors induces down-regulation by an increased receptor degradation. In SHR, this increased receptor degradation is not compensated with an adaptive increase in receptor synthesis which results in a permanent receptor down-regulation.

The time-dependent modulation of brain α_2-adrenoceptor density by chronic treatment with clorgyline in SD rats is consistent with the reported decrease in the density of brain α_2-adrenoceptors and desensitization of associated functional responses (e.g. clonidine-induced mydriasis) after long-term administration of various antidepressant drugs (including clorgyline), suggesting further that sustained stimulation of α_2-adrenoceptors by the endogenous agonist NA results in down-regulation of the receptor (Smith & Hollingsworth, 1984; Giralt & García-Sevilla, 1989; Menargues *et al.*, 1990; Barturen & García-Sevilla, 1992). In line with these findings, chronic clorgyline treatment in WKY rats also resulted in down-regulation of brain α_2-adrenoceptors. In contrast, the native lower density of brain α_2-adrenoceptors in SHR was not down-regulated further by treatment with the MAO inhibitor. In this context, clorgyline treatment in WKY rats markedly accelerated the turnover of brain α_2-adrenoceptors with the expected increased receptor degradation and shorter half life, but also with a greater receptor synthesis. The greater increase in receptor degradation over receptor synthesis could explain the down-regulation of brain α_2-adrenoceptor density induced by clorgyline, as the greater receptor degradation in SHR explains the lower native brain receptor density in this strain. Similarly to the reported increase in the turnover of brain α_2-adrenoceptors as a consequence of desipramine treatment (Barturen & García-Sevilla, 1992), as well as those of α_1-adrenoceptors (Hughes & Insel, 1986), β-adrenoceptors (Snavely *et al.*, 1985) and benzodiazepine receptors (Miller *et al.*, 1991) as a consequence of exposure to an agonist, one can suggest that sustained

stimulation of α_2-adrenoceptors by endogenous NA, after inhibition of MAO activity by clorgyline (present study) or neuronal uptake by desipramine (Barturen & García-Sevilla, 1992), increases receptor degradation, leading to an initial reduction in receptor number. Also, the increase in receptor synthesis induced by clorgyline treatment in WKY rats could be viewed as a later compensatory mechanism that would lead to restoration of brain α_2-adrenoceptor density (see Discussion in Barturen & García-Sevilla, 1992). In marked contrast to WKY rats, chronic clorgyline treatment in SHR did not accelerate significantly the turnover of brain α_2-adrenoceptors, indicating that these genetically desensitized α_2-adrenoceptors cannot be further down-regulated by clorgyline treatment, probably due to the higher rate of receptor degradation in SHR compared to WKY rats and to the lack of the expected adaptative increase in receptor synthesis (see above). In this sense, it is noteworthy that chronic treatment with the imidazoline drugs, idazoxan and cirazoline, that in normotensive SD and WKY rats resulted in a significant up-regulation of brain I_2-imidazoline sites, did not modify the density of these sites in the brain of SHR rats (Olmos *et al.*, 1992). Together these results could reflect the existence of a relevant abnormality in common receptor regulatory mechanisms controlling receptor synthesis in this genetic model of hypertension.

Little is known about the basic biochemical mechanisms of agonist (NA)-induced down-regulation of α_2-adrenoceptors. In contrast, homologous desensitization and down-regulation of β_2-adrenoceptors in cultured cells is a well characterized phenomenon (Schwinn *et al.*, 1992). Thus, two major mechanisms involved in down-regulation of β_2-adrenoceptors have been elucidated: a decreased receptor synthesis (via destabilization of mRNA levels) and an increased receptor degradation (via receptor phosphorylation), and both mechanisms could explain a loss of receptors (Schwinn *et al.*, 1992). With respect to α_2-adrenoceptors in brain tissue, previous studies with desipramine (Barturen & García-Sevilla, 1992) and the present results with clorgyline clearly demonstrate that only an increased receptor degradation is the relevant mechanism involved in down-regulation of brain α_2-adrenoceptor density, indicating that this accelerated degradation is the first change in the metabolism of the receptor induced by these two prototypical antidepressant drugs. In this context, the consistent increase in receptor synthesis induced by chronic desipramine and clorgyline might represent a later compensatory mechanism that would lead to restoration of brain α_2-adrenoceptor density (Barturen & García-Sevilla, 1992).

In the rat brain, α_2-adrenoceptors are heterogeneous in nature and the existence of at least two receptor subtypes (α_{2A} and α_{2B}) has been documented in the various brain regions (Bylund, 1985; Brown *et al.*, 1990) with a preponderance of the α_{2A} subtype in the cerebral cortex (Uhlén & Wikberg, 1991; Barturen & García-Sevilla, 1992). In the present study, the radioligand used to quantify α_2-adrenoceptors, [^{3}H]-UK 14304, is a mixed $\alpha_{2A/B}$ agonist and the alkylating agent EEDQ does not discriminate between α_2-adrenoceptor subtypes (Barturen & García-Sevilla, 1992). Recently, however, the mechanisms of agonist-induced down-regulation of α_2-adrenoceptors have been shown to be the same for α_{2A}- and α_{2B}-adrenoceptors (Eason & Liggett, 1992; Liggett *et al.*, 1992). Thus in cultured cells, adrenaline induces homologous desensitization through phosphorylation by β_2-adrenoceptor kinase of α_{2A}- and α_{2B}-subtypes, which is followed by uncoupling from G_i proteins (rightward shifts for adrenaline-mediated inhibition of adenylyl cyclase and decreases in agonist high affinity binding), and in the long-term by a decrease in the density of cellular G_i proteins (important component of chronic desensitization), receptor sequestration (translocation from the cell surface to the interior) and finally receptor down-regulation (proteolytic receptor degradation) (Eason & Liggett, 1992; Liggett *et al.*, 1992). These same mechanisms, leading to α_2-adrenoceptor down-regulation after sustained stimulation by endogenous NA, could operate in the rat brain after chronic treatment with desipramine (Barturen & García-Sevilla, 1992) and clorgyline (present study). Moreover, in line with the above mechanisms, preliminary results from this laboratory indicate that chronic treatment with the MAO inhibitor, clorgyline, decreases by about 20% the density of specific G_i protein subunits ($G_{\alpha_{i1/2}}$) in the rat cerebral cortex. In this context, the genetic model of down-regulation of brain α_2-adrenoceptors in SHR together with an accelerated receptor turnover (increased receptor degradation), and an apparent lack of receptor down-regulation and turnover acceleration induced by clorgyline in these rats, suggest the existence of relevant altered patterns of α_2-adrenoceptor regulatory mechanisms (e.g. increased receptor phosphorylation, abnormal G_i proteins and/or dysfunction of receptor synthesis) in this genetic model of hypertension.

This study was supported by DGICYT Grant PM 91-0069, FIS Grant 93/0641 and by CDTI-S.A. LASA Laboratorios Grant 92-0178. C.R. was supported by a fellowship from MEC, Spain.

References

BARTUREN, F. & GARCIA-SEVILLA, J.A. (1992). Long-term treatment with desipramine increases the turnover of α_2-adrenoceptors in the rat brain. *Mol. Pharmacol.*, **42**, 846–855.

BELLEAU, B., DITULLIO, V. & GODIN, D. (1969). The mechanism of irreversible adrenergic blockade by N-carbethoxydihydroquinolines-model studies with typical serine hydrolases. *Biochem. Pharmacol.*, **18**, 1039–1044.

BROWN, C.M., MACKINNON, A.C., MCGRATH, J.C., SPEDDING, M. & KILPATRICK, A.T. (1990). Heterogeneity of α_2-adrenoceptors in rat cortex but not in human platelets can be defined by 8-OH-DPAT, RU 24969 and methysergide. *Br. J. Pharmacol.*, **99**, 481–486.

BRUNS, R.F., LAWSON-WENDLING, K. & PUGSLEY, T.A. (1983). A rapid filtration assay for soluble receptor using polyethylenimine-treated filters. *Anal. Biochem.*, **132**, 74–81.

BYLUND, B.D. (1985). Heterogeneity of alpha-2 adrenergic receptors. *Pharmacol. Biochem. Behav.*, **22**, 835–843.

EASON, M.G. & LIGGETT, S.B. (1992). Subtype-selective desensitization of α_2-adrenergic receptors. *J. Biol. Chem.*, **267**, 25473–25479.

GARCIA-SEVILLA, J.A., GUIMON, J., GARCIA VALLEJO, P. & FUSTER, M.J. (1986). Biochemical and functional evidence of supersensitive platelet α_2-adrenoceptor in major effective disorder: effect of long-term lithium carbonate treatment. *Arch. Gen. Psychiatry*, **43**, 51–57.

GARCIA-SEVILLA, J.A., PADRO, D., GIRALT, M.T., GUIMON, J. & ARESO, P. (1990). α_2-Adrenoceptor-mediated inhibition of platelet adenylate cyclase and induction of aggregation in major depression. *Arch. Gen. Psychiatry*, **47**, 125–132.

GIRALT, M.T. & GARCIA-SEVILLA, J.A. (1989). Acute and long-term regulation of brain α_2-adrenoceptors after manipulation of noradrenergic transmission in the rat. *Eur. J. Pharmacol.*, **164**, 455–466.

HUGHES, R.C. & INSEL, P.A. (1986). Agonist-mediated regulation of alpha1- and beta2-adrenergic receptor metabolism in a muscle cell line BC3H-1. *Mol. Pharmacol.*, **29**, 521–530.

KUBO, T., GOSHIMA, Y., UEDA, H. & MISU, Y. (1986). Diminished α_2-adrenoceptor-mediated modulation of noradrenergic neurotransmission in the posterior hypothalamus of spontaneously hypertensive rats. *Neurosci. Lett.*, **65**, 29–34.

LEATHERBARROW (1990). *GraFit, version 2.0.* Staines, U.K.: Erithacus Software Ltd.

L'HEUREUX, R., DENNIS, T., CURET, O. & SCATTON, B. (1986). Measurement of endogenous noradrenaline release in the rat cerebral cortex in vivo by transcortical dialysis: effects of drugs affecting noradrenergic transmission. *J. Neurochem.*, **46**, 1794–1801.

LIGGETT, S.B., OSTROWSKI, E.J., CHESNUT, L.C., KUROSE, H., RAYMOND, J.R., CARON, M.G. & LEFKOWITZ, R.J. (1992). Sites in the third intracellular loop of the α_{2A}-adrenergic receptor confer short term agonist-promoted desensitization. *J. Biol. Chem.*, **267**, 4740–4746.

LOWRY, O.H., ROSEBROUGH, N.F., FARR, A.G. & RANDALL, R.J. (1951). Protein measurement with the Folin phenol reagent. *J. Biol. Chem.*, **193**, 265–275.

MAHAN, L.C., MCKERNAN, R.M. & INSEL, P.A. (1987). Metabolism of alpha- and beta-adrenergic receptors in vitro and in vivo. *Annu. Rev. Pharmacol. Toxicol.*, **27**, 215–235.

MAUGER, J.P., SLADECZEK, F. & BOCKAERT, J. (1982). Characteristics and metabolism of α_1-adrenergic receptors in a nonfusing muscle cell line. *J. Biol. Chem.*, **257**, 875–879.

MCPHERSON, G.A. (1985). Analysis of radioligand binding experiments: a collection of computer programs for IBM PC. *J. Pharmacol. Methods*, **14**, 213–228.

MEANA, J.J., BARTUREN, F. & GARCIA-SEVILLA, J.A. (1989). Characterization and regional distribution of α_2-adrenoceptors in postmortem human brain using the full agonist [^{3}H]UK 14304. *J. Neurochem.*, **52**, 1210–1217.

MEANA, J.J., BARTUREN, F. & GARCIA-SEVILLA, J.A. (1992). α_2-Adrenoceptors in the brain of suicide victims: increased receptor density associated with major depression. *Biol. Psychiatry*, **31**, 471–490.

MENARGUES, A., OBACH, R. & GARCIA-SEVILLA, J.A. (1990). Modulation by antidepressant drugs of CNS postsynaptic α_2-adrenoceptors mediating mydriasis in the rat. *Naunyn-Schmied. Arch. Pharmacol.*, **341**, 101–107.

MICHEL, M.C., BRODDE, O.-E. & INSEL, P.A. (1990). Peripheral adrenergic receptors in hypertension. *Hypertension*, **16**, 107–120.

MILLER, L.G., LUMPKIN, M., GREENBLATT, D.J. & SHADER, R.I. (1991). Accelerated benzodiazepine receptor recovery after lorazepam discontinuation. *FASEB J.*, **5**, 93–97.

MIRALLES, A., OLMOS, G., SASTRE, M., BARTUREN, F., MARTIN, I. & GARCIA-SEVILLA, J.A. (1993). Discrimination and pharmacological characterization of I_2-imidazoline sites with [^{3}H]-idazoxan and alpha-2 adrenoceptors with [^{3}H]RX 821002 (2-methoxy idazoxan) in the human and rat brains. *J. Pharmacol. Exp. Ther.*, **264**, 1187–1197.

MUNSON, P.J. & RODBARD, D. (1980). Ligand: a versatile computerized approach for the characterization of ligand binding system. *Anal. Biochem.*, **107**, 220–239.

OLMOS, G., MIRALLES, A., BARTUREN, F. & GARCIA-SEVILLA, J.A. (1991). Decreased density and sensitivity of α_2-adrenoceptors in the brain of spontaneously hypertensive rats. *Eur. J. Pharmacol.*, **205**, 93–96.

OLMOS, G., MIRALLES, A., BARTUREN, F. & GARCIA-SEVILLA, J.A. (1992). Characterization of brain imidazoline receptors in normotensive and hypertensive rats: differential regulation by chronic imidazoline drug treatment. *J. Pharmacol. Exp. Ther.*, **260**, 1000–1007.

RIBAS, C., MIRALLES, A. & GARCIA-SEVILLA, J.A. (1992). Long-term treatment with clorgyline accelerates the turnover of brain α_2-adrenoceptors in normotensive (WKY) but not in hypertensive (SHR) rats. *Br. J. Pharmacol.*, **107**, 377P.

ROUTLEDGE, C. & MARSDEN, C.A. (1987). Comparison of the effects of selected drugs on the release of hypothalamic adrenaline and noradrenaline measured in vivo. *Brain Res.*, **426**, 103–111.

SCHWINN, D.A., CARON, M.C. & LEFKOWITZ, R.J. (1992). The beta-adrenergic receptor as a model for molecular structure-function relationships in G-protein-coupled receptors. In *The Heart and Cardiovascular System.* ed. Fozzard, H.A. pp. 1657–1684. New York: Raven Press, Ltd.

SMITH, C.B. & HOLLINGSWORTH, P.J. (1984). α_2-Adrenoceptor and antidepressant treatments. In *Proceedings of the 9th IUPHAR Congress.* ed. Paton, W. Vol. 3. pp. 131–136. London: MacMillan Press Ltd.

SNAVELEY, M.D., ZIEGLER, M.G. & INSEL, P.A. (1985). A new approach to determine rates of receptor appearance and disappearance in vivo: application to agonist-mediated down-regulation of rat renal corticoid β_1- and β_2-adrenergic receptors. *Mol. Pharmacol.*, **27**, 19–26.

TSUDA, K., TSUDA, S., GOLDSTEIN, M. & MASUYAMA, Y. (1990). Effect of neuropeptide Y on norepinephrine release in hypothalamic slices of spontaneously hypertensive rats. *Eur. J. Pharmacol.*, **182**, 175–180.

UHLEN, S. & WIKBERG, J.E.S. (1991). Rat spinal cord α_2-adrenoceptors are of the α_{2A}-subtype: comparison with α_{2A}- and α_{2B}-adrenoceptors in rat spleen, cerebral cortex and kidney using [^{3}H]-RX821002 ligand binding. *Pharmacol. Toxicol.*, **69**, 341–350.

(Received February 8, 1993
Revised April 2, 1993
Accepted April 22, 1993)

Br. J. Pharmacol. (1993), **110**, 107–112

Effect of heparin and a low-molecular weight heparinoid on PAF-induced airway responses in neonatally immunized rabbits

Masahiro Sasaki, Caroline M. Herd & [1]Clive P. Page

Department of Pharmacology, King's College London, Manresa Road, London SW3 6LX

1 We have investigated the effect of an unfractionated heparin preparation, a low-molecular weight heparinoid (Org 10172) and the polyanionic molecule polyglutamic acid against PAF-induced airway hyperresponsiveness and pulmonary cell infiltration in neonatally immunized rabbits *in vivo*.

2 Exposure of neonatally immunized rabbits to aerosolized platelet activating factor (PAF) (80 $\mu g\ ml^{-1}$ for 60 min) elicited an increase in airway responsiveness to inhaled histamine 24 h and 72 h following challenge which was associated with an infiltration of inflammatory cells into the airways, as assessed by bronchoalveolar lavage (BAL).

3 A significant increase in the total numbers of cells recovered from BAL fluid was associated with significantly increased cell numbers of neutrophils, eosinophils and mononuclear cells 24 h following PAF exposure. The numbers of eosinophils and neutrophils in the airways remained elevated 72 h after challenge.

4 The intravenous administation of an unfractionated preparation of heparin (100 units kg^{-1}) or Org 10172 (100 $\mu g\ kg^{-1}$) 30 min prior to PAF exposure significantly inhibited the airway hyperresponsiveness induced by PAF, 24 h and 72 h following challenge. PAF-induced hyperresponsiveness was not significantly affected by prior intravenous administration of polyglutamic acid (100 $\mu g\ kg^{-1}$).

5 The intravenous administration of unfractionated heparin (100 units kg^{-1}), Org 10172 (100 $\mu g\ kg^{-1}$) or polyglutamic acid (100 $\mu g\ kg^{-1}$) 30 min prior to PAF exposure significantly inhibited the expected increase in total cell infiltration.

6 This study shows that unfractionated heparin and a low-molecular weight heparinoid, Org 10172, are capable of inhibiting both the airway hyperresponsiveness and pulmonary cell infiltration induced by PAF in the rabbit.

Keywords: Heparin; low-molecular weight heparin; PAF; airways; inflammation; airway hyperresponsiveness; neonatally immunized rabbit

Introduction

Bronchial asthma is now recognised as an inflammatory disease which is characterized by bronchial hyperresponsiveness, excessive mucus production, mucosal oedema and recruitment of inflammatory cells into the airways. Much attention has been focussed on the role of inflammatory cells such as mast cells, and more recently circulating T-lymphocytes (Corrigan *et al.*, 1988; Kay, 1991; Robinson *et al.*, 1992), in allergic inflammation. Heparin, a major component of the mast cell granule matrix, is widely known as a polyanionic anticoagulant; however, comparatively little work has been done with respect to its anti-inflammatory effects.

It was reported in 1928 that heparin could inhibit features of anaphylaxis (Van der Carr & Williams, 1928), a phenomenon confirmed later by clinical studies which showed that heparin could modulate allergic responses in the skin and respiratory system (Dolowitz & Dougherty, 1960; Dahl, 1962; Boyle *et al.*, 1964; Bowler *et al.*, 1993). In addition, an increased level of an endogenous 'heparin-like material' has been reported in the plasma of allergic subjects (Lasser *et al.*, 1987). Heparin has been shown to inhibit activation of the complement system (Kazatchkine *et al.*, 1981; Ekre *et al.*, 1986), neutrophil chemotaxis (Matzner *et al.*, 1984) and eosinophil infiltration (Hanss *et al.*, 1989; Seeds & Page, 1992). Furthermore, heparin protects against tissue damage induced by cationic leukocyte-derived cationic mediators (Motojima *et al.*, 1989), such as the specific eosinophil-derived mediators major basic protein (MBP), eosinophilic cationic protein and eosinophil perioxidase (Frigas & Gleich, 1986). Heparin has also been shown to inhibit the increased vascular permeability induced by a variety of inflammatory mediators including histamine, bradykinin, prostaglandin E_1 (Carr, 1979) and cationic proteins (Needham *et al.*, 1988; Antunes *et al.*, 1990; Sasaki *et al.*, 1991). Evidence suggests that heparin can inhibit T-lymphocyte activation (Frieri & Metcalfe, 1983), trafficking (Sy *et al.*, 1983; Willenborg & Parish, 1988; Lider *et al.*, 1990) and delayed hypersensitivity responses (Frieri & Metcalfe, 1983; Sy *et al.*, 1983; Lider *et al.*, 1990) via a mechanism unrelated to its anti-coagulant properties.

Heparin is a mixture of anionic sulphated mucopolysaccharide chains with an average molecular weight of 10,000–15,000 Da, composed of sulphated disaccharides. It is heterogeneous with respect to its affinity for anti-thrombin III (AT-III), the most important heparin cofactor present in plasma (Rosenberg *et al.*, 1978). Org 10172, a low-molecular weight heparinoid, is a mixture of sulphated glycosaminoglycans derived from animals intestinal mucosa, with a mean molecular weight of approximately 6,000 Da. Org 10172 consists of approximately 80% low-molecular weight heparin sulphate, 10% dermatan sulphate and approximately 5% each of chondroitin sulphate and a low molecular weight heparin-like component with high affinity for AT-III. In animals studies Org 10172 displayed anti-thrombotic activity with only a small dose-dependent bleeding enhancing capacity compared with equipotent antithrombotic doses of standard heparin (Bradbrook *et al.*, 1987). Org 10172 has been used to investigate the contribution of molecular weight to the activity of heparin on PAF-induced airway changes.

It has been suggested that the ether-linked phospholipid

[1] Author for correspondence.

platelet activating factor (PAF), plays an important role in the pathogenesis of asthma as it can reproduce many of the features of the disease, both in experimental animals and man (reviewed in Page, 1988). PAF has been employed in this study to induce airway hyperresponsiveness in rabbits as we have previously reported that this is a useful test system for the evaluation of pharmacological agents and is simpler and more robust method than antigen challenge. We have utilized antigen-immunized rabbits in this study as we have previously shown that PAF can induce airway hyperresponsiveness to inhaled histamine in all neonatally immunized rabbits to some degree (Herd *et al.*, 1992), whereas only in some, but not all *normal* rabbits (Coyle *et al.*, 1990; Herd *et al.*, 1992).

Therefore, in the present study we have investigated the effects of heparin and related compounds on PAF-induced airway hyperresponsiveness and pulmonary cell infiltration in neonatally antigen-immunized rabbits *in vivo*.

Methods

Animals

New Zealand White (NZW) rabbits (Froxfield Farms, Petersfield, Hants) of either sex were used throughout the study. The immunization procedure of neonatal rabbits was that described previously (Herd *et al.*, 1992). Briefly, rabbits were injected intraperitoneally (0.5 ml) within 24 h of birth with *Alternaria tenuis* extract (1 mg ml^{-1}) in aluminium hydroxide ($Al(OH)_3$) moist gel. Antigen administration was repeated weekly for the first month and then biweekly for the next two months. The methods described in this study was subject to Home Office approval and performed under the Animals (Scientific Procedures) Act, 1986.

Pulmonary function measurements

Immunized rabbits (2.0–3.75 kg) were pre-medicated with diazepam (5 mg ml^{-1}, 5 mg kg^{-1}, i.p.) and were subsequently treated with Hypnorm (0.4 ml kg^{-1}, i.m.; a mixture of fentanyl citrate 0.315 mg ml^{-1} and fluanisone 10 mg ml^{-1}), a regime which produces neuroleptanalgesia and is recommended for recovery experiments in laboratory rabbits (Flecknall, 1987). Neuroleptanalgesia was maintained throughout the course of the experiment by administration of 0.2–0.3 ml Hypnorm i.m. approximately every 30 min (Flecknall, 1987). Animals were intubated with an endotracheal tube (3.0 mm i.d., Mallinckrodt Laboratories, Athlone, Ireland), which was connected to a heated Fleisch pneumotachograph (size 00). Measurements of flow, pleural pressure, transpulmonary pressure (the difference between thoracic and pleural pressure) and tidal volume were made according to Herd *et al.* (1992). Measurements of total lung resistance (R_L) and dynamic compliance (C_{dyn}) were calculated by an online respiratory analyser (PMS Version 4.1 Mumed Ltd., London).

Experimental protocol

On Day 1, airway responsiveness to aerosolized histamine was determined as a measure of lung function, as previously described (Herd *et al.*, 1992). Cumulative dose-response curves were established and the provocation concentration (PC) of histamine which produced 50% increase in R_L (PC_{50}) and 35% decrease in C_{dyn} (PC_{35}) was determined for each rabbit. These calculated values were used as indices of airway responsiveness.

On Day 2, rabbits were injected with 0.5 ml sterile saline (control), unfractionated heparin (100 u kg^{-1}), Org 10172 (100 μg kg^{-1}) or polyglutamic acid (100 μg kg^{-1}) intravenously 30 min prior to exposure of a 2 min aerosol of 0.25% bovine serum albumin (BSA) (the carrier molecule for PAF). PAF aerosol (80 μg ml^{-1}) was then administered over the following hour, after which time respiratory function was recorded. On Days 3 and 5, airway responsiveness to histamine was determined as on Day 1.

Control studies were performed whereby heparin (100 u kg^{-1}) and Org 10172 (100 μg kg^{-1}) were administered intravenously 30 min prior to a 1 h aerosol challenge of 0.25% BSA. In these experiments, respiratory parameters (R_L and C_{dyn}) were recorded before and 1, 15 and 30 min following the drug administration.

Bronchoalveolar lavage

Bronchoalveolar lavage (BAL) was performed immediately following histamine challenge on Days 1, 3 and 5 as previously described (Herd *et al.*, 1992). Both total and differential cell counts were enumerated from BAL fluid.

Analysis of results

Results of the lung function studies are expressed as mean ± s.e.mean. *In vivo* histamine potency values were derived from measurements of airway resistance (R_L) (PC_{50}) and dynamic compliance (C_{dyn}) (PC_{35}) and are expressed as the geometric means together with upper and lower values for s.e.mean. For statistical purposes PC_{50} and PC_{35} values were $\log_{10}$ transformed. One-way analysis of variance was used to analyse the bronchoconstriction data (R_L and C_{dyn}) (expressed as percentage change). Two-way analysis of variance for repeated measures was employed to analyse the histamine potency data prior to and at the 2 time points following PAF administration. The total cell counts and mononuclear cell, eosinophil and neutrophil counts obtained from BAL before, 24 h and 72 h after PAF challenge were analysed by Kruskall-Wallis one-way analysis of variance as the variances were found to be non-homogeneous. Tukey's HSD test was used to determine differences in means when multiple comparisons were made for the parametric data (with analysis of variance) and distribution-free multiple comparisons were used to determine differences in means when multiple comparisons were made for the non-parametric data (Kruskall-Wallis one-way analysis of variance). Results were considered significant if $P < 0.05$.

Drugs

Alternaria tenuis extract was obtained from Greer Laboratories Inc., Lenoir, N.C., U.S.A. (40,000 PNU ml^{-1}, 1 mg ml^{-1}) and aluminium hydroxide ($Al(OH)_3$) moist gel from FSA Laboratory supplies, Loughborough, Leicestershire. Histamine diphosphate, bovine serum albumin (low endotoxin) and polyglutamic acid (60,000–90,000 mol. wt.) were obtained from Sigma (Poole, Dorset). Platelet activating factor (PAF, C16) was obtained from Novabiochem (Nottingham). Unfractionated heparin was obtained from C.P. Pharmaceuticals. Org 10172 was a gift from Dr T. Moelker, Organon B.V., Oss, The Netherlands. Diazepam was purchased from Roche (UK) and fentanyl citrate (Hypnorm) from Janssen Pharmaceutical Ltd., UK.

Results

Airway responses

Airway responsiveness to inhaled histamine (both airway resistance R_L and dynamic compliance C_{dyn}) determined on Day 1 were not significantly different in groups of immunized rabbits that received heparin (100 u kg^{-1}), Org 10172 (100 μg kg^{-1}) or polyglutamic acid (100 μg kg^{-1}) compared with the control saline group (Tables 1A and B). The combined mean values were R_L PC_{50}: 11.15 ± 1.14 mg ml^{-1} and C_{dyn} PC_{35}: 7.96 ± 1.19 mg ml^{-1} ($n = 27$). There were no

significant differences in baseline absolute values of R_L or C_{dyn} between any of the study days (Table 2).

Single intravenous doses of saline, heparin (100 u kg^{-1}), Org 10172 (100 $\mu g\ kg^{-1}$) or polyglutamic acid (100 $\mu g\ kg^{-1}$) caused small changes in baseline lung function (R_L or C_{dyn}) measured 1, 15 or 30 min following administration (Table 3).

Table 1 The effect of saline, heparin (100 u kg^{-1}), Org 10172 (100 $\mu g\ kg^{-1}$) and polyglutamic acid (100 $\mu g\ kg^{-1}$) on airway responsiveness to histamine prior to, and 24 h and 72 h following PAF challenge (80 $\mu g\ ml^{-1}$) in immunized rabbits.

A Histamine PC_{50} is the concentration of histamine (aerosol) (mg ml^{-1}) required to cause a 50% increase in airway resistance (R_L).

		Histamine PC_{50} (mg ml^{-1})		
		Pre	24 h	72 h
Saline	*n*	9	9	8
	mean	12.11	4.26*	3.78*
	s.e.mean	1.32	1.15	1.24
Heparin	*n*	6	6	6
	mean	9.29	15.14*†	16.83*†
	s.e.mean	1.35	1.40	1.42
Org 10172	*n*	6	6	6
	mean	10.21	16.41*†	18.11*†
	s.e.mean	1.33	1.32	1.23
Polyglutamic acid	*n*	6	6	6
	mean	12.97	4.96*	5.13*
	s.e.mean	1.14	1.14	1.21

*$P<0.05$ compared with Pre value of same treatment group
†$P<0.05$ compared with appropriate saline control group

B Histamine PC_{35} is the concentration of histamine (aerosol) (mg ml^{-1}) required to cause a 35% fall in dynamic compliance (C_{dyn}).

		Histamine PC_{35} (mg ml^{-1})		
		Pre	24 h	72 h
Control	*n*	9	9	8
	mean	9.23	2.99*	3.63*
	s.e.mean	1.37	1.24	1.29
Heparin	*n*	6	6	6
	mean	5.31	9.55†	9.12
	s.e.mean	1.48	1.35	1.33
Org 10172	*n*	6	6	6
	mean	5.90	10.14†	9.91†
	s.e.mean	1.53	1.32	1.39
Polyglutamic acid	*n*	6	6	6
	mean	13.06	4.64*	3.45*
	s.e.mean	1.14	1.18	1.20

*$P<0.05$ compared with Pre value of same treatment group
†$P<0.05$ compared with appropriate saline control group

These changes were significantly less than those achieved following PAF administration (Table 4). The acute bronchoconstriction induced by PAF was not significantly different from groups of rabbits pretreated with saline, heparin (100 u kg^{-1}), Org 10172 (100 $\mu g\ kg^{-1}$) or polyglutamic acid (100 $\mu g\ kg^{-1}$) (Table 4).

Airway responses to inhaled histamine (PC_{50} or PC_{35}) were not significantly different in animals treated with heparin (100 u kg^{-1}), Org 10172 (100 $\mu g\ kg^{-1}$) or polyglutamic acid (100 $\mu g\ kg^{-1}$) 30 min prior to BSA aerosol at 24 h or 72 h following challenge compared with Pre-BSA values (Table 5).

There was a significant increase in airway responsiveness to inhaled histamine (R_L and C_{dyn}) in immunized rabbits 24 h and 72 h after PAF exposure compared to pre-PAF level in the control saline-treated group ($P<0.05$) (Tables A and B). In rabbits pretreated with either heparin (100 u kg^{-1}) or Org 10172 (100 $\mu g\ kg^{-1}$), PC_{50} and PC_{35} values were significantly different from saline control values 24 h following PAF challenge (Tables 1A and B). Furthermore, in rabbits that received heparin or Org 10172, PC_{50} values 24 h and 72 h post PAF were significantly increased. Pretreatment of rabbits with polyglutamic acid (100 $\mu g\ kg^{-1}$) had no significant effect on PAF-induced hyperresponsiveness. R_L and C_{dyn} were significantly different at 24 h and 72 h compared with Pre-PAF values (Tables 1A and B). PC_{50} and PC_{35} values were not significantly different from the saline control group at 24 h and 72 h following PAF challenge (Tables 1A and B).

Bronchoalveolar lavage

There were no significant differences in total or differential cell counts between any of the pretreatment groups prior to PAF exposure (Table 6). Total cell counts were significantly elevated in BAL fluid 24 h and 72 h after PAF exposure in control saline-treated rabbits ($P<0.05$). This was reflected as significant increases in the numbers of neutrophils, eosinophils and mononuclear cells at 24 h and 72 h following challenge ($P<0.05$, Table 6).

In rabbits pretreated with heparin and Org 10172, total cell counts in BAL fluid at 24 h and 72 h after PAF exposure were significantly reduced compared with the saline-treated controls ($P<0.05$, Table 6). Numbers of neutrophils and eosinophils were significantly less than those observed in the control group 24 h and 72 h following PAF challenge ($P<0.05$, Table 6).

In rabbits pretreated with polyglutamic acid, numbers of total cells and eosinophils were significantly different from those in the control animals 24 h and 72 h following PAF exposure ($P<0.05$, Table 6). The number of neutrophils recovered from polyglutamic acid-treated rabbits was significantly less than that recovered from control animals at 24 h following PAF challenge only ($P<0.05$, Table 6).

No significant differences in mononuclear cell numbers were evident following PAF in any of the 3 drug treatment

Table 2 Absolute values for baseline lung function (airway resistance R_L) and dynamic compliance (C_{dyn}), Pre, 24 h and 72 h following PAF aerosol (80 $\mu g\ ml^{-1}$) in immunized rabbits pretreated with saline, heparin (100 u kg^{-1}), Org 10172 (100 $\mu g\ kg^{-1}$) and polyglutamic acid (PGA) (100 $\mu g\ kg^{-1}$)

		R_L ($cmH_2O/(l\ s^{-1})$)			C_{dyn} (ml cmH_2O^{-1})		
		Pre	24 h	72 h	Pre	24 h	72 h
Total	mean	33.38	32.73	32.22	7.46	7.75	7.58
($n=27$)	s.e.mean	1.97	2.06	2.18	0.49	0.46	0.42
Saline	mean	26.05	28.05	31.67	7.47	7.60	7.77
($n=9$)	s.e.mean	2.57	2.63	5.41	0.90	0.96	0.71
Heparin	mean	33.49	36.18	33.06	7.02	7.27	6.23
($n=6$)	s.e.mean	3.90	2.57	3.93	0.94	0.94	0.90
Org	mean	40.04	40.34	36.33	6.59	7.54	7.40
($n=6$)	s.e.mean	4.27	5.79	3.61	0.50	0.74	0.41
PGA	mean	34.63	28.70	30.91	9.20	8.62	8.86
($n=6$)	s.e.mean	1.41	3.06	1.49	0.94	0.57	0.95

Table 3 Percentage change in airway resistance (R_L) and dynamic compliance (C_{dyn}), 1, 15 and 30 min following i.v. administration of heparin (100 μg kg^{-1}) and Org 10172 (100 μg kg^{-1}) in immunized rabbits

		R_L (cmH$_2$O/(1 s^{-1}))			C_{dyn} (ml cmH$_2$O^{-1})		
		1 min	15 min	30 min	1 min	15 min	30 min
Heparin	mean	5.13	11.70	15.90	− 3.73	− 8.68	− 7.23
(n = 3)	s.e.mean	1.27	4.65	1.35	8.07	10.28	9.16
Org	mean	2.32	0.30	4.03	− 8..80	− 11.00	− 3.60
(n = 3)	s.e.mean	3.19	7.67	10.70	3.83	3.62	6.74

Table 4 Percentage change in airway resistance (R_L) and dynamic compliance (C_{dyn}) following PAF aerosol (80 μg ml^{-1}) in immunized rabbits pretreated with saline, heparin (100 u kg^{-1}), Org 10172 (100 μg kg^{-1}) and polyglutamic acid (100 μg kg^{-1})

		R_L	C_{dyn}
Saline	mean	65.88	− 44.84
(n = 9)	s.e.mean	6.85	5.50
Heparin	mean	38.18	− 27.22
(n = 6)	s.e.mean	7.03	7.87
Org 10172	mean	40.60	− 32.47
(n = 6)	s.e.mean	13.34	7.28
Polyglutamic acid	mean	56.37	− 38.77
(n = 6)	s.e.mean	9.57	7.90

groups. Numbers of mononuclear cells in these groups of animals were all significantly less than numbers recovered from control rabbits at 24 h and 72 h following PAF ($P < 0.05$, Table 6).

Therefore, the total cell infiltration induced by PAF was significantly inhibited by heparin, Org 10172 and polyglutamic acid treatment at 24 h and 72 h post challenge, as was the recruitment of eosinophils and mononuclear cells. The infiltration of neutrophils was similarly inhibited by all drug pretreatments at 24 h and 72 h following PAF with the exception of that observed 72 h post PAF in animals that received polyglutamic acid ($P < 0.05$, Table 6). In addition, no significant differences were found to exist between the effects of heparin, Org 10172 or polyglutamic acid on PAF-induced cell infiltration.

Table 5 The effect of saline, heparin (100 u kg^{-1}) and Org 10172 (100 μg kg^{-1}) on airway responsiveness to histamine prior to, and 24 h and 72 h following BSA challenge (0.25%) in immunized rabbits.

		PC_{50} R_L (mg ml^{-1})			PC_{35} C_{dyn} (mg ml^{-1})		
		Pre	24 h	72 h	Pre	24 h	72 h
Saline	mean	10.66	11.24	12.69	5.56	5.92	4.77
	s.e.mean	1.52	1.22	1.04	1.33	1.14	1.11
	n	6	6	6	6	6	6
Heparin	mean	9.08	8.53	6.28	5.83	6.20	5.61
	s.e.mean	1.24	1.25	1.24	1.14	1.12	1.17
	n	7	7	5	7	7	5
Org	mean	7.36	7.77	8.03	7.50	7.38	7.59
	s.e.mean	1.06	1.06	1.08	1.10	1.09	1.10
	n	5	5	5	5	5	5

PC_{50} is the concentration of histamine (aerosol) (mg ml^{-1}) required to cause a 50% increase in airway resistance (R_L). PC_{35} is the concentration of histamine (aerosol) (mg ml^{-1}) required to cause a 35% fall in dynamic compliance (C_{dyn}).

Table 6 Number of total cells and different cell counts recovered from bronchoalveolar lavage (BAL) fluid before (Pre) and 24 h and 72 h following exposure of PAF (80 μg ml^{-1}) in immunized rabbits pretreated with saline, heparin (100 u kg^{-1}), Org 10172 (100 μg kg^{-1}) and polyglutamic acid (PGA) (100 μg kg^{-1})

			× 10^5 cells ml^{-1}							
			Total		*Neutrophils*		*Eosinophils*		*Mononuclear cells*	
Control (saline)	Pre	(n = 9)	1.01	(0.3–2.0)	0.024	(0.002–0.09)	0.007	(0.0–0.054)	0.99	(0.30–1.98)
	24 h	(n = 9)	5.94	(0.9–12.6)*	3.451	(0.38–8.42)*	0.141	(0.032–0.253)*	2.40	(0.49–5.88)*
	72 h	(n = 8)	3.25	(0.9–5.8)*	1.146	(0.19–3.63)*	0.101	(0.023–0.464)*	2.01	(0.68–4.21)*
Heparin	Pre	(n = 6)	0.94	(0.45–1.8)	0.049	(0.005–0.143)	0.003	(0.0–0.009)	0.89	(0.44–1.73)
	24 h	(n = 6)	1.37	(0.6–2.4)*†	0.608	(0.15–0.96)*†	0.021	(0.003–0.048)*†	0.78	(0.45–1.63)†
	72 h	(n = 6)	1.23	(0.7–2.1)†	0.557	(0.34–1.01)*†	0.015	(0.0–0.024)*†	0.66	(0.32–1.07)†
Org 10172	Pre	(n = 6)	0.85	(0.4–1.4)	0.008	(0.004–0.018)	0.001	(0.0–0.06)	0.84	(0.39–1.39)
	24 h	(n = 6)	1.47	(0.6–2.4)*†	0.943	(0.32–1.62)*†	0.020	(0.007–0.032)*†	0.56	(0.28–0.78)†
	72 h	(n = 6)	1.33	(0.8–1.8)*†	0.400	(0.04–0.81)*†	0.007	(0.0–0.018)*†	0.94	(0.75–1.35)†
PGA	Pre	(n = 6)	0.92	(0.4–2.1)	0.035	(0.006–0.06)	0.001	(0.0–0.006)	0.90	(0.34–2.07)
	24 h	(n = 6)	1.35	(0.7–1.8)*†	0.754	(0.51–1.12)*†	0.011	(0.0–0.042)*†	0.57	(0.18–1.12)†
	72 h	(n = 6)	1.58	(1.1–2.4)*†	0.658	(0.41–0.92)*	0.007	(0.0–0012)*†	0.92	(0.52–1.46)†

Results are expressed as means with range in parentheses
*$P < 0.05$ compared with Pre value of same treatment group.
†$P < 0.05$ compared with respective control value (saline treated group).

Discussion

Our results show that unfractionated heparin and the low-molecular weight heparinoid Org 10172 can inhibit airway hyperresponsiveness induced by aerosolized PAF in neonatally immunized adult rabbits. It has been reported that heparin can bind histamine, which possibly may explain the effect we have seen *in vivo* since we have used histamine as a marker of airway responsiveness. Nonetheless, neither heparin nor Org 10172 had any effect on the airway responsiveness to histamine following BSA challenge, suggesting that the observed inhibitory action of heparin and Org 10172 is not attributable merely to the ability of these drugs to bind histamine. Furthermore, from our results we suggest that the ability of heparin to inhibit airway hyperresponsiveness is unlikely to be related solely to its highly anionic nature since similar inhibitory effects were not observed with the linear anionic molecule polyglutamic acid. However, we cannot rule out the contribution of the negatively charged nature of heparin as it is plausible that any charge effect is dependent on the charge being presented in a conformationally constrained manner.

Heparin has been previously shown to inhibit PAF-induced airway hyperresponsiveness and eosinophil infiltration in guinea-pigs (Hanss *et al.*, 1989). While in the present study both heparin and Org 10172 inhibited the infiltration of inflammatory cells into the airways following PAF challenge, it appears that the inhibitory effect of heparin on PAF-induced airway hyperresponsiveness is not dependent on this anti-inflammatory effect as polyglutamic acid substantially inhibited cell infiltration without inhibiting the associated airway hyperresponsiveness. These results, separating the induction of bronchial hyperresponsiveness from inflammatory cell infiltration, support previous work in this model with other drug classes (Spina *et al.*, 1991; Herd *et al.*, 1992) and in other experimental (Ladenius & Biggs, 1989; Kings *et al.*, 1990; Sanjar *et al.*, 1990; Matsuse *et al.*, 1991) and clinical (Lundgren *et al.*, 1988; Gibson *et al.*, 1989) situations, showing that eosinophils may not be a prerequisite for the induction of airway hyperresponsiveness.

Others have reported that heparin can modulate allergen-induced airway hyperresponsiveness in the guinea-pig via a mechanism related to reversing the effects of the eosinophil-derived cationic protein MBP on M_2 receptor function on airway ganglia (Fryer & Jacoby, 1991). Again it is unlikely that such a mechanism explains the inhibitory effect of heparin on PAF-induced airway hyperresponsiveness in the present study as, unlike the experiments in guinea-pigs, the inhibitory effect of heparin against airway hyperresponsiveness could not be modulated by polyglutamic acid. Furthermore, the experiments in the guinea-pig used very high doses of heparin in comparison with those reported here. Recently heparin has been reported to inhibit Type 1 hypersensitivity reactions in allergic sheep, which has been suggested to be via an inhibitory effect on mast cell degranulation (Ahmed *et al.*, 1992). However, such a mechanism is unlikely to account for the inhibitory effects of heparin on PAF-induced airway hyperresponsiveness as rabbits have very few mast cells and their Type I hypersensitivity reactions are mediated principally by basophils or 'basophiloid' cells.

Heparin has also been reported to inhibit both exercise and antigen-induced bronchoconstriction, possibly by altering inositol trisphosphate (IP_3) levels (Ahmed & Danta, 1992). In the present experiments however, these observations were not supported as heparin did not inhibit PAF-induced bronchoconstriction. These findings furthermore suggest that the inhibition of PAF-induced airway hyperresponsiveness and cell infiltration by heparin cannot be explained by heparin acting merely as a PAF antagonist. We have previously reported that PAF-induced airway hyperresponsiveness and eosinophil infiltration in the rabbit is platelet dependent, being substantially reduced in animals rendered thrombocytopaenic (Coyle *et al.*, 1990). It is therefore of interest that two platelet-derived products, platelet factor 4 (PF_4) (Chihara *et al.*, 1988) and the related member of the IL-8 supergene family, RANTES (Kameyoshi *et al.*, 1992) have been recently reported to be chemoattractant for eosinophils. Heparin has long been known to inhibit the actions of the PF_4 (Block *et al.*, 1980), a cationic protein shown to be released following antigen challenge in sensitized rabbits (McManus *et al.*, 1979) and human asthmatics (Knauer *et al.*, 1981; Averill *et al.*, 1992), raising the possibility that part of the inhibitory actions of heparin on PAF-induced eosinophil infiltration is via the neutralization of PF_4.

In summary, our results provide clear evidence that heparin and Org 10172 possess anti-inflammatory activity in the lung and the ability to inhibit PAF-induced airway hyperresponsiveness in the rabbit.

References

AHMED, T., ABRAHAM, W.M. & D'BROT, J. (1992). Effects of inhaled heparin on immunologic and nonimmunologic bronchoconstrictor responses in sheep. *Am. Rev. Respir. Dis.*, **145**, 566–570.

AHMED, T. & DANTA, I. (1992). Prevention of exercise-induced bronchoconstriction (EIB) by inhaled heparin. *Am. Rev. Respir. Dis.*, **145**, A462.

ANTUNES, E., MARIANO, M., CIRINO, G., LEVIN, S. & DE NUCCI, G. (1990). Pharmacological characterisation of polycation-induced rat hind paw oedema. *Br. J. Pharmacol.*, **101**, 986–990.

AVERILL, F.J., HUBBARD, W.C., PROUD, D., GLEICH, G.J. & LIU, M.C. (1992). Platelet activation in the lung after antigen challenge in a model of allergic asthma. *Am. Rev. Respir. Dis.*, **145**, 571–576.

BLOCK, P.E., LUSCOMB, M., MARSHALL, S.E., PEPPER, D.S. & HOLBROOK, J.J. (1980). The multiple complexes formed by the interaction of platelet factor 4 with heparin. *Biochem. J.*, **191**, 769–776.

BOWLER, S.D., SMITH, S.M. & LAVERCOMBE, P.S. (1993). Heparin inhibits the immediate response to antigen in the skin and lungs of allergic subjects. *Am. Rev. Respir. Dis.*, **147**, 160–163.

BOYLE, J.P., SMART, R.H. & SHIREY, J.K. (1964). Heparin in the treatment of chronic obstructive bronchopulmonary disease. *Am. J. Cardiol.*, **14**, 25–28.

BRADBROOK, I.D., MAGNANI, H.N., MOELKER, H.T.C., MORRISON, P.J., ROBINSON, J., ROGERS, H.J., SPECTOR, R.G., VAN DINTHER, T. & WIJNAND, H. (1987). ORG 10172: a low molecular weight heparinoid anticoagulant with a long half life in man. *Br. J. Clin. Pharmacol.*, **23**, 667–675.

CARR, J. (1979). The anti-inflammatory action of heparin: Heparin as an antagonist to histamine, bradykinin and prostaglandin E_1. *Thromb. Res.*, **16**, 507–516.

CHIHARA, J., FUKUDA, K., YASUBA, H., KISHIGARA, N., SUGIHARA, R., KUBO, H. & NAKAJIMA, S. (1988). Platelet factor 4 enhances eosinophil IgG and IgE-Fc receptors and has eosinophil chemotactic activity. *Am. Rev. Respir. Dis.*, **137**, A421.

CORRIGAN, C.J., HARTNELL, A. & KAY, A.B. (1988). T Lymphocyte activation in acute severe asthma. *Lancet*, **i**, 1129–1131.

COYLE, A.J., SPINA, D. & PAGE, C.P. (1990). PAF-induced bronchial hyperresponsiveness in the rabbit: contribution of platelets and airway smooth muscle. *Br. J. Pharmacol.*, **101**, 31–38.

DAHL, S.V. (1962). Heparin und asthma. *Z. Tuberk*, **118**, 255–262.

DOLOWITZ, D.A. & DOUGHERTY, T.F. (1960). The use of heparin as an anti-inflammatory agent. *Laryngoscope*, **70**, 873–884.

EKRE, H.-P.T., FJELLNER, B. & HAGERMARK, O. (1986). Inhibition of complement dependent experimental inflammation in human skin by different heparin fractions. *Int. J. Immunopharmacol.*, **8**, 277–286.

FLECKNALL, P.A. (1987). In *Laboratory Animal Anaesthesia: An Introduction for Research Workers*, pp. 98–100. London: Academic Press.

FRIERI, M. & METCALFE, D.D. (1983). Analysis of the effect of mast cell granules on lymphocyte blastogenesis in the absence and presence of mitogens: Identification of heparin as a granule-associated suppressor factor. *J. Immunol.*, **131**, 1942–1947.

FRIGAS, E. & GLEICH, G.J. (1986). The eosinophil and the pathophysiology of asthma. *J. Allergy Clin. Immunol.*, **77**, 527–537.

FRYER, A.D. & JACOBY, D.B. (1991). Antigen-induced pulmonary M_2 muscarinic receptor dysfunction in guinea-pigs is reversed by heparin and poly-L-glutamate. *Br. J. Pharmacol.*, **104**, 292P.

GIBSON, P.G., DOLOVICH, J., DENBERG, J., RAMSDALE, E.H. & HARGREAVE, F.E. (1989). Chronic cough: Eosinophilic bronchitis without asthma. *Lancet*, **ii**, 1346–1348.

HANSS, J.G., WOODS, M.A., COYLE, A.J. & PAGE, C.P. (1989). The effect of heparin and related molecules on PAF induced bronchial hyperreactivity and eosinophil infiltration in the guinea-pig. *Am. Rev. Respir. Dis.*, **139**, A134.

HERD, C.M., DONIGI-GALE, D., SHOUPE, T.S. & PAGE, C.P. (1992). Effect of a 5-lipoxygenase inhibitor and leukotriene antagonist (PF 5901) on PAF-induced airway responses in neonatally immunized rabbits. *Br. J. Pharmacol.*, **107**, 1108–1115.

KAMEYOSHI, Y., DORSCHNER, A., MALLET, A.I., CHRISTOPHERS, E. & SCHRODER, J.-M. (1992). Cytokine RANTES released by thrombin-stimulated platelets is a potent attractant for human eosinophils. *J. Exp. Med.*, **176**, 587–592.

KAY, A.B. (1991). Lymphocytes in asthma. *Resp. Med.*, **85**, 87–90.

KAZATCHKINE, M.D., FEARON, D.T., METCALFE, D.D., ROSENBERG, R.D. & AUSTEN, K.F. (1981). Structural determinants of the capacity of heparin to inhibit the formation of the human amplification C3 convertase. *J. Clin. Invest.*, **67**, 223–228.

KINGS, M.A., CHAPMAN, I.D., KRISTERSSON, A., SANJAR, S. & MORLEY, J. (1990). Human recombinant lymphokines and cytokines induce pulmonary eosinophilia in the guinea pig which is inhibited by ketotifen and AH 21-132. *Int. Arch. Allergy Appl. Immunol.*, **91**, 354–361.

KNAUER, K.A., LICHTENSTEIN, L.M., ADKINSON, N.F.JNR. & FISH, J.E. (1981). Platelet activation during antigen-induced airway reactions in asthmatic subjects. *New Engl. J. Med.*, **304**, 1404–1406.

LADENIUS, A.R.C. & BIGGS, D.F. (1989). Capsaicin prevents the induction of airway hyperresponsiveness in a guinea-pig model of asthma. *Am. Rev. Respir. Dis.*, **139**, A232.

LASSER, E.C., SIMON, R.A., LYON, S.G., HAMBLIN, A.W. & STEIN, R. (1987). Heparin-like anticoagulants in asthma. *Allergy*, **42**, 619–625.

LIDER, O., MEKORI, Y.A., MILLER, T., BAR-TANA, R., VLODAVSKY, I., BAHARAV, E., COHEN, I.R. & NAPARSTEK, Y. (1990). Inhibition of T lymphocyte heparanase by heparin prevents T cell migration and T cell-mediated immunity. *Eur. J. Immunol.*, **20**, 493–499.

LUNDGREN, R., SODERBERG, M., HORSTEDT, P. & STENLING, R. (1988). Morphological studies of bronchial mucosal biopsies from asthmatics before and after ten years of treatment with inhaled steroids. *Eur. Respir. J.*, **1**, 883–889.

MATSUSE, T., THOMSON, R.J., CHEN, X.-R., SALARI, H. & SCHELLENBERG, R.R. (1991). Capsaicin inhibits airway hyperresponsiveness but not lipoxygenase activity or eosinophilia after repeated aerosolized antigen in guinea pigs. *Am. Rev. Respir. Dis.*, **144**, 368–372.

MATZNER, Y., MARX, G., DREXLER, R. & ELDOR, E. (1984). The inhibitory effect of heparin and related glycosaminoglycans on neutrophil chemotaxis. *Thromb. Res.*, **52**, 134–137.

MCMANUS, L.M., MORLEY, C.A., LEVINE, S.P. & PINCKARD, R.N. (1979). Platelet activating factor (PAF) induced release of platelet factor 4 (PF_4) in vitro during IgE anaphylaxis in the rabbit. *J. Immunol.*, **123**, 2835–2841.

MOTOJIMA, S., FRIGAS, E., WEGERING, D.A. & GLEICH, G.J. (1989). Toxicity of eosinophil cationic protein from guinea-pig tracheal epithelium *in vitro*. *Am. Rev. Respir. Dis.*, **139**, 801–805.

NEEDHAM, L., HELLEWELL, P.J., WILLIAMS, T.J. & GORDON, J.L. (1988). Endothelial cell functional responses and increased vascular permeability induced by polycations. *Lab. Invest.*, **59**, 538–548.

PAGE, C.P. (1988). The role of platelet activating factor in asthma. *J. Allergy Clin. Immunol.*, **81**, 144–152.

ROBINSON, D.S., HAMID, Q., YING, S., TSICOPOULOS, A., BARKANS, J., BENTLEY, A.M. CORRIGAN, C., DURHAM, S.R. & KAY, A.B. (1992). Predominant T_{H2}-like bronchoalveolar T lymphocyte population in atopic asthma. *N. Engl. J. Med.*, **326**, 298–304.

ROSENBERG, R.D., ARMAND, G. & LAM, L. (1978). Structure-function relationships of heparin species. *Proc. Natl. Acad. Sci. U.S.A.*, **75**, 3065–3069.

SANJAR, S., AOKI, S., KRISTERSSON, A., SMITH, D. & MORLEY, J. (1990). Antigen challenge induces pulmonary airway eosinophil accumulation and airway hyperreactivity in sensitised guinea pigs. *Br. J. Pharmacol.*, **99**, 679–686.

SASAKI, M., PAUL, W., DOUGLAS, G.J. & PAGE, C.P. (1991). Cutaneous responses to poly-L-lysine in the rabbit. *Br. J. Pharmacol.*, **104**, 444P.

SEEDS, E.A.M. & PAGE, C.P. (1992). The effect of heparin and related molecules on PAF and antigen induced eosinophil infiltration in guinea pigs. *Am. Rev. Respir. Dis.*, **145**, A697.

SPINA, D., MCKENNIFF, M.G., COYLE, A.J., SEEDS, E.A.M., TRAMONTANA, M., PERRETTI, F., MANZINI, S. & PAGE, C.P. (1991). Effect of capsaicin on PAF-induced bronchial hyperresponsiveness and pulmonary cell accumulation in the rabbit. *Br. J. Pharmacol.*, **103**, 1268–1274.

SY, M.S., SCHNEEBERGER, E., MCCLUSKEY, R., GREENE, M.I., ROSENBERG, R.D. & BENACERRAF, B. (1983). Inhibition of delayed type hypersensitivity by heparin depleted of anticoagulant activity. *Cell Immunol.*, **82**, 23–32.

VAN DER CARR, F.R. & WILLIAMS, O.B. (1928). Further studies on the influence of heparin on anaphylactic shock in the guinea pig. *J. Immunol.*, **15**, 13–20.

WILLENBORG, D.O. & PARISH, C.R. (1988). Inhibition of allergic encephalomyelitis in rats by treatment with sulfated polysaccharides. *J. Immunol.*, **140**, 3401–3405.

(Received November 16, 1992
Revised April 20, 1993
Accepted April 22, 1993)

Br. J. Pharmacol. (1993), **110**, 113–118

The effect of platelet-activating factor on the responsiveness of the human nasal airway

C.E. Austin & [1]J.C. Foreman

Department of Pharmacology, University College London, Gower Street, London WC1E 6BT

1 The effects of inhaled platelet-activating factor (PAF) on responsiveness of the human nasal airway were examined in normal subjects by measuring nasal airway resistance in response to histamine and bradykinin at 2, 6, 24, 48 h and 7 d after PAF administration. Eosinophil cationic protein (ECP) in nasal secretions was also measured.

2 Intranasal aerosol administration of PAF, 30 or 60 μg per nostril to normal human subjects induced an increased responsiveness to inhaled histamine, 50 to 400 μg and bradykinin, 100 μg per nostril at 2, 6 and 24 h following PAF treatment. However the effect was not apparent at 48 h or 7 days after PAF administration.

3 Intranasal administration of lyso-PAF, 60 μg by aerosol did not increase the reactivity of the nasal airway in response to histamine, 200 μg.

4 There was no difference in the time course of the PAF-induced hyperresponsiveness to histamine or bradykinin.

5 PAF-induced nasal hyperresponsiveness at 2 and 6 h was associated with increases in the ECP concentration of the nasal lavage fluid.

6 Vitamin E pretreatment of subjects resulted in the attenuation of the PAF-induced hyperresponsiveness to histamine, and a decrease in ECP levels of the nasal lavage fluid.

7 The results suggest that in the human nasal airway, PAF induces a non-specific hyperresponsiveness which is accompanied by eosinophil activation in the nasal cavity. Free radical production induced by PAF may contribute to the hyperresponsiveness and the activation of eosinophils.

Keywords: Platelet-activating factor; human nasal airway; hyperresponsiveness; histamine; bradykinin; vitamin E; eosinophil cationic protein

Introduction

Platelet-activating factor or PAF (1-O-hexadecyl-2-acetyl-*sn*-glycero-3-phosphocholine), is a membrane-derived phospholipid that has been shown to have a wide variety of biological activities. It increases vascular permeability, is chemoattractant for neutrophils and eosinophils, activates these cells and it induces superoxide anion production and leukotriene synthesis (O'Flaherty & Wylkle, 1983). In the lower airways, PAF has been implicated in the pathogenesis of asthma. It has been shown to cause immediate bronchoconstriction (Chung *et al.*, 1986; Cuss *et al.*, 1986) as well as inducing a non-specific bronchial hyperresponsiveness in both animals (Patterson *et al.*, 1984; Chung *et al.*, 1986; Robertson *et al.*, 1988) and man (Cuss *et al.*, 1986).

The mechanism of this hyperresponsiveness is not known. Previous studies have indicated that inflammation is an important factor and that the hyperresponsiveness may involve the release of cytotoxic mediators from eosinophils, such as eosinophil cationic protein (Frigas & Gleich, 1986). However, more recently Webber *et al.* (1992) have provided evidence for PAF-induced hyperresponsiveness *in vitro*, predominantly in the absence of circulating inflammatory cells. This hyperresponsiveness was suggested to be produced by the receptor-mediated release of oxygen free radicals.

Hyperresponsiveness is also seen in the upper airway in patients with allergic rhinitis (Andersson *et al.*, 1987). In order to determine whether PAF might be a potential mediator of hyperresponsiveness in the upper airway, we have studied the effect of inhaled PAF on responsiveness of the human nasal airway in normal subjects towards histamine and bradykinin. We have also investigated, by employing vitamin E as an oxygen free radical scavenger, the possibility that oxygen free radicals may mediate PAF-induced changes in nasal airway reactivity.

[1] Author for correspondence.

Methods

Subjects

The study was approved by the local Ethics Committee at University College London and all subjects gave their informed consent. For all experiments, normal, healthy volunteers with an age range of 21 to 40 years were used. Subjects suffering from a cold or reporting nasal symptoms were excluded and subjects were taking no medication at the time of, or in the 2 weeks prior to, an experiment. Experiments were performed in conditions kept as constant as possible with respect to temperature and humidity.

Nasal airway resistance measurements

Nasal airways resistance (NAR) was measured by active posterior rhinomanometry using a Mercury Electronics (Glasgow, UK) NR6 Rhinomanometer. The instrument was programmed to calculate nasal resistance at a reference pressure of 75Pa. The subject held a mask, with airtight seal, over the nose and mouth and breathed through the nose. Airflow was monitored by a pneumotachograph, and pressure within the oropharynx was monitored by an oral pressure cannula placed over the tongue and held through sealed lips.

The instrument was programmed to give the mean NAR over four nasal cycles, and for each subject, three consecutive series of breaths were used to calculate an overall mean of 12

breaths. Readings were only accepted if the coefficient of variation of the overall mean NAR for a subject was less than 20%.

Study design

In each experiment, subjects were first challenged with saline, then three measurements each of four nasal cycles were taken every 5 min by active posterior rhinomanometry (NAR) over a 15 min period to provide the baseline. To begin with, subjects were challenged with either four doses of histamine (50, 100, 200 and 400 μg) or bradykinin, 100 μg to each nostril. This dose of bradykinin had previously been shown to produce a significant decrease in nasal airway conductance (Proud *et al.*, 1988). After each dose, NAR was measured at 2, 5, 10, 15 and 20 min. Subjects were then treated with vehicle or PAF, 30 or 60 μg to each nostril and subsequent histamine or bradykinin challenges were performed at 2, 6, 24, 48 h and 7 days later. Subjects were allocated to PAF or vehicle treatment groups on a randomized basis. At least 1 week later, subjects were given vehicle or PAF: vehicle if they had previously had PAF and PAF if they had previously had vehicle. Histamine or bradykinin challenges were performed again at 2, 6, 24, 48 h and 7 days after vehicle or PAF administration. In addition, subjects underwent a nasal lavage on each challenge occasion.

In the study with vitamin E, 5 subjects received orally, vitamin E, 400 u daily for 14 days. A blood sample was taken from each subject immediately prior to starting the vitamin E treatment, and another sample was taken on day 14. At this time subjects were treated with PAF, 60 μg to each nostril, as before, and histamine challenges were performed at 2, 6 and 24 h after PAF administration. Nasal lavages were also performed on these occasions.

Nasal lavage

Nasal lavages were performed by a previously described method (Naclerio *et al.*, 1983). Subjects were in a sitting position with the head extended 30° from the horizontal. Warmed sterile saline (5 ml) was instilled in the nostril while the subject abstained from breathing or swallowing. After 10 s the subject leaned forward and expelled the lavage fluid into a collection vessel, which was stored on ice until the completion of the experiment. Approximately 4 ml of the wash was recovered on each occasion. In each experiment, three initial washes were collected in order to remove pre-existing nasal secretions and the third of these was retained and served as a baseline.

The lavage fluid was centrifuged at 4°C for 10 min at 1000 *g*, after which the supernatants were separated, and stored at −20°C until analysis.

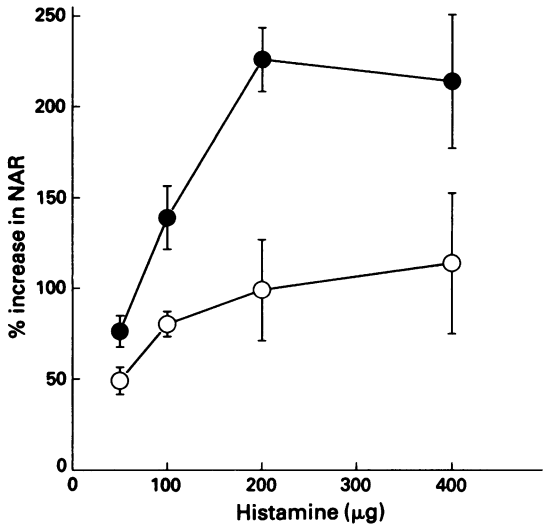

Figure 2 Dose-response curve for histamine and increased nasal airway resistance (NAR) 6 h after pretreatment. (○) Vehicle pretreatment; (●) PAF, 60 μg pretreatment. Changes in NAR are expressed as a percentage of the baseline value which was 0.381 ± 0.021 Pa.s.cm^{-3}. The data are the means with s.e.mean from 5 separate experiments. *Significant difference ($P<0.05$) by paired t test between PAF and vehicle administration.

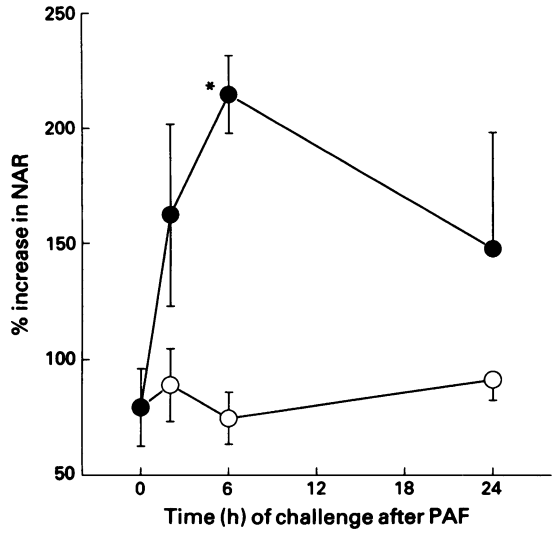

Figure 1 Responses to histamine (200 μg), expressed as maximal percentage increase in nasal airway resistance (NAR) above baseline in the post-challenge period, pre-PAF (0 h) and at 2, 6 and 24 h following vehicle or treatment with PAF, 60 μg. (○) Vehicle pretreatment; (●) PAF pretreatment. The baseline NAR was 0.317 ± 0.016 Pa.s.cm^{-3}. The data are the means with s.e.mean from 5 separate experiments. *Significant difference ($P<0.05$) by paired t test between PAF and vehicle pretreatment.

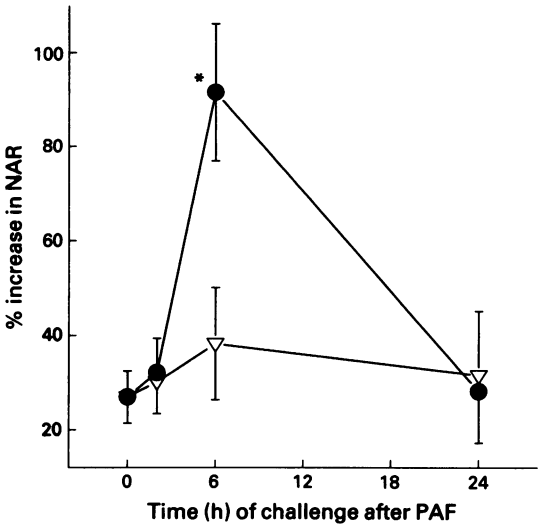

Figure 3 Responses to bradykinin (100 μg) expressed as maximal percentage increase in nasal airway resistance (NAR) above baseline in post-challenge period, pre-PAF (0 h) and at 2, 6 and 24 h following vehicle or PAF administration. (▽) Vehicle treatment; (●) treatment with PAF, 60 μg. The baseline NAR was 0.343 ± 0.013 Pa.s.cm^{-3}. The data are the means with s.e.mean from 5 separate experiments. *Significant difference ($P<0.05$) by paired t test between vehicle and PAF administration.

Vitamin E measurements

Blood (5 ml) was obtained by superficial venepuncture of the antecubital fossa, and left to clot at room temperature. The blood was then centrifuged at 1400 *g* for 10 min, the serum aspirated off, then stored at − 20°C until analysis. Vitamin E was assayed by the Department of Chemical Pathology, University College London. The vitamin E was assayed by measuring its fluorescence in hexane (excitation 290 nm; emission 330 nm). The serum samples were saponified with potassium hydroxide in the presence of ascorbic acid, as an anti-oxidant, and ethanol to reduce the extraction of interfering substances (Taylor *et al.*, 1976).

Nasal challenge

Nasal challenge was undertaken with a nasal pump spray (Perfect-Valois, UK Ltd), delivering 100 µl per activation. The spray was placed in one nostril and activated once, then repeated for the opposite nostril. All solutions were at room temperature, and doses of substances were controlled by the concentration of the solutions. Fresh solutions of all challenge agents were made each day from stock solutions stored at − 20°C.

Histamine as the diphosphate salt was dissolved in saline (NaCl 154 mM) to make solutions ranging from 1 mg ml^{-1} to 10 mg ml^{-1}. Bradykinin was dissolved in saline to make a 1 mg ml^{-1} solution. PAF was dispersed in distilled water to make a suspension of 0.6 mg ml^{-1}.

Eosinophil cationic protein (ECP) assay

ECP was measured, as previously described (Venge *et al.*, 1977), by a radioimmunoassay.

Data analysis

Changes in NAR in response to each substance were expressed as the percentage change from the NAR values obtained with vehicle challenge. The response to each substance was expressed as the maximal change in NAR for each dose during the post-challenge period.

All data were expressed as mean ± s.e.mean. Student's *t* tests for paired or independent samples, as appropriate, were applied when comparing the differences between mean values obtained with the various treatments. A probability value $P<0.05$ was considered significant.

Materials

Bradykinin was obtained from Peninsula Laboratories, St Helens, Merseyside. Platelet-activating factor (C_{16}) and the lyso form were obtained from Novabiochem, Nottingham. Histamine diphosphate was obtained from Sigma, Poole, Dorset. Vitamin E was manufactured by Pharmadas Ltd, Greenford, Middlesex. The ECP assay kit was produced by Pharmacia Diagnostics, Uppsala, Sweden. All other substances used were of Analar or simliar quality.

Results

Following PAF inhalation, no significant change in NAR was measured in any of the subjects. No response was obtained to vehicle alone. All subjects sneezed and experienced nasal itching and nasal blockage after histamine challenge. However, Figure 1 shows that histamine challenge with 200 µg per nostril prior to PAF administration and at 2, 6 and 24 h following PAF resulted in increases in NAR of 79%, 162%, 215%, and 148% respectively, whereas responses to histamine, 200 µg after vehicle treatment were 79%, 89%, 74% and 91% respectively ($n = 5$).

In a separate experiment, when subjects were challenged with histamine, 200 µg the increase in NAR was 71 ± 17% above baseline (0.315 ± 0.015 Pa.s.cm^{-3}) prior to administration of lyso-PAF and 68 ± 25% above baseline (0.326 ± 0.017 Pa.s.cm^{-3}) 6 h after intranasal administration of lyso-PAF, 60 µg ($n = 5$).

The maximum hyperresponsiveness induced by PAF was observed at 6 h, when the percentage increase in NAR following histamine challenge was significantly larger than that obtained before PAF administration ($P<0.05$) (Figure 2). Subjects challenged with bradykinin experienced nasal blockage without other symptoms and this too was augmented following PAF treatment. Bradykinin-induced increases in NAR prior to PAF administration and at 2, 6 and 24 h after

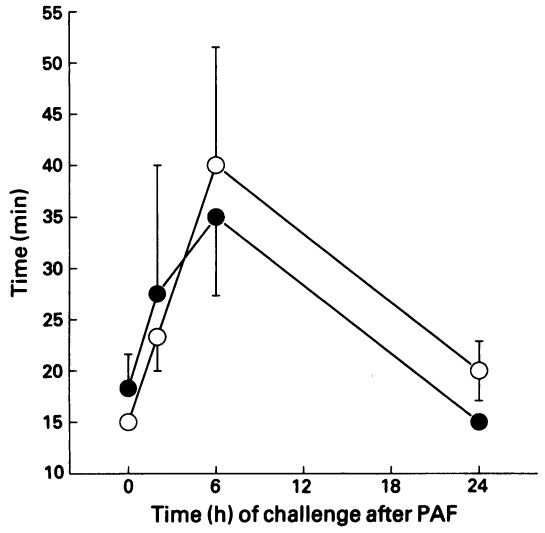

Figure 4 Duration of responses to histamine and bradykinin, pre-PAF (0 h) and at 2, 6 and 24 h after administration of PAF, 60 µg. (○) Bradykinin, 100 µg; (●) histamine, 200 µg. The data are the means with s.e.mean from 5 separate experiments.

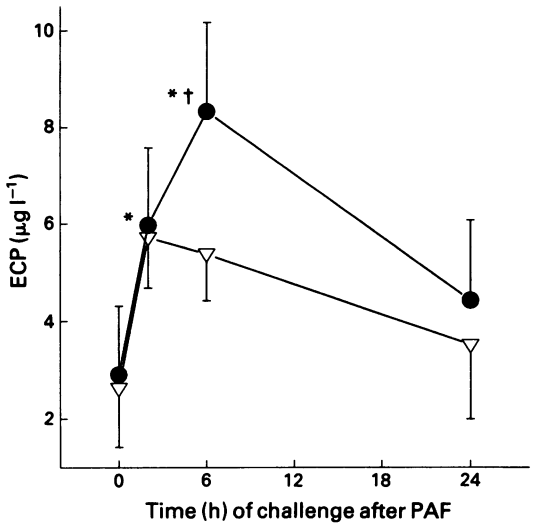

Figure 5 The effect of PAF administration on the eosinophil cationic protein (ECP) concentration of nasal lavage fluid taken pre-PAF (0 h) and at 2, 6 and 24 h after administration. (●)-PAF, 60 µg; (▽)-PAF 60 µg and vitamin E treatment. The data are the means with s.e.mean from 3 separate experiments. *Significant change by paired *t* test in ECP concentration compared with that before PAF administration (0 h). †Significant difference by unpaired *t* test in ECP concentration between the untreated subjects and those treated with vitamin E.

PAF were 27%, 32%, 92% and 28% respectively ($n = 5$), as compared with increases of 27%, 30%, 38% and 31% when subjects received vehicle (Figure 3). There was no difference in the duration of the hyperresponsiveness induced by PAF between subjects challenged with histamine and those challenged with bradykinin (Figure 4).

The ECP concentrations in nasal lavage after PAF administration were significantly increased at 2 h and 6 h when compared with the ECP concentrations in the nasal lavage prior to PAF administration. The maximal increase in ECP concentration of the nasal lavage fluid, which occurred at 6 h after PAF administration, was 8.3 $\mu g\,l^{-1}$ compared with 2.9 $\mu g\,l^{-1}$ before PAF treatment (Figure 5). Nasal blockage following histamine challenge at 48 h and 7 days after PAF treatment was not significantly different from that without PAF administration (Figure 6).

The effect of the PAF dose required to produce this hyperresponsiveness was investigated and it appeared that the hyperresponsiveness was dose-related (Figure 7).

To study the effect of vitamin E on the PAF-induced hyperresponsiveness, subjects were pretreated with vitamin E 400 u for 14 days. In all subjects, serum levels increased significantly from a mean of $13.2 \pm 1.02\,mg\,l^{-1}$ to a mean of $18.2 \pm 1.44\,mg\,l^{-1}$: a mean increase of $37.4 \pm 5.2\%$ ($P < 0.01$). On day 14, the PAF-induced hyperresponsiveness to histamine was inhibited (Figure 8), and there was also a corresponding reduction in ECP levels of nasal lavage fluid from 8.3 $\mu g\,l^{-1}$ without vitamin E pretreatment, to 5.3 $\mu g\,l^{-1}$ after vitamin E but this was only significant at the 6 h time point (Figure 5).

Discussion

In this paper, we have demonstrated a non-specific increase in responsiveness induced by PAF in the human nasal airway. This hyperresponsiveness is non-specific, as demonstrated by the increase in responses to both histamine and bradykinin following PAF administration. It occurred between 2 and 24 h after PAF administration and was maximal at 6 h. The dose of PAF was chosen from pilot experiments which we conducted and also on the basis of the studies by Andersson & Pipkorn (1988). The effects of the doses we have studied in the nasal airway are consistent with effects of PAF reported in studies on the human lower airway (Cuss *et al.*, 1986), in primates (Patterson *et al.*, 1984), dogs (Chung *et al.*, 1986) and guinea-pigs (Chapman *et al.*, 1991). However, the precise mechanism of PAF-induced airway hyperresponsiveness is unknown. A variety of mechanisms have been suggested. The PAF-induced hyperresponsiveness has been shown to be dependent on platelet activation (Chapman *et al.*, 1985; Coyle *et al.*, 1990), and is thought to be linked to mediator release from inflammatory cells, particularly eosinophils (Frigas & Gleich, 1986; Sanjar *et al.*, 1990). So in addition to the NAR measurements, we also investigated the possibility of eosinophil activation in this study.

We have shown increases in ECP levels of nasal lavage fluid which have a similar time course to the PAF-induced hyperresponsiveness. This suggests that activation of eosinophils with subsequent release of ECP may contribute to the development of hyperresponsiveness. The interest in examining eosinophil activation in these experiments arose from suggestions that airway hyperresponsiveness may, at least in part, be due to a change in the barrier function of the epithelium (Hogg, 1981), which may be brought about by the release of cytotoxic constituents of eosinophils. A previous study indicated a relationship between ECP levels in nasal secretions and allergen-induced nasal hyperresponsiveness (Linder *et al.*, 1987). However, others (Andersson *et al.*, 1989) found no clear-cut relationship between ECP levels and the induction of hyperresponsiveness. It seems, therefore, that eosinophil recruitment and activation might play a role in nasal hyperresponsiveness, but it is unlikely that it is solely responsible.

Recently, evidence of PAF-induced hyperresponsiveness occurring *in vitro*, largely in the absence of inflammatory cells, has been reported. This is not affected by indomethacin, FPL55712 or mepyramine and cimetidine, but is prevented by catalase, superoxide dismutase (SOD) and WEB2086 (Webber *et al.*, 1992). It has been suggested that a receptor-mediated release of oxygen free radicals may be responsible for this effect, since SOD is a potent scavenger for O_2^-. The protective effect of SOD in other pathological conditions has previously been demonstrated (Rubanyi & Vanhoutte, 1986). In the airway, several reports suggest that oxygen free radicals may be linked to the development of non-specific airway hyperresponsiveness: ozone inhalation can induce hyperresponsiveness in animals (Murlas & Roum, 1985) and

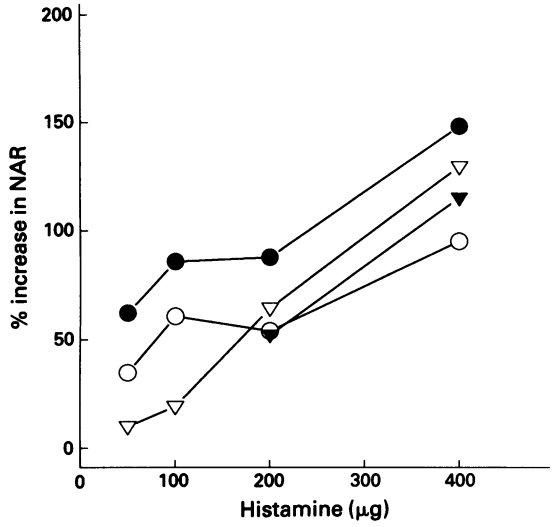

Figure 6 Dose-response curve for histamine and increased nasal airway resistance (NAR) pre-PAF (0 h) and at 24, 48 h and 7 days after PAF, 30 μg. (○) Pre-PAF (0 h); (●) 24 h after PAF; (▽) 48 h after PAF; (▼) 7 days after PAF. The baseline NAR was $0.339 \pm 0.016\,Pa.s.cm^{-3}$. The data are the means with s.e.mean from 6 separate experiments and bars representing the s.e.mean having been omitted for clarity.

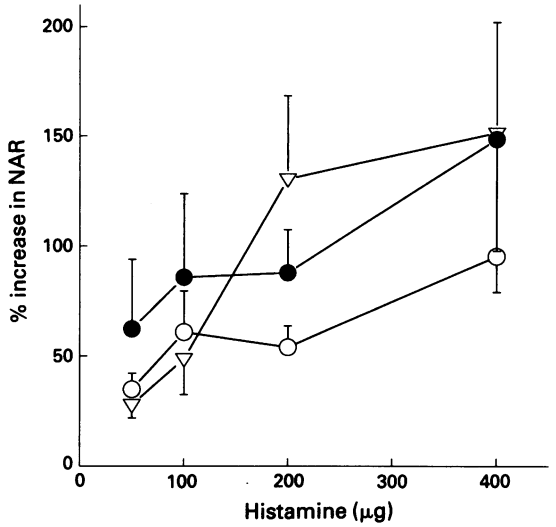

Figure 7 Dose-response curve for histamine and increased nasal airway resistance (NAR) at 24 h after PAF administration. (○) Control; (●) PAF, 30 μg; (▽) PAF, 60 μg. The baseline NAR was $0.301 \pm 0.014\,Pa.s.cm^{-3}$. The data are the means from 6 separate experiments and the vertical bars represent the s.e.mean.

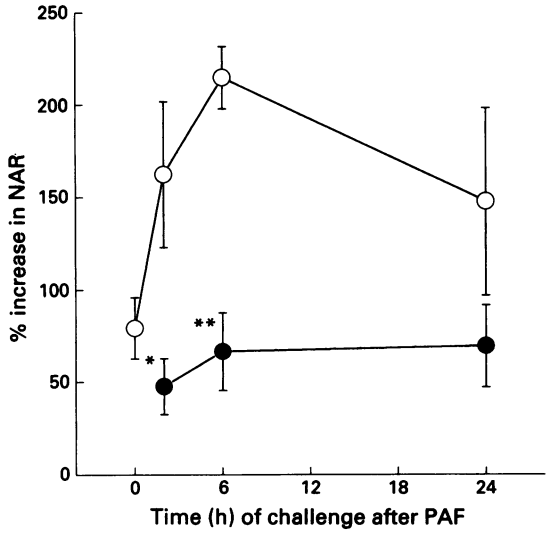

Figure 8 Responses to histamine, 200 μg, pre-PAF (0 h) and at 2, 6 and 24 h after PAF, 60 μg administration, expressed as the maximal percentage increase in nasal airway resistance (NAR) above baseline during period after challenge with histamine. (○) Control group; (●) vitamin E-treated group. The baseline NAR was 0.295 ± 0.022 Pa.s.cm^{-3}. The data are the means with s.e.mean from 5 separate experiments. Significant differences by paired t test (*$P<$ 0.05 and **$P<0.01$) between no treatment and vitamin E treatment.

man (Seltzer *et al.*, 1986); inhalation of xanthine and xanthine oxidase (an oxygen free radical generating system) has been reported to induce airway hyperresponsiveness in anaesthetized cats (Katsumata *et al.*, 1990); hydrogen peroxide can induce potentiation of contractile responses in isolated rat airway which can be inhibited by catalase (Szarek & Schmidt, 1990), and xanthine oxidase activation is associated with respiratory viral infection (Akaike *et al.*, 1990). We have attempted to examine the role of free radicals in PAF-induced hyperresponsiveness in the nasal airway by use of vitamin E as a free radical scavenger. We have shown that treatment with vitamin E inhibits the PAF-induced increase in responsiveness to histamine and also the accompanying increase in ECP. The dose of vitamin E used has previously been shown to produce a maximum increase in serum levels (Szczeklik, 1987). Vitamin E is a well-documented, effective antioxidant; protecting unsaturated lipids against peroxidation and free radical formation. There is evidence that vitamin E has a similar protective effect in tissues (McCay *et al.*, 1972). It acts by stabilizing and reacting with free radicals to prevent the chain of events by which they lead to cell damage (Fragata & Bellemare, 1980). Assuming that the levels of vitamin E we have produced in the subjects are blocking only free radical formation, then our data suggest that PAF-induced free radical formation is responsible for both hyperresponsiveness and also eosinophil activation. As mentioned above, it is possible that hyperresponsiveness can occur independently of eosinophil activation and support for this comes from experiments showing that hyperresponsiveness occurs *in vitro* where eosinophils are unlikely to be present (Webber *et al.*, 1992). Furthermore, pulmonary eosinophilia has been demonstrated in guinea-pigs, without attendant hyperresponsiveness (Chapman *et al.*, 1991) and *vice versa* (Spina *et al.*, 1991; Herd *et al.*, 1992). However, we cannot exclude the possibility that eosinophil activation acts in concert with other, as yet unknown, mechanisms to produce hyperresponsiveness in the human nasal airway.

C.E.A. holds an S.E.R.C. Case Award with Pfizer Central Research, Sandwich, Kent as the industrial collaborators. We thank all those who gave generously of their time to act as subjects for these experiments.

References

AKAIKE, T., ANDO, M., ODA, T., DOI, T., IJIRI, S., ARAKI, S. & MAEDA, H. (1990). Dependence on O_2^- generation by xanthine oxidase of pathogenesis of influenza virus infection in mice. *J. Clin. Invest.*, **85**, 739–745.

ANDERSSON, M., ANDERSSON, P., VENGE, P. & PIPKORN, U. (1989). Eosinophils and eosinophil cationic protein in nasal lavages in allergen-induced hyperresponsiveness: effects of topical glucocorticosteroid treatment. *Allergy*, **44**, 342–348.

ANDERSSON, M. & PIPKORN, U. (1988). The effect of platelet activating factor on nasal hypersensitivity. *Eur. J. Clin. Pharmacol.*, **35**, 231–235.

ANDERSSON, M., VON KOGERER, B., ANDERSSON, P. & PIPKORN, U. (1987). Allergen-induced nasal hyperreactivity appears unrelated to the size of the nasal and dermal immediate allergic reaction. *Allergy*, **42**, 631–637.

CHAPMAN, I.D., BOUBEKEUR, K. & MORLEY, J. (1991). Airway eosinophilia and airway hyperreactivity are parallel rather than sequential events in the guinea-pig. *Agents Actions*, **34**, 445–456.

CHUNG, K.F., AIZCIWA, H., LEIKAUF, G.D., UEKI, I.F., EVANS, T.W. & NADEL, J.A. (1986). Airway hyperresponsiveness induced by platelet-activating factor: role of thromboxane generation. *J. Pharmacol. Exp. Ther.*, **236**, 580–584.

COYLE, A.J., SPINA, D. & PAGE, C.P. (1990). PAF-induced bronchial hyperresponsiveness in the rabbit: contribution of platelets and airway smooth muscle. *Br. J. Pharmacol.*, **101**, 31–38.

CUSS, F.M., DIXON, C.M.S. & BARNES, P.J. (1986). Effects of inhaled platelet-activating factor on pulmonary function and bronchial responsiveness in man. *Lancet*, **ii**, 189–192.

FRAGATA, M. & BELLEMARE, F. (1980). Model of singlet oxygen scavenging by α-tocopherol in biomembranes. *Chem. Phys. Lipids*, **27**, 93–99.

FRIGAS, E. & GLEICH, F.J. (1986). The eosinophil and the pathophysiology of asthma. *J. Allergy Clin. Immunol.*, **77**, 527–537.

HOGG, J.C. (1981). Bronchial mucosal permeability and its relationship to airway hyperreactivity. *J. Allergy Clin. Immunol.*, **67**, 421–425.

HERD, C.M., DONIGI-GALE, D., SHOUPZ, T.S. & PAGE, C.P. (1992). Effect of a combined 5-lipoxygenase inhibitor and leukotriene antagonist (PF 5901) on PAF-induced airway responsiveness and cellular infiltration in neonatally immunised rabbit. *Br. J. Pharmacol.*, **107**, 1108–1115.

KATSUMATA, U., MIURA, M., ICHINOSE, M., KIMURA, K., TAKAHASHI, Y., INOUE, H. & TAKISHIMA, T. (1990). Oxygen radicals produce airway constriction and hyperresponsiveness in anaesthetised cats. *Am. Rev. Respir. Dis.*, **141**, 1158–1161.

LINDER, A., VENGE, P. & DEUSCHL, H. (1987). Eosinophil cationic protein and myeloperoxidase in nasal secretions as markers of inflammation in allergic rhinitis. *Allergy*, **42**, 583–590.

MCCAY, P.B., PFEIFER, P.M. & STIPE, W.H. (1972). Vitamin E protection of membrane lipids during electron transport functions. *Ann. N. Y. Acad. Sci.*, **203**, 62–73.

MURLAS, C.G. & ROUM, J.H. (1985). Sequence of pathologic changes in the airway mucosa of guinea pigs during ozone-induced bronchial hyperreactivity. *Am. Rev. Respir. Dis.*, **131**, 314–320.

NACLERIO, R.M., MEIER, H.L., KAGEY-SOBOTKA, A., ADKINSON, N.F., MEYERS, D.A., NORMAN, P.S. & LICHTENSTEIN, L.M. (1983). Mediator release after nasal airway challenge with allergen. *Am. Rev. Respir. Dis.*, **128**, 597–602.

O'FLAHERTY, J.T. & WYLKLE, R.L. (1983). Biology and biochemistry of platelet activating factor. *Clin. Rev. Allergy*, **1**, 353–367.

PATTERSON, R., BERNSTEIN, P.R., HARRIS, K.E. & KRELL, R.D. (1984). Airway responses to sequential challenge with platelet-activating factor and leukotriene D_4 in rhesus monkeys. *J. Lab. Clin. Med.*, **104**, 340–345.

PROUD, D., REYNOLDS, C.J., LACAPRA, S., KAGEY-SOBOTKA, A., LICHTENSTEIN, J.M. & NACLERIO, R.M. (1988). Nasal provocation with bradykinin induces symptoms of rhinitis and a sore throat. *Am. Rev. Respir. Dis.*, **137**, 613–616.

ROBERTSON, D.N., COYLE, A.J., RHODEN, K.J., GRANDORDY, B., PAGE, C.P. & BARNES, P.J. (1988). The effect of platelet activating factor on histamine and muscarinic receptor function in guinea-pig airways. *Am. Rev. Respir. Dis.*, **137**, 1317–1322.

RUBANYI, G.M. & VANHOUTTE, P.M. (1986). Superoxide anions and hyperoxia inactivate endothelium-derived relaxing factor. *Am. J. Physiol.*, **250**, H822–827.

SANJAR, J.L., AOKI, S., BOUBEKEUR, K., CHAPMAN, I.D., SMITH, D., KINGS, M.A. & MORLEY, J. (1990). Eosinophil accumulation in pulmonary airways of guinea-pigs induced by exposure to an aerosol of platelet-activating factor: effect of anti-asthma drugs. *Br. J. Pharmacol.*, **99**, 267–272.

SELTZER, J., BIGBY, B.G., STULBARG, M., HOLTZMAN, M.J., NADEL, J.A., UEKI, I.F., LEIKAUF, G.D. & GOETZL, E.J. (1986). O_3^- induced change in bronchial reactivity to methacholine and airway inflammation in humans. *J. Appl. Physiol.*, **60**, 1321–1326.

SPINA, D., MCKENNIFF, M.G., COYLE, A.J., SEEDS, E.A.M., TRAMONTANA, M., PERRETTI, F., MANZINI, S. & PAGE, C.P. (1991). Effect of capsaicin on PAF-induced bronchial hyperresponsiveness and pulmonary cell accumulation in the rabbit. *Br. J. Pharmacol.*, **103**, 1268–1274.

SZAREK, J.L. & SCHMIDT, N. (1990). Hydrogen peroxide-induced potentiation of contractile responses in isolated rat airways. *Am. J. Physiol.*, **258**, L232–L237.

SZCZEKLIK, A. (1987). Antioxidant effect of vitamin E in hyperlipoproteinemias. *Agents Actions*, **22**, 359.

TAYLOR, S.C., LAMDEN, M.P. & TAPPEL, A.L. (1976). Sensitive fluorimetric method for tissue tocopherol analysis. *Lipids*, **11**, 530–538.

VENGE, P., ROXIN, L.E. & OLSSON, I. (1977). Radioimmunoassay of human eosinophil cationic protein. *Br. J. Haematol.*, **37**, 331–335.

WEBBER, S.E., MORIKAWA, T. & WIDDICOMBE, J.G. (1992). PAF-induced muscarinic cholinoceptor hyperresponsiveness of ferret tracheal smooth muscle and gland secretion *in vitro*. *Br. J. Pharmacol.*, **105**, 230–237.

(Received February 1, 1993
Revised March 30, 1993
Accepted April 22, 1993)

Br. J. Pharmacol. (1993), **110**, 119–126

RS 23597-190: a potent and selective 5-HT_4 receptor antagonist

[1]R.M. Eglen, K. Bley, D.W. Bonhaus, *R.D. Clark, S.S. Hegde, L.G. Johnson, E. Leung & E.H.F. Wong

Institutes of Pharmacology and *Organic Chemistry, Syntex Discovery Research, 3401 Hillview Ave., Palo Alto, CA 94304, U.S.A.

1 The pharmacological properties of RS 23597-190 (3-(piperdine-1-yl)-propyl-4-amino-5-chloro-2-methoxy benzoate hydrochloride) have been studied *in vitro* and *in vivo*.

2 RS 23597-190 competitively antagonized 5-HT_4 receptor-mediated relaxations of rat, carbachol precontracted oesophageal muscularis mucosae, ($pA_2 = 7.8 \pm 0.1$; Schild slope $= 1.2 \pm 0.2$). Affinity estimates ($-\log K_B$) at 5-HT_4 receptors using either renzapride or SC-53116 as agonists yielded a $-\log K_B$ value of 8.0 ± 0.01. In contrast, RS 23597-190 failed to antagonize contractile responses to 5-HT of guinea-pig ileal 5-HT_3 receptors, even at concentrations up to 10 μM.

3 Increases in short-circuit current, induced by 5-HT, were studied in guinea-pig ileal mucosal sheets. Concentration-response curves to 5-HT were biphasic, with the high potency phase to 5-HT inhibited by RS 23597-190 and mimicked by 5-methoxytryptamine. The $-\log K_B$ value for RS 23597-190 at the high potency phase was 7.3 confirming that 5-HT_4 receptors mediated the high potency phase.

4 In rat isolated vagus nerve, 5-HT elicited a slow, maintained depolarization at low concentrations and a rapid, transient depolarization at higher concentrations. The high potency, slow depolarizing phase to 5-HT was abolished selectively in the presence of 1 μM RS 23597-190 and the low potency phase was abolished selectively in the presence of 1 μM ondansetron. These data confirm that 5-HT_4 and 5-HT_3 receptors mediated slow and fast depolarization responses, respectively.

5 At 5-HT_3 binding sites in membranes from NG 108-15 cells, labelled by [^{3}H]-quipazine, RS 23597-190 exhibited an apparent affinity ($-\log K_i$) of 5.7 ± 0.1. At 5-HT_3 receptors in membranes from rat cerebral cortex, labelled by [^{3}H]-RS 42358-197, the apparent affinity ($-\log K_i$) of RS 23597-190 was also 5.7 ± 0.1. In both studies, Hill coefficients were not significantly different from unity. At 5-HT_{1A}, 5-HT_2, muscarinic M_1, M_2, M_3, M_4 and dopamine D_1 and D_2 receptors, RS 23597-190 exhibited low apparent affinities, with all $-\log K_i$ values less than 5.5.

6 Intravenous infusion of RS 23597-190 in the conscious, restrained rat antagonized the von Bezold Jarisch reflex induced by 2-methyl 5-HT, with an ID_{50} of 300 $\mu g\,kg^{-1}\,min^{-1}$, i.v. In the anaesthetized, bilaterally vagotomized micropig, RS 23597-190 (6 $mg\,kg^{-1}$, i.v.) antagonized 5-HT-induced tachycardia with a half-life of 77 (63–99) min. Transient arrhythmic effects were noted after administration of the compound.

7 In conclusion, RS 23597-190 acts as a high affinity, selective competitive antagonist at 5-HT_4 receptors. Thus, the compound appears to be a useful tool for 5-HT_4 receptor identification *in vitro*. *In vivo*, the compound is rapidly metabolized in pigs such that 5-HT_4 blockade is not maintained. However, in the rat, when given by infusion, RS 23597-190 antagonizes 5-HT_3 mediated responses, at doses consistent with a low affinity 5-HT_3 receptor. These data suggest that, under appropriate experimental conditions, RS 23597-190 may also be used *in vivo* to characterize further 5-HT_4 receptor function.

Keywords: 5-HT_4 receptors; 5-HT_3 receptors; rat oesophagus; rat vagus; guinea-pig ileal mucosa; short-circuit current; NG 108-15 cells; rat cerebral cortex; rat von Bezold-Jarisch reflex; micropig tachycardia

Introduction

Receptors for 5-hydroxytryptamine (5-HT) are classified currently as 5-HT_1, 5-HT_2, 5-HT_3 and 5-HT_4 (Bockaert *et al.*, 1992). The 5-HT_4 receptor is defined by sensitivity to indole agonists such as 5-HT and 5-methoxytryptamine, substituted benzamides such as renzapride and SC-53116 or substituted benzimidazolones such as BIMU-8 (see Bockaert *et al.*, 1992 for review; Flynn *et al.*, 1992). Characterization of the receptor using antagonists can be accomplished with the benzamide, SDZ 205,557 ($pA_2 = 7.5$; Buchheit *et al.*, 1992), the tropane, tropisetron (ICS 205-930; $-\log K_B = 6.5$; Dumuis *et al.*, 1988), indazole derivatives of tropisetron (e.g. SB 203186 $pA_2 = 7.2$; Kaumann *et al.*, 1992a) and the benzimidazolone, DAU 6285 ($pA_2 = 6.8$; Dumuis *et al.*, 1992).

Differential antagonist affinities are important criteria to define novel receptor sites (Kenakin *et al.*, 1992), although no antagonist described so far is an ideal tool for characterization of the 5-HT_4 receptor. Tropisetron, for example, has a higher affinity for the 5-HT_3 receptors than 5-HT_4 receptors. SDZ 205,557 and DAU 6285, in contrast, exhibit similar affinities for these two receptors (see Bockaert *et al.*, 1992 for review; Eglen *et al.*, 1993a). Furthermore, the apparent selectivity of these compounds is enhanced if the affinity at the 5-HT_4 receptor is compared with the affinity at 5-HT_3 receptors in guinea-pig tissue (Eglen *et al.*, 1993a). The guinea-pig contains a species variant of the 5-HT_3 receptor, at which the majority of 5-HT_3 antagonists exhibit a low affinity (see Kilpatrick & Tyers, 1992, for review; Wong *et al.*, 1992; 1993).

There is clearly a need, therefore, for a potent and selective 5-HT_4 receptor antagonist. In this paper, the pharmacology of an analogue of the 5-HT_4 receptor partial agonist, metoclopramide (a partial 5-HT_4 antagonist), is described. RS 23597-190 (3- (piperidine-1-yl) -propyl-4-amino-5-chloro-2 methoxy benzoate hydrochloride; Figure 1) displays high affinity and reduced intrinsic efficacy relative to metoclopramide at the 5-HT_4 receptor. By contrast with the related

[1] Author for correspondence.

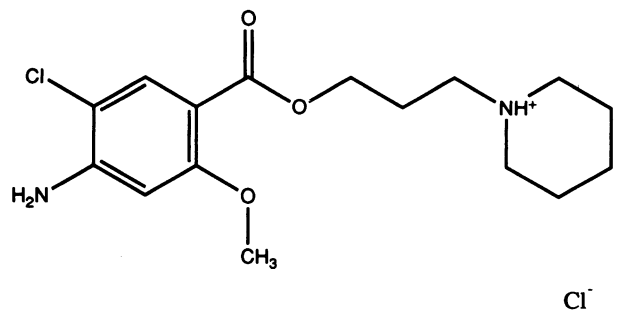

Figure 1 The structure of RS 23597-190 (3-piperidine-1-yl)-propyl-4-amino-5-chloro-2 methoxybenzoate HCl).

compound SDZ 205,557, RS 23597-190 offers clear selectivity for this receptor.

Preliminary accounts of these data have been presented to the British Pharmacological Society (Eglen *et al.*, 1993b) and the 2nd International Symposium on Serotonin, Houston, (Leung *et al.*, 1992a).

Methods

In vitro *studies*

The affinity of RS 23597-190 at 5-HT_4 receptors was determined on the rat isolated oesophageal muscularis mucosae (Baxter *et al.*, 1991). All tissues were suspended in Krebs physiological salt solution of the following composition (mM): NaCl 139.0, KCl 2.7, $MgCl_2.6H_2O$ 1.1, NaH_2PO_4 0.4, glucose 5.6, $NaHCO_3$ 11.8 and $CaCl_2.6H_2O$ 1.8. When precontracted with carbachol (3 μM), this preparation is relaxed by 5-HT via 5-HT_4 receptor-mediated stimulation of adenosine 3':5'-cyclic monophosphate (cyclic AMP) production (Baxter *et al.*, 1991; Ford *et al.*, 1992). After construction of a control cumulative concentration-response curve to 5-HT, preparations were washed and equilibrated for 75 min with RS 23597-190 (0.1–10 μM). A second concentration-response curve to 5-HT was then established in the presence of the antagonist. A third concentration-response curve to the agonist was constructed in the presence of 10 μM 5-methoxytryptamine to desensitize the 5-HT_4 receptor. Relaxant responses under these conditions were mediated by mechanisms other than the 5-HT_4 receptor (Baxter *et al.*, 1991). These experiments were repeated with the non-indole 5-HT_4 agonists, renzapride and SC-53116 in order to assess the agonist dependence of the affinity for RS 23597-190. In these studies, a single concentration of RS 23597-190 (0.1 μM) was employed.

The affinity of RS 23597-190 for 5-HT_3 receptors was assessed both functionally, in quiescent guinea-pig ileum (Craig *et al.*, 1990), and in radioligand binding studies, with EDTA-washed membranes from NG108-15 cells and rat cerebral cortex (Sharif *et al.*, 1991). In guinea-pig ileum (Eglen *et al.*, 1990), concentration-response curves to 5-HT were constructed in the presence of 10 μM 5-methoxytryptamine and 1 μM methysergide to desensitize the 5-HT_4 receptor (Craig *et al.*, 1990) and antagonize 5-HT_1 and 5-HT_2 receptors, respectively. The curves were constructed in either the presence or absence of RS 23597-190 (0.1–10 μM).

In radioligand binding studies, 5-HT_3 receptor sites in NG108-15 cell (a mouse neuroblastoma cell line) membranes were labelled with 0.5 nM [^{3}H]-quipazine and in membranes from rat cerebral cortex, 5-HT_3 receptors were labelled with the more selective 5-HT_3 radioligand, [^{3}H]-RS 42358-197 (Wong *et al.*, 1992; 1993). Non-specific binding in both studies was defined by the presence of 1 μM (S)-zacopride. The affinity of RS 23597-190, was also determined at 5-HT_{1A} ([^{3}H]-8-OH-DPAT; rat cerebrocortical membranes), 5-HT_2 ([^{3}H]-ketanserin; rat cerebrocortical membranes), D_1 ([^{3}H]-SCH 23390; rat striatal membranes), D_2 ([^{3}H]-spiperone; rat striatum), M_1 ([^{3}H]-pirenzepine; rat cerebrocortical membranes), M_2 ([^{3}H]-N-methyl scopolamine (NMS); rat myocardium), M_3 ([^{3}H]-NMS; rat submaxilliary gland) and M_4 ([^{3}H]-NMS; rabbit lung) receptors. (Further details of these assays can be found in Wong *et al.*, 1993 and references therein).

It has been suggested that 5-HT_4 receptors mediate tetrodotoxin-insensitive, 'maintained', changes in short-circuit current in guinea-pig ileal mucosa, (Scott *et al.*, 1992). Male, Hartley guinea-pigs (300–350 g) were killed by CO_2 asphyxiation and approximately 20 cm of distal ileum was removed starting 2.0 cm from the ileocaecal junction. Ileal mucosal sheets were prepared and mounted in Ussing chambers (window area 0.6 cm^2) as described by Bunce & Spraggs (1989) and Scott *et al.* (1992). The tissues were voltage-clamped at zero potential by passage of current using a voltage clamp amplifier (WPI, Sarasota, FL, U.S.A.) and the resulting short circuit current continuously recorded. This was used as an indirect measure of electrogenic chloride transport (see Scott *et al.*, 1992 for references).

The tissues were bathed on both sides with 12.5 ml Krebs solution with glucose (10 mM) added to the serosal solution and mannitol (10 mM) to the mucosal solution; the latter to reduce differences in osmotic pressure. Glucose was omitted from the mucosal side in order to prevent coupled electrogenic sodium absorption which might have affected subsequent measurements of short-circuit current. Compounds were added to the serosal side of the tissue only and antagonists were added 60 min before the construction of the agonist cumulative concentration-response curve. Only one concentration-response curve, in either the presence or absence of antagonist, was constructed for each tissue.

Rhodes *et al.* (1992) have suggested that 5-HT_3 and 5-HT_4 receptors mediate depolarization of rat vagus. To investigate this effect, extracellular voltage recordings from rat isolated vagus nerves were made according to the method of Marsh *et al.* (1987). Briefly, 15–20 mm lengths of vagus nerve from male Sprague-Dawley rats (200–250 g) were desheathed in cold Krebs solution and transferred to two compartments 'grease-gap' perspex baths for extracellular recording of 5-HT-induced changes in potential differences. One side of the bath was continuously perfused at a rate of 4 ml min^{-1} with Krebs solution (pH 7.4, 35°C). In some studies this solution contained antagonists which were equilibrated with the tissues for 45 min. At 12 min intervals, the flow was switched for 1 min to superfusate containing varying concentrations of 5-HT (including, where appropriate, antagonists). Spiperone 1 μM was present in all solutions to antagonize responses mediated by 5-HT_{1A} and 5-HT_2 receptors. The data were displayed, stored and analyzed on a computer using Axotape software (Axon Instruments).

In vivo *studies*

To determine the duration of action of RS 23597-190 *in vivo*, the time course for blockade of 5-HT_4-receptor-mediated tachycardia in anaesthetized, bilaterally vagotomized micropig, was determined (Villalon *et al.*, 1990; Eglen *et al.*, 1993a). Yucatan micropigs (male and female, 17.3 ± 4.3 kg, S & S Farms, Ranchita, CA, U.S.A.) were anaesthetized with pentobarbitone sodium (20 mg kg^{-1}) via a marginal ear vein following pretreatment with ketamine (approx. 30 mg kg^{-1}, i.m.). Following tracheal intubation, the pigs were mechanically ventilated with room air using an animal respirator (Harvard Instruments, Model 613). A cannula was inserted into a femoral artery and advanced into the abdominal aorta for measurement of aortic blood pressure via a Gould/Statham pressure transducer (P23ID). Dual cannulae were inserted into the ipsilateral femoral vein, one for continuous infusion of supplemental anaesthetic (pentobarbitone sodium,

8–15 mg kg^{-1} h^{-1}) and the second for compound administration. A limb lead II electrocardiogram (ECG) was monitored using subcutaneously-placed electrodes. Heart rate was determined by a cardiotachometer triggered by the aortic pressure. The vagus nerve were bilaterally transected. Blood gas parameters were periodically monitored via a blood gas analyzer (nova Stat Profile 3) with blood gas values stabilized within normal physiological ranges (pH, 7.45 ± 0.17; Po_2, 95.6 ± 1.9 mmHg; Pco_2, 35.2 ± 1.2 mmHg) before continuing an experiment.

5-HT and RS 23597-190 were each dissolved in 0.15 M NaCl and administered in base equivalent doses. A full tachycardiac dose-response curve to 5-HT was run in each animal, utilizing half-log interval intravenous doses of 1–100 μg kg^{-1} (10–15 min intervals between doses; 0.05 ml kg^{-1} $dose^{-1}$). An ED_{50} dose for 5-HT was determined visually for each animal from its dose-response curve. Animals were assigned randomly to either the RS 23597-190 or vehicle-treatment group (4 animals per group). The tachycardic ED_{50} dose of 5-HT, determined previously in the animal, was repeated 3 times at 10–15 min intervals with the heart rate responses averaged to determine a control response. Following administration of either RS 23597-190 (6.0 mg kg^{-1}, i.v.) or vehice (0.15 M NaCl; 0.1 ml kg^{-1}, i.v.), the ED_{50} dose of 5-HT (3 or 10 μg kg^{-1}) was administered intravenously at 3, 10, 20, 30, 45 and 60 min during the first hour, and then at 15 min intervals for the next 2 h.

The potency of RS 23597-190 in antagonizing 5-HT_3 receptors in conscious restrained rats, was assessed by its ability to inhibit the von Bezold Jarisch reflex, elicited by bolus administration of 2-methyl-5-HT (Richardson *et al.*, 1985). Under ether anesthesia, two femoral veins and one femoral artery were cannulated with PE-50 tubing for drug administration and blood pressure measurement respectively. The animals were placed in a Bollman cage and allowed to recover consciousness. Heart rate was derived from a limb lead II ECG monitored via subdermal platinum electrodes and was recorded using ECG/Biotech amplifiers connected to a Gould recorder (RS 3800). Arterial pressure was measured with Gould tranducers (P23XL). Three reproducible bradycardiac responses to 2-methyl 5-HT (10 μg kg^{-1}, i.v.) were initially obtained in each animal. Since RS 23597-190 is an ester, like SDZ 205,557, it was expected to be hydrolyzed rapidly *in vivo*. Thus, RS 23597-190 was infused via a femoral vein, at doses ranging from 0.01–3 mg kg^{-1} min^{-1}. The animals were challenged with 2-methyl 5-HT 10 min during infusion of each dose of RS 23597-190.

Analysis of data

Concentration-response data were analyzed by non-linear iterative curve fitting procedures (Leung *et al.*, 1992b), using the relationship described by Parker & Waud (1971). The apparent affinity of RS 23597-190, in functional *in vitro* studies was calculated by the method of Arunlakshana & Schild (1959), using at least three concentrations of antagonist. In studies where only a single concentration of antagonist was used the apparent affinity was calculated according to Furchgott (1972). All competition binding data were analyzed by non-linear iterative curve fitting procedures (Munson & Rodbard, 1980), and the affinity estimate (– log K_i) was calculated from IC_{50} values by the method of Cheng & Prusoff (1973). All values quoted are mean ± s.e.mean, $n = 4–8$ assays. Statistically significant differences were assessed by an unpaired Student's t test and $P < 0.05$ was considered significant.

To study the duration of 5-HT_4 antagonism in the micropig, variances of test compound and vehicle treatment group data were compared for homogeneity with Bartlett's test for heteroscedasticity. Finding no evidence of variance heterogeneity, a parametric repeated measures two-way analysis of variance (ANOVA) was used for an over-all analysis of the data (expressed as percentage inhibition of control 5-HT-induced tachycardiac response) to test the effects of treatment, time, and their interaction. Subsequently, a one-way ANOVA was run at each time point to compare treatments. Paired contrasts were adjusted for multiple comparisons using Dunn's procedure (i.e., if no overall significant treatment of treatment by time effect was detected, the critical value for each pairwise comparison was adjusted using a Bonferroni correction). The half-life for 5-HT_4 antagonist activity of RS 23597-190 was determined by non-linear iterative curve fitting procedures (Leung *et al.*, 1992b), using a model for exponential decay of the percentage inhibition of the 5-HT-induced change in heart rate. In the von Bezold-Jarisch reflex studies, data were expressed as percentage inhibition of the 2-methyl 5-HT-induced bradycardia (mean ± s.e.mean, $n = 8$ animals). Statistical analysis was performed by an unpaired Student's t test, with $P < 0.05$ being considered significant.

Compounds used

RS 23597-190 (3-(piperidine-1-yl)-propyl-4-amino-5-chloro-2-methoxy benzoate hydrochloride), 2-methyl-5-HT, renzapride and (S)-zacopride were synthesized in the Institute of Organic Chemistry, Syntex Discovery Research, Palo Alto, CA, U.S.A. SC-53116 was generously donated by Searle (Skokie, IL., U.S.A.). All remaining unlabelled compounds were obtained from Sigma Chemical Co., St. Louis, MO, U.S.A. [^{3}H]-RS 42358-197 (specific activity 60 Ci $mmol^{-1}$) was synthesized in the Institute of Organic Chemistry, Syntex Discovery Research, Palo Alto, CA, U.S.A. Other radioligands were obtained from DuPont NEN (Boston, MA, U.S.A.).

Results

5-HT relaxed the precontracted oesophageal muscularis mucosae in a concentration-dependent manner (– log EC_{50} = 8.2 ± 0.06). RS 23597-190 (0.1 nM–10 μM), by itself, failed to modify its contractile response to carbachol. However, RS 23597-190 antagonized competitively responses to 5-HT, resulting in parallel rightward shift in the concentration-response curve with no depression in maxima (Figure 2). The pA_2 value calculated was 7.5 ± 0.2 and slope of the Schild regression was 1.2 ± 0.2 (Figure 3). Since the slope of the Schild regression was not significantly different from one, the slope was constrained to one, resulting in a – log K_B value of 7.8 ± 0.1. SC-53116 and renzapride also evoked con-

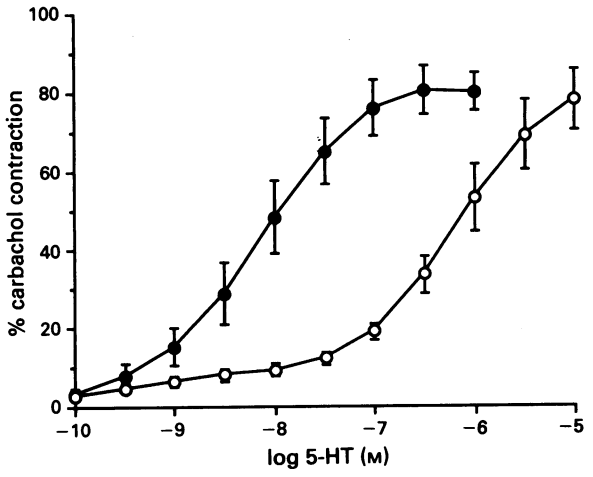

Figure 2 Antagonism of 5-HT concentration-response curves, by RS 23597-190 (1 μM), in rat isolated oesophagus. (●) Control concentration-response curves; (○) curves constructed in the presence of RS 23597-190. Values are mean ± s.e.mean, $n = 4–8$ animals.

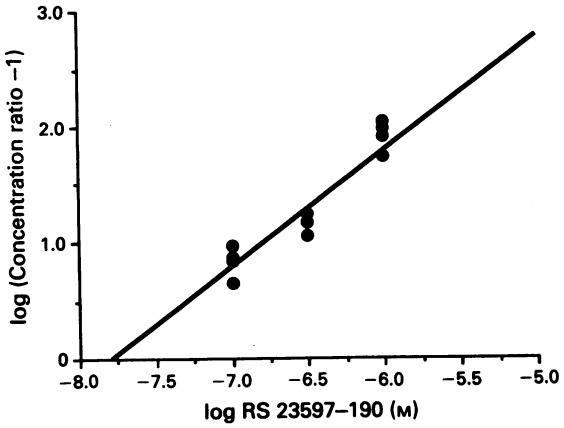

Figure 3 Schild analysis of the antagonism by RS 23597-190 of relaxant responses to 5-HT in rat isolated oesophagus. Values shown are concentration-ratios from individual tissues.

centration-dependent relaxations ($-\log EC_{50}$ values were 7.8 ± 0.1, and 7.6 ± 0.12, respectively, data not shown). RS 23597-190, at 0.1 μM, antagonized these responses, resulting in a parallel rightward shift of the concentration-response curves. The $-\log K_B$ values for RS 23597-190 were 8.0 ± 0.01 against renzapride and 8.0 ± 0.1 against SC-53116. These were not significantly different from each other or from the constrained $-\log K_B$ value observed for RS 23597-190 against 5-HT (see above).

Contractile responses of the guinea-pig ileum to 5-HT in the presence of 5-methoxytryptamine (10 μM) are mediated solely by 5-HT_3 receptors (Craig *et al.*, 1990). RS-23597-190 at concentrations up to and including 10 μM did not antagonize contractile responses to 5-HT (Figure 4). The apparent affinity ($-\log K_B$) at this site was therefore less than 5.0.

At 5-HT_3 receptors in NG108-15 cells labelled by [^{3}H]-quipazine, RS 23597-190 exhibited an affinity ($-\log K_i$) of 5.7 ± 0.1 and a Hill slope of 1.1 ± 0.2, the latter value being not significantly different from one. At 5-HT_3 sites in membranes from rat cerebral cortex, labelled with [^{3}H]-RS 42358-197, RS 23597-190 exhibited an identical affinity ($-\log K_i$) of 5.7 ± 0.1 and a Hill slope of 1.1 ± 0.3. Again the Hill slope was not significantly different from one. Taken together, the selectivity of RS 23597-190 for 5-HT_3 receptors in rat oesophagus, relative to 5-HT_4 receptors in guinea-pig ileum was greater than 1000 fold. The selectivity, when compared to the 5-HT_3 sites in NG108-15 cells or rat cerebral cortex membranes, was reduced to 125 fold.

The affinity of RS 23597-190 at 5-HT_{1A} and 5-HT_2 receptors was assessed in binding studies, and the $-\log K_i$ values determined were 5.2 ± 0.12 and 5.2 ± 0.04, respectively. The $-\log K_i$ values at D_1 and D_2 dopamine receptors were less than 4 and less than 5.3, respectively. At M_1, M_2, M_3 and M_4 muscarinic receptors, RS 23597-190 exhibited affinities of less than 4.5.

In the rat isolated vagus nerve, 5-HT (1 nM–0.1 mM) evoked depolarizations that, at low concentrations developed slowly but were sustained and at higher concentrations depolarizations exhibited a fast component in addition to the sustained plateau. At 0.1 mM 5-HT, the fast depolarization responses declined. The concentration-response curve for 5-HT was biphasic with a phase of desensitization observed at high concentrations (Figure 5). In the presence of ondansetron (1 μM), the initial high potency phase (0.1 nM–0.1 μM) was unaffected, but the maximum response was reduced from 442 ± 29 μV to 150 ± 14 μV. In the presence of RS 23597-190 (1 μM), the maximum response to 5-HT was unaffected, but the initial high potency phase was abolished (Figure 5).

In guinea-pig isolated ileal mucosa, 5-HT causes a biphasic increase in short-circuit current due to an increase in electrogenic chloride secretion (Scott *et al.*, 1992). The sustained phase of this response has been attributed to a heterogeneous population of 5-HT receptors, one of which has some characteristics of the 5-HT_4 receptor (Scott *et al.*, 1992). The sustained phase of this short-circuit current was stimulated by 5-HT over a wide range of concentrations (0.1 nM–10 μM) and the concentration-response curve to 5-HT showed a biphasic relationship (Figure 6a). Tetrodotoxin (0.3 μM) abolished both phases of the response to 5-HT (Figure 6b). Methysergide (1 μM) did not affect responses to 5-HT whereas 5-methoxytryptamine caused an increase in short-circuit current of similar magnitude to the first, high potency phase of the 5-HT concentration-response curve (data not shown). RS 23597-190 (1 μM) had no effect on the second, low potency phase of the 5-HT concentration-response curve. However, the first, high potency phase of the concentration response curve was abolished (Figure 6a) and the affinity ($-\log K_B$) ranged from 7.3 to 7.7. RS 23597-190 also shifted the concentration-response curve to 5-methoxytryptamine

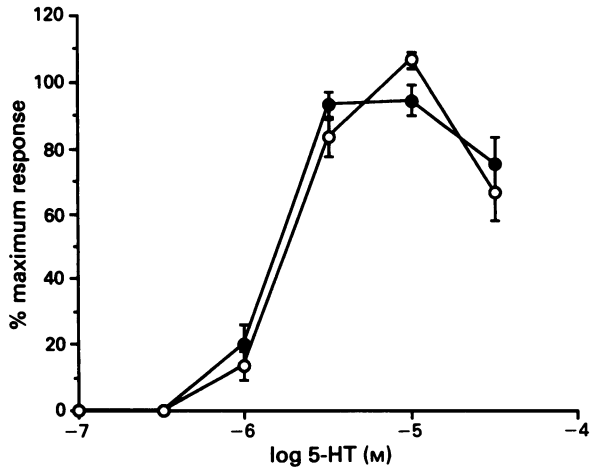

Figure 4 Antagonism of 5-HT concentration-response curves, by RS 23597-190, in guinea-pig isolated ileum. (●) Control concentration-response curves; (○) curves constructed in the presence of 10 μM RS 23597-190. Values are mean ± s.e.mean, $n = 4–8$ animals.

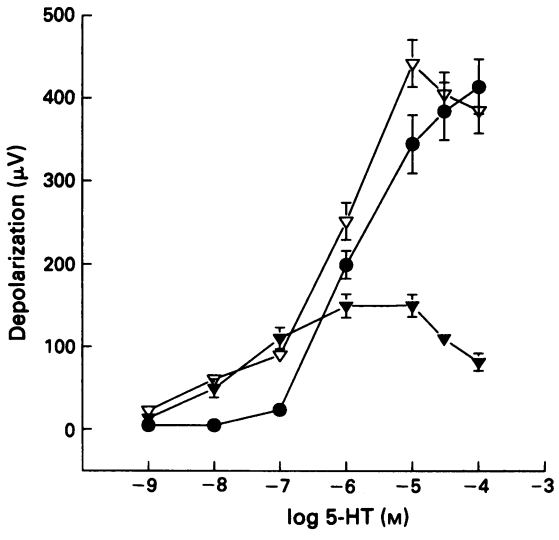

Figure 5 Concentration-response curves for the depolarization of the rat isolated vagus nerve by 5-HT. (△) Control responses; (▼) in the presence of 1 μM ondansetron; or (●) 1 μM RS 23597-190. Spiperone (1 μM) was present throughout to inhibit 5-HT_{1A} receptor function. Values are mean ± s.e.mean, $n = 5–8$ animals.

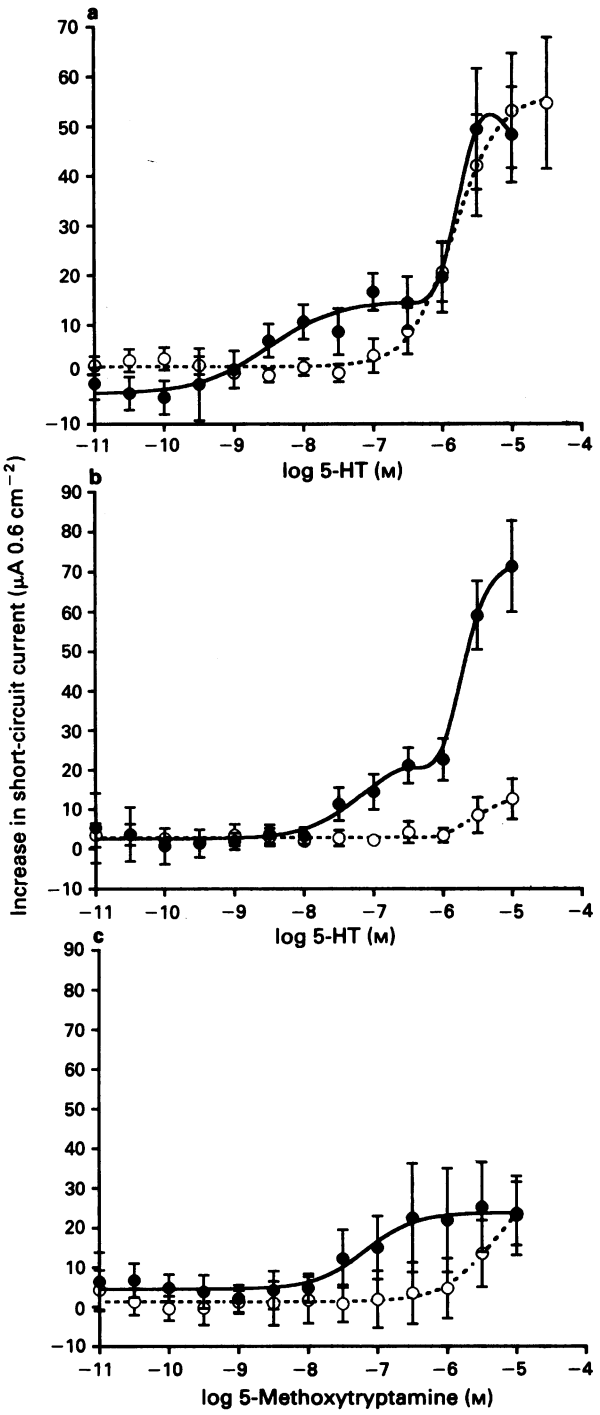

Figure 6 Concentration-dependent increases in short-circuit current, induced by 5-HT in guinea-pig isolated mucosa. The effects of RS 23597-190 1 μM on responses to 5-HT are shown in (a). The effect of tetrodotoxin (0.3 μM) on responses to 5-HT is shown in (b). (●) Responses to 5-HT; (○) responses to 5-HT in the presence of RS 23597-190 (a) or tetrodotoxin (b). Responses to 5-methoxytryptamine in the absence (●) or presence (○) of RS23597-190 1 μM are shown in (c). Values are mean ± s.e.mean, $n = 4-8$ animals.

dextrally and in a parallel manner although due to the small response and high variability a $-\log K_B$ was not calculated (Figure 6c).

In vivo *studies*

In the anaesthetized micropig, treatment by RS 23597-190 ($P<0.05$), time ($P<0.01$), and treatment by time interaction ($P<0.01$) were all significant. The pairwise comparisons at each time point showed that RS 23597-190, administered at 6.0 mg kg^{-1} i.v., significantly ($P<0.05$) inhibited the tachycardiac response to 5-HT at all times studied up to 150 min following compound administration (Figure 7). The maximal inhibition of 5-HT-induced tachycardia (87 ± 8%) occurred 10 min after addition of RS 23597-190 and the effective half-life for the compound was 77 (63–99) min (mean and 95% confidence intervals). At this dose, RS 23597-190 induced severe, transient but variable ECG changes with periods of ventricular tachycardia in 2 animals and episodes of premature ventricular contractions in each animal, which were generally resolved after 10–15 min. Associated with ECG abnormalities were periods of electrical-mechanical dissociation, in which inefficient heart function resulted in severe hypotension (decreases of 60 to 70 mmHg). The effects of RS 23597-190 on basal heart rate were variable with increases observed in 1 pig but decreases in 3 pigs (mean decrease of 36 ± 15 beats min^{-1} for the 4 animals).

In the anaesthetized rat, RS 23597-190 had no effect on resting heart rate or arterial pressure at doses up to 1 mg kg^{-1} min^{-1}. At 3 mg kg^{-1} min^{-1}, the drug produced a significant hypotensive response (decrease of 30 mmHg). As shown in Figure 8, RS 23597-190 dose-dependently inhibited the bradycardia elicited by 2-methyl 5-HT with a potency (ID_{50}) of 300 μg kg^{-1} min^{-1}.

Discussion

The aim of the present study was to characterize a novel ester analogue of metoclopramide, RS 23597-190. Antagonists available for the characterization of 5-HT$_4$ receptors include tropisetron, DAU 6285 and SDZ 205,557 (see introduction for references). Tropisetron and the indazole derivative have a high affinity for 5-HT$_3$ receptors, whereas DAU 6285 and SDZ 205,557 exhibit similar affinities for both the 5-HT$_4$ and 5-HT$_3$ receptor.

The affinity estimate (pA_2) of RS 23597-190 at the 5-HT$_4$ receptor (7.8) was higher than that for tropisetron (6.5), DAU 6285 (6.8) and SDZ 205,557 (7.5) (see Bockaert *et al.*, 1992 for references). The surmountable nature of the antagonism and unity slope of the Schild plot suggest a competitive interaction at 5-HT$_4$ receptors. The affinity of the antagonist appeared to be independent of the agonist, as similar $-\log K_B$ estimates were estimated with renzapride and SC-53116. This is in contrast to SDZ 205,557, where pA_2 values at 5-HT$_4$ receptors in guinea-pig ileum were found to be lower against zacopride than 5-HT (Buchheit *et al.*, 1992). Similar observations with SDZ 205,557 have been observed against 5-HT$_4$-mediated responses to renzapride and 5-HT in

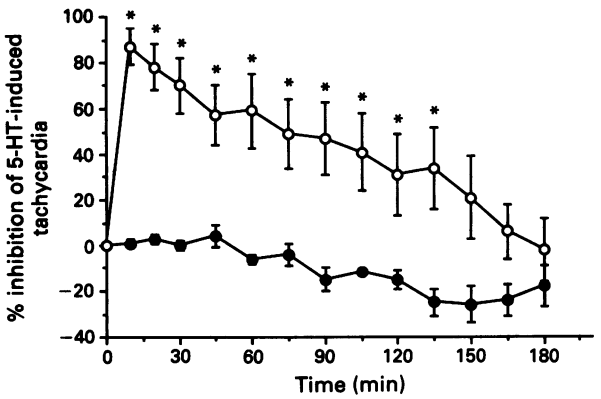

Figure 7 Time course of the inhibitory effect of RS 23597-190 (6 mg kg^{-1}, i.v.) on tachycardia elicited by 3–10 μg kg^{-1}, i.v., 5-HT, in the anaesthetized, bilaterally vagotomized micropig. (○) Animals pretreated with RS 23597-190; (●) animals pretreated with vehicle. Values are mean ± s.e.mean, $n = 5$ animals. *$P<0.05$, when compared to vehicle-treated animals.

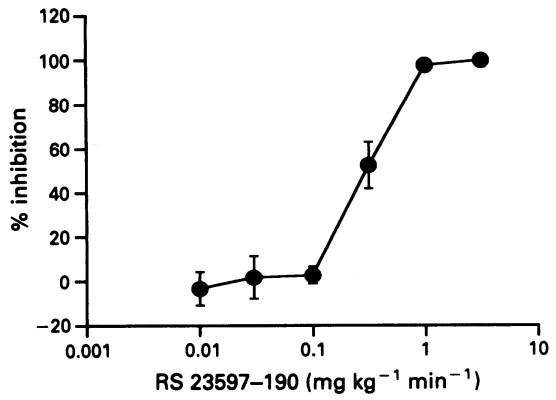

Figure 8 The inhibitory effect of RS 23597-190 (infused via the femoral vein) on the von Bezold Jarisch reflex elicited by 2-methyl 5-HT in conscious, restrained rats. Values are mean ± s.e.mean, $n = 8$ animals.

rat oesophagus (Eglen *et al.*, 1993a). The reasons for the deviations for competitiveness with SDZ 205,557 require further investigation.

The selectivity of RS 23597-190 between 5-HT_4 and 5-HT_3 receptors was determined to be greater than 1000 fold if guinea-pig 5-HT_3 affinity estimates were considered or 125 fold if rat, or mouse 5-HT_3 affinity estimates are used. The greater selectivity observed with guinea-pig data reflects a species variant of the 5-HT_3 receptor at which antagonists exhibit a low affinity (Wong *et al.*, 1993). The selectivity of RS 23597-190 was not observed with either SDZ 205,557 or DAU 6285 (see introducton for references) and highlights the advantage of the compound in characterizing 5-HT_4 receptors *in vitro*. This is particularly important in preparations where both 5-HT_3 and 5-HT_4 receptors mediate 5-HT responses such as contractile responses of guinea-pig ileum (Eglen *et al.*, 1990) enhancement of short-circuit current (Scott *et al.*, 1992), or depolarization of the rat vagus nerve (Rhodes *et al.*, 1992). Antagonists of lower or reverse selectivity have proved difficult to use for definitive characterization of the roles of these two receptors (see Bockaert *et al.*, 1992 for review).

Regarding other 5-HT receptors, RS 23597-190 lacked meaningful affinity toward 5-HT_{1A}, 5-HT_2, and dopamine D_1 and D_2 receptors. In this respect, it differed from metoclopramide which has an affinity at the D_2 receptor of 7.12 ± 0.14 (Wong & Hsu, 1992, unpublished observation). The inability of RS 23597-190 to antagonize 5-HT_3 mediated (cholinergic) contractions in guinea-pig ileum (Kilbinger & Wolf, 1992), or to affect the carbachol-induced contracture in rat oesophagus at concentrations up to 10 μM, was consistent with the low affinity of RS 23597-190 for muscarinic receptors (less than 5.0), as demonstrated directly in the binding studies at M_1, M_2, M_3 and M_4 receptors.

In guinea-pig ileal mucosa, 5-HT increases the short-circuit current, due to electrogenic chloride secretion (see Hendricks *et al.*, 1985; Scott *et al.*, 1992 for references). In the presence of tetrodotoxin, Scott *et al.* (1992) suggested that part of the response was mediated by 5-HT_4 receptors and the data obtained with RS 23597-190 in the present paper confirms this. In the present study, by contrast, the response was abolished by tetrodotoxin suggesting that 5-HT_4 receptors were located neuronally. Paradoxically, Scott *et al.* (1992) also reported that the 5-HT_4 mediated component was insensitive to high concentrations of tropisetron (10 μM), which exhibits an affinity (pA_2) of ~6.5 at 5-HT_4 receptors (Bockaert *et al.*, 1992). In our hands, RS 23597-190 antagonized the initial high potency phase of the response with similar $-\log K_B$ values to those found at 5-HT_4 receptors in oesophagus. The remainder of the enhancement of the short-circuit current by 5-HT was unaffected either by RS 23597-190 or methysergide, excluding 5-HT_4, 5-HT_1 and 5-HT_2 receptor stimulation. Preliminary data suggest that this phase, in part, is also resistant to granisetron 1 μM (Blissard & Leung, unpublished observations). This is in accordance with Scott *et al.* (1992) who also noted a response phase resistant to 5-HT_1, 5-HT_2, 5-HT_3 or 5-HT_4 blockade. Additional studies are evidently required to elucidate the nature of this site.

Rhodes *et al.* (1992) have suggested that 5-HT_4 receptors, in addition to 5-HT_3 receptors (Ireland & Tyers, 1987) mediate 5-HT-induced depolarizations of rat isolated vagus. The data obtained in the present paper support this contention. The presence of 5-HT_4 receptors on vagal afferents accords with the ability of zacopride (a mixed 5-HT_4 agonist/5-HT_3 antagonist) to induce emesis resistant to ondansetron (Bhandari & Andrews, 1991). The nature of the depolarization responses (5-HT_4 receptor: slow, sustained depolarization; 5-HT_3, fast, transient depolarization) probably reflects the nature of the coupling of the receptors since 5-HT_3 receptors are part of the ligand-gated ion channel superfamily (Maricq *et al.*, 1991), whereas 5-HT_4 receptors, as they stimulate adenylyl cyclase, are probably G protein coupled (Bockaert *et al.*, 1992) although Bley & Eglen, (1993) suggest that the 5-HT_4 receptor in rat vagus nerve may couple differently. Taken together, these studies illustrate the advantages of using a selective 5-HT_4 antagonist to define the role in preparations where more than one 5-HT receptor is involved.

A good correlation has been shown (Fozard, 1989) to exist between 5-HT_3 receptor affinity of compounds and potency at antagonizing 2-methyl 5-HT induced bradycardia (the von Bezold Jarisch reflex). Consequently, the low potency of RS 23597-190 at blocking this reflex in rat (300 μg kg^{-1} min^{-1}) accords with its low affinity at the 5-HT_3 receptor as estimated in the binding studies (5.7). The potency of infused RS 23597-190 at inhibiting the reflex was similar to that reported for a bolus dose of DAU 6285 (231 μg kg^{-1}, i.v.; Dumuis *et al.*, 1992), which is also a weak 5-HT_3 antagonist ($-\log K_i = 6.5$ nM; Dumuis *et al.*, 1992). In contrast, the potency of tropisetron in antagonizing the reflex is much higher (less than 1 μg kg^{-1}, i.v.; Richardson *et al.*, 1985), which accords with the high affinity of tropisetron for the 5-HT_3 receptor ($-\log K_i = 9.1$; Sharif *et al.*, 1991; Wong *et al.*, 1993).

Thus *in vivo* studies in the rat permitted identification of doses of RS 23597-190 at which 5-HT_3 antagonism is evident. Since the affinity at 5-HT_4 receptors is higher, it is reasonable to suggest that 5-HT_4 receptor blockade occurred at lower doses. To confirm this, however, an unambiguous *in vivo* assay for 5-HT_4 receptor function in the rat will be required. Such an assay has not yet been reported. In the pig and micropig, atrial 5-HT_4 receptor stimulation gives rise to tachycardia (Villalon *et al.*, 1990; Eglen *et al.*, 1993a). In the micropig, RS 23597-190, which is an ester, appeared to be subjected to rapid plasma hydrolysis, a property also inherent in a close structure analogue, SDZ 205,557 (Eglen *et al.*, 1993a). The half-life for the duration of action of SDZ 205,557 at inhibiting 5-HT_4-mediated tachycardia was approximately 23 min (Eglen *et al.*, 1993a). RS 23597-190, 6.0 mg kg^{-1}, i.v., produced approximately a 3 fold longer duration of 5-HT_4 receptor antagonist activity (77 min) than SDZ 205,557 (23 min), consistent with the higher affinity of the compound for the receptor. However, more serious cardiovascular side-effects (ECG, heart rate, and blood pressure effects) with RS 23597-190 were evident. The reason behind these effects are unknown. Cisapride, a partial 5-HT_4 agonist, has been shown to induce tachycardia in man (Olsson & Edwards, 1992) and 5-HT_4 antagonists have been suggested to possess potential as antiarrhythmic agents (Bockaert *et al.*, 1992). The disrhythmic activity of RS 23597-190 at this dose may argue against this contention.

Recently, other 5-HT_4 antagonists have been described which also have high affinity for the 5-HT_4 receptor. These

include LY297582 (Krushinski *et al.*, 1992), SB 203186 (Kaumann *et al.*, 1992b) and GR 113808 (Grossman *et al.*, 1992). LY297582 is structurally similar to RS 23597-190, although the selectivity between rat oesophageal 5-HT_4 receptors and guinea-pig ileal 5-HT_3 receptors is lower (240 fold). GR 113808 is structurally different, has a notably higher affinity for the 5-HT_4 receptor ($pA_2 = 9.2-9.5$; Grossman *et al.*, 1992) than RS 23597-190 and has formed the basis of a radioligand binding assay. However, it is also an ester, with a very short plasma half-life (Grossman *et al.*, 1992). SC-63606 (Yang *et al.*, 1992), by contrast, is more stable *in vivo* but is less selective (8 fold) than RS 23597-190 for the 5-HT_4 receptor over 5-HT_3 receptors. DAU 6285 (Bockaert *et al.*, 1992) is also stable *in vivo* (Johnson & Eglen, unpublished observations), but is only 5 fold selective for the 5-HT_4 receptor.

To conclude, present data support the contention of Krushinski *et al.* (1992) that esteric derivatives of metoclopramide, such as RS 23597-190, LY297582 or LY297524 are potent 5-HT_4 antagonists. RS 23597-190, and most recently GR 113808, represent major advances in the pharmacology of the 5-HT_4 receptor, since they are antagonists with a high affinity for the receptor and a genuine selectivity over the 5-HT_3 receptor from several species, not solely the guinea-pig. The availability of such pharmacological tools will allow more unambiguous definition of 5-HT_4 receptors in various preparations. *In vivo*, however, the situation is more complex due to the short half-lives of those antagonists and in this regard DAU 6285 or SC 53606 may be preferable. Thus, precise characterization of the function of the 5-HT_4 receptor awaits development of more stable, high affinity, selective antagonists.

The authors wish to thank D. Blissard, W. Lachnit, L. Perkins, M. Perry, E. Stefanich, S. Wallace and A. Wong, for their valuable assistance in performing these studies. Drs D.E. Clarke, A.P.D.W. Ford and R.M. Johnson provided valuable advice in the preparation of the manuscript.

References

ARUNLAKSHANA, O. & SCHILD, H.O. (1959). Some quantitative uses of drug antagonist. *Br. J. Pharmacol. Chemother.*, **14**, 48–58.

BAXTER, G.S., CRAIG, D.A. & CLARKE, D.E. (1991). 5-Hydroxytryptamine$_4$ receptors mediate relaxation of the rat oesophageal tunica muscularis mucosae. *Naunyn-Schmied. Arch. Pharmacol.*, **343**, 439–446.

BHANDARI, P. & ANDREWS, P.L.R. (1991). Preliminary evidence for the involvement of the putative 5-HT_4 receptor in zacopride- and copper-sulphate induced vomiting in the ferret. *Eur. J. Pharmacol.*, **204**, 273–280.

BLEY, K.R. & EGLEN, R.M. (1993). Characterization of serotoninergic depolarizations in the isolated rat vagus nerve. *B. J. Pharmacol.*, **108**, 246P.

BOCKAERT, J., FOZARD, J., DUMUIS, A. & CLARKE. D.E. (1992). The 5-HT_4 receptor: a place in the sun. *Trends Pharmacol. Sci.*, **13**, 141–145.

BUCHHEIT, K.-H., GAMSE, R. & PFANNKUCHE, H.-J. (1992). SDZ 205,557, a selective surmountable antagonist for 5-HT_4 receptors in the isolated guinea-pig ileum. *Naunyn-Schmied. Arch. Pharmacol.*, **343**, 387–393.

BUNCE, K.T. & SPRAGGS, C.F. (1989). Stimulation of electrogenic chloride secretion by prostaglandin E_2 in guinea-pig isolated gastric mucosa. *J. Physiol.*, **400**, 381–394.

CHENG, Y.-C. & PRUSOFF, W.M. (1973). Relationship between inhibitors constant (K_i) and the concentration of inhibitor which causes 50 percent inhibition (IC_{50}) of an enzymatic reaction. *Biochem. Pharmacol.*, **92**, 881–894.

CRAIG, D.A., EGLEN, R.M., WALSH, L.K.M., PERKINS, L.A., WHITING, R.L. & CLARKE, D.E. (1990). 5-methoxytryptamine and 2-methyl 5-hydroxytryptamine induced desensitization as discriminative tools for the 5-HT_3 and putative 5-HT_4 receptors in guinea-pig ileum. *Naunyn-Schmied. Arch. Pharmacol.*, **342**, 9–16.

DUMUIS, A., BOUHELAL, R., SEBBEN, M. & BOCKAERT, J. (1988). A 5-HT receptor in the central nervous system postively coupled with adenylate cyclase is antagonized by ICS 205,930. *Eur. J. Pharmacol.*, **146**, 187–188.

DUMUIS, A., GOZLAN, H., SEBBEN, M., ANSANAY, H., RIZZI, C.A., TURCONI, M., MONFERINI, E., GIRALDO, E., SCHIANTARELLI, P., LADINSKY, H. & BOCKAERT, J. (1992). Characterization of a novel 5-HT_4 receptor antagonist of the azabicyclobenzimidazolone class: DAU 6285. *Naunyn-Schmied. Arch. Pharmacol.*, **345**, 264–269.

EGLEN, R.M., ALVAREZ JOHNSON, L.G. & WONG, E.M.F. (1993a). The action of SDZ 205,557 5-hydroxytryptamine (5-HT_3 and 5-HT_4) receptors. *Br. J. Pharmacol.*, **108**, 376–382.

EGLEN, R.M., BONHAUS, D.W., HEGDE, S., LEUNG, E. & WHITING, R.L. (1993b). RS 23597-190: a potent and selective 5-HT_4 receptor antagonist. *Br. J. Pharmacol.*, **107**, 439P.

EGLEN, R.M., SWANK, S.R., WALSH, L.K.M. & WHITING, R.L. (1990). Characterization of 5-HT_3 and atypical 5-HT receptors mediating ileal contractions *in vitro*. *Br. J. Pharmacol.*, **101**, 513–520.

FLYNN, D.L., ZABROWSKI, D.L., BECKER, D.P., NOSAL, R., VILLANIL, C.I., GULLIKSON, G.W., MOUMMI, C. & YANG, D.-C. (1992). SC-53116: The first selective agonist at the newly identified serotonin 5-HT_4 receptor subtype. *J. Med. Chem.*, **35**, 1486–1489.

FORD, A.P.D.W., BAXTER, G.S., EGLEN, R.M. & CLARKE, D.E. (1992). 5-hydroxytryptamine (5-HT) stimulates cyclic AMP formation in the tunica muscularis mucosae (TMM) of the rat oesophagus. *Eur. J. Pharmacol.*, **225**, 105–112.

FOZARD, J.R. (1989). The development and early clinical evaluation of selective 5-HT_3 receptor antagonists. In *The Peripheral Actions of 5-Hydroxytryptamine*, ed. Fozard, J.R. New York: Oxford University Press.

FURCHGOTT, R.F. (1972). The classification of adrenoreceptors (adrenergic receptors). An evaluation for the standpoint of receptor theory. In *Handbook of Experimental Pharmacology, Catecholamines*, vol. 33, ed. Blashko, H. & Muscholl, E. pp. 283–335. New York: Springer-Verlag.

GROSSMAN, C.J., KILPATRICK, G.J., BUNCE, K.T., OXFORD, A.W., GALE, J.D., WHITEHEAD, J.F. & HUMPHREY, P.P.A. (1992). Development of a radioligand binding assay for the 5-HT_4 receptor: use of a novel antagonist. Abstract *2nd International Symposium on Serotonin*, Houston, U.S.A. p. 31.

HENDRICKS, R., BORNSTEIN, J.C. & FURNESS, J.B. (1985). Evidence for two types of 5-hydroxytryptamine receptor on secretomotor neurones of the guinea-pig ileum. *Naunyn-Schmied. Arch. Pharmacol.*, **339**, 409–414.

IRELAND, S.J. & TYERS, M.B. (1987). Pharmacological characterization of 5-hydroxytryptamine-induced depolarization of the rat isolated vagus nerve. *Br. J. Pharmacol.*, **90**, 229–238.

KAUMANN, A.J., KING, F.D. & YOUNG, R.C. (1992a). Indazole as an indole bioisostere: 5-HT_4 receptor antagonism. *Biorgan. Med. Chem. Letts.*, **2**, 419–420.

KAUMANN, A.J., MEDHURST, A., BOYLAND, P., VIMAL, M. & YOUNG, R.C. (1992b). SB 203186, a potent and selective 5-HT_4 receptor antagonist. Abstract *2nd International Symposium on Serotonin*, Houston, U.S.A. p. 44.

KENAKIN, T.P., BOND, R.A. & BONNER, T.I. (1992). Definition of pharmacological receptors. *Pharmacol. Rev.*, **44**, 351–362.

KILBINGER, H. & WOLF, D.R. (1992). Effects of 5-HT_4 receptor stimulation on basal and electrically evoked release of acetylcholine from guinea-pig myenteric plexus. *Naunyn-Schmied. Arch. Pharmacol.*, **345**, 270–275.

KILPATRICK, G. & TYERS, M.B. (1992). Interspecies variants of the 5-HT_3 receptor. *Biochem. Soc. Trans.*, **20**, 118–123.

KRUSHINSKI, J.M., SUSEMICHEL, A., ROBERTSON, D.W. & COHEN, M.L. (1992). Interaction of metoclopramide analogues at 5HT_4 receptors. Abstract, *203rd National Meeting of the American Chemical Society*, San Francisco, USA.

LEUNG, E., PERKINS, L.A., BONHAUS, D.W., LOURY, D.N., CLARK, R. & EGLEN, R.M. (1992a). RS 23597-190: a selective high affinity antagonist for 5-HT_4 receptors. Abstracts, *2nd International Meeting on Serotonin*, Houston, USA, p. 49.

LEUNG, E., MICHELSON, S., VILLARUBIA, C., PERKINS, L.A. & EGLEN, R.M. (1992b). Analysis of concentration-response relationships by seemingly unrelated nonlinear regression (SUNR) technique. *J. Pharmacol. Methods*, **4**, 209–216.

MARSH, S.J., STANSFELD, C.E., BROWN, D.A., DAVEY, R. & MCCARTHY, D. (1987). The mechanism of action of capsaicin on sensory C-type neurons and their axons *in vitro*. *Neuroscience*, **23**, 275–289.

MARICQ, A.T., PETTERSON, A.S., BRAKE, A.J., MYERS, R.M. & JULIUS, D. (1991). Primary structure and functional expression of the 5-HT_3 receptor, a serotonin-gated ion channel. *Science*, **254**, 432–437.

MUNSON, P.J. & RODBARD, D. (1980). Ligand: a versatile computerized approach for characterization of ligand-binding systems. *Anal. Biochem.*, **107**, 220–239.

OLSSON, S. & EDWARDS, I.R. (1992). Tachycardia during cisapride treatment. *Br. Med. J.*, **305**, 748–749.

PARKER, R.B. & WAUD, D.R. (1971). Pharmacological estimation of drug-receptor dissociation constants. Statistical analysis. I. Agonists. *J. Pharmacol. Exp. Ther.*, **177**, 1–12.

RICHARDSON, B.P., ENGEL, D., DONATSCH, P. & STADLER, P.A. (1985). Identification of serotonin M-receptor subtypes as their specific blockade by a new class of drugs. *Nature*, **316**, 126–131.

RHODES, K.F., COLEMAN, J. & LATTIMER, N. (1992). A component of 5-HT-evoked depolarization of the rat isolated vagus nerve in vitro is mediated by a putative 5-HT_4 receptor. *Naunyn-Schmied Arch. Pharmacol.*, **346**, 496–503.

SCOTT, C.M., BUNCE, K.T. & SPAGGS, C.F. (1992). Investigation of the 5-hydroxytryptamine receptor mediating the 'maintained' short-circuit current response in guinea-pig ileal mucosa. *Br. J. Pharmacol.*, **106**, 877–882.

SHARIF, N.A., WONG, E.H.F., LOURY, D.N., STEFANICH, E., MICHEL, A.D., EGLEN, R.M. & WHITING, R.L. (1991). Characteristics of 5-HT_3 binding sites in NG108-15, NCB-20 neuroblastoma cells and rat cerebral cortex using [^{3}H]quipazine and [^{3}H]-GR 65630 binding. *Br. J. Pharmacol.*, **102**, 919–925.

VILLALON, C.M., DEN BOER, M.O., HEILIGERS, J.P.C. & SAXENA, P.R. (1990). Mediation of 5-hydroxytryptamine induced tachycardia in the pig. *Br. J. Pharmacol.*, **100**, 665–667.

WONG, E.H.F., BONHAUS, D.W., WU, I., STEFANICH, E. & EGLEN, R.M. (1993). Labelling of 5-HT_3 receptors with a novel 5-HT_3 receptor ligand, [^{3}H]RS 42358-197. *J. Neurochem.*, **60**, 921–930.

WONG, E.H.F., WU, I., EGLEN, R.M. & WHITING, R.L. (1992). Labelling of species variants of 5-hydroxytryptamine$_3$ (5-HT_3) receptors by a novel 5-HT_3 receptor ligand [^{3}H]RS 42358-197. *Br. J. Pharmacol.*, **105**, 33P.

YANG, D.-C., MOORMANN, A.E., FLYNN, D.L. & GULLIKSON, G.W. (1992). SC-53606: a selective potent serotonin-5-HT_4 receptor antagonist. Abstract, *2nd International Symposium on Serotonin*, Houston, USA, p. 48.

(Received December 7, 1992
Revised March 4, 1993
Accepted April 23, 1993)

Br. J. Pharmacol. (1993), **110**, 127–132

Leukotriene D_4- and prostaglandin $F_{2\alpha}$-induced airflow obstruction and airway plasma exudation in guinea-pig: role of thromboxane and its receptor

Hirokazu Arakawa, [1]Jan Lötvall, Ivana Kawikova, Claes-Göran Löfdahl & Bengt-Eric Skoogh

Lung Pharmacology Group, Division of Clinical Pharmacology (Department of Pharmacology), and Division of Pulmonary Medicine (Department of Internal Medicine), Göteborg University, Göteborg, Sweden

1 We studied the effects of a thromboxane A_2 receptor (TP receptor) antagonist, ICI-192,605 (0.5 mg kg^{-1}, i.v.) and a selective thromboxane (Tx) synthetase inhibitor, OKY-046 (30 mg kg^{-1}, i.v.), on airway responses induced by leukotriene D_4 (LTD_4; 0.2 nmol) or prostaglandin $F_{2\alpha}$ ($PGF_{2\alpha}$; 20 nmol) instilled via the airways route to anaesthetized guinea-pigs. For a comparison, airway responses to a TxA_2-mimetic, U-46619 (0.02 nmol) were also studied. We measured both lung resistance (R_L) to monitor airflow obstruction, and extravasation of Evans Blue dye to quantify airway plasma exudation.

2 Instilled LTD_4 into the tracheal lumen induced an immediate peak and subsequently persistent increase in R_L and produced a large amount of extravasation of Evans Blue dye at all airway levels. Both ICI-192,605 and OKY-046 significantly attenuated the persistent increase in R_L following the immediate response and reduced LTD_4-induced extravasation of Evans Blue dye in the trachea and proximal intrapulmonary airway. Instilled LTD_4 produced significant increases in immunoreactive TxB_2 in bronchoalveolar lavage fluid obtained 1.5 min after instillation of LTD_4.

3 Instilled $PGF_{2\alpha}$ into the tracheal lumen induced an immediate increase in R_L which peaked at approximately 15 s. We also observed a delayed sustained increase in R_L, reaching a second peak at approximately 4 min. $PGF_{2\alpha}$ produced small but significant increases in the amount of Evans Blue dye at all airway levels. As with $PGF_{2\alpha}$, instillation of U-46619 produced a biphasic increase in R_L and extravasation of Evans Blue dye. The potency of $PGF_{2\alpha}$ in inducing these airway responses was about 1000 times less than U-46619. ICI-192,605 abolished both the immediate and the delayed increase in R_L after $PGF_{2\alpha}$, and also blocked $PGF_{2\alpha}$-induced extravasation of Evans Blue dye. However, OKY-046 had no inhibitory effects on these responses.

4 We conclude that airflow obstruction and airway plasma exudation induced by instilled LTD_4 is, in part, mediated via TxA_2 generation and subsequent activation of TP-receptors. On the other hand, instilled $PGF_{2\alpha}$, while inducing similar responses, does so primarily by direct activation of TP receptors, rather than via TxA_2 generation.

Keywords: Asthma; airway oedema; arachidonic acid; vascular permeability

Introduction

The role of thromboxane A_2 (TxA_2) in bronchial asthma remains unclear, despite several studies designed to evaluate this (Barnes *et al.*, 1988; O'Byrne & Manning, 1992). Recent *in vivo* studies in guinea-pigs have revealed that a TxA_2-mimetic, U-46619 (9,11-dideoxy methanoepoxy-9α, 11α-prostaglandin $F_{2\alpha}$), induces airflow obstruction and airway plasma exudation (Lötvall *et al.*, 1992). In addition, TxA_2 may, in this species, be one of the final pathways of airflow obstruction and airway plasma exudation induced by platelet activating factor (Tokuyama *et al.*, 1991) and bradykinin (Arakawa *et al.*, 1992; Kawikova *et al.*, 1992). In guinea-pigs, allergen-induced airflow obstruction is mediated in part via TxA_2 production (Beasley *et al.*, 1989; Arakawa *et al.*, 1993), and an increased level of TxB_2 is found in bronchoalveolar lavage after allergen challenge (Fujimura *et al.*, 1991).

The role of cyclo-oxygenase products in leukotriene D_4 (LTD_4)-induced airway responses in guinea-pigs is controversial. Both Hamel *et al.* (1982) and Birch *et al.* (1988) have suggested that TxA_2 mediates bronchoconstrictor responses to i.v. LTD_4 in guinea-pigs. However, cyclo-oxygenase products were found not to mediate either bronchoconstriction (Hamel *et al.*, 1982) or airway plasma exudation (Woodward *et al.*, 1983) induced by LTD_4 given via the airway route in guinea-pigs.

$PGF_{2\alpha}$ causes airflow obstruction (Birch *et al.*, 1988) and weak airway plasma exudation (Persson, 1992). Bronchoconstriction induced by $PGF_{2\alpha}$ or PGD_2 is mediated through activation of TxA_2 receptors (TP receptors) (Birch *et al.*, 1988). Also, *in vitro* studies have demonstrated that $PGF_{2\alpha}$ acts in part through TP receptors to induce contraction of lung parenchymal strips from guinea-pigs (McKenniff *et al.*, 1991). However, to our knowledge there is no information available concerning the inhibitory effects of TP-receptor antagonists on $PGF_{2\alpha}$-induced airway plasma exudation.

The aims of this study were first to evaluate whether TxA_2 is involved in airway responses to instilled LTD_4, and secondly, to investigate whether $PGF_{2\alpha}$-induced airway plasma exudation is mediated through activation of TP receptors. We studied the effects of ICI-192,605, a TP receptor antagonist, and OKY-046, a selective Tx synthetase inhibitor, on both airflow obstruction and airway plasma exudation induced by either LTD_4 or $PGF_{2\alpha}$. For comparison, we also studied the effects of a TxA_2-mimetic, U-46619, instilled into the tracheal lumen.

Methods

Experiments were performed on male Dunkin Hartley guinea-pigs weighing 450–670 g. The animals were anaesthetized with a 3:2 mixture of ketamine (50 mg ml^{-1}) and xyalzine (20 mg ml^{-1}) intramuscularly (1 ml kg^{-1}). Additional anaes-

[1] Author for correspondence.

thetic was given to an appropriate level of anaesthesia as evidenced by a disappearance of corneal reflex and withdrawal response to foot pad pinching. Anaesthesia was subsequently monitored by these means until the time when suxamethonium was administered to avoid artefacts induced by spontaneous breathing. Thereafter, systemic blood pressure was monitored throughout the experiment. A tracheal cannula (10 mm length and 2.7 mm inner diameter) was inserted into the lumen of the cervical trachea through a tracheostomy, and secured with a suture. A polyethylene catheter was inserted into the left carotid artery to monitor blood pressure with a pressure transducer (model P23XL, Viggo-Spectramed, Helsingborg, Sweden). The right external jugular vein was cannulated for the administration of drugs and Evans Blue dye. All animals were pretreated with suxamethonium (5 mg kg^{-1}, i.v.) to avoid artefacts induced by spontaneous breathing.

Measurement of airway function

Guinea-pigs were placed on a heated blanket (Harvard model 50-7061, Harvard Apparatus Ltd., Edenbridge, Kent) which maintained body temperature at 37°C, with the intratracheal cannula connected to a constant volume mechanical ventilator (Harvard model 50-1718, Harvard Apparatus Ltd.). A tidal volume of 10 ml kg^{-1} and a frequency of 60 breaths min^{-1} was used. Transpulmonary pressure was measured with a pressure transducer (Model FCO40; ± 1000 mmH_2O; Furness Controls Ltd., Bexhill, Sussex), with one side attached to a catheter inserted into the right pleural cavity and the other side attached to a catheter connected to a side port of the intratracheal cannula. The ventilatory circuit had a total volume of 18 ml. Airflow was measured with a pneumotachograph (Model F1L; Mercury Electronics Ltd., Glasgow) connected to a transducer (Model FCO40; ± 20 mmH_2O; Furness Controls Ltd.). The signal from the blood pressure transducer was amplified with an analog preamplifier (Kungsbacka mät & reglerteknik AB, Sweden). All signals were digitalized with a 12-bit analog digital board (National Instruments, Austin, Tx, U.S.A.) connected to a Macintosh II computer (Apple computer Inc., Cupertino, U.S.A.) and analyzed with a software (LabView, National Instruments), which was programmed to calculate instantaneously lung resistance (R_L) by the method of von Neergaard & Wirz (1927). Mean blood pressure was also monitored throughout the experiments.

Protocol

The animals were divided into six groups in order to study the effects of pretreatment with ICI-192,605 (0.5 mg kg^{-1}; Lötvall *et al.*, 1992) or OKY-046 (30 mg kg^{-1}; Arakawa *et al.*, 1992) on both airway plasma exudation and increase in R_L up to 6 min after instillation of LTD_4 (0.2 nmol; $n = 7$ and $n = 6$, respectively) or $PGF_{2\alpha}$ (20 nmol; $n = 6$ and $n = 4$, respectively), compared to untreated animals (LTD_4, $n = 9$; $PGF_{2\alpha}$, $n = 9$). For comparison, we also studied the effects of a TxA_2 mimetic, U-46619 (0.02 nmol, $n = 5$) or vehicle (0.9% NaCl, $n = 6$) instilled into the tracheal lumen of untreated guinea-pigs in two groups (Table 1). Furthermore, we measured TxB_2, a stable metabolite of TxA_2, in bronchoalveolar lavage fluid (BALF) of guinea-pigs 1.5 min after instilled LTD_4 or saline (0.9% NaCl) in another two groups.

Ten minutes after pretreatment with suxamethonium, either ICI-192,605 (0.5 mg kg^{-1}) or OKY-046 (30 mg kg^{-1}) was given intravenously. Five minutes later, or 15 min after suxamethonium (untreated animals), Evans Blue dye (20 mg kg^{-1}) was administered i.v. over 1 min. Another minute later, 100 µl of LTD_4 (2 µM), $PGF_{2\alpha}$ (200 µM), U-46619 (0.2 µM) or vehicle (0.9% NaCl) was instilled into the airways. Airway instillation was performed by flushing 100 µl volumes with 1 ml of air, directly into the tracheal lumen via the tracheal cannula. At that time, the animals were disconnected from the ventilator for a few seconds. Transpulmonary pressure, R_L and mean blood pressure were monitored by the computer.

Determination of plasma extravasation

Six minutes after administration of LTD_4, $PGF_{2\alpha}$, U-46619 or vehicle, the animals were disconnected from the ventilator, and the thoracic cavity was opened. A catheter was inserted into the aorta through the left ventricle, and the animal was perfused with 50 ml of 0.9% NaCl to remove dye within the bronchial circulation. After perfusion through this route, another catheter was inserted into the pulmonary artery, and the pulmonary circulation was then perfused with 20 ml of saline. The trachea and lungs were dissected out en bloc, the parenchyma carefully scraped off, and extraneous tissue removed. The trachea, main bronchi and intrapulmonary airways were separated from each other, and the intrapulmonary airways were then divided into two lengthwise equal portions, arbitrarily named proximal and distal. All airway tissues were dried, with a freeze dryer (MicroModulyo, Edwards High Vacuum International, West Sussex) for 24 h. All tissues were weighed dry, and Evans Blue dye was extracted in 2 ml of formamide in a 40°C water bath for 24 h. Absorption at 620 nm was measured in a spectrophotometer (PU8670 VIS/NIR, Philips, Cambridge, U.K.). The extracted Evans Blue dye was quantified by interpolation on a standard curve of dye concentrations in the range of 0–10 µg ml^{-1}, and expressed as ng mg^{-1} dry tissue. Evans Blue dye measurement has been previously shown to correlate highly with the extravasation of radiolabelled albumin in guinea-pig airways (Rogers *et al.*, 1989).

Measurement of TxB_2 in BALF

Ninety seconds after instillation of LTD_4 (0.2 nmol) or vehicle (0.9% NaCl), 10 ml kg^{-1} saline at 37°C was instilled through the tracheal cannula and sequentially removed by gentle manual aspiration. The recovered BALF was immediately put into a tube with indomethacin (final concentration, 10 µM) and centrifuged for 10 min at 400 *g* to separate fluid from cells and debris. The supernatant was stored at − 25°C for measurement of TxB_2 concentration. TxB_2 concentration in BALF was measured by radioimmunoassay kit (Amersham, Stockholm, Sweden), using ^{125}I TxB_2 as standard, and an antibody to TxB_2. The activity was counted in a gamma counter (LKB Wallac, Wallac, Sollentuna, Sweden), and the amount of TxB_2 expressed as pM. The percentage cross-reactivity of this kit with leukotriene D_4 was less than 0.35, in preliminary experiments. Briefly, we found an apparent value of TxB_2 of 31 pg ml^{-1} after adding 10,000 pg LTD_4 to the solution.

Drugs and chemicals

The following drugs and chemicals were used: ketamine hydrochloride (Park-Davis S.A., Barcelona, Spain); xylazine chloride (Bayer Sverige AB, Göteborg, Sweden); suxamethonium chloride (KabiVitum AB, Stockholm, Sweden); Evans Blue dye (Aldrich Chemical Co., Milwaukee, U.S.A.); leukotriene D_4 (Sarva, Germany); prostaglandin $F_{2\alpha}$, U-46119 (Sigma, St Louis, U.S.A.). ICI-192,605: 4(Z)-6-(2-*o*-chlorophenyl-4-*o*-hydroxyphenyl-1,3-dioxan-*cis*-5-yl) and OKY-046; (E)-3- [*p*-(4-imidazol-methyl) phenyl]-2-propenoic acid hydrochloride were kindly donated by ICI Pharmaceutical Co. (USA) and Kissei Pharmaceutical Co. (Japan). ICI-192,605 was at first diluted with 100 mM $NaHCO_3$ to give a concentration of 5 mg ml^{-1}, and further dilutions were made with 0.9% NaCl to give a final concentration of 0.5 mg ml^{-1} (Lötvall *et al.*, 1992). In a previous study, ICI-192,605

administration alone had no effect on baseline R_L or extravasation of Evans Blue dye (Tokuyama *et al.*, 1991). OKY-046 was diluted in saline. All drugs injected intravenously were given at a dose volume of 1 ml kg^{-1}.

Data analysis

Data are given as mean ± s.e.mean. Non-parametric analysis of variance (Kruskal-Wallis method) was used to determine any significant variance among groups. If a significant variance was found, a Mann-Whitney U-test was used to test for significant differences between individual groups. A P value less than 0.05 was considered significant. Data were analyzed by a Macintosh computer using standard statistical packages (StatView II).

Results

R_L-changes induced by LTD$_4$, PGF$_{2\alpha}$ and U-46119

There were no significant differences in body weight and baseline R_L between any of the groups studied (Table 1). In untreated animals, instilled LTD$_4$ (0.2 nmol) produced an immediate and subsequently persistent increase in R_L, with an immediate peak at approximately 45 s (3.5 ± 0.5 cmH$_2$O ml^{-1} s) (Figure 1). R_L was significantly higher after LTD$_4$ than after instillation of saline at all time points. Neither ICI-192,605 nor OKY-046 significantly affected the immediate increase in R_L induced by LTD$_4$. However, the persistent increase in R_L following the immediate response was significantly attenuated by pretreatment with both ICI-192,605 and OKY-046 at all time points longer than 1.5 min after instillation of LTD$_4$.

In untreated animals, instilled PGF$_{2\alpha}$ (20 nmol) produced a biphasic increase in R_L, with an immediate peak at approximately 15 s (2.2 ± 0.8 cmH$_2$O ml^{-1} s) and a delayed sustained increase in R_L which peaked at approximately 4 min (2.2 ± 0.2 cmH$_2$O ml^{-1} s) (Figure 2). R_L was significantly higher after PGF$_{2\alpha}$ than after instillation of saline at all time points. Instillation of U-46619 (0.02 nmol) also induced a biphasic increase in R_L, with similar levels of increased R_L compared with those after PGF$_{2\alpha}$ (Figure 2). ICI-192,605 abolished both the immediate and the delayed sustained increase in R_L induced by PGF$_{2\alpha}$. However, OKY-046 did not affect these responses (Figure 2).

Evans Blue dye extravasation induced by LTD$_4$, PGF$_{2\alpha}$ and U-46619

In untreated animals, instillation of LTD$_4$ (0.2 nmol) caused pronounced extravasation of Evans Blue dye at all airway levels (Figure 3). Both ICI-192,605 and OKY-046 reduced extravasation of dye after LTD$_4$, with a significant inhibition

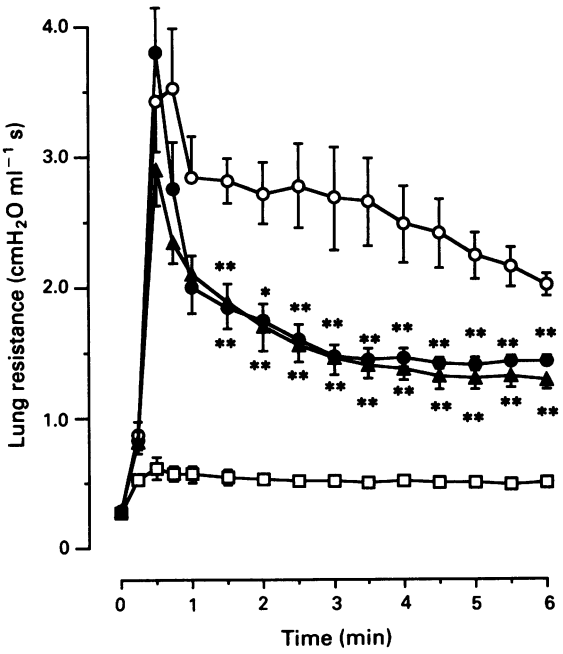

Figure 1 Effect of ICI-192,605 (●: 0.5 mg kg^{-1}, $n = 7$) or OKY-046 (▲: 30 mg kg^{-1}, $n = 6$) given i.v. 5 min before instillation of leukotriene D$_4$ (LTD$_4$, 0.2 nmol) on the time-course of increased lung resistance (R_L), compared with untreated guinea-pigs given instilled LTD$_4$ (○: $n = 9$) or saline (□: 0.9% NaCl, $n = 6$). *$P < 0.01$, **$P < 0.005$ compared to untreated animals given instilled LTD$_4$.

in trachea ($P < 0.01$ and $P < 0.05$, respectively) and proximal intrapulmonary airways ($P < 0.01$ after ICI-192,605). These values after ICI-192,605 or OKY-046 were, however, still significantly higher than in animals given vehicle instillation. In untreated animals, instillation of PGF$_{2\alpha}$ (20 nmol) caused a small but significant increase in extravasation of Evans Blue dye at all airway levels (Figure 3). U-46619 (0.02 nmol) also produced significant extravasation of Evans Blue dye at all airway levels (Figure 3). The amount of extravasated dye was larger after U-46619 than PGF$_{2\alpha}$, with a significant difference in trachea ($P < 0.05$). ICI-192,605 significantly blocked extravasation of dye after PGF$_{2\alpha}$ at all airway levels, except for distal intrapulmonary airways. However, OKY-046 did not influence PGF$_{2\alpha}$-induced extravasation of Evans Blue dye (Figure 3).

Blood pressure-changes induced by LTD$_4$, PGF$_{2\alpha}$ and U-46619

There were no significant differences in baseline mean systemic blood pressure between any of the groups studied

Table 1 Body weight, baseline data for lung resistance (R_L), mean systemic blood pressure, and percentage change in mean systemic blood pressure after either leukotriene D$_4$ (LTD$_4$) or prostaglandin F$_{2\alpha}$ (PGF$_{2\alpha}$)

			LTD$_4$ (0.2 nmol)			PGF$_{2\alpha}$ (20 nmol)		
Group	*Saline* (0.9% NaCl)	*U-46619* (0.02 nmol)	*Untreated*	*ICI-192,605* (0.5 mg kg^{-1})	*OKY-046* (30 mg kg^{-1})	*Untreated*	*ICI-192,605* (0.5 mg kg^{-1})	*OKY-046* (30 mg kg^{-1})
Body weight (g)	512 ± 5	532 ± 7	612 ± 12	611 ± 13	592 ± 17	523 ± 15	535 ± 9	513 ± 15
Number	$n = 6$	$n = 5$	$n = 9$	$n = 7$	$n = 6$	$n = 9$	$n = 6$	$n = 4$
Baseline R_L (cmH$_2$O ml^{-1} s)	0.27 ± 0.01	0.25 ± 0.01	0.29 ± 0.02	0.29 ± 0.01	0.28 ± 0.01	0.31 ± 0.02	0.27 ± 0.01	0.29 ± 0.02
Blood pressure baseline (mmHg)	53 ± 1	52 ± 2	51 ± 2	49 ± 2	50 ± 3	52 ± 2	47 ± 1	47 ± 3
% change	− 10.8 ± 5.2	− 62.3 ± 2.8	− 61.3 ± 2.0	− 64.5 ± 2.3	− 65.8 ± 2.6	− 59.9 ± 1.4	− 14.9 ± 3.5 *	− 56.8 ± 2.7

Values are expressed as mean ± s.e.mean.
*$P < 0.001$ as compared to untreated animals given instilled PGF$_{2\alpha}$.

(Table 1). In untreated animals, instillation of LTD_4 (0.2 nmol) caused an immediate fall and subsequently transient increase in mean systemic blood pressure approximately 1 min after LTD_4 administration (Figure 4). ICI-192,605 and OKY-046 blocked the transient increase in mean systemic blood pressure induced by LTD_4, with a significant difference from 0.5 to 1 min until 4 min after instillation of LTD_4 ($P<0.005$ and $P<0.01$ at 2.5 min after LTD_4, respectively) (Figure 4). Instilled $PGF_{2\alpha}$ (20 nmol) and U-46619 (0.02 nmol) caused a significant fall in systemic mean blood pressure (Table 1). However, an instillation of saline also caused a small fall. ICI-192,605 abolished the $PGF_{2\alpha}$-induced fall in blood pressure. In contrast, OKY-046 had no inhibitory effect on $PGF_{2\alpha}$-induced changes in blood pressure.

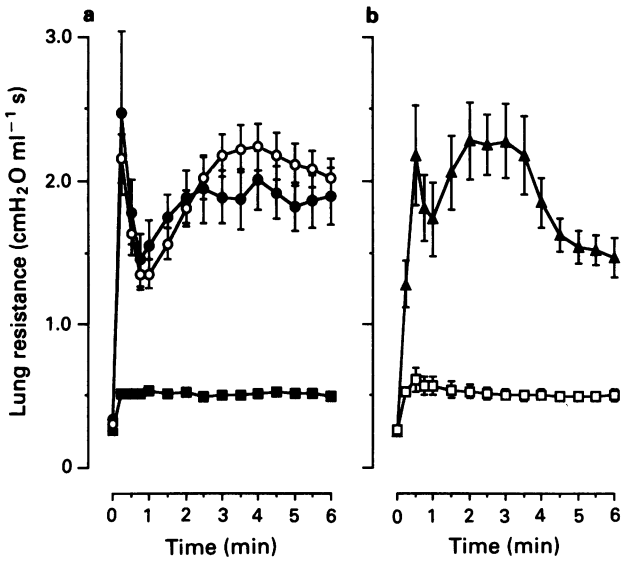

Figure 2 (a) Effect of ICI-192,605 (■: 0.5 mg kg^{-1}, $n=6$) or OKY-046 (●: 30 mg kg^{-1}, $n=4$) given i.v. 5 min before instillation of prostaglandin $F_{2\alpha}$ ($PGF_{2\alpha}$, 20 nmol) on the time-course of changes in R_L, compared with untreated guinea-pigs given instilled $PGF_{2\alpha}$ (○: $n=9$). (b) Time course of effect of instilled U-46619 (▲: 0.02 nmol; $n=5$) or saline (□: 0.9% NaCl, $n=6$) on R_L in untreated animals.

TxB_2 concentration in BALF after instilled LTD_4

The recovery percentage of BALF was 27 ± 2 and 44 ± 0.2% in animals given either instilled LTD_4 or vehicle respectively. Instilled LTD_4 induced a significant increase in TxB_2 (14.6 ± 2.0 pM, $P<0.01$) in bronchoalveolar lavage fluid obtained 1.5 min after challenge, compared to the animals given instilled vehicle (1.0 ± 0.1 pM).

Discussion

We have shown that both airflow obstruction and airway plasma exudation induced by LTD_4 instilled directly into the airways are significantly attenuated by both ICI-192,605, a thromboxane A_2 receptor (TP receptor) antagonist, and OKY-046, a thromboxane (Tx) synthetase inhibitor, in anaesthetized guinea-pigs. In addition, instilled LTD_4 resulted in a large increase of the level of TxB_2 in bronchoalveolar lavage fluid (BALF). ICI-192,605, but not OKY-046, also blocked both the biphasic increase in R_L and airway plasma

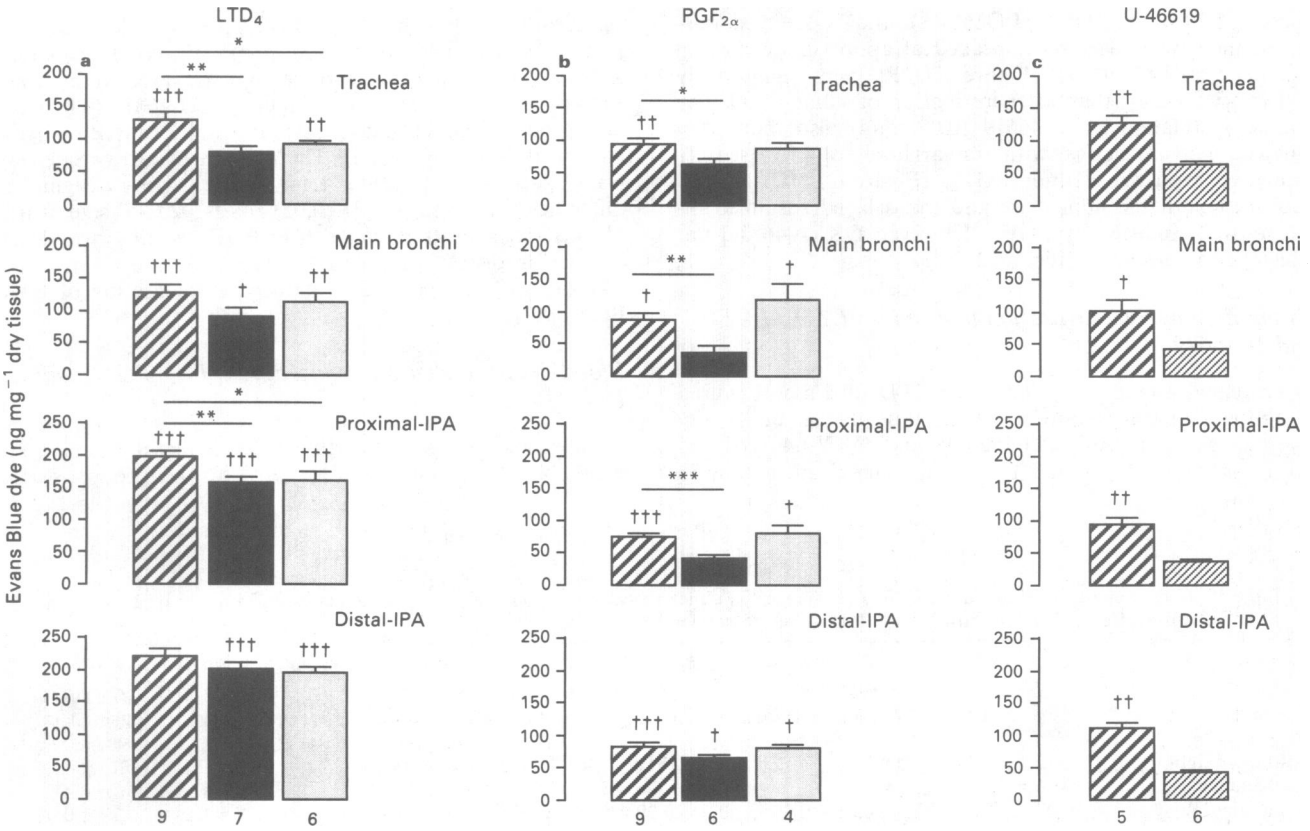

Figure 3 Extravasation of Evans Blue dye induced by instilled leukotriene D_4 (LTD_4, a), prostaglandin $F_{2\alpha}$ ($PGF_{2\alpha}$, b), and U-46619 or saline (c) at different airway levels in untreated animals (thickly hatched columns), compared to animals given instilled saline (thinly hatched columns). Animals were also pretreated with either ICI-192,605 (0.5 mg kg^{-1}, i.v.; solid columns) or OKY-046 (30 mg kg^{-1}, i.v.: stippled columns). IPA = intrapulmonary airways. *$P<0.05$; **$P<0.001$; ***$P<0.005$ compared to untreated animals given instilled LTD_4 or $PGF_{2\alpha}$. †$P<0.05$; ††$P<0.01$; †††$P<0.005$ compared to animals given instilled saline. $n=4$–9 as indicated at the foot of each column.

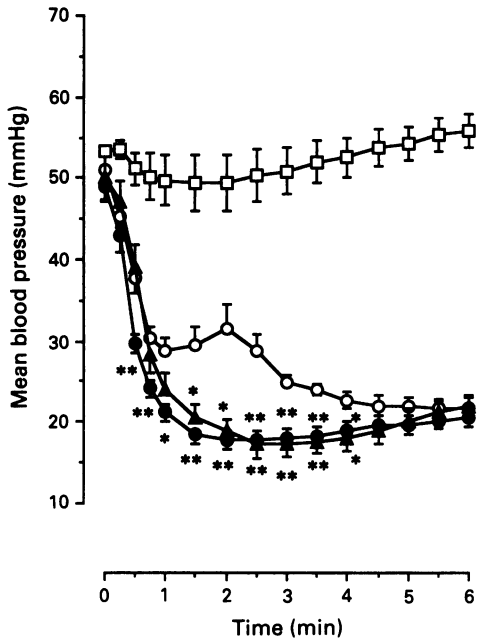

Figure 4 Effect of ICI-192,605 (●: 0.5 mg kg^{-1}, $n = 7$) and OKY-046 (▲: 30 mg kg^{-1}, $n = 6$) given i.v. 5 min before instillation of leukotriene D_4 (LTD_4, 0.2 nmol) on the time-course of the decrease in systemic blood pressure induced by LTD_4, compared with untreated animals given instilled LTD_4 (○: $n = 9$) or saline (□: 0.9% NaCl, $n = 6$). $^*P < 0.05$; $^{**}P < 0.005$ compared to untreated animals.

exudation induced by $PGF_{2\alpha}$ instilled into the tracheal lumen. These findings suggest that LTD_4-induced airway plasma exudation and airflow obstruction may be mediated in part, via TxA_2 generation, but that the airway responses to $PGF_{2\alpha}$ may be mediated via direct activation of TP receptors, rather than via TxA_2 generation.

Bronchoconstriction produced by LTD_4 administered through the intratracheal route may be due to one or more of the following mechanism: (1) reflex stimulation via vagal pathways, (2) release of local mediators, such as cyclo-oxygenase products, (3) via direct effects (Smith *et al.*, 1987). In the present study, instillation of LTD_4 produced an immediate and subsequently persistent increase in R_L, with an immediate peak at 45 s. Neither ICI-192,605 nor OKY-046 significantly affected the initial increase in R_L, suggesting that the immediate airflow obstruction after LTD_4 may be mediated via cholinergic reflexes (Hirshman *et al.*, 1983) or due to a direct effect on airway smooth muscle (Smith *et al.*, 1987). Hamel *et al.* (1982) found that bronchoconstriction produced by aerosolized LTD_4 was not attentuated by cyclo-oxygenase inhibitors, although the effect of i.v. LTD_4 was. In the present study, the persistent increase in R_L following the immediate response after LTD_4 was significantly attenuated by both ICI-192,605 and OKY-046, strongly arguing for a role of TxA_2 in the airway responses to instilled LTD_4. Furthermore, we found in the present study that instilled LTD_4 resulted in a large increase in TxB_2, a stable TxA_2 metabolite, in BALF. Thus, our study strongly suggests that LTD_4-induced airflow obstruction in guinea-pigs may be mediated in part via TxA_2, in accord with the findings of Vincent *et al.* (1984) and Birch *et al.* (1988) who studied the effects of i.v. LTD_4. The discrepancy from the previous findings of Hamel *et al.* (1982) may be explained by different methods of administration and use of different inhibitors of the cyclo-oxygenase pathway (they used indomethacin). After intratracheal administration, it is possible that higher local concentrations of LTD_4 induce TxA_2 synthesis, compared with aerosolized LTD_4. Another possibility is that LTD_4 given as aerosol causes production of bronchodilator prostaglandins as well as TxA_2. Therefore, a reduction of both the synthesis of TxA_2 and bronchodilator prostaglandins after indomethacin may explain the lack of attenuation of LTD_4-induced bronchoconstriction in the previous study (Hamel *et al.*, 1982). However, airway plasma exudation induced by aerosolized LTD_4 may well be attenuated by a cyclo-oxygenase inhibitor, because bronchodilator prostaglandins such as PGE_2 are known to enhance mediator-induced plasma exudation in the skin (Williams, 1979).

Woodward *et al.* (1983) found that indomethacin did not alter the increase in tracheal vascular permeability produced by intratracheal injection of LTD_4. By contrast, we found in the present study that both ICI-192,605 and OKY-046 significantly reduced instilled LTD_4-induced extravasation of dye in the trachea and proximal intrapulmonary airways, suggesting that LTD_4-induced airway plasma exudation may be mediated in part via TxA_2 generation. The discrepancy with the previous study of Woodward *et al.* (1983) may be explained by complete blockade of the TxA_2 receptors on the endothelial cells with ICI-192,605 and inhibition of TxA_2 synthesis with OKY-046, whereas the dose of indomethacin (5 mg kg^{-1}) used by Woodward *et al.* (1983) may have been insufficient to inhibit cyclo-oxygenase in the airways completely. In guinea-pigs, indomethacin may also have had the theoretical effect of shunting of arachidonic acid to the lipoxygenase pathway resulting in the synthesis of leukotrienes (Beasley *et al.*, 1989).

In the present study, instillation of $PGF_{2\alpha}$ into the trachea in guinea-pigs produced an immediate increase in R_L, peaking at approximately 15 s. The response to exogenously administered $PGF_{2\alpha}$ has been shown to be due in part, to cholinergic reflexes (Patel, 1975; Hadhazy *et al.*, 1982). We also found a delayed sustained increase in R_L, peaking at approximately 4 min. This biphasic response to $PGF_{2\alpha}$ was quite similar to that found with instilled U-46619 in the present study, although $PGF_{2\alpha}$ was about 1000 times less potent than U-46619 in producing a similar increase in R_L. As with instillation of U-46619, we have previously found that i.v. U-46619 produces an immediate and a delayed increase in R_L, both of which are abolished in animals pretreated with the TP receptor antagonist used in the present study, ICI-192,605 (Lötvall *et al.*, 1992). Furthermore, TP receptor antagonists block both $PGF_{2\alpha}$-induced contraction in lung parenchymal strip in guinea-pigs *in vitro* (McKeniff *et al.*, 1991) and bronchoconstriction induced by intravenous administration of $PGF_{2\alpha}$ *in vivo* (Birch *et al.*, 1988). In the present study, we found that both the immediate and the delayed sustained increase in R_L after $PGF_{2\alpha}$ were abolished by pretreatment with ICI-192,605, but not with OKY-046. Therefore, it is unlikely that $PGF_{2\alpha}$ induces TxA_2 release from inflammatory cells to cause airflow obstruction, because a Tx synthetase inhibitor did not affect this response. The mechanism underlying the observed biphasic R_L response is not known, but our data provide evidence that $PGF_{2\alpha}$-induced airflow obstruction may be mediated through activation of TP receptors. Alternatively, it is possible that ICI-192,605 may antagonize not only TP receptors but also other prostanoid receptor types such as DP, FP and EP_1 receptors (mediating the effects of PGD_2, $PGF_{2\alpha}$ and PGE, respectively; McKenniff *et al.*, 1991).

We have previously shown that i.v. U-46619 (2–200 nmol kg^{-1}) produces pronounced extravasation of Evans Blue dye at all airway levels, which is most prominent in intrapulmonary airways. In addition, this effect may be mediated via TP receptors, because extravasated dye was abolished in animals pretreated with the same dose of ICI-192-605 (Lötvall *et al.*, 1992) used in the present study. In the current study instillation of U-46619 (0.02 nmol) produced significant but rather small extravasation of dye at all airway levels. This may be explained by use of a lower dose of U-46619 or the different route of administration. Instilled $PGF_{2\alpha}$ produced a similar amount of extravasation of Evans Blue dye compared with U-46619, although the potency in inducing the effect was about 1000 times lower than with U-46619.

ICI-192,605 blocked the extravasation of Evans Blue dye induced by $PGF_{2\alpha}$, suggesting that $PGF_{2\alpha}$-induced airway plasma exudation is mediated through TP receptors. It is again considered unlikely that $PGF_{2\alpha}$ induces TxA_2 release from inflammatory cells to cause airway plasma exudation, since OKY-046 did not affect dye extravasation. Another possibility is that $PGF_{2\alpha}$ induces the release of other prostanoids, such as PGD_2 which activate TP receptors (McKenniff *et al.*, 1991).

We found that instillation of LTD_4 caused an immediate fall and subsequently a transient increase in mean systemic blood pressure approximately 1 min after administration. Both ICI-192,605 and OKY-046 blocked the transient increase in mean systemic blood pressure induced by LTD_4. This suggests that TxA_2 generation induced by instilled LTD_4 may be responsible for this effect, since TxA_2 is a potent vasoconstrictor (Lötvall *et al.*, 1992). Instilled U-46619 induced a significant fall in systemic blood pressure. Also, instilled $PGF_{2\alpha}$ caused a significant fall in systemic blood pressure, which was blocked with ICI-192,605, but not OKY-046, suggesting that blood pressure fall after $PGF_{2\alpha}$ may be mediated via TP receptor. It is likely that the effects of instilled U-46619 and $PGF_{2\alpha}$ on the blood pressure response is secondary to their airway effect. The transient partial recovery of blood pressure induced by instilled LTD_4 may be explained by TxA_2 generation after an immediate peak airway response following the instillation.

In asthmatics, a recent double-blind, placebo-controlled trial of a TP receptor antagonist (GR32191) failed to demonstrate any decrease in airway responsiveness to acetylcholine (Stenton *et al.*, 1992). However, of particular interest to our present study is the finding that enhanced airway responsiveness to histamine following inhalation of LTE_4 in asthmatics is inhibited by prior ingestion of indomethacin (Christie *et al.*, 1992), implying that LTE_4-induced hyperresponsiveness in part is due to the release of TxA_2, or possibly some other cyclooxygenase product. In conclusion, our data suggest that airflow obstruction and airway plasma exudation induced by instilled $PGF_{2\alpha}$ may be mediated via activation of TP-receptors. Airway responses to instilled LTD_4 may in part, be produced by generation of TxA_2. However, from our present study, it is not possible to elucidate which cell is producing the thromboxane in response to exogenous leukotriene. Furthermore, the interactions between TxA_2, $PGF_{2\alpha}$ and LTD_4 in plasma exudation in human airways are not known, and deserve further investigation.

This study was supported by the Swedish Heart & Lung foundation and the Swedish Medical Research Council. The authors would like to thank Mrs Maud Pettersson for performing the RIA for TxB_2.

References

ARAKAWA, H., KAWIKOVA, I., LÖFDAHL, C.G. & LÖTVALL, J. (1992). Bradykinin-induced airway responses in guinea-pig: effects of inhibition of cyclooxygenase and thromboxane synthetase. *Eur. J. Pharmacol.*, **229**, 131–136.

ARAKAWA, H., KAWIKOVA, I., SKOOGH, B.E., HAYES, J., MORIKAWA, A., LÖFDAHL, C.G. & LÖTVALL, J. (1993). Role of arachidonic acid metabolites in trimellitic anhydride induced airway responses in actively sensitized guinea pigs. *Am. Rev. Respir. Dis.*, (in press).

BARNES, P.J., CHUNG, K.F. & PAGE, C.P. (1988). Inflammatory mediators and asthma. *Pharmacol. Rev.*, **40**, 49–84.

BEASLEY, R.C.W., FEATHERSTONE, R.L., CHURCH, M.K., RAFFERTY, P., VARLEY, J.G., HARRIS, A., ROBINSON, C. & HOLGATE, S.T. (1989). Effect of a thromboxane receptor antagonist on PGD_2- and allergen-induced bronchoconstriction. *J. Appl. Physiol.*, **66**, 1685–1693.

BIRCH, J., BROWN, E., CALNAN, C., JESSUP, C.L., JESSUP, R. & WAYNE, M. (1988). Studies in the guinea-pig with ICI 185,282: a thromboxane A_2 receptor antagonist. *J. Pharm. Pharmacol.*, **40**, 706–710.

CHRISTIE, P.E., HAWKSWORTH, R., SPUR, B.W. & LEE, T.H. (1992). Effect of indomethacin on leukotriene E_4-induced histamine hyperresponsiveness in asthmatic subjects. *Am. Rev. Respir. Dis.*, **146**, 1506–1510.

FUJIMURA, M., SAKAMOTO, S., NISHI, K., SAITO, M., MIYAKE, Y. & MATSUDA, T. (1991). Inhibitory effect of inhaled procaterol on anaphylactic bronchonstriction and thromboxane A_2 production in guinea-pigs. *Clin. Exp. Allergy*, **21**, 189–194.

HADHAZY, P., QUACH-VAN, B., MALOMVOLGYI, B. & MAGYAR, K. (1982). Nanomolar concentrations of prostaglandin F2 alpha potentiate cholinergic contractions of rabbit isolated tracheal muscle. *Eur. J. Pharmacol.*, **24**, 207–212.

HAMEL, R., MASSON, P., FORD-HUTCHINSON, A.W., JONES, T.R., BRUNET, G. & PIECHUTA, H. (1982). Differing mechanism for leukotriene D_4-induced bronchoconstriction in guinea pigs following intravenous and aerosol administration. *Prostaglandins*, **24**, 419–432.

HIRSHMAN, C.A., DARNELL, M., BRUGMAN, T. & PETERS, J. (1983). Airway constrictor effects of leukotriene D_4 in dogs with hyperreactive airways. *Prostaglandins*, **25**, 481–490.

KAWIKOVA, I., ARAKAWA, H., LÖFDAHL, C.G., SKOOGH, B.E. & LÖTVALL, J. (1992). Bradykinin induced bronchoconstriction and airway microvascular leakage: effects of drugs that inhibit acetylcholine, thromboxane A_2 or leukotrienes. *Am. Rev. Respir. Dis.*, **145**, A612.

LÖTVALL, J.O., ELWOOD, W., TOKUYAMA, K., SAKAMOTO, T., BARNES, P.J. & CHUNG, K.F. (1992). A thromboxane mimetic, U-46619, produces plasma exudation in airways of the guinea pigs. *J. Appl. Physiol.*, **72**, 2415–2419.

McKENNIF, M.G., NORMAN, P., CUTHBERT, N.J. & GARDINER, P.J. (1991). BAY u3405, a potent and selective thromboxane A_2 receptor antagonist on airway smooth muscle *in vitro*. *Br. J. Pharmacol.*, **104**, 585–590.

O'BYRNE, P.M. & MANNING, P.J. (1992). Clinical relevance of lipid mediators in asthma. *J. Asthma*, **29**, 153–163.

PATEL, K.R. (1975). Atropine, sodium cromoglycate and thymoxamine in $PGF_{2\alpha}$-induced bronchoconstriction in extrinsic asthma. *Br. Med. J.*, **2**, 360–362.

PERSSON, C.G.A. (1992). Plasma exudation into airway tissue and lumen. In *Asthma: Basic Mechanisms and Clinical Management*. 2nd ed. Barnes, P.J., Rodger, I.W. & Thomson, N.C. pp. 207–224. London: Academic Press.

ROGERS, D.F., BOSCHETTO, P. & BARNES, P.J. (1989). Plasma exudation: correlation between Evans Blue dye and radiolabelled albumin in guinea-pig airways *in vivo*. *J. Pharmacol. Methods*, **21**, 309–315.

SMITH, L.J., KERN, R., PATTERSON, R., KRELL, R.D. & BERNSTEIN, P.R. (1987). Mechanism of Leukotriene D4-induced bronchoconstriction in normal subjects. *J. Allergy Clin. Immunol.*, **80**, 338–345.

STENTON, S.C., YOUNG, C.A., HARRIS, A., PALMER, J.B.D., HENDRICK, D.J. & WALTERS, E.H. (1992). The effect of GR32191 (a thromboxane receptor antagonist) on airway responsiveness in asthma. *Pulmon. Pharmacol.*, **5**, 199–202.

TOKUYAMA, K., LÖTVALL, J.O., MORIKAWA, A., BARNES, P.J. & CHUNG, K.F. (1991). Role of thromboxane A_2 in airway microvascular leakage induced by inhaled platelet-activating factor. *J. Appl. Physiol.*, **71**, 1729–1734.

VINCENT, J.E., ZIJLSTRA, F.J. & BONTA, I.L. (1984). The effect of inhibitors on the LTD_4-induced contractions and release of thromboxane A_2 in the guinea-pig lung parenchymal strip. *Agents Actions*, **14**, 69–81.

VON NEERGAARD, K. & WIRZ, K. (1927). Die messung der strömungswiderstände in den atemwegen des menschen, insbesondere bei asthma und emphysem. *Z. Klin. Med.*, **105**, 51–82.

WOODWARD, D.F., WEICHMAN, B.M., GILL, C.A. & WASSERMAN, M.A. (1983). The effect of synthetic leukotrienes on tracheal microvascular permeability. *Prostaglandins*, **25**, 131–142.

WILLIAMS, T.J. (1979). Prostaglandin E_2, prostaglandin I_2 and the vascular permeability in inflammation. *Br. J. Pharmacol.*, **65**, 517–524.

(Received January 4, 1993
Revised April 14, 1993
Accepted April 23, 1993)

Br. J. Pharmacol. (1993), **110**, 133–138

Characterization of P_2-purinoceptor mediated cyclic AMP formation in mouse C2C12 myotubes

Robert H. Henning, Marry Duin, Adriaan den Hertog & Adriaan Nelemans

Department of Pharmacology/Clinical Pharmacology, University of Groningen, Bloemsingel 1, 9713 BZ Groningen, The Netherlands

1 The formation of adenosine 3':5'-cyclic monophosphate (cyclic AMP) and inositol(1,4,5)tris-phosphate (Ins(1,4,5)P_3), induced by ATP and other nucleotides was investigated in mouse C2C12 myotubes.

2 ATP (100 μM) and ATPγS (100 μM) caused a sustained increase in cyclic AMP content of the cells, reaching a maximum after 10 min. The cyclic AMP content reached a maximum in the presence of 100 μM ATP, followed by a decline at higher ATP concentrations. ATP-induced cyclic AMP formation was inhibited by the P_2-purinoceptor antagonist, suramin.

3 Myotubes hydrolysed ATP to ADP at a rate of 9.7 ± 1.0 nmol mg^{-1} protein min^{-1}. However, further hydrolysis of ADP to AMP and adenosine was negligible.

4 The cyclic AMP formation induced by ADP (10 μM–1 mM) showed similar characteristics to that induced by ATP, but a less pronounced decline was observed than with ATP. ADP-induced cyclic AMP formation was blocked by suramin, while cyclic AMP formation elicited by adenosine (10 μM–1 mM) was insensitive to suramin.

5 The ATP analogue, α,β-methylene-ATP also induced a suramin-sensitive cyclic AMP formation, while 2-methylthio-ATP and the pyrimidine, UTP, did not affect cyclic AMP levels.

6 Stimulation of the myotubes with ATP or UTP (10 μM–1 mM) caused a concentration-dependent increase in the Ins(1,4,5)P_3 content of the cells. ADP (100 μM–1 mM) was less effective. Adenosine did not affect Ins(1,4,5)P_3 levels.

7 Incubation of the cells with UTP (30 μM–1 mM) inhibited the ATP- and ADP-induced cyclic AMP formation, suggesting that stimulation of the 'nucleotide' type P_2-receptor inhibits P_2-purinoceptor mediated cyclic AMP formation in C2C12 myotubes. In contrast, UTP (30 μM–1 mM) enhanced adenosine-induced cyclic AMP formation.

8 Adenosine-sensitive P_1-purinoceptors activating cyclic AMP formation were found in C2C12 myotubes. Further, a novel P_2-purinoceptor is postulated, sensitive to ATP, ADP and ATPγS, which also activates the formation of cyclic AMP in C2C12 myotubes.

Keywords: Cyclic AMP; Ins(1,4,5)P_3; P_2-purinoceptor; P_1-purinoceptor; cross-talk; nucleotide receptor; C2C12 myotubes

Introduction

It is known that adenosine 3':5'-cyclic monophosphate (cyclic AMP) affects the nicotinic acetylcholine receptors (AChRs) of skeletal muscle and myotubes. An acute increase in intracellular cyclic AMP accelerates desensitization of these receptors (Albuquerque *et al.*, 1986; Miles *et al.*, 1987) most likely via cyclic AMP-dependent phosphorylation of the δ-subunit of the nicotinic AChR (Miles *et al.*, 1989; Huganir & Greengard, 1983; Changeux, 1991). A sustained increase in cyclic AMP level induced up-regulation of nicotonic AChRs (Betz & Changeux, 1979), mediated by transcriptional (Fontaine *et al.*, 1987; Moss *et al.*, 1991), and post-transcriptional (Green *et al.*, 1991) effects on nicotinic AChR biosynthesis. Only a few primary messengers possibly involved in the regulation of the cyclic AMP level of skeletal muscle have been established. Calcitonin gene-related peptide, a peptide that is co-released with acetylcholine-(ACh) at the neuromuscular junction (Changeux, 1991), elevates intracellular levels of cyclic AMP (Mulle *et al.*, 1988) and induces the related desensitization (Takami *et al.*, 1986) and up-regulation (Fontaine *et al.*, 1987) of nicotinic AChRs.

Another co-transmitter with ACh at the neuromuscular junction, ATP (Silinsky, 1975), activates phosphoinositide signalling in skeletal myotubes by stimulation of P_2-purinoceptors (Häggblad & Heilbronn, 1988). In C2C12 myotubes, this signalling pathway is activated through the 'nucleotide' type P_2-purinoceptor, which also responds to UTP (Henning *et al.*, 1992). It has been shown that ATP affects the cyclic AMP level via stimulation of P_2-purinoceptors in hepatic and aortic cells (Okajima *et al.*, 1987; Tada *et al.*, 1992). It is also known that adenosine, the hydrolysis product of ATP, modulates cyclic AMP levels through stimulation of P_1-purinoceptors (Londos *et al.*, 1980). The contribution of ATP and derivatives in the regulation of cyclic AMP and the interaction with the phospholipase C (PLC) pathway was studied by measuring the formation of cyclic AMP and inositol(1,4,5)tris-phosphate (Ins(1,4,5)P_3) in C2C12 myotubes.

Methods

Cell culture

C2C12 cells, a murine myoblast cell line (Yaffee & Saxel, 1977) were obtained from the American Tissue Type Collection, Rockville, U.S.A. and cultured in 9.6 cm^2 plastic wells as described by Henning *et al.* (1992). Myotubes were used 7 days after initiating myoblast fusion.

Cyclic AMP measurement

The cyclic AMP content of the myotubes was assessed by mass measurement using a radioligand binding assay. Before the experiment, the cells were washed three times with a buffer of the following composition (mM): NaCl 125, KCl 6, $CaCl_2$ 1.2, $MgCl_2$ 2.5, NaH_2PO_4 1.2, glucose 11, HEPES 10

(pH 7.4). The reaction was started by the addition of one of the nucleotides and stopped by addition of trichloroacetic acid (TCA: 5%, 350 µl) after removing the buffer. Experiments were conducted at 20°C. The TCA was extracted (three times) with water-saturated diethylether, the samples were neutralized with KOH and stored at −40°C. Cyclic AMP mass was determined essentially according to Brown *et al.* (1971). To reach equilibrium, 50 µl sample was incubated for at least 2 h at 4°C with 1.7 mg bovine adrenal binding protein and 10 µl [^{3}H]-cyclic AMP (190 nM; specific activity: 40 Ci mmol^{-1}) in a buffer of 50 mM Tris-HCl and 4 mM EDTA (pH 7.4) in a final volume of 300 µl. The incubation was terminated by adding a charcoal suspension (Norit A special, 3.5 g l^{-1}), mixing, and subsequent centrifugation to remove excess [^{3}H]-cyclic AMP, all at 4°C. The radioactivity in the supernatant was determined by scintillation counting. A standard curve for determination of cyclic AMP mass was constructed using ether-extracted TCA solution.

Adenine nucleotides

Single wells (9.6 cm^2) containing 7 days differentiated C2C12 myotubes were incubated at 20°C for 5 or 10 min with 2 ml extracellular medium containing ATP 300 µM. Adenine nucleotides (adenosine, AMP, ADP and ATP) in the extracellular medium were separated by high-performance liquid chromatography (h.p.l.c.), using a Zorbax SAX Bioseries column (Du Pont, Wilmington, DE, U.S.A.) and detected by light absorption at 259 nm. Separation of adenine nucleotides was accomplished by use of a programmed gradient of $NH_4H_2PO_4$ in water at a flow rate of 1.5 ml min^{-1}. Injection of samples (100 µl) was followed by a 2-min flow of water and a 14 min flow of linearly increasing $NH_4H_2PO_4$ (1 M; pH 3.7) in water to a final concentration of 40% (v/v). Retention times of adenosine, AMP, ADP and ATP were 2, 6, 8 and 12 min, respectively.

Ins(1,4,5)P_3 measurement

Experiments were conducted in a similar way to those described for cyclic AMP. The samples were assayed for Ins-(1,4,5)P_3 content by a radioligand binding assay as described in detail by Den Hertog *et al.* (1992).

Data analysis

Data are presented as mean ± s.e.mean unless stated otherwise and were considered statistically different at $P<0.05$ (unpaired Student's t test).

Drugs

Adenosine 3':5'-cyclic monophosphate (cyclic AMP), adenosine, adenosine 5'-diphosphate (ADP), adenosine 5'-O-(3-thiotriphosphate) (ATPγS) and α,β-methylene-adenosine 5'-triphosphate (α,β-MeATP) were obtained from Boehringer, Mannheim, Germany. Adenosine 5'-triphosphate (ATP), adenosine 5'-monophosphate (AMP) and uridine 5'-triphosphate (UTP) were obtained from Serva, Heidelberg, Germany. Suramin was obtained from Bayer, Leverkusen, Germany. 2-(Methylthio)-adenosine 5'-triphosphate (2-MeSATP) was obtained from Research Biochemicals Inc., Natick, Mass., U.S.A. and pertussis toxin (PTx) from Sigma, St. Louis, U.S.A. [2,8-^{3}H]-adenosine 3':5'-cyclic monophosphate ([^{3}H]-cyclic AMP) and D-[2-^{3}H]-inositol 1,4,5-trisphosphate were obtained from Du Pont-New England Nuclear U.S.A.

Results

ATP and cyclic AMP formation

The basal cyclic AMP content of the C2C12 myotubes, as measured by radioligand binding assay, was 10.5 ± 0.9 pmol mg^{-1} protein (n = 72). The myotubes responded to application of ATP (100 µM) with a slowly developing but marked increase in cyclic AMP content, becoming manifest after 30 s. A further increase in cyclic AMP content was found after prolonged stimulation with ATP (up to 60 min), approaching a maximum at about 10 min (Figure 1a). Application of the stable ATP analogue ATPγS (100 µM) also induced an increase in cyclic AMP content of the cells, showing a similar time course as observed with ATP (not shown).

The formation of cyclic AMP in myotubes stimulated with different ATP concentrations was used to plot a concentration-response curve. The cyclic AMP content increased until a maximum was reached at 100 µM ATP, followed by a decline at higher concentrations. Consequently, the concentration-response curves obtained after 5, 10 and 30 min ATP stimulation were bell-shaped (Figure 1b). Pretreatment (15 min) of the cells with the P_2-purinoceptor antagonist, suramin (500 µM) prevented the increase of cyclic AMP content of the cells as evoked by ATP (Figure 1b).

To investigate whether the slow increase in cyclic AMP content could be caused by ATP derivatives, hydrolysis of ATP was investigated by measuring the accumulation of the adenine nucleotides ATP, ADP, AMP and adenosine in the incubating medium in the presence of C2C12 myotubes. During incubation ATP (300 µM; 10 min) was hydrolysed to ADP at 9.7 ± 1.0 nmol mg^{-1} protein min^{-1}. Further hydrolysis of ADP to AMP or adenosine was not observed (Table 1).

An action of ADP on the cyclic AMP level can be expected in view of its formation from ATP in the incubation medium (Table 1). Stimulation of the cells with ADP (10 µM−1 mM) induced an increase in cyclic AMP with a similar time course as observed for ATP (not shown). The concentration-response curve obtained at optimal stimulation periods (10 min), showed a small decline at a high agonist concentration (Figure 2a). The ADP-induced increase in cyc-

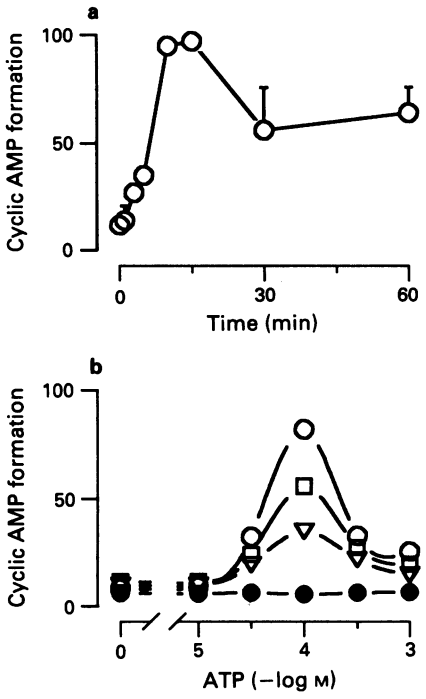

Figure 1 The effect of ATP on cyclic AMP formation in C2C12 myotubes. (a) Time-dependent increase in cyclic AMP content upon stimulation with ATP (100 µM). (b) Concentration-dependent changes in cyclic AMP content of the myotubes measured after 5 min (▽), 10 min (○) and 30 min (□) stimulation. The increase in cyclic AMP content observed after 10 min was blocked by suramin (500 µM, ●). Data are expressed as pmol mg^{-1} protein (mean ± s.e.) and were obtained from 4 or more experiments.

Table 1 Hydrolysis of extracellular ATP by C2C12 myotubes

	Medium without cells (nmol/well)	*Incubation 5 min* (nmol/well)	*Incubation 10 min* (nmol/well)	*Hydrolysis* (nmol mg^{-1} protein min^{-1})
ATP	545 ± 8	497 ± 4	436 ± 43	+ 9.7 ± 1.0
ADP	34 ± 4	88 ± 2	129 ± 27	− 9.6 ± 0.8
AMP	20 ± 5	19 ± 1	35 ± 16	− 0.6 ± 0.3
Adenosine	<0.5	<0.5	<0.5	-
Total	599 ± 10	604 ± 5	594 ± 33	

Single wells containing differentiated C2C12 myotubes were incubated with 600 nmol of ATP in 2 ml medium (300 μM) for 5 or 10 min. Control experiments were performed in wells in the absence of myotubes (medium without cells). Data are expressed as nmol of recovered nucleotides (mean ± s.e., $n = 3$). Rate of hydrolysis was calculated by pooling data from 5 and 10 min incubation ($n = 6$). Average protein content per well was 1.06 ± 0.10 mg protein/well.

lic AMP content was blocked by suramin (500 μM; Figure 2a). It was found that ADP was about equipotent to ATP as judged by the onset of the ascending phase of their respective concentration-response curves (Figures 1b, 2a).

Although hydrolysis of ATP to adenosine was not detected in the incubation medium (Table 1), adenosine might be produced at the cell surface very near its receptor. The presence of P_1-purinoceptors on the myotubes was investigated by measuring the change of cyclic AMP content evoked by adenosine. Stimulation with adenosine (10 μM–1 mM) induced the formation of cyclic AMP with a similar time course as observed for ATP. However, adenosine-induced cyclic AMP formation was not affected by suramin and reached a lower maximal level compared to that induced by ATP or ADP (Figure 2b).

By convention, a purinoceptor sensitive to ATP and ADP, has to be classified as a P_2-purinoceptor. To examine whether this receptor can be recognized as one of the established P_2-purinoceptor subclasses, the action of ATP analogues was studied. The selective P_{2X}-agonist, α,β-MeATP, evoked a concentration-dependent increase in cyclic AMP content of the myotubes; this response was also blocked by suramin (Figure 2c). The concentration-response curve of α,β-MeATP ascended at a similar agonist concentration as found with ATP and ADP, but in the presence of α,β-MeATP consistently lower values of cyclic AMP were found compared to ATP and ADP (Figures 1b, 2a,c). The selective agonist for the P_{2Y}-purinoceptor, 2-MeSATP did not affect cyclic AMP levels (Figure 2c). To examine whether the ATP-evoked increase in cyclic AMP content was mediated by the nucleotide type P_2-purinoceptor present in C2C12 myotubes (Henning *et al.*, 1992), the action of the pyrimidine, UTP, on cyclic AMP formation was examined. It was found that stimulation of the myotubes with UTP (10 μM–1 mM) did not affect their cyclic AMP content (Figure 2d). To investigate whether ATP- and ADP-induced formation of cyclic AMP was mediated through the same purinoceptor, simultaneous stimulation of the myotubes by these compounds was examined. Stimulation of the cells (10 min) by ATP (100 μM) and ADP (100 μM) respectively induced a similar formation of cyclic AMP (89.6 ± 8.3 pmol mg^{-1} protein and 82.4 ± 9.7 pmol mg^{-1} protein; $n = 4$). However, formation of cyclic AMP elicited by simultaneous addition of the nucleotides was significantly diminished (36.5 ± 2.1 pmol mg^{-1} protein, $n = 4$).

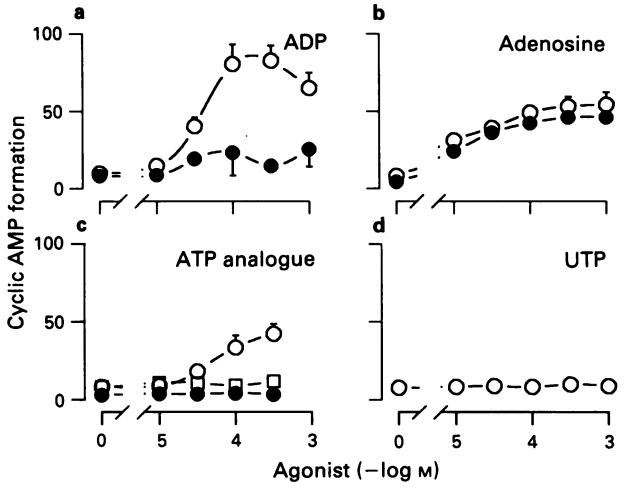

Figure 2 Concentration-dependent changes in cyclic AMP content of C2C12 myotubes after 10 min stimulation with different nucleotides. (a) The increase in cyclic AMP content induced by ADP (○) was blocked by suramin (500 μM; ●). (b) The increase in cyclic AMP content induced by adenosine (○) was not affected by suramin (500 μM; ●). (c) The increase in cyclic AMP content induced by α,β-MeATP (○) was blocked by suramin (500 μM; ●); 2-MeSATP (□) did not affect cyclic AMP content. (d) The cyclic AMP content was not changed in the presence of UTP. Suramin was added 15 min prior to stimulation. Data are expressed as pmol mg^{-1} protein (mean ± s.e.) and were obtained from 4 or more experiments.

Ins(1,4,5)P_3 formation

In C2C12 myotubes, both ATP (10 μM–1 mM) and UTP (10 μM–1 mM) induced a four fold increase in the Ins(1,4,5)P_3 content of the cells after 45 s stimulation (Table 2). In contrast to the generation of cyclic AMP, ADP (10 μM–1 mM) was less effective in producing Ins(1,4,5)P_3 than ATP, while adenosine was ineffective (Table 2). Further, it was observed that the maximal increase of Ins(1,4,5)P_3 elicited by ATP (1 mM) and UTP (1 mM) were not additive (3.36 ± 0.81 pmol mg^{-1} protein; $n = 4$).

Inhibition of P_2-purinoceptor-mediated cyclic AMP formation

The decline in formation of cyclic AMP at high ATP concentrations was further examined in ATP-stimulated myotubes pretreated for 14 h with pertussis toxin (PTx; 100 ng ml^{-1}). Pretreatment of the cells with PTx enhanced the maximum formation of cyclic AMP, but did not affect the decline in cyclic AMP formation at higher ATP concentrations (Figure 3).

Inhibition of cyclic AMP formation at higher ATP concentrations might be caused by simultaneous stimulation of the 'nucleotide' receptor. UTP stimulated the nucleotide receptor (Table 2; Henning *et al.*, 1992), but did not affect cyclic AMP formation in contrast to ATP (Figure 2d). Therefore, this compound was used to study the effect of 'nucleotide' receptor stimulation on cyclic AMP formation in the myotubes. When added simultaneously, UTP (30 μM–1 mM) progressively decreased the cyclic AMP formation in myotubes elicited with an optimal concentration of ATP or ADP (100 μM; Figure 4a,b). In contrast, UTP enhanced the adenosine (100 μM) induced cyclic AMP formation (Figure 4c). The inhibitory effect of UTP on ATP-induced cyclic AMP formation was further studied by constructing concentration-re-

Table 2 The increase in Ins(1,4,5)P_3 content of C2C12 myotubes following stimulation by variouis nucleotides

Agonist concentration	*Increase in Ins(1,4,5)P_3* (pmol mg^{-1} protein)			
	ATP	*UTP*	*ADP*	*Adenosine*
10 μM	0.52 ± 0.07	− 0.05 ± 0.12	− 0.12 ± 0.07	–
30 μM	1.69 ± 0.13	1.02 ± 0.09	0.26 ± 0.07	–
100 μM	2.90 ± 0.12	2.10 ± 0.10	0.44 ± 0.11	0.07 ± 0.13
300 μM	3.34 ± 0.29	2.68 ± 0.14	1.05 ± 0.13	− 0.19 ± 0.30
1 mM	3.41 ± 0.12	3.22 ± 0.06	3.01 ± 0.10	− 0.10 ± 0.14

Myotubes were stimulated for 45 s in the presence of the nucleotide concentrations indicated. Data are expressed as the increase in Ins(1,4,5)P_3 content over basal level (1.06 ± 0.12 pmol mg^{-1} protein, mean ± s.e., $n \geq 4$).

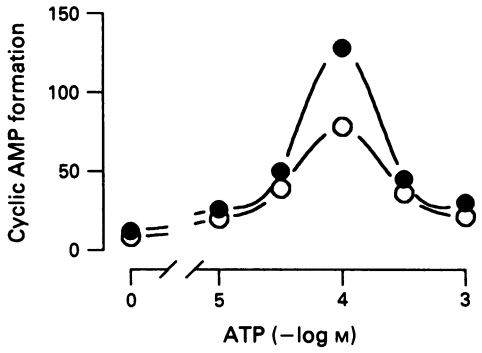

Figure 3 The effect of pretreatment of C2C12 myotubes with pertussis toxin (PTx) on ATP-induced formation of cyclic AMP. Stimulation of the cells with ATP for 10 min in control cells (○) and after pretreatment with PTx (100 ng ml^{-1}) for 14 h (●). Data are expressed as pmol mg^{-1} protein (mean ± s.e.) and were obtained from 4 or more experiments.

sponse curves to ATP at various UTP (100 μM–1 mM) concentrations, showing a progressive decrease in the ATP-induced formation of cyclic AMP, without an apparent shift in the concentration-response curve (Figure 5).

Discussion

Extracellular ATP caused a relatively slow formation (10 min) of cyclic AMP in C2C12 myotubes, which was characterized by a prominent bell-shaped concentration-response relationship. Application of adenosine also induced a concentration-dependent increase in cyclic AMP formation, which was characterized by a regular concentration-response relationship. For several reasons, however, it seems likely that cyclic AMP formation induced by ATP in C2C12 myotubes is mediated via P_2-purinoceptors, rather than caused by stimulation of P_1-purinoceptors by its hydrolysis product, adenosine. This is supported by the finding that the ATP-induced cyclic AMP formation was completely blocked by the P_2-purinoceptor antagonist, suramin (Dunn & Blakely, 1988; Den Hertog *et al.*, 1989; Henning *et al.*, 1992), while adenosine-induced cyclic AMP formation was insensitive to suramin. Further, the formation of cyclic AMP was also observed with the stable ATP analogue, ATPγS. Moreover, during the incubation period, negligible amounts of AMP and adenosine were generated, in contrast to ATP hydrolysis to ADP. These observations strongly suggest that ATP-induced formation of cyclic AMP is caused by stimulation of a P_2-purinoceptor in C2C12 myotubes, while adenosine-induced cyclic AMP formation is presumably mediated through an A_2-type P_1-purinoceptor as found in other cells (Londos *et al.*, 1980).

The nucleotides ATP or ADP showed a similar potency with respect to the formation of cyclic AMP. The action of both nucleotides was not additive and was blocked by suramin. Formation of cyclic AMP was also induced by the P_{2X}-purinoceptor agonist, α,β-MeATP. However, since α,β-MeATP did not exceed ATP or ADP potency with respect to cyclic AMP formation, the ATP-sensitive receptor cannot be classified as P_{2X}-purinoceptor (Cusack & Hourani, 1990). Moreover, the P_2-purinoceptor was not sensitive to 2-MeSATP or UTP, excluding the involvement of P_{2Y}-purinoceptors (Cusack & Hourani, 1990) and the nucleotide type P_2-purinoceptor (O'Connor *et al.*, 1991). Other P_2-purinoceptors, i.e. P_{2T}- and P_{2Z}-purinoceptors have to be excluded in view of the agonistic action of both ATP and ADP on cyclic AMP formation (Cusack & Hourani, 1990). Thus, it is concluded that a novel type of P_2-purinoceptor is linked to the cyclic AMP formation in C2C12 myotubes. This P_2-

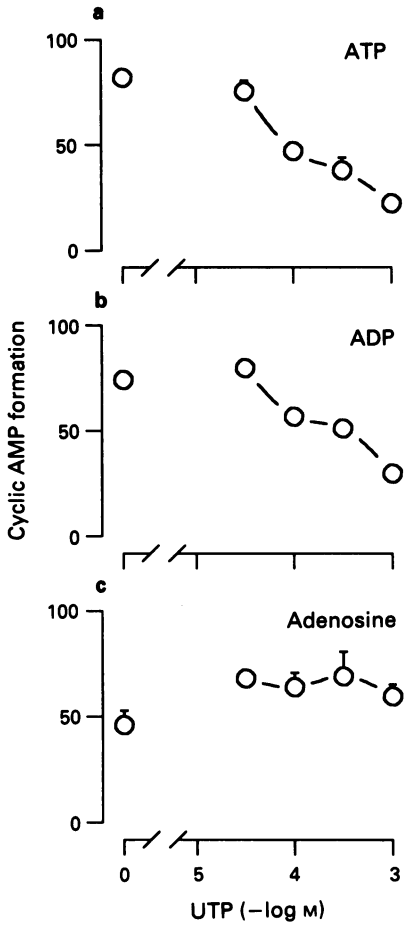

Figure 4 Concentration-dependent effect of UTP on cyclic AMP formation induced by adenine nucleotides. UTP and adenine nucleotides were added simultaneously. UTP (30 μM–1 mM) evoked a progressive decline in cyclic AMP formation of myotubes stimulated with ATP (100 μM; a) and ADP (100 μM; b). The cyclic AMP formation was enhanced in myotubes stimulated with adenosine (100 μM; c). Cells were stimulated for 10 min. Data are expressed as pmol mg^{-1} protein (mean ± s.e.) and were obtained from 4 or more experiments.

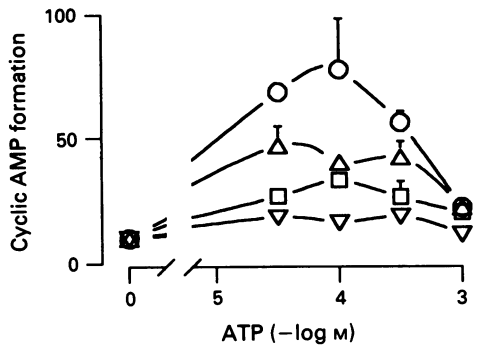

Figure 5 Inhibition of ATP-induced cyclic AMP formation by UTP. The concentration-dependent cyclic AMP formation evoked by ATP at 10 min (○) was progressively inhibited by UTP 100 μM (△), 300 μM (□) and 1 mM (▽). Both nucleotides were added simultaneously. Data are expressed as pmol mg^{-1} protein (mean ± s.e.) and were obtained from 4 or more experiments.

purinoceptor of C2C12 myotubes resembles the P_2-purinoceptor mediating cyclic AMP formation in bovine aortic smooth muscle cells (Tada *et al.*, 1992). The ATP-induced cyclic AMP formation in the aortic cells, however, was not inhibited by suramin, suggesting the presence of different P_2-purinoceptor subtypes in bovine aortic cells and C2C12 myotubes.

The concentration-dependent ATP-induced cyclic AMP formation showed a substantial decline at high agonist concentrations. This decline was not caused by activation of a PTx-sensitive G_i-protein at higher agonist concentrations. C2C12 myotubes have been shown to possess a nucleotide type P_2-purinoceptor (Henning *et al.*, 1992) activating the PLC pathway, besides the P_2-purinoceptor mediating cyclic AMP formation. Simultaneous stimulation of the myotubes with UTP, not affecting cyclic AMP formation, inhibited the ADP- and ATP-induced formation of cyclic AMP. The effect of progressively higher concentrations of UTP on the ATP-induced concentration-response relationship for cyclic AMP formation was characterized by a decrease in the maximum effect without an apparent shift in the curve. This observation demonstrates that the action of UTP in reducing the ATP-induced response cannot be explained solely by a competitive antagonism of UTP on the P_2-purinoceptor mediating the ATP-induced cyclic AMP formation. The inhibition of the P_2-purinoceptor-mediated cyclic AMP formation by UTP might be related to the stimulation of the PLC pathway by this compound. A similar Ins(1,4,5)P_3 formation was produced by UTP and ATP in the myotubes, while ADP was less effective. The cyclic AMP content of myotubes optimally stimulated by ATP or ADP but inhibited by maximal concentrations of UTP, was similar to that of myotubes stimulated with the maximal ATP concentration. However, cyclic AMP formation induced by maximum ADP concentrations was inhibited to a lesser extent. These observations suggest that the activation of the PLC pathway via the nucleotide receptor inhibits P_2-purinoceptor-mediated cyclic AMP formation. In contrast to the reduction of P_2-purinoceptor mediated cyclic AMP formation found in the presence of UTP, enhancement of adenosine-induced cyclic AMP formation by UTP was observed, possibly also dependent on nucleotide-receptor mediated activation of the PLC pathway. At this stage, the involvement of nucleotide receptor-mediated PLC activation in either the inhibition of P_2-purinoceptor-mediated cyclic AMP formation or stimulation of P_1-purinoceptor-mediated cyclic AMP formation by UTP remains speculative. PLC-activated modulation of the cyclic AMP pathway has been studied extensively in non-skeletal muscle cells and is attributed to the activation of the phosphorylating enzyme protein kinase C (PKC) (Houslay, 1991). Activation of PKC is associated with stimulation (Garte & Belman, 1980; Goureau *et al.*, 1990) as well as with inhibition of cyclic AMP formation, due to phosphorylation of different components of the cyclic AMP pathway (Katada *et al.*, 1985; Bell & Brunton, 1986; Irvine *et al.*, 1986; Yoshimasa *et al.*, 1987; Abou-Samra *et al.*, 1987; Convents *et al.*, 1989). Modulation of cyclic AMP formation by receptor-mediated PLC activation, however, may also be dependent on mechanisms other than PKC-mediated phosphorylation, such as Ca^{2+}-dependent activation of phosphodiesterase (Boyajian & Cooper, 1990) or involvement of different heteromeric G protein subunits (cf. Birnbaumer, 1992). The opposite action of UTP on P_1- and P_2-purinoceptor-activated cyclic AMP formation in C2C12 myotubes would suggest that the inhibitory effect of UTP is not exerted on adenylate cyclase or phosphodiesterase. However, multiple isoenzymes, possessing different sensitivity to the UTP-activated mechanism may be present in these cells. Therefore, to establish the mechanisms involved in the modulation of cyclic AMP formation by UTP in C2C12 myotubes needs further study.

It has been shown that cyclic AMP regulates important cellular functions in myotubes, including desensitization (Albuquerque *et al.*, 1986; Miles *et al.*, 1987) and expression (Betz & Changeux, 1979; Fontaine *et al.*, 1987; Moss *et al.*, 1991; Green *et al.*, 1991) of nicotinic AChRs. In this study we identified two receptor types, an ATP-sensitive P_2-purinoceptor mediating cyclic AMP formation, and a P_1-purinoceptor sensitive to adenosine, both mediating the generation of cyclic AMP. So far, only calcitonin gene-related peptide had been identified as a possible primary messenger in the regulation of intracellular levels of cyclic AMP in myotubes (Mulle *et al.*, 1988; Changeux, 1991). As ATP is excreted from the motor nerve endings in conjunction with acetylcholine (Silinksy, 1975), the existence of multiple purinoceptors coupled to the cyclic AMP pathway suggests that a primary messenger role for ATP needs to be considered.

In summary, P_1-purinoceptor-induced cyclic AMP formation was established in C2C12 myotubes. Further, a novel ATP- and ADP-sensitive P_2-purinoceptor is proposed, also activating the formation of cyclic AMP. Activation of these cellular pathways by ATP in C2C12 myotubes suggests that this co-transmitter may serve as a primary messenger to regulate intracellular signalling in skeletal muscle.

This study was partly sponsored by grant 900-549-133 from The Netherlands Organisation for Scientific Research (NWO).

References

ABOU-SAMRA, A.B., HARWOOD, J.P., MANGANIELLO, V.C., KATT, K.J. & AGUILERA, G. (1987). Phorbol 12-myristate 13-acetate and vasopressin potentiate the effect of corticotropin-releasing factor on cyclic AMP production in rat anterior pituitary cells. Mechanisms of action. *J. Biol. Chem*,. **262**, 1129–1136.

ALBUQUERQUE, E.X., DESHPANDE, S.S., ARACAVA, Y., ALKONDON, M. & DALEY, J.W. (1986). A possible involvement of cyclic AMP in the expression of desensitization of the nicotinic acetylcholine receptor. *FEBS Lett.*, **199**, 113–120.

BELL, J.D. & BRUNTON, L.L. (1986). Enhancement of adenylate cyclase activity in S49 lymphoma cells by phorbol esters. Withdrawal of GTP-dependent inhibition. *J. Biol. Chem.*, **261**, 12036–12041.

BETZ, H. & CHANGEUX, J.P. (1979). Regulation of muscle acetylcholine receptor synthesis *in vitro*, by cyclic nucleotide derivatives. *Nature*, **278**, 749–752.

BIRNBAUMER, L. (1992). Receptor-to-effector signaling through G proteins: roles for βγ dimers as well as α subunits. *Cell*, **71**, 1069–1072.

BOYAJIAN, C.D. & COOPER, D.M.F. (1990). Potent and cooperative feedback inhibition of adenylate cyclase activity by calcium in pituitary-derived GH_3 cells. *Cell Calcium*, **11**, 299–307.

BROWN, B.L., ALBANO, J.D.M., EKINS, R.P., SGHERZI, A.M. & TAMPION, W. (1971). A simple and sensitive saturation assay method for the measurement of adenosine-3':5'-cyclic monophosphate. *Biochem. J.*, **121**, 561–562.

CHANGEUX, J.P. (1991). Compartimentalized transcription of acetylcholine receptor genes during motor endplate epigenesis. *New Biologist*, **3**, 413–429.

CONVENTS, A., DE BACKER, J.P., ANDER, C. & VAUQUELIN, G. (1989). Desensitization of alpha 2-adrenergic receptors in NG 108 15 cells by (−)-adrenaline and phorbol 12-myristate 13-acetate. *Biochem. J.*, **262**, 245–251.

CUSACK, N.J. & HOURANI, S.M.O. (1990). Subtypes of P_2-purinoceptors. *Ann. NY Acad. Sci.*, **603**, 172–181.

DEN HERTOG, A., NELEMANS, A. & VAN DEN AKKER, J. (1989). The inhibitory action of suramin on the P_2-purinceptor response in smooth muscle cells of guinea-pig taenia caeci. *Eur. J. Pharmacol.*, **166**, 531.

DEN HERTOG, A., HOITING, B., MOLLEMAN, A., VAN DER AKKER, J., DUIN, M. & NELEMANS, S.A. (1992). Calcium release from separate receptor-specific intracellular stores induced by histamine and ATP in a hamster cell line. *J. Physiol.*, **454**, 591–607.

DUNN, P.M. & BLAKELY, A.G. (1988). Suramin: a reversible P_2-purinoceptor antagonist in mouse vas deferens. *Br. J. Pharmacol.*, **93**, 243.

FONTAINE, B., KLARFELD, A. & CHANGEUX, J.P. (1987). Calcitonine gene-related peptide and muscle activity regulate acetylcholine receptor α-subunit mRNA levels by distinct intracellular pathways. *J. Cell. Biol.*, **105**, 1337–1342.

GARTE, S.J. & BELMAN, S. (1980). Tumour promoter uncouples β-adrenergic receptor from adenyl cyclase in mouse epidermis. *Nature*, **284**, 171–173.

GOUREAU, O., TANFIN, Z. & HARBON, S. (1990). Prostaglandins and muscarinic agonists induce cyclic AMP attenuation by two distinct mechanisms in the pregnant-rat myometrium. *Biochem. J.*, **271**, 667–673.

GREEN, W.N., ROSS, A.F. & CLAUDIO, T. (1991). cAMP stimulation of acetylcholine receptor expression is mediated through post-translational mechanisms. *Proc. Natl. Acad. Sci. U.S.A.*, **88**, 854–858.

HÄGGBLAD, J. & HEILBRONN, E. (1988). P_2-purinoceptor-stimulated phosphoinositide turnover in chick myotubes. *FEBS Lett.*, **235**, 133–136.

HENNING, R.H., NELEMANS, S.A., VAN DEN AKKER, J. & DEN HERTOG, A. (1992). The nucleotide receptors on mouse C2C12 myotubes. *Br. J. Pharmacol.*, **106**, 853–858.

HOUSLAY, M.D.(1991). 'Crosstalk': a pivotal role for protein kinase C in modulating relationships between signal transduction pathways. *Eur. J. Biochem.*, **195**, 9–27.

HUGANIR, R.L. & GREENGARD, P. (1983). cAMP-dependent protein kinase phosphorylates the nicotinic acetylcholine-receptor. *Proc. Natl. Acad. Sci. U.S.A.*, **80**, 1130–1134.

IRVINE, F.J., PYNE, N.J. & HOUSLAY, M.D. (1986). The phorbol ester TPA inhibits cyclic AMP phosphodiesterase activity in intact hepatocytes. *FEBS Lett.*, **208**, 455–459.

KATADA, T., GILMAN, A.G., WATANABE, Y., BAUER, S. & JAKOBS, K.H. (1985). Protein kinase C phosphorylates the inhibitory guanine-nucleotide binding regulatory component and apparently suppresses its function in hormonal inhibition of adenylate cyclase. *Eur. J. Biochem.*, **151**, 431–437.

LONDOS, C.D., COOPER, M.F. & WOLFF, J. (1980). Subclasses of external adenosine receptors. *Proc. Natl. Acad. Sci. U.S.A.*, **77**, 2551–2554.

MILES, K., ANTHONY, D.T., RUBIN, L.L., GREENGARD, P. & HUGANIR, R.L. (1987). Regulation of nicotinic acetylcholine receptor phosphorylation in rat myotubes by forskolin and cAMP. *Proc. Natl. Acad. Sci. U.S.A.*, **84**, 6591–6595.

MILES, K., GREENGARD, P. & HU, R.L. (1989). Calcitonin gene-related peptide regulates phosphorylation of the nicotinic acetylcholine receptor in rat myotubes. *Neuron*, **2**, 1517–1524.

MOSS, S.J., HARKNESS, P.C., MASON, I.J., BERNARD, E.A. & MUDGE, A.W. (1991). Evidence that CGRP and cAMP increase transcription of AChR α-subunit gene, but not of other subunits genes. *J. Mol. Neurosci.*, **3**, 101–108.

MULLE, C., BENOIT, P., PINSET, C., ROA, M. & CHANGEUX, J.P. (1988). Calcitonine gene-related peptide enhances the rate of desensitization of the nicotinic acetylcholine receptor in cultured mouse muscle cells. *Proc. Natl. Acad. Sci. U.S.A.*, **85**, 5728–5732.

O'CONNOR, S.E., DAINTY, I.A. & LEFF, P. (1991). Further subclassification of ATP receptors based on agonist studies. *Trends Pharmacol. Sci.*, **12**, 137–141.

OKAJIMA, F., TOKUMITSU, Y., KONDO, Y. & UI, M. (1987). P_2-purinergic receptors are coupled to two signal transduction systems leading to inhibition of cAMP generation and to production of inositol trisphosphate in rat hepatocytes. *J. Biol. Chem.*, **252**, 13483–13490.

SILINSKY, E.M. (1975). On the association between transmitter secretion and the release of adenine nucleotides from mammalian motor nerve terminals. *J. Physiol.*, **247**, 145–162.

TADA, S., OKAJIMA, F., MITSUI, Y., KONDO, Y. & UI, M. (1992). P_2 purinoceptor mediated cyclic AMP accumulation in bovine vascular smooth muscle cells. *Eur. J. Pharmacol.*, **227**, 25–31.

TAKAMI, K., HASHIMOTO, K., UCHIDA, S., TOKOYAMA, M., SHIOTANI, Y., HOSHIDA, H., EMSON, P.C., GIRGIS, S.H., HILLYARD, C.J. & MACINTYRE, I. (1986). Effect of calcitonine gene-related peptide on the cyclic AMP level of isolated mouse diaphragm. *Jpn. J. Pharmacol.*, **42**, 345–350.

YAFFEE, D. & SAXEL, O. (1977). Serial passage and differentiation of myogenic cells isolated from dystrophic mouse muscle. *Nature*, **270**, 725–727.

YOSHIMASA, T., SIBLEY, D.R., BOUVIER, M., LEFKOWITZ, R.J. & CARON, M.G. (1987). Cross-talk between second messenger systems: phorbol esters induce phosphorylation of the catalytic unit of adenylate cyclase and enhancement of its activity. *Nature*, **327**, 67–70.

(Received February 15, 1993
Revised April 22, 1993
Accepted April 26, 1993)

Br. J. Pharmacol. (1993), **110**, 139–144

Partial inhibition by epithelium of tracheal smooth muscle relaxation induced by the potassium channel activator, BRL 38227

Dragan Pavlovic, Eveline Brione, *Dominique De Vernejoul & [1]Michel Aubier

Laboratoire de Pathologie Expérimentale, Unité INSERM 226, Faculté Xavier Bichat, Paris, France and *Laboratoires Beecham SmithKline, France

1 A method is described whereby either the serosal (Out) or epithelial (In) sides of rat isolated tracheae were selectively perfused. Perfusion with BRL 38227 (10^{-8}–5×10^{-6} M; In/Out) of preparations with intact epithelium (+ EP) precontracted with carbachol (10^{-6} M; Out/In) produced complete relaxation. Perfusion with aminophylline (10^{-5}–10^{-3} M; In) of + EP preparations precontracted with carbachol (10^{-6} M; Out) also produced complete relaxation.

2 In preparations precontracted with carbachol (10^{-6} M) epithelium removal (– EP) increased the sensitivity to the relaxant effect of BRL 38227 (In), but not BRL 38227 (Out) [– log EC_{50}, + EP/ – EP; carbachol (In), BRL 38227 (Out): 6.76 ± 0.11 vs 6.67 ± 0.15; carbachol (Out), BRL 38227 (In): 5.93 ± 0.06 vs 6.25 ± 0.07]. Removal of the epithelium increased also the sensitivity to BRL 38227 (In) of preparations precontracted with a lower concentration (5×10^{-7} M) of carbachol (Out). [– log EC_{50}, + EP/ – EP, carbachol (Out), BRL 38227 (In): 6.19 ± 0.14 vs 6.58 ± 0.17].

3 Removal of the epithelium did not affect the sensitivity to BRL 38227 (In) of preparations precontracted with a higher concentration (5×10^{-6} M) of carbachol (Out).

4 In both + EP and – EP preparations precontracted with carbachol (10^{-6} M; Out), BRL 38227 (In) had a more potent relaxant effect than aminophylline (In) (EC_{50}, BRL 38227 vs aminophylline, + EP/ – EP: 5.93 ± 0.06 vs 3.66 ± 0.11/6.25 ± 0.07 vs 3.77 ± 0.11).

5 In preparations precontracted with carbachol (10^{-6} M; Out), removal of the epithelium did not affect the sensitivity to aminophylline (In) but increased the degree of precontraction (T_{max}) following epithelial but not serosal stimulation with carbachol.

6 We conclude that BRL 38227, a K^+ channel activator, is a potent relaxant of rat tracheal smooth muscle precontracted with carbachol, and that the effect can be partially inhibited by the presence of an intact tracheal epithelium, whereas the relaxant effect of aminophylline is not.

Keywords: Smooth muscle; tracheal epithelium; potassium channel activator; BRL 38227 (lemakalim)

Introduction

Potassium (K^+) channels have been associated with the recovery of the resting potential of excitable cells after depolarization. Indeed, drugs that block K^+ channels have been shown to cause an increase in cellular excitability. In airway smooth muscle, application of K^+ channel blocking drugs results in spontaneous action potentials and a reduced threshold of excitation (Davis *et al.*, 1982; Kannan *et al.*, 1983). These changes appear to be similar to the electrophysiological changes described in asthmatic airways (Akasaka *et al.*, 1975). The recent development of drugs that open K^+ channels in smooth muscle reawakened interest in these channels because these drugs relax airway smooth muscle and thus might reduce airway hyperreactivity which is the main feature of asthma.

Although most attention has been focussed on the role of K^Q channels in airway smooth muscle, these channels have also been shown to be present on many different cell types such as nerve terminals, ganglia, macrophages and epithelial cells (Hall *et al.*, 1988; Kakuta *et al.*, 1988; McCaig & Jonckheere, 1989). This may be relevant in airway disease in which these cells have been shown to play an important role in the mechanism of airway hyperreactivity. In this connection, the role played by airway epithelial cells should be pointed out. Indeed, it has been shown that airway epithelium can modulate bronchial smooth muscle contraction (Cuss & Barnes, 1987; Pavlovic *et al.*, 1989, Vanhoutte, 1988). It is therefore possible that K^+ channels on airway epithelial cells may be implicated in the control of airway tone by the bronchial epithelium. Furthermore, in asthma the bronchial epithelium is often damaged which may influence the effect of some bronchodilator compounds and particularly K^+ channel opening agents which have been shown to inhibit the excitatory NANC (non-adrenergic non-cholinergic) response (Ichinose & Barnes, 1990). The aims of this study were, therefore: (i) to test the relaxant effect in airway smooth muscle of a new K^+ channel opening agent BRL 38227 (lemakalim, (–)-enantiomer of cromakalim) on rat trachea *in vitro* and to compare its potency with another smooth muscle relaxant, aminophylline; (ii) to determine whether the relaxant effect of BRL 38227 in this tissue was influenced by the presence of airway epithelium.

Methods

The method used to prepare rat isolated tracheal smooth muscle preparations has been described by Pavlovic *et al.* (1989). Tracheae were taken from male Sprague-Dawley rats (300–350 g body weight) that had been stunned by a blow on the head and quickly exsanguinated. The tracheae were immersed in Krebs solution (composition mM: NaCl 137, KCl 4, $MgCl_2$ 1, KH_2PO_4 1, $NaHCO_3$ 12, $CaCl_2$ 2, glucose 6.5) and cleaned of all surrounding tissue. Proximal ends (10 rings long) were used for the experiments and distal ends

[1] Author for correspondence at: Service de Pneumologie, Hôpital Bichat, 46 rue Henri Huchard, 75018 Paris, France.

were discarded. In one-half of the preparations the epithelium was removed (– EP) by gently rubbing with a cotton-wrapped metal stick; in the other half of the preparations the epithelium was left intact (+ EP).

An organ bath was constructed that permitted independent circulation of fluid within the lumen of the tracheal segment (In, epithelial side) or around the exterior (Out, serosal side) of the tracheal segment (Figure 1). A modified 5 ml syringe with top and lateral openings served as the organ bath. The piston served as a support for the tubing system used to intubate and secure the tracheal segments in place. Mounting of tracheal segments involved the following.

Under microscopic control two stainless steel hooks were passed through the tracheal wall around two adjacent cartilaginous rings as close as possible to the muscle insertions. The tracheal segments were then longitudinally connected to the steel tubes built in the piston and firmly tightened with silk thread. The lower hook was attached below, serving as a fixed point. Its length was adjusted such that it did not pull down the tracheal wall.

The piston was then introduced into the syringe and the upper hook connected to a force transducer (UC2, Gould Cleveland, OH, U.S.A.). The latter was attached to a micromanipulator (Prior PO 22, Prior Scientific Instruments, Herts, UK) that enabled the displacement of the upper hook along a strict vertical axis. Any change of tension at the level of the tracheal muscle was registered by the recorder (Gould AT 550) to which the transducer was connected.

Krebs solution (at 37°C, pH 7.4, gassed with 95% O_2:5% CO_2) was perfused at a constant flow rate (2 ml min^{-1}) through the syringe organ bath (outer perfusion) and through the lumen of the tracheal segment (inner perfusion) by using peristaltic pumps (Watson Marlow 5025, Falmouth, Cornwall, UK).

Fluid tightness of preparation

To ensure that the hooks did not induce a fluid leak through the tracheal wall, a solution of methylene blue was perfused into the tracheal lumen or the organ bath in separate experiments. No cross-staining was observed.

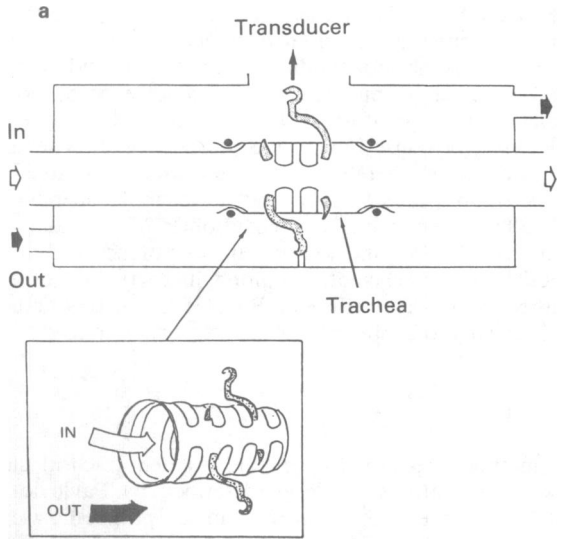

Figure 1 (a) Schematic representation of the experimental apparatus. Inner (In) and outer (Out) perfusions are maintained at 37°C, bubbled with 95% O_2–5% CO_2 and a constant flow rate of 2 ml min^{-1} is maintained.

Procedure

The tracheal muscle was stretched transversely to its optimal length which had been established in preliminary experiments. After a period of stabilization (40–50 min) the preparations were precontracted by perfusing either the epithelial (In) or the serosal (Out) surface of the trachea with a solution of carbachol at a concentration (10^{-6} M) corresponding to the EC_{50}, determined in a preliminary series of experiments (data not shown). In the other series of experiments, the tracheae were perfused with lower (5×10^{-7} M) or higher (5×10^{-6} M) concentrations of carbachol. When the response to carbachol reached a plateau, in a first series of experiments (Table 1), cumulative concentrations (10^{-8} to 5×10^{-6} M) of BRL 38227 were administered either outside or inside the trachea. In this series of experiments, concentration-effect curves for BRL 38227 were constructed. The order of perfusion was such that the bronchoconstrictor agent (carbachol) was always perfused from one side and the bronchodilator agent (BRL 38227) from the other side. To determine whether the relaxant effect was reversible, when the effect of the relaxant agent was maximal, the side where the relaxant agent had been perfused was washed with Krebs solution and then, when the tracheal muscle regained tension, the other side of the trachea which had been perfused with carbachol was washed with Krebs solution until the preparation relaxed completely.

In a second series of experiments (also shown in Table 1) a similar protocol was used. Preparations, precontracted with carbachol, 10^{-6} M (Out), were perfused from the epithelial side (In) with cumulative concentrations (10^{-5} to 10^{-3} M) of aminophylline to compare the relaxant effect of BRL 38227 with that of another smooth muscle relaxant compound. These experiments were performed in preparations with or without epithelium.

After completion of the experiments, 10 tracheal segments without epithelium (– EP) and 10 with epithelium (+ EP) taken at random, were removed from the organ bath and fixed in 2.5% glutaraldehyde. Semi-thin sections from plastic-embedded blocks were then prepared, stained with toluene blue and examined microscopically for the presence of epithelium and/or possible damage of the tracheal wall and epithelium caused by the hooks. A quantification of the epithelium present was performed by estimating the number of nuclei of epithelial cells in the whole circumference of the cross-section of the tracheal segment (intact circumference was taken to be 100%) (Pavlovic *et al.*, 1989).

Materials

The following substances were used: carbachol (carbamylcholine chloride, Sigma Chimie S.a.r.l., 38299 St. Quentin Fallavier, France), BRL 38227 (Beecham Pharmaceuticals, Brockham Park, Betchworth, Surrey), aminophylline (theophylline-ethylene-diamine, Pharmacie Centrale des Hôpitaux, Paris, France). Stock solutions were prepared just before the experiments in distilled water while final dilutions were made with Krebs solution. An initial stock solution (10^{-1} M) of BRL 38227 was made in 70% ethanol.

Analysis of results

The data (changes in tension) are expressed as a percentage of maximal response and in absolute values (g). The results are given as means ± s.e.mean. Half maximal concentrations (EC_{50} values) were calculated from regression analysis of probit-transformed data, and results are given as geometric means of the log EC_{50} obtained. Statistical analysis was conducted by use of Student's t test for paired or unpaired samples. A probability value less than 0.05 was regarded as being statistically significant.

Table 1 Experimental protocol

Preparation	n	*Protocol* (time →)
+EP	10	C ——— P - - - - - - - - W in (10^{-6}) BRL, out (10^{-8} to 5×10^{-6})
+EP	10	C ——— P - - - - - - - - W out (10^{-6}) BRL, in (10^{-8} to 5×10^{-6})
−EP	10	C ——— P - - - - - - - - W in (10^{-6}) BRL, in (10^{-8} to 5×10^{-6})
−EP	10	C ——— P - - - - - - - - W out (10^{-6}) BRL, in (10^{-8} to 5×10^{-6})
+EP	10	C ——— P - - - - - - - - W out (5×10^{-6}) BRL, in (10^{-8} to 5×10^{-6})
+EP	10	C ——— P - - - - - - - - W out (5×10^{-7}) BRL, in (10^{-8} to 5×10^{-6})
−EP	9	C ——— P - - - - - - - - W out (5×10^{-6}) BRL, in (10^{-8} to 5×10^{-6})
−EP	10	C ——— P - - - - - - - - W out (5×10^{-7}) BRL, in (10^{-8} to 5×10^{-6})
+EP	9	C ——— P - - - - - - - - W out (10^{-6}) Aminophylline, in (10^{-5} to 10^{-3})
−EP	10	C ——— P - - - - - - - - W out (10^{-6}) Aminophylline, in (10^{-5} to 10^{-3})

+EP = with epithelium; −EP = without epithelium; C = carbachol; W = wash, in = inside (epithelial side); out = outside (serosal side); P = plateau; (- - -) = carbachol perfusion; (———) = BRL 38227 or aminophylline perfusion (see text for details).

Results

Histology

Twenty preparations, of which ten had been rubbed for epithelium removal, were selected at random for histological evaluation. In (− EP) preparations 60–80% of the epithelium was removed without any obvious damage to the underlying submucosa or muscle layer. After 3 h in the organ bath, 60–80% of the epithelium remained intact in the control tissues (+ EP).

Contractility

In + EP preparations, BRL 38227 (In) produced a concentration-dependent relaxation of rat tracheal muscle precontracted with 10^{-6} M carbachol (Out). Complete relaxation was obtained with 5×10^{-5} M BRL 38227 (Figure 2). This figure also shows that under the same precontraction conditions, BRL 38227 (In) was much more potent ($P < 0.001$) than aminophylline (In), for which complete relaxation was observed with a concentration of 10^{-3} M (EC_{50}, BRL 38227 vs aminophylline, +/− epithelium: 5.93 ± 0.06 vs 3.66 ± 0.11/6.25 ± 0.07 vs 3.77 ± 0.11, $P < 0.001$).

As shown in Figure 3a and Table 2, in + EP preparations the relaxant effect of BRL 38227 was signficantly more pronounced ($P < 0.001$) when the agent was perfused outside rather than inside the trachea. However, in − EP preparations this difference was abolished (Figure 3b, Table 2).

Removal of the epithelium also increased the sensitivity to BRL 38227 of the preparations precontracted with a lower concentration (5×10^{-7} M) of carbachol but not of preparations precontracted with a higher concentration (5×10^{-6} M) of carbachol (Figure 4, Table 3).

By contrast, as shown in Figure 5, epithelium removal had no effect on the relaxant action of aminophylline, no significant difference in potency being observed with or without epithelium when the drug was perfused inside the trachea.

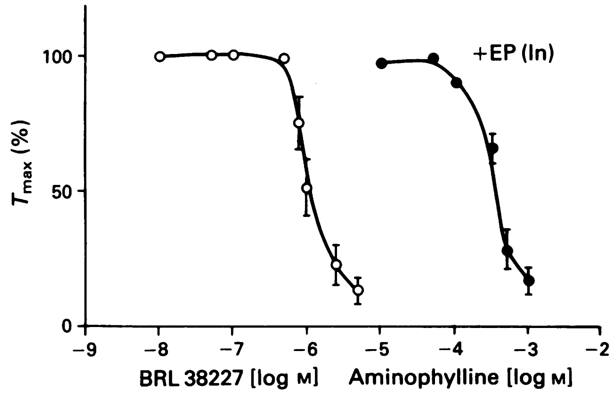

Figure 2 Cumulative concentration-response curves for relaxation induced by either BRL 38277 (○, $n = 10$) or aminophylline (●, $n = 10$) perfused from the epithelial side (In) of the trachea with epithelium precontracted with 10^{-6} M carbachol solution. Tension is expressed as a percentage of the maximal tension (T_{max}) obtained with 10^{-6} M carbachol before administration of BRL 38277 or aminophylline and presented as mean data. Values are mean ± 1 s.e.mean. The two curves represent the results obtained in two different sets of experiments.

The degree of precontraction (T_{max}) obtained by perfusing carbachol 10^{-6} M was not affected by the presence or absence of the epithelium in the preparations exposed to carbachol (Out) but was significantly increased in the preparations exposed to carbachol (In) in − EP preparations (Table 4).

Discussion

The results of the present study indicate that BRL 38227, a K^+ channel activator, is a potent relaxant of rat tracheal smooth muscle precontracted with carbachol and that this effect is partially inhibited by the tracheal epithelium.

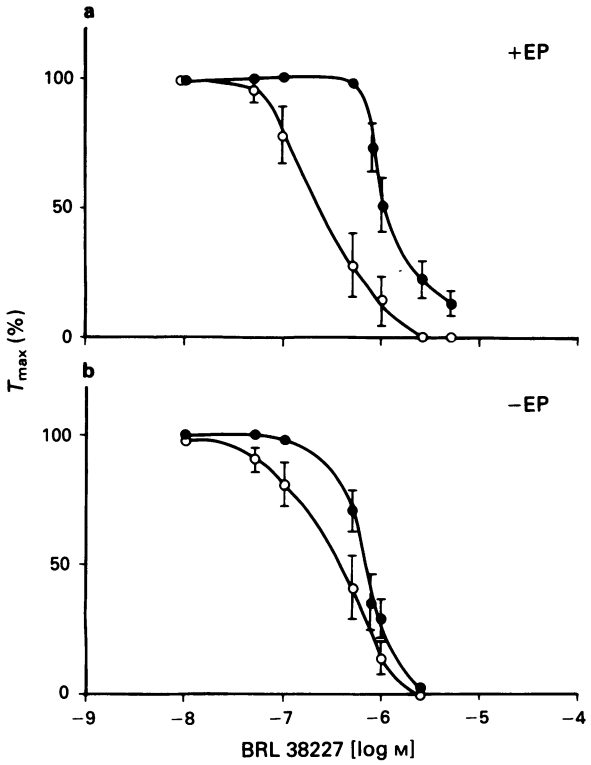

Figure 3 Cumulative concentration-responses curves constructed after administration of BRL 38277 in rat isolated trachea with (a; +EP) and without epithelium (b; −EP). In both preparations BRL 38277 was administered inside (In) (●, $n = 10$) or outside (Out) (○, $n = 10$) the trachea. Tension is expressed as a percentage of the maximal tension (T_{max}) obtained with 10^{-6} M carbachol before administration of BRL 38277 and presented as mean data ± s.e.mean.

Table 2 EC_{50} values for BRL 38227

	BRL In	*BRL Out*	P *(BRL In/BRL Out)*
+EP	5.93 ± 0.06	6.76 ± 0.11	0.001
−EP	6.25 ± 0.07	6.67 ± 0.15	0.01
P (+EP/−EP)	0.005	NS	

Geometric means (± s.e.means) of −log EC_{50} values for relaxation obtained in preparations with (+EP) and without epithelium (−EP) following perfusion from epithelial (In) or serosal sides (Out) with cumulative concentrations of BRL 38227 (BRL). The preparations were precontracted with carbachol 10^{-6} M (NS = non significant).

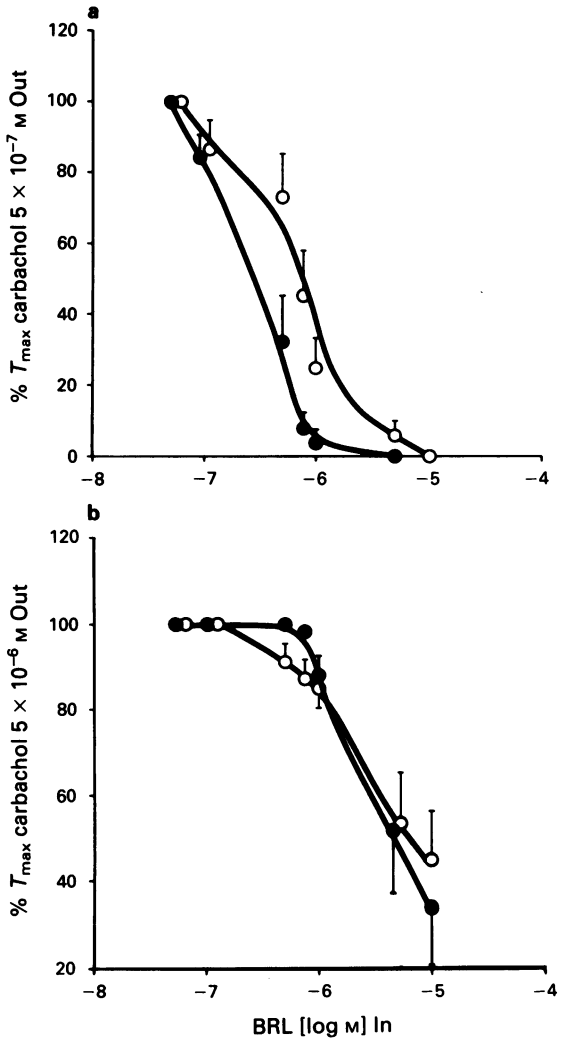

Figure 4 Cumulative concentration-response curves for the relaxant effect of BRL 38227 administered from epithelial side (In) in rat isolated tracheal preparations with (+EP, ○) and without epithelium (−EP, ●). Tension is expressed as a percentage of the maximal (T_{max}) obtained with 5×10^{-7} M carbachol ($n = 9$) (a), or 5×10^{-6} M carbachol ($n = 10$) (b), perfused from the serosal side (Out) and presented as mean data ± s.e.mean.

Table 3 EC_{50} values for BRL 38227 at different carbachol concentrations

	Carbachol Out	
BRL In	5×10^{-7}	5×10^{-6}
+EP	6.19 ± 0.14	5.27 ± 0.18
−EP	6.58 ± 0.07	5.18 ± 0.17
P	<0.03	NS

Geometric means (± s.e.mean) of −log EC_{50} values obtained in preparations with (+EP) and without epithelium (−EP) following epithelial (In) perfusion with cumulative concentrations of BRL 38227. The preparations were precontracted with carbachol 5×10^{-7} and 5×10^{-6} M from the serosal side (Out) (NS = not significant).

The relaxation of rat tracheal smooth muscle that we observed following BRL 38227 administration was similar to that previously described for this compound in guinea-pig (Ichinose & Barnes, 1990) and human isolated bronchi (Black *et al.*, 1990). In the latter study, BRL 38227 was equally effective against contractions induced by carbachol, histamine, or neurokinin A. The maximal relaxation obtained in human bronchi *in vitro* with BRL 38227 amounted to 60–80% of that induced by a maximal concentration of isoprenaline (Black *et al.*, 1990). In our study, the magnitude of the relaxant effect of BRL 38227 was compared to that of aminophylline. However, when compared to aminophylline, BRL 38227 was much more potent, whether the agent was administered inside or outside the trachea. A xanthine compound was used instead of a stimulator of adrenoceptors because rat tracheal smooth muscle has very few β-adrenoceptors (O'Donnell *et al.*, 1987). Indeed, in previous experiments using the same preparation as in the present study we were unable to obtain with salbutamol, (a β_2-agonist) a significant relaxation in rat trachea precontracted with carbachol (unpublished data).

The relaxant effect of BRL 38227 in our model was significantly influenced by the presence of the tracheal epithelium and, when the epithelium was intact, by the route

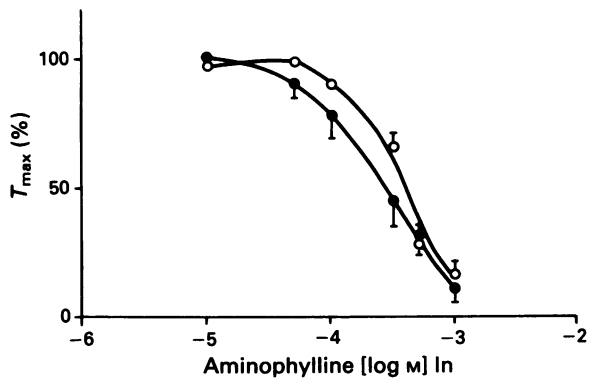

Figure 5 Cumulative concentration-response curve for the relaxant effect of aminophylline perfused from the epithelial side (In) ($n = 10$) in rat isolated tracheal preparations with epithelium (+EP, ○) and without epithelium ($n = 10$) (−EP, ●). Tension is expressed as a percentage of the maximal tension (T_{max}) obtained with 10^{-6} M carbachol before administration of aminophylline and presented as mean data ± s.e.mean.

Table 4 Effects of epithelial removal on carbachol T_{max}

Carbachol (M)	5×10^{-7} Out ($n = 9$)	10^{-6} Out ($n = 10$)	10^{-6} In ($n = 10$)	5×10^{-6} Out ($n = 10$)
−EP	1.1 ± 0.1	1.14 ± 0.08	1.62 ± 0.19	1.4 ± 0.12
+EP	1.32 ± 0.09	1.36 ± 0.12	1.03 ± 0.11	1.68 ± 0.17
P	NS	NS	<0.03	NS

Maximal tension (T_{max}) in g obtained following stimulation with low (5×10^{-7} M), intermediate (10^{-6} M, equivalent to EC_{50}), and high concentrations (5×10^{-6} M) of carbachol perfused from the serosal side (Out) or (for carbachol 10^{-6} M only) also from epithelial (In) side in tracheal preparations with or without epithelium (+EP, −EP) (mean ± s.e.mean, NS = non significant).

of BRL 38227 administration (inside or outside the trachea). Indeed, when the drug was perfused inside the trachea, the relaxant effect of BRL 38227 in tracheae precontracted with carbachol was much less potent in the preparations with epithelium than in those without epithelium. Furthermore, it was also found that BRL 38227 was more effective if administered outside (serosal side) than inside (epithelial side) the trachea with the epithelium intact.

These results suggest that the epithelium may act as a diffusion barrier, limiting access of the drug to the smooth muscle. Indeed, in the same model, we have previously shown that the time course of tension development was longer when carbachol was administered inside the trachea rather than outside, an effect that was abolished when the epithelium was removed (Pavlovic *et al.*, 1989). In the present study, the relaxant effect of BRL 38227 was more pronounced when the epithelium had been removed; no difference was observed when BRL 38227 was administered inside or outside the trachea, contrary to what was noted in the intact preparations. This suggests that the epithelium could act as a diffusion barrier when BRL 38227 was perfused inside the trachea in the preparations with intact epithelium. This hypothesis is further supported by the results obtained in experiments where we tested the effects of BRL 38227 in preparations precontracted with different (higher and lower) concentrations of carbachol. Indeed, it has been suggested (Stuart-Smith & Vanhoutte, 1990) that the type of contractile agent and the level of the excitation might be important in explaining the modulatory effects of bronchial epithelium on airway smooth muscle tone. However, we found that maximal tension of precontraction was changed (increased) only in preparations without epithelium when carbachol was perfused from the epithelial side and BRL 38227 from the serosal side. In this series of experiments we did not observe an effect of epithelium removal on the sensitivity to BRL 38227. Indeed, in the preparations precontracted with low concentrations of carbachol (5×10^{-7} M) the sensitivity to BRL 38227 (In) was strongly influenced by the presence of the bronchial epithelium. By contrast, in the preparations precontracted with the high concentration of carbachol (5×10^{-6} M), the sensitivity to BRL 38227 was not affected by the epithelium removal. The fact that we did not find a difference in sensitivity to BRL 38227 in preparations with or without epithelium precontracted with higher concentrations of carbachol (5×10^{-6} M) further supports our hypothesis that the tracheal epithelium could play the role of a diffusion barrier. At a high level of contractile excitation such as that obtained with a high carbachol concentration, higher concentrations of BRL 38227 are also necessary to obtain the relaxant effect. Assuming that the epithelium has a limited capacity to act as a diffusion barrier, in the presence of high concentrations of BRL 38227 which largely overcome the capacity of the epithelium layer, the effect of a diffusion barrier would be practically unobservable.

Another explanation underlying the modulation of the drug effect by the tracheal epithelium could be a direct effect of BRL 38227 on the epithelial cells or on the release of neuropeptides from sensory nerve terminals. In the latter case, it has been shown that another potassium channel activator, cromakalim, inhibited the excitatory NANC response in guinea-pig airways, probably by reducing the release of neuropeptides from sensory nerve terminals (Ichinose & Barnes, 1990). This effect may be more pronounced when the epithelium had been removed, facilitating the access of BRL 38227 to the sensory nerve terminals. Finally, BRL 38227 may stimulate tracheal epithelial cells to produce some unknown constricting factor. Or, increased permeability of the cell membrane could affect production of the putative EpDIF (epithelium-derived inhibitory factor). Indeed, it has been suggested that potassium exchange at the cell membrane level could be important for the regulation of tracheal smooth muscle tone through various mechanisms which are still not fully elucidated (Fedan *et al.*, 1988; Black & Barnes, 1990).

The present results are difficult to compare with experiments performed earlier by other investigators who used different *in vitro* models, such as bronchial rings (Stuart-Smith & Vanhoutte, 1990) or tracheal spirals (Arch *et al.*, 1988). In these models both sides of the bronchial smooth muscle (epithelial and serosal) were perfused simultaneously. The specific effect of epithelium removal may have been missed by the presence of the agent not only on the epithelial but on the serosal side as well. In our experiments the effect of agents that were examined were perfused exclusively from either the epithelial or serosal side.

By contrast to what was observed with BRL 38227, the relaxant effect of aminophylline was not influenced by the removal of the epithelium. Thus although it has been previously suggested that the relaxant effect of aminophylline depends on the presence of epithelium (Papadimikiou *et al.*, 1988) our results do not confirm this observation. This discrepancy may be explained by the preparation we used in which we could separate the application of aminophylline to the epithelial and serosal sides of the trachea.

Whatever the mechanisms by which the relaxant effect of BRL 38227 is influenced by the tracheal epithelium, this observation may be important in asthma since it has been shown that in these patients, airway epithelium is damaged (Laitinen *et al.*, 1985). Our finding that the relaxant effect of BRL 38227 is more potent after epithelium removal may therefore have a therapeutic interest, particularly if the compound is given by inhalation.

References

AKASAKA, K., KONNO, K., ONO, Y., MUES., ABE, C., KUNAGAI, M. & ISE, T. (1975). Electromyographic study of bronchial smooth muscle in bronchial asthma. *Tokoshu. J. Exp. Med.*, **117**, 55–59.

ARCH, J.R.S., BUCKLE, D.R., BUMSTEAD, J., CLARKE, G.D., TAYLOR, J.F. & TAYLOR, S.G. (1988). Evaluation of the potassium channel activator cromakalim (BRL 38277) as bronchodilatator in the guinea pig: comparison with nifedipine. *Br. J. Pharmacol.*, **95**, 763–770.

BLACK, J.L., ARMON, C.L., JOHNSON, P.R., ALOUAN, L.A. & BARNES, P.J. (1990). The action of potassium channel activator BRL 38277 (Lemakalim) on human airway smooth muscle. *Am. Rev. Respir. Dis.*, **142**, 1384–1389.

BLACK, J.L. & BARNES, P.J. (1990). Potassium channels and airway function: new therapeutic prospects. *Thorax*, **45**, 213–218.

CUSS, F.M. & BARNES, P.J. (1987). Epithelial mediators. *Am. Rev. Resp. Dis.*, **136**, 32–35.

DAVIS, C., KANNAN, M.S., JONES, T.R. & DANIEL, E.E. (1982). Control of human airway muscle: in vitro studies. *J. Appl. Physiol.*, **153**, 1080–1087.

FEDAN, J.S., HAY, D.W.P., FARMER, S.G. & REABURN, D. (1988). Epithelial sells: modulation of airway smooth muscle reactivity. ed. Barnes, P.J., Rodger, I.W. & Thompson, N.C. In: *Asthma, Basic Mechanics and Clinical Management*. New York: Academic Press.

HALL, A.K. & MACLAGAN, J. (1988). Effect of cromakalim on cholinergic neurotransmission in the guinea-pig trachea. *Br. J. Pharmacol.*, **96**, 792P.

ICHINOSE, M. & BARNES, P.J. (1990). A potassium channel activator modulates both excitatory noncholinergic and cholinergic neurotransmission in guinea pig airways. *J. Pharmacol. Exp. Ther.*, **252**, 1207–1212.

KAKUTA, Y., OKAYAMA, H. & AIKAWA, T. (1988). K+ channels of human alveolar macrophages. *J. Allergy Clin. Immunol.*, **81**, 460–468.

KANNAN, M.S., JAGER, L.P., DANIEL, E.E. & GARFIELD, R.E. (1983). Effects of 4-amynopiridine and tetraaethylammonium chloride on the electrical activity and cable properties of canine tracheal smooth muscle. *J. Pharmacol. Exp. Ther.*, **227**, 706–715.

LAITINEN, L.A., HEINO, M., LAITINEN, A., KAVA, T. & HAAHTELA, T. (1985). Damage of the airway epithelium and bronchial reactivity in patients with asthma. *Am. Rev. Resp. Dis.*, **131**, 599–606.

MCCAIG, D.J. & DE JONCKHEERE, B. (1989). Effect of cromakalim on bronchoconstriction evoked by cholinergic nerve stimulation in guinea-pig isolated trachea. *Br. J. Pharmacol.*, **98**, 662–668.

O'DONNELL, S., WANSTALL, J.C. & MUSTAFA, M.B.H. (1987). Influence of thyroid status on responses of rat isolated pulmonary artery, vas deferens and trachea to smooth muscle relaxant drugs. *Br. J. Pharmacol.*, **92**, 221–229.

PAPADIMIKIOU, J.M., PATERSON, J.W., RIGHY, P.J. & SPINA, D. (1988). Influence of the epithelium on responsiveness of guinea-pig isolated trachea to contractile and relaxant agonists. *Br. J. Pharmacol.*, **87**, 5–14.

PAVLOVIC, D., FOURNIER, M., AUBIER, M. & PARIENTE, R. (1989). Epithelial vs. serosal stimulation of tracheal muscle: role of epithelium. *J. Appl. Physiol.*, **67**, 2522–2526.

STUART-SMITH, K. & VANHOUTTE, P.M. (1990). Epithelium, bronchial tone and responses to relaxing agonists in canine bronchi. *J. Appl. Physiol.*, **69**, 678–685.

VANHOUTTE, P.M. (1988). Epithelium derived relaxing factor: myth or reality. *Thorax*, **43**, 665–668.

(Received October 26, 1992
Revised April 13, 1993
Accepted April 26, 1993)

Br. J. Pharmacol. (1993), **110**, 145–150

Kinetics of rate-dependent slowing of intraventricular conduction by the class Ib antiarrhythmic agent tocainide *in vivo*

[1]Hannes Todt, Niklas Zojer & Gerhard Raberger

Pharmakologisches Institut der Universität Wien, Währingerstr. 13a, 1090 Vienna, Austria

1 The effects of the class I antiarrhythmic agent, tocainide, on intraventricular conduction were assessed in guinea-pigs, anaesthetized with pentobarbitone sodium 60 mg kg^{-1}, i.p.

2 After electrical ablation of the sinus node, heart rate was controlled by atrial pacing. His bundle electrograms were recorded by means of an epicardial bipolar electrode.

3 During continuous stimulation, comparison of HV intervals measured at a cycle length of 475 ms, with HV intervals measured at a cycle length of 250 ms yielded the following results: 25.26 ± 0.64 ms versus 25.02 ± 0.70 ms (NS), at baseline, 26.65 ± 0.80 ms versus 29.88 ± 1.13 ms ($P<0.001$) after i.v. administration of 30 mg kg^{-1} tocainide, and 28.04 ± 0.64 ms versus 36.24 ± 1.31 ms ($P<0.001$), after addition of 20 mg kg^{-1} tocainide. Thus, tocainide caused HV intervals to increase in a strictly rate-dependent fashion.

4 In order to characterize the rate-dependent class I activity of tocainide in terms of its binding kinetics to sodium channels, fractional sodium channel block was estimated from drug induced reductions of intraventricular conduction velocity ($\Delta\theta$). On abruptly changing the drive cycle length from 500 ms to 250 ms, $\Delta\theta$ reached a new steady state with rate constants of 1.23 ± 0.09 beat^{-1} and 1.28 ± 0.09 beat^{-1}, after administration of 30 mg kg^{-1} and addition of 20 mg kg^{-1} tocainide, respectively. At a basic drive cycle length of 250 ms $\Delta\theta$ recovered with time constants of 250.29 ± 23.32 ms and 183.04 ± 8.03 ms after administration of 30 mg kg^{-1} and addition of 20 mg kg^{-1} tocainide, respectively.

5 The experimentally determined kinetic parameters were implemented into a mathematical model that assumes drug binding to sodium channels in terms of a periodical two-state process. Rate-dependent reductions in conduction velocity during continuous stimulation after administration of tocainide were closely approximated by steady state reductions in sodium channel availability as calculated on the basis of the aforementioned model.

6 In agreement with previously published *in vitro* studies, our data, obtained *in vivo*, confirm the classification of tocainide as a class I antiarrhythmic agent with fast onset and offset kinetics. The kinetic parameters obtained *in vivo* can be used in order to predict steady state reductions in conduction velocity at a wide range of frequencies.

Keywords: Tocainide; lignocaine; antiarrhythmic drugs; bundle of His; rate-dependent; mathematical models

Introduction

Class I antiarrhythmic drugs have been shown to reduce sodium channel availability in a rate-dependent fashion (Heistracher, 1971; Campbell, 1983b). Mathematical models have been developed which describe the rate-dependent nature of sodium channel block by class I antiarrhythmic drugs in terms of a restriction of drug binding to certain conformational channel states (Hondeghem & Katzung, 1977; Starmer *et al.*, 1984; Starmer & Grant, 1984; Starmer, 1986). With regard to the kinetics of binding to the high-affinity state, class I antiarrhythmic agents can be subdivided into agents with 'fast' and 'slow' onset-offset kinetics (for review see Campbell, 1992). On the basis of experimental data and theoretical models it has recently been suggested that class Ib drugs, which exhibit fast onset-offset kinetics (e.g. lignocaine, tocainide and mexiletine) are likely to cause less proarrhythmic events than slow kinetic agents (Starmer *et al.*, 1991; Nesterenko *et al.*, 1992; Campbell, 1983a). The present study was designed to investigate the use-dependent action of the class Ib antiarrhythmic drug, tocainide, an oral congener of lignocaine, on intraventricular conduction velocity *in vivo*. To date, the rate-dependent class I action of tocainide has only been characterized *in vitro* (Oshita *et al.*, 1980; Borchard *et al.*, 1985; Kodama *et al.*, 1987). Since both antiarrhythmic and proarrhythmic actions of class I agents are mediated via depression of conduction velocity on a multicellular level (Wald *et al.*, 1980; Spinelli & Hoffman, 1989; Nesterenko *et al.*, 1992), the characterization of rate-dependent drug effects on intraventricular conduction *in vivo* may be of considerable clinical relevance.

Furthermore, we wished to determine whether rate-dependent depression of conduction by tocainide *in vivo* can be characterized on the basis of an established theoretical model of periodical ligand binding to sodium channels (Starmer & Grant, 1984; Starmer *et al.*, 1984; Starmer, 1986). Because the onset-offset kinetics of rate-dependent suppression of conduction by sodium channel blockers depends upon fibre orientation (Turgeon *et al.*, 1992), we chose to assess conduction time within the well defined physiological conduction pathway of the His-Purkinje system. For this purpose we used the recently described method of epicardial His bundle recording in the guinea-pig (Todt & Raberger, 1992; Todt *et al.*, 1992a).

Methods

The animals used in this study were handled in accordance with the animal welfare regulations of the University of

[1] Author for correspondence.

Vienna. The method and the experimental protocol were approved by the Animal Subjects Committee of the University of Vienna and by the Austrian Ministry of Science.

Guinea-pigs of either sex (300–500 g, $n = 11$) were anaesthetized with pentobarbitone sodium (60 mg kg^{-1}, i.p.) and respired artificially by a small animal ventilator (Type 874072, Braun Melsungen AG, FRG). Using needle electrodes, standard limb leads I–III were recorded by means of Grass 7P4F EKG preamplifiers and Grass model 7DAG driver amplifiers (Grass Instrument Co., Quincy, Mass., U.S.A.). The right jugular vein was dissected and a catheter was inserted for drug application. Following sternotomy the heart was exposed and sinus rhythm was abolished by application of high frequency alternating current (1.8 MHz; Siemens Radiotom 612) to the junction of the Superior vena cava with the right atrium. Thereafter heart rate was controlled by bipolar pacing of the left atrium with a Medtronic Model 5328 programmable stimulator and a Grass S48 Stimulator. The cycle length of stimulation was set at the value of spontaneous sinus rhythm before ablation of the sinus node. The electrical activity of the bundle of His was recorded by means of an epicardial bipolar electrode which was placed in the aortic-right atrial groove (Todt & Raberger, 1992; Todt *et al.*, 1992a). The electrode was connected to a Gould model 11 G412301 amplifier (Gould Inc., Cleveland, Ohio, U.S.A.) using a filter setting of 30 Hz–20 kHz. Both His bundle and standard limb ECG recordings were stored on magnetic tape (portable instrumentation recorder model 17-6500-00, Gould Inc., Cleveland, Ohio, U.S.A.). For measurement of HV intervals, the recordings were displayed on a digital storage oscilloscope (OS 4200, Gould Inc., Cleveland, Ohio, U.S.A.).

HV intervals were measured from the H-deflection in His bundle electrograms to the earliest peak of the R wave in any of the recorded leads. Usually the earliest R-peak was registered in the His-bundle electrogram. This measurement technique encompasses the ventricular activation time (MacFarlane & Veitch Lawrie, 1989) and thus allows assessment of the time span from the beginning of activation of the specialized ventricular conduction system until ventricular activation reaches its maximum. No measurements were performed if any change of the conduction pathway was indicated by alterations of the QRS vector in standard limb leads I–III.

Atrial stimulation for assessment of steady state conduction slowing (protocol 1)

The right atrium was continuously paced at selected cycle lengths between 200 ms and a cycle length 10 ms below the cycle length of spontaneous AV nodal rhythm. HV interval measurements were performed on beats 11–15 of each train and the mean value of all 5 measurements was calculated.

Atrial stimulation for assessment of onset of conduction slowing (protocol 2)

Eight basic drive beats, paced at a cycle length of 500 ms, were followed by a rapid train of 11 beats, paced at a cycle length of 250 ms.

Atrial stimulation for assessment of recovery from conduction slowing (protocol 3)

After a basic drive train of 8 depolarizations at a cycle length of 250 ms, an extrastimulus was introduced at a coupling interval of 225 ms. Thereafter the coupling interval was increased by 25 ms steps until interference of the spontaneous pacemaker was encountered. Because the excitation wave elicited by atrial stimulation has to pass the AV node before activating the ventricular conduction system, AV nodal accommodation may cause differences between the cycle length of stimulation (S_1S_2) and the cycle length of ventricular activation (H_1H_2 intervals). Differences between S_1S_2 and H_1H_2 were usually encountered only at coupling intervals of less than 275 ms. If present, such disparities were compensated by adjustment of coupling intervals to yield the desired H_1H_2 interval. The same applies to drug-induced changes in AV conduction. Subsequently the terms cycle length, activation rate, coupling interval etc. refer to activation of the ventricular conduction system.

Drug administration

The stimulation protocol was performed during a drug-free baseline period and following cumulative i.v. infusion of tocainide (30 mg kg^{-1} and 20 mg kg^{-1}, each over 30 min). The protocol was started 10 min after the end of each drug administration. The interval between administration of the two doses was 60 min.

Data evaluation

Percentage sodium channel block, b, was calculated from measurements of HV intervals by the formula

[eq 1] $$b = \Delta\theta = [1 - (HV_b/HV_d)]*100$$

where HV_b denotes the mean HV interval at baseline and HV_d indicates the HV interval during a given activation following drug administration (Packer *et al.*, 1989). Under the assumption of a stable conduction pathway, eq 1 yields the drug induced fractional reduction of conduction velocity within the His-Purkinje system ($\Delta\theta$).

The onset rate constant of block (λ^*) was estimated by fitting $\Delta\theta$ of every depolarization following an abrupt decrease in cycle length to the single exponential equation (Packer *et al.*, 1989):

[eq 2] $$b_n = b_{ss} + (b_0 - b_{ss})e^{-n\lambda^*}$$

where b_n is the block associated with the n^{th} stimulus, b_{ss} is the steady state block during the rapid train, and b_0 is the initial block prior to the abrupt beginning of rapid pacing.

In order to calculate the time constant of recovery from block, τ_{rec}, the $\Delta\theta$ values of each extrastimulus after the basic train were plotted against the respective coupling interval. The time course of recovery from steady state block at a cycle length of 250 ms is then given by

[eq 3] $$b(t) = (b_{250} - r_\infty)*(e^{-(t-250)/\tau rec}) + r_\infty$$

where b_{250} is the amount of block at a coupling interval of 250 ms and r_∞ denotes the final level of block that is approached if the recovery pause was extended for infinite time.

Analytical procedure

Starmer developed a theoretical model of drug binding to sodium channels by assuming a periodical two-state binding process (Starmer, 1986). Accordingly, sodium channels are considered to switch between high affinity and low affinity states during the cardiac cycle. Thus, steady state block (b_{ss}), which is present if heart rate is maintained stable during a prolonged period of time, can be described by:

[eq 4] $$b_{ss} = \frac{a_\infty(1-e^{-\frac{t_a}{\tau_{on}}})e^{-\frac{t_r}{\tau_{rec}}} + r_\infty(1-e^{-\frac{t_r}{\tau_{rec}}})}{1-e^{\lambda^*}}$$

where t_a and t_r are the durations of high and low affinity states, respectively. a_∞ and r_∞ denote the fractional block that would be achieved if channels were held for infinite time in high and low affinity states, respectively. Since tocainide has been shown to bind to both activated and inactivated sodium channels (Borchard *et al.*, 1985; Kodama *et al.*, 1987), t_a roughly corresponds to the duration of the action

potential (APD) and t_r corresponds to the interval between action potentials.

τ_{on}, the time constant of drug binding during the high affinity state, can be calculated from the relationship:

[eq 5] $$\lambda^* = \frac{t_a}{\tau_{on}} + \frac{t_r}{\tau_{rec}}$$

where λ^* and τ_{rec} are determined from eq 2 and 3.

a_∞ was calculated by the following approach: during a rapid train according to protocol 2, the amount of block at the end of any action potential ($b_{n(APD)}$) is given by

[eq 6] $$b_{n(APD)} = (a_\infty - b_n)(1\text{-}e^{-APD/\tau on}) + b_n$$

where b_n is the initial block at depolarization. $b_{n(APD)}$ can also be estimated by a modification of eq 3:

[eq 7] $$b_{n(APD)} = (b_{n+1} - r_\infty)^*(e^{-(APD-250)/\tau rec}) + r_\infty$$

Once $b_{n(APD)}$ has been determined from eq 7, a_∞ can be calculated from eq 6. In the present study $b_{n(APD)}$ was calculated from the $\Delta\theta$ values of beats 10 ($= b_n$) and 11 ($= b_{n+1}$) of the rapid train according to protocol 2.

r_∞ is estimated from eq 3.

Because APD of the His-Purkinje system cannot be measured *in vivo*, we estimated APD by means of the equation:

[eq 8] $$APD = 0.045^*CL + 152$$

where CL = cycle length. This equation was derived by linear regression analysis of previously published plots relating APD in isolated guinea-pig Purkinje fibres to cycle lengths between 300 ms and 1000 ms ($r = 0.96$) (Aomine, 1989). Although the relationship between cardiac repolarization and cycle length becomes hyperbolic if cycle lengths >1000 ms are included (Aomine, 1989; Surawicz, 1992), linear regression can be fitted equally well to the relationship if only the range of cycle lengths pertinent to this study are considered (Todt *et al.*, 1992b).

Statistics

Unless otherwise stated, data are given as mean ± s.e.mean. Statistical comparisons were performed using Student's *t* test for paired data with Bonferroni adjustment for multiple comparisons (Wallenstein *et al.*, 1980).

Results

Steady state decrease in conduction velocity

At baseline, steady state HV intervals were independent of changes in stimulation cycle length (25.26 ± 0.64 versus 25.02 ± 0.70 ms, NS, at stimulation cycle lengths of 475 and 250 ms, respectively). After administration of tocainide the rate of spontaneous AV-nodal rhythm decreased, thus allowing the assessment of lower frequencies than at baseline. The longest cycle length that could be achieved in all animals both during baseline and after tocainide was 475 ms (rate = 126.3 beats min^{-1}). At this cycle length HV intervals were only moderately prolonged when compared to the respective baseline values (26.65 ± 0.80 ms, NS, and 28.04 ± 0.64 ms, $P<0.001$, after administration of 30 mg kg^{-1} and subsequent addition of 20 mg kg^{-1} tocainide, respectively). At a cycle length of 250 ms (rate = 240 beats min^{-1}) both doses of tocainide caused very pronounced increases in HV intervals when compared to the respective baseline values (29.88 ± 1.13 ms, $P<0.001$, and 36.24 ± 1.31 ms, $P<0.001$, after administration of 30 mg kg^{-1} and subsequent addition of 20 mg kg^{-1} tocainide, respectively). At both dosages of tocainide, HV intervals measured at cycle lengths of 250 ms were significantly longer than HV intervals measured at cycle lengths of 475 ms ($P<0.001$).

The relationship between drive cycle length and $\Delta\theta$ values at all assessed cycle lengths is shown in Figure 1. The drug-induced increase in $\Delta\theta$ was tonic at long cycle lengths but became strongly rate-dependent at short cycle lengths. The longest cycle length that caused $\Delta\theta$ values to increase significantly was 400 ms (rate = 150 beats min^{-1}) and 475 ms (rate = 126.3 beats min^{-1}) after 30 mg kg^{-1} and after additional 20 mg kg^{-1}, respectively. Increasing the dosage of tocainide had little effect upon $\Delta\theta$ values at long cycle lengths but induced an extensive additional increase in $\Delta\theta$ at short cycle lengths.

Onset of conduction slowing

Although in some animals spontaneous AV-nodal rhythm interfered with sustained pacing at a cycle length of 500 ms

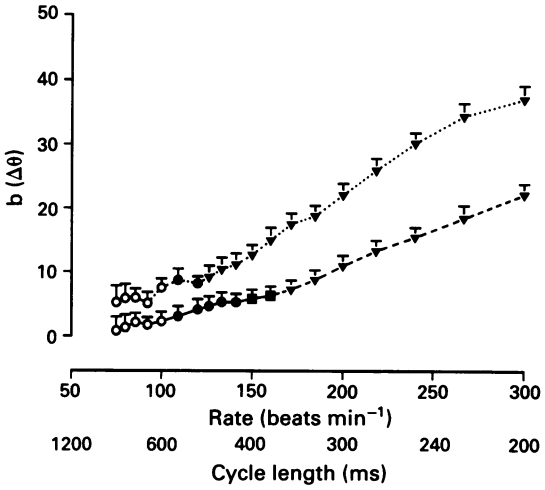

Figure 1 Relationship between sodium channel block (b), as reflected by conduction slowing ($\Delta\theta$), and cycle length (rate) during continuous stimulation. The points connected by dashed lines are measurements after 30 mg kg^{-1} tocainide; the points connected by dotted lines indicate measurements after addition of 20 mg kg^{-1} tocainide. Symbols indicate the level of significance when compared with baseline values: (▼): $P<0.001$; (■): $P<0.05$; (●): NS; (○): no comparison (because of interference of AV-nodal rhythm with stimulated rhythm at baseline).

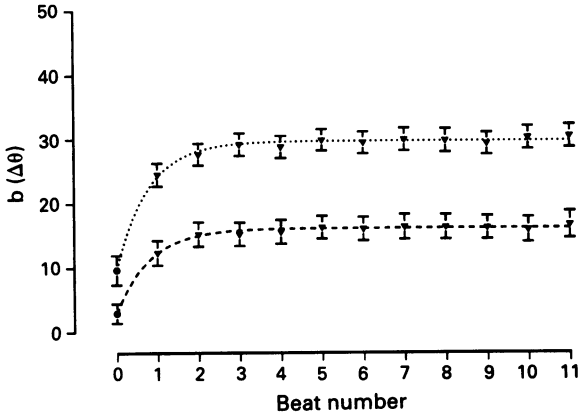

Figure 2 Onset of sodium channel block (b), as reflected by conduction slowing ($\Delta\theta$), during a rapid train paced at a cycle length of 250 ms. The beats of the rapid train are numbered consecutively (abscissa scale). The rapid train was preceded by 8 basic stimuli paced at a cycle length of 500 ms (not shown). The points fitted by dashed lines are measurements after 30 mg kg^{-1} tocainide, the points fitted by dotted lines indicate measurements after addition of 20 mg kg^{-1} tocainide. Symbols indicate the level of significance when compared with baseline values: (▼): $P<0.001$; (●): NS.

(protocol 1), such interference was not encountered during the short 8-beat basic drive train before abruptly decreasing the cycle length to 250 ms. Figure 2 shows the effect of a sudden change of cycle length from 500 ms to 250 ms on $\Delta\theta$ values after tocainide. Tocainide induced a small but non-significant increase in $\Delta\theta$ at a cycle length of 500 ms. As the cycle length was abruptly reduced to 250 ms, $\Delta\theta$ values increased to a new steady state within 2–3 beats. Although the amount of steady state block at a cycle length of 250 ms was dose-dependent, the time course of onset of block was similar for the two applied doses of tocainide. Thus, the calculated rate constants of drug induced onset of $\Delta\theta$ are in the same order of magnitude (Table 1).

Recovery from conduction slowing

An original registration demonstrating the recovery from tocainide-induced HV-prolongation is presented in Figure 3. Figure 4 shows the effect of administration of tocainide on the time course of recovery from drug-induced increase in $\Delta\theta$. Recovery of $\Delta\theta$ exhibited a monoexponential time course that allowed estimation of τ_{rec} and r_∞ (Table 1). τ_{rec} was found to be in the same order of magnitude (<300 ms) following both doses of tocainide. r_∞ was unaffected by 30 mg kg^{-1} tocainide but exhibited a slight increase following addition of 20 mg kg^{-1} tocainide.

Comparison with model predictions

In order to test whether the rate-dependent steady state increase in $\Delta\theta$ after tocainide can be predicted by a mathematical model of periodical two-state ligand binding to sodium channels (eq 4), the model parameters τ_{on} and a_∞ were calculated according to eqs 5, 6 and 7. APD within the His-Purkinje system cannot be measured *in vivo* and was therefore estimated by means of eq 8, which describes the relationship between APD and cycle length under drug free conditions *in vitro*. However, the administration of tocainide has been shown to shorten APD (Oshita *et al.*, 1980). In order to take such a potential shortening of APD into consideration, we calculated the APD-dependent model parameters τ_{on} and a_∞, as well as predicted steady state values of $\Delta\theta$ under the assumption of various degrees of shortening of APD (Table 2). The calculated values of steady state block were only negligibly changed by the assumption of drug-induced reductions in APD. This is the case because reductions in steady state $\Delta\theta$, as would be predicted if only APD was shortened in eq 4, are counteracted by concomitant increases in the calculated value of a_∞. Figure 5 shows the predicted curves, relating $\Delta\theta$ to steady state cycle length. Again, for each dosage, separate curves were calculated by assuming drug induced shortening of APD by 0%, −5%, −10%, −15%, −20%. Because these assumptions of APD shortening had little influence on shape and position of the calculated relationship between $\Delta\theta$ and steady cycle length, the respective curves in Figure 5 are superimposed, giving the impression of a single curve for each dosage of tocainide. Also shown in Figure 5 are the experimentally determined steady state values of $\Delta\theta$ at selected cycle lengths. Clearly, measured values of $\Delta\theta$ are in good agreement with the predicted relationship between $\Delta\theta$ and steady state cycle length. This is also indicated by the residual sum of squares (SS) of predicted values and experimental data, presented in Table 2.

Table 1 Binding kinetics of tocainide as determined from measurements of HV intervals

	λ^* (beat^{-1})	τ_{rec} (ms)	r_∞ (Δ%)
Tocainide 30 mg kg^{-1}	1.23 ± 0.09	250.29 ± 23.32	0.00 ± 0.63
+ Tocainide 20 mg kg^{-1}	1.28 ± 0.09	183.04 ± 8.03	5.79 ± 0.36

Values are mean ± s.e.mean.

Discussion

It has been recently shown that the slow binding kinetic properties of quinidine and procainamide can be characterized from measures of impulse propagation within the framework of a mathematical model suggesting periodical drug binding to Na^+-channels (Packer *et al.*, 1989; Villemaire *et al.*, 1992). The present study provides an *in vivo* analysis of rate-dependent conduction slowing induced by tocainide, which exhibits fast kinetic binding properties *in vitro* (Oshita *et al.*, 1980; Borchard *et al.*, 1985; Kodama *et al.*, 1987).

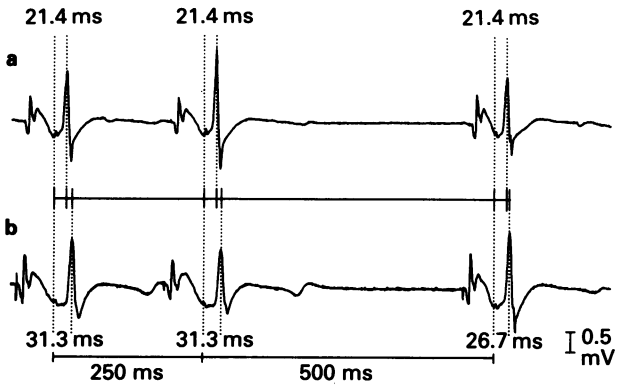

Figure 3 Original registration of epicardial His Bundle electrograms at baseline (a) and following cumulative administration of 30 mg kg^{-1} and 20 mg kg^{-1} tocainide (b). Shown are the two last beats of a basic train consisting of 8 beats, paced at a cycle length of 250 ms, and one extra beat after a longer coupling interval which is adjusted for differences in AH-intervals to yield a 500 ms interval between the His activations before and after the pause. Measurements of HV intervals are indicated by dotted lines. Clearly, introduction of a 500 ms pause has no effect upon HV intervals at baseline. Administration of tocainide prolongs HV intervals during the rapid train. After the pause, HV prolongation recovers partially.

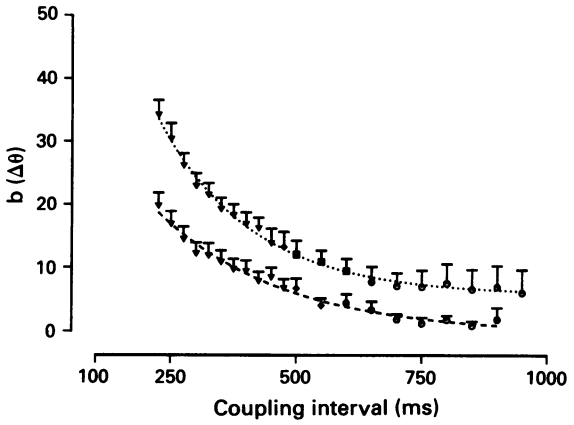

Figure 4 Time course of recovery from sodium channel block (b), as reflected by conduction slowing ($\Delta\theta$). A conditioning train of 8 depolarizations at a cycle length of 250 ms was followed by a test stimulus at variable coupling intervals. $\Delta\theta$ of the test depolarization is displayed for each coupling interval. The points fitted by dashed lines are measurements after 30 mg kg^{-1} tocainide, the points fitted by dotted lines indicate measurements after addition of 20 mg kg^{-1} tocainide. Symbols indicate the level of significance when compared with baseline values: (▼): $P<0.001$; (◆): $P<0.01$; (■): $P<0.05$; (●): NS; (○): no comparison (because of interference of AV-nodal rhythm with stimulated beats at baseline).

Table 2 Binding kinetics of tocainide as calculated from a mathematical model that assumes drug binding to sodium channels in terms of a periodical two-state process

	Tocainide (30 mg kg^{-1})					+ *Tocainide* (20 mg kg^{-1})				
APD (Δ%)	0	− 5	− 10	− 15	− 20	0	− 5	− 10	− 15	− 20
τ_{on} (ms)	185.25	182.75	180.05	177.12	173.94	201.59	202.67	203.88	205.26	206.82
a_{∞} (Δ%)	28.82	30.49	32.30	34.28	36.43	57.26	61.65	66.61	72.26	78.74
b_{200} (Δ%)	22.38	22.37	22.36	22.34	22.33	41.85	41.82	41.79	41.76	41.72
b_{250} (Δ%)	16.92	16.92	16.92	16.92	16.92	30.47	30.46	30.46	30.46	30.46
b_{475} (Δ%)	5.96	5.98	5.99	6.01	6.03	12.03	12.05	12.07	12.10	12.12
b_{800} (Δ%)	1.65	1.66	1.67	1.68	1.69	6.91	6.92	6.93	6.94	6.95
SS	38.3	38.78	39.34	39.97	40.69	55.59	56.05	56.6	57.23	57.97

Model parameters (τ_{on}, a_{∞}) and values of rate-dependent steady state block are calculated under assumptions of variable degrees of drug induced reductions of APD. b_{200}, b_{250}, b_{475}, b_{800} denote calculated block values at steady state cycle lengths of 200, 250, 475 and 800 ms respectively. SS = residual sum of squares between all measured steady state values of Δθ and predicted values.

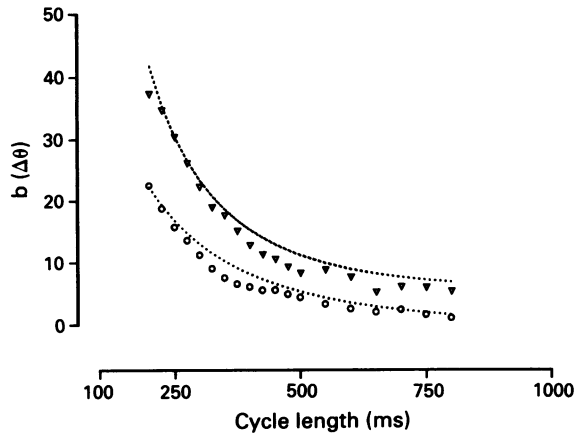

Figure 5 Comparison of experimentally determined steady state values of sodium channel block (b), as reflected by conduction slowing (Δθ), after 30 mg kg^{-1} tocainide (○) and additional 20 mg kg^{-1} (▽), with respective predictions as calculated from eq 4 (dotted lines). Analogously to the data presented in Table 3, steady state reductions in Δθ are predicted under the assumption of drug-induced reductions in APD by 0%, − 5%, − 10%, − 15% and − 20%. The respective predicted curves are superimposed. However, the deviations of the predicted curves from each other are negligible, thus giving the impression of a single curve for each dosage of tocainide. The residual sum of squares (SS) of predicted values and experimental data are presented in Table 2.

In our model, the chosen procedure of atrial pacing following ablation of the sinus node not only allows the assessment of HV-conduction at slow rates without interference with sinus rhythm, but also of HV intervals at activation rates pertinent to the frequency pattern of ventricular tachycardia in man. Because of the reported difficulties in achieving selective His bundle pacing *in vivo* (Williams *et al.*, 1976), we did not attempt to pace directly the bundle of His. Furthermore, in small animals like the guinea-pig, atrial frequencies higher than 200 beats min^{-1} are conducted in a 1:1 pattern to the ventricles thus eliminating the need to pace the bundle of His in order to assess HV conduction at high rates. By contrast, *in vitro* techniques, such as microelectrode impalements of the papillary muscle are limited with regard to the assessment of high frequencies by the increasing mechanical activity of the preparations (Weirich & Antoni, 1988). On the other hand, resting membrane potential, an important modulator of sodium channel block, can only be controlled *in vitro*. In the present study we avoided pacing at cycle lengths <200 ms in order to exclude phase 3 block. Nevertheless, any characterization of the dynamics of sodium channel block from data obtained *in vivo* is limited by the inability to exclude shifts in resting membrane potential, which contribute to drug binding.

Tocainide depresses HV-conduction in a strictly rate-dependent manner, pronounced depression of intraventricular conduction only occurring at short cycle lengths. Increasing the dosage caused an increase in rate-dependent block as well as a shift in significant conduction slowing to longer cycle lengths. As illustrated in Figure 1, a substantial increase in dosage of tocainide may produce little extra increase in block at long cycle lengths, but may be associated with a very profound additional depression of conduction velocity at short cycle lengths. Thus, as the dosage of tocainide is increased, the amount of additional conduction slowing that may be encountered during a period of tachycardia appears to be essentially unpredictable if only cycle lengths of >500 ms (rates of <120 beats min^{-1}) are considered.

The steady state relationship between Δθ and heart rate was approximately linear for both dosages (Figure 1). These dynamics of frequency-dependent steady state block are in excellent agreement with previously published calculations using *in vitro* kinetic data (Weirich & Antoni, 1990).

Steady state Δθ after tocainide was reached within two beats of a rapid train at a cycle length of 250 ms. In guinea-pig ventricular muscle, the rate-dependent reduction of V_{max} induced by tocainide has been reported to occur with an onset rate constant of 0.277 AP^{-1} (Campbell, 1983a), which is lower than the values of 1.23 (30 mg kg^{-1} tocainide) and 1.28 beat^{-1} (30 + 20 mg kg^{-1} tocainide) obtained in the present study. This difference may be accounted for by the longer APD within the His-Purkinje system than in ventricular muscle. Upon cessation of continuous stimulation, steady state block induced by tocainide recovered rapidly. The recovery time constants that were found in the present study reasonably agree with those reported *in vitro* (Oshita *et al.*, 1980; Borchard *et al.*, 1985; Kodama *et al.*, 1987) and, thus, confirm the classification of tocainide as a fast sodium channel blocker within the novel framework of the 'Sicilian gambit' ($\tau_{rec}<300$ ms; Task Force of the Working Group on Arrhythmias of the European Society of Cardiology, 1991). An additional slower recovery time constant of 2.1–3.8 s was found by Oshita *et al.* (1980) in guinea-pig isolated papillary muscle. Because of the limited range of coupling intervals that can be assessed *in vivo*, estimation of time constants >1 s would have required an extrapolation far beyond the measured data points and might have been associated with considerable variance. We, therefore, decided to apply a monoexponential fit to the recovery data. Furthermore, from visual inspection of the recovery curves, the contribution of a second (slower) time constant to the overall amount of conduction slowing was regarded as only minimal.

As a major finding of our study, the relationship between drug-induced slowing of conduction and cycle length closely follows the model of a two-state process of drug binding to

Na^+-channels proposed by Starmer (1986). Thus, depression of conduction occurring during continuous stimulation over a wide range of cycle lengths can be predicted, if a limited number of kinetic parameters is provided (λ^*, τ_{rec}, a_∞, r_∞). Increasing the dosage of tocainide induced a pronounced increase in rate-dependent block although the parameters λ^* and τ_{rec} remained in the same order of magnitude. Thus, within the framework of the described mathematical model, the dose-dependent increase in frequency-dependent block resulted predominantly from a substantial increase in a_∞ (and to a lesser extend in r_∞). In the clinical setting r_∞ could be approximated by the steady state decrease in conduction velocity at normal (low) heart rates. Using the mathematical approach described in the methods section (eqs 6 and 7), a_∞ can be estimated from reductions in conduction velocity measured during a short period of rapid stimulation. Thus, once the values of λ^* and τ_{rec} of an agent exhibiting class I action have been determined *in vivo*, steady state reductions of conduction velocity can be predicted for a large range of frequencies using a simple stimulation protocol (protocol 2).

We thank Professor Dr W. Schütz for critical correction of the manuscript and Miss G. Brugger for graphical work. We are grateful to Astra Hässle AB, Sweden, for the gift of tocainide. This study was supported by the Anton Dreher-Gedächtnisschenkung für Medizinische Forschung.

References

AOMINE, M. (1989). Electrophysiological effects of lidocaine on isolated guinea pig Purkinje fibers: comparison with its effects on papillary muscle. *Gen. Pharmacol.*, **20**, 99–104.

BORCHARD, U., HAFNER, D. & EWERBACK, S. (1985). Electrophysiological and antiarrhythmic actions of tocainide in isolated heart preparations of the guinea pig. *Drug Res.*, **35**, 1367–1374.

CAMPBELL, T.J. (1983a). Importance of physico-chemical properties in determining the kinetics of the effects of class I antiarrhythmic drugs on maximum rate of depolarization in guinea-pig ventricle. *Br. J. Pharmacol.*, **80**, 33–40.

CAMPBELL, T.J. (1983b). Kinetics of rate-dependent effects of class I antiarrhythmic drugs are important in determining their effects on refractoriness in guinea pig ventricle, and provide a theoretical basis for their subclassification. *Cardiovasc. Res.*, **17**, 344–352.

CAMPBELL, T.J. (1992). Subclassification of class-I antiarrhythmic drugs – enhanced relevance after CAST. *Cardiovasc. Drugs Ther.*, **6**, 519–528.

HEISTRACHER, P. (1971). Mechanisms of action of antifibrillatory drugs. *Naunyn Schmied. Arch. Pharmacol.*, **269**, 199–211.

HONDEGHEM, L.M. & KATZUNG, B.G. (1977). Time- and voltage-dependent interactions of antiarrhythmic drugs with cardiac sodium channels. *Biochim. Biophys. Acta*, **472**, 373–398.

KODAMA, I., TOYAMA, J., TAKANAKA, C. & YAMADA, K. (1987). Block of activated and inactivated sodium channels by class-I antiarrhythmic drugs studied by using the maximum upstroke velocity (V_{max}) of action potential in guinea-pig cardiac muscles. *J. Mol. Cell. Cardiol.*, **19**, 367–377.

MACFARLANE, P.W. & VEITCH LAWRIE, T.D. (1989). The normal electrocardiogram and vectorcardiogram. In *Comprehensive Electrocardiography. Theory and Practice in Health and Disease.* ed. Macfarlane, P.W. & Veitch Lawrie, T.D. pp. 407–457. New York: Pergamon Press.

NESTERENKO, V.V., LASTRA, A.A., ROSENSHTRAUKH, L.V. & STARMER, C.F. (1992). A proarrhythmic response to sodium channel blockade – modulation of the vulnerable period in guinea pig ventricular myocardium. *J. Cardiovasc. Pharmacol.*, **19**, 810–820.

OSHITA, S., SADA, S., KOJIMA, M. & BAN, T. (1980). Effects of tocainide and lidocaine on the transmembrane action potentials as related to external potassium and calcium concentrations in guinea-pig papillary muscles. *Naunyn Schmied. Arch. Pharmacol.*, **314**, 67–82.

PACKER, D.L., GRANT, A.O., STRAUSS, H.C. & STARMER, C.F. (1989). Characterization of concentration- and use-dependent effects of quinidine from conduction delay and declining conduction velocity in canine Purkinje fibers. *J. Clin. Invest.*, **83**, 2109–2119.

SPINELLI, W. & HOFFMAN, B.F. (1989). Mechanisms of termination of reentrant atrial arrhythmias by class I and class II antiarrhythmic agents. *Circ. Res.*, **65**, 1565–1579.

STARMER, C.F. (1986). Theoretical characterization of ion channel blockade: ligand binding to periodically accessible receptors. *J. Theor. Biol.*, **119**, 235–249.

STARMER, C.F. & GRANT, A.O. (1984). Phasic ion channel blockade. A kinetic model and parameter estimation procedure. *Mol. Pharmacol.*, **46**, 15–27.

STARMER, C.F., GRANT, A.O., & STRAUSS, H.C. (1984). Mechanisms of use-dependent block of sodium channels in excitable membranes by local anesthetics. *Biophys. J.*, **46**, 15–27.

STARMER, C.F., LASTRA, A.A., NESTERENKO, V.V. & GRANT, A.O. (1991). Proarrhythmic response to sodium channel blockade. Theoretical model and numerical experiments. *Circulation*, **84**, 1364–1377.

SURAWICZ, B. (1992). Role of potassium channels in cycle length dependent regulation of action potential duration in mammalian cardiac Purkinje and ventricular muscle fibers. *Cardiovasc. Res.*, **26**, 1021–1029.

TASK FORCE OF THE WORKING GROUP ON ARRHYTHMIAS OF THE EUROPEAN SOCIETY OF CARDIOLOGY (1991). The Sicilian Gambit. *Circulation*, **84**, 1831–1851.

TODT, H., FISCHER, G., GROHS, J. & RABERGER, G. (1992a). Use dependent effects of tocainide on His-to-ventricular conduction in the guinea pig myocardium in vivo. *J. Mol. Cell. Cardiol.*, **24** (Suppl I), S263.

TODT, H., KRUMPL, G., KREJCY, K. & RABERGER, G. (1992b). Mode of QT correction for heart rate: implications for the detection of inhomogeneous repolarization after myocardial infarction. *Am. Heart J.*, **124**, 602–609.

TODT, H. & RABERGER, G. (1992). Epicardial His bundle recordings in the guinea pig in vivo. *J. Pharmacol. Methods*, **27**, 191–195.

TURGEON, J., WISIALOWSKI, T.A., WONG, W., ALTEMEIER, W.A., WIKSWO, J.P. & RODEN, D.M. (1992). Suppression of longitudinal versus transverse conduction by sodium channel block. Effects of sodium bolus. *Circulation*, **85**, 2221–2226.

VILLEMAIRE, C., SAVARD, P., TALAJIC, M. & NATTEL, S. (1992). A quantitative analysis of use-dependent ventricular conduction slowing by procainamide in anesthetized dogs. *Circulation*, **85**, 2255–2266.

WALD, R.W., WAXMAN, M.B. & DOWNAR, E. (1980). The effect of antiarrhythmic drugs on depressed conduction and unidirectional block in sheep Purkinje fibers. *Circ. Res.*, **46**, 612–619.

WALLENSTEIN, S., ZUCKER, C.L. & FLEISS, J.L. (1980). Some statistical methods useful in circulation research. *Circ. Res.*, **47**, 1–9.

WEIRICH, J. & ANTONI, H. (1988). Evaluation and interpretation of voltage- and frequency-dependent electrophysiologic effects of a new class I antiarrhythmic agent (nicainoprol) on guinea pig papillary muscle and isolated heart. *J. Cardiovasc. Pharmacol.*, **12**, 664–671.

WEIRICH, J. & ANTONI, H. (1990). Differential analysis of the frequency-dependent effects of class 1 antiarrhythmic drugs according to periodical ligand binding: implications for antiarrhythmic and proarrhythmic efficacy. *J. Cardiovasc. Pharmacol.*, **15**, 998–1009.

WILLIAMS, D.O., SCHERLAG, B.J., HOPE, D.R., EL-SHERIF, N., LAZZARA, R. & SAMET, P. (1976). Selective versus non-selective His bundle pacing. *Cardiovasc. Res.*, **10**, 91–100.

(Received February 11, 1993
Revised April 26, 1993
Accepted April 27, 1993)

Br. J. Pharmacol. (1993), **110**, 151–158

Involvement of nitric oxide in the endothelium-dependent relaxation induced by hydrogen peroxide in the rabbit aorta

[1]Artur Zembowicz, [2]Richard J. Hatchett, Andrzej M. Jakubowski & Richard J. Gryglewski

Department of Pharmacology, Copernicus Academy of Medicine, ul. Grzegórzecka 16, 31-531 Kraków, Poland

1 The effects of hydrogen peroxide (H_2O_2, 0.1–1 mM) on the tone of the rings of rabbit aorta precontracted with phenylephrine (0.2–0.3 μM) were studied.

2 H_2O_2 induced a concentration-dependent relaxation of both the intact and endothelium-denuded rings. However, in the presence of intact endothelium, H_2O_2-induced responses were 2–3 fold larger than in its absence, demonstrating the existence of endothelium-independent and endothelium-dependent components of the vasorelaxant action of H_2O_2.

3 The endothelium-dependent component of H_2O_2-induced relaxation was prevented by N^G-nitro-L-arginine methyl ester (L-NAME, 30 μM) or N^G-monomethyl-L-arginine (300 μM), inhibitors of nitric oxide synthase (NOS), in a manner that was reversible by L-, but not by D-arginine (2 mM). The inhibitors of NOS did not affect the responses of denuded rings.

4 Methylene blue (10 μM), an inhibitor of soluble guanylate cyclase, blocked H_2O_2-induced relaxation of both the intact and denuded rings.

5 H_2O_2 (1 mM) enhanced the efflux of cyclic GMP from both the endothelium-intact and denuded rings. The effect of H_2O_2 was 4 fold greater in the presence of intact endothelium and this endothelium-dependent component was abolished after the inhibition of NOS by L-NAME (30 μM).

6 In contrast to the effects of H_2O_2, the vasorelaxant action of stable organic peroxides, *tert*-butyl hydroperoxide or cumene hydroperoxide, did not have an endothelium-dependent component. Moreover, they did not potentiate the efflux of cyclic GMP from the rings of rabbit aorta.

7 Exogenous donors of NO, specifically, 3-morpholinosydnonimine (SIN-1), glyceryl trinitrate or sodium nitroprusside were used to decrease the tone of denuded rings to the level induced by endogenous NO released from intact endothelium. This procedure did not influence the vasorelaxant activity of H_2O_2, showing that H_2O_2 does not potentiate the vasorelaxant action of NO within the smooth muscle.

8 Thus, H_2O_2-induced relaxation in the rabbit aorta has both endothelium-dependent and independent components. The endothelium-dependent component of the relaxant action of H_2O_2 is due to enhanced endothelial synthesis of NO.

Keywords: Nitric oxide; hydrogen peroxide; endothelium; L-arginine; nitric oxide synthase; nitric oxide synthase inhibitors; methylene blue; polymorphonuclear leukocytes

Introduction

Endothelium-derived relaxing factor (EDRF), a mediator of endothelium-dependent relaxation in the rabbit aorta (Furchgott & Zawadzki, 1980), has recently been identified as nitric oxide (NO) (Palmer *et al.*, 1987). NO also plays a significant role in the cytotoxicity of activated macrophages (reviewed by Nathan & Hibbs, 1991) and is a neuromediator in both the central and peripheral nervous system (reviewed by Snyder & Bredt, 1991). The formation of NO from L-arginine (Palmer *et al.*, 1988a) is catalyzed by a family of FAD and FMN containing haemoproteins (White & Marletta, 1992; Stuehr & Ikeda-Saito, 1992) referred to as NO synthases. These enzymes are dioxygenases (Kwon *et al.*, 1990; Leone *et al.*, 1991), the activity of which depends on NADPH and tetrahydrobiopterin (reviewed by Nathan, 1992). Isoforms of NO synthase present in vascular endothelial (Förstermann *et al.*, 1991) and neuronal cells (Bredt & Snyder, 1990) are expressed constitutively and their activity is calcium- and calmodulin-dependent. In contrast, the macrophage isoform is expressed in cells only following their activation by cytokines and bacterial products and generates NO independently of calcium or calmodulin (Marletta *et al.*, 1988). The activity of NO synthases can be inhibited by N^G-substituted analogues of L-arginine (L-Arg), such as N^G-nitro-L-arginine methyl ester (L-NAME) or N^G-monomethyl-L-arginine (L-NMMA) (Palmer *et al.*, 1988b; Mülsch & Busse, 1990).

The inhibitors of NO synthase cause a pronounced and long lasting elevation of blood pressure and increase the resistance of various vascular beds, indicating that the continuous generation of NO plays a crucial role in the regulation of vascular tone (Rees *et al.*, 1989; Gardiner *et al.*, 1990a,b). Moreover, the release of NO from the endothelium plays an important role in the interactions between the vessel wall and circulating blood cells. Activated platelets release substances such as ADP or 5-hydroxytryptamine which enhance the release of NO from the endothelium (Houston *et al.*, 1985). The released NO relaxes vascular smooth muscle and serves as a negative feedback mechanism, exerting an inhibitory action on the activated platelets resulting in reduced platelet adhesion and aggregation (Radomski *et al.*, 1987a,b).

Several lines of evidence suggest that NO is also an endogenous modulator of certain functions of polymorphonuclear leukocytes (PMNs), including the generation of O_2^-, enzyme release (Schröder *et al.*, 1990) and adhesion to the endothelial cells (Kubes *et al.*, 1991). Conversely, activated PMNs affect the activity of endothelium-derived

[1] Author for correspondence at present address: Division of Hematology, University of Texas Medical School, 6431 Fannin, Houston, Texas 77030, U.S.A.

[2]On leave from Vanderbilt University School of Medicine, Nashville, Tennessee 37232, U.S.A.

NO. Stimulation of PMNs leads to a rapid increase in the consumption of oxygen and the concomitant release of large amounts of oxygen-derived reactive species including O_2^- and H_2O_2 (Babior *et al.*, 1973). O_2^- shortens the half-life of endothelium-derived NO (Gryglewski *et al.*, 1986). Consistent with these observations are reports showing that activated PMNs induce an endothelium-dependent contraction that can be inhibited by superoxide dismutase (Ohlstein & Nichols, 1989). Less is known about the regulation of vascular tone by H_2O_2. Early studies investigating the effects of H_2O_2 on the vascular endothelium established that H_2O_2 is responsible for PMN-induced damage of endothelial cells (Weiss *et al.*, 1981). However, at lower than lethal concentrations, H_2O_2 stimulates the biosynthesis of prostaglandins, including vasodilator prostacyclin, by cultured endothelial cells (Harlan & Callahan, 1984; Ager & Gordon, 1984). Finally, H_2O_2 induces the relaxation of bovine pulmonary artery via the stimulation of soluble guanylate cyclase, through a process dependent on the metabolism of H_2O_2 by catalase (Wolin & Burke, 1987).

We investigated the effects of H_2O_2 on the tone of endothelium-intact and denuded rings of rabbit aorta. We have shown that H_2O_2, at concentrations that do not impair the functional integrity of endothelial cells, induces relaxation in both types of rings; that H_2O_2-induced relaxation has both endothelium-dependent and independent components and that the endothelium-dependent component of the relaxant action of H_2O_2 is due to the enhanced endothelial synthesis of NO.

Methods

Organ bath experiments

New Zealand rabbit of either sex (2–2.5 kg) were killed with an overdose of pentobarbitone (Verbutal, Biowet, Poland, 50 mg kg^{-1}, i.v.) and their thoracic aortae were isolated and cut into rings of 3 mm width, which were then suspended between stainless steel hooks and mounted in 5 ml organ baths filled with warmed (37°C) and oxygenated (95% O_2, 5% CO_2) Krebs solution containing 5.6 μM indomethacin. The Krebs solution had the following composition (mM): NaCl 118, KCl 4.7, KH_2PO_4 1.2, $MgSO_4$ 1.17, $CaCl_2$ 2.5, $NaHCO_3$ 25, and glucose 5.6. Denuded rings were prepared by gently rotating the rings on a stainless steel wire prior to mounting. Isometric force was measured with Biegestab K30 type 351 transducers (Hugo Sachs Elektronic, Germany). A tension of 4 g was applied and the rings were equilibrated (60–90 min) by changing the Krebs solution and adjusting the preload to 4 g every 15 min. After a stable baseline was obtained (1.5 h), the rings were contracted with KCl (60 mM) followed by 30 min equilibration in fresh Krebs buffer. The rings were then contracted with phenylephrine at concentrations of 0.2–0.3 μM, which typically produced 80% of KCl-induced contraction, and acetylcholine (ACh, 0.3 μM) was added to the baths to test the functional integrity of the endothelium. Only tissues which relaxed by more than 50% of the phenylephrine-induced tone after addition of ACh were considered to have undamaged endothelium. ACh (0.3 μM) either did not change the tone of endothelium-denuded rings or slight contractions were observed. After replacing the contents of the baths with fresh buffer 5 times every 10 min, the rings were contracted with phenylephrine (0.2–0.3 μM) and the responses of tissues induced by H_2O_2 (0.1–1 mM) were recorded. L-NAME (30 μM), L-NMMA (300 μM) or MeB (10 μM) were added to the baths 20 min before addition of H_2O_2 or after maximal H_2O_2-induced relaxation was obtained. Relaxations were expressed as a percentage of the tone induced by phenylephrine. Contractions were expressed as a percentage of the tone induced by KCl (60 mM).

Determination of the efflux of cyclic GMP from the rings of rabbit aorta

Rings of rabbit aorta were obtained as described above. Before the experiments some of the rings were gently rotated on a stainless steel rod to remove their endothelium. The rings were transferred to 1.5 ml Eppendorf tubes containing 0.5 ml of oxygenated Krebs buffer and 0.1 mM isobutylmethylxanthine (IBMX), an inhibitor of phosphodiesterases. After 30 min of incubation at 37°C the rings were transferred to another set of Eppendorf tubes containing H_2O_2, cumene hydroperoxide (CumHP), *tert*-butyl hydroxperoxide (*t*-ButHP) (all at 1 mM) or ACh (0.3 μM) diluted in 0.5 ml of oxygenated Krebs buffer containing 0.1 mM IBMX. The incubation was continued for another 20 min. In some experiments, both the initial and final incubations were carried out in the presence of L-NAME at a concentration of 30 μM. Following incubation, the rings were removed from the tubes, quickly dried on blotting paper, and weighed. The weights of the rings were typically between 12 and 20 mg. The tubes containing the incubation buffer were stored in a deep freezer (− 70°C) until the concentrations of guanosine 3′:5′-cyclic monophosphate (cyclic GMP) in the buffer were assayed with a specific radioimmunoassay (Amersham, U.K.). The amount of cyclic GMP released from the rings during 20 min of incubation was expressed as fmol mg^{-1} of tissue weight. The net change of the extravascular release of cyclic GMP by peroxides or ACh was calculated by subtracting the concentrations of cyclic GMP in the presence of tested compounds from the concentration obtained in their absence.

Materials

Indomethacin, acetylcholine HCl (ACh), L-phenylephrine HCl, N^G-nitro-L-arginine methyl ester (L-NAME), N^G-monomethyl-L-arginine (L-NMMA), methylene blue (MeB), sodium nitroprusside, catalase (thymol free from bovine liver), superoxide dismutase, isobutylmethylxanthine (IBMX), cumene hydroperoxide (CumHP) and *tert*-butyl hydroperoxide (*t*-ButHP) were purchased from Sigma, H_2O_2 (3% solution) was obtained from a local pharmacy. Glyceryl trinitrate was from Lipha Pharmaceuticals Ltd. (West Drayton, U.K.). SIN-1 (3-morpholinosydnonimine) was a gift from GEA Ltd. (Copenhagen, Denmark). Lipid peroxidation inhibitor U-83836E ((−)-2-[[4-(2,6-Di-1-pyrrolidinyl-4-pirymidinyl)-1-piperazinyl]methyl]-3,4-dichloro-2,5,7,8-tetramethyl-2H-1-benzopyran-6-ol, dihydrochloride) was a generous gift from The Upjohn Company (Kalmazoo, MI, U.S.A.).

Statistical analysis

Results are expressed as mean ± s.e.mean of *n* observations. In organ bath experiments, *n* is the number of separate rabbits from which arterial rings used in a particular procotol were obtained. The measurements of the efflux of cyclic GMP were performed in duplicate; consequently, *n* is the number of rings obtained from *n*/2 different rabbits. Statistical differences between means were assessed by two-way unpaired Student's *t* test or, in the case of multiple means, one-way analysis of variance followed by the *post hoc* Bonferroni test or LSD test. In appropriate situations an unpaired two-way one sample *t* test was used. In all cases, a *P* value of 0.05 was considered statistically significant.

Results

Endothelium-dependent and endothelium-independent components of H_2O_2-induced relaxation

Addition of H_2O_2 (0.1–1 mM) to baths containing intact rings of rabbit aorta precontracted with phenylephrine (0.2–0.3 μM)

caused a biphasic response consisting of a small, brief contraction followed by a pronounced, sustained relaxation. In rings denuded of endothelium only the relaxant response was observed. As shown in Figure 1, the relaxant effects of H_2O_2 (0.1–1 mM) were concentration-dependent. The removal of endothelium resulted in a 2–3 fold decrease of H_2O_2-induced relaxation suggesting the existence of endothelium-dependent and endothelium-independent components of H_2O_2-induced relaxation.

The effect of inhibitors of nitric oxide synthase and methylene blue on H_2O_2-induced relaxation

Relaxations induced by H_2O_2 (0.75 mM) in intact rings were partially reversed when L-NAME (30 μM) or L-NMMA (300 μM) were added to the baths after H_2O_2-induced relaxation attained its maximum. These inhibitors of NO synthase did not reverse H_2O_2-induced relaxation in endothelium-denuded rings. In contrast, MeB (10 μM) reversed the relaxations induced by H_2O_2 in both intact and denuded tissues (Figure 2).

In a separate series of experiments, L-NAME (30 μM) or L-NMMA (300 μM) given alone or in combination with L-Arg or D-Arg (both at 2 mM), or MeB (10 μM) was added 20 min before the addition of H_2O_2 (0.75 mM). Both inhibitors of NO synthase abolished the endothelium-dependent component of

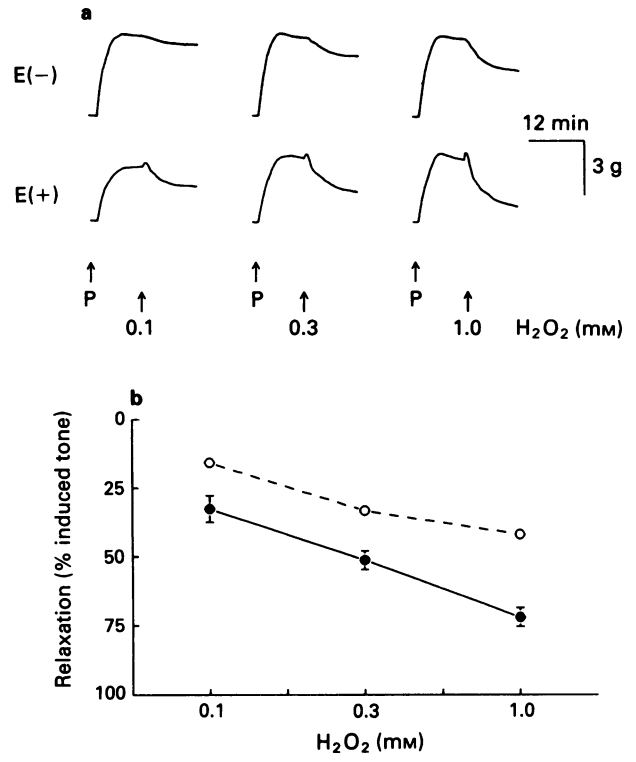

Figure 1 H_2O_2-induced relaxation of intact and endothelium-denuded rings of rabbit aorta. For experimental details refer to Methods: (a) shows original traces of six rings of rabbit aorta obtained from a single animal. The rings were precontracted with phenylephrine (P, 0.3 μM). Increasing concentrations of H_2O_2 (0.1–1 mM) elicited a concentration-dependent relaxation both in rings denuded of endothelium (upper 3 traces, E (−)) as well as in those with intact endothelium (lower 3 traces, E (+)). The relaxant responses of the endothelium-intact rings were 2–3 fold larger than those of denuded ones. Addition of H_2O_2 to the baths containing intact rings elicited a biphasic response in which a small, brief contraction was followed by a long, pronounced relaxation. The trace is representative of $n = 7$ identical experiments which are summarized in (b). The responses of rings containing endothelium are depicted as (●———●), those of denuded rings are shown (O - - - O). Points represent means ± s.e.mean of $n = 7$ different rings.

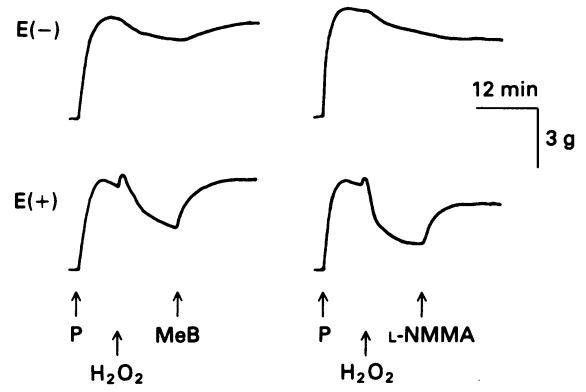

Figure 2 Reversal by inhibitors of NO synthase and methylene blue of the endothelium-dependent component of H_2O_2-induced relaxation. For experimental details refer to Methods. Original traces of four rings of rabbit aorta obtained from a single animal are shown. The rings were precontracted with phenylephrine (P, 0.3 μM). H_2O_2 (0.75 mM) induced the relaxation of the rings denuded of endothelium (E (−)). Addition of H_2O_2 (0.75 mM) to the baths containing intact rings (E (+)) elicited a biphasic response. A small, brief contraction was followed by a pronounced relaxation. Methylene blue (MeB, 10 μM) reversed the relaxation of both intact and denuded ring ($n = 6$). N^G-monomethyl-L-arginine (L-NMMA, 300 μM) had no effect on the H_2O_2-induced relaxation of the denuded ring ($n = 7$). However, it partially reversed H_2O_2-induced relaxation of endothelium-intact rings ($n = 7$). N^G-nitro-L-arginine methyl ester (L-NAME, 30 μM) exerted effects similar to those of L-NMMA (300 μM). L-NAME reversed the relaxations induced by H_2O_2 in intact rings and did not affect the relaxations of rings containing no endothelium ($n = 5$, not shown). Traces are typical of n different experiments.

the relaxant action of H_2O_2 and their inhibitory action was reversed in the presence of 2 mM L-Arg, but not D-Arg. H_2O_2-induced relaxations of intact rings in the presence of MeB (10 μM) were reduced as compared to those of rings denuded of endothelium, indicating that MeB inhibited both the endothelium-dependent and endothelium-independent components of the relaxant action of H_2O_2 (Figure 3). H_2O_2 did not affect the tone of intact or denuded rings in the presence of catalase (100 u ml^{-1}, $n = 3$, data not shown). In contrast, superoxide dismutase (50 u ml^{-1}, $n = 6$) did not change the relaxant activity of H_2O_2 (0.3–1 mM) in either intact or denuded rings. Interestingly, in the presence of L-NAME (30 μM, $n = 11$), L-NMMA (300 μM, $n = 11$) or MeB (10 μM, $n = 7$) the initial contraction induced by H_2O_2 was also abolished (data not shown).

The effect of H_2O_2 on the functional integrity of endothelium

In order to establish whether concentrations of H_2O_2 used in this study affect the functional integrity of endothelium of the rabbit aorta, we investigated the effects of pretreatment of the rings of rabbit aorta with H_2O_2 (1 mM) on the endothelium-dependent relaxation induced by ACh. In these experiments, the H_2O_2-induced relaxation of intact rings precontracted with phenylephrine (0.2–0.3 μM) was recorded. In control rings the addition of H_2O_2 was omitted. Afterwards, the rings were washed for 1 h with fresh Krebs buffer and, after again contracting the rings with phenylephrine (0.2–0.3 μM), concentration-response curves to ACh (0.01–3 μM) were obtained. As shown on Figure 4, pretreatment of the rings with H_2O_2 did not affect subsequent ACh-induced relaxation.

Because we suspected that H_2O_2-induced peroxidation of lipids might contribute to the effects we had observed we investigated the effect of the active (−)-racemate (U-83836E) of a potent 2-methylaminochroman lipid peroxidation inhibitor U-78517F (Hall *et al.*, 1991) on the vasorelaxant

activity of H_2O_2. U-83836E (1–50 μM) did not affect the tone of either intact or endothelium-denuded rings of rabbit aorta ($n = 4$, data not shown). The preincubation of rings for 20 min with U-83836E at concentrations (30–50 μM) which effectively inhibit iron-catalysed lipid peroxidation (Hall et al., 1991), did not affect the relaxant responses elicited by H_2O_2 (1 mM) in either intact and denuded rings ($n = 4$, data not shown).

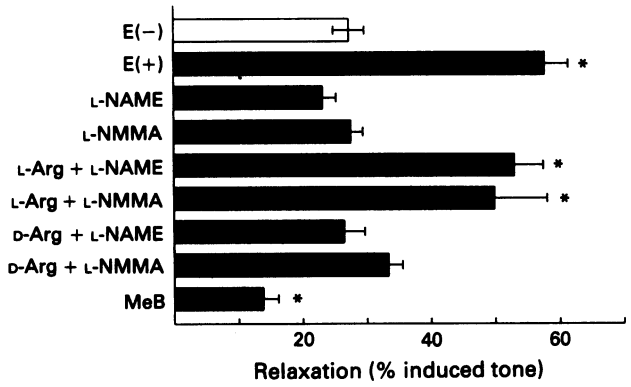

Figure 3 Prevention of inhibitors of NO synthase and methylene blue of endothelium-dependent component of H_2O_2-induced relaxation. For experimental details see Methods. The responses of phenylephrine (0.3 μM)-precontracted rings of rabbit aorta induced by H_2O_2 (0.75 mM) are shown. The H_2O_2-induced relaxations of rings containing undamaged endothelium (E (+), solid bars) were significantly greater than those of rings denuded of endothelium (E (−), open bar) ($n = 15$). Preincubation of the intact rings (20 min) with the inhibitors of NO synthase, N^G-monomethyl-L-arginine (L-NMMA, 300 μM, $n = 11$) or N^G-nitro-L-arginine methyl ester (L-NAME, 30 μM, $n = 11$), blocked the endothelium-dependent component of the relaxant action of H_2O_2. The inhibitory action of both L-NAME and L-NMMA was reversed in the presence of L-arginine (L-Arg, 2 mM, $n = 5$). D-Arginine (D-Arg, 2 mM) did not affect the inhibitory action of L-NAME or L-NMMA ($n = 6$). Preincubation of intact rings with methylene blue (MeB, 10 μM) inhibited the H_2O_2-induced relaxation to the level below that observed in the tissues denuded of endothelium ($n = 7$) indicating that MeB blocks both the endothelium-dependent and the endothelium-independent components of the relaxation induced by H_2O_2. Bars represent means ± s.e.mean of n different experiments. *Bonferroni $P < 0.01$ as compared to E(−).

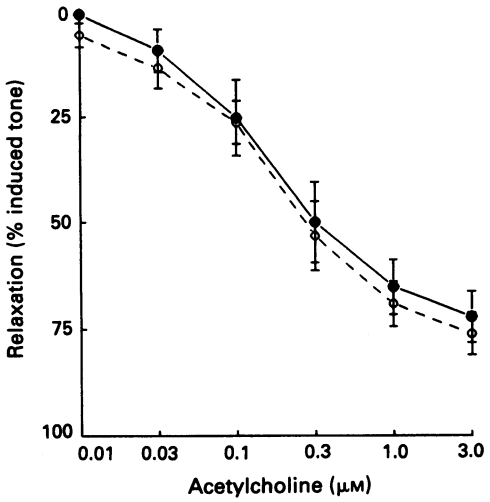

Figure 4 The lack of toxic effect of H_2O_2 on the endothelium on the rabbit aorta. For experimental details see Methods. Rings of rabbit aorta were precontracted with phenylephrine (0.2 μM) and H_2O_2 (1 mM) was added to some of the baths. After recording the relaxations induced by H_2O_2, the rings were washed with fresh Krebs buffer for 1.5 h. Then, following contraction of tissues with phenylephrine (0.2 μM), the relaxant responses induced by increasing concentrations of acetylcholine (ACh, 0.01–3 μM) were recorded. The ACh-induced relaxations of the rings treated with H_2O_2 (1 mM, O - - - O) were not different from those of the control rings (●——●). Values represent means ± s.e.mean of $n = 5$ experiments.

The effect of H_2O_2 on the efflux of cyclic GMP from the rings of rabbit aorta

Incubation of rings of rabbit aorta in Krebs buffer containing IBMX (0.1 mM), an inhibitor of phosphodiesterases, resulted in the accumulation of cyclic GMP in the incubation buffer. As depicted in Figure 5, the concentrations of cyclic GMP attained after 20 min incubation were 5 fold higher if intact endothelium was present. H_2O_2 (1 mM) augmented the efflux of cyclic GMP from denuded rings and, to a significantly greater extent, from rings with intact endothelium. Moreover, the endothelium-dependent component of cyclic GMP efflux was abolished in the presence of L-NAME (30 μM) (Figure 5). As seen in Table 1, the presence of intact endothelium resulted in 4 fold larger net stimulation of cyclic GMP release induced by H_2O_2. Importantly, ACh (0.3 μM) did not affect the efflux of cyclic GMP from denuded rings, demonstrating the complete removal of endothelium. ACh (0.3 μM) did, however, potentiate the efflux of cyclic GMP from rings with intact endothelium (Table 1).

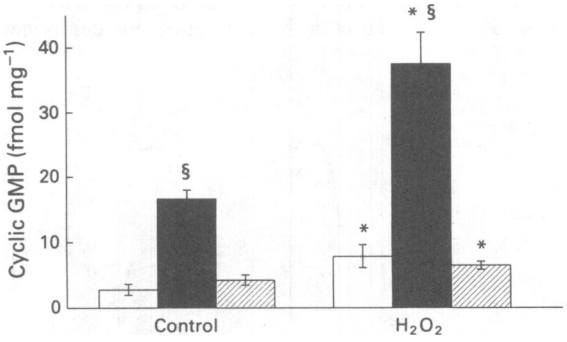

Figure 5 Enhancement by H_2O_2 of the efflux of cyclic GMP from rings of rabbit aorta. The results of experiments are shown (described in detail in Methods), in which the concentration of cyclic GMP released from the rings of rabbit aorta into the incubation medium was measured by RIA. Columns represent the concentrations of cyclic GMP, expressed as means ± s.e.means of $n = 12–18$ experiments, for intact (solid columns) and endothelium-denuded rings (open columns). Hatched columns represent results of experiments performed in the presence of N^G-nitro-L-arginine methyl ester (L-NAME, 30 μM). Incubation of the rings in the presence of the phosphodiesterase inhibitor isobutylmethylxanthine (0.1 mM) for 20 min resulted in detectable levels of extravascular cyclic GMP which were significantly enhanced if intact endothelium was present. H_2O_2 (1 mM) resulted in enhanced efflux of cyclic GMP from denuded rings and, to a significantly greater extent, from endothelium-intact rings. The endothelium-dependent component of the efflux of cyclic GMP was abolished in the presence of L-NAME (30 μM). *$P < 0.05$ when compared to the appropriate control; §$P < 0.05$ as compared to rings without endothelium.

Table 1 Net stimulation of cyclic GMP efflux from the rings of rabbit aorta by H_2O_2 and acetylcholine (ACh)

Presence of endothelium	*H_2O_2* (1 mM)	*ACh* (0.3 μM)
Denuded [E (−), $n = 12$]	5.1 ± 1.2*	0.6 ± 0.4
Intact [E (+), $n = 18$]	21.7 ± 4.2*§	6.7 ± 1.5*§

For experimental details refer to Methods. Values represent net increases in the concentration of extravascular cyclic GMP (fmol mg^{-1}), as compared with the appropriate controls, and are expressed as means ± s.e.means of n rings. H_2O_2 (1 mM) caused a significant increase in the release of cyclic GMP from both the intact and endothelium-denuded rings, while ACh (0.3 μM) increased cyclic GMP efflux only in the presence of endothelium. *$P < 0.002$ as different from 0 by two-tailed one sample t test, §$P < 0.01$ as compared to E (−) by two-way unpaired t test.

Comparison of the relaxant action of H_2O_2 with the effects of organic peroxides

Stable organic peroxides, *t*-ButHP (0.1–1 mM) and CumHP (0.1–1 mM), caused relaxations of denuded rings similar to those induced by H_2O_2 ($n = 5$). When endothelium was present, the addition of *t*-ButHP or CumHP to the baths induced a biphasic response, consisting of a pronounced contraction followed by relaxation. However, in contrast to the effects of H_2O_2, the relaxant effects of *t*-ButHP or CumHP were not enhanced in the presence of endothelium ($n = 5$, Figure 6).

Comparison of the effects of H_2O_2 and those of organic peroxides on the efflux of cyclic GMP from the rabbit aorta

As depicted in Figure 7, CumHP (1 mM) did not affect the release of cyclic GMP from the denuded rings and significantly reduced its release from the rings containing intact endothelium. *t*-ButHP (1 mM) slightly enhanced the release of cyclic GMP from denuded rings. Its effect was ca. 50% of that of H_2O_2. In the presence of endothelium, *t*-ButHP (1 mM) also decreased the efflux of cyclic GMP. These results suggest that the initial contraction of the endothelium-intact rings of rabbit aorta induced by organic peroxides was due to the inhibition of endothelial NO production, most likely through damage caused to the endothelium. Consistent with this notion are observations that ACh-induced relaxations of intact rings treated with CumHP (1 mM) were completely abolished, and those of rings treated with *t*-ButHP (1 mM) were significantly attenuated ($n = 3$, data not shown).

The effect of exogenous donors of NO on H_2O_2-induced relaxation in the rabbit aorta

Smooth muscle of rings containing intact endothelium is under the continuous influence of basally released NO, which attenuates the contraction induced by phenylephrine. Thus, we tested the hypothesis that the endothelium-dependent component of H_2O_2-induced relaxation is due to the potentiation by H_2O_2 of the vasorelaxant action of basally released NO within the smooth muscle. To accomplish this, we investigated the vasorelaxant activity of H_2O_2 (1 mM) in endothelium-denuded rings after the titration of their tone to levels approximating that of rings obtained from the same animals and possessing an intact endothelium. Titrations were performed by the sequential addition of the NO donors SIN-1 (30–60 nM), glyceryl trinitrate (30–80 nM) or sodium nitroprusside (30 nM). However, as shown in Figure 8, the vasorelaxant action of H_2O_2 (1 mM) in the presence of NO donors was not different from that of control rings without endothelium.

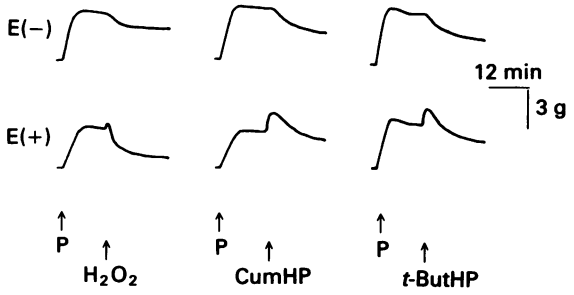

Figure 6 Comparison of the relaxant effects of H_2O_2 and the stable organic peroxides *tert*-butyl hydroperoxide and cumene hydroperoxide. For experimental details refer to Methods. Original traces of six rings of rabbit aorta obtained from a single animal are shown. The rings were precontracted with phenylephrine (P, 0.3 μM). The upper traces show the responses of rings denuded of endothelium (E (−)), while those of rings with intact endothelium (E (+)) are shown below. H_2O_2 (1 mM), *tert*-butyl hydroperoxide (*t*-ButHP, 1 mM) and cumene hydroperoxide (CumHP, 1 mM) elicited comparable relaxation of the denuded rings. In the presence of intact endothelium, addition of all tested peroxides resulted in a biphasic response, which consisted of a contraction followed by relaxation. In the presence of H_2O_2, this initial contraction was small and of short duration while the following relaxation was pronounced and 2–3 fold larger than in the absence of endothelium. In contrast, *t*-ButHP- and CumPH-induced contractions were of much greater extent and duration and were followed by relaxations of a magnitude similar to those induced by organic peroxides in the denuded rings. This figure is representative of $n = 5$ similar experiments.

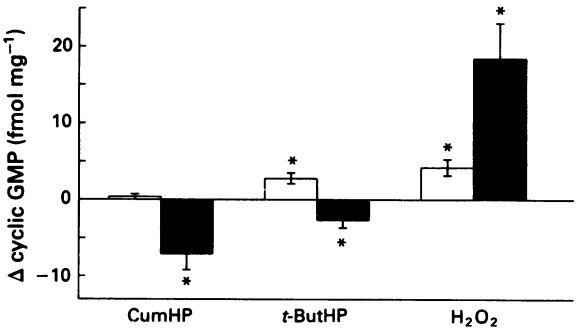

Figure 7 Comparison of the effects of H_2O_2 and those of organic peroxides on the efflux of cyclic GMP from the rings of rabbit aorta. The results of a series of experiments are shown (described in detail in Methods), in which the concentration of cyclic GMP released from the rings of rabbit aorta into the incubation medium was measured by RIA. Columns represent net change of cyclic GMP concentration in the incubation buffer in the presence of cumene hydroperoxide (CumHP, 1 mM), *tert*-butyl hydroperoxide (*t*-ButHP, 1 mM) or H_2O_2 (1 mM) and are expressed as means ± s.e.means of $n = 12$ rings. CumHP (1 mM) did not affect the efflux of cyclic GMP from denuded rings (open columns) while it significantly reduced the efflux from rings containing intact endothelium (solid columns). *t*-ButHP (1 mM) slightly enhanced the release of cyclic GMP from denuded rings. In the presence of endothelium, *t*-ButHP (1 mM) decreased the efflux of cyclic GMP. H_2O_2 (1 mM), on the other hand, significantly enhanced cyclic GMP efflux from both intact and denuded rings. $^*P < 0.05$ as different from 0 by two-way, unpaired one sample *t* test.

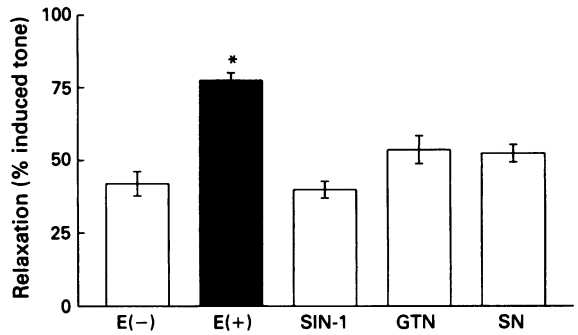

Figure 8 Lack of effect of NO donors on H_2O_2-induced relaxation in the rabbit aorta. For experimental details see Methods. The relaxant responses induced by H_2O_2 (1 mM) in endothelium-intact (E (+), solid column) and denuded (E(−), open column) rings of rabbit aorta are shown. In this series of experiments, the tone of denuded rings (99.7 ± 12.8% of KCl-induced contraction, $n = 5$) was reduced to the level of rings containing endothelium (71.9 ± 4.5% KCl; $n = 10$ from 5 separate animals) by the addition of increasing concentrations of 3-morpholinosydnonimine (SIN-1, 30–60 nM; 68.0 ± 10.2% KCl; $n = 5$), glyceryl trinitrate (GTN, 30–80 nM; 73.2 ± 12.6% KCl; $n = 5$) or sodium nitroprusside (SN, 30 nM; 67.8 ± 10.8% KCl; $n = 5$). H_2O_2-induced relaxation was enhanced in rings with intact endothelium but not in the denuded rings relaxed with NO-donors. Values represent means ± s.e.means of *n* different rings. *Bonferroni $P < 0.01$, as compared to E(−) as well as SIN-1, GTN or SN.

Discussion

Within the cardiovascular system, the major source of H_2O_2 is the activated PMN. A significant, so called marginated, pool of PMNs remains in close contact with endothelial cells. Importantly, in response to tissue mediators of inflammation, PMNs adhere to endothelial cells and crawl along their surface towards interendothelial junctions. The adhesion of PMNs is concomitant with their activation and leads to a massive release of H_2O_2 and other oxygen-derived species into a microcompartment between plasma membranes of adjacent cells. Therefore, the endothelial cells may be exposed to very high local concentrations of H_2O_2.

We have investigated the effects of H_2O_2 on the tone of intact and endothelium-denuded rings of rabbit aorta. H_2O_2, at concentrations of 0.1–1 mM, elicits a concentration-dependent relaxation of both intact and denuded rings. However, the relaxant responses of rings containing undamaged endothelium were 2–3 fold larger than those of denuded rings. This indicates that in the rabbit aorta, the relaxant action of H_2O_2 has endothelium-dependent and endothelium-independent components.

The major novel finding of this paper is that the endothelium-dependent component of the relaxant action of H_2O_2 is mediated through endogenous NO. This conclusion is well supported by several lines of experimental data. The relaxation of endothelium-intact rings induced by H_2O_2 was reversed by L-NAME or L-NMMA, inhibitors of NO synthase (Palmer *et al.*, 1988b; Mülsch & Busse, 1990), while the relaxation of denuded rings was unaffected. Preincubation of endothelium-intact rings with L-NAME or L-NMMA abolished the endothelium-dependent component of H_2O_2-induced relaxation. The effects of inhibitors of NO synthase were specific because their action could be reversed in the presence of high concentrations of L-Arg, a physiological substrate for NO synthase, while the D-stereoisomer of arginine was inactive. It is important to note that preincubation with L-NAME and L-NMMA did not affect the relaxant responses of denuded rings. Moreover, the relaxations induced by H_2O_2 were also blocked by MeB, an inhibitor of the soluble guanylate cyclase, activation of which is responsible for the vasorelaxant action of NO. However, in contrast to the inhibitors of NO synthase, MeB blocked both the endothelium-dependent and endothelium-components of the relaxant action of H_2O_2, the implication being that both components depend upon the stimulation of guanylate cyclase within the vessel wall.

Conclusions derived from our bioassay experiments are supported by the measurements of the release of cyclic GMP from rabbit aortic rings. It is well established that a portion of cyclic GMP escapes the action of phosphodiesterases and can be detected extracellularly. The extracellular accumulation of cyclic GMP following stimulation of guanylate cyclase has been observed in isolated segments of rat aorta (Schini *et al.*, 1989), bovine cultured endothelial and rat vascular smooth muscle cells (Hamet *et al.*, 1989; Feelisch & Kelm, 1991), dog kidney epithelial cell line MDCK (Woods & Houslay, 1991), rat cerebellar (Tjörnhammar *et al.*, 1986), and liver slices (Tjörnhammar *et al.*, 1983) as well as rat pineal glands (O'Dea *et al.*, 1978). Moreover, the release of cyclic GMP from aortic rings is closely correlated with intracellular levels of cyclic GMP (Zembowicz *et al.*, unpublished observations). Consistent with these observations are our results showing that the incubation of rings of rabbit aorta in the presence of an inhibitor of phosphodiesterases resulted in an accumulation of cyclic GMP in the incubation buffer which was markedly enhanced in the presence of intact endothelium. H_2O_2 enhanced the levels of cyclic GMP released from the denuded rings which indicates that H_2O_2 enhances the activity of a soluble guanylate cyclase present in the smooth muscle cells of the rabbit aorta. In the presence of intact endothelium, H_2O_2-induced efflux of cyclic GMP was significantly augmented, an observation which supports the proposed endothelium-dependent component of guanylate cyclase stimulation induced by H_2O_2. This endothelium-dependent component of H_2O_2-induced release of cyclic GMP, like that of the endothelium-dependent component of H_2O_2-induced relaxation, was abolished after the inhibition of endothelial NO synthase by L-NAME.

It is known that H_2O_2 activates the soluble guanylate cyclase present in the smooth muscle of the bovine aorta by a mechanism that involves its metabolism by catalase (Wolin & Burke, 1987). Consistent with this hypothesis is the inhibition of H_2O_2-induced relaxation of bovine pulmonary artery by ethanol (Burke-Wolin & Wolin, 1990), which decreases the formation of compound I species of catalase. It is not implausible that the mechanism of endothelium-independent relaxation induced by H_2O_2 in the rabbit aorta also involves the catalase-dependent activation of the soluble guanylate cyclase.

The results of our experiments discussed above clearly establish that the endothelium-dependent component of the vasorelaxant action of H_2O_2 was dependent on the activity of endothelial NO synthase. This effect could be due to the enhancement of the activity of endothelial NO synthase by H_2O_2 or due to a potentiation of vasorelaxant action of basally released NO at the level of the smooth muscle. In order to resolve this, we investigated the relaxant activity of H_2O_2 in denuded rings, the tone of which was decreased by the exogenous donors of NO, SIN-1, glyceryl trinitrate or sodium nitroprusside, to the level induced by NO released from the endothelium of control tissues. Donors of NO did not affect H_2O_2-induced relaxation. These results strongly support the hypothesis that H_2O_2 enhances endothelial biosynthesis of NO rather than its action in the vascular smooth muscle and implies an augmentation of the activity of NO synthase.

Like H_2O_2, the stable organic peroxides CumHP and *t*-ButHP induced an endothelium-dependent contraction of the intact rings of rabbit aorta that was followed by a relaxation. However, the initial contractile response induced by organic peroxides was much larger than that induced by H_2O_2. In contrast to H_2O_2, the vasorelaxant activity of *t*-ButHP and CumHP was not augmented in the presence of intact endothelium. Thus, the activation of NO synthase induced by H_2O_2 is not a general property of peroxides, but is a phenomenon specific to H_2O_2. Interestingly, both CumHP and *t*-ButHP reduced the efflux of cyclic GMP from the intact rings. These results may reflect damage to the endothelium induced by these organic peroxides. Finally, CumHP did not affect and *t*-ButHP only slightly enhanced, the efflux of cyclic GMP from denuded rings. This finding suggests that mechanisms other than the activation of soluble guanylate cyclase are involved in the endothelium-independent relaxation induced by organic peroxides.

As already discussed, our results demonstrate that H_2O_2 enhances endothelial synthesis of NO. However, the exact mechanism responsible for the activation of NO synthase by H_2O_2 has not yet been established. It is known that many biological actions of H_2O_2 are mediated by hydroxyl radicals formed during the iron-catalyzed Haber-Weiss reaction of H_2O_2 with O_2^- (Haber & Weiss, 1934; McCord & Day, 1978). However, in contrast to catalase, superoxide dismutase did not affect H_2O_2-induced endothelial NO synthesis. This implies that the effects of H_2O_2 are not due to the production of hydroxyl radicals as a consequence of its interactions with O_2^- present in oxygenated Krebs buffer.

Exposure of porcine cultured endothelial cells to H_2O_2 at concentrations as low as 100 μM caused a time-dependent augmentation of cytosolic calcium concentration which was attenuated in the presence of a lipid peroxidation inhibitor U-78517F (Kimura *et al.*, 1992). Thus, we considered lipid peroxidation-induced increase in cytosolic calcium concentration as a possible mechanism of the augmentation of endothelial NO synthase activity by H_2O_2. However, the active racemate of U-78517F, U-83836E (Hall *et al.*, 1991),

did not affect endothelium-dependent or endothelium-independent components of H_2O_2-induced relaxation. It should be noted that these results do no exclude the possibility that H_2O_2 activates endothelial cells and increases levels of intracellular calcium by a mechanism not involving lipid peroxidation.

Another possibility is suggested by the experiments of Boucher *et al.* (1992) who demonstrated that a number of haemoproteins in the presence of H_2O_2 or other peroxides can catalyze the formation of NO and citrulline from L-HOArg, an intermediate in the biosynthesis of NO from L-arginine (Stuehr *et al.*, 1991; Zembowicz *et al.*, 1991). Consistently, L-HOArg can be metabolized to NO in cultured bovine endothelial cells by a pathway that is not blocked by inhibitors of NO synthase (Zembowicz *et al.*, 1991; 1992). Thus, H_2O_2 may act upon L-HOArg formed by NO synthase and convert it to NO in a haem-dependent manner. Interestingly, NO synthase is also a haemoprotein (White & Marletta, 1992; Stuehr & Ikeda-Saito, 1992). Thus, the haem involved in this putative reaction might be the one present in NO synthase.

Whatever mechanisms are involved, H_2O_2-induced augmentation of endothelial NO synthesis may be part of the complex physiological or pathophysiological interactions between activated PMNs and the vessel wall. NO released by H_2O_2 may react with O_2^- to form peroxynitrite which then produces cytotoxic hydroxyl radicals (Beckman *et al.*, 1990) thereby contributing to H_2O_2-induced endothelial injury. However, the NO-dependent relaxation induced by H_2O_2 occurred before any irreversible impairment of endothelial cell function, assessed as the ability of endothelial cells to release NO after subsequent stimulation with ACh, could be observed. This suggests that H_2O_2-induced release of NO may also play a regulatory role. NO may oppose the vasoconstrictor effects of other PMN-derived mediators such as O_2^-, thromboxane A_2, peptidoleukotrienes (Goldstein *et al.*, 1978; Mullane *et al.*, 1987; Ohlstein & Nichols, 1989) or vasoactive peptides such as angiotensin II or endothelin-1 generated in the circulation of PMN-derived proteases (Wintroub *et al.*, 1984; Dzau *et al.*, 1987; Kaw *et al.*, 1992). Moreover, NO exerts an inhibitory action on many functions of the PMN. SIN-1, an exogenous donor of NO, inhibits the release of lysosomal enzymes and the generation of superoxide anion (O_2^-) by human PMNs stimulated by the chemotactic peptide N-formyl-methionyl-leucyl-phenylalanine (fMLP) (Schröder *et al.*, 1990). Inhibitors of NO synthase have been shown to enhance adhesion of PMNs to the endothelium of the mesenteric venules in the cat *in vivo* (Kubes *et al.*, 1991). Moreover, nitric oxide inhibits the chemotaxis and adhesion to cultured endothelial cells of fMLP-stimulated monocytes (Bath *et al.*, 1991). Thus, the augmentation of the formation of NO by H_2O_2 may serve as a negative feedback mechanism by which the activation of PMNs adhering to the endothelium is modulated by endothelium-derived NO.

We conclude that H_2O_2-induced relaxation in the rabbit aorta has both endothelium-dependent and independent components. The endothelium-dependent component of the relaxant action of H_2O_2 is due to enhanced endothelial synthesis of NO. These findings also suggest that H_2O_2-induced release of NO may play a role in interactions between PMNs and the vessel wall.

We are indebted to Mrs Maria Pyrka for excellent technical assistance with bioassay experiments. This work was supported by a grant from the Commission P 2.7 of the Committee for Scientific Investigation of Polish Government. R.J.H. was supported by an American Heart Association Student Research Fellowship.

References

AGER, A. & GORDON, J.L. (1984). Differential effects of hydrogen peroxide on indices of endothelial cell functions. *J. Exp. Med.*, **159**, 592–603.

BABIOR, B.M., KIPNES, R.S. & CUNUTTE, J.T. (1973). The production by leukocytes of superoxide anion, a potential bactericidal agent. *J. Clin. Invest.*, **52**, 741–744.

BATH, P.M.W., HASSALL, D.G., GALDWIN, A.-M., PALMER, R.M.J. & MARTIN, J.F. (1991). Nitric oxide and prostacyclin. Divergence of inhibitory effects on monocyte chemotaxis and adhesion of endothelium in vitro. *Atheroscler. Thromb.*, **11**, 254–260.

BECKMAN, J.S., BECKMAN, T.W., CHÉN, J., MARSHALL, P.A. & FREEMAN, B.A. (1990). Apparent hydroxyl radical formation from peroxynitrite: implications for endothelial injury from nitric oxide and superoxide. *Proc. Natl. Acad. Sci. U.S.A.*, **87**, 1620–1624.

BOUCHER, J.L., GENET, A., VADON, S., DELAFORGE, M. & MANSUY, D. (1992). Formation of nitrogen oxides and citrulline upon oxidation of N^G-hydroxy-L-arginine by hemoproteins. *Biochem. Biophys. Res. Commun.*, **184**, 1158–1164.

BREDT, D.S. & SNYDER, S.H. (1990). Isolation of nitric oxide synthase, a calmodulin requiring enzyme. *Proc. Natl. Acad. Sci. U.S.A.*, **87**, 682–685.

BURKE-WOLIN, T.M. & WOLIN, M.S. (1990). Inhibition of cGMP-associated pulmonary arterial relaxation to H_2O_2 and O_2 by ethanol. *Am. J. Physiol.*, **258**, H1267–H1273.

DZAU, V.J., GONZALES, D., KAEMPFER, C., DUBIN, D. & WINTROUB, B.U. (1987). Human neutrophils release serine proteases capable of activating prorenin. *Circ. Res.*, **60**, 595–601.

FEELISCH, M. & KELM, M., (1991). Biotransformation of organic nitrates to nitric oxide by vascular smooth muscle and endothelial cells. *Biochim. Biophys. Res. Commun.*, **180**, 286–293.

FÖRSTERMANN, U., GORSKY, L.D., POLLOCK, J.S., SCHMIDT, H.H.H.W., HELLER, M. & MURAD, F. (1991). Calmodulin-dependent endothelium-derived relaxing factor/nitric oxide synthase activity is present in the particular and cytosolic fractions of bovine aortic endothelial cell. *Proc. Natl Acad. Sci. U.S.A.*, **88**, 1788–1792.

FURCHGOTT, R.F. & ZAWADZKI, J.V. (1980). The obligatory role of endothelial cells in the relaxation of arterial smooth muscle by acetylcholine. *Nature*, **286**, 373–376.

GARDINER, S.M., COMPTON, A.M., BENNET, T., PALMER, R.M.J. & MONCADA, S. (1990a). Control of regional blood flow by endothelium-derived relaxing factor. *Hypertension*, **15**, 486–492.

GARDINER, S.M., COMPTON, A.M., BENNET, T., PALMER, R.M.J. & MONCADA, S. (1990b). Persistent haemodynamic changes following prolonged infusions of N^G-monomethyl-L-arginine (L-NMMA) in conscious rats. In *Nitric Oxide from L-arginine: A Bioregulatory System.* ed. Moncada, S & Higgs, E.A. pp.489–491. Amsterdam: Elsevier.

GOLDSTEIN, I.M., MALMSTEN, C.L., KINDAHL, H., KAPLAN, H.B., RADMARK, O., SAMUELSSON, B. & WEISSMAN, G. (1978). Thromboxane generation by human peripheral blood polymorphonuclear leukocytes. *J. Exp. Med.*, **148**, 787–792.

GRYGLEWSKI, R.J., PALMER, R.M.J. & MONCADA, S. (1986). Superoxide is involved in the breakdown of endothelium-derived relaxing factor. *Nature*, **320**, 454–456.

HABER, F. & WEISS, J. (1934). The catalytic decomposition of hydrogen peroxide by iron salts. *Proc. R. Soc.*, **147**, 332–351.

HALL, E.D., BRAUGHLER, J.M., YONKERS, P.A., SMITH, S.L., LINSEMAN, K.L., MEANS, E.D., SCHERCH, H.M., VON VOIGTLANDER, P.F., LAHTI, R.A. & JACOBSEN, E.J. (1991). U-78517F: a potent inhibitor of lipid peroxidation with activity in experimental brain injury and ischemia. *J. Pharmacol. Exp. Ther.*, **258**, 688–694.

HAMET, P., PANG, S.C. & TREMBLAY, J. (1989). Atrial natriuretic factor-induced eggression of cyclic guanosine 3':5'-monophosphate in cultured vascular smooth muscle and endothelial cells. *J. Biol. Chem.*, **264**, 12364–12369.

HARLAN, J.M. & CALLAHAN, K. (1984). The role of hydrogen peroxide in the neutrophil-mediated release of PGI_2 from cultured endothelial cells. *J. Clin. Invest.*, **74**, 442–448.

HOUSTON, D.S., SHEPHERD, J.T. & VANHOUTTE, P.M. (1985). Adenine nucleotides, serotonin and endothelium-dependent relaxation to platelets. *Am. J. Physiol.*, **248**, H389–H395.

KAW, S., HECKER, M. & VANE, J.R. (1992). The two-step conversion of big endothelin 1 to endothelin 1 and degradation of endothelin 1 by subcellular fractions from human polymorphonuclear leukocytes. *Proc. Natl. Acad. Sci. U.S.A.*, **89**, 6886–6890.

KIMURA, M., MAEDA, K. & HYASHI, S. (1992). Cytosolic calcium increase in coronary endothelial cells after H_2O_2 exposure and the inhibitory effects of U78517F. *Br. J. Pharmacol.*, **107**, 488–493.

KUBES, P., SUZUKI, M. & GRANGER, D.N. (1991). Nitric oxide: an endogenous modulator of leukocyte adhesion. *Proc. Natl. Acad. Sci. U.S.A.*, **88**, 4651–4655.

KWON, N.S., NATHAN, C.F., GILKER, C., GRIFFITH, O.W., MATTHEWS, D.E. & STUEHR, D.J. (1990). L-Citrulline production from L-arginine by macrophage nitric oxide synthase: the ureido oxygen derives from oxygen. *J. Biol. Chem.* **265**, 13442–13445.

LEONE, A.M., PALMER, R.M.J., KNOWLES, R.G., ASHTON, D.S. & MONCADA, S. (1991). Constitutive and inducible nitric oxide synthases incorporate molecular oxygen into both nitric oxide and citrulline. *J. Biol. Chem.*, **266**, 23790–23795.

MARLETTA, M.A., YOON, P.S., IYENGAR, R., LEAF, C.D. & WISHNOK, J.S. (1988). Macrophage oxidation of L-arginine to nitrite and nitrate: nitric oxide is an intermediate. *Biochemistry*, **27**, 8706–8711.

MCCORD, J.M. & DAY, D.E. Jr. (1978). Superoxide-dependent production of hydroxyl radical catalyzed by iron-EDTA complex. *FEBS Lett.*, **86**, 139–142.

MULLANE, K.M., SALMON, J.A. & KRAEMER, R. (1987). Leukocyte-derived metabolites of arachidonic acid in ischemia-reperfusion myocardial injury. *Fed. Proc.*, **46**, 2422–2433.

MÜLSCH, A. & BRUSSE, R. (1990). N^G-nitro-l-arginine (N^G-[imino(nitroamino)methyl]-l-ornithine) impairs endothelium-dependent dilations by inhibiting cytosolic nitric oxide synthesis from l-arginine. *Naunyn-Schmied. Arch. Pharmacol.*, **341**, 143–147.

NATHAN, C.F. 1992) Nitric oxide as a secretory product of mammalian cells. *FASEB J.*, **6**, 3051–3064.

NATHAN, C.F. & HIBBS, J.B. (1991). Role of nitric oxide synthesis in macrophage antimicrobial activity. *Curr. Opin. Immunol.*, **3**, 65–70.

O'DEA, R.F., GAGNON, C. & ZATZ, M. (1978). Regulation of guanosine 3',5'-cyclic monophosphate in the rat pineal and posterior pituitary gland. *J. Neurochem.*, **31**, 733–738.

OHLSTEIN, E.H. & NICHOLS, A.J. (1989). Rabbit polymorphonuclear neutrophils elicit endothelium-dependent contraction in vascular smooth muscle. *Circ. Res.*, **65**, 917–924.

PALMER, R.J.M., ASHTON, D.S. & MONCADA, S. (1988a). Vascular endothelial cells synthesize nitric oxide from L-arginine. *Nature*, **333**, 664–666.

PALMER, R.J.M., FERRIDGE, A.G. & MONCADA, S. (1987). Nitric oxide release from vascular endothelial cells accounts for the biological activity of endothelium-derived relaxing factor. *Nature*, **327**, 524–526.

PALMER, R.M.J., REES, D.D., ASHTON, D.S. & MONCADA, S. (1988b). L-Arginine in the physiological precursor for the formation of nitric oxide in endothelium-dependent relaxation. *Biochem. Biophys. Res. Commun.*, **153**, 1251–1256.

RADOMSKI, M.W., PALMER, R.M.J. & MONCADA, S. (1987a). Comparative pharmacology of endothelium-derived relaxing factor, nitric oxide and prostacyclin in platelets. *Br. J. Pharmacol.*, **92**, 181–187.

RADOMSKI, M.W., PALMER, R.M.J. & MONCADA, S. (1987b). Endogenous nitric oxide inhibits human platelet adhesion to vascular endothelium. *Lancet*, **ii**, 1057–1058.

REES, D.D., PALMER, R.M.J. & MONCADA, S. (1989). Role of endothelium-derived nitric oxide in the regulation of blood pressure. *Proc. Natl. Acad. Sci. U.S.A.*, **86**, 3375–3378.

SCHINI, V., SCHOEFFER, P. & MILLER, R.C. (1989). Effect of endothelium on basal and stimulated accumulation and efflux of cyclic GMP in rat isolated aorta. *Br. J. Pharmacol.*, **97**, 853–865.

SCHRÖDER, H., NEY, P., WOODITCH, I. & SCHRÖR, K. (1990). Cyclic GMP mediates SIN-1 induced inhibition of human polymorphonuclear leukocytes. *Eur. J. Pharmacol.*, **182**, 211–218.

SNYDER, S.H. & BREDT, D.S. (1991). Nitric oxide as a neuronal messenger. *Trends Pharmacol. Sci.*, **12**, 125–128.

STUEHR, D.J. & IKEDA-SAITO, M. (1992). Spectral characerization of brain and macrophage nitric oxide synthases. Cytochrome P-450-like hemoproteins that contain a flavin semiquinone radical. *Biol Chem.*, **267**, 20547–20550.

STUEHR, D.J., KWON, N.S., NATHAN, C.F., GRIFFITH, O.W., FELDMAN, P.L. & WISEMAN, J. (1991). N^G-hydroxy-L-arginine is an intermediate in the biosynthesis of nitric oxide from L-arginine. *J. Biol. Chem.*, **266**, 6259–6253.

TJÖRNHAMMAR, M.-L., LAZARDIS, G. & BARTFAI, T. (1983). Cyclic GMP efflux from liver slices. *J. Biol. Chem.*, **258**, 6882–6886.

TJÖRNHAMMAR, M.-L., LAZARDIS, G. & BARTFAI, Y. (1986). Efflux of cyclic guanosine 3':5'-monophosphate from cerebellar slices stimulated by L-glutamate or high K^+ or N-methyl-N'-nitro-N-nitrosoguanidine. *Neurosci. Lett.*, **68**, 95–99.

WEISS, S.J., YOUNG, J., LOBUGLIO, A.F., SLIVKA, A. & NIMEH, N.F. (1981). Role of hydrogen peroxide in neutrophil-mediated destruction of cultured endothelial cells. *J. Clin. Invest.*, **68**, 714.

WHITE, K.A. & MARLETTA, M.A. (1992). Nitric oxide synthase is a cytochrome P450 type hemoprotein. *Biochemistry*, **31**, 6627–6631.

WINTROUB, B.U., KLICKSTEIN, L.B., DZAU, V.J. & WATT, K.W.K. (1984). Granulocyte-angiotensin system: identification of angiotensinogen as the plasma protein substrate of leukocyte cathepsin G. *Biochemistry*, **23**, 227–232.

WOLIN, M.S. & BURKE, T.M. (1987). Hydrogen peroxide elicits activation of bovine pulmonary arterial soluble guanylate cyclase by a mechanism associated with is metabolism by catalase. *Biochem. Biophys. Res. Commun.*, **143**, 20–25.

WOODS, M. & HOUSLAY, M.D. (1991). Desensitization of atriopeptin stimulated accumulation and extrusion of cyclic GMP from a kidney epithelial cells line (MDCK). *Biochem. Pharmacol.*, **41**, 385–394.

ZEMBOWICZ, A., HECKER, M., MACARTHUR, H., SESSA, W. & VANE, J.R. (1991). Nitric oxide and another vasodilator are formed from N^G-hydroxy-L-arginine by cultured endothelial cells. *Proc. Natl. Acad. Sci. U.S.A.*, **88**, 11172–11176.

ZEMBOWICZ, A., ŚWIERKOSZ, T.A., SOUTHAN, G.J., HECKER, M. GRYGLEWSKI, R.J. & VANE, J.R. (1992). Mechanisms of the endothelium-dependent relaxation induced by N^G-hydroxy-L-arginine. *J. Cardiovasc. Pharmacol.*, **20** (Suppl. 12), S57–S59.

(Received February 2, 1993
Revised March 22, 1993
Accepted April 28, 1993)

Br. J. Pharmacol. (1993), **110**, 159–162

Regional haemodynamic effects of angiotensin II (3-8) in conscious rats

[1]S.M. Gardiner, P.A. Kemp, J.E. March & T. Bennett

Department of Physiology & Pharmacology, University of Nottingham Medical School, Queen's Medical Centre, Nottingham, NG7 2UH

1 It has been reported that angiotensin II (AII) (3-8) causes endothelium-dependent renal cortical vasodilatation, in anaesthetized rats, through interaction with a novel receptor that shows no affinity for the AT_1-receptor antagonist, losartan. Therefore in order to get a fuller profile of the regional haemodynamic effects of AII (3-8) in conscious rats we assessed its renal, mesenteric and hindquarters vascular effects, and compared them to the responses elicited by AII and AIII.

2 AII and AIII (1.25, 12.5 and 125 pmol kg^{-1}) caused dose-dependent pressor and renal and mesenteric vasoconstrictor effects. At doses up to 125 pmol kg^{-1}, AII (3-8) was without any cardiovascular effects, but with doses of 1.25 and 12.5 nmol kg^{-1} there were dose-dependent increases in mean arterial blood pressure and reductions in renal and mesenteric flows and vascular conductances. The responses to AII (3-8) (12.5 nmol kg^{-1}) were abolished by losartan (20 μmol kg^{-1}).

3 Since it has been found that pretreatment with L-arginine can reveal a vasodilator effect of AII (3-8) on rabbit pial arterioles, we assessed responses to AII (3-8) (12.5 nmol kg^{-1}) before and 5 min after onset of a primed infusion of L-arginine (1.4 mmol kg^{-1} bolus, 1.4 mmol kg^{-1} h^{-1} infusion). Responses to AII (3-8) were unchanged by L-arginine.

4 The results are consistent with AII (3-8) being a less effective agonist than AII (or AIII) at the AT_1-receptor, but provide no evidence for AII (3-8) interacting with a novel receptor that shows no affinity for losartan.

Keywords: Angiotensin II; angiotensin II (3-8); losartan; L-arginine; haemodynamics

Introduction

Recently, Swanson *et al.* (1992) described a specific binding site for angiotensin II (AII) (3-8), distinct from the AT_1- or the AT_2- receptor. Swanson *et al.* (1992) found that AII (3-8) injected into the renal artery in anaesthetized rats caused an increase in superficial renal blood flow, as assessed by a laser Doppler flowmeter. Under the same conditions, Swanson *et al.* (1992) found that AII caused a reduction in renal cortical blood flow consistent with the potent renal vasoconstrictor effect of this peptide seen in conscious rats (Gardiner *et al.*, 1988). In support of their findings, Swanson *et al.* (1992) cited the work of Haberl *et al.* (1991), showing that AII (3-8) could cause cerebral vasodilatation. However, in the latter study, AII (3-8) only caused vasodilatation after L-arginine pretreatment, whereas AII and AIII both caused dilatation when applied topically to pial arterioles. Since the vasodilator effects of AII and AIII were inhibited by amastatin (which blocks enzymatic degradation of AII and AIII), Haberl *et al.* (1991) suggested that release of the AII degradation products, AII (3-8) and L-arginine, 'specifically produce endothelium-dependent dilation of cerebral resistance vessels.'

Against this background, we compared the effects of AII (3-8), AII and AIII on renal, mesenteric and hindquarters haemodynamics in conscious rats. In addition, we assessed the effects of pretreatment with L-arginine, or the AT_1-receptor-selective antagonist, losartan (Timmermans *et al.*, 1991), on responses to AII (3-8).

Methods

Male Long Evans rats (350–450 g), bred in our Animal Unit, were used in this study. Under sodium methohexitone anaesthesia (Brietal, Lilly; 60 mg kg^{-1}, i.p. supplemented as required), pulsed Doppler flow probes (Haywood *et al.*, 1991) were sutured around the left renal and superior mesenteric arteries, and the distal abdominal aorta (to monitor hindquarters flow). Animals were given an i.m. injection of ampicillin (7 mg kg^{-1}) and were kept in individual home cages to recover for 7–14 days with free access to food (Biosure GLP grade 41B) and water. After that time, the animals were anaesthetized again (sodium methohexitone, 40 mg kg^{-1}, i.p.), and those with acceptable signals (signal: noise $>$20:1) from all 3 probes had a catheter implanted in the distal abdominal aorta (via the ventral caudal artery), and 3 separate catheters implanted in the right jugular vein. The catheters ran subcutaneously to emerge at the back of the neck, with the probe wires. These wires were soldered into a microconnector (Microtech Inc, Boothwyn, U.S.A.) that was clamped in a harness fitted to the rat. The harness was connected to a flexible spring through which the catheters were threaded for protection. The spring and all connections to the rat were supported by a counter-balanced lever system that allowed the animal free movement in its home cage to which it was returned, with free access to food and water, until experiments began at least 1 day after catheter implantation. The following experiments were performed:-

Responses to AII and AII (3-8)

The same animals ($n = 7$) were given increasing bolus doses of AII (1.25, 12.5 and 125 pmol kg^{-1}) or AII (3-8) (0.125, 1.25 and 12.5 nmol kg^{-1}) in random order, in the morning or afternoon of the same experimental day. Injections were separated by at least 20 min to allow variables to return to baseline. In pilot experiments, we found that AII (3-8) had no consistent effects over the range of doses used for AII, so we used the highest dose employed for AII (i.e., 125 pmol kg^{-1}) as the lowest dose of the range for AII (3-8).

Effects of L-arginine on responses to AII (3-8)

Since there is some evidence that L-arginine promotes the vasodilator effects of AII (3-8) applied topically to rabbit pial

[1] Author for correspondence.

arterioles (Haberl et al., 1991), we assessed regional haemodynamic responses to AII (3-8) before, and 5 min after, the onset of a primed infusion of L-arginine (1.4 mmol kg^{-1} bolus, 1.4 mmol kg^{-1} h^{-1} infusion) in 3 of the animals studied above; this experiment was carried out on a separate day to that above.

Responses to AIII

In order to determine if responses to AII (3-8) resembled those to AIII more than those to AII, another three of the animals used in the first experiment also received increasing bolus doses (1.25, 12.5 and 125 pmol kg^{-1}) of AIII; this experiment was carried out on the same day as the first experiment, but at least 1 h before or after administration of AII or AII (3-8).

Responses to AII (3-8) before and after administration of the AT_1-receptor antagonist, losartan

Swanson et al. (1992) reported that the site which bound AII (3-8) showed no affinity for losartan, but they did not assess the effects of losartan on functional responses to AII (3-8). Therefore, in a separate group of rats ($n = 5$) we measured regional haemodynamic responses to AII (3-8) (12.5 nmol kg^{-1}) before, and 5 min after i.v. bolus injection of losartan (20 μmol kg^{-1}). Elsewhere we have shown this dose of losartan completely abolishes the AT_1-receptor-mediated haemodynamic effects of AII for several hours (Batin et al., 1991a,b).

Data analysis

Throughout an experiment, continuous recordings were made of instantaneous heart rate, mean and phasic arterial blood pressure, and mean and phasic Doppler shift signals with a modified (Gardiner et al., 1990) VF-1 pulsed Doppler flowmeter (Crystal Biotech, Hopkinton, U.S.A.). At time points representative of the profile of response to any particular intervention, variables were averaged over 20 s epochs. Changes relative to baseline were assessed by Friedman's test (Theodorsson-Norheim, 1987), applied to the areas under or over curves. Because the duration of responses to AII and AII (3-8) differed (see Results), areas were calculated over the 5 min period following AII and over the 2 min period after AII (3-8) administration. A P value <0.05 was taken as significant.

Drugs

AII (H_2N-Asp-Arg-Val-Tyr-Ile-His-Pro-Phe-OH), AIII (H_2N-Arg-Val-Tyr-Ile-His-Pro-Phe-OH) and AII (3-8) (H_2N-Val-Tyr-Ile-His-Pro-Phe-OH), were obtained from Bachem (U.K.). Peptides were dissolved in sterile isotonic saline (154 mmol l^{-1} NaCl) containing 1% bovine serum albumin (Sigma). L-Arginine hydrochloride (Sigma) and losartan potassium (gift from Dr R. Smith, DuPont U.S.A.) were dissolved in isotonic saline. All injections were given in a volume of 100 μl and flushed in with 100 μl of saline. Administration of saline alone in these volumes had no consistent cardiovascular effects.

Results

AII caused dose-dependent pressor effects and reductions in renal and mesenteric flows and vascular conductances (Figure 1, Table 1). Only the highest dose of AII caused significant bradycardia and hindquarters vasoconstriction (Figure 1, Table 1).

AII (3-8) also caused dose-dependent pressor effects, but these were of shorter duration than those seen with AII (Figure 1, Table 1). Moreover, although with the doses chosen the peak pressor effects of AII and AII (3-8) were similar, the doses of the latter were 100 fold higher than those of AII (Figure 1, Table 1).

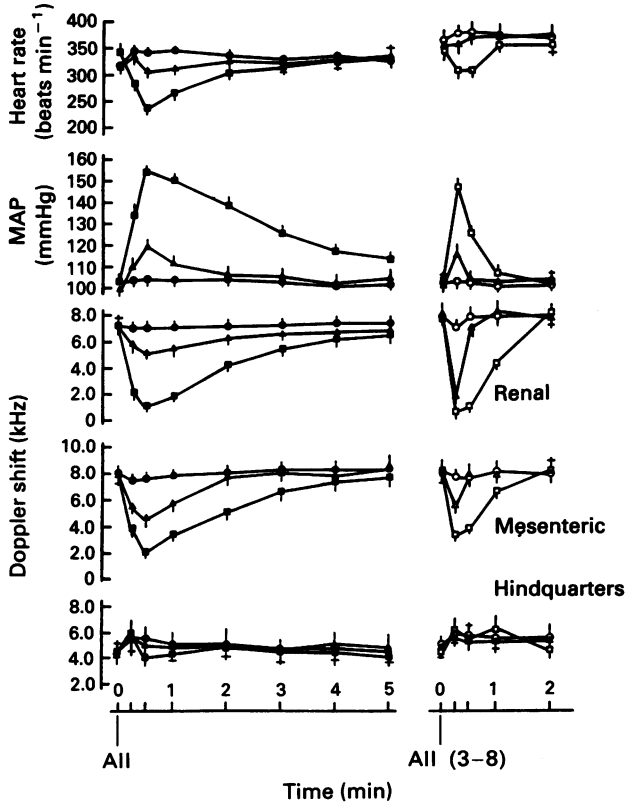

Figure 1 Cardiovascular responses to angiotensin II (● 1.25; ▲ 12.5; ■ 125 pmol kg^{-1}; left-hand panels) or angiotensin II (3-8) (○ 0.125; △ 1.25; □ 12.5 nmol kg^{-1}; right-hand panels) in the same conscious Long Evans rats ($n = 7$). Values are mean with s.e.mean. Statistics for the integrated changes are shown in Table 1.

The pressor effects of AII (3-8) were accompanied by dose-dependent reductions in renal and mesenteric flows and vascular conductances, but the dose-effect relation was particularly steep in the renal vascular bed (Figure 1, Table 1). As with AII, the changes in heart rate and hindquarters haemodynamics in response to AII (3-8) were variable (Figure 1, Table 1).

Pretreatment with L-arginine ($n = 3$) had no consistent effects on responses to AII (3-8) (12.5 nmol kg^{-1}) (Table 2). However, losartan abolished the effects of AII (3-8) (Figure 2).

Cardiovascular responses to AIII were very similar to those seen with AII, and over the same dose-range (Figure 3).

Discussion

The present work has provided no evidence for AII (3-8) acting as a vasodilator agent in the renal (Swanson et al., 1992) or in the mesenteric vascular bed. Although AII (3-8) was capable of causing an increase in hindquarters flow, this effect was not different from that seen with AII, and, as with the latter, was probably, in part, due to release of adrenal medullary adrenaline, causing activation of β_2-adrenoceptors in the hindquarters vascular bed (Gardiner et al., 1988). However, the effects of AII (3-8) (and of AII) on hindquarters haemodynamics and heart rate were less reproducible or prominent than its pressor and renal and mesenteric vasoconstrictor actions, which were abolished by the AT_1-receptor antagonist, losartan.

These results do not agree with those of Swanson et al. (1992), who considered that AII (3-8) interacted with 'an

Table 1 Integrated (areas under or over curves) cardiovascular responses to incremental bolus doses of angiotensin II (AII) or AII (3-8) in the same conscious, Long Evans rats ($n = 7$)

	AII (pmol kg^{-1})			*AII (3-8)* (nmol kg^{-1})		
	1.25	12.5	125	0.125	1.25	12.5
Δ Heart rate (beats)	66 ± 19*	68 ± 29	− 253 ± 47*	23 ± 7*	27 ± 13	− 43 ± 17*
Δ Mean arterial blood pressure (mmHg min)	3 ± 1	38 ± 5*	146 ± 15*	1 ± 1	8 ± 1*	23 ± 3*
Δ Renal flow (kHz min)	− 1.0 ± 0.2	− 5.4 ± 0.8*	− 15.7 ± 2.0*	− 0.6 ± 0.1	− 3.1 ± 0.3*	− 8.8 ± 0.6*
Δ Mesenteric flow (kHz min)	− 1.2 ± 0.5	− 5.2 ± 0.8*	− 12.9 ± 1.6*	− 0.5 ± 2	− 1.6 ± 0.2*	− 4.4 ± 0.5*
Δ Hindquarters flow (kHz min)	2.2 ± 1.3	3.1 ± 1.3	2.5 ± 1.1	1.2 ± 0.4	1.3 ± 0.3*	2.9 ± 0.7*
Δ Renal conductance ([kHz mmHg^{-1} min] 10^3)	− 6 ± 2	− 74 ± 10*	− 189 ± 19*	− 5 ± 1	− 32 ± 4*	− 88 ± 6*
Δ Mesenteric conductance ([kHz mmHg^{-1} min] 10^3)	− 11 ± 4	− 69 ± 9*	− 172 ± 19*	− 4 ± 2	− 20 ± 4*	− 50 ± 6*
Δ Hindquarters conductance ([kHz mmHg^{-1} min] 10^3)	22 ± 12	47 ± 21	− 109 ± 26*	22 ± 6*	11 ± 4	16 ± 6*

Values are mean ± s.e.mean.
*$P < 0.05$ versus baseline.

Table 2 Integrated (areas under or over curves) cardiovascular responses to angiotensin II (3-8) (AII (3-8) (12.5 nmol kg^{-1}) in the same conscious, Long Evans rats ($n = 3$) in the absence (control) or presence of L-arginine (1.4 mmol kg^{-1} bolus, 1.4 mmol kg^{-1} h^{-1} infusion)

	Control	*+ L-Arginine*
Δ Heart rate (beats)	− 69 ± 27	− 55 ± 16
Δ Mean arterial blood pressure (mmHg min)	23 ± 4	37 ± 12
Δ Renal flow (kHz min)	− 9.3 ± 1.2	− 7.6 ± 0.5
Δ Mesenteric flow (kHz min)	− 4.5 ± 1.1	− 6.2 ± 1.4
Δ Hindquarters flow (kHz min)	− 1.7 ± 0.5	1.1 ± 0.2
Δ Renal conductance ([kHz mmHg^{-1} min] 10^3)	− 95 ± 10	− 79 ± 7
Δ Mesenteric conductance ([kHz mmHg^{-1} min] 10^3)	− 55 ± 14	− 76 ± 21
Δ Hindquarters conductance ([kHz mmHg^{-1} min] 10^3)	21 ± 13	4 ± 2

Values are mean ± s.e.mean

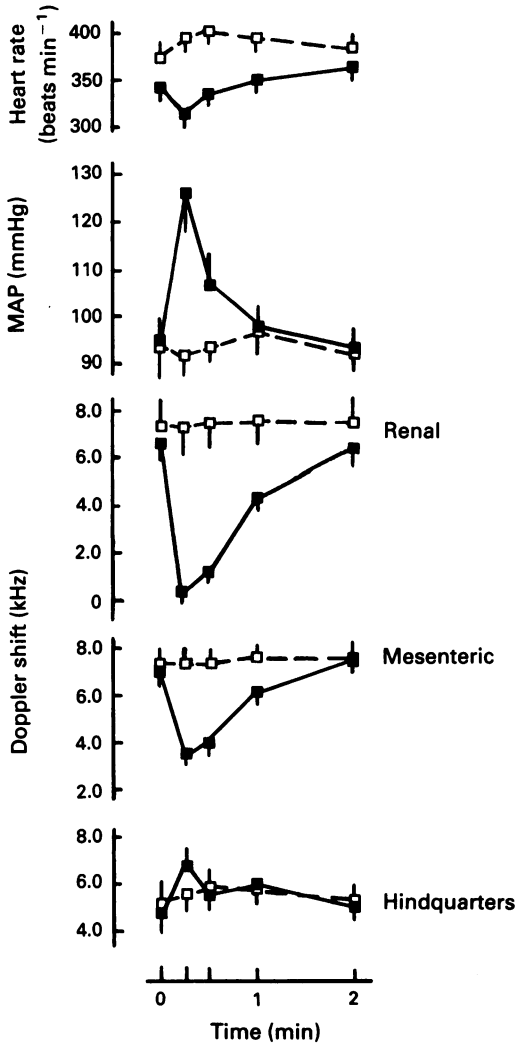

Figure 2 Cardiovascular responses to angiotensin II (3-8) (12.5 nmol kg^{-1}) in the same conscious Long Evans rats ($n = 5$) in the absence (■) or presence (□) of losartan (20 μmol kg^{-1}). Values are mean ± s.e.mean.

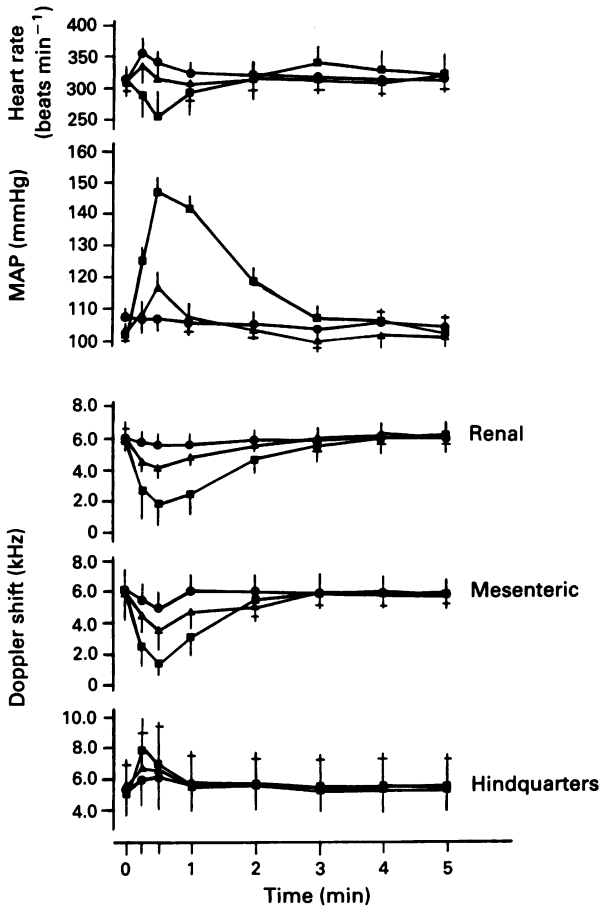

Figure 3 Cardiovascular responses to angiotensin III (● 1.25; ▲ 12.5; ■ 125 pmol kg^{-1}) in the same conscious Long Evans rats ($n = 3$). Values are mean ± s.e.mean.

entirely new angiotensin receptor with unique specificity, distribution and functional characteristics'. Swanson *et al.* (1992) speculated that the interaction of AII (3-8) with its receptor on endothelial cells stimulated the synthesis and release of endothelium-derived relaxing factor (EDRF). In support of their findings, Swanson *et al.* (1992) cited the work of Haberl *et al.* (1991) which, they claimed, showed that AII (3-8) acted as a vasodilator in rat cerebral arteries via an EDRF-mediated mechanism. In fact, Haberl *et al.* (1991) studied anaesthetized rabbits, and showed that AII (3-8) was without effect on pial arterioles, whereas AII and AIII caused vasodilatation. However, when AII (3-8) (which differs from AIII only in the absence of the amino-terminal L-arginine residue) was applied after L-arginine, vasodilatation was seen. As mentioned in the Introduction, Haberl *et al.* (1991) considered that their results indicated availability of L-arginine and AII (3-8) was necessary for endothelium-dependent cerebral vasodilatation. However, there is no clear evidence that L-arginine can enhance the release of nitric oxide (NO) contingent upon receptor-mediated activation of constitutive NO synthase, and in the present work, L-arginine had no effect on responses to AII (3-8). Moreover, AIII had effects very like AII, causing marked renal and mesenteric vasoconstrictions. A similar pattern of response was seen with AII (3-8) although it was about 100 fold less potent than AII, and its duration of action was considerably shorter. Thus, our results are consistent with AII (3-8) being a less effective agonist at the receptor with which AII interacts.

Considering the findings of Swanson *et al.* (1992), showing that AII (3-8) caused marked renal cortical vasodilatation, it is particularly notable that, in our model, the effects of AII (3-8) were characterized by dramatic renal vasoconstriction. One difference between our study and that of Swanson *et al.* (1992) is that we gave i.v. bolus injections of AII (3-8) to conscious animals, whereas they infused the peptide into the renal artery of anaesthetized rats. Thus, it is possible that our assessment of total renal flow masked a specific vasodilator effect of AII (3-8) in the renal cortex. It is also feasible that, given i.v., AII (3-8) activated mechanisms that concealed its direct vasodilator effects, Indeed, it could be suggested that the short duration of the pressor and vasoconstrictor action of AII (3-8), compared to AII, was due to concurrent activation of vasodilator mechanisms, possibly also in vascular beds not studied by us. However, these arguments are difficult to reconcile with our finding that losartan blocked all the effects of AII (3-8), unless the former was not acting as a selective antagonist of AT_1-receptors, but was also inhibiting the action of AII (3-8) on a distinct AII-receptor subtype. In that case, one is left with the problem of aligning this proposal with the finding of Swanson *et al.* (1992) that AII (3-8) interacted with a receptor that showed no affinity for losartan. Whatever the explanation of the disparities between our findings and those of Swanson *et al.* (1992), the present work provides no evidence for AII (3-8) exerting acute effects, other than through activation of AT_1-receptors.

References

BATIN, P., GARDINER, S.M., COMPTON, A.M. & BENNETT, T. (1991a). Differential regional haemodynamic effects of the non-peptide angiotensin II antagonist, DuP 753, in water-replete and water-deprived Brattleboro rats. *Life Sci.*, **48**, 733–739.

BATIN, P., GARDINER, S.M., COMPTON, A.M., KEMP, P.A. & BENNETT, T. (1991b). Cardiac haemodynamic effects of the non-peptide, angiotensin II-receptor antagonist, DuP 753, in conscious Long Evans and Brattleboro rats. *Br. J. Pharmacol.*, **103**, 1585–1591.

GARDINER, S.M., BENNETT, T. & COMPTON, A.M. (1988). Regional haemodynamic effects of neuropeptide Y, vasopressin and angiotensin II in conscious, unrestrained, Long Evans and Brattleboro rats. *J. Auton. Nerv. Syst.*, **24**, 15–27.

GARDINER, S.M., COMPTON, A.M., BENNETT, T. & HARTLEY, C.J. (1990). Can pulsed Doppler technique measure changes in aortic flow in conscious rats? *Am. J. Physiol,*. **259**, H448–H456.

HABERL, R.L., DECKER, P.J. & EINHÄUPL, K.M. (1991). Angiotensin degradation products mediate endothelium-dependent dilation of rabbit brain arterioles. *Circ. Res.*, **68**, 1621–1627.

HAYWOOD, J.R., SHAFFER, R., FASTENOW, C, FINK, G.D. & BRODY, M.J. (1981). Regional blood flow measurement with pulsed Doppler flowmeter in conscious rat. *Am. J. Physiol.*, **241**, H273–H278.

SWANSON, G.N., HANESWORTH, J.M., SARDINIA, M.F., COLEMAN, J.K.M., WRIGHT, J.-W., HALL, K.L., MILLER-WING, A.V., STOBB, J.W., COOK, V.I., HARDING, E.C. & HARDING, J.W. (1992). Discovery of a distinct binding site for angiotensin II (3-8), a putative angiotensin IV receptor. *Regul. Pept.*, **40**, 409–419.

THEODORSSON-NORHEIM, E. (1987). Friedman and Quade tests: BASIC computer program to perform non-parametric two-way analysis of variance and multiple comparisons on ranks of several related samples. *Comput. Biol. Med.*, **17**, 85–99.

TIMMERMANS, P.B.M.W.M., WONG, P.C., CHIU, A.T. & HERBLIN, W.F. (1991). Non-peptide angiotensin II receptor antagonists. *Trends Pharmacol. Sci.*, **12**, 55–62.

(Received February 25, 1993
Revised March 26, 1993
Accepted April 28, 1993)

Br. J. Pharmacol. (1993), **110**, 163–168

Blockade by 2,2′,2″-tripyridine of the nicotinic acetylcholine receptor channels in embryonic *Xenopus* muscle cells

K.S. Hsu, W.M. Fu & [1]S.Y. Lin-Shiau

Institutes of Pharmacology and Toxicology, College of Medicine, National Taiwan University, Taipei, Taiwan

1 The effects of 2,2′,2″-tripyridine on the nicotinic acetylcholine (ACh) receptor channels were studied in the cultured myocytes of 1-day-old *Xenopus* embryos.

2 2,2′,2″-Tripyridine depressed the amplitude of iontophoretic ACh-induced current at a low frequency of 0.7 Hz stimulation and it not only decreased the initial responses but also enhanced the run-down of ACh-induced current at higher frequency stimulation of 7 Hz and 30 Hz.

3 Single ACh channel recordings showed that 2,2′,2″-tripyridine decreased the channel conductance, the opening frequency and mean open time of both types of low- and high-conductance channels.

4 These results suggest that the blocking actions of 2,2′,2″-tripyridine on ACh receptor channels in the skeletal muscle may contribute to the depression of the nerve-evoked contraction of the mouse diaphragm as reported previously.

Keywords: 2,2′,2″-Tripyridine; nicotinic ACh receptor channel; *Xenopus* muscle cell

Introduction

2,2′,2″-Tripyridine is a pyridine derivative that has been found to be a synthetic by-product of the herbicide, paraquat and to be a strong mutagen (Kuo *et al.*, 1986; Lin *et al.*, 1988). Epidemiological studies showed that the incidence of skin cancer of paraquat manufacturers was much higher than that of the general population of Taiwan (Wang *et al.*, 1986). In addition 2,2′,2″-tripyridine was more potent than paraquat in producing carcinogenic actions and DNA damage (Lin *et al.*, 1988).

In our previous study, we have shown a curare-like action of 2,2′,2″-tripyridine in the mouse phrenic nerve-diaphragm preparation (Lin-Shiau *et al.*, 1992). At the mouse neuromuscular junction, 2,2′,2″-tripyridine not only depressed the amplitudes but also shortened the decay time constant of both endplate potentials (e.p.ps) and miniature endplate potentials (m.e.p.ps). In addition, it produced a fade of tetanic muscle tension and a run down of successive endplate potentials (e.p.ps) during repetitive stimulation in cut muscle preparations of mouse phrenic nerve-diaphragm (Lin-Shiau *et al.*, 1992). The present study was aimed at the exploration of the action of 2,2′,2″-tripyridine on the acetylcholine receptor channel of *Xenopus* muscle cells in culture, and attempted to distinguish the actions of the neuromuscular blocking agent, 2,2′,2″-tripyridine on the ACh receptor and its associated ionic channel.

Methods

Preparation of Xenopus *nerve-muscle cultures*

The *Xenopus* nerve-muscle cultures were prepared as previously reported (Spitzer & Lamborghini, 1976; Sanes & Poo, 1989). Briefly, the neural tube and the associated myotomal tissues of 1-day-old *Xenopus* embryos (stage 20–22) were dissociated in the Ca^{2+}- and Mg^{2+}-free saline. The cells were plated on clean glass coverslips and were used for experiments after 24 h at room temperature (20–22°C). The culture medium consisted of 50% (vol/vol) Ringer solution (composition mM: NaCl 115, $CaCl_2$ 2, KCl 2.5, HEPES 10 (pH 7.6), 49% L-15 Leibovitz's medium (Sigma), and 1% foetal bovine serum (Gibco).

Electrophysiological recording and analysis

Gigaohm-seal whole-cell and cell-attached patch clamp recording methods followed those described previously (Hamill *et al.*, 1981; Young & Poo, 1983). Recordings were made at room temperature in culture medium. The solution inside the whole-cell recording pipettes contained (mM): KCl 150, NaCl 1, $MgCl_2$ 1 and HEPES 10, pH 7.2. Iontophoresis of ACh was applied to the surface of the myocytes by conventional glass microelectrodes filled with 3 M ACh (resistance, 100–200 MΩ). The iontophoretic ACh pulses of 2 ms duration were supplied by a Grass stimulator (SD9) through a microelectrode amplifier (WPI S-7061A), which provides a breaking current between 2 to 10 nA. For cell-attached recording, the pipette was filled with Ringer solution containing low concentrations of ACh (3–5 nM) to avoid the simultaneous opening of the multiple channels. In all recordings, the membrane currents were monitored by a patch-clamp amplifier (EPC-7), and the single channel current signal was filtered at 3 kHz. The data were digitalized by a digitizing unit (Neurocorder DR-384) and stored on a videotape recorder. For single channel analysis, the current signals were digitized at 100 μs intervals and analysed with a PClamp programme (Axon Instruments). Events corresponding to opening of more than one channel were excluded from the open time analysis. Events with open time shorter than 500 μs were not analysed because of possible attenuation and distortion. Open duration histograms were fitted with a single exponential and the amplitude histograms were fitted with Gaussian distribution curves, using least-squares methods in both cases. Effects of drugs were compared from different patches of the same myocyte.

Drugs

All of the chemical compounds listed above for the test experiments were purchased from Sigma Chemical Company, St. Louis, Missouri, U.S.A.

Results

Effects of 2,2′,2″-tripyridine on the ACh-induced whole-cell currents

ACh channels were found on the surface of isolated myocytes of *Xenopus* at relatively high density and uniform

[1] Author for correspondence.

distribution (Poo, 1982; Young & Poo, 1983). Repetitive iontophoretic applications of identical ACh pulses at one spot on the myocyte surface resulted in transient inward membrane currents. Figure 1 shows an example of whole-cell voltage-clamp recording of membrane currents induced by iontophoretic ACh pulses. The ACh-induced currents remained relatively constant at 0.7 Hz and 7 Hz application, but showed gradual decline at 30 Hz. Bath application of 43 μM 2,2',2''-tripyridine inhibited the ACh-induced currents when the iontophoretic ACh pulses were applied at 0.7 Hz (Figure 1b). In addition, 2,2',2''-tripyridine not only reduced the amplitude of initial responses but also enhanced the rate of decline at either 7 Hz or 30 Hz stimulation within 10 min (Figures 1c and d). The decay time constant of ACh-induced current recorded at a holding potential of − 60 mV was significantly shorter in myocytes treated with 43 μM 2,2',2''-tripyridine ($\tau = 2.7 \pm 0.4$ ms as compared with control; $\tau = 4.1 \pm 0.3$ ms, $n = 12$) (Figure 1a). 2,2',2''-Tripyridine decreased whole-cell ACh-induced currents in a concentration-dependent manner when ACh pulses were applied at 0.7 Hz (Figure 2). As shown in Figure 3, the amplitude and decay time constant of ACh-induced currents were linearly related to the membrane potential. 2,2',2''-Tripyridine inhibited the ACh-induced currents more effectively at hyperpolarized membrane potential but did not significantly affect the reversal potential of ACh-induced whole-cell currents.

Effects of 2,2',2''-tripyridine on ACh single channel currents

Cell-attached patch clamp recordings were made on isolated myocytes in 1-day-old *Xenopus* cultures. The cultured myocytes possess two populations of ACh channels, i.e. embryonic-type channels (low-conductance channels) which have a prolonged mean open time and lower current amplitude and adult-type channels (high-conductance channels) which have 50% greater unitary conductance than embryonic-type channels and shorter mean open time. A representative example of the single channel recordings is shown in Figure 4. The average channel opening frequency, the amplitude of single channel events, and mean channel

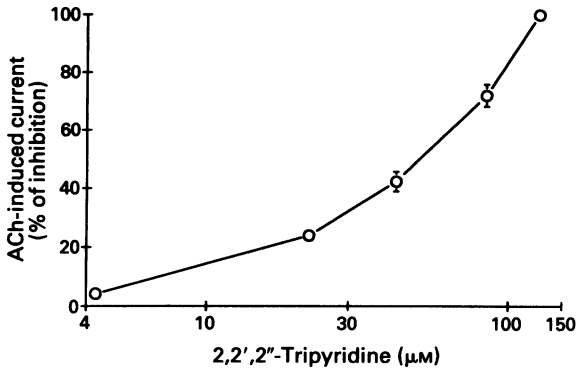

Figure 2 Concentration-dependent inhibition of acetylcholine (ACh)-induced current of the *Xenopus* muscle cells by 2,2',2''-tripyridine. The ACh-induced membrane currents were recorded by whole-cell recording from the myocytes before and 20 min after bath application of various concentrations ($n = 3-6$) of 2,2',2''-tripyridine. The ACh-induced current was recorded by repetitive iontophoretic ACh pulses on the surface of the myocyte at 0.7 Hz.

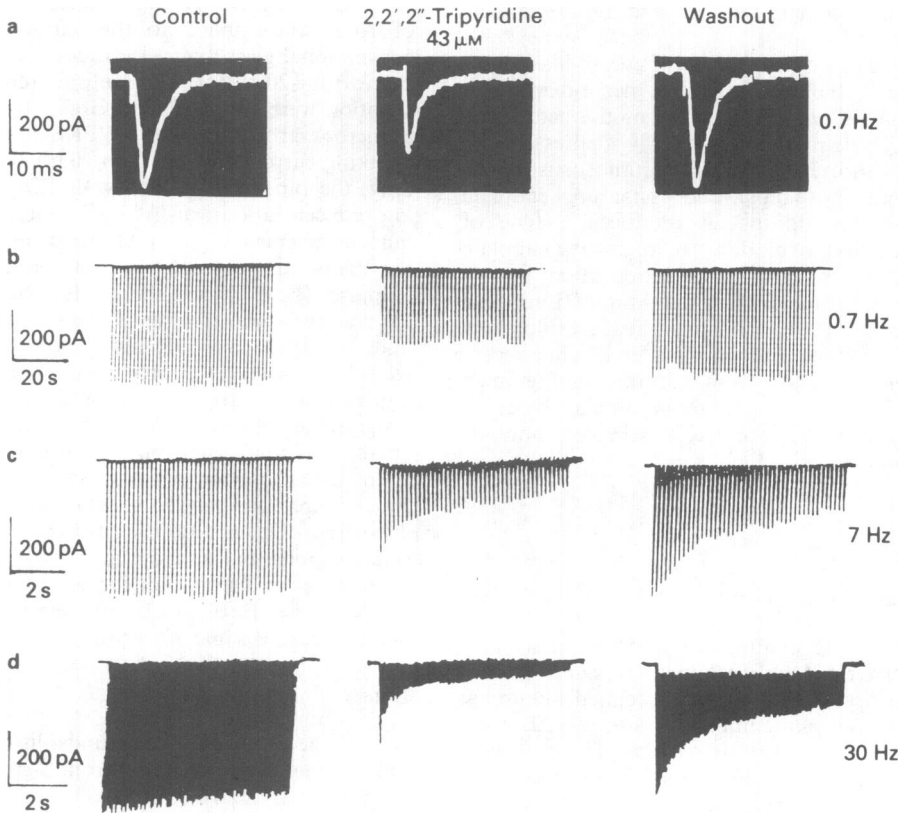

Figure 1 Effects of 2,2',2''-tripyridine on the acetylcholine (ACh)-induced whole-cell currents in *Xenopus* cultured myocytes. The myocytes were voltage-clamped at a holding potential of − 60 mV. Continuous traces showed the membrane currents recorded by whole-cell recording from the same myocyte before (left), 20 min after bath application of 43 μM 2,2',2''-tripyridine (middle) and 20 min after washout (right). The identical iontophoretic ACh pulses were applied on the surfae of the myoctye at a frequency of 0.7 (b), 7 (c) and 30 Hz (d), respectively (filtered at 150 Hz). Samples of current are shown on the upper trace at higher time resolution (filtered at 10 kHz). Note that 2,2',2''-tripyridine inhibited the initial responses of ACh-induced currents and enhanced the run-down of the currents at higher frequency of stimulation.

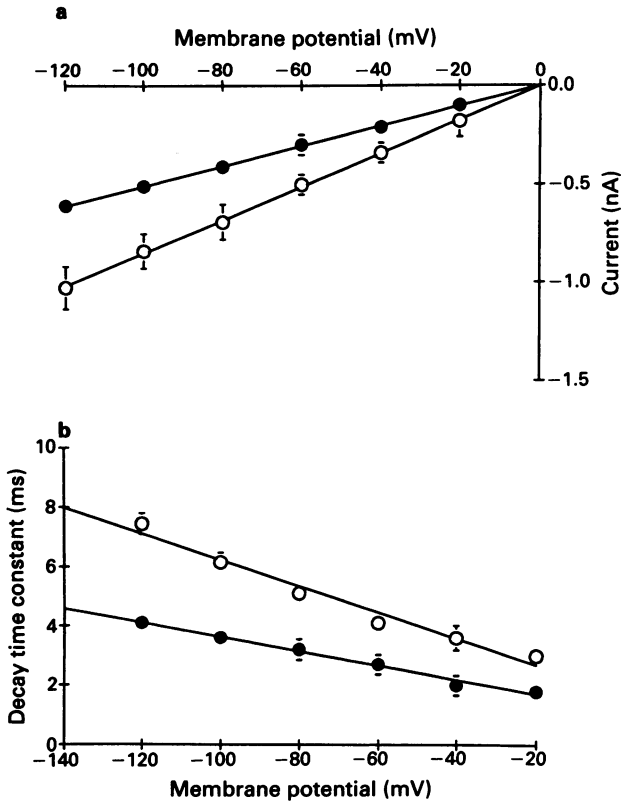

Figure 3 Inhibitory action of 2,2',2''-tripyridine on the acetylcholine (ACh)-induced current as a function of membrane potential. The ACh-induced membrane currents were recorded by whole-cell recording from the myocytes in the absence (○) or 20 min after bath application of 43 μM 2,2',2''-tripyridine (●). The ACh-induced currents were recorded by repetitive iontophoretic ACh pulses on the surface of the myocyte at 0.7 Hz. Note that more pronounced inhibitory effects of 2,2',2''-tripyridine on both the amplitude (a) and decay time constant (b) of ACh-induced currents at hyperpolarizing potentials. The symbols show mean ± s.e.means for the six experiments. The reversal potentials were estimated at 0 mV (control) and − 2 mV (43 μM 2,2',2''-tripyridine) respectively. Resting membrane potentials in these cells were from − 75 mV to − 80 mV.

Table 1 Comparison of the kinetics of acetylcholine single channel between control and 2,2',2''-tripyridine-treated *Xenopus* embryonic myocytes in culture

Channel property	*Control*	*2,2',2''-Tripyridine (43 μM)*
Low-conductance ACh channel		
Amplitude (pA)	5.21 ± 0.06 (12)	3.64 ± 0.09 (12)*
Mean open time (ms)	4.92 ± 0.17 (12)	3.68 ± 0.14 (12)*
Opening frequency (s^{-1})	7.4 ± 0.4 (12)	2.7 ± 0.3 (12)*
High-conductance ACh channel		
Amplitude (pA)	7.71 ± 0.11 (12)	5.59 ± 0.10 (12)*
Mean open time (ms)	1.96 ± 0.05 (12)	1.60 ± 0.04 (12)*
Opening frequency (s^{-1})	4.0 ± 0.3 (12)	1.8 ± 0.2 (12)*

Single ACh channel currents were obtained from cell-attached patch recording on the surface of isolated *Xenopus* muscle cells and the patch was hyperpolarized to 60 mV from rest.
Pipettes were filled with Ringer solution containing acetylcholine (3–5 nM).
*$P < 0.05$ as compared with control.
Data are presented as mean ± s.e.mean (n).
n represents the number of myocytes examined.

open time before and after 2,2',2''-tripyridine treatment were analysed from different patches of the same myocyte. As shown in Figure 4b, 2,2',2''-tripyridine reduced the current amplitude, mean open time as well as average opening frequency of both types of low- and high-conductance ACh channels. Results obtained from 12 cells are summarized in Table 1. Similar to the reversible blockade of 2,2',2''-tripyridine on the ACh-induced whole-cell current, the inhibitory effects of 2,2',2''-tripyridine (43 μM) on the single ACh channel were restored by washout (Figure 4c). As shown in Figure 5, the amplitude of single channel currents, activated by ACh, was linearly related to the membrane potential and the linear regression yielded one high-conductance channel of 61.8 ± 0.9 pS ($n = 12$) and another low-conductance channel of 42.6 ± 0.8 pS ($n = 12$). After exposure to 2,2',2''-tripyridine (43 μM), the conductance decreased to 42.8 ± 1.2 pS and 31.4 ± 0.7 pS for high- and low-conductance channel, respectively. The reversal potentials of single ACh channels were correlated with the data obtained from ACh-induced whole-cell currents and 2,2',2''-tripyridine did not significantly affect the reversal potential of ACh channels. This reduction of channel activity may indicate that 2,2',2''-tripyridine blocks the open conformation of the nicotinic ACh receptor channels.

Discussion

The action of the nondepolarizing neuromuscular blocking agents, (+)-tubocurarine and lobeline on both the ACh receptor and ACh receptor-activated ionic channel at the neuromuscular junction have been studied in some detail (Katz & Miledi, 1978; Lambert *et al.*, 1980; 1981; Gibb & Marshall, 1984). Initial work indicated that (+)-tubocurarine competitively blocked ACh receptors with no effect on the channel lifetime (Katz & Miledi, 1978), despite some earlier evidence that the drug shortened endplate current (e.p.c) decay (Beranek & Vyskocil, 1968) and blocked ACh-activated channels in *Aplysia* neurone (Marty *et al.*, 1976). Manalis (1977) demonstrated that the e.p.c. produced by iontophoretic application of ACh at frog endplates was shortened by (+)-tubocurarine, which produced a voltage-dependent decrease of peak e.p.c. amplitude. This effect became more pronounced at hyperpolarizing potentials. These observations led to a 'reexamination' of the action of (+)-tubocurarine by Katz & Miledi (1978), who confirmed the voltage-dependent channel-blocking action of the drug; in contrast, this effect was not seen with α-bungarotoxin.

The present results clearly showed that 2,2',2''-tripyridine not only depressed the amplitude but also shortened the decay time constant of ACh-induced whole-cell current in *Xenopus* myocyte. The reduction in peak amplitude of the ACh-induced current could be due to the inhibition of either or both the ACh receptor and its associated ionic channel. The sudden rise of the ACh concentration at the *Xenopus* myocyte causes a number of channels to open. Each channel will stay opened for a random, experimentally distributed period of time. The rising phase of the current reflects the number of channels opening as a function of time and the falling phase reflects the distribution of channel closing. The exponential time constant of the current decay is a measure of mean channel open time, a finding that has been confirmed by independent techniques such as noise analysis and patch clamp (Anderson & Stevens, 1973; Neher & Steinbach, 1978). In our experiments, the decay time constant of ACh-induced current recorded at a holding potential of − 60 mV was 4.1 ± 0.3 ms in control compared with 2.7 ± 0.4 ms in the presence of 43 μM 2,2',2''-tripyridine. From the result of single channel recording, 2,2',2''-tripyridine reduced the mean open time of both types of low- and high-conductance ACh channels which could explain the effects of 2,2',2''-tripyridine on the shortening of ACh-induced current decay time constant. Furthermore, the total

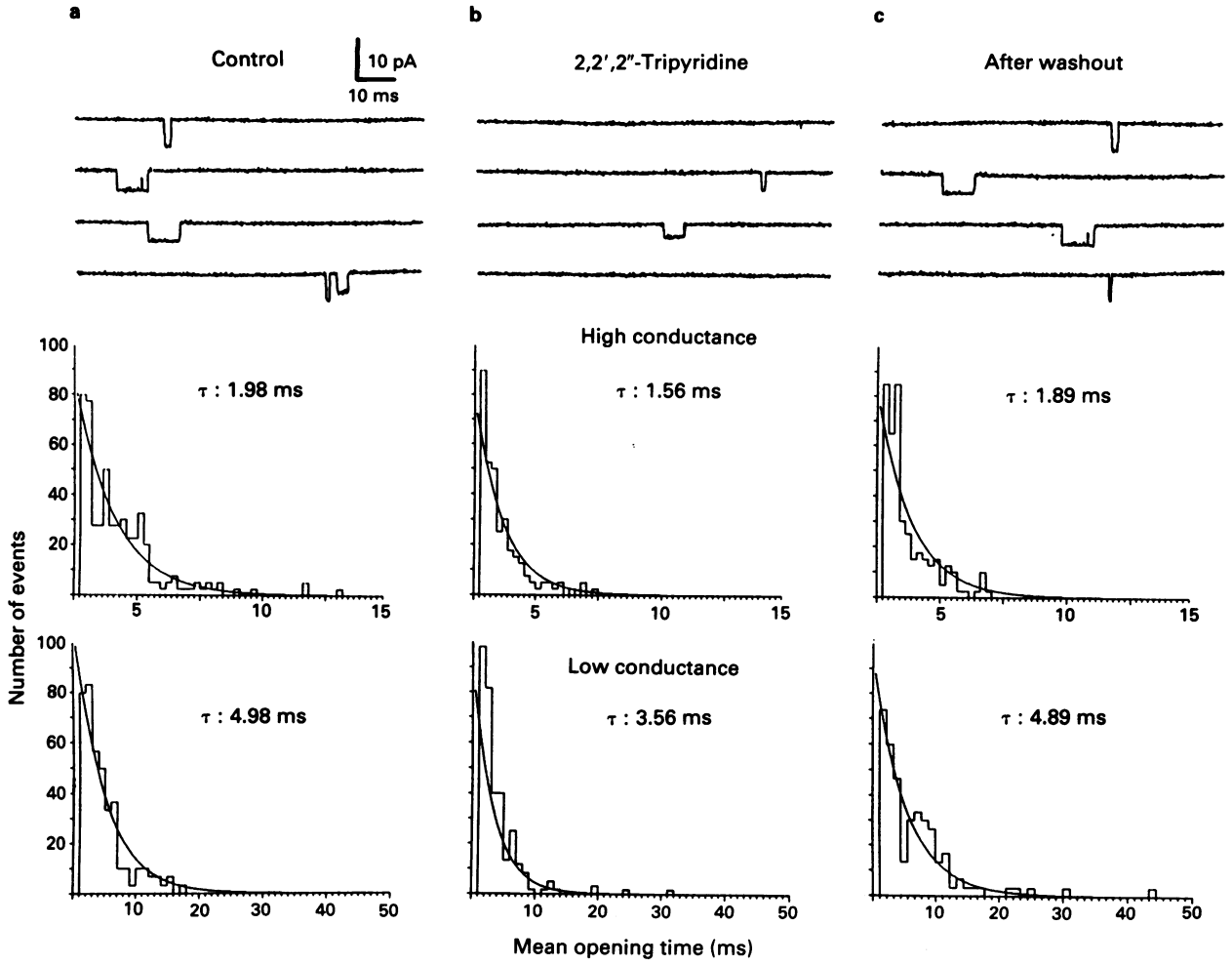

Figure 4 Effects of 2,2',2''-tripyridine on single acetylcholine (ACh) channel currents. Samples of recordings of single ACh channel currents and histograms of channel open time before (a) and after (b) treatment with 2,2',2''-tripyridine (43 μM) and 20 min after washout (c) were obtained from different cell-attached patches of the same *Xenopus* myocyte. Pipettes were filled with Ringer containing 3 nM ACh. The records were low-pass-filtered at 3 kHz and the patch was hyperpolarized to 60 mV from rest. Note that 2,2',2''-tripyridine decreased the open time and opening frequency of both classes of ACh channels.

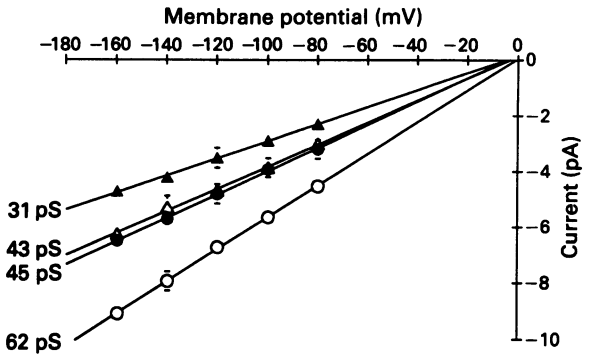

Figure 5 Effects of 2,2',2''-tripyridine on the conductance of acetylcholine (ACh) channels. This figure showed the current-voltage relations for high- (○,●) and low- (△,▲) conductance of ACh-activated channels in *Xenopus* muscle cells in culture. The open symbols (control) and filled symbols (20 min after bath application of 43 μM 2,2',2''-tripyridine) were recorded from the five cells. The indicated conductances were computed by the inverse slope of the line fitted by least squares of the five data points. Note that 2,2',2''-tripyridine reduced the conductance of both classes of ACh channels to the same degree. The symbols show mean ± s.e.means for the five experiments. The reversal potentials of the currents were estimated at − 3 mV (high conductance) and − 6 mV (low conductance) for the control condition and at − 4 mV (high conductance) and − 7 mV (low conductance) for the application of 43 μM 2,2',2''-tripyridine. Resting membrane potentials in these cells were − 75 mV to − 80 mV.

conductance of the membrane induced by ACh is supposed to be the sum of the conductance of individual channels and that each channel can show multiple open states (Sakmann *et al.*, 1980). The peak amplitude of ACh-induced currents in the whole cell recording was reduced by 2,2',2''-tripyridine in a concentration-dependent manner which corresponded to the depression of both types of low- and high-conductance ACh channels in the single channel recordings. Similar effects have been reported for (+)-tubocurarine (Katz & Miledi, 1978; Lambert *et al.*, 1980; 1981; Gibb & Marshall, 1984) and other neuromusclar blocking agents (Colquhoun & Sheridan, 1981).

2,2',2''-Tripyridine increased the run-down of ACh-induced currents at higher frequency stimulations of 7 Hz and 30 Hz, which could be accounted for either by enhancement of the rate of agonist-induced desensitization or by a direct action on the receptor-activated ionic channel. From the data of single channel recording, it seems unlikely that the enhancement of run-down of trains of ACh-induced current by 2,2',2''-tripyridine can be accounted for by postulating enhancement of desensitization of the receptor-channel complex (Bowman *et al.*, 1986; Wilson & Thomsen, 1991) since the conductance of ACh-activated single channels appeared to be independent of ACh receptor desensitization (Sakmann *et al.*, 1980); however, 2,2',2''-tripyridine could decrease the conductance of both types of low- and high-conductance ACh-activated channels. Furthermore, if 2,2',2''-tripyridine possessed an ability to enhance desensitization of the receptor-channel complex, it could potentiate the occurrence

of grouping or clustering of ACh channels opening in the presence of higher concentrations of ACh (> 1 μM). While, in our experiments with 2,2',2''-tripyridine on the patch pipettes with 1 μM ACh on cell attached patches, we saw less evidence for grouping or clustering of openings than in the absence of 2,2',2''-tripyridine. Thus, it was considered that 2,2',2''-tripyridine probably inhibited the nicotinic acetylcholine channels which resulted in the reduction of conductance of both types of ACh channel in the *Xenopus* muscle cells. Furthermore, 2,2',2''-tripyridine decreased the opening frequency and the mean open time of both types of low- and high-conductance ACh channel in *Xenopus* muscle cells. These decreasing effects on ACh channel activity were compared with those of typical blockers of nicotinic ACh receptor channels: bupivacaine as an open channel blocker (Aracava *et al.*, 1984), chlorpromazine as a closed or nonconducting channel blocker (Carp *et al.*, 1983) and phencyclidine as an open and closed channel blocker (Aguayo *et al.*, 1986). These three drugs manifested different blocking actions on single channel currents (Kimura *et al.*, 1991). 2,2',2''-Tripyridine was shown to be a mixed type of channel blocker of open and closed conformation of the ionic channel (like phencylidine) because of the simultaneous decrease of both the open time and open frequency.

2,2',2''-Tripyridine exerted two effects on the endplate potentials (e.p.ps) on the mouse phrenic nerve-diaphragm preparations: a depression in the peak amplitude and a decrease in decay time constant. Both effects seemed to be affected independently for the following reasons: (a) the onset of the depression of decay time constant was much faster than the depression of the peak amplitude; (b) the peak amplitude but not the decay time constant was progressively reduced by the repetitive stimulations. It is not known whether this dichotomy in the actions of the toxin reflects two different binding sites or a single topographical site possessing two conformations, one of which alters the decay time constant and the other immobilizes the ACh receptor in its closed form (Hsu *et al.*, 1992). A similar result was found in the present study. ACh-induced whole-cell current shows as a function of membrane potential under control and in the presence of 2,2',2''-tripyridine. 2,2',2''-Tripyridine reduces the peak amplitudes and decay time constant of ACh-induced whole-cell current in a voltage-dependent manner. Like (+)-tubocurarine, 2,2',2''-tripyridine is more effective in reducing ACh-induced whole-cell currents at hyperpolarized potentials. Furthermore, the reversal potential for both ACh-induced whole-cell currents and single ACh channel currents were not altered by 2,2',2''-tripyridine. In addition, 2,2',2''-tripyridine has no effect on the membrane potential of myocytes. These observed effects of 2,2',2''-tripyridine on the *Xenopus* muscle cells were correlated with findings on the mouse phrenic nerve-diaphragm preparations.

In conclusion, these results together with our previous report (Lin-Shiau *et al.*, 1992) which showed that 2,2',2''-tripyridine inhibited the binding of α-bungarotoxin in the mouse diaphragm, suggest that 2,2',2''-tripyridine, like (+)-tubocurarine, has at least two distinct postjunctional actions. 2,2',2''-Tripyridine appears to interact with both the ACh receptor and its ionic channel. It would be of interest to compare the binding characteristics of these two sites and to determine if 2,2',2''-tripyridine, (+)-tubocurarine and local anaesthetics share common channel binding sites.

This work was supported by a research grant from the National Science Council, Republic of China (NSC81-0412-B002-06z).

References

ANDERSON, C.R. & STEVENS, C.F. (1973). Voltage clamp analysis acetylcholine produced end-plate current fluctuations at frog neuromuscular junction. *J. Physiol.*, **235**, 665–691.

AGUAYO, L.G., VITKOP, B. & ALBUQUERQUE, E.X. (1986). Voltage- and time dependent effects of phencyclidines on the endplate current arise from open and closed channel blockade. *Proc. Natl. Acad. Sci. U.S.A.*, **83**, 3523–3527.

ARACAVA, Y. & ALBUQUERQUE, E.X. (1984). Meproadifen enhances activation and desensitization of the acetylcholine receptor-ionic channel complex (AChR), single channel studies. *FEBS Lett.*, **174**, 267–274.

BERANEK, R. & VYSKOCIL, F. (1968). The effect of atropine on the frog sartorius neuromuscular junction. *J. Physiol.*, **195**, 493–503.

BOWMAN, W.C., GIBB, A.J., HARVEY, A.L. & MARSHALL, I.G. (1986). Prejunctional actions of cholinoceptor agonists and antagonists, and of anticholinesterase drugs. In *New Neuromuscular Blocking Agents. Handb. Exp. Pharmacol.*, Vol. 79, ed. Kharkevich, D.A. pp. 141–170. Berlin: Springer-Verlag.

CARP, J.S., ARONSTAM, R.S., WITKOP, B. & AIBUOUEROUE, E.X. (1983). Electrophysiological and biochemical studies on enhancement of desensitization by phenothiazine neuroleptics. *Proc. Natl. Acad. Sci. U.S.A.*, **80**, 310–314.

COLQUHOUN, D. & SHERIDAN, R.E. (1981). The modes of action of gallamine. *Proc. R. Soc. B*, **211**, 181–203.

GIBB, A.J. & MARSHALL, I.G. (1984). Pre- and post-junctional effects of d-tubocurarine and other nicotinic antagonists during repetitive stimulation in the rat. *J. Physiol.*, **351**, 275–297.

HAMILL, O.P., MARTY, A., NEHER, E., SAKMANN, B. & SIGWORTH, F.J. (1981). Improved patch-clamp techniques for high-resolution current recording from cell and cell-free membrane patches. *Pflügers Arch.*, **391**, 85–100.

HSU, K.S., FU, W.M. & LIN-SHIAU, S.Y. (1992). Further studies on the mode of twitch depression induced by 2,2',2''-tripyridine in mouse phrenic nerve-diaphragm. *Joint Annual Conference Neurosci.* Oct. 30–31, Taipei, Taiwan. Abs.p. 8.

KATZ, B. & MILEDI, R. (1973). The binding of acetylcholine to receptors and its removal from the synaptic cleft. *J. Physiol.*, **231**, 549–574.

KATZ, B. & MILEDI, R. (1978). A re-examination of curare action at the motor endplate. *Proc. R. Soc. B*, **203**, 119–133.

KIMURA, M., NOJIMA, H., MUROI, M. & KIMURA, I. (1991). Mechanisms of the blocking action of β-eudesmol on the nicotinic acetylcholine receptor channel in mouse skeletal muscles. *Neuropharmacol.*, **30**, 835–841.

KUO, M.L., WANG, L.D. & LIN, J.K. (1986). Mutagenicity and cytotoxicity of dipyridyl derivatives and waste water discharged from paraquat manufactory. *J. Chin. Oncol. Soc.*, **2**, 1–8.

LAMBERT, J.J., VOLLE, R.L. & HENDERSON, E.G. (1980). An attempt to distinguish between the actions of neuromuscular blocking drugs on the acetylcholine receptor and on its associated ionic channel. *Proc. Natl. Acad. Sci. U.S.A.*, **77**, 5003–5007.

LAMBERT, J.J., DURANT, N.N., REYNOLDS, L.S., VOLLE, R.L. & HENDERSON, E.G. (1981). Characterization of endplate conductance in transected frog muscle: modification by drugs. *J. Pharmacol. Exp. Ther.*, **216**, 62–69.

LIN, J.K., KUO, M.L., LEE, K.W. & LIN-SHIAU, S.Y. (1988). DNA cleavage effect and cytotoxicity of the waste water discharged from paraquat manufactory. *J. Chin. Oncol. Soc.*, **4**, 1–12.

LIN-SHIAU, S.Y., HSU, K.S. & FU, W.M. (1992). Studies on the curare-like action of 2,2',2''-tripyridine in the mouse phrenic nerve-diaphragm. *Br. J. Pharmacol.*, **106**, 55–60.

MANALIS, R.S. (1977). Voltage-dependent effect of curare at the frog neuromuscular junction. *Nature*, **267**, 366–368.

MARTY, A., NEILD, T. & ASCHER, P. (1976). Voltage sensitivity of acetylcholine currents in *Aplysia* neurons in the presence of curare. *Nature*, **261**, 501–503.

NEHER, E. & STEINBACH, J.H. (1982). Local anaesthetics transiently block currents through single acetylcholine-receptor channels. *J. Physiol.*, **227**, 153–176.

POO, M.M. (1982). Rapid lateral diffusion of functional ACh receptors in embryonic muscle cell membrane. *Nature*, **299**, 332–334.

SAKMANN, B., PATLAK, J. & NEHER, E. (1980). Single acetylcholine-activated channels show burst-kinetics in presence of desensitizing concentrations of agonist. *Nature*, **286**, 71–73.

SANES, D.H. & POO, M.M. (1989). In vitro analysis of position- and lineage-dependent selectivity in the formation of neuromuscular synapse. *Neuron*, **2**, 1237–1244.

SPITZER, N.C. & LAMBORGHINI, J.C. (1976). The development of the action potential mechanisms of amphibian neurons isolated in culture. *Proc. Natl. Acad. Sci. U.S.A.*, **73**, 1641–1645.

WANG, J.D., LI, W.M., HU, F.C. & HU, K.H. (1987). The occupational risk and the development of premalignant skin lesions among paraquat manufacturers. *Br. J. Indust. Med.*, **44**, 196–200.

WILSON, D.F. & THOMSEN, R.H. (1991). Nicotinic receptors on the phrenic nerve: evidence for negative feedback. *Neurosci. Lett.*, **132**, 163–166.

YOUNG, S.H. & POO, M.M. (1983). Topographical rearrangement of ACh receptor alters channel kinetics. *Nature*, **304**, 161–163.

YOUNG, S.H. & POO, M.M. (1983a). Spontaneous release of transmitter from growth cones of embryonic neurons. *Nature*, **305**, 634–637.

(Received April 16, 1993
Accepted April 29, 1993)

Br. J. Pharmacol. (1993), **110**, 169–176

Effects of the central analgesic tramadol and its main metabolite, O-desmethyltramadol, on rat locus coeruleus neurones

[1]Jan Sevcik, Karen Nieber, Bernd Driessen & [2]Peter Illes

Department of Pharmacology, University of Freiburg, Hermann-Herder-Strasse 5, D-7800 Freiburg, Germany

1 Tramadol is a centrally acting analgesic with low opioid receptor affinity and, therefore, presumably additional mechanisms of analgesic action. Tramadol and its main metabolite O-desmethyltramadol were tested on rat central noradrenergic neurones of the nucleus locus coeruleus (LC), which are involved in the modulation of nociceptive afferent stimuli.

2 In pontine slices of the rat brain the spontaneous discharge of action potentials of LC cells was recorded extracellularly. (−)-Tramadol (0.1–100 μM), (+)-tramadol (0.1–100 μM), (−)-O-desmethyltramadol (0.1–100 μM) and (+)-O-desmethyltramadol (0.01–1 μM) inhibited the firing rate in a concentration-dependent manner. (+)-O-desmethyltramadol had the highest potency, while all other agonists were active at a similar range of concentrations.

3 (−)-Tramadol (10, 100 μM) was less inhibitory in brain slices of rats pretreated with reserpine (5 mg kg^{-1}, 5 h before decapitation) than in controls.

4 The effect of (−)-tramadol (10 μM) was abolished in the presence of the α_2-adrenoceptor antagonist, rauwolscine (1 μM), whilst that of (+)-O-desmethyltramadol (0.3 μM) virtually disappeared in the presence of the opioid antagonist, naloxone (0.1 μM). (+)-Tramadol (30 μM) and (−)-O-desmethyltramadol (10 μM) became inactive only in the combined presence of naloxone (0.1 μM) and rauwolscine (1 μM).

5 In another series of experiments, the membrane potential of LC neurones was determined with intracellular microelectrodes. (−)-Tramadol (100 μM) inhibited the spontaneous firing and hyperpolarized the cells; this effect was abolished by rauwolscine (1 μM). (+)-O-desmethyltramadol (10 μM) had a similar but somewhat larger effect on the membrane potential than (−)-tramadol. The (+)-O-desmethyltramadol- (10 μM) induced hyperpolarization was abolished by naloxone (0.1 μM).

6 The hyperpolarizing effect of noradrenaline (30 μM) was potentiated in the presence of (−)-tramadol (100 μM), but not in the presence of (+)-O-desmethyltramadol (10 μM). There was no potentiation of the noradrenaline (30 μM) effect, when the cells were hyperpolarized by current injection to an extent similar to that produced by (−)-tramadol (100 μM).

7 Both noradrenaline (100 μM) and (−)-tramadol (100 μM) decreased the input resistance.

8 The results confirm that the analgesic action of tramadol involves both opioid and non-opioid components. It appears that (−)-tramadol inhibits the uptake of noradrenaline and via a subsequent increase in the concentration of endogenous noradrenaline indirectly stimulates α_2-adrenoceptors. (+)-O-desmethyltramadol seems to stimulate directly opioid μ-receptors. The effects of (+)-tramadol and (−)-O-desmethyltramadol consist of combined μ-opioid and α_2-adrenergic components.

Keywords: Tramadol; O-desmethyltramadol; locus coeruleus neurones; firing rate; membrane potential; noradrenaline uptake blockade

Introduction

Tramadol is a centrally acting analgesic (Friderichs *et al.*, 1978) with a limited range of side effects (Vogel *et al.*, 1978; Flohe *et al.*, 1978). It binds to opioid μ-receptors with an approximately 100-times lower affinity than morphine (Hennies *et al.*, 1988), while there is a much smaller difference between the analgesic potencies of these compounds (Friderichs *et al.*, 1978). Hence, it was concluded that non-opioid mechanisms are likely to be involved in tramadol analgesia (see e.g. Carlsson & Jurna, 1987). In fact this opioid has been shown to inhibit the uptake of noradrenaline and 5-hydroxytryptamine (Driessen & Reimann, 1992; Raffa *et al.*, 1992) thereby increasing the concentration of the two neurotransmitters in the central nervous system (CNS). Endogenous noradrenaline and 5-hydroxytryptamine participate in pain modulation (Besson & Chaouch, 1987; Jones, 1991) and may, in consequence, mediate the analgesic effect of tramadol.

The nucleus locus coeruleus (LC) is situated in the pons and consists of a compact group of noradrenergic cell bodies, which project into various areas of the central nervous system (Foote *et al.*, 1983). LC neurones possess somatic (and/or dendritic) α_2-adrenoceptors (Aghajanian & Vander-Maelen, 1982; Williams *et al.*, 1985) and opioid μ-receptors (Williams & North, 1984). Stimulation of either receptor-type increases the same potassium conductance (North & Williams, 1985) and, subsequently, leads to hyperpolarization and inhibition of spontaneous firing. α_2-Adrenoceptors may be tonically activated by endogenous noradrenaline after uptake blockade by desipramine (Egan *et al.*, 1983) or cocaine (Surprenant & Williams, 1987).

The LC is involved in the control of various cognitive and vegetative functions (Olpe *et al.*, 1985), including the modulation of pain perception (Jones, 1991). The aim of the present study was two fold. Firstly, the effects of tramadol and its main metabolite O-desmethyltramadol (Lintz *et al.*, 1981) were investigated on the firing rate and membrane potential of LC neurones. Secondly, the possible involvements of α_2-adrenoceptors and opioid μ-receptors in the effects of

[1] Permanent address: Institute of Pharmacology, CSAV, Albertov 4, 128 00 Prague 2, The Czech Republic.
[2] Author for correspondence.

tramadol and O-desmethyltramadol were studied. Both (−)- and (+)-enantiomers of tramadol and O-desmethyltramadol were used, since opioid receptors (Höllt & Wüster, 1978) and the noradrenaline carrier (Graefe & Bönisch, 1988) bind ligands in a stereoselective manner.

Methods

Brain slice preparation

Midpontine slices of the rat brain were prepared and maintained as described earlier (Henderson *et al.*, 1982; Regenold & Illes, 1990). In brief, male Wistar rats (150–220 g) were anaesthetized with ether and decapitated. Slices of 400 μm thickness, containing the caudal part of the LC were prepared in oxygenated medium at 1–4°C with a Lancer vibratome. A single slice was transferred to the recording chamber and was superfused at a rate of 2 ml min^{-1} with medium saturated with 95% O_2 plus 5% CO_2 and maintained at 35–36°C. The medium was of the following composition (in mM): NaCl 126, KCl 2.5, NaH_2PO_4 1.2, $MgCl_2$ 1.3, $CaCl_2$ 2.4, $NaHCO_3$ 25, glucose 11, EDTA 0.03 and ascorbic acid 0.3.

Recording techniques

Extracellular recording Glass microelectrodes filled with 4 M NaCl and having a tip resistance of 2–4 MΩ were used to record the firing rate. The electrode signals were passed through a Grass P16 high impedance amplifier, filtered and displayed on a Tektronix 5113 oscilloscope. The spikes were gated and counted by means of a WPI 121 window discriminator coupled to an electronic ratemeter and a Watanabe WTR 311 pen-recorder. Firing rate was recorded as consecutive 30 s samples.

Intracellular recording Recordings were carried out with glass microelectrodes filled with KCl 2 M (tip resistance 60–100 MΩ) using a high impedance pre-amplifier and a bridge-circuit (Axoclamp 2 A). In some experiments LC cells were constantly hyperpolarized (about 15 mV) by injecting current through the microelectrode. In addition, hyperpolarizing current pulses of constant amplitude and 250 ms duration were delivered at a frequency of 0.5 Hz. The input resistance was calculated from the peak potential change produced. The membrane potential was determined on withdrawal of the microelectrode from the cell at the end of each experiment. Changes in the membrane potential were displayed on a Gould RS 3200 pen-recorder and in addition stored on tape (Racal Store 4).

Identification of LC neurones

The LC could be easily identified under a binocular microscope as a translucent oval area at the ventrolateral border of the fourth ventricle. LC cells spontaneously fire with a constant rate of 0.2–5 Hz. The neurones were identified on the basis of their electrophysiological properties and their sensitivity to noradrenaline (Illes & Nörenberg, 1990; Regenold & Illes, 1990).

Application of drugs and evaluation of data

Drugs were applied by changing the superfusion medium by means of three-way taps. At the constant flow rate of 2 ml min^{-1} about 30 s were required for the drug to reach the bath.

Extracellular recording A first series of experiments was designed in order to find out whether the inhibitory effect of (−)-tramadol (10 μM) reaches a steady-state within 10 min. The depression of firing rate was measured 10 and 20 min after addition of tramadol (average of two counting periods each). These effects were expressed as percentages of the average firing during the 2 min immediately before addition of (−)-tramadol (average of 4 counting periods). (−)-Tramadol (10 μM) decreased the discharge of action potentials 10 min after its application to 44.0 ± 5.4% of the pre-drug value; the effect of (−)-tramadol did not increase further during the next 10 min of incubation (41.2 ± 5.2%; $n = 7$; $P > 0.05$). A few preliminary experiments indicated that the effects of (+)-tramadol (30 μM), as well as (−)- and (+)-O-desmethyltramadol (10 μM and 0.3 μM, respectively) also reached a maximum within 10 min of superfusion. Therefore, cumulative concentration-response curves of (−)- and (+)-tramadol as well as (−)- and (+)-O-desmethyltramadol were determined by applying increasing concentrations of each drug for 10 min. The depression of firing rate was measured again at its maximum. In every experiment, the IC_{50} value, i.e. the concentration that produced 50% inhibition of the spike discharge, was graphically estimated. Only one concentration-response curve for one drug was determined on a single cell of a brain slice. Concentration-response curves for (−)-tramadol were determined also by using brain slices of rats pretreated with reserpine (5 mg kg^{-1}, i.p., 5 h before decapitation).

The interaction of the agonists [(−)- and (+)-tramadol; (−)- and (+)-O-desmethyltramadol] with naloxone or rauwolscine was tested as follows. A concentration of the respective agonist was used that inhibited the discharge of action potentials by about 80%, as estimated from the concentration-response curves. At first the agonist was applied for 10 min. Then either naloxone (0.1 μM) or rauwolscine (1 μM) were co-applied in the continuous presence of the agonist for another 10 min. Finally, both antagonists together with the agonist were present in the medium for an additional 10 min; this period was followed by washout.

Intracellular recording (−)-Tramadol (100 μM) was applied to spontaneously firing LC neurones at the resting membrane potential. When the (−)-tramadol-induced hyperpolarization did not increase further, rauwolscine (1 μM) was added in the continued presence of the agonist until a complete recovery was achieved. In analogous experiments (+)-O-desmethyltramadol (10 μM) was used as an agonist and naloxone (0.1 μM) as an antagonist. Agonists were present for about 10 min alone and then for another 10 min in the presence of the respective antagonist.

The effect of noradrenaline (30 μM) was tested before, during and after the application of (−)-tramadol (100 μM) or (+)-O-desmethyltramadol (10 μM). At first noradrenaline (30 μM) was applied for 1.5 min. Then (−)-tramadol (100 μM) or (+)-O-desmethyltramadol (10 μM) was added for 10 min without, and subsequently for 1.5 min with noradrenaline (30 μM). After a washout period, during which the firing rate and membrane potential of LC neurones recovered to their pre-drug level, noradrenaline (30 μM) was applied again for 1.5 min. In some additional experiments, LC neurones were hyperpolarized (about 15 mV) by passing constant current through the microelectrode. The effect of noradrenaline (30 μM) was tested before, during and after hyperpolarization.

The effects of (−)-tramadol (100 μM; 10 min superfusion) and noradrenaline (100 μM; 1.5 min superfusion) on the apparent input resistance of LC neurones were determined on constantly hyperpolarized non-firing neurones (for experimental details see 'Recording techniques'). The two compounds were added in random order to the same cell; between applications sufficient time was allowed for full recovery of the membrane potential and input resistance. When the response to either drug reached a steady-state, the membrane potential was temporarily restored to its pre-drug value by depolarizing current injection. The input resistance measured during this procedure (manual clamp) was compared with the input resistance determined before the

application of noradrenaline (100 μM) or (−)-tramadol (100 μM).

Materials

The following drugs were used: reserpine (Serpasil, 0.1%; Ciba-Geigy, Wehr, Germany); naloxone hydrochloride (Du Pont, Wilmington, DE, U.S.A.); (−)- and (+)-tramadol hydrochloride [(1**RS**;2**RS**)-2-[(dimethylamino)methyl]-1-(3-methoxyphenyl)-cyclohexanol hydrochloride], (−)- and (+)-O-desmethyltramadol hydrochloride (Dr W. Reimann; Grünenthal, Aachen, Germany); (−)-noradrenaline hydrochloride (Hoechst, Frankfurt am Main, Germany); rauwolscine hydrochloride (Roth, Karlsruhe, Germany).

Stock solutions (1–10 mM) of all drugs were prepared with distilled water. Further dilutions were made with medium. Equivalent quantities of the solvent had no effect.

Statistics

Arithmetic means ± s.e.mean are given throughout except in the case of IC_{50} values, when geometric means and 95% confidence limits are presented. The paired or unpaired Student's *t* test (as appropriate) was used for comparison of the means, and the paired Student's *t* test was used for comparison of the means with zero. A probability level of 0.05 or less was considered to be statistically significant.

Results

Extracellular recording

Effects of (−)-tramadol, (+)-tramadol, (−)-O-desmethyltramadol and (+)-O-desmethyltramadol on the discharge of action potentials All LC neurones included in this extracellular study fired spontaneously with an average rate of 1.00 ± 0.04 Hz ($n = 88$). (−)-Tramadol (0.1–100 μM) and (+)-tramadol (0.1–100 μM) inhibited the firing rate in a concentration-dependent manner and with similar potencies (Figure 1a). When the experiments were performed on brain slices of rats pretreated with reserpine (5 mg kg^{-1}), both 10 μM and 100 μM (−)-tramadol produced less inhibition than on brain slices of untreated rats (Figure 1a). (−)-O-desmethyltramadol (0.1–100 μM) and (+)-O-desmethyltramadol (0.01–1 μM) also depressed the discharge of action potentials in a concentration-dependent manner. The (+)-isomer had a considerably higher potency than the (−)-isomer (Figure 1b). The highest concentrations of all agonists abolished the firing. The IC_{50} values determined from the concentration-response curves were 6.0 (2.6–13.4) μM for (−)-tramadol ($n = 5$), 11.6 (5.7–23.7) μM for (+)-tramadol ($n = 8$), 2.1 (0.3–14.2) μM for (−)-O-desmethyltramadol ($n = 5$) and 0.15 (0.11–0.22) μM for (+)-O-desmethyltramadol ($n = 6$). Thus, (+)-O-desmethyltramadol had the highest potency, while all other agonists were active at a similar range of concentrations.

Interaction of tramadol with rauwolscine and naloxone Based on the concentration-response curves (Figure 1a), concentrations of (−)-tramadol (10 μM) and (+)-tramadol (30 μM) were chosen that inhibited the firing rate by about 80%. The effect of (−)-tramadol (10 μM) was not changed in the presence of naloxone (0.1 μM), but was abolished in the combined presence of naloxone (0.1 μM) and rauwolscine (1 μM) (Figure 2a, left panel) as well as in the presence of rauwolscine (1 μM) alone (Figure 2a, right panel). On the other hand, the effect of (+)-tramadol (30 μM) was greatly reduced in the presence of naloxone (0.1 μM) (Figure 2b, right panel) and abolished in the combined presence of naloxone (0.1 μM) and rauwolscine (1 μM) (Figure 2b, left and right panels). However, rauwolscine (1 μM) failed to attenuate the effect of (+)-tramadol (30 μM), when there was no naloxone (0.1 μM) in the perfusion medium (Figure 2b, left panel).

Interaction of O-desmethyltramadol with rauwolscine and naloxone The experimental schedule was the same as described above. The effect of (+)-O-desmethyltramadol (0.3 μM) was not influenced by rauwolscine (1 μM), but was abolished in the combined presence of rauwolscine (1 μM) and naloxone (0.1 μM) (Figure 3a, left panel). When naloxone (0.1 μM) was applied first, the effect of (+)-O-desmethyltramadol (0.3 μM) was nearly fully antagonized, and there was only a very slight further antagonism by rauwolscine (1 μM) (Figure 3a, right panel).

The effect of (−)-O-desmethyltramadol (10 μM) was only moderately attenuated in the presence of rauwolscine (1 μM), but disappeared in the combined presence of rauwolscine (1 μM) and naloxone (0.1 μM) (Figure 3b, left panel). On the other hand, naloxone on its own was capable of markedly diminishing the effect of (−)-O-desmethyltramadol (10 μM) (Figure 3b, right panel).

In accordance with previous results (Illes & Nörenberg, 1990) neither rauwolscine (1 μM) nor naloxone (0.1 μM) altered the firing on its own (not shown).

Intracellular recording

Effects of (−)-tramadol and (+)-O-desmethyltramadol on the membrane potential; interaction with rauwolscine and naloxone, respectively. The resting membrane potential (RMP) of the 30 LC neurones impaled by intracellular microelectrodes was −52.9 ± 1.5 mV. In 5 cells (RMP,

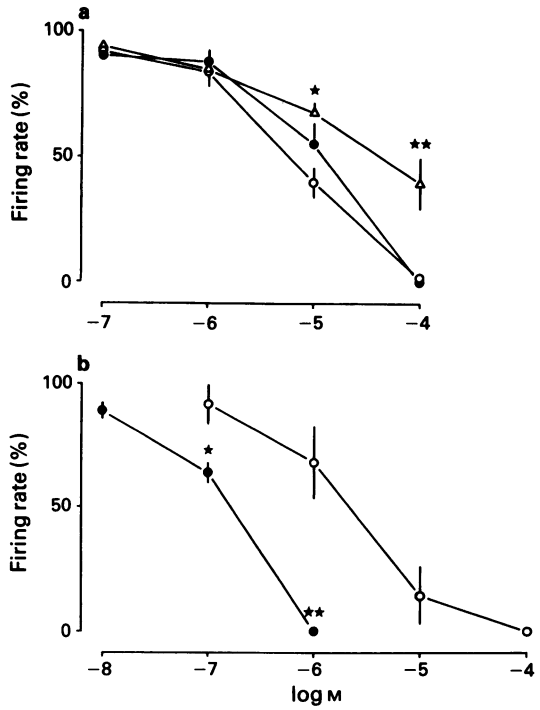

Figure 1 Inhibitory effects of (−)- and (+)-tramadol, and (−)- and (+)-O-desmethyltramadol on the firing rate of rat LC neurones. Extracellular recording. (a) Concentration-response curves of (−)-tramadol (○, $n = 5$) and (+)-tramadol (●, $n = 8$) on brain slices of untreated rats. Concentration-response curve of (−)-tramadol on brain slices of rats pretreated with reserpine (5 mg kg^{-1}) 5 h before decapitation (△, $n = 5$). Asterisks indicate significant differences from the effects of (−)-tramadol on brain slices of untreated rats (*$P < 0.05$; **$P < 0.01$). (b) Concentration-response curves of (−)-O-desmethyltramadol (○, $n = 5$) and (+)-O-desmethyltramadol (●, $n = 6$). Asterisks indicate significant differences from the effect of (−)-O-desmethyltramadol (*$P < 0.05$; **$P < 0.01$). Means ± s.e.mean from *n* slices each.

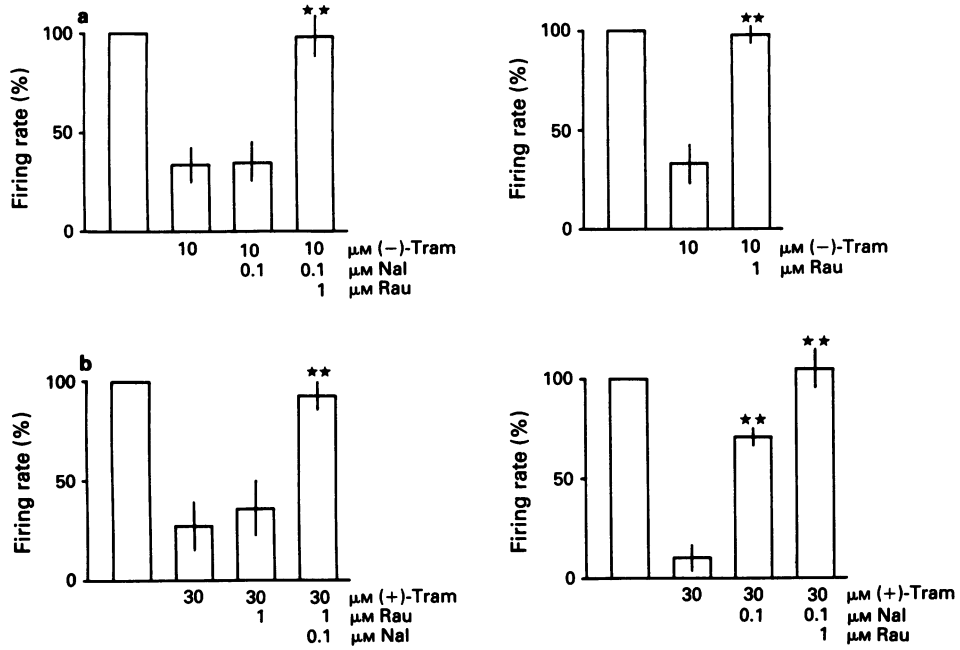

Figure 2 Inhibitory effects of (−)- and (+)-tramadol on the firing rate of LC neurones and antagonism by naloxone or rauwolscine. Extracellular recording. In this and the subsequent figure, the average firing rate during the 2 min immediately before addition of agonists was taken as 100% in each experiment (1st column). (a) Interaction between (−)-tramadol (Tram) and naloxone (Nal) or rauwolscine (Rau) (or both antagonists). Effect of naloxone (0.1 μM), and naloxone (0.1 μM) plus rauwolscine (1 μM) on the (−)-tramadol- (10 μM) induced inhibition (left panel). Asterisks indicate significant differences between the 3rd and 4th columns (**$P<0.01$). Means ± s.e.mean from 5 slices. Effect of rauwolscine (1 μM) on the (−)-tramadol- (10 μM) induced inhibition (right panel). Asterisks indicate significant differences between the 2nd and 3rd columns (**$P<0.01$). Means ± s.e.mean from 5 slices. (b) Interaction between (+)-tramadol, and rauwolscine or naloxone (or both antagonists). Effect of rauwolscine (1 μM), and rauwolscine (1 μM) plus naloxone (0.1 μM) on the (+)-tramadol- (30 μM) induced inhibition (left panel). Asterisks indicate significant differences between the 3rd and 4th columns (**$P<0.01$). Means ± s.e.mean from 6 slices. Effect of naloxone (0.1 μM), and naloxone (0.1 μM) plus rauwolscine (1 μM) on the (+)-tramadol- (30 μM) induced inhibition (right panel). Asterisks indicate significant differences between the 2nd and 3rd (**$P<0.01$) as well as between the 3rd and 4th columns (**$P<0.01$). Means ± s.e.mean from 6 slices.

− 57.8 ± 1.1 mV), (−)-tramadol (100 μM) abolished the firing and caused a hyperpolarization of 12.3 ± 2.4 mV ($P<0.01$), which was abolished in the presence of rauwolscine (1 μM) (Figure 4) the membrane potential returning to its original value (RMP, − 53.5 ± 3.9 mV). Similarly, (+)-O-desmethyltramadol (10 μM) hyperpolarized another 4 cells (RMP, − 53.0 ± 3.8 mV) by 19.5 ± 1.7 mV ($P<0.01$); this effect was abolished by naloxone (0.1 μM) (RMP, − 53.2 ± 4.8 mV).

Interaction of (−)-tramadol and (+)-O-desmethyltramadol with noradrenaline Noradrenaline (30 μM) caused in 6 LC neurones a quickly developing hyperpolarization (14.2 ± 2.3 mV) (Figure 5). Subsequently applied (−)-tramadol (100 μM) evoked a hyperpolarization of comparable amplitude (12.3 ± 1.9 mV) but slower onset and offset. The effect of noradrenaline (30 μM) was more marked (19.1 ± 2.3 mV; $P<0.01$) and longer lasting in the presence of (−)-tramadol (100 μM) than in its absence. After the washout of (−)-tramadol (100 μM), the original sensitivity of LC cells to noradrenaline (30 μM) recovered (15.0 ± 2.8 mV hyperpolarization).

In another 5 neurones, (+)-O-desmethyltramadol (10 μM) produced a hyperpolarization of 14.2 ± 2.7 mV. Noradrenaline had the same effect before (9.7 ± 1.8 mV), during (7.3 ± 0.7 mV; $P>0.05$ from the preceding value) and after (8.3 ± 0.8 mV) the application of (+)-O-desmethyltramadol (10 μM). Finally, in 5 LC cells the membrane potential was hyperpolarized (about 15 mV) by passing current through the microelectrode. The effects of noradrenaline before (11.1 ± 1.4 mV), during (10.7 ± 1.3 mV; $P>0.05$ from the preceding value) and after (11.1 ± 1.0 mV) current injection did not change.

Effects of noradrenaline and (−)-tramadol on the input resistance Five LC cells were constantly hyperpolarized (about 15 mV) by injecting current through the microelectrode (Figure 6). In addition, hyperpolarizing current pulses of constant amplitude and 250 ms duration were delivered at a frequency of 0.5 Hz. The apparent input resistance of these neurones was 176.4 ± 16.9 MΩ. (−)-Tramadol (100 μM) caused a slowly developing hyperpolarization (10.8 ± 0.9 mV) and in addition decreased the input resistance by 18.4 ± 2.6% ($P<0.01$). Noradrenaline (100 μM) evoked a hyperpolarization of faster onset (13.3 ± 0.9 mV) than (−)-tramadol (100 μM), and decreased the input resistance by 34.6 ± 6.2% ($P<0.01$).

Discussion

The present experiments demonstrate that tramadol and its main metabolite, O-desmethyltramadol, depress the firing rate of rat LC neurones. This effect is stereospecific and consists of two components, one of them mediated by opioid μ-receptors and the other one by α_2-adrenoceptors. Two antagonists were used as experimental tools, namely naloxone and rauwolscine. Rauwolscine exhibits a high selectivity for α_2- over α_1-adrenoceptors (Weitzell *et al.*, 1979), while naloxone has only a slight preference for μ- over δ- and κ-opioid receptors (Illes, 1989). However, the limited selectivity of naloxone does not constitute a major problem, since LC neurones of rats are endowed with a homogeneous population of opioid μ-receptors (Williams & North, 1984). Furthermore, it is noteworthy that the only adrenoceptors present in the rat LC belong to the α_2-type (Williams *et al.*, 1985).

Noradrenaline released from dendrites or recurrent axon collaterals of LC neurones may regulate under *in vivo* conditions the spontaneous discharge of the action potentials (Aghajanian & VanderMaelen, 1982). However, under *in vitro* conditions there is probably no major α_2-adrenoceptor-mediated tonic control of neuronal activity, since rauwolscine did not increase the firing rate when given alone (Illes & Nörenberg, 1990). This may be due to the disruption of excitatory inputs to LC cells during the preparation of brain slices and the subsequent depression of the spontaneous dendritic release of noradrenaline. We suggest that (−)-tramadol induces an increase in the concentration of noradrenaline in

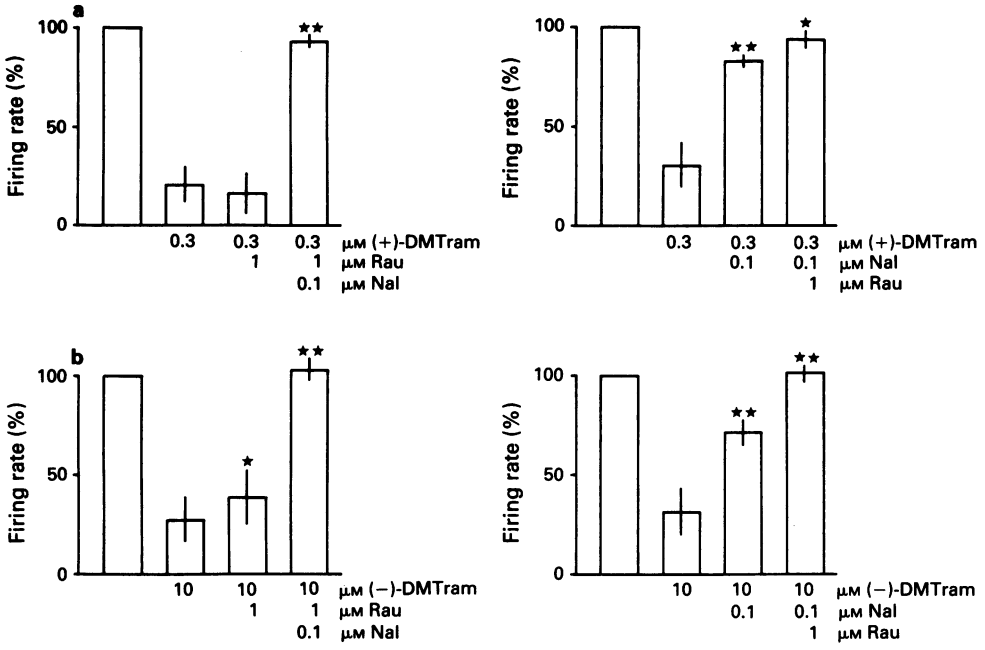

Figure 3 Inhibitory effects of (+)- and (−)-O-desmethyltramadol on the firing rate of LC neurones and antagonism by naloxone or rauwolscine. Extracellular recording. (a) Interaction between (+)-O-desmethyltramadol (DMTram) and rauwolscine (Rau) or naloxone (Nal) (or both antagonists). Effect of rauwolscine (1 μM), and rauwolscine (1 μM) plus naloxone (0.1 μM) on the (+)-O-desmethyltramadol- (0.3 μM) induced inhibition (left panel). Asterisks indicate significant differences between the 3rd and 4th columns (**$P<0.01$). Means ± s.e.mean from 8 slices. Effect of naloxone (0.1 μM), and naloxone (0.1 μM) plus rauwolscine (1 μM) on the (+)-O-desmethyltramadol- (0.3 μM) induced inhibition (right panel). Asterisks indicate significant differences between the 2nd and 3rd columns (**$P<0.01$) as well as between the 3rd and 4th columns (*$P<0.05$). Means ± s.e.mean from 7 slices. (b) Interaction between (−)-O-desmethyltramadol, and rauwolscine or naloxone (or both antagonists). Effect of rauwolscine (1 μM), and rauwolscine (1 μM) plus naloxone (0.1 μM) on the (−)-O-desmethyltramadol- (10 μM) induced inhibition (left panel). Asterisks indicate significant differences between the 2nd and 3rd columns (*$P<0.05$) as well as between the 3rd and 4th columns (**$P<0.01$). Means ± s.e.mean from 7 slices. Effect of naloxone (0.1 μM), and naloxone (0.1 μM) plus rauwolscine (1 μM) on the (−)-O-desmethyltramadol- (10 μM) induced inhibition (right panel). Asterisks indicate significant differences between the 2nd and 3rd (**$P<0.01$) as well as between the 3rd and 4th columns (**$P<0.01$). Means ± s.e.mean from 8 slices.

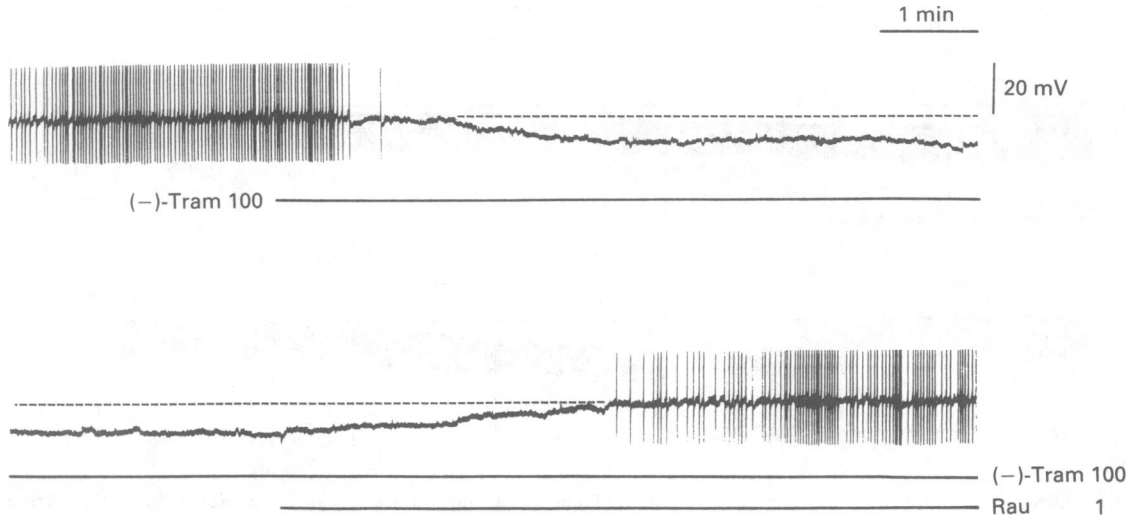

Figure 4 Effect of (−)-tramadol (Tram) on LC neurones. Intracellular recording. (−)-Tramadol (100 μM) abolished the spontaneous firing and hyperpolarized the neurone; its effect was antagonized by rauwolscine (Rau, 1 μM). The full height of action potentials was not reproduced by the pen-recorder. The resting membrane potential is indicated by the broken line. Representative experiment from 5 slices. Drugs were present for the periods indicated by the horizontal bars.

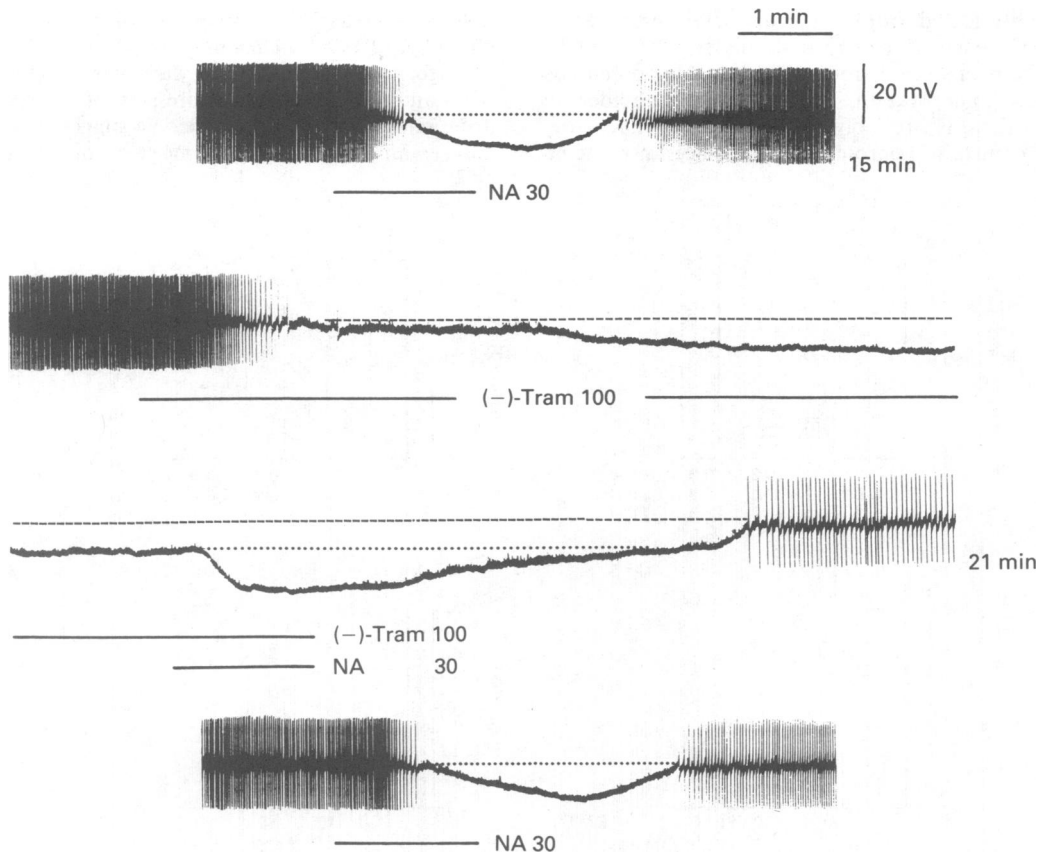

Figure 5 Potentiation of the effect of noradrenaline in LC neurones. Intracellular recording. Noradrenaline (NA, 30 μM) had a larger and longer-lasting effect during, than before or after the application of (−)-tramadol (Tram, 100 μM). The resting membrane potential is indicated by the broken line. The steady-state effect of (−)-tramadol is designated by the dotted line. Representative experiment from 6 slices. Drugs were present for the periods indicated by the horizontal bars. The intervals between the traces are shown.

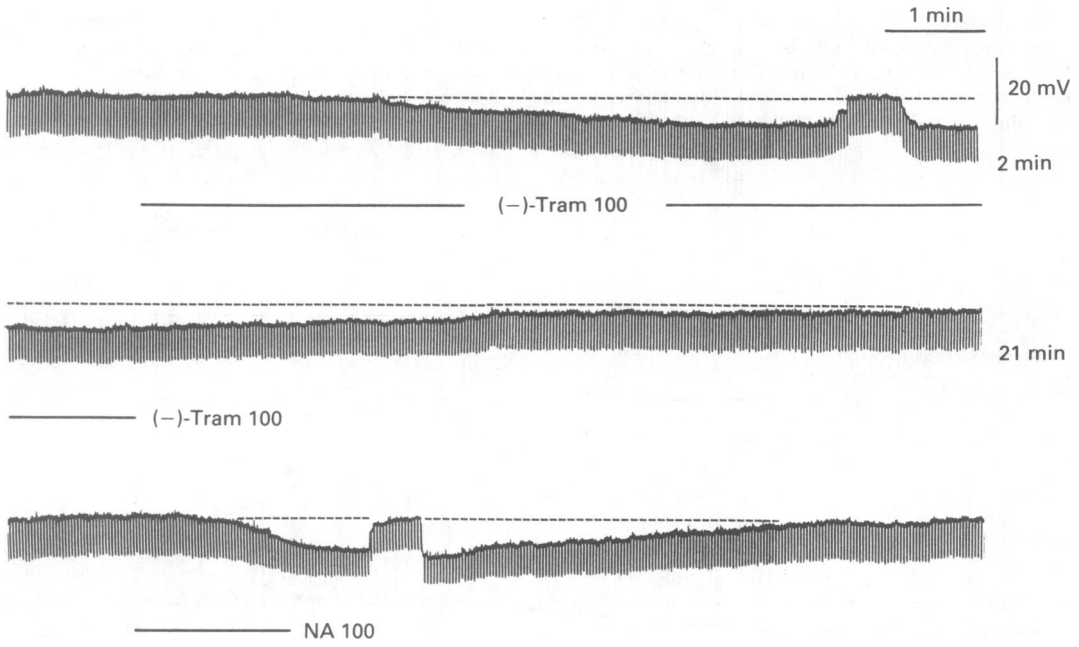

Figure 6 Effects of noradrenaline (NA) and (−)-tramadol (Tram) on the input resistance of LC neurones. Intracellular recording. The resting membrane potential of the neurone was slightly raised by continuous current injection in order to suppress spontaneous firing; this raised membrane potential is indicated by the broken line. Downward deflections represent electrotonic potentials caused by hyperpolarizing current pulses of constant amplitude. The electrotonic potentials are directly proportional to the input resistance. At the steady-states of the (−)-tramadol (100 μM) and noradrenaline (100 μM) responses the membrane potential was temporarily restored to its pre-drug value with depolarizing current. Representative experiment from 5 slices. Drugs were present for the periods indicated by the horizontal bars. The intervals between the traces are shown.

the vicinity of the α_2-adrenoceptors, and thereby inhibits the firing rate. In fact, the inhibitory potency of (−)-tramadol decreased in brain slices of rats pretreated with reserpine, a compound known to deplete noradrenaline pools. Moreover, (−)-tramadol caused a slowly developing depression of the firing, which was antagonized by rauwolscine, but not naloxone. The prototypic uptake inhibitor, desipramine, has been shown to cause a similar rauwolscine-sensitive inhibitory effect on LC neurones (Illes & Nörenberg, 1990).

Intracellular recordings in LC cells also suggest that (−)-tramadol acts by the blockade of noradrenaline uptake. Such a mode of action is favoured by three fold evidence. Firstly, the effects of (−)-tramadol on the membrane potential and firing rate were abolished by rauwolscine. Hyperpolarizations sensitive to α_2-adrenoceptor antagonists developed in LC neurones also in the presence of the uptake inhibitors, desipramine (Egan *et al.*, 1983) and cocaine (Surprenant & Williams, 1987). Secondly, the hyperpolarizing effect of noradrenaline was potentiated in the presence of (−)-tramadol. In good accordance with this finding, the uptake inhibitor cocaine was reported to facilitate the noradrenaline-induced outward current (Surprenant & Williams, 1987). Since (−)-tramadol causes hyperpolarization when given alone, we shifted the membrane potential to a similar extent by passing constant current via the microelectrode. Under these conditions the effect of noradrenaline was the same as in the absence of (−)-tramadol at the original resting membrane potential. It is unclear, why the expected slight depression of the noradrenaline-induced response after hyperpolarizing current injection was not noticed (Williams *et al.*, 1985). Thirdly, (−)-tramadol may act in LC neurones by the same mechanism as noradrenaline. Both compounds caused hyperpolarization and a reduction of input resistance, which persisted when the membrane potential was manually clamped to its pre-drug value. Input resistance changes that are secondary to hyperpolarization are thereby eliminated (Williams *et al.*, 1984). The ions involved in the (−)-tramadol effect might be potassium and not chloride as the microelectrodes were filled with KCl. When Cl^- diffuses from the microelectrode into the cells, an increased permeability of the membrane to Cl^- depolarizes rather than hyperpolarizes LC neurones (Cherubini *et al.*, 1988).

(+)-O-desmethyltramadol depressed the firing rate of LC neurones in a naloxone-reversible manner; rauwolscine had only a slight antagonistic effect. The (+)-O-desmethyltramadol-induced hyperpolarization was also abolished by naloxone. In contrast to (−)-tramadol, (+)-O-desmethyltramadol did not potentiate the effect of noradrenaline. Hence, (+)-O-desmethyltramadol seems to stimulate directly opioid μ-receptors, while the activation of α_2-adrenoceptors by (−)-tramadol is indirect. This proposal is in good agreement with the previously published high binding affinity of (±)-O-desmethyltramadol to opioid μ-sites and its correspondingly strong analgesic potency (Hennies *et al.*, 1988). In contrast, (±)-tramadol blocked the neuronal uptake of noradrenaline with a dissociation constant of approximately 1 μM, although even much higher concentrations of the compound did not bind to α_2-adrenoceptors (Raffa *et al.*, 1992). Furthermore, (±)-tramadol facilitated the electrically-evoked release of [^{3}H]-noradrenaline from rat brain cortex slices in the absence, but not in the presence of the uptake inhibitor cocaine (Driessen *et al.*,1993).

The use of naloxone and rauwolscine demonstrated that (−)-tramadol acts exclusively via α_2-adrenoceptors, whereas (+)-O-desmethyltramadol activates mostly opioid μ-receptors (see above). The effects of (+)tramadol and (−)-O-desmethyltramadol consist of both opioid and noradrenergic components. The relative contribution of these components to the effect of agonists was determined by the application of rauwolscine or naloxone, and the subsequent application of both antagonists. With this experimental schedule the noradrenergic components of both (+)-tramadol and (−)-O-desmethyltramadol appear to be smaller, when rauwolscine is applied alone, than when rauwolscine and naloxone are present together in the medium (see Figures 2b, 3b). The underestimation of the noradrenergic component may be due to the unidirectional interaction between α_2-adrenoceptors and opioid μ-receptors (Illes & Nörenberg, 1990; Illes *et al.*, 1990): blockade of α_2-adrenoceptors enhanced μ-receptor-mediated effects, while blockade of μ-receptors did not alter α_2-adrenoceptor-mediated effects. Thus, rauwolscine may, on the one hand, potentiate the opioid component, and, on the other hand, counteract the noradrenergic component of both (+)-tramadol and (−)-O-desmethyltramadol.

Although O-desmethyltramadol is the main metabolite of tramadol in most species, in man there is only a slow biotransformation, and tramadol is excreted mainly unchanged (Lintz *et al.*, 1981). Hence, the production of metabolites with strong opioid activity (i.e. O-desmethyltramadol) occurs in man only to a minor extent.

Drugs that manipulate noradrenergic activity markedly influence opioid-induced antinociception (Bläsig & Herz, 1980). The LC is a main source of the ascending and descending noradrenergic systems in the CNS (Moore & Card, 1984). Noradrenaline administered into the spinal subarachnoidal space produces powerful analgesic effects (Reddy *et al.*, 1980). Electrical or chemical stimulation of the LC also causes analgesia of spinal origin (Segal & Sandberg, 1977; Jones & Gebhart, 1988). It is difficult to reconcile these data with the finding that opioids depress the firing rate of LC neurones both *in vivo* (Bird & Kuhar, 1977) and *in vitro* (Pepper & Henderson, 1980; North & Williams, 1985). The most likely explanation is that noradrenaline plays opposite roles in the brain and spinal cord; the descending noradrenergic system facilitates analgesia, while the ascending system inhibits it (Kuraishi *et al.*, 1987). Ascending nociceptive projections from the spinal cord transmit information via collaterals to the LC (Jones, 1991). Opioids, including tramadol may interrupt the subsequent noradrenergic activation of higher brain centres necessary for the perception of pain.

Potentiation of opioid analgesia by noradrenaline uptake blockers is a well documented clinical finding (Jaffe & Martin, 1990). It has been shown that the inhibitory effect of tramadol on the uptake of noradrenaline occurs at serum concentrations which are achieved with analgesic doses in the mouse tail-flick test (Friderichs & Becker, 1991). These observations support the proposal that inhibition of the activity of LC neurones by a combined stimulation of opioid μ-receptors and α_2-adrenoceptors may be one of the mechanisms by which tramadol exerts antinociception. Of course additional transmitter systems (e.g. 5-hydroxytryptamine; Driessen & Reimann, 1992) may also be involved.

J.S. is the recipient of a research fellowship from the Alexander von Humboldt-Stiftung. We are grateful to Drs W. Reimann and W. Nörenberg for many helpful discussions and to Dr U. Trendelenburg for critically reading the manuscript. The excellent technical assistance of Mr E. Schöffel is acknowledged with thanks. This work was supported by the Deutsche Forschungsgemeinschaft (SFB 325).

References

AGHAJANIAN, G.K. & VANDERMAELEN, C.P. (1982). α_2-Adrenoceptor-mediated hyperpolarization of locus coeruleus neurones: intracellular studies *in vivo*. *Science*, **215**, 1394–1396.

BESSON, J.M. & CHAOUCH, A. (1987). Descending serotonergic systems. In *Pain and Headache*. Vol. 9. ed. Gildenberg, P.L. pp. 64–100. Basel: Karger.

BIRD, S.J. & KUHAR, M.J. (1977). Iontophoretic application of opiates to the locus coeruleus. *Brain Res.*, **122**, 523–533.

BLÄSIG, J. & HERZ, A. (1980). Interactions of opiates and endorphins with cerebral catecholamines. In *Adrenergic Activators and Inhibitors. Handbook of Experimental Pharmacology*. Vol. 54/I. ed. Szekeres, L. pp. 463–497. Berlin: Springer.

CARLSSON, K.-H. & JURNA, I. (1987). Effects of tramadol on motor and sensory responses of the spinal nociceptive system in the rat. *Eur. J. Pharmacol.*, **139**, 1–10.

CHERUBINI, E., NORTH, R.A. & WILLIAMS, J.T. (1988). Synaptic potentials in rat locus coeruleus neurones. *J. Physiol.*, **406**, 431–442.

DRIESSEN, B. & REIMANN, W. (1992). Interaction of the central analgesic, tramadol, with the uptake and release of 5-hydroxytryptamine in the rat brain *in vitro*. *Br. J. Pharmacol.*, **105**, 147–151.

DRIESSEN, B., REIMANN, W. & GIERTZ, H. (1993). Effects of the central analgesic tramadol on the uptake and release of noradrenaline and dopamine *in vitro*. *Br. J. Pharmacol.*, **108**, 806–811.

EGAN, T.M., HENDERSON, G., NORTH, R.A. & WILLIAMS, J.T. (1983). Noradrenaline-mediated synaptic inhibition in rat locus coeruleus neurones. *J. Physiol.*, **345**, 477–488.

FLOHE, L., AREND, I., COGAL, A., RICHTER, W. & SIMON, W. (1978). Klinische Prüfung der Abhängigkeitsentwicklung nach Langzeitapplikation von Tramadol. *Arzneim. Forsch./Drug Res.*, **28**, 213–217.

FOOTE, S.L., BLOOM, F.E. & ASTON-JONES, G. (1983). Nucleus locus coeruleus: new evidence of anatomical and physiological specifity. *Physiol. Rev.*, **63**, 844–915.

FRIDERICHS, E. & BECKER, R. (1991). Correlation of tramadol and M_1 serum levels with antinociceptive activity in mice. *Naunyn-Schmied. Arch. Pharmacol.*, **343**, R9.

FRIDERICHS, E., FELGENHAUER, F., JONGSCHAAP, P. & OSTERLOH, G. (1978). Pharmakologische Untersuchungen zur Analgesie, Abhängigkeits- und Toleranzentwicklung von Tramadol, einem stark wirkenden Analgetikum. *Arzneim. Forsch./Drug Res.*, **28**, 122–134.

GRAEFE, K.-H. & BÖNISCH, H. (1988). The transport of amines across the axonal membranes of noradrenergic and dopaminergic neurones. In *Catecholamines. Handbook of Experimental Pharmacology*. Vol. 90/I. ed. Trendelenburg, U. & Weiner, N. pp. 193–245. Berlin: Springer.

HENDERSON, G., PEPPER, C.M. & SHEFNER, S.A. (1982). Electrophysiological properties of neurones contained in the locus coeruleus and mesencephalic nucleus of the trigeminal nerve *in vitro*. *Exp. Brain Res.*, **45**, 29–37.

HENNIES, H.-H., FRIDERICHS, E. & SCHNEIDER, J. (1988). Receptor binding, analgesic and antitussive potency of tramadol and other selected opioids. *Arnzeim. Forsch./Drug Res.*, **38**, 877–880.

HÖLLT, V. & WÜSTER, M. (1978). The opiate receptors. In *Developments in Opiate Research. Modern Pharmacology-Toxicology*. Vol. 14. ed. Herz, A. pp. 1–65. New York: Marcel Dekker.

ILLES, P. (1989). Modulation of transmitter and hormone release by multiple neuronal opioid receptors. *Rev. Physiol. Biochem. Pharmacol.*, **112**, 139–233.

ILLES, P. & NÖRENBERG, W. (1990). Blockade of α_2-adrenoceptors increases opioid μ-receptor-mediated inhibition of the firing rate of rat locus coeruleus neurones. *Naunyn-Schmied. Arch. Pharmacol.*, **342**, 490–496.

ILLES, P., WEBER, H.D., NEUBURGER, J., BUCHER, B., REGENOLD, J.T. & NÖRENBERG, W. (1990). Receptor interactions at noradrenergic neurones. *Ann. N.Y. Acad. Sci.*, **604**, 197–210.

JAFFE, J.H. & MARTIN, W.R. (1990). Opioid analgesics and antagonists. In *The Pharmacological Basis of Therapeutics*. ed. Goodman Gilman, A., Rall, T.W., Nies, A.S. & Taylor, P. pp. 485–521. New York: Pergamon.

JONES, S.L. (1991). Descending noradrenergic influences on pain. *Progr. Brain Res.*, **88**, 381–394.

JONES, S.L. & GEBHART, G.F. (1988). Inhibition of spinal nociceptive transmission from the midbrain, pons and medulla in the rat: activation of descending inhibition by morphine, glutamate and electrical stimulation. *Brain. Res.*, **460**, 281–296.

KURAISHI, Y., SATOH, M. & TAKAGI, H. (1987). The descending noradrenergic system and analgesia. In *Pain Headache*. Vol. 9. ed. Gildenberg, P.L. pp. 101–128. Basel: Karger.

LINTZ, W., ERLACIN, S., FRANKUS, E. & URAGG, H. (1981). Metabolismus von Tramadol bei Mensch und Tier. *Arzneim-Forsch./Drug Res.*, **31**, 1932–1943.

MOORE, R.Y. & CARD, J.P. (1984). Noradrenaline-containing neuron systems. In *Classical Transmitters in the CNS. Handbook of Chemical Neuroanatomy*. Vol. 2. ed. Björklund, A & Hökfelt, T. pp. 123–156. Amsterdam: Elsevier.

NORTH, R.A. & WILLIAMS, J.T. (1985). On the potassium conductance increased by opioids in rat locus coeruleus neurones. *J. Physiol.*, **364**, 265–280.

OLPE, H.-R., STEINMANN, M.W. & JONES, R.S.G. (1985). Electrophysiological perspectives on locus coeruleus: its role in cognitive and vegetative functions. *Physiol. Psychol.*, **13**, 179–187.

PEPPER, C.M. & HENDERSON, G. (1980). Opiates and opioid peptides hyperpolarize locus coeruleus neurons *in vitro*. *Science*, **209**, 394–396.

RAFFA, R.B., FRIDERICHS, E., REIMANN, W., SHANK, R.P., CODD, E.E. & VAUGHT, J.L. (1992). Opioid and nonopioid components independently contribute to the mechanism of action of tramadol, an 'atypical' opioid analgesic. *J. Pharmacol. Exp. Ther.*, **260**, 275–285.

REDDY, S.V.R., MADERDRUT, J.L. & YAKSH, T.L. (1980). Spinal cord pharmacology of adrenergic agonist-mediated antinociception. *J. Pharmacol. Exp. Ther.*, **213**, 525–533.

REGENOLD, J.T. & ILLES, P. (1990). Inhibitory adenosine A_1-receptors on rat locus coeruleus neurones. An intracellular electrophysiological study. *Naunyn-Schmied. Arch. Pharmacol.*, **341**, 225–231.

SEGAL, M. & SANDBERG, D. (1977). Analgesia produced by electrical stimulation of catecholamine nuclei in the rat brain. *Brain Res.*, **123**, 369–372.

SURPRENANT, A. & WILLIAMS, J.T. (1987). Inhibitory synaptic potentials recorded from mammalian neurones prolonged by blockade of noradrenaline uptake. *J. Physiol.*, **382**, 87–103.

VOGEL, W., BURCHARDI, H., SIHLER, K. & VALIC, L. (1978). Über die Wirkung von Tramadol auf Atmung und Kreislauf. *Arzneim. Forsch./Drug Res.*, **28**, 183–186.

WEITZELL, R., TANAKA, T. & STARKE, K. (1979). Pre- and postsynaptic effects of yohimbine stereoisomers on noradrenaline transmission in the pulmonary artery of the rabbit. *Naunyn-Schmied. Arch. Pharmacol.*, **308**, 127–136.

WILLIAMS, J.T. & NORTH, R.A. (1984). Opiate-receptor interactions on single locus coeruleus neurones. *Mol. Pharmacol.*, **26**, 489–497.

WILLIAMS, J.T., NORTH, R.A., SHEFNER, S.A., NISHI, S. & EGAN, T.M. (1984). Membrane properties of rat locus coeruleus neurones. *Neuroscience*, **13**, 137–156.

WILLIAMS, J.T., HENDERSON, G. & NORTH, R.A. (1985). Characterization of α_2-adrenoceptors which increase potassium conductance in rat locus coeruleus neurones. *Neuroscience*, **14**, 95–101.

(Received January 18, 1993
Revised March 30, 1993
Accepted April 29, 1993)

Br. J. Pharmacol. (1993), **110**, 177–182

Role of tumour necrosis factor in the induction of nitric oxide synthase in a rat model of endotoxin shock

[1]Christoph Thiemermann, Chin-Chen Wu, Csaba Szabó, Mauro Perretti & John R. Vane

The William Harvey Research Institute, St. Bartholomew's Hospital Medical College, Charterhouse Square, London, EC1M 6BQ

1 This study investigates the role of tumour necrosis factor (TNF) in the induction of nitric oxide synthase (NOS) by bacterial endotoxin (lipopolysaccharide; LPS) in a rat model of endotoxin shock.

2 In anaesthetized rats, pretreatment with a monoclonal antibody for TNF (TNF_{ab}; 20 mg kg^{-1}, s.c., at 16 h prior to LPS) ameliorated the fall in mean arterial blood pressure (MAP) in response to LPS (2 mg kg^{-1}, i.v.). For instance, endotoxaemia for 180 min resulted in a fall in MAP from 114 ± 6 (control) to 84 ± 5 mmHg ($P<0.01$; $n=7$). In contrast, animals pretreated with TNF_{ab} prior to LPS injection maintained significantly higher MAP when compared to LPS-control (MAP at 180 min; 118 ± 3 mmHg; $P<0.01$, $n=5$).

3 Three hours of endotoxaemia was also associated with a significant reduction of the contractile effects of noradrenaline (NA) (10^{-8}–10^{-6} M) on the thoracic aorta *ex vivo*. This hyporeactivity to NA was partially restored by *in vitro* treatment of the vessels with N^G-nitro-L-arginine methyl ester (L-NAME, 20 min, 3×10^{-4} M). Pretreatment of rats with TNF_{ab} (20 mg kg^{-1}; at 16 h prior to LPS) significantly ($P<0.05$) attenuated the LPS-induced hyporeactivity of rat aortic rings *ex vivo*. L-NAME did not enhance the contractions of aortic rings obtained from TNF_{ab} pretreated LPS-rats.

4 At 180 min after LPS there was a significant elevation of the induced NOS activity in the lung (5.14 ± 0.57 pmol citrulline mg^{-1} min^{-1}, $n=8$). TNF_{ab} pretreatment significantly attenuated this induction of NOS in response to LPS by 37 ± 6% ($n=5$; $P<0.05$).

5 We conclude that the formation of endogenous TNF contributes to the induction of the calcium-independent isoform of NOS in response to LPS *in vivo*. Thus, the beneficial effects of agents which inhibit either the release or the action of TNF in circulatory shock may be, in part, due to inhibition of NOS induction.

Keywords: Nitric oxide; endotoxin shock; vasodilatation; contraction; aorta; noradrenaline

Introduction

Tumour necrosis factor (TNF) is a primary mediator of circulatory shock (Tracey *et al.*, 1986; 1987; see Billiau & Vanderkerchove, 1991, for review). Administration of TNF alone, or in combination with low (otherwise ineffective) doses of endotoxin mimics several cardiovascular features of circulatory shock, including hypotension, peripheral vasodilatation, and organ damage (for review see Billiau & Vanderkerchove, 1991). Elevated plasma concentrations of TNF are found in endotoxaemia (Beutler *et al.*, 1985; Waage, 1987; Michie *et al.*, 1988; Feuerstein *et al.*, 1990; Klosterhafen *et al.*, 1992). In addition, antibodies directed against TNF (Tracey *et al.*, 1987; Mathison *et al.*, 1988; Hinshaw *et al.*, 1990; Silva *et al.*, 1990; Walsh *et al.*, 1992), or agents which inhibit the release of TNF, such as pentoxyfilline (Schade, 1990), exert protective effects in animal models of endotoxin shock.

An enhanced formation of NO in response to LPS is an important mediator of hypotension, peripheral vasodilatation and vascular hyporeactivity to vasoconstrictor agents in endotoxaemia (Julou-Schaeffer *et al.*, 1990; Thiemermann & Vane, 1990; Kilbourn *et al.*, 1990; Wright *et al.*, 1992; Meyer *et al.*, 1992; Szabó *et al.*, 1993a). LPS induces a calcium-independent nitric oxide (NO) synthase (NOS) in various cells (including macrophages and vascular smooth muscle cells *in vitro*), as well as in whole organs such as lung, liver and spleen *in vivo*, resulting in an enhanced formation of NO (see Moncada *et al.*, 1991; Kilbourn & Griffith, 1992; Nathan, 1992). Corticosteroids, which inhibit the induction of this calcium-independent isoform of NO synthase (NOS) in response to LPS (Radomski *et al.*, 1990; Knowles *et al.*, 1990) exert beneficial effects in circulatory shock (Wright *et al.*, 1992; Szabó *et al.*, 1993a).

Like LPS, TNF also induces the calcium-independent isoform of NOS *in vitro* (Drapier *et al.*, 1988; Kilbourn & Belloni, 1990). Systemic administration of TNF increases NO production (Kosaka *et al.*, 1992) and causes NO-mediated vasodilatation (Kilbourn *et al.*, 1990) and vascular hyporeactivity to vasoconstrictors *in vivo* (Vicaut & Baundry, 1992) and *ex vivo* (Takahashi *et al.*, 1992; Foulkes & Shaw, 1992).

Thus, there is strong experimental evidence suggesting that (i) TNF is a key mediator of endotoxin shock; (ii) TNF can induce NOS *in vitro* and (iii) NOS induction leading to an enhanced formation of NO contributes to the cardiovascular failure in endotoxin shock. The importance of TNF in the induction of NOS *in vivo*, however, has not yet been adequately studied. Here we investigate whether the endogenous production of TNF contributes to the induction of NOS in response to LPS in the anaesthetized rat.

Methods

Haemodynamic measurements

Male Wistar rats (250–290 g; Glaxo Laboratories Ltd., Greenford, Middx.) were anaesthetized with thiopentone sodium (Trapanal; 120 mg kg^{-1}, i.p.). The trachea was cannulated to facilitate respiration and rectal temperature was maintained at 37°C with a homeothermic blanket (Bio-Sciences, Sheerness, Kent). The right carotid artery was cannulated and connected to a pressure transducer (P23XL,

[1] Author for correspondence.

Spectramed, Statham, U.S.A.) for the measurement of phasic and mean arterial blood pressure (MAP) and heart rate (HR) which were displayed on a Grass model 7D polygraph recorder (Grass Instruments, Quincy, Mass, U.S.A.). Left or right femoral veins were cannulated for the administration of drugs.

Upon completion of the surgical procedure, cardiovascular parameters were allowed to stabilize for 15 min. After recording baseline haemodynamic parameters, animals received *E. coli* LPS (2 mg kg^{-1}, i.v.; in 0.3 ml saline) as a slow injection over 2 min and were monitored for 180 min. The above protocol was used in vehicle-treated control rats and in rats pretreated subcutaneously with monoclonal antibody for TNF_α (TNF_{ab}; 20 mg kg^{-1}, 16 h prior to LPS). Such treatment produces maximal plasma concentrations at 16 h (Perretti & Flower, 1993). Moreover, this pretreatment with TNF_{ab} neutralizes the TNF_α-mediated cytotoxic effect of plasma obtained from rats at 60 min after *E. coli* LPS (1 mg kg^{-1}, i.p.) in L-929 fibroblasts (Perretti & Peers, unpublished observation).

Organ bath experiments

At 180 min after the injection of LPS, thoracic aortae were obtained from rats pretreated either with vehicle (control) or with TNF_{ab}. In addition, control aortic rings were obtained from male Wistar rats anaesthetized as above and subsequently exsanguinated. The vessels were rapidly removed, cleared of adhering periadventitial fat and cut into rings of 2 mm width. The endothelium was removed by rubbing. The rings were mounted in 20 ml organ baths filled with warmed (37°C), oxygenated (95% O_2/5% CO_2) Krebs solution (pH 7.4) consisting of (mM): NaCl 118, KCl 4.7, KH_2PO_4 1.2, $MgSO_4$ 1.17, $CaCl_2$ 2.5, $NaHCO_3$ 25 and glucose 5.6. Isometric force was measured with Biegestab K30 type 351 transducers (Hugo Sachs Elektronik, Germany) and recorded on a Grass model 7D polygraph recorder (Grass Instruments, Quincy, Mass, U.S.A.). A tension of 2 g was applied and the rings were equilibrated for 60 min, changing the Krebs solution every 15 min. In every experimental group, dose-response curves to noradrenaline (10^{-9}–10^{-6} M) were obtained before and after N^G-nitro-L-arginine methyl ester (L-NAME; 20 min, 3×10^{-4} M).

Nitric oxide synthase assay

Lungs from animals treated with LPS (in the absence [control] or in the presence of TNF_{ab} pretreatment) were removed at 180 min and frozen in liquid nitrogen. Lungs from sham-operated rats were also prepared for determination of baseline NOS activity. Lungs were stored for no more than 2 weeks at −80°C before assay. Frozen lungs were homogenized on ice with an Ultra-Turrax T 25 homogenizer (Janke & Kunkel, IKA Labortechnik, Staufen i. Br., Germany) in a buffer composed of (mM): Tris-HCl 50, EDTA 0.1 mM, EGTA 0.1 mM, 2-mercaptoethanol 12 mM and phenylmethylsulphonyl fluoride 1 mM (pH 7.4). Conversion of [^{3}H]-arginine to [^{3}H]-citrulline was measured in the homogenates as described by Mitchell *et al.* (1991) and Szabó *et al.* (1993a). Briefly, tissue homogenates (50 µl, approx. 100 µg protein) were incubated in the presence of [^{3}H]-L-arginine (10 µM, 5 kBq/tube), NADPH (1 mM), calmodulin (30 nM), tetrahydrobiopterin (5 µM) and calcium (2 mM) for 35 min at 37°C in HEPES buffer (pH 7.5). Reactions were stopped by dilution with 1 ml of ice cold HEPES buffer (pH 5.5) containing EGTA (2 mM) and EDTA (2 mM). Reaction mixtures were applied to Dowex 50W (Na^+ form) columns and the eluted [^{3}H]-L-citrulline activity was measured by scintillation counting (Beckman, LS3801; Fullerton, CA, U.S.A.). Experiments performed in the absence of NADPH determined the extent of [^{3}H]-L-citrulline formation independent of a specific NOS activity. Experiments in the presence of NADPH, without calcium and with EGTA (5 mM), determined the calcium-independent (i.e. induced) NOS activity.

Protein concentration was measured spectrophotometrically in 96-well plates with Bradford reagent (Bradford, 1976), using bovine serum albumin as standard.

Materials

Calmodulin, bacterial lipopolysaccharide (*E. coli* serotype 0.127:B8), NADPH, N^G-nitro-L-arginine methyl ester, noradrenaline bitartrate, and Dowex 50W anion exchange resin were obtained from Sigma Chemical Co. (Poole, Dorset). Monoclonal antibody for murine TNF_α (raised in hamster; TN3.19.12) was supplied by Celltech (Slough, Bucks). All solutions were made in saline. L-[2,3,4,5-^{3}H] arginine hydrochloride was obtained from Amersham (Buckinghamshire, U.K.). Tetrahydrobiopterin (6R-L-erythro-5,6,-7,8,tetrahydrobiopterin) was obtained from Dr B. Schircks Laboratories (Jona, Switzerland).

Statistical evaluation

All values in the figures and text are expressed as mean ± standard error of the mean of n observations, where n represents the number of animals, or the number of blood vessels studied. Student's paired or unpaired t tests were used to compare means among or between groups, respectively. A P-value less than 0.05 was considered to be statistically significant.

Results

TNF_{ab} protects against LPS-induced cardiovascular changes in the anaesthetized rat

Baseline values for MAP and HR of the vehicle- and TNF_{ab}-pretreated animal groups were 114 ± 6 (n = 7) and 118 ± 6 (n = 5) mmHg and 423 ± 9 (n = 7) and 422 ± 17 (n = 5) beats min^{-1}, respectively and were not significantly different between groups. Administration of LPS (2 mg kg^{-1}, i.v.) induced a fall in MAP from 114 ± 6 mmHg to 84 ± 5 mmHg (n = 7, P<0.01) at 60 min. Thereafter, MAP remained significantly reduced throughout the 180 min experimental period; e.g. at 180 min, MAP was 84 ± 5 mmHg (n = 7) (Figure 1a). LPS injection did not cause a significant change in HR (Figure 1b). LPS-treated animals which had been pretreated with TNF_{ab} maintained higher MAP values when compared to rats treated with LPS alone at 90–180 min (Figure 1a). TNF_{ab} pretreatment of LPS-rats did not affect HR (Figure 1b).

TNF_{ab} prevents the LPS-induced vascular hyporeactivity to noradrenaline ex vivo

In rat aortic rings obtained from sham-operated rats (control), NA caused a dose-dependent increase in vascular tone. Rat aortic rings obtained from rats subjected to a 180 min period of endotoxaemia showed a significant reduction of the contractile responses to NA (P<0.01 at 10^{-9}–10^{-6} M; Figure 2a). TNF_{ab} pretreatment of LPS-rats significantly attenuated the vascular hyporeactivity to NA of rat aortic rings *ex vivo* (P<0.05 at 10^{-8}–10^{-6} M; Figure 2a). However, contractions of the rat aortic rings produced by NA obtained from TNF_{ab} pretreated LPS-rats were still significantly reduced when compared to control responses (P<0.05 at 10^{-8}–10^{-7} M; Figure 2a).

In vitro treatment of vessels with L-NAME, an inhibitor of NO synthase (Moore *et al.*, 1990) (3×10^{-4} M), did not enhance the contractions to NA in control rings (Figure 2b). In contrast, L-NAME significantly enhanced the contractile responses to NA in aortic rings obtained from vehicle-treated LPS-rats (P<0.05 at 10^{-8}–10^{-6} M) (Figure 2c). However, even after L-NAME the contractile responses of these vessels

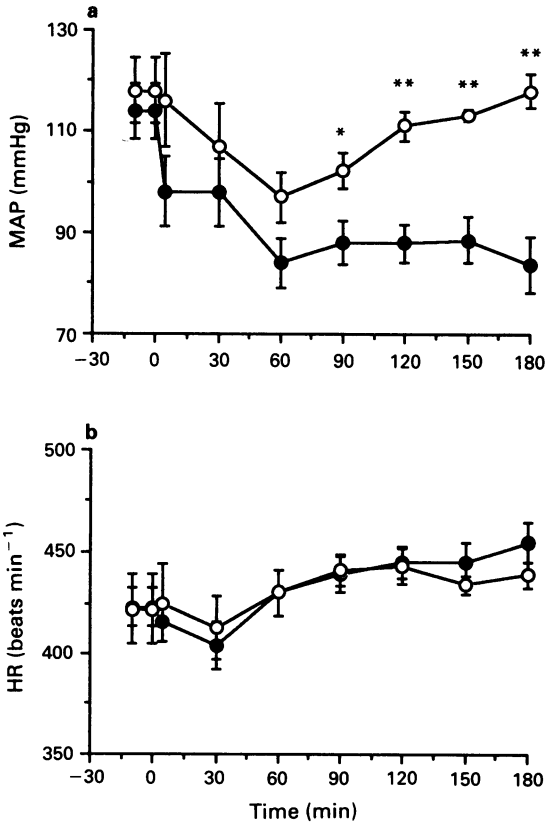

Figure 1 Tumour necrosis factor antibody (TNF_{ab}) ameliorates the delayed hypotension in endotoxic shock in the anaesthetized rat. Depicted are the changes in (a) mean arterial blood pressure and (b) heart rate in rats subjected to *E. coli* lipopolysaccharide (LPS, 2 mg kg^{-1}, i.v.). Groups of animals were pretreated either with vehicle (●, $n = 7$), or TNF_{ab} (20 mg kg^{-1}, s.c. for 16 h; ○, $n = 5$). LPS was administered at time 0. Data are expressed as means ± s.e.mean of n observations. $*P<0.05$ and $**P<0.01$ represent significant differences when compared to control at the same time point.

to NA were still significantly smaller when compared to control ($P<0.05$ at 10^{-9}–10^{-6} M). In contrast, L-NAME did not enhance the NA-induced contractions of rat aortic rings obtained from TNF_{ab}-pretreated LPS-rats (Figure 2d).

TNF_{ab} inhibits the induction of nitric oxide synthase by LPS in vivo

A small, calcium-independent NOS activity was detectable in lung homogenates obtained from sham-operated control animals. After 180 min of endotoxaemia there was a substantial induction of NOS activity in lung homogenates (Figure 3). The activity of this induced NOS was significantly reduced (by 37 ± 6%, $n = 5$, $P<0.05$) in lungs obtained from TNF_{ab} pretreated LPS-rats (Figure 3).

Discussion

The present study demonstrates that TNF_{ab} attenuates the induction of NOS by LPS in lung homogenates *ex vivo* and it protects against the vascular hyporeactivity of rat aortic rings *ex vivo*. The inhibition of NOS induction by TNF_{ab} was associated with a significant protection against the fall in MAP. Indeed, at 180 min there was a complete recovery of MAP, as compared to LPS alone. Thus, our data suggest that TNF is one of the endogenous mediators of NOS induction by LPS in the lung and aorta of the anaesthetized rat.

LPS treatment results in reduced contractile responsiveness

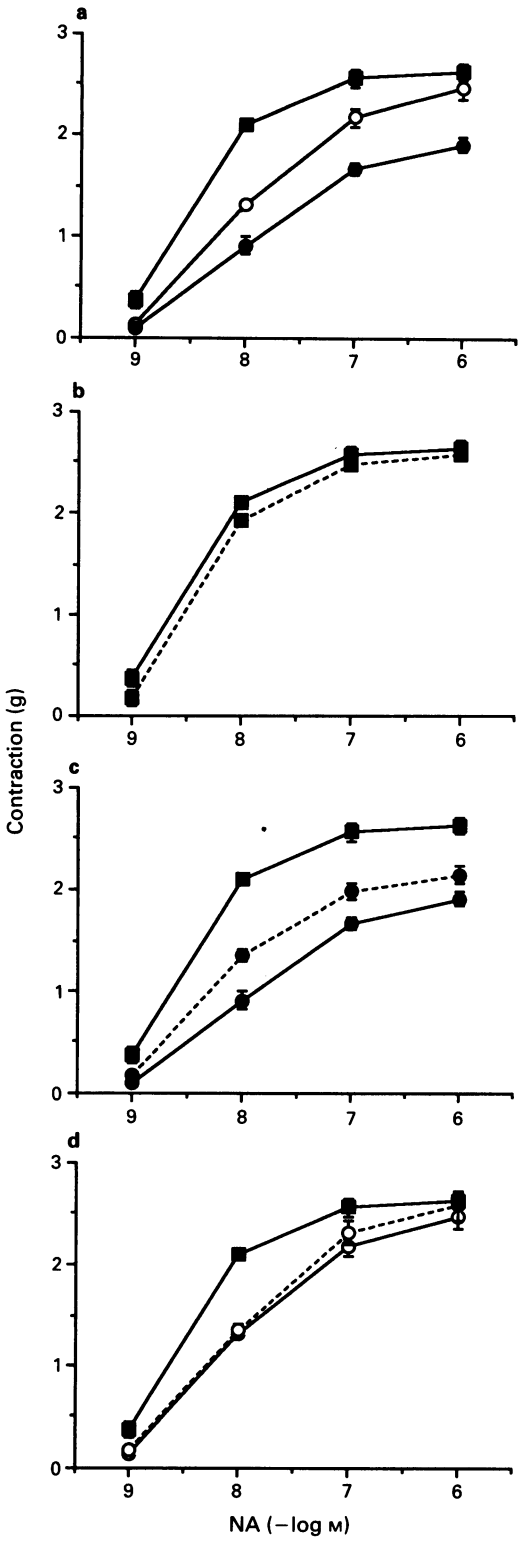

Figure 2 Tumour necrosis factor antibody (TNF_{ab}) protects against the development of vascular hyporeactivity to noradrenaline (10^{-8}–10^{-6} M) after lipopolysaccharide (LPS) injection *ex vivo* (a) Dose-response curves to noradrenaline (10^{-9}–10^{-6} M) in aortic rings without endothelium obtained from control rats (■, $n = 5$), from LPS-treated rats (●, $n = 12$) and from LPS-treated rats pretreated with TNF_{ab} (○, $n = 9$). (b–d) Dose-response curves to noradrenaline (10^{-9}–10^{-6} M) in aortic rings without endothelium obtained from control rats (■), from LPS-treated rats (●) and from LPS-treated rats pretreated with TNF_{ab} (○) before (solid line) and after (dotted line) *in vitro* L-NAME (3×10^{-4} M) treatment. Data are expressed as means ± s.e.mean.

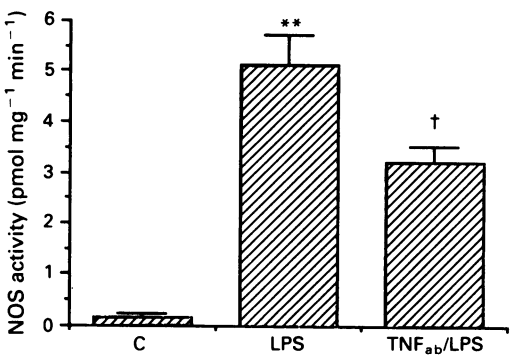

Figure 3 Tumour necrosis factor antibody (TNF_{ab}) inhibits induction of the calcium-independent nitric oxide synthase in lung homogenates *ex vivo*. Calcium-independent (induced) nitric oxide synthase (NOS) activity was measured in lung homogenates obtained from control rats (C, $n = 3$) and from rats pretreated with vehicle (LPS, $n = 7$) or TNF_{ab} (20 mg kg^{-1}, s.c. 16 h prior to LPS; TNF_{ab}/LPS $n = 5$) at 180 min after LPS administration (2 mg kg^{-1}, i.v.). **Represents a significant ($P < 0.01$) increase in NOS activity after 180 min of endotoxaemia (LPS) when compared to controls (C); † represents a significant ($P < 0.05$) reduction in the LPS-induced NOS activity in TNF_{ab}-treated animals. Data are expressed as means ± s.e.mean.

to NA in blood vessels such as the rat thoracic aorta *ex vivo*, which is mediated by an enhanced formation of NO by the inducible NOS (Julou-Schaeffer *et al.*, 1990; Rees *et al.*, 1990). The present findings demonstrate that pretreatment of LPS-treated rats with TNF_{ab} significantly attenuated the hyporeactivity to NA in aortic rings *ex vivo*. However, L-NAME only partially restored the contractile response to NA in LPS-treated rats, suggesting that the vascular hyporeactivity to NA following systemic LPS administration is only partially mediated by NO. These results reinforce the contribution made by mechanisms independent of NOS induction to the vascular hyporeactivity to NA. For instance, LPS induces an isoform of cyclo-oxygenase (COX-2) resulting in an enhanced formation of cyclo-oxygenase metabolites including vasodilator prostanoids (Masferrer *et al.*, 1992). The subsequent enhanced formation of adenosine 3':5'-cyclic monophosphate (cyclic AMP) in the vascular smooth muscle and an impairment of the NA-mediated signal transduction (see Suba *et al.*, 1992) may also contribute to the vascular hyporeactivity in response to endotoxin. Nevertheless, TNF_{ab} significantly attenuated the hyporeactivity to NA in aortic rings *ex vivo*, and L-NAME did not further enhance the contractions to NA in rats pretreated with TNF_{ab} prior to LPS. This suggests that TNF_{ab} may completely prevent NOS induction in the aorta.

Thus, the endogenous release of TNF in endotoxaemia contributes to the induction of NOS by LPS *in vivo*. Although the inhibition of NOS induction by TNF_{ab} in the lung was only partial, pretreatment with TNF_{ab} prevented the fall in MAP observed at 180 min after LPS. Similarly, dexamethasone administration prior to LPS injection results in an incomplete inhibition of NOS induction in the lung, but abolishes NOS induction in the aorta (Szabó *et al.*, 1993a). Moreover in anaesthetized rats, the calcium antagonist, nifedipine (Szabó *et al.*, 1993b) and the platelet-activating factor antagonist, WEB 2086 (Szabó *et al.*, 1993c) only partially inhibit NOS induction in the lung. However, both drugs cause a near-complete prevention of the delayed fall in blood pressure associated with endotoxaemia in the anaesthetized rat.

The present data provide a rational basis for recent observations demonstrating that the platelet-activating factor antagonist, WEB 2086 (Szabó *et al.*, 1993c) and certain prostaglandins such as prostacyclin and prostaglandin E_2 (Marotta *et al.*, 1992) inhibit NOS induction, for PAF antagonists (Floch *et al.*, 1989; Rabinovici *et al.*, 1990) and prostaglandin E_2 (Renz *et al.*, 1988; Ferreri *et al.*, 1992) inhibit the release of TNF in response to LPS. In addition, the present data support the view that elevations of plasma TNF levels in the absence of endotoxaemia are involved in the induction of NOS in haemorrhagic shock (Thiemermann *et al.*, 1993).

Although TNF_{ab} attenuated both NOS induction and the delayed fall in MAP in rats subjected to LPS, TNF_{ab} did not affect the immediate hypotension caused by LPS injection. This is consistent with the view that approximately 30–60 min are required for an increase in plasma concentrations of TNF after LPS injection (Feuerstein *et al.*, 1990; Klosterhafen *et al.*, 1992). In contrast, the immediate hypotension in response to LPS can be prevented by NO synthase inhibitors (Thiemermann & Vane, 1990; Lambert *et al.*, 1992) and platelet-activating factor antagonists (Casals-Stenzel, 1987; Szabó *et al.*, 1993c). As PAF can release NO (Schmidt *et al.*, 1989; Moritoki *et al.*, 1992), it is conceivable that the immediate hypotension to LPS in the rat is due to an enhanced formation of NO which is triggered by activation of the constitutive NOS by PAF.

Glucocorticosteroids such as dexamethasone inhibit the LPS-mediated induction of NOS *in vitro* and *in vivo* (Radomski *et al.*, 1990; Knowles *et al.*, 1990). Glucocorticosteroid pretreatment also ameliorates the delayed fall in MAP after LPS administration (Wright *et al.*, 1992; Szabó *et al.*, 1993a). As glucocorticosteroids inhibit the release of TNF (Waage, 1987; Zuckerman *et al.*, 1989), the present study suggests that this may be one of the mechanisms by which glucocorticosteroids inhibit the induction of NOS.

NO, when produced in large amounts (e.g. following NOS induction), acts as a cytotoxic effector molecule (Stuehr & Nathan, 1989) which can mediate or enhance cellular damage in endotoxaemia. Thus, NO is likely to participate in the TNF-induced cellular damage. Indeed, TNF-induced endothelial cell damage can be blocked by NO synthase inhibitors (Estrada *et al.*, 1992). In additon, both NO (Geng *et al.*, 1992) and TNF (Stadler *et al.*, 1992) inhibit mitochondrial respiration. It is conceivable that NO also participates in the inhibitory effect of TNF on mitochondrial respiration.

Although the prevention of the LPS-induced circulatory failure with antibodies directed against TNF appears to be an important approach for the therapy of endotoxin shock, it should be stressed that the beneficial cardiovascular effects of TNF antibodies, when administered following LPS, are limited (Tracey *et al.*, 1987; Mathison *et al.*, 1988; Hinshaw *et al.*, 1990; Silva *et al.*, 1990). Similarly, inhibition of NOS induction with corticosteroids (Radomski *et al.*, 1990; Knowles *et al.*, 1990), prevents the cardiovascular failure caused by LPS, but does not exert beneficial cardiovascular effects once NOS induction has occurred (Wright *et al.*, 1992; Szabó *et al.*, 1993a; Paya *et al.*, 1993). This is consistent with the hypothesis that NOS induction contributes importantly to the delayed cardiovascular failure in endotoxaemia (Wright *et al.*, 1992; Szabó *et al.*, 1993a) and haemorrhagic shock (Thiemermann *et al.*, 1993). This observation also suggests that at a later stage of endotoxin shock, when the induction of NOS has already occurred, inhibitors of the inducible isoform of NOS may be therapeutically important.

This work was supported by a grant from Glaxo Group Research Ltd. C.T. is supported by a grant from the Commission of the European Communities (Biomed I, BMHI, CT 92/1893). C.C.W. is supported by the NDMC of Taiwan, C.S. is a fellow of Lloyd's of London Tercentenary Foundation. The authors wish to thank Celltech (Slough, U.K.) for the generous gift of the anti-TNF monoclonal antibody.

References

BEUTLER, B.A., MULSARK, I.W. & CERAMI, A. (1985). Cachectin/tumor necrosis factor: production, distribution and metabolic fate in vivo. *J. Immunol.*, **135**, 3972–3977.

BILLIAU, A. & VANDEKERCHOVE, F. (1991). Cytokines and their interactions with other inflammatory mediators in the pathogenesis of sepsis and septic shock. *Eur. J. Clin. Invest.*, **21**, 559–573.

BRADFORD, M.M. (1976). A rapid and sensitive method for the quantification of protein dye binding. *Anal. Biochem.*, **72**, 248–254.

CASALS-STENZEL, J. (1987). Protective effect of WEB 2086, a novel antagonist of platelet activating factor, in endotoxin shock. *Eur. J. Pharmacol.*, **135**, 117–122.

DRAPIER, J., WIETXERBIN, J. & HIBBS, J.B. (1988). Interferon gamma and tumor necrosis factor induce the L-arginine-dependent cytotoxic effector mechanism in murine macrophages. *Eur. J. Immunol.*, **18**, 1587–1591.

ESTRADA, C., GOMEZ, C., MARTIN, C., MONCADA, S. & GONZALEZ, C. (1992). Nitric oxide mediates tumour necrosis factor-α cytotoxicity in endothelial cells. *Biochem. Biophys. Res. Commun.*, **186**, 475–482.

FERRERI, N.R., SARR, T., ASKENASE, P.W. & RUDDLE, N.H. (1992). Molecular regulation of tumor necrosis factor-α and lymphotoxin production in T cells. *J. Biol. Chem.*, **267**, 9443–9449.

FEUERSTEIN, G., HALLENBECK, J.M., VANATTA, B., RABINOVICI, R., PERERA, P.Y. & VOGEL, S.N. (1990). Effect of gram-negative endotoxin on levels of serum corticosterone, TNF_α, circulating blood cells, and the survival of rats. *Circ. Shock*, **30**, 265–278.

FLOCH, A., BOUSSEAU, A., HETIER, E., FLOCH, F., BOST, P.E. & CABERO, I. (1989). RP 55778, a PAF receptor antagonist, prevents and reverses hemoconcentration and TNF release. *J. Lipid Med.*, **1**, 349–360.

FOULKES, R. & SHAW, S. (1992). The cardiodepressant and vasodepressant effects of tumour necrosis factor in rat isolated atrial and aortic tissues. *Br. J. Pharmacol.*, **106**, 942–947.

GENG, Y., HANSSON, G.K. & HOLME, E. (1992). Interferon-γ and tumor necrosis factor synergize to induce nitric oxide production and inhibit mitochondrial respiration in vascular smooth muscle cells. *Circ. Res.*, **71**, 1268–1276.

HINSHAW, L.B., TEKAMP-OLSEN, P., CHANG, A.C.K., LEE, A.P., TAYLOR, F.B., MURRAY, C.K., PEER, G.T., EMERSON, T.E., PASSEY, R.B. & KUO, G.C. (1990). Survival of primates in LD100 septic shock following therapy with antibody to tumor necrosis factor (TNF). *Circ. Shock*, **30**, 279–292.

JULOU-SCHAEFFER, G., GRAY, G.A., FLEMING, I., SCHOTT, C., PARRATT, J.R. & STOCLET, J.C. (1990). Loss of vascular responsiveness induced by endotoxin involves the L-arginine pathway. *Am. J. Physiol.*, **259**, H1038–H1043.

KILBOURN, R.G. & BELLONI, P. (1990). Endothelial cell production of nitrogen oxides in response to interferon in combination with tumor necrosis factor, interleukin-1 or endotoxin. *J. Natl. Cancer Inst.*, **82**, 772–776.

KILBOURN, R.G. & GRIFFITH, O.W. (1992). Overproduction of nitric oxide in cytokine-mediated and septic shock. *J. Natl. Cancer Inst.*, **84**, 827–877.

KILBOURN, R.G., GROSS, S.S., JUBRAN, A., ADAMS, J., GRIFFITH, O.W., LEVI, R. & LODATO, R.F. (1990). N^G-methyl-L-arginine inhibits tumor necrosis factor-induced hypotension: implications for the involvement of nitric oxide. *Proc. Natl. Acad. Sci. U.S.A.*, **87**, 3629–3632.

KLOSTERHAFEN, B., HORSTMENN-JUNGEMANN, K., VOGEL, P., FLOHE, S., OFFNER, F., KIRKPATRICK, C.J. & HEINRICH, P.C. (1992). Time course of various inflammatory mediators during recurrent endotoxaemia. *Biochem. Pharmacol.*, **43**, 2103–2109.

KNOWLES, R.G., SALTER, M., BROOKS, S.L. & MONCADA, S. (1990). Anti-inflammatory glucocorticoids inhibit the induction by endotoxin of nitric oxide synthase in the lung, liver and aorta of the rat. *Biochem. Biophys. Res. Commun.*, **172**, 1042–1048.

KOSAKA, H., HARADA, N., WATANABE, M., YOSHIHARA, H., KATSUKI, Y. & SHIGA, T. (1992). Synergistic stimulation of nitric oxide hemoglobin production in rats by recombinant interleukin 1 and tumor necrosis factor. *Biochem. Biophys. Res. Commun.*, **189**, 392–397.

LAMBERT, L.E., FRENCH, J.F., WHITTEN, J.P., BARON, B.M. & McDONALD, I.A. (1992). Characterization of cell selectivity of two novel inhibitors of nitric oxide synthesis. *Eur. J. Pharmacol.*, **216**, 131–134.

MAROTTA, P., SAUTEBIN, L. & DI ROSA, M. (1992). Modulation of the induction of nitric oxide synthase by eicosanoids in the murine macrophage cell line J774. *Br. J. Pharmacol.*, **107**, 640–641.

MASFERRER, J.L., SEIBERT, K., ZWEIFEL, B.S. & NEEDLEMAN, P. (1992). Endogenous glucocorticoids regulate an inducible cyclooxygenase enzyme. *Proc. Natl. Acad. Sci. U.S.A.*, **89**, 3917–3921.

MATHISON, J.C., WOLFSON, E. & ULEVITCH, R.J. (1988). Participation of tumour necrosis factor in the mediation of gram negative bacterial lipopolysaccharide-induced injury in rabbits. *J. Clin. Invest.*, **81**, 1925–1931.

MEYER, J., TRABER, L.D., NELSON, S., LENTZ, C.W., NAKAZAWA, H., HERNDON, D.N., NODA, H. & TRABER, D.L. (1992). Reversal of hyperdynamic response to continuous endotoxin administration by inhibition of NO synthesis. *J. Appl. Physiol.*, **73**, 324–328.

MICHIE, H.R., MANOGUE, K.R., SPRIGGS, D.R., REVAUG, A., O'DWYER, S., DINARELLO, C., CERAMI, A., WOLFF, S.M. & WILMORE, D.W. (1988). Detection of circulating tumor necrosis factor after endotoxin administration. *N. Engl. J. Med.*, **318**, 1481–1486.

MITCHELL, J.A., SHENG, H., FORSTERMANN, U. & MURAD, F. (1991). Characterization of nitric oxide synthase in non-adrenergic-non-cholinergic nerves containing rat anococcygeus. *Br. J. Pharmacol.*, **104**, 289–291.

MONCADA, S., PALMER, R.M.J. & HIGGS, E.A. (1991). Nitric oxide: physiology, pathophysiology, and pharmacology. *Pharmacol. Rev.*, **43**, 109–141.

MOORE, P.K., AL-SWAYEH, O.A., CHONG, N.W.S., EVANS, R.A. & GIBSON, A. (1990). L-N^G-nitroarginine (L-NOARG), a novel, L-arginine-reversible inhibitor of endothelium-dependent vasodilatation *in vitro*. *Br. J. Pharmacol.*, **99**, 408–412.

MORITOKI, H., HISAYAMA, T., TAKEUCHI, S., MIYANO, H. & KONDOH, W. (1992). Involvement of nitric oxide in the PAF-induced relaxation of rat thoracic aorta. *Br. J. Pharmacol.*, **107**, 196–201.

NATHAN, C. (1992). Nitric oxide as a secretory product of mammalian cells. *FASEB J.*, **6**, 3051–3064.

PAYA, D., GRAY, G.A., FLEMING, I. & STOCLET, J.C. (1993). Effect of dexamethasone on the onset and persistence of vascular hyporeactivity induced by E. Coli lipopolysaccharide in rats. *Circ. Shock*, (in press).

PERRETTI, M. & FLOWER, R.J. (1993). Modulation of IL-1-induced neutrophil migration by dexamethasone and lipocortin-1. *J. Immunol.*, **150**, 992–999.

RABINOVICI, R., YUE, T.L., FARHAR, M., SMITH III, E., ESSER, K.M., SLIVJAK, M. & FEUERSTEIN, G. (1990). Platelet-activating factor (PAF) and tumour necrosis factor-α (TNFα) interactions in endotoxemic shock: studies with BN 50739, a novel PAF antagonist. *J. Pharmacol. Exp. Ther.*, **255**, 256–263.

RADOMSKI, M.W., PALMER, R.M.J. & MONCADA, S. (1990). Glucocorticoids inhibit the expression of an inducible, but not the constitutive nitric oxide synthase in vascular endothelial cells. *Proc. Natl. Acad. Sci. U.S.A.*, **87**, 10043–10047.

REES, D.D., CELLEK, S., PALMER, R.M.J. & MONCADA, S. (1990). Dexamethasone prevents the induction of a nitric oxide synthase and the associated effects on the vascular tone: an insight into endotoxic shock. *Biochem. Biophys. Res. Commun.*, **173**, 541–547.

RENZ, H., GONG, J.H., SCHMIDT, A., NAIN, H. & GEMSA, D. (1988). Release of tumor necrosis factor-α from macrophages. Enhancement and suppression are dose-dependently regulated by prostaglandins E_2 and cyclic nucleotides. *J. Immunol.*, **141**, 2388–2393.

SCHADE, U.F. (1990). Pentoxyfilline increases survival in murine endotoxin shock and decreases formation of tumor necrosis factor. *Circ. Shock*, **31**, 171–181.

SCHMIDT, H.H.H.W., SEIFERT, R. & BOHME, E. (1989). Formation and release of nitric oxide from human neutrophils and HL-60 cells induced by a chemotactic peptide, platelet-activating factor and leukotriene B_4. *FEBS Lett.*, **244**, 357–360.

SILVA, A.T., BAYSTON, K.F. & COHEN, J. (1990). Prophylactic and therapeutic effects of a monoclonal antibody to tumour necrosis factor-α in experimental gram-negative septic shock. *J. Infect. Dis.*, **162**, 421–427.

STADLER, J., BENTZ, B.G., HARBRECHT, B.G., SILVIO, M.D., CURRAN, R.D., BILLIAR, T.R., HOFFMAN, R.A. & SIMMONS, R.L. (1992). Tumor necrosis factor alpha inhibits hepatocyte mitochondrial respiration. *Ann. Surg.*, **216**, 5539–5546.

STUEHR, D.J. & NATHAN, C.F. (1989). Nitric oxide: a macrophage product responsible for cytostasis and respiratory inhibition in tumour target cells. *J. Exp. Med.*, **169**, 1543–1555.

SUBA, E.A., MCKEENNA, T.M. & WILLIAMS, T.J. (1992). In vivo and in vitro effects of endotoxin on vascular responsiveness to noradrenaline and signal transduction in the rat. *Circ. Shock*, **36**, 127–133.

SZABÓ, C., MITCHELL, J.A., THIEMERMANN, C. & VANE, J.R. (1993a). Nitric-oxide mediated hyporeactivity to noradrenaline precedes nitric oxide synthase induction in endotoxin shock. *Br. J. Pharmacol.*, **108**, 786–792.

SZABÓ, C., MITCHELL, J.A., GROSS, S.S., THIEMERMANN, C. & VANE, J.R. (1993b). Nifedipine inhibits the induction of nitric oxide synthase by bacterial lipopolysaccharide. *J. Pharmacol. Exp. Ther.*, **265**, 674–680.

SZABÓ, C., MITCHELL, J.A., GROSS, S.S., THIEMERMANN, C. & VANE, J.R. (1993c). An antagonist of platelet-activating factor (WEB 2086) inhibits the induction of nitric oxide synthase by bacterial lipopolysaccharide. *Br. J. Pharmacol.*, (in press).

TAKAHASHI, K., ANDO, K., ONO, A., SHIMOSAWA, T., OGATA, E. & FUJITA, T. (1992). Tumor necrosis factor-α induces vascular hyporesponsiveness in Sprague-Dawley rats. *Life Sci.*, **50**, 1437–1444.

THIEMERMANN, C., SZABÓ, C., MITCHELL, J.A. & VANE, J.R. (1993). Vascular hyporeactivity to vasoconstrictor agents and haemodynamic decompensation in hemorrhagic shock is mediated by nitric oxide. *Proc. Natl. Acad. Sci. U.S.A.*, **90**, 267–271.

THIEMERMANN, C. & VANE, J.R. (1990). Inhibition of nitric oxide synthesis reduces the hypotension induced by bacterial lipopolysaccharides in the rat in vivo. *Eur. J. Pharmacol.*, **182**, 591–595.

TRACEY, K.J., FONG, Y., HESSE, D.G., MANOGUE, K.R., LEE, A.T., KUO, G.C., LOWRY, S.F. & CERAMI, A. (1987). Anti-cachetin/TNF monoclonal antibodies prevent septic shock during lethal bateraemia. *Nature*, **330**, 662–664.

TRACEY, K.J., GEUTLER, B., LOWRY, S.F., MERRYWEATHER, J., WOLPE, S., MILSARK, I.W., HARIRI, R.J., FAHEY III, T.J., ZENTELLA, A., ALBERT, J.D., SHIRES, G.T. & CERAMI, A., (1986). Shock and tissue injury induced by recombinant human cachectin. *Science*, **234**, 470–474.

VICAUT, E. & BAUDRY, N. (1992). Nitric oxide and tumour necrosis factor in terminal arterioles of rat skeletal muscle. In *The Biology of Nitric Oxide*, Vol 1, ed. Moncada, S., Marletta, M.A., Hibbs Jr., J.B. & Higgs, E.A. pp. 216–218. London & Chapel Hill: Portland Press Inc.

WAAGE, A. (1987). Production and clearance of tumor necrosis factor exposed to endotoxin and dexamethasone. *Clin. Immunol. Immunopathol.*, **45**, 348–355.

WALSH, C.J., SUGERMAN, H.J., MULLEN, P.G., CAREY, P.D., LEEPER-WOODFORD, S.K., JESMOK, G.J., ELLIS, E.F. & FLOWER, A.A. (1992). Monoclonal antibody to tumor necrosis factor α attenuates cardiopulmonary dysfunction in porcine gram-negative sepsis. *Arch. Surg.*, **127**, 138–145.

WRIGHT, C.E., REES, D.D. & MONCADA, S. (1992). Protective and pathological roles of nitric oxide in endotoxin shock. *Cardiovasc. Res.*, **26**, 48–57.

ZUCKERMAN, S.H., STELLHAAS, J. & BUTLER, L.D. (1989). Differential regulation of lipopolysaccharide-induced interleukin-1 and tumour necrosis factor synthesis: effects of endogenous and exogenous glucocorticoids and the role of the pituitary-adrenal axis. *Eur. J. Immunol.*, **19**, 301–305.

(Received March 29, 1993
Revised April 29, 1993
Accepted April 30, 1993)

Br. J. Pharmacol. (1993), **110**, 183–192

Use-dependent block of Na^+ currents by mexiletine at the single channel level in guinea-pig ventricular myocytes

Akihiko Sunami, Zheng Fan, Tohru Sawanobori & [1]Masayasu Hiraoka

Department of Cardiovascular Diseases, Medical Research Institute, Tokyo Medical and Dental University, 1-5-45 Yushima, Bunkyo-ku, Tokyo 113, Japan

1 The mechanism of use-dependent block of Na^+ current by mexiletine was studied at the single channel level in guinea-pig ventricular myocytes by the patch-clamp techniques. All experiments were performed using stimulation protocols to enable us to analyze the strict dependence of changes in channel properties on channel use.

2 In cell-attached patches, bath or pipette application of mexiletine (40 μM) produced a use-dependent reduction of the peak average current without changes in single channel conductance. Null sweeps were increased and the number of openings per sweep decreased with successive pulses, whereas no significant change in the mean open time was detected during the train.

3 Block by mexiletine became greater when pulse duration was extended beyond the period in which channels were open, suggesting that block progressed without channel opening.

4 At near threshold potentials, mexiletine decreased the later occurrence of first openings. Additionally, late openings were reduced in a use-dependent way.

5 We conclude that mexiltine binds to the inactivated closed states of the Na^+ channel and then causes a failure of late openings as well as early, which results in null sweeps on subsequent depolarization.

Keywords: Single Na^+ channel current, inactivated states of the Na^+ channels; mexiletine; cell-attached patches

Introduction

Mexiletine has been shown to exert suppressive effects against a variety of experimental and clinical arrhythmias (Chew *et al.*, 1979; Hondeghem & Katzung, 1984). It is a class I antiarrhythmic agent the main action of which is to inhibit the fast Na^+ current (I_{Na}) for excitation. However, there have been few studies that examine the action of mexiletine on cardiac Na^+ channels by direct measurement of I_{Na} using the whole-cell patch-clamp technique (Hering *et al.*, 1983; Yatani & Akaike, 1985) and, so far, no detailed reports are available to deal with its action at the single channel level. Therefore, its precise mechanism of action has not been clarified.

Recordings of single Na^+ channel currents have provided direct information on the mechanism by block by class I antiarrhythmic agents (Nilius *et al.*, 1987; Kohlhardt & Fichtner, 1988; Grant *et al.*, 1989; McDonald *et al.*, 1989; Undrovinas *et al.*, 1989) and on the drug binding site in cardiac Na^+ channels (Carmeliet *et al.*, 1989; Baumgarten *et al.*, 1991; Gruber *et al.*, 1991). The class I agents are also characterized by use-dependent block of I_{Na}. The mechanism of use-dependent block by these agents has been explained by either the modulated receptor hypothesis (Hille, 1977; Hondeghem & Katzung, 1977) or the guarded receptor hypothesis (Starmer *et al.*, 1984; Starmer & Grant, 1985) based on studies using the maximum rate of rise ($\dot{V}_{max}$) of the action potential and macroscopic I_{Na} measurements. However, there have been few detailed studies on single Na^+ channel block that is strictly dependent on channel use (Grant *et al.*, 1989; McDonald *et al.*, 1989). This is in part due to the difficulty of setting a recovery interval long enough for drug unbinding because of time-dependent shifts of gating which are commonly seen during single channel recordings from cell-attached and inside-out patches (Cachelin *et al.*, 1983; Kunze *et al.*, 1985; Patlak & Ortiz, 1985; Kimitsuki *et al.*, 1990). Therefore, we used a fast kinetic drug (Campbell, 1983), mexiletine and performed all the experiments in cell-attached and inside-out patches using the protocol proposed by Grant *et al.* (1989), applying trains of pulses separated by an interval to attain a full recovery. This enabled us to analyze the dependence of change in gating parameters on channel use and clarify the precise mechanisms of use-dependent block of the Na^+ channel by mexiletine at the single channel level.

Methods

Myocyte preparation

Single ventricular myocytes from guinea-pig hearts were prepared by an enzymatic dissociation procedure as described previously (Hirano & Hiraoka, 1988).

Solutions

For cell-attached recordings, the bath solution was Tyrode of the following composition (mM): NaCl 144.0, KCl 4.0, $CaCl_2$ 1.8, $MgCl_2$ 0.53, glucose 5.5, NaH_2PO_4 0.33, and HEPES 5.0; the pH was adjusted to 7.3 by addition of NaOH. In some experiments, the isolated myocytes were superfused with a high-K^+ solution of the following composition (mM): K-aspartate 140.0, NaCl 4.5, $MgCl_2$ 0.5, EGTA 1.0, glucose 5.5 and HEPES 5.0. The pH was adjusted to 7.3 with KOH. This high-K^+ solution was used to depolarize cells to approximately 0 mV. The pipette solution contained (mM): NaCl 140.0, KCl 4.0, $MgCl_2$ 1.0, $CaCl_2$ 0.1, glucose 5.5, and HEPES 5.0; the pH was adjusted to 7.3 by adding NaOH (Sunami *et al.*, 1993).

For inside-out patch recordings, the high-K^+ solution was used to perfuse the bath.

Single channel recordings

Single Na^+ channel currents were recorded at room temperature (22–25°C) in the cell-attached and inside-out patch configurations (Hamill *et al.*, 1981) using a patch-clamp amplifier (AXOPATCH-1C, Axon Instruments, Foster City, Calif., U.S.A.). At the start of each experiment, the junction

[1] Author for correspondence.

potential of each electrode was nulled to zero. It was checked again at the end of each experiment. The shift of the junction potential was usually less than ± 2 mV. Current signals were stored on a video cassette recorder (HR-S 7000, Victor Co., Tokyo, Japan) through a PCM converter system (RP-880, NF Instruments, Yokohama, Japan). The recorded signals were filtered by an active 16-pole Bessel filter (FV-665, NF Instruments) using a -3dB cutoff point at 2 kHz. The analog signals were converted into digital signals with an AD converter (TL-1 DMA INTERFACE, Axon Instruments) at a sampling frequency of 8 kHz and were stored in an IBM-PS/2 personal computer (Sunami *et al.*, 1993).

Experimental protocols

Stimulation protocols were designed to examine use-dependent block of single Na^+ channel currents by mexiletine. Trains of five or ten 20- or/and 200 ms pulses with an interpulse interval of 500 ms were applied. Each pulse train was followed by a recovery interval of 7 s, which was sufficient to permit full recovery from mexiletine block. We applied a total of 100 such trains, giving a total of 500 or 1000 voltage steps in each condition. Voltage steps were applied to test potentials ranging from − 70 to − 40 mV or from 15 mV positive to the resting potential (Vr + 15 mV) to Vr + 40 mV. The holding potential usually was set at − 120 mV or Vr − 40 mV.

Mexiletine (mexiletine HCl, a gift from Boehringer Japan, Kawanishi City, Japan) was applied to the bath solution or in the pipette solution in concentrations of 40 μM. This concentration was chosen to produce moderate degrees of use-dependent block under the stimulation protocols described above and similar to those in previous studies using isolated cardiac myocytes (Hering *et al.*, 1983; Yatani & Akaike, 1985). In the case of bath-application of mexiletine in cell-attached (external application) or inside-out patch recording (internal application), the usual approach was to obtain the control and then the mexiletine data in the same patch. The bath solution could be replaced completely within 30 s by changing from one solution to another. We describe results of experiments under both conditions. As another mode of external application for mexiletine, the outside of the membrane was also exposed to the drug in the pipette for cell-attached patch recording.

Data analysis

Single Na^+ channel records were analyzed using the software package, pCLAMP 5.5.1 on a computer (IBM-PS/2). The capacitive transient was partially compensated by analog circuitry and the residual transient was removed by subtracting the average current from steps to the same potential without openings. Ensemble average currents were obtained by averaging 100 sweeps, that is, the set of *n*th pulses of all trains. Channel openings were detected using a half-amplitude threshold. Open time histograms were obtained from open events that did not overlap with other open-channel currents and could be fitted to a single exponential after exclusion of the first bin (0.125 ms). The number of channels in a patch was estimated by counting the maximum number of overlapping events. Since patches always had more than one channel, closed times were not determined. First latency was measured as the time from the start of depolarization to the first channel opening. 'Active time' was defined as the interval between the first opening and the last closure. For the measurement of the first latency and active time, we included overlapping events as well as non-overlapping events. All the time histograms were constructed from uncorrected data and bin sizes for those were set as multiples of the sampling interval. In addition to the analysis of total sweeps, parameters of open time, first latency and active time were analyzed in every set of *n*th pulses of all trains. All the values are expressed as mean ± s.e. Statistical analysis was by the paired *t* test for the comparison between two groups of mean values, and $P < 0.05$ was considered significant.

Results

Use-dependent block by mexiletine

We examined the use-dependent block of single cardiac Na^+ channels by mexiletine applied to the bath solution in cell-attached patches. Figures 1 and 2 show 10 consecutive sweeps of each train and ensemble average currents obtained from 100 sweeps for the *n*th pulses of each train, before and after adding 40 μM mexiletine to the bath solution. In the control, the patterns of single channel activity did not reveal any striking differences in different pulses and the peak amplitude of the average current was stable over 10 pulses during the train (Figure 1b,c). This indicated that the interpulse interval of 500 ms was enough time for channels to recover from inactivation. During exposure to mexiletine, single channel activity decreased with increasing pulse numbers and the average currents declined progressively during the train (Figure 2a). There was a 48.1% decline in the average currents between the 1st and 10th pulses (Figure 2b). In other words, use-dependent Na^+ channel block could be observed at the single channel level.

Under these conditions, use-dependent block of single channel currents was confirmed in all of five patches tested. This was also true in two patches of the cells superfused with a high-K^+ bath solution including 40 μM mexiletine. Similar effects were obtained on two patches when 40 μM mexiletine was added to the pipette solution but not to the bath solution. Figure 3 shows an example of the effect of mexiletine added to the pipette solution on single channel currents in a cell-attached patch. During exposure of mexiletine to the outside of the membrane patch, single channel activity decreased as the pulse number of train increased (Figure 3a) and the average currents declined progressively during the train (Figure 3c). There was a 42.7% decline in the peak average currents between the 1st and 5th pulses (Figure 3b). In Figure 4, the effects of 40 μM mexiletine on single Na^+ channel currents were examined with inside-out patches when the drug was added to the bath solution. From the examples of consecutive current records (Figure 4a) and the ensemble average currents (Figure 4b,c), mexiletine did not block the channels in a use-dependent manner. Lack of block by internal application of mexiletine was confirmed in three inside-out patches, which might be due to gating changes caused by the replacement of the cytoplasm by the internal solution after excision (Horn & Vandenberg, 1986; Kirsch & Brown, 1989). Therefore, the following experiments were carried out on cell-attached patches.

In the presence of mexiletine, sweeps without channel openings (null sweeps) could be seen as shown in the middle column of Figure 2a. There was a question whether use-dependent block by mexiletine was associated with the number of nulls between the pulses within a train. Figure 5 shows the relation between the average currents and number of nulls in a different patch from that shown in Figures 1 and 2. Under the same stimulation protocol as that shown in Figure 1a, mexiletine produced a use-dependent reduction of the average currents. At this time, the number of nulls increased progressively during the train and consequently the number of openings per sweep decreased with pulse number. In this way, use-dependent block by mexiletine reflected a decrease in the number of open events.

Modulation of channel kinetics by mexiletine

The effect of mexiletine on the fast gating process was analyzed with open time histograms. Probability density histograms of the open times measured at Vr + 20 mV are shown in Figure 6. The open time histograms, which were

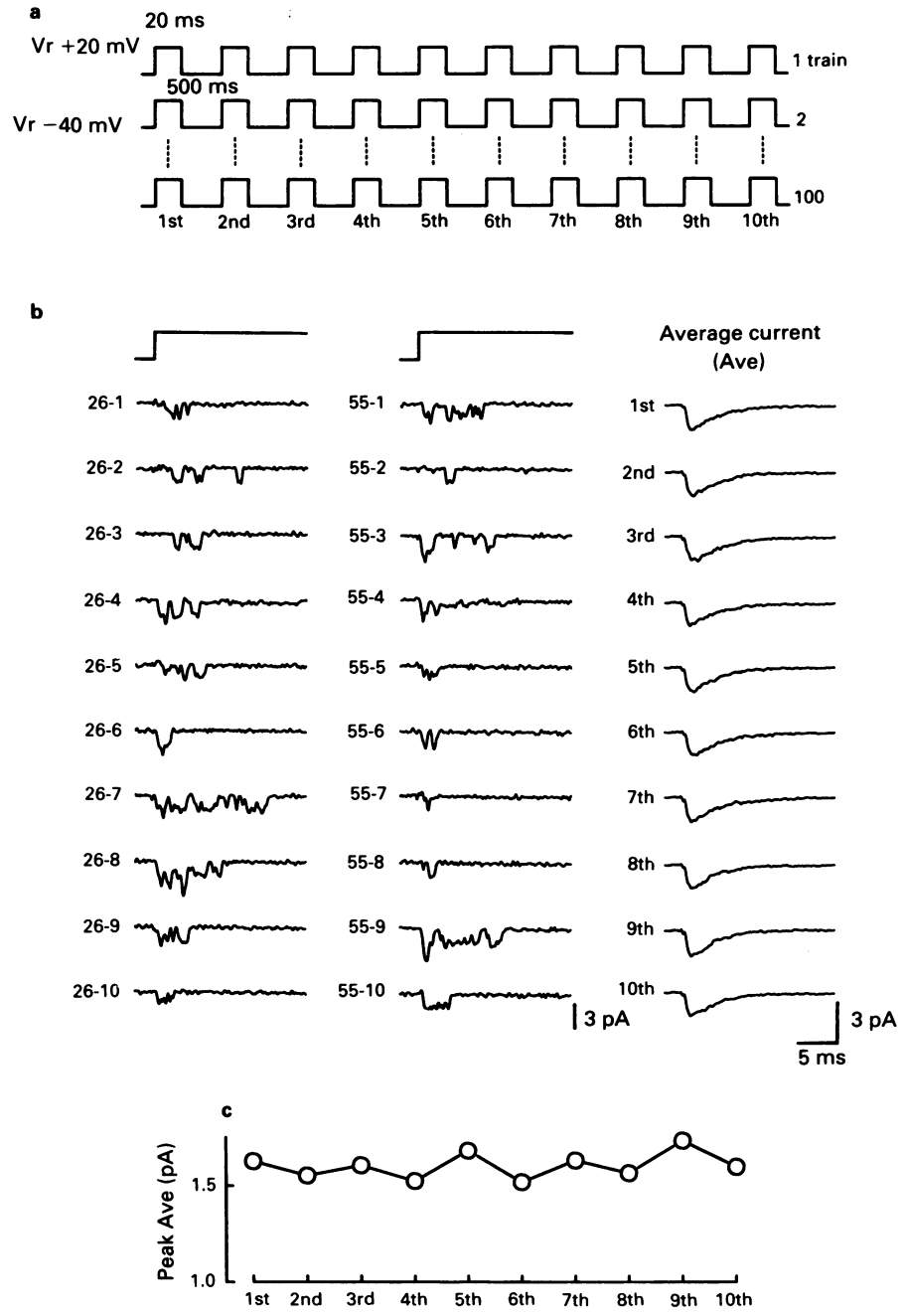

Figure 1 Single Na^+ channel currents recorded from a cell-attached patch in the control. (a) Voltage protocols. Currents were elicited by 100 trains of ten pulses of 20 ms duration. Pulses were applied from a holding potential at 40 mV negative to the resting potential (Vr − 40 mV) to Vr + 20 mV. An interpulse interval was 500 ms and each train was followed by a recovery interval of 7 s. The pulses were grouped according to the sequence in each train. The *n*th means the set of *n*th pulses of all trains. (b) Single channel currents and ensemble average current records. In the left and middle column, the top panels show the voltage protocols and the bottom 10 consecutive traces illustrate current records. The number to the left of each current trace represents the train and pulse numbers which are separated by a bar (−). Current records of the left and middle column were obtained from 10 consecutive depolarizations in the 26th and 55th train, respectively. The right column shows ensemble average currents (Ave) obtained from 100 sweeps for each set. Sequence numbers of sets are indicated as *n*th at the left side of each average current trace. (c) Plot of amplitude of average currents vs. the sequence of the pulses within the train. The ordinate scale indicates the peak amplitude of average currents (Peak Ave) in each set (1st, 2nd, 3rd, 4th . . .) of the train pulses and the abscissa scale represents the *n*th pulse of the trains. The patch contained four channels.

analyzed for the 1st and 5th pulses of trains, revealed a single exponential distribution with a time constant of 0.55 ms for the 1st pulses and 0.56 ms for the 5th pulses in control. After application of 40 μM mexiletine, the open time constants for the 1st and 5th pulses were not changed and their values did not differ from those in the control condition ($\tau_0 = 0.57$ and 0.59 ms for 1st and 5th pulses, respectively). No differences in the open time constants for the 1st and 5th pulses in the presence of 40 μM mexiletine were confirmed in three other patches at Vr + 20 mV (1st vs. 5th; 0.53 ± 0.04 ms vs. 0.52 ± 0.04 ms, not significant). In other voltages, there were no systematic changes in open times between the groups of the first and last pulses in the train during exposure to mexiletine. The single channel current-voltage relation was linear

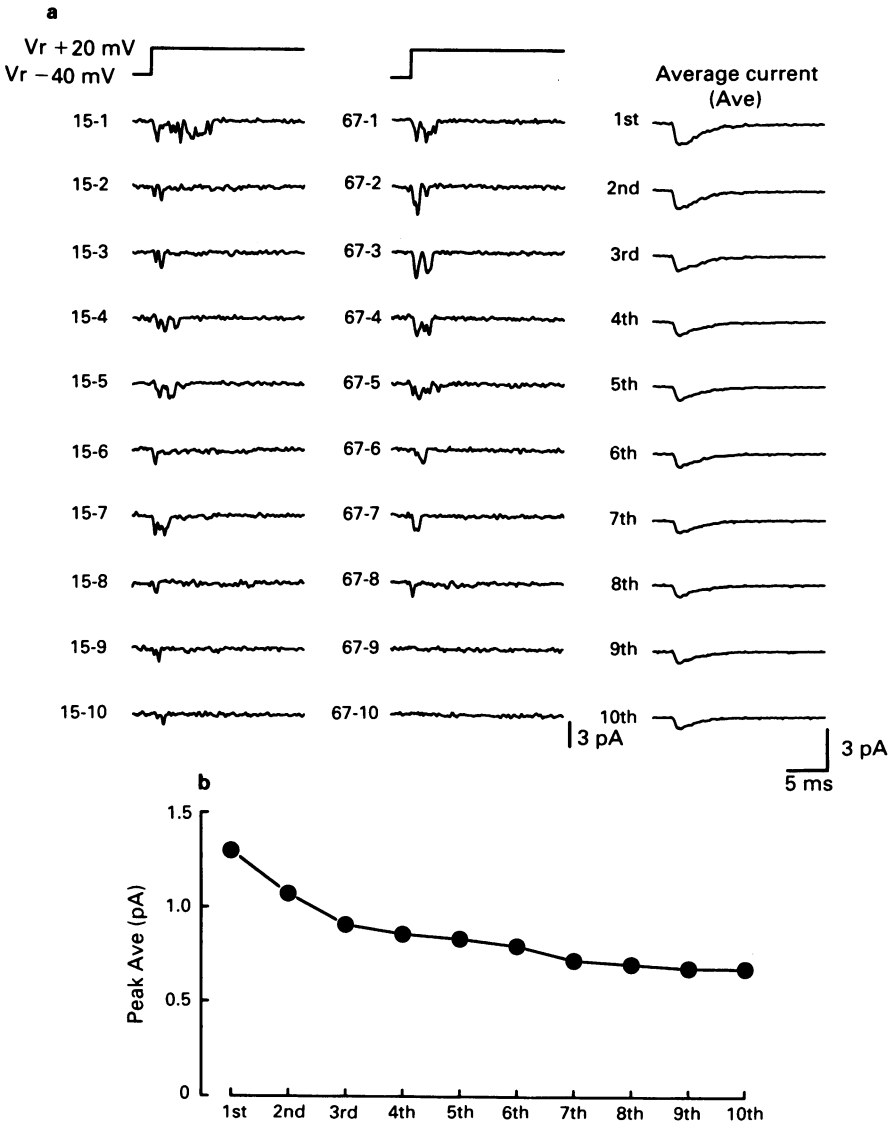

Figure 2 Use-dependent block of single Na^+ channel currents in a cell-attached patch by mexiletine. (a) Single channel currents and ensemble average current records in the presence of 40 μM mexiletine in the bath solution. This patch was the same patch shown in Figure 1. After control records of Figure 1, 40 μM mexiletine was added to the bath solution and currents were elicited by the same protocol shown in Figure 1a. The left and middle column illustrate 10 consecutive traces in the 15th and 67th train, respectively. Single channel activities of the later traces are obviously less than those of the earlier traces in both trains. Consequently, use-dependent reduction of the peak average currents (Peak Ave) from 100 sweeps is evident between pulses (right column). (b) Plot of amplitude of average currents vs. the sequence of the pulses within the train with mexiletine in the bath. The peak amplitude of average currents (Peak Ave) in each set from the right column of (a) is indicated.

between Vr + 15 and Vr + 40 mV with a slope of 16 pS and was not affected by mexiletine. In this way, use-dependent block of single Na^+ channel currents by mexiletine was caused by a progressive decrease in the number rather than the duration of open events.

It has been reported that local anaesthetics affect the time course of the Na^+ current decay (Bennet, 1987; Nilius *et al.*, 1987; Baumgarten *et al.*, 1991; Gruber *et al.*, 1991). Therefore, we examined the effects of mexiletine on the ensemble current decay. Figure 7a shows a typical example of the mexiletine effect on ensemble average currents. After application of 40 μM mexiletine, peak current decreased from 1.82 to 0.58 pA and the ensemble current decayed faster. The decay time constants from single exponential fits were 4.2 ms for the control and 3.2 ms with 40 μM mexiletine. In the five patches, the decay time constants of control and mexiletine were 3.1 ± 0.3 and 2.7 ± 0.2 ms, respectively (significantly different, $P<0.05$). The waiting time to the first opening (first latency) is correlated with the time course of decay as well as activation (Aldrich *et al.*, 1983). A previous study of cardiac Na^+ channel block by ethacizin showed that the drug caused a decrease in the peak open probability with an increase in the first latency (Undrovinas *et al.*, 1989). We therefore examined the effects of mexiletine on the first latency. Figure 7b depicts the influence of mexiletine on the first latency distribution. As previously noted (Patlak & Horn, 1982; Kunze *et al.*, 1985; Scanley *et al.*, 1990), the observed first latencies revealed biphasic distributions during the control and mexiletine exposure. After application of 40 μM mexiletine to the bath solution, the mean first latency multiplied by the number of channels in the patch decreased from 8.60 to 6.60 ms. Such a decrease in the first latency induced by mexiletine was observed in five other patches at Vr + 20 mV (control vs. 40 μM mexiletine; 9.83 ± 0.66 ms vs. 7.55 ± 0.52 ms, $P<0.001$, $n=6$).

Since mexiletine decreased the first latency at voltages near

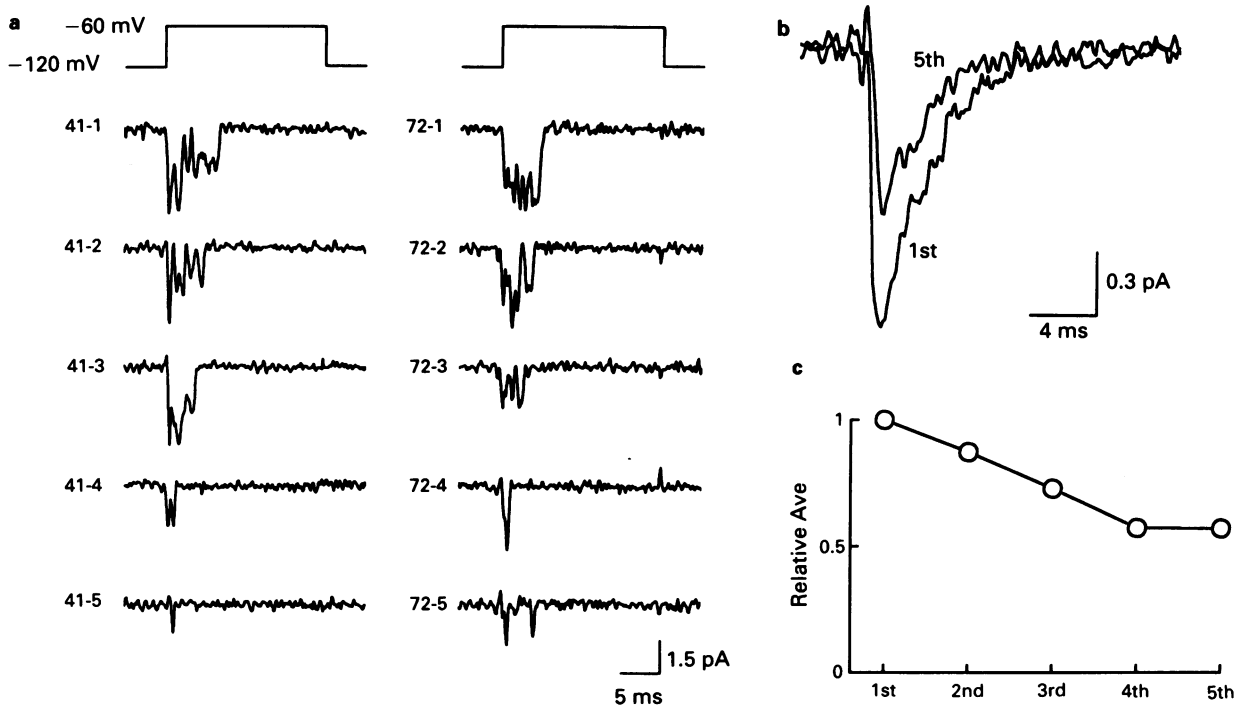

Figure 3 Effects of mexiletine applied to the outside of the membrane patch on single Na^+ channel currents recorded from a cell-attached patch. A high-K^+ bath solution was used to depolarize the cell to approximately 0 mV. (a) Single channel current records from a cell-attached patch in the presence of 40 μM mexiletine in the pipette solution. Currents were elicited by the protocol similar to that shown in Figure 1a except that test pulses were applied to − 60 mV from a holding potential of − 120 mV and the number of pulses during a train was five. The left and right column show 5 consecutive traces in the 41st and 72nd train, respectively. (b) Superimposed ensemble average current records for the 1st and 5th pulses. Average currents were obtained from 100 sweeps for each sets. (c) Plot of amplitude of average currents vs. the sequence of the pulses within the train. The peak amplitude of average currents (Ave) in each set was normalized by that in the 1st set. The patch contained four channels.

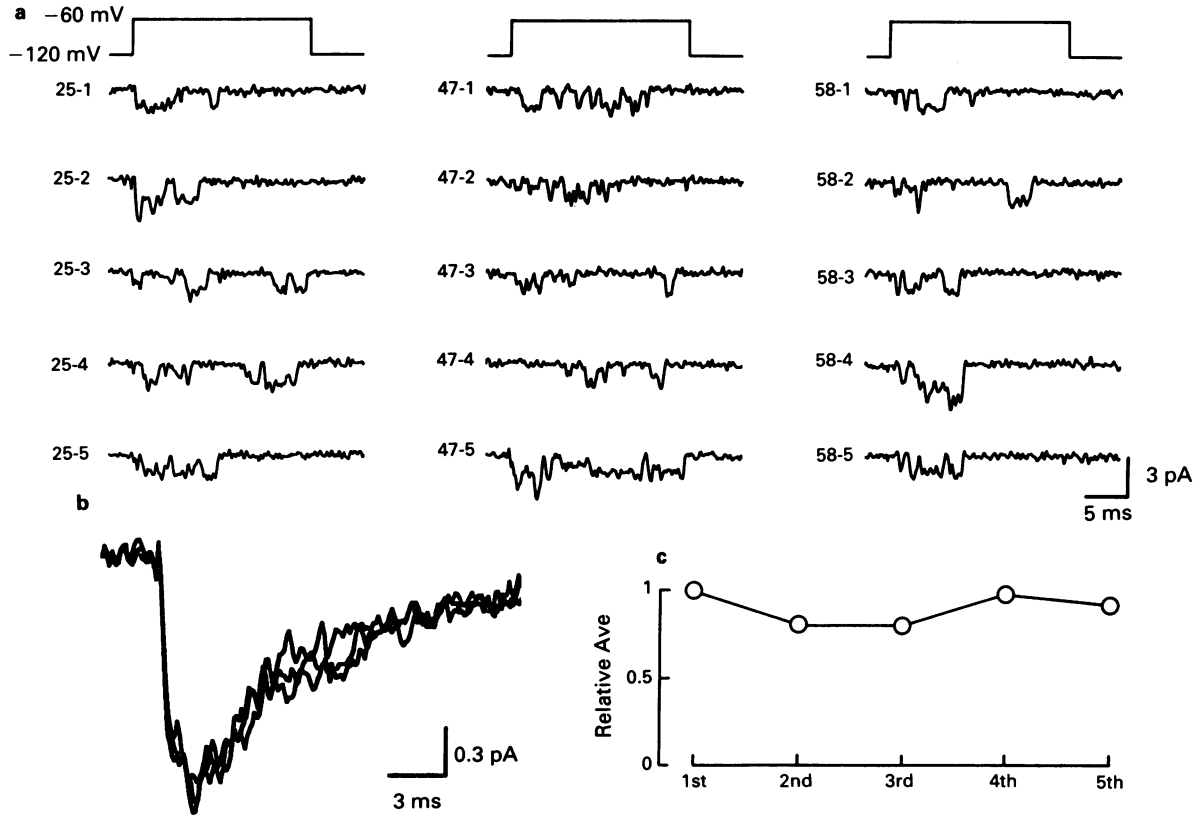

Figure 4 Effects of mexiletine applied to the intracellular solution on single Na^+ channel currents recorded from an inside-out patch. (a) Single channel current records from an inside-out patch in the presence of 40 μM mexiletine in the bath solution. Currents were elicited by the protocol similar to that shown in Figure 1a except that test pulses were applied to − 60 mV from a holding potential of − 120 mV and the number of pulses during a train was five. The left, middle and right column show 5 consecutive traces in the 25th, 47th and 58th train, respectively. (b) Superimposed ensemble average currents records for the 1st, 4th and 5th pulses. Average currents were obtained from 100 sweeps for each set. (c) Plot of amplitude of average currents vs. the sequence of the pulses within the train. The peak amplitude of average currents (Ave) in each set was normalized by that in the 1st set. The patch contained three channels.

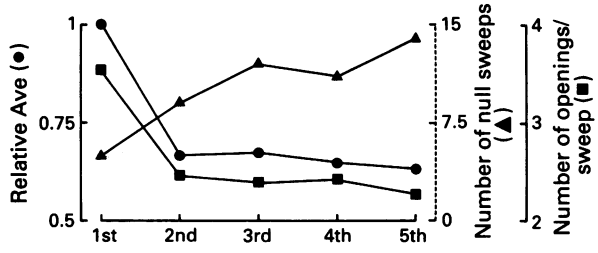

Figure 5 Use-dependent appearance of null sweeps and reduction of open events by mexiletine. The data were obtained from a cell-attached patch during exposure to 40 μM mexiletine in the bath solution. This patch was different from that in Figures 1 and 2, and contained five channels. The pulse protocol was similar to that shown in Figure 1a, but the number of pulses during a train was five. Normalized peak amplitude of average currents (Ave) (●), numbers of sweeps without openings of the channel (null sweeps) (Δ) and open events per sweep (■) were plotted against the sequence of the pulses within the train.

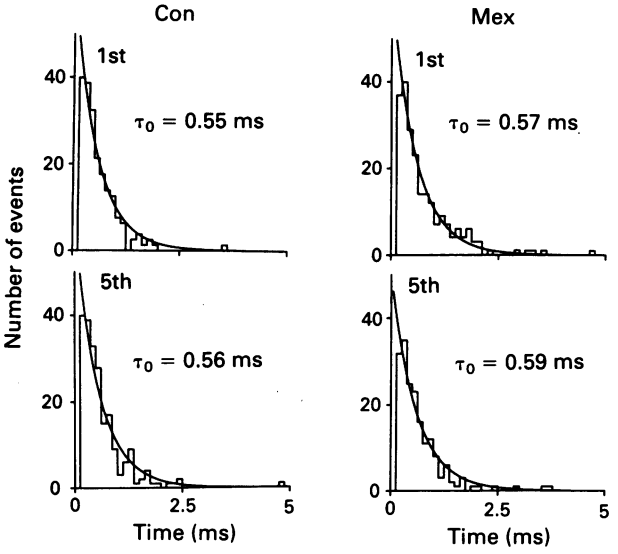

Figure 6 Effects of mexiletine on the open time of single Na^+ channel currents recorded from a cell-attached patch. The left column shows the open time histograms under control conditions (Con) and the right those in the presence of 40 μM mexiletine applied to the bath solution (Mex). Open time distributions were analyzed for the 1st pulses (upper panel) and 5th pulses (lower panel) within the train. The time constants (τ_0) of the open time were obtained from single exponential fits for all the cases. Currents were elicited by a protocol similar to that shown in Figure 1a except that there were five pulses during a train. The patch contained four channels.

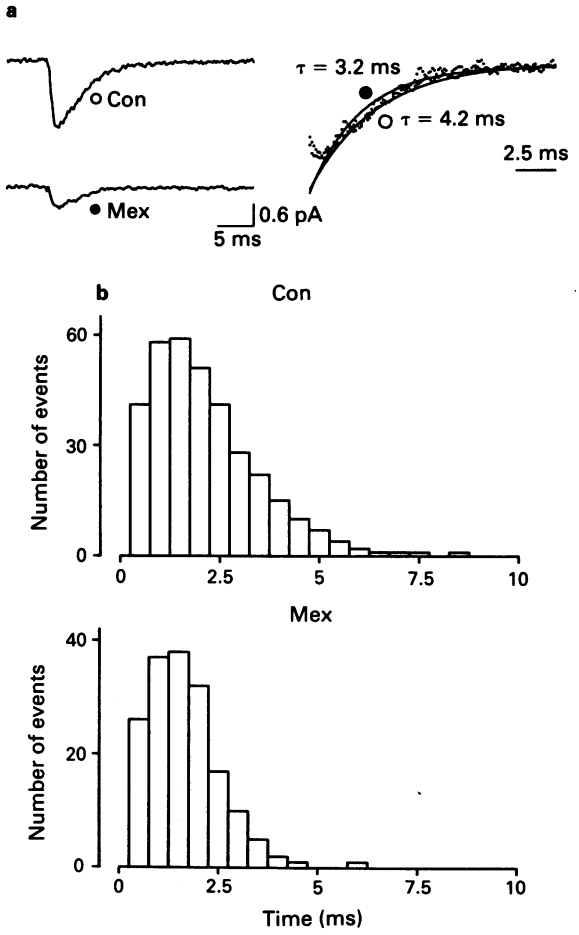

Figure 7 Effects of mexiletine on the first latency of single Na^+ channel currents recorded from a cell-attached patch. The data were obtained with a voltage protocol similar to that shown in Figure 1a except that there were 200-ms pulses within a train before and after application of 40 μM mexiletine to the bath solution. (a) Ensemble average currents in the absence and presence of mexiletine. The left column shows ensemble average currents obtained from 1000 sweeps for control (Con, ○) and 40 μM mexiletine (Mex, ●). The right column shows the decay phase of the ensemble currents during control (○) and mexiletine exposure (●). The smooth curves in average currents are fit to a single exponential function using a least-squares procedure and the decay time constants (τ) are indicated. Average currents were arbitrarily scaled and superimposed for comparison. (b) First latency distribution during control and mexiletine exposure. The first latency histogram was obtained from all sweeps with activity for 1000 depolarizations producing the average currents in (a) under control conditions (Con) (upper panel) and in the presence of 40 μM mexiletine (Mex) (lower panel).

threshold but a decrease in time to peak current was not observed, it seemed likely that mexiletine suppressed the first openings occurring at later times during a voltage step. Reopening is an important source of Na^+ current for cardiac cells near threshold potentials (Kunze *et al.*, 1985) and the ensemble is a convolution of the all latency distribution and the mean open time (Scanley *et al.*, 1990). In order to evaluate further the effects of mexiletine on the late openings, we defined 'active time' as the interval between the first opening and the last closure as shown with the 'shadow' in Figure 8a. Figure 8b shows the active time distribution from total sweeps during the control and 40 μM mexiletine exposure. In the control, the active time histogram demonstrated the rising and declining phase with time to peak of 4.04 ms and an arithmetic mean was 6.46 ms. After application of mexiletine, the time to peak markedly decreased and an arithmetic mean of active time was decreased to 3.23 ms. Figure 9 shows a test of whether the shortening of the active time during exposure to mexiletine was use-dependent or not. Under control conditions, active times revealed biphasic distributions both for the 1st and 10th pulses and their mean values did not differ substantially from each other (6.75 and 6.25 ms for the 1st and 10th pulses, respectively). After application of mexiletine, the peak values of active times in the 10th pulses was strikingly decreased compared to that in the 1st pulses and consequently active times of the 10th pulses were distributed in one phase, whereas those of the 1st pulses were distributed in two phases. Here, in the 100th pulses, the numbers of sweeps with activity were decreased and the mean value of active times was shortened (1st vs. 10th, 4.43 vs. 2.90 ms, a mean of 81 and 71 traces). Such use-dependent shortening of active times by mexiletine was observed in five

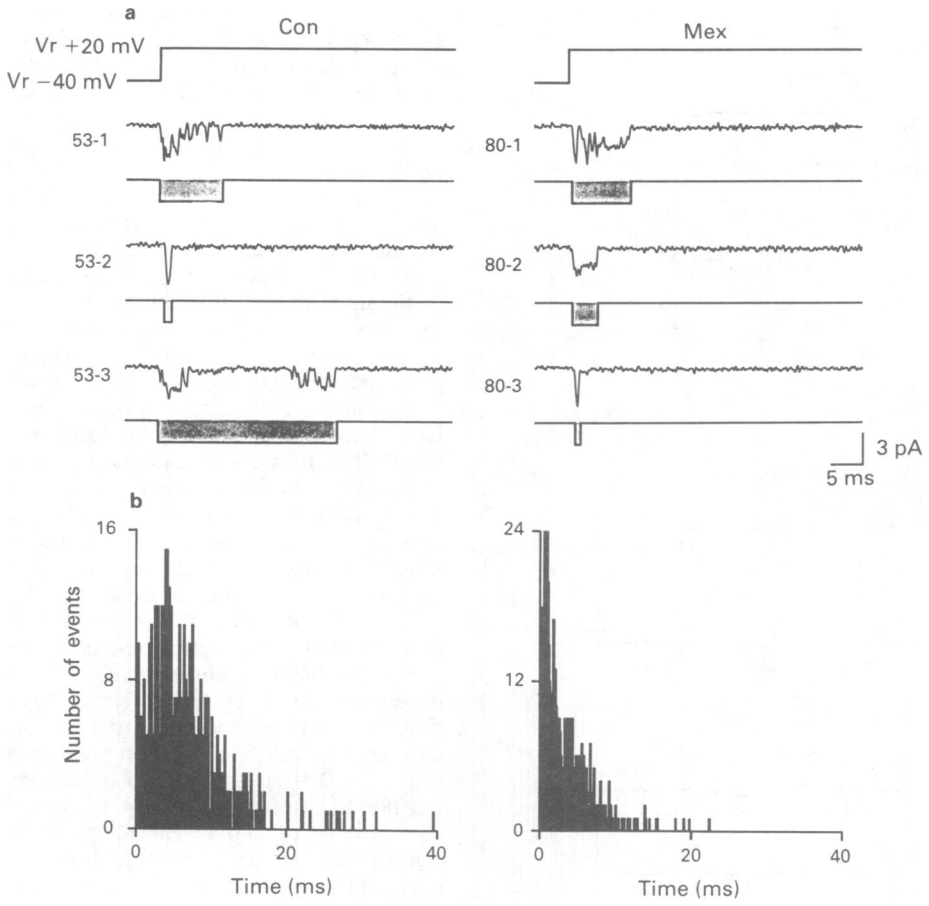

Figure 8 Effects of mexiletine on the active time of single Na^+ channel currents recorded from a cell-attached patch. (a) Estimation of the active time. Active was defined as the time from the first channel opening to the end of the last opening and indicated with shaded area in response to 3 consecutive traces before (Con) (left column) and after application of 40 μM mexiletine to the bath solution (Mex) (right column). (b) Active time distribution during control and mexiletine exposure. The left column shows the active time histogram obtained from the total sweeps with openings including 3 traces in (a) for 1000 depolarizations under control conditions and the right column shows that in the presence of 40 μM mexiletine. The data were obtained from the same protocol as shown in Figure 7.

other patches. On average, the mean value of active times significantly decreased from 5.79 ± 0.30 (the 1st pulses, $n = 6$) to 3.18 ± 0.09 ms (the 5th or 10th pulses) ($P < 0.001$).

Interaction of mexiletine with inactivated closed state

We have described above the effects of mexiletine on the patches near threshold potentials and in which open events occurred even at late times during a voltage step. Under these conditions, it is not clear if the cumulative block by mexiletine is dependent on the open events. Therefore, we used patches in which events closed at earlier times during some voltage steps and compared the extent of block produced by short and long pulses applied to the same potential. Figure 10 shows a typical example of such experiments. In the absence of drug, for 100 trains giving a total of 500 voltage steps, channel openings never appeared later than 15 ms after depolarization at Vr + 30 mV (Figure 10a). After application of 40 μM mexiletine, 200 ms-pulses produced a greater decline in the average currents than 20 ms-pulses between the 1st and 5th pulses (Figure 10c) in spite of no open events at a later time than 20 ms after depolarization at this voltage. This demonstrated a prominent development of block by mexiletine when the channel was still in an inactivated closed state.

Recently, several groups (Patlak & Ortiz, 1985; Grant & Starmer, 1987) have identified slow gating kinetics in a low

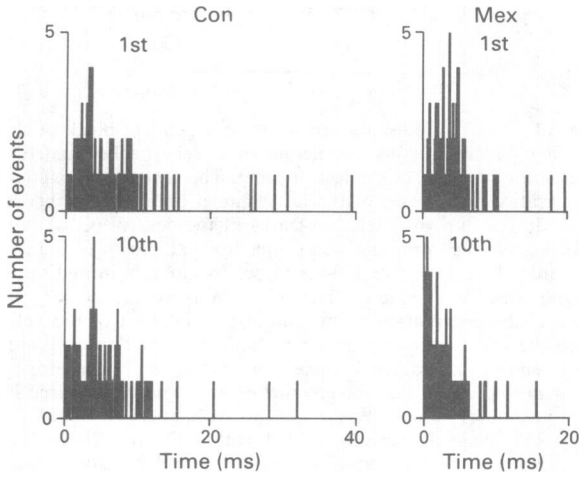

Figure 9 Use-dependent shortening of the active time of single Na^+ channel currents in a cell-attached patch by mexiletine. The left column shows the active time histograms under control conditions (Con) and the right column shows those in the presence of 40 μM mexiletine applied to the bath solution (Mex). Active time distributions were analyzed for 1st pulses (upper panel) and 10th pulses (lower panel) within the train. The data were obtained from the same experiments as that shown in Figure 8.

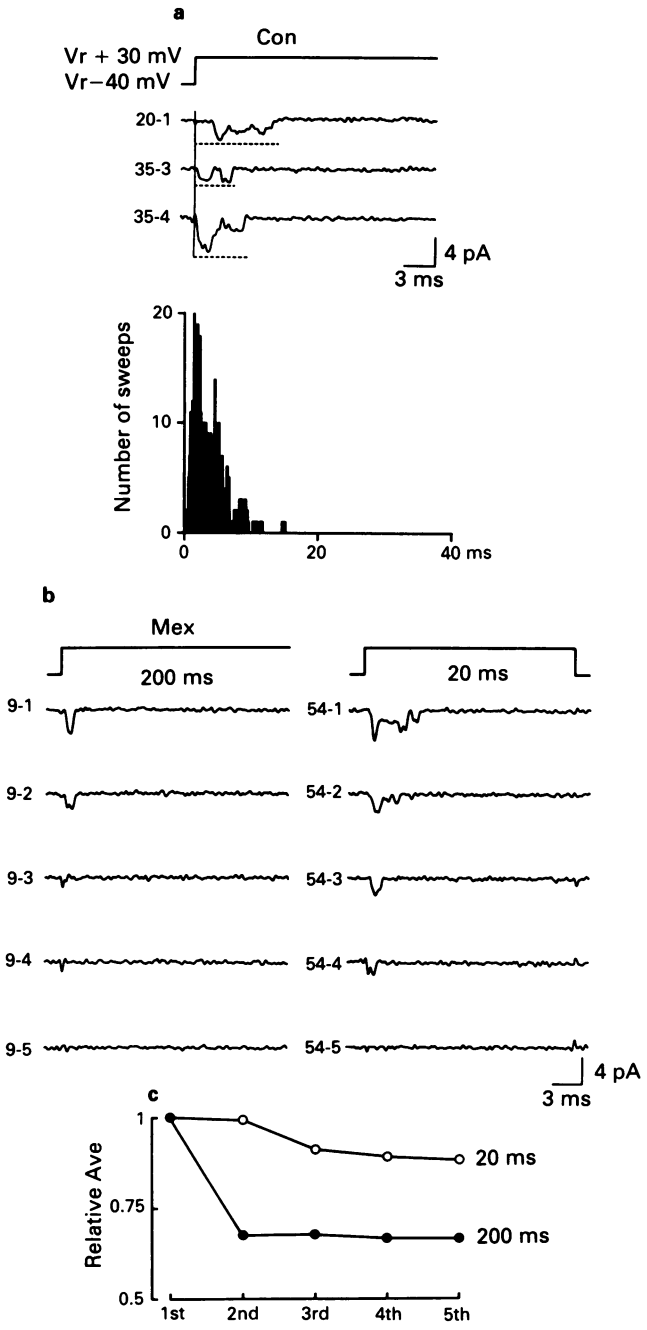

Figure 10 Effect of pulse duration on use-dependent block of single Na^+ channel currents by mexiletine in a cell-attached patch. (a) Estimation of the end of the last opening. The time from the start of depolarization to the end of the last channel opening was indicated with a 'dotted line' in 3 selected traces in the control (Con) (upper panel). The voltage protocol was similar to that shown in Figure 1a except that there were five 200-ms pulses within a train and the test potential was Vr + 30 mV. The histogram in the lower panel represents the distribution of the time from the start of the voltage step to the end of the last opening obtained from the total sweeps with openings including 3 traces in the upper panel for 500 depolarizations. Note that the channel openings never appeared later than 15 ms after depolarization at this voltage (Vr + 30 mV). (b) Single Na^+ channel currents elicited with 200- and 20-ms pulses during exposure to mexiletine. After the control records shown in (a), 40 μM mexiletine (Mex) was applied to the bath solution and currents were first elicited with 200-ms pulses and then with 20-ms pulses. The left column illustrates 5 consecutive traces in the 9th train with 200-ms pulses and the right column illustrates those in the 54th train with 20-ms pulses. (c) Plot of amplitude of average currents vs. the sequence of the pulses within the train in the presence of 40 μM mexiletine in the bath. Normalized peak amplitude of average currents (Ave) with 200- (●) and 20-ms (○) pulses was plotted against the sequence of the pulses within the train. The patch contained three channels.

percentage (< 1%) of depolarizing sweeps in ventricular cells. However, because of the low probability of observing bursts of opening, we were unable to study effects of mexiletine on such bursts before and after drug exposure in the same patch.

Discussion

The present study demonstrated the use-dependent block of cardiac Na^+ channels by mexiletine at the single channel level. The use-dependent block was manifested as an increase in the number of null sweeps and consequently a decrease in the number of open events, whereas the unitary current amplitude and mean open times were not affected. Furthermore, late openings were reduced in a use-dependent manner.

Time-dependent voltage shifts in the Na^+ channel gating have been suggested in single channel recordings of the cell-attached and inside-out patches (Cachelin *et al.*, 1983; Kunze *et al.*, 1985; Patlak & Ortiz, 1985; Kimitsuki *et al.*, 1990). These changes confuse the drug effects and limit the usefulness of detailed kinetic data. Previous studies on the block kinetics of single Na^+ channel currents by class I agents were carried out under long-term periods of recordings (Nilius *et al.*, 1987; Kohlhardt & Fichtner, 1988). Recently, Undrovinas *et al.* (1989) and Baumgarten *et al.* (1991) observed use-dependent block of single channel currents from frequency-dependent effects or the difference between initial and the final segments of successive depolarizations. Similarly, the use-dependence of the blocking action of the drug was presented in DPI 201-106 modified Na^+ channels (Carmeliet *et al.*, 1989). All of the above reports, however, did not mention the appearance and extent of the voltage shifts occurring during the drug exposure, and how much the voltage shift effects affected the observed use-dependent block. To depict the manner of use-dependent block observed in whole-cell and action potential recordings, we designed a stimulation protocol similar to the one used for single channel recordings (Grant *et al.*, 1989). Using these protocols, any time-dependent changes should affect the groups of the train pulses in a similar manner. Moreover, in most cases, the time difference between first and last pulses in trains was within 2.08–6.3 s, during which time-dependent gating shifts were negligible. However, when we compared the total data in one condition with those in another, we could not exclude any interference of time-dependent shifts.

Previous studies of Na^+ channel block by class I agents showed a reduction in open channel probability (P_o) without change in single channel conductance (Nilius *et al.*, 1987; Kohlhardt & Fichtner, 1988; Carmeliet *et al.*, 1989; Grant *et al.*, 1989; McDonald *et al.*, 1989; Undrovinas *et al.*, 1989; Baumgarten *et al.*, 1991; Gruber *et al.*, 1991). We also observed this change for mexiletine. During exposure to mexiletine, channel openings decreased as pulses progressed. That is, use-dependent binding of mexiletine decreased the probability of channel openings (P_o). However, we could not detect any significant change in the mean open time during the train. A shortening of mean open time has been reported for diprafenone (Kohlhardt & Fichtner, 1988) and penticainide (Carmeliet *et al.*, 1989; Gruber *et al.*, 1991) having a high affinity for the activated state of the channel. On the other hand, there is a conflict among the reports as to lignocaine having a high affinity for the inactivated state of the channel. A shortening (Nilius *et al.*, 1987; McDonald *et al.*, 1989; Baumgarten *et al.*, 1991) and no change (Grant *et al.*, 1989) of mean open time have been observed for lignocaine. In the present study, use-dependent block of the Na^+ channel by mexiletine did not require a shortening of open time. This is the first demonstration that use-dependent block by mexiletine is caused by a progressive decrease in the number (open channel probability, P_o) rather than the duration of open events. Here, we assume that a channel is blocked when the drug is bound and that it conducts only when the drug 'unbinds'. If binding occurs rapidly during the

time course of an opening, mean open time should be shortened. Recently, it was suggested that drug-bound channels can still open and conduct with different gating kinetics from drug-free channels (McDonald *et al.*, 1989; Baumgarten *et al.*, 1991). McDonald *et al.* (1989) and Baumgarten *et al.* (1991) postulated this from quantitative analysis of two-pulse protocols and the existence of two exponentials of open time distributions in the presence of lignocaine. We cannot exclude this hypothesis completely but we failed to find evidence that drug-bound channels conduct with altered kinetics. In addition, if apparent shortening of the mean open time occurs, it should make the time to peak of the ensemble current earlier than the control. But we did not observe any consistent changes in time to peak current. Therefore, lack of effects on mean open time might be due to a slow binding of mexiletine relative to gating events of the channels.

Preferential binding of mexiletine to the inactivated state of the channel was suggested from the macroscopic current (Courtney, 1981; Hering *et al.*, 1983) and $\dot{V}_{max}$ experiments (Kodama *et al.*, 1987). Our single channel results demonstrated that block by mexiletine continued to accumulate and became greater when pulse duration was extended beyond the period in which channels were open. This result might indicate accumulation of drug-bound channels in an absorbing inactivated state since the number of nulls increased progressively during the train. These results further imply that use-dependent block of the Na^+ channel by mexiletine does not require channel openings.

From the data on the first latency near threshold potentials, mexiletine seemed to suppress the first openings at later times. However, an ensemble cannot be sufficiently accounted for by the first latencies (Kunze *et al.*, 1985) but is a combination of the all latency distribution and the open time distribution (Scanley *et al.*, 1990). On the other hand, the drug did not change the mean open times as described above. Therefore, to estimate effects of mexiletine on the late openings, we tried to quantify simply the late opening behaviour by using the active time histogram instead of the all latency histogram. Active time is the time from the first channel opening to the end of the last channel reopening in the case of patches, including a single level of the channel. In the case of multi-channel patches, we cannot be sure to ascertain reopenings of the channels, since the persistent channel activity may include later openings of any channel. Active time histograms during control demonstrated the rising and declining phase as shown in Figures 8 and 9, similar to the previous reports on all latency (Scanley *et al.*, 1990), reopening (Scanley *et al.*, 1990) and first latency histograms (Patlak & Horn, 1982; Kunze *et al.*, 1985; Scanley *et al.*, 1990) (see also Figure 7), which might also be able to support the presence of a series of closed states prior to the open state. Here, we saw consistent evidence for reductions of late opening events by mexiletine, as others have reported for lignocaine (Bennet, 1987; Baumgarten *et al.*, 1991). In those studies, however, time-dependent gating shifts could not be completely excluded, although we observed a use-dependent reduction of late openings by mexiletine during the train of depolarizations under conditions minimizing time-dependent shifts of gating. To our knowledge, the present study is the first single channel study demonstrating the use-dependent suppression of late openings.

In conclusion, mexiletine exhibits slow binding to the inactivated closed states of the Na^+ channel causing a failure of late as well as early openings, which results in null sweeps on subsequent depolarization.

This work was supported by the grants from the Ministry of Education, Science and Culture of Japan and the Fugaku Trust for Scientific Research to M.H. The authors express their thanks to Dr J.C. Makielski (University of Chicago) for reading and commenting on the manuscript. The technical assistance by Ms Y. Sugimoto and the secretarial assistance by Ms N. Fujita are also acknowledged.

References

ALDRICH, R.W., COREY, D.P. & STEVENS, C.F. (1983). A reinterpretation of mammalian sodium channel gating based on single channel recording. *Nature*, **306**, 436–441.

BAUMGARTEN, C.M., MAKIELSKI, J.C. & FOZZARD, H.A. (1991). External site for local anesthetic block of cardiac Na^+ channels. *J. Mol. Cell. Cardiol.*, **23**(Suppl I), 85–93.

BENNET, P.B. (1987). Mechanisms of antiarrhythmic drug action: block of sodium channels in voltage clamped cardiac cell membranes. *J. Appl. Cardiol.*, **2**, 463–488.

CACHELIN, A.B., DEPEYER, J.E., KOKUBUN, S. & REUTER, H. (1983). Sodium channels in cultured cardiac cells. *J. Physiol.*, **340**, 389–401.

CAMPBELL, T.J. (1983). Importance of physico-chemical properties in determining the kinetics of the effects of Class I antiarrhythmic drugs on maximum rate of depolarization in guinea-pig ventricle. *Br. J. Pharmacol.*, **80**, 33–40.

CARMELIET, E., NILIUS, B. & VEREECKE, J. (1989). Properties of the block of single Na^+ channels in guinea-pig ventricular myocytes by the local anaesthetic penticainide. *J. Physiol.*, **409**, 241–262.

CHEW, C.Y.C., COLLETT, J. & SINGH, B.N. (1979). Mexiletine: A review of its pharmacological properties and therapeutic efficacy in arrhythmias. *Drugs*, **17**, 161–181.

COURTNEY, K.R. (1981). Comparative actions of mexiletine on sodium channels in nerve, skeletal and cardiac muscle. *Eur. J. Pharmacol.*, **74**, 9–18.

GRANT, A.O., DIETZ, M.A., GILLIAM, F.R. III & STARMER, C.F. (1989). Blockade of cardiac sodium channels by lidocaine: single-channel analysis. *Circ. Res.*, **65**, 1247–1262.

GRANT, A.O. & STARMER, C.F. (1987). Mechanisms of closure of cardiac sodium channels in rabbit ventricular myocytes: single-channel analysis. *Circ. Res.*, **60**, 897–913.

GRUBER, R., VEREECKE, J. & CARMELIET, E. (1991). Dual effect of the local anaesthetic penticainide on the Na^+ current of guinea-pig ventricular myocytes. *J. Physiol.*, **435**, 65–81.

HAMILL, O.P., MARTY, A., NEHER, E., SAKMANN, B. & SIGWORTH, F.J. (1981). Improved patch-clamp techniques for high-resolution current recording from cells and cell-free membrane patches. *Pflügers Arch.*, **391**, 85–100.

HERING, S., BODEWEI, R. & WOLLENBERGER, A. (1983). Sodium current in freshly isolated and in cultured single rat myocardial cells: frequency and voltage-dependent block by mexiletine. *J. Mol. Cell. Cardiol.*, **15**, 431–444.

HILLE, B. (1977). Local anesthetics: hydrophilic and hydrophobic pathways for the drug-receptor reaction. *J. Gen. Physiol.*, **69**, 497–515.

HIRANO, Y. & HIRAOKA, M. (1988). Barium-induced automatic activity in isolated ventricular myocytes from guinea-pig hearts. *J. Physiol.*, **395**, 455–472.

HONDEGHEM, L.M. & KATZUNG, B.G. (1977). Time- and voltage-dependent interactions of antiarrhythmic drugs with cardiac sodium channels. *Biochim. Biophys. Acta*, **472**, 373–398.

HONDEGHEM, L.M. & KATZUNG, B.G. (1984). Antiarrhythmic agents: the modulated receptor mechanism of action of sodium and calcium channel-blocking drugs. *Annu. Rev. Pharmacol. Toxicol.*, **24**, 387–423.

HORN, R. & VANDENBERG, C.A. (1986). Inactivation of single sodium channels. In *Ion Channels in Neural Membranes*. ed. Ritchie, J.M., Keynes, R.D. & Bolis, L. pp. 71–83. New York: Alan R. Liss.

KIMITSUKI, T., MITSUIYE, T. & NOMA, A. (1990). Negative shift of cardiac Na^+ channel kinetics in cell-attached patch recordings. *Am. J. Physiol.*, **258**, H247–H254.

KIRSCH, G.E. & BROWN, A.M. (1989). Kinetic properties of single sodium channels in rat heart and rat brain. *J. Gen. Physiol.*, **93**, 85–99.

KODAMA, I., TOYAMA, J., TAKANAKA, C. & YAMADA, K. (1987). Block of activated and inactivated sodium channels by class-I antiarrhythmic drugs studied by using the maximum upstroke velocity ($\dot{V}_{max}$) of action potential in guinea-pig cardiac muscles. *J. Mol. Cell. Cardiol.*, **19**, 367–377.

KOHLHARDT, M. & FICHTNER, H. (1988). Block of single cardiac Na^+ channels by antiarrhythmic drugs: the effect of amiodarone, propafenone and diprafenone. *J. Membr. Biol.*, **102**, 105–119.

KUNZE, D.L., LACERDA, A.E., WILSON, D.L. & BROWN, A.M. (1985). Cardiac Na currents and the inactivating, reopening and waiting properties of single cardiac Na channels. *J. Gen. Physiol.*, **86**, 691–719.

MCDONALD, T.V., COURTNEY, K.R. & CLUSIN, W.T. (1989). Use-dependent block of single sodium channels by lidocaine in guinea pig ventricular myocytes. *Biophys. J.*, **55**, 1261–1266.

NILIUS, B., BENNDORF, K. & MARKWARDT, F. (1987). Effects of lidocaine on single cardiac sodium channels. *J. Mol. Cell. Cardiol.*, **19**, 865–874.

PATLAK, J. & HORN, R. (1982). Effects of N-bromoacetamide on single sodium channel currents in excised membrane patches. *J. Gen. Physiol.*, **79**, 333–351.

PATLAK, J.B. & ORTIZ, M. (1985). Slow currents through single sodium channels of the adult rat heart. *J. Gen. Physiol.*, **86**, 89–104.

SCANLEY, B.E., HANCK, D.A., CHAY, T. & FOZZARD, H.A. (1990). Kinetic analysis of single sodium channels from canine cardiac Purkinje cells. *J. Gen. Physiol.*, **95**, 411–437.

STARMER, C.F. & GRANT, A.O. (1985). Phasic ion channel blockade: a kinetic model and parameter estimation procedure. *Mol. Pharmacol.*, **28**, 348–356.

STARMER, C.F., GRANT, A.O. & STRAUSS, H.C. (1984). Mechanisms of use-dependent block of sodium channels in excitable membranes by local anesthetics. *Biophys. J.*, **46**, 15–27.

SUNAMI, A., SASANO, T., MATSUNAGA, A., FAN, Z., SAWANOBORI, T. & HIRAOKA, M. (1993). Properties of veratridine-modified single Na^+ channels in guinea pig ventricular myocytes. *Am. J. Physiol.*, **264**, H454–H463.

UNDROVINAS, A.I., BURNASHEV, N.A., NESTERENKO, V.V., MAKIELSKI, J.C., FLEIDERVISH, I.A., FOZZARD, H.A. & ROSENSHTRAUKH, L.V. (1989). Single channel sodium current in rat cardiomyocytes: use-dependent block by ethacizin. *J. Pharmacol. Exp. Ther.*, **248**, 1138–1145.

YATANI, A. & AKAIKE, N. (1985). Blockage of the sodium currents in isolated single cells from rat ventricle with mexiletine and disopyramide. *J. Mol. Cell. Cardiol.*, **17**, 467–476.

(Received January 5, 1993
Revised April 29, 1993
Accepted May 4, 1993)

Br. J. Pharmacol. (1993), **110**, 193–198

Evidence for participation of B_1 and B_2 kinin receptors in formalin-induced nociceptive response in the mouse

Clóvis R. Corrêa & [1]João B. Calixto

Deparment of Pharmacology, CCB, Universidade Federal de Santa Catarina, Rua Ferreira Lima, 82-88015-420, Florianópolis-SC, Brazil

1 This study was designed to investigate the role of bradykinin (BK), as well as the subtype of BK receptors involved, in formalin-induced hindpaw pain in the mouse by use of selective B_1 and B_2 receptor antagonists. In addition, we have analysed whether or not BK may be involved in formalin-induced hindpaw oedema in the mouse.

2 The pretreatment of animals with captopril (2 and 5 mg kg^{-1}, s.c.) significantly increase the first and the second phases of formalin-induced pain.

3 Co-injection of the selective B_1 receptor antagonist des-Arg^9[Leu^8]-BK (0.2–0.4 nmol/paw), together with formalin, caused graded and similar inhibitions of both phases of formalin-induced pain. Similar results were obtained with the B_2 antagonists NPC 349 (D-Arg[Hyp^3,Thi^{5,8}-D-Phe^7]-BK) and NPC 567 (D-Arg[Hyp^3, D-Phe^7]-BK) (0.2 and 0.6 nmol/paw). Higher concentrations of these antagonists (1 nmol/paw) failed to antagonize formalin-induced pain.

4 The new potent and selective B_2 receptor antagonists, Hoe 140 (D-Arg[Hyp^3,Thi^5,D-Tic^7,Oic^8]-BK), NPC 17731 (D-Arg[Hyp^3, *trans*-4-propoxy-D-proline (*trans*propyl)^7, Oic^8]-BK), and NPC 17761 (D-Arg[Hyp^3, *trans*-4-propoxy-D-proline (*trans* thiophenyl)^7, Oic^8]-BK) (0.02 to 1.0 nmol/paw), also caused significant inhibitions of both phases of formalin-induced pain. When Hoe 140 was injected subcutaneously 30 min before formalin injection (9.9 and 99 nmol kg^{-1}), it significantly attenuated both phases of formalin-induced pain. The putative non-peptide BK antagonist, MV 8612 (1.6 to 9.6 nmol/paw), but not MV 8608 (5.5 to 33 nmol/paw), caused a graded inhibition of both phases of formalin-induced pain, being, however, more active against the first phase.

5 The pretreatment of animals with morphine (2.6 to 13 μmol kg^{-1}, s.c.) caused dose-dependent and equipotent inhibitions of both phases of formalin-induced pain. In contrast, indomethacin (2.7 to 27 μmol kg^{-1}) antagonized only the second phase of formalin-induced pain.

6 The B_2 receptor antagonists, Hoe 140, NPC 17731, NPC 17761, NPC 349 and NPC 567, all caused a significant inhibition of formalin-induced hindpaw oedema. A similar inhibition was also observed with indomethacin but not with captopril or morphine.

7 Our results provide strong evidence for the important role of endogenous BK, acting through both B_1 and B_2 receptors, in the genesis of both phases of formalin-induced persistent pain in the mouse. In addition, the current results also demonstrate that the inflammatory oedema associated with the later phase of formalin-induced pain seems to be mediated by endogenous BK, via activation of B_2 receptors.

Keywords: Formalin test; pain; oedema; kinins; B_1 and B_2 bradykinin antagonists; *Mandevilla velutina* compounds

Introduction

The nonapeptide bradykinin (BK) and its related kinins are generated in plasma and in several tissues following tissue damage or infection. Once released, BK may induce pain and is thought to be involved in many inflammatory states (for review see: Marceau *et al.*, 1983; Proud & Kaplan, 1988; Steranka & Burch, 1991). Exogenous BK produces pain by activating and/or sensitizing nociceptive afferent A-δ and C fibres (Collier & Lee, 1963; Franz & Mense, 1975; Mense, 1975; Besson & Chaouch, 1987; Szolcsányi, 1987).

Considerable biochemical and functional evidence indicates that the effects of BK result from stimulation of specific membrane receptors B_1 and/or B_2, widely distributed in the peripheral and central nervous system (for review see: Regoli & Barabé, 1980; Steranka *et al.*, 1988a,b; Burch *et al.*, 1990; Bathon & Proud, 1991; Farmer & Burch, 1992). With the development of more selective and competitive BK antagonists, many biochemical and pharmacological studies have suggested that kinins are involved in inflammatory pain, acting mainly by stimulation of B_2 receptors (for review see: Proud & Kaplan, 1988; Steranka *et al.*, 1988b; Steranka & Burch, 1991). Thus, BK and its related kinins may play an important role as physiological mediators of pain and inflammatory hyperalgesia.

Formalin induces a long lasting nociceptive response in the mouse paw, and this effect has been widely used to model persistent tonic pain of moderate intensity which involves chemical irritation, some tissue damage, and formation of oedema due to release of inflammatory mediators (Hunskaar *et al.*, 1985; Hunskaar & Hole, 1987; Murray *et al.*, 1988). This nociceptive model usually involves two distinct phases: an early transient phase, which occurs in the first 5 min and a late tonic phase, evident 15 to 30 min after injection. It has been proposed that the early phase reflects direct stimulation of nociceptors, while the late phase may be associated with release of inflammatory mediators (Dubuisson & Dennis, 1977; Hunskaar *et al.*, 1985; 1986; Rosland *et al.*, 1990). In addition, formalin-induced persistent pain is thought to resemble clinical pain due to its tonic nature (Dennis & Melzack, 1979; Abbott *et al.*, 1982; Abbott & Franklin, 1986).

A recent electrophysiological study suggested that BK may be involved in the second phase of formalin-induced tonic pain in the mouse (Haley *et al.*, 1989). As the nociceptive response to formalin was markedly inhibited by the NPC 349 (D-Arg[Hyp^3,Thi^{5,8},D-Phe^7]-BK), but not by the selective B_1 antagonist des-Arg^9-[Leu^8]-BK, the authors concluded that

[1] Author for correspondence.

activation of B_2 receptors may underlie formalin-induced pain. In contrast, Shibata *et al.* (1989) reported that the first and second phases of pain elicited by formalin in the mouse were significantly antagonized by the B_1 selective antagonist des-Arg^9[Leu^8]-BK.

In the present study we have attempted to examine further the possible participation of BK in formalin-induced peripheral persistent pain in mice, and to characterize the subtype of BK receptors involved, by use of selective and competitive B_1 and B_2 receptor antagonists. In addition, we have also investigated whether BK is involved in formalin-induced hindpaw oedema in mice.

Methods

Formalin-induced pain

Male Swiss mice (25–35 g) were housed at 22–24°C under a 12 h light/12 h dark cycle and were given access to water and purina chow *ad libitum*. The procedure used was essentially similar to that described by Hunskaar & Hole (1987) and Murray *et al.* (1988), with minor modifications. Briefly, animals of the same strain were lightly anaesthetized with ether, except when used to analyse the first phase of formalin-induced pain, and 20 µl of 2.5% formalin solution (0.92% of formaldehyde), made up in PBS (phosphate-buffered solution containing: NaCl 137 mM; KCl 2.7 mM and phosphate buffer 10 mM), was injected s.c. under the plantar surface of the left hindpaw with a Hamilton microsyringe. Animals were acclimatized to the laboratory for at least 24 h before the experiments. Usually, two mice (control and treated) were observed simultaneously for 0 to 30 min following formalin injection. All experiments were carried out during the light period at 23 ± 2°C (Rosland *et al.*, 1990).

The amount of time (s) that animals spent licking the injected paw was timed with a chronometer and was considered as an index of pain. The initial nociceptive response normally peaked about 5 min after formalin injection (first phase), and was followed by a second peak that occurred 15 to 30 min after formalin injection (second phase). This later phase was usually accompanied by inflammation due to release of inflammatory mediators (Hunskaar & Hole, 1987). To avoid the influences of pharmacokinetics in the action of the drugs studied, different groups of animals were used to analyse each phase of formalin-induced pain. The animals were treated topically (in association with formalin) or by the s.c. route (0.1 ml 10 g^{-1} weight) with several selective B_1 and B_2 antagonists, or with functional BK antagonists isolated from the rhizome of the plant *Mandevilla velutina* (Calixto *et al.*, 1988). For the purpose of comparison in a separate set of experiments, the animals were treated with morphine (2.6–13 µmol kg^{-1}, s.c.) or with indomethacin (2.7–27 µmol/paw, i.p.), 30 and 60 min before formalin injection, respectively. Other groups of animals were treated with captopril (2 and 5 mg kg^{-1}, s.c.) 2 h before subplantar injection of formalin. Control animals received only the vehicle used to dilute these drugs (PBS or NaCl solution containing 5% w/v $NaHCO_3$; 0.1 ml 10 g^{-1} weight). Following intraplantar injection of formalin, the animals were immediately placed into the glass cylinder 20 cm in diameter and the time spent licking the injected paw was determined.

Effect of bradykinin antagonists on formalin-induced hindpaw oedema in the mouse

We measured the oedema by comparing the difference in weight of the formalin-treated paw and the weight of the control paw (untreated paw). For this purpose, the animals were killed 30 min after formalin injection by cervical dislocation, and the paw was cut at the knee joint and weighed on an analytical balance.

Statistical analysis

The results are presented as the mean ± s.e.mean, and statistical significance of differences between groups was analysed by means of analysis of variance followed by Dunnett's test or by the unpaired t test where indicated. P values less than 0.05, were considered as indicative of significance. When possible, the ID_{50} or IC_{50} (i.e. the dose or concentrations of drugs that reduced formalin pain by 50% relative to control values), were estimated from individual experiments by using the least squares method in a computer programme, produced in our laboratory (Armando Dettemer).

Drugs

The following drugs were used: des-Arg^9-[Leu^8]-BK, captopril, indomethacin (from Sigma Chemical Company, St. Louis, U.S.A.), formalin, morphine sulphate (Merck, Germany), NPC 349 (D-Arg-[Hyp^3, Thi^{5,8}, D-Phe^7]-BK), NPC 567 (D-Arg-[Hyp^3, D-Phe^7]-BK) (Peninsula Laboratories, U.S.A.), Hoe 140 (D-Arg-[Hyp^3,Thi^5,D-Tic^7,Oic^8]-BK) was kindly supplied by the Department of Pharma Synthesis, Hoechst, Frankfurt Main, Germany; NPC 17731 [D-Arg^9,Hyp^3,*trans*-4-propoxy-D-proline (*trans* propyl)^7,Oic^8]-BK and NPC 17761 [D-Arg^9, Hyp^3,*trans*-4-propoxy-D-proline (*trans* thiophenyl)^7, Oic^8]-BK were kindly supplied by Nova Pharmaceutical Corporation, Baltimore, U.S.A. The *Mandevilla velutina* compounds (MV 8608, molecular weight of 326 and MV 8612, molecular weight of 1182) were obtained in our laboratory as described previously (Calixto *et al.*, 1988). The stock solution for all peptides used was prepared in PBS (1–10 mM) and kept in siliconized plastic tubes, maintained in a freezer at – 18°C. The other drugs were prepared just before use in 0.9% w/v of NaCl solution, except indomethacin (NaCl solution plus 5% w/v of $NaHCO_3$) and *M. velutina* compounds (absolute ethanol). The final ethanol concentration did not exceed 5%.

Results

Effects of drugs on formalin-induced pain

Figure 1 (a and b) shows that the pretreatment of animals with captopril (2 and 5 mg kg^{-1}, s.c.) 2 h beforehand caused a significant enhancement of both the first and the second phases of formalin-induced pain. Figure 2 (a and b) illustrates that the co-injection of the selective B_1 receptor

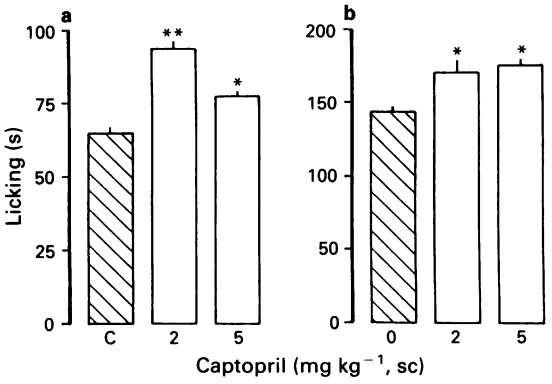

Figure 1 Effect of pretreatment with subcutaneous captopril on the formalin-induced pain in mice. In this and subsequent figures the total time (s, mean ± s.e.mean) spent licking the hindpaw was measured in the first (0–5 min, a) and the second phase (15–30 min, b), after intradermal injection of formalin in the hindpaw. Each column represents the mean with s.e.mean of 5 to 8 animals. C indicates the control animals (injected with the vehicle) and the asterisks denote the significance levels. Significantly different from controls: $*P<0.05$; $**P<0.01$.

antagonist des-Arg^9-[Leu^8]-BK (0.2 and 0.4 nmol/paw), together with formalin, caused a graded and similar degree of inhibition of the first and the second phases of the formalin-induced pain (maximal inhibition of about 40%). Nevertheless, at a higher concentration (0.6 nmol/paw) its analgesic effect against both phases of formalin-induced pain was absent. Very similar results were obtained when animals were pretreated with the B_2 antagonists NPC 349 (0.2 and 0.6 nmol/paw) and NPC 567 (0.2 and 0.6 nmol/paw) (Figure 3). Both BK antagonists consistently inhibited both phases of formalin-induced pain (maximum inhibition of about 45 to 50%). However, higher concentrations of these antagonists (1 nmol/paw) failed to antagonize the formalin-induced algesia (Figure 3).

The new generation of selective B_2 receptor antagonists, NPC 17731 (0.02 to 0.2 nmol/paw) and 17761 (0.1 to 1 nmol/paw), also caused a significant inhibition of both phases of the formalin-induced nociceptive response (Figure 4). NPC 17731 was more potent than NPC 17761, and their antinociceptive effects were not dose-dependent. At higher concentrations NPC 17731 (0.2 and 0.4 nmol/paw) did not cause any significant analgesic effect (Figure 4). The maximal inhibition produced by NPC 17731 and NPC 17761 was about 40–45%, against the first and the second phase of formalin-induced pain. Figure 5 shows that Hoe 140, a selective B_2 antagonist (0.19 to 1.9 nmol/paw), caused discrete, but significant inhibition of both phases of the formalin-induced persistent nociceptive response (maximal inhibition

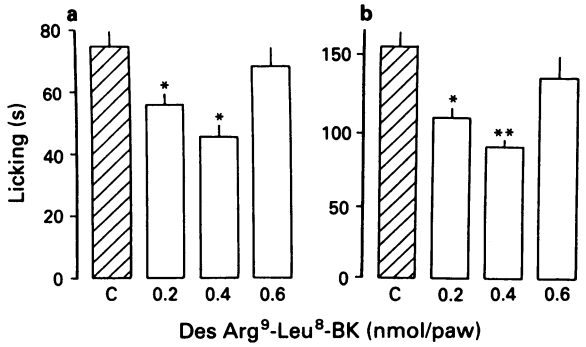

Figure 2 Effect of intradermal injection of the selective B_1 antagonist, des-Arg^9-[Leu^8]-bradykinin, on formalin-induced pain in mice. Each column represents the mean with s.e.mean of 5 to 8 animals. C indicates control animals. Significantly different from controls: $P<0.05$; $^{**}P<0.01$.

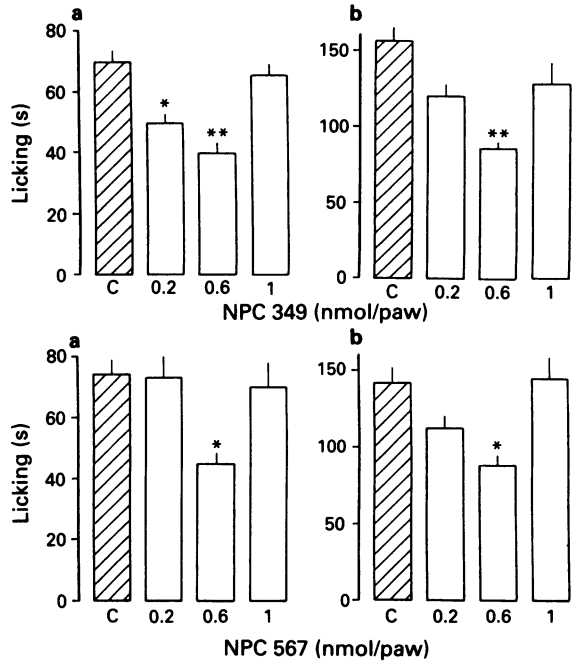

Figure 3 Effect of intradermal injection of B_2 bradykinin receptor antagonists, NPC 349 (upper panel) and NPC 567 (lower panel), in formalin induced pain in mice. Each column represents the mean with s.e.mean of 5 to 7 animals. C indicates control animals. Significantly different from controls; $^{*}P<0.05$; $^{**}P<0.01$.

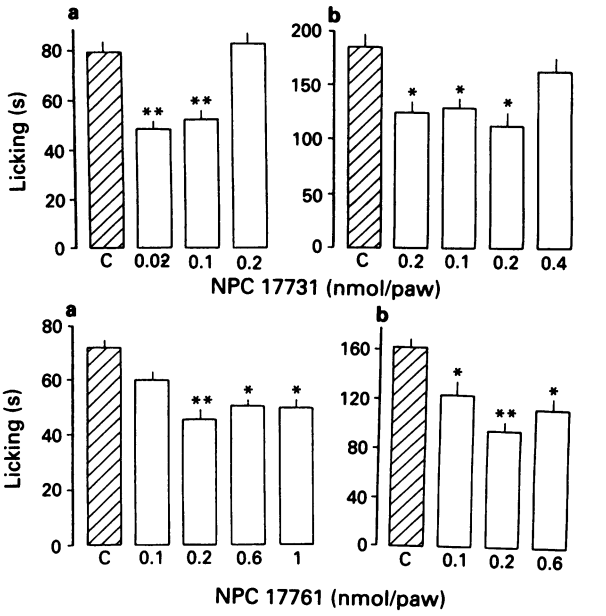

Figure 4 Effect of intradermal injection of B_2 bradykinin receptor antagonists NPC 17731 (upper panel) and NPC 17761 (lower panel) on formalin-induced pain in the mice. Each column represents the mean with s.e.mean of 5 to 8 animals. C indicates control animals. Significantly different from controls; $^{*}P<0.05$; $^{**}P<0.01$.

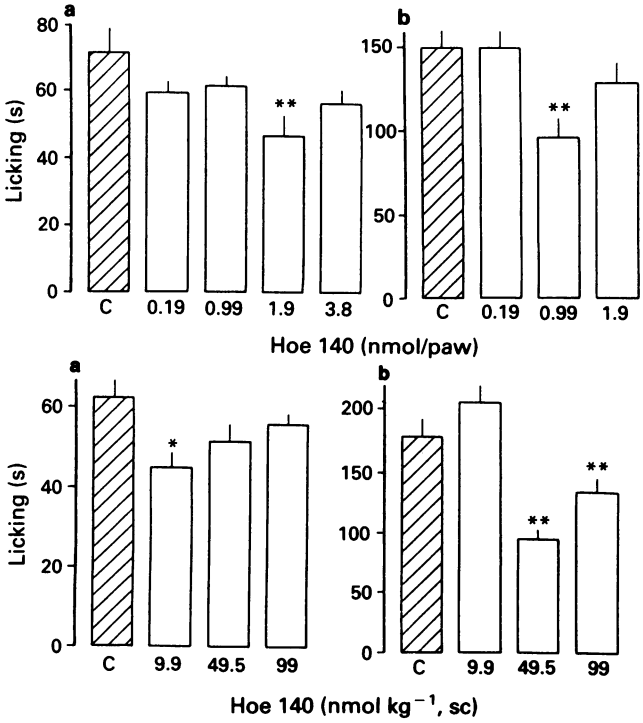

Figure 5 Effect of intradermal (upper panel) of subcutaneous (lower panel) injection of B_2 bradykinin receptor antagonist Hoe 140 on the formalin-induced pain in the mice. Each column represents the mean with s.e.mean of 5 to 9 animals. C indicates control animals. Significantly different from controls; $^{*}P<0.05$; $^{**}P<0.01$.

of about 40%). On the other hand, when Hoe 140 was administered subcutaneously 30 min before formalin injection (9.9 to 99 nmol kg^{-1}) it was markedly more effective in inhibiting the second phase of formalin-induced pain (maximal inhibition of 50%), than the first phase of formalin-induced pain. The nonpeptide BK antagonist isolated from *M. velutina*, compound MV 8612 (1.6 to 9.6 nmol/paw) caused graded and potent inhibitions of both phases of formalin-induced pain, being however much more effective against the first phase, with maximal inhibitions of 50 and 20%, respectively (Figure 6). Compound MV 8608 (5.5 to 33 nmol/paw) was completely ineffective against both phases of the formalin-induced nociceptive response (Figure 6).

The pretreatment of mice with morphine (2.6–13 μmol/kg, s.c.) caused dose-dependent and equipotent inhibition of both phases of formalin-induced pain, with an ID_{50} of about 3.5 μmol kg^{-1} (against both phases) and caused about 90% to 100% inhibition of formalin-induced pain (Figure 7). In contrast, indomethacin (2.7 to 27 μmol kg^{-1}, i.p.) dose-dependently antagonized only the second phase of formalin-induced pain, with an ID_{50} of about 10 μmol kg^{-1} (Figure 7).

Effects of drugs on formalin-induced paw oedema

The results summarized in Table 1 show that the selective B_1 receptor antagonist, des-Arg^9-[Leu^8]-BK, did not significantly inhibit formalin-induced hindpaw oedema. The B_2 antagonists NPC 349 and NPC 567 caused a discrete but significant inhibition of formalin-induced oedema (Table 1). However, the most potent and selective B_2 receptor antagonists, NPC 17731, NPC 17761 and Hoe 140 were all very effective and significantly inhibited formalin-induced paw oedema. Similar inhibition of formalin-induced paw oedema was observed in animals pretreated with indomethacin (Table 1). In contrast, *M. velutina* compounds, captopril and morphine all failed to inhibit significantly formalin-induced oedema (results not shown).

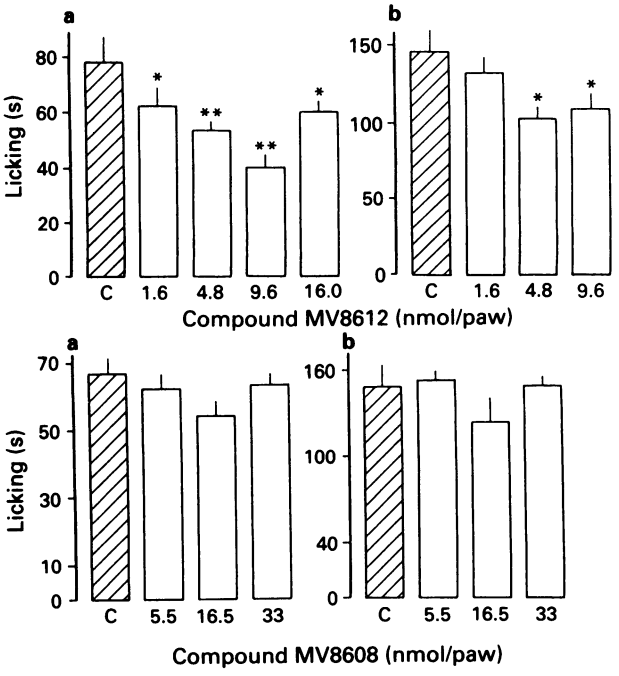

Figure 6 Effect of intradermal injection of compounds from *Mandevilla velutina* MV 8612 (upper panel) and MV 8608 (lower panel) on the formalin-induced pain in the mice. Each column represents the mean with s.e.mean of 5 to 10 animals. C indicates control animals. Significantly different from controls; $*P<0.05$; $**P<0.01$.

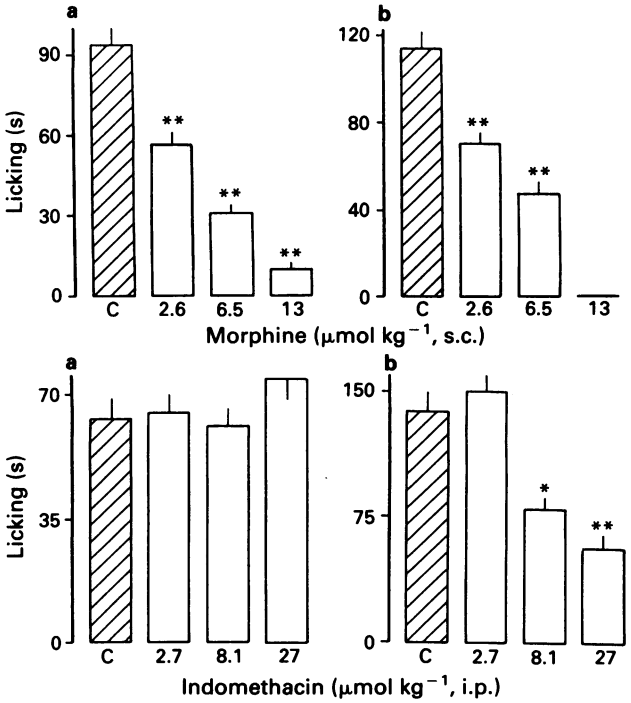

Figure 7 Effect of pretreatment with morphine given subcutaneously (upper panel) or with indomethacin given intraperitoneally (lower panel) on the formalin-induced pain in the mice. Each column represents the mean with s.e.mean of 5 to 12 animals. C indicates control animals. Significantly different from controls; $*P<0.05$; $**P<0.01$.

Discussion

The present study clearly demonstrates that selective and competitive BK receptor antagonists caused a pronounced antinociceptive effect in a model of persistent pain. This strongly supports the view that endogenous BK plays an important role in the genesis of both the first and second phases of the peripheral nociceptive response caused by intradermal injection of formalin in the mouse hindpaw. In addition, our results also indicate that both BK receptor subtypes, B_1 and B_2, are involved in both phases of formalin-induced tonic nociceptive response in mice. These views are substantiated by the fact that the selective B_1 receptor antagonist, des-Arg^9-[Leu^8]-BK, as well as the most potent and selective B_2 receptor antagonists, including NPC 349, NPC 567 (Burch *et al.*, 1990; Bathon & Proud, 1991), Hoe 140 (Hook *et al.*, 1991; Lembeck *et al.*, 1991), NPC 17761 and NPC 17731 (Kyle *et al.*, 1991a,b; Kyle & Burch, 1992), when co-injected with formalin or given subcutaneously, caused a pronounced inhibition of both phases of the pain caused in mice by formalin. Similar inhibition has been previously observed with selective B_2 antagonists, including Hoe 140 (Chapman & Dickenson, 1992), NPC 349 (Haley *et al.*, 1989), and with the selective B_1 receptor antagonist, des-Arg^9-[Leu^8]-BK (Shibata *et al.*, 1989). Interestingly, higher doses of most of the BK antagonists, failed to affect formalin-induced pain. These data are consistent with the view that BK antagonists may exhibit agonist activity (Steranka *et al.*, 1988a;b; 1989; Kindsen-Mells & Klement, 1992; Farmer & Burch, 1992). However, our results agree well with previously reported data, indicating that neither of the selective BK receptor antagonists was able to abolish completely the formalin-induced nociceptive response. These findings are consistent with the notion that other inflammatory mediators besides BK also participate in this response (Shibata *et al.*, 1986; 1989; Haley *et al.*, 1989; Dray & Dickenson, 1991; Murray *et al.*, 1991; Moore *et al.*, 1991). Another clear piece of evidence suppor-

Table 1 Effect of several peptide bradykinin receptor antagonists on formalin-induced oedema in the mice paw

Group	Dose: Systemic (nmol kg^{-1})	Dose: Local (nmol/paw)	*Oedema* (mg)	% *Inhibition*
Control	–	–	63 ± 4	–
Des-Arg^9-[Leu^8]-BK	–	0.2	57 ± 3	10
	–	0.4	52 ± 3	18
	–	0.6	63 ± 5	00
Hoe 140	9.9	–	67 ± 3	00
D-Arg-[Hyp^3,Thi^5,D-Thi^7,Oic^8]-BK	49.5	–	48 ± 3	26*
	99.0	–	56 ± 4	11
	–	0.1	52 ± 5	21*
	–	0.99	63 ± 5	00
NPC 567	–	0.2	58 ± 2	08
D-Arg-[Hyp^3,D-Phe^7]-BK	–	0.4	47 ± 2	26*
	–	1.0	55 ± 4	12
NPC 349	–	0.2	53 ± 2	16
Arg-[Hyp^3,Thi^{5,8},D-Phe^7]-BK	–	0.6	49 ± 3	22*
	–	1.0	54 ± 5	15
NPC 17731	–	0.02	53 ± 2	16
D-[Arg^0,Hyp^3,*trans*-4-propoxy-proline	–	0.1	39 ± 3	38**
(*trans*propyl)^7,Oic^8]-BK	–	0.2	42 ± 3	33**
	–	0.4	53 ± 2	16
NPC 17761	–	0.1	63 ± 3	00
D-[Arg^0,Hyp^3,*trans*-4-propoxy-proline-	–	0.2	46 ± 1	28**
(*trans* thiophenyl)^7,Oic^8]-BK	–	0.6	53 ± 1	16
Indomethacin[a]	2.7	–	66 ± 5	00
	8.4	–	56 ± 2	14*
	27.0	–	49 ± 3	25**

[a]μmol kg^{-1}, i.p.
Each group represents the mean of 5 to 12 animals. Oedema was measured 30 min after formalin injection.
Significantly different from controls: *$P<0.05$; **$P<0.01$.

ting a role of BK in formalin-induced tonic pain was the significant potentiation of formalin-induced licking by systemic captopril, a kininase II inhibitor (Ondetti *et al.*, 1977). However, captopril failed to affect the paw oedema associated with late phase of formalin-induced pain. Thus, we cannot rule out the possibility that the potentiation caused by captopril in formalin-induced pain may be, at least in part, secondary to the fall in blood pressure. The potent antinociceptive effect caused by morphine against both phases of formalin-induced pain, and the inhibition of the second phase of the formalin-induced pain by indomethacin are in good agreement with previous evidence reported in the literature (Hunskaar *et al.*, 1985; Murray *et al.*, 1988; Shibata *et al.*, 1989; Dray & Dickenson, 1991; Moore *et al.*, 1991; Oluyomi *et al.*, 1992; Chapman & Dickenson, 1992).

An interesting aspect investigated in the present study was whether the oedema associated with the later phase of formalin-induced pain, was also mediated by BK. Our results clearly show that the most potent and selective B_2 receptor antagonists such as Hoe 140, NPC 17731 and NPC 17761, and to a lesser extent the less potent B_2 antagonists such as NPC 349 and NPC 567, but not the selective B_1 antagonist, des-Arg^9[Leu^8]-BK, were found to be effective in antagonizing formalin-induced hindpaw oedema. This supports the view that only B_2 receptors appear to be involved in the formalin-induced inflammatory response. Our results are in agreement with a great deal of experimental evidence that suggests the involvement of the B_2 but not B_1 receptors in many experimental inflammation models (see for review: Marceau *et al.*, 1983; Proud & Kaplan, 1988; Burch *et al.*, 1990; Bathon & Proud, 1991; Steranka & Burch, 1991).

Concerning the potent antinociceptive effect of the functional BK antagonist isolated from *Mandevilla velutina*, compound MV 8612 but not MV 8608 was found very active in inhibiting both phases of formalin-induced pain, being more effective against the first phase of the formalin-induced pain. These findings provide additional evidence supporting our previous view that this compound may interfere with some stage of BK action (Calixto *et al.*, 1985; 1987; 1988; 1991).

In conclusion, our current data show that the selective and competitive BK receptor antagonists caused a pronounced antinociceptive effect against formalin-induced persistent pain in mice, thus providing strong evidence supporting the notion that endogenous BK, acting through B_1 and B_2 receptors, contributes to the genesis of both phases of peripheral nociceptive response. In addition, these results also demonstrate that the inflammatory response associated with the late phase of formalin-induced pain in mice seems to be mediated, at least in part, by endogenous BK via stimulation of the B_2 receptors.

We are grateful to Josane R. de Andrada and Elizabet T. Ramos for secretarial help in preparing this manuscript and to Dr G.A. Rae for his critical comments. C.R.C. is an undergraduate medical student receiving a grant from CNPq (n. 801285/86-0-BF). This work was supported by grants from CNPq and FINEP (Brazil).

References

ABBOTT, F.V., MELZACK, R. & SAMMUEL, C. (1982). Morphine analgesia in the tail-flick and formalin pain tests is mediated by different neural systems. *Exp. Neurol.*, **75**, 644–651.

ABBOTT, F.V. & FRANKLIN, K.B.J. (1986). Noncompetitive antagonism of morphine analgesia by diazepam in the formalin test. *Pharmacol. Biochem. Behav.*, **24**, 319–321.

BATHON, P.J. & PROUD, D. (1991). Bradykinin antagonists. *Annu. Rev. Pharmacol. Toxicol.*, **31**, 129–162.

BESSON, J.-M. & CHAOUCH, A. (1987). Peripheral and spinal mechanisms of nociception. *Physiol. Rev.*, **67**, 67–186.

BURCH, R.M., FARMER, G.S. & STERANKA, R.R. (1990). Bradykinin receptor antagonists. *Med. Res. Rev.*, **10**, 237–270.

CALIXTO, J.B., NICOLAU, M. & YUNES, R.A. (1985). The selective antagonism of bradykinin action on rat isolated uterus by crude *Mandevilla velutina* extract. *Br. J. Pharmacol.*, **85**, 729–731.

CALIXTO, J.B., NICOLAU, M., PIZZOLATTI, M.G. & YUNES, R.A. (1987). Kinin antagonist activity of compounds from *Mandevilla velutina* in the rat isolated uterus. *Br. J. Pharmacol.*, **91**, 199–204.

CALIXTO, J.B., PIZZOLATTI, M.G. & YUNES, R.A. (1988). The competitive antagonistic effect of compounds from *Mandevilla velutina* on kinin-induced contractions of rat uterus and guinea-pig ileum *in vitro*. *Br. J. Pharmacol.*, **91**, 1133–1142.

CALIXTO, J.B., YUNES, R.A., RAE, G.A. & MEDEIROS, Y.S. (1991). Nonpeptide bradykinin antagonists. In *Bradykinin Antagonists: Basic and Clinical Research*. ed. Burch, R.M. pp. 97–129. New York: Marcel Dekker Inc.

CHAPMAN, V. & DICKENSON, A.H. (1992). The spinal and peripheral roles of bradykinin and prostaglandins in nociceptive processing in the rat. *Eur. J. Pharmacol.*, **219**, 427–433.

COLLIER, H.O. & LEE, I.R. (1963). Algesic actions of bradykinin. *Br. J. Pharmacol.*, **21**, 151–158.

DENNIS, S.G. & MELZACK, R. (1979). Comparison of phasic and tonic pain in animals. *Adv. Pain Res. Ther.*, **3**, 747–760.

DRAY, A. & DICKENSON, A. (1991). Systemic capsaicin and olvanil reduce the acute algogenic and the late inflammatory phase following formalin injection into rodent paw. *Pain*, **47**, 78–83.

DUBUISSON, D. & DENNIS, S.G. (1977). The formalin test: a quantitative study of the analgesic effects of morphine, meperidine and brain stem stimulation in rats and cats. *Pain*, **4**, 161–174.

FARMER, S.G. & BURCH, R.M. (1992). Biochemical and molecular pharmacology of kinin receptors. *Annu. Rev. Pharmacol. Toxicol.*, **32**, 511–536.

FRANZ, M. & MENSE, S. (1975). Muscle receptors with group IV afferent fibres responding to application of bradykinin. *Brain Res.*, **92**, 369–383.

HALEY, J.E., DICKENSON, A.H. & SCHACHTER, M. (1989). Electrophysiological evidence for a role of bradykinin in chemical nociception in the rat. *Neurosci. Lett.*, **97**, 198–202.

HOOK, F.J., WIRTH, K., ALBUS, U., LINZ, W., GERHARDS, H.J., WIEMER, G., ST. HENKE, G., BREIPOHL, W., KÖNIG, W., KNOLLE, J. & SCHÖLKENS, B.A. (1991). Hoe 140 a new potent and long acting bradykinin-antagonist: *in vitro* studies. *Br. J. Pharmacol.*, **102**, 769–773.

HUNSKAAR, S., FASMAR, O.B. & HOLE, K. (1985). Formalin test in mice: a useful technique for evaluating mild analgesics. *J. Neurosci. Methods*, **14**, 69–76.

HUNSKAAR, S., BERGE, O.G. & HOLE, K. (1986). Dissociation between antinociceptive and anti-inflammatory effects of acetylsalicylic acid and indomethacin in the formalin test. *Pain*, **25**, 125–132.

HUNSKAAR, S. & HOLE, K. (1987). The formalin test in mice: dissociation between inflammatory and non-inflammatory pain. *Pain*, **30**, 103–114.

KINDGEN-MILLES, D. & KLEMENT, W. (1992). Pain and inflammation evoked in human skin by bradykinin receptors antagonists. *Eur. J. Pharmacol.*, **218**, 183–185.

KYLE, J.D. & BURCH, R.M. (1992). Recent advances toward novel bradykinin antagonists. *Drugs of the Future*, **17**, 305–312.

KYLE, D.J., MARTIN, J.A., FARMER, S.G. & BURCH, R.M. (1991a). Design and conformational analysis of several highly potent bradykinin receptor antagonists. *J. Med. Chem.*, **34**, 1230–1233.

KYLE, D.J., MARTIN, J.A., BURCH, R.M., CARTER, J.P., LU, S., MEEKER, S., PROSSER, J.C., SULLIVAN, J.P., TOGO, J., NORONHA-BLOB, L., SINSKO, J.A., WALTERS, R.F., WHALEY, L.W. & HINER, R.N. (1991b). Probing the bradykinin receptor: mapping the geometric topography using ethers of hydroxyproline in novel peptides. *J. Med. Chem.*, **34**, 2649–2653.

LEMBECK, F., GRIESBACHER, T., ECKHARDT, M., HENKE, S., BREIPOHL, G. & KNOLLE, J. (1991). New, long acting potent bradykinin antagonists. *Br. J. Pharmacol.*, **102**, 297–304.

MARCEAU, F., LUSSIER, A., REGOLI, D. & GIROUD, J.P. (1983). Pharmacology of kinins: their relevance to tissue injury and inflammation. *Gen. Pharmacol.*, **14**, 209–229.

MENSE, S. (1982). Reduction of the bradykinin-induced activation of feline group III and IV muscle receptors by acetylsalicyclic acid. *J. Physiol.*, **326**, 269–283.

MOORE, P.K., OLUYOMI, A.O., BABBEDGE, R.C., WALLACE, P. & HART, M.L. (1991). L-N^G-nitro arginine methyl ester exhibits antinociceptive activity in mouse. *Br. J. Pharmacol.*, **102**, 198–202.

MURRAY, C.W., PORRECA, F. & COWAN, A. (1988). Methodological refinements of the mouse paw formalin test – an animal model of tonic pain. *J. Pharmacol. Methods*, **20**, 175–186.

MURRAY, C.W., COWAN, A. & LARSON, A.A. (1991). Neurokinin and NMDA antagonists (but not a kainic acid anatagonist) are antinociceptive in the mouse formalin model. *Pain*, **44**, 179–185.

OLUYOMI, A.O., HART, S.L. & SMITH, T.W. (1992). Differential antinociceptive effects of morphine and methylmorphine in the formalin test. *Pain*, **49**, 415–418.

ONDETTI, M.A., RUBIN, N.J. & CUSHING, D.W. (1977). Design of specific inhibitors of angiotensin-converting enzyme: new class of orally active antihypertensive agents. *Science*, **196**, 441–444.

PROUD, D. & KAPLAN, A.P. (1988). Kinin formation: mechanisms and role in inflammatory disorders. *Annu. Rev. Immunol.*, **6**, 49–83.

REGOLI, D. & BARABÉ, J. (1980). Pharmacology of kinins. *Pharmacol. Rev.*, **32**, 1–46.

ROSLAND, J.H., TJØLSEN, A., MÆHLE, B. & HOLE, K. (1990). The formalin test in mice: effect of formalin concentration. *Pain*, **42**, 235–242.

SHIBATA, M., OHKUBO, T., TAKAHASHI, H. & INOKI, R. (1986). Interaction of bradykinin with substance P on vascular permeability and pain response. *Jpn. J. Pharmacol.*, **41**, 427–429.

SHIBATA, M., OHKUBO, T., TAKAHASHI, H. & INOKI, R. (1989). Modified formalin test: characteristic biphasic pain response. *Pain*, **38**, 347–352.

STERANKA, L.R. & BURCH, R.M. (1991). Bradykinin antagonists in pain and inflammation. In *Bradykinin Antagonists: Basical and Clinical Research*. ed. Burch, R.M. pp. 191–211. New York: Marcel Dekker Inc.

STERANKA, L.R., FARMER, S.G. & BURCH, R.M. (1989). Antagonists of B_2 bradykinin receptors. *FASEB J.*, **3**, 2019–2025.

STERANKA, L.R., MANNING, D.C., DEHAAS, C.J., FERKANY, J.W., BOROSKI, S.A., CONNOR, J.R., VAVREK, R.J., STEWART, J.M. & SNYDER, S.H. (1988a). Bradykinin as a pain mediator: receptors are localized to sensory neurons, and antagonists have analgesic actions. *Proc. Natl. Acad. Sci. U.S.A.*, **85**, 3245–3249.

STERANKA, L.R., BURCH, R.M., VAVREK, R., STEWART, J.M. & ENNA, S.J. (1988b). Multiple bradykinin receptors: results of studies using a novel class of receptor antagonists. In *Neuroreceptors and Signal Transduction*. ed. Kito, S., Segawa, T., Kuriyama, K. & Olsen, R.W. pp. 11–127. New York: Plenum Publishing Co.

SZOLCSÁNYI, J. (1987). Selective responsiveness of polymodal nociceptors of rabbit ear to capsaicin, bradykinin and ultraviolet irradiation. *J. Physiol.*, **388**, 9–23.

(Received March 1, 1993
Revised May 4, 1993
Accepted May 5, 1993)

Br. J. Pharmacol. (1993), **110**, 199–206

Effects of hydroxyethylrutosides on the permeability of microvessels in the frog mesentery

S. Kendall, *R. Towart & [1]C.C. Michel

Department of Physiology & Biophysics, St Mary's Hospital Medical School, Imperial College of Science, Technology & Medicine, Norfolk Place, London W2 1PG and *Zyma SA, CH1260 Nyon, Switzerland

1 We have investigated the effects of a standardised mixture of hydroxyethylrutosides (HR, Venoruton), a mixture of five of its main components (M) and each of the five components separately (7-mono-HR, 7,4'-di-HR, 7,3',4'-tri-HR, 5,7,3',4'-tetra-HR and 7,3'4'-tri HQ) upon the permeability of single perfused capillaries and venules in the mesenteries of pithed frogs.

2 In each experiment, the hydraulic permeability (L_p) of a single perfused microvessel and the effective osmotic pressure ($\sigma\Delta\pi$) exerted by macromolecules across its walls were estimated by a microcclusion technique, first during control perfusion and then in the presence of a known concentration of test substance.

3 HR, M and 7,4'-di-HR reduced L_p in a similar concentration-dependent manner over the range of 1 $\mu g\,ml^{-1}$ to 1 $mg\,ml^{-1}$ (maximum reduction was to 40% of control L_p at 1 $mg\,ml^{-1}$). At perfusate concentrations greater than 1 $mg\,ml^{-1}$, these substances reduced L_p to a lesser extent. While the four other test substances reduced L_p significantly when their perfusate concentrations equalled or exceeded 100 $\mu g\,ml^{-1}$, they were all less potent than 7,4'-di-HR.

4 The reduction in L_p induced by the mixture of flavonoids was only slightly reversed by subsequent perfusion with flavonoid-free solutions.

5 When permeability was increased by perfusing with protein-free solutions, both HR and 7,4'-di-HR reduced and then reversed the increase in L_p in a concentration-dependent manner over the range of 1 $\mu g\,ml^{-1}$ to 100 $\mu g\,ml^{-1}$. None of the other component flavonoids was effective in restoring L_p under these conditions.

Keywords: Capillaries; flavonoids; hydroxyethylrutosides; microcirculation; microvascular permeability; vascular permeability

Introduction

O-(β-hydroxyethyl)-rutosides (oxerutins, Venoruton), abbreviated to HR, is a standardized mixture of hydroxyethyl derivatives of rutin which is widely used in patients with chronic venous insufficiency to reduce leg oedema and its related symptoms (Pulvertaft, 1983; Balmer & Limoni, 1989; Nocker *et al.*, 1989; de Jongste *et al.*, 1989, Wadworth & Faulds, 1992). Although HR has been shown to lower microvascular filtration rates in human limbs (Roztocil *et al.*, 1971; 1977; Cesarone *et al.*, 1992), the mechanism of its action is obscure.

Studies on experimental animals suggest that HR reduces microvascular permeability. It has been shown to reduce the leakage of plasma macromolecules in burns in anaesthetized dogs (Arturson, 1972; Hilton, 1982) and to diminish the accumulation of albumin in rats after local injection of histamine and bradykinin (Gerdin & Svensjo, 1983). Previous studies in our laboratory (Blumberg *et al.*, 1989; Michel *et al.*, 1990) showed that HR reduced the hydraulic permeability (L_p) of single perfused frog capillaries in both normal and inflamed mesenteric tissues. In inflamed tissues where permeability to plasma proteins was increased, HR was found to raise the effective osmotic pressure ($\sigma\Delta\pi$) exerted across the microvascular walls by perfusate macromolecules (Blumberg *et al.*, 1989). In preliminary experiments we also observed that the increase in vascular permeability which follows perfusion of these vessels with solutions free of plasma proteins (Mason *et al.*, 1977; Michel & Phillips 1985), could be partially (and sometimes completely) reversed by perfusion with solutions containing HR (Michel *et al.*, 1990).

The present paper describes experiments which address three issues arising from our previous studies. The first of these is to establish the relation between the reduction in L_p induced by HR and the concentration of HR in the perfusate. While Blumberg *et al.* (1989) showed that the effect of HR was concentration-dependent, they failed to establish a clear dose-response relation, possibly because they pooled data from both normal and inflamed vessels. To minimize the range of 'control' values of permeability in the present study, we have investigated only vessels that appeared normal at the outset of an experiment.

The second issue arises from HR's being a mixture of O-(β-hydroxyethyl)-rutosides. The potency of its separate components has not been investigated previously and in this paper we describe the permeability-reducing effects of five of the principal constituents of HR.

The third set of experiments described in this paper was designed to investigate the range of perfusate concentration of HR over which it would reverse the increase in permeability induced by perfusion with protein-free solutions. We extended these experiments to examine the effectiveness of some of the principal components of HR in reducing permeability under these conditions. The effects of 7,4'-di-O-(β-hydroxyethyl)-rutoside, the constituent that reduced permeability most effectively in our preparation, were examined also over a range of perfusate concentrations. The effects of the other principal components were examined only at a single perfusate concentration.

Like Blumberg *et al.* (1989) we carried out our experiments on single perfused frog mesenteric capillaries and venules. By using this preparation we were able to apply techniques (Michel *et al.*, 1974; Michel, 1980) which yield values for both the L_p and the molecular sieving properties of vessel walls to macromolecules ($\sigma\Delta\pi$) in the same microvessel before, during and after perfusion with HR or one of its components. Working on single perfused microvessels reduces the ambiguities involved in interpreting changes in

[1] Author for correspondence.

blood tissue transport in terms of changes in permeability. In the capillary beds of intact organs and tissues, however, changes in blood-tissue transport may result from changes in the distribution of flow (and pressure) between different microvascular units as well as from changes in permeability.

Methods

Preparation

The experiments were performed on single mesenteric capillaries and venules of frogs (*R. temporaria* and *R. pipiens*) in which brains and upper spinal cords had been destroyed by pithing. The frog was laid in a perspex tray and a loop of intestine was delivered through a lateral incision through the abdominal wall and the mesentery laid over the polished upper surface of a short perspex pillar. The mesentery was then transilluminated through the pillar and viewed through a Wild M8 stereomicroscope while the tissue was kept cool, moist and well oxygenated by continuous superfusion of its upper surface with frog Ringer solution bubbled with 97% O_2, 3% CO_2. A thermistor bead on the upper surface of the pillar in contact with the base of the mesentery, allowed tissue temperature to be monitored continuously.

Solutions

The Ringer solution used as a superfusate had the following constituents (mM): NaCl 111.1, KCl 2.4, $MgSO_47H_2O$ 1.1, glucose 5.5, $CaCl_21.1$, $NaHCO_3$ approximately 10 but adjusted so that pH was between 7.2 and 7.4 when the solution was bubbled with 97% O_2 and 3% CO_2. Single microvessels were perfused with control and test Ringer solutions to which had been added bovine serum albumin (10 mg ml^{-1}) and the neutral macromolecule, Ficoll 70 (40 mg ml^{-1}). The concentrations of small molecules in the control perfusates were identical to those in the superfusates except the perfusates contained no $NaHCO_3$ and pH was adjusted by titration with 0.23 M NaOH immediately before being used. The test perfusates were made by adding a known mass of test substance to a measured volume of control perfusate. For the experiments described below in Sections 2 and 3 of Results, seven test substances were supplied to the experimenters (S.K. and C.C.M.) under ten different code numbers.

In some cases the same substance was supplied under a different code number. The code was revealed to the experimenters only after these experiments had been completed. The test substances were: (a) a standard preparation of HR (O-(β-hydroxyethyl)-rutosides, (lot number 2634, Zyma SA); (b) 7-mono-O-(β-hydroxyethyl)-rutoside (7-mono-HR); (c) 7,4'-di-O-(β-hydroxyethyl-rutoside (7,4'-di-HR); (d) 7,3'4'-tri-O-(8-hydroxyethyl)-rutoside (7,3',4'-tri-HR); (e) 5,7,3',4'-tetra-O-(β-hydroxyethyl)-rutoside (5,7,3',4'-tetra-HR); (f) 7,3',4'-trio-O-(β-hydroxyethyl)-quercetin (7,3',4'-tri-HQ): (g) an artificial mixture (M) consisting of the above five pure compounds, in the same proportions in which they occur in HR (3: 32: 57: 7.5: 0.5). The structures of these flavonoid derivatives are shown in Table 1.

The oncotic pressure of both control and test perfusates, measured in a Hansen type membrane osmometer fitted with an Amicon PM-10 membrane, lay in the range of 20–23 cmH_2O. A few washed human red cells were added to all the perfusate solutions to act as markers of fluid flow. For the experiments described in Section 5 of Results, the second perfusate was a Ringer solution containing Ficoll 70 (40 mg ml^{-1}) but no bovine serum albumin (BSA). The third perfusate in these experiments was a similar Ringer solution (containing Ficoll 70 but not BSA) to which the test substance was added at a known concentration. Test substances were not coded in these later experiments.

Measurement of microvascular permeability

Microvascular permeability was assessed from the hydraulic permeability coefficient (L_p) and the effective oncotic pressure exerted across the microvascular walls by perfusate macromolecules ($\sigma\Delta\pi$). Fluid movements through unit area of vessel wall (J_v/A) are related to the transmural hydrostatic pressure difference (ΔP) across them through the relation:

$$J_v/A = L_p\ (\Delta P - \sigma\Delta\pi) \quad \ldots\ldots\ 1.$$

Since L_p is independent of capillary hydrostatic pressure in these vessels over a wide range, the relation between J_v/A and ΔP, at constant $\sigma\Delta\pi$, is linear with a slope of L_p and an intercept of $\sigma\Delta\pi$. Thus measurements of J_v/A at two values of ΔP allow both L_p and $\sigma\Delta\pi$ to be estimated.

J_v/A and ΔP were measured by the method of Michel *et al.* (1974). In this technique a long, straight and unbranched microvessel (diameter 15–25 μm) is cannulated with a sharpened micropipette and perfused with a Ringer solution

Table 1 Structure of the flavonoid derivatives tested

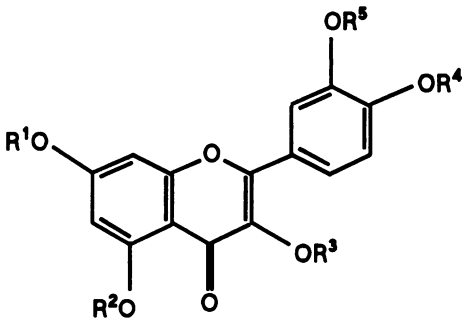

No.*	R^1	R^2	R^3	R^4	R^5
1	$HOCH_2CH_2$	H	Rutinose	H	H
2	$HOCH_2CH_2$	H	Rutinose	$HOCH_2CH_2$	H
3	$HOCH_2CH_2$	H	Rutinose	$HOCH_2CH_2$	$HOCH_2CH_2$
4	$HOCH_2CH_2$	$HOCH_2CH_2$	Rutinose	$HOCH_2CH_2$	$HOCH_2CH_2$
5	$HOCH_2CH_2$	H	H	$HOCH_2CH_2$	$HOCH_2CH_2$
6	Mixture of compounds 1, 2, 3 and 4				

*1 7-Mono-hydroxyethyl rutoside. 2 7,4'-Di-hydroxyethyl rutoside. 3 7,3',4'-Tri-hydroxyethyl rutoside. 4 5,7,3',4'-Tetra-hydroxyethyl rutoside. 5 7,3',4'-Tri-hydroxyethyl quercetin.

containing a few suspended red cells at constant pressure. After 5–10 min of perfusion, the outflow from the microvessel is interrupted by occlusion with a fine microneedle, some distance downstream from the cannulation site. The movements of red cells in the occluded segment then reflect fluid movements through the capillary walls between the marker red cells and the site of occlusion. From the velocity of a red cell (which is determined from a video recording) and the dimensions of the microvessel, J_v/A can be calculated. Such measurements of red cell velocity are made over the period 2 s to 10 s after microocclusion when the pressure applied to the microvessel through the pipette can be switched to a second value (Michel, 1980). While changes in the volume of the occluded segment interfere with the red cell movements immediately after occlusion or immediately after step changes in pipette pressure during occlusion, these compliance changes are complete within a second providing the microvascular pressure remains higher than 10 cmH_2O (Michel *et al.*, 1974; Levick & Michel, 1977; Swayne & Smaje, 1989). No attempt to estimate microvascular compliance was made in the present experiments.

Because the pressure applied to the micropipette approximates within 0.1 cmH_2O to the pressure inside the microvessels during occlusion, values of J_v/A can be estimated at different values of microvascular pressure which in turn approximates closely to ΔP. Thus both L_p and $\sigma\Delta\pi$ may be determined.

Protocol

In each experiment a single chosen capillary or venule was perfused with the control perfusate and L_p and $\sigma\Delta\pi$ were determined. The micropipette was then removed and the vessel was recannulated with a second micropipette filled with the test perfusate. L_p and $\sigma\Delta\pi$ were redetermined after at least 5 min perfusion with the second (test) solution. In the determination of dose-response curves, estimates of L_p and $\sigma\Delta\pi$ were made on 12 different vessels in the absence and presence of a given concentration of the test substance.

To investigate the effects of test substances in the absence of plasma proteins, L_p and $\sigma\Delta\pi$ were determined during each of three successive perfusions on the same microvessel. The first perfusate was the standard control perfusate containing Ficoll 70 and BSA; the second perfusate contained Ficoll 70 but no BSA; the third perfusate contained Ficoll 70 plus a known concentration of a test substance but no BSA. L_p and $\sigma\Delta\pi$ were determined between 5 and 10 min after the start of the first and third perfusions but it was found necessary to perfuse for 20 min with the second solution (protein-free) in order to obtain a reproducible increase in L_p over its control value.

Statistics

L_p was estimated from the slope of the regression line relating J_v/A to capillary pressure during perfusion with either control or test solution. The intercept of this relation with the pressure axis was taken as $\sigma\Delta\pi$.

Paired *t* tests were used to assess the significance of differences between L_p and $\sigma\Delta\pi$ in the absence and presence of test substances.

Results

(1) Reproducibility of estimates of L_p and $\sigma\Delta\pi$ in the same vessel

At the outset of the investigation, the reproducibility of the technique was assessed by determining the values for L_p and $\sigma\Delta\pi$ in a capillary or venule perfused with a control solution and then removing the micropipette, recannulating the vessel with a second micropipette filled with the same control perfusate and remeasuring L_p and $\sigma\Delta\pi$. Seventeen experiments of this kind were carried out. The mean value ($\pm$ s.e.mean) of L_p during the first perfusion was 3.97 ($\pm$ 0.45) $\times 10^{-7}$ cm s^{-1} cmH_2O^{-1} and during the second perfusion was 3.71 ($\pm$ 0.44) $\times 10^{-7}$ cm s^{-1} cmH_2O^{-1}. A paired *t* test revealed no significant difference between the first and second estimates of L_p.

The mean value ($\pm$ s.e.mean) of $\sigma\Delta\pi$ was 12.85 ($\pm$ 0.47) cmH_2O during the first perfusion and 11.35 ($\pm$ 0.43) cmH_2O during the second perfusion. The difference was not significant.

(2) Reduction of permeability by varying concentrations of mixtures of flavonoids

Figure 1a–d show the effects of various concentrations of Venoruton (HR) upon the relation between J_v/A and P_c in four single perfused capillaries. Each part of Figure 1 represents the results of a single experiment at one concentration of HR. It is seen that as the test perfusate contained increasing concentrations of HR, the slope of the relation between J_v/A and capillary pressure was reduced to a greater extent relative to its control value. There was, however, no change in the intercept of the relation, $\sigma\Delta\pi$. These four experiments were representative of the general response of microvessels to perfusion with HR. A clear concentration-dependent lowering of L_p could be observed as the HR concentration in the perfusate was raised from 10 $\mu g\ ml^{-1}$ to 1 $mg\ ml^{-1}$. Perfusion with a test solution containing 10 mg HR ml^{-1}, however, reduced L_p to a smaller extent than perfusion at 1.0 $mg\ ml^{-1}$. In Figure 2a, each closed circle is the mean value of 12 determinations of L_p in vessels perfused with solutions containing a given concentration of HR. The open circles represent mean control values of L_p for the same microvessels later investigated at that concentration of HR. Thus the effect of a particular concentration of HR can be assessed from the difference in L_p between the open and closed-circles at that concentration. A paired *t* test revealed that the differences were significant ($P<0.001$) at all perfusate concentrations of HR equal to or greater than 10 $\mu g\ ml^{-1}$. Figure 2b is a similar representation of the data obtained from experiments where the second perfusate contained M, the reconstituted mixture of five components of HR. Here each point in based on 24 determinations of L_p as M was investigated on two separate occasions under two different code numbers.

The general pattern is very similar to that seen for HR namely that increasing concentrations of the mixture reduce L_p to an increasing extent up to a concentration of 1 $mg\ ml^{-1}$ when L_p is lowered to less than half its control value. At a concentration of 10 $mg\ ml^{-1}$, both HR and the reconstituted mixture reduce L_p to smaller extent than at 1 $mg\ ml^{-1}$. Nevertheless a paired *t* test revealed the reduction in L_p was highly significant ($P<0.001$) at this concentration as it was at all perfusate concentrations of M equal to or greater than 10 $\mu g\ ml^{-1}$. Like HR, the reconstituted mixture did not effect the value of $\sigma\Delta\pi$.

(3) Reduction of permeability by varying concentrations of five purified components of HR

When each of the five purified components was tested on their own, they were all found to reduce L_p ($P<0.02$, paired *t* test) once their concentration in the perfusate had exceeded 100 $\mu g\ ml^{-1}$. None of the components significantly affected the values of $\sigma\Delta\pi$. There were, however, marked quantitative differences in their effectiveness. Thus at concentrations of 1 $mg\ ml^{-1}$, 7-mono-HR, 7,3′,4′-tri-HR, and 5,7,3′,4′-tetra-HR reduced L_p by only 10%–13% ($P<0.001$) and at concentrations to 10 $mg\ ml^{-1}$ lowered L_p further to 14–20% below its control value ($P<0.001$). Thus they were considerably less effective than either HR or the reconstituted

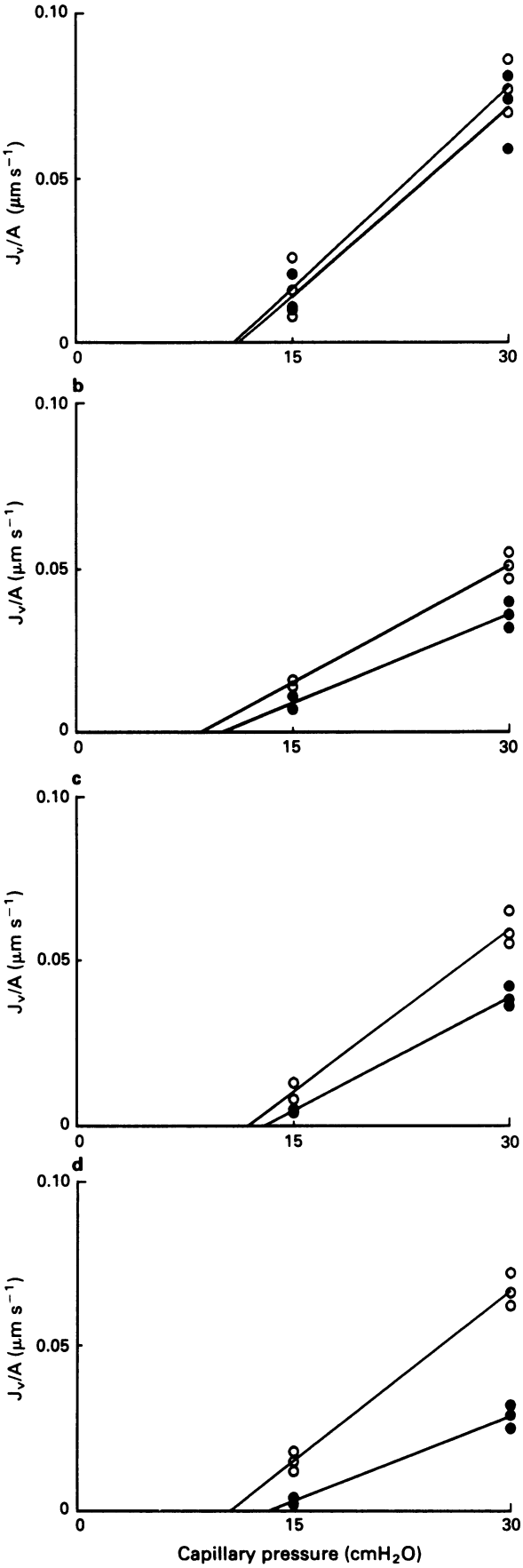

Figure 1 (a–d) The relation between fluid filtration per unit area of capillary wall (J_v/A) and capillary pressure in four experiments on single mesenteric capillaries of frog. Each diagram shows the results from a vessel which was perfused first with the control perfusate (○) and then with a perfusate containing HR (●). The concentrations of HR in the second perfusate were (a) 0; (b) 10 $\mu g\ ml^{-1}$; (c) 100 $\mu g\ ml^{-1}$; (d) 1.0 $mg\ ml^{-1}$.

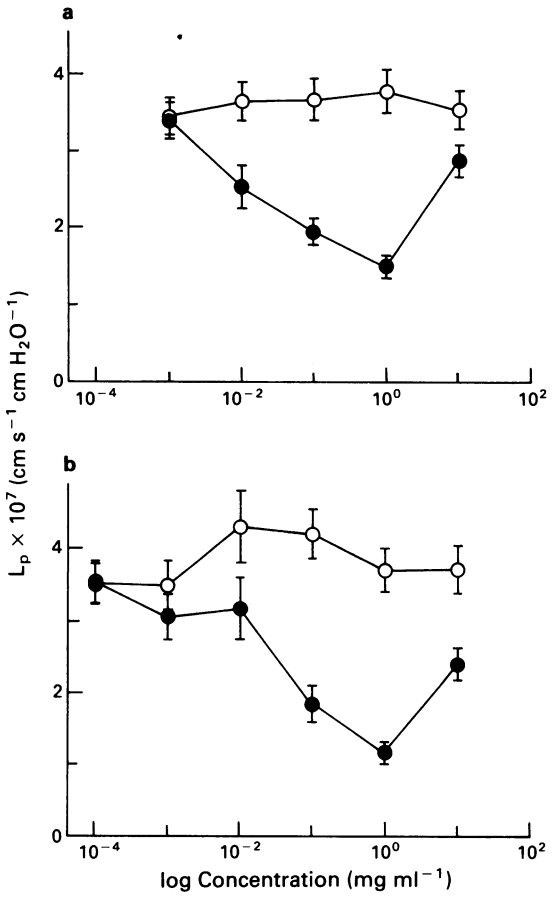

Figure 2 The effects of varying concentrations of HR and the reconstituted mixture of five of its components upon the L_p of single microvessels of frog. (a) Mean values ± s.e.mean of L_p in the absence (○) and presence (●) of HR ($n = 12$). (b) Mean values ± s.e.mean of L_p in the absence (○) and presence (●) of M, the reconstituted mixture of five components of HR ($n = 24$).

mixture. 7,4′-di-HR, however, reduced L_p when it was present at all concentrations greater than 10 $\mu g\ ml^{-1}$ ($P < 0.001$). When its perfusate concentration was 1.0 $mg\ ml^{-1}$, L_p was reduced to 40% of its control value (a reduction of 60%) and as with HR itself, raising the perfusate concentration of 7,4′-di-HR to 10 $mg\ ml^{-1}$ reduced the magnitude by which it lowered L_p. 7,3′,4′-tri-HQ was less effective than 7,4′-di-HR but more effective than the other three β-hydroxyethyl rutosides significantly reducing L_p ($P < 0.001$) when present in the perfusate at concentrations greater than 10 $\mu g\ ml^{-1}$. At a concentration of 1 $mg\ ml^{-1}$, 7,3′,4′-tri-HQ lowered L_p to 74% of its control value (i.e. a 26% reduction).

The dose-response curves for the five components are shown in Figure 3. Here the effect on L_p is shown as the mean value of L_p in the presence of a given concentration of the test substance divided by the mean control value of L_p for the same microvessels. Each point is based on paired test and control measurements on 12 microvessels.

(4) Reversibility of effects of reconstituted mixture on L_p

To investigate the reversibility of the effects of the reconstituted mixture upon permeability, 12 experiments were carried out in which a microvessel was perfused with (i) control perfusate, (ii) perfusate containing the mixture at a concentration of 1.0 $mg\ ml^{-1}$, (iii) control perfusate. Estimates of L_p and $\sigma\Delta\pi$ were made during each perfusion and continued for at least 20 min (and usually 30–40 min) during the final control perfusion. It was found that L_p which was reduced

from an initial value (± s.e.mean) of 4.56 (± 0.47) × 10^{-7} cm s^{-1} cmH_2O^{-1} to one of 0.94 (± 0.11) × 10^{-7} cm s^{-1} cmH_2O^{-1} during perfusion with the mixture, was increased only slightly after 20 min–40 min of the third perfusion when it had a mean value of 1.11 (± 0.14) × 10^{-7} cm s^{-1} cmH_2O^{-1}. The small rise in L_p during the final perfusion was reproducible and a paired t test revealed it was significant ($P<0.01$).

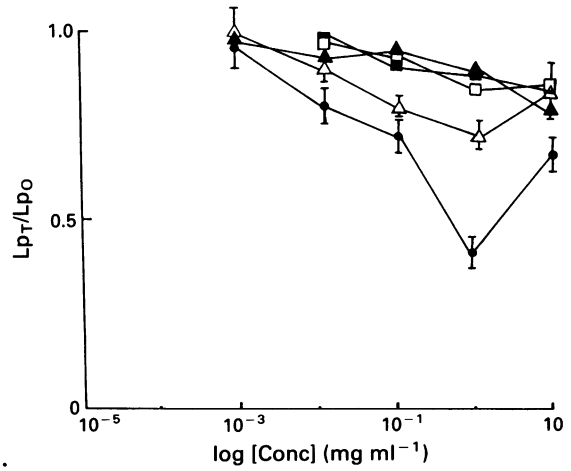

Figure 3 The effects of varying concentrations of five purified components of HR upon the L_p of frog single microvessels: (■) 7-mono-HR; (●) 7,4′-di-HR; (▲) 7,3′,4′-tri-HR; (△) 7,3′,4′-triHQ; (□) 5,7,3′,4′-tetra-HR. Each point represents the mean (± s.e.mean) value of L_p in the presence of a given concentration of the test substance divided by the mean value of L_p for the paired controls ($n = 12$).

(5) Effects of HR and its principal components on L_p of vessels in which permeability has been increased by protein-free perfusions

Perfusion with albumin-free solutions consistently increased L_p to approximately twice its value in the presence of 1% BSA and reduced the effective osmotic pressure exerted by Ficoll 70 in the perfusate. HR reversed the increase in L_p when added to the perfusate at concentrations equal to or greater than 6 μg ml^{-1}. Figure 4a–d shows the changes in fluid filtration rate per unit area of microvascular wall (J_v/A) with changes in microvascular pressure in four experiments each with a different concentration of HR in the third perfusate. Each part of Figure 4 relates J_v/A to microvascular pressure during the three perfusions of a single experiment. The slope of each line yields the value for L_p during that perfusion while the intercept with the pressure axis gives the value for $\sigma\Delta\pi$. It is seen that removal of BSA from the perfusate (solution b) increases the slope of the relation (L_p) and reduces the value of $\sigma\Delta\pi$ in all experiments. Whereas HR has no effect when present at a concentration of 1 μg ml^{-1}, it restores L_p to its control value at 0.006 mg ml^{-1} and takes it below control when its concentration is 0.1 mg ml^{-1}. HR, however, does not appear to restore $\sigma\Delta\pi$ to its initial value.

Between 8 and 10 experiments were carried out for each concentration of HR in the third perfusate and the results are summarized in Table 2. It is seen that removal of BSA from the perfusate consistently increased L_p and the increase was reversed by HR in a dose-dependent fashion. The changes in $\sigma\Delta\pi$, however, are less clear. While perfusion with albumin-

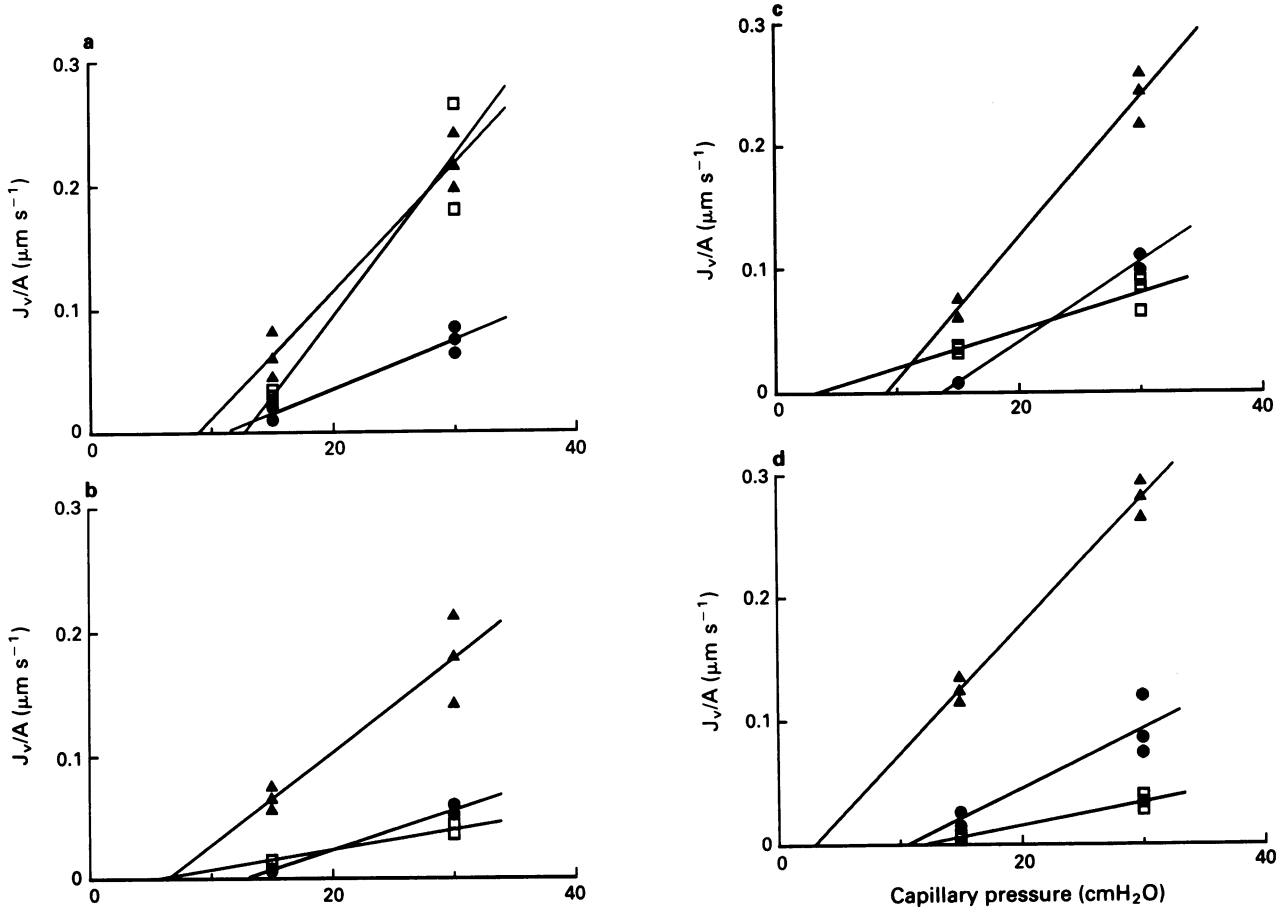

Figure 4 (a–d) The relations between fluid filtration (J_v/A) and capillary pressure in four experiments on single mesenteric capillaries of frog. Each diagram shows the results of a single experiment when the vessel was perfused first with a control perfusate containing Ficoll 70 and serum albumin (●), then with a similar solution containing Ficoll 70 but no albumin (▲) and finally with a solution containing Ficoll 70 and HR (□). The concentrations of HR in the third perfusate were as follows: (a) 1 μg ml^{-1}; (b) 6 μg ml^{-1}; (c) 10 μg ml^{-1}; (d) 100 μg ml^{-1}.

Table 2 Reversal of the effects of removal of serum albumin by hydroxethyl-rutosides (HR)

		Ringer perfusate solutions							
Concentrations of HR in solution (iii) (mg ml^{-1})		(i) *Perfusate with 4% Ficoll 70 + 1% BSA*		(ii) *Perfusate with 4% Ficoll 70*		(iii) *Perfusate with 4% Ficoll 70 + HR*			
	n	L_{p1}	$(\sigma\Delta\pi)_1$	L_{p2}	$(\sigma\Delta\pi)_2$	L_{p3}	$(\sigma\Delta\pi)_3$	L_{p1}/L_{p2}	L_{p3}/L_{p2}
0.1	10	3.36 (± 0.31)	11.11 (± 0.38)	7.0 (± 0.88)	9.10 (± 0.73)	1.65 (± 0.73)	10.18 (± 0.48)	0.48	0.24
0.01	10	3.81 (± 0.51)	10.9 (± 0.43)	7.57 (± 0.79)	6.35 (± 0.70)	3.06 (± 0.49)	9.37 (± 0.64)	0.50	0.40
0.006	8	3.27 (± 0.34)	10.71 (± 0.81)	8.69 (± 0.45)	5.78 (± 0.70)	2.64 (± 0.29)	7.15 (± 0.52)	0.38	0.3
0.003	10	4.5 (± 0.77)	10.34 (± 0.76)	8.48 (± 0.51)	6.43 (± 0.46)	7.91 (± 0.54)	6.08 (± 0.53)	0.53	0.93
0.001	10	4.33 (± 0.31)	11.53 (± 0.36)	8.72 (± 0.51)	6.51 (± 0.87)	8.75 (± 0.38)	7.10 (± 0.62)	0.5	1.00

All figures for L_p and $\sigma\Delta\pi$ are mean values ± s.e.mean. Values for L_p are expressed as $10^{-7} \times$ cm s^{-1}H$_2$O^{-1}; values for $\sigma\Delta\pi$ are in cmH$_2$O

Table 3 Reversal of permeability increase (induced by removal of serum albumin) by 7,4'-di-HR

Concentration of di-HR in solution (iii) (mg ml^{-1})	(i) *Perfusate with 4% Ficoll 70 + 1% BSA*		(ii) *Perfusate with 4% Ficoll 70 (protein-free)*		(iii) *Perfusate with 4% Ficoll 70 + di-HR*			
	L_{p1}	$(\sigma\Delta\pi)_2$	L_{p2}	$(\sigma\Delta\pi)_2$	L_{p3}	$(\sigma\Delta\pi)_3$	L_{p1}/L_{p2}	L_{p3}/L_{p2}
0.1	4.58 (± 0.51)	11.33 (± 0.27)	9.44 (± 0.42)	5.86 (± 0.83)	3.15 (± 0.43)	6.94 (± 1.07)	0.49	0.33
0.01	4.58 (± 0.65)	11.30 (± 0.19)	9.13 (± 0.84)	7.61 (± 0.87)	4.4 (± 1.00)	7.91 (± 0.64)	0.50	0.48
0.001	4.05 (± 0.83)	11.00 (± 0.38)	8.04 (± 0.65)	5.70 (± 0.72)	7.86 (± 0.85)	6.03 (± 0.63)	0.50	0.98

All figures are mean values of experiments ± s.e.mean. Values for L_p are expressed as $10^{-7} \times$ cm s^{-1}cmH$_2$O^{-1}; values for $\sigma\Delta\pi$ are in cmH$_2$O.
For abbreviations, see text.

Table 4 Effects of 7-mono-HR, 7,3',4'-tri-HR and 5,7,3',4'-tetra-HR in single vessels where permeability has been increased by perfusion with protein-free solutions

Test substance in perfusate (iii)		(i) *Perfusate with 4% Ficoll 70 + 1% BSA*		(ii) *Perfusate with 4% Ficoll 70 alone*		(iii) *Perfusate with 4% Ficoll + test substance*			
	n	L_{p1}	$(\sigma\Delta\pi)_1$	L_{p2}	$(\sigma\Delta\pi)_2$	L_{p3}	$(\sigma\Delta\pi)_3$	L_{p1}/L_{p2}	L_{p3}/L_{p2}
mono-HR 10 μg ml^{-1}	6	3.53 (± 0.50)	10.23 (± 0.17)	8.21 (± 0.80)	5.95 (± 0.70)	8.33 (± 0.69)	6.17 (± 0.86)	0.43	1.01
tri-HR 10 μg ml^{-1}	6	4.22 (± 0.62)	11.48 (± 0.60)	8.28 (± 0.63)	5.07 (± 1.29)	8.50 (± 0.66)	5.20 (± 1.21)	0.51	1.03
tetra-HR 10 μg ml^{-1}	6	3.00 (± 0.25)	10.25 (± 0.60)	8.03 (± 0.56)	4.40 (± 0.27)	7.95 (± 0.67)	4.47 (± 0.713)	0.37	0.99

All values of L_p and $(\sigma\Delta\pi)$ represent means of 6 experiments ± s.e.mean. Values of L_p are expressed as $10^{-7} \times$ cm s^{-1} cmH$_2$O^{-1} and $\sigma\Delta\pi$ in cmH$_2$O.
For abbreviations, see text.

free solutions reduced $\sigma\Delta\pi$, perfusion with HR at concentrations $\geqslant 6\,\mu g\,ml^{-1}$ raised $\sigma\Delta\pi$ from a mean (± s.e.mean) of 5.78 (± 0.70) cmH$_2$O to one of 7.15 (± 0.52) cmH$_2$O but did not restore it to its control value (10.71 cmH$_2$O).

When varying concentrations of 7,4'-di-HR were present in the third perfusate, the effects on L_p were similar to those found with HR. The data are summarised in Table 3 which also shows that 7,4'-di-HR had no significant effect upon $\sigma\Delta\pi$.

The effects of the other three principal constituents of HR were investigated at the single concentration of $10\,\mu g\,ml^{-1}$. Six experiments were carried out with each of these compounds as the test substance and the results are summarized in Table 4.

Although near maximal effects of HR and 7,4'-di-HR were seen when they were present at a concentration of $10\,\mu g\,ml^{-1}$, none of the other rutosides were found to affect permeability at this concentration.

Discussion

Effects of HR and its constituents on vessels of normal permeability

Our findings, which confirm many of the observations of Blumberg *et al.* (1989), show that HR reduces the L_p of frog mesenteric microvessels in a concentration-dependent manner. Maximum effects of HR are seen in the range of 0.1 mg ml^{-1} to 1.0 mg ml^{-1}. We have also shown that a mixture of five components of HR reproduces the permeability lowering properties of HR in frog mesenteric capillaries. This suggested that at least one of the constituents of the mixture was responsible for the effects of HR on permeability. An examination of the effects of the individual components revealed that 7,4'-di-HR was largely responsible for the reduction of L_p by HR. The other four components had smaller but significant effects in reducing L_p. It is, of course, quite possible that in the mixture and in HR itself, they have a synergistic influence on the actions of 7,4'-di-HR. Such synergism would account for the slightly greater potency of the mixtures than 7,4'-di-HR in reducing L_p.

The effects of a wide range of concentrations of HR and 7,4'-di-HR upon L_p are described by bell-shaped dose-response curves. It is of particular interest that the purified single compound, 7,4'-di-HR, is less effective in reducing L_p when its perfusate concentration rises above 1 mg ml^{-1}. One possible explanation would be that 7,4-di-HR binds to two different receptors which initiate opposite effects on permeability. Providing the interaction of these effects is non-competitive and the affinity for the receptor that promotes a reduction of L_p is greater than that which leads to a permeability increase, the overall dose-response curve would be bell shaped (e.g. Young *et al.*, 1992).

We did not observe any effects of HR (or its constituents) on $\sigma\Delta\pi$ in vessels of normal permeability. This is consisent with the observations of Blumberg *et al.* (1989). While they reported that HR raised $\sigma\Delta\pi$, the effects were restricted to inflamed vessels where $\sigma\Delta\pi$ was initially low and $\sigma\Delta\pi$ was raised to values in the normal range but not above it.

We have also confirmed that the effects of HR on L_p reversed very slowly. This characteristic effect of HR has restricted our experimental protocols in that the effects of test substances on permeability had to be assessed by comparing the value of L_p (and $\sigma\Delta\pi$) for a given vessel in the presence of the test substance with its value for the same vessel during the preceding control perfusion only. Justification for this general protocol is derived from observations that there were no significant changes in L_p when the second perfusate was identical in composition to the first.

The slow reversibility of the effects of HR on permeability may be of considerable significance in maintaining therapeutic levels of these substances in the tissues during their long term administration. In this context it is worth noting that the concentrations of HR and 7, 4'-di-HR which clearly reduced permeability, are comparable with levels which might be achieved if the recommended oral dose of HR were diluted in a volume equivalent to that of the plasma or blood (500 mg in 3 litres or 5 litres). While the incomplete absorption of HR from the gastrointestinal tract and its hepatobiliary clearance from portal venous blood might seriously reduce the levels of HR in the systemic arterial blood, the slow reversibility of the effects of HR raise the possibility that repeated oral doses may allow potent levels of HR to accumulate in the target areas (Neumann *et al.*, 1992).

Effects of HR and its components on vessels perfused with protein-free solutions

In this study we have shown that both HR and 7,4'-di-HR reverse the increase in L_p which is induced by perfusion with protein free solutions. The fall in $\sigma\Delta\pi$ to Ficoll 70, which accompanied the increase in L_p, was incompletely reversed by HR and little affected by 7,4'-di-HR.

Our preliminary investigation of the effects of HR on vessels in which permeability had been increased by protein-free perfusion (Michel *et al.*, 1990), arose from the observation that HR reduced the permeability of inflamed frog microvessels in spite of the persistance of gaps in the endothelium (Blumberg *et al.*, 1989).

The increase in permeability which occurs in inflammation or that resulting from mediators such as histamine, is associated with the development of gaps in the endothelium. By contrast, perfusion with protein-free solutions raises permeability without the development of gaps (Mason *et al.*, 1979). The raised permeability associated with removal of protein can be readily and completely reversed by perfusion with albumin containing solutions (Mason *et al.*, 1979; Michel & Phillips, 1985). Furthermore, there is strong evidence that serum albumin binds reversibly to the luminal surface of the endothelium (Schneeberger & Hamelin, 1984; Schnitzer *et al.*, 1988), and since its removal from this site is associated with the permeability increase, it has been proposed that the ultrafilter of capillary walls and a major component of the hydraulic resistance of the pathways through them, reside in a lattice-like structure formed by the interaction of plasma proteins with the luminal endothelial glycocalyx (Curry & Michel, 1980; see Michel, 1988, for review). Thus when Blumberg *et al.* (1989) observed a reduction of permeability without the disappearance of the endothelial gaps, they suggested that HR might reduce the permeability of an extracellular barrier such as the glycocalyx. Our observation that HR can reverse the rise in L_p associated with removal of albumin is consistent with this hypothesis. It seem unlikely, however, that the flavonoids act in the same way as albumin itself. The action of albumin is dependent upon its positively charged arginine residues (Michel *et al.*, 1985) and it is believed to reduce L_p by occupying space within the surface coat and by ordering the fibrous molecules of glycocalyx into an evenly spaced lattice (Michel, 1988). It is unlikely that HR and 7,4'-di-HR, which are small molecules, can have a direct action of this kind. Furthermore, we should note that HR and 7,4'-di-HR failed to reverse the fall in $\sigma\Delta\pi$.

An alternative mechanism would be for 7,4'-di-HR (and possibly other as yet unidentified components of HR) to act on the endothelial cell and for intracellular mechanisms to order the molecules of the glycocalyx or promote its secretion. It is of considerable interest that Curry & Lenz (1987) reported that noradrenaline reduced the L_p of frog mesenteric capillaries in the absence of BSA but not in its presence. Recent work by He & Curry (1991) has shown that depolarizing the endothelium with high extracellular K^+ concentrations reduces L_p. The depolarization reduces Ca^{2+} influx into the endothelial cells (He & Curry, 1991) and preliminary reports suggest that the raised L_p following protein-free perfusion may be reduced by high concentrations of extracellular K^+ (He *et al.*, 1991). At present it is unclear how changes within the endothelial cell can modify permeability except where this is associated with the development of gaps between adjacent endothelial cells. Against this background the possible mechanism of actions of HR and other flavonoids on vascular permeability remains highly speculative.

We thank Dr H. Keberle for helpful suggestions and discussions, and Dr A. Albert and Dr E. Moret for synthesizing and purifying the pure compounds and Mrs R. Haddleton for typing the manuscript.

References

ARTURSON, G. (1972). Effects of O-(beta-hydroxyethyl)-rutosides (HR) on the increased microvascular permeability in experimental skin burn. *Acta Chir. Scand.*, **138**, 111–117.

BALMER, A. & LIMONI, C. (1980). A double-blind placebo-controlled clinical trial of Venoruton in the symptoms and signs of chronic venous insufficiency. The importance of patient selection. *Vasa*, **9**, 76–82.

BLUMBERG, S., CLOUGH, G. & MICHEL, C.C. (1989). Effects of hydroxyethyl rutosides upon the permeability of single capillaries in the frog mesentery. *Br. J. Pharmacol.*, **96**, 913–919.

CESARONE, M.R., LAUROVA, G., RICCA, A., BEKARO, G., CANDIANI, D., LEON, M. & NICOLAIDES, A.N. (1992). Acute effect of hydroxyethylrutosides on capillary filtration in normal volunteers, patients with venous hypertension and in patients with diabetic microangiopathy. A dose comparison study. *Vasa*, **21**, 76–80.

CURRY, F.E. & LENZ, J. (1987). The effect of norepinephrine on hydraulic conductivity of Ringer perfused microvessels in frog mesentery. *Fed. Proc.*, **46**, Abst M53.

CURRY, F.E. & MICHEL, C.C. (1980). A fiber matrix model of capillary permeability. *Microvasc. Res.*, **20**, 96–99.

CURRY, F.E., MICHEL, C.C. & PHILLIPS, M.E. (1987). Effects of albumin on the osmotic pressure exerted by myoglobin across capillary walls in frog mesentery. *J. Physiol.*, **387**, 69–82.

DE JONGSTE, A.B., JONKER, J.J.C., HÚISMAN, M.V., TENCATE, J.W. & AZAR, A.J. (1989). A double blind three centre clinical trial on the short-term efficiency of O-(beta-hydroxyethyl)-rutosides in patients with post-thrombotic syndrome. *Thromb. Haemost.*, **62**, 826–829.

GERDIN, B. & SVENSJO, E. (1983). Inhibitory effect of the flavonoid O-(β-hydroxyethyl)-rutoside on increased microvascular permeability induced by various agents in rat skin. *Int. J. Microcirc: Clin. Exp.*, **2**, 39–46.

HE, P. & CURRY, F.E. (1991). Depolarisation modulates endothelial cell calcium influx and microvessel permeability. *Am. J. Physiol.*, **261**, H21246–H1254.

HE, P., KAJIMURA, M. & CURRY, F.E. (1991). Depolarisation reduces endothelial cell calcium influx and permeability increase after albumin is removed from the perfusate of single perfused microvessels. *Proc. Fifth World Congress for Microcirculation*, Abst. 217.

HILTON, J.G. (1982). Effects of β-hydroxyethylrutosides (HR) administered post burn after thermal-injury-induced plasma volume loss in the non-resuscitated dog. *Burns*, **8**, 391–394.

LEVICK, J.R. & MICHEL, C.C. (1977). A densitometric method for determining the filtration coefficients of single capillaries in the frog mesentery. *Microvasc. Res.*, **13**, 141–15.

MASON, J.C., CURRY, F.E. & MICHEL, C.C. (1977). The effects of proteins upon the filtration coefficient of individually perfused frog mesenteric capillaries. *Microvasc. Res.*, **13**, 185–202.

MICHEL, C.C. (1980). Filtration coefficients and osmotic reflexion coefficients of the walls of single frog mesenteric capillaries. *J. Physiol.*, **309**, 341–355.

MICHEL, C.C. (1988). Capillary permeability and how it may change. *J. Physiol.*, **404**, 1–29.

MICHEL, C., BLUMBERG, S. & CLOUGH, G. (1990). Hydroxyethylrutosides (HR) reduce permeability of frog mesenteric microvessels. *Phlebology*, **5**, (Suppl. 1) 3–7.

MICHEL, C.C., MASON, J.C., CURRY, F.E. & TOOKE, J.E. (1974). A development of the Landis technique for measuring the filtration coefficient of individual capillaries in the frog mesentery. *Q. J. Exp. Physiol.*, **59**, 283–309.

MICHEL, C.C., PHILLIPS, M.E. & TURNER, M.R. (1985). The effects of native and modified bovine serum albumin on the permeability of frog mesenteric capillaries. *J. Physiol.*, **360**, 333–346.

MICHEL, C.C. & PHILLIPS, M.E. (1985). The effects of bovine serum albumin and a form of cationised ferritin upon the molecular selectivity of the walls of single frog capillaries. *Microvasc. Res.*, **29**, 190–203.

NEUMANN, H.A.M., CARLSON, K. & BROWN, G.H.M. (1992). Uptake and localisation of O-(β-hydroxyethyl)-rutosides in the venous wall, measured by laser scanning microscopy. *Eur. J. Clin. Pharmacol.*, **43**, 423–426.

NOCKER, W., DIEBSCHLAG, W. & LEHMACHER, W. (1989). Three-month randomised, double-blind, dose-response study with O-(beta-hydroxyethyl)-rutosides drinking solution. *Vasa*, **18**, 235–238.

PULVERTAFT, T.B. (1983). General practice treatment of symptoms of venous insufficiency with oxerutins. Results of a 660 patient multicentre study in the UK. *Vasa*, **12**, 373–376.

ROZTOCIL, K., FISCHER, A., NOVAK, P. & RAZGOVA, L. (1971). The effects of O-(beta-hydroxyethyl)-rutosides (HR) on the peripheral circulation in patients with chronic venous insufficiency. *Eur. J. Clin. Pharmacol.*, **3**, 243–246.

ROZTOCIL, K., PREROVSKY, I. & OLIVA, I. (1977). The effects of hydroxyethylrutosides on capillary filtration rate in the lower limbs of man. *Eur. J. Clin. Pharmacol.*, **11**, 435–438.

SCHNEEBERGER, E.E. & HAMELIN, M. (1984). Interaction of circulating proteins with pulmonary endothelial glycocalyx and its effects on endothelial permeability. *Am. J. Physiol.*, **247**, H206–H217.

SCHNITZER, J.E., CARLEY, W.W. & PALADE, G.E. (1988). Albumin interacts specifically with a 60-kDa microvascular endothelial glycoprotein. *Proc. Natl. Acad. Sci. U.S.A.*, **85**, 6773–6777.

SWAYNE, G.T.G. & SMAJE, L.H. (1989). Dynamic compliance of single perfused frog mesenteric capillaries and rat venules: a filtration coefficient correction. *Int. J. Microcirc.: Clin. Exp.*, **8**, 43–52.

WADWORTH, A.N. & FAULDS, D. (1992). Hydroxyethylrutosides. A review of its pharmacology and therapeutic efficacy in venous insufficiency and related disorders. *Drugs*, **44**, 1013–1032.

YOUNG, A.A., GEDULIN, B., WOLFE-LOPEZ, D., GREENE, H.E., RINK, T.J. & COOPER, G.J.S. (1992). Amylin and insulin in rat soleus muscle: dose responses for cosecreted non-competitive antagonists. *Am. J. Physiol.*, **263**, E274–E281.

(Received February 22, 1993
Revised April 28, 1993
Accepted May 5, 1993)

Br. J. Pharmacol. (1993), **110**, 207–212

Relation between α_1-adrenoceptor subtypes and noradrenaline-induced contraction in rat portal vein smooth muscle

Irène Sayet, Ghislaine Neuilly, Lala Rakotoarisoa, [1]Chantal Mironneau & Jean Mironneau

Laboratoire de Physiologie Cellulaire et Pharmacologie Moléculaire, URA CNRS 1489, Université de Bordeaux II, 3 place de la Victoire, 33076 Bordeaux, France

1 In vascular smooth muscle, α_1-adrenoceptors have been classified recently into two or three subtypes. We examined which α_1-adrenoceptor subtypes are involved in the noradrenaline-induced contraction of rat portal vein smooth muscle.

2 Binding studies with [^{3}H]-prazosin in membranes from equine portal vein smooth muscle revealed the presence of two distinct affinity binding sites. The high-affinity site for [^{3}H]-prazosin was also identified in intact strips of rat portal vein. Prazosin, HV723 (α-ethyl-3,4,5-trimethoxy-α-(3-((2-(2-methoxyphenoxy)ethyl)-amino)-propyl) benzene-acetonitrile fumarate), WB4101 (2-(2,6-dimethoxyphenoxyethyl)aminomethyl-1,4-benzodioxane), 5-methylurapidil, phentolamine and yohimbine antagonized [^{3}H]-prazosin binding at both types of sites. Pretreatment with 50 μM chloroethylclonidine (CEC) eliminated the high-affinity sites for prazosin but had no effect on the low-affinity sites.

3 Noradrenaline produced a concentration-dependent contraction in the rat portal vein. Pretreatment with 50 μM CEC induced a slight rightward displacement of the concentration-response curve but the maximal contraction was not significantly affected suggesting that the CEC-sensitive α_1-adrenoceptors played a minor role in the noradrenaline-induced contraction. Prazosin, WB4101 and HV723 produced a concentration-dependent inhibition of noradrenaline-induced contractions. The inhibition curves were little affected by CEC-pretreatment and yielded a relative order of potency of WB4101 > prazosin > HV723.

4 In the presence of 0.1 μM isradipine to block voltage-dependent Ca^{2+} channels, the noradrenaline-induced contraction is due to release of Ca^{2+} ions from agonist-sensitive intracellular Ca^{2+} stores. Under these conditions, the noradrenaline-induced contraction was not significantly affected by pretreatment with 50 μM CEC but was inhibited by the antagonists mentioned above with affinities different from those in the absence of isradipine. The rank order of potency became HV723 ≥ WB4101 > prazosin.

5 The present results indicate the existence of two distinct α_1-adrenoceptor subtypes in rat portal vein smooth muscle, which show high- and low-affinities respectively for each of prazosin, WB4101 and HV723 and correspond to α_{1H}- and α_{1L}-adrenoceptor subtypes. According to recent α_1-adrenoceptor subclassifications, the α_{1H}-adrenoceptor subtype which is sensitive to inactivation by CEC may correspond to the α_{1B}-adrenoceptor subtype. The contraction induced by noradrenaline seems to be predominantly mediated through the α_{1L}-adrenoceptor subtypes which may include the α_{1N}-adrenoceptor subtype, as recently proposed.

Keywords: α_1-Adrenoceptor subtypes; noradrenaline-induced contraction; [^{3}H]-prazosin binding; rat portal vein

Introduction

Two subtypes of α_1-adrenoceptors have been defined on the basis of both binding and functional experiments (Morrow & Creese, 1986; Minneman, 1988; Hanft & Gross, 1989; Oshita *et al.*, 1991). The α_{1A}-adrenoceptor subtype shows high affinity for 2-(2,6-dimethoxyphenoxyethyl)aminomethyl-1,4-benzodioxane (WB4101), 5-methylurapidil and phentolamine and is relatively insensitive to an alkylating agent, chloroethylclonidine (CEC), while the α_{1B}-adrenoceptor subtype has low affinity for the antagonists mentioned above and is potently inactivated by chloroethylclonidine. Both α_{1A}- and α_{1B}-adrenoceptor subtypes have a high affinity for prazosin. On the other hand, another subclassification has been proposed, where the α_1-adrenoceptors can be separated into three subtypes (α_{1H}, α_{1L} and α_{1N}) (Flavahan & Vanhoutte, 1986; Muramatsu *et al.*, 1990a,b; Oshita *et al.*, 1991). Prazosin has a higher affinity for the α_{1H}-adrenoceptor subtype than for the α_{1L}- and α_{1N}-adrenoceptor subtypes. The α_{1N}-adrenoceptor, the third subtype, is distinguished by its higher affinity for α-ethyl-3,4,5-trimethoxy-α-(3-((2-(2-methoxyphenoxy)ethyl)-amino)-propyl) benzeneacetonitrile fumarate (HV723) compared with the other α_1-adrenoceptor subtypes. In addition, the α_{1H} and α_{1N}-adrenoceptor subtypes show a higher affinity for yohimbine than the α_{1L}-adrenoceptor subtype (Muramatsu *et al.*, 1990b).

Molecular cloning studies have confirmed the existence of three or four α_1-adrenoceptor subtypes. The α_{1B}-adrenoceptor subtype isolated from DDT1 MF-2 cells is predominantly expressed in rat liver, heart and cerebral cortex (Cotecchia *et al.*, 1988; Lomasney *et al.*, 1991). As recently proposed by Schwinn & Lomasney (1992) the α_{1A}-adrenoceptor subtype family would be composed of at least three members: the cloned rat α_{1A}-adrenoceptor or α_{1D}-adrenoceptor (Perez *et al.*, 1991), the cloned bovine α_{1C}-adrenoceptor (Schwinn *et al.*, 1990), and the classical α_{1A}-adrenoceptor, as defined by pharmacological studies, which has not yet been identified by molecular cloning techniques. However, the relationship between these cloned receptors and those identified by pharmacological means has not been clarified in all tissues.

In the present study, we examined which α_1-adrenoceptor subtypes contribute to the noradrenaline-induced contraction of rat portal vein by using both contraction and binding studies. The results obtained show that noradrenaline-induced contraction of the rat portal vein is, at least, mediated through two distinct α_1-adrenoceptor subtypes (α_{1L}

[1] Author for correspondence.

and α_{1N}) and that the other α_1-adrenoceptor subtype (α_{1H} or α_{1B}) has a restricted role in mediating contraction.

Methods

[^{3}H]-prazosin binding study

Microsomes from fresh equine portal vein were prepared as previously described (Dacquet *et al.*, 1988) and protein concentration was determined according to Bradford (1976). Membrane proteins (0.1–0.2 mg ml^{-1}) in duplicate were incubated for 45 min at 25°C with various concentrations of [^{3}H]-prazosin in 2 ml of 20 mM HEPES buffer (pH 7.4) containing 0.1% bovine serum albumin. Non-specific binding was defined as the amount of radioligand bound in the presence of 2 μM unlabelled prazosin and accounted for 25–30% of the total binding with 2 nM [^{3}H]-prazosin.

Binding to longitudinal strips of rat portal vein (0.5–1.5 mg wet weight) was measured by incubating the strips for 60 min at 37°C in a physiological solution (composition, mM): NaCl 130, KCl 5.6, $CaCl_2$ 2, $MgCl_2$ 0.24, HEPES 8.3, glucose 11, pH 7.4, with various concentrations of the radioligand (Rakotoarisoa *et al.*, 1990). At the end of the incubation period each strip was dried on filter paper, and then weighed. Radioactivity was measured by dissolving the vein strips in 100 μl of NaOH (0.1 M). Non-specific binding was defined as indicated above and accounted for 45–50% of the total binding at a concentration of 0.5 nM [^{3}H]-prazosin.

Contraction experiments

Isometric contractions of longitudinal strips from rat portal vein were recorded in an experimental chamber described previously (Mironneau *et al.*, 1980) by means of a highly sensitive isometric force transducer (Akers 801 AME, Norten, Norway). The physiological solution was similar to that used for binding of intact strips but contained yohimbine (10 nM) and propranolol (0.1 μM) in order to inhibit α_2- and β-adrenoceptors. The circulating solution was maintained at 37 ± 1°C. Vein strips were first contracted with noradrenaline (30 μM; maximal response) followed by a washing period of 30 min. Subsequent contractions to noradrenaline in the presence of various antagonists were expressed as a percentage of this maximal contraction to noradrenaline.

Chloroethylclonidine treatment

In order to inactivate the α_{1B}-adrenoceptor subtype, the membrane protein preparation (usually 5–7 mg ml^{-1}) was incubated for 15 min at 37°C with or without 50 μM CEC. The reaction was stopped by dilution with 200 ml cold HEPES buffer and centrifuging at 100,000 *g* for 20 min. Each final pellet was resuspended in 7.5 ml HEPES buffer.

Strips of rat portal vein were incubated for 30 min at 37°C with 50 μM CEC and then washed for 30 min in physiological solution before contraction or binding assays.

Chemicals

[^{3}H]-prazosin (specific activity 80–85 Ci mmol^{-1}) was obtained from Amersham (Les Ulis, France). Noradrenaline, phentolamine, yohimbine, prazosin were from Sigma (St Louis, MO, U.S.A.). WB4101 (2-(2,6-dimethoxyphenoxyethyl)aminomethyl-1,4-benzodioxane), 5-methylurapidil, chloroethylclonidine dihydrochloride were from RBI (Natick, MA, U.S.A.). HV723 (α-ethyl-3,4,5-trimethoxy-α-(3-((2-(2-methoxyphenoxy)ethyl)-amino)-propyl) benzene-acetonitrile fumarate) from Hokuriku Seiyaku (Katsuyama, Fukui, Japan) was a gift from Dr Muramatsu.

Analysis of data

The apparent dissociation constant (K_D) and maximal number of binding sites (B_{max}) for [^{3}H]-prazosin were estimated by Scatchard analysis of the saturation data. The ability of antagonists to inhibit specific [^{3}H]-prazosin binding or contraction induced by 3 μM noradrenaline was estimated from the IC_{50} value which was the concentration which inhibited 50% of the maximal response. A value for the inhibition constant K_i was calculated from the equation, $K_i = IC_{50}/(1 + L/K_D)$, where L equals the concentration of [^{3}H]-prazosin and K_D is the apparent dissociation constant (Cheng & Prusoff, 1973). The Hill coefficient for inhibition by a drug was obtained by Hill plot analysis. The data obtained from saturation, kinetic and competition studies were analysed by a programme derived from nonlinear least-squares curve fitting programme LIGAND (Munson & Rodbard, 1980). The data were first fitted to a one- then a two-site model and if the residual sums of squares were statistically less for a two-site fit of the data than for a one-site, as determined by an *F*-test comparison, the two-site model was accepted. The experimental results were expressed as mean ± s.e.mean and significance was tested by Student's *t* test. *P* values less than 0.05 were considered as significant.

Results

Equilibrium binding of [^{3}H]-prazosin to portal vein membranes

[^{3}H]-prazosin, at concentrations ranging from 0.01 to 4 nM, was used to label α_1-adrenoceptors on vascular membranes (Figure 1). The specific binding was approximately 80% of the total binding at 0.1 nM [^{3}H]-prazosin. A Scatchard plot of the specific binding component indicates the existence of both high and low affinity binding sites. The dissociation constants (K_D) and maximal binding capacities (B_{max}) were: K_D = 0.018 ± 0.002 nM and B_{max} = 73 ± 9 fmol mg^{-1} of protein for the high-affinity site and K_D = 2.42 ± 0.27 nM and B_{max} = 295 ± 37 fmol mg^{-1} of protein for the low-affinity site (n = 9). Heat treatment (65°C, 20 min) or trypsin treatment (0.1 mg ml^{-1}) of vascular membranes resulted in a large reduction (85–95%) in the population of the two families of sites.

High- and low-affinity binding sites for [^{3}H]-prazosin in vascular membranes

The properties of the high-affinity binding site were examined by use of 0.1 nM [^{3}H]-prazosin. Under these conditions, about 85% of the signal originated from binding to the high-affinity binding site and 15% from binding to the low-affinity binding site. Typical kinetics of association of [^{3}H]-prazosin are presented in Figure 2a. Figure 2b shows that the semilogarithmic representation of the data is linear, as expected for a pseudo-first-order reaction (Weiland & Molinoff, 1981). The experimental association rate constant measured was K_{obs} = 0.147 ± 0.015 min^{-1} (n = 6). Furthermore, $K_{obs} = k_1$ ([^{3}H]-prazosin) + k_{-1}, in which k_1 and k_{-1} represent, respectively, the rate constants of association and dissociation of the [^{3}H]-prazosin-receptor complex. Figure 3a shows that [^{3}H]-prazosin bound to vascular membranes can be displaced by unlabelled prazosin. Because of the large excess of unlabelled prazosin (10 μM), the reassociation of [^{3}H]-prazosin with the receptor was prevented, and then the dissociation was a first-order reaction. As expected, the semilogarithmic representation of the dissociation data was linear, as shown in Figure 3b, and gave a constant for dissociation (k_{-1}) of 0.041 ± 0.003 min^{-1} (n = 6). The calculated value of k_{-1} was 1.18 ± 0.07 nM^{-1} min^{-1} (n = 6) and the dissociation constant from kinetic data ($K_D = k_{-1}/k_1$) was estimated to be 0.034 ± 0.002 nM (n = 6). This value is in

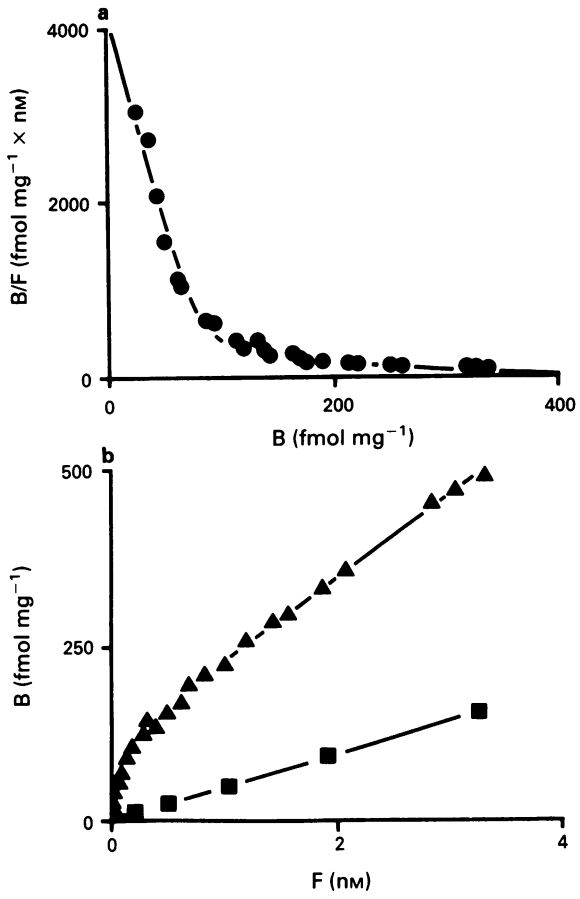

Figure 1 Scatchard plot (a) and saturation binding (b) of [^{3}H]-prazosin to portal vein membranes. Portal vein smooth muscle membranes (0.1 mg ml^{-1} protein) were incubated with increasing concentrations of [^{3}H]-prazosin (25 Ci mmol^{-1}) for 45 min at 25°C. Non specific binding was defined as that which was not displaceable by 2 μM unlabelled prazosin. Scatchard analysis of specific binding was done with the nonlinear least-square programme LIGAND (Munson & Rodbard, 1980). The best fit was determined with a two-site model. The data shown are means of duplicate determinations in a representative experiment. Similar estimations were obtained from 9 separate experiments. (▲) Total binding; (■) non-specific binding; (●) specific binding. B/F, bound/free.

good agreement with the value of K_D obtained from equilibrium binding measurements (Figure 1).

The properties of the low-affinity prazosin site were examined with 5 nM [^{3}H]-prazosin. Under these conditions about 75% of the total bound ligand was associated with the low-affinity binding site. The rate constants for association and dissociation were 0.011 ± 0.004 nM^{-1} min^{-1} and 0.061 ± 0.012 min^{-1}, respectively ($n = 4$). The calculated dissociation constant from kinetic data was estimated to be 4.97 ± 0.86 nM ($n = 4$), a value similar to that obtained from equilibrium binding experiments (Figure 1).

The pharmacological profile of high- and low-affinity sites for prazosin was examined in displacement experiments. [^{3}H]-prazosin, 0.1 nM, was used to label the high-affinity site. Unlabelled prazosin, HV723, WB4101, 5-methylurapidil, phentolamine and yohimbine displaced the binding in a monophasic manner with increasing inhibition constant values (Table 1). The rank order of potency was, therefore, prazosin > HV723, WB4101 > 5-methylurapidil, phentolamine > yohimbine. To elucidate the mode of binding of the α-adrenoceptor antagonists, Scatchard plots of the [^{3}H]-prazosin binding were carried out in the presence of two concentrations of α-adrenoceptor antagonists. These data which show an increase of the apparent K_D value without

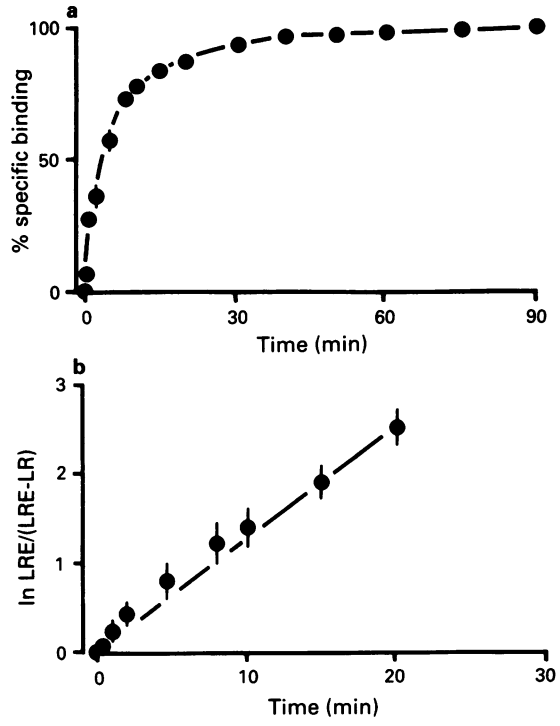

Figure 2 Association kinetics for the specific high-affinity binding of [^{3}H]-prazosin to portal vein membranes. (a) Association was initiated by addition of 0.1 nM [^{3}H]-prazosin (85 Ci mmol^{-1}) to an assay mixture containing 0.1 mg ml^{-1} protein. At the indicated times an aliquot of the mixture was withdrawn, and the association was terminated by rapid filtration. Non-specific binding, determined with 2 μM unlabelled prazosin, was constant. (b) Pseudo-first-order representation of the data. LR_E, concentration of [^{3}H]-prazosin-receptor complex at equilibrium; LR, concentration of the complex at time t. Each point represent the mean of 6 experiments ± s.e.mean.

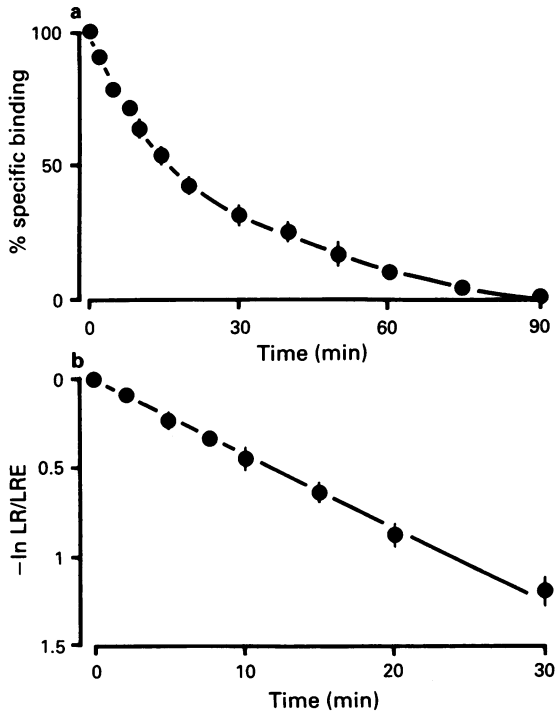

Figure 3 Dissociation kinetics for the specific high-affinity binding of [^{3}H]-prazosin to portal vein membranes. (a) After equilibrium had been reached, dissociation was monitored after addition of 10 μM unlabelled prazosin. (b) First-order representation of binding. LR_E, concentration of [^{3}H]-prazosin-receptor complex at equilibrium; LR, concentration of the complex at time t. Each value is the mean of 6 experiments ± s.e.mean.

Table 1 Inhibition of [^{3}H]-prazosin binding to membranes and intact strips of portal vein by α-adrenoceptor antagonists: high-affinity sites and low-affinity sites are labelled with 0.10–0.15 nM and 5 nM [^{3}H]-prazosin, respectively

	High-affinity sites		*Low-affinity sites*	
	Membranes	*Intact strips*	*Membranes*	
Antagonist	K_i (nM)	K_i (nM)	IC_{50} (nM)	*nH*
Prazosin	0.04 ± 0.01	0.08 ± 0.01	30 ± 7	0.60 ± 0.03*
HV723	0.32 ± 0.07	1.61 ± 0.29	348 ± 125	0.60 ± 0.06*
WB4101	0.68 ± 0.09	0.53 ± 0.09	223 ± 55	0.60 ± 0.10*
5-Methylurapidil	12.00 ± 4.00	3.66 ± 0.87	354 ± 144	0.95 ± 0.05
Phentolamine	7.50 ± 0.90	8.20 ± 2.10	15560 ± 3100	0.50 ± 0.01*
Yohimbine	82 ± 6	290 ± 68	13280 ± 3350	0.96 ± 0.04

Each value is mean ± s.e.mean of 3–7 experiments, each done in duplicate. K_i values were calculated from inhibition curves according to the equation of Cheng & Prusoff (1973). nH = pseudo-Hill coefficient.
*Significant change ($P<0.001$).

Table 2 Parameters of [^{3}H]-prazosin (0.01–0.4 nM) binding to portal vein membranes in the presence of α-adrenoceptor antagonists

Ligand	K_D *app* (nM)	B_{max} (fmol mg^{-1})
Prazosin		
0 nM	0.026 ± 0.002	63.6 ± 2.0
0.03 nM	0.065 ± 0.002*	63.2 ± 1.9
0.10 nM	0.125 ± 0.023*	63.0 ± 0.1
HV723		
0 nM	0.018 ± 0.001	64.4 ± 2.3
0.2 nM	0.037 ± 0.008*	67.3 ± 3.8
1.0 nM	0.064 ± 0.002*	62.2 ± 0.2
WB4101		
0 nM	0.021 ± 0.002	63.8 ± 1.8
0.5 nM	0.044 ± 0.007*	63.7 ± 4.0
2.0 nM	0.092 ± 0.011*	63.2 ± 1.8
5-Methylurapidil		
0 nM	0.019 ± 0.001	63.3 ± 1.9
10 nM	0.033 ± 0.002*	58.0 ± 1.6
30 nM	0.078 ± 0.004*	61.4 ± 4.0

Each value is mean ± s.e.mean of 3–4 experiments, each done in duplicate.
*Significant change ($P<0.05$).

any significant variation of the B_{max} value are compatible with competition (Table 2).

[^{3}H]-prazosin binding, at 5 nM, was used to label the low-affinity site. Displacement curves for prazosin, HV723, WB4101 and phentolamine had pseudo-Hill coefficients that deviated significantly from unity (Table 1). Thus, these agents appear to have interacted with more than two sites for [^{3}H]-prazosin. Only yohimbine and 5-methylurapidil antagonized [^{3}H]-prazosin binding with a Hill coefficient close to unity. The rank order of potency was prazosin > WB4101, HV723, 5-methylurapidil > yohimbine, phentolamine. For example, Scatchard plots of the binding data in the presence of 5-methylurapidil (200 nM) resulted in a significant increase of the apparent K_D value (control: 0.70 ± 0.01 nM; 5-methylurapidil: 1.65 ± 0.01 nM, $n = 3$, $P<0.05$) without any effects on the B_{max} value (control: 226 ± 10 fmol mg^{-1} of protein; 5-methylurapidil: 207 ± 13 fmol mg^{-1} of protein, $n = 3$) suggesting a competitive behaviour.

Effects of CEC treatment on [^{3}H]-prazosin binding to vascular membranes

Pretreatment of membrane preparations from a variety of tissues with chloroethylclonidine (CEC) has previously been reported to inactivate selectively the α_{1B}-subtype (Minneman, 1988; Mante & Minneman, 1991). Pretreatment with increasing doses of CEC (10 to 50 μM) caused a concentration-dependent loss of high-affinity binding sites without any significant effect on apparent prazosin affinity. After pretreatment with 50 μM CEC, the B_{max} value of the high-affinity sites was decreased from 84.2 ± 4.1 fmol mg^{-1} of protein in control to 11.3 ± 0.9 fmol mg^{-1} of protein ($n = 5$, $P<0.001$) while the B_{max} value of the low-affinity sites was unchanged (control: 320 ± 14 fmol mg^{-1} of protein, CEC-pretreated: 309 ± 11 fmol mg^{-1} of protein, $n = 3$).

[^{3}H]-prazosin binding to intact strips of rat portal vein

The specific binding of [^{3}H]-prazosin (0.03–1.0 nM) was concentration-dependent and saturated at 0.5 nM. At this concentration, the specific binding accounted for 50–55% of the total binding. Scatchard plots of the binding data resulted in a straight line, suggesting a single class of binding sites ($K_D = 0.13 \pm 0.01$ nM, $B_{max} = 15.1 \pm 1.0$ fmol mg^{-1} wet wt, $n = 4$). The K_D value obtained from kinetic experiments (0.230 ± 0.045 nM, $n = 5$) is similar to that obtained from equilibrium binding experiments. In the strips pretreated with 50 μM CEC, [^{3}H]-prazosin bound to a single site with an affinity ($K_D = 0.14 \pm 0.01$ nM, $n = 4$) similar to that of CEC-untreated strips, but the number of binding sites was reduced by about 70% (4.6 ± 0.4 fmol mg^{-1} wet wt, $n = 4$).

Unlabelled prazosin, WB4101, HV723, 5-methylurapidil, phentolamine and yohimbine displaced the specific binding of 0.15 nM [^{3}H]-prazosin in a monophasic manner (Table 1). The rank order of potency: prazosin > WB4101, HV723 > 5-methylurapidil, phentolamine > yohimbine was similar to that obtained with portal vein microsomes for the high-affinity binding sites.

Effects of prazosin, WB4101, HV723, and chloroethylclonidine on noradrenaline-induced contractions

Noradrenaline produced concentration-dependent contractions in isolated strips from rat portal vein, the maximal effect being obtained at 30 μM (Figure 4a). CEC (50 μM) increased the spontaneous myogenic activity in rat portal vein (Schwietert *et al.*, 1991). In the preparations pretreated with 50 μM CEC, noradrenaline produced a concentration-response curve with a concentration producing half-maximal contraction (EC_{50}) of 0.78 ± 0.14 μM ($n = 5$) similar to that obtained in control (0.62 ± 0.04 μM, $n = 5$, Figure 4a). The contraction obtained at 3 μM noradrenaline was not significantly modified after CEC treatment (control: 97 ± 1.5% of maximal contraction; CEC-pretreated: 89 ± 3%). Prazosin, WB4101 and HV723 inhibited the noradrenaline-induced contraction in a concentration-dependent manner. The concentrations required to produce 50% of inhibition (IC_{50}) of the maximal contraction were: WB4101, 1.97 ± 0.51 nM; prazosin, 3.90 ± 0.35 nM; HV723, 9.96 ± 0.50 nM ($n = 3$–4). The rank order of potency was, therefore, WB4101 > prazosin > HV723. After pretreatment with 50 μM

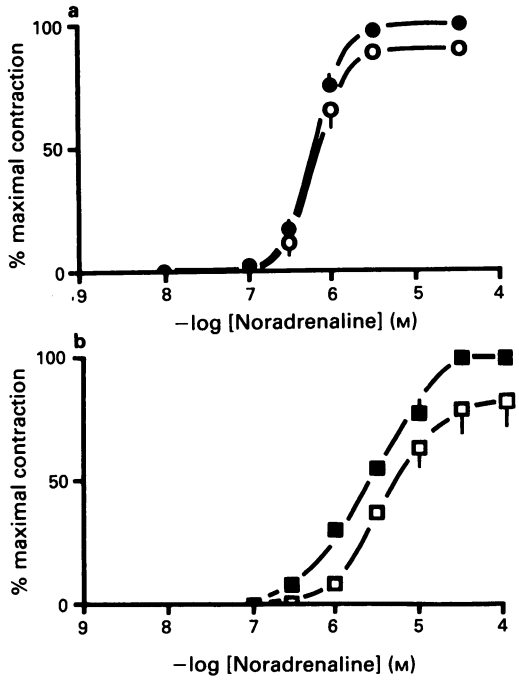

Figure 4 Effect of chloroethylclonidine (CEC) on the response to noradrenaline in intact strips from rat portal vein. (a) Concentration-response curves to noradrenaline in control conditions (●), and after a pretreatment with 50 μM CEC (○). (b) Concentration-response curves to noradrenaline in the presence of 0.1 μM isradipine (control, ■) and after pretreatment with 50 μM CEC (□). Each value is the mean of 3 to 5 experiments ± s.e.mean. Values are referred to the maximal contraction induced by 30 μM noradrenaline in the control curve.

CEC, the IC_{50}s for each α-antagonist were approximately doubled. For example, the IC_{50} for HV723 was 16.7 ± 0.5 nM ($n = 3$).

In the presence of 0.1 μM isradipine to block voltage-dependent calcium channels, the noradrenaline-induced contraction is due to release of Ca^{2+} ions from agonist-sensitive intracellular Ca^{2+} stores. After pretreatment with 50 μM CEC, the concentration-response curve for noradrenaline (Figure 4b) had an EC_{50} (3.90 ± 0.10 μM, $n = 3$) similar to that obtained in control (2.60 ± 0.08 μM, $n = 3$). The maximal response obtained at 30 μM noradrenaline was not significantly reduced (81 ± 9%, $n = 3$) compared to the maximal contraction in control conditions (Figure 4b). The noradrenaline-induced contraction obtained after pretreatment with 50 μM CEC and in the presence of 0.1 μM isradipine was concentration-dependently inhibited by WB4101, prazosin and HV723. The most important point was that HV723 inhibited the contraction dependent on Ca^{2+} release from intracellular stores with a higher affinity (IC_{50} = 2.21 ± 0.17 nM, $n = 4$), so that the rank order of potency became HV723 ⩾ WB4101 > prazosin. Finally, when α_{1H}- and α_{1N}-adrenoceptor subtypes were inhibited by pretreatment with 50 μM CEC and addition of 0.1 μM HV723, noradrenaline was unable to produce a contractile response ($n = 5$).

Discussion

α_1-Adrenoceptor sites in membranes prepared from equine portal vein smooth muscle have been identified and characterized by a radioligand assay using [^{3}H]-prazosin. [^{3}H]-prazosin has been demonstrated to bind to portal vein smooth muscle in a rapid, specific, reversible and saturable manner with both high- and low-affinity. The high-affinity site for [^{3}H]-prazosin is also present in intact strips of rat portal vein. The fact that the high-affinity binding sites for prazosin are inactivated in a concentration-dependent manner by pretreatment with CEC in membrane preparations as well as in intact strips of rat portal vein clearly suggests that the α_{1H}-adrenoceptor subtype may correspond to the α_{1B}-adrenoceptor subtype. In the displacement curves, the high-affinity and low-affinity sites for prazosin are inhibited by the six α-adrenoceptor antagonists used. The rank order of potency for the most effective antagonists is prazosin > HV723, WB4101. The most intriguing aspect of their competition with [^{3}H]-prazosin was the ability of these agents to distinguish between two different [^{3}H]-prazosin low-affinity binding sites. This is evident from the pseudo-Hill coefficients of displacement curves which are smaller than unity (Table 1), confirming the reports of several investigators that these agents have different affinities for α_1-adrenoceptor subtypes (Piascik *et al.*, 1991; Ohmura *et al.*, 1992; Satoh *et al.*, 1992).

The contraction study reveals that selective inhibition of the α_{1H}-adrenoceptor subtype by pretreatment with low concentrations of prazosin or 50 μM CEC does not modify significantly the maximal contraction to noradrenaline as well as the noradrenaline concentration producing half-maximal response. These results indicate that the noradrenaline-induced contraction in rat portal vein is mediated through activation of α_{1L}-adrenoceptors. In CEC-pretreated strips, prazosin, HV723 and WB4101 antagonize the contractile response to noradrenaline with low affinities. Although a contribution of the α_{1A}-adrenoceptor cannot be ruled out completely, the low-affinity of prazosin for inhibition of the noradrenaline response supports the idea that the response to noradrenaline is predominantly mediated through the α_{1L}- or α_{1N}-adrenoceptor subtypes. In the presence of 0.1 μM isradipine to block voltage-dependent calcium channels, the noradrenaline-induced contraction is mainly due to release of Ca^{2+} ions from the intracellular stores (Dacquet *et al.*, 1987). Under these conditions, the IC_{50} for HV723 is decreased from 16.7 nM in the absence of isradipine to 2.2 nM in the presence of isradipine. As the inhibitory characteristics of prazosin and WB4101 remain unchanged, these results suggest that in isradipine-containing solution, the α_{1N}-adrenoceptor subtype would be predominantly involved in the noradrenaline-induced contraction.

It has been previously proposed that the diversity of α_1-adrenoceptor-induced responses may be, in part, related to the distinct subtypes of receptors which may activate different mechanisms of signal transduction (Minneman, 1988). The α_{1B}-adrenoceptor subtype has been associated with formation of inositol 1,4,5-trisphosphate ($InsP_3$) and mobilization of intracellular calcium (Han *et al.*, 1987) but, recent publications indicate that this subtype can also activate Ca^{2+} influx (Han *et al.*, 1992). The α_{1A}-adrenoceptor subtype has been shown to gate Ca^{2+} influx, sometimes through L-type Ca^{2+} channels but it has also been reported that the α_{1A}-adrenoceptor subtype could stimulate the formation of inositol phosphates (Han *et al.*, 1990). In portal vein smooth muscle, the sequence of events induced by noradrenaline can be summarized as follows: (i) noradrenaline releases intracellular Ca^{2+} stores through $InsP_3$ production; (ii) the calcium released opens chloride channels producing outward chloride current and membrane depolarization (Byrne & Large, 1988); (iii) this depolarization produces Ca^{2+} entry through voltage-dependent Ca^{2+} channels; (iv) the open probability of Ca^{2+} channels is enhanced by noradrenaline (Pacaud *et al.*, 1991). As activation of the α_{1L}-adrenoceptor subtype alone is unable to elicit contraction, these results suggest that both α_{1L}- and α_{1N}-adrenoceptors mediate the noradrenaline-induced contraction in physiological conditions. Furthermore, the isradipine-resistant contraction induced by noradrenaline is more sensitive to HV723 than that obtained in the absence of isradipine, suggesting that the α_{1N}-adrenoceptor subtype may

be involved in the mobilization of intracellular Ca^{2+} stores and further activation of chloride channels.

In conclusion, the present study indicates that three distinct subtypes of α_1-adrenoceptors can be identified in portal vein smooth muscle by combining binding and functional experiments. These subtypes fit with the subclassification proposed by Muramatsu *et al.* (1990a,b). Therefore, it is proposed that in rat portal vein, the contractile response to noradrenaline is predominantly caused through activation of both α_{1L}- and α_{1N}-adrenoceptor subtypes.

This work was supported by grants from Région Aquitaine, Centre National des Etudes Spatiales, and Institut National de la Santé et de la Recherche Médicale, France. We thank Ms N. Biendon for excellent assistance.

References

BRADFORD, M.M. (1976). A rapid and sensitive method for the quantitation of microgram quantities of protein utilizing the principle of protein-dye binding. *Anal. Biochem.*, **72**, 248–254.

BYRNE, N.G. & LARGE, W.A. (1988). Membrane ionic mechanisms activated by noradrenaline in cells isolated from the rabbit portal vein. *J. Physiol.*, **404**, 557–573.

CHENG, Y.C. & PRUSOFF, W.H. (1973). Relationship between the inhibition constant (Ki) and the concentration of inhibitor which causes 50 percent inhibition (I_{50}) of an enzymatic reaction. *Biochem. Pharmacol.*, **22**, 3099–3108.

COTECCHIA, S., SCHWINN, D.A., RANDALL, R.R., LEFKOWITZ, R.F., CARON, M.G. & KOBILKA, B.K. (1988). Molecular cloning and expression of cDNA for hamster α_1-adrenergic receptor. *Proc. Natl. Acad. Sci. U.S.A.*, **85**, 7159–7163.

DACQUET, C., MIRONNEAU, C. & MIRONNEAU, J. (1987). Effects of calcium entry blockers on calcium-dependent contractions of rat portal vein. *Br. J. Pharmacol.*, **92**, 203–211.

DACQUET, C., PACAUD, P., LOIRAND, G., MIRONNEAU, C. & MIRONNEAU, J. (1988). Comparison of binding affinities and calcium current inhibitory effects of a 1,4-dihydropyridine derivative (PN 200-110) in vascular smooth muscle. *Biochem. Biophys. Res. Commun.*, **152**, 1165–1172.

FLAVAHAN, N.A. & VANHOUTTE, P.M. (1986). α_1-Adrenoceptor subclassification in vascular smooth muscle. *Trends Pharmacol. Sci.*, **7**, 347–349.

HAN, C., ABEL, P.W. & MINNEMAN, K.P. (1987). α_1-Adrenoceptor subtypes linked to different mechanisms for increasing intracellular Ca^{2+} in smooth muscle. *Nature*, **329**, 333–335.

HAN, C., ESBENSHADE, T.A. & MINNEMAN, K.P. (1992). Subtypes of α_1-adrenoceptors in DDT1 MF-2 and BC3H-1 clonal cell lines. *Eur. J. Pharmacol. Mol. Pharmacol. Section*, **226**, 141–148.

HAN, C., WILSON, K.M. & MINNEMAN, K.P. (1990). α_1-Adrenergic receptors subtypes and formation of inositol phosphates in dispersed hepatocytes and renal cells. *Mol. Pharmacol.*, **37**, 903–910.

HANFT, G. & GROSS, G. (1989). Subclassification of α_1-adrenoceptor recognition sites by urapidil derivatives and other selective antagonists. *Br. J. Pharmacol.*, **97**, 691–700.

LOMASNEY, J.W., COTECCHIA, S., LEFKOWITZ, R.J. & CARON, M.G. (1991). Molecular biology of α-adrenergic receptors: implications for receptor classification and for structure-function relationships. *Biochim. Biophys. Acta*, **1095**, 127–139.

MANTE, S. & MINNEMAN, K.P. (1991). The alkylating prazosin analog SZL-49 inactivates both α_{1A}- and α_{1B}-adrenoceptors. *Eur. J. Pharmacol.*, **208**, 113–117.

MINNEMAN, K.P. (1988). α_1-Adrenergic receptor subtypes, inositol phosphates, and sources of cell Ca^{2+}. *Pharmacol. Rev.*, **40**, 87–119.

MIRONNEAU, J., MIRONNEAU, C., GROSSET, A., HAMON, G. & SAVINEAU, J.P. (1980). Action of angiotensin II on the electrical and mechanical activity of rat uterine smooth muscle. *Eur. J. Pharmacol.*, **68**, 275–285.

MORROW, A.L. & CREESE, I. (1986). Characterization of α_1-adrenergic receptor subtypes in rat brain: a reevaluation of [^{3}H]WB4101 and [^{3}H]prazosin binding. *Mol. Pharmacol.*, **29**, 321–330.

MUNSON, P.J. & RODBARD, D. (1980). Ligand: a versatile computerized approach for characterization of ligand binding systems. *Anal. Biochem.*, **107**, 220–239.

MURAMATSU, I., KIGOSHI, S. & OSHITA, M. (1990a). Two distinct alpha$_1$-adrenoceptor subtypes involved in noradrenaline contraction of the rabbit thoracic aorta. *Br. J. Pharmacol.*, **101**, 662–666.

MURAMATSU, I., OHMURA, T., KIGOSHI, S., HASHIMOTO, S. & OSHITA, M. (1990b). Pharmacological subclassification of alpha$_1$-adrenoceptors in vascular smooth muscle. *Br. J. Pharmacol.*, **99**, 197–201.

OHMURA, T., OSHITA, M., KIGOSHI, S. & MURAMATSU, I. (1992). Identification of alpha$_1$-adrenoceptor subtypes in the rat vas deferens. Binding and functional studies. *Br. J. Pharmacol.*, **107**, 697–704.

OSHITA, M., KIGOSHI, S. & MURAMATSU, I. (1991). Three distinct binding sites for [^{3}H]-prazosin in the rat cerebral cortex. *Br. J. Pharmacol.*, **104**, 961–965.

PACAUD, P., LOIRAND, G., BARON, A., MIRONNEAU, C. & MIRONNEAU, J. (1991). Ca^{2+} channel activation and membrane depolarization mediated by Cl^- channels in response to noradrenaline in vascular myocytes. *Br. J. Pharmacol.*, **104**, 1000–1006.

PEREZ, D.M., PIASCIK, M.T. & GRAHAM, R.M. (1991). Solution phase library screening for the identification of rare clones: isolation of an α_{1D}-adrenergic receptor cDNA. *Mol. Pharmacol.*, **40**, 876–883.

PIASCIK, M.T., SPARKS, M.S., PRUITT, T.A. & SOLTIS, E.E. (1991). Evidence for a complex interaction between the subtypes of the α_1-adrenoceptor. *Eur. J. Pharmacol.*, **199**, 279–290.

RAKOTOARISOA, L., SAYET, I., MIRONNEAU, C. & MIRONNEAU, J. (1990). Selective modulation by membrane potential of desmethoxyverapamil binding to calcium channels in rat portal vein. *J. Pharmacol. Exp. Ther.*, **255**, 942–947.

SATOH, M., KOJIMA, C. & TAKAYANAGI, I. (1992). Characterization of alpha$_1$-adrenoceptor subtypes labeled by [^{3}H]-prazosin in single cells prepared from rabbit thoracic aorta. *Eur. J. Pharmacol.*, **221**, 35–41.

SCHWIETERT, H.R., GOUW, M.A.M., WILHELM, D., WILFFERT, B. & VAN ZWIETEN, P.A. (1991). The role of α_1-adrenoceptor subtypes in the phasic and tonic responses to phenylephrine in the longitudinal smooth muscle of the rat portal vein. *Naunyn-Schmied. Arch. Pharmacol.*, **343**, 463–471.

SCHWINN, D.A. & LOMASNEY, J.W. (1992). Pharmacologic characterization of cloned α_1-adrenoceptor subtypes: selective antagonists suggests the existence of a fourth subtype. *Eur. J. Pharmacol. Mol. Pharmacol. Section*, **227**, 433–436.

SCHWINN, D.A., LOMASNEY, J.W., LORENZ, W., SZKLUT, P.J., FREMEAU, R.T.Jr., YANG-FENG, T.L., CARON, M.G., LEFKOWITZ, R.J. & COTECCHIA, S. (1990). Molecular cloning and expression of the cDNA for a novel alpha$_1$- adrenergic receptor subtype. *J. Biol. Chem.*, **265**, 8183–8189.

WEILAND, G.A. & MOLINOFF, P.B. (1981). Quantitative analysis of drug receptor interactions. Determination of kinetic and equilibrium properties. *Life Sci.*, **29**, 313–330.

(Received August 5, 1992
Revised May 4, 1993
Accepted May 5, 1993)

Br. J. Pharmacol. (1993), **110**, 213–218

Effects of L- and D-arginine and some related esters on the cytosolic mechanisms of α-thrombin-induced human platelet activation

[1]Paola Failli, Enrica Cecchi, C. Ruocco, A. Fazzini & A. Giotti

Dipartimento di Farmacologia Preclinica e Clinica 'M. Aiazzi Mancini' and Centro Interuniversitario 'Ipossie', V. le G.B. Morgagni, 65, University of Florence, 50134 Florence, Italy

1 In Fura-2 preloaded human platelets, the increase in cytosolic calcium induced by α-thrombin was reduced by some L- and D-arginine ester compounds the IC_{50} (μM) values of which were 7.4 for TAEE, 56.9 for BAEE, 77.6 for TAME, 560 for T(d)AME, 656.3 for L-ArgOMe and 2206.7 for D-ArgOMe. α-tosyl-L-Arginine, L- and D-arginine were inactive.

2 The inhibitory activity of the L-arginine esters was not modified when platelets were pretreated with 100 μM N^{ω}-monomethyl-L-arginine.

3 The L-arginine esters did not increase cyclic GMP content in platelets either in the presence or absence of indomethacin and apyrase at rest and after α-thrombin stimulation.

4 The kinetic parameters of platelet Na^+/H^+ antiporter (amiloride-inhibitable, evaluated after cytosolic nigericin-induced acidification) were modified by L- and D-arginine esters, while the native amino acids were ineffective.

5 The inhibitory effects of the L- and D-arginine esters on platelet activation appear to be mainly due to their inhibitory effect on Na^+/H^+ antiporter.

Keywords: Human platelets; α-thrombin activation; cytosolic calcium concentration; Na^+/H^+ antiporter activity; L-arginine; D-arginine; L-arginine esters; D-arginine esters; N^{ω}-monomethyl-L-arginine

Introduction

Recent data from many laboratories point to the role of L-arginine in a wide range of physiological functions (Moncada *et al.*, 1991), including platelet aggregation (Radomski *et al.*, 1987; 1990a,b). L-Arginine has been found to be directly linked to the production of endothelial-derived relaxing factor (EDRF), which has been identified as nitric oxide (Palmer *et al.*, 1987; Ignarro *et al.*, 1987), one of the two nitrogen atoms of the guanidine group of the amino acid being oxidized to produce nitric oxide. The biochemical pathway for synthesizing nitric oxide from L-arginine is competitively inhibited by guanidine-substituted L-arginine derivatives such as N^{ω}-monomethyl-L-arginine (L-NMMA) (Hibbs *et al.*, 1987; Moncada *et al.*, 1991). Nitric oxide appears to exert its action through activation of a soluble guanylate cyclase and hence an increase in guanosine 3′:5′-cyclic monophosphate (cyclic GMP) formation.

It has been proposed not only that L-arginine might be the substrate for the production of nitric oxide, but also that some L-arginine derivatives may induce endothelium-dependent relaxation in different vascular beds by increasing nitric oxide synthesis (Thomas & Ramwell, 1988; Al-Swayeh & Moore, 1989; Thomas *et al.*, 1990; Busija *et al.*, 1990; Farhat *et al.*, 1990a,b). More recently it has been reported that the vasorelaxation induced by N-α-benzoyl-L-arginine ethyl ester (BAEE) is either not nitric oxide-dependent (Al-Swayeh & Moore, 1989; Fasehun *et al.*, 1990; Schmidt *et al.*, 1990) or is only partially so (Farhat *et al.*, 1990b), while N-α-tosyl-L-arginine methyl ester (TAME) has been described as a nitric-oxide-independent vasorelaxant (Schmidt *et al.*, 1990) or an endothelium-independent inhibitor of contraction induced by several agents in human umbilical arteries (White, 1988).

Some of the L-arginine esters also inhibit platelet aggregation (Salzman & Chambers, 1964; Aoki *et al.*, 1978; Failli *et al.*, 1990; Spurej *et al.*, 1990). Preliminary data obtained in our laboratory show that L- and D-arginine esters inhibit aggregation induced by α-thrombin, while concentrations up to 500 μM are ineffective against collagen-induced aggregation. In order to investigate the antiaggregatory mechanism of arginine esters in human platelets stimulated by α-thrombin, we have studied their effects against the increases in cytosolic free calcium induced by α-thrombin: the experimental conditions were chosen to rule out the amplification mechanisms due to either arachidonic acid metabolites (in particular thromboxane A_2), or ADP by inhibiting arachidonic acid cyclo-oxygenase with indomethacin and by hydrolyzing extraplatelet ADP with apyrase. The possible role of L-arginine esters as nitric oxide precursors has also been investigated, by measuring cyclic GMP platelet content. This set of experiments was performed either in the presence of indomethacin and apyrase or in their absence. Finally, we have monitored Na^+/H^+ antiporter activity and its modification by the L- and D-arginine esters.

Some of these results were presented at the XIth International Congress of Pharmacology (Failli *et al.*, 1990).

Methods

Platelet preparation

Blood was collected by venipuncture from healthy human volunteers and immediately diluted 1/5 with citric acid: trisodium citrate:glucose (1.5%:2.5%:2% w/v). Platelet-rich plasma (PRP) was prepared by centrifugation at 500 *g* at 25°C for 15 min and incubated with 3 μM Fura-2-AM or 2 μM BCECF-AM at 37°C for 45 min.

Platelets were then washed twice by centrifugation and resuspended in HEPES buffer of the following composition (mM): NaCl 140, HEPES 10, $NaHCO_3$ 12, KCl 2.9, $MgCl_2$ 0.9, NaH_2PO_4 0.5 and glucose 10. Apyrase (100 u l^{-1}) was added to hydrolyze ATP to ADP and ADP to AMP (Molnar & Lorand, 1961) and indomethacin (10 μM) was added to inhibit arachidonic acid cyclo-oxygenase. In experiments to explore the effect of the D- and L-arginine esters on Na^+/H^+

[1] Author for correspondence.

antiporter activity, BCECF-loaded platelets were washed twice and suspended in a modified (nominally Na^+ and K^+-free) N-methylglucamine buffer of the following composition (mM): N-methylglucamine 138, HEPES 10, glucose 10, $MgCl_2$ 0.1, HCl 140 (adjusted to pH 7.4 with choline carbonate) (HEPES-*N*-methyl-glucamine buffer). D- and L-Arginine esters were dissolved in either HEPES-$NaHCO_3$ or HEPES-N-methylglucamine buffer; the pH of the solutions was measured and, if necessary, carefully adjusted.

Internal cytosolic free calcium concentrations ($[Ca^{2+}]_i$) were estimated in HEPES buffer 1 mM $CaCl_2$ according to the method of Pollock & Rink (1986), using a Shimadzu RF-5000 spectrofluorimeter (equipped with a thermostated cuvette holder and magnetic stirrer), wavelength settings being 345 nm for excitation and 500 nm for emission. α-Thrombin was added directly to the cuvette in the presence or absence of the test compound.

The Na^+/H^+ antiporter activity was determined by the spectrofluorimetric technique described by Grinstein *et al.* (1989). Briefly, BCECF-loaded platelets suspended in nominally Na^+- and K^+-free N-methylglucamine buffer were acidified by addition of nigericin. A typical acid-loading experiment is shown in Figure 1. The decrease in fluorescence (ordinate scale, arbitrary units) indicates the decrease in intracytosolic pH (pH_i). When the fluorescence value had stabilized, the administration of 30 mM NaCl brought about a rapid cytosolic alkalinization, indicating restored Na^+/H^+ antiporter activity. At the end of each experiment, the pH of the buffer was measured in order to verify that the pH of the medium had remained constant. Intracytosolic pH was then calculated after platelet lysis, and the kinetic parameters of the first phase of alkalinization were calculated after measuring specific fluorescence of the BCECF at various pH values and expressed as $\Delta pH_i \times min^{-1}$.

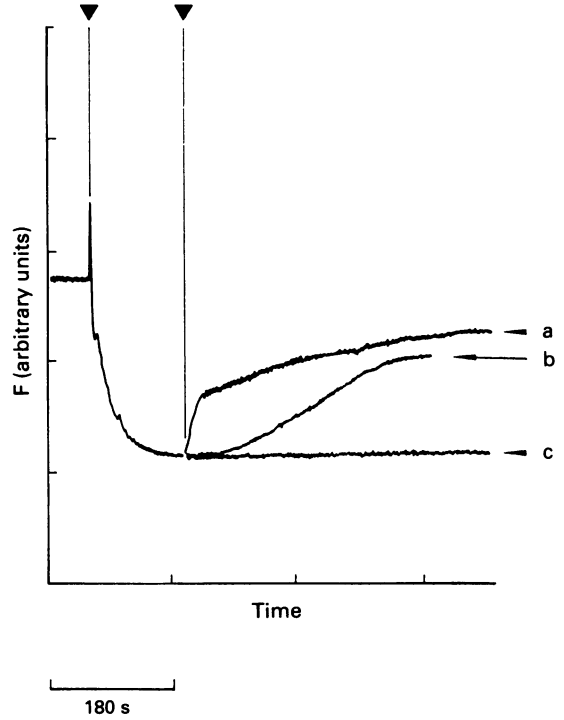

Figure 1 Acid-loading and activation of Na^+/H^+ antiporter of BCECF-loaded platelets suspended in nominally Na^+ and K^+-free N-methylglucamine buffer. Nigericin, 2 μM, was added to begin acid loading in the absence of Na^+ (first arrow). Na^+/H^+ antiporter was then activated by addition of 30 mM NaCl (second arrow) in the absence (a) or in the presence (b) of 1 mM amiloride. The bottom trace (c) was obtained when, instead of NaCl, 30 mM choline chloride was added at the second arrow (osmotic control). Abscissa scale: time. Ordinate scale: fluorescence (arbitrary units), excitation 505 nm, emission 530 nm.

Test molecules were preincubated with platelet suspensions for 2 min prior to adding α-thrombin.

Cyclic GMP measurement

Measurements of cyclic GMP were performed by radioimmunoassay, using kits supplied by Amersham International. In brief, twice-washed platelets were suspended at a density of 10^8-10^9 platelets per 100 μl in indomethacin/apyrase HEPES/$NaHCO_3$ buffer, 1 mM $CaCl_2$, containing isobutylmethylxanthine (30 μM). In some experiments, indomethacin and apyrase were not added. Test molecules were preincubated with platelets at 37°C for 20 min and then 0.03 u ml^{-1} α-thrombin (final concentration) or the same volume of buffer was added. Incubation was continued for an additional 5 min and then the reaction stopped by addition of 50 μl cold 20% $HClO_4$ and transfer of the samples onto ice for 5 min. The reaction mixture was neutralized with 110 μl 1.08 M K_3PO_4, tubes were centrifuged and 3 aliquots of supernatant (100 μl) were used for cyclic GMP determination.

Reagents

Amiloride HCl, N-methyl-D-glucamine, digitonin, D-arginine (D-Arg), N-α-*p*-tosyl-L-arginine (α-tosyl-L-arginine), N-α-*p*-tosyl-L-arginine methyl ester HCl (TAME), isobutylmethylxanthine (IBMX), N-α-benzoyl-L-arginine ethyl ester HCl (BAEE) and N^{ω}-monomethyl-L-arginine acetate salt (L-NMMA) were obtained from Sigma; L-arginine (L-Arg) and sodium nitroprusside (NP) from Merck; L-arginine methyl ester.2HCl (L-ArgOMe) from Fluka; nigericine (sodium salt), Fura-2 and BCECF were from Calbiochem; Fura-2-AM, BCECF-AM from Molecular Probes; α-thrombin from Boehringer-Mannheim. All other reagents were of analytical grade. D-Arginine methyl ester 2HCl (D-ArgOMe), N-α-*p*-tosyl-D-arginine methyl ester HCl (T(d)AME), N-α-benzoyl-D-arginine methyl ester HCl (B(d)AME) and N-α-*p*-tosyl-L-arginine ethyl ester HCl (TAEE) were the kind gift of Drs Buzzetti and Sala of Italfarmaco (Milano, Italy).

Statistical analysis

All values are expressed as mean ± s.e.mean of the number of experiments indicated and were compared by Student's *t* test for paired data, with $P<0.05$ considered as statistically significant. IC_{50} values were estimated from at least 4 separate dose-effect curves by computerized linear regression analysis.

Results

Internal calcium

The average value for basal $[Ca^{2+}]_i$, measured within the 5 h duration of experiments, was 145 ± 4 nM ($n = 33$). Addition of α-thrombin induced a rapid, sustained and dose-dependent increase in $[Ca^{2+}]_i$ (Figure 2). A concentration-response curve for α-thrombin was performed for each separate sample of platelets in order to choose a suitable agonist concentration for studying potential antagonists at equivalent activation levels, i.e. around the half-maximal response. The concentration selected was between 0.03 u ml^{-1} and 0.01 u ml^{-1} (final).

L- or D-Arginine esters, added 2 min before stimulation, did not influence basal $[Ca^{2+}]_i$ values, but reduced the $[Ca^{2+}]_i$ response induced by α-thrombin in a concentration-dependent way; IC_{50} values are shown in Table 1. Esterification of the parent amino acids engendered an antithrombin activity in the compounds, with L-arginine esters being more active than D-arginine esters. Sodium nitroprusside also concentration-dependently inhibits the $[Ca^{2+}]_i$ response induced by α-thrombin, dose-dependently ($IC_{50} = 497.4$ μM – Table

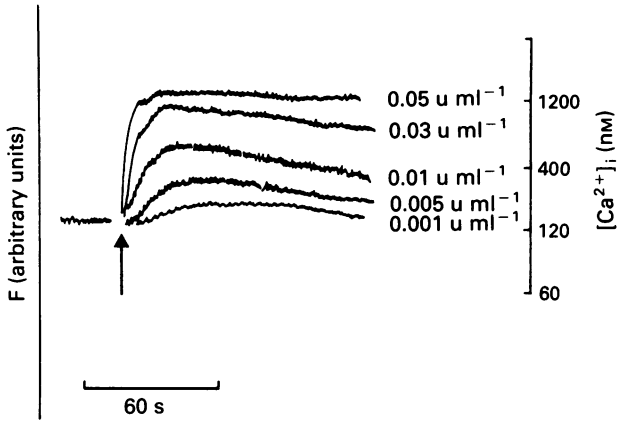

Figure 2 Increases in internal free calcium ($[Ca^{2+}]_i$) induced by α-thrombin on Fura-2 loaded platelets. α-Thrombin (0.05 u ml^{-1}–0.001 u ml^{-1}) was added at the arrow. Abscissa scale: time. Left ordinate scale: fluorescence (arbitrary units), excitation 345 nm, emission 500 nm; right ordinate scale: $[Ca^{2+}]_i$ calibration scale.

Table 1 IC_{50} values (μM) of L- and D-arginine compounds and sodium nitroprusside (NP) on the α-thrombin-induced increase of $[Ca^{2+}]_i$ in human platelets

Compounds	*IC_{50} (μM)*
L-Arg	No effect
D-Arg	No effect
L-ArgOMe	656.3 (608–712)
D-ArgOMe	2206.7 (1834–2769)
TAME	77.6 (50–138)
T(d)AME	560.0 (430–810)
TAEE	7.4 (5–12)
BAEE	56.9 (47–71)
B(d)AME	No effect
α-tosyl-L-arginine	No effect
NP	497.4 (339–932)

Confidence limits in parentheses.
For abbreviations, see text.

1). Unesterified L-arginine was ineffective, even when preincubated at a high concentration (10 mM) with platelets for 30 min at 37°C. The increase in $[Ca^{2+}]_i$ induced by α-thrombin was not modified by preincubating platelets (30 min at 37°C) with 100 μM L-NMMA, the increase being 701 ± 51 nM and 692 ± 51 nM with and without L-NMMA respectively (mean of at least 17 different determinations). N^{ω}-monomethyl-L-arginine (100 μM) did not diminish the inhibitory effect of L-arginine esters TAEE, BAEE, TAME tested in the ratios 1:1, 1:10, 1:100. Figure 3 shows results for the most effective compound, TAEE. Inhibition by one of the least active esters, L-ArgOMe (1 mM) was also not modified by L-NMMA (36.3 ± 12% inhibition in the absence and 45.3 ± 10% inhibition in the presence of 100 μM L-NMMA; mean of 4 experiments).

Cyclic GMP content

Experiments in the presence of indomethacin and apyrase Cyclic GMP content of human platelets was 0.67 ± 0.14 pmol per 10^8 platelets in basal conditions and 0.73 ± 0.1 pmol per 10^8 platelets after α-thrombin stimulation in indomethacin/apyrase HEPES/$NaHCO_3$ buffer, 1 mM $CaCl_2$. These values were increased in a dose-dependent manner by 1, 10 and 100 μM sodium nitroprusside. At the maximal concentration tested (100 μM), sodium nitroprusside increased the basal content of cyclic GMP to 1.5 ± 0.25 pmol per 10^8 platelets ($P<0.05$ vs no drugs at rest) and 1.9 ± 0.45 pmol per 10^8 platelets ($P<0.05$ vs no drugs after α-thrombin

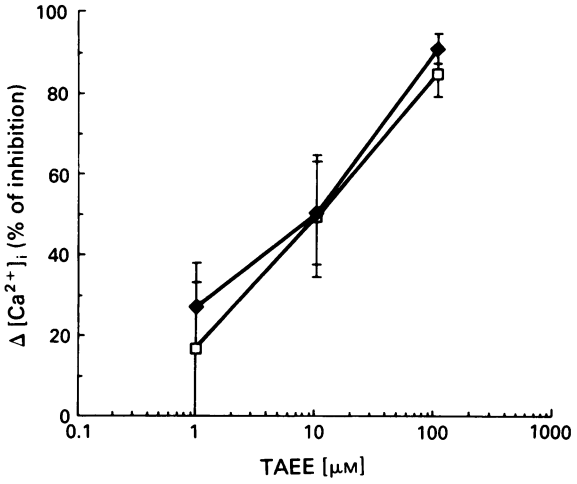

Figure 3 Effect of N-α-*p*-tosyl-L-arginine ethyl ester (TAEE) in the presence (◆) or absence (□) of 100 μM N^{ω}-monomethyl-L-arginine (L-NMMA). Each point is the mean (± s.e.mean) of at least 3 experiments.

administration), respectively, at rest and after α-thrombin stimulation (Figure 4a). Neither L-arginine esters (at concentrations near to their IC_{50} values for inhibition of α-thrombin-induced $[Ca^{2+}]_i$ increase) nor 100 μM L-arginine increased platelet cyclic GMP content (Figure 4a).

Experiments in the absence of indomethacin and apyrase In these experimental conditions, cyclic GMP content of human platelets was 0.5 ± 0.13 pmol per 10^8 platelets in basal conditions and 0.97 ± 0.18 pmol per 10^8 platelets after α-thrombin stimulation. Sodium nitroprusside (100 μM) increased cyclic GMP content in unstimulated platelets by about 18 fold ($P<0.001$ vs no drugs at rest) and by about 9 fold after α-thrombin stimulation ($P<0.0001$ vs no drugs after α-thrombin stimulation, Figure 4b). However, L-arginine esters did not increase this content either at rest or after α-thrombin stimulation (Figure 4b). Preincubation with L-arginine (100 μM) did not increase cyclic GMP content in unstimulated platelets (0.63 ± 0.13 and 0.5 ± 0.13 pmol per 10^8 platelets L-arginine and no drugs at rest respectively, $P<0.5$, not significant), while α-thrombin (administered after 20 min preincubation with 100 μM L-arginine) increased it (0.63 ± 0.13 pmol per 10^8 platelets to 1.25 ± 0.14 pmol per 10^8 platelets, $P<0.05$ vs L-arginine at rest, Figure 4b). However, platelet cyclic GMP content after L-arginine (100 μM) and α-thrombin did not differ from that in α-thrombin-treated platelets, being 1.25 ± 0.14 pmol per 10^8 platelets and 0.97 ± 0.18 pmol per 10^8 platelets, respectively ($P<0.295$, not significant).

Na^+/H^+ antiporter activity

After the administration of 30 mM Na^+ ions in acid-loaded platelets, the pH_i began to increase rapidly (1.20 ± 0.12 pH units min^{-1}, Figure 1 and Table 2, control). Amiloride (1 mM) strongly modified this response (Figure 1 and Table 2), while choline chloride did not induce any changes in pH_i (Figure 1 and Table 2). The effects of L- and D-arginine esters on Na^+/H^+ antiporter activity are summarized in Table 2. The most active compound was TAEE, its effect being concentration-dependent in the range 0.5–0.01 mM. L-Arginine and D-arginine, although tested at 20 mM, were inactive (Table 2).

Discussion

Our data show that some methyl- and ethyl esters of both D- and L-arginine inhibit the $[Ca^{2+}]_i$ increase induced in Fura-2

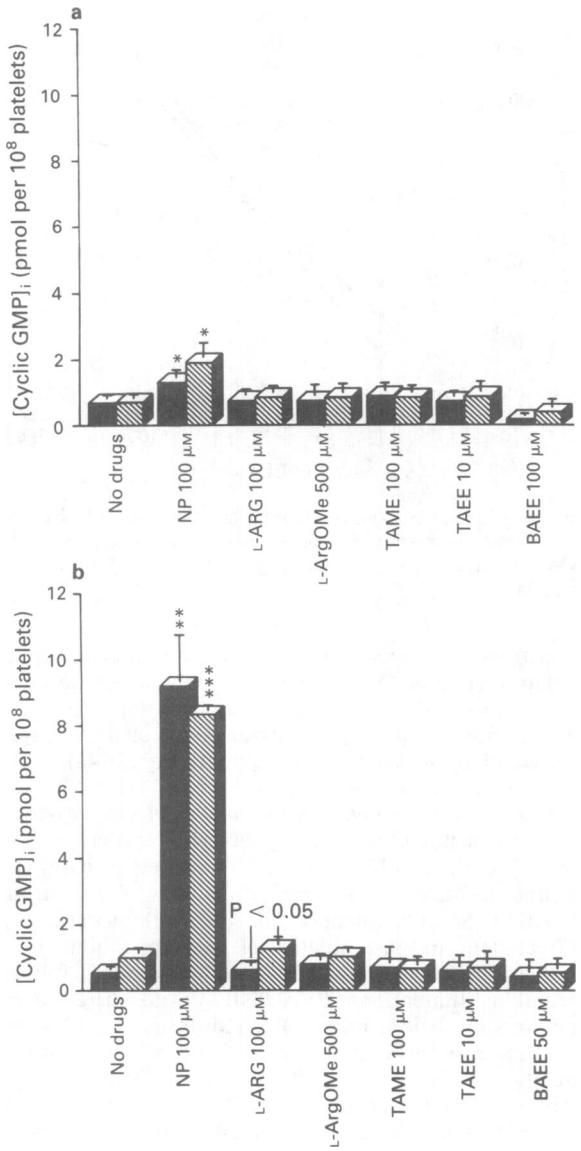

Figure 4 (a) Effect of L-arginine esters (tested at concentrations near their IC_{50} values for inhibition of α-thrombin-induced $[Ca^{2+}]_i$ increase) in comparison with 100 μM sodium nitroprusside (NP) and 100 μM L-arginine on cyclic GMP concentration measured in human platelets suspended in HEPES/$NaHCO_3$ buffer containing 1 mM $CaCl_2$, 10 μM indomethacin, 100 u ml^{-1} apyrase and 30 μM isobutyl methyl xanthine (IBMX), estimated either at rest (solid columns) or after stimulation by α-thrombin (0.03 u ml^{-1}) (hatched columns). Values are the mean (± s.e.mean) of at least 3 experiments. $^*P<0.05$ vs no drugs. (b) Effect of L-arginine esters (tested at concentrations near their IC_{50} values for inhibition of α-thrombin-induced $[Ca^{2+}]_i$ increase) in comparison with 100 μM sodium nitroprusside (NP) and 100 μM L-arginine on cyclic GMP concentration measured in human platelets suspended in HEPES/$NaHCO_3$ buffer containing 1 mM $CaCl_2$ and 30 μM isobutyl methyl xanthine (IBMX), estimated either at rest (solid columns) or after stimulation by α-thrombin (0.03 u ml^{-1}) (hatched columns). Values are the mean (± s.e.mean) of at least 3 experiments. $^{**}P<0.001$ vs no drugs; $^{***}P<0.0001$ vs no drugs.

loaded human platelets by α-thrombin. The inhibitory activities of these esters are increased by substitutions on the primary α-amino group, tosyl substitution being more effective than benzoyl. It is also interesting to note that ethyl esters are more effective than methyl esters (TAME< TAEE).

In the same experimental conditions, sodium nitroprusside, which increases cyclic GMP content through a direct activation of soluble NO-sensitive guanylate cyclase, reduced

Table 2 Effects of amiloride, L- and D-arginine and L- and D-arginine esters on Na^+/H^+ antiporter activity in human platelets

No drugs	*Δ pH min^{-1}*
Control (30 mM NaCl)	1.20 ± 0.12
Choline chloride (30 mM)	0.00
Compounds	
Amiloride (1 mM)	0.37 ± 0.08*
Amiloride (0.1 mM)	0.64 ± 0.25
TAEE (0.5 mM)	0.29 ± 0.10**
TAEE (0.1 mM)	0.41 ± 0.13**
TAEE (0.01 mM)	0.51 ± 0.08*
BAEE (0.5 mM)	0.67 ± 0.13*
BAEE (0.1 mM)	0.71 ± 0.14
TAME (1 mM)	0.29 ± 0.10***
TAME (0.1 mM)	0.33 ± 0.12*
L-ArgOMe (10 mM)	0.29 ± 0.06**
D-ArgOMe (10 mM)	0.34 ± 0.15*
L-Arg (20 mM)	1.04 ± 0.31
D-Arg (20 mM)	0.66 ± 0.26

For abbreviations, see text.
Values are mean ± s.e.mean of at least 3 different experiments.
$^*P<0.05$; $^{**}P<0.01$; $^{***}P<0.001$.

α-thrombin-induced $[Ca^{2+}]_i$ increase in platelets in a dose-dependent way, suggesting that an increase in platelet cyclic GMP content (Figure 4a) reduces $[Ca^{2+}]_i$ increase induced by α-thrombin stimulation.

The suggestion that some L-arginine esters might influence cellular function by increasing nitric oxide synthesis (see Introduction) seems an unsatisfactory explanation of the inhibitory effects observed in our experimental conditions. In fact, a high concentration (100 μM) of the NO-synthase inhibitor L-NMMA did not modify the inhibition induced by the compounds. Moreover, L-arginine esters did not increase platelet cyclic GMP content either in the presence of indomethacin and apyrase or in their absence (Figure 4a and b).

On the other hand, in the experimental conditions in which we measured $[Ca^{2+}]_i$ (i.e. in the presence of indomethacin and apyrase), the NO-synthase pathway from L-arginine seems not to be activated. L-Arginine did not in fact inhibit the $[Ca^{2+}]_i$ increase induced by α-thrombin, either with or without a 30 min preincubation time at 37°C. Moreover, 100 μM L-NMMA did not modify α-thrombin-induced $[Ca^{2+}]_i$ increase. Furthermore, although 100 μM L-arginine (preincubated 20 min) and α-thrombin induced an increase in platelet cyclic GMP content in the absence of indomethacin and apyrase (Figure 4b), this increase seems to be too small to reduce α-thrombin-induced $[Ca^{2+}]_i$ increase. In fact, a small dose of sodium nitroprusside (1 μM), which induced a similar increase in platelet cyclic GMP content (52%, measured in the same experimental conditions as $[Ca^{2+}]_i$ determination) hardly affected α-thrombin-induced $[Ca^{2+}]_i$ increase (⩽ 10% inhibition). This result is compatible with the weak inhibition by L-arginine of thrombin-induced aggregation of human platelets (Radomski *et al.*, 1990a,b).

We have shown that some of the L- and D-arginine esters inhibit Na^+/H^+ antiporter activity, as demonstrated by analysing the early phase of Na^+/H^+ activation. Furthermore, the potencies for the inhibition of the Na^+/H^+ antiporter were correlated with potencies for inhibiting the $[Ca^{2+}]_i$ increase induced by α-thrombin, the most effective of the esters being TAEE. More intriguing is the inhibitory effect of T(d)AME on the $[Ca^{2+}]_i$ increase induced by α-thrombin, as the Na^+/H^+ antiporter activity was not affected by 1 mM or 0.1 mM T(d)AME (94% and 92% of the control, respectively). Further research will be necessary in order to clarify the effect of this compound.

Although the role of Na^+/H^+ antiporter activation in the induction of aggregation and $[Ca^{2+}]_i$ increase in platelets is a matter of debate (Siffert & Akkermann, 1987; Simpson & Rink, 1987; Hunyady *et al.*, 1987; Zavoico & Cragoe, 1988; Ghigo *et al.*, 1988; Sanchez *et al.*, 1988; Siffert *et al.*, 1989), we suggest that the effect of L-arginine esters on the Na^+/H^+ antiporter activity may be the basis of their inhibitory action on α-thrombin-induced $[Ca^{2+}]_i$ increase and aggregation; indeed the prototype inhibitor of the Na^+/H^+ antiporter, amiloride, also inhibits platelet aggregation (Siffert *et al.*, 1986).

The L-arginine esters were also inhibitors of α-thrombin-induced aggregation, IC_{50} values being 15.2 μM, 18.0 μM and 26.3 μM for TAEE, TAME and BAEE, respectively (results not shown). In contrast, concentrations up to 500 μM of TAEE, TAME and BAEE were completely ineffective as inhibitors of collagen-induced aggregation, a mechanism of platelet activation which is independent of the activation of the Na^+/H^+ antiporter (Joseph *et al.*, 1990). All these data support the hypothesis that the mechanism of action of L-arginine esters is the inhibition of Na^+/H^+ antiporter activity.

Recently, the thrombin human platelet receptor has been cloned and functionally characterized (Vu *et al.*, 1991). It seems that thrombin binding with its receptor sites is characterized by a partial proteolytic digestion of an extraplatelet domain. Although we cannot rule out the possibility that the antithrombin effect of L-arginine esters is an antiproteolytic process, preliminary results indicate that L-arginine esters inhibit the proteolytic effect of α-thrombin only at concentrations which are 10 times greater than those required to inhibit the $[Ca^{2+}]_i$ increase after α-thrombin (unpublished observations). Therefore, this property is unlikely to explain the inhibitory effect of the compounds. In fact, subthreshold antiproteolytic concentrations are fully active in inhibiting the $[Ca^{2+}]_i$ increase induced by α-thrombin. Moreover, in PRP, BAEE inhibits thrombin-induced platelet aggregation without inhibiting fibrin clot formation (Spurej *et al.*, 1990).

In conclusion, our observations are consistent with the interpretation that pharmacological actions of some arginine esters may be linked to their inhibitory effect on platelet Na^+/H^+ antiporter activity. For instance, this property might also explain some of the endothelium-independent (or only partially endothelium-dependent) effects of L-arginine esters described by other authors (White, 1988; Schmidt *et al.*, 1990; Farhat *et al.*, 1990; Fasehun *et al.*, 1990).

We would like to thank Sir John Vane and Prof. Giuseppe Nisticò for reading the manuscript and for their useful suggestions and Ms Susan Charlton for her editing of the English.

This work was supported by a MURST 60% grant.

References

AL-SWAYEH, O.A. & MOORE, P.K. (1989). Amino acids dilate resistance blood vessels of the perfused rat mesentery. *J. Pharm. Pharmacol.*, **41**, 723–726.

AOKI, N.A., NAITA, K. & YOSHDA, N. (1978). Inhibition of platelet aggregation by protease inhibitors. Possible involvement of proteases in platelet aggregation. *Blood*, **52**, 1–12.

BUSIJA, D.W., LEFFLER, C.W. & WAGERLE, L.C. (1990). Mono-L-arginine-containing compounds dilate piglet pial arterioles via an endothelium-derived relaxing factor-like substance. *Circ. Res.*, **67**, 1374–1380.

FAILLI, P., FRANCONI, F., GIOTTI, A., MICELI, M., POLENZANI, L. & STENDARDI, I. (1990). Effects of arginine and arginine derivatives on human platelets. *Eur. J. Pharmacol.*, **183**, 639.

FARHAT, M.Y., RAMWELL, P.W. & THOMAS, G. (1990a). Endothelium-mediated effects of N-substituted arginine on the isolated perfused rat kidney. *J. Pharmacol. Exp. Ther.*, **255**, 473–477.

FARHAT, M.Y., THOMAS, G., CUNARD, C.M., COLE, E., MYERS, A.M. & RAMWELL, P.W. (1990b). Vasodilatory property of N-alpha benzoyl-L-arginine ethyl ester in rat isolated pulmonary artery and perfused lung. *J. Pharmacol. Exp. Ther.*, **254**, 289–293.

FASEHUN, O.A., GROSS, S.S., RUBIN, L.E., JAFFE, E.A., GRIFFITH, O.W. & LEVI, R. (1990). L-Arginine, but not N alpha-benzoyl-L-arginine ethyl ester, is a precursor of endothelium-derived relaxing factor. *J. Pharmacol. Exp. Ther.*, **255**, 1348–1353.

GHIGO, D., TREVES, S., TURRINI, F., PANNOCCHIA, A., PESCARMONA, G. & BOSIA, A. (1988). Role of Na^+/H^+ exchange in thrombin- and arachidonic acid-induced Ca^{2+} influx in platelets. *Biochim. Biophys. Acta*, **940**, 141–148.

GRINSTEIN, S., COHEN, S., GOETZ-SMITH, J.D. & DIXON, S.J. (1989). Measurements of cytoplasmic pH and cellular volume for detection of Na^+/H^+ exchange in lymphocytes. In *Methods in Enzymology*, ed. Fleischer, S. & Fleischer, B. Vol. 173, pp. 777–790. S. Diego, CA: Academic Press Inc.

HIBBS, J.B.Jr., TAINTOR, R.R. & VAVRIN, Z. (1987). Macrophage cytotoxicity: role for L-arginine deiminase and imino nitrogen oxidation to nitrite. *Science*, **235**, 473–476.

HUNYADY, L., SARKADI, B., CRAGOE, E.J. Jr., SPÄT, A. & GÁRDOS, G. (1987). Activation of sodium-proton exchange is not a prerequisite for Ca^{2+} mobilization and aggregation in human platelets. *FEBS Lett.*, **225**, 72–76.

IGNARRO, L.J., BUGA, G.M., WOOD, K.S., BYRNS, R.E. & CHAUDHIRI, G. (1987). Endothelium-derived relaxing factor produced and released from artery and vein is nitric oxide. *Proc. Natl. Acad. Sci. U.S.A.*, **84**, 9265–9269.

JOSEPH, S., SIFFERT, W., GORTER, G. & AKKERMAN, J.W.N. (1990). Stimulation of human platelets by collagen occurs by a Na^+/H^+ exchanger independent mechanisms. *Biochim. Biophys. Acta*, **1054**, 26–32.

MOLNAR, J. & LORAND, L. (1961). Studies on apyrases. *Arch. Biochem. Biophys.*, **93**, 353–363.

MONCADA, S., PALMER, R.M.J. & HIGGS, E.A. (1991). Nitric oxide: physiology, pathophysiology and pharmacology. *Pharmacol. Rev.*, **43**, 109–141.

PALMER, R.M.J., FERRIGE, A.G. & MONCADA, S. (1987). Nitric oxide release accounts for the biological activity of endothelium-derived relaxing factor. *Nature*, **327**, 524–526.

POLLOCK, W.K. & RINK, T.J. (1986). Thrombin and ionomycin can raise platelet cytosolic Ca^{2+} to micromolar levels by discharge of internal Ca^{2+} stores: studies using fura-2. *Biochem. Biophys. Res. Commun.*, **139**, 308–314.

RADOMSKI, M.W., PALMER, R.M.J. & MONCADA, S. (1987). Comparative pharmacology of endothelium-derived relaxing factor, nitric oxide and prostacyclin in platelets. *Br. J. Pharmacol.*, **92**, 181–187.

RADOMSKI, M.W., PALMER, R.M.J. & MONCADA, S. (1990a). An L-arginine to nitric oxide pathway in human platelets regulates aggregation. *Proc. Natl. Acad. Sci. U.S.A.*, **87**, 5193–5197.

RADOMSKI, M.W., PALMER, R.M.J. & MONCADA, S. (1990b). Characterization of the L-arginine: nitric oxide pathway in human platelets. *Br. J. Pharmacol.*, **101**, 325–328.

SALZMAN, E.W. & CHAMBERS, D.A. (1964). Inhibition of ADP-induced platelet aggregation by substituted amino-acids. *Nature*, **204**, 698–700.

SANCHEZ, A., ALONSO, M.T. & COLLAZOS, J.M. (1988). Thrombin-induced changes of intracellular $[Ca^{2+}]$ and pH in human platelets. Cytoplasmic alkalinization is not a prerequisite for calcium mobilization. *Biochim. Biophys. Acta*, **938**, 497–500.

SCHMIDT, H.H.H.W., BAEBLICH, S.E., ZERNIKOW, B.C., KLEIN, M.M. & BOHME, E. (1990). L-Arginine and arginine analogues: effects on isolated blood vessels and cultured endothelial cells. *Br. J. Pharmacol.*, **101**, 145–151.

SIFFERT, W. & AKKERMAN, J.N.W. (1987). Activation of sodium-proton exchange is a prerequisite for Ca^{2+} mobilization in human platelets. *Nature*, **325**, 456–458.

SIFFERT, W., GENGENBACH, S. & SHEID, P. (1986). Inhibition of platelet aggregation by amiloride. *Thromb. Res.*, **44**, 235–240.

SIFFERT, W., SIFFERT, G., SCHIED, P. & AKKERMAN, J.N.W. (1989). Activation of Na^+/H^+ exchange and Ca^{2+} mobilization start simultaneously in thrombin-stimulated platelets. Evidence that platelet shape change disturbs early rises of BCECF fluorescence which causes an underestimation of actual cytosolic alkalinization. *Biochem. J.*, **258,** 521–527.

SIMPSON, A.W.M. & RINK, T.J. (1987). Elevation of pH_i is not an essential step in calcium mobilization in fura-2-loaded human platelets. *FEBS Lett.*, **222,** 144–148.

SPUREJ, E., SNEDDON, J.M. & VANE, R.J. (1990). The influence of pH on aggregation of human washed platelets induced by thrombin or collagen. *Blood Coagul. Fibrinolysis*, **1,** 47–53.

THOMAS, G., FARHAT, M., MYERS, A.M. & RAMWELL, P.W. (1990). Effect of Nα-benzoyl-L-arginine ethyl ester on coronary perfusion pressure in isolated guinea-pig heart. *Eur. J. Pharmacol.*, **178,** 251–254.

THOMAS, G. & RAMWELL, P.W. (1988). Vasodilatory properties of mono L-arginine containing compounds. *Biochem. Biophys. Res. Commun.*, **154,** 332–338.

VU, T.K.H., HUNG, D.T., WHEATON, V.I. & COUGHLIN, S.R. (1991). Molecular cloning of a functional thrombin receptor reveals a novel proteolytic mechanism of receptor activation. *Cell*, **64,** 1057–1068.

WHITE, R.P. (1988). Pharmacodynamic effects of tosyl-arginine methyl ester (TAME) on isolated human arteries. *Gen. Pharmacol.*, **19,** 387–392.

ZAVOICO, G.B. & CRAGOE, E.J. (1988). Ca^{2+} mobilization can occur independent of acceleration of Na^+/H^+ exchange in thrombin-stimulated human platelets. *J. Biol. Chem.*, **263,** 9635–9639.

(Received November 26, 1992
Revised May 5, 1993
Accepted May 6, 1993)

Br. J. Pharmacol. (1993), **110**, 219–224

Characterization of the novel nitric oxide synthase inhibitor 7-nitro indazole and related indazoles: antinociceptive and cardiovascular effects

[1]P.K. Moore, P. Wallace, Z. Gaffen, S.L. Hart & R.C. Babbedge

Pharmacology Group, Biomedical Sciences Division, King's College, University of London, Manresa Road, London SW3 6LX

1 7-Nitro indazole (7-NI, 10–50 mg kg^{-1}), 6-nitro indazole and indazole (25–100 mg kg^{-1}) administered i.p. in the mouse produce dose-related antinociception in the late phase of the formalin-induced hindpaw licking and acetic acid-induced abdominal constriction assays. The ED_{50} values (mg kg^{-1}) were as follows: 7-NI (27.5 and 22.5), 6-nitro indazole (62.5 and 44.0) and indazole (41.0 and 48.5) in the two assays respectively. 3-Indazolinone, 6 amino indazole and 6-sulphanilimido indazole (all 50 mg kg^{-1}) were without effect. With the exception of 5-nitro indazole (50 mg kg^{-1}) which produced sedation, none of the other indazole derivates examined caused overt behavioural changes.

2 The antinociceptive effect of 7-NI (25 mg kg^{-1}, i.p.) in the late phase of the formalin-induced hindpaw licking assay was partially (46.7 ± 16.2%, $n = 18$) reversed by pretreatment with L- but not D-arginine (both 50 mg kg^{-1}, i.p.).

3 The time course of 7-NI induced antinociception in the mouse was correlated with inhibition of brain (cerebellum) nitric oxide synthase (NOS) activity. Maximum antinociceptive activity and NOS inhibition were detected 18–30 min following i.p. administration. In contrast, no antinociceptive effect or inhibition of cerebellar NOS was detected 75 min post-injection.

4 7-NI, 6-nitro indazole, indazole, 3-indazolinone and 6-amino indazole (all 50 mg kg^{-1}) failed to influence mean arterial pressure (MAP) over the 45 min after i.p. administration in the anaesthetized mouse. Similarly, 7-NI (25 mg kg^{-1}) administered i.v. in the anaesthetized rat did not increase MAP or influence the vasodepressor effect of i.v. injected acetylcholine (ACh) over the same period.

5 7-NI (100 μM) did not influence the vasorelaxant effect of ACh (IC_{50}, 0.2 ± 0.04 μM, cf. 0.16 ± 0.06 μM, $n = 6$) in phenylephrine-precontracted rabbit aortic rings.

6 These data provide further evidence that antinociception following administration of 7-NI in the mouse results from inhibition of central NOS activity and is not associated with inhibition of *in vivo* vascular endothelial cells NOS. Accordingly, 7-NI (or a derivative thereof) may provide an alternative approach to the development of novel antinociceptive drugs.

Keywords: 7-Nitro indazole; substituted indazole derivatives; antinociception; anaesthetized mouse; anaesthetized rat; rabbit aorta; nitric oxide; nitric oxide synthase

Introduction

The selective inhibitor of nitric oxide synthase (NOS), L-N^G-nitro arginine methyl ester (L-NAME), exhibits potent antinociceptive activity in the mouse (Moore *et al.*, 1991). Antinociception is both naloxone-insensitive and partially reversed by L- (but not D-) arginine implying a role for nitric oxide (NO) in central nociceptive pathways which is unrelated to the release of endogenous opioids. Essentially similar results have been obtained in the mouse following i.p. administration of L-NAME (Mustafa, 1992).

The precise site of action of the antinociceptive effect of L-NAME within the central nervous system is not clear. However, several experimental observations suggest a spinal mechanism of action (Meller & Gebhart, 1993). Thus: (i) immunochemical staining using an antibody raised against brain NOS reveals large amounts of this enzyme in the intermediolateral cell column and superficial and deeper laminae of the rat dorsal spinal cord with no activity detected in the ventral spinal cord (Dun *et al.*, 1992; Valtschanoff *et al.*, 1992). (ii) Inflammation of the rat hindpaw is associated with an increase in NADPH diaphorase (reportedly identical with NOS; Hope *et al.*, 1991) in the rat dorsal spinal cord (Solodkin *et al.*, 1992). (iii) Intrathecal administration of L-NAME prevents the dorsal horn expression of Fos protein (a marker for nociceptive pathways in the central nervous system; Bullitt, 1990), following mechanical (pinch) stimulation of the rat hindpaw (Lee *et al.*, 1992). (iv) Intrathecal administration of L-NAME reduces N-methyl-D-aspartate (NMDA)-induced hyperalgesia in the rat (Meller *et al.*, 1992) and mouse (Kitto *et al.*, 1992). (v) Electrophysiological responses of dorsal horn neurones following activation of sensory C-fibres by formalin injection in the rat hindpaw are inhibited by spinal application of L-NAME (Haley *et al.*, 1992). Cumulatively these data strongly indicate that NO plays a part in nociceptive events occurring in the spinal cord in response to peripheral noxious stimuli and, furthermore, suggest a rational basis for the antinociceptive effect of drugs which inhibit NOS.

Unfortunately, the sustained vasopressor effect of L-NAME (for review see Moncada *et al.*, 1991) effectively precludes its use as an analgesic in man. We have recently reported that 7-nitro indazole (7-NI) inhibits both rat and mouse brain NOS and exhibits potent antinociceptive activity in the mouse without significantly increasing blood pressure in this species (Moore *et al.*, 1993). Accordingly, we have proposed that 7-NI, or a chemically related compound, may provide a good starting point for the development of novel, clinically useful analgesics.

We have now studied further the antinociceptive and cardiovascular activity of 7-NI and a range of chemically related mono- and di-substituted indazole derivatives.

Methods

Assessment of antinociceptive effect

Male mice (LACA, 28–35 g) were allowed food and water *ad libitum* and transported to the laboratory at least 2 h prior to

[1] Author for correspondence.

the study. Experiments were carried out in the period between 13 h 00 min and 17 h 00 min in normal room light and temperature (22 ± 2°C). All experiments were performed with appropriate Home Office approval.

The antinociceptive effect of indazole derivatives was assessed by the formalin-induced hindpaw licking procedure of Hunskaar & Hole (1987). Animals were injected sub-plantar in one hindpaw with formalin (5% v/v, 10 μl) and the duration of paw licking monitored in the periods 0–5 min (early phase) and 15–30 min (late phase) thereafter. Drugs or an appropriate volume of vehicle (arachis oil, 0.1 ml 10 g^{-1}) were administered i.p. 15 min prior to formalin administration. In experiments to determine the ability of L-arginine to reverse the antinociceptive effects of 7-NI, either L- or D-arginine (both 50 mg kg^{-1}) or an appropriate volume of vehicle (0.9% w/v NaCl) were administered i.p. to mice 20 min prior to subplantar formalin injection. These animals subsequently received a second i.p. injection of 7-NI or vehicle (arachis oil) 15 min prior to formalin injection. Results are expressed as % inhibition of hindpaw licking time compared with licking time in the appropriate control group of animals.

In separate experiments, indazole derivatives or vehicle were administered i.p. 15 min prior to i.p. administration of acetic acid (0.6% v/v, 10 ml kg^{-1}). The resulting abdominal constrictions were counted for 30 min thereafter. Results are expressed as % inhibition of acetic acid-induced abdominal constrictions over this period compared with control, vehicle-pretreated, animals.

Effect of 7-NI on mouse cerebellar NOS: correlation with antinociceptive effect

Mice (LACA, 28–35 g) were pretreated with 7-NI (25 mg kg^{-1}, i.p.) or an appropriate volume of vehicle either 3, 15, 60 or 120 min prior to subplantar formalin (5% v/v, 10 μl) injection as described above; 15 min later (i.e. at the start of the late phase of the paw licking response) animals were killed by cervical dislocation. Cerebella were removed and weighed and either rapidly frozen and stored at − 70°C until required or immediately homogenized in an Ultra-Turrax (type 18/2N) homogenizer in 10 volumes of 20 mM Tris HCl buffer (pH 7.4) containing 2 mM EDTA. Homogenates were centrifuged (10,000 *g*, 15 min, 4°C) and the crude supernatant used for assay of NOS as below.

Conversion of [^{3}H]-arginine to [^{3}H]-citrulline was determined as described by Dwyer *et al.* (1991). Incubations (15 min at 0°C followed by 15 min at 37°C) contained 25 μl cerebellar (1:10 w/v) supernatant, 0.5 μCi [^{3}H]-L-arginine (concentration = 120 nM), 0.75 mM $CaCl_2$, 0.5 mM NADPH and 5 μl water or drug solution in a total volume of 105 μl. Assays were terminated by addition of 3 ml HEPES buffer (pH 5.5) containing 2 mM EDTA and were applied to 0.5 ml columns of Dowex AG50WX-8 (Na^+ form) followed by 0.5 ml distilled water. [^{3}H]-citrulline was quantified by liquid scintillation spectroscopy of a 1 ml aliquot of the flow-through. In control experiments cerebellar supernatant was added to the incubation after stopping the reaction with HEPES buffer. Protein concentration was measured according to the procedure of Lowry *et al.* (1951) and NOS activity calculated in terms of pmol mg^{-1} protein 15 min^{-1}. Results are shown as % inhibition of cerebellar NOS in 7-NI-treated compared with control vehicle-injected animals.

Effect of indazole derivatives on rat and mouse blood pressure

Mice were anaesthetized with urethane (10 g kg^{-1}, i.p.) and a cannula inserted into the carotid artery. Blood pressure was monitored via a Bell & Howell pressure transducer connected to a Devices 2-channel pen recorder. 7-NI, 6-nitro indazole, indazole, 6-amino indazole or 3-indazolinone were administered i.p. and MAP monitored for up to 45 min thereafter. Control animals received an appropriate volume of arachis oil. In separate experiments, rats were anaesthetized with urethane (10 g kg^{-1}, i.p.) and cannulae inserted both into the carotid artery for blood pressure recording as described above and into the jugular vein for drug injection. Dose-response curves to the vasodepressor effect of acetylcholine (0.05–3.0 μg i.v.) were constructed and a single dose (1 μg) representing approximately 70% of the maximum effect chosen and repeated 4 times at 5 min intervals. Thereafter, 7-NI (25 mg kg^{-1}) was administered i.v. and the response to the standard dose of ACh determined at timed intervals over the following 45 min.

Effect of 7-NI on rabbit aorta

Male New Zealand White rabbits (2.5–3.5 kg) were killed by an overdose of pentobarbitone (60 mg kg^{-1}) administered into a marginal ear vein. Aortae were removed, cleared of connective tissue, cut into rings (approx. 2–3 mm diameter) and mounted in 20 ml organ baths containing warmed (37°C), oxygenated (95% O_2: 5% CO_2) Krebs solution (composition, mM: NaCl 121, KCl 4.7, $CaCl_2$ 2.7, $NaHCO_3$ 25, KH_2PO_4 1.18, $MgSO_4$ 0.7, glucose 11.1, pH 7.4) under an initial resting tension of 2 g. Changes in tension were monitored by means of Grass FT-03 force transducers connected to a Devices pen recorder. Preparations were pre-equilibrated in the organ bath for 1 h and thereafter contracted with an EC_{70} concentration of phenylephrine (PE, 0.75 μM). Endothelium-dependent relaxation in response to acetylcholine (ACh 0.01–1.0 μM) was determined before and 12 min after addition of 7-NI (100 μM).

Drugs and chemicals

Indazole, 5-nitro indazole, 6-nitro indazole, 6-amino indazole, 3-indazolinone and 6-sulphanilimido indazole were purchased from Aldrich Ltd. 7-Nitro indazole was obtained from MTM Lancaster Ltd. Radiolabelled [^{3}H]-arginine (sp. act. 62 Ci $mmol^{-1}$) was obtained from Amersham, U.K. All other drugs and chemicals were purchased from Sigma Ltd. Dowex AG50WX-8 H^+ form (Sigma Ltd.) was converted into the Na^+ form by soaking for 2 h in 2 M NaOH. For *in vivo* experiments indazole and its derivatives were dissolved in arachis oil with the exception of i.v. administered 7-NI in rats in which Na_2CO_3 (0.5%, w/v) was the vehicle. For *in vitro* experiments 7-NI was dissolved in Na_2CO_3 (0.5%, w/v). Drugs stocks were prepared fresh on the morning of each experiment.

Statistical analysis

Results indicate mean ± s.e.mean. Statistical significance of differences between groups was determined by unpaired Student's *t* test. A probability (*P*) value of 0.05 or less was taken to indicate statistical significance.

Results

Antinociceptive effect of indazole derivatives

Pretreatment of mice with 7-NI (10–50 mg kg^{-1}), 6-nitro indazole (25–100 mg kg^{-1}) or indazole (25–100 mg kg^{-1}) resulted in a dose-related inhibition of late phase formalin-induced hindpaw licking behaviour (Figure 1) and acetic acid-induced abdominal constrictions (Figure 2). None of the drugs tested significantly influenced first phase formalin-induced hindpaw licking time. Calculated ED_{50} values for the three indazole derivatives were 27.5 mg kg^{-1}, 62.5 mg kg^{-1} and 41.0 mg kg^{-1} in the formalin assay and 22.5 mg kg^{-1}, 44.0 mg kg^{-1} and 48.5 mg kg^{-1} in the acetic acid assay respectively. In contrast, 3-indazolinone, 6 amino indazole and 6-sulphanilimido indazole (all 50 mg kg^{-1}) were without antinociceptive activity in either assay (data not shown).

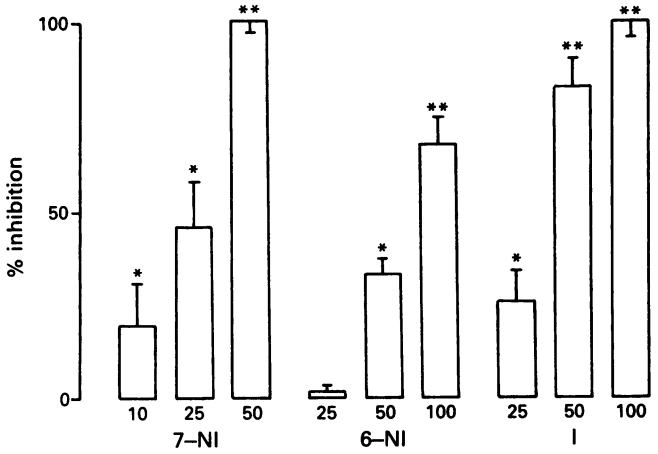

Figure 1 Antinociceptive effect of i.p. administered 7-nitro indazole (7-NI), 6-nitro indazole (6-NI) and indazole (I) assessed by the formalin-induced hindpaw licking assay in the mouse. Figures beneath each column represent dose administered (mg kg^{-1}). Results indicate % inhibition of late phase (15–30 min following subplantar formalin injection) hindpaw licking time compared with licking time in control, vehicle-injected animals and are mean ± s.e.mean, n = 6–14. *P<0.05; **P<0.01.

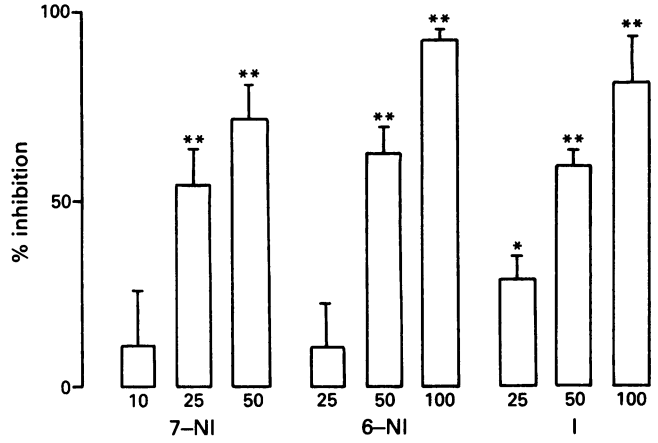

Figure 2 Antinociceptive effect of i.p. administered 7-nitro indazole (7-NI), 6-nitro indazole (6-NI) and indazole (I) assessed by the acetic acid-induced abdominal constriction assay in the mouse. Figures beneath each column represent dose administered (mg kg^{-1}). Results indicate % inhibition of abdominal constrictions observed over a 30 min period following i.p. injection of acetic acid compared with results obtained in control (vehicle-injected) animals and are mean ± s.e.mean, n = 6–8. *P<0.05; **P<0.01.

5-Nitro indazole (50 mg kg^{-1}) produced sedation in all mice and was subsequently excluded from further study. With the exception of 5-nitro indazole none of the other derivatives tested produced sedation or other overt behavioural changes.

Reversal of 7-NI induced antinociception by L-arginine

Control animals receiving saline (20 min) plus arachis oil (15 min) prior to subplantar administration of formalin exhibited early phase (late phase in parenthesis) paw licking times of 99.2 ± 15.7 s (156.3 ± 19.2 s, n = 7). Neither L-arginine (50 mg kg^{-1}, early phase: 76.3 ± 9.6 s, late phase: 132.8 ± 9.9 s, n = 7) nor D-arginine (50 mg kg^{-1}, early phase: 86.1 ± 6.9 s, late phase: 170.3 ± 18.6 s, n = 10) significantly (P>0.05) influenced hindpaw licking time in either phase of the response when administered on their own. However, prior administration of L-arginine (50 mg kg^{-1}) significantly (P<0.05) reversed the late phase anti-nociceptive effect of i.p. administered 7-NI (25 mg kg^{-1}) by 46.7 ± 16.2% (n = 18). In contrast, D-arginine (50 mg kg^{-1}) administration resulted in a non-significant (P>0.05) reversal of 7-NI induced late phase antinociception of 13.6 ± 11.1% (n = 12) (Figure 3).

Correlation between antinociceptive effect of 7-NI and its effect on mouse brain NOS activity

Preliminary analysis of the time course of effect of i.p. administered 7-NI revealed significant antinociceptive activity when injected 3 min prior to formalin (Table 1). Similar antinociceptive activity was still apparent when the pretreatment time was extended to 15 min whilst no antinociception could be detected in mice injected with 7-NI either 60 or 120 min before formalin injection. In separate experiments, i.p. administration of 7-NI resulted in a broadly similar

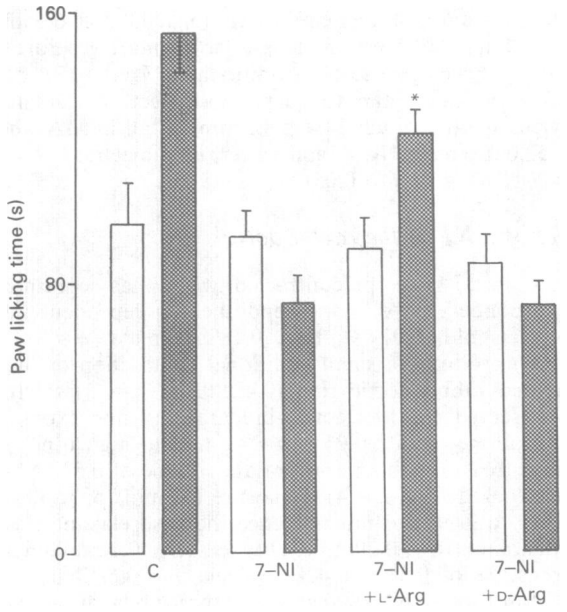

Figure 3 Effect of L- and D-arginine (50 mg kg^{-1}) pretreatment on antinociceptive effect of i.p. administered 7-nitro indazole (7-NI, 25 mg kg^{-1}). Open columns represent early phase (0–5 min following subplantar formalin injection) hindpaw licking time (s) while stippled columns indicate late phase (15–30 min following subplantar formalin injection) hindpaw licking time (s). Results indicate mean ± s.e.mean, n = 10–18. L-Arginine pretreatment significantly (*P< 0.05) reverses the late phase antinociceptive effect of 7-NI.

Table 1 Antinociception and inhibition of cerebellar nitric oxide synthase (NOS) following 7-nitro indazole (7-NI) administration in the mouse

Time (min)	*Antinocicepton* (% inhibition)	*% inhibition of NOS*
3	53.8 ± 11.1*	40.5 ± 1.2*
15	44.6 ± 14.6*	57.2 ± 0.7*
60	0	29.7 ± 1.9*
120	5.7 ± 6.2	0.7 ± 0.7

7-NI was administered i.p. at timed intervals (3–120 min) prior to subplantar formalin injection. Antinociceptive activity is expressed as % inhibition of hindpaw licking time in the late phase (15–30 min) compared with control animals receiving an appropriate volume of arachis oil. Results show mean ± s.e.mean, n = 6–10, *P<0.05. In separate experiments mice pretreated with 7-NI at timed intervals as above, were injected subplantar with formalin and killed 15 min thereafter. Results show % inhibition of cerebellar NOS compared with activity in control, vehicle-injected animals and are mean ± s.e.mean, n = 6, *P<0.05.

time-related inhibition of mouse cerebellar NOS. Again, significant inhibition of cerebellar NOS was evident at both 3 and 15 min prior to formalin administration which declined by approximately 50% at 60 min and was not apparent at 120 min (Table 1).

Effect of indazole derivatives on mouse and rat blood pressure

Administration of 7-NI, 6-nitro indazole, indazole, 6-amino indazole or 3-indazoline (all 50 mg kg^{-1}, i.p.) failed to influence MAP in the anaesthetized mouse at timed intervals up to 45 min (Table 2). A time-related increase in heart rate was observed both in vehicle-injected and in non-injected animals (data not shown) and is consequently most likely a response to the anaesthetic. No additional effect was seen in response to indazole derivatives. 7-NI dissolved in 0.5% Na_2CO_3 and administered i.v. to rats at a dose (25 mg kg^{-1}) which represents the limit of solubiltiy of this compound under these conditions, did not increase MAP (e.g. 149.9 ± 6.5 mmHg 45 min after 7-NI injection cf. 154.9 ± 7.0 mmHg before 7-NI injection, $n = 6$, $P > 0.05$). Additionally, 7-NI (25 mg kg^{-1}) failed to influence the vasodepressor effect of i.v. injected acetylcholine (e.g. 1 μg; 54.4 ± 8.2 mmHg fall in MAP before and 52.0 ± 6.6 mmHg 45 min after i.v. injection of 25 mg kg^{-1} 7-NI, $n = 6$, $P > 0.05$).

Effect of 7-NI on the rabbit aorta

Rabbit aortic rings precontracted with phenylephrine (0.7 μM) responded to ACh with endothelium-dependent relaxation (threshold, 0.01 μM; IC_{50}, 0.18 ± 0.05 μM, $n = 8$). 7-NI (100 μM) produced a small additional contraction of the PE-pretreated rabbit aortic ring (0.4 ± 0.2 g, $n = 6$) which was also observed in 'low tone' preparations not exposed to phenylephrine (0.75 ± 0.25 g, $n = 4$) and in 'high tone' preparations treated with an appropriate volume of 0.5% Na_2CO_3 vehicle (0.3 ± 0.2 g, $n = 4$). Exposure (12 min) of rabbit aortic rings to 7-NI did not influence the vasorelaxant effect of acetylcholine (IC_{50}, 0.20 ± 0.04 μM, cf. IC_{50}, 0.16 ± 0.06 μM in the presence of 0.5% Na_2CO_3 vehicle, $n = 6$, $P > 0.05$). Higher doses of 7-NI (300 μM) produced relaxation of the phenylephrine-pretreated rabbit aortic ring. However, this is again unlikely to represent a pharmacological effect of 7-NI since control aortic rings exposed to an equivalent volume of 0.5% Na_2CO_3 vehicle were similarly relaxed. For this reason the effect of higher concentrations of 7-NI were not evaluated.

Discussion

To date the indazole nucleus (see Figure 4) has not featured prominently in medicinal chemistry. Of the simpler indazole compounds to appear in the literature, micromolar concentrations of 6-amino indazole have been shown to inhibit both

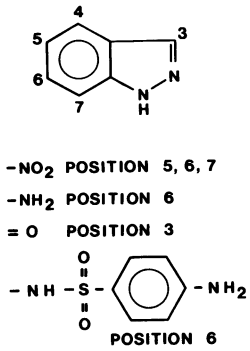

Figure 4 Structure of indazole showing points of substitution of derivatives used in this study.

the effect of pilocarpine on the guinea-pig isolated trachea and the effect of histamine on the guinea-pig isolated ileum whilst 5-amino indazole is a relatively potent inhibitor of carbachol-induced gastric acid secretion in the rat (Pinelli *et al.*, 1989). More chemically complex indazole derivatives which inhibit lipoxygenase enzyme activity (Foster *et al.*, 1989) or antagonize either leukotriene (Yee *et al.*, 1990) or 5-HT_3 (Robertson *et al.*, 1990) receptors have also been synthesized. Perhaps of greater relevance to the present study is benzydamine, an indazole derivative, with pronounced antinociceptive activity which has been recognised for over two decades (Silvestrini *et al.*, 1966; Lisciani *et al.*, 1968).

The present study illustrates the antinociceptive effect in the mouse of a series of mono-substituted indazoles. Of the various structures examined, 7-NI exhibited greatest activity in both the formalin-induced hindpaw licking and acetic acid-induced abdominal constriction assays. In the former assay 7-NI inhibited the late phase but not the early phase hindpaw licking response which is consistent with reports of the involvement of NO in the phenomenon of 'wind-up' in dorsal horn neurones following activation of sensory C fibres (Meller & Gebhart, 1993). It is clear that antinociceptive activity within the indazole series is not confined to 7-NI but is also apparent following administration of both indazole and 6-nitro indazole. It should be made clear that observation of mice treated with indazole, 6-nitro indazole or 7-NI did not reveal any overt changes in locomotor activity or sedative effect which might have interfered with the interpretation of these data. In contrast, 5-nitro indazole proved to be a powerful sedative and was thus not studied further.

Evidence presented in this paper indicates that 7-NI, like L-NAME (Moore *et al.*, 1991), is antinociceptive by virtue of inhibiting central NOS. Thus, 7-NI induced antinociception is partially reversed by L- but not D-arginine. Furthermore, the time course of 7-NI-induced antinociception is correlated with inhibition of brain (cerebellar) NOS. Interestingly, and unlike L-NAME, which produces a long-lasting (>24 h)

Table 2 Effect of indazole derivatives on mouse mean arterial pressure (MAP)

	MAP (mmHg)			
	0 min	15 min	30 min	45 min
Vehicle	52.1 ± 4.9	54.3 ± 3.9	47.9 ± 5.5	49.8 ± 6.1
7-NI, 25 mg kg^{-1}	51.6 ± 4.4	54.5 ± 4.2	50.5 ± 4.2	47.4 ± 5.1
7-NI, 80 mg kg^{-1}	49.5 ± 2.9	48.1 ± 3.3	44.9 ± 4.4	43.9 ± 5.3
6-NI, 50 mg kg^{-1}	54.3 ± 3.4	54.9 ± 3.3	43.5 ± 3.3	43.0 ± 4.5
3-I, 50 mg kg^{-1}	43.2 ± 5.4	43.7 ± 5.0	47.8 ± 5.2	44.5 ± 3.2
6-AI, 50 mg kg^{-1}	49.0 ± 4.7	49.5 ± 5.8	44.7 ± 5.6	41.5 ± 3.4
I, 50 mg kg^{-1}	46.7 ± 5.4	51.2 ± 4.4	46.7 ± 4.0	49.8 ± 3.2

Indazole derivatives (7-NI, 7-nitro indazole; 6-NI, 6-nitro indazole; 3-I, 3-indazolinone; 6-AI, 6-amino indazole; I, indazole) were suspended in arachis oil and administered i.p. MAP (mmHg) was determined for up to 45 min thereafter. Control animals received 0.1 ml kg^{-1} arachis oil vehicle. Results show mean ± s.e.mean, $n = 6$.

antinociception in the mouse (Moore *et al.*, 1991), the effect of 7-NI is more short-lived with all activity dissipated within 60 min. One explanation for this difference in time course may be the nature of the NOS inhibitory activity of the two drugs. Thus, L-NAME is reportedly an irreversible inhibitor of brain NOS (Dwyer *et al.*, 1991) whilst 7-NI appears to compete with L-arginine for the substrate site of the rat cerebellar NOS (Babbedge *et al.*, 1993). In light of these results it is not surprising that of all the indazoles tested for antinociceptive activity 7-NI is the most potent NOS inhibitor (Babbedge *et al.*, 1993). Furthermore, 3-indazolinone, 6 amino indazole and 6-sulphanilimido indazole are devoid of antinociceptive activity in the present study and exhibited no or only negligible NOS inhibitory activity (Babbedge *et al.*, 1993).

An equally intriguing aspect of the present study is the lack of biological activity of 7-NI within the cardiovascular system. Thus, 7-NI (100 μM) failed to inhibit endothelium-dependent relaxation of the rabbit isolated aorta in response to acetylcholine. In contrast, we have previously reported that L-NAME (1.5 and 15 μM) produces approximately 20% and 70% inhibition of the response of the rabbit aorta to acetylcholine (Moore *et al.*, 1990). An accurate determination of relative potency is not possible since at doses in excess of 100 μM, 7-NI causes blood vessel relaxation via a vehicle effect. In addition, 7-NI (plus related antinociceptive indazole derivatives) do not increase MAP in the anaesthetized mouse following i.p. administration thus confirming the results of a previous study (Moore *et al.*, 1993). In the anaesthetized rat i.v. administered 7-NI neither increases MAP nor reduces the vasodepressor effect of acetylcholine. Again these results are in contrast to a number of published studies in which established NOS inhibitors such as L-NAME and L-NMMA have been shown to elicit a powerful and sustained vasopressor effect in both experimental animals and man (e.g. Aisaka *et al.*, 1989; Rees *et al.*, 1989; Petros *et al.*, 1991).

The lack of vasopressor effect of 7-NI and other indazoles presumably reflects an inability to inhibit endothelial NOS in these circumstances. In the accompanying paper (Babbedge *et al.*, 1993) we provide evidence that 7-NI potently inhibits bovine endothelial NOS *in vitro*. Although we cannot rule out the possibility of species differences in the effect of 7-NI on endothelial NOS the most likely explanation for the lack of vasopressor effect of 7-NI in the rat and mouse *in vivo* and in the rabbit aorta *in vitro* is an inability to access the cytosolic NOS across endothelial membranes. It might be argued that the lack of effect of 7-NI on MAP reflects inadequate absorption. However, this is clearly not the case since i.p. administration in mice (this study) and rats (Babbedge *et al.*, 1993) effectively inhibits cerebellar NOS activity. It is perhaps surprising that 7-NI, while clearly capable of crossing the blood brain barrier to access neuronal NOS, does not pass across endothelial membranes. It is tempting to speculate that 7-NI is taken up into the central nervous system by a carrier mechanism perhaps similar to that for L-tryptophan which has a chemically similar indole ring structure. Clearly, more information about the absorption and tissue distribution of 7-NI and related indazoles following parenteral administration is required.

The present data highlight the potential importance of 7-NI and perhaps other indazole derivatives as selective inhibitors of NOS in the central nervous system. In this context, 7-NI (or a derivative thereof) may provide an alternative approach to clinical analgesia. Furthermore, 7-NI may prove to be a useful tool with which to probe the functions of NO in the brain and or spinal cord. For example, one potential application of 7-NI is in the study of the role of NO in the phenomenon of neurodegeneration which, in recent years, has proved controversial. Thus, L-NAME has been reported to reduce infarct size in models of focal cerebral ischaemia in the rat (Buisson *et al.*, 1992; Trifiletti, 1992) and mouse (Nowicki *et al.*, 1991) and to attenuate NMDA-induced damage to hippocampal neurones in cell culture (Dawson *et al.*, 1991). In contrast, several researchers have either failed to identify a neuroprotective effect of L-NAME or have reported enhanced neuronal damage following administration of this inhibitor (Dawson *et al.*, 1992; Haberny *et al.*, 1992; Weissman *et al.*, 1992). As a further complication, Morikawa and colleagues (1992) have reported that L-arginine pretreatment also decreases infarct size following cerebral ischaemia in the rat. The precise reason for this divergence of data is not clear. However, locally produced NO is believed to play an important part in the control of cerebrovascular blood flow (Faraci, 1990). Furthermore, vasoconstriction induced by L-NAME in this vascular bed is reported to result in the uncoupling of cerebral blood flow and metabolism (Goadsby *et al.*, 1992; Dirnagl *et al.*, 1993) thereby exacerbating neuronal damage and masking any beneficial effect which may result from inhibition of neuronal NOS. Clearly, the lack of vasoconstrictor activity coupled with potent brain NOS inhibitory activity makes 7-NI the NOS inhibitor of choice when studying the role of NO in neurodegeneration and most probably in other central functions in which NO may play a part.

We would like to thank the MRC for financial support. R.C.B. is an SERC-CASE scholar with Wellcome Research Laboratories.

References

AISAKA, K., GROSS, S.S., GRIFFITH, O.W. & LEVY, R. (1989). N^G-methyl arginine, an inhibitor of endothelium-derived nitric oxide synthesis, is a potent pressor agent in the guinea pig; does nitric oxide regulate blood pressure in vivo? *Biochem. Biophys. Res. Commun.*, **160**, 881–886.

BABBEDGE, R.C., BLAND-WARD, P.A., HART, S.L. & MOORE, P.K. (1993). Inhibition of nitric oxide synthase by 7-nitro indazole and related substituted indazoles. *Br. J. Pharmacol.*

BUISSON, A., PLOTKINE, M. & BOULU, R.G. (1992). The neuroprotective effect of a nitric oxide inhibitor in a rat model of focal cerebral ischaemia. *Br. J. Pharmacol.*, **106**, 766–777.

BULLITT, E. (1990). Expression of a c-fos-like protein as a marker for neuronal activity following noxious stimulation in the rat. *J. Comp. Neurol.*, **296**, 517–530.

DAWSON, V.L., DAWSON, T.M., LONDON, E.D. & REIS, D.J. (1991). Nitric oxide mediates glutamate neurotoxicity in primary cortical cultures. *Proc. Natl. Acad. Sci. U.S.A.*, **88**, 6368–6371.

DAWSON, D.A., KUSUMOTO, K., GRAHAM, D.I. & MCCULLOCH, J. (1992). Inhibition of nitric oxide synthesis does not reduce infarct volume in a rat model of focal cerebral ischaemia. *Neurosci. Letts.*, **142**, 151–154.

DIRNAGL, U., LINDAUER, U. & VILLRINGER, A. (1993). Role of nitric oxide in the coupling of cerebral blood flow to neuronal activation in rats. *Neurosci. Letts.*, **149**, 43–46.

DUN, N.J., DUN, S.L., FORSTERMANN, U. & TSENG, L.F. (1992). Nitric oxide synthase immunoreactivity in rat spinal cord. *Neurosci. Letts.*, **147**, 217–220.

DWYER, M.A., BREDT, D.S. & SNYDER, S.H. (1991). Nitric oxide synthase: irreversible inhibition by L-N^G-nitro arginine in brain *in vitro* and *in vivo*. *Biochem. Biophys. Res. Commun.*, **176**, 1136–1141.

FARACI, F.M. (1990). Role of nitric oxide in regulation of basilar artery tone *in vivo*. *Am. J. Physiol.*, **259**, H1216–H1221.

FOSTER, S.J., BRUNEAU, P., WALKER, E.R.H. & MCMILLAN, R.M. (1989). 2-Substituted indazolinones: orally active and selective 5-lipoxygenase inhibitors with anti-inflammatory activity. *Br. J. Pharmacol.*, **99**, 113–118.

GOADSBY, P.J., KAUBE, H. & HOSKIN, K.L. (1992). Nitric oxide synthesis couples cerebral blood flow and metabolism. *Brain Res.*, **595**, 167–170.

HABERNY, K.A., POU, S. & ECCLES, C.U. (1992). Potentiation of quinolinate-induced hippocampal lesions by inhibition of NO synthesis. *Neurosci. Letts.*, **146**, 187–191.

HALEY, J.E., DICKINSON, A.H. & SCHACTER, M. (1992). Electrophysiological evidence for a role of nitric oxide in prolonged chemical nociception in the rat. *Neuropharmacology*, **31**, 251–258.

HOPE, B.E., MICHAEL, G.J., KNIGGE, K.M. & VINCENT, S.R. (1991). Neuronal NADPH diaphorase is a nitric oxide synthase. *Proc. Natl. Acad. Sci. U.S.A.*, **88**, 2811–2814.

HUNSKAAR, S. & HOLE, K. (1987). The formalin test in mice: dissociation between inflammatory and non-inflammatory pain. *Pain*, **30**, 103–114.

KITTO, K.F., HALEY, J.E. & WILCOX, G.L. (1992). Involvement of nitric oxide in spinally mediated hyperalgesia in the mouse. *Neurosci. Letts*, **148**, 1–5.

LEE, J.-H., WILCOX, G.L. & BEITZ, A.J. (1992). Nitric oxide mediates Fos expression in the spinal cord induced by mechanical noxious stimulation. *NeuroReport*, **3**, 841–844.

LISCIANI, R., SCORZA, BARCELLONA, P. & SILVESTRINI, B. (1968). Researches on the topical activity of benzydamine. *Eur. J. Pharmacol.*, **3**, 157–162.

LOWRY, O.H., ROSEBROUGH, N.J., FARR, A.L. & RANDALL, R.J. (1951). Protein measurement with Folin-phenol reagent. *J. Biol. Chem.*, **193**, 265–275.

MELLER, S.T., DYKSTRA, C. & GEBHART, G.F. (1992). Production of endogenous nitric oxide and activation of soluble guanylate cyclase are required for NMDA produced facilitation of the nociceptive tail flick reflex. *Eur. J. Pharmacol.*, **214**, 93–96.

MELLER, S.T. & GEBHART, G.F. (1993). Nitric oxide (NO) and nociceptive processing in the spinal cord. *Pain*, **52**, 127–136.

MONCADA, S., PALMER, R.M.J. & HIGGS, E.A. (1991). Nitric oxide: physiology, pathophysiology and pharmacology. *Pharmacol. Rev.*, **43**, 109–142.

MOORE, P.K., AL-SWAYEH, O.A., CHONG, N.W.S., EVANS, R.A. & GIBSON, A. (1990). L-N^G-nitro arginine (L-NOARG), a novel, L-arginine-reversible inhibitor of endothelium-dependent vasodilatation *in vitro*. *Br. J. Pharmacol.*, **99**, 408–412.

MOORE, P.K., OLUYOMI, A.O., BABBEDGE, R.C., WALLACE, P. & HART, S.L. (1991). L-N^G-nitro arginine methyl ester exhibits antinociceptive activity in the mouse. *Br. J. Pharmacol.*, **102**, 198–202.

MOORE, P.K., WALLACE, P., GAFFEN, Z., HART, S.L. & BABBEDGE, R.C. (1993). 7-nitro indazole, an inhibitor of nitric oxide synthase, exhibits antinociceptive activity in the mouse without increasing blood pressure. *Br. J. Pharmacol.*, **108**, 296–297.

MORIKAWA, E., HUANG, Z. & MOSKOWITZ, M.A. (1992). L-arginine decreases infarct size caused by middle arterial occlusion in SHR. *Am. J. Physiol.*, **263**, H1632–H1635.

MUSTAFA, A.A. (1992). Mechanisms of L-N^G-nitro arginine methyl ester-induced antinociception in mice: a role for serotonergic and adrenergic neurones. *General Pharmacol.*, **23**, 1177–1182.

NOWICKI, J.P., DUVAL, D., POIGENT, H. & SCATTON, B. (1991). Nitric oxide mediates neuronal death after focal cerebral ischaemia in the mouse. *Eur. J. Pharmacol.*, **204**, 339–340.

PETROS, A., BENNETT, D. & VALLANCE, P. (1991). Effect of nitric oxide synthase inhibitors on hypotension in patients with septic shock. *Lancet*, **338**, 1557–1558.

PINELLI, A., TRIVULZIO, S., MALVEZZI, L., ROSSONI, G. & BERTI, F. (1989). Antisecretory activity of 6-aminoindazole in rats. *Arzneim. Forsch.*, **39**, 361–365.

REES, D.D., PALMER, R.M.J. & MONCADA, S. (1989). Role of endothelium-derived nitric oxide in the regulation of blood pressure. *Proc. Natl. Acad. Sci. U.S.A.*, **86**, 3375–3378.

ROBERTSON, D.W., BLOOMQUIST, W., COHEN, M.L., REID, L.R. & SCHENK, K. (1990). Synthesis and biochemical evaluation of tritium labelled 1-methyl-N-(8-methyl-8-azabicyclo 3,2,1 oct-3-yl)-1H-indazole-3-carboxamide, a useful radioligand for 5-HT_3 receptors. *J. Med. Chem.*, **33**, 3176–3181.

SILVESTRINI, B., GARAU, A., POZZATTI, V., CIOLI, V. & CATANESE, B. (1966). Additional pharmacological studies of benzydamine. *Arch. Int. Pharmacodyn.*, **163**, 61–69.

SOLODKIN, A., TRAUB, R.J. & GEBHART, G.F. (1992). Unilateral hindpaw inflammation produces a bilateral increase in NADPH diaphorase histochemical staining in the rat lumbar spinal cord. *Neurosci.*, **51**, 495–500.

TRIFILETTI, R. (1992). Neuroprotective effect of N^G-nitro-L-arginine in focal stroke in the 7-day old rat. *Eur. J. Pharmacol.*, **218**, 197–198.

VALTSCHANOFF, J.G., WEINBERG, R.J., RUSTIONE, A. & SCHMIDT, H.W.W.W. (1992). Nitric oxide synthase and GABA co-localise in lamina II of rat spinal cord. *Neurosci. Letts.*, **148**, 6–10.

WEISSMAN, B.A., KADAR, T., BRANDEIS, R. & SHAPIRA, S. (1992). N(G)-Nitro-L-arginine enhances neuronal death following transient forebrain ischaemia in gerbils. *Neurosci. Letts.*, **146**, 139–143.

YEE, Y.K., BERNSTEIN, P.R., ADAMS, E.J., BROWN, F.J., CRONK, L.A., HEBBEL, K.C., VACEK, E.P., KRELL, R.D. & SNYDER, D.W. (1990). A novel series of selective leukotriene antagonists: exploration and optimisation of the acidic region in 1,6-disubstituted indoles and indazoles. *J. Med. Chem.*, **33**, 2443–2446.

(Received February 10, 1993
Revised April 26, 1993
Accepted May 6, 1993)

Br. J. Pharmacol. (1993), **110**, 225–228

Inhibition of rat cerebellar nitric oxide synthase by 7-nitro indazole and related substituted indazoles

R.C. Babbedge, P.A. Bland-Ward, S.L. Hart & [1]P.K. Moore

Pharmacology Group, Biomedical Sciences Division, King's College, University of London, Manresa Road, London SW3 6LX

1 7-Nitro indazole (7-NI) produces potent inhibition of rat cerebellar nitric oxide synthase (NOS) with an IC_{50} of 0.9 ± 0.1 μM ($n = 6$). NOS activity is dependent on the presence of both exogenous $CaCl_2$ and NADPH. The inhibitory potency of 7-NI remained unaltered in the presence of different concentrations of either $CaCl_2$ (0.75–7.5 mM) or NADPH (0.05–5.0 mM).

2 Kinetic (Lineweaver-Burke) analysis of the effect of 7-NI on rat cerebellar NOS revealed that inhibition was of a competitive nature with a K_i value of 5.6 μM. The K_m of cerebellar NOS with respect to L-arginine was 2.5 μM.

3 The following indazole derivatives (IC_{50} values shown in parentheses, all $n = 6$) caused concentration-related inhibition of rat cerebellar NOS *in vitro*: 6-nitro indazole (31.6 ± 3.4 μM), 5-nitro indazole (47.3 ± 2.3 μM), 3-chloro indazole (100.0 ± 5.5 μM), 3-chloro 5-nitro indazole (158.4 ± 2.1 μM) and indazole (177.8 ± 2.1 μM). The IC_{50} values for 5-amino indazole, 6-amino indazole and 6-sulphanilimido indazole were in excess of 1 mM; 3-indazolinone was inactive.

4 7-NI (10 mg kg^{-1}) administered i.p. to rats produced 60 min thereafter a significant inhibition of NOS activity in cerebellum ($31.1 \pm 3.2\%$, $n = 6$), cerebral cortex ($38.2 \pm 5.6\%$, $n = 6$), hippocampus ($37.0 \pm 2.8\%$, $n = 6$) and adrenal gland ($23.7 \pm 3.0\%$, $n = 6$). NOS activity in olfactory bulb and stomach fundus were unchanged.

5 These results indicate that 7-NI is a potent and competitive inhibitor of rat brain NOS *in vitro* and also inhibits NOS in different brain regions and in the adrenal gland *in vivo*. Inhibition of NOS is a characteristic property of the indazole nucleus. Nitration of the indazole ring at positions 5, 6 and 7 results in a graded increase in inhibitory potency. Indazole-based inhibitors of NOS may prove useful tools with which to evaluate the biological roles of nitric oxide in the central nervous system.

Keywords: 7-Nitro indazole; substituted indazole derivatives; cerebellar nitric oxide synthase; nitric oxide; rat cerebellum; rat spleen; bovine endothelial cells

Introduction

We have recently shown that 7-nitro indazole (7-NI) inhibits rat and mouse cerebellar nitric oxide synthase (NOS) with equivalent potency to established inhibitors of this enzyme such as L-N^G-nitro arginine methyl ester (L-NAME) and L-N^G-monomethyl arginine (L-NMMA) (Moore *et al.*, 1993a). In the accompanying paper (Moore *et al.*, 1993b) we provide evidence that 7-NI, 6-nitro indazole and indazole elicit antinociception in the mouse utilising the formalin-induced hindpaw licking and acetic acid induced-abdominal constriction assays. None of the indazole derivatives investigated influenced mouse blood pressure. In this paper we have compared the ability of indazole plus nine mono- or di-substituted derivatives of indazole to inhibit rat brain cerebellar NOS *in vitro* and have further characterized the mechanism of action and isoform selectivity of 7-NI both *in vitro* and following i.p. administration in the rat.

Methods

Preparation and assay of rat cerebellar NOS

Male rats (Sprague-Dawley, 200–300 g) were killed by a blow to the head and exsanguination. Cerebella were removed, weighed and homogenized in an Ultra-Turrax (type 18/2N) homogenizer in 10 volumes of 20 mM Tris HCl buffer (pH 7.4) containing 2 mM EDTA. In some experiments, cerebella were stored at − 70°C until required. Homogenates were centrifuged (10,000 *g*) for 15 min at 4°C. NOS was assayed by monitoring the conversion of [^{3}H]-arginine to [^{3}H]-citrulline as described by Dwyer *et al.* (1991). Incubations (15 min at 0°C followed by 15 min at 37°C) routinely contained 25 μl cerebellar supernatant, 0.5 μCi [^{3}H]-L-arginine (concentration = 120 nM), 0.75 mM $CaCl_2$, 0.5 mM NADPH and 5 μl water or drug solution in a total volume of 105 μl. In some experiments the concentrations of NADPH and $CaCl_2$ were varied from 0.5–5.0 mM and 0.37–7.5 mM respectively. In order to determine the K_m of rat cerebellar NOS for L-arginine and the K_i for 7-NI against this enzyme the concentration of L-arginine in the incubation medium was also varied in some experiments from 0.1–10 μM. Preliminary investigation of the time course of NOS activity under these conditions revealed that [^{3}H]-citrulline formation was linear up to 5 min.

Accordingly, for these experiments incubations were carried out at 37°C for 3 min. All assays were terminated by addition of 3 ml HEPES buffer (pH 5.5) containing 2 mM EDTA and incubates applied to 0.5 ml columns of Dowex AG50WX-8 (Na^+ form) followed by 0.5 ml distilled water to remove unchanged [^{3}H]-arginine. [^{3}H]-citrulline was quantified by liquid scintillation spectroscopy of a 1 ml aliquot of the combined flow-through. Protein concentration was measured by the method of Lowry *et al.* (1951).

Preparation of rat spleen and bovine endothelial cell NOS

Male rats (Sprague-Dawley, 220–250 g) were anaesthetized by i.p. administration of urethane (10 g kg^{-1}). Spleen NOS enzyme was induced by i.p. administration of 5.0 mg kg^{-1} *E. coli* lipopolysaccharide (serotype 0127:B8) and animals killed by cervical dislocation 6 h later. The spleen was removed, weighed, homogenized in 20 mM Tris-HCl buffer (pH 7.4) and assayed for NOS as described above with the exception

[1] Author for correspondence.

that $CaCl_2$ was omitted from the incubation medium. Bovine aortae were obtained from a local slaughterhouse. Vascular endothelial cells were removed by careful rubbing of the intimal surface with a scalpel blade. The crude cell suspension was washed twice with phosphate buffered saline, centrifuged (1000 *g*, 5 min, 4°C) and endothelial cells subsequently homogenized in 50 mM Tris-HCl buffer (pH 7.4) containing 0.1 mM EDTA, 0.1 mM EGTA and 0.1% 2-mercaptoethanol with 25 passes of a glass teflon Dounce homogenizer. Crude homogenate was subsequently assayed for NOS as described above.

Pretreatment of rats with 7-NI

Male rats (Sprague-Dawley, 200–220 g) were injected i.p. with 7-NI (10 mg kg^{-1}) or an appropriate volume of vehicle (arachis oil, 0.1 ml 100 g^{-1}) and killed 60 min later by a blow to the head and exsanguination. Brains were removed and the cerebellum, hippocampus, cerebral cortex and olfactory bulb dissected. Stomach fundus and adrenal medulla were also removed. All brain regions/organs were weighed and homogenized in 20 mM Tris-HCl buffer (pH 7.4). In preliminary experiments low levels of NOS were detected in cerebral cortex, stomach fundus and adrenal gland. In order to optimize [^{3}H]-citrulline production all brain regions/organs used in this part of the study were applied to 0.3 ml columns of Dowex AG50WX-8 to remove endogenous L-arginine prior to assay for NOS as described above.

Drugs and chemicals

Indazole, 5-nitro indazole, 6-nitro indazole, 5-amino indazole, 6-amino indazole, 3-chloro indazole, 3-chloro 5-nitro indazole, 3-indazolinone and 6-sulphanilimido indazole were purchased from Aldrich Ltd. 7-Nitro indazole was obtained from MTM Lancaster Ltd. Radiolabelled [^{3}H]-arginine (sp. act. 62 Ci $mmol^{-1}$) was obtained from Amersham. L-N^G-nitro arginine methyl ester hydrochloride (L-NAME), L-arginine hydrochloride and NADPH were purchased from Sigma Ltd. Dowex AG50WX-8 H^+ form (Sigma Ltd.) was converted into the Na^+ form by soaking for 2 h in 2 M NaOH. For *in vivo* experiments 7-NI was dissolved in arachis oil. For *in vitro* experiments 7-NI and all other indazole derivatives were dissolved in Na_2CO_3 (0.5%, w/v). Drug stocks were prepared fresh on the morning of each experiment.

Statistical analysis

Results indicate mean ± s.e.mean. Statistical significance of differences between groups was determined by unpaired Student's *t* test. A probability (*P*) value of 0.05 or less was taken to indicate statistical significance.

Results

Effect of indazole derivatives on rat cerebellar NOS

Three of the ten indazole derivatives examined in this study (5-amino indazole, 6-amino indazole and 6-sulphanalimido indazole) failed to achieve > 50% inhibition of NOS activity at the highest concentration employed (1 mM). Calculated IC_{15}s for these derivatives were 237.1 ± 20.9 μM, 501.2 ± 25.4 μM and 133.3 ± 9.9 μM (all $n = 6$) respectively. A fourth compound, 3-indazolinone, failed to inhibit rat cerebellar NOS at a concentration of 1 mM. Concentration-inhibition curves for the remaining indazole derivatives examined are shown in Figure 1a, b. The rank order of potency with IC_{50} concentrations shown in parentheses (all $n = 6$) were as follows: 7-nitro indazole (0.9 ± 0.1 μM) > 6-nitro indazole (31.6 ± 3.4 μM) > 5-nitro indazole (47.3 ± 2.3 μM) > 3-chloro indazole (100.0 ± 5.5 μM) > 3-chloro 5-nitro indazole (158.4 ± 2.1 μM) > indazole (177.8 ± 2.1 μM). For comparison, the IC_{50}s for other inhibitors of NOS under identical experimental conditions were L-NAME, 0.9 ± 0.08 μM and L-NMMA, 3.4 ± 0.4 μM ($n = 6$).

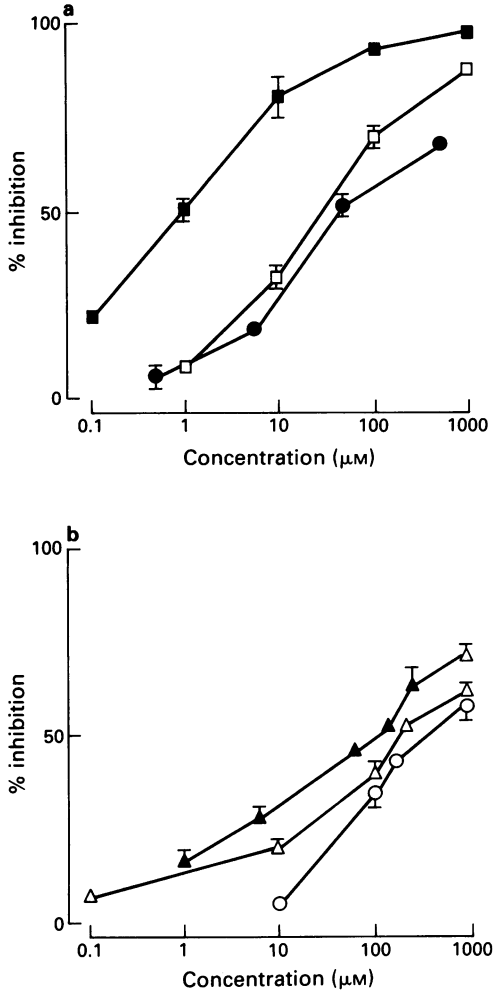

Figure 1 Concentration-response curves for inhibition of rat cerebellar nitric oxide synthase (NOS) activity by (a), 7-nitro indazole 7-NI (■); 6-nitro indazole (□); 5-nitro indazole (●) and (b), 3-chloro indazole (▲); 3-chloro 5-nitro indazole (△) and indazole (○). Results show % inhibition of NOS and are mean ± s.e.mean, $n = 6$.

Effect of substrate and cofactor concentration on inhibition of rat cerebellar NOS by 7-NI

In an attempt to obtain further information about the mechanism of action of 7-NI, additional experiments were undertaken to examine the NOS inhibitory effect of this derivative in the presence of varying concentrations of NADPH, $CaCl_2$ and L-arginine.

In the absence of added NADPH, rat cerebellar NOS activity was reduced by > 99% (0.04 ± 0.02 pmol citrulline mg^{-1} 15 min^{-1}, cf. 17.3 ± 0.4 pmol citrulline mg^{-1} 15 min^{-1} in the presence of 0.5 mM NADPH, $n = 6$, $P < 0.005$). A lower concentration of NADPH (0.05 mM) did not significantly alter NOS activity (17.9 ± 0.6 pmol citrulline mg^{-1} 15 min^{-1}, $n = 6$, $P > 0.05$) whilst at higher concentration (5 mM) NOS activity was reduced (9.5 ± 0.5 pmol mg^{-1} 15 min^{-1}, $n = 6$, $P < 0.01$). An approximate IC_{50} concentration of 7-NI (1 μM) produced similar % inhibition of NOS regardless of the concentration of NADPH in the incubation (e.g. 0.05 mM, 51.6 ± 0.5%; 0.5 mM, 53.9 ± 2.7%; 5.0 mM, 50.3 ± 2.3%, all $n = 6$). Reducing the concentration of added

$CaCl_2$ in the incubation to 0.37 mM or 0.17 mM completely abolished rat cerebellar NOS activity (data not shown). It should be emphasised that these values do not reflect free calcium concentration in the incubation which were not measured in the present study but would be expected to be considerably lower. At higher $CaCl_2$ concentrations, 7-NI (10 μM) produced similar inhibition of rat cerebellar NOS regardless of the concentration of $CaCl_2$ in the incubation (e.g. 0.75 mM, 76.4 ± 0.7%; 1.8 mM, 74.6 ± 0.7%; 3.7 mM, 87.2 ± 2.0%; 7.5 mM, 82.8 ± 0.6%, all $n = 6$). Clearly, it was not possible to assess the effect of 7-NI in the presence of $CaCl_2$ concentrations lower than 0.75 mM.

In order to investigate the possible interaction of 7-NI with a substrate binding site on rat cerebellar NOS, experiments were conducted in the presence of 0.1–10.0 μM L-arginine. A double reciprocal (Lineweaver-Burke) plot of cerebellar NOS in the presence and absence of 7-NI (10 μM) is shown in Figure 2. The calculated K_m for L-arginine was 2.5 μM whilst the K_i for 7-NI was 5.6 μM.

Effect of 7-NI on NOS from other tissue sources

Both spleen removed from endotoxin pretreated (induced) rats and bovine endothelial cells exhibited significant NOS activity (0.98 ± 0.14 pmol citrulline mg^{-1} $15\ min^{-1}$ and 3.7 ± 0.14 pmol citrulline mg^{-1} $15\ min^{-1}$, respectively, $n = 6$). 7-NI inhibited rat spleen (IC_{50}, 57.0 ± 5.5 μM, $n = 6$) and bovine endothelial cell (IC_{50}, 0.7 ± 0.2 μM, $n = 6$) NOS. 7-NI was more potent than L-NAME as an inhibitor of the endothelial cell (cf. IC_{50} for L-NAME, 6.5 ± 1.1 μM, $n = 6$) but less potent as an inhibitor of the induced spleen enzyme (cf. IC_{50} for L-NAME, 9.0 ± 0.7 μM, $n = 6$).

Inhibition of NOS following administration of 7-NI in the intact rat

NOS activity in cerebellum, cerebral cortex and hippocampus was reduced by approximately 30–38% 60 min after i.p. administration of 7-NI (10 mg kg^{-1}). In contrast, adrenal NOS activity was reduced by only 23.9 ± 2.8% ($n = 6$). Olfactory bulb and stomach fundus NOS activity were unchanged (Table 1).

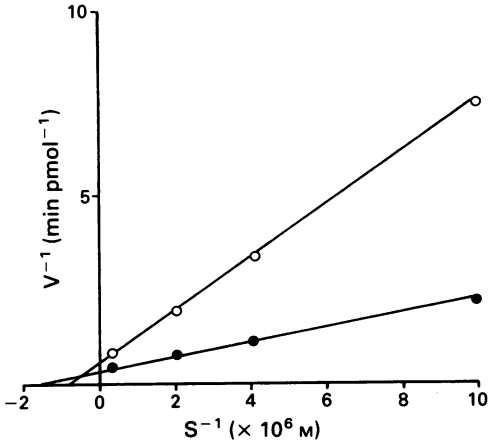

Figure 2 Double reciprocal analysis of the inhibitory effect of 7-NI (10 μM) against rat cerebellar NOS using increasing concentrations of L-arginine (0.1–10 μM) as substrate: (●) experiments carried out in the absence and (○) in the presence of 7-NI. Results show the reciprocal of the initial rate of [^{3}H]-citrulline formation monitored over the first 3 min incubation plotted against the reciprocal of L-arginine concentration in μM. Data indicate the mean results from 3 separate experiments in which NOS activity was monitored in triplicate. Standard errors fall within the dimensions of the symbols.

Table 1 Effect of 7-nitro indazole (7-NI) administered i.p. in rats on nitric oxide synthase (NOS) activity in different brain regions/organs

	Citrulline biosynthesis	
	Control	*7-NI*
Cerebellum	40.5 ± 1.8	27.9 ± 1.3*
Cerebral cortex	8.9 ± 0.3	5.5 ± 0.5*
Hippocampus	10.8 ± 0.5	6.8 ± 0.3*
Olfactory bulb	16.4 ± 0.8	17.7 ± 0.8
Adrenal gland	13.5 ± 0.4	10.3 ± 0.4*
Stomach fundus	7.1 ± 0.4	7.6 ± 0.5

NOS activity is expressed as citrulline formation (pmol mg^{-1} protein $15\ min^{-1}$) in organs removed from rats 60 min following i.p. injection of 7-NI (10 mg kg^{-1}) or arachis oil (0.1 ml kg^{-1}, control). Results show mean ± s.e.mean of 6 observations.
*$P < 0.05$.

Discussion

The present data indicate that 7-NI inhibits rat cerebellar NOS with a potency similar to that of L-NAME and L-NMMA (Moore *et al.*, 1993a). The principal aim of the present investigation has been to provide a more detailed characterization of the NOS inhibitory effect of 7-NI and related indazole compounds and to investigate the effect of 7-NI on NOS activity in a range of organs *in vivo*.

Preliminary experiments demonstrated that the crude (10,000 *g*) rat cerebellar NOS used in this study required exogenous NADPH and Ca^{2+} for activity. Optimum enzyme activity occurred at a concentration of 0.05–0.5 mM NADPH and 0.75 mM $CaCl_2$. The absolute dependence of brain NOS on exogenous calcium has been noted previously (Knowles *et al.*, 1989; Mayer *et al.*, 1990) although the finding that high concentrations of NADPH inhibit cerebellar NOS does not appear to have been reported. The explanation of this phenomenon is not clear although it is conceivable that crude rat cerebellar supernatant may contain additional enzymes capable of oxidising NADPH into NADP which, in turn, may inhibit NOS. Kinetic analysis of cerebellar NOS revealed a K_m for L-arginine of 2.5 μM which is similar to previously published data for this enzyme from rat cerebellum (Schmidt *et al.*, 1991), rat cerebral cortex (Knowles *et al.*, 1989), bovine endothelial cells (Pollock *et al.*, 1991) and mouse macrophages (Stuehr *et al.*, 1991).

Reported inhibitors of NOS generally fall into one of three main classes, (a) guanidino-monosubstituted substrate analogues such as L-NAME and L-NMMA, (b) calmodulin antagonists (Bredt & Snyder, 1990) and (c) agents which interfere with the binding of cofactor, NADPH, such as diphenylene iodonium and its derivatives (Stuehr *et al.*, 1991). To this list may be added agents which sequester free Ca^{2+} since, as indicated in these experiments, rat cerebellar NOS has an absolute requirement for this cation. Of these possible mechanisms of action of 7-NI, an interaction with the NADPH binding site can be excluded since varying the concentration of NADPH in the incubation medium did not influence the inhibitory potency of 7-NI. Furthermore, inhibition of NOS by 7-NI was unaltered in the presence of a range of $CaCl_2$ concentrations implying that sequestration of Ca^{2+} ions (i.e. an EDTA-like effect) is not involved. Although not investigated in the present study we also believe it unlikely that calmodulin antagonist activity contributes to the mechanism of action of 7-NI since the concentration of calmodulin antagonists required to inhibit NOS are considerably greater than the equi-effective concentration of 7-NI (Bredt & Synder, 1990). Furthermore, chlorpromazine, a known calmodulin antagonist, exhibits only very weak inhibition of rat cerebellar NOS (e.g. 100 μM, 22.6 ± 0.8% inhibition of [^{3}H]-citrulline formation, Babbedge & Moore, unpublished).

In contrast, we present here direct evidence from double reciprocal analysis of the inhibitory effect of 7-NI in the presence of varying concentrations of L-arginine that inhibition results from a competitive interaction of 7-NI with the L-arginine binding site on cerebellar NOS. The calculated K_i for 7-NI is in the low micromolar range. It could also be argued that the relatively short-lived inhibition of cerebellar NOS following i.p. administration of 7-NI in the mouse (Moore *et al.*, 1993b) provides further evidence for a competitive (reversible) mechanism of action although, of course, we cannot exclude the possibility that this apparently transient effect of 7-NI relates not to its interaction with NOS but to rapid metabolic breakdown.

The effect of 7-NI on NOS in supernatants prepared from a variety of tissue sources has also been investigated. Compared with L-NAME, 7-NI has equivalent or greater potency as an inhibitor of the constitutive isoform of this enzyme found in rat cerebellum and bovine endothelial cells. In contrast, 7-NI is some 6 times less potent than L-NAME against the inducible isoform of the enzyme located in the spleen from endotoxin-pretreated rats. Clearly, further experiments are required to determine the ability of 7-NI to inhibit the inducible isoform of NOS in, for example, leucocytes or vascular smooth muscle cells.

Administration of 7-NI to intact rats has provided further information about the tissue-specific effect of this inhibitor on a number of different NOS enzymes within the body. Thus, 60 min after i.p. administration of 7-NI (10 mg kg^{-1}), NOS activity was reduced to an almost equal extent in rat cerebral cortex, cerebellum and hippocampus and to a lesser extent in adrenal gland. In contrast, NOS activity in olfactory bulb and stomach fundus were not significantly reduced. At first sight these data appear to provide further evidence for a differential inhibitory effect of 7-NI on NOS in different target organs. However, we cannot rule out the possibility that inhibition of NOS following 7-NI administration reflects the relative blood flow and/or uptake (and hence exposure to 7-NI) or individual brain regions as well as stomach fundus and adrenal gland. Clearly, a better understanding of the uptake and distribution of 7-NI following parenteral administration in different species is necessary. Such experiments in the mouse and rat are currently in progress in this laboratory. Whatever the precise mechanism it is clear from this study that 7-NI administration *in vivo* preferentially inhibits NOS in selected brain regions.

Preliminary evaluation of the structure-activity relationship for inhibition of rat cerebellar NOS using a series of chemically related indazole derivatives has been undertaken. Examination of the ability of ten indazole derivatives to inhibit NOS reveals that nitration of the benzene ring at the 5, 6 or 7 positions results in the production of potent inhibitors of this enzyme. Ring substitution with an $-NO_2$ group has an electron withdrawing effect from the benzene ring and may therefore lead to the formation of a more polarised molecule. The precise position of the $-NO_2$ within the ring is also clearly of importance with 7-NI some 35 times and 55 times more potent than the corresponding 6-nitro and 5-nitro derivatives respectively. Interestingly, amination of the benzene ring at position 5 or 6 effectively removes the residual NOS inhibitory effect of the parent molecule, indazole, whilst chlorination at position 3 of the pyrazole ring significantly reduces the inhibitory effect of 5-nitro indazole. Since ring substitution with either $-NO_2$ or $-Cl$ groups has the opposite effect to nitration viz. an electron donating function, it is tempting to suggest that indazole derivatives substituted with alternative electron withdrawing groups such as a tertiary amine or perhaps cyanoindazole derivatives may also exhibit potent NOS inhibitory activity.

The present study provides evidence that 7-NI is a competitive inhibitor of rat cerebellar NOS with potency similar to or greater than that of L-NAME and L-NMMA. Of the indazole compounds tested, 7-NI is the most potent NOS inhibitor. This observation, coupled with potent antinociceptive activity and lack of cardiovascular and other side effects *in vivo* within this group provides additional impetus for the development of novel indazole-based NOS inhibitors with which to study the central pharmacology of the NO system. Moreover, the possibility that 7-NI, or a chemically related compound, may also prove of clinical benefit in analgesia has been discussed in the accompanying paper (Moore *et al.*, 1993b). Information provided here concerning the structure-activity relationship for indazole based NOS inhibitors may prove useful in the search for such novel therapeutic agents.

We would like to thank the MRC for financial support. R.C.B. is an SERC-CASE scholar with Wellcome Research laboratories. P.B.-W. is supported by a studentship from Glaxo Group Research.

References

BREDT, D.S. & SNYDER, S.H. (1990). Isolation of nitric oxide, synthetase, a calmodulin-requiring enzyme. *Proc. Natl. Acad. Sci. U.S.A.*, **87**, 682–685.

DWYER, M.A., BREDT, D.S. & SNYDER, S.H. (1991). Nitric oxide synthase: irreversible inhibition by L-N^G-nitro arginine in brain in vitro and in vivo. *Biochem. Biophys. Res. Commun.*, **176**, 1136–1141.

KNOWLES, R.G., PALACIOS, M., PALMER, R.M.J. & MONCADA, S. (1989). Formation of nitric oxide from L-arginine in the central nervous system: a transduction mechanism for stimulation of the soluble guanylate cyclase. *Proc. Natl. Acad. Sci. U.S.A.*, **86**, 5159–5162.

LOWRY, O.H., ROSEBROUGH, N.J., FARR, A.L. & RANDALL, R.J. (1951). Protein measurement with Folin-phenol reagent. *J. Biol. Chem.*, **193**, 265–275.

MAYER, B., JOHN, M. & BOHME, E. (1990). Purification of a Ca^{2+}/calmodulin dependent nitric oxide synthase from porcine cerebellum. *FEBS Letts.*, **277**, 215–219.

MOORE, P.K., WALLACE, P., GAFFEN, Z., HART, S.L. & BABBEDGE, R.C. (1993a). 7-nitro indazole, an inhibitor of nitric oxide synthase, exhibits anti-nociceptive activity in the mouse without increasing blood pressure. *Br. J. Pharmacol.*, **108**, 296–297.

MOORE, P.K., WALLACE, P., GAFFEN, Z., HART, S.L. & BABBEDGE, R.C. (1993b). Characterization of the novel nitric oxide synthase inhibitor 7-nitro indazole and related indazoles: antinociceptive and cardiovascular effects. *Br. J. Pharmacol.*, **110**, 219–224

POLLOCK, J.S., FORSTERMANN, U., MITCHELL, J.A., WARNER, T.D., SCHMIDT, H.H.H.W., NAKANE, M. & MURAD, F. (1991). Purification and characterisation of particulate endothelium-derived relaxing factor synthase from cultured and native bovine aortic endothelial cells. *Proc. Natl. Acad. Sci. U.S.A.*, **88**, 10480–10484.

SCHMIDT, H.H.H.W., POLLOCK, J.S., NAKANE, M., GORSKY, L.D., FORSTERMANN, U. & MURAD, F. (1991). Purification of a soluble isoform of guanylyl cyclase-activating factor synthase. *Proc. Natl. Acad. Sci. U.S.A.*, **88**, 365–369.

STUEHR, D.J., CHO, H.J., KWON, N.S., WEISE, M. & NATHAN, C.F. (1991). Purification and characterisation of the cytokine induced macrophage nitric oxide synthase: an FAD and FMN-containing flavoprotein. *Proc. Natl. Acad. Sci. U.S.A.*, **88**, 7773–7777.

(Received February 10, 1993
Revised April 29, 1993
Accepted May 6, 1993)

Br. J. Pharmacol. (1993), **110**, 229–234

Interaction of nitric oxide and salivary gland epidermal growth factor in the modulation of rat gastric mucosal integrity

[1]B.L. Tepperman & B.D. Soper

Department of Physiology, Faculty of Medicine, University of Western Ontario, London, Ontario, Canada N6A 5C1

1 The interaction between endogenous nitric oxide (NO) and factors from the rat submandibular salivary gland such as epidermal growth factor (EGF) on gastric mucosal integrity in the rat has been investigated.

2 Bolus administration of the NO synthase inhibitor, N^G nitro-L-arginine methyl ester (L-NAME; 6.25–50 mg kg^{-1}, i.v.) to animals treated intraluminally with 0.15 N HCl resulted in a significant increase in the area of mucosal haemorrhagic damage at doses 12.5 and 50 mg kg^{-1}. Concurrent administration of indomethacin (5 mg kg^{-1}, i.v.) resulted in a significant haemorrhagic mucosal damage in response to L-NAME (12.5–50 mg kg^{-1}). Administration of the highest dose of L-NAME resulted in an increase in histological damage to the rat gastric mucosa.

3 When compared to control animals, the extent of damage produced by L-NAME or L-NAME in combination with indomethacin was significantly exacerbated in rats which had been sialoadenectomized (SALX) by removal of the submandibular salivary glands. The mucosal damage in SALX rats was ameliorated by treatment with EGF (5 and 10 $\mu g\ kg^{-1}$, i.v.).

4 L-NAME administration resulted in a small reduction of gastric mucosal blood flow as assessed by laser Doppler flowmetry (LDF). The reduction in LDF by 25 and 50 mg kg^{-1} L-NAME was significantly greater in SALX rats than in rats with intact salivary glands. Pretreatment of SALX rats with indomethacin did not augment this large decrease in LDF suggesting that endogenous prostanoids do not interact with NO and salivary factors in regulating mucosal microcirculation.

5 Mucosal NO biosynthesis as assessed by [^{14}C]-citrulline formation was reduced in SALX rats when compared to control animals. Pretreatment of SALX animals with parenterally-administered EGF (10 $\mu g\ kg^{-1}$) was associated with an increase in [^{14}C]-citrulline formation in the gastric mucosa to levels observed in control SALX rats.

6 These data suggest that factors which originate from the salivary gland such as EGF interact with NO in the maintenance of mucosal integrity. The effects may be mediated at least in part by changes in gastric mucosal blood flow. Salivary glands and EGF may mediate these effects to some extent via changes in mucosal NO biosynthesis.

Keywords: Nitric oxide; salivary gland; epidermal growth factor; gastric mucosal integrity; gastric mucosal blood flow; N^G-nitro-L-arginine methyl ester; prostanoids

Introduction

The endothelium-derived vasodilator, nitric oxide, NO (Palmer *et al.*, 1987; Khan & Furchgott, 1987) plays a role in the regulation of the gastric microcirculation (Pique *et al.*, 1989; Whittle & Tepperman, 1991; Tepperman & Whittle, 1992). Furthermore, NO has been shown to interact with prostanoids and with sensory neuropeptides in the modulation of mucosal integrity (Whittle *et al.*, 1990; Tepperman & Whittle, 1991) and this may involve effects on both mucosal blood flow and the continuity of the microvasculature.

Epidermal growth factor (EGF) is a polypeptide originally isolated from the rodent submandibular salivary gland (Cohen, 1962). EGF administration has been shown to promote healing of duodenal ulcers and attenuate gastric mucosal damage in response to ethanol (Pilot *et al.*, 1979; Olsen *et al.*, 1984). Removal of the salivary glands in rats has been shown to increase the susceptibility of the gastric mucosa to ulcerogens and this damage could be reduced by EGF treatment (Skinner *et al.*, 1981; Olsen *et al.*, 1984). EGF has also been shown to contract isolated strips of vascular smooth muscle (Berk *et al.*, 1985; Muramatsu *et al.*, 1985) and to exert vasodilator actions on the splanchnic circulation (Gan *et al.*, 1987a,b). Therefore EGF may influence mucosal integrity via an action on the gastric microcirculation. Furthermore EGF has been shown to interact with sensory neuropeptides in the maintenance of gastric mucosal integrity (Evangelista *et al.*, 1991a,b). Since it is known that NO, prostanoids and neuropeptides from capsaicin-sensitive afferent fibres interact to influence gastric microcirculation and integrity, it is possible that similar interactions between NO and factors of salivary gland origin may also occur.

In the present study we have examined the possible interaction between endogenous NO, and EGF from the salivary gland. In order to examine these interactions we have investigated the pro-ulcerogenic actions of an inhibitor of NO formation, N^G-nitro-L-arginine methyl ester (L-NAME) in animals in which the submandibular salivary glands have been surgically extirpated.

Methods

Animal preparation

Male Sprague Dawley rats (200–250 g) were used in these studies. Sialoadenectomy (SALX) was performed under pentobarbitone anaesthesia (60 mg kg^{-1}, i.p.) by removal of the submandibular-sublingual salivary gland complexes after ligation of the ducts as previously described (Skinner & Tepperman, 1981; Skinner *et al.*, 1984). Sham-operated rats served as controls. Animals were used 2–3 weeks after surgery. Effective sialoadenectomy was confirmed by the observation of an increase in prandial drinking by approx-

[1] Author for correspondence.

imately 200% compared to control animals (Epstein *et al.*, 1964). All experimental procedures were subsequently done on rats which were deprived of food but not water for 18–20 h before the experiments. For each experiment, rats were anaesthetized with sodium pentobarbitone (60 mg kg^{-1}, i.p.). All agents were administered intravenously via a catheter inserted into the tail vein.

Measurement of gastric mucosal damage

In anaesthetized rats, the stomach was exposed by a mid-line incision. After ligating the oesophagus and pylorus, 2 ml of acid saline (150 mN HCl in 150 mM NaCl) was instilled into the gastric lumen through the forestomach, followed by bolus intravenous administration of the agents under investigation. L-NAME was administered in a dose of 6.25–50 mg kg^{-1} via the tail vein. In some experiments indomethacin (5 mg kg^{-1}, i.v.) was given and 5 min later L-NAME was injected. Finally in some experiments epidermal growth factor (EGF) was injected intravenously (5 or 10 μg kg^{-1}) 15 min before administration of indomethacin and L-NAME. All injections were made in volumes of 0.5 ml or less. Thirty min after the last injection the animals were killed by cervical dislocation, the stomachs were excised and opened along the greater curvature, pinned to a wax block with the mucosal side up, immersed in neutral buffered formalin and then photographed on colour transparency film. The extent of macroscopically-visible damage was determined from these projected transparencies via computerized planimetry by the Sigma Scan programme (Mandel Scientific, Corte Madera, Calif., U.S.A.). The area of haemorrhagic mucosal damage was calculated as the % of the total gastric mucosal area.

A sample of gastric corpus (0.5 × 1.5 cm) was excised from either the dorsal or ventral aspect of the corpus mucosa, 0.5 cm below the limiting ridge, and was processed by routine techniques before being embedded in paraffin. Sections (4 μm) were stained with haematoxylin and eosin and examined under a light microscope. A 1 cm length of each histological section was assessed for epithelial cell damage (a score of 1 being assigned); glandular disruption, vasocongestion or oedema in the upper mucosa (a score of 2 being assigned); haemorrhagic damage in the mid to lower mucosa (a score of 3) and deep necrosis and ulceration (a score of 4). Each section was evaluated on a cumulative basis to give the histological damage index, the maximum score thus being 10. All determinations were performed in a randomized manner with both transparencies and histological sections coded to eliminate observer bias.

Assessment of gastric mucosal blood flow

In a separate group of experiments, the effects of L-NAME (6.25–50 mg kg^{-1}, i.v.) gastric mucosal blood flow in the presence or absence of indomethacin was assessed by laser Doppler flowmetry. Experiments were done on pentobarbitone-anaesthetized rats. The stomach was exposed by a mid-line incision. A small bore (8.5 mm o.d.) plastic cannula was then inserted via a small incision in the forestomach and tied in place, to allow free access to the gastric lumen. Gastric blood flow was recorded continuously with a laser Doppler blood flow monitor (Periflux 3; Perimed, Piscataway New Jersey, U.S.A.). A stainless steel laser optic probe (1.9 mm o.d.; Perimed) was inserted into the gastric lumen via the plastic cannula and was allowed to rest gently on the gastric corpus mucosa. Changes in laser Doppler flow (LDF) were assessed in response to intravenous bolus injection (0.5 ml kg^{-1}) of isotonic saline or the compound under investigation. Average LDF values in sham-operated and SALX rats were determined for a 3 min period prior to administration of L-NAME, indomethacin and/or EGF. Similarly the average LDF was calculated for a 3 min period, 15 min after injection of the agents where values of LDF had stabilized. Changes in LDF from pretreatment values were estimated with a software programme designed for use with the PeriFlux laser Doppler flowmeter (Perisoft; Perimed). The mean systemic arterial blood pressure (BP) was also measured from a cannula inserted into a carotid artery connected to a pressure transducer (Cobe CDX3, Lakewood, Colo., U.S.A.) and a chart researcher (Grass, model 79C).

Estimation of NO synthase activity

Experiments were done *in vitro* using segments of excised gastric mucosa. Gastric tissue was taken from pentobarbitone-anaesthetized sham-operated or SALX rats treated with saline or EGF (10 μg kg^{-1}, i.v.) as previously described. After treatment, rats were killed by cervial dislocation. The excised stomach was opened along the greater curvature. The mucosa was rinsed in ice-cold saline, scraped free of the underlying muscle with a blunt scalpel, weighed and placed in a preparative buffer consisting of 10 mM HEPES, 0.32 M sucrose, 0.1 mM EDTA, 1 mM dithiothreitol, 10 μg ml^{-1} soybean trypsin inhibitor, 10 μg ml^{-1} leupeptin, and 2 μg ml^{-1} aprotinin (pH 7.4). Samples were homogenized for 15 s in a Tekmar Ultra-Turrax homogenizer (Model SDT; Cincinnati, Ohio, U.S.A.) and then centrifuged at 10,000 *g* for 20 min at 4°C. NO synthase activity was estimated from the conversion of [^{14}C]-arginine to the NO co-product citrulline as described by Knowles *et al.* (1990). Briefly, the assay system (50 μl total volume, pH 7.2) contained 20 μl of broken cell supernatant and the following components (final concentrations): 30 mM potassium phosphate, 150 μM $CaCl_2$, 15 μM [^{14}C]-L-arginine (700,000 d.p.m. ml^{-1}), 0.7 mM NADPH, as well as 7 mM L-valine to inhibit any arginase. Incubations proceeded for 10 min at 37°C, after which time 1 ml of a 1:1 suspension of Dowex 50W in water was added to bind arginine. The resin was allowed to settle, and the supernatant was removed for estimation of the radiolabelled products by liquid scintillation counting. Product formation that was inhibited by removal of Ca^{2+} (1 mM EGTA in the assay system) or by 100 μM N^G monomethyl-L-arginine (L-NMMA) determined constitutive NO synthase activity (Knowles *et al.*, 1990).

Materials

L-NAME (Sigma Chemical, St. Louis, U.S.A.) was dissolved in isotonic saline immediately before use. Indomethacin (Sigma) was dissolved in 5% w/v Na_2CO_3 solution and diluted to 1.25% with distilled water. EGF (Receptor grade; Biomedical Technologies, Stoughton, Mass, U.S.A.) was dissolved in isotonic saline immediately before use. [^{14}C]-L-arginine monohydrochloride (319 mCi $mmol^{-1}$) was purchased from Amersham Canada, Oakville, Ontario. L-NMMA was purchased from Calbiochem (LaJolla, Calif., U.S.A.). All other components of the NO synthase assay were purchased from Sigma.

Statistical analysis

All data are expressed as the mean ± s.e.mean. Comparisons between SALX and sham-operated rats were made by Student's *t* test for unpaired data while comparisons within groups and between vehicle and indomethacin-treatment were made by analysis of variance (ANOVA) and Duncan's Multiple Range Test. *P* values of less than 0.05 were taken as significant.

Results

Gastric mucosal damage

In response to intraluminal instillation of 150 mM HCl there was no significant difference in the extent of haemorrhagic damage between SALX and sham-operated rats treated

parenterally with saline (Figure 1). L-NAME administration (12.5 and 50 mg kg^{-1}) resulted in a small but significant increase in the extent of haemorrhagic damage in sham-operated rats when compared to saline-treatment (Figure 1). In sialoadenectomized (SALX) rats the area of haemorrhagic damage in response to some doses of L-NAME (12.5–50 mg kg^{-1}) was significantly greater than that observed in the corresponding group of sham-operated control rats. By itself, indomethacin did not result in a significant increase in the area of mucosal damage in control or SALX rats when compared to similar groups of rats treated with vehicle. Indomethacin pretreatment was associated with a significant exacerbation of haemorrhagic damage in sham-operated rats given 12.5–25 mg kg^{-1} L-NAME. The area of haemorrhagic damage in SALX rats treated with indomethacin was signficantly greater than similarly treated sham-operated rats in response to all doses of L-NAME except 12.5 mg kg^{-1}. In indomethacin-treated SALX rats, only damage in response to 50 mg kg^{-1} L-NAME was greater than was observed in SALX control animals.

Pretreatment of SALX rats receiving the combination of indomethacin and L-NAME (50 mg kg^{-1}) with EGF (5 μg kg^{-1} or 10 μg kg^{-1}, i.v.) resulted in a significant dose-dependent decrease in mucosal haemorrhage damage from 12.7 ± 0.8% to 8.1 ± 0.7% and 6.5 ± 1.6% respectively (n = 5–7 for each group). In sham-operated rats treated with indomethacin and L-NAME (50 mg kg^{-1}), EGF (10 μg kg^{-1}) did not significantly reduce the extent of haemorrhagic damage (9.9 ± 0.5% vs 8.3 ± 1.4%; n = 5–7 each group).

Similarly the histological damage index, in response to individual administration of these agents, was greater in SALX rats than in control animals (Figure 2). In control rats the combination of indomethacin and L-NAME (50 mg kg^{-1}) resulted in a significant increase in the histological damage index compared to that observed when this dose of L-NAME was administered alone (Figure 2). There was a further and significant increase in both types of microscopic damage in SALX rats treated with the combination of L-NAME and indomethacin.

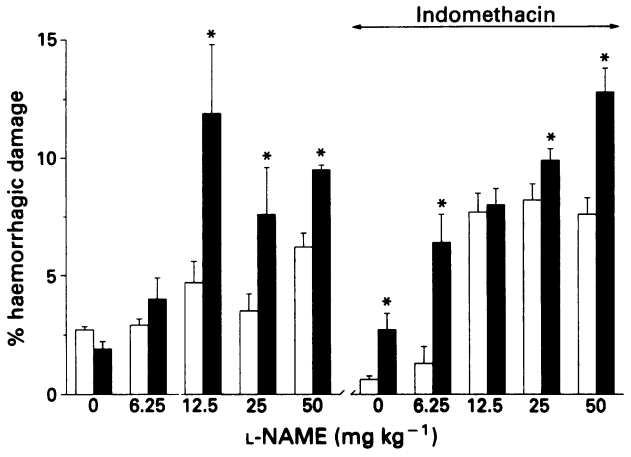

Figure 1 Percentage of the gastric mucosal area displaying haemorrhagic damage in response to intravenous injection of N^G-nitro-L-arginine methyl ester (L-NAME) alone or in combination with indomethacin (5 mg kg^{-1}, i.v.). Experiments were done using sialoadenectomized (SALX, solid columns) or sham-sialoadenectomized (open columns) rats. Results shown as mean ± s.e.mean. Asterisks (*) indicate significant differences between SALX and sham-operated animals receiving similar doses of L-NAME as determined by Student's t test for unpaired data within groups. L-NAME produced significant damage in sham-operated control animals (50 mg kg^{-1}) and sham-operated, indomethacin-treated animals (12.5–50 mg kg^{-1}) as determined by ANOVA and Duncan's multiple range test (n = 6–9 per group).

Gastric mucosal blood flow

In response to saline, LDF was not significantly changed in either SALX or sham-control rats (Figure 3). In sham-operated rats, L-NAME administration resulted in a small decrease in LDF. In SALX rats the decrease in LDF in response to L-NAME was significantly greater in response to 25 and 50 mg kg^{-1} L-NAME (Figure 3). There was no significant effect of indomethacin alone on LDF in sham-

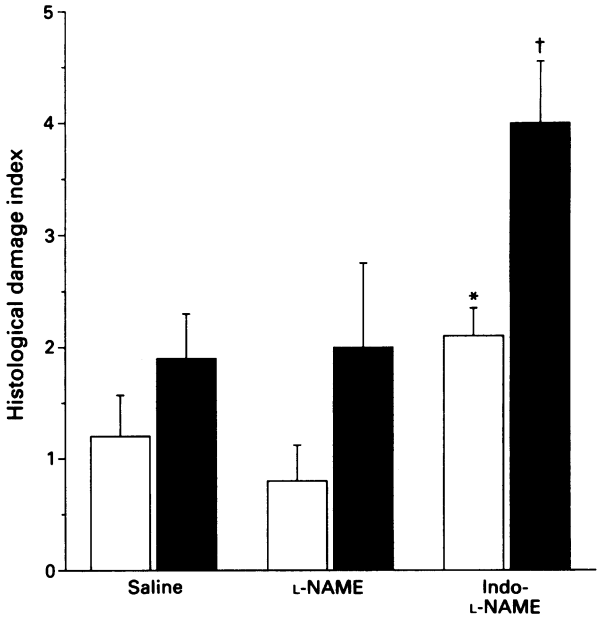

Figure 2 Histological damage index of the gastric mucosa of sialoadenectomized (SALX, solid columns) or sham sialoadenectomized (open columns) rats treated intravenously with saline, N^G-nitro-L-arginine methyl ester (L-NAME; 50 mg kg^{-1}) alone or indomethacin (5 mg kg^{-1}) in combination with L-NAME. Histological index was assessed as described in Methods. Results shown as mean ± s.e.mean. Asterisks (*) indicate significant increases over saline-treated sham-operated rats. Crosses (†) indicate significant differences between similarly treated sham-operated and SALX rates. Statistical significance was determined by ANOVA and Duncan's Multiple Range Test. (n = 5–7 per group).

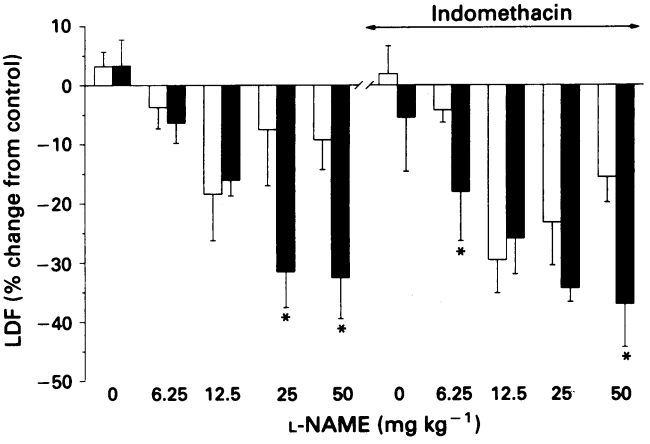

Figure 3 Laser Doppler flow (LDF) in sialoadenectomized (SALX, solid columns) or sham-operated (open columns) rats treated with N^G-nitro-L-arginine methyl ester (L-NAME, i.v.). LDF was calculated as a % change from basal LDF values. Results shown as mean ± s.e.mean. Asterisks (*) indicate significant differences between correspondingly treated sham-operated and SALX animals within groups as determined by Student's t test for unpaired data. (n = 5–7 per group).

operated or SALX rats. While indomethacin-treatment resulted in a further reduction in LDF in sham-operated rats in response to 25 and 50 mg kg^{-1} L-NAME, the decline in LDF was not greater in SALX rats when compared to SALX rats receiving vehicle in place of indomethacin.

EGF administration (10 μg kg^{-1}, i.v.) resulted in a small but significant ($P<0.05$) increase in LDF above basal values in sham-operated (4.2 ± 0.3%, $n=6$) and SALX (3.1 ± 0.1%, $n=6$) rats. When EGF was administered to sham-operated or SALX rats treated concurrently with indomethacin and L-NAME (50 mg kg^{-1}), LDF values were not significantly different from zero (− 8.9 ± 7.6%, $n=4$ and 3.3 ± 11.5%, $n=4$ respectively).

Effects on systemic arterial blood pressure

Intravenous administration of L-NAME (6.25–50 mg kg^{-1}) induced a dose-dependent rise in systemic arterial blood pressure (Figure 4) above resting values (89 ± 6 mmHg; $n=25$). The hypertensive response was significantly augmented in SALX rats over the entire dose range of L-NAME examined. Indomethacin-treatment of sham-operated rats further increased the hypertensive response to L-NAME. In indomethacin-treated SALX rats, arterial pressure was elevated to the same degree regardless of the dose of L-NAME examined.

Mucosal NO synthase activity

NO synthase activity as estimated by [^{14}C]-citrulline formation was detected in the mucosa of sham-operated and SALX rats (Figure 5). The activity was significantly ($P<0.05$) in both groups by *in vitro* addition of 1 mM EGTA (− 92 ± 4%, sham-operated; − 87 ± 6%, SALX) or 100 μM L-NMMA (− 81 ± 8%, sham operated; − 83 ± 6%, SALX). Total NO formation was significantly less in SALX rats than in sham-operated animals (Figure 5). In rats pretreated with EGF (10 μg kg^{-1}, i.v.), NO synthase activity was not significantly affected in sham-operated rats (Figure 5). Furthermore, in SALX rats the amount of [^{14}C]-citrulline formed in response to EGF administration was not significantly different from that observed in sham-operated rats treated with saline.

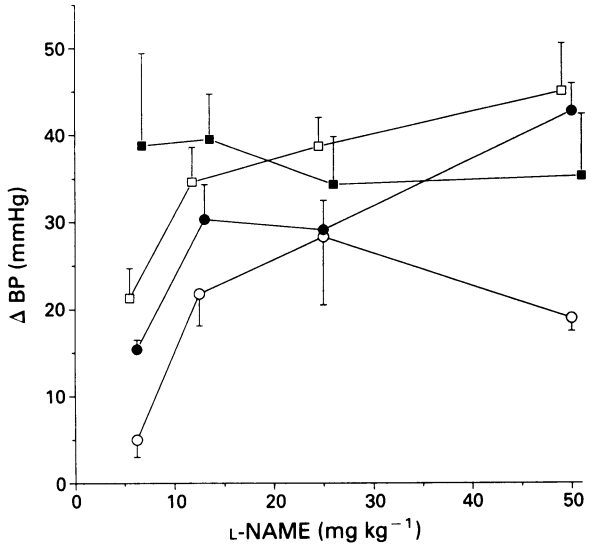

Figure 4 Effects of N^{G}-nitro-L-arginine methyl ester (L-NAME, 6.25–50 mg kg^{-1}, i.v) on changes (Δ) in systemic arterial blood pressure (BP) in sham-operated (○) and sialoadenectomized (□) control rats or after treatment with indomethacin (5 mg kg^{-1}, i.v.; ●, ■). *Results shown as mean ± s.e.mean. $n=4$–5 experiments for each group.

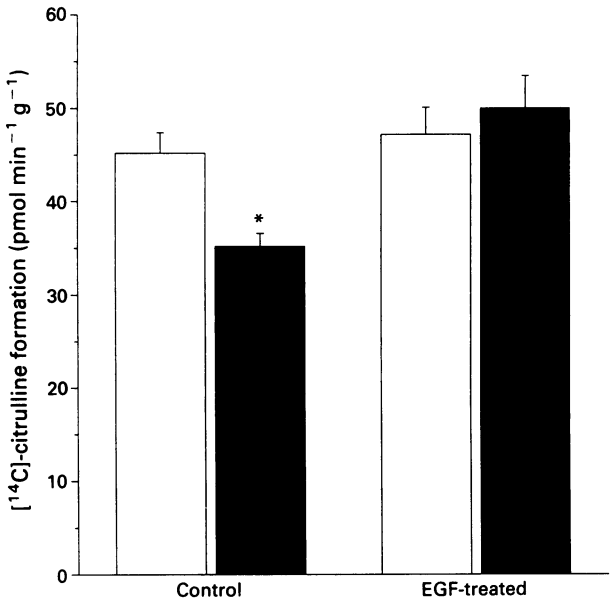

Figure 5 Nitric oxide synthase activity of rat gastric mucosa as assessed by [^{14}C]-citrulline formation. Experiments were done in sialoadenectomized (SALX, solid columns) or sham-operated (open columns) rats treated parenterally with saline (control) or epidermal growth factor, (EGF, 10 μg kg^{-1}). Results shown as mean ± s.e. mean. Asterisks (*) indicate significant differences between sham-operated and SALX control animals as determined by Student's *t* test for unpaired data. [^{14}C]-citrulline formation in EGF-treated SALX rats was significantly ($P<0.05$) greater than the levels determined in SALX control animals as determined by Student's *t* test for unpaired data. ($n=6$–7 per group).

Discussion

The present study demonstrates that in control rats, the inhibitor of NO synthase activity N^{G} nitro-L-arginine methyl ester, L-NAME, by itself resulted in a small degree of macroscopically or histologically detectable gastric mucosal damage. This finding is similar to what has been previously reported by Whittle *et al.* (1990) and Whittle & Tepperman (1991) using the NO synthase inhibitor N^{G} monomethyl-L-arginine (L-NMMA). However a key finding in the present study was that under conditions of sialoadenectomy (SALX) both macroscopic and microscopic damage induced by administration of L-NAME were significantly enhanced. Furthermore the present data also demonstrated that this augmentation in damage could be reversed by pretreatment with EGF. These data suggest that some factors from the salivary gland, possibly EGF, interacts with NO to influence gastric mucosal integrity.

The role of the salivary glands in gastric mucosal integrity has been examined previously. Removal of the salivary glands in rats has been shown to increase the susceptibility of the gastric mucosa to a number of ulcerogens including cysteamine, bile salts and ethanol (Skinner & Tepperman, 1981; Olsen *et al.*, 1984). This increased susceptibility to damage could be reversed by administration of exogenous EGF. In animals with intact salivary glands, EGF has been shown to exert a protective influence on the gastric mucosa (Pilot *et al.*, 1979; Konturek *et al.*, 1981) and levels of EGF in saliva have been shown to increase if the mucosa is damaged (Gysin *et al.*, 1988). The results of these studies suggest that endogenous EGF, released from the salivary gland, plays a role in maintaining mucosal integrity.

The mechanism by which salivary factors such as EGF affect mucosal integrity is uncertain. Konturek and colleagues (1981; 1988) have speculated that the protective

action of EGF may be due to a mitogenic effect while Sarosiek *et al.* (1988) have demonstrated that salivary EGF maintains the gastric mucus coat. In addition, a role for salivary EGF in the gastric microvasculature has been suggested. EGF can influence splanchnic blood flow (Gan *et al.*, 1987a,b) and recently in a preliminary study EGF has been shown to increase gastric mucosal blood flow (Hui *et al.*, 1991). In addition Namiki & Akatsuka (1990) have demonstrated that the vasoactive effect of EGF on rat aorta depends on intact endothelial layer. In the present study, the reduction in LDF to high doses of L-NAME (>12.5 mg kg^{-1}) was augmented in SALX rats. Furthermore, parenterally administered EGF resulted in an increase in mucosal blood flow as assessed by LDF and EGF treatment reversed the LDF fall in response to L-NAME in SALX rats. These data suggest that a factor from the salivary glands, possibly EGF, interacts with NO to modulate mucosal blood flow and hence tissue integrity.

The maintenance of mucosal integrity depends critically on the status of the microcirculation. Reduction in microvascular perfusion can lead to development of mucosal damage (Whittle, 1977). Removal of an endogenous vasodilator such as NO can lead to reductions in blood flow. Whittle and colleagues (Whittle *et al.*, 1990; Whittle & Tepperman 1991) have demonstrated that an inhibitor of NO biosynthesis such as L-NMMA reduced gastric mucosal blood flow. In the present study we have observed that by itself L-NAME at doses of 12.5–50 mg kg^{-1} did not consistently reduce mucosal blood flow. In a previous study Tepperman & Whittle (1992) have demonstrated that doses of 6.25 and 12.5 mg kg^{-1} L-NAME significantly reduced blood flow. The reasons for these differences are uncertain although we have used a different laser Doppler flowmeter and flow probe to estimate blood flow than was used in the study cited above. However Lippe & Holzer (1992) have demonstrated that the effect of NO synthesis inhibition on mucosal blood flow depends critically on the level of systemic arterial blood pressure. Blockade of NO formation lowered blood flow only if blood pressure was above a critical value. Thus the differences between studies may be due to the resting mean arterial pressures in the anaesthetized rats used in these studies.

The present study also confirms that L-NAME induced a dose-dependent increase in systemic blood pressure. The hypertensive action of all doses of L-NAME examined here were augmented in SALX rats. Since gastric microvascular changes in SALX rats were only seen at the higher doses of L-NAME, this suggests the interactions between endogenous NO and salivary gland factors on the gastric mucosa are not exclusively the result of changes in systemic arterial blood pressure.

Indomethacin pretreatment significantly augmented macroscopic mucosal damage in sham-operated rats in response to 12.5 and 25 mg kg^{-1} doses of L-NAME. These responses are similar to those observed by Whittle *et al.* (1990), Tepperman & Whittle (1992) and Whittle & Tepperman (1991) in which indomethacin enhanced mucosal injury in rats treated with L-NMMA. Furthermore in these animals, mucosal blood was further reduced in response to the highest dose of L-NAME. These present findings suggest that under the present conditions, endogenous prostanoids interact to some extent with NO to influence mucosal integrity by a modulation of mucosal blood flow, although direct effects on the microvascular endothelium cannot be excluded. In contrast, in indomethacin-treated SALX rats, neither damage nor LDF values were significantly different from control SALX animals suggesting that endogenous prostanoids do not interact with salivary gland factors and NO on the maintenance of mucosal integrity and vascular perfusion.

In the present study, using radiolabelled citrulline formation as an index of enzyme activity, NO synthase was found to be present in homogenates of rat gastric mucosa. This confirms findings by Whittle *et al.* (1991) using spectrophotometric determinations of NO synthase activity. In the present study, we have observed that SALX was associated with a reduction in NO synthesis. Furthermore, EGF pretreatment resulted in a restoration of mucosal NO biosynthesis to levels observed in sham sialoadenectomized rats. These data could suggest that SALX exacerbates mucosal damage in part by a further reduction in endogenous NO production and thereby influences mucosal blood flow. The mechanism(s) whereby SALX and salivary gland factors such as EGF affect mucosal NO synthase activity is currently under investigation in this laboratory.

Our data are comparable to results produced by Evangelista *et al.* (1991a,b). In those studies, sialoadenectomy was shown to interact with capsaicin-sensitive afferent fibres to augment water immersion stress-induced ulcers in rats. Previous studies have shown that sensory afferent nerves interact with NO in the maintenance of mucosal blood flow and integrity. Thus the present investigation confirms and extends these previous studies by the demonstration that factors from the salivary gland such as EGF may also interact with NO in the maintenance of gastric mucosal integrity. The interaction appears to be mediated, at least in part, by an action on the gastric microvasculature.

This work was supported by a grant from the Medical Research Council of Canada, No. MT6426.

References

BERK, B.C., BROCK, T.A., WEBB, R.C., TAUBMAN, M.B., ATKINSON, W.J., GIMBRONE, M.A. Jr. & ALEXANDER, R.W. (1985). Epidermal growth factor, a vascular smooth muscle mitogen, induces rat aortic contraction. *J. Clin. Invest.*, **75**, 1083–1086.

COHEN, S. (1962). Isolation of a mouse submaxillary gland protein accelerating incisor eruption and eyelid opening in the new-born animals. *J. Biol. Chem.*, **237**, 1555–1562.

EPSTEIN, A.N., SPECTOR, D., SAMMAN, A. & GOLDBLUM, C. (1964). Exaggerated prandial drinking in the rat without salivary glands. *Nature*, **201**, 1342–1343.

EVANGELISTA, S., RENZI, D., GUZZI, P. & MAGGI, C.A. (1991a). Interaction between sialoadenectomy and capsaicin sensitive afferent fibres in gastric acid secretion in rat. *Life Sci.*, **48**, PL37–PL41.

EVANGELISTA, S., RENZI, D., SURRENTI, C. & MAGGI, L.A. (1991b). Capsaicin-sensitive afferents and sialoadenectomy interact in stress-ulcers and gastric acid secretion in rats. *Gastroenterology*, **100**, A62.

GAN, B.S., HOLLENBERG, M.D., MACCANELL, K.L., LEDERIS, K., WINKLER, M.E. & DERYNCK, R. (1987a). Distinct vascular actions of epidermal growth factor-urogastrone and transforming growth factor-α. *J. Pharmacol. Exp. Ther.*, **242**, 331–337.

GAN, B.S., MACCANNELL, K.L. & HOLLENBERG, M.D. (1987b). Epidermal growth factor-urogastrone causes vasodilatation in the anesthetized dog. *J. Clin. Invest.*, **80**, 199–206.

GYSIN, B., MULLER, R.K.M., OTTEN, U. & FISCHLI, A.E. (1988). Epidermal growth factor content of submandibular glands is increased in rats with experimentally induced gastric lesions. *Scand. J. Gastroenterol.*, **23**, 665–671.

HUI, W.M., CHEN, B.W., CHO, C.H., LUK, C.T. & LAM, S.K. (1991). The effect of epidermal growth factor (EGF) on gastric mucosal blood flow. *Gastroenterology*, **100**, A86.

KHAN, M.T. & FURCHGOTT, R.F. (1987). Additional evidence that endothelium-derived relaxing factor is nitric oxide. In *Pharmacology*. ed. Rand, M.J. & Raper, C. pp. 341–344. New York: Elsevier.

KNOWLES, R.G., MERRETT, M., SALTER, M. & MONCADA, S. (1990). Differential induction of brain lung and liver nitric oxide synthase by endotoxin in the rat. *Biochem J.*, **270**, 833–836.

KONTUREK, S.J., DEMBINSKI, A., WAZECHA, S., BRZOZOWSKI, T. & GREGORY, H. (1988). Role of epidermal growth factor in healing of chronic gastroduodenal ulcers in rats. *Gastroenterology*, **94**, 1300–1307.

KONTUREK, S.J., RADECKI, T., BRZOZOWSKI, T., PIASTUCKI, I., DEMBINSKI, A., DEMBINSKI-KIEC, A., ZMUDA, A., GREJGLEWSKI, R. & GREGORY, H. (1981). Gastric cytoprotection by epidermal growth factor: role of endogenous prostaglandins and DNA synthesis. *Gastroenterology*, **81**, 438–443.

LIPPE, I. Th. & HOLZER, P. (1992). Participation of endothelium-derived nitric oxide but not prostacyclin in the gastric mucosal hyperaemia due to acid back-diffusion. *Br. J. Pharmacol.*, **105**, 708–714.

MURAMATSU, I., HOLLENBERG, M.D. & LEDERIS, K. (1986). Stimulation by epidermal growth factor-urogastrone of contraction in isolated canine helical mesenteric arterial strips. *Can. J. Physiol. Pharmacol.*, **64**, 1561–1565.

NAMIKI, A. & AKATSUKA, N. (1990). Vascular smooth muscle relaxation induced by epidermal growth factor is endothelium-dependent. *Eur. J. Pharmacol.*, **180**, 247–254.

OLSEN, P.S., POULSEN, S.S., KIRKEGAARD, P. & NEXO, E. (1984). Role of submandibular saliva and epidermal growth factor in gastric cytoprotection. *Eur. J. Pharmacol.*, **180**, 247–254.

PALMER, R.M.J., FERRIGE, A.G. & MONCADA, S. (1987). Nitric oxide release accounts for the biological activity of endothelium-derived relaxing factor. *Nature*, **327**, 524–526.

PILOT, M.A., DEREGNANCOURT, J. & CODE, C.F. (1979). Epidermal growth factor increases the resistance of the gastric mucosal barrier to ethanol in rats. *Gastroenterology*, **76**, 1217.

PIQUE, J.M., WHITTLE, B.J.R. & ESPLUGUES, J.V. (1989). The vasodilator role of endogenous nitric oxide in the rat gastric microcirculation. *Eur. J. Pharmacol.*, **174**, 293–296.

SAROSIEK, J., BILSKI, J., MURTY, V.L.N., SLOMIANY, A. & SLOMIANY, B.L. (1988). Role of salivary epidermal growth factor in the maintenance of physiochemical characteristics of oral and gastric mucosal mucus coat. *Biochem. Biophys. Res. Comm.*, **152**, 1421–1427.

SKINNER, K.A., SOPER, B.D. & TEPPERMAN, B.L. (1984). Effect of sialoadenectomy and salivary gland extracts on gastrointestinal mucosal growth and gastrin levels in the rat. *J. Physiol.*, **351**, 1–12.

SKINNER, K.A. & TEPPERMAN, B.L. (1981). Influence of desalivation on acid secretory output and gastric mucosal integrity in the rat. *Gastroenterology*, **81**, 335–339.

TEPPERMAN, B.L. & WHITTLE, B.J.R. (1992). Endogenous nitric oxide and sensory neuropeptides interact in the modulation of the rat gastric microcirculation. *Br. J. Pharmacol.*, **105**, 171–175.

WHITTLE, B.J.R. (1977). Mechanisms underlying gastric mucosal damage induced by indomethacin and bile salts and the actions of prostaglandins. *Br. J. Pharmacol.*, **60**, 455–460.

WHITTLE, B.J.R., BERRY, S., LOPEZ-BELMONTE, J., BOUGHTON-SMITH, N.K. & MONCADA, S. (1991). Detection of the synthase enzyme that forms the endogenous vasodilator, nitric oxide in the rat gastric mucosa. *Gastroenterology*, **100**, A184.

WHITTLE, B.J.R., LOPEZ-BELMONTE, J. & MONCADA, S. (1990). Regulation of gastric mucosal integrity by endogenous nitric oxide: interactions with prostanoids and sensory neuropeptides in the rat. *Br. J. Pharmacol.*, **99**, 607–611.

WHITTLE, B.J.R. & TEPPERMAN, B.L. (1991). Role of the endogenous vasoactive mediators, nitric oxide, prostanoids and sensory neuropeptides in the regulation of gastric blood flow and mucosal integrity. In *Mechanisms of Injury, Protection and Repair of the Upper Gastrointestinal Tract*, ed. Garner, A. & O'Brien, P.E. pp. 127–137. New York: Wiley and Sons.

(Received August 24, 1992
Revised March 18, 1993
Accepted May 7, 1993)

Br. J. Pharmacol. (1993), **110**, 235–238

Eicosanoid-dependence of responses of pre- but not postglomerular vessels to noradrenaline in rat isolated kidneys

Bei-Li Zhang & [1]Jean Sassard

Department of Physiology and Clinical Pharmacology, URA CNRS 1483, Faculty of Pharmacy, 8 avenue Rockefeller, 69373 Lyon Cedex 08, France

1 We investigated the role of nitric oxide (NO) and of vasoactive eicosanoids in the control of renal vascular resistance (RVR) and glomerular filtration rate (GFR) and of their responses to noradrenaline (NA). This study was conducted in single-pass perfused, isolated kidney preparations of the rat.

2 NA (63, 110 and 160 nM) dose-dependently increased RVR and to a lesser degree GFR.

3 In baseline conditions, N^{ω}-nitro-L-arginine methylester (L-NAME, 100 μM) increased GFR more than RVR, thus demonstrating a basal release of NO which predominates in postglomerular vessels.

4 In kidneys stimulated with NA, L-NAME potentiated the increases in RVR but not in GFR. Indomethacin (1.5, 150 nM and 15 μM) did not alter GFR but markedly and dose-dependently reduced the NA-induced increase in RVR. Similar results were obtained with GR 32191B (10 and 100 μM), a prostaglandin H_2/thromboxane A_2 (PGH_2/TxA_2) receptor antagonist.

5 Indomethacin (15 μM) suppressed the enhancing effects of L-NAME on RVR responses to NA but did not affect those on GFR.

6 It is concluded that the mechanisms of the response to NA differ among pre- and postglomerular vessels. In preglomerular vessels the vasoconstrictor action and the NO release depend upon the activation of PGH_2/TxA_2 receptors, while both are eicosanoid-independent in the postglomerular vessels.

Keywords: Rat isolated kidney; nitric oxide; cyclo-oxygenase; prostaglandin H_2; thromboxane A_2

Introduction

It is well known that kidneys markedly influence the long-term blood pressure level through the pressure-natriuresis mechanism (Cowley, 1992). This mechanism which allows urinary sodium excretion to equilibrate sodium intake is partly dependent upon the preglomerular vascular resistance which limits the amount of filtered sodium. In that respect, recent experiments highlighted the possible role of nitric oxide (NO) and of prostanoids. NO decreases renal vascular resistance and enhances glomerular filtration rate and natriuresis both *in vitro* (Mattson *et al.*, 1992; Johnson & Freeman, 1992; Salazar *et al.*, 1992; Majid & Gabriel Navar, 1992) and in isolated kidney preparations (Radermacher *et al.*, 1990; Welch *et al.*, 1991; Gardes *et al.*, 1992). Concerning prostanoids, the vasoconstrictor effects of prostaglandin $(PG)H_2$ and of thromboxane $(Tx)A_2$ are well known and have been shown to participate in the control of renal vascular resistance in genetically hypertensive rats of the Japanese (Dai *et al.*, 1992) and of the Lyon strains (Liu *et al.*, 1991).

The present work aimed to assess the role of NO in the control of renal functions. In order to avoid the interference of circulating vasoactive substances, the study was conducted in the single-pass perfused isolated kidney preparation. In addition, to eliminate the possible influence of co-released eicosanoids by endothelial cells (Fulton *et al.*, 1992) the experiments were repeated in the presence of indomethacin which blocks cyclo-oxygenase.

Methods

Animals

Eight-week old male Sprague-Dawley rats (Iffa-Credo, Les Oncins, France) were used. Animals were housed under constant conditions of temperature (21 ± 1°C), lighting (08 h 00 min to 20 h 00 min) and humidity (60 ± 10%). They were fed a standard diet (Elevage UAR, AO3 Villemoisson s/Orge, France) and had free access to tap water.

Isolated kidney preparations

After rats were anaesthetized with sodium pentobarbitone (45 mg kg^{-1}, i.p.), the right kidney was isolated according to Schmidt & Imbs (1980). Briefly, after a midline abdominal incision, the right adrenal artery and small lumbar arteries were tied off. The right kidney was removed from peripheral fat pads and transferred without interruption of the renal blood flow to a small metallic double-walled cup maintained at 37°C. After an injection of heparin (1,000 iu, i.v.), polyethylene catheters were inserted into (1) the superior mesenteric artery, facing the origin of the right renal artery, to ensure perfusion of the kidney; (2) the infrarenal aorta to allow the measurement of the renal perfusion pressure (RPP, mmHg); (3) the suprarenal vena cava to collect the renal venous effluent and (4) the ureter for collecting urine samples. The left renal artery was then ligated and immediately after the beginning of the perfusion the suprarenal aorta and the infrarenal vena cava were tied off. The whole right kidney was then excised, trimmed of adhering tissue and completely isolated. The left kidney was removed and weighed.

Perfusion medium

The perfusate was a blood-free modified Krebs-Henseleit solution containing 35 g l^{-1} of a gelatin derivative (Haemaccel, Behring, Marburg, Germany) as a colloid osmotic agent. The final electrolyte composition of the perfusate was as follows (mM): NaCl 100, KCl 3.8, $CaCl_2$ 1.1, $MgCl_2$ 0.6, KH_2PO_4 1.2 and $NaHCO_3$ 25.0. In addition, the medium contained (mM) D-glucose 10.0, sodium pyruvate 2.0, oxaloacetic acid 1.0, sodium DL-lactate 5.0, L-glutamic acid 5.0 and urea 6.0. Just before use, the perfusate was filtered

[1] Author for correspondence at: URA CNRS 1483, Faculty of Pharmacy, 8 avenue Rockefeller, 69373 Lyon Cedex 08, France.

through a millipore filter (0.8 μm) and polyfructosan (Inutest, Laevosan, Linz, Austria) (0.5 g l^{-1}) added for determination of the glomerular filtration rate (GFR). The solution was continuously bubbled with 95% O_2 and 5% CO_2 mixture and single-pass perfused in an open thermostatically controlled circuit with a peristaltic pump (Minipuls 2, Gilson, Paris, France) at a constant flow rate.

Renal function parameters

The RPP was continuously recorded (Model BS 273, Statham Instrument Division, Gould Inc. Cleveland, Ohio, U.S.A.) at the aorto-renal artery junction through a pressure transducer (model P231D, Statham Instrument Division, Gould Inc., Oxnard, Calif., U.S.A.). Renal perfusion flow rate (RPF, ml min^{-1} g^{-1}) was measured by weighing the venous effluent. Renal vascular resistance (RVR, mmHg ml^{-1} min^{-1} g^{-1}) was calculated as the ratio RPP/RPF. GFR (ml min^{-1} g^{-1}) was determined by polyfructosan clearance (Technicon autoanalyzer). All these parameters were corrected for the weight of the unperfused left kidney, since the weight of the right kidney increased after the perfusion. The venous release of PGE_2 and TxB_2, the stable derivative of TxA_2 was measured by specific immunoassays after high performance liquid chromatography separation (Benzoni *et al.*, 1981).

Protocols

Experiment 1 Seven kidneys were perfused at a RPP of 88 ± 1 mmHg. After a 30 min stabilization period, urines were collected during a baseline period of 10 min and venous effluent during the last min of this baseline period. Then three concentrations (63, 110, and 160 nM) of noradrenaline (NA) were infused for 3 min each, separated by a 17 min interval. These NA infusions were repeated 20 min after the beginning of an infusion of N^{ω}-nitro-L-arginine methyl ester (L-NAME), a specific inhibitor of nitric oxide synthesis, at a concentration of 100 μM (Radermacher *et al.*, 1990). As previously described (Liu *et al.*, 1991), urines were collected for 7 min before (control) and 6 min after the start of each NA infusion. The venous effluent was collected for 1 min before (control) and during the last min of each NA infusion.

Experiment 2 In 7 kidneys, indomethacin, a cyclo-oxygenase inhibitor, was added to the perfusate at a final concentration of 15 μM, and the preparations were studied according to the above protocol.

Experiment 3 In 9 kidneys, after a 30 min stabilization period, NA (160 nM) was infused for 3 min before (control) and 30 min after the beginning of an infusion of indomethacin (1.5 nM, 150 nM and 15 μM). Each kidney received randomly in a cumulative way 2 of these 3 concentrations. Therefore each of them was studied in 6 kidneys. Urine and venous effluent were obtained according to experiment 1.

Experiment 4 In 6 kidneys, after a 30 min stabilization period, NA (160 nM) was administered for 3 min before (control) and 30 min after the infusion of two cumulative concentrations (10 and 100 μM) of GR32191B, a prostaglandin H_2/thromboxane A_2 (PGH_2/TxA_2) receptor antagonist. These two concentrations were chosen after pilot experiments which showed that they efficiently inhibited the contractile effects of U46619 (270 nM), a PGH_2/TxA_2 receptor agonist (ΔRPP of controls: + 14 ± 1.1 mmHg; GR32191B 10 μM: + 2 ± 0.3 mmHg and GR32191B 100 μM: 0 ± 0 mmHg). Urine and venous effluents were collected according to Experiment 1.

Statistics

Data are mean ± s.e.mean. The nonparametric Wilcoxon test was used to assess the effects of NA. One way analysis of variance was used to determine the differences among groups.

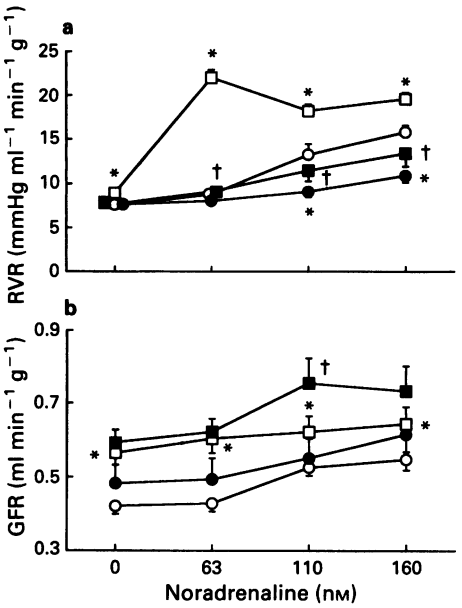

Figure 1 Effects of N^{ω}-nitro-L-arginine methyl ester (L-NAME), (100 μM) on the responses to noradrenaline of rat isolated kidneys in the absence and in the presence of indomethacin (Ind, 15 μM) on renal vascular resistance (RVR, a) and glomerular filtration rate (GFR, b). Controls (○, $n = 7$); L-NAME (□, $n = 7$); Ind (●, $n = 7$); L-NAME + Ind (■, $n = 7$). *$P < 0.05$ L-NAME or Ind vs controls; †$P < 0.05$ L-NAME + Ind vs L-NAME.

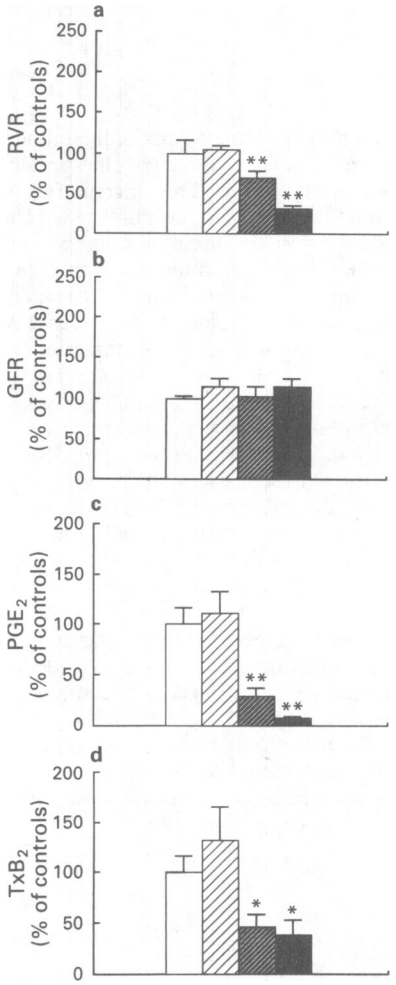

Figure 2 Effects of indomethacin (▨, 1.5 nM; ▨, 150 nM; ■, 15 μM; $n = 6$ in each group) on renal vascular resistance (RVR, a), glomerular filtration rate (GFR, b) and the venous release of prostaglanin E_2 (PGE_2, c) and thromboxane B_2 (TxB_2, d) in rat isolated kidneys challenged with noradrenaline (160 nM). *$P < 0.05$ and **$P < 0.01$ vs controls (□, $n = 9$).

Drugs

NA, L-NAME, indomethacin and U46619 (9,11-dideoxy-11α, 9α-epoxymethano-prostaglandin $F_{2\alpha}$) were from Sigma chemical Co., St. Louis, MO, U.S.A. GR32191B ([1R-[1α(Z),2β,3β,5α]]-(+)-7-[5-[[(1,1'-biphenyl)-4-yl] methoxy]-3-hydroxy-2-(1-piperidinyl) cyclopentyl]-4-heptenoic acid, hydrochloride) was a generous gift from Glaxo Group Research Limited, Ware, Hertfordshire, UK.

Results

As shown by Figure 1, L-NAME significantly ($P<0.05$) increased baseline RVR from 7.3 ± 0.3 to 8.8 ± 0.4 mmHg $ml^{-1} min^{-1} g^{-1}$ and more markedly GFR. NA dose-dependently elevated both parameters. L-NAME enhanced only the NA-induced increase in RVR. Indomethacin did not change baseline RVR and GFR. It did not significantly alter the NA effects on GFR but blunted those on RVR. When given together with L-NAME, indomethacin almost completely suppressed the potentiation by L-NAME of NA-induced vasoconstrictor effects, leaving GFR values unchanged.

Figure 2 indicates that in kidneys infused with NA, indomethacin did not alter GFR but dose-dependently reduced RVR. This reduction was marked with indomethacin at a concentration of 15 μM which profoundly inhibited the venous release of PGE_2 ($-92 \pm 2\%$) and TxB_2 ($-62 \pm 15\%$).

Figure 3 shows that a PGH_2/TxA_2 receptor antagonist exerted similar effects to those of indomethacin as it did not change the baseline RVR and GFR, but markedly opposed the effects of NA on RVR leaving GFR unchanged.

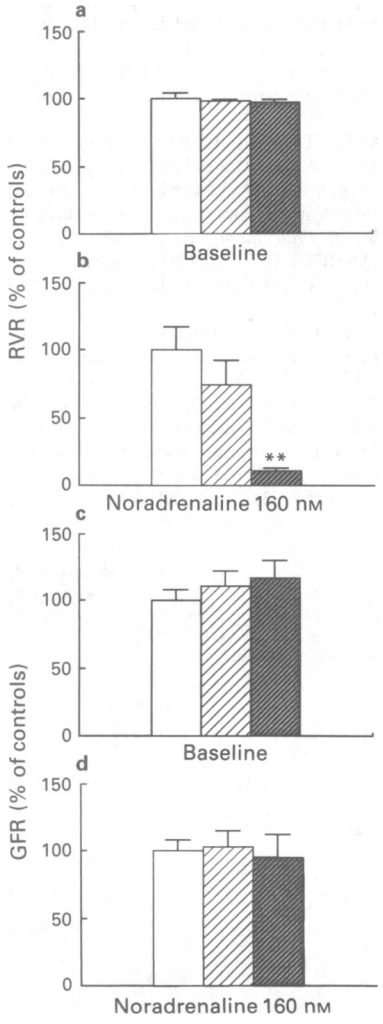

Figure 3 Effects of a prostaglandin H_2/thromboxane A_2 (PGH_2/TxA_2) receptor antagonist (GR32191B; ▨, 10 μM; ▨, 100 μM) on renal vascular resistance (RVR a,b), glomerular filtration rate (GFR c,d) in 6 isolated rat kidneys before (baseline) and after the infusion of noradrenaline (160 nM). $^{**}P<0.01$ vs controls (□).

Discussion

The present work aimed to assess the role of NO in the control of renal vascular resistance and glomerular filtration rate. In order to eliminate the influence of uncontrolled circulating vasoactive substances, it was carried out in single-pass perfused isolated kidneys. This preparation was shown to be valuable for the study of renal vessels responses. In that respect, comparison of the simultaneous changes in RVR and in GFR made it possible to differentiate between the effects which predominate on the pre- or on the postglomerular vasculature. Despite its numerous advantages, single-pass perfused isolated kidneys are not fully satisfactory for the study of tubular functions since the sodium reabsorption never exceeded 90%. In addition, since in baseline conditions the vessels of such a preparation are almost maximally vasodilated it is interesting to challenge them with known concentrations of a vasoconstrictor agent. In the present work, we used low concentrations of NA, infused for short period of times and separated by long intervals to avoid the development of desensitization (Liu *et al.*, 1991). As usual, NA dose-dependently enhanced RVR and to a lower degree GFR.

The functional role of NO release was assessed by use of L-NAME at a concentration (100 μM) which fully blocks NO synthesis (Radermacher *et al.*, 1990). In baseline conditions, L-NAME increased RVR and to a greater extent GFR, thus demonstrating that a basal NO release exists which predominates in postglomerular vessels. Such a basal NO release is likely to be due to shear stress activation of endothelial cells in the kidney as already demonstrated in other vascular beds (Koller & Kaley, 1991; Lamontagne *et al.*, 1992). A more important release by post- than by preglomerular vessels is in accordance with the data of Tolins & Raij (1991) and of Majid & Gabriel Navar (1992) who reported that NO synthase blockade decreases renal blood flow more than GFR. After stimulation with NA, L-NAME produced dramatic increases in RVR leaving the response of GFR unchanged. This indicates that, unlike shear stress, NA induces a more important NO release in pre- than in postglomerular vessels.

To avoid the possible interferences of the vasoactive eicosanoids which are released by NA in the kidneys (Liu *et al.*, 1991) the experiments were repeated in the presence of indomethacin at a concentration (15 μM) that we found to decrease the overall renal release of the vasoconstrictor PGE_2 and TxA_2 by more than 60%. It was observed that indomethacin did not affect the NA effects on GFR, but dose-dependently and markedly inhibited those on RVR. Therefore it appears that in pre- but not in postglomerular vessels, NA may provoke the release of vasoconstrictor eicosanoids which play an important part in the contractile response. There are few reports of the inhibitory effects of cyclo-oxygenase inhibitors on vasoconstriction. However, similar findings were made in isolated lung (Shaw *et al.*, 1992) in coronary vascular beds (Lee *et al.*, 1991) stimulated with 5-hydroxytryptamine, vasopressin or phenylephrine, as well as in rat isolated aortae constricted with endothelin (Taddei & Vanhoutte, 1993). Taken as whole, these data suggest that our observation is not specific for NA. In order to approach the nature of the eicosanoids which are important in the contractile response to NA, we used a specific PGH_2/TxA_2 receptor antagonist GR32191B, at two concentrations (10 and 100 μM) that were chosen after the demonstration that they blocked the vasoconstrictor effect of

U46619, an agonist at these PGH_2/TxA_2 receptors. Interestingly, as well as indomethacin, GR32191B dose-dependently reduced the response on RVR to NA, leaving GFR values unchanged. Therefore it is possible to conclude that the eicosanoids released by NA acting on preglomerular vessels are PGH_2 and/or TxA_2. When considering preparations submitted to L-NAME, it was observed that indomethacin did not consistently affect GFR but blunted the potentiating action of L-NAME on the RVR responses to NA. These data suggest that the NA-induced release of PGH_2 and/or TxA_2 is an important intermediate step which leads to the release of NO. This indicates an interaction within the preglomerular vessels between eicosanoids and NO as has been described in macrophages (Marotta *et al.*, 1992).

In conclusion, the present work shows that, in rat isolated kidney preparations the mechanisms involved in the contractile effects of NA differ between the pre- and the postglomerular vascular beds. In preglomerular vessels both vasoconstriction and the release of NO which partly opposes it, depend upon the release of PGH_2 and/or TxA_2. In postglomerular vessels both are eicosanoid-independent. Although difficult to extrapolate to *in vivo* conditions, these data may be of interest for *in vitro* investigations.

We are grateful to J. Sacquet for prostanoid measurements, Professor D. Benzoni for stimulating comments, and Glaxo Research laboratories for their generous gift of the compound GR32191B.

References

BENZONI, D., VINCENT, M. & SASSARD, J. (1981). Radioimmunoassay for urinary prostaglandins E and Falpha: normal values in different age groups. *Clin. Chem. Acta*, **111**, 9–16.

COWLEY, A.W. Jr. (1992). Long-term control of arterial blood pressure. *Physiol. Rev.*, **72**, 231–300.

DAI, F.X., SKOPEC, J., DIEDERICH, A. & DIEDERICH, D. (1992). Prostaglandin H_2 and thromboxane A_2 are contractile factors in intrarenal arteries of spontaneously hypertensive rats. *Hypertension*, **19**, 795–798.

FULTON, D., MCGIFF, J.C. & QUILLEY, J. (1992). Contribution of NO and cytochrome P450 to the vasodilator effect of bradykinin in the rat kidney. *Br. J. Pharmacol.*, **107**, 722–725.

GARDES, J., POUX, J.M., GONZALEZ, M.F., ALHENC-GELAS, F. & MENARD, J. (1992). Decreased renin release and constant kallikrein secretion after injection of L-NAME in isolated perfused rat kidney. *Life Sci.*, **50**, 987–993.

JOHNSON, R.A. & FREEMAN, R.H. (1992). Pressure natriuresis in rats during blockade of the L-arginine/nitric oxide pathway. *Hypertension*, **19**, 333–338.

KOLLER, A. & KALEY, G. (1991). Endothelial regulation of wall shear stress and blood flow in skeletal muscle microcirculation. *Am. J. Physiol.*, **260**, H862–H868.

LAMONTAGNE, D., POHL, U. & BUSSE, R. (1992). Mechanical deformation of vessel wall and shear stress determine the basal release of endothelium-derived relaxing factor in the intact rabbit coronary vascular bed. *Cir. Res.*, **70**, 123–130.

LEE, S.-L., LEVITSKY, S. & FEINBERG, H. (1991). Endogenous vasoconstrictor prostanoids: role in serotinin and vasopressin-induced coronary vasoconstriction. *J. Pharmacol. Exp. Ther.*, **258**, 292–298.

LIU, K.L., HADJ AISSA, A., LAREAL, M.C., BENZONI, D., VINCENT, M. & SASSARD, J. (1991). Adrenergic stimulation of renal prostanoids in the Lyon hypertensive rat. *Hypertension*, **17**, 296–302.

MAJID, D.S.A. & NAVAR, L.G. (1992). Suppression of blood flow autoregulation plateau during nitric oxide blockade in canine kidney. *Am. J. Physiol.*, **262**, F40–F46.

MAROTTA, P., SAUTEBIN, L. & DI ROSA, M. (1992). Modulation of the induction of nitric oxide synthesis by eicosanoids in the murine macrophage cell line J774. *Br. J. Pharmacol.*, **107**, 640–641.

MATTSON, D.L., ROMAN, R.J. & COWLEY, A.W. Jr. (1992). Role of nitric oxide in renal papillary blood flow and sodium excretion. *Hypertension*, **19**, 766–769.

RADERMACHER, J., FORSTERMANN, U. & FROLICH, J.C. (1990). Endothelium-derived relaxing factor influences renal vascular resistance. *Am. J. Physiol.*, **259**, F9–F17.

SALAZAR, F.J., PINILLA, J.M., LOPEZ, F., ROMERO, J.C. & QUESADA, T. (1992). Renal effects of prolonged synthesis inhibition of endothelium-derived nitric oxide. *Hypertension*, **20**, 113–117.

SCHMIDT, M. & IMBS, J.L. (1980). Pharmacological characterization of renal vascular dopamine receptor. *J. Cardiovasc. Pharmacol.*, **2**, 595–605.

SHAW, A.M., BARKELL, E., ROURKE, S., BARFARAZ, A.R., POLLOCK, D. & MCGRATH, J.C. (1992). A comparison of the effects of L-N^{ω}-nitro arginine methyl ester and flurbiprofen on responses to vasoconstrictors in the pulmonary circulation of the rat perfused lung. *Br. J. Pharmacol.*, **107**, 197P.

TADDEI, S. & VANHOUTTE, P.M. (1993). Role of endothelium in endothelin-evoked contractions in the rat aorta. *Hypertension*, **21**, 9–15.

TOLINS, J.P. & RAIJ, L. (1991). Effects of amino acid infusion on renal hemodynamics: role of endothelium-derived relaxing factor. *Hypertension*, **17**, 1045–1051.

WELCH, W.J., WILCOX, C.S., AISAKA, K., GROSS, S.S., GRIFFITH, O.W., FONTOURA, B.M.A., MAACK, T. & LEVI, R. (1991). Nitric oxide synthesis from L-arginine modulates renal vascular resistance in isolated perfused and intact rat kidneys. *J. Cardiovasc. Pharmacol.*, **17** (Suppl. 3), S165–S168.

(Received April 21, 1993
Accepted May 7, 1993)

Br. J. Pharmacol. (1993), **110**, 239–244

Estimation of partial agonist affinity by interaction with a full agonist: a direct operational model-fitting approach

P. Leff, [1]I.G. Dougall & D. Harper

Department of Pharmacology, Fisons plc, Bakewell Road, Loughborough, Leicestershire, LE11 0RH

1 The operational model of agonism (Black & Leff, 1983) has been extended to describe the interaction between a partial agonist and a full agonist at the same receptor. The derived equation explicitly describes the interaction and allows the affinity (and efficacy) of the partial agonist to be estimated by direct fitting of raw experimental agonist concentration-effect (E/[A]) curve data.

2 The model was used to analyse experimental E/[A] curve data generated for the interaction between pilocarpine (partial agonist) and carbachol (full agonist) at the M_3-muscarinic receptor mediating contraction of the guinea-pig isolated trachea. Pilocarpine affinity estimates obtained by operational model-fitting were compared with those obtained by use of the null method (Stephenson, 1956). These analyses demonstrated that the two methods gave comparable results (mean pK_B estimates were 5.79 and 5.86 for the operational model and null method respectively).

3 When multiple concentrations of partial agonist are used, simultaneous operational model-fitting of all the E/[A] curve data allows the competitive nature of the interaction to be studied.

4 We conclude that operational model-fitting is a valid and analytically simple alternative to the conventional null method of analysing full/partial agonist interactions.

Keywords: Guinea-pig trachea; muscarinic receptor; partial agonist; affinity; efficacy; operational model; null method

Introduction

The commonly used pharmacological approaches to estimating agonist affinities and efficacies are the receptor inactivation method (Furchgott, 1966) which allows quantification of either full or partial agonists and the comparative method (Barlow *et al.*, 1967) which allows quantification of partial agonists. A less frequently used means of estimating these drug-receptor parameters for a partial agonist is to study its interaction with a full agonist (Stephenson, 1956). This method has the advantage of allowing confirmation, in a single tissue, that the effects of the full and partial agonist are mediated by the same receptor. The comparative method makes this assumption but does not test it. Conventionally, estimation of affinity and efficacy by the interaction method (as well as by the other methods) utilises the null equation approach, as originally described by Stephenson (1956) and later advanced by Marano & Kaumann (1976). An alternative approach which has been successfully applied to the receptor inactivation and comparative methods, is to analyse data directly by operational model-fitting (Black *et al.*, 1985; Leff *et al.*, 1990). In this paper we show how this approach can be extended to the interaction method. Initially, we advance the operational model to describe interactions between a partial agonist and a full agonist at the same receptor. Then, we explain how the derived equation is applied in practice to estimate affinity and efficacy of the partial agonist. This analysis is illustrated with experimental E/[A] curve data generated for the interaction between pilocarpine (partial agonist) and carbachol (full agonist) at the M_3-muscarinic receptor mediating contraction of the guinea-pig isolated trachea. Finally, the results of operational model-fitting analysis are compared with those using the null method. A preliminary account of this work was presented to the British Pharmacological Society (Dougall *et al.*, 1993).

Methods

Guinea-pig isolated trachea

Male albino Dunkin-Hartley guinea-pigs (400–550 g) were killed by cervical dislocation and the whole trachea removed. After removing the adherent connective tissue, the trachea was cut into five segments, each three cartilage bands wide and then suspended in 10 ml organ baths containing Krebs solution of the following composition (mM): NaCl 117.56, KCl 5.36, NaH_2PO_4 1.15, $MgSO_4$ 1.18, glucose 11.10, $NaHCO_3$ 25.00 and $CaCl_2$ 2.55. This was maintained at 37°C and continually gassed with 5% CO_2 in oxygen. Indomethacin (2.8 μM), hexamethonium (300 μM) and propranolol (1 μM) were added to the Krebs solution: indomethacin to prevent development of smooth muscle tone due to the synthesis of cyclo-oxygenase products, hexamethonium to block any nicotinic actions of the muscarinic agonists used and propranolol to prevent any possible interference of catecholamines released by stimulation of ganglionic M_1-muscarinic receptors. The tracheal rings were suspended between two tungsten wire hooks, one attached to an Ormed Beam isometric force transducer and the other to a stationary support in the organ bath. Changes in isometric force were recorded on 3-channel Advance Bryans flat bed recorders.

Experimental protocols

General At the beginning of each experiment a force of 1.0 g was applied to the tissues. Subsequently each tissue was exposed to the irreversible antagonist phenoxybenzamine (Pbz) (1 μM) for a period of 10 min. This procedure was employed because preliminary experiments indicated that in untreated tissues pilocarpine produced a maximum response that was on average approximately 70% of that achieved with carbachol (data not shown); that is, the intrinsic activity of pilocarpine was 0.7. The decrease in functional muscarinic receptor reserve that resulted from Pbz treatment allowed well-defined carbachol E/[A] curves in the presence of pilocarpine to be constructed. At the end of the incubation period the tissues were washed four times at 5 min intervals to remove the Pbz. The force of 1.0 g was reinstated at this time point and 30 min later tissues were exposed to 10 μM carbachol, to assess tissue viability. All subsequent contractile agonist concentration-effect, E/[A], curves were constructed by cumulative additions of carbachol at 0.5 $\log_{10}$ unit increments. In all experiments a paired curve design was used with a period of 60 min elapsing between the first and

[1] Author for correspondence.

second curves. Responses were recorded as percentage maximum of the first curve.

Analysis of carbachol by the receptor inactivation method In each tissue a carbachol E/[A] curve was constructed. After washing, tissues were incubated with Pbz (10 μM) or vehicle (ethanol) for 10 min. Following removal of the irreversible antagonist by four changes of the organ bath Krebs solution at 5 min intervals, a second carbachol E/[A] curve was obtained.

Pilocarpine affinity estimation by the interaction method In each tissue a carbachol E/[A] curve was constructed. Tissues were subsequently exposed to pilocarpine (10 μM, 30 μM or 100 μM). When the responses had stabilized a second carbachol E/[A] curve was constructed on top of the response to pilocarpine.

Drugs

The following drugs were used: carbachol chloride (Sigma Chemical Company), pilocarpine hydrochloride (Sigma Chemical Company), phenoxybenzamine hydrochloride (Research Biochemicals Inc.), indomethacin (Sigma Chemical Company), hexamethonium bromide (Sigma Chemical Company) and (±)-propranolol hydrochloride (Sigma Chemical Company).

Indomethacin was dissolved in 10% w/v Na_2CO_3 and Pbz was dissolved in ethanol. Pbz solutions were made up just prior to use. All other drugs were dissolved in distilled water.

Data analysis

Logistic curve fitting In control experiments designed to determine any time-dependent changes in tissue sensitivity, and in the null analysis (see below), individual E/[A] curves were fitted to a logistic of the form:

$$E = \beta + \frac{\alpha[A]^p}{[A_{50}]^p + [A]^p} \quad (1)$$

where β is the basal effect level and α, $[A_{50}]$ and p are the asymptote, location and slope parameters respectively. In the present study, A refers to the full agonist carbachol and β is the effect level produced by the partial agonist pilocarpine.

Analyses of full/partial agonist interactions

Operational model-fitting By extending the operational model of agonism (Black & Leff, 1983; see equation (3) below) to describe the interaction between a partial agonist and a full agonist it can be shown (see Appendix) that the mathematical relationship between pharmacological effect (E) and the concentrations of a full agonist ([A]) and a partial agonist ([B]) is described by the following equation:

$$E = \frac{E_m([A]K_B + \tau_B[B][A_{50}])^n}{[A_{50}]^n\ (K_B + [B])^n + ([A]K_B + \tau_B[B][A_{50}])^n} \quad (2)$$

in which E_m is the maximum possible effect; n determines the steepness of the occupancy-effect relation; K_B is the dissociation constant of the partial agonist; τ_B is the efficacy of the partial agonist: $[A_{50}]$ is the midpoint location of the control full agonist E/[A] curve.

The analysis involves simultaneously fitting the E/[A] curve data for the full agonist obtained in the absence ([B] = 0) and presence of the partial agonist to equation 2. This allows the parameters of interest, namely K_B and τ_B to be estimated and also provides estimates of, E_m, n and $[A_{50}]$. In practice, K_B, τ_B and $[A_{50}]$ are estimated as logarithms. Figure 1 illustrates the fitting procedure for typical experimental E/[A] curve data obtained in a single tissue employing one concentration of partial agonist.

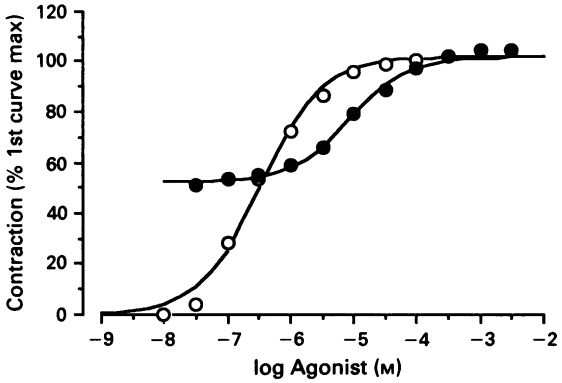

Figure 1 Operational model-fitting of full/partial agonist interaction data. Carbachol E/[A] curves were obtained in the absence (○) and presence of 30 μM pilocarpine (●). The symbols represent the data from a single tissue. The lines drawn through the data are the results of operational model-fitting. For this particular tissue the estimated model parameters were as follows: $E_m = 101.84$; $n = 0.90$; $\tau_B = 1.17$ ($\log \tau_B = 0.07$); $pK_B = 5.49$; $p[A_{50}]$ (control) = 6.47.

Null method analyses The null method was carried out by fitting logistics to each pair of curves (control and in the presence of 10 μM, 30 μM or 100 μM pilocarpine) using equation (1). Equi-effective carbachol concentrations were then interpolated at the 0.1, 0.2, 0.3, 0.4, 0.5, 0.6 and 0.7 fractional levels of the second curve asymptote. Linear regressions of these interpolated values, [A] and [A'] (the equi-effective concentrations of carbachol in the absence and presence of pilocarpine) were performed and K_B was estimated as [pilocarpine] × slope/(1-slope).

Testing for simple competition The operational model-fitting procedure also allows data from tissues in which different concentrations of partial agonist are used to be fitted simultaneously, thus providing an estimate of a model parameter, m, which is analogous to the slope parameter of a Schild plot. That is, the model tests if the interaction between the full and partial agonist is consistent with simple competition. This fitting procedure involves raising the concentration of partial agonist to the power m, each time it appears in equation 2 (i.e. $[B]^m$ replaces [B]) and then simultaneously fitting the control curves and the curves in the presence of the different concentrations of partial agonist to this modified equation. This analysis was carried out for each of the six experiments.

Estimation of the efficacy of the reference full agonist In order to apply the above methods to the analysis of partial agonists it was necessary to ensure that the reference agonist was truly full under the experimental conditions employed. To estimate the efficacy (and affinity) of the full agonist carbachol, experimental E/[A] curve data were fitted using the operational model of agonism (Black & Leff, 1983; Black *et al.*, 1985):

$$E = \frac{E_m\tau^n[A]^n}{(K_A + [A])^n + \tau^n[A]^n} \quad (3)$$

in which E_m and n are as defined above and τ and K_A are the efficacy and dissociation constant respectively of the full agonist, A. This analysis allows τ values before and after Pbz treatment to be estimated as well as K_A, E_m and n.

Experimental design

A single experiment consisted of a carbachol control pair, a carbachol analysis by the inactivation method and three pilocarpine analyses by the interaction method. This pro-

cedure was repeated with tissues from six different animals. All the data obtained in these experiments were analysed as paired curves.

All data fitting procedures were carried out using the statistical package BMDP and a Vax 11/780 mainframe computer. Differences were assessed by Student's t test and considered significant at the level of $P<0.05$.

Results

Carbachol efficacy estimation by the receptor inactivation method

E/[A] curves for carbachol were obtained before and after Pbz-treatment (10 μM for 10 min). Control experiments showed that paired carbachol E/[A] curves were not significantly different in terms of slope (p). In contrast, small but significant differences in asymptote (α) and location ($p[A_{50}]$) occurred between first and second curves, the second curves being depressed and right-shifted (see Figure 3a). These time-dependent changes were not corrected for (see Discussion). The mean logistic parameters (± s.e.; $n = 6$) of curves were as follows: 1st curve: $\alpha = 99.40$ (± 0.35); $p = 1.15$ (± 0.12; $p[A_{50}] = 6.63$ (± 0.09). 2nd curve: $\alpha = 93.25$ (± 0.82); $p = 1.21$ (± 0.11); $p[A_{50}] = 6.40$ (± 0.10).

Figure 2 illustrates typical results obtained in a single Pbz-treated tissue. The lines drawn through the data are the results of operational model-fitting. The substantial rightward shift and depression of the carbachol E/[A] curve produced by Pbz treatment indicated that the agonist has a high efficacy in this tissue. Analysis of 6 experiments gave an average estimate of efficacy (τ) of 64.6 ($\log \tau = 1.81$ (± 0.05)) and an estimate of affinity (pK_A) of 4.78 (± 0.09). The high efficacy confirmed that carbachol was indeed a full agonist in this system.

Analysis of full/partial agonist interactions

Operational model-fitting Figure 3 illustrates the results of a typical interaction experiment. The control data in panel (a) illustrates the small changes in location and asymptote of the second carbachol E/[A] curve. The lines drawn through the data in panels (b), (c) and (d) are the results of fitting the paired E/[A] curve data from each individual tissue to equation (2) and illustrate the goodness-of-fit of the data to the model. The affinity (pK_B) estimates obtained in all six experiments are given in Table 1. The average pK_B value was 5.79 ± 0.05 (mean ± s.e.; $n = 18$).

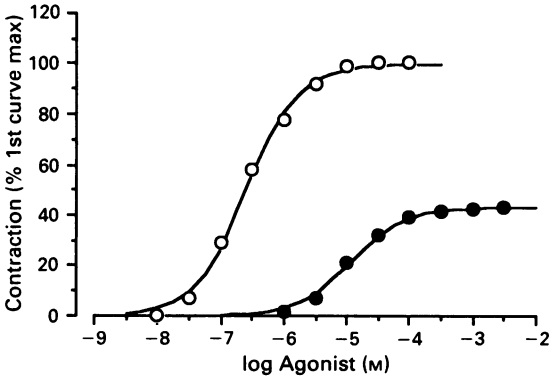

Figure 2 Effect of phenoxybenzamine (Pbz) treatment on carbachol E/[A] curves. Carbachol E/[A] curves were obtained before (○) and following 10 min exposure to 10 μM (●) Pbz. The symbols represent the data from a single tissue. The lines drawn through the data are the results of operational model-fitting. For this particular tissue the estimated model parameters were as follows: $E_m = 100.72$; $n = 1.07$; τ_1 (control) = 72.4 ($\log \tau_1 = 1.86$); τ_2 (10 μM Pbz) = 0.76 ($\log \tau_2 = -0.12$); $pK_A = 4.73$.

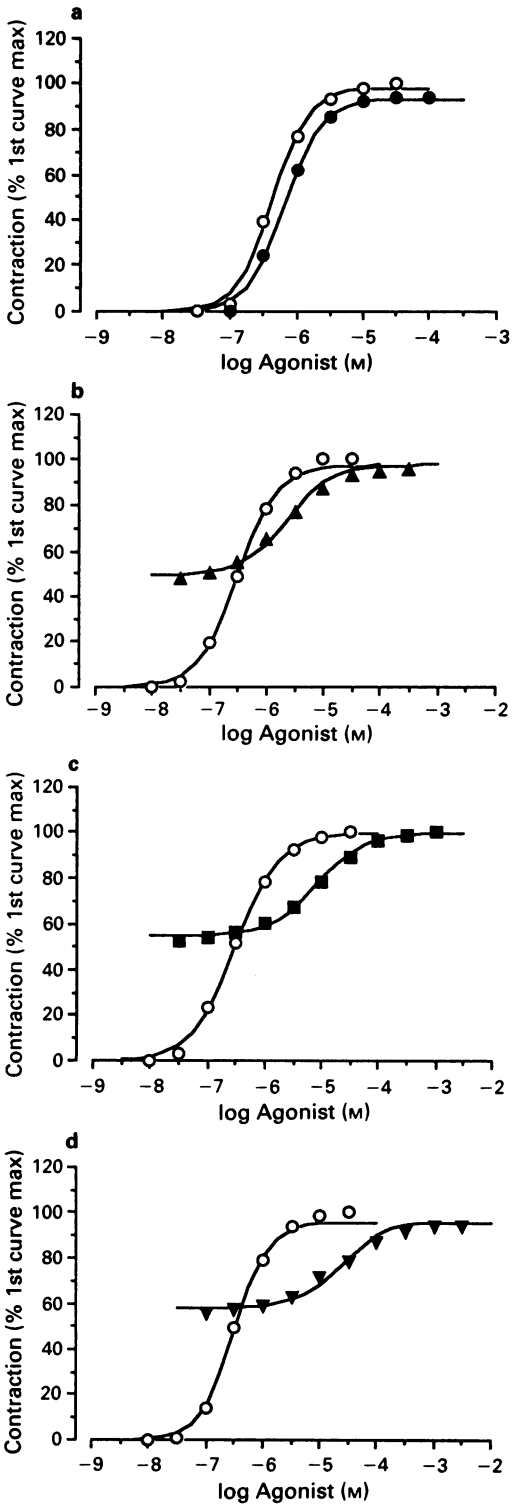

Figure 3 Operational-model fitting analyses of pilocarpine by the interaction method. The data shown are from a single experiment (experiment 5). In all panels (○) represents the carbachol E/[A] curve data in the absence of pilocarpine. In (a) (●) represents the 2nd control carbachol curve. In (b), (c) and (d) (▲), (■), and (▼) illustrate the carbachol E/[A] curve data in the presence of 10 μM, 30 μM and 100 μM pilocarpine respectively. The lines drawn through the data are the results of logistic fitting (a) and operational model-fitting (b, c and d). The model parameter estimates were as follows: panel (b) $E_m = 96.72$; $n = 1.30$; $\tau_B = 1.26$ ($\log \tau_B = 0.10$); $pK_B = 5.66$; $p[A_{50}]$ (control) = 6.51: panel (c) $E_m = 99.59$; $n = 1.14$; $\tau_B = 1.26$ ($\log \tau_B = 0.10$); $pK_B = 5.69$; $p[A_{50}]$ (control) = 6.51: panel (d) $E_m = 95.82$; $n = 1.47$; $\tau_B = 1.34$ ($\log \tau_B = 0.13$; $pK_B = 5.79$; $p[A_{50}]$ (control) = 6.50).

Table 1 Comparison of pilocarpine affinity (pK_B) estimates obtained by operational model-fitting and the null method

Pilocarpine concentration	*Method*	*pK_B Estimate*						*Mean* (± s.e.)
10 μM	Operational	5.55	5.70	5.96	5.75	5.66	5.55	5.70 ± 0.06
	Null	5.63	5.79	6.03	5.79	5.72	5.63	5.77 ± 0.06
	Difference	0.08	0.09	0.07	0.04	0.06	0.08	0.07 ± 0.01
30 μM	Operational	5.48	5.91	5.79	5.92	5.69	5.49	5.71 ± 0.08
	Null	5.52	5.97	5.91	6.00	5.79	5.55	5.79 ± 0.09
	Difference	0.04	0.06	0.12	0.08	0.10	0.06	0.08 ± 0.01
100 μM	Operational	5.91	6.06	5.99	6.17	5.79	5.86	5.96 ± 0.06
	Null	5.96	6.11	6.06	6.21	5.89	5.93	6.03 ± 0.05
	Difference	0.05	0.05	0.07	0.04	0.10	0.07	0.06 ± 0.01

All figures in a given column are from the same experiment; the first column refers to experiment 1, the last to experiment 6.

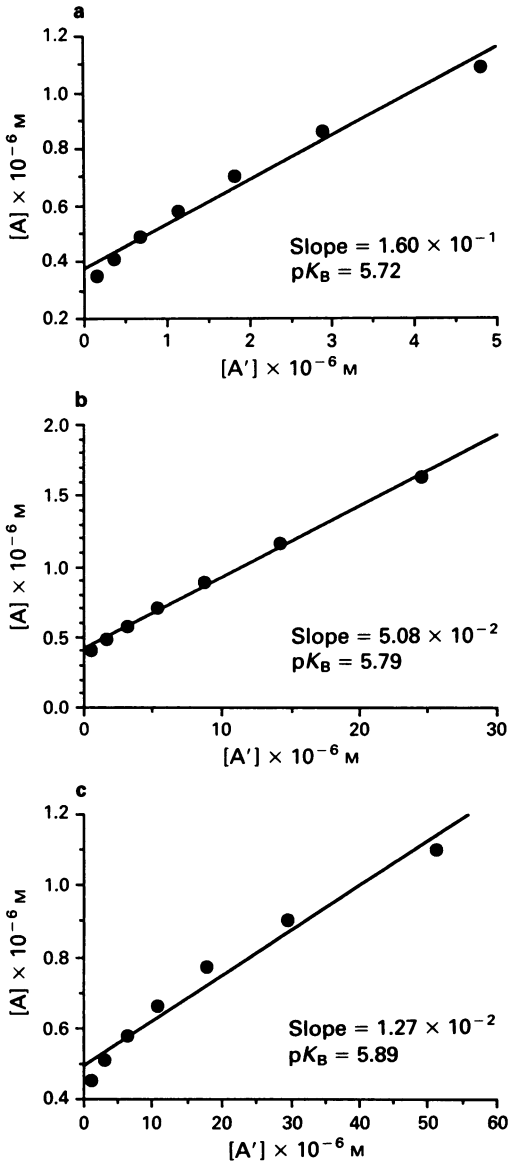

Figure 4 Plots of equi-effective concentrations of carbachol in the absence ([A]) and presence ([A']) of pilocarpine. The regression analyses were performed on the same data set as shown in Figure 3. Panels (a), (b) and (c) show plots for 10 μM, 30 μM and 100 μM pilocarpine respectively. K_B was estimated as [pilocarpine] × slope/(1-slope).

Table 2 Testing for competitive behaviour: results of simultaneously fitting experimental carbachol E/[A] curve data obtained in the presence of different concentrations of pilocarpine to the operational model

Experiment No.	*pK_B*	*Slope* (m)
1	8.19	1.58
2	8.22	1.52
3	5.85	0.99
4	9.11	1.70
5	6.05	1.07
6	6.77	1.25
Mean(± s.e.)	7.37 ± 0.54	1.35 ± 0.12

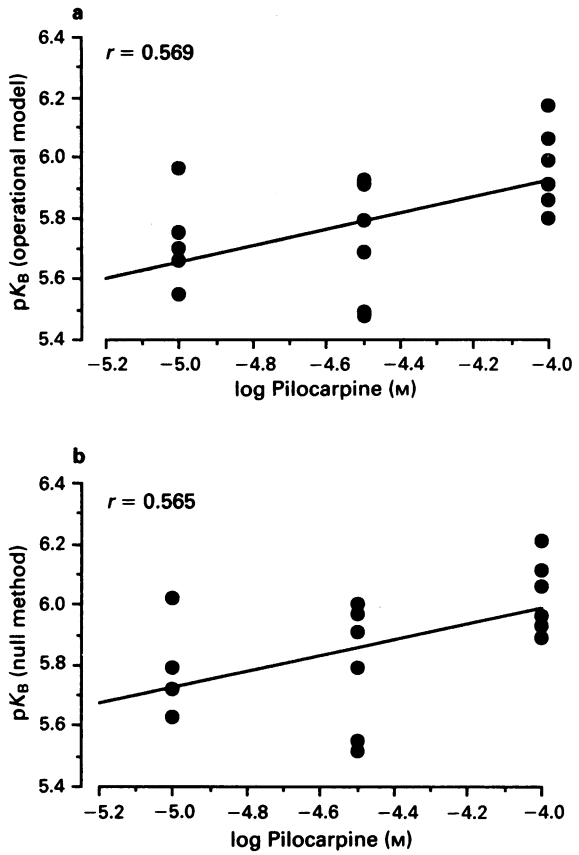

Figure 5 Correlation diagrams of pK_B estimates and pilocarpine concentration; (a) illustrates the correlation for pK_B estimates obtained by operational model fitting; (b) illustrates the correlation obtained for the null method. A significant correlation was seen in both cases.

Null method analyses The E/[A] curve data shown in Figure 3 were used to produce the plots of [A] against [A'] that are shown in Figure 4. The complete set of pK_B estimates obtained from such analyses are shown in Table 1 with the corresponding estimates obtained by operational model-fitting. The average pK_B value was 5.86 ± 0.05 (mean ± s.e.; $n = 18$). The affinities obtained by the two methods were significantly different, the null method giving a small but consistently higher estimate (mean difference = 0.07 log units; $n = 18$).

Testing for simple competition

The results of simultaneously fitting all the interaction E/[A] curve data from each experiment to the modified version of equation 2 are shown in Table 2. The mean slope parameter (m) estimate was 1.35 ± 0.12 (± s.e.; $n = 6$). This value was significantly greater than unity indicating that the interaction was not consistent with simple competitive behaviour. This lack of adherence to simple competition is also evident when the individual pK_B estimates (Table 1) obtained by both the operational model and null method are plotted as a function of the pilocarpine concentration (Figures 5a and b respectively). There is a significant correlation in both plots; for simple competitive behaviour the estimated pK_B values should be independent of the pilocarpine concentration. These plots also show that it is the data obtained with the highest concentration of pilocarpine (100 μM) that are responsible for the observed deviation from competitive behaviour; the pK_B estimates obtained using 10 μM and 30 μM are not significantly different (see Table 1).

Discussion

Previous publications (Black *et al.*, 1985; Leff *et al.*, 1990) have shown how the operational model of agonism is used to estimate agonist affinities and efficacies when the receptor inactivation method (Furchgott, 1966) and the comparative method (Barlow *et al.*, 1967) are employed.

The aim of this study was to extend the operational model to describe the interaction between a partial agonist and a full agonist. This method is important in pharmacology as the displacement of the control full agonist E/[A] curve by the partial agonist confirms that the two agonists interact with the same receptor type. The interaction method thus confirms mechanism and establishes that the partial agonist has genuine low efficacy. In contrast, the comparative method, which is also used to analyse partial agonists makes the assumption that the full and partial agonist interact with the same receptor type but does not test it.

The derived equation (equation 2) was used to analyse experimental E/[A] curve data generated for the interaction between pilocarpine (partial agonist) and carbachol (full agonist) at the M_3-receptor mediating contraction of the guinea-pig isolated trachea. The goodness-of-fit of the model-fitted curves to the experimental data (see Figures 1 and 3) suggest that the operational model accounts quantitatively and qualitatively for the data presented here. The other criterion by which the model can be judged quantitatively is in its ability to determine accurately the partial agonist dissociation constant, K_B. To this end the data were analysed by the method of Stephenson (1956). This null approach, in principle should provide the most assumption-free pragmatic estimate of K_B. Comparison of the estimates obtained by the two methods showed small but significant differences, the null method producing a higher affinity estimate than the operational model (mean difference = 0.07 log units; see Table 1). It is likely that part of this difference can be explained by the different fitting procedures employed by the two methods since analysis of simulated data resulted in a higher affinity estimate by the null method (mean difference = 0.03 log units; $n = 6$, data not shown) than by the operational model. Whatever the reason for the small differences observed, the similarity of the results obtained by the two methods leads us to conclude that the model can be used to provide reliable estimates of the dissociation constant of a partial agonist.

For the purposes of data analysis such a model-fitting approach has several advantages. In the null method a number of choices have to be made regarding data to be analysed and the means by which to analyse them. Equi-effective concentrations of full agonist in the absence and presence of the partial agonist are interpolated between curves, either drawn by eye or produced by logistic fitting. In neither case do the interpolated concentrations necessarily correspond to 'real' data points and differences in the choice of interpolations introduces differences in precision of K_B estimation. Having calculated equi-effective agonist concentrations by whatever means they are typically analysed by linear regression, which may be inappropriate as both sets of concentration data are estimated with error. The direct-fitting approach using the operational model not only eliminates the need for all these considerations but also uses the raw E/[A] curve data without transformation. Furthermore, this direct treatment of the data means they can be displayed along with the model-fitted lines on the scale on which the responses are recorded (in contrast to a plot of equieffective concentrations for the null method). This facilitates assessment of goodness-of-fit.

We analysed the experimental data by both a single curve (using the second curve obtained in each tissue) analysis (results not shown) and a paired curve (using both curves from each tissue) analysis. The paired curve analyses were preferred despite the small right shift and depression observed in the second carbachol control curves (see Results and Figure 3a). The reasons for this preference were as follows. Firstly, this is analytically the simplest way to treat the data since it allows a single estimate of K_B (and τ_B) to be made in each tissue. Individual estimates obtained in different tissues can then be averaged. Such analysis also encompasses the effect of τ_B on K_B estimation in different tissues. Secondly, in the null method a single curve design would necessitate using the same control E/[A] curve to analyse the effects of different concentrations of partial agonist. This would have the effect of overweighting the control data; in the case of the operational model simultaneous fitting of the data allows each curve to be given similar weight in the analysis.

When multiple concentrations of partial agonist are used, as in this study, the fitting procedure can be extended to allow the competitive nature of the interaction to be studied. An equivalent test of competition for the null method has been described (Kaumann & Marano, 1982) but involves plotting the slope of the regression analyses of individual null plots as a function of partial agonist concentration; that is log(1/slope-1) is plotted against log [B]. Use of the operational model simply involves fitting all the data simultaneously to a modified version of equation (2) in which the term [B] is raised to the power m, the order of the reaction of the partial agonist with its receptors. The model parameter m is thus analogous to the slope parameter of a Schild plot.

When the data were analysed in this way the estimated slope parameter (m) was found to be significantly greater than unity (1.35) (see Table 2) indicating that the interaction was not consistent with simple competition. This deviation from competitive behaviour was also evident when the individual pK_B estimates were plotted as a function of pilocarpine concentration (see Figure 5). Furthermore, it was evident from these plots that it was the data obtained with the highest concentration of pilocarpine (100 μM) that caused the deviation from competitive behaviour. The reason for this is unclear at present but will be the subject of future investigations. In conclusion, the results of this study suggest that the operational model may be fitted directly to E/[A] curve data to estimate partial agonist dissociation constants

and that this model-fitting approach is a valid and analytically simple alternative to the conventional null method.

Appendix: *Derivation of equation (2)*

A two-agonist-one receptor model

Following the nomenclature of Furchgott (1966) the system under consideration may be represented by the scheme:

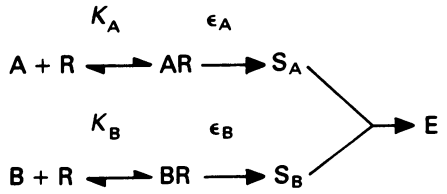

The full agonist, A and the partial agonist, B occupy receptors R to form agonist-receptor complexes AR and BR respectively. The affinities of the agonists for the receptors are defined by K_A and K_B, the agonist dissociation constants. The agonist-receptor complexes impart stimuli, S_A and S_B to the system that are proportional to the agonists respective intrinsic efficacies (ε_A and ε_B). The measured pharmacological effect (E) is some function of the total stimulus ($S_{tot} = S_A + S_B$). The derivation of equation (2) therefore necessitates finding E as a function of S_{tot}.

From the above:

$$S_{tot} = S_A + S_B = \varepsilon_A[AR] + \varepsilon_B[BR] \quad (i)$$

The equilibrium concentrations or receptors occupied by A and B in the presence of each other are given by the following equations:

$$[AR] = \frac{[R_0][A]}{[A] + K_A(1 + [B]/K_B)} \quad (ii) \qquad [BR] = \frac{[R_0][B]}{[B] + K_B(1 + [A]/K_A)} \quad (iii)$$

where $[R_0]$ represents the total functional receptor concentration in the tissue.

Substituting (ii) and (iii) into (i) gives:

$$S_{tot} = \frac{\varepsilon_A[A][R_0]K_B + \varepsilon_B[B][R_0]K_A}{[A]K_B + K_AK_B + K_A[B]} \quad (iv)$$

Let

$$E = \frac{E_m(S_{tot})^n}{1 + (S_{tot})^n} \quad (v)$$

thus E is a logistic function of (S_{tot}), n accounts for non-hyperbolic agonist concentration-effect curves and when $S_{tot} = 1$, $E = 0.5\,E_m$.

Inserting equation (iv) into equation (v) gives:

$$E = \frac{E_m(\varepsilon_A[A][R_0]K_B + \varepsilon_B[B][R_0]K_A)^n}{([A]K_B + K_AK_B + K_A[B])^n + (\varepsilon_A[A][R_0]K_B + \varepsilon_B[B][R_0]K_A)^n} \quad (vi)$$

The terms $\varepsilon_A[R_0]$ and $\varepsilon_B[R_0]$ are equivalent to the operational model parameters τ_A and τ_B therefore equation (vi) can be rewritten as:

$$E = \frac{E_m(\tau_A[A]K_B + \tau_B[B]K_A)^n}{([A]K_B + K_AK_B + K_A[B])^n + (\tau_A[A]K_B + \tau_B[B]K_A)^n} \quad (vii)$$

For a full agonist $K_A >> [A]$ therefore equation (vii) reduces to:

$$E = \frac{E_m(\tau_A[A]K_B + \tau_B[B]K_A)^n}{K_A^n(K_B + [B])^n + (\tau_A[A]K_B + \tau_B[B]K_A)^n} \quad (viii)$$

Dividing throughout by τ_A^n and defining K_A/τ_A as $[A_{50}]$ gives:

$$E = \frac{E_m([A]K_B + \tau_B[B][A_{50}])^n}{[A_{50}]^n(K_B + [B])^n + ([A]K_B + \tau_B[B][A_{50}])^n} \quad (ix)$$

This model describes the interaction of a partial agonist and a full agonist in terms of 5 parameters, E_m the maximum possible effect; n the slope index of the common transducer function linking agonist occupancy to effect; K_B the dissociation constant of the partial agonist; τ_B the efficacy of the partial agonist and $[A_{50}]$ the midpoint location of the control full agonist E/[A] curve.

References

BARLOW, R.B., SCOTT, N.C. & STEPHENSON, R.P. (1967). The affinity and efficacy of onium salts on frog rectus abdominis. *Br. J. Pharmacol.*, **31**, 188–196.

BLACK, J.W. & LEFF, P. (1983). Operational models of pharmacological agonism. *Proc. R. Soc. B*, **220**, 141–162.

BLACK, J.W., LEFF, P., SHANKLEY, N.P. & WOOD, J. (1985). An operational model of agonism: the effect of E/[A] curve shape on agonist dissociation constant estimation. *Br. J. Pharmacol.*, **84**, 561–571.

DOUGALL, I.G., HARPER, D. & LEFF, P. (1993). A direct operational model-fitting approach to the estimation of partial agonist affinity by the interaction method. *Br. J. Pharmacol.*, (in press).

FURCHGOTT, R.F. (1966). The use of β-haloalkylamines in the differentiation of dissociation constants of receptor-agonist complexes. *Adv. Drug Res.*, **3**, 21–55.

KAUMANN, A.J. & MARANO, M. (1982). On equilibrium dissociation constants for complexes of drug-receptor subtypes. *Naunyn-Schmied. Arch. Pharmacol.*, **318**, 192–201.

LEFF, P., PRENTICE, D.J., GILES, H., MARTIN, G.R. & WOOD, J. (1990). Estimation of agonist affinity and efficacy by direct, operational model-fitting. *J. Pharmacol. Methods*, **23**, 225–237.

MARANO, M. & KAUMANN, A.J. (1976). On the statistics of drug-receptor constants for partial agonists. *J. Pharmacol. Exp. Ther.*, **198**, 518–525.

STEPHENSON, R.P. (1956). A modification of receptor theory. *Br. J. Pharmacol. Chemother.*, **11**, 379–393.

(Received February 8, 1993
Revised May 5, 1993
Accepted May 10, 1993)

Br. J. Pharmacol. (1993), **110**, 245–252

Pharmacological characterization of the novel nonpeptide angiotensin II receptor antagonist, BIBR 277

W. Wienen, N. Hauel, J.C.A. Van Meel, B. Narr, U. Ries & [1]M. Entzeroth

Department of Pharma Research, Dr. Karl Thomae GmbH P.O. Box 1755, D-7950 Biberach 1, Germany

1 The pharmacological profile of BIBR 277, 4'-[(1,4'-dimethyl-2'-propyl[2,6'-bi-1H-benzimidazol]-1'-yl)methyl]-[1,1'-biphenyl]-2-carboxylic acid, a novel, nonpeptide angiotensin II receptor antagonist has been investigated by use of receptor binding studies, enzymatic assays, functional *in vitro* assays in rabbit aorta as well as *in vivo* experiments in pithed, anaesthetized and conscious rats.

2 BIBR 277 potently interacted with rat AT_1 receptors (K_i 3.7 nM). Competitive receptor interaction was shown by radioligand saturation experiments performed in the presence of BIBR 277. The failure to inhibit radioligand binding to AT_2 sites demonstrates the selectivity of BIBR 277 for AT_1 receptors. This is further substantiated by the findings that BIBR 277 neither interacted with other receptor systems investigated nor affected the activity of components of the human renin-angiotensin system, such as plasma renin or serum converting enzyme.

3 In rabbit aorta, BIBR 277 had no agonistic properties and was shown to be an insurmountable antagonist of angiotensin II-induced contractions (K_B 0.33 nM). The antagonistic effect persisted even after several wash-out procedures. However, this interaction was not irreversible since the insurmountable antagonism was concentration-dependently reversed when BIBR 277 (0.1 μM) and the surmountable antagonist, losartan (0.1 and 1.0 μM) were incubated simultaneously. The specificity of BIBR 277 for the AT_1 receptor was further substantiated in this preparation since micromolar concentrations of BIBR 277 neither affected potassium chloride and noradrenaline-induced contractions nor acetylcholine-mediated tissue relaxation.

4 In pithed rats, i.v. administration of BIBR 277 (0.1, 0.3 and 1.0 mg kg^{-1}) shifted the dose-pressor response curve to angiotensin II dose-dependently to the right with ED_{50} values of 0.23 μg kg^{-1} (control) and 1.4 μg kg^{-1}, 4.7 μg kg^{-1} and 20 μg kg^{-1}, respectively. As observed in the *in vitro* experiments no agonistic effect was detected and the maximum of the blood pressure response to angiotensin II at the highest dose of BIBR 277 was decreased by 29%.

5 In anaesthetized rats, bolus i.v. administration of 0.1, 0.3 and 1.0 mg kg^{-1} BIBR 277 attenuated the blood pressure response to bolus i.v. injections of angiotensin II (0.1 μg kg^{-1}). At the highest dose an almost complete blockade was observed even after 2 h.

6 Single oral administration of BIBR 277 (0.3 and 1.0 mg kg^{-1}) to conscious, chronically instrumented renovascular hypertensive rats dose-dependently decreased the mean arterial blood pressure by 15 and 30 mmHg, respectively. At the higher dose a significant antihypertensive effect was maintained for more than 24 h. Moreover, consecutive daily dosing of 1 mg kg^{-1} orally resulted in a sustained reduction in blood pressure over the 4 day observation period.

7 It is concluded that BIBR 277 is an effective and selective angiotensin II antagonist with antihypertensive activity after oral administration.

Keywords: Angiotensin II receptor; BIBR 277; losartan

Introduction

The renin-angiotensin system (RAS) is of principal importance for the regulation of cardiovascular function and body fluid composition (Peach, 1977; Valloton, 1987). Angiotensin II (AII), the primary biologically active peptide hormone of the RAS, elicits multiple pharmacological effects such as, for example, an increase in blood pressure and vascular contraction (Catt *et al.*, 1984; Fujii *et al.*, 1985), release of aldosterone from the adrenals (Mendelson & Kachel, 1980) and modulation of central effects such as drinking behaviour (Phillips, 1987). The hormone exerts these effects through interaction with specific AII membrane receptors (Bumpus *et al.*, 1991) of which two subtypes, namely AT_1 and AT_2, have thus far been identified clearly.

The potential pathophysiological involvement of the RAS in hypertension and congestive heart failure in animals and man has been shown by the introduction of inhibitors of angiotensin I converting enzyme (ACE) (Antonaccio & Wright, 1987; Packer, 1987; Robertson & Tillman, 1987). However, there is evidence to suggest that unwanted side effects of ACE inhibitors such as cough or angioedema (Wood *et al.*, 1987; Gavras & Gavras, 1988) result from the lack of specificity of ACE for angiotensin I. In addition, the metabolism of other peptides such as bradykinin is affected. More recently, it has been shown (Okunishi *et al.*, 1987; Kinoshita *et al.*, 1991) that AII can also be formed by a chymotrypsin like proteinase in man which is not affected by ACE inhibitors. A logical approach to overcome those unwanted side effects is the specific blockade of AII receptors. Early attempts with peptide analogues of AII were unsuccessful due to their partial agonistic activity and their poor oral availability (Pals *et al.*, 1971). The recent discovery of the nonpeptide, imidazole-like AII antagonists, the prototype of which is losartan (DuP 753, MK954) (for review see Wong *et al.*, 1991), provided new tools to explore the physiological and pathophysiological role of AII and its receptors and also to generate new therapeutic agents for the treatment of cardiovascular diseases.

In the present study, we report on the *in vitro* and *in vivo* pharmacology of a novel, highly potent and selective AT_1 receptor antagonist, BIBR 277, 4'-[(1,4'-dimethyl-2'-propyl-[2,6'-bi-1H-benzimidazol]-1'-yl)methyl]-[1,1'-biphenyl]-2-carboxylic acid (Figure 1). Preliminary accounts of this work

[1] Author for correspondence.

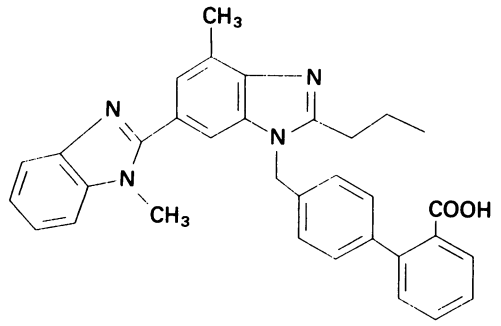

Figure 1 Chemical structure of BIBR 277.

have been presented to the British Pharmacological Society (Entzeroth *et al.*, 1993; Van Meel *et al.*, 1993).

Methods

Binding studies

Membrane preparations from rat lung and adrenal medulla were obtained as follows: male Wistar rats (strain Chbb:THOM, 200–220 g) were killed by a blow to the neck. The tissues were dissected out, cleaned and homogenized in Tris-buffer (50 mM Tris, 150 mM NaCl, 5 mM EDTA, pH 7.20) by use of an Ultra Turrax at maximal setting for 30 s. The homogenate was centrifuged for 10 min at 1 000 *g* and the resulting supernatant was recentrifuged twice for 20 min at 48 000 *g*. The final pellet was resuspended in incubation buffer (50 mM Tris, 5 mM $MgCl_2$, 0.2% bovine serum albumin, pH 7.20) before performing binding experiments in triplicate. For competition experiments protein (lung: 40–100 μg, adrenal medulla: 1–10 μg) was incubated with 50 pM [^{125}I]-AII and increasing concentrations of the competitor at 37°C for 60 min in a total volume of 0.2 ml. For saturation experiments 40–100 μg lung protein was incubated under identical conditions with vehicle or BIBR 277 (3 nM or 10 nM) and increasing concentrations of [^{125}I]-AII (10–10 000 pM). The incubations were terminated by rapid filtration through glass fibre filters using a Scatron cell harvester. The filters were washed twice in ice-cold buffer and particle-bound radioligand was assayed in a γ-counter. Non-specific binding was defined as radioactivity bound in the presence of 1 μM AII in the incubation medium. Protein was determined according to the method of Lowry *et al.* (1951) with bovine serum albumin used as standard. In addition, the affinity of BIBR 277 for other receptors was investigated according to standard procedures. The radioligands, tissue preparations and incubation conditions used are summarized in Table 1.

Plasma renin activity

The interaction of BIBR 277 with plasma renin was determined with a commercial test kit (Isotopen Diagnostik, Dreieich, Germany): 500 μl human EDTA plasma samples, obtained from healthy volunteers, were incubated for 150 min at 37°C with the test compounds (H142 (H-Pro-His-Pro-Phe-His-Leu(CH_2NH)Val-Ile-His-Lys-OH) 0.1 μM, BIBR 277 10 μM) according to the instructions of the manufacturer. Angiotensin I generated was determined by a radioimmunoassay which shows a high selectivity for AI, i.e. cross-reactions with AII and AII fragments of $<0.1\%$, and a detection limit of 0.13 ng AI ml^{-1}.

Angiotensin converting enzyme activity

Angiotensin converting enzyme activity was determined following the procedure of Neels *et al.* (1983). In brief, 10 μl human serum was incubated with 100 μl substrate solution (50 mM HEPES, 300 mM NaCl, 400 mM Na_2SO_4, 30 mM hippuryl-glycyl-glycine, pH 8.15) and the test compounds (captopril: 0.1 μM, BIBR 277, 10 μM) for 30 min at 37°C. The reaction was terminated by the addition of 100 μl 10% sodium tungstate solution and 100 μl 0.33 M H_2SO_4. After centrifugation and addition of 2,4,6-trinitrobenzene sulphonic acid, the amount of substrate hydrolyzed was determined photometrically (420 nm) in a Shimadzu UV-120-02 spectrophotometer.

In vitro *experiments in rabbit aortic rings*

Female New Zealand white rabbits (strain Chbb/NZW; 1.5 kg) were killed by cervical dislocation and exsanguinated. The descending thoracic aorta was dissected free, transferred to prewarmed (37°C) and oxygenated Krebs bicarbonate buffer solution, and cleaned of adherent fat and connective tissue. The aorta was cut into 5 mm rings, and the rings were mounted in 30 ml organ baths, containing Krebs bicarbonate solution of the following composition (in mM): NaCl 118, KCl 4.7, $MgSO_4$ 1.2, $NaHCO_3$ 25, KH_2PO_4 1.2, glucose 10

Table 1 Affinity profile of BIBR 277 SE in different receptor assays for peptide and nonpeptide ligands

Binding site	*Radioligand, tissue, incubation conditions*	K_i (nM)
Adenosine A_1	[^{3}H]-DPCPX (0.1 nM), rat brain, 1 h/room temperature	15 000
Adenosine A_2	[^{3}H]-NECA (0.5 nM)/50 nM cyclopentyl-adenosine, calf striatum, 1 h/room temperature	> 100 000
α_1	[^{3}H]-prazosin (0.5 nM), rat heart, 1 h/ room temperature	> 100 000
α_2	[^{3}H]-clonidine (0.5 nM), rat cerebral cortex, 1 h/room temperature	> 100 000
β_1	[^{3}H]-(−)-CGP 12177 (0.2 nM), rat heart, 3 h/room temperature	> 30 000
β_2	[^{3}H]-(−)-CGP 12177 (0.2 nM), rat lung, 3 h/room temperature	> 30 000
Dopamine D_1	[^{3}H]-SCH 23390 (250 pM), rat striatum, 1 h/room temperature	15 000
Dopamine D_2	[^{3}H]-spiperone (250 pM), rat striatum, 1 h/room temperature	> 100 000
Endothelin ET_A	[^{125}I]-endothelin-1 (10 pM), bovine heart, 24 h/0°C	> 100 000
Histamine H_1	[^{3}H]-pyrilamine (1 nM), rat brain, 1 h/room temperature	> 70 000
Imipramine	[^{3}H]-imipramine (2 nM), rat cerebral cortex, 1 h/0°C	> 100 000
Muscarinic M_1	[^{3}H]-pirenzepine (1 nM), rat cerebral cortex, 90 min/room temperature	78 000
Muscarinic M_2	[^{3}H]-NMS (300 pM), rat heart, 45 min/room temperature	> 50 000
Muscarinic M_3	[^{3}H]-NMS (300 pM), rat submandibular gland, 45 min/room temperature	> 50 000
Neurokinin NK_1	[^{125}I]-substance P (10 pM), rat submandibular gland, 45 min/room temperature	20 000
Neurokinin NK_2	[^{125}I]-neurokinin A (50 pM), rat bladder, 90 min/room temperature	20 000
Neuropeptide Y	[^{125}I]-neuropeptide Y (10 pM), rabbit kidney cortex, 2 h/room temperature	> 10 000
5-HT_2	[^{3}H]-ketanserin (2 nM), rat cerebral cortex, 1 h/room temperature	> 50 000

K_i values were obtained according to Cheng & Prusoff (1972) from the respective IC_{50} values determined in radioligand displacement experiments.

and $CaCl_2$ 2.5. The Krebs solution was kept at 37°C and pH 7.4 while being bubbled continuously with 5% CO_2 in O_2. Isometric contraction was recorded with Statham UC-2 force transducers. Initial resting tension was set to 2.0 g, and the rings were allowed to equilibrate for approximately 90 min. During this period, the rings were stimulated twice by the addition of AII to the bath, in a final concentration of 30 nM. An interval of 30 min was left between each stimulation. After the maximum contractile response was reached, the rings were rinsed three times and were allowed to return to baseline tension. A control cumulative concentration-contractile response curve for AII (0.3 nM to 100 nM) was first determined. The tissue was washed three times until base line was reached. Fifteen min later, BIBR 277 at 10 to 1000 nM was added and the tissue was incubated with the drug for 90 min. The concentration-contractile response curve was then repeated in the presence of BIBR 277. To exclude any influence of multiple dosing with BIBR 277 on the concentration-contractile response curve, each tissue was incubated with only one concentration of the antagonist. Responses were expressed as a percentage of the maximal AII response obtained from the first cumulative concentration-response curve. As BIBR 277 was found to exert non-competitive AII antagonism, the dissociation constant K_B (= [B]/(slope-1); [B] is the concentration of the antagonist) was derived from the double-reciprocal regression as described by Kenakin (1987). For receptor protection studies rabbit aortic rings were incubated for 90 min with BIBR 277 (0.1 μM) either in the absence or presence of two different concentrations (0.1 and 1 μM) of losartan. The concentration-response curve to AII was then repeated in the presence of the test compounds.

In additional experiments we studied the washout kinetics of BIBR 277 in this preparation. After the equilibration period, the tissues were again challenged with a single AII dose, in a final concentration of 30 nM. The maximum contractile force from this challenge was taken as the control response to AII. Tissues were then incubated for 90 min with either the solvent or BIBR 277 (10 nM) and were again challenged with AII (30 nM). Thereafter, BIBR 277 (or vehicle) was removed from the tissues by thorough washing. The tissues were again equilibrated for an additional 40 min, during which the medium was exchanged five times with fresh buffer. Additional challenges with AII (30 nM) were performed 40, 80, and 120 min after removal of the antagonist (or vehicle).

The concentration-contractile response for noradrenaline and KCl was also examined in the presence or absence of BIBR 277 at 10 μM to test the specificity of this antagonist. Furthermore, the effect of BIBR 277 (1 μM) on acetylcholine-induced, endothelium-dependent relaxation was investigated in rabbit aortic rings with intact endothelium, precontracted with noradrenaline (0.3 μM).

Pithed rats

Male rats (strain Chbb: THOM, 220–250 g) were anaesthetized with hexobarbitone-sodium (150 mg kg^{-1}, i.p.) and the trachea was cannulated for artificial respiration by a positive pressure pump. Subsequently, the animals were pithed and the jugular vein and a carotid artery were cannulated for intravenous administration and registration of arterial blood pressure, respectively. Body temperature was kept constant by a heating pad. BIBR 277 was dissolved in 1 M NaOH and the solution was stabilized with 1.8 (w/v)% hydroxypropyl-β-cyclodextrin. The pH of the solution was adjusted to pH 10–11 with 1 M HCl. BIBR 277 was administered in a dose of 0.1, 0.3 and 1 mg kg^{-1}. Two min after injection of BIBR 277 AII was cumulatively injected (0.03–300 μg kg^{-1}) to construct dose-response curves. These curves were compared with a control curve which was obtained after administration of the vehicle. The volume administered per dose AII was 0.05 ml 100 g^{-1} body weight.

AII pressor response in anaesthetized rats

Male rats (strain Chbb: THOM, 230–260 g) were anaesthetized with pentobarbitone-sodium (60 mg kg^{-1}, i.p.) and placed on a heating pad to keep body temperature constant. The trachea was exposed and cannulated with a polyethylene tube and both the left carotid artery and the contralateral jugular vein were catheterized for measurement of arterial blood pressure and administration of AII or BIBR 277, respectively. The arterial catheter was connected to a pressure transducer (Braun Melsungen/Germany) coupled to a polygraph (IFD, Mühlheim/Germany) for monitoring arterial blood pressure. Anaesthesia was kept at a constant level during the experiment by an intraperitoneal infusion of pentobarbitone-sodium at a rate of 0.27 mg kg^{-1} min^{-1}. After a 30 min stabilization period, AII at 0.1 μg kg^{-1} was given i.v. twice prior to administration of BIBR 277 or vehicle. The AII challenge was then repeated after 2, 5, 10, 20, 40, 60, 90, and 120 min in the presence of BIBR 277 or vehicle, respectively. BIBR 277 was dissolved in 1 M HCl. This solution was further stabilized wth 1.8% (w/v) hydroxypropyl-β-cyclodextrin and adjusted to physiological pH. BIBR 277 was administered at doses of 0.1, 0.3 and 1 mg kg^{-1}.

Renovascular hypertensive rats

Male rats (Chbb: THOM; 140–150 g) were anaesthetized with pentobarbitone-sodium (50 mg kg^{-1}, i.p.). The abdominal cavity was opened by a midline incision. A solid silver clip with an internal diameter of 0.20 mm was applied to the left renal artery as close as possible to the aorta. Care was taken that the artery rested at the base of the slit and that a visible blood flow remained in the artery behind the clip. The contralateral kidney was not disturbed. The catheter of a pressure transmitter (TA11PA-C40, Data Sciences Inc., St. Paul, MN, U.S.A.) was inserted in the abdominal aorta and the transmitter was fixed to abdominal musculature. The abdomen was closed with Mersilene (Avalon, Norderstedt, Germany) sutures. The animals were allowed to recover for 2 weeks and housed in individual cages with free access to standard rat chow and tap water *ad libitum*, with 12-h light/dark cycles. After the implantation of the device blood pressure and heart rate were transmitted by telemetry and the signals received by a RA 1010 General Purpose Receiver (Data Sciences Inc., St. Paul, MN, U.S.A.). Data were acquired with the Dataquest IV 1.11 System on a Hewlett Packard Vectra ES/12 386 computer. BIBR 277 was dissolved in 1 M NaOH. The pH was adjusted to 10 with 1 M HCl and the solution was further diluted with saline. For single administration 0.3 and 1.0 mg kg^{-1} BIBR 277 were given orally in a total volume of 2.0 mg kg^{-1}. For repeated dosing the animals were treated with 1 mg kg^{-1} day^{-1} BIBR 277 over a period of 4 days.

Data analysis

Results are given as mean ± s.e.mean. Binding data were analysed by a computer-assisted non-linear least-square curve fitting method using the RS/1 software package (BBN Research Systems, Cambridge, MA, U.S.A.). IC_{50} values were corrected for the radioligand occupancy shift to obtain the inhibition constant (K_i) according to Cheng & Prusoff (1973). Saturation experiments were analysed according to Scatchard (1949). *In vitro* and *in vivo* data were fitted by non-linear regression using GraphPad Inplot software (GraphPad Software Inc., SanDiego, CA, U.S.A.). Competitive antagonist-receptor interaction was analysed according to Arunlakshana & Schild (1959). Statistical analysis were performed by two-tailed analysis of variance, Student's t test. Differences were considered statistically significant at $P \leqslant 0.05$.

Materials

Radioligands were obtained from Amersham (Braunschweig, Germany), New England Nuclear (Dreieich, Germany), and Biotrend (Cologne, Germany). Angiotensin II was purchased from Bachem Biochemica (Heidelberg, Germany), H142 from Novabiochem (Bad Soden, Germany). Hydroxypropyl-β-cyclodextrin was obtained from Sigma (Steinheim, Germany). Pentobarbitone-sodium and hexobarbitone-sodium were obtained from Sanofi (Hannover, Germany) and Serva (Heidelberg, Germany). Captopril, losartan and PD 123.177 (1-(4-amino-3-methyl-benzyl)-5-diphenylacetyl-4,5,6,7-tetrahydro-imidazole[4,5]pyridine-6-carboxylic acid) were synthesized in the chemistry department of Dr Karl Thomae GmbH. All other chemicals were the best grade commercially available.

Results

Receptor binding studies

The inhibition of specific [^{125}I]-AII binding to rat lung membranes by unlabelled AII was concentration-dependent with an inhibition constant (K_i) of 1.2 ± 0.4 nM ($n = 3$) (Figure 2a). The Hill coefficient of 1.09 ± 0.04 was not significantly different from unity indicating the interaction with a single class of binding sites. Inhibition of radioligand binding by BIBR 277 revealed a high affinity of this compound to AII receptors in rat lung tissue preparations with a K_i value of 3.7 ± 0.7 nM. Analysis of the competition curve indicated binding to a single class of binding sites with a Hill coefficient of 0.87 ± 0.07, which was not significantly different from unity. The AT_1 selective antagonist losartan inhibited radioligand binding with a K_i value of 23.7 ± 2.5 nM. The Hill coefficient was 0.99 ± 0.01. In contrast, the AT_2 selective antagonist PD 123.177 did not affect [^{125}I]-AII binding in nanomolar concentrations and had a K_i value of > 10 000 nM.

Interaction of the compounds with AT_2 receptors was investigated in [^{125}I]-AII competition experiments in rat adrenal medulla tissue preparations (Figure 2b). AII inhibited specific radioligand binding with a K_i value of 0.31 ± 0.01 nM. The Hill coefficient was 1.01 ± 0.02. PD 123 177 completely inhibited [^{125}I]-AII binding with a K_i value of 76.0 ± 16.6 nM and a Hill coefficient 0.86 ± 0.06. BIBR 277 and losartan were ineffective in nanomolar concentrations and had K_i values of > 10 000 nM.

The effect of BIBR 277 on the binding of [^{125}I]-AII to AT_1 receptors was further investigated in saturation experiments in rat lung preparation. As shown by Scatchard analysis of the binding data (Figure 3), 3 nM and 10 nM BIBR 277 increased the K_d of the radioligand from 0.51 ± 0.03 nM ($n = 4$) to 0.82 ± 0.12 nM and 1.9 ± 0.98 nM, respectively, whereas the corresponding B_{max} remained unchanged.

In additional binding experiments we investigated the interaction of BIBR 277 with other receptor systems. As shown in Table 1, in sub-micromolar concentrations BIBR 277 neither interacted with other receptors for non-peptide ligands (acetylcholine, adenosine, catecholamines, histamine, imipramine or 5-hydroxytryptamine) nor with other receptors for peptide ligands such as endothelin, neurokinins or neuropeptide Y.

Effect on ACE and plasma renin activity

The possible interference of BIBR 277 with components of the human RAS was determined in enzymatic assays. The renin activity in human plasma was not affected by 10 μM BIBR 277 (106 ± 8.5% of control) whereas it was potently attenuated by the renin inhibitor H142 (0.1 μM) to 2.4 ± 0.03% of control values (3.4 ± 0.1 ng AI ml^{-1} h^{-1}, $n = 3$). Furthermore, BIBR 277 (10 μM) did not affect the activity of human serum ACE (280 ± 3.5 u l^{-1} vs. control, 287 ± 6.9 u l^{-1}, $n = 3$) whereas it was decreased to 16.4 ± 0.3% ($n = 3$) of control values in the presence of 0.1 μM captopril.

Rabbit aortic rings

In rabbit aorta, BIBR 277 (10, 100, and 1000 nM) produced rightward shifts in the concentration-contractile response curve for AII (Figure 4). However, a significant decrease of the Hill-slope from control (2.12 ± 0.08; $n = 18$) to 1.76 ±

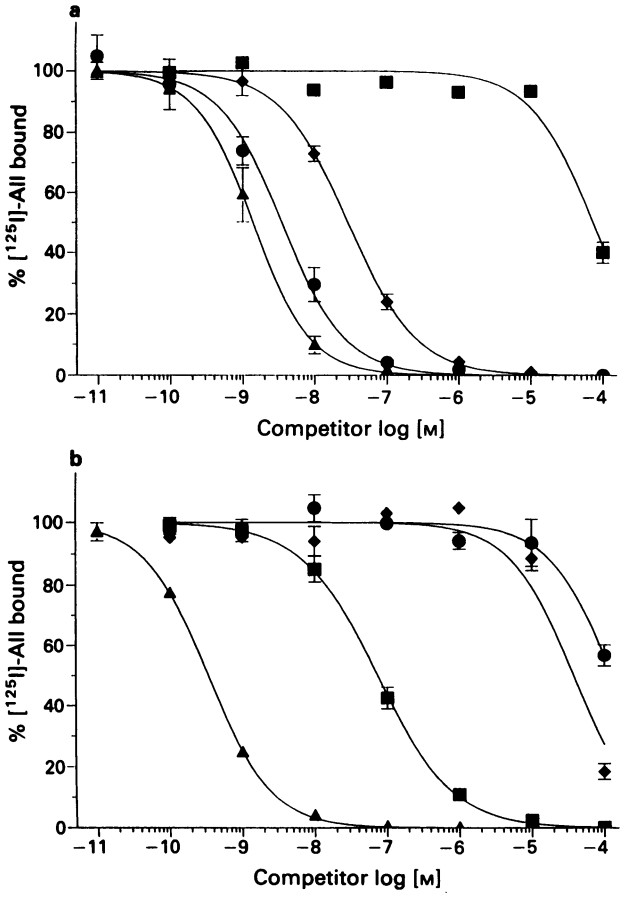

Figure 2 Inhibition of [^{125}I]-angiotensin II binding to (a) rat lung and (b) rat adrenal medulla membrane preparations by angiotensin II (▲), BIBR 277 (●), losartan (◆) and PD 123.177 (■). Data represent the mean of three experiments run in triplicate.

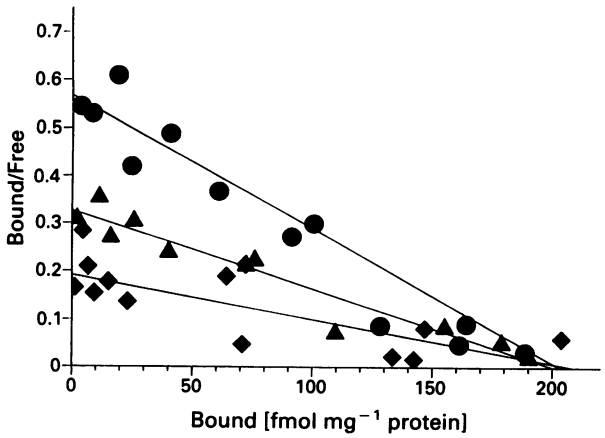

Figure 3 Scatchard transformations of saturation binding data for [^{125}I]-angiotensin II binding to membrane preparations from rat lung in the absence (●) or presence of 3 nM (▲) and 10 nM BIBR 277 (◆). The values are taken from a typical experiment ($n = 4$) done in triplicate.

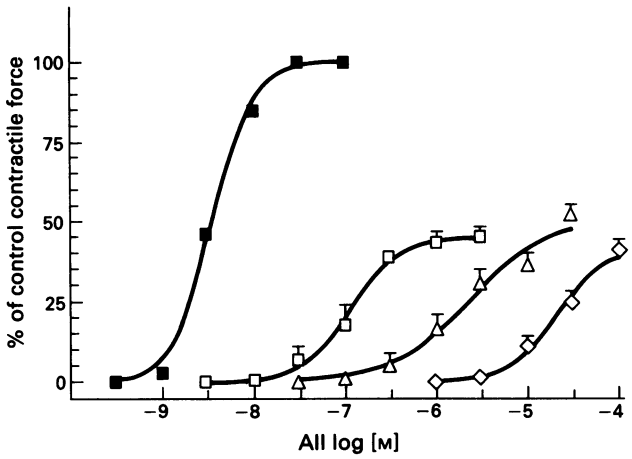

Figure 4 Effect of 10 nM (□), 100 nM (△) and 1000 nM BIBR 277 (◇) on the log concentration-contractile response curve for angiotensin II (■) in rabbit isolated aortic rings (control: $n = 18$; BIBR 277: $n = 6$ each). All values are given as the mean ± s.e. of the maximum contractile force obtained under control conditions before addition of the antagonist.

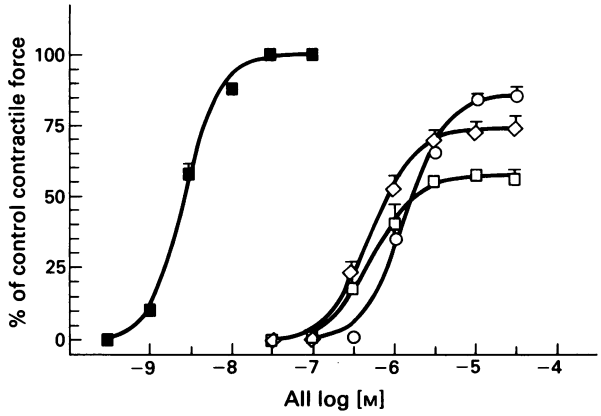

Figure 5 Effect of BIBR 277 (0.1 μM) alone (□) and in the presence of 0.1 μM (◇) or 1 μM (○) losartan on the log concentration-contractile response curve for angiotensin II (■) in rabbit aortic rings. Values are mean ± s.e.

0.22, 1.37 ± 0.08 and 1.66 ± 0.09 (each $n = 6$) in the presence of 10, 100, and 1000 nM BIBR 277, respectively, was seen together with a decrease in the maximum response of 40–50%. The calculated K_B was 0.33 ± 0.09 nM. No agonistic activity was observed at any concentration.

The washout kinetics of the inhibitory effect of BIBR 277 on AII-mediated contraction after several washout cycles is shown in Table 2. In solvent-treated tissues the response to AII, at a concentration of 30 nM that produces maximum contraction, remained stable during the entire experimental period and no tachyphylaxis was observed. The response to AII was significantly depressed to 35 ± 5% ($n = 6$) of the control response in the presence of BIBR 277 (10 nM). Moreover, this inhibitory effect remained unchanged during several subsequent wash-out procedures.

To investigate further the nature of the insurmountable antagonism of BIBR 277, we performed receptor protection experiments by incubating BIBR 277 simultaneously with the surmountable antagonist, losartan. In the presence of 100 nM BIBR 277 the maximum contractile force to angiotensin II was restored to 74% and 85% of the control by 0.1 and 1 μM losartan, respectively (Figure 5).

At higher concentrations of 1 and 10 μM BIBR 277 did not change the concentration-response curve for noradrenaline and KCl in rabbit aortic rings, nor did it interfere with endothelium-dependent relaxation induced by acetylcholine in noradrenaline-precontracted (0.3 μM) rings (Figure 6a,b,c). Furthermore, in guinea-pig ileum, unlike ACE inhibitors, BIBR 277 (10 μM) did not potentiate the contractile response to bradykinin (0.1 μM) (data not shown).

Pithed rats

The angiotensin II antagonism of BIBR 277 was further investigated *in vivo* in pithed rats. Vehicle-treated pithed rats (control) had a mean diastolic blood pressure value of 37 ± 4 mmHg ($n = 6$). Cumulative administration of angiotensin II induced a maximal increase in diastolic blood pressure by 100 ± 3 mmHg ($n = 6$) (Figure 7) with an ED_{50} of 0.23 μg kg^{-1}. Diastolic blood pressure after i.v. administration of 0.1, 0.3 and 1.0 mg kg^{-1} BIBR 277 was 34 ± 1 mmHg ($n = 5$), 30 ± 1 mmHg ($n = 6$) and 33 ± 3 mmHg ($n = 7$), respectively. The compound not only caused a dose-dependent rightward shift of the dose-response curve to AII with ED_{50} values of 1.4 μg kg^{-1}, 4.7 μg kg^{-1} and 20 μg kg^{-1}, respectively, but also significantly decreased the maximum blood pressure response to AII. The maximal increases in diastolic blood pressure were 92 ± 2 mmHg, 78 ± 5 mmHg and 71 ± 4 mmHg, respectively. BIBR 277 did not show an agonistic effect in this model.

Inhibition of the AII pressor response in anaesthetized rats

The duration of action of BIBR 277 after i.v. administration to anaesthetized rats as well as its potency in inhibiting the AII pressor response is shown in Figure 8. Compared to the vehicle-treated group ($n = 7$), bolus i.v. injection of BIBR 277 at 0.1, 0.3 and 1 mg kg^{-1} inhibited the pressor response to AII (0.1 μg kg^{-1}, i.v.) dose-dependently. Maximal inhibitory effects were observed at 5, 5, and 2 min post injection, respectively, and at all doses this inhibitory effect was still significant at 2 h post drug administration.

Renovascular hypertensive rats

In the first series BIBR 277 (0.3 mg kg^{-1} ($n = 4$) and vehicle ($n = 3$); 1.0 mg kg^{-1} ($n = 6$)) and vehicle ($n = 6$) was given as a single oral administration to renal hypertensive rats. Pretreatment values of mean arterial blood pressure and heart rate were 197 ± 15 mmHg and 429 ± 30 beats min^{-1} for the 0.3 mg kg^{-1}-treated group ($n = 4$) and 195 ± 11 mmHg and 382 ± 15 beats min^{-1} for the vehicle-treated group ($n = 3$); pretreatment values of mean arterial blood pressure

Table 2 Effect of wash-out of BIBR 277 on angiotensin II (30 nM)-induced contractile response in rabbit aortic rings

	1st challenge (control)	*2nd challenge* + drug	*3rd challenge* 40′ wash-out	*4th challenge* 80′ wash-out	*5th challenge* 120′ wash-out
Solvent ($n = 8$)	100	97 ± 2	99 ± 3	103 ± 3	103 ± 3
BIBR 277 (10 nM, $n = 6$)	100	35 ± 5*	30 ± 7*	29 ± 6*	33 ± 8*

Values were calculated as a percentage of the maximum contractile force obtained during the first (control) challenge and are given as mean ± s.e. The maximum control forces in both the solvent and the BIBR 277-treated groups was 46 ± 4 mN.
*$P < 0.05$ vs control response.

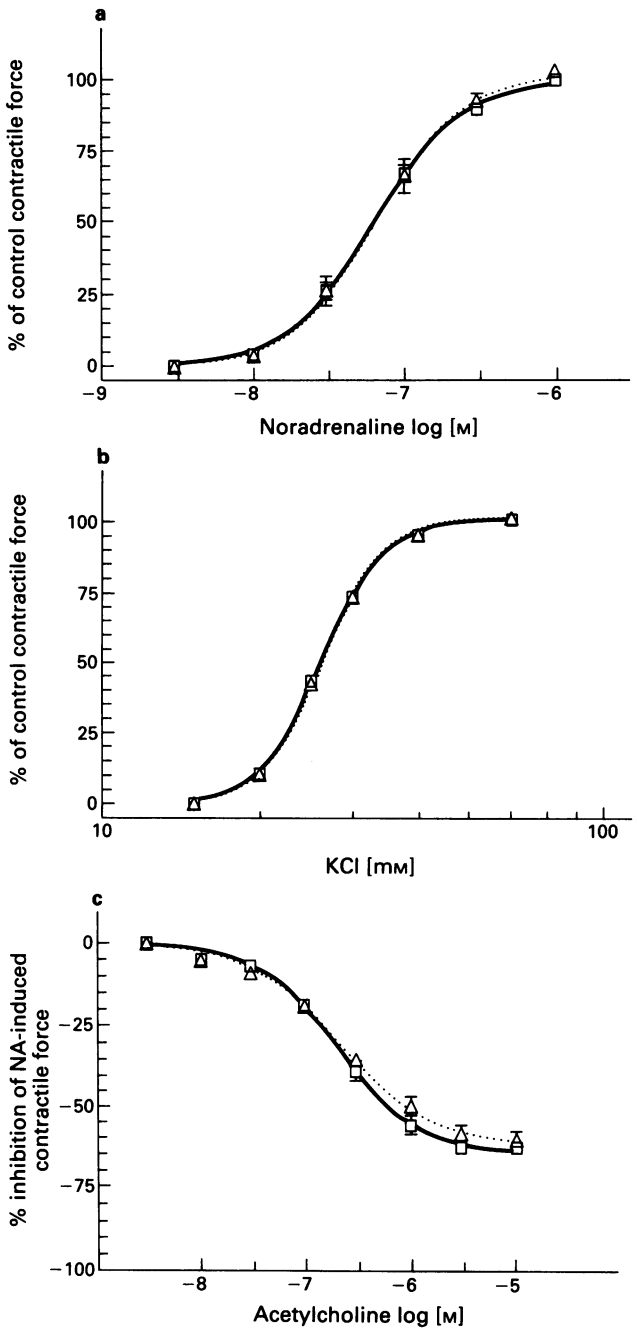

Figure 6 Effect of BIBR 277 (10 μM) on the log concentration-contractile response curve to noradrenaline (a), potassium chloride (b) and on endothelium-dependent relaxation by acetylcholine in rabbit aortic rings (c). Data represent the mean ± s.e. of 4–9 experiments; (□): control curve; (△): in the presence of 10 μM BIBR 277.

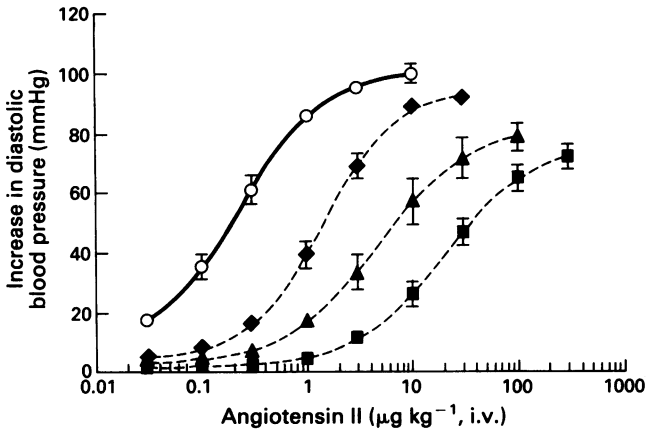

Figure 7 Effects of BIBR 277 on the log dose-pressor response curve of angiotensin II in pithed rats. Vehicle treatment (○, $n = 6$), 0.1 mg kg^{-1} (◆, $n = 5$), 0.3 mg kg^{-1} (▲, $n = 6$) and 1 mg kg^{-1} (■, $n = 7$). Data represent mean values ± s.e.

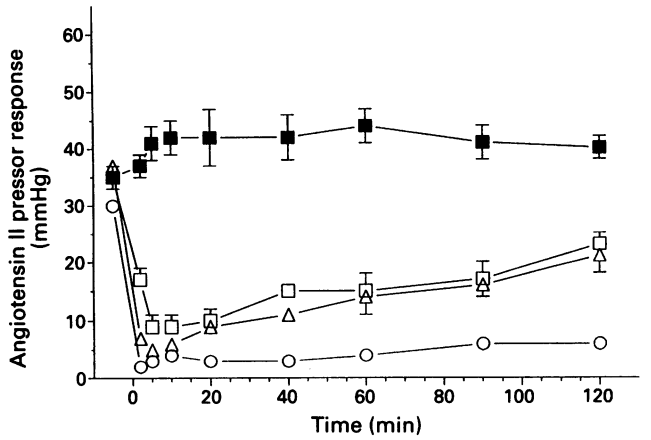

Figure 8 Blood pressure response to angiotensin II (0.1 μg kg^{-1}, i.v.) after i.v. administration of vehicle (■, $n = 7$) or BIBR 277 (0.1 mg kg^{-1} (□, $n = 3$), 0.3 mg kg^{-1} (△, $n = 6$) and 1 mg kg^{-1} (○, $n = 3$)) to pentobarbitone-anaesthetized, normotensive rats. All data points are mean values ± s.e.

and heart rate were 188 ± 12 mmHg and 386 ± 14 beats min^{-1} for the 1 mg kg^{-1}-treated group ($n = 6$) and 187 ± 10 mmHg and 393 ± 19 beats min^{-1} for the vehicle-treated group ($n = 6$). BIBR 277 reduced the mean arterial blood pressure in these animals in a dose-dependent manner by maximally 14 ± 3 (data not shown) and 30 ± 6 mmHg (Figure 9a), respectively, without having any significant effect on heart rate. After single administration the mean blood pressure remained significantly decreased for approximately 22 h, after which it returned to control values within the following 9 h. Repeated administration of 1 mg kg^{-1} day^{-1} over a period of 4 days (Figure 9b) resulted in a significant and sustained reduction in mean blood pressure by 35 to 60 mmHg. The pretreatment values of mean arterial blood pressure and heart rate were 212 ± 6 mmHg and 402 ± 15 beats min^{-1} for the BIBR 277-treated animals ($n = 6$) and 202 ± 6 mmHg and 407 ± 14 beats min^{-1} for the vehicle-treated animals ($n = 6$), respectively.

Discussion

Specific inhibitors of the RAS are useful tools for the determination of the physiological role of this system and for diagnosis and/or treatment of related diseases such as hypertension and congestive heart failure. Blockade of angiotensin AT_1 receptors has recently been demonstrated for losartan, a nonpeptide AII receptor antagonist (Chiu *et al.*, 1990) and in clinical trials this drug was shown to inhibit the AII-induced increase in blood pressure in man (Munafo *et al.*, 1992). In the present study we describe the pharmacology of BIBR 277, a novel, highly selective AII receptor antagonist with oral activity.

The affinity of BIBR 277 for AII receptors was assessed in radioligand binding studies. The compound totally displaced specifically bound [^{125}I]-AII from binding sites in rat lung, previously shown to be solely of the AT_1 subtype (Entzeroth & Hadamovsky, 1991), with low-nanomolar affinity indicating that BIBR 277 is six times more potent than losar-

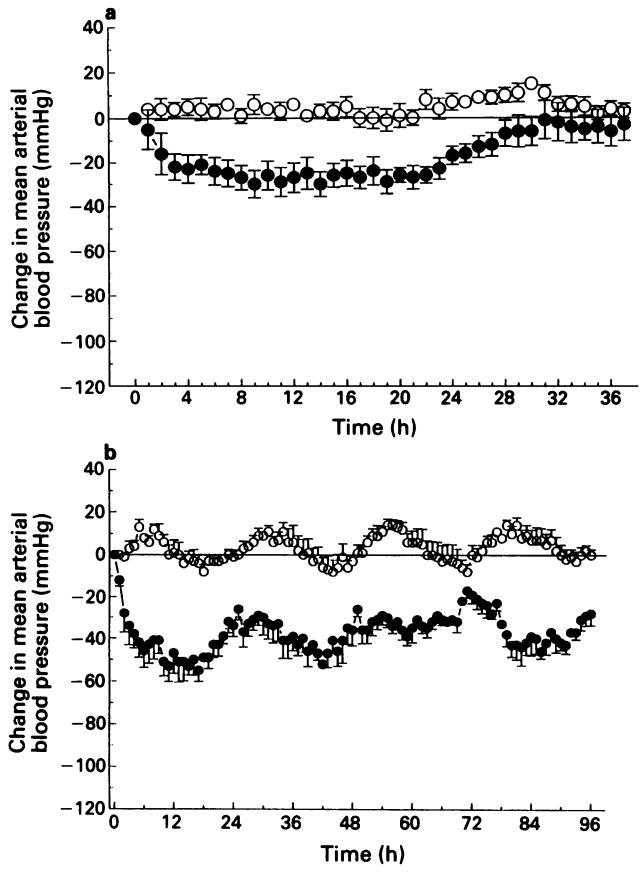

Figure 9 Blood pressure in conscious, chronically instrumented renovascular hypertensive rats after single oral administration (a) of vehicle (○, $n = 6$) or 1.0 mg kg^{-1} BIBR 277 (●, $n = 6$) and (b) after repeated oral administration of vehicle (○, $n = 6$) or 1.0 mg kg^{-1} day^{-1} BIBR 277 (●, $n = 6$). Data represent the mean ± s.e. The arrows indicate compound or vehicle administration.

tan. In contrast, up to 10 μM BIBR 277 had no interaction with AII receptors in adrenal medulla which are of the AT_2 subtype (Whitebread *et al.*, 1989; Chiu *et al.*, 1989), could be demonstrated while the AT_2-selective antagonist, PD 123177, inhibited [^{125}I]-AII binding to these sites with nanomolar affinity. Thus, BIBR 277 is selective for AT_1 receptor sites.

Several functional *in vitro* studies were performed to characterize the mode of interaction of BIBR 277 with AT_1 receptors. In rabbit aorta, BIBR 277 was shown to be an insurmountable antagonist of AII-induced contraction. This unusual pharmacological behaviour has also been reported previously for other nonpeptide AT_1 antagonists such as EXP3174 or GR 117289 (Wienen *et al.*, 1992; Robertson *et al.*, 1992). However, in contrast to results obtained with those compounds we did not detect a reduction in AII binding sites in radioligand saturation experiments performed in the presence of BIBR 277. These data provide strong evidence that BIBR 277 competitively interacts with AT_1 receptors. A further support for a competitive and reversible antagonism was provided by our findings in rabbit aorta that the insurmountable antagonism of BIBR 277 was reversed when the tissue was incubated simultaneously in the presence of the surmountable antagonist, losartan. Similar results have been reported previously for other insurmountable AII antagonists (Wong & Timmermans, 1991; Liu *et al.*, 1992; Robertson *et al.*, 1992; Wienen *et al.*, 1992).

The specificity of BIBR 277 was further confirmed in a number of other binding assays. In concentrations lower than 1 μM BIBR 277 lacked any affinity for other receptors for peptide and nonpeptide ligands relevant for cardiovascular regulation. The selective and specific interaction of BIBR 277 with AII receptors was further substantiated by the results from the functional experiments demonstrating no interference of the compound with other contractile (noradrenaline, KCl) or relaxant (ACh) tissue stimuli. Furthermore, BIBR 277 did not interfere with either human renin or human angiotensin I converting enzyme. Thus, it may be that BIBR 277 is unlikely to exhibit side-effects associated with renin inhibitors (Schaffer *et al.*, 1990) or converting enzyme inhibitors (Wood *et al.*, 1987; Gavras & Gavras, 1988).

The AII antagonistic properties of BIBR 277 described for the *in vitro* experiments were also observed *in vivo*. In the pithed rat increasing doses of antagonists resulted in non-parallel shifts in the dose-pressor response curve to AII. In these experiments, as in the *in vitro* assays, BIBR 277 was shown to be significantly more potent than losartan (Wong *et al.*, 1990a).

The duration of action of BIBR 277 was investigated in several *in vivo* models. In the anaesthetized rats BIBR 277 dose-dependently antagonized the blood pressure response to AII with a long duration of action (> 2 h) for all doses. Furthermore, in contrast to losartan, which is known to be converted *in vivo* to the active metabolite EXP3174 (Wong *et al.*, 1990a,b), we observed a rapid and sustained inhibition of the AII response with no evidence for a biphasic mode of activity. So far our data do not provide evidence that the pharmacological effects of BIBR 277 are to be assigned to the presence of an active metabolite.

To study the duration of action and the antihypertensive potential of BIBR 277 in a renin-dependent model of hypertension we investigated its effect in renal-artery ligated rats (Cangiano *et al.*, 1979). BIBR 277 given orally caused a potent, dose-dependent antihypertensive effect, which at the highest dose persisted for more than 24 h. Despite the decrease in blood pressure, no reflex tachycardia was observed in these animals. Thus the haemodynamic responses to BIBR 277 reported here, as well as those for other AII antagonists described earlier (Wong *et al.*, 1990b; Siegl *et al.*, 1992), clearly differ from those observed with vasodilator drugs such as hydralazine (Zacest *et al.*, 1972). A long duration of action of BIBR 277 was further demonstrated after repeated oral administration of the drug which produced a pronounced and sustained reduction in blood pressure.

In summary, the data presented here demonstrate that BIBR 277 is a highly selective and potent nonpeptide angiotensin II receptor antagonist with preference for the AT_1 receptor subtype. In contrast to peptide antagonists and as shown for other nonpeptide inhibitors (Wong *et al.*, 1990c), BIBR 277 lacks any agonistic activity. Given orally, BIBR 277 was shown to be an effective antihypertensive agent. A slow off-rate from the receptors may account for its long duration of action demonstrated *in vivo*. Therefore, BIBR 277 might be a new tool for the investigation of the physiology and pathophysiology of the renin-angiotensin system in the regulation of arterial pressure. The therapeutic potential of the drug will be evaluated in clinical studies.

The authors wish to thank J. Haller, C. Karg, D. Lefevre, I. Moll, D. Rühl, H. Seidel and U. Schmid for their excellent technical assistance.

References

ANTONACCIO, M.J. & WRIGHT, J.J. (1987). Enzyme inhibitors of the renin-angiotensin system. *Prog. Drug Res.*, **31**, 161–191.

ARUNLAKSHANA, A.D. & SCHILD, H.O. (1959). Some quantitative uses of drug agonists. *Br. J. Pharmacol. Chemother.*, **14**, 265–175.

BUMPUS, F.M., CATT, K.J., CHIU, A.T., DEGASPARO, M., GOODFRIEND, T., HUSAIN, A., PEACH, M.J., TAYLOR, D.G.Jr. & TIMMERMANS, P.B.M.W.M. (1991). Nomenclature for angiotensin receptors. *Hypertension (Dallas)*, **17**, 720–721.

CANGIANO, J.L., RODRIGUEZ-SARGENT, C. & MARTINEZ-MALDONADO, M. (1979). Effects of antihypertensive treatment on systolic blood pressure and renin in experimental hypertension in rats. *J. Pharmacol. Exp. Ther.*, **208**, 310– 313.

CATT, K.J., MENDELSON, F.A.O., MILLAN, M.A. & AGUILERA, G. (1984). The role of angiotensin II receptors in vascular regulation. *J. Cardiovasc. Pharmacol.*, **6** (Suppl. 4), 5575–5586.

CHENG, Y.C. & PRUSOFF, W.H. (1973). Relationship between the inhibition constant (K_i) and the concentration of inhibitor which causes 50 per cent inhibition (IC_{50}) of an enzymatic reaction. *Biochem. Pharmacol.*, **22**, 3099–3108.

CHIU, A.T., MCCALL, D.E., PRICE, W.A., WONG, P.C., CARINI, D.J., DUNCIA, J.V., WEXLER, R.R., YOO, S.E., JOHNSON, A.L. & TIMMERMANS, P.B.M.W.M. (1990). Nonpeptide angiotensin II antagonists. VII. Cellular and biochemical pharmacology of DuP 753, an orally active antihypertensive agent. *J. Pharmacol. Exp. Ther.*, **252**, 711–718.

CHIU, A.T., HERBLIN, W.F., MCCALL, D.E., ARDECKY, R.J., CARINI, D.J., DUNCIA, J.V., PAESE, L.J., WONG, P.C., WEXLER, R.R., JOHNSON, A.L. & TIMMERMANS, P.B.M.W.M. (1989). Identification of angiotensin II receptor subtypes. *Biochem. Biophys. Res. Commun.*, **165**, 196–203.

ENTZEROTH, M. & HADAMOVSKY, S. (1991). Angiotensin II receptors in the rat lung are of the AII-1 subtype. *Eur. J. Pharmacol. -Mol. Pharmacol. Sect.*, **206**, 237–241.

ENTZEROTH, M., HAIGH, R., HAUEL, N., VAN MEEL, J.C.A. & WIENEN, W. (1993). *In vitro* pharmacology of BIBR 277, a potent and highly selective nonpeptide angiotensin antagonist. *Br. J. Pharmacol.*, **108** (Suppl.), P240.

FUJII, A.M. & VATNER, S.F. (1985). Direct versus indirect actions of angiotensin in conscious dogs. *Hypertension*, **7**, 253–261.

GAVRAS, H. & GAVRAS, I. (1988). Angiotensin converting enzyme inhibitors. Properties and side effects. *Hypertension (Dallas)*, **11** (Suppl. II), II-37–II-41.

KENAKIN, T.P. (1987). Drug antagonism. In *Pharmacological Analysis of Drug Receptor Interaction*. ed. Kenakin, T.P. pp. 205–244. New York: Raven Press.

KINOSHITA, A., URATU, H., BUMPUS, F.M. & HUSAIN, A. (1991). Multiple determinants for the high substrate specificity of an angiotensin II-forming chymase from human heart. *J. Biol. Chem.*, **266**, 19192–19197.

LIU, Y.J., SHANKLEY, N.P., WELSH, N.J. & BLACK, J.W. (1992). Evidence that the apparent complexity of receptor antagonism by angiotensin II is due to a reversible and syntopic action. *Br. J. Pharmacol.*, **106**, 233–241.

LOWRY, O.H., ROSEBROUGH, N.J., FARR, A.L. & RANDALL, R.J. (1951). Protein measurement with the Folin phenol reagent. *J. Biol. Chem.*, **193**, 265–275.

MENDELSON, F.A.O. & KACHEL, C.D. (1980). Action of angiotensins I, II, and III on aldosterone production by isolated rat adrenal zona glomerulosa cells. Importance of metabolism and conversion of peptides in-vitro. *Endocrinology*, **106**, 1760–1768.

MUNAFO, A., CHRISTEN, Y., NUSSBERGER, J., SHUM, L.Y., BORLAND, M., LEE, R.J., WAEBER, B., BIOLLAZ, J. & BRUNNER, H.R. (1992). Drug concentration response in normal volunteers after oral administration of losartan, an angiotensin II receptor antagonist. *Clin. Pharmacol. Ther.*, **51**, 513–521.

NEELS, H.M., VAN SANDE, M.E. & SCHARPÉ, S.L. (1983). Sensitive colorometric assay for angiotensin converting enzyme in serum. *Clin. Chem.*, **29**, 1399–1403.

OKUNISHI, H., MIYAZAKI, M., OKAMURA, T. & TODA, N. (1987). Different distribution of two types of angiotensin II-generating enzymes in the aortic wall. *Biochem. Biophys. Res. Commun.*, **149**, 1186–1192.

PACKER, M. (1987). Converting enzyme inhibition in the management of severe chronic congestive heart failure: physiologic concepts. *J. Cardiovasc. Pharmacol.*, **10** (Suppl. 7), S83–S87.

PALS, D.T., MASUCCI, F.D., DENNINGS, G.S.Jr., SIPOS, F. & FESSLER, D.C. (1971). Role of the pressor action of angiotensin II in experimental hypertension. *Circ. Res.*, **29**, 673–681.

PEACH, M.J. (1977). Renin-angiotensin system: biochemistry and mechanism of action. *Physiol. Rev.*, **57**, 313–370.

PHILIPPS, P.I. (1987). Functions of angiotensin in the central nervous system. *Annu. Rev. Physiol.*, **49**, 413–435.

ROBERTSON, J.I.S. & TILLMAN, D.M. (1987). Converting enzyme inhibitors in the treatment of hypertension. *J. Cardiovasc. Pharmacol.*, **10** (Suppl. 7), S43–S48.

ROBERTSON, M.J., BARNES, J.C., DREW, G.M., MARSHALL, F.H., MICHEL, A., MIDDLEMISS, D., ROSS, B.C., SCOPES, D. & DOWLE, M.D. (1992). Pharmacological profile of GR 117289 in-vitro: a novel, potent and specific non-peptide angiotensin AT_1 receptor antagonist. *Br. J. Pharmacol.*, **107**, 1173–1180.

SCATCHARD, G. (1949). The attraction of proteins for small molecules and ions. *Ann. N.Y. Acad. Sci.*, **51**, 660–672.

SCHAFFER, L.W., SCHORN, T.W., WINQUIST, R., STROUSE, J.F., PAYNE, L., CHAKRAVARTY, P., DE LAZIO, S.E., TENBROEKE, J., VEBER, D.F., GREENLEE, W.J. & SIEGL, P.K.S. (1989). Acute hypotensive responses to peptide inhibitors of renin in conscious monkeys: an effect on blood pressure independent of plasma renin inhibition. *J. Hypertens.*, **8**, 251–259.

SIEGL, P.K.S., CHANG, R.S.L., MANTLO, N.B., CHAKRABARTY, P.K., ONDEYKA, D.L., GREENLEE, W.J., PATCHETT, A.A., SWEET, C.S. & LOTTI, V.J. (1992). In-vivo pharmacology of L-158,809, a new highly potent and selective nonpeptide angiotensin II receptor antagonist. *J. Pharmacol. Exp. Ther.*, **262**, 139–144.

VALLOTON, M.B. (1987). The renin-angiotensin system. *Trends Pharmacol. Sci.*, **8**, 69–74.

VAN MEEL, J.C.A., HAUEL, N., ENTZEROTH, M., HAIGH, R. & WIENEN, W. (1993). Antihypertensive effects of the angiotensin receptor antagonist BIBR 277 in conscious renal hypertensive and spontaneously hypertensive rats. *Br. J. Pharmacol.*, **108** (Suppl.), P191.

WHITEBREAD, S., MELE, M., KAMBER, B. & DE GASPARO, M. (1989). Preliminary characterization of two angiotensin II receptor subtypes. *Biochem. Biophys. Res. Commun.*, **163**, 284–291.

WIENEN, W., MAUZ, A.B.M., VAN MEEL, J.C.A. & ENTZEROTH, M. (1992). Different types of receptor interaction of peptide and nonpeptide angiotensin II antagonists revealed by receptor binding and functional studies. *Mol. Pharmacol.*, **41**, 1081–1088.

WONG, P.C., BARNES, T.B., CHIU, A.T., CHRIST, D.D., DUNCIA, J.V., HERBLIN, W.F. & TIMMERMANS, P.B.M.W.M. (1991). Losartan (DuP 753), an orally active nonpeptide angiotensin II receptor antagonist. *Cardiovasc. Drug Rev.*, **9**, 317–339.

WONG, P.C., PRICE, W.A., CHIU, A.T., DUNCIA, J.V., CARINI, D.J., WEXLER, R.R., JOHNSON, A.L. & TIMMERMANS, P.B.M.W.M. (1990a). Nonpeptide angiotensin II receptor antagonists. VIII. Characterization of functional antagonism displayed by DuP 753, an orally active antihypertensive agent. *J. Pharmacol. Exp. Ther.*, **252**, 719–725.

WONG, P.C., PRICE, W.A., CHIU, A.T., DUNCIA, J.V., CARINI, D.J., WEXLER, R.R., JOHNSON, A.L. & TIMMERMANS, P.B.M.W.M. (1990b). Nonpeptide angiotensin II receptor antagonists. XI. Pharmacology of EXP3174: an active metabolite of DUP 753, an orally active antihypertensive agent. *J. Pharmacol. Exp. Ther.*, **255**, 211–217.

WONG, P.C., PRICE, W.A., CHIU, A.T., DUNCIA, J.V., CARINI, D.J., WEXLER, R.R., JOHNSON, A.L. & TIMMERMANS, P.B.M.W.M. (1990c). Nonpeptide angiotensin II receptor antagonists. IX. Antihypertensive activity in rats of DuP 753, an orally active antihypertensive agent. *J. Pharmacol. Exp. Ther.*, **252**, 726–732.

WONG, P.C. & TIMMERMANS, P.B.M.W.M. (1991). Nonpeptide angiotensin II receptor antagonists: insurmountable angiotensin II antagonism of EXP3892 is reversed by the surmountable antagonist DuP 753. *J. Pharmacol. Exp. Ther.*, **258**, 49–57.

WOOD, S.M., MANN, R.D. & RAWLINS, M.D. (1987). Angio-oedema and urticaria associated with angiotensin converting enzyme inhibitors. *Br. Med. J.*, **294**, 91–92.

ZACEST, R., GILMOREK, E. & KOCH-WESER, J. (1972). Treatment of essential hypertension with combined vasodilation and beta-adrenergic blockade. *N. Engl. J. Med.*, **286**, 617–622.

(Received January 15, 1993
Revised April 30, 1993
Accepted May 10, 1993)

Br. J. Pharmacol. (1993), **110**, 253–256

Centrally administered ouabain aggravates rapid-eye-movement-sleep-related bradyarrhythmias in freely moving rats

[1]Takayuki Sato & Katsuo Seto

Department of Physiology, Kochi Medical School, Nankoku, Kochi 783, Japan

1 The effects of continuous infusions of ouabain on bradyarrhythmias (cardiac pauses for 0.5 s or longer) during sleep were examined in freely moving Wistar-Kyoto rats.

2 In a control group ($n = 7$), saline was infused into both the lateral ventricle and the femoral vein. In an intracerebroventricular (i.c.v.) ouabain group ($n = 7$), ouabain was infused centrally, such that each rat received three stepped doses of 1, 10, and 100 ng kg^{-1} h^{-1} for 3 days at each dose, while saline was infused systemically. In an intravenous (i.v.) ouabain group ($n = 7$), ouabain was infused systemically at the same doses as the i.c.v. ouabain received, while the simultaneous i.c.v. infusion of saline was carried out.

3 Three-day i.c.v. infusions of the three stepped doses of ouabain caused a dose-dependent increase in the frequency of bradyarrhythmias during rapid-eye movement (REM) sleep without affecting the time spent in REM sleep, arterial pressure, average heart rate, or the frequency of bradyarrhythmias during non-REM sleep. Intravenous ouabain or i.c.v. saline had no effects on the frequency of bradyarrhythmias.

4 Intrinsic CNS activity during REM sleep may be involved in the centrally mediated arrhythmogenic properties of ouabain during sleep.

Keywords: Ouabain-induced arrhythmia; rapid-eye-movement sleep; central nervous system; limbic system; freely moving rat

Introduction

Digitalis-induced arrhythmias occur more often during sleep than during daytime (Otsuka, 1980). Their diurnal distribution does not correspond to the diurnal change in the serum concentrations of digitalis agents (Otsuka, 1980). The central nervous system (CNS) activity during sleep may be of significance in the arrhythmogenic properties of digitalis. The CNS-mediated effects of digitalis on cardiac rhythm have been examined extensively (Somberg & Smith, 1979; Gillis & Quest, 1980) but the high incidence of digitalis-induced arrhythmias during sleep cannot be explained by the findings obtained from earlier experimental studies in which anaesthetized animals or large doses of digitalis enough to induce seizures in conscious animals were used.

The objectives of this study were to examine the CNS-mediated effects of the digitalis agent, ouabain, on the cardiac rhythm during sleep in freely moving rats. In a preliminary study (Tadokoro *et al.*, 1991), we have confirmed that the chronic intracerebroventricular (i.c.v.) infusion of ouabain at a dose of 1 μg kg^{-1} h^{-1} induces epileptic discharges on the electroencephalogram (EEG) only during rapid-eye-movement (REM) sleep without arousing rats. We therefore selected smaller doses that do not result in any EEG abnormalities for the present study.

Methods

Surgical preparation

Twenty-one male Wistar-Kyoto rats from Charles River Japan, 12–14 weeks of age, weighing 280–290 g, were used. The care of the animals was in strict accordance with the guiding principles of the Physiological Society of Japan. The following electrodes and tubes were implanted under pentobarbitone anaesthesia (40 mg kg^{-1}, i.p.): for the monitoring of the EEG, two stainless-steel screws into the bilateral frontal bones; for recording the electrooculogram (EOG), two small loops of stainless-steel wire beneath the skin at the inner and outer canthi of one eye; for recording the electrocardiogram (ECG), two vinyl tubes containing saturated salt solution and 0.5% agar, plugged bipolarly with Ag-AgCl electrodes, under the skin at the right foreleg and the left hindleg; for measurement of arterial pressure, a Teflon tube into the abdominal aorta through the femoral artery; for the i.c.v. infusion of drugs, a 24-gauge, 20-mm-long stainless-steel tube into the lateral ventricle; for the intravenous (i.v.) infusion of drugs, a Teflon tube into the femoral vein. The leads and tubes from peripheral sites were tunnelled subcutaneously into an opening on the head. All the leads were soldered to the pins of a miniature male socket cemented on the skull. A female socket and miniature electrical swivel with three fluid channels was connected to the male socket and the three tubes. After surgery, the rat was transferred to a plastic box in an electrically shielded and soundproof room where fluorescent lights provided 100-lux illumination under a 14 h/10 h light-dark schedule. The temperature in the room was kept at 24 ± 1°C. The animals were allowed free access to normal rat chow (CRF-1, Charles River Japan) and distilled water, and were allowed to recover for 10 days before polygraphic recordings.

Infusion protocols

Twenty-one rats were divided into control ($n = 7$), i.c.v. ouabain ($n = 7$), and i.v. ouabain ($n = 7$) groups. The infusion study was started after the recovery period.

In the control group, saline was infused both intracerebroventricularly and intravenously for 15 days.

In the i.c.v. ouabain group, for the first 3 days saline was infused intracerebroventricularly; for the next 9 days ouabain dissolved in saline was infused intracerebroventricularly, such that each rat received three stepped doses of 1, 10, and

[1] Author for correspondence.

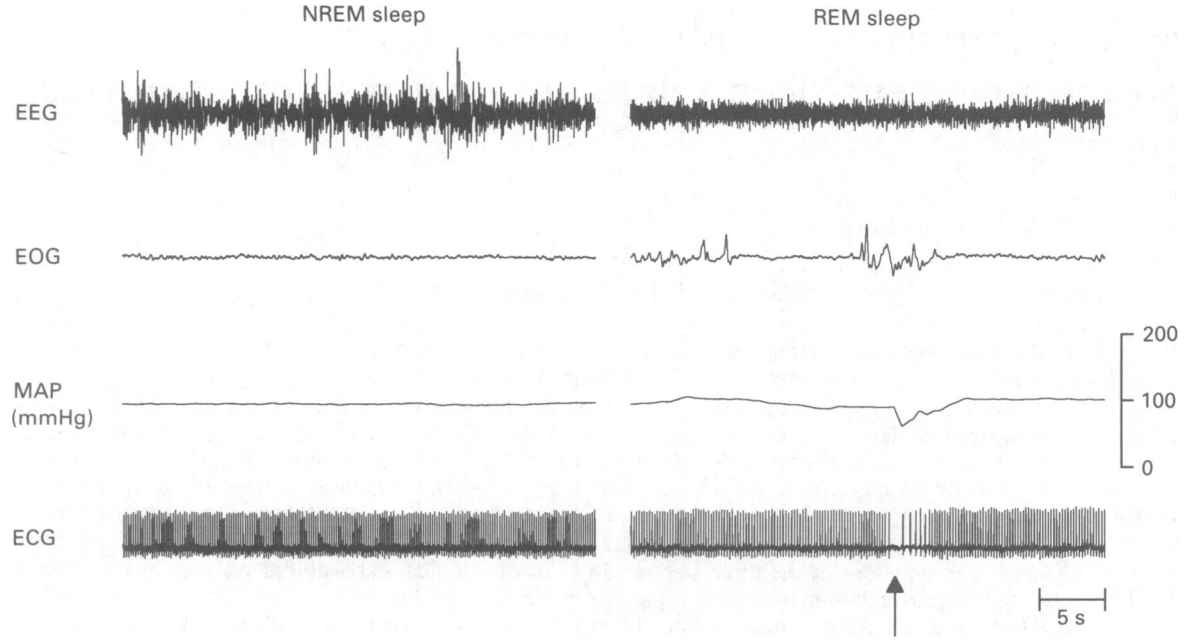

Figure 1 Typical polygraph recordings during non-rapid-eye-movement (NREM) sleep and REM sleep. Shown are the electroencephalogram (EEG), electrooculogram (EOG), mean arterial pressure (MAP), and electrocardiogram (ECG). An arrow indicates a bradyarrhythmia episode.

100 ng kg^{-1} h^{-1} for 3 days at each dose; for the next 3 days saline was infused intracerebroventricularly. For these 15 days, a simultaneous i.v. infusion of saline was carried out.

In the i.v. ouabain group, for the first 3 days saline was infused intravenously; for the next 9 days ouabain dissolved in saline was infused intravenously at the same doses as the i.c.v ouabain group received; for the next 3 days saline was infused intravenously. For these 15 days, a simultaneous i.c.v. infusion of saline was carried out.

All the infusions were at a flow rate of 1.6 μl h^{-1}, which is 1/75 of the rate of cerebrospinal fluid production in rats (Mann *et al.*, 1978). The positions of all the i.c.v. tubes were confirmed at *post-mortem* examination.

Polygraphic recordings

The EEG, EOG, mean arterial pressure (MAP), and ECG were recorded on polygraph paper and FM magnetic tape. The electrical signals of the arterial pressure were digitized through an analog-to-digital converter mounted in a personal computer, which automatically calculated and stored the 3-day averages of the MAP and heart rate (HR) every 3 days.

Sleep staging

According to our previous criteria (Saito *et al.*, 1983), sleep states were identified in 10 s epochs and were divided into the following three states from the EEG and EOG: wakefulness, non-REM (NREM) sleep, and REM sleep.

Definition of cardiac arrhythmias

The definition of tachyarrhythmias was the same as the criteria for man. Bradyarrhythmias were defined as cardiac pauses for 0.5 s or longer; as the normal HR of rats is 300–350 beats min^{-1} (Otsuka *et al.*, 1986), they are equivalent to cardiac arrests lasting 3 s or longer in man.

Statistical analysis

The physiological parameters and the frequency of cardiac arrhythmias were tested by a mixed model analysis of

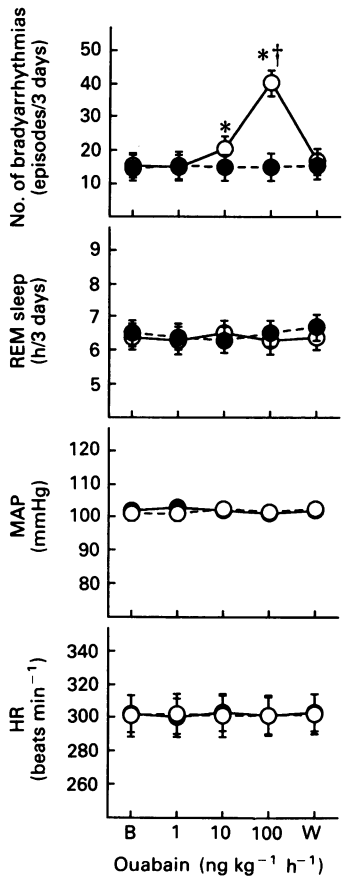

Figure 2 Effects of intracerebroventricular (○) or intravenous (●) ouabain infusion on the frequency of bradyarrhythmias during rapid-eye-movement (REM) sleep, on the time spent in REM sleep, on mean arterial pressure (MAP), and on heart rate (HR). Values are mean ± 95% simultaneous confidence intervals (overall $\alpha < 0.05$). *$P < 0.05$ from baseline period (B); †$P < 0.01$ from middle-dose infusion period (Tukey-studentized range method for a least significant difference test). W, withdrawal period.

variance. A 95% simultaneous confidence interval for the mean (overall $\alpha < 0.05$) was estimated from 5% point of the studentized form of the largest variance. A *post-hoc* analysis for multiple comparisons was performed by a Tukey studentized range method for a least significant difference test. Durations of cardiac pauses in bradyarrhythmia episodes were examined by a Kruskal-Wallis test, because a normal distribution of them could not be assumed. Differences were considered significant at $P < 0.05$.

Drugs

Ouabain was purchased from Sigma Chemical, St Louis, MO, U.S.A., and pentobarbitone sodium from Abbott Laboratories, IL, U.S.A.

Results

Examples of polygraph recordings are presented in Figure 1. No cardiac tachyarrhythmias were observed. In every rat, bradyarrhythmias such as sinus arrest, sinoatrial block, and type I (Wenckebach) second-degree atrioventricular block were found only during REM sleep.

In the control group, no time-dependent changes in the physiological parameters or the frequency of bradyarrhythmias were found during saline infusion into both the lateral ventricle and the femoral vein (data not shown). The effects of i.c.v. or i.v. ouabain infusion are summarized in Figure 2. Three-day i.c.v. infusions of the three stepped doses of ouabain caused a dose-dependent increase in the frequency of bradyarrhythmias during REM sleep without affecting the time spent in NREM or REM sleep, MAP, or HR. In the i.v. ouabain group, no effects of ouabain were found on the physiological parameters or the frequency of bradyarrhythmias. The frequency of bradyarrhythmias in the control group did not differ from baseline conditions in the two ouabain groups.

Types of bradyarrhythmias and durations of cardiac pauses in bradyarrhythmia episodes were analysed in the i.c.v ouabain group. Ouabain infusion had no effects on these characteristics of bradyarrhythmias (Figure 3).

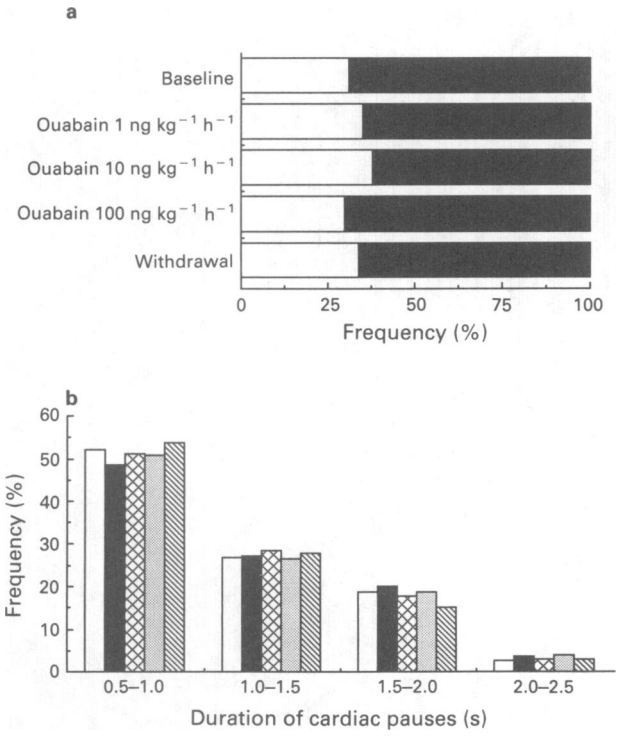

Figure 3 (a) Effects of intracerebroventricular ouabain infusion on the types of bradyarrhythmias. Open bars, sinus arrest and sinoatrial block; solid bars, type I (Wenckebach) atrioventricular block. (b) Effects of intracerebroventricular ouabain infusion on the frequency distribution of durations of cardiac pauses in bradyarrhythmia episodes. Open columns, baseline; solid columns, 1 ng kg^{-1} h^{-1} ouabain; cross-hatched columns, 10 ng kg^{-1} h^{-1} ouabain; stippled columns, 100 ng kg^{-1} h^{-1} ouabain; hatched columns, withdrawal.

Discussion

The actions of 'cardiac' glycosides, digitalis agents, on CNS functions have been studied for many years; they are also recognized as 'neural' glycosides (Gillis & Quest, 1980). Digitalis agents affect the release, uptake, synthesis, degradation, and storage of neurotransmitters such as noradrenaline, dopamine, 5-hydroxytryptamine, acetylcholine and γ-aminobutyric acid (Gillis & Quest, 1980). Digitalis-induced arrhythmias have been examined extensively; centrally administered digitalis induces tachyarrhythmias through sympathetic activation. However, the high incidence of digitalis-induced arrhythmias during sleep cannot be explained by the findings obtained from the earlier experimental studies in which anaesthetized animals or doses of digitalis large enough to induce seizures in conscious animals were used. Much attention must be given to whether the chronic i.c.v. infusion of a small dose that does not induce convulsions or EEG abnormalities produces arrhythmias. The present study shows that centrally administered ouabain induces bradyarrhythmias during REM sleep without increasing the time spent in REM sleep or changing arterial pressure.

The distribution of Na^+, K^+-adenosinetriphosphatase in the rat brain is not uniform; relatively high activity of this enzyme is found in the limbic system (Donaldson *et al.*, 1971). An autoradiographic study has revealed that [^{3}H]-ouabain administered intraventricularly is accumulated preferentially in this region; the inhibitory effect of ouabain injected into the lateral cerebral ventricle on the enzyme activity is also observed most significantly in this region. These findings indicate that this region may be a major site for both binding and action of i.c.v. ouabain.

The sensitivity of the limbic system to ouabain is different among sleep states. Baldy-Moulinier *et al.* (1973) have shown that the limbic system of cats becomes most sensitive to ouabain during REM sleep. A low dose of ouabain induces epileptic discharges on the EEG only during REM sleep without arousing the animal; the high dose causes epileptic phenomena during any sleep state and lethal convulsive seizures. In a preliminary study (Tadokoro *et al.*, 1991), we also have confirmed that the chronic i.c.v. infusion of ouabain at a dose of 1 μg kg^{-1} h^{-1} induces epileptic discharges on the EEG only during REM sleep without arousing rats. We therefore selected the smaller doses of 1–100 ng kg^{-1} h^{-1} that do not result in any EEG abnormalities for the present study.

Our previous studies have shown that REM-sleep-related bradyarrhythmias such as sinus arrest, sinoatrial block, and type I (Wenckebach) second-degree atrioventricular block are observed in normal rats (Saito *et al.*, 1983; Otsuka *et al.*, 1986; 1987), and that the frequency of bradyarrhythmias is decreased by vagotomy (Otsuka *et al.*, 1986). Many earlier electrophysiological studies have suggested the importance of the neural activity generated phasically during REM sleep in REM-sleep-related changes in the activity of the autonomic nervous system (Calvo & Fernández-Guardiola, 1984; Kline *et al.*, 1986; Otsuka *et al.*, 1987); the phasic neural activity spreads from the brain stem to the visual cortex and the limbic system. It may be speculated that the phasic neural activity stimulates limbic structures and results in bradyarrhythmias occasionally through drastic vagal activation. Ouabain may prime the genesis of bradyarrhythmias during REM sleep through a permissive action. We therefore speculate that centrally infused ouabain can make limbic

structures prone to be more activated by the phasic neural activity. This proposed mechanism may also explain why 'continuously' infused ouabain increases 'sudden' cardiac pauses only during REM sleep and does not affect average HR. The present study may provide a new view of mechanisms for digitalis-induced arrhythmias during sleep.

In conclusion, centrally administered ouabain aggravated arrhythmias during REM sleep in freely moving rats. We suggest that the CNS activity during REM sleep may be involved in the centrally mediated arrhythmogenic properties of ouabain.

We are grateful to Hiroyoshi Takatsuji of the Medical Research Laboratory for excellent technical assistance.

References

BALDY-MOULINIER, M., ARIAS, L.P. & PASSOUANT, P. (1973). Hippocampal epilepsy produced by ouabain. *Eur. Neurol.*, **9**, 333–348.

CALVO, J.M. & FERNÁNDEZ-GUARDIOLA, A. (1984). Phasic activity of the basolateral amygdala, cingulate gyrus, and hippocampus during REM sleep in the cat. *Sleep*, **7**, 202–210.

DONALDSON, J., ST-PIERRE, T., MINNICH, J. & BARBEAU, A. (1971). Seizures in rats associated with divalent cation inhibition of Na^+-K^+-ATP'ase. *Can. J. Biochem.*, **49**, 1217–1224.

GILLIS, R.A. & QUEST, J.A. (1980). The role of the nervous system in the cardiovascular effects of digitalis. *Pharmacol. Rev.*, **31**, 19–97.

KLINE, L.R., HENDRICKS, J.C., DAVIES, R.O. & PACK, A.I. (1986). Control of activity of the diaphragm in rapid-eye-movement sleep. *J. Appl. Physiol.*, **61**, 1293–1300.

MANN, J.D., BUTLER, A.B., ROSENTHAL, J.E., MAFFEO, C.J., JOHNSON, R.N. & BASS, N.H. (1978). Regulation of intracranial pressure in rat, dog, and man. *Ann. Neurol.*, **3**, 156–165.

OTSUKA, K. (1980). Studies of digitalis-induced arrhythmias by recordings of twenty-four hour continuous electrocardiograms. *Fukuoka Acta Medica*, **71**, 631–649.

OTSUKA, K., IKARI, M., ICHIMARU, Y., SAITO, H., KAWAKAMI, T., OTSUKA, K., KABA, H. & SETO, K. (1986). Experimental study on the relationship between cardiac arrhythmias and sleep states by ambulatory ECG-EEG monitoring. *Clin. Cardiol.*, **9**, 305–313.

OTSUKA, K., OZAWA, T., SAITO, H. & SETO, K. (1987). REM sleep and bradyarrhythmias. *Jiritsusinkei*, **24**, 96–100.

SAITO, H., OTSUKA, K., SATO, T., YOSHIMATSU, K., KABA, H., SETO, K., ICHIMARU, Y., SATO, Y. & YANAGA, T. (1983). Arrhythmogenic properties of paradoxical sleep. *Am. Heart J.*, **105**, 875–877.

SOMBERG, J.C. & SMITH, T.W. (1979). Localization of the neurally mediated arrhythmogenic properties of digitalis. *Science*, **204**, 321–323.

TADOKORO, M., SATO, T., SAITO, H., TAKATSUJI, H. & SETO, K. (1991). Effects of chronic intracerebroventricular infusion of ouabain on blood pressure and sleep in freely moving rats. *Jpn. J. Physiol.*, **41**, S178 (Abstract).

(Received January 8, 1993
Revised April 29, 1993
Accepted May 10, 1993)

Br. J. Pharmacol. (1993), **110**, 257–262

Effects of morphine metabolites on micturition in normal, unanaesthetized rats

[1]*Yasuhiko Igawa, **Dagmar Westerling, *Anders Mattiasson & †Karl-Erik Andersson

Departments of *Urology, **Anaesthesiology, and †Clinical Pharmacology, Lund University Hospital, Lund, Sweden, and [1]Department of Urology, Shinshu University School of Medicine, Matsumoto, Japan

1 By means of continuous cystometry in normal, unanaesthetized rats, the effects on micturition of intrathecally (i.t.) administered morphine-3-glucuronide (M3G) and morphine-6-glucuronide (M6G), the two main metabolites of morphine, were studied and compared with those of i.t. morphine.

2 Both M6G (0.01, 0.1, and 0.5 μg) and M3G (5 μg) were found to have significant effects on micturition. Like morphine (0.1, 0.5, and 10 μg), M6G was able to inhibit the micturition reflex, and produce urinary retention and dribbling incontinence in a dose-dependent manner. The potency of M6G for inhibiting micturition was approximately 10 times higher than that of morphine, and the duration of its effect was longer. All effects of M6G could be reversed by naloxone.

3 M3G (5 μg) facilitated the micturition reflex, resulting in decreases in bladder capacity and micturition volume, and an increase in spontaneous contractile activity. Pretreatment with naloxone (10 μg), which by itself had no effect on micturition, enhanced the facilitatory effects of M3G. In addition, M3G tended to counteract the inhibitory effects of both morphine and M6G on micturition. M3G (5 μg) also produced an excitatory behavioural syndrome.

4 It is concluded that in rats, i.t. M3G has excitatory effects on micturition and behaviour, probably not mediated via opioid receptors. I.t M6G has a potent inhibitory effect on micturition mediated by stimulation of opioid receptors. It may have effects on somatosensory afferent input in lower doses than those required for effects on micturition.

Keywords: Morphine; morphine-3-glucuronide; morphine-6-glucuronide; naloxone; intrathecal administration; micturition; cystometry; unanaesthetized rat

Introduction

It is well known that urinary retention may occur following epidural administration of morphine and other opiates (Bromage *et al.*, 1982; Rawal *et al.*, 1983; Stenseth *et al.*, 1985). This is due to complex effects on central and may be also peripheral neurogenic mechanisms controlling the micturition reflex (Dray & Metsch, 1984a,b,c,d; Hisamitsu & de Groat, 1984; Dray *et al.*, 1985; Dray & Nunan, 1987; Sheldon *et al.*, 1987; 1988; Berggren *et al.*, 1992).

Morphine is metabolized predominantly to morphine-3-glucuronide (M3G) and to a minor extent to morphine-6-glucuronide (M6G; Boerner *et al.*, 1975). These metabolites are active and believed to contribute to the pharmacological effects of morphine. Higher concentrations of M6G than of morphine itself were found in plasma (Säwe *et al.*, 1983; Poulain *et al.*, 1990) and cerebro-spinal fluid (Poulain *et al.*, 1990) after oral administration of morphine in man. M6G was shown to have analgesic effects in mice (Shimomura *et al.*, 1971), and clinically, it produced long-lasting analgesia when given to cancer patients (Osborne *et al.*, 1992). M6G binds to μ and δ receptors with apparent affinities similar to those of morphine (Christensen & Jorgensen, 1987; Pasternak *et al.*, 1987; Frances *et al.*, 1990). After administration of M6G into the central nervous system, it has been reported to have a 9 to 650 fold greater analgesic effect than morphine administered via the same route (Pasternak *et al.*, 1987; Abbott & Palmour, 1988; Sullivan *et al.*, 1989; Paul *et al.*, 1989; Gong *et al.*, 1991; Frances *et al.*, 1990; 1992). In contrast, M3G does not bind to any opioid receptor subtype (Pasternak *et al.*, 1987), and is devoid of analgesic activity (Shimomura *et al.*, 1971; Yoshimura *et al.*, 1973; Pasternak *et al.*, 1987). However, the metabolite has been shown to produce hyperaesthesia/hyperalgesia via non-opioid related mechanisms in rats when administered intrathecally (i.t.; Woolf, 1981; Yaksh *et al.*, 1986; Yaksh & Harty, 1988) and intracerebroventricularly (i.c.v.; Labella *et al.*, 1979). It may antagonize some pharmacological effects of morphine (Smith *et al.*, 1990) and M6G (Gong *et al.*, 1991; 1992).

The effects of morphine on micturition in unanaesthetized rats have been reported previously (Durant & Yaksh, 1988; Igawa *et al.*, 1992; Soulard *et al.*, 1992). However, the effects of M3G and M6G on micturition do not seem to have been established. Particularly, if there is a separation between its analgesic potency (high) and its potency for inhibiting the micturition reflex (low), M6G, which has a longer duration of analgesic action than morphine, would be an interesting alternative for i.t. opioid treatment of pain.

In the present study, we have by means of continuous cystometries in normal unanaesthetized rats, attempted to define the potency of i.t. M6G for inhibiting the micturition reflex, and compared it to that of i.t. morphine. We have also investigated how i.t. M3G by itself influences micturition, and whether the effects of i.t. morphine and M6G are antagonized by i.t. M3G.

Methods

Animals

Female Sprague-Dawley rats, weighing 200–240 g, were used in this study. The experimental protocol was approved by the Animals Ethics Committee, University of Lund.

Surgical procedures

The rats were anaesthetized with ketamine (75 mg kg^{-1}, i.m.) and xylazine (15 mg kg^{-1}, i.m.). A polyethylene catheter

[1] Author for correspondence at: Department of Urology, Lund University Hospital, S-221 85 Lund, Sweden.

(Clay-Adams PE-10, NJ, U.S.A.) was implanted into the subarachnoid space at the level of L_6–S_1 spinal cord segments for i.t. administration of drugs as described in detail previously (Igawa *et al.*, 1993b). Thereafter, the abdomen was opened through a midline incision, and a polyethylene catheter (Clay-Adams PE-50, NJ, U.S.A.) was implanted into the bladder through the dome as described previously (Malmgren *et al.*, 1987). The catheters were tunnelled subcutaneously and orifices were made on the back of the animal. After implantation of the catheters, rats were housed individually in cages on a 12 h/12 h, light/dark photo cycle. The injection sites in the spinal cord and the extent of dye distribution were confirmed by injection of dye (methylene blue) in every animal at the end of the experiment.

Cystometric investigations

Cystometric investigations were performed without any anaesthesia three days after the surgical preparation. The bladder catheter was connected via a T-tube to a pressure transducer (P23 DC, Statham Instrument Inc., CA, U.S.A.) and a microinjection pump (CMA 100, Carnegie Medicine AB, Sweden). The conscious rat was placed, without any restraint, in a metabolic cage which also enabled measurements of micturition volumes by means of a fluid collector connected to a Grass force displacement transducer (FT 03 C, Grass Instrument Co., Quincy, Mass, U.S.A.). Room-temperature saline was infused into the bladder at a rate of 10 ml h^{-1}. Intravesical pressure and micturition volumes were recorded continuously on a Grass polygraph (Model 7E, Grass Instrument Co., Quincy, Mass, U.S.A.; recording speed: 10 mm min^{-1}). Three reproducible micturition cycles, corresponding to a 20 min period, were recorded before drug administration. After each drug administration, recording was continued for at least another 120 min. The following cystometric parameters were investigated (Malmgren *et al.*, 1987): basal pressure (the lowest bladder pressure during filling), threshold pressure (bladder pressure immediately prior to micturition), micturition pressure (the maximum bladder pressure during micturition), bladder capacity (residual volume at the latest previous micturition plus volume of infused saline at the micturition), micturition volume (volume of expelled urine), residual volume (bladder capacity minus micturition volume), and spontaneous contractile activity (mean amplitude and frequency of bladder pressure fluctuations during 2 min prior to micturition). Analysis was performed for a 20 min period before drug administration. Drug effects on cystometric parameters were assessed for 120 min, and the two most effective micturition cycles were subjected to analysis.

Administration of drugs

The following drugs were used for i.t. administration: morphine-3β-glucuronide (M3G), morphine-6β-glucuronide (M6G), naloxone hydrochloride (Sigma Chemical Co., St. Louis, Mo, U.S.A.), and morphine sulphate (Gacell Laboratories, Malmö, Sweden). Drugs were dissolved in redistilled water, and then stored at −70°C. Subsequent dilutions of the drugs were made on the day of experiments with saline. Drugs were administered i.t. in 10 μl of saline followed by a flush of 15 μl of saline for 10 s; 10 μl of saline was injected i.t. as control, prior to drug administration. Neither the placement of the i.t. catheter itself, nor i.t. injection of saline, affects the cystometric pattern (Igawa *et al.*, 1992; 1993b).

Statistical analysis

The results are given as mean values ± s.e.mean. Statistical comparisons for experiments were based on doses expressed as micrograms per rat. Student's paired two-tail t test was used for comparison between before and after treatments. Comparison between drugs was performed by using factorial analysis of variance, and followed by Scheffe's F test. To evaluate the antagonistic effects of M3G on the effects of morphine or M6G, the incidence of urinary retention produced by these drugs were compared in the presence and absence of M3G by using the Chi-square test. A probability level <0.05 was accepted as significant.

Results

Effects of morphine

Morphine, administered i.t. in doses of 0.1 ($n = 7$), 0.5 ($n = 9$), 10 μg ($n = 8$), dose-dependently inhibited micturition, eventually ending with urinary retention and dribbling incontinence (Figure 1). After 0.1 μg, threshold pressure, bladder capacity and micturition volume increased ($P<0.05$; Table 1), but dribbling incontinence did not occur. The onset time of the effects of morphine (0.1 μg) was approximately 20 min. The maximum effect was seen 30 to 40 min after the injection. Dribbling incontinence was observed after 0.5 (6 out of 9 animals) and 10 μg (8 out of 8; Figure 2). The onset times of dribbling incontinence after 0.5 ($n = 6$) and 10 μg ($n = 8$) were 43 ± 7 and 19 ± 2 min, respectively. The duration of dribbling incontinence after 0.5 μg was 51 ± 8 min ($n = 5$).

Effects of morphine-6-glucuronide

M6G, administered i.t. in doses of 0.01 ($n = 7$), 0.05 ($n = 10$), and 0.5 μg ($n = 7$), inhibited micturition in a dose-dependent manner (Figure 3). Dribbling incontinence was observed after 0.01 (1 out of 7 animals), 0.05 (7 out 10), and 0.5 μg (7 out of 7; Figure 2). After 0.01 μg, threshold pressure, bladder capacity, and micturition volume increased ($P<0.01$; Table 1). The onset time of the effects of M6G (0.01 μg) was approximately 15 min. The maximum effect was seen within 30 min after the injection. The onset time of dribbling incon-

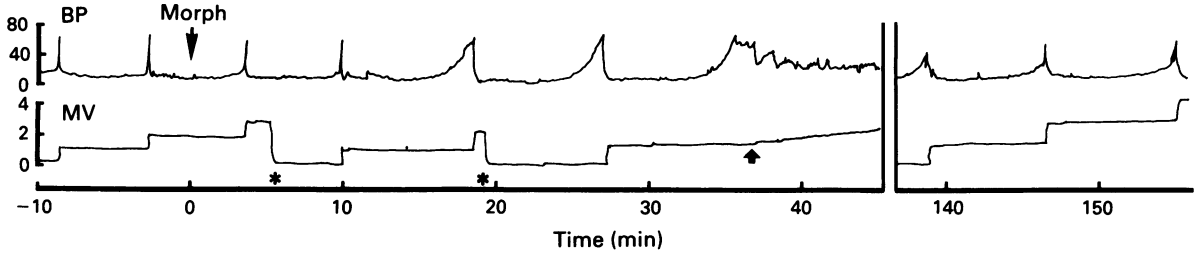

Figure 1 Effects of morphine administered intrathecally (i.t.) on bladder pressure (BP cmH_2O) and micturition volume (MV ml) during cystometry in a normal rat. Morphine (Morph 0.5 μg) inhibited micturition, and produced dribbling incontinence. The cystometric pattern was restored to the pre-administration state about 140 min after the administration. *and ↑ indicate adjustment to baseline position and initiation of dribbling incontinence, respectively.

tinence after M6G (0.05 μg; $n = 7$) was 20 ± 2 min, which was significantly ($P < 0.01$) shorter than the corresponding value (43 ± 7 min) after morphine (0.5 μg; $n = 6$). The duration of dribbling incontinence after M6G (0.05 μg; $n = 5$) was 165 ± 29 min. This was significantly ($P < 0.01$) longer than that (51 ± 8 min) after morphine (0.5 μg; $n = 5$).

Table 1 Effects of intrathecal administration of morphine (0.1 μg; $n = 7$) and morphine-6-glucuronide (M6G 0.01 μg; $n = 6$) on cystometric parameters in normal, unanaesthetized rats

	Morphine		*M6G*	
	before	after	before	after
Th P	10.7 ± 2.1	19.2 ± 3.6*	15.0 ± 2.5	39.0 ± 5.4**
M P	66.7 ± 15.9	40.5 ± 5.4	63.8 ± 15.7	61.5 ± 16.7
B C	1.15 ± 0.09	1.51 ± 0.13*	0.81 ± 0.09	1.49 ± 0.16**
M V	1.11 ± 0.06	1.48 ± 0.13*	0.75 ± 0.10	1.29 ± 0.15**
R V	0.03 ± 0.03	0.03 ± 0.02	0.06 ± 0.02	0.20 ± 0.08

Th P: threshold pressure (cmH_2O); M P: micturition pressure (cmH_2O); BC: bladder capacity (ml); MV: micturition volume (ml); R V: residual volume (ml). Results are expressed as mean ± s.e.mean. Before vs after: *$P < 0.05$; **$P < 0.01$.

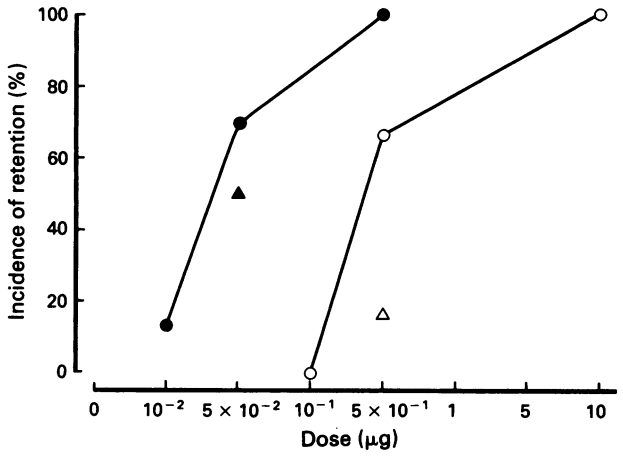

Figure 2 Dose-response relations for the inhibition of micturition produced by morphine (○; $n = 7-10$) and morphine-6-glucuronide (M6G, ●, $n = 7-10$) administered intrathecally (i.t.). The effects of morphine-3-glucuronide (M3G, 0.5 μg administered i.t. 30 min before morphine or M6G) on the effects of morphine (△; $n = 6$) and M6G (▲; $n = 6$) are included.

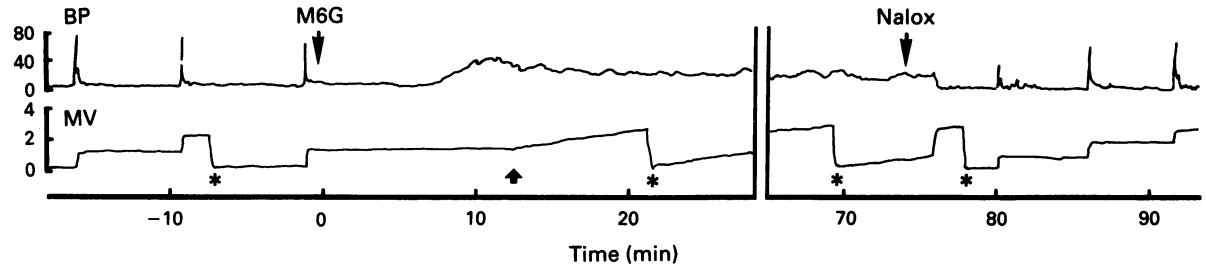

Figure 3 Effects of morphine-6-glucuronide administered intrathecally (i.t.) on bladder pressure (BP cmH_2O) and micturition volume (MV ml) during cystometry in a normal rat. Morphine-6-glucuronide (M6G 0.05 μg) inhibited micturition, and produced dribbling incontinence. Naloxone (Nalox 10 μg, i.t.) reversed the effects of M6G. *and ↑ indicate adjustment to baseline position and initiation of dribbling incontinence, respectively.

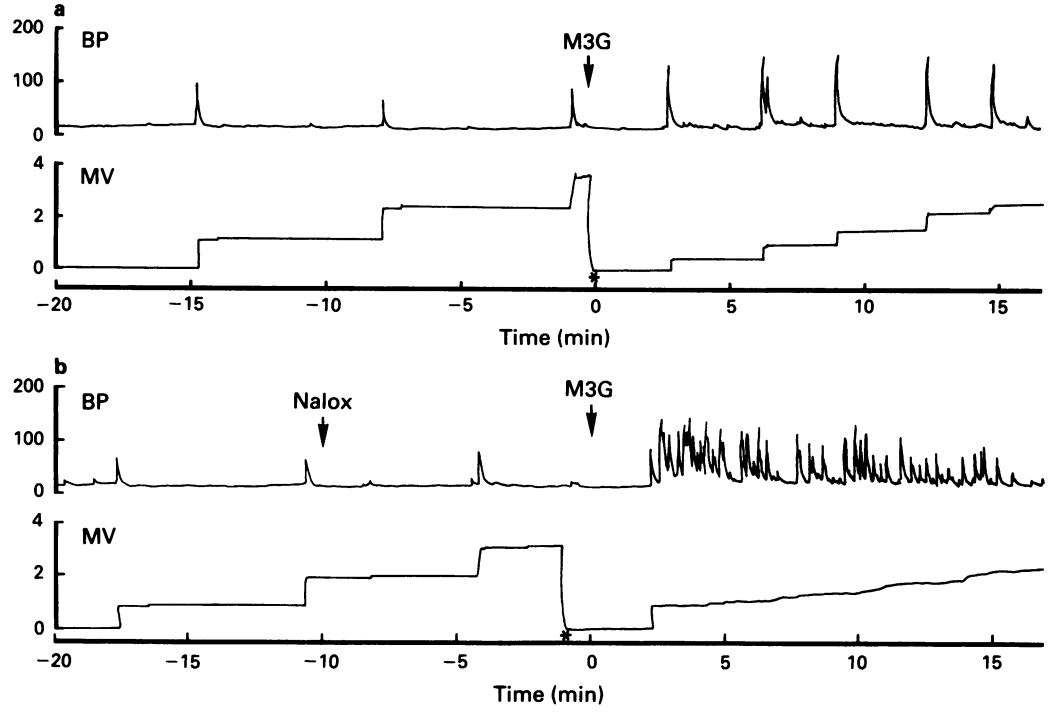

Figure 4 Effects of intrathecal (i.t.) administration of morphine-3-glucuronide (M3G 5 μg) on bladder pressure (BP cmH_2O) and micturition volume (MV ml) during cystometry in a normal rat in the absence (a) and presence (b) of naloxone (Nalox; 10 μg, i.t.). (a) In the absence of naloxone, M3G decreased bladder capacity and micturition volume, and facilitated the spontaneous bladder activity. (b) In the presence of naloxone (administered 10 min before M3G), the facilitatory effects of M3G were enhanced and dribbling incontinence was induced. *indicates adjustment to baseline position.

Table 2 Effects of intrathecal administration of morphine-3-glucuronide (5 μg) in the absence ($n = 7$) and presence ($n = 4$) of naloxone (10 μg i.t.) on cystometric parameters in normal, unanaesthetized rats

	Absence of naloxone		*Presence of naloxone*	
	before	after	before	after
ThP	16.3 ± 3.2	13.0 ± 2.0	13.8 ± 3.1	17.8 ± 2.7*
MP	65.0 ± 2.0	91.6 ± 20.6	61.8 ± 12.8	82.2 ± 12.5*
BC	0.94 ± 0.11	0.41 ± 0.04**	0.68 ± 0.09	0.16 ± 0.04*
MV	0.87 ± 0.08	0.39 ± 0.04***	0.61 ± 0.10	0.15 ± 0.04*
RV	0.07 ± 0.04	0.01 ± 0.01	0.06 ± 0.03	0.01 ± 0.01
ASA	1.7 ± 1.1	8.0 ± 1.4***	4.8 ± 2.1	13.2 ± 2.7*
FSA	0.4 ± 0.3	2.1 ± 0.2***	0.6 ± 0.3	3.6 ± 0.4*†

ThP: threshold pressure (cmH_2O); MP: micturition pressure (cmH_2O); BC: bladder capacity (ml); MV: micturition volume (ml); RV: residual volume (ml); ASA: amplitude of spontaneous activity (cmH_2O); FSA : frequency of spontaneous activity (min^{-1}). Results are expressed as mean ± s.e.mean. Before vs after *$P < 0.05$; **$P < 0.01$; ***$P < 0.001$. Absence of naloxone vs presence of naloxone †$P < 0.05$.

Effects of morphine-3-glucuronide

M3G, administered i.t. in doses of 0.1 ($n = 5$) and 0.5 μg ($n = 5$), by itself had no consistent effects on the cystometric pattern (data not shown). After 5 μg, i.t. ($n = 7$), on the other hand, bladder capacity and micturition volume decreased. M3G also increased both the amplitude and frequency of the spontaneous contractile activity (Figure 4a; Table 2). The onset time of the effects of M3G was within 5 min. The maximum effect was seen approximately 5 to 10 min after the injection. The cystometric pattern was restored to the pre-administration state within 60 min after injection. After 5 μg, i.t. a behavioural syndrome, characterized by agitation, biting, vocalization and jumping, was also observed in all animals. In the presence of M3G (0.5 μg, i.t., 30 min before morphine or M6G), morphine (0.5 μg, i.t.) and M6G (0.05 μg, i.t.) produced dribbling incontinence in 1 out of 6 animals and 3 out of 6, respectively (Figure 2). The changes were not statistically significant. In these animals, the onset time of dribbling incontinence was 75 min (morphine) and 14 ± 3 min (M6G), and the duration 24 min (morphine) and 136 ± 28 min (M6G).

Effects of naloxone

Naloxone, administered i.t. in doses of 10 ($n = 7$) and 100 μg ($n = 6$), by itself had no effects on the cystometric pattern (Figure 4b). However, naloxone (10 μg, i.t.) immediately reversed the inhibitory effects of morphine (0.5 and 10 μg; $n = 12$) and M6G (0.05 and 0.5 μg; $n = 5$; Figure 3) on each occasion tested. In the presence of naloxone (10 μg, i.t., 10 min before M3G), the frequency of the spontaneous contractile activity induced by M3G (5 μg, i.t.; $n = 4$) was enhanced (Table 2). In three out of seven animals, M3G in the presence of naloxone, caused a pronounced bladder hyperactivity leading to dribbling incontinence (Figure 4b).

Discussion

The present study shows that M6G, and M3G, the two main metabolites of morphine, when given i.t., have significant effects on micturition in normal, unanaesthetized rats. Like morphine, M6G was able to inhibit the micturition reflex, and produce urinary retention and dribbling incontinence in a dose-dependent manner, whereas M3G facilitated the micturition reflex, resulting in decreases in bladder capacity and micturition volume. M3G also induced an increase in spontaneous contractile activity and counteracted the inhibitory effects of both morphine and M6G on micturition. An inhibitory effect of i.t. morphine on micturition in unanaesthetized rats has been reported previously (Durant & Yaksh 1988; Igawa *et al.*, 1992; Soulard *et al.*, 1992), but to the best of our knowledge the micturition effects of M6G have not been described. The effects of M6G on micturition, like those of morphine, may be mediated via opioid receptors, since the opioid antagonist naloxone reversed its effects. Supporting this view, M6G has been found to bind to μ- and δ-sites with apparent affinities similar to those of morphine (Christensen & Jørgensen, 1987; Pasternak *et al.*, 1987; Frances *et al.*, 1990).

In the present study, the potency of i.t. M6G for inhibition of micturition was approximately 10 times higher than that of i.t. morphine (see Figure 2). With regard to antinociception, a higher potency of M6G than of morphine has been established in different tests including tail-flick, hot-plate, and writhing tests performed in rats and mice (Pasternak *et al.*, 1987; Abbott & Palmour, 1988; Paul *et al.*, 1989; Gong *et al.*, 1991; Frances *et al.*, 1990; 1992). However, the degree of relative antinociceptive potency of M6G is dependent on the pharmacological test chosen and the method of administration. The writhing test is thought to represent the response to noxious visceral stimulation (Schmauss & Yaksh; 1984; Porreca *et al.*, 1987), while both tail-flick and hot-plate tests may reflect the responses to somatosensory cutaneous pain (Groossman *et al.*, 1973; Holmgren *et al.*, 1986). Interestingly, the relative potency of i.t. M6G for inhibition of micturition observed in the present study, is almost the same as that of i.c.v. M6G for visceral antinociception, as judged by writhing test (9 times; Gong *et al.*, 1991) and for depression of ventilation (10 times; Gong *et al.*, 1991). This value is considerably lower than that for somatosensory antinociception as judged by tail-flick and/or hot-plate tests via the i.c.v. route (20–360 times; Pasternak *et al.*, 1987; Paul *et al.*, 1989; Gong *et al.*, 1991; Frances *et al.*, 1992) and via the i.t. route (650 times; Paul *et al.*, 1989). Thus, i.t. M6G may have a more selective effect on somatosensory antinociception than on micturition and ventilation. If this is the case also in man, it may be of clinical interest, since M6G would then be an interesting alternative for i.t. opioid treatment of certain types of pain.

In the rat, distinct μ and δ, but not κ, receptors are known to be involved in central opioid modulation of bladder motility, both at supraspinal (Dray & Metsch, 1984a,b; Dray *et al.*, 1985; Dray & Nunan, 1987; Sheldon *et al.*, 1987) and spinal (Dray & Metsch, 1984c,d; Dray *et al.*, 1985; Dray & Nunan, 1987; Sheldon *et al.*, 1988) sites. However, Sheldon *et al.* (1987; 1988) demonstrated in the rat that the identical inhibitory effects of several μ-receptor agonists on bladder motility could be antagonized differently. This suggested the presence of μ receptor subtypes (μ-isoreceptors) in the rat spinal cord and brain. Such receptors may be involved in the regulation of bladder function, and it may be speculated that the subtype of μ receptor involved in spinal and/or supraspinal modulation of bladder motility is different from that involved in somatosensory antinociception. Supporting such a view, Hucks *et al.* (1992) found that M6G had a 4 to 5 fold lower binding affinity for the μ_2 receptor subtype than morphine. The μ_2 receptor is believed to mediate, e.g., respiratory depression (Ling *et al.*, 1985). In line with this, spinal and/or supraspinal μ_2 receptors may be involved also in the inhibitory action of M6G on micturition.

The present study demonstrated that M3G by itself facilitated the micturition reflex, and functionally tended to antagonize the effects of both morphine and M6G on micturition. After a high dose of i.t. M3G, an excitatory behavioural syndrome was observed. The excitatory effects of M3G, and its antagonistic effect on the opioid-induced inhibition of micturition may not be related to an opioid-mediated mechanism, since M3G has been found not to bind to any type of opioid receptor (Pasternak *et al.*, 1987). This is in line with the view that M3G may induce hyperalgesia,

respiratory stimulation and behavioural excitation by non-opioid mechanisms (Yaksh *et al.*, 1986; Yaksh & Harty, 1988; Pelligrino *et al.*, 1989; Gong *et al.*, 1991). The finding that M3G-induced contractile activity in the bladder was enhanced by naloxone does not contradict this view. Even if naloxone by itself had no stimulatory effects on bladder activity, the drug can be expected to counteract any existing endogenous opioid inhibitory tone, and thus enhance the stimulatory actions of M3G. The excitatory actions of M3G have been postulated to be due to a block of γ-aminobutyric acid (GABA)-mediated inhibition (Robinson & Deadwyler, 1980), or to interference with glycine (Woolf, 1981). We have found that bicuculline, a $GABA_A$ antagonist given i.t. to normal, unanaesthetized rats, produced an excitatory effect on micturition (Igawa *et al.*, 1993a), which resembled the effect of M3G found in the present study. It may therefore be speculated that M3G facilitates the micturition reflex due to inhibition of central GABA-ergic transmission. Whether or not this is the case is currently under investigation.

This project was supported by the Swedish Medical Research Council (no 6837 & 10399), and by the Medical Faculty of Lund, Sweden.

References

ABBOTT, F.V. & PALMOUR, R.M. (1988). Morphine-6-glucuronide: analgesic effects and receptor binding profile in rats. *Life Sci.*, **43**, 1685–1695.

BERGGREN, A., RUBENSSON, A. & SILLEN, U. (1992). Involvement of opioid mechanisms in peripheral motor control of detrusor muscle. *Pharmacol. Toxicol.*, **71**, 179–184.

BOERNER, U., ABBOTT, S. & ROE, R.L. (1975). The metabolism of morphine and heroin in man. *Drug Metab. Rev.*, **4**, 39–73.

BROMAGE, P.R., CAMPORESI, E.M., DURANT, P.A.C. & NIELSEN, C.H. (1982). Nonrespiratory side effects of epidural morphine. *Anesth. Analg.*, **61**, 490–495.

CHRISTENSEN, C.B. & JORGENSEN, L.N. (1987). Morphine-6-glucuronide has high affinity for the opioid receptor. *Pharmacol. Toxicol.*, **60**, 75–76.

DRAY, A. & METSCH, R. (1984a): Morphine and the centrally-mediated inhibition of urinary bladder motility in the rat. *Brain Res.*, **297**, 191–195.

DRAY, A. & METSCH, R. (1984b). Opioid receptor subtypes involved in the central inhibition of urinary bladder motility. *Eur. J. Pharmacol.*, **104**, 47–53.

DRAY, A. & METSCH, R. (1984c). Inhibition of urinary bladder contractions by a spinal action of morphone and other opioids. *J. Pharmacol. Exp. Ther.*, **231**, 254–260.

DRAY, A. & METSCH, R. (1984d). Spinal opioid receptors and inhibition of urinary bladder motility in vivo. *Neurosci. Lett.*, **47**, 81–84.

DRAY, A. & NUNAN, L. (1987). Supraspinal and spinal mechanisms in morphine-induced inhibition of reflex urinary bladder contractions in the rat. *Neurosci.*, **22**, 281–287.

DRAY, A., NUNAN, L. & WIRE, W. (1985). Central δ-opioid receptor interactions and the inhibition of reflex urinary bladder contractions in the rat. *Br. J. Pharmacol.*, **85**, 717–726.

DURANT, P.A.C. & YAKSH, T.L. (1988). Drug effects on urinary bladder tone during spinal morphine-induced inhibition of the micturition reflex in unanesthetized rats. *Anesthesiology*, **68**, 325–334.

FRANCES, B., GOUT, R., CAMPISTRON, G., PANCONI, E. & CROS, J. (1990). Morphine-6-glucuronide is more mu-selective and potent in analgesic tests than morphine. *Prog. Clin. Biol. Res.*, **328**, 477–480.

FRANCES, B., GOUT, R., MONSARRAT, B., CROS, J. & ZAJAC, J.-M. (1992). Further evidence that morphine-6β-glucuronide is a more potent opioid agonist than morphine. *J. Pharmacol. Exp. Ther.*, **262**, 25–31.

GONG, Q.-L., HEDNER, J., BJÖRKMAN, R. & HEDNER, T. (1992). Morphine-3-glucuronide may functionally antagonize morphine-6-glucuronide induced antinociception and ventilatory depression in the rat. *Pain*, **48**, 249–255.

GONG, Q.-L., HEDNER, T., HEDNER, J., BJÖRKMAN, R. & NORDBERG, G. (1991). Antinociceptive and ventilatory effects of the morphine metabolites: morphine-6-glucuronide and morphine-3-glucuronide. *Eur. J. Pharmacol.*, **193**, 47–56.

GROOSSMAN, W., JURNA, I., NELL, T. & THERES, C. (1973). The dependence of the anti-nociceptive effect of morphine and other analgesic agents on spinal motor activity after central monoamine depletion. *Eur. J. Pharmacol.*, **24**, 67–77.

HISAMITSU, T. & DE GROAT, W.C. (1984). The inhibitory effect of opioid peptides and morphine applied intrathecally and intracerebroventricularly on the micturition reflex in the cat. *Brain Res.*, **298**, 51–65.

HOLMGREN, M., HEDNER, T., MELLSTRAND, G., NORDBERG, G. & HEDNER, TH. (1986). Characterization of the antinociceptive effects of some adenosine analogues in the rat. *Naunyn-Schmied. Arch. Pharmacol.*, **334**, 290–293.

HUCKS, D., THOMPSON, P.I., MCLOUGHLIN, L., JOEL, S.P., PATEL, N., GROSSMAN, A., REES, L.H. & SLEVIN, M.L. (1992). Explanation at the opioid receptor level for differing toxicity of morphine and morphine 6-glucuronide. *Br. J. Cancer*, **65**, 122–126.

IGAWA, Y., ANDERSSON, K.-E., POST, C., UVELIUS, B. & MATTIASSON, A. (1992). A rat model for investigation of spinal mechanisms in detrusor instability associated with infravesical outflow obstruction. *J. Urol.*, **147**, 349A (abstract no. 546).

IGAWA, Y., MATTIASSON, A. & ANDERSSON, K.-E. (1993a). Effects of GABA-receptor stimulation and blockade on micturition in normal rats and rats with bladder outflow obstruction. *J. Urol.*, (in press).

IGAWA, Y., PERSSON, K., ANDERSSON, K.-E., UVELIUS, B. & MATTIASSON, A. (1993b). Facilitatory effect of vasoactive intestinal polypeptide on spinal and peripheral micturition reflex pathways in conscious rats with and without detrusor instability. *J. Urol.*, **149**, 884–889.

LABELLA, F.S., PINSKY, C. & HAVILICEK, V. (1979). Morphine derivatives with diminished opiate receptor potency show enhanced central excitatory activity. *Brain Res.*, **174**, 263–271.

LING, G.S., SPIEGEL, K., LOCKHART, S.H. & PASTERNAK, G.W. (1985). Separation of opioid analgesia from respiratory depression: evidence for different receptor mechanisms. *J. Pharmacol. Exp. Ther.*, **232**, 149–155.

MALMGREN, A., SJÖGREN, C., UVELIUS, B., MATTIASSON, A., ANDERSSON, K.-E. & ANDERSSON, P.O. (1987). Cystometrical evaluation of bladder instability in rats with infravesical outflow obstruction. *J. Urol.*, **137**, 1291–1294.

OSBORNE, R., THOMPSON, P., JOEL, S., TREW, D., PATEL, N. & SLEVIN, M. (1992). The analgesic activity of morphine-6-glucuronide. *Br. J. Clin. Pharmacol.*, **34**, 130–138.

PASTERNAK, G.W., BODNAR, R.J., CLARK, J.A. & INTURRISI, C.E. (1987). Morphine-6-glucuronide: a potent mu agonist. *Life Sci.*, **41**, 2845–2849.

PAUL, D., STANDIFER, K.M., INTURRISI, C.E. & PASTERNAK, G.W. (1989). Pharmacological characterization of morphine-6β-glucuronide, a very potent morphine metabolite. *J. Pharmacol. Exp. Ther.*, **251**, 477–483.

PELLIGRINO, D.A., RIEGLER, F.X. & ALBRECHT, R.F. (1989). Ventilatory effects of fourth cerebroventricular infusions of morphine-6- or morphine-3-glucuronide in the awake dog. *Anesthesiology*, **71**, 936–940.

PORRECA, F., MOSBERG, H.I., OMNAAS, J.R., BURKS, T.F. & COWAN, A. (1987). Supraspinal and spinal potency of selective opioid agonists in the mouse writhing test. *J. Pharmacol. Exp. Ther.*, **240**, 890–894.

POULAIN, P., RIBON, A.M., HANKS, G.W., HOSKIN, P.J., AHERNE, G.W. & CHAPMAN, D.J. (1990). CSF concentrations of morphine-6-glucuronide after oral administration of morphine. *Pain*, **41**, 115–116.

RAWAL, N., MÖLLEFORS, K., AXELSSON, K., LINGÅRDH, G. & WIDMAN, B. (1983). An experimental study of urodynamic effects of epidural morphine and of naloxone reversal. *Anesth. Analg.*, **62**, 641–647.

ROBINSON, J.H. & DEADWYLER, S.A. (1980). Morphine excitation: effects on field potentials recorded in the in vitro hippocampal slice. *Neuropharmacol.*, **19**, 507–514.

SCHMAUSS, C. & YAKSH, T.L. (1984). In vivo studies on spinal opiate receptor systems mediating antinociception. II. Pharmacological profiles suggesting a differential association of mu, delta and kappa receptors with vesceral chemical and cutaneous thermal stimuli in the rat. *J. Pharmacol. Exp. Ther.*, **228**, 1–12.

SHELDON, R.J., NUNAN, L. & PORRECA, F. (1987). Mu antagonist properties of kappa agonists in a model of rat urinary bladder motility in vivo. *J. Pharmacol. Exp. Ther.*, **243**, 234–240.

SHELDON, R.J., NUNAN, L. & PORRECA, F. (1988). U50,488H differentially antagonizes the bladder effects of μ agonists at spinal sites. *Eur. J. Pharmacol.*, **146**, 229–235.

SHIMOMURA, K., KAMATA, O., UEKI, S., IDA, S., OGURI, K., YOSHIMURA, H. & TSUKAMOTO, H. (1971). Analgesic effect of morphine glucuronides. *Tohoku J. Exp. Med.*, **105**, 45–52.

SMITH, M.T., WATT, J.A. & CRAMOND, T. (1990). Morphine-3-glucuronide – a potent antagonist of morphine analgesia. *Life Sci.*, **47**, 579–585.

SOULARD, C., PASCAUD, F., ROMAN, F.J., GROUHEL, A. & JUNIEN, J.L. (1992). Pharmacological evaluation of JO 1870: relation to the potential treatment of urinary bladder incontinence. *J. Pharmacol. Exp. Ther.*, **260**, 1152–1158.

STENSETH, R., SELLEVOLD, O. & BREIVIK, H. (1985). Epidural morphine for postoperative pain: Experience with 1085 patients. *Acta Anesthesiol. Scand.*, **29**, 148–156.

SULLIVAN, A.F., MCQUAY, H.J., BAILEY, D. & DICKENSON, A.H. (1989). The spinal antinociceptive actions of morphine metabolites, morphine-6-glucuronide and normorphine, in the rat. *Brain Res.*, **482**, 219–224.

SÄWE, J., SVENSSON, J.O. & RANE, A. (1983). Morphine metabolism in cancer patients on increasing doses – no evidence for autoinduction or dose-dependence. *Br. J. Clin. Pharmacol.*, **16**, 85–93.

WOOLF, C.J. (1981). Intrathecal high dose morphine produces hyperalgesia in the rat. *Brain Res.*, **209**, 491–495.

YAKSH, T.L., HARTY, G.J. & ONOFRIO, B.M. (1986). High doses of spinal morphine produce a nonopiate receptor-mediated hyperesthesia: clinical and theoretic implications. *Anesthesiology*, **64**, 590–597.

YAKSH, T.L. & HARTY, G.J. (1988). Pharmacology of the allodynia in rats evoked by high dose intrathecal morphine. *J. Pharmacol. Exp. Ther.*, **244**, 501–508.

YOSHIMURA, H., IDA, S., OGURI, K. & TSUKAMOTOR, H. (1973). Biochemical basis for analgesic activity of morphine-6-glucuronide. I. penetration of morphine-6-glucuronide in the brain of rats. *Biochem. Pharmacol.*, **22**, 1423–1430.

(Received January 27, 1993
Revised April 30, 1993
Accepted May 10, 1993)

Br. J. Pharmacol. (1993), **110**, 263–268

The effects of ATP and α,β-methylene-ATP on cytosolic Ca^{2+} level and force in rat isolated aorta

[1]Satoshi Kitajima, Hiroshi Ozaki & Hideaki Karaki

Department of Veterinary Pharmacology, Faculty of Agriculture, The University of Tokyo, Bunkyo-ku, Yayoi 1-1-1, Tokyo 113, Japan

1 The effects of a non-selective P_2-receptor agonist ATP and a selective P_{2x}-receptor agonist α,β-methylene-ATP on intracellular free Ca^{2+} level ($[Ca^{2+}]_i$) and force were examined in rat isolated aorta without endothelium.

2 Both ATP (1–1000 μM) and α,β-methylene-ATP (0.1–100 μM) induced transient increase followed by small sustained increase in $[Ca^{2+}]_i$ in a concentration-dependent manner. Compared with the force induced by a high concentration of KCl, the force induced by α,β-methylene-ATP was smaller and that induced by ATP was much smaller at a given $[Ca^{2+}]_i$.

3 An L-type Ca^{2+} channel blocker, verapamil (10 μM), completely inhibited the high K^+-stimulated $[Ca^{2+}]_i$ and force. Verapamil partially inhibited the transient and sustained increases in $[Ca^{2+}]_i$ induced by 10 μM α,β-methylene-ATP and the sustained increase but not the transient increase induced by 1 mM ATP.

4 In the absence of extracellular Ca^{2+} (with 0.5 mM EGTA) 1 mM ATP caused transient increase in $[Ca^{2+}]_i$ while 10 μM α,β-methylene-ATP was ineffective

5 ATP, but not α,β-methylene-ATP, increased the tissue adenosine 3':5'-cyclic monophosphate (cyclic AMP) level.

6 These data suggest that ATP and α,β-methylene-ATP increase $[Ca^{2+}]_i$ by an activation of both L-type and non-L-type Ca^{2+} channels. In addition, ATP, but not α,β-methylene-ATP, increases $[Ca^{2+}]_i$ by a release of Ca^{2+} from an intracellular Ca^{2+} store. Possible reasons are discussed as to why the increase in $[Ca^{2+}]_i$ due to ATP and α,β-methylene-ATP resulted in only a small contraction.

Keywords: ATP; α,β-methylene-ATP; vascular smooth muscle; cytosolic Ca^{2+} level; contraction; Ca^{2+} sensitivity

Introduction

In smooth muscles, ATP is released from purinergic nerve endings as a transmitter or from cholinergic and adrenergic nerve endings as a cotransmitter and is involved in the physiological regulation of smooth muscles (for review, see Burnstock, 1990; Olsson & Pearson, 1990; El-Moatassim *et al.*, 1992). Although the responses mediated by ATP are usually inhibitory in oesophagus, stomach, small and large intestines, they are excitatory in vas deferens and urinary bladder (see, Gordon, 1986). In blood vessels, ATP induces either contraction or relaxation (Kennedy *et al.*, 1985; Kennedy & Burnstock, 1985; Ralevic *et al.*, 1991). The diversity of the effects of ATP on smooth muscle contractility may be due to the multiple receptor subtypes coupled to different signal transduction pathways.

Purinoceptors are classified into P_1 and P_2 subtypes. P_2 receptors are further classified into P_{2X} and P_{2Y} subtypes (Burnstock & Kennedy, 1985). P_{2X} receptors are linked to non-selective cation channels whereas P_{2Y} receptors are linked to phospholipase C (Kennedy, 1990). ATP also activates a 'nucleotide' receptor in vascular smooth muscle (Chinellato *et al.*, 1992) which is also coupled to phospholipase C (O'Connor, 1992). In the phaeochromocytoma-derived PC12 cell line, ATP has been shown to elicit an inward current (Nakazawa *et al.*, 1990), Ca^{2+} influx and inositol 1,4,5-trisphosphate (IP_3) accumulation (Fasolato *et al.*, 1990). The existence of an ATP-activated Ca^{2+}-permeable cation channel has recently been reported in smooth muscles (Benham & Tsien, 1987; Honore *et al.*, 1989). Rembold *et al.* (1991) have demonstrated that ATP transiently increases $[Ca^{2+}]_i$ as measured by aequorin-luminescence, myosin light chain phosphorylation and force in swine carotid artery and suggested that ATP induces contraction by an increase in transmembrane Ca^{2+} influx through activation of the P_{2X} receptor. On the other hand, in rat cultured aortic smooth muscle cells, ATP has been shown to mobilize intracellular Ca^{2+} by an increase in IP_3 (Tawada *et al.*, 1988). In canine gastric smooth muscle, ATP increases both Ca^{2+} release and protein kinase C activity (Ozaki *et al.*, 1992). In this muscle, products of phosphatidylinositol turnover inhibit spontaneous rhythmic contractions by reducing Ca^{2+} channel activity, possibly through the activation of Ca^{2+}-dependent K^+ channels (IP_3-induced Ca^{2+} release from sarcoplasmic reticulum) and/or the direct inhibition of Ca^{2+} channels (phosphorylation by protein kinase C). These results suggest that different subtypes of purinoceptors in smooth muscle are coupled to different signal transduction pathways.

In order to examine further the role of purinoceptors in vascular smooth muscle, we observed the effects of ATP on $[Ca^{2+}]_i$, force, and Ca^{2+} sensitivity of contractile elements. For these purposes, we compared the effects of ATP with α,β-methylene-ATP, a poorly hydrolyzable and P_{2X}-specific analogue of ATP.

Methods

Male Wistar rats (250–300 g) were stunned and bled and the thoracic aorta was dissected. After removal of fat and connective tissues, the aorta was cut into helical strips approximately 2 mm in width and 8 mm in length. The endothelium was removed by gently rubbing the intimal surface with a finger moistened with physiological salt solution (PSS). This procedure changed neither the magnitude of high K^+-induced contraction nor the threshold concentration of KCl required to induce contraction, suggesting that the smooth muscle layer was not damaged. In such tissue, 1 μM car-

[1] Author for correspondence.

bachol, a releaser of endothelium-derived relaxing factor, did not change the contraction induced by 0.1 μM noradrenaline, suggesting that the endothelium had been removed. Normal PSS contained (mM): NaCl 136.9, KCl 5.4, $CaCl_2$ 1.5, $MgCl_2$ 1.0, $NaHCO_3$ 20.0, glucose 5.5 and EDTA 0.01. A solution with elevated K^+ was made by replacing NaCl with equimolar KCl. A Ca^{2+}-free solution was made by removing $CaCl_2$ and adding 0.5 mM EGTA. These solutions were maintained at 37°C and aerated with 95% O_2 and 5% CO_2. Muscle force was recorded isometrically with a force displacement transducer.

$[Ca^{2+}]_i$ was measured according to the method described by Ozaki et al. (1987) and Sato et al. (1988) using fura-2 (Grynkiewicz et al., 1985). Muscle strips were exposed to the acetoxymethyl ester of fura-2 (5 μM) in the presence of 0.02% cremophor EL for 3 to 4 h at room temperature. The muscle strip was then transferred to the muscle bath integrated in the fluorimeter (CAF-100) and illuminated alternately (48 Hz) with two excitation wave lengths (340 nm and 380 mm). Fluorescence at 500 nm was measured, and the ratio of the fluorescence induced by these two wavelengths was calculated and used as a indicator of $[Ca^{2+}]_i$. Absolute $[Ca^{2+}]_i$ was not calculated because the dissociation constant of fura-2 for Ca^{2+} may change in smooth muscle cells (Konishi et al., 1988; Karaki, 1989). Ratios of fluorescence in the resting muscle and that in the depolarized muscle with elevated external K^+ (72.4 mM) were considered as 0 and 100%, respectively.

Tissue adenosine 3':5'-cyclic monophosphate (cyclic AMP) content was measured with a competitive radioimmunoassay (Abe & Karaki, 1988). Subsequent to an incubation, muscle strips were frozen in liquid nitrogen and homogenized in 6% trichloroacetic acid solution. After centrifugation twice at 3,000 r.p.m., trichloroacetic acid in the supernatant was removed by washing with water-saturated ether, and the succinylated cyclic AMP was assayed by a competitive radioimmunoassay (Yamasa Shoyu, Tokyo, Japan). Tissue guanosine 3',5'-cyclic monophosphate (cyclic GMP) content was measured by competitive radioimmunoassay.

Chemicals used were verapamil hydrochloride, α,β-methylene-adenosine 5'-triphosphate (α,β-methylene-ATP) (Sigma Chemicals, St. Louis, U.S.A.), adenosine 5'-triphosphate (ATP) (Yamasa Shoyu, Tokyo, Japan), forskolin (Nihon Kayaku, Tokyo, Japan), acetoxymethyl esters of fura-2 (Dojindo Laboratories, Kumamoto, Japan) and cremophor EL (Nacarai Chemicals, Tokyo, Japan). The pH of ATP and α,β-methylene-ATP stock solutions was adjusted to 7.4 by addition of NaOH.

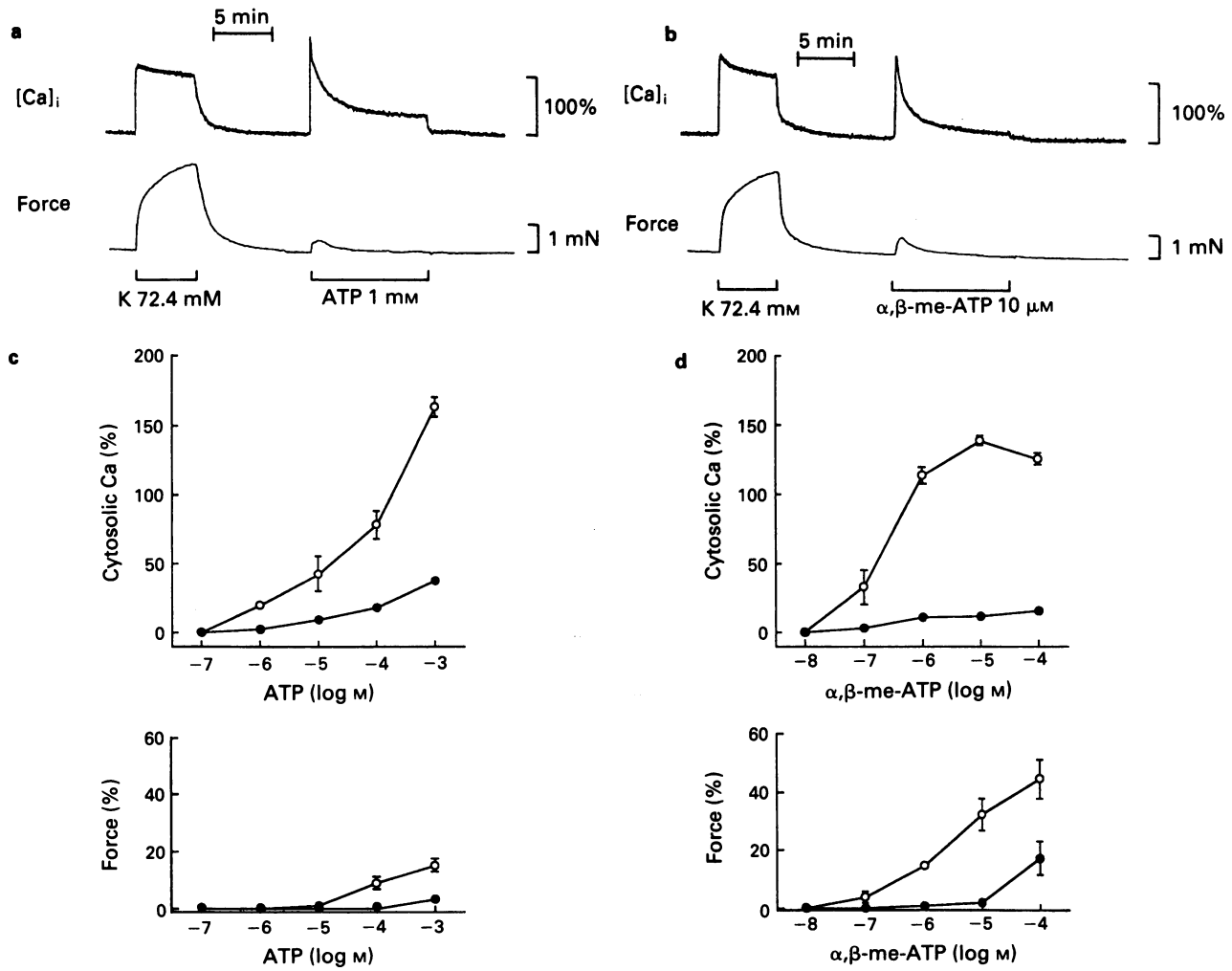

Figure 1 Typical recordings of the effects of ATP (a) and α,β-methylene-ATP (b) on $[Ca^{2+}]_i$ (upper trace) and contraction (lower trace) in rat isolated aorta loaded with a Ca^{2+} indicator, fura-2. ATP (1 mM) and α,β-methylene-ATP (10 μM) induced transient increase in $[Ca^{2+}]_i$ followed by sustained increase. As compared with the effects of high K^+, ATP and α,β-methylene-ATP induced sustained increases in $[Ca^{2+}]_i$ with smaller contractions. Lower panels show concentration-dependent effects of ATP (c) and α,β-methylene-ATP (d) on $[Ca^{2+}]_i$ and force. The peak $[Ca^{2+}]_i$ (○) and force (○) and the values of $[Ca^{2+}]_i$ (●) and force (●) at 10 min are plotted against the concentrations. Each point represents mean ± s.e.mean of 4 experiments.

The numerical data are expressed as mean ± s.e.mean. Differences were evaluated by Student's t test, and a P value less than 0.05 was considered to be statistically significant.

Results

Effects of ATP and α,β-methylene-ATP on $[Ca^{2+}]_i$ and force

Figure 1 shows the typical changes in $[Ca^{2+}]_i$ and force in response to 1 mM ATP and 10 μM α,β-methylene-ATP in rat isolated aorta. ATP (1 mM) induced a rapid increase in $[Ca^{2+}]_i$ (162.8 ± 7.0%, $n = 4$) followed by a small sustained increase which reached a plateau after about 10 min (37.7 ± 2.0%, $n = 4$). Although 1 mM ATP increased $[Ca^{2+}]_i$ to a level higher than that induced by high K^+ solution, it induced only a small transient force (15.2 ± 2.5%, $n = 4$). α,β-Methylene-ATP (10 μM) also induced a rapid increase in $[Ca^{2+}]_i$ (138.4 ± 4.2%, $n = 4$) followed by a small sustained increase which reached a plateau after about 10 min (11.5 ± 1.7%, $n = 4$). As with ATP, α,β-methylene-ATP induced a smaller force (32.1 ± 5.5%, $n = 4$) than high K^+.

Figure 1c and d shows the effects of various concentrations of ATP (0.1–1000 μM) and α,β-methylene-ATP (0.01–100 μM) on $[Ca^{2+}]_i$ and force. Peak Ca^{2+} transient and force increased with the increase in the concentrations of ATP and α,β-methylene-ATP.

Effects of verapamil on $[Ca^{2+}]_i$ and force induced by ATP or α,β-methylene-ATP

The mechanism of the increases in $[Ca^{2+}]_i$ due to ATP and α,β-methylene-ATP was examined by use of the L-type Ca^{2+} channel blocker, verapamil (Figure 2a,b). Verapamil (10 μM) completely inhibited the high K^+ (72.4 mM)-induced increase in $[Ca^{2+}]_i$ and force ($n = 4$, data not shown). In the presence of 10 μM verapamil, 1 mM ATP-induced peak $[Ca^{2+}]_i$ and force were not affected. Verapamil, on the other hand, inhibited the 10 μM α,β-methylene-ATP-induced peak $[Ca^{2+}]_i$ from 138.4 ± 4.2 to 79.3 ± 4.1% ($n = 4$, $P < 0.01$) and force from 32.1 ± 5.5 to 7.4 ± 1.6% ($n = 4$, $P < 0.01$). Verapamil also inhibited the sustained component of $[Ca^{2+}]_i$ in the presence of α,β-methylene-ATP more strongly (from 11.5 ± 1.7 to 3.8 ± 0.3%, $n = 4$, at 10 min) than those in the presence of ATP (from 37.7 ± 2.0 to 31.3 ± 1.4%, $n = 4$, at 10 min), although the sustained component of force was not affected by verapamil.

Effects of ATP and α,β-methylene-ATP on $[Ca^{2+}]_i$ and force in Ca^{2+}-free solution

Muscle strips were first treated with high K^+ (72.4 mM) for 5 min to load Ca^{2+} in storage sites (Karaki *et al.*, 1979). After the Ca^{2+} loading, external Ca^{2+} was removed which decreased $[Ca^{2+}]_i$ below the resting level. As shown in Figure 3, ATP (1 mM) induced a transient increase in $[Ca^{2+}]_i$ (116.2 ± 22.1%, $n = 4$) and force (7.0 ± 1.8%, $n = 4$) in the absence of external Ca^{2+}. Sequential addition of α,β-methylene-ATP (10 μM) did not change $[Ca^{2+}]_i$ or force.

In the absence of external Ca^{2+}, 10 μM α,β-methylene-ATP induced only a small increase in $[Ca^{2+}]_i$ (6.7 ± 3.5%, $n = 4$) with no detectable force. Sequential addition of ATP (1 mM) induced a transient increase in $[Ca^{2+}]_i$, (122.1 ± 14.2%, $n = 4$) with a small increase in force (9.8 ± 3.1%, $n = 4$).

Effects of ATP after the desensitization of the P_{2X} receptor

It has been shown that α,β-methylene-ATP has the ability to desensitize P_{2X} purinoceptors (Burnstock & Kennedy, 1985). As demonstrated in Figure 4, the increase in $[Ca^{2+}]_i$ and force induced by α,β-methylene-ATP (10 μM) became smaller

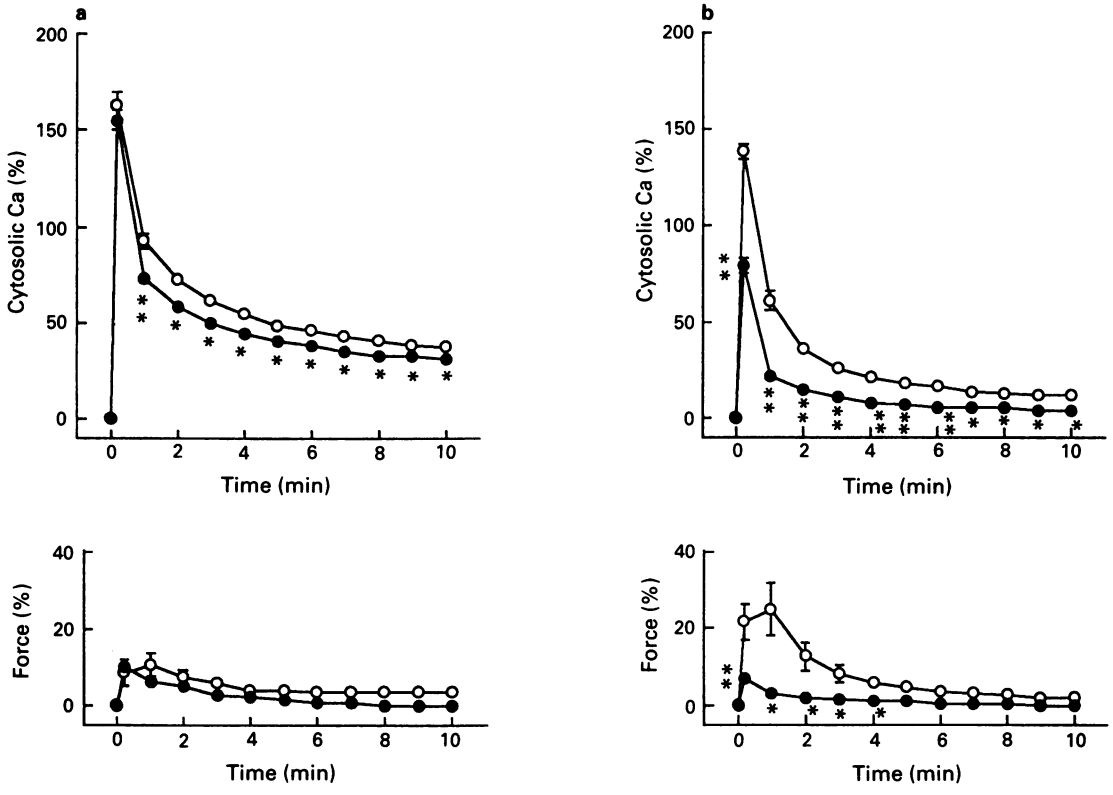

Figure 2 Effects of verapamil (●) on the increases in $[Ca^{2+}]_i$ and force induced by ATP (○) (a) and α,β-methylene-ATP (○) (b). After treatment of the muscle with verapamil (10 μM) for 7 min, ATP (1 mM) or α,β-methylene-ATP (10 μM) was added. Each point represents mean ± s.e.mean of 4 experiments. Significantly different from respective control with $*P < 0.05$ and $**P < 0.01$.

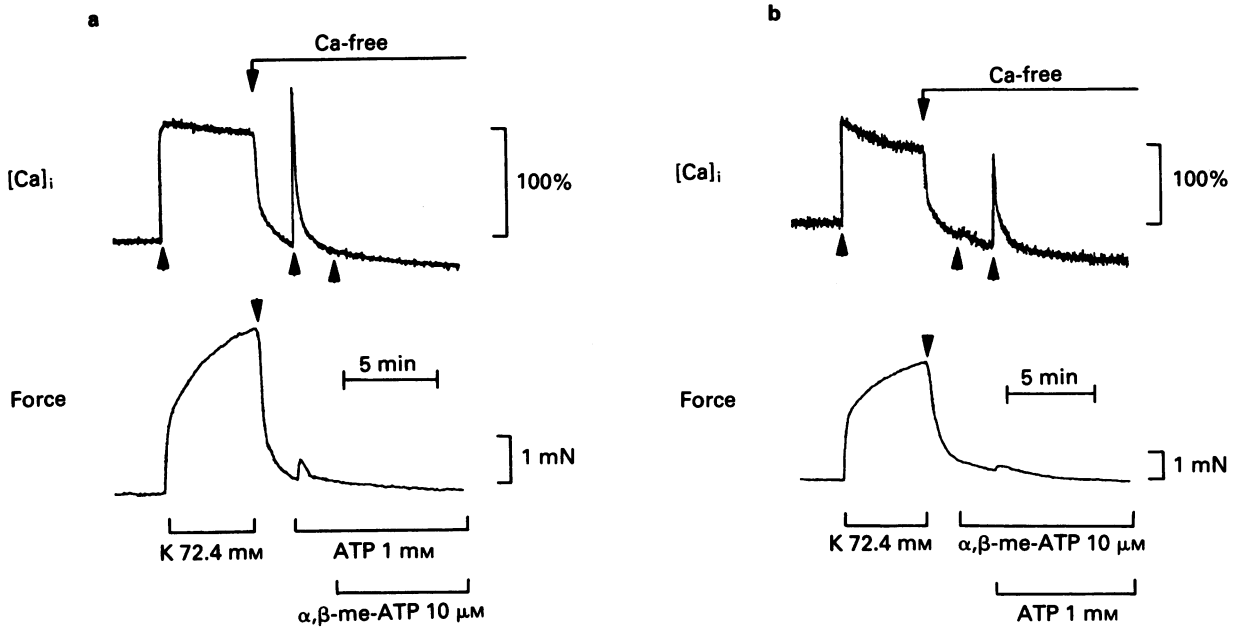

Figure 3 Effects of ATP (a) and α,β-methylene-ATP (b) on $[Ca^{2+}]_i$ (upper trace) and contraction (lower trace) in the absence of external Ca^{2+}. After treatment of tissue with high K^+ (72.4 mM) for 5 min, external Ca^{2+} was removed (with 0.5 mM EGTA) for 2 min. ATP (1 mM) and α,β-methylene-ATP (10 μM) were then added. ATP transiently increased $[Ca^{2+}]_i$ although α,β-methylene-ATP showed little effect. In the presence of ATP or α,β-methylene-ATP, α,β-methylene-ATP or ATP, respectively, was added sequentially. ATP transiently increased $[Ca^{2+}]_i$ even after treatment of the tissue with α,β-methylene-ATP.

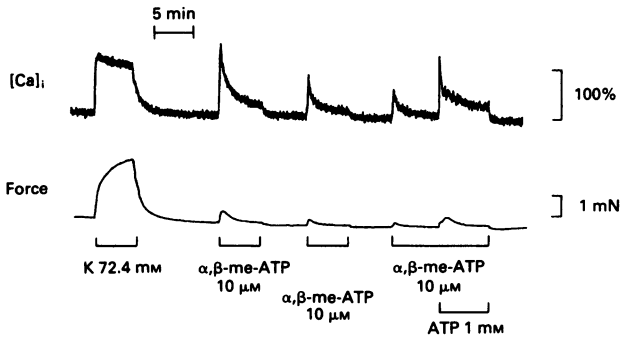

Figure 4 Effects of ATP on $[Ca^{2+}]_i$ and contraction after repeated application of α,β-methylene-ATP (10 μM) for 5 min at 5 min intervals. During the third application of α,β-methylene-ATP, ATP (1 mM) was added which produced an additional increase in $[Ca^{2+}]_i$ and contraction.

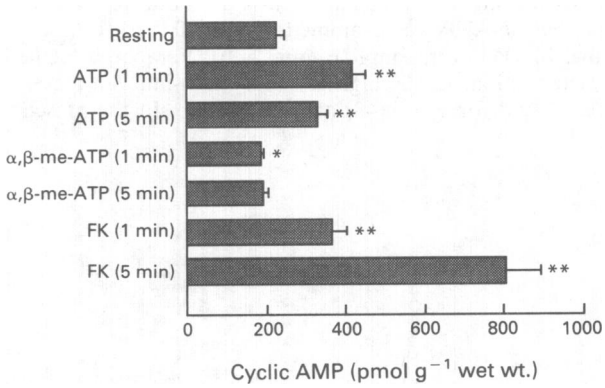

Figure 5 Effects of ATP and α,β-methylene-ATP on cyclic AMP contents. Muscle strips were treated with ATP (1 mM), α,β-methylene-ATP (10 μM) or forskolin (FK, 1 μM) for 1 or 5 min. Significantly different from the control with $*P<0.05$ and $**P<0.01$, respectively.

during repeated applications. The peak $[Ca^{2+}]_i$ and the peak force due to the third application of α,β-methylene-ATP were only 51.9 ± 4.9% ($n = 4$) and 57.4 ± 14.8% ($n = 4$), respectively, of those due to the first applications of α,β-methylene-ATP. Addition of 1 mM ATP during the third application of α,β-methylene-ATP induced additional increase in $[Ca^{2+}]_i$ to 78.4 ± 6.4% and force to 177.6 ± 50.0% ($n = 4$) of those obtained without α,β-methylene-ATP pretreatment.

Effects of ATP and α,β-methylene-ATP on cyclic AMP and cyclic GMP levels

Figure 5 summarizes the effects of ATP (1 mM) and α,β-methylene-ATP (10 μM) on cyclic AMP content. ATP (1 mM) increased cyclic AMP content (to 183.4% in 1 min and 145.3% in 5 min). In contrast, α,β-methylene-ATP (10 μM) did not increase cyclic AMP content. Treatment of the muscle for 5 min with an activator of adenylate cyclase, forskolin (1 μM), increased cyclic AMP content to 352.8%.

Cyclic GMP content of resting tissue was 139.2 ± 0.7 pmol g^{-1} tissue ($n = 5$). ATP (1 mM) did not change the cyclic GMP content (131.1 ± 13.1 pmol g^{-1} tissue 1 min^{-1}, $n = 5$ and 161.4 ± 6.4 pmol g^{-1} tissue 5 min^{-1}, $n = 5$). α,β-methylene-ATP also did not change the cyclic GMP content (139.2 ± 12.6 pmol g^{-1} tissue 1 min^{-1}, $n = 5$ and 127.8 ± 8.1 pmol g^{-1} tissue 5 min^{-1}, $n = 5$).

Discussion

The results of the present study demonstrated that ATP elicited a large and transient increase followed by a small and sustained increase in $[Ca^{2+}]_i$. Verapamil did not inhibit the ATP-induced initial transient increase in $[Ca^{2+}]_i$ but it partially (by approximately 15%) inhibited the sustained increase. It has been demonstrated that, in rat aorta, noradrenaline, prostaglandin $F_{2\alpha}$ and endothelin-1 induced sustained increases in $[Ca^{2+}]_i$ and verapamil almost complete-

ly inhibited these increases (>80%; Hori *et al.*, 1992). These results suggest that the mechanism by which ATP increases $[Ca^{2+}]_i$ is different from that activated by other receptor agonists. It has been shown that ATP opens non-selective cation channels which are permeable to Ca^{2+} and not sensitive to Ca^{2+} channel blockers (Benham & Tsien, 1987; Honore *et al.*, 1989). Thus, it is possible that the ATP-induced increase in $[Ca^{2+}]_i$ may be partly mediated by the opening of this type of channel. In the absence of external Ca^{2+}, ATP induced a rapid and transient increase in $[Ca^{2+}]_i$. These results suggest that ATP releases Ca^{2+} from intracellular storage sites and this may partly be responsible for the initial phase of the ATP-induced response. This ATP-induced Ca^{2+} release might be induced by the increase in IP_3, as has been reported in cultured vascular smooth muscle cells (Tawada *et al.*, 1988). Although we did not identify the type of non-P_{2X} receptor in the present experiments, either the P_{2Y} purinoceptor or nucleotide receptor may be mediating the Ca^{2+} release due to ATP (see Introduction). However, the P_{2Y} purinoceptors seem to be less likely because this type of receptor is generally found on the vascular endothelium (Burnstock & Kennedy, 1985) which was removed in the present study.

α,β-Methylene-ATP also induced an initial transient increase in $[Ca^{2+}]_i$ followed by a sustained increase. In contrast to the effects of ATP, verapamil partially inhibited $[Ca^{2+}]_i$ at the initial phase. Another difference was that α,β-methylene-ATP did not induce a transient increase in $[Ca^{2+}]_i$ in Ca^{2+}-free solution. These results suggest that α,β-methylene-ATP does not release Ca^{2+} from storage sites and that it activates a non-selective cation channel. It was also found that repeated application of α,β-methylene-ATP induced partial desensitization which is one of the characteristics of P_{2X} purinoceptors (Burnstock & Kennedy, 1985). These results suggest that α,β-methylene-ATP activates mainly P_{2X} receptors, opens non-selective cation channels, and increases influx of Ca^{2+} (and possibly other cations) through this type of channel that in turn depolarizes membrane to activate voltage-dependent Ca^{2+} channels. The transient increase in $[Ca^{2+}]_i$ may partly be due to the rapid desensitization of P_{2X} receptors. In the muscle strips pretreated with α,β-methylene-ATP, $[Ca^{2+}]_i$ and force stimulated by α,β-methylene-ATP decreased to 51.9% and 57.4%, respectively. In these desensitized muscle strips, ATP induced an additional increase in $[Ca^{2+}]_i$ and force even in the presence of α,β-methylene-ATP. The increase in $[Ca^{2+}]_i$ was 78.4% of that in the absence of pretreatment with α,β-methylene-ATP. These results support the suggestion that ATP activates not only P_{2X} purinoceptors but also other type of receptors.

Although, ATP and α,β-methylene-ATP induced large increases in $[Ca^{2+}]_i$, these stimulants induced only small contractions. Since it has been shown that ATP is metabolized to adenosine possibly by smooth muscle ecto-nucleotidase (Rembold *et al.*, 1991); that adenosine activates P_1 receptors to increase cyclic AMP (Burnstock & Kennedy, 1985), and that cyclic AMP decreases Ca^{2+} sensitivity of smooth muscle contractile elements (Karaki, 1989), we measured cyclic nucleotide contents. Results indicated that ATP but not α,β-methylene-ATP increased cyclic AMP content without changing cyclic GMP content. These results suggest that the dissociation between $[Ca^{2+}]_i$ and force stimulated by ATP may be partly explained by the cyclic AMP-induced Ca^{2+} desensitization of contractile elements. However, this is unlikely to be an important mechanism in dissociation since α,β-methylene-ATP also caused similar dissociation without increasing cyclic AMP content. An alternative possibility has been suggested by Himpens *et al.* (1992) in cultured smooth muscle cells; ATP may increase Ca^{2+} in the nucleus. Further studies are necessary to determine whether fura-2 detects not only the cytosolic free Ca^{2+} level but also the Ca^{2+} level in the nucleus.

In conclusion, ATP and α,β-methylene-ATP increase $[Ca^{2+}]_i$ by an activation of L-type (verapamil-sensitive) and non-L-type (verapamil-insensitive) Ca^{2+} channels possibly through activation of P_{2X} purinoceptors whereas ATP, but not α,β-methylene-ATP, has an additional effect, releasing Ca^{2+} from storage sites.

This work was supported by Grant-in-Aid for Scientific Research from the Ministry of Education, Science and Culture, Japan and a research grant from Ciba-Geigy Foundation (Japan).

References

ABE, A. & KARAKI, H. (1988). Inhibitory effects of forskolin on vascular smooth muscle of rabbit aorta. *Jpn. J. Pharmacol.*, **46**, 293–301.

BENHAM, C.D. & TSIEN, R.W. (1987). A novel receptor-operated Ca^{2+} channel activated by ATP in smooth muscle. *Nature*, **328**, 275–278.

BURNSTOCK, G. (1990). Purinergic mechanisms. *Ann. N.Y. Acad. Sci.*, **603**, 1–17.

BURNSTOCK, G. & KENNEDY, C. (1985). Is there a basis for distinguishing two types of P_2-purinoceptor? *Gen. Pharmacol.*, **16**, 433–440.

CHINELLATO, A., RAGAZZI, E., PANDOLFO, L., FROLDI, G., CAPARROTTA, L. & FASSINA, G. (1992). Pharmacological characterization of a new purinergic receptor site in rabbit aorta. *Gen. Pharmacol.*, **23**, 1067–1071.

EL-MOATASSIM, C., DORNAND, J. & MANI, J. (1992). Extracellular ATP and cell signalling. *Biochim. Biophys. Acta*, **1134**, 31–45.

FASOLATO, C., PIZZO, P. & POZZAN, T. (1990). Receptor mediated calcium influx in PC12 cells. *J. Biol. Chem.*, **265**, 20351–20355.

GORDON, J.L. (1986). Extracellular ATP: effects, sources and fate. *Biochem. J.*, **233**, 309–319.

GRYNKIEWICZ, G., POENIE, M. & TSIEN, R.Y. (1985). A new generation of Ca^{2+} indicators with greatly improved fluorescence properties. *J. Biol. Chem.*, **260**, 3340–3450.

HIMPENS, B., DE SMEDT, H., DROOGMANS, G. & CASTEELS, R. (1992). Differences in regulation between nuclear and cytoplasmic Ca^{2+} in cultured smooth muscle cells. *Am. J. Physiol.*, **263**, C95–C105.

HONORE, E., MARTIN, C., MIRONNEAU, C. & MIRONNEAU, J. (1989). An ATP-sensitive conductance in cultured smooth muscle cells from pregnant rat myometrium. *Am. J. Physiol.*, **257**, C297–C305.

HORI, M., SATO, K., SAKATA, K., OZAKI, H., TAKANO-OHMURO, H., TSUCHIYA, T., SUGI, H., KATO, I. & KARAKI, H. (1992). Receptor agonists induce myosin phosphorylation-dependent and phosphorylation-independent contraction in vascular smooth muscle. *J. Pharmacol. Exp. Ther.*, **261**, 506–512.

KARAKI, H. (1989). Ca^{2+} localization and sensitivity in vascular smooth muscle. *Trends Pharmacol. Sci.*, **10**, 320–325.

KARAKI, H., KUBOTA, H. & URAKAWA, N. (1979). Mobilization of stored calcium for phasic contraction induced by norepinephrine in rabbit aorta. *Eur. J. Pharmacol.*, **56**, 237–245.

KENNEDY, C. (1990). P_1- and P_2-purinoceptor subtypes – an update. *Arch. Int. Pharmacodyn. Ther.*, **303**, 30–50.

KENNEDY, C. & BURNSTOCK, G. (1985). ATP produces vasodilation via P_1 purinoceptors and vasoconstriction via P_2 purinceptors in the isolated rabbit central ear artery. *Blood Vessels*, **22**, 145–155.

KENNEDY, C., DELBRO, D. & BURNSTOCK, G. (1985). P_2-purinoceptors mediate both vasodilation (via the endothelium) and vasoconstriction of the isolated rat femoral artery. *Eur. J. Pharmacol.*, **107**, 161–168.

KONISHI, M., OLSON, A., HOLLINGWORTH, S. & BAYLOR, S.M. (1988). Myoplasmic binding of fura-2 investigated by steady state fluroescence and absorbance measurement. *Biophys. J.*, **54**, 1089–1104.

NAKAZAWA, K., FUJIMORI, K., TAKANAKA, A. & INOUE, K. (1990). Reversible and selective antagonism by suramin of ATP-induced inward current in PC12 phaeochromocytoma cells. *Br. J. Pharmacol.*, **101**, 224–226.

O'CONNOR, S.E. (1992). Recent developments in the classification and functional significance of receptors for ATP and UTP, evidence for nucleotide receptors. *Life Sci.*, **50**, 1657–1664.

OLSSON, R.A. & PEARSON, J.D. (1990). Cardiovascular purinoceptors. *Physiol. Rev.*, **70**, 761–849.

OZAKI, H., SATO, K. & KARAKI, H. (1987). Simultaneous recordings of calcium signals and mechanical activity using fluorescent dye fura 2 in isolated strips of vascular smooth muscle. *Jpn. J. Pharmacol.*, **45**, 429–433.

OZAKI, H., ZHANG, L., BUXTON, I.L.O., SANDERS, K.M. & PUBLICOVER, N.G. (1992). Negative-feedback regulation of excitation-contraction coupling in gastric smooth muscle. *Am. J. Physiol.*, **263**, C1160–C1171.

RALEVIC, V., MATHIE, R.T., ALEXANDER, B. & BURNSTOCK, G. (1991). Characterization of P_{2X}- and P_{2Y}-purinoceptors in the rabbit hepatic arterial vasculature. *Br. J. Pharmacol.*, **103**, 1108–1113.

REMBOLD, C.M., WEAVER, B.A. & LINDEN, J. (1991). Adenosine triphosphate induces a low $[Ca^{2+}]_i$ sensitivity of phosphorylation and an unusual form of receptor desensitization in smooth muscle. *J. Biol. Chem.*, **266**, 5407–5411.

SATO, K., OZAKI, H. & KARAKI, H. (1988). Changes in cytosolic calcium level in vascular smooth muscle strip measured simultaneously with contraction using fluorescent calcium indicator fura-2. *J. Pharmacol. Exp. Ther.*, **246**, 294–300.

TAWADA, Y., FURUKAWA, K. & SHIGEKAWA, M. (1988). Cyclic AMP enhances inositol triphosphate-induced mobilization of intracellular Ca^{2+} in cultured aortic smooth muscle cells. *J. Biochem.*, **104**, 795–800.

(Received November 24, 1992
Revised April 14, 1993
Accepted May 10, 1993)

Br. J. Pharmacol. (1993), **110**, 269–274

Desensitization of histamine H_1 receptor-mediated inositol phosphate accumulation in guinea pig cerebral cortex slices

[1]D.R. Bristow, P.C. Banford, I. Bajusz, *A. Vedat & *J.M. Young

Department of Physiological Sciences, University of Manchester, Stopford Building, Oxford Road, Manchester M13 9PT and *Department of Pharmacology, University of Cambridge, Tennis Court Road, Cambridge, CB2 1QJ

1 Histamine stimulated the production of [^{3}H]-inositol phosphates in untreated (control) guinea-pig cerebral cortex slices with a best-fit EC_{50} of $17 \pm 4\,\mu M$, and a best-fit maximum response of $385 \pm 23\%$ over basal accumulation.

2 Histamine pretreatment desensitized guinea-pig cortex slices to a subsequent challenge with histamine, which was observed as a reduction in the best-fit maximum response to $182 \pm 32\%$ over basal accumulation.

3 The time-course for the histamine-induced production of [^{3}H]-inositol phosphates was approximately linear over 90 min of stimulation in both control and histamine pretreated slices. The rate of production in pretreated slices was significantly slowed compared to control, such that by 90 min of histamine stimulation the desensitized slices produced 2.8 times the basal [^{3}H]-inositol phosphate accumulation compared to 5.3 fold the basal [^{3}H]-inositol phosphate accumulation in the control slices.

4 Displacement of [^{3}H]-mepyramine binding to homogenates of guinea-pig cerebral cortex by mepyramine and histamine revealed that histamine pretreatment did not alter the apparent affinity of the H_1 receptor for histamine (control $K_d = 6.3 \pm 0.7\,\mu M$, desensitized $K_d = 7.9 \pm 1.6\,\mu M$) or mepyramine (control $K_d = 3.4 \pm 0.8$ nM, desensitized $K_d = 3.4 \pm 1.3$ nM), nor was there any reduction in the calculated maximum number of [^{3}H]-mepyramine binding sites (control $B_{max} = 192 \pm 31$ fmol mg^{-1} protein, desensitized $B_{max} = 220 \pm 50$ fmol mg^{-1} protein).

5 The histamine-mediated desensitization of response in guinea-pig slices was mediated by the H_1 receptor subtype, since the attentuated maximum histamine-stimulated [^{3}H]-inositol phosphate accumulation could not be prevented by inclusion of an H_2- (ranitidine) and an H_3- (thioperamide) receptor antagonist during the pretreatment period.

6 The desensitized histamine-stimulated [^{3}H]-inositol phosphate accumulation recovered to 90% of control levels over a period of 150 min after the removal of the conditioning dose of histamine, with a half-time of recovery of about 95 min.

Keywords: Histamine H_1 receptors; desensitization; [^{3}H]-inositol phosphates; guinea-pig cerebral cortex

Introduction

It is well known that many hormone- and neurotransmitter-induced signalling pathways are desensitized after persistent agonist stimulation. This ubiquitous regulatory mechanism is manifest as an attenuation of cellular responsiveness to continued or subsequent receptor activation and plays a pivotal role in regulating cellular homeostasis. In addition, *in vivo* receptor desensitization has clinical implications, being purported to have a role in the aetiology of several diseases (Brodde & Michel, 1989) and suggested to be responsible for the tolerance to certain drugs after long-term treatment (Brodde & Michel, 1989; Rickels *et al.*, 1983).

The molecular mechanisms underlying receptor desensitization appear multifaceted and can be divided into two phases: homologous desensitization (receptor-specific) which involves the selective loss of response to the stimulated receptor only, and heterologous desensitization (receptor non-specific) which in addition to a reduced responsiveness of the stimulated receptor, also involves an attenuation of responses induced by other receptor systems. The molecular basis for agonist-induced desensitization has been characterized in detail for the catecholamine-induced desensitization of the β-adrenoceptor system. Here, both phases of desensitization can be observed that appear to be mediated, at least in part, by protein phosphorylation (Huganir & Greengard, 1990). In contrast to the β-adrenoceptor-adenylate cyclase pathway, much less information is available on the mechanisms of agonist-induced desensitization of receptors coupled to phospholipase C (PLC). There is evidence that receptors coupled to PLC, such as muscarinic acetylcholine receptors, α_1-adrenoceptors, angiotensin II and histamine H_1 receptors, desensitize by both homologous and heterologous mechanisms and that modulation of the activity of protein kinase C can affect the development of desensitization (Hepler *et al.*, 1988; Mitsuhashi & Payan, 1988; Cowlen *et al.*, 1990), implicating a role for phosphorylation in this process (Huganir & Greengard, 1990).

Histamine is an established neurotransmitter in the mammalian CNS, where it is found in discrete pathways (Pollard & Schwartz, 1987). It interacts with three pharmacologically distinct receptors subtypes in the CNS, H_1, H_2 and H_3, to regulate a plethora of physiological actions, such as arousal state, locomotor activity, brain energy metabolism, neuroendocrine, autonomic and vestibular functions, feeding, drinking, sexual behaviour and analgesia (Wada *et al.*, 1991). Much work in the brain has focused on the histamine H_1 receptor which is coupled to inositol phospholipid hydrolysis, and thus to the mobilization of intracellular calcium (Hill, 1990). The responses induced by H_1 receptors can be desensitized after prolonged agonist stimulation in both a homologous (Nakahata & Harden, 1987; Dillon-Carter & Chuang, 1989; Cowlen *et al.*, 1990) and heterologous (Brown *et al.*, 1986; McDonough *et al.*, 1988) manner. Previous studies have shown that the histamine-induced hydrolysis of membrane inositol phospholipids (Nakahata & Harden, 1987; Cowlen *et al.*, 1990) is desensitized by agonist pretreatment, as well as the intracellular pathways distal to calcium mobilization, such as histamine-stimulated guanosine 3′:5′-cyclic monophosphate (cyclic GMP) formation (Taylor & Richelson, 1979), -glycogen

[1] Author for correspondence.

hydrolysis (Quach et al., 1981) and -calcium fluxes (Brown et al., 1986). However, the H_1 agonist-induced desensitization of histamine-stimulated inositol 1,4,5-trisphosphate (IP_3) production has only been characterized in cultured cells and not in more complex CNS tissue preparations, such as brain slices, which contain a heterogeneous populations of communicating cells. In this paper we describe the desensitization of H_1 receptor-mediated inositol phosphate production in guinea-pig cerebral cortex slices.

Methods

Accumulation and extraction of [^{3}H]-inositol phosphates

Guinea-pig cerebral cortices (male, Dunkin Hartley strain, 350–500 *g*) were cross-chopped into 350 × 350 μm slices (McIlwain tissue chopper), dispersed and washed 3 times in Krebs-Henseleit medium (composition in mM: NaCl 116, KCl 4.7, $MgSO_4$ 1.1, KH_2PO_4 1.2, $NaHCO_3$ 25, $CaCl_2$ 2.5, D-glucose 11). The slices were then incubated at 37°C in continuously gassed (95% O_2:5% CO_2) Krebs-Henseleit medium for 60 min with 4 changes of medium. A proportion of the slices were preincubated in histamine (100 μM) containing Krebs-Henseleit medium and the remainder preincubated in Krebs-Henseleit medium alone for 30 min at 37°C with continuous gassing (95% O_2:5% CO_2). In experiments to determine the receptor subtype mediating the desensitization effect, ranitidine (100 μM, H_2 antagonist) and thioperamide (1 μM, H_3 antagonist) were included in both the control and histamine pretreatment mediums. The slices were washed thoroughly (4 × 50 ml Krebs-Henseleit medium) and transferred to an Eppendorf Multipipette tip and allowed to settle under gravity. Aliquots of the slices (50 μl, approx 1.5 mg protein) were added to 190 μl of Krebs-Henseleit medium containing 0.33 μM *myo*-[2-^{3}H]-inositol (1 μCi per incubation) and 10 mM LiCl, in insert vials. The vials were gassed (95% O_2:5% CO_2), capped and incubated for 30 min in a shaking water bath (37°C) before the addition of 10 μl solution of Krebs-Henseleit medium or histamine (10^{-6}–10^{-3} M). After incubation for a further 45 min, the reaction was terminated by addition of 250 μl of an ice-cold solution of 10% perchloric acid containing EDTA (1 mM) and phytic acid (1 mg ml^{-1}). Tubes were then allowed to stand on ice for 20 min before addition of 400 μl of freshly prepared trioctylamine/1,1,2 trichlorotrifluoroethane mixture (1:1 v:v) to extract the inositol phosphates (Sharpes & McCarl, 1982). The samples were then vortex mixed for 15 s and centrifuged at 1500 *g* for 3 min. The upper aqueous phase (350 μl) was transferred to new insert vials and neutralized with 3 ml of HEPES (100 mM, pH 7.5), and each sample was then applied to an AG1-X8 (formate form, 100–200 mesh, Biorad) anion-exchange column. [^{3}H]-inositol and [^{3}H]-glycerophosphoinositol were eluted with 10 ml water and 10 ml 60 mM ammonium formate/5 mM sodium tetraborate, respectively, and [^{3}H]-inositol mono-, bis- and tris-phosphates ([^{3}H]-IP_n) were collectively eluted with 10 ml 800 mM ammonium formate/100 mM formic acid. Quicksafe scintillation fluid (10 ml, Zinsser Analytic) was added to each fraction and tritium determined by scintillation counting.

Inhibition of [^{3}H]-mepyramine binding

Guinea-pig cerebral cortex slices were prepared and pretreated as described above. The histamine preincubated and control slices were then washed thorougly with ice-cold Krebs-Henseleit medium (2 × 50 ml) followed by ice-cold *N*-Tris-(hydroxymethyl)-methyl-2-amino-ethanesulphonic acid (TES-KOH) buffer (10 mM, pH 7.5, 2 × 50 ml), prior to homogenization (Teflon-glass homogenizer, 3 passes). Measurement of the binding of [^{3}H]-mepyramine to the cerebral cortex homogenates (385 ± 39 μg protein, $n = 8$) was performed immediately. [^{3}H]-mepyramine (1 nM) binding and inhibition by various concentrations of competing ligand (mepyramine: 1×10^{-12}–1×10^{-7} M and histamine 1×10^{-8}–1×10^{-2} M) was allowed to come to equilibrium at 30°C for 60 min before the reaction was terminated by rapid filtration (Brandel 24-place cell harvester) through GF/B filters (presoaked in 0.3% polyethylenimine), essentially as described by Treherne & Young (1988). The buffer used was 10 mM TES-KOH (pH 7.5) and the non-specific binding component was defined by use of 1 μM temelastine in each experiment. For each experiment the concentration of [^{3}H]-mepyramine was determined by scintillation spectrometry and the protein concentration determined according to Lowry *et al.* (1951).

Analysis of data

The histamine-induced concentration-response curves for [^{3}H]-inositol phosphate accumulation in cerebral cortex slices were expressed as a percentage increase above basal values (unstimulated) in each experiment and fitted to a Hill equation (logistic equation) according to Crawford *et al.* (1990). Each point was weighted according to the reciprocal of the variance associated with it. The errors associated with the best-fit parameters are appreciable with this approach, since the number of points on each curve is limited by the need to obtain curves for both histamine-pretreated and control slices within the same experiment. However, fitting the curves in this way does have the advantage of giving unbiased estimates of EC_{50} and maximum response.

To obtain a best-fit value of the IC_{50} ± estimated s.e.mean for curves of mepyramine and histamine inhibition of [^{3}H]-mepyramine binding to cerebral cortex homogenates, the curves were fitted as above to the equation:

$$\%\text{ of the uninhibited binding of [}^3\text{H]-mepyramine} = \frac{100-\text{NSB}}{((A/IC_{50})^n + 1)} + \text{NSB}$$

with IC_{50}, n and NSB as variables. A is the concentration of inhibitor, IC_{50} the inhibitor concentration giving 50% inhibition of specific binding, n the Hill coefficient and NSB non-specific binding. Analysis of statistical significance of differences between observations was performed by the Student's *t* test (unpaired data) using MultiStat statistics package implemented on a Macintosh LCII computer.

Chemicals

[^{3}H]-*myo*-inositol (specific activity 15–18 Ci mmol^{-1}) was obtained from New England Nuclear and histamine dihydrochloride and mepyramine maleate were purchased from Sigma. Ranitidine was a gift from Glaxo and Thioperamide was purchased from Cookson Chemicals. All other compounds were analytical grade and purchased mainly from BDH and Sigma

Results

Effect of histamine pretreatment on histamine-stimulated [^{3}H]-inositol phosphate accumulation in guinea-pig cerebral cortex slices

The concentration-response curve for histamine-stimulated [^{3}H]-inositol phosphate ([^{3}H]IP_n) accumulation in guinea pig cerebral cortex slices in the presence of 10 mM Li^+ is shown in Figure 1. Histamine stimulated the production of [^{3}H]-inositol phosphates in untreated (control) guinea-pig cerebral cortex slices with a best-fit EC_{50} of 17 ± 4 μM (mean ± s.e.mean, 6 experiments), with a 1 mM histamine response of 385 ± 24% over basal accumulation. The histamine response is mediated by the H_1 receptor subtype, since mepyramine (1 μM), a selective H_1 antagonist, complete-

ly abolished (99.6% inhibition, mean of 2 experiments) the response to 100 μM histamine, whereas the H_2 receptor antagonist, ranitidine (100 μM, 6% inhibition, mean of 2 experiments), and a selective H_3 receptor antagonist, thioperamide (1 μM, 7% inhibition, mean of 2 experiments), were ineffective. The antagonist results and the EC_{50} value for the histamine-stimulated [^{3}H]-IP_n accummulation in untreated slices of 17 μM are in accordance with previous reports (Daum *et al.*, 1983; 1984).

Preincubation of the cerebral cortex slices for 30 min with 100 μM histamine resulted in a subsequent concentration-response curve for histamine with an EC_{50} of 23 ± 19 μM (4 experiments); this value is not significantly different from the EC_{50} value from control slices. The best-fit maximum histamine-stimulated [^{3}H]-IP_n production in histamine-pretreated slices was 182 ± 32% (4 experiments) over basal accumulation (Figure 1). Significant differences were obtained at the two highest histamine concentrations tested, 10^{-4} M ($P<0.002$, Student's t test) and 10^{-3} M ($P<0.009$), between the response induced in control compared to pretreated brain slices. In several experiments we observed in both control and desensitized slices that histamine concentrations of above 10^{-3} M induce an [^{3}H]-IP_n accumulation less than that obtained with 10^{-3} M histamine.

Time-course of histamine-stimulated [^{3}H]-inositol phosphate accumulation in guinea-pig cerebral cortex slices

The rate of histamine-stimulated (100 μM) and basal (unstimulated) accumulation of [^{3}H]-IP_n in untreated and histamine-pretreated guinea-pig cerebral cortex slices is shown in Figure 2. The accumulation of [^{3}H]-IP_n ([^{3}H]-inositol mono-, bis- and trisphosphates) in non-pretreated slices of guinea-pig cerebral cortex rises at a near linear rate, reaching 5.3 fold over basal by 90 min of histamine stimulation. In histamine-pretreated slices the time course of accumulation of [^{3}H]-IP_n also rises at a near linear rate, but the rate of accumulation of [^{3}H]-IP_n is significantly reduced ($P<0.03$, Student's t test) and by 90 min of stimulation the response is only 2.8 times basal levels. The basal levels for both untreated and pretreated slices steadily increase at approximately the same rate over the 90 min stimulation period (Figure 2). Note that there is a slight increase in the basal accumulation of [^{3}H]-IP_n in pretreated compared to control slices, but this difference is insignificant relative to the attenuation of histamine-stimulated response in treated compared to control tissue.

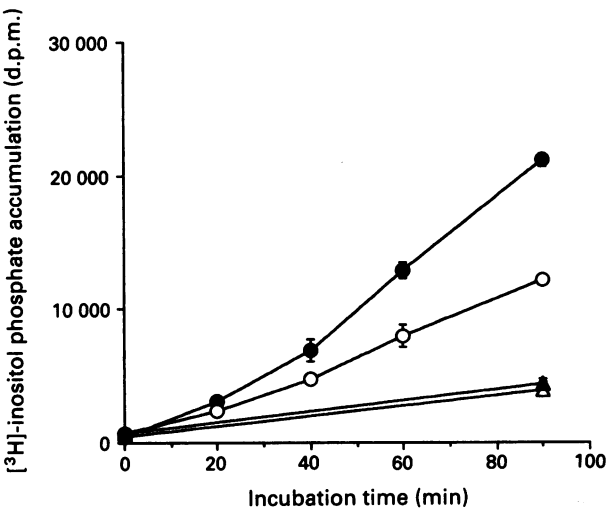

Figure 2 Time course of histamine-induced (100 μM) and basal accumulation of [^{3}H]-inositol mono-, bis- and tris phosphates ([^{3}H]-IP_n) in guinea-pig cerebral cortex slices. Cerebral cortex slices were prepared, preincubated, prelabelled with [^{3}H]-*myo*-inositol, and stimulated with histamine (10^{-4} M) or Krebs-Henseleit medium (basal) in the presence of LiCl (10 mM), and the [^{3}H]-IP_n extracted and measured as described under Methods. The graph is expressed as mean d.p.m. values ± s.e.mean of triplicate determinations from a representative experiment. Very similar results were obtained on a further two occasions. At all time points the histamine-treated slices were significantly lower (to at least $P<0.03$) than the corresponding control slices. At 90 min incubation the basal [^{3}H]-IP_n accumulation was not significantly different under the two conditions. The lines represent histamine-induced response in control (●) and histamine-pretreated (○) slices and basal (Krebs-Henseleit medium) response in control (▲) and histamine-pretreated (△) slices.

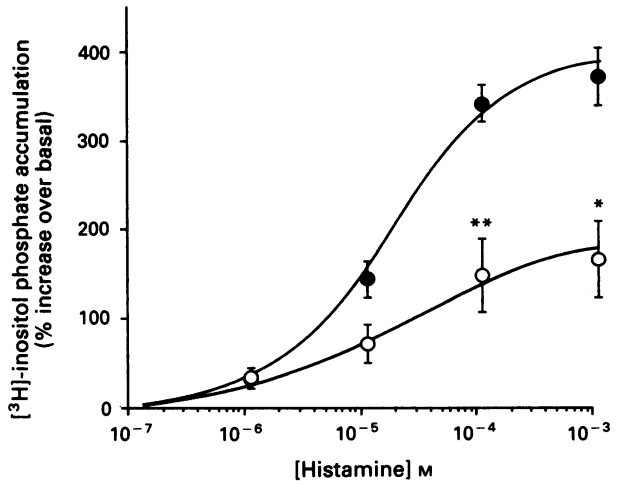

Figure 1 Concentration-response curve for histamine-induced [^{3}H]-inositol mono-, bis- and tris-phosphates ([^{3}H]-IP_n) formation in control (●) and desensitized (○) guinea-pig cerebral cortex slices. Cerebral cortex slices were prepared, preincubated, prelabelled with [^{3}H]-*myo*-inositol, and stimulated with histamine (10^{-6} M–10^{-3} M) in the presence of LiCl (10 mM), and the accumulated [^{3}H]-IP_n extracted and measured as described under Methods. In order to allow for variations in cellular response between experiments, values were standardized against [^{3}H]-IP_n accumulation in cells without histamine stimulation (basal). Each point is expressed as % increase over basal and is the mean ± s.e.mean of 6 (control) and 4 (histamine-pretreated) independent experiments.

Significantly different from control at $*P<0.009$ and $**P<0.002$, respectively. The basal [^{3}H]-IP_n accumulation ranged from 1455–2051 d.p.m. in control slices and 2307–3023 d.p.m. in desensitized slices. Note that these values are not corrected for variations in protein concentrations (i.e. number of brain slices per incubation) between control and histamine-pretreated preparations.

Inhibition of [^{3}H]-mepyramine binding to untreated (control) and desensitized guinea-pig cortex homogenates by mepyramine and histamine

The inhibition of [^{3}H]-mepyramine binding to untreated (control) and desensitized guinea-pig cortex homogenates by mepyramine and histamine is shown in Figure 3. The displacement of [^{3}H]-mepyramine (1 nM) binding to untreated and desensitized guinea-pig cortex homogenates by unlabelled mepyramine occurs with an apparent equilibrium dissociation constant, K_d, of 3.4 ± 0.8 nM (mean ± s.e.mean, 4 experiments) and 3.4 ± 1.3 nM, respecticely. However, both mepyramine inhibition curves had Hill coefficients less than unity (0.44 ± 0.04 and 0.58 ± 0.1, respectively) which may be a consequence of the experimental protocol adopted, although the reason for the low slope is not clear. The calculated maximum number of binding sites, B_{max}, for [^{3}H]-mepyramine was 192 ± 31 fmol mg^{-1} protein (untreated) and 220 ± 50 fmol mg^{-1} protein (desensitized). Histamine displacement of [^{3}H]-mepyramine binding to untreated and desensitized guinea-pig cortex homogenates reveals apparent

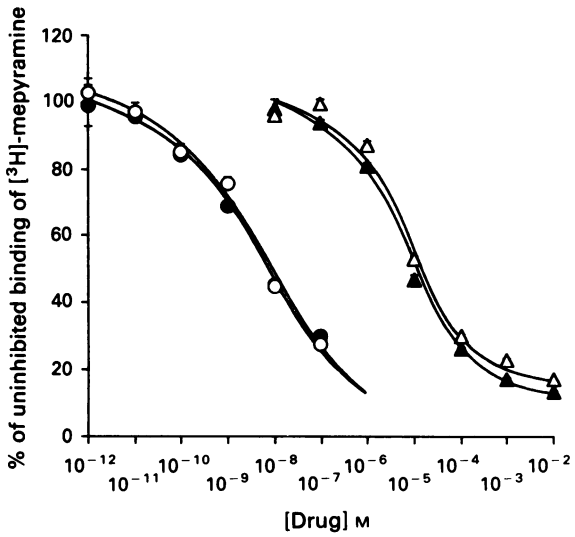

Figure 3 Inhibition of [^{3}H]-mepyramine binding to guinea-pig cortex homogenates by mepyramine and histamine. Guinea-pig cortex slices were prepared and pretreated with histamine (100 μM, 30 min) or untreated (control), and homogenized as described under Methods. Results are expressed as % of the total binding of [^{3}H]-mepyramine and are means ± s.e.mean of triplicate determinations from 4 experiments. The lines represent control homogenates displaced by mepyramine (●) and histamine (▲) and histamine pretreated homogenates displaced by mepyramine (○) and histamine (△).

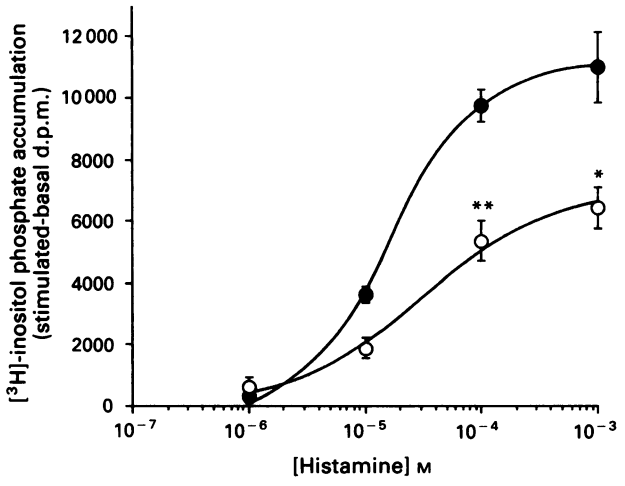

Figure 4 Effect of histamine H_2 and H_3 receptor antagonists on the development of histamine-mediated desensitization of [^{3}H]-inositol mono-, bis and tris phosphates ([^{3}H]-IP$_n$) accumulation in guinea-pig cerebral cortex slices. Cortical slices were prepared according to the Methods section and then pretreated with histamine (100 μM) in the presence of ranitidine (100 μM) and thioperamide (1 μM) (○, histamine + inhibitors) or pretreated with ranitidine (100 μM) and thioperamide (1 μM) alone (●, control + inhibitors). After extensive washing the slices were rechallenged with histamine (10^{-6}–10^{-3} M) for 45 min before the extraction and measurement of [^{3}H]-IP$_n$ accumulation as described under Methods. Each point is given as the stimulated – basal [^{3}H]-IP$_n$ accumulation in d.p.m. values (mean ± s.e.mean of triplicate determinations) from a representative experiment. The same experiment was repeated on two other occasions with similar results. Significantly different from control- + inhibitors at $^*P<0.007$ and $^{**}P<0.004$, respectively.

K_d values of 6.3 ± 0.7 μM (mean ± s.e.mean, 4 experiments; Hill coefficient 0.64 ± 0.03) and 7.9 ± 1.6 μM (Hill coefficient 0.65 ± 0.06), respectively. In all cases the parameters determined for the untreated guinea-pig cortex homogenates were not significantly different from those obtained in histamine-pretreated homogenates.

Effects of H_2 and H_3 receptor antagonists on histamine-induced desensitization

The histamine concentration-response curve for the accumulation of [^{3}H]-IP$_n$ in guinea-pig cortex slices pretreated with histamine (30 min) in the presence of ranitidine (100 μM) and thioperamide (1 μM) (histamine + inhibitors) and pretreated with ranitidine and thioperamide alone (control- + inhibitors) is shown in Figure 4. The EC_{50} for histamine of 18 ± 1 μM (mean ± s.e.mean, 3 experiments) derived from the control + inhibitors slices is not significantly different (Student's t test) from that obtained in non-pretreated (control) slices. The EC_{50} value for histamine in the histamine- + inhibitors pretreated brain slices of 30 ± 16 is also not significantly different from the EC_{50} value derived from slices pretreated with histamine alone (Figure 1), nor is it significantly different from the control + inhibitors EC_{50} value. The response to both 1 mM and 0.1 mM histamine in guinea-pig cerebral cortex slices pretreated with histamine (100 μM) in the presence of ranitidine and thioperamide were significantly ($P<0.007$ and $P<0.004$, respectively, Student's t test) attenuated compared to control + inhibitors brain slices (Figure 4), consistent with the involvement of histamine H_1 receptors in the desensitization process.

Recovery from histamine-induced desensitization of [^{3}H]-inositol phosphate accumulation in guinea-pig cerebral cortex slices

Histamine-stimulated [^{3}H]-IP$_n$ accumulation was measured in untreated and histamine-pretreated slices at various times

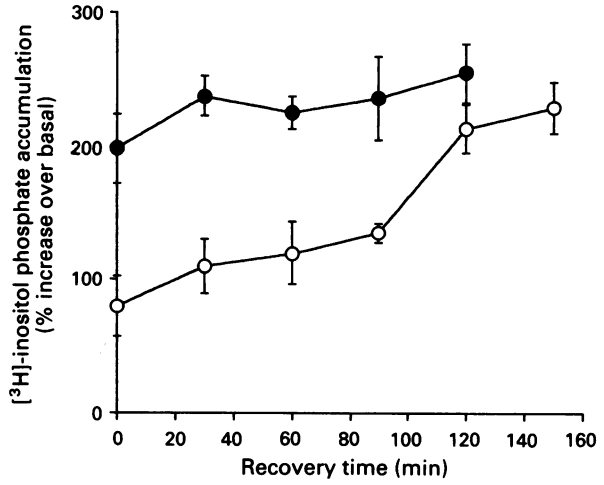

Figure 5 Time-course for recovery from desensitization of [^{3}H]-inositol mono-, bis- and tris-phosphates ([^{3}H]-IP$_n$) accumulation in guinea-pig cortex slices. Cerebral cortex slices were prepared, histamine preincubated, and prelabelled with [^{3}H]-*myo*-inositol as described under Methods. Slices from both control (●) and histamine-pretreated (○) preparations were allowed to recover for between 0 and 150 min (in Krebs-Henseleit medium at 37°C continuously gassed with 95% O_2:5%CO_2) before being stimulated with histamine (10^{-4} M) for 45 min and the [^{3}H]-IP$_n$ extracted and measured as described under Methods. Values at each time-point were calculated as a % increase over basal [^{3}H]-IP$_n$ accumulation and are the mean ± s.e.mean of three independent experiments. The histamine-stimulated [^{3}H]-IP$_n$ accumulation was significantly reduced in the desensitized slices (○) compared to controls at 0, 30, 60 and 90 min of recovery at $P<0.03$, 0.007, 0.01 and 0.03, respectively (Student's t test).

(0–150 min) after the removal of histamine (pretreated) and the washing procedure to assess the recovery of the histamine response (Figure 5). The histamine response was relatively constant at 230 ± 9% (mean ± s.e.mean, 5 experiments) increase over basal throughout 150 min of the experiment in the untreated (control) slices. In the desensitized slices the histamine-induced response was only 80 ± 23% over basal immediately after the removal of histamine ($t = 0$), before recovery of the response occurred over the following 150 min. The histamine-induced response in the desensitized slices was significantly lower (Student's test) than the corresponding control slices at 0 ($P < 0.03$), 30 ($P < 0.007$), 60 ($P < 0.01$) and 90 ($P < 0.03$) min of recovery. After removal of histamine the desensitized tissue had recovered to 84% of the control response by 120 min and to 90% by 150 min and was not significantly different from the histamine response measured in the control slices (at 120 min). The half-time for the recovery of the histamine-mediated [^{3}H]-IP_n accumulation was estimated at 95 min.

Discussion

The results presented here show clearly that histamine H_1 receptor-mediated [^{3}H]-IP_n accumulation in guinea-pig cerebral cortex slices can be desensitized by a prior acute treatment of the cells with histamine. The desensitization effect is mediated by histamine acting on H_1 and not H_2 or H_3 receptors and is manifest as a reduction in the maximum histamine-stimulated IP_n accumulation and an attenuated time-course for [^{3}H]-IP_n production. This desensitization effect is essentially the same as that observed for histamine H_1 receptor-induced [^{3}H]-IP_n accumulation in HeLa cells (Bristow & Young, 1991; Bristow & Zamani, 1993) and the P_{2Y} purinoceptor-coupled phosphoinositidase C system in Turkey erythrocytes (Martin & Harden, 1989). The slowed time course for [^{3}H]-IP_n production is a very subtle way of desensitizing the system to agonist stimulation, but the effect of this reduced rate of [^{3}H]-IP_n formation on the intracellular calcium mobilization and the ultimate cellular function is unknown and awaits further investigation. The desensitization of the response does not appear to involve a reduction in the affinity of the H_1 receptor for histamine or the antagonist mepyramine, nor does it seem to be the result of a reduction in the number of H_1 receptors in the cerebral cortex slice preparation. Characterization of the histamine-mediated desensitization phenomenon shows that the effect is reversible with an almost full recovery of the response after removal of the desensitizing stimulus.

Histamine pretreatment of rat cerebellar granule cells (Dillon-Carter & Chuang, 1989), N1E-115 mouse neuroblastoma cells (Taylor & Richelson, 1979), HeLa cells (Bristow & Zamani, 1993), BC3H-1 muscle cells (Brown *et al.*, 1986), 1321N1 human astrocytoma cells (McDonough *et al.*, 1988), DDT_1 MF-2 cells (Cowlen *et al.*, 1990), guinea-pig ileum (Donaldson & Hill, 1986), rabbit aorta (Lurie *et al.*, 1985), guinea-pig jejunum (Leurs *et al.*, 1990) and also of mouse cerebral cortex slices (Quach *et al.*, 1981) has been shown to attenuate histamine-induced intracellular responses. We are able to extend this list to include the H_1 receptor-mediated [^{3}H]-IP_n production in guinea-pig cerebral cortex slices. The type of desensitization mechanism shown in the previous studies varies, with both homologous and heterologous forms of H_1 receptor desensitization being reported. Homologous desensitization is thought to involve an alteration at the level of the receptor molecules, perhaps by phosphorylation, although no evidence has been presented to date to support this contention for H_1 receptors. Some evidence does support the role of PKC in regulating H_1 receptor responsiveness (Mitsuhashi & Payan, 1988; Murray *et al.*, 1989; Cowlen *et al.*, 1990) and acute histamine stimulation of cells does appear to cause protein phosphorylation (Levin & Santel, 1991; Raymond *et al.*, 1991). However, the PKC-mediated attenuation of H_1 receptor responses may be a non-selective desensitization mechanism, since in HeLa cells the agonist-mediated desensitization of histamine H_1 receptors appears to occur independently of PKC activation (Smit *et al.*, 1992; Zamani & Bristow, unpublished observations).

Here we show that H_1 receptor desensitization in guinea-pig cerebral cortex involves a reduction in the maximum histamine-induced response, an effect that has also been found in NIE-115 neuroblastoma cells (Taylor & Richelson, 1979), BC3H-1 muscle cells (Brown *et al.*, 1986), DDT_1 MF-2 smooth muscle cell line (Cowlen *et al.*, 1990) and HeLa cells (Bristow & Zamani, 1993). We observe about a 60% desensitization of the 10^{-3} M histamine-stimulated [^{3}H]-IP_n production, which is of similar magnitude to the degree of desensitization of response observed in mouse brain slices (Quach *et al.*, 1981), NIE-115 cells (Taylor & Richelson, 1979) and DDT_1 MF-2 smooth muscle cells (Cowlen *et al.*, 1990). However, due to the delay inherent in our experimental procedure, [^{3}H]-IP_n accumulation was measured 70 min after the removal of the desensitizing stimulus, and considering our findings that the desensitization process is reversible (Figure 5), the actual maximum extent of desensitization of this system may be greater than the earliest measurable value of 60% inhibition.

Our study of guinea-pig cortex slices and homogenates do not show any significant alteration in the EC_{50} values for histamine-induced [^{3}H]-IP_n accumulation, the maximum number of binding sites (B_{max}) for [^{3}H]-mepyramine, nor was there any change in the apparent affinity of the H_1 receptor for histamine and mepyramine. However, histamine inhibition of [^{3}H]-mepyramine binding may not be a sensitive measure of receptor-effector coupling, since GTP, GPPNHP or GTPγS produce only a small, or no, shift in the histamine inhibition curves in membranes from guinea-pig whole brain (Chang & Snyder, 1980), guinea-pig cerebellum (Bristow & Young, unpublished observations) or HeLa cells (Arias-Montaño & Young, unpublished observations). The [^{3}H]-mepyramine binding evidence suggests that the desensitization process in guinea-pig cortex does not involve an alteration in H_1 receptor affinity for agonists or antagonists. Thus, the attenuation of the response is likely to occur at sites distal to the initial agonist binding interaction and may involve a change in the activity of the transduction pathway.

The lack of a reduction in the B_{max} for [^{3}H]-mepyramine binding to histamine-pretreated cerebral cortex homogenates does not exclude the possibility that the reduction in response is due to a loss of functional H_1 receptors from the cell surface. In fact our results are in contrast to the situation reported in mouse cerebral cortex, where a small (18%) reduction in [^{3}H]-mepyramine binding sites was observed after a similar desensitization protocol to that used here (Quach *et al.*, 1981). We believe that our findings of an unchanged B_{max} are more consistent with the mechanism involved in acute (< 2 h stimulation) agonist desensitization of other receptor systems, which do not appear to involve receptor down-regulation and degradation (Huganir & Greengard, 1990). Furthermore, a result indicating a reduction in the B_{max} of H_1 receptors using [^{3}H]-mepyramine should be viewed with caution, since the physiochemical nature of this ligand make it freely accessible to both cell-surface and intracellular compartments, and thus it is unlikely to detect H_1 receptor down-regulation. A reduction in [^{3}H]-mepyramine binding sites would only be observed if desensitization involved the concomitant degradation of H_1 receptors, and the report of Quach *et al.* (1981) clearly shows that this is not the case.

It is clear from previous research that histamine-induced H_1 receptor desensitization can occur by different processes that seem to be dependent on the tissue preparation. For instance, homologous desensitization occuring at the level of the H_1 receptor has been shown to occur in the DDT_1 MF-2 smooth muscle cell line (Cowlen *et al.*, 1990) and mouse cerebral cortex slices (Quach *et al.*, 1981), whereas the

heterologous type of receptor desensitization involving the H_1 receptor and the attenuation of other receptor-mediated events after prolonged histamine pretreatment has also been reported in HeLa cells (Bristow & Zamani, 1993), BC3H-1 smooth muscle cells (Brown *et al.*, 1986) and 1321N1 human astrocytoma cells (McDonough *et al.*, 1988). In guinea-pig cerebral cortex slices the homologous or heterologous nature of the histamine H_1 receptor desensitization is unresolved. Preliminary studies on the effect of histamine pretreatment on either carbachol- (muscarinic acetylcholine receptor agonist) or noradrenaline (α_1-adrenoceptor agonist) induced $[^3H]$-IP_n accumulation in guinea-pig cortex slices have to date failed to provide consistent answers (Bristow and Banford, unpublished observation) and the mechanism of histamine-induced desensitization must remain a target for future studies.

The authors wish to express their thanks to the Medical Research Council for financial support and to Glaxo Group Research for the gift of ranitidine.

References

BRISTOW, D.R. & YOUNG, J.M. (1991). Characterisation of histamine-induced inositol phospholipid hydrolysis in HeLa Cells. In *New Perspectives in Histamine Research: Agents and Actions Supplements*. ed. Timmerman, H. & van der Goot, H. pp. 387–392. Basel: Birkhauser Verlag.

BRISTOW, D.R. & ZAMANI, M.R. (1993). Desensitization of histamine H_1 receptor-mediated inositol phosphate production in HeLa cells *Br. J. Pharmacol.* (in press).

BRODDE, O. & MICHEL, M.C. (1989). Disease states can modify both receptor number and signal transduction pathways. *Trends Pharmacol. Sci.*, **10**, 383–384.

BROWN, D.R., PRENDIVILLE, P. & CAIN, C. (1986). α_1-Adrenergic and H_1-histamine receptor control of intracellular Ca^{2+} in a muscle cell line: the influence of prior agonist exposure on receptor responsiveness. *Mol. Pharmacol.*, **29**, 531–539.

CHANG, R.S.L. & SNYDER, S.H. (1980). Histamine H_1-receptor binding sites in guinea pig brain membranes: regulation of agonist interactions by guanine nucleotides and cations. *J. Neurochem.*, **34**, 916–922.

COWLEN, M.S., BARNES, R.M. & TOEWS, M.L. (1990). Regulation of histamine H_1 receptor-mediated phosphoinositide hydrolysis by histamine and phorbol esters in DDT_1 MF-2 cells. *Eur. J. Pharmacol. Mol. Pharmacol. Sec.*, **188**, 105–112.

CRAWFORD, M.L.A., CARSWELL, H. & YOUNG, J.M. (1990). γ-Aminobutyric acid inhibition of histamine-induced inositol phosphate formation in guinea pig cerebellum: comparison with guinea pig and rat cerebral cortex. *Br. J. Pharmacol.*, **100**, 867–873.

DAUM, P.R., DOWNES, C.P. & YOUNG, J.M. (1983). Histamine-induced inositol phospholipid breakdown mirrors H_1-receptor density in brain. *Eur. J. Pharmacol.*, **87**, 497–498.

DAUM, P.R., DOWNES, C.P. & YOUNG, J.M. (1984). Histamine stimulation of inositol-1-phosphate accumulation in lithium-treated slices from regions of guinea-pig brain. *J. Neurochem.*, **43**, 25–32.

DILLON-CARTER, O. & CHUANG, D.-M. (1989). Homologous desensitization of muscarinic cholinergic, histaminergic, adrenergic and serotonergic receptors coupled to phospholipase C in cerebellar granule cells. *J. Neurochem.*, **52**, 598–603.

DONALDSON, J. & HILL, S.J. (1986). Selective enhancement of histamine H_1-receptor responses in guinea-pig ileal smooth muscle by 1,4-dithiothreitol. *Br. J. Pharmacol.*, **87**, 191–199.

HEPLER, J.R., EARP, H.S. & HARDEN, T.K. (1988). Long-term phorbol ester treatment down-regulates protein kinase C and sensitises the phosphoinositide signalling pathway to hormone and growth factor stimulation: evidence for a role of protein kinase C in agonist-induced desensitization. *J. Biol. Chem.*, **263**, 7610–7620.

HILL, S.J. (1990). Distribution, properties, and functional characteristics of three classes of histamine receptor. *Pharmacol. Rev.*, **42**, 45–83.

HUGANIR, R.L. & GREENGARD, P. (1990). Regulation of neurotransmitter receptor desensitisation by protein phosphorylation. *Neuron*, **5**, 555–567.

LEURS, R., SMIT, M.J., BAST, A. & TIMMERMAN, H. (1990). Different profiles of desensitisation dynamics in guinea-pig jejunal smooth muscle after stimulation with histamine and methacholine. *Br. J. Pharmacol.*, **101**, 881–888.

LEVIN, E.G. & SANTELL, L. (1991). Thrombin- and histamine-induced signal transduction in human endothelial cells. *J. Biol. Chem.*, **266**, 174–181.

LOWRY, O.H., ROSEBROUGH, N.J., FARR, A.L. & RANDALL, R.J. (1951). Protein measurement with the Folin phenol reagent. *J. Biol. Chem.*, **193**, 265–275.

LURIE, K.G., TSUJIMOTO, G. & HOFFMAN, B.B. (1985). Desensitization of alpha-1 adrenergic receptor-mediated vascular smooth muscle contraction. *J. Pharmacol. Exp. Ther.*, **234**, 147–

MARTIN, M.W. & HARDEN, T.K. (1989). Agonist-induced desensitisation of a $P_{2\gamma}$-purinergic receptor-regulated phospholipase C. *J. Biol. Chem.*, **264**, 19535–19539.

McDONOUGH, P.M., EUBANKS, H.J. & BROWN, J.H. (1988). Desensitisation and recovery of muscarinic and histaminergic Ca^{2+} mobilisation in 1321N1 astrocytoma cells. *Biochem. J.*, **249**, 135–141.

MITSUHASHI, M. & PAYAN, D.G. (1988). Phorbol ester-mediated desensitisation of histamine H_1 receptors on a cultured smooth muscle cell line. *Life Sci.*, **43**, 1433–1440.

MURRAY, R.K., BENNETT, C.F., FLUHARTY, S.J. & KOTLIKOFF, M.I. (1989). Mechanism of phorbol ester inhibition of histamine-induced IP_3 formation in cultured airway smooth muscle. *Am. J. Physiol.*, **257**, L209–L216.

NAKAHATA, N. & HARDEN, T.K. (1987). Regulation of inositol trisphosphate accumulation by muscarinic cholinergic and H_1-histamine receptors on human astrocytoma cells. *Biochem. J.*, **241**, 337–344.

POLLARD, H. & SCHWARTZ, J.-C. (1987). Histamine neuronal pathways and their functions. *Trends Neurosci.*, **10**, 86–89.

QUACH, T.T., DUCHEMIN, A., ROSE, C. & SCHWARTZ, J. (1981). Specific desensitization of histamine H_1 receptor-mediated $[^3H]$glycogen hydrolysis in brain slices. *Mol. Pharmacol.*, **20**, 331–338.

RAYMOND, J.R., ALERS, F.J., MIDDLETON, J.P., LEFKOWITZ, R.J., CARON, M.G., OBEID, L.M. & DENNIS, V.W. (1991). 5-HT_{1A} and histamine H_1 receptors in HeLa cells stimulate phosphoinositide hydrolysis and phosphate uptake via distinct G protein pools. *J. Biol. Chem.*, **266**, 372–379.

RICKELS, K., CASE, W., DOWNING, R. & WINNKUR, A. (1983). Long-term diazepam therapy and clinical outcome. *J. Am. Med. Assoc.*, **250**, 767–771.

SHARPES, E.S. & McCARL, R.L. (1982). A high-performance liquid chromatographic method to measure ^{32}P incorporation into phosphorylated metabolites in cultured cells. *Anal. Biochem.*, **124**, 421–424.

SMIT, M.J., BLOEMERS, S.M., LEURS, R., TERTOOLEN, L.G.J., BAST, A. DE LAAT, S.W. & TIMMERMAN, H. (1992). Short-term desensitization of the histamine H_1 receptor in human HeLa cells: involvement of protein kinase C dependent and independent pathways. *Br. J. Pharmacol.*, **107**, 448–455.

TAYLOR, J.E. & RICHELSON, E. (1979). Desensitization of histamine H_1 receptor-mediated cyclic GMP formation in mouse neuroblastoma cells. *Mol. Pharmacol.*, **15**, 462–471.

TREHERNE, J.M. & YOUNG, J.M. (1988). $[^3H]$-(+)-N-methyl-4-methyldiphenhydramine, a quaternary radioligand for the histamine H_1-receptor. *Br. J. Pharmacol.*, **94**, 797–810.

WADA, H., INAGAKI, N., YAMATODANI, A. & WATANABE, T. (1991). Is the histaminergic neuron system a regulatory center for whole-brain activity? *Trends Neurosci.*, **14**, 415–418.

(Received March 3, 1993
Revised April 30, 1993
Accepted May 11, 1993)

Br. J. Pharmacol. (1993), **110**, 275–280

Dissociation of the anti-ischaemic effects of cloricromene from its anti-platelet activity

[1]Paul S. Lidbury, [2]Rocco Cirillo & John R. Vane

The William Harvey Research Institute, St Bartholomew's Hospital Medical College, Charterhouse Square, London EC1M 6BQ

1 Cloricromene is a non-anticoagulant coumarin derivative with anti-platelet and anti-leukocyte properties, which has beneficial effects in various models of ischaemia and shock.

2 We have assessed the effects of cloricromene on (a) *ex vivo* platelet aggregation, and (b) infarct size using a model of myocardial ischaemia in the anaesthetized rabbit.

3 Cloricromene (1–1000 $\mu g\ kg^{-1}\ min^{-1}$ for 15 min) induced a dose-dependent inhibition of *ex vivo* platelet aggregation, causing only a minimal increase in heart rate and no change in mean arterial blood pressure. The inhibitory activity was considerably stronger when platelet aggregation was induced by collagen than by ADP.

4 Cloricromene inhibited *ex vivo* platelet aggregation in rabbits pretreated with indomethacin (5 $mg\ kg^{-1}$) and this inhibition persisted for 30–60 min.

5 The model of myocardial ischaemia involved 1 h occlusion of the first antero-lateral branch of the left coronary artery followed by 2 h of reperfusion. Infusion of cloricromene (30 or 300 $\mu g\ kg^{-1}\ min^{-1}$), ibuprofen (80 $\mu g\ kg^{-1}\ min^{-1}$) or vehicle began 15 min prior to occlusion, and continued throughout the experiment.

6 While area at risk was similar for all groups studied, cloricromene (30 or 300 $\mu g\ kg^{-1}\ min^{-1}$) or ibuprofen caused a reduction in infarct size, and decreased myeloperoxidase activity in the tissue of the infarcted myocardium.

7 Cloricromene at 300 $\mu g\ kg^{-1}\ min^{-1}$ also reduced the occlusion-induced elevation of the ST-segment of the rabbit electrocardiogram, and inhibited platelet aggregation *ex vivo*. Ibuprofen or cloricromene at 30 $\mu g\ kg^{-1}\ min^{-1}$ had no effect on either the ST-elevation or platelet reactivity.

8 Thus, cloricromene exhibits a cardioprotective activity via an inhibition of leukocyte infiltration, in the presence (300 $\mu g\ kg^{-1}\ min^{-1}$) or absence (30 $\mu g\ kg^{-1}\ min^{-1}$) of inhibition of platelet activity *ex vivo*. The anti-aggregatory activity of cloricromene acts via a mechanism that is either different from, or in addition to, inhibition of cyclo-oxygenase, and is of long duration.

Keywords: Cloricromene; myocardial infarction; platelet; leukocyte

Introduction

The myocardial damage induced by ischaemia and reperfusion is a dynamic process accompanied by the accumulation of neutrophils and platelets in the ischaemic area (Laws *et al.*, 1983; Mullane *et al.*, 1984; Dinerman & Mehta, 1990). Numerous pharmacological approaches to modify the progression of myocardial tissue injury to irreversible necrosis have been made. Leukocytes (PMNs) are a potential therapeutic target in myocardial ischaemia, since they characteristically become activated and subsequently release cytotoxic and vasoconstrictor substances that may exacerbate myocardial injury (Schmid-Schonbein & Engler, 1986; Forman *et al.*, 1990; Lucchesi, 1990).

Cloricromene, a coumarin derivative (8-monochloro-3-β-diethylaminoethyl-4-methyl-7-ethoxy-carbonylmethoxycoumarin) was originally evaluated as an anti-thrombotic and is at present used in patients with microcirculatory disease (Lazzaro *et al.*, 1992). Cloricromene weakly stimulates prostacyclin production in human cultured endothelial cells and rat thoracic aortic rings (Dejana *et al.*, 1982), reduces thromboxane B_2 release from platelets and inhibits platelet aggregation induced by various agents (Galli *et al.*, 1980; Prosdocimi *et al.*, 1985; 1986). In addition, cloricromene inhibits both polymorphonuclear adhesion to endothelial cells and superoxide generation (Bertocchi *et al.*, 1989), and causes coronary dilatation in the dog (Aporti *et al.*, 1978).

Pathophysiologically, cloricromene has protective activity in rat models of shock caused by splanchnic artery occlusion (Sturniolo *et al.*, 1989), haemorrhage (Sturniolo *et al.*, 1991), endotoxin (Squadrito *et al.*, 1992) or peripheral ischaemia in the rabbit hindlimb (Cirillo *et al.*, 1992).

The present study was designed to evaluate the effects of cloricromene on infarct size in a rabbit model of acute myocardial ischaemia and reperfusion, while monitoring platelet reactivity *ex vivo*. Ibuprofen was also evaluated for comparative purposes.

Methods

Ex vivo *platelet aggregation*

Surgical procedure Male New Zealand white rabbits (2–3 kg) receiving a standard diet and water *ad libitum* were used. Ten minutes before surgery all rabbits were premedicated with Hypnorm (0.1 $ml\ kg^{-1}$, i.m.; containing 0.315 mg ml^{-1} fentanyl citrate and 10 mg ml^{-1} fluanisone). General anaesthesia was induced with Sagatal (sodium pentobarbitone, 30 $mg\ kg^{-1}$) injected into the left marginal ear vein and maintained with supplementary doses as required. Lignocaine (Xylocaine 2%) was also used for local anaesthesia. Body temperature was monitored and maintained at 37–38°C by means of a rectal probe thermometer attached to a homeothermic blanket control unit (Bioscience).

The trachea was cannulated and the rabbit ventilated

[1] Author for correspondence.
[2] Permanent address: Fidia Research Laboratories, 35031 Abano Terme, Italy.

(Harvard) with air at 45 strokes min^{-1} and a tidal volume of 6 ml kg^{-1}. The left femoral artery was cannulated and connected to a pressure transducer to monitor mean arterial blood pressure (MAP) and for the withdrawal of blood samples. The right femoral vein was cannulated for drug administration. Whilst monitoring pressure another catheter was placed in the left ventricle, via the right carotid artery, for measurement of left ventricular systolic pressure (LVSP) and heart rate (HR; derived from LVSP).

Platelet aggregation Arterial blood samples (1.8 ml) were withdrawn from the left femoral artery and collected into 3.15% w/v tri-sodium citrate (0.2 ml) and immediately centrifuged at 1 400 *g* (4 000 r.p.m.) for 20 s (Heraeus, Biofuge 15) to produce platelet-rich plasma (PRP). The blood was further centrifuged at 14 900 *g* (12 000 r.p.m.) for 1 min to obtain platelet-poor plasma (PPP). Platelet aggregation was studied in a dual channel aggregometer (Payton) calibrated using PRP (0%) and PPP (100%) with respect to the degree of light transmission. Aliquots of PRP (0.4 ml) were added to siliconized cuvettes, warmed to 37°C and stirred at 1 000 r.p.m. After incubation for 30 s, a sub-maximal dose of adenosine diphosphate (ADP; 2 μg ml^{-1}) or collagen (8 μg ml^{-1}) was added and the extent of aggregation measured as peak increase in light transmission.

The inhibition of platelet aggregation induced by a drug was calculated using peak increase in light transmission observed over a 4 min period after addition of a sub-maximal dose (70–80% maximum response) of the aggregating agent, as compared to that of a control.

Experimental protocol and drug regimen Cloricromene was infused (i.v.) for 15 min periods at increasing concentrations (1–1 000 μg kg^{-1} min^{-1}; $n = 4–8$). At the end of each infusion period a blood sample was withdrawn and the PRP tested for platelet reactivity. Thus, the effects of cloricromene on haemodynamic parameters and platelet aggregation *ex vivo* were monitored concomitantly.

Since cloricromene had an effect on platelets similar to that of cyclo-oxygenase inhibitors, its effects were also investigated in the presence of indomethacin ($n = 6$). Indomethacin (5 mg kg^{-1}; i.v.) was injected and the effect on platelet activity reassessed after a further 20 min. In the presence of indomethacin, collagen-induced aggregation was much reduced as expected and so challenges with higher doses of collagen (16 μg ml^{-1}) were performed to counteract this effect. The ADP-induced aggregation remained uneffected. Subsequently, cloricromene (300 μg kg^{-1} min^{-1}) was administered as a 15 min infusion (i.v.), and the effect on platelets determined. Further blood samples were withdrawn at 5, 10, 20 and 40 min post-infusion and tested for platelet reactivity.

Myocardial ischaemia and reperfusion

The method of coronary artery occlusion/reperfusion in the anaesthetized rabbit was performed according to Thiemermann *et al.* (1989).

Coronary artery isolation and occlusion Rabbits were surgically prepared as described above for haemodynamic recording and sampling. A 3–4 cm left thoracotomy through the 4th intercostal space was performed to expose the heart. The pericardium was opened and a snare occluder was placed around the first antero-lateral branch of the left coronary artery (LAL) 1 cm distal from its origin, taking care to avoid veins. In contrast to other species, the rabbit LAL supplies much of the left ventricular myocardium including most of the septum and apex (Flores *et al.*, 1984). The rabbits were allowed to stabilize for 30 min before LAL ligation.

At time 0, the LAL was occluded. After 1 h the occluder was released to allow 2 h of reperfusion.

Haemodynamic measurements and electrocardiograms Haemodynamic parameters such as MAP, LVSP and HR, were continuously recorded on a polygraph recorder (Grass Instruments, 7D). Lead II electrocardiograms (ECGs) were monitored with subdermal platinum electrodes, thus determining changes in ST-segment as well as changes in R-wave and Q-wave amplitude.

Measurement of area at risk and infarct size After the 2 h reperfusion period the LAL was reoccluded and Evans blue dye solution (4 ml of 2% w/v) injected into the left ventricle to distinguish between perfused and non-perfused (myocardium at risk) sections of the heart. The Evans blue solution stains the perfused myocardium while the occluded vascular bed remains uncoloured. The dose of Evans blue dye is well within the range reported for nearly exclusive binding to plasma albumin or other proteins in the rabbit (Lindner & Heinle, 1982). The rabbits were killed with an overdose of anaesthetic. The heart was excised and sectioned into 4–5 mm thick slices. After removing the right ventricular wall, the area at risk and non-ischaemic myocardium were separated by following the line of demarcation between blue stained and unstained tissue.

To distinguish between ischaemic and infarcted tissue, the area at risk was chopped into pieces and incubated with *p*-nitroblue tetrazolium (NBT, 0.5 mg ml^{-1}) for 20 min at 37°C. NBT stains pieces with intact dehydrogenase enzyme systems (normal myocardium), while areas of necrosis lack dehydrogenase activity and therefore do not stain (Nachlas & Shnitka, 1963). Pieces were separated according to staining and weighed in order to determine the infarct as a percentage of the area at risk. All tissues were then stored at − 20°C for later analysis of myeloperoxidase activity.

Myeloperoxidase activity Neutrophil-specific myeloperoxidase (MPO) was recovered by a modification of the method of Krawisz *et al.* (1984). Briefly, the myocardial tissues were homogenized in 6 ml of 50 μM potassium phosphate (pH 6) containing 10 mM EDTA, 0.5% w/v hexadecyltrimethylammonium bromide by means of a Potter homogenizer. The samples were sonicated for 1 min and the released enzyme was separated from insoluble cellular debris by centrifugation at 40,000 *g* for 30 min at 4°C.

MPO activity was assayed by an adaptation of the Renlund method (1980) in a 96-well plate by measuring the H_2O_2-dependent oxidation of *o*-dianisidine di-hydrochloride. The MPO reagent consisted of 0.53 M *o*-dianisidine, 0.3 mM H_2O_2 and 0.1 M citrate-phosphate buffer. The reaction mixture for analysis consisted of 200 μl of MPO reagent added to 20 μl tissue sample/per well. After 5 min of incubation the reaction was stopped with the addition of 55 μl 1 M HCl to each well. One unit of enzyme activity was defined as the amount of MPO that caused a change in one absorbance unit min^{-1} at 405 nm at 37°C. To ensure linearity during this reaction time, human leukocytes were included (as MPO standard) in each assay. The assay was linear between $10^4–10^6$ cell ml^{-1}.

Experimental protocol and drug regimen All drugs were administered as infusions commencing 15 min prior to LAL occlusion and continuing throughout the experiment.

The test groups received cloricromene at 30 ($n = 9$) or 300 μg kg^{-1} min^{-1} ($n = 7$) in saline or ibuprofen at 80 μg kg^{-1} min^{-1} ($n = 6$) in 5% w/v sodium bicarbonate, adjusted to pH 7.5 with HCl. The vehicle control group ($n = 14$) contained rabbits treated with saline ($n = 10$) or with 5% w/v sodium bicarbonate ($n = 4$). All drugs were infused at 0.1 ml min^{-1} except ibuprofen which was infused at 0.2 ml min^{-1}.

Statistical comparison

All values in the text, figures and tables are expressed as the

mean ± s.e.mean of n observations. Where repeated measurements were made the results were analysed by a one-way analysis of variance followed by the Bonferoni's test. End-point determinations were analysed by Student's t test. A P value of less than 0.05 was considered statistically significant.

Materials

Cloricromene was provided by Fidia Research Laboratories. Purchased drugs included ibuprofen, ADP, Evans blue, NBT, dextran (Sigma Chemical Company), Hypnorm (Janssen Pharmaceuticals), Sagatal (May and Baker), Xylocaine (Astra) and collagen (Hormon-Chemie).

Results

Ex vivo *platelet aggregation*

Haemodynamic data In an anaesthetized rabbit cumulative infusions of cloricromene for 15 min (1–1 000 $\mu g\,kg^{-1}\,min^{-1}$) caused no change in MAP and only a minimal increase in HR at 100–1 000 $\mu g\,kg^{-1}\,min^{-1}$. Cloricromene had no significant effects on LVSP or the lead II ECG.

Platelet aggregation In blood samples withdrawn during these studies, platelet aggregation induced by ADP was only partially inhibited by cloricromene at 100–1 000 $\mu g\,kg^{-1}\,min^{-1}$, whereas collagen-induced aggregation was more readily inhibited, with partial inhibition at 100 $\mu g\,kg^{-1}\,min^{-1}$ and full inhibition at 300 $\mu g\,kg^{-1}\,min^{-1}$ and above (Figure 1).

After pretreatment with indomethacin and with the use of higher doses of collagen, cloricromene (300 $\mu g\,kg^{-1}\,min^{-1}$) still caused inhibition of collagen-induced aggregation. Furthermore, post-infusion determinations showed that the inhibitory effect of cloricromene persisted for 30–60 min (Figure 2).

Myocardial ischaemia and reperfusion

Of the 50 rabbits which underwent LAL occlusion, 12 died within the experimental period due either to ventricular fibrillation or to cardiac failure and these were excluded from the study. Ten of these died within 8–15 min of the ischaemic period (6 rabbits receiving vehicle, 1 rabbit receiving cloricromene at 30 $\mu g\,kg^{-1}\,min^{-1}$ and 3 rabbits receiving cloricromene at 300 $\mu g\,kg^{-1}\,min^{-1}$) and 2 others during reperfusion (both receiving vehicle).

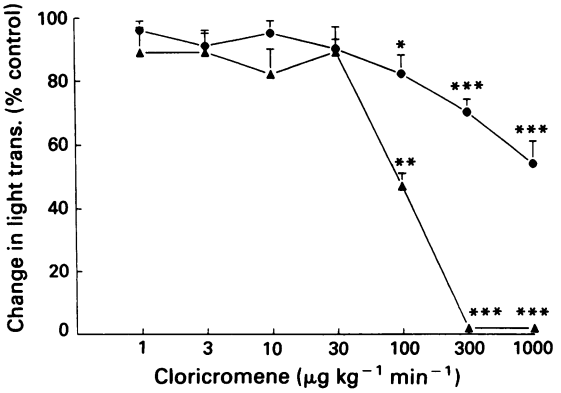

Figure 1 Cloricromene administration (1–1 000 $\mu g\,kg^{-1}\,min^{-1}$; 15 min; $n = 4–8$) to anaesthetized rabbits partially inhibited platelet aggregation *ex vivo* induced by ADP (●, 2 $\mu g\,ml^{-1}$) but totally inhibited that induced by collagen (▲, 8 $\mu g\,ml^{-1}$). Results are expressed as mean ± s.e.mean of n observations. $^{*}P<0.01$, $^{**}P<0.01$ and $^{***}P<0.001$ when compared to control.

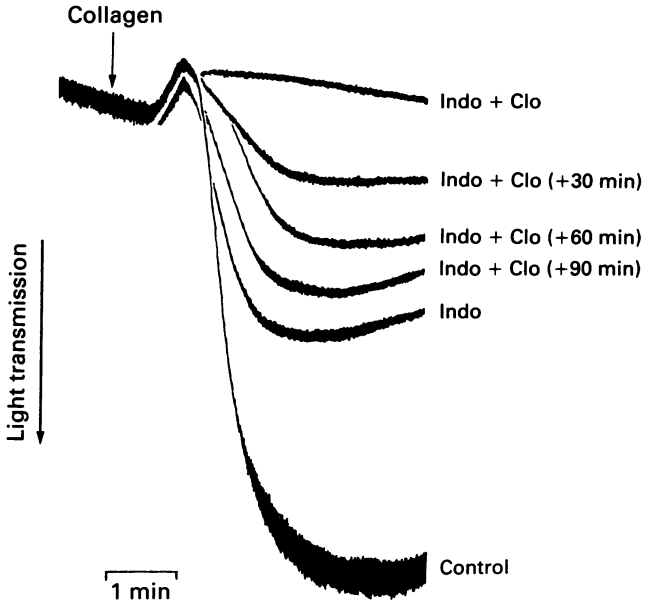

Figure 2 In rabbits pretreated with indomethacin (Indo, 5 mg kg^{-1}) 20 min before infusion of cloricromene (Clo, 300 $\mu g\,kg^{-1}\,min^{-1}$ for 15 min; $n = 6$) caused a prolonged inhibition of collagen (16 $\mu g\,ml^{-1}$)-induced *ex vivo* platelet aggregation. Aggregation was determined by change in light transmission, measured at 30, 60 and 90 min after cloricromene infusion.

Haemodynamic data Table 1 shows values for HR, LVSP and pressure-rate index (PRI). Basal data (– 15 min) and data at time 0 were similar in all groups investigated.

In comparison to the vehicle control group, the only significant change in the general haemodynamics was a slight decrease in LVSP at the end of the reperfusion period with cloricromene at 300 $\mu g\,kg^{-1}\,min^{-1}$ and ibuprofen at 80 $\mu g\,kg^{-1}\,min^{-1}$. With cloricromene there was a concomitant rise in HR. Indeed, although cloricromene at 300 $\mu g\,kg^{-1}\,min^{-1}$ and ibuprofen at 80 $\mu g\,kg^{-1}\,min^{-1}$ induced a gradual decrease in MAP, the changes were not statistically significant, emphasized by the fact that none of the groups studied had altered myocardial oxygen consumption as shown by PRI (Baller *et al.*, 1981).

Table 1 Heart rate (HR, beat min^{-1}), left ventricular systolic pressure (LVSP, mmHg), pressure-rate index (PRI, mmHg $min^{-1} \times 10^3$) in rabbits subjected to 1 h coronary artery occlusion and 2 h reperfusion

Group/Dose		*– 15 min*	*0 min*	*60 min*	*180 min*
Control	HR	245 ± 4	243 ± 4	240 ± 4	241 ± 5
	LVSP	95 ± 4	96 ± 3	94 ± 4	83 ± 5
	PRI	16 ± 1	16 ± 1	15 ± 1	14 ± 1
Clo 30	HR	226 ± 6	224 ± 5	229 ± 5	228 ± 5
	LVSP	87 ± 4	90 ± 3	90 ± 4	89 ± 3
	PRI	14 ± 1	14 ± 1	15 ± 1	15 ± 1
Clo 300	HR	226 ± 9	234 ± 10	254 ± 7	261 ± 8*
	LVSP	82 ± 5	80 ± 5	78 ± 4**	72 ± 4
	PRI	14 ± 1	14 ± 2	14 ± 1	12 ± 1
Ibu 80	HR	246 ± 12	241 ± 9	240 ± 9	229 ± 11
	LVSP	83 ± 7	81 ± 8	74 ± 7*	69 ± 7
	PRI	15 ± 1	14 ± 1	12 ± 1	11 ± 1

Rabbits received either vehicle (control, $n = 14$), cloricromene at 30 $\mu g\,kg^{-1}\,min^{-1}$ (Clo 30, $n = 9$), or at 300 $\mu g\,kg^{-1}\,min^{-1}$ (Clo 300, $n = 7$) or ibuprofen at 80 $\mu g\,kg^{-1}\,min^{-1}$ (Ibu 80, $n = 6$).
Values are given as mean ± s.e.mean of n observations for each group.
$^{*}P<0.05$ and $^{**}P<0.01$, when compared to control.

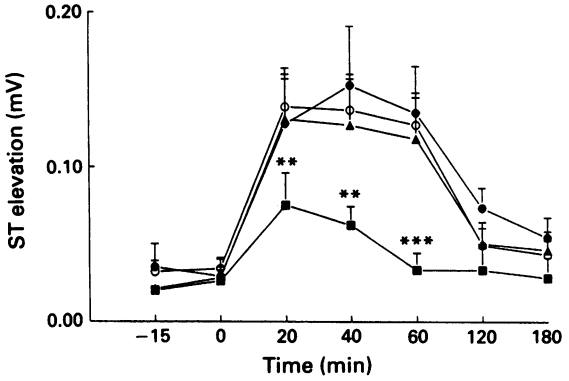

Figure 3 Changes in ST-segment (lead II) induced in rabbits by 1 h coronary artery occlusion and 2 h reperfusion. Rabbits received either vehicle (○, $n = 14$), cloricromene at 30 μg kg^{-1} min^{-1} (▲, $n = 9$), cloricromene at 300 μg kg^{-1} min^{-1} (■, $n = 6$) or ibuprofen at 80 μg kg^{-1} min^{-1} (●, $n = 6$). Results are expressed as mean ± s.e.mean of n observations. $^{**}P < 0.01$ and $^{***}P < 0.001$ when compared to control.

Electrocardiogram changes In vehicle-treated rabbits, LAL occlusion produced an increase in the ST-segment of the lead II ECG from 0.03 ± 0.01 mV to 0.14 ± 0.02 mV after 20 min which remained elevated for the 1 h occlusion period. Upon reperfusion the ST-segment gradually returned to basal, with values of 0.05 ± 0.01 mV at 2 h and 0.04 ± 0.01 mV at 3 h (Figure 3).

At 300 μg kg^{-1} min^{-1}, cloricromene significantly reduced the occlusion-induced ST elevation to 0.08 ± 0.02 mV ($P <$ 0.01) after 20 min (Figure 3). This was gradually attenuated further during the occlusion period reaching basal values at 1 h (0.03 ± 0.01 mV, $P < 0.01$; Figure 3). In sham-operated rabbits receiving cloricromene at 300 μg kg^{-1} min^{-1} there was no effect on the ECG.

No attenuation of the ST elevation was observed with the lower dose of cloricromene or with ibuprofen (Figure 3). Furthermore, none of the groups tested showed any significant changes in the amplitude of either the Q-wave or R-wave of the lead II ECG complex.

Platelet aggregation ex vivo Consistent aggregation to ADP or collagen was obtained in rapidly prepared PRP from anaesthetized rabbits undergoing the occlusion/reperfusion procedure. Addition of a sub-maximal dose of collagen to the PRP resulted in irreversible aggregation, while the aggregation induced by ADP was reversible. Unlike its effects in human PRP, high doses of ADP did not induce biphasic or irreversible aggregations when added to rabbit PRP. Accordingly, in control samples the peak change in light transmission was approximately 60% with collagen and 45% with ADP.

During the course of the experiment only cloricromene at 300 μg kg^{-1} min^{-1} demonstrated significant inhibition of platelet aggregation *ex vivo* (Figure 4a and b). This inhibition was considerably greater against aggregation induced by collagen than that by ADP. Moreover, the degree of inhibition increased as the infusion of cloricromene proceeded. After 15 min of infusion of cloricromene (just prior to occlusion at time 0) there was no significant inhibition of the aggregation induced by either aggregating agent. However, by the end of the ischaemic period the aggregations had been reduced to 57% for collagen and 74% for ADP. These responses were further reduced to 13% with collagen and 53% with ADP after 2 h of reperfusion.

Cloricromene at 30 μg kg^{-1} min^{-1} or ibuprofen at 80 μg kg^{-1} min^{-1} did not inhibit platelet aggregation induced by either aggregating agent.

Area at risk and infarct size As expected, the area of the left ventricle at risk was approximately 30%, and this was similar in all groups studied. In rabbits treated with vehicle alone the infarct size was 67.1 ± 2.4% of the area at risk (Figure 5).

Administration of cloricromene resulted in a dose-dependent reduction in infarct size, to 40.8 ± 7.9% ($P < 0.01$) at 30 μg kg^{-1} min^{-1} and 32.4 ± 6.6% ($P < 0.001$) at 300 μg kg^{-1} min^{-1}. Ibuprofen (80 μg kg^{-1} min^{-1}) infusion also produced a decrease in infarct size to 45.5 ± 11.7% ($P < 0.05$; Figure 5).

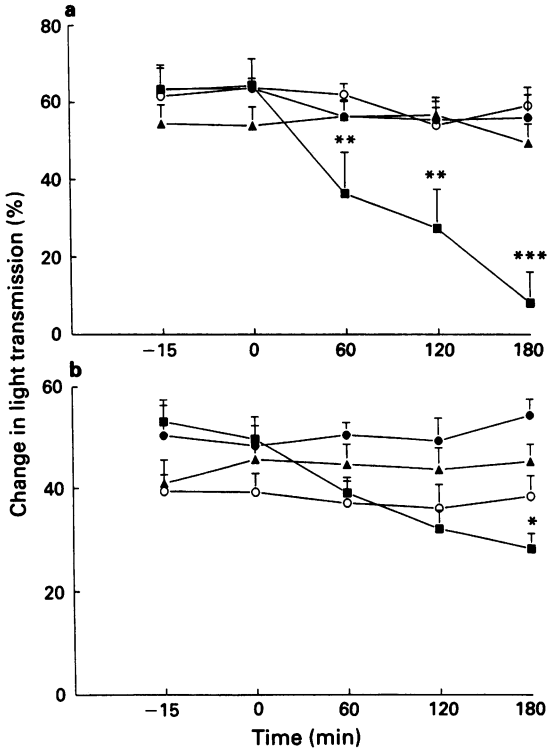

Figure 4 Changes in *ex vivo* platelet aggregation in rabbits with 1 h coronary artery occlusion and 2 h reperfusion. Platelet reactivity as determined in platelet-rich plasma by challenge with either (a) collagen or (b) ADP. Rabbits received either vehicle (○, $n = 14$), cloricromene at 30 μg kg^{-1} min^{-1} (▲, $n = 9$), cloricromene at 300 μg kg^{-1} min^{-1} (■, $n = 7$) or ibuprofen at 80 μg kg^{-1} min^{-1} (●, $n = 6$). Results are expressed as mean ± s.e.mean of n observations. $^{*}P < 0.05$, $^{**}P < 0.01$ and $^{***}P < 0.001$ when compared to control.

Myeloperoxidase activity The measurement of myeloperoxidase (MPO) activity as a marker for the presence of PMNs confirmed the infiltration of leukocytes into myocardial tissue subjected to ischaemia. In vehicle-treated animals the MPO

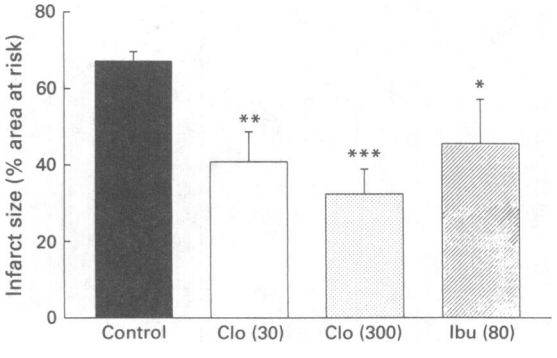

Figure 5 Infarct size expressed as a percentage of the area at risk. Rabbits received either vehicle (control; $n = 4$), cloricromene at 30 μg kg^{-1} min^{-1} (Clo 30, $n = 9$), cloricromene at 300 μg kg^{-1} min^{-1} (Clo 300, $n = 7$) or ibuprofen at 80 μg kg^{-1} min^{-1} (Ibu 80, $n = 6$). Results are expressed as mean ± s.e.mean of n observations. $^{*}P < 0.05$, $^{**}P < 0.01$ and $^{***}P < 0.001$ when compared to control.

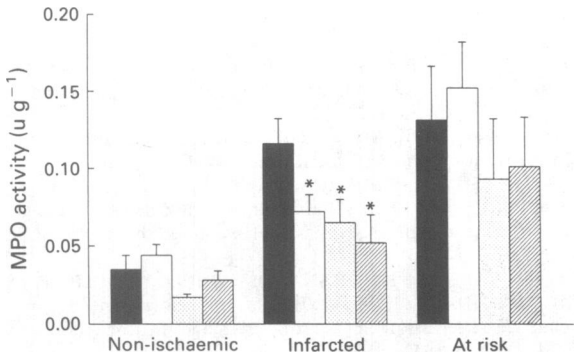

Figure 6 Changes in myeloperoxidase (MPO) activity determined in non-infarcted tissue, and infarcted tissue within the area at risk as designated by Evans blue dye and nitroblue tetrazolium staining. Rabbits received either vehicle (solid columns, $n = 5$), cloricromene at 30 $\mu g\,kg^{-1}\,min^{-1}$ (open columns, $n = 8$), cloricromene at 300 $\mu g\,kg^{-1}\,min^{-1}$ (stippled columns, $n = 5$), or ibuprofen at 80 $\mu g\,kg^{-1}\,min^{-1}$ (hatched columns, $n = 5$). Results are expressed as mean ± s.e.mean of n observations. $^*P < 0.05$ when compared to control.

activity within the area at risk was 0.131 ± 0.035 u g^{-1} for non-infarcted tissue and 0.115 ± 0.016 u g^{-1} for infarcted tissue, as compared to only 0.035 ± 0.009 u g^{-1} measured in tissue outside the area at risk (Figure 6).

The MPO activity in the infarcted tissue was significantly reduced with cloricromene at 30 and 300 $\mu g\,kg^{-1}\,min^{-1}$, and IBU at 80 $\mu g\,kg^{-1}\,min^{-1}$. However, the non-infarcted tissue did not demonstrate a significant reduction in MPO activity in the presence of either of the drugs (Figure 6).

Discussion

Administration of cloricromene reduced infarct size in a model of myocardial ischaemia and reperfusion in the anaesthetized rabbit. To substantiate this cardioprotective activity we have monitored an attenuation of the ST-segment elevation, an accepted indicator of ischaemic injury (Kjekshus *et al.*, 1972; Ross, 1976). The degree of cardioprotection exhibited by cloricromene is similar to that reported for iloprost (Chiariello *et al.*, 1988), defibrotide (Thiemermann *et al.*, 1989) and superoxide dismutase/catalase (Downey *et al.*, 1987) using occlusion of the same branch of the coronary artery in the rabbit. Collectively, these results indicate that a reduction in infarct size of about 50% may represent the maximum protection achievable in this experimental model of severe myocardial ischaemia.

The mechanisms through which cloricromene elicits this beneficial activity and indeed that responsible for protection in other models of myocardial ischaemia (Milei *et al.*, 1992; 1993), peripheral ischaemia (Cirillo *et al.*, 1992) or shock (Sturniolo *et al.*, 1989; 1991; Squadrito *et al.*, 1992) have essentially remained unknown. However, while cloricromene at 30 and 300 $\mu g\,kg^{-1}\,min^{-1}$ significantly reduced infarct size, the determination of platelet and MPO activity in this study clearly supports inhibition of leukocyte infiltration as the primary mode of action of cloricromene.

Cloricromene at both 30 and 300 $\mu g\,kg^{-1}\,min^{-1}$ significantly reduced the number of leukocytes present in the infarcted myocardium as determined by measurement of MPO activity, while only the high dose infusion of cloricromene inhibited platelet aggregation *ex vivo*. The cardioprotection elicited by cloricromene was similar to that of ibuprofen, which decreased infarct size and inhibited the infiltration of leukocytes into the necrotic tissue without affecting the platelet response. These results corroborated data from a previous study of experimental myocardial infarction in the anaesthetized dog in which radiolabelled platelets and leukocytes were used (Romson *et al.*, 1982) that showed cardioprotection with ibuprofen. This was accompanied by a reduction in leukocyte infiltration, without altering the accumulation of platelets in infarcted myocardium. Although it is unclear why neither cloricromene nor ibuprofen caused a reduction in MPO activity measured in the non-infarcted tissue of the area at risk, a similar profile of MPO activity has also been shown for interleukin 8 in a model of infarction in the anaesthetized rabbit (Lefer *et al.*, 1991).

It is clear from the reduction in ischaemia-induced elevation of the ST-segment that cloricromene at 300 $\mu g\,kg^{-1}\,min^{-1}$ expresses a cardioprotective action during the occlusion period. However, at the lower dose of cloricromene, and indeed with ibuprofen, no amelioration of the ST elevation was observed during the occlusion period. Thus, the reduction in myocardial damage observed with the low dose of cloricromene may be related to a modification of processes that occurred during reperfusion alone. Furthermore, a contribution of coronary vasodilatation (Aporti *et al.*, 1978) to the anti-ischaemic effects of cloricromene cannot be excluded.

With respect to anti-aggregatory activity, while cloricromene demonstrated cardioprotection at both 30 and 300 $\mu g\,kg^{-1}\,min^{-1}$, only the high dose of cloricromene caused an inhibition of ADP or collagen-induced platelet aggregation. The short delay between blood sample withdrawal and challenge with the aggregating agents is unlikely to result in a loss of anti-platelet activity since the effect of cloricromene on platelets is long-acting (Prosdocimi *et al.*, 1985; Lazzaro *et al.*, 1992). Therefore, while cloricromene clearly possesses anti-platelet properties *ex vivo*, the data presented here suggest that little if any of the activity on platelets is responsible for the cardioprotective action of cloricromene. Similarly, it may be argued that cloricromene at 30 $\mu g\,kg^{-1}\,min^{-1}$ reduced myocardial damage in the absence of significant prostacyclin release into the circulation, for an affect on platelet aggregation would have been observed. Thus, cloricromene can reduce infarct size without inhibition of platelet aggregation or reduction in systemic blood pressure. Interestingly, the protection obtained is equivalent to that for iloprost (1.2 $\mu g\,kg^{-1}\,min^{-1}$) which expressed strong anti-platelet activity, though this activity may have been accompanied by biologically relevant reductions in blood pressure and may also have been related to an effect on leukocytes (Chiariello *et al.*, 1988).

Cloricromene was considerably more effective against collagen-induced aggregation than against challenge with ADP. This observation alone, while perhaps having little relevance to the attentuation of myocardial infarction, suggests inhibition of pro-aggregatory metabolites of the arachidonic acid cascade. However, in the studies using rabbits pretreated with indomethacin, cloricromene caused an additional inhibition of *ex vivo* platelet aggregation, which was of long duration. Therefore, cloricromene exerts anti-aggregatory activity via a mechanism that is either different from, or in addition to, the inhibition of cyclo-oxygenase. Other mechanisms by which cloricromene has been proposed to act include, inhibition of phospholipase A_2, inhibition of the cyclic GMP-specific phosphodiesterase, and attenuation of tumour necrosis factor or myocardial depressant factor release during experimental shock (Squadrito *et al.*, 1992). However, it remains to be determined whether these events are a direct result of cloricromene administration or are indirect consequences of its administration.

While the absolute mechanism has still to be defined it is clear that, in the rabbit heart, cloricromene has a protective effect against infarction. Furthermore, the anti-ischaemic effect of cloricromene was accompanied by a reduction in leukocyte infiltration into the ischaemic myocardium either in the presence or in the absence of an inhibition of *ex vivo* platelet activation.

The authors are indebted to Dr E. Salvatico for the myeloperoxidase assay.

References

APORTI, F., FINESSO, M. & GRANATA, L. (1978). Effects of 8-monochloro-3-beta-diethylaminoethyl-4-methyl-7-ethyoxycarbonyl methoxy coumarin (AD_6) on coronary circulation in the dog. *Pharmacol. Res. Commun.*, **10**, 469–477.

BALLER, D., BRETSCHNEIDER, H.J. & HELLIGE, G. (1981). A critical look at currently used indices of myocardial oxygen consumption. *Basic Res. Cardiol.*, **76**, 163–181.

BERTOCCHI, F., BREVIARIO, F., PROSERPIO, P., JI MING WANG, GHEZZI, P., TRAVAGLI, R.A., PROSDOCIMI, M. & DEJANA, E. (1989). *In vitro* inhibition of human polymorphonuclear cell function by cloricromene. *Naunyn Schmied. Arch. Pharmacol.*, **339**, 697–703.

CHIARIELLO, M., GOLINO, P., CAPPELLI-BIGAZZI, M., AMBROSIO, G., TRITTO, I. & SALVATORE, M. (1988). Reduction in infarct size by the prostacyclin analogue iloprost (ZK 36374) after experimental coronary artery occlusion-perfusion. *Am. Heart J.*, **115**, 499–504.

CIRILLO, R., SALVATICO, E., ALIEV, G. & PROSDOCIMI, M. (1992). The effect of cloricromene during ischaemia and reperfusion of rabbit hindlimb: evidence for an involvement of leukocytes in reperfusion-mediated tissue and vascular injury. *J. Cardiovasc. Pharmacol.*, **20**, 969–975.

DEJANA, E., DE CASTELLARNAU, C., BALCONI, G., ROTILIO, D., PIETRA, A. & DE GAETANO, G. (1982). AD_6, a coronary dilating agent, stimulates, PGI_2 production in rat aorta *ex vivo* and in human endothelial cells in culture. *Pharmacol. Res. Commun.*, **14**, 719–724.

DINERMAN, Y.L. & MEHTA, J.L. (1990). Endothelial, platelet and leukocyte interactions in ischemic heart disease: insights into potential mechanisms and their clinical relevance. *J. Am. Coll. Cardiol.*, **16**, 207–221.

DOWNEY, J.M., MIURA, T., EDDY, L.J., CHAMBERS, D.E., MELLERT, T., HEARSE, D.J. & YELLON, D.M. (1987). Xanthine oxidase is not a source of free radicals in the ischemic rabbit heart. *J. Mol. Cell. Cardiol.*, **19**, 1053–1060.

FLORES, N.A., DAVIES, R.L., PENNY, W.J. & SHERIDAN, D.J. (1984). Coronary microangiography in the guinea-pig, rabbit and ferret. *Int. J. Cardiol.*, **6**, 459–471.

FORMAN, M.B., VIRMANI, R. & PUETT, D.W. (1990). Mechanisms and therapy of myocardial reperfusion injury. *Circulation*, **81**, IV69–IV78.

GALLI, C., AGRADI, E., PETRONI, A. & SOCINI, A. (1980). Effects of 8-monochloro-3-beta-diethylaminoethyl-4-methyl-7-ethoxycarboxyl methoxy coumarin (AD_6) on aggregation, arachidonic acid metabolism and thromboxane B_2 formation in human platelets. *Pharmacol. Res. Commun.*, **12**, 329–337.

KJEKSHUS, J.K., MAROKO, P.R. & SOBEL, B.E. (1972). Distribution of myocardial injury and its relation to epicardial ST-segment changes after coronary artery occlusion in dogs. *Cardiovasc. Res.*, **6**, 490–499.

KRAWISZ, J.E., SHARON, P. & STENSON, F. (1984). Quantitative assay for acute intestinal inflammation based on myeloperoxidase activity. *Gastroenterology*, **87**, 1344–1350.

LAWS, K.H., CLANTON, J.A., STARNES, V.A., LUPINETTI, L.M., COLLINS, J.C., OATES, J.A. & HAMMON, J.W. (1983). Kinetics and imaging of indium-111-labelled autologous platelets in experimental myocardial infarction. *Circulation*, **67**, 110–116.

LAZZARO, M.P., LATTANZIO, M.T., ALVINO, S., TESSARI, F., MARIOT, R., ZANGIROLAMI, L. & BELLATO, P. (1992). Pharmacokinetics and pharmacodynamics of cloricromene in patients with cerebral ischemia. *Thromb. Res.*, **65** (Suppl. 1), S145.

LEFER, A.M., JOHNSON III, G., MA, X., TSAO, P.S. & THOMAS, G.R. (1991). Cardioprotective and endothelial protective effects of $[Ala\text{-}IL8]_{77}$ in a rabbit model of myocardial ischaemia and reperfusion. *Br. J. Pharmacol*, **103**, 1153–1159.

LINDNER, V. & HEINLE, H. (1982). Binding properties of circulating Evans' blue dye in rabbits as determined by disc electrophoresis. *Atherosclerosis*, **43**, 417–422.

LUCCHESI, B.R. (1990). Myocardial ischaemia, reperfusion and free radical injury. *Am. J. Cardiol.*, **65**, 14I–23I.

MILEI, J., LLESUY, S., FERREIRA, R., GRANA, D., PROSDOCIMI, M. & BOVERIS, A. (1992). Reduction of myocardial damage by cloricromene during ischemia-reperfusion in the rabbit. *Cardioscience*, **3**, 97–105.

MILEI, J., FERREIRA, R., GRANA, D., CIRILLO, R., LLESUY, S. & PROSDOCIMI, M. (1993). Effects of cloricromene on the ischaemia-reperfusion myocardial damage in the rabbit. *Cardiology*, (in press).

MULLANE, K.M., READ, N., SALMON, J.A. & MONCADA, S. (1984). Role of leukocytes in acute myocardial infarction in anaesthetised dog: relationship to myocardial salvage by anti-inflammatory drugs. *J. Pharmacol. Exp. Ther.*, **228**, 510–522.

NACHLAS, M.M. & SHNITKA, T.K. (1963). Macroscopic identification of early myocardial infarct by alterations in dehydrogenase system. *Am. J. Pathol.*, **43**, 379–405.

PROSDOCIMI, M., FINESSO, M., TESSARI, F., GORIO, A., LANGUINO, L.R., DE GAETANO, G. & DEJANA, E. (1985). Inhibition of AD_6 (8-monochloro-3-beta-diethylaminoethyl-4-methyl-7-ethyoxycarbonyl methoxy coumarin) of platelet aggregation in dog stenosed coronary artery. *Thromb. Res.*, **39**, 399–409.

PROSDOCIMI, M., ZATTA, A., GORIO, A., ZANETTI, A. & DEJANA, E. (1986). Action of AD_6 (8-monochloro-3-beta-diethylaminoethyl-4-methyl-7-ethyoxycarbonyl methoxy coumarin) on human platelets *in vitro*. *Naunyn Schmied. Arch. Pharmacol.*, **332**, 305–310.

RENLUND, D.G. MACFARLANE, J.L., CHRISTENSEN, R.D., LYNCH, R.E. & ROTHSTEIN, G. (1980). A quantitative and sensitive method for measurement of myeloperoxidase. *Clin. Res.*, **28**, 75A.

ROMSON, J.L., HOOK, B.G., RIGET, V.H., SCHORK, M.A., SWANSON, D.P. & LUCCHESI, B.R. (1982). The effect of ibuprofen on accumulation of indium-111-labelled platelets and leucocytes in experimental myocardial infarction. *Circulation*, **66**, 1002–1011.

ROSS, J. (1976). Electrocardiographic characterisation of myocardial ischaemic injury and infarction. *Circulation*, **53**, 73–86.

SCHMID-SCHONBEIN, G.W. & ENGLER, R.L. (1986). Granulocytes as active participants in acute myocardial ischaemia and infarction. *Am. J. Cardiovasc. Pathol.*, **1**, 15–30.

SQUADRITO, F., ALTAVILLA, D., CAMPO, G.M., CALAPAI, G., IOCULANO, M., ZINGARELLI, B., SAITTA, A., PROSDOCIMI, M. & CAPUTI, A.P. (1992). Cloricromene, a coumarine derivative, protects against lethal endotoxin shock in rats. *Eur. J. Pharmacol.*, **210**, 107–113.

STURNIOLO, R., SQUADRITO, F., ALTAVILLA, D., TRIMARCHI, G.R., PROSDOCIMI, M. & CAPUTI, A.P. (1989). Cloricromene improves survival rate and peritoneal macrophage function in splanchnic artery occlusion shock in rats. *Circ. Shock*, **28**, 267–277.

STURNIOLO, R., SQUADRITO, F., CAMPO, G.M., VINCI, R., CALATRONI, A., PROSDOCINI, M. & CAPUTI, A.P. (1991). Protective effect of cloricromene, a coumarine derivative, in hypovolemic hemorrhagic shock in the rat. *J. Cardiovasc. Pharmacol.*, **17**, 261–266.

THIEMERMANN, C., THOMAS, R.G. & VANE, J.R. (1989). Defibrotide reduces infarct size in a rabbit model of experimental myocardial ischaemia and reperfusion. *Br. J. Pharmacol.*, **97**, 401–408.

(Received January 29, 1993
Revised April 15, 1993
Accepted May 12, 1993)

Br. J. Pharmacol. (1993), **110**, 281–288

Involvement of pertussis toxin-sensitive and -insensitive mechanisms in α-adrenoceptor modulation of noradrenaline release from rat sympathetic neurones in tissue culture

C.E. Hill, [1]D.A. Powis & I.A. Hendry

Division of Neuroscience, John Curtin School of Medical Research, Australian National University, Canberra, ACT, 2600, Australia

1 Sympathetic neurones derived from superior cervical ganglia of neonatal rats and maintained in tissue culture were used to investigate the modulation of neurotransmitter release by presynaptic receptors. Three week old cultures of neurones were loaded with [^{3}H]-noradrenaline to label endogenous neurotransmitter stores. Release of noradrenaline was evoked by depolarization with raised extracellular K^+ in the presence of desipramine and corticosterone to prevent uptake of released catecholamine.

2 Potassium (55 mmol l^{-1}) depolarization for 30 s caused more than a four fold increase in ^{3}H overflow from basal levels but this increase was reduced by up to 40% in the presence of exogenous noradrenaline (1 μmol l^{-1}). The inhibition by noradrenaline of depolarization-evoked overflow was blocked by the α_1/α_2-adrenoceptor antagonist, phentolamine. Phentolamine alone did not increase K^+-evoked ^{3}H overflow.

3 The α_2-adrenoceptor antagonist, yohimbine, produced a concentration-dependent block of the inhibition by noradrenaline of K^+-evoked overflow, while the α_1-adrenoceptor antagonist, prazosin, was without effect at concentrations up to 0.1 μmol l^{-1}.

4 The β-adrenoceptor antagonist, propranolol, neither reduced K^+-evoked overflow nor increased the degree of inhibition caused by the addition of 1 μmol l^{-1} noradrenaline.

5 The α_2-adrenoceptor agonist, clonidine (1 μmol l^{-1}) was less effective than noradrenaline at inhibiting K^+-evoked overflow, while the α_1-adrenoceptor agonist, phenylephrine (1 μmol l^{-1}) had no significant effect.

6 The L-channel calcium blocker, nicardipine (1 μmol l^{-1}) significantly inhibited ^{3}H overflow evoked by K^+. In the presence of L-channel block, however, noradrenaline still inhibited residual evoked overflow.

7 In the presence or absence of nicardipine, pertussis toxin pretreatment (1 nmol l^{-1}) reduced, but did not prevent, the effect of noradrenaline (1 μmol l^{-1}). Pertussis toxin alone caused a significant enhancement of K^+-evoked ^{3}H overflow.

8 The data indicate that on postganglionic neurones of cultured rat sympathetic ganglia there are α_2-adrenoceptors that modulate neurotransmitter release, but no functional β-adrenoceptors that mediate an enhancement of transmitter release. The data suggest further that in this preparation the mechanism of α_2-adrenoceptor modulation may involve pertussis toxin sensitive and insensitive G-proteins and effects on calcium channels other than L-type.

Keywords: Sympathetic neurone; noradrenaline release; presynaptic modulation; rat superior cervical ganglion; α-adrenoceptor; tissue culture; pertussis toxin

Introduction

For the past twenty years the notion has been advanced that the quanitity of neurotransmitter released at nerve terminals in response to an invading action potential is modified by substances present in the synaptic cleft. These substances include the neurotransmitter, or co-transmitter, released by the nerve terminal itself or by adjacent nerve terminals, and hormones and drugs (Starke *et al.*, 1989; Langer & Arbilla, 1990). For example, noradrenaline released by sympathetic nerve terminals acts on α-adrenoceptors to depress further release (see Starke, 1987). Use of more specific pharmacological tools has shown that α-adrenoceptors are not a homogeneous population (Starke, 1972; Dubocovich & Langer, 1974) but can be subdivided: the suggested terminology of the major subdivisions being α_1 and α_2 (Langer, 1974). Initially it was considered that α_1-adrenoceptors were located postsynaptically and α_2-adrenoceptors were presynaptic (Langer, 1974; Arbilla & Langer, 1978). However there is now clear evidence for a functional postsynaptic presence of α_2-adrenoceptors (McGrath, 1982). On the other hand, with regard to the possibility that there are, likewise, functional α_1-adrenoceptors located presynaptically, Starke (1987) has reviewed the literature and remains sceptical that there are such that operate to modulate neurotransmitter release, at least from sympathetic nerve terminals. His scepticism is based partly on the observation that in the experiments reviewed, either high concentrations of α_1-adrenoceptor agonists and antagonists were used, thereby raising the question of their specificity of action, or that even when low concentrations of the α_1-adrenoceptor antagonist, prazosin, were used its known reserpine-like neurotransmitter releasing action was not taken into account (e.g. Cubeddu & Weiner, 1975). Subsequent studies however have continued to suggest the presence of functional presynpatic α_1-adrenoceptors (Hicks *et al.*, 1986; Murphy & Majewski, 1989; 1990; Rump *et al.*, 1992; see also Wilson & Minneman, 1991) although Shinozuka *et al.* (1991) have attributed these effects to postjunctional α_1 receptors and the release of purines which in turn act prejunctionally.

[1] Author for correspondence at: Neuroscience Group, Faculty of Medicine, University of Newcastle, New South Wales 2308, Australia.

Other studies have suggested presynaptic receptors which have properties that do not conform precisely with those of either α_1- or α_2-adrenoceptor subtypes (Elliott *et al.*, 1989; Kawasaki *et al.*, 1989; Lipscombe *et al.*, 1989; Harsing & Vizi, 1991).

The present studies were undertaken with neonatal rat superior cervical ganglion neurones in tissue culture in order to determine the type of adrenoceptors which have a role in modulating noradrenaline release and to determine also aspects of second messenger coupling between receptor and exocytotic mechanism.

Some of these data have been presented in preliminary form elsewhere (Powis *et al.*, 1989a,b; Hill *et al.*, 1990; Hill & Powis, 1991; Hill, 1991).

Methods

Preparation of sympathetic neuronal cultures

Superior cervical ganglia were removed from neonatal rats, stripped of their connective tissue sheaths and teased into several small fragments. The ganglionic fragments were incubated at 37°C with 0.1% collagenase for 30 min followed by six successive 5 min incubations in 0.1% trypsin. After each treatment with trypsin the fragments were triturated with pipettes of decreasing bore. Supernatants were collected from the last four trypsinizations. The resulting suspension of neuronal and non-neuronal cells was centrifuged and resuspended in Dulbecco's modified Eagle's medium (DMEM) supplemented with 26 mmol l^{-1} NaH_2CO_3, 2 mmol l^{-1} pyruvate, 4 mmol l^{-1} L-glutamine, additional vitamins ('Vitamin Supplement': Commonwealth Serum Laboratories, Melbourne, Victoria, Australia), 100 iu ml^{-1} penicillin, 0.1 mg ml^{-1} streptomycin sulphate, 38 mmol l^{-1} glucose, 10% (v/v) foetal calf serum and 1 μg ml^{-1} β-nerve growth factor (prepared according to the method of Mobley *et al.*, 1976). Corticosterone (1 μmol l^{-1} from 10 mmol l^{-1} stock in ethanol) was added to the medium to maintain the neurones in an adrenergic phenotype (McLennan *et al.*, 1980). The cells were seeded at a density of 10^3 cells per well into 96 wells plates which had been previously coated with either rat tail collagen or poly-L-lysine. The medium was changed every 3–4 days and the cultures grown for 2 to 3 weeks at 37°C.

Some experiments were performed on cultures which contained only neurones, the non-neuronal cells, e.g., fibroblasts having been removed by treatment for several days with 20 μmol l^{-1} fluorodeoxyuridine and 20 μmol l^{-1} uridine. However, it was found that the extensive washing and incubation steps involved in the release experiments resulted in the neuronal nerve networks becoming detached from the bottom of the culture wells and frequently being removed from the wells together with wash solutions before the end of the incubations. This problem was not encountered with the cultures containing non-neuronal cells as these were more firmly attached to the substrate.

At the time the experiments described here were performed, the neurones were readily visible either isolated or in small clusters and had formed extensive networks over a background of non-neuronal cells (Figure 1).

Noradrenaline overflow studies

All overflow experiments were carried out in the 96 well plates at 37°C. Loading of neurones with labelled noradrenaline was achieved by incubating the cultures for 1 h with DMEM containing 10 μCi ml^{-1} [^{3}H]-noradrenaline (0.5–0.75 μmol l^{-1}; 1 μCi per well), 30 μmol l^{-1} corticosterone (10 mmol l^{-1} stock in ethanol) to prevent uptake of noradrenaline by any non-neuronal cells and 120 μmol l^{-1} pargyline to prevent noradrenaline degradation by monoamine oxidase. Excess noradrenaline was removed with 3 rinses of minimal salt solution (MSS, see below). To confirm that uptake of the labelled noradrenaline was mainly confined to the neurones, desipramine (1–100 μmol l^{-1}) was added to the [^{3}H]-noradrenaline containing loading medium. In experiments using pertussis toxin, cells were pretreated with the toxin (1 nmol l^{-1}) for 17 or 40 h in control medium at 37°C before incubation in [^{3}H]-noradrenaline.

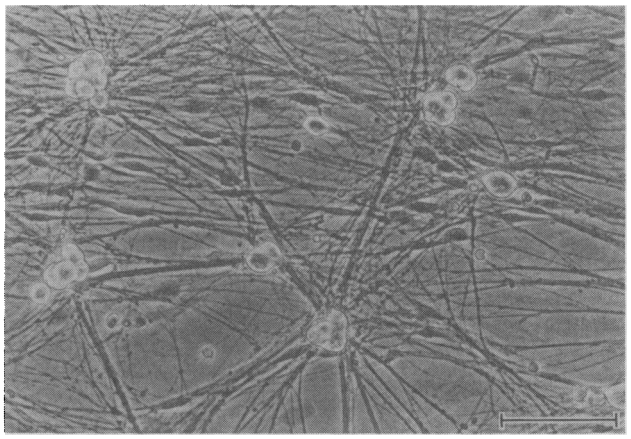

Figure 1 Photomicrograph of sympathetic neurones derived from rat superior cervical ganglion after 21 days in tissue culture showing extensive neuritic outgrowth from the dissociated cell bodies. Calibration bar = 100 μm

All test compounds were made up in MSS containing (mmol l^{-1}): NaCl 140, KCl 5.4, $CaCl_2$ 1.2, $MgCl_2$ 1.0, glucose 10, ascorbic acid 0.1, HEPES 15, Na_2HCO_3 10, desipramine 0.01 (to prevent reuptake of released noradrenaline by the neurones, see Table 1); and 30 μmol l^{-1} corticosterone to prevent uptake of noradrenaline by non-neuronal cells. High potassium depolarizing solution contained 55 mmol l^{-1} KCl and 90 mmol l^{-1} NaCl, while low calcium solution contained 0.12 mmol l^{-1} $CaCl_2$ and 5 mmol l^{-1} $MgCl_2$. The pH of all solutions was adjusted to 7.2. Stock solutions of drugs ($10^3\times$ or $10^4\times$) were made up in distilled water, except for nicardipine which was made up as 10 mmol l^{-1} in ethanol and noradrenaline which was made up as 10 mmol l^{-1} in 100 mmol l^{-1} ascorbic acid.

Pharmacological agents were added to both MSS and high-K^+ solutions. Cells were preincubated for 45 min with receptor antagonists or with nicardipine following the incubation in [^{3}H]-noradrenaline. Receptor agonists, on the other hand, were added for only a short (30 s) preincubation to prevent receptor desensitization. Wells were rinsed briefly and the basal overflow of labelled noradrenaline measured (by β scintillation spectrometry) in the supernatant from each well after 30 s exposure to MSS containing the appropriate drug. The MSS was replaced in the same well by high-K^+ solution containing the appropriate drug and the K^+-evoked overflow measured by removing the supernatant after 30 s.

At the end of each experiment the cells were lysed with 1% sodium dodecylsulphate and the residual intracellular radioactivity determined for each well by β-scintillation spectrometry.

Basal and K^+-evoked transmitter overflow were expressed as a percentage of the total amount of [^{3}H]-noradrenaline within the cells at the start of the basal overflow period, i.e.,

Table 1 Effect of desipramine upon [^{3}H]-noradrenaline accumulation by rat superior cervical ganglion cell cultures

Concentration of desipramine (μmol l^{-1})	*% reduction in uptake**
1	91 ± 1.4 (10)
10	94 ± 1.0 (11)
100	97 ± 0.5 (11)

*Mean ± s.e.mean of (*n*) determinations, being 3 or 4 determinations in each of 3 different preparations of cells

residual content + total ^3H released. All data are expressed as mean ± s.e.mean of n wells. Basal and K^+-evoked overflow were determined as described in the same wells and basal overflow was subtracted from the overflow obtained during the K^+ stimulation period to give evoked overflow. Each pair of measurements (basal and K^+-evoked) were made in 3–6 wells in at least 3 experiments, each using different batches of cells. Each experiment had its own separate control evoked overflow (no drug) and evoked overflow in the presence of noradrenaline in addition to the drugs tested. Thus, each Figure is based on its own internal data set. Statistical analyses were performed with Student's t test; P values less than 0.05 were considered to be significant.

Materials

(±)-[7-^{3}H]-noradrenaline (specific activity 13.3–19.2 Ci mmol^{-1}) was obtained from Amersham International (UK). All materials for preparation and maintenance of cells in culture were obtained from Flow Laboratories (Sydney, N.S.W., Australia). Clonidine hydrochloride, corticosterone, desipramine hydrochloride, nicardipine hydrochloride, (−)-noradrenaline hydrochloride, pargyline hydrochloride, pertussis toxin, (−)-phenylephrine hydrochloride, yohimbine hydrochloride, ascorbic acid and HEPES were obtained from Sigma (St Louis, MO, U.S.A.). Phentolamine (mesylate; Regitine) was obtained from Ciba Geigy (Sydney, N.S.W., Australia). Prazosin hydrochloride was a gift from Pfizer (Sydney, N.S.W., Australia). All other reagents used were of analytical grade.

Results

Uptake of [^{3}H]-noradrenaline into sympathetic postganglionic neurones

Cell cultures exposed to [^{3}H]-noradrenaline for 1 h accumulated substantial radioactivity. In the presence of desipramine (1–100 μmol l^{-1}) and corticosterone (30 μmol l^{-1}) parallel cultures accumulated only between 3–9% of that measured in the absence of desipramine (Table 1). In subsequent experiments 10 μmol l^{-1} desipramine was included routinely to all incubation solutions after loading the cells with [^{3}H]-noradrenaline.

Overflow of ^{3}H from cultured neurones

In all experiments described here, K^+ caused at least a four fold increase in ^{3}H overflow over basal levels. Depolarization-evoked ^{3}H-overflow was dependent upon the presence of external calcium since a reduction in the Ca^{2+} concentration of MSS to 0.12 mmol l^{-1} and an increase of Mg^{2+} to 5 mmol l^{-1} reduced K^+-evoked overflow to 19% of that obtained with a medium containing 1.2 mmol l^{-1} Ca^{2+} and 1.0 mmol l^{-1} Mg^{2+} ($n = 12$). Furthermore addition of 0.3 mmol l^{-1} $CdCl_2$ to normal MSS reduced K^+-evoked overflow to 5% of that obtained in normal MSS ($n = 12$).

Effects of adrenoceptor agonists and antagonists upon K^+-evoked ^{3}H overflow

Noradrenaline (1 μmol l^{-1}) caused a significant reduction in K^+-evoked overflow (Figure 2). The extent to which overflow was modulated by noradrenaline varied between different experiments: from 20–40% of control evoked overflow.

The α-adrenoceptor antagonist, phentolamine (1 μmol l^{-1}), did not itself increase K^+-evoked ^{3}H overflow, but did prevent the reduction of evoked overflow by noradrenaline (Figure 2).

The β-adrenoceptor antagonist, propranolol (1 μmol l^{-1}), did not alter K^+-evoked ^{3}H overflow, suggesting that endogenous noradrenaline released from the neurones during depolarization was not sufficient to stimulate β-adrenoceptors. In addition, in the presence of propranolol, there was no change in the size of the reduction in evoked overflow produced by exogenous noradrenaline (1 μmol l^{-1}, Figure 3). This suggested that there were no β-adrenoceptors present on the neurones, as stimulation of these receptors would be expected to counteract the inhibitory effect of noradrenaline on evoked overflow via the α-adrenoceptors. Subsequent block of the β-adrenoceptors would be expected to increase the inhibition of overflow produced by noradrenaline.

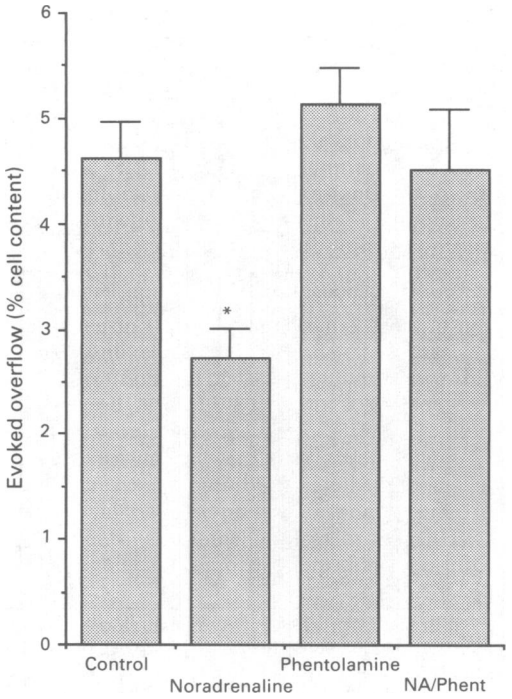

Figure 2 Noradrenaline reduces K^+-evoked ^{3}H overflow by an action that is blocked by phentolamine. Columns show ^{3}H overflow over a 30 s period evoked by K^+ (55 mmol l^{-1}) in the absence ($n = 11$ wells in 3 experiments) or presence of either noradrenaline (NA, 1 μmol l^{-1}, $n = 11$), phentolamine (Phent, 1 μmol l^{-1}, $n = 8$) or both together ($n = 7$). Data shown (mean ± s.e.mean) represent K^+-evoked overflow minus basal overflow for the same wells. The mean basal overflow for the no drug wells in these experiments was 1.3 ± 0.2% ($n = 11$) of cell ^{3}H content. *$P < 0.05$ (compared with control, no drug).

Cultured neurones were exposed to a range of concentrations of the α_1 and α_2-adrenoceptor antagonists, prazosin and yohimbine, to determine their effects upon the inhibition by noradrenaline of evoked ^{3}H overflow. Neither drug had any effect on evoked overflow when added alone suggesting that the amount of endogenous noradrenaline released by K^+ was insufficient to stimulate these receptors.

Yohimbine caused a concentration-dependent reduction in the magnitude of the noradrenaline inhibition of evoked overflow while prazosin up to a concentration of 0.1 μmol l^{-1}, the highest concentration that can be justified for preferential blockade of α_1-adrenoceptors, was without effect (Figure 4).

The α_1-adrenoceptor agonist, phenylephrine (1 μmol l^{-1}), failed to reduce the K^+ evoked ^{3}H-overflow while the α_2-adrenoceptor agonist, clonidine (1 μmol l^{-1}), reduced K^+-evoked overflow by 12% ($P < 0.05$); a smaller degree of inhibition than that caused by the same concentration of noradrenaline in these experiments (Figure 5).

Effects of calcium channel blockers on K^+-evoked ^{3}H-overflow

Nicardipine (1 μmol l^{-1}) reduced K^+ evoked ^{3}H overflow by 20% (Figure 6, $P < 0.05$). The result suggests a small contri-

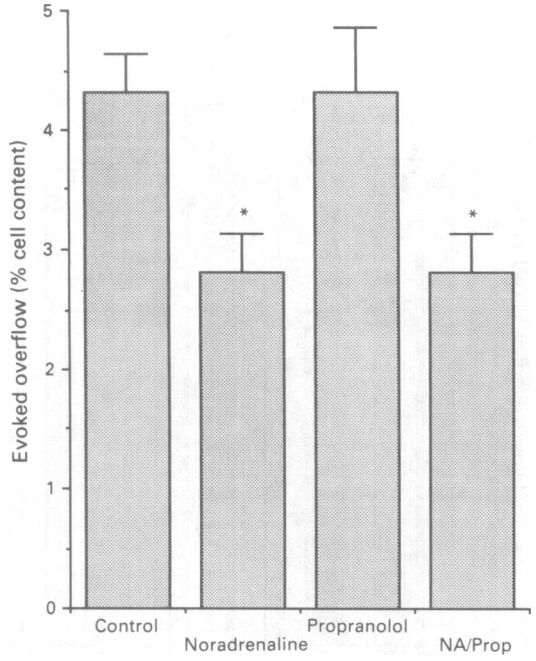

Figure 3 Propranolol neither increases nor does it alter the reduction by noradrenaline of K^+-evoked ^3H overflow. Columns show overflow over a 30 s period evoked by K^+ (55 mmol l^{-1}) in the absence ($n = 17$ wells in 3 experiments) or presence of either propranolol (Prop, 1 μmol l^{-1}, $n = 15$), noradrenaline (NA, 1 μmol l^{-1}, $n = 17$) or both together ($n = 14$). The mean basal overflow for the no drug wells in these experiments was 1.1 ± 0.1% of cell ^3H content. $^*P < 0.05$ (compared with corresponding control).

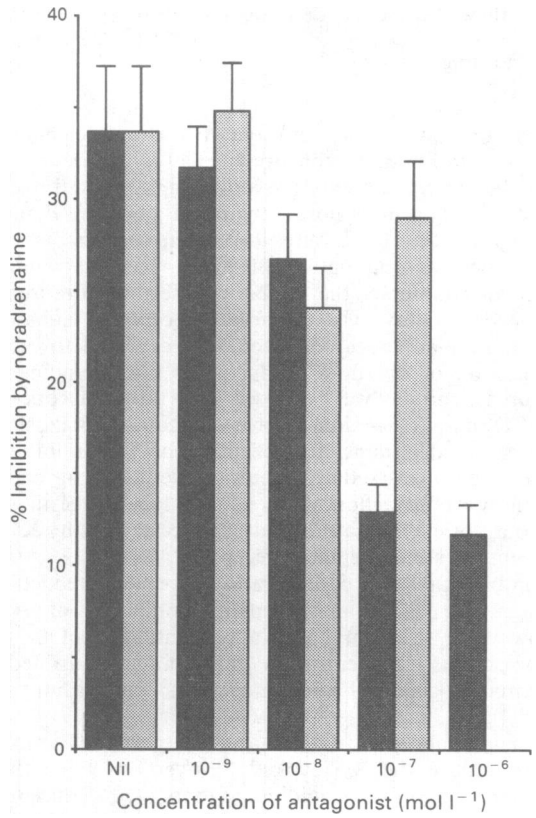

Figure 4 Yohimbine but not prazosin reduces the inhibition by noradrenaline of K^+-evoked ^3H overflow in a concentration-dependent manner. The inhibition by noradrenaline (1 μmol l^{-1}) of K^+-evoked ^3H overflow is expressed as a % reduction from that evoked in the absence of noradrenaline. The effects on this inhibition of increasing concentrations of the α_1-adrenoceptor antagonist, prazosin (light columns), or the α_2-adrenoceptor antagonist, yohimbine (dark columns), are shown. Each column is the mean ± s.e.mean of at least 12 wells in 4 experiments.

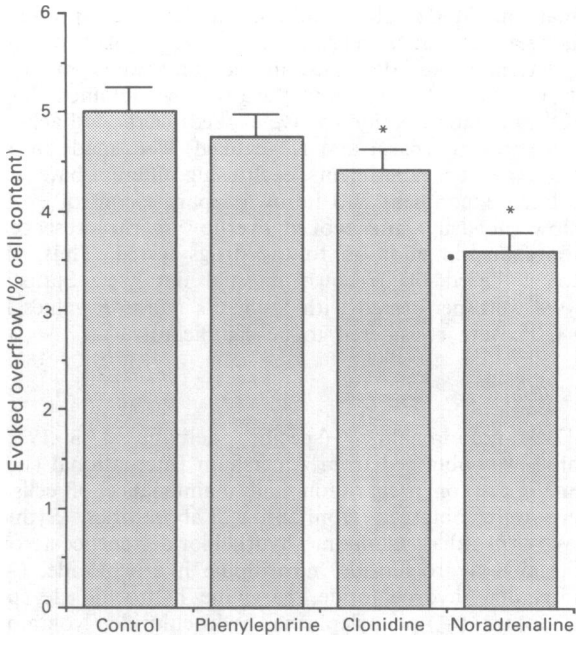

Figure 5 Clonidine but not phenylephrine reduces K^+-evoked ^3H overflow. Columns show overflow over a 30 s period evoked by K^+ (55 mmol l^{-1}) in the absence ($n = 14$ wells in 3 experiments) or presence of phenylephrine (1 μmol l^{-1}, $n = 19$), clonidine (1 μmol l^{-1}, $n = 18$) or noradrenaline (1 μmol l^{-1}, $n = 6$). The mean basal overflow for the no drug wells in these experiments was 1.0 ± 0.2% ($n = 14$) of cell ^3H content. $^*P < 0.05$ (compared with control, no drug).

bution by L-type calcium channels to transmitter overflow evoked by K^+-depolarization in this experimental preparation. In the presence of nicardipine, noradrenaline still inhibited significantly the residual evoked ^3H overflow (Figure 6). At higher concentrations (10 μmol l^{-1}), nicardipine appeared to have deleterious effects on the cells, as the basal overflow of ^3H was increased and the evoked overflow was greatly reduced. Evoked overflow was frequently less than twice basal overflow making the results difficult to interpret.

Effects of pertussis toxin on inhibition of K^+-evoked overflow by noradrenaline

Pretreatment of neuronal cultures for 17 h with pertussis toxin (1 nmol l^{-1}) caused a significant increase in the magnitude of K^+-evoked ^3H overflow (Figure 7, $P < 0.05$). The percentage inhibition by noradrenaline of the corresponding evoked overflow was, however, unaffected by the toxin pretreatment (Figure 7). Longer pretreatment with pertussis toxin (40 h) also failed to abolish the inhibitory effects of noradrenaline upon evoked overflow (data not shown).

When cultures were pretreated with pertussis toxin and the evoked overflow measured in the presence of nicardipine (1 μmol l^{-1}) to block L-type calcium channels, pertussis toxin was still unable to abolish the effect of noradrenaline although the absolute magnitude of the inhibition (−24%) was significantly reduced in the presence compared with that in the absence (−32%) of pertussis toxin ($P < 0.05$; Figure 8).

Discussion

The superior cervical ganglion of the neonatal rat is a widely used source of experimental neuronal tissue. From neurones dissociated from such ganglia sprout viable postganglionic sympathetic neurites which, in culture, in the presence of corticosterone, continue to express an adrenergic phenotype (McLennan *et al.*, 1980). O'Lague *et al.* (1978) showed that

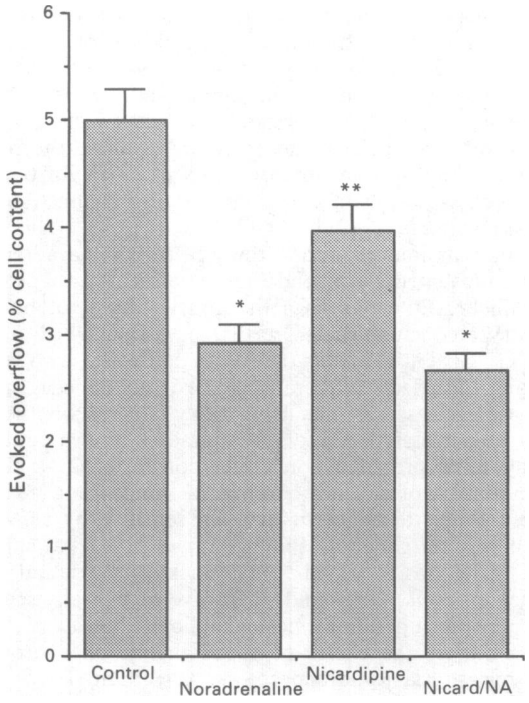

Figure 6 Nicardipine does not alter the reduction by noradrenaline of K^+-evoked ^3H overflow. Columns show overflow over a 30 s period evoked by K^+ (55 mmol l^{-1}) in the absence ($n = 18$ wells in 4 experiments) or presence of either nicardipine (Nicard, 1 μmol l^{-1}, $n = 20$), noradrenaline (NA, 1 μmol l^{-1}, $n = 19$) or both together ($n = 18$). The mean basal overflow for the no drug wells in these experiments was $1.6 \pm 0.3\%$ ($n = 18$) of cell ^3H content. $^*P < 0.05$ (compared with relevant control, i.e., with or without nicardipine). $^{**}P < 0.05$ (compared with control, no drug).

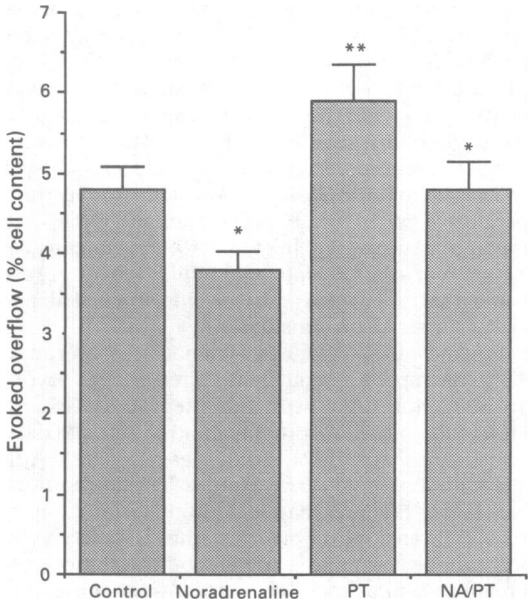

Figure 7 Pertussis toxin does not prevent the inhibition by noradrenaline of evoked overflow. Columns show overflow over a 30 s period evoked by K^+ (55 mmol l^{-1}) in the absence ($n = 16$ wells in 3 experiments), or presence of either noradrenaline (NA, 1 μmol l^{-1}, $n = 17$), pertussis toxin (PT, preincubation in 1 nmol l^{-1} for 17 h, $n = 16$) or both together ($n = 16$). Basal overflow for control no drug $1.2 \pm 0.2\%$ ($n = 16$) of cell ^3H content. $^*P < 0.05$ compared with corresponding control, either with or without preincubation in pertussis toxin. $^{**}P < 0.05$ compared with control, no drug.

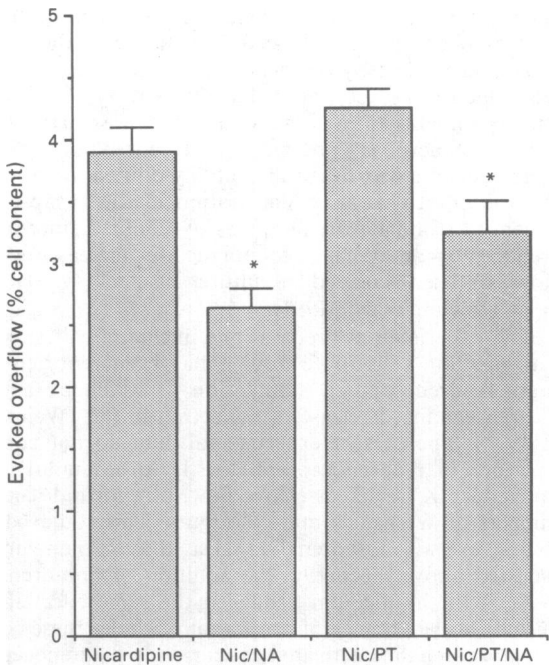

Figure 8 In the presence of nicardipine, pertussis toxin does not prevent the reduction by noradrenaline of K^+-evoked ^3H overflow. Columns show overflow over a 30 s period evoked by K^+ (55 mmol l^{-1}) in the presence of nicardipine alone (1 μmol l^{-1}, $n = 18$ determinations in 4 experiments) or nicardipine plus noradrenaline (Nic/NA, 1 μmol l^{-1}, $n = 18$) nicardipine plus pertussis toxin (Nic/PT, preincubation 1 nmol l^{-1} for 17 h, $n = 18$), or nicardipine, pertussis toxin and noradrenaline together (Nic/PT/NA) ($n = 18$). Basal overflow in nicardipine control was $1.1 \pm 0.1\%$ of cell ^3H content. $^*P < 0.05$ (compared with corresponding control, i.e., nicardipine with or without pertussis toxin).

cultured principal sympathetic neurones dissociated from this source have electrophysiological properties similar to those of sympathetic neurones of adult rats. Furthermore, these neurones are able to synthesize neurotransmitter and accumulate, store and release radiolabelled neurotransmitter (Burton & Bunge, 1975; Patterson *et al.*, 1976; Sweadner, 1985). The present data show clearly that such preparations, after two to three weeks in tissue culture, have extensive neuritic outgrowth and that only the neuronal components accumulate and therefore subsequently release [^3H]-noradrenaline. Furshpan *et al.* (1986) state that 'the high innervation density in microcultures (of rat superior cervical ganglion neurones) enhances the probability of detecting weak synaptic effects'. This suggests the preparation should be ideal for investigating presynaptic modulation of neurotransmitter release.

We have previously reported that neonatal rat sympathetic neurones in tissue culture continue to release ^3H in response to K^+ depolarization over at least a 5 h period but that the rate of release declines after the first few minutes (Powis *et al.*, 1989a). When measured over a 30 s period, the basal (spontaneous) overflow was enhanced more than four fold by depolarization with 55 mmol l^{-1} K^+. Furthermore the overflow evoked by K^+ was dependent upon the presence of external calcium. The results indicate that the calcium required for release enters the neurones predominantly through non-L type calcium channels (presumably N-channels) since the presence of the dihydropyridine L-channel blocker nicardipine reduced evoked ^3H overflow by only 20%. These results correspond well with the results of other studies. For example Hirning *et al.* (1988) have shown that L-channels relative to N-channels contribute in only a minor way to the calcium influx that precedes neurotransmitter release from rat sympathetic neurones.

Noradrenaline caused a significant inhibition of K^+-evoked ^3H overflow and this inhibition was prevented by the

α-adrenoceptor antagonist, phentolamine. Unexpectedly, addition of phentolamine alone did not increase the release of transmitter evoked by the depolarizing stimulus. This was probably due to the fact that in the culture dishes used in the present experiments the volume of medium was many times the volume of neurones present. The noradrenaline released from the neurones was thus substantially diluted, quite probably to the point that its concentration in the synapse was insufficient to stimulate the receptors. A similar failure of the α_2-adrenoceptor antagonist, yohimbine, to increase evoked overflow has been reported in cultures of chick sympathetic neurones (Boehm *et al.*, 1991).

In some experimental preparations, including rat superior cervical ganglion cells in culture, it has been reported that there are β-adrenoceptors, stimulation of which by agonist leads to an enhanced release of neurotransmitter (Weinstock *et al.*, 1978). The present experimental data do not confirm the presence of β-adrenoceptors. Firstly, propranolol alone did not reduce K^+-evoked ^3H overflow, but nor did it in the experiments of Weinstock and colleagues. This could be due to the low levels of noradrenaline released from the neurones as discussed above. Secondly, the addition of noradrenaline (1 μmol l^{-1}) to the medium produced the same effect in the presence as in the absence of propranolol. Under these conditions, if noradrenaline activated concurrently β-adrenoceptors and α-adrenoceptors, blockade of the β-adrenoceptors with propranolol would have been expected to augment the inhibition of evoked overflow by exogenous noradrenaline, but this was not observed. Thus we find no evidence for functional β-adrenoceptors in our cultures.

The inhibition by noradrenaline of K^+-evoked ^3H overflow was reduced in a concentration-dependent manner by the α_2-adrenoceptor antagonist, yohimbine. The α_1-adrenoceptor antagonist, prazosin, even at a concentration of 0.1 μmol l^{-1}, did not significantly reduce the inhibitory effect of noradrenaline. These results are consistent with the notion that the modulatory adrenoceptors on postganglionic sympathetic nerves are predominantly of the α_2 type as has been reported for other systems (Starke, 1987; Lipscombe *et al.*, 1989; Schofield, 1990; Brock *et al.*, 1990). It is interesting to note that in a number of studies, including the present one, yohimbine was unable to antagonize fully the effects of noradrenaline, even at very high concentrations (Kawasaki *et al.*, 1989; Lipscombe *et al.*, 1989). The reduced sensitivity to yohimbine in the present study suggests a similarity of the receptor to the α_{2D} subtype (Simonneaux *et al.*, 1991; Limberger *et al.*, 1992). Alternatively, the results may suggest the involvement of more than one α-adrenoceptor subtype as has been previously postulated (Docherty, 1983; Hicks *et al.*, 1986; Daly *et al.*, 1988; Kawasaki *et al.*, 1989; Murphy & Majewski, 1989; 1990; Harsing & Vizi, 1991; Wilson & Minneman, 1991; Rump *et al.*, 1992).

Consistent with the involvement of an α_2-adrenoceptor modulating evoked noradrenaline release in this tissue, the α_1-adrenoceptor agonist, phenylephrine, was ineffective. On the other hand, the α_2-adrenoceptor agonist, clonidine, was also less effective than noradrenaline. These findings, however, may simply be a reflection of the partial agonist properties of clonidine. Clonidine has been noted by others to have a smaller effect than noradrenaline in reducing calcium currents and/or neurotransmitter release from isolated sympathetic neurones (Lipscombe *et al.*, 1989; Schofield, 1990; Boehm *et al.*, 1992).

In the present study, the K^+-evoked overflow of noradrenaline from the sympathetic neurones was predominantly dependent on calcium entering via non-L type channels, presumably N-channels. In the presence of L-channel blockers, noradrenaline was still able to inhibit evoked overflow. This suggests that the modulatory action of noradrenaline is mediated by N-channels. A similar conclusion was reached by others (Lipscombe *et al.*, 1989; Akasu *et al.*, 1990; see also Wanke *et al.*, 1987), although in their (electrophysiological) studies only calcium (current) movement through channels located on the nerve cell bodies was being monitored, i.e., remote from the sites at which neurotranmitter is released. In the present study the neurones were intact, having regenerated long axons during the culture period. Our measurements would thus reflect the net effects over the entire membrane surface and therefore confirm the importance of calcium movements through N-channels for both the release process and its modulation by noradrenaline (see also Kongsamut *et al.*, 1989).

The modulation of transmitter release by noradrenaline was not prevented by extended pretreatment with pertussis toxin which ADP-ribosylates the alpha subunit of both G_o and G_i. We conclude therefore that pathways which involve either G_o or G_i are not the only pathways involved in mediating the effects of noradrenaline in modulating neurotransmitter release. Results from other studies on the sensitivity to pertussis toxin of the noradrenaline modulatory pathway have provided conflicting conclusions. Noradrenaline inhibition of calcium currents in sympathetic neurones has been found to be pertussis-toxin sensitive by some (rat superior cervical ganglion: Plummer *et al.*, 1991; rat superior cervical ganglion: Schofield, 1991; chick paravertebral ganglion: Boehm *et al.*, 1992) and insensitive or partially sensitive by others (rat superior cervical ganglion: Song *et al.*, 1989; 1991). Similarly the effects of noradrenaline on neurotransmitter release via α_2-adrenoceptors have been described as pertussis toxin-sensitive (Allgaier *et al.*, 1985; Boehm *et al.*, 1992) and insensitive (Musgrave *et al.*, 1987; Docherty, 1990; Murphy & Majewski, 1990). It is of interest that, in the presence of L-type calcium channel blockade, the modulation of transmitter release by noradrenaline was reduced but not prevented by pertussis toxin, suggesting that there may be pertussis toxin-sensitive and -insensitive components to the response. Beech *et al.* (1992) have described effects of noradrenaline on (N-channel) calcium currents in rat superior cervical ganglia neurones that have both pertussis toxin-sensitive and -insensitive components (see also Song *et al.*, 1991). Their results were interpreted as providing evidence for participation of multiple G-proteins in modulating ion channel function (see Elmslie, 1992). It is possible therefore that the presynaptic α-adrenoceptor that mediates the noradrenaline inhibition of transmitter release can be coupled to both pertussis toxin-sensitive and -insensitive G-proteins with the functional mix perhaps determined by the environment to which the cells are exposed. Our results suggest that the culture conditions used in the present study favour coupling of the α-adrenoceptor to both a pertussis toxin-sensitive and a pertussis toxin-insensitive G-protein (or, in this latter case, perhaps even to no G-protein at all). Note here the conclusions of Murphy & Majewski (1990) who consider that both α_1- and α_2-adrenoceptors modulate neurotransmitter release and that it is the α_1-adrenoceptor-mediated pathway which is pertussis toxin sensitive.

Pretreatment of the cultured sympathetic neurones with pertussis toxin caused a significant increase in K^+-evoked ^3H overflow suggesting that neurotramitter release is normally under tonic inhibitory G-protein control (see Ikeda, 1991; Ohara-Imaizumi *et al.*, 1991; Sontag *et al.*, 1991). Although this tonic inhibition could be explained by released noradrenaline acting on the presynaptic α_2-adrenoceptors linked to pertussis toxin-sensitive G-proteins, this is unlikely because exposure to phentolamine or yohimbine did not result in any increase in evoked overflow, as discussed above. Furthermore, the inhibitory effect of exogenous noradrenaline on evoked overflow in the present study was not prevented by treatment with pertussis toxin.

In summary, our data suggest that neurotransmitter release can be evoked from rat sympathetic neurones grown in cell culture by K^+-depolarization via a calcium-dependent process. Calcium influx through dihydropyridine-sensitive L-channels plays only a minor role in this release mechanism. A pertussis toxin-sensitive G-protein appears to cause tonic inhibition of evoked overflow under control conditions but this G-protein

is not part of the α-adrenoceptor-mediated modulation pathway. Noradrenaline causes a reduction in K^+-evoked overflow through an α_2-adrenoceptor mechanism which is independent of L-type calcium channels. This mechanism may involve pertussis toxin-sensitive and -insensitive G-proteins.

The expert technical assistance of Jenny Meaney, Eleanor Oyston and Mary Preston is gratefully acknowledged. Thanks are offered to Pfizer Pty (Dr Harry Wooller) for a gift of prazosin.

References

AKASU, T., TSURUSAKI, M. & TOKIMASA, T. (1990). Reduction of the N-type calcium current by noradrenaline in neurones of rabbit vesical parasympathetic ganglia. *J. Physiol.*, **426**, 439–452.

ALLGAIER, C., FEUERSTEIN, T.J., JACKISCH, R. & HERTTING, G. (1985). Islet-activating protein (pertussis toxin) diminishes α_2 adrenoceptor mediated effects on noradrenaline release. *Naunyn-Schmied. Arch. Pharmacol.*, **331**, 235–239.

ARBILLA, S. & LANGER, S.Z. (1978). Differences between presynaptic and postsynaptic α-adrenoceptors in the isolated nictitating membrane of the cat: effects of metanephrine and tolazoline. *Br. J. Pharmacol.*, **64**, 259–264.

BEECH, D.J., BERNHEIM, L. & HILLE, B. (1992). Pertussis toxin and voltage dependence distinguish multiple pathways modulating calcium channels of rat sympathetic neurons. *Neuron*, **8**, 97–106.

BOEHM, S., HUCK, S., DROBNY, H. & SINGER, E.A. (1991). Electrically evoked noradrenaline release from cultured chick sympathetic neurons: modulation via α_2-adrenoceptors and lack of autoinhibition. *Naunyn-Schmied. Arch. Pharmacol.*, **344**, 130–132.

BOEHM, S., HUCK, S., DROBNY, H. & SINGER, E.A. (1992). Pertussis toxin abolishes the inhibition of Ca^{2+} currents and of noradrenaline release via α_2-adrenoceptors in chick sympathetic neurons. *Naunyn-Schmied. Arch. Pharmacol.*, **345**, 606–609.

BROCK, J.A., CUNNANE, T.C., STARKE, K. & WARDELL, C.F. (1990). α_2-Adrenoceptor-mediated autoinhibition of sympathetic transmitter release in guinea-pig vas deferens studied by intracellular and focal extracellular recording of junction potentials and currents. *Naunyn-Schmied. Arch. Pharmacol.*, **342**, 45–52.

BURTON, H. & BUNGE, R.P. (1975). A comparison of the uptake and release of [^{3}H]norepinephrine in rat autonomic and sensory ganglia in tissue culture. *Brain Res.*, **97**, 157–162.

CUBEDDU, L.X. & WEINER, N. (1975). Release of norepinephrine and dopamine-beta-hydroxylase by nerve stimulation. V. Enhanced release associated with a granular effect of a benzoquinolizine derivative with reserpine-like properties. *J. Pharmacol. Exp. Ther.*, **193**, 757–774.

DALY, C.J., MCGRATH, J.C. & WILSON, V.G. (1988). Pharmacological analysis of postjunctional α-adrenoceptors mediating contractions to (−)-noradrenaline in the rabbit isolated lateral saphenous vein can be explained by interacting responses to simultaneous activation of α_1- and α_2-adrenoceptors. *Br. J. Pharmacol.*, **95**, 485–500.

DOCHERTY, J.R. (1983). An investigation of presynaptic α-adrenoceptor subtypes in the pithed rat heart. *Br. J. Pharmacol.*, **78**, 655–657.

DOCHERTY, J.R. (1990). No effect of pertussis toxin in peripheral prejunctional α_2-adrenoceptor-mediated responses and on endothelium-dependent relaxations in the rat. *Br. J. Pharmacol.*, **100**, 348–352.

DUBOCOVICH, M.L. & LANGER, S.Z. (1974). Negative feed-back regulation of noradrenaline release by nerve stimulation in the perfused cat's spleen: differences in potency of phenoxybenzamine in blocking the pre- and post-synaptic adrenergic receptors. *J. Physiol.*, **237**, 505–519.

ELLIOTT, P., MARSH, S.J. & BROWN, D.A. (1989). Inhibition of Ca-spikes in rat preganglionic cervical sympathetic nerves by sympathomimetic amines. *Br. J. Pharmacol.*, **96**, 65–76.

ELMSLIE, K.S. (1992). Calcium current modulation in frog sympathetic neurones: multiple neurotransmitters and G proteins. *J. Physiol.*, **451**, 229–246.

FURSHPAN, E.J., LANDIS, S.C., MATSUMOTO, S.G. & POTTER, D.D. (1986). Synaptic functions in rat sympathetic neurons in microcultures. I. Secretion of norepinephrine and acetylcholine. *J. Neurosci.*, **6**, 1061–1079.

HARSING, L.G. Jr. & VIZI, E.S. (1991). Evidence that two stereochemically different alpha-2 adrenoceptors modulate norepinephrine release in rat cerebral cortex. *J. Pharmacol. Exp. Ther.*, **256**, 44–49.

HICKS, P.E., NAJAR, M., VIDAL, M. & LANGER, S.Z. (1986). Possible involvement of presynaptic α_1-adrenoceptors in the effects of idazoxan and prazosin on ^{3}H-noradrenaline release from tail arteries of SHR. *Naunyn-Schmied. Arch. Pharmacol.*, **333**, 354–361.

HILL, C.E. (1991). Modulation of neurotransmitter release from sympathetic neurones by pertussis toxin sensitive and insensitive mechanisms. *Proc. Third IBRO World Congress of Neurosci.*, p. 270.

HILL, C.E., HENDRY, I.A. & POWIS, D.A. (1990). Prejunctional modulation of neurotransmitter release from rat sympathetic neurones in tissue culture. *Proc. Aust. Neurosci. Soc.*, **1**, 86.

HILL, C.E. & POWIS, D.A. (1991). Involvement of α_1- and α_2-adrenoceptors in modulating transmitter release in rat sympathetic neurones. *J. Neurochem.*, **57**, S75.

HIRNING, L.D., FOX, A.P., MCCLESKEY, E.W., OLIVERA, B.M., THAYER, S.A., MILLER, R.J. & TSIEN, R.W. (1988). Dominant role of N-type Ca^{2+} channels in evoked release of norepinephrine from sympathetic neurons. *Science*, **239**, 57–61.

IKEDA, S.R. (1991). Double-pulse calcium channels current facilitation in adult rat sympathetic neurones. *J. Physiol.*, **439**, 181–214.

KAWASAKI, H., URABE, M. & TAKASAKI, K. (1989). Presynaptic α_2-adrenoceptor modulation of 5-hydroxytryptamine and noradrenaline release from vascular adrenergic nerves. *Eur. J. Pharmacol.*, **164**, 35–43.

KONGSAMUT, S., LIPSCOMBE, D. & TSIEN, R.W. (1989). The N-type Ca channel in frog sympathetic neurons and its role in α-adrenergic modulation of transmitter release. *Ann. N.Y. Acad. Sci.*, **560**, 312–333.

LANGER, S.Z. (1974). Presynaptic regulation of catecholamine release. *Biochem. Pharmacol.*, **23**, 1793–1800.

LANGER, S.Z. & ARBILLA, S. (1990). Presynaptic receptors on peripheral noradrenergic neurons. *Ann. N.Y. Acad. Sci.*, **604**, 7–16.

LIMBERGER, N., TRENDELENBURG, A.-U. & STARKE, K. (1992). Pharmacological characterization of presynaptic α_2-autoreceptors in rat submaxillary gland and heart atrium. *Br. J. Pharmacol.*, **107**, 246–255.

LIPSCOMBE, D., KONGSAMUT, S. & TSIEN, R.W. (1989). α-Adrenergic inhibition of sympathetic neurotransmitter release mediated by modulation of N-type calcium-channel gating. *Nature*, **340**, 639–642.

MCGRATH, J.C. (1982). Evidence for more than one type of postjunctional α-adrenoceptor. *Biochem. Pharmacol.*, **31**, 467–484.

MCLENNAN, I.S., HILL, C.E. & HENDRY, I.A. (1980). Glucocorticoids modulate transmitter choice in developing superior cervical ganglion. *Nature*, **283**, 206–207.

MOBLEY, W.C., SCHENKER, A. & SHOOTER, E. (1976). Characterization and isolation of proteolytically modified nerve growth factor. *Biochemistry*, **15**, 5543–5551.

MURPHY, T.V. & MAJEWSKI, H. (1989). Modulation of noradrenaline release in slices of rat kidney cortex through α_1- and α_2-adrenoceptors. *Eur. J. Pharmacol.*, **169**, 285–295.

MURPHY, T.V. & MAJEWSKI, H. (1990). Pertussis toxin differentiates between α_1- and α_2-adrenoceptor-mediated inhibition of noradrenaline release from rat kidney cortex. *Eur. J. Pharmacol.*, **179**, 435–439.

MUSGRAVE, I.F., MARLEY, P. & MAJEWSKI, H. (1987). Pertussis toxin does not attenuate α_2-adrenoceptor mediated inhibition of noradrenaline release in mouse atria. *Naunyn-Schmied. Arch. Pharmacol.*, **336**, 280–286.

OHARA-IMAIZUMI, M., KAMEYAMA, K., KAWAE, N., TAKEDA, K., MURAMATSU, S. & KUMAKURA, K. (1992). Regulatory role of the GTP-binding protein, G_o, in the mechanism of exocytosis in adrenal chromaffin cells. *J. Neurochem.*, **58**, 2275–2284.

O'LAGUE, P.H., POTTER, D.D. & FURSHPAN, E.J. (1978). Studies on rat sympathetic neurons developing in cell culture. I. Growth characteristics and electrophysiological properties. *Dev. Biol.*, **67**, 384–403.

PATTERSON, P.H., REICHARDT, L.F. & CHUN, L.L.Y. (1976). Biochemical studies on the development of primary sympathetic neurons in cell culture. *Cold Spring Harbor Symp. Quant. Biol.*, **40**, 389–397.

PLUMMER, M.R., RITTENHOUSE, A., KANEVSKY, M. & HESS, P. (1991). Neurotransmitter modulation of calcium channels in rat sympathetic neurons. *J. Neurosci.*, **11**, 2339–2348.

POWIS, D.A., HENDRY, I.A. & HILL, C.E. (1989a). Some characteristics of neurotransmitter release from rat sympathetic neurones in tissue culture. *Proc. Int. Cong. Physiol. Sci.*, **17**, 408–409.

POWIS, D.A., HENDRY, I.A. & HILL, C.E. (1989b). Neurotransmitter release from rat sympathetic neurones in tissue culture. *Proc. Aust. Physiol. Pharmacol. Soc.*, **20**, 167P.

RUMP, L.C., WOLK, V., RUFF, G. & SCHOLLMEYER, P. (1992). Activation of α_1- and α_2-adrenoceptors inhibits noradrenaline release in rabbit renal arteries: effects of pertussis toxin and N-ethylmaleimide. *J. Auton. Pharmacol.*, **12**, 97–108.

SCHOFIELD, G.G. (1990). Norepinephrine blocks a calcium current of adult rat sympathetic neurons via an α_2-adrenoceptor. *Eur. J. Pharmacol.*, **180**, 37–47.

SCHOFIELD, G.G. (1991). Norepinephrine inhibits a Ca^{2+} current in rat sympathetic neurons via a G-protein. *Eur. J. Pharmacol.*, **207**, 195–207.

SHINOZUKA, K., SEDAA, K.O., BJUR, R.A. & WESTFALL, D.P. (1991). Participation by purines in the modulation of norepinephrine release by methoxamine. *Eur. J. Pharmacol.*, **192**, 431–434.

SIMONNEAUX, V., EBADI, M. & BYLUND, D.B. (1991). Identification and characterization of α_{2D}-adrenergic receptors in bovine pineal gland. *Mol. Pharmacol.*, **40**, 235–241.

SONG, S.-Y., SAITO, K., NOGUCHI, K. & KONISHI, S. (1989). Different GTP-binding proteins mediate regulation of calcium channels by acetylcholine and noradrenaline in rat sympathetic neurons. *Brain Res.*, **494**, 383–386.

SONG, S.-Y., SAITO, K., NOGUCHI, K. & KONISHI, S. (1991). Adrenergic and cholinergic inhibition of Ca^{2+} channels mediated by different GTP-binding proteins in rat sympathetic neurones. *Pflügers Arch.*, **418**, 592–600.

SONTAG, J.-M., THIERSE, D., ROUOT, B., AUNIS, D. & BADER, M.-F. (1991). A pertussis-toxin-sensitive protein controls exocytosis in chromaffin cells at a step distal to the generation of second messengers. *Biochem. J.*, **274**, 339–347.

STARKE, K. (1972). Alpha sympathomimetic inhibition of adrenergic and cholinergic transmission in the rabbit heart. *Naunyn-Schmied. Arch. Pharmacol.*, **274**, 18–45.

STARKE, K. (1987). Presynaptic α-autoreceptors. *Rev. Physiol. Biochem. Pharmacol.*, **107**, 73–146.

STARKE, K., GÖTHERT, M. & KILBINGER, H. (1989). Modulation of neurotransmitter release by presynaptic autoreceptors. *Physiol. Rev.*, **69**, 864–989.

SWEADNER, K.J. (1985). Ouabain-evoked norepinephrine release from intact rat sympathetic neurons: evidence for carrier-mediated release. *J. Neurosci.*, **5**, 2397–2406.

WANKE, E., FERRONI, A., MALGAROLI, A., AMBROSINI, A., POZZAN, T. & MELDOLISI, J. (1987). Activation of a muscarinic receptor selectively inhibits a rapidly inactivated Ca^{2+} current in rat sympathetic neurons. *Proc. Natl. Acad. Sci. U.S.A.*, **84**, 4313–4317.

WEINSTOCK, M., THOA, N.B. & KOPIN, I.J. (1978). β-Adrenoceptors modulate noradrenaline release from axonal sprouts in cultured rat superior cervical ganglia. *Eur. J. Pharmacol.*, **47**, 297–302.

WILSON, K.M. & MINNEMAN, K.P. (1991). Synergistic interactions between α_1- and α_2-adrenergic receptors in activating ^{3}H-inositol phosphate formation in primary glial cell cultures. *J. Neurochem.*, **56**, 953–960.

(Received October 21, 1992
Revised May 4, 1993
Accepted May 13, 1993)

Br. J. Pharmacol. (1993), **110**, 289–296

A facilitatory effect of anti-angiotensin drugs on vagal bradycardia in the pithed rat and guinea-pig

M. Rechtman & [1]H. Majewski

Prince Henry's Institute of Medical Research, P.O. Box 152, Clayton, 3168, Victoria, Australia

1 In pithed rats, preganglionic vagal nerve stimulation (at 5 Hz) elicited a bradycardia. This bradycardia was potentiated by the angiotensin converting enzyme inhibitor, captopril (1 mg kg^{-1}, i.v.) by about 40%. Subsequent angiotensin II infusion (0.03 $\mu g\ kg^{-1}\ min^{-1}$) reversed this effect. A similar facilitatory effect was also seen with the angiotensin receptor antagonist, losartan (10 mg kg^{-1}, i.v.). These results suggest a tonic inhibitory effect of endogenous angiotensin II on vagal transmission.

2 The effect of captopril in potentiating vagal bradycardia appears to be at the level of vagal neurones, since the bradycardia elicited by the muscarinic agonist, methacholine was unaffected.

3 After the pithed rats were nephrectomized, captopril had no effect on vagally-induced bradycardia, suggesting that the formation of the endogenous angiotensin II responsible for the effect was dependent on renin release from the kidney.

4 When the sympathetic nerves of the pithed rat were electrically stimulated there was a tachycardia, and this was unaffected by captopril. However, when the sympathetic and vagus nerves were activated concurrently, the resulting tachycardia was inhibited by captopril.

5 In pithed guinea-pigs, captopril also potentiated the bradycardia caused by vagal nerve stimulation. This appears to be a tissue-selective effect since the bronchoconstriction due to the vagal stimulation was not affected by captopril.

6 These results suggest that endogenous angiotensin II can have a tonic inhibitory effect on cardiac vagal transmission. Disruption of this mechanism by anti-angiotensin drugs may attenuate the reflex tachycardia associated with the fall in blood pressure in anti-hypertensive therapy.

Keywords: Acetylcholine release; angiotensin II; angiotensin receptor; bradycardia; heart; vagus

Introduction

In clinical antihypertensive therapy, angiotensin converting enzyme inhibitors decrease blood pressure without causing reflex tachycardia (Johnston *et al.*, 1984; Campbell *et al.*, 1985; Guidicelli *et al.*, 1985). Although some effects on the baroreceptor reflex with converting enzyme inhibitors have been observed in animals (Kirkman & Scott, 1985), many studies show that baroreceptor reflex sensitivity is unaltered in the clinical situation (Guidicelli *et al.*, 1985; Mancia *et al.*, 1988; Kondowe *et al.*, 1988). Thus, alternative explanations for the lack of reflex tachycardia must be sought.

Angiotensin II is known to enhance action-potential evoked sympathetic transmitter release *in vitro* (see Starke, 1977; Zimmerman, 1978) and *in vivo* (Majewski *et al.*, 1984) by activating release-enhancing presynaptic angiotensin II receptors at the sympathetic terminals. However, although converting enzyme inhibitors decrease whole body noradrenaline release in the pithed rat with stimulated sympathetic outflow (Majewski, 1989), they appear to have no effect on the tachycardia exerted by either electrical stimulation of the cardiac sympathetic nerves (Boura *et al.*, 1983a,b; Rose'Meyer *et al.*, 1989) or the tachycardia due to cardiac sympathetic nerve activation by the ganglion stimulant McNeil A343 (Boura *et al.*, 1983a) in this model.

Converting enzyme inhibitors appear to have facilitatory effects on the vagus. For example, the vagal bradycardia induced by the diving reflex in humans with essential hypertension is increased by captopril (Sturani *et al.*, 1982). This may indicate an inhibitory effect of endogenous angiotensin II on vagal transmission. Indeed, there is some evidence to suggest that angiotensin II can inhibit vagal effects in animals by either a central action (Scroop & Lowe, 1969; Lumbers *et al.*, 1979; Lee *et al.*, 1980) or a peripheral effect (Potter, 1982a,b). However, the physiological relevance of these observations remains unclear. Indeed, in anaesthetized ferrets it has been suggested that angiotensin II has no inhibitory effect on vagal transmission (Andrews *et al.*, 1984).

In the present study we set out to examine the effects of the converting enzyme inhibitor captopril and the recently developed AT_1 receptor antagonist, losartan (DuP 753) (Chiu *et al.*, 1989; 1991; Wong *et al.*, 1991) on vagal bradycardia in the pithed rat. Parasympathetic nerve actions can also effect sympathetic tachycardia. When parasympathetic and sympathetic nerves are stimulated simultaneously the resulting response is not accounted for by the simple addition of the effects of the two opposing stimuli and there appears to be an accentuated antagonism whereby vagal stimulation reduces sympathetic effects by a factor greater than the addition of the opposing effects (Levy & Martin, 1981). To some extent this appears to be due to the activation of presynaptic muscarinic receptors on sympathetic nerves by neuronally-released acetylcholine (Loffelholz & Muscholl, 1970; Muscholl, 1980). However, the important consequence is that changes in vagal transmitter release can affect sympathetic function. Therefore the aim of the latter part of the study was to determine whether in the presence of concomitant vagal and sympathetic stimulation there was an effect of captopril on cardiac autonomic nerve responses which was not evident on sympathetic stimulation alone.

Methods

Pithed rat preparation

Male Sprague Dawley rats (250–375 g) were anaesthetized with an intra-peritoneal injection of a combination of sodium amylobarbitone (63 mg kg^{-1}) and sodium methohexitone (25 mg kg^{-1}). The right carotid artery was tied and the trachea cannulated. The animals were then pithed with a

[1] Author for correspondence.

stainless steel rod (Gillespie *et al.*, 1970) and connected to a ventilator and artificially respired (5 ml per stroke, 58 strokes per min). The left carotid artery was cannulated for measuring blood pressure via a transducer connected to a Maclab recording system (ADI, Sydney, Australia). Heart rate was measured by a ratemeter triggered from the blood pressure record. The right and left jugular veins were cannulated for administration of drugs as a bolus or by infusion. Temperature was maintained at 35–37°C. In one group of rats, acute bilateral nephrectomy was performed through a midline incision in the abdomen. After the renal arteries, veins and ureters were ligated close to the hilum, both kidneys were removed and the incision closed. Animals were then pithed and experiments commenced. A period of at least 45 min elapsed after nephrectomy before responses were measured to allow plasma renin activity to decline (de Jonge *et al.*, 1982).

Vagus nerve stimulation Before initiating any stimulation, the pithed rats were pretreated with the β-adrenoceptor antagonist, propranolol (3 mg kg^{-1}, i.v.) and the α_2-adrenoceptor antagonist, idazoxan (3 mg kg^{-1}, i.v.). Bipolar platinum electrodes were placed beneath the right vagus nerve in the cervical region for parasympathetic stimulation (5 Hz, 0.5 ms pulses of square wave 20 V for 15 s) delivered by a Grass stimulator S88. Intervals of 2–5 min were allowed between stimuli. After obtaining two reproducible responses the effect of drugs was investigated.

Dual sympathetic-vagus stimulation In these experiments rats were pretreated with (+)-tubocurarine (0.5 mg kg^{-1}, i.v.) to prevent neuromuscular activity. Electrodes were placed under both the vagus nerve and the cervical sympathetic fibres running alongside it. The stimulation parameters were (5 Hz, 0.5 ms pulses for 15 s, 20 V) giving a resultant tachycardia of approximately 40 beats per min. Ten min between successive stimuli was allowed.

Sympathetic stimulation of the heart Rats were pretreated with (+)-tubocurarine (0.5 mg kg^{-1}, i.v.) and atropine (1 mg kg^{-1}, i.v.) to prevent neuromuscular activity and parasympathetic effects respectively. The vagus and sympathetic nerves were placed on platinum electrodes and stimulated electrically (0.5 Hz, 0.5 ms, 20 V for 15 s), with 5 min between stimuli.

Pithed guinea-pig preparation

Male Dunkin-Hartley guinea-pigs (430–610 g) were anaesthetized with halothane (4%) in nitrous oxide and oxygen (1 l min^{-1}, each). Blood vessels, right vagus nerve and trachea were isolated and cannulated as appropriate as for rats. Pithing with a steel rod was performed through a hole made with a punch in the sagittal fissure between the orbits (Rechtman *et al.*, 1990) and the animals immediately ventilated mechanically (10 ml per kg, 60 strokes per min). Insufflation pressure was recorded via a pressure transducer connected to a side arm of the inflow circuit and this was used as an index of bronchial resistance. The right vagus nerve in the cervical region was stimulated electrically (1–3 Hz, 0.5 ms pulses at 20 V for 15 s). The parameters used caused both changes in heart rate and bronchial tone.

Drugs

(Asn^1,Val^8) Angiotensin II acetate and methacholine (acetyl beta methacholine chloride) were obtained from Sigma, St Louis, U.S.A.; atropine sulphate from Abbott Laboratories, Sydney, Australia; methohexitone sodium and sodium isoamylethylbarbiturate (amylobarbitone) from Eli Lilly, Sydney, Australia; (+)-tubocurarine chloride from Wellcome, Sydney, Australia. Captopril was a gift from Squibb, Melbourne, Australia; (±)-propranolol hydrochloride was a gift from ICI, Melbourne, Australia; idazoxan was a gift from Reckitt and Colman, Hull, U.K. and losartan was a gift from DuPont Merck Pharmaceutical Co, Wilmington, U.S.A. All doses are expressed as mass of the salt used.

Vehicle experiments were done with appropriate volumes/infusions of saline (0.9% sodium chloride).

Calculation of results and statistics

In all experimental groups of rats, repetitive stimulations were carried out and all results were expressed as a percentage of the mean of the first two reproducible stimulations which were carried out in the absence of drugs. Drug effects were compared with vehicle experiments and significance assessed by two way analysis of variance. In some cases Student's *t* tests were used where appropriate. When successive responses were compared back to a pre-drug value Dunnett's test was used.

Results

Effects of captopril and angiotensin infusion on heart rate responses to vagus nerve stimulation

In pithed rats treated with propranolol (3 mg kg^{-1}) and idazoxan (3 mg kg^{-1}), vagal stimulation (5 Hz, 0.5 ms 20 V) of 15 s duration caused bradycardia of about 46 beats min^{-1} (Table 1). After captopril (1 mg kg^{-1}, i.v.), there was a gradual enhancement of the vagally induced bradycardia over the next four stimuli (Figure 1a). When angiotensin II (0.03 μg kg^{-1} min^{-1}, i.v.) was infused over the subsequent four stimuli, the enhanced bradycardia to vagal stimulation produced by captopril was decreased (Figure 1a). However, it should be noted that the fourth vagal response after angiotensin infusion commenced did not differ significantly from the pre-angiotensin II infusion value (see Figure 1a). When the angiotensin II infusion was stopped and four more stimuli applied, there was some recovery of the bradycardia to pre-angiotensin levels. The basal heart rate and basal mean arterial pressure at the commencement of the experiments is shown in Table 1. There was no statistically significant changes in basal heart rate by drugs when compared to control (Figure 1b). Captopril decreased mean arterial pressure and angiotensin II infusion enhanced mean arterial pressure (Figure 1c).

In another series of experiments, angiotensin II was infused in animals in the absence of captopril (Figure 2a). In this case, the angiotensin II (0.03 μg kg^{-1} min^{-1}, i.v.) had no effect on vagally induced bradycardia (Figure 2a) or basal heart rate (Figure 2b) but it did increase mean arterial pressure which returned to basal levels when the infusion ceased (Figure 2c). The absolute values of these parameters at the beginning of the experiment are given in Table 1.

Effect of captopril and angiotensin infusion on heart rate responses in nephrectomized pithed rats

In nephrectomized pithed rats treated with propranolol (3 mg kg^{-1}) and idazoxan (3 mg kg^{-1}), captopril had no significant effect on vagally-induced bradycardia (Figure 3a), nor did it affect basal heart rate (Figure 3b). Whilst mean arterial pressure was slightly reduced (Figure 3c), the hypotensive effect of captopril was much less than that in pithed rats with intact kidneys (cf. Figure 1c). The basal mean blood pressure was significantly lower in nephrectomized rats than in rats with intact kidneys (Table 1) but basal heart rate was not significantly different (Table 1).

Effect of captopril and subsequent AII infusion on chronotropic responses to methacholine

In pithed rats treated with propranolol (3 mg kg^{-1}) and

Table 1 Cardiovascular parameters of rats and guinea-pigs in different experimental groups

	Initial heart rate response (beats min^{-1})	*Pre-drug basal rate* (beats min^{-1})	*Pre-drug mean pressure* (mmHg)	*Basal insufflation pressure* (mmHg)
Pithed rats: vagal stimulation				
Vehicle ($n = 5$)	46 ± 8	316 ± 12	78.6 ± 5	
Captopril/AII ($n = 8$)	41 ± 6	307 ± 7	70.1 ± 4	
Saline/AII ($n = 8$)	36 ± 4	339 ± 8	64.0 ± 6	
Vehicle ($n = 7$)	45 ± 6	335 ± 8	66.8 ± 4	
Losartan ($n = 10$)	39 ± 4	326 ± 10	62.5 ± 5	
Nephrectomized and pithed rats: vagal stimulation				
Vehicle ($n = 8$)	46 ± 5	321 ± 10	52.8 ± 6	
Captopril ($n = 7$)	32 ± 3	340 ± 17	48.3 ± 5	
Pithed rats: methacholine administration				
Vehicle ($n = 6$)	57 ± 12	311 ± 14	72.0 ± 2	
Captopril/AII ($n = 10$)	43 ± 5	317 ± 10	76.5 ± 3	
Pithed rats: sympathetic alone stimulation				
Captopril ($n = 6$)	40 ± 6	338 ± 10	62.1 ± 5	
Pithed rats: vago-sympathetic stimulation				
Vehicle ($n = 6$)	35 ± 4	336 ± 25	63.2 ± 1	
Captopril ($n = 8$)	37 ± 4	343 ± 6	57.8 ± 4	
Pithed guinea-pigs: vagal stimulation				
Vehicle ($n = 4$)	36.3 ± 14	179.4 ± 6	34.4 ± 1	16.1 ± 1
Captopril ($n = 5$)	52.2 ± 7	186.5 ± 12	34.4 ± 4	21.9 ± 4

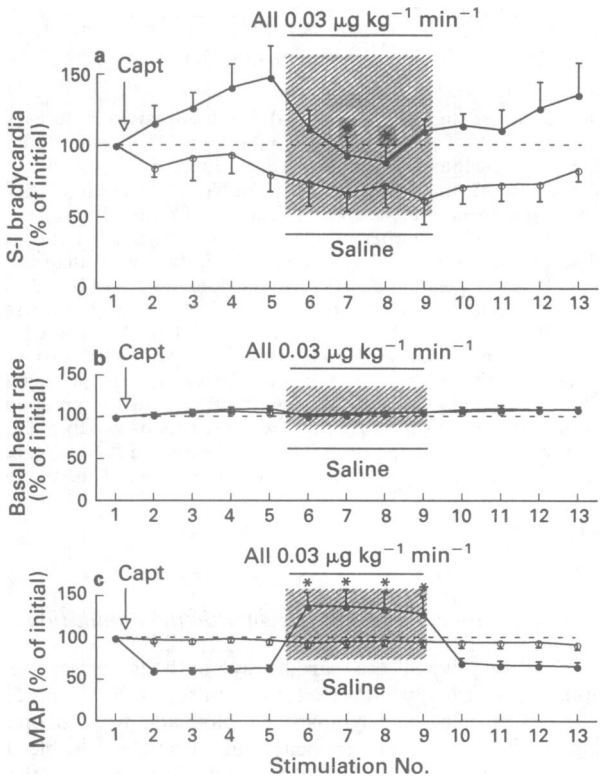

Figure 1 Effect of captopril on bradycardia induced by vagal nerve stimulation in pithed rats. There were 13 consecutive vagal stimulations (each 5 Hz for 15 s). All results are expressed as a percentage of the initial values at stimulation No. 1. Absolute values for all initial parameters are shown in Table 1. Captopril (Capt, 1 mg kg^{-1}, i.v.) given immediately after stimulation 1, significantly increased stimulation-induced bradycardia ($P < 0.05$, two way analysis of variance). Subsequent application of angiotensin II (AII, 0.03 μg kg^{-1} min^{-1}) significantly reduced the S-I bradycardia compared to the pre-angiotensin II value (*$P < 0.05$, Dunnett's test). None of the drugs affected basal heart rate ($P > 0.05$, two way analysis of variance or Dunnett's test). However, captopril significantly lowered mean arterial pressure (MAP) ($P < 0.05$, two way analysis of variance), and angiotensin II significantly increased mean arterial pressure compared to the pre-angiotensin II value (*$P < 0.05$, Dunnett's test). $n = 8$ for captopril (●), $n = 5$ for vehicle (○). In vehicle experiments neither captopril nor angiotensin II was administered.

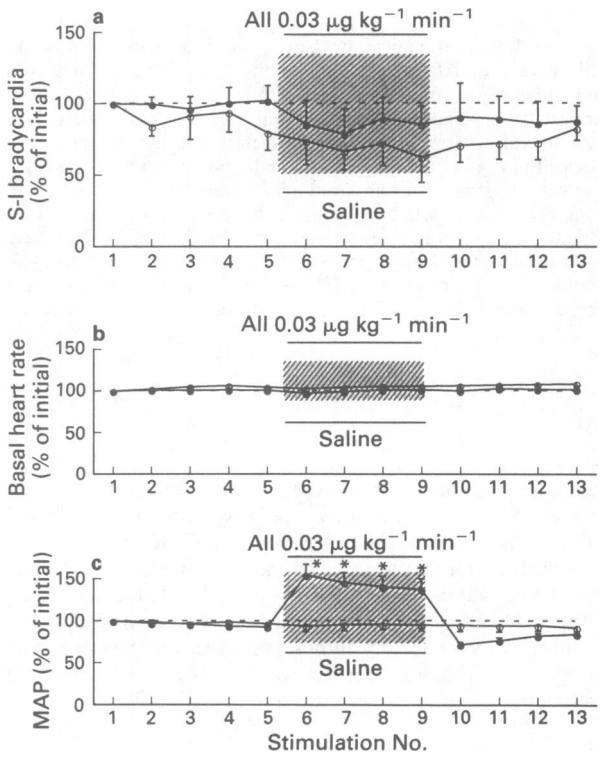

Figure 2 Effect of angiotensin II (AII) on bradycardia induced by vagal nerve stimulation in pithed rats. There were 13 consecutive vagal stimulations (each 5 Hz for 15 s). All results are expressed as a percentage of the initial values at stimulation No. 1. Absolute values for all initial parameters are shown in Table 1. Subsequent application of angiotensin II (AII, 0.03 μg kg^{-1} min^{-1}) did not significantly affect the stimulation-induced (S-I) bradycardia compared to vehicle (*$P < 0.05$, two way analysis of variance and Dunnett's test). Basal heart rate was unaltered by angiotensin II ($P > 0.05$, two way analysis of variance and Dunnett's test). However, angiotensin II significantly elevated mean arterial pressure (MAP) (*$P < 0.05$, two way analysis of variance and Dunnett's test). $n = 8$ for angiotensin II series (●), $n = 5$ for vehicle (○). In vehicle experiments no angiotensin II was administered.

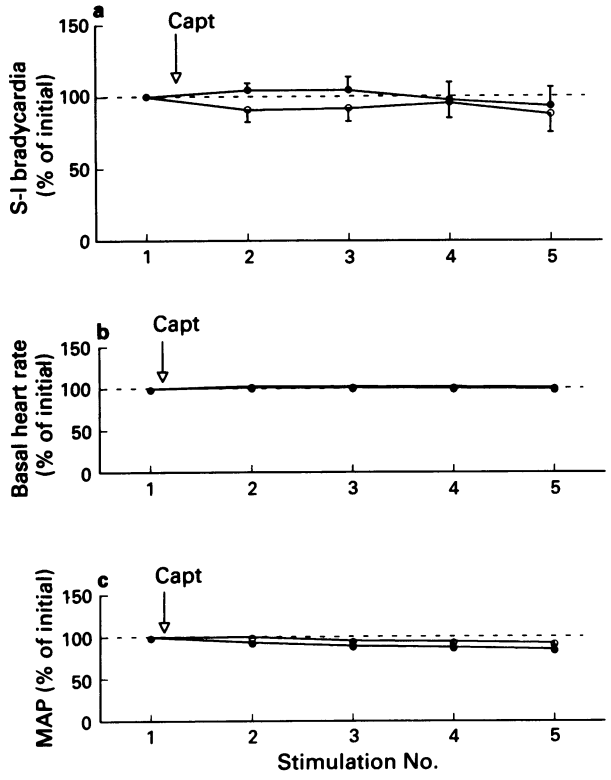

Figure 3 Effect of captopril (Capt), on bradycardia induced by vagal nerve stimulation in nephrectomized pithed rats. There were 5 consecutive vagal stimulations (each 5 Hz for 15 s). All results are expressed as a percentage of the initial values at stimulation No. 1. Absolute values for all initial parameters are shown in Table 1. Captopril (1 mg kg^{-1}, i.v.) given immediately after stimulation 1 had no effect on stimulation-induced (S-I) bradycardia ($P > 0.05$, two way analysis of variance). Captopril did not affect basal heart rate ($P > 0.05$, two way analysis of variance), but caused a slight reduction in mean arterial pressure (MAP) ($P < 0.05$, two way analysis of variance). $n = 7$ for captopril (●), $n = 8$ for vehilce (○). In vehicle experiments no captopril was administered.

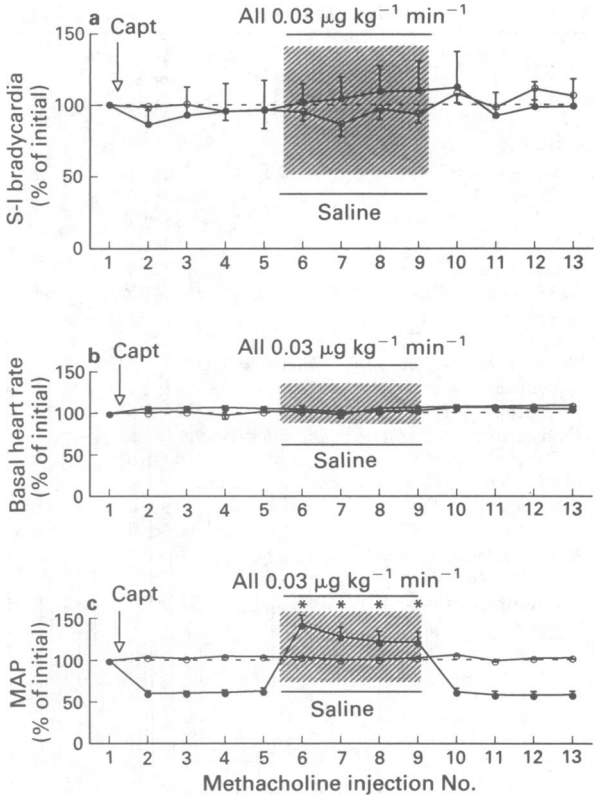

Figure 4 Effect of captopril (Capt) on bradycardia induced by methacholine (3–10 μg kg^{-1}, i.v.) in pithed rats. There were 13 consecutive methacholine injections. All results are expressed as a percentage of the initial values at injection No. 1. Absolute values for all initial parameters are shown in Table 1. Captopril (1 mg kg^{-1}, i.v.) given immediately after injection 1 had no significant effect on methacholine-induced bradycardia ($P < 0.05$, two way analysis of variance). Subsequent application of angiotensin II (AII, 0.03 μg kg^{-1} min^{-1}) had no effect on methacholine-induced bradycardia compared to the pre-angiotensin II value (*$P > 0.05$, Dunnett's test). None of the drugs affected basal heart rate ($P > 0.05$, two way analysis of variance or Dunnett's test). However, captopril significantly lowered and angiotensin II significantly elevated mean arterial pressure respectively (*$P < 0.05$, two way analysis of variance, Dunnett's test). $n = 10$ for captopril (●), $n = 6$ for vehicle (○). In vehicle experiments neither captopril nor angiotensin II was administered.

idazoxan (3 mg kg^{-1}) bradycardia was induced by methacholine. The dose of intravenously administered methacholine was adjusted in each experiment to give an initial bradycardia of comparable magnitude to electrical stimulation of the vagus (range 3–10 μg kg^{-1}) (Table 1). Neither captopril (1 mg kg^{-1}, i.v.) or angiotensin II infusion (0.03 μg kg^{-1} min^{-1}, i.v.) had any significant effect on the bradycardia caused by methacholine (Figure 4a). The initial basal cardiovascular parameters are shown in Table 1.

Effect of losartan and subsequent AII infusion on chronotropic responses to vagus nerve stimulation

In pithed rats treated with propranolol (3 mg kg^{-1}) and idazoxan (3 mg kg^{-1}), the angiotensin receptor blocking drug, losartan (10 mg kg^{-1}, i.v.) significantly enhanced bradycardic responses to vagal nerve stimulation (Figure 5a) over eight successive vagal stimulations. Angiotensin II infusion (0.03 μg kg^{-1} min^{-1}, i.v.) had no significant effect on these enhanced responses. Losartan had a slight enhancing effect on basal heart rate (Figure 5b) but markedly reduced mean arterial pressure (Figure 5c). The pressor effect of angiotensin II was attenuated by losartan ($P < 0.05$, two way analysis of variance; compare Figures 2c and 5c). The initial basal cardiovascular parameters are shown in Table 1.

Effect of captopril on cardiac sympathetic stimulation

In pithed rats when the cardiac sympathetic nerves were stimulated electrically (0.5 Hz, 0.5 ms pulses at 20 V for 15 s) in the presence of parasympathetic blockade with atropine (1 mg kg^{-1}), an increase in heart rate occurred (Table 1). Captopril (1 mg kg^{-1}, i.v.) had no significant effect on these responses (Figure 6a). Propranolol (1 mg kg^{-1}, i.v.) markedly inhibited tachycardia to electrical stimulation confirming that the nerves being stimulated were of sympathetic origin (Figure 6a). The initial basal cardiovascular parameters are shown in Table 1.

Effect of combined vagus and sympathetic nerve stimulation on heart rate and the effect of captopril

In pithed rats without autonomic antagonist pretreatment, combined sympathetic and parasympathetic nerve stimulation (5 Hz, 0.5 ms pulses at 20 V for 15 s) increased heart rate (Table 1). This tachycardia was reduced by captopril (1 mg kg^{-1}) (Figure 7a). Addition of atropine (1 mg kg^{-1}, i.v.) at the end of the experiment increased heart rate responses to electrical stimulation indicating that there was an

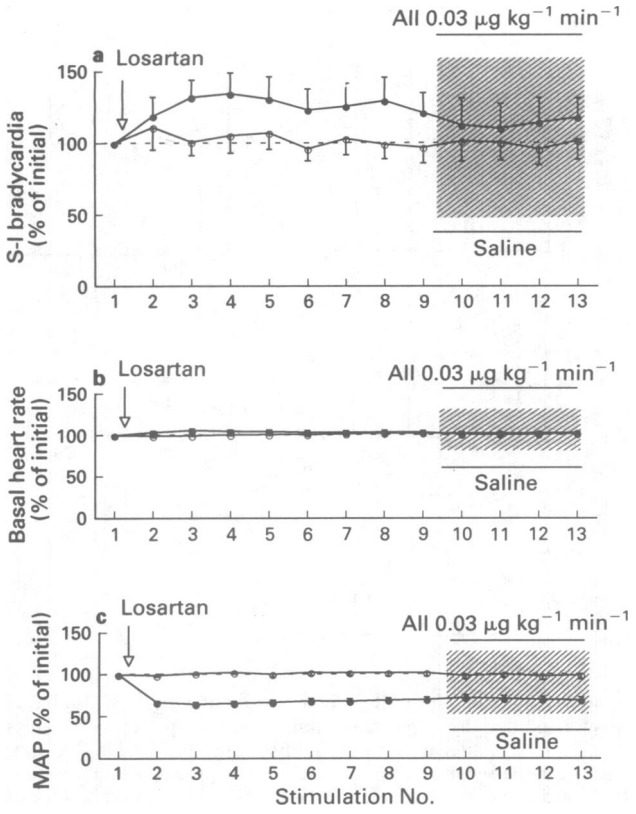

Figure 5 Effect of losartan on bradycardia induced by vagal nerve stimulation in pithed rats. There were 13 consecutive vagal stimulations (each 5 Hz for 15 s). All results are expressed as a percentage of the initial values at stimulation No. 1. Absolute values for all initial parameters are shown in Table 1. Losartan (10 mg kg^{-1}, i.v.) given after stimulation 1 significantly increased stimulation-induced bradycardia ($P<0.05$, two way analysis of variance). Subsequent application of angiotensin II (AII, 0.03 μg kg^{-1} min^{-1}) had no significant effect on the S-I bradycardia compared to the pre-angiotensin II value (*$P>0.05$, Dunnett's test). Losartan slightly but significantly enhanced basal heart rate ($P<0.05$, two way analysis of variance). but angiotensin II had no effect ($P>0.05$, Dunnett's test). Losartan significantly lowered mean arterial pressure ($P<0.05$, two way analysis of variance), but subsequent angiotensin infusion had no significant effect on mean arterial pressure (*$P>0.05$, Dunnett's test). $n=10$ for losartan (●), $n=7$ for vehicle (○). In vehicle experiments neither losartan nor angiotensin II was administered.

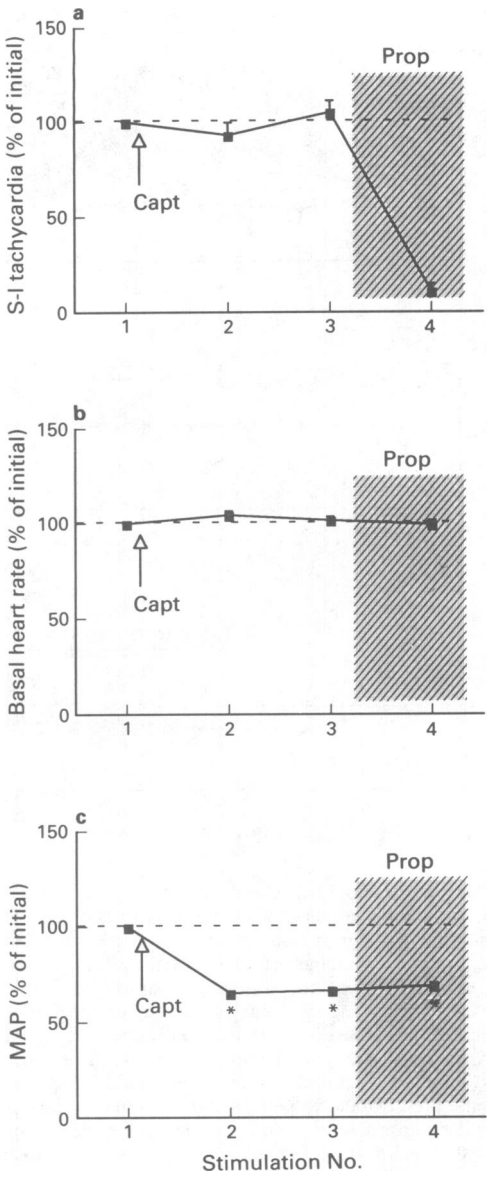

Figure 6 Effect of captopril (Capt) on tachycardia induced by sympathetic nerve stimulation in pithed rats. There were 4 consecutive sympathetic stimulations (each 5 Hz for 15 s). All results are expressed as a percentage of the initial values at stimulation No. 1. Absolute values for all initial parameters are shown in Table 1. Captopril (1 mg kg^{-1}, i.v.) given immediately after stimulation 1 had no significant effect on stimulation-induced (S-I) tachycardia ($P>0.05$, Dunnett's test). Subsequent application of propranolol (Prop, 1 mg kg^{-1}) after stimulation 3 significantly reduced the S-I tachycardia compared to the pre-propranolol value (*$P<0.05$, unpaired Student's t test). None of the drugs affected basal heart rate ($P>0.05$, Dunnett's test or unpaired Student's t test). However, captopril significantly lowered mean arterial pressure (MAP) ($P<0.05$, Dunnett's test). $n=6$.

underlying vagal tone (Figure 7a). The initial basal cardiovascular parameters are shown in Table 1.

Effect of captopril on vagally induced bradycardia and bronchoconstriction in pithed guinea pigs

In guinea-pigs treated with propranolol (3 mg kg^{-1}, i.v.) and idazoxan (3 mg kg^{-1}, i.v.), electrical stimulation of the vagus nerve (1–3 Hz, 20 V) caused an increase of airway insufflation pressure of 8.6 ± 1 mmHg ($n=5$) and a bradycardia (see Table 1). The bradycardia induced by vagal stimulation was potentiated by captopril (1 mg kg^{-1}, i.v.) (Figure 8a). In contrast, captopril did not affect the change in insufflation pressure induced by vagal nerve stimulation (Figure 8b). Basal heart rate (Figure 8c) and basal insufflation pressure (Figure 8d) did not change after captopril. Captopril significantly lowered mean arterial pressure (Figure 8e). The initial basal cardiovascular and pulmonary parameters are shown in Table 1.

Discussion

The pithed rat has a high circulating renin activity (de Jonge *et al.*, 1982), presumably because of the low blood pressure inducing renin release from the kidney. In the present study, the angiotensin converting enzyme inhibitor, captopril, had a marked hypotensive action in pithed rats which was not seen in pithed rats which had been nephrectomized. This is similar to previous studies (Boura *et al.*, 1983b; Majewski, 1989) and indicates that endogenous angiotensin II, which is dependent on renin release from the kidney, has appreciable effects in this model.

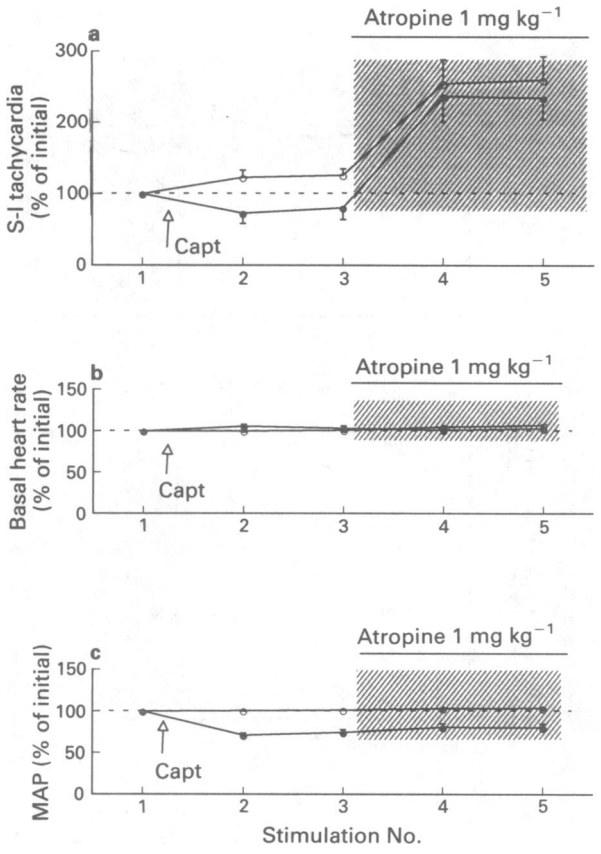

Figure 7 Effect of captopril (Capt) on tachycardia induced by combined sympathetic/vagal nerve stimulation in pithed rats. There were 5 consecutive vagal stimulations (each 5 Hz for 15 s). All results are expressed as a percentage of the initial values at stimulation No. 1. Absolute values for all initial parameters are shown in Table 1. Captopril (1 mg kg^{-1}, i.v.) given immediately after stimulation 1 significantly decreased stimulation-induced (S-I) tachycardia ($P<0.05$, two way analysis of variance). Subsequent application of atropine (1 mg kg^{-1}) significantly increased the S-I tachycardia compared to the pre-atropine value ($P<0.05$, Dunnett's test) in both the vehicle and captopril series. None of the drugs affected basal heart rate ($P>0.05$, two way analysis of variance or Dunnett's test). However, captopril significantly lowered mean arterial pressure (MAP) ($P<0.05$, two way analysis of variance). $n=8$ for captopril (●), $n=6$ for vehicle (○). In vehicle experiments atropine but not captopril was administered.

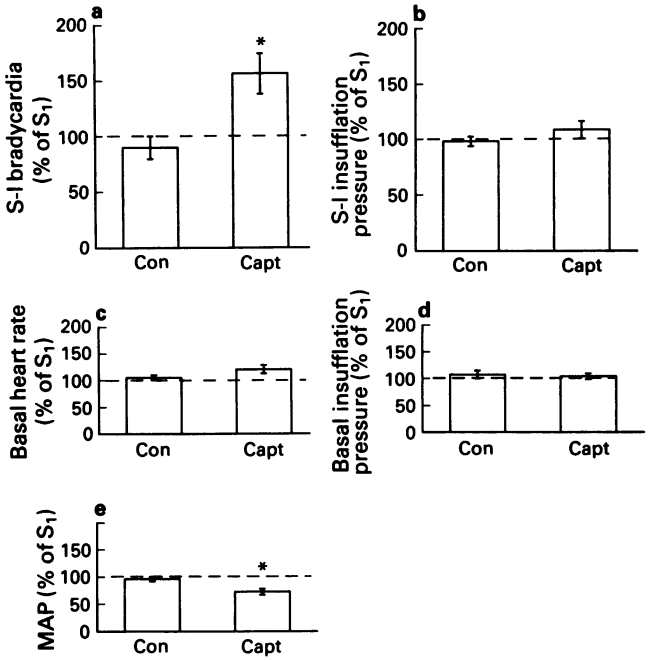

Figure 8 Effect of captopril on bradycardia and airways insufflation pressure induced by vagal nerve stimulation in pithed guinea-pigs. There were 2 consecutive vagal stimulations (each 5 Hz for 15 s). Results for the second stimulation (S_2) are expressed as a percentage of the initial values of stimulation No. 1 (S_1). Absolute values for all initial parameters are shown in Table 1. Captopril (Capt, 1 mg kg^{-1}, i.v.) given immediately after stimulation 1 significantly increased stimulation-induced (S-I) bradycardia ($P<0.05$, unpaired Student's t test), but did not affect basal heart rate ($P>0.05$, unpaired Student's t test). However, captopril significantly lowered mean arterial pressure (MAP) ($P<0.05$, unpaired Student's t test). Captopril had no significant effect on either basal or stimulation-induced airways insufflation pressure ($P>0.05$, unpaired Student's t test), $n=5$ for captopril experiments, $n=4$ for control (Con) experiments.

In the present study in the pithed rat, the vagus nerve was electrically stimulated at 5 Hz for 15 s to elicit a submaximal bradycardia which was blocked by atropine, indicating that it was mediated by acetycholine activation of muscarinic receptors. In these experiments propranolol and idazoxan were given to block β-adrenoceptors and α_2-adrenoceptors respectively. Captopril significantly enhanced the bradycardia induced by vagal nerve stimulation. The most likely explanation for this finding is that there was a reduction in endogenous angiotensin II formation after captopril and this removed an inhibitory effect of endogenous angiotensin on vagal transmission. Indeed, subsequent infusion of angiotensin II reversed the inhibitory effect of captopril, although this reversal seemed to decline with time. In the absence of captopril, angiotensin II infusion did not inhibit vagal bradycardia. This probably indicates that endogenous angiotensin II already maximally activated the angiotensin II receptors in the pithed rat as has been previously suggested for angiotensin effects on sympathetic transmission in this model (Majewski, 1989).

Previously, Potter (1982a,b) had shown that a bolus injection of angiotensin II inhibits both the effects of vagal nerve stimulation in the heart in the dog and in guinea-pig isolated atria, although the physiological relevance of this observation was unclear. Since the pithed rat is a high renin model, the present result with captopril suggests that endogenous angiotensin II also has a physiologically significant inhibitory effect on vagal transmission. Although inhibition of converting enzyme by captopril can affect the levels of the many peptides (e.g. bradykinin, enkephalins, substance P) which may be metabolized by this system (Soffer, 1976; Erdos *et al.*, 1978; Subissi *et al.*, 1990), this is unlikely to explain the enhanced vagal bradycardia after captopril, since the enhancement was reversed by subsequent angiotensin II infusion. Furthermore, the angiotensin II receptor (AT_1) blocking drug, losartan (DuP 753) (Chui *et al.*, 1989; Wong *et al.*, 1991) also enhanced vagally induced bradycardia. Losartan is thought to be metabolized to EXP3174 which is also a potent angiotensin II antagonist (Wong *et al.*, 1990; Christ *et al.*, 1990). However in the present study the facilitation of vagal bradycardia was evident as early as 5 min after losartan administration and did not increase over the subsequent 30 min when it may be expected that EXP3174 would be formed. Angiotensin II infusion did not significantly inhibit vagal bradycardia after losartan which is in contrast to its inhibitory effects after captopril. This is probably an indication that angiotensin II was not able to overcome the receptor blockade produced by losartan, which contrasts with the captopril situation where the receptor remains free for activation.

By stimulating the cervical vagal trunk both pre and postganglionic nerves are activated. Thus there are many possible sites of endogenous angiotensin II action for inhibiting vagal

bradycardia. However, the effect is not postjunctional at the myocardium since the bradycardia evoked by the muscarinic agonist methacholine, was not affected by captopril or subsequent angiotensin II infusion after captopril administration. Similarly, Potter (1982a,b) found that exogenous angiotensin II did not inhibit the bradycardia caused by acetylcholine in guinea-pig atria. This implies that the effect must be neuronal or at the ganglia.

Classically, angiotensin II formation depends on renin release from the kidney, but a local renin angiotensin generating system has been described in some tissues including the heart and vasculature (Dzau, 1988; Lindpaintner & Ganten, 1991). The source of the endogenous angiotensin II which inhibits vagal transmission in the present study (as evidenced by the facilitatory effect of captopril) probably involves kidney release of renin, since in the acutely nephrectomized pithed rat, captopril did not enhance vagal bradycardia. It should be noted however, that in contrast to expectations, the absolute magnitude of the vagal bradycardia in nephrectomized animals was not significantly greater than in non-nephrectomized animals. This may be because of a marked 'between animal' variability in the absolute responses or may indicate that other factors are involved after nephrectomy.

There are many reports indicating a facilitatory action of angiotensin II on peripheral noradrenergic transmission (see Rand *et al.*, 1990). In the present study, captopril had no effect on sympathetic stimulation of the heart in the pithed rat even though facilitatory angiotensin II receptors on sympathetic terminals have been demonstrated in rat atria (see Mian *et al.*, 1989) and captopril decreased whole body noradrenaline release in the pithed rat with stimulated sympathetic outflow (Majewski, 1989). In other studies in the pithed rat, cardiac sympathetic nerve stimulation was also not affected by captopril (Hatton & Clough, 1982; Boura *et al.*, 1983a,b). However, it is likely that in the physiological situation both the vagus and the sympathetic nerves are activated at the same time. When we stimulated sympathetic and parasympathetic nerves to the heart simultaneously at a frequency (5 Hz) which caused an overall tachycardia, this was potentiated by atropine showing that there was an underlying vagal tone. In this situation of dual autonomic activation, captopril inhibited the tachycardia. This, we propose, is due to the enhancement of the vagal effect and indicates that the vagal potentiating effect of captopril can lead to changes in net autonomic influences in the heart.

It is possible that the facilitatory effect on vagal transmission by anti-angiotensin drugs applies to branches of the vagus nerve in regions other than the heart. Indeed, Potter (1982b) demonstrated that angiotensin II inhibited vagal responses in the intact rabbit stomach. In the present study, we examined the effect of captopril on vagal transmission to the lung. In our rat model, vagal stimulation did not significantly alter pulmonary insufflation pressure. We therefore repeated the experiment in the guinea-pig where insufflation pressure is increased by vagal stimulation (Grundström & Andersson, 1985). In pithed guinea-pigs, captopril potentiated bradycardic responses to vagal nerve stimulation as in the rat. However, the lung insufflation pressure increases which were simultaneously measured, were not altered. Thus, as far as endogenous angiotensin effects are concerned, the vagal transmission to the lung is not functionally altered. The side-effect profile of converting enzyme inhibitors also agree with this finding. Although, cough is a commonly reported side effect with converting enzyme inhibitors (Sebastian *et al.*, 1991), there is little evidence that bronchoconstriction is a problem with angiotensin converting enzyme inhibitors in clinical practice (Edwards & Padfield, 1985; Weber, 1988; Boulet *et al.*, 1989).

The results of the present study suggest that endogenous angiotensin II has an inhibitory effect on vagal transmission in both the rat and guinea-pig. This agrees with human data on the potentiating effects of captopril on bradycardia induced by the diving reflex (Sturani *et al.*, 1982). In the clinical situation, angiotensin converting enzyme inhibitors cause little reflex tachycardia (see Introduction) and the results of the present study offer one explanation of this phenomenon.

This work was supported by a grant from the National Health and Medical Research Council of Australia.

References

ANDREWS, P.L., DUTIA, M.B. & HARRIS, P.J. (1984). Angiotensin II does not inhibit vagally-induced bradycardia or gastric contractions in the anaesthetized ferret. *Br. J. Pharmacol.*, **82**, 833–837.

BOULET, L.P., MILOT, J., LAMPRON, N. & LACOURCIERE, Y. (1989). Pulmonary function and airway responsiveness during long-term therapy with captopril. *J. Am. Med. Assoc.*, **261**, 413–416.

BOURA, A.L.A., HUI, S.-C.G., ISHAC, E.J.N., RECHTMAN, M.P. & WALTERS, W.A.W. (1983a). Attenuation by captopril of pressor responses to peripheral sympathetic nerve stimulation in rats is abolished after bilateral nephrectomy and during mineralocorticoid hypertension. *Clin. Exp. Pharmacol. Physiol.*, **10**, 283–287.

BOURA, A.L.A., RECHTMAN, M.P. & WALTERS, W.A.W. (1983b). Attenuation by captopril of pressor responses to sympathetic stimulii: effects of procedures reducing activity of the renin-angiotensin system. *J. Auton. Pharmacol.*, **3**, 203–211.

CAMPBELL, B.C., STURANI, A. & REID, J.L. (1985). Evidence of parasympathetic activity of the angiotensin converting enzyme inhibitor, captopril, in normotensive man. *Clin. Sci.*, **68**, 49–56.

CHIU, A.T., HERBLIN, W.F., MCCALL, D.E., ARDECKY, R.J., CARINI, D.J., DUNCIA, J.V., PEASE, L.J., WONG, P.C., WEXLER, R.R., JOHNSON, A.L. & TIMMERMANS, P.B.M.W.M. (1989). Identification of angiotensin II receptor subtypes. *Biochem. Biophys. Res. Commun.*, **165**, 196–203.

CHIU, A.T., MCCALL, D.E., PRICE, W.A.Jr., WONG, P.C., CARINI, D.J., DUNCIA, J.V., WEXLER, R.R., YOO, S.E., JOHNSON, A.L. & TIMMERMANS, P.B.M.W.M. (1991). In vitro pharmacology of DuP 753. *Am. J. Hypertens.*, **4**, 282 S–287 S.

CHRIST, D., KILKSON, T., WONG, N. & LAM, G. (1990). Formation and disposition of EXP3174, a pharmacologically active metabolite of the novel angiotensin II receptor antagonist DuP 753. Abstract of the *3rd North American Meeting of the International Society for the Study of Xenobiotics.*

DE JONGE, A., KNAPE, J.TH.A., VAN MEEL, J.C.A., KALKMAN, H.O., WILFFERT, B., THOOLEN, M.J.M.C., TIMMERMANS, P.B.M.W.M. & VAN ZWIETEN, P.A. (1982). Effect of converting enzyme inhibition and angiotensin receptor blockade on the vasoconstriction mediated by α_1 and α_2-adrenoceptor stimulation in pithed normotensive rats. *Naunyn-Schmied. Arch. Pharmacol.*, **321**, 309–313.

DZAU, V.J. (1988). Vascular renin-angiotensin system in hypertension. New insights into the mechanisms of action of angiotensin converting enzyme inhibitors. *Am. J. Med.*, **84** (Suppl. 4A) 4–8.

EDWARDS, C.R.W. & PADFIELD, P.L. (1985). Angiotensin-converting enzyme inhibitors: past, present, and bright future. *Lancet*, **i**, 30–34.

ERDOS, E.G., JOHNSON, A.R. & BOYDEN, N.T. (1978). Hydrolysis of enkephalin by cultured human endothelial cells and by purified peptidyl dipeptidase. *Biochem. Pharmacol.*, **27**, 843–848.

GILLESPIE, J.S., MACLAREN, A. & POLLOCK, D. (1970). A method of stimulating different segments of the autonomic outflow from the spinal column to various organs in the pithed cat and rat. *Br. J. Pharmacol.*, **40**, 257–267.

GRUNSTRÖM, N. & ANDERSON, R.G.G. (1985). In vivo demonstration of alpha-2-adrenoceptor-mediated inhibition of the excitatory non-cholinergic neurotransmission in guinea pig airways. *Naunyn-Schmied. Arch. Pharmacol.*, **328**, 236–240.

GUIDICELLI, J.F., BERDEAUX, A., EDOUARD, A., RICHER, C. & JACOLOT, D. (1985). The effect of enalapril on baroreceptor mediated reflex function in normotensive subjects. *Br. J. Clin. Pharmacol.*, **20**, 211–218.

HATTON, R. & CLOUGH, D.P. (1982). Captopril interferes with neurogenic vasoconstriction in the pithed rat by angiotensin-dependent mechanisms. *J. Cardiovasc. Pharmacol.*, **4**, 116–123.

JOHNSTON, C.I., ARNOLD, A.L. & HIWATARI, M. (1984). Angiotensin-converting enzyme inhibitors in the treatment of hypertension. *Drugs*, **27**, 271–277.

KIRKMAN, E. & SCOTT, E.M. (1985). The effect of captopril on the baroreflex in the cat. *Br. J. Pharmacol.*, **84**, 21P.

KONDOWE, G.B., DEERING, A.H., RIDDELL, J.G., JOHNSTON, G.D. & HARRON, D.W.G. (1988). The effect of acute and chronic captopril therapy on baroreflex function in man. *Br. J. Clin. Pharmacol.*, **25**, 315–321.

LEE, W.B., ISMAY, M.J. & LUMBERS, E.R. (1980). Mechanisms by which angiotensin II affects the heart rate of the conscious sheep. *Circ. Res.*, **47**, 286–292.

LEVY, M.N. & MARTIN, P.J. (1981). Neural regulation of the heart beat. *Annu. Rev. Physiol.*, **43**, 443–453.

LINDPAINTNER, K. & GANTEN, D. (1991). Tissue renin-angiotensin systems and their modulation: the heart as a paradigm for new aspects of converting enzyme inhibition. *Cardiology*, **79** (Suppl. 1), 32–44.

LOFFELHOLZ, K. & MUSCHOLL, E. (1970). Inhibition by parasympathetic nerve stimulation of the release of the adrenergic transmitter. *Naunyn-Schmied. Arch. Pharmacol.*, **267**, 181–184.

LUMBERS, E.R., MCCLOSKEY, D.I. & POTTER, E.K. (1979). Inhibition by angiotensin II of baroreceptor-evoked activity in cardiac vagal efferent nerves in the dog. *J. Physiol.*, **294**, 69–80.

MAJEWSKI, H. (1989). Angiotensin II and noradrenergic transmission in the pithed rat. *J. Cardiovasc. Pharmacol.*, **14**, 622–630.

MAJEWSKI, H., HEDLER, L., SCHURR, L. & STARKE, K. (1984). Modulation of noradrenaline release in the pithed rabbit: a role for angiotensin II. *J. Cardiovasc. Pharmacol.*, **6**, 888–896.

MANCIA, G., GIANNATTASIO, C., GRASSI, G., MORGANTI, A. & ZANCHETTI, A. (1988). Reflex control of circulation and angiotensin converting enzyme inhibition in man. *J. Hypertension*, **6**, (Suppl. 3), S45–S49.

MIAN, M.A., MAJEWSKI, H. & RAND, M.J. (1989). Facilitation of noradrenaline release by isoprenaline in rat isolated atria does not involve angiotensin II formation. *Clin. Exp. Pharmacol. Physiol.*, **16**, 905–911.

MUSCHOLL, E. (1980). Peripheral muscarinic control of norepinephrine release in the cardiovascular system. *Am. J. Physiol.*, **239**, H713–H720.

POTTER, E.K. (1982a). Angiotensin inhibits action of vagus nerve at the heart. *Br. J. Pharmacol.*, **75**, 9–11.

POTTER, E.K. (1982b). Peripheral inhibition of the parasympathetic nervous system by angiotensin. *Clin. Exp. Pharmacol. Physiol.*, **1**, Suppl. 7, 51–55.

RAND, M.J., MAJEWSKI, H. & STORY, D.F. (1990). Modulation of neuroeffector transmission. In *Cardiovascular Pharmacology*, 3rd edition, ed. Antonaccio, M. pp. 229–292. New York: Raven Press.

RECHTMAN, M.P., BOURA, A.L.A., KING, R.G., OLLEY, J.E. & SCHILLER, P.W. (1990). Effects of morphine, H-Tyr-D-Arg-Phe-Lys-NH_2(DALDA) and B-HT920 on cholinergic nerve mediated bronchoconstriction in pithed guinea pigs. *Br. J. Pharmacol.*, **101**, 269–272.

ROSE'MEYER, C.M., RECHTMAN, M.P., BOURA, A.L.A. & KING, R.G. (1989). Presynaptic α_2-adrenoceptors affecting terminal synaptic transmission by the nervi cardiaci accelerantes in the rat. *J. Auton. Pharmacol.*, **9**, 119–127.

SCROOP, G.C. & LOWE, R.D. (1969). Efferent pathways of the cardiovascular response to vertebral artery infusions of angiotensin in the dog. *Clin. Sci.*, **37**, 605–619.

SEBASTIAN, J.L., MCKINNEY, W.P., KAUFMAN, J. & YOUNG, M.J. (1991). Angiotensin-converting enzyme inhibitors and cough. Prevalence in an outpatient medical clinic population. *Chest*, **99**, 36–39.

SOFFER, R.L. (1976). Angiotensin converting enzyme and the regulation of vasoactive peptides. *Annu. Rev. Biochem.*, **45**, 73–94.

STARKE, K. (1977). Regulation of noradrenaline release by presynaptic receptor systems. *Rev. Physiol. Biochem. Pharmacol.*, **77**, 1–124.

STURANI, A., CHIARINI, C., DEGLI ESPOSTI, E., SANTORO, A., ZUCCALA, A. & ZUCCHELLI, P. (1982). Heart rate control in hypertensive patients treated by captopril. *Br. J. Clin. Pharmacol.*, **14**, 849–855.

SUBISSI, A., GUELFI, M. & CRISCUOLI, M. (1990). Angiotensin converting enzyme inhibitors potentiate the bronchoconstriction induced by substance P in the guinea pig. *Br. J. Pharmacol.*, **100**, 502–506.

WEBER, M.A. (1988). Safety issues during antihypertensive treatment with angiotensin converting enzyme inhibitors. *Am. J. Med.*, **84** (Suppl. 4A), 16–23.

WONG, P.C., PRICE, W.A.Jr., CHIU, A.T., DUNCIA, J.V., CARINI, D.J., WEXLER, R.R., JOHNSON, A.L. & TIMMERMANS, P.B.M.W.M. (1990). Nonpeptide angiotensin II receptor antagonists. XI. Pharmacology of EXP3174: an active metabolite of DUP 753, an orally active antihypertensive agent. *J. Pharmacol. Exp. Ther.*, **255**, 211–217.

WONG, P.C., PRICE, W.A.Jr., CHIU, A.T., DUNCIA, J.V., CARINI, D.J., WEXLER, R.R., JOHNSON, A.L. & TIMMERMANS, P.B.M.W.M. (1991). In vivo pharmacology of DUP 753. *Am. J. Hypertens.*, **4**, 288S–298S.

ZIMMERMAN, B.G. (1978). Actions of angiotensin on adrenergic nerve endings. *Fed. Proc.*, **37**, 199–202.

(Received February 2, 1993
Revised May 10, 1993
Accepted May 17, 1993)

Br. J. Pharmacol. (1993), **110**, 297–302

Effect of adrenoceptor agonists on striated muscle strips of the canine oesophagus

Taigo Tokuhara, *Ann L. Meulemans, *Walter J.E. De Ridder, Masayuki Higashino, Hiroaki Kinoshita & [1]Jan A.J. Schuurkes

2nd Department of Surgery, Osaka City University Medical School, 1-5-7, Asahimachi, Abenoku, Osaka, Japan and *Department of Gastrointestinal Pharmacology, Janssen Research Foundation, B-2340 Beerse, Belgium.

1 Acute psychological stress, which could be related to the release of a large amount of catecholamines, may cause oesophageal motility disorders. Therefore, the aim of our study was to elucidate the influence of adrenoceptor agonists on the striated muscle portion of the oesophagus by use of isolated strips from dogs.

2 Contractions were evoked in isolated striated muscle strips by electrical field stimulation (1 pulse min^{-1}, 1 ms/pulse, submaximal voltage). The effects induced by administration of adrenoceptor agonists alone or in the presence of antagonists were tested to determine the nature of the adrenoceptors on this muscle preparation.

3 The administration of both the natural adrenoceptor agonists, adrenaline and noradrenaline, and the synthetic β-adrenenoceptor agonists, isoprenaline ($\beta_1 + \beta_2$), dobutamine (β_1) or ritodrine (β_2), enhanced the amplitude of the contractions induced by electrical stimulation in a concentration-dependent manner. The maximum responses were 82.6 (adrenaline), 66.2 (noradrenaline), 86.2 (isoprenaline), 34.6 (dobutamine) and 80.8% (ritodrine). The EC_{20} values obtained were respectively 2 nM, 0.2 μM, 0.91 nM, 3 μM and 80 nM. The administration of the α_1-adrenoceptor agonist, phenylephrine, also enhanced the contractile response in a concentration-dependent manner (EC_{20} value = 0.3 μM) and the maximum response was 64.6%, but the administration of the α_2-adrenoceptor agonist, clonidine, did not influence the contractile response. These data suggest the involvement of β_2- and possibly α_1-adrenoceptors in the responses of these adrenoceptor agonists.

4 The selective β_2-adrenoceptor antagonist ICI 118551 (3–100 nM) shifted the concentration-effect curves for noradrenaline, phenylephrine and ritodrine to the right in a concentration-dependent manner. ICI 118551 (3 nM) also shifted the concentration-effect curves for adrenaline and isoprenaline to the right, but increasing the concentration of ICI 118551 did not cause any further antagonist activity until a concentration of 100 nM, when a further rightward shift was obtained.

5 The selective α_1-adrenoceptor antagonist, prazosin (30–300 nM), did not affect the increased contractile responses induced by adrenaline, noradrenaline, phenylephrine, isoprenaline or ritodrine.

6 In conclusion, it appears that β_2-adrenoceptors are present in the striated muscle portion of the canine oesophagus, where they mediate an enhancement of contractile responses evoked by electrical stimulation. The α_1-agonist, phenylephrine, appears to interact with β_2-adrenoceptors on this preparation. β_3-Adrenoceptors have already been demonstrated in smooth muscle from various parts of the gastrointestinal tract, and our study does not exclude the possibility that there is an additional population of β_3-receptors in the canine striated muscle part of the oesophagus.

Keywords: Stress; striated muscle; oesophagus; β_2-adrenoceptor; adrenoceptor agonists; contractile response

Introduction

Previous studies suggest that acute psychological stress causes oesophageal motility disorders. Cook and his colleagues (Cook *et al.*, 1987) have demonstrated that the resting pressure of the upper oesophageal sphincter (UES), which is composed entirely of striated muscle, was increased by a stressful listening task in human volunteers. Furthermore, the amplitude of the oesophageal contractions was increased in stressed normal subjects and in patients with noncardiac chest pain or the nutcracker oesophagus (Anderson *et al.*, 1989). Recent clinical studies indicate that high-amplitude peristaltic contractions or abnormal peristaltic sequences in the distal oesophagus could be related to symptoms of noncardiac chest pain (Benjamin *et al.*, 1979; 1983; Peters *et al.*, 1988). In fact, it has been suggested that psychological characteristics, such as anxiety and depression, cause peristaltic abnormalities, an increase in wave amplitude, in wave duration or in frequency of abnormal peristaltic waves (Clouse & Lustman, 1983). However, how acute psychological stress could induce such an abnormality of oesophageal function is incompletely understood.

Acute stress may release large amounts of catecholamines and adrenocorticotropic hormone. Therefore, investigating the influence of adrenoceptor agonists on oesophageal function is important clinically. This has already been evaluated for the smooth muscle portion of the oesophagus. In the distal oesophageal body, α-adrenoceptor agonists enhance the contractile response (Christensen *et al.*, 1979; Tøttrup *et al.*, 1990), whereas β-adrenoceptor agonists inhibit the peristaltic contraction (Cohen, 1975; Dimarino & Cohen, 1982; Koch *et al.*, 1982; Lyrenas & Abrahamsson, 1986). Similar results have been obtained for the lower oesophageal sphincter (LES) (Dimarino & Cohen, 1975; Goyal & Rattan, 1978). Although many studies on the effects of adrenoceptor agonists on the smooth muscle portion of the oesophagus (including the LES) have been performed, only a few reports, describing the histology (Christensen & Percy, 1984; Marsh & Bieger, 1987) or *in vivo* experiments (Dodds *et al.*, 1979; Lyrenas & Abrahamsson, 1986), have been published on the adrenoceptor-mediated effects on the striated muscle portion. It has been suggested that neither α-adrenoceptor agonists

[1] Author for correspondence at: Dept. of Gastrointestinal Pharmacology, Janssen Research Foundation, Turnhoutseweg 30, B 2340 Beerse, Belgium.

nor β-adrenoceptor agonists induce an effect on the striated muscle portion of the opossum oesophagus *in vivo* (Dodds *et al.*, 1979). But the exact influence of adrenoceptor agonists on the striated muscle portion of the oesophagus is still unclear.

This *in vitro* study was therefore performed to investigate the effects of adrenoceptor agonists on oesophageal function by use of striated muscle strips isolated from dog oesophagus, and to attempt to elucidate the nature of the receptors involved.

Methods

Mongrel dogs of either sex were used for this experiment. After rapid removal of the upper oesophagus combined with the lower pharynx, this tissue was placed immediately in Krebs-Henseleit buffer at room temperature (composition in mM: KCl 4.69, $CaCl_2 \cdot 2H_2O$ 2.51, $NaHCO_3$ 25, KH_2PO_4 1.18, $MgSO_4 \cdot 7H_2O$ 1.18, NaCl 118.06, glucose 5.55). The musculature of the oesophagus was freed from the adherent mucosa care being taken not to damage the underlying muscle layer; 8 longitudinal strips (length 4–5 cm, width 2 mm) were prepared from the zone directly below the pharyngoesophageal junction. Each strip was mounted between two platinum electrodes (8 cm long and 0.5 cm apart) and placed in a 100 ml organ bath filled with Krebs-Henseleit buffer, gassed with a mixture of 95% O_2 and 5% CO_2 and maintained at 37°C.

The strips were connected to an isometric force transducer under a preload of approximately 3 g, which had been previously evaluated as the mean optimal preload for this kind of preparation. The preparations were then allowed to stabilize for at least 40 min. After this stabilization procedure, electrical stimulation was applied over the entire length of the strip by means of 2 platinum electrodes (JSI power stimulator). The stimulation parameters were: 1 pulse min^{-1}, 1 ms/pulse. The voltage was increased by steps of 2 V, from 7 V up to 13 V. Contractions were measured isometrically (Statham UC2 force transducer) and recorded with a polygraph (BD9; Kipp & Zonen). When the maximum amplitude of the contraction was obtained, the voltage was reduced until a submaximal level (50% of the maximum amplitude) was reached. The strips were allowed to stabilize again for at least 15 min until reproducible twitch responses could be observed, after which drugs were administered to the organ bath.

In the first set of experiments, several adrenoceptor agonists were administered cumulatively to the organ bath: adrenaline (1 nM–3 μM), noradrenaline (30 nM–10 μM), phenylephrine (30 nM–30 μM), clonidine (300 nM–10 μM), isoprenaline (0.3 nM–1 μM), dobutamine (100 nM–30 μM) or ritodrine (3 nM–3 μM). In a control experiment, performed in parallel, similar preparations were treated with the appropriate type and amount (0.01–1.0 ml) of vehicle for each of the agonists.

In the next protocol, agonists were administered cumulatively in the presence of a single concentration of an antagonist (prazosin: 30 nM, 100 nM, 300 nM or 1 μM, or ICI 118551: 3 nM, 10 nM, 30 nM or 100 nM), or, in a control experiment, in the presence of solvent (distilled water). The effects which could be induced by the administration of the antagonists or solvent were followed for at least 15 min before administration of the agonists. The agonists adrenaline, noradrenaline, phenylephrine, isoprenaline and ritodrine were then administered in the same concentration ranges as in the first series.

Drugs

The following drugs were used: adrenaline, noradrenaline, phenylephrine and isoprenaline (Janssen Chimica, Belgium), clonidine (Boehringer, Germany), dobutamine (Shionogi, Japan), ritodrine (Duphar, The Netherlands), prazosin (Pfizer, U.S.A.), ICI 118551 (1-[2,3-dihydro-4-methyl-1H-inden-7yl oxy]-3-[(1-methylethyl)amino]-2butanol hydrochloride, Imperial Chemical Industries, UK). Adrenaline was dissolved in 0.03% HCl. Noradrenaline and isoprenaline were dissolved in 0.9% NaCl. Ascorbic acid (2.5×10^{-7} M in the stock solution) was added to adrenaline, noradrenaline and the isoprenaline solution. The other drugs were dissolved in distilled water.

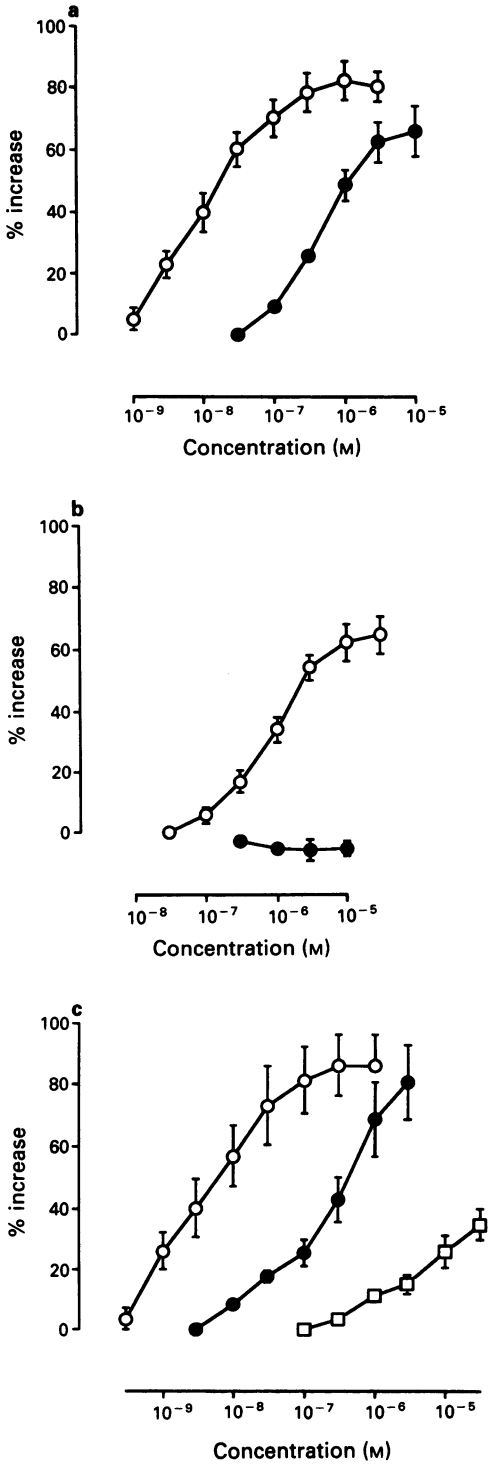

Figure 1 Effect of adrenoceptor agonists on contractions of the striated muscle strips of the canine oesophagus. (a) Concentration-response curves for adrenaline (○) and noradrenaline (●). (b) Concentration-response curves for phenylephrine (○) or clonidine (●). (c) Concentration-response curves for isoprenaline (○), ritodrine (●) and dobutamine (□). Mean ± s.e.mean (vertical lines) ($n = 5$) expressed as % increase of initial value.

Statistical analysis

All data are expressed for graphic presentation as mean percentage increase of initial values i.e. before the administration of the agonists (mean ± s.e.mean). Differences between mean values or EC_{20} values were tested with the ANOVA and Dunnett's *t* test. *P* values less than 0.05 were considered to indicate a significant effect.

For calculation of the EC_{20} value, the concentration of an agonist required to produce 20% of the maximal effect observed with isoprenaline was used.

EC_{20} values were calculated by linear regression analysis.

Results

Effect of adrenoceptor agonists on isolated striated muscle strips

Cumulative administration of adrenaline, noradrenaline, isoprenaline, dobutamine and phenylephrine enhanced the amplitude of the contractions elicited by electrical stimulation in a concentration-dependent manner whereas clonidine was without effect (see Figure 1). Typical responses to adrenaline, noradrenaline and phenylephrine are illustrated in Figure 2.

The rank order of agonist potency was: isoprenaline > adrenaline > ritodrine > noradrenaline > phenylephrine > dobutamine > clonidine. The EC_{20} values for the agonists had the same order of potency: isoprenaline [0.91 (0.65–1.3) nM], adrenaline [2 (1.4–2.7) nM], ritodrine [80 (44–130) nM], noradrenaline [0.17 (0.16– 0.18) μM], phenylephrine [0.3 (0.18–0.51) μM], dobutamine [3 (2.0–4.7) μM]. The maximal effects obtained were respectively: 86.2 ± 9%, 82.6 ± 6.3%, 80.8 ± 11.9%, 66.2 ± 8.1%, 64.6 ± 6.2%, 34.6 ± 5.1%.

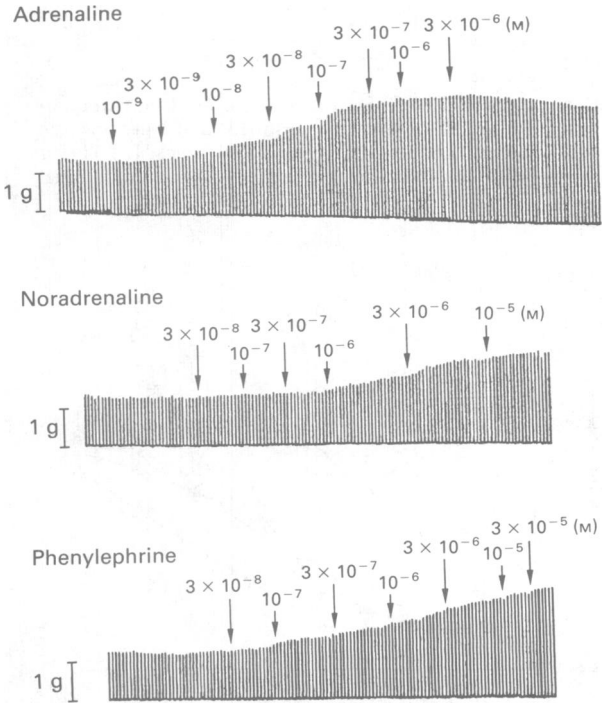

Figure 2 Representative examples of the effects induced by adrenoceptor agonists on contractions of the isolated striated muscle strips of the canine oesophagus elicited by electrical stimulation (1 pulse min^{-1}, 1 ms/pulse, submaximal voltage).

Effect of adrenoceptor agonists in the presence of prazosin or ICI 118551 on isolated striated muscle strips

Addition of prazosin (up to 1 μM) did not affect the contractile responses to electrical stimulation. Furthermore, in concentrations of 30–300 nM, prazosin had no effect on concentration-effect curves for adrenaline, noradrenaline, isoprenaline or ritodrine, and in concentrations of 100–1000 nM, it was similarly ineffective with reference to concentration-effect curves to phenylephrine (Figures 3a, 4a, 5a, 6a and 7a).

Addition of ICI 118551 (up to 100 nM) did not affect the contractile responses to electrical stimulation. However, ICI 118551 significantly shifted to the right the concentration-effect curves for adrenaline, noradrenaline, phenylephrine, isoprenaline or ritodrine (Figures 3b, 4b, 5b, 6b and 7b). This antagonism was associated with some apparent flattening of the agonist curves

ICI 118551 inhibited the response to noradrenaline, phenylephrine and ritodrine in a concentration-dependent manner, whereas its effect on adrenaline and isoprenaline was not concentration-dependent. With adrenaline and isoprenaline, the lowest concentration of ICI 118551 (3 nM) caused a marked rightward shift of agonist concentration-effect curves, but increasing the concentration to 10 and 30 nM caused no further shift. Only when a concentration of ICI 118551 of 100 nM was achieved was a further rightward shift obtained.

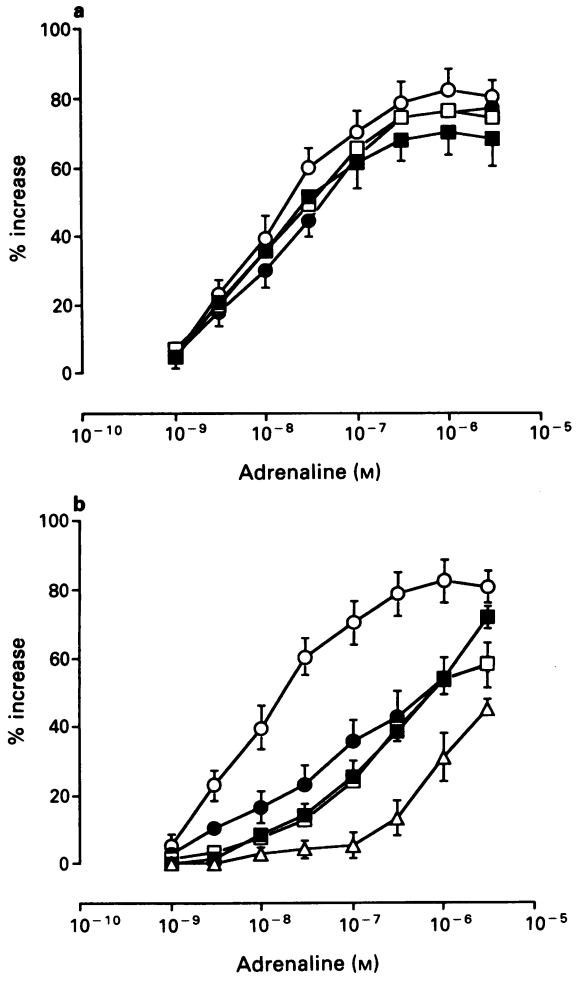

Figure 3 Effect of adrenaline on contractions of the striated muscle strips of the canine oesophagus. (a) Concentration-response curves for adrenaline in the presence of solvent (○), 30 nM prazosin (●), 100 nM prazosin (□) and 300 nM prazosin (■). (b) Concentration-response curves for adrenaline in the presence of solvent (○), 3 nM ICI 118551 (●), 10 nM ICI 118551 (□), 30 nM ICI 118551 (■) and 100 nM ICI 118551 (△). Mean ± s.e.mean (vertical lines) ($n = 5$) expressed as % increase of initial value.

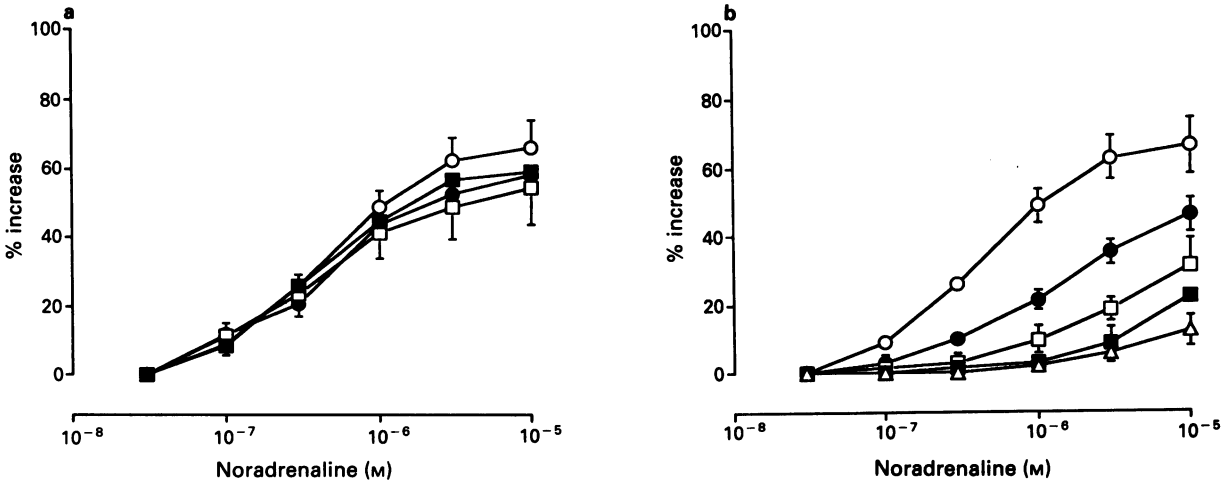

Figure 4 Effect of noradrenaline on contractions of the striated muscle strips of the canine oesophagus. (a) Concentration-response curves for noradrenaline in the presence of solvent (○), 30 nM prazosin (●), 100 nM prazosin (□) and 300 nM prazosin (■). (b) Concentration-response curves for noradrenaline in the presence of solvent (○), 3 nM ICI 118551 (●), 10 nM ICI 118551 (□), 30 nM ICI 118551 (■) and 100 nM ICI 118551 (△). Mean ± s.e.mean (vertical lines) ($n = 5$) expressed as % increase of initial value.

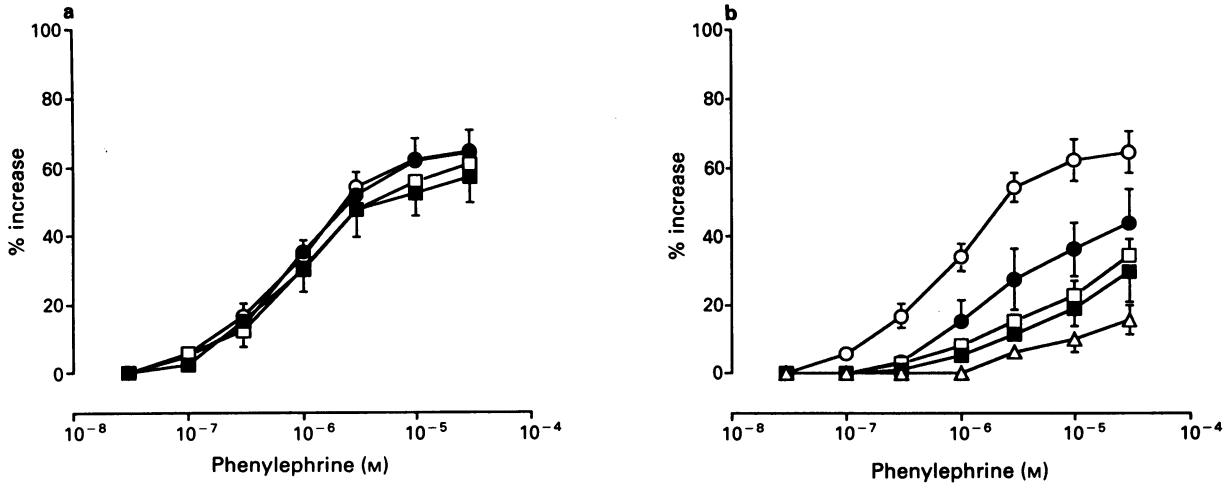

Figure 5 Effect of phenylephrine on contractions of the striated muscle strips of the canine oesophagus. (a) Concentration-response curves for phenylephrine in the presence of solvent (○), 100 nM prazosin (●), 300 nM prazosin (□) and 1 μM prazosin (■). (b) Concentration-response curves for phenylephrine in the presence of solvent (○), 3 nM ICI 118551 (●), 10 nM ICI 118551 (□), 30 nM ICI 118551 (■) and 100 nM ICI 118551 (△). Mean ± s.e.mean (vertical lines) ($n = 5$) expressed as % increase of initial value.

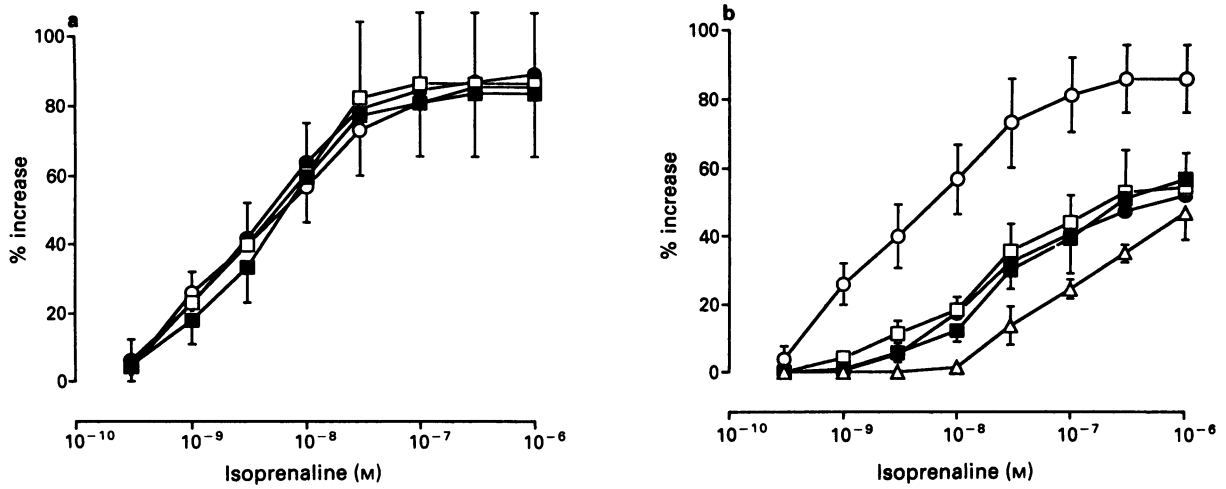

Figure 6 Effect of isoprenaline on contractions of the striated muscle strips of the canine oesophagus. (a) Concentration-response curves for isoprenaline in the presence of solvent (○), 30 nM prazosin (●), 100 nM prazosin (□) and 300 nM prazosin (■). (b) Concentration-response curves for isoprenaline in the presence of solvent (○), 3 nM ICI 118551 (●), 10 nM ICI 118551 (□), 30 nM ICI 118551 (■) and 100 nM ICI 118551 (△). Mean ± s.e.mean (vertical lines) ($n = 5$) expressed as % increase of initial value.

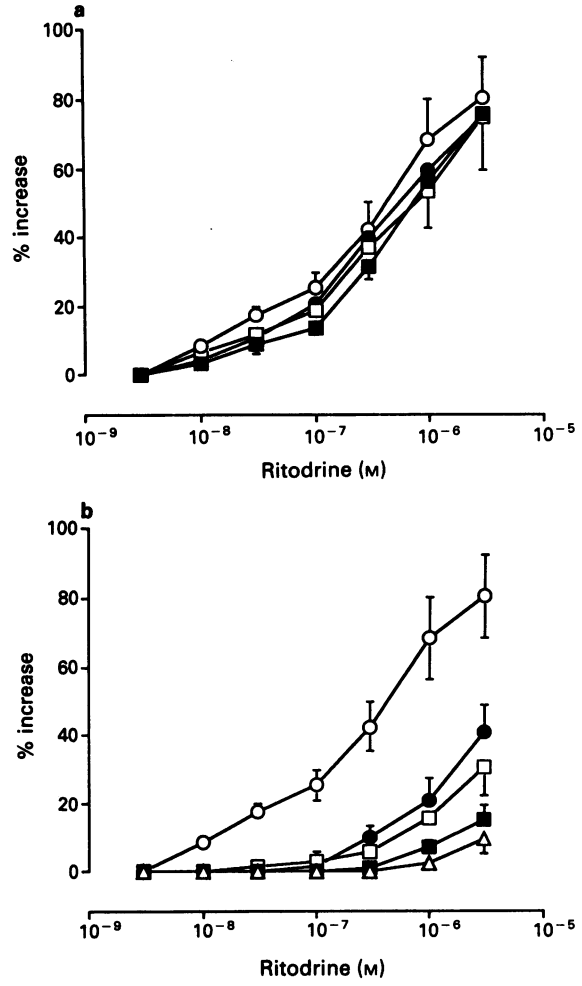

Figure 7 Effect of ritodrine on contractions of the striated muscle strips of the canine oesophagus. (a) Concentration-response curves for ritodrine in the presence of solvent (○), 30 nM prazosin (●), 100 nM prazosin (□) and 300 nM prazosin (■). (b) Concentration-response curves for ritodrine in the presence of solvent (○), 3 nM ICI 118551 (●), 10 nM ICI 118551 (□), 30 nM ICI 118551 (■) and 100 nM ICI 118551 (△). Mean ± s.e.mean (vertical lines) ($n = 5$) expressed as % increase of initial value.

Discussion

The neural control mechanism of peristalsis in the striated muscle portion of the oesophagus differs from that in the smooth muscle portion (Roman & Gonella, 1987). In manometric studies, however, peristalsis induced in the different portions shows a similar coordinated profile. Two control mechanisms for peristalsis exist in the smooth muscle portion: one is the central control mechanism mediated via the vagal nerve and the other is the peripheral control mechanism which can be regulated by the myenteric plexus (Diamant & El-Sharkawy, 1977). The myenteric plexus is also present in the striated muscle portion, although less well developed (Diamant, 1989). Therefore, the action of this muscle portion might be modulated mainly by extrinsic nerves (Roman & Gonella, 1987).

The importance of the cholinergic effects in the striated muscle portion of the oesphagus has been demonstrated extensively (Dodds *et al.*, 1979; 1981; Crist *et al.*, 1984; Marsh & Bieger, 1987; Taylor, 1990).

Concerning the adrenoceptor, previous studies *in vivo* and *in vitro* have demonstrated that α-adrenoceptor agonists enhance the contractile response of the LES to electrical stimulation. β-Agonists reduce the contractile response. None of the adrenoceptor agonists influence the relaxation of the LES (Dimarino & Cohen, 1975; Goyal & Rattan, 1978). In the striated muscle portion, however, it has been demonstrated that phenylephrine and isoprenaline do not induce any enhancement or inhibition in the peristaltic contraction of the opossum oesophagus. There is no evidence for ganglionic synapses in the neural pathway (Dodds *et al.*, 1979). Our study was designed to elucidate the action of adrenoceptor agonists on the striated muscle portion by the use of isolated oesophageal strips of dogs as a model.

Adrenaline and noradrenaline, which have agonist activity at both α- and β-adrenoceptors, enhanced the contractile responses, noradrenaline being less potent than adrenaline. This suggests that the effect is induced via β-adrenoceptors, since adrenaline has been shown to be a more potent β-agonist than noradrenaline and a less potent α-agonist. A range of agonists specific for α- and β-adrenoceptors were also tested in an attempt to identify the subtype of the adrenoceptor involved. The results, obtained with the selective α_1-agonist phenylephrine or the selective α_2-agonist clonidine, suggest that α_1-adrenoceptors are involved. However, in other experiments we conducted, a range of β-adrenoceptor agonists, isoprenaline ($\beta_1 + \beta_2$-agonist), dobutamine (selective β_1-agonist) and ritodrine (selective β_2-agonist) were tested; ritodrine increased the contractile response, suggesting the presence of β_2-adrenoceptors on the striated muscle portion. On the other hand, dobutamine only moderately increased the contractile response and only at high concentrations. It is known that high concentrations of dobutamine can activate both β_1- and β_2-adrenoceptors (Hoffman & Lefkowitz, 1990). The results from this series of experiments are consistent with the presence of β_2-adrenoceptors, and there is no convincing evidence for the involvement of β_1-adrenoceptors.

In another series of experiments, agonists were administered cumulatively in the presence of the selective α_1-antagonist prazosin (Berthelsen & Pettinger, 1977; Doxey *et al.*, 1977) or the selective β_2-antagonist ICI 118551 (Bilski *et al.*, 1980; Wilffert *et al.*, 1982a). Whereas prazosin did not block any of the agonists, ICI 118551 inhibited the increases in contractile responses induced by all of the agonists tested.

The mechanism by which ICI 118551 inhibits the effect induced by phenylephrine is unclear. In vascular smooth muscle, ICI 118551 did not influence the electrical stimulation-induced increase in diastolic pressure which was strongly attenuated by the α_1-antagonist prazosin (Wilffert *et al.*, 1982b), suggesting that ICI 118551 is devoid of α_1 blocking properties. We, therefore, may suppose that phenylephrine acts via a β_2-adrenoceptor in the striated muscle portion of the oesophagus. Stimulation of β-adrenoceptors by phenylephrine has been observed, but only at a much higher concentration (Hoffman & Lefkowitz, 1990). Therefore, the interaction of ICI 118551 with the responses to phenylephrine is still difficult to explain.

On the other hand, addition of ICI 118551 did not induce a concentration-related antagonism. The effects induced after addition of adrenaline and isoprenaline, and also to a degree after addition of phenylephrine, could be reduced in the presence of 3 nM ICI 118551. At 10 and 30 nM ICI 118551, no further effect was observed. Only after addition of 100 nM could a further antagonism be seen. These results could be explained by the presence of a mixed receptor population, one receptor type being blocked by the lower concentrations of ICI 118551, the other only sensitive to blockade by the highest concentration tested (100nM). Atypical or β_3-adrenoceptors have already been demonstrated in the smooth muscle part of the guinea-pig ileum (Taneja & Clarke, 1992), in the rat ileum (Van der Vliet *et al.*, 1990) and in the rat colon (McLaughlin & MacDonald, 1990) but they mediate inhibitory activity on smooth muscle. It is possible that they also exist in canine oesophagus and that they mediate an excitatory effect. More experiments, however, are needed to confirm the importance of the β_3-receptor in this model.

In conclusion, in our study adrenaline, noradrenaline, phenylephrine, isoprenaline and ritodrine enhanced the con-

tractile response of isolated striated muscle strips, an action which was suppressed by low concentrations of the β_2-adrenoceptor antagonist ICI 118551. These results suggest that facilitatory β_2-adrenoceptors are present in the striated muscle portion of the oesophagus, and that in this region the α_1-agonist phenylephrine acts via β_2-adrenoceptors. We hypothesize that acute psychological stress may cause oesophageal motility disorders via adrenoceptors, predominantly of the β_2-subtype in the striated muscle portion of the oesophagus.

The authors wish to thank Janssen-Kyowa Co. Ltd. in Japan for financial support.

References

ANDERSON, K.O., DALTON, C.B., BRADLEY, L.A. & RICHTER, J.E. (1989). Stress induces alteration of oesophageal pressures in healthy volunteers and non-cardiac chest pain patients. *Dig. Dis. Sci.*, **34**, 83–91.

BENJAMIN, S.B., GERHARDT, D.C. & CASTELL, D.O. (1979). High amplitude, peristaltic oesophageal contractions associated with chest pain and/or dysphagia. *Gatroenterology*, **77**, 478–483.

BENJAMIN, S.B., RICHTER, J.E., CORDOVA, C.M., KNUFF, T.E. & CASTELL, D.O. (1983). Prospective manometric evaluation with pharmacologic provocation of patients with suspected oesophageal motility dysfunction. *Gastroenterology*, **84**, 893–901.

BERTHELSEN, S. & PETTINGER, W.A. (1977). A functional basis for classification of α-adrenergic receptors. *Life Sci.*, **21**, 595–606.

BILSKI, A., DORRIES, S., FITZGERALD, J.D., JESSUP, R., TUCKER, H. & WALE, J. (1980). ICI118,551, a potent β_2 adrenoceptor antagonist. *Br. J. Pharmacol.*, **69**, 292p–293p.

CHRISTENSEN, J., ARTHUR, C. & CONKLIN, J.L. (1979). Some determinants of latency of off-response to electrical field stimulation in circular layer of smooth muscle of opossum oesophagus. *Gastroenterology*, **77**, 677–681.

CHRISTENSEN, J. & PERCY, W.H. (1984). A pharmacological study of oesophageal muscularis mucosa from the cat, dog and American opossum (*Didelphis virginiana*). *Br. J. Pharmacol.*, **83**, 329–336.

CLOUSE, R.E. & LUSTMAN, P.J. (1983). Psychiatric illness and contraction abnormalities of the oesophagus. *New Engl. J. Med.*, **309**, 1337–1342.

COHEN, S. (1975). Force velocity characteristics of oesophageal muscle: interaction of isoprenaline and calcium. *Eur. J. Clin. Invest.*, **5**, 259–265.

COOK, I.J., DENT, J., SHANNON, S. & COLLINS, S.M. (1987). Measurement of upper oesophageal sphincter pressure: effect of acute emotional stress. *Gastroenterology*, **93**, 526–532.

CRIST, J., GIDDA, J.S. & GOYAL, R.K. (1984). Intramural mechanism of oesophageal peristalsis: roles of cholinergic and noncholinergic nerves. *Proc. Natl. Acad. Sci. U.S.A.*, **81**, 3595–3599.

DIAMANT, N.E. (1989). Physiology of oesophageal motor function. *Gastroenterol. Clin. North Am.*, **18**, 179–194.

DIAMANT, N.E. & EL-SHARKAWY, T.Y. (1977). Neural control of oesophageal peristalsis: a conceptual analysis. *Gastroenterology*, **72**, 546–556.

DIMARINO, A.J. & COHEN, S. (1975). The adrenergic control of lower oesophageal sphincter function: response to beta$_2$ adrenergic agonists. *Proc. Soc. Exp. Biol. Med.*, **148**, 1265–1269.

DIMARINO, A.J. & COHEN, S. (1982). Effect of an oral beta$_2$-adrenergic agonist on lower oesophageal sphincter pressure in normals and in patients with achalasia. *Dig. Dis. Sci.*, **27**, 1063–1066.

DODDS, W.J., CHRISTENSEN, J., DENT, J., ARNDORFER, R.C. & WOOD, J.D. (1979). Pharmacologic investigation of primary peristalsis in smooth muscle portion of opossum oesophagus. *Am. J. Physiol.*, **237**, E561–E566.

DODDS, W.J., DENT, J., HOGAN, W.J. & ARNDORFER, R.C. (1981). Effect of atropine on oesophageal motor function in humans. *Am. J. Physiol.*, **240**, G290–G296.

DOXEY, J.C., SMITH, C.F.C. & WALKER, J.M. (1977). Selectivity of blocking agents for pre- and postsynaptic α-adrenoceptors. *Br. J. Pharmacol.*, **60**, 91–96.

GOYAL, R.K. & RATTAN, S. (1978). Neurohumoral, hormonal, and drug receptors for the lower oesophageal sphincter. *Gastroenterology*, **74**, 598–619.

HOFFMAN, B.B. & LEFKOWITZ, R.J. (1990). Catecholamines and sympathomimetic drugs. In *The Pharmacological Basis of Therapeutics*, ed. Gilman, A.G., Rall, T.W., Nies, A.S. & Taylor, P. pp. 187–220. New York: Pergamon Press.

KOCH, K.L., CURRY, R.C., FELDMAN, R.L., PEPINE, C.J., LONG, A. & MATHIAS, J.R. (1982). Ergonovine-induced oesophageal spasm in patients with chest pain resembling angina pectoris. *Dig. Dis. Sci.*, **27**, 1073–1080.

LYRENAS, E. & ABRAHAMSSON, H. (1986). Beta adrenergic influence on oesophageal peristalsis in man. *Gut*, **27**, 260–266.

MCLAUGHLIN, D.P. & MACDONALD, A. (1990). Evidence for the existence of 'atypical' beta-adrenoceptors (beta 3-adrenoceptors) mediating relaxation in the rat distal colon *in vitro*. *Br. J. Pharmacol.*, **101**, 569–574.

MARSH, D.C. & BIEGER, D. (1987). Cholinoceptor-mediated mechanical and electrical responses of rat oesophageal striated musculature: a comparison of two *in vitro* methods. *Gen. Pharmacol.*, **18**, 657–663.

PETERS, L., MAAS, L., PETTY, D., DALTON, C., PENNER, D., WU, W., CASTELL, D. & RICHTER, J. (1988). Spontaneous noncardiac chest pain evaluation by 24 hour ambulatory oesophageal motility and pH monitoring. *Gastroenterology*, **94**, 878–886.

ROMAN, C. & GONELLA, J. (1987). Extrinsic control of digestive tract motility. In *Physiology of the Gastrointestinal Tract*, ed. Johnson, L.R. Vol. 1. pp. 507–554. New York: Raven Press.

TANEJA, D.T. & CLARKE, D.E. (1992). Evidence for a noradrenergic innervation to 'atypical' beta adrenoceptors (or putative beta-3 adrenoceptors) in the ileum of guinea-pig. *J. Pharmacol. Exp. Ther.*, **260**, 192–200.

TAYLOR, P. (1990). Agents acting at the neuromuscular junction and autonomic ganglia. In *The Pharmacological Basis of Therapeutics*, ed. Gilman, A.G., Rall, T.W., Nies, A.S. & Taylor, P. pp. 166–186. New York: Pergamon Press.

TØTTRUP, A., FORMAN, A., JENSEN, P.F., RAUNDAHL, U. & ANDERSSON, K.E. (1990). Effects of transmural field stimulation in isolated muscle strips from human oesophagus. *Am. J. Physiol.*, **258**, G344–G351.

VAN DER VLIET, A., RADEMAKER, B. & BAST, A. (1990). A beta adrenoceptor with atypical characteristics is involved in the relaxtion of the rat small intestine. *J. Pharmacol. Exp. Ther.*, **255**, 218–226.

WILFFERT, B., GOUW, M.A.M., DE JONGE, A., TIMMERMANS, P.B.M.W.M. & VAN ZWIETEN, P.A. (1982a). Indications for vascular alpha- and beta-2 adrenoceptors in synapse of the muscarinic pathway in the pithed normotensive rats. *J. Pharmacol. Exp. Ther.*, **223**, 219–223.

WILFFERT, B., TIMMERMANS, P.B.M.W.M. & VAN ZWIETEN, P.A. (1982b). Extrasynaptic location of alpha-2 and non-innervated beta-2 adrenoceptors in the vascular system of the pithed normotensive rat. *J. Pharmacol. Exp. Ther.*, **221**, 762–768.

(Received July 3, 1992
Revised January 26, 1993
Accepted January 31, 1993)

Br. J. Pharmacol. (1993), **110**, 303–309

Functional evidence for multiple receptor activation by κ-ligands in the inhibition of spinal nociceptive reflexes in the rat

Juan F. Herrero & [1]P. Max Headley

Department of Physiology, The School of Medical Sciences, University of Bristol, University Walk, Bristol BS8 1TD

1 The evidence for κ-receptor heterogeneity is equivocal. We have now investigated this question by comparing the effects of five putatively selective κ-agonists. The parameters examined were: the relative potencies in depressing hindlimb flexor muscle reflexes to noxious pinch stimuli in both spinalized and sham-spinalized rats; the reversibility of these effects by naloxone; and the effects on blood pressure.

2 Two types of drug effect was discriminated. One drug group, represented by U-50,488, U-69,593 and PD-117,302, had a potency ratio between sham and spinalized rats approximately 10 fold lower than the other group, which comprised GR103545 and CI-977.

3 Under sham-spinalized conditions, CI-977 and GR103545 at high doses caused only sub-maximal reductions of spinal reflexes. U-50,488 was still active when superimposed on these high doses of GR103545.

4 Naloxone reversed all effects, but different doses were required between compounds, with GR103545 taking some 20 times higher doses of naloxone to cause reversal than did U-50,488.

5 The effects on mean arterial pressure were opposite between groups.

6 The results imply that more than one type of naloxone-sensitive non-μ opioid receptor must be involved in mediating these complex actions of ligands that have been claimed to be selective for κ-receptors.

Keywords: κ-Opioid agonist; nociception; naloxone; mean arterial pressure; spinal reflex

Introduction

The suggestion of κ-opioid receptor subtypes was initially based on binding experiments. Multiple κ binding sites have been defined in terms either of [D-Ala^2,D-Leu^5]enkephalin (DADLE)-sensitive or insensitive sites (Attali *et al.*, 1982; Audigier *et al.*, 1982; Castanas *et al.*, 1985) or of dynorphin A(1-17) sensitive or insensitive sites (Pfeiffer *et al.*, 1981; Morre *et al.*, 1983). In functional studies Iyengar *et al.* (1986) reported two different kinds of action of κ agonists in modulating the levels of corticosterone, thyroid-stimulating hormone (TSH), 3,4-dihydroxyphenylacetic acid (DOPAC) and homovanillic acid (HVA) in plasma, and the reversibility of these effects by high doses of naloxone and WIN 4441-3, a long acting non-selective narcotic antagonist. Since then evidence has been presented either for up to four different κ-receptor subtypes (Clark *et al.*, 1989; Rothman *et al.*, 1990), or for different affinity states of the same receptor (Wood *et al.*, 1989; Traynor, 1989).

No clear conclusions can be drawn from these reports other than that there have been three major difficulties: (a) the lack of specific and selective κ-opioid agonists, (b) the lack of selective κ antagonists that have consistent effects *in vitro* and *in vivo*, and (c) the lack of physiological models *in vivo* on which κ-opioid systems can be studied convincingly.

We have previously shown that the κ-agonist U-50,488 i.v. mediates clear antinociceptive effects within the spinal cord, reducing nociceptive reflexes (Headley *et al.*, 1989; Parsons & Headley, 1989; Herrero & Headley, 1991) and dorsal horn neuronal responses (Dong *et al.*, 1990). This antinociceptive effect was potentiated by surgery affecting the spinal column, whether the spinal cord was intact (Herrero & Headley, 1991) or sectioned (Hartell & Headley, 1991). Naloxone reversed these effects at doses about ten times those reversing the actions of μ-ligands (Parsons *et al.*, 1989).

We have now used this model of κ-sensitive nociceptive responses to study the relative effects of five agonists that are claimed to be selective for κ-receptors: U-50,488 (Von Voigtlander *et al.*, 1983), U-69,593 (Lahti *et al.*, 1985), PD-117,302 (Clark *et al.*, 1988), CI-977 (Hunter *et al.*, 1990) and GR103545 (Hayes *et al.*, 1990). We have compared the agonist properties of the compounds in terms of (1) the potency-ratio of the agonists on nociceptive reflexes in spinalized versus sham spinalized animals; (2) the slope of the dose-response curves obtained; and (3) effects of blood pressure.

The definition of receptor subtypes, as opposed to affinity substates, is however most convincingly demonstrated by the use of antagonists, which do not show such substates. The only selective κ-antagonist available, norbinaltorphimine (Portoghese *et al.*, 1987) has unpredictable kinetics under *in vivo* conditions; we have therefore used the non-selective opioid antagonist, naloxone, to assess whether the κ-agonists show similar or different sensitivity to antagonism.

Some of these data have been presented in preliminary form (Headley & Herrero, 1991; Herrero & Headley, 1992).

Methods

Animal preparation

The preparation of rats for reflex recording has been described previously in detail (Hartell & Headley, 1990; Herrero & Headley, 1991). Briefly, male Wistar rats weighing 300–390 g were anaesthetized with halothane in O_2 and the trachea, right carotid and right jugular vein were cannulated. After infiltration of lignocaine (2%) with adrenaline, a laminectomy was performed from thoracic 10 to 8 vertebrae. The dura mater was then opened and the spinal cord was either kept intact (sham spinalized group) or transected at thoracic segment 8 or 9 (spinalized group). Sham spinalization was performed because the surgery of spinalization itself enhances κ-opioid potency (Herrero & Headley, 1991). The

[1] Author for correspondence.

incision was closed. Anaesthesia was then changed to α-chloralose (50 mg kg^{-1}, i.v., initial dose and 20 mg kg^{-1}, i.v., approximately every hour) and the animal was moved to an appropriate recording frame. Core temperature was maintained close to 37°C by means of feedback-controlled blanket and lamp systems. The experiment was terminated if systolic arterial pressure fell below 100 mmHg. All animals were left for at least 1 h after surgery before recording was started.

Recording system

Nociceptive flexor reflexes were elicited by means of a pneumatically controlled pincher device applied to one toe for 15 s every 3 min. All stimuli were of 2.5 N force applied between 4 mm diameter jaws. This is about 3 times the force causing a withdrawal reflex in awake rats when using the same stimulator (N.A. Hartell, personal communication).

Responses to stimuli were recorded as single motor unit (SMU) discharges by means of a bipolar teflon-coated tungsten electrode, inserted percutaneously into a flexor muscle (Hartell & Headley, 1990). Unit firing rate (see Figure 1), force applied to the pincher, and blood pressure were recorded on a chart recorder. The quantitative analysis presented below is based on counts of spikes evoked during the last 10 s of each pinch stimulus (see Parsons & Headley, 1989).

Drug administration and analysis of drug effects

The following drugs were used in these experiments: U-50,488H (*trans*-3,4-dichloro-*N*-methyl-*N*[2-(1 pyrrolidinyl)-cyclohexyl] benzeneacetamide (Upjohn): U-69,593 ((5 alpha, 7 alpha, 8 beta)-(−)-*N*-methyl-N-[7-(1-pyrrolidinyl)-1-oxaspiro (4,5) dec-8-yl]benzene-acetamide (Upjohn); PD-117,302 ((+)-*trans*-N-methyl-*N*-[2(1-pyrrolidinyl)-cyclohexyl]benzo[b]thiophene-4-acetamide monohydrochloride) (Parke-Davis); CI-977 ((5**R**)-(5 alpha, 7 alpha, 8 beta)-N-methyl-*N*-[7-(1-pyrrolidinyl)-1-oxaspiro[4,7]dec-8-yl]-4-benzo- furanacetamide monohydrochloride (Parke-Davis); GR103545 ((**R**)-methyl 4-[(3,4-dichlorophenyl)acetyl]-3-(1-pyrrolidinyl-methyl)-1-piperazinecarboxylate fumarate) (Glaxo); and naloxone (Sigma). U-50,488H, CI-977 and GR103545 were dissolved in isotonic saline whereas U-69,593 and PD-117,302 were dissolved in a few microlitres of absolute ethanol which was then diluted in distilled water or isotonic saline. Controls with the equivalent amount of solvent used in each case were always done either before or after the administration of the drug. All drugs were given i.v. in a constant volume of 0.3 ml, and were injected in a dose-doubling cumulative regime. The starting dose used in spinalized animals was 1 mg kg^{-1} for U-50,488H, U-69,593 and PD-117,302; 10 μg kg^{-1} for CI-977 and 20 μg kg^{-1} for GR103545. In sham-spinalized animals the starting dose usually had to be lower. In most cases doses were increased at intervals of 6 min until the response was reduced to below 25% of control (but see below). Most animals were tested with only one agonist, but if more than one opioid was administered, an interval of at least 30 min after full recovery from the previous drug was allowed before any further drug administration. Comparison of data showed no differences between results of single vs. multiple tests; data have therefore been pooled.

Data on nociceptive reflexes are expressed as a percentage of pre-drug control values, where control is the mean of the three responses preceding the administration of the drug. Data were only accepted for analysis if the response recovered by at least 80% of the maximum effect of the drug, or were reversed by naloxone to this degree. Estimates of ED_{50} are based on regression analysis of pooled data of responses reduced to between 20 and 80% control values; this has limitations (Parsons & Headley, 1989) but is the only feasible method under these *in vivo* conditions. Statistical significance was determined on pooled data by the non-parametric two-tailed Mann-Whitney U test (Siegel & Castellan, 1988). The effect produced by the κ-opioids on blood pressure was quantified as the change produced by each dose with respect to the preceding value, in mean arterial pressure (MAP mmHg). Statistical significance was determined on pooled data by Student's *t* test.

Naloxone was used to assess any difference in the sensitivity of the opioids to an antagonist. Practical limitations in this type of electrophysiological experiment preclude assessing antagonist effects under equilibrium conditions. To gain some idea of the effectives doses of naloxone, the antagonist was administered i.v. after the last dose of the agonist, in a cumulative regime. (The doses depended on the effect assessed in initial experiments; see Table 1). The degree of reversal by naloxone was assessed by comparing the recovery of responses in those animals tested with naloxone with the recovery seen in control animals not tested with naloxone. The quantification of percentage reversal is expressed as:

[(% pre-drug control with naloxone) − (% pre-drug without naloxone) / (100 − % pre-drug control without naloxone)] × 100%.

Results

General

Experiments were performed on 107 rats; 48 of them were spinalized whereas 59 were kept with the spinal cord intact. Data were obtained from 130 SMU; 63 in transected and 67 in sham spinalized animals. The pre-drug neuronal firing rate was a little higher in sham spinalized (24 spikes per second) than in spinalized rats (19 spikes per second), but this difference was not significant. Spontaneous activity was absent or very low. The MAP in sham operated rats was 121 ± 3 mmHg (mean ± s.e.mean), whereas in spinalized rats it was 98 ± 2 mmHg. This difference was significant (*t* test, $P<0.001$).

All five κ-agonists reduced the responses to nociceptive mechanical stimulation in a dose-dependent manner and these effects were reversed by naloxone. In the cases in which ethanol/saline or ethanol/water were used as solvents for the agonists, control tests showed no significant action.

The five κ-agonists did, however, affect both nociceptive flexor responses and blood pressure to different degrees. U-50,488 had similar effects to U-69,593 and PD-117,302, whereas CI-977 and GR103545 were different in several respects.

Group 1 agonists: U-50,488, U-69,593 and PD-117,302

Figure 1 shows sample records of SMU discharge rates and the effects on them of the three κ-agonists, to illustrate the relative potencies and timecourses of these agents. Figure 2 shows pooled data for both spinalized (a) and sham spinalized rats (b). All three compounds produced an inhibition of the nociceptive responses over a similar dose range (1 to 16 mg kg^{-1}).

All three agonists were more potent in those animals with the spinal cord intact (Figure 2b). The estimated ED_{50} values for spinalized versus sham spinalized rats are shown in Table 1. The ratio of ED_{50} between spinalized and sham spinalized rats was 5 fold for U-50,488, 6 fold for U-69,593 and 1.5 fold for PD-117,302. These differences were statistically significant for all three agents ($P<0.05$, Mann-Whitney U-test).

Figure 5a shows the actions of these three κ-agonists on blood pressure. In spinalized rats the initial dose of all three compounds (1 mg kg^{-1} in each case) increased the MAP to a small but significant degree (*t* test, $P<0.02$). The effect was of 13 ± 4 mmHg for U-50,488; 12 ± 4 mmHg for U-69,593 and 11 ± 4 mmHg for PD-117,302. This hypertensive effect shifted to hypotension at doses that caused near maximal block of the reflexes. The hypotensive action was significant ($P<0.01$) for U-69,593 16 mg kg^{-1} (24 ± 1 mmHg) and for

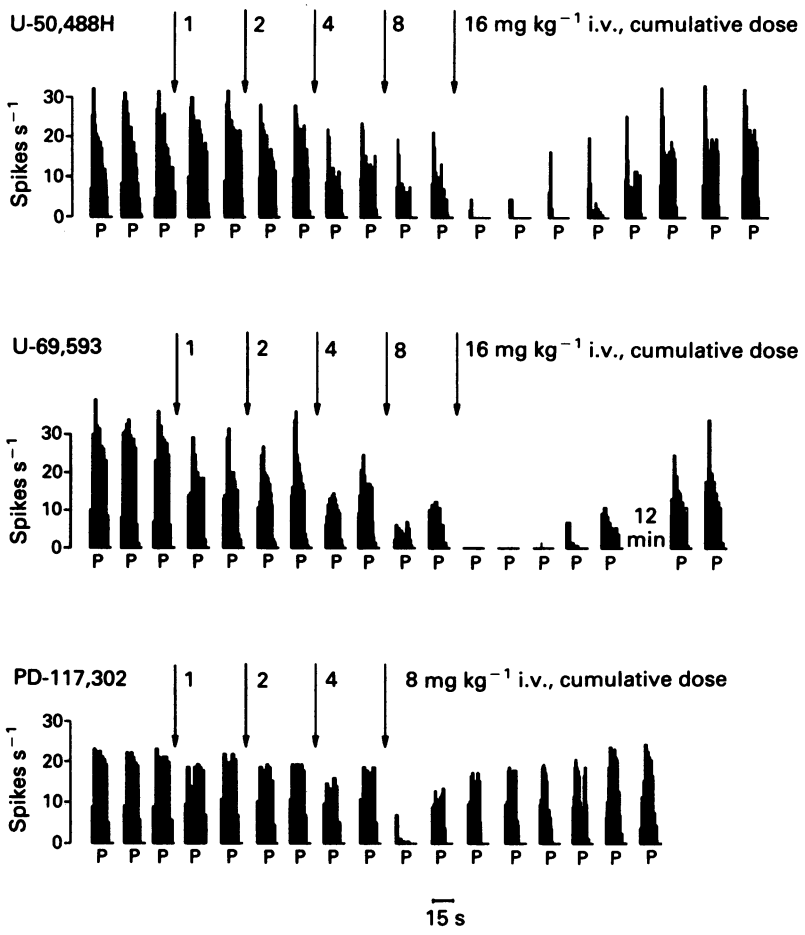

Figure 1 Effects of the κ-opioids U-50,488, U-69,593 and PD-117,302 on reflex responses to noxious pinch stimuli. The figure shows traces of original records of the firing rate of single motor units (SMU) in hindlimb flexor muscles in response to 15 s noxious pinch stimuli (P) repeated every 3 min. The chart recorder was halted between stimuli; there was no spontaneous activity. One test is shown for each opioid in different animals. Agonists were injected in a dose-doubling cumulative regime at 6 min intervals until the response was reduced to below 25% of control. α-Chloralose anaesthetized, spinalized rats.

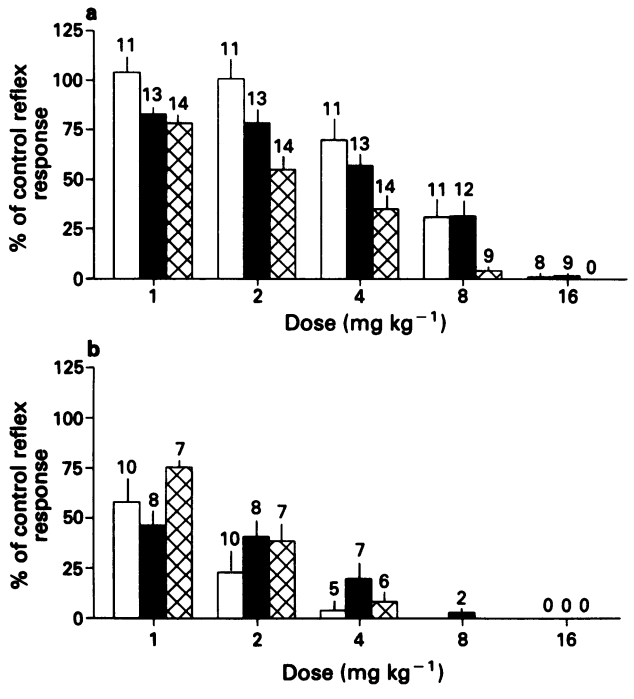

PD-117,302 8 mg kg^{-1} (42 ± 5 mmHg) but not for U-50,488 16 mg kg^{-1} (11 ± 6 mmHg). In spinally intact rats, blood pressure was affected less at the (lower) doses that blocked reflexes: in no case was MAP changed to a significant degree.

Group 2 agonists: CI-977 and GR103545

Data obtained with CI-977 and GR103545 are shown in Figure 3 (layout as for Figure 2) and Table 1. These agonists, as those in group 1, were more potent in sham spinalized than in spinalized rats. The situation is, however, complicated because in sham spinalized animals, different potencies were obtained in experiments performed with different initial doses. When the starting dose in the cumulative dose-response regime was sufficient to cause a reduction of responses to 50–70% control, the slope of the dose-response curve was similar to that seen in spinalized rats; the ratio of ED_{50} values between spinalized and intact groups was 40 for

Figure 2 Pooled data of the effects of the group 1 κ-agonists, U-50,488 (open columns), U-69,593 (solid columns) and PD-117,302 (cross-hatched columns), on SMU responses to peripheral noxious pinch stimuli, in spinalized (a) and sham spinalized rats (b). The data are shown as percentages of pre-drug control responses at each cumulative dose. Error bars show s.e.mean and numbers above columns indicate the number of units tested at each dose of drug. Note that the three agonists were more effective in sham spinalized rats.

Table 1 ED_{50} values for five κ-agonists

Agonist	*Initial dose tested*	*Spinalized ED_{50}*	*Sham spinalized ED_{50}*
U-50,488 (mg kg^{-1}, i.v.)	1	6.8	1.2
U-69,593 (mg kg^{-1}, i.v.)	1	5.0	0.7
PD-117,302 (mg kg^{-1}, i.v.)	1	2.8	1.7
CI-977 (μg kg^{-1}, i.v.)	10	180	
	2.5		62
	5		4.7
GR103545 (μg kg^{-1}, i.v.)	20	400	
	0.625		⩾ 25*
	2.5		5.1

ED_{50} values were related to spinal cord section (spinalized and sham spinalized) and to initial dose tested (note the varied starting doses for CI-977 and GR103545 in sham spinalized rats). ED_{50} values were estimated from regression analysis of pooled data (see Methods).
*This value cannot be specified further since the maximal reduction was only to around 50% control.

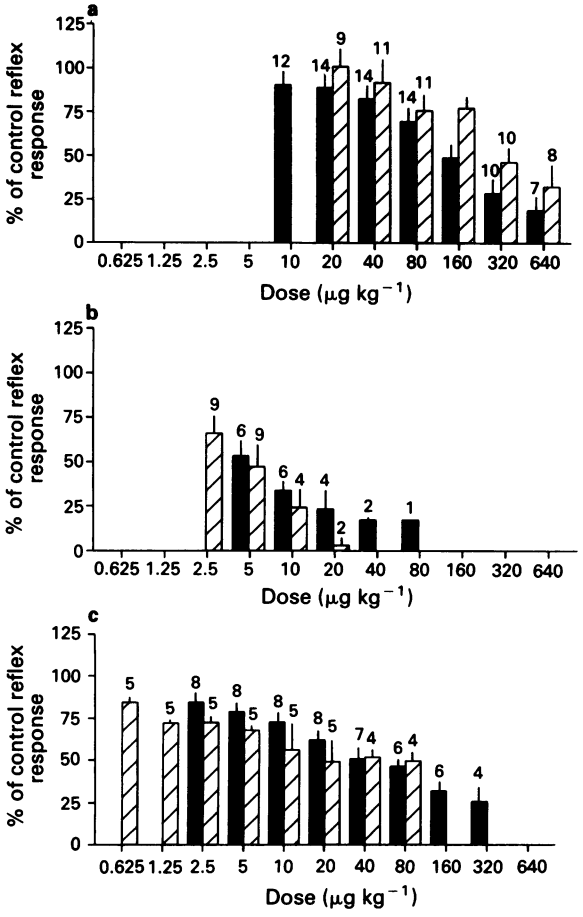

Figure 3 Pooled data of the effects of the group 2 κ-agonists, CI-977 (solid columns) and GR103545 (hatched columns), on SMU responses to peripheral noxious pinch stimuli, in spinalized (a) and sham spinalized animals (b and c). Format as in Figure 2. Note that, as with the agonists shown in Figure 2, these compounds were more potent in spinalized rats; however, the difference of potency, and the slope of the dose-response curve, depended on the starting dose used in the cumulative dose regime (compare b and c).

CI-977 and 56 for GR103545. However, when the starting dose was decreased such that responses were reduced only to about 80% control, the slope of the doses-response curve was markedly shallower and the estimated ED_{50} values were increased (Table 2). For CI-977 the ED_{50} was increased from 5 to 60 μg kg^{-1}; for GR103545 the ED_{50} was again increased,

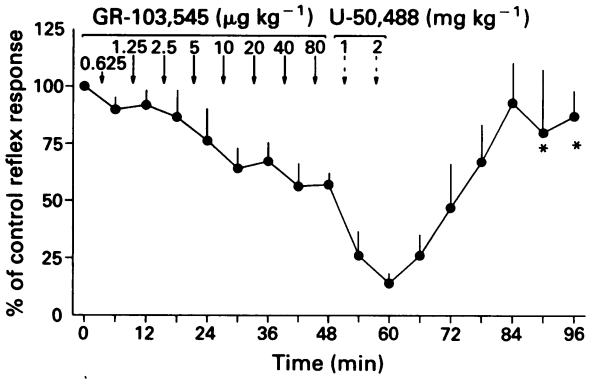

Figure 4 Effectiveness of U-50,488 in the presence of GR103545. GR103545 was administered with the same protocol as that shown in Figure 3c, and caused a maximal reduction to 57% control. Low doses of U-50,488 were then tested for efficacy. S.e.mean shown of $n = 6$ (or $*n = 5$).

but as the maximal reduction was only to approximately 50% of control, no meaningful ED_{50} value can be given.

To investigate the relationship between group 1 and group 2 compounds further, an independent group of 6 experiments was performed in sham spinalized animals. U-50,488 was administered 5 min after the last dose of GR103545; at 2 mg kg^{-1} it readily reduced the responses further, with a potency apparently similar to that seen in naive animals (Figure 4, cf. Figure 2).

The actions of CI-977 and GR103545 on blood pressure (Figure 5b) were different from those of group 1 agonists. In spinalized rats neither GR103545 nor CI-977 had any significant effect on MAP. In sham spinalized animals, in contrast, all doses decreased MAP to a significant degree ($P < 0.01$), although the effect was not dose-dependent over the dose-range causing reduction of spinal reflexes. The mean maximal reduction was 27 ± 3 mmHg for CI-977 and 19 ± 3 mmHg for GR103545.

Reversal of actions by naloxone

The agonist most sensitive to naloxone was U-50,488 (Table 2). The antagonist at 0.02 mg kg^{-1} produced a significant effect and 0.05 mg kg^{-1} reversed the action of this agonist by over 50% in both spinalized and intact rats. With U-69,593, PD-117,302 and CI-977 doses of 0.2–0.5 mg kg^{-1} of naloxone were required to produce a substantial reversal. With GR103545, doses greater than 1 mg kg^{-1} of naloxone were needed to cause reversal.

Comparing the doses of naloxone needed in spinalized and spinally intact groups, there were again some differences between the agonists. With U-50,488 and U-69,593 reversal at any given dose was somewhat greater in sham spinalized animals; with PD-117,302 and GR103545 there was no difference; and with CI-977 the reversal was greater in spinalized animals.

Naloxone also appeared to reverse the cardiovascular effects of the κ-agonists; MAP had always recovered to control at the end of a naloxone test. Since these cardiovascular effects were generally shorter-lasting than the effects on neuronal responses, recovery towards control MAP was often occurring before naloxone was administered, particularly with CI-977; quantification of the reversal could therefore not be performed.

Discussion

All five compounds tested reduced the flexor reflexes elicited by noxious mechanical stimulation of the hindpaw receptive field. U-50,488, PD-117,302 and U-69,593 were effective in

Table 2 Antagonism by intravenous naloxone of the actions of five κ-agonists

Agonist	Naloxone Dose (mg)	Spinalized % reversal	s.e.mean	n	Sham spinalized % reversal	s.e.mean	n
U-50,488	0.01	20	3.8	6			
	0.02	43	4.7	6	45	12.9	6
	0.05	76	9.2	6	91	6.6	6
	0.1	82	11.8	4			
U-69,593	0.05				46	6.6	4
	0.1	31	14.5	7	62	7.1	5
	0.2	54	14.6	6	71	17.7	6
	0.5	70	3.4	5	97	3.3	6
	1	88	6.3	4			
PD-117,302	0.05				39	8.6	5
	0.1	68	7.8	5	59	14.9	5
	0.2	71	15	5	76	17.1	5
	0.5	95	10.2	4	97	8.9	4
CI-977	0.1	65	9	9	51	8.5	11
	0.2	92	8	6	65	9.5	10
	0.5				94	6.3	8
GR103545	0.1	32	11.6	8	24	5.4	9
	1	57	14.9	8	64	8.0	8
	10	126	15	6	104	8.7	7

Percentage reversal was calculated comparing the recovery phase of the agonist in the presence of naloxone with that in the absence of the antagonist (see Methods). s.e.mean = standard error of the mean; n = number of units tested at each dose of naloxone.

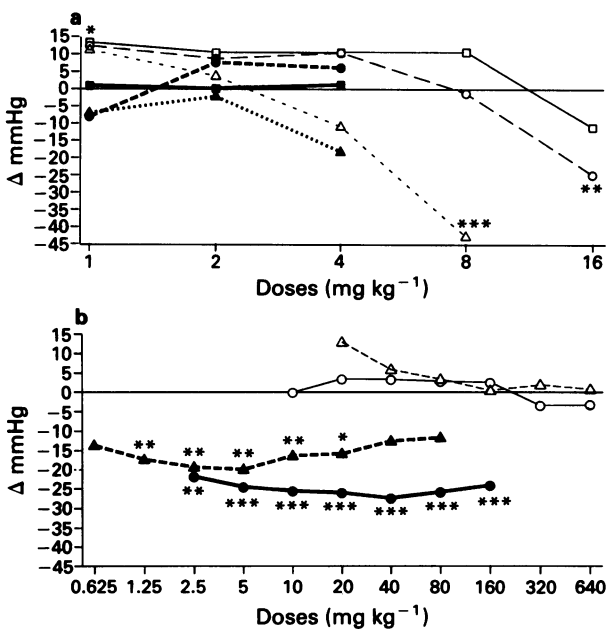

Figure 5 Effects of all five κ-agonists on blood pressure. Pooled data are expressed as the change in MAP, in mmHg, with each dose of drug, compared with pre-drug control values. Data are shown for both spinalized (open symbols) and sham spinalized animals (closed symbols). (a) U-50488 (□, ■); U-69,593 (○, ●) and PD-117,302 (△, ▲). (b) CI-977 (○, ●), GR-103545 (△, ▲). Note that there were differences not only for each agent between spinalized and sham-spinalized rats, but also between agonists of group 1 (a) and group 2 (b). Data were compared with pre-drug values of MAP by Student's t test (*$P<0.02$, **$P<0.01$, ***$P<0.001$).

spinally intact (sham spinalized) rats at doses similar to those reported for the paw-pressure test in awake animals (Leighton *et al.*, 1988; Hunter *et al.*, 1990). The same is true with CI-977 if paw pressure test data (Hunter *et al.*, 1990) are compared with the results shown in Figure 3c, i.e. when the starting doses were kept low; the drug was however more potent when higher starting doses were used (Figure 3b). GR103545 was slightly weaker in the present experiments than in paw pressure tests (Rogers *et al.*, 1992).

All five opioids were effective in spinalized as well as in spinally intact (sham operated) animals. This implies that the agents have an action within the spinal cord, which tallies with previous results using U-50,488 (Parsons & Headley, 1989; Dong *et al.*, 1990; Herrero & Headley, 1991).

All the agonists were less potent in spinalized than in spinally intact (sham operated) animals, as has been reported for U-50,488 (Herrero & Headley, 1991). The ratios of ED_{50} values were, however, not the same for the five compounds; there appear to be two types of result. The first was seen with U-50,488, U-69,593 and PD-117,302, where potency ratios were less than 6. The second occurred with CI-977 or GR103545, where the ratios were over 40 when larger starting doses were used in the cumulative dose regime.

The antinociceptive effects were dose-dependent. In spinalized animals the dose-response curves for all agents were relatively parallel, although the potencies varied over a 40 fold range. In sham spinalized animals, however, the picture is more complex and less easy to interpret. This arises from the finding that the cumulative-dose response curves varied with the starting dose for some but not all agents. This effect was only seen with CI-977 and GR103545, which had a shallower shape when the starting dose was lower (Figure 3b vs 3c). The low variability in potency of the other agonists between SMU was such that this effect would have been seen had it been present with the other agonists.

The shallower dose-response curves following lower starting doses could have been caused by progressive desensitization of receptors. However, since U-50,488 was still effective following cumulative doses of GR103545 that caused a plateau reduction of only some 50%, any desensitization could only have been of a sub-set of receptors upon which U-50,488 does not act.

Two types of effect were again seen on blood pressure, with the same grouping of κ-agonists. Over the range of antinociceptive doses tested, U-50,488, U-69,593 and PD-117,302 modified the MAP only in spinally transected animals; presumably they have complex central cardiovascular effects that are normally compensated by sympathetic vasoconstriction that is compromized in spinalized animals.

CI-977 and GR103545 had the opposite effect: blood pressure was reduced only in spinally intact animals. This hypotension was not dose-dependent over the antinociceptive dose-range, nor was its duration related to the time course of the antinociceptive effects.

The effects of naloxone were more disparate between compounds. In both groups of animals, 50% reversal of U-50,488 was elicited with doses of naloxone of 0.05 mg kg^{-1} or less (see also Parsons *et al.*, 1989; Herrero & Headley, 1991). As stated previously (Parsons *et al.*, 1989) it is unlikely that U-50,488 at these doses is acting on μ-receptors, both because μ-agonists were still ten fold more sensitive to naloxone and because U-50,488 does not have μ-like cardiovascular depressant effects. At the other extreme, the naloxone ED_{50} against GR103545 was approaching 1 mg kg^{-1}, i.e. almost 20 times greater. This high dose is comparable with results on the structurally related compound GR38414 (Hayes *et al.*, 1990). The other three compounds, however, fell between these extremes in a manner that did not closely parallel the groupings seen with the other parameters (Table 2).

These differences in antagonist potency probably reflect different affinities of more than one receptor type; alternatively they might reflect different rates of agonist dissociation. The resistance of GR103545 to antagonism cannot however be explained in this manner since the agonist U-50,488 was still as potent in the presence as in the absence of GR103545 (see above and Figure 4).

Comparison of the data gathered in the four paradigms, i.e. antinociception in spinally intact rats, in spinally sectioned animals, naloxone reversibility, and blood pressure, all indicate that there are qualitative and quantitative differences between these five agonists. Whilst it remains true that many differences between κ-agonists can be due to varying affinity states of the same receptor (Wood *et al.*, 1989; Traynor, 1989; see also Clark *et al.*, 1989), the different ED_{50} values obtained with naloxone indicate that receptor differences must contribute to the different functional effects observed with these five κ agonists. For reasons stated above, as well as because of other binding and pharmacological data, it is unlikely that any of the differences are due to actions of some of the agonists on μ-receptors. The most likely explanation is therefore that these agonists act to differing degrees on an unknown variety of opioid receptor subtypes; they may in addition interact differently with different affinity states of such receptor subtypes to yield the complex picture obtained here. It is not clear whether these multiple sites can all be classified as κ-receptors; final resolution of this situation must await a combination of molecular genetics data on gene sequences and pharmacological investigations with satisfactory and selective κ-antagonists.

In conclusion, two different behaviours of κ agonists have been discriminated in relation to spinal nociceptive and cardiovascular parameters. One type is represented by U-50,488, U-69,593 and PD-117,302, the other by GR103545 and perhaps CI-977. The data can only be explained if there is more than one population of κ-opioid receptors on which these agonists act. It is not, however, possible to relate the receptor populations seen here to the κ-receptor terminology proposed by others (Clark *et al.*, 1989).

We thank Upjohn for the gift of U-50,488 and U-69,593, Parke-Davis for the gift of PD-117,302 and CI-977, and Glaxo for the gift of GR103545. We also thank the Wellcome Trust and the Spanish Ministry of Education who provided financial support.

References

ATTALI, B., GOUARDERES, C., MAZARGUIL, H., AUDIGIER, Y. & CROS, J. (1982). Evidence for multiple 'kappa' binding sites by use of opioid peptides in the guinea-pig lumbo-sacral spinal cord. *Neuropeptides*, **3**, 53–64.

AUDIGIER, Y., ATTALI, B., MAZARGUIL, H. & CROS, J. (1982). Characterization of [^{3}H]etorphine binding in guinea pig striatum after blockade of mu and delta sites. *Life Sci.*, **31**, 1287–1290.

CASTANAS, E., BOURHIM, N., GIRAUD, P. BOUDOURESQUE, F., CANTAU, P. & OLIVER, C. (1985). Interaction of opiates with opioid binding sites in the bovine adrenal medulla: II. Interaction with kappa sites. *J. Neurochem.*, **45**, 688–699.

CLARK, C.R., BIRCHMORE, B., SHARIF, N.A., HUNTER, J.C., HILL, R.G. & HUGHES, J. (1988). PD 117302: a selective agonist for the κ-opioid receptor. *Br. J. Pharmacol.*, **93**, 618–626.

CLARK, J.A., LIU, L., PRICE, M., HERSH, B., EDELSON, M. & PASTERNAK, G.W. (1989). Kappa opiate receptor multiplicity: evidence for two U-50,488-sensitive κ_1 subtypes and a novel κ_3 subtype. *J. Pharmacol. Exp. Ther.*, **251**, 461–468.

DONG, X.W., PARSONS, C.G. & HEADLEY, P.M. (1991). Effects of intravenous μ and κ receptor agonists on sensory responses of convergent neurones in the dorsal horn of spinalized rats. *Br. J. Pharmacol.*, **103**, 1230–1236.

HARTELL, N.A. & HEADLEY, P.M. (1990). Spinal effects of four injectable anaesthetics on nociceptive reflexes in rats: a comparison of electrophysiological and behavioural measurements. *Br. J. Pharmacol.*, **101**, 563–568.

HARTELL, N.A. & HEADLEY, P.M. (1991). Preparative surgery enhances the direct spinal actions of three injectable anaesthetics in the anaesthetized rat. *Pain*, **46**, 75–80.

HAYES, A.G., BIRCH, P.J., HAYWARD, N.J., SHEEHAN, M.J., ROGERS, H., TYERS, M.B., JUDD, D.B., SCOPES, D.I.C. & NAYLOR, A. (1990). A series of novel, highly potent and selective agonists for the κ-opioid receptor. *Br. J. Pharmacol.*, **101**, 944–948.

HEADLEY, P.M. & HERRERO, J.F. (1991). Do different kappa opioids mediate analgesia via different receptors at spinal and supraspinal sites? *Soc. Neurosci. Abst.*, **17**, 121.4.

HEADLEY, P.M., PARSONS, C.G., WEST, D.C. & DONG, X.-W. (1989). On the influence of anaesthesia, stimulus intensity and drug access in pharmacological tests of sensory processing in the superficial dorsal horn. In *Processing of Sensory Information in the Superficial Dorsal Horn of the Spinal Cord.* ed. Cervero, F., Bennett, G.J. & Headley, P.M. NATO ASI Series A. Life Sciences, Vol. 176, pp. 499–511. New York: Plenum Press.

HERRERO, J.F. & HEADLEY, P.M. (1991). The effects of sham and full spinalization on the systemic potency of μ- and κ-opioids on spinal nociceptive reflexes in rats. *Br. J. Pharmacol.*, **104**, 166–170.

HERRERO, J.F. & HEADLEY, P.M. (1992). Functional evidence for kappa receptor heterogeneity between spinal and supraspinal sites. *Br. J. Pharmacol.*, **105**, 140P.

HUNTER, J.C., LEIGHTON, G.E., MEECHAM, K.G., BOYLE, S.J., HORWELL, D.C., REES, D.C. & HUGHES, J. (1990). CI-977, a novel and selective agonist for the κ-opioid receptor. *Br. J. Pharmacol.*, **101**, 183–189.

IYENGAR, S., KIM, H.S. & WOOD, P.L. (1986). Effects of kappa opiate agonists on neurochemical and neuroendocrine indices: evidence for kappa receptor subtypes. *Life Sci.*, **39**, 637–644.

LAHTI, R.A., MICKELSON, M.M., MCCALL, J.M. & VON VOIGTLANDER, P.F. (1985). [^{3}H]U-69593, a highly selective ligand for the opioid κ-receptor. *Eur. J. Pharmacol.*, **109**, 281–284.

LEIGHTON, G.E., RODRIGUEZ, R.E., HILL, R.G. & HUGHES, J. (1988). κ-Opioid agonists produce antinociception after i.v. and i.c.v. but not intrathecal administration in the rat. *Br. J. Pharmacol.*, **93**, 553–560.

MORRE, M., BACHY, A., GOUT, B., BOIGEGRAIN, R., ARNONE, M. & RONCUCCI, R. (1983). κ-binding sites in guinea-pig brain membranes: evidence for a dynorphin resistant subtype. *Life Sci.*, **33** Suppl. 1, 179–182.

PARSONS, C.G. & HEADLEY, P.M. (1989). Spinal antinociceptive actions of μ and κ-opioids: the importance of stimulus intensity in determining 'selectivity' between reflexes to different modalities of noxious stimulus. *Br. J. Pharmacol.*, **98**, 523–532.

PARSONS, C.G., WEST, D.C. & HEADLEY, P.M. (1989). Spinal antinociceptive actions and naloxone reversibility of intravenous μ- and κ-opioids in spinalised rats: potency mismatch with values reported for spinal administration. *Br. J. Pharmacol.*, **98**, 533–544.

PFEIFFER, A., PASI, A., MEHRAEIN, P. & HERZ, A. (1981). A subclassification of kappa sites in human brain by use of dynorphin 1-17. *Neuropeptides*, **2**, 89–97.

PORTOGHESE, P.S., LIPKOWSKI, A.W. & TAKEMORI, A.E. (1987). Binaltorphimine and nor-binaltorphimine, potent and selective κ-opioid receptor antagonists. *Life Sci.*, **40**, 1287–1292.

ROGERS, H., BIRCH, P.J., HARRISON, S.M., PALMER, E., MANCHEE, G.R., JUDD, D.B., NAYLOR, A., SCOPES, D.I.C. & HAYES, A.G. (1992). GR94839, a κ-opioid agonist with limited access to the central nervous system, has antinociceptive activity. *Br. J. Pharmacol.*, **106**, 783–789.

ROTHMAN, R.B., BYKOV, V., COSTA, B.R., JACOBSON, A.E., RICE, K.C. & BRADY, L.S. (1990). Interaction of endogenous opioid peptides and other drugs with four kappa opioid binding sites in guinea pig brain. *Peptides*, **11**, 311–331.

SIEGEL, S. & CASTELLAN, N.J. (1988). *Non-parametric Statistics for the Behavioural Sciences*. 2nd edition. New York: McGraw-Hill.

TRAYNOR, J. (1989). Subtypes of the κ-opioid receptor: fact or fiction? *Trends Pharmacol. Sci.*, **10**, 52–53.

VON VOIGTLANDER, P.F., LAHTI, R.A. & LUDENS, J.H. (1983). U-50,488: a selective and structurally novel non-mu (kappa) opioid agonist. *J. Pharmacol. Exp. Ther.*, **224**, 7–12.

WOOD, M.S., RODRIGUEZ, F.D. & TRAYNOR, J.R. (1989). Characterisation of κ-opioid binding sites in rat and guinea-pig spinal cord. *Neuropharmacol.*, **28**, 1041–1046.

(Received November 16, 1992
Revised March 11, 1993
Accepted March 22, 1993)

Br. J. Pharmacol. (1993), **110**, 310–316

Mechanical and electrophysiological studies on the positive inotropic effect of 2-phenyl-4-oxo-hydroquinoline in rat cardiac tissues

[1]Ming Jai Su, Gwo Jyh Chang & *Sheng Chu Kuo

Department of Pharmacology, College of Medicine, National Taiwan University, Taipei and *Institute of Pharmaceutical Chemistry, China Medical College, Taichung, Taiwan

1 The pharmacological and electrophysiological effect of 2-phenyl-4-oxo-hydroquinoline (YT-1), a new synthetic agent, were determined in rat isolated cardiac tissues and ventricular myocytes.

2 YT-1 was found to have a positive inotropic effect in both atria and ventricular muscles but did not cause significant increases in the spontaneously beating rate of right atria.

3 The positive inotropic effect of YT-1 was antagonized neither by β-nor by α-adrenoceptor antagonists but was partially antagonized by a Ca^{2+} channel blocker (verapamil) and a K^+ channel blocker (4-AP).

4 The action potential duration and amplitude of ventricular cells were progressively increased as the concentration of YT-1 was increased from 3 to 30 μM.

5 A voltage clamp study revealed that the prolongation of action potential duration by YT-1 was associated with a prominent inhibition of 4-AP-sensitive transient outward current (I_{to}). At potentials negative to the reversal potential of K_1-channels, the inward current through these channels was partially reduced by YT-1. At potentials positive to the reversal potential, the outward current through these channels was affected very little.

6 Although YT-1 blocked the amplitude of I_{to}, the voltage-dependence of the steady-state inactivation of I_{to}, was unaffected.

7 Apart from the inhibition of K^+ currents, YT-1 also inhibited the sodium inward current.

8 The evidence suggests that YT-1 increases the slow inward Ca^{2+} current (I_{Ca}) significantly.

9 It is concluded that the positive inotropic effect of YT-1 is due predominantly to the increase of I_{Ca} and inhibition of I_{to}.

Keywords: 2-Phenyl-4-oxo-hydroquinoline; positive inotropic action; transient outward current; sodium inward current; calcium inward current; myocytes

Introduction

Digitalis is the standard inotropic agent for the enhancement of myocardial contractility and improvement of heart function in congestive heart failure. The primary limitation of digitalis is the associated toxicity due to alteration of impulse generation and conduction in the heart and the resultant narrow margin of safety. Digitalis has other limitations including peripheral vasoconstriction and questionable efficacy during chronic therapy (Mikkelsen *et al.*, 1979). Therefore, many candidates for a digitalis substitute have been developed in recent years (Farah *et al.*, 1984). 2-Phenyl-4-oxo-hydroquinoline (YT-1) is a newly synthesized compound with structure partially similar to quinidine (Figure 1).

Following an observation that YT-1 stimulated heart muscle *in vitro*, the present experiments were carried out to investigate the cardiac effect and possible mechanism of the positive inotropic effect of YT-1 and the detailed mode of action of YT-1 on membrane currents in single rat ventricular myocytes.

Methods

Mechanical response

Right atria, left atria and right ventricular strips (4 × 6 mm) were quickly dissected from the hearts of male WKY rats (weighing 250–300 g) and placed in an organ bath containing 10 ml Tyrode solution gassed with 95% O_2 plus 5% CO_2 kept at 36 ± 0.2°C. The composition of the Tyrode solution was (in mM): NaCl 137.0, KCl 5.4, $MgCl_2$ 1.1, $NaHCO_3$ 11.9, NaH_2PO_4 0.33, dextrose 11.0 and $CaCl_2$ 2.0. Contractions of spontaneously beating right atria and electrically driven left atria and right ventricular strips were measured by connecting one end of the preparations using a fine silk thread to a force displacement transducer (Type BG 25, Gould Inc., Cleveland, Ohio, U.S.A.) and tension was recorded on a Gould 2200s recorder. A preload of 500 mg was used. Both left atria and right ventricular strips were stimulated at a frequency of 2 Hz by rectangular pulses of 1 ms duration at supramaximal intensity via a Grass SD9 isolated stimulator (Grass Instruments Co., Quincy, MA, U.S.A.).

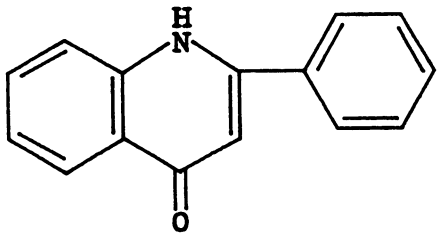

Figure 1 Chemical structure of 2-phenyl-4-oxo-hydroquinoline (YT-1).

[1] Author for correspondence.

Single-cell isolation

Single myocytes were isolated from adult rats by enzymatic dissociation, as described previously (Mitra & Morad, 1985). Briefly, the heart was rapidly excised from pentobarbitone-anesthetized rats. The aorta was canulated and retrogradely perfused with Ca^{2+}-free Tyrode solution containing (in mM): NaCl 137.0, KCl 5.4, $MgCl_2$ 1.1, dextrose 11.0, and N-2-[hydroxyethyl] piperazine-*N'*-[2-ethane sulphonic acid] (HEPES)-NaOH buffer (pH 7.4) 10.0. The perfusate was oxygenated and maintained at 37 ± 0.2°C. After 5 min, the perfusate was changed to the same solution containing 1 mg ml^{-1} collagenase (Type I, Sigma Chemical Co., St. Louis, MO, U.S.A.) and 0.3 mg ml^{-1} protease (Type XIV, Sigma). After 20–30 min digestion, the residual enzyme-containing solution was cleared by 5 min perfusion with 0.2 mM Ca^{2+} Tyrode solution. Thereafter, the left and right ventricles were separated from the atria, dispersed and stored in 0.2 mM Ca^{2+} Tyrode solution for later use. Only rod-like relaxed ventricular myocytes showing clear striations were used for the experiments.

Whole-cell recording

Transmembrane voltages and currents were recorded by the single-pipette whole-cell patch clamp technique (Hamill *et al.*, 1981). Rat ventricular cells were transferred to a chamber mounted on an inverted microscope (Nikon Diaphot, Nikon Co., Tokyo, Japan) for electrophysiological recording and were bathed in Tyrode solution containing (mM): NaCl 137.0, KCl 5.4, $CaCl_2$ 2.0, $MgCl_2$ 1.1, dextrose 11.0 and HEPES-NaOH buffer (pH 7.4) 10.0. All experiments were performed at room temperature (23–25°C). Action potentials were elicited by intracellularly applied stimuli (4 ms duration of 1 nA) through a heat-polished patch electrode with resistance between 2 and 5 Mohm when filled with an internal solution of the following composition (mM): KCl 120.0, NaCl 10.0, MgATP 5.0, K_2EGTA 5.0, cyclic AMP 0.03, dextrose 5.0, and HEPES-KOH buffer (pH 7.4) 10.0. The maximum rate of rise of the action potential upstroke (V_{max}) was obtained from electronic differentiation of the action potential. Electrode junction potentials (5 to 10 mV) were measured and nulled before impalement of the cell. The formation of a high resistance seal was monitored by applying 1 nA current from a digital pulse generator. A high resistance seal (5 to 10 gigaohm) was obtained before the disruption of the membrane patch. The cells were dialyzed with the electrode solution for 3–5 min to reach a state of equilibrium after disruption of the membrane patch. In voltage clamp experiments, series resistance compensation was used to offset the series resistance due to the pipette tip resistance. During measurement of potassium outward currents, the contamination of calcium inward current (I_{Ca}) was prevented by adding 1.0 mM Co^{2+} to the bathing medium. In this condition, 200 ms depolarization of membrane potential to a level positive to −40 mV usually resulted in a generation of a fast sodium inward current (I_{Na}) followed by a transient outward potassium current. In order to eliminate the contamination of inward current completely, 30 μM TTX was added to inhibit the I_{Na}. The magnitude of the transient outward current was measured at 10 ms after the start of the 200 ms depolarizing pulses.

During measurement of I_{Na} and I_{Ca}, the potassium currents were prevented by adding 2–4 mM Cs^+ to the bathing medium and internal dialysis of the cells with Cs^+-containing internal solution of the following composition (mM): CsCl 130.0, EGTA 5.0, tetraethylammonium (TEA) chloride 15.0, cyclic AMP 0.03, dextrose 5.0, HEPES-CsOH buffer (pH 7.4) 10.0. Under such circumstances inward and outward K^+ currents were almost abolished within 4 to 6 min (Iijima *et al.*, 1985). The cells bathed in normal Tyrode solution, I_{Na} elicited by depolarization to −40 mV was larger than 20 nA. In this condition, the spatial and voltage control of membrane potential was not satisfactory. To improve the clamp efficiency, the I_{Na} was reduced by bathing the cells in low Na^+ Tyrode solution (122 mM NaCl was substituted with choline chloride) and internal dialysis of the cell with Na^+ containing (5 mM) Cs^+ pipette solution to reduce the transmembrane Na^+ concentration gradient and to prevent the contamination of potassium outward currents. Since the I_{Na} evoked by the depolarizing step was completely inhibited by 30 μM TTX (not shown), the possible contamination of this current by inward current through T-type Ca^{2+} channels could be excluded. For measurement of I_{Ca}, the I_{Na} was inactivated by the first step depolarization of membrane potential to −40 mV (Weidmann, 1955; Lee *et al.*, 1981), the I_{Ca} could then be activated by the second step depolarization to levels positive to −20 mV. In order to evaluate the concentration and time-dependent effect of YT-1 on I_{Ca}, 10, 30 and 100 μM YT-1 were added cumulatively and sequentially at 3, 6 and 9 min after disruption of the membrane patch.

Recording and data analysis

Recording was made through a Dagan 8900 voltage clamp amplifier (Dagan Co., Minneapolis, MN, U.S.A.), displayed on a storage oscilloscope (Model 511A, Tektronix Inc., Beaverton, OR, U.S.A.) and photographaged for subsequent analysis. Data are presented as mean ± s.e. (n = no. of preparations). A Student's t test was used to compare test and control values. Comparison of mean values among groups was done by a repeated-measure analysis of variance. A P value of less than 0.05 was regarded as statistically significant. Each of the results illustrated in the figures is representative of at least four complete experiments of the same design.

Drugs and chemicals

YT-1 (2-phenyl-4-oxo-hydroquinoline) was synthesized by Dr S.C. Kuo. Quinidine, lignocaine, 4-aminopyridine (4-AP), (±)-verapamil hydrochloride, propranolol hydrochloride, prazosin hydrochloride and tetrodotoxin (TTX) were purchased from Sigma Chemical Company (St. Louis, Mo., U.S.A.). Both YT-1 and quinidine were dissolved in dimethylsulphoxide (DMSO) as a stock solution. The stock solutions were diluted by the bathing solution to a given concentration. In control experiments DMSO (up to 0.1%) alone had no discernible effect on the electrophysiological parameters.

Results

Positive inotropic effect

The effects of YT-1 on both twitch tension in rat atria and ventricular strips and spontaneously beating rate in right atria are shown in Figure 2. The control values for contractile force of right atria, left atria, right ventricular strips and spontaneously beating rate of right atria were 0.21 ± 0.01 ($n = 8$), 0.18 ± 0.02 ($n = 8$), 0.22 ± 0.02 g ($n = 7$) and 232 ± 8 beats min^{-1} ($n = 8$), respectively. YT-1 (23-204 μM) concentration-dependently increased contractile force in both atria and ventricular muscles but without significantly increasing the spontaneously beating rate. The percentage increase of twitch tension by YT-1 was antagonized neither by propranolol (2 μM) nor prazosin (0.1 μM) but was significantly antagonized by the Ca^{2+} channel blocker verapamil, 1 μM and partially but insignificantly antagonized by the K^+ channel blocker 4-AP, 1 mM (Figure 3).

Effect of YT-1 on action potential

The action potential duration (APD) and amplitude of ventricular cells were progressively increased as the concentration

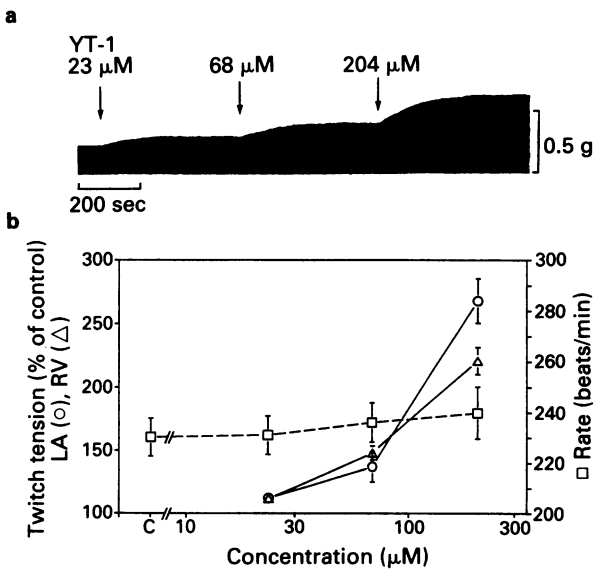

Figure 2 Effect of YT-1 on isometric contractions and spontaneously beating rate of rat cardiac tissues. (a) Positive inotropic effect of YT-1 on rat isolated left atrium. (b) Concentration-response curves for YT-1 on contractions of left atria (○), right ventricular strips (△) and spontaneously beating rate of right atria (□), $n = 6-8$. Twitch tension after YT-1 treatment is expressed as percentage of control. Values are mean ± s.e.mean.

of YT-1 was increased from 3 to 30 μM as illustrated in Figure 4. Effects of YT-1 (10 μM) on various parameters of the ventricular action potential are summarized in Table 1. YT-1 significantly increased action potential amplitude and prolonged APD_{50} and APD_{90} without affecting either the resting membrane potential or the maximum upstroke velocity (V_{max}).

Effects of YT-1 on Na^+ current (I_{Na}) and Ca^{2+} current (I_{Ca})

The ventricular myocytes were depolarized from a holding potential of − 80 mV to − 40 mV for 10 ms to evoke the I_{Na}, and then to 0 mV for 30 ms to evoke the I_{Ca}. In the absence of K^+ currents, YT-1 clearly decreased the inward Na^+ currents concentration-dependently in all cells tested (Figure 5). However, L-type Ca^{2+} currents ($I_{Ca,L}$) were increased by YT-1. Control values for I_{Na} and I_{Ca} were 4.6 ± 0.4 and 1.9 ± 0.1 nA, respectively. The IC_{50} of YT-1, lignocaine, and quinidine on I_{Na} were 63.3 ± 1.2, 10.0 ± 0.8 and 2.8 ± 0.1 μM, respectively (Figure 5). It is noteworthy that the reduction of $I_{Ca,L}$ due to the 'run-down' phenomenon with time (Belles *et al.*, 1988) was observed in the absence of YT-1. In our control study, I_{Ca} measured at 6, 9 and 12 min after disruption of the membrane patch were 74.3 ± 2.8, 62.5 ± 2.3 and 56.4 ± 2.7% ($n = 6$) of that measured at 3 min after disruption, respectively (Figure 5c). In the presence of 10, 30 and 100 μM YT-1, the value of I_{Ca} measured at 6, 9 and 12 min after disruption were 140.3 ± 6.1, 162 ± 6.8 and 109.2 ± 5.0% ($n = 11$) of that measured at 3 min after the disruption, respectively.

Effects of YT-1 on the transient outward (I_{to}) and the inward rectifying (I_{k1}) potassium current

As shown in Figure 6, the I_{Na} and I_{Ca} were abolished by TTX (30 μM) and Co^{2+} (1 μM), respectively, and the transient outward currents were elicited by depolarizing pulses in 20 mV increments between − 40 and + 60 mV from a holding potential of − 80 mV. Figure 6a shows that when the myocytes were exposed to 10 μM YT-1, the initial amplitude

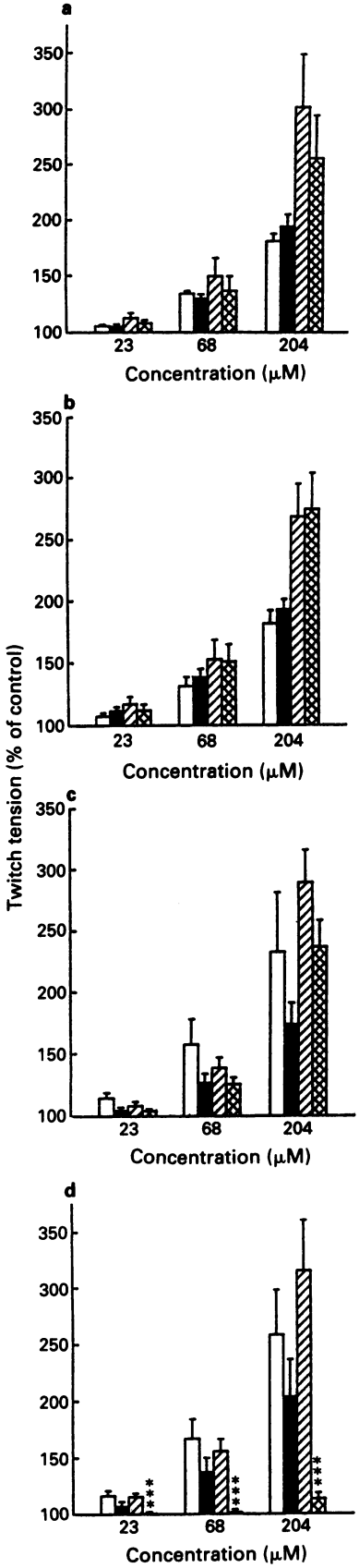

Figure 3 Effect of 2 μM propranolol (a), 0.1 μM prazosin (b), 1 mM 4-aminopyridine (c) and 1 μM verapamil (d) on positive inotropism of YT-1 in rat isolated left atria and right ventricular strips. Open column and hatched columns represent the effect of YT-1 alone on right ventricular strips and left atria, respectively, while solid columns and cross-hatched columns represent the effect of YT-1 after pretreatment with each drug as indicated above on right ventricular strips and left atria, respectively. Mean from 6 to 8 preparations; values are mean with s.e.mean. ***$P < 0.001$ as compared with tissues not treated with verapamil by a repeated-measure analysis of variance.

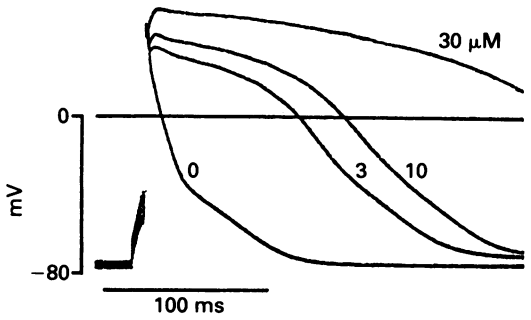

Figure 4 Effect of YT-1 on the action potential of rat ventricular cell. The superimposed action potentials show the progressive effect of 3, 10 and 30 μM YT-1 at a constant stimulation rate of 0.1 Hz. Horizontal line indicates zero potential.

Table 1 Effects of 2-phenyl-4-oxo-hydroquinoline (YT-1) on the action potential parameters in rat ventricular myocytes

	Control	*YT-1* (10 μM)
APA (mV)	115.3 ± 3.7	127.3 ± 4.1*
RMP (mV)	− 79.5 ± 1.3	− 79.4 ± 1.6
V_{max} (V s^{-1})	240.4 ± 9.0	236.2 ± 10.2
APD_{50} (ms)	13.4 ± 0.9	67.4 ± 4.7***
APD_{90} (ms)	36.0 ± 3.1	137.9 ± 4.4***

Data are expressed as mean ± s.e. of 8 cells. APA, action potential amplitude; RMP, resting membrane potential; V_{max}, maximum rate of rise of the action potential upstroke; APD_{50} and APD_{90}, action potential duration measured at 50% and 90% repolarization, respectively. * indicates a significant difference (Student's *t* test, $P<0.05$) between the YT-1-treated cells and control cells, ***$P<0.001$.

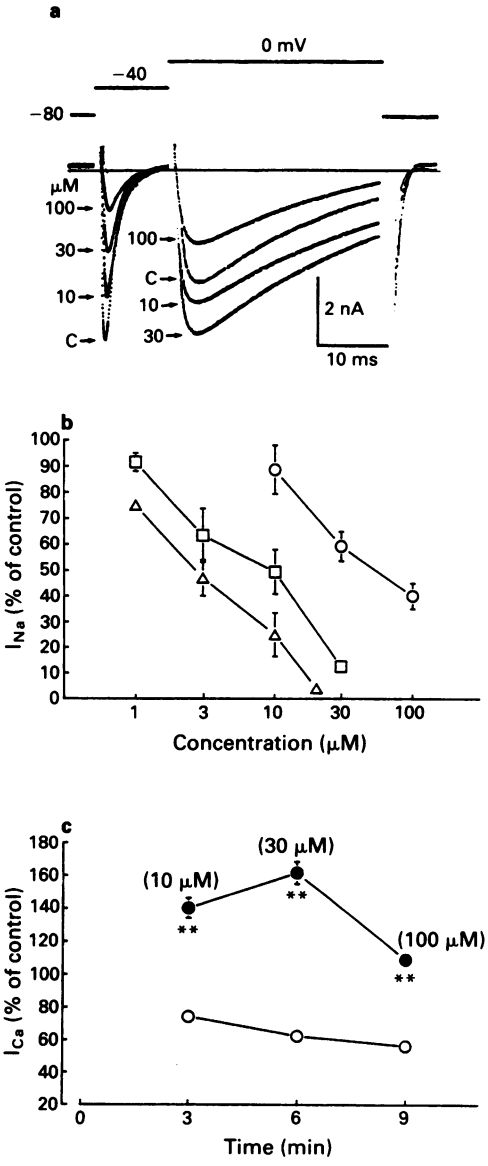

Figure 5 Effect of YT-1 on I_{Na} and I_{Ca} of the rat ventricular cells. (a) The typical current traces of I_{Na} and I_{Ca} before and after treatment with YT-1 in a cumulative fashion. C: control. Horizontal line indicates zero-current level. The experimental conditions are described in the text. (b) The concentration-dependent effects of YT-1 (○), lignocaine (□) and quinidine (△) on I_{Na} . I_{Na} after drug treatment were normalized and expressed as a percentage of those before drug treatment. Mean ± s.e.mean from 4 to 7 cells. (c) Concentration- and time-dependent effect of YT-1 on I_{Ca} . Spontaneous run down (○) and after YT-1 treatment (●) are shown. Values are means ± s.e.mean from 11 cells.

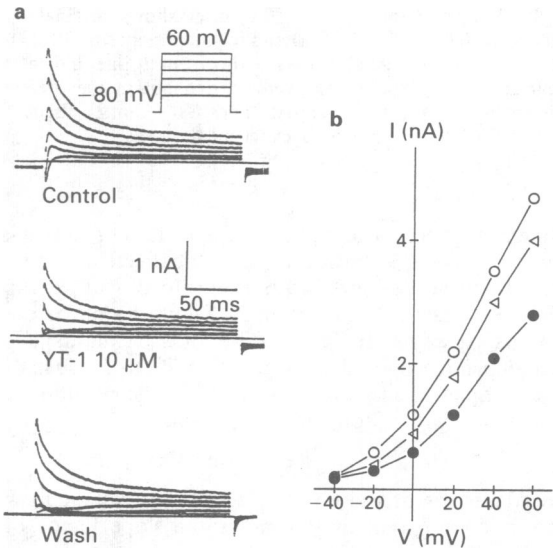

Figure 6 Voltage-dependence of I_{to} in the absence, presence and washout of 10 μM YT-1. (a) Typical current traces activated by 200 ms depolarizing pulses in 20 mV increments between − 40 and + 60 mV from a holding potential of − 80 mV before (upper panel), 3 min after exposure (middle panel) and 5 min washout (lower panel) of YT-1. Horizontal lines indicate zero-current level. TTX (30 μM) and Co^{2+} (1 mM) were added to the external solution to block I_{Na} and I_{Ca} , respectively. I_{to} was measured as the net current at its initial spike. (b) *I-V* curves of I_{to} : (○) control; in presence of 10 μM YT-1 (●); after washout of YT-1 (△).

of I_{to} measured 5–10 ms after the onset of the clamp pulse was reduced. I_{to} recovered significantly upon washout, regaining 85% of its control value in 3 to 5 min. Figure 6b shows the current-voltage relationship to I_{to} in the absence and presence of YT-1. The initial amplitude of I_{to} was increased linearly with potential. YT-1 suppressed the initial amplitude of I_{to} (Figure 6b). Figure 7 shows concentration-dependent inhibition of I_{to} by YT-1. Under control conditions I_{to} at + 40 mV had an initial peak value of 3.0 ± 0.2 nA ($n = 8$). The concentration-response curve for the inhibition of I_{to} induced by 3–100 μM YT-1 was determined as the integral of the current measured from the first 200 ms of the current after the depolarization. The response is consistent with a first-order reaction with a dissociation constant of 14.9 ± 1.3 μM ($n = 8$ cells). This value was calculated by fitting the experimental data to the equation:

$$\text{Response} = 1/\{1 + (Kd/[D])\}$$

where *K*d is the dissociation constant and [D] is the concentration of YT-1. YT-1 decreased I_{to} in a concentration-

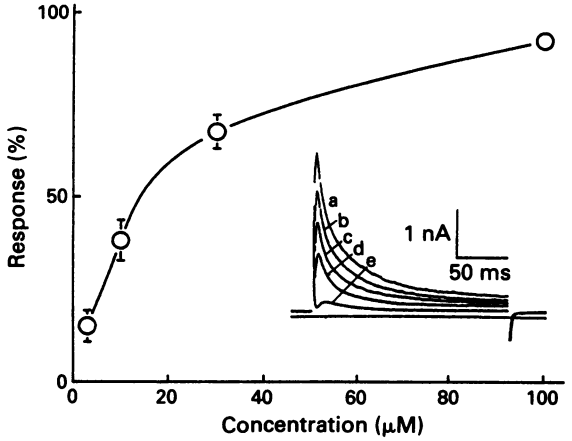

Figure 7 Concentration-response curve for the inhibition of the I_{to} induced by YT-1 measured as the integral of the first 200 ms of the current elicited by a 200 ms depolarizing clamp pulse from − 80 mV to + 40 mV applied once every 20 s. Inset shows original current records at + 40 mV in control (a) and in the presence of 3 (b), 10 (c), 30 (d) and 100 (e) μM YT-1. The horizontal line indicates the zero-current level. Experiments were carried out in the presence of tetrodotoxin (30 μM), Co^{2+} (1 mM) and Cs^+ (2 mM). Each point represents the mean value of 8 experiments.

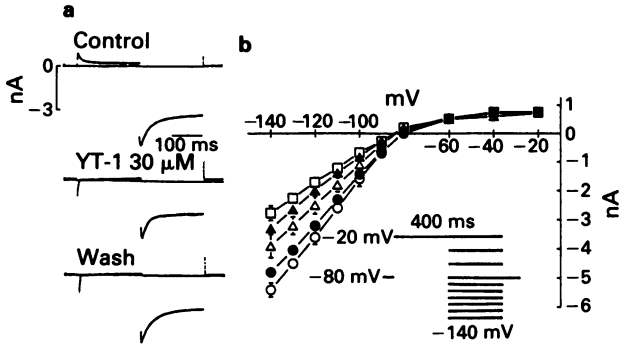

Figure 9 Effect of YT-1 on I_{k1} in rat ventricular cells. I_{k1} was initially deactivated by a 200 ms prepulse to − 20 mV then activated by 200 ms test pulses to potentials from − 20 to − 140 mV as shown in the inset of (b). (a) Typical inward current through inward rectifier activated by a hyperpolarizing pulse to − 120 mV before (upper panel), 3 min after exposure to (middle panel) and 5 min washout (lower panel) of 30 μM YT-1. I_{k1} was measured as the net current at the initial start of test pulse to levels between − 20 and − 140 mV. (b) *I-V* curves of I_{k1} in the absence (○) and presence of 3 μM (●), 10 μM (△), 30 μM (▲) and 100 μM (□) YT-1. Each point represents the mean value ± s.e.mean of 8 experiments.

dependent manner. The voltage-dependence of steady-state inactivation of I_{to}, however, was unaffected. This was evaluated with a standard two pulse protocol (for description see Figure 8 inset). As is shown in Figure 8c under control conditions, steady-state inactivation of I_{to} exhibits a steep voltage-dependence in the range of − 70 to − 50 mV and almost completely inactive at − 40 mV. The resulting curve was then fit by the Boltzmann equation:

$$I/I_{max} = 1/\{1 + \exp[(Vm - Vh)/s]\}$$

Where Vm is the prepulse potential, Vh the voltage at which the normalized I_{to} equals 0.5 and s the slope factor of the curve. Vh and s were − 58.9 ± 1.7 mV and 7.0 ± 0.5 mV for control and − 61.3 ± 1.5 mV and 7.3 ± 0.6 mV in the presence of 10 μM YT-1 (mean of 6 cells). This suggests that a concentration of 10 μM YT-1 did not affect the voltage-dependent inactivation curve of I_{to}. Apart from the inhibition of I_{to}, YT-1 could inhibit inward current through inward rectifier. As shown in Figure 9b, 100 μM YT-1 reduced 50% inward current through the K_1-channel. However the outward current through the K_1-channel was unaffected.

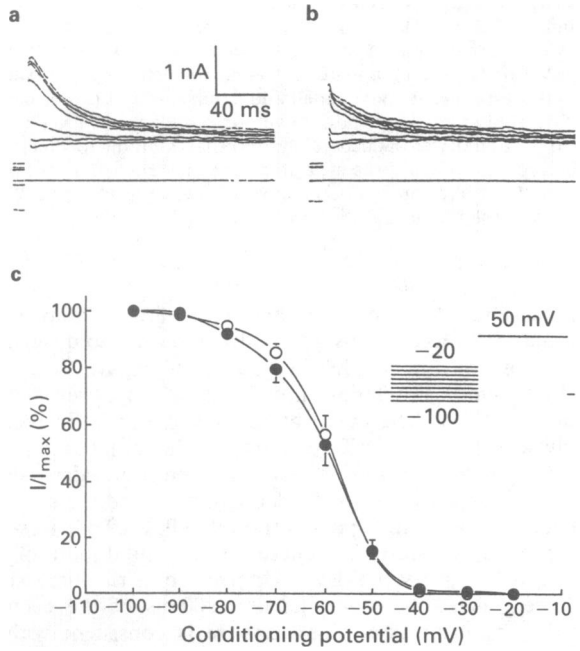

Figure 8 Effect of YT-1 on the potential-dependent inactivation curve of I_{to}. The effect of 200 ms prepulse on potentials in the range from − 100 to − 20 mV was examined in the absence (○) and presence (●) of 10 μM YT-1. I_{to} was measured at + 60 mV and was plotted in (c) after normalization, which was performed independently in the absence and presence of YT-1. External solution contained Co^{2+} (1 mM) and tetrodotoxin (30 μM).

Discussion

The best described and most often used cardiotonic agents are the sympathomimetic amines (such as dobutamine) and cardiac glycosides. Both classes of agents increase cardiac contractility by an increase of calcium influx or inhibition of Na^+–Ca^{2+} exchange via suppression of the sodium pump. However, serious problems have arisen concerning their usefulness in long term therapy to increase cardiac output. The increase in intracellular Ca^{2+} produced by these agents can aggravate the effects of ischaemia and cause arrhythmias (Smith, 1975; Hamer, 1979). Most of the currently available cardiotonic agents are hindered by the difficulties associated with Ca^{2+} overload and have a low therapeutic index. Therefore, positive inotropic agents which act by other mechanisms have been considered in recent years (Farah *et al.*, 1984). In the present study we found that YT-1 increased contractile force of rat cardiac tissues concentration-dependently. Since this effect was not antagonized by propranolol, it cannot be mediated by activation of classical β-adrenoceptors. It is well known that in most mammalian cardiac tissue, such as in rat (Wagner & Brodde, 1978), rabbit (Hescheler *et al.*, 1988), and human cardiac tissues, activation of α-adrenoceptors increases contractility. More recently, it has been reported that in the rat ventricular cell (Apkon & Nerbonne, 1988) and rabbit atrial cell (Fedida *et al.*, 1990), the activation of α_1-adrenoceptor may result in prolongation of the APD through inhibition of the transient outward current (I_{to}). Since the positive inotropic effect of YT-1 was not retarded by an α_1-adrenoceptor antagonist, it suggests that this effect also cannot be mediated by the activation of α-adrenoceptors. In the heart, the action potential duration may be prolonged by an increase of inward currents, e.g., Na^+ current (Honerjager & Reiter, 1977) or Ca^{2+} current (Schramm *et al.*, 1983), and/or a decrease of outward currents (Frank & Flom, 1978), either of which is

expected to increase the force of contraction. In the twitch tension study, the positive inotropic effect of YT-1 was partially but insignificantly attenuated by pretreatment of the preparations with a K^+ channel blocker (4-AP) and significantly attenuated by a Ca^{2+} channel blocker (verapamil). These results suggest that the positive inotropic effect of YT-1 may be mediated by the suppression of K^+ outward current and/or an increase of Ca^{2+} inward current. This consideration was further substantiated by the electrophysiological study which found that the increase of contractile force by YT-1 is consistent with its prolongation of action potential duration (APD) through the inhibition of K^+ outward current and the increase of Ca^{2+} current (Figures 4, 5 and 6). Wahler & Sperelakis (1984) showed that Bay K 8644 possesses both positive inotropic and chronotropic effects. In contrast to Bay K 8644, the increase of contractile force by YT-1 was not associated with any significant increase of the spontaneously beating rate in right atria preparations. It is possible that the enhancement of heart rate by YT-1 through the activation of Ca^{2+} current may be counteracted by the opposite effect through the inhibition of the K^+ outward current.

The effects of YT-1 on action potential configuration are similar to those of 4-AP (Kenyon & Gibbons, 1979) with an inhibition of phase 1 repolarization and an enhancement of action potential plateau. This suggests that YT-1 may act on the currents responsible for the repolarization process and/or the plateau phase of the action potential. Although YT-1 could also reduce I_{Na}, the maximum upstroke velocity of the action potential was only slightly inhibited or almost unchanged (Table 1), this effect was more similar to lignocaine (Hondeghem & Katzung, 1977; Brennan *et al.*, 1978) than quinidine (Chen *et al.*, 1975; Nawrath, 1981). The IC_{50} of YT-1, lignocaine, and quinidine on I_{Na} was 63.3 ± 1.2, 10.0 ± 0.8 and $2.8 \pm 0.5\,\mu M$, respectively. These results suggest that YT-1 is less potent in inhibiting Na^+ channels than lignocaine and quinidine.

In the heart, the most predominant voltage-activated outward currents are the transient outward current (I_{to}) and the delayed outward current (I_K). It is well known that ionic currents responsible for the repolarization of the cardiac action potential show important species-dependence. The I_{to} appears to be the major current activated at plateau potentials in sheep (Kenyon & Gibbons, 1979), calf (Siegelbaum & Tsien, 1980), and dog (Gilmour *et al.*, 1986) Purkinje fibres, rat ventricle (Josephson *et al.*, 1984), and most mammalian atrial tissues, including human (Escande *et al.*, 1987). In other mammalian ventricular tissues, the most prominent voltage-activated outward current is I_k (Jewell, 1981). I_{to} is assumed to be partly responsible for a marked phase of rapid early repolarization and for a low level of plateau of action potential in Purkinje fibres (Carmeliet & Vereecke, 1979). Studies in Purkinje fibres (Kenyon & Gibbons, 1979) and rat ventricular myocytes (Watanabe *et al.*, 1983) showed that 1 mM 4-AP caused an increase in action potential amplitude and a marked lengthening of the APD_{25}. In the present study, YT-1 causes a prominent suppression of phase 1 repolarization of action potential in a concentration-dependent manner (Figure 4); this effect is consistent with its suppression effect on I_{to}. In rat ventricular myocytes, 10 mM 4-AP was required to block I_{to} completely (Dukes & Morad, 1991), whereas 80 to $100\,\mu M$ YT-1 was effective in causing an equivalent reduction in the current (Figure 7). This phenomenon suggests that YT-1 was much more potent than the well-studied K^+ channel blocker 4-AP.

Since the delayed, time-dependent current is either absent or insignificant in rat ventricular myocytes (Jewell, 1981), whether YT-1 can affect I_k or not needs further investigation in cardiomyocytes of another animal species, such as guinea-pig ventricular myocytes, in which a large delayed outward K^+ current is activated at a positive potential range. The inward rectifying current I_{k1} is responsible for a considerable fraction of the outward K^+ current between -40 mV and the resting potential; any reduction in this current leads to a slowing of the late phase 3 repolarization and a decrease of the resting potential level in Purkinje fibres (Dudel *et al.*, 1967; Isenberg, 1976). Since the current-voltage relationship of I_{k1} in rat ventricular myocytes does not exhibit a negative slope region compared to that in guinea-pig ventricular myocytes, the decrease of I_{k1} by drugs may contribute less to the increase in action potential duration. Though the outward current through K_1 channels is less important in the regulation of action potential duration of rat ventricular cells, it is important in the control of resting membrane potential. In this study, although the inward current through K_1 channels was reduced significantly by YT-1, the outward current through K_1 channels measured at potentials between -80 and -20 mV was unaffected by YT-1. This result is correlated with the insignificant change of resting membrane potential.

We conclude that YT-1 is a novel positive inotropic agent which acts by its prolongation of action potential duration and exhibits a different mechanism of action to sympathomimetic amines (such as dobutamine) and cardiac glycosides. Since prolongation of the cardiac action potential has long been regarded as a potential antiarrhythmic mechanism (Vaughan Williams, 1984), whether YT-1 may also exert this effect or not needs further study.

This work was supported by a grant from the National Science Council (NSC80-0420-B002-19) of Taiwan. We also thank Mr I.S. Peng for skilled secretarial assistance.

References

APKON, M. & NERBONNE, J.M. (1988). α_1-Adrenergic agonists selectively suppress voltage dependent K^+ currents in rat ventricular myocytes. *Proc. Natl. Acad. Sci. U.S.A.*, **85**, 8756–8760.

BELLES, B., MALECOT, C.O., HESCHELER, J. & RAUTWEIN, W. (1988). 'Rundown' of the Ca current during long whole-cell recordings in guinea pig heart cells: role of phosphorylation and intracellular calcium. *Pflügers Arch.*, **411**, 353–360.

BRENNAN, F.J., CRANEFIELD, P.F. & WIT, A.L. (1978). Effects of lidocaine on slow response and depressed fast response action potentials of canine cardiac Purkinje fibers. *J. Pharmacol. Exp. Ther.*, **204**, 312–324.

CARMELIET, E. & VEREECKE, J. (1979). Electrogenesis of the action potential and automaticity. In *Handbook of Physiology. The Cardiovascular System*, I. ed. Berne, R.M. & Geiger, S.R. pp. 269–334, Bethesda, Maryland: American Physiological Society.

CHEN, C., GETTES, L.S. & KATZUNG, B.G. (1975). Effect of lidocaine and quinidine on steady-state characteristics and recovery kinetics of $(dv/dt)_{max}$ in guinea pig ventricular myocardium. *Cir. Res.*, **37**, 20–29.

DUDEL, J., PEPER, K., RUDEL, R. & TRAUTWEIN, W. (1967). The potassium component of membrane current in Purkinje fibres. *Pflügers Arch.*, **296**, 308–327.

DUKES, I.D. & MORAD, M. (1991). The transient K^+ current in rat ventricular myocytes: evaluation of its Ca^{2+} and Na^+ dependence. *J. Physiol.*, **435**, 395–420.

ESCANDE, D., COULOMBE, A., FAIVRE, J.R., DEROUBAIX, E. & CORABOEUF, E. (1987). Two types of transient outward currents in adult human atrial cells. *Am. J. Physiol.*, **252**, H142–H148.

FARAH, A.E., ALOUSI, A.A. & SCHWARZ, R.P. Jr. (1984). Positive inotropic agents. *Annu. Rev. Pharmacol. Toxicol.*, **24**, 275–328.

FEDIDA, D., SHIMONI, Y. & GILES, W.R. (1990). α-Adrenergic modulation of the transient outward current in rabbit atrial myocytes. *J. Physiol.*, **423**, 257–277.

FRANK, M. & FLOM, L.L. (1978). Effects of 2,4,6-triaminopyrimidine on the electromechanical properties of guinea pig myocardium. *J. Pharmacol. Exp. Ther.*, **204**, 175–182.

GILMOUR, R.F., SALATA, J.I. & DAVIS, J.R. (1986). Effect of 4-aminopyridine on rate related depression of cardiac action potentials. *Am. J. Physiol.*, **251**, H297–H306.

HAMER, J. (1979). The paradox of the lack of the efficacy of digitalis in congestive heart failure with sinus rhythm. *Br. J. Clin. Pharmacol.*, **8**, 109–113.

HAMILL, O.P., MARTY, A., NEHER, E., SAKMANN, B. & SIGWORTH, F.J. (1981). Improved patch-clamp techniques for high resolution current recording from cells and cell-free membrane patches. *Pflügers Arch.*, **391**, 85–100.

HESCHELER, J., NAWRATH, H., TANG, M. & TRAUTWEIN, W. (1988). Adrenoceptor-mediated changes of excitation and contraction in ventricular heart muscle from guinea-pigs and rabbits. *J. Physiol.*, **397**, 657–670.

HONDEGHEM, L.M. & KATZUNG, B.G. (1977). Time and voltage-dependent interactions of antiarrhythmic drugs with cardiac sodium channels. *Biochem. Biophys. Acta*, **472**, 373–398.

HONERJAGER, P. & REITER, M. (1977). Sarcolemmal sodium permeability and contractile force of guinea pig papillary muscle: effects of germitrine. *Circ. Res.*, **40**, 90–98.

IIJIMA, T., IRISAWA, H. & KAMEYAMA, M. (1985). Membrane currents and their modification by acetylcholine in isolated single atrial cells of the guinea-pig. *J. Physiol.*, **359**, 485–501.

ISENBERG, G. (1976). Cardiac Purkinje fibres: cesium as a tool to block inward rectifying potassium currents. *Pflügers Arch.*, **365**, 99–106.

JEWELL, B. (1981). Rate dependent control of action potential duration. *Progr. Biophys. Mol. Biol.*, **15**, 125–179.

JOSEPHSON, I.R., SANCHEZ-CHAPULA, J. & BROWN, A.M. (1984). Early outward current in rat single ventricular cells. *Circ. Res.*, **54**, 157–162.

KENYON, J.L. & GIBBONS, W.R. (1979). 4-Aminopyridine and the early outward current of sheep cardiac Purkinje fibers. *J. Gen. Physiol.*, **73**, 139–157.

LEE, K.S., HUME, J.R., GILES, W. & BROWN, A.M. (1981). Sodium current depression by lidocaine and quinidine in isolated ventricular cells. *Nature*, **291**, 325–327.

MIKKELSEN, E., ANDERSSON, K.E. & PEDERSON, O.L. (1979). Effects of digoxin on isolated human peripheral arteries and veins. *Acta Pharmacol. Toxicol.*, **45**, 249–256.

MITRA, R. & MORAD, M. (1985). A uniform enzymatic method for the dissociation of myocytes from heart and stomach of vertebrates. *Am. J. Physiol.*, **249**, H1056–H1060.

NAWRATH, H. (1981). Action potential, membrane currents and force of contraction in mammalian heart muscle fibers treated with quinidine. *J. Pharmacol. Exp. Ther.*, **216**, 176–182.

SCHRAMM, M., THOMAS, G., TOWART, R. & FRANCKOWIAK, G. (1983). Activation of calcium channels by novel 1,4-dihydropyridines. *Arzneimittel Forsch*, **33**, 1268–1272.

SIEGELBAUM, S.A. & TSIEN, R.W. (1980). Calcium-activated transient outward current in cardiac Purkinje fibres. *J. Physiol.*, **299**, 485–506.

SMITH, T.W. (1975). Digitalis toxicity: epidemiology and clinical use of serum concentration measurements. *Am. J. Med.*, **58**, 470–476.

VAUGHAN WILLIAMS, E.M. (1984). A classification of antiarrhythmic actions reassessed after a decade of new drugs. *J. Clin. Pharmacol.*, **24**, 129–147.

WAGNER, J. & BRODDE, O.E. (1978). On the presence and distribution of α-adrenoceptors in the heart of various mammalian species. *Naunyn-Schmied. Arch. Pharmacol.*, **302**, 239–254.

WAHLER, G.M. & SPERELAKIS, N. (1984). New Ca^{2+} agonist (Bay K 8644) enhances and induces cardiac slow action potentials. *Am. J. Physiol.*, **247**, H337–H340.

WATANABE, T., DELBRIDGE, L.M. BUSTAMANTE, J.O. & MCDONALD, T.F. (1983). Heterogeneity of the action potential in isolated rat ventricular myocytes and tissue. *Circ. Res.*, **52**, 280–290.

WEIDMANN, S. (1955). Effects of calcium ions and local anesthetics on electrical properties of Purkinje fibers. *J. Physiol.*, **129**, 568–582.

(Received July 7, 1992
Revised March 25, 1993
Accepted April 5, 1993)

Br. J. Pharmacol. (1993), **110**, 317–325

Effects of excitatory neurotransmitters on Ca^{2+} channel current in smooth muscle cells isolated from guinea-pig urinary bladder

S. Nakayama

University Department of Pharmacology, Mansfield Road, Oxford, OX1 3QT

1 A whole-cell voltage clamp technique was used to examine the effects of purinoceptor and muscarinic receptor agonists on voltage-sensitive Ca^{2+} channels in guinea-pig isolated urinary bladder cells.

2 When the cell membrane was clamped at the holding potential, rapid application of ATP elicited a large inward current in normal solution containing 2.5 mM Ca^{2+}, and reduced the subsequent Ca^{2+} channel current evoked by a depolarizing pulse (0 mV). Carbachol (CCh) elicited little membrane current, but similarly reduced the Ca^{2+} current.

3 When purinoceptor agonists were rapidly applied during conditioning depolarizations at +80 mV, an outward current was elicited, and the Ca^{2+} channel current evoked by the subsequent test potential of 0 mV was not affected. Application of CCh at +80 mV also elicited an outward current, but it reduced the subsequently evoked Ca^{2+} current.

4 The inhibitory effect of muscarinic agonists on the Ca^{2+} channel current was attenuated by caffeine (10 mM).

5 In Ca^{2+}-free, low-Mg^{2+} solution, a Na^+ current flowing through voltage-dependent Ca^{2+} channels was evoked by depolarization. This current was not reduced by bath application of purinoceptor agonists (ATP and α,β-methylene ATP).

6 These results suggest that the main effect of purinoceptor stimulation is opening of non-selective cation channels, and that muscarinic stimulation triggers Ca^{2+} release from intracellular stores. Voltage-sensitive Ca^{2+} channels are inactivated through an increase in intracellular Ca^{2+} induced by either activation of purinoceptor or muscarinic receptors.

Keywords: Smooth muscle; urinary bladder; Ca^{2+} channels; non-selective cation channels; purinoceptors; muscarinic receptors

Introduction

In the urinary bladder of most mammals, contraction elicited by nerve stimulation is diminished, but not completely abolished by atropine, a muscarinic antagonist (Langley & Anderson, 1885; Henderson & Roepke, 1934). In the guinea-pig, the response to local application of adenosine 5'-triphosphate (ATP) mimics that to non-cholinergic nerve stimulation (Burnstock *et al.*, 1972), and ATP is released from intramural nerves (Burnstock *et al.*, 1978). Thus, in urinary bladders of various species both ATP and acetylcholine (ACh) have been proposed as excitatory neurotransmitters (Fujii, 1988). However, the underlying mechanism involved in the action of these neurotransmitters seems to be quite different. Purinoceptor agonists depolarize the cell membrane (Fujii, 1988), whereas muscarinic agonists produce little or no change in membrane potential (Creed, 1971; Creed *et al.*, 1983).

Recently, in smooth muscle cells isolated from guinea-pig urinary bladder, patch clamp techniques have revealed a transient activation of non-selective cation channels by ATP (Inoue & Brading, 1990). Inward current through these channels is carried by Ca^{2+} ions as well as other monovalent cations. ACh is also known to activate a non-selective cation conductance in many mammalian smooth muscle cells (Benham *et al.*, 1985). In guinea-pig ileum, the ACh-induced cation conductance is facilitated by depolarization and intracellular Ca^{2+} (Inoue & Isenberg, 1990a,b). In canine gastric smooth muscle cells (Sims, 1992), and in canine and guinea-pig tracheal smooth muscle cells (Janssen & Sims, 1992), it has recently been suggested that ACh-induced Ca^{2+} release from intracellular stores triggers activation of the non-selective cation current. However, in guinea-pig detrusor cells, an ACh-activated conductance has not yet been clearly demonstrated.

Voltage-dependent Ca^{2+} channels are also known to play an important role in excitation-contraction coupling. Previously, we described the activation and inactivation properties of the Ca^{2+} channels in guinea-pig detrusor cells (Nakayama & Brading, 1993a,b). In the present study, the membrane currents evoked by these two excitatory neurotransmitters, and their interaction with the voltage-dependent Ca^{2+} channels have been examined. The experiments were carried out with only a low concentration of Ca^{2+} chelator (0.1 mM EGTA) in the pipette, to allow the effects of changes in $[Ca^{2+}]_i$ on membrane currents to be observed. To investigate the involvement of Ca^{2+} entry in the responses, in some experiments the agonists were applied in the absence of extracellular Ca^{2+}, or during large depolarizations (+ 80 mV) to reduce the driving force for Ca^{2+} entry.

Methods

Single detrusor cells

Male guinea-pigs (450–750 g) were killed either by stunning, or cervical dislocation, or decapitation after anaesthesia by halothane. The urinary bladder was immediately dissected. Muscle strips (total approximately 0.1 g wet weight), from which the epithelium had been removed, were incubated in a nominally Ca^{2+}-free solution for 60 min (at 35°C). Subsequently, the strips were digested in an enzyme-containing (0.05% collagenase and 0.1% pronase) Ca^{2+}-free solution for 10–20 min, and then agitated with a glass pipette. Some of the cell suspension was stored at 5°C and used for up to 6 h.

Whole-cell voltage clamp

A conventional whole-cell configuration of the patch clamp method was used (Hamill *et al.*, 1981). Single smooth muscle

[1] Author for correspondence.

cells were allowed to settle in a recording bath, and continuously superfused with physiological saline. The resistance of the patch pipette used was in the region of 5 MΩ. The membrane potential was clamped with a List amplifier (EPC 7, Germany). Unless otherwise stated, the membrane potential was clamped at − 60 mV (holding potential). An AD/DA converter (DT 2801A, Data Translation, U.K.) was used for voltage step generation and on-line data acquistion. Data were collected on an IBM compatible personal computer using the Quick Basic software package. The membrane current was also monitored by a digital storage oscilloscope (DSO1602, Gould, U.K.) and a brush pen recorder (Gould). A cut-off frequency of 10 kHz (3 pole Bessel filter) was applied to reduce the noise.

Most smooth muscle cells used had a membrane capacitance between 40 and 70 pF. The initial sealing between the patch pipette and cell was performed in Ca^{2+}-free solution, to avoid contraction of the cell induced by ATP contained in the pipette. Subsequently, in normal solution, high seal resistance (= 10 GΩ) was obtained by repeated gentle suction. After rupture of the cell membrane, the series resistance was less than 10 MΩ. The capacitive surge was electrically compensated. In most experiments, particularly when large inward tail currents were evoked by application of extremely high (+ 80 mV) conditioning potentials, the series resistance was partially compensated (by 50–70%). All experiments were performed at room temperature (24–26°C).

Application of agonists

A pressure ejector (Picospritzer II, General Valve, U.S.A.) was used to apply rapidly purinoceptor and muscarinic receptor agonists, except in Ca^{2+}-free, low-Mg^{2+} solution. Glass pipettes filled with the agonist had resistance of around 10 MΩ. The tip of the pipette was positioned approx. 100 to 200 μm from the cell so that it was against the flow of the bathing solution. Upon application of the agonists, an air pressure of 4000 kPa was charged for several hundred ms.

When effects of purinoceptor stimulation were examined in Ca^{2+}-free, low-Mg^{2+} solution, which allows Na^+ current to flow through the voltage-dependent Ca^{2+} channels, the agonists were applied to the bathing solution. This application method was chosen, because the stability of the membrane seal resistance is poor during exposure to solutions containing low concentration of divalent cations, and the mechanical shock upon pressure ejection can break the seal.

Data analysis and statistics

Curve fitting of the decay of the purinoceptor agonist-activated membrane currents was by fitting the digital data points iteratively with single or multiple exponential terms using a modified 'simplex' programme. The total residual current were used as a criterion for the convergence. At convergence, the mean residual currents were usually less than 8 pA or 2% of the peak inward current. When the decay was fitted by two exponential terms, the faster time constant (150 to 230 ms) was nearly the same as that obtained by single exponential fitting. The second exponential had a time constant of 3 to 6 s, and the amplitude was small and its sign was opposite to that of the first exponential term. Thus, the single exponential was judged to be appropriate in the present experiments.

Current traces of slow time base were drawn using an X–Y plotter (7470A, Hewlett-Packard, U.S.A.)

Numerical data were expressed as means ± standard deviation (s.d.)

Solutions

Normal (bathing) solution for superfusion of smooth muscle cells had the following composition (mM): NaCl 125, KCl 5.9, $CaCl_2$ 2.5, $MgCl_2$ 1.2, glucose 11.8 and HEPES (N-2-hydroxyethylpiperadine-*N*-2-ethanesulphonic acid), 11.8. The pH of the solution was adjusted to 7.4 (25°C) with Tris base. Modification of the solution was made by iso-osmotic substitution of NaCl. When monovalent cation (Na^+) currents through Ca^{2+} channels were measured, Ca^{2+} was removed and Mg^{2+} was reduced to 0.1 mM by iso-osmotically substituting with Na^+ and 1 mM EGTA (ethyleneglycol-*bis*-(β-aminoethylether) *N*, *N*, *N'*, *N'*-tetraacetic acid) was added.

The composition of the pipette solution was (mM): CsCl 141, $MgCl_2$ 1.4, ATP 1, GTP (guanosine 5'-triphosphate 0.1, EGTA 0.1, HEPES/Tris 10 (pH 7.2 at 25°C). The pipette solutions were kept frozen before use.

In preliminary experiments, when a relatively high concentration (2 mM) of Ca^{2+} chelator (EGTA) was used in the patch pipette, although application of ATP elicited a large inward current, which involved Ca^{2+} influx (Inoue & Brading, 1990), the subsequently evoked Ca^{2+} channel current was not reduced in size. Thus, in the present experiments, the pipette solution contained only 0.1 mM EGTA in order to demonstrate the effects of changes in $[Ca^{2+}]_i$ more clearly.

Drugs and chemicals

The following chemicals were used: ATP (disodium salt), α,β-methylene ATP (lithium salt), guanosine 5'-triphosphate (GTP) (sodium salt), carbamylcholine chloride (carbachol, CCh), caffeine, collagenase (type 1, all from Sigma) and pronase (Fluka).

Results

Effects of excitatory agonist application at the holding potential

Figure 1 shows an example of the effect of ATP on the Ca^{2+} channel current. Single smooth muscle cells were continuously superfused with normal solution containing 2.5 mM Ca^{2+}. The tip of a glass pipette containing 0.1 mM ATP was set close to a detrusor cell which was voltage-clamped. While the membrane potential of the recording cell was held at − 60 mV, ATP was rapidly applied by pressure ejection. The application of ATP transiently elicited a large inward current (arrow in a) (1.6 ± 0.9 nA, $n = 7$).

In the same experiment, voltage-dependent Ca^{2+} channel currents were evoked every 30 s by depolarizing the cell membrane to 0 mV. The peak amplitude of the Ca^{2+} channel current evoked approx. 1.5 s after application of ATP was decreased by 21% (ii) but after 30 s, the current had recovered (iii). Similar effects of ATP were observed in three other cells.

It has been shown that the ATP-activated inward current flowing through non-selective cation channels involves Ca^{2+} influx as well as monovalent cations (Inoue & Brading, 1990). As voltage-dependent Ca^{2+} channels are known to inactivate through increases in $[Ca^{2+}]_i$ (Ca^{2+}-dependent inactivation), the reduction of the Ca^{2+} current (ii) could be due to this mechanism (Schneider *et al.*, 1991).

In the present experiments, the patch pipette contained only 0.1 mM EGTA in order to demonstrate effects of changes in $[Ca^{2+}]_i$ clearly. When 2 mM EGTA was used in some cells, application of purinoceptor agonists similarly elicited a transient, large inward current, but caused little changes in the subsequent Ca^{2+} channel current. In some cells there was a small reduction of the Ca^{2+} current, however it failed to recover upon washout (data not shown).

In Figure 2, carbachol (CCh, 1 mM in the pressure ejection pipette) was rapidly applied. In five cells, application of CCh (arrow in a) elicited a very small (< 50 pA) or no inward current at − 60 mV. However, there was a marked reduction in the subsequent Ca^{2+} channel current (Figure 2a(ii)) (by 20 to 45%, on average 30.3 ± 12.2%, $n = 5$). Recovery of the

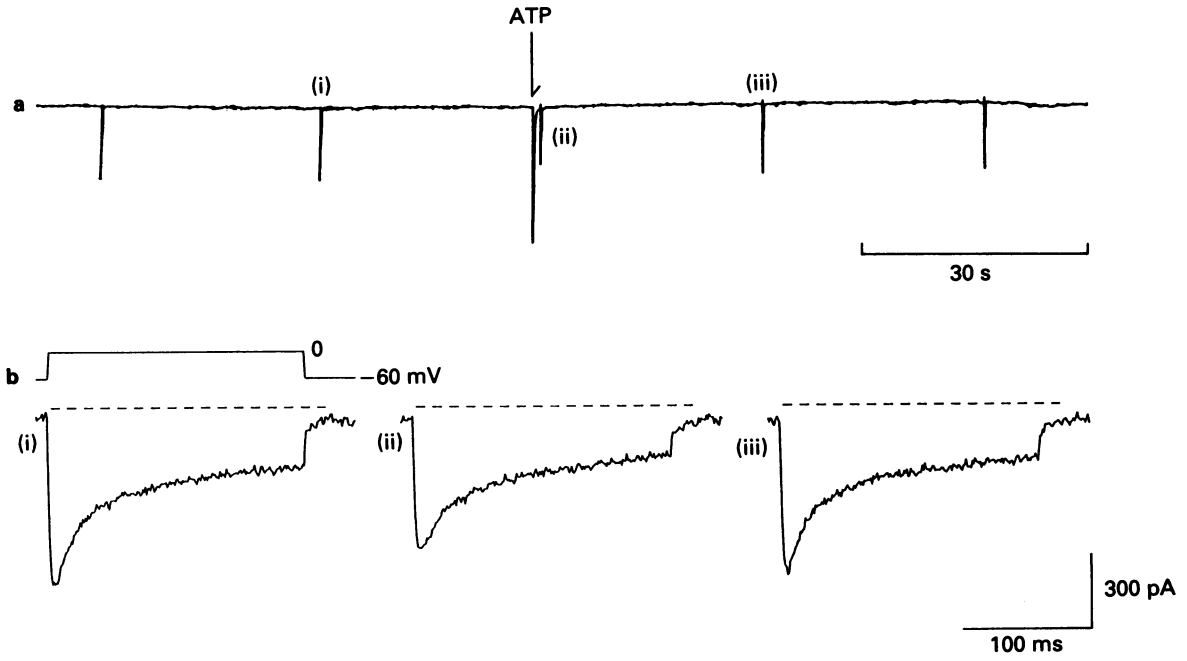

Figure 1 Effects of ATP on membrane current at the holding potential and on depolarization-activated Ca^{2+} channel current. The membrane potential was clamped at −60 mV, and a transient depolarizing pulse to 0 mV (200 ms) was repeated at 30 s intervals. ATP was applied by a pressure ejector for 500 ms just before (approx. 1.5 s) the Ca^{2+} channel current (ii) was evoked. The glass pipette for pressure ejection was filled with a normal solution containing 0.1 mM ATP. Pen recording of the membrane current is shown in (a). The voltage-dependent Ca^{2+} channel currents (i) to (iii) are shown expanded in (b). Zero current level is indicated by the dotted line. Note the transient inward current elicited by ATP (in a) and the reduction of the subsequently evoked Ca^{2+} channel current ((ii) in a and b).

Ca^{2+} current was slow after CCh application, and sometimes incomplete. Since there is no detectable Ca^{2+} influx observed upon application of muscarinic agonists, if the reduction of Ca^{2+} current is due to Ca^{2+}-dependent inactivation, the source of Ca^{2+} must be intracellular stores.

Purinoceptor stimulation in the absence of extracellular Ca^{2+}

Purinoceptor agonists were applied in the absence of Ca^{2+}, in order to address whether inactivation of voltage-dependent Ca^{2+} channels is due to Ca^{2+} influx upon purinoceptor stimulation. After observing Ca^{2+} channel current evoked by depolarization to 0 mV in normal solution (2.5 mM Ca^{2+}), extracellular Ca^{2+} was removed from the perfusate. In nominally Ca^{2+}-free solution (1.2 mM Mg^{2+}), the Ca^{2+} channel current was completely eliminated. However, addition of 1 mM EGTA and reduction of Mg^{2+} to 0.1 mM yielded an inward current upon depolarization of the cell membrane. During exposure to solutions containing low concentrations of divalent cations, the voltage-dependent Ca^{2+} channels become permeable to monovalent cations (Fukushima & Hagiwara, 1985). Therefore in this case, inward currents evoked by depolarizations are carried mainly by Na^{+}. When the holding potential was −60 mV, the voltage-dependent Ca^{2+} channel current was gradually reduced with time, pos-

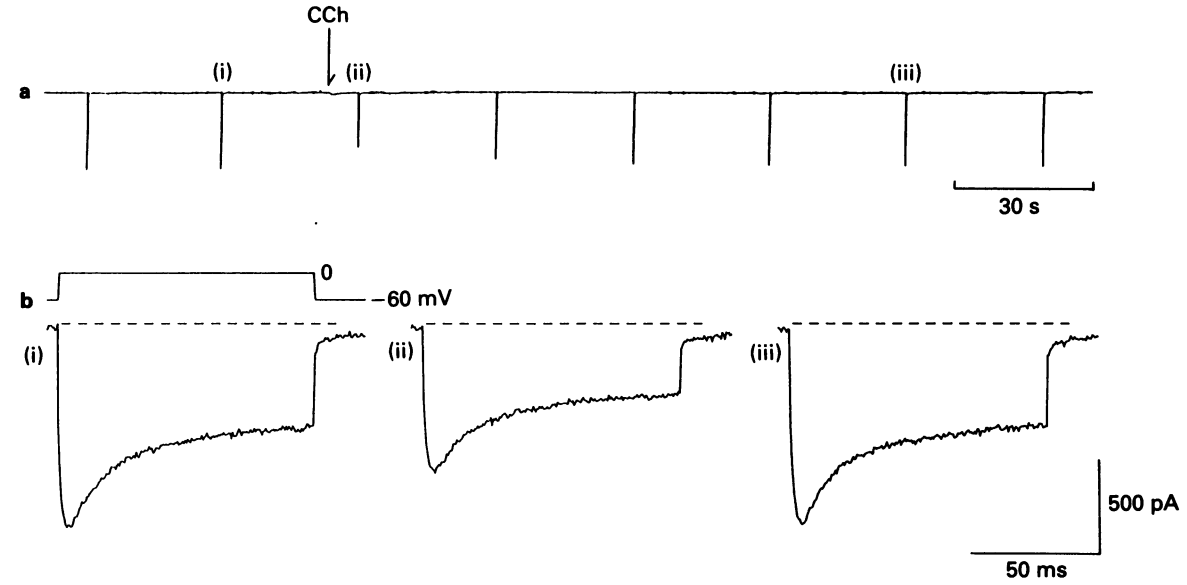

Figure 2 Effects of carbachol (CCh) application at the holding potential (−60 mV). The cell membrane was transiently (100 ms) depolarized to 0 mV every 30 s. Pressure ejection (900 ms) of CCh was applied approx. 8 s before (ii). The glass pipette for pressure ejection was filled with a normal solution containing 1 mM CCh. (a) Pen recording; (b) (i) to (iii) shown expanded.

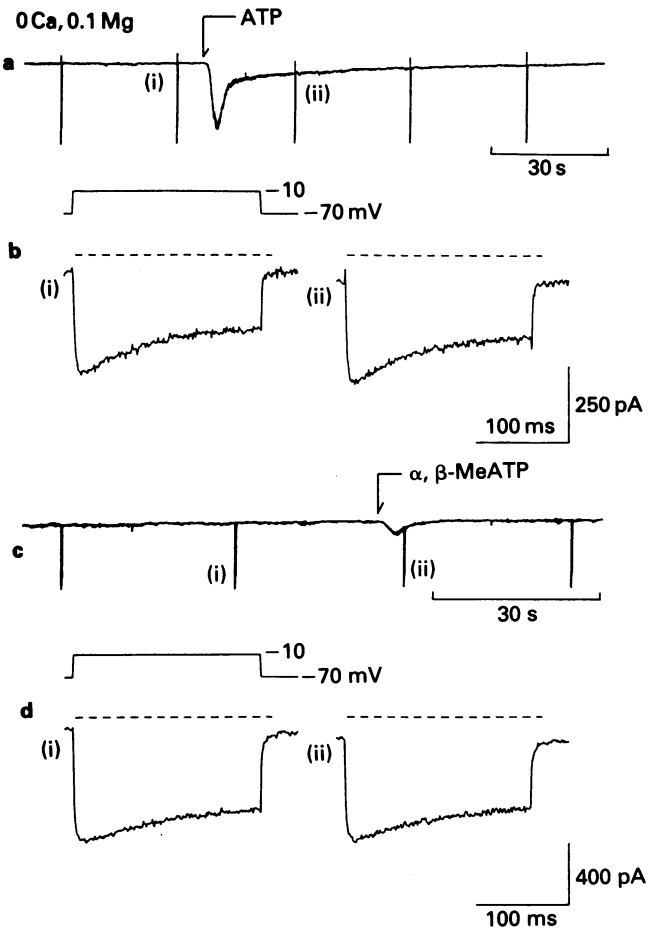

Figure 3 Effects of purinoceptor stimulation in the absence of extracellular Ca^{2+}. In low-Mg^{2+} (0.1 mM), EGTA-containing (1 mM) solution, the cell membrane was transiently depolarized to − 10 mV (200 ms) every 30 s. The holding potential was − 70 mV. ATP (30 μM: a, b) or α,β-methylene ATP (10 μM: c, d) was added to the bathing solution for approx. 5 min. The Ca^{2+} channel currents (i) and (ii) in (a) are shown expanded in (b). The same for (c) and (d).

sibly due to changes in surface charge (being identical to the effects of mild depolarization of the cell membrane). Thus, in the following experiments, a more negative holding potential (− 70 mV) was applied.

Figure 3 shows effect of purinoceptor agonist application in the absence of Ca^{2+} (low-Mg^{2+}, EGTA-containing solution). Voltage-dependent Ca^{2+} channel current was evoked every 30 s by depolarizing the membrane to − 10 mV. Bath application of 30 μM ATP still elicited a large inward current in the absence of external Ca^{2+} (Figure 3a) (the peak amplitude varied from 150 to 900 pA, 409 ± 308 pA, $n = 5$). This inward current decayed during appliation of ATP, but the time course was much slower than that elicited by rapid application. However, reduction of the Ca^{2+} channel current was not observed after application of ATP (Figure 3b). In three cells, similar results were reproduced by application of α,β-methylene ATP (10 μM) (Figure 3c,d). These results suggest that the main effect of purinoceptor stimulation is opening of non-selective cation channels in the plasma membrane. In these experiments, the lack of inactivation of the Ca^{2+} channel current upon application of purinoceptor agonists could be attributed to the fact that there was no Ca^{2+} entry.

When ATP (30 μM) was applied in the absence of Ca^{2+} (low-Mg^{2+}, EGTA-containing solution), the amplitude of the Na^+ current through the voltage-dependent Ca^{2+} channels slightly increased (Figure 3b, by 19 ± 9% $n = 5$) throughout the 5 min application, and was reversed on washout (data not shown). This small increase induced by ATP application was also observed after purinoceptor desensitization with α,β-methylene ATP (10 μM), despite the fact that the ATP-induced current was eliminated at the holding potential (data not shown). The persistent enhancement of the Ca^{2+} channel current and the lack of effect of desensitization by α,β-methylene ATP suggest that this effect of ATP is not through purinoceptor stimulation, but probably through chelation of extracellular Mg^{2+} (divalent cation block of Ca^{2+} channel current carried by monovalent cations: Fukushima & Hagiwara, 1985). In rabbit portal vein, a similar phenomenon has been reported (Xiong *et al.*, 1991).

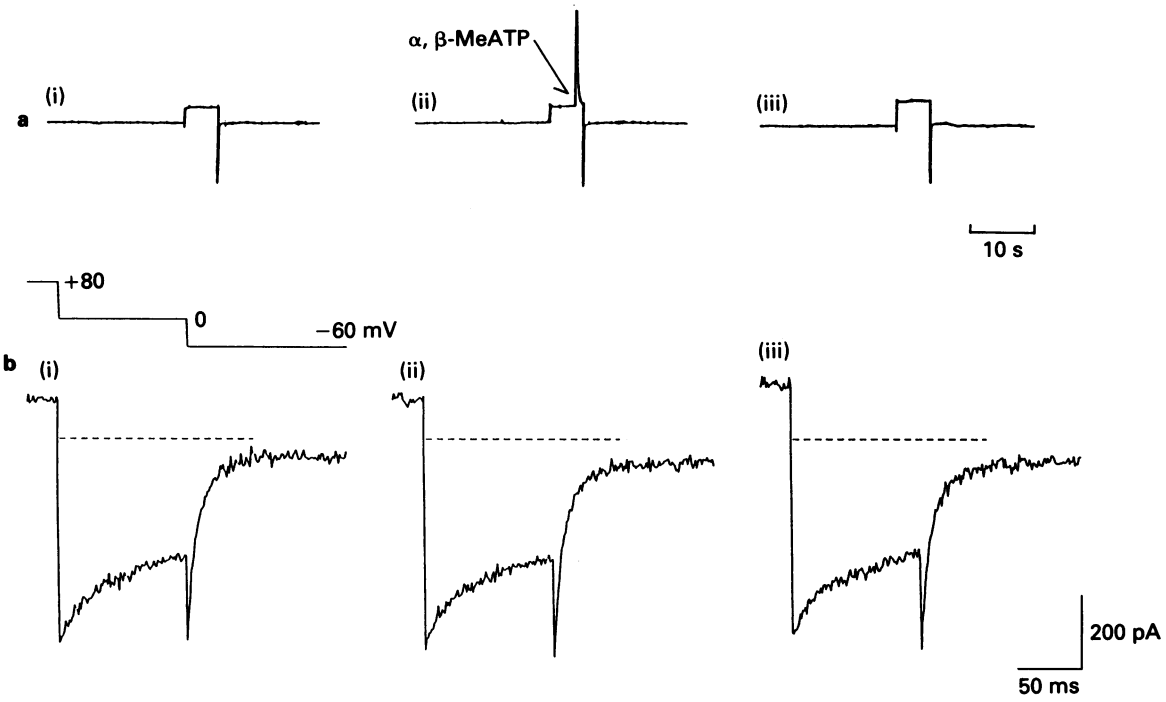

Figure 4 Purinoceptor stimulation during large depolarizations. The cell membrane was clamped at + 80 mV for 5 s, then switched to 0 mV (100 ms) and − 60 mV. This step pulse protocol was repeated at 2 min intervals. During the large depolarization in (ii), α,β-methylene ATP was applied by pressure ejection (400 ms). (a) Slow time base (pen recording) of current. In (b), the membrane currents evoked by repolarizations are shown expanded. The last 25 ms of the + 80 mV step is shown.

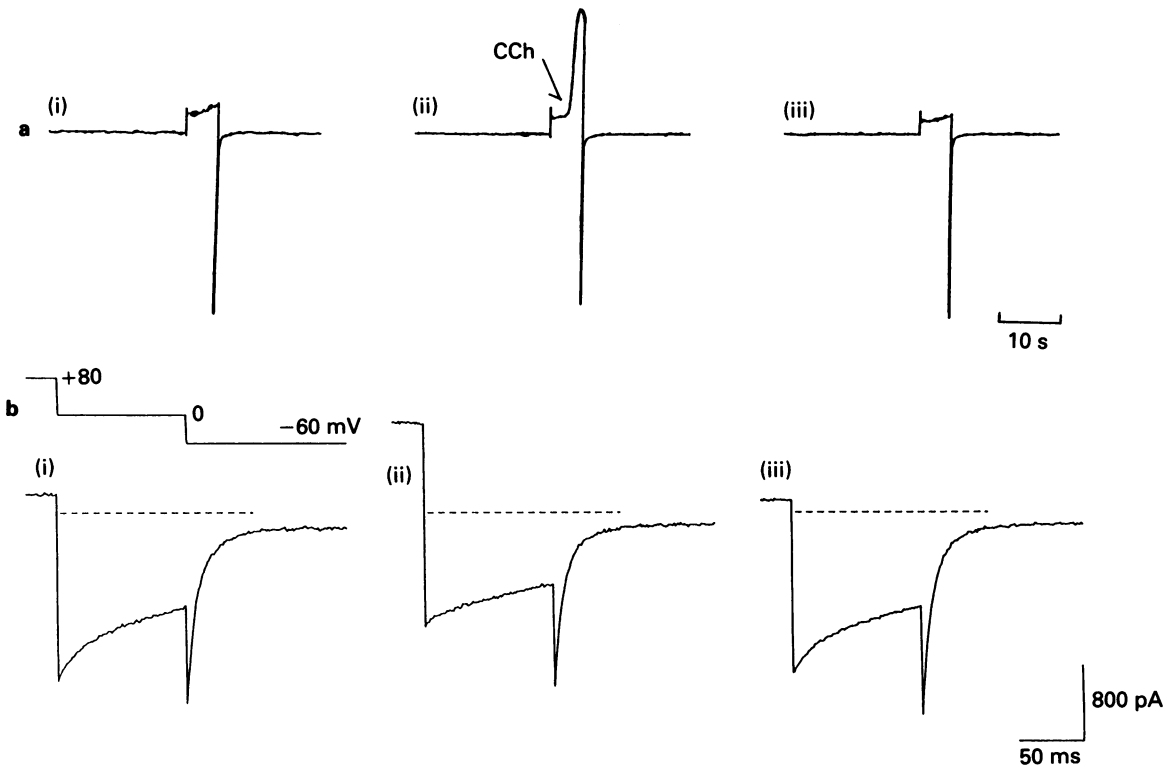

Figure 5 Muscarinic stimulation during large depolarizations. The same experimental protocol as Figure 4 was applied, but carbachol (CCh, 1 mM in the pressure ejection pipette, 500 ms) was used as the agonist. Note the reduction of inward current evoked by returning the membrane potential to 0 mV after application of CCh.

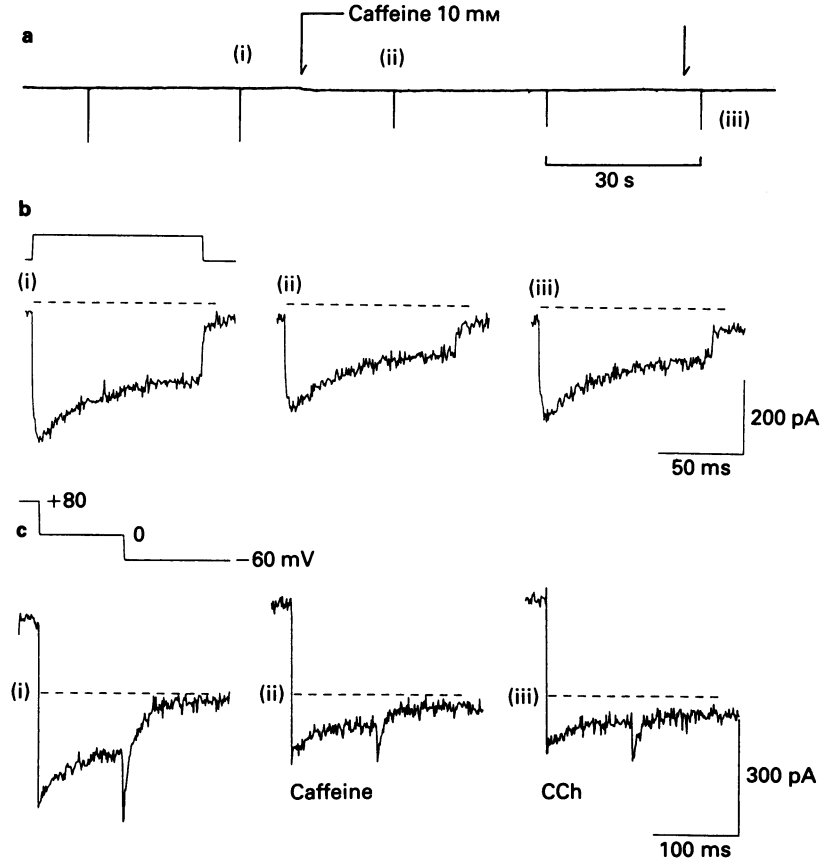

Figure 6 Effects of caffeine on carbachol (CCh)-induced effects. In (a), step depolarization (0 mV, 100 ms) was repeated at 30 s intervals. The holding potential was −60 mV. In the presence of caffeine (10 mM, bath application), pressure ejection (900 ms) of CCh (1 mM) was applied. The Ca^{2+} channel currents (i) to (iii) in (a) are shown expanded in (b). In (c), the same voltage steps shown in Figure 4 (conditioning step: +80 mV, 5 s; test step: 0 mV, 100 ms) were repeated at 2 min intervals. the last 25 ms of the conditioning step is shown. After observing control membrane currents (i), caffeine (10 mM) was applied to the bathing solution; (ii) was obtained approx. 1 min after the caffeine application. In the continuous presence of caffeine, CCh (1 mM) was applied by pressure ejection (900 ms), when the membrane was clamped at +80 mV (iii).

Agonist application during large depolarizations

With large depolarizations of the cell membrane, there is little inward driving force for Ca^{2+}. Therefore, we can neglect Ca^{2+} influx during such depolarizing steps (> +80 mV), if agonists open non-selective cation channels during large depolarizations. Figure 4 shows the effect of purinoceptor stimulation during a large depolarization. The cell membrane was clamped at + 80 mV for 5 s, during which α,β-methylene ATP (0.1 mM in the pressure ejection pipette) was rapidly applied by pressure ejection (Figure 4a(ii)). The membrane potential was then switched to 0 mV (100 ms) and subsequently to − 60 mV (holding potential). In Figure 4b, the membrane currents evoked at 0 and − 60 mV steps are shown expanded. The voltage-dependent Ca^{2+} channel currents show little inactivation after large depolarizations (Nakayama & Brading, 1993b). Application of α,β-methylene ATP immediately elicited a large outward, rapidly declining current at + 80 mV. The time course was very similar to that observed on application of ATP at the holding potential (Figure 1a). However, the subsequently evoked Ca^{2+} channel current was not reduced.

The same experiments were repeated using CCh as the agonist (Figure 5). Pressure ejection of CCh (1 mM) at + 80 mV similarly elicited a large outward current, but its rising time course was much slower and the membrane current lasted longer (Figure 5a(ii)). The Ca^{2+} channel current evoked by returning the membrane potential to 0 mV (from the preconditioning step at 80 mV) was reduced by approx. 30% after CCh application. Similar reduction of the Ca^{2+} current was observed in two other cells (on average 28%).

Effects of caffeine on muscarinic receptor stimulation

In order to assess whether intracellular Ca^{2+} stores were involved in particular functions, the effects of caffeine on responses induced by stimulation of muscarinic cholinoceptors were examined (Figure 6). After observing control Ca^{2+} current evoked by depolarizations to 0 mV, 10 mM caffeine was added to the bathing solution (Figure 6a). The bath application of caffeine elicited a small (20 to 30 pA) inward current at the holding potential, and reduced the Ca^{2+} current (Figure 6a and b(ii)) (by 24%). In the presence of caffeine, a pressure ejection of CCh (1 mM) failed to reduce the subsequently evoked Ca^{2+} current (Figure 6a and b(iii)). Caffeine also inhibited further reduction of Ca^{2+} channel current after application of CCh at + 80 mV (Figure 6c).

Agonist-induced membrane currents at different potentials

Membrane currents elicited by purinoceptor or muscarinic receptor stimulation at different potentials are shown in Figure 7. In (a), α,β-methylene ATP (0.1 mM, in the pipette) was applied by pressure ejection (500 ms). Outward and inward currents were immediately elicited at the membrane potentials of + 80 mV and − 60 mV, respectively. Since the α,β-methylene ATP-activated current became smaller on repeated application, it was difficult to quantify the difference in current recorded at these two potentials. However, when the purinoceptor-operated current was alternately elicited at the potentials, the amplitude at − 60 mV was consistently, considerably larger than that at + 80 mV. The decay time constants were similar at both of the membrane potentials. In the same cell, α,β-methylene ATP was also applied at − 40 and − 80 mV (data not shown). The decay time courses of the α,β-methylene ATP-activated current were well fitted by a single exponential ($\tau = 150 \sim 210$ ms), and the time constant was not systematically changed by changing the membrane potential.

Pressure ejection (500 ms) of CCh (1 mM) was applied in Figure 7b. At − 60 mV, application of CCh caused no detectable change in membrane current. In contrast, when the

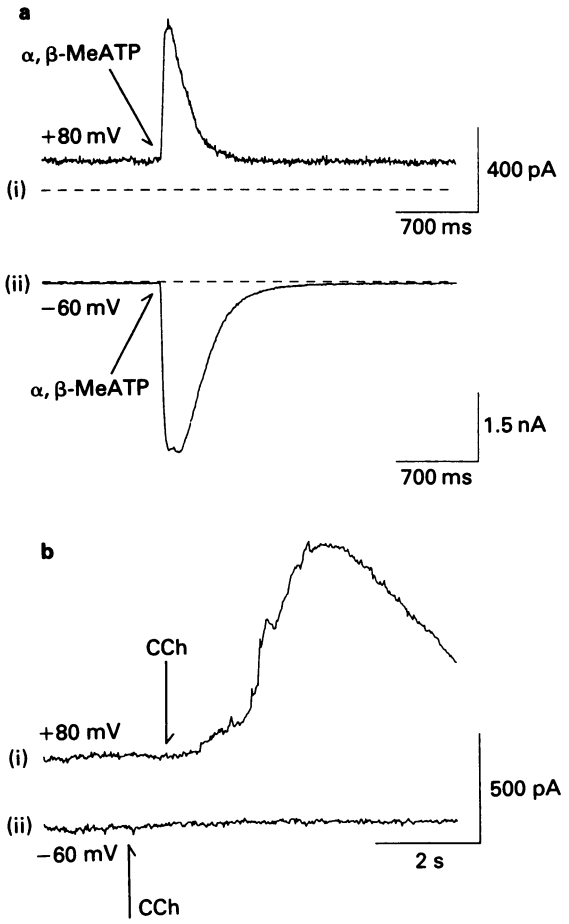

Figure 7 Membrane currents elicited by either pressure ejection (500 ms) of purinoceptor (a) or muscarinic receptor agonists (b) at potentials of + 80 (a) and − 60 mV (ii). The pressure ejection pipette contained 0.1 mM α,β-methylene ATP or 1 mM carbachol (CCh). The membrane currents shown in (a) and (b) were obtained from the same cells. Dotted line corresponds to zero current level. Note, in (a), each current trace has its own scale. In (b), the zero level for the current (i) is almost identical to the level of the current (ii).

membrane was held at + 80 mV, CCh elicited a large outward current (1.5 ± 0.5 nA) which was activated very slowly (time to peak, 2.5 ± 0.4 s, $n = 5$) and had a long duration. Figure 8 shows the effect of depolarization after CCh application. CCh was applied approx. 2 s before depolarization to + 80 mV. Rapid application of CCh did not induce any

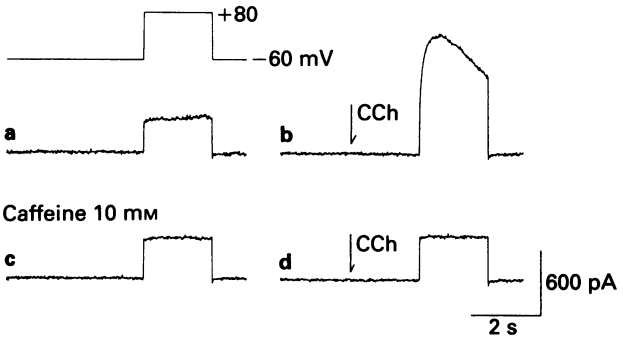

Figure 8 The effects of large depolarizations after carbachol (CCh) application (1 mM, 900 ms) at the holding potential (− 60 mV). After a control depolarization to + 80 mV (2 s) was observed in normal solution (a), CCh was applied approx. 2 s before the second depolarization (b). Depolarization 1 min after application of 10 mM caffeine (c). CCh was applied in the continuous presence of caffeine (d). The depolarizing pulse (a) to (d) was repeated at 2 min intervals. Note, the outward current induced by CCh was attenuated in the presence of caffeine (10 mM).

membrane current while the cell was clamped at the holding potential, but the subsequent depolarization elicited a large outward current (b). Caffeine resulted in a small increase in outward current at + 80 mV (c), but attenuated the CCh response (d).

Discussion

Application of purinoceptor agonists (ATP and α,β-methylene ATP) by pressure ejection activated inward and outward currents at negative (− 60 mV) and positive membrane potentials (+ 80 mV), respectively. The membrane currents developed immediately, and decayed rapidly during application. These properties were very similar to those described by Inoue & Brading (1990), although the application methods and ionic composition of the pipette solutions were different. In the present experiments, the decay time constants observed were similar over a wide voltage-range. At the holding potential (− 60 mV), Ca^{2+} entry is involved in the purinoceptor-induced current, but does not occur during large depolarizations (+ 80 mV), because there is little inward driving force for Ca^{2+} ions. These results suggest that the ATP-induced current is not modulated by intracellular Ca^{2+}. This deduction is also consistent with the previous observation that intracellular perfusion with high concentration of Ca^{2+} chelator or pretreatment with caffeine did not significantly change the ATP-induced current (Inoue & Brading, 1990). These authors also defined the decay time course of the (α,β-methylene) ATP-activated non-selective cation channel current as the sum of two exponential terms. In the present study, however, the decay of the purinoceptor-induced current is well fitted by a single exponential term, the time constant corresponding to the faster of the two exponential terms obtained previously. The discrepancy could be due to the shorter exposure time of the agonists used in the present study.

Bath application of ATP elicited a large inward current at the holding potential in Ca^{2+}-free, low-Mg^{2+} solution. However, the rising and the decay time courses were much slower compared to pressure ejection. In normal solution, similar inward currents were observed (data not shown). Since this inward current was not elicited after prior desensitization with α,β-methylene ATP, it is presumably identical to the non-selective cation channel current activated by pressure ejection of purinergic agonists. The slow decay time course may correspond to the second exponential obtained using the concentration jump methods (Inoue & Brading, 1990).

Pressure ejection of muscarinic agonists caused little change in membrane current at the holding potential. On the other hand, CCh elicited a large outward current during a depolarizing step to + 80 mV. However, the development and the decay of the outward membrane current were much slower than those of the ATP-activated current, implying involvement of different processes. CCh application at both − 60 and + 80 mV reduced the subsequently evoked Ca^{2+} channel current. From these results, we can deduce that the reduction of the Ca^{2+} current is due to Ca^{2+}-dependent inactivation, and the source of Ca^{2+} is the intracellular stores. The slow rise time of the outward current may reflect the increase in $[Ca^{2+}]_i$. Application of caffeine, which is known to release Ca^{2+} from the sarcoplasmic reticulum (SR) (Ebashi, 1976; Endo, 1977; Karaki & Weiss, 1988) attenuated all of the CCh-induced responses, supporting the hypothesis that the main source of Ca^{2+} upon muscarinic receptor stimulation is the intracellular stores. The release of Ca^{2+} from the intracellular store (the SR) could be through production of inositol trisphosphate (IP_3), because flash photolysis of caged IP_3, which had been introduced through the patch pipette, produced similar results to those obtained by CCh application (A. Zholos & S. Nakayama, unpublished observation).

If depolarization to + 80 mV was preceded by CCh application, the depolarization resulted in a large outward current. However, it was not elicited by either procedure alone. This suggests that the large outward current observed is due to ion channels which possess both Ca^{2+}- and voltage-sensitivities, e.g. Ca^{2+}-activated Cl^--channels (Amédée *et al.*, 1990; Evans & Marty, 1986), Ca^{2+}-activated non-selective cation channels (Inoue & Isenberg, 1990a,b; Loirand *et al.*, 1991). Outward Cs^+ current through Ca^{2+}-activated K^+ channels may also have some contribution. The CCh-induced current was quite small at negative potentials compared to the ATP-induced current, and would therefore be much less effective for depolarization of the cell membrane. However, it is possible that ion channels activated through muscarinic transduction may be depressed by perfusion of the pipette solution due to changes in intracellular Ca^{2+}-buffering power etc (Amédée *et al.*, 1990; Wang & Large, 1991). Further identification of the CCh-induced current was not undertaken in the present study.

Two activation mechanisms have been proposed for voltage-dependent Ca^{2+} channels (voltage-dependent and Ca^{2+}-dependent inactivation: reviewed by Pelzer *et al.*, 1990). Previously, we described Ca^{2+} channels in guinea-pig detrusor cells that were inactivated through both of the inactivation mechanisms (Nakayama & Brading, 1993b). In the same smooth muscle, Schneider *et al.* (1990) have shown that bath application of ATP induced an inward current and an increase in $[Ca^{2+}]_i$. The authors suggested that the reduction of the Ca^{2+} channel current during application is due to Ca^{2+}-dependent inactivation. The present results obtained by pressure ejection of purinoceptor agonists at the holding potential agree well with their results. However, in arterial smooth muscle cells, it has also been reported that ATP triggered Ca^{2+} release from the sarcoplasmic reticulum (SR), and subsequently activated Cl^- channels (Droogmans *et al.*, 1991). One would suspect that Ca^{2+} released from the SR would also inactivate the voltage-dependent Ca^{2+} channels upon purinoceptor stimulation in detrusor cells. In the present study, there are two pieces of evidence which exclude this possibility. Firstly, in Ca^{2+}-free, low-Mg^{2+} solution, the Na^+ current through Ca^{2+} channels was not reduced by application of ATP. Secondly, in normal solution (2.5 mM Ca^{2+}), application of purinoceptor agonists during a + 80 mV conditioning depolarization hardly affected the Ca^{2+} current subsequently evoked by the test potential (0 mV). Although in the former case, intracellular Ca^{2+} stores might have been depleted during the exposure to Ca^{2+}-free solution before agonist application, in the latter case, such a depletion is unlikely. Therefore, the fact that Ca^{2+} channel current was not inactivated is attributed solely to lack of Ca^{2+} influx due to the absence of a significant inward driving force.

Thus, we can infer that the main effect of purinoceptor activation is opening non-selective cation channels in the plasma membrane. Recently, Ganitkevich & Isenberg (1992) have reported that depolarization-mediated Ca^{2+} channel current triggers Ca^{2+} release from the SR through a Ca^{2+}-induced Ca^{2+} release mechanism. Similarly, it is possible that Ca^{2+} influx upon purinoceptor stimulation may induce Ca^{2+} release. A possibility that Ca^{2+}-induced Ca^{2+} release also contributed to inactivation of the Ca^{2+} channel still remains. On the other hand, the Ca^{2+} channel current was reduced by muscarinic agonist application at both − 60 mV and + 80 mV. Caffeine also reduced the Ca^{2+} channel current; however, it attenuated further reduction of the Ca^{2+} current following CCh application. It is likely that upon muscarinic receptor stimulation, Ca^{2+} released from intracellular stores, which can be depleted by caffeine, inactivates the Ca^{2+} channels through a Ca^{2+}-dependent inactivation mechanism. The caffeine-induced reduction of the Ca^{2+} current may also involve direct block of voltage-dependent Ca^{2+} channels (Martin *et al.*, 1989; Hughes *et al.*, 1990; Zholos *et al.*, 1991).

Muscarinic receptor activation triggers Ca^{2+} release from the SR probably through the IP_3 pathway. However, the present experiments do not imply that the IP_3-sensitive Ca^{2+}

store is also caffeine sensitive, because it has been reported that Ca^{2+} release from this store is potentiated by a small increase in $[Ca^{2+}]_i$, (biphasic Ca^{2+} dependence of IP_3-induced Ca^{2+} release: $[Ca^{2+}]_i > 300$ nM inhibits the Ca^{2+} release: Iino, 1990). In the presence of caffeine, a small reduction of the Ca^{2+} channel current was observed 30 s after CCh application (data not shown). This may be due to slower IP_3-induced Ca^{2+} release in the presence of a greater Ca^{2+} concentration (Iino, 1990) or other mechanisms induced by muscarinic receptor activation (e.g. possible inhibition of the Ca^{2+} current through activation of protein kinase C: Ozaki *et al.*, 1992).

Previously, we showed lack of inactivation of the Ca^{2+} current after a depolarization at +80 mV for 5 s, a duration often used to achieve a steady state (Nakayama & Brading, 1993a,b). This was explained by lack of voltage-dependent inactivation of a long open state induced by large depolarizations, as well as little Ca^{2+} influx at +80 mV. In the present study, application of α,β-methylene ATP at +80 mV little affected, while CCh reduced the subsequent Ca^{2+} channel current, although both applications elicited large outward currents during the +80 mV step. The contrast of the effects between purinoceptor and muscarinic agonists on the subsequently evoked Ca^{2+} channel current supports the hypothesis that the sources of Ca^{2+} are different for these two agonists. The persistent effect of muscarinic agonists can be explained since the Ca^{2+} release mechanism triggered by muscarinic stimulation is not affected by the membrane potential. This effect could also be evidence that Ca^{2+} channels in the long open state can be inactivated by a Ca^{2+}-dependent inactivation mechanism, and also support the notion that voltage-dependent and Ca^{2+}-dependent inactivation mechanisms operate separately (Hadley & Lederer, 1991). After a large depolarization, tail currents were evoked by returning the membrane potential to −60 mV. When the patch pipette contained a high concentration (2 mM) of EGTA, the tail current and the inward current evoked at 0 mV were reduced by dihydropyridine Ca^{2+} antagonists in the same manner, suggesting that the tail current was also flowing through L-type Ca^{2+} channels (Nakayama & Brading, 1993a). However, in the present experiments, since EGTA was reduced to 0.1 mM to demonstrate clearly Ca^{2+}dependent inactivation, the tail current may be contaminated by other Ca^{2+}-dependent conductances.

In microelectrode recording of the membrane potential, guinea-pig urinary bladder smooth muscle shows spontaneous action potential generation. Purinoceptor agonists evoke depolarizations, while muscarinic agonists cause only small changes in membrane potential (Fujii, 1988). The results shown in the present study (a large inward current upon purinoceptor activation; little membrane current induced by muscarinic agonists) are consistent with the microelectrode recordings. Although action potential frequency is increased by application of purinoceptor and muscarinic receptor agonists, the amplitude is often reduced (Personal communication from N. Bramich). The reduction of action potential amplitude can be explained by Ca^{2+}-dependent inactivation of voltage-dependent Ca^{2+} channels.

In conclusion, activation of purinoceptors results in opening of non-selective cation channels in the plasma membrane. Stimulation of muscarinic receptors triggers Ca^{2+} release from intracellular stores. Voltage-operated Ca^{2+} channels are inactivated by an increase in intracellular Ca^{2+}, irrespective of the channel state. Activation of either purinoceptors or muscarinic receptors can contribute to Ca^{2+}-dependent inactivation.

This work was carried out during the tenure of a grant from Bristol Myers Squibb. The author is grateful to Drs A. Brading, N. Bramich and T. Cunnane, Oxford University, for their pertinent help, discussion and critical reading of this manuscript, and also to Dr A. Zholos and Prof T. Bolton, St George's Hospital Medical School, for supporting experiments on caged compounds.

References

AMÉDÉE, T., LARGE, W.A. & WANG, Q. (1990). Characteristics of chloride current activated by noradrenaline in rabbit ear artery cells. *J. Physiol.*, **428**, 501–516.

BENHAM, C.D., BOLTON, T.B. & LANG, R.J. (1985). Acetylcholine activates an inward current in single mammalian smooth muscle cells. *Nature*, **316**, 345–347.

BURNSTOCK, G., COCKS, T., CROWE, R. & KASAKOV, L. (1978). Purinergic innervation of the guinea-pig bladder. *Br. J. Pharmacol.*, **63**, 125–138.

BURNSTOCK, G., DUMSDAY, B.H. & SMYTHE, A. (1972). Atropine resistant excitation of the urinary bladder: the possibility of transmission via nerves releasing a purine nucleotide. *Br. J. Pharmacol.*, **44**, 451–467.

CREED, K.E. (1971). Effects of ions and drugs on the smooth muscle cell membrane of the guinea-pig urinary bladder. *Pflügers Arch.*, **326**, 127–141.

CREED, K.E., ISHIKAWA, S. & ITO, Y. (1983). Electrical and mechanical activity recorded from rabbit urinary bladder in response to nerve stimulation. *J. Physiol.*, **338**, 149–164.

EBASHI, S. (1976). Excitation-contraction coupling. *Annu. Rev. Physiol.*, **38**, 293–311.

ENDO, M. (1977). Calcium release from sarcoplasmic reticulum. *Phsyiol. Rev.*, **57**, 71–108.

EVANS, M.G. & MARTY, A. (1986). Calcium-dependent chloride currents in isolated cells from rat lacrimal glands. *J. Physiol.*, **378**, 437–460.

DROOGMANS, G., GALLEWAERT, G., DECLERCK, I. & CASTEELS, R. (1991). ATP-induced Ca^{2+} release and Cl^- current in cultured smooth muscle cells from pig aorta. *J. Physiol.*, **440**, 623–634.

FUJII, K. (1988). Evidence for adenosine triphosphate as an excitatory transmitter in guinea-pig, rabbit and pig urinary bladder. *J. Physiol.*, **404**, 39–52.

FUKUSHIMA, Y. & HAGIWARA, S. (1985). Current carried by monovalent cations through calcium channels in mouse neoplastic B lymphocytes. *J. Physiol.*, **358**, 255–284.

GANITKEVICH, V.YA & ISENBERG, G. (1992). Contribution of Ca^{2+}-induced Ca^{2+} release to the $[Ca^{2+}]_i$ transients in myocytes from guinea-pig urinary bladder. *J. Physiol.*, **458**, 119–137.

HADLEY, R.W. & LEDERER, W.J. (1991). Ca^{2+} and voltage inactivate Ca^{2+} channels in guinea-pig ventricular myocytes through independent mechanisms. *J. Physiol.*, **444**, 257–268.

HAMILL, O.P., MARTY, A., NEHER, E., SAKMANN, B. & SIGWORTH, F.J. (1981). Improved patch-clamp techniques for high-resolution current recording from cells and cell-free membrane patches. *Pflügers Arch.*, **391**, 85–100.

HENDERSON, V.E. & ROEPKE, M.H. (1934). The role of acetylcholine in bladder contractile mechanisms and in parasympathetic ganglia. *J. Pharmacol. Exp. Ther.*, **51**, 97–111.

HUGHES, A.D., HERING, S. & BOLTON, T.B. (1990). The action of caffeine on inward barium current through voltage-dependent calcium channels in single rabbit ear artery cells. *Pflügers Arch.*, **416**, 462–466.

IINO, M. (1990). Biphasic Ca^{2+}dependence of inositol 1,4,5-trisphosphate-induced Ca^{2+} release in smooth muscle cells of the guinea-pig taenia caeci. *J. Gen. Physiol.*, **95**, 1103–1122.

INOUE, R. & BRADING, A.F. (1990). The properties of the ATP-induced depolarization and current in single cells isolated from guinea-pig urinary bladder. *Br. J. Pharmacol.*, **100**, 619–625.

INOUE, R. & ISENBERG, G. (1990a). Effect of membrane potential on acetylcholine-induced inward current in guinea-pig ileum. *J. Physiol.*, **424**, 57–71.

INOUE, R. & ISENBERG, G. (1990b). Intracellular calcium ions modulate acetylcholine-induced inward current in guinea-pig ileum. *J. Physiol.*, **424**, 73–92.

JANSSEN, L.J. & SIMS, S.M. (1992). Acetylcholine activates non-selective cation and chloride conductances in canine and guinea-pig tracheal cells. *J. Physiol.*, **453**, 197–218.

KARAKI, H. & WEISS, G.B. (1988). Calcium release in smooth muscle. *Life Sci.*, **42**, 111–122.

LANGLEY, K.N. & ANDERSON, H.K. (1885). The innervation of the pelvic and adjoining viscera. Part II. The bladder. *J. Physiol.*, **19**, 71–84.

LOIRAND, G., PACAUD, P., BARON, A., MIRONNEAU, C. & MIRONNEAU, J. (1991). Large conductance calcium-activated non-selective cation channel in smooth muscle cells isolated from rat portal vein. *J. Physiol.*, **437**, 461–475.

MARTIN, C., DACQUET, C., MIRONNEAU, C. & MIRONNEAU, J. (1989). Caffeine-induced inhibition of calcium channel current in cultured smooth muscle cells from pregnant rat myometrium. *Br. J. Pharmacol.*, **98**, 493–498.

NAKAYAMA, S. & BRADING, A.F. (1993a). Evidence for multiple open states of the Ca^{2+} channels in smooth muscle cells isolated from the guinea-pig detrusor. *J. Physiol.*, (in press).

NAKAYAMA, S. & BRADING, A.F. (1993b). Inactivation of the voltage-dependent Ca^{2+} channel current in smooth muscle cells isolated from the guinea-pig detrusor. *J. Physiol.*, (in press).

OZAKI, H., ZHANG, L., BUXTON, I.L.O., SANDERS, K.M. & PUBLICOVER, N.G. (1992). Negative-feedback regulation of excitation-contraction coupling in gastric smooth muscle. *Am. J. Physiol.*, **263**, C1160–1171.

PELZER, D., PELZER, S. & McDONALD, T.F. (1990). Properties and regulation of calcium channels in muscle cells. *Rev. Physiol. Biochem. Pharmacol.*, **114**, 107–207.

SCHNEIDER, P., HOPP, H.H. & ISENBERG, G. (1991). Ca^{2+} influx through ATP-gated channels increments $[Ca^{2+}]_i$ and inactivates I_{Ca} in myocytes from guinea-pig urinary bladder. *J. Physiol.*, **440**, 479–496.

SIMS, S.M. (1992). Cholinergic activation of a non-selective cation current in canine gastric smooth muscle is associated with contraction. *J. Physiol.*, **449**, 377–398.

WANG, Q. & LARGE, W.A. (1991). Noradrenaline-evoked cation conductance recorded with the nystatin whole-cell method in rabbit portal vein cells. *J. Physiol.*, **435**, 21–39.

XIONG, Z., KITAMURA, K. & KURIYAMA, H. (1991). ATP activates cationic currents and modulates the calcium current through GTP-binding protein in rabbit portal vein. *J. Physiol.*, **440**, 143–165.

ZHOLOS, A.V., BAIDAN, L.V. & SHUBA, M.F. (1991). The inhibitory action of caffeine on calcium currents in isolated intestinal smooth muscle cells. *Pflügers Arch.*, **419**, 267–273.

(Received March 1, 1993
Revised March 22, 1993
Accepted April 14, 1993)

Br. J. Pharmacol. (1993), **110**, 326–330

Post-receptor pathway of the ATP-induced relaxation in smooth muscle of the mouse vas deferens

[1]Ph. Gailly, B. Boland, C. Paques, *B. Himpens, *R. Casteels & J.M. Gillis

Department of Physiology, U.C. Louvain, 1200 Bruxelles, Belgium and *Physiological Laboratory, K.U. Leuven, 3000 Leuven, Belgium

1 The post-receptor pathway of the ATP relaxant effect in K^+-precontracted vas deferens smooth muscle (VD) was examined.

2 The relaxation to ATP was not antagonized either by 10 μM methylene blue, a cyclic GMP inhibitor, by 10 μM indomethacin, an inhibitor of prostaglandin synthesis or by 100 μM N^G-nitro-L-arginine, an inhibitor of NO production.

3 The Rp-diastereomer of adenosine 3':5'-cyclic monophosphorothioate (Rp-cAMPS) 200 μM, a competitive inhibitor of cyclic AMP significantly diminished the relaxant response to ATP.

4 Isoprenaline 10 μM, a β-adrenoceptor agonist, produced a sustained relaxation, inhibited by Rp-cAMPS, without a significant change in $[Ca^{2+}]_i$, thereby mimicking the ATP-induced relaxant effect.

5 The level of the phosphorylated myosin light chain in the precontracted VD was significantly lowered by 1000 μM ATP.

6 ATP (1000 μM) and isoprenaline (10 μM) produced the same increase (+ 50%) of [cyclic AMP] when applied to a resting VD.

7 The effect of simultaneous increases of $[Ca^{2+}]_i$ and of [cyclic AMP] produced by externally applied ATP are discussed.

8 These results suggest that ATP-induced relaxation in K^+-precontracted VD is mediated by the activation of adenylyl cyclase.

Keywords: ATP; P_2-purinoceptors; cyclic AMP; myosin phosphorylation; relaxation; smooth muscle; vas deferens

Introduction

Co-transmission of adenosine 5'-triphosphate (ATP) and noradrenaline was initially observed in the sympathetic nerves of the rodent vas deferens (Sneddon & Westfall, 1984). In this tissue, ATP induces contraction through the so called P_{2X}-purinoceptors (Fedan *et al.*, 1982; Burnstock *et al.*, 1985), the activation of which triggers opening of non-selective ion channels, membrane depolarization and calcium influx (Friel, 1988). The contractile effect of externally applied ATP is however very weak and transient (Fedan *et al.*, 1982; Hourani *et al.*, 1986; Wilkund & Gustafsson, 1988; von Kügelen *et al.*, 1990). We recently reported that, in the mouse vas deferens (VD), ATP induced a large rise of the cytoplasmic free calcium concentration ($[Ca^{2+}]_i$), as large as that produced by massive depolarization with isotonic K^+ solution. We also observed that ATP could induce relaxation of a K^+-depolarized preparation. Therefore, it was suggested that the calcium-force dissociation could be due to the simultaneous binding of ATP to both P_{2X}-purinoceptors, mediating contraction and P_{2Y}-purinoceptors, mediating relaxation (Boland *et al.*, 1992). We describe here our attempts to identify the post-receptor signal for the ATP-induced relaxant response. Several possible messengers were excluded on the basis of pharmacological experiments. Results show that externally applied ATP not only produces an intracellular rise of $[Ca^{2+}]_i$, but also of adenosine 3':5'-cyclic monophosphate (cyclic AMP). The latter seems to be the post-receptor signal for the relaxant response. However, as discussed, this may not be sufficient to explain fully the observed calcium-force dissociation induced by ATP when applied to the resting VD.

[1] Author for correspondence.

Methods

Muscle preparation and measurements of cytosolic Ca^{2+} concentration and of force

We essentially followed the procedures previously described (Boland *et al.*, 1992) except for fura-2 fluorescence measurements. Adult male albino mice (NMRI) of 3–4 months were killed by cervical dislocation after anaesthesia with ether. The end segment of the prostatic portion of the VD was isolated and opened longitudinally; its thick mucosal layer was then scraped away by gentle rubbing. VD preparations were stretched to 2 mN passive tension and isometric contraction force was measured by use of a strain gauge (type FLA-3-11, Tokyo Sokki Kenkyujo Co. Ltd). Isometric force was expressed in mN on the original traces. In the text, the force relaxation produced in raised-tone preparations by ATP or isoprenaline is normalized to the steady raised tone level maintained by prolonged stimulation with the high K^+ solution. All experiments were performed at room temperature.

Fura-2 fluorescence was measured with inverted fluorescence microscopic equipment (from Nikon and Deltascan, PTI) where the emission intensity was collected at a 510 nm by a photon counting tube (PTI). Calculation of $[Ca^{2+}]_i$ was performed by internal calibration of the fura-2 fluorescence signal, according to a procedure designed by Himpens and co-workers (1988). In order to verify that the $[Ca^{2+}]_i$ rise upon application of ATP, essentially came from muscle cells and not from nerve endings (known to be numerous in VD; Swedin, 1971), we checked that this $[Ca^{2+}]_i$ rise was unaffected either after incubation with ω-conotoxin (1 μM, 30 min), a blocking agent specific for the neuronal calcium channels (McCleskey *et al.*, 1987) or after pharmcological destruction of nerve endings (Wakade, 1979). In the latter case, mice were injected intraperitoneally with 6-hydroxydopamine (6-OHDA), three times at two days interval. This treatment totally abolished the response to electrical stimulation.

Measurement of cyclic AMP

The concentration of the cytoplasmic cyclic AMP was determined by radioimmunoassay, as described (Barnette *et al.*, 1989; McHenry *et al.*, 1991). After 5 min incubation in the experimental solution, VD strips were rapidly frozen in liquid nitrogen and homogenized in 1 ml of 6% trichloracetic acid (TCA) on ice. Precipitated proteins were removed by 2000 *g* centrifugation for 15 min. TCA was removed from the supernatant by four extractions with water-saturated ether (3 ml), and the samples were evaporated. The measurement of cyclic AMP was by radioimmunoassay (Amersham kit, U.K.). The results are expressed in femtomoles per milligram (fmol mg^{-1}) of frozen muscle.

Determination of the myosin light chain phosphorylation

Phosphorylation of the 20 kDa myosin light chain (LC) was determined by two dimensional electrophoresis. The frozen VD preparations were ground in a mortar precooled with liquid nitrogen, in 300 µl 0.5 M perchloric acid. After thawing at room temperature, 400 µl perchloric acid was added and the whole extract was centrifugated for 5 min at 5000 r.p.m. The pellet was dissolved in 10 µl of the lysis buffer (9.5 M urea, 2% (w/v) nonidet P40 (NP 40), 1.6% ampholine pH 5–7, 0.4% ampholine pH 3–10, 5% β-mercaptoethanol) and 10 µl of glycerol, for a first separation by isoelectrofusing (IEF). We used two different methods: (1) capillary gels containing 7% acrylamide, 3% NP 40, 0.3% ampholine pH 4–6, 0.3% ampholine pH 3.5–10 and 0.3% ampholine pH 5–8; IEF was run at 800 V, for 3 h. (2) Precoated commercial strips providing an immobilized pH gradient 4–7 (IPG), from Pharmacia (Righetti, 1990). In this case, focusing was run under the cover of paraffin oil and, in order to get good penetration of the sample into the gel, voltage was very progressively increased to 3.3 kV, then maintained overnight. Some samples were analyzed by both methods and identical results were obtained. For the second dimension, gels or strips were transferred to the top of a polyacrylamide slab gel (stacking gel: 3% polyacrylamide in 0.5 M Tris-HCl, sodium dodecylsulphate (SDS) 0.4%, pH 6.8; separating gel: 15% polyacrylamide in 1.5 M Tris-glycine, SDS 0.4%, pH 8.8) and covered with the running buffer (20 mM Tris, 192 mM glycine, 0.1% SDS). A sample of purified myosin from soleus muscle was run simultaneously. After staining, densitometry was integrated over the spot areas (Lecphor image analysis programme of Biocom, 91942 Les Ulis, France). The results are given as the percentage of phosphorylated (PMLC) and unphosphorylated forms of the total amount of the 20 kDa myosin light chains.

Drugs and solutions

The normal HEPES-Krebs solution contained in mM: Na^+ 135.5, K^+ 5.9, Mg^{2+} 1.2, Ca^{2+} 1.5, Cl^- 143.8, HEPES 11.6 and glucose 11.5. The pH was 7.3. K^+ 140 mM solutions were obtained by replacing external Na^+ by an equivalent amount of K^+. Isoprenaline, ATP, indomethacin, ionomycin, 6-OHDA, ω-conotoxin and N^G-nitro-L-arginine were from Sigma. Methylene blue was obtained from Merck (Darmstadt, Germany) and adenosine 3′:5′-cyclic monophosphorothioate (Rp diastereomer, Rp-cAMPS) from Biolog (Bremen, Germany). Fura-2/AM was from Molecular Probes (Eugene, Oregon, U.S.A.). All other reagents were of analytical grade. Drugs were dissolved in Krebs solution, except ionomycin which was dissolved in ethanol (stock solution 5 mM), and indomethacin, solubilized in 80% methanol containing 0.2 M NaOH (Griffith *et al.*, 1981) and used at the 1/1000 dilution of the stock solution.

Statistics

The data were evaluated for differences by Student's *t* test (paired two-tailed *t* test). A probability of less than 0.05 was considered significant. The results are presented as means ± s.e.mean, and *n* is the number of experiments.

Results

Factors affecting the ATP-induced relaxation

We previously showed that the mechanical counterpart of the P_{2Y} activation could be revealed on pre-contracted and depolarized preparations (15 min in 140 mM K^+ solution): in these conditions, after a transient P_{2X}-related contraction, ATP produced a sustained and reversible relaxation induced by P_{2Y} activation (Boland *et al.*, 1992). The relaxant effect was maximal for a concentration of ATP of 1 mM. We describe here how this relaxation can be affected by various pharmacological interventions.

The relaxation induced by 1 mM ATP was unaffected by pre-incubation of the preparations, for 30 min, with 10 µM methylene blue, 10 µM indomethacin, or 100 µM N^G-nitro-L-arginine, agents known to inhibit the synthesis of cyclic GMP (Gruetter *et al.*, 1981), of prostaglandin (Vane, 1971), and of nitric oxide (Moore *et al.*, 1990; Toda *et al.*, 1990; Ishii *et al.*, 1990), respectively (Table 1). On the other hand, after 1 h incubation in the presence of 200 µM Rp-cAMPS, a cyclic AMP competitive inhibitor (Botelho *et al.*, 1988), the relaxant effect of ATP was significantly diminished (Table 1). The effect of Rp-cAMPS was further studied on the relaxation induced by 500 µM ATP. As illustrated in Figure 1, force contraction of VD maintained in 140 mM K^+ stabilized at about one-fifth of its peak contraction, while $[Ca^{2+}]_i$ remained between 200 and 250 nM. In this condition, 500 µM ATP produced a rise of $[Ca^{2+}]_i$ followed by a return to its previous level after 3 min. This calcium increase was accompanied by a transient contraction followed within 30 s by a force decrease of about 35 ± 3.9% below the steady plateau level ($n = 7$). Thus, relaxation started while $[Ca^{2+}]_i$ was still well above its previous level (before ATP addition). This relaxation was maintained as long as ATP was applied, and was not associated with any further decrease of $[Ca^{2+}]_i$. After 1 h incubation in presence of 200 µM Rp-cAMPS, the transient contraction induced by ATP was not significantly modified but the relaxant effect of ATP significantly diminished from 35 ± 3.9% to 10.7 ± 3.5% ($n = 7$) (Figure 1).

Isoprenaline (10 µM) mimicked the effect of ATP 500 µM as it induced a relaxation of 35 ± 5% ($n = 7$) after 30 s, which was maintained as long as isoprenaline was applied (Figure 1), without affecting the level of $[Ca^{2+}]_i$. This β-agonist is well known to produce an increase of [cyclic AMP] in smooth muscle (Scheid *et al.*, 1979). As expected, we found that the relaxation induced by isoprenaline was completely abolished by pre-incubation with 200 µM Rp-cAMPS ($n = 5$).

Changes of cyclic AMP concentration

The similarity of the relaxant effects of ATP and isoprenaline on force and the sensitivity of these effects to the Rp-cAMPS

Table 1 The effect of various agents on ATP-induced relaxation of the vas deferens

Pre-incubation conditions	*ATP-(1 mM)-induced relaxation*†
Control (K^+ 140 mM)	− 56 ± 6%, $n = 7$
Indomethacin 10 µM	− 58 ± 7%, $n = 4$
Methylene blue 10 µM	− 50 ± 9%, $n = 3$
N^G-nitro-L-arginine 100 µM	− 51 ± 2%, $n = 4$
Rp-cAMPS 200 µM	− 19 ± 3%, $n = 4$*

†Drop in tension, expressed as % of the steady tone level maintained by prolonged K^+-depolarization.
*$P < 0.01$: *t* test.

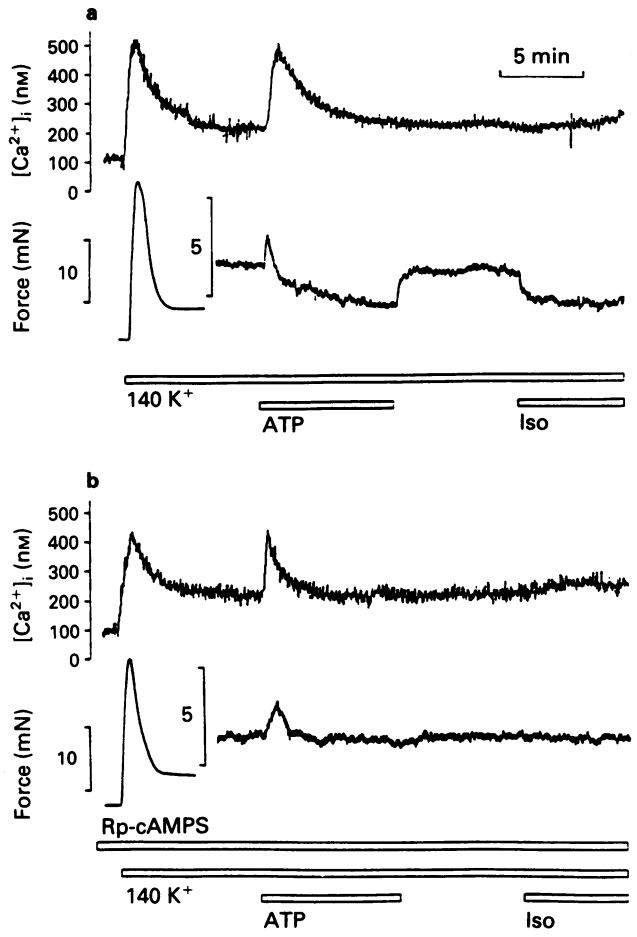

Figure 1 (a) Shows the changes in $[Ca^{2+}]_i$ (upper trace) and force (lower trace) in the vas deferens in response to superfusion with K^+ 140 mM, ATP 500 μM and isoprenaline 10 μM (Iso). (b) Presents the same experiment after 1 h incubation with Rp-cAMPS. Horizontal bars indicate the timing of the superfusions.

inhibitor suggested the participation of cyclic AMP in the relaxation of the depolarized preparation. Therefore, we measured [cyclic AMP] directly in muscle extracts. In control, resting conditions, [cyclic AMP] was 636 ± 18 fmol mg^{-1} of wet muscle ($n = 16$). A similar basal level was reported by others (Diamond & Janis, 1978; Heller *et al.*, 1989). After 5 min in 100 μM ATP, [cyclic AMP] rose to 760 ± 46 fmol mg^{-1} ($n = 16$), and to 939 ± 113 fmol mg^{-1} ($n = 5$), in 1000 μM ATP. As a point of comparison, isoprenaline (10 μM, 5 min) produced an increase of [cyclic AMP] to 937 ± 87 fmol mg^{-1} ($n = 6$). All these increases were significantly higher than the basal level.

Myosin light chain phosphorylation

At rest, the relative amount of phosphorylation of the 20 kDa myosin light chain (PMLC) amounted to 5.4 ± 2.9% ($n = 8$). At the initial peak of contraction during depolarization with 140 mM K^+, PMLC reached 31.8 ± 4.1% ($n = 7$); after 25 min, PMLC had declined to 16.85 ± 1.4% ($n = 19$, control situation). When ATP (1000 μM) was added to the pre-contracted VD, after 15 min in 140 mM K^+, and the muscle frozen 10 min later (total duration in 140 mM K^+: 25 min), PMLC had decreased to 12.75 ± 1.2% ($n = 20$). The difference compared with the control situation was significant. Thus in pre-contracted and depolarized VD, ATP produced a force relaxation and a myosin LC dephosphorylation of about the same relative amplitude.

Test of the two antagonistic pathways hypothesis

We previously suggested that calcium-force dissociation observed in resting VD with ATP (Boland *et al.*, 1992) might be explained by an overlap of contracting and relaxing influences; the latter was shown, here, to be related to cyclic AMP production. Two experiments were designed to test this hypothesis.

(i) If the ATP-induced synthesis of cyclic AMP is responsible for the calcium-force dissociation in VD, then incubation of resting VD with Rp-cAMPS would be expected to improve the calcium-force coupling, and thereby to increase the amplitude of the contraction produced by ATP. Stimulation with 100 μM ATP, which induces an obvious calcium-force dissociation (Boland *et al.*, 1992), significantly elevated [cyclic AMP] (see above) and induced a contraction of only 3 ± 1% ($n = 9$) of the maximal force developed in response to 140 mM K^+ depolarization. This force response was not increased by pre-incubation with 200 μM Rp-cAMPS (2.25 ± 0.75%, $n = 4$).

(ii) The simple model of overlapping increases of $[Ca^{2+}]_i$ and of $[\text{cyclic AMP}]_i$ can be mimicked by combining K^+ depolarization (Boland *et al.*, 1992) with the presence of isoprenaline (see above). We found that K^+-induced contraction was not significantly affected by concomitant addition of 10 μM isoprenaline (97 ± 6.5% of the K^+ reference peak, $n = 4$). However, after a pre-incubation with 20 μM isoprenaline for 2.5 min, the peak contraction induced by K^+ depolarization attained 76 ± 2% ($n = 7$) of the reference value. Obviously, an antagonistic effect of Ca^{2+} and cyclic AMP on the force response can be detected in the latter condition, but it is not of the required magnitude to explain the very weak force observed in the presence of ATP.

Discussion

We previously showed that ATP can induce a transient contraction followed by a sustained relaxation in depolarized preparations and that the latter effect probably involved P_{2Y}-purinoceptors (Boland *et al.*, 1992). In this paper, different intracellular mechanisms able to induce smooth muscle relaxation were investigated.

ATP-induced relaxation could be mediated by a decrease of $[Ca^{2+}]_i$ but the finding that relaxation started during the peak of calcium and was maintained at an elevated and steady $[Ca^{2+}]_i$ (around 250 nM, see Figure 1) does not support this interpretation. ATP can also induce opening of K^+-channels and hence hyperpolarization, in guinea-pig taenia coli (Tomita & Watanabe, 1973) and in ileum circular layers (Crist *et al.*, 1992). Obviously, membrane hyperpolarization is not involved here as K^+-depolarized VD showed relaxation in response to ATP. Prostaglandin synthesis and ATP-induced relaxation are linked in guinea-pig taenia coli (Brown & Burnstock, 1981); but, as relaxation of VD was unaffected by indomethacin, this pathway seems unlikely. In vascular smooth muscle, relaxation can also be mediated through the P_{2Y}-induced release of nitric oxide by endothelium, producing an activation of the smooth muscle guanylyl cyclase. Recently, NO has also been reported as a neurotransmitter in non vascular (Li & Rand, 1990; Boeckxstaens *et al.*, 1991; Lefebvre *et al.*, 1992) and vascular smooth muscle (Toda & Okamura, 1992). Muscle tissue could even directly generate a muscle-derived relaxing factor (MDRF) similar to NO (Wood *et al.*, 1990). In our preparation, we found that relaxation was unaffected by inhibitors of NO production. Stimulation of cyclic GMP synthesis, independent of the NO pathway, can also be excluded, as relaxation was insensitive to methylene blue.

P_{2Y}-purinoceptors are linked to a G protein (Kennedy, 1990) and could activate cytosolic adenylyl cyclase. Three observations support the proposal that cyclic AMP is mediating the ATP-induced relaxation in the K^+-pre-

contracted VD. (1) Relaxation is partially inhibited by Rp-cAMPS, a competitive antagonist of cyclic AMP. (2) We observed some similarities of the responses to ATP and to isoprenaline, a β-adrenoceptor agonist, well known to induce relaxation by the synthesis of cyclic AMP (Scheid *et al.*, 1979): in K^+-depolarized preparations, both isoprenaline and ATP caused sustained relaxations of comparable amplitudes, which occurred in spite of an elevated $[Ca^{2+}]_i$, and were significantly inhibited by Rp-cAMPS. (3) In physiological conditions, direct measurements showed that externally applied ATP produced a rise of the cyclic AMP concentration similar to that produced by isoprenaline.

ATP-induced relaxation of depolarized VD was correlated with a reduction of the level of PMLC. Most likely this reflected the inhibition of the myosin light chain kinase (MLCK) when it is phosphorylated by a cyclic AMP-dependent protein kinase A (Adelstein *et al.*, 1978; Kerrick & Hoar, 1981; Nishimura & van Bremen, 1989; Ozaki *et al.*, 1992)

On the basis of the rank order of potency of different ATP analogues, of the absence of tachyphylaxis and of the action of selective antagonists, it was proposed that ATP-induced relaxation implies a P_{2Y}-like purinoceptor (Boland *et al.*, 1992). Our results suggest that this effect is linked to the activation of adenylyl cyclase. This pathway is well documented for P_1-purinoceptors (A_2 subclass; for review, see Kennedy, 1990) but has not been reported for P_{2Y}-purinoceptors. However, the possibility that the receptor could be another sub-type of P_2-purinoceptor (P_{2Z}, P_{2T} or unknown) cannot be definitely excluded (for review, see Olson & Pearson, 1990).

Together, these and our previous results indicate that externally applied ATP gives rise to two intracellular messengers, Ca^{2+} and cyclic AMP. The first one, in combination with calmodulin, would lead to activation of MLCK, while the second, through the cyclic AMP-protein kinase A cascade, to the inhibition of MLCK (for review, see Rasmussen & Rasmussen, 1990). As these two antagonistic influences overlap somewhat in time, the force response would reflect the net result of these influences at the level of MLCK. This could be the basis of the calcium-force dissociation we previously reported. A similar model of two antagonistic influences has been proposed by Watanabe and co-workers (1992) to explain the calcium-force dissociation observed in caffeine-treated aorta. However, in the case of the VD, it seems that the simultaneous elevation of $[Ca^{2+}]_i$ and [cyclic AMP] would not be sufficient to explain fully the calcium-force dissociation. Indeed, when the cyclic AMP pathway was inhibited, the weak ATP-induced force was not potentiated, contrary to expectations. Moreover, in experiments meant to mimic the simultaneous increases of $[Ca^{2+}]_i$ and [cyclic AMP] (stimulation with K^+ and isoprenaline), the observed antagonistic influence of the two second messengers on the force response was much too small to explain the calcium-force dissociation induced by ATP.

Ph.G. and B.B. are research assistants of the FNRS (Belgium). The assistance of Prof. J.M. Ketelslegers, Mrs M.L. Cao and Mrs P. Lison is gratefully acknowledged.

References

ADELSTEIN, R.S., CONTI, M.A., HATHAWAY, D.R. & KLEE, C.B. (1978). Phosphorylation of smooth muscle myosin light chain kinase by the catalytic subunit of adenosine 3', 5'-monophosphate-dependent protein kinase. *J. Biol. Chem.*, **253**, 8347–8350.

BARNETTE, M.S., GROUS, M., TORPHY, T.J. & ORMSBEE, H.S. (1990). Activation of cyclic AMP-dependent protein kinase during canine lower esophageal sphincter relaxation. *J. Pharmacol. Exp. Ther.*, **252**, 1160–1166.

BOECKXSTAENS, G.E., PELCKMANS, P.A., BULT, H., DE MAN, J.G., HERMAN, A.G. & VAN MAERCKE, Y.M. (1990). Non-adrenergic non-cholinergic relaxation mediated by nitric oxide in the canine ileocolonic junction. *Eur. J. Pharmacol.*, **190**, 239–246.

BOLAND, B., HIMPENS, B., GILLIS, J.M. & CASTEELS, R. (1992). ATP activates both contracting P2x- and relaxing P2y-purinoceptors in the smooth muscle of mouse the vas deferens. *Br. J. Pharmacol.*, **107**, 1152–1158.

BOTELHO, L.H.P., ROTHERMEL, J.D., COOMBS, R.V. & JASTORFF, B. (1988). cAMP analog antagonists of cAMP action. *Methods Enzymol.*, **159**, 159–172.

BROWN, C.M. & BURNSTOCK, G. (1981). The structural conformation of the polyphosphate chain of the ATP molecule is critical for its promotion of prostaglandin biosynthesis. *Eur. J. Pharmacol.*, **69**, 81–86.

BURNSTOCK, G., CUSACK, N.J. & MELDRUM, L.A. (1985). Studies on the stereoselectivity of the P_2-purinoceptor in the guinea-pig vas deferens. *Br. J. Pharmacol.*, **84**, 431–434.

CRIST, J.R., XUE, D.H.E. & GOYAL, R.K. (1992). Both ATP and the peptide VIP are inhibitory neurotransmitters in guinea-pig ielum circular muscle. *J. Physiol.*, **447**, 119–131.

DIAMOND, J. & JANIS, R.A. (1978). Increases in cyclic GMP levels may not mediate relaxant effects of sodium nitroprusside, verapamil and hydralazine in rat vas deferens. *Nature*, **271**, 472–473.

FEDAN, J.S., HIGABOOM, G.K., WESTFALL, D.P. & O'DONNELL, J.P. (1982). Comparison of contractions of the smooth muscle of the guinea-pig vas deferens induced by ATP related nucleotides. *Eur. J. Pharmacol.*, **81**, 193–204.

FRIEL, D.D. (1988). An ATP-sensitive conductance in single smooth muscle cells from the rat vas deferens. *J. Physiol.*, **401**, 361–380.

GRIFFITH, S.G., MEGHJI, P., MOODY, C.J. & BURNSTOCK, G. (1981). 8-Phenyltheophylline: a potent P_1-purinoceptor antagonist. *Eur. J. Pharmacol.*, **75**, 61–64.

GRUETTER, C.A., KADOWITZ, P.J. & IGNARRO, L.J. (1981). Methylene blue inhibits coronary arterial relaxation and guanylate cyclase activation by nitroglycerin, sodium nitrite, and amyl nitrite. *Can. J. Physiol. Pharmacol.*, **59**, 150–156.

HELLER, T., KÖCHER, M., NEUMANN, J., SCHMITZ, W., SCHOLTZ, H., STEMMILDT, V. & STÖRZEL, K. (1989). Effects of adenosine analogues on force and cAMP in the heart. Influence of adenosine deaminase. *Eur. J. Pharmacol.*, **164**, 179–187.

HIMPENS, B., MATTIJS, G., SOMLYO, A.V., BUTLER, T.M. & SOMLYO, A.P. (1988). Cytoplasmic free calcium, myosin light chain phosphorylation and force in phasic and tonic smooth muscle. *J. Gen. Physiol.*, **92**, 489–503.

HOURANI, S.M.O., LOIZOU, G.D. & CUSACK, N.J. (1986). Pharmacological effects of L-AMP-PC P on ATP receptors on smooth muscle. *Eur. J. Pharmacol.*, **131**, 99–103.

ISHII, K.B., CHANG, B., KERWIN, J.F., HUANG, Z.-J. & MURAD, F. (1990). N^{ω}-nitro-L-arginine: a potent inhibitor of endothelium-derived relaxing factor formation. *Eur. J. Pharmacol.*, **176**, 219–223.

KENNEDY, C. (1990). P1- and P2-purinoceptor subtypes – an update. *Arch. Int. Pharmacodyn.*, **303**, 30–50.

KERRICK, W.G.L. & HOAR, P.E. (1981). Inhibition of smooth muscle tension by cyclic AMP-dependent protein kinase. *Nature*, **292**, 253–255.

LEFEBVRE, R.A., BAERT, E. & BARBIER, A.J. (1992). Influence of N^G-nitro-arginine on non-adrenergic non-cholinergic relaxation in the guinea-pig gastric fundus. *Br. J. Pharmacol.*, **106**, 173–179.

LI, C.G. & RAND, M.J. (1991). Evidence that part of the NANC relaxant response of guinea-pig trachea to electrical field stimulation is mediated by nitric oxide. *Br. J. Pharmacol.*, **102**, 91–94.

MCCLESKEY, E.W., FOX, A.P., FELDMAN, D.H., CRUZ, L.J., OLIVERA, B.M., TSIEN, R.W. & YOSHIKAMI, D. (1987). ω-Conotoxin: direct and persistant blockade of specific types of calcium channels in neurons but not muscles. *Proc. Natl. Acad. Sci. U.S.A.*, **84**, 4327–4331.

MCHENRY, L., MURTHY, K.S., GRIDER, J.R. & MAKHLOUF, G.M. (1991). Inhibition of muscle cell relaxation by somatostatin: tissue-specific, cAMP-dependent, pertussis toxin-sensitive. *Am. J. Physiol.*, **261**, G45–49.

MOORE, P.K., AL-SWAYEH, O.A., CHONG, N.W.S., EVANS, R.A. & GIBSON, A. (1990). L-N^G-nitro-arginine (L-NOARG), a novel, L-arginine-reversible inhibitor of endothelium-dependent vasodilation *in vitro*. *Br. J. Pharmacol.*, **99**, 408–412.

NISHIMURA, J. & VAN BREEMEN, C. (1989). Direct regulation of smooth muscle contractile elements. *Biochem. Biophys. Res. Commun.*, **163**, 929–935.

OLSON, R.A. & PEARSON, J.D. (1990). Cardiovascular purinoceptors. *Physiol. Rev.*, **70**, 761–845.

OZAKI, H., BLONDFIELD, D.P., HORI, M., SANDERS, K.M. & PUBLICOVER, N.G. (1992). Cyclic AMP-mediated regulation of excitation-contraction coupling in canine gastric smooth muscle. *J. Physiol.*, **447**, 351–372.

RASMUSSEN, H. & RASMUSSEN, J.E. (1990). Calcium as intracellular messenger: from simplicity to complexity. *Current Topics Cell. Reg.*, **31**, 1–109.

RIGHETTI, P.G. (1990). Immobilized pH gradient: theory and methodology. In *Laboratory Techniques in Biochemistry and Molecular Biology*. ed. Burdon, R.H. & Van Knippenberg, P.H. Vol. 20, pp. 183–205. Amsterdam: Elsevier.

SCHEID, C.R., HONEYMAN, T.W. & FAY, F.S. (1979). Mechanism of β-adrenergic relaxation of smooth muscle. *Nature*, **277**, 32–36.

SNEDDON, P. & WESTFALL, D.P. (1984). Pharmacological evidence that adenosine triphosphate and noradrenaline are co-transmitters in the guinea-pig vas deferens. *J. Physiol.*, **346**, 561–580.

SWEDIN, G. (1971). Studies on the neurotransmission mechanisms in the rat and guinea-pig vas deferens. *Acta Physiol. Scand.*, **369**, suppl 1–34.

TODA, N. & OKAMURA, T. (1992). Regulation by nitroxidergic nerve of arterial tone. *N.I.P.S.*, **7**, 148–152.

TODA, N., MINAMI, Y. & OKAMURA, T. (1990). Inhibitory effect of L-N^G-nitro-arginine on the synthesis of EDRF and the cerebro-arterial response to vasodilator nerve stimulation. *Life Sci.*, **47**, 345–355.

TOMITA, T. & WATANABE, H. (1973). A comparison of the effects of adenosine triphosphate with noradrenaline and with the inhibitory potential of the guinea-pig taenia coli. *J. Physiol.*, **231**, 167–177.

VANE, J.R. (1971). Inhibition of prostaglandin synthesis as a mechanism of action of aspirin like drugs. *Nature*, **231**, 232.

VON KÜGELGEN, I., BÜLTMAN, R. & STARKE, K. (1990). Interaction of adenine nucleotides, UTP and suramine in mouse vas deferens: suramin-sensitive and suramin-insensitive components in the contractile effect of ATP. *Naunyn Schmied. Arch. Pharmacol.*, **342**, 198–205.

WAKADE, A.R. (1979). Recent developments in degradation of the sympathetic neurone. *Gen. Pharmacol.*, **10**, 35–57.

WATANABE, C., YAMAMOTO, H., HIRANO, K., KOBAYASHI, S. & KANAIDE, H. (1992). Mechanisms of caffeine-induced contraction and relaxation of rat aortic smooth muscle. *J. Physiol.*, **456**, 193–213.

WILKUND, N.P. & GUSTAFSSON, L.E. (1988). Indications for P2-purinoceptors subtypes in guinea-pig smooth muscle. *Eur. J. Pharmacol.*, **148**, 361–370.

WOOD, K.S., BUGA, G.M., BYRNS, R.E. & IGNARRO, L.J. (1990). Vascular smooth-derived relaxing factor (MDRF) and its close similarity to nitric oxide. *Biochem. Biophys. Res. Commun.*, **170**, 80–88.

(Received February 8, 1993
Revised March 15, 1993
Accepted April 15, 1993)

Br. J. Pharmacol. (1993), **110**, 331–337

Comparison of the cardiovascular and neural activity of endothelin-1, -2, -3 and respective proendothelins: effects of phosphoramidon and thiorphan

[1]Giovan G. Mattera, Anthony Eglezos, Anna Rita Renzetti & [2]Jacques Mizrahi

Pharmacology Department, Laboratori Guidotti SpA, Via Livornese 402, San Piero a Grado, 56122, Pisa, Italy

1 In the anaesthetized, ganglion-blocked rat, intravenous boluses of endothelin-1, endothelin-2 and endothelin-3 induced a transient hypotensive effect followed by a potent long lasting pressor response ($ED_{50\,mmHg}$: 0.72 ± 0.05, 1.8 ± 0.2 and 2.7 ± 0.3 nmol kg^{-1}, respectively). The maximal effect for the three peptides was of a similar order of magnitude (ΔMAP: 84 to 89 mmHg). Neither of these effects was influenced by phosphoramidon or thiorphan (10 mg kg^{-1}, i.v.).

2 Intravenously administered big-endothelin-1 and -2 induced a transient (1–2 min) hypotension followed by a potent long lasting (>25 min) vasopressor effect ($ED_{50\,mmHg}$: 1.8 ± 0.2 and 6.7 ± 0.4 nmol kg^{-1}, respectively), with a similar maximal activity (Δ MAP: 85 ± 4 and 81 ± 2.4 mmHg, respectively). The onset of the big-endothelin-1 vasopressor effect was more rapid (5–6 min) than that of big-endothelin-2 (10–13 min). Big-endothelin-3 was found to induce only a potent, long lasting (>35 min) hypertension, with a maximal effect of 75 ± 4.6 mmHg at 10 nmol kg^{-1} and an $ED_{50\,mmHg}$ of 6.5 ± 0.4 nmol kg^{-1}. The onset of this effect was much slower (20–25 min) than that of the other proendothelins. Pressor responses induced by big-endothelin-1, -2 and -3 (3, 15 and 10 nmol kg^{-1}, respectively) were markedly reduced (60, 80 and 100%) in the presence of phosphoramidon (10 mg kg^{-1}, i.v.). Thiorphan (10 mg kg^{-1}, i.v.) did not inhibit the effects of big-endothelin-1, -2 and -3.

3 In the electrically stimulated rat vas deferens, endothelin-1 and -2 were found to be equipotent enhancers of the twitch response ($EC_{100\%}$: 4.0 ± 0.4 nM and 7.9 ± 4.8 nM, respectively), both about 3–4 fold as active as endothelin-3 ($EC_{100\%}$: 19 ± 2.5 nM). Endothelin-1 and -3 showed a comparable maximal stimulatory effect (E_{max}: 296 ± 30 and 262 ± 24%) while endothelin-2 was less active (E_{max}: 194 ± 30%).

4 Big-endothelin-1 and -2 were potent enhancers of the twitch reponse too ($EC_{100\%}$: 10.0 ± 2.6 nM and 21.6 ± 3.2 nM, respectively), with a comparable maximal stimulatory effect (E_{max}: 254 ± 22 and 264 ± 24%). Big-endothelin-3 was found to be less potent ($EC_{100\%}$: 275 ± 21 nM), but retained a marked potentiating effect (E_{max}: 200 ± 38%). Phosphoramidon, but not thiorphan, concentration-dependently (10 and 100 μM) reduced big-endothelin-1 (58 and 86% respectively) and big-endothelin-2 (21 and 56%) -mediated responses. Conversely, the big-endothelin-3 effect was reduced by phosphoramidon only at 100 μM (− 70%), while thiorphan acts concentration-dependently (31 and 71% at 10 and 100 μM respectively); thus, in the rat vas deferens, big-endothelin-1 and -2 were as potent as their corresponding endothelins, while big-endothelin-3 was about 20 times less potent than endothelin-3.

5 The increasing effect of endothelin-2 (194 ± 30% over baseline) was significantly enhanced by either 10 μM phosphoramidon (277 ± 42%) or thiorphan (318 ± 15%). The endothelin-1 and endothelin-3-mediated twitch enhancement was not affected by the two protease inhibitors (10 μM).

6 These results suggest that *in vivo* big-endothelin-1, -2 and -3, are processed through a similar phosphoramidon-sensitive enzymatic pathway although with different apparent affinity. This enzymatic process is probably attributable to a neutral endoprotease, distinct from neutral-endopeptidase 24.11 (NEP). On the other hand, a NEP-like enzymatic activity may be involved, in the rat vas deferens, in the activation of big-endothelin-3 to endothelin-3 and in the metabolism of endothelin-2, but not of endothelin-1 or endothelin-3.

Keywords: Endothelins; proendothelins; phosphoramidon, thiorphan; mean arterial pressure; rat vas deferens

Introduction

Endothelin-1, endothelin-2 and endothelin-3 are members of the endothelin peptide family, which have a distinct distribution and represent the agonists for a related family of endothelin receptors, namely ET_A and ET_B (Kloog & Sokolovsky, 1989; Arai *et al.*, 1990; Sakurai *et al.*, 1990). These receptors are distributed in peripheral tissues (Power *et al.*, 1989) and the central nervous system (Jones *et al.*, 1989). Endothelin-1 is one the most potent vasopressors known (Yanagisawa *et al.*, 1988) and it is now widely accepted that endothelin-1 exerts its activities not only as a potent constrictor of the vascular smooth muscle but also as a modulator of the release of circulating hormones from kidney, atria and adrenal glands (Miller *et al.*, 1989; Jaffer *et al.*, 1990; Gomez-Sanchez *et al.*, 1990). Further, endothelin-1 was shown to be a modulator of neuronal activity (Yanagisawa & Masaki, 1989), inducing a potent facilitation of the nerve-mediated twitch response at the post-junctional level on the rat vas deferens (Maggi *et al.*, 1989; Télémaque & D'Orléans-Juste, 1991; Hiley *et al.*, 1989) and inhibiting the twitch response in the guinea-pig vas deferens (Wiklund *et al.*, 1990) by a pre-junctional mechanism; these observations underline the possible role of the endothelins as neuromodulator peptides.

Endothelin-1 is derived from proendothelin (big-endothelin-1) by a putative endothelin converting enzyme (ECE) that cleaves the 38-mer at the bond between Trp^{21}-Val^{22} (Yanag-

[1] Author for correspondence.
[2] Present address: Italfarmaco, S.p.A., Via dei Lavoratori, 54 20092 Cinisello Balsamo, Milano, Italy.

isawa et al., 1988). Since big-endothelin-1 has only 1/100th of the rat aorta contractile activity of endothelin-1 (Kashiwabara et al., 1989), inhibition of the ECE should effectively block the biological activities involving conversion of big-endothelin-1 to endothelin-1. This was the case in functional studies *in vitro* (D'Orléans-Juste et al., 1991a,b; Hisaki et al., 1991) and *in vivo* (Fukuroda et al., 1990; Matsumura et al., 1990b; Pollock & Opgenorth, 1991; McMahon et al., 1991; Pons et al., 1991; Mattera et al., 1992a,b). Further, ECE has been described as a phosphoramidon-sensitive neutral endopeptidase distinct from the thiorphan/phosphoramidon-sensitive neutral endopeptidase (NEP 24.11).

Haemodynamic effects of big-endothelin-2 have been described by Gardiner et al. (1992a). These effects were similar and phosphoramidon-sensitive, like those of big-endothelin-1, though less potent.

On the other hand, big-endothelin-3 was previously described as a very poor substrate for ECE (Okada et al., 1990, 1991; Takada et al., 1991; D'Orléans-Juste et al., 1991a; Mattera et al., 1992b), suggesting that the enzymatic cleavage of the proendothelins was facilitated when Trp^{21}-Val^{22} bond is present. More recently these data have been contradicted by observations *in vitro* (Matsumura et al., 1992) and *in vivo* (Gardiner et al., 1992a,b). Matsumura and coworkers have found, in membranes from cultured vascular endothelial cell, a phosphoramidon-sensitive conversion of big-endothelin-3 to its active form, while Gardiner and coworkers, in conscious Long Evans rats, have found that big-endothelin-3 exerts clear pressor and vasoconstrictor effects which are big-endothelin-1-like and phosphoramidon-sensitive.

Endothelin-1, -2 and -3 were all described as good substrates for NEP 24.11 (Vijayaraghavan et al., 1990). On the other hand, McKay et al. (1992) reported that the metabolism of the endothelins is apparently compound and species-specific, since only the endothelin-3 mediated contractile effect was potentiated by phosphoramidon in rabbit and man, but not in canine bronchus, while endothelin-1 remained unaffected. To our knowledge *in vivo* data to support these findings have not been reported so far.

In the present study we have investigated the biological effects of the endothelins and their precursors, in the presence and in the absence of phosphoramidon and thiorphan, in two systems representative of two different actions of endothelins: one *in vivo* model, for the cardiovascular effects, and one *in vitro* model, for the neuromodulatory effects.

Methods

In vivo: *pressure changes in anaesthetized, ganglion-blocked rat*

All experiments were carried out on male Sprague-Dawley rats (220–250 g, Charles River, Italy), fasted overnight, and anaesthetized with ethyl urethane (1.25 g kg^{-1}, i.m.). Rats were placed on a heating pad to maintain a constant body temperature (37 ± 0.5°C). Both femoral veins were catheterized (PE-50) for infusion of the ganglion-blocking agent and for protease inhibitor administration. Catheters (PE-50) were implanted in the left carotid artery and right jugular vein for monitoring arterial pressure and for injection of peptides, respectively. The trachea was cannulated to allow free breathing. Mean arterial pressure (MAP) was measured with a Bentley Trantec 800 pressure transducer connected with a pre-amplifer (BM614, Biomedica Mangoni) and recorded on an Astromed MT 9500 polygraph. Following a 20 min post-operative recovery period, ganglion-blockade was produced in rats with a constant infusion of pentolinium (0.1 mg^{-1} kg^{-1} min^{-1}) throughout the experiment.

Rat treatment protocols were as follows: three groups of rats received 5–6 i.v. doses of big-endothelin-1 (0.1, 0.3, 1.0, 3.0, 5.0 and 10.0 nmol kg^{-1}, $n = 6$), big-endothelin-2 (0.1, 0.3, 1.0, 3.0, 10 and 15 nmol kg^{-1}, $n = 4$) or big-endothelin-3 (0.3, 1.0, 3.0 and 10 nmol kg^{-1}, $n = 4$). Another three groups of rats were used for cumulative-dose response curves to endothelin-1 (0.03, 0.1, 0.3, 0.5, 1.0 and 2.0 nmol kg^{-1}, $n = 6$), endothelin-2 (0.4, 0.8, 1.8, 2.5, 3.0 and 5 nmol kg^{-1}, $n = 4$) or endothelin-3 (0.1, 0.3, 1, 3, 5 and 9 nmol kg^{-1}, $n = 5$). All the doses are expressed as actual dose injected. Cumulative dose-response curves were constructed by administering the next dose when the effect of the preceding one had reached a stable response, for at least 5 min, or the response started to fall.

To determine the effect of the protease inhibitors on the pressor responses induced by big-endothelin-1 (3 nmol kg^{-1}), big-endothelin-2 (15 nmol kg^{-1}), big-endothelin-3 (10 nmol kg^{-1}), endothelin-1 (1 nmol kg^{-1}), endothelin-2 (1.5 nmol kg^{-1}) and endothelin-3 (4 nmol kg^{-1}); phosphoramidon (Pho) and thiorphan (Thi), both at 10 mg kg^{-1} or vehicle (saline or 0.5% dimethylsulphoxide (DMSO), respectively) were administered (0.5 ml kg^{-1}) 5 min prior to peptide challenge.

In vitro: *electrically-stimulated rat vas deferens*

Male Sprague Dawley rats (250–300 g, Charles Rivers, Italy) were killed by cervical dislocation and the *vasa deferentia pars prostatica* (RVD) were rapidly removed, cleaned and placed in tissue baths containing warm (37°C), oxygenated (95% O_2, 5% CO_2) Krebs solution of the following composition (mM): NaCl 118, KCl 4.69, $MgSO_4$ 1.18, KH_2PO_4 1.20, glucose 11, $NaHCO_3$ 25 and $CaCl_2$ 2.52.

Activity was recorded along the longitudinal axis of RVD (1.5 cm) with an isotonic transducer (Ugo Basile, Italy) under a resting tension of 0.5 g. The tissues were electrically stimulated submaximally (10 V, 0.25 ms pulse width, 200 ms pulse interval, 5 s trains every 60 s) by means of platinum electrodes connected to a digital stimulator (3T Biomedica Mangoni).

Following a 60–90 min equilibration period, cumulative concentration-response curves ($n = 4$–6) for big-endothelin-1 (0.1, 1, 5, 10, 50, 100 and 500 nM), big-endothelin-2 (0.1, 1, 5, 10, 50 and 100 nM) and big-endothelin-3 (0.01, 0.05, 0.1, 0.2, 0.35, 0.5, 0.75 and 1 μM) and their corresponding endothelins (0.1, 1, 5, 10, 50 and 100 nM; $n = 7$–11) were constructed. Only one curve was carried out in each tissue. When studying the effects of peptidase inhibitors (Pho and Thi 10 and 100 μM), tissues were incubated for 30 min in the presence of the test substance, followed by cumulative addition of one of the three endothelins (0.1, 1, 5, 10, 50 and 100 nM, $n = 3$), or a single dose of the proendothelin (big-endothelin-1 and -2: 100 nM; big-endothelin-3: 500 nM, $n = 3$).

Drugs

Human isoforms of proendothelins and endothelins were used. Peptides were purchased from the Peptide Institute (Osaka, Japan). Stock solutions of peptides (0.1 mM), prepared in isotonic saline or 0.1% acetic acid (big-endothelin-3) for *in vivo* experiments and in water for *in vitro* experiments (all peptides), were stored at − 20°C and thawed only once, immediately prior to use. Stock solutions were tested for purity by high performance liquid chromatography (h.p.l.c.) analysis (using a 5 μm Vydac C18 column, with ultraviolet detection at 215 nm). In all cases a single peak corresponding to each peptide was detected.

Protease inhibitors were obtained from Novabiochem (Laufelfingen, Switzerland) or Sigma Chemicals (St. Louis, Mo, U.S.A.) and dissolved either in DMSO (0.5%) or isotonic saline.

Data analysis

In vitro and *in vivo*, results are presented as mean ± s.e.mean. $EC_{100\%}$ (the concentration of peptide that induces a 100% increase of twitch response over basal response) or $ED_{50\,mmHg}$ (the dose of peptide that induces an increase of 50 mmHg of

MAP) values were calculated using the Macintosh Allfit Programme version 1.0. E_{max} respresents the maximal effect induced by the highest concentration or dose tested for each peptide. Comparison between means was carried out by Student's unpaired t-test. A value of $P<0.05$ was taken as significant.

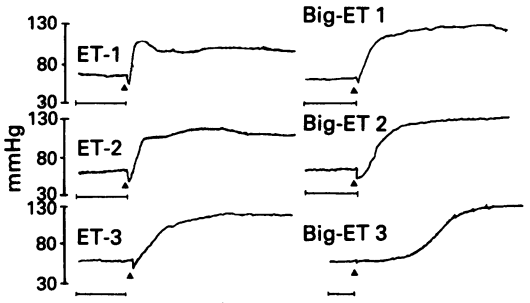

Figure 1 Typical tracings representing the mean arterial pressure (MAP) effects of intravenous endothelins (ET-1: 1 nmol kg^{-1}; ET-2; 1.5 nmol kg^{-1} and ET-3: 4 nmol kg^{-1}) and related proendothelins (Big-ET1: 3 nmol kg^{-1}; Big-ET2 15 nmol kg^{-1} and Big-ET3: 10 nmol kg^{-1}) in anaesthetized ganglion-blocked rats. Animals received peptide as a bolus at the time indicated by black arrow points; the horizontal bars represent 5 min in each case.

Results

In vivo: *MAP changes in the anaesthetized ganglion-blocked rat*

Dose-response curves Basal MAP of the ganglion-blocked rats was 57 ± 1 mmHg (n = 30). Endothelins induced a transient (1–3 min) fall in systemic pressure followed by a long lasting (>25 min) rise of MAP (Figure 1). The hypotensive effect was a dose-dependent and a maximum fall of − 31 ± 2 and − 25 ± 2 mmHg at 2 and 3 nmol kg^{-1} for endothelin-1 and -2 respectively, was reached (Figure 2a). Endothelin-3 also induced a significant hypotension at an intermediate dose (− 13 ± 2 mmHg at 3 nmol kg^{-1}), whereas the highest dose (9 nmol kg^{-1}) was devoid of any depressor activity (Figure 2a).

The endothelin-1-induced vasopressor effect had an $EC_{50\,mmHg}$ of 0.7 ± 0.05 nmol kg^{-1}. Endothelin-2 and -3 were about 2 and 4 fold less active than endothelin-1, with ED_{50mmHg} values of 1.8 ± 0.2 and 2.7 ± 0.3 nmol kg^{-1}, respectively (Figure 2b). The E_{max} obtained at the highest doses tested of each peptide, was of similar magnitude (ΔMAP 84 ± 4.2; 84 ± 3.8 and 89 ± 4.7 mmHg above basal values for endothelin-1, -2 and -3, respectively).

Big-endothelin-1 and -2 induced a rapid, short-lived (1–3 min) hypotensive effect (Figure 1) which was consistently observed in all animals tested and was found to be dose-dependent with a maximum fall of − 18 ± 2.8 and − 31 ± 9 mmHg respectively (Figure 3a). Big-endothelin-3 also showed a hypotensive effect, but without a clear dose-dependency and only in experiments to determine cumulative dose-response curves. The maximal pressure fall was of − 7 ± 2.8 mmHg at a dose of 10 nmol kg^{-1} (Figure 3a).

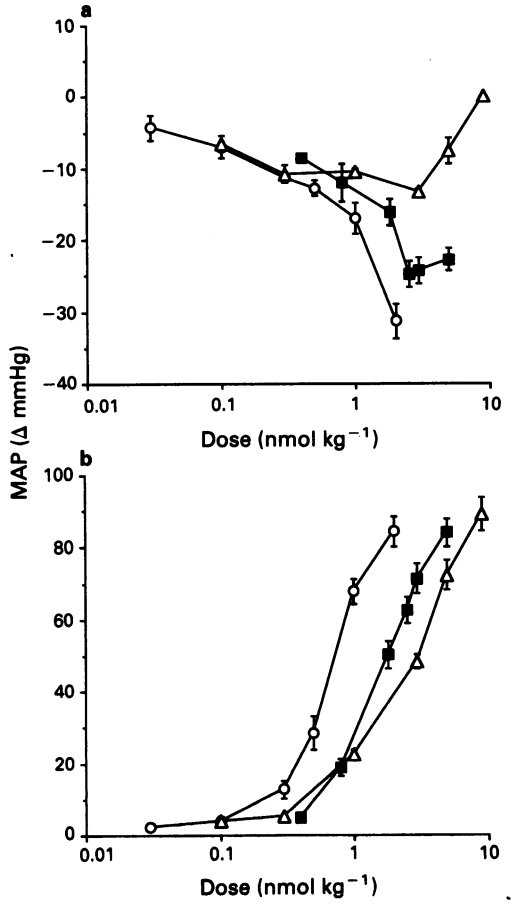

Figure 2 Dose-response curves to endothelin-1 (○), endothelin-2 (■) and endothelin-3 (△), showing hypotensive (a) and hypertensive (b) phases of mean arterial pressure (MAP), in anaesthetized ganglion-blocked rat. Values are mean ± s.e.mean; n = 4–6.

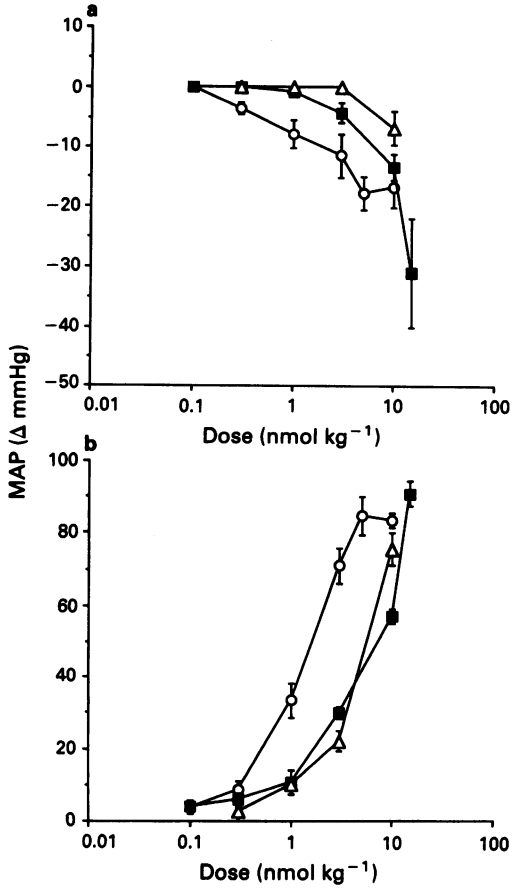

Figure 3 Dose-response curves to big-endothelin-1 (○), big-endothelin-2 (■) and big-endothelin-3 (△), showing hypotensive (a) and hypertensive (b) phases of mean arterial pressure (MAP), in anaesthetized ganglion-blocked rat. Values are mean ± s.e.mean; n = 3–6.

Proendothelins induced a potent long lasting (25–35 min) vasopressor effect (Figure 1). Big-endothelin-1 was more active than big-endothelin-2 ($ED_{50\,mmHg}$: 1.8 ± 0.2 and 6.7 ± 0.4 nmol kg^{-1} respectively) while having similar E_{max} (ΔMAP: 85 ± 4 and 91 ± 2.4 mmHg). The effect of big-endothelin-2 was slower in onset than that of big-endothelin-1 (10–13 *vs* 5–6 min). Although the dose-response curve for big-endothelin-3 was incomplete, this peptide showed an activity close to that of big-endothelin-2, in the range of the tested doses, with an $ED_{50\,mmHg}$ 6.5 ± 0.4 nmol kg^{-1} for an E_{max} of 75 ± 4.6 mmHg at 10 nmol kg^{-1} (Figure 3b). In our model the pressor response of big-endothelin-3 showed the longest latency (25–30 min).

Single-dose: effects of phosphoramidon and thiorphan Pho and Thi were found to be devoid of any significant effect *per se*.

The transient hypotensive effects of 3 nmol kg^{-1} big-endothelin-1 and 15 nmol kg^{-1} big-endothelin-2 were not significantly affected by a 10 mg kg^{-1} bolus of Pho (ΔMAP: − 5.0 ± 1.3 and − 12.0 ± 4.2 mmHg with Pho versus − 4.3 ± 0.9 and − 9.0 ± 2.6 mmHg without Pho, respectively). In this condition big-endothelin-3 (10 nmol kg^{-1}) did not produce any hypotension. On the contrary, the vasopressor response induced by the three proendothelins was reduced from 60 ± 1.7 to 25 ± 3.7 mmHg ($P<0.001$ *vs* control), from 59 ± 3.1 to 11.7 ± 2.8 mmHg ($P<0.001$ *vs* control) and from 69 ± 7.5 to 1.5 ± 1.5 mmHg ($P<0.001$ *vs* control) respectively (Figure 4a).

Pho had no significant effect on either endothelin-1 (1 nmol kg^{-1}, ΔMAP: 49 ± 1.9 *vs* 52 ± 2.2 mmHg), endothelin-2 (1.5 nmol kg^{-1}, ΔMAP: 49 ± 2.9 *vs* 46 ± 3.2 mmHg), or endothelin-3 (4 nmol kg^{-1}, ΔMAP: 59 ± 2.9 *vs* 67 ± 1.8 mmHg) -induced pressor response (Figure 4b). The transient vasodepressor effects induced by either endothelin-1 (ΔMAP: − 11.0 ± 1.7 *vs* − 12.0 ± 1.3 mmHg), endothelin-2 (ΔMAP: − 11.0 ± 1.5 *vs* − 11.0 ± 0.6 mmHg) or endothelin-3 (Δ MAP: − 9.0 ± 2.4 *vs* − 10.0 ± 1.4 mmHg) were not changed in the presence of Pho.

Thi, under the same conditions, was inactive against the effects of the three endothelins and related proendothelins (data not shown).

In vitro: *electrically-stimulated rat vas deferens*

Effect of endothelins on rat vas deferens twitch response Electrical stimulation before addition of peptides induced a stable contractile response (12 ± 3 mm). The twitch response to electrical stimulation was not affected by enzyme inhibitors and, in the presence or absence of peptides, it could be abolished by tetrodotoxin (1 μM) indicating its neural origin (data not shown).

Endothelin-1, -2 and -3 increased, concentration-dependently, the RVD twitch response to electrical stimulation; the threshold concentration of the endothelins that significantly enhanced the twitch response was between 0.1 and 1 nM (Figure 5a). Endothelin-1 and -2 were equipotent ($EC_{100\%}$: 4.0 ± 0.4 and 7.9 ± 4.8 nM, respectively), both being three–four fold more active than endothelin-3 ($EC_{100\%}$; 19 ± 2.5 nM). All three peptides induced a maximum stimulatory

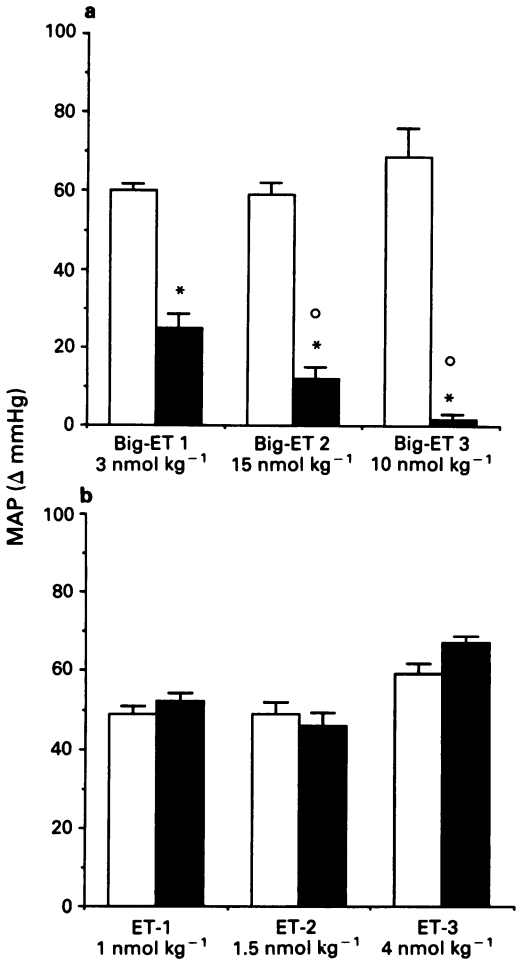

Figure 4 Effects of (a) big-endothelin-1 (Big-ET 1: 3 nmol kg^{-1}), big-endothelin-2 (Big-ET 2: 15 nmol kg^{-1}) and big-endothelin-3 (Big-ET 3: 10 nmol kg^{-1}), or (b) endothelin-1 (ET-1: 1 nmol kg^{-1}), endothelin-2 (ET-2: 1.5 nmol kg^{-1}) and endothelin-3 (ET-3: 4 nmol kg^{-1}), in the absence (open columns) or in the presence (closed columns) of phosphoramidon (10 mg kg^{-1}), on mean arterial pressure (MAP) in anaesthetized, ganglion-blocked rat. Values are mean ± s.e.mean; $n = 6$. *$P<0.05$ unpaired t test vs control; °$P<0.05$ unpaired t test vs big-ET-1.

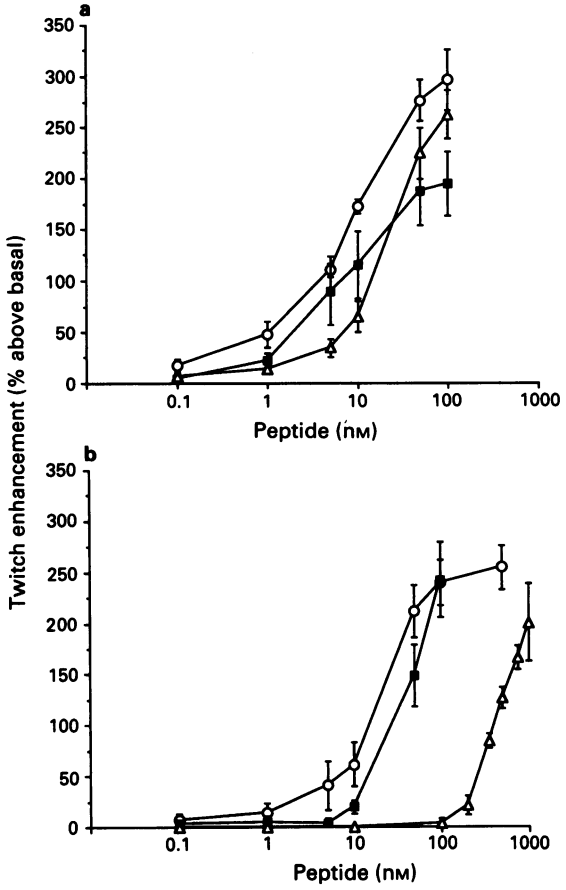

Figure 5 Concentration-response curves to (a) endothelin-1 (○), endothelin-2 (■) and endothelin-3 (△), and (b) related proendothelins on electrically stimulated twitch response of rat vas deferens. Results are presented as % above basal. Each point represents the mean ± s.e.mean of 4–11 experiments.

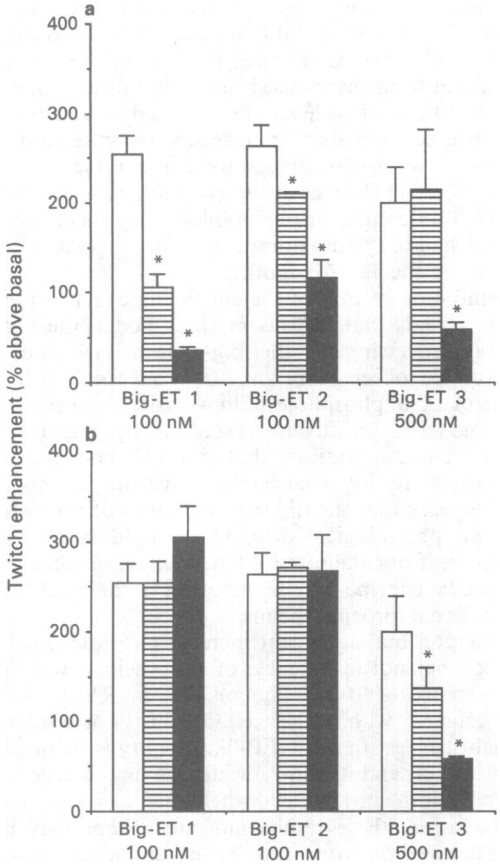

Figure 6 Effects of (a) phosphoramidon or (b) thiorphan at concentrations of 10 μM (hatched columns) or 100 μM (closed columns) on the enhancement of the twitch response of the electrically stimulated vas deferens of the rat induced by big-endothelin-1 (Big-ET 1, 100 nM), big-endothelin-2 (Big-ET 2, 100 nM) and big-endothelin-3 (Big-ET 3, 500 nM). Results are presented as % above basal. Each column represents the mean ± s.e.mean of at least 3 determinations. *$P<0.05$, unpaired t test.

effect at 100 nM: endothelin-1 and -3 were equally effective (296 ± 30 and 262 ± 24% above baseline, respectively), while endothelin-2 was less active, with a maximal stimulation of 194 ± 30%. Endothelins dose-dependently increased RVD basal tone (data not shown).

Effect of the proendothelins on the rat vas deferens twitch response Big-endothelin-1 enhanced (E_{max}: 254 ± 21.5%) RVD twitch response in a concentration-dependent manner ($EC_{100\%}$: 10.0 ± 2.6 nM), with a threshold concentration around 1 nM (Figure 5b). In our model, big-endothelin-1 was only two times less effective than endothelin-1. Big-endothelin-2 was also an effective enhancer of the twitch response with a threshold around 10 nM and with an $EC_{100\%}$ value of 21.6 ± 3.2 nM and an E_{max} of 264 ± 24%, being three times less potent than endothelin-2. Big-endothelin-3 enhanced the RVD twitch response with a threshold around 200 nM and an $EC_{100\%}$ of 275.3 ± 20.7 nM and an E_{max} of 200 ± 38% (Figure 6b). Big-endothelin-3 was therefore at least 20 times less potent than its related endothelin. Proendothelins enhance basal tone too, but only at higher doses (data not shown).

Effects of phosphoramidon and thiorphan Both Pho and Thi up to 100 μM had no effect on electrical induced twitch response.

In the presence of either Pho or Thi (10 μM), the effects of endothelin-1 or -3 remained unchanged, whereas a significant potentiation of the E_{max} of endothelin-2, to 277 ± 42% and 318 ± 15% respectively, was observed (Table 1). Pho inhibited significantly and concentration-dependently the twitch enhancement mediated by both big-endothelin-1 and -2 (Figure 6a). Thi, under the same conditions was totally ineffective (Figure 6b). Conversely Thi (10 and 100 μM) was able to reduce big-endothelin-3 twitch response enhancement (31 ± 14 and 71 ± 5%, respectively; $P<0.05$). In contrast, Pho was found effective ony at 100 μM (70 ± 12%, $P<0.05$).

Table 1 Effect of phosphoramidon (Pho) and thiorphan (Thi) on endothelin-induced facilitation of the twitch response in the electrically stimulated vas deferens of the rat

		$EC_{100\%}$ (nM)	E_{max} (% above basal)
Endothelin-1		4.0 ± 0.4	296 ± 30
	Pho	5.2 ± 0.7	249 ± 25
	Thi	3.5 ± 0.8	298 ± 14
Endothelin-2		7.9 ± 4.8	194 ± 30
	Pho	10.5 ± 0.1	277 ± 42*
	Thi	5.1 ± 2.0	318 ± 15*
Endothelin-3		19.2 ± 2.5	262 ± 24
	Pho	22.5 ± 1.1	252 ± 16
	Thi	17.9 ± 3.1	220 ± 11

E_{max} = maximal effect obtained at the highest concentration tested for each peptide (see methods); Pho = phosphoramidon 10 μM; Thi = thiorphan 10 μM.
*$P<0.05$, unpaired Student's t test.

Discussion

The *in vivo* results of the present work show that endothelins, in the anaesthetized ganglion-blocked rat, induce a rapid, profound and transient hypotension followed by a long lasting hypertensive effect confirming the data previously obtained in a number of different models (Inoue *et al.*, 1989; Douglas & Hiley, 1990; Le Monnier de Gouville & Cavero, 1991; Randall, 1991; Mattera *et al.*, 1992a,b). The hypotensive effect induced by endothelin-1 and 2 has a similar overall profile, whereas that of endothelin-3 appears to be weaker, and is probably subject to rapid tachyphylaxis. The hypertensive effect is dose-dependent and characterized by a similar onset time. The rank order of potency is: endothelin-1 > endothelin-2 > endothelin-3. The E_{max} of the three endothelins is very similar, a finding in contrast with the results reported by Inoue *et al.* (1989), who described a smaller maximal response for endothelin-3.

Although less potent than the respective endothelins, big-endothelin-1 and -2 retain similar pressor activity in terms of maximal effect. The time to reach the maximum increase in blood pressure, for each dose, was about the same for endothelin-1 and big-endothelin-1, in accordance with previously reported findings (Kashiwabara *et al.*, 1989; Douglas *et al.*, 1991), while the onset of big-endothelin-2 effect is definitely slower.

In our *in vivo* model, big-endothelin-3 shows a clear vasopressor activity characterized by the slowest onset among all peptides tested and not preceded by a dose-dependent hypotensive effect. These data suggest that the presence of a Trp^{21}-Ile^{22} bond, instead of the Trp^{21}-Val^{22} one, in big-endothelin-3, may reduce the affinity for ECE, and decrease the velocity of enzymatic conversion. This reduction may not permit a rapid achievement of an efficacious concentration of active peptide at receptor sites, thus producing the observed slow onset. These results are in accordance with recent biochemical (Matsamura *et al.*, 1992) and functional (Gardiner *et al.*, 1992a,b), studies, but in sharp contrast to a number of previous studies (Okada *et al.*, 1990, 1991; Télémaque & D'Orléans-Juste, 1991; D'Orléans-Juste *et al.*, 1991a,b; Mattera *et al.*, 1992a; Takada *et al.*, 1992) in which

no vasopressor activity had been shown for big-endothelin-3. At the moment no exhaustive explanation can be given for this important discrepancy, but it may be supposed that difference in the source of the peptide and in its handling (i.e. different way of solubilization in either buffer saline or acetic acid, storage, etc.) plays an important role. Moreover species-specificity of big-endothelin cleavage could be advocated in some instances (e.g. D'Orléans-Juste *et al.*, 1991a,b, used guinea-pigs instead of rats), as well as interference originating from the pharmacological manipulation of animals (anaesthetics, ganglion-blocking agents). In order to obtain a better defined picture of the physiologically important roles of big-endothelin-3 a careful study seems to be necessary to explore these hypotheses systematically. However, the data produced in the present work seem to reinforce the concept that the *in vivo* biological actions of the proendothelins are mediated through the corresponding endothelins.

Conversion of the proendothelins to their active forms is generally agreed to involve a neutral Pho-sensitive metalloendopeptidase (Matsumura *et al.*, 1990a,b; 1991; LeMonnier de Gouville & Cavero, 1991; Yano *et al.*, 1991; Mattera *et al.*, 1992a,b; Gardiner *et al.*, 1992a). Accordingly, in this study, Pho significantly reduced the responses to the three proendothelins. The following rank order of inhibition: big-endothelin-3 > big-endothelin-2 > big-endothelin-1 was found. Such strong inhibition of the conversion of big-endothelin-3 by Pho, as well as the difference in the behaviour of big-endothelin-3 compared to that of big-endothelin-1 and -2 (slower onset of the hypertensive effect and the absence of the early hypotension) pointed out before, might suggest that the big-endothelin-1 and -2 are more efficiently converted than big-endothelin-3.

Thi was unable to block proendothelin-induced pressor responses, in contrast with a previous study (McMahon *et al.*, 1991) that showed a weak, but dose-dependent inhibition of porcine big-endothelin-1 pressor response by Thi. Most likely this discrepancy is related to the lower dose used in this work and/or to the different peptide isoform (human *vs* porcine).

Finally, the sensitiveness to Pho and insensitiveness to Thi of proendothelin-induced pressor response support the concept that all three proendothelins are converted by the same enzyme *in vivo*. On the other hand, neither Pho nor Thi have any significant influence on the pressor responses to endothelin-1, -2 or -3. This finding does not support the involvement of a NEP-like activity in the metabolism of the endothelins *in vivo*, as has been described *in vitro* (Vijayaraghavan *et al.*, 1990; Fagny *et al.*, 1991).

As regards the *in vitro* model, both proendothelins and endothelins have been shown to be potent enhancers of the twitch response to electrical stimulation, with potency values in agreement with previous studies (Maggi *et al.*, 1989; Télémaque & D'Orléans-Juste, 1991). However, in contrast to Télémaque & D'Orléans-Juste (1991), in our experimental conditions we observed that: (a) all peptides exerted a concentration-related increase of the basal tone and (b) big-endothelin-3 behaved as a full agonist similarly to the related endothelin. The first difference may be due to the different type of force transducers used: isotonic in our study, isometric in the study of Télémaque & D'Orléans-Juste. In fact, when we used isometric transducers in a separate set of experiments, we obtained results comparable to those of Télémaque & D'Orléans-Juste (unpublished observations). The second difference, in our opinion, may be chiefly related to peptide handling and storage or animal species as already discussed for the *in vivo* model.

The inhibition of Pho of the enhancing effect of the proendothelins reveals that, in this *in vitro* model, the profile for enzymatic processing of the big-endothelin-1 and -2 was similar to that observed *in vivo*, the conversion being under the control of a phosphoramidon-sensitive process. On the other hand, the sensitiveness showed by big-endothelin-3 activity to Thi may indicate that in RVD there is a different enzymatic activity involved in the processing of this peptide. Thus it appears that the different activities of proendothelins in different physiological districts are modulated essentially by a similar, if not the same, ECE, even if, in some cases, an organ-specific enzyme may be involved in the local activation of the different proendothelins.

A moderate, but significant increase (1.5 fold) in the maximal effect, but not in potency, of endothelin-2 was observed in the presence of 10 μM Pho or Thi, in RVD. No similar effect occurred with either endothelin-1 or endothelin-3. This might suggest that a NEP-like activity is involved in the degradation of endothelin-2, while having minimal or no effect on endothelin-1 or endothelin-3.

In conclusion, these results indicate a homology between the *in vivo* and *in vitro* activity of endothelin converting enzyme. This enzymatic activity is probably not NEP 24.11, as indicated by the inconsistent activity of thiorphan. Further, the previously described selectivity of endothelin converting enzyme for the conversion of big-endothelin-1 is more likely to be related to the selectivity for the Trp^{21}-Val^{22} bond, a bond also present in big-endothelin-2, but not in big-endothelin-3 (Trp^{21}-Ile^{22}). Moreover, in the rat vas deferens another enzyme, different from vascular ECE, may be involved in the big-endothelin-3 enzymatic processing. The degradation of the endothelins is possibly tissue- and isopeptide-dependent, since only endothelin-2 was susceptible to thiorphan or phosphoramidon *in vitro*, while *in vivo* these neutral protease inhibitors seem to be totally inactive.

This work was supported by IMI grant No 55202. The authors thank Mr M. Bachi and Mr M. Guelfi for their excellent technical assistance and express their gratitude to Drs M. Criscuoli, G. D'Agostino and A. Subissi for their support and suggestions during the preparation of this manuscript.
Laboratori Guidotti SpA is part of A. Menarini Pharmaceuticals, Firenze, Italy.

References

ARAI, H., HORI, S., ARAMOI, I., OHKUBO, H. & NAKANISHI, S. (1990). Cloning and expression of a cDNA encoding an endothelin receptor. *Nature*, **348**, 730–732.

D'ORLÉANS-JUSTE, P., TÉLÉMAQUE, S. & CLAING, A. (1991a). Different pharmacological profiles of big-endothelin-3 and big-endothelin-1 in vivo and also in vitro through a phosphoramidon-sensitive conversion to endothelin-1. *Br. J. Pharmacol.*, **104**, 440–444.

D'ORLÉANS-JUSTE, P., LINDBURY, P.S., TÉLÉMAQUE, S., WARNER, T.D. & VANE, J.R. (1991b). Human big-endothelin releases prostacyclin in vivo and in vitro. *J. Cardiovasc. Pharmacol.*, **17** (Suppl 7), S251–S255.

DOUGLAS, S.A. & HILEY, C.R. (1990). Responses to endothelin-1, human proendothelin (1-38) and porcine proendothelin (1-39) in the rat on intravenous administration and in the blood perfused mesentery. *Neurochem. Int.*, **4**, 445–454.

FAGNY, C., MICHEL, A., LEONARD, I., BERKENBOOM, G., FONTAINE, J. & DESCHODT-LANCKMAN, M. (1991). In vitro degradation of endothelin-1 by endopeptidase 24.11 (enkephalinase). *Peptides*, **12**, 773–778.

FUKURODA, T., NOGUCHI, K., TSUCHIDA, S., NISHIKIBE, M., IKEMOTO, F., OKADA, K. & YANO, M. (1990). Inhibition of biological actions of big endothelin-1 by phosphoramidon. *Biochem. Biophys. Res. Commun.*, **172**, 390–395.

GARDINER, S.M., KEMP, P.A. & BENNETT, T. (1992a). Inhibition by phosphoramidon of the regional haemodynamic effects of proendothelin-2 and -3 in conscious rats. *Br. J. Pharmacol.*, **107**, 584–590.

GARDINER, S.M., KEMP, P.A., COMPTON, A.M. & BENNETT, T. (1992b). Coeliac haemodynamic effects of endothelin-1, endothelin-3, proendothelin-1[1-38] and proendothelin-3[1-41] in conscious rats. *Br. J. Pharmacol.*, **106**, 483–488.

GOMEZ-SANCHEZ, C.E., COZZA, E.N., FOECKLING, M.F., CHIOU, S. & FERRIS, M.W. (1990). Endothelin receptor subtypes and stimulation of aldosterone secretion. *Hypertension*, **15**, 744–747.

HILEY, C.R., PELTON, J.T. & MILLER, R.C. (1989). Effects of endothelin on field stimulated rat vas deferens and guinea pig ileum. *Br. J. Pharmacol.*, **96**, 104P.

HISAKI, K., MATSUMURA, Y., IKEGAWA, R., NISHIGUCHI, S., HASASHI, K., TAKAOKA, M. & MOROMOTO, S. (1991). Evidence for Phosphoramidon-sensitive conversion of big endothelin-1 to endothelin-1 in isolated rat mesenteric artery. *Biochem. Biophys. Res. Commun.*, **177**, 1127–1132.

INOUE, A., YANAGISAWA, M., KIMURA, S., KASUYA, Y., MIYAUCHI, K., GOTO, K. & MASAKI, T. (1989). The human endothelin family; three structurally and pharmacologically distinct isopeptides predicted by three separate genes. *Proc. Natl. Acad. Sci. U.S.A.*, **86**, 2863–2867.

JAFFER, F.E., KNAUSS, C., POPTIC, E. & ABBOUD, H.E. (1990). Endothelin stimulates PDGF secretion in cultured human mesangial cells. *Kidney Int.*, **38**, 1193–1198.

JONES, C.R., HILEY, C., PELTON, J.T. & MOHR, M. (1989). Autoradiographic visualization of the binding sites for [I^{125}] endothelin in rat and human brain. *Neurosci. Lett.*, **97**, 276–279.

KASHIWABARA, T., INAGAKI, Y., OHTA, H., IWAMATSU, A., NOMIZU, M., MORITA, A. & NISHIKORI, K. (1989). Putative precursors of endothelin have less vasoconstrictor activity in vitro but a potent pressor effect in vivo. *FEBS Lett.*, **247**, 73–76.

KLOOG, Y. & SOKOLOVSKY, M. (1989). Similarities in mode and sites of action of sarafotoxins and endothelins. *Trends Pharmacol. Sci.*, **10**, 212–214.

LE MONNIER DE GOUVILLE, A.C. & CAVERO, I. (1991). Differential pharmacological profile of endothelin-1 and its precursor, big endothelin. *J. Cardiovasc. Pharmacol.*, **17** (Suppl. 7), S362–365.

MAGGI, C.A., GIULIANI, S., PATACCHINI, R., ROVERO, P., GIACHETTI, A. & MELI, A. (1989). The activity of peptides of the endothelin family in various mammalian smooth muscle preparations. *Eur. J. Pharmacol.*, **174**, 23–31.

MATSUMURA, Y., IKEGAWA, R., TAKAOKA, M. & MORIMOTO, S. (1990a). Conversion of porcine big endothelin to endothelin by an extract from the porcine aortic endothelial cells. *Biochem. Biophys Res. Commun.*, **167**, 203–210.

MATSUMURA, Y., HISAKI, K., TAKAOKA, M. & MORIMOTO, S. (1990b). Phosphoramidon, a metalloproteinase inhibitor, suppresses the hypertensive effect of big endothelin-1. *Eur. J. Pharmacol.*, **185**, 103–106.

MATSUMURA, Y., IKEGAWA, R., TSUKAHARA, Y., TAKAOKA, M. & MORIMOTO, S. (1991). n-Ethylmaleimide differentiates endothelin converting activity by two types of metalloproteinases derived from vascular endothelial cells. *Biochem. Biophys. Res. Commun.*, **178**, 531–538.

MATSUMURA, Y., TSUKAHARA, Y., KUNINOBU, K., TAKAOKA, M. & MORIMOTO, S. (1992). Phosphoramidon sensitive endothelin-converting enzyme in vascular endothelial cells converts big endothelin-1 and big endothelin-3 to their mature form. *FEBS Lett,*. **305**, 86–90.

MATTERA, C.G., EGLEZOS, A., CUCCHI, P., RENZETTI, A.R. & MISRAHI, J. (1992a). Phosphoramidon-sensitive conversion of human proendothelin in vivo: effect on pressure and plasma prostacyclin. *Br. J. Pharmacol.*, **107**, 161P.

MATTERA, C.G., RENZETTI, A.R. & MIZRAHI, J. (1992b). Metalloprotease dependent conversion of human proendothelin in vivo. *Pharmacol. Res.*, **26** (Suppl. 1), 159.

MCKAY, K.O., BLACK, J.L. & ARMOUR, C.L. (1992). Phosphoramidon potentiates the contractile response to endothelin-3, but not endothelin-1 in isolated airway tissue. *Br. J. Pharmacol.*, **105**, 929–932.

MCMAHON, E.G., PALOMO, M.A., MOORE, W.M., MCDONALD, J.F. & STERN, M.K. (1991). Phosphoramidon blocks the pressor activity of porcine big endothelin 1(1-39) in vivo and conversion of big endothelin 1 (1-39) to endothelin 1 (1-21) in vitro. *Proc. Natl. Acad. Sci. U.S.A.*, **88**, 703–707.

MILLER, V.M., REDFIELD, M.M. & BURNETT, J.C. (1989). Integrated cardiac, renal and endocrine action of endothelin. *J. Clin. Invest.*, **83**, 317–320.

OKADA, K., MIYAZAKI, J., TAKADA, J., ARAI, Y., MATSUYAMA, K., YAMAKI, T. & YANO, M. (1990). Conversion of Big-endothelin-1 by membrane-bound metalloendopeptidase in cultured bovine endothelial cells. *Biochem. Biophys. Res. Commun.*, **171**, 1192–1198.

OKADA, K., TAKADA, J., ARAI, Y., MATSUYAMA, K. & YANO, M. (1991). Importance of the C-terminal region of Big-endothelin-1 for specific conversion by phosphoramidon-sensitive endothelin converting enzyme. *Biochem. Biophys. Res. Commun.*, **180**, 1019–1023.

POLLOCK, D.M. & OPGENORTH, T.J. (1991). Evidence for metalloprotease involvement in the in vivo effects of big Endothelin 1. *Am J. Physiol,*. **261**, R257–R263.

PONS, F., TOUVAY, C., LAGENTE, V., MENCIA-HUERTA, J.M. & BRAQUET, P. (1991). Bronchopulmonary and pressor activities of endothelin-1 (ET-1), ET-2, ET-3 and Big ET-1 in the Guinea Pig. *J. Cardiovasc. Pharmacol,*. **17** (Suppl. 7), S326–S328.

POWER, R.F., WHARTON, J., SALAS, S.P., KANSE, S., GHATEI, M., BLOOM, S.R. & POLAK, J.M. (1989). Autoradiographic localisation of endothelin binding sites in human and porcine coronary arteries. *Eur. J. Pharmacol.*, **160**, 199–200.

RANDALL, M.D. (1991). Vascular activities of the endothelins. *Pharmacol. Ther.*, **50**, 73–93.

SAKURAI, T., YANAGISAWA, M., TAUWA, Y., MIYAZAKI, H., KIMURA, S., GOTO, K. & MASAKI, T. (1990). Cloning of cDNA encoding a non-isopeptide selective sub-type of the endothelin receptor. *Nature*, **348**, 732–735.

TAKADA, J., OKADA, K., IKEGAWA, T., MATSUYAMA, K. & YANO, M. (1991). Phosphoramidon-sensitive endothelin-converting enzyme in the cytosol of cultured bovine endothelial cells. *Biochem. Biophys. Res. Commun.*, **176**, 860–865.

TÉLÉMAQUE, S. & D'ORLÉANS-JUSTE, P. (1991). Presence of a phosphoramidon-sensitive endothelin-converting enzyme which converts Big-Endothelin-1, but not Big-Endothelin-3 in the rat vas deferens. *Naunyn-Schmied. Arch. Pharmacol.*, **344**, 500–507.

VIJAYARAGHAVAN, J., SCICLI, A.G., CARRETTERO, O.A., SLAUGHTER, C., MOOMAW, C. & HERSH, L.B. (1990). The hydrolysis of endothelins by neutral endopeptidase 24.11 (enkefalinase). *J. Biol. Chem.*, **265**, 14150–14155.

WIKLUND, N.P., OHLEN, A., WIKLUND, C.U., HEDQVIST, P. & GUSTAFSSON, L.E. (1990). Endothelin modulation of neuroeffector transmission in rat and guinea pig vas deferens. *Eur. J. Pharmacol.*, **185**, 25–33.

YANAGISAWA, M., KURIHARA, H., KIMURA, S., TONOBE, Y., KOBAYASHI, M., MITSUI, Y,. YAZAKI, Y,. GOTO, K. & MASAKI, T. (1988). A novel potent vasoconstrictor peptide produced by vascular endothelial cells. *Nature*, **32**, 411–415.

YANAGISAWA, M. & MASAKI, T. (1989). Endothelin, a novel endothelium-derived peptide. *Biochem. Pharmacol.*, **38**, 1877–1883.

YANO, M., OKADA, K., TAKADA, J,. HIOKI, Y., MATSUYAMA, K., FUKURODA, T., NOGUCHI, K., NISHIKIBE, M. & IKEMOTO, F. (1991). Endothelin-converting enzyme and its in vitro and in vivo inhibition. *J. Cardiovasc. Pharmacol.*, **17** (Suppl. 7), S26–S28.

(Received January 11, 1993
Revised April 14, 1993
Accepted April 19, 1993)

Br. J. Pharmacol. (1993), **110**, 338–342

Evidence for sympathetic neurotransmission through presynaptic N-type calcium channels in human saphenous vein

Fulvia Fabi, *Mario Chiavarelli, Livio Argiolas, *Roberto Chiavarelli & [1]Paola del Basso

Department of Pharmacology, Istituto Superiore di Sanità, Viale Regina Elena 299, 00161 Rome, Italy, and *Department of Cardiovascular Surgery, Università di Roma, 'La Sapienza', Rome, Italy

1 The specific type(s) of voltage-sensitive calcium channels (VSCCs) involved in sympathetic neurotransmission have not yet been characterized in human vascular tissues. We therefore examined the functional role of the N- and L-type VSCCs in human saphenous veins.

2 Contractile response curves for transmural nerve stimulation (TNS) and for exogenously administered noradrenaline (NA) were obtained in superfused saphenous vein rings. The contractions induced by TNS, but not by NA, were inhibited by 1 μM tetrodotoxin and by 10 μM guanethidine. Both responses were substantially reduced by 1 μM phentolamine, indicating that the contractions evoked by TNS were mediated by endogenous NA released from noradrenergic nerves.

3 In the presence of 2 μM ω-conotoxin GVIA (omega *Conus Geographus* toxin, fraction VI A; ω-CgTx), a polypeptide with specific inhibitory activity on N- and L-type calcium channels, the neurally evoked contractions were almost completely abolished. In contrast, the responses induced by exogenous NA were not affected by the neurotoxin, thus providing evidence of the exclusive presynaptic action of ω-CgTx.

4 In the presence of the calcium antagonist verapamil (10 μM), which selectively blocks L-type VSCCs, the contractions induced by both TNS and NA were diminished to the same extent, suggesting that the organic calcium blocker is active only at the postjunctional level.

5 It is concluded that N-type calcium channels are the main pathway of calcium entry controlling the functional responses induced by activating sympathetic nerves; the role of L-type channels appears to be limited to the postjunctional level, modulating smooth muscle contractions.

Keywords: Calcium channels; human saphenous veins; sympathetic neurotransmission; ω-conotoxin GVIA; verapamil

Introduction

Transmitter release from presynaptic nerve endings is regulated by the influx of extracellular calcium ions (Augustine *et al.*, 1985) flowing through voltage-sensitive calcium channels (VSCCs). Electrophysiological studies have shown that in the nervous system, VSCCs may be subdivided into L-, N-, P- and T-types, which differ in their voltage and time-dependence of inactivation as well as in their single-channel conductance (Nowycky *et al.*, 1985; Sher & Clementi, 1991). These VSCCs may also be characterized by pharmacological means (Miller, 1987). Recent patch-clamp studies have clearly demonstrated that ω-conotoxin GVIA (ω-CgTx), a 27-amino acid peptide isolated from the venom of the marine snail *Conus geographus*, is able to block N- and L-, but not T-type calcium channels at presynaptic level (Olivera *et al.*, 1984; McCleskey *et al.*, 1987; Olivera *et al.*, 1991), thus emerging as a valuable tool in the investigation of the specific type of VSCCs involved in neuronal function. Conversely, the organic Ca^{2+} channel antagonists, such as dihydropyridine compounds and verapamil, do not influence N- and T-type channels but selectively block L-channels (Miller, 1987; Ferrante & Triggle, 1990).

In sympathetic neurones of experimental animals both N- and L-channels are present (Marrion *et al.*, 1987; Lipscombe *et al.*, 1988) and appear to be involved in neurotransmitter release. N-type VSCCs have been shown to be the dominant type of Ca^{2+} entry pathway in the depolarization-evoked release of noradrenaline (NA) from rat (Hirning *et al.*, 1988) and frog (Lipscombe *et al.*, 1989) sympathetic neurones and from the sympathetic nerves in rat isolated iris (Rittenhouse & Zigmond, 1991). Furthermore, N-type channels have been demonstrated to be involved in the vasoconstrictor responses induced by sympathetic nerve stimulation in rat isolated kidney (El-Din & Malik, 1988) and in rat small mesenteric arteries (Pruneau & Angus, 1990). However, since organic calcium channel blockers have been shown to decrease both the release of tritium and the contractile response induced by transmural nerve stimulation (TNS) in the canine saphenous vein (Jayakody *et al.*, 1986; Takata & Kato, 1988), an involvement of L-channels in sympathetic neurotransmission may also be hypothesized. Consequently, at least as far as the sympathetic innervation of the vasculature is concerned, discrepancies exist on the type of VSCCs involved in neurotransmitter release, thus suggesting that Ca^{2+} channels at noradrenergic nerve terminals probably differ in various tissues and species. In addition, although sympathetic neurotransmission in human vascular tissues has been extensively studied, the VSCCs involved in transmitter release have not yet been characterized.

The present work was undertaken to elucidate the type and the functional role of the VSCCs involved in the sympathetic neurotransmission in human vascular tissue.

A preliminary account of this work was presented at the 3rd Joint Meeting of Hungarian, Italian and Polish Pharmacological Societies, at Modena, in 1992 (Del Basso *et al.*, 1992).

Methods

Tissue preparation

Segments of macroscopically normal human saphenous veins were obtained from 41 to 60 year old male patients undergoing surgery for aorta-coronary bypass grafting. The patients were not treated with adrenoceptor agonists or antagonists or with drugs influencing the storage or release of noradrenaline. The vessel specimen was placed in an oxygenated Krebs solution at 4°C and transported immediately to the laboratory. Most of the vessels were used on the day of surgery and all the tissues were used within 18 h. The vessels

[1] Author for correspondence.

were cleaned of the adherent connective tissue and cut into rings 4–5 mm wide. The vein segments were mounted in an organ chamber on L shaped stainless steel rods, so that it was possible to record the smooth muscle force. The preparations were superfused with Krebs oxygenated solution at 37°C by a constant perfusion pump (Gilson Minipuls II) at a flow rate of 5 ml min^{-1}; the resting tension was adjusted to 2 g and a period of 90–120 min was allowed for equilibration. The composition of the Krebs solution was (mM): $NaHCO_3$ 25, NaCl 118, KCl 4.7, $CaCl_2 \cdot 2H_2O$ 2.5, KH_2PO_4 1.2, $MgSO_4 \cdot 7H_2O$ 1.17 and glucose 5.6; the solution was aerated with a mixture of 95% O_2 and 5% CO_2. The tension of the circular muscle layer was recorded with an isometric strain gauge transducer (Grass FT 0.3 T) coupled to a polygraph (Grass 7 P). TNS was delivered for 1 min through platinum wire electrodes placed on either side of the vessel. The rectangular pulses applied by an electronic stimulator (Grass S 11) were 0.3 ms in duration, of supramaximal voltage (14 V measured across the electrodes) and were applied at 1–16 Hz.

Experimental protocol

After the preparations had been allowed to equilibrate and a stable tension obtained, they were stimulated with a bolus injection of NA (40 μg), which caused near maximal contraction in pilot experiments. The contractile responses of vein rings to TNS lasting 1 min were obtained at 1, 2, 4, 8 and 16 Hz, with a period of at least 10 min between each stimulation. NA was then administered by superfusing the vessel segment for one minute with Krebs solution containing NA (0.1, 0.3, 1, 3 μM). After the control series of TNS and NA responses were elicited, antagonists were added to the superfusing medium and allowed to bathe the blood vessels for 30 min. A second series of TNS and NA was repeated in the presence of antagonists. Control experiments ($n = 4$; data not shown) demonstrated reproducible contractile responses to TNS and to exogenous NA in two experimental periods separated by at least 30 min. In order to normalize the data, the contractile responses were expressed as the percentage of the maximum force generated in response to 40 μg NA in each tissue.

Statistical evaluation

Data are expressed as means ± standard error of the means. Frequency-response curves to transmural nerve stimulation and concentration-response curves to noradrenaline (with and without the antagonists) were compared by analysis of variance with repeated measures (Winer, 1971). The potency-ratios were estimated according to parallel line or slope ratio assays (Finney, 1952). Results were considered statistically significant when $P < 0.05$. Confidence limits were calculated at 0.05 probability.

Drugs

(−)-Noradrenaline bitartrate, guanethidine sulphate, phentolamine hydrochloride, verapamil hydrochloride, tetrodotoxin, ω-conotoxin-GVIA were all obtained from Sigma. Noradrenaline was dissolved in 0.9% saline containing 0.1% ascorbic acid and kept in the refrigerator. Stock solutions of tetrodotoxin and ω-conotoxin were stored frozen and diluted daily in saline and discarded after use. All other drugs were dissolved in distilled water and dilutions were made in the Krebs solution.

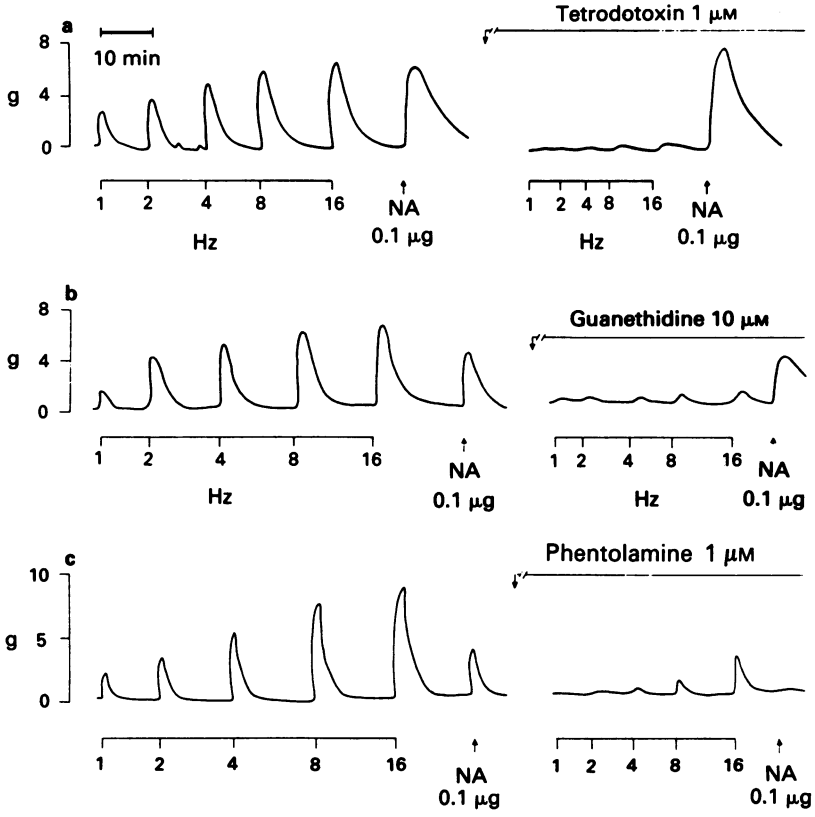

Figure 1 Typical recordings of the effects of transmural nerve stimulation (1–16 Hz, 14 V, 0.3 ms, 1 min) and noradrenaline (NA; 0.1 μg by bolus injection) in superfused human saphenous vein ring segments. After a control series of TNS- and NA-induced responses was obtained, drugs were added to the superfusing Krebs solution for 30 min before and during the second series of responses. Responses to TNS and NA in the absence and in the presence of 2 μM tetrodotoxin (a), 10 μM guanethidine (b) and 1 μM phentolamine (c) are shown.

Results

Characterization of the contractile responses to transmural nerve stimulation of human isolated saphenous veins

In these experiments, the results described refer to at least three vessels. As shown in Figure 1, TNS of the saphenous rings produced frequency-dependent contractile responses, which started at 0.5 Hz and reached maximum at 16–20 Hz. Since the contractions were almost completely abolished by 2 μM tetrodotoxin and since the veins still responded to a bolus injection of 0.1 μg NA (Figure 1a), it was assumed that the responses must be due to activation of intramural nerves. These neurogenic contractions, but not those corresponding to exogenous NA, were virtually abolished by 10 μM guanethidine (Figure 1b), thus indicating their sympathetic nature. Adding 1 μM phentolamine to the perfusing medium (Figure 1c) substantially reduced the contractile responses evoked by both TNS and by exogenously administered NA.

Effect of ω-conotoxin GVIA on the contractile responses to TNS and to exogenous NA

As shown in Figure 2, after the first series of TNS- and NA-induced contractile responses were performed, adding 2 μM ω-CgTx to the perfusing medium did not cause any change in the resting tone of the vessel. However, the neurally evoked contractions decreased considerably in the presence of the neurotoxin, whereas the contractile responses to increasing concentrations of superfused NA were not affected. In 6 experiments, log frequency- and log concentration-contractile response relationships were obtained (Figure 3). In the control period, the contractile responses to TNS at all frequencies used were significantly higher than those obtained in the presence of the neurotoxin ($P<0.001$). In the same preparations, the concentration-response curve to NA appeared to be enhanced in the presence of ω-CgTx, even though no significant differences ($P>0.05$) were found with and without the neurotoxin.

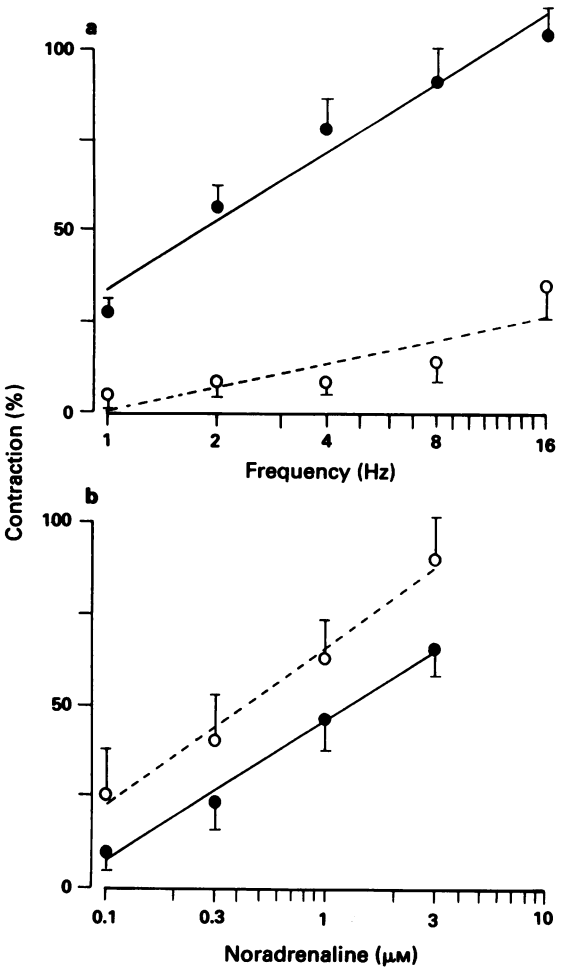

Figure 3 Frequency- (a) and concentration-response curves (b) of the contractile responses to transmural nerve stimulation (Hz) and to noradrenaline (μM) in the absence (●) and in the presence (○) of 2 μM ω-conotoxin in human saphenous veins. Each point indicates the mean ± s.e.mean of 6 experiments. Contractions are expressed as a percentage of the maximum response to 40 μg noradrenaline at the start of experiments.

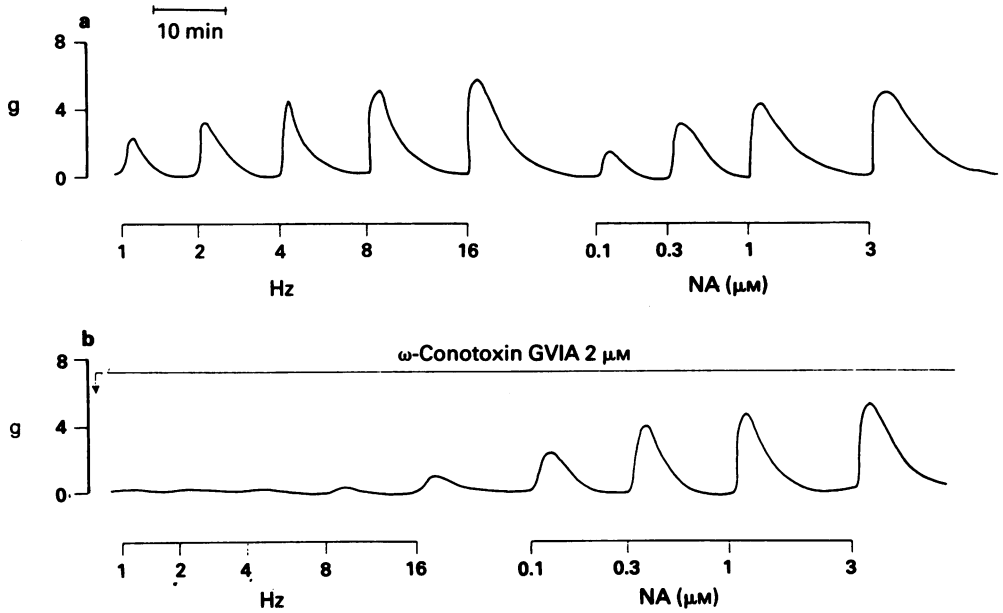

Figure 2 A representative tracing from one saphenous vein ring showing the effect of 2 μM ω-conotoxin-GVIA on the frequency-dependent contractile responses induced by 1 min transmural nerve stimulation (1–16 Hz) and on the concentration-dependent responses produced by noradrenaline (NA) superfusion. (a) Control series of responses; (b) responses in the presence of ω-conotoxin. ω-Conotoxin was added to the superfusing physiological solution 30 min before and during the second series of responses.

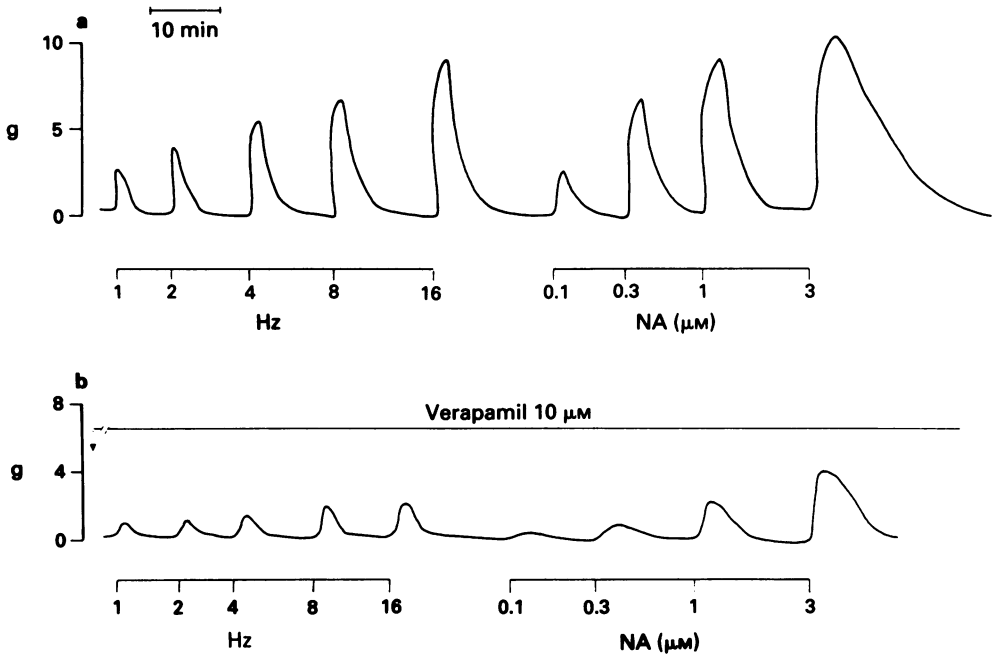

Figure 4 (a) A typical recording of the contractile responses evoked by transmural nerve stimulation (1–16 Hz) and by noradrenaline superfusion (NA, 0.1–3 μM) in one superfused human saphenous vein. (b) Electrical field stimulation and NA superfusion repeated in the same vein ring after exposure to 10 μM verapamil.

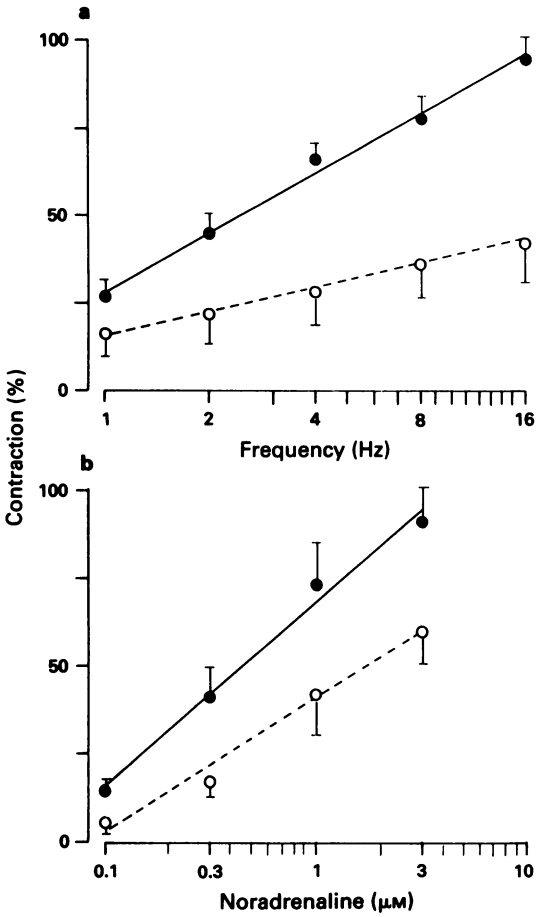

Figure 5 The effect of 10 μM verapamil on the frequency- (a) and concentration-curves (b) of the contractile responses induced by transmural nerve stimulation (Hz) and noradrenaline (μM). The mean responses ± s.e.mean of 6 experiments before (●) and after (○) verapamil are shown.

Effect of verapamil

In the presence of the organic calcium entry blocker, verapamil (10 μM), the contractile responses of the venous rings induced by both TNS and exogenous NA were reduced (Figure 4 and Figure 5). Accordingly, the neurally mediated contractions at all tested frequencies were significantly reduced by the presence of verapamil ($P<0.01$). As in the case of TNS-induced contractions, a significant difference between the control and the second series of contractile responses carried out in the presence of the antagonist was also found for the concentration-response curves to exogenous NA ($P<0.05$).

In order to compare the blocking effect of verapamil on the contractile responses to endogenous and exogenous NA, their relative potency-ratio was determined. Actually, the ratio of 0.16 (confidence limits 0.04–0.35) between equiactive nerve stimulations, with and without the calcium blocker, overlapped the corresponding ratio between the equiactive concentration of exogenous NA (0.31; confidence limits 0.16–0.58). This indicated that verapamil reduced equally both TNS- and NA-induced contractions.

Discussion

Even though it is now well established that different types of VSCCs are present in sympathetic neurones from experimental animals (Hirning *et al.*, 1988; Tsien *et al.*, 1988), no previous data were available on the type of VSCCs involved in the noradrenergic transmission of human vessels.

Our results show that ω-CgTx, the specific blocker of N- and L-type VSCCs, inhibits sympathetic neurotransmission in human saphenous veins without affecting the responses of the smooth muscle cells to exogenous NA. The inhibitory action of ω-CgTx on the sympathetic neurogenic responses of experimental animals has been demonstrated in the isolated kidney (El-Din & Malik, 1988), in various non vascular peripheral tissues (Maggi *et al.*, 1988) and in the vas deferens (Brock *et al.*, 1989). An inhibitory action on the responses

evoked by sympathetic stimulation, but not to exogenous noradrenaline, has already been shown in rat small mesenteric arteries (Pruneau & Angus, 1990). Hence these data, together with our results, provide direct evidence of the exclusive presynaptic action in vascular tissue of the neurotoxin, which, acting on VSCCs, probably inhibits NA release. Furthermore, these studies make it possible to define the specific type of VSCCs involved in this process. Indeed, recent studies in chick sensory neurones (Aosaki & Kasai, 1989) and in rat phaeochromocytoma PC12 cells (Usowicz *et al.*, 1990) imply a rather selective inhibition of N-type Ca^{2+} channels by ω-CgTx, although previous patch-clamp studies on chicken embryo DRG neurones demonstrated the ability of the toxin to interact with dihydropiridine-resistant, N-type channels, as well as dihydropiridine-sensitive, L-type channels (McCleskey *et al.*, 1987).

In the canine saphenous vein, the organic calcium channel antagonists verapamil, nicardipine and diltiazem have been shown to block both the contractile responses induced by TNS and NA release (Takata & Kato, 1988). Furthermore, verapamil (Godfraind *et al.*, 1986), was shown to inhibit more effectively depolarization-evoked contractions than [^{3}H]-NA overflow in canine saphenous veins (Takata & Kato, 1985). In contrast to these results, calcium antagonists were unable to block [^{3}H]-NA overflow and contractile responses to electrical stimulation in rabbit aorta (Karaki *et al.*, 1984) or in rat isolated kidney (El-Din & Malik, 1988) and iris (Rittenhouse & Zigmond, 1991). Different types of VSCCs may therefore regulate noradrenergic transmission in a species- and tissue-specific manner.

Our study showed that the contractile responses induced by both TNS and exogenous NA were reduced by verapamil. It is therefore difficult to determine if verapamil had any prejunctional action. We found, however, that responses to TNS and NA were depressed to a similar degree, suggesting a postjunctional action only.

In conclusion, the present work provides evidence that in human saphenous veins ω-CgTx sensitive Ca^{2+} channels, probably N-type VSCCs, are present at the presynaptic level and modulate the vasoconstrictor responses to sympathetic activation by regulating the release of noradrenaline. Verapamil-sensitive L-type Ca^{2+} channels are functionally active only at the postjunctional level.

References

AOSAKI, T. & KASAI, H. (1989). Characterization of two kinds of high-voltage-activated Ca-channel currents in chick sensory neurons. *Pflügers Arch.*, **414**, 150–156.

AUGUSTINE, G.J., CHARLTON, M.P. & SMITH, S.J. (1985). Calcium entry and transmitter release at voltage-clamped nerve terminals of squid. *J. Physiol.*, **369**, 163–181.

BROCK, J.A., CUNNANE, T.C., EVANS, R.J. & ZIOGAS, J. (1989). Inhibition of transmitter release from sympathetic nerve endings by ω-conotoxin. *Clin. Exp. Pharmacol. Physiol.*, **16**, 333–339.

DEL BASSO, P., FABI, F., CHIAVARELLI, M. & CHIAVARELLI, R. (1992). Differential effects of verapamil and ω-conotoxin-GVIA on adrenergic mechanisms in human saphenous veins. *Pharmacol. Res.*, **25**, Suppl. 2, 190–191.

EL-DIN, M.M.M. & MALIK, K.U. (1988). Differential effect of ω-conotoxin on release of the adrenergic transmitter and the vasoconstrictor response to noradrenaline in the rat isolated kidney. *Br. J. Pharmacol.*, **94**, 355–362.

FERRANTE, J. & TRIGGLE, D.J. (1990). Drug- and disease-induced regulation of voltage-dependent calcium channels. *Pharmacol. Rev.*, **42**, 29–44.

FINNEY, D.J. (1952). *Statistical Methods in Biological Assay*. pp. 99–117, 187–213. London: C. Griffin.

GODFRAIND, T., MILLER, R. & WIBO, M. (1986). Calcium antagonism and calcium entry blockade. *Pharmacol. Rev.*, **38**, 321–416.

HIRNING, L.D., FOX, A.P., MCCLESKEY, E.W., OLIVERA, B.M., THAYER, S.A., MILLER, R.J. & TSIEN, R.W. (1988). Dominant role of N-type Ca^{2+} channels in evoked release of norepinephrine from sympathetic neurons. *Science*, **239**, 57–61.

JAYAKODY, R.L., KAPPAGODA, C.T. & SENARATNE, M.P.J. (1986). Effect of calcium antagonists on adrenergic mechanisms in canine saphenous veins. *J. Physiol.*, **372**, 25–39.

KARAKI, H., NAKAGAWA, H. & URAKAWA, N. (1984). Effects of calcium antagonists on release of ^{3}H noradrenaline in rabbit aorta. *Eur. J. Pharmacol.*, **101**, 177–183.

LIPSCOMBE, D., KONGSAMUT, S. & TSIEN, R.W. (1989). α-Adrenergic inhibition of sympathetic neurotransmitter release mediated by modulation of N-type calcium-channel gating. *Nature*, **340**, 639–642.

LIPSCOMBE, D., MADISON, D.V., POENIE, M., REUTER, H., TSIEN, R.Y. & TSIEN, R.W. (1988). Spatial distribution of calcium channels and cytosolic calcium transients in growth cones and cell bodies of sympathetic neurons. *Proc. Natl. Acad. Sci. U.S.A.*, **85**, 2398–2402.

MAGGI, C.A., PATACCHINI, R., SANTICIOLI, P., LIPPE, I.T., GIULIANI, S., GEPPETTI, P., DEL BIANCO, E., SELLERI, S. & MELI, A. (1988). The effect of omega conotoxin GVIA, a peptide modulator of the N-type voltage sensitive calcium channels, on motor responses produced by activation of efferent and sensory nerves in mammalian smooth muscle. *Naunyn-Schmied. Arch. Pharmacol.*, **338**, 107–113.

MARRION, N.V., SMART, T.G. & BROWN, D.A. (1987). Membrane currents in adult rat superior cervical ganglia in dissociated tissue culture. *Neurosci. Lett.*, **77**, 55–60.

MCCLESKEY, E.W., FOX, A.P., FELDMAN, D.H., CRUZ, L.J., OLIVERA, B.M., TSIEN, R.W. & YOSHIKAMI, D. (1987). ω-Conotoxin: direct and persistent blockade of specific types of calcium channels in neurons but not muscle. *Proc. Natl. Acad. Sci. U.S.A.*, **84**, 4327–4331.

MILLER, R.J. (1987). Multiple calcium channels and neuronal function. *Science*, **235**, 46–52.

NOWYCKY, M.C., FOX, A.P. & TSIEN, R.W. (1985). Three types of neuronal calcium channel with different calcium agonist sensitivity. *Nature*, **316**, 440–443.

OLIVERA, B.M., MCINTOSH, J.M., CRUZ, L.J., LUQUE, F.A. & GRAY, W.R. (1984). Purification and sequence of a presynaptic peptide toxin from *Conus geographus* venom. *Biochemistry*, **23**, 5087–5090.

OLIVERA, B.M., IMPERIAL, J.S., CRUZ, L.J., BINDOKAS, V.P., VENEMA, V.J. & ADAMS, M.E. (1991). Calcium channel-targeted polypeptide toxins. *Ann. N.Y. Acad. Sci.*, **635**, 114–122.

PRUNEAU, D. & ANGUS, J.A. (1990). ω-Conotoxin GVIA is a potent inhibitor of sympathetic neurogenic responses in rat small mesenteric arteries. *Br. J. Pharmacol.*, **100**, 180–184.

RITTENHOUSE, A.R. & ZIGMOND, R.E. (1991). ω-Conotoxin inhibits the acute activation of tyrosine hydroxylase and the stimulation of norepinephrine release by potassium depolarization of sympathetic nerve endings. *J. Neurochem.*, **56**, 615–622.

SHER, E. & CLEMENTI, F. (1991). ω-Conotoxin-sensitive voltage-operated calcium channels in vertebrate cells. *Neuroscience*, **42**, 301–307.

TAKATA, Y. & KATO, H. (1985). Effects of Ca antagonists on the norepinephrine release and contractile responses of isolated canine saphenous veins to high KCl. *Jpn. J. Pharmacol.*, **37**, 381–394.

TAKATA, Y. & KATO, H. (1988). Differential effects of verapamil, nicardipine and diltiazem on Ca^{2+}-dependent and Ca^{2+}-independent noradrenaline release and contraction in isolated canine saphenous veins. *Pharmacology*, **37**, 24–37.

TSIEN, R.W., LIPSCOMBE, D., MADISON, D.V., BLEY, K.R. & FOX, A.P. (1988). Multiple types of neuronal calcium channels and their selective modulation. *Trends Neurosci.*, **11**, 431–438.

USOWICZ, M.M., PORZIG, H., BECKER, C. & REUTER, H. (1990). Differential expression by nerve growth factor of two types of Ca^{2+} channels in rat phaeochromocytoma cell lines. *J. Physiol.*, **426**, 95–116.

WINER, B.J. (1971). *Statistical Principles in Experimental Design*. pp. 514–603. New York: McGraw-Hill.

(Received January 20, 1993
Revised March 29, 1993
Accepted April 21, 1993)

Br. J. Pharmacol. (1993), **110**, 343–349

Inhibitory actions of ZENECA ZD7288 on whole-cell hyperpolarization activated inward current (I_f) in guinea-pig dissociated sinoatrial node cells

Robert E. BoSmith, [1]Ian Briggs & Nicholas C. Sturgess

Cardiovascular Research Department, ZENECA Pharmaceuticals, Alderley Park, Macclesfield, SK10 4TG

1 ZENECA ZD7288 (4-(*N*-ethyl-*N*-phenylamino)-1,2-dimethyl-6-(methylamino) pyrimidinium chloride) is a sinoatrial node (SAN) modulating agent which produces a selective slowing of the heart rate. Its effects have been studied in single, freshly dissociated guinea-pig SAN cells, by standard patch clamp procedures.

2 Whole-cell inward currents were evoked by hyperpolarizing voltage clamp steps from a holding potential of −40 mV. ZD7288 inhibited the hyperpolarization activated cationic current (I_f) in a concentration-dependent manner. The 'selective bradycardic agents' alinidine and UL-FS 49 (zatebradine) both also inhibited I_f.

3 The activation of I_f was investigated by measuring tail current amplitudes at +20 mV after hyperpolarizing steps to different potentials to activate the current. The reduction in I_f resulted from both a shift in the I_f current activation curve in the negative direction on the voltage axis, and also a reduction in the activation curve amplitude.

4 ZD7288 did not affect the ion selectivity of the I_f channel, since the tail current reversal potential was unchanged in the presence of the drug.

5 With ZD7288 the inhibition of I_f was not use-dependent, whereas UL-FS 49 displayed use-dependence in the block of the I_f current.

6 Whereas ZD7288 had no significant effect on the delayed rectifier current (I_k) in these cells, both alinidine and UL-FS 49 significantly reduced I_k at the same concentrations which reduced I_f.

7 The data show that ZD7288 reduces I_f by affecting the activation characteristics of the I_f current; this inhibition may account for this agent's selective bradycardic properties.

Keywords: Sinoatrial node; hyperpolarization activated current; I_f; specific bradycardic agent; ZD7288; alinidine; zatebradine; patch clamp; UL-FS 49

Introduction

In the presence of a restricted coronary blood supply to the heart, an increase in beating rate is an important contributory factor in myocardial ischaemia (Guth *et al.*, 1987a). The use of β-adrenoceptor antagonists in coronary angina is based on their ability to attenuate increases in heart rate by reducing the effects of sympathetic activity (Guth *et al.*, 1987b). However, the non-cardiac actions of these agents have disadvantages, and drugs have been identified recently which have the ability to reduce heart rate while allowing the occurrence of responses to exercise, without the non-cardiac side effects of β-adrenoceptor blockade. Alinidine and UL-FS 49, which have been termed 'specific bradycardic agents' (Kobinger *et al.*, 1979; Kobinger & Lillie, 1984; Lillie & Kobinger, 1986), are examples of this type of drug. By improving blood flow and reducing the metabolic demand of the heart, these agents should have beneficial actions in the treatment of myocardial ischaemia.

ZENECA ZD7288 (4-(*N*-ethyl-*N*-phenylamino)-1,2-dimethyl-6-(methylamino) pyrimidinium chloride; Figure 1; known as ICI D7288 in previous publications) is a new heart rate modulating agent (Hargreaves *et al.*, 1992). It slows the beating rate of the guinea-pig right atrium *in vitro* without affecting the force of contraction of the paced left atrium (Marshall *et al.*, 1992; 1993), and in the anaesthetized dog, reduces the beating rate without directly affecting inotropy (Rouse & Johnson, 1992). Its effects on the action potentials of guinea-pig sinoatrial node (SAN) cells in isolated intact tissues have been described, in comparison with the effects of the known bradycardic agents alinidine and UL-FS 49 (Briggs & Heapy, 1992). This paper describes the effects of ZD7288 on whole-cell currents of isolated single SAN cells and compares them with the effects of alinidine and UL-FS 49. Some of these data have been published in abstract form (BoSmith *et al.*, 1992).

[1] Author for correspondence.

Methods

Sinoatrial node cell dissociation

Single SAN cells were dissociated from guinea-pig nodal tissues by the method of Denyer & Brown (1990a) with minor modifications. The procedure was as follows. Two or three guinea-pigs (Duncan Hartley) each weighing 250–300 g were killed by cervical dislocation. The hearts were removed

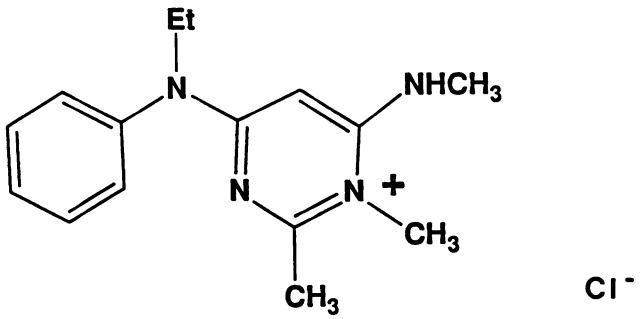

Figure 1 Chemical structure of ZD7288.

and placed in oxygenated Tyrode solution at 33–37°C. Each node was dissected out, cut into four strips (0.5–1.0 mm wide), and placed in oxygenated Ca^{2+}-free Tyrode solution containing 50 μM ethyleneglycol-*bis*-(β-amino-ethyl ether)-*N,N'*-tetra-acetic acid (EGTA) for 5 min after which the tissue was washed in Ca^{2+}-free Tyrode solution without EGTA for a further 2 min. The tissue strips were incubated in oxygenated low Ca^{2+} Tyrode solution containing 20 mM taurine, 169 units ml^{-1} collagenase (Worthington), 16 units ml^{-1} elastase (Sigma Type IV), 30 units ml^{-1} hyaluronidase (Sigma Type I-S) and 2.5 mg ml^{-1} bovine serum albumin (Miles Diagnostics) at 37°C for 25–35 min. After this time, the strips were placed in a 'KB' recovery solution (Isenberg & Klöckner, 1982) with the addition of 5 mM D-fructose-1,6-diphosphate (Sigma) for 60 min at 4°C. The tissue was gently teased apart with fine forceps in 2.5 ml of 'KB' solution in a petri-dish to release single cells. Aliquots of the suspension of SAN cells were plated onto 35 mm plastic petri-dishes (Falcon 3080, Becton Dickinson), which were stored at 4°C for 20 min to allow the cells to settle. Petri-dishes containing dissociated SAN cells were then transferred to an Open Perfusion Micro Incubator (PDMI-2; Medical Systems Corp.), mounted on the stage of an inverted microscope (Nikon Diaphot).

Cells were superfused with a Ca^{2+} containing Tyrode solution, at 1 to 2.5 ml min^{-1}, either by a gravity-fed or peristaltic pump perfusion systems. Excess solution was continuously aspirated from the side of the petri-dish opposite to the inflow tube. The solution temperature in the centre of the petri-dish was maintained at 34–36°C. The volume of the fluid in the dish was 2 ml.

Solutions and drugs

The solutions used had the following compositions (in mM): Tyrode solution: NaCl 140, KCl 5.4, $CaCl_2$ 1.8, $MgCl_2$ 0.5, N-2-hydroxyethylpiperazine-*N'*-2-ethanesulphonic acid (HEPES) 5 and glucose 10; pH 7.2 with NaOH. Low Ca^{2+} Tyrode solution: NaCl 140, KCl 5.4, $CaCl_2$ 0.06, $MgCl_2$ 3.5, taurine 20, HEPES 5 and glucose 10; pH 7.2 with NaOH. Ca^{2+}-free Tyrode solution: NaCl 140, KCl 5.4, $MgCl_2$ 3.5, taurine 20, HEPES 5, glucose 10 and EGTA 0.05; pH 7.2 with NaOH. 'KB' solution: KCl 70, adenosine triphosphate (ATP; dipotassium salt) 5, $MgSO_4$ 5, potassium glutamic acid 5, taurine 20, trisphosphocreatine 5, succinic acid 5, KH_2PO_4 20, glucose 10 and HEPES 5; pH 7.0 with KOH. Electrode solution: KCl 140, $MgCl_2$ 3, ATP 3, guanosine triphosphate (GTP; sodium salt) 0.4, trisphosphocreatine 5 and HEPES 11; pH 7.2 with KOH.

In some instances when I_f tail currents were recorded, the Tyrode solution also contained 2 mM $BaCl_2$ (Sigma), 1 mM $NiCl_2$ (Sigma) and 0.3 μM tetrodotoxin (Sigma) in order to block any contaminating outward K^+ (delayed rectifier), Ca^{2+} and Na^+ currents respectively (Denyer & Brown, 1990a; Frace *et al.*, 1992).

ZD7288, UL-FS 49 (1,3,4,5-tetrahydro-7,8-dimethoxy-3-[3-[[2-(3,4-dimethoxyphenyl)ethyl]methylimino]propyl]-2H-3-benzazepin-2-on hydrochloride) and alinidine (2-[N-allyl-N-(2,6-dichlorophenyl)-amino]-2-imidazoline hydrochloride) were all synthesized at ZENECA Pharmaceuticals. ZD7288, UL-FS 49 and alinidine were all made up as stock solutions of 1 mM in Tyrode solution, and were appropriately diluted to give final concentrations of 0.1–10 μM. All water used to prepare solutions was of reagent grade from a Millipore water purification system.

Electrical recording and analysis

Whole-cell patch clamp recordings under voltage and current clamp were performed by standard procedures (Hamill *et al.*, 1981). Recording electrodes were pulled from borosilicate glass (GC120-10; Clark Electromedical Instruments) with a Sutter P-87 electrode puller. When filled with the internal recording solution, they had resistances of 1–6 MΩ. Currents were recorded with an EPC-7 (List Electronics) or Axopatch 1D (Axon Instruments) patch clamp amplifier employing capacitance and series resistance compensation, and voltage clamp steps were controlled and applied using a Tandon PCA/12 PC microcomputer and pClamp 5.5.1 software via a TL-1 DMA Interface A-D/D-A Converter (Axon Instruments). The currents were low-pass filtered by a 3 or 4-pole Bessel filter with a cut-off frequency (3 dB down) of 3 or 2 kHz respectively. Current or voltage data were stored on hard or floppy disc for later analysis and/or recorded simultaneously onto magnetic tape (Racal 4DS), digital audio tape using a DTR1200 digital tape recorder (Biologic) or video tape using a TEAC XR-310 cassette data recorder. Current amplitudes were measured with pClamp 5.5.1 software (Axon Instruments), and hard copies produced with a Hewlett Packard 7475A digital plotter or Laserjet IIID printer. Voltage recordings of cell action potentials were obtained under current clamp conditions, and plotted on an Astromed Dash IV thermal array recorder.

Under whole-cell recording conditions, peak membrane currents for I_f and I_k (delayed rectifier) were measured at the end of the voltage clamp pulses, at 5 min intervals until stable amplitudes were established. Consistent current amplitude readings were required before the addition of any drugs. In the presence of the drugs, data were considered acceptable if at least 3 consecutive stable current amplitudes were measured, typically after some 15–40 min of drug application. The drug effects were thus always assessed after attainment of a steady state of inhibition.

All data in text and tables are presented as mean values ± standard error. The statistical significance of differences between experimental groups were assessed by Student's *t* test for unpaired data.

Results

Inhibition of I_f *by ZD7288*

When the single, dissociated SAN cells were whole-cell voltage clamped at − 40 mV and hyperpolarizing step voltage pulses applied, a time-dependent, inward current was evoked at voltages more hyperpolarized than − 60 mV (Figure 2). This hyperpolarization activated current was recognized as being the cationic I_f current observed in single SAN cells by other workers (Denyer & Brown, 1990a; DiFrancesco, 1987). The principal effect of ZD7288 was to inhibit this current, in a concentration-dependent manner. Concentrations of 0.1, 0.3 and 1.0 μM ZD7288 inhibited the I_f current measured at − 120 mV by 44 ± 4% ($n = 15$), 65 ± 4% ($n = 14$) and 78 ± 4% ($n = 9$) respectively (e.g. Figure 2). The current-voltage curves for I_f in the absence and presence of 0.3 μM ZD7288 revealed that the current was inhibited over the range of voltages − 60 to − 120 mV (Figure 2b). We found that it was essential to establish stable current amplitudes in response to the voltage steps before drug administration in all experiments, because over the initial period of recording after establishing the whole-cell configuration, run-down of I_f was often seen. It would therefore have been difficult to differentiate any drug effects from spontaneous changes. In the majority of cells the evoked current at − 120 mV was found to stabilize, and all the data used were from cells in which the amplitudes of the evoked currents reached stability before and during drug application. The time course of the inhibition of the I_f current by ZD7288 was slow; equilibration of the drug effect required some 35 min of drug application. This meant that a stable whole-cell configuration had to be maintained for 1 h or more in order to ascertain the effects of a single concentration of drug on I_f and I_k.

Although a comprehensive study was not attempted, in three cells where action potentials were examined as well as membrane currents, the reduction of I_f by 0.1 or 1 μM

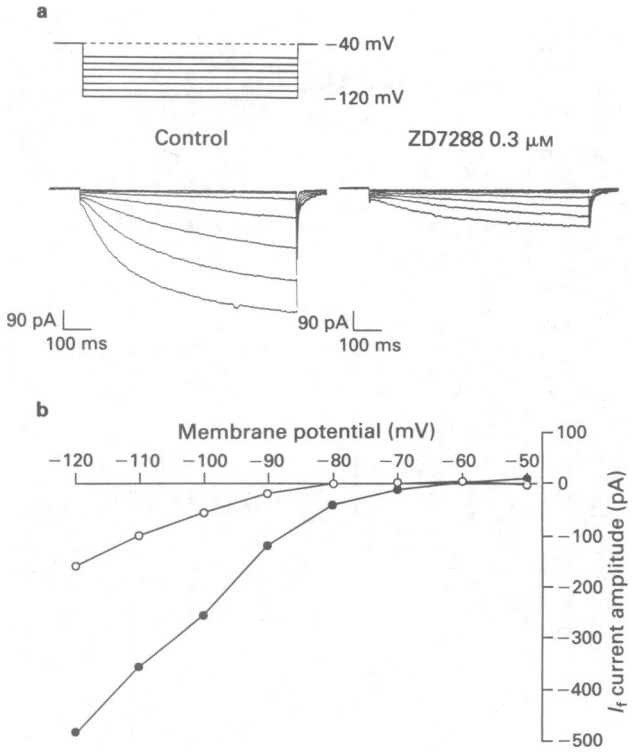

Figure 2 Inhibition of the whole-cell hyperpolarization activated current, I_f, by 0.3 μM ZD7288 in a SAN cell. The cell was voltage-clamped at a holding potential of − 40 mV and stepped to − 120 mV in 10 mV intervals. The current was measured at the end of the clamp pulses, and the percentage inhibition was calculated from the currents evoked at − 120 mV. (a) Superimposed current records showing inhibition by 0.3 μM ZD7288; 62% inhibition. (b) Current-voltage relationship of the I_f currents in (a) in the absence (●) and presence (○) of 0.3 μM ZD7288.

ZD7288 was accompanied by a slowing of the spontaneous action potential firing rate and decreased rate of diastolic depolarization (Figure 3). In one cell, 0.1 μM ZD7288 increased mean cycle length (CL) from 580 to 624 ms (+ 8%), and in two others, 1 μM ZD7288 increased CL from 524 to 780 ms (+ 48%) and from 430 to 890 ms (+ 107%) respectively. These drug concentrations had similar effects on the firing rate and the rate of diastolic depolarization of cells in guinea-pig isolated SAN tissue (Briggs & Heapy, 1992).

The reduction in I_f by ZD7288 resulted from both a concentration-dependent shift in the current activation curve in a negative direction on the voltage axis, and also a reduction in the activation curve amplitude. Activation curves for

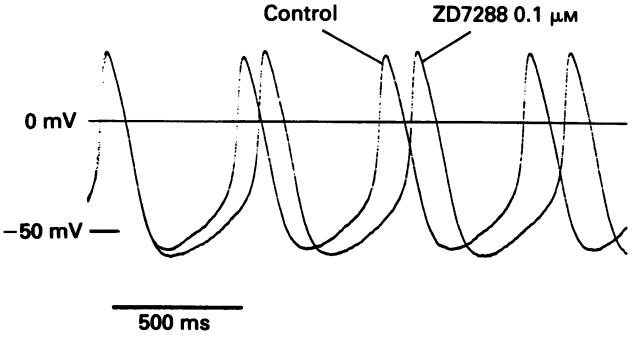

Figure 3 Action potentials recorded from a single isolated SAN cell in current-clamp mode in the absence and presence of 0.1 μM ZD7288. Waveforms are superimposed to show the reduction, by ZD7288, of diastolic depolarization rate and the slowing of action potential generation.

I_f were constructed by measuring the peak tail current amplitudes at + 20 mV from various test potentials in the absence and presence of the drug (Figure 4). In the absence of ZD7288 the mean half-maximal activation potential was − 98.4 ± 0.8 mV ($n = 32$). ZD7288 (0.1 μM) shifted the I_f half-maximal activation by − 6.1 ± 1.1 mV ($n = 8$) and reduced the activation curve maximum by 35 ± 3% ($n = 8$); 0.3 μM produced a shift of − 16.2 ± 1.8 mV ($n = 5$) in the half-maximal activation, and reduced the maximum by 52 ± 6% ($n = 5$).

The reversal potential for I_f was determined by constructing fully activated current-voltage relationships (data not shown). This involved hyperpolarizing the cell to − 120 mV (to activate I_f) and then returning to more positive voltages (− 80 mV to + 30 mV) in 10 mV increments. The resulting tail current amplitudes gave a mean control reversal potential of − 30.6 ± 1.0 mV ($n = 16$). Similar values have been reported for I_f under similar ionic conditions (DiFrancesco, 1987; van Ginneken & Giles, 1991; Frace *et al.*, 1992). ZD7288 (0.3 μM) reduced the slope of the current-voltage relationship, but did not alter the reversal potential for I_f (− 32.3 ± 3.9 mV; $n = 3$; $P > 0.5$), indicating that the drug does not alter the I_f channel selectivity properties.

The inhibitory effect on I_f of ZD7288 was compared with those of alinidine and UL-FS 49. Alinidine (10 μM) and UL-FS 49 (0.3 μM) also decreased I_f by 51 ± 5% ($n = 8$) and 37 ± 4% ($n = 11$) respectively (Figure 5).

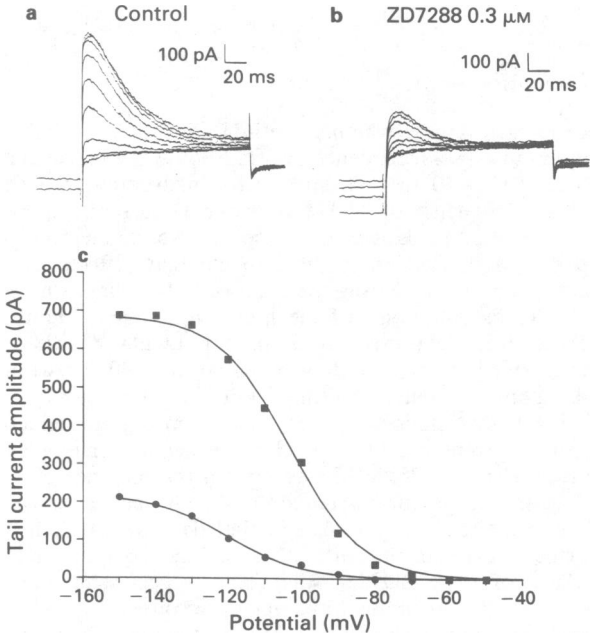

Figure 4 Action of ZD7288 on the I_f current activation characteristics. The SAN cell was voltage clamped at − 40 mV and I_f activated by successive hyperpolarizing steps (− 70 mV to − 150 mV shown) in 10 mV intervals. Each hyperpolarizing step was followed by a depolarizing step to + 20 mV to elicit I_f tail currents and then returned to the holding potential. (a) Superimposed control I_f tail currents recorded at + 20 mV. (b) I_f tail currents recorded from the same SAN cell in the presence of 0.3 μM ZD7288. (c) Activation curves for I_f in control conditions (■) and in the presence of 0.3 μM ZD7288 (●), obtained by plotting peak I_f tail current amplitudes against the potentials (− 50 to − 150 mV) of test hyperpolarization. The activation curves (continuous lines) were obtained by least squares fitting of the data with a Boltzmann equation ($I = \{1 + \exp[(V_t - V_{0.5})K^{-1}]\}^{-1}$ where I = peak tail current amplitude; V_t = hyperpolarizing test voltage; $V_{0.5}$ = half-maximal activation voltage; K = slope factor). The half-maximal activation potential was − 103 mV in the control and − 120 mV in the presence of 0.3 μM ZD7288. The amplitude of the activation curve was reduced by 69% in the presence of the drug.

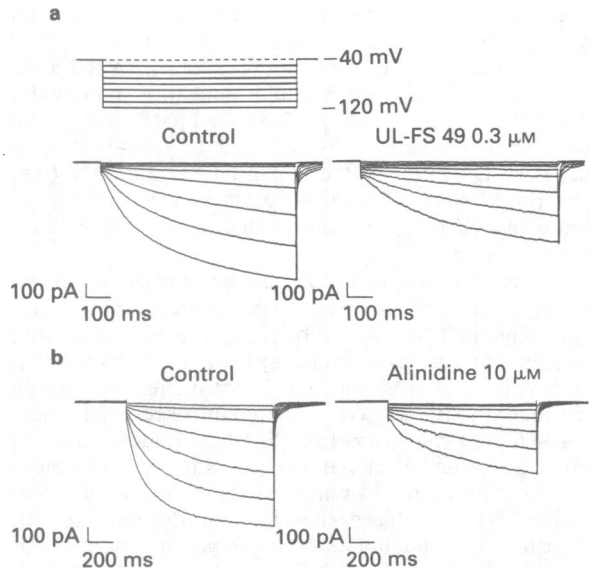

Figure 5 Effect of UL-FS 49 and alinidine on I_f currents in two separate SAN cells. The cells were clamped at a holding potential of − 40 mV and stepped to − 120 mV in 10 mV intervals. The first step in record (b) was to − 60 mV. Percentage inhibition of I_f was measured at − 120 mV. (a) Superimposed current records showing inhibition of I_f by 0.3 μM UL-FS 49; 29% inhibition. (b) Current records showing inhibition by 10 μM alinidine; 43% inhibition. Compare these inhibitions with the effect of 0.3 μM ZD7288 shown in Figure 2.

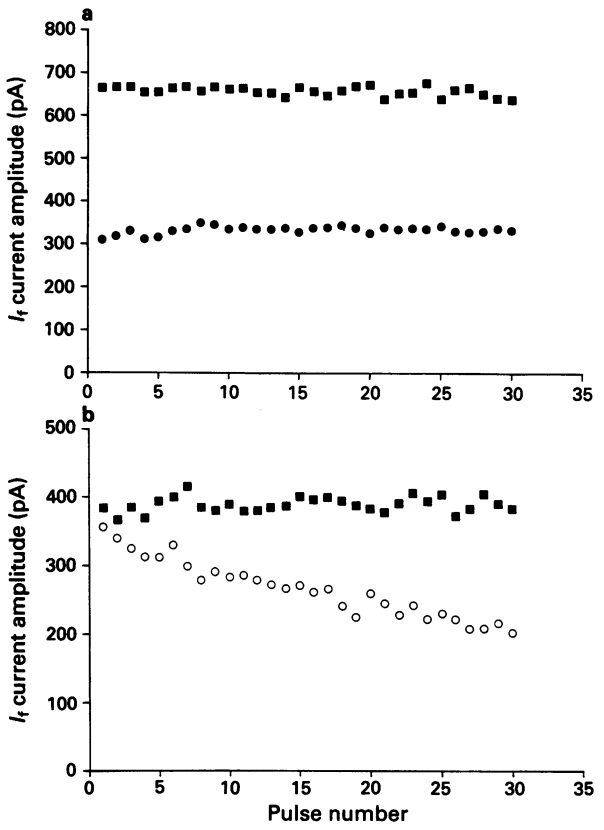

Figure 6 Use-dependence of I_f blockade: 30 voltage clamp pulses from − 40 mV to a potential of − 120 mV were applied as a train at a rate of 0.2 Hz. The amplitude of the I_f current is plotted. (a) Lack of use-dependence of ZD7288. I_f current amplitude in drug-free Tyrode solution (■) and after 35 min exposure to 1 μM ZD7288 (●). (b) Use-dependence of UL-FS 49. I_f current amplitude in drug-free Tyrode solution (■) and after 35 min exposure to 1 μM UL-FS 49 (○).

Examination of use-dependence

In order to examine whether the inhibition of I_f by ZD7288 showed any use-dependence, a train of 30 voltage clamp pulses from − 40 to − 120 mV, 1.8 s in duration, were applied at a frequency of 0.2 Hz, to evoke 30 current responses. The train of 30 pulses was only applied after stable I_f current responses had been established, to eliminate effects due to possible run-down. During the train of pulses there was little change in the amplitude of the I_f current evoked (Figure 6). The cell was then exposed to 0.3 or 1.0 μM ZD7288 for 35 min, and kept at a holding potential of − 40 mV without evoking any currents. Another train of 30 voltage clamp pulses was then imposed. There was an immediate reduction of the I_f current amplitude evoked during the first pulse of the train (e.g. to 47% of the control in the presence of 1 μM ZD7288), with no further reduction during the successive 29 pulses in the train (Figure 6a). Similar data were obtained in a further 3 experiments with ZD7288. This indicates that the blockade of I_f by ZD7288 was not use-dependent, and did not require the I_f channel to be open to produce its inhibitory effect. When the experiments were repeated with 1 μM UL-FS 49 ($n = 3$), the amplitude of the evoked current from the first pulse of the train after addition of the drug was the same as in the control conditions, but successive pulses in the train elicited progressively less current until the final pulse in the train activated only 54% of the amplitude of I_f evoked during the first pulse of the train (Figure 6b). This clearly illustrates the use-dependent nature of the inhibition of I_f by UL-FS 49 in SAN cells.

Selectivity of ZD7288

Effects of ZD7288 on other currents tested were absent or not significant at the concentrations which markedly decreased I_f. The inward rectifier current (I_{k1}) was observed in some cells as an instantaneous component of current evoked during hyperpolarization, which was distinguishable from I_f in these cells by the slower development of the latter. This instantaneous current was not reduced significantly (− 4.1 ± 6.1%; $n = 4$) by ZD7288 (1 μM) even when I_f was inhibited profoundly in the same cells (− 90 ± 3%; e.g. Figure 7).

Calcium current (I_{Ca}) was observed as an inward current during depolarizing clamp steps from a holding potential of − 60 mv which was used in a few experiments. In most of these cells, this current showed run-down which prevented studies of the effect of ZD7288, but in two cells it was possible to demonstrate that the compound (0.1 or 1.0 μM) affected I_{Ca} much less than I_f measured in the same cell: I_{Ca} was reduced by 18% and 14% while I_f was reduced by 66% and 82% respectively. This inward current rapidly inactivated and an outward current developed during the clamp pulse. In most cells, which were held at − 40 mV, the initial inward component was not seen, presumably because of inactivation or rapid run-down, and the delayed outward rectifier component (I_k) was seen alone. ZD7288 (0.1, 0.3 and 1.0 μM) did not significantly affect this outward current: changes of − 1 ± 6% ($n = 10$), − 12 ± 8% ($n = 8$) and + 9 ± 15% ($n = 3$) were observed at these concentrations respectively (Figure 8).

In contrast to ZD7288, alinidine (10 μM) and UL-FS 49 (0.3 μM) caused reductions in the delayed rectifier (I_k) of 45 ± 11% ($n = 6$) and 33 ± 7% ($n = 11$) respectively. The reductions in I_k by alinidine and UL-FS 49 were significantly greater than the effects of ZD7288 at 0.1 μM, which had a similar inhibitory effect on I_f. For the effects on I_k of alinidine compared with ZD7288, $P < 0.01$, and for UL-FS 49 compared with ZD7288, $P < 0.005$, by Student's t test. The inhibitory effects of alinidine and UL-FS 49 on I_k current-voltage relationships are illustrated in Figure 8.

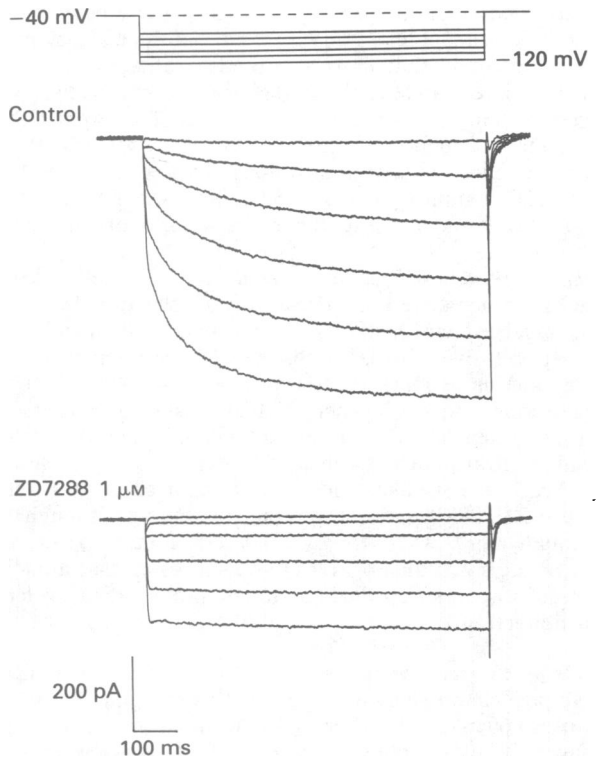

Figure 7 Lack of effect of 1 μM ZD7288 on the inward rectifier, I_{k1}, in a SAN cell with prominent I_{k1} and I_f currents together. The cell was clamped at a holding potential of − 40 mV and stepped to − 70, − 80, − 90, − 100, − 110 and − 120 mV. The amplitude of the I_{k1} (instantaneous) current remained unchanged in the presence of 1 μM ZD7288, whilst the time-dependent I_f current was inhibited by 91% when measured at − 120 mV.

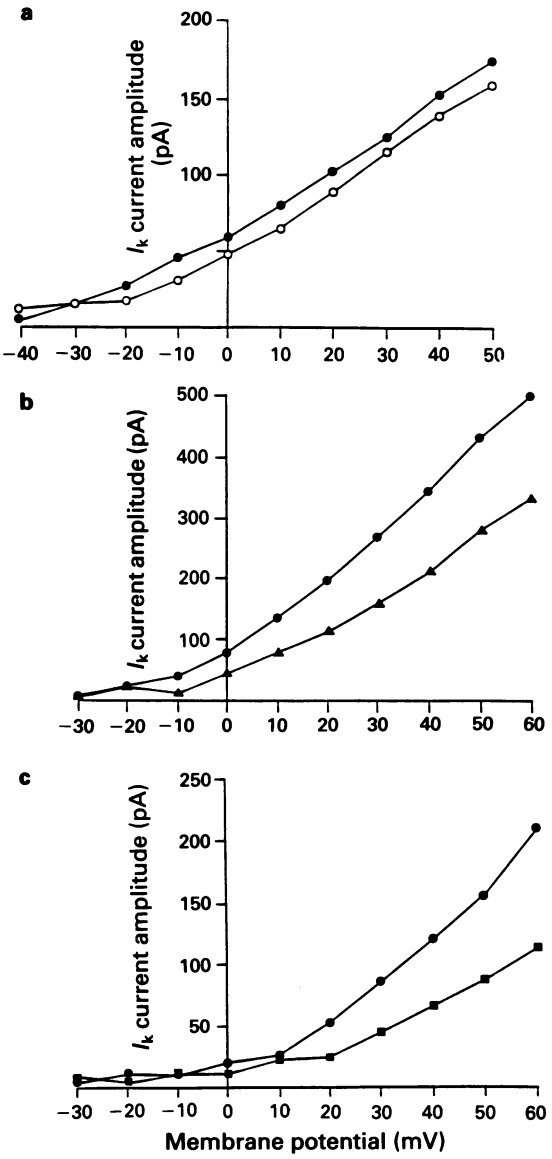

Figure 8 Effect of ZD7288, UL-FS 49 and alinidine on delayed outward (I_k) currents. Current-voltage relationships of peak currents are shown. (a) Lack of effect of ZD7288 on I_k currents elicited from a cell clamped at a holding potential of − 60 mV and stepped to − 40 mV to + 50 mV; (●) control; (○) 0.3 μM ZD7288. (b) Inhibition by UL-FS 49 of I_k currents elicited from a cell clamped at a holding potential of − 40 mV and stepped to − 30 mV to + 60 mV; (●) control; (▲) 0.3 μM UL-FS 49. (c) Inhibition by alinidine of I_k currents elicited from a cell clamped at a holding potential of − 40 mV and stepped to − 30 mV to + 60 mV; (●) control; (■) 10 μM alinidine.

Discussion

Inhibition of I_f *by ZD7288*

The principal effect of ZD7288 in this study was on the hyperpolarization-activated current (I_f) of the SAN cells. The effects on this current were seen at concentrations which reduced the rate of diastolic depolarization recorded with intracellular microelectrodes in cells in isolated SAN tissue preparations (Briggs & Heapy, 1992) and in isolated cells in the present series of experiments. Noma *et al.* (1983) and Hagiwara & Irisawa (1989) have questioned whether I_f has a role in pacemaking. However, many workers have concluded that I_f is indeed functional in pacemaking in the SAN, though other currents are also involved (DiFrancesco *et al.*, 1986; Oei *et al.*, 1989; Denyer & Brown, 1990a,b; DiFrancesco, 1991; van Ginneken & Giles, 1991). It seems reasonable to conclude therefore that the inhibitory action of ZD7288 on the pacemaker activity of the sinoatrial node is probably mediated by its selective reduction of the I_f current of the pacemaker cells.

The prolonged time to reach equilibrium for the inhibition of I_f by ZD7288, even in single cells, suggests that the compound may have an intracellular site of action, to which it penetrates only slowly, or that it causes slow changes in some factor which modulates the I_f current. In this it appears to resemble UL-FS 49 (Van Bogaert *et al.*, 1990; Van Bogaert, 1992). The ZD7288 molecule has a positive charge which is likely to be distributed between the different nitrogens of the structure; its quaternary properties would hinder penetration into cells, but the distribution of the charge may render it less impermeable than would a non-distributed charge.

The present data clearly show that the reduction in I_f at a given membrane potential by ZD7288 is not due to any changes in the ionic selectivity of the I_f channel, since the I_f reversal potential remained unchanged in the presence of the drug. The I_f current-voltage curve did however have a reduced slope in the presence of ZD7288, showing that the drug had reduced the I_f conductance. The effects of the drug on the activation characteristics of I_f suggest that ZD7288 reduces the current in a number of ways. The reduction in the activation curve amplitude (maximum evokable current; I_{max}) may reflect either a reduction in the channel conductance or a reduced probability of opening. The negative shift of the I_f activation curve, which results in the activation of a reduced fraction of I_{max} at a given potential, may indicate an action by the drug on the voltage sensor mechanism of the channel.

There is some controversy about the effects of alinidine

on the activation characteristics of I_f; Snyders & Van Bogaert (1987) found a negative shift of the activation curve and also a reduction of the fully activated I_f in Purkinje fibres, but in SAN cells, DiFrancesco (1987) found little change in I_f at -98 mV with 50 μM alinidine. UL-FS 49 was found not to alter the I_f half-maximal activation potential (E_y) in sheep Purkinje fibres, even when I_{max} was reduced by more than 70% (Van Bogaert *et al.*, 1990). In contrast, acetylcholine (ACh) is reported to shift the I_f activation curve without reducing the maximum evokable I_f current (DiFrancesco & Tromba, 1988a). ACh acts by reduction of basal adenylate cyclase activity via a G protein link (DiFrancesco & Tromba, 1988b). It is not yet known whether the selective bradycardic drugs also affect the gating of I_f directly or by an action on the G-protein and cyclic nucleotide-modulated mechanism. More detailed studies of single channel kinetics and of possible interactions with G-protein modulation of the channels might help to elucidate the mechanism further.

The lack of use-dependence in the blockade of I_f by ZD7288 illustrates a further difference between this compound and UL-FS 49. Use-dependent blockade of I_f by UL-FS 49 has been shown in sheep Purkinje fibres (Van Bogaert & Goethals, 1987; Van Bogaert *et al.*, 1990), and the experiments reported in the present paper clearly demonstrate that this compound blocks I_f in SAN cells in a similar manner. The absence of use-dependence in the action of ZD7288 on I_f could indicate an affinity of the drug for the closed or resting state of the channel, resulting in the development of block even in the absence of activation, whereas UL-FS 49 shows little or no inhibition of the current in the absence of activation. This may mean that UL-FS 49 can only block the I_f channel in its open state. The action of alinidine on I_f resembles that of ZD7288, since it has also been reported not to show any use-dependence in its blockade of I_f in Purkinje fibres (Van Bogaert & Goethals, 1987); however, its effects on SAN cells remain to be investigated.

It has previously been noted that I_f run-down is seen in many cells, and makes accurate quantitative comparison between current-voltage relations unreliable (DiFrancesco *et al.*, 1986). The long durations of the recordings which were necessary in the present experiments made it essential that the current amplitudes were stable before the drugs were applied, since the tendency to run down would otherwise have given misleading results. Doerr & Trautwein (1990) failed to find any inhibition of I_f in guinea-pig SAN cells by UL-FS 49. This is in striking contrast to our data; the explanation for this discrepancy is not clear, although these authors commented that it was difficult to separate the effects of the drug from those of run-down of I_f in their experiments. The short durations of the drug applications used by these authors may explain some of the differences in degree of effect; if stability of the responses was not attained before the drug was applied, the small drug effect likely to be obtained during a short period would be difficult to separate from the run-down. In our experiments both ZD7288 and UL-FS 49 required prolonged applications before equilibration was attained, but the effects were clear, using the protocol described.

Selectivity of action of ZD7288

Effects on the delayed rectifier current, I_k In inhibiting I_f, ZD7288 resembles alinidine and UL-FS 49. However, ZD7288 appears to have a greater degree of selectivity for I_f than the other agents, in that they can have inhibitory effects on the delayed rectifier current I_k in addition to their actions on I_f. These data provide a probable explanation for the effects of the compounds on the action potential waveforms of sinoatrial cells *in situ*: ZD7288 resembles the other compounds in reducing the rate of diastolic depolarization of the cells, but causes less prolongation of the action potential duration than alinidine or UL-FS 49 (Briggs & Heapy, 1992). Snyders & Van Bogaert (1987) and Satoh & Hashimoto (1986) also found that I_k was reduced by alinidine, in sheep Purkinje fibres and rabbit SAN cells respectively. Van Bogaert & Goethals (1987) and Doerr & Trautwein (1990) also found a reduction of outward current by UL-FS 49, but only at relatively high concentrations. This contrasts with its effect in the guinea-pig SAN cells in our experiments, in which both I_f and I_k were affected at similar concentrations.

Effects on the inward rectifier current, I_{kl} The cells used in these experiments were almost always of the spindle shaped type, regarded as being primary/transitional nodal cells (Denyer & Brown, 1990a). Cells with less prominent nuclear bulges and more marked striations were also found in the preparations, but they generally had smaller I_f currents (if any) and often had a large instantaneous hyperpolarization activated inward current, which we interpret as I_{k1}. A few of these cells were studied, and no significant effect was found of 1 μM ZD7288 on this instantaneous current, though the accompanying I_f was strongly inhibited (Figure 7). In contrast, Snyders & Van Bogaert (1987) suggested that alinidine did reduce I_{k1} in sheep Purkinje fibres, though their evidence was indirect.

Effects on the calcium current, I_{Ca} In some cells, depolarizing voltage clamp steps were imposed from a holding potential of -60 mV, which caused an initial inward current (thought to be I_{Ca}) followed by a slowly developing outward current (I_k). Denyer & Brown (1990a) reported that this inward current was stable for a period, after which it rapidly ran down. However, in our experiments, in most of the cells in which it was seen, this current disappeared rapidly during the early stages of recording, thus preventing studies of the drug effects. In two cells, which did have stable inward currents, there were only slight reductions by ZD7288 at concentrations which markedly inhibited I_f. We cannot exclude the possibility that a proportion of the apparent reduction of I_{Ca} was in fact due to run-down, but this possibility does not invalidate the relative lack of effect on I_{Ca}, and may even cause an overestimation of any effect. We have not investigated the actions of the other agents using this protocol, but Doerr & Trautwein (1990) found that the most prominent effect of UL-FS 49 was a use-dependent block of L-type calcium channels. However, Tytgat *et al.* (1990) found that UL-FS 49 was not a specific L- or T-type calcium channel blocker, as it acts only at much higher concentrations on Ca channels than on pacemaker current. It is thus not clear whether ZD7288 is significantly different from UL-FS 49 with respect to its relative lack of effect on the calcium current. In current-clamp recordings, no slowing by ZD7288 of the later part of diastolic depolarization or of the upstroke was observed, further suggesting that no inhibition of I_{Ca} had occurred.

The selective action of ZD7288 on the hyperpolarization-activated current produces a limited slowing of heart rate, since this current is only one of several components which contribute to the pacemaker activity of the sinoatrial node cells (DiFrancesco, 1991; van Ginneken & Giles, 1991). It is difficult to quantify whether the inhibitory effect of ZD7288 on I_f is sufficient to account fully for its action on heart rate *in vivo*, since the contribution of I_f to pacemaker activity *in vivo* is unknown. However, since the effect of I_f inhibition in single cells is a slowing of beating rate similar to that seen in isolated SAN tissues *in vitro*, and *in vivo*, and no other action of the compound has been observed which could have this effect, it seems reasonable to conclude that these actions are related. If the actions of ZD7288 are shown finally to be as selective as they appear from the present series of experiments, the effects of this compound on the diastolic depolarization provide further evidence that I_f is important in the modulation of pacemaker function in the guinea-pig SAN.

We are pleased to acknowledge the valuable assistance of Petra Danks in the early stages of this work, especially in the development of the cell dissociation methodology.

We would also like to express our appreciation to Prof. N.B. Standen for his useful comments on the manuscript.

References

BOSMITH, R.E., BRIGGS, I., DANKS, P. & STURGESS, N.C. (1992). Actions of ICI D7288 on sinoatrial node cellular electrophysiology: whole-cell currents. *Br. J. Pharmacol.*, **107**, 381P.

BRIGGS, I. & HEAPY, C.G. (1992). Actions of ICI D7288 on sinoatrial node cellular electrophysiology: action potentials. *Br. J. Pharmacol.*, **107**, 382P.

DENYER, J.C. & BROWN, H.F. (1990a). Rabbit sino-atrial node cells: isolation and electrophysiological properties. *J. Physiol.*, **428**, 405–424.

DENYER, J.C. & BROWN, H.F. (1990b). Pacemaking in rabbit isolated sino-atrial node cells during Cs^+ block of the hyperpolarization-activated current i_f. *J. Physiol.*, **429**, 401–409.

DIFRANCESCO, D. (1987). The pacemaker current in the sinus node. *Eur. Heart J.*, **8**, (Supplement L), 19–23.

DIFRANCESCO, D. (1991). The contribution of the 'pacemaker' current (i_f) to generation of spontaneous activity in rabbit sino-atrial node myocytes. *J. Physiol.*, **434**, 23–40.

DIFRANCESCO, D., FERRONI, A., MAZZANTI, M. & TROMBA, C. (1986). Properties of the hyperpolarizing-activated current (i_f) in cells isolated from the rabbit sino-atrial node. *J. Physiol.*, **377**, 61–88.

DIFRANCESCO, D. & TROMBA, C. (1988a). Inhibition of the hyperpolarization-activated current (i_f) induced by acetylcholine in rabbit sino-atrial node myocytes. *J. Physiol.*, **405**, 477–491.

DIFRANCESCO, D. & TROMBA, C. (1988b). Muscarinic control of the hyperpolarization-activated current (i_f) in rabbit sino-atrial node myocytes. *J. Physiol.*, **405**, 493–510.

DOERR, TH. & TRAUTWEIN, W. (1990). On the mechanism of the 'specific bradycardic action' of the verapamil derivative UL-FS 49. *Naunyn-Schmied. Arch. Pharmacol.*, **341**, 331–340.

FRACE, A.M., MARUOKA, F. & NOMA, A. (1992). Control of the hyperpolarization-activated cation current by external anions in rabbit sino-atrial node cells. *J. Physiol.*, **453**, 307–318.

GUTH, B.D., HEUSCH, G., SEITELBERGER, R. & ROSS, J.Jr. (1987a). Elimination of exercise-induced regional myocardial dysfunction by a bradycardic agent in dogs with chronic coronary stenosis. *Circulation*, **75**, 661–669.

GUTH, B.D., HEUSCH, G., SEITELBERGER, R. & ROSS, J.Jr. (1987b). Mechanism of beneficial effect of β-adrenergic blockade on exercise-induced myocardial ischemia in conscious dogs. *Circ. Res.*, **60**, 738–746.

HAGIWARA, N. & IRISAWA, H. (1989). Modulation by intracellular Ca^{2+} of the hyperpolarization-activated inward current in rabbit single sino-atrial node cells. *J. Physiol.*, **409**, 121–141.

HAMILL, O.P., MARTY, A., NEHER, E., SAKMANN, B. & SIGWORTH, F.J. (1981). Improved patch-clamp techniques for high-resolution current recording from cells and cell-free membrane patches. *Pflügers Arch.*, **391**, 85–100.

HARGREAVES, R.B., MILLS, S.D., MCLOUGHLIN, B.J. & MARSHALL, P.W. (1992). ICI D7288, a novel sino-atrial node modulator: synthesis and pharmacological activity. *23rd National Medicinal Chemistry Symposium. American Chemical Society*. Buffalo, June, 1992; abstract 21.

ISENBERG, G. & KLÖCKNER, U. (1982). Calcium tolerant ventricular myocytes prepared by preincubation in a 'KB medium'. *Pflügers Arch.*, **395**, 6–18.

KOBINGER, W. & LILLIE, C. (1984). Cardiovascular characterization of UL-FS 49, 1,3,4,5-tetrahydro-7,8-dimethoxy-3-[3-[[2-[3,4-dimethoxyphenyl)ethyl]methylimino]propyl]-2H-3-benzazepin-2-on hydrochloride, a new 'specific bradycardic agent'. *Eur. J. Pharmacol.*, **104**, 9–18.

KOBINGER, W., LILLIE, C. & PICHLER, L. (1979). N-Allyl-derivative of clonidine, a substance with specific bradycardic action at a cardiac site. *Naunyn-Schmied. Arch. Pharmacol.*, **306**, 255–262.

LILLIE, C. & KOBINGER, W. (1986). Investigations into the bradycardic effects of UL-FS 49 (1,3,4,5-tetrahydro-7,8-dimethoxy-3-[3-[[2-[3,4-dimethoxyphenyl)-ethyl] methylimino]propyl]-2H-3-benzazepin-2-on hydrochloride) in isolated guinea pig atria. *J. Cardiovasc. Pharmacol.*, **8**, 791–797.

MARSHALL, P.W., BRAMLEY, J. & BRIGGS, I. (1992). The effects of ICI D7288 – a novel sino-atrial node modulating agent – on guinea pig isolated atria. *Br. J. Pharmacol.*, **107**, 134P.

MARSHALL, P.W., ROUSE, W., BRIGGS, I., HARGREAVES, R.B., MILLS, S.D. & MCLOUGHLIN, B.J. (1993). ICI D7288 – a novel sino-atrial node modulator. *J. Cardiovasc. Pharmacol.*, (in press).

NOMA, A., MORAD, M. & IRISAWA, H. (1983). Does the 'pacemaker current' generate the diastolic depolarization in the rabbit s.a. node cells? *Pflügers Arch.*, **397**, 190–194.

OEI, H.I., VAN GINNEKEN, A.C.G., JONGSMA, H.J. & BOUMAN, L.N. (1989). Mechanisms of impulse generation in isolated cells from the rabbit sinoatrial node. *J. Mol. Cell. Cardiol.*, **21**, 1137–1149.

ROUSE, W. & JOHNSON, I.R. (1992). Haemodynamic actions of ICI D7288, a novel sino-atrial node modulator. *Br. J. Pharmacol.*, **107**, 383P.

SATOH, H. & HASHIMOTO, K. (1986). Electrophysiological study of alinidine in voltage clamped rabbit sino-atrial node cells. *Eur. J. Pharmacol.*, **121**, 211–219.

SNYDERS, D.J. & VAN BOGAERT, P.-P. (1987). Alinidine modifies the pacemaker current in sheep Purkinje fibres. *Pflügers Arch.*, **410**, 83–91.

TYTGAT, J., VAN BOGAERT, P.P., VEREECKE, J. & CARMELIET, E. (1990). On the mechanism of action of the bradycardic agent UL-FS 49 on ventricular Ca channels. *Pharmacodyn. Ther.*, **9**, 19–27.

VAN BOGAERT, P.-P. (1992). Kinetics of the blocking and unblocking processes of the i_f pacemaker current by bradycardic agents injected into isolated sheep cardiac Purkinje fibres. *J. Physiol.*, **446**, 342P.

VAN BOGAERT, P.-P. & GOETHALS, M. (1987). Pharmacological influence of specific bradycardic agents on the pacemaker current of sheep cardiac Purkinje fibres. A comparison between three different molecules. *Eur. Heart J.*, **8**, Supplement L, 35–42.

VAN BOGAERT, P.-P., GOETHALS, M. & SIMOENS, C. (1990). Use- and frequency-dependent blockade by UL-FS 49 of the i_f pacemaker current in sheep cardiac Purkinje fibres. *Eur. J. Pharmacol.*, **187**, 241–256.

VAN GINNEKEN, A.C.G. & GILES, W. (1991). Voltage clamp measurements of the hyperpolarization-activated inward current I_f in single cells from rabbit sino-atrial node. *J. Physiol.*, **434**, 57–83.

(Received February 3, 1993
Revised April 4, 1993
Accepted April 21, 1993)

Br. J. Pharmacol. (1993), **110**, 350–354

Effect of endopeptidase-24.11 inhibition and of atrial natriuretic peptide clearance receptor ligand on the response to rat brain natriuretic peptide in the conscious rat

Jane E. Kirk & [1]M.R. Wilkins

Department of Clinical Pharmacology, Royal Postgraduate Medical School, Du Cane Road, London W12 0NN

1 The present studies examined the effect of (a) a specific endopeptidase-24.11 (E-24.11) inhibitor (candoxatrilat) and (b) a ligand for the atrial natriuretic peptide (ANP) clearance receptor (SC 46542) on the renal and blood pressure response to brain natriuretic peptide (BNP) in conscious rats.

2 Infusion of BNP 200 ng kg^{-1} min^{-1} for 60 min produced a small rise in urinary sodium and guanosine 3':5'-cyclic monophosphate (cyclic GMP) excretion with a non-significant fall in mean arterial blood pressure.

3 Candoxatrilat (3 mg kg^{-1}) alone had no significant effect on sodium excretion or blood pressure but markedly potentiated the natriuretic response to BNP.

4 Similarly SC 46542 (68 μg kg^{-1}; 6.8 μg kg^{-1} min^{-1}) which produced no significant effect on its own, potentiated the natriuresis-induced by BNP, although the effect was of shorter duration compared to that of candoxatrilat.

5 The data indicate two approaches to the potentiation of the renal activity of BNP and suggest that BNP may mediate some of the activity of E-24.11 inhibitors reported in cardiac failure.

Keywords: Brain natriuretic peptide; endopeptidase 24.11; clearance receptor

Introduction

First isolated from porcine brain (Sudoh *et al.*, 1989), it is now clear that brain natriuretic peptide (BNP) is most abundant in cardiac tissue (Saito *et al.*, 1989; Aburaya *et al.*, 1989; Kambayashi *et al.*, 1989). The molecular form of the cardiac peptide varies considerably between species. In man, BNP is synthesized as a 108 amino acid prohormone; the C-terminal 32 residues are cleaved and secreted into the circulation (Sudoh *et al.*, 1989; Kambayashi *et al.*, 1990b). Two forms of BNP are found in the rat heart; pro-BNP 1-95 and BNP-45 (Aburaya *et al.*, 1989; Nakao *et al.*, 1990). The latter has been shown to be the major storage, secretory and circulating form of BNP in rat plasma (Nakao *et al.*, 1990; Aburaya *et al.*, 1991).

BNP displays considerable sequence homology to atrial natriuretic peptide (ANP) and has a similar profile of biological activity (Sudoh *et al.*, 1988; Kambayashi *et al.*, 1990a; Kita *et al.*, 1991). Both peptides exhibit a 17 amino acid ring formed by a disulphide bond and both produce a natriuresis and a reduction in blood pressure when infused into animals and man (McGregor *et al.*, 1990; Yoshimura *et al.*, 1991). It has been proposed that the two peptides act in concert to regulate sodium balance and blood pressure.

In addition to filtration at the glomerulus, two other pathways are thought to participate in the clearance of ANP; namely, metabolism by endopeptidase-24.11 (E-24.11) and receptor-mediated endocytosis (Ruskoaho, 1992). E-24.11 opens the 17 amino acid ring and inactivates ANP (Stephenson & Kenny, 1987; Olins *et al.*, 1989). The clearance receptors for ANP are distinct from guanylyl cyclase linked receptors for this peptide in that they have not been clearly linked to any second messenger system but have been shown to internalise ANP in cell culture (Maack, 1992). Inhibition of either pathway alone has been shown to enhance the natriuretic response to ANP (Wilkins *et al.*, 1992) and this observation has therapeutic potential: E-24.11 inhibitors are currently under evaluation as novel agents for treating patients with cardiac failure (Northridge *et al.*, 1989).

There is increasing evidence that BNP is also cleared by E-24.11 and may therefore contribute to the pharmacological actions of E-24.11 inhibitors. Rat and human BNP are hydrolysed by this enzyme, although the cleavage site differs between the two peptides (Norman *et al.*, 1991). Recently, Seymour *et al.* (1992) have reported that co-infusion of the E-24.11 inhibitor, SQ 28,603, enhances the natriuretic response to rat BNP-32 in the spontaneously hypertensive rat and human BNP-32 in the cynomolgus monkey. It must be noted, however, that SQ-28,603 is not specific for E-24.11 as it has also been reported to inhibit the transformation of big endothelin-1 (1-38) to endothelin-1 (1-21) (Gardiner *et al.*, 1992), a property not shared by all E-24.11 inhibitors (McMahon *et al.*, 1991; Pollock & Opgenorth, 1991).

The role of receptor-mediated clearance of BNP *in vivo* also needs to be addressed. Studies *in vitro* have shown that human BNP exhibits a 14 fold lower affinity for the human clearance receptor than ANP (Nakao *et al.*, 1991). Similarly, rat BNP-45 has a 6 fold lower affinity than rat ANP for the rat clearance receptor (Suga *et al.*, 1992). It has been suggested that this may contribute to the longer half-life of circulating BNP compared to ANP. However, there are no studies of the effect of clearance receptor ligands on the biological activity of BNP *in vivo*.

Accordingly, the present study examined the effect of a specific E-24.11 inhibitor, candoxatrilat, and the clearance receptor ligand, SC 46542, on the renal and hypotensive response to an exogenous infusion of rat BNP-45 in the conscious rat.

Methods

Infusion protocol

Studies were performed on male Wistar rats (275–300 g). Under Hypnorm (fentanyl/fluanisone) anaesthesia, cannulae (portex 0.58 mm) were placed in a femoral artery, femoral vein and bladder. The animals were allowed to regain consciousness in individual restraining cages. An infusion of sodium chloride 150 mM (2.38 ml h^{-1}) containing [^{3}H]-inulin

[1] Author for correspondence.

(Amersham) 2 μCi ml^{-1} was given via the femoral vein, which was also used to administer drugs, and continued for the study duration. Observations were started 3 h after beginning the infusion. Urine was collected at 15 min intervals into preweighed tubes for determination of volume, sodium, guanosine 3':5'-cyclic monophosphate (cyclic GMP) and [^{3}H]-inulin concentrations. Blood pressure was measured via the femoral artery every 15 min (MacLab instruments). Arterial blood samples (200 μl) were taken into lithium-haematocrit tubes for [^{3}H]-inulin measurement 30 and 90 min from the start of observations.

Studies

Effect of candoxatrilat To investigate the effect of E-24.11 inhibition on the response to BNP, animals were divided into one of the following treatment groups: (a) BNP-45, 200 ng kg^{-1} min^{-1} for 60 min ($n = 6$); (b) saline vehicle alone ($n = 6$); (c) candoxatrilat 3 mg kg^{-1} (in 100 μl saline) as a single bolus injection over 1 min ($n = 6$); (d) candoxatrilat 3 mg kg^{-1} (in 100 μl saline) at the start of the 60 min BNP-45 infusion ($n = 7$). The treatments were commenced after two baseline urine collections. The dose of BNP was chosen as one which would produce only a small natriuresis when given alone. Groups (a) and (b) received 100 μl saline in place of candoxatrilat at the appropriate time. Doses of ≥ 3 mg kg^{-1} candoxatrilat represent the top of the dose-response curve for natriuresis in hydrated rats (Shepperson *et al.*, 1991; Wilkins *et al.*, 1992).

Effect of SC 46542 To investigate the effect of a clearance receptor ligand on the response to BNP, the following additional treatment groups were studied: a) SC 46542 68 μg kg^{-1} bolus (in 100 μl saline); followed by 6.8 μg kg^{-1} min^{-1} for 60 min ($n = 6$); b) as in a) but combined with BNP-45 200 ng kg^{-1} min^{-1} ($n = 6$); c) SC 46542 680 μg kg^{-1} bolus (in 100 μl saline); then 68 μg kg^{-1} min^{-1} for 60 min ($n = 7$); d) as in c) but combined with BNP-45 200 ng kg^{-1} min^{-1} ($n = 7$).

Assays

Urine volume was measured gravimetrically. Sodium concentration was measured by flame photometry (Corning 480). [^{3}H]-inulin level were determined by liquid scintillation counting in Insta-gel (Packard). Urinary cyclic GMP concentration was measured by radioimmunoassay on appropriately diluted samples as previously described (Wilkins *et al.*, 1990a).

Drugs and peptides

Rat BNP-45 was purchased from Peninsula Laboratories. Candoxatrilat is a specific E-24.11 inhibitor (Danilewicz *et al.*, 1989) and was a gift from Pfizer UK. SC 46542 is des(Phe^{106}Gly^{107}Ala^{115}Gln^{116})-ANP(5-28) and was synthesized by Monsanto Company, St Louis, U.S.A.; it binds specifically to the ANP clearance receptor (Koepke *et al.*, 1989).

Statistics

Data are presented as mean ± s.e.mean. Blood pressure and renal responses were examined by analysis of variance with respect to treatment and time (urine collection). Statistical significance was assessed by Scheffes' test. Statistical significance was assumed when the P value was <0.05. All calculations were made with Complete Statistical System (StatSoft) software.

Results

Sodium excretion

Infusion of BNP 200 ng kg^{-1} min^{-1} produced a modest 2 to 3 fold increase in urinary sodium excretion compared to baseline but this did not differ significantly from the gradual 2 fold rise seen in the vehicle-treated group during the period of observation (Figure 1). Candoxatrilat alone had no significant effect on sodium excretion with respect to baseline or to vehicle controls (Figure 1a). When co-infused with BNP, however, there was a 5 fold increase in the natriuretic response; both the peak and duration of the natriuresis were significantly greater than seen with BNP alone ($P<0.01$). Similarly, infusion of SC 46542 (68 μg kg^{-1}, followed by 6.8 μg kg^{-1} min^{-1}) alone did not significantly affect sodium excretion but enhanced the response to BNP (Figure 1b). There were significant differences in the time-course of the response to the two combination treatments. The peak response to candoxatrilat and BNP occurred slightly later than that with SC 46542 and BNP, but was more prolonged. Increasing the dose of SC 46542 10 fold (680 μg kg^{-1}, then 68 μg kg^{-1} min^{-1}) produced no further potentiation of the effect of BNP beyond that seen with the lower dose of clearance receptor ligand.

Cyclic GMP excretion

BNP alone produced a significant rise in urinary cyclic GMP excretion compared to vehicle treated controls ($P<0.01$, Figure 2). This response was enhanced by candoxatrilat and

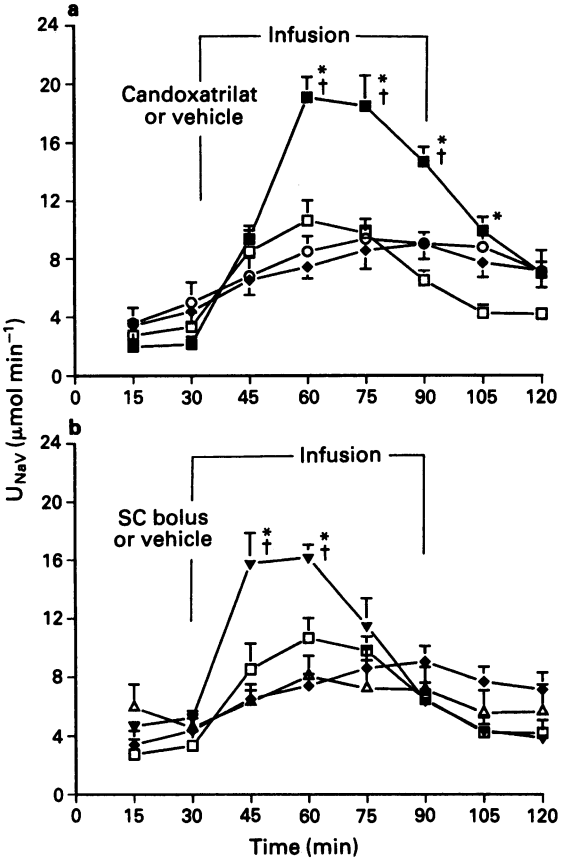

Figure 1 (a) Effect of brain natriuretic peptide (BNP) infusion (200 ng kg^{-1} min^{-1}, □), candoxatrilat (3 mg kg^{-1}, ○), vehicle (saline, ◆) and BNP after candoxatrilat (■) on urinary sodium excretion in conscious rats. (b) Effect of SC 46542 (68 μg kg^{-1} bolus, then 6.8 μg kg^{-1} min^{-1}, △), BNP (200 ng kg^{-1} min^{-1}, □), vehicle (saline, ◆) and BNP with SC 46542 (▼) on urinary sodium excretion in conscious rats. Data are mean with s.e.mean. *$P<0.01$, compared to BNP infusion alone group and †$P<0.01$ compared to vehicle. BNP in combination with candoxatrilat is significantly different ($P<0.01$) from the SC 46542 and BNP combination at times 45, 75, 90, 105 min.

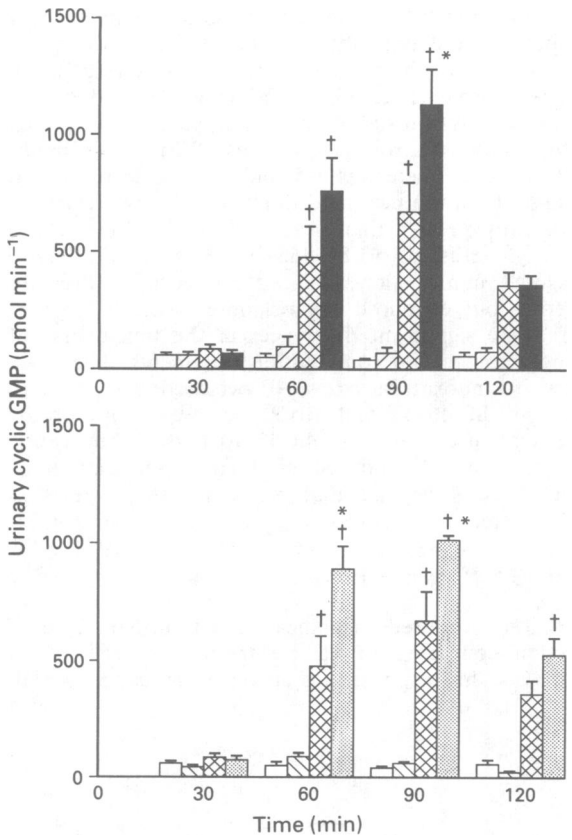

Figure 2 Urinary cyclic GMP excretion during treatment with: (a) vehicle (open columns), candoxatrilat (3 mg kg^{-1}) alone (hatched columns), BNP 200 ng kg^{-1} min^{-1} infusion (cross hatched columns), and candoxatrilat (3 mg kg^{-1}) prior to BNP infusion (solid columns); and (b) vehicle, (open columns), SC 46542 (68 μg bolus then 6.8 μg kg^{-1} min^{-1}) alone (hatched columns) BNP 200 ng kg^{-1} min^{-1} infusion (cross hatched columns), and the combination of SC 46542 and BNP (stippled columns). Data are mean with s.e.mean. †$P<0.01$ compared to vehicle and *$P<0.05$ compared to BNP alone.

by SC 46542. Neither candoxatrilat nor SC 46542 alone significantly affected cyclic GMP excretion.

GFR and blood pressure There was a small rise in GFR on initiating the BNP infusion in all the treatment groups, but in no group was it sustained after the first 15 min of the infusion (Table 1). This transient rise in GFR is probably an artifact due to the wash-out of [^{3}H]-inulin from the 'dead-space', constituted by the bladder stump and cannula, following the rapid increase in urine flow and is unlikely to be representative of increased glomerular filtration.

Mean arterial blood pressure showed a gradual downward drift during infusion of BNP alone compared to the vehicle-treated group, but this did not reach statistical significance (Table 1). Neither candoxatrilat nor SC 46542 alone significantly affected blood pressure; in combination with BNP, a significant ($P<0.05$) fall in blood pressure was observed at the end of the peptide infusion (Table 1).

Discussion

Inhibition of E-24.11 and infusion of a specific ligand for the ANP clearance receptor are two approaches used to inhibit the clearance of ANP and enhance its natriuretic action (Wilkins *et al.*, 1992). This study shows that both manipulations also potentiate the renal response to BNP in the rat.

Several authors have shown that BNP is a substrate for E-24.11 *in vitro* (Vogt-Schaden *et al.*, 1989; Norman *et al.*, 1991). The site of hydrolysis of BNP differs from that for ANP and, like the molecular form, varies between species. E-24.11 cleaves ANP at the Cys-Phe bond within the ring in all mammalian species studied to date but this bond is not the primary site of hydrolysis in BNP. Instead, rat BNP-32 is hydrolysed at the Arg-Leu bond within the ring and the Arg-Leu bond in the C-terminus. The primary site of attack on human BNP-32 is the Met-Val bond in the N-terminal sequence followed by the Arg-Ile bond in the ring.

The 17 amino acid ring is essential for the biological activity of ANP and BNP, and so hydrolysis of bonds within the ring would be expected to inactivate the peptide. Recently, Seymour *et al.* (1992) reported that the E-24.11 inhibitor, SQ 28,603, potentiates the renal response to human BNP-32 in cynomolgus monkeys and rat BNP-32 in the SHR. The structural diversity of BNP means that it is essential to use the peptide appropriate to the test species (Kambayashi *et al.*, 1990a). We have examined the effect of E-24.11 inhibition on the response to rat BNP-45, the circulating form of the peptide in this species. Our observations support and extend those of Seymour *et al.* (1992) and strengthen the thesis that E-24.11 is an important enzyme in the inactivation and clearance of circulating BNP.

Data on the contribution of the ANP clearance receptor to the regulation of BNP activity are limited. Nakao *et al.* (1991) have reported that the binding affinity of human BNP for human ANP clearance receptors is only 7% that of human ANP. These authors suggest that the clearance receptor is less active in removing BNP than ANP from the circulation and that this contributes to its longer half-life *in*

Table 1 Glomerular filtration rate and mean arterial blood pressure

	Time (min)							
	15	30	45	60	75	90	105	120
GFR (ml min^{-1})								
Saline	3.7 ± 0.3	3.8 ± 0.3	4.1 ± 0.2	3.7 ± 0.2	3.6 ± 0.4	3.5 ± 0.2	3.4 ± 0.3	3.3 ± 0.6
BNP	2.9 ± 0.3	3.4 ± 0.3	4.1 ± 0.4	3.2 ± 0.2	2.9 ± 0.2	2.9 ± 0.2	2.3 ± 0.3	3.2 ± 0.3
BNP + candoxatrilat	3.3 ± 0.3	3.1 ± 0.2	3.9 ± 0.3	3.2 ± 0.1	3.1 ± 0.2	3.1 ± 0.2	2.7 ± 0.2	3.1 ± 0.2
BNP + SC 46542	3.4 ± 0.2	3.4 ± 0.2	3.9 ± 0.4	3.1 ± 0.1	3.1 ± 0.1	2.9 ± 0.3	2.5 ± 0.3	3.1 ± 0.3
BP (mmHg)								
Saline	108 ± 2	107 ± 2	108 ± 2	109 ± 3	110 ± 4	111 ± 4	111 ± 4	114 ± 5
BNP	110 ± 3	111 ± 3	110 ± 3	109 ± 2	105 ± 3	105 ± 3	106 ± 4	108 ± 3
BNP + candoxatrilat	107 ± 2	110 ± 2	110 ± 3	109 ± 3	107 ± 2	104 ± 2*	106 ± 3	106 ± 3
BNP + SC 46542	113 ± 5	113 ± 4	112 ± 4	108 ± 4	105 ± 4	104 ± 3*	104 ± 4	104 ± 3

Data are mean ± s.e.mean. Brain natriuretic peptide (BNP) was infused from 30 ± 90 min. Candoxatrilat (3 mg kg^{-1}) was given prior to BNP 200 ng kg^{-1} min^{-1}. SC 46542 was given as 68 μg kg^{-1} bolus then 6.8 μg kg^{-1} min^{-1} during BNP 200 ng kg^{-1} min^{-1}. *$P<0.05$ compared to saline.

vivo compared to ANP. This is difficult to test in man with currently available agents. In an attempt to circumvent this problem, Lang *et al.* (1992) infused ANP into patients with heart failure in a dose which they calculated would 'swamp' the ANP clearance receptor and saw no change in plasma BNP levels. Our data support a role for the clearance receptor in the regulation of BNP activity *in vivo* in the rat. Nonetheless, a useful comparison can be made between the present experiments and a comparable study with ANP, in which an approximately equimolar dose of ANP was used in place of BNP (Wilkins *et al.*, 1992). In the present study, maximum potentiation of the natriuretic effect of BNP with SC 46542 was obtained with the lower dose used (68 $\mu g\ kg^{-1}$, 6.8 $\mu g\ kg^{-1}\ min^{-1}$) and the response was similar, although of shorter duration, to that produced by candoxatrilat (3 mg kg^{-1}). In the ANP study, this dose of SC 46542 caused sub-maximal potentiation; a 10 fold higher dose of SC 46542 (680 $\mu g\ kg^{-1}$, 68 $\mu g\ kg^{-1}\ min^{-1}$) produced significantly greater potentiation of the natriuretic effect of ANP than the lower dose and exceeded the maximal response that could be obtained with candoxatrilat (Wilkins *et al.*, 1992). These observations would be consistent with the idea that SC 46542 is more effective at competing with BNP than ANP for the clearance receptor and that, compared to E-24.11, the clearance receptor plays a smaller role in clearing BNP than ANP.

The effects of candoxatrilat and SC 46542 on the hypotensive response to BNP were small, and observed at the end of the BNP infusion, when the animals are significantly hypovolaemic from the diuretic actions of these treatments, and perhaps increased extravasation of fluid. Candoxatrilat and SC 46542 have little effect on the fall in blood pressure during ANP infusion (Wilkins *et al.*, 1992), and Seymour *et al.* (1992) observed no potentiation of the depressor effect of BNP in the monkey or SHR with their E-24.11 inhibitor. The kidneys are a rich source of both E-24.11 and clearance receptors and play an important role in clearing ANP. It seems that inhibition of these clearance pathways preferentially enhance the local effects of ANP and BNP on the kidney, rather than their systemic actions.

The present study is clinically relevant as E-24.11 inhibitors are undergoing trials in the treatment of heart failure. Plasma BNP levels are elevated in this condition (Mukoyama *et al.*, 1991). Indeed the incremental rise is greater than that seen with ANP. As the two peptides are equipotent (Kambayashi *et al.*, 1990a) this suggests that BNP plays as important a role in this condition as ANP. Interestingly, several authors have commented on the observation that E-24.11 inhibitors are more effective natriuretic agents in heart failure than would be predicted from the rise in plasma ANP level (Wilkins *et al.*, 1990b; Cavero *et al.*, 1990). Given that the response to BNP is also potentiated by E-24.11 inhibitors, a component of the response to these drugs in heart failure may be due to BNP.

In summary, this study suggests that BNP can be potentiated by pharmacological manipulations used to inhibit the clearance of ANP and may contribute to the therapeutic effect of these manipulations in heart failure.

This work was supported by the British Heart Foundation. The authors are grateful to Pfizer U.K. for candoxatrilat and Monsanto Co, St Louis, U.S.A. for SC 46542.

References

ABURAYA, M., HINO, J., MINAMINO, N., KANGAWA, K. & MATSUO, H. (1989). Isolation and identification of rat brain natriuretic peptides in cardiac atrium. *Biochem. Biophys. Res. Commun.*, **163**, 226–232.

ABURAYA, M., SUZUKI, E., MINAMINO, N., KANGAWA, K., TANAKA, K. & MATSUO, H. (1991). Concentration and molecular forms of brain natriuretic peptide in rat plasma and spinal cord. *Biochem. Biophys. Res. Commun.*, **177**, 40–47.

CAVERO, P.G., MARGULIES, K.B., WINAVER, J., SEYMOUR, A.A., DELANEY, M.G. & BURNETT, J.C. (1990). Cardiorenal actions of neutral endopeptidase inhibition in experimental congestive heart failure. *Circulation*, **82**, 196–201.

DANILEWICZ, J.C., BARCLAY, P.L., BARNISH, I.T., BROWN, D., CAMPBELL, S.F., JAMES, K., SAMUELS, G.M.R., TERRETT, N.K. & WHYTHES, M.J. (1989). UK-69, 578, a novel inhibitor of EC 3.4.24.11 which increases endogenous ANF levels and is natriuretic and diuretic. *Biochem. Biophys. Res. Commun,*. **164**, 58–65.

GARDINER, S.M., KEMP, P.A. & BENNETT, T. (1992). Effects of the neutral endopeptidase inhibitor, SQ 28,603, on regional haemodynamic responses to atrial natriuretic peptide or proendothelin-1 [1-38] in conscious rats. *Br. J. Pharmacol,*. **106**, 180–186.

KAMBAYASHI, Y., NAKAO, K., ITOH, H., HOSODA, K., SAITO, Y., YAMADA, T., MUKOYAMA, M., ARAI, H., SHIRAKAMI, G., SUGA, S., OGAWA, Y., JOUGASAKI, M., MINAMINO, N., KANGAWA, K., MATSUO, H., INOUYE, K. & IMURA, H. (1989). Isolation and sequence determination of rat cardiac natriuretic peptide. *Biochem. Biophys. Res. Commun.*, **163**, 33–240.

KAMBAYASHI, Y., NAKAO, K., KIMURA, H., KAWABATA, T., NAKAMURA, M., INOUYE, K., YOSHIDA, N. & IMURA, H. (1990a). Biological characterization of human brain natriuretic peptide (BNP) and rat BNP: species-specific actions of BNP. *Biochem. Biophys. Res. Commun.*, **173**, 599–605.

KAMBAYASHI, Y., NAKAO, K., MUKOYAMA, M., SAITO, Y., OGWA, Y,. SHIONO, S., INOUYE, K., YOSHIDA, N. & IMURA, H. (1990b). Isolation and sequence determination of human brain natriuretic peptide in human atrium. *FEBS Lett*, **259**, 341–345.

KITA, T., KIDA, O., YOKOTA, N., ETO, T., MINAMINO, N., KANGAWA, K., MATSUO, H. & TANAKA, K. (1991). Effects of brain natriuretic peptide-45, a circulating form of rat brain natriuretic peptide, in spontaneously hypertensive rats. *Biochem. Biophys. Res. Commun,*. **202**, 73–79.

KOEPKE, J.P., TYLER, L.D., TRAPANI, A.J., BOVY, P.R., SPEAR, K.L., OLINS, G.M. & BLAINE, E.D. (1989). Interaction of non-guanylate cyclase-linked atriopeptin receptor ligand and endopeptidase inhibitor in conscious rats. *J. Pharmacol. Exp. Ther.*, **249**, 172–176.

LANG, C.C., MOTWANI, J.G., COUTIE, W.J.R. & STRUTHERS, A.D. (1992). Clearance of brain natriuretic peptide in patients with chronic heart failure: indirect evidence for a neutral endopeptidase mechanism but against an atrial natriuretic peptide clearance receptor mechanism. *Clin. Sci.*, **82**, 619–623.

MAACK, T. (1992). Receptors for atrial natriuretic factor. *Annu. Rev. Physiol.*, **54**, 11–27.

MCGREGOR, A., RICHARDS, M., ESPINER, E., YANDLE, T. & IKRAM, H. (1990). Brain natriuretic peptide administered to man: actions and metabolism. *J. Clin. Endocrinol. Metabol.*, **70**, 1103–1107.

MCMAHON, E.G., PALOMO, M., MOORE, W.M., MCDONALD, J.F. & STEARN, M.K. (1991). Phosphoramidon blocks the pressor activity of porcine big endothelin-1 (1-39) *in vivo* and conversion of big endothelin-1 (1-39) to endothelin-1 (1-21) *in vitro*. *Proc. Natl. Acad. Sci. U.S.A.*, **88**, 703–707.

MUKOYAMA, M., NAKAO, K., HOSODA, K., SUGA, S., SAITO, Y., OGAWA, Y., SHIRAKAMI, G., JOUGASAKI, M., OBATA, K., YASUE, H. *et al.* (1991). Brain natriuretic peptide as a novel cardiac hormone in humans. Evidence for an exquisite dual natriuretic peptide system, atrial natriuretic peptide and brain natriuretic peptide. *J. Clin. Invest.*, **87**, 1402–1412.

NAKAO, K., ITOH, H., KAMBAYASHI, Y., HOSHODA, K., SAITO, Y., YAMADA, T., MUKOYAMA, M., ARAI, H., SHIRAKAMI, G., SUGA, S.-I., JOUGASAKI, M., OGAWA, Y., INOUYE, K. & IMURA, H. (1990). Rat brain natriuretic peptide isolation from rat heart and tissue distribution. *Hypertension*, **15**, 774–778.

NAKAO, K., MUKOYAMA, M., HOSODA, K., SUGA, K.-I., OGAWA, Y., SAITO, Y., SHIRAKAMI, G., ARAI, H., JOUGASAKI, M. & IMURA, H. (1991). Synthesis, secretion, and receptor selectivity of human brain natriuretic peptide. *Can. J. Physiol. Pharmacol.*, **69**, 1500–1506.

NORMAN, J.A., LITTLE, D., BOLGAR, M. & DI DONATO, G. (1991). Degradation of brain natriuretic peptide by neutral endopeptidase: species specific sites of proteolysis determined by mass spectrometry. *Biochem. Biophys. Res. Commun.*, **175**, 22–30.

NORTHRIDGE, D.B., ALABASTER, C.T., CONNELL, J.M.C., DILLY, S.G., LEVER, A.F., JARDINE, A.G., BARCLAY, P.L., DARGIE, H.J., FINDLAY, I.N. & SAMMUEL, G.M.R. (1989). Effect of UK 69 578: A novel atriopeptidase inhibitor. *Lancet*, **ii**, 591–593.

OLINS, G.M., KRIETER, P.A., TRAPANI, A.J., SPEAR, K.L. & BOVY, P.R. (1989). Specific inhibitors of endopeptidase 24.11 inhibit the metabolism of atrial natriuretic peptides in vitro and in vivo. *Mol. Cell. Endocrinol.*, **61**, 201–208.

POLLOCK, D.M. & OPGENORTH, T.J. (1991). Evidence for metalloproetase involvement in the *in vivo* effects of big endothelin-1. *Am. J. Physiol.*, **261**, R257–R263.

RUSKOAHO, H. (1992). Atrial natriuretic peptide: Synthesis, release and metabolism. *Pharmacol. Rev.*, **44**, 479–602.

SAITO, Y., NAKAO, K., ITOH, H., YAMADA, T., MUKOYAMA, M., ARAI, H., HOSODA, K., SHIRAKAMI, G., SUGA, S., MINAMINO, N., KANGAWA, K., MATSUO, H. & IMURA, H. (1989). Brain natriuretic peptide is a novel cardiac hormone. *Biochem. Biophys. Res. Commun.*, **158**, 360–368.

SEYMOUR, A.A., ASAAD, M.M., ABBOA-OFFEI, B.E., ROVNYAK, P.L., FENNELL, S. & ROGERS W.L. (1992). Potentiation of brain natriuretic peptides by SQ 28,603, an inhibitor of neutral endopeptidase 3.4.24.11, in monkeys and rats. *J. Pharmacol. Exp. Ther.*, **262**, 60–70.

SHEPPERSON, N.B., BARCLAY, P.L., BENNETT, J.A. & SAMUELS, G.M.R. (1991). Inhibition of neutral endopeptidase (EC 3.4.24.11) leads to an atrial natriuretic factor-mediated natriuretic diuretic and antihypertensive response in rodents. *Clin. Sci.*, **80**, 265–269.

STEPHENSON, S.L. & KENNY, A.J. (1987). The hydrolysis of α-human atrial natriuretic peptide by pig kidney microvillar membranes is initiated by endopeptidase-24.11. *Biochem. J.*, **243**, 183–187.

SUDOH, T., KANGAWA, K., MINAMINO, N. & MATSUO, H. (1988). A new natriuretic peptide in porcine brain. *Nature*, **332**, 78–81.

SUDOH, T., MAEKAWA, K., KOJIMA, M,. MINAMINO, N., KANGAWA, K. & MATSUO, H. (1989). Cloning and sequence analysis of cDNA encoding a precursor for human brain natriuretic peptide. *Biochem. Biophys. Res. Commun.*, **159**, 1427–1434.

SUGA, S.-I., NAKAO, K,. HOSODA, K., MUKOYAMA, M., OGAWA, Y., SHIRAKAMA, G., ARAI, H., SAITO, Y., KAMBAYASHI, Y., INOUYE, K. & IMURA, H. (1992). Receptor selectivity of natriuretic peptide family, atrial natriuretic peptide, brain natriuretic peptide, and C-type natriuretic peptide. *Endocrinol.*, **130**, 229–239.

VOGT-SCHADEN, M., GAGELMANN, M., HOCK, D., HERBST, F. & FORSSMANN, W.G. (1989). Degradation of porcine brain natriuretic peptide (pBNP-26) by endopeptidase-24.11 from kidney cortical membranes. *Biochem. Biophys. Res. Commun,*. **161**, 1177– 1183.

WILKINS, M.R., SETTLE, S.L. & NEEDLEMAN, P. (1990a). Augmentation of the natriuretic activity of exogenous and endogenous atriopeptin in rats by inhibition of guanosine 3'-5'cyclic monophosphate degradation. *J. Clin. Invest.*, **85**, 1274–1279.

WILKINS, M.R., SETTLE, S.L., STOCKMANN, P. & NEEDLEMAN, P. (1990b). Maximizing the natriuretic effect of endogenous atriopeptin in a rat model of heart failure. *Proc. Natl. Acad. Sci. U.S.A.*, **87**, 6465–6469.

WILKINS, M.R., SETTLE, S.L., KIRK, J.E., TAYLOR, S.A., MOORE, K.P. & UNWIN, R.J. (1992). Response to atrial natriuretic peptide, endopeptidase-24.11 inhibitor and C-ANP receptor ligand in the rat. *Br. J. Pharmacol.*, **107**, 50–57.

YOSHIMURA, M., YASUA, H., MORITA, E., SAKAINO, N, JOUGASAKI, M., KUROSE, M., MUKOYAMA, M., SAITO, Y., NAKAO, K. & IMURA, H. (1991). Hemodynamic, renal, and hormonal responses to brain natriuretic peptide infusion in patients with congestive heart failure. *Circulation*, **84**, 1581–1588.

(Received March 8, 1993
Revised April 13, 1993
Accepted April 21, 1993)

Br. J. Pharmacol. (1993), **110**, 355–359

The effects of single and repeated anorectic doses of 5-hydroxytryptamine uptake inhibitors on indole levels in rat brain

[1]Silvio Caccia, Marina Anelli, Anna Maria Codegoni, Claudia Fracasso & Silvio Garattini

Istituto di Ricerche Farmacologiche 'Mario Negri', Via Eritrea 62, 20157 Milan, Italy

1 The effects of acute and repeated equiactive anorectic doses (ED_{50}) of recently marketed 5-hydroxytryptamine (5-HT) uptake inhibitors on the content of brain indoles were compared in rats in relation to the brain regional concentrations of unchanged drug and its known active metabolite.

2 Single intraperitoneal (i.p.) doses of the anorectic ED_{50} of fluoxetine (35 μmol kg^{-1}), fluvoxamine (60 μmol kg^{-1}), paroxetine (20 μmol kg^{-1}) and sertraline (49 μmol kg^{-1}) slightly reduced brain 5-hydroxyindoleacetic acid (5-HIAA), with regional differences, this being compatible with 5-HT uptake blockade. Only fluvoxamine and sertraline significantly enhanced the content of 5-HT in the cortex.

3 The regional sensitivity to the acute effect of a given drug was not related to any preferential drug distribution, as these compounds distributed almost uniformly in the brain areas considered (cortex, striatum and hippocampus).

4 Repeating the same doses twice daily, i.p. for 14 days, however gave a different picture, fluvoxamine having little or no effect on the content of indoles and fluoxetine, paroxetine and sertraline lowering both 5-HT and 5-HIAA in all the brain regions compared to pair-fed control animals, 1 h after the last dose.

5 One week later only fluoxetine-treated animals still had reduced brain 5-HT, this probably being related to the accumulation of its main metabolite norfluoxetine in rat brain after chronic dosing.

6 Further studies on the relationship between the long-term neurochemical changes and anorectic activity are required but it appears from these results that anorectic drugs with similar acute effects on 5-HT uptake may differ in their long-term effects on 5-HT mechanisms.

Keywords: Fluoxetine; fluovoxamine; paroxetine; sertraline; anorectic drugs; brain; indoles; 5-hydroxytryptamine

Introduction

Recent studies indicate that an inhibitory 5-hydroxytryptaminergic system is involved in the control of mechanisms concerned with feeding. Accordingly many agents that increase the availability of 5-hydroxytryptamine (5-HT) show anorectic activity (Nathan & Rolland, 1987; Wong & Fuller, 1987; Garattini *et al.*, 1988; 1991; Samanin & Garattini 1990). They include several 5-HT uptake inhibitors which have proved effective in a number of experimental conditions of hyperphagia (see the above reviews) and some have also been reported to reduce body weight in man (Simpson *et al.*, 1981; Smedegaard *et al.*, 1981; Ferguson & Feighner 1987).

Consistent with an inhibition of reuptake, 5-HT uptake blockers given acutely at pharmacologically effective doses generally rapidly lower the concentrations of 5-hydroxyindoleacetic acid (5-HIAA) in whole brain or selected brain areas of rats, without appreciably affecting the levels of its precursor 5-HT (Ross *et al.*, 1981; Koe *et al.*, 1983; Schmidt *et al.*, 1988; Caccia *et al.*, 1992a).

Only fragmentary studies are available on the neurochemical effects of these drugs after repeated dosing in animals, which would allow a better assessment of the inhibition of amine uptake in relation to the therapeutic activity of the drugs. However, sertraline was reported to have no effect on 5-HIAA (and 5-HT) in selected rat brain areas after repeated administration, suggesting that its effect on 5-HT turnover is relatively short-lived (Leonard, 1988).

Fluvoxamine reduced 5-HT turnover in rat brain after short-term treatment (25 mg kg^{-1} day^{-1} × 7 days) but this effect was not apparent after three weeks of repeated dosing (5-HIAA was not measured) (Benfield & Ward, 1986).

Zimeldine, now withdrawn from the market, dose-dependently depleted both 5-HIAA and 5-HT after prolonged treatment (Ross *et al.*, 1981). Fluoxetine increased cortical 5-HT and lowered 5-HIAA when given for three days at a relatively high dose (30 mg kg^{-1}) (Sarkissian *et al.*, 1990) but reduced both indoles in cortex, hippocampus and striatum when given for longer times in the range of the anorectic ED_{50} (7.5–15 mg kg^{-1} for 7–21 days) (Caccia *et al.*, 1992b). Repeated full anorectic doses of (+)-fenfluramine, the prototype of the so called anorectic drugs which block 5-HT reuptake and enhance its release from nerve terminals, also reduce both 5-HT and 5-HIAA in animals, the effect being particularly marked and long-lasting at higher doses (Garattini *et al.*, 1988; 1991).

All these findings suggest that each 5-HT uptake inhibitor may affect 5-hydroxytryptaminergic mechanisms in rats differently, depending on its dose and treatment schedule, although a certain biochemical effect on 5-HT content and metabolism does not necessarily mean that it is essential to a functional effect such as the anorectic action. Hence our interest in comparing the acute and chronic effects on the central 5-hydroxytryptaminergic system of recently marketed 5-HT uptake inhibitors when given at anorectic doses to rats, in order to assess differences and similarities in their neurochemical behaviour.

The present study compared the effects of fluvoxamine, paroxetine and sertraline at equal anorectic doses (ED_{50}) on concentrations of 5-HT and 5-HIAA in discrete areas of the rat brain, in relation to the treatment schedule. The relationships between neurochemical effects on indole contents and the brain uptake and distribution of these drugs after acute and repeated administration of the ED_{50} were also examined. Fluoxetine was used as a reference drug for interaction with these aspects of 5-HT biochemistry.

[1] Author for correspondence.

Methods

Animals and drug treatment

Male CD-COBS rats weighing 150–175 g (Charles River, Italy) were used. Procedures involving animals and their care were conducted in conformity with the institutional guidelines that are in compliance with national and international laws and policies (EEC Council Directive 86/609, OJ L 358, 1, Dec. 12, 1987; NIH Guide for the Care and Use of Laboratory Animals, NIH Publication No. 85–23, 1985).

Fluoxetine hydrochloride (E. Lilly, Florence, Italia), fluvoxamine maleate (Unione Chimica Medicamenti, Solvay, Turin, Italia), paroxetine acetate (Ferrosan, Malmoe, Sweden) and sertraline hydrochloride (Roering Farmaceutici Italiana, Pfizer, Rome, Italy) were dissolved in deionised water and injected intraperitoneally (i.p.). In separate experiments, animals were trained to eat their daily ration in 4 h.

On the day of the experiment the test drugs were injected i.p. and food was made available after 30 min. The amount of food eaten during the next 60 min was measured, as described before (Garattini *et al.*, 1991; Caccia *et al.*, 1992a; Anelli *et al.*, 1992).

The ED_{50} (± 95% confidence limits), calculated on five drug doses with four rats per group at each dose, according to the method of De Lean *et al.* (1978) adapted to a Macintosh computer (V. Guardabasso, personal communication) were 34.7 (± 14.9) μmol kg^{-1} (12.0 mg kg^{-1}) for fluoxetine; 59.9 (± 37.8) μmol kg^{-1} (22.2 mg kg^{-1}) for fluvoxamine, 20.4 (± 5.7) μmol kg^{-1} (7.9 mg kg^{-1}) for paroxetine and 48.7 (± 25.4) μmol kg^{-1} (16.7 mg kg^{-1}) for sertraline. These doses were then given to other groups of rats which were killed by decapitation 60 min thereafter for determination of the indole content and drug concentrations in selected brain areas (cortex, hippocampus and striatum).

Finally in other studies, the animals received i.p. injections of either vehicle or the test drug at approximately 12-h intervals for 14 days and were killed 60 min or 7 days after the last dose; the brains were immediately removed, as described above.

Since repeated treatment with 5-HT uptake inhibitors may reduce food intake (Wong & Fuller, 1987), the control animals were 'pair-fed'. i.e. the amount of food treated animals ate was measured each day and given to controls the next day. According to this schedule, pair-fed animals started with the vehicle one day later than the test drug groups.

Chemical analysis

Concentrations of 5-HT, 5-HIAA, noradrenaline (NA), dopamine and its acidic metabolites homovanillic acid (HVA) and dihydroxyphenylacetic acid (DOPAC) in brain areas were measured by high-performance liquid chromatography (h.p.l.c.) with electrochemical detection based on the method described by Achilli *et al.* (1985).

Plasma and brain concentrations of fluoxetine and sertraline and their nor-derivatives nor-fluoxetine and nor-sertraline were determined as described respectively by Caccia *et al.* (1990) and Tremaine *et al.* (1989). Fluvoxamine was extracted from plasma and brain homogenate (acetone-formic acid 85:15, v/v, as for fluoxetine), after adding fluoxetine as internal standard, and quantified by h.p.l.c. with ultraviolet detection (u.v.) as described by Foglia *et al.* (1989), with minor modifications (i.e. the chromatographic column was a μBondapack C_{18}, 30 cm × 3.9 mm i.d., particle size 10 μm, Waters Assoc., maintained at room temperature). With these experimental conditions, approximate retention times were 10 min for fluvoxamine and 15 min for fluoxetine. The limit of detection, precision and reproducibility in plasma were similar to those reported by Foglia *et al.* (1989). The limit of detection in brain was 250 ng g^{-1} (about 0.8 nmol g^{-1}), using approximately 0.1 g of brain tissue. At this concentration the coefficient of variation (C.V.) was 13% ($n = 4$) and all higher concentrations gave C.V. less than 10%.

Paroxetine was extracted from plasma and brain homogenate as above and quantified by h.p.l.c. with u.v. detection at 240 nm. The analytical column was as for fluvoxamine but the mobile phase was 0.01 M KH_2PO_4-CH_3CN-CH_3OH (60:35:5) buffered to pH 3 with H_3PO_4, delivered isocratically at a flow-rate of 1 ml min^{-1}. Under these conditions, approximate retention times were 13 min for paroxetine and 22 min for fluoxetine (internal standard). The limit of detection was 25 ng ml^{-1} or 250 ng g^{-1}, using 1 ml of plasma or approximately 100 mg of tissue, and the C.V. were generally below 10% for identical samples containing 25–100 ng ml^{-1} or 250–2000 ng g^{-1} (i.e. the range of the calibration graphs for plasma and brain analysis, respectively).

Statistical analysis

Statistical analysis was done by one-way analysis of variance or two-way analysis of variance (when examining the effects of two factors, the brain areas and treatment schedule) and probabilities (P) less than 0.05 were considered statistically significant.

Results

Table 1 shows the effect of equiactive anorectic doses of fluoxetine, fluvoxamine, paroxetine and sertraline on the regional content of indoles 1 h after a single dose. Fluoxetine and paroxetine slightly lowered 5-HIAA in cortex (by

Table 1 Concentrations of indoles after equi-active anorectic doses (ED_{50}) of fluoxetine, fluvoxamine, paroxetine and sertraline to male rats

Drug[a]	*ED_{50}* (μmol kg^{-1}, i.p.)	*Brain area*	*Content (% of control)* 5-HT	5-HIAA
Fluoxetine	35	Cortex	95 ± 12	76 ± 7**
		Hippocampus	95 ± 8	83 ± 14*
		Striatum	106 ± 13	87 ± 16
Fluvoxamine	60	Cortex	120 ± 7**	68 ± 7**
		Hippocampus	107 ± 19	77 ± 11*
		Striatum	104 ± 13	74 ± 4*
Paroxetine	20	Cortex	102 ± 11	83 ± 14*
		Hippocampus	102 ± 19	94 ± 19
		Straitum	110 ± 11	85 ± 14
Sertraline	49	Cortex	116 ± 9*	80 ± 14*
		Hippocampus	111 ± 17	76 ± 10*
		Striatum	100 ± 13	80 ± 7*

[a]Results are means ± s.d. of 5 animals.
**$P < 0.01$; *$P < 0.05$ compared to vehicle.

approximately 20% compared to the $0.26 \pm 0.04\ \mu g\ g^{-1}$ 5-HIAA content of controls) with smaller or no effects (paroxetine) in hippocampus (controls $0.46 \pm 0.04\ \mu g\ g^{-1}$) and striatum (controls $0.51 \pm 0.08\ \mu g\ g^{-1}$); fluvoxamine and sertraline caused comparable reductions in all the brain regions examined. Brain 5-HT increased significantly only in the cortex of fluvoxamine- (0.53 ± 0.03 vs $0.43 \pm 0.03\ \mu g\ g^{-1}$) and sertraline-treated rats (0.51 ± 0.04 vs $0.43 \pm 0.03\ \mu g\ g^{-1}$). Cortical and hippocampal NA, striatal and cortical dopamine and striatal HVA and DOPAC were not affected 60 min after these doses of fluoxetine, fluvoxamine, paroxetine and sertraline (data not shown).

Twice-daily doses of fluoxetine, fluvoxamine, paroxetine and sertraline for 14 days slightly slowed the gain in body weight because food intake was reduced compared to controls, as expected. Final body weight averaged respectively 209 ± 12 g, 231 ± 5, 240 ± 4 g and 244 ± 15 g in the groups treated with fluoxetine, fluvoxamine, paroxetine and sertraline, being 77–85% of that of the respective vehicle-treated groups (275–293 g). Food intake in the pair-fed control animals mimicked that of the drug-treated groups (with a delay of one day) over the period of drug administration and their final body weights (227 ± 10, 235 ± 14, 242 ± 14 and 257 ± 15 g for the pair-fed controls of fluoxetine, fluvoxamine, paroxetine and sertraline respectively) were comparable to the drug-treated group.

The content of indoles in the cortex, hippocampus and striatum, 1 h after the last dose of the 14-day regimen of fluoxetine, fluvoxamine and paroxetine are set out in Table 2. Daily fluoxetine markedly reduced the brain content of 5-HT and 5-HIAA (30–60% reduction, depending on the indole and the brain region examined), compared to pair-fed control animals. This effect was shared by paroxetine (pair-fed control values 0.39 ± 0.02, 0.21 ± 0.04 and $0.30 \pm 0.06\ \mu g\ g^{-1}$ and 0.22 ± 0.02, 0.26 ± 0.05 $0.51 \pm 0.13\ \mu g\ g^{-1}$ for 5-HT and 5-HIAA in cortex, hippocampus and striatum respectively) and sertraline (pair-fed control values $0.40 \pm 0.02\ \mu g\ g^{-1}$, 0.21 ± 0.04 and $0.28 \pm 0.06\ \mu g\ g^{-1}$ and 0.22 ± 0.02, 0.26 ± 0.05, $0.51 \pm 0.13\ \mu g\ g^{-1}$, respectively) but not by fluvoxamine which tended to reduce only 5-HIAA in the cortex (0.17 ± 0.01 vs $0.23 \pm 0.05\ \mu g\ g^{-1}$). Concentrations of NA in cortex and hippocampus and dopamine and its metabolites DOPAC and HVA were not affected by the 14-day twice daily regimen of the four compounds, as after the single doses (data not shown).

The distribution of these drugs in cortex, hippocampus and striatum 1 h after the first and last injection of the ED_{50} is illustrated in Table 3. The 'anorectic' brain concentrations differed for the various compounds but fluvoxamine, paroxetine and sertraline distributed almost uniformly in the brain areas considered ($P > 0.05$, two-way analysis of variance), as previously reported for fluoxetine (Caccia *et al.*, 1990; 1992a). They all concentrated in brain tissues, achieving mean brain-to-plasma ratios ranging from 32–39 for fluvoxamine, 8–13 for paroxetine, and 70–80 for sertraline (80–90 for norsertraline) at the end of the 14-day regimen, when presumably pseudo-equilibrium between plasma and brain was achieved for all compounds.

Table 2 Content of indoles in cortex, hippocampus and striatum after repeated anorectic doses of fluoxetine, fluvoxamine, paroxetine and sertraline

Drug ($\mu mol\ kg^{-1}$; twice daily)	*Brain area*	*Content (% of control) of:* 5-HT	5-HIAA
Fluoxetine	Cortex	47 ± 13**	34 ± 6**
(35)	Hippocampus	39 ± 8**	39 ± 5**
	Striatum	69 ± 12**	46 ± 10**
Fluvoxamine	Cortex	99 ± 11	73 ± 5*
(60)	Hippocampus	94 ± 11	96 ± 13
	Striatum	110 ± 14	93 ± 7
Paroxetine	Cortex	55 ± 7**	61 ± 11**
(20)	Hippocampus	49 ± 10**	40 ± 5**
	Striatum	53 ± 11**	48 ± 10**
Sertraline	Cortex	80 ± 6**	60 ± 5**
(49)	Hippocampus	86 ± 6**	62 ± 8**
	Striatum	84 ± 11**	70 ± 8**

Drugs were injected intraperitoneally at approx 12 h intervals for 14 days. Assays were done 1 h after the last dose. Results are presented as percentage of the pair-fed control ($n = 5$). $^{**}P < 0.01$; $^{*}P < 0.05$ vs pair-fed control.

Table 3 Drug concentrations in brain areas after single and repeated anorectic doses of fluoxetine, fluvoxamine paroxetine and sertraline to male rats

Drug	($\mu mol\ kg^{-1} \times$ days)	*Drug concentration* (nmol g^{-1}) *Cortex*	*Hippocampus*	*Striatum*
Fluoxetine[a]	35 × 1	36 ± 13	38 ± 13	40 ± 14
		(14 ± 5)	(13 ± 7)	(16 ± 4)
	35, b.i.d., × 14	97 ± 17**	94 ± 14**	100 ± 28**
		(318 ± 35)**	(312 ± 56)**	(324 ± 64)**
Fluvoxamine	60 × 1	47 ± 18	45 ± 21	50 ± 23
	60, b.i.d., × 14	74 ± 31	72 ± 24	65 ± 34
Paroxetine	20 × 1	13 ± 2	13 ± 2	16 ± 5
	20, b.i.d., × 14	23 ± 9	20 ± 7	28 ± 15
Sertraline[a]	49 × 1	98 ± 26	74 ± 21	80 ± 18
		(16 ± 5)	(14 ± 2)	(15 ± 5)
	49, b.i.d., × 14	77 ± 29	68 ± 9	71 ± 18
		(49 ± 11)**	(45 ± 13)**	(44 ± 18)**

[a]Brain concentrations of the active nor-metabolite nor-fluoxetine and nor-sertraline are shown in parentheses.
Each value is the mean ± s.d. of five rats. The determinations were made 60 min after the last dose.
$^{**}P < 0.01$; $^{*}P < 0.05$ compared to acute dosing.

After repeated sertraline the mean plasma (data not shown) and brain concentrations of unchanged drug tended to decrease ($P>0.05$) and those if its metabolite nor-sertraline increased ($P<0.05$), changing the metabolite-to-parent drug ratio in all brain regions compared to the acute dosing (0.6 vs 0.2). Although repeated treatment with fluvoxamine and paroxetine gave slightly higher mean plasma and brain concentrations than single doses in all tissues, the difference did not reach significance based on two-way analysis of variance ($P>0.05$). In contrast, repeated doses of fluoxetine led to marked accumulation of the unchanged compound and its metabolite nor-fluoxetine in rat plasma and brain compared to acute dosing ($P<0.05$) (Table 3).

Finally, additional groups of rats were given the anorectic ED_{50} of fluoxetine, paroxetine and sertraline or the vehicle twice daily for 14 days and were killed a week after the last doses for the measurement of the drug and indole concentrations in the brain. Fluvoxamine was not included in these studies because it has negligible effect on brain indole concentrations 1 h after the last dose (anorectic ED_{50}).

As shown in Table 4, the content of 5-HT in cortex and hippocampus (and other brain areas, data not shown) was still reduced by approximately 20–30% one week after fluoxetine (pair-fed controls 0.27 ± 0.02 and $0.35 \pm 0.04\ \mu g\ g^{-1}$ for cortex and hippocampus) but not after paroxetine and sertraline. 5-HIAA was unchanged or even tended to be higher than the pair-fed control values (fluoxetine and paroxetine), although the differences did not always reach significance, probably because of the wide variability. By one week the drugs were undetectable in rat brain within the limits of sensitivity of the h.p.l.c. procedures. However, about $1\ nmol\ g^{-1}$ of the active metabolite of fluoxetine, norfluoxetine, were still detected in the cortex and hippocampus of fluoxetine-treated rats.

Discussion

In agreement with previous pharmacological observations on 5-HT uptake blockers (Nathan & Rolland, 1987; Wong & Fuller, 1987; Samanin & Garattini, 1990; Garattini *et al.*, 1988; 1991) fluoxetine, fluvoxamine, paroxetine and sertraline showed dose-dependent anorectic activity in overnight food-deprived rats. On a molar dose basis, and taking into account the i.p. ED_{50}, paroxetine ($20\ \mu mol\ kg^{-1}$) was slightly more active than fluoxetine ($35\ \mu mol\ kg^{-1}$) and sertraline ($49\ \mu mol\ kg^{-1}$) which in turn were slightly more active than fluvoxamine ($60\ \mu mol\ kg^{-1}$) in this acute test in rats. These ED_{50} for anorexia are 2–5 times those inhibiting [^{3}H]-5-HT uptake *ex vivo*, with the exception of fluoxetine which shows comparable efficacy in inhibiting 5-HT uptake and causing anorexia (ED_{50} about $30\ \mu mol\ kg^{-1}$) (Leonard, 1988; Johnson, 1989).

Paroxetine was also the most active compound in terms of the brain concentrations necessary to achieve an anorectic effect (10–20 μM) in rats, with sertraline giving the highest (70–100 μM) and fluvoxamine and fluoxetine intermediate 'anorectic' brain concentrations (40–50 μM), at the middle of the food intake period. Attempts to correlate brain concentrations with the *in vitro* potency in inhibiting 5-HT uptake (see Dechant & Clissold, 1991; Murdoch & McTavish, 1992 for a comparison of the relative potency) are unfortunately limited by the fact that fluoxetine and sertraline are biotransformed by hepatic N-dealkylation to the nor-derivatives norfluoxetine and nor-sertraline (Schmidt *et al.*, 1988; Tremaine *et al.*, 1989) and these fully retain the parent drug's anorectic activity in animals despite their lower efficacy in inhibiting 5-HT reuptake (Garattini *et al.*, 1991; Caccia *et al.*, 1992a; Anelli *et al.*, 1992). However, metabolites of fluvoxamine and paroxetine do not appear to have significant uptake inhibiting properties *in vitro* in animals (Benfield & Ward, 1986; Dechant & Clissold, 1991), although their activity in relation to 5-HT mechanisms other than uptake inhibition, and to the anorectic action, is still unknown.

Interestingly, brain concentrations of all these drugs (and their known active metabolites) are several hundred times the IC_{50} for inhibiting 5-HT uptake *in vitro* (ranging from 0.1–0.5 μM for fluoxetine to less than 0.01 μM for paroxetine) (Benfield & Ward, 1986; Leonard, 1988; Garattini *et al.*, 1991; Caccia *et al.*, 1992a), making it unlikely that they reduce food intake in rats by specifically blocking 5-HT neuronal uptake. Evidence now exists that fluoxetine, sertraline and their nor-derivatives (Garattini *et al.*, 1991) and paroxetine (T. Mennini, personal communication) can all release 5-HT from synaptosomes *in vitro* besides inhibiting 5-HT uptake. Fluoxetine (Gobbi *et al.*, 1992), sertraline and their active metabolites (T. Mennini, personal communication) induce tritium release from synaptosomes preloaded with [^{3}H]-5-HT, through a mechanism different from that of (+)-fenfluramine. The concentrations active on 5-HT release are in the same range as those reached after anorectic doses, suggesting another potential mechanism of action.

The neurochemical results of the present study confirm and extend previous findings on the effects of 5-HT uptake inhibitors on the content of indoles in rat brain. Acute treatment with anorectic doses of all these compounds typically reduces the content of 5-HIAA, although to different degrees and with regional differences in sensitivity. Fluvoxamine and sertraline, however, also tended to increase brain 5-HT, with regional differences again, an effect not shared by the other 5-HT uptake inhibitors mentioned, at least at doses in the range of anorectic activity. These findings also indicate that the regional sensitivity to the acute effect of a given drug was not due to differences in distribution as 5-HT uptake inhibitors distributed almost uniformly in the brain regions examined after either single or repeated doses.

After repeated doses of these compounds, however, the interaction with the 5-hydroxtryptaminergic system was different from after single doses. Fluvoxamine caused only a slight fall in the cortical content of 5-HIAA without appreciably affecting 5-HT. This was not related to any pharma-

Table 4 The effects of repeated administration of fluoxetine, paroxetine and sertraline on the content of indoles in cortex and hippocampus, 1 week after the last dose

Treatment ($\mu mol\ kg^{-1}$, twice daily)	*Brain area*	*Indole content* (% of control) *5-HT*	*5-HIAA*	*Drug concentration* ($nmol\ g^{-1}$)
Fluoxetine (35)	Cortex	75 ± 5**	127 ± 35	ND (0.9 ± 0.2)[a]
	Hippocampus	82 ± 9*	124 ± 11*	ND (1.2 ± 0.5)[a]
Paroxetine (20)	Cortex	106 ± 10	131 ± 36	ND
	Hippocampus	99 ± 14	106 ± 14	ND
Sertraline (49)	Cortex	97 ± 9	106 ± 12	ND (ND)[a]
	Hippocampus	99 ± 8	105 ± 9	ND (ND)[a]

Drugs were injected at the dose indicated, twice daily for 14 days. Each value is the mean ± s.d. of five animals.
(ND) = Below the level of quantitation ([a]brain concentrations of the nor-metabolite).
**$P<0.01$; *$P<0.05$ vs pair-fed control.

cokinetic tolerance because the drug concentrations were, if anything, slightly higher in animals given the repeated schedule.

By contrast, paroxetine and sertraline caused pronounced decreases in the brain content of both 5-HT and 5-HIAA, as already known for fluoxetine (Caccia *et al.*, 1992b). Unlike fluoxetine, paroxetine accumulated only slightly in the brain with this schedule of repeated administration so the variations found should be mainly related to the different treatment schedule, as in the case of fluvoxamine. Brain concentrations of the active metabolite of sertraline, norsertraline, differed after repeated and acute dosing. In this case, therefore, the different neurochemical effects of acute and repeated sertraline may depend partly on kinetic factors leading to different metabolite-to-parent drug ratios at the site of action.

Sertraline and paroxetine, however, had no significant long-term effects in rat brain, indicating that their depleting effects on 5-HT content and metabolism are short-lasting. Fluoxetine on the other hand reduced 5-HT for at least a week after the last dose, although the content of 5-HIAA recovered fully or even tended to overshoot.

Kinetic factors may be partly responsible for these differences because at that time paroxetine, sertraline and its metabolite norsertraline were no longer measurable in rat brain whereas the active nor-metabolite of fluoxetine was still detectable. This is in agreement with previous findings of a progressive dose-related accumulation of the parent compound and particularly of nor-fluoxetine in rats, possibly due to saturation of their clearance mechanisms on repeated dosing (Caccia *et al.*, 1992b).

In conclusion, drugs belonging to the well-defined class of 5-HT uptake inhibitors, when employed at repeated anorectic doses, have different effects on the levels of 5-HT and 5-HIAA in various brain areas making them a heterogeneous group of drugs. This implies that other mechanisms than just the inhibition of 5-HT uptake are probably operative in reducing food intake.

M.A. is the recipient of a fellowship from Centrobanca di Milano, Italy. The skilful technical assistance of Miss Alessandra Bergami is acknowledged. This study was supported by Consiglio Nazionale delle Ricerche, Rome, Convenzione Psicofarmacologia.

References

ARCHILLI, G., PEREGO, C. & PONZIO, F. (1985). Application of the dual-cell coulometric detector: a method for assaying monoamines and their metabolites. *Anal. Biochem.*, **148**, 1–9.

ANELLI, M., BIZZI, A., CACCIA, S., CODEGONI, A.M. FRACASSO, C. & GARATTINI, S. (1992). Anorectic activity of fluoxetine and norfluoxetine in mice, rats and guinea-pigs. *J. Pharm. Pharmacol.*, **44**, 696–698.

BENFIELD, T. & WARD, A. (1986). Fluvoxamine. A review of its pharmacodynamic and pharmacokinetic properties, and therapeutic efficacy in depressive illness. *Drug*, **32**, 313–334.

CACCIA, S., BIZZI, A., COLTRO, G., FRACASSO, C., FRITTOLI, E., MENNINI, T. & GARATTINI, S. (1992a). Anorectic activity of fluoxetine and norfluoxetine in rats: relationship between brain concentrations and in-vitro potencies on monoaminergic mechanisms. *J. Pharm. Pharmacol.*, **44**, 250–254.

CACCIA, S., CAPPI, M., FRACASSO, C. & GARATTINI, S. (1990). Influence of dose and route of administration on the kinetics of fluoxetine and its metabolite norfluoxetine in the rat. *Psychopharmacology* (Berl), **100**, 509–514.

CACCIA, S., FRACASSO, C., GARATTINI, S., GUISO, G. & SARATI, S. (1992b). Effects of short- and long-term administration of fluoxetine on the monoamine content of rat brain. *Neuropharmacology*, **31**, 343–347.

DECHANT, K.L. & CLISSOLD, S.P. (1991). Paroxetine. A review of its pharmacodynamic and pharmacokinetic properties, and therapeutic potential in depressive illness. *Drugs*, **41**, 225–253.

DELEAN, A., MUNSON, P.J. & RODBARD, D. (1978). Simultaneous analysis of families of sigmoidal curves: application to bioassay, radioligand assay, and physiological dose-response curves. *Am. J. Physiol.*, **235**, E97–E102.

FERGUSON, J.M. & FEIGHNER, J.P. (1987). Fluoxetine-induced weight loss in overweight non-depressed humans. *Int. J. Obes.*, **11**, Suppl. 3, 163–170.

FOGLIA, J.P., BIRDER, L.A. & PEREL, J.M. (1989). Determination of fluvoxamine in human plasma by high-performance liquid chromatography with ultraviolet detection. *J. Chromatogr.*, **495**, 295–302.

GARATTINI, S., BIZZI, A., CACCIA, S., MENNINI, T. & SAMANIN, R. (1988). Progress in assessing the role of serotonin in the control of food intake. *Clin. Neuropharmacol.*, **11**, Suppl. 1, S8–S32.

GARATTINI, S., CACCIA, S., MENNINI, T. & SAMANIN, R. (1991). Progress report on drugs inducing anorexia by affecting brain serotonin. In *Obesity and Cachexia: Physiological Mechanisms and New Approaches to Pharmacological Control.* ed. Rothwell, N.J. & Stock, M.J. pp. 227–240. Chichester: Wiley.

GOBBI, M., FRITTOLI, E., MENNINI, T. & GARATTINI, S. (1992). Releasing activities of d-fenfluramine and fluoxetine on rat hippocampal synaptosomes preloaded with [^{3}H]serotonin. *Naunyn Schmied. Arch. Pharmacol.*, **345**, 1–6.

JOHNSON, A.M. (1989). An overview of the animal pharmacology of paroxetine. *Acta Psychiatr. Scand.*, **80**, Suppl. 350, 14–20.

KOE, B.K., WEISSMAN, A., WELCH, W.M. & BROWNE, R.G. (1983). Sertraline, 1S, 4S-N-methyl-4-(3,4-dichlorophenyl)-1,2,3,4-tetrahydro-1-naphtylamine, a new uptake inhibitor with selectivity for serotonin. *J. Pharmacol. Exp. Ther.*, **226**, 686–700.

LEONARD, B.E. (1988). Pharmacological effects of serotonin reuptake inhibitors. *J. Clin. Psychiatry*, **49**, Suppl., 12–17.

MURDOCH, D. & MCTAVISH, D. (1992). Sertraline. A review of its pharmacodynamic and pharmacokinetic properties, and therapeutic potential in depression and obsessive-compulsive disorder. *Drugs*, **44**, 604–624.

NATHAN, C. & ROLLAND, Y. (1987). Pharmacological treatments that affect CNS activity: serotonin. *Ann. N.Y. Acad. Sci.*, **499**, 277–296.

ROSS, S.B., HALL, H., RENYI, A.L. & WESTERLUND, D. (1981). Effects of zimelidine on serotoninergic and noradrenergic neurons after repeated administration in the rat. *Psychopharmacology* (Berl), **72**, 219–225.

SAMANIN, R. & GARATTINI, S. (1990). The pharmacology of serotoninergic drugs affecting appetite. In *Nutrition and the Brain*, ed. Wurtman, R.J. & Wurtman, J.J. pp. 163–192. New York: Raven Press.

SARKISSIAN, C.F., WURTMAN, R.J., MORSE, A.N. & GLEASON, R. (1990). Effect of fluoxetine or D-fenfluramine on serotonin release from, and levels in, rat frontal cortex. *Brain Res.*, **529**, 294–301.

SCHMIDT, M.J., FULLER, R.W. & WONG, D.T. (1988). Fluoxetine, a highly selective serotinin reuptake inhibitor: a review of preclinical studies. *Br. J. Psychiatry*, **153**, Suppl. 3, 40–46.

SIMPSON, R.J., LAWTON, D.J., WATT, M.H. & TIPLADY, B. (1981). Effect of zimelidine, a new antidepressant, on appetite and body weight. *Br. J. Clin. Pharmacol.*, **11**, 96–98.

SMEDEGAARD, J., CHRISTIANSEN, P. & SKRUMSAGER, B. (1981). Treatment of obesity by femoxetine a selective 5 HT reuptake inhibitor. *Int. J. Obes.*, **5**, 377–378.

TREMAINE, L.M., WELCH, W.M. & RONFELD, R.A. (1989). Metabolism and disposition of the 5-hydroxytryptamine uptake blocker sertraline in the rat and dog. *Drug. Metab. Dispos.*, **17**, 542–550.

WONG, D.T. & FULLER, R.W. (1987). Serotonergic mechanisms in feeding. *Int. J. Obes.*, **11**, Suppl. 3, 125–133.

(Received March 5, 1993
Revised April 21, 1993
Accepted April 22, 1993)

Br. J. Pharmacol. (1993), **110**, 360–368

Comparison of contractile responses to 5-hydroxytryptamine and sumatriptan in human isolated coronary artery: synergy with the thromboxane A_2-receptor agonist, U46619

[1]T.M. Cocks, B.K. Kemp, [2]D. Pruneau & J.A. Angus

Baker Medical Research Institute, Melbourne, Victoria 3181, Australia

1 The interaction between the thromboxane A_2 receptor agonist, U46619 and two 5-hydroxytryptamine (5-HT) receptor agonists, the non-selective, naturally occurring agonist, 5-HT and the selective 5-HT_1-like agonist, sumatriptan were studied in human epicardial coronary arteries *in vitro*.

2 Coronary artery rings (2–4 mm in diameter) were prepared from epicardial arteries from explant hearts of patients undergoing heart transplant (cardiomyopathy, $n = 13$; ischaemic heart disease, $n = 10$) and unused donor hearts ($n = 5$). Each ring of artery was set at optimal resting conditions to record changes in isometric force.

3 The majority of artery rings developed phasic, rhythmic contractions either spontaneously or in response to all vasoconstrictor agonists tested. Both the spontaneous and agonist-induced phasic contractions were abolished by nifedipine (0.1 μM).

4 Concentration-contraction curves to 5-HT-receptor agonists and noradrenaline (NA), were first constructed in artery rings that did not develop phasic activity. 5-HT and ergometrine were the most potent agonists with EC_{50} values of 6.8 ± 0.2 and 7.7 ± 0.2 ($-\log$ M) respectively. Potencies (EC_{50}'s) to sumatriptan, methysergide and noradrenaline could not be determined due to their poor ability to contract the coronary artery. Maximum contractions (E_{max}; normalized as a percentage of the contraction to a maximum-depolarizing concentration of K^+ in physiological salt solution (KPSS)) for 5-HT, ergometrine, sumatriptan, methysergide and noradrenaline were 40 ± 10, 9 ± 3, <5, <5 and $<5\%$ respectively.

5 In arteries without phasic activity, U46619 (1 nM) caused an increase in force of $3.8 \pm 1\%$ KPSS. With U46619 present, the E_{max} values for 5-HT, ergometrine, sumatriptan and methysergide were all markedly increased. For 5-HT and sumatriptan, E_{max} values were $92 \pm 4\%$ and $49 \pm 14\%$ KPSS respectively. The presence of U46619 did not significantly change the sensitivity (EC_{50}) to 5-HT.

6 In a separate series of arteries, nifedipine (0.1 μM) was used to block phasic, contractile activity. The synergy observed between U46619 and 5-HT or sumatriptan still occurred although the E_{max} values for each agonist were depressed but the EC_{50} values were again unaffected.

7 In conclusion, these *in vitro* studies indicate that the normally poor contractions to sumatriptan, in human coronary arteries are significantly enhanced when active force is induced with a thromboxane A_2-receptor agonist, U46619. The enhanced response is not specific for either sumatriptan or 5-HT_1-like receptors since contractions to 5-HT, ergometrine and methysergide were also potentiated by U46619.

Keywords: Human coronary artery; sumatriptan; thromboxane A_2; 5-hydroxytryptamine; synergy

Introduction

Sumatriptan (GR43175), first characterized as a selective 5-HT_1-like receptor agonist (see Bradley *et al.*, 1986; Van Heuven-Nolsen, 1988) in the contraction assay of dog saphenous vein (Humphrey *et al.*, 1988), has been developed as a treatment for migraine (Humphrey *et al.*, 1990 and see Perrin *et al.*, 1989; Ferrari *et al.*, 1991). Whilst the precise mechanism by which sumatriptan relieves migraine is unknown, it may involve stimulation of a population of 5-HT_1-like receptors located on intracerebral vessels. During a migrainous headache, distension, oedema and extravasation of the intracranial vessels occurs partly due to the nociceptive impulses from the Vth cranial nerve. Sumatriptan may constrict these vessels, therefore reducing the release of the inflammatory mediators or it may have a separate action on neuropeptide release from sensory nerve terminals (Humphrey & Feniuk, 1991; Moskowitz, 1992). In other vasculature studied, sumatriptan has been shown to constrict cranial arteriovenous anastomoses (AVA shunts) of anaesthetized cats (Feniuk *et al.*, 1987; Perren *et al.*, 1989) and pigs (den Boer *et al.*, 1990), constrict the carotid arterial bed of the anaesthetized dog (Brittain *et al.*, 1987; Feniuk *et al.*, 1989a), cause a small dilatation of the coronary vasculature in the anaesthetized dog (Feniuk *et al.*, 1989b), contract human (Parsons *et al.*, 1989), canine and primate (Connor *et al.*, 1989a) basilar arteries and cause a general lack of contraction of peripheral arteries in man (Nielsen & Tfelt-Hansen, 1989).

Sumatriptan contracts human isolated large coronary arteries via 5-HT_1-like receptors (Chester *et al.*, 1990). However, these arteries are thought to possess only few 5-HT_1-like receptors since compared with 5-HT, the contractions to sumatriptan are poor (Connor *et al.*, 1989b; Chester *et al.*, 1990). Also, contractions to 5-HT in this tissue were found to be substantially antagonized by the selective 5-HT_2-receptor antagonist, ketanserin (Connor *et al.*, 1989b; Toda & Okamura, 1990). Furthermore, *in vivo* evidence in man to support this came from a clinical study by Golino *et al.* (1991). They found that ketanserin blocked completely both the decrease in large coronary diameter and the increase in flow to the distal bed to intracoronary infusions of 5-HT in patients with and without angiographic evidence of atherosclerosis. In a similar study, however, McFadden *et al.* (1991) included patients with Prinzmetal's angina (diagnosed previously by intracoronary challenge with ergometrine (ergonovine)) and

[1] Author for correspondence.
[2] Present address: Centre de Recherches, Laboratoires Fournier, 50 rue de Dijon 2112, Fontaine-les-Dijon, France

found that intracoronary infusions of 5-HT caused spasm (zero flow) which was resistant to ketanserin (McFadden *et al.*, 1992). Ketanserin does not prevent either ergometrine-induced ischaemia (Freedman *et al.*, 1984) or spontaneous attacks of variant angina (De Caterina *et al.*, 1984) in man and although ergometrine activates many different types of receptors including α-adrenoceptors (Feniuk *et al.*, 1989b), both it (Muller-Schweinitzer, 1980; Sakanashi & Yonemura, 1980; Brazenor & Angus, 1981; Holtz *et al.*, 1982), and the antimigraine drug methysergide (Saxena, 1974; Brazenor & Angus, 1981), cause contractions via receptors other than α-adrenoceptors. Thus, in the dog isolated coronary artery, ergometrine was found to be a potent agonist at unspecified 5-HT receptors (Brazenor & Angus, 1981) whilst in the rabbit saphenous vein, ergometrine was demonstrated to be a potent 5-HT_1-like receptor agonist (MacLennan & Martin, 1990). Also, Kawachi *et al.* (1984), found selective hyperreactivity to ergometrine in canine coronary arteries *in vivo* with intimal thickening induced by balloon catheter denudation followed by high cholesterol diet. In addition, Egashira *et al.* (1992) found that ergometrine mediated hyperconstriction of endothelium-denuded coronary arteries in the conscious dog was resistant to block by ketanserin, prazosin and indomethacin and suggested that non-5-HT_2 receptors may play a role in ergometrine-induced hyperconstriction.

In the present study, we compared the concentration-contraction curves to 5-HT and sumatriptan in the presence and absence of another vasoconstrictor agent, the thromboxane A_2-receptor agonist, U46619. This agent was chosen for three reasons. First, since conditions of organ bath experiments are necessarily devoid of blood and extrinsic factors such as circulating hormones and neural control, addition of one putative factor (U46619) in a concentration-controlled manner may in part resemble conditions within the artery wall *in vivo* and thus influence contractility of other vasoconstrictor agents (Angus, 1989). Second, thromboxane A_2 and 5-HT are released from aggregating platelets and intracoronary thrombus formation has been shown to result in focal vasoconstriction in patients with coronary artery disease (Zeiher *et al.*, 1991b). Finally, MacLennan & Martin (1992) showed marked synergy between U46619 and 5-HT contractile responses in the rabbit femoral artery with evidence that 5-HT_1-like rather than 5-HT_2 receptors were involved. Our results show that the normally poor contractions to the selective 5-HT_1-like agonist sumatriptan and the non-selective agonist 5-HT in human, isolated, coronary arteries, are markedly enhanced in the presence of U46619 which is in close agreement with the findings of MacLennan & Martin (1992) in the rabbit femoral artery.

Methods

Tissue source

Human large coronary arteries were obtained from 28 hearts, 23 of which were from patients undergoing heart transplantation and 5 unused normal donor hearts (3 from patients undergoing heart-lung transplants for cystic fibrosis and primary pulmonary hypertension). The diseased hearts were obtained from patients diagnosed with cardiomyopathy (13 patients) and ischaemic heart disease (10 patients).

Artery preparation

Approximately 10–20 min after removal of the heart, the large distal right coronary artery, left anterior descending artery, circumflex artery and the first branches of these vessels were dissected free of adhering connective tissue and fat and placed in cold, oxygenated Krebs solution (see below). After dissection, arteries were cut into 3 mm ring segments with a fixed double-bladed scapel. Ring segments were suspended on stainless steel wire hooks, 500 or 350 μm in diameter, in 25 ml jacketed glass organ baths. The upper wire hook was suspended from a force transducer (Grass FT03C) via which isometric force was amplified and monitored on a single-channel, flat-bed chart recorder. The lower hook was fixed to an inert support leg attached to a micrometer. The tissues were maintained in modified Krebs solution of the following composition (in mM): Na^+ 144, K^+ 5.9, Ca^{2+} 2.5, Mg^{2+} 1.2, Cl^- 128.7, HCO_3^- 25, SO_4^{2-} 1.2, glucose 11, pH 7.4, at 37 ± 0.1°C and saturated with 5% CO_2 in oxygen. Up to 30 rings from the same heart were set up simultaneously.

Normalization

In order to compare the reactivity of arteries with different internal diameters, each ring segment was set to the same passive stretch conditions by a normalization procedure prior to construction of concentration-response curves. The normalization procedure was adapted from that developed by Mulvany & Halpern (1977) and involves setting the arteries at a passive tension equivalent to 90% of their internal circumference (0.9 L_{100}) if they had been relaxed and perfused with a transmural pressure of 100 mmHg in the absence of constrictor tone. This wall tension (T) (at 0.9 L_{100}) can be used to estimate the equivalent transmural pressure (P) assuming a thin walled sphere from Laplace, $T = r.P$ where radius (r) is circumference $(L)/2\pi$. P is a useful measure of whether the arteries of different size have been normalized to similar equivalent distending pressures. The procedure has been described previously (Angus *et al.*, 1986). During the normalization stretch procedure, some coronary artery rings developed spontaneous contractions, making normalization difficult (see Figure 1). Consequently, sodium nitroprusside (SNP; 10 μM) was added 5 min prior to normalization to reduce this activity. SNP was washed out once the tissues had been normalized at 0.9 L_{100}.

Experimental protocols

Two experimental protocols were followed. Initially, artery rings were normalized and left resting at 0.9 L_{100} for 1 h before they were contracted with a potassium depolarizing solution (potassium physiological salt solution, KPSS, 124 mM K^+). Once the contraction to KPSS had plateaued, the tissues were washed with normal Krebs solutions and the force allowed to return to baseline. Only one concentration-contraction curve to a single agonist was obtained for any one ring of artery by cumulative addition of the agonist. The 5-HT receptor agonists tested were 5-HT, sumatriptan, methysergide and ergometrine as well as the α-adrenoceptor agonist, noradrenaline. In some experiments, the responses to the agonists were obtained in the presence of low concentrations of the thromboxane A_2-mimetic, U46619, added 5–10 min previously. The contraction curves to noradrenaline were always generated in the presence of propranolol (1 μM) to prevent β-adrenoceptor-mediated smooth muscle relaxation.

In the second protocol, ring segments were normalized to 0.9 L_{100} and contracted with KPSS followed by washout as previously described. To prevent any phasic contractile activity developing either spontaneously or in response to constrictor agonists, nifedipine (0.1 μM) was added and concentration-contraction curves to the 5-HT receptor agonists were generated in the absence or presence of U46619 (1 nM).

Drugs

Drugs used and their sources were: sumatriptan (Glaxo Group Research, Ware, U.K.); U46619 ([1,5,5-hydroxy-11, 9-(epoxymethano)prosta-5z, 13E-dienoic acid], Upjohn, Kalamazoo, MI, U.S.A.); (−)-noradrenaline bitartrate (Sigma, St. Louis, MO, U.S.A.); 5-hydroxytryptamine creatinine sulphate (5-HT, Sigma, St. Louis, MO, U.S.A.); methysergide

maleate (Sandoz S.A., Basle, Switzerland); sodium nitroprusside dihydrate (Roche, Dee Why, NSW, Australia); ergometrine maleate (David Bull Laboratories, Mulgrave, Victoria, Australia); propranolol HCl (ICI, Villawood, NSW, Australia) and nifedipine (Bayer A.G., Wuppertal, Germany). All drugs were diluted in distilled water with the exception of U46619 and nifedipine which were made up as 1 mM and 10 mM stock solutions respectively in absolute ethanol. Further dilutions of these drugs were made in distilled water.

Data analysis

Parameters at normalization and maximum contractions to KPSS of vessels obtained from hearts with different aetiologies were analyzed in a subset of 19 patients. The maximum response to KPSS in each artery ring was normalized for diameter and expressed as F_{max}/unit diameter (g mm^{-1}; see Table 1). All contractile responses were measured as a percentage of the maximum increase in force to KPSS. When phasic activity occurred, the response was taken as the peak of each contraction. When vessels were precontracted with low concentrations of U46619, the contractile responses to the additional agonist were measured above the U46619-induced contraction and expressed as a percentage of the total KPSS contraction in the absence of U46619.

The individual contraction curves were fitted to the sigmoidal logistic equation, $Y = P_1 + P_2/[1 + e^{P3(\log X - P4)}]$, where X = agonist concentration, P_1 = lower plateau response, P_2 = range between the lower and the maximal plateau of the concentration-response curve, P_3 = a negative curvature index indicating the slope independently of the range and P_4 = log dose required to produce a half maximal response (EC_{50}) (Elghozi & Head, 1990). From this relationship, computer estimates of the concentrations required to give, 10, 30, 50, 70 and 90% (EC_{10} – EC_{90}) of the maximum response were determined. The individual EC_{50} values were averaged and the mean and standard error of the mean calculated.

Student's unpaired *t* tests were used to compare the EC_{50} and maximum values of the agonists in the absence and presence of U46619. For the comparison of passive vessel parameters and KPSS (see Table 1), a one-way analysis of variance was used to make multiple comparisons of EC_{50} values and maximum responses between the independent groups. When the ANOVA indicated that differences existed between all groups, Scheffe's test was applied to determine the source of variation (Wallenstein *et al.*, 1980). Statistical significance was accepted at $P<0.05$ for both tests and values are given as mean ± s.e.mean.

Results

A summary of vessel parameters grouped for hearts with different aetiologies is given in Table 1. The vessels obtained from ischaemic hearts were approximately 20% smaller in internal diameter than those from cardiomyopathic hearts. They also had lower transmural pressures, levels of resting force, levels of force developed 60 min following normalization and maximal contractions to KPSS (F_{max}) compared with the latter two groups (Table 1). When F_{max} was normalized for vessel diameter, no difference was noted between the ischaemic and cardiomyopathy groups (3.1 vs 3.4 g mm^{-1}, $P>0.05$). The normalized F_{max} value for the ischaemic group was significantly smaller than that obtained for unused donor hearts (3.1 vs 4.0 g mm^{-1}; $P<0.05$; see Table 1). In addition, normalization of rings from cardiomyopathic hearts in the presence of SNP to prevent development of phasic activity during this procedure resulted in a significant increase in internal diameter, resting force and, level of force 60 min after normalization (Table 1).

Phasic activity

In 6 of the 28 hearts, spontaneous phasic activity developed during the normalization procedure in 8% of all rings of artery (Fgiure 1). In 10 of the hearts, a further 5% of rings developed phasic contractions after the vessels had been set at their optimal resting passive force (Figure 1). This activity consisted of large all-or-none type rhythmical contractions each of which were maintained for 1–2 min. SNP (10 μM)

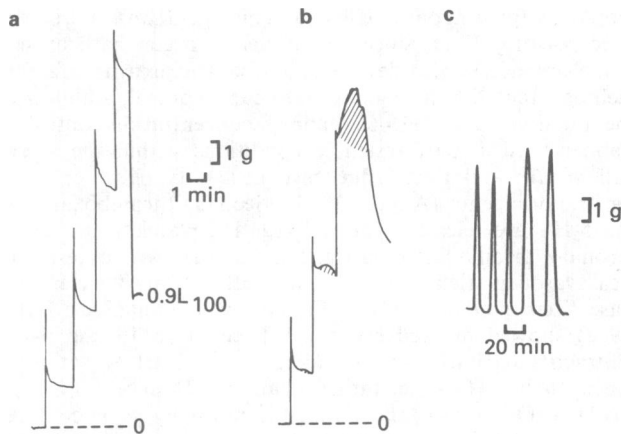

Figure 1 Original chart recordings depicting changes in passive and active isometric force during (a and b) and after (c) the stretch procedure at normalization. The shaded areas in (b) represent development of active force during the passive stretch procedure at normalization (see Methods). The artery in (c) shows a typical pattern of spontaneous phasic contractile activity following normalization. 0 represents zero force on the tissue prior to stretch. 0.9 L_{100} is the normalised internal circumference of each artery (see Methods).

Table 1 Human coronary artery – summary of initial vessel parameters at normalization and contraction in response to K^+ depolarization

Disease	*Number of patients*	*Number† of rings*	*D* (mm)	*P* (mmHg)	*Resting force* F_1(g)	*Force at 60 min* (g)	*KPSS* (F_{max}) (g)	F_{max}/*Diam* (g mm^{-1})
Cardiomyopathy	6	41	3.84 ± 0.15[1]	59.0 ± 1.3[1]	5.6 ± 0.3[1]	6.5 ± 0.5[1]	12.5 ± 0.5[1]	3.42 ± 0.17[1,2]
Ischaemic heart disease	6	55	3,03 ± 0.09[2,3]	53.4 ± 1.1*	4.3 ± 0.2[2]	4.6 ± 0.2[2]	9.3 ± 0.6[2]	3.09 ± 0.19[1]
Unused donor hearts	4	35	3.47 ± 0.12[1,2]	59.5 ± 0.7[1]	5.9 ± 0.3[1]	6.3 ± 0.3[1]	13.3 ± 0.8[1]	4.02 ± 0.32[2]
Cardiomyopathy (– SNP)	3	38	2.83 ± 0.11[3]	60.6 ± 1.4[1]	4.1 ± 0.3[2]	4.3 ± 0.3[2]	11.5 ± 0.7[1,2]	4.12 ± 0.24[2]

D is internal diameter at 0.9 L_{100} (see text). P is equivalent transmural pressure at 0.9 L_{100} (see text).
*Mean significantly different from means of all other groups ($P<0.05$, Scheffe's test).
Values marked with the same number are not significantly different ($P>0.05$, Scheffe's test).
†Minimum of 4 rings per heart.
– SNP: ring segments normalized in the absence of sodium nitroprusside.

was added prior to normalization in artery rings from 16 of the hearts in an attempt to inhibit this spontaneous phasic activity during the normalization procedure. It was successful in 92% of rings but of these, 33% then developed phasic contractions once sodium nitroprusside had been washed out. In 66% of all artery rings from 28 hearts, phasic contractions were also triggered by addition of constrictor agonists such as U46619, sumatriptan, 5-HT and noradrenaline. Generally then, vasoconstrictors increased the level of tonic, active force in the tissues until an apparent threshold level was reached at which point phasic activity was induced (Figure 2). Consequently, concentration-contraction curves with maintained plateaus could only be generated in rings from a small number of patients (see below).

Agonist responses in the absence of phasic activity

5-HT (0.001–30 μM), sumatriptan (0.003–30 μM), methysergide (0.003–30 μM), ergometrine (0.001–30 μM) and noradrenaline (0.001–30 μM) caused concentration-dependent contractions in the human coronary artery with an apparent order of potency of ergometrine > 5-HT > noradrenaline = methysergide > sumatriptan (Figure 3). Ergometrine and 5-HT were the most potent agonists tested with EC_{50} values of 7.7 ± 0.2 (− log M; 7 rings from 3 patients) and 6.8 ± 0.2 (− log M; 7 rings from 3 patients) respectively. In this subgroup of rings, 5-HT also generated the highest maximal response of 40 ± 10% KPSS. The remaining agonists studied were weak constrictors. Ergometrine contracted the vessels to 7–21% of the maximum contraction to KPSS and noradrenaline, in the presence of propranolol (1 μM), generated maximal responses ranging from 3–18% KPSS. Sumatriptan and methysergide either failed to contract the vessels or contracted them to less than 5% of the maximum KPSS contraction (see Table 2 and Figures 3 and 4).

Phasic contractions induced by agonists

In most rings of artery that did not develop phasic activity after normalization, 5-HT and the less efficacious agonists like sumatriptan, ergometrine and methysergide were able to cause marked contraction of the coronary artery due to their induction of phasic activity. For example, 5-HT and sumatriptan generated peak phasic responses of 82 ± 7% KPSS (12 rings, 6 patients) and 71 ± 18% KPSS (6 rings, 3 patients) respectively (see Figure 2). In one patient, methysergide and ergometrine caused maximum phasic contractions of 75% and 78% KPSS respectively and in a further two patients, noradrenaline generated maximal phasic contractions of 42% and 75% KPSS.

Nifedipine abolished the phasic contractions that developed following normalization (data not shown) and in response to exogenously applied constrictor agonists. Thus, in the presence of nifedipine, agonists like 5-HT always caused concentration-dependent contractions with maintained plateaus.

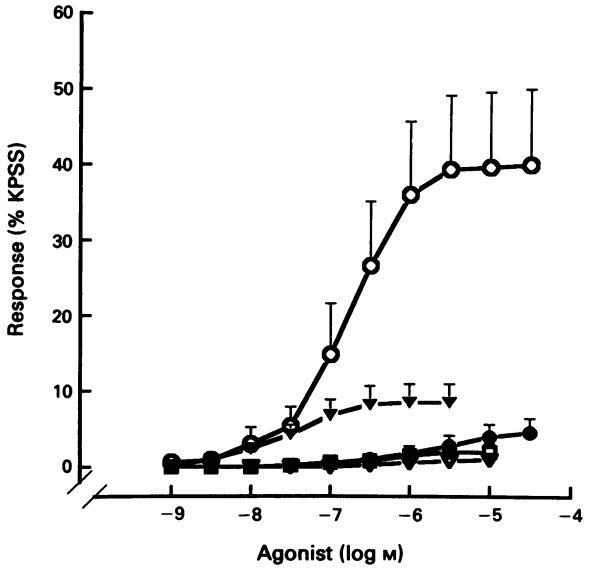

Figure 3 Concentration-contraction curves to 5-hydroxytryptamine (5-HT, ○, $n = 7$), sumatriptan (▽, $n = 7$), methysergide (●, $n = 5$), ergometrine (▼, $n = 7$) and noradrenaline (□, $n = 4$) in isolated rings of human coronary artery that did not develop phasic contractile activity either spontaneously or in response to the added agonists. Values are mean ± 1 s.e.mean and are normalized to the maximal contraction to KPSS.

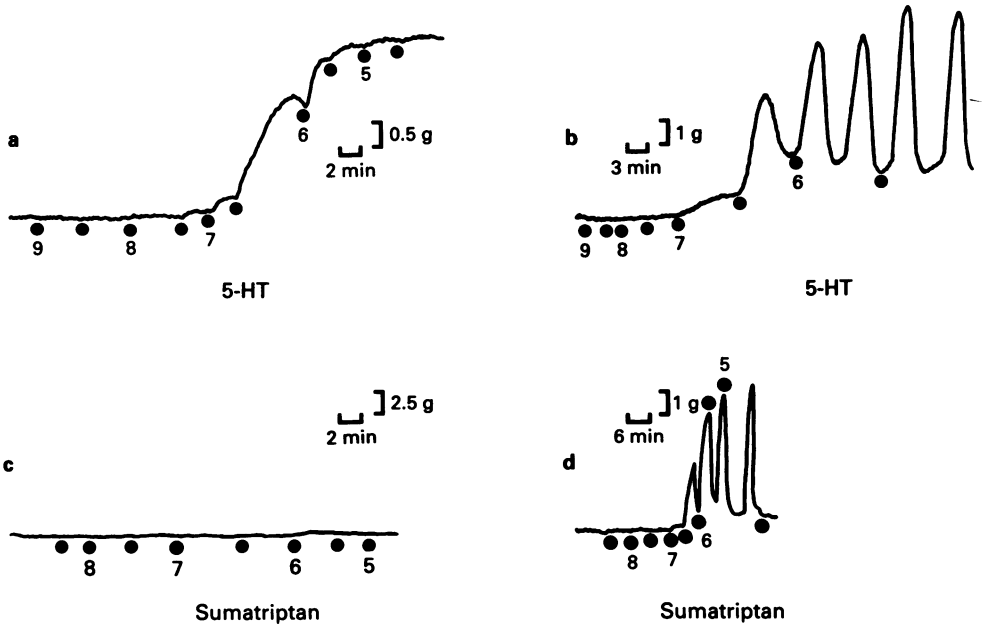

Figure 2 Representative chart recordings from four rings of coronary artery from the same patient. Rings were exposed to cumulative concentrations (− log M) of 5-hydroxytryptamine (5-HT) (a and b) and sumatriptan (c and d). Traces on the right (b and d) developed phasic contractile activity during the addition of each agonist.

Agonist responses in the presence of U46619

U46619 (1 nM) caused a contraction of 3.8 ± 1.1% KPSS (24 rings from 12 patients) in arteries that did not develop phasic contractile activity in response to constrictor agonists. Under these conditions, the maximal contraction responses to 5-HT, sumatriptan, ergometrine and methysergide were markedly increased (Figure 4). A quantitative comparative study was conducted to examine the effect of U46619 on responses to 5-HT and sumatriptan in these rings without phasic activity. U46619 (1 nM) generated a contraction of 6.6 ± 2.4% KPSS (6 rings, 3 patients) and caused a significant increase ($P < 0.05$, Student's unpaired t test) in the maximum contraction response to 5-HT from 40.2 ± 10% KPSS (7 rings, 3 patients) to 92.3 ± 4% KPSS (3 rings, 3 patients; see Figure 5 and Table 2). The maximum response to sumatriptan was also significantly increased from 4.6 ± 1.9% KPSS (10 rings, 5 patients) to 48.5 ± 14% KPSS (3 rings, 3 patients) in the presence of U46619 (Figure 5 and Table 2). Sensitivity to 5-HT was unaffected by U46619 (see Table 2).

In the presence of nifedipine (0.1 μM), U46619 (1.0 nM) caused a contraction of 2.6 ± 0.7% KPSS (7 rings, 3 patients) that was not significantly different from the group not treated with nifedipine (Table 2). Under these conditions U46619 increased significantly the maximum contractions to 5-HT from 22.8 ± 6.4% KPSS (8 rings, 4 patients) to 49.0 ± 6.5% KPSS (3 rings, 3 patients) and sumatriptan from 2.5 ± 1.1% KPSS (6 rings, 3 patients) to 11.4 ± 3.5% KPSS (4 rings 3 patients; see Figure 5 and Table 2). No change in sensitivity to either agonist was observed in the presence of U46619 and nifedipine as compared with U46619 alone (Table 2).

Discussion

The main finding from this study was that in the presence of U46619, human epicardial coronary arteries *in vitro* showed a marked increase in contractility to both 5-HT and the selective 5-HT_1-like receptor agonist, sumatriptan. This synergistic

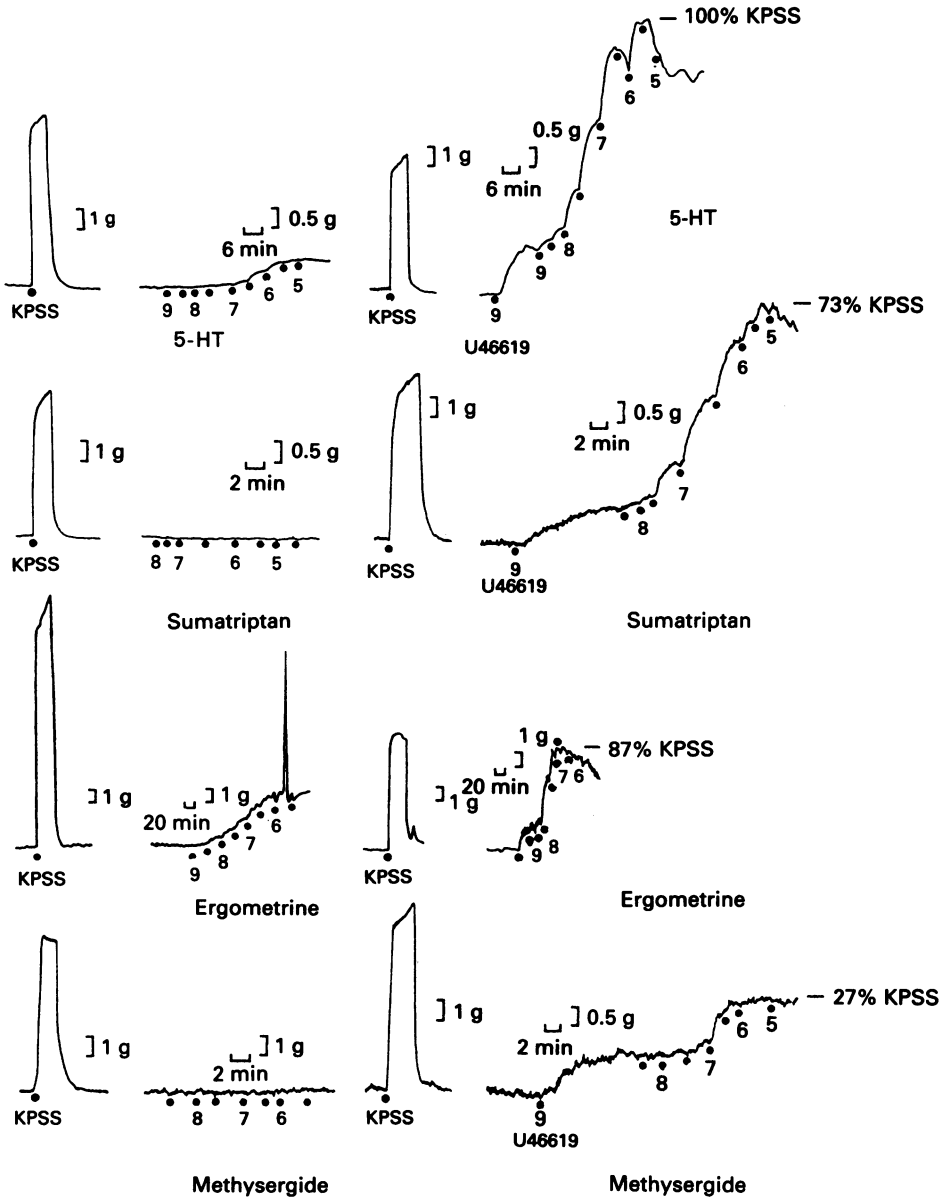

Figure 4 Original chart recordings from rings of coronary artery from a single patient showing synergistic effects of U46619 (right panels) on contractions to cumulative additions (− log M) of 5-hydroxytryptamine (5-HT), sumatriptan, ergometrine and methysergide (left panels) in rings of artery without phasic activity (except note the one phasic contraction to ergometrine in the absence of U46619). Maximal contractions to each agent were compared to the KPSS maximum in each case. Note the gain change in some of the traces in the presence of U46619 (right panels).

interaction did not appear to be specific for either sumatriptan or 5-HT_1-like receptors since contractions to 5-HT, ergometrine, and methysergide were also potentiated by U46619. Nor was the synergy likely to have been specific for the thromboxane A_2 analogue (U46619) as the agonist used to induce threshold levels of active force, since Yang *et al.* (1990) showed that threshold concentrations of endothelin-1 (Yanagisawa *et al.*, 1988) enhanced the contractions to noradrenaline and 5-HT in human isolated coronary and internal mammary arteries. Indeed there are numerous reports in the literature where subthreshold or threshold concentrations of one constrictor agonist can readily amplify the response to a second agent. For example in rabbit femoral artery, MacLennan & Martin (1992) reported anecdotally that both histamine and angiotensin II amplified the contraction to 5-HT, and in rat mesenteric small arteries contraction to sympathetic nerve stimulation was enhanced by as much as 500% by threshold concentrations of vasopressin, neuropeptide Y, endothelin-1 and methoxamine (Lew & Angus, 1992).

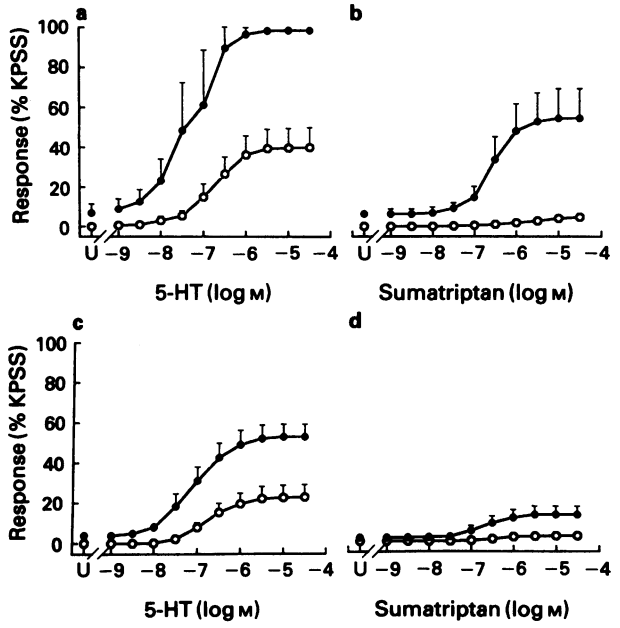

Figure 5 Effects of nifedipine (0.1 μM) on the synergism between U46619 (U: 1 nM) and 5-hydroxytryptamine (5-HT) or sumatriptan in isolated rings of human coronary artery: (○) absence and (●) presence of U46619. Cumulative contraction curves to 5-HT and sumatriptan were constructed in the absence (a, b) and presence (c,d) of nifedipine. All contraction curves in the absence of nifedipine were from artery rings without phasic activity. Values are means ± 1 s.e.mean and are normalized to the tissues' maximal contraction to KPSS.

In the absence of both U46619-induced tone and phasic contractile activity (see below), we found similar results as those reported by Connor *et al.* (1989b) and Chester *et al.* (1990) who found 5-HT to be more potent and cause significantly greater contractions compared with sumatriptan in human, isolated, coronary arteries. Unlike these studies, we did not attempt to determine the EC_{50} for sumatriptan in vessels without any U46619-induced tone because of the poor contractions generated under these conditions. With tone increased with U46619, however, the potency of 5-HT was unaltered and that to sumatriptan was approximately an order of magnitude less than that for 5-HT in the presence of U46619 which agrees with previous studies (Connor *et al.*, 1989b). Although our studies were not performed in the presence of ketanserin, other studies have shown that 5-HT activates both 5-HT_2 and 5-HT_1-like receptors (see Connor *et al.*, 1989b; Chester *et al.*, 1990) and sumatriptan 5-HT_1-like receptors only (Chester *et al.*, 1990).

Whilst the synergy observed between U46619 and 5-HT receptor agonists may not be specific for these two classes of constrictor agents, our results highlight the importance of vascular tone when comparing absolute contractions to vasoconstrictor agonists with apparently different efficacies. Martin *et al.* (1986) also pointed this out in the rabbit isolated aorta where they showed that removal of the endothelium resulted in a much greater enhancement of contractions to partial as compared to full adrenoceptor agonists, presumably due to removal of basal EDRF release (see Moncada *et al.*, 1991). We used the thromboxane A_2-mimetic, U46619, to increase the level of tone since not only is thromboxane A_2 released together with 5-HT and other compounds upon activation of platelets (Golino *et al.*, 1989) but it has also been reported to potentiate contractions to 5-HT in a variety of isolated blood vessels including the rabbit femoral artery (MacLennan & Martin, 1992), guinea-pig iliac artery (Sahin-Erdemli *et al.*, 1991) and human digital arteries (Young *et al.*, 1986). Also, thromboxane A_2 and 5-HT have been postulated to be the mediators of coronary vasoconstriction triggered by local platelet activation in the dog *in vivo* (Golino *et al.*, 1989) and in man (Zeiher *et al.*, 1991b). Furthermore, Ashton *et al.* (1987) found that thromboxane A_2 and 5-HT acted cooperatively to induce cyclic flow variations in anaesthetized dogs with severe coronary artery stenosis and Quillen *et al.* (1991) found that long-term cholesterol feeding in adult cynomolgus monkeys caused coronary artery hyperreactivity to both U46619 and 5-HT. Therefore, the *in vitro* conditions of assay used in our study may represent conditions that in part occur within the artery wall *in vivo*.

Table 2 Sensitivity and maximum contractions to 5-hydroxytryptamine (5-HT) and sumatriptan in human coronary artery in the absence and presence of U46619

Agonist	*U46619* (nM)	*Δ U46619* (% KPSS)	n	*EC_{50} value* (− log M)	*Maximum response* (% KPSS)
5-HT	0	–	7	6.80 ± 0.17	40.2 ± 10.1
	1	6.8 ± 4.6	3	7.41 ± 0.26	92.3 ± 4.0*
5-HT +	0	–	8	6.67 ± 0.10	22.8 ± 6.4
nifedipine (0.1 μM)	1	3.8 ± 0.4	3	7.08 ± 0.16	49.0 ± 6.5*
Sumatriptan	0	–	10	†	4.6 ± 1.9
	1	6.3 ± 1.8	3	6.51 ± 0.09	48.5 ± 13.9*
Sumatriptan +	0	–	6	†	2.5 ± 1.1
nifedipine (0.1 μM)	1	1.7 ± 0.9	4	6.65 ± 0.11	11.4 ± 3.5*

n = number of rings; values are given as mean ± s.e.mean.
*Mean significantly different from control ($P<0.05$, Student's unpaired t test)
†The EC_{50} value for sumatriptan was not calculated in the absence of U46619 as the maximum contraction to the agonist was less than 5% KPSS.
ΔU46619: increase in force to U46619 (1 nM) expressed as a % of the contraction to KPSS.

Other local and circulating substances may also contribute to the synergy observed here between 5-HT receptor agonists and U46619. These include endothelin-1, vasopressin, angiotensin II, kinins and the level of neuronal activity, which for large arteries as those considered here, would be expected to be minimal. Also, the endothelium's ability to release endothelium-derived relaxing factors like prostacyclin and nitric oxide (see Moncada *et al.*, 1991) is another important consideration not only in terms of the inhibitory effects of these dilators on constrictor activity, but also in terms of their antithrombotic effects since both factors themselves synergize to inhibit platelet aggregation (see Moncada *et al.*, 1991). Conditions that have been reported to enhance reactivity of human coronary arteries both *in vitro* and *in vivo* include the presence and location of atherosclerotic lesions (Golino *et al.*, 1991; McFadden *et al.*, 1991), intracoronary thrombus formation (Zeiher *et al.*, 1991b) and endothelial cell dysfunction (Berkenboom *et al.*, 1991; Drexler & Zeiher, 1991; Zeiher *et al.*, 1990a).

The human coronary artery exhibited a tendency to develop large all-or-none type phasic contractions either spontaneously or in response to vasoconstrictors such as U46619, 5-HT and sumatriptan (see also Golenhofen, 1978; Ross *et al.*, 1980; Kalsner, 1985; Kimura *et al.*, 1989) although Connor *et al.* (1989b) and Chester *et al.* (1990) did not report this type of activity. Whilst the reasons for the discrepancy between the studies is unclear, the type and duration of the patients' drug therapy prior to transplantation may be important. Drugs prescribed to patients in this study included diuretics, anticoagulants, cardiac glycosides, angiotensin converting enzyme inhibitors and antiarrhythmic drugs. It was noted, however, that the cardiomyopathic, ischaemic and unused donor hearts exhibited the same trends and degree of reactivity and were therefore comparable.

The inhibition of phasic contractile activity by nifedipine in this study suggests voltage-operated Ca^{2+} channels may be involved both in the spontaneous and agonist-induced phasic activity. Nifedipine also reduced the tonic maximum contractions to 5-HT and sumatriptan. Sumner *et al.* (1992) also showed a similar depression of maximum contractions to 5-HT and sumatriptan in the dog isolated saphenous vein, a tissue that is known to contract sensitively and maximally to sumatriptan (Humphrey *et al.*, 1988). Interestingly, the tonic contractions to other constrictor agonists like U46619 and endothelin-1 in the human coronary artery were unaffected by nifedipine (Cocks & Stork, unpublished data). This is an important point, given that the ability to demonstrate synergy between U46619 and 5-HT in the presence of nifedipine relied on the tonic response to U46619 being unaffected.

A possible explanation for the synergy between 5-HT receptor agonists and U46619 may be due to the absence or dysfunction of the endothelium, since earlier studies in pig and dog coronary arteries indicated that contractile responses to 5-HT and noradrenaline are enhanced in the absence of endothelium (Cocks & Angus, 1983; Cohen *et al.*, 1983). This is unlikely, however, as histological examination of selected vessels revealed no disruption of endothelium integrity and endothelium-dependent vasodilators such as substance P and histamine caused potent relaxation (Cocks & Kemp, unpublished data). A more likely explanation is that U46619 facilitates the transducer mechanisms of these agonists. Angus & Brazenor (1983) found that the constrictor response to U46619 in dog isolated coronary arteries, were not altered by the Ca^{2+}-entry blockers, nifedipine, D600 and verapamil, therefore suggesting that the contractions generated by U46619 are largely dependent on release of intracellular calcium. In addition, Young *et al.* (1986), have shown that the potentiation of the contractile effect of 5-HT by U46619 in human digital arteries was a result of increased mobilization of intracellular calcium stores. In the present study, low concentrations of U46619 did not always cause contraction yet in all cases contractions to other agonists were potentiated. Release of intracellular calcium may account for these observations. Thus, in the human coronary artery there may be a threshold level of calcium at which contractions are triggered. Pretreatment with concentrations of U46619 that failed to cause contraction, could bring the cellular levels of calcium closer to threshold, such that other agonists now cause release of more intracellular Ca^{2+} from the same or different stores or influx of extracellular Ca^{2+} through receptor or voltage-operated channels. Even with concentrations of U46619 that caused significant contractions, the increase in reactivity to 5-HT and sumatriptan probably reflected sensitization to further increases in intracellular calcium. Thus, in the rabbit femoral artery, MacLennan & Martin (1992) showed marked potentiation of the contractions to 5-HT in the presence of 5-HT_2 receptor blockade even when U46619 itself caused a large contraction.

An important question that arises from the present study relates to the possible clinical relevance of coronary 5-HT_1-like receptors, particularly in instances of advanced atherosclerosis and vasospastic disease. McFadden *et al.* (1992) showed that in patients with variant angina where 5-HT induced spasm at the sites of stenoses as well as in patients with stable angina where 5-HT constricted the distal epicardial coronary arteries, these responses to 5-HT were resistance to ketanserin. While McFadden *et al.* (1992) discussed the limitations of their study, they speculated that more direct evidence for a role of 5-HT_1-like receptors in coronary vasospasm may be determined by the use of selective 5-HT_1-like agonists such as sumatriptan. In fact, a recent study in man found that intravenous infusion of sumatriptan significantly reduced coronary artery diameter (MacIntyre *et al.*, 1992). This issue, however, will be more convincingly resolved with the development of a selective 5-HT_1-like antagonist. Nevertheless, there is a case report of a patient with migraine who, in response to subcutaneous sumatriptan, developed severe chest pain and ECG changes (marked ST elevation) characteristic of coronary vasospasm (Willett *et al.*, 1992). In addition, there have been two case reports of ventricular arrhythmias (Curtin *et al.*, 1992) associated with subcutaneous sumatriptan. These isolated reports, however, should be considered against the international post marketing experience of treating 3 million attacks of migraine. Nevertheless, in their replies to these case reports, the company has acknowledged that there are circumstances where sumatriptan should be avoided (Castle & Simmons, 1992) and emphasised that sumatriptan should be contraindicated in patients with ischaemic heart disease and related cardiac disorders (Pilgrim *et al.*, 1992).

In conclusion, our study demonstrates that inherent active force or tone as well as receptor populations are crucial in determining the reactivity to vasoconstrictor agents in human coronary artery *in vitro*. It also highlights the importance of *in vitro* assay conditions when comparing contractile activities of agonists with different apparent efficacies (see also Martin *et al.*, 1986; MacLennan & Martin, 1992). Thus, given appropriate conditions, 5-HT_1-like receptor agonists like sumatriptan can cause relatively potent and powerful contractions in human large coronary arteries *in vitro*.

This work was supported by an Institute Grant from the National Health and Medical Research Council of Australia and Glaxo Australia. We would like to thank sincerely Mr Don Esmore, Mr Bruce Davis, Dr Frank Rosenfeldt, Ms Anne Griffith, Mr Robin McEgan, Mr Arthur Preovolos and all members of the Heart-Lung Transplant Unit at the Alfred Hospital for their assistance.

References

ANGUS, J.A. (1989). 5-HT receptors in the coronary circulation. *Trends Pharmacol. Sci.*, **10**, 89–90.

ANGUS, J.A. & BRAZENOR, R.M. (1983). Relaxation of large coronary artery by verapamil, D600 and nifedipine is constrictor selective: comparison with glyceryl trinitrate. *J. Cardiovasc. Pharmacol.*, **5**, 321–328.

ANGUS, J.A., COCKS, T.M. & SATOH, K. (1986). α_2-Adrenoceptors and endothelium-dependent relaxation in canine large arteries. *Br. J. Pharmacol.*, **88**, 767–777.

ASHTON, J.H., OGLETREE, M.L., MICHEL, I.M., GOLINO, P., MCNATT, J.M., TAYLOR, A.L., RAHEJA, S., SCHMITZ, J., BUJA, L.M., CAMPBELL, W.B. & WILLERSON, J.T. (1987). Cooperative mediation by serotonin S_2 and thromboxane A_2/prostaglandin H_2 receptor activation for cyclic flow variations in dogs with severe coronary artery stenoses. *Circulation*, **76**, 952–959.

BERKENBOOM, G., UNGER, P., FANG, Z.Y. & FONTAINE, J. (1991). Endothelium-derived relaxing factor and protection against contraction to norepinephrine in isolated canine and human coronary arteries. *J. Cardiovasc. Pharmacol.*, **17** (Suppl. 3), S127–S132.

BRADLEY, P.B., ENGEL, G., FENIUK, W., FOZARD, J.R., HUMPHREY, P.P.A., MIDDLEMISS, D.N., MYLECHARANE, E.J, RICHARDSON, B.P. & SAXENA, P.R. (1986). Proposals for the classification and nomenclature of functional receptors for 5-hydroxytryptamine. *Neuropharmacology*, **25**, 563–576.

BRAZENOR, R.M. & ANGUS, J.A. (1981). Ergometrine contracts canine coronary arteries by a serotonergic mechanism: no role for alpha adrenoceptors. *J. Pharmacol. Exp. Ther.*, **218**, 530–536.

BRITTAIN, R.T., BUTINA, D., COATES, I.H., FENIUK, W., HUMPHREY, P.P.A., JACK, D., OXFORD, A.W. & PERREN, M.J. (1987). GR43175 selectively constricts the canine carotid arterial bed via stimulation of 5-HT_1-like receptors. *Br. J. Pharmacol.*, **92**, 618P.

CASTLE, W.M. & SIMMONS, V.E. (1992) Coronary vasospasm and sumatriptan. *Br. Med. J..*, **305**, 117–118.

CHESTER, A.H., MARTIN, G.R., BODELSSON, M., ARNEKLO-NOBIN, B., TADJKARIMI, S., TORNEBRANDT, K. & YACOUB, M.H. (1990). 5-Hydroxytryptamine receptor profile in healthy and diseased human epicardial coronary arteries. *Cardiovasc. Res.*, **24**, 932–937.

COCKS, T.M. & ANGUS, J.A. (1983). Endothelium-dependent relaxation of coronary arteries by noradrenaline and serotonin. *Nature*, **305**, 627–630.

COHEN, R.A., SHEPHERD, J.T. & VANHOUTTE, P.M. (1983). 5-Hydroxytryptamine can mediate endothelium-dependent relaxation of coronary arteries. *Am. J. Physiol.*, **245**, H1077–H1080.

CONNOR, H.E., FENIUK, W. & HUMPHREY, P.P.A. (1989a). Characterization of 5-HT receptors mediating contraction of canine and primate basilar artery by use of GR43175, a selective 5-HT_1-like receptor agonist. *Br. J. Pharmacol.*, **96**, 379–387.

CONNOR, H.E., FENIUK, W. & HUMPHREY, P.P.A. (1989b). 5-Hydroxytryptamine contracts human coronary arteries predominantly via 5-HT_2 receptor activation. *Eur. J. Pharmacol.*, **161**, 91–94.

CURTIN, T., BROOKS, A.P. & ROBERTS, J. (1992). Cardiorespiratory distress after sumatriptan given by injection. *Br. Med. J.*, **305**, 713–714.

DE CATERINA, R., CARPEGGIANI, C. & L'ABBATE, A. (1984). Evidence against a role for serotonin in the genesis of coronary vasospasm. *Circulation*, **69**, 889–894.

DEN BOER, M.O., VILLALÓN, C.M., HEILIGERS, J.P.C., SAXENA, P.R. & HUMPHREY, P.P.A. (1990). The craniovascular effects of sumatriptan in the pig. *Br. J. Pharmacol.*, **99**, 37P.

DREXLER, H. & ZEIHER, A.M. (1991). Importance of the functional integrity of the endothelium in coronary vasomotion in humans. *J. Cardiovasc. Pharmacol.*, **17** (Suppl. 3), S273–S278.

EGASHIRA, K., TOMOIKE, H., HAYASHI, Y., YAMADA, A., NAKAMURA, M. & TAKESHITA, A. (1992). Mechanism of ergonovine-induced hyperconstriction of the large epicardial coronary artery in conscious dogs a month after arterial injury. *Circ. Res.*, **71**, 435–442.

ELGHOZI, J. & HEAD, G.A. (1990). Spinal noradrenergic pathways and pressor responses to central angiotensin II. *Am. J. Physiol.*, **258**, H240–H246.

FENIUK, W., HUMPHREY, P.P.A. & PERREN, M.J. (1987). Selective vasoconstrictor action of GR43175 on arteriovenous anastomoses (AVAS) in the anaesthetised cat. *Br. J. Pharmacol.*, **92**, 756P.

FENIUK, W., HUMPHREY, P.P.A. & PERREN, M.J. (1989a). The selective carotid arterial vasoconstrictor action of GR43175 in anaesthetized dogs. *Br. J. Pharmacol.*, **96**, 83–90.

FENIUK, W., HUMPHREY, P.P.A. & PERREN, M.J. (1989b). GR43175 does not share the complex pharmacology of the ergots. *Cephalagia*, **9** (Suppl. 9), 35–39.

FERRARI, M.D., MELAMED, E., GAWEL, M.J., NAPPI, G., LUBEN, V., TRANCHANT, C., DONOGHUE, S., DURHAM, J., PILGRIM, A. & TANSEY, M.J.B. (1991). Treatment of migraine attacks with sumatriptan. *N. Engl. J. Med.*, **325**, 316–321.

FREEDMAN, S.B., CHIERCHIA, S., RODRIGUEZ-PLAZA, L., BUGIARDINI, R., SMITH, G. & MASERI, A. (1984). Ergonovine-induced myocardial ischemia: no role for serotonergic receptors? *Circulation*, **70**, 178–183.

GOLENHOFEN, K. (1978). Activation mechanisms in smooth muscle of human coronary arteries and their selective inhibition. *Naunyn Schmied Arch. Pharmacol.*, **302** Suppl. R36.

GOLINO, P., ASHTON, J.H., BUJA, M., ROSOLOWSKY, M., TAYLOR, A.L., MCNATT, J., CAMPBELL, W.B. & WILLERSON, J.T. (1989). Local platelet activation causes vasconstriction of large epicardial canine coronary arteries in vivo. Thromboxane A_2 and serotonin are possible mediators. *Circulation*, **79**, 154–166.

GOLINO, P., PISCIONE, F., WILLERSON, J.T., CAPPELLI-BIGAZZI, M., FOCACCIO, A., VILLARI, B., INDOLFI, C., RUSSOLILLO, E., CONDORELLI, M. & CHIARIELLO, M. (1991). Divergent effects of serotonin on coronary-artery dimensions and blood flow in patients with coronary atherosclerosis and control patients. *N. Engl. J. Med.*, **324**, 641–648.

HOLTZ, J., HELD, W., SOMMER, O., KUHNE, G. & BASSENGE, E. (1982). Ergonovine-induced constrictions of epicardial coronary arteries in conscious dogs: α-adrenoceptors are not involved. *Basic Res. Cardiol.*, **77**, 278–291.

HUMPHREY, P.P.A., APPERLEY, E., FENIUK, W. & PERREN, M.J. (1990). A rational approach to identifying a fundamentally new drug for the treatment of migraine. In *Cardiovascular Pharmacology of 5-Hydroxytryptamine*. ed. Saxena, P.R., Wallis, D.I., Wouters, W. & Bevan, P. pp. 417–431, Dordrecht: Kluwer Academic Publishers.

HUMPHREY, P.P.A. & FENIUK, W. (1991). Mode of action of the anti-migraine drug sumatriptan. *Trends Pharmacol. Sci.*, **12**, 444–446.

HUMPHREY, P.P.A., FENIUK, W., PERREN, M.J., CONNOR, H.E., OXFORD, A.W., COATES, I.H. & BUTINA, D. (1988). GR43175, a selective agonist for the 5-HT_1-like receptor in dog isolated saphenous vein. *Br. J. Pharmacol.*, **94**, 1123–1132.

KALSNER, S. (1985). Coronary artery reactivity in human vessels: some questions and answers. *Fed. Proc.*, **44**, 321–325.

KAWACHI, Y., TOMOIKE, H., MARUOKA, Y., KIKUCHI, Y., ARAKI, H., ISHII, Y., TANAKA, K. & NAKAMURA, M. (1984). Selective hypercontraction caused by ergonovine in the canine coronary artery under conditions of induced atherosclerosis. *Circulation*, **69**, 441–450.

KIMURA, T., YASUE, H., SAKAINO, N., ROKUTANDA, M., JOUGASAKI, M. & ARAKI, H. (1989). Effects of magnesium on the tone of isolated human coronary arteries – comparison with diltiazem and nitroglycerin. *Circulation*, **79**, 1118–1124.

LEW, M.J. & ANGUS, J.A. (1992). Vascular responses to sympathetic nerve stimulation *in vitro* are enhanced by vasoconstrictors at subthreshold concentrations. In *Proceedings of the Australian Physiology and Pharmacological Society*, 46P.

MCFADDEN, E.P., CLARKE, J.G., DAVIES, G.J., KASKI, J.C., HAIDER, A.W. & MASERI, A. (1991). Effects of intracoronary serotonin on coronary vessels in patients with stable angina and patients with variant angina. *N. Engl. J. Med.*, **324**, 648–655.

MCFADDEN, E.P., BAUTERS, C., LABLANCHE, J.M., LEROY, F., CLARKE, J.G., HENRY, M., SCHANDRIN, C., DAVIES, G.J., MASERI, A. & BERTRAND, M.E. (1992). Effect of ketanserin on proximal and distal coronary constrictor responses to intracoronary infusion of serotonin in patients with stable angina, patients with variant angina, and control patients. *Circulation*, **86**, 187–195.

MACINTYRE, P.D., BHARGAVAE, B., HOGG, K.J., GEMMILL, J.D. & HILLIS, W.S. (1992). The effect of i.v. sumatriptan, a selective 5-HT_1-receptor agonist on central haemodynamics and the coronary circulation. *Br. J. Clin. Pharmacol.*, **34**, 541–546.

MACLENNAN, S.J. & MARTIN, G.R. (1990). Actions of non-peptide ergot alkaloids at 5-HT_1-like and 5-HT_2 receptors mediating vascular smooth muscle contraction. *Naunyn Schmied Arch. Pharmacol.*, **342**, 120–129.

MACLENNAN, S.J. & MARTIN, G.R. (1992). Effect of the thromboxane A_2-mimetic U-46619 on 5-HT_1-like and 5-HT_2 receptor-mediated contraction of the rabbit isolated femoral artery. *Br. J. Pharmacol.*, (in press).

MARTIN, W., FURCHGOTT, R.F., VILLANI, G.M. & JOTHIANANDAN, D. (1986). Depression of contractile responses in rat aorta by spontaneously released endothelium-derived relaxing factor. *J. Pharmacol. Exp. Ther.*, **237**, 529–537.

MONCADA,S., PALMER, R.M.J. & HIGGS, E.A. (1991). Nitric oxide: physiology, pathophysiology and pharmacology. *Pharmacol. Rev.*, **43**, 109–142.

MOSKOWITZ, M.A. (1992). Neurogenic versus vascular mechanisms of sumatriptan and ergot alkaloids in migraine. *Trends Pharmacol. Sci.*, **13**, 307–311.

MULLER-SCHWEINITZER, E. (1980). The mechanism of ergometrine-induced coronary arterial spasm: *in vitro* studies on canine arteries. *J. Cardiovasc. Pharmacol.*, **2**, 645–655.

MULVANY, M.J. & HALPERN, W. (1977). Contractile properties of small arterial resistance vessels in spontaneously hypertensive and normotensive rats. *Circ. Res.*, **41**, 19–26.

NIELSEN, T.H. & TFELT-HANSEN, P. (1989). Lack of effect of GR43175 on peripheral arteries in man. *Cephalgia*, **9** (Suppl. 9), 93–95.

PARSONS, A.A., WHALLEY, E.T., FENIUK, W., CONNOR, H.E. & HUMPHREY, P.P.A. (1989). 5-HT_1-like receptors mediate 5-hydroxytryptamine-induced contraction of human isolated basilar artery. *Br.J. Pharmacol.*, **96**, 434–449.

PERREN, M.J., FENIUK, W. & HUMPHREY, P.P.A. (1989). The selective closure of feline carotid arteriovenous anastomoses (AVAs) by GR43175. *Cephalagia*, **9** (Suppl. 9), 41–46.

PERRIN, V.L., FARKKILA, M., GOASGUEN, J., DOENICKE, A., BRAND, J. & TFELT-HANSEN, P. (1989). Overview of initial clinical studies with intravenous and oral GR43175 in acute migraine. *Cephalagia*, **9** (Suppl. 9), 63–72.

PILGRIM, A.J., LLOYD, D.K. & SIMMONS, V.E. (1992). Reply to case reports by T. Curtin *et al. Br. Med. J.*, **305**, 714.

QUILLEN, J.E., SELLKE, F.W., ARMSTRONG, M.L. & HARRISON, D.G. (1991). Long-term cholesterol feeding alters the reactivity to primate coronary microvessels to platelet products. *Arteriosclerosis Thrombosis*, **11**, 639–644.

ROSS, G., STINSON, E., SCHROEDER, J. & GINSBURG, R. (1980). Spontaneous phasic activity of isolated human coronary arteries. *Cardiovasc. Res.*, **14**, 613–618.

SAHIN-ERDEMLI, I., HOYER, D., STOLL, A., SEILER, M.P. & SCHOEFFTER, P. (1991). 5-HT_1-like receptors mediate 5-hydroxytryptamine-induced contraction of guinea-pig isolated iliac artery. *Br. J. Pharmacol.*, **102**, 386–390.

SAKANASHI, M. & YONEMURA, K. (1980). On the mode of action of ergometrine in the isolated dog coronary artery. *Eur. J. Pharmacol.*, **64**, 157–160.

SAXENA, P.R. (1974). Selective vasoconstriction in carotid vascular bed by methysergide: possible relevance to its antimigraine effect. *Eur. J. Pharmacol.*, **27**, 99–105.

SUMNER, M.J., FENIUK, W., MCCORMICK, J.D. & HUMPHREY, P.P.A. (1992). Studies on the mechanism of 5-HT_1 receptor-induced smooth muscle contraction in dog saphenous vein. *Br. J. Pharmacol.*, **105**, 603–608.

TODA, N. & OKAMURA, T. (1990). Comparison of the response to 5-carboxamidotryptamine and serotonin in isolated human, monkey and dog coronary arteries. *J. Pharmacol. Exp. Ther.*, **253**, 676–682.

VANHEUVEN-NOLSEN, D. (1988). 5-HT receptor subtype-specific drugs and the cardiovascular system. *Trends Pharmacol. Sci.*, **9**, 423–425.

WALLENSTEIN, S., ZUCKER, C.L. & FLEISS, J.L. (1980). Some statistical methods useful in circulation research. *Circ. Res.*, **47**, 1–9.

WILLETT, F., CURZEN, N., ADAMS, J. & ARMITAGE, M. (1992). Coronary vasospasm induced by subcutaneous sumatriptan. *Br. Med. J.*, **304**, 1415.

YANG, Z., RICHARD, V., VON SEGESSER, L., BAUER, E., STULZ, P., TURINA, M. & LUSCHER, T.F. (1990). Threshold concentrations of endothelin-1 potentiate contractions to norepinephrine and serotonin in human arteries. *Circulation*, **82**, 188–195.

YANAGISAWA, M., KURIHARA, H., KIMURA, S., TOMOBE, T., KOBAYASHI, M., MITSUI, Y., YAZAKI, Y., GOTO, K. & MASAKI, T. (1988). A novel potent vasoconstrictor peptide produced by vascular endothelial cells. *Nature*, **332**, 411–415.

YOUNG, M.S., IWANOV, V. & MOULDS, R.F.W. (1986). Interaction between platelet-released serotonin and thromboxane A_2 on human digital arteries. *Clin. Exp. Pharmacol. Physiol.*, **13**, 143–152.

ZEIHER, A.M., DREXLER, H., WOLLSCHLAGER, H. & JUST, H. (1991a). Modulation of coronary vasomotor tone in humans: progressive endothelial dysfunction with different early stages of coronary atherosclerosis. *Circulation*, **83**, 391–401.

ZEIHER, A.M., SCHACHINGER, V., WEITZEL, S.H., WOLLSCHLAGER, H. & JUST, H. (1991b). Intracoronary thrombus formation causes focal vasoconstriction of epicardial arteries in patients with coronary artery disease. *Circulation*, **83**, 1519–1525.

(Received January 4, 1993
Revised March 26, 1993
Accepted April 22, 1993)

Br. J. Pharmacol. (1993), **110**, 369–377

Calcium antagonist and antiperoxidant properties of some hindered phenols

[1]G.P. Sgaragli, M. Valoti, B. Gorelli, F. Fusi, M. Palmi & P. Mantovani

Istituto di Scienze Farmacologiche, Via E.S. Piccolomini 170, Villa Betlem, 53100 Siena, Italy

1 The calcium antagonist and antioxidant activities of certain synthetic and natural phenols, related to BHA (2-*t*-butyl-4-methoxyphenol), were evaluated in rat ileal longitudinal muscle and in lipid peroxidation models respectively.

2 Compounds with a phenol or a phenol derivative moiety, with the exception of 2,2'-dihydroxy-3,-3'-di-*t*-butyl-5,5'-dimethoxydiphenyl (di-BHA), inhibited in a concentration-dependent manner the $BaCl_2$-induced contraction of muscle incubated in a Ca^{2+}-free medium. Calculated pIC_{50} (M) values ranged between 3.32 (probucol) and 4.96 [3,5-di-*t*-butyl-4-hydroxyanisole (di-*t*-BHA)], with intermediate activity shown by khellin < gossypol < quercetin < 3-*t*-butylanisole < BHA < nordihydroguaiaretic acid (NDGA) < 2,6-di-*t*-butyl-4-methylphenol (BHT) and papaverine.

3 The Ca^{2+} channel activator Bay K 8644 overcame the inhibition sustained by nifedipine, BHA and BHT, while only partially reversing that of papaverine.

4 BHA, BHT, nifedipine and papaverine also inhibited in a concentration-dependent fashion $CaCl_2$ contractions of muscle depolarized by a K^+-rich medium. This inhibition appeared to be inversely affected by the Ca^{2+}-concentration used.

5 The inhibitory effects of nifedipine, papaverine, BHA and BHT were no longer present when muscle contraction was elicited in skinned fibres by 5 μM Ca^{2+} or 500 μM Ba^{2+}, suggesting a plasmalemmal involvement of target sites in spasmolysis.

6 Comparative antioxidant capability was assessed in two peroxyl radical scavenging assay systems. These were based either on the oxidation of linoleic acid initiated by a heat labile azo compound or on lipid peroxidation of rat liver microsomes promoted by Fe^{2+} ions. Across both model systems, di-*t*-BHA, NDGA, BHT, di-BHA, BHA and quercetin ranked as the most potent inhibitors of lipid oxidation, with calculated pIC_{50} (M) values ranging between 7.4 and 5.7.

7 Of the 32 compounds studied only 15 phenolic derivatives exhibited both antispasmogenic and antioxidant activity. Within this subgroup a linear and significant correlation was found between antispasmogenic activity and antioxidation. These bifunctional compounds were characterized by the presence of at least one hydroxyl group on the aromatic ring and a highly lipophilic area in the molecule.

8 Di-*t*-BHA is proposed as a lead reference compound for future synthesis of new antioxidants combining two potentially useful properties in the prevention of tissue damage after ischaemia-reperfusion injury.

Keywords: Phenol derivatives; calcium antagonist; antioxidant; 2-*t*-butyl-4-methoxyphenol (BHA); 2,6-di-*t*-butyl-4-methylphenol (BHT)

Introduction

Superoxide formation ($O_2^{\cdot-}$) appears central to the pathological process attendant on ischaemia-reperfusion injury. In experimental animals, free radicals are generated in two main ways during ischaemia: when xanthine oxidase is formed subsequent to a calcium-triggered proteolytic attack on xanthine dehydrogenase (Battelli *et al.*, 1972; Della Corte & Stirpe, 1972) and during disorders of electron transport in anoxic-reoxygenated mitochondria (Boveris & Turrens, 1981; Naqui *et al.*, 1986). The direct effects of $O_2^{\cdot-}$ include membrane de-esterification of the apolar regions, lipid peroxidation after Fe^{2+} release (Deby & Goutier, 1990) and a redox cycle when hydrogen peroxide is converted to the reactive hydroxyl radical. This circular process perpetuates the formation of $O_2^{\cdot-}$ and an increased release of non-esterified fatty acids. This, in turn, may promote intracellular increase in calcium concentration due to anoxia. The formation of hypochlorous acid from reactive oxygen species may also contribute to tissue damage.

It is now recognized that disturbances in the homeostasis of intracellular Ca^{2+} may underlie a variety of toxicological and pathological processes. Several potential mechanisms have been identified whereby changes in intracellular free calcium trigger cytotoxic processes. Calcium ions activate phospholipase A_2 (PLA_2) and a number of proteinases and nucleases. The observation that sustained increase of intracellular Ca^{2+} causes membrane breakdown and subsequent cell damage is supported by the fact that PLA_2 inhibitors prevent ischaemic cell damage in liver and heart and by the finding that phospholipid hydrolysis is enhanced during tissue injury. Evidence that calcium ions mediate or propagate ischaemic cell damage (Nayler *et al.*, 1979; Katz & Reuter, 1979) is borne out by reports that Ca^{2+} increases the damage caused by oxygen free radicals to the mitochondrial electron transport chain (Malis & Bonventre, 1986). All these observations suggest that reperfusion or post-ischaemic tissue injury is a complex phenomenon to which several interrelated factors may contribute.

Different protective strategies might be envisaged to curtail tissue damage. There is some evidence for the clinical effectiveness of the enzyme superoxide dismutase, which catalyzes the dismutation of $O_2^{\cdot-}$ to form hydrogen peroxide and oxygen (Fridovich, 1986; Michelson, 1986; Marklund, 1986). This would not eliminate the noxious effects of hydrogen peroxide, itself a source of oxygen-derived radicals, in the presence of transition metals, though supplement with catalase might regress this problem. Tissue integrity is also

[1] Author for correspondence.

challenged by the hypochlorous acid released by reactive oxygen species. Though xanthine oxidase inhibitors such as allopurinol and oxypurinol may be of value in certain cases, their applicability to man is still unclear (McCord, 1985).

From a strictly pharmacological point of view, tissue damage may be countered either upstream by compounds that scavenge the free radicals or downstream by limiting the increase of free intracellular calcium.

The effectiveness of hydroxyl or peroxyl radical scavengers has been established in animal models by the novel butylated hydroxytoluene (BHT) derivatives, such as the thiazolidinone derivative LY256548 (Ruterbories & Lindstrom, 1990), *p*-(pyrrolidinylmethylene)butylated hydroxytoluene (E-5110) (Shirota *et al.*, 1987) and 2-(allyl-1-piperazinyl)-4-n-amyloxyquinazoline fumarate (KB-5666) (Hara & Kogure, 1990).

Downstream protection may be afforded by calcium channel blockers such as verapamil and nifedipine which reduce calcium uptake from the extracellular space during or after ischaemia. Though some evidence has been marshalled for the clinical effectiveness of calcium antagonists (the Danish Study Group on Verapamil in Myocardial Infarction, 1990; the Multicenter Diltiazem Postinfarction Trial Research Group, 1988), the precise means by which they prevent ischaemia-reperfusion damage remains a matter for further elucidation (Cheung *et al.*, 1986; Nayler, 1992).

Results obtained in this laboratory (Sgaragli *et al.*, 1989) indicate that 2-*t*-butyl-4-methoxyphenol (BHA), besides its well-known antioxidant effect may also exhibit nifedipine-like spasmolytic activity. Molecules which combine both scavenging and calcium antagonist properties may be of particular value in protecting against ischaemia-reperfusion tissue damage. The focus of this paper is directed at identifying such dual-purpose molecules and comparing their performance against those that act simply as either calcium channel blockers or radical scavengers.

Methods

Animals

Male Sprague-Dawley rats (200–370 g body weight) were purchased from Società S. Morini S.p.a., S. Polo d'Enza, Italy. They were housed in a normal environmentally controlled animal room (20–22°C) with a 12 h alternating light/dark cycle, and had free access to food pellets and water. One kg of rat pellets contained: vitamin A 15,000 iu; vitamin D_3 1,500 iu; vitamin K_3 2 mg; vitamin E 30 mg; vitamin B_1 3 mg; vitamin B_2 5 mg; vitamin C 40 mg; vitamin B_6 3 mg; B_{12} 0.03 mg; D-pantothenic acid 15 mg; folic acid 1 mg; vitamin PP 30 mg; choline chloride 400 mg; manganese 60 mg; iron 150 mg; copper 5 mg; zinc 30 mg; iodine 1 mg; cobalt 0.2 mg; BHT 10 mg (Società S. Morini S.p.a., S. Polo d'Enza, Italy).

Assays on intact rat ileum longitudinal muscle preparations

These preparations were used in two distinct series of contractility experiments under isometric conditions (Basile, Comerio, Italy). In the first series, segments of longitudinal muscle (1.5–2.0 cm, in length; 60–80 mg, weight) were suspended under 500 mg tension in a 6 ml chamber filled with a modified Krebs-Henseleit solution containing (mM final concentration): NaCl 118, KCl 4.7, $MgCl_2$ 1.2, $NaHCO_3$ 25, glucose 5, $CaCl_2$ 2.5 and gassed with a 95% O_2:5% CO_2 mixture at 37°C. After 30 min equilibration, contractility was tested by stimulating the tissue electrically or chemically with acetylcholine (ACh). Five s train stimuli (60 V at 10 Hz for 2 ms) were delivered through two silver electrodes placed at the top and bottom of the bath chamber. After washing with the incubation solution, ACh was added at three different final concentrations (0.2, 1.6 and 10 μM). Muscle contraction was then elicited by the addition of $BaCl_2$ at different final concentrations. The subsequent assays were performed in the same medium deprived of $CaCl_2$. The omission of $CaCl_2$ from the bathing solution abolished any spontaneous activity as well as any electrically stimulated muscle contractions. Muscle contraction was elicited by the addition of $BaCl_2$ at different final concentrations every 15 min; between each addition extensive washing reduced tissue tension to baseline values. $BaCl_2$-induced responses were concentration-dependent and rapid in onset, an initial peak (phasic) being followed by a more sustained contraction (tonic).

The addition of Ba^{2+} to both incubation solutions, whether free or supplemented by Ca^{2+}, caused a concentration-dependent contraction of muscle tissue. ED_{50} (phasic phase) was 1.71 ± 0.14 mM ($n = 6$) in the presence of Ca^{2+} and 5.34 ± 0.06 mM ($n = 7$) in its absence. The synergistic action of Ca^{2+}, however, disappeared at the highest concentration of Ba^{2+} leaving the maximal tension unaltered. The presence of Ca^{2+} affected the constancy of response over time. Contractility with 2.5 mM Ca^{2+} decreased in a steady, and progressive manner in response to Ba^{2+}, dropping by approximately 40% over 4 h of incubation. In the absence of Ca^{2+}, this decrease took place in the first 90 min and stabilized thereafter.

In a separate series of experiments, the addition of 35 mM dimethylsulphoxide (DMSO) for up to 4 h had no effect on Ba^{2+}-elicited responses in a Ca^{2+}-deprived medium.

In the second experimental series, segments of longitudinal muscle were initially subjected to 500 mg tension and bathed by a MOPS-buffered physiological salt solution (MOPS-PSS) composed as follows (mM final concentration): NaCl 129.7, KCl 5.9, $CaCl_2$ 2.54, $MgCl_2$ 1.19, MOPS 10 and glucose 11.1. The pH of the solution was adjusted to 7.4 with NaOH. After equilibration the bath fluid was changed to a K^+-rich, Ca^{2+}-free MOPS-PSS which contained K^+ at 40 mM, sufficient to depolarize intestinal smooth muscle (Spedding, 1982). This produced a spasm which was dissipated by regular changes of the K^+-rich, Ca^{2+}-free bath fluid. The spasmogenic response to $CaCl_2$ was studied by constructing cumulative concentration-effect curves. The 15 min contact time for each concentration of $CaCl_2$ was sufficient to attain optimal isometric tension.

An initial concentration-effect curve was derived for $CaCl_2$ followed by two others. In test tissues, calcium antagonists were present for 30 min before and throughout the second and the third concentration-effect curves and increased 30 min before the third curve. Control tissues were treated similarly, without exposure to calcium antagonists. The inhibitory effect of all antagonists at the two concentrations was measured as the reduction (%) of the initial spasmogenic effect of $CaCl_2$ 0.1–10 mM.

Assays on skinned rat ileum longitudinal muscle preparations

Segments of rat ileum longitudinal muscle were skinned of their plasmalemma according to a procedure prescribed for vascular smooth muscle from rabbit renal arteries (Kreye *et al.*, 1983). Pieces of tissue (0.5 mm wide, 3–5 mm length) were attached with acrylate glue (Loctite) by both ends to the small part of two L-shaped stainless steel rods and kept in a vertical position under 200 mg tension. The skinning procedure consisted of an initial 30 min incubation in an aqueous solution (pH 7.4) containing 5 mM EGTA, 20 mM imidazole, 50 mM KCl, and 150 mM sucrose at 4°C, and a subsequent 1 h incubation in the same solution with the addition of 1% Triton X-100 and 0.5 mM dithioerythritol at 4°C, and followed by a final 30 min incubation in a solution containing 50% glycerol (v/v), 10 mM imidazole, 2 mM EGTA, 5 mM $MgCl_2$, 0.5 mM NaN_3, 3.75 mM ATP, 5 mM creatine phosphate and 0.5 mM dithioerythritol at − 20°C. The preparations were stored in the latter solution at − 20°C for up to 6 weeks. For the isometric contraction and relaxation studies,

the preparations, still attached to the rods, were transferred into 10 ml thermostatted organ bath chambers and connected to high sensitivity isometric transducers (Basile, Comerio, Varese, Italy). Contractile change was induced by alternating the 'relaxing' and 'contracting solution'. The relaxing solution (pCa > 8, pH 6.7) contained 20 mM imidazole, 4 mM EGTA, 10 mM $MgCl_2$, 1 mM NaN_3, 2 mM dithioerythritol, 7.5 mM ATP, 10 mM creatine phosphate and 10 units ml^{-1} of creatine kinase. The contracting solution, containing 5 μM $CaCl_2$, was a Krebs-Henseleit solution. For Ba^{2+}-induced contractions the contracting solution was nominally Ca^{2+}- and phosphate-free but contained 500 μM $BaCl_2$. The electrical transduction signals were amplified and displayed on a Basile strip recorder (Mod. Gemini). All contraction studies were performed at room temperature.

Comparative assessment of the antioxidant properties of phenol compounds: inhibition of lipid peroxidation

Phenol derivatives were assessed for their capacity to prevent lipid peroxidation by two experimental model systems. The first was based on the oxidation of linoleic acid initiated by 2,2'-azobis-2-amidinopropane hydrochloride (ABAP), a thermolabile azo compound which, on decomposition, forms radicals that abstract hydrogen atoms from linoleic acid. ABAP (11 mM) was added to a suspension of linoleic acid (33 mM) in 50 mM Na phosphate buffer pH 7.4, in the chamber of an O_2 electrode (Model 5300 Biological Oxygen monitor, Yellow Spring Instrument Co., Inc. Yellow Spring, Ohio, U.S.A.) thermostatted at 37°C (Wayner *et al.*, 1987). O_2 consumption was monitored for approximately 6 min before adding the antioxidant at different concentrations. O_2 consumption due to ABAP decomposition was determined separately and subtracted from the peroxidation rate of linoleic acid. In the second model, peroxidation of rat liver microsomes, by a peroxidizing mixture of 100 μM Fe^{2+}/Fe^{3+} and 100 μM ascorbic acid, was measured at 37°C as O_2 consumption. Reaction mixtures in a final volume of 3 ml contained 0.5 mg microsomal protein, with 57 mM ethanol or 47 mM DMSO vehicle and 20 mM KH_2PO_4-KOH buffer, pH 6.0.

Drugs: commercial sources and synthetic procedures

Phenol from Merk (Darmstadt, Germany) and phenol derivatives 3,5-di-*t*-butyl-4-hydroxyanisole (di-*t*-BHA) and 2,4,6-tri-*t*-butylphenol (TTP) from Aldrich-Chemie (Steinheim, Germany) were recrystallized once prior to use from ethanol. BHA and BHT from Fluka Chemie AG (Buchs, Switzerland) were recrystallized once prior to study from petroleum ether and ethanol respectively. 2,2'-Dihydroxy-3,3'-di-*t*-butyl-5,5'-dimethoxydiphenyl (di-BHA, dimer of BHA) was synthesized by direct oxidation of BHA as described elsewhere (Sgaragli *et al.*, 1980). 3-*t*-Butylanisole was synthesized from 3-*t*-butylphenol by methylation with diazomethane. After 24 h incubation at room temperature and normal pressure the mixture was washed with 2 N NaOH to remove the unreacted phenol. 3-*t*-Butylanisole was consequently purified by vacuum distillation. 1,4-Dimethoxy-2-*t*-butylbenzene was synthesized from BHA by methylation with CH_3I in the presence of Na methanolate. After 24 h incubation at room temperature and normal pressure the mixture was washed with 2 N NaOH to remove unreacted BHA. 1,4-Dimethoxy-2-*t*-butylbenzene was subsequently purified by vacuum distillation. Nifedipine, nordihydroguaiaretic acid (NDGA), gossypol and linoleic acid were purchased from Sigma Chemical Company (U.S.A.). Aldrich-Chemie (Steinheim, Germany) supplied 2,6-di-*t*-butyl-*p*-benzoquinone, 3,5-di-*t*-butyl-1,2-benzoquinone, 2-*t*-butylphenol, 3-*t*-butylphenol, 4-*t*-butylphenol, 4-*t*-butylphenyl-2,3-epoxypropylether, quercetin, khellin, eugenol, 2,4-di-*t*-butyl-6-(4-methoxybenzil) phenol, 3-hydroxyanisole, 1,8-dihydroxyanthraquinone, caffeic acid, trolox, anthraquinone, 4-*t*-butylbenzoic acid, 4-*t*-butylpyridine, *t*-butylbenzene and *t*-butylcyclohexane. Papaverine was purchased from Merk (Darmstadt, Germany). ABAP was purchased from Polysciences Inc. (U.S.A.). Silymarin, a mixture of three isomers (silybin, silidianin and silicristin) was a generous gift of Istituto Biochimico Italiano 'Giovanni Lorenzini' S.p.a. (Milan, Italy). Probucol was obtained from Lepetit S.p.a. (Milan, Italy). Bay K 8644 (methyl-1,4-dihydro-2,6-dimethyl-3-nitro-4-(2-trifluoromethylphenyl)-pyridine-5-carboxylate) was a generous gift of Dr Franckoviack. All other compounds were of analytical grade and were used without further purification.

Compounds were diluted in DMSO or ethanol or water to give stock solutions stored at 4°C until use. All stock solutions were shielded from light with aluminium foil. Because of the known photosensitivity of the dihydropyridines, the experiments with nifedipine and Bay K 8644 were performed in the dark. The water used to prepare the calcium- and phosphate-free Krebs-Henseleit solution was first distilled and then passed through a NANOpure II deionization system (Barnstead-Sybron, Boston, U.S.A.), to obtain Type I Reagent Grade water (resistivity 18 MΩ).

Statistical analyses

Data are presented as means ± s.e.mean; n is the number of independent experiments. Statistical analysis was performed by Student's t test (paired to compare drug effects at different Ba^{2+} concentrations). P values < 0.05 were considered significant. The pharmacological response to each substance was described, where possible, by the pIC_{50} value (the negative $\log_{10}$ of the molar concentration at which the substance inhibits 50% of the maximum response). pIC_{50} values were estimated by linear regression analysis.

Results

Inhibiting effects of hindered phenols in ileal smooth muscle: structure-activity

In a structure-activity relation study various model phenol compounds (see Table 1) were assessed to ascertain the requirements for inhibiting Ba^{2+}-induced muscle contraction in a nominally Ca^{2+}-free solution.

Table 2 shows pIC_{50} (M) values for some of the tested compounds (less than 10% inhibition was considered meaningless). Compounds which exhibited antispasmogenic activity were, at least, three orders of magnitude less potent than nifedipine ($pIC_{50} = 8.02 \pm 0.01$; $n = 5$). When either the hydroxyl- and *t*-butyl-moieties were present on the aromatic ring, compounds showed antispasmogenic properties, with pIC_{50} values ranging between 4.56 (2-*t*-butylphenol) and 4.08 (4-*t*-butylphenol). Compounds with only one of these groups on the ring were ineffective (phenol, *t*-butylcyclohexane, *t*-butylbenzene and 4-*t*-butylpyridine). This demonstrates that the presence of both groups is essential for activity. Additional tests included the study of the three different series of phenol derivatives obtained by substitution in the *o*-, *m*- and *p*-position. Among the *p*-substituted compounds, activity increased when the hydroxyl group was derivatized, even with a bulky moiety such as 2,3-epoxypropyl, but disappeared when the hydroxyl group was replaced by a carboxyl one as in the case of 4-*t*-butylbenzoic acid. Other carboxylic compounds, such as caffeic acid and trolox, were shown to be inactive. In the *m*-substituted series, activity was still maintained after derivatization of the hydroxyl group (3-*t*-butylanisole), while the substitution of the *t*-butyl moiety with a methoxy one made the 3-hydroxyanisole compound inactive. Finally, in the *o*-substituted derivatives (the closest series to our lead compounds BHA and BHT), the introduction of a *p*-methoxyl moiety into 2-*t*-butylphenol did not appreciably change the activity of the resulting BHA with

Table 1 General structures of phenol derivatives studied

		X
1	*t*-Butylcyclohexane	C
2	*t*-Butylbenzene	C
3	4-*t*-Butylpyridine	N

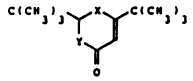

		X	Y
4	2,6-di-*t*-Butyl-*p*-benzoquinone	C=O	H
5	3,5-di-*t*-Butyl-1,2-benzoquinone	H	C=O

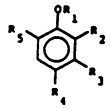

		R_1	R_2	R_3	R_4	R_5
6	Phenol	H	H	H	H	H
7	2-*t*-Butylphenol	H	$C(CH_3)_3$	H	H	H
8	BHA	H	$C(CH_3)_3$	H	OCH_3	H
9	1,4-Dimethoxy--2-*t*-butylbenzene	CH_3	$C(CH_3)_3$	H	OCH_3	H
10	3-*t*-Butylphenol	H	H	$C(CH_3)_3$	H	H
11	3-*t*-Butylanisole	CH_3	H	$C(CH_3)_3$	H	H
12	3-Hydroxyanisole	H	H	OCH_3	H	H
13	4-*t*-Butylphenol	H	H	H	$C(CH_3)_3$	H
14	4-*t*-Butylphenyl-2,3--epoxypropylether	CH_2-CH-CH_2 (O)	H	H	$C(CH_3)_3$	H
15	4-*t*-Butylbenzoic acid	COOH	H	H	$C(CH_3)_3$	H
16	TTP	H	$C(CH_3)_3$	H	$C(CH_3)_3$	$C(CH_3)_3$
17	di-*t*-BHA	H	$C(CH_3)_3$	H	OCH_3	$C(CH_3)_3$
18	BHT	H	$C(CH_3)_3$	H	CH_3	$C(CH_3)_3$
19	di-BHA	H	$C(CH_3)_3$	H	OCH_3	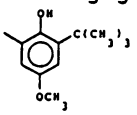
20	2,4-di-*t*-Butyl-6-(4--methoxybenzil)phenol	H	$C(CH_3)_3$	H	$C(CH_3)_3$	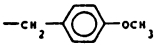
21	Probucol	H	$C(CH_3)_3$	H	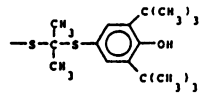	$C(CH_3)_3$
22	Caffeic acid	H	OH	H	CH=CH-COOH	H
23	Eugenol	H	OCH_3	H	CH_2-CH=CH_2	H
24	NDGA	H	OH	H	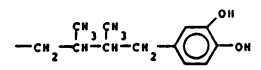	H

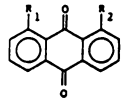

		R_1	R_2
25	Anthraquinone	H	H
26	1,8-Dihydroxyanthraquinone	OH	OH

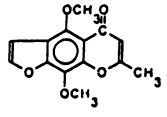

27 Khellin

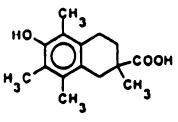

28 Trolox

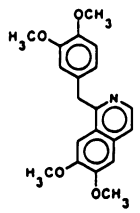

29 Papaverine

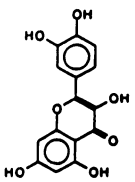

30 Quercetin

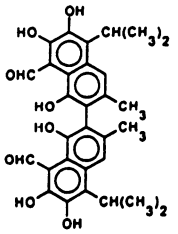

31 Gossypol

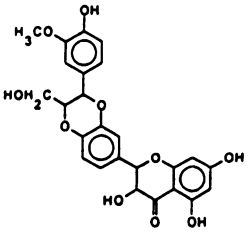

32 Silymarin

Table 2 Inhibition of Ba^{2+}-induced contractions in rat ileum longitudinal muscle preparations

Compounds	pIC_{50} (M)
Mono substituted hydrocarbons	
4-*t*-Butylpyridine	Inactive at 100 μM
t-Butylcyclohexane	Inactive at 200 μM
t-Butylbenzene	Inactive at 200 μM
Phenols	
Phenol	Inactive at 400 μM
o-*Substituted*	
2-*t*-Butylphenol	4.56 ± 0.07
BHA	4.34 ± 0.05
1,4-Dimethoxy-2-*t*-butylbenzene	4.30 ± 0.08
Khellin	4.03 ± 0.06
m-*Substituted*	
3-*t*-Butylanisole	4.29 ± 0.14
3-*t*-Butylphenol	4.24 ± 0.12
3-Hydroxyanisole	Inactive at 100 μM
p-*Substituted*	
4-*t*-Butylphenyl-2,3-epoxypropylether	4.39 ± 0.01
4-*t*-Butylphenol	4.08 ± 0.01
4-*t*-Butylbenzoic acid	Inactive at 200 μM
o-*di-Substituted*	
di-*t*-BHA	4.96 ± 0.06
BHT	4.68 ± 0.05
2,4-di-*t*-Butyl-6-(4-methoxybenzil)phenol	3.64 ± 0.31
TTP	3.34 ± 0.24
Probucol	3.32 ± 0.03
di-BHA	Inactive at 200 μM
poly-Substituted	
Trolox	Inactive at 1 mM
Natural polyphenol derivatives	
Papaverine	4.78 ± 0.08
NDGA	4.57 ± 0.03
Quercetin	4.26 ± 0.08
Gossypol	4.24 ± 0.08
Eugenol	3.87 ± 0.04
Silymarin	3.74 ± 0.13
Caffeic acid	Inactive at 5 mM
Quinones	
2,6-di-*t*-Butyl-p-benzoquinone	4.67 ± 0.01
3,5-di-*t*-Butyl-1,2-benzoquinone	4.66 ± 0.01
1,8-Dihydroxyanthraquinone	3.40 ± 0.68
Anthraquinone	Inactive at 200 μM

$BaCl_2$-induced contractions were developed at 37°C in a $CaCl_2$-free, modified Krebs-Henseleit solution gassed with a 95% O_2:5% CO_2 mixture. The various agents were added 5 min before $BaCl_2$ (6.25 mM). For further details see Methods section. Figures represent mean values ± s.e.mean ($n = 3-12$).

respect to the parent compound. Similarly little change occurred when the phenolic hydroxyl moiety was derivatized, giving rise to 1,4-dimethoxy-2-*t*-butylbenzene. Though lacking a *t*-butyl group, we considered khellin a lipophilic *p*-dimethoxy-benzene derivative of 1,4-dimethoxy-2-*t*-butylbenzene which showed a comparable pIC_{50} value to its parent compound. Compounds of a broader hindrance than BHA, namely BHT and di-*t*-BHA, characterized by the presence of 2,6-di-*t*-butyl groups, were among the most effective spasmolytics. Though diminished activity was still present when the *p*-methyl group was substituted by a *t*-butyl one (TTP) or by another BHT-analogue attached via an isopropylidenedithio bridge (probucol). This loss of activity might be a consequence of increased molecular size. In fact when di-*t*-BHA was substituted by a BHA radical in 2-position, the enlarged di-BHA molecule proved devoid of activity. However, molecular size alone could not account for suppression of activity as could be seen when the 2-*t*-butyl group of TTP was replaced by a 4-methoxybenzil radical, giving a 2,4-di-*t*-butyl-6-(4-methoxybenzil)phenol of greater efficacy than the parent compound.

Among the quinone derivatives, only those with two *t*-butyl groups were effective. The other test compounds were a series of natural polyphenolic derivatives. Of these the catechol-derivatizated papaverine and the catechol derivative NDGA were the most potent antispasmogenics and performed equivalently to BHT.

Mechanism of the antispasmogenic action of BHA, BHT and papaverine: reversal of the inhibition by Bay K 8644

As summarized in Figure 1, nifedipine, papaverine, BHA and BHT markedly inhibited in decreasing order of potency the Ba^{2+}-induced contraction of ileal preparations. Nifedipine was the strongest suppressor at concentrations three orders of magnitude lower than that of the other compounds.

When the same test was performed after addition of 1 μM Bay K 8644 there was an approximate 50% increase over control conditions in responsiveness to Ba^{2+}. The addition of Bay K 8644 to the preparations pre-incubated with BHA, BHT and nifedipine, abolished any inhibition except in the case of papaverine where inhibition was only partially reversed.

Studies with depolarized muscles

In K^+-depolarized tissues, $CaCl_2$ caused concentration-dependent contraction which became maximal at 10 mM. In control tissues the $CaCl_2$ concentration-effect curve showed no appreciable changes when repeated over time. The effects of BHA, BHT, papaverine and nifedipine are depicted in Figure 2. DMSO and ethanol, used to dissolve the drugs, had different effects on the preparations (data not shown). While DMSO, at 14.1 mM concentration had no effect, ethanol at 17.1 mM concentration increased the sensitivity of the preparation to $CaCl_2$ as could be seen in the leftward and upward shift of the $\log_{10}$ concentration-response curve. BHA (17.5 and 35 μM), BHT (10 and 20 μM), papaverine (8 and 25 μM) and nifedipine (5 and 10 nM) each antagonized $CaCl_2$ in a concentration-dependent manner. Figure 2 (a–d) shows that this antagonism comprised both a shift to the right of the log concentration-effect curve for $CaCl_2$ and a depression of the maximal response. The calculated mean pIC_{50} values were 4.47, 4.94, 4.84 and 9.01 for BHA, BHT, papaverine and nifedipine, respectively.

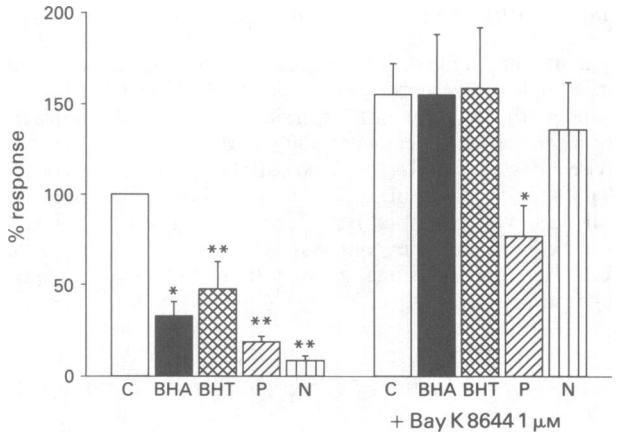

Figure 1 Inhibition of Ba^{2+}-induced contractions in rat ileum longitudinal muscle preparations and its reversal by Bay K 8644. Responses (%) were calculated with respect to paired controls (C). Columns represent mean values with s.e.mean ($n = 4-15$). BHA 50 μM, BHT 25 μM, papaverine 25 μM (P) (in 35 mM DMSO, final concentration) and nifedipine 50 nM (N; in 29 mM ethanol) were always present in the physiological solution, while Bay K 8644 was added 5 min before $BaCl_2$ (6.25 mM). For Methods see Table 2. The significance of differences was calculated by use of Student's *t* test. For abbreviations, see text. $^*P<0.05$; $^{**}P<0.01$. Tension developed in control + Bay K 8644 (1.01 ± 0.11 g) was significantly different ($P<0.01$; $n = 15$) from that developed in control alone (0.65 ± 0.09 g).

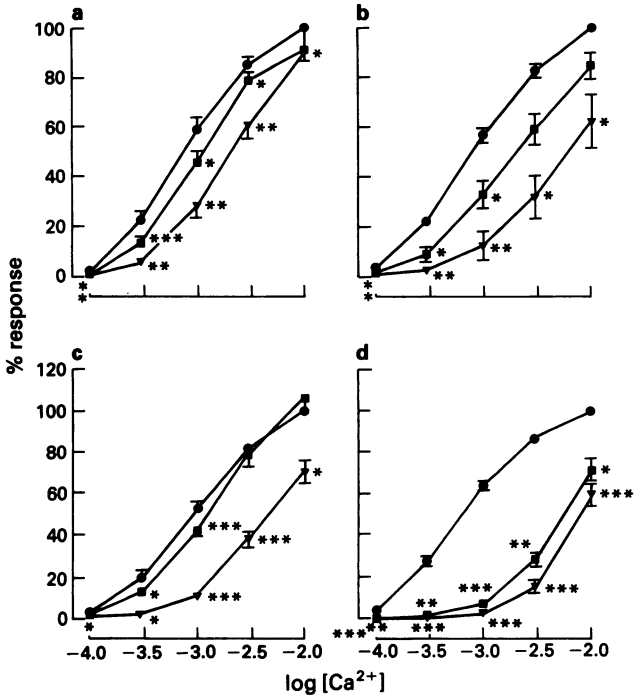

Figure 2 The effect of BHA, BHT, papaverine and nifedipine on the response to $CaCl_2$ of rat ileum longitudinal muscle in K^+-rich (40 mM), Ca^{2+}-free, MOPS-PSS. The abscissae indicate the concentration of $CaCl_2$ (M) on a $\log_{10}$ scale. The ordinates indicate spasm as a % of the maximal response to $CaCl_2$ in the absence of antagonists. Points represent mean values ± s.e.mean, ($n = 4-8$): (●) initial $\log_{10}$ concentration-effect curve for $CaCl_2$ in the presence of vehicles (DMSO for BHA, BHT and papaverine; ethanol for nifedipine), control; (■) second $\log_{10}$ concentration-effect curve for $CaCl_2$ obtained after tissue equilibration for 30 min in (a) BHA 17.5 μM, (b) BHT 10 μM, (c) papaverine 8 μM, (d) nifedipine 5 nM; (▼) third $\log_{10}$ concentration-effect curve for $CaCl_2$ obtained after an additional 30 min period of equilibration in (a) BHA 35 μM, (b) BHT 20 μM, (c) papaverine 25 μM, (d) nifedipine 10 nM. The significance of differences was calculated by use of Student's t test. $^*P<0.05$; $^{**}P<0.01$; $^{***}P<0.001$.

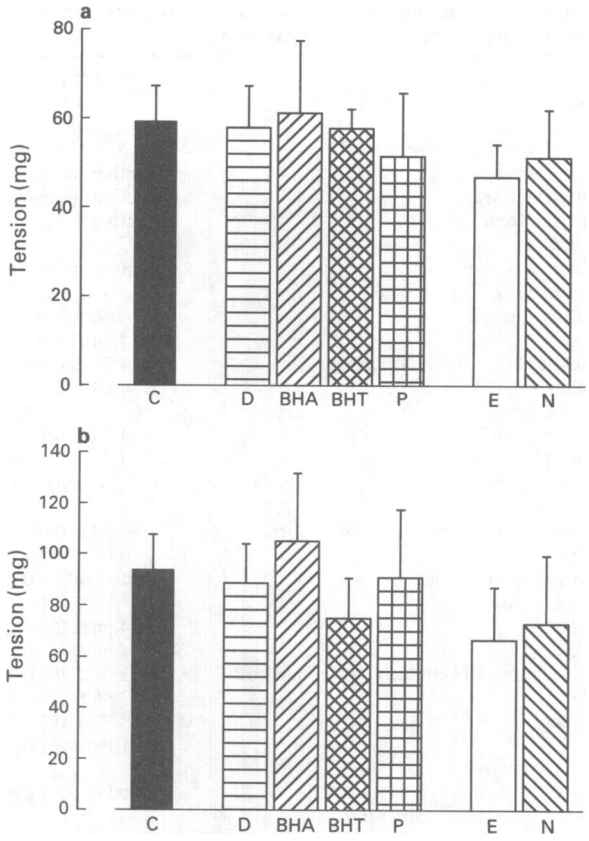

Figure 3 Effects of various agents on (a) Ba^{2+}- and (b) Ca^{2+}-induced contractions of rat ileum longitudinal skinned muscle. Contractions were developed at room temperature in a Krebs-Henseleit solution containing 0.5 mM Ba^{2+} or 5 μM Ca^{2+} gassed with 95% O_2:5% CO_2 mixture. Columns represent mean values with s.e.mean ($n = 4-14$). BHA 10 μM, BHT 50 μM, papaverine 50 μM (P) [in 140 mM DMSO (D) final concentration] and nifedipine 50 nM (N) [in 172 mM ethanol (E)] were added 5 min before $BaCl_2$ or $CaCl_2$ (C). The significance of differences was calculated by use of Student's t test.

Studies with skinned ileal preparations

Segments of skinned longitudinal ileum contracted in response to low concentrations of both Ba^{2+} and Ca^{2+}.

Under the experimental conditions, maximal contractile response was obtained with 500 μM Ba^{2+} or 5 μM Ca^{2+}.

The effects of BHA (100 μM), BHT (50 μM), papaverine (50 μM) and nifedipine (50 nM) on skinned preparations challenged with Ca^{2+} or Ba^{2+}, are summarized in Figure 3. As may be seen, the compounds were without inhibitory effects at concentrations greater than the IC_{50}s in intact preparations.

Antioxidant properties of hindered phenols: inhibition of lipid peroxidation

Among the group of antispasmogenic phenols, 27 compounds were assessed for their prevention of lipid peroxidation. Two model systems were employed as described previously (see Methods). Almost all compounds showed some degree of inhibition of lipid peroxidation as seen in Table 3. The degree of inhibition in linoleic acid was greater than that in the microsomal system. Ranking of inhibition according to potency was almost the same in both model systems, and with a wide range of potency (IC_{50}s 0.04–120 and 0.13–933 μM, respectively).

t-Butylbenzene, 1,8-dihydroxyanthraquinone, 4-*t*-butylphenyl-2,3-epoxypropylether, papaverine, khellin, 2,6-di-*t*-butyl-*p*-benzoquinone, 3-*t*-butylanisole and 1,4-dimethoxy-2-*t*-butylbenzene were inactive at concentrations ⩾ 100 μM. The vehicle, whether DMSO or ethanol, exerted no significant effect (data not shown) at the concentrations used.

Di-*t*-BHA, the most potent of the compounds tested, with antiperoxidant IC_{50} values of 0.04 and 0.13 μM in the linoleate and microsome system respectively, showed 100% inhibition at concentrations of 0.56 and 10 μM, respectively. BHA and BHT displayed IC_{50} values of 0.45 and 2.30 and 0.17 and 1.50 μM in the two model systems, respectively. Fifty percent inhibition of peroxidation by di-BHA required 0.22 and 1.0 μM concentration in both models. This indicates that the dimer maintains the antiperoxidant activity of the parent BHA. Quercetin and gossypol also exhibited remarkable antiperoxidant activity. The other compounds, in particular eugenol, silymarin, trolox and probucol showed IC_{50} values approximately two orders of magnitude higher than di-*t*-BHA.

The dihydropyridine derivative, nifedipine, protected the lipids against oxidation, but only at very high concentrations.

Discussion

This work demonstrates the dual action of some phenol derivatives – namely their antispasmogenic activity on longitudinal ileum musculature and their antioxidant property on microsomal and linoleate systems.

Table 3 Inhibition of lipid peroxidation (peroxyl radical scavenging property)

	Radical generating system/substrate	
	ABAP/linoleic acid	*Fe-ascorbic acid/microsomes*
Antioxidant	pIC_{50} (M)	pIC_{50} (M)
di-*t*-BHA	7.38	6.89
NDGA	6.80	6.01
BHT	6.77	5.82
di-BHA	6.66	6.00
3,5-di-*t*-Butyl-1,2-benzoquinone		5.98
BHA	6.35	5.64
Quercetin	6.30	5.66
TTP		5.63
2,4-di-*t*-Butyl-6-(4-methoxy-benzil)phenol		5.43
Gossypol	5.96	5.70
2-*t*-Butylphenol		4.91
3-*t*-Butylphenol		4.23
Eugenol	5.59	4.17
Trolox	5.31	4.17
4-*t*-Butylphenol		4.15
Probucol	5.09	3.51
Silymarin	5.03	4.43
Nifedipine	3.92	3.19
Caffeic acid		3.03
t-Butylbenzene	Inactive at 100 μM	
Papaverine	Inactive at 100 μM	
1,8-Dihydroxyanthraquinone	Inactive at 100 μM	
Khellin	Inactive at 150 μM	
2,6-di-*t*-Butyl-p-benzoquinone	Inactive at 313 μM	
4-*t*-Butylphenyl-2,3-epoxy-propylether	Inactive at 1 mM	
3-*t*-Butylanisole	Inactive at 1 mM	
1,4-Dimethoxy-2-*t*-butylbenzene	Inactive at 1 mM	

In the ABAP/linoleic acid assay samples containing a suspension of linoleic acid (33 mM) were incubated in 50 mM phosphate buffer pH 7.4 at 37°C. Peroxidation was initiated by 11 mM ABAP and the O_2 consumption was monitored by an O_2 electrode. After 6 min antioxidant was added at different concentrations.

In the Fe-ascorbic acid/microsomes assay samples containing rat liver microsomes (0.5 mg microsomal proteins) were incubated in 20 mM phosphate buffer pH 6.0 at 37°C. Peroxidation was started by adding 100 μM Fe^{2+}-Fe^{3+} and 100 μM ascorbic acid. After 6 min antioxidant was added at different concentrations.

Whereas previous research has focused on these two properties in isolation, our study points to a correlation between the two activites. It has been suggested that some phenol derivatives possess calcium antagonistic properties and other authors have shown how this restricts Ca^{2+} availability both in smooth muscle contraction (khellin, Ubeda *et al.*, 1991; quercetin, Abdalla *et al.*, 1989) and in immune response regulation (quercetin, kaempferol, myricetin and silymarin, Middleton & Kandaswami, 1992). Recent electrophysiological research provides evidence of some effects of NDGA on calcium channels. This compound, in fact, was shown to produce a reversible, concentration-dependent inhibition of Ca^{2+} channel currents with a pIC_{50} of 4.73 on two clonal anterior pituitary cell lines (Korn & Horn, 1990). The authors suggested that NDGA blocked Ca^{2+} currents by simply partitioning into the plasmalemma and interacting either directly with channel proteins, or with other membrane-bound Ca^{2+} channel modulators.

In the present study, muscle contraction was elicited by Ba^{2+} in a Ca^{2+}-free incubation medium and less, systematically, by Ca^{2+} in a K^+-rich medium.

Ba^{2+} induces phasic contraction via passage through voltage-operated Ca^{2+} channels of plasma membranes (Bülbring & Tomita, 1969; Inomata & Kao, 1985; Benham *et al.*, 1985) and/or by releasing Ca^{2+} from sarcoplasmic store sites (Northover, 1968; Somlyo *et al.*, 1974; Chi-Ming & Murphy, 1987). Phenol derivatives may exert antispasmogenic effects by inhibiting either or both of these mechanisms. Alternatively, phenols may inhibit the direct action of Ba^{2+}/Ca^{2+} on the contractile machinery. These possible *loci* of antispasmogenic action were examined by studying the effects of BHA, BHT and nifedipine on skinned fibres. The skinning procedure we adopted, based on Triton X-100, not only disrupts the plasma membrane (Cortijo *et al.*, 1987) but has also been found to destroy the functional integrity of both the sarcoplasmic reticulum and the mitochondria (Meisheri & Rüegg, 1983).

Failure to inhibit contraction in skinned fibres demonstates that an intact cell membrane or sarcoplasmic reticulum, or indeed both, are functional prerequisites for BHA and BHT action. Ca^{2+} and Ba^{2+} induce contractions by initially binding to calmodulin (Satoh *et al.*, 1987); the Ba^{2+}/Ca^{2+} thus complexed activates the contractile proteins (Rüegg *et al.*, 1984), so by-passing the binding sites seemingly required by BHA and BHT. Consequently, our results suggest that BHA and BHT act at the sarcoplasmic reticulum or certain plasmalemma components in close structural association with the voltage-operated Ca^{2+} channels.

Experiments with the Ca^{2+} channel activator, Bay K 8644 further narrowed the target site options for BHA and BHT to the plasmalemma alone. Bay K 8644 was found to reverse completely inhibition caused by the antioxidants and by nifedipine. It is now established that Bay K 8644 binds to the same pore site as nifedipine, but acts in an opposite fashion, that is, Bay K 8644 promotes the opening of the voltage-operated Ca^{2+} channels (Schramm *et al.*, 1983), thus pinpointing the plasmalemma as the main target site for the two antioxidants.

Though plasmalemma calcium channels seem therefore to be the main target sites of BHA and BHT antispasmogenic action, they seem less likely to be the unique means whereby papaverine exerts its effects. Bay K 8644, in fact, only partly reverses the antispasmogenic action, in support of the proposal that papaverine acts by a combination of phosphodiesterase inhibition (as with methylxanthines) and block of calcium channels.

Within the framework of spasmolytic function, it is well to remember that at concentrations one order of magnitude greater than those used here, BHA and BHT were shown to disrupt membrane structure (Sgaragli *et al.*, 1977). Among their pleiotypic effects on mitochondria we found that BHA increases the proton leak through the mitochondrial inner membrane and weakens the Δp generating system (proton motive force across the mitochondrial inner membrane), but has no effect on phosphorylation (Fusi *et al.*, 1992). The disruption of biomembranes or the inhibition of mitochondrial respiration (Fusi *et al.*, 1991) does not seem to occur at the antispasmogenic concentrations described here. In closing the discussion on BHA and BHT we suggest that spasmolytic action is a common feature of phenol derivatives and that this pharmacological property is exerted via the inhibition of Ca^{2+} influx into the cells through the voltage-operated Ca^{2+} channels. This mechanism, however, requires clarification.

Aside from their effects on contractility, the phenolic compounds also exhibited their more familiar distinctive antiperoxidant property. It is well established that phenols, in their capacity as hydrogen donors (Burton & Ingold, 1981), form stable phenoxy radicals and are therefore effective antioxidants (Valoti *et al.*, 1989). Experiments using the two model systems of lipid peroxidation, gave comparable results despite the higher complexity of the microsomal system as compared to the linoleate. In the microsomal system, the greater the degree of lipophilicity, the more effective the antioxidant agent was shown to be. Therefore it is conceivable that the compounds behaved in an equivalent pharmacokinetic manner in both model systems and that the differences in potency observed are a real reflection of their intrinsic antiperoxidant capability. While di-*t*-BHA, NDGA, BHT and di-BHA were the most potent, nifedipine and caffeic acid were the least effective scavengers of peroxyl radicals. Though the antiperoxidant action of nifedipine, described elsewhere (Janero *et al.*, 1988; Janero & Burghardt, 1989), is difficult to interpret because it was used only at stronger concentrations than those required for effective calcium antagonism, caffeic acid might be of more than theoretical interest as an antioxidizing agent. In mammals, in fact, caffeic acid might be found in sufficient concentrations as a metabolite of chlorogenic and neochlorogenic acid, abundant components of many foodstuffs, to be a reliable and readily forming antioxidant resource, though devoid of spasmolytic activity.

A highly significant ($P<0.01$) linear correlation was found when plotting the antispasmogenic versus antioxidant activity of the fifteen phenolic derivatives showing dual activity (Figure 4). The fifteen effective 'dual action' compounds all presented at least one hydroxyl group on the aromatic ring and a highly lipophilic area on the molecule. The compounds which exhibited only spasmolytic effects or only antioxidant effects did not and were therefore excluded from the correlation. Of the excluded compounds, those with no phenol moiety were bereft of antioxidant capability, whereas the highly polar phenol derivatives (e.g. caffeic acid and trolox) were devoid of antispasmogenic capacity. Di-BHA, though possessing both structural requirements for the dual activity,

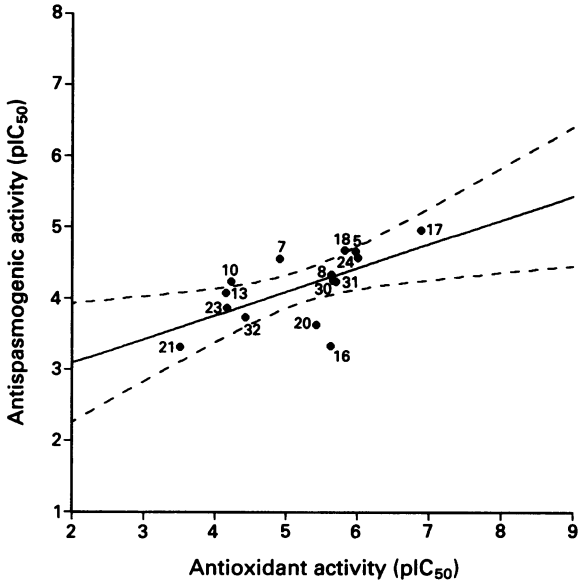

Figure 4 Comparison of pIC_{50} values for certain phenol derivatives. Antispasmogenic activity (intact musculature) versus peroxidation blockade (rat liver microsomal system). See Table 1 for key to compound numbers. Dashed lines represent 95% confidence intervals. Regression and correlation analysis showed $P<0.01$ and $r=0.62323$.

constitutes the exception i.e. though having lipophilic *t*-butyl and phenol moieties, this compound preserved the antioxidant capability of the parent without BHA's attendant antispasmogenic feature. This would seem to suggest that the phenol function, sterically hindered by a lipophilic moiety, is a necessary but insufficient condition for conferring dual action.

As to the linear correlation between the two activities in Figure 4, though significance was high the coefficient was low and the antispasmogenic property, though in an orderly relationship, consistently was less than the antioxidant behaviour of the compounds. Nevertheless, this suggests that some distinguishing structural feature determines dual behaviour and that di-*t*-BHA – structurally the simplest of all the bi-functional compounds – is of especial interest. This lead compound provides a fruitful starting point in the design of new drugs of high antioxidant and Ca^{2+}-blocking capabilities, thus potentially offering dual protection against tissue damage in ischaemia-reperfusion injury.

We are grateful to Mr Alberto Benocci and Roberto Borghi for invaluable technical assistance and to Mrs Gabriella Pacchierotti for typing the manuscript; also to Dr Rio Raikes for a critical reading and discussion of the manuscript.

This work was supported by the MURST and C.N.R., Roma, Italy.

References

ABDALLA, S., ZARGA, M.A., AFIFI, F., AL-KHALIL, S., MAHASNEH, A. & SABRI, S. (1989). Effects of 3,3'-di-o-methylquercetin on guinea-pig isolated smooth muscle. *J. Pharm. Pharmacol.*, **41**, 138–141.

BATTELLI, M.G., DELLA CORTE, E. & STIRPE, F. (1972). Xanthine oxidase type D (dehydrogenase) in the intestine and other organs of the rat. *Biochem. J.*, **126**, 747–749.

BENHAM, C.D., BOLTON, T.B., LANG, R.J. & TAKEWAKI, T. (1985). The mechanism of action of Ba^{2+} and TEA on single Ca^{2+}-activated K^+-channels in arterial and intestinal smooth muscle cell membranes. *Pflügers Arch.*, **403**, 120–127.

BOVERIS, A. & TURRENS, J.F. (1981). Production of superoxide anion by the NADH-dehydrogenase of mammalian mitochondria. In *Chemical and Biochemical Aspects of Superoxide and Superoxide Dismutase*. ed. Bannister, J.V. & Hill, H.A.O. pp. 84–92. Amsterdam: Elsevier, North Holland.

BÜLBRING, E. & TOMITA, T. (1969). Effect of calcium, barium and manganese on the action of adrenalin in the smooth muscle of guinea-pig taenia. *Proc. R. Soc. B*, **172**, 121–136.

BURTON, G.W. & INGOLD, K.U. (1981). Autoxidation of biological molecules. 1. The antioxidant activity of vitamin E and related chain-breaking phenolic antioxidants in vitro. *J. Am. Chem. Soc.*, **103**, 6472–6477.

CHEUNG, J.Y., BONVENTRE, J.V., MALIS, C.D. & LEAF, A. (1986). Calcium and ischemic injury. *N. Engl. J. Med.*, **314**, 1670–1676.

CHI-MING, H. & MURPHY, R.A. (1987). Ba^{2+} induces contraction in swine carotid artery by mobilizing intracellular Ca^{2+}. *Am. J. Physiol.*, **252**, C378–C384.

CORTIJO, J., DIXON, J.S., FOSTER, R.W. & SMALL, R.C. (1987). Influence of some variables in the Triton X-100 method of skinning the plasmalemmal membrane from guinea-pig trachealis muscle. *J. Pharmacol. Methods*, **18**, 253–266.

DEBY, C. & GOUTIER, R. (1990). New perspectives on the biochemistry of superoxide anion and the efficiency of superoxide dismutases. *Biochem. Pharmacol.*, **39**, 399–405.

DELLA CORTE, E. & STIRPE, F. (1972). The regulation of rat liver xanthine oxidase. Involvement of thiol groups in the conversion of the enzyme activity from dehydrogenase (type D) to oxidase (type O) and purification of the enzyme. *Biochem. J.*, **126**, 739–745.

FRIDOVICH, I. (1986). Biological effects of the superoxide radical. *Arch. Biochem. Biophys.*, **247**, 1–11.

FUSI, F., VALOTI, M., SGARAGLI, G.P. & MURPHY, M.P. (1991). The interaction of antioxidants and structurally related compounds with mitochondrial oxidative phosphorylation. *Meth. Find. Exp. Clin. Pharmacol.*, **13**, 599–603.

FUSI, F., SGARAGLI, G.P. & MURPHY, M.P. (1992). Interaction of butylated hydroxyanisole with mitochondrial oxidative phosphorylation. *Biochem. Pharmacol.*, **43**, 1203–1208.

HARA, H. & KOGURE, K. (1990). Prevention of hippocampus neuronal damage in ischemic gerbils by a novel lipid peroxidation inhibitor (quinazoline derivative). *J. Pharmacol. Exp. Ther.*, **255**, 906–913.

INOMATA, H. & KAO, C.Y. (1985). Actions of B^{++} on ionic currents of the guinea-pig taenia coli. *J. Pharmacol. Exp. Ther.*, **233**, 112–124.

JANERO, D.R. & BURGHARDT, B. (1989). Antiperoxidant effects of dihydropyridine calcium antagonists. *Biochem. Pharmacol.*, **38**, 4344–4348.

JANERO, D.R., BURGHARDT, B. & LOPEZ, R. (1988). Protection of cardiac membrane phospholipid against oxidative injury by calcium antagonists. *Biochem. Pharmacol.*, **37**, 4197–4203.

KATZ, A.M. & REUTER, H. (1979). Cellular calcium and cardiac cell death. *Am. J. Cardiol.*, **44**, 188–190.

KORN, S.J. & HORN, R. (1990). Nordihydroguaiaretic acid inhibits voltage-activated Ca^{2+} currents independently of lipoxygenase inhibition. *Mol. Pharmacol.*, **38**, 524–530.

KREYE, V.A.W., RUEGG, J.C. & HOFMANN, F. (1983). Effect of calcium-antagonist and calmodulin-antagonist drugs on calmodulin-dependent contractions of chemically skinned vascular smooth muscle from rabbit renal arteries. *Naunyn-Schmied. Arch. Pharmacol.*, **323**, 85–89.

MALIS, C.D. & BONVENTRE, J.V. (1986). Mechanism of Ca^{2+} and oxygen free radical injury to the mitochondrial electron transport chain. *Kidney Int.*, **29**, 305.

MARKLUND, S.L. (1986). Superoxide dismutase in human tissues, cells, and extracellular fluids: clinical applications. In *Free Radicals, Aging and Degenerative Diseases*. ed. Johnson, J.E., Walford, R., Harman, D. & Miquel, J. pp. 509–526. New York: Alan R. Liss.

MCCORD, J.M. (1985). Oxygen-derived free radicals in postischemic tissue injury. *N. Engl. J. Med.*, **312**, 159–163.

MEISHERI, K.D. & RÜEGG, J.C. (1983). Dependence of cyclic-AMP induced relaxation on Ca^{2+} and calmodulin in skinned smooth muscle of guinea pig taenia coli. *Pflügers Arch.*, **399**, 315–320.

MICHELSON, A.M. (1986). Free radicals and disease: treatment and clinical application with superoxide dismutase. In *Free Radicals, Aging and Degenerative Diseases*. ed. Johnson, J.E., Walford, R., Harman, D. & Miquel, J. pp. 263–291. New York: Alan R. Liss.

MIDDLETON, E.Jr. & KANDASWAMI, C. (1992). Effects of flavonoids on immune and inflammatory cell functions. *Biochem. Pharmacol.*, **43**, 1167–1179.

NAQUI, A., CHANCE, B. & CADENAS, E. (1986). Reactive oxygen intermediates in biochemistry. *Annu. Rev. Biochem.*, **55**, 137–166.

NAYLER, W.G. (1992). Calcium channels and their involvement in cardiovascular disease. *Biochem. Pharmacol.*, **43**, 39–46.

NAYLER, W.G., POOLE-WILSON, P.A. & WILLIAMS, A. (1979). Hypoxia and calcium. *J. Mol. Cell. Cardiol.*, **11**, 683–706.

NORTHOVER, B.J. (1968). The effect of drugs on the constriction of isolated depolarized blood vessels in response to calcium or barium. *Br. J. Pharmacol.*, **34**, 417–428.

RUEGG, J.C., SPARROW, M.P., MRWA, U., SCHNEIDER, M. & PFITZER, G. (1984). Calcium and calmodulin dependent regulatory mechanisms in chemically skinned smooth muscle. In *Smooth Muscle Contraction*. ed. Stephens, N.L. pp. 361–372. New York: Marcel Dekker Inc.

RUTERBORIES, K.J. & LINDSTROM, T.D. (1990). Pharmacokinetics of a novel butylated hydroxytoluene-thiazolidinone CNS anti-ischemic agent LY256548 in rats, mice, dogs and monkeys. *Drug Metab. Disp.*, **18**, 674–679.

SATOH, S., KUBOTA, Y., ITOH, T. & KURIYAMA, H. (1987). Mechanisms of the Ba^{2+}-induced contraction in smooth muscle cells of the rabbit mesenteric artery. *J. Gen. Physiol.*, **89**, 215–237.

SCHRAMM, M., THOMAS, G., TOWART, R. & FRANCKOWIAK, G. (1983). Novel dihydropyridines with positive inotropic action through activation of Ca^{2+} channels. *Nature*, **303**, 535–537.

SGARAGLI, G.P., DELLA CORTE, L., PULITI, R., DE SARLO, F., FRANCALANCI, R., GUARNA, A., DOLARA, P. & KOMARYNSKY, M. (1980). Oxidation of 2-t-butyl-4-metoxyphenol (BHA) by horseradish and mammalian peroxidase systems. *Biochem. Pharmacol.*, **29**, 763–769.

SGARAGLI, G.P., DELLA CORTE, L., RIZZOTTI-CONTI, M. & GIOTTI, A. (1977). Effects of monocyclic compounds on biomembranes. *Biochem. Pharmacol.*, **26**, 2145–2149.

SGARAGLI, G.P., VALOTI, M., PALMI, M. & MANTOVANI, P. (1989). Nifedipine-like activity of 2-t-butyl-4-methoxyphenol (BHA) on rat ileum longitudinal muscle preparation. *Pharmacol. Res.*, **21**, 649–650.

SHIROTA, H., CHIBA, K., ONO, H., YAMAMOTO, H., KOBAYASCHI, S., TERATO, K., IKUTA, H., YAMATSU, I. & KATAYAMA, K. (1987). Pharmacological properties of the novel non-steroidal anti-inflammatory agent N-methoxy-3-(3,5-di-tert-butyl-4-hydroxybenzylidene)pyrrolidin-2-one. *Arzneim-Forsch.*, **37**, 930–936.

SOMLYO, A.P., SOMLYO, A.V., DEVINE, C.E., PETERS, P.D. & HALL, T.A. (1974). Electron microscopy and electron probe analysis of mitochondrial cation accumulation in smooth muscle. *J. Cell. Biol.*, **61**, 723–742.

SPEDDING, M. (1982). Assessment of 'Ca^{2+}-antagonist' effects of drugs in K^+-depolarized smooth muscle. Differentiation of antagonist subgroups. *Naunyn-Schmied. Arch. Pharmacol.*, **318**, 234–240.

THE DANISH STUDY GROUP ON VERAPAMIL IN MYOCARDIAL INFARCTION (1990). Effect of verapamil on mortality and major events after acute myocardial infarction (The Danish Verapamil Infarction Trial II-DAVIT II). *Am. J. Cardiol.*, **66**, 779–785.

THE MULTICENTER DILTIAZEM POSTINFARCTION TRIAL RESEARCH GROUP (1988). The effect of diltiazem on mortality and reinfarction after myocardial infarction. *N. Engl. J. Med.*, **319**, 385–392.

UBEDA, A., TEJERINA, T., TAMARGO, J. & VILLAR, A. (1991). Effects of khellin on contractile responses and $^{45}Ca^{2+}$ movements in rat isolated aorta. *J. Pharm. Pharmacol.*, **43**, 46–48.

VALOTI, M., SIPE, H.J.Jr., SGARAGLI, G.P. & MASON, R. (1989). Free radical intermediates during peroxidase oxidation of 2-t-butyl-4-methoxyphenol, 2,6-di-t-butyl-4-methylphenol, and related phenol compounds. *Arch. Biochem. Biophys.*, **269**, 423–432.

WAYNER, D.D.M., BURTON, G.W., INGOLD, K.U., BARCLAY, L.R.C. & LOCKE, S.J. (1987). The relative contributions of vitamin E, urate, ascorbate and proteins to the total peroxyl radical-trapping antioxidant activity of human blood plasma. *Biochim. Biophys. Acta*, **924**, 408–419.

(Received December 29, 1992
Revised April 18, 1993
Accepted April 22, 1993)

Br. J. Pharmacol. (1993), **110**, 378–384

Involvement of cholecystokinin receptor types in pathways controlling oxytocin secretion

[1]Simon M. Luckman, Mitsuko Hamamura, Irina Antonijevic, Sandra Dye & Gareth Leng

Department of Neurobiology, AFRC Babraham Institute, Babraham, Cambridge CB2 4AT

1 Intravenous administration of cholecystokinin (CCK) results in a transient activation of oxytocin neurones in the rat, and hence to oxytocin secretion: this activation is followed by expression of c-*fos* mRNA and of Fos-like immunoreactivity (Fos-LI) in magnocellular oxytocin neurones. Fos-like immunoreactivity is also induced in the regions of the brainstem that are thought to relay information from the periphery to the hypothalamus.

2 Administration of the selective CCK_A receptor antagonist MK-329, but not the CCK_B receptor antagonist L-365,260, prior to CCK injection, prevented oxytocin release as measured by radioimmunoassay and oxytocin neuronal activation as measured by electrophysiology and by the lack of induction of c-*fos* mRNA.

3 MK-329 abolished the release of adrenocorticotrophic hormone (ACTH) following injection of CCK.

4 MK-329 prevented the expression of Fos-LI in the hypothalamic magnocellular nuclei and in the area postrema and dorsal vagal complex of the brainstem.

5 L-365,260 had no effect on the expression of Fos-LI in the brainstem, but attenuated that seen in the hypothalamic magnocellular nuclei.

6 We conclude that CCK acts on CCK_A receptors, either in the area postrema or on peripheral endings of the vagus nerve, to cause the release of hypothalamic oxytocin and ACTH. Information may be carried to the hypothalamus in part by CCK acting at CCK_B receptors.

Keywords: Adrenocorticotrophic hormone; CCK_A receptors; c-*fos*; cholecystokinin; oxytocin

Introduction

The magnocellular oxytocin neurones of the rat supraoptic and paraventricular nuclei respond to intravenous administration of cholecystokinin octapeptide (CCK) with a highly reproducible excitation, lasting 10–15 min and with a mean peak response of about 2 spikes s^{-1} above basal firing rates. The neuronal excitation (see Renaud *et al.*, 1987; Leng & Dyball, 1991) results in an elevation of plasma oxytocin concentrations, rising 5 min after CCK injection to about 50 pg ml^{-1} above basal levels (Verbalis *et al.*, 1986a,b; Blackburn & Leng, 1990). Systemically administered CCK also activates centrally-projecting oxytocin neurones, which form one limb of a gastric reflex arc, and also corticotrophin-releasing factor (CRF) neurones, that results in the release of ACTH (Verbalis *et al.*, 1991b; Kamilaris *et al.*, 1992). The profile of neuronal activation in the hypothalamus following systemic administration of CCK has been studied using products of the immediate-early gene c-*fos* as a marker. Within 10 min of CCK injection, c-*fos* mRNA is expressed in neurones of the supraoptic and paraventricular nuclei (Hamamura *et al.*, 1991). In the supraoptic nucleus, Fos-like immunoreactivity (Fos-LI) is found exclusively in magnocellular oxytocin neurones following CCK injection, while in the paraventricular nucleus at least three neuronal populations express Fos-LI: the CRF neurones, and both magnocellular and parvocellular oxytocin neurones (Verbalis *et al.*, 1991b).

There are two distinct CCK receptor types that are present in both the central nervous system and peripheral tissues (Hill *et al.*, 1987). In the periphery, CCK_A receptors predominate, though they are also present in the medial nucleus tractus solitarii (NTS) and the area postrema of the brainstem. The brain possesses mainly the CCK_B type of receptor. Though the supraoptic and paraventricular nuclei themselves possess CCK receptors (Day *et al.*, 1989; Blackburn *et al.*, 1990), systemically administered CCK is unlikely to access them directly, since these sites are within the blood-brain barrier. Instead CCK probably influences hormone secretion by a primary action at one of the circumventricular sites which lack an effective blood-brain barrier, or at the peripheral endings of the afferent vagus (Verbalis *et al.*, 1986b; Carter & Lightman, 1987). Thus, it has been possible to show the induction of Fos-LI in the area postrema, a circumventricular organ, and in the dorsal vagal complex, that contains the NTS, following administration of CCK (Luckman, 1992). The afferent pathway to the hypothalamus has been proposed to involve a direct vagal projection to noradrenergic neurones within the NTS, and thence either directly to the hypothalamus or indirectly via, for example, the parabrachial nucleus. CCK and CCK receptors are present in neurones throughout this proposed pathway, and it has therefore been suggested that CCK activates a chain of CCK-coding neurones, which may utilize CCK as a central neurotransmitter.

The present study employed two potent CCK receptor antagonists, one selective for CCK_A receptors and one for CCK_B receptors, to establish which receptor type was involved in neuroendocrine activation following systemic administration of CCK. We measured plasma concentrations of oxytocin and of ACTH, the electrical activity of magnocellular oxytocin neurones and the expression of c-*fos* mRNA in the hypothalamus after CCK following receptor antagonism. To determine possible sites of action of the antagonists, the expression of Fos-LI was examined throughout the brain. Preliminary results have been published in abstract form (Leng *et al.*, 1992; Luckman *et al.*, 1993).

Methods

Rats from the AFRC Babraham Wistar colony (body weight 250–300 g) were used in all studies. CCK-8 (CCK26-33,

[1] Author for correspondence.

sulphated; Sigma, UK) was dissolved in isotonic saline (1 mg ml^{-1}). MK-329 (3S(−)-N-(2,3-dihydro-1-methyl-2-oxo-5-phenyl-1H-1,4-benzodiazepine-3-yl)-1H-indole-2-carboxyamide; also known as L-364,718 or devazepide) and L-365,260 (3R(+)-N-(2,3-dihydro-1-methyl-2-oxo-5-phenyl-1H-1,4-benzodiazepine-3-yl)-N′-(3-methylphenyl)urea) (both Merck Sharp & Dohme, UK), selective antagonists for the CCK_A and CCK_B receptor types, were dissolved in 20% absolute ethanol/80% propan-1,2-diol.

For the electrophysiological study, female rats were anaesthetized with urethane (ethyl carbamate; 1.25 g kg^{-1}, i.p.). The supraoptic nucleus and the neural stalk were exposed by ventral surgery (Leng & Dyball, 1991); a bipolar stimulating electrode was placed upon the neural stalk and a microelectrode introduced into the nucleus by direct visual control. Single neurones, recorded extracellularly from the supraoptic nucleus region were identified antidromically as projecting to the neural lobe and as putative oxytocin neurones by their continuous pattern of discharge activity, and by their lack of response to i.v. injection of phenylephrine (10 μg; Sigma, UK): phenylephrine injections result in a selective transient inhibition of vasopressin neurones mediated by baroreceptor activation (see Leng & Dyball, 1991). Three injections of CCK-8 were given (20 μg kg^{-1}, i.v.), which were separated by injections of L-365,260 (1 mg kg^{-1}, i.v.) and MK-329 (1 mg kg^{-1}). Only one neurone was tested for these effects in each rat.

To assess the effects of the antagonists on the release of oxytocin induced by CCK, female rats were anaesthetized with urethane to allow cannulation of jugular and femoral veins. Two hours after surgery, rats were given two injections of CCK-8 (20 μg kg^{-1}, i.v.) 40 min apart; 30 min after the first CCK injection MK-329 or L-365,260 were administered at doses of 0.001, 0.01, 0.1 or 1 mg kg^{-1}. Blood samples of 0.3 ml, replaced with an equal volume of heparinized saline, were taken immediately before and 5, 10 and 30 min after each CCK injection. Oxytocin in the plasma was measured by specific radioimmunoassay (Higuchi *et al.*, 1985).

For the *in situ* hybridization study, male rats had a jugular vein cannulated with polyethylene tubing under brief tribromoethanol (10 ml kg^{-1}, i.p.) anaesthesia. The following day the conscious, freely-moving rats were injected with MK-329 (1 mg kg^{-1}, i.v.) or vehicle; 15 min later CCK-8 was injected (50 μg kg^{-1}, i.v.) and the rats were subsequently decapitated at 0, 10, 30 and 240 min. Two control groups were killed 30 min after injection of the antagonist or vehicle without injection of CCK. Oxytocin was measured as described by Higuchi *et al.* (1985) and ACTH was determined by kits derived from Diagnostic Corp (DPC, Los Angeles CA, U.S.A.) in a single assay.

The *in situ* hybridization technique for measurement of c-*fos* mRNA has been described in full elsewhere (Hamamura *et al.*, 1991; 1992). The probe was a synthetic oligonucleotide (48-mer) complementary to rat c-*fos* mRNA (Curran *et al.*, 1987), 3′ end-labelled using α[^{35}S]-dATP (New England Nuclear, UK) and terminal deoxynucleotidyl transferase (Pharmacia, UK). Northern analysis has confirmed that probe binding is specifically to mRNA corresponding in size to that reported for rat c-*fos* mRNA (Wisden *et al.*, 1990). Hybridization in the hypothalamus is localized to neuronal cell bodies, and is blocked in the presence of an excess of cold oligonucleotide and by RNase A pretreatment of tissue sections (Hamamura *et al.*, 1991; 1992). Coronal sections of the hypothalamus (20 μm) were fixed, prehybridized and hybridized overnight with the probe, and treated sections were apposed to autoradiographic film (Amersham, UK) for 3 weeks. The apposition time was selected so that the optical density of film images did not exceed 0.7, as above this level the film response deviates from linearity. For quantification of the c-*fos* mRNA signal, the optical density of the autoradiographic film image was measured by a Magiscan Image Analysis System (Joyce-Loebl, UK). The autoradiographic film was viewed under a microscope, and a circular-counting frame (125 μm diameter) was centred on the region of most intense signal. The mean optical density within each such counting frame, after subtraction of the background optical density, was calculated for each paraventricular and supraoptic nucleus on each section, and the mean values calculated for each animal.

For the functional mapping study using Fos-LI as an activity marker, male rats had a jugular vein cannulated under tribromoethanol anaesthesia 2 days prior to experimentation. On the day of experimentation the conscious, freely-moving rats were injected i.v. with either MK-329, L-365,260 (each at 100 μg kg^{-1}) or vehicle (100 μl kg^{-1}); 20 min later rats were injected with CCK-8 (20 μg kg^{-1}, i.v.) or isotonic saline. After a further 90 min the rats were anaesthetized with sodium pentobarbitone (50 mg kg^{-1}, i.v.) and

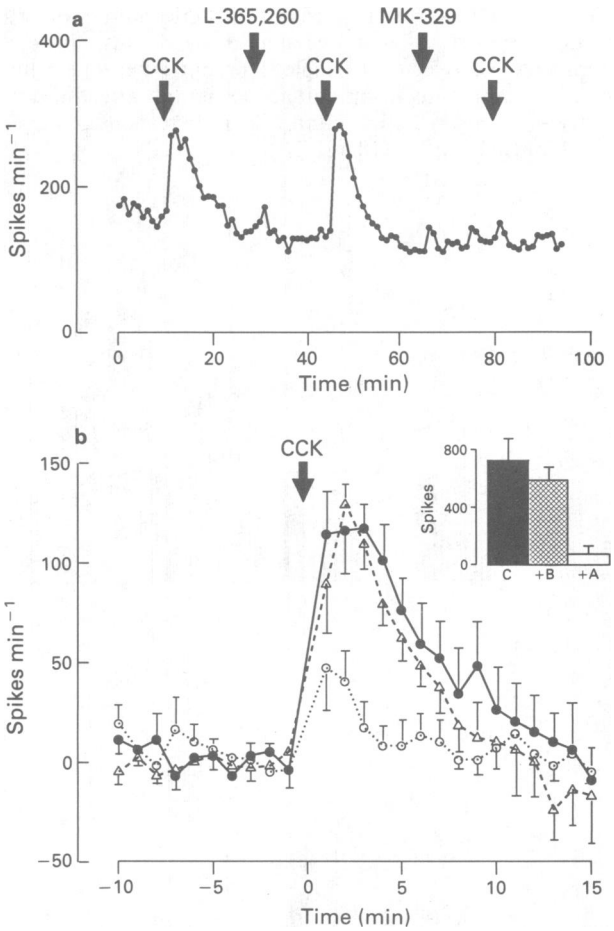

Figure 1 (a) Electrical activity of a single oxytocin neurone recorded from the supraoptic nucleus of a urethane-anaesthetized rat, showing responses to three injections of CCK-8 (20 μg kg^{-1}, i.v.), separated by i.v. injection of the CCK_B receptor antagonist L-365,260 and the CCK_A receptor antagonist MK-329 (1 mg kg^{-1}, i.v.). The CCK_B receptor antagonist was ineffective, while the CCK_A receptor antagonist abolished CCK-induced excitation. (b) Mean responses of four oxytocin neurones, each recorded from the supraoptic nucleus of different urethane-anaesthetized rats. Each neurone was tested as in (a). The data for each cell was first expressed as total spikes in each minute of recording. Firing rates were then normalized by subtraction of the mean basal firing rate, calculated separately for each test exposure as the mean firing rate in the 10 min prior to CCK injection. The figure gives the mean ± s.e.mean of the normalized counts, to show the mean neuronal activation following CCK in each of the three tests. The CCK_A receptor antagonist virtually eliminated the neuronal response to CCK, whereas the CCK_B receptor antagonist at the same dose was ineffective. The inset gives the mean neuronal response, calculated as the mean additional number of spikes recorded in the 10 min following each CCK injection compared to the control period, for the initial injection of CCK (C); CCK injection following the CCK_B receptor antagonist (+ B); and CCK injection following the CCK_A receptor antagonist (+ A).

perfused with fixative for standard immunocytochemistry using a polyclonal antibody raised against the N-terminal amino acids 2–17 of the Fos protein, as previously described (Luckman, 1992). The mean number of Fos-LI nuclear profiles per 30 μm section was counted in a variety of brain regions. These figures were then further meaned to give a value for each experimental group.

The Mann Whitney U-test (two tailed) was used for all statistical comparisons.

Results

Effects of CCK antagonists on the electrical activity of supraoptic neurones

The electrical activity of supraoptic neurones, identified antidromically as projecting to the posterior pituitary, was recorded from four urethane-anaesthetized rats. In each experiment, we selected a single supraoptic neurone which showed a continuous firing pattern, excitation after injection of CCK-8 (20 μg kg^{-1}, i.v.), and a lack of response to injection of phenylephrine (10 μg, i.v.).

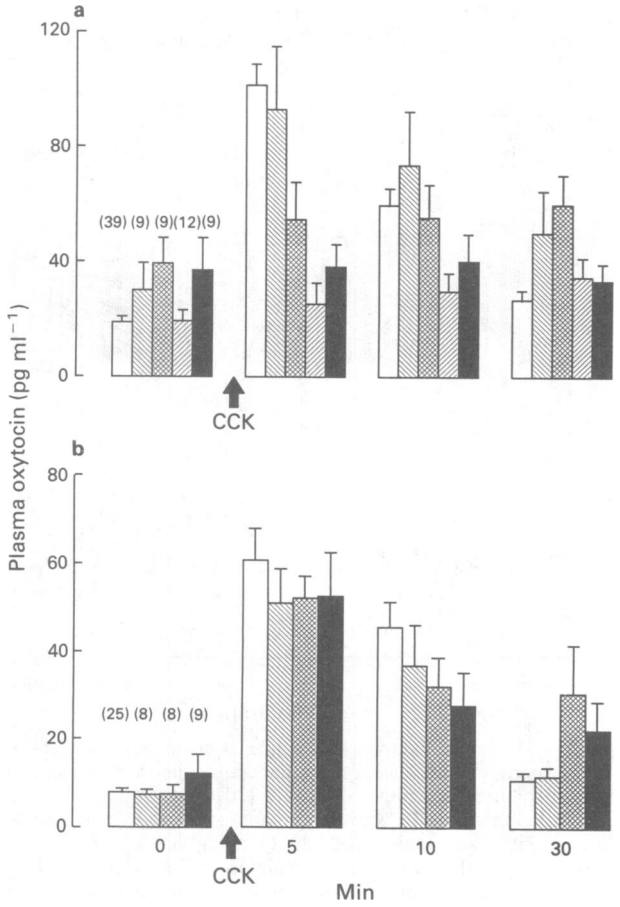

Figure 2 Oxytocin release following i.v. injections of CCK-8 (20 μg kg^{-1}) in anaesthetized rats, measured following administration of CCK_A receptor antagonist MK-329 (a) and the CCK_B receptor antagonist L-364,260 (b) at various concentrations. In (a) concentration of receptor antagonist; □; 0; ▨ 0.001; ▩ 0.01; ▨ 0.1; ■ 1 mg kg^{-1}, in (b): □, 0; ▨ 0.01; ▩ 0.1; ■ 1 mg kg^{-1}. Columns are means ± s.e.mean plasma oxytocin at 0, 5, 10 and 30 min after CCK injection, $n \geq 9$ for each group of rats (numbers in each group is in parentheses). CCK-induced oxytocin release was unaffected by the CCK_B receptor antagonist but blocked in a dose-related manner by the CCK_A receptor antagonist at similar concentrations. The open columns show oxytocin release in response to the first (control) CCK injection given to all rats. Attenuation of CCK-evoked release is significant ($P<0.01$) at all doses of the CCK_A receptor antagonist above 0.001 mg kg^{-1}.

Injection of CCK-8 (20 μg kg^{-1}, i.v.) transiently and significantly increased the firing rate of each of the oxytocin neurones (Figure 1a; $P<0.01$ comparison of pre- and post-injection firing rates). Injection of L-365,260 had no significant effect either on the basal firing rate or on the excitatory response to CCK. On the other hand, MK-329 clearly suppressed the excitatory response in each neurone without affecting spontaneous discharge rate. Figure 1b shows the averaged response to CCK with or without prior injection of MK-329 or L-365,260. For each cell the CCK-induced excitation after injection of MK-329 was significantly smaller than the responses observed before and after injection of L-365,260 ($P<0.01$).

Effects of CCK receptor antagonist on plasma concentrations of oxytocin

In 39 urethane-anaethetized female rats, injection of CCK (20 μg kg^{-1}, i.v.) increased significantly ($P<0.001$) the immunoreactive oxytocin concentration in the plasma (Figure 1a). This initial injection of CCK was followed by the CCK_A antagonist MK-329 i.v. at doses of 0.001, 0.01, 0.1 or 1 mg kg^{-1} (Figure 2a). Injection of MK-329 itself had no effect on the plasma oxytocin concentration at any dose used. The oxytocin release in response to a subsequent injection of CCK was attenuated in a dose-dependent manner by MK-329; the attenuation was significant at a dose of 0.01 mg kg^{-1} ($P<0.01$), and higher doses ($P<0.001$) abolished the response.

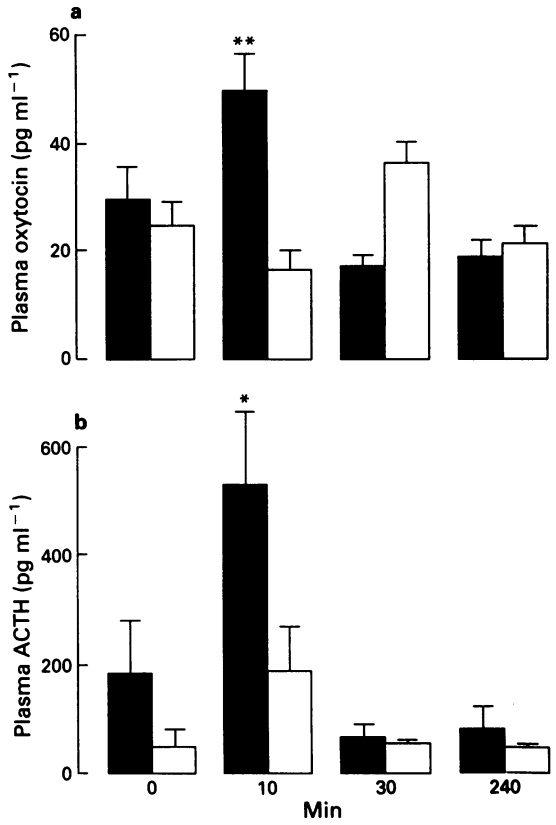

Figure 3 Mean concentrations of oxytocin (a) and ACTH (b) in trunk blood of rats killed for analysis of c-*fos* mRNA expression in the hypothalamus. Rats were given an i.v. injection of either the CCK_A receptor antagonist, MK-329 (1 mg kg^{-1}, open columns) or vehicle (solid columns), followed 30 min later by i.p. injection of CCK-8 (50 μg kg^{-1}). Rats were killed 10, 30 or 240 min later, or were killed without CCK injection; $n = 5$ or 6 in each group. CCK induced significant increases in oxytocin and ACTH in rats killed 10 min after injection in the vehicle pretreated, but not the antagonist pretreated group. $^*P<0.05$, $^{**}P<0.01$ compared to rats killed immediately after CCK.

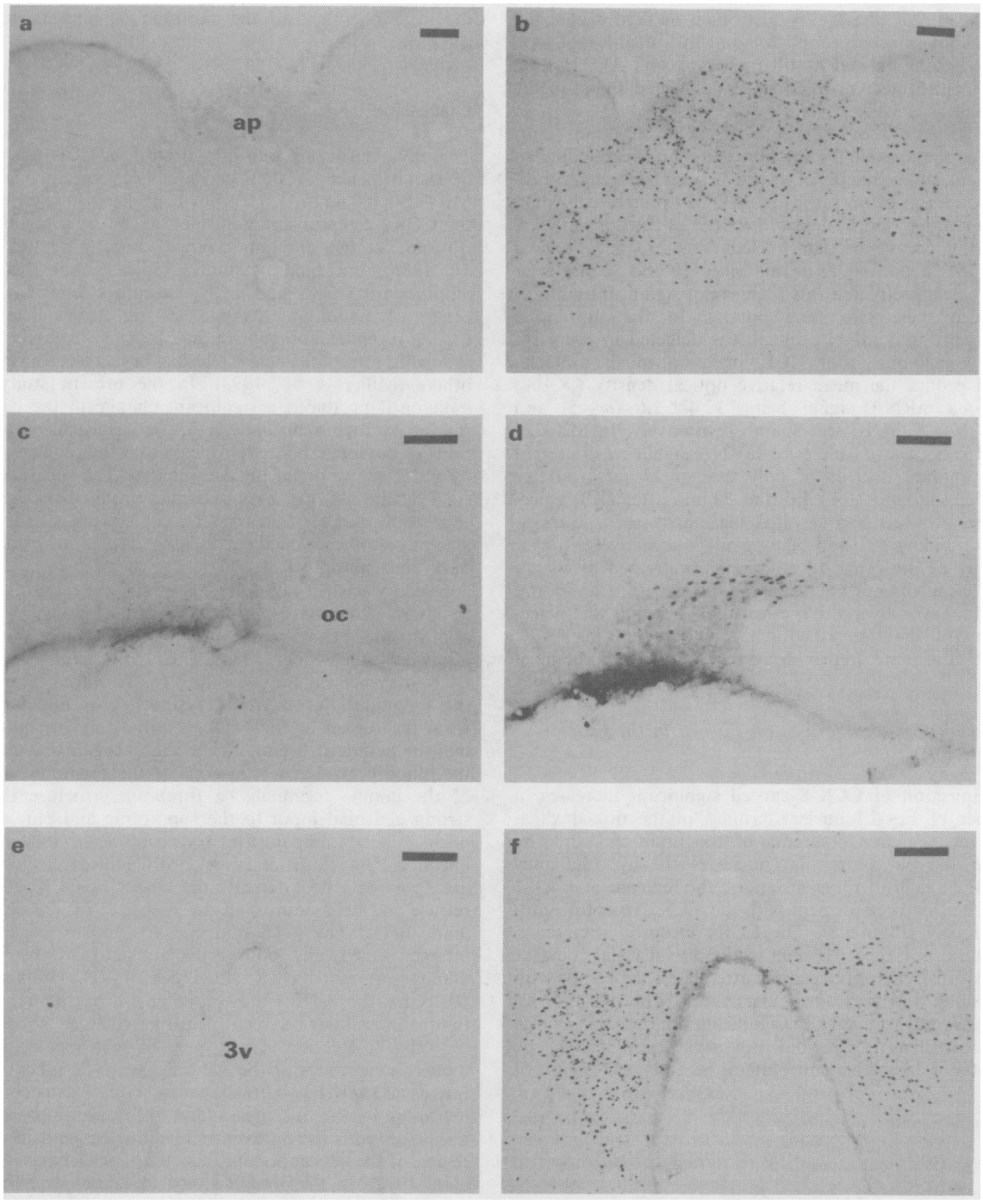

Figure 4 Photomicrographs showing Fos-LI before (a,c,e) and 90 min after (b,d,f) injection of CCK-8 (20 $\mu g\,kg^{-1}$, i.v.). (a and b) Brainstem at level of area postrema (ap); the NTS lies between the area postrema and the central canal. (c and d) Supraoptic nucleus; Fos-LI nuclear profiles are in the dorsal region of the supraoptic nucleus of the stimulated brain, the area in which oxytocin neurones predominate; oc = optic chiasm. (e and f) Paraventricular nuclei on either side of the third ventricle (3v). Bars represent 10 μm.

A second group of 25 female rats similarly showed a significant increase in plasma oxytocin concentration following an initial injection of CCK (20 $\mu g\,kg^{-1}$, i.v.). Thirty minutes after the first injection, the CCK_B receptor antagonist L-365,260 was administered i.v. at doses of 0.01, 0.1 or 1 $mg\,kg^{-1}$. L-365,260 had no significant effect either upon basal oxytocin release or upon the oxytocin release in response to CCK at any dose (Figure 2b).

Effects of CCK_A receptor antagonism on c-fos mRNA expression in the hypothalamus

Radioimmunoassay of the trunk blood samples confirmed significant elevation of both oxytocin ($P<0.01$) and ACTH ($P<0.05$) plasma concentrations 10 min after CCK in the vehicle pre-treated rats, but not in the MK-329 pre-treated rats (Figure 3).

In the two control groups not injected with CCK, no c-*fos* mRNA signal was detected in any of 6 rats pretreated with MK-329, but measurable signal was present in two of six rats pre-treated with vehicle. In these two rats, the relative optical densities ($\times$ 100) of the c-*fos* mRNA signal in the supraoptic nucleus were 21.8 and 17.5 respectively and in the paraventricular nucleus were 19.7 and 24.6 respectively. These two rats had elevated concentrations of oxytocin in the circulation at the time of killing (39.5 and 53.4 $pg\,ml^{-1}$ respectively, the highest values of this group and higher than any rat in the vehicle pretreated group killed 30 min or 4 h after CCK

injection). One of these rats also had markedly elevated plasma ACTH concentration (249.4 ng ml^{-1}), although one rat in this group showed a still higher plasma ACTH level (638 ng ml^{-1}) not accompanied by any detected signal in the paraventricular nucleus.

In rats killed 10 or 30 min after CCK injection, c-*fos* mRNA was measurable on the film images corresponding to the paraventricular nuclei of every rat in the vehicle pretreated group, but of no rat in the MK-329 pretreated group. The mean relative optical density (× 100) of the c-*fos* mRNA signal in the paraventricular nucleus was 21.0 ± 1.9 ($n = 5$ rats) and 20.2 ± 2.4 ($n = 5$) in rats killed 10 and 30 min after CCK in vehicle pretreated rats (values not significantly different between these two time points). In the supraoptic nucleus, again c-*fos* mRNA signal was detected in every rat killed 10 or 30 min after CCK injection in the vehicle-pretreated group: the mean relative optical density (× 100) of the c-*fos* mRNA signal being 12.4 ± 2.6 ($n = 5$) and 16.1 ± 1.8 ($n = 5$) at 10 and 30 min respectively. In MK-329 pretreated rats, measurable c-*fos* mRNA signal was detected in the supraoptic nucleus of only two of 12 rats (relative O.D. × 100, 14.0 and 16.8), both at 30 min after CCK injection. These two rats had elevated plasma oxytocin levels at the time of killing (67 and 50.9 pg ml^{-1} respectively, higher than in any of the other 18 antagonist-pretreated rats), but ACTH levels in the normal range for this experiment (40 and 63.7 ng ml^{-1} respectively). No c-*fos* mRNA signal was detected in any of the rats killed 4 h after injection of CCK, whether in rats pretreated with vehicle ($n = 5$) or antagonist ($n = 5$).

Effect of receptor antagonists on Fos-LI in the brain following CCK

Systemic injection of CCK-8 caused significant increases in the number of Fos-LI nuclear profiles in the dorsal vagal complex and the area postrema of the brainstem and the supraoptic and paraventricular nuclei of the hypothalamus (Figure 4). In each of these instances, the increase in Fos-LI was abolished by pretreatment with the CCK_A receptor antagonist MK-329 (Figure 5). The CCK_B receptor antagonist, L-365,260 did not affect staining in the dorsal vagal complex or the area postrema, but severely attenuated the response in the supraoptic and paraventricular nuclei. The effect of L-365,260 was only statistically significant in the case of the supraoptic nucleus. CCK did not significantly alter the amount of Fos-LI in the ventrolateral medulla, the region of the locus coeruleus or the parabrachial nucleus (results not shown).

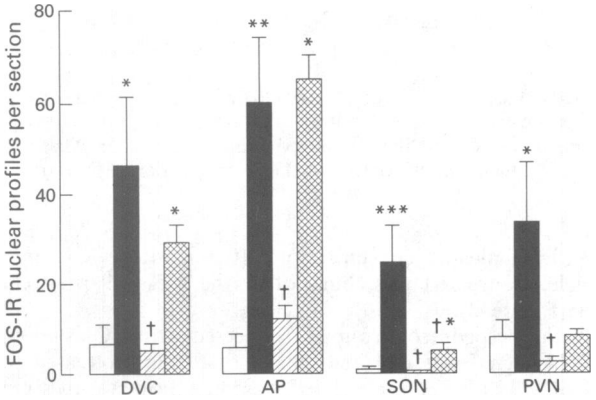

Figure 5 Number of Fos-LI nuclear profiles in four brain areas following injections of isotonic saline, CCK-8 alone (20 μg kg^{-1}, i.v.), or CCK with prior injection of MK-329 or L-365,260 (100 μg kg^{-1}, i.v.). Columns represent means ± s.e.mean, $n = 5$–6. ☐ Saline; ■ CCK; ▨ MK-329; ▩ L-365,260. DVC, dorsal vagal complex; AP, area postrema; SON, supraoptic nucleus; PVN, paraventricular nucleus. *$P < 0.05$; **$P < 0.01$, ***$P < 0.005$ compared to isotonic saline; †$P < 0.05$ compared to CCK only.

Discussion

The oxytocin response to i.v. injection of CCK-8 is abolished in the presence of the specific CCK_A receptor antagonist MK-329 (100 μg μg^{-1}, i.v.) but unaffected in the presence of the CCK_B receptor antagonist L-365,260 at a higher concentration. The two antagonists are chemically related (Evans *et al.*, 1986), but binding studies indicate that their relative affinities for CCK_A and CCK_B receptors differ by over two orders of magnitude (Lotti & Chang, 1989). The effect of CCK_A receptor antagonism in blocking oxytocin secretion following intraperitoneal CCK has been recently reported by others (Miller *et al.*, 1993). In the present study, neither antagonist produced a significant change in the basal firing rate of oxytocin neurones, or in the basal plasma concentrations of oxytocin, hence it appears that the pathway activated by CCK may not be tonically active. The measurements of ACTH and of the hypothalamic profile of c-*fos* mRNA expression indicate that CCK_A receptors are also involved in activation of parvocellular neurosecretory neurones in the paraventricular nucleus.

Selective gastric vagotomy eliminates the oxytocin response to CCK (Verbalis *et al.*, 1986b) and lesions of the NTS abolish the behavioural effects of CCK on food intake (Crawley & Schwaber, 1984). Thus, peripherally administered CCK may act via the ascending gastric vagus, and influence the magnocellular oxytocin system via a direct projection from the region of the NTS. Alternatively, peripheral CCK may be acting at a circumventricular organ that lies outside the blood-brain barrier. Lesions of the organum vasculosum of the lamina terminalis, a forebrain structure that has a strong neuronal input to the supraoptic and paraventricular nuclei, do not impair the oxytocin release following CCK injection (Blackburn & Leng, 1990). However, lesions of the area postrema do attenuate the effects of CCK on oxytocin release and behaviour (Van der Kooy, 1984; Carter & Lightman, 1987). The NTS and the area postrema are heavily interconnected, and both areas are activated by peripheral administration of CCK (Luckman, 1992). Unlike the area postrema, the NTS is the source of a direct afferent input to the magnocellular oxytocin neurones (Day & Sibbald, 1988a, b; Raby & Renaud, 1989), part of which comprises noradrenergic neurones of the A2 cell group. Peripheral administration of CCK has been shown to activate catecholaminergic neurones in the A2 group and to result in noradrenaline release in both the paraventricular nucleus and in the dorsal region of the supraoptic nucleus (Kendrick *et al.*, 1991; Luckman, 1992). In the present study, no increase in Fos-LI was seen in the ventrolateral medulla, the region of the locus coeruleus or parabrachial nucleus, all of which are possible relay sites on the pathway between the brainstem and the hypothalamus. However, Fos-LI is present in these areas in all animals and therefore it is possible that changes in the activation of specific neuronal populations, for example noradrenergic neurones in the ventrolateral medulla or locus coeruleus, may be masked by absolute cell counts. It should also be noted that many of the neurones activated in the NTS are non-catecholaminergic (Luckman, 1992), and thus a recently described peptidergic innervation of oxytocin neurones from the NTS (Sawchenko *et al.*, 1988) may also be involved.

An additional target for peripheral CCK is believed to be the neural lobe of the pituitary, since CCK induces oxytocin and vasopressin release from the neural lobe *in vitro* (Bondy *et al.*, 1989). This *in vitro* finding has many unusual and intriguing aspects. The release occurs only after a long latency, and is independent of extracellular calcium entry. As yet, it appears to have no parallel *in vivo*, where observed release is immediate and selective for oxytocin.

Since CCK is present in afferent vagal neurones, in neurones of the NTS, and in magnocellular oxytocin neurones (Vanderhaeghen *et al.*, 1980), it is possible that centrally released CCK participates in coding the neuronal responses to peripheral CCK injection. The apparent effect of the CCK_B receptor antagonist ($100\,\mu g\,kg^{-1}$) on Fos-LI in the hypothalamus would suggest a role for central CCK receptors in the mediation of the effects of CCK. This is surprising since this and higher concentrations of the CCK_B antagonist were ineffective at inhibiting the electrical and secretory activity of oxytocin neurones. It remains possible that several neurotransmitters are involved in these central pathways, and that the expression of Fos in these neurones is more sensitive to antagonism than is their electrical activity.

The physiological role of the pathway activated by CCK is not known. One of the postulated functions of oxytocin in the rat is to promote sodium excretion (Balment *et al.*, 1986; Verbalis *et al.*, 1991a), hence the pathway may initiate a reflex natriuresis following feeding. Since there is little evidence of significant oxytocin release following feeding, this hypothesis is so far unsupported. An alternative interpretation comes from the evidence that in the rat, oxytocin release is activated by diverse acute stressors, including immobilization, ether inhalation and fear-related emotional stress (Lang *et al.*, 1983; Gibbs, 1986; Onaka & Yagi, 1990). Link *et al.* (1992) have shown a synergistic effect of oxytocin and CRF on the release of ACTH at the level of the pituitary, though it is more likely that oxytocin released from the median eminence is involved, rather than that released by the magnocellular system into the general circulation. It is clearly possible, however, that the activation of oxytocin and CRF neurones following CCK administration may be via a common 'stress' pathway.

The authors would like to thank Merck Sharp and Dohme for their kind gift of the specific CCK receptor antagonists, and Drs Takashi Higuchi and Gerard Evan for their gifts of oxytocin and Fos antisera, respectively.

References

BALMENT, R.J., BRIMBLE, M.J., FORSLING, M.L., KELLY, L.P. & MUSABAYANE, C.T. (1986). A synergistic effect of oxytocin and vasopressin on sodium excretion in the neurohypophysectomized rat. *J. Physiol.*, **381**, 453–464.

BLACKBURN, R.E., DAY, N.C., LENG, G. & HUGHES, J. (1990). The effect of anteroventral third ventricular lesions on the changes in cholecystokinin receptor density in the rat supraoptic nucleus following saline drinking. *J. Neuroendocrinol.*, **2**, 323–328.

BLACKBURN, R.E. & LENG, G. (1990). Ablation of the region anterior and ventral to the third ventricle (AV3V region) in the rat does not abolish the release of oxytocin in response to systemic cholecystokinin. *Brain Res.*, **508**, 156–160.

BONDY, C.A., JENSEN, R.T., BRADY, L.S. & GAINER, H. (1989). Cholecystokinin evokes secretion of oxytocin and vasopressin from rat neural lobe independent of external calcium. *Proc. Natl. Acad. Sci. U.S.A.*, **886**, 5198–5201.

CARTER, D.A. & LIGHTMAN, S.L. (1987). A role for the area postrema in mediating cholecystokinin-stimulated oxytocin secretion. *Brain Res.*, **435**, 327–330.

CRAWLEY, J.N. & SCHWABER, J.S. (1984). Abolition of the behavioural effects of cholecystokinin following bilateral radiofrequency lesions of the parvocellular subdivision of the nucleus tractus solitarius. *Brain Res.*, **295**, 289–299.

CURRAN, T., GORDON, M.B., RUBINO, K.L. & SAMBUCETTI, L.C. (1987). Isolation and characterisation of c-*fos* (rat) cDNA and analysis of post-transcriptional modification *in vitro*. *Oncogene*, **2**, 79–84.

DAY, N.C., HALL, M.D. & HUGHES, J. (1989). Modulation of hypothalamic cholecystokinin receptor density with changes in magnocellular activity: a quantitative autoradiographic study. *Neuroscience*, **29**, 371–383.

DAY, T. & SIBBALD, J.R. (1988a). Direct catecholaminergic projection from nucleus tractus solitarii to supraoptic nucleus. *Brain Res.*, **454**, 387–392.

DAY, T. & SIBBALD, J.R. (1988b). Solitary nucleus excitation of supraoptic vasopressin cells via adrenergic afferents. *Am. J. Physiol,*. **254**, R711–R716.

EVANS, B.E., BOCK, M.G., RITTLE, K.E., DIPARDO, R.M., WHITTER, W.L., VEBER, D.F., ANDERSON, P.S. & FREIDINGER, R.M. (1986). Design of potent, orally effective, nonpeptidal antagonists of the peptide hormone cholecystokinin. *Proc. Natl. Acad. Sci. U.S.A.*, **83**, 4918–4922.

GIBBS, D.M. (1986). Vasopressin and oxytocin: hypothalamic modulators of the emotional stress response: a review. *Psychoneuroendocrinol,*. **11**, 131–140.

HAMAMURA, M., LENG, G., EMSON, P.C. & KIYAMA, H. (1991). Electrical activation and c-fos mRNA expression in rat neurosecretory neurones after systemic administration of cholecystokinin. *J. Physiol,*. **444**, 51–63.

HAMAMURA, M., NUNEZ, D.J.R., LENG, G., EMSON, P.C. & KIYAMA, H. (1992). C-fos may be a common transcription factor within the hypothalamic neural circuits involved in osmoregulation. *Brain Res.*, **572**, 42–51.

HIGUCHI, T., HONDO, K., FUKUOKA, T., NEGORO, H. & WAKABAYISHI, K. (1985). Release of oxytocin during suckling and parturition in the rat. *J. Endocrinol.*, **105**, 339–346.

HILL, D.R., CAMPBELL, N.J., SHAW, T.M. & WOODRUFF, G.N. (1987). Autoradiographic localization and biochemical characterization of peripheral type CCK receptors in rat CNS using highly selective nonpeptide CCK antagonists. *J. Neurosci.*, **7**, 2967–2976.

KAMILARIS, T.C., JOHNSON, E.O., CALOGERO, A.E., KALOGERAS, K.T., BERNARDINI, R., CHROUSOS, G.P. & GOLD, P.W. (1992). Cholecystokinin-octapeptide stimulates hypothalamic-pituitary-adrenal function in rats: role of corticotropin-releasing hormone. *Endocrinology*, **130**, 1764–1774.

KENDRICK, K., LENG, G. & HIGUCHI, T. (1991). Noradrenaline, dopamine and serotonin release in the paraventricular and supraoptic nuclei of the rat in response to cholecystokinin injections. *J. Neuroendocrinol.*, **3**, 139–144.

LANG, R.E., HEIL, J.W.E., GANTEN, D., HERMANN, K., UNGER, T. & RASCHER, W. (1983). Oxytocin unlike vasopressin is a stress hormone in the rat. *Neuroendocrinol.*, **37**, 353–356.

LENG, G. & DYBALL, R.E.J. (1991). Functional identification of magnocellular neuroendocrine neurones. In *Neuroendocrine Research Methods*, Vol. 2. ed. Greenstein, B. pp. 769–791. Reading: Harwood Academic Publishers.

LENG, G., HAMAMURA, M., BACON, J. & EMSON, P.C. (1992). CCK-induced activation of oxytocin neurones is blocked by a selective CCK_A receptor antagonist. In *Multiple Cholecystokinin Receptors in the CNS*. ed. Dourish, C.T., Cooper, S.J., Iversen, S.D. & Iversen, L.L. pp. 315–318. Oxford: Oxford Science Publications.

LINK, H., DAYANITHI, G., FOHR, K.J. & GRATZL, M. (1992). Oxytocin at physiological concentrations evokes adrenocorticotropin (ACTH) release from corticotrophs by increasing intracellular free calcium mobilized mainly from intracellular stores. Oxytocin displays synergistic or additive effects on ACTH-releasing factor or arginine vasopressin-induced ACTH secretion, respectively. *Endocrinology*, **130**, 2183–2191.

LOTTI, V.J. & CHANG, R.S.L. (1989). A new potent and selective non-peptide gastrin antagonist and brain cholecystokinin receptor (CCK-B) ligand: L-365,260. *Eur. J. Pharmacol.*, **162**, 273–280.

LUCKMAN, S.M. (1992). Fos-like immunoreactivity in the brainstem of the rat following peripheral administration of cholecystokinin. *J. Neuroendocrinol.*, **4**, 149–152.

LUCKMAN, S.M., ANTONIJEVIC, I. & DYE, S. (1993). The peripheral-type cholecystokinin receptor antagonist, MK-329, blocks induction of Fos-like immunoreactivity in the rat brain following systemic administration of cholecystokinin. *J. Physiol.*, **459**, 483P.

MILLER, T.R., BIANCHI, B.R., WITTE, D.G. & LIN, C.W. (1993). Peripheral cholecystokinin type A receptors mediate oxytocin secretion in vivo. *Regul. Pept.*, **43**, 107–112.

ONAKA, T. & YAGI, K. (1990). Differential effects of naloxone on neuroendocrine responses to fear-related emotional stress. *Exp. Brain Res.*, **81**, 53–58.

RABY, W.N. & RENAUD, L.P. (1989). Dorsomedial medulla stimulation activates rat supraoptic oxytocin and vasopressin neurones through different pathways. *J. Physiol.*, **417**, 279–294.

RENAUD, L.P., TANG, M., MCCANN, M.J., STRICKER, E.M. & VERBALIS, J.G. (1987). Cholecystokinin and gastric distension activate oxytocinergic cells in rat hypothalamus. *Am. J. Physiol.*, **253**, 661–665.

SAWCHENKO, P.E., PLOTSKY, P.M., CUNNINGHAM, E.T., VAUGHAN, J., RIVIER, J. & VALE, W. (1988). Inhibin β in central neural pathways involved in the control of oxytocin secretion. *Nature*, **344**, 315–317.

VANDERHAEGHEN, J.J., LOTSTRA, F., DE MEY, J. & GILLES, C. (1980). Immunohistochemical localization of cholecystokinin- and gastrin-like peptides in the brain and hypophysis of the rat. *Proc. Natl. Acad. Sci. U.S.A.*, **77**, 1190–1194.

VAN DER KOOY, D. (1984). Area postrema: site where cholecystokinin acts to decrease food intake. *Brain Res.*, **295**, 345–347.

VERBALIS, J.G., MANGIONE, M.P. & STRICKER, E.M. (1991a). Oxytocin produces natriuresis in rats at physiological plasma concentrations. *Endocrinology*, **128**, 1317–1322.

VERBALIS, J.G., MCCANN, M.J., MCHALE, C.M. & STRICKER, E.M. (1986a). Oxytocin and vasopressin secretion in response to stimuli producing learned taste aversions in rats. *Behav. Neurosci.*, **100**, 466–475.

VERBALIS, J.G., MCCANN, M.J., MCHALE, C.M. & STRICKER, E.M. (1986b). Oxytocin secretion in response to cholecystokinin and food: differentiation of nausea from satiety. *Science*, **232**, 1417–1419.

VERBALIS, J.G., STRICKER, E.M., ROBINSON, A.G. & HOFFMAN, G.E. (1991b). Cholecystokinin activates c-*fos* expression in hypothalamic oxytocin and corticotropin-releasing hormone neurons. *J. Neuroendocrinol.*, **3**, 205–214.

WISDEN, W., ERRINGTON, M.L., WILLIAMS, S., DUNNETT, S.B., WATERS, C., HITCHCOCK, D., EVANS, G., BLISS, T.V.P. & HUNT, S.P. (1990). Differential expression of immediate early genes in the hippocampus and spinal cord. *Neuron*, **4**, 603–614.

(Received February 25, 1993
Revised April 7, 1993
Accepted April 23, 1993)

Br. J. Pharmacol. (1993), **110**, 385–391

The interaction of the NK_1 receptor antagonist CP-96,345 with L-type calcium channels and its functional consequences

[1]S. Guard, S.J. Boyle, K.-W. Tang, K.J. Watling, A.T McKnight & G.N. Woodruff

Parke-Davis Neuroscience Research Centre, Addenbrookes Hospital Site, Hills Road, Cambridge, CB2 2QB

1 We investigated the effects of the non-peptide NK_1 receptor antagonist, CP-96,345, its inactive enantiomer CP-96,344, and the racemic mixture (±)-CP-96,345, on the binding of [^{3}H]-nimodipine and [^{3}H]-diltiazem to L-type calcium channels in rat cerebral cortex membranes. In isolated peripheral tissues containing tachykinin receptors, the effects of (±)-CP-96,345 have been compared with those of diltiazem.

2 In guinea-pig trachea, (±)-CP-96,345 produced antagonism of responses to the selective NK_1 agonists [Sar^9, Met(O$_2$)^{11}]SP and substance P-methyl ester that was apparently competitive in nature (pK_B 7.0–7.5), while in guinea-pig ileum the antagonism was not surmountable.

3 The reduction of maximum responses by (±)-CP-96,345 in the guinea-pig ileum was not selective; it was obtained with muscarinic agonists and other agents, and was also observed in the portal vein of the rat where NK_1 receptors are not present.

4 The tissue-specific reduction of maximum responses by (±)-CP-96,345 in ileum was reproduced by diltiazem.

5 (±)-CP-96,345 produced a concentration-dependent enhancement of [^{3}H]-nimodipine binding to rat cerebral cortex membranes with a maximal stimulation of 186 ± 29% above control (EC_{50} 83.2 nM). Scatchard analysis revealed that (±)-CP-96,345 increased the affinity of [^{3}H]-nimodipine for its binding sites without affecting B_{max} (control: K_D = 0.32 nM; with 100 nM (±)-CP-96,345: K_D = 0.074 nM).

6 CP-96,345, CP-96,344, and the racemate all inhibited [^{3}H]-diltiazem binding in rat cerebral cortex membranes with K_i values of 22.5 nM, 34.5 nM and 29.9 nM respectively; a similar value was obtained for diltiazem itself (33.6 nM). In comparison, CP-96,345 and (±)-CP-96,345 inhibited the binding of [^{125}I]-Bolton-Hunter-conjugated substance P in this tissue with K_i values of 59.6 nM and 82.0 nM respectively, while CP-96,344 had no measurable affinity ($IC_{50} > 10\ \mu M$).

7 Substance P and a range of ligands selective for NK_1, NK_2, or NK_3 receptors had no significant effect at 10 μM on either [^{3}H]-diltiazem or [^{3}H]-nimodipine binding.

8 The results indicate that in addition to possessing affinity for the NK_1 receptor, the non-peptide antagonist, CP-96,345, displays high affinity for [^{3}H]-diltiazem binding sites on L-type calcium channels. The functional effect that may be observed in integrated models will be a consequence of either property, or be a composite effect of NK_1 receptor antagonism and L-channel blockade.

Keywords: Tachykinin receptors; NK_1 receptor antagonists; L-type calcium channels; CP-96,345

Introduction

Substance P (SP) and the structurally-related mammalian peptides neurokinin A (NKA), neurokinin B (NKB), neuropeptide K (NPK) and neuropeptide-γ (NP-γ), belong to the tachykinin family of neuropeptides and are believed to mediate a variety of physiological processes, both centrally and in the periphery (see Pernow, 1983; Maggio 1988). It is now widely accepted that these neuropeptides interact with at least three types of tachykinin receptor, termed NK_1, NK_2 and NK_3 (see Guard & Watson, 1991).

Earlier studies on the biological effects of these peptides relied on the use of the naturally occurring agonists SP, NKA and NKB, although more recently receptor-selective synthetic agonists have been employed. Nonetheless, the elucidation of the precise role(s) of tachykinins in physiological and pathological processes has been hindered by the lack of high affinity, receptor-selective and metabolically stable antagonists. The recent discovery of CP-96,345, a selective non-peptide antagonist with high affinity for the NK_1 receptor (Snider *et al.*, 1991), thus represents a major advance towards this end. However, while CP-96,345 has been reported in functional and binding studies to possess high selectivity for the NK_1 receptor (Beresford *et al.*, 1991; Lecci *et al.*, 1991; Rouissi *et al.*, 1991; Snider *et al.*, 1991), on closer examination its pharmacological profile, both *in vitro* and *in vivo*, appears to be more complicated than originally suggested. Thus, non-specific depression of NK_3 receptor-mediated contraction of the rat portal vein *in vitro* was reported initially by Snider and co-workers (1991) for both CP-96,345 and its inactive (2**R**,3**R**) enantiomer, CP-96,344. This observation was confirmed by us using the racemic mixture (±)-CP-96,345, and extended to other tissues in a preliminary study (Boyle *et al.*, 1991). Similarly 'unspecific' effects with (±)-CP-96,345 in several *in vitro* smooth muscles have been reported (Lecci *et al.*, 1991; Wang & Håkanson, 1991; Legat *et al.*, 1992). Furthermore, both CP-96,345 and CP-96,344 have been reported to be equally effective in producing a marked transient hypotensive response when administered *in vivo* to anaesthetized dogs (Constantine *et al.*, 1991), rats (Donnerer *et al.*, 1992), and rabbits (Griesbacher *et al.*, 1992).

These observations, with the findings that (±)-CP-96,345 depresses smooth muscle contraction to a variety of non-tachykinin agonists, suggested a non-specific action of this compound, possibly via an interaction with depolarization-contraction coupling processes. In this study we describe our findings with (±)-CP-96,345 in peripheral tissues. We have also investigated whether these non-specific properties may be due to an interaction with voltage-sensitive calcium channels by examining the effects of CP-96,345, CP-96,344 and

[1] Author for correspondence.

the racemic mixture, (±)-CP-96,345, on the binding of the 1,4-dihydropyridine radioligand [^{3}H]-nimodipine and the benzothiazepine radioligand [^{3}H]-diltiazem to L-type calcium channels in cerebral cortex membranes. Finally we have compared the actions of (±)-CP-96,345 and diltiazem in the functional studies.

Preliminary accounts of this work have been presented to the British Pharmacological Society (Boyle *et al.*, 1991; Guard & Watling, 1992).

Methods

Functional studies

Tissue preparation Adult male Dunkin-Hartley guinea-pigs (330–400 g, B & K Universal), with free access to food and water, were killed by cervical dislocation and the ileum and trachea rapidly removed. The distal ileum was discarded and sections of longitudinal muscle from remaining sections were mounted in siliconized 3 ml organ baths containing Krebs-Henseleit solution of the following composition (mM): NaCl 118, KCl 5.9, $MgSO_4$ 1.2, $CaCl_2$ 2.5, NaH_2PO_4 1.2, $NaHCO_3$ 25.5 and glucose 11.1. The solution was maintained at 37°C and was gassed continuously with a mixture of 95% O_2/5% CO_2. For studies with NK_1 receptor-selective agonists the solution included indomethacin 5 μM, and atropine, mepyramine and methysergide all at 1 μM; with other agonists only indomethacin was present. Spiral strips of trachea were mounted in 3 ml baths containing Krebs-Henseleit solution to which was added indomethacin 5 μM and phosphoramidon 10 μM. Isometric contractile responses were measured with Grass FT.03 force-displacement transducers and recorded on Graphtec Linearcorders (Mark VII).

Adult male Wistar rats (200–400 g, B & K Universal), with free access to food and water, were killed and the portal vein rapidly removed, cleared of connective tissue and mounted in 3 ml baths containing Krebs-Henseleit solution as above, for isometric recording of myogenic activity.

Experimental procedure Tissues were placed under 1 g tension and allowed to equilibrate for 30 min after which time they were contracted with a submaximal concentration of agonist. For the guinea-pig ileum a 12-min dose cycle was employed and concentration-response curves were generated for a range of agonists that included substance P-methyl ester (SPOMe), [Sar^9, Met(O$_2$)^{11}]SP, senktide, histamine and carbachol. For the guinea-pig trachea concentration-response curves to tachykinin agonists were constructed cumulatively. In rat portal vein, a 10-min dose cycle was used in concentration-response work with senktide, carbachol or noradrenaline.

Drugs were added in volumes not exceeding 10 μl. For antagonism studies, tissues were exposed to antagonists for 15 min before re-exposure to agonists.

Analysis of results Contractile responses to exogenously applied agonists were expressed as absolute changes in tension and then transformed to a percentage of the maximal response achieved for that agonist. Responses obtained to agonists in the presence of antagonists were expressed as a percentage of the control maximum response obtained in the same tissue preparation. Agonist concentration-response curves in the absence and presence of increasing concentrations of antagonists were obtained from the best fit to the function $f(x) = b.x^n/(x^n + c^n)$, where b is the maximal asymptote, n is the slope factor ('Hill slope') and c is the location parameter (EC_{50}). Where appropriate, the method of Arunlakshana & Schild (1959) was used to derive affinity constants for the agonist-antagonist interaction; where this analysis indicated a competitive nature for the antagonism, values for pK_B were obtained by constraining the slope of the Schild plot to unity.

Binding studies

Membrane preparation Cerebral cortices from male Sprague-Dawley rats (200–250 g B & K Universal), and from 300–500 g male guinea-pigs (B & K Universal) were dissected on ice and placed in ice-cold 10% (w/v) sucrose solution. Pooled tissues were homogenized in 10 volumes of 10% sucrose with a teflon glass homogenizer (10–12 strokes, 800 r.p.m.). The homogenate was centrifuged at 1,600 *g* for 10 min and the resulting supernatant centrifuged at 48,000 *g* for 30 min. The crude synaptosomal pellet was resuspended in 10 volumes of ice-cold 50 mM Tris-HCl solution, pH 7.4 (Tris-buffer), by Polytron (position 6 for 5 s) and centrifuged for a further 30 min. The resulting pellet was washed once more with Tris-buffer, and centrifuged as above. The final pellet was resuspended in a small volume (5–10 ml) of Tris-buffer to give a final protein concentration of 3–5 mg ml^{-1}. Protein concentration was determined by the method of Bradford (1976) using bovine serum albumin (BSA) as a standard.

[^{3}H]-nimodipine binding assays [^{3}H]-nimodipine binding assays were performed essentially as described for [^{3}H]-nitrendipine binding by Bolger *et al.* (1983). Rat cerebral cortex membranes (a 200 μl aliquot of membrane suspension equivalent to 75 μg protein) were incubated in a final volume of 4 ml of Tris-buffer, with 0.1 nM [^{3}H]-nimodipine in the presence or absence of various test substances for 60 min at room temperature (22–25°C). Where appropriate, 0.01% (w/v) BSA and a mixture of peptidase inhibitors (bacitracin 40 μg ml^{-1}, leupeptin 4 μg ml^{-1}, chymostatin 2 μg ml^{-1}, phosphoramidon 2 μM) were added to the incubation buffer. The incubation was terminated by rapid filtration over Whatman GF/C filters (presoaked in an aqueous solution of 0.3% (v/v) polyethylenimine/0.5% (v/v) Triton X-100) using a Brandel Cell Harvester, and the filters washed three times with 5 ml of ice-cold Tris-buffer. [^{3}H]-nimodipine specific binding was defined by use of 1 μM nifedipine or 1 μM nimodipine (both gave similar values for non-specific binding). Bound radioactivity was determined by liquid scintillation spectrometry.

[^{3}H]-diltiazem binding assays [^{3}H]-diltiazem binding assays were performed essentially as described by Schoemaker & Langer (1989), with minor modifications. Rat or guinea-pig cerebral cortex membranes (a 200 μl aliquot of 1 mg ml^{-1} suspension) were incubated in a final volume of 1 ml in Tris-buffer, with 4 nM [^{3}H]-diltiazem in the presence or absence of various test substances for 120 min under conditions identical to those for [^{3}H]-nimodipine binding. The incubation was similarly terminated by rapid filtration through GF/C filters and the bound radioactivity determined by liquid scintillation spectrometry. [^{3}H]-diltiazem specific binding was defined by use of 10 μM unlabelled diltiazem.

[^{125}I]-Bolton Hunter-substance P binding assays The binding of [^{125}I]-Bolton Hunter-conjugated substance P ([^{125}I]-BHSP) to rat cerebral cortex membranes was performed essentially as described by Lee *et al.* (1986). Briefly, rat cerebral cortex membranes (a 150 μl aliquot corresponding to approximately 50 μg protein) were incubated with 0.1 nM [^{125}I]-BHSP for 60 min at room temperature in a final volume of 0.3 ml in Tris-buffer, containing 2 mM $MnCl_2$, 0.01% BSA and peptidase inhibitors (as before) in the presence or absence of test substances. Non-specific binding was defined by use of 1 μM SP. Incubations were terminated by rapid filtration through GF/C filters and bound radioactivity measured in a Hewlett-Packard gamma counter.

Data analysis The ability of compounds to inhibit or enhance radioligand binding was determined by use of at least 9 test concentrations (3 pM–10 μM), assayed in duplicate. Drug effects on radioligand binding were analysed using a non-linear least-squares iterative curve fitting programme

(RS1 Bolt, Beranek & Newman Inc.). Data were expressed as the maximal effect observed as a percentage of control specific binding (100%), and the concentration at which a half-maximal effect was observed (IC_{50} or EC_{50} for inhibition or enhancement of radioligand binding, respectively).

K_i values were calculated according to the Cheng & Prussoff (1973) relationship. Data are expressed as geometric mean (− s.e.mean, + s.e.mean) for K_i values, or otherwise as arithmetic means ± s.e.mean.

The affinity of [^{3}H]-nimodipine for rat cerebral cortex dihydropyridine binding sites was determined by saturation analysis of [^{3}H]-nimodipine binding over a concentration range of 0.01–1.5 nM. The K_D was determined by using a non-linear regression programme on RS1. The affinity (K_D) of [^{3}H]-diltiazem binding to rat cerebral cortex membranes was determined by Scatchard transformation of data obtained for the displacement of [^{3}H]-diltiazem specific binding by diltiazem.

Materials

CP-96,345 ((2S,3S)-[*cis*-2-(diphenylmethyl)-*N*-[(2-methoxyphenyl)-methyl]-1-azabicyclo[2.2.2.]octan-3-amine]) was supplied by Dr R.M. Snider, Pfizer Central Research, Groton, CT, U.S.A. The (2R,3R)-enantiomer, CP-96,344, and the racemic mixture were synthesized in the Medicinal Chemistry Department of the Parke-Davis Neuroscience Research Centre, Cambridge. Diltiazem and nifedipine were obtained from Research Biochemicals Inc., Natick, MA, U.S.A. Nimodipine was obtained from Bayer AG, Germany. Substance P, SPOMe, [Sar^9, Met(O$_2$)^{11}]SP, [Glp^6, L-Pro^9]SP(6–11), senktide and L-659,877 (cyclo(Gln-Trp-Phe-Gly-Leu-Met)) were purchased from Bachem U.K. Ltd. [β-Ala^8]NKA(4–10) was purchased from Novabiochem, Switzerland. L-668,169 (cyclo (Gln-D-Trp-*N*-Me-Phe-(R)-Gly[ANC-2]Leu-Met)$_2$) was obtained from Cambridge Research Biochemicals, U.K. GR64349 ([Lys^3, Gly^8-R-γ-lactam-Leu^9]NKA(3–10)) and GR82334 ([D-Pro^9(spiro-γ-lactam)Leu^{10},Trp^{11}]-physalæmin(1–11)) were obtained from Neosystem Laboratoire, Strasbourg, France. Carbachol, indomethacin, atropine, noradrenaline, histamine, bacitracin, chymostatin, leupeptin and BSA were from the Sigma Chemical Co. Phosphoramidon was from the Peptide Research Foundation (Osaka).

D-*cis*[Methyl-^{3}H]-diltiazem (162–166 Ci mmol^{-1}) and [^{125}I]-Bolton Hunter substance P (2,000 Ci mmol^{-1}) were purchased from Amersham International plc, U.K. [Isopropyl-1,3-^{3}H]-nimodipine (126–157 Ci mmol^{-1}) was obtained from New England Nuclear, Boston, MA, U.S.A.

Results

Effects of (±)-CP-96,345 at NK$_1$ receptors

In the guinea-pig isolated trachea the response to the selective NK$_1$-receptor agonist [Sar^9, Met(O$_2$)^{11}]SP was blocked by (±)-CP-96,345, with the antagonism appearing competitive (Figure 1a). The slope of the Schild plot for the interaction was not significantly different from unity (1.14, s.d. 0.15), and the pK_B was 7.10 (95% c.l. 6.97, 7.24). Qualitatively similar observations were made in a less extensive study with the agonist SPOMe (mean apparent pK_B = 7.39 ± 0.17, n = 8); against the NK$_2$ receptor-selective agonist [β-Ala^8]NKA (4–10), (±)-CP-96,345 was a weak antagonist (mean apparent pK_B = 5.35 ± 0.13, n = 4).

In contrast to the findings in the guinea-pig trachea, increasing concentrations of (±)-CP-96,345 produced a non-competitive antagonism of responses to the NK$_1$-selective agonists in the longitudinal muscle of the ileum of the same species (Figure 1b). At the lower concentrations of (±)-CP-96,345 (≤ 100 nM) in the ileum the maximum response to the agonists was largely unaffected, and rightward shifts in the concentration-response curve to the NK$_1$ agonist were observed, consistent with an apparent pK_B for (±)-CP-96,345 of around 8. If concentrations greater than 100 nM (±)-CP-96,345 were used a concentration-dependent reduction in the maximum response to [Sar^9, Met(O$_2$)^{11}]SP or SPOMe was observed, along with further rightward shifts in the concentration-response curve.

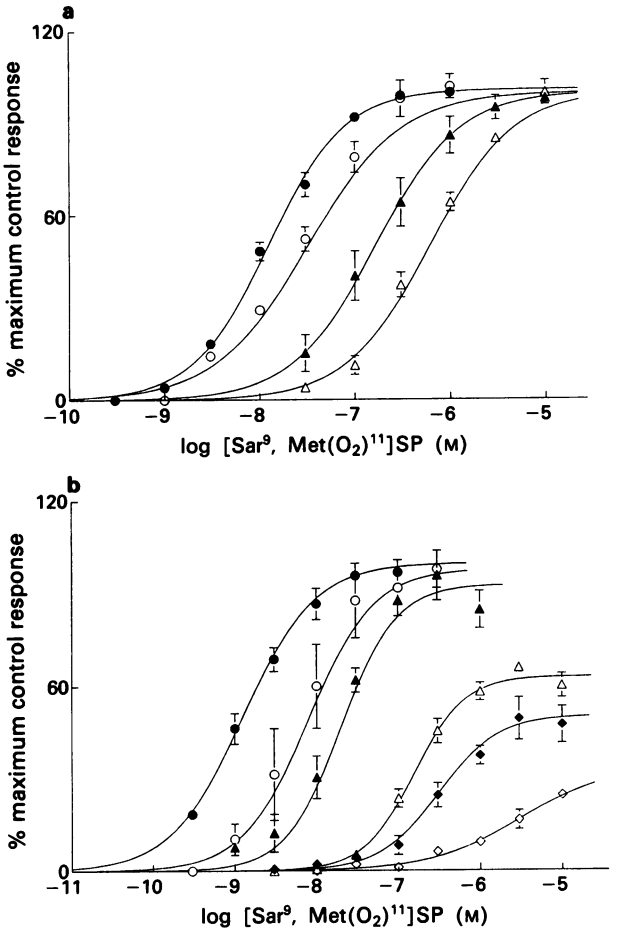

Figure 1 (a) Inhibitory effect of (±)-CP-96,345 on control concentration-response curves to the NK$_1$ receptor agonist [Sar^9, Met(O$_2$)^{11}]SP in guinea-pig isolated trachea. Increasing concentrations of (±)-CP-96,345 0.3 μM (○), 1 μM (▲) and 3 μM (△) resulted in a concentration-dependent rightward shift of the [Sar^9, Met(O$_2$)^{11}]SP concentration-response curve. Data are expressed as percentage of control (●) maximum response to [Sar^9, Met(O$_2$)^{11}]SP and each point represents the mean ± s.e.mean of not less than 4 observations. (b) Non-competitive blockade of [Sar^9, Met(O$_2$)^{11}]SP concentration-response curve by increasing concentrations of (±)-CP-96,345 in guinea-pig ileum longitudinal muscle. The maximum response was reduced in a concentration-dependent manner by 30 nM (○), 100 nM (▲), 300 μM (△), 1 μM (◆) and 3 μM (◇) (±)-CP-96,345. Data are expressed as percentage of control (●) maximum response to [Sar^9, Met(O$_2$)^{11}]SP and each point represents the mean of not less than 4 observations. Vertical bars represent s.e.mean.

In the ileum the racemate reduced the maximum response to the NK$_3$ receptor-selective agonist senktide (to 58 ± 12% of control at 0.1 μM, and 23 ± 8.1% at 1 μM, n = 4), apparently without affecting the sensitivity of the preparation to this agonist (values for pEC_{50} (95% c.l.) 8.41 (8.24, 8.59) and 8.60 (8.07, 9.26) in control preparations, and in the presence of 1 μM (±)-CP-96,345 respectively). Similarly with the cholinoceptor agonist, carbachol (Figure 2a), or with histamine (not shown) the effect in the guinea-pig ileum longitudinal muscle was to produce a concentration-related reduction in the maximum response to either agonist, without affecting significantly the location parameter for the log concentration-response curve (Figure

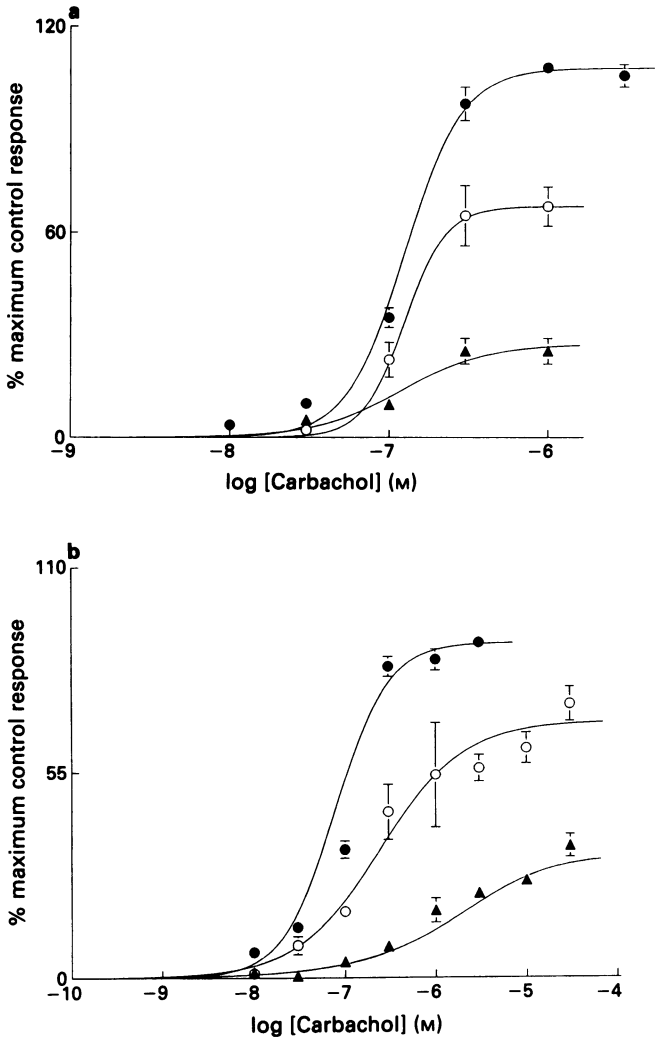

Figure 2 (a) Non-competitive blockade of carbachol concentration-response curve in guinea-pig ileum longitudinal muscle by (±)-CP-96,345, 300 nM (○) and 3 μM (▲). Data are expressed as percentage of control (●) maximum response to carbachol and each point represents the mean ± s.e.mean of not less than 4 observations. (b) Non-competitive blockade of carbachol concentration-response curve in guinea-pig ileum longitudinal muscle by diltiazem, 300 nM (○) and 3 μM (▲). Data are expressed as percentage of control (●) maximum response to carbachol and each point represents the mean ± s.e.mean of not less than 4 observations.

2a). In the rat portal vein a reduction in the maximum response to senktide by (±)-CP-96,345 was again obtained, without an effect on the sensitivity of the preparation to the agonist (maximum response reduced to 23.3 ± 4.3% of control by 0.3 μM (±)-CP-96,345, pEC_{50} values 8.56 (8.45, 8.68) and 8.26 (7.91, 8.63) in control, and in the presence of 0.3 μM (±)-CP-96,345 respectively). Qualitatively similar effects against the response to noradrenaline were seen in this preparation (maximum response reduced to 14.4 ± 3.9% of control by 3 μM (±)-CP-96,345, pEC_{50} values 6.53 (6.43, 6.63) and 6.82 (6.78, 6.86) in control, and in the presence of (±)-CP-96,345).

[^{3}H]-nimodipine binding

Both unlabelled nimodipine and nifedipine inhibited the specific binding of [^{3}H]-nimodipine with K_i values of 0.33 nM (− 0.03, + 0.03) and 1.03 nM (− 0.16, + 0.17), respectively ($n = 3$; Figure 3), confirming that the [^{3}H]-nimodipine binding was a dihydropyridine binding site on L-type calcium channels. In contrast, (±)-CP-96,345 produced a concentration-dependent enhancement of [^{3}H]-nimodipine binding in this tissue with a maximal potentiation of 186 ± 29% above basal and an EC_{50} value for this effect of 83.2 nM (− 22.9, + 31.6; $n = 4$; Figure 3). Scatchard analysis of [^{3}H]-nimodipine binding to rat cerebral cortex membranes in the absence and presence of 100 nM (±)-CP-96,345 revealed that (±)-CP-96,345 increased the affinity of [^{3}H]-nimodipine for its binding sites (control: $K_D = 0.32$ nM; in the presence of (±)-CP-96,345: $K_D = 0.074$ nM) while the number of [^{3}H]-nimodipine binding sites was not significantly altered (control: $B_{max} = 511$ fmol mg^{-1} protein; in the presence of (±)-CP-96,345: $B_{max} = 498$ fmol mg^{-1} protein, $n = 2$, Figure 4). A range of tachykinin receptor ligands including NK_1- and NK_2-selective agonists and antagonists, and the NK_3-selective agonist senktide, did not produce any appreciable effect on [^{3}H]-nimodipine specific binding (data not shown).

[^{3}H]-diltiazem binding

Unlabelled diltiazem, CP-96,345, CP-96,344 and (±)-CP-96,345 inhibited the binding of [^{3}H]-diltiazem in rat cerebral cortex membranes with K_i values around 30 nM (Table 1). Similar affinities were obtained for the inhibition of [^{3}H]-diltiazem binding to guinea-pig cerebral cortex membranes (not shown). As with [^{3}H]-nimodipine binding, NK_1, NK_2 and NK_3 receptor-selective ligands did not produce any significant inhibition of [^{3}H]-diltiazem binding in rat cerebral cortex membranes (Table 1).

[^{125}I]-BHSP binding

In agreement with previous findings, CP-96,345 and the racemate, (±)-CP-96,345, inhibited the binding of [^{125}I]-Bolton-Hunter-labelled substance P to NK_1 binding sites in rat cortex membranes with K_i values of 59.6 nM (− 5.0, + 5.5; $n = 3$) and 82.0 nM (− 9.4, + 11.5; $n = 4$), respectively, while 10 μM CP-96,344 was without effect (Table 1). In addition, 1 μM diltiazem had no significant effect on [^{125}I]-BHSP binding to rat cortex membranes (Table 1).

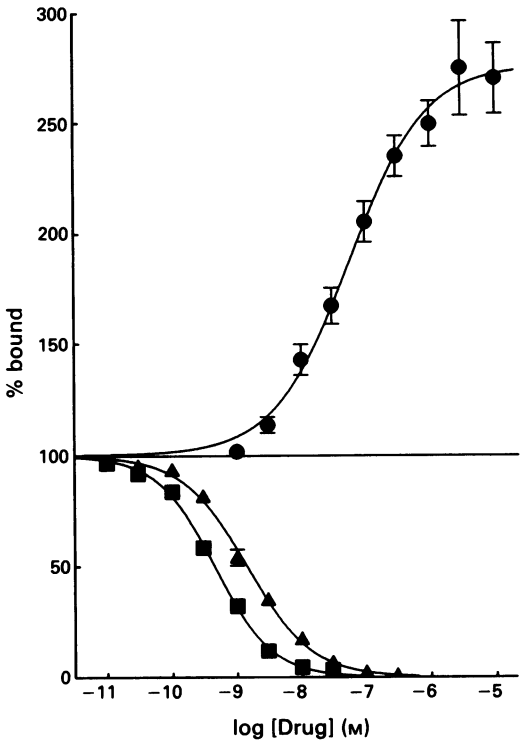

Figure 3 The effect of nimodipine (■), nifedipine (▲) and (±)-CP-96,345 (●) on [^{3}H]-nimodipine specific binding to rat cerebral cortex membranes. Curves were fitted by non-linear regression using RS1. Each point represents the mean ± s.e.mean of 3–4 separate experiments performed in duplicate. Where no vertical lines are shown the s.e.mean is contained within the symbol.

Effects of diltiazem in functional assays

The maximum response of the muscarinic agonist carbachol in longitudinal muscle from guinea-pig ileum was reduced in a concentration-dependent manner by diltiazem (Figure 2b). As with (±)-CP-96,345 a 70% reduction in the maximum response to carbachol was observed with 3 μM diltiazem. When diltiazem was examined against the NK_1 receptor selective agonist SPOMe in guinea-pig ileum longitudinal muscle (Figure 5a) it was found to reduce the maximum response of the agonist in a concentration-dependent manner without any apparent effect on the affinity of the agonist. Diltiazem was without effect on the NK_1 receptor in the guinea-pig trachea; 10 μM diltiazem affected neither the maximum response nor the affinity of SPOMe in this preparation (Figure 5b).

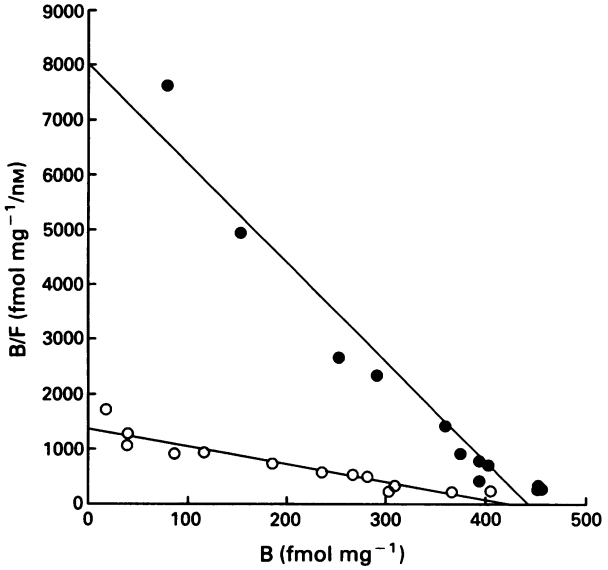

Figure 4 Effect of 100 nM (±)-CP-96,345 on the specific binding of [^{3}H]-nimodipine to rat cerebral cortex membranes. Membranes were incubated in the absence (○) or presence (●) of 100 nM (±)-CP-96,345 with increasing concentrations of [^{3}H]-nimodipine (0.01–1.5 nM). Data are shown as a Scatchard plot and values represent the means of duplicate determinations from a single representative experiment that was repeated once with similar results. Best-fit lines were calculated by linear regression using RS1. See text for mean K_D and B_{max} values.

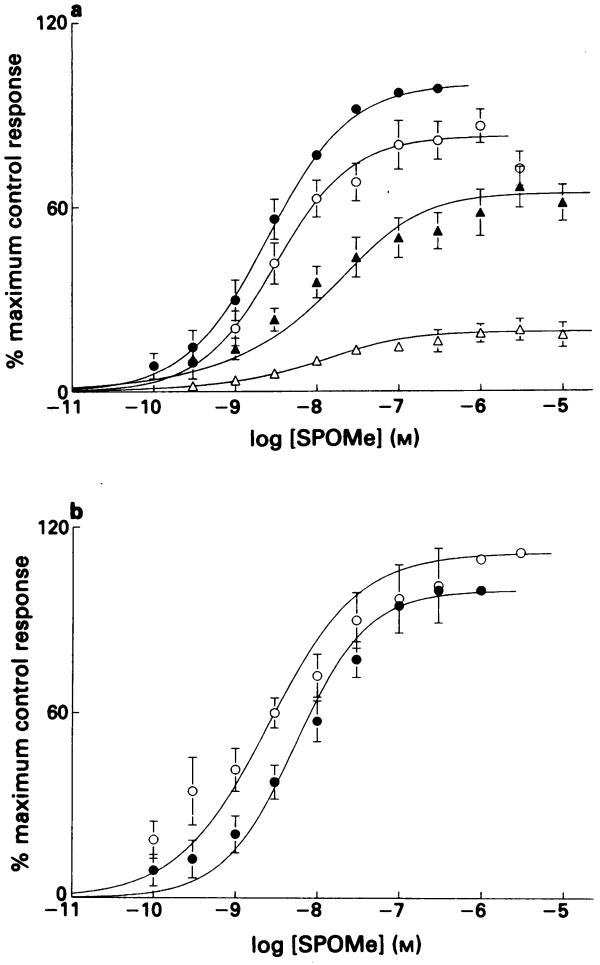

Figure 5 (a) Non-competitive blockade of the response to the NK_1 receptor agonist substance P-methyl ester (SPOMe) in guinea-pig ileum longitudinal muscle by diltiazem, 100 nM (○), 1 μM (▲) and 10 μM (△). Data are expressed as percentage of control (●) maximum response to SPOMe and each point represents the mean ± s.e.mean of not less than 4 observations. (b) Lack of effect of diltiazem on the response of the guinea-pig isolated trachea to SPOMe. 10 μM diltiazem (○) did not affect the ability of the trachea to contract on exposure to the agonist. Data are expressed as percentage of control (●) maximum response to SPOMe and each point represents the mean ± s.e.mean of not less than 4 obervations.

Table 1 K_i values for the inhibition of [^{3}H]-diltiazem and [^{125}I]-Bolton-Hunter-conjugated substance P ([^{125}I]-BHSP) specific binding to rat cerebral cortex membranes

Compound	*[^{3}H]-diltiazem* K_i (nM)	*[^{125}I]-BHSP* K_i (nM)
Diltiazem	33.6 (− 4, + 4.7)	> 1,000
Substance P	> 10,000	0.07 (− 0.01, + 0.01)
CP-96,345	22.5 (− 2.2, + 2.4)	59.6 (− 5.0, + 5.5)
CP-96,344	37.3 (− 0.7, + 0.7)	> 10,000
(±)-CP-96,345	29.2 (− 2.3, + 2.4)	82.0 (− 9.4, + 11.5)
[Sar^9, Met(O$_2$)^{11}]SP	> 10,000	0.23 (− 0.04, + 0.06)
GR82334	> 10,000	3978 (− 563, + 656)
L-668,169	> 10,000	1125 (− 161, + 187)
[β-Ala^8]NKA(4–10)	> 10,000	> 10,000
GR64349	> 10,000	> 10,000
L-659,877	> 10,000	> 10,000
Senktide	> 10,000	> 10,000

Data are expressed as K_i values (nM) and are the geometric means (− s.e.mean, + s.e.mean) of 3–6 separate experiments. IC_{50} values were converted to K_i using the Cheng & Prussoff relationship; apparent Hill slopes were not significantly different from unity.

Discussion

The results of this study demonstrate that the non-peptide NK_1 receptor antagonist (±)-CP-96,345 interacts with L-type calcium channels in rat cerebral cortex membranes in agreement with the findings of Schmidt *et al.* (1992).

In competition experiments against the binding of the 1,4-dihydropyridine radioligand [^{3}H]-nimodipine (0.1 nM), (±)-CP-96,345 produced almost a 200% increase in binding, and saturation analysis of [^{3}H]-nimodipine binding to rat cortex membranes in the absence or presence of (±)-CP-96,345 indicated that the racemate increased the affinity of [^{3}H]-nimodipine, rather than affecting the maximum number of sites. This potentiation of [^{3}H]-nimodipine binding by (±)-CP-96,345 is characteristic of the positive allosteric modulation by compounds such as diltiazem that interact with the benzothiazepine site on L-type calcium channels (Depover *et al.*, 1982; Boles *et al.*, 1984).

When the affinities at [^{3}H]-diltiazem binding sites in rat cortex were determined for CP-96,345, the (2**R**,3**R**) enantiomer CP-96,344 and the racemate, all had appreciable affinity with K_i values comparable to that obtained for unlabelled diltiazem itself. The potentiation by (±)-CP-96,345 of [^{3}H]-nimodipine binding can be presumed to be a result of a direct action at the diltiazem site on the calcium channel. CP-96,345 and CP-96,344 have also recently been reported to interact with [^{3}H]-diltiazem binding sites in rat heart membranes and to produce a concentration-dependent enhancement of [^{3}H]-nimodipine binding to rat cerebral cortex membranes (Schmidt *et al.*, 1992).

Although the interaction of CP-96,345 with the NK_1 receptor is stereoselective, the ability of the racemate to displace [^{3}H]-diltiazem binding is not, since both CP-96,345 and CP-96,344 possess similar affinities for the latter site. The lack of an involvement of tachykinin receptors in the modulation of calcium channel binding by CP-96,345 is shown by the lack of an effect on the binding of either [^{3}H]-nimodipine or [^{3}H]-diltiazem by a range of NK_1-selective ligands, both agonists and antagonists. Furthermore, nifedipine, nimodipine and diltiazem did not produce any significant inhibition of [^{125}I]-BHSP binding to NK_1 receptor sites in rat cortex membranes.

The affinity of CP-96,345 for NK_1 receptors exhibits marked differences between species (Beresford *et al.*, 1991; Gitter *et al.*, 1991; Snider *et al.*, 1991; Watling *et al.*, 1991). Thus, CP-96,345 displays approximately 100 fold higher affinity for NK_1 receptor sites in bovine, guinea-pig and human brain tissue, compared to rat or mouse. However, the affinities of CP-96,345, CP-96,344 and (±)-CP-96,345 for [^{3}H]-diltiazem binding sites in guinea-pig cerebral cortex were comparable to those observed in the rat. Similar observations have recently been reported by Schmidt *et al.* (1992) who have shown that CP-96,345 and CP-96,344 possess similar affinities for [^{3}H]-desmethoxyverapamil binding sites in rat and guinea-pig heart.

The finding that CP-96,345 possesses (presumed) calcium channel binding properties in addition to NK_1 receptor antagonist activity will account for many of the apparently non-specific effects observed e.g. on smooth muscle contraction *in vitro*. Thus while the rightward shifts in the concentration-response curves to selective NK_1-receptor agonists are explained as a consequence of the affinity of the active isomer CP-96,345 at the NK_1 receptor, the reduction in maximum response may be associated with the blockade of the L-type calcium channel. It may be concluded that the effect of diltiazem in the ileum, being only to reduce the maximum response to the NK_1 agonist, is analogous to the effect of (±)-CP-96,345 in reducing the maximum responses to senktide and carbachol in this tissue (and in the rat portal vein) without affecting the potency of these agonists. Consequently in the trachea where the antagonism by (±)-CP-96,345 of the response to the NK_1 agonist appears competitive, and is surmountable, there was no effect of the racemate (±)-CP-96,345 on the response to other agonists, and diltiazem had no effect on the response to the NK_1 agonist.

These findings are pertinent to the interpretation of data obtained with CP-96,345 *in vitro* and *in vivo* studies on NK_1 receptors. Accordingly, caution should be exercised in studies of NK_1 receptor function in the rat or mouse where the affinities of CP-96,345 for NK_1 receptors and calcium channels are very similar. Thus the recent report that (±)-CP-96,345 blocked the hyperalgesia and œdema caused by intraplantar injection of carrageenin in the rat, and was active in blocking the nociceptive response in the formalin test (Birch *et al.*, 1992), cannot now be taken as evidence that activation of the NK_1 receptor occurred in these tests, with the subsequent report that these actions were obtained with both of the separate enantiomers CP-96,345 and CP-96,344 (Nagahisha *et al.*, 1992). Similarly the conclusion that substance P acting via the NK_1 receptor mediates thermal nociception, based on the observation that (±)-CP-96,345 is antinociceptive after intrathecal administration in the mouse hot-plate test (Lecci *et al.*, 1991), must be reconsidered. Particularly pertinent to such uses of this compound, in tests for antinociceptive activity after local administration, is the recent report that (±)-CP-96,345 blocks voltage-dependent sodium currents, and is 50 times more active than lignocaine in this respect (Caesar *et al.*, 1993).

References

ARUNLAKSHANA, O. & SCHILD, H.O. (1959). Some quantitative uses of drug antagonists. *Br. J. Pharmacol. Chemother.*, **14**, 48–58.

BERESFORD, I.J.M., BIRCH, P.J., HAGAN, R.M. & IRELAND, S.J. (1991). Investigation into species variants in tachykinin NK_1 receptors by use of the non-peptide antagonist, CP-96,345. *Br. J. Pharmacol.*, **104**, 292–293.

BIRCH, P.J., HARRISON, S.M., HAYES, A.G., ROGERS, H. & TYERS, M.B. (1992). The non-peptide NK_1 antagonist, (±)-CP-96,345, produces antinociceptive and anti-oedema effects in the rat. *Br. J. Pharmacol.*, **105**, 508–510.

BOLES, R.G., YAMAMURA, H.I., SCHOEMAKER, H. & ROESKE, W.R. (1984). Temperature dependent modulation of [^{3}H]-nitrendipine binding by the calcium channel antagonists verapamil and diltiazem in rat brain synaptosomes. *J. Pharmacol. Exp. Ther.*, **229**, 333–339.

BOLGER, G.T., GENGO, P., KLOCKOWSKI, R., LUCHOWSKI, H., SIEGEL, H., JANIS, R.A., TRIGGLE, A.M. & TRIGGLE, D.J. (1983). Characterization of binding of the Ca^{++} channel antagonist [^{3}H]-nitrendipine to guinea-pig ileal smooth muscle. *J. Pharmacol. Exp. Ther.*, **225**, 291–309.

BOYLE, S.J., HOWSON, W. & MCKNIGHT, A.T. (1991). An examination of the selectivity of a new non-peptide tachykinin antagonist. *Br. J. Pharmacol.*, **104**, 146P.

BRADFORD, M.M. (1976). A rapid and sensitive method for the quantitation of microgram quantities of protein utilizing the principle of protein-dye binding. *Anal. Biochem.*, **72**, 248–254.

CAESAR, M., SEABROOK, G.R. & KEMP, J.A. (1993). Block of voltage-dependent sodium currents by the substance P receptor antagonist (±)-CP-96,345 in neurones cultured from the rat cortex. *J. Physiol.*, **459**, 397P.

CHENG, Y.C. & PRUSSOFF, W.H. (1973). Relationship between the inhibition constant (K_i) and the concentration of inhibitior which causes 50% inhibition (I_{50}) of an enzymatic reaction. *Biochem. Pharmacol.*, **22**, 3099–3108.

CONSTANTINE, J.W., LEBEL, W.S. & MOODY, H.A. (1991). Inhibition of tachykinin-induced hypotension in dogs by CP-96,345, a selective blocker of NK-1 receptors. *Naunyn-Schmied. Arch. Pharmacol.*, **344**, 471–477.

DEPOVER, A., MATLIB, M.A., LEE, S.W., DUBE, G.P., GRUPP, I.L., GRUPP, G. & SCHWARTZ, A. (1982). Specific binding of [^{3}H]-nitrendipine to membranes from coronary arteries and heart in relation to pharmacological effects. Paradoxical stimulation by diltiazem. *Biochem. Biophys. Res. Commun.*, **108**, 110–117.

DONNERER, J., STARK, U., TRITTHART, H.A. & LEMBECK, F. (1992). CP-96,345, a non-peptide antagonist of substance P. III. Cardiovascular effects in mammals unrelated to actions on substance P receptors. *Naunyn-Schmied. Arch. Pharmacol.*, **346,** 328–332.

GITTER, B.D., WATERS, D.C., BRUNS, R.F., MASON, N.R., NIXON, J.A. & HOWBERT, J.J. (1991). Species differences in affinities of non-peptide antagonists for substance P receptors. *Eur. J. Pharmacol.*, **197,** 237–238.

GRIESBACHER, T., DONNERER, J., LEGAT, F.J. & LEMBECK, F. (1992). CP-96,345, a non-peptide antagonist of substance P: II. Actions on substance P-induced hypotension and bronchoconstriction, and on depressor reflexes in mammals. *Naunyn-Schmied. Arch. Pharmacol.*, **346,** 323–327.

GUARD, S. & WATLING, K.J. (1992). Interaction of the non-peptide NK_1 tachykinin receptor antagonist (±)-CP-96,345 with L-type calcium channels in rat cerberal cortex. *Br. J. Pharmacol.*, **105,** 37P.

GUARD, S. & WATSON, S.P. (1991). Tachykinin receptor types: classification and transmembrane signalling mechanisms. *Neurochem. Intl.*, **18,** 149–165.

LECCI, A., GIULLIANI, S., PATACCHINI, R., VITI, G. & MAGGI, C.A. (1991). Role of NK_1 tachykinin receptors in thermonociception: effect of (±)-CP-96,345, a non-peptide substance P antagonist, on the hot plate test in mice. *Neurosci. Letts.*, **129,** 299–302.

LEE, C.M., CAMPBELL, N.J., WILLIAMS, B.J. & IVERSEN, L.L. (1986). Multiple tachykinin binding sites in peripheral tissues and brain. *Eur. J. Pharmacol.*, **130,** 209–217.

LEGAT, F.J., GRIESBACHER, T. & LEMBECK, F. (1992). CP-96,345, a non-peptide antagonist of substance P: I. Effects on the actions mediated by substance P and related tachykinins on guinea-pig ileum and rabbit jejunum. *Naunyn-Schmied. Arch. Pharmacol.*, **346,** 315–322.

MAGGIO, J.E. (1988). Tachykinins. *Annu. Rev. Neurosci.*, **11,** 13–28.

NAGAHISHA, A., ASAI, R., KANAI, Y., MURASE, A., TSUCHIYA-NAKAGAKI, M., NAKAGAKI, T., SHIEH, T.-C. & TANIGUCHI, K. (1992). Non-specific activity of (±)-CP-96,345 in models of pain and inflammation. *Br. J. Pharmacol.*, **107,** 273–275.

PERNOW, B. (1983). Substance P. *Pharmacol. Revs.*, **35,** 85–141.

ROUISSI, N., GITTER, B.D., WATERS, D.C., HOWBERT, J.J., NIXON, J.A. & REGOLI, D. (1991). Selectivity and specificity of new, non-peptide, quinuclidine antagonists of substance P. *Biochem. Biophys. Res. Commun.*, **176,** 894–901.

SCHMIDT, A.W., MCLEAN, S. & HEYM, J. (1992). The substance P receptor antagonist CP-96,345 interacts with Ca^{2+} channels. *Eur. J. Pharmacol.*, **215,** 351–352.

SCHOEMAKER, H. & LANGER, S. (1989). Effects of Ca^{++} on ^{3}H-diltiazem binding and its allosteric interaction with dihydropyridine calcium channel binding sites in the rat cortex. *J. Pharmacol. Exp. Ther.*, **248,** 710–715.

SNIDER, R.M., CONSTANTINE, J.W., LOWE, J.A., LONGO, K.P., LEBEL, W.S., WOODY, H.A., DROZDA, S.E., DESAI, M.J., VINICK, F.J., SPENCER, R.W. & HESS, H.-J. (1991). A potent non-peptide antagonist of the substance P (NK_1) receptor. *Science*, **251,** 435–437.

WANG, Z.-Y. & HÅKANSON, R. (1992). (±)-CP-96,345, a selective tachykinin NK_1 receptor antagonist has non-specific actions on neurotransmission. *Br. J. Pharmacol.*, **107,** 762–765.

WATLING, K.J., GUARD, S., HOWSON, W. & WALTON, L. (1991). Inhibition of binding to tachykinin NK_1 receptor sites in rat, guinea-pig and human brain by the non-peptide substance P antagonist (±)-CP-96,345. *Br. J. Pharmacol.*, **104,** 27P.

(Received March 4, 1993
Revised April 22, 1993
Accepted April 23, 1993)

Br. J. Pharmacol. (1993), **110**, 392–398

Endothelin-induced contraction and mediator release in human bronchus

[1]Douglas W.P. Hay, *Walter C. Hubbard & *Bradley J. Undem

Department of Inflammation & Respiratory Pharmacology, SmithKline Beecham Pharmaceuticals, P.O. Box 1539, King of Prussia, PA 19406, U.S.A. and *Division of Allergy and Clinical Immunology, Johns Hopkins Asthma & Allergy Center, 301 Bayview Boulevard, Baltimore, MD 21224, U.S.A.

1 To elucidate the role of acetylcholine and various autacoids in endothelin-1 (ET-1)-induced contraction in human bronchus, the effects of various receptor antagonists were examined. In addition, the ability of ET-1 to stimulate the release of histamine, peptidoleukotrienes and prostanoids was determined.

2 ET-1 was a potent and effective contractile agonist in human bronchus, possessing similar potency and efficacy to leukotriene D_4 (LTD_4); EC_{50} ($-\log M$): ET-1 = 7.76 ± 0.09, $n = 7$; LTD_4 = 8.46 ± 0.53, $n = 7$; $P > 0.2$; maximum response (% 10 μM pre-carbachol): ET-1 = 103.8 ± 17.4, $n = 7$; LTD_4 = 95.5 ± 9.3, $n = 7$; $P > 0.6$.

3 The cyclo-oxygenase inhibitor, sodium meclofenamate (1 μM) or the potent and selective thromboxane receptor antagonist, SQ 29,548 (1 μM) were without significant effect on ET-1 concentration-response curves.

4 In the presence of sodium meclofenamate (1 μM), the muscarinic receptor antagonist, atropine (1 μM), the platelet activating factor (PAF) receptor antagonist, WEB 2086 (1 μM) or the combination of the H_1-histamine receptor antagonist, mepyramine (10 μM) and the leukotriene receptor antagonist, SK&F 104353 (10 μM), were without marked effect on ET-1 concentration-response curves. In addition, the combination of all four receptor antagonists did not antagonize ET-1-induced contraction.

5 ET-1 (0.3 μM) did not stimulate the release of histamine or immunoreactive leukotrienes from human bronchus.

6 ET-1 (0.3 μM) significantly stimulated the release of prostaglandin D_2 (PGD_2), 9α, 11β PGF_2 (PGD_2 metabolite), PGE_2, 6-keto $PGF_{1\alpha}$ (PGI_2 metabolite), $PGF_{2\alpha}$ and thromboxane B_2 (TxB_2) a lower concentration, 10 nM, was without effect on prostanoid release. The production of PGD_2 was increased 7.5 fold, whereas the release of the other prostanoids was stimulated only about 1.6 to 2.7 fold.

7 These data provide evidence that ET-1 elicits contraction of human isolated bronchus predominantly via a direct mechanism with no significant involvement of the release of acetylcholine, leukotrienes, histamine or PAF. Although ET-1 increased the release of several prostanoids they did not have a significant modulatory effect on the smooth muscle contraction.

Keywords: Endothelin-1; human bronchus; SK&F 104353; mepyramine; WEB 2086; SQ 29,548; peptidoleukotriene release; histamine release; sodium meclofenamate; prostanoid release

Introduction

Yanagisawa and co-workers described the isolation, purification, cloning and pharmacological characterization of a potent vasoconstrictor peptide, designated endothelin, which was released from porcine aortic endothelial cells (Yanagisawa *et al.*, 1988). Endothelin is a 21-amino acid peptide, with two sets of intrachain disulphide bridges, which bears a close structural homology with the sarafotoxins, a group of snake venom toxins (Lee & Chiappinelli, 1988; Kloog *et al.*, 1988). Subsequent research indicated that endothelin, named endothelin-1 (ET-1), is only one member of a family of mammalian endothelins: Thus, Inoue and co-workers cloned three distinct ET-related genes by screening a human genomic DNA library (Inoue *et al.*, 1989). These three 21-amino acid peptides, which have only minor differences in amino acid sequence, were designated ET-1 (the orginal porcine/human ET), ET-2 (two amino acid substitution from ET-1) and ET-3 (six amino acid substitution from ET-1) (Yanagisawa & Masaki, 1989a,b).

Although the focus of the research to date on the endothelins has been on their effects and potential pathophysiological relevance in the cardiovascular system, they produce an array of activities in a variety of other systems (Yanagisawa & Masaki, 1989a,b). For example, shortly after its discovery, ET-1 was reported to be a potent contractile agonist of guinea-pig trachea (Uchida *et al.*, 1988). This observation has been confirmed (Hay, 1989; Maggi *et al.*, 1989; Henry *et al.*, 1990) and extended to isolated airway tissues from a variety of species including rat (Turner *et al.*, 1989), ferret (Lee *et al.*, 1990), rabbit (Grunstein *et al.*, 1991) and man (Henry *et al.*, 1990; Hemsén *et al.*, 1990; Advenier *et al.*, 1990; Brink *et al.*, 1991; McKay *et al.*, 1991). In fact, it has been proposed that the endothelins play a role in the pathophysiology of pulmonary disorders including asthma and pulmonary hypertension (Cernacek & Stewart, 1989; Mattoli *et al.*, 1991a; Springall *et al.*, 1991; Hay *et al.*, 1993).

By use of [^{125}I]-ET-1, specific binding sites of high density were detected in smooth muscle of human isolated trachea (Power *et al.*, 1989) and bronchus (Henry *et al.*, 1990; McKay *et al.*, 1991), in human cultured bronchial smooth muscle cells (Mattoli *et al.*, 1990) and in human lung membranes (Brink *et al.*, 1991). The ET-1 EC_{50} in human bronchus is generally in the 10–30 nM range (Henry *et al.*, 1990; Hemsén *et al.*, 1990; Advenier *et al.*, 1990; Brink *et al.*, 1991; McKay *et al.*, 1991).

The role of indirect mechanisms in endothelin-induced airway smooth muscle contraction is controversial. *In vivo* studies have indicated that endothelin-induced bronchocon-

[1] Author for correspondence.

striction in guinea-pigs can be substantially inhibited by cyclo-oxygenase or thromboxane synthase inhibitors (Payne & Whittle, 1988; Nambu *et al.*, 1990). However, there is conflicting information on the effects of cyclo-oxygenase inhibitors (Maggi *et al.*, 1989; Sarriá *et al.*, 1990; Henry *et al.*, 1990; Hay, 1990) or thromboxane receptor antagonists (Filep *et al.*, 1990; Hay, 1990) on endothelin-induced contraction of guinea-pig isolated trachea. ET-1 elicits histamine release from guinea-pig isolated lung parenchymal mast cells (Uchida *et al.*, 1992), and in preliminary reports it was proposed that the mast-cell derived products, histamine and the peptidoleukotrienes, played a role in endothelin-induced responses in guinea-pig isolated trachea (Ninomiya *et al.*, 1989; Nomura *et al.*, 1990). However, a later study, which included direct measurement of the release of these mediators from the trachea, failed to corrobate this hypothesis (Hay & Undem, 1993). There is little information about potential indirect mechanisms in endothelin-induced contraction of human airways. Several investigations, however, have demonstrated that indomethacin is without effect on contraction elicited by ET-1 in human bronchus (Henry *et al.*, 1990; Advenier *et al.*, 1990; McKay *et al.*, 1991). The purpose of this study was to examine further the potential role of secondary mediators in ET-1-induced contraction in human bronchus. This was conducted by evaluating the effects of various potent and selective receptor antagonists for inflammatory mediators on the contractile response to ET-1 and also by measuring directly the effect of ET-1 on the release of histamine, the leukotrienes and various prostanoids. A preliminary account of the results has been presented by Hay *et al.* (1992).

Methods

Tissue preparation for contraction studies

Human lung tissue from organ donors was obtained from the International Institute for the Advancement of Medicine (IIAM, Exton, PA, U.S.A.) and the National Disease Research Interchange (NDRI, Philadelphia, PA, U.S.A.). Lungs were received within 24 h of removal. The donors had no known respiratory disorders. The bronchi were removed from the lung by carefully placing a glass probe within individual segments and dissecting away lung parenchymal and vascular tissue. First- and fifth-generation bronchial strips (4–15 mm diameter) were prepared and each one was placed in a 10 ml water-jacketed tissue bath containing modified Krebs-Henseleit solution which was maintained at 37°C and continuously aerated with 95% O_2/5% CO_2; according to this classification, the main bronchus is regarded as the first generation airway. The composition of the Krebs-Henseleit solution was (mM): NaCl 113, KCl 4.8, $MgSO_4$ 1.2, $CaCl_2$ 2.5, $NaHCO_3$ 25, KH_2PO_4 1.2 and glucose 5.5. One end of each preparation was attached with a silk suture to a glass tissue holder and the other end was tied to a Grass model FT03C force-displacement transducer (Grass Instrument Co., Quincy, MA, U.S.A.) for the recording of isometric tension on multichannel Grass polygraphs. The tissues were then placed under about 2 g of passive tension and equilibrated for 60 min, during which they were washed every 15 min with fresh physiological solution, before the start of each experiment.

Concentration-response curves

After the equilibration period, and before construction of ET-1 concentration-response curves, tissues were exposed to 10 μM carbachol. After this reference contraction had reached a plateau, which in preliminary experiments was shown to represent 89.0 ± 4.6% ($n = 4$) of the maximum contractile response to carbachol (100 μM), tissues were washed several times over 15–30 min until the tension returned to baseline level. The preparations were then left for at least 30 min before the start of the experiment. Agonist concentration-response curves were obtained by their cumulative addition to the organ bath in 3 fold increments according to the technique of Van Rossum (1963). Each drug concentration was left in contact with the preparation until the response reached a plateau before addition of the subsequent agonist concentration. In most experiments examining the effects of drugs, tissues were exposed to these agents for 30 min before addition of ET-1. ET-1 concentration-response curves were generally conducted in the presence of 1 μM sodium meclofenamate, the cyclo-oxygenase inhibitor, which was added 45 min before initiation of the curves. Only one agonist concentration-response curve was generated per tissue. The receptor antagonists, and their concentrations, employed in this study were 10 μM SK&F 104353 (a peptidoleukotriene receptor antagonist; Hay *et al.*, 1987), 10 μM mepyramine (an H_1-histamine receptor antagonist), 1 μM atropine (a muscarinic receptor antagonist), 1 μM SQ 29,548 (a thromboxane receptor antagonist; Ogletree *et al.*, 1985) and 10 μM WEB 2086 (a PAF receptor antagonist; Casals-Stenzel, 1987a,b). The concentration of SK&F 104353 used has been observed previously to produce marked, competitive antagonism of leukotriene-induced contraction in human bronchus ($pK_B > 8$), and, in combination with 10 μM mepyramine, to abolish antigen-induced contraction in this tissue (Hay *et al.*, 1987). SQ 29,548 has been shown to be a potent antagonist of contractions in guinea-pig trachea elicited by U-46619, the thromboxane-mimetic, or PGD_2 ($pA_2 = 8.2$ and 8.3, respectively; Ogletree *et al.*, 1985). WEB 2086 (1 μM) was reported to inhibit substantially contractions elicited by PAF in human bronchus (Johnson *et al.*, 1990). Furthermore, in the present series of experiments, in four human bronchi, mepyramine (10 μM) and atropine (1 μM) produced marked inhibition of contractions produced by histamine or carbachol, respectively (data not shown); the estimated pK_Bs were 8.5 for mepyramine and 9.3 for atropine.

Tissue preparation for mediator release studies

Human lung tissue was obtained from organ donors as described above. In addition, tissues were obtained from lung resections of anonymous lung cancer patients. The lungs were immediately placed in RPMI 1640 (4°C) solution (Gibco Co., Grand Isle, NY, U.S.A.) and transported to the laboratory. Within 24 h the bronchi (2–12 mm inner diameter) were dissected free of parenchymal tissue with the aid of a dissecting microscope. The bronchi were cut into small pieces and divided into aliquots each containing approximately 175 mg (wet weight). The bronchial tissues were incubated in 2 ml of Krebs-Henseleit solution, which was gassed with 95% O_2/5% CO_2 and maintained at 37°C. The physiological buffer was replaced at 15 min intervals for 90 min. Following this equilibration period, 2 ml of Krebs-Henseleit, containing or lacking ET-1 (10 nM or 0.3 μM), was added for 15 min. After this time the supernatant was taken to assay histamine and eicosanoid release. In addition, to determine the total tissue content of histamine, 2 ml of 0.4 N perchloric acid was added to the tissue, which was then placed in a hot water bath for 15 min. The supernatant fluid was assayed to measure the total histamine content.

Measurement of mediator release

Histamine was assayed by the automated fluorometric technique described by Siraganian (1974). Histamine release is expressed as a percentage of the total histamine content.

Leukotrienes released from bronchi were assayed by the radioimmunoassay previously described by Undem *et al.* (1987). Aliquots (100 μl) were stored at 4°C and assayed without prior purification within 48 h of each experiment. The limit of sensitivity of this assay was approximately

0.03 pmol, as defined by that amount required to inhibit [^{3}H]-LTC_4 binding by 10%. The anti-peptidoleukotriene antibody is highly selective with little affinity (cross-reactivity $<1\%$) for a variety of heterologous eicosanoids. The antibody does not, however, distinguish markedly between LTC_4, LTD_4 and LTE_4; accordingly the data indicate the levels of immunoreactive LTs (i-LTs). Standard curves with authentic LTC_4, LTD_4 and LTE_4 were parallel; the amounts of LTC_4, LTD_4 and LTE_4 required to inhibit [^{3}H]-LTC_4 binding by 50% were found to be approximately 0.4, 0.5 and 0.6 pmol/0.1 ml, respectively.

Prostanoid release into the supernatant fluid was assayed by combined gas chromatography (negative ion chemical ionization) mass spectrophotometry (GC/MS) as previously described (Hubbard *et al.*, 1986). Briefly, a 100 µl aliquot of the supernatant was added to 250 µl of acetone in a silanized vial. A mixture containing a known quantity (about 1 ng) of 3,3,4,4-tetradeuterated PGE_2, PGD_2, $PGF_{2\alpha}$, TxB_2 and 6-keto $PGF_{1\alpha}$ was added to provide internal standards for the identification and quantification of these prostanoids. In addition, the identification of 9α, 11β-PGF_2, was based on its retention to the tetradeuterated $PGF_{2\alpha}$. Samples were then dried down under a stream of nitrogen and the residue was treated with 2% methoxymine hydrochloride dissolved in pyridine. Excess pyridine was evaporated under nitrogen and the residue was subjected to sequential procedures for the synthesis of pentafluorobenzyl ester and trimethylsilyl ether derivatives as previously described (Hubbard *et al.*, 1986). CG/MS analysis of the derivatized samples (1 µl volume) was performed with a Finnigan Model 9611 gas chromatograph interfaced with a Finnigan MAT 4610B EI/CI mass spectrophotometer (Finnigan MAT Corp., San Jose, CA, U.S.A.) supplied with a Superincos data system. The sensitivity of this technique is <0.1 fmol/injection for each of the six prostanoids assayed.

Analysis of data

Agonist-induced responses for each tissue were expressed as a percentage of the reference carbachol-induced contraction added at the beginning of the experiment ('pre-carbachol'). Geometric mean EC_{50} values were calculated from linear regression analyses of data. In some tissues, due to insufficient supply of ET-1 because of cost constraints, a true maximum response could not be obtained. In these instances the contractile response to the maximum concentration of ET-1 used, 0.3 µM, was regarded as the maximum response for data analyses. Results for control- and treated-tissues were analysed for differences in both the EC_{50}s and also the maximum contractile response produced by ET-1. Mediator release is expressed as a function of the wet weight of tissues. In addition, histamine release is expressed as a percentage of total content. All data are given as the mean ± s.e.mean. Statistical analysis was conducted by ANOVA or two-tailed Student's *t* test for paired or unpaired samples where appropriate; a probability value less than 0.05 was regarded as significant.

Drugs

The following drugs were used: endothelin-1 (human, porcine) was purchased from Peninsula Laboratories (Belmont, CA, U.S.A.) or Sigma Chemical Co. (St. Louis, MO, U.S.A.). SK&F 104353 (2(S)-hydroxy-3(R)-(2-carboxyethylthio)-3-[2-(8-phenyloctyl)phenyl]-propanoic acid) was synthesized at SmithKline Beecham Pharmaceuticals (King of Prussia, PA, U.S.A.). Carbachol and mepyramine were obtained from Sigma Chemical Co. and WEB 2086 (3-(4-(2-chlorophenyl)-9-methyl-6H-thieno-(3,2-f) (1,2,4)-triazolo-(4,3-a) (1,4)-diazepine-2-yl)-1-(4-morpholinyl)-1-propanone), SQ 29,548 ([1S-[1α,2β(5Z),3β,4α]]-7-[3-[[2-[(phenylamino) carbonyl]hydrazino]methyl]-7-oxabicyclo[2.2.1]hept-2-yl]-5-heptenoic acid), sodium meclofenamate and zileuton were generous gifts from Boehringer Ingelheim (Richfield, CT, U.S.A.), Squibb Institute of Medical Research (Princeton, NJ, U.S.A.), Warner Lambert (Ann Arbor, MI, U.S.A.) and Abbott Laboratories (Chicago, IL, U.S.A.), respectively.

Results

Contractile studies

As shown in Figure 1, ET-1 was a potent and effective contractile agonist in human bronchus with an EC_{50} = 17.4 nM. In some tissues, due to insufficient supply of ET-1, a true maximum contractile response could not be obtained. Notwithstanding this caveat, and based on the contraction to 0.3 µM ET-1, the highest concentration used, representing the maximum response for data analyses, ET-1 possessed a similar potency and efficacy as LTD_4; EC_{50} (− log M): ET-1 = 7.76 ± 0.09, $n = 7$; LTD_4 = 8.46 ± 0.53, $n = 7$; $P > 0.05$; maximum response (% 10 µM pre-carbachol): ET-1 = 10.38 ± 17.4, $n = 7$; LTD_4 = 95.5 ± 9.3, $n = 7$; $P > 0.05$. Both ET-1 and LTD_4 were less efficacious agonists than carbachol: carbachol contraction at the end of the experiment ('post-carbachol') = 166 ± 8.4% of pre-carbachol ($P < 0.05$, compared to ET-1 or LTD_4).

Sodium meclofenamate (1 µM), the cyclo-oxygenase inhibitor, although it increased the contractile response to 10 nM and 30 nM ET-1, was without significant effect on the ET-1 EC_{50} or maximum contractile response; EC_{50} (− log M): control = 7.35 ± 0.09, $n = 7$; + sodium meclofenamate = 7.59 ± 0.05, $n = 7$; $P > 0.05$; maximum contractile response (% 10 µM pre-carbachol): control = 99.2 ± 25.8, $n = 7$; + sodium meclofenamate = 98.7 ± 12.4, $n = 7$; $P > 0.05$ (Figure 2a). Furthermore, in the absence of sodium meclofenamate, the potent and selective thromboxane receptor antagonist, SQ 29,548 (1 µM), had no effect on ET-1 concentration-responses curves (Figure 2b).

A series of studies, conducted in the presence of sodium meclofenamate, was performed to examine the effects of various receptor antagonists on ET-1-induced contraction. Previous studies in our laboratory have indicated that SK&F 104353 or mepyramine generally had minor effects on antigen-induced contraction of guinea-pig trachea or human bronchus, whereas the combination of the antagonists essentially abolished the response (Hay *et al.*, 1987). In this experi-

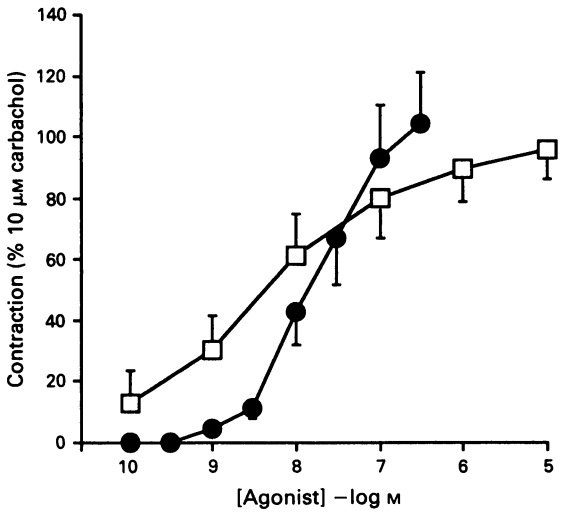

Figure 1 Comparison of endothelin-1 (ET-1) and leukotriene D_4 (LTD_4) concentration-response curves in human isolated bronchus. Results are expressed as a percentage of the response to 10 µM pre-carbachol and are the mean ± s.e.mean of 4 experiments. (●) ET-1; (□) LTD_4. Studies were conducted in the presence of 1 µM sodium meclofenamate.

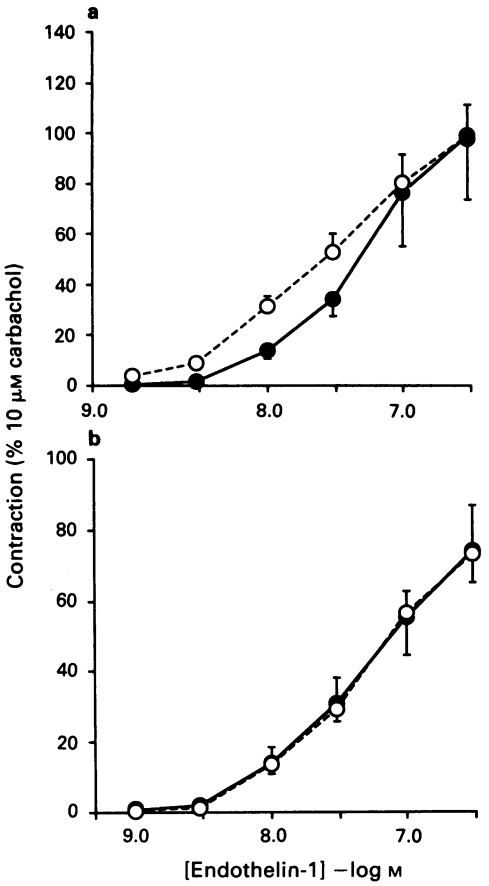

Figure 2 Effects of (a) the cyclo-oxygenase inhibitor, sodium meclofenamate (1 μM), or (b) the thromboxane receptor antagonist, SQ 29,548 (1 μM) on endothelin-1 (ET-1) concentration-response curves in human isolated bronchus. Results are expressed as a percentage of the response to 10 μM pre-carbachol and are the mean ± s.e.mean of (a) 7 or (b) 6 experiments; (a) (●) control; (○) + 1 μM sodium meclofenamate; (b) (●) control; (○) + 1 μM SQ 29,548.

ment the combination of SK&F 104353 (10 μM) and mepyramine (10 μM) had no effect on contraction elicited by ET-1 (Figure 3a). In addition, WEB 2086 (10 μM) or atropine (1 μM) had no significant effect on ET-1 concentration-response curves (Figures 3b and c). Furthermore, the combination of SK&F 104353 (10 μM), mepyramine (10 μM), WEB 2086 (1 μM) and atropine (1 μM) also was without effect on ET-1-induced contractions (Figure 4).

Mediator release

The ability of 0.3 μM ET-1, the highest concentration of ET-1 used in contractile studies, to elicit the release of leukotrienes (measured by RIA), histamine (measured fluorometrically) and six prostanoids (measured by GC/MS methods) from human bronchus was examined. All the mediators were found to be released under basal conditions (Table 1). The two major prostanoids released under basal conditions were PGE_2 and the prostacyclin metabolite, 6-keto $PGF_{1\alpha}$. The spontaneous release of immunoreactive LTs (i-LTs) was relatively high, averaging 14 ng g^{-1} tissue. The immunoreactivity was not further evaluated regarding the authenticity of the reactant; however, in a separate series of 9 experiments the spontaneous release of i-LT was only marginally inhibited by 10 μM zileuton, the 5-lipoxygenase inhibitor (Carter *et al.*, 1989); control = 8.6 ± 2.0 ng g^{-1} tissue; + zileuton = 6.5 ± 1.8 ng g^{-1} tissue ($P = 0.053$). The spontaneous release of histamine was less than 1% of total histamine content.

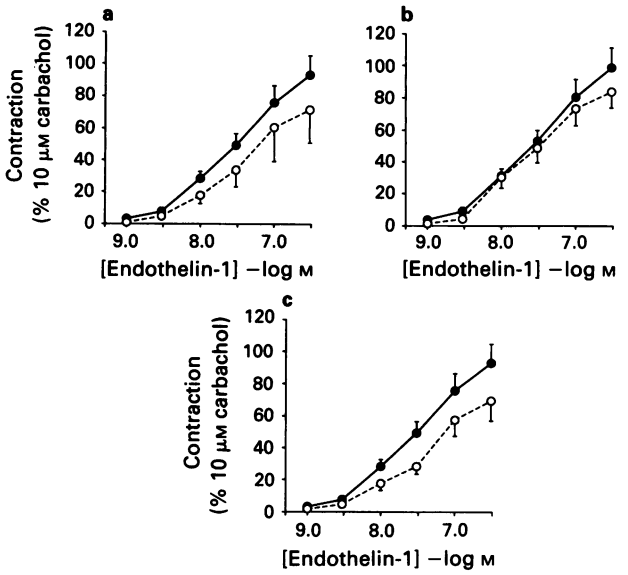

Figure 3 Effects of (a) the combination of the leukotriene receptor antagonist, SK&F 104353 (10 μM) and the H_1-histamine receptor antagonist, mepyramine (10 μM); (b) the PAF receptor antagonist, WEB 2086 (1 μM), or (c) the muscarinic receptor antagonist, atropine (1 μM) on endothelin-1 (ET-1) concentration-response curves in human isolated bronchus. Results are expressed as a percentage of the response to 10 μM pre-carbachol and are the mean ± s.e.mean of (a) 8, (b) 7 and (c) 8 experiments; (a) (●) control; (○) + 10 μM SK&F 104353 and 10 μM mepyramine; (b) (●) control; (○) + 1 μM WEB 2086; (c) (●) control; (○) + 1 μM atropine. Studies were conducted in the presence of 1 μM sodium meclofenamate.

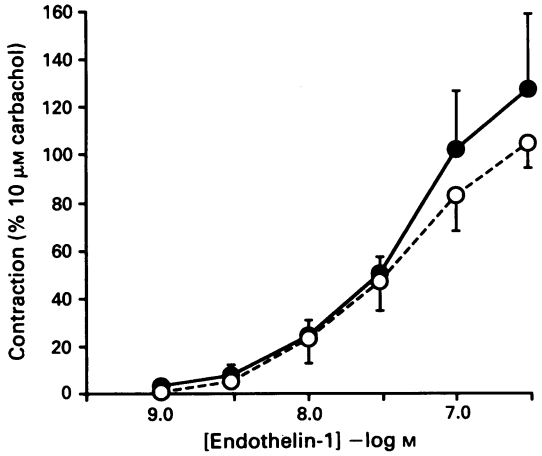

Figure 4 Effects of the combination of the leukotriene receptor antagonist, SK&F 104353 (10 μM), the H_1-histamine receptor antagonist, mepyramine (10 μM), the PAF receptor antagonist, WEB 2086 (1 μM) and the muscarinic receptor antagonist, atropine (1 μM) on endothelin-1 (ET-1) concentration-response curves in human isolated bronchus. Results are expressed as a percentage of the response to 10 μM pre-carbachol and are the mean ± s.e.mean of 5 experiments. (●) control; (○) + receptor antagonists. Studies were conducted in the presence of 1 μM sodium meclofenamate.

ET-1 (0.3 μM; 15 min exposure) had no significant effect on the release of histamine or i-LT from the bronchi. In contrast, ET-1 produced a marked increase in the production of each of the six prostanoids analysed. The most robust effect was on the production of PGD_2 where a 7.5 fold increase was observed. Approximately 10% of the PGD_2 was released from the tissue as its metabolite 9α, 11β PGF_2. The increase in the other prostanoids averaged about 1.6 to 2.7 fold over spontaneous release levels. These data are summarized in Table 1. Note, a lower concentration of ET-1, 10 nM, did not elicit a significant increase in the release of any of the prosta-

Table 1 Endothelin-1 (ET-1)-induced autacoid release from human isolated bronchus[a]

Autacoid	Spontaneous	Release ET-1 (0.3 μM)	n[c]
Eicosanoids (ng g^{-1})			
PGD_2	0.73 ± 0.31	5.51 ± 2.11**[b]	12
9α, 11β PGF_2	0.09 ± 0.03	0.56 ± 0.19**	12
TxB_2	0.17 ± 0.07	0.45 ± 0.17**	12
PGE_2	3.11 ± 0.87	6.07 ± 1.20**	12
6-keto $PGF_{1\alpha}$	2.26 ± 0.81	3.77 ± 0.90**	12
$PGF_{2\alpha}$	0.60 ± 0.17	0.94 ± 0.22*	12
i-LT	14.1 ± 9.3	10.4 ± 3.7 NS	6
Histamine (%)	0.76 ± 0.12	1.32 ± 0.21 NS	7

[a]The release of various autacoids during a 15 min period, from human isolated bronchial tissue in the absence or presence of ET-1 (0.3 μM) was quantified as outlined in Methods. Briefly, human bronchi were cut into small fragments and equilibrated at 37°C in 2 ml of buffer solution, which was replaced at 15 min intervals. After 60 min vehicle was added for a 15 min period and the solution was analysed for 'spontaneous' mediator release. The buffer was again replaced and ET-1 or vehicle was added for 15 min and the supernatant fluids analysed for ET-1-induced mediator release values or time-control values, respectively. There was no significant difference between two consecutive 15 min spontaneous release values for any mediator except prostaglandin E_2 (PGE_2), $PGF_{2\alpha}$ and 6-keto $PGF_{1\alpha}$. With respect to these mediators the increase in release over time averaged 1.4, 1.2 and 1.3 fold, respectively. The release of the prostanoids and i-LT are expressed as ng g^{-1} tissue wet weight. The release of histamine is expressed as a percentage of total histamine content which averaged 4.1 μg g^{-1} ($n = 7$).

[b]Denotes a statistically significant difference (*$P < 0.05$; **$P < 0.01$) between the amount of autacoid released in the absence (spontaneous release) and presence of ET-1, based on Student's t test for paired observations. For PGE_2, $PGF_{2\alpha}$ and 6-keto $PGF_{1\alpha}$ (prostanoids whose release was found to increase with the 15 min incubation time used, see above), the asterisk denotes that the mediator release after ET-1 was significantly greater than that observed with time alone (Student's t test for unpaired data). NS denotes no significant increase.

[c]n indicates the number of experiments (each lung provided tissue for a single experiment).

noids ($n = 4$, data not shown). In two separate experiments 1 μM sodium meclofenamate abolished ET-1-induced release of all the prostanoids (data not shown).

Discussion

The results confirmed that ET-1 is a potent contractile agonist of human bronchus with an EC_{50} of approximately 17 nM, which is in agreement with values reported previously (Advenier *et al.*, 1990; Hemsén *et al.*, 1990; Henry *et al.*, 1990; Brink *et al.*, 1991; McKay *et al.*, 1991). The potency of ET-1 observed in this study is similar to that which has been reported generally for guinea-pig isolated trachea (Hay, 1989; 1990; Maggi *et al.*, 1989; Henry *et al.*, 1990).

The functional data from the present study also demonstrate that the contractile response to ET-1 in human bronchus does not appear to involve the release of significant amounts of acetylcholine, histamine, leukotrienes, PAF or thromboxane. Thus, atropine, the classical muscarinic receptor antagonist, WEB 2086, the PAF receptor antagonist (Casals-Stenzel, 1987a,b), SQ 29,548, the thromboxane receptor antagonist (Ogletree *et al.*, 1985), or the combination of mepyramine, the H_1-histamine receptor antagonist, and SK&F 104353, the leukotriene receptor antagonist (Hay *et al.*, 1987), were without marked effect on ET-1 concentration-response curves. The concentrations of these receptor antagonists employed in this study were those which had been observed to inhibit markedly contractions produced by the natural ligands in human bronchus and/or guinea-pig trachea (see above). It has been demonstrated previously that the combination of mepyramine and SK&F 104353 was much more effective than either agent alone at inhibiting antigen-induced, mast cell-dependent contraction of human bronchus or guinea-pig trachea, suggesting that in the presence of the antagonist of one mediator, there is a sufficient quantity of the other mediator released to elicit the maximum, or close to the maximum, contractile response (Hay *et al.*, 1987). It is possible that a similar, or even more complex, scenario may occur with ET-1-induced contraction of human bronchus, such that ET-1 may stimulate the release of multiple mediators which contribute to the contractile response. However, this does not appear to be the case, as the combination of atropine, mepyramine, SK&F 104353 and WEB 2086, in the presence of sodium meclofenamate, the cyclo-oxygenase inhibitor, was without marked effect on ET-1 concentration-response curves. In agreement with functional studies, 0.3 μM ET-1, which is close to the maximally effective concentration, did not stimulate the release of histamine or i-LTs from human bronchus. In contrast to these findings it has been reported recently that ET-1 potently stimulates histamine release from guinea-pig lung parenchymal, but not peritoneal mast cells (Uchida *et al.*, 1992).

We have previously reported that ET-1 did not stimulate the release of histamine and various potent and selective receptor antagonists were without effect on contraction elicited by ET-1 in guinea-pig trachea (Hay & Undem, 1983). These and the present data suggest that ET-1 contracts human isolated bronchus and guinea-pig trachea by a similar, direct mechanism(s) which does not involve the release of secondary mediators. However, other studies have provided evidence that ET-1-induced contraction of guinea-pig trachea is in part mediated via the release of histamine, PAF and/or thromboxane (Ninomiya *et al.*, 1989; Nomura *et al.*, 1990; Battistini *et al.*, 1990; Filep *et al.*, 1990; Uchida *et al.*, 1992).

Contractile responses to ET-1 in human bronchus and guinea-pig trachea have a similar resistance to inhibition by voltage-dependent calcium channel inhibitors and appear to involve comparable calcium translocation mechanisms, i.e. predominantly the release of intracellular calcium (Maggi *et al.*, 1989; Hay, 1990; Sarriá *et al.*, 1990; Advenier *et al.*, 1990; McKay *et al.*, 1991). Thus, in both tissues ET-1-induced contraction appears to be mediated via an interaction with specific ET receptors and subsequent stimulation of the phosphatidylinositol pathway (Hay, 1990; Mattoli *et al.*, 1991b). Collectively, the above data indicate that the guinea-pig trachea is a good *in vitro* model tissue for human isolated airways to examine the bronchoconstrictor effects of ET-1.

Sodium meclofenamate, a cyclo-oxygenase inhibitor was without marked effect on ET-1 concentration-response curves. This finding is similar to those of previous studies which indicated that indomethacin had no effect on ET-1-induced contraction of human bronchi (Henry *et al.*, 1990; Advenier *et al.*, 1990; McKay *et al.*, 1991) and suggests that cyclo-oxygenase products do not significantly modulate ET-1-induced contraction in human bronchus.

Despite cyclo-oxygenase inhibitors exerting no effect on the ET-1-induced contractile responses. ET-1, albeit in a high concentration of 0.3 μM, was an effective stimulant of prostaglandin production in the human bronchus, enhancing the release of all six prostanoids measured. ET-1 caused a 7.5 fold increase in the production of PGD_2 in human isolated bronchus. The cellular source of the PGD_2 or the other prostanoids cannot be discerned from our results. Mast cells and macrophages are two types of cell capable of producing PGD_2 in the human airways (Lewis *et al.*, 1981; Balter *et al.*, 1988; Yoss *et al.*, 1990). The fact that ET-1 failed to enhance significantly histamine or i-LT production suggests either mast cells were not stimulated, or they were stimulated in a

unique manner such that only cyclo-oxygenase metabolites were formed. ET-1-induced PGD_2 production, in the absence of histamine release, is consistent with its effect on guinea-pig isolated trachea (Hay, Hubbard & Undem, unpublished observations), and canine bronchoalveolar lavage preparations (Ninomiya *et al.*, 1992). Although the human lung macrophages produce PGD_2, the major prostanoid produced upon stimulation of this cell is thromboxane A_2 (Balter *et al.*, 1988; Yoss *et al.*, 1990). In contrast, ET-1 in the present study stimulated the release of about 17 times more PGD_2 than thromboxane. The microvasculature may be a source for some of the ET-1 induced prostanoid production in the airway. Thus, ET-1 has been found to stimulate the production of prostacyclin from bovine cultured aortic endothelial cells (Filep *et al.*, 1991). In guinea-pig trachea experiments using epithelium-containing and epithelium-denuded tissues provided evidence to suggest that the epithelium is not the source of the prostanoids released by ET-1 (Hay, Hubbard & Undem, unpublished observations).

In summary, the present data provide evidence that ET-1 produces potent contraction of human bronchus predominantly via a direct action, which does not involve a significant contribution of the release of acetylcholine, histamine, leukotrienes or PAF. ET-1 does not evoke the release of histamine or i-LT from the human bronchus, but is an effective stimulus for prostanoid production. However, the released prostanoids exert no significant modulatory influence on ET-1-induced contraction in human bronchus, although the possibility remains that these autacoids may play a significant role in mediating or modulating other effects of ET-1 in the respiratory system.

The authors thank Dotti Lavan for secretarial assistance, Roseanna Muccitelli, Mark Luttmann and Sonya Meeker for excellent technical help and Boehringer Ingelheim, Warner Lambert and Squibb Institute of Medical Research and Abbott Laboratories for their gifts of WEB 2086, sodium meclofenamate, SQ 29,548 and zileuton, respectively. We would also like to thank the International Institute for the Advancement of Medicine and the National Disease Research Interchange for their valuable assistance in obtaining human tissue and Dr Roy Goldie for helpful discussions and critique of the manuscript.

References

ADVENIER, C., SARRIA, B., NALINE, E., PUYBASSET, L. & LAGENTE, V. (1990). Contractile activity of three endothelins (ET1, ET-2 and ET-3) on the human isolated bronchus. *Br. J. Pharmacol.*, **100**, 168–172.

BALTER, M.S., ESCHENBACHER, W.L. & PETERS-GOLDEN, M. (1988). Arachidonic acid metabolism in cultured alveolar macrophages from normal, atopic, and asthmatic subjects. *Am. Rev. Respir. Dis.*, **138**, 1134–1142.

BATTISTINI, B., SIROIS, P., BRAQUET, P. & FILEP, J.G. (1990). Endothelin-induced constriction of guinea-pig airways; role of platelet-activating factor. *Eur. J. Pharmacol.*, **186**, 307–310.

BRINK, C., GILLARD, V., ROUBERT, P., MENCIA-HUERTA, J.M., CHABRIER, P.E., BRAQUET, P. & VERLEY, J. (1991). Effects of specific binding sites of endothelin in human lung preparations. *Pulmon. Pharmacol.*, **4**, 54–59.

CARTER, G.W., YOUNG, P.R., ALBERT, D.H., BOUSKA, J.B., DYER, R.D., BELL, R.L., SUMMERS, J.B., BROOKS, D.W., GUN, B.P., RUBIN, P. & KESTERSON, J. (1989). A-64077, a new potent orally active 5-lipoxygenase inhibitor. In *Leukotrienes and Prostanoids in Health and Disease. New Trends Lipid Mediators Research.* ed. Zor, U., Naot, Z. & Danon, A., vol. 3, pp. 50–55. Basel: Karger.

CASALS-STENZEL, J. (1987a). Effects of WEB 2086, a novel antagonist of platelet activating factor, in active and passive anaphylaxis. *Immunopharmacol.*, **13**, 117–124.

CASALS-STENZEL, J. (1987b). Protective effect of WEB 2086, a novel antagonist of platelet activating factor, in endotoxin shock. *Eur. J. Pharmacol.*, **135**, 117–122.

CERNACEK, P. & STEWART, D.J. (1989). Immunoreactive endothelin in human plasma: marked elevations in patients in cardiogenic shock. *Biochem. Biophys. Res. Commun.*, **161**, 562–567.

FILEP, J.G., BATTISTINI, B., COTÉ, Y.P., BEAUDOIN, A.R. & SIROIS, P. (1991). Endothelin-1 induces prostacyclin release from bovine aortic endothelial cells. *Biochem. Biophys. Res. Commun.*, **177**, 171–176.

FILEP, J.G., BATTISTINI, B. & SIROIS, P. (1990). Endothelin induces thromboxane release and contraction of isolated guinea-pig airways. *Life Sci.*, **47**, 1845–1850.

GRUNSTEIN, M.M., ROSENBERG, S.M., SCHRAMM, C.M. & PAWLOWSKI, N.A. (1991). Mechanisms of action of endothelin 1 in maturing rabbit airway smooth muscle. *Lung Cell. Mol. Physiol.*, **4**, L434–L443.

HAY, D.W.P., MUCCITELLI, R.M., TUCKER, S.S., VICKERY-CLARK, L.M., WILSON, K.A., GLEASON, J.G., HALL, R.F., WASSERMAN, M.A. & TORPHY, T.J. (1987). Pharmacologic profile of SK&F 104353: a novel, potent and selective peptidoleukotriene receptor antagonist in guinea pig and human airways. *J. Pharmacol. Exp. Ther.*, **243**, 474–481.

HAY, D.W.P. (1989). Guinea-pig tracheal epithelium and endothelin. *Eur. J. Pharmacol.*, **171**, 241–245.

HAY, D.W.P. (1990). Mechanism of endothelin-induced contraction of isolated guinea-pig trachea: comparison with rat aorta. *Br. J. Pharmacol.*, **100**, 383–392.

HAY, D.W.P., HENRY, P.J. & GOLDIE, R.G. (1993). Endothelin and the respiratory system. *Trends Pharmacol. Sci.*, **14**, 29–32.

HAY, D.W.P. & UNDEM, B.J. (1993). Does endothelin contract guinea-pig trachea via a direct mechanism? *Am. Rev. Resp. Dis.*, **143**, A160 (Abstract).

HAY, D.W.P., LUTTMANN, M.A., HUBBARD, W. & UNDEM, B. (1992). Endothelin-1 (ET-1)-induced smooth muscle contraction and mediator release in human bronchus. *Am. Rev. Resp. Dis.*, **145**, A373. (Abstract).

HEMSÉN, A., FRANCO-CERECEDA, A., MATRAN, R., RUDEHILL, A. & LUNDBERG, J.M. (1990). Occurrence, specific binding sites and functional effects of endothelin in human cardiopulmonary tissue. *Eur. J. Pharmacol.*, **1991**, 319–328.

HENRY, P.J., RIGBY, P.J., SELF, G.J., PREUSS, J.M. & GOLDIE, R.G. (1990). Relationship between endothelin-1 binding site densities and constrictor activities in human and animal airway smooth muscle. *Br. J. Pharmacol.*, **100**, 786–792.

HUBBARD, W.C., LITTERST, C.C., LIU, M.C., BLEECKER, E.R., EGGLESTON, P.C., MCLEMORE, T.C. & BOYD, M.R. (1986). Profiling of prostaglandin biosynthesis in biopsy fragments of human lung carcinoma and normal human lung by capillary gas chromatography-negative ion chemical ionization mass spectrometry. *Prostaglandins*, **32**, 889–906.

INOUE, A., YANAGISAWA, M., KIMURA, S., KASUYA, Y., MIYAUCHI, T., GOTO, K. & MASAKI, T. (1989). The human endothelin family: three structurally and pharmacologically distinct isopeptides predicted by three separate genes. *Proc. Natl. Acad. Sci. U.S.A.*, **86**, 2863–2867.

JOHNSON, P.R.A., ARMOUR, C.L. & BLACK, J.L. (1990). The action of platelet activating factor and its antagonism by WEB 2086 on human isolated airways. *Eur. Respir. J.*, **3**, 55–60.

KLOOG, Y., AMBAR, I., SOKOLOVSKY, M., KOCHVA, E., WOLLBERG, S. & BDOLAH, A. (1988). Sarafotoxin, a novel vasoconstrictor peptide: phosphoinositide hydrolysis in rat heart and brain. *Science*, **242**, 268–270.

LEE, C.Y. & CHIAPPINELLI, V.A. (1988). Similarity of endothelin to snake venom toxin. *Nature*, **335**, 303.

LEE, H.-K., LEIKAUF, G.D. & SPERELAKIS, N. (1990). Electromechanical effects of endothelin on ferret bronchial and tracheal smooth muscle. *J. Appl. Physiol.*, **68**, 417–420.

LEWIS, R.A., ROBERTS, L.J.II, HOLGATE, S.T., OATES, J.A. & AUSTEN, K.F. (1981). Preferential generation of prostaglandin D_2 by rat and human mast cells. In *Biochemistry of Acute Allergic Reactions; 4th International Symposium.* ed. Becker, E.L., Simon, A.S. & Austen, K.F. pp. 239–254. New York: Liss.

MAGGI, C.A., PATACCHINI, S. & MELI, A. (1989). Potent contractile effect of endothelin in isolated guinea-pig airways. *Eur. J. Pharmacol.*, **160**, 179–182.

MATTOLI, S., MEZZETTI, M., RIVA, G., ALLEGRA, L. & FASOLI, A. (1990). Specific binding of endothelin on human bronchial smooth muscle cells in culture and secretion of endothelin-like material from bronchial epithelial cells. *Am. J. Respir. Cell Mol. Biol.*, **3**, 145–151.

MATTOLI, S., SOLOPERTO, M., MARINI, M. & FASOLI, A. (1991a). Levels of endothelin in the bronchoalveolar lavage fluid of patients with symptomatic asthma and reversible airflow obstruction. *J. Allergy Clin. Immunol.*, **88**, 376–384.

MATTOLI, S., SOLOPERTO, M., MEZZETTI, M. & FASOLI, A. (1991b). Mechanisms of calcium mobilization and phosphoinositide hydrolysis in human bronchial smooth muscle cells by endothelin 1. *Am. J. Respir. Cell. Mol. Biol.*, **5**, 424–430.

MCKAY, K.O., BLACK, J.L. & ARMOUR, C.L. (1991). The mechanism of action of endothelin in human lung. *Br. J. Pharmacol.*, **102**, 422–428.

NAMBU, F., YUBE, N., OMAWARI, N., SAWADA, M., OKEGAWA, T., KAWASAKI, A. & IKEDA, S. (1990). Inhibition of endothelin-induced bronchoconstriction by OKY-046, a selective thromboxane A_2 synthetase inhibitor, in guinea pigs. *Adv. Prost. Thromb. Leuk. Res.*, **21**, 453–456.

NINOMIYA, N., UCHIDA, Y., SAOTOME, M., NOMURA, A. & HASEGAWA, S. (1989). Histamine release from guinea pig mast cells in endothelin-induced tracheal constriction. *Am. Rev. Resp. Dis.*, **139**, A118 (Abstract).

NINOMIYA, N., YU, X.Y., HASEGAWA, S. & SPANNHAKE, E.W. (1992). Endothelin-1 induces stimulation of prostaglandin synthesis in cells obtained from canine airways by bronchoalveolar lavage. *Prostaglandins*, **43**, 401–411.

NOMURA, A., NIMONIYA, H., SAOTOME, M., OHSE, N., ISHII, Y., UCHIDA, Y., HIRATA, F. & HASEGAWA, S. (1990). Multiple mechanisms of bronchoconstrictive response to endothelin-1. *J. Vasc. Med. Biol.*, **2**, 199 (Abstract).

OGLETREE, M.L., HARRIS, D.N., GREENBERG, R., HASLANGER, M.F. & NAKANE, M. (1985). Pharmacological actions of SQ 29,548, a novel selective thromboxane antagonist. *J. Pharmacol. Exp. Ther.*, **234**, 435–441.

PAYNE, A.N. & WHITTLE, B.J.R. (1988). Potent cyclo-oxygenase-mediated bronchoconstrictor effects of endothelin in the guinea-pig in vivo. *Eur. J. Pharmacol.*, **158**, 303–304.

POWER, R.F., WHARTON, J., ZHAO, Y., BLOOM, S.R. & POLAK, J.M. (1989). Autoradiographic localization of endothelin-1 binding sites in the cardiovascular and respiratory systems. *J. Cardiovasc. Pharmacol.*, **13**, S50–S56.

SARRIA, B., NALINE, E., MORCILLO, E., CORTIJO, J., ESPLUGUES, J. & ADVENIER, C. (1990). Calcium dependence of the contraction produced by endothelin (ET-1) in isolated guinea-pig trachea. *Eur. J. Pharmacol.*, **187**, 445–453.

SIRAGANIAN, R.P. (1974). An automated continuous-flow system for the extraction and fluorometric analysis of histamine. *Anal. Biochem.*, **57**, 383–394.

SPRINGALL, D.R., HOWARTH, P.H., COUNIHAN, H., DJUKANOVIC, R., HOLGATE, S.T. & POLAK, J.M. (1991). Endothelin immunoreactivity of airway epithelium in asthmatic patients. *Lancet*, **337**, 697–701.

TURNER, N.C., POWER, R.F., POLAK, J.M., BLOOM, S.R. & DOLLERY, C.T. (1989). Endothelin-induced contractions of tracheal smooth mucle and identification of specific endothelin binding sites in the trachea of the rat. *Br. J. Pharmacol.*, **98**, 361–366.

UCHIDA, Y., NINOMIYA, S., SAOTOME, M., NOMURA, A., OHTSUKA, M., YANAGISAWA, M., GOTO, K., MASAKI, T. & HASEGAWA, S. (1988). Endothelin, a novel vasoconstrictor peptide, as potent bronchoconstrictor. *Eur. J. Pharmacol.*, **154**, 227–228.

UCHIDA, Y., NINOMIYA, H., SAKAMOTO, T., LEE, J.Y., ENDO, T., NOMURA, A., HASEGAWA, S. & HIRATA, F. (1992). ET-1 released histamine from guinea pig pulmonary but not peritoneal mast cells. *Biochem. Biophys. Res. Commun.*, **189**, 1196–1201.

UNDEM, B.J., PICKETT, W.C. & ADAMS, G.III (1987). Antigen-induced sulfidopeptide leukotriene release from the guinea pig superfused trachea. *Eur. J. Pharmacol.*, **142**, 31–37.

VAN ROSSUM, J.M. (1963). Cumulative dose-response curves. II. Technique for the making of dose-response curves in isolated organs and the evaluation of drug parameters. *Arch. Int. Pharmacodyn.*, **143**, 299–330.

YANAGISAWA, M., KURIHARA, H., KUMURA, S., TOMOBE, Y., KOBAYASHI, M., MITSUI, T., YASAKI, Y., GOTO, K. & MASAKI, T. (1988). A novel potent vasoconstrictor peptide produced by vascular endothelial cells. *Nature*, **332**, 411–415.

YANAGISAWA, M. & MASAKI, T. (1989a). Endothelin, a novel endothelium-derived peptide. Pharmacological activities, regulation and possible roles in cardiovascular control. *Biochem. Pharmacol.*, **38**, 1877–1883.

YANAGISAWA, M. & MASAKI, T. (1989b). Molecular biology and biochemistry of the endothelins. *Trends Pharmacol. Sci.*, **10**, 374–378.

YOSS, E.B., SPANNHAKE, E.W., FLYNN, J.T., FISH, J.E. & PETERS, S.P. (1990). Arachidonic acid metabolism in normal human alveolar macrophages: stimulus specificity for mediator release and phospholipid metabolism, and pharmacological modulation *in vitro* and *in vivo*. *Am. J. Respir. Cell Mol. Biol.*, **2**, 69–80.

(Received April 21, 1993
Accepted April 28, 1993)

Br. J. Pharmacol. (1993), **110**, 399–403

Effect of trimebutine on voltage-activated calcium current in rabbit ileal smooth muscle cells

[1]Masaaki Nagasaki, Seiichi Komori & Hidenori Ohashi

Laboratory of Pharmacology, Department of Veterinary Science, Faculty of Agriculture, Gifu University, Gifu 501-11, Japan

1 The effect of trimebutine on the voltage-dependent inward Ca^{2+} current was investigated by the whole-cell voltage-clamp technique in single smooth muscle cells from rabbit ileum.

2 Trimebutine (3–100 μM) reduced the Ca^{2+} current in a concentration-dependent manner. The inhibitory effect on the Ca^{2+} current was also dependent on the holding potential. The Ca^{2+} current after a low holding potential was inhibited to a greater extent than that after a high membrane potential: the IC_{50} values were 7 μM and 36 μM at holding potentials of −40 mV and −60 mV, respectively. The Ca^{2+} current elicited from a holding potential of −80 mV could not be reduced by as much as 50% of the control by trimebutine at concentrations as high as 100 μM.

3 Trimebutine (30 μM) shifted the voltage-dependent inactivation curve for the Ca^{2+} current by 18 mV in the negative direction. The affinity of the drug for Ca^{2+} channels was calculated to be 36 times higher in the inactivated state than in the closed-available state.

4 Blockade of the Ca^{2+} current by trimebutine, unlike verapamil, was not use-dependent.

5 The results suggest that trimebutine inhibits the voltage-dependent inward Ca^{2+} current through a preferential binding to Ca^{2+} channels in the inactivated state in the smooth muscle cell from rabbit ileum. The inhibitory effect of trimebutine on gastrointestinal motility is discussed in the light of the present findings.

Keywords: Trimebutine; Ca^{2+} current; ileal smooth muscle cells; whole-cell voltage-clamp

Introduction

Trimebutine has been used for treatment of both hypermotility and hypomotility disorders of the gastrointestinal tract including irritable bowel syndrome, gastritis and dyspepsia (Abei *et al.*, 1977; Moshal & Herron, 1979; Mazzone *et al.*, 1980; Luttecke, 1980). Trimebutine has been demonstrated to stimulate and inhibit the spontaneous contractions during respective low and high contractile activities in the isolated intestine from the guinea-pig and rabbit (Takenaga *et al.*, 1984; 1986). The mechanism underlying the duality of the action of trimebutine is not clear.

Our recent studies on single voltage-clamped smooth muscle cells of the rabbit intestine revealed that trimebutine inhibits both Ca^{2+}-dependent and independent K^+ currents evoked upon depolarization, with little selectivity for them, and there is neither voltage- nor use-dependence in the current inhibition (Nagasaki *et al.*, 1993). The inhibition of K^+ current could lead to stimulation of contractile activity. In intestinal smooth muscles, trimebutine possesses a Ca^{2+} antagonist-like action which contributes to the inhibitory effect on contractile activity: trimebutine interacts in a negative allosteric manner with 1,4-dihydropyridine ([^{3}H]-nitrendipine) binding sites (Nagasaki *et al.*, 1990), and inhibits both cytosolic Ca^{2+} elevation and tension development produced by high K^+ solution (Nagasaki *et al.*, 1991). Further, whole-cell voltage-clamp experiments revealed that trimebutine inhibits the voltage-dependent Ba^{2+} current through Ca^{2+} channels in rabbit ileal smooth muscle cells (Shimada *et al.*, 1990).

In the present study, we have investigated the effect of trimebutine on the voltage-dependent Ca^{2+} inward current which sustains generation and conduction of the smooth muscle action potential in single smooth muscle cells from rabbit ileum, using the whole-cell voltage-clamp technique.

[1] Author for correspondence at present address: Pharmacological Research Laboratory, Tanabe Seiyaku Co., Ltd., 2-2-50, Kawagishi, Toda, Saitama 335, Japan.

Methods

Male rabbits (Japanese White; 1.5–2.5 kg) were killed by injecting an overdose of sodium pentobarbitone into the ear vein. A segment of the ileum was removed and some pieces of the longitudinal muscle layer were peeled from the underlying circular muscle. They were cut into smaller pieces of (2 × 2 mm) and incubated in a low-Ca^{2+} (30 μM) physiological salt solution (PSS; composition given below) at 37°C for 10 min, and then incubated in a mixture of collagenase (0.5–0.8 mg ml^{-1}, Amano), papain (12–15 u ml^{-1}, Sigma type III) and bovine serum albumin (2 mg ml^{-1}, Wako) in the low-Ca^{2+} PSS at 37°C for 30–40 min. After the enzymatic digestion, tissue fragments were suspended in a fresh 120 μM Ca^{2+}-containing PSS and gently agitated. The resulting suspension was centrifuged at 100 *g* for 2 min and the cells were resuspended in a 0.8 mM Ca^{2+}-containing PSS. Small aliquots of cell suspension were placed on glass coverslips and stored in a moist atmosphere at 4°C.

Whole-cell Ca^{2+} current was recorded at room temperature by the whole-cell voltage-clamp technique (Hamill *et al.*, 1981). Patch pipettes had a resistance of 4–7 MΩ when filled with pipette solution. Current recordings were made through a patch-clamp amplifier (Nihon Khoden; CEZ-2300). Voltage command pulses were delivered through this amplifier, and the recorded currents were stored on a digital audio tape and replayed onto a thermal array recoder (Nihon Khoden; RTA-1100) for analysis and illustration. Measurements of the amplitude of Ca^{2+} currents were corrected for background membrane current by subtraction of currents obtained when voltage command pulses were applied to the cells in the extracellular presence of Cd^{2+} (100 μM) (Lang *et al.*, 1991).

The experimental values obtained were expressed as means ± s.e.mean. IC_{50} values were determined by a probit method from cumulative dose-response relationships. Statistical significance was tested by Student's *t* test and differences considered significant when $P<0.05$.

PSS used for the bath solution had the following composition (mM): NaCl 126, KCl 6, $CaCl_2$ 2, $MgCl_2$ 1.2, glucose 14

and HEPES 10.5 (titrated to pH 7.2 with NaOH). The patch pipette solution had the following composition (mM): CsCl 134, $MgCl_2$ 1.2, ATP 1, GTP 0.1, EGTA 0.05, glucose 14 and HEPES 10.5 (titrated to pH 7.2 with NaOH).

Drugs and chemicals used were trimebutine maleate (Tanabe) and verapamil hydrochloride (Nacalai tesque). All other chemicals used were of reagent grade.

Results

In cells held by voltage-clamp at a potential of − 80 to − 40 mV with inclusion of CsCl-rich solution in the pipette (see Methods), depolarization by command pulses (300 ms in duration) to − 30 mV or more positive, elicited a transient inward current carried by Ca^{2+}. The inward current was completely abolished after external application of Cd^{2+} (100 μM) (see Figure 2).

Figure 1 shows current traces obtained by command pulses from − 60 mV holding potential to − 20 to + 60 mV in 20 mV increments before and after application of trimebutine (30 μM). Trimebutine reduced the amplitude of the Ca^{2+} current evoked at every command potential, but did not change the time course of its time-dependent inactivation (Figure 1). The inhibitory effect of trimebutine was readily reversible. When the holding potential was − 40 mV, command pulses with the same parameters as at − 60 mV elicited smaller Ca^{2+} currents. The Ca^{2+} current evoked from a depolarized holding potential was preferentially reduced by trimebutine, as shown in Figure 2. In Figure 3, the current-voltage relationships for the peak Ca^{2+} current before and after application of trimebutine (10 μM) obtained at a holding potential of − 40 mV are illustrated to compare with those before and after application of trimebutine (30 μM), obtained at a holding potential of − 60 mV. A greater reduction of the current amplitude at − 40 mV can be seen over a wide range of command potentials. Indeed, the peak current evoked by a depolarizing pulse from − 40 mV to + 10 mV was decreased by 68% and the peak current evoked by a depolarizing pulse from − 60 mV to + 10 mV was decreased by 36%. It can be also seen in Figure 3 that regardless of the holding potential, the apparent reversal potential of the Ca^{2+} current remained unchanged after application of trimebutine.

Dose-response curves for the inhibitory action of trimebutine on the Ca^{2+} current evoked by a command pulse (200 ms in duration) to 0 mV from three different holding potentials of − 40, − 60 and − 80 mV are shown in Figure 4. At − 40 mV and − 60 mV, trimebutine (3–100 μM) reduced the peak current in a concentration-dependent manner

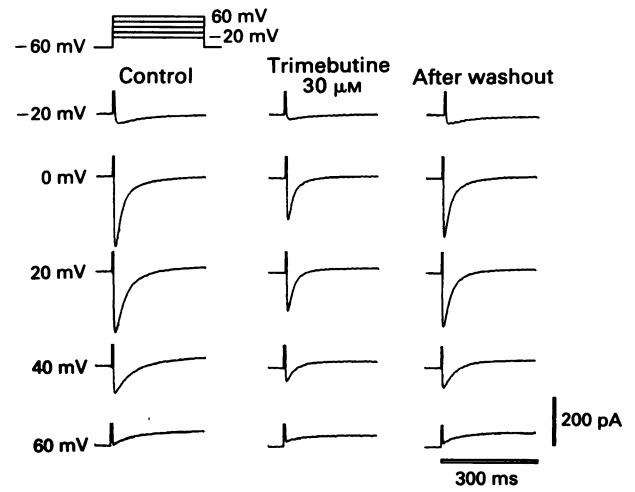

Figure 1 The effect of trimebutine on inward Ca^{2+} currents elicited by stepping from a holding potential of − 60 mV to test potentials of − 20 to + 60 mV in 20 mV increments for 300 ms in a single Cs-filled cell bathed in physiological salt solution. Current traces before and after addition of trimebutine (30 μM) and after its washout are shown from left to right.

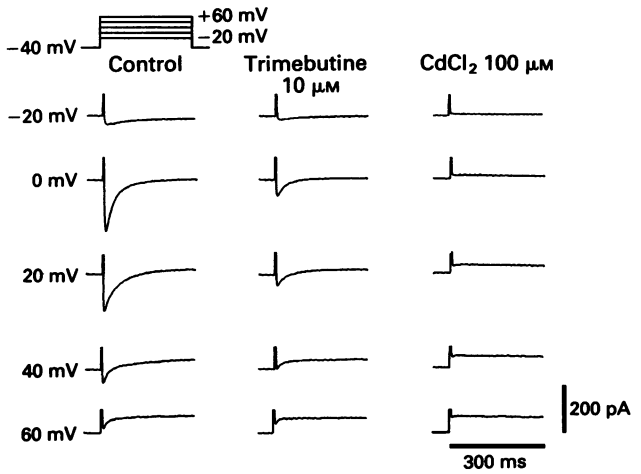

Figure 2 The effect of trimebutine on inward Ca^{2+} currents elicited by stepping from a holding potential of − 40 mV to test potentials of − 20 to + 60 mV in 20 mV increments for 300 ms. Current traces before and after addition of trimebutine (10 μM) are shown (left and middle rows). Addition of $CdCl_2$ (100 μM) abolished the inward currents (right row).

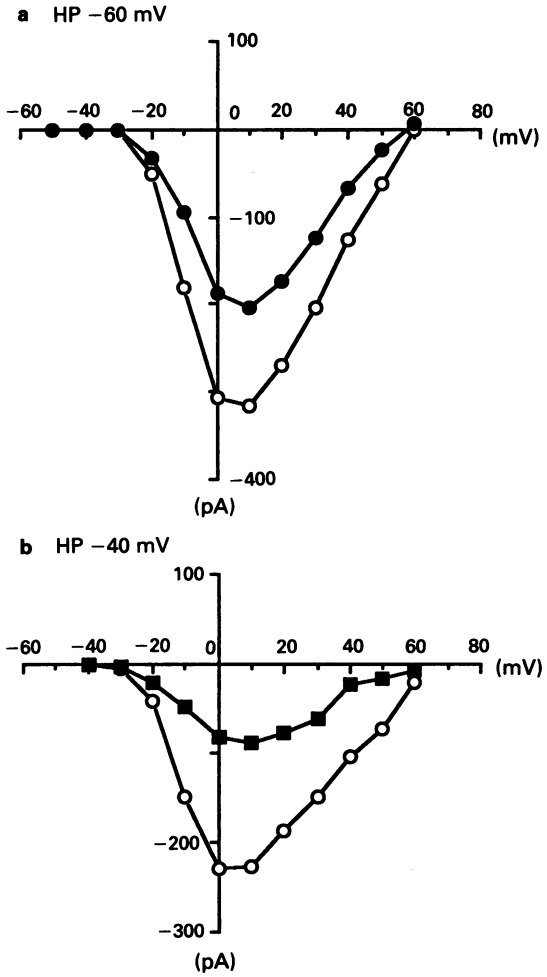

Figure 3 Current-voltage relationships for the peak inward Ca^{2+} current activated from holding potentials of − 60 mV (a) and − 40 mV (b). The peak amplitude of the Ca^{2+} current evoked by stepping to different potentials from the holding potential is plotted against the potential. Control (○) and in the presence of trimebutine (10 μM, ■; 30 μM, ●).

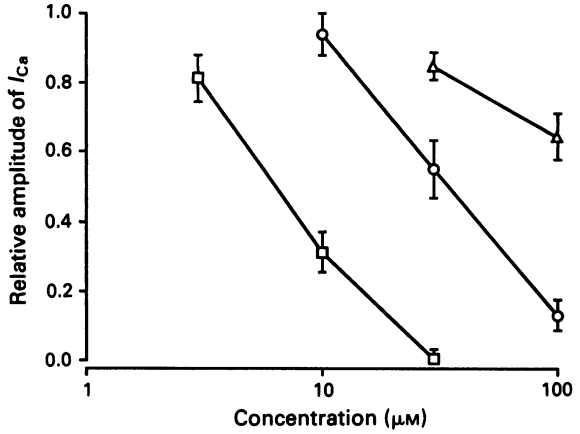

Figure 4 Relationships between the concentration of trimebutine (3–100 μM) and the relative amplitude of the Ca^{2+} current activated from three different holding potentials (– 40 mV, □; – 60 mV, ○; – 80 mV, △). The Ca^{2+} current was evoked by stepping from the holding potentials to 0 mV for 200 ms and the amplitude of the current before cumulative application of the drug was normalized as 1.0. Each point indicates the mean ± s.e.mean of 6–7 experiments.

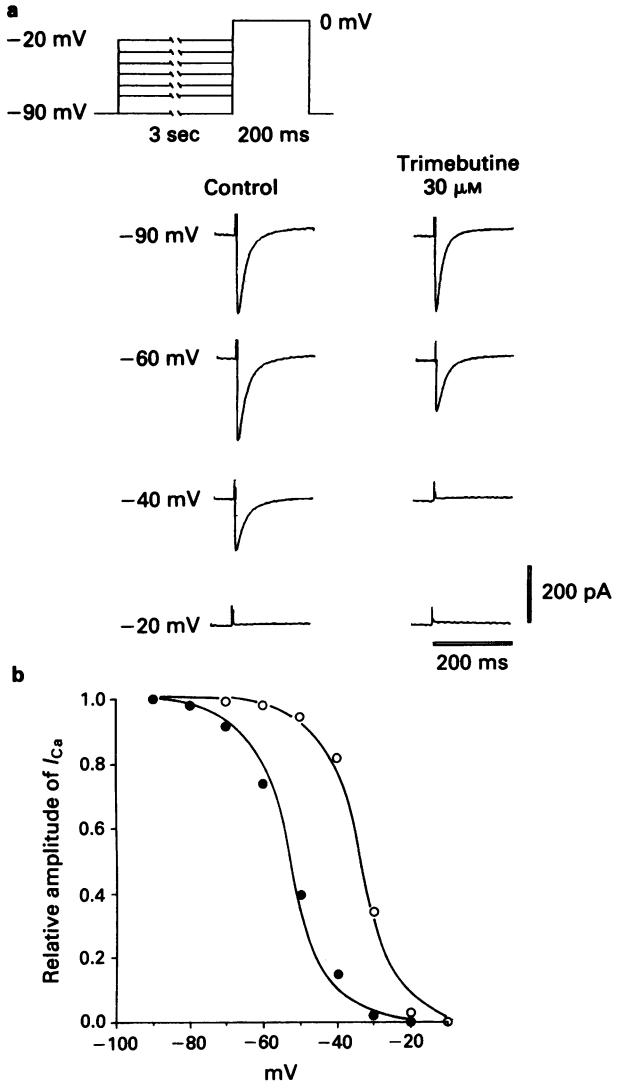

Figure 5 The effect of trimebutine on the voltage-dependent inactivation of the Ca^{2+} current. (a) Current traces recorded from a cell of which the membrane potential was held at different levels (– 90 to – 20 mV) during a 3 s conditioning pulse and then stepped to 0 mV for 200 ms. Left row, the control; right row, in the presence of trimebutine (30 μM). (b) The relationships between the relative peak amplitude of the Ca^{2+} current and the membrane potential attained by the conditioning pulse in the absence (○) and presence of trimebutine (30 μM, ●). The peak amplitudes of the Ca^{2+} current evoked by stepping to 0 mV from – 90 mV in the absence and presence of the drug were normalized as 1.0, respectively. Points were fitted by the Boltzmann equation (see text). The inward current was 50% inactivated at – 34 mV in the control and at – 52 mV in the presence of 30 μM trimebutine.

with respective IC_{50} values of 7.3 ± 1.2 μM ($n = 6$) and 35.8 ± 6.2 μM ($n = 7$). However, at – 80 mV, 50% inhibition of the peak current could not be obtained even by 100 μM trimebutine (the highest concentration used in the present study). In fact, 100 μM trimebutine reduced the current amplitude only by 35.5 ± 6.7% ($n = 6$) (Figure 4). These results indicate a strong dependence of the inhibitory action of trimebutine on the membrane potential at which the cell is held before eliciting the current.

To clarify the voltage-dependent inhibitory action of trimebutine, steady-state inactivation curves of the Ca^{2+} current were obtained before and after application of 30 μM trimebutine by means of a conventional double-pulse protocol. Application of a 3 s conditioning pulse, varying from – 90 mV to – 20 mV in 10 mV increments, was followed by a constant test pulse (200 ms in duration) to 0 mV. The Ca^{2+} current evoked by the test pulse was decreased in amplitude as the potential of the conditioning pulses was increased. No inward current was evoked by the test pulse when the conditioning potential was – 20 mV (Figure 5a). The voltage-dependent inactivation of the Ca^{2+} current was quantified as follows. The amplitude of the current (I) evoked by the test pulse was normalized by taking the amplitude of the current (I_{max}) evoked by the test pulse with a conditioning pulse of – 90 mV as 1.0. Figure 5b shows a plot of the ratio of I to I_{max} against the conditioning potential (V). The data could be fitted by a least squares method with a Boltzmann equation of the form: $I/I_{max} = 1/\{1 + \exp[(V - V_{0.5})/V_s]\}$, where $V_{0.5}$ is the conditioning potential at which the ratio of I/I_{max} was 0.5 and V_s the slope factor. The sigmoid inactivation curve was shifted by about 18 mV in the negative direction without any appreciable change in the slope after application of trimebutine (30 μM). Four experiments gave mean values for $V_{0.5}$ and for V_s in the absence of trimebutine as – 33.8 ± 1.8 mV and 7.1 ± 0.6 mV, respectively, and corresponding mean values in the presence of trimebutine (30 μM) as – 52.0 ± 3.2 mV and 6.5 ± 0.5 mV, respectively. The difference between the $V_{0.5}$ values was statistically significant ($P < 0.01$).

In cells held at – 60 mV, the Ca^{2+} current was repeatedly evoked at 30 s intervals by a 100 ms pulse to 0 mV. Pulse application was interrupted and trimebutine (30 μM) or verapamil (3 μM) applied. Three minutes after the drug application, pulses were restarted for 2 min to evoke the first series of Ca^{2+} currents, interrupted for 3 min, and restarted again to evoke the second series of Ca^{2+} currents. As shown in Figure 6, reduction of the current amplitude reached about 50% during the early 3 min of exposure to trimebutine and was only slightly reduced by repeated application of pulses (ten times with a 3 min interruption). In contrast, during exposure to verapamil, the extent of current reduction was small for the first pulse (7%), but increased progressively on repetition of the pulse (five times) and reached about 40% for the 5th Ca^{2+} current. The current reduction in the second series of the Ca^{2+} currents during the exposure to verapamil developed to a greater extent than, but in a similar manner to, that in the first series of the Ca^{2+} currents. Similar effects were obtained in four other cells with trimebutine and two cells with verapamil. These results suggest that the inhibitory action of trimebutine on the Ca^{2+} current is not conspicuously use-dependent.

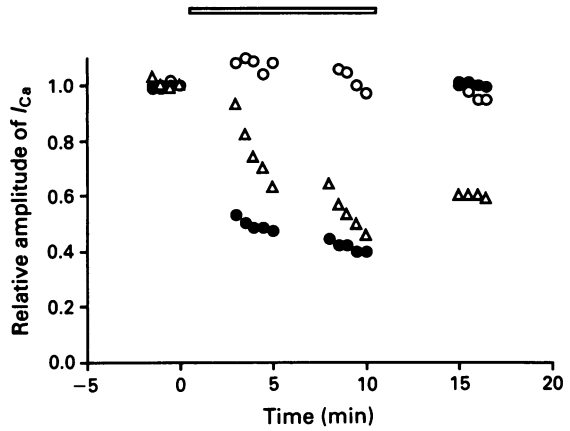

Figure 6 Comparison of the time courses of the inhibition of Ca^{2+} current by trimebutine and verapamil. Control (○) and in the presence of trimebutine (30 μM, ●) and verapamil (3 μM, Δ). The drug was added at time 0 in the horizontal scale and removed at 10 min. A depolarizing pulse (100 ms in duration) to 0 mV from the holding potential of − 60 mV was applied at 30 s intervals for 2 min and then the drug was added without application of the pulses. Three minutes later, a train of pulses was applied twice with a 3 min quiescent period. The amplitude of the Ca^{2+} current evoked by the pulse immediately before application of the drug was normalized as 1.0.

Discussion

The present results show that trimebutine dose-dependently inhibits whole-cell Ca^{2+} current evoked by depolarization in single smooth muscle cells isolated from rabbit ileum. Trimebutine exerted a stronger inhibitory effect on the Ca^{2+} currents elicited from lower holding potentials and caused a parallel shift in the voltage-dependent inactivation curve for the Ca^{2+} current in the negative direction. These characteristics of the action of trimebutine may be attributed to varying affinities of the drug for the Ca^{2+} channels in different channel states. Membrane depolarization induces an inactivated state of the Ca^{2+} channels in which trimebutine binding is favoured. According to Bean *et al.* (1983) and Sanguinetti & Kass (1984), the dissociation constant for trimebutine binding to the Ca^{2+} channels in the inactivated state (K_i) can be calculated from the equation: $\Delta V_{0.5} = V_s \times \ln(1 + [D]/K_i)/(1 + [D]/K_r)$, where $\Delta V_{0.5}$ and V_s are the shifted amplitude by trimebutine in the voltage-dependent inactivation curve and the slope factor of the inactivation curve, respectively, [D] is the concentration of trimebutine and K_r is the dissociation constant for trimebutine binding to the Ca^{2+} channels in the close-available state. Using the values of 18.2 mV for $\Delta V_{0.5}$ and 6.5 mV for V_s obtained with 30 μM trimebutine (Figure 5b) and 35.8 μM for Kr (IC_{50} of trimebutine for the Ca^{2+} current at a holding potential of − 60 mV which can be used, assuming that the Ca^{2+} channels are all in the closed-available state at the holding potential of − 60 mV (Figure 5b)), a value for K_i is calculated to be 1.0 μM, suggesting about 36 times higher affinity of trimebutine for the inactivated than the closed-available state of the Ca^{2+} channels. However, trimebutine was much less effective in reducing the current amplitude at the holding potential of − 80 mV than at − 60 mV. This cannot be simply explained by a possible underestimate caused by assuming that the channels are all in the closed-available state at − 60 mV. The channels might be in another state at − 80 mV in which trimebutine could not readily bind to them.

The lack of use-dependence of the inhibition of the Ca^{2+} current by trimebutine suggests that the drug may hardly enter the Ca^{2+} channels in the open state. In contrast, verapamil enters the open-state Ca^{2+} channels since blockade of the channels by the drug was use-dependent, as previously described (Terada *et al.*, 1987a). Furthermore, the use-dependent inhibition of ion channel current is suggested to be related to the p*K*a value for drugs: a drug in charged form can enter ion channels in their open state in which it acts (Sanguinetti & Kass, 1984; Terada *et al.*, 1987a). According to this view, as the p*K*a value for trimebutine is 6.2, the drug is almost unionized at pH 7.2 in PSS and expected to exhibit no use-dependent block of the Ca^{2+} current. The prediction is consistent with the present result.

On the basis of a comparison of IC_{50} values for the Ca^{2+} current and Ca^{2+}-independent K^+ current, Terada *et al.* (1987a,b) assessed the selectivity of various Ca^{2+} antagonists for the voltage-dependent Ca^{2+} channel in smooth muscle cells of rabbit small intestine. The ratio of the IC_{50} for the K^+ current to that for the Ca^{2+} current was 190 for nicardipine, 21 for diltiazem and 11 for verapamil. The ratio of the IC_{50} of trimebutine for Ca^{2+}-independent K^+ current (7.6 μM) (Nagasaki *et al.*, 1993) to that for the Ca^{2+} current (35.8 μM) was 0.2, and in addition the ratio of the IC_{50} for Ca^{2+}-dependent K^+ current (23.5 μM) (Nagasaki *et al.*, 1993) to that for the Ca^{2+} current was 0.7. Thus, trimebutine may be considered as a member of a family of non-specific organic Ca^{2+} antagonists (Godfraind *et al.*, 1986).

The voltage-dependent Ca^{2+} current and K^+ current in smooth muscles are responsible for the upstroke and repolarization phases of the action potential, respectively, and the K^+ current also may participate in determination of the resting membrane potential. Our present and previous (Nagasaki *et al.*, 1993) results, that trimebutine inhibits both Ca^{2+} current and K^+ current evoked by depolarization with little selectivity for them, provide some insight into the mechanism by which trimebutine stimulates or inhibits the mechanical activity in the isolated stomach and intestine over the same concentration-range, and exerts the dual action dependent on the level of the mechanical activity (Takenage *et al.*, 1982; 1984; 1986). The stimulation of the mechanical activity, when it is low, may be due in part to block of the K^+ current leading to the membrane depolarization which allows an increased discharge rate of action potentials, and the inhibition of the mechanical activity, when it is high, may be due in part to block of the Ca^{2+} current leading to suppression of generation and conduction of the action potential accompanied by reduction of tension. The membrane potential-dependent inhibition of the Ca^{2+} current by trimebutine would support this idea. Thus the stimulatory effect on the hypomotile gastrointestinal tract and the inhibitory effect in hypermotility could be explained.

References

ABEI, T., ISOGAI, S., ONUKI, T., OKADA, T., OSADA, M., KAWAMURA, A., KIRYU, Y,. KOIZUMI, H., SUZUKI, K., TAKAGI, S., TAKASHASHI, H., TSUCHIYA, M., NAKAMURA, K., NAMUBA, T., MURAOKA, M., YOKOI, Y. & YOKOTA, A. (1977). A multi-institutional double blind control study to compare the effectiveness of TM-906 and metoclopramide in controlling functional gastrointestinal symptoms. *Clin. Eval.*, **5**, 189–203 (Abstr. in English).

BEAN, B.P., COHEN, C.J. & TSIEN, R.W. (1983). Lidocaine block of cardiac sodium channels. *J. Gen. Physiol.*, **81**, 613–642.

GODFRAIND, T., MILLER, R. & WIBO, M. (1986). Calcium antagonism and calcium entry blockade. *Pharmacol. Rev.*, **38**, 321–416.

HAMILL, O.P., MARTY, A., NEHER, E., SAKMANN, B. & SIGWORTH, F.J. (1981). Improved patch-clamp techniques for high-resolution current recording from cells and cell-free membrane patches. *Pflügers Arch.*, **391**, 85–100.

LANG, R.J., OZOLINS, I.Z. & PAUL, R.J. (1991). Effects of okadaic acid and ATPγ S on cell length and Ca^{2+}-channel currents recorded in single smooth muscle cells of the guinea-pig taenia caeci. *Br. J. Pharmacol.*, **104**, 331–336.

LUTTECKE, K. (1980). A three-part controlled study of trimebutine in the treatment of irritable colon syndrome. *Curr. Med. Res. Opin.*, **6**, 437–443.

MAZZONE, O., TROVATO, G.M., MANDALA, M.L. & MONELLO, S. (1980). Trimebutina e motilita gastrica: studio tensiografico. *Clin. Ther.*, **95**, 629–635.

MOSHAL, M.G. & HERRON, M. (1979). A clinical trial of trimebutine (Mebutine) in spastic colon. *J. Int. Med. Res.*, **7**, 231–234.

NAGASAKI, M., KOBAYASHI, T. & TAMAKI, H. (1991). Effects of trimebutine on cytosolic Ca^{2+} and force transitions in intestinal smooth muscle. *Eur. J. Pharmacol.*, **195**, 317–321.

NAGASAKI, M., KOMORI, S., TAMAKI, H. & OHASHI, H. (1993). Effect of trimebutine on K^+ current in rabbit ileal smooth muscle cells. *Eur. J. Pharmacol.*, **235**, 197–203.

NAGASAKI, M., KUROSAWA, H., NAITO, K. & TAMAKI, H. (1990). Allostric interaction of trimebutine maleate with dihydropyridine binding sites. *Eur. J. Pharmacol. Mol. Pharmacol. Sect.*, **189**, 71–76.

SANGUINETTI, M.C. & KASS, R.S. (1984). Voltage-dependent block of calcium channel current in the calf cardiac Purkinje fiber by dihydropyridine calcium channel antagonists. *Circ. Res.*, **55**, 336–348.

SHIMADA, T., KURACHI, A., TERANO, A. & SUGIMOTO, T. (1990). Trimebutine maleate has inhibitory effects on the voltage-dependent Ca^{2+} inward current and other membrane currents in intestinal smooth muscle cells. *Gastroenterol. Jpn.*, **25**, 175–179.

TAKENAGA, H., MAGARIBUCHI, T. & TAMAKI, H. (1982). Effects of trimebutine maleate (TM-906) on the spontaneous contraction of isolated guinea-pig stomach. *Folia Pharmacol. Jpn.*, **80**, 163–168. (Abstr. in English).

TAKENAGA, H., MAGARIBUCHI, T. & TAMAKI, H. (1984). Effects of trimebutine maleate (TM-906) on the spontaneous contraction of isolated guinea-pig colon. *Jpn. J. Pharmacol.*, **34**, 177–181.

TAKENAGA, H., MAGARIBUCHI, T. & TAMAKI, H. (1986). Effects of trimebutine maleate (TM-906) on the spontaneous contraction of isolated duodenum and ileum in both guinea pigs and rabbits. *Jpn. J. Pharmacol.*, **40**, 13–20.

TERADA, K., KITAMURA, K. & KURIYAMA, H. (1987a). Blocking actions of Ca^{2+} antagonists on the Ca^{2+} channels in the smooth muscle cell membrane of rabbit small intestine. *Pflügers Arch.*, **408**, 552–557.

TERADA, K., KITAMURA, K. & KURIYAMA, H. (1987b). Different inhibitions of the voltage-dependent K^+ current by Ca^{2+} antagonists in the smooth muscle cell membrane of rabbit small intestine. *Pflügers Arch.*, **408**, 558–564.

(Received March 1, 1993
Revised April 14, 1993
Accepted April 28, 1993)

Br. J. Pharmacol. (1993), **110**, 404–410

Nitric oxide-dependent and -independent hyperaemia due to calcitonin gene-related peptide in the rat stomach

[1]P. Holzer, I.Th. Lippe, M. Jocič, Ch. Wachter, R. Erb & A. Heinemann

University of Graz, Department of Experimental and Clinical Pharmacology, A-8010 Graz, Austria

1 Calcitonin gene-related peptide (CGRP) potently enhances mucosal blood flow in the rat stomach. The aim of this study was to examine whether CGRP also dilates extramural arteries supplying the stomach and whether the vasodilator action of CGRP involves nitric oxide (NO).

2 Rat CGRP-α (0.03–1 nmol kg^{-1}, i.v.) produced a dose-dependent increase in blood flow through the left gastric artery (LGA) as determined by an ultrasonic transit time technique in urethane-anaesthetized rats. Blockade of NO synthesis by N^G-nitro-L-arginine methyl ester (L-NAME, 20 and 60 μmol kg^{-1}, i.v.) significantly reduced basal blood flow (BF) in the LGA and attenuated the hyperaemic activity of CGRP by a factor of 2.8–4. D-NAME tended to enhance basal BF in the LGA but had no influence on the dilator activity of CGRP. The ability of vasoactive intestinal polypeptide to increase left gastric arterial blood flow remained unaltered by L-NAME.

3 L-NAME (20 and 60 μmol kg^{-1}, i.v.) evoked a prompt and sustained rise of mean arterial blood pressure (MAP) and caused a slight decrease in the hypotensive activity of CGRP. In contrast, D-NAME induced a delayed and moderate increase in MAP and did not influence the hypotensive activity of CGRP.

4 Rat CGRP-α dilated the isolated perfused bed of the rat LGA precontracted with methoxamine and was 3 times more potent in this respect than rat CGRP-β. The dilator action of rat CGRP-α in this preparation was not affected by L-NAME or D-NAME (40 μM).

5 L-NAME (60 μmol kg^{-1}, i.v.) reduced gastric mucosal blood flow as assessed by laser Doppler flowmetry and diminished the hyperaemic activity of rat CGRP-α in the gastric mucosa by a factor of 4.5, whereas D-NAME was without effect.

6 These data show that CGRP is a potent dilator of mucosal and extramural resistance vessels in the rat stomach. Its dilator action involves both NO-dependent and NO-independent mechanisms.

Keywords: Calcitonin gene-related peptide (CGRP); vasoactive intestinal polypeptide; blood flow; rat stomach; gastric mucosa; left gastric artery; vasodilatation; hypotension; nitric oxide; N^G-nitro-L-arginine methyl ester (L-NAME); D-NAME; inhibition of nitric oxide synthase

Introduction

Calcitonin gene-related peptide (CGRP) is a potent dilator of submucosal arterioles in the rat stomach (Chen *et al.*, 1992), an action by which it augments gastric mucosal blood flow (MBF) (Holzer & Guth, 1991). This and other findings suggest that CGRP plays a regulatory role in the gastric mucosal microcirculation. Arteries and arterioles in the rat stomach are surrounded by a dense plexus of primary afferent nerve fibres containing CGRP (Green & Dockray 1988; Sternini & Anderson, 1992). Activation of these neurones causes release of CGRP into the vascular bed of the stomach (Holzer *et al.*, 1990), and there is pharmacological evidence that CGRP participates in the gastric hyperaemic response to sensory nerve stimulation with capsaicin (Li *et al.*, 1991). The first objective of the present study was to investigate whether the vasodilator action of CGRP in the rat stomach is confined to the mucosal microvessels or whether CGRP also dilates extramural resistance vessels. This question was addressed by measuring blood flow in the gastric mucosa and in the left gastric artery (LGA) of anaesthetized rats and by use of the isolated perfused bed of the LGA.

The second objective was to inquire into the mechanism of the vasodilator action of CGRP in the rat stomach. In addition to a direct action on vascular smooth muscle, transmitter substances can regulate blood flow via release of vasodilator mediators such as nitric oxide (NO) (Moncada *et al.*, 1991). There is evidence that NO plays an important role in the regulation of gastric MBF (Walder *et al.*, 1990; Pique *et al.*, 1992; Lippe & Holzer, 1992; Tepperman & Whittle, 1992). CGRP-evoked dilatation of various extragastric vascular beds differs with regard to the involvement of NO and the endothelium, an important source of NO (Gardiner *et al.*, 1991; Abdelrahman *et al.*, 1992; Gray & Marshall, 1992), and there is a preliminary report suggesting that the hyperaemic action of CGRP in the rat gastric mucosa depends to some extent on NO (Whittle *et al.*, 1992). The question whether the vasodilator action of CGRP in the rat stomach involves NO was examined by the use of N^G-nitro-L-arginine methyl ester (L-NAME), a specific blocker of the constitutive NO synthase (Moore *et al.*, 1990; Rees *et al.*, 1990).

Methods

Surgical preparation of the animals for the in vivo *experiments*

All experiments were performed on female Sprague-Dawley rats, weighing 190–220 g. They were fasted for about 20 h before experimentation but allowed free access to water. After the induction of anaesthesia with urethane (1.5 g kg^{-1}, s.c.) the rats were fitted with a tracheal cannula to facilitate spontaneous respiration. The body temperature was kept at 36–37°C by means of a water-perfused heating pad. Mean arterial blood pressure (MAP) was recorded from a cannula in the right carotid artery. In many experiments the MAP signal was fed into a heart ratemeter and the heart rate (HR) and MAP were displayed on a chart recorder. For the i.v. administration of drugs a catheter was placed in a jugular

[1] Author for correspondence at: Department of Experimental and Clinical Pharmacology, University of Graz, Universitätsplatz 4, A-8010 Gaz, Austria

vein through which saline (0.9% NaCl, wt/wt) was continuously infused at a rate of 1.5 ml h^{-1} to avoid dehydration. In some experiments the drugs were administered close arterially to the stomach, in which case the abdominal aorta was cannulated with a catheter (PE-20) in a retrograde direction so that the tip of the catheter lay just above the branching of the coeliac artery (Lippe *et al.*, 1989). After completion of surgery a period of at least 30 min was allowed for equilibration until the experiments were started.

Measurement of blood flow in the LGA

Blood flow in the LGA was determined by the ultrasonic transit time shift technique. This method involves a flow sensor, which contains two ultrasonic transducers passing a plane wave of ultrasound back and forth over the full width of the vessel alternately intersecting the flowing blood in upstream and downstream directions (Burton & Gorewit, 1984; Wang *et al.*, 1989). The shift in transit time which results from the flow of blood is integrated over the full width of the vessel and used to calculate the volume of blood flow (μl min^{-1}). After a midline laparotomy the LGA was separated from the surrounding tissue over a length of 4–5 mm under a binocular microscope. Care was taken to remove any fat tissue from the vessel. Blood flow was measured by an ultrasonic flow sensor (model 1RB, Transonic, Ithaca, New York, U.S.A.) which was placed around the LGA and connected to a small animal flowmeter (model T106, Transonic).

The experiments were started by priming the animals with i.v. injections of rat CGRP-α (100 pmol kg^{-1}) or vasoactive intestinal polypeptide (VIP, 300 pmol kg^{-1}) at 15 min intervals. Once the hyperaemic actions of these peptides were stable, saline (1 ml kg^{-1}), D-NAME (20 or 60 μmol kg^{-1}) or L-NAME (20 or 60 μmol kg^{-1}) was injected into the jugular vein. After a wait of 30 min, dose-response curves for the hyperaemic actions of CGRP and/or VIP were recorded. This was done by injecting increasing doses of CGRP (0.03–1 nmol kg^{-1}) and VIP (0.3–1 nmol kg^{-1}) at 15 min intervals. All peptide doses were injected at a volume of 1 ml kg^{-1}, the vehicle being saline.

Measurement of gastric mucosal blood flow with laser Doppler flowmetry

The stomach was exposed by a midline laparotomy, and a small bore (4 mm o.d.) plastic cannula was inserted via a small incision in the forestomach and tied in place, to allow free access to the gastric lumen (Tepperman & Whittle, 1992). Gastric MBF was recorded continuously with a laser Doppler flow monitor (model MBF3D, Moor Instruments, Devon) and an endoscopic laser optic probe (model P6B, 1.25 mm o.d.; Moor Instruments) which was inserted into the gastric lumen via the plastic cannula and allowed to rest gently on the gastric corpus mucosa (Tepperman & Whittle, 1992). Drug-induced changes in the laser Doppler flux readings were expressed as a percentage of the average flux recorded over a 3 min period immediately before administration of the drug. The experimental protocol was identical with that used for the measurement of blood flow in the LGA.

Measurement of gastric mucosal blood flow with the hydrogen gas clearance technique

The clearance of hydrogen from the gastric tissue was measured by a platinum needle electrode which, after a midline laparotomy, was inserted from the serosa into the basal portion of the gastric corpus mucosa and positioned at the submucosal border of the muscularis mucosae (Lippe & Holzer, 1992). MBF was estimated by computer-assisted analysis of the hydrogen clearance curves and expressed as μl min^{-1} g^{-1} (Lippe & Holzer, 1992). The experimental protocol involved alternating 15 min periods of saturation, and desaturation, of the tissue with hydrogen gas. Measurements of MBF were taken during the periods of 45–60 min, 75–90 min, 105–120 min, 135–150 min, and 165–180 min after the start of the experiments. Since MBF measured by the hydrogen clearance technique represents flow averaged over a period of 15 min, only prolonged changes in blood flow can be measured. CGRP was infused, therefore, close arterially to the stomach via a catheter in the abdominal aorta. This catheter was continuously perfused with Krebs buffer pH 7.4 containing 0.2 mM acetic acid (i.e., the vehicle for CGRP) at a rate of 1.5 ml min^{-1} to keep the catheter patent and to avoid dehydration of the rat (no infusion of saline via a jugular vein was carried out in these experiments). At 60 min, D-NAME or L-NAME (20 μmol kg^{-1}, 1 ml kg^{-1}) was administered to the stomach by slow injection into the aortic catheter. Rat CGRP-α (60 pmol min^{-1}, 0.03 ml min^{-1}) was infused via the same route during the period of 160–180 min.

Perfusion of the isolated bed of the LGA

Twenty minutes after the induction of anaesthesia with pentobarbitone (50 mg kg^{-1}, i.p.) the rats were laparotomized to expose the stomach. After cannulation of the LGA with a catheter (PE-20) the preparation was slowly flushed with 20 ml of Krebs buffer pH 7.4 containing heparin (20 iu ml^{-1}). The perfused stomach was excised and cut open along the greater curvature. The preparation thus was drained via the plexus of submucosal arterioles that had been cut during dissection. The preparation was transferred to a perfusion apparatus which consisted of an inclined pad maintained at 37°C. The stomach was placed on the pad with the mucosal side downwards and covered with parafilm to avoid dehydration. Oxygenated Krebs buffer pH 7.4 enriched with dextran F70 (3%, wt/wt) (Kwok *et al.*, 1988) was perfused through the preparation by means of a peristaltic pump at a rate of 1.35 ml min^{-1}. Proper perfusion of the preparation was checked visually by injecting 0.05 ml of Evans blue (10 mg ml^{-1}). The perfusion pressure was measured by way of a pressure transducer connected to the inflow cannula and displayed on a chart recorder.

After an initial equilibration period of 20 min the α-adrenoceptor agonist, methoxamine, was added to the perfusion solution to enhance perfusion pressure and thereby facilitate the study of dilator responses (Kawasaki *et al.*, 1990). The concentration of methoxamine (25–90 μM) was such that perfusion pressure rose by about 80–100 mmHg. After allowing a further 20 min for equilibration in the presence of methoxamine, two sets of experiments were carried out. In the first set of experiments the dilator responses to rat CGRP-α and CGRP-β were compared. To this end, increasing doses of the two peptides (3–100 pmol) were injected at volumes of 0.1 ml at 20 min intervals. The dilator response to 100 pmol CGRP-α was used to standardize the preparations at the end of each experiment and all other dilator responses were expressed as a percentage of that response. In the second set of experiments the effect of D-NAME and L-NAME on the dilator response to rat CGRP-α was investigated. For this purpose, a dose of CGRP (usually 10 pmol) causing approximately half-maximal relaxation of the methoxamine-contracted preparations was chosen as test dose and administered at 20 min intervals. After reproducible dilator responses to the test dose of CGRP had been obtained (usually after 3 dosings), D-NAME (40 μM) was added to the perfusion medium. Following 3 applications of the test dose of CGRP, D-NAME was replaced with L-NAME (40 μM), and CGRP was tested 3 times in the presence of L-NAME.

Substances and solutions

Rat CGRP-α, rat CGRP-β, and rat VIP (Peninsula, Heidelberg, Germany) were dissolved in 0.02 M acetic acid to give stock solutions of 0.1 mM. For intravascular administration,

the stock solutions were diluted with Krebs buffer pH 7.4 (i.a. infusion) or saline (i.v. injection). D-NAME (N^G-nitro-D-arginine methyl ester) and L-NAME (N^G-nitro-L-arginine methyl ester) came from Bachem (Bubendorf, Switzerland) and were dissolved (20 or 60 mM) in saline. Methoxamine (Sigma, Deisenhofen, Germany) was dissolved (0.7 M) in saline. Heparin was provided by Sandoz (Vienna, Austria) and dextran F70 was obtained from Serva (Heidelberg, Germany).

Calculation of data and statistics

Since D-NAME and L-NAME caused changes in gastric blood flow and MAP, all actions of CGRP and VIP on these parameters were expressed as percentage changes in order to account for the change in the baseline values (Abdelrahman *et al.*, 1992). All data are presented as mean ± s.e.mean. Statistical evaluation of the results was performed with the Mann-Whitney U test, Kruskal-Wallis H test or Wilcoxon test for pair differences as appropriate. Probability values of $P<0.05$ were regarded as significant.

Results

Effect of L-NAME and D-NAME on blood flow in the LGA, MAP and HR

The basal levels of blood flow in the LGA and gastric mucosa, MAP and HR as measured before administration of saline, L-NAME or D-NAME are given in Table 1. There were no significnat differences in these parameters between the different groups of rats used in the present study.

L-NAME (20 and 60 μmol kg^{-1}, i.v.) led to an immediate and sustained increase in MAP, which was accompanied by a significant decrease in HR and blood flow through the LGA (Table 2). The dose of 20 μmol kg^{-1} L-NAME appeared to be maximally effective, because the effects of a 3 times higher dose of the drug (60 μmol kg^{-1}) were not different from those of 20 μmol kg^{-1} L-NAME (Table 2). The vehicle (saline, 1 ml kg^{-1}) had no influence on MAP, HR and blood flow through the LGA (Table 2).

D-NAME (20 and 60 μmol kg^{-1}, i.v.) caused a delayed and moderate increase in MAP but failed to change HR (Table 2). Whilst the hypertensive effect of L-NAME was fully developed within 5–10 min after injection of the drug, it took more than 15 min until the hypertensive effect of D-NAME reached the level of statistical significance. The increase in MAP caused by 20 μmol kg^{-1} D-NAME did not differ from that caused by 60 μmol kg^{-1} D-NAME (Table 2). Unlike L-NAME, D-NAME tended to increase blood flow through the LGA, but this effect reached statistical significance only in the experiments involving 20 μmol kg^{-1} D-NAME (Table 2).

Table 1 Basal values of mean arterial blood pressure (MAP), heart rate (HR), blood flow in the left gastric artery (BF/LGA), gastric MBF measured by laser Doppler flowmetry (LDF Flux/GM) and gastric MBF measured by the hydrogen gas clearance technique (Gastric MBF) as measured before administration of N^G-nitro-L-arginine methyl ester (L-NAME), D-NAME or their vehicle (saline)

Parameter	*Unit*	*Value*	n
MAP	mmHg	90 ± 1.1	81
HR	min^{-1}	431 ± 5.7	58
BF/LGA	μl min^{-1}	530 ± 30	58
LDF Flux/GM	arbitrary units	98 ± 7.1	21
Gastric MBF	μl min^{-1} g^{-1}	546 ± 35	14

The values shown are mean ± s.e.mean.

Effect of L-NAME and D-NAME on the hyperaemic action of CGRP in the LGA

Intravenous injection of rat CGRP-α (0.03 to 1 nmol kg^{-1}), but not of the vehicle (saline, 1 ml kg^{-1}), evoked an immediate and transient increase in blood flow through the LGA (Figure 1a). This action of CGRP was dose-dependent (Figure 2).

L-NAME (20 and 60 μmol kg^{-1}, i.v.) reduced the potency of CGRP in augmenting blood flow through the LGA when compared with the activity of CGRP in rats treated with saline (1 ml kg^{-1}), whereas D-NAME (20 and 60 μmol kg^{-1}) had no effect (Figure 2). Following injection of L-NAME the CGRP dose-response curve was shifted to the right in a parallel manner, with no depression of the maximal hyperaemic response to CGRP (Figure 2). The doses of 20 and 60 μmol kg^{-1} L-NAME did not differ in their ability to attenuate the hyperaemic activity of CGRP (Figure 2). Graphical extrapolation at the level of 140% increase in LGA blood flow showed that 20 μmol kg^{-1} L-NAME shifted the CGRP dose-response curve by a factor of 4 (Figure 2a) compared with a shift of 2.8 caused by 60 μmol kg^{-1} L-NAME (Figure 2b). This observation indicates that the dose of 20 μmol kg^{-1} L-NAME is maximally effective in antagonizing the dilator action of CGRP in the LGA.

Effect of L-NAME and D-NAME on the hypotensive action of CGRP

Intravenous injection of rat CGRP-α (0.03 to 1 nmol kg^{-1}) induced an immediate and transient fall in MAP which was accompanied by a transient increase in the heart rate (HR) (Figure 1a). The hypotensive (Figure 2) and tachycardiac (data not shown) actions of CGRP were dose-dependent; the vehicle (saline, 1 ml kg^{-1}) was devoid of any effect (data not shown).

L-NAME (20 and 60 μmol kg^{-1}, i.v.) diminished the hypotensive potency of CGRP when compared with the activity of CGRP in rats treated with saline (1 ml kg^{-1}) (Figure 2). The effect of L-NAME consisted of a parallel rightward shift of the CGRP dose-response curve, the magnitude of the shift (1.8–2 fold) being independent of whether 20 or 60 μmol

Table 2 Effect of i.v. injected saline (1 ml kg^{-1}), N^G-nitro-L-arginine methyl ester (L-NAME) and D-NAME (20 and 60 μmol kg^{-1}) on mean arterial blood pressure (MAP), heart rate (HR), blood flow in the left gastric artery (BF/LGA), and laser Doppler flux readings in the gastric mucosa (LDF Flux/GM) as measured 30 min post-drug injection

Parameter	*Saline* (1 ml kg^{-1})	*L-NAME* (20 μmol kg^{-1})	*L-NAME* (60 μmol kg^{-1})	*D-NAME* (20 μmol kg^{-1})	*D-NAME* (60 μmol kg^{-1})
MAP	102 ± 1% (21)	160 ± 4% (13)**	169 ± 5% (17)**	116 ± 3% (13)**	120 ± 3% (16)**
HR	103 ± 1% (14)	93 ± 3% (13)**	94 ± 3% (8)*	102 ± 1% (13)	100 ± 1% (9)
BF/LGA	100 ± 4% (15)	67 ± 5% (13)**	65 ± 7% (8)**	128 ± 12% (13)*	120 ± 13% (9)
LDF Flux/GM	104 ± 7% (7)	ND	76 ± 7% (7)**	ND	106 ± 4% (7)

The values shown are expressed as a percentage of the values recorded immediately before administration of saline, L-NAME or D-NAME and are mean ± s.e.mean. The number of observations (animals) is given in parentheses.
*$P<0.05$, **$P<0.01$ versus saline. ND, not determined.

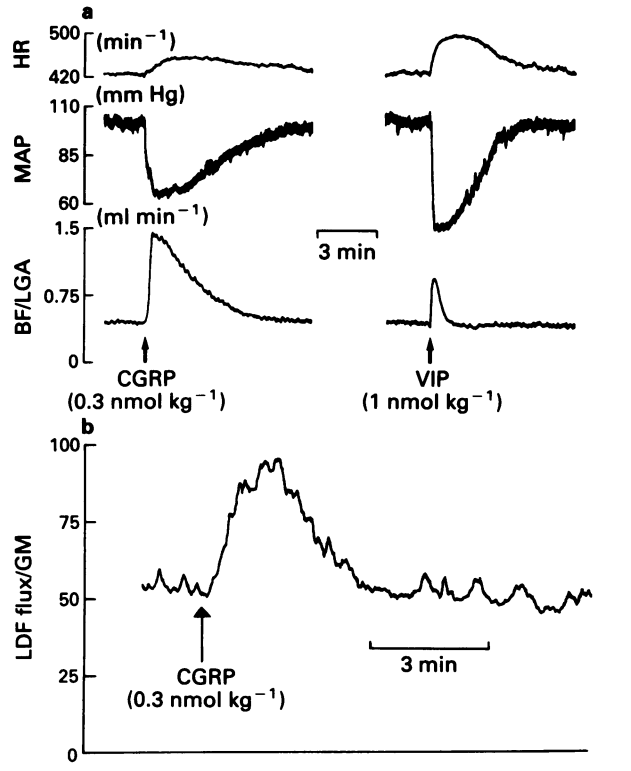

Figure 1 (a) Recordings of the actions of rat calcitonin gene-related peptide-α (CGRP) and vasoactive intestinal polypeptide (VIP), injected i.v., on heart rate (HR), mean arterial blood pressure (MAP) and blood flow in the left gastric artery (BF/LGA). (b) Recording of the action of rat CGRP, injected i.v., on blood flow in the gastric mucosa as determined by laser Doppler flowmetry (LDF flux/GM).

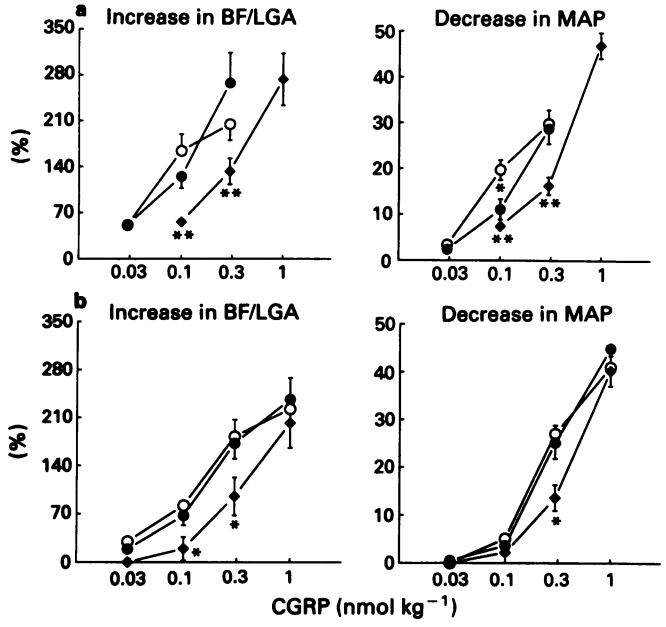

Figure 2 Dose-response relationship for the ability of i.v. injected rat calcitonin gene-related peptide-α (CGRP) to increase blood flow in the left gastric artery (BF/LGA) and to decrease mean arterial blood pressure (MAP) in rats pretreated with (a) saline (NaCl, 1 ml kg^{-1} ○), N^{G}-nitro-D-arginine methyl ester (D-NAME, (20 μmol kg^{-1} ●) or L-NAME 20 μmol kg^{-1} ◆) or (b) with saline (NaCl, 1 ml kg^{-1} ○), D-NAME (60 μmol kg^{-1} ●) or L-NAME (60 μmol kg^{-1} ◆). These drugs were injected i.v. 30 min before the recording of the dose-response curve to CGRP was begun. The ordinate scale shows the percentage changes in BF/LGA and MAP. Results are mean with s.e.mean shown by vertical bars; $n = 7$–9. *$P < 0.05$, **$P <$ 0.01 versus respective values recorded in rats treated with saline.

kg^{-1} L-NAME had been administered (Figure 2). The tachycardiac action of CGRP was not altered by L-NAME in any consistent manner (data not shown).

D-NAME (20 and 60 μmol kg^{-1}, i.v.) failed to influence the hypotensive potency of CGRP (Figure 2), with the only exception that the fall in MAP evoked by 0.1 nmol kg^{-1} CGRP was significantly inhibited by 20 μmol kg^{-1} D-NAME (Figure 2a). The tachycardic response to CGRP was unchanged by D-NAME (data not shown).

Effect of L-NAME on the hyperaemic action of VIP in the LGA

Experiments involving VIP were carried out to test whether or not the action of a vasodilator peptide other than CGRP is changed by L-NAME as compared with the action of the peptide in the presence of D-NAME. Like CGRP, i.v. injection of VIP (0.3 to 1 nmol kg^{-1}) caused an immediate fall in MAP associated with an increase in HR and blood flow through the LGA (Figure 1a). The potency of VIP in dilating the LGA was lower than that of CGRP (compare Figure 2 with Figure 3), and the duration of the actions of VIP on the cardiovascular system was shorter than that of the actions of CGRP (Figure 1a). The ability of VIP to augment blood flow through the LGA did not differ between rats treated with D-NAME or L-NAME (20 μmol kg^{-1}, i.v.) as was the case for the tachycardic action of VIP (data not shown). However, L-NAME tended to reduce the hypotensive action of VIP when compared with the hypotensive responses to VIP in rats treated with D-NAME, although this effect of L-NAME did not consistently reach the level of statistical significance (Figure 3).

Effect of L-NAME and D-NAME on the hyperaemic action of CGRP in the gastric mucosa

Intravenous injection of rat CGRP-α (0.1 to 1 nmol kg^{-1}) caused an immediate and transient increase in blood flow through the gastric mucosa as measured by laser Doppler flowmetry (LDF) (Figure 1b). The hyperaemic action of CGRP in the gastric mucosa was dose-dependent (Figure 4) but the amplitude of the CGRP-evoked hyperaemia in the gastric mucosa was considerably smaller than that in the LGA (Figure 2). Injection of the vehicle (saline, 1 ml kg^{-1}, i.v.) was devoid of any effect (data not shown).

L-NAME (60 μmol kg^{-1}, i.v.) led to a sustained decrease in blood flow through the gastric mucosa as measured by LDF whereas the same dose of D-NAME or the vehicle (saline, 1 ml kg^{-1}) did not alter the LDF signal (Table 2). The

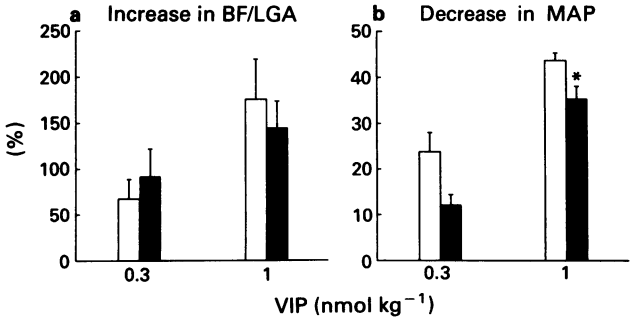

Figure 3 (a) Dose-dependent increase in blood flow in the left gastric artery (BF/LGA) and (b) decrease in mean arterial blood pressure (MAP) in response to i.v. injection of vasoactive intestinal polypeptide (VIP) in rats treated with N^{G}-nitro-D-arginine methyl ester (D-NAME, 20 μmol kg^{-1}, open columns) or L-NAME (20 μmol kg^{-1}, solid columns). These drugs were injected i.v. 30 min before the recording of the actions of VIP was begun. The ordinate scale shows the percentage changes in BF/LGA and MAP. Results are mean with s.e.mean shown by vertical bars; $n = 8$. *$P < 0.05$ versus respective values recorded in rats treated with D-NAME.

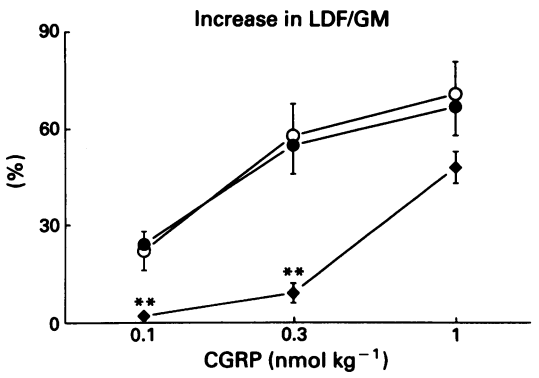

Figure 4 Dose-response relationship for the ability of i.v. injected rat calcitonin gene-related peptide-α (CGRP) to increase blood flow in the gastric mucosa as measured by laser Doppler flowmetry (LDF/GM) in rats pretreated with saline (NaCl, 1 ml kg^{-1} ○), N^{G}-nitro-D-arginine methyl ester (D-NAME, 60 μmol kg^{-1} ●) or L-NAME (60 μmol kg^{-1} ◆). These drugs were injected i.v. 30 min before the recording of the dose-response curve to CGRP was begun. The ordinate scale shows the percentage changes in BF/LGA. Results are mean with s.e.mean; $n = 7$. $^{**}P < 0.01$ versus respective values recorded in rats treated with saline.

potency of CGRP in augmenting blood flow through the gastric mucosa was reduced by L-NAME when compared with the activity of CGRP in rats treated with saline (Figure 4). Graphical extrapolation at the level of 40% increase in the LDF signal showed that L-NAME caused a 4.5 fold shift of the CGRP dose-response curve to the right, with no apparent depression of the maximal action of the peptide (Figure 4). In contrast, D-NAME failed to affect the hyperaemic activity of CGRP in the gastric mucosa (Figure 4).

The inhibitory effect of L-NAME on the CGRP-evoked hyperaemia in the gastric mucosa was confirmed in experiments in which gastric MBF was measured by the hydrogen gas clearance technique (Table 3). Close arterial injection of L-NAME (20 μmol kg^{-1}) to the stomach reduced gastric MBF by about 40%, whereas the same dose of D-NAME had no influence on MBF (Table 3). L-NAME prevented the gastric hyperaemia evoked by close arterial infusion of CGRP (60 pmol min^{-1}) to the stomach, which resulted in a 70% increase in gastric MBF in rats treated with D-NAME (Table 3). Saline-treated rats were not used in these experiments which were conducted solely to confirm that L-NAME, relative to D-NAME, inhibits the vasodilator action of CGRP in the gastric mucosa.

Effect of L-NAME and D-NAME on the dilator action of CGRP in the isolated bed of the LGA

Injection of rat CGRP-α reduced the perfusion pressure in the left gastric arterial bed precontracted with methoxamine (Figure 5a). The CGRP-induced decline in the perfusion

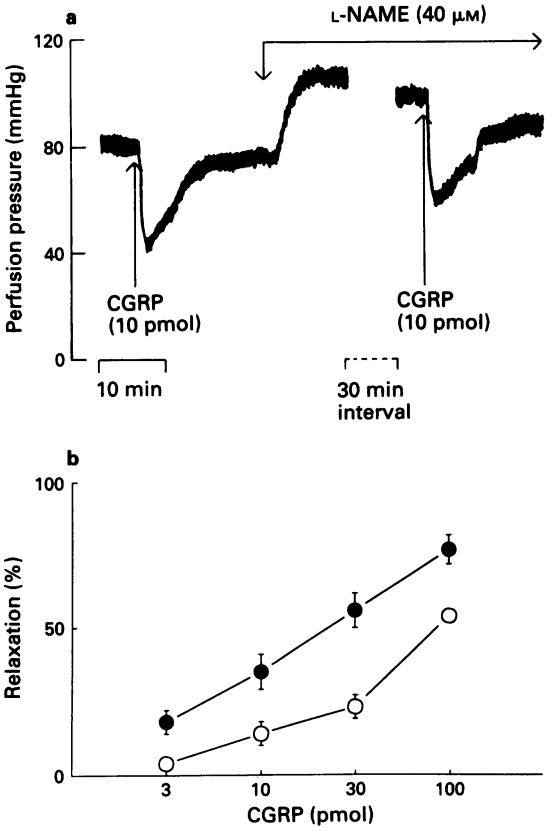

Figure 5 (a) Recording of the action of rat calcitonin gene-related peptide-α (CGRP) on the perfusion pressure in the isolated bed of the rat left gastric artery in the presence of N^{G}-nitro-D-arginine methyl ester (D-NAME, 40 μM; first injection of CGRP) and L-NAME (40 μM; second injection of CGRP). Ordinate scale: perfusion pressure generated by the addition of methoxamine (50 μM). (b) Dose-dependent actions of rat CGRP-α (●) and rat CGRP-β (○), given as bolus injections, on the perfusion pressure in the isolated bed of the left gastric artery precontracted with methoxamine (25–90 μM). Ordinate scale: reduction of the perfusion pressure, expressed as a percentage of the perfusion pressure generated by methoxamine. Results are mean ± s.e.mean; $n = 8$.

Table 3 Effect of N^{G}-nitro-D-arginine methyl ester (D-NAME) and L-NAME (20 μmol kg^{-1}, i.a.) on basal blood flow (Basal MBF) and calcitonin gene-related peptide (CGRP)-evoked hyperaemia (CGRP hyperaemia) in the gastric mucosa as measured by the hydrogen gas clearance technique

Parameter	*D-NAME*	*L-NAME*
Basal GMBF	94 ± 14% (7)	59 ± 4% (7)*
CGRP hyperaemia	173 ± 25% (7)	103 ± 11% (7)*

D-NAME and L-NAME (20 μmol kg^{-1}) were injected close arterially to the stomach 100 min before close arterial infusion of CGRP (60 pmol min^{-1}) to the stomach. The values shown are expressed as a percentage of the values recorded immediately before administration of L-NAME or D-NAME (Basal MBF) or immediately before administration of CGRP (CGRP hyperaemia) and are mean ± s.e.mean. The number of observations (animals) is given in parentheses.
*$P < 0.05$ versus D-NAME.

Table 4 Effect of saline, N^{G}-nitro-D-arginine methyl ester (D-NAME) and L-NAME on the perfusion pressure and the relaxant action of calcitonin gene-related peptide (CGRP) in the isolated bed of the rat left gastric artery precontracted with methoxamine

Treatment	*Perfusion pressure* (mmHg)	*Hypotension induced by CGRP (%)*
Saline	92 ± 9	47 ± 3
D-NAME	99 ± 11	47 ± 4
L-NAME	115 ± 11	43 ± 6

Results are mean ± s.e.mean; $n = 7$. No significant differences. The preparations were continuously perfused with saline containing methoxamine. D-NAME and L-NAME (40 μM) were administered by perfusion, the perfusion pressure being measured 20 min after their infusion was started and immediately before a bolus injection of rat CGRP-α (10–30 pmol) was performed. The relaxant action of CGRP is expressed relative to the perfusion pressure generated by methoxamine.

pressure, i.e. vasodilatation, was reproducible for up to 5 h when successive injections of rat CGRP-α (10–30 pmol) were carried out at 20 min intervals. The dilator responses to rat CGRP-α and rat CGRP-β were dose-dependent, rat CGRP-α being at least 3 times more potent than rat CGRP-β (Figure 5b). Perfusion of D-NAME (40 μM) did not significantly alter the perfusion pressure and failed to influence the vasodilator action of rat CGRP-α (Table 4). Perfusion of L-NAME (40 μM) increased the perfusion pressure (Figure 5a), an effect that slowly waned with time (Table 4). The vasodilator action of CGRP was not significantly changed in the presence of L-NAME (Table 4).

Discussion

The present data confirm that pmol doses of CGRP increase blood flow in the rat gastric mucosa (Holzer & Guth, 1991) and, in addition, show that CGRP is at least as potent in dilating extramural arterial vessels of the rat stomach as it is in dilating mucosal microvessels. The gastric hyperaemic action of CGRP was demonstrated both *in vivo* and in the isolated perfused bed of the LGA *in vitro*. This isolated preparation, which is drained via submucosal arterioles that have been cut during dissection, was used to measure the resistance of extramucosal arterial vessels in the stomach. Rat CGRP-α was chosen as the molecular form of CGRP to be tested in the *in vivo* experiments, since this variant of CGRP prevails in the primary afferent nerve fibres that supply the splanchnic arterial bed (Mulderry *et al.*, 1988; Sternini & Anderson, 1992). Additional experiments revealed that rat CGRP-α is about 3 times more potent than rat CGRP-β in reducing the resistance of the left gastric arterial bed *in vitro*, which is consistent with the finding that human CGRP-α is more active in increasing blood flow in the rabbit stomach than human CGRP-β (Bauerfeind *et al.*, 1989).

L-NAME and D-NAME were employed to examine whether the CGRP-evoked hyperaemia in the LGA and gastric mucosa of the rat involves NO as a secondary vasodilator mediator. As shown previously, inhibition of NO synthesis by L-NAME resulted in hypertension and bradycardia (Gardiner *et al.*, 1990; Rees *et al.*, 1990) and in a decline of gastric blood flow (Lippe & Holzer, 1992; Tepperman & Whittle, 1992; Whittle *et al.*, 1992). In contrast, D-NAME was without influence on HR and tended to increase blood flow in the LGA rather than to decrease it. D-NAME, though, enhanced MAP albeit this effect of D-NAME was delayed and less pronounced than that of L-NAME. The present finding of a hypertensive effect of D-NAME corroborates the study of Abdelrahman *et al.* (1992) but is at odds with the negative findings of Gardiner *et al.* (1990) and Rees *et al.* (1990).

Although D-NAME, the enantiomer believed to be inactive on the NO synthase (Gardiner *et al.*, 1990; Rees *et al.*, 1990; Moncada *et al.*, 1991), changed MAP and blood flow in the LGA to some extent, it did not alter the action of CGRP in inducing hypotension and increasing gastric blood flow. In contrast, L-NAME caused a small reduction of the CGRP-evoked fall in MAP, as has been reported previously (Abdelrahman *et al.*, 1992), and a more pronounced inhibition of the CGRP-induced hyperaemia in the LGA and gastric mucosa. The enantiomer specificity of the effect of L-NAME in inhibiting the vasodilator activity of CGRP indicates that L-NAME interfered with CGRP-evoked hyperaemia by way of inhibition of NO formation and not by way of its vasoconstrictor effect. The validity of this conclusion is supported by a number of other findings. (i) The hypotensive action of CGRP is not blunted when the α-adrenoceptor agonist phenylephrine is used to augment MAP (Abdelrahman *et al.*, 1992). (ii) The antagonistic effect of L-NAME on the CGRP-induced gastric hyperaemia *in vivo* was overcome by increasing the dose of CGRP. (iii) The dilator action of VIP on the LGA *in vivo* was left unaltered by L-NAME. VIP is present in nerve fibres around splanchnic blood vessels (Della *et al.*, 1983), and the present results show that, as in other vascular beds (Burnstock, 1990), VIP dilates the LGA in a NO-independent manner. (iv) Hyperaemia in the gastric mucosa evoked by glyceryl trinitrate remains unaltered by blockade of NO formation (Walder *et al.*, 1990). Thus, inhibition of the L-arginine:NO system does not cause general suppression of the dilator capacity of gastric resistance vessels but counteracts the hyperaemic responses to CGRP (this study) and pentagastrin (Walder *et al.*, 1990; Pique *et al.*, 1992) in a selective manner.

The data obtained with L-NAME signify, therefore, that the dilator action of CGRP on the gastric circulation *in vivo* involves two mechanisms, a NO-dependent process that is activated by low doses of the peptide and a NO-independent process that becomes apparent with higher doses of CGRP. This inference is affirmed by the fact that the doses of L-NAME used here (20 and 60 $\mu mol\ kg^{-1}$) appeared to be maximally effective. The contribution of NO to the hyperaemic action of CGRP was similar in the LGA and gastric mucosa, as in both tissues L-NAME caused a parallel rightward shift of the CGRP dose-response curves by a factor of 2.8–4.5, abolishing the dilator action of low doses of CGRP. This means that, if the low levels of circulating CGRP (Diez Guerra *et al.*, 1988) were to regulate blood flow through the stomach, they would do so in a primarily NO-dependent manner. Further evidence for a contribution of NO to the hyperaemic action of CGRP in the gastric mucosa comes from a study in which a low dose of L-NAME (8 $\mu mol\ kg^{-1}$) was found to attenuate the vasodilator action of CGRP (Whittle *et al.*, 1992) and from the present experiments in which gastric MBF was measured by the hydrogen gas clearance technique.

Unlike *in vivo*, L-NAME failed to inhibit significantly the dilator action of CGRP in the isolated bed of the LGA *in vitro*, an observation that is in line with a report that the relaxant action of the peptide on LGA strips does not require the presence of the endothelium, an important source of NO (Brâtveit *et al.*, 1991). Although the discrepancy between the *in vivo* and *in vitro* observations cannot yet be explained conclusively, it is conceivable that the system which forms NO in response to CGRP either is no longer present or is functionally damaged in the *in vitro* preparations. Whatever the reason, our findings point to a potential limitation in the use of isolated perfused vascular preparations for the study of the L-arginine:NO system.

In conclusion, the hyperaemic action of CGRP in the rat gastric circulation involves both NO-dependent and NO-independent mechanisms. This dual mode of action is in keeping with the dual distribution of CGRP receptors to both endothelium and smooth muscle of gastrointestinal arteries and arterioles in the rat (Sternini *et al.*, 1991). CGRP released from sensory nerve endings participates in the rise of MBF caused by capsaicin-induced sensory nerve stimulation (Li *et al.*, 1991), hyperaemia strengthening the resistance of the gastric mucosa to experimental injury (Lippe *et al.*, 1989; Holzer *et al.*, 1991). The mucosal hyperaemic responses to CGRP (this study) and sensory nerve stimulation by capsaicin (Whittle *et al.*, 1992) or acid back-diffusion (Lippe & Holzer, 1992) as well as the gastric mucosal protective actions of CGRP (Lambrecht & Peskar, 1992) and capsaicin-induced sensory nerve stimulation (Peskar *et al.*, 1991) all depend on NO. These findings indicate that NO is a major secondary mediator of the hyperaemic and protective actions of CGRP released from sensory nerve endings in the stomach.

This work was supported by the Jubiläumsfonds of the Austrian National Bank (grant 4207) and by the Austrian Scientific Research Council (grants P7845-MED and P9473-MED). The authors thank Wolfgang Schluet for technical assistance and Irmgard Russa for secretarial help.

References

ABDELRAHMAN, A., WANG, Y.-X., CHANG, S.D. & PANG, C.C.Y. (1992). Mechanism of the vasodilator action of calcitonin gene-related peptide in conscious rats. *Br. J. Pharmacol.*, **106**, 45–48.

BAUERFEIND, P., HOF, R., HOF, A., CUCALA, M., SIEGRIST, S., VON RITTER, C., FISCHER, J.A. & BLUM, A.L. (1989). Effects of hCGRP I and II on gastric blood flow and acid secretion in anesthetized rabbits. *Am. J. Physiol.*, **256**, G145–G149.

BRÅTVEIT, M., HAUGAN, A. & HELLE, K.B. (1991). Effects of calcitonin gene-related peptide (CGRP) on regional haemodynamics and on selected hepato-splanchnic arteries from the rat: a comparison with VIP and atriopeptin II. *Scand. J. Clin. Lab. Invest.*, **51**, 167–174.

BURNSTOCK, G. (1990). Local mechanisms of blood flow control by perivascular nerves and endothelium. *J. Hypertens.*, **8**, S95–S106.

BURTON, R.G. & GOREWIT, R.C. (1984). Ultrasonic flowmeter uses wide beam transit-time technique. *Med. Electron.*, **15**, 68–73.

CHEN, R.Y.Z., LI, D.-S. & GUTH, P.H. (1992). Role of calcitonin gene-related peptide in capsaicin-induced gastric submucosal arteriolar dilation. *Am. J. Physiol.*, **262**, H1350–H1355.

DELLA, N.G., PAPKA, R.E., FURNESS, J.B. & COSTA, M. (1983). Vasoactive intestinal peptide-like immunoreactivity in nerves associated with the cardiovascular system of guinea-pigs. *Neuroscience*, **9**, 605–619.

DIEZ GUERRA, F.J., ZAIDI, M., BEVIS, P., MACINTYRE, I. & EMSON, P.C. (1988). Evidence for release of calcitonin gene-related peptide and neurokinin A from sensory nerve endings in vivo. *Neuroscience*, **25**, 839–846.

GARDINER, S.M., COMPTON, A.M., KEMP, P.A. & BENNETT, T. (1990). Regional and cardiac haemodynamic effects of N^G-nitro-L-arginine methyl ester in conscious, Long Evans rats. *Br. J. Pharmacol.*, **101**, 625–631.

GARDINER, S.M., COMPTON, A.M., KEMP, P.A., BENNETT, T., FOULKES, R. & HUGHES, B. (1991). Haemodynamic effects of human α-calcitonin gene-related peptide following administration of endothelin-1 or N^G-nitro-L-arginine methyl ester in conscious rats. *Br. J. Pharmacol.*, **103**, 1256–1262.

GRAY, D.W. & MARSHALL, I. (1992). Human α-calcitonin gene-related peptide stimulates adenylate cyclase and guanylate cyclase and relaxes rat thoracic aorta by releasing nitric oxide. *Br. J. Pharmacol.*, **107**, 691–696.

GREEN, T. & DOCKRAY, G.J. (1988). Characterization of the peptidergic afferent innervation of the stomach in the rat, mouse and guinea-pig. *Neuroscience*, **25**, 181–193.

HOLZER, P. & GUTH, P.H. (1991). Neuropeptide control of rat gastric mucosal blood flow. Increase by calcitonin gene-related peptide and vasoactive intestinal polypeptide, but not substance P and neurokinin A. *Circ. Res.*, **68**, 100–105.

HOLZER, P., LIVINGSTON, E.H., SARIA, A. & GUTH, P.H. (1991). Sensory neurons mediate protective vasodilatation in rat gastric mucosa. *Am. J. Physiol.*, **260**, G363–G370.

HOLZER, P., PESKAR, B.M., PESKAR, B.A. & AMANN, R. (1990). Release of calcitonin gene-related peptide induced by capsaicin in the vascularly perfused rat stomach. *Neurosci. Lett.*, **108**, 195–200.

KAWASAKI, H., NUKI, C., SAITO, A. & TAKASAKI, K. (1990). Role of calcitonin gene-related peptide containing nerves in the vascular adrenergic neurotransmission. *J. Pharmacol. Exp. Ther.*, **252**, 403–409.

KWOK, Y.N., MCINTOSH, C.H.S., SY, H. & BROWN, J.C. (1988). Inhibitory effects of tachykinins and neurokinins on release of somatostatin-like immunoreactivity from the isolated perfused rat stomach. *J. Pharmacol. Exp. Ther.*, **246**, 726–731.

LAMBRECHT, N. & PESKAR, B.M. (1992). Nitric oxide (NO) in calcitonin gene-related peptide (CGRP)-induced gastroprotection. *Gastroenterology*, **102**, A105.

LI, D.-S., RAYBOULD, H.E., QUINTERO, E. & GUTH, PH. (1991). Role of calcitonin gene-related peptide in gastric hyperemic response to intragastric capsaicin. *Am. J. Physiol.*, **261**, G657–G661.

LIPPE, I.T. & HOLZER, P. (1992). Participation of endothelium-derived nitric oxide but not prostacyclin in the gastric mucosal hyperaemia due to acid back-diffusion. *Br. J. Pharmacol.*, **105**, 708–714.

LIPPE, I.T., LORBACH, M. & HOLZER, P. (1989). Close arterial infusion of calcitonin gene-related peptide into the rat stomach inhibits aspirin- and ethanol-induced hemorrhagic damage. *Regul. Pept.*, **26**, 35–46.

MONCADA, S., PALMER, R.M.J. & HIGGS, E.A. (1991). Nitric oxide: physiology, pathophysiology, and pharmacology. *Pharmacol. Rev.*, **43**, 109–142.

MOORE, P.K., AL-SWAYEH, O.A., CHONG, N.W.S., EVANS, R.A. & GIBSON, A. (1990). L-N^G-nitro arginine (L-NOARG), a novel, L-arginine-reversible inhibitor of endothelium-dependent vasodilatation in vitro. *Br. J. Pharmacol.*, **99**, 408–412.

MULDERRY, P.K., GHATEI, M.A., SPOKES, R.A., JONES, P.M., PIERSON, A.M., HAMID, Q.A., KANSE, S., AMARA, S.G., BURRIN, J.M., LEGON, S., POLAK, J.M. & BLOOM, S.R. (1988). Differential expression of α-CGRP and β-CGRP by primary sensory neurons and enteric autonomic neurons of the rat. *Neuroscience*, **25**, 195–205.

PESKAR, B.M., RESPONDEK, M., MÜLLER, K.M. & PESKAR, B.A. (1991). A role for nitric oxide in capsaicin-induced gastroprotection. *Eur. J. Pharmacol.*, **198**, 113–114.

PIQUE, J.M., ESPLUGUES, J.V. & WHITTLE, B.J.R. (1992). Endogenous nitric oxide as a mediator of gastric mucosal vasodilatation during acid secretion. *Gastroenterology*, **102**, 168–174.

REES, D.D., PALMER, R.M.J., SCHULZ, R., HODSON, H.F. & MONCADA, S. (1990). Characterization of three inhibitors of endothelial nitric oxide synthase *in vitro* and *in vivo*. *Br. J. Pharmacol.*, **101**, 746–752.

STERNINI, C. & ANDERSON, K. (1992). Calcitonin gene-related peptide-containing neurons supplying the rat digestive system: differential distribution and expression pattern. *Somatosens. Motor Res.*, **9**, 45–59.

STERNINI, C., ANDERSON, K., SOTTILI, M. & LAI, M. (1991). Distribution of calcitonin gene-related peptide receptor binding sites (CGRP-RB) in the rat gastrointestinal tract. *Gastroenterology*, **100**, A668.

TEPPERMAN, B.L. & WHITTLE, B.J.R. (1992). Endogenous nitric oxide and sensory neuropeptides interact in the modulation of the rat gastric microcirculation. *Br. J. Pharmacol.*, **105**, 171–175.

WALDER, C.E., THIEMERMANN, C. & VANE, J.R. (1990). Endothelium-derived relaxing factor participates in the increased blood flow in response to pentagastrin in the rat stomach mucosa. *Proc. R. Soc. B.*, **241**, 195–200.

WANG, B.C., BIE, P., LEADLEY, R.J. & GOETZ, K.L. (1989). Cardiovascular effects of calcitonin gene-related peptide in conscious dogs. *Am. J. Physiol.*, **257**, R726–R731.

WHITTLE, B.J.R., LOPEZ-BELMONTE, J. & MONCADA, S. (1992). Nitric oxide mediates rat mucosal vasodilatation induced by intragastric capsaicin. *Eur. J. Pharmacol.*, **218**, 339–341.

(Received February 23, 1993
Revised April 23, 1993
Accepted April 28, 1993)

Br. J. Pharmacol. (1993), **110**, 411–415

Bradykinin-induced release of PGI_2 from aortic endothelial cell lines: responses mediated selectively by Ca^{2+} ions or a staurosporine-sensitive kinase

[1]Heydar Parsaee, [2]Jean R. McEwan & [3]John MacDermot

Department of Clinical Pharmacology, Royal Postgraduate Medical School, Du Cane Road, London W12 0NN

1 Bradykinin (100 nM) triggers release of nitric oxide and prostacyclin from both AG07680A and AG04762 bovine cultured aortic endothelial cells. The exposure of these cells to bradykinin is in each case associated with a striking rise in intracellular calcium ion concentration.

2 Exposure of AG07680A cells to 250 nM ionomycin was followed also by a significant release of prostacyclin, whereas 250 nM ionomycin had no capacity to stimulate release of prostacyclin from AG04762 cells.

3 There was a similar concentration-dependent increase in intracellular calcium ion concentration on exposure of AG07680A and AG04762 cells to ionomycin.

4 Exposure of AG04762 cells for 10 min to staurosporine produced a concentration-dependent inhibition (IC_{50} = 107 ± 14 nM) in bradykinin-stimulated prostacyclin release. There was no similar inhibitory effect of staurosporine in AG07680A cells.

5 Bradykinin (10 nM) triggered release of nitric oxide from both AG07680A and AG04762 cells, and the effect was not inhibited by 500 nM staurosporine. There was a similar ionomycin-dependent release of nitric oxide from both cell types.

6 These results identify a common pathway for bradykinin-dependent nitric oxide release from both AG07680A and AG04762 cells, involving increases in intracellular calcium ion concentration. In contrast, the bradykinin-dependent release of prostacyclin may involve one of two pathways (involving an increase in intracellular calcium or activation of a staurosporine-sensitive kinase), and the two pathways are selectively exploited in AG07680A and AG04762 cells, respectively.

Keywords: Endothelial cells; prostacyclin; bradykinin; calcium; protein kinase C; nitric oxide; endothelium-derived relaxing factor

Introduction

A monolayer of endothelial cells lines the luminal surface of blood vessels and provides a physical barrier between the circulating blood and underlying vascular smooth muscle. Endothelial cells also serve a role in regulating vascular smooth muscle tone by release of dilator substances such as prostacyclin (epoprostenol, PGI_2; Moncada *et al.*, 1976) and nitric oxide (endothelium-derived relaxing factor, NO; Furchgott & Zawadzki, 1980; Palmer *et al.*, 1987; Ignarro, 1991), or constrictor substances such as endothelin (Yanagisawa *et al.*, 1988). The release of PGI_2 and NO from endothelial cells may be triggered by hormones or vasoactive mediators whose receptors are coupled to phospholipase C (PLC). Examples include bradykinin, angiotensin II and acetylcholine (reviewed in Jacob *et al.*, 1990). Receptor-dependent hydrolysis of phosphatidylinositol 4,5-bisphosphate (PIP_2) by PLC yields inositol 1,4,5-trisphosphate and diacylglycerol which are implicated in release of Ca^{2+} from endoplasmic reticulum to the cytosol, and activation of protein kinase C (PKC) respectively (Berridge, 1987). The receptor-dependent release of NO involves activation of the constitutively expressed NO synthase, an effect which is mediated by increases in intracellular Ca^{2+} concentration, $[Ca^{2+}]_i$ (Moncada *et al.*, 1991). In contrast, the release of PGI_2 may involve more than one pathway of transduction, with complex patterns of interaction between these pathways (reviewed in Jacob *et al.*, 1990). PGI_2 release may be triggered by Ca^{2+}-dependent activation of PLA_2 (with subsequent release of arachidonic acid) (Hallam *et al.*, 1988). Alternatively, PGI_2 release may involve activation of PKC, with little or no significant rise in $[Ca^{2+}]_i$ (Carter *et al.*, 1989). The mechanism of PKC-dependent release of PGI_2 appears to involve altered sensitivity to $[Ca^{2+}]_i$, mediated by phosphorylation of an unidentified substrate, which (it has been proposed) might be PLA_2 itself, or perhaps a G protein that couples activated cell-surface receptors to PLC (Carter *et al.*, 1989).

In primary human endothelial cultures, the release of PGI_2 appears to be mediated by a variable contribution from both signalling pathways, although the consensus view suggests a primary role for receptor-dependent elevations in $[Ca^{2+}]_i$ (Hallam *et al.*, 1988). However, we have now identified two related bovine aortic endothelial lines, which are available from the Institute of Aging Cell Repository (U.S.A.), in which the two pathways involved in receptor-dependent release of PGI_2 segregate between the two cell lines. These cell lines provide a unique resource for further examination of the complex signalling pathways involved in release of PGI_2 from endothelium.

Methods

Cells

Bovine aortic endothelial cells were obtained from the National Institute of Aging Cell Repository (Institute for Medical Research, Copewood and Davis Streets, Camden, NJ 08103, U.S.A.). Two cell lines were obtained, namely

Present addresses: [1]Department of Pharmacology, Ghaem Hospital, Ahmad Abad St., Mashad, Iran 91375.
[2] Hatter Institute for Cardiovascular Studies, University College London Medical School, University College Hospital, London WC1E 6AU.
[3] Author for correspondence.

AG04762 (previously listed as AG4762) and AG07680A (previously listed as AG7680). These cells were obtained originally by collagenase digestion of a bovine thoracic aortic segment (Holstein breed), and they are known to express factor VIII immunoreactivity and angiotensin converting enzyme. AG04762 is reported to be a later passage of the AG07680A cell line.

The cells were cultured in 75 cm^2 flasks or 3.5 cm (diameter) wells in Dulbecco's modified Eagle's medium (DMEM, Gibco) containing 15% (v/v) foetal calf serum (Gibco), 1.5 mM glutamine, 60 u ml^{-1} penicillin, 50 $\mu g\ ml^{-1}$ streptomycin and 25 $\mu g\ ml^{-1}$ gentamicin. The culture medium in each flask was changed twice a week.

Confluent cells were divided in a ratio 1:4. The medium was aspirated and the cells washed once with Dulbecco's phosphate-buffered saline (without Ca^{2+} or Mg^{2+} ions, Gibco). Thereafter the cells were exposed to 0.05% (w/v) trypsin and 0.02% (w/v) EDTA in PBS (Flow Laboratories) for 1–2 min at 37°C. The detached cells were pelleted by centrifugation at 150 g for 3 min, resuspended in culture medium and plated into new flasks or dishes, or on to cover slips for fluorescence measurements.

For some experiments, cells were sub-cultured on to microcarrier beads which were then loaded on to 2 ml columns (described fully in Parsaee *et al.*, 1992). This arrangement allowed perfusion of the cells on the column with Krebs-Henseleit buffer (gassed with 5% CO_2 and 95% air) at 2 ml min^{-1}. The eluate from these columns was then analysed for its content of PGI_2 and NO. Although it was not possible to measure exactly the cell number on each column, similar numbers of confluent beads were loaded on to all columns, and the cell number approximated 2×10^7. The release of PGI_2 was also measured from endothelial cells cultured in 3.5 cm plates as described previously (Carter *et al.*, 1988; Parsaee *et al.*, 1992).

Bioassay for NO

NO was measured by a modification (described fully in Parsaee *et al.*, 1992) of the method of Furchgott & Zawadzki (1980). Briefly, eluate from the columns was allowed to superfuse a rat aortic ring, preconstricted with 1 μM phenylephrine. Measurements were then made of the relaxation of the ring. In pilot experiments, endothelial cell-dependent relaxation of the aortic ring was shown to be inhibited by prior perfusion of the column with N^{ω}-monomethyl-L-arginine (L-NMMA), or simultaneous superfusion of the aortic ring with haemoglobin. These findings confirmed the identity of NO in the column eluate.

Prostacyclin determination

Prostacyclin was measured as its stable hydrolysis product 6-oxo-prostaglandin $F_{1\alpha}$ ($PGF_{1\alpha}$) in 50 μl fractions taken from the column eluate. The analysis was by radioimmunoassay, and the antibody was a generous gift from Dr Susan Barrow (UMDS, University of London).

Measurement of free intracellular calcium ion concentration $[Ca^{2+}]_i$

The method employed was a modification (Parsaee *et al.*, 1992) of that described by Hallam *et al.* (1988). Briefly, fluorescence intensity was measured in Fura 2-loaded endothelial cells cultured on 10 mm glass cover slips (Chance Proper). Recordings were made at 37°C in a Shimadzu RF5000 spectrophotofluorimeter, with excitation at 340 nm and 380 nm, and emission measured at 500 nm. The value of $[Ca^{2+}]_i$ was calculated from the ratio of the two fluorescence signals according to the equation of Grynkiewicz *et al.* (1985).

The results were analysed with GraphPAD InPlot computer software, and curves were fitted to a simple one-site model, assuming Michaelis-Menton kinetics. [^{3}H]-6-oxo-$PGF_{1\alpha}$ was obtained from Amersham International (UK); Fura 2-AM was obtained from Calbiochem (UK). 6-Oxo-prostaglandin $F_{1\alpha}$ (free acid), ionomycin (Ca^{2+} salt), bradykinin (triacetate salt), phenylephrine (free base) and staurosporine were obtained from Sigma (UK). General reagents were also obtained from Sigma (UK) except where indicated.

Results

The release of 6-oxo-$PGF_{1\alpha}$ from AG07680A cells was measured. Figure 1a shows that exposure of these cells to a saturating (100 nM) concentration of bradykinin was followed by a rapid release of 6-oxo-$PGF_{1\alpha}$ which was sustained for about 5–10 min. In similar experiments, AG04762 cells were also shown to release 6-oxo-$PGF_{1\alpha}$ following exposure to 100 nM bradykinin (Figure 1b). Figure 1a and b is representative of three similar experiments. Basal release from AG07680A and AG04762 cells was 6.0 ± 3.6 and 10.4 ± 3.0 pg 6-oxo-$PGF_{1\alpha}$ 50 μl^{-1}, and stimulated release reached a maximum of 1698 ± 87 and 523 ± 112 pg 6-oxo-$PGF_{1\alpha}$ 50 μl^{-1} respectively ($n = 3$).

In contrast to the effect of bradykinin on the two endothelial cell lines, there was a striking difference in their sensitivity to ionomycin. In separate experiments ($n = 3$ for each cell line) AG07680A or AG04762 cells were exposed to 250 nM ionomycin, and measurements made of the release of

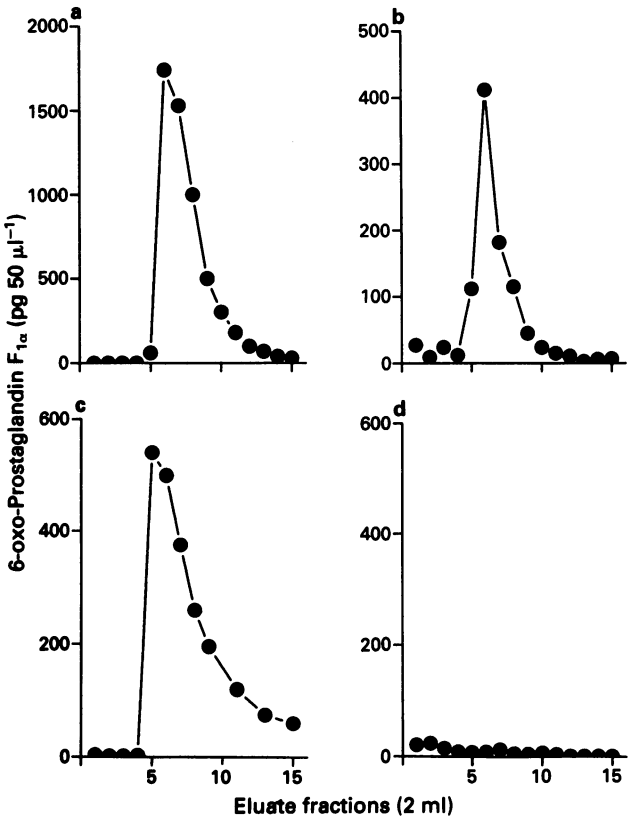

Figure 1 Release of prostacyclin (PGI_2) (measured as 6-oxo-$PGF_{1\alpha}$) from cultured endothelial cells. AG07680A cells (a and c) or AG04762 cells (b and d) were subcultured on to microcarrier beads and perfused on columns with Krebs-Henseleit buffer. Prior to any measurements or stimulation of the cells, the system was allowed to settle at a perfusion rate of 2 ml min^{-1} for at least 30 min.The cells were then exposed to 100 nM bradykinin (a and b) or 250 nM ionomycin (c and d) in the perfusate during the interval of collection of fractions 2–4 (3 min). Eluate factions (2 ml) from the columns were collected and analysed for their content of 6-oxo-$PGF_{1\alpha}$/50 μl. The results are representative of 3 similar experiments.

6-oxo-$PGF_{1\alpha}$. Figure 1c and d shows representative examples of the responsiveness of AG07680A cells to ionomycin, with absolutely no response seen in AG04762 cells.

These results prompted further experiments in which the capacity of bradykinin or ionomycin to trigger rises in $[Ca^{2+}]_i$ was measured. The resting $[Ca^{2+}]_i$ levels in AG07680A and AG04762 cells were 141 ± 12 nM ($n = 11$) and 172 ± 26 nM ($n = 6$), and increased on exposure to 500 nM bradykinin to 517 ± 56 nM ($n = 9$) and 548 ± 41 nM ($n = 6$) respectively. The response to bradykinin is concentration-dependent in AG07680A cells, and the bradykinin concentration (EC_{50}) required for the half-maximum increase in $[Ca^{2+}]_i$ has been reported previously by us as 4.8 nM (Parsaee *et al.*, 1992). A similar result was obtained with AG04762 (data not presented).

In later experiments, cells of both endothelial cell lines were exposed to ionomycin at concentrations between 10 nM and 500 nM, and the results are shown in Figure 2. There was no difference between the two cell lines in the rise in $[Ca^{2+}]_i$ with increasing ionomycin concentrations, notwithstanding their striking difference in sensitivity to ionomycin in terms of 6-oxo-$PGF_{1\alpha}$ release.

These findings prompted us to compare the effect of staurosporine on bradykinin-dependent release of 6-oxo-$PGF_{1\alpha}$ in the two cell lines. Exposure of AG04762 cells for 10 min to 500 nM staurosporine attenuated by about 55% the increase in 6-oxo-$PGF_{1\alpha}$ triggered by 100 nM bradykinin (Figure 3b). In contrast, the same concentration of staurosporine had no capacity to reduce bradykinin-dependent release of 6-oxo-$PGF_{1\alpha}$ from AG07680A cells (Figure 3a). Exposure of AG04762 cells to selected concentrations of staurosporine revealed a concentration-dependent inhibition of 6-oxo-$PGF_{1\alpha}$ release triggered by bradykinin, and the IC_{50} value for this effect was 107 ± 14 nM (Figure 4). Analysis of the data in Figure 4 revealed that the bradykinin-dependent effect could only be inhibited by staurosporine under these experimental conditions by 65.2%.

Finally, measurements were made of the capacity of bradykinin or ionomycin to release NO. In these experiments no differences were observed between NO release from AG07680 or AG04762 cells. The bradykinin-dependent release of NO is shown in Figure 5, and the effect was unaltered by the prior exposure of these cells to 500 nM staurosporine. Exposure of AG07680A cells to selected concentrations of bradykinin revealed a concentration-dependent response, with an EC_{50} value reported previously by us (Parsaee *et al.*, 1992) of 0.70 ± 0.14 nM ($n = 3$). Similar results were obtained with AG04762 cells (data not presented). Ionomycin has been reported previously by us to trigger release of NO from AG07680A cells (Parsaee *et al.*, 1992), and once again similar results were obtained with AG04762 cells (data not presented).

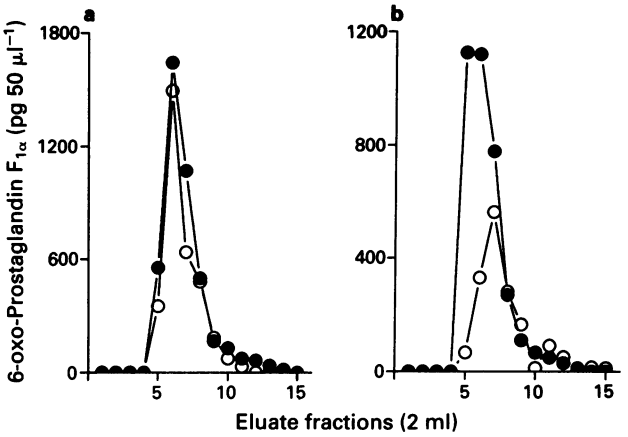

Figure 3 Bradykinin-dependent release of prostacyclin (measured as 6-oxo-$PGF_{1\alpha}$) from endothelial cells. AG07680A cells (a) or AG04762 cells (b) were perfused on columns as described in the legend to Figure 1. Prior to exposure of the cells to 100 nM bradykinin (during collection of fractions 2–4), the column was perfused for 10 min with Krebs-Henseleit buffer containing 500 nM staurosporine (○), or Krebs-Henseleit buffer alone (●). Individual 2 ml fractions from the columns were analysed for their content of 6-oxo-$PGF_{1\alpha}$. The results are typical of 3 similar experiments.

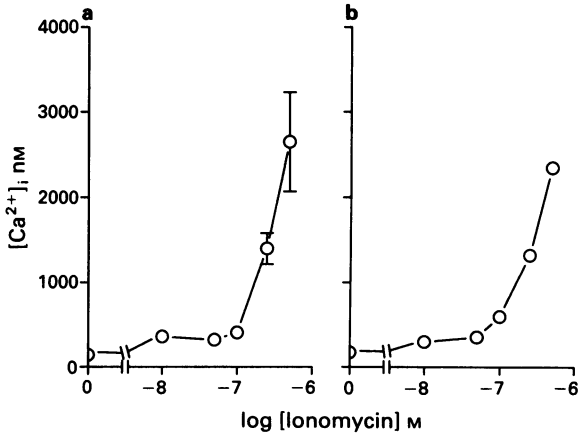

Figure 2 Concentration-response relationships of ionomycin-dependent increases in $[Ca^{2+}]_i$ in cultured endothelial cells. AG07680A cells (a) or AG04762 cells (b) were subcultured on to glass cover slips and loaded with Fura-2. The cells were then exposed to selected concentrations of ionomycin, and fluorescence intensity measured in a spectrophotofluorimeter. The results show mean values for increases in $[Ca^{2+}]_i$ ($n = 3$–6, ± s.e.mean. When omitted, the error bars are incorporated into the symbol).

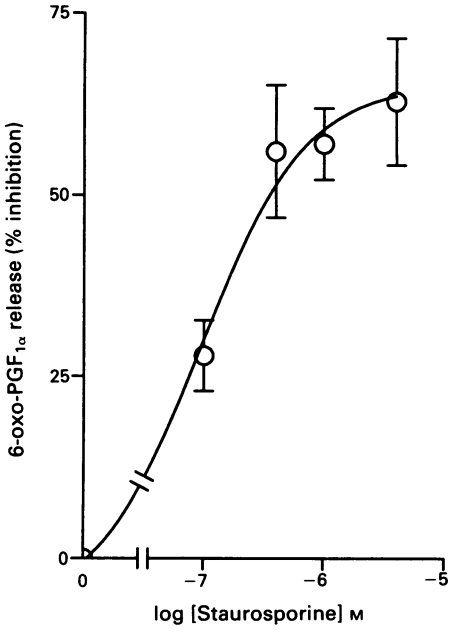

Figure 4 Concentration-response relationship for staurosporine-dependent inhibition of 6-oxo-$PGF_{1\alpha}$ release from AG04762 cells following exposure to bradykinin. Cells were cultured in 3.5 cm (diam.) dishes, and then exposed to selected concentrations of staurosporine (or culture medium control) for 10 min. Thereafter, the medium was changed, the cells washed, and the cells then exposed to 100 nM bradykinin for 5 min. The culture medium was then analysed for its content of 6-oxo-$PGF_{1\alpha}$, and the results are expressed as the mean staurosporine-dependent inhibition of the bradykinin-dependent increase in 6-oxo-$PGF_{1\alpha}$ release ($n = 4$; values given ± s.e.mean).

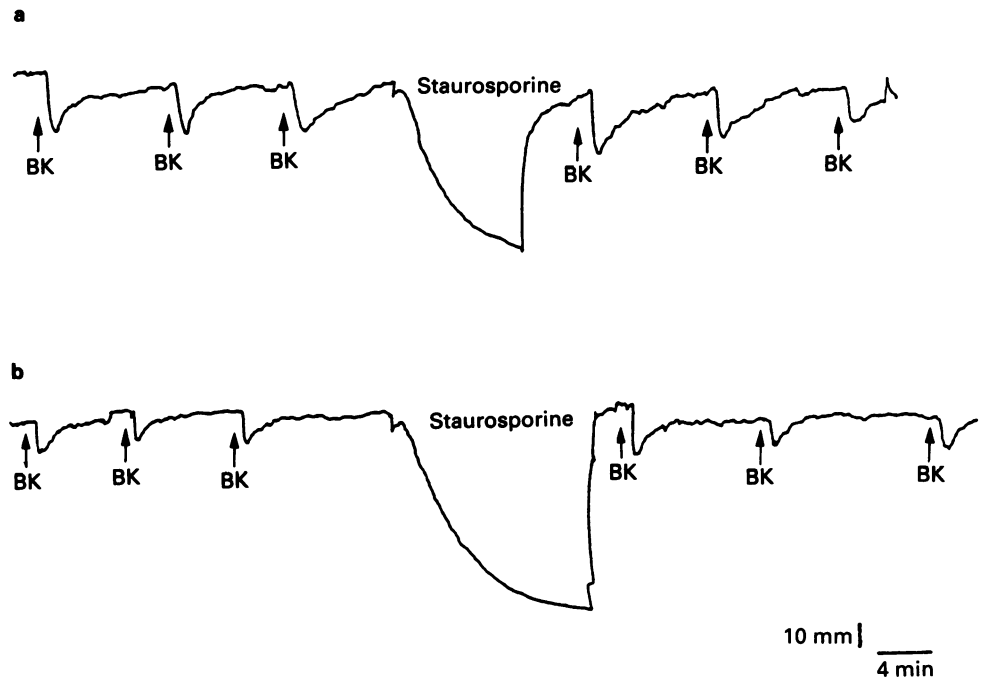

Figure 5 The release of nitric oxide from cultured endothelial cells. AG04762 cells (a) or AG07680A cells (b) were perfused on columns as described in the legend to Figure 1. The column eluates were superfused on to rat aortic rings, which had been pre-constricted with 1 μM phenylephrine. The results show the relaxation mediated by repeated exposure to 10 nM bradykinin for 45 s. At a point shown on the curve, the eluate from the column was temporarily diverted, and the ring allowed to relax. The endothelial cells were then exposed to 500 nM staurosporine for 10 min. The ring then contracted again with 1 μM phenylephrine, and the eluate from the column used to superfuse the ring. The results show the nitric oxide-dependent relaxations of the rings mediated by subsequent exposure of the endothelial cells to 10 nM bradykinin. The relaxations produced by 10 nM bradykinin were 19.2 ± 1.7 before, and 18.3 ± 3.0 mm ($n = 3$) after exposure of AG04762 cells to staurosporine. The bradykinin-dependent relaxations were 12.8 ± 0.6 before, and 13.7 ± 2.0 mm ($n = 3$) after exposure of AG07680A cells to staurosporine (results are means ± s.e.mean).

Discussion

Results published previously have suggested that the release of PGI_2 from endothelial cells may be triggered either by increases in $[Ca^{2+}]_i$ (Hallam *et al.*, 1988), or by a complex pathway involving reduced sensitivity to $[Ca^{2+}]_i$ mediated by activation of PKC (Carter *et al.*, 1989). Either (or both) pathways might be activated by receptor-dependent activation of PLC (reviewed in Jacob *et al.*, 1990), and results are now presented which show that two closely related endothelial cell lines exploit selectively a rise in $[Ca^{2+}]_i$ or activation of a staurosporine-sensitive kinase in bradykinin-dependent release of PGI_2. In contrast, we confirm earlier reports that the release of NO from endothelial cells appears to be coupled in all cases to rises in $[Ca^{2+}]_i$, most probably by direct activation of NO synthase (Moncada *et al.*, 1991). Intriguingly, the threshold of $[Ca^{2+}]_i$ required for activation of NO synthase is substantially lower than that involved in activation of PLA_2 and release of PGI_2 (Parsaee *et al.*, 1992).

Bradykinin triggers a rapid and significant rise in $[Ca^{2+}]_i$ in both AG07680A and AG04762 cells, and these changes in $[Ca^{2+}]_i$ are accompanied by a very striking increase in the release PGI_2. Ionomycin also increased $[Ca^{2+}]_i$, and to very high levels when the cells were exposed to ionomycin at concentrations above 100nM. However, despite $[Ca^{2+}]_i$ at concentrations above 2 μM in both cell types, ionomycin triggered release of PGI_2 from only AG07680A cells and not from AG04762 cells.

It followed that bradykinin-dependent release of 6-oxo-$PGF_{1\alpha}$ from AG04762 cells was not simply dependent on increases in $[Ca^{2+}]_i$. Further experiments revealed that the bradykinin-dependent release of 6-oxo-$PGF_{1\alpha}$ from these cells was inhibited by staurosporine, which suggests the involvement of a staurosporine-sensitive kinase. In view of the previous work on endothelial cell signalling, this kinase is identified most probably as one of the many PKC isoforms. The finding that staurosporine inhibited bradykinin-dependent release of PGI_2 only partially (about 60%) also suggests the possibility that other signalling pathways may be involved (perhaps in a cascade of protein phosphorylation). Further extensive studies will be required to identify with confidence the individual kinase(s), and these are not included in the present report. There are now upwards of 11 PKC isoenzymes that have been identified or sequenced, some of which are insensitive to phorbol ester, and for many of which no specific inhibitors are currently available. The published evidence to date suggests, at least in the rat, that the most abundant PKC isoenzyme in endothelial cells is PKC_α (Mattila, 1991).

Details of the pathways implicated in receptor-dependent release of PGI_2 have proved very difficult to examine experimentally in endothelial cells, most particularly because of the variable involvement of $[Ca^{2+}]_i$. Exploitation of these two cell lines in further studies may permit more precise assignment of the biochemical pathways involved.

This work was supported in part by a Programme Grant from the Wellcome Trust. H.P. was in receipt of a scholarship from the Ministry of Health and Medical Education, Iran.

References

BERRIDGE, M.J. (1987). Inositol trisphosphate and diacylglycerol: two interacting second messengers. *Annu. Rev. Biochem.*, **56**, 159–193.

CARTER, T.D., HALLAM, T.J., CUSACK, N.J. & PEARSON, J.D. (1988). Regulation of P_{2y} purinoceptor-mediated prostacyclin release from human endothelial cells by cytoplasmic calcium concentration. *Br. J. Pharmacol.*, **95**, 1181–1190.

CARTER, T.D., HALLAM, T.J. & PEARSON, J.D. (1989). Protein kinase C activation alters the sensitivity of agonist-stimulated endothelial-cell prostacyclin production to intracellular Ca^{2+}. *Biochem. J.*, **262**, 431–437.

FURCHGOTT, R.F. & ZADAWZKI, J.V. (1980). The obligatory role of endothelial cells in the relaxation of smooth muscle by acetylcholine. *Nature*, **288**, 373–376.

GRYNKIEWICZ, G., POENIE, M. & TSIEN, R.Y. (1985). A new generation of Ca^{2+} indicators with greatly improved fluorescence properties. *J. Biol. Chem.*, **260**, 3440–3450.

HALLAM, T.J., PEARSON, J.D. & NEEDHAM, L.A. (1988). Thrombin-stimulated elevation of human endothelial-cell cytoplasmic free calcium concentration causes prostacyclin production. *Biochem. J.*, **251**, 243–249.

IGNARRO, L.J. (1991). Signal transduction mechanisms involving nitric oxide. *Biochem. Pharmacol.*, **41**, 485–490.

JACOB, R., SAGE, S.O. & RINK, T.J. (1990). Aspects of calcium signalling in endothelium. In *Endothelium: an Introduction to Current Research*. ed. Warren, J.B. pp. 33–44. New York: Wiley-Liss.

MATTILA, P. (1991). Protein kinase C subtypes in endothelial cells. *FEBS Lett.*, **289**, 86–90.

MONCADA, S., GRYGLEWSKI, R.J., BUNTING, S. & VANE, J.R. (1976). An enzyme isolated from arteries transforms prostaglandin endoperoxide to an unstable substance that inhibits platelet aggregation. *Nature*, **263**, 663–665.

MONCADA, S., PALMER, R.M.J. & HIGGS, E.A. (1991). Nitric oxide: physiology, pathophysiology, and pharmacology. *Pharmacol. Rev.*, **43**, 109–142.

PALMER, R.M.J., FERRIGE, A.G. & MONCADA, S. (1987). Nitric oxide release accounts for the biological activity of endothelium-derived relaxing factor. *Nature*, **327**, 524–526.

PARSAEE, H., MCEWAN, J.R. & MACDERMOT, J. (1992). Differential sensitivities of the prostacyclin and nitric oxide biosynthetic pathways to cytosolic calcium in bovine aortic endothelial cells. *Br. J. Pharmacol.*, **107**, 1013–1019.

YANAGISAWA, M., KURIHARA, H., KIMURA, S., TOMOBE, Y., KOBAYASHI, M., MITSUI, Y., YAZAKI, Y., GOTO, K. & MASAKI, T. (1988). A novel potent vasoconstrictor peptide produced by vascular endothelial cells. *Nature*, **332**, 411–415.

(Received March 8, 1993
Revised April 19, 1993
Accepted April 29, 1993)

Br. J. Pharmacol. (1993), **110**, 416–422

E-type prostaglandins enhance local oedema formation and neutrophil accumulation but suppress eosinophil accumulation in guinea-pig skin

[1]M.M. Teixeira, T.J. Williams & P.G. Hellewell

Department of Applied Pharmacology, National Heart and Lung Institute, Dovehouse Street, London SW3 6LY

1 Prostaglandins possess both pro- and anti-inflammatory actions depending on their route of administration and the experimental model used. In this study, we have investigated the effect of locally injected prostaglandins on oedema formation, neutrophil accumulation and eosinophil accumulation in inflammatory responses in guinea-pig skin.

2 Prostaglandin E_1 (PGE_1) significantly enhanced local oedema formation induced by zymosan-activated plasma (ZAP), bradykinin and in a passive cutaneous anaphylatic (PCA) reaction. The accumulation of ZAP-induced ^{111}In-labelled neutrophils was also significantly enhanced by PGE_1. In addition, the prostacyclin analogue, iloprost, enhanced ZAP-induced responses.

3 In contrast PGE_1 decreased the accumulation of ^{111}In-labelled eosinophils in skin sites. This was demonstrated on eosinophil accumulation and local eodema formation induced by PAF, compound 48/80 and in the PCA reaction. PGE_2 also suppressed eosinophil accumulation while iloprost had no detectable effect.

4 Isoprenaline inhibited eosinophil accumulation in a dose-dependent manner with no effect on local oedema formation, except in the case of responses to ZAP where suppression was observed.

5 The vasodilator neuropeptide, calcitonin gene-related peptide (CGRP), enhanced local oedema formation but had no detectable effect on eosinophil accumulation.

6 In conclusion, the magnitude of a given response to an inflammatory mediator *in vivo* depends on the net effect of stimulation of several cell types e.g. arteriolar smooth muscle cells, microvascular endothelial cells, mast cells and accumulating leukocytes. In this study, we have demonstrated that different components of the inflammatory response in guinea-pig skin can be differentially modulated by E-type prostaglandins and isoprenaline, suggesting that cyclic AMP has an important regulatory role.

Keywords: Prostaglandins; eosinophils; neutrophils, inflammation; isoprenaline; oedema

Introduction

Chemical signals are generated in tissues in response to an inflammatory stimulus and these mediators induce the features of the inflammatory process. One such group of mediators are the prostaglandins, which have been shown to mimic some of the features of inflammation when administered *in vivo* (Williams & Peck, 1977; Salmon & Higgs, 1987) and have been shown to be present in various experimental models of inflammation (Salmon & Higgs, 1987). The inhibition of prostaglandin synthesis by aspirin-like drugs is widely and effectively used for the treatment of some of the symptoms of inflammation, further substantiating the importance of prostaglandins as mediators of the inflammatory process (Vane, 1971; Insel, 1990).

Intradermal (i.d.) injection of prostaglandins potentiates the oedema-inducing activity of other mediators (Moncada *et al.*, 1973; Williams & Morley, 1973; Williams & Peck, 1977; Wedmore & Williams, 1981). This effect is thought to be related to the action of prostaglandins on the arterial side of the microcirculation where they cause vasodilatation and increase local blood flow. This leads to an elevated hydrostatic pressure in the post-capillary venules and it is from these vessels that the leakage of plasma protein occurs (Majno & Palade, 1961). In rabbit skin, i.d. injection of prostaglandin E_2 (PGE_2) also potentiates the rate of accumulation of ^{111}In-labelled neutrophils induced by N-formyl-methionyl-leucyl-phenylalanine or zymosan activated plasma (ZAP) (Issekutz, 1981). This effect is also thought to be due to a local increase in blood flow which would enhance the delivery of cells available for accumulation at the site of inflammation (Issekutz, 1981).

Prostaglandins have also been shown to have anti-inflammatory effects both *in vivo* and *in vitro* (Morikawa *et al.*, 1992; Anastassiou *et al.*, 1992). For example, it has been shown that PGE_2 can inhibit eosinophil degranulation, an effect which is enhanced by co-incubation with a phosphodiesterase inhibitor (Kita *et al.*, 1991). Neutrophil function is also inhibited by prostaglandins of the E series (Takenawa *et al.*, 1986; Chopra & Webster, 1988). Interestingly, the systemic administration of a stable PGE_1 analogue was able to suppress inflammation in a model of cutaneous vasculitis and to other mediators (Kunkel *et al.*, 1979; Fantone *et al.*, 1980). These inhibitory effects were related to the capacity of a PGE_1 analogue to inhibit neutrophil activation. In a model of inflammation in rabbit skin, Rampart & Williams (1986) have shown that prostaglandins can either enhance (when given locally) or inhibit (when given sytemically) neutrophil-dependent oedema. Thus, it seems that prostaglandins can possess either inflammatory or anti-inflammatory properties depending on the route of administration.

In this study, we have investigated the effect of locally injected prostaglandins on oedema formation and leukocyte (neutrophils and eosinophils) accumulation in inflammatory responses in guinea-pig skin. We have found that locally-injected prostaglandins of the E series, whilst enhancing oedema formation and neutrophil accumulation induced by different mediators, unexpectedly suppress the accumulation of eosinophils in response to the same mediators.

[1] Author for correspondence.

Methods

Preparation of zymosan-activated plasma

Zymosan-activated plasma (ZAP) was used as a source of guinea-pig C5a des-Arg. ZAP was prepared by incubating guinea-pig heparinized (10 u ml^{-1}) plasma with zymosan (5 mg ml^{-1}) for 30 min at 37°C. Zymosan was removed by centrifugation (2 × 10 min at 3000 *g*). The activated plasma was desalted on a PD-10 sephadex G-25M column and stored in aliquots at − 20°C.

Preparation of passive cutaneous anaphylaxis sera and reactions

Details of the preparation of IgG_1-rich sera are described elsewhere (Weg *et al.*, 1991). Briefly, male guinea-pigs (Harlan Porcellus, 350–400 g) were immunized with bovine gamma-globulin (BGG) in Freund's complete adjuvant (0.2 mg BGG 0.2 ml^{-1} of adjuvant s.c.). These animals received a boost of antigen in Freund's incomplete adjuvant on day 21 and the serum was prepared on day 30. Recipient animals received an injection of 50 µl of a 1/50 dilution of the anti-sera i.d., followed 16–20 h later by the i.d. injection of antigen (BGG).

Induction, purification and radiolabelling of guinea-pig eosinophils

The method is described in detail elsewhere (Faccioli *et al.*, 1991). Briefly, horse serum (1 ml) was injected i.p. in ex-breeder female guinea-pigs (Harlan Porcellus, Oxon; 700–800 g) every other day for two weeks and a boost was given the day prior to collection of the cells. The animals were killed by exposure to CO_2 and their peritoneal cavities washed with heparinized saline (10 u ml^{-1}). These cells were layered onto a discontinuous percoll-HBSS (calcium and magnesium-free) gradient prepared on the day of the procedure and the eosinophils collected from the 1.085/1.090 and 1.090/1.095 interfaces. The purity of the cells used was always greater than 95%. The main contaminating cells were mononuclear cells and the presence of neutrophils (>1% contamination) was a major exclusion criterion for the use of the preparation. Viability, assessed by trypan blue exclusion, was greater than 98%. The purified eosinophils (2–3 × 10^7 cells) were incubated with ^{111}Indium (100 µCi in 10 µl) chelated to 2-mercaptopyridine-*N*-oxide (40 µg in 0.1 ml of 50 mM PBS, pH 7.4) for 15 min at room temperature. The cells were then washed twice in HBSS (Ca^{2+} and Mg^{2+}-free) containing 10% guinea-pig platelet poor plasma and re-suspended at a final concentration of 10^7 cells ml^{-1} prior to injection.

Induction, purification and radiolabelling of guinea-pig neutrophils

Neutrophils were elicited in the peritoneal cavity of naive ex-breeder guinea-pigs by the i.p. injection of 20 ml of 0.2% (w/v) glycogen. After 8–12 h, the animals were killed and the peritoneal cavity washed with heparinized saline (10 u ml^{-1}). The rest of the procedure was as described for the eosinophils. The cells were also collected from the 1.085/1.090 and 1.090/1.095 interfaces and were used only if over 95% pure. The major contaminants were eosinophils (3–4%) and mononuclear cells (2–3%). Viability tested by trypan blue exclusion was greater than 98%.

Measurements of local oedema formation and leukocyte accumulation in guinea-pig skin

Radiolabelled leukocyte infiltration and oedema formation were measured simultaneously. ^{125}I-human serum albumin (~5 µCi) was added to the ^{111}In-labelled eosinophils or neutrophils and these were injected intravenously (5 × 10^6 cells per animal) into recipient guinea-pigs (350–400 g) anaesthetized with Hypnorm (0.15 ml, i.m.). After 5 min, inflammatory mediators or antigen were injected i.d. into the dorsal skin of shaved animals with or without prostaglandins, calcitonin-gene related peptide or isoprenaline. All drugs were mixed before the injection. Each animal received a duplicate of each treatment following a randomized injection plan and the inflammatory response (^{111}In-labelled cell accumulation and oedema formation) was assessed after 2 h. This time point was chosen based on previous experiments showing that most of the ^{111}In-labelled leukocyte accumulation occurred during the first 2 h (Faccioli *et al.*, 1991; Teixeira *et al.*, unpublished observations). At this time, a blood sample was obtained by cardiac puncture, the animals were killed by an overdose of sodium pentobarbitone, the dorsal skin was removed, cleaned free of excess blood and the skin sites punched out with a 17 mm punch. The samples were counted in an automatic 5-head gamma-counter (Canberra Packard Ltd, Pangbourne, Berks) and the counts were cross-channel corrected for the two isotopes.

Leukocyte numbers are expressed as the number of ^{111}In-labelled cells per skin site and oedema formation as the ratio of ^{125}I counts of the skin sample divided by the ^{125}I counts in 1 µl of plasma.

Reagents

The following compounds were purchased from Sigma Chemical Company (Poole, Dorset): bradykinin, glycogen, bovine gamma globulin, compounds 48/80, (−)-isoprenaline, zymosan. Hanks solutions, HEPES and horse serum were purchased from Gibco Limited (Paisley, Renfrewshire). Percoll was purchased from Pharmacia (Milton Keynes, Bucks), PAF and calcitonin-gene related peptide (CGRP) from Bachem (Saffron Walden, Essex) and prostaglandins E_1 and E_2 from Janssen Pharmaceuticals (Belgium). Iloprost was a gift from Dr F. McDonald (Schering AG, Berlin, Germany).

Statistics

Data were analysed by Student's paired *t* test. Multiple comparisons were evaluated by two-way analysis of variance on normally distributed data. Values of $P<0.05$ were considered significant.

Results

The percentages of ^{111}In-labelled neutrophils and eosinophils circulating 2 h after i.v. injection were 5.8 ± 1.9 ($n = 9$) and 7.8 ± 0.7% ($n = 31$), respectively. At 2 h, over 95% of the total plasma ^{111}In was bound to the infused circulating leukocytes. Previous studies have shown that the radiolabelled leukocytes accumulated extravascularly at sites of cutaneous inflammation (Faccioli *et al.*, 1991; Weg *et al.*, unpublished observations). Each recipient animal received an i.v. injection of 5 × 10^6 ^{111}In-eosinophils or ^{111}In-neutrophils. Thus, approximately 60% of the total circulating eosinophil population was radiolabelled after the i.v. injection while the ^{111}In-neutrophils represented about 6% of the total.

Effect of PGE_1 on neutrophil accumulation

The coinjection of PGE_1 (3 × 10^{-11} and 3 × 10^{-10} mol per site) significantly enhanced the oedema formation induced by 10% ZAP and bradykinin (BK 10^{-10} mol per site) (Figure 1b). These doses of PGE_1, which have been previously shown to potentiate oedema formation in guinea-pig skin (Williams & Morley, 1973), had no effect when injected alone (Figure 1b). The accumulation of ^{111}In-labelled neutrophils measured in the same sites was slightly, but significantly, enhanced by PGE_1 (Figure 1a). BK did not induce a significant accumula-

tion of neutrophils above saline background (Figure 1a). In the same experiments, PGE_1 had no effect on PCA (1 μg of BGG per site)-induced neutrophil accumulation, but significantly enhanced PCA-induced oedema formation (data not shown). The prostacyclin analogue, iloprost (10^{-9} mol per site), also enhanced the accumulation of neutrophils induced by ZAP by 55.7 ± 14.2% ($n = 6$, $P < 0.01$). Oedema responses in the same sites were enhanced by 254 ± 92% ($n = 6$, $P < 0.01$). Iloprost did not alter the accumulation of neutrophils induced by PCA (BGG, 1 μg per site, 4321 ± 1644 ^{111}In-neutrophils; BGG + iloprost, 4472 ± 1847 ^{111}In-neutrophils, $n = 6$).

Effect of PGE_1 on eosinophil accumulation

Surprisingly, while PGE_1 (3×10^{-10} mol per site) enhanced ZAP-induced oedema formation, it significantly inhibited in the same sites ZAP-induced eosinophil accumulation (Figure 2). Further analysis of the effects of PGE_1 (10^{-12} to 3×10^{-8} mol per site) on ZAP-induced responses is shown in Figure 3. PGE_1 dose-dependently inhibited ZAP-induced eosinophil accumulation whilst potentiating oedema formation in the same sites. The ED_{50} values for PGE_1-mediated inhibition of eosinophil accumulation and potentiation of oedema formation were approximately 3×10^{-11} mol per site and 2×10^{-11} mol per site, respectively.

PGE_1 (3×10^{-10} mol per site) also potentiated oedema formation while suppressing eosinophil accumulation induced by other mediators of inflammatory stimuli (Table 1). For example, PGE_1 suppressed eosinophil accumulation induced in the PCA reaction (1 μg of BGG per site) and PAF (10^{-9} mol per site) by 35% and 48%, while oedema formation in the same sites was potentiated by 49% and 64%, respectively (Table 1). In addition, PGE_1 significantly inhibited eosinophil accumulation induced by compound 48/80 (3–30 μg per site) while potentiating oedema formation in the same sites (Table 1).

Effect of PGE_2 and iloprost on eosinophil accumulation and oedema formation

Another E-type prostaglandin, PGE_2 (3×10^{-10} mol per site) had similar effects to PGE_1. Coinjection of PGE_2 with ZAP, enhanced oedema formation (29.4 ± 4.7 μl without PGE_2 and 36.6 ± 4.3 μl with PGE_2, $n = 6$, $P < 0.05$) and suppressed eosinophil accumulation (2507 ± 218 ^{111}In-eosinophils without PGE_2 and 1312 ± 147 ^{111}In-eosinophils with PGE_2, $n = 6$, $P < 0.01$). Nevertheless, it was without effect against PCA (1 μg of BGG per site)-induced eosinophil accumulation or oedema formation (data not shown).

The stable prostacyclin analogue, iloprost (10^{-9} mol per site), was capable of potentiating oedema formation induced by ZAP and BK (10^{-10} mol per site) but it had no effect on ZAP-induced eosinophil accumulation (Figure 4). PCA-induced oedema formation appeared to be enhanced by iloprost, but this did not reach significance ($P = 0.06$) (Figure 4b). Iloprost had no effect on PCA-induced eosinophil accumulation (Figure 4a).

Effect of isoprenaline on eosinophil accumulation and oedema formation

Since some of the effects of E-series prostaglandins are thought to occur through a G-protein linked receptor leading

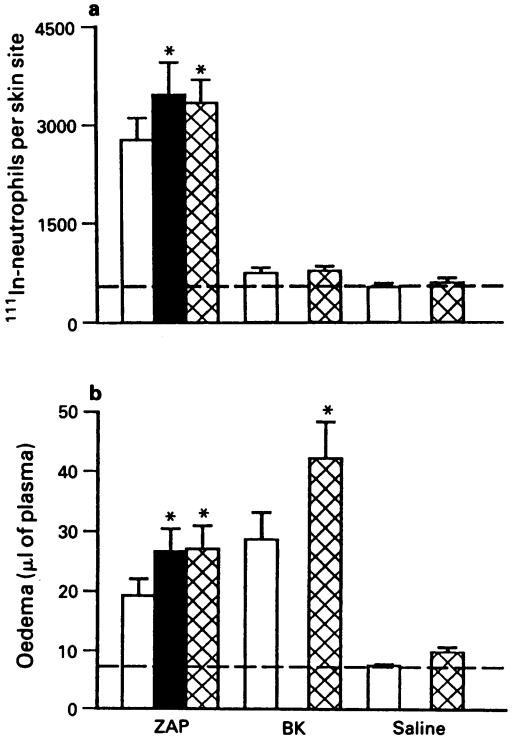

Figure 1 Effect of prostaglandin E_1 (PGE_1) on the accumulation of ^{111}In-labelled neutrophils (a) and local oedema formation (b) induced by zymosan-activated plasma (ZAP, 10% in saline) and bradykinin (BK, 10^{-10} mol per site). ^{111}In-neutrophil accumulation and oedema formation were assessed over a 2 h period. Results are expressed as the mean ± s.e.mean of 4–8 animals in control sites (open columns), sites injected with PGE_1 3×10^{-11} mol per site (solid columns) or PGE_1 3×10^{-10} mol per site (cross-hatched columns). The dashed lines represent the background values in sites injected with saline alone. *$P < 0.05$.

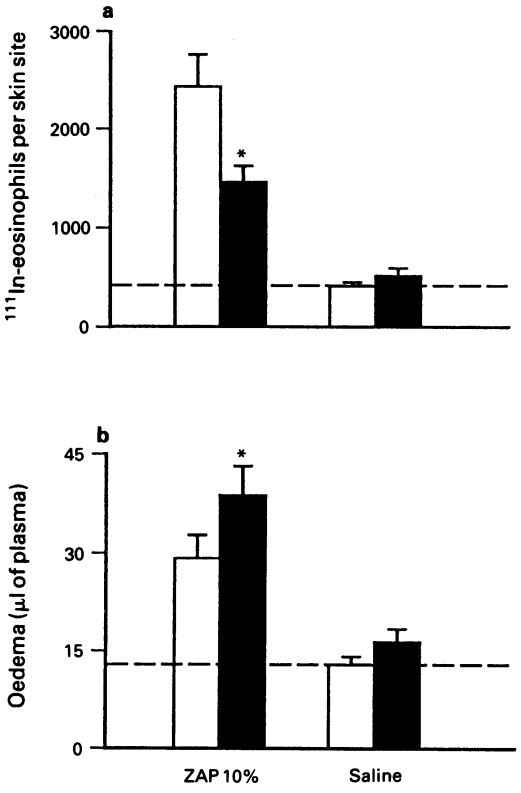

Figure 2 Effect of prostaglandin E_1 (PGE_1) on the accumulation of ^{111}In-labelled eosinophils (a) and oedema formation (b) induced by zymosan-activated plasma (ZAP, 10% in saline). ^{111}In-eosinophil accumulation and oedema formation were assessed over a 2 h period. Results are expressed as the mean ± s.e.mean of 9 animals in control sites (open columns) or sites injected with PGE_1 3×10^{-10} mol per site (solid columns). The dashed lines represent the background values in sites injected with saline alone. *$P < 0.05$.

to an increase in the adenosine 3':5'-cyclic monophosphate (cyclic AMP) content of cells (Coleman & Humphrey, 1993), we used the β-agonist isoprenaline which also increases intracellular cyclic AMP (Goldie *et al.*, 1991). Isoprenaline (10^{-10} to 10^{-8} mol per site) caused a dose-dependent inhibition of ZAP-, PCA- and PAF-induced eosinophil accumulation, but also inhibited ZAP-induced oedema formation (Table 2); PCA- and PAF-induced oedema formation were not significantly affected. ZAP-induced ^{111}In-neutrophil accumulation was not significantly altered by isoprenaline (ZAP alone, 6386 ± 2532 ^{111}In-neutrophils; ZAP + 10^{-9} mol isoprenaline per site, 6729 ± 2511; ZAP + 10^{-8} mol isoprenaline per site, 7133 ± 2693, $n = 6$).

Effect of calcitonin gene-related peptide (CGRP) on eosinophil accumulation and oedema formation

Neuropeptides have been shown to be potent vasodilators in animal and human skin (Brain *et al.*, 1985). Since these peptides may also act through an increase in cyclic AMP in different cell types (Goldie *et al.*, 1991), we tested the effect of CGRP on ZAP- and PCA-induced eosinophil accumulation and oedema formation. CGRP caused a dose-dependent increase in oedema formation in these reactions (Figure 5b), while eosinophil accumulation was unaltered (Figure 5a). CGRP also effectively potentiated oedema formation induced by BK (Figure 5b).

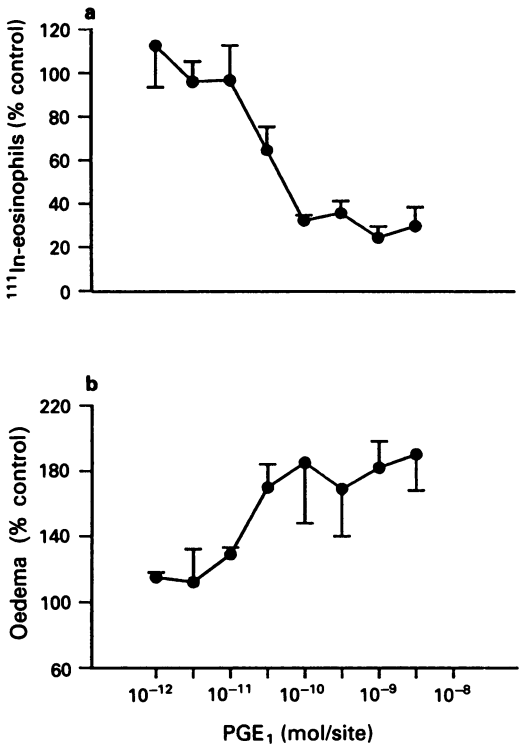

Figure 3 Dose-dependent effect of prostaglandin E_1 (PGE_1) on the eosinophil accumulation (a) and oedema formation (b) induced by zymosan-activated plasma (ZAP 10% in saline). ^{111}In-eosinophil accumulation and oedema formation were assessed over a 2 h period. Results are expressed as a percentage of the control response to ZAP. Responses in control sites were 2840 ± 223 ^{111}In-labelled neutrophils per site and 28.2 ± 3.5 μl of plasma per site. Values are means ± s.e.mean of 4–6 animals.

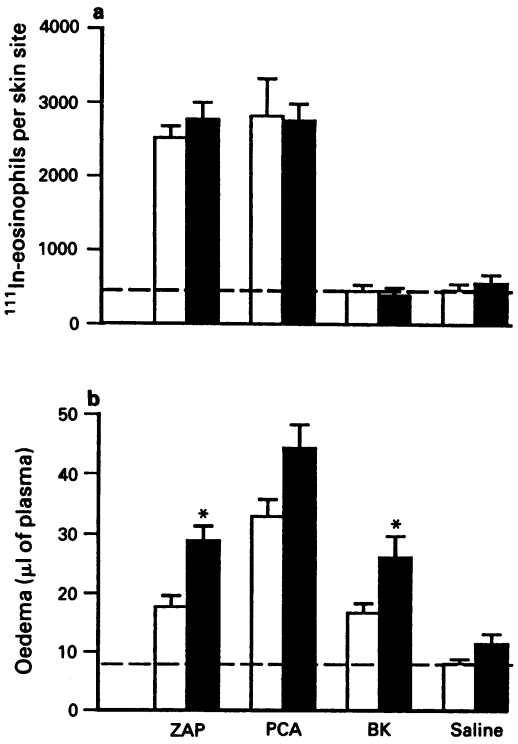

Figure 4 Effect of iloprost on the accumulation of ^{111}In-labelled eosinophils (a) and oedema formation (b) induced by zymosan-activated plasma (ZAP, 10% in saline), the passive cutaneous anaphylaxis (PCA) reaction (0.1 μg of BGG per site) and bradykinin (BK, 10^{-10} mol per site). ^{111}In-eosinophil accumulation and oedema formation were assessed over a 2 h period. Results are expressed as the mean ± s.e.mean of 4–7 animals in control sites (open columns) or sites injected with iloprost 10^{-9} mol per site (solid columns). The dashed lines represent the background values in sites injected with saline alone. *$P < 0.05$.

Table 1 Effect of prostaglandin E_1 (PGE_1, 3×10^{-10} mol per site) on the eosinophil accumulation and oedema formation induced by the passive cutaneous anaphylaxis reaction (PCA), platelet-activating factor (PAF) and compound 48/80 (C48/80) in guinea-pig skin

	^{111}In-eosinophils		*Oedema (μl of plasma)*	
	Control	*+ PGE_1*	*Control*	*+ PGE_1*
PCA 0.1 μg	2049 ± 170	1334 ± 427*	21.1 ± 1.0	25.0 ± 2.9
1.0 μg	4353 ± 712	2969 ± 512	26.1 ± 2.3	33.9 ± 2.9*
PAF 10^{-10} moles	1535 ± 239	866 ± 189*	35.6 ± 3.8	64.1 ± 5.3*
3×10^{-10} moles	2498 ± 670	1655 ± 471*	45.8 ± 4.7	72.1 ± 5.8*
10^{-9} moles	3590 ± 583	2071 ± 241*	53.1 ± 4.4	82.2 ± 7.6*
C48/80 3 μg	3797 ± 920	1648 ± 866*	42.7 ± 3.6	49.4 ± 4.2*
10 μg	5693 ± 810	2933 ± 722*	50.6 ± 2.6	64.7 ± 3.5*
30 μg	8589 ± 1505	5486 ± 835*	55.2 ± 2.6	72.3 ± 3.6*
Saline	441 ± 65	418 ± 55	13.1 ± 1.4	14.6 ± 1.3

The PCA reaction was induced by 0.1 or 1.0 μg BGG per site. ^{111}In-eosinophil accumulation and oedema formation were assessed over a 2 h period. Results are expressed as the mean ± s.e.mean, $n = 5–7$ experiments.
*$P < 0.05$.

Table 2 Effect of isoprenaline (10^{-10} to 10^{-8} mol per site) on the eosinophil accumulation and oedema formation induced by zymosan-activated plasma (ZAP), passive cutaneous anaphylaxis reaction (PCA) and platelet-activating factor (PAF) in guinea-pig skin

	^{111}In-eosinophils per site				*Oedema* (μl of plasma per site)			
	Isoprenaline (mol per site)				*Isoprenaline* (mol per site)			
	Control	10^{-10}	10^{-9}	10^{-8}	Control	10^{-10}	10^{-9}	10^{-8}
ZAP	2006 ± 248	1781 ± 528	1597 ± 211*	1221 ± 142*	30.5 ± 4.6	23.1 ± 2.5*	25.2 ± 5.3*	24.9 ± 2.0*
PCA	2309 ± 313	2452 ± 445	1701 ± 212*	1548 ± 346*	27.1 ± 2.7	22.8 ± 3.5	28.1 ± 3.3	28.3 ± 3.8
PAF	1395 ± 120	884 ± 164*	740 ± 92*	692 ± 30*	38.9 ± 11.1	31.1 ± 5.2	30.4 ± 5.8	31.0 ± 5.9
Saline	496 ± 47	461 ± 21	412 ± 64	440 ± 38	15.5 ± 1.5	12.8 ± 3.0	16.3 ± 0.92	15.6 ± 1.7

ZAP was diluted 10% in saline, the PCA reaction induced by 1 μg BGG per site and PAF used at 10^{-9} mol per site. ^{111}In-eosinophil accumulation and oedema formation were assessed over a 2 h period. Results are expressed as the mean ± s.e.mean, $n = 4-6$ experiments.
*$P < 0.05$.

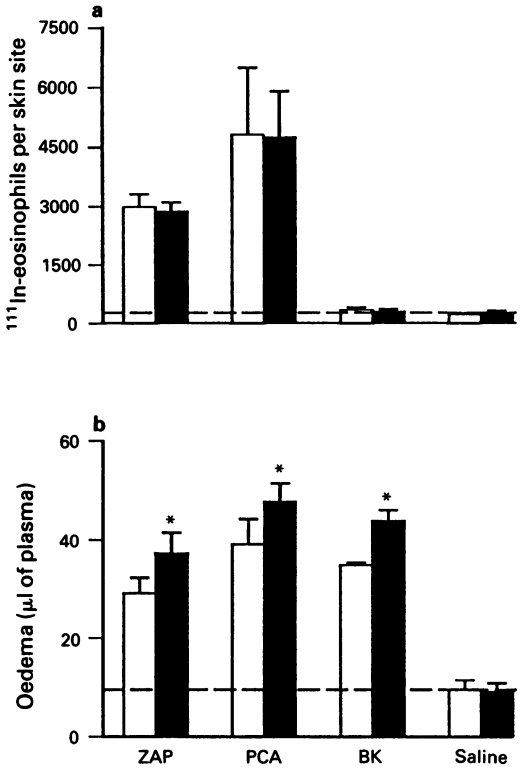

Figure 5 Effect of calcitonin gene-related peptide (CGRP) on the accumulation of ^{111}In-labelled eosinophils (a) and oedema formation (b) induced by zymosan-activated plasma (ZAP 10% in saline), passive cutaneous anaphylaxis (PCA) reaction (0.1 μg of BGG per site) and bradykinin (BK, 10^{-10} mol per site). ^{111}In-eosinophil accumulation and oedema formation were assessed over a 2 h period. Results are expressed as the mean ± s.e.mean of 4 animals in control sites (open columns) and sites injected with CGRP 10^{-11} mol per site (solid solumns). The dashed lines represent the background values in sites injected with saline alone. *$P < 0.05$.

Discussion

The capacity of different vasodilator prostaglandins to potentiate cutaneous oedema formation induced by different mediators of inflammation has been demonstrated extensively *in vivo* (Williams & Morley, 1973; Williams & Peck, 1977). This synergism is explained by a local increase in blood flow which is thought to enhance hydrostatic pressure in postcapillary venules, thus facilitating the extravasation of plasma proteins leading to oedema formation. Neutrophil accumulation at local sites of inflammation in skin is also enhanced by intradermal administration of vasodilators such as PGE_2 and CGRP and this has been attributed to increased delivery of inflammatory cells to the lesion (Issekutz, 1981; Issekutz & Movat, 1982; Buckley *et al.*, 1991).

In the present study, local administration of PGE_1 with various stimuli (ZAP, PCA, compound 48/80 and PAF) potentiated oedema formation and neutrophil accumulation in guinea-pig skin. However, eosinophil accumulation was suppressed by PGE_1 in sites at which local oedema formation was enhanced. The capacity of PGE_1 to inhibit eosinophil accumulation was partially mimicked by PGE_2. The lower efficacy of PGE_2 at inhibiting the PCA-induced eosinophil accumulation may be at least partially explained by its lesser potency *in vivo* to potentiate oedema formation in guinea-pig skin (Williams & Morley, 1973). PGE_2 has also been shown to be less effective than PGE_1 as an inhibitor of leukocyte function (Zurier, 1982). In contrast to the effects of PGE_1, the prostacyclin analogue, iloprost, while potentiating oedema formation and neutrophil accumulation, did not inhibit eosinophil accumulation. Since some of the biological effects of prostaglandin E_1 and E_2 are thought to be mediated by an increase of cyclic AMP within the target cell (Coleman & Humphrey, 1993), we used a β-adrenoceptor agonist, which also increases cyclic AMP within cells through a G-protein linked receptor (Goldie *et al.*, 1991), to test if this pathway was important. Interestingly, the β-agonist, isoprenaline, dose-depedently inhibited the accumulation of eosinophils induced by ZAP, PAF and in the PCA reaction. ZAP-induced oedema formation was also partially reduced by isoprenaline. The inhibition of oedema by isoprenaline has been previously shown, and is thought to be related to its action on endothelial cells (Beets & Paul, 1980). Indeed, isoprenaline acts on cultured endothelial cells to increase the levels of intracellular cyclic AMP (McEwan *et al.*, 1990). Prostaglandins of the E-series also increase cyclic AMP levels in endothelial cells (Hopkins & Gorman, 1981; Allison *et al.*, 1986), however, their effect on vascular smooth muscle cell cyclic AMP may be greater and the net effect is to increase local blood flow. We have also found that certain phosphodiesterase inhibitors suppress eosinophil accumulation in the guinea-pig skin, providing additional support for a role of cyclic AMP in the inhibitory effect of prostaglandins and isoprenaline (Teixeira *et al.*, unpublished observations). If elevation of cyclic AMP does have a role in the inhibitory effects of PGE_1, the receptor most likely to be involved is the EP_2 receptor (Coleman & Humphrey, 1993). Nevertheless, further studies are necessary to define unequivocally the prostanoid receptor(s) involved.

There are several possible cell targets on which prostaglandins and isoprenaline may be acting to inhibit the accumulation of eosinophils *in vivo*. Eosinophil function has been shown to be directly inhibited *in vitro* by prostaglandins (Giembycz *et al.*, 1990; Kita *et al.*, 1991), an effect which appears to be mediated by an increase in cyclic AMP, and this may explain the inhibitory effects that we observe *in vivo*. However, the fact that neutrophil functions (including chemotaxis) are also inhibited by different prostaglandins or

prostaglandin analogues *in vitro* (Takenawa *et al.*, 1986; Chopra & Webster, 1988) argues against a direct effect of prostaglandins on either the eosinophil or the neutrophil in our experimental model. It has been reported that, compared with other leukocytes, neutrophils are less responsive to agonists that activate adenylate cyclase (Plaut *et al.*, 1980) but whether this is true and relevant *in vivo* for the accumulation of guinea-pig neutrophils is not known. The mast cell is another possible cellular target particularly if one considers the inhibition of compound 48/80- and PCA-induced eosinophil accumulation by PGE_1. However, one would expect an inhibition of both eosinophil accumulation and oedema formation if the mast cell were a target for the inhibitory effects of PGE_1 since, at least for the PCA and compound 48/80, both functions are thought to be related to the activation of the mast cell.

Platelets have been shown to release eosinophil chemoattractants (Kameyoshi *et al.*, 1992; Burgers *et al.*, 1993) and they may also have a role in allergic states in guinea-pig lung (Lellouch-Tubiana *et al.*, 1988). If platelets are important in eosinophil accumulation in our skin model, then inhibition of platelet secretion by prostaglandins may explain the inhibitory effect on eosinophil accumulation.

Leukocytes express different adhesion molecules which are thought to be important for regulating their influx into the tissue (Williams & Hellewell, 1992). The integrin VLA-4 is expressed on the cell surface of the eosinophil, but not the neutrophil, and its presence appears to be important for eosinophil migration into sites of cutaneous inflammation (Weg *et al.*, 1993). VCAM-1, one of the ligands for VLA-4, is expressed after several hours on the surface of activated endothelial cells *in vitro* (Williams & Hellewell, 1992). Interestingly, the expression of endothelial cell VCAM-1 *in vitro* is inhibited by agents which elevate cyclic AMP (Pober *et al.*, 1992). However, it is not known whether VCAM-1 is expressed on venular endothelial cells in skin under our acute experimental procedure, or if prostaglandins of the E series and isoprenaline can inhibit this expression through an increase in cyclic AMP.

CGRP, a neuropeptide which has been shown to be a potent vasodilator in the microcirculation (Brain *et al.*, 1985), significantly enhanced oedema formation induced by ZAP, the PCA reaction and bradykinin. Nevertheless, it had no effect on ZAP- or PCA-induced eosinophil accumulation. Since CGRP may ultimately lead to an increase of cyclic AMP within various cells (Goltzman & Mitchell, 1985; McEwan *et al.*, 1991), it was surprising that it did not inhibit the accumulation of eosinophils. Neuropeptides, such as CGRP and substance P, have been recently shown to modulate chemotaxis of eosinophils from allergic subjects (Numao & Agrawal, 1992). Nevertheless the mechanism of modulation was not investigated in that study. It is possible that the receptor for CGRP may be lacking on the cells responsible for the inhibitory effects on eosinophil accumulation, eg. venular endothelial cells.

Human airways have been shown to release eicosanoids both *in vitro* (Schulman *et al.*, 1982) and *in vivo* (Wenzel *et al.*, 1989). It is suggested that asthmatic subjects produce relatively few 'bronchoprotective' eicosanoids as opposed to bronchoconstrictors and that the generation of prostaglandins may help preserve patency of the airways (Wenzel *et al.*, 1989). In animal models, a decrease in the production of PGE_2 has been suggested to be responsible for airways hyperreactivity (Folkert *et al.*, 1989; Gray *et al.*, 1992). PGE_2 is also partially responsible for the beneficial effects of frusemide against exercise-induced asthma (Pavord *et al.*, 1992). These data support a role for prostaglandin synthesis and protection in asthma. Eosinophils have been identified as important effector cells in allergic diseases such as asthma (Djukanovic *et al.*, 1990). If prostaglandins also inhibit the accumulation of eosinophils in the lungs of asthmatic subjects, this may prove to be another possible protective mechanism exerted by prostaglandins. It also implies that drugs which act similarly, such as the phosphodiesterase inhibitors, may have a role as anti-inflammatory drugs in asthma (Kuehl *et al.*, 1987; Torphy & Undem, 1991).

In summary, we have shown that prostaglandins of the E series enhance oedema formation and neutrophil accumulation, but significantly inhibit eosinophil accumulation into inflammatory sites. Isoprenaline partially mimics these effects suggesting that the inhibitory actions of both β-agonist and prostaglandins may be through an increase of cyclic AMP within the target tissue.

We thank the National Asthma Campaign and Sandoz, Switzerland for support.

References

ALLISON, A.C., KOWALSKI, W.J. & STRULOVICI, B. (1986). Effects of enprostil on platelets, endothelial cells, and other cell types, and second messenger systems by which these effects are mediated. *Am. J. Med.*, **81**, 34–39.

ANASTASSIOU, E.D., PALIOGIANNI, F., BALOW, J.P., YAMADA, H. & BOUMPAS, D.T. (1992). Prostaglandin E_2 and other cyclic AMP elevating agents modulate IL-2 and IL-2Rα gene expression at multiple levels. *J. Immunol.*, **148**, 2845–2852.

BEETS, J.L. & PAUL, W. (1980). Actions of locally administered adrenoceptor agonists on increased plasma protein extravsation and blood flow in guinea-pig skin. *Br. J. Pharmacol.*, **70**, 461–467.

BRAIN, S.D., WILLIAMS, T.J., TIPPINS, J.R., MORRIS, H.R. & MACINTYRE, I. (1985). Calcitonin gene-related peptide (CGRP) is a potent vasodilator. *Nature*, **313**, 54–56.

BUCKLEY, T.L., BRAIN, S.D., COLLINS, P.D. & WILLIAMS, T.J. (1991). Inflammatory edema induced by interactions between interleukin-1 and the neuropeptide calcitonin gene-related peptide. *J. Immunol.*, **146**, 3424–3430.

BURGERS, J.E., SCHWEIZER, R.C., KOENDERMAN, L., BRUIJNZEEL, P.L.B. & AKKERMAN, J.W.N. (1993). Human platelets secrete chemotatic activity for eosinophils. *Blood*, **81**, 49–55.

CHOPRA, J. & WEBSTER, R.O. (1988). PGE_1 inhibits neutrophil adherence and neutrophil-mediated injury to cultured endothelial cells. *Am. Rev. Respir. Dis.*, **138**, 915–920.

COLEMAN, R.A. & HUMPHREY, P.P.A. (1993). Prostanoid receptors: their function and classification. In *Therapeutic Applications of Prostaglandins*. ed. Vane, J. & O'Grady, J. London: Edward Arnold (in press).

DJUKANOVIC, R., ROCHE, W.R., WILSON, J.W., BEASLEY, C.R.W., TWENTYMAN, O.P., HOWARTH, P.H. & HOLGATE, S.T. (1990). Mucosal inflammation in asthma. *Am. Rev. Respir. Dis.*, **142**, 434–457.

FACCIOLI, L.H., NOURSHARGH, S., MOQBEL, R., WILLIAMS, F.M., SEHMI, R., KAY, A.B. & WILLIAMS, T.J. (1991). The accumulation of ^{111}In-eosinophils induced by inflammatory mediators in vivo. *Immunology*, **73**, 222–227.

FANTONE, J.C., KUNKEL, S.L., WARD, P.A. & ZURIER, R.B. (1980). Suppression by prostaglandin E_1 of vascular permeability by vasoactive inflammatory mediators. *J. Immunol.*, **125**, 2591–2596.

FOLKERT, G., ENGELS, F. & NIJKAMP, F.P. (1989). Endotoxin-induced hyperreactivity of the guinea-pig isolated trachea coincides with decreased prostaglandin E_2 production by the epithelial layer. *Br. J. Pharmacol.*, **96**, 388–394.

GIEMBYCZ, M.A., KROEGEL, C. & BARNES, P.J. (1990). Prostaglandin E_2 inhibits platelet activating factor-induced eosinophil activation. *Am. Rev. Respir. Dis.*, **141**, A396.

GOLDIE, R.G., PATERSON, J.W. & LULICH, K.M. (1991). Pharmacology and therapeutics of Beta-adrenoceptor agonists. In *Pharmacology of Asthma*. ed. Page, C.P. & Barnes, P.J. pp. 167–205. Berlin: Springer-Verlag.

GOLTZMAN, D. & MITCHELL, J. (1986). Interaction of calcitonin and calcitonin gene-related peptide at receptor sites in target tissues. *Science*, **227**, 1343–1345.

GRAY, P.R., DERKSEN, F.J., BROADSTONE, R.V., ROBINSON, N.E. & PETERS-GOLDEN, M. (1992). Decreased airway mucosal prostaglandin E_2 production during airway obstruction in an animal model of asthma. *Am. Rev. Respir. Dis.*, **146**, 586–591.

HOPKINS, N.K. & GORMAN, R.R. (1981). Regulation of endothelial cell cyclic nucleotide metabolism by prostacyclin. *J. Clin. Invest.*, **67**, 540–546.

INSEL, P.A. (1990). Analgesic-antipyretics and anti-inflammatory agents: drugs employed in the treatment of rheumatoid arthritis and gout. In *Goodman and Gilman's The Pharmacological Basis of Therapeutics*. ed. Gilman, A.G. Rall, T.W., Nies, A.S. & Taylor, P. pp. 638–681. New York: Pergamon Press.

ISSEKUTZ, A.C. (1981). Effect of vasoactive agents on polymorphonuclear leukocyte emigration in vivo. *Lab. Invest.*, **45**, 234–240.

ISSEKUTZ, A.C. & MOVAT, H.Z. (1982). The effect of vasodilator prostaglandins on polymorphonuclear leukocyte infiltration and vascular injury. *Am. J. Pathol.*, **107**, 300–309.

KAMEYOSHI, Y., DORSCHNER, A., MALLET, A.I., CHRISTOPHERS, E. & SCHRODER, J.-M. (1992). Cytokine RANTES released by thrombin-stimulated platelets is a potent attractant for human eosinophils. *J. Exp. Med.*, **176**, 587–592.

KITA, H., ABU-GHAZALEH, R.I., GLEICH, G.J. & ABRAHAM, R.T. (1991). Regulation of Ig-induced eosinophil degranulation by adenosine 3',5'-cyclic monophosphate. *J. Immunol.*, **146**, 2712–2718.

KUEHL, F.A., ZANETTI, M.E., SODERMAN, D.D., MILLER, D.K. & HAM, E.A. (1987). Cyclic AMP-dependent regulation of lipid mediators in white cells. A unifying concept for explaining the efficacy of theophylline in asthma. *Am. Rev. Respir. Dis.*, **136**, 210–213.

KUNKEL, S.L., THRALL, R.S., KUNKEL, R.G., MCCORMICK, J.R., WARD, P.A. & ZURIER, R.B. (1979). Suppression of immune complex vasculitis in rats by prostaglandin. *J. Clin. Invest.*, **64**, 1525–1529.

LELLOUCH-TUBIANA, A., LEFORT, J., SIMON, M.-T., PFISTER, A. & VARGAFTIG, B.B. (1988). Eosinophil recruitment into guinea pig lungs after PAF-acether and allergen administration. Modulation by prostacyclin, platelet depletion, and selective antagonists. *Am. Rev. Respir. Dis.*, **137**, 948–954.

MAJNO, G. & PALADE, G.E. (1961). Studies on inflammation. 1. The effect of histamine and serotonin on vascular permeability: an electron microscopic study. *J. Biol. Physiol. Biochem. Cytol.*, **11**, 571–605.

MCEWAN, J.R., PARSAEE, H., LEFROY, D.C. & MACDERMOTT, J. (1990). Receptors linked to adenylate cyclase on endothelial cells. In *The Endothelium: An Introduction to Current Research*. ed. Warren J.B. pp. 45–52. New York: Wiley-Liss.

MONCADA, S., VANE, J. & FERREIRA, S.H. (1973). Prostaglandins, aspirin-like drugs and the oedema of inflammation. *Nature*, **246**, 217–219.

MORIKAWA, M., AIKAWA, T., SEKIZAWA, K., OHRUI, T., SASAKI, H. & TAKISHIMA, T. (1992). Inhibitory actions of prostaglandin E_1 on neurogenic plasma extravasation in rat airways. *Eur. J. Pharmacol.*, **217**, 31–35.

NUMAO, T. & AGRAWAL, D.K. (1992). Neuropeptides modulate human eosinophil chemotaxis. *J. Immunol.*, **149**, 3309–3315.

PAVORD, I.D., WISNIEWSKI, A. & TATTERSFIELD, A.E. (1992). Inhaled frusemide and exercise induced asthma: evidence of a role for inhibitory prostanoids. *Thorax*, **47**, 797–800.

PLAUT, M., MARONE, G., THOMAS, L.L. & LICHTENSTEIN, L.M. (1980). Cyclic nucleotides in immune responses and allergy. In *Advances in Cyclic Nucleotide Research*. Vol. 12. ed. Hamet, P. & Sands, H. pp. 161–172. New York: Raven Press.

POBER, J.S., SLOWICK, M., DELUCA, L. & RITCHIE, A.J. (1992). Elevated cAMP inhibits endothelial expression of ELAM-1 and VCAM-1 but not ICAM-1. *FASEB. J.*, **6**, A1592.

RAMPART, M. & WILLIAMS, T.J. (1986). Polymorphonuclear leukocyte-dependent plasma leakage in the rabbit skin enhanced or inhibited by prostacyclin, depending on the route of administration. *Am. J. Pathol.*, **124**, 285–296.

SALMON, J.A. & HIGGS, G.A. (1987). Prostaglandins and leukotrienes as inflammatory mediators. *Br. Med. Bull.*, **43**, 285–296.

SCHULMAN, E.S., ADKINSON, N.F. & NEWBALL, H.H. (1982). Cyclooxygenase metabolites in human lung anaphylaxis: airway vs parenchyma. *J. Appl. Physiol.*, **53**, 589–595.

TAKENAWA, T., ISHITOYA, J. & NAGAI, Y. (1986). Inhibitory effect of prostaglandin E_2, forskolin, and dibutyryl cAMP on arachidonic acid release and inositol phospholipid metabolism in guinea pig neutrophils. *J. Biol. Chem.*, **261**, 1092–1098.

TORPHY, T.J. & UNDEM, B.J. (1991). Phosphodiesterase inhibitors: new opportunities for the treatment of asthma. *Thorax*, **46**, 512–523.

VANE, J.R. (1971). Inhibition of prostaglandin synthesis as a mechanism of action for aspirin-like drugs. *Nature, New Biol.*, **231**, 232–235.

WEDMORE, C.V. & WILLIAMS, T.J. (1981). Control of vascular permeability by polymorphonuclear leukocytes in inflammation. *Nature*, **289**, 646–650.

WEG, V.B., WATSON, M.L., CORDEIRO, R.S.B. & WILLIAMS, T.J. (1991). Histamine, leukotriene D_4 and platelet activating factor in guinea pig passive cutaneous anaphylaxis. *Eur. J. Pharmacol.*, **204**, 157–163.

WEG, V.B., WILLIAMS, T.J., LOBB, R.R., NOURSHARGH, S. (1993). A monoclonal antibody recognising very late activation antigen-4 (VLA-4) inhibits eosinophil accumulation in vivo. *J. Exp. Med.*, **177**, 561–566.

WENZEL, S.E., WESTCOTT, J.Y., SMITH, H.R. & LARSEN, G.L. (1989). Spectrum of prostanoid release after bronchoalveolar challenge in atopic asthmatics and in control groups. An alteration in the ratio of bronchoconstrictive to bronchoprotective mediators. *Am. Rev. Respir. Dis.*, **139**, 450–457.

WILLIAMS, T.J. & HELLEWELL, P.G. (1992). Adhesion molecules involved in the microvascular inflammatory response. *Am. Rev. Respir. Dis.*, **146**, S45–S50.

WILLIAMS, T.J. & MORLEY, J. (1973). Prostaglandins as potentiators of increased vascular permeability in inflammation. *Nature*, **246**, 215–217.

WILLIAMS, T.J. & PECK, M.J. (1977). Role of prostaglandin-mediated vasodilatation in inflammation. *Nature*, **270**, 530–532.

ZURIER, R.B. (1982). Prostaglandins immune responses and murine lupus. *Arthritis Rheum.*, **25**, 804–809.

(Received March 22, 1993
Revised April 27, 1993
Accepted April 30, 1993)

Br. J. Pharmacol. (1993), **110**, 423–427

Specific inhibition of leukotriene B_4 (LTB_4)-induced neutrophil emigration by 20-hydroxy LTB_4: implications for the regulation of inflammatory responses

[1]E.R. Pettipher, E.D. Salter, R. Breslow, L. Raycroft & H.J. Showell

Department of Immunology and Infectious Diseases, Central Research Division, Pfizer Inc., Groton, CT 06340, U.S.A.

1 The interaction between leukotriene B_4 (LTB_4) and its metabolite, 20-hydroxy LTB_4 in the control of neutrophil emigration was examined in guinea-pig skin.

2 Leukotriene B_4 (10–300 ng) elicited a dose-dependent increase in neutrophil infiltration (as measured by myeloperoxidase activity) 4 h after injection into guinea-pig skin. In contrast, 20-hydroxy LTB_4 (30–1000 ng) displayed only weak inflammatory activity in this assay.

3 Although 20-hydroxy LTB_4 had low agonist activity, this metabolite caused a potent dose-dependent inhibition of responses to LTB_4 (100 ng), when administered systemically ($ED_{50} = 1.3\ \mu g\ kg^{-1}$, s.c.) without significantly affecting neutrophil infiltration in response to C5a (2 μg). Systemic administration of 20-carboxy LTB_4 (10 μg) did not affect neutrophil accumulation in response to LTB_4 or C5a. In addition, neither 15(S)-hydroxy 5(S)-HPETE(10 μg) nor lipoxin A_4 (10 μg) inhibited responses to LTB_4.

4 Addition of 20-hydroxy LTB_4 (10^{-11}–10^{-8} M) to human blood prior to isolation of the neutrophils led to concentration-dependent decrease in the number of LTB_4 receptors and decreased chemotactic responsiveness to LTB_4 without affecting responses to C5a. Incubation of blood with 20-carboxy LTB_4 (10^{-8} M) did not reduce LTB_4 receptor number of chemotactic responsivness to LTB_4.

5 These data indicate that although 20-hydroxy LTB_4 is a weak agonist at LTB_4 receptors, it can desensitize neutrophils to the effects of LTB_4 via down-regulation of the high affinity receptor and thus provides evidence for a mechanism whereby inflammatory responses may be regulated.

Keywords: Leukotriene B_4; neutrophils; inflammation; 20-hydroxy LTB_4

Introduction

Leukocyte adhesion and emigration are cellular hallmarks of acute inflammation which can be elicited by a variety of neutrophil chemotactic factors. One such factor is leukotriene B_4 (LTB_4), an arachidonic acid metabolite of the 5-lipoxygenase pathway (Borgeat & Samuelsson, 1979). *In vitro*, LTB_4 causes neutropil adhesion to endothelial cells (Gimbrone *et al.*, 1984; Hoover *et al.*, 1984) and stimulates neutrophil chemotaxis (Ford-Hutchinson *et al.*, 1980). *In vivo*, application of LTB_4 stimulates neutrophil adhesion in postcapillary venules (Dahlen *et al.*, 1981), emigration of neutrophils into tissues (Bray *et al.*, 1981; Higgs *et al.*, 1981; Movat *et al.*, 1984) and increased vascular permeability (Wedmore & Williams, 1981; Bjork *et al.*, 1982). LTB_4 is produced by PMN and other cell-types and has been detected at sites of experimentally-induced inflammation (Simmons *et al.*, 1983; Ford-Hutchinson *et al.*, 1984) and in several inflammatory disease states including psoriasis (Brain *et al.*, 1984), gout (Rae *et al.*, 1982), rheumatoid arthritis (Davidson *et al.*, 1983) and inflammatory bowel disease (Sharon & Stenson, 1984). The reduction in neutrophil infiltration by agents which inhibit the production of or antagonize the action of LTB_4 suggest that this mediator can play a central role in the recruitment of leukocytes to sites of inflammation (Salmon *et al.*, 1983; Foster *et al.*, 1990; Fretland *et al.*, 1990; Carter *et al.*, 1991).

Neutrophils also have the unique capacity to metabolize LTB_4 via ω-oxidation to 20-hydroxy LTB_4 and further to 20-carboxy LTB_4 (Hansson *et al.*, 1981). 20-carboxy LTB_4 is essentially biologically inactive while 20-hydroxy LTB_4 is reported to bind to the LTB_4 receptor and possess limited biological activity (Ford-Hutchinson *et al.*, 1983; Clancy *et al.*, 1984). Nanomolar concentrations of these ω-oxidation products have been detected in patients with conditions such as purulent peritonitis and acute respiratory distress syndrome (Kikawa *et al.*, 1986; Seeger *et al.*, 1991), suggesting that this may be an important pathway of LTB_4 inactivation at sites of inflammation *in vivo*.

In the present study we have compared the inflammatory activities of 20-hydroxy LTB_4 with those of LTB_4 after injection into guinea-pig skin. We have also investigated the possibility that 20-hydroxy LTB_4 may desensitize responses to LTB_4 *in vivo*.

Methods

Induction of inflammatory responses in guinea-pig skin

Male Hartley guinea-pigs (400–450 g) were anaesthetized in an atmosphere of Metofane (methoxyflurane) and their backs shaved. Leukotriene B_4, 20-hydroxy LTB_4, 20-carboxy LTB_4 (all from Biomol, Plymouth Meeting, PA, U.S.A.) and human recombinant C5a (Franke *et al.*, 1988) were dissolved in saline containing 0.25% bovine serum albumin (BSA). Duplicate intradermal injections of saline or mediators were given in a volume of 0.1 ml in a randomized fashion such that there were a maximum of 6 sites per guinea-pig. Four hours after injection animals were killed, skin removed and sites punched out with a 13 mm gasket punch. 20-Hydroxy LTB_4 or 20-carboxy LTB_4 were either co-injected with LTB_4 or C5a or given subcutaneously in the nape of the neck.

Extraction and assay of myeloperoxidase activity in skin samples

Skin sites were homogenized and assayed for myeloperoxidase by a modification of the method described by Lundberg & Arfors (1983). Skin samples were homogenized in phosphate-buffered saline (pH 7.2), containing 0.5% hexadecyltri-

[1] Author for correspondence.

methylammonium bromide with a Polytron homogenizer (Brinkman, New York, U.S.A.). After homogenization, and 2 freeze/thaw cycles, the homogenates were centrifuged at 2,500 *g* for 30 min. Myeloperoxidase activity was then assayed in the supernatant by incubating 50 μl of diluted sample with 150 μl potassium phosphate buffer (pH 6.0) containing O-dianisidine (0.2 mg ml^{-1}) and hydrogen peroxide (0.001%) at 37°C for 15 min. The reaction was terminated by the addition of 100 μl 0.4 M glycine (pH 10) and the absorbance read at 450 nm using a 96-well plate reader (Molecular Devices, Menlo Park, CA, U.S.A.). Known numbers of guinea-pig neutrophils (harvested from the peritoneal cavity after injection of casein) were included in each assay as a standard curve and the data expressed as numbers of neutrophils per skin site.

In vitro *desensitization (chemotaxis and [^{3}H]-LTB$_4$ binding) experiments using neutrophils isolated from whole blood*

Aliquots (10 ml) of heparinized human blood were incubated with log dilutions of 20-hydroxy LTB$_4$ (10^{-11}–10^{-8} M final concentrations) for 5 min at 37°C. Neutrophils were then isolated as described below and the capacity to respond in the chemotaxis assay to either LTB$_4$ (5 nM) or C5a (5 nM) was evaluated (see below). In parallel, the ability of neutrophils to bind specifically [^{3}H]-LTB$_4$ was evaluated according to a method adapted from Lin *et al.* (1984). Briefly, neutrophils at a density of 2.5×10^6 cells per ml were incubated with 0.25–0.75 nM [^{3}H]-LTB$_4$ (195 Ci mmol^{-1}, DuPont/NEN, Boston, MA, U.S.A.) in Hanks buffered saline (containing Ca^{2+} and Mg^{2+}, 10 mM HEPES pH 7.25, 0.04% sodium bicarbonate) in the absence and presence of 1 μM unlabelled LTB$_4$ at 4°C for 30 min. The assay was performed in triplicate in microtiter plates (Costar, Cambridge, MA, U.S.A.) with a total volume of 200 μl and bound ligand was separated from free ligand using the betaplate apparatus (Pharmacia LKB, Piscataway, NJ, U.S.A.). The wash buffer was the same buffer as used for the incubation. Specific binding represents the value obtained when non-specific binding is subtracted from total binding.

Measurement of human neutrophil chemotaxis in vitro

Neutrophils were isolated from anticoagulated (heparin, Squibb-Monsam, Inc., Cherry Hill, N.J., U.S.A., 30 units ml^{-1} final concentration) human blood obtained from normal donors according to the method of Ferrante & Thong (1978). Isolated neutrophils were resuspended (2.5×10^6 cells ml^{-1}) in HBSS (supplemented with 10 mM HEPES) containing 0.7 mM Mg^{2+} and 1.6 mM Ca^{2+} and recrystallized bovine serum albumin (BSA; 2 mg ml^{-1} Sigma) and adjusted to pH 7.2. The chemotaxis assay was performed in a 48 well chamber apparatus (Neuroprobe, Cabin John, MD, U.S.A.) with cellulose nitrate filters (pore size, 3.0 μm) as described (Harvath *et al.*, 1987). The total number of cells (observed at × 400 magnification) migrating from 20 μm from beneath the surface monolayer to the leading front (usually ~100– 120 μm per 45 min at optimal chemotactic factor concentration) in response to various concentrations of LTB$_4$, 20-hydroxy LTB$_4$ or 20-carboxy LTB$_4$ were summed with the aid of an Optimax image analyzer (Optimax, Hollis, N.H., U.S.A.) and provided an index of the chemotactic response. Each experimental condition was performed in duplicate and three to five fields were assessed for cell migration. Results are expressed as the percentage maximum response where 100 per cent was equal to the peak response seen in the presence of the most efficacious concentration of LTB$_4$. The number of cells migrating spontaneously (i.e. negative controls) was subtracted from all measurements prior to data transformation.

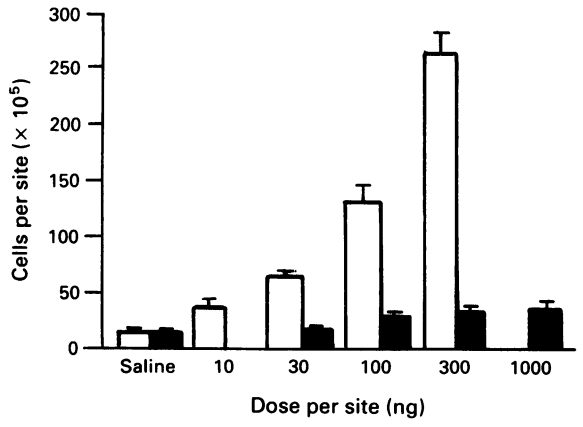

Figure 1 Increase in neutrophil infiltration (as measured by myeloperoxidase activity) after injection of leukotriene B$_4$ (LTB$_4$, open columns bars) or 20-hydroxy LTB$_4$ (solid columns) into the skin of separate groups of guinea-pigs. Results are expressed as the mean ± s.e.mean of data derived from 5 animals.

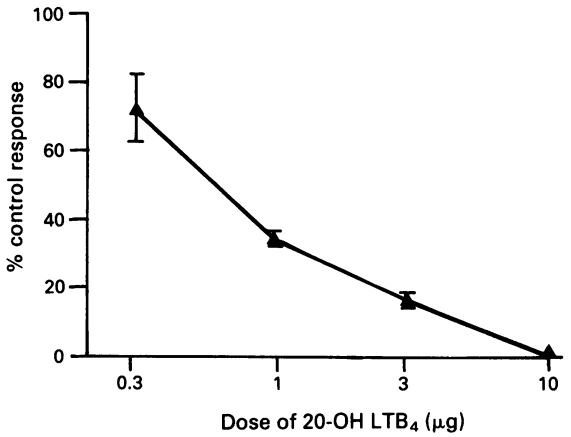

Figure 2 Inhibition of leukotriene B$_4$ (LTB$_4$, 100 ng)-induced neutrophil accumulation in guinea-pig skin by systemic (subcutaneous) administration of 20-hydroxy LTB$_4$. Each point represents the mean ± s.e.mean of data from 5–10 animals.

Results

LTB$_4$ (10–300 ng) caused a dose-dependent increase in neutrophil infiltration 4 h after injection into guinea-pig skin (Figure 1). In contrast, 20-hydroxy LTB$_4$ was much less active, producing inflammatory responses of similar magnitude to the saline controls. 20-carboxy LTB$_4$ also showed very little inflammatory activity when injected *in vivo*. In the experiments shown in Figure 1, the LTB$_4$ and 20-hydroxy LTB$_4$ were injected in separate groups of animals. Initially, LTB$_4$ and 20-hydroxy LTB$_4$ were injected at different sites in the same animals and we observed unexpectedly low control responses to LTB$_4$. These results prompted us to determine whether systemic injection of 20-hydroxy LTB$_4$ (injected subcutaneously at a distant site from the LTB$_4$ injections) could suppress the responses to LTB$_4$.

The results shown in Figure 2 indicate that 20-hydroxy LTB$_4$ inhibited neutrophil responses to LTB$_4$ (100 ng) *in vivo* at extremely low doses (ED_{50} = 1.3 μg kg^{-1}, s.c.). However, 20-hydroxy LTB$_4$ did not significantly affect neutrophil emigration in response to C5a (2 μg) in animals where responses to LTB$_4$ were inhibited (Figure 3). This dose of C5a was submaximal and chosen because it gave a similar magnitude of response as 100 ng LTB$_4$. The inhibitory property of 20-hydroxy LTB$_4$ was not shared with 20-carboxy LTB$_4$ which did not affect responses to LTB$_4$ or C5a (Figure 4).

In addition, neither 15(S)-hydroxy (5(S)-HPETE nor lipoxin

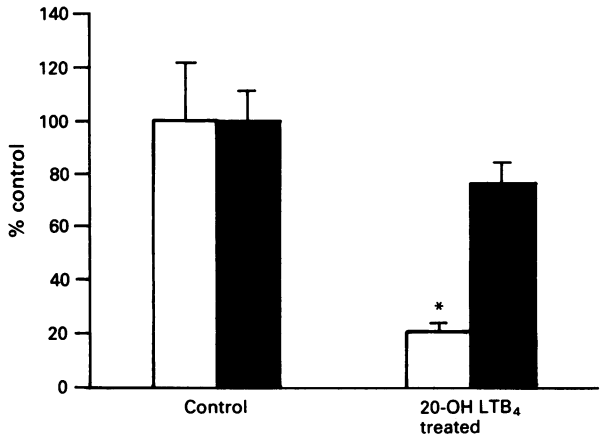

Figure 3 Effect of systemic administration of 20-hydroxy leukotriene B_4 (20-OH-LTB_4) (3 μg) on accumulation of neutrophils in guinea-pig skin in response to LTB_4 (100 ng, open columns) or C5a (2 μg, solid columns) in the same animals. Each point represents the mean ± s.e.mean of data from 5 animals per group. $*P < 0.01$ vs. control.

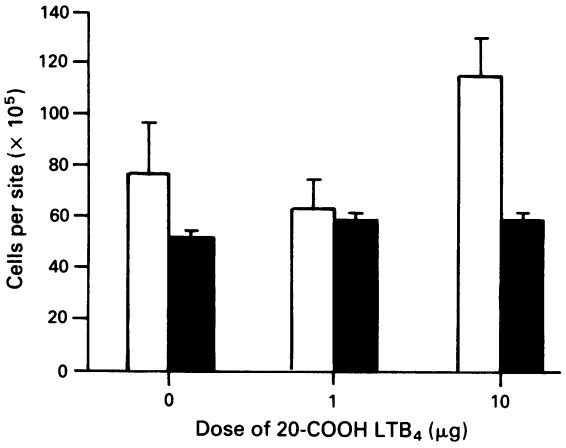

Figure 4 Effect of systemic administration of 20-carboxy leukotriene B_4 (20-COOH LTB_4) on accumulation of neutrophils in guinea-pig skin in response to LTB_4 (100 ng, open columns) or C5a (2 μg, solid columns). Results are expressed as the mean ± s.e.mean of data from 5 animals per group.

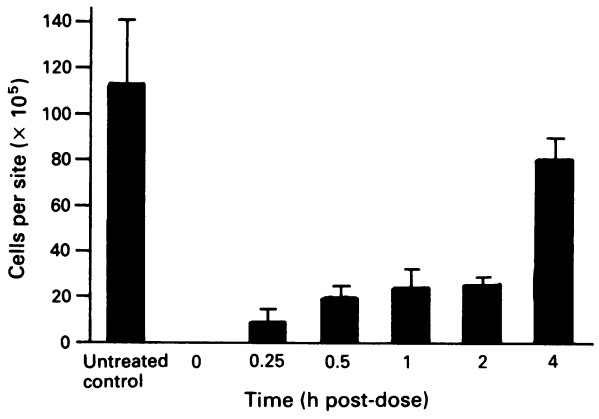

Figure 5 Inhibition of leukotriene B_4 (LTB_4)-induced inflammatory responses by 20-hydroxy LTB_4 (10 μg) at various times after dosing. Results are expressed as the mean ± s.e.mean of data from 5 animals per group.

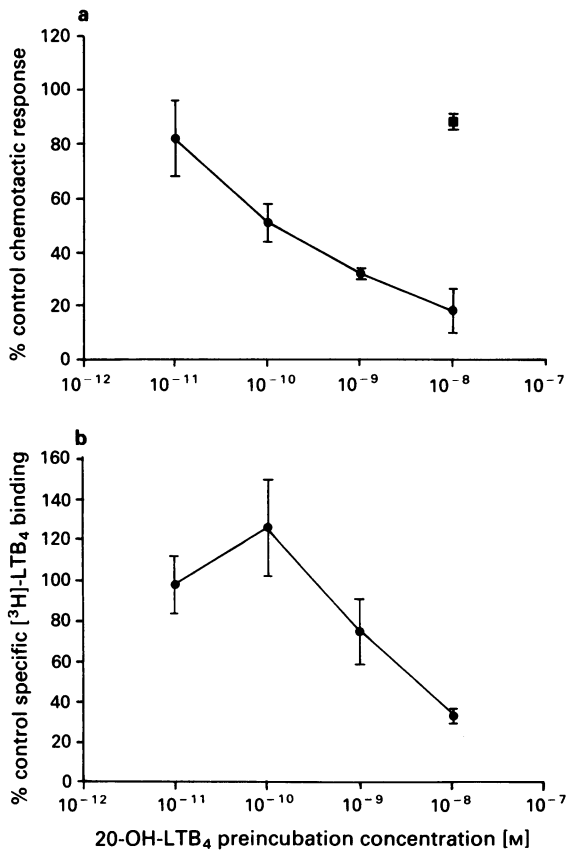

Figure 6 Inhibition of leukotriene B_4 (LTB_4)-mediated neutrophil chemotaxis (a) and specific [^{3}H]-LTB_4 binding to isolated neutrophils (b) pre-exposed to 20-hydroxy LTB_4 in whole blood. Log dilutions of 20-hydroxy LTB_4 were added to whole human blood and incubated at 37°C for 5 min. Neutrophils were then isolated as described in the methods section and assayed for their ability to respond in the chemotaxis assay to LTB_4 (5 nM) (●) or C5a (5 nM) (■) (a) and to bind specifically [^{3}H]-LTB_4 (b). The values shown represent the mean ± s.e.mean for 3 independent experiments.

A_4 inhibited responses to LTB_4 when administered under the same conditions as 20-hydroxy LTB_4 at doses up to 10 μg (for 15(S)-hydroxy 5(S)-HPETE % control response = 88.3 ± 17.3, $n = 5$; for lipoxin A_4, % control response = 102.7 ± 10.6, $n = 5$). Figure 5 shows that the effect of 20-hydroxy LTB_4 was longlasting (responses still maximally inhibited at 2 h after dosing), but reversible (responses were not significantly reduced at 4 h after dosing). When 20-hydroxy LTB_4 was coadministered locally with LTB_4 no inhibition was observed at doses which were devoid of systemic activity.

In vitro, pretreatment of human neutrophils in whole blood with 20-hydroxy LTB_4 led to a concentration-dependent and specific inhibition of the chemotactic response to LTB_4 ($IC_{50} = 0.15 \pm 0.07$ nM) and loss of high affinity receptors for [^{3}H]-LTB_4 ($IC_{50} = 4.0 \pm 1.8$ mM) (Figure 6). No inhibition of either chemotaxis (% control response = 101 ± 3.6) or receptor expression (% control response = 93.0 ± 7.6) was noted in response to 20-carboxy LTB_4 (10^{-8} M). Moreover, pre-exposure of neutrophils to 20-hydroxy LTB_4 in blood did not inhibit chemotaxis in response to the complement fragment, C5a (Figure 6).

Discussion

There is increasing evidence that LTB_4 plays a central role in leukocyte recruitment and the ensuing tissue damage that occurs in inflammatory diseases. Leukotriene B_4 has been detected at sites of inflammation, both in laboratory animals

(Simmons et al., 1983; Ford-Hutchinson et al., 1984) and in human diseases (Rae et al., 1982; Davidson et al., 1983; Brain et al., 1984; Sharon & Stenson, 1984) and has been shown to possess potent leukocyte chemotactic properties *in vitro* and *in vivo*. Treatments which lower LTB_4 pharmacologically (Foster et al., 1990; Carter et al., 1991; Salmon et al., 1983) or by dietary means (Lefkowith, 1988) have been demonstrated to diminish leukocyte recruitment *in vivo*. In addition, agents which antagonize LTB_4 at its receptor have also displayed anti-inflammatory activity (Fretland et al., 1990; 1991).

Further evidence to support a role for LTB_4 in inflammation can be inferred from the finding that an effective mechanism exists for its inactivation at sites of inflammation. Thus, LTB_4 can be metabolized by neutrophils and possibly other cell types via ω-oxidation to products which have much reduced biological activity (Hansson et al., 1981; Ford-Hutchinson et al., 1983; O'Flaherty et al., 1986). Furthermore, these products (20-hydroxy LTB_4 and 20-carboxy LTB_4) have been detected in inflammatory exudates (Kikawa et al., 1986; Seeger et al., 1991), suggesting that ω-oxidation is an important pathway of LTB_4 inactivation *in vivo*.

In the present study we have confirmed that 20-hydroxy LTB_4 and 20-carboxy LTB_4 have significantly reduced inflammatory activities compared to LTB_4. As 20-hydroxy LTB_4 has been shown to bind to LTB_4 receptors on neutrophils with 10–20 times less affinity than LTB_4 (Clancy et al., 1984; O'Flaherty et al., 1986; Jackson et al., 1992), we also investigated the possibility that 20-hydroxy LTB_4 may antagonize the inflammatory effects of LTB_4 *in vivo*. Surprisingly, when 20-hydroxy LTB_4 was co-injected with LTB_4 in guinea-pig skin, the LTB_4 responses at distant control sites were also diminished. Consequently, we found that systemic (subcutaneous) administration of extremely low doses of 20-hydroxy LTB_4 can effectively block inflammatory responses to LTB_4. 20-Carboxy LTB_4 did not possess this property of 20-hydroxy LTB_4 and the effect was specific for LTB_4 since 20-hydroxy LTB_4 administration did not inhibit neutrophil infiltration in response to C5a. However, 20-hydroxy LTB_4 also caused a small (but nonsignificant) reduction in the myeloperoxidase signal in response to C5a which we believe reflects a LTB_4-dependent component to the eosinophil infiltration that occurs in response to C5a. As eosinophils contain myeloperoxidase-like activity the low numbers infiltrating the skin sites may make a small contribution to the signal and would account for the slight reduction caused by 20-hydroxy LTB_4 in response to C5a. Studies are underway to investigate the LTB_4-dependent component of C5a-induced eosinophil infiltration using selective markers of eosinophil infiltration.

Doses of 20-hydroxy LTB_4 which were devoid of systemic activity did not inhibit responses to LTB_4 when co-injected locally. These data suggest that 20-hydroxy LTB_4 acted by desensitizing neutrophils to the action of LTB_4 in the circulation and did not inhibit responses to LTB_4 by local antagonism. This concept is supported by *in vitro* data where pre-exposure of neutrophils in whole blood to 20-hydroxy LTB_4 selectively inhibited neutrophil chemotaxis to LTB_4 and reduced the number of high affinity receptors for LTB_4 which have previously been shown to transduce the chemotactic response and can be eliminated by chemotactic deactivation of neutrophils to LTB_4 (Goldman & Goetzl, 1984). In fact *in vitro* it has already been shown that 20-hydroxy LTB_4 can desensitize neutrophil responses to LTB_4 and *vice versa* (O'Flaherty et al., 1986). However, 20-hydroxy LTB_4 appears to be more potent as an inhibitor in the functional chemotaxis assay than in inhibiting receptor expression which may reflect a redistribution of receptors on the cell surface that are functionally uncoupled for chemotaxis but are still capable of binding ligand. A distribution of N-formyl peptide receptors into specialised membrane domains has previously been shown to occur upon ligand binding and may be relevant to the above finding with LTB_4 receptors (Jesaitis et al., 1988). This selective desensitization of LTB_4-mediated function is similar to that which occurs in neutrophils from patients with cystic fibrosis (Lawrence & Sorrell, 1992).

These data indicate that although 20-hydroxy LTB_4 possesses only weak inflammatory activity it can cause specific desensitization to the inflammatory effects of LTB_4 and therefore may serve as a probe to investigate the role of LTB_4 in animal models of inflammatory disease. A similar proposal was recently put forward by Marleau et al. (1993) where infusion of LTB_4 itself was used to induce a state of desensitization in the rabbit. Furthermore, as 20-hydroxy LTB_4 has been detected at sites of inflammation in concentrations sufficient to produce these inhibitory effects, this process of desensitization may serve as a mechanism to regulate inflammatory processes and a reduced capacity to metabolize LTB_4 via ω-hydroxylation may predispose to chronic inflammatory disease.

References

BJORK, J., HEDQVIST, P. & ARFORS, K.-E. (1982). Increase in vascular permeability induced by leukotriene B_4 and the role of polymorphonuclear leukocytes. *Inflammation*, **6**, 189–200.

BORGEAT, P. & SAMUELSSON, B. (1979). Transformation of arachidonic acid by rabbit polymorphonuclear leukocytes: formation of a novel dihydroxyeicosatetraenoic acid. *J. Biol. Chem.*, **254**, 2643–2650.

BRAIN, S.D., CAMP, R., DOWD, P., KOBZA BLACK, A. & GREAVES, M.W. (1984). The release of leukotriene B_4-like material in biologically active amounts from the lesional skin of patients with psoriasis. *J. Invest. Dermatol.*, **83**, 70–73.

BRAY, M.A., FORD-HUTCHINSON, A.W. & SMITH, M.J.H. (1981). Leukotriene B_4: an inflammatory mediator *in vivo*. *Prostaglandins*, **22**, 213–222.

CARTER, G.W., YOUNG, P.R., ALBERT, D.H., BOURKA, J., DYER, R., BELL, R.L., SUMMERS, J.B. & BROOKS, D.W. (1991). 5-Lipoxygenase inhibitory activity of zileuton. *J. Pharmacol. Exp. Ther.*, **256**, 929–937.

CLANCY, R.M., DAHINDEN, C.A. & HUGLI, T.E. (1984). Oxidation of leukotrienes at the ω end: demonstration of a receptor for the 20-hydroxy derivative of leukotriene B_4 on human neutrophils and implications for the analysis of leukotriene receptors. *Proc. Natl. Acad. Sci. U.S.A.*, **81**, 5729–5733.

DAHLEN, S.-E., BJORK, J., HEDQVIST, P., ARFORS, K.-E., HAMMARSTROM, S., LINDGREN, J.-A. & SAMUELSSON, B. (1981). Leukotrienes promote leakage and leukocyte adhesion in post capillary venules: *In vivo* effects with relevance to the acute inflammatory response. *Proc. Natl. Acad. Sci. U.S.A.*, **78**, 3887–3891.

DAVIDSON, E.M., RAE, S.A. & SMITH, M.J.H. (1983). Leukotriene B_4, a mediator of inflammation present in synovial fluid in rheumatoid arthritis. *Ann. Rheum. Dis.*, **42**, 677–679.

FERRANTE, A. & THONG, Y.H. (1978). A rapid one-step procedure for purification of mononuclear and polymorphonuclear leukocytes from human blood using a modification of the hypaque-ficoll technique. *J. Immunol. Methods*, **24**, 389–393.

FORD-HUTCHINSON, A.W., BRAY, M.A., DOIG, M.V., SHIPLEY, M.E. & SMITH, M.J.H. (1980). Leukotriene B: a potent chemokinetic and aggregating substance released from polymorphonuclear leukocytes. *Nature*, **286**, 264–265.

FORD HUTCHINSON, A.W., BRUNET, G., SAVARD, P. & CHARLESON, S. (1984). Leukotriene B_4, polymorphonuclear leukocytes and inflammatory exudates in the rat. *Prostaglandins*, **28**, 13–27.

FORD-HUTCHINSON, A.W., RACKHAM, A,. ZAMBONI, R., ROKACH, J. & ROY, S. (1983). Comparative biological activities of synthetic leukotriene B_4 and its ω-oxidation products. *Prostaglandins*, **25**, 29–37.

FOSTER, S.J., BRUNEAU, P., WALKER, E.R.H. & MCMILLAN, R.M. (1990). 2-Substituted indazolinones: orally active and selective 5-lipoxygenase inhibitors with anti-inflammatory activity. *Br. J. Pharmacol.*, **99**, 501–503.

FRANKE, A.E., ANDREWS, G.C., STIMLER-GERARD, N.P., GERARD, C.J. & SHOWELL, H.J. (1988). Human anaphylatoxin: gene synthesis, expression and recovery of biologically active material from *Escherichia coli*. *Meth. Enzymol.*, **162**, 653–668.

FRETLAND, D.J., WIDOMSKI, D.L., SHONE, R.L., LEVIN, S. & GAGINELLA, T.S. (1991). Effect of the leukotriene B_4 receptor antagonist, SC 41930, on experimental allergic encephalomyelitis (EAE) in the guinea pig. *Agents Actions*, **34**, 172–174.

FRETLAND, D.J., WIDOMSKI, D.L., ZEMAITIS, J.M., WALSH, R.E., LEVIN, S., DJURIC, S.W., SHONE, R.L., TSAI, B.S & GAGINELLA, T.S. (1990). Inflammation of guinea pig dermis: effects of leukotriene B_4 receptor antagonist SC 41930. *Inflammation*, **14**, 727–739.

GIMBRONE, M.A., BROCK, A.F. & SCHAFER, A.I. (1984). Leukotriene B_4 stimulates polymorphonuclear leukocyte adhesion to cultured vascular endothelial cells. *J. Clin. Invest.*, **74**, 1552–1555.

GOLDMAN, D.W. & GOETZL, E.J. (1984). Heterogeneity of human polymorphonuclear leukocyte receptors for leukotriene B_4. Identification of a subset of high affinity receptors that transduce the chemotactic response. *J. Exp. Med.*, **159**, 1027– 1041.

HANNSON, G., LINDGREN, J.A., DAHLEN, S.-E., HEDQVIST, P. & SAMUELSSON, B. (1981). Identification and biological activity of novel omega-oxidized metabolites of leukotriene B_4 from human leukocytes. *FEBS Lett.*, **130**, 107–112.

HARVATH, L., MCCALL, C.E., BASS, D.A. & MCPHAIL, L.C. (1987). Inhibition of human neutrophil chemotaxis by the protein kinase inhibitor, 1-(5-isoquinolinesulfonyl) piperazine. *J. Immunol.*, **139**, 3055–3061.

HIGGS, G.A., SALMON, J.A. & SPAYNE, J.A. (1981). The inflammatory effects of hydroperoxy and hydroxy acid products of arachidonate lipoxygenase in rabbit skin. *Br. J. Pharmacol.*, **74**, 429–433.

HOOVER, R.L., KARNOFSKY, M.J., AUSTEN, K.F., COREY, E.J. & LEWIS, R.A. (1984). Leukotriene B_4 action on endothelium mediates augmented neutrophil/endothelial adhesion. *Proc. Natl. Acad. Sci. U.S.A.*, **81**, 2191–2193.

JESAITIS, A.J., BOKOCH, G.M., TOLLEY, J.O. & ALLEN, R.A. (1988). Lateral segregation of neutrophil chemotactic receptors in actin- and fodrin-rich plasma membrane microdomains depleted in guanyl nucleotide regulatory proteins. *J. Cell Biol.*, **107**, 921–928.

JACKSON, R.H., MORRISSEY, M.M., SILLS, M.A. & JARVIS, M.F. (1992). Comparison of antagonist binding to the leukotriene receptor on intact human polymorphonuclear neutrophils (PMN). *J. Pharmacol. Exp. Ther.*, **262**, 80–89.

KIKAWA, Y., SHIGEMATSU, Y. & SUDO, M. (1986). Leukotriene B_4 and 20-OH-LTB$_4$ in purulent peritoneal exudates demonstrated by GC-MS. *Prostaglandins, Leukt. Med.*, **23**, 85–94.

LAWRENCE, R.H. & SORRELL, T.C. (1992). Decreased polymorphonuclear leucocyte chemotactic response to leukotriene B_4 in cystic fibrosis. *Clin. Exp. Immunol.*, **89**, 321–324.

LEFKOWITH, J.B. (1988). Essential fatty acid deficiency inhibits the *in vivo* generation of leukotriene B_4 and suppresses levels of resident and elicited leukocytes in acute inflammation. *J. Immunol.*, **140**, 228–233.

LIN, A.H., RUPPEL, P.L. & GORMAN, R.R. (1984). Leukotriene B_4 binding to human neutrophils. *Prostaglandins*, **28**, 837–849.

LUNDBERG, C. & ARFORS, K.-E. (1983). Polymorphonuclear leukocyte accumulation in inflammatory dermal sites as measured by ^{51}Cr-labelled cells and myeloperoxidase. *Inflammation*, **7**, 247–255.

MARLEAU, S., FORTIN, C., POUBELLE, P.E. & BORGEAT, P. (1993). *In vivo* desensitization to leukotriene B_4 (LTB$_4$) in the rabbit. *J. Immunol.*, **150**, 206–213.

MOVAT, H.Z., RETTL, C., BURROWES, C.E. & JOHNSTON, M.G. (1984). The *in vivo* effect of leukotriene B_4 on polymorphonuclear leukocytes and the microcirculation. *Am. J. Pathol.*, **115**, 233–244.

O'FLAHERTY, J., KOSFELD, S. & NISHIHIRA, J. (1986). Binding and metabolism of leukotriene B_4 by neutrophils and their subcellular organelles. *J. Cell. Physiol.*, **126**, 359–370.

RAE, S.A., DAVIDSON, E.M. & SMITH, M.J.H. (1982). Leukotriene B_4, an inflammatory mediator in gout. *Lancet*, **ii**, 1122–1124.

SALMON, J.A., SIMMONS, P.M. & MONCADA, S. (1983). The effects of BW 755C and other anti-inflammatory drugs on eicosanoid concentrations and leukocyte accumulation in experimentally-induced acute inflammation. *J. Pharm. Pharmacol.*, **35**, 808–813.

SEEGER, W., GRIMMINGER, F., BORDEN, M., BECKER, G., LOHMEYER, J., HEINRICH, D. & LARCH, H.-G. (1991). Omega-oxidized leukotriene B_4 detected in the broncho-alveolar lavage fluid of patients with non-cardiogenic pulmonary edema, but not in those with cardiogenic edema. *Intensive Care Med.*, **17**, 1–6.

SHARON, P. & STENSON, W.F. (1984). Enhanced synthesis of leukotriene B_4 by colonic mucosa in inflammatory bowel disease. *Gastroenterology*, **86**, 453–460.

SIMMONS, P.M., SALMON, J.A. & MONCADA, S. (1983). The release of leukotriene B_4 during experimental inflammation. *Biochem. Pharmacol.*, **32**, 1353–1359.

WEDMORE, C.V. & WILLIAMS, T.J. (1981). Control of vascular permeability by polymorphonuclear leukocytes in inflammation. *Nature*, **289**, 646–650.

(Received March 23, 1993
Revised April 23, 1993
Accepted May 4, 1993)

Br. J. Pharmacol. (1993), **110**, 428–434

Cerebral blood flow and cerebrovascular reactivity after inhibition of nitric oxide synthesis in conscious goats

N. Fernández, J.L. García, A.L. García-Villalón, L. Monge, B. Gómez & [1]G. Diéguez

Departamento de Fisiología, Facultad de Medicina, Universidad Autónoma, Arzobispo Morcillo 1, 28029 Madrid, Spain

1 The role of nitric oxide in the cerebral circulation under basal conditions and after vasodilator stimulation was studied in instrumented, conscious goats, by examining the action of inhibiting endogenous nitric oxide production with N^G-nitro-L-arginine methyl ester (L-NAME).

2 In 6 unanaesthetized goats, blood flow to one brain hemisphere (electromagnetically measured), systemic arterial blood pressure and heart rate were continuously recorded. L-NAME (35 mg kg^{-1} by i.v. bolus) decreased resting cerebral blood flow by 43 ± 3%, increased mean arterial pressure by 21 ± 2%, and decreased heart rate by 41 ± 2%; cerebrovascular resistance increased by 114 ± 13% ($P<0.01$); the immediate addition of i.v. infusion of L-NAME (0.15–0.20 mg kg^{-1} during 60–80 min) did not significantly modify these effects. Cerebral blood flow recovered at 72 h, arterial pressure and cerebrovascular resistance at 48 h, and heart rate at 6 days after L-NAME treatment.

3 A second treatment with L-NAME scheduled as above reproduced the immediate haemodynamic effects of the first treatment, which (except bradycardia) reversed with L-arginine (200–300 mg kg^{-1} by i.v. bolus).

4 Acetylcholine (0.01–0.3 μg), sodium nitroprusside (3–100 μg) and diazoxide (0.3–9 mg), injected into the cerebral circulation of 5 conscious goats, produced dose-dependent increases in cerebral blood flow, and decreases in cerebrovascular resistance; sodium nitroprusside (30 and 100 μg) also caused hypotension and tachycardia.

5 The reduction in cerebrovascular resistance from resting levels (in absolute values) to lower doses, but not to the highest dose, of acetylcholine was diminished, to sodium nitroprusside was increased, and to diazoxide was unaffected after L-NAME, compared to control conditions. The effects on cerebrovascular resistance to acetycholine normalized within 24 h and to sodium nitroprusside within 48 h after L-NAME treatment.

6 This study provides information about the evolution of the changes in cerebral blood flow and cerebrovascular reactivity after inhibition of endogenous nitric oxide in conscious animals. The results suggest: (a) endogenous nitric oxide is involved in regulation of the cerebral circulation by producing a resting vasodilator tone, (b) the cerebral vasodilatation to acetylcholine is mediated, at least in part, by nitric oxide release, and (c) inhibition of nitric oxide production induces supersensitivity of cerebral vasculature to nitrovasodilators.

Keywords: Endothelium; N^G-nitro-L-arginine methyl ester (L-NAME); cerebral blood vessels; vasodilator tone; acetylcholine; nitrovasodilators; supersensitivity

Introduction

Nitric oxide, or a closely related compound, seems to be at least one type of endothelium-derived relaxing factor that is synthesized from L-arginine and relaxes vascular smooth musculature via the stimulation of guanylate cyclase (Ignarro, 1990; Moncada *et al.*, 1991a). The synthesis of endothelial nitric oxide can be inhibited by several L-arginine analogues and this inhibition induces vascular contraction *in vitro* and *in vivo* (Moncada & Higgs, 1990), and increases resistance in several vascular beds (Gardiner *et al.*, 1990; 1991b). Thus, the basal release of nitric oxide (Martin *et al.*, 1986; Rees *et al.*, 1989a) appears to be responsible for maintaining a vasodilator tone in the cardiovascular system (Rees *et al.*, 1989b; Gardiner *et al.*, 1990).

In the cerebral circulation, experimental observations suggest that nitric oxide mediates the dilatation of cerebral blood vessels to acetylcholine (Fujiwara *et al.*, 1986; Faraci, 1990; Fischer-Nakielski *et al.*, 1990; Rosenblum *et al.*, 1990) and could play a role in maintaining cerebrovascular tone *in vivo* (Faraci, 1990; Fischer-Nakielski *et al.*, 1990; Rosenblum *et al.*, 1990). Studies measuring cerebral blood flow have been performed in anaesthetized animals and have produced controversial results as inhibition of nitric oxide synthesis decreases (Kovách *et al.*, 1992; Kozniewska *et al.*, 1992; Pellegrino *et al.*, 1992) or does not change (Faraci & Heistad, 1992; Iadecola, 1992) resting cerebral blood flow. Thus, more studies are necessary to clarify the role of nitric oxide in the regulation of basal cerebral blood flow, as well as in cerebrovascular reactivity. Since anaesthetics can modify cerebrovascular response, the use of conscious animals could contribute to the elucidation of this issue.

The present study was carried out to analyse the role of endogenous nitric oxide in basal cerebral blood flow and in dilatation of the cerebral circulation. The experiments were performed by using an experimental model in goats that permits the blood supply to one brain hemisphere to be continuously measured on a beat-to-beat basis in the unanaesthetized animal, a situation that is near to normal conditions (Reimann *et al.*, 1972; Gómez *et al.*, 1977; García *et al.*, 1991). Inhibition of endogenous nitric oxide production was induced by i.v. administration of N^G-nitro-L-arginine methyl ester (Moore *et al.*, 1990; Rees *et al.*, 1990) and acetylcholine, sodium nitroprusside and diazoxide were used as vasodilators. This study allowed us to evaluate throughout several days the time course of the effects of inhibition of nitric oxide production on basal cerebral blood flow, systemic arterial blood pressure and heart rate, as well as on cerebral vasodilatation.

[1] Author for correspondence.

Methods

The present experiments were performed in six female goats (32 to 49 kg weight). In this species, each internal maxillary artery, a branch of the external carotid artery, provides the total blood flow to each cerebral hemisphere via the rete mirabile; the vertebral arteries do not contribute to brain blood flow, and the extracranial internal carotid artery is absent (Daniel *et al.*, 1953; Reimann *et al.*, 1972). The circle of Willis in the goat is similar to that in man except that the blood flows in a caudal direction in the basilar artery (Daniel *et al.*, 1953; Reimann *et al.*, 1972). Analysis of the distribution of radioactively labelled microspheres in the cerebral circulation of the goat after the surgical procedure described by Reimann *et al.* (1972) indicates that nearly all of the blood carried by the internal maxillary artery passes directly to cerebral tissue (Miletich *et al.*, 1975). Extracerebral blood flow is minimal, $<5\%$ of total flow.

The operative procedure has been described elsewhere (Reimann *et al.*, 1972). Briefly, the extracerebral vessels from one of the internal maxillary arteries were ligated and thrombosed with 1 000 units of thrombin (Thrombostat, Parke Davis, Morris Plains, NJ, U.S.A.) dissolved in 1 ml of 0.9% NaCl solution. This manoeuvre produces an almost immediate obliteration of the ethmoidal, ophthalmic, and buccinator arteries and thus eliminates blood flow to the eye and other facial structures. This is confirmed on recovery from surgery by the presence of ipsilateral blindness. However, obliteration of the extracerebral vessels from the internal maxillary artery does not cut off vascular supply to half of the face. The areas supplied by the ethmoidal, buccinator, dental, and temporal arteries are nourished by anastomotic channels that are normally in a state of dynamic balance but in which the direction of blood flow can be quickly changed, depending on the pressure differential from one side of the union to the other (Daniel *et al.*, 1953; Reimann *et al.*, 1972). There is no necrosis, and the functions related to these areas such as eating, drinking, and rumen are intact. Obliteration and thrombosis of the ophthalmic artery permanently cuts off vascular supply to the ipsilateral eye. This procedure becomes necessary for the successful isolation of the cerebral circulation (Reimann *et al.*, 1972; Miletich *et al.*, 1975). The ipsilateral blindness that ensues does not seem to alter normal behaviour and the physical condition of the animals.

An electromagnetic flow transducer (Biotronex, Silver Spring, MD, U.S.A.) was placed on the internal maxillary artery to measure blood flow to the ipsilateral cerebral hemisphere. A polyethylene catheter (PE-90) inserted in the temporal artery permitted the injection of drugs directly into the internal maxillary artery in the conscious goat; the same catheter was used to measure arterial blood pressure with a Statham P 23 ID transducer. A snare-type occluder was placed on the external carotid, close to the temporal artery, to obtain zero-flow base lines. The external connecting leads from the flow transducer and occluder, and the temporal artery catheter were led out subcutaneously and secured to the horn of the goat.

Heart rate was measured from the arterial pressure pulse with a ratemeter. Flow measurements were made with a Biotronex electromagnetic flowmeter (model BL-610). Cerebral blood flow systemic arterial blood pressure, and heart rate were recorded on a Dynograph Recorder (model R611, Sensor Medics, Bilthoven, The Netherlands).

The experiments on the conscious goats were started 2–3 days after the operative procedure, at which time the goats had fully recovered and were in good condition. The various measurements were made with the goat unrestrained in a large cage, except for a Lucite stock fitting loosely around the neck that limited forward and backward motion. Once placed in the cage the animal stood quietly during the experiments and showed no signs of disturbance. However, the experiments were stopped whenever the animals showed signs of excitation or uneasiness as also evidenced by alterations in the recordings of blood pressure and heart rate. In this event, the goat was brought back to the animal quarters, and a period of $\geqslant 24$ h was allowed before attempting a new experiment. The administration of small amounts of drugs into the internal maxillary artery can be carried out with reproducible results on different days in the conscious state without causing any discomfort to the animal (Lluch *et al.*, 1975; García *et al.*, 1991).

In this work the following experiments were performed: (1) after resting control measurements were recorded, all the animals received an i.v. bolus of N^G-nitro-L-arginine methyl ester (L-NAME, 35 mg kg^{-1} during 15–18 min), and 5 min after the haemodynamic variables had reached a new steady state, animals received an i.v. infusion of L-NAME (0.15–0.20 mg kg^{-1} during 60–80 min); the animals received in total 47 mg kg^{-1} of this substance. The effects of L-NAME were continuously recorded during about 2 h after stopping the infusion, and periodically during the subsequent 6–8 days; (2) four of these animals received a second treatment with L-NAME 8–10 days after the first treatment in the same way and doses as indicated above; these four goats, immediately after stopping the infusion of L-NAME, were also treated with L-arginine by i.v. route (200–300 mg kg^{-1} during 15–20 min), the haemodynamic variables being recorded during about 2 h. L-NAME and L-arginine were dissolved in isotonic saline at 5 mg ml^{-1} and 40 mg ml^{-1}, respectively; and (3) the effects of acetylcholine (0.01, 0.03, 0.1 and 0.3 μg), sodium nitroprusside (3, 10, 30 and 100 μg) and diazoxide (0.3, 1, 3 and 9 mg) were recorded in 5 goats. These substances, dissolved in isotonic saline, were given in volumes of 0.3 ml through the catheter placed into the temporal artery, and their effects were evaluated under control conditions, during the infusion and periodically after administration of the first treatment of L-NAME.

Arterial blood P_{O_2}, P_{CO_2} and pH were measured before and after injection of L-NAME by standard electrometric methods (Radiometer, ABL 300, Copenhagen, Denmark). Cerebrovascular resistance was calculated as the mean systemic arterial blood pressure (mmHg) divided by blood flow to one brain hemisphere (ml min^{-1}). In previous experiments (unpublished observations) and in 2 animals of the present study, we found that the goat intracranial pressure (intracranial venous pressure) in the cisterna magna is 0–3 mmHg under control conditions. Also, as in the 2 animals of the present study intracranial pressure did not appreciably change during the experimental conditions, we considered cerebral venous pressure to be of minor relevance for cerebrovascular resistance calculations.

Drugs used were: N^G-nitro-L-arginine methyl ester (Sigma), acetylcholine chloride (Sigma), sodium nitroprusside (Nitroprussiat Fides, Barcelona, Spain), and diazoxide (Hyperstat, Schering Corporation, NJ, U.S.A.). Administration of isotonic saline alone intravenously or into the internal maxillary artery at the volumes employed in the present study had no systemic or cerebrovascular effects.

Statistics

All haemodynamic measurements before and after L-NAME treatment were compared using the same animal as its own control. An analysis of variance for repeated measures, followed by Dunnett's test was applied to the results with L-NAME, acetylcholine, sodium nitroprusside, diazoxide and L-arginine. Percentage changes in cerebral blood flow and cerebrovascular resistance after L-NAME or L-arginine, and decreases in cerebrovascular resistance from resting levels taken in absolute values for the effects of acetylcholine, sodium nitroprusside and diazoxide before and after L-NAME were used. $P<0.05$ was considered statistically significant.

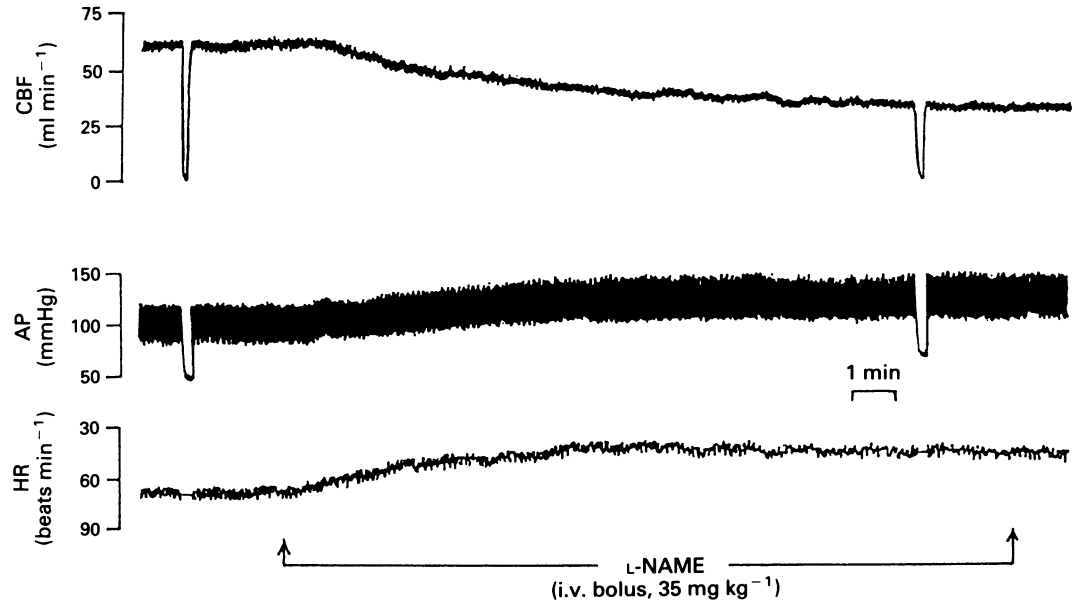

Figure 1 Actual recordings of the mean cerebral blood flow (CBF), systemic arterial blood pressure (AP) and heart rate (HR) obtained before and during administration of N^G-nitro-L-arginine methyl ester (L-NAME) in one conscious goat. Deflections of CBF and AP records correspond to occlusions of external carotid artery to obtain zero flow.

Results

Effects of L-NAME

With the first treatment, the i.v. bolus of L-NAME induced arterial hypertension, bradycardia and decreases in cerebral blood flow in all 6 goats. These effects began to be evident at 2–3 min after beginning the injection, the systemic and cerebral blood flow changes being practically simultaneous (Figure 1). The maximal effects of the i.v. bolus were reached at about 3–5 min after ending the injection, and cerebral blood flow decreased by 43 ± 3%, mean systemic arterial blood pressure increased by 21 ± 2%, heart rate decreased by 41 ± 2%, and calculated cerebrovascular resistance increased by 114 ± 13% ($P<0.01$). These effects were not significantly modified by adding the i.v. infusion of L-NAME (cerebral blood flow decreased by 48 ± 4%, mean arterial pressure increased by 28 ± 3%, heart rate decreased by 37 ± 4% and cerebrovascular resistance increased by 156 ± 27%) and remained for at least 2 h after stopping the infusion. The haemodynamic variables returned to control values after treatment with L-NAME, arterial pressure was the first variable to do so at about 48 h, cerebral blood flow at about 72 h, and heart rate at about 6 days (Figure 2).

The second treatment with L-NAME (i.v. bolus and infusion) in 4 of the 6 goats produced immediate systemic and cerebral blood flow effects comparable to those induced by the first treatment. In these 4 animals, the administration of L-arginine following infusion of L-NAME reversed the effects of L-NAME on systemic arterial pressure and cerebral blood flow, but not on heart rate (Table 1). The systemic arterial pressure and cerebral blood flow normalized at 10–20 min after stopping the administration of L-arginine and they remained within the control values during at least 4–6 days. Bradycardia persisted for this period in spite of L-arginine treatment.

We also observed that the first or second treatment with L-NAME produced clinical impairment in all the animals, which were moderately obtunded and less responsive to laboratory stimuli during 6–8 days after drug administration, an effect that was not apparently affected by L-arginine. Administration of L-NAME or L-arginine did not modify significantly arterial blood gases and pH.

Reactivity of the cerebral circulation

Figure 3 summarizes the absolute values for cerebrovascular resistance obtained before and after administration of acetylcholine, sodium nitroprusside and diazoxide in the animals

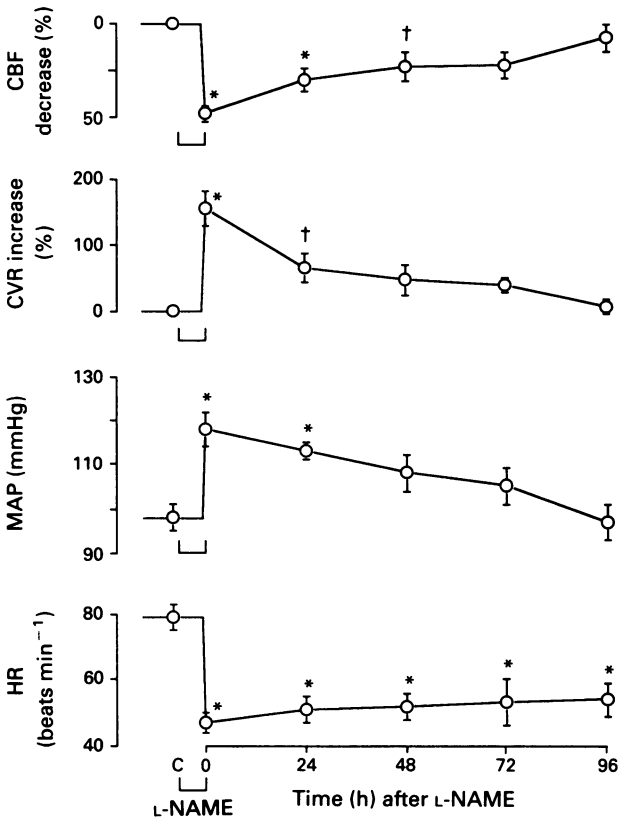

Figure 2 Summary of changes in cerebral blood flow (CBF), cerebrovascular resistance (CVR), mean systemic arterial blood pressure (MAP) and heart rate (HR) induced by the first treatment (i.v. bolus and infusion) with N^G-nitro-L-arginine methyl ester (L-NAME) in 6 conscious goats. *$P<0.01$, †$P<0.05$ compared with the control (C).

Table 1 Haemodynamic values (means ± s.e.mean) obtained before (control), immediately after the second N^G-nitro-L-arginine methyl ester (L-NAME) treatment (i.v. bolus + i.v. infusion) and after i.v. administration of L-arginine following L-NAME in 4 unanaesthetized goats

	Control	*L-NAME* (47 mg kg^{-1})	*L-Arginine* (200–300 mg kg^{-1})
CBF (ml min^{-1})	66 ± 3.2	39 ± 3.6 *	69 ± 3.4
CVR (mmHg ml^{-1} min^{-1})	1.51 ± 0.12	3.21 ± 0.20*	1.61 ± 0.13
MAP (mmHg)	101 ± 5.1	126 ± 7.3 †	110 ± 3.6
HR (beats min^{-1})	65 ± 3.8	45 ± 2.7 *	51 ± 3.4†

CBF = cerebral blood flow; CVR = cerebrovascular resistance; MAP = mean systemic arterial blood pressure; HR = heart rate. *$P<0.01$ and †$P<0.05$ compared to control.

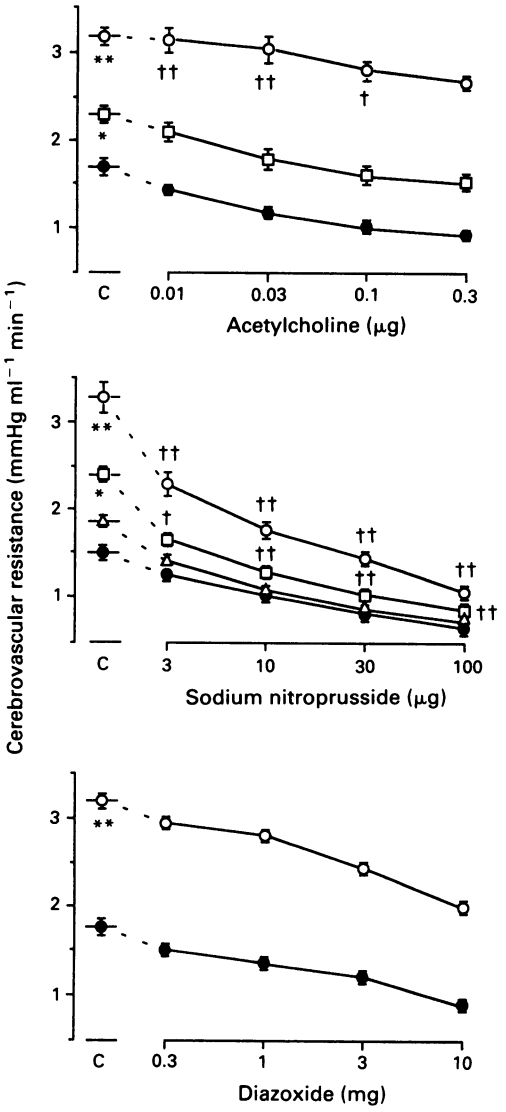

Figure 3 Values (mean ± s.e.mean) for cerebrovascular resistance under resting conditions in control (C) and after effects of acetylcholine, sodium nitroprusside and diazoxide obtained before (●), during treatment with N^G-nitro-L-arginine methyl ester (L-NAME) (○), at 24 h (□), and at 48 h (△) after L-NAME treatment. *$P<0.05$ and **$P<0.01$ for resting values before and after L-NAME. †$P<0.05$ and ††$P<0.01$ for decreases in resistance from resting values before and after L-NAME.

with and without L-NAME. Resting cerebrovascular resistance under control (without any treatment) was about 1.55 ± 0.11 mmHg ml^{-1} min^{-1}, and after L-NAME treatment were 3.45 ± 0.35 (immediate, $P<0.01$), 2.51 ± 0.30 (at 24 h, $P<0.5$) and 2.15 ± 0.25 (at 48 h, $P>0.05$) mmHg ml^{-1} min^{-1}.

Acetylcholine (0.01–0.3 μg), injected into the internal maxillary artery, produced dose-dependent increases in cerebral blood flow and decreases in cerebrovascular resistance, without affecting systemic variables. However, the decreases in cerebrovascular resistance (in absolute values) by the three lower doses of acetylcholine were significantly lower during the i.v. infusion of L-NAME; the reduction in cerebrovascular resistance by the highest dose (0.3 μg) of acetylcholine was comparable before and after L-NAME. At 24 h after L-NAME, the effects of acetylcholine were not significantly different from the control situation.

Sodium nitroprusside (3–100 μg), injected into the internal maxillary artery, produced marked, dose-dependent increases in cerebral blood flow and decreases in cerebrovascular resistance; and the doses of 30 and 100 μg also caused a small hypotension and tachycardia. These effects of sodium nitroprusside, however, were significantly higher after than before L-NAME. The decreases in cerebrovascular resistance (in absolute values) induced by sodium nitroprusside were significantly higher during and at 24 h after L-NAME than under control conditions; at 48 h after L-NAME these decreases were comparable to those obtained in controls.

Diazoxide (0.3–9 mg), injected into the internal maxillary artery, caused dose-dependent increases in cerebral blood flow and decreases in cerebrovascular resistance, without affecting systemic arterial pressure or heart rate. The decreases in cerebrovascular resistance (in absolute values) produced by diazoxide were not significantly different before and after treatment with L-NAME.

Discussion

The present study shows that i.v. administration of L-NAME reduced considerably resting cerebral blood flow by increasing cerebrovascular resistance in unanaesthetized animals, and these effects were accompanied by systemic arterial hypertension and bradycardia. The effects of L-NAME on cerebral blood flow and systemic variables reversed spontaneously and were reproduced when a second treatment was administered to the animals after recovery from the first treatment. Also, the cerebrovascular effects and systemic hypertension, but not bradycardia, induced by L-NAME were reversed by L-arginine. As L-NAME has proved to be a potent inhibitor of nitric oxide production (Moore *et al.*, 1990; Rees *et al.*, 1990), and the observed effects of this

substance were reversed by L-arginine, precursor of endothelial nitric oxide synthesis (Ignarro, 1990; Moncada *et al.*,1991a), our results suggest that the reduction in cerebral blood flow by L-NAME is due to decreases in basal nitric oxide production and, consequently, to inhibition of nitric oxide-mediated basal vasodilator tone in the cerebral vasculature under normal conditions. This is in line with observations by others in the cerebral blood flow of anaesthetized animals (Gardiner *et al.*, 1991b; Kovách *et al.*,1992; Kozniewska *et al.*, 1992; Pellegrino *et al.*, 1992) and supports the idea that an important basal vasodilator tone mediated by nitric oxide is present in the cerebral circulation as in other vascular beds (Moncada *et al.*, 1991a). Systemic hypertension and bradycardia have been previously observed with nitric oxide inhibitors (Moncada & Higgs, 1990). Results found in anaesthetized animals suggest that bradycardia after administration of inhibitors of nitric oxide synthesis is mainly caused by an increased vagal efferent activity (Aisaka *et al.*, 1989; Rees *et al.*, 1989b; Widdop *et al.*, 1992), whereas data from conscious rats suggest that it is related to inhibition of sympathetic activity, rather than potentiation of parasympathetic nerve activity (Wang & Pang, 1991). Widdop *et al.* (1992) observed that in the presence of supramaximal doses of atropine and atenolol, a small bradycardia persisted following L-NAME administration in anaesthetized rats, and they suggest that this persistent bradycardia could be due to coronary vasoconstriction induced by L-NAME. Other studies in conscious animals show that L-NAME (Gardiner *et al.*, 1991a) or N^G-nitro-L-arginine (L-NOARG) (Du *et al.*, 1992) did not affect the cardiac baroreflex sensitivities to pressor or depressor stimuli. Interestingly, we found that bradycardia remained for relatively longer periods than the reduction in cerebral blood flow and hypertension after treatment with L-NAME, and that it did not reverse with L-arginine. Du *et al.* (1992) also observed in conscious rabbits that bradycardia persisted for a longer period than hypertension after L-NOARG treatment. Although we have no confident data for the observed clinical effects after L-NAME, we can speculate that this substance may induce a sedative effect by depressing the central nervous system, including the basal nervous activity on the heart. This depression might account for the prolonged bradycardia found in our experiments. Data from mice suggest that L-NAME produces a long-lasting antinociception most probably by a direct effect within the central nervous system (Moore *et al.*, 1991).

The reduction in resting cerebral blood flow by L-NAME remained during 48 h and these effects were of longer duration than those on systemic arterial blood pressure, thus suggesting that cerebral blood vessels are particularly sensitive to the blockade of nitric oxide production, and that this substance plays a major role in regulating cerebral blood flow.

Therefore, the present experimental model permitted us to evaluate the time course of the changes in cerebral blood flow after inhibition of endogenous nitric oxide formation in the animals without anaesthesia, in conditions near to the normal situation. However, this model has potential limitations. First, with respect to cerebrovascular resistance, we cannot determine the vascular segments (arteries, microvessels, veins) of the cerebral circulation where changes in cerebrovascular resistance take place, as the changes in cerebral blood flow induced by L-NAME reflect the effects on the cerebral circulation as a whole. Also, because we do not consider outflow (venous) pressure, an error probably exists in our calculations of cerebrovascular resistance. However, this error should be small since in two animals we did not find appreciable changes in intracranial pressure during the experiments. In addition, it is accepted that changes in cerebrovascular resistance occur mainly in the arterial side when vasoactive stimuli are applied and that changes in cerebral venous caliber affect cerebral blood volume rather than cerebral blood flow (Auer & MacKenzie, 1984). Second, in the goat an arterial rete (carotid rete mirabile) is interposed between the internal maxillary artery and the circle of Willis. Thus, the changes in cerebral blood flow after L-NAME could reflect the overall effects of this substance on nitric oxide synthesis in retial and cerebral vessels. In our laboratory we have observed (unpublished observations) that the i.v. administration of L-NAME also reduces resting blood flow in the middle cerebral artery, thus suggesting that nitric oxide produces a vasodilator tone in cerebral vessels under basal conditions. Therefore, the reduction in cerebral blood flow observed in the present study after L-NAME could be due, at least in part, to the reduction of nitric oxide production in the cerebral vasculature. Retial vessels, however, could also contribute to these effects and this should be taken into account. The last point is related to the interpretation of the increase in cerebrovascular resistance after L-NAME. One could argue that the increase in cerebrovascular resistance represents an intrinsic vascular response to the simultaneous hypertension. However, if this were the case, cerebral blood flow probably would remain at the same level as before the raise in arterial pressure. On the other hand, if the intrinsic vascular response were disturbed, then one would expect an increase and not a decrease in cerebral blood flow. Therefore, although we cannot exclude the possibility that part of the increase in cerebrovascular resistance may be due to an intrinsic cerebrovascular response to hypertension after L-NAME, the decrease in cerebral blood flow found in the present study is not.

With regard to the site(s) of the cerebral circulation where synthesis of nitric oxide takes place, experimental data show the cerebral microvessels do not release (Kontos *et al.*, 1988) or release a minimal amount (Rosenblum, 1986) of nitric oxide, and that basal production of this substance seems to be dependent on cerebral vessels size, being greater in large than in small arteries (Faraci, 1991). Also, although the endothelium appears to be a main source of nitric oxide, other sources of this vasodilator such as cerebral arterial nerves (Bredt *et al.*, 1990) and cerebrovascular musculature (Katusic, 1991) seem also to exist. Thus, the reduction in cerebral blood flow by L-NAME in our study could be due to inhibition of nitric oxide production in the different sources of formation, the importance of which we cannot determine. The reduction in brain metabolism during L-NAME treatment might also be involved in the observed changes in cerebral blood flow.

In evaluating the effects of the vasodilators acetylcholine, sodium nitroprusside and diazoxide on cerebral circulation before and after L-NAME administration, the fact that basal haemodynamic conditions before and after L-NAME are different, should be taken into account as this might influence the subsequent responses to vasodilators. In Figure 3 we present the values for cerebrovascular resistance obtained before and after the vasodilators used, and the cerebrovascular responses to these vasodilators can be evaluated as follows: (1) by expressing the changes in cerebrovascular resistance as a percentage of the immediately preceding basal resistance; this approach could be questionable when changes in vascular resistance are analysed, as it could lead to underestimation of the effects of the vasodilators during L-NAME administration, when vascular resistance is higher than under control conditions; (2) by expressing the changes as the level of resistance reached after each dose of the vasodilators, and (3) by expressing the response as the resistance changes in absolute values induced by vasodilators from the preceding basal resistance level before and after L-NAME. When the second approach (levels of resistance reached) is considered, the comparison before and after L-NAME could present a problem as cerebrovascular resistance is considerably higher after L-NAME. In this case, it may be reasonable to expect that the cerebrovascular resistance reached after vasodilators frequently will remain more elevated after than before L-NAME, and it would not mean necessarily that vasodilator responses were lower after L-

NAME. The third approach considered could be the least dependent on the preceding basal resistance level of the three approaches. In addition, it seems that increases in arterial pressure would not, necessarily, enhance the response to vasodilator agents (Gardiner *et al.*, 1991b). Thus, evaluation of reductions in cerebrovascular resistance from resting levels in absolute values as in Figure 3 may be a more appropriate approach to analyse specific interactions between the effects of L-NAME and of vasodilators. Using this approach we found that absolute reductions in cerebrovascular resistance induced by diazoxide were comparable before and after L-NAME, indicating that effects of this vasodilator are not affected by the basal cerebrovascular resistance, and suggesting that cerebral vasodilatation by diazoxide is not related to nitric oxide. Diazoxide, a benzothiadiazine derivative, seems to produce relaxation of the vascular smooth muscle by hyperpolarizing arterial smooth muscle cells through activation of ATP-sensitive K^+ channels (Standen *et al.*, 1989). The results with acetylcholine and sodium nitroprusside, however, differed from those with diazoxide. The reduction of resistance caused by lower doses, but not by the highest dose, of acetylcholine were attenuated after L-NAME, suggesting that at least a component of the cerebral vasodilatation to acetylcholine is mediated by nitric oxide. This suggestion agrees with that previously proposed by others (Fujiwara *et al.*, 1986; Faraci, 1990; Fischer-Nakielski *et al.*, 1990; Rosenblum *et al.*, 1990). Although basal release of nitric oxide in the cerebral circulation could be greater in large arteries than in small vessels, the role of nitric oxide in mediating responses to acetylcholine in the cerebral circulation seems to be similar in large arteries and the microcirculation (Faraci, 1991). However, other factors distinct to the L-arginine-nitric oxide pathway could be involved because in the present study, L-NAME did not affect the cerebral vasodilatation to the highest dose of acetylcholine used. This feature has also been observed by recording internal carotid blood flow of rats, where L-NAME reduced the effects of lower, but not of higher dose, of acetylcholine (Gardiner *et al.*, 1991b). Our data also indicate that the duration of the changes in reactivity of the cerebral circulation to acetylcholine was shorter than that of the changes in cerebral blood flow after L-NAME. Thus after inhibition of nitric oxide synthesis, the ability of cerebral blood vessels to release nitric oxide upon stimulation appears to normalize more quickly than the capacity for nitric oxide release under basal conditions.

The reductions in cerebrovascular resistance induced by sodium nitroprusside were increased during and at 24 h, and normalized at 48 h, after L-NAME treatment suggesting that cerebral vasodilatation to sodium nitroprusside is increased after inhibition of nitric oxide synthesis. Sodium nitroprusside, a nitrous compound used as a donor of exogenous nitric oxide, produces vasodilatation in a similar way to nitric oxide (Ignarro, 1990), and enhanced vasorelaxant responses to sodium nitroprusside and other nitrous compounds have been found in the absence of a functional endothelium or in the presence of L-arginine analogues (Shirasaki & Su, 1985; Lüscher *et al.*, 1989; Moncada *et al.*, 1991b; García *et al.*, 1992). This enhanced response has been related to an increased sensitivity of guanylate cyclase in vascular smooth muscle to exogenous nitric oxide when endogenous nitric oxide production is reduced (Gardiner *et al.*, 1991b; Moncada *et al.*, 1991b). Thus, it appears that the removal of endogenous nitric oxide in the vasculature could lead to supersensitivity to vasodilators that act by stimulating soluble guanylate cyclase (Gardiner *et al.*, 1991b; Moncada *et al.*, 1991b) and this phenomenon could also occur in the cerebral circulation of the unanaesthetized animals as suggested from our study. We also observed that supersensitivity of cerebral vasculature to sodium nitroprusside remained for a shorter period than that required for the cerebral blood flow to recover.

In conclusion, the present study performed in the conscious goat suggests that endogenous nitric oxide plays an important role in regulating cerebral blood flow by producing a basal vasodilator tone in the cerebral circulation under normal conditions. It also suggests that the cerebral vasodilatation to acetylcholine is mediated, at least in part, by nitric oxide release, and that inhibition of endogenous nitric oxide production induces supersensitivity of cerebral vasculature to nitrovasodilators.

The authors are grateful to H. Fernández-Lomana and E. Martínez for technical assistance.

This work was supported, in part, by FIS (92/0289), DGICYT (PM 91/0020) and CAM (C 109/91).

References

AISAKA, K., GROSS, S.S., GRIFFITH, O.W. & LEVI, R. (1989). N^G-methylarginine, an inhibitor of endothelium-derived nitric oxide synthesis, is a potent pressor agent in the guinea pig: does nitric oxide regulate blood pressure in vivo? *Biochem. Biophys. Res. Commun.*, **160**, 881–886.

AUER, L.M. & MACKENZIE, E.T. (1984). Physiology of the cerebral venous system. In *The Cerebral Venous System and Its Disorders*. ed. Kapp, J.P. & Shmidek, H.M. pp. 169–227. New York: Grune & Stratton.

BREDT, D.S., HWANG, P.M. & SNYDER, S.H. (1990). Localization of nitric oxide synthase indicating a neural role for nitric oxide. *Nature*, **347**, 768–770.

DANIEL, P.M., DAWES, J.D.K. & PRICHARD, M.M.L. (1953). Studies of the carotid rete and its associated arteries. *Phil. Trans. R. Soc. B. Biol. Sci.*, **273**, 173–208.

DU, Z.-Y., DUSTING, G.J. & WOODMAN, O.L. (1992). Baroreceptor reflexes and vascular reactivity during inhibition of nitric oxide synthesis in conscious rabbits. *Eur. J. Pharmacol.*, **214**, 21–26.

FARACI, F.M. (1990). Role of nitric oxide in regulation of basilar artery tone in vivo. *Am. J. Physiol.*, **259**, H1216–H1221.

FARACI, F.M. (1991). Role of endothelium-derived relaxing factor in cerebral circulation: large arteries vs. microcirculation. *Am. J. Physiol.*, **261**, H1038–1042.

FARACI, F.M. & HEISTAD, D.D. (1992). Does basal production of nitric oxide contribute to regulation of brain-fluid balance? *Am. J. Physiol.*, **262**, H340–H344.

FISCHER-NAKIELSKI, H. & SCHRÖR, K. (1990). Nitric oxide is the endothelium-derived relaxing factor in bovine pial arterioles. *Stroke*, **21**, IV-46–IV-48.

FUJIWARA, S., KASSELL, N.F., SASAKI, T., NAKAGOMI, T. & LEHMAN, R.M. (1986). Selective hemoglobin inhibition of endothelium-dependent vasodilation of rabbit basilar artery. *J. Neurosurg.*, **64**, 445–452.

GARCÍA, J.L., FERNÁNDEZ, N., GARCÍA-VILLALÓN, A.L., MONGE, L., GÓMEZ, B. & DIÉGUEZ, G. (1992). Effects of nitric oxide synthesis inhibition on the goat coronary circulation under basal conditions and after vasodilator stimulation. *Br. J. Pharmacol.*, **106**, 563–567.

GARCÍA, J.L., GÓMEZ, B., MONGE, L., GARCÍA-VILLALÓN, A.L. & DIÉGUEZ, G. (1991). Endothelin action on cerebral circulation in unanesthetized goats. *Am. J. Physiol.*, **261**, R581-R587.

GARDINER, S.M., COMPTON, A.M., BENNETT, T., PALMER, R.M.J. & MONCADA, S. (1990). Control of regional blood flow by endothelium-derived nitric oxide. *Hypertension*, **15**, 486–492.

GARDINER, S.M., COMPTON, A.M., KEMP, P.A. & BENNETT, T. (1991a). Effects of N^G-nitro-L-arginine methyl ester or indomethacin on differential regional and cardiac haemodynamic actions of arginine vasopressin and lysine vasopressin in conscious rats. *Br. J. Pharmacol.*, **102**, 65–72.

GARDINER, S.M., KEMP, P.A. & BENNETT, T. (1991b). Effects of N^G-nitro-L-arginine methyl ester on vasodilator responses to acetylcholine, 5'-N-ethylcarboxamidoadenosine or salbutamol in conscious rats. *Br. J. Pharmacol.*, **103**, 1725–1732.

GÓMEZ, B., VALLEJO, A.R., ALBORCH, E., DIÉGUEZ, G. & LLUCH, A. (1977). Cerebral blood flow during hemorrhagic hypotension in the unanesthetized goat. *Stroke*, **4**, 50–56.

IADECOLA, C. (1992). Does nitric oxide mediate the increases in cerebral blood flow elicited by hypercapnia? *Proc. Natl. Acad. Sci. U.S.A.*, **89**, 3913–3916.

IGNARRO, L.J. (1990). Biosynthesis and metabolism of endothelium-derived nitric oxide. *Annu. Rev. Pharmacol. Toxicol.*, **30**, 535–560.

KATUSIC, Z.S. (1991). Basal activity of L-arginine nitric oxide pathway in smooth muscle cells of canine basilar artery (Abstract). *FASEB J.*, **5**, A399.

KONTOS, H.A., WEI, E.P. & MARSHALL, J.J. (1988). In vivo bioassay of endothelium-derived relaxing factor. *Am. J. Physiol.*, **255**, H1259–H1262.

KOVÁCH, R.G.B., SZABÓ, C., BENYÓ, Z., CSÁKI, C., GREENBERG, J.H. & REIVICH, M. (1992). Effects of N^G-nitro-L-arginine and L-arginine on regional cerebral blood flow in the cat. *J. Physiol.*, **449**, 183–196.

KOZNIEWSKA, E., OSEKA, M. & STYS, T. (1992). Effects of endothelium-derived nitric oxide on cerebral circulation during normoxia and hypoxia in the rat. *J. Cereb. Blood Flow Metab.*, **12**, 311–317.

LLUCH, S., GÓMEZ, B., ALBORCH, E. & URQUILLA, P.R. (1975). Adrenergic mechanisms in cerebral circulation of the goat. *Am. J. Physiol.*, **228**, 985–989.

LÜSCHER, T.F., RICHARD, V. & YANG, Z. (1989). Interaction between endothelium-derived nitric oxide and SIN-1 in human and porcine blood vessels. *J. Cardiovasc. Pharmacol.*, **14**, Suppl. 11, S76–S80.

MARTIN, W., FURCHGOTT, R.F., VILLANI, G.M. & JOTHIANANDAN, D. (1986). Depression of contractile responses in rat aorta by spontaneously released endothelium-derived relaxing factor. *J. Pharmacol. Exp. Ther.*, **237**, 529–538.

MILETICH, D.J., IVANKOVIC, A.D., ALBRECH, R.F. & TOYOOKA, E.T. (1975). Cerebral hemodynamics following internal maxillary artery ligation in the goat. *J. Appl. Physiol.*, **38**, 942–945.

MONCADA, S. & HIGGS, E.A. (1990). *Nitric Oxide from L-Arginine: A Bioregulatory System*. Amsterdam: Excerpta Medica.

MONCADA, S., PALMER, R.M.J. & HIGGS, E.A. (1991a). Nitric oxide: physiology, pathophysiology, and pharmacology. *Pharmacol. Rev.*, **43**, 109–142.

MONCADA, S., REES, D.D., SCHULZ, R. & PALMER, R.M.J. (1991b). Development and mechanism of a specific supersensitivity to nitrovasodilators after inhibition of vascular nitric oxide synthesis in vivo. *Proc. Natl. Acad. Sci. U.S.A.*, **88**, 2166–2170.

MOORE, P.K., AL-SWAYEH, O.A., CHONG, N.W.S., EVANS, R.A. & GIBSON, A. (1990). L-N^G-nitro arginine (L-NOARG), a novel L-arginine-reversible inhibitor of endothelium-dependent vasodilatation in vitro. *Br. J. Pharmacol.*, **99**, 408–412.

MOORE, P.K., OLUYOMI, A.O., BABBEDGE, R.C., WALLACE, P. & HART, S.L. (1991). L-N^G-nitro arginine methyl ester exhibits antinociceptive activity in the mouse. *Br. J. Pharmacol.*, **102**, 198–202.

PELLIGRINO, D.A., MILETICH, D.J. & ALBRECHT, R.F. (1992). Diminished muscarinic receptor-mediated cerebral blood flow response in streptozotocin-treated rats. *Am. J. Physiol.*, **262**, E447–E454.

REES, D.D., PALMER, R.M.J., HODSON, H.F. & MONCADA, S. (1989a). A specific inhibitor of nitric oxide formation from L-arginine attenuates endothelium-dependent relaxation., *Br. J. Pharmacol.*, **96**, 418–424.

REES, D.D., PALMER, R.M.J. & MONCADA, S. (1989b). Role of endothelium-derived nitric oxide in the regulation of blood pressure. *Proc. Natl. Acad. Sci. U.S.A.*, **86**, 3375–3378.

REES, D.D., PALMER, R.M.J., SCHULZ, R., HODSON, H.R. & MONCADA, S. (1990). Characterization of three inhibitors of endothelial nitric oxide synthase *in vitro* and *in vivo*. *Br. J. Pharmacol.*, **101**, 746–752.

REIMANN, C., LLUCH, S. & GLICK, G. (1972). Development and evaluation of an experimental model for the study of the cerebral circulation in the unanesthetized goat. *Stroke*, **3**, 322–328.

ROSENBLUM, W.I. (1986). Endothelial dependent relaxation demonstrated in vivo in cerebral arterioles. *Stroke*, **17**, 494–497.

ROSENBLUM, W.I., NISHIMURA, H. & NELSON, G.H. (1990). Endothelium-dependent L-Arg- and L-NAME-sensitive mechanisms regulate tone of brain microvessels. *Am. J. Physiol.*, **259**, H1396–H1401.

SHIRASAKI, Y. & SU, C. (1985). Endothelium removal augments vasodilation by sodium nitroprusside and sodium nitrite. *Eur. J. Pharmacol.*, **114**, 93–96.

STANDEN, N.B., QUAYLE, J.M., DAVIS, N.W., BRAYDEN, J.E., HUANG, Y. & NELSON, M.T. (1989). Hyperpolarizing vasodilators activate ATP-sensitive K^+ channels in arterial smooth muscle. *Science*, **245**, 177–180.

WANG, Y.-X. & PANG, C.C.Y. (1991). Possible dependence of pressor and heart rate effects of N^G-nitro-L-arginine on autonomic nerve activity. *Br. J. Pharmacol.*, **103**, 2004–2008.

WIDOPP, R.E., GARDINER, S.M., KEMP, P.A. & BENNET, T. (1992). The influence of atropine and atenolol on the cardiac haemodynamic effects of N^G-nitro-L-arginine methyl ester in conscious, Long Evans rats. *Br. J. Pharmacol.*, **105**, 653–656.

(Received November 12, 1992
Revised April 5, 1993
Accepted May 4, 1993)

Br. J. Pharmacol. (1993), **110**, 435–441

Endothelin-1 (ET-1)-induced contraction in rat isolated trachea: involvement of ET_A and ET_B receptors and multiple signal transduction systems

Peter J. Henry

Department of Pharmacology, University of Western Australia, Nedlands, 6009, Australia

1 Quantitative autoradiographic, biochemical and functional studies were performed to investigate the endothelin receptor subtypes and signal transduction systems that mediate endothelin-1 (ET-1)-induced contraction in rat isolated tracheal smooth muscle.

2 Specific binding of 0.5 nM [^{125}I]-ET-1 to tracheal smooth muscle was inhibited by at least 40% in the presence of either the ET_A receptor selective ligand BQ-123 (1 μM) or the ET_B receptor-selective ligand sarafotoxin S6c (30 nM), indicating the presence of both ET_A and ET_B receptors in this tissue.

3 ET-1 and sarafotoxin S6c were both potent spasmogens of rat isolated tracheal smooth muscle preparations. Sarafotoxin S6c-induced contractions were unaffected in the presence of the ET_A receptor antagonist BQ-123 (10 μM), but were markedly attenuated in tissue previously exposed to 100 nM sarafotoxin S6c to induce ET_B receptor desensitization. ET-1-induced contractions were, at most, only partially attenuated either by blocking the ET_A receptor-effector system (with 10 μM BQ-123) or by desensitizing the ET_B receptor-effector system with sarafotoxin S6c. However, ET-1-induced contractions were markedly attenuated by blocking both receptor-effector systems simultaneously. These findings suggest that ET-1 could induce contraction by stimulating either ET_A or ET_B receptors.

4 ET-1 (10 μM) induced a 7 fold increase in intracellular [^{3}H]-inositol phosphate accumulation over basal levels in rat isolated tracheal smooth muscle. In contrast, sarafotoxin S6c (2.5 μM) increased intracellular [^{3}H]-inositol phosphate accumulation by only 2 fold. ET-1-induced accumulation of [^{3}H]-inositol phosphates was abolished by 10 μM BQ-123.

5 In Ca^{2+}-free Krebs bicarbonate solution, 100 nM ET-1 induced a significantly larger contraction than that induced by 100 nM sarafotoxin S6c (46.6 ± 5.6% C_{max} versus 8.8 ± 2.8% C_{max}, $n = 5-7$). This presumed intracellular Ca^{2+}-dependent phase of contraction induced by ET-1 was significantly inhibited by 10 μM BQ-123 (7.5 ± 1.0% C_{max}). Subsequent addition of 2.5 mM Ca^{2+} induced a second phase of contraction. The extracellular Ca^{2+}-dependent phase of contraction induced by ET-1 was similar in magnitude to that induced by sarafotoxin S6c (63.6 ± 4.5% C_{max} versus 58.0 ± 3.7% C_{max}) and was not inhibited by BQ-123. Sarafotoxin S6c-induced contractions were not inhibited by the L-type Ca^{2+}-channel antagonists, nicardipine or verapamil.

6 In summary, ET_A and ET_B receptors coexist in rat isolated tracheal smooth muscle and stimulation of both receptor subtypes contributes to ET-1-induced contraction in this tissue. However, stimulation of these receptor subtypes appears to induce contraction by activating different second messenger pathways; ET_A receptor stimulation induces phosphoinositide turnover and subsequent release of intracellular Ca^{2+} whereas stimulation of ET_B receptors facilitates the influx of extracellular Ca^{2+}.

Keywords: Endothelin-1; endothelin receptors; BQ-123; sarafotoxin S6c; airway smooth muscle; inositol phosphates; calcium

Introduction

Endothelin-1 (ET-1) is a potent spasmogen of airway smooth muscle (Uchida *et al.*, 1988; Henry *et al.*, 1990; Hay, 1992). The mechanism of action of ET-1-induced contraction has not been fully elucidated, but the initial step involves the activation of specific receptors for endothelin located on the plasma membrane of the airway smooth muscle cells (Mattoli *et al.*, 1990; 1991). Recent studies in a variety of cells and tissues have provided evidence for the existence of two distinct endothelin receptors, designated ET_A and ET_B. Whereas ET-1 has a similar affinity for both receptor subtypes, several recently developed compounds show selectivity for ET_A or ET_B receptors. For example, the ET receptor antagonist BQ-123 is a cyclic pentapeptide [cyclo(D-Trp,D-Asp,L-Pro,D-Val, L-Leu)] that shows a 33,000 fold selectivity for binding to ET_A receptors (Ihara *et al.*, 1992a; Molenaar *et al.*, 1992; 1993). On the other hand, sarafotoxin S6c, [Ala^{1,3,11,15}]ET-1 and BQ3020 are agonists that selectively stimulate ET_B receptors (Williams *et al.*, 1991; Saeki *et al.*, 1991; Ihara *et al.*, 1992b). Using this approach, Hay (1992) has recently shown that ET-1-induced contraction in guinea-pig bronchus is predominantly mediated via activation of the ET_B receptor subtype.

Stimulation of ET receptors in airway smooth muscle activates several signal transduction pathways which may lead to the mobilization of intracellular Ca^{2+} and also the influx of extracellular Ca^{2+} (Mattoli *et al.*, 1991). Both of these pathways may contribute to ET-1-induced contraction. ET-1-induced mobilization of intracellular Ca^{2+} occurs via a cascade of events including the stimulation of phospholipase C and the generation of the inositol 1,4,5-triphosphate, which induces the release of Ca^{2+} from the sarcoplasmic reticulum into the cell cytosol (Mattoli *et al.*, 1991; Henry *et al.*, 1992). ET-1-induced entry of extracellular Ca^{2+} into airway smooth muscle cells is poorly understood, but appears to occur primarily through receptor-operated rather than voltage-dependent Ca^{2+} channels (Hay, 1990; Ninomiya *et al.*, 1992). Although it is likely that ET-1-induced contraction of airway smooth muscle uses intracellular and extracellular Ca^{2+}, it is not known whether both of these effects are mediated via a single endothelin receptor subtype.

In the current study, selective ligands of ET_A and ET_B receptors were used in a series of functional, biochemical and autoradiographic studies designed to investigate the mechan-

ism of ET-1-induced contraction in rat isolated tracheal smooth muscle. Results indicate that ET_A and ET_B receptors coexist within rat isolated tracheal smooth muscle and that these receptor subtypes mediate ET-1-induced contractions by activating different signal transduction pathways.

Methods

Autoradiography

Autoradiographs of [^{125}I]-ET-1 binding to rat tracheal sections were prepared as described previously (Henry *et al.*, 1990). Briefly, male Wistar rats (10–12 weeks) were stunned and killed by cervical dislocation and exsanguination. The trachea was excised and placed in Krebs bicarbonate solution (KBS). The composition of the KBS was (in mM); NaCl 117, KCl 5.36, $NaHCO_3$ 25.0, KH_2PO_4 1.03, $MgSO_4.7H_2O$ 0.57, $CaCl_2.H_2O$ 2.5 and glucose 11.1. Trachea were cleaned of adhering connective tissue, submerged in Macrodex and frozen by immersion in isopentane, quenched with liquid nitrogen. Transverse sections (10 μm) of trachea were cut at − 20°C and thaw-mounted onto gelatin-chrome alum-coated glass slides (four tracheal sections from different rats per slide). Slide-mounted tracheal sections were incubated for 60 min with 0.5 nM [^{125}I]-ET-1 in the presence and absence of the competing ligands, 1 μM BQ-123 (ET_A receptor-selective) or 30 nM sarafotoxin S6c (ET_B receptor-selective). Non-specific binding was determined in the presence of 1 μM unlabelled ET-1. Autoradiographic grain densities over the tracheal smooth muscle band were determined with an automated grain detection and counting system (Henry *et al.*, 1990). Five separate fields (4 over smooth muscle and one over a non-tissue area) were viewed from each tracheal section and duplicate slides were analysed. Thus, a total of 160 fields were analysed [(5 fields per section) × (4 rat tracheal sections per slide) × (2 slides per treatment) × (4 treatments)]. Autoradiographic densities were expressed as grains per 1000 μm^2.

Functional studies using tracheal segments

Trachea were excised and cleaned as described above. Six to eight ring segments (2 mm long) were obtained from each trachea and denuded of epithelium (Goldie *et al.*, 1986). Tracheal segments were suspended under a resting tension of 500 mg and placed in organ baths containing 3 ml of KBS at 37°C, bubbled continuously with 5% CO_2 in O_2. Changes in isometric tension were recorded via FT03 force-displacement transducers (Grass Instruments). Tracheal segments were allowed to equilibrate for 45 min before exposure to the cumulative addition of 0.3 and 10 μM carbachol. Upon reaching contraction plateaus the preparations were washed in drug-free KBS for 15 min. Concentration-effect curves were constructed to ET-1 and sarafotoxin S6c in the presence and absence of the ET_A receptor antagonist BQ-123, and various Ca^{2+}-channel inhibitors (nicardipine and verapamil). In these experiments, preparations were exposed for 20 min to one of these agents or its solvent (paired control preparation) and then to cumulative additions (0.5 log-concentration increments) of ET-1 or sarafotoxin S6c (1 nM to 300 nM). Only one concentration-effect curve was constructed from each preparation. ET-1- and sarafotoxin S6c-induced contractions were plotted as a percentage of the initial contraction induced by 10 μM carbachol (C_{max}). The concentration of ET-1 and sarafotoxin S6c that produced 50% C_{max} was estimated by fitting the concentration-effect curve to a logistic function by computer-assisted non-linear least squares regression analysis.

In some experiments, preparations were exposed to 100 nM sarafotoxin S6c for 45 min to desensitize the ET_B receptor-effector system (for protocol see also Figure 3a). Following this desensitizing period, preparations were washed five times over a 10 min period and rested for a further 20 min. Some preparations were incubated with 10 μM BQ-123 during this 20 min rest period and for the remainder of the experiment. Preparations were then exposed to either 100 nM ET-1 or 100 nM sarafotoxin S6c and contractile responses measured.

The relative contribution of intracellular and extracellular Ca^{2+} to the contractions induced by ET-1 and sarafotoxin S6c were determined in the following manner (see also Figure 4a). Firstly, extracellular Ca^{2+} was removed by washing the preparations four times (over a 5 min period) with Ca^{2+}-free KBS containing 10 μM EGTA and then for 20 min with Ca^{2+}-free KBS (no EGTA). The preparations were then exposed to either 100 nM ET-1 or 100 nM sarafotoxin S6c, and contractile responses measured. The first phase of contraction, obtained in the absence of extracellular Ca^{2+}, is presumed to be due to the release of intracellular Ca^{2+} (Shimamoto *et al.*, 1992). When the peptide-induced contraction had reached its plateau, calcium chloride was added to the Ca^{2+}-free KBS at a final concentration of 2.5 mM and a second phase of contraction was observed. This response is due to the influx of extracellular Ca^{2+}. In some additional studies, the influence of BQ-123 on the intracellular and extracellular Ca^{2+}-dependent phases of ET-1 and sarafotoxin S6c-induced contractions was determined. In these experiments, preparations were exposed to 10 μM BQ-123 at the beginning of the 20 min equilibration period in Ca^{2+}-free KBS and for the remainder of the experiment.

[^{3}H]-inositol phosphate generation

ET-1- and sarafotoxin S6c-induced generation of inositol phosphates in rat tracheal smooth muscle was determined as described previously (Henry *et al.*, 1992). Briefly, the tracheal smooth muscle band, which lies between the cartilage horns along the posterior membrane of the trachea was dissected from the trachea and cut transversely into 4 pieces of equivalent size. The tracheal smooth muscle pieces from 7 rats were pooled and randomly divided into 14 groups. Each tissue group was weighed, preincubated for 30 min in 5 ml of KBS at 37°C and then incubated with [^{3}H]-*myo*-inositol (5 μCi) in 1 ml of carbogen-aerated KBS for 3 h at 37°C with gentle shaking. Tissues were washed twice with 5 ml KBS for 15 min to remove excess [^{3}H]-*myo*-inositol and a third time for a further 15 min. After washing, the tissues were incubated for a further 15 min in 1 ml KBS containing 5 mM LiCl to inhibit the breakdown of inositol monophosphate to inositol and thus enhance the accumulation of inositol phosphates. The tissues were stimulated for 15 min by the addition of 20 μl ET-1 (10 nM to 10 μM) or sarafotoxin S6c (100 nM to 2.5 μM) and the stimulation terminated by the addition of 1.5 ml chloroform:methanol (1:2, v/v) with vigorous shaking. After standing for 15 min, chloroform (0.5 ml) and water (0.5 ml) were added sequentially. The entire upper methanol/water phase was applied to an anion exchange chromatography column (1 ml of Dowex AG1-X8 in formate form). Inositol was eluted with 10 ml of water and glycerophosphoinositol with 15 ml of a buffer containing 5 mM sodium tetraborate and 60 mM sodium formate. [^{3}H]-inositol phosphates were eluted with a buffer containing 0.1 mM formic acid and 0.75 M ammonium formate. Three 1 ml aliquots of the final fraction were mixed with 10 ml of scintillant (5.8 g l^{-1}, 2,5-diphenyloxazol (PPO) in Triton × 10:toluene, 1:2) and radioactivity counted in a Tricarb liquid scintillation counter (Packard, Model 1500). Total [^{3}H]-inositol phosphate accumulation was expressed as d.p.m. mg^{-1} wet wt. tracheal smooth muscle.

Drugs

Drugs used were; [^{125}I]-ET-1, ET-1, sarafotoxin S6c, (Auspep, Melbourne, Australia), carbamylcholine chloride (±)-verapamil hydrochloride, nicardipine hydrochloride, EGTA (Sigma Chemical Company, St Louis, U.S.A.), BQ-123

(gift from Dr D.W.P. Hay of SmithKline Beecham Laboratories). Stock solutions of ET-1 and sarafotoxin S6c, both 50 μM, were prepared in 0.1 M acetic acid and dilutions made in saline. BQ-123 was prepared in 100 mM Na_2CO_3. Nicardipine hydrochloride and (±)-verapamil hydrochloride were dissolved in water. All other drugs were dissolved in saline. Drugs were kep on ice and protected from light. In Ca^{2+}-free KBS, $CaCl_2$ was omitted.

Statistical analyses

In functional studies, contractile potency is expressed in terms of the concentration of ET-1 or sarafotoxin S6c required to produce 50% of the maximal response to 10 μM carbachol (50% C_{max}). For statistical comparisons, data were transformed to mean [−log (concentration of drug producing 50% C_{max})] ± s.e.mean from n different animals. In all studies, differences between treatment means were assessed by analysis of variance followed by a modified t statistic (Wallenstein *et al.*, 1980). P values less than 0.05 were considered to be statistically significant.

Results

Autoradiographic studies

Rat isolated tracheal smooth muscle contained specific binding sites for [^{125}I]-ET-1 (total grain density, 135 ± 16 grains per 1000 μm^2, $n = 4$ versus nonspecific grain density, 12 ± 1 grains per 1000 μm^2; $n = 4$; Figures 1a and 1d). [^{125}I]-ET-1 binding was inhibited by the ET_A receptor-selective ligand BQ-123 (1 μM; 81.9 ± 8.2 grains per 1000 μm^2, 43.2% inhibition of specific grain density; Figure 1b) and by the ET_B receptor-selective ligand sarafotoxin S6c (30 nM; 84.1 ± 6.4 grains per 1000 μm^2, 41.4% inhibition of specific grain density; Figure 1c), indicating the coexistence of ET_A and ET_B receptors in rat tracheal smooth muscle.

Functional studies

Selective inhibition of ET_A and ET_B receptor function ET-1 and the ET_B receptor-selective agonist, sarafotoxin S6c, induced concentration-dependent contractions of rat isolated

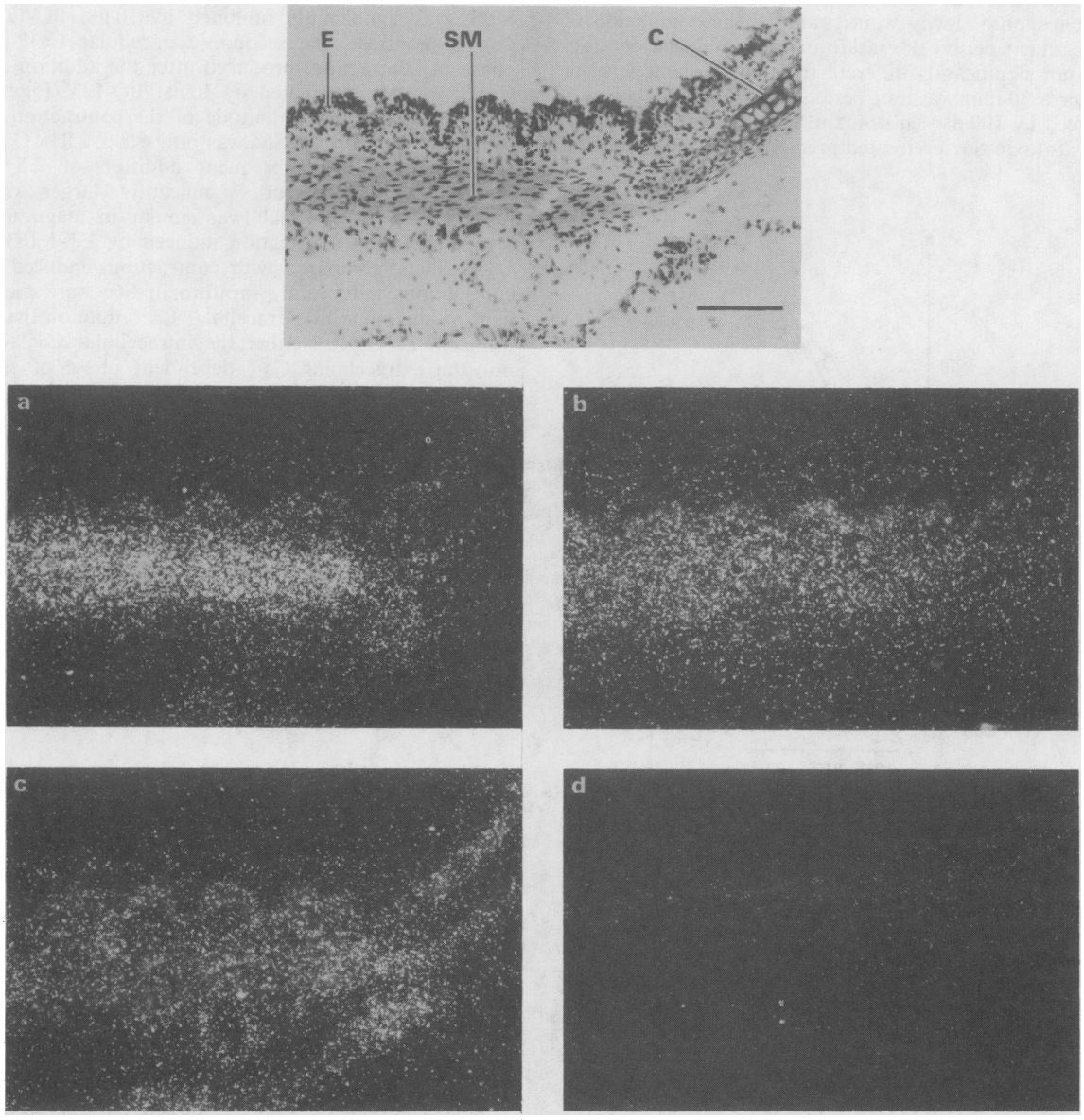

Figure 1 Density and distribution of [^{125}I]-endothelin-1 ([^{125}I]-ET-1) binding sites in rat isolated trachea. The upper panel of the montage is a lightfield photomicrograph of a transverse section of rat isolated trachea. E, epithelium; SM, smooth muscle; C, cartilage. Panel (a) is a darkfield autoradiograph of this section and depicts total [^{125}I]-ET-1 binding to rat trachea. The majority of binding sites was associated with the tracheal smooth muscle band. In serial sections, the binding of [^{125}I]-ET-1 was inhibited by both BQ-123 (1 μM, b) and sarafotoxin S6c (30 nM, c), indicating the presence of both ET_A and ET_B receptors. Panel (d) shows nonspecific binding determined in the presence of 1 μM ET-1. The calibration bar is 100 μm long.

tracheal smooth muscle (Figure 2a). Sarafotoxin S6c was slightly more potent than ET-1 (concentrations producing 50% C_{max} (95% confidence limits) were 9.7 nM (3.4–27 nM) and 18 nM (10–32 nM), respectively). However, ET-1 induced a significantly greater maximal contraction than sarafotoxin S6c. The ET_A receptor antagonist, BQ-123 (10 μM), had no significant inhibitory effect on the contractile responses induced by low concentrations of ET-1 (< 10 nM) (Figure 2b). However, contractile responses to higher concentrations of ET-1 (> 10 nM) were clearly attenuated by 10 μM BQ-123. In contrast, 10 μM BQ-123 has no inhibitory effect on contractile responses to sarafotoxin S6c (Figure 2c).

The functional experiments described above suggest that ET-1-induced contractions of rat isolated tracheal smooth muscle may involve activation of both ET_A and ET_B receptors. Further evidence for the involvement of ET_A receptors in ET-1-induced contractions was obtained from studies in which preparations were desensitized to the ET_B receptor agonist, sarafotoxin S6c (Figure 3). In these studies, rat tracheal smooth muscle preparations were pretreated for 45 min to 100 nM sarafotoxin S6c or solvent (Figure 3a). During this pretreatment period, a peak contractile response to sarafotoxin S6c was observed after 5 to 10 min. However, this peak response slowly waned and by the completion of the pretreatment period the sarafotoxin S6c-induced contraction was not significantly different from the baseline level of tone. After a 30 min washout period with KBS, the contraction induced by 100 nM sarafotoxin S6c was significantly less in the sarafotoxin S6c-pretreated preparations than in control preparations (Figure 3b). In contrast, contractions observed in response to 100 nM ET-1 were similar in control and sarafotoxin S6c-pretreated preparations. However, as shown in Figure 3c, ET-1-induced contractions were inhibited by BQ-123 to a significantly greater extent in sarafotoxin S6c-pretreated preparations than in control preparations. That is, in the presence of 10 μM BQ-123, the contraction induced by 100 nM ET-1 was reduced by 63.4 ± 8.2% C_{max} in sarafotoxin S6c-pretreated preparations, but by only 22.3 ± 8.8% C_{max} in control preparations.

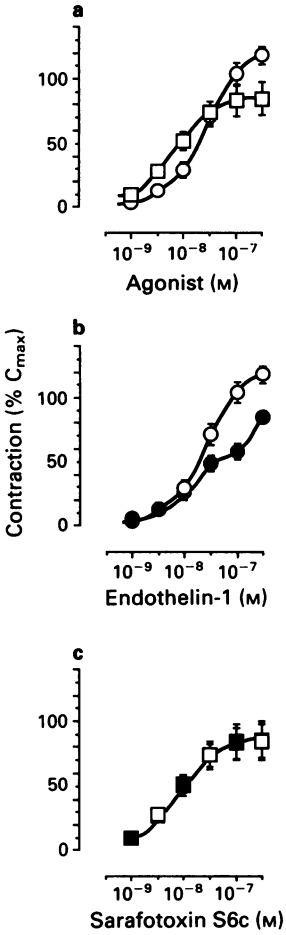

Figure 2 (a) Mean concentration-effect curves to endothelin-1 (ET-1, ○) and sarafotoxin S6c (□) in rat tracheal smooth muscle. The effects of the ET_A receptor antagonist BQ123 (10 μM, ●, ■) on contractile responses to ET-1 (○, control) and sarafotoxin S6c (□, control) are shown in (b) and (c), respectively. Shown are the mean ± s.e.mean values from 5–7 animals.

Intracellular and extracellular Ca^{2+} pools

Experiments were performed in Ca^{2+}-free KBS to examine the relative contributions that intracellular and extracellular Ca^{2+} make to contractions induced by ET-1 and sarafotoxin S6c (Figure 4a). In Ca^{2+}-free KBS, 100 nM ET-1 induced a contraction of 46.6 ± 5.6% C_{max} (Figure 4b). The subsequent addition of 2.5 mM Ca^{2+} induced a second phase of contraction of slightly greater magnitude (63.6 ± 4.5% C_{max}, Figure 4b). Thus, ET-1-induced contractions appear to use both intracellular and extracellular Ca^{2+}. The intracellular Ca^{2+}-dependent phase of contraction, produced in the Ca^{2+}-free KBS, was significantly inhibited by 10 μM BQ-123 (Figure 4b). In contrast, the second, extracellular Ca^{2+}-dependent phase of contraction, produced after the addition of 2.5 mM Ca^{2+}, was not attenuated by 10 μM BQ-123 (Figure 4b). In Ca^{2+}-free KBS, the magnitude of the contraction produced by 100 nM sarafotoxin S6c was only 8.8 ± 2.8% C_{max} (Figure 4c). However, the subsequent addition of 2.5 mM Ca^{2+} induced a second and significantly larger contraction (58.0 ± 3.7% C_{max}) which was similar in magnitude to the second phase of contraction induced by ET-1 (63.6 ± 4.5% C_{max}). Thus, compared with contractions induced by ET-1, contractions induced by sarafotoxin S6c were more dependent on the influx of extracellular Ca^{2+} than on the release of intracellular Ca^{2+}. Neither the intracellular Ca^{2+}-dependent nor the extracellular Ca^{2+}-dependent phase of sarafotoxin S6c-induced contraction was inhibited by 10 μM BQ-123 (Figure 4c). In control experiments, the magnitude of the contraction induced by the depolarizing spasmogen KCl (60 mM) in Ca^{2+}-free KBS was 12.6 ± 2.5% C_{max} and addition of 2.5 mM Ca^{2+} induced a second contraction of 83.2 ± 4.7% C_{max} ($n = 6$).

To examine further the type of plasma membrane Ca^{2+}-channels that are linked to the ET_B receptor, the influence of L-type Ca^{2+}-channel inhibitors (nicardipine and verapamil) on sarafotoxin S6c-induced contractions was investigated. Despite significant inhibitory effects on KCl-induced contractions, neither 1 μM nicardipine nor 10 μM verapamil had any significant inhibitory effects on sarafotoxin S6c-induced contractions (Figure 5).

[^{3}H]-inositol phosphate generation

ET-1 caused a concentration-dependent accumulation of [^{3}H]-inositol phosphates in rat isolated tracheal smooth muscle (Figure 6a). At the highest concentration of ET-1 used (10 μM), the mean increase in [^{3}H]-inositol phosphate accumulation was 7.03 ± 0.55 fold above basal levels. In comparison, sarafotoxin S6c was a weak stimulator of [^{3}H]-inositol phosphate accumulation and at a concentration of 2.5 μM produced a 2.05 ± 0.46 fold increase above basal levels (Figure 6a). ET-1-induced accumulation of [^{3}H]-inositol phosphates was significantly attenuated by 1 and 10 μM BQ-123 (Figure 6b). In the presence of 10 μM BQ-123, ET-1-induced accumulation of [^{3}H]-inositol phosphates (1.37 ± 0.22 fold increase, $n = 6$) was not significantly above basal levels. BQ-123 produced no significant inhibition of sarafotoxin S6c-induced [^{3}H]-inositol phosphate accumulation (Figure 6b). BQ-123 (10 μM) alone had no significant effect on basal levels of [^{3}H]-inositol phosphate accumulation (1.13 ± 0.18 fold increase, $n = 3$).

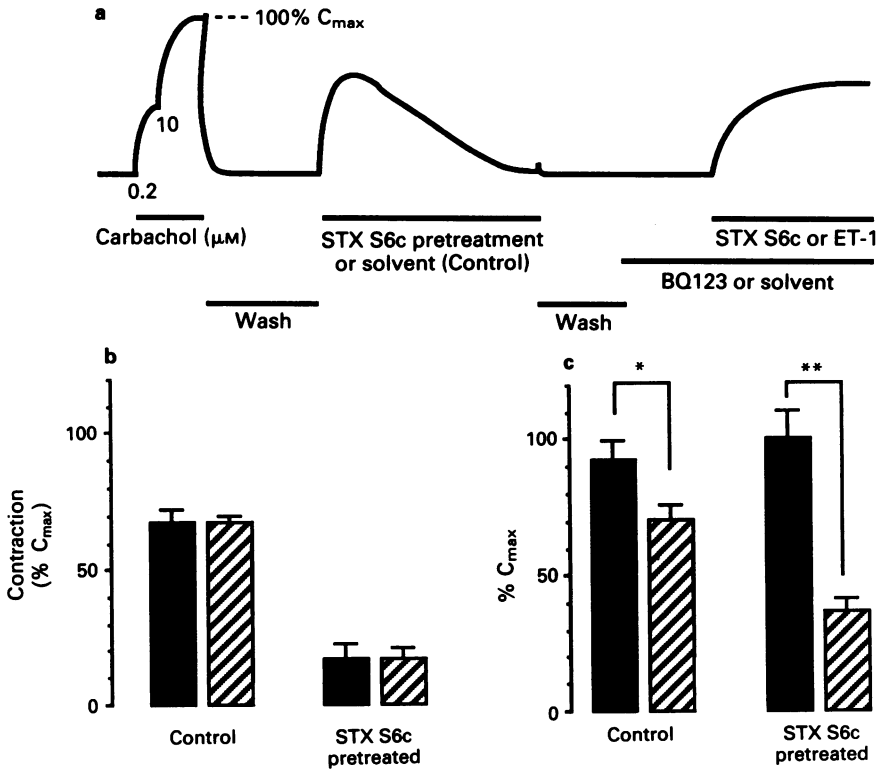

Figure 3 (a) Experimental protocol for sarafotoxin S6c (STX S6c)-desensitization studies, as described in the Methods section. (b) Contractile responses to 100 nM STX S6c in control and STX S6c-pretreated preparations (solid columns). These contractions were not inhibited by 10 μM BQ-123 (hatched columns). (c) Contractile responses to 100 nM ET-1 in control and STX S6c-pretreated preparations (solid columns). These contractions were differentially inhibited by 10 μM BQ-123 (hatched columns). Shown are the mean ± s.e.mean values from 6 animals. $*P < 0.05$; $**P < 0.01$.

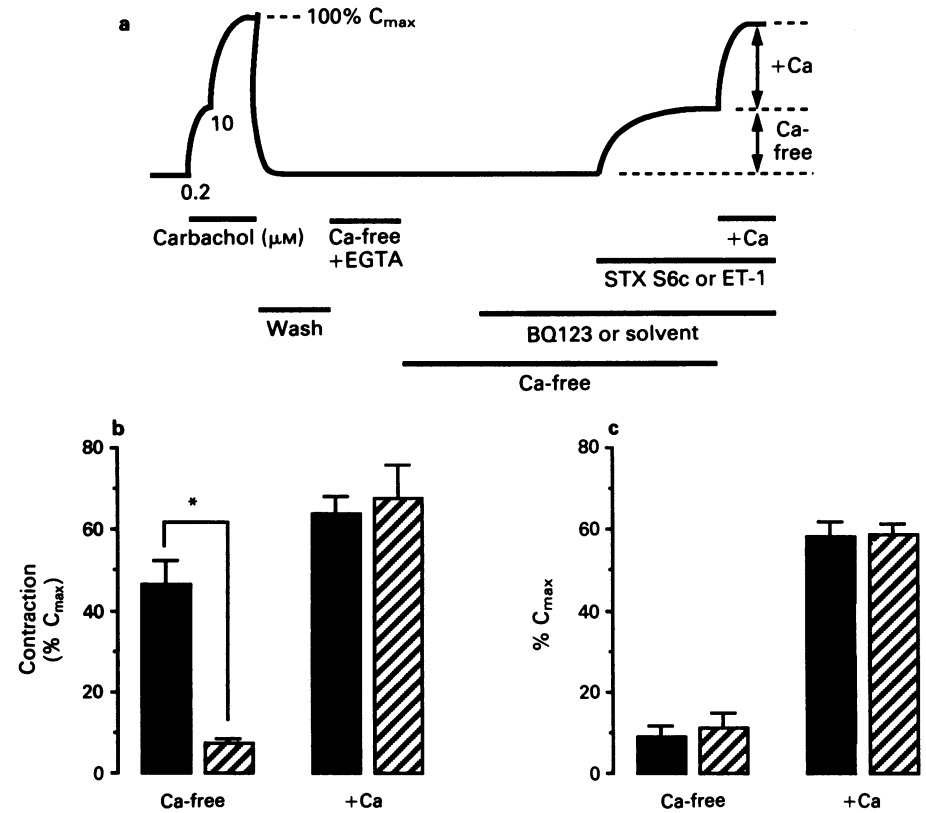

Figure 4 (a) Experimental protocol used to study the dependence of sarafotoxin S6c (STX S6c)- and endothelin-1 (ET-1)-induced contractions on intracellular and extracellular Ca^{2+}. (b) Contractions induced by 100 nM ET-1 in Ca^{2+}-free Krebs bicarbonate solution (KBS) and after the addition of 2.5 mM Ca^{2+} (solid columns). BQ-123 10 μM inhibited the contraction induced by ET-1 in Ca^{2+}-free KBS ($*P < 0.01$) but not the second phase of contraction produced by the addition of 2.5 mM Ca^{2+} (hatched columns). (c) Contractions induced by 100 nM STX S6c in Ca^{2+}-free Krebs bicarbonate solution (KBS) and after the addition of 2.5 mM Ca^{2+} (solid columns). BQ-123 had no inhibitory effect on either phase of the STX S6c-induced contraction (hatched columns). Shown are the mean ± s.e.mean values from 5–7 animals.

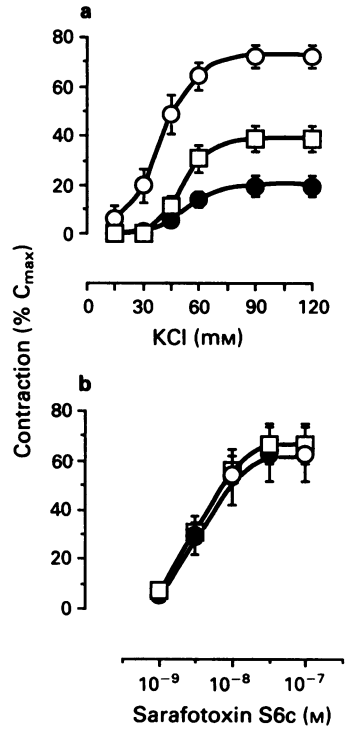

Figure 5 Mean concentration-effect curves to (a) KCl and (b) sarafotoxin S6c in the absence (○) and presence of 10 μM verapamil (●) or 1 μM nicardipine (□). Shown are the mean ± s.e.mean values from 5 animals.

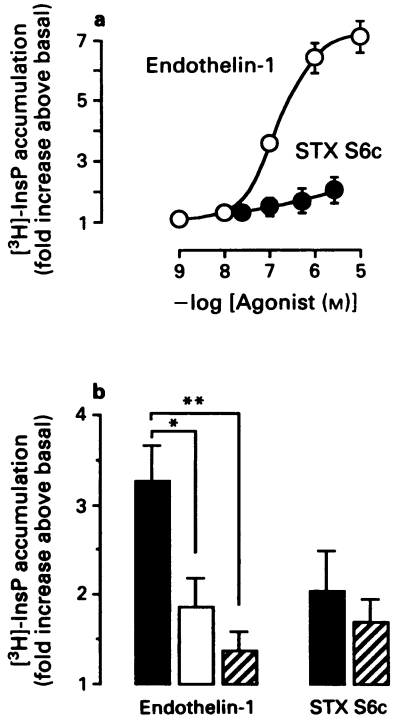

Figure 6 (a) Mean concentration-effect curves describing endothelin-1 (ET-1, ○) and sarafotoxin S6c (STX S6c, ●)-induced accumulation of [^{3}H]-inositol phosphates ([^{3}H]-InsP) in rat isolated tracheal smooth muscle. (b) [^{3}H]-inositol phosphate accumulation induced by 100 nM ET-1 (solid column) was significantly inhibited by 1 μM (open column; $*P < 0.05$) and 10 μM BQ-123 (hatched column; $**P < 0.01$). However, the small accumulation of [^{3}H]-inositol phosphates produced in the presence of 2.5 μM STX S6c (open column) was not significantly inhibited by 10 μM BQ-123 (hatched column). Shown is the mean ± s.e.mean value obtained from 3–5 experiments.

Discussion

In the current investigation, quantitative autoradiographic analyses of [^{125}I]-ET-1 binding to rat tracheal smooth muscle suggest the coexistence of ET_A and ET_B receptors in this tissue. Furthermore, isometric tension recordings indicate that ET_A and ET_B receptors are both linked to rat isolated tracheal smooth muscle contraction. However, the contractions induced following stimulation of ET_A and ET_B receptors appear to be mediated via different signal transduction systems. Functional and biochemical data from the current study suggest that stimulation of ET_A receptors is associated with the activation of phospholipase C, the generation of inositol phosphates and the release of intracellular Ca^{2+}, whereas stimulation of ET_B receptors appears to be linked to the influx of extracellular Ca^{2+}, via non-L-type Ca^{2+}-channels.

Although our group and others have previously reported the presence of high densities of binding sites for [^{125}I]-ET-1 in airway smooth muscle from many animal species including man (Turner *et al.*, 1989; Henry *et al.*, 1990; McKay *et al.*, 1991), it was not possible in these previous studies to distinguish clearly between binding to ET_A and ET_B receptors. However, with the recent introduction of highly selective ligands for ET_A and ET_B receptors it is now possible to investigate the presence of ET receptor subtypes in airway smooth muscle. In the current study, [^{125}I]-ET-1 binding to rat isolated smooth muscle was partially inhibited by an ET_A receptor-selective ligand, BQ-123 and also by an ET_B receptor-selective ligand, sarafotoxin S6c, indicating the presence of both ET_A and ET_B receptors in this tissue. These findings are in agreement with recent studies which demonstrated the presence of two endothelin receptor subtypes in guinea-pig tracheal smooth muscle (Tschirhart *et al.*, 1991) and rat lung (Cioffi *et al.*, 1992). Although from the current study it is not possible to document accurately the relative proportions of ET_A and ET_B receptors in rat tracheal smooth muscle, both subtypes clearly coexist in this tissue.

This study also indicates that both ET_A and ET_B receptors were functionally linked to the generation of tracheal smooth muscle contraction. The findings that ET-1 and the ET_B receptor-selective agonist, sarafotoxin S6c, were both potent spasmogens, either in the presence or absence of the ET_A receptor antagonist, BQ-123, was a clear indication of a functional link between ET_B receptor stimulation and smooth muscle contraction in rat isolated tracheal smooth muscle. These data are consistent with recent studies using sarafotoxin S6c in guinea-pig isolated bronchi (Hay, 1992). Furthermore, evidence for a functional link between ET_A receptor stimulation and smooth muscle contraction was provided by the findings that ET-1-induced contractions were partially inhibited by the ET_A receptor antagonist, BQ-123. Although neither a selective ET_A receptor agonist nor a selective ET_B receptor antagonist was available for the present study, further evidence that the ET_A receptor was linked to contraction was obtained from a series of desensitization studies. In these experiments, smooth muscle preparations were pretreated for 45 min with 100 nM sarafotoxin S6c to desensitize selectively the ET_B receptor-effector system. Desensitization was confirmed by the very low spasmogenic activity of subsequently administered sarafotoxin S6c in these preparations. In contrast, the spasmogenic activity of ET-1, which stimulates both ET_A and ET_B receptors, was not significantly attenuated by ET_B receptor desensitization. The additional findings that ET-1-induced contractions observed in these sarafotoxin S6c desensitized preparations were markedly attenuated by BQ-123 provides further confirmatory evidence that ET_A receptors were predominantly mediating these ET-1-induced contractions.

The findings that ET-1-induced contractions in rat tracheal smooth muscle can be mediated by the ET_A receptors is consistent with the preliminary *in vitro* and *in vivo* studies on allergic sheep (Noguchi *et al.*, 1992). Thus, in some species

such as sheep, ET-1-induced contractions of airway smooth muscle appear to be mediated primarily via the stimulation of ET_A receptors (Noguchi *et al.*, 1992), but in other species including the guinea-pig, via the stimulation of ET_B receptors (Hay, 1992). Functional studies performed in the current investigation indicate that ET-1-induced contractions in rat isolated tracheal smooth muscle can be induced by stimulating either ET_A or ET_B receptors.

Although stimulation of either ET_A or ET_B receptors will produce smooth muscle contraction in rat trachea, the results of the current study suggest that these receptor subtypes are coupled to different signal transduction systems. Several lines of evidence suggest that ET_A receptors are coupled to phosphoinositide turnover and the release of Ca^{2+} from intracellular stores. Firstly, ET-1, but not the ET_B receptor-selective agonist sarafotoxin S6c, induced marked accumulation of [^{3}H]-inositol phosphates in rat tracheal smooth muscle. Secondly, ET-1-induced accumulation of [^{3}H]-inositol phosphates was inhibited by the ET_A receptor antagonist, BQ-123. Thirdly, ET-1, but not sarafotoxin S6c, induced significant smooth muscle contractions in the absence of extracellular Ca^{2+}. Fourthly, this intracellular Ca^{2+}-dependent phase of ET-1-induced contraction was inhibited by BQ-123. Furthermore, it is unlikely that ET_B receptors are linked to inositol (1,4,5)-trisphosphate-induced release of intracellular Ca^{2+} because sarafotoxin S6c was, at best, a very poor stimulant of [^{3}H]-inositol phosphate generation in this preparation. Thus, the ET_A receptor, but not the ET_B receptor appears to mediate the ET-1-induced generation of inositol phosphates and release of intracellular Ca^{2+} in rat tracheal smooth muscle.

In contrast, ET_B receptors in rat tracheal smooth muscle seem to be linked to the influx of extracellular Ca^{2+}. Thus, sarafotoxin S6c-induced contractions were almost entirely dependent upon the presence of extracellular Ca^{2+}. Conversely, the ET_A receptor was apparently not linked to the influx of extracellular Ca^{2+}, because the extracellular-Ca^{2+}-dependent phase of ET-1-induced contractions was not attenuated by BQ-123. At present it is not clear which type of Ca^{2+}-channel is linked to ET_B receptors and activated by sarafotoxin S6c. However, as sarafotoxin S6c-induced contractions were not inhibited by either verapamil or nicardipine, the ET_B receptor-linked Ca^{2+}-channel cannot be of the L-type. The results of these studies indicate that the ET_B receptor, but not the ET_A receptor, mediates ET-1 and sarafotoxin S6c-induced influx of extracellular Ca^{2+}.

In summary, ET_A and ET_B receptors coexist in rat tracheal smooth muscle and are both functionally linked to smooth muscle contraction. However, these receptor subtypes are linked to different signal transduction systems. Whereas ET_A receptor-mediated contraction seems to involve activation of the phosphoinositide pathway and utilization of intracellular Ca^{2+}, ET_B receptor-mediated contractions appear to result from the influx of extracellular Ca^{2+} via non-L-type Ca^{2+}-channels. ET-1-induced contraction uses both receptor-effector pathways.

This research was supported by grants from the National Health and Medical Research Council of Australia and the Child Health Research Foundation of Western Australia. The author would like to acknowledge Dr Douglas Hay of SmithKline Beecham Pharmaceuticals for the generous gift of BQ-123 and Dr Roy Goldie for helpful and constructive discussion during the preparation of this manuscript.

References

CIOFFI, C.L., NEALE, R.F., JACKSON, R.H. & SILLS, M.A. (1992). Characterization of rat lung endothelin receptor subtypes which are coupled to phosphoinositide hydrolysis. *J. Pharmacol. Exp. Ther.*, **262**, 611–618.

GOLDIE, R.G., PAPADIMITRIOU, J.M., PATERSON, J.W., RIGBY, P.J., SELF, H.M. & SPINA, D. (1986). Influence of the epithelium on responsiveness of guinea-pig isolated trachea to contractile and relaxant agonists. *Br. J. Pharmacol.*, **87**, 5–14.

HAY, D.W.P. (1990). Mechanism of endothelin-induced contraction in guinea-pig trachea: comparison with rat aorta. *Br. J. Pharmacol.*, **100**, 383–392.

HAY, D.W.P. (1992). Pharmacological evidence for distinct endothelin receptors in guinea-pig bronchus and aorta. *Br. J. Pharmacol.*, **106**, 759–761.

HENRY, P.J., RIGBY, P.J., SELF, G.J., PREUSS, J.M. & GOLDIE, R.G. (1990). Relationship between endothelin-1 binding site densities and constrictor activities in human and animal airway smooth muscle. *Br. J. Pharmacol.*, **100**, 786–792.

HENRY, P.J., RIGBY, P.J., SELF, G.J., PREUSS, J.M. & GOLDIE, R.G. (1992). Endothelin-1-induced [^{3}H]-inositol phosphate accumulation in rat trachea. *Br. J. Pharmacol.*, **105**, 135–141.

IHARA, M., NOGUCHI, K., SAEKI, T., FUKURODA, T., TSUCHIDA, S., KIMURA, S., FUKAMI, T., NISHIKIBE, M. & YANO, M. (1992a). Biological profiles of highly potent novel endothelin antagonists selective for the ET_A receptor. *Life Sci.*, **50**, 247–255.

IHARA, M., SAEKI, T., FUKURODA, T., KIMURA, S., OZAKI, S., PATEL, A.C. & YANO, M. (1992b). A novel radioligand [125I]BQ-3020 selective for endothelin (ETB) receptors. *Life Sci.*, **51**, PL47–PL52.

MATTOLI, S., MEZZETTI, M., RIVA, G., ALLEGRA, L. & FASOLI, A. (1990). Specific binding of endothelin on human bronchial smooth muscle cells in culture and secretion of endothelin-like material from bronchial epithelial cells. *Am. J. Respir. Cell. Mol. Biol.*, **3**, 145–151.

MATTOLI, S., SOLOPERTO, M., MEZZETTI, M. & FASOLI, A. (1991). Mechanisms of calcium mobilisation and phosphoinositide hydrolysis in human bronchial smooth muscle cells by endothelin-1. *Am. J. Respir. Cell. Mol. Biol.*, **5**, 424–430.

McKAY, K.O., BLACK, J.L. & ARMOUR, C.L. (1991). The mechanism of action of endothelin in human lung. *Br. J. Pharmacol.*, **102**, 422–428.

MOLENAAR, P., KUC, R.E. & DAVENPORT, A.P. (1992). Characterization of two new ET_B selective ligands, [^{125}I]-BQ3020 and [^{125}I]-[Ala^{1,3,11,15}]ET-1 in human heart. *Br. J. Pharmacol.*, **107**, 637–639.

MOLENAAR, P., O'REILLY, G., SHARKEY, A., KUC, R.E., HARDING, D.P., PLUMPTON, C., GRESHAM, G.A. & DAVENPORT, A.P. (1993). Characterization and localization of endothelin receptor subtypes in the human atrioventricular conducting system and myocardium. *Circ. Res.*, **73**, 526–538.

NINOMIYA, N., UCHIDA, Y., SAOTOME, M., NOMURA, A., OHSE, H., MATSUMOTO, H., HIRATA, F. & HASEGAWA, S. (1992). Endothelins constrict guinea-pig tracheas by multiple mechanisms. *J. Pharmacol. Exp. Ther.*, **262**, 570–576.

NOGUCHI, K., ISHIKAWA, K., YANO, M., ADMED, A., CORTES, A., HALLMON, J. & ABRAHAM, W.M. (1992). An endothelin (ET_A) receptor antagonist, BQ-123, blocks ET-1 induced bronchoconstriction and tracheal smooth muscle (TSM) contraction in allergic sheep. *Am. Rev. Respir. Dis.*, **145**, A858.

SAEKI, T., IHARA, M., FUKURODA, T., YAMAGIWA, M. & YANO, M. (1991). [Ala^{1,3,11,15}]Endothelin-1 analogs with ET_B agonistic activity. *Biochem. Biophys. Res. Commun.*, **179**, 286–292.

SHIMAMOTO, H., KWAN, C.-Y. & DANIEL, E.E. (1992). Pharmacological assessment of Ca^{2+}-dependence of endothelin-1-induced response in rat aorta. *Eur. J. Pharmacol.*, **216**, 225–233.

TSCHIRHART, E.J., DRIJHOUT, J.W., PELTON, J.T., MILLER, R.C. & JONES, C.R. (1991). Endothelins: functional and autoradiographic studies in guinea-pig trachea. *J. Pharmacol. Exp. Ther.*, **258**, 381–387.

TURNER, N.C., POWER, R.F., POLAK, J.M., BLOOM, S.R. & DOLLERY, C.T. (1989). Endothelin-induced contractions of tracheal smooth muscle and identification of specific endothelin binding sites in the trachea of the rat. *Br. J. Pharmacol.*, **98**, 361–366.

UCHIDA, Y., NINOMIYA, H., SAOTOME, M., NOMURA, A., OHTSUKA, M., YANAGISAWA, M., GOTO, K., MASAKI, T. & HASEGAWA, S. (1988). Endothelin, a novel vasoconstrictor peptide, as potent bronchoconstrictor. *Eur. J. Pharmacol.*, **154**, 227–228.

WALLENSTEIN, S., ZUCKER, C.L. & FLEISS, J.L. (1980). Some statistical methods useful in circulation research. *Circ. Res.*, **47**, 1–9.

WILLIAMS, D.L. Jr, JONES, K.L., PETTIBONE, D.J., LIS, E.V. & CLINESCHMIDT, B.V. (1991). Sarafotoxin S6c; an agonist which distinguishes between endothelin receptor subtypes. *Biochem. Biophys. Res. Commun.*, **175**, 556–561.

(Received March 19, 1993
Revised April 30, 1993
Accepted May 5, 1993)

Br. J. Pharmacol. (1993), **110**, 442–446

The β-adrenoceptors mediating relaxation of rat oesophageal muscularis mucosae are predominantly of the β_3-, but also of the β_2-subtype

[1]Robert E.P. de Boer, Frans Brouwer & Johan Zaagsma

Department of Pharmacology and Therapeutics, University of Groningen, Antonius Deusinglaan 2, 9713 AW Groningen, The Netherlands

1 β-Adrenoceptor-mediated relaxation of rat oesophageal smooth muscle was investigated by studying the effects of β_1- and β_2-selective antagonists on the relaxation induced by (−)-isoprenaline, the β_2-selective agonists fenoterol and clenbuterol and the β_3-agonist, BRL 37344.

2 The highly β_1-selective antagonist CGP 20712A did not antagonize (−)-isoprenaline- or BRL 37344-induced relaxations in concentrations up to 10 μM. Only at 100 μM of CGP 20712A were clear rightward shifts of the agonist concentration-response curves (CRCs) observed, with pA_2 values of 4.70 and 4.97 against (−)-isoprenaline and BRL 37344, respectively.

3 ICI 118,551, a potent and selective β_2-antagonist, at 100 nM caused moderate rightward shifts of the CRCs of (−)-isoprenaline, fenoterol and clenbuterol; with fenoterol and clenbuterol, this was accompanied by a clear steepening of the curve. Only at the highest concentration (100 μM ICI 118,551) did the shifts to the right further increase substantially. Resulting Schild-plots were clearly biphasic. BRL 37344-induced relaxations were only antagonized at 100 μM ICI 118,551, yielding a pA_2 value of 5.48.

4 These results clearly demonstrate that the BRL 37344-induced relaxation of rat oesophageal muscularis mucosae is mediated solely through β_3-adrenoceptors, whereas (−)-isoprenaline-, fenoterol- and clenbuterol-induced relaxations were shown to involve both β_2- and, predominantly, β_3-adrenoceptors.

Keywords: β_3-Adrenoceptors; rat oesophagus; muscularis mucosae; BRL 37344; ICI 118,551; CGP 20712A

Introduction

During the past few years, both pharmacological and molecular studies have revealed that β-adrenoceptors are more heterogeneous than believed thus far. In a number of tissues, especially adipose and gastrointestinal tissue, responses appeared to be mediated by a receptor with distinct characteristics, different from classical β_1-and/or β_2-adrenoceptors. Recently, a human gene was cloned that encoded for a third (β_3-) adrenoceptor which, after transfection into Chinese Hamster Ovary (CHO) cells, revealed similar properties (Emorine *et al.*, 1989). Although this receptor was shown to exhibit clear atypical characteristics, it did not completely correspond to functional human and rat adipocyte β-adrenoceptors (Zaagsma & Nahorski, 1990). Furthermore, cloning of the rat β_3-adrenoceptor and subsequent expression in CHO cells revealed a pharmacological profile different from that reported for the human β_3-receptor, but similar to the properties exhibited by the atypical receptors in rat adipocytes (Granneman *et al.*, 1991). This would indicate species differences and/or the existence of multiple atypical receptor subtypes.

In addition to adipose tissue, atypical β-adrenoceptors have been shown to exist in a number of gastrointestinal smooth muscle preparations, for example guinea-pig ileum (Bond & Clarke, 1988); rat proximal colon (Croci *et al.*, 1988); rat distal colon (McLaughlin & MacDonald, 1990); rat jejunum (Van der Vliet *et al.*, 1990); and rat gastric fundus (McLaughlin & MacDonald, 1991). Also, the presence of atypical β-adrenoceptors has been indicated in other non-gastrointestinal tissues, for example in skeletal muscle (Challiss *et al.*, 1988) and in tracheal epithelium (Webber & Stock, 1992).

In rat oesophageal smooth muscle, Buckner & Christopherson (1974) have reported unusually low potencies of β-adrenoceptor antagonists in antagonizing isoprenaline-induced relaxations. Because this is now an established hallmark of an atypical, β_3-type adrenoceptor (Zaagsma & Nahorski, 1990), we decided to study the β-adrenoceptor-mediated relaxation of rat oesophageal muscularis mucosae in detail by comparing the potencies of (−)-isoprenaline, the selective β_3-adrenoceptor agonist BRL 37344 and the β_2-adrenoceptor agonists fenoterol and clenbuterol, using CGP 20712A and ICI 118,551 as selective β_1- and β_2-adrenoceptor antagonists, respectively. The results show that both β_2- and β_3-adrenoceptors are involved in the relaxation of rat oesophageal muscularis mucosae, the β_3-adrenoceptor playing the predominant role.

[1] Author for correspondence.

Methods

Tissue preparation

Male Wistar rats (250–300 g) were killed by a blow on the head and exsanguinated. Oesophagi were rapidly removed and placed in a water-jacketed preparation dish filled with Krebs-Henseleit solution at 37°C, composed of (mM): NaCl 117.5, KCl 5.6, $MgSO_4$ 1.18, $CaCl_2$ 2.52, NaH_2PO_4 1.28, $NaHCO_3$ 25.0, glucose 5.5, gassed with 95% O_2 and 5% CO_2, pH 7.4. The preparation was divided into two parts, cervical and thoracic, each with a length of 10–15 mm. Both parts were cut longitudinally and pinned on a silicon mat with the outer, striated muscle coat up. After dissection of the striated muscle, the remaining muscularis mucosae was divided into 4 (5 × 2 mm, thoracic part) and 6 (5 × 1.5 mm, cervical part) strips. Strips from different parts showed no differences in pharmacological behaviour. The preparations were mounted in 20 ml water-jacketed organ baths filled with Krebs-Henseleit buffer solution, gassed with 95% O_2/5% CO_2, pH 7.4, 37°C, for isotonic recording under 0.2 g load. After equilibration for a period of at least 30 min, tissues showed neither resting tone nor spontaneous activity throughout the experiments.

Concentration-response curves

An initial methacholine concentration-response curve (CRC) (0.1, 1, 10 μM) was constructed for each preparation which, after a washing period of 30 min, was followed by a second curve (0.1, 1, 10, 100 μM) to determine the maximal contraction. The preparations were then washed twice and, before the cumulative addition of a β-adrenoceptor agonist, contracted with methacholine in two concentration-steps, starting with 0.1 μM methacholine and supplemented to a final concentration of 1 μM, which induced approximately 50% of the maximal contraction.

With each preparation, only single CRCs to each agonist were constructed. When studying the effects of antagonists, two untreated strips (i.e. without antagonist) always served as controls. Antagonists were added 40 min prior to the beginning of each agonist-CRC.

(−)-Isoprenaline and fenoterol were added in 0.5 log increments. As relaxations by BRL 37344 and clenbuterol developed more slowly, these compounds were added in log intervals. At the end of each CRC, preparations were washed twice to obtain basal tone again.

All experiments were performed in duplicate each day using strips from the same animal, providing one data-set for the mean results.

Data analysis

CRCs of all β-adrenoceptor agonists were expressed as a percentage of the (1 μM) methacholine-induced contraction. Schild plots were constructed according to Arunlakshana & Schild (1959) using the agonist-concentrations producing half-maximal relaxation in the absence and the presence of different concentrations of the antagonist. In cases where the Schild plot was biphasic, the slope was calculated from the steep part of the plot only, discounting the constant log (DR-1) values obtained with low antagonist concentrations (Bond & Clarke, 1988); if the slope was not significantly different from unity (two-tailed Student's t test, $\alpha < 0.05$), pA_2 values were calculated from each antagonist concentration, using the formula $pA_2 = -\log\{[\text{antagonist}]/(DR-1)\}$ (MacKay, 1978). This formula was also used when the Schild-plot consisted of only one data point.

All data are given as mean ± s.e.mean of (n) determinations.

Drugs

(−)-Isoprenaline hydrochloride was purchased from Sigma (St. Louis, U.S.A.). BRL 37344 (4-[2-[(2-hydroxy-2-(3-chlorphenyl)ethyl)amino]-propyl]-phenoxyacetic acid), ICI 118,551 (erythro-1-(7-methylindan-4-yloxy)-3-(isopropylamine)-butan-2-ol), CGP 20712A (1-[2-((3-carbamoyl-4-hydroxy)-phenoxy)-ethylamino]-3-[4-(1-methyl-4-trifluoromethyl-2-imidazolyl) phenoxy]-propan-2-ol), fenoterol and clenbuterol were kind gifts from SmithKline Beecham (Epsom, U.K.), ICI (Macclesfield, U.K.), Ciba-Geigy (Basel, Switzerland) and Boehringer Ingelheim (Ingelheim, Germany). Phentolamine was donated by Ciba-Geigy (Arnhem, The Netherlands) and corticosterone was from Organon (Oss, The Netherlands). All buffer salts were from Merck (Amsterdam, The Netherlands).

Results

All β-adrenoceptor agonists produced concentration-dependent relaxations of oesophageal smooth muscle. Addition of phentolamine (1 μM) or corticosterone (10 μM) to block classical α-adrenoceptor effects and extraneuronal uptake, respectively, did not affect agonist-induced relaxations (data not shown).

Relaxations to BRL 37344 were slow compared to (−)-isoprenaline-induced relaxations (Figure 1). In addition, with BRL 37344 a clear tachyphylaxis was observed, a second CRC being shifted to the right 10–30 fold. Therefore, only one CRC to each agonist was constructed per tissue.

With ICI 118,551 at the highest concentration (100 μM) only, some depression of the methacholine-induced contraction was observed, which may indicate some antimuscarinic effect; this depression amounted to 21.6 ± 1.3% (mean ± s.e.mean; $n = 29$) of the maximal (0.1 mM methacholine) con-

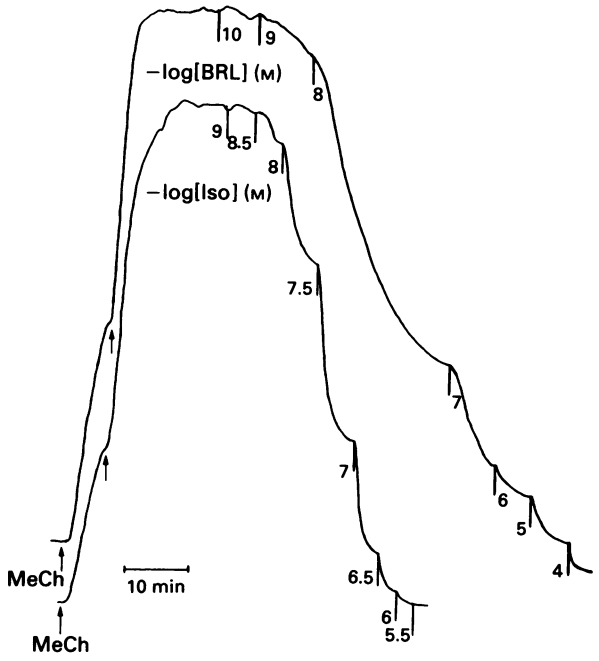

Figure 1 Typical traces showing BRL 37344 (upper curve) and (−)-isoprenaline (Iso) (lower curve)-induced relaxations of rat oesophageal muscularis mucosae. Smooth muscle tone was elevated by step-wise additions of 0.1 and 0.9 μM methacholine (MeCh) (arrows).

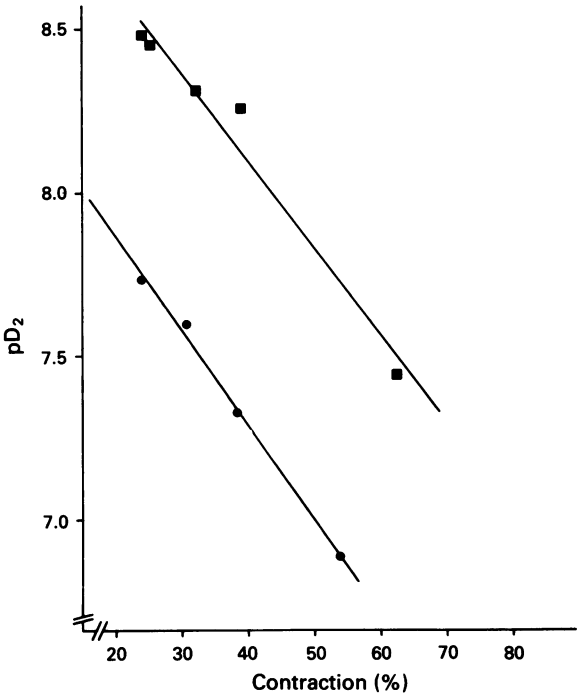

Figure 2 Correlation between methacholine-induced contraction and pD_2 values for BRL 37344 (■) ($r = -0.980$, $P < 0.01$) and fenoterol (●) ($r = -0.996$, $P < 0.01$). Datapoints correspond to methacholine-concentrations (in downward direction) of: 0.2, 0.4, 0.8, 1, and 3 μM (BRL 37344) and 0.4, 0.8, 1, and 3 μM (fenoterol). Data represent the mean from at least three observations.

traction. Because lowering the tone induced by contractile agonists can enhance the responsiveness of a smooth muscle to a β-adrenoceptor agonist, shifting the CRC to the left (Van Amsterdam *et al.*, 1989), the relationship between the size of the methacholine-induced contraction and the pD_2 ($-\log EC_{50}$) value for relaxation induced by the β_3-adrenoceptor agonist BRL 37344, and the β_2-adrenoceptor agonist fenoterol was established (Figure 2). For both compounds linear relationships with identical slopes were found. Hence, the spontaneous leftward-shift, due to the decrease of the methacholine-induced contraction by 100 μM ICI 118,551, could be corrected for. This procedure was applied to all agonists to correct the individual log(DR-1) values, obtained at 100 μM ICI 118,551.

Antagonism of (−)-isoprenaline-induced relaxation by CGP 20712A is shown in Figure 3a. Only at 100 μM CGP 20712A was a clear rightward shift observed, from which a pA_2 value of 4.70 ± 0.16 ($n = 5$) was calculated.

ICI 118,551 at 10 nM caused a moderate shift to the right of the (−)-isoprenaline CRC, which hardly increased at 100 nM to 10 μM. Only at 100 μM did the shift increase substantially (Figure 3b). The resulting Schild-plot (inset) was clearly biphasic. From the steep part of this plot, having a slope of 1.09 ± 0.09, which was not significantly different from unity, a pA_2 value of 5.31 ± 0.10 ($n = 13$) was calculated.

Responses to BRL 37344 were not affected by CGP 20712A or ICI 118,551 in concentrations up to 10 μM. Only at 100 μM of both antagonists was the CRC to BRL 37344 clearly shifted (Figure 4). From the 100 μM data-points pA_2 values were calculated, yielding 4.97 ± 0.12 ($n = 3$) for CGP 20712A and 5.48 ± 0.10 ($n = 12$) for ICI 118,551.

With fenoterol as the (β_2-selective) agonist, a moderate shift and clear steepening of the CRC was seen at 100 nM ICI 118,551 (Figure 5a). A marked further shift was observed only at 100 μM ICI 118,551. From the steep part of the biphasic Schild plot (inset), with a slope not significantly different from unity (1.15 ± 0.05), a pA_2 value of 5.30 ± 0.11 ($n = 10$) was calculated.

Clenbuterol, the least potent of the agonists used, showed a markedly shallow CRC (Figure 5b). As with fenoterol, the CRC to clenbuterol was shifted and clearly steepened at 100 nM ICI 118,551. Again, only at 100 μM of the antagonist was a substantial further shift to the right observed. The inset shows the biphasic Schild plot, of which the steep part has a slope of 1.02 ± 0.23, which was not significantly different from unity, yielding an apparent pA_2 value of 5.48 ± 0.35 ($n = 11$).

Discussion

The existence of atypical or β_3-adrenoceptors has now been generally accepted. Although a selective β_3-adrenoceptor antagonist is still lacking, low potencies and stereoselectivities of classical β-adrenoceptor antagonists (Harms *et al.*, 1977; Bojanic *et al.*, 1985), together with the high potency of a novel class of β-adrenoceptor agonists (Arch *et al.*, 1984) has provided strong support for the occurrence of atypical β-adrenoceptors. These receptors were shown to be abundantly

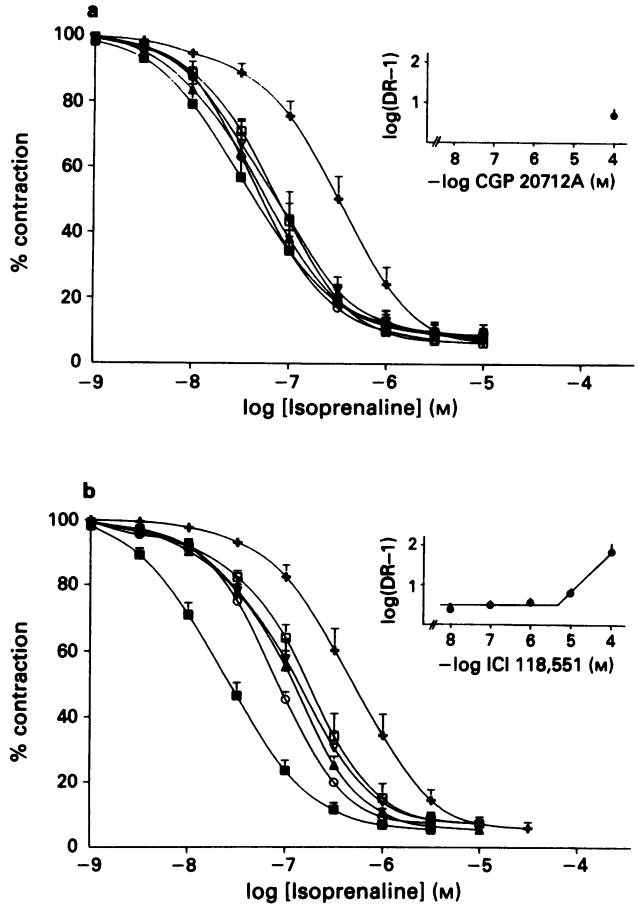

Figure 3 Antagonism of (−)-isoprenaline-induced relaxation by CGP 20712A (a) and ICI 118,551 (b). Control (■), CGP 20712A/ICI 118,551 10 nM (○), 100 nM (▲), 1 μM (▽), 10 μM (□), and 100 μM (+). Shown are the mean of five to eight experiments each performed in duplicate. The inset shows the corresponding Schild plot.

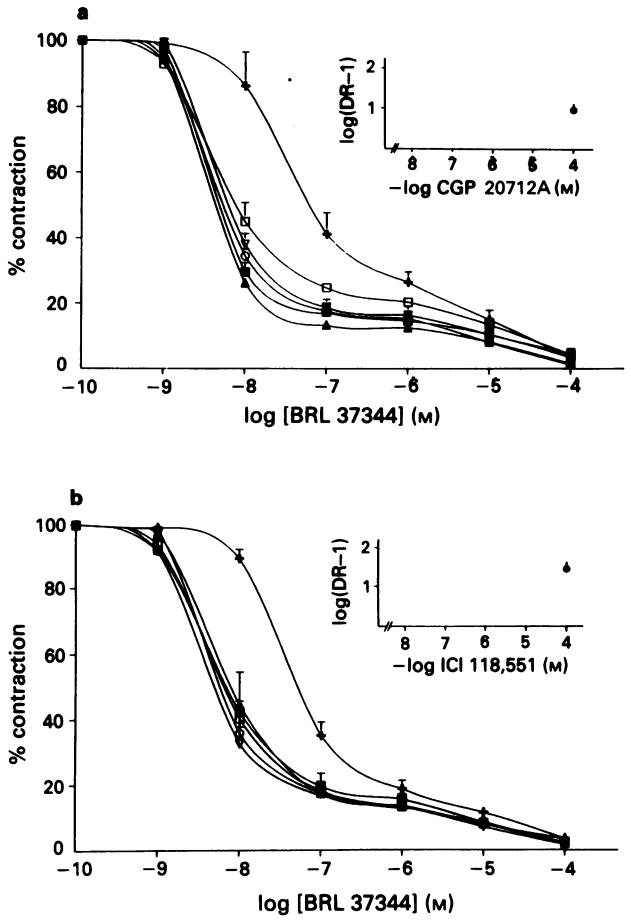

Figure 4 Antagonism of BRL 37344-induced relaxation by CGP 20712A (a) and ICI 118,551 (b). Control (■), CGP 20712A/ICI 118,551 10 nM (○), 100 nM (▲), 1 μM (▽), 10 μM (□), and 100 μM (+). Shown are the mean of three to five (CGP 20712A) and eight to thirteen (ICI 118,551) experiments each performed in duplicate. The inset shows the corresponding Schild plot.

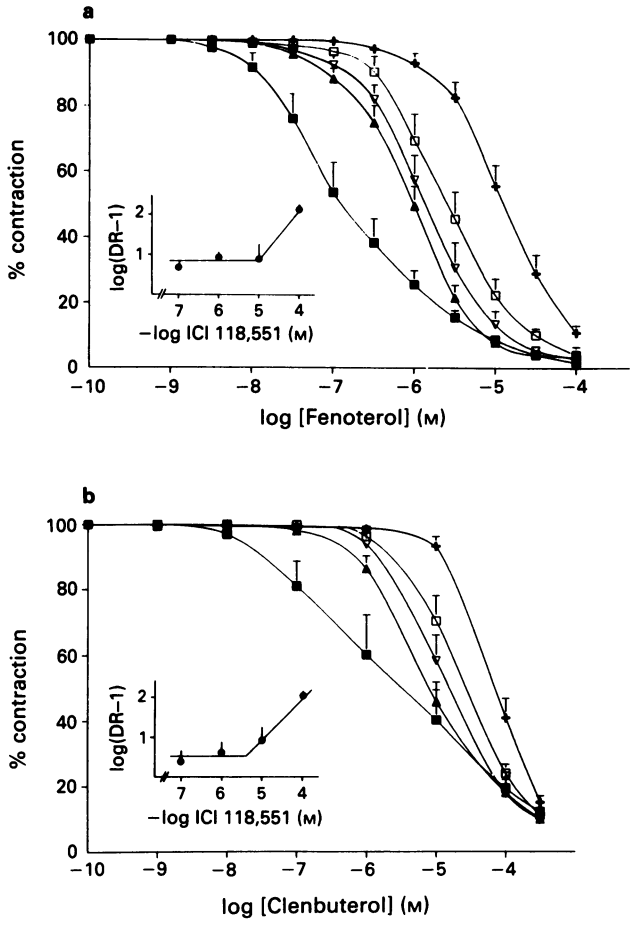

Figure 5 Antagonism of fenoterol- (a) and clenbuterol- (b) induced relaxation by ICI 118,551. Control (■), ICI 118,551 100 nM (▲), 1 μM (▽), 10 μM (□) and 100 μM (+). Shown are the mean of five to seven experiments each performed in duplicate. The inset shows the corresponding Schild plot.

present in adipose and gastrointestinal tissue (for a review, see Zaagsma & Hollenga, 1991).

The present study was undertaken to characterize the β-adrenoceptor(s) mediating relaxation of rat oesophageal muscularis mucosae by performing complete concentration-response curves with (−)-isoprenaline, BRL 37344, fenoterol and clenbuterol. Isoprenaline was almost a full agonist with a potency which was very similar to values reported for lipolysis (Hollenga & Zaagsma, 1989) and colonic relaxation (McLaughlin & MacDonald, 1990). The (−)-isoprenaline-induced relaxation was not antagonized by low CGP 20712A concentrations. Since CGP 20712A is a very potent and highly β_1-selective antagonist (Dooley *et al.*, 1986), it can be concluded that β_1-adrenoceptors are not involved in (−)-isoprenaline-induced relaxation of oesophageal smooth muscle. The pA_2 value of 4.70, derived from the highest CGP 20712A concentration is similar to the value of 4.80 for antagonizing (−)-isoprenaline-induced lipolysis in rat adipocytes (Hollenga & Zaagsma, 1989), indicating the involvement of similar atypical adrenoceptors as in rat adipocytes. With 100 nM ICI 118,551, some steepening and a small rightward shift of the (−)-isoprenaline CRC indicates the involvement of a β_2-adrenoceptor population, particularly at the lower concentrations of the agonist. With the marked rightward shift at 100 μM ICI 118,551, the participation of atypical receptors is clearly indicated as well. The pA_2 value for ICI 118,551 calculated from the steep part of the Schild plot (5.31) is similar to the value of 5.49 for antagonizing (−)-isoprenaline-induced lipolysis in rat adipocytes (Hollenga & Zaagsma, 1989).

BRL 37344-induced relaxation of oesophageal muscularis mucosae was mediated almost exclusively by atypical receptors. As shown in Figure 4, responses to BRL 37344 were not antagonized by either CGP 20712A or ICI 118,551 at concentrations up to 10 μM. Only at 100 μM was a clear rightward shift observed for both compounds. Again, pA_2-values (4.97 and 5.48, respectively) were similar to the pA_2 values for CGP 20712A and ICI 118,551 obtained in rat adipocytes (4.61 and 5.33; Hollenga & Zaagsma, 1989). The relaxing potency of BRL 37344 was 6.5 fold higher than (−)-isoprenaline, which is somewhat lower than the 10 fold potency difference, reported for lipolysis in rat adipocytes (Hollenga & Zaagsma, 1989). This may be explained by the small, but significant contribution of β_2-adrenoceptors in the (−)-isoprenaline-induced relaxation of rat muscularis mucosae, in contrast to the mere subordinate role of the β_1-adrenoceptor population in rat adipocytes.

As compared with the other agonists used, the relaxation by BRL 37344 was less complete. The effects observed at the highest concentrations of BRL 37344 (10 and 100 μM) appeared to be non-specific and not due to a β_2- (or β_3-) adrenoceptor-mediated relaxation, as increasing concentrations of the β_2-antagonist ICI 118,551 were without any effect on this part of the CRC.

BRL 37344-induced relaxations were slow, compared to (−)-isoprenaline-induced relaxations. Complete CRCs to BRL 37344 lasted about 2 times longer than comparable CRCs with (−)-isoprenaline as the agonist. In addition, BRL 37344 caused tachyphylaxis. This phenomenon has also been observed in other gastrointestinal tissues, like guinea-pig gastric fundus with BRL 35135 (Coleman *et al.*, 1987) and with BRL 37344 in rat distal colon (McLaughlin & MacDonald, 1990) and rat gastric fundus (McLaughlin & MacDonald, 1991). The mechanism of this desensitization however, is unclear.

As suggested recently for the cloned human β_3-adrenoceptor (Emorine *et al.*, 1991), agonist-induced regulation of this receptor might be different from that of β_1- and β_2-adrenoceptors, due to the absence of protein kinase A (PKA) phosphorylation sites, together with the absence of several serine and threonine-rich regions in the C-terminal region involved in β-adrenoceptor kinase (βARK)-mediated desensitization (Hausdorff *et al.*, 1990). These structural differences have also been reported for the rat β_3-adrenoceptor (Granneman *et al.*, 1991). According to these findings, the observed desensitization in our study would indicate a mechanism, other than phosphorylation by PKA or βARK, or phosphorylation at different positions within the receptor.

With fenoterol and clenbuterol as β_2-selective agonists, the moderate rightward shifts and clear steepening of the CRCs at 100 nM ICI 118,551 confirmed the presence of a functional β_2-adrenoceptor population, particularly at the lower concentrations of the agonists. This shift increased substantially only at 100 μM, indicating the contribution of a major, atypical β-adrenoceptor population. Interestingly, the pD_2 values for fenoterol and clenbuterol are again very similar to the values reported for rat adipocytes (6.95 and 5.40 for fenoterol and clenbuterol, respectively; Hollenga *et al.*, 1990), suggesting that at concentrations producing half-maximal relaxation, the atypical β-adrenoceptor already predominates. This would be in line with the recent observation in adipocytes that the transduction efficiency (i.e. the relationship between cyclic AMP generation and cellular response) is much higher for the atypical than for the typical β-adrenoceptor (Hollenga *et al.*, 1991). Therefore, it can be predicted that selective blockade of the less efficient β_2-adrenoceptor (by low concentrations of ICI 118,551) in rat oesophagus would steepen the CRCs of β_2-selective agonists like fenoterol and clenbuterol. Thus, although we realize that the construction of Schild plots, in cases where steepening of the CRCs is indicative for the involvement of more than one receptor type, is questionable, it is evident from both the CRCs and the Schild analyses, that β_2-, and predominantly

β_3-adrenoceptors, are involved in the β-adrenoceptor-mediated relaxation of rat muscularis mucosae by fenoterol, clenbuterol as well as (−)-isoprenaline. As expected, the BRL 37344-mediated relaxation was shown to be mediated solely by β_3-adrenoceptors.

Using CGP 20712A as the antagonist, no evidence for any contribution of a β_1-adrenoceptor was found. The pA_2 values of the antagonists as well as the pD_2 values of the agonists clearly indicate that the nature of the β_3-adrenoceptor population in rat oesophageal muscularis mucosae is identical to that of rat adipocytes.

BRL 37344 was kindly supplied by SmithKline Beecham Pharmaceuticals (Epsom, U.K.). We are also grateful to ICI (Macclesfield, U.K.) for ICI 118,551, to Ciba Geigy (Basel, Switzerland) for CGP 20712A and to Boehringer Ingelheim (Ingelheim, Germany) for fenoterol and clenbuterol.

References

ARCH, J.R.S., AINSWORTH, A.T., CAWTHORNE, M.A., PIERCY, V., SENNITT, M.V., THODY, V.E., WILSON, C. & WILSON, S. (1984). Atypical β-adrenoceptor on brown adipocytes as target for anti-obesity drugs. *Nature*, **309**, 163–165.

ARUNLAKSHANA, O. & SCHILD, H.O. (1959). Some quantitative uses of drug antagonists. *Br. J. Pharmacol. Chemother.*, **14**, 48–58.

BOJANIC, D., JANSEN, J., NAHORSKI, S.R. & ZAAGSMA, J. (1985). Atypical characteristics of the β-adrenoceptor mediating cyclic AMP generation and lipolysis in the rat adipocyte. *Br. J. Pharmacol.*, **84**, 131–137.

BOND, R.A. & CLARKE, D.E. (1988). Agonist and antagonist characterization of a putative adrenoceptor with distinct pharmacological properties from the α- and β-subtypes. *Br. J. Pharmacol.*, **95**, 723–734.

BUCKNER, C.K. & CHRISTOPHERSON, R.C. (1974). Adrenergic receptors of rat esophageal smooth muscle. *J. Pharmacol. Exp. Ther.*, **189**, 467–475.

CHALLISS, R.A.J., LEIGHTON, B., WILSON, S., THURLBY, P.L. & ARCH, J.R.S. (1988). An investigation of the β-adrenoceptor that mediates metabolic responses to the novel agonist BRL 28410 in rat soleus muscle. *Biochem. Pharmacol.*, **37**, 947–950.

COLEMAN, R.A., DENYER, L.H. & SHELDRICK, K.E. (1987). β-Adrenoceptors in guinea pig gastric fundus – are they the same as the 'atypical' β-adrenoceptors in rat adipocytes? *Br. J. Pharmacol.*, **90**, 40P.

CROCI, T., CECCHI, R., TARANTINO, A., AUREGGI, G., BIANCHETTI, A., BOIGEGRAIN, R. & MANARA, L. (1988). Inhibition of rat colon motility by stimulation of atypical β-adrenoceptors with new gut-specific agents. *Pharmacol. Res. Commun.*, **20**, 147–151.

DOOLEY, D.J., BITTIGER, H. & REYMANN, N.C. (1986). CGP 20712A: a useful tool for quantitating β_1- and β_2-adrenoceptors. *Eur. J. Pharmacol.*, **130**, 137–139.

EMORINE, L.J., FEVE, B., PAIRAULT, J., BRIEND-SUTREN, M.-M., MARULLO, S., DELAVIER-KLUTCHKO, C. & STROSBERG, D.A. (1991). Structural basis for functional diversity of β_1-, β_2- and β_3-adrenergic receptors. *Biochem. Pharmacol.*, **41**, 853–859.

EMORINE, L.J., MARULLO, S., BRIEND-SUTREN, M.-M., PATEY, G., TATE, K., DELAVIER-KLUTCHKO, C. & STROSBERG, A.D. (1989). Molecular characterization of the human β_3-adrenergic receptor. *Science*, **245**, 1118–1121.

GRANNEMAN, J.G., LAHNERS, K.N. & CHAUDHRY, A. (1991). Molecular cloning and expression of the rat β_3-adrenergic receptor. *Mol. Pharmacol.*, **40**, 895–899.

HARMS, H.H., ZAAGSMA, J. & DE VENTE, J. (1977). Differentiation of β-adrenoceptors in right atrium, diaphragm and adipose tissue of the rat using stereoisomers of propranolol, alprenolol, nifenalol and practolol. *Life Sci.*, **21**, 123–128.

HAUSDORFF, W.P., CARON, M.G. & LEFKOWITZ, R.J. (1990). Turning off the signal: desensitization of β-adrenergic receptor function. *FASEB J.*, **4**, 2881–2889.

HOLLENGA, CH., BROUWER, F. & ZAAGSMA, J. (1991). Relationship between lipolysis and cyclic AMP generation mediated by atypical β-adrenoceptors in rat adipocytes. *Br. J. Pharmacol.*, **102**, 577–580.

HOLLENGA, CH., HAAS, M., DEINUM, J.T. & ZAAGSMA, J. (1990). Discrepancies in lipolytic activities induced by β-adrenoceptor agonists in human and rat adipocytes. *Horm. Metab. Res.*, **22**, 17–21.

HOLLENGA, CH. & ZAAGSMA, J. (1989). Direct evidence for the atypical nature of functional β-adrenoceptors in rat adipocytes. *Br. J. Pharmacol.*, **98**, 1420–1424.

MACKAY, D. (1978). How should values of pA_2 and affinity constants for pharmacological competitive antagonists be estimated? *J. Pharm. Pharmacol.*, **30**, 312–313.

MCLAUGHLIN, D.P. & MACDONALD, A. (1990). Evidence for the existence of 'atypical' β-adrenoceptors (β_3-adrenoceptors) mediating relaxation in the rat distal colon in vitro. *Br. J. Pharmacol.*, **101**, 569–574.

MCLAUGHLIN, D.P. & MACDONALD, A. (1991). Characterization of catecholamine-mediated relaxations in rat isolated gastric fundus: evidence for an atypical β-adrenoceptor. *Br. J. Pharmacol.*, **103**, 1351–1356.

VAN AMSTERDAM, R.G.M., MEURS, H., BROUWER, F., POSTEMA, J.-B., TIMMERMANS, A. & ZAAGSMA, J. (1989). Role of phosphoinositide metabolism in functional antagonism of airway smooth muscle contraction by β-adrenoceptor agonists. *Eur. J. Pharmacol. Mol. Pharmacol.*, **172**, 175–183.

VAN DER VLIET, A., RADEMAKER, B. & BAST, A. (1990). A beta adrenoceptor with atypical characteristics is involved in the relaxation of the rat small intestine. *J. Pharmacol. Exp. Ther.*, **255**, 218–226.

WEBBER, S.E. & STOCK, M.J. (1992). Evidence for an atypical, or β_3-adrenoceptor in ferret tracheal epithelium. *Br. J. Pharmacol.*, **105**, 857–862.

ZAAGSMA, J. & HOLLENGA, CH. (1991). Distribution and function of atypical β_3-adrenoceptors. In *Adrenoceptors: Structure, Mechanisms, Function.* ed. Szabadi, E. & Bradshaw, C.M., pp. 47–58. Basel: Birkhäuser Verlag.

ZAAGSMA, J. & NAHORSKI, S.R. (1990). Is the adipocyte β-adrenoceptor a prototype for the recently cloned atypical 'β_3-adrenoceptor'? *Trends Pharmacol. Sci.*, **11**, 3–7.

(Received August 4, 1992
Revised May 4, 1993
Accepted May 6, 1993)

Br. J. Pharmacol. (1993), **110**, 447–453

Suppression of inflammatory responses to 12-*O*-tetradecanoylphorbol-13-acetate and carrageenin by YM-26734, a selective inhibitor of extracellular group II phospholipase A_2

[1]Akira Miyake, Hirokazu Yamamoto, Emi Kubota, Katsuhiko Hamaguchi, Akio Kouda, Kazuo Honda & Hiroyuki Kawashima

Molecular and Cellular Pharmacology Dept., Central Research Laboratories, Yamanouchi Pharmaceutical Co. Ltd., 1–8 Azusawa 1-chome, Itabashi-ku, Tokyo 174, Japan

1 YM-26734 [4-(3,5-didodecanoyl-2,4,6-trihydroxyphenyl)-7-hydroxy-2-(4-hydroxyphenyl)chroman] dose-dependently inhibited the activities of extracellular phospholipase A_2 (PLA_2): rabbit platelet-derived group II and porcine pancreas-derived group I PLA_2, with IC_{50} values of 0.085 (0.056–0.129, $n = 5$) and 6.8 (5.0–9.6, $n = 5$) μM, respectively.

2 In contrast, YM-26734 did not reduce the activity of intracellular PLA_2 prepared from mouse macrophages, which preferentially hydrolyzed arachidonoyl phospholipids at concentrations up to 50 μM. YM-26734 also showed no effect against either sheep seminal vesicle cyclo-oxygenase or rat leukocyte 5-lipoxygenase.

3 Lineweaver-Burk analysis showed that YM-26567-1 behaved as a competitive inhibitor of group II PLA_2 derived from rabbit platelets, with a K_i value of 48 nM.

4 In mice, YM-26734 inhibited 12-*O*-tetradecanoylphorbol-13-acetate (TPA, 1 μg/ear)-induced ear oedema in a dose-dependent manner, with ED_{50} values of 45 (30–67) μg/ear ($n = 5$) and 11 (4–32) mg kg^{-1}, i.v. ($n = 5$), but did not decrease arachidonic acid (4 mg/ear)-induced ear oedema at 1 mg/ear and 30 mg kg^{-1}, i.v.

5 In rats, the accumulation of exudate fluids and leukocytes in the pleural cavity in response to carrageenin injection (2 mg) was significantly less in a group treated with YM-26734 (20 mg kg^{-1}, i.v.) than in the control group (0.43 ± 0.02 vs 0.59 ± 0.03 g per cavity and 3.8 ± 0.2 vs 4.9 ± 0.3 × 10^7 cells per cavity, respectively; $n = 5$).

6 These results suggest that YM-26734 is a potent and competitive inhibitor of extracellular PLA_2 with selectivity for group II PLA_2, and that the inhibition of group II enzymes activity may cause the suppression of inflammatory responses to TPA and carrageenin.

Keywords: YM-26734; phospholipase A_2; mouse ear oedema; rat pleurisy

Introduction

Phospholipase A_2 [EC3.1.1.4] (PLA_2) catalyzes the hydrolysis of the acyl-ester bound to the *sn*-2 position of membrane phospholipids, resulting in the formation of fatty acids and lysophospholipids. Arachidonic acid (AA) and 1-*O*-aklyl-2-lyso-glycero-3-phosphorylcholine are two such products which can be converted into potent proinflammatory lipid mediators: the eicosanoids (prostaglandin and leukotriene) and platelet activating factor (PAF), respectively (Waite 1985). These mediators (Salmon & Higgs 1987; Chan *et al.*, 1985; Braquet *et al.*, 1987) each promote the inflammatory process by inducing leukocyte infiltration (PAF and leukotriene B_4 (LTB_4)), epidermal proliferation (LTB_4 and 12-hydroxyeicosatetraenoic acid (HETE)), vascular permeability (PAF, LTC_4 and LTD_4), and vasodilatation (prostaglandin E_2 (PGE_2) and PGI_2).

Mammalian cells contain multiple forms of PLA_2 which can be classified into extracellular and intracellular forms. Extracellular PLA_2 can be further divided into two groups based on their amino acid sequence (Waite, 1987). In mammals, group I PLA_2 occurs mainly in the pancreas, whereas group II PLA_2 is distributed in cells such as platelets (Kramer *et al.*, 1989) and neutrophils (Wright *et al.*, 1990). Group II enzyme is released by platelets into the extracellular space in response to thrombin and PAF (Horigome *et al.*, 1987), and is found in the soluble form at inflammatory sites such as in human synovial fluid from patients with rheumatoid arthritis (Kramer *et al.*, 1989). In addition to these findings, purified group II PLA_2 elicits or exacerbates inflammatory responses when injected into the tissue of mice (Chang *et al.*, 1989), rats (Murakami *et al.*, 1990) and rabbits (Bomalaski *et al.*, 1991). Regulation of group II enzyme may therefore achieve important therapeutic effects, particularly in inflammatory disease. Regarding intracellular PLA_2, Clark *et al.* (1991) recently reported the cloning of a cDNA encoding a novel PLA_2 in human monocytic cell line U937. This PLA_2 is distributed in the cytosol of macrophages (Wijkander & Sundler 1989; Clark *et al.*, 1990), platelets (Takayama *et al.*, 1991) and the kidney (Gronich *et al.*, 1990), and preferentially hydrolyzes phospholipids containing an arachidonoyl residue at the *sn*-2 position. The finding that this cytosolic PLA_2 is activated by intracellular concentrations of Ca^{2+} in response to receptor occupancy suggests that this PLA_2 type may operate intracellularly and regulate eicosanoid production in cells exposed to inflammatory stimuli. It remains to be determined which of the PLA_2 isoforms are biologically significant in inflammatory processes, particularly with regard to extracellular group II or intracellular PLA_2. Selective inhibitors of each isoform are required to solve this problem.

Previously we reported that YM-26567-1 [(+)-*trans*-4-(3-dodecanoyl-2,4,6-trihydroxyphenyl)-7-hydroxy-2-(4-hydroxyphenyl)chroman], a natural product isolated from the fruit of *Horsefieldia amygdaline*, competitively inhibits extracellular group II PLA_2 prepared from rabbit platelets (Miyake *et al.*, 1992). We screened YM-26567-1 derivatives to find an inhibitor which selectively targets the group II isoform. YM-26734 (Figure 1) was the result of this process. In the present

[1] Author for correspondence.

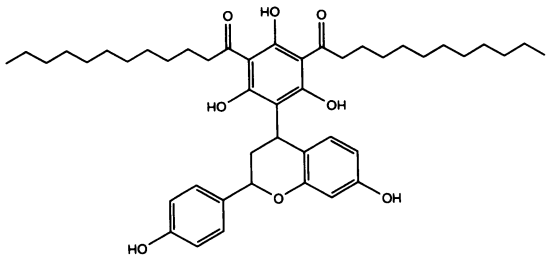

Figure 1 Chemical structure of YM-26734, [4-(3,5-didodecanoyl-2,4,6-trihydroxyphenyl)-7-hydroxy-2-(4-hydroxyphenyl)chroman].

paper, we characterize the effects of YM-26734 on not only extracellular (group I and II) but also intracellular PLA_2. In addition, we also describe the effects of this compound on enzymes related to AA cascade and inflammatory responses in animal models.

Methods

Assay of PLA_2

Extracellular PLA_2 activities were measured by established methods (Pepinsky *et al.*, 1986) using the substrate [^{3}H]-oleic acid-labelled autoclaved *Escherichia coli* (*E. coli*) which was prepared according to the method of Elsbach & Weiss (1990). Phospholipids in radiolabelled *E. coli* were quantified on the basis of inorganic phosphate according to the method of Bartlett (1959). The specific radioactivity of these lipids was approximately $1-2 \times 10^5$ c.p.m. nmol^{-1} inorganic phosphate. The incubation mixture for standard assay of PLA_2 activity contained 150 µl of Tris-HCl buffer (100 mM, pH 8.0), Ca^{2+} (10 mM), bovine serum albumin (BSA, 0.2 mg ml^{-1}), and [^{3}H]-oleic acid-labelled autoclaved *E. coli* (5 µM). Test compounds were dissolved in methanol and added to the reaction mixture just before the addition of the enzyme solution. The final concentration of methanol in the reaction mixture was less than 1% which showed no effect on the enzyme activities. The reaction was started by adding the enzyme solution and stopped after 10 min incubation at either 6°C or 37°C by adding 25 µl of 4 N HCl and 25 µl of 40 mg ml^{-1} BSA. As enzyme sources, rabbit platelet and porcine pancreas PLA_2 were added at 130 and 1.0 ng for incubation at 6°C, or at 1.0 and 0.01 ng for incubation at 37°C, respectively. Tubes were kept on ice for 30 min and then *E. coli* was pelleted by centrifugation for 5 min at 10,000 *g*. Radioactivity of each supernatant was counted with a liquid scintillation counter. For experiments in which substrate concentration-dependence was determined, the reaction was performed at 6°C for 5 min in the presence of 65 ng of rabbit platelet enzyme.

Intracellular PLA_2 activity was measured as the release of radiolabeled AA from 1-palmitoyl-2-[^{14}C]-arachidonoyl phosphatidylcholine according to the methods of Clark *et al.* (1990). 1-Palmitoyl-2-[^{14}C]-arachidonoyl phosphatidylcholine (10 µM) was dried under nitrogen, then suspended in 0.1 ml of 100 mM glycine buffer, pH 9.0, containing 200 µM Triton X-100, 10 mM $CaCl_2$, 0.25 mg ml^{-1} BSA, and 40% glycerol. The suspension was then sonicated to form mixed micellea of phospholipid and Triton X-100. The reaction was started by adding the enzyme solution (approximately 5 µg protein of cytosolic fraction from macrophages) and stopped after a 60 min incubation period at 37°C by mixing with 0.5 ml of isopropyl alcohol:heptane:0.5 M H_2SO_4 (10:5:1). Heptane (0.3 ml) and water (0.2 ml) were then added, and the solution was vigorously mixed for 15 s. The heptane phase was mixed with silica (40 mg) and centrifuged, and the radioactivity in each supernatant was counted by liquid scintillation spectrometry.

Phospholipid hydrolysis was expressed as velocity (micromol of free fatty released per minute per milligram protein), calculated from the specific activities of the radiolabelled phospholipids and the protein concentration of the enzyme. The percentage of enzyme inhibition was obtained by comparison with vehicle control hydrolysis.

Preparation of extracellular PLA_2

Extracellular group I PLA_2 derived from porcine pancreas was purchased from Sigma Chemical Co. (St. Louis, MO, USA). Extracellular group II PLA_2 was prepared from rabbit platelets according to a modification of the methods of Horigome *et al.* (1987). Blood from rabbits anaesthetized with sodium pentobarbitone (20 mg kg^{-1}, i.v.) was collected in a plastic syringe containing 3.8% (w v^{-1}) sodium citrate, and centrifuged for 10 min at 270 *g* at room temperature to prepare platelet-rich plasma. The platelets were pelleted from the plasma by further centrifugation at 1,200 × *g* for 10 min, resuspended at 2×10^9 cells ml^{-1}, and incubated at 37°C for 5 min with 2.5 units ml^{-1} thrombin in the presence of 2 mM Ca^{2+}. The mixture was centrifuged at 3,000 *g* for 10 min at 4°C, and the supernatant was applied to a heparin-Sepharose CL-6B column. After extensive washing, the column was eluted with a linear concentration gradient of NaCl and the eluted fractions were assayed for PLA_2 activity. The PLA_2 activity was eluted at a molarity of approximately 0.8 to 1.1 M NaCl. Fractions showing high PLA_2 activity were pooled and condensed by ultrafiltration with a centricon-10 and stored at − 80°C until use.

Preparation of intracellular PLA_2

Intracellular PLA_2 was prepared from mouse peritoneal resident macrophages according to the method of Wijkander & Sundler (1989). Resident macrophages were collected from mice by peritoneal lavage, plated onto culture dishes (2×10^5 cells cm^{-2}) and allowed to adhere for 2 h at 37°C. The adherent cells were collected by scraping, then homogenized with a Dounce homogenizer in 10 mM HEPES buffer, pH 7.4, containing 80 mM KCl, 5 mM dithiothreitol and 1 mM EGTA. The homogenate was centrifuged at 700 *g* for 5 min and the resulting supernatant was further centrifuged at 100,000 *g* for 60 min to obtain the cytosolic fraction. The cytosolic fraction was stored at 4°C in the presence of 10% (v v^{-1}) glycerol and used within 1 week.

Assay of cyclo-oxygenase

Cyclo-oxygenase activity was measured in 0.1 ml incubations with sheep seminal vesicle microsome (4 mg ml^{-1}) and [^{14}C]-AA (50 µM) in 0.1 M Tris-HCl buffer, pH 7.6, containing 2 mM tryptophan, 4 mM reduced glutathione and the test compound. After incubation at 37°C for 10 min, the reaction was terminated by adding 0.3 ml of diethyl ether:methanol: 1 M citric acid (30:4:1). The samples were centrifuged at 1,000 *g* for 1 min, then dehydrated by the addition of 0.5 *g* of Na_2SO_4. The organic phases were analyzed by thin layer chromatography (t.l.c.) on silica gel 60 plates using benzene:dioxane:acetic acid (50:50:2.5) as solvent. The amount of radioactivity migrating at the AA and PGE_2 positions was determined by liquid scintillation spectrometry. Cyclo-oxygenase activity was expressed as the percentage of conversion of AA to PGE_2. The percentage of enzyme inhibition was obtained by comparison with vehicle controls.

Assay of 5-lipoxygenase

The activity of 5-lipoxygenase was measured from the conversion of [^{14}C]-AA to 5-HETE using t.l.c. to resolve the products of the reaction (Skoog *et al.*, 1986). 5-Lipoxygenase was prepared from polymorphonuclear leukocytes in rat peritoneal exudates collected 18–20 h after a 10 ml injection

of 8% (w v^{-1}) casein. The leukocytes were lysed at 4°C by sonication at a concentration of 2×10^8 cells ml^{-1} in 10 mM HEPES buffer, pH 7.3, containing 2 mM EDTA and 1 mM mercaptoethanol. The soluble fraction (100,000 *g* supernatant) was used as the enzyme preparation. The incubation mixture of the assay of 5-lipoxygenase activity contained 0.1 ml of 25 mM phosphate buffer, pH 7.3, 1 mM ATP, 1 mM Ca^{2+}, the enzyme preparation (0.6 mg ml^{-1}), and test compound. The enzyme was preincubated at 37°C for 2 min before initiation of the reaction by the addition of [^{14}C]-AA (final 5 μM). After incubation for 10 min at 37°C, the reaction was stopped by adding 0.4 ml of diethyl ether:methanol: 1 M citric acid (30:4:1). The samples were centrifuged at 1,000 *g* for 1 min, then dehydrated by the addition of 0.5 *g* of Na_2SO_4. The organic phases were analyzed by t.l.c. on silica gel 60 plates using ethyl acetone:iso-octane:acetic acid:H_2O (100:50:20:100) as solvent. The amount of radioactivity migrating at the positions of AA and 5-HETE was determined with a liquid scintillation spectrometer. 5-Lipoxygenase activity was expressed as the percentage of conversion of AA to 5-HETE. The percentage of enzyme inhibition was obtained by comparisons with vehicle control conversion.

Induction of mouse ear oedema

A modification of the methods of Young *et al.* (1983) was used. 12-*O*-tetradecanoyl-phorbol-13-acetate (TPA) and AA were dissolved in acetone at concentrations of 100 μg ml^{-1} and 400 mg ml^{-1} respectively, and applied to the right ears of mice by an automatic pipette in a volume of 10 μl; vehicle was applied to the left ears. After the indicated time, mice were killed and the ears were excised and weighed. For topical evaluation, all drugs were dissolved in acetone and applied 30 min prior to TPA or AA application, except prednisolone which was applied 3 h beforehand. For systemic evaluation, YM-26734 was dissolved in equimolar NaOH with 0.1 N solution, diluted with saline, and injected into the saphenous vein 30 s before application of either TPA or AA. Ear oedema was calculated from the formula, (R-L)/L × 100, where R and L were the weight of the right and left ears. The percentage inhibition was calculated by comparing individual values in treatment groups to the mean value of the control group.

Induction of rat pleurisy

Pleurisy was induced in rats by intrapleural injection of 0.1 ml of 2% (w v^{-1}) λ-carrageenin under light anaesthesia with ether (Miyasaka & Mikami, 1982). Four hours later, rats were killed with chloroform. The pleural cavity was lavaged twice with 2.0 ml of saline containing 2 units ml^{-1} heparin and the exudate harvested on ice. The weight of exudate fluids was measured and the number of migrated leukocytes was counted in a Coulter Counter (Coulter Electronics). YM-26734 was dissolved as described before and injected into the saphenous vein 30 s before carrageenin injection. Indomethacin was suspended in 0.5% methylcellulose solution and administered orally 60 min before carrageenin injection.

Materials and animals

YM-26734 was chemically synthesized in our laboratories. Other materials were purchased from the following sources: λ-carrageenin, bovine serum albumin (BSA, fatty acid-free), indomethacin and TPA from Sigma Chemical Co. (St. Louis, MO, U.S.A.); heparin from Novo Industry (Denmark); thrombin from Mochida Pharmaceutical Co. Ltd. (Japan); heparin-Sepharose CL-6B from Pharmacia (Sweden); Centricon-10 from Amicon (Danvers, MA, U.S.A.); AA from Nakarai Tesque Co. (Japan); casein sodium, reduced glutathione, manoalide, prednisolone and phenidone (1-phenyl-3-pyrazolidone) from Wako Chemical Co. (Japan); sheep seminal vesicle microsomes from Funakoshi Co. (Japan); and [^{3}H]-oleic acid, [^{14}C]-AA, 1-palmitoyl-2-[^{14}C]-arachidonoyl phosphatidylcholine and 1-palmitoyl-2-[^{14}C]-oleoyl phosphatidylcholine from New England Nuclear (Boston, MA, U.S.A.). Male ICR mice (25–35 g) and male Wistar rats (140–180 g) were purchased from Japan SLC Co. (Japan), and female Japanese white rabbits (3.0–3.5 kg) were purchased from Clean Experimental Animal Center (Japan), they were maintained on a standard pellet chow and distilled water *ad libitum*.

Statistical analysis

Data are expressed as the mean ± s.e.mean or the mean with 95% confidence limits. Statistical differences were determined by ANOVA. The level of significance was set at 5% ($P<0.05$). The ED_{50} or IC_{50} values were determined by probit analysis.

Results

Inhibitory effects of YM-26734 on extracellular PLA_2 activities

Figure 2 shows the effect of YM-26734 on the initial rates of PLA_2 hydrolysis of *E. coli* phospholipids at 6°C. YM-26734 dose-dependently inhibited both rabbit platelet and porcine pancreas PLA_2. In the presence of a fixed concentration of phospholipids, IC_{50} values for hydrolysis of rabbit platelet and porcine pancreas PLA_2 were 0.085 (0.056–0.129) and 6.8 (5.0–9.6) μM, respectively. YM-26734 showed approximately 100 fold more potent inhibition against group II than group I PLA_2 in mammals. To determine whether the action of YM-26734 against PLA_2 was affected by incubation temperature, we examined its inhibitory effects on extracellular PLA_2 activities at 37°C. YM-26734 inhibited rabbit platelet and porcine pancreas PLA_2 activity at 37°C, with IC_{50} values of 0.12 (0.08–0.19) and 7.6 (5.5–10.5) μM, respectively. Thus, the potency of YM-26734 for each enzyme was independent of incubation temperature.

Effect of YM-26734 on intracellular PLA_2

Cytosolic fraction prepared from mouse peritoneal resident macrophages was used as a source of intracellular PLA_2. In contrast to extracellular PLA_2, the cytosolic fraction prepared from mouse peritoneal macrophages showed PLA_2 activity with an approximately 11 fold higher preference for 1-palmitoyl-2-arachidonoyl- than for 1-palmitoyl-2-oleoyl-phosphatidylcholine, and was insensitive to the reductive

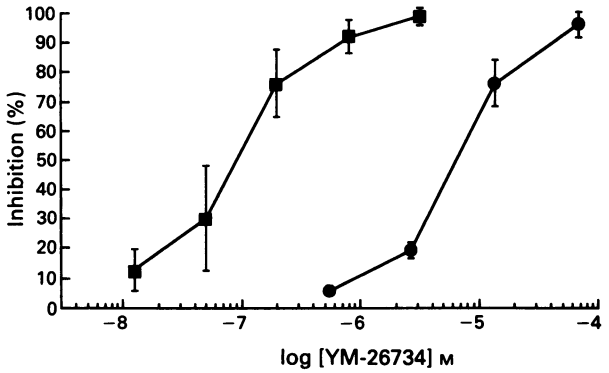

Figure 2 Dose-response curves for YM-26734 on activities of phospholipase A_2 (PLA_2) prepared from rabbit platelets (■) and porcine pancreas (●). Each value represents the mean ± s.e.mean of five independent experiments.

agent, dithiothreitol (data not shown). These findings accord with information published by Wijkander & Sundler (1989) and Clark et al. (1990). Manoalide, used as a reference compound, inhibited intracellular PLA_2 activity (81% inhibition at 50 μM), whereas YM-26734 did not affect enzyme activity (− 14% inhibition at 50 μM).

Lineweaver-Burk analysis of inhibition by YM-26734 of group II PLA_2

The dependence of inhibition on substrate concentration was examined for PLA_2 hydrolysis. Figure 3 shows double-reciprocal plots of kinetic data for the hydrolysis of phospholipids in *E. coli* plasma membrane by rabbit platelet PLA_2 at different concentrations of YM-26734. In the concentration-range used here, rabbit platelet PLA_2 was shown to give linear double-reciprocal plots that conformed well to Michaelis-Menten kinetics ($\gamma = 0.991$). Similar kinetics have been demonstrated with group II PLA_2 in human synovial fluid (Jacobson et al., 1990). Lineweaver-Burk analysis revealed that YM-26734 behaved as a competitive inhibitor of rabbit platelet PLA_2, with K_i values of 48 nM.

Effect of YM-26734 on cyclo-oxygenase and 5-lipoxygenase

The inhibitory selectivity of YM-26734 for enzymes associated with metabolic pathways leading from phospholipids to eicosanoids was evaluated by assessing its activity against sheep seminal vesicle microsomal cyclo-oxygenase and rat leukocyte 5-lipoxygenase. Indomethacin and phenidone were used as reference inhibitors of cyclo-oxygenase and 5-lipoxygenase, respectively. Table 1 shows that YM-26734 inhibited neither sheep seminal vesicle cyclo-oxygenase nor rat leukocyte 5-lipoxygenase.

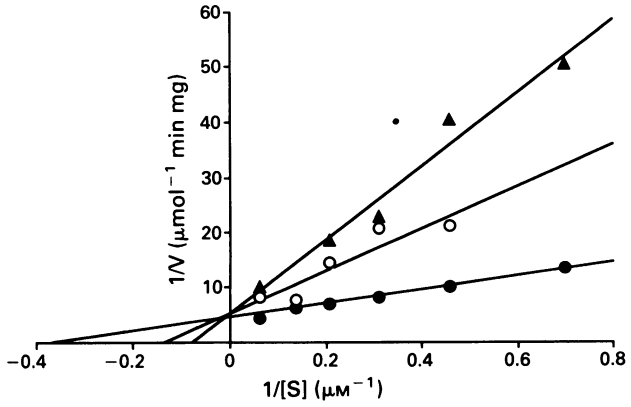

Figure 3 Lineweaver-Burk analysis of phospholipase A_2 (PLA_2) derived from rabbit platelet incubated with YM-26734. Rabbit platelet PLA_2 activity was measured in the presence of 0 (●), 0.1 (○) and 0.2 μM (▲) YM-26734. Each value represents the mean of two determinations.

Table 1 Effect of YM-26734 and reference compounds on cyclo-oxygenase and 5-lipoxygenase

Compound	IC_{50} (μM)[a] Cyclo-oxygenase	5-Lipoxygenase
YM-26734	− 12% at 100[b]	3% at 10[b]
Indomethacin	6.3	NT
Phenidone	NT	1.1

[a]Each value is the mean of two independent determinations.
[b]Percentage of inhibition at the highest concentration tested.
NT: not tested.

Inhibitory effect of YM-26734 on TPA-induced mouse ear oedema

The anti-oedema activity of YM-26734 was evaluated by use of a TPA-induced ear oedema model. Data for YM-26734 against TPA-induced ear oedema are presented in Figure 4. Topical administration of YM-26734 caused a dose-dependent inhibition of swelling with an ED_{50} value of 45 (31–67) μg/ear (Figure 4a). As shown in Table 2, YM-26734 was approximately 3, 5 and 40 fold more potent than the irreversible PLA_2 inhibitor manoalide, the cyclo-oxygenase inhibitor, indomethacin and the eicosanoid synthesis inhibitor, phenidone, respectively, and about one tenth as active as prednisolone, a strong anti-inflammatory steroid which induces PLA_2-inhibitory protein (Flower 1988; Suwa et al., 1990). Further, its effectiveness in systemic administration was evaluated using TPA-induced mouse ear oedema. Intravenous administration of YM-26734 inhibited ear oedema in response to TPA application in a dose-dependent manner ($ED_{50} = 11$ mg kg^{-1}, Figure 4b).

Effect of YM-26734 on AA-induced mouse ear oedema

The anti-oedema selectivity of YM-26734 was evaluated by assessing its activity against another ear oedema model, AA-induced ear oedema. The ear oedema was measured at 60 min after application of AA at 4 mg/ear, generating a submaximal response. Topical application (1 mg/ear) of the eicosanoid synthesis inhibitor, phenidone and the cyclo-oxygenase inhibitor, indomethacin, significantly inhibited AA-induced ear oedema (Table 2). In contrast, YM-26734

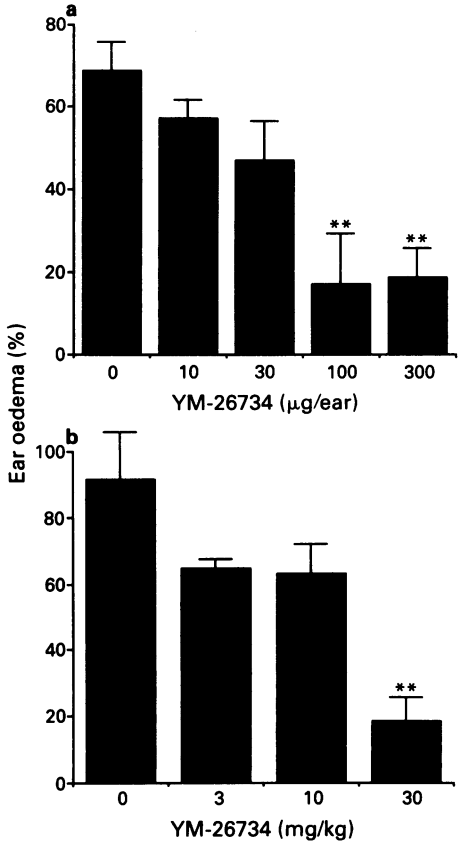

Figure 4 Inhibitory effect of YM-26734 on TPA-induced mouse ear oedema. YM-26734 was topically administrated 30 min (a), or intravenously injected 30 s (b), prior to the application of TPA at 1 μg/ear. Ear oedema was measured 4 h after TPA application. Each value represents the mean ± s.e.mean of 5 mice. $*P<0.05$, $**P<0.01$ compared with respective controls.

Table 2 Inhibition of mouse ear oedema induced by application of either 12-*O*-tetradecanoylphorbol-13-acetate (TPA) or arachidonic acid (AA)

Compound[b]	ED_{50} (μg/ear)[a] *TPA*	*AA*
YM-26734	45 (31–67)	NS at1000[c]
Prednisolone	3.3 (1.8–6.2)[d]	NT
Manoalide	119 (90–158)[d]	NT
Indomethacin	201 (174–231)[d]	70% at 1000[d,e]
Phenidone	1900 (1600–2300)[d]	62% at 1000[d,e]

[a]Ear oedema was measured 1 and 4 h after application of AA 4 mg/ear and TPA 1 μg/ear, respectively. Numbers in parentheses show 95% confidence limits ($n \geq 5$ per dose, dose = 3,4 points). [b]Compounds were applied to the mouse ear 30 min prior to TPA or AA application, except prednisolone which was applied 3 h beforehand. [c]No significant inhibition at the highest concentration tested. [d]Data from Miyake *et al.* (1992). [e]Percentage of statistically significant inhibition. NT: not tested.

did not significantly inhibit ear swelling caused by AA at 1 mg/ear. Moreover, intravenous administration of YM-26734 with 30 mg kg^{-1} also showed no effect on the oedema.

Inhibitory effect of YM-26734 on carrageenin-induced rat pleurisy

The anti-inflammatory action of YM-26734 was further investigated in a carrageenin-induced rat inflammation model. The pleural cavity was selected as the inflammatory site, in which accumulation of both exudate fluids and leukocytes can be observed as inflammatory responses to carrageenin. As shown in Figure 5, intrapleural carrageenin

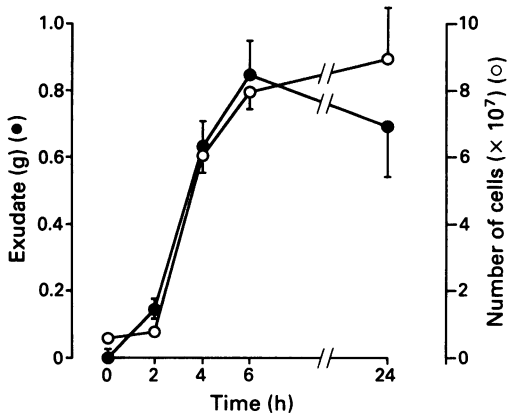

Figure 5 Time course of accumulation of exudate fluid (●) and leukocytes (○) in the pleural cavity in response to carrageenin injection in rats; 2 mg carrageenin was injected intrapleurally. Each value represents the mean ± s.e.mean of 5 rats.

(2 mg) rapidly induced exudate and leukocyte accumulation in the cavity 2 to 4 h after injection, with levels plateauing at 6 to 24 h. The effects of YM-26734 on these responses were measured at 4 h after injection, using the cyclo-oxygenase inhibitor indomethacin as a reference. As shown in Table 3, intravenous administration of YM-26734 at 20 mg kg^{-1} significantly inhibited the accumulation of both exudate fluids and leukocytes in the pleural cavity in response to carrageenin injection.

Discussion

In this study, we found that YM-26734 inhibited extracellular group II PLA_2 from rabbit platelets 100 fold more potently than extracellular group I PLA_2 from porcine pancreas, and had no effect on intracellular PLA_2 from mouse peritoneal macrophages. The high selectivity of YM-26734 for extracellular over intracellular PLA_2 may be explained by the difference in amino acid sequence of the enzyme, as reported by Clark *et al.* (1991). It has been shown that intracellular PLA_2 preferentially hydrolyzes arachidonoyl phospholipids, whereas phospholipids containing two saturated fatty acids, such as dipalmitoyl phosphatidylcholine, are poor substrates for the enzyme. YM-26734 has two saturated alkyl chains which may hinder access to the catayltic site of the intracellular PLA_2. Against this, the 100 fold preferential inhibition of group II over group I PLA_2 is surprising, since the extracellular PLA_2s are reported to share a highly conserved amino acid sequence as the catalytic site: His^{48}, Asp^{99}, Tyr^{62} and Tyr^{73} (Kramer *et al.*, 1989), and all PLA_2 inhibitors reported so far show poor selectivity between the two types of extracellular PLA_2. In this regard, YM-26734 may represent a unique tool in the investigation of differences in catalytic site between the two enzymes, as well as of the physiological significance of extracellular group II PLA_2.

Several inhibitors of PLA_2 activity prepared from various sources (snake venom, bee venom or porcine pancreas) and their anti-inflammatory effects have been reported. However, it is not clear which type of enzyme plays a role in inflammatory responses, as none of these inhibitors has been selective. Moreover, many reported PLA_2 inhibitors affect enzymes metabolizing AA to eicosanoids, which are involved in the inflammatory process. Manoalide, a natural marine product isolated from the sponge *Luffariella variabilis*, inhibits not only extracellular group II PLA_2 purified from human synovial fluid (Jacobson *et al.*, 1990) and rabbit platelets (Miyake *et al.*, 1992), but also intracellular PLA_2 isolated from the cytosol of human monocytic cell line, U937 (Marshall *et al.*, 1991b). Although manoalide shows an anti-inflammatory effect on TPA-induced mouse ear oedema (Burley *et al.*, 1982), this compound also potently inhibits 5-lipoxygenase prepared from rat basoleukaemia cell line RBL-1 (De Vries *et al.*, 1988) in addition to its PLA_2 inhibitory effects. Nordihydroguaiaretic acid also inhibits human synovial fluid PLA_2 (Marshall *et al.*, 1991a) and acts

Table 3 Inhibitory effect of YM-26734 on accumulation of exudate fluid and leukocytes in rat carrageenin-induced pleurisy.

Compound	*Dose*[a] (mg kg^{-1})	*n*	*Exudate fluid* *Weight* (mg)	*Inhibition* (%)	*Leukocytes migration* *Number* (× 10^7)	*Inhibition* (%)
Control		5	587 ± 27		4.91 ± 0.31	
YM-26734	5	5	566 ± 11	4	4.57 ± 0.20	7
	10	5	545 ± 28	7	4.20 ± 0.29	14
	20	5	429 ± 23**	27	3.81 ± 0.21*	22
Control		9	639 ± 31		4.66 ± 0.44	
Indomethacin	3	9	362 ± 25**	43	3.10 ± 0.25**	34

[a]YM-26734 was intravenously injected 30 s prior to carrageenin injection. Indomethacin was administered orally 60 min prior to carrageenin injection. *$P < 0.05$, **$P < 0.01$ compared with respective controls.

as an anti-inflammatory agent, but this agent also potently inhibits cyclo-oxygenase and 5-lipoxygenase. The anti-inflammatory effects of these inhibitors may therefore be due to inhibition of PLA_2, of other enzymes within the AA cascade or both. In contrast, YM-26734 does not inhibit sheep seminal vesicle cyclo-oxygenase or rat leukocyte 5-lipoxygenase as enzymes within the AA cascade, indicating it to be a selective inhibitor of extracellular group II PLA_2, which can be used to investigate the significance of extracellular group II PLA_2 in inflammatory responses and pathology.

Two animal models were used to investigate extracellular group II PLA_2 in inflammatory responses, the TPA-induced mouse ear oedema model and the carrageenin-induced rat pleurisy model. The former is widely used to evaluate the anti-inflammatory activity of PLA_2 inhibitors, TPA induces AA release and eicosanoids synthesis in cultured macrophages *in vitro* (Humes *et al.*, 1982), and TPA challenge to the mouse ear causes PGE_2 to accumulate in parallel with the swelling of the ear (Inoue *et al.*, 1989). However, it is not clear if this inflammation is regulated primarily by PLA_2 activity, or more specifically by extracellular group II enzymes. The present observation that the selective group II PLA_2 inhibitor, YM-26734, strongly inhibited TPA-induced ear oedema suggests a positive relationship between group II PLA_2 activity and inflammatory responses to TPA. As a control study, we evaluated the effect of YM-26734 in an AA-induced mouse ear oedema model, in which both cyclo-oxygenase (PGE_2) and lipoxygenase products (LTC_4/D_4) are implicated (Opas *et al.*, 1985). As expected, YM-26734 failed to inhibit AA-induced ear oedema.

We next examined the effect of YM-26734 on a carrageenin-induced rat pleurisy model. This model allows direct assessment of the effects of various classes of anti-inflammatory agents on plasma exudation and leukocyte migration. The accumulation of exudate fluid and leukocytes into the pleural cavity in response to carrageenin injection appears to be regulated by metabolites of AA for the following reasons. Carrageenin injection causes accumulation of PGE_2 (Katori *et al.*, 1978), LTB_4 (Flower *et al.*, 1986) and LTC_4/D_4 (Ueno *et al.*, 1983), and many inhibitors of cyclo-oxygenase, 5-lipoxygenase, or both suppress both plasma exudation and leukocyte migration induced by carrageenin (Ashida *et al.*, 1983; Ku *et al.*, 1988). YM-26734 also inhibited accumulation of exudate fluid and leukocytes into the pleural cavity, suggesting that extracellular group II PLA_2 may play a role in this inflammatory process. As for inflammatory factors other than eicosanoids, it is possible that such factors may also be involved in the anti-inflammatory effect of YM-26734 in this study. Although we cannot rule out such a possibility, it is reasonable to say, based on our present study, that the anti-inflammatory effect of YM-26734 can be explained, at least in part, by its action on the group II PLA_2.

In conclusion, we have demonstrated that YM-26734 is a potent and competitive PLA_2 inhibitor which is selective for extracellular group II PLA_2 and that inhibition of group II PLA_2 activity may suppress inflammatory responses to TPA and carrageenin by decreasing substrates for cyclo-oxygenase and 5-lipoxygenase.

The authors wish to thank Ms Toshie Hanazato for her excellent technical assistance, and Drs Takeshi Saito and Noriyoshi Inukai for their helpful discussions.

References

ASHIDA, Y., SAIJO, H., KURIKI, H., MAKINO, H., TERAO, S. & MAKI, Y. (1983). Pharmacological profile of AA-861, a lipoxygenase inhibitor. *Prostaglandins*, **26**, 966–972.

BARTLETT, G.R. (1959). Phosphorus assay in column chromatography. *J. Biol. Chem.*, **234**, 466–468.

BOMALASKI, J.S., LAWTON, P. & BROWNING, J.L. (1991). Human extracellular recombinant phospholipase A_2 induces an inflammatory response in rabbit joints. *J. Immunol.*, **146**, 3904–3910.

BRAQUET, P., TOUQUI, L., SHEN, T.Y. & VARGAFTIG, B.B. (1987). Perspectives in platelet-activating factor research. *Pharmacol. Rev.*, **39**, 97–145.

BURLEY, E.S., SMITH, B., CUTTER, G., AHLEM, J.K. & JACOBS, R.S. (1982). Antagonism of phorbol 12-myristate 13-acetate (PMA)-induced inflammation by the marine natural product, manoalide. *Pharmacologist*, **24**, 117–25.

CHAN, C.C., DUHAMEL, L. & FORD-HUTCHINSON, A.W. (1985). Leukotriene B_4 and 12-hydroxyeicosatetraenoic acid stimulate epidermal proliferation *in vivo* in the guinea pig. *J. Invest. Dermatol.*, **85**, 333–334.

CHANG, J., MARSHALL, L.M. & CARLSON, R.P. (1989). Proinflammatory effects phospholipase A_2 (PLA_2) in several in vitro and in vivo systems. In *Advances in Prostaglandin, Thromboxane and Leukotriene Research*, vol. 19, ed. Samuelsson, B., Wong, P.Y.-K., Sun, F.F. pp. 594–597. New York: Raven Press.

CLARK, J.D., LIN, L., KRIZ, R.W., RAMESHA, C.S., SULTMAN, L.A., LIN, A.Y., MILONA, N. & KNOPF, J.L. (1991). A novel arachidonic acid-selective cytosolic PLA_2 contains a Ca^{2+}-dependent translocation domain with homology to PKC and GAP. *Cell*, **65**, 1043–1051.

CLARK, J.D., MILONA, N. & KNOPF, J.L. (1990). Purification of a 110-kilodalton cytosolic phospholipase A_2 from the human monocyclic cell line U937. *Proc. Natl. Acad. Sci. U.S.A.*, **87**, 7708–7712.

DE VRIES, G.W., AMDAHL, L., MOBASSER, A., WENZEL, M. & WHEELER, L.A. (1988). Preferential inhibition of 5-lipoxygenase activity by manoalide. *Biochem. Pharmacol.*, **37**, 2899–2905.

ELSBACH, P. & WEISS, J. (1990). Utilization of labeled *Escherichia coli* as phospholipase substrate. In *Phospholipases, Methods in Enzymology*, vol. 197, ed. Abelson, J.M. & Simon, M.I. pp. 24–30. New York: Academic Press.

FLOWER, R.J. (1988). Lipocortin and the mechanism of the action of glucocorticoids. *Br. J. Pharmacol.*, **94**, 987–1015.

FLOWER, R.J., PARENTE, L., PERSICO, P. & SALMON, J.A. (1986). A comparison of the acute inflammatory response in adrenalectomized and sham-operated rats. *Br. J. Pharmacol.*, **87**, 57–62.

GRONICH, J.H., BONVENTRE, J.V. & NEMENOFF, R.A. (1990). Purification of a high-molecular-mass form of phospholipase A_2 from rat kidney activated at physiological calcium concentrations. *Biochem. J.*, **271**, 37–43.

HORIGOME, K., HAYAKAWA, M., INOUE, K. & NOJIMA, S. (1987). Purification and characterization of phospholipase A_2 released from rat platelets. *J. Biochem.*, **101**, 625–631.

HUMES, J.L., SADWSKI, S., GLAVAGE, M., GOLDENBERG, M., SUBERS, E., BONNEY, R.J. & KUEHL, F.A. (1982). Evidence for two sources of arachidonic acid for oxidative metabolism by mouse peritoneal macrophages. *J. Biol. Chem.*, **257**, 1591–1594.

INOUE, H., MORI, T., SHIBATA, S. & KOSHIHARA, Y. (1989). Modulation by glycyrrhetinic acid derivatives of TPA-induced mouse ear edema. *Br. J. Pharmacol.*, **96**, 204–210.

JACOBSON, P.B., MARSHALL, L.A., SUNG, A. & JACOBS, R.S. (1990). Inactivation of human synovial fluid phospholipase A_2 by the marine natural product, manoalide. *Biochem. Pharmacol.*, **39**, 1557–1564.

KATORI, M., IKEDA, K., HARADA, Y., UCHIDA, Y., TANAKA, K. & OH-ICHI, S. (1978). A possible role of prostaglandins and bradykinin as a trigger of exudation in carrageenin-induced rat pleurisy. *Agents Actions*, **8**, 108–112.

KRAMER, R.M., HESSION, C., JOHANSEN, B., HAYES, G., MCGRAY, P., PINCHANG CHOW, E., TIZARD, R. & PEPINSKY, R.B. (1989). Structure and properties of a human non-pancreatic phospholipase A_2. *J. Biol. Chem.*, **264**, 5768–5775.

KU, C.E., RAYCHAUDHURI, A., GHAI, G., KIMBLE, E.F., LEE, W.H., COLOMBO, C., DOTSON, R., OGLESBY, T.D. & WASLEY, J.W. (1988). Characterization of CGS 8515 as a selective 5-lipoxygenase inhibitor using *in vitro* and *in vivo* models. *Biochem. Biophys. Acta.*, **959**, 332–342.

MARSHALL, L.A., BAUER, J., SUNG, M.L. & CHANG, J.Y. (1991a). Evaluation of antirheumatic drugs for their effect *in vitro* on purified human synovial fluid phospholipase A_2. *J. Rheumatology*, **18**, 59–65.

MARSHALL, L.A., BOLOGNESE, B., YUAN, W. & GLEB, M. (1991b). Phosphonate-phospholipid analogues inhibit human phospholipase A_2. *Agents Actions*, **34**, 106–109.

MIYAKE, A., YAMAMOTO, H., TAKEBAYASHI, Y., IMAI, H. & HONDA, K. (1992). The novel natural product YM-26567-1 [(+)-*trans*-4-(3-dodecanoyl-2,4,6-trihydroxyphenyl)-7-hydroxy-2-(4-hydroxyphenyl)chroman]: a competitive inhibitor of group II phospholipase A_2. *J. Pharmacol. Exp. Ther.*, **263**, 1302–1307.

MIYASAKA, K. & MIKAMI, T. (1982). Comparison of the anti-inflammatory effects of dexamethasone, indomethacin and BW755C on carrageenin-induced pleurisy in rats. *Eur. J. Pharmacol.*, **77**, 229–236.

MURAKAMI, M.. KUDO, I., MAKAMURA, H., YOKOYAMA, Y., MORI, H. & INOUE, K. (1990). Exacerbation of rat adjuvant arthritis by intradermal injection of purified mammalian 14-KDa group II phospholipase A_2. *FEBS*, **268**, 113–116.

OPAS, E.E., BONNEY, R.J. & HUMES, J.L. (1985). Prostaglandin and leukotriene synthesis in mouse ears inflamed by arachidonic acid. *J. Invest. Dermatol.*, **84**, 253–256.

PEPINSKY, R.B., SINCLAIR, L.K., BROWNING, J.L., MATTALIANO, R.J., SMART, J.E., CHOW, E.P., FALBEL, T., RIBOLINI, A., GARWIN, J.L. & WALLNER, B.R. (1986). Purification and partial sequence analysis of a 37-kDa protein that inhibits phospholipase A_2 activity from rat peritoneal exudates. *J. Biol. Chem.*, **261**, 4239–4246.

SALMON, J.A. & HIGGS, J.A. (1987). Prostaglandins and leukotrienes as inflammatory mediators. *Br. Med. Bull.*, **43**, 285–296.

SKOOG, M.T., NICHOLS, J.A. & WISEMAN, J.S. (1986). 5-Lipoxygenase from rat PMN lysate. *Prostaglandins*, **31**, 561–576.

SUWA, Y., KUDO, I., IMAIZUMI, A., OKADA, M., KAMIMURA, T., SUZUKI, Y., CHANG, H.W., HARA, S. & INOUE, K. (1990). Proteinaceous inhibitors of phospholipase A_2 purified from inflammatory sites in rats. *Proc. Natl. Acad. Sci. U.S.A.*, **87**, 2395–2399.

TAKAYAMA, K., KUDO, I., KIM, D.K., NAGATA, K., NOZAWA, Y. & INOUE, K. (1991). Purification and characterization of human platelet phospholipase A_2 which preferentially hydrolyzes an arachidonoyl residue. *FEBS*, **282**, 326–330.

UENO, A., TANAKA, K. & KATORI, M. (1983). Detection of leukotriene C_4 and D_4 in the exudate of rat carrageenin-induced pleurisy. *Prostaglandins*, **26**, 493–504.

WAITE, M.J. (1985). Approaches to the study of mammalian cellular phospholipases. *Lipid Res.*, **26**, 1379–1388.

WAITE, M. (1987). Pancreatic and snake venom phospholipase A_2. In *The Phospholipases, Handbook of Lipid Research*, vol. 5 ed. Hanahan, D.J. pp. 155–190. New York and London: Plenum Press.

WIJKANDER, J. & SUNDLER, R. (1989). A phospholipase A_2 hydrolyzing arachidonoyl-phospholipids in mouse peritoneal macrophages. *FEBS*, **244**, 51–56.

WRIGHT, G.W., OOI, C.E., WEISS, J. & ELSBACH, P. (1990). Purification of a cellular (granulocyte) and an extracellular (serum) phospholipase A_2 that participate in the destruction of Escherichia coli in a rabbit inflammatory exudate. *J. Biol. Chem.*, **265**, 6675–6681.

YOUNG, J.M., WAGNER, B.M. & SPIRES, D.A. (1983). Tachyphylaxis in 12-*O*-tetradecanoylphorbol acetate- and arachidonic acid-induced ear edema. *J. Invest. Dermatol.*, **80**, 48–52.

(Received November 30, 1992
Revised April 14, 1993
Accepted May 7, 1993)

Br. J. Pharmacol. (1993), **110**, 454–460

Vascular actions of purines in the foetal circulation of the human placenta

[1]M.A. Read, *A.L.A. Boura & *W.A.W. Walters

Department of Obstetrics & Gynaecology, John Hunter Hospital, Lookout Drive, Rankin Park NSW 2305, Australia and *Discipline of Reproductive Medicine, The University of Newcastle, University Drive, Callaghan NSW 2308, Australia

1 The vasoactive effects of adenosine triphosphate (ATP), adenosine and other purines in the foetal circulation of the human placenta were examined. Single lobules of the placenta were bilaterally perfused *in vitro* with Krebs buffer (maternal and foetal sides 5 ml min^{-1} each, 95% O_2:5% CO_2, 37°C). Changes in foetal vascular tone were assessed by recording perfusion pressure during constant infusion of each purine. To allow recording of the vasodilator effects, submaximal vasoconstriction was induced by concomitant infusion of prostaglandin $F_{2\alpha}$ (0.7–2.0 μmol l^{-1}).

2 ATP (1.0–100 μmol l^{-1}) usually caused concentration-dependent reductions in perfusion pressure. However, biphasic with initial transient increases, or only increases in pressure were sometimes observed. Falls in pressure caused by ATP were significantly reduced by addition to the perfusate of N^G-nitro-L-arginine (L-NOARG) (100 μmol l^{-1}) but not N^G-nitro-D-arginine (D-NOARG) (100 μmol l^{-1}). They were not influenced by addition of indomethacin (10 μmol l^{-1}) or L-arginine (100 μmol l^{-1}).

3 Adenosine (0.01–1.0 mmol l^{-1}) consistently caused concentration-dependent reductions in perfusion pressure, this effect not being influenced by indomethacin. L-NOARG, but not D-NOARG, reduced the potency of adenosine approximately three fold. L-Arginine, but not D-arginine enhanced its potency by a similar amount.

4 2-Methylthio-ATP, a selective P_{2y} agonist was approximately 50 times more potent than ATP as a vasodilator agent, always causing decreases in perfusion pressure.

5 β-γ-Methylene ATP, a selective P_{2x} agonist, was approximately 100 times more potent than ATP as a vasoconstrictor, but only caused transient increases in perfusion pressure.

6 The rank order of vasodilator potencies of a selection of adenosine receptor agonists was, 2-chloroadenosine>>5-(N-cyclopropyl)-carboxamidoadenosine, >5-N-ethylcarboxamidoadenosine, >2-chloro-N^6-cyclopentyladenosine, >CGS-21680>N^6-cyclohexyladenosine = adenosine. Vasodilatation due to adenosine was inhibited by the P_1-A_2 receptor antagonist 3,7-dimethyl-1-propargylxanthine (DMPX).

7 These results suggest that ATP may cause an endothelium-dependent vasodilatation in the foetal vessels of the human placenta via activation of a P_{2y} receptor linked to the formation of nitric oxide (NO). Vasodilatation caused by ATP may mask an accompanying vasoconstrictor effect mediated, via a P_{2x} receptor, in the villous vascular smooth muscle. Adenosine acting on P_1-A_2 receptors, which are also present in the foetal vasculature, may require synergistic interaction with NO to achieve a maximal vasodilator response.

Keywords: Purinoceptors; ATP; adenosine; placenta; villous vessels; nitric oxide; endothelium

Introduction

The cardiovascular effects of adenine and adenosine nucleotides were first reported by Drury & Szent-Györgyi (1929). Subsequently adenosine was reported to produce dilatation in all vascular beds studied except the kidney and placenta (Kenakin & Pike, 1987; Olsson & Pearson, 1990). In the foetal circulation of the human placenta, adenosine has been associated with vasoconstriction during hypoxia although the exact mechanism causing the vasoconstriction remains to be determined (Kitagawa *et al.*, 1987). Large amounts of adenosine are released into the foetal effluent from the placenta perfused with Krebs solution *in vitro* in response to hypoxia, with concomitant foetal vasoconstriction. It has been suggested that adenosine may participate in this response because it can be blocked by the adenosine antagonist, theophylline (Howard *et al.*, 1987; Slegel *et al.*, 1988). Importantly, these studies were performed using placentae with basal foetal vascular tone, which is normally very low (Boura & Walters, 1991). Detection of any vasodilator responses to adenosine under these conditions would be difficult.

Activation of endothelial P_{2y} purinoceptors by ATP results in endothelium-dependent dilatation of the majority of blood vessels (Kennedy & Burnstock, 1985; Kennedy *et al.*, 1985; Houston *et al.*, 1987; Olsson & Pearson, 1990; Mathie *et al.*,1991; Ralevic *et al.*, 1991). The vasodilatation may be mediated through release of either prostacyclin (PGI_2) or NO or perhaps a combination of the two (Carter *et al.*, 1988; Mathie *et al.*, 1991; Martin *et al.*, 1991). However, ATP-induced vasodilatation is not endothelium-dependent in all vessels (Kennedy & Burnstock, 1985; Mathieson & Burnstock, 1985). The mechanism of ATP-induced vasodilatation is variable and appears to be vessel- and species-specific.

Hence the present study was undertaken to examine the vasoactive effects of adenosine and ATP in the submaximally preconstricted foetoplacental circulation *in vitro*, a situation which may reveal possible vasodilator as well as vasoconstrictor effects. A high oxygen tension was also maintained in the perfusing fluid in order to inhibit placental release of adenyl purines which might have influenced responses to the exogenously administered substances. Efforts were also made to characterize the types of purinoceptor present in the foetoplacental vasculature and to determine whether any vasodilator effects of ATP or adenosine were dependent on formation of prostaglandins or NO.

[1] Author for correspondence.

Methods

Collection of placentae

Placentae were obtained within 20 min of vaginal or Caesarean delivery from women (aged 17–42 years) who had normal uncomplicated pregnancies. Some, but not all, of the patients had received one or more of the following drugs during labour, oxytocin (2 iu over 6–8 h), pethidine hydrochloride (100 mg, i.m.), promethazine maleate (12.5–25.0 mg, i.m.) or inhaled 70% N_2O and 30% O_2. These drugs have no apparent effects on responses of the foetal vascular tissues under the conditions used (Mak *et al.*, 1984). Placentae from women with blood pressures of $>140/90$ mmHg or who had experienced an increase of >20 mmHg diastolic pressure during pregnancy were not used, nor were those from women who smoked more than 10 cigarettes per day.

Placental lobule perfusion

Placental lobules were perfused by a technique originally described by Penfold *et al.* (1981) as modified by Mak *et al.* (1984). A suitable paired artery and vein, typically third or fourth branches of the chorionic plate vessels, to a peripheral placental lobule were chosen. The artery was cannulated with plastic tubing and the vein cut at a convenient point to allow blood and perfusate to escape. The cannula, which was inserted to the point where the artery disappeared below the surface of the chorionic plate, was connected to a Gilson Minipuls 3 (Gilson Medical Electronics, Villiers-le Bel, France) peristalic pump and the lobule perfused with Krebs solution containing (mmol l^{-1}): NaCl 97.0, $NaHCO_3$ 24.0, KCl 3.0, KH_2PO_4 1.2, $CaCl_2$ 1.89, $MgSO_4$ 1.0, D-glucose 5.5, pH 7.3) maintained at 37°C and gassed with 95% O_2:5% CO_2. The oxygen tension of the perfusing fluid was 400–500 mmHg. Each lobule was initially perfused at 1 ml min^{-1} for 5 min and thereafter with a constant flow rate of 5 ml min^{-1}. A venous cannula was inserted only after all visible blood had been flushed out of the lobule. The maternal side of the lobule was also perfused with Krebs solution under similar conditions to those used for perfusion of the foetal circulation. Perfusate was delivered into the maternal side of the placenta by two cannulae inserted into the spiral arterioles of the basal plate. Placentae were bathed in Krebs solution at 37°C.

Experimental design

Changes in foetoplacental vascular resistance were monitored by recording the inflow pressure to the lobule, with a Gould Statham P23D transducer (Cleveland, Ohio, U.S.A.), connected via a T-junction to the foetal arterial perfusion line. Signal conditioning and amplification was performed by a J-RAK PA-2 module (Melbourne, Australia) and displayed on a Kontron 330 flat-bed recorder (Eching, Germany). Inflow pressure at the start of perfusion was typically 80–100 mmHg, declining to a stable baseline pressure between 20–40 mmHg within a period of 1 h. Drug infusions were not started until a stable baseline pressure was achieved. Preparations having baseline pressures greater than 60 mmHg were discarded. Vasoconstriction was induced in the foetal circulation with $PGF_{2\alpha}$ (0.7–2.0 μmol l^{-1}) infused into the arterial cannula with a Gilson Minipuls 3 peristaltic pump. The concentration was adjusted so that a stable pressure of 100–120 mmHg was maintained prior to establishing concentration-responses curves to the purines.

Effects of adenosine and ATP

Adenosine, ATP or their analogues were infused into the foetal circulation in a logarithmic series of gradually increasing concentrations, with a third Gilson Minipuls 3 pump, at flow rates between 5–250 μl min^{-1}. Starting with a concentration causing a threshold effect, the concentration was increased by approximately 0.5 $\log_{10}$ intervals, after each effect obtained became constant. The highest concentration used was either that causing a maximal response or that which could be achieved due to the constraint of lack of sufficient solubility in the solution being infused. Concentration-response curves were obtained to both adenosine and ATP in the same placenta, the order of administration of the purines being alternated between successive experiments. Responses were expressed as the percentage change in the $PGF_{2\alpha}$-induced pressure (maximum pressure minus basal pressure) obtained prior to the start of infusion of the purine.

Effects of other purines

Further experiments also using cross-over designs were conducted to compare either adenosine or ATP with other various agonists. The order of administration of agonist and endogenous ligand was alternated in successive experiments. Cumulative concentration-response curves were obtained with the exception of that for the constrictor effects of ATP and β-γ-methylene-ATP which were transient. In these instances, an increased concentration of each agonist was administered only after a stable baseline perfusion pressure had been re-established. When various agonists were dissolved in any vehicle other than distilled water or Krebs solution, the vehicle was examined independently for possible vascular effects.

Indirect effects of adenosine and ATP

The contribution of prostanoids or NO to the vasodilator effects of adenosine and ATP were examined by use of the cyclo-oxygenase inhibitor indomethacin (10 μmol l^{-1}) and the NO synthase inhibitor N^G-nitro-L-arginine (L-NOARG 100 μmol l^{-1}) (Mulsch & Busse, 1990). For the latter series of experiments N^G-nitro-D-arginine (D-NOARG) was used in the same concentration, for control purposes, in further preparations. L-Arginine (100 μmol l^{-1}), the precursor of NO (Palmer *et al.*, 1988) was also used in attempts to enhance any NO-mediated vasoactivity shown by either adenosine or ATP and compared with the effect of D-arginine as a control A crossover design was used to study their effects. Concentration-response curves in the presence of L-arginine and D-arginine were obtained either before or after their respective control curves had been obtained. Indomethacin, L-NOARG, D-NOARG, L-arginine and D-arginine were administered in the perfusion fluid and delivered to both foetal and maternal circulations for 60 min before establishment of concentration-response curves to the purine being studied. Concentration-response curves in the presence of indomethacin and L-NOARG were obtained after control curves.

Effects of antagonists at P_1-A_1 and P_1-A_2 receptors on response to adenosine

To study the effects of either P_1-A_1 or P_1-A_2 receptor blockade on vasodilator responses to adenosine, XAC (Rossi *et al.*, 1987) and DMPX (Seale *et al.*, 1988) were used respectively. A control concentration-response curve was determined in groups of 3–4 placentae, each concentration being infused until the effect became constant; 30 min after commencing infusion of the antagonist (80 μmol l^{-1}) a second concentration-response curve to adenosine was obtained. The curves, in the absence and presence of antagonist, were compared. Comparisons were also made with a series of control curves to adenosine obtained over 0.5–4.0 h in the absence of antagonist on both occasions.

Drugs and chemicals

Chemicals used in the Krebs solution were of analytical grade (Analar BDH, Australia). Adenosine, ATP (Boeh-

ringer Mannheim, Germany). β-γ-methylene ATP, L-arginine, D-arginine, N^G-nitro-L-arginine (L-NOARG), N^G-nitro-D-arginine (D-NOARG), (Sigma, St Louis, U.S.A.), 2-methylthio-ATP, N^6-cyclohexyladenosine (CHA), 3,7-dimethyl-1-propargylxanthine (DMPX), 8-[4-[[[[(2-aminoethyl)amino]carbonyl]methyl]oxy]phenyl]-1,3-dipropylxanthine (XAC) (Research Biochemicals, Natick, U.S.A), CGS-21680 (2-[4-(-2-carboxyethyl)-phenethylamino]-5'-N-ethylcarboxamido adenosine HCl) (Ciba Geigy, Pharmaceuticals Division, Summit, New Jersey, U.S.A.), 2-chloroadenosine (2-CADO) and 2-chloro-N^6-cyclopentyladenosine (2-CCPA) (Research Biochemicals) were dissolved in distilled water. 5'-N-ethylcarboxamidoadenosine (5-NECA) and 5'-(N-cyclopropyl)-carboxamidoadenosine (5-CPCA) (Research Biochemicals) were dissolved in 0.02 mol l^{-1} HCl. Indomethacin (Sigma, St Louis, U.S.A.) was dissolved in 5% $NaHCO_3$. Prostaglandin $F_{2\alpha}$ was supplied as its trometamol salt (Dinoprost, Upjohn, Sydney, Australia) at a concentration of 5 mg ml^{-1} in sterile distilled water and diluted as required in distilled water.

Statistical analysis

All values are expressed as means (± s.e.mean) unless otherwise stated. Linear regression analysis was performed on all concentration-response cruves using Minitab (Pasadena, U.S.A.). Differences in the linear portions of the curves were compared and tested for significant displacement and parallelism, as described by Bowman & Rand (1980). Unless otherwise stated a probability value of <0.05 was considered significant. Non-parallel curves were tested for differences by two-way analysis of variance. Pairwise comparisons were made by use of Student's paired t test where indicated.

Results

Effects of adenosine and ATP

Both ATP and adenosine caused concentration-dependent reductions in perfusion pressure when infused into isolated placental lobules. These effects developed slowly, maximal responses to each being seen 20–30 min after the start of infusion. Adenosine was significantly less potent in reducing perfusion pressure than ATP (Figure 1). It consistently reduced the perfusion pressure in every placenta examined ($n = 48$). In contrast, ATP caused variable effects. Usually ATP produced concentration-dependent falls in perfusion pressure ($n = 16$). In others ($n = 5$) only concentration-dependent transient increases in pressure occurred. Additionally, biphasic effects due to ATP were observed in further preparations, with an initial rise in pressure being followed by a fall ($n = 8$). Reductions in perfusion pressure at low concentrations but increases in response to higher concentrations also occurred ($n = 5$). For comparison of the relative vasodilator potencies of ATP and adenosine (Figure 1) data were used only from those placentae responding solely by vasodilatation to ATP.

Control experiments were performed to determine whether responses to ATP or adenosine changed with time, because of the slow responses to each concentration of the purines. Following establishment of an initial concentration-response curve to either ATP or adenosine, subsequent concentration-response curves were obtained over a period of 0.5–4.0 h. No statistically significant differences from their respective controls were observed in responses to either adenosine or ATP following these time intervals (data not shown).

Effects of other purines

The selective P_{2y} receptor agonist, 2-methylthio-ATP, caused concentration-dependent reductions in perfusion pressure (Figure 2) and was significantly more potent than ATP. A comparison of the curve for 2-methylthio-ATP with that for ATP showed that 2-methylthio-ATP was approximately 50 times more potent (Table 1a). Unlike ATP, 2-methylthio-ATP caused only reductions in perfusion pressure in all preparations ($n = 6$). However, the differences found between the vasodilator potencies of ATP and the other purines could fail to reflect accurately their true relative activities. The data used to assess the potency of ATP were obtained from placentae responding only by vasodilatation. Nevertheless its vasoconstrictor effect, seen more prominently in other preparations, could have concomitantly opposed to variable extents the vasodilator responses recorded, thus reducing its apparent vasodilator potency.

The selective P_{2x} receptor agonist, β-γ-methylene ATP, exclusively produced concentration-dependent increases in perfusion pressure (Figure 2). No vasodilator responses to this agonist were observed ($n = 6$). The increases in perfusion pressure caused by β-γ-methylene ATP or ATP were transient and showed fade, maximum responses being achieved approximately 5 min after starting infusion. Compared to ATP, β-γ-methylene-ATP was approximately 100 times more potent as a vasoconstrictor agent (Table 1a). The maximum effective concentration of β-γ-methylene ATP could not be determined, high concentrations causing very large increases in perfusion pressure (>200 mmHg) and complete cessation of the venous outflow, suggesting that leakage was occurring between the foetal and maternal compartments.

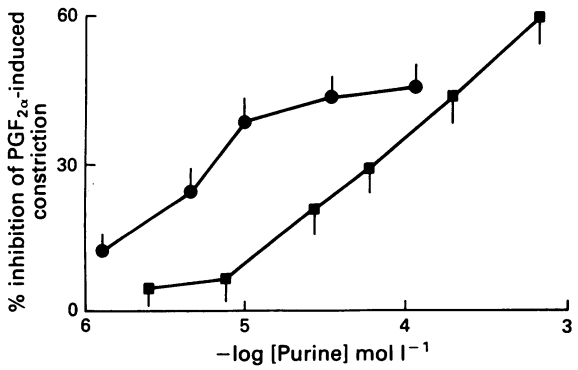

Figure 1 Concentration-response curves for the vasodilator effects of ATP (●) and adenosine (■) in blood vessels of the human placenta. Each point is the mean ± s.e.mean of at least 16 determinations. Curves do not differ significantly from parallelism and are significantly displaced, $P<0.05$.

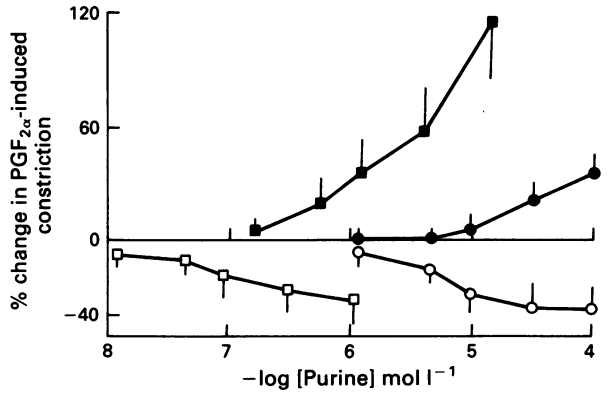

Figure 2 Concentration-response curves for vasoconstriction caused by ATP (●) and β-γ-methylene-ATP (■) and vasodilatation caused by ATP (○) and 2-methylthio-ATP (□). Each point is the mean ± s.e.mean of at least 6 determinations. The vasodilator response curves to ATP and 2-methylthio-ATP do not differ significantly from parallelism and are significantly displaced, $P<0.05$. The vasoconstrictor response curves to ATP and β-γ-methylene-ATP do not differ significantly from parallelism and are significantly displaced, $P<0.05$.

2-CADO, an agonist with activity at both P_1-A_1 and P_1-A_2 receptors (Olsson & Pearson, 1990), was the most potent purine examined for effects mediated by P_1 receptors, causing reductions in perfusion pressure. As a vasodilator agent, 2-CADO was approximately 40 times more potent than adenosine, as indicated by comparison of the linear portions of their respective concentration-response curves (Table 1c).

5-CPCA, a selective P_1-A_2 receptor agonist (Daly, 1982) also caused concentration-dependent reductions in perfusion pressure. Comparison of the regression lines obtained indicated that 5-CPCA was approximately 7 times more potent than adenosine (Table 1c). 2-CCPA, a selective P_1-A_1 receptor agonist (Lohse *et al.*, 1988) was found to be 4 times more potent as a vasodilator than adenosine in the placenta (Table 1c). 5-NECA, a non-selective adenosine agonist (Olsson & Pearson, 1990) also caused reductions in perfusion pressure. Comparison of the concentration-response curve obtained with that for adenosine indicated that 5-NECA was approximately 5 times more potent than adenosine (Table 1c). CGS-21680, a selective P_1-A_2 agonist (Olsson & Pearson, 1990) was approximately 2.5 times more potent than adenosine in causing dilatation, the difference being significant (Table 1c).

CHA, a selective P_1-A_1 receptor agonist (Olsson & Pearson, 1990) produced concentration-dependent reductions in perfusion pressure, but the concentration-response curve was not significantly different from that of adenosine (Table 1c).

Indirect effects of adenosine and ATP

Indomethacin (10.0 μmol l^{-1}) had no effect on the vasodilator activities of adenosine and ATP ($n = 6$) (Table 1b). L-NOARG (100 μmol l^{-1}) significantly inhibited ATP-induced reductions in perfusion pressure (Figure 3; $n = 6$) and had a smaller, but statistically significant inhibitory effect on adenosine-induced falls in perfusion pressure (Figure 4; $n = 6$). In further preparations, reductions in perfusion pressure caused by ATP (1.34–436 μmol l^{-1}) or adenosine (2.5–823 μmol l^{-1}) were not significantly affected by infusion of D-NOARG (100 μmol l^{-1}) ($n = 5$ and 4 respectively). L-NOARG had no effect on the increases in perfusion pressure caused by ATP, when they occurred. In instances when biphasic responses to ATP were observed initially, during infusion of L-NOARG relaxant responses were absent ($n = 3$). Infusion of L-NOARG in a number of preparations

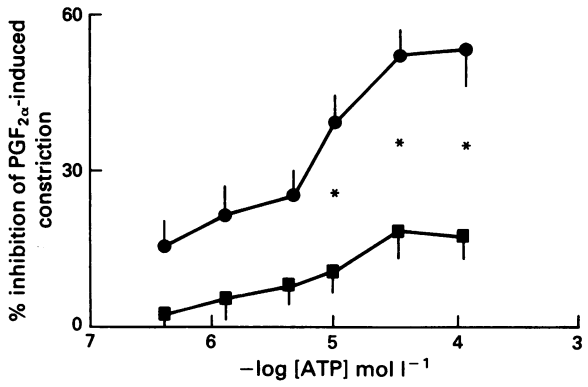

Figure 3 Effects of N^G-nitro-L-arginine (L-NOARG) (100 μmol l^{-1}) on ATP-mediated vasodilatation in foetal vessels. Concentration-response curves (± s.e.mean) to ATP in the absence (●) and presence (■) of L-NOARG. Curves differ from parallelism and are significantly displaced, $P < 0.05$. *$P < 0.05$, Student's t test between mean responses to the same concentration of agonist.

Table 1 Effects and relative potencies of purines in the foetal circulation of the placenta

a

Agonist	*Vasodilatation*	*Vasoconstriction*	*Potency* (cf. ATP)
ATP	+	+	1.0
Adenosine	+		0.16 (0.15–0.17)*
2-methylthio-ATP	+		50 (36–70)*
β-γ-methylene ATP		+	112 (87–144)*

*Significantly different from ATP (95% confidence limits)
(+ vasoactive effect, refer to text)

b

Agonist	*Potency* (cf. control)
ATP + L-arginine 100 μmol l^{-1}	1.3 (0.4–7.8)
ATP + L-NOARG 100 μmol l^{-1}	inhibited (see Fig 2b)
ATP + indomethacin 10 μmol l^{-1}	1.4 (0.7–3.8)
Adenosine + L-arginine 100 μmol l^{-1}	3.01 (2.52–3.56)*
Adenosine + L-NOARG 100 μmol l^{-1}	0.38 (0.27–0.52)*
Adenosine + indomethacin 10 μmol l^{-1}	2.4 (0.5–4.0)

*Significantly different from control (95% confidence limits)

c

Agonist	*P_1-A_2*	*P_1-A_1*	*Potency* (cf. Adenosine)
Adenosine	+	+	1.0
2-CADO	+	+	38.9 (35.5–42.6)*
5-CPCA	+		7.2 (6.4–8.1)*
5-NECA	+	+	5.2 (4.6–6.6)*
2-CCPA		+	3.8 (3.4–4.3)*
CGS-21680	+		2.4 (2.1–2.7)*
CHA		+	1.5 (1.0–2.4)

*Significantly different from adenosine (95% confidence limits)
(+ reported agonist selectivity, refer to text)

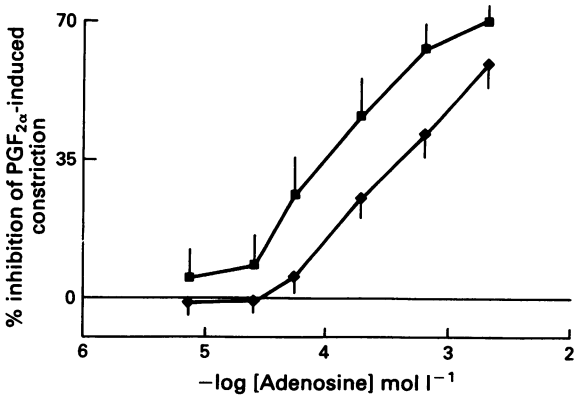

Figure 4 Concentration-dependent vasodilatation caused by adenosine in the absence (■) and presence (◆) of N^G-nitro-L-arginine (100 μmol l^{-1}). Each point is the mean ± s.e.mean of 6 determinations. Curves do not differ significantly from parallelism but are significantly displaced, $P<0.05$.

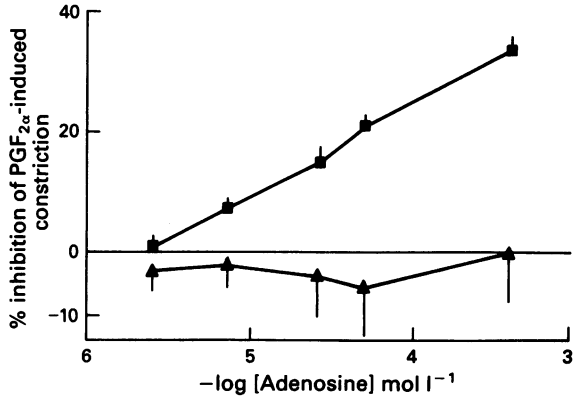

Figure 6 Vasodilatation caused by adenosine in the absence (■) and presence (▲) of the P_1-A_2 antagonist 3,7-dimethyl-1-propargylxanthine (DMPX, 80 μmol l^{-1}) ($n=4$). The curves are significantly different ($P<0.05$, two way analysis of variance) and are not parallel.

($n=3$) was followed by increases in perfusion pressure (up to 30 mmHg). This effect, however, was absent in the remainder ($n=9$). When perfusion pressures increased in the presence of L-NOARG the concentration of $PGF_{2\alpha}$ being infused concomitantly was reduced so that the pressure fell back to the basal level before infusing either ATP or adenosine.

L-Arginine (100 μmol l^{-1}), when infused through the foetal circulation for 60 min did not change the basal perfusion pressure significantly ($n=12$) and was without effect on ATP-induced reductions in perfusion pressure (Table 1b). In contrast, a significant potentiation of adenosine-induced reduction in perfusion pressure (Figure 5) was observed during infusion of this amino acid. In further experiments there was no significant change in the potency of adenosine when a similar concentration of D-arginine was infused ($n=4$).

Effects of antagonists at P_1-A_1 and P_1-A_2 receptors on responses to adenosine

Addition of DMPX, an antagonist selective for P_1-A_2 purinoceptors (Seale *et al.*, 1988) to the Krebs solution (80 μmol l^{-1}) perfusing the placental lobules markedly reduced vasodilator responses to adenosine (Figure 6). In the presence of the XAC (80 μmol l^{-1}), which has high affinity but moderate selectivity as an antagonist at P_1-A_1 receptors (Rossi *et al.*, 1987), the mean vasodilator responses to adenosine (3–300 μmol l^{-1}) were not significantly different from those of the concentration-response curve to adenosine obtained in its absence (linear regression analysis, $P>0.05$). In addition, neither curve differed significantly in position from that of the control curve to adenosine obtained when examining DMPX, as shown in Figure 6.

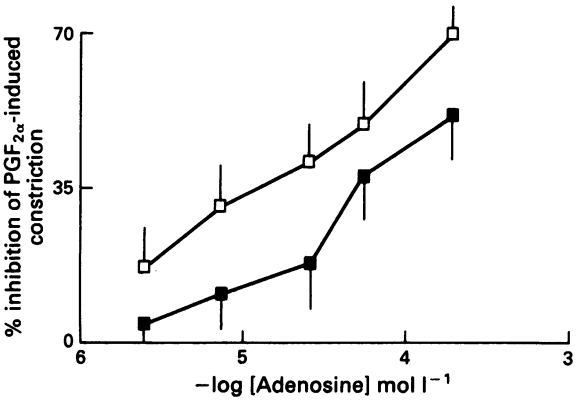

Figure 5 Concentration-dependent vasodilatation caused by adenosine in the absence (■) and presence (□) of L-arginine (100 μmol l^{-1}). Each point is the mean ± s.e.mean of 6 determinations. Curves do not differ significantly from parallelism but are significantly displaced, $P<0.05$.

Discussion

The importance of endogenous adenyl purines in the control of vascular resistance and foetal blood flow in the placenta is not known. However purines, interacting with autacoids both locally released and circulating in the umbilical blood, are likely to have important roles in the control of villous vascular tone, particularly as neural mechanisms do not influence the foetal extracorporeal vasculature (Boura & Walters, 1991). Adenosine concentrations in the placenta increase 100 fold during delivery (Sim & Maguire, 1972) and it is released from perfused placental tissues into the foetal circulation during ischaemia (Kitagawa *et al.*, 1987). Adenosine and its metabolites are also found in umbilical cord blood after delivery (Irestedt *et al.*, 1989) and during perinatal hypoxia (O'Connor *et al.*, 1981).

The present study has shown that adenyl purines in the foetal circulation of the human placenta cause both vasoconstriction and vasodilatation, the relative prominence of which depended on the purine. Thus, adenosine, 2-CADO, 5-CPCA, 2-CCPA, 5-NECA, CHA and CGS -21680 caused only vasodilatation and β-γ-methylene-ATP only vasoconstriction in all placental preparations. In contrast, ATP exerted both effects, the prominence of each depending on the preparation. In particular, the vasodilatation always seen in the present study during infusion of adenosine contrasted with its reported ability to cause placental foetal vasoconstriction (Kitagawa *et al.*, 1987; Slegel *et al.*, 1988). However, this apparent anomaly is capable of explanation. In the present work the normal very low tone of the villous vasculature was increased with $PGF_{2\alpha}$ to permit any vasodilator responses to be seen. The oxygen tension of the Krebs solution was also high. In the other reported studies the tone of the vasculature was low and vasoconstrictor responses to reducing oxygen tension examined. The combined findings may have physiological implications. Release of adenosine in local areas of ischaemia in the placenta may contribute to the ensuing vasoconstrictor response, so directing blood to placental villi having higher oxygen tensions where its vasodilator effect could help sustain adequate blood flow.

Unequivocal identification of the receptors involved in mediating the vascular effects of purines is difficult, due to lack of highly specific antagonists of their actions and the ability of cells to vary the concentration of an individual

purine at receptor sites by uptake and metabolism. Nevertheless, Burnstock (1978) classified receptors for purines into two groups, P_1 and P_2, based on their relative potencies and various preparations. The rank order of potency for agonists at the P_1 receptor is adenosine > AMP > ADP > ATP, while the reverse potency order defines P_2 receptors. The latter were subsequently further divided into two subgroups, P_{2x} and P_{2y} (Burnstock & Kennedy, 1985). The P_{2y} receptor which is found on the vascular endothelium, has been linked to the production of NO (Mathie *et al.*, 1991) and prostacyclin (Carter *et al.*, 1988). The P_{2x} receptor, found on vascular smooth muscle cells,may be directly coupled to activation of calcium channels (Benham & Tsien, 1987). P_1 receptors have also been divided into two sub-groups, A_1 and A_2, primarily on their ability, when activated, to inhibit or stimulate adenylate cyclase respectively (Olsson & Pearson, 1990).

The present study demonstrated the probable existence of the P_{2x}, P_{2y} and P_1-A_2 subgroups of purine receptor in the foetal resistance vessels of the human placenta. In this respect human placental vessels appear to be similar to human subcutaneous and omental resistance vessels which also contain P_{2x}, P_{2y} and P_1 receptors (Martin *et al.*, 1991). The activity of ATP and the much higher potency of the selective agonist 2-methylthio-ATP indicates that the vasodilatation caused by ATP in the foetoplacental vascular bed is probably mainly due to activation of P_{2y} receptors. Presumably, these are located on the vascular endothelium (Kennedy *et al.*, 1985; Needham *et al.*, 1987) since ATP-induced vasodilatation appeared dependent on formation of NO, being substantially inhibited by L-NOARG. Mathie *et al.* (1991) have also shown that ATP vasodilatation in the rabbit hepatic arterial vascular bed is mediated by NO. No evidence was found for prostacyclin, or other vasodilator prostaglandins, being involved in the vasodilator effects of ATP in the placenta since the cyclo-oxygenase inhibitor indomethacin did not modify responses to ATP.

The presence of P_{2x} receptors in the resistance vessels of the foetoplacental vascular bed was indicated by the finding that the P_{2x} agonist, β-γ-methylene-ATP, was a potent constrictor agent. At times, ATP also caused vasoconstriction. Sometimes this action preceded its vasodilator action whereas in other preparations it was the sole effect. The dilator and constrictor responses to ATP suggest that it has the ability to interact with both P_{2y} and P_{2x} receptor subtypes. P_{2y} receptor-mediated vasorelaxation appeared to be the predominant effect, otherwise masking vasoconstriction mediated by P_{2x} receptors. Variability in responses to ATP, in what appeared to be identical preparations, could have been due to changes in endothelial cell function. A vascular endothelium with reduced function, due to ischaemia before perfusion or to other factors, may tend to reduce dilator responses to ATP. Support for this idea came from the observation that when biphasic responses to ATP were obtained, L-NOARG inhibited the secondary dilatation.

Formation of NO by the foetal vasculature also contributed to the vasodilator responses to adenosine. The precursor of NO, L-arginine, potentiated vasodilator responses to this purine whereas responses were reduced during inhibition of NO synthesis with L-NOARG. It may be that concomitant production of NO by the foetal vascular endothelial cells during the vasoconstriction caused by prostaglandin $F_{2\alpha}$ administration contributed to the vascular dilator response to adenosine. Basal NO release has been demonstrated in the foetal circulation of the human perfused placenta (Gude *et al.*, 1990) and endogenous NO reduces foetal vascular responses to endothelin, U44619 and 5-hydroxytryptamine (Gude *et al.*, 1993).

L-Arginine was found to potentiate vasodilatation caused by adenosine but not that caused by ATP. This finding, bearing in mind the evidence obtained indicating that NO release contributed to responses to both purines, can perhaps be related to the method used for selecting placentae. For those experiments studying the effects of L-arginine on responses to ATP, the placentae used were those that responded to ATP solely by vasodilatation, no vasoconstrictor responses being seen. Thus placental endothelial cell function in the ATP experiments was likely to be good and addition of L-arginine unlikely to increase further the output of NO. On the other hand, the variable nature of responses to ATP, dilatation and vasoconstriction, indicated possible reduced endothelial cell function in some placentae. The latter could not have been identified in the group in which adenosine was used, as this purine consistently caused vasodilatation, presumably mainly due to a direct action on the foetal vascular smooth muscle, as in other vessels (Olsson & Pearson, 1990). In the latter circumstances there could have been some depression of endothelial cell function causing less than optimal output of NO which improved when the availability of L-arginine was increased.

The probable existence of P_1-A_2 receptors mediating the action of adenosine in the foetal vessels of the placenta was obtained by the finding that DMPX, an antagonist at these receptors (Seale *et al.*, 1988), inhibited responses to the purine. In contrast, a relatively high concentration of XAC had no effect on responses to adenosine, this agent being a moderately selective antagonist at P_1-A_1 receptors (Rossi *et al.*, 1987). A_2 binding sites have been identified on human placental cell membranes (Fox & Kurpis, 1983). The rank order of potencies found for the P_1 receptor agonists used also indicated that, in keeping with other studies (Edvinsson & Fredholm, 1983; Kusachi *et al.*, 1983; Leung *et al.*, 1985; Mustafa & Askan, 1985; Hutchison *et al.*, 1988) relaxation of human placental foetal vascular smooth muscle in response to purines can additionally be mediated through an A_2 receptor subtype. On the other hand, 5-NECA was not as potent as a vasodilator in the placenta as reported in other vascular preparations (Olsson & Pearson, 1990) and was found to be less potent than 2-CADO. CGS-21680 was less potent than 5-NECA and only slightly more potent than adenosine despite being reported to be a highly selective P_1-A_2 agonist in the rat brain (Jarvis *et al.*, 1989). CGS-21680 has also been found to be less potent than 5-NECA in causing relaxation of the human coronary artery *in vitro* (Makujina *et al.*, 1992). Variation in the relative potencies of the various A_2 agonists between preparations appears to be common (Olsson & Pearson, 1990).

In summary, the results of this study indicate that in foetal blood vessels in the human placenta, in the presence of high oxygen tensions, both ATP and adenosine cause vasodilatation, the magnitude of these responses being modified by changes in endothelial NO output. Vasodilatation to ATP is probably mediated by P_{2y} receptors located on the endothelium. ATP can also cause vasoconstriction probably mediated via a P_{2x} receptor, perhaps located on the vascular smooth muscle. Therefore, the overall response to ATP may be critically dependent on endothelial cell function. On the other hand, vasodilatation caused by adenosine may be predominantly mediated by a P_1-A_2 receptor and may require synergistic interaction with endogenously produced NO to exert its full effect.

We gratefully acknowledge the co-operation of the nursing and medical staff of the Department of Obstetrics, John Hunter Hospital in obtaining placentae and Dr R.D. Robson of Ciba Geigy (Pharmaceuticals Research Laboratory, Summit, New Jersey, U.S.A.) for the kind gift of CGS-21680. This work was supported by The University of Newcastle (Grant No 45/200/204R) and NH&MRC (Grant No 920922).

References

BENHAM, C.D. & TSIEN, R.W. (1987). A novel receptor-operated Ca^{2+} permeable channel activated by ATP in smooth muscle. *Nature*, **328**, 275–278.

BOURA, A.L.A. & WALTERS, W.A.W. (1991). Review article: autacoids and the control of vascular tone in the human umbilical-placental circulation. *Placenta*, **12**, 453–477.

BOWMAN, W.C. & RAND, M.J. (1980). In *Textbook of Pharmacology*. 2nd ed. ed. Bowman, W.C. & Rand, M.J. pp. 41.1–41.48. Oxford: Blackwell.

BURNSTOCK, G. (1978). A basis for distinguishing two types of purinergic receptors. In *Cell Membrane Receptors for Drugs and Hormones: A Multidisciplinary Approach*. ed. Staub, R.W. & Bolis, L. pp. 107–118. New York: Raven Press.

BURNSTOCK, G. & KENNEDY, C. (1985). Is there a basis for distinguishing two types of P_2-purinoceptor? *Gen. Pharmacol.*, **16**, 433–440.

CARTER, T.D., HALLAM, T.J., CUSACK, N.J. & PEARSON, J.D. (1988). Regulation of P_{2y}-purinoceptor-mediated prostacyclin release from human endothelial cells by cytoplasmic calcium concentration. *Br. J. Pharmacol.*, **95**, 1181–1190.

DALY, J.W. (1982). Adenosine receptors: targets for future drugs. *J. Med. Chem.*, **25**, 197–207.

DRURY, A.N. & SZENT-GYÖRGYI, A. (1929). The physiological activity of adenine compounds with especial reference to their action upon the mammalian heart. *J. Physiol.*, **68**, 213–237.

EDVINSSON, L. & FREEDHOLM, B.B. (1983). Characterization of adenosine receptors in isolated cerebral arteries of the cat. *Br. J. Pharmacol.*, **80**, 631–637.

FOX, I.H. & KURPIS, L. (1983). Binding characteristics of an adenosine receptor in the human placenta. *J. Biol. Chem.*, **258**, 6952–6955.

GUDE, N.M., BOURA, A.L.A., BRENNECKE, S.P., JAMAL, O., SMITH, R. & WALTERS, W.A.W. (1992). Evidence for inhibition by endothelium derived relaxing factor of thromboxane A_2 receptor mediated vasoconstriction in fetal vessels of human perfused placental lobules. *Placenta*, **13**, 597– 605.

GUDE, N.M, KING, R.G. & BRENNECKE, S.P. (1990). Role of endothelium-derived nitric oxide in maintenance of low fetal vascular resistance in placenta. *Lancet*, **336**, 1589–1590.

HOUSTON, D.S., BURNSTOCK, G. & VANHOUTTE, P.M. (1987). Different P_2 purinergic receptor sub-types of endothelium and smooth muscle in canine blood vessels. *J. Pharmacol. Exp. Ther.*, **241**, 501–506.

HOWARD, R.B., HOSOKAWA, T. & MAGUIRE, M.H. (1987). Hypoxia-induced fetoplacental vasoconstriction in perfused human placental cotyledons. *Am. J. Obstet. Gynecol.*, **157**, 1261–1266.

HUTCHISON, A.J., WEBB, R.L., OEI, H.H., GHAI, G.R., ZIMMERMAN, M.B. & WILLIAMS, M. (1989). CGS 21,680C, an A_2 selective adenosine receptor agonist with preferential hypotensive activity. *J. Pharmacol. Exp. Ther.*, **251**, 47–55.

IRESTEDT, L., DAHLIN, I., HERTZBERG, T., SOLLEVI, A. & LAGERCRANTZ, H. (1989). Adenosine concentration in umbilical cord blood of newborn infants after vaginal delivery and Cesarean section. *Pediatr. Res.*, **26**, 106–108.

JARVIS, M.F., SCHULZ, R., HUTCHISON, A.J., DO, U.H., SILLS, M.A. & WILLIAMS, M. (1989). [^{3}H]CGS-21680, a selective A_2 agonist directly labels A_2 receptors in rat brain. *J. Pharmacol. Exp. Ther.*, **251**, 888–891.

KENAKIN, T.P. & PIKE, N.B. (1987). An *in vitro* analysis of purine mediated renal vasoconstriction in rat isolated kidney. *Br. J. Pharmacol.*, **90**, 373–381.

KENNEDY, C. & BURNSTOCK, G. (1985). Evidence for two types of P_2-receptor in longitudinal muscle of the rabbit portal vein. *Eur. J. Pharmacol.*, **111**, 49–56.

KENNEDY, C., DELBRO, D. & BURNSTOCK, G. (1985). P_2-receptors mediate both vasodilatation (via the endothelium) and vasoconstriction of the isolated rat femoral artery. *Eur. J. Pharmacol.*, **107**, 161–168.

KITAGAWA, H., SLEGEL, P.H. & MACGUIRE, M.H. (1987). Ischaemia induced vasoconstriction and adenosine release in perfused human placental cotyledons. *Pharmacologist*, **29**, 197.

KUSACHI, S., THOMPSON, R.D. & OLSSON, R.A. (1983). Ligand selectivity of dog coronary adenosine receptor resembles that of adenylate cyclase stimulatory $R_{(a)}$ receptors. *J. Pharmacol. Exp. Ther.*, **227**, 316–322.

LEUNG, E.C., JOHNSTON, C.I. & WOODCOCK, E.A. (1985). An investigation of the receptors involved in the coronary vasodilatory effect of adenosine analogues. *Clin. Exp. Pharmacol. Physiol.*, **12**, 515–519.

LOHSE, M.J., KLOTZ, K.N., SCHWABE, U., CRISTALLI, G., VITTORI, S. & GRIFANTINI, M. (1988). 2-Chloro-N^6-cyclopentyladenosine: a highly selective agonist at A_1 adenosine receptors. *Naunyn Schmied. Arch. Pharmacol.*, **337**, 687–689.

MAK, K.K.-W., GUDE, N.M., WALTERS, W.A.W. & BOURA, A.L.A. (1984). Effects of vasoactive autacoids on the human umbilical-fetal placental vasculature. *Br. J. Obstet. Gynaecol.*, **91**, 99–106.

MAKIJINA, S.R., SABOUNI, M.H., BHATIA, S., DOUGLAS, F.L. & MUSTAFA, S.J. (1992). Vasodilatory effects of adenosine A_2 receptor agonists CGS 21680 and CGS 22492 in human vasculature. *Eur. J. Pharmacol.*, **221**, 243–247.

MARTIN, G.N., MCG.THOM, S.A. & SEVER, P.S. (1991). The effects of adenosine triphosphate (ATP) and related purines on human isolated subcutaneous and omental resistance arteries. *Br. J. Pharmacol.*, **102**, 645–650.

MATHIE, R.T., RALEVIC, V., ALEXANDER, B. & BURNSTOCK, G. (1991). Nitric oxide is the mediator of ATP-induced dilatation of the rabbit hepatic arterial vascular bed. *Br. J. Pharmacol.*, **103**, 1602–1606.

MATHIESON, J.J.I. & BURNSTOCK, G. (1985). Purine mediated relaxation and constriction of isolated rabbit mesenteric artery are not endothelium dependent. *Eur. J. Pharmacol.*, **118**, 221–229.

MULSCH, A. & BUSSE, R. (1990). N^G-nitro-L-arginine (N^5-[imino-(nitroamino methyl]-L-orthinine) impairs endothelium dependent dilatations by inhibitory cytosolic nitric oxide synthesis from L-arginine. *Naunyn Schmied. Arch. Pharmacol.*, **341**, 143–147.

MUSTAFA, S.J. & ASKAN, A.O. (1985). Evidence suggesting an $R_{(a)}$-type adenosine receptor in bovine coronary arteries. *J. Pharmacol. Exp. Ther.*, **232**, 49–56.

NEEDHAM, L., CUSACK, N.J., PEARSON, J.D. & GORDON, J.L. (1987). Characteristics of the P_2 purinoceptor that mediates endothelial prostacyclin production by pig aortic endothelial cells. *Eur. J. Pharmacol.*, **143**, 199–209.

O'CONNOR, M.C., HARKNESS, R.A., SIMMONDS, R.J. & HYTTEN, F.E. (1981). The measurement of hypoxanthine, xanthine, inosine and uridine in umbilical cord blood and fetal scalp blood samples as a measure of fetal hypoxia. *Br. J. Obstet. Gynaecol.*, **88**, 381–390.

OLSSON, R.A. & PEARSON, J.D. (1990). Cardiovascular purinoceptors. *Physiol. Rev.*, **70**, 761–845.

PALMER, R.M.J., REES, D.D., ASHTON, D.S. & MONCADA, S. (1988). L-arginine is the physiological precursor for the formation of nitric oxide in endothelium dependent relaxation. *Biochem. Biophys. Res. Commun.*, **1553**, 1251–1256.

PENFOLD, P., DRURY, L., SIMMONDS, R. & HYTTEN, F.E. (1981). Studies on a single placental cotyledon in vitro: 1. The preparation and its viability. *Placenta*, **2**, 149–154.

RALEVIC, V., MATHIE, R.T., ALEXANDER, B. & BURNSTOCK, G. (1991). Characterisation of P_{2x} and P_{2y}-purinoceptors in the rabbit hepatic arterial vasculature. *Br. J. Pharmacol.*, **103**, 1108–1113.

ROSSI, N.F., CHURCHILL, P.C., JACOBSON, K.A. & LEAHY, A.E. (1987). Further characterization of the renovascular effects of N^6-cyclohexyladenosine in the isolated perfused rat kidney. *J. Pharmacol. Exp. Ther.*, **240**, 911–915.

SEALE, T.W., ABLA, K.A., SHAMIM, M.T., CARNEY, J.M. & DALY, J.W. (1988). 3,7-Dimethyl-1-propargylxanthine: a potent and selective *in vivo* antagonist of adenosine analogs. *Life Sci.*, **43**, 1671–1684.

SIM, M.K. & MAGUIRE, M.H. (1972). Presence of adenosine in the human term placenta: determination of adenosine content and pathways of adenosine metabolism. *Circ. Res.*, **31**, 779–788.

SLEGEL, P., KITAGAWA, H. & MAGUIRE, M.H. (1988). Determination of adenosine in fetal perfusates of human placental cotyledons using fluorescence derivatization and reversed-phase high-performance liquid chromatography. *Anal. Biochem.*, **171**, 124–134.

(Received February 22, 1993
Revised April 23, 1993
Accepted May 7, 1993)

Br. J. Pharmacol. (1993), **110**, 461–469

The effect of ions and second messengers on long-term potentiation of chemical transmission in avian ciliary ganglia

T.R.D. Scott & [1]M.R. Bennett

The Neurobiology Laboratory, Department of Physiology, The University of Sydney, N.S.W. 2006, Australia

1 The effects of tetanic stimulation of the oculomotor nerve on transmission through the avian ciliary ganglion have been determined by use of the amplitude of the compound action potential recorded in the ciliary nerve, in the presence of hexamethonium (300 μM), as a measure of synaptic efficacy.

2 Tetanic stimulation for 20 s at 30 Hz potentiated the chemical phase of the compound action potential by at least 100% of its control level. This potentiation, reflecting an increase in synaptic efficacy, decayed over two distinct time courses: firstly, a rapid decay with a time constant in the order of minutes, and secondly, a slower decay, representing a smaller potentiation, with a time constant in the order of an hour. The large increase in synaptic efficacy is attributed to post-tetanic potentiation (PTP) whereas the smaller but longer lasting increase is attributed to long-term potentiation (LTP).

3 Higher frequencies of tetanic stimulation gave increased PTP and LTP.

4 In order to test whether the influx of calcium ions into the nerve terminal during the tetanus is likely to be involved in potentiation, facilitation was measured during PTP and LTP. Facilitation was reduced to approximately zero during PTP but recovered to normal values about 15 min into LTP. A requirement for the induction of LTP was shown to be the presence of calcium in the bathing solution. However, blocking synaptic transmission with a high concentration of hexamethonium (3 mM) during the tetanic stimulation did not block the induction of LTP.

5 Application of the muscarinic inhibitor, atropine (2 μM), did not affect the magnitude of PTP or LTP.

6 The activator of protein kinase C, phorbol 12,13-dibutyrate (2 μM) potentiated synaptic transmission and reduced the potentiation due to PTP although it did not affect that due to LTP, but the inhibitor of this kinase, staurosporine (0.5 μM), partially blocked the appearance of LTP without affecting PTP after the tetanus.

7 An inhibitor of calmodulin, W-7 (5 μM), reversibly blocked the appearance of LTP significantly after a tetanus although the size of PTP was not affected.

8 The results presented here suggest that the initiation of LTP in the ciliary ganglion is due to an influx of calcium ions into the calyciform nerve terminal during the tetanus and that the mechanism for LTP involves a calcium-calmodulin-dependent process.

Keywords: Synapse; long-term potentiation; avian ciliary ganglia; calcium ions

Introduction

If sympathetic preganglionic axons are stimulated at a relatively high frequency (> 5 Hz) for several seconds, the fast excitatory postsynaptic potential is increased in amplitude for periods of the order of an hour (Dunant & Dolivo, 1968; Zengel *et al.*, 1980; Brown & McAfee, 1982; Koyano *et al.*, 1985). The discovery of long-term potentiation (LTP) in the peripheral nervous system made available a relatively simple preparation for the analysis of at least one form of LTP compared with the preparations available from the central nervous system (Kuba & Kumamoto, 1990). This LTP is likely to be due to an enhanced probability of secretion of quanta from the nerve terminal as there is no change in the sensitivity of the postsynaptic membrane to applied acetylcholine (Briggs & McAfee, 1988) and an accompanying increase in quantal content (Briggs *et al.*, 1985; Koyano *et al.*, 1985). This LTP is thought to be the result of an elevated calcium concentration in the preganglionic nerve terminals of both amphibia and mammals following a tetanus, as short term facilitation is substantially decreased during LTP (Minota *et al.*, 1991); the amplitude of LTP is also dependent on the level of the extracellular calcium concentration (Briggs *et al.*, 1985).

Post-tetanic potentiation (PTP), like LTP, involves an increase in the efficacy of synaptic transmission following tetanic stimulation but unlike LTP, it has a duration in the order of minutes. PTP has been described in both peripheral and central synapses including the ciliary ganglion (Martin & Pilar, 1964c), the hippocampus (Racine & Milgram, 1983) and the neuromuscular junction (Magleby & Zengel, 1975; Delaney *et al.*, 1989). The level of PTP has been shown to be directly related to the extracellular calcium concentration (Erulkar & Rahamimoff, 1978; but see Tanabe & Kijima, 1992). It has been suggested that PTP may be the result of the activation of calcium channels during a tetanic stimulation causing a calcium ion acccumulation as a consequence of the saturation of calcium pumps or their run-down due to limited energy resources in the presence of high calcium loads (Zucker, 1989). A role in PTP for sodium accumulation in the presynaptic nerve terminal during tetanic stimulation (Rahamimoff *et al.*, 1980; Zucker, 1989) has also been suggested.

The avian ciliary ganglion is an ideal preparation for studying forms of LTP and PTP that are due to changes in the properties of presynaptic nerve terminals (Martin & Pilar, 1963; 1964c). The giant calyciform nerve terminal, the largest terminal in the vertebrata (Marwitt *et al.*, 1971), is accessible for both imaging the movements of calcium ions in the terminal after loading it with a suitable calcium indicator (Delaney *et al.*, 1989; Swandulla *et al.*, 1991; Larkum *et al.*, 1992), as well as for measuring the calcium currents in the terminal responsible for transmitter release (Stanley, 1992). Ciliary neurones receive a monosynaptic input (Martin & Pilar, 1963; Hess, 1965), thereby making investigations into their mechanisms simpler than at other synapses. The present

[1] Author for correspondence.

work shows that LTP and PTP exist in the ciliary ganglion following a tetanus and that their initiation involves an elevation of the calcium concentration in the presynaptic calyciform terminal. The involvement of a calcium-calmodulin-dependent mechanism for LTP is implied.

Methods

One to five day post-hatch white leghorn chicks (*Gallus gallus*) were used in all experiments. Animals were decapitated and a craniectomy performed to expose the right ciliary ganglion. The ciliary ganglia with the attached right eye and oculomotor nerve were then removed. The right eye was dissected to free it from the ciliary nerve from within the eye (see Pilar & Tuttle, 1982 for a further description of the dissection). Ciliary ganglia with attached oculomotor and ciliary nerves were then placed in a tissue bath. The bath was perfused at a rate of approximately 2 ml min^{-1} with Tyrode solution of the following composition (in mM): Na^+ 140, K^+ 5, Mg^{2+} 1, Ca^{2+} 3, Cl^- 153, glucose 10, HEPES 10, equilibrated by bubbling with 95% O_2, 5% CO_2 and pH adjusted to 7.2–7.4 by adding NaOH. Stimulation was applied to the oculomotor nerve through a glass suction electrode. The application of the stimulating pulse (a square wave of height 14 V and duration 0.09 ms) was through a radio-frequency isolation unit. Experiments were conducted at room temperature (17 to 20°C).

Recordings of compound action potentials were made by applying a fine suction electrode to the postganglionic ciliary nerve. Signals obtained from this nerve were amplified by an Axoclamp 2A amplifier (Axon Instruments). These signals were digitized using a Labmaster A-D board and recorded and analysed on an IBM compatible computer using the pCLAMP (Fetchex, Fetchan) software package (Axon Instruments).

Drugs used were hexamethonium chloride, phorbol 12,13-dibutyrate (PDBu), staurosporine (SS) and N-(6-aminohexyl)-5-chloro-1-naphthalenesulphonamide hydrochloride (W-7). These were purchased from Sigma Chemical Company. PDBu, SS and W7 were dissolved in dimethyl sulphoxide (DMSO) as a stock solution. The stock was then diluted with perfusing solution such that the overall concentration of DMSO used in the experiments was never greater than 0.01%.

The compound action potential in the ciliary ganglion due to nerve stimulation is biphasic (Figure 1): the first phase is due to electrical transmission through the ganglion (Figure 1) whereas the second is due to chemical transmission (Martin & Pilar, 1964a,b). Hexamethonium (300 μM), a nicotinic cholinergic antagonist, was routinely added to the bathing solution in order to reduce the size of the chemical component of the biphasic compound action potential. Supramaximal stimulation was applied to the preganglionic oculomotor nerve. The reduction in the compound action potential by hexamethonium permitted measurement of an increase in synaptic efficacy. Hexamethonium made, to a large extent, the synaptic responses within the ganglion subthreshold (the chemical component of the compound action potential reduced by at least 60% of its original size). An increase in the synaptic efficacy, such as that which might happen following tetanic stimulation during PTP and LTP, was reflected by a significant increase in the number of the postsynaptic population reaching action potential firing threshold. This was indicated by an increase in the height of the chemical component of the compound action potential.

Protocols for the measurement of LTP and PTP were followed routinely. Upon the attachment of the suction electrodes to the pre- and post-ganglionic nerves, the preganglionic oculomotor nerve was stimulated at a frequency of 0.033 Hz. Only preparations with evoked compound action potentials larger than 1 mV were used. Hexamethonium (300 μM) was then added to the bathing solution. This was allowed to perfuse the ganglion for at least 60 min so that the chemical phase of the compound action potential could be reduced (by at least 60% of its original value) and a control measurement for its height established. The preparation was stimulated at 0.033 Hz during this period. Tetanic stimulation of 30 Hz for 20 s was applied following the establishment of the control. It has been shown that the frequency of this tetanic stimulation occurs within the normal operating range of ciliary ganglia (Fujii, 1992).

Following tetanic stimulation of the ciliary ganglion, recordings of the PTP and LTP time courses were made by measuring the heights of the chemical phase of the evoked compound action potential. Any subsequent tetanic stimulation of the ganglion or addition of a drug to the bathing solution was carried out at least 60 min after the previous tetanic stimulation. Any drug added to the bathing solution was allowed to perfuse the ganglion for at least 60 min before tetanic stimulation was applied.

Some experiments were conducted where the stimulation protocol was varied. In such an experiment, the same ganglion was stimulated tetanically at 10 Hz, then at 20 Hz and then at 30 Hz while maintaining the number of pulses applied to the oculomotor nerve during tetanic stimulation constant. Each tetanic stimulation was separated by at least 1 h in order to allow the return of the response to control levels. Between each tetanic stimulation, evoked compound action potentials were measured at a frequency of 0.033 Hz. The expression of the frequency-dependent levels of tetanic stimulation was compared between different ganglia by normalizing the increase in the chemical phase of the compound action potential. This was done by making that increase following the 30 Hz tetanic stimulation as the unit value and describing the potentiation due to lower frequency stimulation as a fraction of this normalized value.

The ordinates of many of the figures are expressed in terms of percentage of control. A control value (V_{ctl}) was obtained by averaging the heights of the chemical component of the compound action potential for the 15 min before tetanic stimulation (measured by evoking compound action potentials at a frequency of 0.033 Hz). Following tetanic stimulation, compound action potentials were again evoked at a frequency of 0.033 Hz. The amplitudes of these post-tetanic compound action potentials (V) were measured. The percentage increase was calculated as:

$$\text{Percentage of control} = 100 \times \frac{V}{V_{ctl}}$$

In the case of the measurements involving paired-pulse facilitation, the value for V, in this formula, was calculated as the difference between the heights of the chemical phase of the compound action potential evoked from the conditioning and then the test pulse. V_{ctl} represents the difference between the heights of the chemical phase of the compound action potential evoked from the conditioning and then the test pulse averaged over the 15 min prior to tetanic stimulation.

Data are expressed as mean ± standard error of the mean (s.e.mean) and n gives the number of experiments. The significance of the difference between n pairs of observations made before and after application of a drug was calculated by Student's paired t test. P values of 0.05 or less were considered to represent significant changes.

Results

Characteristics of potentiation of transmission in the ciliary ganglion

When the ciliary ganglion was stimulated with a single impulse through the preganglionic oculomotor nerve, the compound action potential recorded in the ciliary nerve was biphasic (Figure 1a). The first phase of this response was

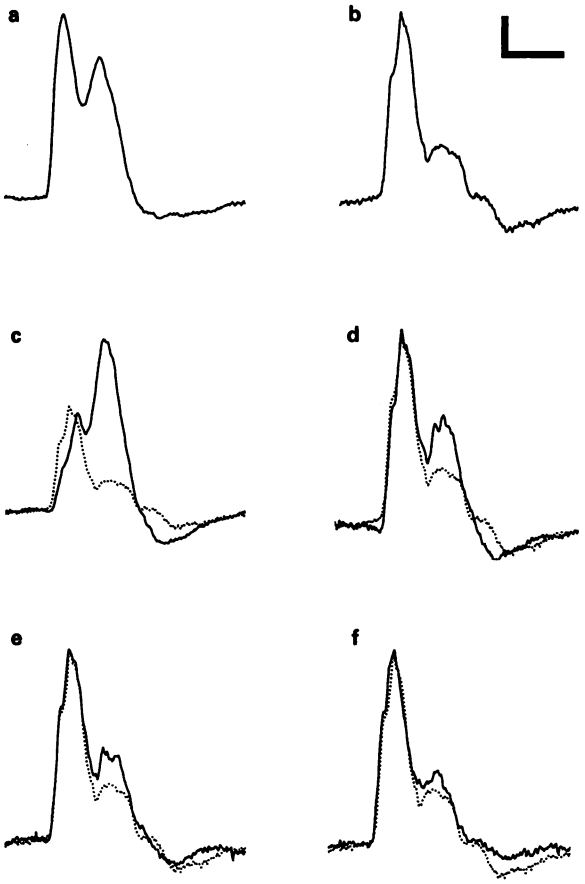

Figure 1 Changes in the amplitude of the chemical and electrical phases of synaptic transmission in the ciliary ganglion following a tetanus (30 Hz, 20 s) applied to the oculomotor nerve. (a) The compound action potential recorded from the ciliary nerve; the first peak indicates the phase due to electrical transmission and the second peak indicates the phase due to chemical transmission. (b) The compound action potential following the perfusion of the ganglion in the hexamethonium (300 μM) for at least 60 min. (c) The compound action potential 20 s after the end of a tetanus, during post-tetanic potentiation (PTP), showing that the chemical component of the compound action potential is approximately 510% of the control level corresponding to (b) but also shown by the dotted line here (on a different scale from signal shown in b). (d) The compound action potential 3 min after the end of the tetanus, nearing the end of the PTP time course, with the chemical component of the compound action potential approximately 190% of the control level from (b) shown by the dotted line. (e) The compound action potential 10 min after the end of the tetanic stimulation with the chemical component of the compound action potential approximately 153% of the control level. (f) The compound action potential 35 min following the tetanic stimulation with the chemical component of the compound action potential approximately 130% of the pretetanic stimulation control level. The scaling bars refer to each of the traces a, b, c, d, e and f and represent in the vertical 0.5, 0.2, 0.5, 0.2, 0.2 and 0.2 mV respectively. The horizontal scaling bar refers to 5 ms in all traces.

usually the larger of the two whilst the second phase could be blocked with high concentrations of hexamethonium (by at least 60% of its original height using 300 μM hexamethonium; Figure 1b). The first phase is due to electrical transmission through the ganglion (Martin & Pilar, 1964a; Hess *et al.*, 1969) whereas the second phase is due to chemical transmission (Martin & Pilar, 1963; 1964b). Stimulation of the oculomotor nerve with a tetanus of 30 Hz for 20 s gave rise to a large increase in the second phase of the compound action potential due to chemical transmission without affecting any significant persistent change in the phase due to electrical transmission (Figure 1c) although often, immediately following the tetanic stimulation, there was a slight decrease in the electrical phase of transmission of no more than 10% that lasted no more than 30 s. It is shown below that the enhancement of the chemical phase is most probably related to an increase in calcium concentration in the nerve terminal; the small but persistent change in the electrical phase may be related to the known dependence of gap junctions that mediate the electrical transmission on intracellular calcium (Rose & Loewenstein, 1975). The chemical phase was still elevated for a long time after the tetanus, returning to control levels usually in the order of an hour (Figure 1d,e and f). Evoked compound action potentials were measured by stimulating the ganglion through the oculomotor nerve at 0.033 Hz before and after the tetanic stimulation. The increase in the amplitude of the chemical phase following tetanic stimulation clearly consisted of two components with different time courses (Figure 2a). The first component consisted of a several hundred percent increase in amplitude of the chemical phase and this lasted for about 4 min; it was followed by a smaller, but more persistent, increase which generally returned to control levels in the order of 1 h (Figure 2a). The electrical phase remained about the same amplitude throughout this period (Figure 2b). The large and relatively fast declining component has the characteristics of post-tetanic potentiation (PTP) observed at other

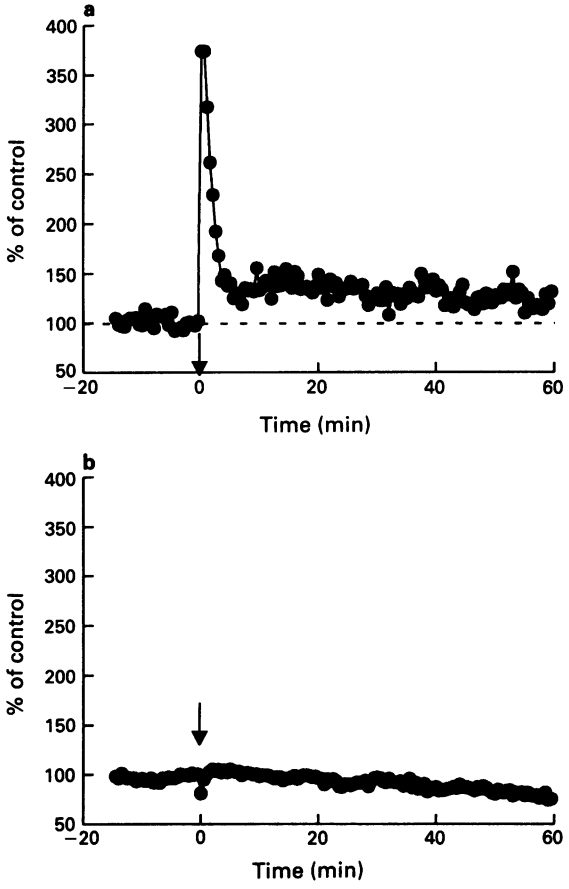

Figure 2 Evidence for the existence of both post-tetanic (PTP) and long-term potentiation (LTP) in the ciliary ganglion following a tetanus. (a) The percentage of the control amplitude of the phase of the compound action potential due to chemical transmission following a tetanus (30 Hz, 20 s); note that the PTP component which is maximal at approximately 375% of control is over in less than 5 min whereas the LTP component, initially about 140% of the control level, lasts for over 1 h. (b) The percentage increase of the electrical phase of neurotransmission through the ciliary ganglion. No significant change in the compound action potential due to electrical transmission is noted at any time following stimulation at time zero. The control amplitude is average over the 15 min prior to tetanic stimulation.

synapses whereas the very slow declining component has the characteristics of long-term potentiation (LTP; Kuba & Kumamoto, 1990).

The time course and amplitude of PTP and LTP were measured by plotting the percentage increase in the amplitude of the chemical phase of the compound action potential every 30 s after a tetanus on log-linear axes as shown in Figure 3a. A least squares linear regression analysis of the points between 10 and 60 min results in a straight line that intercepts the ordinate scale at 50% and has a time constant of 71 min; these values correspond to the amplitude and time constants for LTP. Subtracting this line from the points in Figure 3a between 0 and 4 min produces the points shown in Figure 3b; fitting a least squares linear regression line to these gives an amplitude and time constant for PTP of 280% and 1.5 min respectively. For 50 ciliary ganglia analysed in this way the amplitude and time constant of PTP were $882 \pm 300\%$ and 1.4 ± 0.1 min (mean ± s.e.mean; $n = 50$). For LTP these values were $53 \pm 14\%$ and 50 ± 22 min respectively.

The size of PTP and LTP depended on the frequency of stimulation of the tetanus (Figure 4). PTP decreased significantly ($P < 0.05$ level, $n = 4$), as frequency of tetanic stimulation decreased from 30 Hz to 20 Hz, to $67 \pm 7\%$ of the 30 Hz level, and to $16 \pm 1\%$ of its 30 Hz level for tetanic stimulation at 10 Hz. The magnitude of LTP also decreased as the frequency of tetanic stimulation decreased. Tetanic stimulation at 20 Hz produced LTP of a magnitude that was $40 \pm 7\%$ of that for tetanic stimulation at 30 Hz. Tetanic stimulation of 10 Hz resulted in LTP the magnitude of which was $28 \pm 7\%$ of that resulting from tetanic stimulation of 30 Hz. These results showed a significant ($P < 0.05$, $n = 4$) decrease of the magnitude of LTP as frequency decreased.

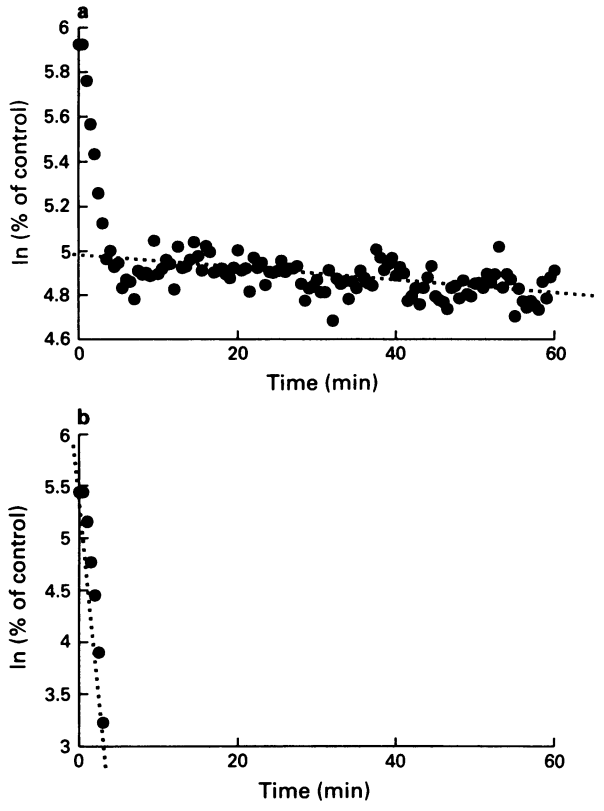

Figure 3 The time course of post-tetanic (PTP) and long-term potentiation (LTP) following a tetanus (30 Hz, 20 s) at time zero. (a) The percentage increase, plotted on a logarithmic ordinate scale in the phase of the compound action potential due to chemical transmission relative to the average of that over 15 min prior to tetanic stimulation at different times after the tetanus; the broken line is drawn according to a least squares regression analysis of the points between 10 and 60 min. (b) The results of subtracting the regression line in (a) from the points between 0 and 3 min; this is also drawn with a logarithmic ordinate scale. The regression line in (a) gives a time constant for the LTP of 71 min and the line in (b) gives a time constant for PTP of 1.5 min. The increase of the signal, with respect to its control level, for the beginning (time zero) of LTP and PTP immediately after the tetanus were 148% and 245% of the control reading respectively in this case.

Mechanisms responsible for PTP and LTP in the ciliary ganglion

It has been suggested that potentiation following tetanic stimulation is caused to a large extent by the presence of residual calcium in the presynaptic nerve terminal (Zucker, 1989). A test that might be used to see if the slow removal of excess calcium in the nerve terminal following a tetanus is responsible for PTP or LTP in this preparation is to measure facilitation during potentiation. Facilitation is most probably due to residual calcium left in the nerve terminal after a conditioning impulse adding to the calcium influx accompanying a test impulse; if the calcium concentration is elevated by potentiation then this residual calcium will be comparatively small and so facilitation will be decreased. Figure 5 shows that facilitation is decreased during PTP and during the beginning of LTP but that it recovers to control values about 15 min after a tetanus. Facilitation was reduced to $-1.8 \pm 1.8\%$ of the control level immediately following tetanic stimulation, $52 \pm 7\%$ at 5 min into LTP and $85 \pm 9\%$ at 15 min into LTP; it returned to control levels about 20 min after tetanic stimulation ($n = 11$). These results sug-

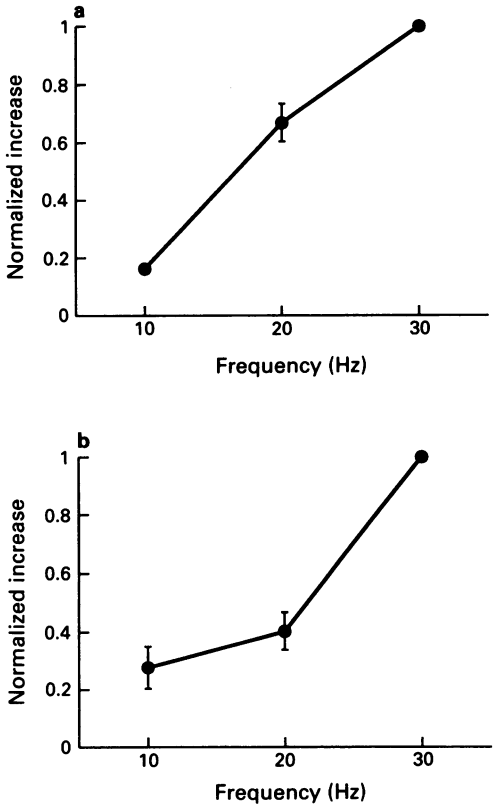

Figure 4 The dependence of post-tetanic (PTP) and long-term potentiation (LTP) on frequency. (a) The increase of the chemical component of the compound action potential during PTP shown as a fraction of the increase of that for 30 Hz stimulation as the frequency of tetanic stimulation is varied. (b) The increase of the chemical component of the compound action potential during LTP shown as the frequency of tetanic stimulation is varied. Each point represents the mean ± s.e.mean of three experiments.

gest that calcium is elevated during PTP and at the beginning of LTP but that it is not elevated during most of the LTP period.

In order to check if the induction of LTP was dependent on the binding of acetylcholine to its postsynaptic receptors, a high concentration of hexamethonium (3 mM) was used to block the receptors prior to a tetanus and then, following the tetanus, the usual low concentration of hexamethonium (300 μM) returned. At the lower concentration of hexamethonium the ganglionic synaptic transmission recovered from the block. The control experiment (Figure 6a) shows the block of chemical synaptic transmission with 3 mM hexamethonium and its subsequent recovery to control levels following the reintroduction of the normal bathing solution at time 15 min ($n = 3$). The control reading at time zero was 108 ± 8% of the average value in the preceding 15 min; following the recovery of the ganglion it was 107 ± 10% at time 60 min. Experiments were then conducted as in the control except that immediately prior to the reintroduction of the bath solution tetanic stimulation of 20 Hz for 30 s was applied. Under these circumstances, a potentiation over the control levels of synaptic transmission was present upon recovery in 4 experiments (Figure 6b) as the level at time zero was 95 ± 5% of control and at time 60 min was 132 ± 16% of control and this increase was statistically significant ($P < 0.05$). This was in contrast to the lack of LTP observed for the control situation (Figure 6a). This indicated that nicotinic cholinergic transmission was not necessary for the induction of LTP.

In order to test further whether the initiation of LTP is likely to be dependent on the influx of calcium ions into the terminal during the tetanus, synaptic transmission through

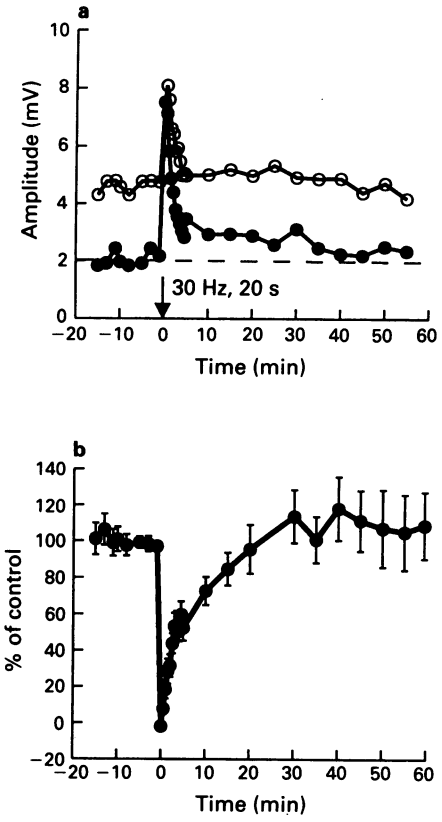

Figure 5 Changes in facilitation during post-tetanic (PTP) and long-term potentiation (LTP). (a) Measurement of the amplitude of conditioning (●) and test (○) pulses, 30 ms apart, during PTP and LTP due to a tetanus of 30 Hz for 20 s at time zero. (b) The average facilitation as a percentage of the pretetanic stimulation control levels, averaged over the 15 min before time zero, for 11 different experiments is shown; for each point the s.e.mean is shown.

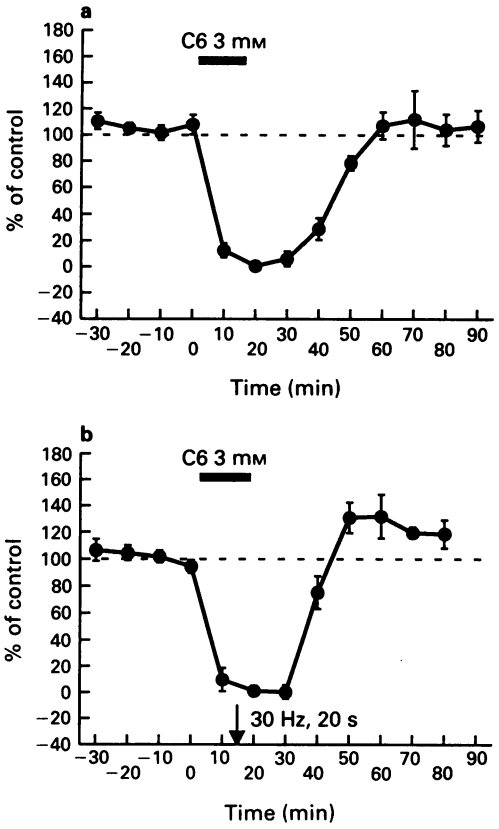

Figure 6 The induction of long-term potentiation (LTP) in the absence of nicotinic cholinergic synaptic transmission. (a) Chemical synaptic transmission through the ganglion was blocked by the application of 3 mM hexamethonium chloride (C6) at time zero for 15 min after which, normal solution was returned to the bath and normal transmission allowed to recover. The percentage of control refers to the size of the chemical component of synaptic transmission relative to its average size over the 15 min prior to time zero. (b) The same protocol as (a), except that tetanic stimulation was applied to the ganglion at time 15 min, immediately before the reintroduction of normal solution to the bath. Upon the recovery of the transmission, the signal was potentiated above control levels indicating that LTP had been induced by the tetanic stimulation during the block of transmission. Each point represents the mean ± s.e.mean for 3 experiments.

the ganglion was blocked with a high magnesium concentration (8 mM) and zero calcium concentrations (0 mM). In a control experiment, synaptic transmission was blocked with 8 mM $[Mg^{2+}]$ and 0 mM $[Ca^{2+}]$. Normal bathing solution was then reapplied to the ganglion at time 15 min and chemical synaptic transmission allowed to recover to control levels (Figure 7a; $n = 3$). In other experiments tetanic stimulation was applied immediately before the reintroduction of normal bath solution (Figure 7b). The results showed that potentiation of the chemical synaptic transmission was not observed following the recovery of the ganglion from the block if calcium was absent during the tetanus in 3 experiments (Figure 7b). This showed that the induction of LTP required the presence of calcium.

To ascertain whether the LTP mechanism shown to occur in ciliary neurones involved muscarinic transmission, a muscarinic antagonist, atropine was used. A control experiment was carried out, initially, involving the usual elicitation of PTP and LTP at time zero (Figure 8a). At least 60 min following the tetanic stimulation, after the completion of the majority of the LTP time course, the ganglion was perfused for at least 60 min with 2 μM atropine sulphate. Following this perfusion, tetanic stimulation of the ganglion was repeated. Again PTP and LTP were observed and these were

not significantly different from those obtained in atropine-free conditions (Figure 8b).

Given that calcium has been shown to play an important role in LTP in the ciliary ganglion, the question arose as to whether the calcium-activated signal transduction mechanisms of protein kinase C or calcium-calmodulin kinase were involved in the initiation or maintenance of LTP. Tetanic stimulation was applied to the ganglion under control conditions (Figure 9a), then, at least 1 h after this stimulation, the protein kinase C activator, phorbol 12,13-dibutyrate (2 μM), was added to the bathing solution and allowed to perfuse the ganglion for at least 60 min. The activator elevated transmission by 158 ± 103% ($n = 5$) but, following a second tetanic stimulation, no significant effect on the levels of LTP ($P > 0.10$; $n = 5$; Figure 9b). PTP was reduced from 356 ± 69% to 221 ± 12% ($n = 5$) indicating that the potentiation produced by PDBu used a similar mechanism to that for PTP. For four separate ganglia, following their tetanic stimulation under control conditions (Figure 10a), the protein kinase C blocker, staurosporine (0.5 μM) was used to perfuse the ganglion. This perfusion did not significantly change the magnitude of PTP but did decrease the magnitude of LTP from 135 ± 12% to 115 ± 2% ($P < 0.05$; $n = 4$; Figure 10b). It is surprising that while

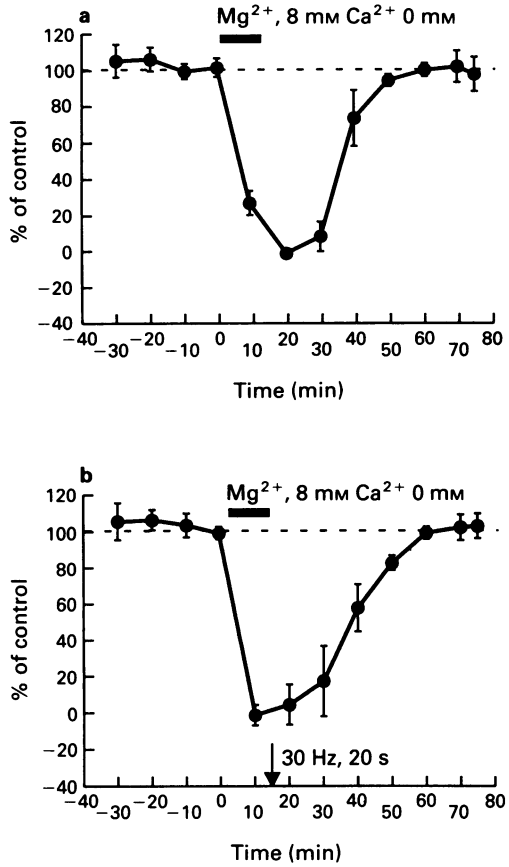

Figure 7 The dependence on calcium for induction of long-term potentiation (LTP). (a) Measurements were made of the chemical component of the compound action potential as a percentage of the average of that 15 min prior to time zero. At time zero a solution containing high magnesium (8 mM) and low calcium (0 mM) was added for 15 min only in order to block chemical transmission before the reintroduction of the normal bathing solution and the subsequent recovery of synaptic transmission. (b) The same protocol as (a) except immediately before the reintroduction of normal bathing solution at time zero, tetanic stimulation was applied to the ganglion. After the recovery of the ganglion no potentiation of synaptic transmission was seen as occurred in Figure 6 indicating a dependence on calcium for the induction of LTP. Each point represents the mean ± s.e.mean for 3 experiments.

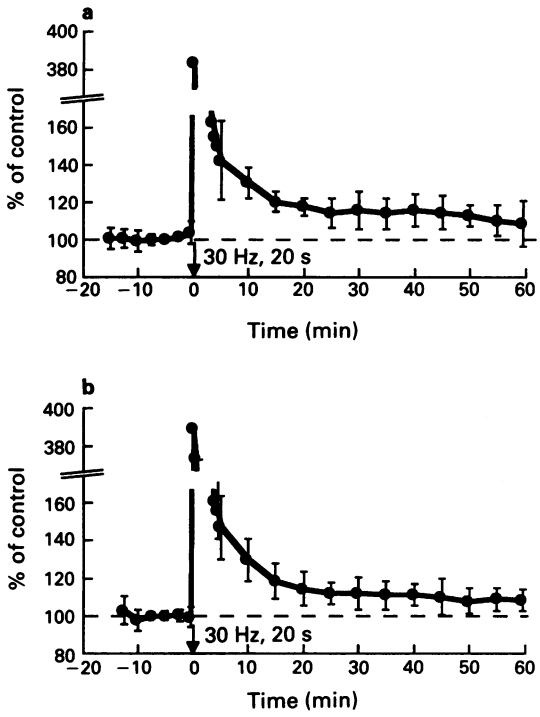

Figure 8 The effect of atropine on long-term (LTP) and post-tetanic potentiation (PTP). (a) Ganglia were stimulated at 30 Hz for 20 s to elicit PTP of 390 ± 52% of the control and LTP of 131 ± 5% of the control (mean ± s.e.mean; $n = 4$). (b) The same ganglia were stimulated after their perfusion with 2 μM atropine sulphate for at least 60 min to give PTP of 362 ± 37% and LTP of 127 ± 6% (mean ± s.e.mean; $n = 4$).

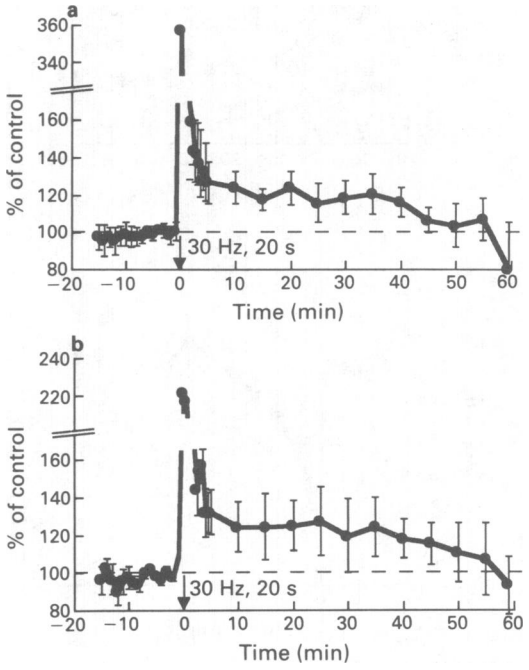

Figure 9 The effect of activating protein kinase C with phorbol 12,13-dibutyrate (PDBu) on post-tetanic (PTP) and long-term potentiation (LTP). (a) The ganglia were stimulated tetanically in the control period ($n = 5$). (b) The same ganglia, after perfusion of the system with PDBu for at least 1 h, were stimulated tetanically.

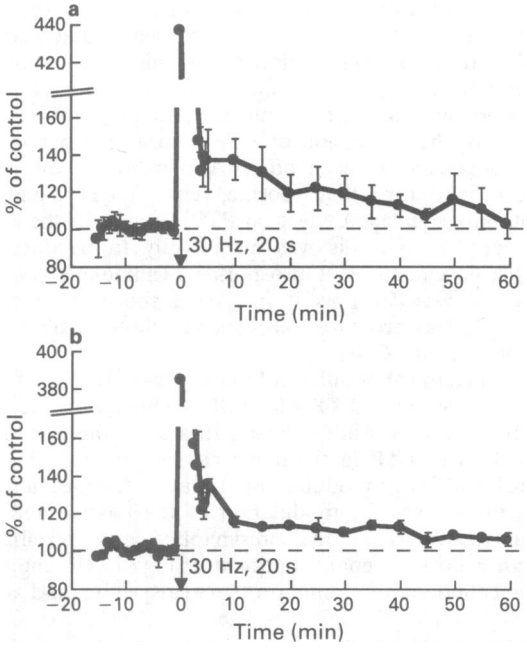

Figure 10 The effect of blocking protein kinase C with staurosporine (SS) on post-tetanic (PTP) and long-term potentiation (LTP). (a) The ganglia were stimulated tetanically in the control period ($n = 4$). (b) The same ganglia, after perfusion of the system with SS for at least 1 h, were stimulated tetanically.

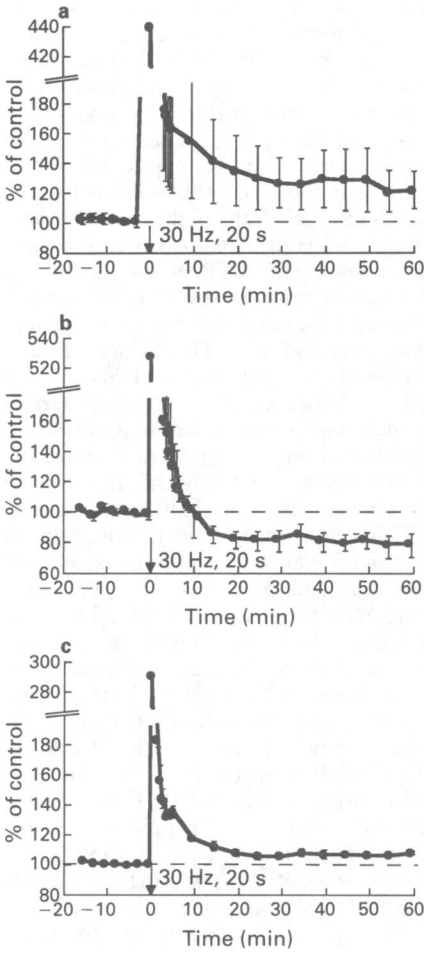

Figure 11 The effect of blocking Ca-calmodulin with N-(6-aminohexyl)-5-chloro-1-naphthalenesulphonamide hydrochloride (W-7) on post-tetanic (PTP) and long-term potentiation (LTP). (a) The ganglion was stimulated tetanically in the control period ($n = 6$). (b) The same ganglia, after perfusion of the system with W-7 for at least 1 h, were stimulated tetanically. (c) Four of the six ganglia analysed in (a) and (b) were washed with normal bathing solution to test the reversibility of the W-7 effect; following washing of at least 1 h, tetanic stimulation was applied.

PDBu effects on PTP implicated a role for protein kinase C, blocking this with staurosporine did not affect PTP.

In a separate experiment, at least 60 min following tetanic stimulation under control conditions (Figure 11a), the calcium-calmodulin kinase blocker W-7 (0.5 μM) was introduced into the bath and allowed to perfuse the ganglion for 60 min. After this time, a decrease in the chemical component of the compound action potential occurred ($-23.4 \pm 6.9\%$; $n = 6$). PTP was not significantly reduced by W-7 whereas LTP was completely inhibited (Figure 11b). Indeed, W-7 reversed the LTP to a long-term depression ($92 \pm 3\%$ in W-7 compared to $150 \pm 32\%$ in control; $n = 6$). This surprising result was maintained for a period of at least 60 min. In six experiments, PTP was $440 \pm 146\%$ during the control period and $526 \pm 86\%$ after the introduction of W-7 ($P < 0.05$). Four experiments continued with a wash of the W-7 from the ganglion with normal bathing solution for at least 60 min. The chemical component of the compound action potential increased slightly ($6.3 \pm 1.5\%$; $n = 4$) although not completely back to control levels. Tetanic stimulation of the washed ganglion gave the usual PTP, with LTP being partially restored to a new level of $113 \pm 3\%$ ($n = 4$; Figure 11c) which was smaller than the control measurement of LTP for these experiments ($166 \pm 47\%$; $n = 4$). In four experiments the PTP for the control was $481 \pm 262\%$; in the presence of W-7 it was $413 \pm 70\%$ and after the wash, it was $290 \pm 27\%$. Although the mean value reduced considerably, this change was not significant.

Discussion

The induction and amplitude of LTP and PTP in the ciliary ganglion showed a dependence on the frequency of impulses during the tetanus and its duration in much the same way as at other preganglionic nerve terminals (Briggs *et al.*, 1985). It has been proposed (Dolphin, 1985) that activity-dependent LTP in sympathetic ganglia is expressed from the presynaptic terminal as the result of increased presynaptic calcium accumulation or sensitivity. As the frequency of tetanic stimulation increases, the inward calcium signals at the terminal overlap and summate, indicating that the calcium level here is dependent on the frequency of stimulation up to the level of saturation. This high calcium level in the terminal accounts for PTP which is a product of residual calcium (Erulkar & Rahamimoff, 1978; see however Tanabe & Kijima, 1992). Also, it is proposed (Kuba & Kumamoto, 1990) that this enlarged calcium influx persistently affects the calcium-dependent second messenger systems in the presynaptic terminal during ganglionic LTP. Therefore, the maximum amplitude of LTP and PTP is directly proportional to the frequency of stimulation as this affects the amount of overlap and summation of the inward presynaptic calcium signal. The PTP following the tetanus of 30 Hz for 20 s declined with a time constant of about 1.5 min, which is similar to that at other ganglionic synapses (Waziri *et al.*, 1969; Zengel *et al.*, 1980), as is the time constant of decline of the LTP of about 50 min (Dunant & Dolivo, 1968; Brown & McAfee, 1982; Briggs *et al.*, 1985; Briggs & McAfee, 1988; Minota *et al.*, 1991).

During potentiation, elevated calcium levels in the presynaptic nerve terminal (Zucker, 1989; Kuba & Kumamoto, 1990; Swandulla *et al.*, 1991) cause impulses to add an equal increment of residual calcium to the presynaptic nerve terminal so that the time course of removal of this residual

calcium following tetanic stimulation described the separate time courses of decay of the different components of potentiation (Zengel & Magleby, 1982; Zucker, 1989). Facilitation, while having a high control level following a tetanus, is reduced to almost zero during PTP and remains depressed for about 15 min during LTP. This suggests that during PTP the presynaptic terminal has a high concentration of calcium and that this is reduced to control levels following the establishment of LTP. This implies that calcium concentration in the presynaptic nerve terminal is raised for the induction but not the maintenance of LTP in the ciliary ganglion.

Short term facilitation is also reduced during LTP at bullfrog sympathetic preganglionic nerve terminals but this lasts for the entire period of LTP (Minota *et al.*, 1991), and therefore suggests that intraterminal calcium is elevated during LTP here. However at mossy fibre terminals on CA3 pyramidal neurones the intraterminal calcium concentration is only elevated during the first few minutes of LTP (Zalutsky & Nicholl, 1990). Certainly the induction of LTP in the calyciform terminal is dependent on calcium ions, as withdrawing calcium ions from the extracellular medium during a tetanus blocks LTP as it does at bullfrog sympathetic ganglia (Koyano *et al.*, 1985; Minota *et al.*, 1991) and rabbit sympathetic ganglia (Briggs *et al.*, 1985). The action of acetylcholine released from the calyciform terminals during a tetanus on either presynaptic or postsynaptic nicotinic receptors does not seem to be involved in the induction of LTP. Blocking these receptors with high concentrations of hexamethonium during a tetanus did not block the subsequent appearance of LTP when the high concentration was washed out (see also Briggs *et al.*, 1985). These results suggest that the chemical activation of the postsynaptic neurone is not required for the induction of LTP. However, it is possible that the activations of the postganglionic neurones through electrical transmission together with the accumulation of intraterminal Ca^{2+} act cooperatively to activate the LTP mechanism in the terminals. Muscarinic transmission is not required for the expression of LTP here as the application of atropine, a muscarinic receptor antagonist, had no significant effect on LTP.

Given that calcium has been shown to be a necessary component in the induction of LTP, an investigation was made into some of the calcium-activated biochemical processes which may be involved in the formation of LTP. The two calcium-activated intracellular transduction mechanisms, both of which have been implicated in the expression of LTP, are protein-kinase C (Bar *et al.*, 1984) and calcium-calmodulin (Minota *et al.*, 1991). Activation of protein kinase C by application of PDBu caused a potentiation of synaptic transmission. Following tetanic stimulation LTP was unaffected, simply adding to the protein-kinase C induced potentiation. It is unlikely that protein-kinase C is involved in the expression of LTP here as the potentiations were independent of each other. Application of the protein-kinase C inhibitor, staurosporine, reduced LTP significantly without any significant effect on PTP. In view of the effect of PDBu application, this was most likely to be due to the non-specific effects of staurosporine (Tamaoki *et al.*, 1986; Minota *et al.*, 1991) as it has been shown to block the activity of other protein kinases such as those involving cyclic AMP and cyclic GMP.

The calcium-calmodulin inhibitor, W-7, produced a significant reduction in LTP with little significant change in the level of PTP. This result indicates that calmodulin is likely to be involved in LTP in the avian ciliary ganglion. Two possible roles which calmodulin might play in the mechanism for LTP here are via the modulation of the passive and active calcium transport at the presynaptic nerve terminals or through a possible conformational change in the interaction of the calmodulin-binding protein, calspectin, and a cytoskeletal protein, F-actin (Sobue *et al.*, 1983). Calcium transport might be modulated by the phosphorylation of calcium-calmodulin-dependent protein kinase II (CaMKII) which inhibits active calcium transports or accelerates passive calcium transports at the presynaptic nerve terminal (Minota *et al.*, 1991). Alternatively, the effectiveness of the protein, calspectin, in its binding to F-actin, in the presence of the calmodulin-binding protein, protein 4.1, is inversely proportional to the terminal calcium concentration; it has been suggested that this process modulates terminal membrane calcium-transporting molecules (Minota *et al.*, 1991). Thus, a very large calcium transient, such as that which follows tetanic stimulation, might cause a persistent change in the calcium-transporting molecules at the presynaptic membrane, so altering the availability of transmitter for secretion from the terminal or the actual excitation-secretion mechanism itself.

LTP in the avian ciliary ganglion has been shown here to be highly dependent on the modulation of the calcium concentration and calcium-dependent mechanisms in the presynaptic nerve terminal. It is likely, here, that the activity-dependent modulation of synaptic efficacy involves calmodulin and, possibly, the phosphorylation of its protein kinase, CaMKII.

References

BAR, P.R., WIEGANT, F., LOPES DE SILVA, F.H. & GISPEN, W.H. (1984). Tetanic stimulation affects the metabolism of phosphonositides in hippocampal slices. *Brain Res.*, **321**, 381–385.

BRIGGS, C.A., BROWN, T.H. & MCAFEE, D.A. (1985). Neurophysiology and pharmacology of long-term potentiation in the rat sympathetic ganglion. *J. Physiol.*, **359**, 503–521.

BRIGGS, C.A. & MCAFEE, D.A. (1988). Long-term potentiation at nicotinic synapses in the rat superior cervical ganglion. *J. Physiol.*, **404**, 129–144.

BROWN, T.H. & MCAFEE, D.A. (1982). Long-term synaptic potentiation in the superior cervical ganglion. *Science*, **215**, 1411–1413.

DELANEY, K.R., ZUCKER, R.S. & TANK, D.W. (1989). Calcium in motor nerve terminals associated with posttetanic potentiation. *J. Neurosci.*, **9**, 3558–3567.

DOLPHIN, A.C. (1985). Long-term potentiation at peripheral synapses. *Trends Neurosci.*, **8**, 376–378.

DUNANT, Y. & DOLIVO, M. (1968). Plasticity of synaptic function in the excised sympathetic ganglion of the rat. *Brain Res.*, **10**, 271–273.

ERULKAR, S.D. & RAHAMIMOFF, R. (1978). The role of calcium ions in tetanic and posttetanic increase of miniature end-plate potential frequency. *J. Physiol.*, **278**, 501–511.

FUJII, J.T. (1992). Repetitive firing properties in subpopulations of the chick edinger westphal nucleus. *J. Comp. Neurology*, **316**, 279–286.

HESS, A. (1965). Developmental changes in the structure of the synapse on the myelinated cell bodies of the chicken ciliary ganglion. *J. Cell Biol.*, **25**, 1–19.

HESS, A., PILAR, G. & WEAKLY, J.N. (1969). Correlation between transmission and structure in avian ciliary ganglion synapses. *J. Physiol.*, **202**, 339–354.

KOYANO, K., KUBA, K. & MINOTA, S. (1985). Long-term potentiation of transmitter release reduced by repetitive presynaptic activities in bull-frog sympathetic ganglia. *J. Physiol.*, **359**, 219–233.

KUBA, K. & KUMAMOTO, E. (1990). Long-term potentiations in vertebrate synapses: a variety of cascades with common subprocesses. *Prog. Neurobiol.*, **34**, 197–269.

LARKUM, M.E., SCOTT, T.R.D. & BENNETT, M.R. (1992). Calcium concentration changes in avian ciliary ganglia during post-tetanic potentiation and long-term potentiation of transmitter secretion. *Proc. Aust. Neurosci. Soc.*, **3**, 73.

MAGLEBY, K.L. & ZENGEL, J.E. (1975). A quantitative description of tetanic and posttetanic potentiation of transmitter release at the frog neuromuscular junction. *J. Physiol.*, **245**, 183–208.

MARTIN, A.R. & PILAR, G. (1963). Dual mode of synaptic transmission in the avian ciliary ganglion. *J. Physiol.*, **168**, 443–463.

MARTIN, A.R. & PILAR, G. (1964a). An analysis of electrical coupling at synapses in the avian ciliary ganglion. *J. Physiol.*, **171**, 454–475.

MARTIN, A.R. & PILAR, G. (1964b). Quantal components of the synaptic potential in the ciliary ganglion of the chick. *J. Physiol.*, **175**, 1–16.

MARTIN, A.R. & PILAR, G. (1964c). Presynaptic and postsynaptic events during post-tetanic potentiation and facilitation in the avian ciliary ganglion. *J. Physiol.*, **175**, 17–30.

MARWITT, R., PILAR, G. & WEAKLEY, J.N. (1971). Characteristics of two ganglion cell populations in avian ciliary ganglia. *Brain Res.*, **25**, 317–334.

MINOTA, S., KUMAMOTO, E., KITAKOGA, O. & KUBA, K. (1991). Long-term potentiation induced by a sustained rise in the intraterminal Ca^{2+} in bull-frog sympathetic ganglia. *J. Physiol.*, **435**, 421–438.

PILAR, G. & TUTTLE, J.B. (1982). A simple neuronal system with a range of uses: the avian ciliary ganglion. In *Progress in Cholinergic Biology: Model Cholinergic Synapses*. ed. Hanin, I. & Goldberg, A.M. pp. 213–247. New York: Raven Press.

RACINE, R.J. & MILGRAM, N.W. (1983). Short-term potentiation phenomena in the rat limbic forebrain. *Brain Res.*, **260**, 201–216.

RAHAMIMOFF, R., LEV-TOV, A. & MEIRI, H. (1980). Primary and secondary regulation of quantal transmitter release: calcium and sodium. *J. Exp. Biol.*, **89**, 5–18.

ROSE, B. & LOEWENSTEIN, W.R. (1975). Permeability of cell junction depends on local cytoplasmic calcium activity. *Nature*, **254**, 250–252.

SOBUE, K., KANDA, K., ADACHI, J. & KAKEUCHI, S. (1983). Calmodulin-binding proteins that interact with actin filaments in a Ca^{2+}-dependent flip-flop manner: survery in brain and secretory tissues. *Proc. Natl. Acad. Sci. U.S.A.*, **80**, 6868–6871.

STANLEY, E.F. (1992). Single calcium channels on a cholinergic presynaptic nerve terminal. *Neuron*, **7**, 585–591.

SWANDULLA, D., HANS, M., ZIPSER, K. & AUGUSTINE, G.J. (1991). role of residual calcium in synaptic depression and posttetanic potentiation: fast and slow calcium signalling in nerve terminals. *Neuron*, **7**, 915–926.

TAMAOKI, T., NOMOTO, H., TAKAHASHIO, I., KATO, Y., MORIMOTO, M. & TOMITA, F. (1986). Staurosporine, a potent inhibitor of phospholipid/Ca^{++} dependent protein kinase. *Biochem. Biophys. Res. Commun.*, **135**, 397–402.

TANABE, N. & KIJIMA, H. (1992). Ca^{2+}-dependent and -independent components of transmitter release at the frog neuromuscular junction. *J. Physiol.*, **455**, 271–290.

WAZIRI, R., KANDEL, E.R. & FRAZIER, W.T. (1969). Organization and inhibition in abdominal ganglion of *Aplysia*. II. Posttetanic potentiation, heterosynaptic depression, and increments in frequency of inhibitory postsynaptic potentials. *J. Neurophysiol.*, **32**, 509–515.

ZALUTSKY, R.A. & NICOLL, R.A. (1990). Comparison of two forms of long-term potentiation in single hippocampal neurons. *Science*, **248**, 1619–1624.

ZENGEL, J.E. & MAGLEBY, K.L. (1982). Augmentation and facilitation of transmitter release. A quantitative description at the frog neuromuscular junction. *J. Gen. Physiol.*, **80**, 583–611.

ZENGEL, J.E., MAGLEBY, K.L., HORN, J.P., MCAFEE, D.A. & YAROWSKY, P.J. (1980). Facilitation, augmentation and potentiation of synaptic transmission at the superior cervical ganglion of the rabbit. *J. Gen. Physiol.*, **76**, 213–231.

ZUCKER, R.S. (1989). Short-term synaptic plasticity. *Annu. Rev. Neurosci.*, **12**, 13–31.

(Received March 4, 1993
Revised April 26, 1993
Accepted May 10, 1993)

Br. J. Pharmacol. (1993), **110**, 470–476

Mediation of the neuroprotective action of R-phenylisopropyladenosine through a centrally located adenosine A_1 receptor

D.G. MacGregor, W.J. Miller & [1]T.W. Stone

Department of Pharmacology, University of Glasgow, Glasgow, G12 8QQ

1 Systemic injections of kainic acid, 10 mg kg^{-1}, into adult rats resulted in lesions in the hippocampus, as assessed by peripheral benzodiazepine ligand binding. Co-administration of clonazepam at 1 mg kg^{-1} or 0.2 mg kg^{-1} prevented major seizures associated with kainate injections, but did not alter significantly the production of hippocampal damage.

2 The co-administration of the adenosine A_1 agonist **R**-phenylisopropyladenosine (**R**-PIA, 25 μg kg^{-1}, i.p.) abolished the lesions induced by kainic acid.

3 The presence of the selective A_1 antagonist, 8-cyclopentyl-1,3-dipropylxanthine (250 or 50 μg kg^{-1}, i.p.) abolished the **R**-PIA neuroprotective action.

4 The A_1/A_2 antagonist, 8-(*p*-sulphophenyl)theophylline (20 mg kg^{-1}, i.p.) which cannot cross the blood brain barrier, did not alter significantly the neuroprotective action of **R**-PIA, indicating that the neuroprotective action of the purine may be predominantly central.

5 The time course of the neuroprotection was also examined. **R**-PIA was effective when administered 2 h before or after kainate administration.

6 The results emphasise the potential utility of systemically active adenosine A_1 receptor ligands in reducing CNS gliosis induced by the activation of excitatory amino acid receptors.

Keywords: Kainic acid; **R**-phenylisopropyladenosine; peripheral benzodiazepine receptor; PK11195; hippocampus; neuroprotection; neurodegeneration; adenosine receptor

Introduction

The striatum and limbic regions of the brain are susceptible to damage caused by chemical or physical changes such as hypoxia, ischaemia or oedema (Leranth & Ribak, 1991; Schmidt-Kastner & Freund, 1991; Freund *et al.*, 1992). Patterns of damage caused by ischaemia can be mimicked by intracranial injections of glutamate agonists acting at receptors for N-methyl-D-aspartate (NMDA) or kainate and the damage can in turn be reduced or abolished by NMDA and non-NMDA antagonists respectively (Bullock *et al.*, 1990; Urban *et al.*, 1990; Uematsu *et al.*, 1991; Bullock & Fujisawa, 1992). The dominant current view on the mechanism of neurotoxicity is that the initial damage is caused by prolonged depolarization, produced by activation of NMDA and non-NMDA receptors with resulting elevated intraceullar calcium concentrations due to the entry of calcium through voltage-operated and NMDA receptor-operated channels (see Choi & Rothman, 1990). This hypothesis is supported by the findings that blockade of either calcium channels or amino acid receptors can suppress ischaemic cell damage (Lin *et al.*, 1990; Ohta *et al.*, 1991; Uematsu *et al.*, 1991).

The kainate receptor agonists, kainic acid and domoic acid, are glutamate agonists which can cross the blood brain barrier and cause neuorotoxicity (Heggli *et al.*, 1981; Schwob *et al.*, 1980; Lothman & Collins, 1981; Heggli & Malthe-Sorenssen, 1982; Altar & Baudry, 1990; Stewart *et al.*, 1990). The systemic administration of kainate produces a pattern of hippocampal damage which differs from that seen in focal ischaemia of the hippocampus, but bears similarities to the pattern seen in global ischaemia or temporal lobe epilepsy (Schwarcz *et al.*, 1984; Coyle, 1987; Franck & Roberts, 1990). Systemic administration has the advantage that surgery is not required and hence the effects of anaesthetics on neurotransmitter release and neurotoxicity can be avoided (Kendall & Minchin, 1982; Richards, 1983; Carla & Moroni, 1992; Sutula *et al.*, 1992). Kainate receptors are located predominantly on presynaptic terminals in the CA3 region of the hippocampus (Ferkany *et al.*, 1982) and studies have shown that stimulation of these kainate receptors causes the release of glutamate *in vivo* and *in vitro* (Ferkany & Coyle, 1983; Notman *et al.*, 1984; Palmer *et al.*, 1992).

The hippocampus also contains high levels of adenosine receptors and various groups have shown that adenosine can hyperpolarize hippocampal neurones (Ameri & Jurna, 1991; Thompson *et al.*, 1992) and reduce glutamate release (Fastbom & Fredholm, 1985; Fredholm & Dunwiddle, 1988; Lupica *et al.*, 1992; see Stone & Simmonds, 1991). It has also been shown that adenosine and its analogues can protect against the neurotoxic effects of NMDA and non-NMDA receptor agonists (Arvin *et al.*, 1989; Connick & Stone, 1989; Finn *et al.*, 1991) as well as against ischaemia (von Lubitz *et al.*, 1989).

We have recently reported that the systemic administration of the stable adenosine analogue **R**-N^6-phenylisopropyladenosine (**R**-PIA) can prevent the hippocampal neurotoxicity produced by systemic kainate, in a dose-dependent manner as assessed by peripheral benzodiazepine receptor binding (MacGregor & Stone, 1993). In the present study we have examined the time course of the neuroprotection, as well as identifying the type of adenosine receptor involved.

Methods

All experiments employed 8 week old male Wistar rats, 190–220 g, which were kept under standard conditions.

Animals were injected intraperitoneally (i.p.) with drugs in a volume not exceeding 1 ml kg^{-1}. Kainic acid, 8-cyclopentyl-1,3-dipropylxanthine (CPX) and 8-(*p*-sulphophenyl)-theophylline (8-PST) were dissolved in saline, and **R**-PIA in methanol. In all cases vehicles were used as control injections. In the antagonist studies animals were pretreated with clonazepam (0.2 mg kg^{-1}) i.p. 10 min prior to kainate injection. The animals were allowed to recover, and were killed 7 days later.

[1] Author for correspondence.

Tissue preparation

The method used was that of Eshleman & Murray (1989) for the preparation of P_2 membranes, as modified by MacGregor & Stone (1993). The animals were killed by stunning followed by cervical dislocation. The hippocampi were removed and homogenized in 5 ml ice-cold 0.27 M sucrose, pH 7.4 with a Braun Homogenizer, 10 strokes × 500 r.p.m. The homogenate was brought to 20 ml with sucrose solution and was then stored at −20°C for 2–4 h. After completing the preparation of tissue from a group of animals the samples were defrosted and centrifuged for 10 min at 4°C, 1000 *g* (IEC DPR 6000 centrifuge). The pellet was discarded and the supernatant centrifuged for 20 min at 4°C, 16000 *g* (Sorval RC 5B Refrigerated Superspeed Centrifuge, SS 34 Rotor). After this step the supernatant was discarded and the pellet resuspended in 20 ml ice-cold 50 mM Tris HCl buffer pH 7.8 and then centrifuged for 20 min at 4°C, 30000 *g* (Sorval RC 5B). The new pellet was resuspended in 5 ml Tris HCl buffer and stored at −20°C, normally for no more than 24 h.

On the day of the assay the samples were defrosted and centrifuged for 20 min at 4°C 30000 *g*, and the supernatant discarded. The pellet was homogenized in 5 ml Tris HCl buffer 7 strokes × 1500 r.p.m., brought to 20 ml with Tris HCl buffer, and stored on ice until needed, this being the P_2 mitochondrial membrane fraction.

[^{3}H]-PK11195 assay

All assays were carried out on ice and samples were incubated for 60 min. The assay was performed in duplicate for both nonspecific and total binding. The volume of the assay chamber was 2 ml, and contained 5 µl [^{3}H]-PK11195, 5 µl cold ligand, with 500 µl P_2 membranes and the volume brought to 2 ml with Tris HCl buffer. Final assay conditions were 1.75 nM [^{3}H]-PK11195 in ethanol (0.25% final), 0.25% dimethylsulphoxide (DMSO) ± 10 µM PK11195 and 100–150 µg protein. The assay samples were vortexed at the start of their incubation and every 20 min before filtration. The incubation was terminated by vacuum filtration, with all of the sample being filtered through prewetted Whatman GF/C glass filters using a Millipore 12 well 1225 Sampling Manifold. Filters were washed twice with 12 ml ice-cold Tris HCl buffer and vacuum dried, before being placed in scintillation vials in 5 ml Ecoscint scintillation fluid. The samples were left overnight and counted in a Packard 2000 Scintillation Counter for d.p.m.

Protein concentrations were measured by the method of Lowry *et al.* (1951), following solubilization with 0.25 M NaOH and with bovine serum albumin used as the standard.

Data analysis

Specific binding was calculated in absolute terms and as percentage of same day control to minimize day to day variations. All values are mean ± s.e.mean. Statistical significance was assessed by an unpaired Student's *t* test (unequal variance), significance being considered when $P < 0.05$.

Neuroprotection was calculated for each rat by the following equation:

$$\frac{(\text{kainate} - \text{test})}{(\text{kainate} - \text{Control})} \times 100$$

Materials

[^{3}H]-PK11195 (1-(2-chlorophenyl)-*N*-methyl-*N*-(1-methylpropyl) -3-isoquinoline carboxamide) (specific activity = 80–86 Ci mmol^{-1}) was purchased from DuPont/NEN (Stevenage, Herts); kainic acid and R-PIA from Sigma Chemical Co. (Poole, Dorset), CPX and 8-PST from RBI/SEMAT Technical Ltd (St. Albans, Hertfordshire). Rivotril (clonazepam for injection) was purchased from Roche Laboratories. Unlabelled PK11195 was a gift from Pharmuka Laboratories.

Results

Clonazepam pilot

In a previous paper (MacGregor & Stone, 1993) about 15% of rats injected with kainic acid 10 mg kg^{-1} died during tonic clonic seizures and a preliminary study was therefore performed to determine whether protection could be afforded against seizures without compromising hippocampal toxicity. Groups of animals were preinjected with 1 mg kg^{-1} clonazepam or 1 ml kg^{-1} vehicle i.p. alone or followed after 10 min by an injection of 10 mg kg^{-1} kainic acid. There was an apparent reduction in the severity of the seizure activity, with a marked sedative effect, but the animals still displayed wet dog shakes, salivation, circling and forepaw treading as reported previously. The [^{3}H]-PK11195 binding was significantly different between the kainate- and vehicle-treated groups, but no significant difference was obtained between clonazepam and vehicle-treated animals in the presence of kainate (Figure 1). When the dose of clonazepam was reduced to 0.2 mg kg^{-1} seizure activity was still prevented but with less apparent sedation and still no effect on [^{3}H]-PK11195 binding. The smaller dose was therefore used routinely in subsequent experiments.

8-Cyclopentyl-1,3-dipropylxanthine (CPX)

Kainate alone induced an almost 300% increase in [^{3}H]-PK11195 binding in these animals, but this could be suppressed by the coinjection of R-PIA 25 µg kg^{-1}, as reported previously. When CPX was administered in addition, the protective effect of R-PIA was inhibited, [^{3}H]-PK11195 binding now showing no significant differences from that with kainate alone (Figure 2). CPX was effective at both the dose levels tested – 50 and 250 µg kg^{-1}.

There was no overall change in the behaviour of the CPX-treated animals when compared to the kainate-treated or kainate/R-PIA-treated animals. Animals injected with 250 µg kg^{-1} CPX and saline showed no increase in [^{3}H]-PK11195 binding when compared to control ($P = 0.494$),

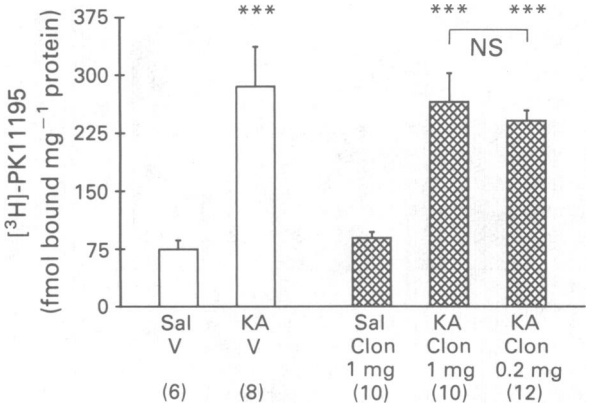

Figure 1 Comparison of clonazepam or vehicle treatment on kainate induced increased in [^{3}H]-PK11195 binding to hippocampal P_2 membranes. Rats were pretreated with clonazepam or vehicle i.p. 10 min before kainate 10 mg kg^{-1} or saline i.p. injection. Animals were left for 7 days and binding performed as in Methods. Columns indicate mean ± s.e.mean. Sal = saline 1 ml kg^{-1}; KA = kainate 10 mg kg^{-1}; V = clonazepam vehicle 1 ml kg^{-1} or 0.2 ml kg^{-1}; Clon = clonazepam. Number of experiments shown in parentheses. ***$P \leq 0.001$ significance versus saline/clonazepam control.

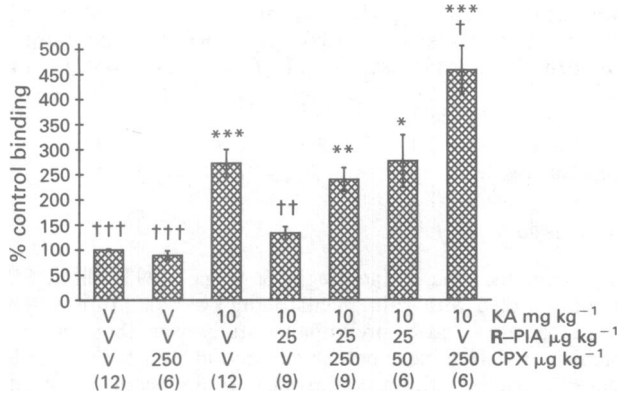

Figure 3 Effect of 8-(*p*-sulphophenyl)theophylline (8-PST) on kainate evoked increase in [^{3}H]-PK11195 binding. Rats were pretreated with 0.2 mg kg^{-1} clonazepam 10 min prior to kainate (10 mg kg^{-1}) and/or **R**-phenylisopropyladenosine (**R**-PIA)/vehicle, 8-PST/saline injection i.p. Hippocampal P_2 membranes were prepared as in Methods. Binding was calculated as % of same day control [^{3}H]-PK11195 binding. Columns indicate mean ± s.e.mean. V = vehicle; KA V = saline; KA = kainate; **R**-PIA V = methanol/saline; 8-PST V = saline. $^{**}P<0.01$; $^{***}P<0.001$ significance versus vehicle control; †$P\leqslant0.05$; ††$P\leqslant0.01$; †††$P\leqslant0.001$ significance versus kainate alone.

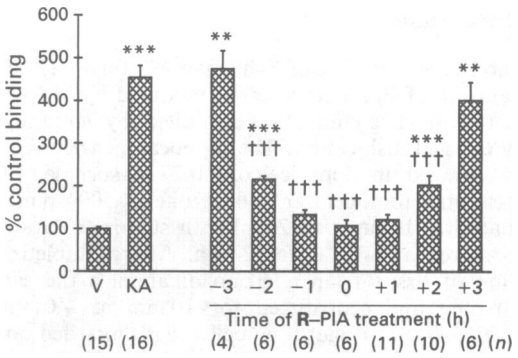

Figure 4 Time course of **R**-phenylisopropyladenosine (**R**-PIA) protection against kainate toxicity. Rats were injected i.p. with a single dose of 25 μg kg^{-1} **R**-PIA at various times before or after kainate injection. Clonazepam (0.2 mg kg^{-1}) was injected i.p. 10 min before i.p. kainate injection (t_o). Tissue preparation and binding as in Methods. Binding as % of same day controls. Columns indicate mean ± s.e.mean. V = saline and methanol/saline treatment (t_o), KA = kainic acid 10 mg kg^{-1} and methanol/saline treatment (t_o). $^{**}P\leqslant0.01$; $^{***}P\leqslant0.001$ significance versus vehicle control; ††$P\leqslant0.01$; †††$P\leqslant0.001$ significance versus 10 mg kg^{-1} kainate.

indicating that there was no induced gliosis or neurodegeneration (Figure 2).

The coadministration of kainate (10 mg kg^{-1}) and CPX (250 μg kg^{-1}) led to a significantly greater degree of neuronal damage than was seen with kainate alone (Figure 2).

8-(p-Sulphophenyl)theophylline (8-PST)

The injection of 20 mg kg^{-1} 8-PST or 1 ml kg^{-1} saline induced no change in the [^{3}H]-PK11195 binding when compared to same day controls ($P=0.638$), though the binding was significantly less than in the kainate/saline group ($P<0.001$) (Figure 3), indicating that there was no gliosis or neuronal damage produced by the xanthine alone. Kainate again produced a 3 fold elevation in [^{3}H]-PK11195 binding, which could be prevented by **R**-PIA at 25 μg kg^{-1}, but the additional presence of 8-PST at 20 mg kg^{-1} did not prevent that protection. The combined administration of kainate and 8-PST resulted in a significantly greater degree of binding than obtained with kainate alone (Figure 3).

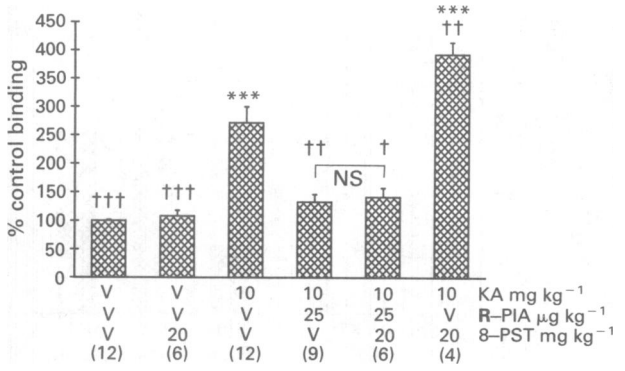

Figure 3 Effect of 8-(*p*-sulphophenyl)theophylline (8-PST) on kainate evoked increase in [^{3}H]-PK11195 binding. Rats were pretreated with 0.2 mg kg^{-1} clonazepam 10 min prior to kainate (10 mg kg^{-1}) and/or **R**-phenylisopropyladenosine (**R**-PIA)/vehicle, 8-PST/saline injection i.p. Hippocampal P_2 membranes were prepared as in Methods. Binding was calculated as % of same day control [^{3}H]-PK11195 binding. Columns indicate mean ± s.e.mean V = vehicle; KA V = saline; KA = kainate; **R**-PIA V = methanol/saline; 8-PST V = saline. $^{**}P<0.01$; $^{***}P<0.001$ significance versus vehicle control; †$P\leqslant0.05$; ††$P\leqslant0.01$; †††$P\leqslant0.001$ significance versus kainate alone.

R-PIA time course

As with the other experiments, clonazepam (0.2 mg kg^{-1}) was co-administered with kainate 10 mg kg^{-1} (t_o), and not with the **R**-PIA administration, which was injected at times up to 3 h preceding or following the kainate administration. Injection of **R**-PIA at 1 or 2 h before or after kainate induced a significant ($P\leqslant0.001$) protection against the neuronal damage (Figure 4), whereas administration at the 3 h time points was ineffective. Protection was greater within 1 h of kainate injection with the maximal protection occurring when **R**-PIA was co-administered with kainate ($P\leqslant0.001$) (see Figure 4).

Discussion

Intraperitoneally administered kainic acid causes an early increase in local cerebral glucose utilisation, increased neuronal firing, transient permeabilization of the blood brain barrier and tonic seizures, with associated behavioural disturbances (see Heggli *et al.*, 1981; Lothman & Collins, 1981). During this stage there is a transient increase in extracellular glutamate, similar to that seen in ischaemia, probably caused by activation of presynaptic receptors (Ferkany *et al.*, 1982; Benveniste *et al.*, 1984; Globus *et al.*, 1988). The released glutamate acts on receptors located both on neurones and glia (Ferkany *et al.*, 1982; Ferkany & Coyle, 1983) to cause the further release of neuroactive substances and depolarization of the postsynaptic membrane through NMDA and non-NMDA receptors (Choi, 1988; Choi & Rothman, 1990). Overstimulation of the NMDA receptor is thought to be a critical step in the initiation of excitotoxicity (Butcher *et al.*, 1990; Globus *et al.*, 1990) and several groups have shown that NMDA antagonists can block kainate evoked neurotoxicity (Fariello *et al.*, 1989; Lerner-Natoli *et al.*, 1991; Wolf *et al.*, 1991). The pattern of cell damage which results from this sequence has been detailed in histological work by several groups (Heggli *et al.*, 1981; Schwob *et al.*, 1980; Lothman & Collins, 1981; Altar & Baudry, 1990).

Use of clonazepam

In the present study clonazepam, at low doses, did not significantly protect against kainate-induced damage measured in the hippocampus, but did abolish the tonic-clonic limbic seizures and reduced the frequency of the mild seizure-like activity such as tremor as reported by several other studies (Heggli *et al.*, 1981; Lothman & Collins, 1981; Braun & Freed, 1990). There was no apparent effect on wet dog shakes or other behavioural effects of kainate suggesting that these may be initiated in a non-limbic locus by a mechanism independent of seizure activity. At the higher dose used (1 mg kg^{-1} clonazepam) there was marked sedation but still a significant increase in [^{3}H]-PK11195 binding with kainate, a result consistent with the interpretation of Heggli *et al.* (1981) that the degree of seizure activity did not correspond to neuronal damage following 12 mg kg^{-1} kainate. Conversely Lerner-Natoli *et al.* (1991) reported that TCP (N-[1-(2-thienyl)cyclohexyl]-piperidine) was able to block kainate damage (i.e. by blockade of the NMDA receptors), but was unable to block the induced seizures.

Several groups have reported that only certain anticonvulsants protect against kainate damage (Zaczek *et al.*, 1978; Fuller & Olney, 1981; Voll & Auer, 1991). Benzodiazepines seem unable to prevent kainate damage in the hippocampus (Ben-Ari *et al.*, 1979; Heggli & Malthe-Sorenssen, 1982) and Koh & Choi (1987) found that diazepam or phenobarbitone were not neuroprotective against glutamate neurotoxicity in cell culture. This separation of convulsions and neuronal damage contradicts the popular view that seizures are needed for the damage (Fuller & Olney, 1981; Lothman & Collins, 1981). One possible explanation for the difference in effect of anticonvulsants may depend on the experimental technique. Several groups have used high doses of anticonvulsants in the presence of anaesthetics, which themselves have been reported to alter the release of amino acids (Kendall & Minchin, 1982; Richards, 1983; Carla & Moroni, 1992). These alterations may enhance the action of anticonvulsants. Since the present study is based on the change in a glial marker with no histology, another possible explanation is that there is an increase either of K_D or B_{max} with no actual neuronal loss. (This technique means that no information could be drawn on the development of damage in different CA areas of the hippocampus.) However, parallel histological studies support the conclusions reached in this paper and indicate that there is still widespread necrosis in the hippocampus 7 days following 10 mg kg^{-1} kainate with 0.2 mg kg^{-1} clonazepam i.p. (unpublished observations) and we have previously reported that kainate increases B_{max} without affecting K_D (MacGregor & Stone, 1993), so it is unlikely that this is the case.

Purine-mediated protection

Adenosine is found in low micromolar concentrations extracellularly in the brain although the levels are raised substantially by ischaemia and glutamate receptor activation (Phillis *et al.*, 1987; Hoehn & White, 1990; Chen *et al.*, 1992; Dagani *et al.*, 1992). Adenosine receptors (both A_1 and A_2) are found on neuronal and non-neuronal cells (Goodman & Snyder, 1982; Deckert & Jorgensen, 1988), as well as the vasculature and there are numerous reports that activation of A_1 receptors reduces ischaemic or excitotoxic brain damage (Arvin *et al.*, 1989; Connick & Stone, 1989; von Lubitz *et al.*, 1989; Alzheimer *et al.*, 1991; Finn *et al.*, 1991; Miller & Hsu, 1992; Rudolphi *et al.*, 1992; Simpson *et al.*, 1992; MacGregor & Stone, 1993).

Adenosine may provide protection by several mechanisms, including vasodilatation of the central and peripheral vasculature, hyperpolarization of neuronal membranes, decreased oxygen consumption by decreased neuronal activity, increased glucose uptake, increased glycolysis in glia, as well as hypothermia (Nehlig *et al.*, 1988; Miller & Hsu, 1992; Rudolphi *et al.*, 1992; Tominaga *et al.*, 1992). In a previous study there was no significant change in rectal temperature following systemic kainate/**R**-PIA treatment in the presence or absence of 8-phenyltheophylline (MacGregor & Stone, 1993), so it seems unlikely that in this model hypothermia had a significant role.

The most likely explanation for the protection by purines is a suppression of glutamate release. Heron *et al.* (1992) have reported that i.p. **R**-PIA (20 μg kg^{-1} given 30 min before and 10 μg kg^{-1} 30 min after) significantly decreased glutamate release following a 20 min period of ischaemia. Cantor *et al.* (1992) reported that A_1 agonists also significantly reduced the ischaemic release of glycine in a dose-dependent manner. The importance of glycine in potentiating glutamate toxicity has been examined by several groups (Lerma *et al.*, 1990; Patel *et al.*, 1990; Wood *et al.*, 1992). Glycine decreases the rate of NMDA receptor desensitization and the reports by Baker *et al.* (1991) and Globus *et al.* (1991) indicate that the elevation of extracellular glycine remains high longer than that of glutamate. The prolonged elevation of glycine may therefore contribute to the delayed neuronal loss reported by other groups (Nakano *et al.*, 1990; Haba *et al.*, 1991). It is unclear whether kainate itself causes the release of glycine.

Xanthine blockade

CPX is a highly selective A_1 antagonist (Bruns *et al.*, 1987) which has low nanomolar affinity for the receptor. A recent report by Baumgold *et al.* (1992) indicates that it can cross the blood-brain barrier. A dose of 250 μg kg^{-1} CPX would be similar to an intracranial injection of 0.34 μM as calculated by Baumgold *et al.* (1992), and should completely block all A_1 receptors with a degree of A_2 blockade as well. At this dose as well as at the lower dose of 50 μg kg^{-1} here, which should block the A_1 sites only, the present results demonstrate a complete inhibition of the neuroprotection produced by **R**-PIA. This would be entirely consistent with the role of A_1 receptors in mediating inhibition of endogenous amino acid release.

8-PST was administered to determine the importance of peripheral vasodilatation on the neuroprotective effect of **R**-PIA, since 8-PST cannot readily cross the blood-brain barrier: Baumgold *et al.* (1992) reported that there was less than 5% penetration into the brain after the administration of 50 mg kg^{-1}. In the present work there was no effect of 8-PST on [^{3}H]-PK11195 binding when administered in the absence of kainate and this dose was unable to block the **R**-PIA protection.

When 8-PST was administered with kainate and clonazepam the elevation in [^{3}H]-PK11195 binding was highly significant when compared to the kainate and clonazepam group. One possible explanation for this could be that 8-PST is causing vasoconstriction which decreases the blood flow to the brain and increases neuronal metabolic stress and cell damage. An alternative explanation might be that as kainate causes a transient permeabilization of the blood brain barrier (Zucker *et al.*, 1983; Saija *et al.*, 1992) this permeabilization would allow the 8-PST to cross the blood-brain barrier and enhance the neurotoxicity in a manner similar to that reported by Rudolphi *et al.* (1987) for theophylline and CPX reported here. The main difficulty with such an explanation is that it does not explain why 8-PST did not prevent the protection by **R**-PIA. We therefore suggest that 8-PST does not penetrate into CNS, but that it is a blockade of vascular adenosine receptors, leading to a degree of vasoconstriction, which enhances kainate toxicity. Such a possibility would be consistent with previous indications that any fall in blood pressure, and thus cerebral perfusion can potentiate excitotoxicity (Connick & Stone, 1989). Since neuronal depolarization by kainate would result in the release of adenosine locally, the greatest influence of 8-PST would be expected to be in areas most susceptible to the

toxin. There may also be some potentiation of damage due to increased reperfusion as the 8-PST blockade of adenosine receptors decays.

Time course

When adenosine A_1 agonists have been used to protect against ischaemic damage thay have been almost invariably administered prior to the onset of ischaemia (von Lubitz *et al.*, 1989; Cantor *et al.*, 1992; Simpson *et al.*, 1992; See Rudolphi *et al.*, 1992 for review). In the present work the effective window of protection was found to span 4 h (− 2 to + 2 h). Protection obtained by **R-PIA** administration before kainate is probably due to the lipophilic properties of the purine and its persistence in the brain. The protection within the first hour after kainate injection is probably due to the reduction in glutamate and glycine efflux reported by other groups (Cantor *et al.*, 1992; Heron *et al.*, 1992). The time course of kainate penetration into the CNS and of induced glutamate release has not been reported, but is probably quite rapid in view of the fact that wet dog shakes are seen in all animals within 40 min of systemic administration (Lothman & Collins, 1981). Seizure activity has a longer onset period than wet dog shakes (Heggli *et al.*, 1981; Lothman & Collins, 1981) and thus may require higher intracranial kainate concentrations.

In summary the present results indicate that the neuroprotective action of systemically administered **R-PIA** is via a centrally located A_1 receptor with little or no contribution from the A_2 or systemic A_1 receptors at the microgram doses used in the present study. The finding that single low doses of **R-PIA** are neuroprotective up to 2 h prior to or following cerebral insult may suggest the use of selective, lipid-soluble A_1 agonists to be used post-ischaemically or prophylactically as they do not affect the basal release of either the excitatory amino acids or glycine (Cantor *et al.*, 1992).

D.G.M. is supported by a Glasgow University Scholarship, W.J.M. by a Scottish Education Department grant. The authors are grateful to Dr K. Hamilton, Miss K. Paisley and Mr J. Younger for technical advice and assistance.

References

ALTAR, C.A. & BAUDRY, M. (1990). Systemic injection of kainic acid: gliosis in olfactory and limbic brain regions quantified with [^{3}H]-PK11195 binding autoradiography. *Exp. Neurol.*, **109**, 333–341.

ALZHEIMER, C., KARGL, L. & BRUGGENCATE, G.T. (1991). Adenosinergic inhibition in hippocampus is mediated by adenosine A_1 receptors very similar to those of peripheral tissues. *Eur. J. Pharmacol.*, **196**, 313–317.

AMERI, A. & JURNA, I. (1991). Adenosine-A1 and non-A1 receptors-intracellular analysis of the actions of adenosine agonists and antagonists in rat hippocampal neurones. *Brain Res.*, **546**, 69–78.

ARVIN, B., NEVILLE, L.F., PAN, J. & ROBERTS, P.J. (1989). 2-Chloroadenosine attenuates kainic acid-induced toxicity within the rat striatum: relationship to release of glutamate and Ca^{2+} influx. *Br. J. Pharmacol.*, **98**, 225–235.

BAKER, A.J., ZORNOW, M.H., GRAFE, M.R. SCHELLER, M.S., SKILLING, S.R., SMULLIN, D.H. & LARSON, A.A. (1991). Hypothermia prevents ischemia-induced increase in hippocampal glycine concentrations in rabbits. *Stroke*, **22**, 666–673.

BAUMGOLD, J., NIKODIJEVIC, O. & JACOBSON, K.A. (1992). Penetration of adenosine antagonists into mouse brain as determined by *ex vivo* binding. *Biochem. Pharmacol.*, **43**, 889–894.

BEN-ARI, Y., TREMBLAY, E., OTTERSEN, O.P. & NAQUET, R. (1979). Evidence suggesting secondary epileptogenic lesions after kainic acid; pretreatment with diazepam reduces distant but not local brain damage. *Brain Res.*, **165**, 362–365.

BENVENISTE, H., DREJER, J., SCHOUSBOE, A. & DEIMER, N.H. (1984). Elevation of extracellular concentrations of glutamate and aspartate in rat hippocampus during transient cerebral ischaemia monitored by intracerebral microdialysis. *J. Neurochem.*, **43**, 1369–1374.

BRAUN, D.E. & FREED, W.J. (1990). Effect of nifedipine and anticonvulsants on kainic acid-induced seizures in mice. *Brain Res.*, **533**, 157–160.

BRUNS, R.F., FERGUS, J.H., BADGER, E.W., BRISTOL, J.A., SANTAY, L.A., HARTMAN, J.D., HAYS, S.J. & HUANG, C.C. (1987). Binding of the A_1-selective adenosine antagonist 8-cyclopentyl-1,3-dipropylxanthine to rat brain membranes. *Naunyn Schmied. Arch. Pharmacol.*, **335**, 59–63.

BULLOCK, R., MCCULLOCH, J., GRAHAM, D.I., LOWE, D., CHEN, M.H. & TEASDALE, G.M. (1990). Focal ischemic damage is reduced by CPP-ene. Studies in two animal models. *Stroke*, **21** (suppl. III), III-32–III-36.

BULLOCK, R. & FUJISAWA, H. (1992). The role of glutamate antagonists for the treatment of CNS injury. *J. Neurotrauma*, **9**, Suppl. 2, S443–S462.

BUTCHER, S.P., BULLOCK, R., GRAHAM, D.I. & MCCULLOCH, J. (1990). Correlation between amino acid release and neuropathologic outcome in rat brain following middle cerebral artery occlusion. *Stroke*, **21**, 1727–1733.

CANTOR, S.L., ZORNOW, M.H., MILLER, L.P. & YAKSH, T.L. (1992). The effect of cyclohexyladenosine on the periischemic increases of hippocampal glutamate and glycine in the rabbit. *J. Neurochem.*, **59**, 1884–1892.

CARLA, V. & MORONI, F. (1992). General anaesthetics inhibit the responses induced by glutamate receptor agonists in the mouse cortex. *Neurosci. Lett.*, **146**, 21–24.

CHEN, Y., GRAHAM, D.I. & STONE, T.W. (1992). Release of endogenous adenosine and its metabolites by the activation of NMDA receptors in the rat hippocampus *in vivo*. *Br. J. Pharmacol.*, **106**, 632–638.

CHOI, D.W. (1988). Calcium mediated neurotoxicity: relationship to specific channel types and role in ischemic damage. *Trends Neurosci.*, **11**, 465–469.

CHOI, D.W. & ROTHMAN, S.M. (1990). The role of glutamate neurotoxicity in hypoxic-ischemic neuronal death. *Annu. Rev. Neurosci.*, **13**, 171–182.

CONNICK, J.H. & STONE, T.W. (1989). Quinolinic acid neurotoxicity, protection by intracerebral PIA and potentiation by hypotension. *Neurosci. Lett.*, **101**, 191–196.

COYLE, J.T. (1987). Kainic acid: insights into excitatory mechanism causing selective neuronal degredation. In *Selective Neuronal Death*. (Ciba Foundation Symposium, 126) pp. 186–203. Chichester: Wiley.

DAGANI, F., CATTABENI, F., CANEVERI, L., FERRARI, R. & ABBRACCHIO, M.P. (1992). Adenosine receptors in rat brain synaptosomes: receptor characterisation and relationships with glutamate release. *Int. J. Purine Pyrimidine Res.*, **3**, 20.

DECKERT J. & JORGENSEN, M.B. (1988). Evidence for pre- and postsynaptic location of adenosine A_1 receptors in the Ca1 region of the rat hippocampus: a quantatitive autoradiographic study. *Brain Res.*, **446**, 161–164.

ESHLEMAN, A.J. & MURRAY, T.F. (1989). Differential binding properties of the peripheral-type benzodiazepine ligands [^{3}H]-PK11195 and [^{3}H]Ro 5-4864 in trout and mouse brain membranes. *J. Neurosci.*, **53**, 494–502.

FARIELLO, R.G., GOLDEN, G.T., SMITH, C.C. & REYES, P.F. (1989). Potentiation of kainic acid epileptogenicity and sparing from neuronal damage by an NMDA receptor antagonist. *Epilepsy Res.*, **3**, 206–213.

FASTBOM, J. & FREDHOLM, B.B. (1985). Inhibition of [^{3}H] glutamate from rat hippocampal slices by L-PIA. *Acta Physiol. Scand.*, **125**, 121–123.

FERKANY, J.W. & COYLE, J.T. (1983). Kainic acid selectively stimulates the release of endogenous excitatory acidic amino acids. *J. Pharmacol. Exp. Ther.*, **225**, 399–406.

FERKANY, J.W., ZACZEK, R. & COYLE, J.T. (1982). Kainic acid stimulates excitatory amino acid neurotransmitters release at presynaptic receptors. *Nature*, **298**, 757–759.

FINN, S.F., SWARTZ, K.J. & BEAL, M.F. (1991). A comparison of excitotoxic lesions of the basal forebrain by kainate, quinolinate, ibotenate, N-methyl-D-aspartate or quisqualate, and the effects on toxicity of 2-amino-5-phosphonovaleric acid and kynurenic acid in the rat. *Neurosci. Lett.*, **126,** 191–194.

FRANCK, J.E. & ROBERTS, D.L. (1990). Combined kainate and ischemia produces 'mesial temporal schlerosis'. *Neurosci. Lett.*, **118,** 159–163.

FREDHOLM, B.B. & DUNWIDDIE, T.V. (1988). How does adenosine inhibit transmitter release? *Trends Pharmacol. Sci.*, **9,** 130–134.

FREUND, T.F., YLINEN, A., MIETTINEN, R., PITKANEN, A., LAHTINEN, H., BAIMBRIDGE, K.G. & RIEKKINEN, P.J. (1992). Pattern of neuronal death in the rat hippocampus after status epilepticus – relationship to calcium binding protein and ischaemic vulnerability. *Brain Res. Bull.*, **28,** 27–38.

FULLER, T. & OLNEY, J.W. (1981). Only certain anticonvulsants protect against kainate neurotoxicity. *Neurobehav. Toxicol. Teratol.*, **3,** 355–361.

GLOBUS, M.Y.-T., BUSTO, R., DIETRICH, W.D., MARTINEZ, E., VALDES, I. & GINSBERG, M.D. (1988). Effect of ischaemia on the *in vivo* release of striatal dopamine, glutamate and GABA studied by intracerebral microdialysis. *J. Neurochem.*, **51,** 1455–1464.

GLOBUS, M.Y.-T., BUSTO, R., MARTINEZ, E., VALDES, I. & DIETRICH, W.D. (1990). Ischemia induced release of glutamate in regions spared from histopathologic damage in the rat. *Stroke*, **21,** (Suppl. III), III-43–III-46.

GLOBUS, M.Y.-T., BUSTO, R., MARTINEZ, E., VALDES, I., DIETRICH, W.D. & GINSBERG, M.D. (1991). Comparative effect of transient global ischemia on extracellular levels of glutamate, glycine and -aminobutyric acid in vulnerable and nonvulnerable brain regions of the rat. *J. Neurochem.*, **57,** 470–478.

GOODMAN, R.R. & SYNDER, S.H. (1982). Autoradiographic localisation of adenosine receptors using [^{3}H] cyclohexyladenosine. *J. Neurosci.*, **2,** 1230–1241.

HABA, K., OGAWA, N., MIZUKAWA, K. & MORI, A. (1991). Time course of changes in lipid peroxidation, pre- and postsynaptic cholinergic indices, NMDA receptor binding and neuronal death in the gerbil hippocampus following transient ischaemia. *Brain Res.*, **540,** 116–122.

HEGGLI, D.A., AAMODT, A. & MALTHE-SORENSSEN, D. (1981). Kainic acid neurotoxicity; effect of systemic injection on neurotransmitter markers in different brain regions. *Brain Res.*, **230,** 253–262.

HEGGLI, D.E. & MALTHE-SORENSSEN, D. (1982). Systemic injection of kainic acid; effect on neurotransmitter markers in piriform cortex, amygdaloid complex and hippocampus and protection by cortical lesioning and anticonvulsants. *Neurosci.*, **7,** 1257–1264.

HERON, A., LASBENNES, F. & SEYLAZ, J. (1992). Effect of two different routes of administration of R-PIA on glutamate release during ischaemia. *Neurosci. Lett.*, **147,** 205–208.

HOEHN, K. & WHITE, T.D. (1990). Glutamate-evoked release of endogenous adenosine from rat cortical synaptosomes is mediated by glutamate uptake and not by receptors. *J. Neurochem.*, **54,** 1716–1724.

KENDALL, T.J.G. & MINCHIN, M.C.W. (1982). The effects of anaesthetics on the uptake and release of amino acid neurotransmitters in thatamic slices. *Br. J. Pharmacol.*, **75,** 219–227.

KOH, J.-J. & CHOI, D.W. (1987). Effect of anticonvulsant drugs on glutamate neurotoxicity in cortical cell culture. *Neurology*, **37,** 319–322.

LERMA, J., ZUKIN, R.S. & BENNET, M.V.L. (1990). Glycine decreases desensitisation of N-methyl-D-apartate (NMDA) receptors expressed in *Xenopus* oocytes and is required for NMDA responses. *Proc. Natl. Acad. Sci. U.S.A.*, **87,** 2354–2358.

LERANTH, C. & RIBAK, C.E. (1991). Calcium-binding proteins are concentrated in the CA2 field of the monkey hippocampus: a possible key to this region's resistance to epileptic damage. *Exp. Brain Res.*, **85,** 129–136.

LERNER-NATOLI, M., RONDOUIN, G., BELAIDI, M., BALDY-MOULINIER, M. & KAMENKA, J.M. (1991). N-[1-(2-Thienyl)cyclohexyl]-piperidine (TCP) does not block kainic acid-induced status epilepticus but reduces secondary hippocampal damage. *Neurosci. Lett.*, **122,** 174–178.

LIN, B., DIETRICH, E.D., BUSTO, R. & GINSBERG, M.D. (1990). (S)-Emopamil protects against global ischemic brain injury in rats. *Stroke*, **21,** 1734–1739.

LOTHMAN, E.W. & COLLINS, R.C. (1981). Kainic acid induced limbic seizures; metabolic, behavoural, electroencephalographic and neuropathological correlates. *Brain Res.*, **218,** 299–318.

LOWRY, O.H., ROSEBROUGH, N.J., FARR, A.L. & RANDALL, R.A. (1951). Protein measurements with the folin phenol reagent. *J. Biol. Chem.*, **193,** 265–275.

LUPICA, C.R., PROCTER, W.R. & DUNWIDDIE, T.V. (1992). Adenosine reduces EPSPs presynaptically by decreasing quantal content and not quantal size in hippocampal CA1 pyramidal neurons. *Int. J. Purine Pyrimidine Res.*, **3,** 16.

MACGREGOR, D.G. & STONE, T.W. (1993). Inhibition by the adenosine analogue (**R**-)-N^6-phenylisopropyladenosine of kainic acid neurotoxicity in rat hippocampus after systemic administration. *Br. J. Pharmacol.*, **109,** 316–321.

MILLER, L.P. & HSU, C. (1992). Therapeutic potential for adenosine receptor activation in ischemic brain injury. *J. Neurotrauma*, **9,** Suppl. 2, S563–S577.

NAKANO, S., KOGURE, K. & FUJIKURA, H. (1990). Ischemia-induced slowly progressive neuronal damage in the rat brain. *Neurosci.*, **38,** 115–124.

NEHLIG, A., PEREIRA DE VASCONCELOS, A., COLLIGNON, A. & BOYET, S. (1988). Comparative effects on caffeine and L-phenylisopropyladenosine on local cerbral glucose utilization in the rat. *Eur. J. Pharmacol.*, **157,** 1–11.

NOTMAN, H., WHITNEY, R. & JHAMANDAS, K. (1984). Kainic acid evoked release of D-[^{3}H] aspartate from rat striatum *in vitro*; characterization and pharmacological modulation. *Can. J. Physiol. Pharmacol.*, **62,** 1070–1077.

OHTA, S., SMITH, M.-L. & SIESJÖ, B.K. (1991). The effect of a selective dihydropyridine calcium antagonist (isradipine) on selective neuronal necrosis. *J. Neurosci.*, **103,** 109–115.

PALMER, A.M., REITER, C.T. & BOTSCHELLER, M. (1992). Comparison of the release of exogenous and endogenous excitatory amino acids from rat cerebral cortex. *Neurotoxins and Neurodegenerative Diseases. Ann. N.Y. Acad. Sci.*, **648,** 361–364.

PATEL, J., ZINKLAND, W.C., THOMPSON, C., KEITH, R. & SALAMA, A. (1990). Role of glycine in the N-methyl-D-aspartate mediated neuronal cytotoxicity. *J. Neurochem.*, **54,** 849–854.

PHILLIS, J.W., WALTER, G.A., O'REGAN, M.H. & STAIR, R.E. (1987). Increases in cerebral cortical perfusate adenosine and inosine concentrations during hypoxia and ischemia. *J. Cereb. Blood Flow Metab.*, **7,** 679–686.

RICHARDS, C.D. (1983). Actions of general anaesthetics on synaptic transmission in the CNS. *Br. J. Anaesth.*, **55,** 201–207.

RUDOLPHI, K.A., SCHUBERT, P., PARKINSON, F.E. & FREDHOLM, B.B. (1992). Neuroprotective role of adenosine in cerbral ischaemia. *Trends Pharmacol. Sci.*, **13,** 439–445.

RUDOLPHI, K.A., KEIL, M. & HINZE, H.J. (1987). Effect of theophylline on ischaemically induced hippocampal damage in Mongolian gerbils; a behavioural and histopathological study. *J. Cereb. Blood Flow Metab.*, **7,** 74–81.

SAIJA, A., PRINCI, P., PISANI, A., SANTORO, G., DE PASQUALE, R., MASSI, M. & COSTA, G. (1992). Blood-brain barrier dysfunctions following systemic injections of kainic acid in the rat. *Life Sci.*, **51,** 467–477.

SCHMIDT-KASTNER, R. & FREUND, T.F. (1991). Selective vulnerability of the hippocampus in brain ischemia. *Neurosci.*, **40,3,** 599–636.

SCHWARCZ, R., FOSTER, A.C., FRENCH, E.D., WHETSELL, W.O. & KÖHLER, C. (1984). II. Excitotoxic models for neurodegenerative disorders. *Life Sci.*, **35,** 19–32.

SCHWOB, J.E., FULLER, T., PRICE, J.L. & OLNEY, J.W. (1980). Widespread patterns of neuronal damage following systemic or intracerebral injections of kainic acid: a histological study. *Neurosci.*, **5,** 991–1014.

SIMPSON, R.E., O'REGAN, M.H., PERKINS, L.M. & PHILLIS, J.W. (1992). Excitatory transmitter amino acid release from the ischemic rat cerebral cortex: effects of adenosine receptor agonists and antagonists. *J. Neurochem.*, **58,** 1683–1690.

STEWART, G.R., ZORUMSKI, C.F., PRICE, M.T. & OLNEY, J.W. (1990). Domoic acid: a dementia-inducing excitotoxic food poison with kainic acid receptor specificity. *Exp. Neurol.*, **110,** 127–138.

STONE, T.W. & SIMMONDS, H.A. (1991). *Purines: Basic and Clinical Aspects.* London: Kluwer Academic Press.

SUTULA, T., CAVAZOS, J. & GOLARAI, G. (1982). Alteration of long-lasting structural and functional effects of kainic acid in the hippocampus by brief treatment with phenobarbital. *J. Neurosci.*, **12,** 4173–4187.

THOMPSON, S.M., HAAS, H.L. & GAHWILER, B.H. (1992). Comparison of the actions of adenosine at presynaptic and postsynaptic receptors in the rat hippocampus *in vitro*. *J. Physiol.*, **451**, 347–363.

TOMINAGA, K., SHIBATA, S. & WATANABE, S. (1992). A neuroprotective effect of adenosine A_1-receptor agonists on ischemia-induced decrease in 2-deoxyglucose uptake in rat hippocampal slices. *Neurosci. Lett.*, **145**, 67–70.

UEMATSU, D., ARAKI, N., GREENBERG, J.H., SLADKY, J. & REIVICH, M. (1991). Combination therapy with MK-801 and nimodipine for protection of ischemic brain damage. *Neurology*, **41**, 88–94.

URBAN, L., NEILL, K.H., CRAIN, B.J., NADLER, J.V. & SOMJEN, G.G. (1990). Postischemic synaptic excitation and N-methyl-D-aspartate receptor activation in gerbils. *Stroke*, **21** (Suppl. III), III-23–III-27.

VOLL, C.L. & AUER, R.N. (1991). Postischemic seizures and necrotizing ischemic brain damage: neuroprotective effect of postischemic diazepam and insulin. *Neurology*, **41**, 423–428.

VON LUBITZ, D.K.E.J., DAMBROSIA, J.M. & REDMOND, D.J. (1989). Protective effect of cyclohexyl adenosine in treatment of cerebral ischemia in gerbils. *Neurosci.*, **30**, 451–462.

WOLF, G., FISCHER, S., HASS, P., ABICHT, K. & KEILHOFF, G. (1991). Magnesium sulphate subcutaneously injected protects against kainate-induced convulsions and neurodegenerations – *in vivo* study on the rat hippocampus. *Neurosci.*, **43**, 31–34.

WOOD, E.R., BUSSEY, T.J. & PHILLIPS, A.G. (1992). A glycine antagonist reduced ischemia-induced CA1 cell loss in vivo. *Neurosci. Lett.*, **145**, 10–14.

ZACZEK, R., NELSON, M.F. & COYLE, J.T. (1978). Effects of anaesthetics and anticonvulsants on the action of kainic acid in the rat hippocampus. *Eur. J. Pharmacol.*, **52**, 323–327.

ZUCKER, D.K., WOOTEN, G.F. & LOTHMAN, E.W. (1983). Blood-brain-barrier changes with kainic acid-induced limbic seizures. *Exp. Neurol.*, **79**, 422–433.

(Received March 8, 1993
Revised April 27, 1993
Accepted May 11, 1993)

Br. J. Pharmacol. (1993), **110**, 477–481

Differential effects of B_2 receptor antagonists upon bradykinin-stimulated phospholipase C and D in guinea-pig cultured tracheal smooth muscle

[1]Susan Pyne & Nigel J. Pyne

Department of Physiology and Pharmacology, University of Strathclyde, Royal College, Glasgow G1 1XW

1 Guinea-pig tracheal smooth muscle cells were isolated and maintained in culture for 14–21 days prior to the study of the effect of a selective bradykinin B_1 agonist and B_2 antagonists upon bradykinin-stimulated phospholipase C and D activities.

2 Bradykinin-stimulated phospholipase C activity was determined by mass measurement of inositol (1,4,5)trisphosphate (Ins(1,4,5)P_3) in unlabelled cells, whereas phospholipase D activity was assayed by the accumulation of [^{3}H]-phosphatidylbutanol ([^{3}H]-PtdBut) in [^{3}H]-palmitate-labelled cells, which were stimulated in the presence of butan-1-ol (0.3%, v/v).

3 Bradykinin elicited the rapid and transient formation of Ins(1,4,5)P_3, in a concentration-dependent manner (log $EC_{50} = -7.55 \pm 0.1$ M, $n = 3$). Bradykinin also rapidly activated the concentration-dependent (log $EC_{50} = -8.3 \pm 0.4$ M, $n = 3$) phospholipase D-catalysed accumulation of [^{3}H]-PtdBut; the accumulation of [^{3}H]-PtdBut was sustained. These effects were not inhibited by pretreatment of the cells with indomethacin (1 μM).

4 The bradykinin B_1 agonist, desArg^9-bradykinin (1 μM) was without effect upon phospholipase C or phospholipase D activity. Bradykinin-stimulated (10 nM, EC_{40}) Ins(1,4,5)P_3 formation was inhibited by B_2 receptor antagonists, D-Arg-[Hyp^3,D-Phe^7]-bradykinin (NPC 567) and D-Arg-[Hyp^3,Thi^{5,8},D-Phe^7]-bradykinin (NPC 349), with log IC_{50} values of -6.3 ± 0.5 M and -6.3 ± 0.4 M, respectively. However, bradykinin-stimulated (10 nM, EC_{100}) [^{3}H]-PtdBut accumulation was poorly inhibited and with low potency by each B_2 receptor antagonist and bradykinin-stimulated phospholipase D activity persisted at concentrations of antagonist that completely blocked bradykinin-stimulated Ins(1,4,5)P_3 formation (30 μM).

5 These observations suggest that the activation of phospholipase C by bradykinin may be mediated through a bradykinin B_2 receptor population, whereas bradykinin-stimulated phospholipase D may be activated via a distinct population of bradykinin receptors that do not appear to be either B_1 or B_2 receptor types, based upon pharmacological specificity. The mechanism of the activation of phospholipase D by bradykinin and the role of the putative B_3 bradykinin receptor are discussed.

Keywords: Bradykinin; phospholipase; receptor; smooth muscle; trachea; B_3 receptor

Introduction

Bradykinin is a potent nonapeptide which is generated in the tracheo-bronchial tree and in plasma during the inflammatory response (Proud & Kaplan, 1988) and may be an important mediator in diseases such as asthma. For example, asthmatics undergo bronchoconstriction in response to bradykinin and exhibit elevated levels of bradykinin in plasma and bronchoalveolar lavage after antigen challenge (Christiansen *et al.*, 1987). Whether the effects of bradykinin via B_2 receptors upon smooth muscle tone are direct or indirect remains ill-defined (Ichinose *et al.*, 1990). However, bradykinin receptors are present in airway smooth muscle (Farmer *et al.*, 1989; 1991; Panettieri *et al.*, 1989; Pyne & Pyne, 1993; Marsh & Hill, 1992).

The molecular mechanism whereby agonists induce airway smooth muscle contraction remains ill-defined. However, the initiation and development of contraction is believed to be due to agonist-stimulated phosphatidylinositol 4,5-biphosphate (PtdIns(4,5)P_2) hydrolysis and the production of inositol (1,4,5)trisphosphate (Ins(1,4,5)P_3) which mobilizes Ca^{2+} from intracellular stores (Somlyo *et al.*, 1988). This leads to the activation of myosin light chain kinase and tension development (Chilvers *et al.*, 1989; Murray *et al.*, 1989). Bradykinin has been shown to elicit phosphoinositide hydrolysis in bovine cultured tracheal smooth muscle (Marsh & Hill, 1992) and the opening of receptor-operated Ca^{2+} channels in human cultured airway smooth muscle (Murray & Kotlikoff, 1991). Protein kinase C has been implicated in the process of sustained contraction since activators of protein kinase C, e.g. phorbol 12-myristate 13-acetate (PMA), synergize with Ca^{2+} to mimic agonist-stimulated contraction (Park & Rasmussen, 1985) and treatment of airway smooth muscle with PMA induces contraction in the absence of an intracellular Ca^{2+} signal (Kotlikoff *et al.*, 1987).

In addition, bradykinin elicits other biochemical responses including the activation of phospholipases A_2 and D (Farmer & Burch, 1992). We have recently demonstrated a bradykinin-stimulated phospholipase D activity in primary cultures of guinea-pig tracheal smooth muscle (Pyne & Pyne, 1993). These cultured cells have been shown to express large numbers of B_2 receptors mediating, for example, prostaglandin synthesis, but are also believed to contain a novel B_3 receptor type, coupled to bradykinin-induced Ca^{2+} efflux (Farmer *et al.*, 1991). This latter receptor type is believed to be involved in airway smooth muscle contraction since B_1 and B_2 antagonists have only a weak effect upon bradykinin-induced contraction of guinea-pig trachealis (Farmer *et al.*, 1989). Furthermore, bradykinin B_2 antagonists failed to displace [^{3}H]-bradykinin from freshly prepared guinea-pig tracheal smooth muscle membranes (Farmer *et al.*, 1989). However, the role of the putative B_3 receptor sub-type in airway smooth muscle contraction and the molecular mechanism involved remain unclear.

In this study, we aimed to characterize the bradykinin receptor type involved in the activation of phospholipase C

[1] Author for correspondence.

and D in guinea-pig cultured tracheal smooth muscle by the use of bradykinin B_2 antagonists and a bradykinin B_1 agonist. We demonstrate that whilst neither phospholipase C nor D is activated by a B_1 agonist, activation of phospholipase C by bradykinin can be completely inhibited by B_2 antagonists whereas bradykinin-stimulated phospholipase D activity is poorly inhibited and persists in the absence of a measurable phospholipase C response.

Methods

Cell culture

Tracheal smooth muscle cells were cultured from male guinea-pigs (Dunkin-Hartley, 450–500 g) by the method of Panettieri *et al.* (1989) and maintained in Dulbecco's Modified Eagle's medium (DME) containing 10% (v/v) foetal calf serum (FCS)/10% (v/v) donor horse serum (DHS) at 37°C in air/CO_2 (95:5, v/v) (Pyne & Pyne, 1993). Cells were passaged by use of trypsin and grown to confluence on 24 well plates for experiments at 14–21 days after the initial preparation (passage 3). Identity of the smooth muscle cells was confirmed by the presence of smooth muscle α-actin using a mouse monoclonal antibody (Pyne & Pyne, 1993).

Measurement of inositol(1,4,5)trisphosphate

Ins(1,4,5)P_3 mass measurement was performed as described previously (Palmer & Wakelam, 1990; Pyne & Pyne, 1993). The cells were washed and preincubated in 250 μl Krebs Ringer bicarbonate buffer containing (mM): NaCl 118, $NaHCO_3$ 25, KCl 5, K_2HPO_4 1, $MgSO_4$ 1, $CaCl_2$ 1.5, glucose 10, pH 7.4) and supplemented with bovine serum albumin (Fraction V, 1% (w/v)) (KRB) for 30 min at 37°C in air/CO_2 (95:5, v/v). This medium was replaced with 100 μl of KRB in the presence and absence of bradykinin as required. In all cases bradykinin was present during the entire time-course of the incubation. Incubations were terminated by the addition of 25 μl of ice-cold perchloric acid (10%, w/v) and the samples placed on ice. Acid extracts were harvested, neutralized by the addition of approx. 25 μl (mM) 1500 KOH, 60 HEPES in the presence of a trace quantity of Universal Indicator and the resulting supernatants assayed for Ins(1,4,5)P_3 by an Ins(1,4,5)P_3-specific radioligand binding assay (Palmer & Wakelam, 1990) employing a crude adrenocortical microsomal fraction as a binding protein preparation. A standard curve of 25 fmol–25 pmol was conducted in parallel.

Incubation of cells with [^{3}H]-palmitate; phospholipase D assay

Confluent tracheal smooth muscle cells were preincubated with [^{3}H]-palmitate (2 μCi ml^{-1}) in DME containing 1% (v/v) FCS and 1% (v/v) DHS for 24–48 h. This procedure has previously been shown to result in the selective incorporation of radioactivity into phosphatidylcholine (PtdCh, which contained 82% of total radioactivity associated with major phospholipids in comparison with only 6% associated with phosphatidylinositol, phosphatidylethanolamine and phosphatidylserine combined (Pyne & Pyne, 1993)).

Phospholipase D activity was determined by a transphosphatidylation assay (Pai *et al.*, 1988). Briefly, [^{3}H]-palmitate-labelled cells were washed and preincubated for 30 min with 500 μl KRB at 37°C in air/CO_2 (95/5, v/v) prior to a further preincubation for 5 min with 250 μl KRB containing butan-1-ol (0.3%, v/v). Bradykinin was added as required and was present during the entire time-course of the incubation. The incubations were terminated by removal of the medium and the addition of ice-cold methanol (200 μl). Organic extracts were prepared and the non-metabolizable [^{3}H]-PtdBut formed determined by its resolution upon thin layer chromatography (t.l.c.) using a solvent of the upper phase of ethyl acetate:2,2,4-trimethylpentane:acetic acid:H_2O (110:50:20:100, v/v) as described previously (Pyne & Pyne, 1993). [^{3}H]-PtdBut, which is a direct indicator of phospholipase D activity (Pai *et al.*, 1988), routinely migrated with an $R_F = 0.35$ and was quantified by excising the appropriate area from each lane and counting the associated radioactivity.

Preincubation of cells with indomethacin or bradykinin B_2 antagonists

For the experiments involving cyclo-oxygenase inhibition, cells were pretreated with indomethacin (1 μM) for 10 min prior to stimulation. In experiments involving the bradykinin B_2 antagonists, D-Arg-[Hyp^3,D-Phe^7]-bradykinin (NPC 567) and D-Arg-[Hyp^3,Thi^{5,8},D-Phe^7]-bradykinin (NPC 349), the cells were preincubated with the appropriate concentration for 2 min prior to the addition of bradykinin (10 nM).

Statistical analysis

All data are expressed as means ± s.d. and significance was determined by Student's *t* test.

Materials

[^{3}H]-palmitate (sp. act. 40–60 Ci mmol^{-1}) and [^{3}H]-inositol (1,4,5)trisphosphate (sp. act. 20–60 Ci mmol^{-1}) were purchased from Amersham International plc (Amersham, U.K.). Tissue culture reagents and plasticware were obtained from Gibco BRL (Paisley, U.K.) and ICN Flow (High Wycombe, U.K.). Bradykinin, bradykinin B_2 antagonists D-Arg-[Hyp^3,D-Phe^7]-bradykinin (NPC 567) and D-Arg-[Hyp^3,Thi^{5,8},D-Phe^7]-bradykinin (NPC 349) and the bradykinin B_1 agonists, des-Arg^9-bradykinin were purchased from Calbiochem (Nottingham, U.K.). Thin layer chromatography plates (LK5D) were obtained from Whatman (Maidstone, U.K.). All other reagents were of the highest purity commercially available.

Results

Bradykinin-stimulated Ins(1,4,5)P_3 formation

Bradykinin stimulated the rapid formation of Ins(1,4,5)P_3 in guinea-pig cultured tracheal smooth muscle cells. Basal levels of Ins(1,4,5)P_3 were 1.82 ± 0.35 pmol/0.25 × 10^6 cells ($n = 13$) and stimulation for 10s with a maximal concentration of bradykinin (100 nM) produced a 10.4 ± 6.1 ($n = 13$) fold increase in Ins(1,4,5)P_3 mass. A representative time course is illustrated in Figure 1a. The Ins(1,4,5)P_3 signal was transient, returning to close to basal levels by 30–60 s stimulation. The bradykinin-stimulated generation of Ins(1,4,5)P_3, measured at 10 s was concentration-dependent (Figure 1b) with a log EC_{50} of −7.55 ± 0.1 M ($n = 3$).

Bradykinin-stimulated phospholipase D

Bradykinin stimulated the activation of phospholipase D-catalysed PtdCh hydrolysis as evidenced by the accumulation of [^{3}H]-PtdBut in [^{3}H]-palmitate-labelled tracheal smooth muscle cells (Pyne & Pyne, 1993). Significant [^{3}H]-PtdBut formation was detected at 1 min and continued to be formed throughout the 10 min time course (Figure 2a). Stimulation with 100 nM bradykinin typically resulted in a 2.68 ± 1.1 ($n = 25$) fold increase in [^{3}H]-PtdBut above basal at 10 min. The bradykinin-stimulated phospholipase D response, measured at 10 min, was concentration-dependent (Figure 2b) with a log EC_{50} of −8.3 ± 0.4 M, which is significantly lower than that for bradykinin-stimulated phospholipase C activation.

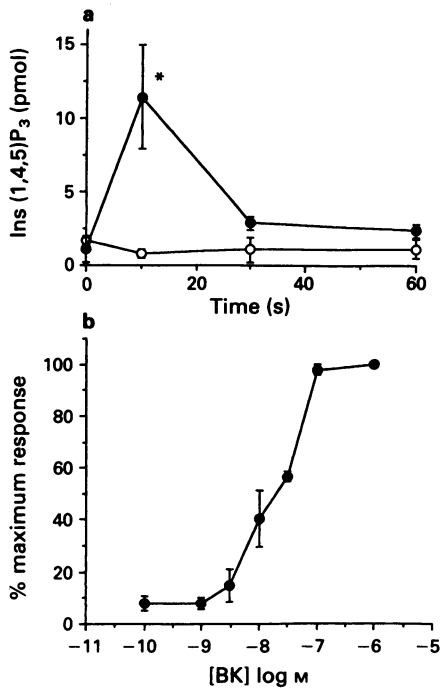

Figure 1 (a) Timecourse of bradykinin-stimulated inositol(1,4,5) trisphosphate (Ins(1,4,5)P_3) mass formation in guinea-pig cultured tracheal smooth muscle cells: (○) control; (●) bradykinin (100 nM). Results are mean ± s.d. ($n = 3$). (b) Bradykinin concentration-dependent Ins(1,4,5)P_3 formation at 10 s stimulation; means ± s.d. ($n = 3$) as % of maximal response. *$P < 0.025$ vs control (Student's t test).

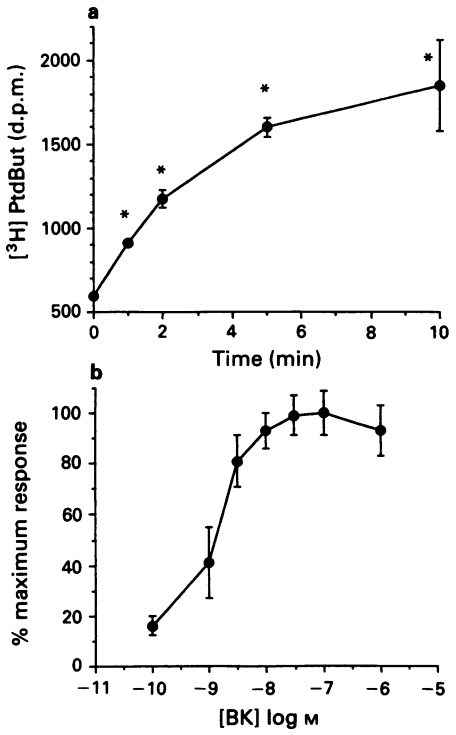

Figure 2 (a) Timecourse of bradykinin-stimulated [^{3}H]-phosphatidylbutanol ([^{3}H]-PtdBut) accumulation in guinea-pig cultured tracheal smooth muscle cells: (●) bradykinin (100 nM). Results are mean ± s.d. ($n = 3$). (b) Bradykinin concentration-dependent [^{3}H]-PtdBut accumulation at 10 min stimulation; means ± s.d. ($n = 3$ incubations) as % of maximal response. *$P < 0.005$ vs zero timepoint (Student's t test).

Effects of indomethacin and bradykinin antagonists

Bradykinin-stimulated phospholipase C was not inhibited by pretreatment of the cells with 1 μM indomethacin, suggesting that the observed effects of bradykinin were not secondary to bradykinin-stimulated prostaglandin synthesis (Figure 3). Similar data have previously been obtained for the bradykinin-stimulated phospholipase D response (Pyne & Pyne, 1993).

The identity of the bradykinin receptor sub-type(s) involved in the activation of these responses was investigated with a bradykinin B_1 agonist, desArg^9-bradykinin, and two bradykinin B_2 antagonists, NPC 567 and NPC 349. Stimulation of the tracheal smooth muscle cells with desArg^9-bradykinin (1 μM) elicited neither a phospholipase C nor phospholipase D response (Figure 3). In contrast, preincuba-

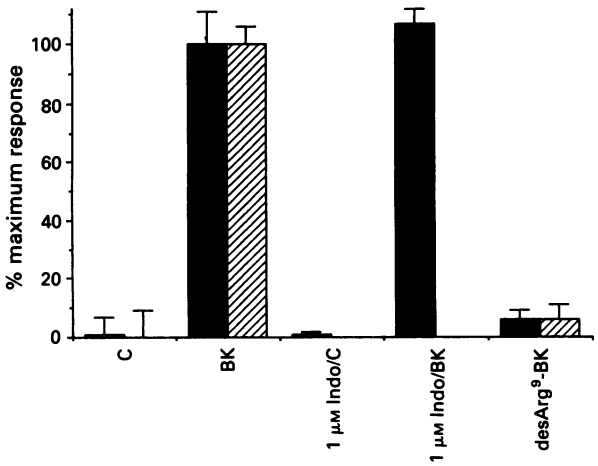

Figure 3 Lack of effect of indomethacin (Indo, 1 μM) upon 100 nM bradykinin (BK)-stimulated inositol(1,4,5)trisphosphate (Ins(1,4,5)P_3) formation at 10 s (solid columns) and the lack of effect of desArg^9-bradykinin (1 μM) upon [^{3}H]-phosphatidylbutanol ([^{3}H]PtdBut) accumulation (hatched columns) at 10 min and Ins(1,4,5)P_3 accumulation (solid columns) at 10 s. Results are means ± s.d. ($n = 3$) as % of maximal response.

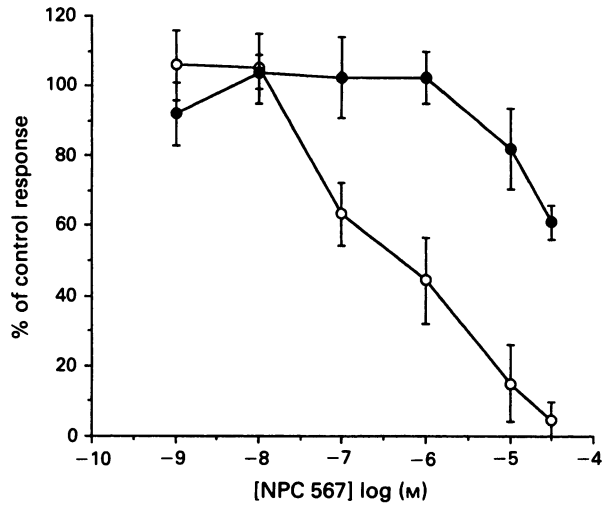

Figure 4 The effect of the bradykinin B_2 antagonist NPC 567 (D-Arg-[Hyp^3,D-Phe^7]-bradykinin) on bradykinin-stimulated (10 nM) inositol(1,4,5)trisphosphate (Ins(1,4,5)P_3) formation (10 s, ○) and [^{3}H]-phosphatidylbutanol ([^{3}H]PtdBut) accumulation (10 min, ●) in guinea-pig cultured tracheal smooth muscle cells. Control values were 0.81 ± 0.26 pmol Ins(1,4,5)P_3/0.25 × 10^6 cells and 750 ± 106 d.p.m. [^{3}H]PtdBut/0.25 × 10^6 cells. Results are means ± s.d. ($n = 3$).

tion of the cells with the bradykinin B_2 antagonist NPC 567 for 2 min prior to stimulation with bradykinin (10 nM) resulted in the inhibition of both Ins(1,4,5)P_3 formation and, at high concentrations (> 10 μM), [^{3}H]-PtdBut accumulation (Figure 4). A second B_2 antagonist, NPC 349, displayed essentially the same characteristics.

The IC_{50} for inhibition of the phospholipase C and phospholipase D responses by these antagonists differed markedly. Log IC_{50} values for the Ins(1,4,5)P_3 response to 10 nM bradykinin were -6.3 ± 0.5 M ($n = 3$) for NPC 567 and -6.3 ± 0.4 M ($n = 3$) for NPC 349. The Ins(1,4,5)P_3 response to 10 nM bradykinin was abolished by 30 μM NPC 567 (Figure 4) or NPC 349 (data not shown). In contrast, preincubation of the cells for 2 min with either bradykinin B_2 receptor antagonist resulted in only limited inhibition of bradykinin-stimulated (10 nM) phospholipase D activation (Figure 4). At 30 μM B_2 antagonist, a concentration which abolished the phospholipase C response, approx. 60% of the phospholipase D response remained and the IC_{50} for bradykinin-stimulated phospholipase D was estimated to be in excess of 100 μM. At these high concentrations of antagonist, non-specific interactions with bradykinin-stimulated phospholipase D may occur.

Discussion

This study provides the first demonstration of bradykinin-stimulated changes in Ins(1,4,5)P_3 mass in airway smooth muscle, although Marsh & Hill (1992) have recently shown bradykinin-stimulated accumulation of [^{3}H]-inositol phosphates. However, this latter technique is not sufficiently sensitive to detect agonist-stimulated changes in phosphoinositide metabolism at functionally important early times. The kinetics of the Ins(1,4,5)P_3 response are similar to those observed for carbachol in bovine cervical trachealis muscle slices (Chilvers *et al.*, 1989) and correlate with the kinetics of bradykinin-stimulated [Ca^{2+}] transients in Fura-2 loaded monolayers of human primary cultured airway smooth muscle (Panettieri *et al.*, 1989). Bradykinin-stimulated Ins(1,4,5)P_3 mass increased rapidly (within seconds) and was transient. This may be due to enhanced metabolism of Ins(1,4,5)P_3 by Ins(1,4,5)P_3 5-phosphatase and 3-kinase (Shears, 1991) or desensitization of agonist-stimulated PtdIns(4,5)P_2 hydrolysis (Palmer *et al.*, 1991) or both. Desensitization of phospholipase C during prolonged bradykinin-stimulation is suggested by the plateau in [^{3}H]-inositol phosphates accumulation in bovine cultured tracheal smooth muscle (Marsh & Hill, 1992).

Bradykinin was a less potent stimulator of Ins(1,4,5)P_3 formation in guinea-pig tracheal smooth muscle when compared to its effect upon [^{3}H]-inositol phosphate accumulation in bovine cultured tracheal smooth muscle cells (Marsh & Hill, 1992). However, both effects were inhibited by B_2 antagonists, suggesting that sensitivity of the bradykinin B_2 receptor coupling to phospholipase C may differ between species. In addition, desArg^9-bradykinin failed to elicit an Ins(1,4,5)·P_3 response (the present study) whereas it weakly activates [^{3}H]-inositol phosphate accumulation in bovine cultured tracheal smooth muscle cells (Marsh & Hill, 1992), indicating that B_1 bradykinin receptors may be differentially expressed between species.

In contrast to the transient Ins(1,4,5)P_3 signal, [^{3}H]-PtdBut accumulation was sustained in response to bradykinin due to the inability of the cells to metabolize phosphatidylalcohols. However, partial desensitization of bradykinin-stimulated phospholipase D activity may occur since the rate of accumulation of [^{3}H]-PtdBut declined after 2–5 min stimulation.

Interestingly, bradykinin-stimulated phospholipase D activity displayed significantly higher potency than that for bradykinin-stimulated phospholipase C activity. This may suggest that distinct bradykinin receptor types are involved in mediating the two responses. However, we cannot exclude from these studies the possibility that receptor-G-protein fidelities are different or that a receptor reserve exists for the phospholipase D response. However, our results from the antagonism experiment would argue against these latter hypotheses.

For example, if one receptor mediates both PLD and PLC responses via distinct G-proteins then, since the affinity of the receptor for antagonist is not dependent upon G-protein association (i.e. guanine nucleotides do not modify the affinity of the receptor for antagonist), both PLC and PLD responses should be blocked with exactly the same concentration-dependence for the antagonist. This clearly does not occur. Thus, if both responses were mediated by the same receptor, we would predict that the PLD response would be inhibited by at least 40% and with an identical antagonist concentration-dependence to that observed for PLC inhibition (in response to an EC_{40} concentration of agonist).

The conditions used in the antagonist experiments reduce the effect of a receptor reserve for PLD to a minimum, i.e. the concentration of agonist used (10 nM) is at the threshold for maximal activation of the PLD response. Thus, if one receptor mediates both responses, then, the occupancy of the 'spare receptors' will be minimal. Under these conditions, the antagonist concentration-dependence for inhibition of both PLD and PLC should be virtually identical since, by the law of mass action, receptor occupancy for both responses will be virtually the same. The fact that the IC_{50} values differ by approximately two orders of magnitude clearly precludes the possibility that a receptor reserve for PLD exists to account for these results.

We conclude that the only reasonable explanation for the large shift in antagonist concentration-dependence for the two responses is to invoke the possibility of a novel receptor mediating PLD activation. Furthermore, phospholipase D activation was detected in the absence of phospholipase C activation, which was completely blocked by B_2 antagonists. This suggests that, in this case, bradykinin-stimulated phospholipase D is not down-stream of phospholipase C activation, as has been suggested for several other agonists (Billah & Anthes, 1991).

We have previously shown that bradykinin-stimulated phospholipase D is down-stream of protein kinase C activation in guinea-pig cultured tracheal smooth muscle cells (Pyne & Pyne, 1993). Bradykinin-stimulated [^{3}H]-PtdBut accumulation is abolished in protein kinase C down-regulated cells or in the presence of a protein kinase C inhibitor, staurosporine. Since phospholipase D can be activated in the absence of PtdIns(4,5)P_2 hydrolysis, protein kinase C must be activated independently of *sn*-1,2-diacylglycerol derived from this source. Multiple isoforms of protein kinase C exist which can be variously activated by 1,2-diacylglycerol, phosphatidate, arachidonate and Ca^{2+} (Bell & Burns, 1991). The identify of the isoform(s) mediating activation of phospholipase D are unknown. However, 1,2-diacylglycerol and phosphatide can be produced by bradykinin-stimulated phospholipase C-catalysed hydrolysis of PtdCh in guinea-pig tracheal smooth muscle cells, independent of prior activation of protein kinase C. This mechanism may provide the source of protein kinase C activator necessary for phospholipase D activation (Pyne & Pyne, unpublished). Furthermore, bradykinin activates the influx of extracellular Ca^{2+} in human cultured airway smooth muscle (Murray & Kotlikoff, 1991), and we have previously demonstrated a requirement for extracellular Ca^{2+} for activation of phospholipase D (Pyne & Pyne, 1993). The arachidonate-activated protein kinase C isoform is unlikely to play a role, since bradykinin-stimulated prostanoid production is also abolished at concentrations of B_2 antagonist at which phospholipase D activity persists (Farmer *et al.*, 1991 and the present study).

Thus, bradykinin-stimulated phospholipase D activation appears to be independent of B_1 and B_2 receptor types. Farmer *et al.* (1989) have proposed the existence of a B_3 receptor which may mediate bradykinin-stimulated contrac-

tion of guinea-pig trachealis (Farmer *et al.*, 1989) and Ca^{2+} efflux from guinea-pig cultured airway smooth muscle (Farmer *et al.*, 1991). The EC_{50} for bradykinin-stimulated phospholipase D activation (the present study) is similar to that observed for Ca^{2+} efflux in guinea-pig cultured tracheal smooth muscle cells (Farmer *et al.*, 1991). Furthermore, the IC_{50} values for inhibition of these responses by NPC 567 are also similar (the present study and Farmer *et al.*, 1991). Therefore, we suggest that the putative B_3 bradykinin receptor may mediate bradykinin-stimulated phospholipase D activation in these cells. However, specific B_3 antagonists are required to prove that this is the case.

In conclusion, bradykinin induces airway smooth muscle contraction (Farmer *et al.*, 1989) and maintains the allergic inflammation of airways in guinea-pigs (Farmer *et al.*, 1992). Whilst the inflammatory response induced by bradykinin is mediated by B_1 and B_2 receptor types *in vivo* (Farmer *et al.*, 1992) and the bronchoconstriction induced by bradykinin *in vivo* is mediated by B_2 receptors (Jin *et al.*, 1989), the direct effects of bradykinin upon sustained smooth muscle contraction *in vitro* are not accounted for by these receptors. In this context, Farmer *et al.* (1991) have clearly shown that B_2 antagonists do not displace bradykinin from freshly prepared tracheal smooth muscle membranes thus identifying that B_2 receptors are unlikely to mediate direct effects of bradykinin upon contraction *in vitro*. However, in the same study, B_2 receptors appear to be 'up-regulated' in culture and this is consistent with the present study and that of Marsh & Hill (1992). The putative B_3 receptor appears to allow Ca^{2+} efflux and is present in both fresh and cultured guinea-pig tracheal smooth muscle cell membranes. Given the ability of PLD to generate activators of PKC and the possible B_3 mediated regulation of extracellular Ca^{2+} flux in these cells, we suggest that the physiological relevance of this receptor may be related to sustained contraction. However, this will only be resolved with the advent of specific B_3 receptor antagonists.

This work was supported by The Wellcome Trust.

References

BELL, R.M. & BURNS, D.J. (1991). Lipid activation of protein kinase C. *J. Biol. Chem.*, **97**, 598–602.

BILLAH, M.M. & ANTHES, J.C. (1990). The regulation and cellular function of phosphatidylcholine hydrolysis. *Biochem. J.*, **269**, 281–291.

CHILVERS, E.R., CHALLISS, R.A.J., BARNES, P.J. & NAHORSKI, S.R. (1989). Mass changes of inositol (1,4,5) trisphosphate in trachealis muscle following agonist stimulation. *Eur. J. Pharmacol.*, **164**, 587–590.

CHRISTIANSON, S.C., PROUD, D. & COCHRAINE, C.G. (1987). Detection of tissue kallikrein in bronchoalveolar lavage fluid of asthmatic subjects. *J. Clin. Invest.*, **79**, 188–197.

FARMER, S.G. & BURCH, R.M. (1992). Biochemical and molecular pharmacology of kinin receptors. *Annu. Rev. Pharmacol. Toxicol.*, **32**, 511–536.

FARMER, S.G., BURCH, R.M., MEEKER, S.N. & WILKINS, D.E. (1989). Evidence for a pulmonary bradykinin B_3 receptor. *Mol. Pharmacol.*, **36**, 1–8.

FARMER, S.G., ENSOR, J.E. & BURCH, R.M. (1991). Evidence that cultured airway smooth muscle cells contain bradykinin B_2 and B_3 receptors. *Am. Rev. Respir. Cell Mol. Biol.*, **4**, 273–277.

FARMER, S.G., WILKINS, D.E., MEEKER, S.A., SEEDS, E.A.M. & PAGE, C.P. (1992). Effects of bradykinin receptor antagonists on antigen-induced respiratory distress, airway hyperresponsiveness and eosinophilia in guinea-pigs. *Br. J. Pharmacol.*, **107**, 653–659.

ICHINOSE, M., BELVISI, M.G. & BARNES, P.J. (1990). Bradykinin-induced bronchoconstriction in guinea pig *in vivo*: role of neural mechanisms. *J. Pharmacol. Exp. Ther.*, **253**, 594–599.

JIN, L.S., SEEDS, E.A.M., PAGE, C.P. & SCHACHTER, M. (1989). Inhibition of bradykinin-induced bronchoconstriction in the guinea-pig by a synthetic B_2 receptor antagonist. *Br. J. Pharmacol.*, **97**, 598–602.

KOTLIKOFF, M.I., MURRAY, R.K. & REYNOLDS, E.E. (1987). Histamine-induced calcium release and phorbol ester antagonism in cultured smooth muscle cells. *Am. J. Physiol.*, **253**, (*Cell Physiol.*, **22**), C561–C566.

MARSH, K.A. & HILL, S.J. (1992). Bradykinin B_2 receptor-mediated phosphoinositide hydrolysis in bovine cultured tracheal smooth muscle cells. *Br. J. Pharmacol.*, **107**, 443–447.

MURRAY, R.K., BENNETT, C.F. & FLUHARTY, S.J. (1989). Mechanism of phorbol ester inhibition of histamine-induced IP_3 formation in cultured airway smooth muscle. *Am. J. Physiol.*, **257**, L209–L216.

MURRAY, R.K. & KOTLIKOFF, M.I. (1991). Receptor-activated calcium influx in human airway smooth muscle cells. *J. Physiol.*, **435**, 123–144.

PAI, J.-K., SIEGEL, M.I., EGAN, R.W. & BILLAH, M.M. (1988). Phospholipase D catalyses phospholipid metabolism in chemotactic peptide-stimulated HL-60 granulocytes. *J. Biol. Chem.*, **263**, 12472–12477.

PALMER, S., PLEVIN, R. & WAKELAM, M.J.O. (1991). Homologous desensitization of bombesin-stimulated Ins(1,4,5,)P_3 production in Swiss 3T3 fibroblasts. *Biochem. Soc. Trans.*, **19**, 101S.

PALMER, S. & WAKELAM, M.J.O. (1990). Mass measurement of Ins(1,4,5)P_3 using a specific binding assay. In *Methods in Inositide Research* ed. Irvine, R.F. pp. 127–134. New York: Raven Press.

PANETTIERI, R.A., MURRAY, R.K., DE PALO, L.R., YADVISH, P.A. & KOTLIKOFF, M.I. (1989). A human airway smooth muscle cell line that retains physiological responsiveness. *Am. J. Physiol.*, **256**, (*Cell. Physiol.*, **25**), C329–C335.

PARK, S. & RASMUSSEN, H. (1985). Activation of tracheal smooth muscle contraction: synergism between Ca^{2+} and C-kinase activators. *Proc. Natl. Acad. Sci. U.S.A.*, **82**, 8835–8839.

PROUD, D. & KAPLAN, A.P. (1988). Kinin formation: mechanisms and role in inflammatory disorders. *Annu. Rev. Immunol.*, **6**, 49–84.

PYNE, S. & PYNE, N.J. (1993). Bradykinin stimulates phospholipase D in primary cultures of guinea-pig tracheal smooth muscle. *Biochem. Pharmacol.*, **45**, 593–603.

SHEARS, S.B. (1991). Regulation of the metabolism of 1,2-diacylglycerols and inositol phosphates that respond to receptor activation. *Pharmacol. Ther.*, **49**, 79–104.

SOMLYO, A.P., WALKER, J.W., GOLDMAN, Y.E., TRENTHAM, D.R., KOBAYASHI, S., KITAZAWA, T. & SOMLYO, A.V. (1988). Inositol trisphosphate, calcium and muscle contraction. *Phil. Trans. R. Soc.*, **320**, 399–404.

(Received January 4, 1993
Revised April 13, 1993
Accepted May 11, 1993)

Br. J. Pharmacol. (1993), **110**, 482–490

Human liver microsomal metabolism of the enantiomers of warfarin and acenocoumarol: P450 isozyme diversity determines the differences in their pharmacokinetics

J.J.R. Hermans & [1]H.H.W. Thijssen

Cardiovascular Research Institute Maastricht, Department of Pharmacology, University of Limburg, PO Box 616, 6200 MD Maastricht, The Netherlands

1 To explain the large differences in (the stereoselectivity of) the clearances of the enantiomers of warfarin and acenocoumarol (4'-nitrowarfarin) their human liver microsomal metabolism has been studied and enzyme kinetic parameters determined. The effects of cimetidine, propafenone, sulphaphenazole, and omeprazole on their metabolism has been investigated.

2 The 4-hydroxycoumarins follow similar metabolic routes and are mainly hydroxylated at the 6- and 7-position (accounting for 63 to 99% of the metabolic clearances).

3 Due to the lower K_m values of **R**- and S-acenocoumarol and higher V_{max} values of S-acenocoumarol, the overall metabolic clearances of **R/S** acenocoumarol exceed those of **R/S** warfarin 6 and 66 times respectively.

4 The metabolism of both compounds is stereoselective for the S-enantiomers, which is 10 times more pronounced in the case of acenocoumarol.

5 Except for the 7-hydroxylation of the **R**-enantiomers ($r = 0.90$; $P < 0.025$), the 6- and 7-hydroxylation rates of **R/S** warfarin do not correlate with those of **R/S** acenocoumarol.

6 Sulphaphenazole competitively inhibits the 7- and in some samples partly (up to 50%) the 6-hydroxylation of S-warfarin as well as the 7-hydroxylation of **R**- and S-acenocoumarol and the 6-hydroxylation of S-acenocoumarol (K_is ranging from 0.5– 1.3 μM).

7 Omeprazole partly (40–80%) inhibits the 6- and 7-hydroxylation of **R**-warfarin ($K_i = 99$ and 117 μM) and of **R**- ($K_i = 219$ and 7.2 μM) and S-acenocoumarol ($K_i = 6.1$ and 7.7 μM) but not S-warfarin in a competitive manner.

8 Differences in the partial (up to 40%) inhibition of the metabolism of the enantiomers of the 4-hydroxycoumarins were also observed for the relatively weak inhibitors, propafenone and eimetidine.

9 The results suggest that the coumarin ring hydroxylations of both compounds are catalysed by different combinations of P450 isozymes. The 7-hydroxylation of **R/S** acenocoumarol and the 6-hydroxylation of S-acenocoumarol are at least partly conducted by (a) P450 isozyme(s) of the 2C subfamily different from P450 2C9 (the main S-warfarin 7- and 6-hydroxylase).

Keywords: Warfarin, acenocoumarol (4'-nitrowarfarin); enantiomers; stereoselectivity; biotransformation; human liver cytochrome P450 2C isozymes: drug-drug interactions

Introduction

The oral anticoagulants warfarin and acenocoumarol (the 4'-nitro analogue of warfarin; Figure 1) are administered as racemates. Although structurally related, these 4-hydroxycoumarins display great differences in their pharmacokinetics. In man, acenocoumarol enantiomers are eliminated much faster than **R/S** warfarin. In addition, the stereoselectivity of the elimination for the S-enantiomer is much more pronounced for acenocoumarol. For example, elimination half lifes are about 24–33 and 35–58 h for S- and **R**-warfarin (Kelly & O'Malley, 1979), whereas those of S- and **R**-acenocoumarol are 0.5–1 and 8–10 h (Thijssen *et al.*, 1986). Since both 4-hydroxycoumarins are eliminated by biotransformation, these pharmacokinetic differences may be explained by disparity in their metabolism.

The enantiomers of warfarin follow different metabolic routes in man (Lewis *et al.*, 1974; Toon *et al.*, 1987). The S-enantiomer is mainly hydroxylated to form 7-hydroxywarfarin (Figure 1), whereas **R**-warfarin is mainly reduced to its **RS** alcohol and hydroxylated at the 6-position. The enantiomers of acenocoumarol are hydroxylated at the 7- and, to a lesser extent, the 6-position to form 7- or 6-hydroxyacenocoumarol respectively (Thijssen *et al.*, 1986).

The *in vitro* metabolism of warfarin is extensively studied and warfarin is often used as a probe for (the stereoselectivity of) cytochromes P450 (Guengerich *et al.*, 1982; Beaune *et al.*, 1986; Kaminsky, 1989). Various P450 isozymes, displaying different regio- and stereoselectivities, have been shown to be involved in the metabolism of warfarin (Guengerich *et al.*, 1982; Rettie *et al.*, 1992). The variety of warfarin metabolizing P450 isozymes offers an explanation for the stereoselective (pharmacokinetic) drug-interactions with **R**-warfarin (Choonara *et al.*, 1986; Toon *et al.*, 1987; Sutfin *et al.*, 1989;), S-warfarin (Lewis *et al.*, 1974; O'Reilly, 1980), as well as non-stereoselective interactions (O'Reilly *et al.*, 1987) that have been observed. The human cytochrome P450 2C9 has

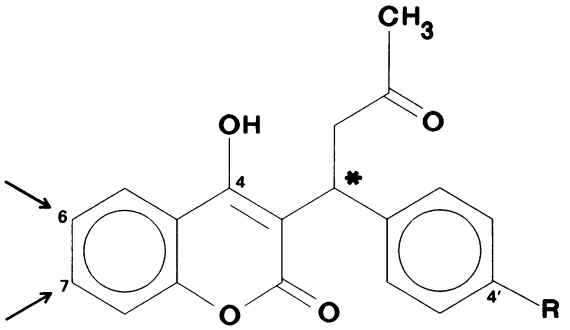

Figure 1 Structural formulae of warfarin (R = H) and acenocoumarol ($R = NO_2$). Arrows indicate the main sites of hydroxylation (6- and 7-positions). *Indicates the stereocentre.

[1] Author for correspondence.

been shown to be a S-warfarin 7- (and to a lesser extent 6-) hydroxylase, and is claimed to be responsible for the bulk of S-warfarin clearance *in vivo* (Rettie *et al.*, 1992). The main metabolic routes of R-warfarin are conducted by other enzymes among which is the human cytochrome P450 1A2 which is able to hydroxylate R-warfarin at the 6- (and to a lesser extent 7-) position (Wang *et al.*, 1983; Rettie *et al.*, 1992). To our knowledge, the *in vitro* human cytochrome P450 mediated metabolism of acenocoumarol has not been studied before.

Previous studies from our laboratory showed that in rats, substitution of the 4'-hydrogen did not only enhance the intrinsic clearances but also generally led to a marked inversion of the stereoselectivity for the S-enantiomers (Thijssen *et al.*, 1985; Baars *et al.*, 1990). With rat liver microsomes, it was found that warfarin and acenocoumarol follow similar metabolic routes. However, the metabolic clearances of R/S acenocoumarol are much higher due to their lower K_m values and unlike warfarin, the rat liver microsomal metabolism of acenocoumarol is stereoselective for the S-enantiomer (Hermans & Thijssen, 1991). Since enzyme inducers and the cytochrome P450 inhibitor cimetidine, showed differential effects on the metabolism of the 4-hydroxycoumarins, it was considered that the kinetic differences between warfarin and acenocoumarol in the rat can be partly attributed to the involvement of different sets of P450 isozymes in the metabolism of the 4-hydroxycoumarins.

In this study, the enzyme kinetic parameters of the human liver microsomal metabolism of warfarin have been compared with those of its 4'-nitro-analogue (acenocoumarol). To investigate whether the set of human liver cytochrome P450 isozymes metabolizing R/S warfarin is similar to that metabolizing R/S acenocoumarol, the inhibiting effects of four drugs (cimetidine, propafenone, sulphaphenazole, and omeprazole) have been studied. Cimetidine and omeprazole were chosen since these compounds are known to decrease the clearance of R-warfarin in man (Choonara *et al.*, 1986; Sutfin *et al.*, 1989; Unge *et al.*, 1992). Sulphaphenazole, was studied because this compound is reported to be a potent inhibitor of human liver cytochrome P450 2C9-mediated S-warfarin 7-hydroxylation (Rettie *et al.*, 1992). Propafenone was chosen because, although this compound is shown to decrease the clearance of warfarin in man (Kates *et al.*, 1987), information on stereochemical aspects is still lacking.

Methods

Preparation of microsomal fractions

Human liver samples (Table 1) were obtained from kidney donors (I, II and V) or were obtained *post mortem* (III, and IV). The use of human liver for the study had the approval of the Ethics Committee of the University Hospital. Liver samples were stored at − 80°C until processing. Data on liver sample sources are shown in Table 1. Microsomes were prepared according to standard procedures as previously described (Hermans & Thijssen, 1991). The final microsomal pellet was resuspended in Tris-KCl-NaCl buffer (0.02 M, 0.15 M and 1.0 M, respectively; pH = 7.4) to contain about 20 mg protein per ml homogenate.

Table 1 Information on the subjects from whom liver samples were obtained

Code	*Sex*	*Age*	*Death cause*	*Drug history*
I	male	52	Traffic accident	
II	male	18	Traffic accident	
III	female	36	Subarachnoidal bleeding	
IV	female	61	Brain damage	Alcohol abuse
V	male	57	Brain tumour	Propranolol

Assay for warfarin and acenocoumarol metabolism

The assay of warfarin and acenocoumarol metabolism was conducted essentially as previously described (Hermans & Thijssen, 1991). Microsomal fractions were incubated in the presence of a NADPH-generating system at 37°C for 15–60 min in test tubes. The incubation mixture consisted of 0.5 to 1.0 mg microsomal protein, substrate, 7.4 mM glucose 6-phosphate, 2.4 mM $MgCl_2$ and 1.0 μunit of glucose 6-phosphate dehydrogenase, 0.5 mM NADPH, and 2 mM $NADP^+$. The amount of metabolites formed increased linearly with time (up to 75 min at saturating substrate concentrations) and protein content (range tested: 0.2 to 2.0 mg per incubation mixture).

Metabolite formation rates and the inhibitor effect for the various microsomal preparations were determined at substrate concentrations of 25 μM and 100 μM and incubation times of 30 and 60 min for acenocoumarol and warfarin enantiomers respectively. Inhibitor concentrations were 25 μM (sulphaphenazole), 100 μM (propafenone and omeprazole), and 1000 μM (cimetidine). At the concentrations chosen, satisfactory inhibition was observed. However, as the extent of inhibition is dependent on substrate- and inhibitor concentrations, inhibition kinetics have been determined in greater detail for microsomal sample 2. The reactions were started by addition of substrate to complete reaction mixtures, containing microsomes, NADPH-generating system and inhibitor (or an equal volume of buffer in the controls) that were briefly preincubated at 37°C.

The enzyme kinetic parameters of the metabolism of acenocoumarol enantiomers by liver microsomes were determined at substrate concentrations ranging from 0.5 to 25 μM (S-acenocoumarol) and 2.5 to 250 μM (R-acenocoumarol) and incubation times of 15–30 min. The enzyme kinetic parameters of warfarin metabolism were determined at substrate concentrations of 25 to 800 μM (R-enantiomer) and 2.5 to 400 μM (S-enantiomer) and an incubation time of 30 min.

Determination of K_i values and types of inhibition were tested at R/S acenocoumarol concentrations of 5–25 μM, S-warfarin concentrations of 50–400 μM, and R-warfarin concentrations of 100–400 μM. Inhibitor concentrations ranged from 1–25 μM for sulphaphenazole, 25–100 μM for omeprazole, 25–250 μM for propafenone, and 50–600 μM for cimetidine.

The metabolites were extracted and analyzed by high performance liquid chromatography (h.p.l.c.) as previously described (Hermans & Thijssen, 1991), except for the omeprazole inhibition experiments in which an additional basic (pH = 8.5) extraction step was introduced to remove omeprazole and some of its metabolites.

Protein content was determined by the method of Lowry *et al.* (1951). Cytochrome P450 content was determined by the DT-difference method as described by Rutten *et al.* (1987). 7-Ethoxycoumarin deethylase and aniline-*p*-hydroxylase activity was determined by Greenlee & Poland (1978) and Macleod *et al.* (1973).

Drugs

Racemic warfarin and racemic propafenone (as the HCl salt) were obtained from Sigma Chemicals (St. Louis, U.S.A.). Racemic acenocoumarol as well as 6- and 7-hydroxyacenocoumarol (used for reference purposes) were a kind gift of Ciba-Geigy (Basel, Switzerland). The 6- and 7-hydroxy metabolites of warfarin (used for reference purposes) were kindly provided by Dr J. de Vries (Univ. Heidelberg, Germany). Cimetidine was from Smith, Kline and French Laboratories (Welwyn Garden City, UK). Sulphaphenazole was kindly provided by Dr T. Vree (Dept. Clin. Pharmacy, Univ. Hospital, Nijmegen, the Netherlands). Racemic omeprazole was from Astra Pharmaceuticals (Rijswijk, the Netherlands). All other chemicals were of analytical grade and were

obtained from Merck (Darmstadt, Germany) unless stated otherwise.

Warfarin and acenocoumarol enantiomers were at our disposal (Hermans & Thijssen, 1991).

Statistical analysis of the data

V_{max} and K_m values were determined by fitting the Michaelis-Menten equation to the data using the GPAD (GraphPAD Software, San Diego, U.S.A.) software package. K_i values and inhibition mechanisms were determined by the use of Dixon plots and double reciprocal plots respectively. The effect of the inhibitors on the 6- and 7-hydroxylation of warfarin and acenocoumarol was tested for significance by the use of a oneway ANOVA and least significant differences (LSD) were calculated. Spearman rank correlation coefficients were tested for significance by transformation to Students t test distribution (Sachs, 1984).

Results

Standard parameters of the human liver samples are shown in Table 2. The obtained values are in the range of data reported in other studies (Beaune *et al.*, 1986).

Table 2 Cytochrome P450 content, 7-ethoxycoumarin-(7-EC-) deethylase activity, and aniline-*p*- (An-*p*-) hydroxylase activity in the human liver microsomal preparations used

Code	*[P450]* (nmol mg^{-1})	*7-EC-deethylase* (nmol mg^{-1} min^{-1})	*An-p-hydroxylation* (nmol mg^{-1} min^{-1})
I	0.45 ± 0.07	0.24 ± 0.01	2.1 ± 0.6
II	0.45 ± 0.15	0.14 ± 0.01	2.5 ± 0.3
III	0.74 ± 0.06	0.21 ± 0.01	1.1 ± 0.6
IV	0.40 ± 0.12	0.21 ± 0.01	1.5 ± 0.4
V	0.51 ± 0.13	0.22 ± 0.04	2.0 ± 0.8

Data are expressed as the mean ± s.d. of three determinations.

Kinetic parameters of the metabolism of warfarin and acenocoumarol enantiomers

Detailed enzyme kinetic parameters V_{max}, K_m and intrinsic formation clearances (Cli) of warfarin and acenocoumarol metabolism have been determined for samples II and V (Tables 3 and 4). For warfarin, next to 6- and 7-hydroxylation, formation of the 4'-hydroxy-, 8-hydroxy-, benzyl-hydroxy-, and dehydrometabolites as well as reduction of the acetonyl side chain to the alcohols occurred. For acenocoumarol, in addition to the 6- and 7-hydroxy metabolites, the 8-hydroxy-, benzyl-hydroxy-, and dehydrometabolites as well as the alcohols were found. However, as shown in Tables 3 and 4, 6- and 7-hydroxylation appeared to be the main metabolic routes, accounting for about 65% and 70% of the total metabolic clearance of **R**-and **S**-warfarin, and about 90% and 99% of the total metabolic clearance of **R**- and **S**-acenocoumarol. Therefore, these reactions have been mainly focussed on. Furthermore, this demonstrates that the higher clearance of **R/S** acenocoumarol *versus* **R/S** warfarin is not due to the fact that the enantiomers of acenocoumarol are able to follow additional metabolic routes.

Table 3 shows that for the 6- and 7-hydroxylation, the (mean) K_m values of **S**-warfarin are 19 and 76 times lower than those of **R**-warfarin. On the other hand, the (mean) V_{max} values are 49 and 14 times higher for **R**-warfarin. As a result, the formation of 6-hydroxywarfarin is stereoselective for the **R**-enantiomer (mean $Cli_R/Cli_S = 2.6$), whereas the formation of 7-hydroxywarfarin is stereoselective for the **S**-enantiomer (mean $Cli_S/Cli_R = 5.4$).

As for warfarin, the (mean) K_m values for the formation of the 6- and 7-hydroxy metabolites are (93 and 17 times) lower for the **S**- than for the **R**-enantiomer of acenocoumarol (Table 4). The (mean) maximal formation rate of the formation of 6-hydroxyacenocoumarol is 4.4 times higher for the **R**-enantiomer, whereas that of the 7-hydroxyacenocoumarol is 2.1 times higher for the S-enantiomer. The mean intrinsic

Table 3 Enzyme kinetics of the human liver (samples II and V) microsomal metabolism of the enantiomers of warfarin

R-*Warfarin*	*Sample*	V_{max} (pmol mg^{-1} min^{-1})	K_m (μM)	*Cli** (nl mg^{-1} min^{-1})	*%Cli*
6-hydroxy	II	13.8	585	23.6	48.5
	V	19.8	580	34.1	32.4
	x̄ ± s.d.	16.8 ± 4.2	583 ± 3.5	28.9 ± 7.4	40.5 ± 11.3
7-hydroxy	II	2.94	336	8.8	18.1
	V	10.9	379	28.8	27.3
	x̄ ± s.d.	6.92 ± 5.6	358 ± 30	18.8 ± 14.1	22.7 ± 6.5
Other	II			16.3	33.5
	V			42.2	40.1
	x̄ ± s.d.			29.3 ± 18.3	36.8 ± 4.7
Total#	II			48.7	
	V			105.1	
	x̄ ± s.d.			76.9 ± 39.8	
S-*Warfarin*	*Sample*	V_{max} (pmol mg^{-1} min^{-1})	K_m (μM)	*Cli* (nl mg^{-1} min^{-1})	*% Cli*
6-hydroxy	II	0.55	30	18.3	11.0
	V	0.13	32	4.1	2.8
	x̄ ± s.d.	0.34 ± 0.30	31 ± 1.4	11.2 ± 10	6.9 ± 5.8
7-hydroxy	II	0.62	5.2	120	71.9
	V	0.35	4.2	83.3	56.3
	x̄ ± s.d.	0.48 ± 0.19	4.7 ± 0.7	102 ± 26	64.1 ± 11.0
Other	II			28.6	17.1
	V			60.6	40.9
	x̄ ± s.d.			54.9 ± 32.8	29.0 ± 16.8
Total	II			167	
	V			148	
	x̄ ± s.d.			158 ± 13.4	

*Intrinsic clearance $Cli = V_{max}/K_m$ #Total = sum of Cli's

Table 4 Enzyme kinetics of the human liver (samples II and V) microsomal metabolism of the enantiomers of acenocoumarol

R-*Acenocoumarol*	*Sample*	V_{max} (pmol mg^{-1} min^{-1})	K_m (μM)	*Cli** (nl mg^{-1} min^{-1})	*%Cli*
6-hydroxy	II	20.6	131	157	35.0
	V	13.3	45.3	294	63.2
	$\bar{x}$ ± s.d.	16.8 ± 4.2	88 ± 61	226 ± 97	49.1 ± 19.9
7-hydroxy	II	3.4	14.4	236	52.6
	V	1.9	14.8	127	27.3
	$\bar{x}$ ± s.d.	2.7 ± 1.1	14.6 ± 0.3	182 ± 77.1	40.0 ± 17.9
Other	II			55.8	12.4
	V			43.7	9.4
	$\bar{x}$ ± s.d.			49.8 ± 8.6	10.9 ± 2.1
Total#	II			449	
	V			465	
	$\bar{x}$ ± s.d.			457 ± 11.3	
S-*Acenocoumarol*	*Sample*	V_{max} (pmol mg^{-1} min^{-1})	K_m (μM)	*Cli* (nl mg^{-1} min^{-1})	*% Cli*
6-hydroxy	II	4.97	1.11	4477	33.7
	V	2.64	0.79	3342	44.4
	$\bar{x}$ ± s.d.	3.80 ± 1.65	0.95 ± 0.23	3910 ± 803	39.1 ± 7.6
7-hydroxy	II	7.95	0.93	8548	64.3
	V	3.48	0.83	4193	55.6
	$\bar{x}$ ± s.d.	5.72 ± 3.16	0.88 ± 0.07	6371 ± 3080	60.0 ± 6.2
Other	II			267	2.0
	V			10	0.1
	$\bar{x}$ ± s.d.			139 ± 181	1.1 ± 1.3
Total	II			13292	
	V			7545	
	$\bar{x}$ ± s.d.			10419 ± 4063	

*Intrinsic clearance Cli = V_{max}/K_m #Total = sum of Cli's

clearances of the formation of these metabolites are 17 and 35 times higher for S-acenocoumarol.

Comparison of Tables 3 and 4 shows that in accordance with *in vivo* observations, the rate of elimination of the enantiomers of acenocoumarol due to metabolism are much higher than those of warfarin (ratios of mean intrinsic clearances of about 6 and 65 for the **R**- and **S**-enantiomers respectively). For the **R**-enantiomers this is attributable to the 6 to 25 times lower K_m values of acenocoumarol. For the **S**-enantiomers this is due to approximately 10 times higher V_{max} values in combination with the lower K_m values for the formation of the 6- and 7-hydroxy metabolites of acenocoumarol. Also in accordance with *in vivo* data, are the observations that the overall metabolism of both 4-hydroxycoumarins is stereoselective for the **S**-enantiomer and that this stereoselectivity is far more pronounced in the case of acenocoumarol. The (mean) sum of intrinsic clearances of the metabolites formed is about 2 times higher for **S**- than for **R**-warfarin and 23 times higher for **S**- than for **R**-acenocoumarol.

Variation in the 6- and 7-hydroxylation rates

Figures 2 and 3 show the rates of the 6- and 7-hydroxylation of **R/S** warfarin and acenocoumarol in 5 human liver microsomal samples. The formation rates of 6-hydroxywarfarin ranged 7 fold (0.5 to 3.5 pmol mg^{-1} min^{-1}) for **R**-warfarin and 11 fold for **S**-warfarin (0.12 to 1.3 pmol mg^{-1} min^{-1}) among the microsomal preparations. The 6-hydroxylation of **R**-acenocoumarol ranged 10 fold (3 to 30 pmol mg^{-1} min^{-1}), whereas that of **S**-acenocoumarol ranged only 4 fold (3 to 12 pmol mg^{-1} min^{-1}). The 6-hydroxylation rate of both 4-hydroxycoumarins is higher for the **R**- than for the **S**-enantiomers at the substrate concentration chosen. This is probably due to the higher V_{max} values of the **R**-enantiomers (Tables 3 and 4). However, during therapy, blood levels range from 1 to 10 μM for warfarin (Holford, 1986) and from 60 to 600 nM for acenocoumarol (Thijssen *et al.*, 1988). The concentration of the unbound drugs will be even lower. Therefore, intrinsic clearances rather than V_{max} values will give an indication of the metabolic profile *in vivo*, since in this parameter, differences in K_m values are accounted for.

The 7-hydroxylation of all substrates appears to be less variable among the microsomes than the 6-hydroxlation. Formation rates of the 7-hydroxy metabolite range 3 to 4 fold. 7-Hydroxylation rates are generally lower for the **S**-enantiomer of warfarin (0.5 to 1.5 pmol mg^{-1} min^{-1}) than for the **R**-enantiomer (0.7 to 2.8 pmol mg^{-1} min^{-1}). In contrast, the 7-hydroxylation rates of **S**-acenocoumarol (4.2 to 13.8 pmol mg^{-1} min^{-1}) are higher than those of **R**-acenocoumarol (1.1 to 4.5 pmol mg^{-1} min^{-1}).

Correlation of the 6- and 7-hydroxylation rates

Table 5 shows a correlation matrix of the 6- and 7-hydroxylation rates of warfarin and acenocoumarol enantiomers in the human liver microsomes. If the correlations between the enantiomers are considered, there appears to be no clear relationship between the 6- and 7–hydroxylation of **R**-warfarin with those of **S**-warfarin. This is in sharp contrast to acenocoumarol for which the 6- and 7-hydroxylation rates of the **R**-enantiomer correlate significantly with those of the S-enantiomer ($P<0.025$). Considering correlations between warfarin and acenocoumarol, only the 7-hydroxylations of the **R**-enantiomers correlate significantly ($P<0.025$). Finally, a significant correlation between the 6- and 7-hydroxylation within and between the enantiomers of acenocoumarol is observed ($P<0.025$). In contrast, these reactions do not correlate for warfarin.

Effect of inhibitors on the 6- and 7-hydroxylation

The effect of sulphaphenazole, propafenone, cimetidine and omeprazole on the 6- and 7-hydroxylation of warfarin and

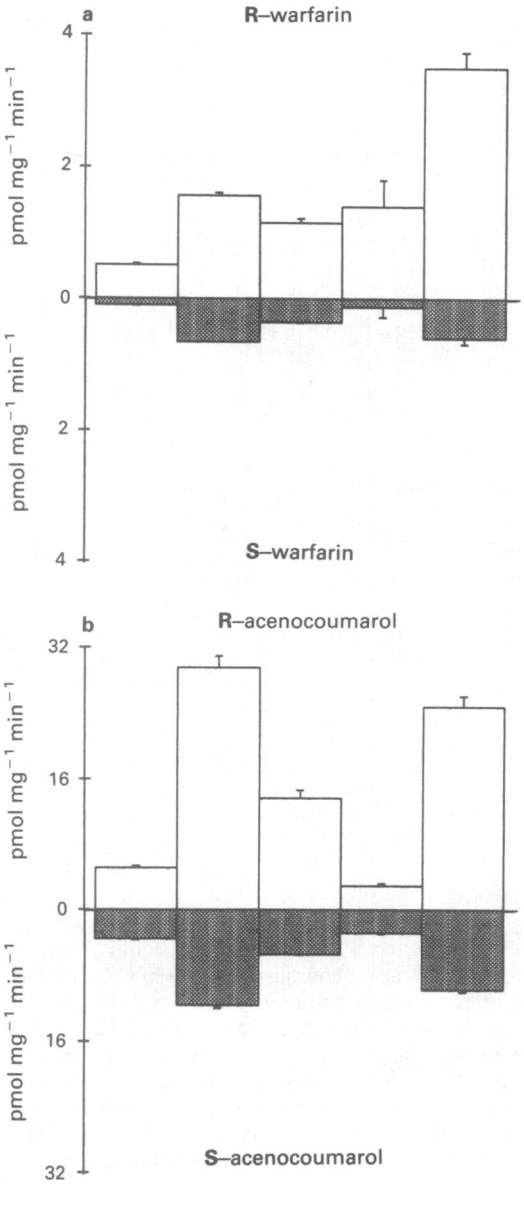

Figure 2 Rates of information of the 6-hydroxy metabolites of the enantiomers of warfarin (a) and acenocoumarol (b) in 5 human liver microsomal preparations. Data are expressed as the mean (pmol metabolite mg^{-1} protein min^{-1}) ± s.e. of two incubations. The five sets of columns represent microsomal fraction I (left) to V (right). Open columns: **R**-enantiomers; cross hatched columns: **S**-enantiomers.

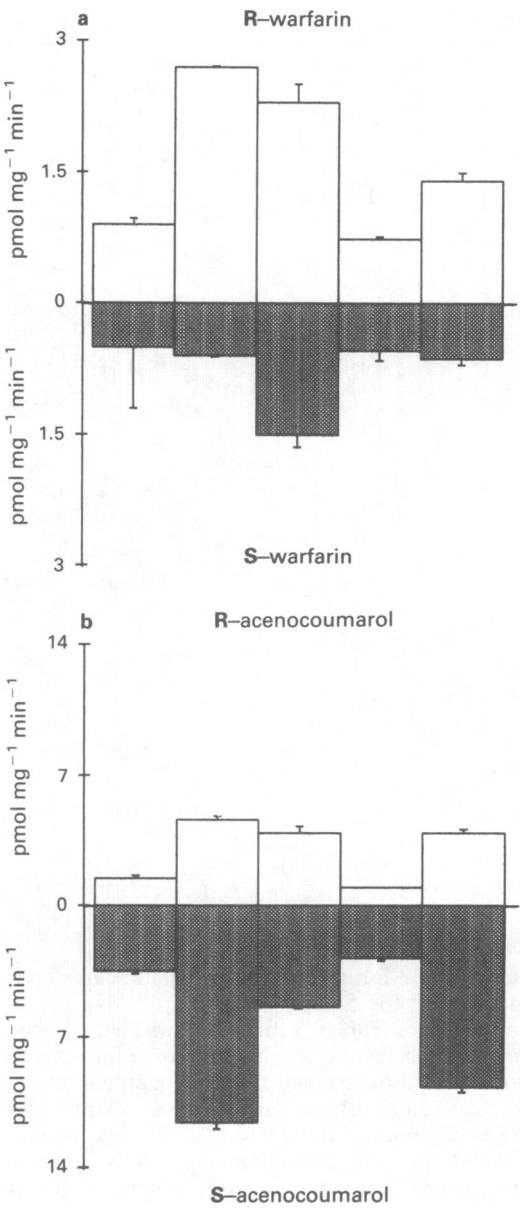

Figure 3 Rates of formation of the 7-hydroxy metabolites of the enantiomers of warfarin (a) and acenocoumarol (b) in 5 human life microsomal preparations. Data are expressed as the mean rate (pmol metabolite mg^{-1} protein min^{-1}) ± s.e. of two incubations. The five sets of columns represent microsomal fraction I (left) to V (right). Open columns: **R**-enantiomers; cross hatched columns: **S**-enantiomers.

acenocoumarol enantiomers by the various microsomal preparations is shown in Figures 4 and 5. These data are expressed as the mean % inhibition ± s.e. Sulphaphenazole inhibits the 6-hydroxylation of S-acenocoumarol ($P<0.05$) about 65% but has no overall significant effect on the 6-hydroxylation of **R**-acenocoumarol or of **R**- and S-warfarin. However, in the case of the 6-hydroxylation of S-warfarin, there was considerable variation in the effect of sulphaphenazole, the inhibition ranging from about 0 (sample V) to 50% (sample II). The rate of 7-hydroxylation is decreased significantly ($P<0.05$) by sulphaphenazole for **R**- and S-acenocoumarol (about 55 and 75%) and for **S**- (about 60%) but not **R**-warfarin.

Propafenone significantly ($P<0.05$) inhibits the formation of the 6- and 7-hydroxy metabolites of **R**- and S-acenocoumarol about 15–20%. In the case of warfarin, only the 7-hydroxylation of the **R**-enantiometer is inhibited ($P<0.05$) about 25%.

Cimetidine decreases ($P<0.05$) the rate of 6- and 7-hydroxylation of **R**-warfarin (about 25%) and **R**-acenocoumarol (about 15 and 20%) but not of the **S**-enantiomers.

Omeprazole is an inhibitor ($P<0.05$) of the 6-hydroxylation of **R**-(21% decrease) and S-acenocoumarol (47% decrease) and of **R**-warfarin (53% decrease) but has no effect on the 6-hydroxylation of S-warfarin. Similarly, the 7-hydroxylation of **R**- and S-acenocoumarol and of **R**-warfarin is decreased significantly ($P<0.05$) by omeprazole (47, 33, and 46% respectively) but the 7-hydroxylation of S-warfarin is not affected by this compound.

Kinetic parameters of the inhibitors

In Table 6, K_i values and types of inhibition of the inhibitors for their effect on the 6- and 7-hydroxylation of warfarin and acenocoumarol are given for sample II. However, these data

Table 5 Correlation matrix of the 6- and 7-hydroxy metabolite formation rates of R- and S-warfarin and -acenocoumarol in human liver microsomes from 5 subjects

	R-6OHW	R-7OHW	S-6OHW	S-7OHW	R-6OHAC	R-7OHAC	S-6OHAC	S-7OHAC
R-6OHW	–	–	–	–	–	–	–	–
R-7OHW	0.05	–	–	–	–	–	–	–
S-6OHW	0.16	−0.37	–	–	–	–	–	–
S-7OHW	0.08	0.31	−0.37	–	–	–	–	–
R-6OHAC	0.64	0.65	−0.24	0.03	–	–	–	–
R-7OHAC	0.45	0.90*	0.12	0.41	0.92*	–	–	–
S-6OHAC	0.59	0.71	0.20	0.06	0.99*	0.89*	–	–
S-7OHAC	0.54	0.75	0.30	0.01	0.99*	0.90*	0.99*	–

*Significant correlation $P<0.025$, as determined by transformation to the Student's t distribution.

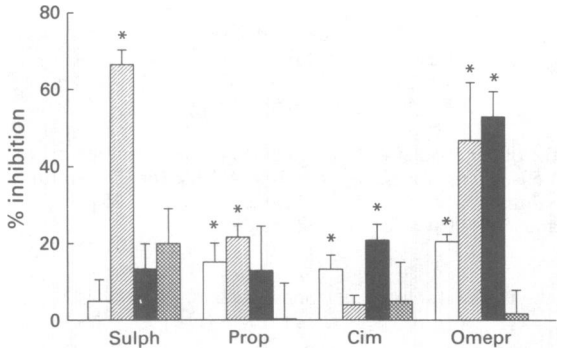

Figure 4 Inhibition of the 6-hydroxylation of the enantiomers of warfarin and acenocoumarol by sulphaphenazole, propafenone, cimetidine, and omeprazole. Open columns: **R**-acenocoumarol; hatched columns: **S**-acenocoumarol; solid columns: **R**-warfarin; cross hatched columns: **S**-warfarin. Inhibitor concentrations were: sulphaphenazole (Sulph): 25 μM, propafenone (Prop): 100 μM, cimetidine (Cim): 1000 μM and omeprazole (Omepr): 100 μM. The concentration of warfarin and acenocoumarol enantiomers were 100 and 25 μM respectively. Data are expressed as the mean ± s.e. of 5 human microsomal samples. *Indicates a significant inhibition: $P<0.05$, ANOVA, LSD.

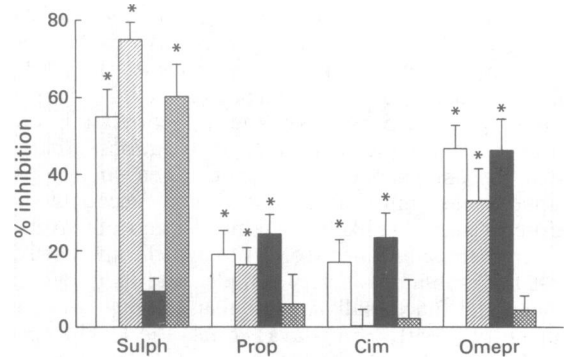

Figure 5 Inhibition of the 7-hydroxylation of the enantiomers of warfarin and acenocoumarol by sulphaphenazole, propafenone, cimetidine, and omeprazole. Key to columns as in Figure 4. Inhibitor concentrations were: sulphaphenazole (Sulph): 25 μM, propafenone (Prop): 100 μM, cimetidine (Cim): 1000 μM, and omeprazole (Omepr): 100 μM. The concentration of warfarin and acenocoumarol enantiomers were 100 and 25 μM respectively. Data are expressed as the mean ± s.e. of 5 human microsomal samples. *Indicates a significant inhibition: $P<0.05$, ANOVA, LSD.

should be interpreted with care since the hydroxylation reactions are probably carried out by multiple P450 isozymes, some of which may not be influenced by the inhibitors. Therefore (although estimated from the linear parts of Dixon plots), K_i values may be overestimated, and quasi mixed type inhibition may actually be a combination of competitive inhibitions. In fact, all inhibitions appeared to be partial (with the exception of the inhibition of the 7-hydroxylation of S-warfarin by sulphaphenazole). For that reason, the maximal inhibition (in %) at the lowest substrate and highest inhibitor concentration is given. Sulphaphenazole appears to be a competitive inhibitor of the 7- and 6-hydroxylation of S-warfarin with similar K_i values (0.6 and 0.7 μM). The 7-hydroxylation is fully inhibited by this compound, the 6-hydroxylation to 45%. In the case of acenocoumarol, sulphaphenazole competitively inhibits the 7-hydroxylation of both enantiomers and the 6-hydroxylation of the S-enantiomer with approximately similar K_i values (1.0–1.3 μM) and maximal inhibitions (70–80%).

The inhibition of the 6- and 7-hydroxylation of R-warfarin by cimetidine appears to be of the mixed type with K_i values of 472 and 1780 μM respectively. In the case of R-acenocoumarol, cimetidine is a mixed type inhibitor of the 6-hydroxylation (up to 35%, $K_i = 1938$ μM) but a competitive inhibitor of the 7-hydroxylation (up to 40%, $K_i = 223$ μM).

Propafenone is a mixed type inhibitor of the 7-hydroxylation of R-warfarin ($K_i = 131$ μM) and of R- and S-acenocoumarol (K_i's of 231 and 236 μM) and these reactions are inhibited up to 40%. The inhibition of the 6-hydroxylation of R- and S-acenocoumarol by propafenone also appears to be of the mixed type with K_i values of 563 and 670 μM and maximal inhibitions of 40 and 30%.

Omeprazole is a competitive inhibitor of the 6- and 7-hydroxylation of R-warfarin (up to 75% inhibition) and R- (up to 40 and 80%) and S-acenocoumarol (up to 60%). The K_i values of the 7-hydroxylation of R- and S-acenocoumarol and the 6-hydroxylation of S-acenocoumarol are all in the same range (6–8 μM). The K_i values of omeprazole of the other reactions that are inhibited are 13–36 times higher: for the 6- and 7-hydroxylation of R-warfarin, K_i values of 99 and 117 μM are observed whereas the K_i value for the 6-hydroxylation of R-acenocoumarol is 219 μM.

Discussion

The results of this study clearly demonstrate that a relatively small change in the structure of a chiral drug may not only have an impact on the rate but also on the stereoselectivity of its metabolism. In human liver microsomes, substitution of the 4'-hydrogen of warfarin by a nitro group enhances the intrinsic clearances of the R- and S-enantiomers 6 and 65 fold respectively and increases the S/R ratio of the intrinsic clearances about 11 fold (Tables 3 and 4), despite the fact that both 4-hydroxycoumarins follow similar metabolic routes. These observed patterns are qualitatively in good agreement with those found *in vivo*, although ketone reduction, an important metabolic route of R-warfarin, has not been fully dealt with, since the enzymes responsible for this reaction are mainly located in the cytosol (Hermans & Thijssen, 1989, 1993). Interestingly, for 4'-chlorowarfarin, we also

Table 6 Inhibitor type and K_i values of the inhibition of the human liver (sample II) microsomal 6- and 7-hydroxylation of the enantiomers of warfarin and acenocoumarol by sulphaphenazole, cimetidine, propafenone, and omeprazole

Inhibitor		*6-OH-warfarin*		*7-OH-warfarin*	
Sulphaphen	R-	NI		NI	
	S-	0.6 ± 0.3	Comp. 45%	0.5 ± 0.3	Comp. 95%
Cimetidine	R-	472 ± 103	Mixed 40%	1780 ± 667	Mixed 35%
	S-	NI		NI	
Propafenone	R-	NI		131 ± 22	Mixed 40%
	S-	NI		NI	
Omeprazole	R-	99 ± 21	Comp. 75%	117 ± 31	Comp. 75%
	S-	NI		NI	
Inhibitor		*6-OH-acenocoumarol*		*7-OH-acenocoumarol*	
Sulphaphen	R-	NI		1.0 ± 0.4	Comp. 70%
	S-	1.3 ± 0.3	Comp. 80%	1.2 ± 0.4	Comp. 80%
Cimetidine	R-	1938 ± 328	Mixed 35%	223 ± 25	Comp. 40%
	S-	NI		NI	
Propafenone	R-	563 ± 97	Mixed 40%	231 ± 22	Mixed 40%
	S-	670 ± 170	Mixed 30%	236 ± 79	Mixed 40%
Omeprazole	R-	219 ± 15	Comp. 40%	6.1 ± 2.6	Comp. 60%
	S-	7.2 ± 3.2	Comp. 80%	7.7 ± 1.8	Comp. 60%

K_i values are given as mean (in μM) ± s.d. calculated from all intersections of the obtained lines in Dixon plots. Type of inhibition were determined from double reciprocal plots. Substrate concentrations range from 50–400 μM for S-warfarin, 100–400 μM for R-warfarin, 0.5–25 μM for S-acenocoumarol and 2.5–250 μM for R-acenocoumarol. Inhibitor concentrations ranged from 1–25 μM for sulphaphenazole, 25–100 μM for omeprazole, 25–250 μM for propafenone and 50–600 μM for cimetidine.
NI = no inhibition as determined by one-way ANOVA.
Comp: competitive inhibition. Mixed: mixed type inhibition.
Percentages indicate the maximal inhibition at the lowest substrate and highest inhibitor concentrations used.

found that the human liver microsomal metabolic clearance is much higher (12 and 120 fold for the R- and S-enantiomers) than that of warfarin, and that the S/R ratio is about 10 times higher (own observations), suggesting that the phenyl ring of warfarin is highly involved in the interaction with (human) liver microsomal monoxygenases.

We previously found that the higher metabolic clearance of acenocoumarol in rat liver microsomes, as well as the inversion of the stereochemical course of its metabolism as compared with warfarin, could partly be explained by the fact that the enantiomers of warfarin and acenocoumarol are metabolized by different sets of cytochrome P450 isozymes (Hermans & Thijssen, 1991). This also appears to be the case in human liver microsomes since the 6- and 7-hydroxylation of R/S warfarin and acenocoumarol show different responses toward inhibitors (Figures 4 and 5; Table 6). For instance, the 7-hydroxylation of R-acenocoumarol but not of R-warfarin is inhibited by sulphaphenazole, whereas the 7-hydroxylation of S-acenocoumarol but not of S-warfarin is inhibited by omeprazole and propafenone. Furthermore, we found that R-enantiomers of warfarin and acenocoumarol mutually did not have any effect on their 6-hydroxylation rates (data not shown). The lack of a clear correlation between the 6-hydroxylation rates of R/S warfarin and the corresponding acenocoumarol enantiomers as well as the absence of any correlation between the 7-hydroxylation of the S-enantiomers (Table 5) also suggests that these reactions are catalysed by different combinations of cytochrome P450 isozymes.

Recently, Rettie *et al.* (1992), in testing various cDNA expressed human liver cytochromes P450 for regio- and stereoselective hydroxylation of R/S warfarin, found that cytochrome P450 2C9 hydroxylates S-warfarin at the 7- and 6-position. Consequently, these authors found the 7- and 6-hydroxylation rates of S-warfarin to be decreased by sulphaphenazole, a selective competitive inhibitor of cytochromes P450 of the 2C subfamily (Guengerich, 1992). In agreement with these data we found that sulphaphenazole almost fully inhibits the 7-hydroxylation of S-warfarin but is without effect on the 7- and 6-hydroxylation of R-warfarin. We did however find that the 6-hydroxylation of S-warfarin could be only partially inhibited by sulphaphenazole in some (but not all) liver samples and we did not find any correlation between the 6- and 7-hydroxylation of S-warfarin. This apparent contradiction may be explained by the fact that at least two enzymes catalyse this reaction (Rettie *et al.*, 1989), so that the ratio at which these enzymes are present (which may show some regional differences) determines the actual effect of sulphaphenazole and the (lack of) correlation.

As the 7-hydroxylation of both R- and S-acenocoumarol and the 6-hydroxylation of S- but not of R-acenocoumarol are inhibited by sulphaphenazole with approximately similar K_i values as the 7- and 6-hydroxylation of S-warfarin, this would suggest that these acenocoumarol hydroxylations are conducted by cytochrome P450 2C9 or closely related P450 isozymes. On the other hand, omeprazole inhibits these reactions only for acenocoumarol and no correlation of the warfarin and acenocoumarol hydroxylations that are inhibited by sulphaphenazole exist, even if the non-sulphaphenazole inhibitable parts are accounted for. Therefore, it seems unlikely that these acenocoumarol hydroxylations can be ascribed (solely) to cytochrome P450 2C9. The P450 2C subfamily is very complex and its isozymes are structually and functionally very similar (Relling *et al.*, 1990; Nebert *et al.*, 1991; Srivastava *et al.*, 1991; Guengerich, 1992). The 5-hydroxylation of omeprazole appears to be linked to the polymorphic S-mephenytoin 4'-hydroxylase, a member of the P450 2C subfamily (Andersson, 1991; Sohn *et al.*, 1992). Because the 7-hydroxylation of R- and S-acenocoumarol and the 6-hydroxylation of S-acenocoumarol are inhibited both by sulphaphenazole and by omeprazole with relatively low K_i values we speculate that these reactions may be conducted partly by the S-mephenytoin 4'-hydroxylase or by a closely related cytochrome P450 isozyme, different from P450 2C9. Further experiments are necessary to elucidate the nature of the acenocoumarol hydroxylases. The 6- and 7-hydroxylation of R-warfarin and the 6-hydroxylation of R-acenocoumarol are also inhibited by omeprazole. It is however unlikely that the omeprazole inhibitable parts of these reactions are carried out by the same P450 since the K_i values of omeprazole are 13–35 times higher and sulphaphenazole has no effect on these reactions.

The fact that omeprazole inhibits more than one single human cytochrome P450 has been described before by Jensen & Gugler (1986).

The effects of omeprazole and cimetidine on the *in vitro* metabolism of warfarin agree well with the interactions of these drugs with warfarin clearance *in vivo*. Omeprazole has been shown to decrease the clearance of only the **R**-enantiomer of warfarin (Sutfin *et al.*, 1989; Unge *et al.*, 1992). In agreement with these observations we find that the human liver microsomal metabolism of **R**- but not **S**-warfarin is inhibited by omeprazole. In the case of acenocoumarol, the *in vitro* data would predict an interaction of omeprazole with both enantiomers, which because of the relatively low K_i values of omeprazole, may be stronger than in the case of warfarin. Cimetidine, is known to decrease the *in vivo* clearance of the **R**-enantiomer of warfarin (Choonara *et al.*, 1986) and acenocoumarol (Gill *et al.*, 1989). For warfarin, this has been attributed to inhibition of the 6-hydroxylation and to a lesser extent of the 7-hydroxylation (Niopias *et al.*, 1991), which is in accordance with the data in Table 6 (lower K_i value of the 6-hydroxylation). In the case of acenocoumarol, cimetidine decreases the clearance of the **R**-enantiomer only if a relatively high dose of this drug is applied (Thijssen *et al.*, 1986; Gill *et al.*, 1989). The enzyme kinetic data and the data of Table 6 offer an explanation for this phenomenon, the K_m over K_i ratios are lower for acenocoumarol than for warfarin, which implies that at equal substrate and inhibitor concentrations the extent of inhibition will be lower for acenocoumarol than for warfarin.

These finding show that by the use of enzyme and inhibition kinetics, qualitative aspects of drug interactions can be predicted. As such, the described experiments would predict the interaction of sulphonamides to be stereoselective for S-warfarin, which is indeed described for trimethoprim-sulphamethoxazole (O'Reilly, 1980). In the case of acenocoumarol the clearance of both enantiomers is expected to be decreased.

Based on the described experiments, the interaction of propafenone with warfarin is likely to occur only for the **R**-enantiomer, whereas in the case of acenocoumarol a (weak) interaction with both enantiomers is possible. The metabolism of propafenone involves two main routes i.e. 5-hydroxylation, produced by P450 2D6 (Kroemer *et al.*, 1989) and N-dealkylation, produced by P450 3A4 and 1A2 (Botsch *et al.*, 1993). Cytochromes P450 3A4 and 1A2 but not 2D6 are known to have warfarin hydroxylase activity (Rettie *et al.*, 1992). The K_m value of propafenone for its human liver microsomal N-dealkylation (Botsch *et al.*, 1993) but not for its 5-hydroxylation (Kroemer *et al.*, 1989) is in the range of the K_i values we found for propafenone in this study. This suggests that the parts of warfarin and acenocoumarol metabolism that are inhibited by propafenone are catalysed by cytochromes P450 3A4 and/or 1A2.

This study demonstrates once again that small differences in the structure of drugs can completely change their pharmacokinetics and stereoselectivity. Since a small structural change may have implications on the relative contribution of P450 isozymes in the metabolism of 4-hydroxycoumarins, these compounds may interact differently when other drugs are coadministered. Finally we found that ring substituted warfarin analogues may serve as probes in exploring subtle differences between the isozymes of the P450 2C subfamily.

References

ANDERSSON, T. (1991). Omeprazole drug interaction studies. *Clin. Pharmacokin.*, **21**, 195–212.

BAARS, L.G.M., SCHEPERS, M.T., HERMANS, J.J.R., DAHLMANS, H.J. & THIJSSEN, H.H.W. (1990). Enantioselective structure-pharmacokinetics relationships of ring substituted warfarin analogues in the rat. *J. Pharmac. Pharmacol.*, **42**, 861–866.

BEAUNE, P.H., KREMERS, P.G., KAMINSKY, L.S. DE GRAEVE, J., ALBERT, A. & GUENGERICH, F.P. (1986). Comparison of monooxygenase activities and cytochrome P450 isozyme concentrations in human liver microsomes. *Drug Metab. Dispos.*, **14**, 437–442.

BOTSCH, S., GAUTIER, J-C., BEAUNE, Ph., EICHELBAUM, M. & KROEMER, H. (1993). Identification and characterization of the cytochrome P450 enzymes involved in N-dealkylation of propafenone: molecular base for interaction potential and variable disposition of active metabolites. *Mol. Pharmacol.*, **43**, 120–126.

CHOONARA, I.A., CHOLERTON, S., HAYNES, B.P., BRECKENRIDGE, A.M. & PARK, B.K. (1986). Stereoselective interaction between the R-enantiomer of warfarin and cimetidine. *Br. J. Clin. Pharmacol.*, **22**, 729–732.

GILL, T.S., HOPKINS, K.J., BOTTOMLEY, J., GUPTA, S.K. & ROWLAND, M. (1989). Cimetidine-nicoumalone interaction in man: stereochemical considerations. *Br. J. Clin. Pharmacol.*, **27**, 469–474.

GREENLEE, W.F. & POLAND, A. (1978). An improved assay of 7-ethoxycoumarin deethylase activity: induction of hepatic enzyme activity in C57BL/J6 and DBA/2J mice by phenobarbital, 3-methylcholanthrene, and 2,3,7,8-tetrachlorodibenzo-p-dioxin. *J. Pharmacol. Exp. Ther.*, **205**, 596–605.

GUENGERICH, F.P. (1992). Characterization of human cytochrome P450 isozymes. *FASEB J.*, **6**, 745–748.

GUENGERICH, F.P., DANNAN, G.A., WRIGHT, S.T., MARTIN, M.V. & KAMINSKY, L.S. (1982). Purification and characterization of microsomal cytochrome P450s. *Xenobiotica*, **12**, 701–716.

HERMANS, J.J.R. & THIJSSEN, H.H.W. (1989). The in vitro ketone reduction of warfarin and analogues. Substrate stereoselectivity, product stereoselectivity, and species differences. *Biochem. Pharmacol.*, **38**, 3365–3370.

HERMANS, J.J.R. & THIJSSEN, H.H.W. (1991). Comparison of the rat liver microsomal metabolism of the enantiomers of warfarin and 4'nitrowarfarin (acenocoumarol). *Xenobiotica*, **21**, 295–307.

HERMANS, J.J.R. & THIJSSEN, H.H.W. (1993). Properties and stereoselectivity of carbonyl reductases involved in the ketone reduction of warfarin and analogues. In *Enzymology and Molecular Biology of Carbonyl Metabolism*, Vol. 4, pp. 351–360. New York: Plenum Publishing Corporation.

HOLFORD, N.H.G. (1986). Clinical pharmacokinetics and pharmacodynamics of warfarin: understanding the dose-effect relationship. *Clin. Pharmacokin.*, **11**, 483–504.

JENSEN, J.C. & GUGLER, R. (1986). Inhibition of human liver cytochrome P-450 by omeprazole. *Br. J. Clin. Pharmacol.*, **21**, 328–330.

KAMINSKY, L.S. (1989). Warfarin as a probe of cytochromes P450 function. *Drug Metab. Rev.*, **20**, 479–487.

KATES, R.E., YEE, Y.-G. & KIRSTEN, A.B. (1987). Interaction between warfarin and propafenone in healthy volunteer subjects. *Clin. Pharmacol. Ther.*, **42**, 301–311.

KELLEY, J.G. & O'MALLEY, K. (1979). Clinical pharmacokinetics of oral anticoagulants. *Clin. Pharmacokin*, **4**, 1–15.

KROEMER, H.K., MIKUS, G., KRONBACH, T., MEYER, U.A. & EICHELBAUM, M. (1989). In vitro characterization of the human cytochrome P-450 involved in polymorphic oxidation of propafenone. *Clin. Pharmacol. Ther.*, **45**, 28–33.

LEWIS, R.J., TRAGER, W.F., CHAN, K.K., BRECKENRIDGE, A., ORME, M., ROWLAND, M. & SCHARY, W. (1974). Warfarin: Stereochemical aspects of its metabolism and the interaction with phenylbutazone. *J. Clin. Invest.*, **53**, 1607–1617.

LOWRY, O.H., ROSEBROUGH, N.J., FARR, A.L. & RANDALL, R.J. (1951). Protein measurement with the Folin phenol reagent. *J. Biol. Chem.*, **193**, 265–275.

MACLEOD, S.M. RENTON, K.W. & EADE, N.R. (1973). Post mortem characteristics of the hepatic microsomal drug oxidizing enzyme system. *Chem-Biol. Interact.*, **7**, 29–37.

NEBERT, D.W., NELSON, D.R., COON, M.J., ESTABROOK, R.W., FEYEREISEN, R., FUJI-KURIYAMA, GONZALEZ, F.J., GUENGERICH, F.P., GUNSALUS, I.C., JOHNSON, E.F., LOPER, J.C., SATO, R., WATERMAN, M.R. & WAXMAN, D.J. (1991). The P450 superfamily: update on new sequences, gene mapping, and recommended nomenclature. *DNA Cell Biol.*, **10**, 1–14.

NIOPIAS, I., TOON, S. & ROWLAND, M. (1991). Further insight into the stereoselective interaction between warfarin and cimetidine in man. *Br. J. Clin. Pharmacol.*, **32**, 508–511.

O'REILLY, R.A. (1980). Stereoselective interaction of trimethoprim-sulfamethoxazole with the separated enantiomorphs of racemic warfarin in man. *New Engl. J. Med.*, **302**, 33–35.

O'REILLY, R.A., TRAGER, W.F., RETTIE, A.E. & GOULART, D.A. (1987). Interaction of amiodarone with racemic warfarin and its separated enantiomorphs in humans. *Clin. Pharmacol. Ther.*, **42**, 290–294.

RELLING, M.V., AOYAMA, T., GONZALEZ, F.J. & MEYER, U.A. (1990). Tolbutamide and mephenytoin hydroxylation by human cytochrome P450s in the CYP2C subfamily. *J. Pharmacol. Exp. Ther.*, **252**, 442–447.

RETTIE, A.E., EDDY, A.C., HEIMARK, L.D., GIBALDI, M. & TRAGER, W.F. (1989). Characteristics of warfarin hydroxylation catalyzed by human liver microsomes. *Drug Metab. Dispos.*, **17**, 265–270.

RETTIE, A.E., KORZEKWA, K.R., KUNZE, K.L., LAWRENCE, R.F., EDDY, A.C., AOYAMA, T., GONZALEZ, F.J., GELBOIN, H.V. & TRAGER, W.F. (1992). Hydroxylation of warfarin by human cDNA-expressed cytochrome P450: a role for P4502C9 in the etiology of (S)-warfarin-drug interactions. *Chem. Res. Toxicol.*, **5**, 54–59.

RUTTEN, A.J.J.L., FLAKE, H.E., CATSBURG, J.F., TOPP, R., BLAAUW-BOER, B.J., v. HOLSTEIJN, I., DOORN, L. & v. LEEUWEN, F.R.X. (1987). Interlaboratory comparison of total cytochrome P450 and protein determinations in rat liver microsomes. *Arch. Toxicol.*, **61**, 27–35.

SACHS, L. (1984). *Angewandte statistik*. 6th edn. pp. 298–342 and pp. 381–426. Berlin: Springer Verlag.

SOHN, D.-R., KOBAYASHI, K., CHIBA, K., LEE, K.-H., SHIN, S.-G. & ISHIZAKI, T. (1992). Disposition kinetics and metabolism of omeprazole in extensive and poor metabolizers of S-mephenytoin 4'-hydroxylation recruited from an oriental population. *J. Pharmacol. Exp. Ther.*, **262**, 1195–1203.

SRIVASTAVA, P.K., YUN, C.-H., BEAUNE, P.H., GED, C. & GUENGERICH, F.P. (1991). Separation of human liver microsomal tolbutamide hydroxylase and (S)-mephenytoin 4'-hydroxylase cytochrome P-450 enzymes. *Mol. Pharmacol.*, **41**, 69–79.

SUTFIN, T., BALMER, K., BOSTROEM, H., ERIKSSON, S., HOEGLUND, P. & PAULSEN, O. (1989). Stereoselective interaction of omeprazole and warfarin in healthy men. *Ther. Drug. Monit.*, **11**, 176–184.

THIJSSEN, H.H.W., BAARS, L.G.M. & DRITTIJ-REIJINDERS, M.J. (1985). Stereoselective aspects in the pharmacokinetics and pharmacodynamics of acenocoumarol and its amino- and acetamido derivatives in the rat. *Drug Metab. Dispos.*, **13**, 593–597.

THIJSSEN, H.H.W., HAMULYAK, K. & WILLIGERS, H. (1988). 4-Hydroxycoumarin oral anticoagulants: pharmacokinetics-response relationship. *Thromb. Haemost.*, **60**, 35–38.

THIJSSEN, H.H.W., JANSEN, G.M.J. & BAARS, L.G.M. (1986). Lack of effect of cimetidine on pharmacodynamics and kinetics of single oral doses of R- and S-acenocoumarol. *Eur. J. Pharmacol.*, **30**, 619–623.

TOON, S., HOPKINS, K.J., GARSTANG, F.M., AARONS, L., SEDMAN, A. & ROWLAND, M. (1987). Enoxacin-warfarin interaction: pharmacokinetic and stereochemical aspects. *Clin. Pharmacol. Ther.*, **42**, 33–41.

UNGE, P., SVEDBERG, L.E., NORDGREN, A., BLOM, H., ANDERSSON, T., LAGERSTRÖM, P.O. & IDSTRÖM, J.P. (1992). A study of the interaction of omeprazole and warfarin in anticoagulated patients. *Br. J. Clin. Pharmacol.*, **34**, 509–512.

WANG, P.P., BEAUNE, P., KAMINSKY, L.S., DANNAN, G.A., KADLUBAR, F.F., LARREY, D. & GUENGERICH, F.P. (1983). Purification and characterization of six cytochrome P450 isozymes from human liver microsomes. *Biochem.*, **22**, 5375–5385.

(Received January 19, 1993
Revised April 21, 1993
Accepted May 13, 1993)

Br. J. Pharmacol. (1993), **110**, 491–495

Antitussive effects of $GABA_B$ agonists in the cat and guinea-pig

[1]Donald C. Bolser, Sultan M. Aziz, Frances C. DeGennaro, William Kreutner, Robert W. Egan, Marvin I. Siegel & Richard W. Chapman

Schering-Plough Research Institute, Kenilworth, NJ 07033-0539, U.S.A.

1 $GABA_B$ agonists inhibit neuronal processes which are important in the pathogenesis of airway disease, such as bronchospasm. Cough is a prominent symptom of pulmonary disease, but the effects of $GABA_B$ agonists on this airway reflex are unknown. Experiments were conducted to determine the antitussive effect of $GABA_B$ receptor agonists in comparison to the known antitussive agents, codeine and dextromethorphan.

2 Unanaesthetized guinea-pigs were exposed to aerosols of 0.3 mM capsaicin to elicit coughing, which was detected with a microphone and counted. Cough also was produced in anaesthetized cats by mechanical stimulation of the intrathoracic trachea and was recorded from electromyograms of respiratory muscle activity.

3 In guinea-pigs, the $GABA_B$ agonists baclofen and 3-aminopropyl-phosphinic acid (3-APPi) produced dose-dependent inhibition of capsaicin-induced cough when administered by subcutaneous or inhaled routes. The potencies of baclofen and 3-APPi compared favourably with codeine and dextromethorphan.

4 The $GABA_B$ antagonist, CGP 35348 (0.3– 30 mg kg^{-1}, s.c.) inhibited the antitussive effect of baclofen (3.0 mg kg^{-1}, s.c.). However, CGP 35348 (10 mg kg^{-1}, s.c.) had no effect on the antitussive activity of codeine (30 mg kg^{-1}, s.c.). The antitussive effect of baclofen was not influenced by the $GABA_A$ antagonist, bicuculline (3 mg kg^{-1}, s.c.) or naloxone (0.3 mg kg^{-1}, s.c.).

5 In the cat, baclofen (0.3–3.0 mg kg^{-1}, i.v.) decreased mechanically-induced cough in a dose-dependent manner. In this model, baclofen (ED_{50} = 0.63 mg kg^{-1}) was less potent than either codeine or dextromethorphan. The antitussive effect of baclofen in the cat was antagonized by the $GABA_B$ antagonists, CGP 35348 (10 mg kg^{-1}, i.v.) and 3-aminopropylphosphonic acid (3 mg kg^{-1}, i.v.).

6 We show that baclofen and 3-APPi have antitussive effects in the guinea-pig and cat and these effects are mediated by $GABA_B$ receptors.

Keywords: $GABA_B$ receptors; cough; antitussive; CGP35348; baclofen; 3-aminopropyl-phosphinic acid

Introduction

Cough is a defensive reflex that is often present during pulmonary diseases such as chronic bronchitis, asthma, pulmonary neoplasm, upper respiratory infections, and pulmonary fibrosis (Braman & Corrao, 1987; O'Connell *et al.*, 1991). The function of this reflex is to remove fluids, mucus, and/or foreign bodies from the respiratory tract by the generation of rapid airflows (Korpas & Tomori, 1979). Cough is generally considered to be a beneficial event, but there are situations in which this reflex is associated with significant morbidity. Chronic cough is associated with exacerbation of asthmatic symptoms, rib fractures, breathlessness, ruptured abdominal muscles, pneumothorax, syncope, second and third degree heart block, and loss of consciousness (Braman & Corrao, 1987; O'Connell *et al.*, 1991; Young *et al.*, 1991). Therapy for chronic cough can include administration of antitussive agents, the most prominent of which are codeine and dextromethorphan (Braman & Corrao, 1987). Other agents known to have antitussive effects in animal models include dopamine receptor agonists (Kamei *et al.*, 1987a), N-methyl-D-aspartate antagonists (Kamei *et al.*, 1989) and the peripherally acting opioid agonist BW 443C (Adcock *et al.*, 1988). Furthermore, the use of 5-hydroxytryptamine (5-HT) receptor antagonists and depletion of brain (5-HT) levels have suggested an inhibitory effect of this monoamine on cough (Kamei *et al.*, 1986; Kamei *et al.*, 1987b).

Another inhibitory neurochemical which has been implicated in depression of the cough reflex is γ-aminobutyric acid (GABA) (Nosalova *et al.*, 1987). GABA is present throughout the peripheral and central nervous systems (Mugnaini & Oertel, 1985; Erdo & Kiss, 1986) and binds to at least two different receptors, termed $GABA_A$ and $GABA_B$ (Bowery, 1989). Gabalineamide, an analogue of GABA, has antitussive effects in the cat (Nosalova *et al.*, 1987). It was not known whether this action was due to an effect of $GABA_A$ or $GABA_B$ receptor stimulation. However, there is good evidence that $GABA_B$ receptors inhibit the activity of peripheral sensory afferents (Green & Cottrell, 1988) such as pulmonary C-fibres (Belvisi *et al.*, 1989) that may influence the production of cough (Forsberg & Karlsson, 1986). Therefore, we speculated that $GABA_B$ agonists would have antitussive activity and we studied this phenomenon in several animal models of cough. A preliminary account of this work has been published (Bolser *et al.*, 1991b).

Methods

Irritant-induced cough in guinea-pigs

Unanaesthetized male Dunkin-Hartley guinea-pigs (250–600 g) were placed in a transparent plastic chamber and exposed to aerosols of capsaicin (0.3 mM) at an airflow of 4 l min^{-1} to elicit coughing. The aerosol was generated by a jet nebulizer and the volume of solution aerosolized was approximately 0.4 ml min^{-1}. This dose of capsaicin will reliably elicit cough under these conditions (Bolser *et al.*, 1991a). Coughs were detected by a microphone placed in the chamber and connected to a audio monitor and chart recorder. The number of coughs elicited during a 4 min exposure to capsaicin were counted by visual inspection of the chart record.

The antitussive effect of codeine, dextromethorphan, GABA, baclofen, and 3-aminopropylphosphinic acid (3-

[1] Author for correspondence.

APPi) was assessed following subcutaneous or aerosol administration of each drug. For the subcutaneous route of administration, animals were dosed 1 h before challenge with capsaicin. For aerosol administration, drugs or vehicle were delivered by inhalation for 4 min immediately before exposure to capsaicin aerosol. This method has been used in this laboratory to demonstrate blockade of capsaicin-induced cough *in vivo* by the capsaicin antagonist, ruthenium red (Bolser *et al.*, 1991a).

The activity of the $GABA_B$ antagonist, 3-aminopropyl (diethoxymethyl) phosphinic acid (CGP 35348), and a $GABA_A$ antagonist, bicuculline, were evaluated by the ability of these compounds to inhibit the antitussive effect of baclofen. These antagonists or vehicle were administered subcutaneously 40 min before challenge with capsaicin. Baclofen was administered subcutaneously 30 min before capsaicin challenge.

Mechanically induced cough in cats

Cats (2.2–4.0 kg) were anaesthetized with sodium pentobarbitone (35 mg kg^{-1}, i.p.). Supplemental anaesthetic (5 mg kg^{-1}, i.v.) was administered as required. Catheters were placed in a femoral vein and artery for administration of drugs and measurement of arterial blood pressure, respectively. A tracheal cannula was placed to allow access to the intrathoracic trachea.

Electromyograms (EMGs) of respiratory muscle activity were recorded via bipolar silver wire electrodes placed in the diaphragm and rectus abdominis muscles. The EMGs were amplified, filtered (0.5–10 kHz), monitored on a oscilloscope, and integrated with a resistance-capacitance circuit (100 ms time constant). These signals were displayed along the blood pressure on a chart recorder.

Cough is produced by coordinated bursts of activity in inspiratory and expiratory muscles (Korpas & Tomori, 1979; Tomori & Widdicombe, 1969). We defined cough as a burst of EMG activity in the diaphragm (inspiratory muscle) immediately followed by or coincident with burst of activity in the rectus abdominis muscle (expiratory muscle). These criteria are consistent with EMG recordings of respiratory muscle activity during coughing reported by other investigators (Tomori & Widdicombe, 1969; Korpas & Tomori, 1979; Van Lunteren *et al.*, 1989). These criteria also will differentiate coughs from apnoeas or apneusis (no expiratory bursts), augmented breaths (no expiratory bursts), or the expiration reflex (no inspiratory burst).

The antitussive activity of codeine, dextromethorphan, or baclofen was evaluated from cumulative dose-response relationships following intravenous administration of each drug. Coughing was elicited by probing the intrathoracic trachea with a thin flexible polyethylene cannula. Each cough trial consisted of continuous probing of the intrathoracic trachea for approximately 10 s. This stimulus only elicits coughs, augmented breaths (sighs), or the expiration reflex (Korpas & Tomori, 1979). Control values were obtained by averaging the number of coughs during five consecutive trials obtained following vehicle administration. One minute was allowed to elapse between trials. A total of five stimulus trials were then applied at 1,2,3,4, and 5 min after each dose of drug. The cough response following each dose of drug was determined by averaging the number of coughs observed during these five trials. Five minutes elapsed between each dose of drug.

$GABA_B$ antagonist activity was evaluated by administration of the $GABA_B$ antagonist CGP 35348 or the mixed agonist/antagonist (Hills & Howson, 1992) 3-aminopropylphosphonic acid (3-APPA) 5 min before baclofen. The antagonists and baclofen were given by the intravenous route. The number of coughs following mechanical stimulation was assessed as described above.

Compounds

Compounds used in this study included capsaicin, bicuculline methiodide (Sigma Chemical Co., St. Louis, MO, U.S.A.), CGP 35348 (Ciba-Geigy Corp., Basel, Switzerland), 3-APPA, dextromethorphan, naloxone HCl, and (±)-baclofen HCl (Research Biochemicals Inc., Natick, MA, U.S.A.), 3-APPi (Schering-Plough Research Institute, Bloomfield, NJ. U.S.A.) and codeine sulphate (Mallinckrodt, St. Louis, MO, U.S.A.). Capsaicin was dissolved in 1% ethanol, 1% Tween 20, and 98% physiological saline. All other drugs were dissolved in 0.9% saline.

Statistics

All data are represented as mean ± s.e.mean. Statistical differences between means were evaluated with Student's *t* test or one-way Analysis of Variance. Effective doses (ED_{50}, ED_{30}) were determined by linear regression analysis of dose-response relationships. Differences were considered significant if $P<0.05$.

Results

Irritant-induced cough in guinea-pigs

Figure 1 shows the antitussive effects of subcutaneous and aerosol administration of codeine, dextromethorphan and the $GABA_B$ agonists baclofen and 3-aminopropylphosphinic acid (3-APPi) against capsaicin-induced cough in the guinea-pig. The maximum inhibition of cough by these compounds in guinea-pigs by either route was 60–70%. Therefore, effective doses are expressed as ED_{30}'s in Table 1. Dose-dependent

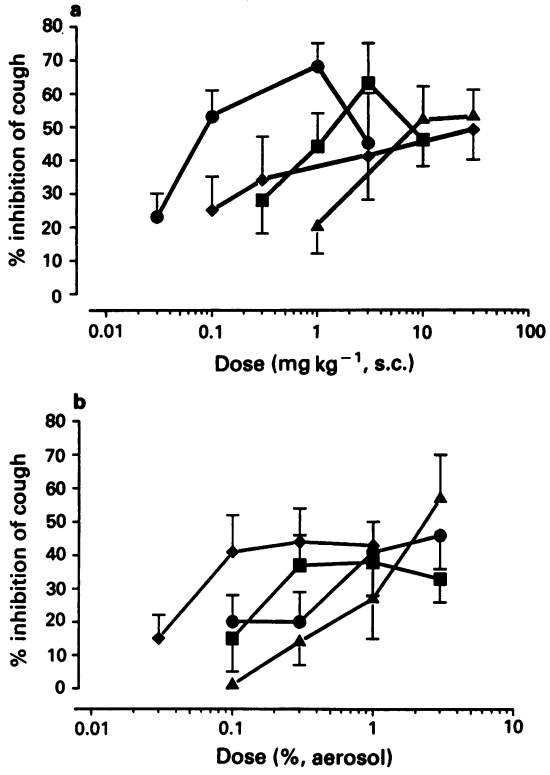

Figure 1 Influence of codeine, dextromethorphan and $GABA_B$ agonists administered via subcutaneous (a) and inhaled (b) routes on capsaicin-induced cough in the guinea-pig. Drugs were administered 1 h before capsaicin challenge in (a). In (b) drugs were delivered by aerosol for 4 min just before capsaicin challenge. Values represent mean ± s.e.mean ($n = 6–18$ animals per dose): (●) baclofen; (■) 3-aminopropylphosphinic acid; (▲) codeine; (◆) dextromethorphan.

Table 1 Antitussive potencies of $GABA_B$ agonists and selected standards in guinea-pigs

Compound[a]	*Inhibition of capsaicin-induced cough*[b] (ED_{30}) subcutaneous (mg kg^{-1})	inhaled (%)
Baclofen	0.04	0.59
3-APPi	0.36	0.22
Codeine	2.20	0.76
Dextromethorphan	0.31	0.08

[a]Compounds administered either 1 h before (subcutaneous) or 4 min before (inhaled) capsaicin challenge. [b]ED_{30} determined by regression analysis. $n = 24-72$ animals for each ED_{30} determination. 3-APPi = 3 aminopropylphosphinic acid.

inhibition was produced by each of these drugs by the subcutaneous route of administration (Figure 1a). Baclofen was apparently more potent than the other drugs by this route of administration (Table 1).

By the inhaled route, baclofen (0.1–3.0%) and 3-APPi (0.1–3.0%) each inhibited capsaicin-induced cough. All drugs had similar potencies to inhibit cough by the inhaled route (Figure 1b, Table 1). In addition, all drugs were equieffective in reducing cough by this route of administration.

The $GABA_B$ antagonist, CGP 35348 (0.3–30 mg kg^{-1}, s.c.) reduced the antitussive effect of baclofen (3 mg kg^{-1}, s.c., Figure 2) but did not alter the antitussive effect of codeine (30 mg kg^{-1}, s.c., Table 2). Conversely, naloxone at a dose (0.3 mg kg^{-1}, s.c.) that significantly inhibited the antitussive effect of codeine (30 mg kg^{-1}, s.c.) had no effect on the antitussive action of baclofen (Table 2). CGP 35348 alone had no effect on cough when delivered at doses up to 15 mg kg^{-1}, s.c. Pretreatment with the $GABA_A$ antagonist, bicuculline, (3 mg kg^{-1}, s.c.) had no effect on the antitussive activity of baclofen (baclofen alone 41 ± 18% inhibition of cough, baclofen + bicuculline 43 ± 13% inhibition).

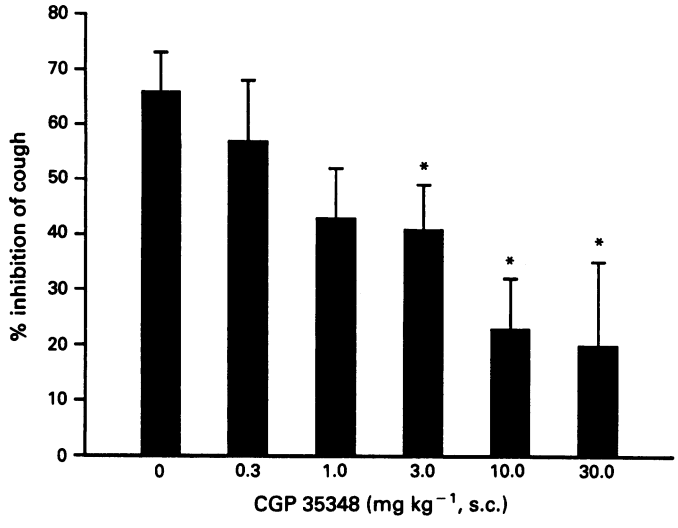

Figure 2 Influence of the $GABA_B$ antagonist CGP 35348 on the antitussive effect of baclofen in the guinea-pig. CGP 35348 was administered subcutaneously 40 min before challenge with capsaicin aerosol. Baclofen (3 mg kg^{-1}) was administered subcutaneously 30 min before challenge with capsaicin aerosol. The inhibition of cough frequency produced by baclofen in the absence of CGP 35348 was 66 ± 7%. Values represent mean ± s.e.mean ($n = 6-18$ per group). *$P < 0.05$ compared to baclofen alone.

Table 2 Effects of selective antagonists on the antitussive effects of baclofen and codeine in guinea-pigs

Treatment *First*[a]	*Second*[b]	*% inhibition of cough (mean ± s.e.mean)*	
CGP35348	Saline	9 ± 21[c]	
Saline	Codeine	44 ± 14	NS
CGP35348	Codeine	61 ± 21	
Naloxone	Saline	27 ± 8[c]	
Saline	Codeine	62 ± 13	*
Naloxone	Codeine	17 ± 6	
Naloxone	Saline	−23 ± 29[c]	
Saline	Baclofen	58 ± 12	NS
Naloxone	Baclofen	68 ± 6	

[a]Naloxone (0.3 mg kg^{-1}, s.c.), CGP35348 (10 mg kg^{-1}, s.c.), or saline was given 40 min before capsaicin challenge. [b]Codeine (30 mg kg^{-1}, s.c.), baclofen (3.0 mg kg^{-1}, s.c.), or saline was given 30 min before capsaicin challenge. [c]Naloxone or CGP35348 had no significant effects on capsaicin-induced cough.
NS = not significant $n = 5-6$ per group. * = $P < 0.05$

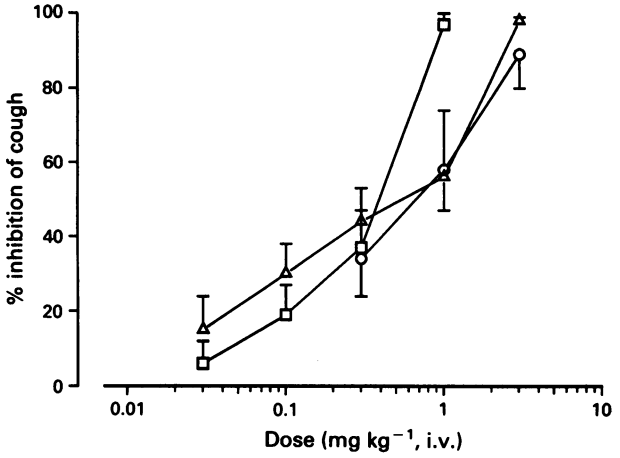

Figure 3 Cumulative dose-response relationships for codeine, dextromethorphan, and baclofen on mechanically-induced cough in the cat: (○) baclofen; (△) codeine; (□) dextromethorphan. Values represent mean ± s.e.mean ($n = 5$ animals per drug).

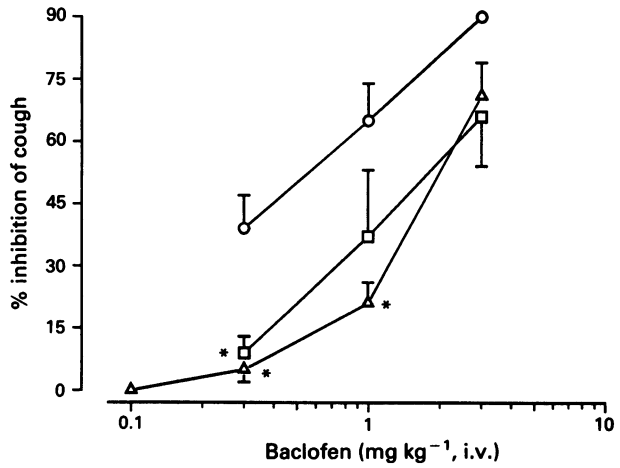

Figure 4 Influence of $GABA_B$ antagonists CGP 35348 and 3-aminopropylphosphonic acid (3-APPA) on antitussive effect of baclofen in the cat. Antagonists or vehicle administered 5 min before first dose of baclofen: (○) vehicle and baclofen; (△) CGP 35348 (10 mg kg^{-1}, i.v.) and baclofen; (□) 3-APPA (3 mg kg^{-1}, i.v.) and baclofen. Values represent mean ± s.e.mean ($n = 5$ animals per drug). *$P < 0.05$ compared to vehicle and baclofen.

Mechanically-induced cough in the cat

Intravenous administration of baclofen (0.3–3 mg kg^{-1}), codeine (0.03–3.0 mg kg^{-1}), or dextromethorphan (0.03–1.0 mg kg^{-1}) reduced mechanically-induced cough in a dose-dependent manner in the cat (Figure 3). The maximum inhibition produced by these drugs was 90–100% and half-maximum inhibition (ED_{50}) was produced by 0.63 mg kg^{-1} baclofen, 0.26 mg kg^{-1} codeine, and 0.27 mg kg^{-1} dextromethorphan.

Prior administration of the $GABA_B$ antagonists, 3-APPA (3 mg kg^{-1}, i.v.) or CGP 35348 (10 mg kg^{-1}, i.v.), shifted the dose-response relationship for baclofen to the right (Figure 4). A higher dose of 3-APPA (10 mg kg^{-1}, i.v.) inhibited the cough response to mechanical stimulation of the trachea, suggestive of agonist activity by this mixed agonist/antagonist.

Discussion

In our studies, baclofen and 3-APPi, which are highly specific $GABA_B$ receptor agonists (Bowery, 1989; Hills & Howson, 1992), inhibited cough in cats and guinea-pigs and the antitussive effect of baclofen was antagonized by selective $GABA_B$ antagonists. In contrast, the $GABA_A$ antagonist, bicuculline, and the opioid antagonist, naloxone, did not influence the antitussive effect of baclofen in the guinea-pig. Likewise, the $GABA_B$ antagonist, CGP 35348, did not alter the antitussive activity of codeine. These observations indicate that the antitussive effects of $GABA_B$ agonists are specific to $GABA_B$ receptors and are independent of $GABA_A$ or opioid receptors. Previously, Nosalova *et al.* (1987) showed that a nonspecific GABA agonist, gabalineamide, had antitussive effects in the cat. But it was not known if the antitussive effect observed by Nosalova *et al.* was due to $GABA_A$ or $GABA_B$ receptors. Our results clearly define a role for inhibition of cough by $GABA_B$ receptor agonists in cats.

Baclofen and 3-APPi had antitussive activity when given systemically or by inhalation to guinea-pigs. This observation contrasts with the findings of Callaway & King (1992) who showed that inhaled baclofen and GABA did not inhibit citric acid-induced cough in guinea-pigs. These differences in results could be due to different protocols and/or the different stimuli (citric acid, capsaicin) used to elicit cough. In our studies, we compared the effects of selective $GABA_B$ agonists to the well-characterized drugs, codeine and dextromethorphan. The antitussive effects of codeine and dextromethorphan that we demonstrated in the guinea-pig are generally consistent with a variety of reports showing similar effects of these drugs on cough induced by inhaled irritants in rats and guinea-pigs (Pickering & James, 1979; Adcock *et al.*, 1988; Karlsson *et al.*, 1990; Kamei & Kasuya, 1992). However caution should be used in comparing antitussive effects of drugs on cough elicited by different irritant stimuli, such as citric acid and capsaicin. Although previous investigators have suggested that citric acid and capsaicin act by the same mechanism on the basis of neuropeptide depletion experiments using capsaicin (Forsberg & Karlsson, 1986), we have recently shown that citric acid can elicit cough by the same or different mechanisms as capsaicin depending upon the dose of citric acid administered (Bolser *et al.*, 1991a). These observations underscore the importance of using the same tussigenic stimulus when comparing activities of antitussive drugs.

The potencies of baclofen and 3-APPi when administered by the subcutaneous or inhaled routes in the guinea-pig compared favourably to that of the standard antitussives, codeine and dextromethorphan. The maximum efficacy of baclofen and 3-APPi in the guinea pig model was approximately 60% inhibition of cough. This observation suggests that it may be difficult to inhibit completely capsaicin-induced cough in this species. However, baclofen and 3-APPi had efficacies equivalent to or greater than codeine and dextromethorphan in this model.

In the cat, the antitussive potencies of codeine and dextromethorphan in the present study are similar to or greater than potencies reported by others (May & Widdicombe, 1954; Chau & Harris, 1980; Kase *et al.*, 1983). In addition, in a model of fictive cough (Bolser, 1991) we have previously reported a potency of codeine (0.1 mg kg^{-1}, i.v.) similar to that found in the present study. Furthermore, dextromethorphan was more potent in our studies (ED_{50} = 0.27 mg kg^{-1}, i.v.) than was reported previously (ED_{50} = 0.82–1.21 mg kg^{-1}; Chau & Harris, 1980; Domino *et al.*, 1985). Therefore, our cat model appears to be very sensitive to the effects of antitussive drugs. In this model, the potency of baclofen was only slightly less than codeine and dextromethorphan.

Previous investigators have suggested peripheral and central sites of action for antitussive drugs (Chou & Wang, 1975; Karlsson *et al.*, 1990). The fact that 3-APPi inhibits cough is consistent with a peripheral site of action, because 3-APPi does not penetrate the CNS (Hills & Howson, 1992). Indeed, we have also found that large doses (30–100 mg kg^{-1}, s.c.) of 3-APPi do not cause respiratory depression in guinea-pigs whereas baclofen (3.0 mg kg^{-1}, s.c.) causes significant respiratory depression (J.A. Hey, G. Mingo & R.W. Chapman; unpublished observations). Therefore, a peripheral site of action of 3-APPi to inhibit cough seems likely. Whether or not baclofen also acts at central sites to inhibit cough is unknown.

The antitussive effects of $GABA_B$ agonists are consistent with their inhibitory effects on other phenomena that are important in the pathogenesis of airway diseases. Baclofen decreases cholinergic and tachykinin-mediated bronchospasm (Belvisi *et al.*, 1989; Chapman *et al.*, 1991) and attenuates airway microvascular leakage induced by stimulation of tachykinin-containing sensory afferents (Danko *et al.*, 1992). Furthermore, baclofen inhibits allergen and histamine-induced bronchospasm in conscious guinea-pigs and attenuates the release of allergic mediators from guinea-pig lungs (Luzzi *et al.*, 1987). Therefore, $GABA_B$ agonists appear to be active in reducing a variety of components that contribute to the pathogenesis of airway diseases, such as asthma.

We thank Carol Battle for typing the manuscript.

References

ADCOCK, J.J., SCHNEIDER, C. & SMITH, T.W. (1988). Effects of codeine, morphine and a novel opioid pentapeptide BW 443C, on cough, nociception and ventilation in the unanesthetized guinea pig. *Br. J. Pharmacol.*, **93**, 93–100.

BELVISI, M.G., ICHINOSE, M. & BARNES, P.J. (1989). Modulation of non-cholinergic neural bronchoconstriction in guinea pig airways via GABA-B receptors. *Br. J. Pharmacol.*, **97**, 1225–1231.

BOLSER, D.C. (1991). Fictive cough in the cat. *J. Appl. Physiol.*, **71**, 2325–2331.

BOLSER, D.C., AZIZ, S.M. & CHAPMAN, R.W. (1991a). Ruthenium red decreases capsaicin and citric acid-induced cough in guinea pigs. *Neuroscience Lett.*, **126**, 131–133.

BOLSER, D.C., AZIZ, S.M., KREUTNER, W. & CHAPMAN, R.W. (1991b). Baclofen has antitussive effects in the cat. *FASEB J.*, **5**, A1244.

BOWERY, N. (1989). GABA-B receptors and their significance in mammalian pharmacology. *Trends Pharmacol. Sci.*, **10**, 401–407.

BRAMAN, S.S. & CORRAO, W.M. (1987). Cough: differential diagnosis and treatment. *Clin. Chest Med.*, **8**, 177–188.

CALLAWAY, J.K. & KING, G. (1992). Effects of inhaled α_2-adrenoreceptor and GABA-B receptor agonists on citric acid induced cough and tidal volume changes in guinea pigs. *Eur. J. Pharmacol.*, **220**, 187–195.

CHAPMAN, R.W., DANKO, G., RIZZO, C., EGAN, R.W. MAUSER, P.J. & KREUTNER, W. (1991). Prejunctional GABA-B inhibition of cholinergic, neurally-mediated airway contractions in guinea pigs. *Pulm. Pharmacol.*, **4**, 218–224.

CHAU, T.T. & HARRIS, L.S. (1980). Comparative studies of the pharmacological effects of the d- and l-isomers of codeine. *J. Pharmacol. Exp. Ther.*, **215**, 668–672.

CHOU, D.T. & WANG, S.C. (1975). Studies on the localization of central cough mechanism; site of action of antitussive drugs. *J. Pharmacol. Exp. Ther.*, **194**, 499–505.

DANKO, G., HEY, J.A., DEL PRADO, M., KREUTNER, W. & CHAPMAN, R.W. (1992). GABA-B inhibition of peptidergic airway microvascular leakage in guinea pigs. *Pharmacol. Commun.*, **1**, 203–209.

DOMINO, E.F., KRUTAK-KROL, H. & LAL, J. (1985). Evidence for a central site of action for the antitussive effects of caramiphen. *J. Pharmacol. Exp. Ther.*, **233**, 249–253.

EDRÖ, S.L. & KISS, B. (1986). Presence of GABA, glutamate decarboxylase, and GABA transaminase in peripheral tissues: a collection of quantitative data. In *GABAergic Mechanisms in the Mammalian Periphery*, ed. Erdö, S.L. & Bowery, N.G., pp. 5–17, New York: Raven Press.

FORSBERG, K. & KARLSSON, J.-A. (1986). Cough induced by stimulation of capsaicin-sensitive sensory neurons in conscious guinea pigs. *Acta Physiol. Scand.*, **128**, 319–320.

GREEN, K.A. & COTTRELL, G.A. (1988). Actions of baclofen on components of the Ca^{++}-current in rat and mouse DRG neurones in culture. *Br. J. Pharmacol.*, **94**, 235–245.

HILLS, J.M. & HOWSON, W. (1992). The GABA-B receptor profile of a series of phosphinic acids-agonist and antagonist activity in a range peripheral tissues. In *GABA Outside the CNS*, ed. Erdö, S.L. pp. 249–260. Berlin, Heidelberg, New York: Springer-Verlag.

KAMEI, J., HOSOKAWA, T., YANAURA, S. & HUKUHARA, T. (1986). Effects of methysergide on the cough reflex. *Jpn. J. Pharmacol.*, **42**, 450–452.

KAMEI, J., HUKUHARA, T. & KASUYA, Y. (1987a). Dopaminergic control of the cough reflex as demonstrated by the effects of apomorphine. *Eur. J. Pharmacol.*, **141**, 511–513.

KAMEI, J. & KASUYA, Y. (1992). Antitussive effects of Ca^{2+} channel antagonists. *Eur. J. Pharmacol.*, **212**, 61–66.

KAMEI, J., OGAWA, M. & KASUYA, Y. (1987b). Monoamines and the mechanisms of action of antitussive drugs in rats. *Arch Int. Pharmacodyn.*, **290**, 117–127.

KAMEI, J., TANIHARA, H., IGARASHI, H. & KASUYA, Y. (1989). Effects of N-methyl-D-aspartate antagonists on the cough reflex. *Eur. J. Pharmacol.*, **168**, 153–158.

KARLSSON, J.-A., LANNER, A.-S. & PERSSON, C.G.A. (1990). Airway opioid receptors mediate inhibition of cough and reflex bronchoconstriction in guinea pigs. *J. Pharmacol. Exp. Ther.*, **252**, 863–868.

KASE, Y., KAWAGUCHI, M., TAKAHAMA, M. MIYATA, T., HIROTSU, I., HIROTSU, T. & OKANO, Y. (1983). Pharmacological studies on dl-glaucine phosphate as an antitussive. *Arzneim-Forsch/Drug Res.*, **33**, 936–944.

KORPAS, J. & TOMORI, Z. (1979). *Cough and other Respiratory Reflexes*. New York: S. Karger.

LUZZI, S., FRANCHI-MICHELI, S., FOLCO, G., ROSSONI, G., CIUFFI, M. & ZILLETTI, L. (1987). Effect of baclofen on different models of bronchial hyperreactivity in the guinea pig. *Agents Actions*, **20**, 307–309.

MAY, A.J. & WIDDICOMBE, J.G. (1954). Depression of the cough reflex by pentobarbitone and some opium derivatives. *Br. J. Pharmacol. Chemother.*, **9**, 335–340.

MUGNAINI, E. & OERTEL, W.H. (1985). An atlas of the distribution of GABAergic neurones and terminals in the rat CNS as revealed by GAD immunohistochemistry. In *Handbook of Chemical Neuroanatomy, GABA and Neuropeptides in the CNS*. ed. Bjorkland, A. & Hokfelt, T. Vol. 4 Part 1, pp. 436–608 Amsterdam: Elsevier.

NOSALOVA, G., VARONOS, D. PAPADOPOULOU-DAIFOTIS, Z., VISNOVSKY, P. & STRAPKOVA, A. (1987). GABA-ergic mechanisms in the central control of cough. *Acta Physiologica Hung*, **70**, 189–194.

O'CONNELL, E.J., ROJAS, A.R. & SACHS, M.I. (1991). Cough-type asthma: a review. *Ann. Allergy*, **66**, 278–286.

PICKERING, R.W. & JAMES, G.W.L. (1979). The antitussive activity of a novel compound RU20201. *Arzneim-Forsch/Drug Res.*, **29**, 287–289.

TOMORI, Z. & WIDDICOMBE, J.G. (1969). Muscular, bronchomotor, and cardiovascular reflexes elicited by mechanical stimulation of the respiratory tract. *J. Physiol.*, **200**, 25–49.

VAN LUNTEREN, E., DANIELS, R., DEAL, E.C. & HAXHIU, M.A. (1989). Role of costal and crural diaphragm and parasternal intercostals during coughing in cats. *J. Appl. Physiol.*, **66**, 135–144.

YOUNG, S., BITSAKOU, H., CARIC, D. & MCHARDY, G.J.R. (1991). Coughing can relieve or exacerbate symptoms in asthmatic patients. *Respir. Med.*, Suppl. A, **85**, 7–12.

(Received January 25, 1993
Revised May 4, 1993
Accepted May 17, 1993)

Br. J. Pharmacol. (1993), **110**, 496–500

The paradoxical vascular interactions between endothelin-1 and calcitonin gene-related peptide in the rat gastric mucosal microcirculation

J. Lopez-Belmonte & [1]B.J.R. Whittle

Department of Pharmacology, Wellcome Research Laboratories, Langley Court, Beckenham, Kent BR3 3BS

1 The interactions between local intra-arterial infusion of endothelin-1 (ET-1) and rat α-calcitonin gene-related peptide (α-CGRP) on gastric mucosal damage and blood flow have been investigated in the pentobarbitone-anaesthetized rat.

2 Close-arterial infusion of ET-1 (2–200 pmol kg^{-1} min^{-1}) induced a significant and dose-dependent increase in gastric mucosal haemorrhagic injury.

3 Close-arterial infusion of the higher doses of ET-1 (100 and 200 pmol kg^{-1} min^{-1}) resulted in a biphasic effect on mucosal blood flow, as determined by laser Doppler flowmetry (LDF). This consisted of an initial transient increase followed by a pronounced and sustained fall in LDF.

4 Local microvascular constriction may thus contribute to the mechanisms underlying the gastric injury induced by these higher doses of ET-1.

5 However, close-arterial infusion of lower doses of ET-1 (2–50 pmol kg^{-1} min^{-1}), that also provoked substantial mucosal damage, induced only a sustained and significant mucosal hyperaemia, which may be secondary to microvascular injury.

6 Concurrent close-arterial administration of rat α-CGRP (50 pmol kg^{-1} min^{-1}) significantly inhibited the extent of gastric mucosal injury induced by ET-1 (5 pmol kg^{-1} min^{-1}).

7 Furthermore, concurrent close-arterial infusion of this dose of α-CGRP, which itself increased mucosal LDF, significantly inhibited the hyperaemic response induced by close-arterial infusion of ET-1 (5 pmol kg^{-1} min^{-1}).

8 These results indicate a damaging action on the gastric mucosa by low doses of ET-1 which is independent of local vasoconstriction, that may involve a direct injury of the microvascular endothelium. The protective action of α-CGRP thus seems unlikely to be due to a local vasodilator effect but may reflect protective actions on the microvascular endothelium

Keywords: Endothelin-1; mucosal blood flow; laser Doppler flowmetry; endothelium; gastric damage; calcitonin gene-related peptide

Introduction

The vascular endothelium synthesizes a variety of vasoactive mediators which act to modulate blood flow through tissues. One such mediator is endothelin-1 (ET-1), a 21 amino-acid peptide originally isolated from the supernatant of cultured porcine aortic endothelial cells, which exhibits potent vasoconstrictor activity both *in vitro* and *in vivo* (Yanagisawa *et al.*, 1988a,b; Inoue *et al.*, 1989). Close-arterial infusion of picomol quantitites of ET-1 induces extensive haemorrhagic injury to the rat gastric mucosa (Whittle & Esplugues, 1988; Whittle *et al.*, 1989b; Whittle & Lopez-Belmonte, 1991). Furthermore, intravenous infusion of ET-1 can significantly enhance the gastric mucosal injury induced in the rat by topical application of ethanol or acid (Wallace *et al.*, 1989). Such ulcerogenic effects of ET-1 were considered to reflect local vasoconstrictor actions on the mucosal microcirculation.

The release of vasodilator neuropeptides from sensory afferent neurones, through a local reflex, has been suggested to be a protective mechanism in the gastric mucosa (Szolcsanyi & Bartho, 1981; Holzer & Sametz, 1986). This proposal was supported by experiments in which chronic capsaicin treatment, to ablate primary afferent neurones and deplete their neuropeptide content, augmented the injury induced by a variety of damaging agents (Szolcsanyi & Bartho, 1981; Holzer & Sametz, 1986; Esplugues *et al.*,1989; Esplugues & Whittle, 1990) including ET-1 (Whittle & Lopez-Belmonte, 1991).

Acute intragastric administration of capsaicin, which stimulates neuropeptide release from sensory nerves, induces mucosal vasodilatation and protects against gastric mucosal injury (Holzer *et al.*,1990; 1991; Li *et al.*, 1991; Whittle *et al.*, 1992). Calcitonin gene-related peptide (CGRP), a potent endothelium-dependent vasodilator (Brain *et al.*, 1985), is the predominant neuropeptide released from afferent sensory nerves in the rat stomach (Green & Dockray, 1988). CGRP is a potent vasodilator in the rat gastric microcirculation following local infusion (Holzer & Guth, 1991; Li *et al.*, 1991; Whittle *et al.*, 1992) and can reduce the haemorrhagic lesions following challenge with aspirin or ethanol (Lippe *et al.*, 1989). Furthermore, close-arterial administration of rat α-CGRP can inhibit the damage induced by local infusion of ET-1 (Whittle & Lopez-Belmonte, 1991). This latter protective effect of CGRP was proposed to reflect local vasodilator actions of the sensory neuropeptide opposing those of the endothelium-derived vasoconstrictor peptide on microvascular tone and gastric mucosal integrity.

In the present study, the effects of local intra-arterial administration of ET-1 and rat α-CGRP on gastric mucosal blood flow have been investigated by the use of laser Doppler flowmetry. Furthermore, these effects have been compared to their actions in gastric mucosal integrity in the anaesthetized rat.

A preliminary account of this work has been presented to the British Pharmacological Society (Lopez-Belmonte & Whittle, 1993).

[1] Author for correspondence.

Methods

Gastric damage induced by local infusion of ET-1

Male Wistar rats (230–260 g body weight) were deprived of food but not water for 18–20 h before the experiment. The animals were anaesthetized with sodium pentobarbitone (60 mg kg^{-1}, i.p.) and the stomach exposed by a mid-line incision. The left gastric artery was then exposed and cannulated with a short 24 gauge teflon cannula (Esplugues *et al.*, 1989). The oesophagus and pylorus were ligated and 2 ml 0.1 M hydrochloric acid was instilled into the gastric lumen via the forestomach. ET-1 (2–200 pmol kg^{-1} min^{-1}) or its vehicle, a 0.1% solution of bovine serum albumin (BSA) in saline, was infused locally via the left gastric artery for 10 min (13 μl min^{-1}) and the stomachs removed 20 min later.

Measurement of gastric mucosal blood flow

Following cannulation of the left gastric artery, a small bore (8.5 mm outer diameter) plastic cannula was inserted in the forestomach and tied in place to allow free access to the gastric lumen for the measurement of mucosal blood flow by laser Doppler velocimetry, as described previously (Tepperman & Whittle, 1992). A teflon-coated laser optic probe (Periflux PF 308, standard probe, 0.25 mm fibre separation) was inserted into the gastric lumen via the forestomach cannula and allowed to rest gently on the corpus mucosa. After a resting period of 20–30 min following surgery, gastric mucosal blood flow was recorded continuously with a laser Doppler flow monitor (Perimed PF3, Stockholm, Sweden; helium-neon laser of wavelength 632.8 nm and power at probe tip of <1 mW) until stable levels were obtained. Changes in laser Doppler flow (LDF) were assessed in response to intra-arterial infusion (13 μl min^{-1}) of 0.1% BSA in saline or the compounds under investigation.

In one study, LDF was also measured with a Moore's MBF3D monitor (Axminster, England), in which the laser beam was generated by a semi-conductor laser diode operating at a wavelength of 782 nm, with approximately 1 mW power at the probe tip. This apparatus also allowed the determination of red cell concentration as well as velocity, upon which the calculation of laser Doppler flux as a measure of blood flow depends.

Effect of ET-1 on gastric mucosal LDF

Endothelin-1 (2–200 pmol kg^{-1} min^{-1}) or its vehicle (0.1% BSA in saline) were infused close-arterially (13 μl min^{-1}) for a period of 10 min. Average LDF values were determined for a 3 min period before ET-1 infusion and similarly for the final 3 min period of the infusion or when LDF values had stabilized. Changes in LDF were expressed as % change from basal values.

Effect of α-CGRP on ET-1 induced mucosal damage and LDF changes

In these studies, an intra-arterial 24 gauge teflon cannula attached to a bifurcated catheter was used, which allowed for the concurrent administration of two substances infused at a rate of 13 μl min^{-1}. In control studies, the vehicle, 0.1% BSA in saline, was infused at 26 μml min^{-1} for 10 min.

Local intra-arterial infusion of rat α-CGRP (50 pmol kg^{-1} min^{-1}) was started 5 min before ET-1 and maintained for the duration of the 10 min infusion of ET-1. This dose of rat α-CGRP was taken from previous dose-response studies as that which produced near-maximal protection against mucosal injury (Whittle & Lopez-Belmonte, 1991). In control experiments, α-CGRP, or its vehicle was infused alone close-arterially for a total period of 15 min at 26 μl min^{-1}.

Assessment of mucosal damage

Twenty min after terminating the local intra-arterial infusion of the drugs, the stomachs were removed from the abdominal cavity, cut open along the greater curvature and gently rinsed with isotonic saline. They were then pinned, mucosal side up, to a wax block and immersed in neutral buffered formalin. Each stomach was photographed on colour transparency film (Kodak EPY 50) and coded to allow for unbiased assessment. The transparencies were then projected and the macroscopically visible damage (identified as vasocongestion, haemorrhagic necrosis and epithelial desquamation) was assessed by computerized planimetry (Apple IIe). The area of damage in each mucosa was expressed as a percentage of the total mucosal area.

Materials

Endothelin-1 (human-porcine) and rat α-CGRP (Peninsula Laboratories, St. Helens, Merseyside) were dissolved in isotonic saline and kept frozen (– 20°C) in aliquots. Samples were freshly diluted when required in isotonic saline for α-CGRP or in a 0.1% solution of bovine serum albumin in saline for ET-1.

Statistical evaluation

Results are expressed as the mean ± s.e.mean, where (n) is the number of animals. The difference between groups was evaluated by analysis of variance with the Bonferroni test for multiple comparisons or by Student's t test for unpaired data where appropriate, a value of $P<0.05$ being taken as significant.

Results

Effect of local ET-1 on gastric mucosal integrity

Local intra-arterial infusion of ET-1 (2–200 pmol kg^{-1} min^{-1} in 0.1% bovine serum albumin) for 10 min induced a dose-dependent increase in gastric mucosal damage, assessed macroscopically 20 min later. This damage was characterized by regions of vasocongestion, epithelial desquamation, haemorrhage and necrosis extending to 30 ± 4% and 96 ± 3% of the total mucosal area at the lowest and highest doses respectively ($n=6$ and 4 respectively, $P<0.001$; Figure 1). The activity of ET-1 in this vehicle was greater than when ET-1 in isotonic saline was locally infused, with damage induced by ET-1 (5 pmol kg^{-1} min^{-1}, i.a.) being 34 ± 3% and 14 ± 5% of total area respectively ($n=5$ for each).

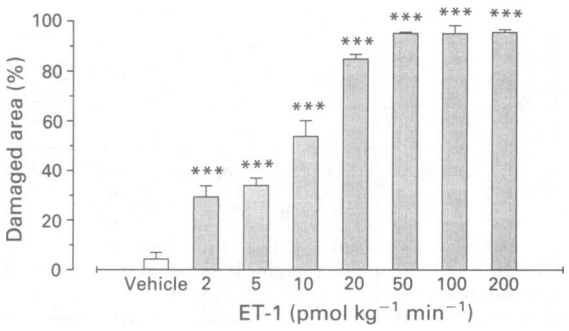

Figure 1 Effect of local intra-arterial infusion (10 min) of endothelin-1 (ET-1, 2–200 pmol kg^{-1} min^{-1}; shaded columns) on gastric mucosal integrity. Macroscopic damage, assessed 20 min after infusion, is shown as the % of the total mucosal area. Results are the mean ± s.e.mean of 4–8 experiments in each group. Statistical significance from damaged area in control studies (vehicle infusion; open column) is given as ***$P<0.001$.

Effect of local ET-1 infusion on gastric mucosal LDF

Local intra-arterial infusion of the higher doses of ET-1 (100 and 200 pmol kg^{-1} min^{-1}) induced a biphasic response in the mucosal LDF signal, determined with the Perimed PF3 monitor. This consisted of an initial significant, but transient, increase in LDF which was followed by a pronounced and sustained fall in LDF (Figure 2). With ET-1 (100 and 200 pmol kg^{-1} min^{-1}), the hyperaemic response lasted 6.5 ± 1.7 and 1.7 ± 0.3 min respectively ($n = 5$ for each). The subsequent reduction in LDF persisted after termination of ET-1 infusion and up to the conclusion of the experiment. Thus, with ET-1 (100 and 200 pmol kg^{-1} min^{-1}) the maximal reduction of LDF of − 38 ± 11% and − 76 ± 6% of basal respectively, achieved at the end of the 10 min infusion, was − 23 ± 11% and − 76 ± 7% of basal, 20 min after the ET-1 infusion.

When lower doses of ET-1 were administered (2–50 pmol kg^{-1} min^{-1}) only an increase in LDF was observed, this response being maximal at a dose of 5 pmol kg^{-1} min^{-1} (Δ111 ± 13% of basal, $n = 15$, $P < 0.01$; Figure 2). This increase in LDF was sustained for the duration of the infusion, and persisted after termination of ET-1 infusion, being Δ80 ± 10% of basal ($n = 15$) 20 min after termination of ET-1 (5 pmol kg^{-1} min^{-1}). As the dose of ET-1 was gradually increased, both the magnitude and duration of this hyperaemic response were diminished until a biphasic response was observed, as shown in Figure 2. Thus, with ET-1 (50 pmol kg^{-1} min^{-1}), the maximal increase in LDF of Δ53 ± 8% of basal ($n = 6$) observed after 10 min of infusion, declined to Δ14 ± 8% of basal, 10 min after terminating the infusion.

Similar findings were observed in a separate series of studies in which LDF was measured with the Moore's MBF3D monitor. Thus, following local infusion of ET-1 (100 pmol kg^{-1} min^{-1}), the initial transient (4 min) increase in LDF of 28 ± 8% was followed by a sustained fall in LDF of − 40 ± 13% ($n = 5$; $P < 0.05$). These changes in LDF were accounted for solely by changes in velocity within the microvasculature, the red blood cell concentration not significantly changing from resting values during the course of the study (change, 1.5 ± 1.9%).

Effect of α-CGRP on ET-1-induced mucosal injury

Local intra-arterial infusion of rat α-CGRP (50 pmol kg^{-1} min^{-1}) alone had no significant effect on macroscopically determined gastric mucosal integrity. However, when co-administered with ET-1 (5 pmol kg^{-1} min^{-1}) there was a significant reduction of the gastric mucosal injury induced by this dose of ET-1 alone (58 ± 11% inhibition, $n = 8$, $P < 0.001$; Figure 3).

Effect of α-CGRP on mucosal hyperaemia induced by ET-1

Local intra-arterial infusion of α-CGRP (50 pmol kg^{-1} min^{-1}) alone induced a significant increase in LDF (Figure 4). However, when this dose of α-CGRP was co-administered with ET-1 (5 pmol kg^{-1} min^{-1}) a significant reduction of the hyperaemic response induced by ET-1 was observed (77 ± 5% inhibition, $n = 6$, $P < 0.001$; Figure 4). Moreover, the remaining hyperaemia was similar in magnitude to that observed with α-CGRP alone, and thus may indicate the complete inhibition of the ET-1 response.

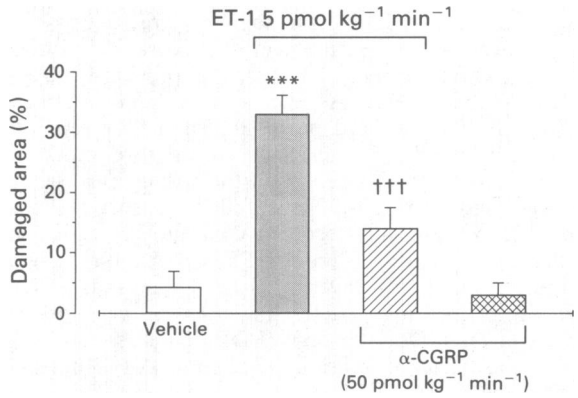

Figure 3 Effect of local intra-arterial infusion of rat α-calcitonin gene-related peptide (α-CGRP, 50 pmol kg^{-1} min^{-1}) on the macroscopic gastric mucosal damage induced by concurrent close-arterial administration (10 min) of endothelin-1 (ET-1, 5 pmol kg^{-1} min^{-1}). Results are shown as the area of damage expressed as a % of the total mucosal area and are the mean ± s.e.mean of 5–6 experiments for each group except for ET-1 alone, where $n = 15$. Statistical significance from control studies (vehicle) is given as $***P < 0.001$. Significant reduction of ET-1 induced damage is given as $†††P < 0.001$.

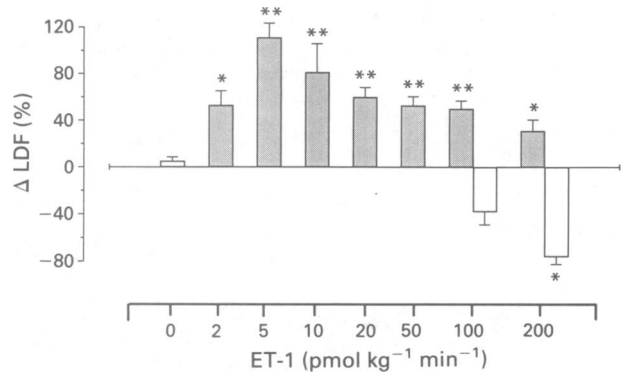

Figure 2 Effect of local intra-arterial infusion (10 min) of endothelin-1 (ET-1, 2–200 pmol kg^{-1} min^{-1}) on gastric mucosal blood flow (as assessed by laser Doppler flowmetry; LDF). Changes in LDF are expressed as the maximal % change from basal values observed during the infusion period. Shaded columns represent vasodilatation and lower open columns vasoconstriction. At the higher doses of ET-1 (100 and 200 pmol kg^{-1} min^{-1}) the transient vasodilatation (lasting 6.5 and 1.7 min respectively) was followed by a sustained vasoconstriction. Results are shown as the mean ± s.e.mean of 4–15 experiments for each group. Statistical significance from LDF values in control studies is given as $*P < 0.05$; $**P < 0.01$.

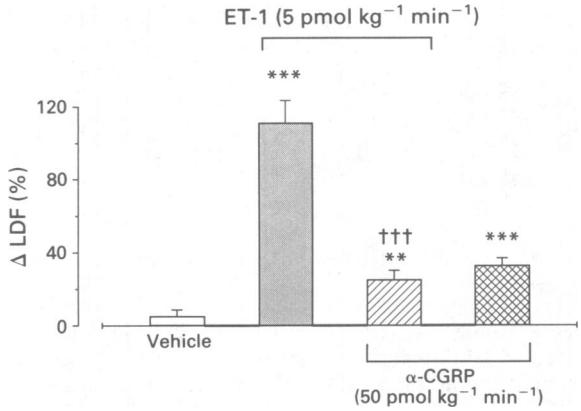

Figure 4 Effect of local intra-arterial infusion of rat α-calcitonin gene-related peptide (α-CGRP, 50 pmol kg^{-1} min^{-1}) on the gastric mucosal hyperaemia induced by concurrent close-arterial administration of endothelin-1 (ET-1, 5 pmol kg^{-1} min^{-1}) as assessed by laser Doppler flowmetry (LDF). Changes in LDF are expressed as the % change from basal values. Results are shown as the mean ± s.e.mean of 5–6 experiments for each group except for ET-1 alone, where $n = 15$. Statistical significance from control studies (vehicle infusion) is given as $**P < 0.01$; $***P < 0.001$. Significant reduction of ET-1-induced hyperaemia is given as $†††P < 0.001$.

Discussion

Local intra-arterial infusion of ET-1 induced dose-dependent gastric mucosal injury. This damage was characterized by widespread areas of vasocongestion and epithelial desquamation, with extensive areas of haemorrhage and necrosis also apparent at the higher doses. The use of bovine serum albumin as a vehicle was found to augment the extent of injury induced by ET-1 when compared to the use of isotonic saline as vehicle as in previous studies (Whittle & Esplugues, 1988; Whittle & Lopez-Belmonte, 1991).

It had been proposed that the induction or augmentation of gastric damage by local or systemic ET-1 administration could be attributed to its potent vasoconstrictor activity in the mucosal microcirculation (Whittle & Esplugues, 1988; Wallace *et al.*, 1989). In the present study, using laser Doppler flowmetry to monitor continuously gastric mucosal blood flow, the higher doses used of ET-1 (100 and 200 pmol kg^{-1} min^{-1}) induced a biphasic response. This consisted of an initial short-lived hyperaemia lasting up to 6 min, which was followed by a pronounced and sustained fall in mucosal blood flow. This profile of events following infusion of these higher doses of ET-1 was also observed using another laser Doppler flow monitor of greater laser wavelength and power and hence with greater tissue penetration. These findings indicate that such blood flow responses are not simply focal response in one area of the microvasculature and probably reflect changes throughout the mucosal microcirculation. The nature of the ET receptor (Arai *et al.*, 1990; Sakurai *et al.*, 1990) involved in this microcirculatory vasoconstrictor response is not yet known; although the ET_A receptor located on vascular smooth muscle mediates the pressor response of ET-1, recent studies have demonstrated the involvement of ET_B-like receptors in vasoconstriction in the rat kidney (Cristol *et al.*, 1993).

Such profound gastric vasoconstrictor effects could contribute to the mucosal injury induced by these higher doses of ET-1. Unexpectedly however, infusion of lower doses of ET-1, which also brought about substantial mucosal injury, induced only mucosal hyperaemia, indicating a dissociation between such mucosal damage and local vasoconstriction. As the dose of ET-1 was increased, this hyperaemia gradually diminished both in magnitude and duration, gradually approaching the biphasic response observed with the higher doses. This transition may reflect an underlying vasoconstriction which gradually opposes and then overcomes the observed hyperaemia. These findings are comparable to previously reported observations on cortical microvascular perfusion in the rat where intracarotid administration of low doses of ET-1 increased cortical perfusion and reduced microvascular resistance, whereas high doses reduced microvascular perfusion and increased resistance (Willette *et al.*, 1989). Furthermore, intravenous administration of ET-1 can decrease, increase or exhibit a biphasic action on rat systemic arterial blood pressure depending on the dose used, the level of anaesthesia or the existing blood pressure (Wright & Fozard, 1988; De Nucci *et al.*,1988; Whittle *et al.*, 1989a,b; Gardiner *et al.*, 1989).

The mechanisms mediating the observed mucosal hyperaemia are not yet clear. However, ET-1 can induce the release of prostacyclin and nitric oxide from the vascular endothelium which accounts for the vasodilatation seen in the isolated mesenteric vascular bed (De Nucci *et al.*, 1988). It will therefore be necessary in future studies to determine if this mucosal vasodilatation or any mediator release is a direct effect of ET-1 in the gastric microcirculation, perhaps through activation of ET_B or other ET receptors (Masaki *et al.*, 1991) or if it occurs secondarily to microvascular injury induced by ET-1.

Local intra-arterial infusion of α-CGRP induced a significant increase in gastric mucosal LDF. This agrees with previous reports where α-CGRP was found to be a potent vasodilator in the gastric microcirculation, determined by use of a variety of techniques including laser Doppler flowmetry and hydrogen gas clearance (Dipette *et al.*, 1987; Bauerfeund *et al.*,1989; Holzer & Guth, 1991; Li *et al.*, 1991; Whittle *et al.*, 1992). Intravenous infusion of α-CGRP can reverse the vasoconstrictor action of ET-1 on the internal carotid vascular bed in the rat (Gardiner *et al.*, 1990), and local α-CGRP administration reduces the vasoconstriction induced by ET-1 in rabbit skin (Brain *et al.*, 1988). Interestingly, the present findings indicate that α-CGRP co-administration can also significantly inhibit the gastric hyperaemic response induced by ET-1. Since this dose of α-CGRP attenuated the mucosal injury induced by ET-1 as shown previously (Whittle & Lopez-Belmonte, 1991), these apparently paradoxical findings again could suggest that the observed hyperaemia in the gastric mucosal microcirculation is a consequence of a damaging action of ET-1 on the vascular endothelium. Thus, prevention of ET-1-induced microvascular injury by CGRP could suppress the subsequent release of local vasodilator mediators.

Such microvascular injury by ET-1 could take place prior to the appearance of gross macroscopic damage in the mucosa. Indeed, injury of the endothelium has been proposed as an initial event in the genesis of mucosal injury induced by a number of agents including topical ethanol (Guth *et al.*, 1984; Szabo *et al.*, 1985) and local generation of free radicals (Parks *et al.*, 1982; Esplugues & Whittle, 1989). Under the present conditions, the ability of α-CGRP to prevent mucosal injury therefore seems unlikely to be due to local vasodilator actions but may involve protective actions in the microvasculature. Thus, it appears that the interactions between ET-1 and CGRP in the mucosal microcirculation are not simply due to opposing vasoactive properties, but reflect complex events involving the release of local mediators and actions on the continuity of the vascular endothelium.

References

ARAI, H., HORI, S., ARAMORI, I., OHKUBO, H. & NAKANISHI, S. (1990). Cloning and expression of a cDNA encoding an endothelin receptor. *Nature*, **348**, 730–732.

BAUERFEUND, P., HOF, R., HOF, A., CUCALA, M., SIEGRIST, S., VON RITTER, C., FISCHER, J.A. & BLUM, A.L. (1989). Effects of hCGRP I and II on gastric blood flow and acid secretion in anaesthetised rabbits. *Am. J. Physiol.*, **256**, G145–G149.

BRAIN, S.D., TIPPINS, J.R. & WILLIAMS, T.J. (1988). Endothelin induces potent microvascular constriction., *Br. J. Pharmacol.*, **95**, 1005–1007.

BRAIN, S.D., WILLIAMS, T.J., TIPPINS, J.R., MORRIS, H.R. & MACINTYRE, I. (1985). Calcitonin gene-related peptide is a potent vasodilator. *Nature*, **313**, 54–56.

CRISTOL, J.P., WARNER, T.D., THIEMERMANN, C. & VANE, J.R. (1993). Mediation via different receptors of the vasoconstrictor effects of endothelin and sarafotoxins in the systemic circulation and renal vasculature of the anaesthetized rat. *Br. J. Pharmacol.*, **108**, 776–779.

DE NUCCI, G., THOMAS, R., D'ORLEANS-JUSTE, P., ANTUNES, E., WALDER, C., WARNER, T.D. & VANE, J.R. (1988). Pressor effects of circulating endothelin are limited by its removal in the pulmonary circulation and by the release of prostacyclin and endothelin-derived relaxing factor. *Proc. Natl. Acad. Sci. U.S.A.*, **85**, 9797–9800.

DIPETTE, D.J., SCHWARZENBERGER, K., KERR, N. & HOLLAND, O.B. (1987). Systemic and regional haemodynamic effects of calcitonin gene-related peptide. *Hypertension*, **9**, Suppl. III, 142–146.

ESPLUGUES, J.V. & WHITTLE, B.J.R. (1989). Gastric damage following local intra-arterial administration of reactive oxygen metabolites in the rat. *Br. J. Pharmacol.*, **97**, 1085–1092.

ESPLUGUES, J.V. & WHITTLE, B.J.R. (1990). Morphine potentiation of ethanol-induced gastric mucosal damage in the rat. Role of local sensory afferent neurones. *Gastroenterology*, **98**, 82–89.

ESPLUGUES, J.V., WHITTLE, B.J.R. & MONCADA, S. (1989). Local opioid-sensitive afferent sensory neurones in the modulation of gastric damage induced by Paf. *Br. J. Pharmacol.*, **97**, 579–585.

GARDINER, S.M., COMPTON, A.M. & BENNETT, T. (1989). Regional haemodynamic effects of endothelin-1 in conscious, unrestrained, Wistar rats. *J. Cardiovasc. Pharmacol.*, **13**, Suppl. 5, S202–S204.

GARDINER, S.M., COMPTON, M., BENNETT, T., KEMP, P.A. & NEY, U. (1990). Synergistic internal carotid vasodilator effects of human α-calcitonin gene-related peptide and nimodipine in conscious rats. *Br. J. Pharmacol.*, **99**, 830–834.

GREEN, T. & DOCKRAY, G.J. (1988). Characterisation of the peptidergic afferent innervation of the stomach in the rat, mouse and guinea-pig. *Neuroscience*, **25**, 181–193.

GUTH, P.H., PAULSEN, G. & NAGATA, H. (1984). Histologic and microcirculatory changes in alcohol-induced gastric lesions in the rat: effect of prostaglandin cytoprotection. *Gastroenterology*, **87**, 1083–1090.

HOLZER, P. & GUTH, P.H. (1991). Neuropeptide control of rat gastric mucosal blood flow. Increase by calcitonin gene-related peptide and vasoactive intestinal polypeptide, but not substance P and neurokinin A. *Circ. Res.*, **68**, 100–105.

HOLZER, P., LIVINGSTON, E.H., SARIA, A. & GUTH, P.H. (1991). Sensory neurones mediate protective vasodilatation in rat gastric mucosa. *Am. J. Physiol.*, **260**, G363–G370.

HOLZER, P., PABST, M.A., LIPPE, I.TH., PESKAR, B.M., PESKAR, B.A., LIVINGSTON, E.H. & GUTH, P.H. (1990). Afferent nerve-mediated protection against deep mucosal damage in the rat stomach. *Gastroenterology*, **98**, 838–848.

HOLZER, P. & SAMETZ, W. (1986). Gastric mucosal protection against ulcerogenic factors in the rat mediated by capsaicin-sensitive afferent neurones. *Gastroenterology*, **91**, 975–981.

INOUE, A., YANAGISAWA, M., KIMURA, S., KASUYA, Y., MIYAUCHI, T., GOTO, K. & MASAKI, T. (1989). The human endothelin family: three structurally and pharmacologically distinct isopeptides predicted by three separate genes. *Proc. Natl. Acad. Sci. U.S.A.*, **86**, 2863–2867.

LI, D.S., RAYBOULD, H.E., QUINTERO, E. & GUTH, P.H. (1991). Role of calcitonin gene-related peptide in gastric hyperaemic response to intragastric capsaicin. *Am. J. Physiol.*, **261**, G657–G661.

LIPPE, I.T., LORBACH, M. & HOLZER, P. (1989). Close arterial infusion in calcitonin gene-related peptide into the rat stomach inhibits aspirin- and ethanol-induced hemorrhagic damage. *Regul. Pept.*, **26**, 35–46.

LOPEZ-BELMONTE, J. & WHITTLE, B.J.R. (1993). Paradoxical interactions between endothelin-1 and calcitonin gene-related peptide in the rat gastric microcirculation. *Br. J. Pharmacol.*, **108**, 113P.

MASAKI, T., KIMURA, S., YANAGISAWA, M. & GOTO, K. (1991). Molecular and cellular mechanism of endothelin regulation. Implication for vascular function. *Circulation*, **84**, 1457–1468.

PARKS, D.A., BUKLEY, G.B., GRANGER, D.N., HAMILTON, S.R. & MCCORD, J.M. (1982). Ischemic injury in the cat small intestine: role of superoxide radicals. *Gastroenterology*, **82**, 9–15.

SAKURAI, T., YANAGISAWA, M., TAKUWA, Y., MIYAZAKI, H., KIMURA, S., GOTTO, K. & MASAKI, T. (1990). Cloning of a cDNA encoding a non-isopeptide selective subtype of the endothelin receptor. *Nature*, **348**, 732–735.

SZABO, S., TRIER, J.S., BROWN, A. & SCHNOOR, J. (1985). Early vascular injury and increased vascular permeability in gastric mucosal injury caused by ethanol in the rat. *Gastroenterology*, **88**, 228–236.

SZOLCSANYI, J. & BARTHO, L. (1981). Impaired defense mechanism to peptic ulcer in the capsaicin-desensitized rat. In *Gastrointestinal Defense Mechanisms*. ed. Mozsik, G., Hanninen, O. & Javor, T. *Adv. Physiol. Sci.*, vol 29, pp. 39–51. Oxford U.K. and Budapest, Hungary: Pergamon Press and Akademiai Kiado.

TEPPERMAN, B.L. & WHITTLE, B.J.R. (1992). Endogenous nitric oxide and sensory neuropeptides interact in the modulation of the rat gastric microcirculation. *Br. J. Pharmacol.*, **105**, 171–175.

WALLACE, J.L., CIRINO, G., DE NUCCI, G., MCKNIGHT, W. & MACNAUGHTON, W.K. (1989). Endothelin has potent ulcerogenic and vasoconstrictor actions in the stomach. *Am. J. Physiol.*, **256**, G661–G666.

WHITTLE, B.J.R. & ESPLUGUES, J.V. (1988). Induction of rat gastric damage by the endothelium-derived peptide, endothelin. *Br. J. Pharmacol.*, **95**, 1011–1013.

WHITTLE, B.J.R. & LOPEZ-BELMONTE, J. (1991). Interactions between the vascular peptide endothelin-1 and sensory neuropeptides in gastric mucosal injury. *Br. J. Pharmacol.*, **102**, 950–954.

WHITTLE, B.J.R., LOPEZ-BELMONTE, J. & MONCADA, S. (1992). Nitric oxide mediates rat mucosal vasodilatation induced by intragastric capsaicin. *Eur. J. Pharmacol.*, **218**, 339–341.

WHITTLE, B.J.R., LOPEZ-BELMONTE, J. & REES, D.D. (1989a). Modulation of the vasodepressor actions of acetylcholine, bradykinin, substance P and endothelin in the rat by a specific inhibitor of nitric oxide formation. *Br. J. Pharmacol.*, **98**, 646–652.

WHITTLE, B.J.R., PAYNE, A.N. & ESPLUGUES, J.V. (1989b). Cardiopulmonary and gastric ulcerogenic actions of endothelin-1 in the guinea-pig and rat. *J. Cardiovasc. Pharmacol.*, **13**, (Suppl. 5), S103–S107.

WILLETTE, R.N., SAUERMELCH, C., EZEKIEL, M., FEUERSTEIN, G. & OHLSTEIN, E.H. (1990). Effect of endothelin on cortical microvascular perfusion in rats. *Stroke*, **21**, 451–458.

WRIGHT, C.E. & FOZARD, J.R. (1988). Regional vasodilation is a prominent feature of the haemodynamic response to endothelin in anaesthetized spontaneously hypertensive rats. *Eur. J. Pharmacol.*, **155**, 201–203.

YANAGISAWA, M., INOUE, A., ISHIKAWA, T., KASUYA, Y., KIMURA, S., KUMAGAYE, S., NAKAJIMA, K., WATANABE, T.X., SAKAKIBARA, S., GOTO, K. & MASAKI, T. (1988a). Primary structure, synthesis and biological activity of rat endothelin, an endothelium-derived vasoconstrictor peptide. *Proc. Natl. Acad. Sci. U.S.A.*, **85**, 6964–6967.

YANAGISAWA, M., KURIHARA, H., KIMURA, S., TOMOBE, Y., KOBAYASHI, M., YAZAKI, Y., GOTO, K. & MASAKI, T. (1988b). A novel potent vasoconstrictor peptide produced by vascular endothelial cells. *Nature*, **323**, 411–415.

(Received March 15, 1993
Revised May 11, 1993
Accepted May 17, 1993)

Br. J. Pharmacol. (1993), **110**, 501–505

Desensitization of the P_2-purinoceptors on the rat colon muscularis mucosae

S.M.O. Hourani, C.R. Johnson & S.J. Bailey

Receptors & Cellular Regulation Research Group, School of Biological Sciences, University of Surrey, Guildford, Surrey GU2 5XH

1 Adenosine 5'-triphosphate (ATP) and adenosine have been shown to contract the rat colon muscularis mucosae, and the receptors at which they act have been classified as P_{2Y} and A_1 respectively. Uridine 5'-triphosphate (UTP) also contracts this tissue, and desensitization was used to investigate the receptors by which it acts, in the light of recent suggestions that specific pyrimidinoceptors may exist for UTP, or that nucleotide receptors may exist which are responsive to both ATP and UTP but not to some ATP analogues such as 2-methylthioadenosine 5'-triphosphate (2-MeSATP).

2 ATP, UTP and adenosine each contracted the rat colon muscularis mucosae in a concentration-dependent manner over the concentration range 0.3–300 μM, although maximal responses to ATP and UTP were not obtained. ATP was approximately 4 times as potent as UTP and approximately equipotent with adenosine although the maximal response to adenosine appeared to be less than that to ATP or UTP.

3 Desensitization of the tissue with ATP (200 μM) given immediately before each concentration of the agonists reduced subsequent contractions induced by ATP itself and also by UTP, but did not reduce contractions induced by adenosine. Desensitization of the tissues with UTP (200 μM) also reduced contractions induced by ATP and UTP but not by adenosine, whereas desensitization with adenosine (200 μM) reduced contractions induced by adenosine itself but not by ATP or UTP.

4 Desensitization of the tissue with 2-MeSATP (200 μM), which is a more potent agonist than ATP at P_{2Y}-purinoceptors, greatly reduced the responses to ATP and to UTP, but had no effect on responses induced by adenosine. Attempts to desensitize the tissue with adenosine 5'-(α,β-methylene)triphosphonate (AMPCPP), which is a more potent agonist than ATP at P_{2X}-purinoceptors but is less potent at P_{2Y}-purinoceptors, were unsuccessful.

5 These results show that cross desensitization to ATP and UTP occurred and was specific for these agonists rather than being due to a general decrease in the ability of the muscle to contract. This implies that ATP and UTP act at the same receptor, which does not support the existence of specific pyrimidinoceptors but which could be taken as evidence for the existence of a nucleotide receptor on this tissue. However, the ability of 2-MeSATP, which is inactive at the proposed nucleotide receptors, also selectively to desensitize this receptor indicates instead that ATP and UTP are both acting at a purinoceptor of the P_{2Y} type in this tissue.

Keywords: Rat colon muscularis mucosae; purinoceptors; pyrimidinoceptors; ATP; UTP; nucleotide receptors; desensitization

Introduction

The classification of P_2-purinoceptors on smooth muscle into P_{2X}, at which adenosine 5'-triphosphate (ATP) acts to cause contraction, and P_{2Y}, at which ATP generally acts to cause relaxation, is now well accepted. These receptors are defined by the potency order of agonists, with 2-methylthioadenosine 5'-triphosphate (2-MeSATP) being more potent than ATP which is more potent than adenosine 5'-(α,β-methylene)triphosphonate (AMPCPP) at P_{2Y}-purinoceptors, while on P_{2X}-purinoceptors AMPCPP is more potent than ATP which is equipotent with 2-MeSATP (Burnstock & Kennedy, 1985; Kennedy, 1990). No selective competitive antagonists are currently available to consolidate this receptor classification, and the best available ATP antagonist, suramin, does not discriminate between P_{2X} and P_{2Y} receptors (Hoyle *et al.*, 1990). The pharmacological actions of adenine nucleotides may be complicated by their breakdown to adenosine which acts via its own receptors of which two major subclasses exist, A_1 which generally mediates contraction of smooth muscle and A_2 which mediates relaxation. The breakdown of ATP and its analogues to adenosine may reduce its potency in some tissues (Welford *et al.*, 1987), and in others may result in ATP acting largely via adenosine receptors rather than P_2-purinoceptors (Bailey & Hourani, 1992). Use of more stable analogues of ATP such as AMPCPP can help to avoid this problem, although they are not as potent as ATP at P_{2Y}-purinoceptors and may not be completely resistant to degradation in some tissues (e.g. Bailey & Hourani, 1992). An additional complication in interpreting results is that the related analogue adenylyl 5'(β,γ-methylene)diphosphonate (AMPPCP) has been shown to act apparently directly via A_1 adenosine receptors in some tissues, showing that one cannot make assumptions about the receptor selectivity of a compound on the basis of its structure (Bailey & Hourani, 1990; Hourani *et al.*, 1991; Von Kügelgen *et al.*, 1992).

Although most research has centred on the actions of adenine nucleotides, there is increasing interest in the effects of other nucleoside triphosphates, in particular the pyrimidine nucleotide uridine 5'-triphosphate (UTP). In many tissues these nucleotides are also active, but there is debate as to whether these actions are via P_{2X} and P_{2Y}-purinoceptors or some other receptor subtype. Pyrimidinoceptors, analogous to purinoceptors but responding to uracil nucleotides, have been proposed to exist largely on the basis of differences in the responses of some tissues to ATP and UTP (reviewed by Seifert & Schultz, 1989). In the absence of selective antagonists, desensitization has been used in an attempt to discriminate between receptors for ATP and for UTP, and in a number of blood vessels which contract to ATP studies of this type have been interpreted as providing some support for the existence of separate UTP receptors (Von Kügelgen *et al.*, 1987; Saïag *et al.*, 1987; 1990; Von Kügelgen & Starke, 1990). However, in other tissues, such as the mouse vas deferens,

there is cross desensitization between ATP and UTP and their contractile responses therefore appear to be mediated by a common receptor (Von Kügelgen et al., 1990). In these tissues the P_2-purinoceptor is of the P_{2X} subtype and may therefore be a receptor-operated cation channel (Benham, 1990; Kennedy, 1990), but recently there has been more interest in the effects of ATP and UTP on cells in which the receptor is linked to phospholipase C activation. These include vascular endothelial cells, which respond to ATP by releasing factors such as nitric oxide which are responsible for the relaxation by ATP of many blood vessels. Because of differences in the structure-activity relationships observed on different cells and in particular the effects of 2-MeSATP, it has been proposed that two types of receptor recognising ATP may be involved. As well as P_{2Y} purinoceptors at which the potency order is 2-MeSATP > ATP > UTP, there may be nucleotide receptors at which the potency order is ATP = UTP >> 2-MeSATP, and some cells may have a mixed population of receptors, which could result in a potency order of 2-MeSATP > ATP = UTP, with a lower maximal response being achieved by 2-MeSATP than by ATP due to the activation of both receptor types by ATP (O'Connor et al., 1991). Phospholipase C-coupled receptors at which UTP and ATP are equipotent, and which are therefore equivalent to nucleotide receptors, have also been called P_{2U}-receptors (Dubyak, 1991).

Although UTP is much less potent than ATP in the guinea-pig taenia caeci (Brown & Burnstock, 1981), which relaxes to ATP via the archetypal P_{2Y}-purinoceptors (Burnstock & Kennedy, 1985; O'Connor et al., 1991), little is known about the effects of UTP and the receptors at which it acts in other non-vascular smooth muscle preparations which contain P_{2Y}-like purinoceptors. P_{2Y}-purinoceptors mediating relaxation of smooth muscle are often resistant to desensitization (Burnstock & Kennedy, 1985), and there are also technical difficulties and problems of interpretation in working with tissues in which the tone has to be raised before addition of nucleotides for detection of relaxation responses. We have recently shown that the rat colon muscularis mucosae contracts to ATP via a P_2-purinoceptor at which the potency order of analogues was 2-MeSATP > ATP > AMPCPP, and which we therefore characterized as P_{2Y} (Bailey & Hourani, 1990). However the maximal response to 2-MeSATP was less than that to ATP, and preliminary studies indicated that UTP was also active here, so it seemed likely that this would be a suitable tissue in which to investigate the possible existence of pyrimidinoceptors or nucleotide receptors using desensitization. This tissue also contracts to adenosine via A_1 receptors (Bailey et al., 1992), so this compound was used as a control agonist to ensure that any desensitization was selective.

Methods

Normally fed Wistar Albino rats (200–250 g), University of Surrey strain, were killed by cervical dislocation. A 40 mm length of the distal colon was removed and placed in warm (32°C) Tyrode buffer of the following composition (mM): NaCl 136.9, KCl 2.8, $CaCl_2$ 1.8, $MgCl_2$ 2.1, $NaHCO_3$ 11.9, NaH_2PO_4 0.3, glucose 5.6, pregassed with 95% O_2/5% CO_2. The tissue was cleared of faecal matter and a glass pipette, external diameter 5 mm, was placed inside the colon. The outer muscularis propria was removed by gently rubbing with moist cotton wool and discarded. From the remaining thick walled tube of mucosal tissue, consisting of epithelial tissue and muscularis mucosae, a 20 mm length was suspended in Tyrode buffer in a 4 ml organ bath bubbled with 95% O_2/5% CO_2 at 32°C. Contractions were recorded isometrically at a resting tension of 1 g with a Grass FT03 transducer and displayed on a Grass 79C polygraph.

The tissues were allowed to equilibrate for 90 min with regular washes at approximately 20 min intervals, following

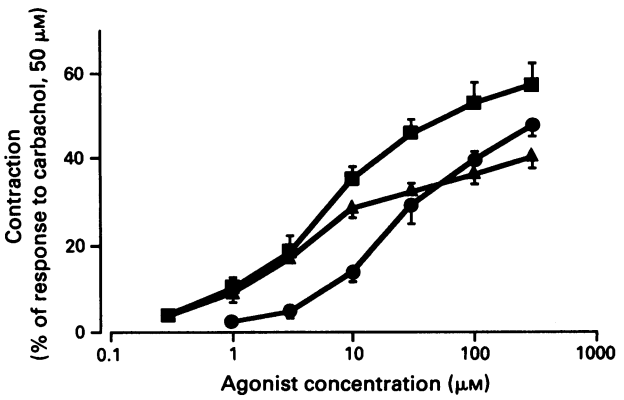

Figure 1 Contraction of the rat colon muscularis mucosae by ATP (■), UTP (●) or adenosine (▲). Each point is the mean ± s.e.mean of four determinations.

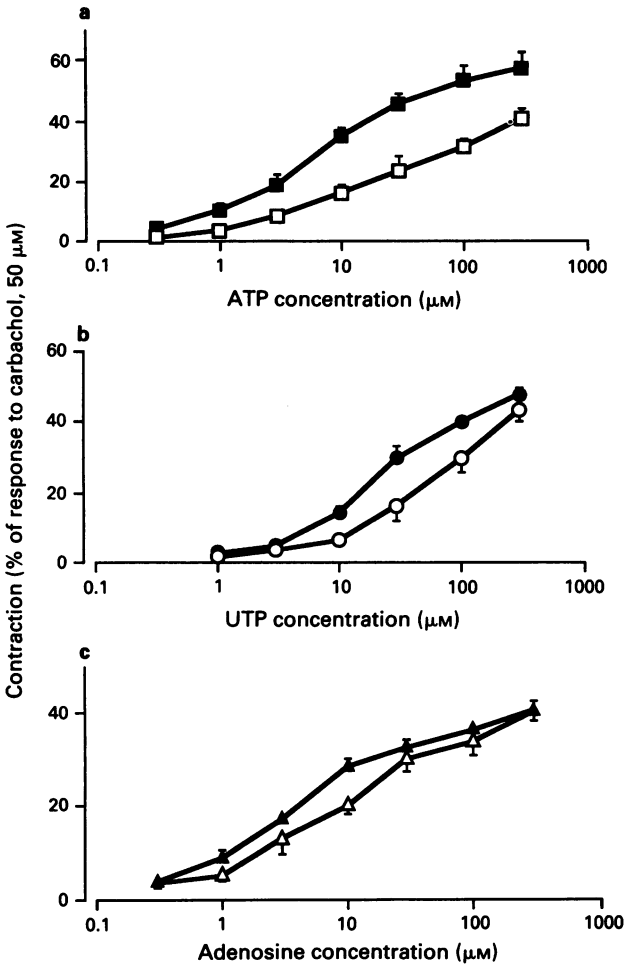

Figure 2 Contraction of the rat colon muscularis mucosae by (a) ATP, (b) UTP or (c) adenosine in the absence (closed symbols) or presence (open symbols) of desensitization by ATP (200 μM). Each point is the mean ± s.e.mean of four determinations.

which concentration-response curves to ATP, UTP or adenosine were determined with or without desensitization with ATP, UTP, adenosine, 2-MeSATP or AMPCPP. For the control concentration-response curves increasing doses of agonist were given non-cumulatively, with a contact time of approximately 1 min, a washout period of 30 s and a recovery period of 10 min for ATP and adenosine and 15 min for UTP. These recovery periods were shown in preliminary experiments to allow repeated administration of the agonists

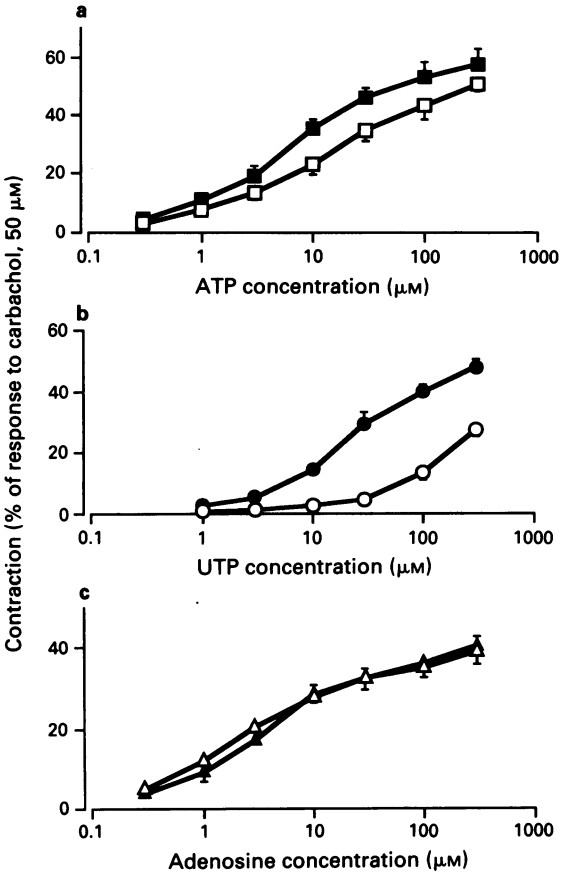

Figure 3 Contraction of the rat colon muscularis mucosae by (a) ATP, (b) UTP or (c) adenosine in the absence (closed symbols) or presence (open symbols) of desensitization by UTP (200 μM). Each point is the mean ± s.e.mean of four determinations.

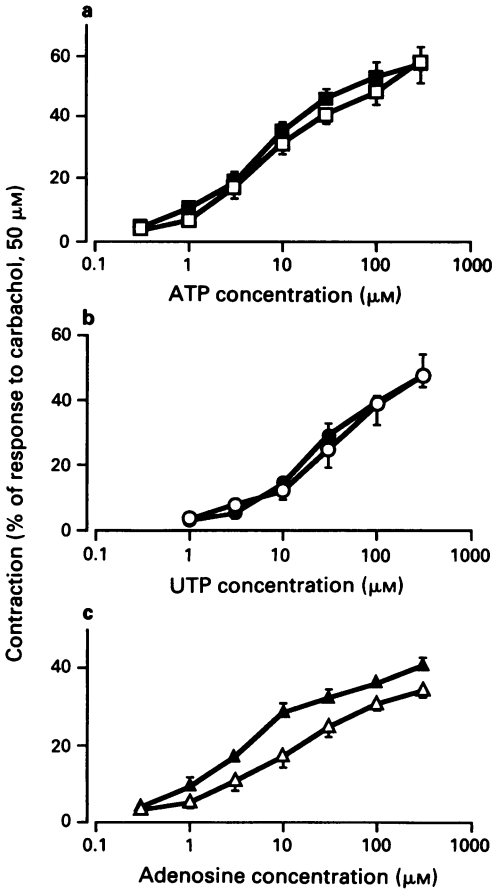

Figure 4 Contraction of the rat colon muscularis mucosae by (a) ATP, (b) UTP or (c) adenosine in the absence (closed symbols) or presence (open symbols) of desensitization by adenosine (200 μM). Each point is the mean ± s.e.mean of four determinations.

(10 μM) to be given without a decrease in the observed responses. Concentration-response curves to ATP and UTP were determined on the same tissue by applying doses of each agonist alternately, and concentration-response curves to adenosine were determined on separate tissues. Desensitization was achieved in separate experiments by applying the agonists at a concentration of 200 μM with a contact time of 5 min (4 min the case of 2-MeSATP) during which time the contraction reached a peak and declined, followed by a 30 s washout to allow the tissue to relax completely before challenging with ATP, UTP or adenosine. The desensitizing agonist was applied before each dose of the test agonists, and a recovery period of 15 min was allowed between doses. All contractions were expressed as a percentage of the contraction induced by carbachol (50 μM) applied at the end of the experiments, and results were expressed graphically as the mean and standard error of the mean (s.e.mean) of the responses obtained. EC_{50} values referred to each agonist's maximal responses could not be obtained because the concentration-response curves did not achieve a plateau. The potency of the agonists was therefore calculated as the pEC_{30} value (the negative log of the concentration required to give 30% of the maximal response to carbachol), calculated by linear regression analysis of the linear portions of the individual log concentration-response curves. The pEC_{30} values were calculated and compared in the presence and absence of desensitization using analysis of variance followed by Dunnett's one-tailed test, and EC_{30} values given in Table 1 were obtained from the mean pEC_{30} values.

Adenosine, ATP, UTP, AMPCPP and carbachol were obtained from Sigma, Poole, Dorset, 2-MeSATP from Research Biochemicals, Natick, MA (U.S.A.), and buffer salts (analytical grade) from BDH, Poole, Dorset.

Results

ATP, UTP and adenosine each contracted the rat colon muscularis mucosae in a dose-dependent manner, although maximal responses were not obtained for ATP and UTP even at a concentration of 300 μM. ATP was approximately 4 times more potent than UTP, and adenosine was of similar potency to ATP but at higher concentrations produced a smaller response than ATP (Figure 1). Pretreatment with ATP (200 μM) significantly reduced responses to ATP and to UTP, increasing the EC_{30} values for these agonists approximately 10 fold and 3 fold respectively (Figure 2a,b). Pretreatment with UTP (200 μM) also reduced responses to both ATP and UTP, increasing the EC_{30} values for these agonists 3 fold and 11 fold respectively, although this increase failed to achieve statistical significance for ATP (Figure 3a,b). Pretreatment with ATP (200 μM) caused a very small (< 2 fold) increase in the EC_{30} value to adenosine, which was not statistically significant ($P > 0.05$) (Figure 2c). Pretreatment with UTP (200 μM) did not affect the concentration-response curve to adenosine (Figure 3c). Pretreatment with adenosine (200 μM) significantly reduced responses to adenosine, increasing the EC_{30} value approximately 4 fold, but did not affect the concentration-response curve to ATP or UTP (Figure 4). Pretreatment with 2-MeSATP (200 μM) greatly reduced the response to both ATP and UTP, increasing the EC_{30} values for these agonists 38 fold and 21 fold respectively

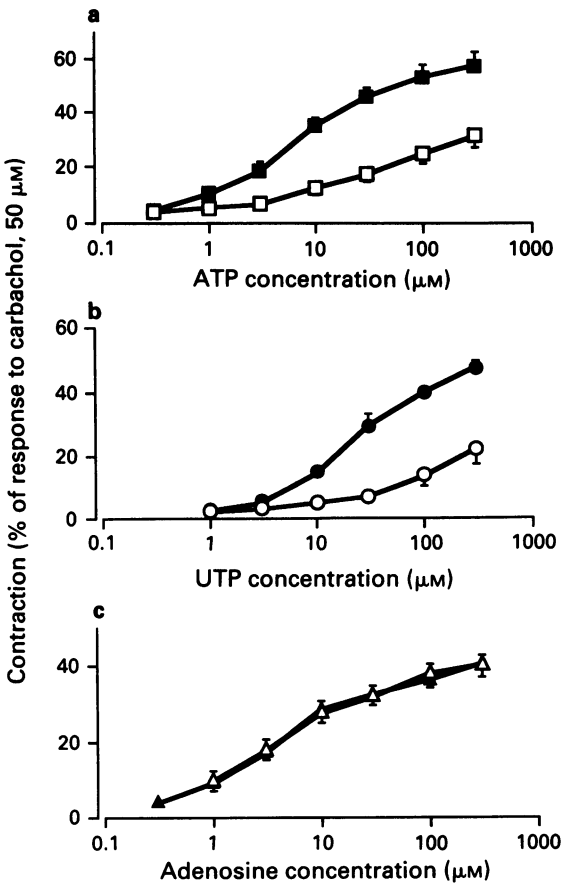

Figure 5 Contraction of the rat colon muscularis mucosae by (a) ATP, (b) UTP or (c) adenosine in the absence (closed symbols) or presence (open symbols) of desensitization by 2-methylthioadenosine 5'-triphosphate (200 μM). Each point is the mean ± s.e.mean of four determinations.

(Figure 5a,b). The responses to adenosine were not affected by pretreatment with 2-MeSATP (200 μM) (Figure 5c). Pretreatment of the tissues with AMPCPP (200 μM) did not significantly affect the concentration-response curves to any of the agonists (results not shown). EC_{30} values for ATP, UTP and adenosine in the presence and absence of desensitization are given in Table 1.

Discussion

These results show that UTP, like ATP, contracts the rat colon muscularis mucosae and is approximately 4 times less potent than ATP itself. We have previously shown that 2-MeSATP is much more potent than ATP on this tissue and had therefore characterized the receptor as a P_{2Y}-purinoceptor (Bailey & Hourani, 1990). The present study, however, indicates that UTP is somewhat more potent here than in other tissues, such as the guinea-pig taenia caeci (Brown & Burnstock, 1981) which have been classified as containing P_{2Y}-purinoceptors. In addition, 2-MeSATP does not achieve the same maximal response as ATP in this tissue (Bailey & Hourani, 1990), in contrast to the guinea-pig taenia caeci (Satchell & Maguire, 1975). In the classification of O'Connor *et al.* (1991), the rat colon muscularis mucosae could therefore contain a mixture of P_{2Y}-purinoceptors and nucleotide receptors, with 2-MeSATP acting on the former, UTP on the latter and ATP on both. Alternatively, this tissue could contain pyrimidinoceptors (see Seifert & Schultz, 1989, for review) on which only UTP acts, together with P_{2Y}-purinoceptors which respond to ATP and 2-MeSATP. In the absence of any antagonist known to be selective for any of these putative receptors we attempted to use desensitization to investigate these possibilities, in the hope that a contractile response might prove easier to manipulate in this way than the relaxations observed in most smooth muscle preparations containing receptors of this type.

Desensitization of the tissue was achieved with ATP, UTP, 2-MeSATP and adenosine, but not with AMPCPP. The failure of this agonist to cause any desensitization probably reflects its relatively low potency in this tissue (Bailey & Hourani, 1990), and is further evidence that ATP does not contract via P_{2X}-purinoceptors here as these receptors are very readily desensitized by AMPCPP (Burnstock & Kennedy, 1985). 2-MeSATP was the most effective desensitizing agonist, again probably reflecting its high potency in this tissue (Bailey & Hourani, 1990). In each case the contractile effect of the desensitizing dose of agonist used was similar except for 2-MeSATP which caused a smaller contraction than the other agonists, so the ability to cause desensitization was not simply related to the size of the contraction and therefore fatigue of the tissue. The desensitization also demonstrated some degree of receptor selectivity, as responses to ATP and UTP were not reduced by desensitization with adenosine and responses to adenosine were not decreased by desensitization with UTP or 2-MeSATP and were only slightly decreased, at low adenosine concentrations, by desensitization with ATP. As part of the desensitization protocol, ATP was left in contact with the tissues for 5 min and we have previously shown that during this time and under these conditions ATP is significantly degraded and adenosine is produced (Bailey & Hourani, 1990). Indeed use of the antagonist, suramin, revealed that contractions induced by high concentrations of ATP had a minor component which was due to interaction with A_1 receptors (Bailey *et al.*, 1992). The effect of desensitization with ATP in reducing the effects of low concentrations of adenosine is therefore most likely to be due to desensitization of the A_1 receptor by the adenosine produced.

The lack of cross-desensitization between adenosine and any of the nucleotides therefore suggested that any reduction in responses was not due to tissue fatigue, but was occurring at some process closer to the receptor interaction. However,

Table 1 Effect of desensitization by ATP, UTP, adenosine (Ado), 2-methylthioadenosine 5'-triphosphate (2-MeSATP) or adenosine 5'-(α,β-methylene)triphosphonate (AMPCPP) (200 μM) on EC_{30} values (μM) for contraction of the rat colon muscularis mucosae induced by ATP, UTP and adenosine

	Control	*Desensitizing agonist*				
		ATP	*UTP*	*Ado*	*2-MeSATP*	*AMPCPP*
ATP	7.5	77**	20	9.5	280**	10
UTP	34	110*	380**	49	710**	57
Adenosine	22	36	20	89*	20	32

Agonist EC_{30} values are calculated from pEC_{30} values which were the mean of 4 determinations.
Values significantly different from control values are indicated.
*$P<0.05$; **$P<0.01$ (Dunnett's one-tailed test).

there was cross-desensitization between ATP and UTP, which suggests that in this tissue ATP and UTP are interacting with the same receptor, and there is therefore no evidence for a separate pyrimidinoceptor. These results are comparable to those found previously in the mouse vas deferens (Von Kügelgen *et al.*, 1990) but not in a number of blood vessels (Von Kügelgen *et al.*, 1987; Saïag *et al.*, 1987; 1990; Von Kügelgen & Starke, 1990), although as mentioned in the introduction, the P_2-purinoceptor in these tissues is of the P_{2X} subtype rather that P_{2Y}. To investigate the possibility that the effects of ATP and UTP may be mediated via nucleotide receptors as proposed by O'Connor *et al.* (1991), we used 2-MeSATP which is a potent agonist at P_{2Y}-purinoceptors but is inactive at the putative nucleotide receptor. 2-MeSATP proved however to be the most effective desensitizing agonist, inhibiting not only responses to ATP but also those to UTP, which does not support the existence of nucleotide receptors.

It is of course possible that the cross-desensitization observed between the nucleotides but not with adenosine may be due to all the nucleotides causing contraction via the same second messenger pathways (e.g. phospholipase C activation), which may be different from that used by the A_1 receptor. In this case the desensitization may not be a true effect at the receptors, but may instead reflect an alteration in the function of this pathway. However, we do not know how adenosine or the nucleotides cause contraction of this tissue, or how the process of desensitization occurs and so these questions remain unanswered. With this reservation however, the results presented here do not support the existence of either pyrimidinoceptors or nucleotide receptors on the rat colon muscularis mucosae, but instead suggest that ATP, UTP and 2-MeSATP all act at the same receptor. There seems no reason at the present time to call this receptor anything other than a P_{2Y}-purinoceptor, although it may not be identical to P_{2Y}-purinoceptors found on other tissues, such as the guinea-pig taenia caeci, at which UTP is considerably less potent.

We thank the MRC for a studentship for C.R.J. and the Wellcome Trust for support for S.J.B.

References

BAILEY, S.J., HICKMAN, D. & HOURANI, S.M.O. (1992). Characterisation of the P_1-purinoceptors mediating contraction of the rat colon muscularis mucosae. *Br. J. Pharmacol.*, **105**, 400–404.

BAILEY, S.J. & HOURANI, S.M.O. (1990). A study of the purinoceptors mediating contraction in the rat colon. *Br. J. Pharmacol.*, **100**, 753–756.

BAILEY, S.J. & HOURANI, S.M.O. (1992). Effects of purines on the longitudinal muscle of the rat colon. *Br. J. Pharmacol.*, **105**, 885–892.

BENHAM, C.D. (1990). ATP-gated channels in vascular smooth muscle cells. *Ann. N. Y. Acad. Sci.*, **603**, 275–286.

BROWN, C.M. & BURNSTOCK, G. (1981). The structural conformation of the polyphosphate chain of the ATP molecule is critical for its promotion of prostaglandin biosynthesis. *Eur. J. Pharmacol.*, **69**, 81–86.

BURNSTOCK, G. & KENNEDY, C. (1985). Is there a basis for distinguishing two types of P_2-purinoceptor? *Gen. Pharmacol.*, **16**, 433–440.

DUBYAK, G.R. (1991). Signal transduction by P_2-purinergic receptors for extracellular ATP. *Am. J. Respir. Cell. Mol. Biol.*, **4**, 295–300.

HOURANI, S.M.O., BAILEY, S.J., NICHOLLS, J. & KITCHEN, I. (1991). Direct effects of adenylyl 5′-(β,γ-methylene)diphosphonate, a stable ATP analogue, on relaxant P_1-purinoceptors in smooth muscle. *Br. J. Pharmacol.*, **104**, 685–690.

HOYLE, C.H.V., KNIGHT, G.E. & BURNSTOCK, G. (1990). Suramin antagonizes responses to P_2-purinoceptor agonists and purinergic nerve stimulation in the guinea-pig urinary bladder and taenia coli. *Br. J. Pharmacol.*, **99**, 617–621.

KENNEDY, C. (1990). P_1- and P_2-purinoceptor subtypes – an update. *Arch. Int. Pharmacodyn.*, **303**, 30–50.

O'CONNOR, S.E., DAINTY, I.A. & LEFF, P. (1991). Further subclassification of ATP receptors based on agonist studies. *Trends Pharmacol. Sci.*, **12**, 137–141.

SAÏAG, B., MILON, D., ALLAIN, H., RAULT, B. & VAN DEN DRIESSCHE, J. (1990). Constriction of the smooth muscle of rat tail and femoral arteries and dog saphenous vein is induced by uridine triphosphate via 'pyrimidinoceptors', and by adenosine triphosphate via P2x purinoceptors. *Blood Vessels*, **27**, 352–364.

SAÏAG, B., MILON, D., GUELOU, M.C., VAN DEN DRIESSCHE, J. & RAULT, B. (1987). Pharmacological evidence for the existence of P2 purinoceptors different from 'pyrimidinoceptors' on arterial and venous smooth muscle. In *Abstracts of the 10th International Congress of Pharmacology, Sydney*, 1987, p959.

SATCHELL, D.G. & MAGUIRE, M.H. (1975). Inhibitory effects of adenine nucleotide analogs on the isolated guinea-pig taenia coli. *J. Pharmacol. Exp. Ther.*, **195**, 540–548.

SEIFERT, R. & SCHULTZ, G. (1989). Involvement of pyrimidinoceptors in the regulation of cell functions by uridine and by uracil nucleotides. *Trends Pharmacol. Sci.*, **10**, 365–369.

VON KÜGELGEN, I., BÜLTMAN, R. & STARKE, K. (1990). Interaction of adenine nucleotides, UTP and suramin in mouse vas deferens: suramin-sensitive and suramin-insensitive components in the contractile effect of ATP. *Naunyn-Schmied Arch. Pharmacol.*, **342**, 198–205.

VON KÜGELGEN, I., HÄUSSINGER, D. & STARKE, K. (1987). Evidence for a vasoconstriction-mediating receptor for UTP, distinct from the P_2 purinoceptor, in rabbit ear artery. *Naunyn-Schmied Arch. Pharmacol.*, **336**, 556–560.

VON KÜGELGEN, I., SPÄTH, L. & STARKE, K. (1992). Stable adenine nucleotides inhibit [^{3}H]-noradrenaline release in rabbit brain cortex slices by direct action at presynaptic adenosine A_1-receptors. *Naunyn-Schmied Arch. Pharmacol.*, **346**, 187–196.

VON KÜGELGEN, I. & STARKE, K. (1990). Evidence for separate vasoconstriction-mediating nucleotide receptors, both distinct from the P_{2X}-receptor, in rabbit basilar artery: a receptor for pyrimidine nucleotides and a receptor for purine nucleotides. *Naunyn-Schmied Arch. Pharmacol.*, **341**, 538–546.

WELFORD, L.A., CUSACK, N.J. & HOURANI, S.M.O. (1987). The structure-activity relationships of ectonucleotidases and of excitatory P_2-purinoceptors: evidence that dephosphorylation of ATP analogues reduces pharmacological potency. *Eur. J. Pharmacol.*, **141**, 123–130.

(Received April 19, 1993
Revised May 14, 1993
Accepted May 17, 1993)

British Journal of Pharmacology

VOLUME 110 (1) SEPTEMBER 1993

BRITISH JOURNAL OF PHARMACOLOGY

The *British Journal of Pharmacology* welcomes contributions in all fields of experimental pharmacology including neuroscience, biochemical, cellular and molecular pharmacology. The Board of Editors represents a wide range of expertise and ensures that well-presented work is published as promptly as possible, consistent with maintaining the overall quality of the journal.

Edited for the British Pharmacological Society by

A.T. Birmingham
(Chairman)

R.W. Horton **W.A. Large**
(Secretaries)

Submission of manuscripts: Manuscripts (two copies) should be sent to The Editorial Office, British Journal of Pharmacology, St. George's Hospital Medical School, Cranmer Terrace, London SW17 0RE.

Authors should consult the Instructions to Authors and the Nomenclature Guidelines for Authors in Vol. **108,** 275–284. These Instructions and Guidelines also appear with the journal Index for Volumes 105–107, 1992. A checklist of the essential requirements is summarised in each issue of the journal on the inside of the back cover.

The *British Journal of Pharmacology* is published monthly by the Scientific & Medical Division, Macmillan Press Ltd.

The journal is covered by *Current Contents*, *Excerpta Medica* and *Index Medicus*.

All business correspondence and reprint requests should be addressed to the Scientific & Medical Division, Macmillan Press Ltd., Houndmills, Basingstoke, Hampshire RG21 2XS, UK. Telephone: (0256) 29242; Fax: (0256) 810526.

Enquiries concerning advertising space or rates should be addressed to: Michael Rowley, Advertisement Manager, Macmillan Press Ltd., 4 Little Essex Street, London WC2R 3LF. Telephone: 071 836 6633; Fax: 071 379 0820.

Annual subscription prices for 1993 EC £455, elsewhere £499/US$923 (sterling rate is definitive). Orders must be accompanied by remittance. Cheques should be made payable to Macmillan Press, and sent to: Macmillan Press Ltd., Subscription Department, Brunel Road, Houndmills, Basingstoke, Hampshire RG21 2XS, UK.
Overseas subscribers may make payments into UK Post Office Giro Account No. 5192455. Full details must accompany the payment.

British Journal of Pharmacology (ISSN 0007–1188) is published monthly by Macmillan Publishers Ltd, c/o Mercury Airfreight International Ltd, 2323 Randolph Avenue, Avenel, NJ 07001, USA. Subscription price is $923.00 per annum. 2nd class postage is paid at Rahway NJ. *Postmaster*: send address corrections to Macmillan Publishers, c/o Mercury Airfreight International Ltd, 2323 Randolph Avenue, Avenel NJ 07001.

ISSN 0007–1188
0007–1188/93 $9.00 + $0.00

PREPARATION OF MANUSCRIPTS

Authors are strongly recommended to read the full *Instructions to Authors* and *Nomenclature Guidelines for Authors* (*Br. J. Pharmacol.* 1993, **108**, 275–284) before submitting a manuscript for publication in the *British Journal of Pharmacology*. The manuscript and cover letter should be checked against the following list before mailing.

The original and one copy of the manuscript must be supplied. Manuscripts must be typed in double-line spacing on one side of A4 paper, in type not smaller than 12 characters per inch or 10 point. Both copies to include Tables and a set of labelled Figures. One set of Figures without numbers or letters is also to be included. The text to be arranged in the following subsections:

1. **Title**—To have no more than 150 characters on a separate page, which should also include a Short Title (50 characters maximum) and the name and address of the author for correspondence.
2. **Summary**—To be arranged in numbered paragraphs (Full Papers) or a single paragraph (Special Reports).
   —to include aims, principal results and conclusions.
   —to include Key words (10 maximum) at end of summary.
3. **Introduction**—To contain concise statements of the problem and the aims of the investigation.
4. **Methods**—To have brief but adequate account of the procedures; *full names of drugs* (*including those referred to by manufacturer's code*), sources of drugs and statistical tests to be stated.
5. **Results**—To have no repetition of data in Figures, Tables and text.
6. **Discussion**—Findings and conclusions to be placed in context of other relevant work.
   NB Simple repetition of results and unwarranted speculation are not acceptable.
7. **Acknowledgments**—Sources of support. Sources of drugs not widely available commercially.
8. **References**—All references in the text to be included in the Reference List and *vice versa*. References in alphabetical order with complete citations; Journals publishing 'in press' papers identified.
   References to manuscripts submitted to other journals but not yet accepted are not allowed.
9. **Tables**—Each on a separate page and prepared in accordance with current requirements of the Journal.
10. **Figures**—Both labelled and non-labelled Figures to be prepared in accordance with current requirements of the Journal (see *Instructions to Authors*, 1993, **108**, 275–281) and provided with Figure Number and Authors' names on back (*in pencil*).
    —each legend to be typed on a separate page and carrying keys to symbols.
    —keys to symbols and histograms must not appear on the figures themselves, but in the respective legends.
    —'box style' figures are not in keeping with the Journal style; line drawings etc must have only left-hand and bottom axes.
11. **Manuscripts**—To be accompanied by a declaration signed by each author that
    (a) results are original
    (b) approval of all persons concerned has been given to submit manuscripts for consideration (see also 12b)
    (c) the same material is neither 'in press' (i.e. is in proof or has definitely been accepted for publication) nor under consideration elsewhere. Furthermore it will not be submitted or published elsewhere before a decision has been reached by the Editorial Board of the *British Journal of Pharmacology* and will not be submitted elsewhere if accepted by the *British Journal of Pharmacology*.
    (d) Copyright assignment is included.
12. **Cover letter**—To state clearly
    (a) Corresponding author's full postal address, telephone, telex or Fax number
    (b) where appropriate, that *either* ethical approval has been given for investigation *or* Company or Institutional permission to publish work has been received.
13. **Reminder**—Packaging to be sufficiently robust to protect Figures and to withstand mailing.

Failure to comply with *Instructions to Authors* may lead to substantial delays in processing, review and publication and may even jeopardize acceptance of the manuscript.

NOMENCLATURE

Authors are reminded that accepted receptor and associated terminology is laid out in *Nomenclature Guidelines for Authors*, as published in the *British Journal of Pharmacology, Br. J. Pharmacol.*, 1993, **108**, 282–284.

SPECIAL REPORTS

The purpose of *Special Reports* is to provide rapid publication for **new** and **important** results which the Editorial Board considers are likely to be of special pharmacological significance. *Special Reports* will have publication priority over all other material and so authors are asked to consider carefully the status of their work before submission.

In order to speed publication there is normally no revision allowed beyond very minor typographical or grammatical corrections. If significant revision is required, the Board may either invite rapid re-submission or, more probably, propose that it be re-written as a Full Paper and be re-submitted for consideration. In order to reduce delays, proofs of *Special Reports* will be sent to authors but **essential corrections must reach the Production Office within 48 hours of receipt.** Authors should ensure that their submitted material conforms exactly to the following requirements.

Special Reports should normally occupy no more than two printed pages of the Journal; two illustrations (Figures or Tables, with legends) are permitted. As a guideline, with type face of 12 pitch and double-line spacing, a page of A4 paper could contain about 400 words. The absolute maximum length of the *Special Report* is 1700 words. For each Figure or Table, please deduct 200 words. The manuscript should comprise a Title page with key words (maximum of 10), a Summary consisting of a single short paragraph, followed by Introduction, Methods, Results, Discussion and References (maximum of 10). In all other respects, the requirements are the same as for Full Papers (see current 'Instructions to Authors').

BRITISH JOURNAL OF PHARMACOLOGY VOLUME 110 (1) 1993

Contents continue inside back cover

Typeset by Elite Typesetting Techniques, Southampton, Hampshire
and printed in Great Britain by Unwin Brothers Ltd., The Gresham Press, Old Woking, Surrey

See last page of issue for PREPARATION OF MANUSCRIPTS